35th ASMS Conference on Mass Spectrometry and Allied Topics

May 24 - 29, 1987
Denver, Colorado

35TH ASMS CONFERENCE ON MASS SPECTROMETRY AND ALLIED TOPICS
MAY 24-29, 1987

TABLE OF CONTENTS

INTRODUCTION v

CORPORATE MEMBERS vi

ASMS BOARD OF DIRECTORS viii

ASMS PAST OFFICERS ix

MEMORIAL PAGE x

35TH ASMS CONFERENCE ON MASS SPECTROMETRY & ALLIED TOPICS

LISTING OF EXTENDED ABSTRACTS xi

MONDAY ORAL SESSIONS
Pharmacology and Drug Metabolism 1
Ionization Methods 21
Symposium: Lasers & Mass Spectrometry II 43
Symposium: An Overview of State-of-the-Art Research 58
High Molecular Weight Biomolecules 64
Symposium: Lasers & Mass Spectrometry, Con't 84

MONDAY POSTER SESSIONS
Environmental/ Polymers 100
Ion Activation & Dissociation/Instrumentation 183

TUESDAY ORAL SESSIONS
Symposium: Dynamics in Biological Systems 267
Instrumentation: New Concepts 275
Desorption and Ionization Methods 300
Symposium: Structural Utility of Negative Ions ... 323
Ion Molecule Reactions 331
Symposium: Dynamics of Ion Processes 347

TUESDAY POSTER SESSIONS
Computational Techniques/LCMS Instrumentation 357
Pharmacology/Drug Metabolism & Natural Products ... 445
Peptides/Ion Molecule Reactions/Fragmentation Mechanisms 538

WEDNESDAY ORAL SESSIONS
LC/MS Applications 634
Symposium: Applications of FTMS to Real Problems . 656
Symposium: Dynamics of Ion Processes, con't 666

WEDNESDAY POSTER SESSION
Metabolism and Toxicology/Ionization Methods 674

THURSDAY ORAL SESSIONS
Feature Lecture: Assessment of the Rise of Environmental Pollutants 759
Symposium: Analytical Epidemiology - Carcinogen Dosimetry in Humans 761
Ion Traps: Instrumentation 767
Collisional Processes & Ion Molecule Reactions 791
Environmental Applications 807
Symposium: Fragmentation of Very Large Molecules . 827
Reaction Mechanisms 836

THURSDAY POSTER SESSIONS
Sugars and Nucleic Acids/Inorganic 856
Biochemical Applications/Fuels and Geoscience/ Inorganic 940

FRIDAY ORAL SESSIONS
Metabolism and Toxicology 1016
Activation and Dissociation of Organic Ions 1036
Symposium: Novel MS for Fuel and Complex Mixture Analysis 1062

FRIDAY POSTER SESSION
LCMS Applications/Instrumentation: ICR et al. ... 1070

INDEX OF AUTHORS 1155

WORKSHOP REPORTS
Chemometrics for Everyone 1171
Applications of MS/MS to Environmental Problems .. 1172
Computerized Ion Optic Design Made Easy 1173
Ionic Clusters: Methods of Generation and Reactions 1174
MS/MS CAD Database: Instrument Design and Operation Apposite to CAD Dynamics 1175
New Techniques for Desorption Ionization of Liquid Samples 1177
Problems in Applications of RIMS to Isotope Ratio Measurements 1178

INTEREST GROUP REPORTS
Biomedical Applications 1179
Computer Applications 1180
Environmental Applications 1181
Fundamentals 1182
Isotope Ratio Measurements 1183
Qualitative Organic Analysis 1184
Quantitative Organic Analysis 1185
Solids and Surface Analysis 1186
Young Mass Spectrometrists 1187

EDUCATION COMMITTEE REPORT 1188

MINUTES OF THE ASMS BUSINESS MEETING 1190

ASMS CONSTITUTION AND BY-LAWS 1192

METASTABLE TABERNACLE CHOIR 1198

1987 ASMS MEMBERS AND/OR CONFERENCE PARTICIPANTS
U.S.A. 1199
Canada 1275
Foreign 1279

INTRODUCTION

This bound volume is the official record of the 35th ASMS Conference on Mass Spectrometry and Allied Topics held in Denver, Colorado, May 24-29, 1987. The extended abstracts provide a timely view of research and innovations in mass spectrometry and a historical record. In the back of this volume are workshop and interest group reports and a directory of names, addresses and telephone numbers of members and conference attendees. The value of this record is a reflection of the care taken by each contributor in preparing the manuscripts and reports, and in meeting the publication deadline.

The efforts of Judith A. Watson of Professional Association Management in compiling the bound volume and arranging for timely printing and distribution in a cost effective manner are gratefully acknowledged. This volume also reflects the dedication of Ronald A. Hites, the Vice President for Programs, in arranging the technical program.

It is the desire of the Board of Directors of ASMS that the Bound Volume be a valuable asset to the members of this Society. Comments or suggestions directed toward making this a more useful resource are appreciated.

Charles N. McEwen
Editor and Member-at-Large
ASMS Board of Directors

CITATION NOTICE

This volume contains the abstracts of papers presented at the 35th ASMS Conference on Mass Spectrometry and Allied Topics. This volume is intended to be distributed only to members of ASMS and conference registrants; therefore, it is not considered to be a publication. The appearance of material in this volume should not jeopardize the author's right to publish the information in scientific journals.

Reference to individual abstracts contained in this volume should be cited as follows:

Author(s); title; Presented at the 35th ASMS Conference on Mass Spectrometry and Allied Topics, Denver, Colorado, May 24-29, 1987.

ASMS GRATEFULLY ACKNOWLEDGES THE SUPPORT OF THE CORPORATE MEMBERS LISTED HERE

BALZERS
8 SAGAMORE PK RD
HUDSON NH 03051
PHONE: 603/889-6888

CAMBRIDGE ISOTOPE LABS
20 COMMERCE WAY
WOBURN MA 01801
PHONE: 617/938-0067

DETECTOR TECHNOLOGY INC
PO BOX K-300
BROOKFIELD MA 01506
PHONE: 617/867-7156

FINNIGAN MAT
355 RIVER OAKS PKWY
SAN JOSE CA 95134
PHONE: 408/946-4848

HEWLETT-PACKARD
1601 CALIFORNIA AVE
PALO ALTO CA 94304
PHONE: 415/857-6090

IONSPEC
ONE LONGSTREET
IRVINE CA 92714
PHONE: 714/857-0793

JOHN WILEY & SONS
605 THIRD AVE
NEW YORK NY 10158
PHONE: 212/850-6518

M-SCAN LTD
SILWOOD PARK
BERKSHIRE SL5 7
PHONE: 302 453 8151

NERMAG
10 KINGSBRIDGE ROAD
FAIRFIELD NJ 07006
PHONE: 201/227-7690

NUCLIDE CORPORATION
642 E COLLEGE AVE
STATE COLLEGE PA 16801
PHONE: 814/238-0541

PERNICKA CORPORATION
112 RACQUETTE DR
FORT COLLINS CO 80524
PHONE: 303/224 0220

R J BRUNFELDT CO
PO BOX 2066
BARTLESVILLE OK 74005
PHONE: 918/336-4467

BIO-ION
PO BOX 15045
UPPSALA S-75215
PHONE: 018-104440

COLORADO GROUP
6385 W 52ND ST #5
ARVADA CO 80002
PHONE: 303/278-9521

EXTREL
250 ALPHA DRIVE
PITTSBURGH PA 15238
PHONE: 412/782-3884

GALILEO ELECTRO-OPTICS
GALILEO PARK
STURBRIDGE MA 01518
PHONE: 617/347-9191

INFICON LEYBOLD-HERAEUS
6500 FLY ROAD
E SYRACUSE NY 13057
PHONE: 315/437-0377

JEOL LTD USA
11 DEARBORN ROAD
PEABODY MA 01960
PHONE: 617/535-5900

KRATOS ANALYTICAL
535 E CRESCENT AVE
RAMSEY NJ 07446
PHONE: 201/934-9000

MSD ISOTOPES
PO BOX 899
QUEBEC H9R 4P7
PHONE: 514/697-2823

NICOLET INSTRUMENT
5225 VERONA RD
MADISON WI 53711
PHONE: 606/271-3333

ONEIDA RESEARCH
ONE HALSEY ROAD
WHITESBORO NY 13492
PHONE: 315/736-3050

PHRASOR SCIENTIFIC
1536 HIGHLAND AVE
DUARTE CA 91010
PHONE: 213/357-3201

SCIENTIFIC GLASS ENGIN
2007 KRAMER LANE
AUSTIN TX 78758
PHONE: 512/837-7190

SCIEX INC
55 GLENCAMERON RD
THORNHILL ONTA L3T 1P2
PHONE: 416/881-4646

SHRADER ANALYTICAL LAB
3814 VINEWOOD
DETROIT MI 48208
PHONE: 313/894-4440

TEKNIVENT CORPORATION
11684 LILBURN PK DR
ST LOUIS MO 63146
PHONE: 314/994-0500

TOFTEC
PO BOX 12877
GAINESVILLE FL 32604
PHONE: 904/472-2668

VESTEC CORP
9299 KIRBY DRIVE
HOUSTON TX 77054
PHONE: 713/521-2599

UTI INSTRUMENTS CO
497 S HILLVIEW DR
MILPITAS CA 95035
PHONE: 408 945 1955

TRACER TECHNOLOGIES
20 ASSEMBLY SQ DRIVE
SOMMERVILLE MA 02145
PHONE:

MASSTRON
6595 ODELL PLACE
BOULDER CO 80301
PHONE: 303/530-7778

WATERS CHROMATOGRAPHY
34 MAPLE STREET
MILFORD MA 01757
PHONE: 617/478-2000

SHIMADZU SCIENTIFIC INSTR
7102 RIVERWOOD DR
COLUMBIA MD 21046
PHONE: 301/997-1227

SPECTROSPIN AG
INDUSTRIESTRASSE 26
CH-8117 FAELLAN
PHONE: 01/825 48 55

TMS ANAL SERVICES
6376 MORENCI TRAIL
INDIANAPOLIS IN 46268
PHONE:

VACUMETRICS
2261 PALMA DRIVE
VENTURA CA 93003
PHONE: 805/644-7461

VG INSTRUMENTS INC
32 COMMERCE CTR
DANVERS MA 01923
PHONE: 203/322-4546

LINDEN-CHROMASSPEC
PO BOX 3451
PRINCETON NJ 08542
PHONE: 609 452 1451

EVENTIDE INC
ONE ALSAN WAY
LITTLE FERRY NJ 47643
PHONE: 201/641-1200

HEYDEN & SON LTD
SPECTRUM HOUSE
LONDON NW4 2JQ
PHONE:

BRUKER INSTRUMENTS
MANNING PARK
BILLERICA MA 01821
PHONE:

AMERICAN SOCIETY FOR MASS SPECTROMETRY
BOARD OF DIRECTORS
1986 - 1987

PRESIDENT	Gerry G. Meisels College of Arts & Sciences 1223 Old Father Hall University of Nebraska Lincoln, NE 68588
VICE-PRESIDENT FOR PROGRAMS	Ronald A. Hites SPEA 410 H Indiana University Bloomington, IN 47405
VICE-PRESIDENT for ARRANGEMENT	Catherine E. Costello Massachusetts Institute of Technology Department of Chemistry Cambridge, MA 02139
SECRETARY	Robert T. McIver, Jr. Department of Chemistry University of California Irvine, CA 92717
TREASURER	Kelsey D. Cook Department of Chemistry University of Tennessee Knoxville, TN 37996
MEMBER at LARGE	Charles N. McEwen E. I. du Pont de Nemours Experimental Station 228 Wilmington, DE 19898
MEMBER at LARGE	Christie G. Enke Department of Chemistry Michigan State University East Lansing, MI 48824
ASTM REPRESENTATIVE	Terrence R. Ashe ESSO Petroleum Post Office Box 3022 Sarnia, Ontario N7T 7M1
PAST PRESIDENT	R. Graham Cooks Department of Chemistry Purdue University West Lafayette, IN 47907
SOCIETY OFFICE	ASMS Post Office Box 1508 East Lansing, MI 48826
Telephone:	517/337-2548

ASMS PAST OFFICERS

YEAR	PRESIDENT	V P PROGRAMS	V P ARRANGEMENTS
1970	J.L. Franklin	R.E. Honig	C.E. Johannsen
1971-2	R.E. Honig	F.H. Field	G.L. Kearns
1972-4	F.H. Field	H.J. Svec	A.H. Struck
1974-6	H.J. Svec	J.H. Futrell	W.H. Brubaker
1976-8	J.H. Futrell	J.A. McCloskey	E.J. Bonelli
1978-9	J.A.McCloskey	B. Munson	E.J. Bonelli
1979-80	" "	" "	W.A. Wolstenholme
1980-1	B. Munson	C.C. Fenselau	" "
1981-2	" "	" "	K.R. Compson
1982-3	C.C. Fenselau	R.G. Cooks	" "
1983-4	" "	" "	M. Grayson
1984-5	R.G. Cooks	G.G. Meisels	" "
1985-6	" "	" "	C.E. Costello
1986-7	G.G. Meisels	R.A. Hites	" "

YEAR	SECTRETARY	TREASURER	MEMBERS-AT-LARGE
1970	J.M. McCrea	H.D. Cook	*H.R. Harless, R.F. Porter, J.T. Herron
1971-2	F.E. Saalfeld	" "	A.G. Sharkey, A.L. Wahrhaftig, *H.R. Harless
1972-4	" "	M.T. Laug	*E. Lumpkin, E.B. Owens, J. Berkowitz
1974-6	J.A. McCloskey	" "	*E.M. Emery, P. Kebarle, J.L. Margrave
1976-7	K.E. McCulloh	" "	H.M. Fales, A.G. Harrison
1977-8	H.M. Fales	M.A. Frisch	*E.G. Carlson A.G. Harrison
1978-9	" "	" "	*M.C. Hamming, C.C. Fenselau, A.G. Harrison
1979-80	" "	" "	*M.C. Hamming, W.L. Fite C.C. Fenselau
1980-1	" "	" "	*M.C. Hamming, W.L. Fite J.T. Watson
1981-2	T.R. Ashe	" "	*T.Aczel, F.W. Lampe, J.T. Watson
1982-3	" "	J. DeCorpo	*T. Aczel, F.W. Lampe, M. Vestal
1983-4	H.S. Hertz	" "	*E. Emery, M. Vestal, R.E. Finnigan
1984-5	" "	" "	*E. Emery, G.W. Wood, R.E. Finnigan
1985-6	R.T. McIver	" "	*T.R. Ashe, G.W. Wood, C.N. McEwen
1986-7	" "	K.D. Cook	*T.R. Ashe, C. Enke, C.N. McEwen

MONDAY ORAL SESSIONS

PHARMACOLOGY AND DRUG METABOLISM

FABMS AND MS/MS ANALYSES OF GLYCOSIDIC TRITERPENES FROM CHINESE MEDICINES 1
*COSTELLO, C E,DOMON, B,ZENG, C-H,DU, S,QIAN, F AND LI, M

THE CHARACTERISATION OF THE TYROTHRICIN COMPLEX BY FAB/MS/MS 3
*BARBER, M,TETLER, L,BYCROFT, B,MONAGHAN, J J AND GREEN B N

METABOLISM OF LEUKOTRIENE E4 IN THE ISOLATED RAT HEPATOCYTE 5
*STENE, D O AND MURPHY, R C

MEASUREMENT OF URINARY 6-KETO-PROTAGLANDIN F1 (6KPGF1) BY GAS CHROMATOGRAPHY TANDEM MASS SPECTROMETRY FOLLOWING PURIFICATION BY IMMUNOAFFINITY CHROMATOGRAPHY 7
*VRBANAC, J J AND KNAPP, D R

GC/MS-MS OF PROSTAGLANDINS--THE ION TRAP VS A SECTOR INSTRUMENT OF BE GEOMETRY 9
*STRIFE, R J,KELLEY, P E AND WEBER-GRABAU, M

BILIARY METABOLITES OF N-FORMYL-N, -DIMETHYL- -PHENYLBENZENEPROPANAMINE IN RATS 11
*SLATTER, J G,ABBOTT, F S AND BURTON, R

A NEW CI-GC-MS METHOD TO MEASURE IMIDAZOLE-ACETIC ACID, A HISTAMINE METABOLITE 13
*KHANDELWAL, J K,PRELL, G D AND GREEN, J P

DETERMINATION OF ANABOLIC STEROIDS BY API SFC/MS AND SFC/MS/MS 15

USING PACKED-COLUMNS
*HENION, J,WEIDOLF, L AND LEE, E D

COMPARISON OF HYPOTHALAMUS-PITUITARY-ADRENAL AXIS SUPRESSION FROM TOPICAL STEROIDS BY STANDARD ENDOCRINE FUNCTION TESTING AND GAS CHROMATOGRAPHY MASS SPECTROMETRY 17
*FENNESSEY, P V,WESTON, W L,PIKE, A W AND GOTLIN, R W

APPLICATIONS OF CHROMATOGRAPHY/SIMS 19
*STANLEY, M S,DOHERTY, S J,DUFFIN, K L AND BUSCH, K L

IONIZATION METHODS

AN EXTERNAL FIELD DESORPTION ION SOURCE FOR ANALYTICAL ION CYCLOTRON RESONANCE SPECTROMETRY 21
LINDEN, H B,KNOLL, H AND *WANCZEK, K P

MECHANISMS OF LASER DESORPTION AS STUDIED BY FOURIER TRANSFORM MASS SPECTROMETRY 23
*CHIARELLI, M P

NEGATIVE ION CI STUDIES OF NITROGEN-SUBSTITUTED AROMATICS BY GC/MS AND FTMS 25
*BUCHANAN, M V AND RUBIN, I B

SURFACE IONIZATION ORGANIC MASS SPECTROMETRY; II. N-CONTAINING CYCLIC ORGANICS 27
*FUJII, T AND JIMBA, H

CHARACTERIZATION OF MIXTURES OF ORGANIC ACIDS BY GLOW-DISCHARGE IONIZATION THERMOSPRAY LC-MS 29
*BENCSATH, F A AND FIELD, F H

DOES THE CHARGING OF A DROPLET ALTER ITS VAPOR PRESSURE? APPLICATIONS TO THERMOSPRAY 31
*ROCKWOOD, A L AND KATTA, V

MULTIPLE CHARGING IN ELECTROSPRAY IONIZATION OF POLYETHYLENE GLYCOLS 33
MENG, C K,WONG, S F AND *FENN, J B

HIGH MASS ION PRODUCTION USING ELECTROHYDRODYNAMIC IONIZATION 35
*LEE, T D,LEGGESSE, K,MAHONEY, J F AND PEREL, J

THERMODYNAMIC AND KINETIC CONTROL OF ION INTENSITIES IN ATMOSPHERIC PRESSURE IONIZATION MASS SPECTROMETRY 37
*SUNNER, J,IKONOMOU, M AND KEBARLE, P

A STUDY OF INVOLATILE AND THERMALLY LABILE MOLECULES BY SPONTANEOUS DESORPTION MASS SPECTROMETRY (SDMS) 39
*SALEHPOUR, M AND HUNT, J E

FAST HEAVY ION INDUCED DESORPTION MASS SPECTROSCOPY STUDY OF LANGMUIR-BLODGETT FILMS 41
*SAVE, G,HAKANSSON, P,SUNDQVIST, B,SODERSTROM, E, LINDQUIST, S-E,BERG, J AND JOHNSON, R E

SYMPOSIUM: LASERS & MASS SPECTROMETRY

INFRARED MULTIPHOTON DISSOCIATION OF GASEOUS IONS 43
*EYLER, J R

PHOTODISSOCIATION STUDIES OF ION SPECTROSCOPY AND STRUCTURE 44
*DUNBAR, R C

HIGH-RESOLUTION LASER PHOTOFRAGMENT SPECTROSCOPY OF SMALL MOLECULAR IONS 46
*SARRE, P J

THE TIME EVOLUTION OF THE MASS SPECTRA AND THE DYNAMICS OF PICOSECOND-LASER MULTIPHOTON IONIZATION-DISSOCIATION 48
*EL-SAYED, M A

NON-RESONANT MULTIPHOTON IONIZATION AND FRAGMENTATION PATTERNS OF SELECTED LOW-MASS HYDROCARBONS 50
*MARTIN, W B AND O'MALLEY, R M

QUANTIFICATION OF PULSED ION CURRENTS PRODUCED IN RESONANCE IONIZATION MASS SPECTROMETRY (RIMS) 52
*FASSETT, J D,WALKER, R J,TRAVIS, J C AND RUEGG, F C

LASER PHOTODISSOCIATION IN A TANDEM QUADRUPOLE FOURIER TRANSFORM MASS SPECTROMETER 54
*SHABANOWITZ, J,HUNT, D F,HAUER, C R AND BRINEGAR, C

SUPERCRITICAL FLUID INJECTION OF SMALL POLAR MOLECULES USING DERIVATIZATION WITH DETECTION BY RESONANT TWO-PHOTON IONIZATION IN SUPERSONIC BEAM-MS 56
*LUBMAN, D M,SIN, C H AND PANG, H M

SYMPOSIUM: AN OVERVIEW OF STATEOF-THE-ART RESEARCH

FUNDAMENTALS - MOLECULAR DYNAMICS 58
*FUTRELL, J H

MASS SPECTROMETRY AND THE LIPID MEDIATOR NETWORK HYPOTHESIS 60
*MURPHY, R C

ISOTOPE RATIO MASS SPECTROMETRY AND YOUR DIET 62
*SCHOELLER, D A,LEITCH, C A AND TAYLOR, P

HIGH MOLECULAR WEIGHT BIOMOLECULES

MECHANISM OF DESORPTION OF INTACT LARGE BIOMOLECULES BY IMPACT OF HIGHLY-IONIZING PARTICLES 64
*WILLIAMS, P AND SUNDQVIST, B

LSIMS ANALYSIS OF TRYPSINIZED CYTOCHROME B5 (MR 10,000) AND ANALOGS WITH AN ARRAY DETECTOR 66
*GIBSON, B W,WALLS, F,COTTRELL, J,WASKELL, L AND LIPKA, J

CLOSING THE GAP BETWEEN keV AND FISSION FRAGMENT SECONDARY ION YIELDS WITH NITROCELLULOSE 68
*LAFORTUNE, F,BEAVIS, R,ENS, W,STANDING, K G AND TANG, X

THE IDENTIFICATION AND CHARACTERIZATION OF NUCLEOTIDES BY LASER IONIZATION FOURIER TRANSFORM MASS SPECTROMETRY 70
*HETTICH, R L AND BUCHANAN, M V

ANALYSIS OF OLIGOSACCHARIDES BY PLASMA DESORPTION MASS SPECTROMETRY 72
*JARDINE, I,SCANLAN, G S,MCNEIL, M,BRENNAN, P J AND LINHARDT, R J

PLASMA-DESORPTION ANALYSIS OF PROTEOLYTIC GLYCOPEPTIDES FROM BOVINE FETUIN TO ELUCIDATE GLYCOSYLATION-SITE MICROHETEROGENEITY 74
*ALAI, M,FENESELAU, C,HARDY, M,LEE, Y C AND TOWNSEND, R R

PROTEIN SEQUENCING BY TANDEM MASS SPECTROMETRY 76
*YATES, J R,HUNT, D F AND SHABANOWITZ, J

RESOLUTION REQUIREMENTS IN THE OPERATION OF A HIGH PERFORMANCE TANDEM MASS SPECTROMETER 78
MARTIN, S A,SCOBLE, H A,COSTELLO, C E AND *BIEMANN, K

PEPTIDE AND PROTEIN MAPPING BY 252Cf-PLASMA DESORPTION MASS SPECTROMETRY 80
*TSARBOPOULOS, A AND JARDINE, I

ADVANTAGES FOR COLLISIONALLY ACTIVATING METAL ION CATIONIZED OLIGONUCLEOTIDES AND PEPTIDES 82
*CERNY, R L AND GROSS, M L

SYMPOSIUM: LASERS AND MASS SPECTROMETRY, con't

STUDIES OF HYPERVALENT RADICALS BY NEUTRALIZATION REIONIZATION MASS SPECTROMETRY 84
SELGREN, S F AND *GELLENE, G I

FORMATION OF LARGE CLUSTER IONS IN FTMS BY DIRECT LASER VAPORIZATION 86
*MCELVANY, S W,NELSON, H H,ROSS, M M AND BARONAVSKI, A P

THE PHYSICS AND CHEMISTRY OF LASER DESORPTION AND ITS APPLICATION TO MASS SPECTROMETRIC ANALYSIS 88
*HILLENKAMP, F,KARAS, M,BAHR, U AND SPENGLER, B

TIME RESOLVED STUDIES OF MOLECULAR ANIONS PRODUCED BY CO2 LASER DESORPTION MASS SPECTROMETRY 90
*DEMIREV, P,OLTHOFF, J K AND COTTER, R J

DETECTION OF NONVOLATILES USING LASER DESORPTION IN ATMOSPHERIC PRESSURE IONIZATION MASS SPECTROMETRY 92
*LUBMAN, D M AND HUANG, S D

POST IONIZATION OF NEUTRALS ABLATED IN LASER MICROPROBE MASS SPECTROMETRY 94
*SCHUELER, B W AND ODOM, R W

GAS PHASE STUDIES OF LASER DESORBED PYRIDINIUM CATIONS 96
*WATSON, C H,BAYKUT, G,KATRITZKY, A R AND EYLER, J R

FAST IMPULSE MEASUREMENT IN RIMS WITH TIME-OF-FLIGHT DETECTION 98
*GREEN, L W,MACDONALD, R G AND SOPCHYSHYN, F C

MONDAY POSTER SESSIONS

ENVIRONMENTAL APPLICATIONS/POLYMERS

APPLICATION OF SEMI-VOST METHODOLOGY TO THE MEASUREMENT OF ORGANIC EMISSIONS FROM HAZARDOUS WASTE INCINERATORS 100
*BURSEY, J,STEGER, J,PALAZZOLO, M,BENSON, D,HOMOLYA, J, MCALLISTER, R,MCGAUGHEY, J,PORCH, R,WAGONER, D AND MARGESON, J

FAB MS/MS TECHNIQUE FOR CERTIFICATION OF PESTICIDE STANDARDS 102
*TONDEUR, Y,SOVOCOOL, G W,NIEDERHUT, W J AND DONNELLY, J R

A DETAILED MASS SPECTROMETRIC STUDY OF DFTPP 104
KINSINGER, J A AND *WEIL, D A

ENVIRONMENTAL MONITORING PROCEDURES FOR BROMINATED DIBENZO-P-DIOXINS AND DIBENZOFURANS 105
*MITCHUM, R K,SOVOCOOL, G W,MUNSLOW, W D,VONNAHME, T L, NUNN, N J,HEDIN, C M AND DONNELLY, J R

'UNUSUAL' ENVIRONMENTAL CONTAMINANTS 107
*FEISTNER, G J,FAULL, K F AND GOLDSTEIN, D B

IDENTIFICATION OF CIS-DIHYDRODIOLS OF THE CARCINOGEN BENZO[a]PYRENE AND ESTIMATION OF 1802 INCORPORATION IN THE GREEN ALGA SELENASTRUM CAPRICORNUTUM 109
WARSHAWSKY, D AND *JAYASIMHULU, K

ANALYSIS OF VOST SAMPLES USING MEGABORE CAPILLARY GC/MS/DS 111
*PORCH, R L,BUEDEL, T A,BURSEY, J T,HOMOLYA, J B,FUERST, R AND LOGAN, T

REAL TIME ENVIRONMENTAL ANALYSES OF VOLATILE ORGANICS IN INDOOR AIR BY TANDEM MASS SPECTROMETRY 113
*KURLICK, N AND PRITCHETT, T

LC/MS AND MS/MS ANALYSES OF CARBAMATE PESTICIDES 115
*CHIU, K S,TANAKA, C AND VANLANGENHOVE, A

CHARACTERIZATION OF HALOGENATED ORGANIC COMPOUNDS IN ESTUARINE BIOTA AND SEDIMENTS BY CHEMICAL IONIZATION TANDEM MASS SPECTROMETRY 117
*ROSTAD, C AND PEREIRA, W E

GC-MS PROCEDURES FOR DETERMINATION OF BROMINATED AND BROMINATED/CHLORINATED DIBENZODIOXINS AND DIBENZOFURANS IN FIRE RETARDANT CHEMICALS 119
*TIERNAN, T O,TAYLOR, M L,WAGEL, D,VANNESS, G F,HARDEN, L, GARRETT, J H AND SOLCH, J G

DEVELOPMENT AND APPLICATION OF A GC-MS TECHNIQUE FOR ACCOMPLISHING RIGOROUS ISOMER-SPECIFIC QUANTITATION OF 2,3,7,8-TETRACHLORODIBENZOFURAN IN EXTRACTS OF ENVIRONMENTAL SAMPLES 121
*TAYLOR, M L,HARDEN, L H,WAGEL, D J,GARRETT, J H,SOLCH, J G, VANNESS, F F AND TIERNAN, T O

NOVEL MASS SPECTROMETRIC METHODS FOR MORE RELIABLE DETERMINATION OF POLYCYCLIC AROMATIC HYDROCARBONS 123
*JAMIESON, W D,BOYD, R K AND SIM, P G

FAB AND FAB-CID-MIKE ANALYSIS OF SULPHONATED DYES. APPLICATION ON ENVIRONMENTAL WATER SAMPLES 125
*RIVERA, J,FRAISSE, D,VENTURA, F,FIGUERAS, A,CAIXACH, J, SALGADO, J G AND JOAN, P S

CORRELATION OF PCB TO PCDD/PCDF IN COMBUSTION ACCIDENTS 127
*AICHELE, D G,DEROOS, F L,SUEPER, C V AND ZIMMERMAN, M L

ANALYSES OF ORGANIC COMPONENTS IN DRILLING FLUIDS, EXPOSURE WATER, FISH, SOIL AND PLANTS 128
*PETERMAN, P H,SCHWARTZ, T R,LEBO, J,JOHNSON, J L AND WOODWARD, D

ANALYSIS OF INSECTICIDES BY THERMOSPRAY LC-MS 130
YANG, L AND VESTAL, C H

NCI MASS SPECTROMETRIC ANALYSIS OF HUMAN ADIPOSE TISSUE FOR PCDDS AND PCDFS 132
*ALLEY, C C,PATTERSON, D G AND ISAACS, S G

SCREENING FOR POLYCHLORINATED DEPHENYL ETHERS AND POLYCHLORINATED BIPHENYLENES WHILE QUANTIFYING POLYCHLORINATED DIOXINS AND DIBENZOFURANS 134
*CZUCZWA, J M,DEROOS, F L,AICHELE, D G AND KATONA, V R

LIQUID CHROMATOGRAPHY-MASS SPECTROMETRY ANALYSES OF NON-VOLATILE ORGANIC ENVIRONMENTAL POLLUTANTS 136
*WILLOUGHBY, R C,MITROVICH, S,DULAK, J G,POEPPEL, F AND SAUTER, D

AMBIENT AIR MONITORING FOR TOXIC CONTAMINANTS BY PROCESS MASS SPECTROMETRY 138
*CESSNA, G,BARTMAN, C AND PATTERSOM, T

ENVIRONMENTAL & BIOMEDICAL APPLICATIONS OF TRACE ANALYSIS BY MS/MS 140
KROLIK, S T AND *PORTER, C J

ADVANCES IN GC-HRMS DATA ACQUISITION TECHNIQUES FOR THE QUANTITATIVE ANALYSIS OF POLYCHLORINATED DIBENZODIOXINS AND DIBENZOFURANS 142
*BILL, J C,GRAY, B W,GREEN, B N AND YOFFE, J A

SPECIFICITY AND SENSITIVITY IN TRACE ANALYSIS BY GAS CHROMATOGRAPHY/MASS SPECTROMETRY 144
*BENOIT, F M

COMPOSITION AND SIZE DISTRIBUTION OF THE ORGANIC CONSTITUENTS OF ATMOSPHERIC PARTICULATE MATTER IN THE PONCE, PR AREA 145
*INFANTE, R,SANTIAGO, N AND CARRASQUILLO, A

ANALYSIS OF SULFUR VESICANTS BY CAPILLARY COLUMN ISOBUTANE CHEMICAL IONIZATION MASS SPECTROMETRY 147
*D'AGOSTINO, P A AND PROVOST, L R

MS/MS ANALYSES OF NITROFLUORANTHENES AND NITROPYRENES 149
*DIETRICH, A M,GUENAT, C R AND BALL, L M

GC/NCI HIGH RESOLUTION MASS SPECTROMETRIC SCREENING FOR PCB'S, PCDD'S AND PCDF'S 151
*DE KANEL, J,HSU, B-H,KELLY, S L AND TANG, S-Y

MASS SPECTROMETRY OF POLYBROMINATED DIBENZODIOXINS USING NEGATIVE CHEMICAL IONIZATION 153
*MARBURY, G D,TURLINGTON, J M AND TUSCHALL, J R

DETERMINATION OF THE PHOTODEGRADATION PRODUCTS OF BASIC YELLOW 2 BY THERMOSPRAY HPLC/MS AND GC/MS 155
*VOYKSNER, R D,PACK, T W,FREEMAN, H S,HSU, W N AND HANEY, C A

ENVIRONMENTAL APPLICATIONS OF THE THERMOSPRAY LC/MS INTERFACE: PART II: DI- AND TETRASULFONATED AZO DYES 157
*FLORY, D A AND MCLEAN, M A

DIRECT EQUILIBRIUM HEAD-SPACE ANALYSIS OF ENVIRONMENTALLY IMPORTANT PURGABLE COMPOUNDS USING GAS CHROMATOGRAPHY WITH ION TRAP DETECTION 159
*PATKIN, A J AND HINSHAW, J V

THE APPLICATION OF ICP/MS TO ENVIRONMENTAL SAMPLES 161
*DONNELLY, J R,CARDENAS, D,HENSHAW, J M,DOBB, D E, HILLMAN, D C,BUTLER, L C,SMIECINSKI, R F,HEITHMAR, E M, MITCHUM, R K AND ROWLAND, C N

ROUTINE ON-SITE GC/MS ANALYSIS: A FULLY MOBILE SYSTEM WITH PRACTICAL APPLICATIONS 163
*WEISS, M AND MATZ, G

LOW LEVEL IMPURITY DETECTION FOR "PURE" GASES 165
*PIZZITOLA, V AND SCHAEFFER, R

DETERMINATION OF MOLECULAR WEIGHT DISTRIBUTIONS OF LOW MOLECULAR WEIGHT POLYMERS USING TIME-OF-FLIGHT SECONDARY ION MASS SPECTROMETRY 167
*BLETSOS, I V,HERCULES, D M,VANLEYEN, D AND BENNINGHOVEN, A

TIME-OF-FLIGHT SECONDARY ION MASS SPECTROMETRY: COPOLYMER SPECTRA FROM THIN FILMS TO POLYMER SPECTRA FROM THICK SAMPLES 169
*BLETSOS, I V,HERCULES, D M,VANLEYEN, D AND BENNINGHOVEN, A

IDENTIFICATION OF ORGANIC COMPONENTS IN UNCURED RUBBER COMPOUNDS USING MASS SPECTROMETRY 171
*LATTIMER, R P,HARRIS, R E,RHEE, C K AND SCHULTEN, H -R

TANDEM MASS SPECTROMETRY (MS/MS) FOR ANALYSIS OF ADDITIVES IN A RUBBER VULCANIZATE 172
*LATTIMER, R P

PYROLYSIS GC/NCIMS OF MALEIC ANHYDRIDE FUNCTIONALIZED POLYETHYLENES 175
*SNOW, T A

POLYMERIZATION OF CYLCOPENTADIENE STUDIED BY FIELD DESORPTION MASS SPECTROMETRY AND PYROLYSIS GC/MS 177
*HSU, C S AND MALATESTA, A

APPLICATION OF MS-MS TO THE ANALYSIS OF UNCURED EPOXY RESIN MIXTURES 179
BLEASE, T G,CATLOW, D A,CLAYTON, E,*MONAGHAN, J J AND SCRIVENS, J H

ANALYTE DETECTION IN SOLID POLYMER MATRICES BY PYROLYSIS-ATMOSPHERIC PRESSURE CHEMICAL IONIZATION-MS/MS 181
*SNYDER, A P,KREMER, J H AND LIEBMAN, S A

ION ACTIVATION AND DISSOCIATION INSTRUMENTATION

LASER-ION BEAM PHOTODISSOCIATION STUDIES: THE Mn2(CO)y+, Fe3(CO)y+, AND Co4(CO)y+ SYSTEMS 183
*TECKLENBURG, R E AND BRICKER, D L

PHOTODISSOCIATION/TANDEM MASS SPECTROMETRY OF METAL CARBONYL CLUSTER IONS 185
*CALLAHAN, J H,TOSS, M M,BARONAVSKI, A P AND FREAS, R B

DISSOCIATION PROCESSES OF METHANOL CLUSTERS FOLLOWING MULTIPHOTON IONIZATION 187
MORGAN, S,*KEESEE, R G AND CASTLEMAN, A W

CID STUDIES OF MIXED HALIDE CLUSTER IONS CONTAINING TETRA-ALKYLAMMONIUM CATIONS 189
*TOLUN, E AND TODD, J F J

IONIZATION AND FRAGMENTATION OF BIOMOLECULES INVESTIGATED BY LASER MASS SPECTROMETRY 191
*GROTEMEYER, J,BOESL, U,WALTER, K AND SCHLAG, E W

UNIMOLECULAR DECAY RATES FROM METASTABLE BROADENING IN A TIME-OF-FLIGHT MASS SPECTROMETER 193
*KINSEL, G R AND JOHNSTON, M V

UNIMOLECULAR DECAY MEASUREMENTS WITH AN ION MIRROR 195
*TANG, X,BEAVIS, R,ENS, W,LAFORTUNE, F,STANDING, K G AND WESTMORE, J B

MS/MS/MS/MS IN A FOUR SECTOR (BE-EB) MASS SPECTROMETER 197
*TOMER, K B,GUENAT, C AND DINO, J

CHARGE SEPARATION PROCESSES OF POLYCYCLIC AROMATIC HYDROCARBON TRICATIONS 199
*KOYANAGI, G K AND MARCH, R E

NEUTRAL DISSOCIATION/REIONIZATION TECHNIQUES AND POSITIVE/NEGATIVE ION CONVERSION IN TANDEM MASS SPECTROMETRY 201
*FENG, R,WESDEMIOTIS, C,ZHANG, M-Y,DRINKWATER, D E AND MCLAFFERTY, F W

DISSOCIATION OF THE ENERGY-SELECTED ETHYL FORMATE ION 203
ZHA, Q,*NISHIMURA, T AND MEISELS, G G

FRAGMENTATION OF ACETIC ACID IONS WITH SELECTED INTERNAL ENERGIES 205
*ZHA, Q,NISHIMURA, T AND MEISELS, G G

ELECTRON-CAPTURE (CHARGE-EXCHANGE) REACTIONS OF MULTIPLY-CHARGED POLYCYCLIC AROMATIC IONS 207
KINGSTON, R G,BRENTON, A G,*HARRIS, F M AND BEYNON, J H

ION KINETIC ENERGY MEASUREMENT ON TANDEM QUADRUPOLE MASS SPECTROMETERS 209
*BEAUGRAND, C,DEVANT, G,JAOUEN, D,MESTDAGH, H AND ROLANDO, C

EVALUATION OF DEUTERIUM ISOTOPE FRACTIONATION IN PROTONATED WATER CLUSTERS WITH A FLOWING AFTERGLOW - TRIPLE QUADRUPOLE 211
*BRICKHOUSE, M D,GRAUL, S T AND SQUIRES, R R

THE GAS-PHASE REACTIONS OF FE+ AND CR+ WITH ALIPHATIC ALCOHOLS: A HIGH ENERGY CAD STUDY 213
*HUANG, S K

INVESTIGATIONS OF ALKOXYPERFLUORO PROPIONATE SALTS: NOVEL DISSOCIATIONS OF FAB GENERATED CARBANIONS 215
*HUNT, S L,LYON, P A AND PELLERITE, M J

CHEMICAL IONIZATION MASS SPECTROMETRY OF K-REGION ARENE OXIDE METHANOLYSIS PRODUCTS 217
*PANNELL, L K,NASHED, N AND GROSSMAN, S

NOVEL MASS SPECTRAL FRAGMENTATION OF SOME CHLOROACETANILIDES 219
*FUJIWARA, H AND MALIK, J M

STUDY OF NON-AQUEOUS COLOR INDICATORS BY ELECTRON IMPACT, LIQUID SECONDARY ION, AND COLLISION-INDUCED-DISSOCIATION MASS SPECTROMETRY 221
*GALE, P J AND BENTZ, B L

ENERGETICS OF REMOTE SITE FRAGMENTATION 223
*WYSOCKI, V H,BIER, M E AND COOKS, R G

WHAT FATTY ACID FUNCTIONAL DERIVATIVES UNDERGO CHARGE REMOTE DECOMPOSITIONS? 225
*DETERDING, L J

COLLISIONAL ACTIVATION OF METAL ION-CATIONIZED PROSTAGLANDINS, STEROLS, FATTY ACID ESTERS, AND VITAMINS 227
*ADAMS, J

KINETIC ENERGY SPECTROSCOPY OF THE IODOMETHANE DICATION 229
*BOYD, R K,CURTIS, J M,BRENTON, A G AND BEYNON, J H

REACTION-INTERMEDIATE MASS SPECTROMETRY ON A KRATOS MS-50TA 231
*GIBLIN, D E AND HOLMAN, R W

A TRIPLE QUADRUPOLE MASS SPECTROMETER WITH FACILITIES FOR CONSECUTIVE RECORDING OF NORMAL AND METASTABLE SCANS 233
SMITH, D C,SWAIN, D,*HINDENLANG, D M AND SEDGWICK, R D

ANALYSIS OF NITROGEN COMPOUNDS IN REFINERY HYDROCARBON STREAMS BY THE USE OF AMMONIA CHEMICAL IONIZATION GC/MS 235
*DZIDIC, I AND BALICKI, M D

AN IMPROVED HYBRID MASS SPECTROMETER FOR COLLISIONALLY ACTIVATED DISSOCIATION STUDIES 237
CURTIS, J E,KAMAR, A,*MARCH, R E AND SCHLUNEGGER, U P

IMPROVED SCANNING MODES USING A MULTIQUADRUPOLE MS/MS/MS INSTRUMENT 239
*BEAUGRAND, C,DEVANT, G,JAOUEN, D,MORIN, N AND ROLANDO, C

POST-SECTOR BEAM DEFLECTION IN TIME-RESOLVED ION MOMENTUM SPECTROMETRY (TRIMS) AND ITS USE WITH TIME ARRAY DETECTION (TAD) FOR MS/MS MAP ACQUISITION 241
*ECKENRODE, B A,NEWCOME, B H,HOLLAND, J F AND ENKE, C G

RESONANT TWO-PHOTON IONIZATION OF SMALL PEPTIDES USING PULSED LASER DESORPTION IN SUPERSONIC BEAM MASS SPECTROMETRY 243
*LUBMAN, D M,LI, L AND TEMBREULL, R

SOURCE DESIGN FOR THERMOSPRAY LC-MS 245
*BUCHNER, J D,WILLOUGHBY, R C AND KETKAR, S N

CONVERSION DYNODE DETECTION BIAS FOR ODD VERSUS EVEN ELECTRON NEGATIVE IONS 247
*SEARS, L J AND GRIMSRUD, E P

MASS DISCRIMINATION IN QUADRUPOLE MASS SPECTROMETERS USED AS MOLECULAR BEAM DETECTORS 249
*GREENE, F T,O'DONNELL, J E AND ROBAUGH, D A

THE CHARACTERISTICS OF A MULTICHANNEL ELECTRO-OPTICAL DETECTION SYSTEM AND ITS APPLICATION TO THE ANALYSIS OF LARGE MOLECULES BY FAB MASS SPECTROMETRY 251
*COTTRELL, J S AND EVANS, S

A NEW HIGH EFFICIENCY HIGH MASS ION DETECTOR 253
*BATEMAN, R H AND BOTT, P A

A SIMPLE ANALOG CIRCUIT FOR IMPROVED PERFORMANCE IN DAC SCANNED MAGNETIC MASS SPECTROMETERS 255
*FREEMAN, J P,HALL, R AND LAY, J O

DESIGN EXPERIENCE WITH AND RECENT ENHANCEMENTS TO THE SIMION PC/AT ELECTROSTATIC LENS DESIGN PROGRAM 257
*DAHL, D A AND DELMORE, J E

APPLICATION OF STORED-WAVEFORM, INVERSE FOURIER TRANSFORM (SWIFT) EXCITATION TO FTMS 259
*CODY, R B,HEIN, R E AND HANNA, D A

APPLICATIONS OF MULTIDIMENSIONAL GAS CHROMATOGRAPHY/HIGH RESOLUTION MASS SPECTROMETRY (GC/GC/HRMS) 261
*LEWIS, S AND CLOTHIER, R

MASS RANGE EXTENSION OF THE ION TRAP MASS SPECTROMETER THROUGH THE APPLICATION OF DC ELECTRIC FIELDS 263
*TODD, J F J,BEXON, J J,WEBER-GRABAU, M,KELLEY, P E, STAFFORD, G C AND SMITH, R D

ENERGETIC CONSIDERATIONS FOR FRAGMENTATION PATHWAYS OBSERVED FOR COLLISIONALLY ACTIVATED MODEL PEPTIDES FORMED BY FAB IONIZATION 265
*MALLIS, L M AND RUSSELL, D H

TUESDAY ORAL SESSIONS

SYMPOSIUM: DYNAMICS IN BIOLOGICAL SYSTEMS

A MASS BALANCE MODEL OF PCBs IN SISKIWIT LAKE, ISLE ROYAL 267
*SWACKHAMER, D L AND HITES, R L

LONG TERM MEASUREMENT OF AMINO ACID TURNOVER AND THE SYNTHESIS OF PLASMA APOLIPOPROTEINS 269
*HACHEY, D L,PATTERSON, B W,GHISELLI, G,MARKS, L, BROWN-BOOTH, L AND KLEIN, P D

MECHANISTIC STUDIES OF XENOBIOTIC METABOLISM AND DRUG-DRUG INTERACTIONS 271
*BAILLIE, T A

INSTRUMENTATION: NEW CONCEPTS

FIRST RESULTS FROM A TIME-OF-FLIGHT MASS SPECTROMETER USING HIGHLY ENERGETIC IONS FROM ARGONNE TANDEM-LINEAR ACCELERATOR SYSTEM (ATLAS) 275
*HUNT, J E,SALEHPOUR, M,KANTER, E,KUTSCHERA, W,ZABRANSKY, B, PARDO, R AND DUNFORD, R

TIME ARRAY DETECTION: MASS SPECTROMETRY'S ANSWER TO HIGH RESOLUTION CHROMATOGRAPHY 277
*HOLLAND, J F,ERICKSON, E,ECKENRODE, B A AND WATSON, J T

SURFACE INDUCED DISSOCIATION IN A NEW TANDEM QUADRUPOLE MASS SPECTROMETER 279
*BIER, M E,COOKS, R G,AMY, J,STAFFORD, G AND CEJA, P C

MOLECULAR IMAGING SECONDARY ION MASS SPECTROMETRY 281
*GILLEN, G AND WILLIAMS, P

CAPILLARY ZONE ELECTROPHORESIS WITH ON-LINE MASS SPECTROMETRIC DETECTION 283
*SMITH, R D,OLIVARES, J A AND NGUYEN, N T

INFRARED SPECTROSCOPY/MASS SPECTROMETRY 285
*PRESSER, D

A LIQUID SAMPLING SYSTEM FOR MASS SPECTROMETRIC STUDY OF CONDENSED-PHASE CHEMICAL REACTIONS 287
*TOU, J C AND DAMODER, R

PARTICLE BEAM-LIQUID CHROMATOGRAPHY-MASS SPECTROMETRY (PB-LC-MS): ADVANTAGES AND APPLICATIONS 289
*WILLOUGHBY, R C AND POEPPEL, F

A NEW ATMOSPHERE SAMPLING ION SOURCE 291
MCLUCKEY, S A AND *GLISH, G L

DESIGN AND CONSTRUCTION OF AN ATMOSPEHERIC PRESSURE ION SOURCE FOR A VG7070E-HF MASS SPECTROMETER 292
*GRANGE, A H,O'BRIEN, R J AND BAROFSKY, D F

DESIGN AND PERFORMANCE OF A NEW API SOURCE COMPATIBLE WITH A COMMERCIAL TANDEM MASS SPECTROMETER 294
*MATUSZAK, K P,HAIL, M E AND JOHNSON, J V

A NEW HIGH RESOLUTION TIME-OF-FLIGHT SECONDARY ION MASS SPECTROMETER 296
*NIEHUIS, E,HELLER, T,FELD, H AND BENNINGHOVEN, A

EFFECTS OF SAMPLE PREPARATION ON MOLECULAR ION FORMATION IN PLASMA DESORPTION MASS SPECTROMETRY OF PEPTIDES AND PROTEINS 298
*ROEPSTORFF, P,NIELSEN, P F,SUNDQVIST, B,HAKANSSON, P AND JONSSON, G

DESORPTION AND IONIZATION METHODS

KINETIC MODELLING OF FAB SPECTRA OF DIETHANOLMINE SOLUTIONS IN GLYCEROL AND MODELS OF DESORPTION IONIZATION 300
*SUNNER, J,MORALES, A AND KEBARLE, P

DIFFERENTIAL APPEARANCE OF ANALYTE AND MATRIX DURING THE FIRST SECONDS OF SPUTTERING BY FAST ATOM BOMBARDMENT 302
*MUSSELMAN, B D,STULTS, J T AND HOLLAND, J F

SURFACE CONCENTRATION IN LIQUID SIMS SAMPLES 304
*TODD, P J

STUDIES OF THE SPUTTERING OF MULTIPLY CHARGED IONS FROM THE LIQUID PHASE 306
*LIGON, W V AND DORN, S B

FAB WITHOUT A LIQUID MATRIX USING A MAGNETIC SECTOR ANALYSER AND PARALLEL DETECTION: A TECHNIQUE FOR REDUCING CHEMICAL NOISE 308
TAYLOR, L C E AND *COTTRELL, J S

LIQUID ASSISTED SIMS WITH A LIQUID METAL ION MICROPROBE 310
JIANG, L,BAROFSKY, E AND *BAROFSKY, D F

STUDIES OF SPUTTERED IONS IN A HIGH-PRESSURE FAST-ATOM BOMBARDMENT ION SOURCE 312
ROSS, M M AND CALLAHAN, J H

SIMS AND CHEMISTRY OF SUBSTITUTED AROMATIC/SULFURIC ACID *SOLUTIONS* 314
*LIEBMAN, C P,TODD, P J AND MAMANTOV, G

A STUDY ON THE FAB-INDUCED ADDUCT FORMATION BETWEEN PEPTIDES AND GLYCEROL 316
*DASS, C AND DESIDERIO, D M

FACTORS INFLUENCING RELATIVE SENSITIVITY FOR SMALL PEPTIDES IN LIQUID SIMS 318
*FALICK, A M,JIANG, K,GIBSON, B W AND WALLS, F C

FAB-MS OF LOW MOLECULAR WEIGHT SLIGHTLY POLAR MOLECULES 320
*ROSEN, R T,HARTMAN, T G,HO, C-T AND ROSEN, J D

TEMPERATURE EFFECTS IN THE BOMBARDMENT MS OF DC704 321
*KATZ, R N AND FIELD, F H

SYMPOSIUM: STRUCTURAL UTILITY OF NEGATIVE IONS

FOURIER TRANSFORM ION CYCLOTRON RESONANCE STUDIES OF NEGATIVE IONS 323
*NIBBERING, N M M

CHEMICAL REACTIONS OF NEGATIVE IONS AS A PROBE OF STRUCTURE 325
*DEPUY, C H AND BIERBAUM, V M

THE FRAGMENTATION OF NEGATIVE IONS FORMED BY ELECTRON CAPTURE NEGATIVE ION MASS SPECTROMETRY 327
*STEMMLER, E A AND HITES, R A

IONIZATION DYNAMICS WITHIN THE HIGH PRESSURE ELECTRON CAPTURE MASS SPECTROMETER 329
SEARS, L J AND *GRIMSRUD, E P

ION MOLECULE REACTIONS

THE USE OF REACTIVE COLLISIONS OCCURRING IN A TRIPLE QUADRUPOLE MASS SPECTROMETER IN DIFFERENTIATION OF ISOMERIC IONS WHICH PRODUCE IDENTICAL CAD SPECTRA 331
*KENTTAMAA, H I AND PACHUTA, R R

AN INVESTIGATION OF ISOMERIC IONS DERIVED FROM ACETONE, DIACETONE ALCOHOL AND MESITYL OXIDE 333
*YOUNG, A AND MARCH, R

IRON ION CHEMISTRY AND ISOMER DISCRIMINATION USING FTMS 335
BJARNASON, A AND *TAYLOR, J W

COLLISION INDUCED DISSOCIATION OF METAL CLUSTER IONS:Al+n(n=3-26), AlnO+m AND AlnD+m 337
*JARROLD, M F AND BOWER, J E

STUDIES OF THE CHEMISTRY OF METAL CLUSTER IONS:Al+n(n=3-26) WITH OXYGEN 339
*JARROLD, M F AND BOWER, J E

PROTONATION OF HEXAMETHYLDISILOXANE (HMDS) IN PARTICULAR AND ORGANOSILICON COMPOUNDS IN GENERAL 341
*STONE, J A AND LI, X

ION/MOLECULE REACTIONS IN A QUADRUPOLE ION TRAP: HALOMETHYLATION 343
*BRODBELT, J S AND COOKS, R G

ION CONFINEMENT IN THE FR-ONLY COLLISION CELL OF A TANDEM QUADRUPOLE INSTRUMENT 345
*BEAUGRAND, C,DEVANT, G,JAOUEN, D,MESTDAGH, H AND ROLANDO, C

SYMPOSIUM: DYNAMICS OF ION PROCESSES

ANOMALOUS EFFECTS IN FRAGMENTATION PATTERNS 347
*LORQUET, J C,DEHARENG, D,LEYH-NIHANT, B,REMACLE, F AND KRIER, C

THE DISSOCIATION RATES OF ION-DIPOLE COMPLEXES - ARE THEY NON-STATISTICAL? 349
*BAER, T,SHAO, J-D,MORROW, J C AND FRASER-MONTEIRO, M

THE ATOMIC OXYGEN ANION AS A CHEMICAL IONIZATION AGENT: MECHANISTIC DETAILS 351
*GRABOWSKI, J J AND MELLY, S J

ISOTOPIC EXCHANGE REACTIONS AS A PROBE OF REACTION DYNAMICS 353
*BIERBAUM, V M,DEPUY, C H,VAN DOREN, J M AND BARLOW, S E

TIME-RESOLVED AND COLLISIONALLY INDUCED DISSOCIATION STUDIES OF GAS PHASE IONS 355
*NIBBERING, N M M

TUESDAY POSTER SESSIONS

COMPUTATIONAL TECHNIQUES/LCMS INSTRUMENTATION

ANALYSIS OF A DIVERSE SET OF BACTERIA BY PYROLYSIS-MASS SPECTROMETRY WITH PATTERN RECOGNITION TECHNIQUES 357
*VOORHEES, K J,DURFEE, S L AND UPDEGRAFF, D

SMALL COMPUTER-DATA SYSTEM FOR RESEARCH APPLICATIONS IN MASS SPECTROMETRY 359
*HADDON, W F,HANDA, M AND LUNDIN, R E

A HIGH SPEED DATA SYSTEM/TIMESHARING SYSTEM LINK 361
BONDAROVICH, H A,*CONE, C,PATEL, S AND STODDART, S

IMPLEMENTATION OF A NON-AUTOCONSOLE KRATOS MS-25/DS-90 SYSTEM TO PERFORM SELECTED ION MONITORING QUANTITATION OF PARTS-PER-TRILLION CONCENTRATIONS OF MULTIPLE ANALYTES DURING A SINGLE ANALYSIS 363
GARRETT, J H,*SOLCH, J G,MILLER, C D,TIERNAN, T O AND TAYLOR, M L

AUTOMATED QUANTITATION OF MULTIPLE ANALYTES IN A LARGE STUDY 365
*FAST, D M,CARDINALI, F L,TODD, G D AND HOLLER, J S

A NEW DATA SYSTEM FOR THE PROCESSING OF ENVIRONMENTAL DATA 367
*KENNERLEY, S,RYAN, P A,MILTON, D J AND SHIEL, D A

DEVELOPMENT OF ON-LINE QC/QA TECHNIQUES FOR STATISTICAL EVALUATION OF GC/MS ENVIRONMENTAL DATA 369
*PRILL, G E AND HEADLEY, J V

QUALITY CONTROL VERIFICATION AND REPORTING OF RESULTS FROM ENVIRONMENTAL ANALYSES 371
*TERWILLIGER, D T,BEHBEHANI, A L AND BUDDE, W L

CHEMICAL INTERPRETATION EMPERICALLY GENERATED SUBSTRUCTURE IDENTIFICATION RULES 373
*HART, K J,WADE, A P,PALMER, P T,NOURSE, B AND ENKE, C G

EVALUATION OF AN AUTOMATED METHOD FOR GENERATING SUBSTRUCTURE IDENTIFICATION OF RULES FROM MS/MS DATA 375
*PALMER, P T,WADE, A P,HART, K J AND ENKE, C G

AN EXPERT PROGRAM FOR THE INTERPRETATION OF GC/MS DATA ON FOSSIL FUEL DISTILLATES 377
*ACZEL, T,COLGROVE, S G AND LAN, L

TQMSTUNE: THE RULES 379
*GREGG, H AND WONG, C

DETERMINATION OF AROCLOR COMPOSITION FROM PCB LEVEL OF CHLORINATION DATA 381
*SLIVON, L E AND SCHUMACHER, P M

PROCESSING OF HIGH RESOLUTION MASS SPECTRAL DATA BY USE OF KENDRICK MASSES IN A RECTANGULAR ARRAY 383
*GRIGSBY, R D

AN EFFICIENT ALGORITHM FOR SEQUENCING PEPTIDES UTILIZING FAST ATOM BOMBARDMENT MASS SPECTRAL DATA 385
*SIEGEL, M M AND BAUMAN, N

PHASE CONSIDERATIONS IN THE EXCITATION OF IONS IN FOURIER TRANSFORM ION CYCLOTRON RESONANCE MASS SPECTROMETRY 387
*BAYKUT, G,WATSON, C H AND EYLER, J R

COMPARISON STUDY OF SEARCH ALGORITHMS AND DATA BASE LIBRARIES FOR COMPOUND IDENTIFICATION FROM MASS SPECTRAL DATA 389
*BURNS, F B AND RODACY, P J

COMPUTER ENHANCEMENT OF MS DATA: MS/MS SPECTRA FROM HADAMARD TRANSFORMS AND COMPOUND IDENTIFICATION USING 130,000 REFERENCE SPECTRA 391
*STAUFFER, D B,LOH, S Y,HENRY, K D,TWISS-BROOKS, A B AND MCLAFFERTY, F W

AN INTERACTIVE APL PROGRAM TO CALCULATE ISOTOPIC PATTERNS IN DAUGHTER IONS 393
*ROACH, J A G,ALBERT, R H AND BRUMLEY, W C

ADDITIONAL ADVANTAGES FOR COMPARING THE MS/MS DAUGHTER ION SPECTRA OF M AND M+1 IONS 395
*BOZORGZADEH, M H

APPLICATIONS OF COLLISION INDUCED DISASSOCIATION (CID) MASS SPECTRA IN THE ANALYSIS OF ANTIBIOTICS 397
*BACZYNSKYI, L AND DUCHAMP, D J

A PROGRAM FOR THE DETERMINATION OF THE AMINO ACID COMPOSITION AND SEQUENCE OF SMALL PEPTIDES FROM THEIR FAST ATOM BOMBARDMENT SPECTRA 399
*BERTRAND, M J,THIBAULT, P,EVANS, M J AND ZIDAROV, D

THE ANALYSIS OF MICROBIAL NATURAL PRODUCTS BY THERMOSPRAY LC-MS 401
*KING, G S,GORDON, L AND RUNNALLS, N

THE IDENTIFICATION OF A SULPHATE CONJUGATE OF A PYRETHROID METABOLITE BY NEGATIVE ION SOFT IONISATION TECHNIQUES 403
*KING, G S,HEATH, J,RUNNALLS, N AND HAMMOND, I

A DIRECT LIQUID AND SUPERCRITICAL FLUID INLET FOR TIME-OF-FLIGHT MASS SPECTROMETRY USING RESONANCE ENHANCED MULTIPHOTON IONIZATION/FRAGMENTATION 405
*KINSEL, G R,SEGAR, K R AND JOHNSTON, M V

CHARACTERISTICS OF LIQUID CHROMATOGRAPH/ATMOSPHERIC PRESSURE IONIZATION MASS SPECTROMETER (LC/API-MS) 407
*SAKAIRI, M AND KAMBARA, H

TRANSPORT PROCESSES, LOSS MECHANISMS AND SIGNALS IN MAGIC-LC/MS 409
*BROWNER, R F,KIRK, D,GARRETT, D A AND PERKINS, D D

HEAT-INDUCED DISSOCIATION IN LC/MS ANALYSES 411
CRAWFORD, J L,*LITTLE, J L AND WILDER, D R

PACKED CAPILLARY LC/MS USING A MOVING BELT INTERFACE 413
*REISER, R W AND BAREFOOT, A C

LC-MS ACCURATE MASS MEASUREMENT USING PLASMASPRAY 415
BATEMAN, R H,*JONES, D AND MAJOR, H

EFFECTS OF SOURCE DESIGN ON THE NATURE OF THERMOSPRAY MASS SPECTRA 417
*COUTANT, J E,ACKERMANN, B L AND VESTAL, M L

DEVELOPMENT OF A NEW INTERFACE FOR COMBINED OPEN-TUBULAR LC/MS 419
*DE WIT, J S M,PARKER, C E,TOMER, K B AND JORGENSON, J W

FUNDAMENTAL STUDIES OF THERMOSPRAY IONIZATION: INVESTIGATION OF THE THERMOSPRAY FLUME 421
*LEE, M S AND YOST, R A

EVALUATION OF A DISPOSABLE MOVING BELT LC-MS INTERFACE 423
*DEMAIO, W

THERMOSPRAY LC/MS INTERFACE FOR TIME-OF-FLIGHT MASS SPECTROMETRY 425
*YERGEY, A L,LAMPE, F W,FISHER, J R,PISERCHIO, M AND MOORE, C B

THERMOSPRAY SPECTRA OF QUATERNARY AMMONIUM SALTS 427
MITCHELL, D,*JENNING, K R AND SCRIVENS, J H

THE APPLICATION OF FAB AND THERMOSPRAY TO THE STRUCTURE DETERMINATION OF -CARBOXY- -AMINO ACIDS 429
*APLIN, R T,DIXON, R R AND FLEET, G J W

THE APPLICATION OF THERMOSPRAY TO CYANAGENIC GLYCOSIDES 431
*APLIN, R T AND ERRINGTON, S G

ION SPRAY API LC/MS AND LC/MS/MS DETERMINATION OF SULFOCONJUGATED ANABOLIC STEROIDS IN THE HORSE 432
*PAWLOWSKI, T M,WEIDOLF, L,LEE, E AND HENION, J

DIRECT INTERFACING OF CAPILLARY SUPERCRITICAL FLUID CHROMATOGRAPHY WITH MASS SPECTROMETRY ELECTRON AND CHEMICAL IONIZATION 434
*HSU, S H,LEE, E D AND HENION, J D

THE FORMATION OF IONS IN THERMOSPRAY LIQUID CHROMATOGRAPHY/MASS SPECTROMETRY 436
*KIDWELL, D A,CALLAHAN, J H AND ROSS, M M

MASS SPECTROMETRY ANALYSIS OF ESPERAMINCINS 438
*DUBAY, G R,GROENEWOLD, G S AND GOLIK, J

DEVELOPMENT OF A MAGIC LC/MS SYSTEM 440
*APFFEL, A AND NORDMAN, B

FIELD LIMIT FOR ION EVAPORATION FROM MOBILITIES OF CHARGED THERMOSPRAY DROPLETS 441
*KATTA, V AND ROCKWOOD, A L

THE UTILITY OF SOLUTION ELECTROCHEMISTRY MS FOR ENHANCING THERMOSPRAY SPECTRA AND ELUCIDATING ELECTROCHEMICAL REDOX PROCESSES 443
*GETEK, T A

PHARMACOLOGY AND DRUG METABOLISM/NATURAL PRODUCTS

APPLICATION OF STABLE-ISOTOPE-CLUSTERS TO VANILLOID METABOLITE IDENTIFICATION 445
*STRIFE, R J,STRATTON, R D,GARDNER, J H AND SIETSEMA, W K

COMPARISON OF VAPOR PHASE METHODOLOGIES FOR DETERMINATION OF PLASMA DEXAMETHASONE 447
*KAYGANICH, K,WATSON, J T AND VRBANAC, J J

DETERMINATION OF 3-QUINUCLIDINYL BENZILATE IN URINE 449
*BYRD, G D,SNIEGOSKI, L T AND WHITE, E

THERMOSPRAY LC/MS STUDIES OF LUPROSTIOL (A PROSTAGLANDIN DERIVATIVE) AND ITS METABOLITES 451
*WEERASINGHE, C A,LOCKE, L A AND WANG, R

THE UTILITY OF THERMOSPRRAY LIQUID CHROMATOGRAPHY/MASS SPECTROMETRY FOR THE DIRECT ANALYSIS OF RAT BILE FOR ACETAMINOPHEN AND TWO OF ITS CONJUGATES 453
*BETOWSKI, L D,KORFMACHER, W A,LAY, J O,POTTER, D W AND HINSON, J A

NEGATIVE ION CHEMICAL IONIZATION GC-MS ANALYSIS OF VALPROIC ACID IN SALIVA AND SERUM 455
ABBOTT, F S,*KASSAHUN, K AND PANESAR, S

GC/MS ASSAY OF PROSTAGLANDINS IN CEREBROSPINAL FLUID 457
*YERGEY, J A,SALEM, N,KARANIAN, J W AND LINNOILA, M

A CANDIDATE DEFINITIVE METHOD FOR THE MEASUREMENT OF SERUM CHOLESTEROL 459
*KINTER, M,HUNDLEY, J,HEROLD, D A,WILLS, M R AND SAVORY, J

QUANTITATION OF CLENBUTEROL IN BIOLOGICAL FLUIDS USING AMMONIA CI AND AUTOMATED CAPILLARY GC-MS 461
ECKER, E M,*FORSTER, H J,WITTROCK, A AND ROMINGER, K L

ANALYTICAL METHODOLOGY TO STUDY THE EFFECTS OF DIETARY METHYLXANTHINES ON THEOPHYLLINE METABOLISM 463
*BUSH, E,LOI, C M,JUE, S G AND VESTAL, R E

QUANTITATIVE METABOLIC PROFILING OF DRUGS BY AUTOMATED GC/MS. APPLICATIONS TO STUDIES ON THE BIODISPOSITION OF VALPROIC ACID IN HUMANS 465
RETTENMEIER, A W,LEVY, R H,WITEK, D J,BAILLIE, T A AND *HOWALD, W N

IDENTIFICATION OF MORPHINE AND CODEINE IN EXTRACTS OF MAMMALIAN BRAIN 467
*FAULL, K F,FEISTNER, G J AND WEITZ, C J

DIFFERENTIATION OF ISOMERIC IONS MASS SPECTRA OF PYRROLIZIDINE ALKALOIDS USING COLLISIONAL ACTIVATION 469
JONES, A D,*KELLEY, R B,WINTER, C K,SEGALL, H J AND SEIBER, J N

THE IDENTIFICATION OF PENICILLINS AND THEIR METABOLITES BY THERMOSPRAY LC/MS 471
SUWANRUMPHA, S AND FLORY, D A

ISOLATION AND CHARACTERIZATION OF THE URINARY METABOLITES OF ARBAPROSTIL IN THE FEMALE DOG AFTER INTRAVENOUS ADMINISTRATION 473
*O'LEARY, I A,GREENFIELD, J C,COOK, K J AND HARPOOTLIAN, H

GC-NICI-MS ANALYSIS OF MACROCYCLIC TRICHOTHECENES 475
*ROSEN, J D,ROSEN, R T AND HARTMAN, T G

GC/MS ANALYSIS OF N-NITROSODIISOPROPANOLAMINE AT THE ng/g LEVEL IN A GEL FORMULATION CONTAINING A NON-STEROID ANTI-FLAMMATORY AGENT 476
JAMES, J C,*PASTEL, M J,LEDOUX, K A AND BALDONI, J M

OFF-LINE SEARCHING OF THE NIH BERDY DATABASE USING MASS SPECTRAL DATA 478
*BOLGAR, M S,WARRACK, B M AND UNGER, S E

DCI MASS SPECTRA OF PEPTIDYL AMINOSTEROIDS 480
WONG, L K,MOKOTOFF, M,ZHAO, M,LIAO, Q-J AND *FU, E W

DETERMINATION OF THE ACTIVE PHOTOSENSITIZER IN THE PHOTODYNAMIC CANCER THERAPY (PDT) DRUG HEMATOPORPHYRIN DERIVATIVE (HPD) 482
*MUSSELMAN, B D,CHANG, C K AND WATSON, J T

INVESTIGATION OF ETHYLENEDIAMINE ANTIHISTAMINES AND THEIR N-OXIDES BY DCI/MS, FAB/MS, AND FAB/MS/MS 484
*LAY, J O,HOLDER, C L,COOPER, W M AND KORFMACHER, W A

DETERMINATION OF MDL-19, 744A AND STABLE ISOTOPE LABELED MDL-19, 744A IN PLASMA BY CAPILLARY GAS CHROMATOGRAPHY/MASS SPECTROMETRY 486
*OLBERDING, E L AND STUHLER, J D

IDENTIFICATION OF BUSPIRONE METABOLITES BY GC/MS 488
*JAJOO, H K,MAYOL, R F,LABUDDE, J AND BLAIR, I A

GC-MS METHOD FOR THE ENANTIOMERS OF RIMANTADINE IN HUMAN PLASMA 490
MIWA, B J,*FUKUDA, E K AND GARLAND, W A

MEASUREMENT OF RIMANTADINE IN PLASMA BY CAPILLARY GAS CHROMATOGRAPHY-MASS SPECTROMETRY 492
*HEROLD, D A,ANONICK, P K,KINTER, M AND HAYDEN, F G

CHARACTERIZATION OF BILIARY METABOLITES OF A SYNTHETIC VASOPRESSIN ANALOGUE 494
*STRAUB, K,GARVIE, C AND LYNN, R K

THERMOSPRAY LC/MS IDENTIFICATION OF MITOMYCIN C AND PORFIROMYCIN DNA ADDUCTS 496
*MUSSER, S M,CALLERY, P S AND PAN, S-S

DIMETHYLFORMAMIDE DIMETHYL ACETAL AS A DERIVITIZING AGENT FOR THE GC-MS DETERMINATION OF UNSTABLE SECONDARY AMINES 498
*KAISER, M F AND CALLERY, P S

LASER DESORPTION-FOURIER TRANSFORM MASS SPECTROMETRY OF ANTIBIOTICS 500
*COATES, M L

IDENTIFICATION OF URINARY RAT METABOLITES OF CGS 15855A UTILIZING LC/MS, GC/MS AND A STABLE ISOTOPE LABEL TRACER 502
*HAYES, M,GAUDRY, D,EGGER, H,MIOTTO, J,BAX, M,IANNUCCI, R AND ALKALAY, D

CHARACTERIZATION OF GLUTATHIONYL CONJUGATES BY FAB/TANDEM MS 504
HUGHES, H,REILLY, M,*GASKELL, S J AND PORTER, C J

QUANTIFICATION OF CGS 16617 IN PLASMA BY COMBINED CAPILLARY GAS CHROMATOGRAPHY/NEGATIVE CHEMICAL IONIZATION MASS SPECTROMETRY 505
*GAUDRY, D,KHEMANI, L,MIOTTO, J AND ALKALAY, D

THE USE OF A HEATABLE-COOLABLE FAB PROBE FOR IMPROVED PERFORMANCE IN FAB MASS SPECTROMETRY 506
*MCCLURE, T D,BAKER, P F AND SCHRAM, K H

CHARACTERIZATION OF LYSOPHOSPHATIDYL CHOLINES USING POSITIVE ION AND NEGATIVE ION FAST ATOM BOMDARDMENT MASS SPECTROMETRY 508
*SWEETMAN, B J,TAMURA, M,HIGASHIMORI, K,INAGAMI, T AND BLAIR, I A

THE USE OF DIMETHYL ETHER CI/MS TO DIFFERENTIATE STRAIGHT FROM BRANCHED CHAIN FATTY ACID METHYL ESTERS (FAMES) 510
*KILLMER, L

ANALYSIS OF GLUTATHIONE CONJUGATES AND RELATED COMPOUNDS BY TSP MS 512
*DE WIT, J S M,PARKER, C E,SMITH, R W,GOPINATHAN, M B, HERNANDEZ, O AND BEND, J R

INVESTIGATION OF ISOQUINOLINE ALKALOIDS USING FAST ATOM BOMBARDMENT MASS SPECTROMETRY 514
*MASUCCI, J A,CALDWELL, G W AND WU, W N

DETERMINATION OF AMINES IN URINE BY GC/MS 516
*AVERY, M AND JUNK, G

MS STUDIES OF ISOMERIC PHENYLPROPANOIDS 518
*PLATTNER, R D AND KLEIMAN, R

IDENTIFICATION OF PLATELET-ACTIVATING FACTOR BY TANDEM MASS SPECTROMETRY 520
*PLATTNER, R D,STACK, R J,SOMMERS, B AND CRIDDLE, R S

SEPARATION AND IDENTIFICATION OF GLUCOSINOLATES FROM BRASSICA VEGETABLES USING HIGH PERFORMANCE CAPILLARY GC-MS 522
*SHAW, G J AND ANDRZEJEWSKI, D

FRAGRANCE ANALYSIS BY CAPILLARY GAS CHROMATOGRAPHY/MASS SPECTROMETRY 524
*WANG, J-S AND ROSENBERG, I E

FAST-ATOM BOMBARDMENT MASS SPECTROMETRY: AN ALTERNATIVE METHODOLOGY FOR THE CHARACTERIZATION OF AMILORIDE ANALOGUES 526
*TONDEUR, Y,NIEDERHUT, W AND CRAGOE, E J

ENHANCEMENT OF MOLECULAR IONS YIELDS IN PLASMA DESORPTION MASS SPECTROMETRY 528
*CRAIG, A G,ENGSTROM, A,BENNICH, H AND KAMENSKY, I

METABOLISM OF HOMOLOGUES OF DELTA-8 AND DELTA-9-TETRAHYDROCANNABINOL IN MICE 530
*HARVEY, D J AND BROWN, N K

THE USE OF NEGATIVE ION CAPILLARY GCMS AND DIRECT EXPOSURE PROBE IN THE QUALITATIVE ANALYSIS OF DELT-9 TETRAHYDROCANNABINOL (D9THC) IN CANNABINOID TREATED HUMAN LYMPHOCYTES AND MONOCYTE CELL LINE 532
*PAPA, V M,OU, D W,ROBBINS, E F AND WIEDERHOLD, M

CHARACTERIZATION OF PROPYLENE OXIDE-DNA ADDUCTS BY MASS SPECTROMETRY. ALKYLATION AT N-3 OF CYTOSINE RESULTS IN DEAMINATION TO A URICAL ADDUCT 534
*SOLOMON, J J,MUKAI, F,DECKER, K AND SEGAL, A

ANALYSIS OF ETHYLENE OXIDE/PROPYLENE OXIDE BIS-PHENOL A ADDUCTS BY THERMOSPRAY LC/MS/MS 536
*RUDEWICZ, P J,COVEY, T R AND MCFADDEN, W H

BIOCHEMISTRY: PEPTIDES/ION MOLECULE REACTIONS

ANALYSIS OF LABILE BIOMOLECULES USING A HIGH-RESOLUTION TIME-OF-FLIGHT MASS SPECTROMETER WITH LASER DESORPTION AND RESONANCE ENHANCED MULTIPHOTON IONISATION 538
*FREY, R,WEISS, G,KAMINSKI, H,BOESL, U,GROTEMEIER, H, WALTER, K AND SCHLAG, E W

ALTERNATIVE PRIMARY ION SOURCES FOR HIGH MASS FAB APPLICATIONS 540
BELL, D AND *GREEN, B N

PROTEIN SEQUENCE ANALYSIS BY TANDEM MAGNETIC DEFLECTION MASS SPECTROMETRY 542
*CARR, S A,ROBERTS, G D,HEMLING, M E AND ANDEREGG, R J

MATRICES FOR PEPTIDE SEQUENCING BY MONITORED ENZYMATIC HYDROLYSIS 544
*BEL, P AND COOK, K D

MAPPING OF PEPTIDES FROM HUMAN SERUM ALBUMIN BY FAB MASS SPECTROMETRY 546
*VAN BREEMEN, R B AND CREECH, J

THE DETERMINATION OF THE PRIMARY STRUCTURE OF A SERUM PROTEASE INHIBITOR BY HIGH PERFORMANCE TANDEM MASS SPECTROMETRY 548
*PAPAYANNOPOULOS, I A AND BIEMANN, K

STRUCTURAL STUDIES ON ALDOLASE REDUCTASE, MITE ALLERGON, AND PHOSPHOPEPTIDES BY TANDEM MASS SPECTROMETRY 550
*GRIFFIN, P R,HUNT, D F,SHABANOWITZ, J,ZHU, N-Z AND HUNT, A M

FAST ATOM BOMBARDMENT AND LOW ENERGY COLLISIONALLY-ACTIVATED DECOMPOSITION OF PEPTIDES USING A HYBRID INSTRUMENT 552
*GASKELL, S J,REILLY, M AND PORTER, C J

EFFECT OF STRUCTURAL VARIATIONS AND CATIONIZATION ON THE COLLISIONALLY ACTIVATED MS/MS SPECTRA OF PEPTIDES 554
*GUENAT, C,DINO, J AND TOMER, K B

MODIFICATION OF THE FRAGMENTATION OF PEPTIDES IN A TANDEM MASS SPECTROMETER BY DERIVATIZATION 556
*JOHNSON, R S AND BIEMANN, K

COLLISIONALLY-ACTIVATED DISSOCIATION SPECTROSCOPY OF NEUROPEPTIDES 558
*DASS, C AND DESIDERIO, D M

MATRIX SELECTION IN THE FABMS ANALYSIS OF PEPTIDES 560
*ACKERMANN, B L AND COUTANT, J E

FAB/MS FOR THE DETERMINATION OF ENDORPHINS 562
*VOYKSNER, R D AND WILLIAMS, F P

THE USE OF FAST ATOM BOMBARDMENT MASS SPECTROMETRY FOR EVALUATION OF SOLID PHASE PEPTIDE SYNTHESIS 564
*WEINTRAUB, S T,KLEBE, R J,KANDA, P AND LANFORD, R E

DETERMINATION OF ENZYMIC REACTION PARAMETERS BY ON-LINE FABMS 566
*MOORE, W T,FAN, T AND CAPRIOLI, R M

A NOVEL C-TERMINUS SPECIFIC PEPTIDE DERIVATIZATION DESIGNED TO ENHANCE FAB-MS SENSITIVITY: CHEMICAL INTRODUCTION OF QUATERNARY AMINE FUNCTIONALITY SPECIFICALLY TO C-TERMINUS VIA AZLACTONE INTERMEDIATE 568
*BENNETT, B D AND DAY, R A

IMPROVEMENTS IN THE SEQUENCING OF PEPTIDES BY GAS CHROMATOGRAPHIC MASS SPECTROMETRY 570
*VATH, J E AND BIEMANN, K

ANALYSIS OF ARGINYL PEPTIDES AT THE 20-200 PICOMOLE LEVEL BY CAPILLARY GAS CHROMATOGRAPHY-MASS SPECTROMETRY 572
*BALLARD, K D AND KNAPP, D R

NEGATIVE ION CHEMICAL IONIZATION MASS SPECTROMETRY OF AMINO ACID THIOHYDANTIONS 574
*WILLIAMS, T D,MORISON, D S AND ANDEREGG, R J

STRUCTURE DETERMINATION OF TRITERPENS FROM LICHENS BY TANDEM MS 576
TSOUPRAS, G,ALLEMAND, P AND *TABUCCHI, R

PLASMA DESORPTION MASS SPECTROMETRY OF HIGH MASS AND THERMALLY 578
LABILE COMPOUNDS
*KAMENSKY, I,CRAIG, A G AND SUNDQVIST, B

A PEPTIDE BOND REARRANGEMENT - FAB MS ANALYSIS OF SOYBEAN 580
LIPOXYGENASE
*YAZDANPARAST, R,STECZKO, J,SHIBATA, D,AXELROD, B
AND DIXON, J

A STUDY OF THE TEMPERATURE DEPENDENCE OF ION-MOLECULE 582
ASSOCIATION REACTIONS
*HERD, C R AND BABCOCK, L M

DIFFERENTIATIAL CROSS-SECTIONS FOR FINE-STRUCTURE TRANSITIONS 584
IN Kr+ [Kr,Kr]Kr+ AND Ar+[Ar,Ar]Ar+
*HOWARD, S,ROCKWOOD, A,TRAFTON, W,FRIEDRICH, B,ANDERSON, S
AND FUTRELL, J

ABSOLUTE CROSS-SECTION MEASUREMENTS IN QQQ INSTRUMENTS: 586
Ar+(Ar,Ar)Ar+ FOR Ar TARGETS
*MARTINEZ, R I AND DHEANDHANOO, S

REACTIONS OF GROUND STATE AND EXCITED STATE ATOMIC METAL IONS 588
WITH HALOGEN MOLECULES. A TANDEM ICR STUDY
*STROBEL, F AND RIDGE, D P

ION-MOLECULE REACTIONS OF GOLD IONS WITH ALIPHATIC AND AROMATIC 590
CARBONS
*CHOWDHURY, A K

ION/MOLECULE REACTIONS OF SILICON CATION CLUSTERS Sin+, N=1 TO 592
6
*CREASY, W R,O'KEEFE, A AND MCDONALD, J R

THE REACTIONS OF TRIALKYLGERMYLIUM (R3Ge+) 594
*STONE, J A AND WYTENBURG, W J

REACTIVITY OF Fe(CO)5 NEGATIVE IONS WITH ACTIVATED OLEFINS, 596
KETONES, AND ALCOHOLS
WEDDLE, G H,WRONKA, J,*MECKSTROTH, W K AND RIDGE, D P

REACTIONS OF C3H3+ AND C5H5+ IONS WITH ACETYLENE AND 598
DIACETYLENE IN THE GAS PHASE
*OZTURK, F,BAYKUT, G,MOINI, M AND EYLER, J R

REACTIONS OF THE CATECHOLATE ANION WITH SELECTED LEWIS ACIDS 600
*TAYLOR, W S AND BABCOCK, L M

SELF-CHEMICAL IONIZATION REACTIONS IN DILUTE DI-I-PROPYL ETHER 602
MIXTURES
*BARRY, R M AND MUNSON, B

SELECTIVE DETERMINATIONS BY LOW ENERGY ION-MOLECULE REACTIONS 604
USING A HYBRID MASS SPECTROMETER
*MISSLER, S R AND FREAS, R B

ION-MOLECULE REACTIONS FOR DISTINGUISHING STRUCTURAL ISOMERS OF 606
ORGANIC IONS IN THE GAS PHASE
*BOZORGZADEH, M H

STRONG HYDROGEN BONDING TO A CARBON-CARBON MULTIPLE BOND 608
*SHALER, T A AND MORTON, T H

KINETICS AND EQUILIBRIA OF ION-MOLECULE ASSOCIATION REACTIONS 610
GALLAGHER, R,MASON, R S,*JENNINGS, K R AND WICKHAM, T J

THE ENERGY DEPENDENCE OF THE REACTIONS OF Ar+ AND Ar2+ WITH METHANE AND CARBON DISULFIDE 612
SHUL, R J,PASSARELLA, R,YANG, X-L,*KEESEE, R G AND CASTLEMAN, A W

SUBSTITUENT EFFECTS ON THE MASS SPECTRAL FRAGMENTATIONS OF METHOXYMETHYLBENZENES 614
*CHIPMAN, G R

ON THE LOSS OF SEVENTEEN MASS UNITS FROM ARYLMETHYLSULFIDES 616
*CHENG, M T

A STUDY OF ADDUCT ION FORMATION: REACTIONS OF THE TRIMETHYLSILYL ION WITH OXYGENATED COMPOUNDS 618
*ORLANDO, R AND MUNSON, B

MASS SPECTROMETRIC STUDY OF BORON TRIAHLIDE MONOAMINES 620
*NG, K,PIATEK, B AND SHIMANSKAS, C

FORMATION OF THE (M+1)- ION IN THE NCI MASS SPECTRUM OF CHLORPROTHIXENE 622
*CALLERY, P S,GARLAND, W A AND FUKUDA, E K

LITHIATED POLYPROPYLENEGLYCOLS FOR CALIBRATION OF TANDEM MASS SPECTROMETERS 624
GILLIAM, J M AND *OCCOLOWITZ, J L

DECOMPOSITION REACTIONS OF ALKYLBENZENE MOLECULAR IONS REVEALED BY MULTI PHOTON IONIZATION MASS SPECTROMETRY: PROPYLBENZENE MOLECULAR IONS 626
*GROTEMEYER, J,BOESL, U,WALTER, K AND SCHLAG, E W

BRANCHING RATIOS AND MECHANISMS OF TWO COMPETING HYDROGEN REARRANGEMENTS IN THE ELECTRON IMPACT FRAGMENTATION OF SUBSTITUTED ACETOACETANILIDES 628
*SHARP, T R

NEW CONSIDERATIONS FOR CHOOSING A LIQUID MATRIX FOR FAST ATOM BOMBARDMENT 630
SCHROEDER, E,PESCH, R AND *DIELMANN, G

SIMULTANEOUS MASS-SELECTIVE EJECT/EXCITE FOR FT/ICR MASS SPECTROMETRY 632
CHEN, L AND *MARSHALL, A G

WEDNESDAY ORAL SESSIONS

LCMS APPLICATIONS

ADAPTION OF THERMOSPRAY LC-MS FOR MICRO LC 634
OSTERMAN, R M,BLAKLEY, C R,FERGUSSON, G J AND *VESTAL, M L

THERMOSPRAY ANALYSIS: STRUCTURAL IDENTIFICATION USING REPELLER CID WITH A TRIPLE STAGE QUADRUPOLE TO OBTAIN CID/MS/MS DATA 636
*MCFADDEN, W H,RUDEWICZ, P J AND GARTEIZ, D A

CONTINUOUS FLOW FAB-MS ANALYSIS OF PEPTIDE DIGESTS 638
HUTCHINSON, D W,WOOLFITT, A R,*JENNINGS, K R AND ASHCROFT, A E

MICROBORE HPLC/MS USING A CONTINUOUS FLOW FAB PROBE INTERFACE 640
*CAPRIOLI, R M,DAGUE, B,FAN, T AND MOORE, W

APPLICATIONS OF CONTINUOUS FLOW FAB-MS AND LC-FAB-MS FOR THE STUDY OF NON POLAR, THERMALLY LABILE MOLECULES 642
*BARBER, M,TETLER, L W,ASHCROFT, A,BROWN, R S AND ELLIOTT, G

RECENT DEVELOPMENTS OF FRIT-FAB LC/MS INTERFACE 644
KOBAYASHI, T,MIZUNA, T,KUBOTA, E,HIGUCHI, T,*ITAGAKI, Y AND ISHII, D

NEW APPROACHES TO THE SUPERCRITICAL FLUID CHROMATOGRAPHY-MASS SPECTROMETRY INTERFACE FOR ANALYSIS OF NONVOLATILE MATERIALS 646
*KALINOSKI, H T,UDSETH, H R,OLIVARES, J A AND SMITH, R D

INTERFACES FOR PACKED AND CAPILLARY COLUMN SFC/MS 648
*BERRY, A J,GAMES, D E,MYLCHREEST, I C,PERKINS, J R AND PLEASANCE, S

SUPERCRITICAL FLUID CHROMATOGRAPHY-MASS SPECTROMETRY USING A "HIGH MASS" QUADRUPOLE MASS SPECTROMETER AND SPLITLESS INJECTION 650
*PINKSTON, J D,OWENS, G D,MILLINGTON, D S,MALTBY, D A, BURKES, L J AND DELANEY, T E

AUTOMATED OFF-LINE LC/MS OF PEPTIDE DIGESTS USING TIME-OF-FLIGHT, SOLID PHASE SIMS 652
*BEAVIS, R C,MAIN, D E,TANG, X,LAFORTUNE, F AND STANDING, K G

ION SPRAY LIQUID CHROMATOGRAPHY/API TANDEM MASS SPECTROMETRY DETERMINATION OF PEPTIDES 654
*LEE, E D,WEIDOLF, L O G AND HENION, J D

SYMPOSIUM: APPLICATIONS OF FTMS TO REAL PROBLEMS

ADVANTAGES AND DIFFICULTIES OF FT/ICR FOR ANALYTICAL MASS SPECTROMETRIC APPLICATIONS 656
*MARSHALL, A G

APPLICATION OF FOURIER TRANSFORM MASS SPECTROMETRY TO STUDY TRANSITION METAL CLUSTER CHEMISTRY 658
*JACOBSON, D B AND DIERS, J

FOURIER TRANSFORM MASS SPECTROMETRY IN THE STRUCTURAL CHARACTERIZATION OF OLIGOPEPTIDES AND PROTEINS 660
*HUNT, D F AND SHABANOWITZ, J

KINETIC CHARACTERIZATION OF IONS DERIVED FROM METAL CARBONYLS 662
REENTS, W,STROBEL, J,WRONKA, J,MECKSTROTH, W AND *RIDGE, D P

PROBLEM-SOLVING APPLICATIONS OF FTMS 664
*CODY, R B

SYMPOSIUM: DYNAMICS OF ION PROCESSES, con't

THE UNIMOLECULAR DECOMPOSITION OF MOLECULAR IONS IN ASSOCIATION WITH INERT GAS CLUSTERS 666
*STACE, A J

ION-DIPOLE AND ELECTRON-DIPOLE REACTIONS 668
*CLARY, D C

NON-ADIABATIC EFFECTS IN ION-MOLECULE PROCESSES 670
*ARMENTROUT, P B

CROSSED BEAM STUDIES OF ION-MOLECULE REACTION DYNAMICS 672
*FARRAR, J M

WEDNESDAY POSTER SESSION

METABOLISM AND TOXICOLOGY/IONIZATION METHODS

URINARY STEROID PROFILES OF ATHLETES 674
*HATTON, C K AND CATLIN, D H

A NEW APPROACH FOR MEASUREMENTS OF URINARY ORGANIC ACIDS IN SMALL VOLUME SAMPLES USING A VARIABLE ION CURRENT ION TRAP DETECTOR 676
*LIN, S-N,CHENG, P-S AND CAPRIOLI, R M

REAL-TIME RESPIRATORY GAS MONITORING WITH QUADRUPOLE MASS SPECTROMETRY IN UNDERWATER RESEARCH 678
*WINBOROUGH, M,CESSNA, G,BARTMAN, C AND PATTERSON, T

STRUCTURE CONFIRMATIONS OF INTERMEDIATES IN THE VITAMIN B12 BIOSYNTHETIC PATHWAY OF PROPIONIBACTERIUM SHERMANII BY FAB MASS SPECTROMETRY 680
SANTANDER, P J,*SHARP, T R AND SCOTT, A I

GC-MS DETERMINATIION OF ISOTOPIC ENRICHMENT AND QUANTITATIVE ANALYSIS OF VITAMIN C: APPLICATION TO HUMAN METABOLIC STUDIES 682
*WAGNER, D A AND ANNAN, M

INTRAMOLECULAR ISOTOPE EFFECTS IN THE DEAMINATION OF DIAMINES BY DIAMINE OXIDASE 684
*SUBRAMANYAM, B,GEELHAAR, L A AND CALLERY, P S

THE METABOLISM OF 2-OCTYNOIC ACID, A SUICIDE SUBSTRATE FOR GENERAL ACYL- COA DEHYDROGENASE, AND ITS EFFECT ON ENDOGENOUS FATTY ACID METABOLISM 686
*MONTGOMERY, J A,MAMER, O A AND COLLE, E

DETERMINATION OF ISOTOPIC ABUNDANCES OF CALCIUM AND MAGNESIUM BY FABMS 688
XIANGYU, J,LIU, Y-M,MARTIN, B,WEAVER, C AND *SMITH, D

DETERMINATION OF SELECTED HERBICIDES AND CHLORINATED PHENOLS IN URINE BY GAS CHROMATOGRAPHY/MASS SPECTROMETRY/MASS SPECTROMETRY 690
*HOLLER, J S,HILL, R H,FAST, D M,CARDINALI, F L,TODD, G D, MCGRAW, J M,BAILEY, S L AND NEEDHAM, L L

SECONDARY METABOLITES OF ERWINIA AMYLOVORA POSSIBLY INVOLVED IN NECROTIC SYMPTOMATOLOGY OF FIREBLIGHT DISEASE 692
*FEISTNER, G J

ANALYSIS OF QUINOLIZIDINE ALKALOIDS IN BIOLOGICAL FLUIDS BY TANDEM MASS SPECTROMETRY 694
*JONES, A D,MEEKER, J E AND KILGORE, W W

TOXICOLOGICAL APPLICATIONS OF THE ION TRAP DETECTOR 696
LIM, H K,*SAKASHITA, C O AND FOLTZ, R L

QUANTIFICATION OF LSD AND NOR-LSD IN URINE BY GAS CHROMATOGRAPHY/NEGATIVE ION CHEMICAL IONIZATION MASS SPECTROMETRY 698
*LIM, H K,FRANCOM, P AND FOLTZ, R L

INVESTIGATION OF GUANINE ADDUCTS BY POSITIVE AND NEGATIVE THERMOSPRAY MASS SPECTROMETRY 700
*CROWLEY, J,O'HARA, M,VALLADIER, P,MARNETT, L J AND HOOD, R

DETECTION AND IDENTIFICATION OF TETRACHLORIDIBENZOFURAN METABOLITES BY GC/MS 701
*PARKER, C E,TOMER, K B,BURKA, L T AND BIRNBAUM, L S

METHODS FOR QUANTITATIVE DETERMINATION OF THE DNA ADDUCT O4-ETHYLTHYMIDINE BY ELECTRON CAPTURE NEGATIVE ION CHEMICAL IONIZATION MASS SPECTROMETRY 703
*TURNER, M J,KOCH, S A M AND SWENBERG, J A

METHANE NEGATIVE ION MASS SPECTROMETRY OF NITRO-POLYCYCLIC AROMATIC HYDROCARBON METABOLITES 705
*KORFMACHER, W A,DJURIC, Z,FIFER, E K AND BELAND, F A

A STUDY OF SOME TRICYCLIC ANTIDEPRESSANT DRUGS USING CAPILLARY GC/CIMS 707
GEIDNER, R M AND *SCHILDCROUT, S M

STIMULATED SURFACE IONIZATION OF ALKALI METALS FROM ALKALI ALUMINUM SILICATES IN THE PRESENCE OF F2 OR Cl2 709
*FUJII, T

APPLICATIONS OF METHANOL THERMOSPRAY IONIZATION TO COMPOUNDS OF PHARMACEUTICAL INTEREST 711
*DAS, P R,MALCHOW, R D AND PRAMANIK, B N

NEGATIVE ION MASS SPECTROMETRY OF POLYCHLORODIBENZO-P-DIOXINS AND POLYCHLORODIBENZOFURANS: CORRELATIONS BETWEEN OBSERVED FRAGMENTATIONS AND CALCULATED TOTAL INTERNAL ENERGIES 713
*LARAMEE, J,ARBOGAST, B AND DEINZER, M

STRUCTURAL ANALYSIS OF UNDERIVATIZED LIPID-A USING LASER DESORPTION (LDMS) AND PLASMA DESORPTION (PDMS) MASS SPECTROMETRY 715
*WANG, R,DEMIREV, P,COTTER, R J,QURESHI, N AND TAKAYAMA, K

THE EFFECT OF PRIMARY BEAM ENERGY ON SECONDARY ION SAMPLE EFFICIENCY IN THE 5-30 KEV ENERGY RANGE 717
*ABERTH, W AND BURLINGAME, A L

POSITIVE AND NEGATIVE ION FABMS OF p-TERT-BUTYLCALIX-8-ARENE TETRAALKYL AMMONIUM SALTS 719
*LEARY, J A,ZEBRE, L E,HOFMEISTER, G E AND PEDERSEN, S F

MASS SPECTROMETRIC STUDIES OF MULTIPLY-CHARGE DIATOMIC SPECIES 721
*HARBOL, K L AND KISER, R W

SOLUTE AGGREGATION IN ELECTROSPRAY IONIZATION OF ARGININE SOLUTIONS 723
*MENG, C K AND FENN, J B

MULTIPHOTON IONIZATION OF CYCLIC KETONES 725
*CORNISH, T AND BAER, T

IONIZATION METHODS FOR FOURIER TRANSFORM MASS SPECTROMETRY OF INVOLATILE MOLECULES 727
*LOO, J A,WILLIAMS, E R,FURLONG, J J P,WANG, B H AND MCLAFFERTY, F W

DERIVATIZATION OF PEPTIDES FOR MULTIPHOTON IONIZATION-FOURIER TRANSFORM MASS SPECTROMETRY 729
*GRESE, R P

BIASED ELECTRON ATTACHMENT MASS SPECTROMETRY (BEAMS) ANAYLSIS OF PERFLUOROCARBONS 731
MALHOTRA, R,ST.JOHN, G A AND *COGGIOLA, M J

K+ IONIZATION OF DESORBED SPECIES(K+IDS) - THE DEPENDENCE OF STRUCTURAL AND MOLECULAR WEIGHT INFORMATION OBRAINED ON THE TEMPERATURE VARIABLE 733
*LIGHT, K J,KASSEL, D B AND ALLISON, J

DESORPTION MECHANISMS USING A NEW LIQUID-SIMS-TOF MASS SPECTROMETER 735
*OLTHOFF, J K,LYS, I AND COTTER, R J

A FOCUSED, FAST NEUTRAL MOLECULAR BEAM PROBE FOR SIMS 737
*APPELHANS, A D,DELMORE, J E AND DAHL, D A

STEREOCHEMICAL EFFECTS IN THE AMMONIA CHEMICAL IONIZATION SPECTRA OF EPIMERIC SECONDARY ALLYLIC ALCOHOLS 739
*MARBURY, G D,CHAMBERS, R J,TABET, J C,GUNAT, C AND ZORETIC, P A

USE OF LEAKY DIELECTRIC END PLATES ON COLLISION CELLS IN TRIPLE QUAD MS/MS 741
*FITE, W L AND KETKAR, S N

THE ADVANTAGES OF PERFLORINATED POLYETHES AS FAB CALIBRATION COMPOUNDS; A STUDY OF CALIBRATION MATERIALS 743
MCCLURE, T D,*BAKER, P F AND SCHRAM, K H

THE ROLE OF MATRIX CHEMISTRY IN "MATRIX-ASSISTED" MASS SPECTROMETRY 745
*REYNOLDS, J D AND COOK, K D

ACETONITRILE AS A SELCTIVE CHEMICAL IONIZATION REAGENT 747
*JALONEN, J

FAB ION YIELD AND SOURCE CONSTRUCTION 749
*MUNSTER, H,THEOBALD, F,BUDZIKIEWICZ, H AND SCHRODER, E

BIOMOLECULAR ION YIELDS FROM SAMPLES PREPARED BY DIFFERENT TECHNIQUES VS ENERGY DENSITY IN THE FAST ION TRACK 751
*JONSSON, G,HAKANSSON, P,SUNDQVIST, B,NIELSEN, P AND ROEPSTORFF, P

THICKNESS AND VOLUME EFFECTS IN MeV ION INDUCED DESORPTION (PDMS) 753
BOLBACH, G,DELLA-NEGRA, S,DEPRUN, C,*LE BEYEC, Y AND STANDING, K G

SPONTANEOUS DESORPTION AND PLASMA DESORPTION MASS SPECTROMETRY, A SIMPLE WAY TO COMPARE keV AND MeV ION INDUCED DESORPTION 755
BOLBACH, G,DELLA-NEGRA, S,DEPRUN, C AND *LE BEYEC, Y

QUANTITATIVE ANALYSIS OF MODIFIED NUCLEOSIDES USING FAST ATOM BOMBARDMENT COMBINED WITH TANDEM MASS SPECTROMETRY 757
*CERNY, R L

THURSDAY ORAL SESSIONS

SYMPOSIUM: ANALYTICAL EPIDEMIOLOGY: CARCINOGEN DOSIMETRY IN HUMANS

FEATURE LECTURE: ASSESSMENT OF THE RISK OF ENVIRONMENTAL POLLUTANTS 759
*HOUK, V N

MOLECULAR DOSIMETRY 761
*WISHNOK, J S

DO DNA ADDUCT MEASUREMENTS IN HUMAN URINE PROVIDE ACCURATE DATA FOR CANCER RISK ASSESSMENT? 763
*GROOPMAN, J D

NUCLEIC ACID-CARCINOGEN ADDUCTS IN HUMAN DOSIMETRY 765
*FARMER, P B

ION TRAPS: INSTRUMENTATION

A FOURIER TRANSFORM QUADRUPOLE ION TRAP MASS SPECTROMETER 767
*SYKA, J E P AND FIES, W J

THE QUADRUPOLE ION TRAP AS A TANDEM MASS SPECTROMETER - INSTRUMENTATION AND APPLICATIONS 769
*LOURIS, J N,COOKS, R G,WEBER-GRABAU, M AND STAFFORD, G

COLLISION ACTIVATED DECOMPOSITION OF NEGATIVE IONS IN AN ION TRAP MASS SPECTROMETER 771
*MCLUCKEY, S A,GLISH, G L AND KELLEY, P E

COMPARISON OF MS/MS WITH TRIPLE QUADRUPOLE AND ION TRAP TANDEM MASS SPECTROMETERS 773
*JOHNSON, J V,YOST, R A,BRADFORD, D AND KELLY, P

ENHANCED SENSITIVITY AND DYNAMIC RANGE ON AN ION TRAP MASS SPECTROMETER WITH AUTOMATIC GAIN CONTROL 775
*STAFFORD, G C,TAYLOR, D M,BRADSHAW, S C AND SYKA, J E P

BIMOLECULAR REACTIONS OF CARBON DIOXIDE MICROCLUSTER IONS WITH WATER, INVESTIGATED WITH A TANDEM MOLECULAR BEAM QUISTOR QUADRUPOLE INSTRUMENT 777
ROMANOWSKI, G,GABLING, R-H AND *WANCZEK, K P

SELECTION OF PARAMETERS FOR ION EXCITATION AND EJECTION IN FOURIER TRANSFORM MASS SPECTROMETRY 779
*CODY, R B,GOODMAN, S D,GHADERI, S AND SHOHET, L

ULTRA-HIGH RESOLUTION FTICR: THEORETICAL CONDITIONS AND EXPERIMENTAL RESULTS 781
*LAUKIEN, F H

LASER DESORPTION FOURIER TRANSFORM MASS SPECTROMETRY USING A DUAL-CELL CONFIGURATION 783
*WEIL, D A,HEIN, R AND CODY, R B

LASER DESORPTION/FOURIER TRANSFORM MASS SPECTROMETRY FOR THE ANALYSIS OF POLYMERIC ADDITIVES 785
*JOHLMAN, C L,WILKINS, C L AND YOUSSEFI, M

STABILITY DIAGRAM DETERMINATION AND ION TRAJECTORY MODELLING FOR THE ION TRAP MASS SPECTROMETER 787
*TODD, J F J,BEXON, J J AND SMITH, R D

PICOGRAM TO MICROGRAM ANALYSIS BY GAS CHROMATOGRAPHY/ION TRAP MASS SPECTROMETRY 789
*YOST, R A,MCCLENNEN, W AND SNYDER, A P

COLLISIONAL PROCESSES AND ION MOLECULE REACTIONS

SLOW UNIMOLECULAR DISSOCIATIONS OF RADICAL CATIONS: ANISOLE AND C6H6 ISOMERS 791
*LIFSHITZ, C,OHMICHI, N,ZIESEL, J -P AND AVIENTE, V

VIBRATIONAL AND ELECTRONIC STATES IN H2+ STUDIED BY FIELD IONIZATION OF RYDBERG H ATOMS 793
BORDAS-NAGY, J AND *HOLMES, J L

ABSOLUTE STATE-TO-STATE CROSS SECTIONS FOR THE REACTIONS: H2++Av AND Av++H2 795
*SHAO, J D,XU, R,LIAO, C L,FLESCH, G D,LI, Y G AND NG, C Y

PRODUCT SELECTION IN ACID-BASE REACTIONS. LEWIS vs. BRONSTED & BRONSTED vs. BRONSTED 797
*MORTON, T H,REDMAN, E W AND STAMS, D A

MODELING THE ELECTROSTATIC INTERACTIONS BETWEEN TRANSITION METAL IONS AND POLAR MOLECULES: THE RELATIONSHIP BETWEEN PREFERRED COMPLEX GEOMETRIES AND PRODUCT DISTRIBUTIONS 799
HANKINSON, D J AND *ALLISON, J

GAS PHASE CHEMISTRY OF THE BENZENE RADICAL CATION: REACTION WITH CYCLIC ALKANES 801
*WARNER, C D,HOLMAN, R W AND GROSS, M L

CHARACTERIZATION AND REACTIVITY OF CARBON CLUSTER IONS USING FTMS 803
*MCELVANY, S W AND NELSON, H H

DO ALKYL CARBANIONS EXIST IN THE GAS PHASE? 805
*GRAUL, S T AND SQUIRES, R R

ENVIRONMENTAL APPLICATIONS

CHARACTERIZATION OF CONSTITUENTS IN TOBACCO SMOKE USING FOURIER TRANSFORM MASS SPECTROMETRY 807
*WISE, M B

DETECTION OF OH-NO2-PAH, OH-NO2-PAK AND OH-NO2-BENZENES/TOLUENES IN AN AMBIENT AIR PARTICULATE EXTRACT BY EI AND NCI GC/MS 809
*NISHIOKA, M G,CONTOS, D A AND LEWTAS, J

FORMATION OF POLYCYCLIC AROMATIC HYDROCARBON ADDUCT IONS IN NEGATIVE ION CHEMICAL IONIZATION 811
*HILPERT, L R AND WHITE, E

A HYBRID HRGC/MS/MS METHOD FOR THE CHARACTERIZATION OF TETRACHLORINATED-p- DIOXINS IN ENVIRONMENTAL SAMPLES 813
*TONDEUR, Y,NIEDERHUT, W N,CAMPANA, J E AND MISSLER, S R

MEASUREMENT OF PHOTO INDUCED LOSS OF LOW VAPOR PRESSURE MOLECULES BY MASS SPECTROMETRY 815
*ORTH, R G AND HILEMAN, F

EVALUATION OF MULTIPLE CARBON-13 LABELED INTERNAL STANDARDS FOR THE GC/MS DETERMINATION OF CHLORINATED DIBENZO-P-DIOXINS AND DIBENZOFURANS 817
*SACK, T M AND STANLEY, J S

HIGH RESOLUTION SELECTED ION MONITORING OF POLYCHLORINATED DIBENZO-P-DIOXINS (PCDD) AND DIBENZOFURANS (PCDF) USING NON-PFK LOCK MASSES 819
*TAGUCHI, V Y,REINER, E J,HALLOS, B AND WANG, D T

ISOMER SPECIFIC GC/MS DETERMINATION OF CHLORINATED DIBENZO-P-DIOXINS 821
SOVOCOOL, G W,*DONNELLY, J R,MUNSLOW, W D AND MITCHUM, R K

A GAS CHROMATOGRAPHY-MASS SPECTROMETRY METHOD FOR SELECTED HERBICIDES IN SURFACE WATER 823
*SMITH R G,TRIEBE, F M,HORNER, L M,LAUER, R,BASZIS, S R AND KLEIN, A J

DETERMINATION OF TRACE LEVELS OF SURFACTANTS IN ENVIRONMENTAL MATRICES USING FAB/MS 825
WARD, S R,SIMMS, J R,MOORE, B L,BANDURRAGA, M M AND *KEOUGH, T

SYMPOSIUM: FRAGMENTATION OF VERY LARGE MOLECULES

TIME AND MASS STUDIES OF UNIMOLECULAR FRAGMENTATION OF LARGE IONS 827
*COTTER, R J

MECHANISMS OF DESORPTION AND FRAGMENTATION OF LARGER MOLECULES AND CLUSTERS FROM SURFACES 829
*TSONG, I S T

SEQUENCE ANALYSIS OF BIOLOGICAL MACROMOLECULES BY TANDEM MAGNETIC DEFLECTION MASS SPECTROMETRY 830
*CARR, S A,HEMLING, M E,ROBERTS, G D,ANDEREGG, R J AND VICKERS, R

TWO COLOR LASER DESORPTION-PHOTOIONIZATION STUDY BY FOURIER TRANSFORM MASS SPECTROMETRY 832
NUWAYSIR, L M,BROWN, R S AND *WILKINS, C L

STUDIES OF THE ACTIVATION AND DISSOCIATION OF LARGE POLYATOMIC IONS 834
*RUSSELL, D H

REACTION MECHANISMS

TRACING REACTION PATHWAYS BY COLLISIONALLY ACTIVATED DISSOCIATION: CH3O=CHCH3 AND CH2=OCH2CH3 836
*MCADOO, D J AND HUDSON, C E

THE METHOXY LOSS FROM IONIZED METHYL ACETATE AND THE KETO/ENOL TAUTOMERIZATION OF VINYL ALCOHOL IN THE GAS PHASE 838
*WESDEMIOTIS, C,FENG, R,ZHANG, M-Y AND MCLAFFERTY, F W

THE STRUCTURE AND GAS PHASE ENERGETICS OF THE C7H7+ ISOMERS: TOLYL, BENZYL, AND TROPYLIUM IONS 840
OLESIK, S,BAER, T,HOLMES, J L AND *MORROW, J C

SECONDARY DEUTERIUM KINETIC ISOTOPE EFFECT ON THE CYCLOREVERSION OF 2,2- DIPHENYL-3-ARYLCYCLOBUTANONE 842
*SMITH, G G AND REDDY, G S

GAS PHASE [4+2] RADICAL CATION CYCLOADDITIONS 844
*CASTLE, L W AND GROSS, M L

HYDROGEN INTERCHANGE PRIOR TO FRAGMENTATION OF PROTONATED MOLECULES 846
*HARRISON, A G

ON THE INTRINSIC PROPERTIES OF ALKYL-SUBSTITUTED BENZENE ARENIUM IONS: A STUDY IN THE GAS PHASE 848
*HOLMAN, R W

MASS SPECTRA OF 3-NITROCHROMENES AND 3-NITROCHROMANS 850
MITCHELL, D,BOWEN, R D,*JENNINGS, K R,VARMA, R S AND KABALKA, G W

EFFECTS OF SITE OF PROTONATION ON LOW AND HIGH ENERGY DAUGHTER ION MS/MS SPECTRA OF PHENOTHIAZINES 852
*MCLUCKEY, S A,GLISH, G L,DIDONATO, G C AND BUSCH, K L

DIFFERENT FRAGMENTATION OF ISOMERIC METHYL ETHYL AND ETHYL METHYL CITRACONATES UNDER ELECTRON IMPACT 854
*MANDELBAUM, A,BORNSTEIN, D,TAMIRI, T AND ZITRIN, S

THURSDAY POSTER SESSIONS

SUGARS AND NUCLEIC ACIDS/INORGANIC

MASS SPECTROMETRY OF L- -ASPARTAMIDO-CARBOHYDRATES ISOLATED FROM OVALBUMIN 856
WANG, T,CHEN, T AND *BAROFSKY, D F

LSIMS SPECTRA AND DAUGHTER ION STUDIES OF SYNTHETIC LACTOSAMINE SERIES OLIGOSACCHARIDES 858
*PAMIDI, K M,JAIN, R K,ABBAS, S A,MATTA, K L AND LAINE, R A

LIQUID SECONDARY ION MASS SPECTROMETRY OF COMPLEX CARBOHYDRATES FROM GLYCOPROTEINS 860
*GILLECE-CASTRO, B,ABERTH, W,KE, J AND BURLINGAME, A L

FAB AND SEQUENTIAL MASS SPECTROMETRY WITH A VG ZAB-EQ: SACCHARIDE STEREOISOMERS 862
WRIGHT, J L C AND *GUEVREMONT. R

CHARACTERIZATION OF GLYCOCONJUGATES BY TANDEM FOUR SECTOR MASS SPECTROMETRY 864
*DOMON, B AND COSTELLO, C E

CHARACTERIZATION OF LIPIDS IN BACTERIA BY CONSTANT NEUTRAL LOSS SCANS 866
*HELLER, D,MARTIN, W,MURPHY, C,UY, M AND FENSELAU, C

DIRECT CHEMICAL IONIZATION MASS SPECTROMETRY OF UNDERIVATIZED ARACHIDONIC ACID METABOLITES: APPLICATION TO LEUKATRIENE BIOSYNTHESIS 868
JAMIESON, G C,GUT, J AND TRUDELL, J R

DETERMINATION OF OLIGOSACCHARIDE ISOMERIC BRANCHING BY CID MASS SPECTROMETRY 870
*SANTIKARN, S,REINHOLD, V,COSTELLO, C E AND WARREN, C D

CHARACTERIZATION OF THE GLYCOLIPID MEMBRANE ANCHOR OF HUMAN ERYTHROCYTE ACETYLCHOLINESTERASE BY FAST ATOM BOMBARDMENT MASS SPECTROMETRY 872
*SANTIKARN, S,REINHOLD, V N,ROSENBERRY, T L AND ROBERTS, W L

STRUCTURE ELUCIDATION OF THE LIPOPOLYSACCHARIDE FROM COXIELLA BURNETII 874
*HER, G R,SANTIKARN, S,REINHOLD, V N AND WILLIAM, J C

THE STRUCTURE DETERMINATION OF NEISSERIA GONOCOCCAL LIPID OLIGOSACCHARIDES BY LSIMS 876
*GIBSON, B W,WEBB, J,FISHER, S,BURLINGAME, A L,YAMASAKI, R AND GRIFFISS, M

ISOLATION AND CHARACTERIZATION OF 3-(3-AMINO 3-CARBOXYPROPYL)URIDINE, A NEW NUCLEOSIDE FROM HUMAN URINE 878
*CHHEDA, G B,TWOREK, H A,BHARGAVAA, A K,MCCLOSKEY, J A, RACHLINT, E,DUTTA, S P AND PATRZYC, H B

CAPILLARY GC AND GCMS OF TRIMETHYLSILYL DERIVATIVES URIDINE, CYTIDINE AND SELECTED ANALOGS 880
SCHRAM, K H AND *REDDY, G S

IMPROVED MATRIX FOR THE DETECTION OF NUCLEOTIDES BY FAB/MS 882
*MOSER, H AND WOOD, G W

DISCRIMINATION OF POSITIONAL ISOMERS OF NUCLEOSIDE MONOPHOSPHATES BY CAD/MIKES 884
*SUZUKI, M,TAKEDA, N,MASUDA, K,HARADA, K,TATEMATSU, A, TAKEDA, T AND SHIRATSUCHI, K

BI-DIRECTIONAL SEQUENCING OF OLIGONUCLEOTIDE-ANALOGS 886
*GRIFFIN, D,STIRCHAK, E,SUMMERTON, J E,WELLER, D AND DEINZER, M

ENHANCED SENSITIVITY OF LITHIUM-OLIGONUCLEOTIDE SALTS USING POSITIVE ION FABMS 888
*LEARY, J A AND OGDEN, S

DIFFERENTIATION BETWEEN ISOMERIC O-ALKYLTHYMIDINES BY TIME-OF-FLIGHT SIMS 890
*LAFORTUNE, F,BEAVIS, R,SCHUELER, B,STANDING, K G,TANG, X AND WESTMORE, J B

PEPTIDE SEQUENCING 892
SCHNEIDER, K,REINER, J AND *SPITELLER, G

IDENTIFICATION OF MODIFIED AND UNMODIFIED BASES AND NUCLEOSIDES USING SELF CHEMICAL IONIZATION FOURIER TRANSFORM ION CYCLOTRON RESONANCE MASS SPECTROMETRY 894
WELLER, R R,*MAYERNIK, J A AND GIAM, C S

MASS SPECTROMETRY OF NEW DIDEOXYNUCLEOSIDES AND 4-THIODIDEOOXYNUCLEOSIDES 896
*KEMPFF, M B,HOOD, R J,HORWITZ, J P AND PALOMINO, E

MASS SPECTRAL ANALYSES OF OLIGONUCLEOTIDES AND PRODUCTS ON BENZO[a]PYRENE REACTIONS WITH DNA IN VITRO 898
*DINO, J J,GUENAT, C R AND KAUFMAN, D G

HPLC-THERMOSPRAY MASS SPECTROMETRIC ANALYSIS OF DNA BASES 900
*DAVIDSON, W C,GREATHEAD, R J,WALDEN, T L,BLAKELY, W F, HOLWITT, E AND DIZDAROGLU, M

FAST ATOM BOMBARDMENT MASS SPECTROMETRY OF THE SODIUM SALT OF THE ANTITUMOR ANTIBIOTIC TETROCARCIN 902
*REDDY, A M AND SCHRAM, K H

REMOVAL OF ISOBARIC INTERFERENCES VIA PULSED LASER RESONANCE IONIZATION MASS SPECTROMETREY FOR LEAD AND BISMUTH MIXTURES 904
*FEAREY, B L,ROWE, M,MILLER, C M AND NOGAR, N S

ANALYSIS OF MONOSUBSTITUTED GROUP VI METAL CARBONYLS BY EI, DCI, FD AND FAB MASS SPECTROMETRY 906
VAN BREEMEN, R B,*MARTIN, L B AND SCHREINER, A F

MASS SPECTROMETRIC DETERMINATION OF STRUCTURAL AND GEOMETRICAL ISOMERS OF CHROMIUM(III)-BETA-DIKETONATES 908
*WENCLAWIAK, B W AND SCHULTZE, P

FAST-ATOM BOMBARDMENT OF MOLTEN BORON TRIOXIDE 910
*DOYLE, R J

EFFECTS OF BORON SUBSTITUENTS ON THE FRAGMENTATION OF PYRAZABOLES (AND THE USE OF SPECTRAL DATA AS A GUIDE TO SYNTHETIC STUDIES) 912
*MOJESKY, M T AND NIEDENZU, K

GAS-PHASE OSMIUM CLUSTER ION STRUCTURES FROM FT/ICR MS/MS AND ION-MOLECULE REACTION KINETICS OF H2Os3(CO)10 AND ITS DIMERS, TRIMERS, AND FRAGMENTS 914
MULLEN, S L AND *MARSHALL, A G

QUANTITATIVE DEPTH PROFILING OF SEMICONDUCTORS 916
*HALL, D J AND CHARALAMBOUS, P M

METAL CARBONYL CLUSTER IONS - FORMATION OF VERY LARGE CLUSTERS AND REACTIONS WITH HYDROCARBONS 918
*WRONKA, J,LAUKIEN, F AND FORBES, R

GAS PHASE PHOTODISSOCIATION OF FERROCENE ION 920
*FAULK, J AND DUNBAR, R C

ISOTOPIC ANALYSIS OF CALCIUM 922
TACKETT, J R AND *ELLEFSON, R E

MASS SPECTROMETRY OF DIMETHYLSILOXANES 924
*EPSTEIN, P S AND CURTIS, M D

DIRECT DETERMINATION OF TRACE ELEMENTS BY LASER MASS SPECTROMETRY 926
*HUANG, L,CONZEMIUS, R J AND HOUK, R S

THE USE OF A COMBINED ASSAY SPIKE AND INTERNAL ISOTOPIC STANDARD FOR THE ISOTOPE DILUTION MASS SPECTROMETRIC ASSAY OF PLUTONIUM 927
*CRAWFORD, D W,LEGEL, M A AND TRAHEY, N M

MATRIX EFFECTS IN SPUTTER ATOMIZATION/RESONANCE IONIZATION MASS SPECTROMETRY OF URANIUM 929
*GOERINGER, D E,CHRISTIE, W H AND VALIGA, R E

METALS ANALYSIS BY GLOW DISCHARGE MASS SPECTROMETRY. FACTORS AFFECTING QUANTITATIVE ANALYSIS 931
*KING, F L AND HARRISON, W W

STRUCTURAL DETERMINATION OF GLYCOPEPTIDE ANTIBIOTICS BY TANDEM MAGNETIC DEFLECTION MASS SPECTROMETRY 933
*ROBERTS, G D,CARR, S A AND CHRISTENSEN, S B

STRUCTURAL ELUCIDATION OF UNKNOWN TRICHOTHEGENES USING CAD FRAGMENTATION MAPS 935
*PAWLOSKY, R,MIROCHA, C J AND ABBAS, H K

A NOVEL METHOD FOR DETERMINING THE ACTIVE HYDROGEN CONTENT OF TRACE QUANTITIES OF BIOLOGICAL MATERIALS 936
*KITSON, F G

CATIONIZATION EFFICIENCY IN LASER DESORPTION FT/ICR MASS SPECTROMETRY 938
SHOMO, R E,VERDUN, F R AND *MARSHALL, A G

BIOCHEMICAL APPLICATIONS/FUELS AND GEOSCIENCE

FAB-MS AND PEPTIDE STRUCTURE DETERMINATION 940
*VAN DORSSELAER, A,LEPAGE, P AND FRAISSE, D

FAB MAPPING PROTEIN STRUCTURAL DETERMINATION OF RECOMBINANT HUMAN INTERFERON GAMMA 942
*GREER, F M,MORRIS, H R,FALLON, T AND BREWER, S J

PEPTIDE MAPPING AT THE SUB-NANOMOLE LEVEL. APPLICATION TO FATTY ACID BINDING PROTEIN 944
GIBSON, B,YU, Z,ABERTH, W,*BURLINGAME, A L AND BASS, N

LOCATION OF CROSS-LINKAGES IN PROTEINS BY FABMS 946
ZHONGRUI, Z,SUN, Y AND *SMITH, D

EXAMINATION OF THE W FRAGMENTATION SERIES IN FAB CAD SPECTRA OF PEPTIDES 948
*STULTS, J T AND WATSON, J T

THE MASS SPECTROMETRIC CHARACTERIZATION OF OLIGOSACCHARIDES RELEASED FROM RED CELL GLYCOPEPTIDES BY ENDO- -GALACTOSIDASE 950
*LAWSON, A M,SCUDDER, P,CARRUTHERS, R A,WILSON, S B, CHILDS, R,HOUNSELL, E F AND FEIZI, T

STRUCTURE ANALYSIS OF BIOLOGICALLY IMPORTANT COMPLEX NUCLEOSIDES BY DIFFERENT IONIZATION MODES COMBINED WITH TANDEM MASS SPECTROMETRY 952
*DAS, B C,COSSON, J P AND DE MAACK, F

STRUCTURAL STUDIES OF OLIGOSACCARIDE ANTIBIOTICS, EVERNINOMICINS BY NEGATIVE ION FAST ATOM BOMBARDMENT (FAB) MASS SPECTROMETRY 954
*PRAMANIK, B N AND GANGULY,A K

STUDIES OF C.GLYCOSIDIC FLAVONOIDS BY FABMS AND MS-MS 956
*FRAISSE, D AND BECCHI, M

THE ROLE OF SERUM PENTITOL CONCENTRATIONS IN THE DIAGNOSIS OF DISSEMINATED VISCERAL CANDIDIASIS 958
*ROBOZ, J,KAPPATOS, D AND HOLLAND, J F

AMMONIA DCI OF DOLICHOLS: QUANTITATION, DETERMINATION OF MOLECULAR WEIGHT AND STRUCTURES 959
*EVANS, J E,ABDEL-MAKSOUD, H M AND DANIEL, P F

IMPURITIES SCREENING OF PHARMACEUTICAL AGENTS USING ON-LINE THERMOSPRAY (TSP) MASS SPECTROMETRY 961
*ROBINS, R H AND ASMUS, P A

DEVELOPMENT OF MS AND MS/MS METHODS FOR THE QUANTIFICATION OF ENKEPHALINS 963
*TOLUN, E,DASS, C AND DESIDERIO, D M

USE OF THE GROWTH MEDUIM TO ANALYZE BACTERIA VIA MS WITH CI 965
*CONWAY, D C,LOPEZ, H AND QUARLES, J M

ANALYSIS OF NAPHTHENIC ACIDS IN CRUDE OILS BY FLUORIDE ION CHEMICAL IONIZATION TECHNIQUE 967
*DZIDIC, I,SOMERVILLE, A C AND RAIA, J C

THE EFFECT OF METAL ATOMS ON ELECTRON IMPACT AND CHEMICAL IONIZATION MASS SPECTRA OF GEOPORPHYRINS 969
*BEATO, B D AND QUIRKE, J M E

TANDEM MASS SPECTROMETRY FOR DETERMINING TRACE LEVELS OF STERANES IN CRUDE SHALE OIL 971
*JOHNSON, J V,WONG, C M AND GREGG, H R
*MISSLER, S R

STRUCTURE AND DISTRIBUTION OF STRAIGHT-CHAIN FATTY ACIDS AND ESTERS IN COAL EXTRACTS STUDIED BY MS/MS AND FD-MS 975
*NIWA, Y AND ISHIKAWA, K

ISOBUTANE CI FOR ON-LINE DETERMINATION OF AMMONIA FROM OIL SHALE PYROLYSIS 977
*CRAWFORD, R W,COBURN, T T,MILLER, P E AND OH, M S

ENERGY-RESOLVED MS/MS SPECTRA OF IONS FORMED FROM TRANSITION METAL ACETYLACETONATES 979
*BUSCH, K L AND DIDONATO, G C

RAPID CHARACTERIZATION OF LIQUID BIOMASS PYROLYSIS PRODUCTS BY MOLECULAR BEAM, MASS SPECTROMETRY AND MULTIVARIATE ANALYSIS TECHNIQUES 981
*EVANS, R J AND MILNE, T A

CHARACTERIZATION AND DETERMINATION OF ALKYL GROUPS OF ZINC DIALKYLDITHIOPHOSPHATES AND OTHER ANTIOXIDANTS IN MOTOR OILS BY PYROLYSIS GAS CHROMATOGRAPHY/MASS SPECTROMETRY 983
*WANG, T H

A NEW INTERNAL STANDARD FOR PYROLYSIS-MS OF FOSSIL FUELS 985
*WINANS, R E,SCOTT, R G AND MCBETH, R L

A COMPARISON OF THE METHODS OF MEDIUM RESOLTUION SELECTED ION RECORDING (SIR) AND MULTIPLE REACTION MONITORING (MRM) WHEN APPLIED TO THE ANALYSIS OF STERANES AND TRITERPHANES IN CRUDE OIL EXTRACTS 987
HARRIMAN, G E,OWEN, R,PARR, V C,WEIR, O AND *WOOD, D

CHEMICAL IONIZATION - PROTEIN EXCHANGE MASS SPECTROMETRIC IDENTIFICATION OF ALKYL BENZENES, TETRALINS, AND INDANS IN A COAL-DERIVED JET FUEL 989
*MILLER, D J AND HAWTHORNE, S B

HYDROCARBON TYPE ANALYSIS OF JET FUEL WITH GAS CHROMATOGRAPHY/MASS SPECTROMETRY 991
*GEHRON, M J AND YOST, R A

ISOTOPIC DETERMINATION OF CALCIUM BY THERMAL IONIZATION USING A VG 354E MASS SPECTROMETER 993
*MUELLER, T R AND WALKER, R L

NEGATIVE IONS IN INDUCTIVELY COUPLED PLASMA MASS SPECTROMETRY (ICP-MS) 994
*FULFORD, J E AND QUAN, E S K

SCINTILLATION-TYPE ION DETECTION FOR INDUCTIVELY COUPLED PLASMA MASS SPECTROMETRY 996
*HUANG, L,JIANG, S AND HOUK, R S

REDUCING MATRIX EFFECTS IN INDUCTIVELY COUPLED PLASMA MASS SPECTROMETRY (ICP-MS) 998
*DOUGLAS, D,BOORN, A,FULFORD, J,GILLSON, G AND HALLIGAN, K

INDUCTIVELY COUPLED PLASMA MASS SPECTROMETRIC DETERMINATION OF MOLYBDENUM IN WHEAT AND RICE FLOURS USING STABLE ISOTOPE DILUTION 1000
*BEARY, E S AND PAULSEN, P J

MATRIX CONSIDERATIONS IN THE ANALYSIS OF NONCONDUCTING POWDER MATERIALS BY GLOW DISCHARGE MASS SPECTROMETRY 1002
TONG, S L AND *HARRISON, W W

TRACE ANALYSES IN SEMICONDUCTOR MATERIALS, HIGH PURITY METALS, AND NUCLEAR MATERIALS BY GLOW DISCHARGE MASS SPECTROMETRY 1004
*CHARALAMBOUS, P M,ROBINSON, K AND BROWN, R

THE USE OF CW LASERS IN RESONANCE IONIZATION MASS SPECTROMETRY 1006
*PARENT, D C,KELLER, R A,FEAREY, B L AND MILLER, C M

FABMS STUDIES OF FORMATION AND STABILITIES OF GASEOUS POLYNUCLEAR LANTHANIDE OXIDES 1008
*KAHWA, I A,HSIEH, T C,PAMIDIMUKKALA, K M,LAINE, R A AND SELBIN, J

LEAD ISOTOPE RATIO ANALYSIS OF THE SACKLER BRONZES 1010
BARNES, I L,CHASE, W T,HOLMES, L L,*JOEL, E C,MEYERS, P AND SAYRE, E V

ION CLUSTERS OF LITHIUM AND TIN EMITTED FROM LIQUID METAL ION SOURCE 1012
*SAITO, Y,WATANABE, M,HAGIWARA, T,INOUE, M,NISHIGAKI, S AND NODA, T

LONG TERM GAIN LOSS OF CHANNEL ELECTRON MULTIPLERS, MEASUREMENTS ON TWO CEMS USED FOR MASS SPECTROMETRY APPLICATIONS 1014
*SOMSSICH, P F

FRIDAY ORAL SESSIONS

METABOLISM AND TOXICOLOGY

AN ISOTOPE DILUTION CAPILLARY COLUMN GC/MS METHOD FOR THE ACCURATE DETERMINATION OF SERUM CHOLESTEROL 1016
*WELCH, M J,COHEN, A,ELLERBE, P,SCHAFFER, R,SNIEGOSKI, L T AND WHITE, E

POSITIVE AND NEGATIVE ION CHEMICAL IONIZATION MASS SPECTROMETRY (NH4+ AND OH-) FOR THE IDENTIFICATION OF PYRROLIZIDINE ALKALOIDS IN EUPATORIUM SPECIES 1018
HENDRIKS, H,HUIZING, H J AND *BRUINS, A P

IDENTIFICATION OF CANNABIDIOL METABOLITES IN HUMAN URINE 1020
*HARVEY, D J AND MECHOULAM, R

SIMULTANEOUS DETERMINATION OF URINARY C-18 OXYGENATED STEROIDS AS ETIOLACTONE DERIVATIVES BY SELECTED ION MONITORING 1022
*CHAN, C AND ULICK, S

DETERMINATION OF GLUTAMINE TURNOVER BY ISOTOPE DILUTION GC/MS 1024
*BLAIR, I A,REDDY, C K,GEER, R AND ABUMRAD, N N

QUALITATIVE SCREENING OF ORGANIC ACIDS IN URINE BY A NEW DESORPTION/ IONIZATION METHOD: K+ IONIZATION OF DESORBED SPECIES(K+IDS) 1026
*KASSEL, D B AND ALLISON, J

A METHOD FOR THE DETERMINATION OF ENDOGENOUS LACTIC AND PYRUVIC ACIDS, AND ENDOGENOUS AND 13C-LABELLED 3-HYDROXYBUTYRIC AND ACETOACETIC ACIDS IN ORGAN PERFUSATES BY SIM-GCMS 1028
*MAMER, O A,MONTGOMERY, J A,BRUNENGRABER, H,DES ROSIERS, C AND DESROCHERS, S

ESSENTIAL OIL FROM THE UNICORN PLANT(PROBOSCIDEA LOUISIANICA): IDENTIFICATION BY MASS SPECTROMETRY AND ALLELOCHEMICAL ACTIVITY 1030
*WALLER, G R,RIFFLE, M S,MURRAY, D S AND SGARAMELLO, R P

ANALYSIS OF CYCLODEXTRINS BY FAB/MS AND FAB/MS/MS 1032
*VOYKSNER, R D,WILLIAMS, F P,KOBLE, D L AND SELTZMAN, H H

DIRECT LIQUID INTRODUCTION (DLI) HIGH PERFORMANCE LIQUID CHROMATOGRAPHY-MASS SPECTROMETRY (HPLC-MS) AND THERMOSPRAY HPLC-MS OF CONJUGATED BENZO(A)PYRENE (B(A)P) METABOLITES 1034
*GREAVES, J AND BIERI, R H

ACTIVATION AND DISSOCIATION OF ORGANIC IONS

ANALYTICALLY USEFUL COLLISION REGIMES IN MS-MS 1036
CATLOW, D A,CLAYTON, E,*MONAGHAN, J J AND SCRIVENS, J H

THE DETERMINATION OF 1,3 SULTONES IN ANIONIC SURFACTANTS BY TANDEM MASS SPECTROMETRY 1038
BLEASE, T G,CATLOW, D,CLAYTON, E,MONAGHAN, J J AND *SCRIVENS, J H

INTERNAL ENERGY AND SITE OF PROTONATION-VARIABLES WHICH EFFECT LOW ENERGY COLLISIONAL ACTIVATION MS/MS ANALYSIS 1040
*HANSEN, G,HATCH, F,FUCHS, V AND FRETER, K

COMPARISON OF ION STRUCTURES USING THREE METHODS FOR COLLISION-INDUCED DISSOCIATION 1042
*BOYD, R K,CURTIS, J M,BRENTON, A G AND BEYNON, J H

PREIONIZATION EFFECTS IN MASS SPECTROMETRY OF AZOXYBENZENES 1044
*BOYD, R K,WADDELL, D S AND BUNCE, N J

ANAMOLOUS ENERGY RELEASE FROM A DISTONIC C3H6O+. ION 1046
*HUDSON, C E,MCADOO, D J AND TRAEGER, J C

RADIATIVE RELAXATION RATES OF HALOBENZENE RADICAL CATIONS 1048
*SO, H Y AND DUNBAR, R C

MOLECULAR STRUCTURE ELUCIDATION USING RESONANCE ENHANCED MULTIPHOTON IONIZATION/FRAGMENTATION 1050
*JOHNSTON, M V,KINSEL, G R,SEGAR, K R AND CHANG, T C

NON-RESONANT MULTIPHOTON IONIZATION/FRAGMENTATION PATTERNS OF N-SUBSTITUTED ANILINES 1052
*ZIMMERMAN, J A AND O'MALLEY, R M

INFRARED MULTIPHOTON DISSOCIATION OF THE NITROBENZENE CATION 1054
*MOINI, M AND EYLER, J R

PHOTODISSOCIATION SPECTROSCOPY (PDS) OF SEVERAL C5H6+ IONS DERIVED FROM NEUTRAL C5H6 ISOMERS AND ANILINE, PHENOL, AND THIOPHENOL 1056
*ASAMOTO, B AND DUNBAR, R C

A NEW APPROACH TO ION DISSOCIATION IN MS-MS 1058
*VESTAL, M L

DISSOCIATION OF CS2+ IONS FORMED IN CHARGE-EXCHANGE REACTIONS OF CS22+ IONS 1060
REID, C J,HARRIS, F M AND BEYNON, J H

SYMPOSIUM: NOVEL MS FOR FUEL AND COMPLEX MIXTURE ANALYSIS

HOMOLOGOUS n-ALKYLBENTHIOPHENES IN ARABIAN HEAVY ASPHALTENES BY PYROLYSIS GC/MS 1062
*GALLEGOS, E J

ANALYSIS OF COMPLEX SURFACTANT MIXTURES 1064
*BOCKHOFF, F M,SHAW, K M,BUDINGER, P A AND ASAMOTO, B

DETAILED CHARACTERIZATION OF HIGH MW SATURATE FRACTIONS BY FDMS AND 13C NMR 1066
*ACZEL, T,REYNOLDS, S D AND DENNIS, L W

APPLICATIOINS OF SUPERCRITICAL FLUID CHROMATOGRAPHY-MASS SPECTROMETRY IN THE ANALYSIS OF FOSSIL FUELS 1068
*CHESS, E K,KALINOSKI, H T,WRIGHT, B W,UDSETH, H R AND SMITH, R D

FRIDAY POSTER SESSION

LCMS APPLICATIONS/INSTRUMENTATION AND OTHER

SUPERCRITICAL FLUID CHROMATOGRAPHY/MASS SPECTROMETRY (SFC/MS) ANALYSIS OF WAXES 1070
*MILLER, D J AND HAWTHORNE, S B

LIQUID CHROMATOGRAPHY-MASS SPECTROMETRY OF BUTYLTIN COMPOUNDS 1072
BELLAR, T A AND BUDDE, W L

FORENSIC COMPARISON OF EXPLOSIVES BY THERMOSPRAY LIQUID CHROMATOGRAPHY- MASS SPECTROMETRY 1074
*BERBERICH, D W AND FETTEROLF, D D

APPLICATIONS OF HIGH RESOLUTION MASS MEASUREMENTS IN THERMOSPRAY LC/MS 1076
*BACZYNSKYI, L AND BRONSON, G E

MASS SPECTROMETRIC ANALYSIS OF ALKYL-SUBSTITUTED NITROSOBENZENES AND METABOLITES OF 2,6-DIETHYLANILINE 1078
*SOLSTEN, R T,FUJIWARA, H AND WRATTEN, S J

DETERMINATION OF IMPURITIES IN RENIN INHIBITOR PEPTIDE BY THERMOSPRAY LC/MS 1080
*CROW, F W,EVANS, K D,MANNING, K S AND ROBINS, R H

THERMOSPRAY LC/MS OF TRIGLYCERIDES 1082
CHARPENTIER, B A,*SANDERS, R A AND VESTAL, C H

THE CHARACTERIZATION OF CAROTENOIDS AND RETINOIDS BY HPLC-MS-MS 1084
*YELLE, L M,FARROW, P E AND TAYLOR, R F

SEPARATION AND IDENTIFICATION OF ACETYLATED MONOGLYSERIDES BY REVERSED-PHASE HIGH PERFORMANCE LIQUID CHROMATOGRAPHY/MASS SPECTROMETRY 1086
*ESPINO, R,NELSON, B AND WEINKAM, R

THERMOSPRAY/MASS SPECTROMETRY AND THERMOSPRAY/MS/MS OF DOXYLAMINE AND PYRILAMINE METABOLITES 1088
*KORFMACHER, W A,BETOWKSI, L D,HOLDER, C L AND MITCHUM, R K

THE ANALYSIS OF DISULFO GLUCOSINOLATES USING THERMOSPRAY LC/MS 1090
*HOGGE, L R,REED, D W AND UNDERHILL, E W

THE USE OF THERMOSPRAY LC/MS FOR THE CHARACTERIZATION OF SURFACTANTS 1092
*GOODLEY, P C

CONTINUOUS FLOW FAST ATOM BOMBARDMENT A NEW LC-MS TECHNIQUE 1094
*ASHCROFT, A E AND CHAPMAN, J R

AN EVALUATION OF THE CONTINUOUS-FLOW FAB PROBE AS AN LC-MS INTERFACE 1096
BATEMAN, R H,JONES, D AND *KROLIK, S T

COMPARISON OF MOVING BELT/FAB, THERMOSPRAY AND CONTINUOUS FLOW FAB PROBE HPLC/MS TECHNIQUES FOR THE ANALYSIS OF PEPTIDES 1098
*VOYKSNER, R D AND WILLIAMS, F P

STUDIES OF NATURAL PRODUCTS BY PACKED COLUMN SFC/MS 1100
BERRY, A J,GAMES, D E,*MYLCHREEST, I C,PERKINS, J R AND PLEASANCE, S

ANALYSIS OF PTH AMINO ACIDS BY THERMOSPRAY LIQUID CHROMATOGRAPHY-MASS SPECTROMETRY 1102
YANG, L AND VESTAL, C H

THERMOSPRAY ANALYSIS OF ACHROMAPHORIC AND CHROMAPHORIC GLUTATHIONE CONJUGATES 1104
*BEAN, M,PALLANTE-MORELL, S,DULIK, D AND FENSELAU, C

CHARACTERISATION OF RADIATION-INDUCED DAMAGE TO POLYADENYLIC ACID USING HPLC-MS-MS 1106
*ALEXANDER, A J,FUCIARELLI, A F,KEBARLE, P AND RALEIGH, J A

THERMOSPRAY LC/MS ANALYSIS OF THE EFFECT OF ALCOHOL ON POLYUNSATURATED PHOSPHOLIPID MOLECULAR SPECIES LEVELS 1108
*KIM, H Y AND SALEM, N

QUANTITATION BY LCMS OF NEUROPEPTIDES ISOLATED BY IMMUNOAFFINITY CHROMATOGRAPHY FROM SPINAL CORD 1110
*LISEK, C A,YAKSH, T L,JARDINE, I,MCDOWALL, M A AND SMITH, D C

FACTORS CONTROLLING ION TRANSFER IN A DUAL CELL FOURIER TRANSFORM ICR 1112
*HONOVICH, J P,MARKEY, S P,WANG, T-C L AND SHIH, M-C

IMPROVED ION TRAP PERFORMANCE WITH NEW CI AND MS/MS SCAN FUNCTIONS 1114
*WEBER-BRABAU, M,KELLEY, P E,SYKA, J E P,BRADSHAW, S C AND BRODBELT, J S

ULTRAHIGH RESOLUTION ION CYCLOTRON RESONANCE SPECTROMETRY 1116
BAMBERG, M AND *WANCZEK, K P

LASER DESORPTION/FOURIER TRANSFORM MASS SPECTROMETRY SPECTRA OF OLIGOPEPTIDES IN THE PRESENCE AND ABSENCE OF CAD 1118
*YANG, C L C

252Cf PLASMA DESORPTION FOURIER TRANSFORM ION CYCLOTRON RESONANCE MASS SPECTROMETRY - IMPROVEMENT IN ION TRAPPING EFFICIENCIES 1120
*VISWANADHAM, S K,WELLER, R R,GIAM, C S AND HERCULES, D M

APPLICATION OF FTICR FREQUENCY CORRECTIONS TO ACCURATE MASS MEASUREMENTS 1122
*MEEK, J T,MILLEN, W G,FRANCL, T J,THOMSON, M L, STOCKTON, G W AND WAYNE, R S

IMPROVED PEAK SHAPES FROM A MODIFIED FTMS CUBIC CELL INCORPORATING SEGMENTED TRAP PLATES 1124
*REMPEL, D L

EFFECTIVENESS OF VELOCITY COMPACTION FOCUSING FOR IMPROVING THE RESOLVING POWER OF A CONVENTIONAL TOF MASS SPECTROMETER 1126
*MUGA, M L

CAPILLARY GAS CHROMATOGRAPHIC/ICR-MASS SPECTROMETRY USING AN EXTERNAL ION SOURCE AND A NOVEL ION TRANSFER SYSTEM 1128
CARAVATTI, P,*GROSSMAN, P,KEFEL, P,ALLEMANN, M AND KELLERHALS, H P

INJECTION OF IONS FROM AN EXTERNAL ION CAGE INTO AN ICR CELL 1130
*KOFEL, P,ALLEMANN, M,KELLERHALS, H AND WANCZEK, K P

WINDOWED EXCITATION SIGNALS FOR FTMS 1132
*HANNA, D A,SPENCER, R B AND GOODMAN, S

HIGH TEMPERATURE MASS SPECTROMETRY AT ENHANCED SENSITIVITY AND AT HIGH RESOLUTION (>3000) 1134
*WAGNER, G AND LASER, B

HIGH MASS ANALYSES USING QUADRUPOLE INSTRUMENTATION 1136
*MADDEN, R,SCHAEFFER, R,BRACKMANN, R T,KETKAR, S N AND POEPPEL, F

MODIFICATION OF THE EI ION SOURCE OF VG-ZAB OR VG-7070 FOR ACQUISITION OF EI/FAB SPECTRA 1138
*METRAL, C J

INSTRUMENTAL MODIFICATIONS TO A MODULAR CHROMATOGRAPHY/SIMS INSTRUMENT 1140
*FLURER, R A,DIDONATO, G C,DUFFIN, K L AND BUSCH, K L

A MICRO-VOLUME CURIE-POINT PYROLYZER FOR RAPID, HIGH RESOLUTION CAPILLARY GC/MS 1142
MEUZELAAR H L C,MCCLENNEN, W H AND *YUN, Y

THE GALILEO PROBE MASS SPECTROMETER 1144
NIEMANN, H B,*HARPOLD, D N,COOLEY, J E AND WAY, S H

252-Cf PLASMA DESORPTION MASS SPECTROMETRY USING THE MAMYRIN REFLECTRON IN A LOW VOLTAGE REGIME 1146
*GENO, P W AND MACFARLANE, R D

COMPUTER MODELING OF SECONDARY ION TRAJECTORIES IN A SIMS/TSQ MASS SPECTROMETER 1148
*BENTZ, B L AND HONIG, R E

NEW SCAN MODES REVEALED BY A SYSTEMATIC EVALUATION OF THE MS/MS EXPERIMENT 1150
*SCHWARTZ, J,ENKE, C C AND WADE, A

A TOF-FTMS SYSTEM FOR PROBING HIGH MASS ANALYSIS BY FT-ICR METHODS 1152
*HANSON, C D AND CASTRO, M E

Presented at the 35th ASMS Conference on Mass Spectrometry and Allied Topics
May 24-29, 1987, Denver, CO

FABMS AND MS/MS ANALYSES OF GLYCOSIDIC TRITERPENES FROM CHINESE MEDICINES

C.E.Costello, B.Domon, and C.-H.Zeng,
Dept. of Chemistry, Mass. Inst. of Technology, Cambridge, MA 02139
and
S. Du, F. Qian and M. Li, Dept. of Chinese Traditional Medicine,
Shanghai Inst. of the Pharmaceutical Industry, Shanghai, PRC.

Saponins are triterpene, steroidal or alkaloidal glycosides produced by higher plants and starfish. The presence of multiple glycosylation sites and the variety of carbohydrate substituents that occur permit almost unlimited complexity in structure and function. The range of biological activities includes, for example, antifungal and bactericidal properties, CNS stimulation, and anti-inflammatory action.

In the present study, FABMS and FAB CID MS/MS in both the positive and negative ion modes were used for the structure determination of a series of cardiovascular active compounds isolated from Chinese traditional medicines. These triterpene saponins are particularly difficult to characterize by the usual techniques, including mass spectrometry, because they contain a complex oligosaccharide moiety and a labile ester-glycosidic linkage. The nature of the aglycone and the types of sugars present were known, but the number of sugars and the location and structure(s) of the oligosaccharides were unknown at the start of this work. The seven saponins thus presented an opportunity to investigate how much structural information could be deduced from CID MS/MS spectra of this class of compounds.

Molecular weights were determined in both the positive and negative ion modes, although in the positive ion spectrum, the abundance of protonated or cationized molecular ions was very low relative to the aglycone ions. Fragmentation in the negative ion spectrum and in the collision spectra of the molecular and fragment ions provided information about the sites of carbohydrate attachment and detailed structure of the carbohydrate moieties. There are some indications of the carbohydrate sequence(s) in the normal FAB mass spectra of these compounds, but the MS/MS spectra are much more useful for this determination. The CID MS/MS spectra of the $(M-H)^-$ and $(M+H)^+$ ions of one of these are shown on the next page.

Even the cationized molecular ions yielded abundant product ions upon collisional activation. There were striking differences between the CID spectra of the $(M + 23)^+$ and $(M + 39)^+$ ions. These can be attributed to differences in charge localization. Because fragmentation of the sugar rings occurred in the MS/MS spectra of the cationized species, they facilitated assignments of sugar substitutions.

It was found possible to determine the structures of all seven saponins. Five of these, numbered HS-1 to HS-5, are derivatives of oleanolic acid. Their structures appear below. The remaining two are derivatives of pomolic acid and contain arabinose and glucose, but no glucuronic acid. Their structures were also determined but are not shown.

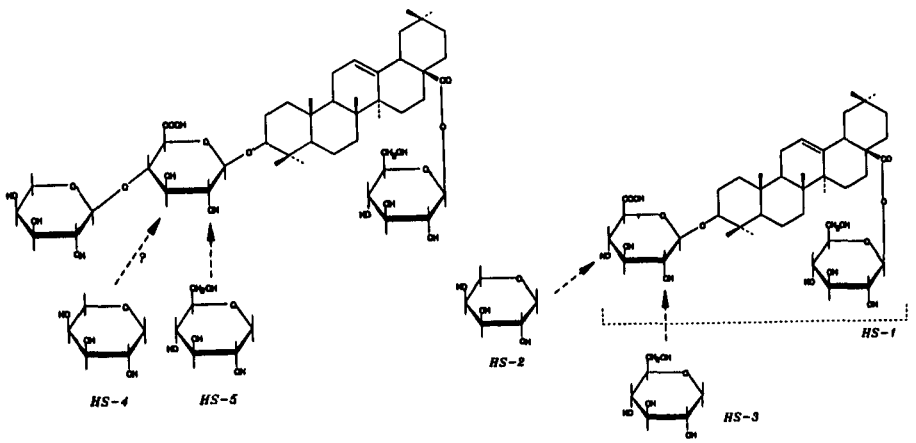

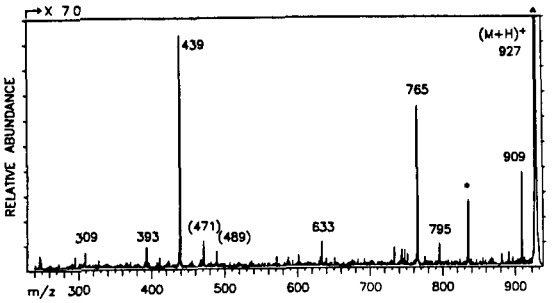

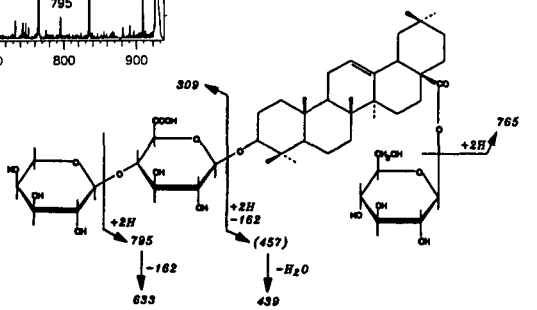

Fig. 1. Positive ion collision mass spectrum of saponin HS-2, $(M+H)^+$ m/z 927.5. Scheme at right shows assignments of product ions.

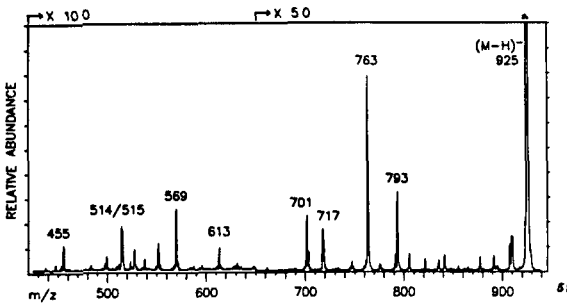

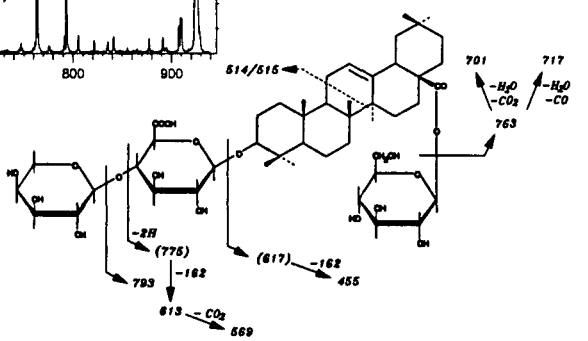

Fig. 2. Negative ion collision mass spectrum of saponin HS-2, $(M-H)^-$ m/z 925.5. Scheme at right shows assignments of product ions.

FAB MS and CID MS/MS spectra were obtained with a JEOL HX110/HX110 4-sector tandem mass spectrometer, operated at 1:1000 resolution in both MS-1 and MS-2. Helium was used as the collision gas, in a cell located between MS-1 and MS-2. Samples were dissolved in DMSO. For FAB(+), glycerol was used as the matrix; for FAB(-), triethanolamine. Accelerating voltage and collision energy were both +/- 10 kV. MS-2 was scanned at constant B/E.

This work was supported by the NIH Division of Research Resources, Grant No. RR00317 (to K. Biemann). B.D. is the recipient of a fellowship from the Swiss Science Foundation.

Presented at the 35th ASMS Conference on Mass Spectrometry and Allied Topics
May 24-29, 1987, Denver, CO

THE CHARACTERISATION OF THE TYROTHRICIN COMPLEX BY FAB/MS/MS:

M. Barber, L. Tetler, D. Bell, UMIST, Sackville Street, Manchester, U.K., B. Bycroft, University of Nottingham, Nottingham, U.K., J. Monaghan, B. Modren, I.C.I. PLC., The Heath, Runcorn, U.K., and B.N. Green, VG Analytical Ltd., Floats Road, Wythenshawe, Manchester, U.K.

Tyrothricin is a mixture of cyclic decapeptides produced by certain species of Bacillus brevis and is widely used as a topical antimicrobiol agent. The structures of the three major components (Tyrocidins A, B & C) were elucidated by 1965 (1) (Fig. 1). However, using FAB/MS we have shown the presence of the three major components as well as an additional six compounds of varying relative abundance (Fig. 2).

Using FAB/MS/MS on the three known Tyrocidins we have delineated a series of cleavages suitable for sequencing the six unknowns. This has allowed us to locate the amino acid changes occurring and hence propose six structures of new, hithertofore, unreported Tyrocidins (Fig. 3).

The instruments used for the MS/MS work were a VG ZAB-SE for MIKES, a VG 70-SE4F tandem instrument for high energy CID and a VG ZAB-HSQ hybrid for low energy CID.

Recent work has shown that biosynthesis of these compounds is non-ribosomal and proceeds via a complex multifunctional enzyme system (2) (Fig. 4). The new structures we have proposed show some interesting substitutional patterns, i.e. the Asn-Gln segment, the Val and the Leu-Phe-Pro being invariant, also only an aromatic amino acid can replace another aromatic amino acid and an aliphatic only another aliphatic unit.

References

(1) Ruttenberg et al., Biochemistry, 4, 11, 1965.

(2) Lipman, F. Advances in Mircobiol. Physiology, 21, 227-266, 1980.

Presented at the 35th ASMS Conference on Mass Spectrometry and Allied Topics
May 24-29, 1987, Denver, CO

STRUCTURE OF THREE MAJOR COMPONENTS ELUCIDATED IN 1968

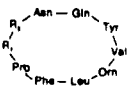

	R_1	R_2	M Wt
Tyrocidin A	Phe	Phe	1289
Tyrocidin B	Tryp	Phe	1308
Tyrocidin C	Tryp	Tryp	1347

Fig 1

MOLECULAR ION REGION OF TYROCIDIN COMPLEX

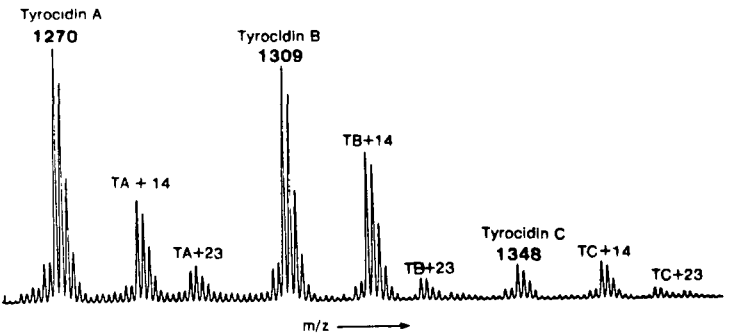

Fig 2

SUBSTITUTIONS

1 Exactly the same substitutions occur in Tyrocidins B and C

2 Summary of proposed new structures

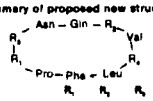

	R_1	R_2	R_3	R_4	M Wt
Tyrocidin A_1	Phe	Phe	Tyr	Lys	1283
Tryptocidin A	Phe	Phe	Tryp	Orn	1292
Tyrocidin B_1	Tryp	Phe	Tyr	Lys	1322
Tryptocidin B	Tryp	Phe	Tryp	Orn	1331
Tryptocidin C_1	Tryp	Tryp	Tyr	Lys	1361
Tryptocidin C	Tryp	Tryp	Tryp	Orn	1370

Fig 3

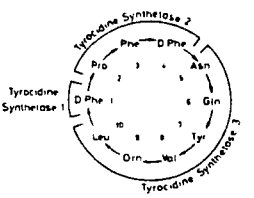

Fig 4

Presented at the 35th ASMS Conference on Mass Spectrometry and Allied Topics
May 24-29, 1987, Denver, CO

METABOLISM OF LEUKOTRIENE E_4 IN THE ISOLATED RAT HEPATOCYTE

Danny O. Stene and Robert C. Murphy
Department of Pharmacology
University of Colorado Health Sciences Center
Denver, Colorado 80262.

Slow reacting substance of anaphylaxis (SRS-A) was described some 45 years ago by Kellaway and Trethwie (1). In 1979, the structure of the major component of SRS-A was elucidated as 5-hydroxy-6-glutathionyl-7,9,11,14-eicosatetraenoic acid acid (LTC_4) (2). This sulfidopeptide leukotriene along with its metabolites LTD_4 and LTE_4 (derived from sequential loss of gamma-glutamate and glycine) have been implicated as important mediators of acute hypersensitivity reactions including asthma. Little is known about the metabolic fate of the sulfidopeptide leukotrienes, but the liver has been reported to be an important organ for metabolism. Furthermore, Keppler has shown that metabolites of LTE_4 can be found in the bile of rats suffering from endotoxin shock (3).

As a model of hepatic metabolism, we have used the isolated rat hepatocyte to examine the fate of LTE_4. Hepatocytes were isolated by perfusion of an isolated liver with collagenase (750 units/250 ml) followed by mechanical dispersion of the cells, then differential centrifugation (4). Hepatocytes at 3 x 10^6 cells/ml suspended in 10 mM Tris buffer were incubated with 20 uM [^{3}H]-LTE_4 for 30 min. After incubation, methanol was used to precipitate proteins and the supernatant partially purified by flash chromatography. Material recovered from the flash chromatography by elution with methanol was further purified by reverse phase HPLC which revealed 5 major components retaining a triene chromophore (UV maximum of 280 nm) (Fig. 1). The component eluting at 41.8 min was characterized as LTE_4 by UV spectroscopy, FAB/MS, and HPLC retention time. The major metabolite (metabolite A) was analyzed by FAB-MS (Fig. 2). The negative ion mass spectrum was in essence a single abundant ion at m/z 480 which was 42 amu above the mass spectrum of LTE_4. After catalytic reduction and derivitization with BSFTA, the positive ion GC/MS revealed a peak with ions at m/z 457, 367, 313, and 261 supporting the structure of 5-hydroxyeicosanoic acid-diTMS. This suggested that this metabolite retained the intact 20-carbon chain with a single hydroxyl moiety at carbon-5. The GC/MS and FAB data was consistent with this metabolite being N-acetyl-LTE_4 which had been previously shown to be a metabolite of LTC_4 in rat (3). Metabolite A had a FAB mass spectrum and HPLC retention time identical to that of synthetic N-acetyl-LTE_4.

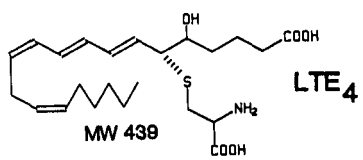

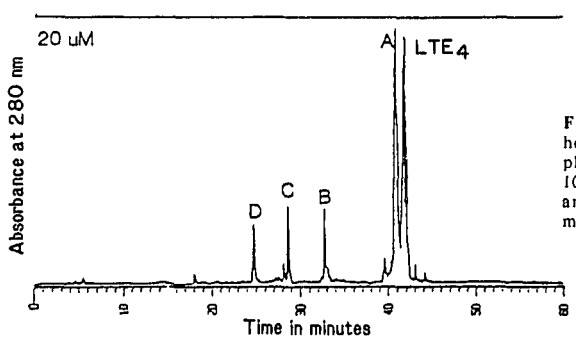

Fig. 1 The RP-HPLC of LTE_4 hepatocyte metabolites. The mobile phase was a gradient from 20% water to 100% methanol each with 50 mM ammonium acetate, pH 4.5; flow=1 ml/min.

The next abundant metabolite (B, retention time 32.8 min) had a UV spectrum consistent with a thioether allylic to a conjugated triene (Fig 3, inset). FAB/MS analysis of this metabolite revealed ions at m/z 510 and 533 among others which suggested the addition of two oxygen atoms and loss of two hydrogen atoms. Catalytic reduction (5) and GC/MS analysis of the resultant methyl ester, pentafluoropropionate derivative by negative ion chemical ionization (NICI) conditions suggested a monohydroxy, C_{20} dicarboxyic acid as the carbon - backbone for this molecule (Fig. 3). This data was consistent with metabolite B being 20-carboxy-N-acetyl-LTE_4. This metabolite would arise by omega-oxidation of the terminal methyl group of N-acetyl-LTE_4, a process known to readily occur for other leukotrienes (6).

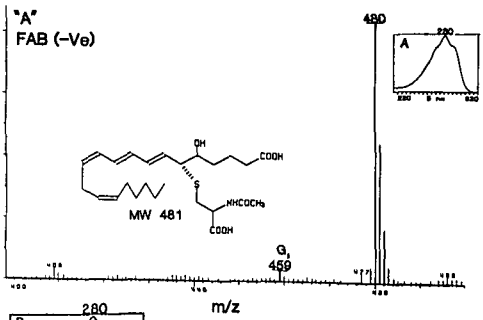

Fig. 2 The negative ion FAB mass spectrum of metabolite A, performed using Xe at 8KV and glycerol as the target matrix. Inset: The UV absorption spectrum of purified metabolite A prior to FAB analysis.

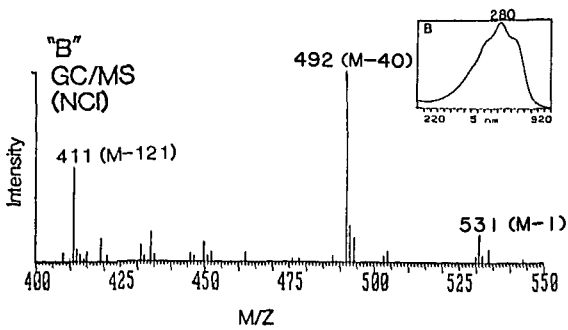

Fig. 3 The NICI mass spectrum of metabolite B. The ions at 531, 492, and 411 are consistent with those expected for a monohydroxy, C_{20} dicarboxylic acid. The spectrum was obtained using methane as the ionization gas. Inset: The UV absorption spectrum of purified metabolite B prior to catalytic reduction.

Acknowledgement. This work was supported in part by a grant from the National Institutes of Health (HL25785)

REFERENCES

1. C.H. Kellaway and E.R. Trethwie. Quart. J. Exp. Physiol. 30:121-145 (1940).
2. R.C. Murphy, S. Hammarstrom, and B Samuelsson. Proc. Natl. Acad. Sci. USA. 76:4275-4279 (1979).
3. W. Hagman, C. Denzlinger, S. Rapp., G. Weckbecker, and D. Keppler. Prostaglandins. 31:239-251.
4. M.N. Berrry and D.S. Friend. J. Cell Physiol. 43:506-520 (1969).
5. M. Balazy and R.C. Murphy. Anal. Chem. 58:1098-1101 (1986).
6. G. Hansson, J. Lindgren, S.e. Dahlen, P. Hedqvist, and B. Samuelsson. FEBS Lett. 130:107-112 (1981).

Presented at the 35th ASMS Conference on Mass Spectrometry and Allied Topics
May 24-29, 1987, Denver, CO

MEASUREMENT OF URINARY 6-KETO-PROSTAGLANDIN $F_{1\alpha}$ ($6KPGF_{1\alpha}$) BY GAS CHROMATOGRAPHY TANDEM MASS SPECTROMETRY FOLLOWING PURIFICATION BY IMMUNOAFFINITY CHROMATOGRAPHY.

J.J. Vrbanac and D.R. Knapp.
Department of Pharmacology, Medical University of South Carolina, Charleston, SC 29425.

One of the research efforts in this laboratory is the development of simplified, rapid yet highly specific mass spectrometric (MS) procedures for the analysis of arachidonic acid metabolites (AAM) in urine. Previously we described an immunoaffinity column which purifies urinary AAM sufficiently that in subsequent analysis by high resolution gas chromatography - negative ion chemical ionization or positive ion electron ionization - mass spectrometry interference free chromatograms were observed. Recently we have directed our efforts towards development of GC-MS-MS methods for the measurement of urinary AAM.

GC-MS-MS analysis was performed using a Nermag R30-10 triple quadrupole tandem mass spectrometer coupled to a Varian 3400 GC. Electron ionization and daughter ion mass spectra of methoxime-pentafluorobenzyl ester-trimethylsilyl (MO-PFB-TMS), MO-methyl ester(ME)-TMS and MO-ME-tert-butyldimethylsilyl (tBDMS) derivatives of $6KPGF_{1\alpha}$, thromboxane B_2(TXB_2) and dinor-TXB_2 were examined. MO-ME-TMS and MO-PFB-TMS derivatives showed extensive fragmentation and weak ion currents for candidate parent ions with the entire $6KPGF_{1\alpha}$ molecule intact. The M^+-57 (M^+-t-butyl; m/z 698) ion of the MO-ME-tBDMS derivative of $6KPGF_{1\alpha}$ represented over 5% of the total ionization and over 50% of the base peak (m/z 115; Figure 1). The base peak of the daughter ion mass spectrum of m/z 698 was m/z 115 (collision energy 35 V; Figure 2). This fragment shifted to m/z 119 in the daughter ion mass spectrum of M^+-57 (m/z 702) of 3,3,4,4-$^2H_4$-$6KPGF_{1\alpha}$ and represents $^+[CH_2CD_2CD_2CH_2COOCH_3]$ (no ion current at m/z 115 was observed). MO-ME-tBDMS derivatives of TXB_2 and dinor-TXB_2 showed a less intense M^+-57 ion and an M^+-(57+32) of equal intensity to M+ -57. Both TXB_2 and dinor-TXB_2 MS showed an intense ion at m/z 385 (this ion was shifted to m/z 389 for $^2H_4$-labeled internal standards). The daughter ion mass spectrum m/z 385 (collision energy 35 V) showed an intense ion at m/z 253 (Figure 3). These parent-daughter ion pairs (m/z 698→115 and 385→253) were evaluated for utility in the analysis of urinary $6KPGF_{1\alpha}$, TXB_2 and dinor-TXB_2.

As expected, GC-MS-MS analysis following immunoaffinity purification provided a highly specific measurement of urinary $6KPGF_{1\alpha}$. Samples were injected at 190°C and the GC oven programmed at 50°C/min. Elution temperatures of $6KPGF_{1\alpha}$ and TXB_2 are labeled (Figures 4 and 5). Figure 4 shows the ion current profile obtained when monitoring 698→115. One peak was obtained for urinary $6KPGF_{1\alpha}$. Figure 5 shows the ion current profile obtained when monitoring 385→253. No interference were noted for urinary dinor-TXB_2 or TXB_2. $6KPGF_{1\alpha}$ and TXB_2 eluted more rapidly and at far lower temperatures (approximately 235° vs. 300°C) using a 1.8 m column compared to a 12 m column. Figure 6 compares MS, bottom trace (m/z 698; M^+ -57) and MS/MS, top trace (m/z 385→253) analysis of the same urine sample. Elution time of TXB_2 is marked with a star in the bottom trace.

In summary, the use of immunoaffinity purification-GC-MS-MS analysis of urinary prostaglandins allowed the use of a shorter capillary GC column (1.8 m) resulting in decreased total analysis time.

Supported in part by NIH grants RR01239 and HL29566.

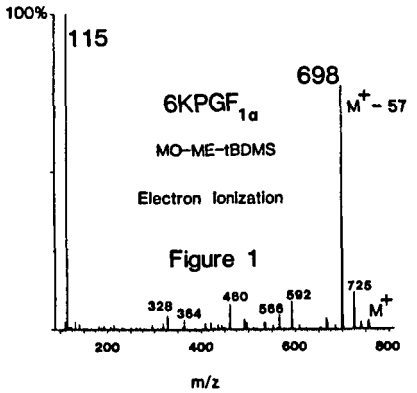
100%
115
698
$M^+ - 57$
6KPGF$_{1\alpha}$
MO-ME-tBDMS
Electron Ionization
Figure 1
725
M^+
460
592
328
364
566
200
400
600
800
m/z

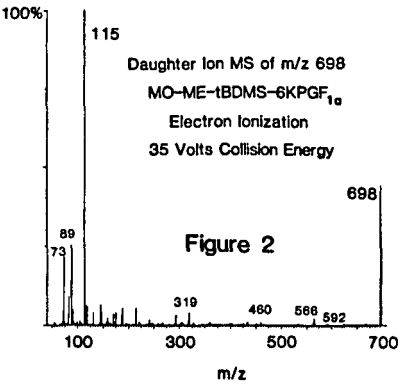
100%
115
Daughter Ion MS of m/z 698
MO-ME-tBDMS-6KPGF$_{1\alpha}$
Electron Ionization
35 Volts Collision Energy
698
89
73
Figure 2
319
460
566
592
100
300
500
700
m/z

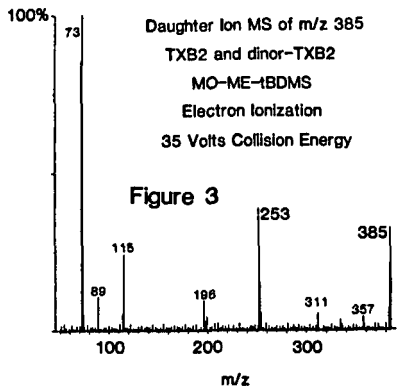
100%
73
Daughter Ion MS of m/z 385
TXB2 and dinor-TXB2
MO-ME-tBDMS
Electron Ionization
35 Volts Collision Energy
Figure 3
253
385
115
89
196
311
357
100
200
300
m/z

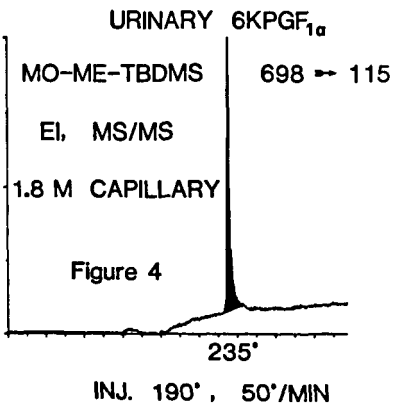
URINARY 6KPGF$_{1\alpha}$
MO-ME-TBDMS
698 → 115
EI, MS/MS
1.8 M CAPILLARY
Figure 4
235°
INJ. 190°, 50°/MIN

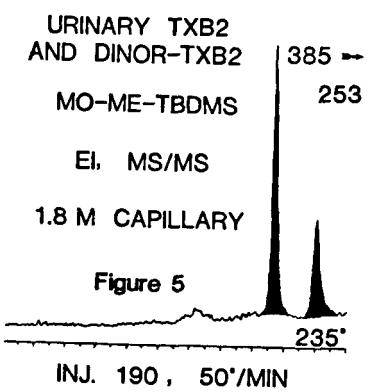
URINARY TXB2
AND DINOR-TXB2
385 →
253
MO-ME-TBDMS
EI, MS/MS
1.8 M CAPILLARY
Figure 5
235°
INJ. 190, 50°/MIN

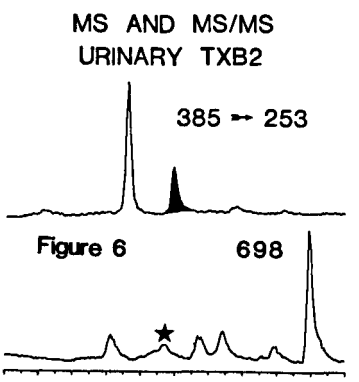
MS AND MS/MS
URINARY TXB2
385 → 253
Figure 6
698

Presented at the 35th ASMS Conference on Mass Spectrometry and Allied Topics
May 24-29, 1987, Denver, CO

GC-MS/MS OF PROSTAGLANDINS-- THE ION TRAP vs. B-E

R. J. Strife*, M. Weber-Grabau+, and P. E. Kelley+
*Procter & Gamble Miami Valley Labs, P.O. Box 39175, Cincinnati,OH 45247 and +Finnigan-MAT, 355 River Oaks Parkway, San Jose, CA 95134

The simplified analysis of prostaglandins (PG's) and leukotrienes (LT's) in vivo and in vitro is of importance for many reasons. These include evaluation of new anti-inflammatory drugs and their effects on the COX and LOX enzymatic pathways. Previously, we demonstrated greatly simplified sample preparation for the GC/MS-MS analysis of PGE_2 in urine at the 200 pg/ml level[1]. This was chosen as a model for: 1) its analytical difficulty by GC/MS, 2) the known structures of major parent ions of PGE_2 derivatives, and 3) the well defined levels of PGE_2 in human female urine.

This previous work had been carried out on an instrument of BE configuration in a reaction-monitoring mode at 6 KeV acceleration potential. The drawbacks of MS-MS of PG's and LT's on this device are the relatively inefficient conversion of parent ions (P) to daughter ions (D) and transmission of (D) to the detector. This limits instrumental sensitivity so that 100 pg of PGE_2 is required on column for a S/N of 10 in the GC/MS-MS (reaction monitoring) mode.

In the ion trap, ion formation and mass analysis occur in the same region. It has unique advantages for high sensitivity MS-MS, including: 1) up to 100% conversion efficiencies of P to D and 2) 50% transmission of D's to the detector because there are no sectors. An investigation was therefore undertaken to compare MS-MS results on the two instruments, dealing first with the types of fragmentation observed (BE vs ITMS).

Mass Spectra and CAD -- The 70 eV EI mass spectrum of PGE_2 as the methyl ester, methoxime, bis-TMS ether shows m/z 73(100), 225 (47), 295(32), 366(8), and 508(8). The spectrum from the ITMS was similar. The four most abundant ions above m/z 200 were selected as parent ions. The ion of m/z 225 is a conjugated oxonium ion. CAD of this ion (BE - 6 keV, fig. 1) gave mostly $(CH_3)_3Si+$ and the neutral dienone. There was also loss of a series of neutral alkanes (C_{15}-C_{20}). Loss of pentene is apparent, though partially obscured by lack of resolution from kinetic energy release.

The daughter ion spectrum on the ITMS (q=.28) was much different (fig. 2). Losses of neutral alkenes from C_{15}-C_{20}, particularly pentene, are most intense. There is also a series of highly unsaturated ions derived from C_8-C_{18}, presumably after loss of TMSOH. These processes are barely evident on the BE instrument. In both spectra, fragmentations reflect a significant degree of rearrangement (e. g. as in loss of TMSOH, m/z 135), or the parent ion structures are not adequately represented by the oxonium ion.

For GC/MS-MS(SRM) assays, several factors are important. Obviously, choice of an intense parent ion, as well as an intense daughter ion, favors the instrumental sensitivity required in PG's and LT's analyses by GC/MS-MS. However, in the case of m/z 225, the observed CAD efficiency is very low (1% - fig. 3) on the BE instrument, with the most intense daughter ion being only .1% of m/z 225 (I_0). Thus, m/z 225 is not a viable parent ion. In contrast, the CAD efficiency on the ITMS is 40 times greater, with over 16% of the original parent ion intensity appearing at m/z 93 (C_7H_9+) and m/z 155 ($-C_5H_{10}$).

It should be noted that these fragmentations are backbone-specific for the eicosanoid skeleton. Previously it was demonstrated that this type of fragmentation confers superior selectivity for biological samples to monitoring loss of TMSOH, a group introduced by derivatization[1]. The ITMS produces an abundance of backbone-specific choices.

Presented at the 35th ASMS Conference on Mass Spectrometry and Allied Topics
May 24-29, 1987, Denver, CO

CI/MS-MS -- The most ideal experiment for SRM of biological samples is CI/MS-MS. On the ITMS, advantage can be taken of the time domain and low partial pressure of reagent gas, to obtain higher ionization efficency than the on the BE instrument. Figure 4 shows the GC/CI-MS-MS analysis of 75 pg of the PGE_2-$MeMoxTMS_2$ derivative, collecting full daughter ion scans.

New Scan Function for Biological Samples -- Many of these results were obtained with a new ITMS scan function designed for samples in biological matrices. Ionization occurs at a low q value, for long times (100 msec), creating a space charge loss in resolution. By proper manipulation of the R_f and DC (q and a values of the ion), the trap is emptied of all ions of lower and higher masses than the parent. The resolution is observed to return, and the rest of the MS-MS experiment is carried out (for a detailed description see these proceedings, "Improved Ion Trap Performance With New CI and MS/MS scan functions", M. Weber Grabau et.al.). We are applying this new scan function to GC/MS-MS assays of crude biological samples at ppb levels.

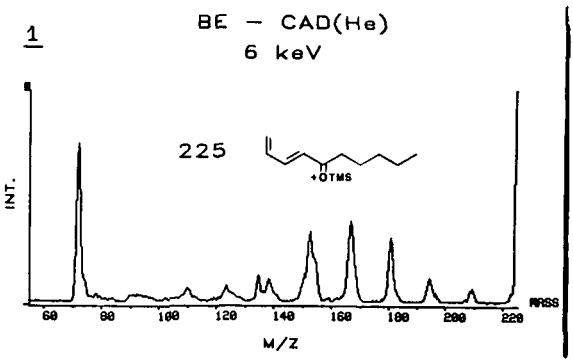

3

CAD EFFICIENCY = $\frac{\Sigma I_{di}}{I_o}$

M/Z	CAD. EFF.(%) BE	CAD. EFF.(%) ITMS
225	1	45
295	2.5	40
540	2	60

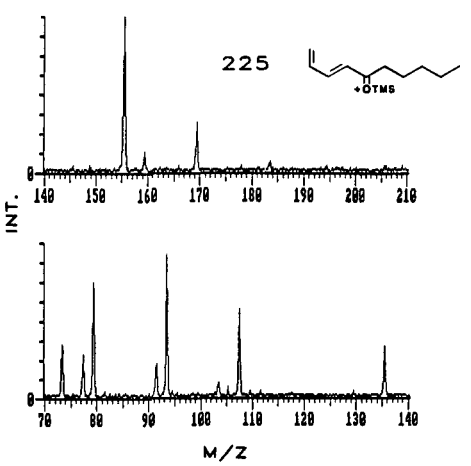

4 < 75 pg

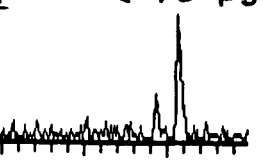

t_R 14:22

$W_{1/2}$ = 5 SEC.

Presented at the 35th ASMS Conference on Mass Spectrometry and Allied Topics
May 24-29, 1987, Denver, CO

BILIARY METABOLITES OF N-FORMYL-N,α-DIMETHYL-γ-PHENYLBENZENEPROPANAMINE IN RATS: Slatter, J.G., Abbott, F.S., and Burton R.; Faculty of Pharmaceutical Sciences, University of British Columbia, Vancouver, B.C., Canada, V6T 1W5.

To investigate a possible pathway in the metabolism of the anticholinergic drug recipavrin[R] (1) to a secondary formamide (2), the metabolites of the tertiary formamide (3) were isolated from the bile of male wistar rats and characterized by positive EI GCMS.

Capillary GCMS was performed on a Hewlett Packard 5987A GCMS using a crosslinked methylsilicone fused silica capillary column, 25 meters by 0.32 mm i.d. Column temperature was programmed from 50° to 150° at 30° per minute , then at 4° per minute to 260° for two minutes. Injections (1 uL) were made in splitless mode with helium back pressure 15 psi. Injection port, interface and source temperatures were 250°. The mass range was 40 to 400 AMU, multiplier voltage 2600, emission current 300 uA and ionization energy 70 eV.

The tertiary formamide was administered to bile duct cannulated rats by s.c. injection at a dose of 40 mg/kg at 1 and 12 hours after recovery from ether anaesthesia. Bile was collected for 24 hours. Metabolites were isolated by solvent extraction prior to and after B-glucuronidase hydrolysis.

In the hydrolyzed fraction, a carbinolamide (4), was observed in intact form ($M^{+\cdot}-H_2O$=265) and as a TMS derivative (5). A carbinolamide phenol (6) and carbinolamide O-methylcatechol (7) were observed as di-TMS derivatives (6a,7a). The carbinolamides are presumed to arise from hydrolysis of glucuronide conjugates of the carbinol OH. On standing, the free carbinolamides decompose with loss of formaldehyde to their respective secondary formamides (2, 8, 9). The structure of the carbinolamide (4) was confirmed by the synthetic condensation of the secondary formamide and formaldehyde in a methanolic suspension of K_2CO_3. Most of the underivatized carbinolamide decomposed to the secondary formamide in the GC inlet. Very little secondary formamide was observed in samples that were extracted and derivatized immediately after hydrolysis.

The carbinolamide (4) and the TMS carbinolamides (5, 6a and 7a) are all characterized by a m/z 85 fragment and m/z 265 (4, 5), m/z 353 (6a) and m/z 383 (7a) which we presume arise by rearrangement/ elimination (*re*) mechanisms (McLafferty, 1980)(Figure 1).

Diagnostic ions arising from the benzylic cleavage of the diphenylmethyl moiety were used to locate phenyl ring intact and phenyl ring oxidized metabolites. In underivatized samples m/z 167, m/z 183 and m/z 213 can be used to locate phenyl ring intact metabolites, phenols and O-methylcatechols respectively. The corresponding ions in BSTFA derivatized samples are m/z 167, m/z 255 and m/z 285.

N-dealkylation via stable, glucuronide conjugated, carbinolamide intermediates is the major metabolic pathway. The tertiary formamide functional group is also N-deformylated to a secondary N-methylamine (10). The amine is further metabolized to an oxime (11) and undergoes oxidative deamination to diphenylbutanone (12) which is in turn reduced to diphenylbutanol (13).

Phenol metabolites of (2, 3, 11 and 12) and O-methylcatechol metabolites of (2, 3, 11, 12 and 13) were also isolated from bile and characterized in intact form and as TMS derivatives.

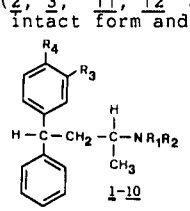

1-10

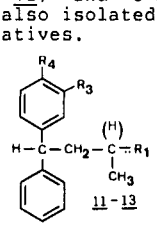

11-13

Presented at the 35th ASMS Conference on Mass Spectrometry and Allied Topics
May 24-29, 1987, Denver, CO

In recipavrin (1) metabolism studies, no carbinolamide (4) or tertiary formamide (3) metabolites were detected, precluding this pathway as a source of the secondary metabolite (2).

Carbinolamide metabolites of lower aliphatic formamides (NMF, DMF) are well documented. Carbinolamides are reactive metabolites which may be important to the toxicity of illicit amphetamines contaminated with arylaliphatic formamide byproducts of the Leuckart reaction.

Table summarizing substituents and GCMS data for metabolites.

	R_1	R_2	R_3	R_4	M^+ (int.)	B.P.[4]	tr[5]
1	Me	Me	H	H	253 (3)	72	12.42
2	CHO	H	H	H	253 (44)	73	18.20
3	CHO	Me	H	H	267 (10)	87	19.32
4	CHO	CH_2OH	H	H	283 (0)	85	20.88
5	CHO	CH_2OTMS	H	H	355 (3)	85	22.92[1]
6	CHO	CH_2OH	H	OH	299 -	--	-d/c-
6a	CHO	CH_2OTMS	H	OTMS	443 -	73	28.84[2]
7	CHO	CH_2OH	OMe	OH	329 -	--	-d/c-
7a	CHO	CH_2OTMS	OMe	OTMS	473 -	73	30.38[2]
8	CHO	H	H	OH	269 -	183	25.70[3]
8a	CHO	H	H	OTMS	341 (15)	255	24.71
9	CHO	H	OMe	OH	299 (30)	213	25.71
9a	CHO	H	OMe	OTMS	371 (33)	285	26.61
10	Me	H	H	H	239 (7)	58	12.02
10a	Me	TMS	H	H	311 (5)	130	15.17
11	=NOH	-	H	H	239 (8)	167	14.81
12	=O	-	H	H	224 (35)	167	10.84
13	OH	-	H	H	226 (2)	167	11.27

Legend: [1]Partial decomposition. [2]M^+ outside scan range. [3]Peak buried [4]Base peak. [5] Retention time (minutes)

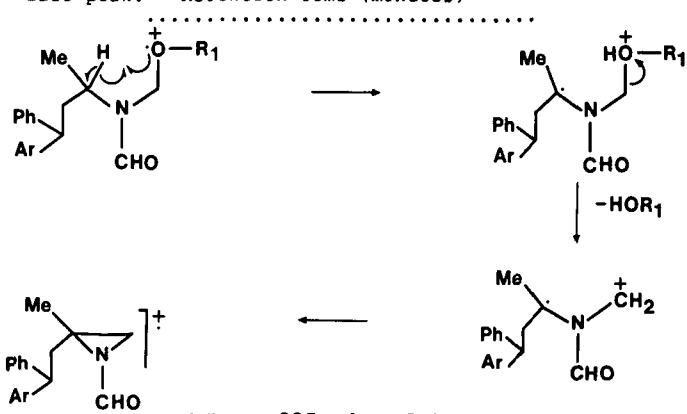

4.5 m/z 265 Ar = C_6H_5
6a m/z 353 Ar = C_6H_4OTMS
7a m/z 383 Ar = $C_6H_3(OTMS)(OMe)$

Figure 1. Alcohol (R_1=H) or TMS ether (R_1=TMS) directed proton rearrangement/elimination to afford m/z 265 (4,5), m/z 353 (6a) and m/z 383 (7a). Transfer of the diphenylethyl moiety in a similar fashion would afford the m/z 85 peak present in all the carbinolamides (4,5,6a,7a).

Presented at the 35th ASMS Conference on Mass Spectrometry and Allied Topics
May 24-29, 1987, Denver, CO

A NEW CI-GC-MS METHOD TO MEASURE IMIDAZOLEACETIC ACID, A HISTAMINE METABOLITE

J.K. Khandelwal, G.D. Prell, and J.P. Green, Department of Pharmacology, Mount Sinai School of Medicine of the City University of New York, New York, NY 10029. U.S.A.

Numerous biological events have been attributed to histamine (HA) which, among other properties, also serves as a neurotransmitter[1]. In one metabolic pathway, HA is methylated to tele-methylhistamine (t-MH) which is oxidatively deaminated to tele-methylimidazoleacetic acid (t-MIAA). In the other pathway, HA undergoes direct oxidative deamination to form imidazoleacetic acid (IAA) which is also formed from histidine without the intervention of HA. Lack of sensitive and specific methods has prevented measurement of IAA in brain and body fluids other than urine. Our recently described EI-GC-MS method to measure IAA in urine as n-butyl ester could not be applied to brain and other body fluids because it lacked sensitivity and showed inconsistent retention time (R_t) on capillary column[2]. To obtain a useful procedure, we derivatized the imidazole ring nitrogen of the n-butyl ester with ethyl chloroformate (ECF) to form n-butyl(n-ethoxycarbonyl)imidazoleacetate. This derivative possesses improved GC characteristics and reproducible R_t and was utilized to develop a new CI-GC-MS method that can measure as little as 1 ng of IAA.

Tissue homogenates and body fluids were subjected to organic extraction and ion exchange column chromatography to separate IAA that was esterified as n-butyl ester by heating with BF_3-BuOH[3,4]. Labeled IAA, ($^{15}N,^{15}N'$)IAA, was used as an internal standard for quantification of IAA. Standards (1-20ng) were run in parallel to obtain standard curve. The n-butyl ester in $CHCl_3$ was reacted with ECF at room temperature to derivatize the ring nitrogen of the ester. The sample was evaporated to dryness and was reconstituted in 15µl of $CHCl_3$. CI-GC-MS analysis was carried out on a 15M x 0.25mm Durabond fused silica capillary column in a splitless mode with CH_4 as reagent gas (1 torr). Protonated molecular ions, m/e 255 and m/e 257, were monitored by SIM corresponding to, respectively, IAA and ($^{15}N,^{15}N'$)IAA derivatives.

Because of tautomerism, IAA formed two chromatographically distinct isomeric derivatives of unequal intensity as was seen in the total ion chromatography. Both the isomeric derivatives exhibited distinct protonated molecular ions at m/e 255. Labeled ($^{15}N,^{15}N'$)IAA also showed similar isomeric derivatives with protonated molecular ions two mass units higher at m/e 257.

Figure 1 shows the EI and CI mass spectra of the bigger isomeric peak of the IAA derivative.

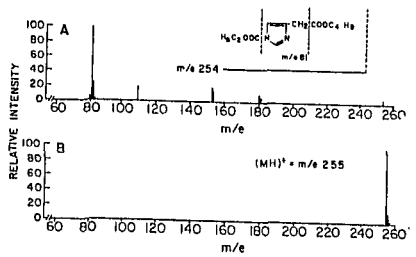

Fig. 1. EI (A) and CI (B) mass spectra of IAA as n-butyl (N-ethoxycarbonyl) imidazole acetate derivative.

The EI mass spectra of both the isomeric derivatives are nearly the same except for ion m/e 154 which shows lower relative abundance for the smaller isomeric peak possessing shorter R_t.

Figure 2 shows the CI-SIM scans of ECF derivatives of authentic IAA and of biological extracts.

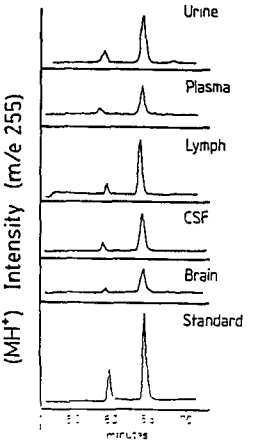

Fig.2. CI-SIM Scans of n-Butyl(N-ethoxycarbonyl)imidazoleacetate derivatives of authentic IAA and biological extracts

The mass ion peak area ratio (IAA/($^{15}N,^{15}N'$)IAA, m/e 255/257) of the bigger isomers at the same R_t was used for quantification. This ratio remained unaffected by isomeric formation of the derivative. This work shows that tautomeric compounds can be quantified if the internal standard is the labeled form of the compound being measured; furthermore, the formation of two isomers can be used to establish the specificity of the assay. CI-GC-MS was used because EI-GC-MS analysis of the biological samples was not satisfactory due to the interfering peaks. Preliminary studies indicate the following levels of unconjugated IAA (ng/g or ml ± S.E.M.): human CSF, 1.38 ± 0.40; sheep lymph, 10.98 ± 0.77; rat brain, 25.43 ± 3.44. [Supported by NIMH grant MH-31805 and training grant 5-T32-DA-07135 to GDP].

We thank Los Alamos National Laboratory (Stable Isotope Resource, Grant No. P41RR00962) for the kind gift of [$^{15}N,^{15}N'$] histidine.

REFERENCES

1. Prell, G.D., and Green, J.P. (1986) Ann. Rev. Neurosci. 9: 209-254.

2. Khandelwal, J.K., Kline, T., and Green, J.P. (1985) J. Chromatogr. 343: 249-257.

3. Khandelwal, J.K., Hough, L.B., Pazhenchevsky, B., Morrishow, A.M., and Green, J.P. (1982) J. Bio. Chem. 257: 12815-12819.

4. Khandelwal, J.K., Hough L.B., and Green, J.P. (1984) J. Neurochem. 42: 519-522.

Presented at the 35th ASMS Conference on Mass Spectrometry and Allied Topics
May 24-29, 1987, Denver, CO

DETERMINATION OF ANABOLIC STEROIDS BY API SFC/MS AND SFC/MS USING PACKED-COLUMNS

Jack D. Henion, Lars Weidolf, Edgar D. Lee and Thomas R. Covey. Drug Testing and Toxicology, New York State College of Veterinary Medicine, Cornell University, 925 Warren Drive, Ithaca, New York 14850

Supercritical fluid chromatography (SFC) is receiving renewed interest today primarily as a result of improved instrumentation. Supporters of the technique argue that SFC "bridges the gap" between the popular chromatographic areas of GC and HPLC. The possible benefits of SFC include better chromatographic efficiency with shorter analysis times than HPLC and high chromatographic efficiency analyses without the temperature extremes of GC. The remaining need for SFC, however, is routine implementation of the mass spectrometer as its detector.

Capillary SFC/MS may be considered reasonably straightforward because the gas volume produced is comparable to that of capillary GC. However, packed-column SFC often utilizes fluid flow rates of 2-4 mL/min which produces much too much gas to introduce directly into a conventional mass spectrometer ion source. We have recently constructed a heated nebulizer-type interface which incorporates a pinhole diaphragm restrictor for use on an atmospheric pressure ionization (API) ion source. The API system can accommodate any fluid flow rate and allows routine use of packed-column SFC features.

EXPERIMENTAL

A Hewlett-Packard Model 1084B HPLC system modified for SFC was connected to a homemade heated pneumatic nebulizer SFC/MS interface. This interface utilized an unchanged Hewlett-Packard direct liquid introduction (DLI) LC/MS interface equipped with a 20 micron stainless steel pinhole diaphragm. Figure 1 shows a schematic drawing of this device. The combination of DLI probe and heated pneumatic nebulizer SFC/MS interface is inserted into the API ion source of a TAGA 6000E tandem triple quadrupole mass spectrometer (Sciex, Thornhill, Ontario, Canada). Ionization occurs via a corona discharge maintained at 6000V while ions are sampled through a 100 micron orifice into the high vacuum region of the MS/MS system. The column used was a 4.6mm x 100mm three micron particle size cyano propyl packed HPLC column (Keystone Scientific, State College, PA) with carbon dioxide doped with methanol as the supercritical fluid maintained at 80 degrees.

The heated pneumatic nebulizer SFC/MS interface is designed to supply sufficient heat to facilitate volatilization of analytes eluting from the pinhole diaphragm prior to ionization. In addition, a makeup gas of nitrogen flowing co-axially through the desolvation region (Figure 1) carries the volatilized analytes towards the ionization region while minimizing contact with the heated quartz surface. Positioning of the SFC/MS interface relative to the ion sampling orifice was not critical.

RESULTS AND DISCUSSION

The API SFC/MS system described here was used to obtain both SFC/MS and SFC/MS/MS data of anabolic steroids isolated from equine urine and bovine tissue samples. Samples of standard dianabol, boldenone, and trenbolone were studied to obtain their mass spectra in the MS and MS/MS modes. Structurally useful full-scan CID spectra were obtained in each case and conditions were optimized for selected reaction monitoring (SRM) determination of low levels of these analytes. In this way boldenone was identified in the full-scan SFC/MS/MS mode from a crude equine urine extract obtained from solid phase extraction of a 10 hour boldenone administration urine. Similarly, trenbolone was identified by SRM SFC/MS/MS of a bovine liver extract fortified with 20 and 30 ppb trenbolone. In each case representative mass spectra for the analytes of interest were obtained.

CONCLUSION

Packed-column API SFC/MS and SFC/MS/MS is an efficient, rapid means of analyzing complex samples for the determination of targeted compounds. Sample volumes up to 20 microliters may be readily injected onto the packed columns and the elution of polar analytes is not often a problem as can be the case with capillary SFC columns. The pinhole diaphragm is rugged and commercially available unlike capillary restrictors. The corona discharge API system is simple and rugged with near universal response to most analytes. Finally, the API ion source readily handles any reasonable packed-column fluid flow rate so all the flexibility of this technique may be utilized. The high sample throughput capability of this system could offset the rather high cost of the MS/MS system.

ACKNOWLEDGEMENT

We thank the Hewlett-Packard Co for the generous loan of the 1084B SFC system, the Harry M. Memorial Fund and the New York State Racing and Wagering Board Equine Drug Testing and Toxicology Program for financial support of this work.

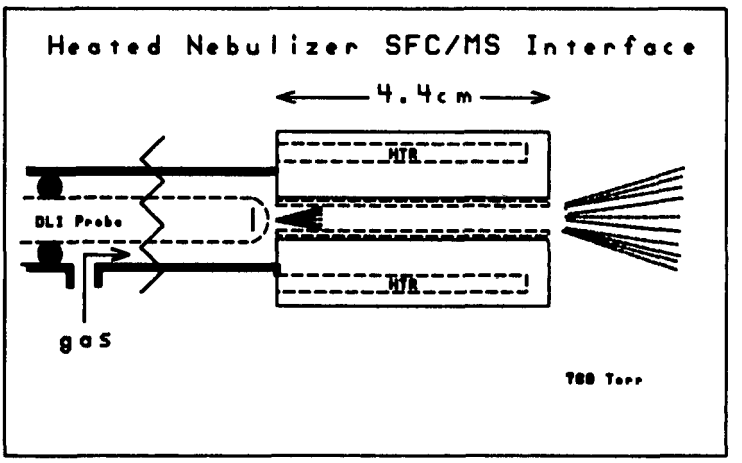

Figure 1

Presented at the 35th ASMS Conference on Mass Spectrometry and Allied Topics
May 24-29, 1987, Denver, CO

COMPARISON OF HYPOTHALAMUS-PITUITARY-ADRENAL AXIS SUPPRESSION FROM TOPICAL STEROIDS BY STANDARD ENDOCRINE FUNCTION TESTING AND GAS CHROMATOGRAPHIC MASS SPECTROMETRY

P.V. Fennessey, W.L. Weston, A.W. Pike, R.W. Gotlin;
University of Colorado School of Medicine, Denver, CO 80262

The development of superpotent topical steroids for the treatment of inflammatory skin disease has allowed dermatologists to achieve dramatic therapeutic responses, but with increased hazards of steroid side effects. In particular, percutaneous absorption of topical steroids may result in systemic suppression of the hypothalamus -pituitary -adrenal axis (HPAS) with resulting adrenal insufficiency. Katz and co-workers recently found a trend towards a difference in HPA-axis suppression1between the two superpotent topical steroids now marketed in the U.S. This difference was detected by morning plasma cortisol determinations and found to be most easily detected in males, since plasma cortisol levels were quite variable in their female subjects.

The purpose of this study was to evaluate the potential for HPAS by superpotent topical steroids. To avoid variations in plasma and urinary cortisol determinations and provide data that could be compared to earlier work, the study was restricted to males. We studies 38 males with psoriasis in a randomized, double-blind, parallel group study, comparing topical betamethasone-dipropionate in an optimized vehicle (BDOV) to clobetasol-17-propionate ointment (CP). For this purpose we compared levels of urinary cortisol metabolites quantitated in 24-hour urines by gas chromatographic mass spectrometry (GCMS) to classical measurements of plasma cortisol, urinary-free cortisol and urinary 17-hydroxy corticosteroids.

The urinary metabolites of cortisone and cortisol, namely, tetrahydrocortisone (THE), tetrahydrocortisol (THF) and allo-tetrahydrocortisol (allo-THF) were used to evaluate steroid suppression. For each patient the percentage difference of the sums of the concentration of THE + THF + a-THF (mg/24h) were compared using similar values determined in the first sample as the baseline.

Efficacy evaluation was based on a score of 1 to 6, and was measured at days 5, 8, 15, and 22. A score of 1 was assigned if the psoriasis had completely cleared; 2, if there was 75% clearing; 4, with less than 50% clearing; and 5, no change with no detectable improvement from baseline; and a score of 6 was assigned if an exacerbation occurred; that is, a flare of the psoriasis within the sites being treated. Efficacy was compared between the two groups by the 2-tailed Fisher's exact test.

Suppression of plasma cortisol levels was observed in 53% of men who received CP (cortisol levels below 7 ug/dl) compared to 17% of men who received BDOV ($p = 0.04$ by Fisher's exact test; two-tailed; Fig. 2). The plasma cortisol suppression did not occur throughout the study period, but was noted at days 4,5,7, & 8. Employing GCMS analysis of total urinary cortisol and cortisone metabolites, we observed suppression of adrenal corticosteroid in 84% of patients receiving CP compared to 22% of those receiving BDOV ($p > 0.01$ by Fisher's exact test) confirming the observations seen in plasma cortisol levels. In every patient in whom the plasma cortisol level was suppressed, the total urinary steroid metabolites as determined by GCMS were also suppressed. In addition, there were 6 patients in the CP group and one additional subject in the BDPV group who were suppressed by criteria for the urinary GCMS determinations. In general when suppression was estimated by plasma cortisol levels, it was confirmed by the mass spectroscopic analysis of urinary cortisone and cortisol metabolites.

The extended suppression observed with GCMS versus plasma cortisol determinations provides a longer time frame in which cortisol suppression can be observed. A secondary advantage of the GCMS technique is that one can observe a complete steroid profile and any perturbations of overall steroid biosynthesis can be simultaneously determined for each patient. By all methods, a differential HPAS was found, despite equal efficacy of the two superpotent topical steroid ointments. Therefore, this study demonstrates that useful information concerning systemic absorption of topical steroid preparations can be gained from readily available adrenal function tests. We found that in men, the measure of a single cortisol value at 8 a.m. under basal conditions provides a useful index of HPA suppression and evidence of restoration of endogenous cortisol production appears to correlate with healing of the skin and return of a normal barrier to steroid absorption. Analysis of urinary cortisol metabolites by GCMS may be more sensitive in detecting differences in HPAS resulting from topical steroid preparations.

These results indicate that we now have a routine urinary method that can be used on an infant population. A group that are not routinely studied for HPAS from topical steroids because of the previously large and repeated blood samples necessary for these studies.

This work was supported by grants NIH RR01152 Clinical Mass Spectrometry Resource and the Hepatobiliary Center at the University of Colorado Health Sciences Center (USPHS #DK34914).

1
Katz HI, Hein NT, Prawer SE, Mastbaum LI, Mooney JJ, Samson CR: Superpotent topical steroid treatment of psoriasis vulgaris - clinical efficacy and adrenal function. J. Am. Acad. Dermatol. (in press, 1987).

Presented at the 35th ASMS Conference on Mass Spectrometry and Allied Topics
May 24-29, 1987, Denver, CO

APPLICATIONS OF CHROMATOGRAPHY/SIMS

M. S. Stanley, S. J. Doherty, K. L. Duffin, and K. L. Busch
Department of Chemistry, Indiana University, Bloomington, IN 47405

A custom-built secondary ion mass spectrometer (SIMS) is used for the direct analysis of components of mixtures separated by planar forms of chromatography, including thin layer and paper chromatography and electrophoresis [1-3]. In contrast to "direct" methods of analysis that rely on an independent location of a sample spot by another detection method, followed by a mass spectral identification that often involves destruction of the chromatogram, the chromatography/SIMS experiments described here use mass spectrometric data to locate the spot on the chromatogram, identify the compound on the basis of its mass spectrum, chart its location on the surface in x and y dimensions, and provide an increased effective resolution of separation for overlapped components. In addition, the intact chromatogram can be retrieved after the analysis and the sample recovered, or stored and reanalyzed at a later date.

The chromatography/SIMS instrument was first used in a study of phenothiazines, psychoactive drugs for which thin layer chromatography (TLC) is often used as a separation method. Using the standard prescribed method of TLC separation, several of the common phenothiazine drugs overlap on the chromatogram. Since the positive ion SIMS spectrum of each contains an abundant signal for the intact cation, the mass spectrometric data can be used to deconvolute the overlapping peaks. A similar problem was encountered in an analysis of phosphonium salts by TLC/SIMS in that several overlapping components could be identified. Figure 1 contains the spatially resolved selected ion monitoring data for phosphonium salts with cation masses of 335 and 339 daltons that have been separated by thin layer chromatography. The x and y coordinates for both halves of the figure are the same, and in fact, one of the phosphonium salts with a mass of 335 daltons co-migrates with the phosphonium salt with a cation mass of 339 daltons. The mass spectral data allows the individual contours of these separated compounds to be distinguished on the basis of the different mass ions in their respective mass spectra. In the plot on the left, two abundance maxima for the ion at m/z 335 are noted. That in the foreground represents the location of a second phosphonium salt with a cation mass of 335 daltons with a lower R_f value. TLC/SIMS has also been used for the separation and detection of steroids and steroid conjugates (as the Girard's derivatives), mixtures of small peptides (up to pentapeptides), and mixtures of organometallic compounds.

Chiral plates (tm) have been used in the separation and detection by mass spectrometry of the d and l forms of 3,4-dihydroxyphenylalanine. The positive secondary ion mass spectra of these two forms of the compound are identical (Figure 2). The data matrix of mass spectra versus x and y parameters therefore contains two distinct regions that produce an identical mass spectrum. When mixtures of compounds present in the d and l forms are separated by chiral plate TLC, the number of discernible spots is twice the number of separated components. The mass spectrometric data is used to link the locations of the separated d and l forms of the sample molecule.

Planar (slab) electrophoresis with aqueous gels is widely used in biochemical and clinical separations. The vapor pressure of water even at reduced temperatures makes the direct analysis of these chromatographic substrates impossible under usual instrument conditions. Persistent secondary ion signals from dried gels could not be obtained. Results are presented that show the spatially-resolved mass spectral data obtained from an electrophoretic gel separation with an intermediate transfer step onto a nitrocellulose support. Blotting techniques are commonly used in the electrophoretic separation and analysis of deoxyribonucleic acids and ribonucleic acids. Blotting by capillary action, by electrophoresis, and by application of a vacuum have all been described in the literature. The medium to which the sample compounds are transferred is typically nitrocellulose, although for special applications, a treated paper support can be used to increase the binding. Our initial experiments have used electrophoresis-SIMS for the separation and analysis of mixtures of organic dyes maintained in their charged forms by a buffer. The bands of separated dye are easily seen on the electrophoretic plate, and the transfer of the dye to the nitrocellulose is also

visually monitored. The development of the gel results in a band of the dye, a structure that is also reflected in the chart of the mass spectrometric data. Electrophoresis-SIMS has also been used for the separation and detection of larger peptides (up to bradykinin) and steroid sulfates. In each case, intermediate transfer by electroblot to a nitrocellulose support has been used. The secondary ion mass spectra of those samples so prepared are identical to those measured for the discrete samples measured in the extraction solvent directly.

1. J. W. Fiola, G. C. DiDonato, and K. L. Busch, Rev. Scient. Instrum., 57 (1986) 2294.
2. G. C. DiDonato and K. L. Busch, Anal. Chem., 58 (1986) 3231.
3. K. L. Busch, J. W. Fiola, G. C. DiDonato, R. A. Flurer, and K. J. Kroha, Adv. Mass Spectrom., 10 (1986) 855.

Figure 1

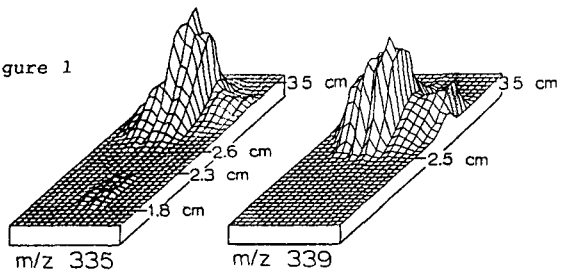

TLC/SIMS of Phosphonium Salts

Figure 2

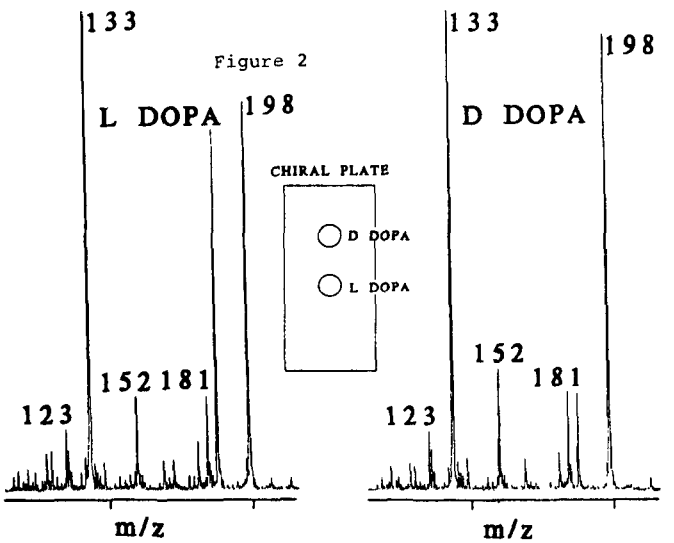

Presented at the 35th ASMS Conference on Mass Spectrometry and Allied Topics
May 24-29, 1987, Denver, CO

An External Field Desorption Ion Source for Analytical Ion Cyclotron Resonance Spectrometry

H. B. Linden, Linden-ChroMasSpec, D-28 Bremen 61
and
H. Knoll, I. Pezsa and K. P. Wanczek, Inorganic Chemistry,
University, D-28 Bremen 33, West Germany

Field desorption/ionization is a well established ionization method in mass spectrometry (1). The characteristics of a field desorption ion source are: Small energy spread of the ions generated, small apparent source size, high brightness, generation of only very small amounts of gas, and soft ionization. The soft ionization has caused the application of the method in the study of fragile compounds of low volatility with great success. The disadvantages of field ionization are the procedure necessary for activating the emitters, the low short term current stability, the total current capability and the effective ion yield due to the small focusing angle.

The ICR technique is characterized by the trapping of the ions generated in the ICR cell and by resonance detection of the trapped ions. With Fourier transform also fast spectrum recording and averaging can be performed. By optimum location of the ion source a large fraction of the ions can be trapped. If the ion source is located in the ICR cell virtually all the ions are trapped. With an external ion source located outside the ICR cell or even outside the room temperature bore of the magnet approximately one third of the ions can be trapped (2). Due to the high electric field used in the FD source only external generation of the ions is possible. With an external ion source the effective sampling time is short, in the 0.1 ms range, two times the flight time of the ions through the ICR cell.

The coupling of the ICR technique with field desorption has great advantages: There is no pressure increase during ion generation, because almost no gas is generated by the FD source, the energy spread of the ions is small, the percentage of the ions trapped is high, the sampling time is small, and signal averaging is possible.

We have coupled a field desorption ion source to an FT ICR spectrometer with a superconducting magnet of 7.02 T field strength and a room temperature bore of 8.9 cm diameter. A Linden ChroMasSpec FDF probe is used with power supply FDF 700. The power supply provides an emitter heating current gradient ranging from 0.5 to 99 mA/min. High voltages between emitter and counter electrode of up to 10 kV can be employed. A cylindrical ICR cell of 4 cm diameter and 6 cm length is used. The FD ion source is introduced into the ultrahigh vacuum system via a solid sample inlet. The experiments show that differential pumping of the FD source vacuum system and the ICR system is not necessary. A pressure below 10^{-8} mbar is maintained during the measurements with one 600 l/s diffusion pump with liquid nitrogen cooled baffle. The FD tip is approximately 25 cm from the front trapping electrode of the ICR cell, which is shielded from the high voltage of the FD source by a grounded shielding electrode. The ions are generated continously with the FD source and sampled by pulsing the front trapping electrode of the ICR cell. In the first experimental setup

described here, no optimization of ion yield for the transfer and trapping has been performed. Therefore due to intensity problems only small band spectra of mass ranges covering up to 15 amu are recorded. For the test of the instrument, alkali salts and d-glucose are employed, all known to give intense FD signals. Very long living field desorption of more than a quarter hour is observed. K^+, Na^+, and Cs^+ ions, the residual gases oxygen, nitrogen and water are seen. From the aqueous solutions the residual solvent is detected with the H_3O^+ ion of larger abundance than the H_2O^+, as expected. No ion-molecule reactions take place in the ICR cell under the experimental conditions. The resolution of the peaks in the small band spectra is medium, up to 80,000. A small band spectrum of the protonated molecule of d-glucose is also obtained. A S/N ratio of greater than 30 is obtained by accumulating approximately 25 to 100 spectra. Strong fluctuations of the signal intensity are observed, which are averaged out by the signal accumulation.
In FD micro-discharges can occur (1) which disturb the ionization and detection and lead to breakdown of the high electric field. In the high magnetic field such micro-discharges are favored by the confining effect of the magnetic field on charged particles. Negative particles are accelerated towards the FD emitter. They can strike the surface and generate secondary ions. This is consistent with the observation of cesium ions without emitter heating current. The discharge is started by the species desorbing first and is maintained until the sample runs out. The generation of ions in the micro-discharge can be developed into a new ionization method.

1. H. D. Beckey, Principles of Field Ionization and Field Desorption Mass Spectrometry, Pergamon Press, Oxford, 1977.
2. P. Kofel, M. Allemann, Hp. Kellerhals and K. P. Wanczek, Int. J. Mass Spectrom. Ion Processes, 65 (1985) 97.

Acknowledgement
Financial support of K.P.W. by the Deutsche Forschungsgemeinschaft is gratefully acknowledged.

Presented at the 35th ASMS Conference on Mass Spectrometry and Allied Topics
May 24-29, 1987, Denver, CO

MECHANISM OF LASER DESORPTION OF THYMIDINE AND URIDINE AS A FUNCTION OF WAVELENGTH: A FTMS STUDY.

M.P. Chiarelli, Dept. of Chemistry, Univ. of Nebraska-Lincoln, Lincoln, NE 68588.

The combination of Laser Desorption (LD) and Fourier Transform Mass Spectrometry may provide a means of analyzing high-mass molecules. The ability of LD to desorb molecules intact combined with the multichannel advantage, high mass resolution, and ion storage capability of FTMS make them a promising combination (1).

Three principal mechanisms of laser desorption elucidated to date have been classified as thermal (2), shockwave-driven (3), and resonant (4). The formation of both $(M-H + 2Na)^+$ and $(M + Na)^+$ ions from thymidine and uridine provides insight into the competition between these mechanisms. At low power densities under thermal desorption conditions both $(M-H + 2Na)^+$ and $(M + Na)^+$ ions are formed, the former in smaller abundance. At 266nm, near threshold, in the power density range of 1-10 X $10^{7W}/cm^2$ the $(M-H + 2Na)^+$ ions predominate and as the power density is raised ca. 30% the ration of $(M-H + 2Na)^+/(M + Na)^+$ ions decreases by a factor of 10 and 4 for thymidine and uridine respectively (Table 1 and Figure I). Near threshold at 266nm direct desorption of $(M-H + 2Na)^+$ is facilitated by resonant desorption driven by an enhancement of acidity due to the formation of an excited state. As the power is increased, desorption proceeds outside the spot in a shockwave process. Further evidence of excited state acid/base effects is sought in the next set of experiments.

Many resonant compounds are known to change their acidity in the excited state (5). 2-Naphthol decreases its pKa from 9 to 3 and 2-naphthoic increases its pKa from 6 to 7 in the first excited singlet state. Both compounds were desorbed independently (Figure II) and in a mixture at the wavelengths specified in order to find evidence of excited state acid/base chemistry. The results are summarized in Table II.

The ratios of the $(M-H)^-$ anions, (m/z 143)/(m/z 171), generated from 2-naphthol and 1-naphthoic acid, were compared for evidence of excited state processes. Column I contains the ratios of the compounds desorbed independently. Column II contains the predicted ratios to be observed when the alcohol and acid were mixed in a 4:3 ratio (wt./wt.). These predicted ratios assume that the two compounds would desorb independently of each lactam forms. Quantum mechanical calculations (5) indicate that the lactim (enol) form is preferred in the triplet state where as the lactam (keto) form is dominant in the ground state. Luminescence experiments (6) with compounds simulating the two tautomers (Figure III) showed the enol form phosphoresced and the keto form did not. These findings support the hypothesis that many of the nucleoside molecules exist as triplets during the process of desorption. Scheme I describes a mechanism by which sodiation at the imide nitrogen may proceed. When the nucleoside is excited the imide hydrogen will migrate to carbonyl oxygen. The triplet state lifetime should be long enough to allow a Na^+ ion to attach to the nitrogen, blocking reprotonation upon relaxation. Adenosine. a purine nucleoside with no imide hydrogen, does not show a $(M-H + 2Na)^+$ ion. The lifetimes of the thymidine and uridine triplets in solution at 300K are ca. 25us and 2us respectively, (7), which parallels the ratios of the $(M-H + 2Na)^+/(M + Na)^+$ of thymidine and uridine at threshold at 266nm (Table I).

1) D.A. McCrery, E.B. Ledford, and M.L. Gross, Anal. Chem., 54, 1437 (1982).
2) R.B. Van Breemen, M. Snow, and R.J. Cotter, IJMSIP, 49, 35 (1982).
3) B. Linder and V.Seydel, Anal. Chem., 57, 2935 (1985).
4) M. Karas, D. Bachmann, and F. Hillenkamp, Anal. Chem., 57, 895 (1985).
5) J.F. Ireland and P.A.H. Wyatt, "Advances in Physical Organic Chemistry", V. Gold and D. Bethell, Eds.; Academic Press: London, 1976; Vol. 12, pp. 131-221.
6) N. K. Kochetkov and E.I. Budovskii, "Organic Chemistry of the Nucleic Acids"; Plenum Press, Inc., New York, 1972, part B, p. 552.
7) J. W. Longworth, et al., J. Chem. Phys., 43, 2930 (1966).

Presented at the 35th ASMS Conference on Mass Spectrometry and Allied Topics
May 24-29, 1987, Denver, CO

Table I: Laser Desorption of Thymidine and Uridine Mixed with An Equal Weight of NaCl, In The Power Density Range Of 1 - 10 x 10^7 W/cm^2.

	5.0 mj	6.5 mj
THYMIDINE (m/z 287)/(m/z 265)	1.7 ± .3	.19 ± .03
URIDINE (m/z 289)/(m/z 267)	1.5 ± .2	.40 ± .04

m/z 287, 289 = $(M-H+2Na)^+$

m/z 267, 265 = $(M+Na)^+$

Figure I

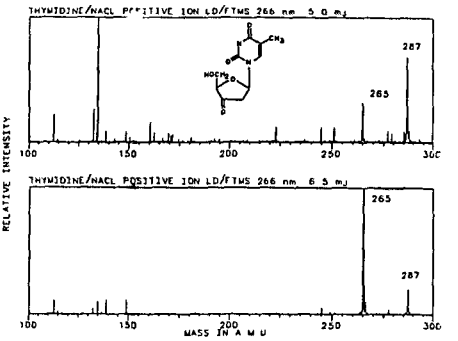

Figure II

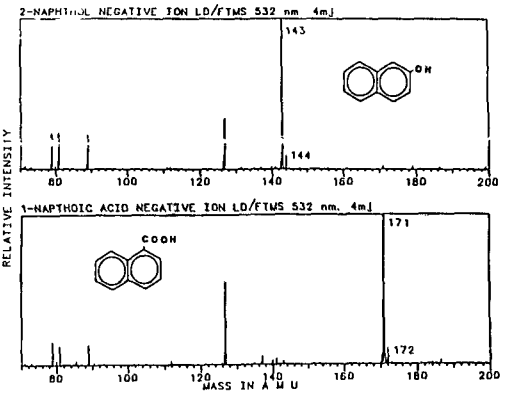

Table II. Intensity Ratios of the $(M - H)^-$ Ions From 2-Naphthol and 1 Naphthoic Acid (m/z 143 / m/z 171) Obtained at Three Wavelengths.

Wavelength	[illegible]	[illegible]	[illegible]
266	.79 ± .06	1.0	.11 ± .02
532	1.1 ± .1	1.4	.50 ± .06
1064	.65 ± .07	.86	.41 ± .08

	pka's	
	Ground State	1st Excited Singlet
2 Naphthol	9	3
1 Naphthoic Acid	6	7

Scheme I

Mechanism for (M-H+Na) Formation at 266 nm.

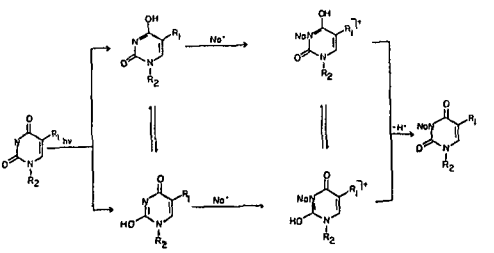

Thymidine R_1 = CH_3, R_2 = 2'-deoxyribose

Uridine R_1 = H, R_2 = Ribose

Figure III

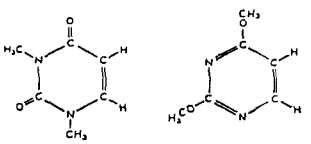

I II

I - N_1, N_3-dimethyluracil

II - 2,4-dimethoxypyrimidine

Presented at the 35th ASMS Conference on Mass Spectrometry and Allied Topics
May 24-29, 1987, Denver, CO.

NEGATIVE ION CI STUDIES OF NITROGEN-SUBSTITUTED AROMATICS BY GC/MS AND FTMS*

M. V. Buchanan, I. B. Rubin, and E. A. Stemmler
Analytical Chemistry Division
Oak Ridge National Laboratory
Oak Ridge, TN 37831-6120

Previous studies in our laboratory have shown that negative ion chemical ionization (NICI) processes are useful for the differentiation of isomeric polycyclic aromatic hydrocarbons (PAH). An apparent ionization threshold of about 0.5 eV exists for the formation of molecular anions, allowing compounds with electron affinity (EA) values on either side of this threshold to be distinguished. Further studies have been undertaken to assess the generality of this trend in ionization. Azaarenes, which have a nitrogen atom within an aromatic ring, were observed to obey this 0.5 eV ionization threshold. Adding a nitrogen to an aromatic ring raises the electron affinity of the compound slightly over that of the parent PAH. Thus acridine (9-azaanthracene) forms a molecular anion under NICI conditions, whereas anthracene (EA -0.49) does not. Further, acridine may be differentiated from its isomer phenanthridine (9-azaphenanthrene), which does not respond under NICI conditions.

Amino-substituted PAH with EA values greater than 0.5 eV also form molecular anions. Amino-PAH with lower EA values respond poorly; however, a number of unusual ions are observed. It was noted that in some cases these anions can yield information about the position of the amine substituent on the aromatic ring. For example, 1-aminoanthracene yields an anion at m/z 207, corresponding to $(M + 14)^-$, as the base peak. On the other hand, 2-aminoanthracene yields an anion at m/z 205, corresponding to $(M + 12)^-$, as the base peak. Similar anions are observed for 1- and 2-aminonaphthalene, allowing them to be differentiated using NICI as well. Another anion observed in the NICI spectra of both 1- and 2-aminoanthracene is m/z 192 $(M - 1)$.

These initial studies were performed with a conventional high pressure (approximately 0.4 torr) CI source on a quadrupole mass spectrometer with the ion source at 200° C. Using this instrument, the identities of the $(M + 14)^-$ and $(M + 12)^-$ ions could not be determined. Fourier transform mass spectrometry (FTMS) was employed to establish the elemental formulae of these anions. In addition, swept double resonance experiments were used to establish the pathways for the formation of some of the anions. The FTMS employed in these studies was equipped with a differentially pumped dual cell. Typically, CI reactions with the FTMS were performed in the source cell using methane as the reagent gas at pressures from 10^{-4} - 10^{-6} torr. However, the anions formed from 1- and 2-aminoanthracene under NICI conditions were not dependent on the use of methane as the CI reagent; these anions were also observed when H_2O or O_2 was used as the CI reagent.

The anion at m/z 192 from 2-aminoanthracene, corresponding to $(M - H)^-$, was found to arise from reaction of the neutral species with OH^- using swept double resonance experiments. An anion corresponding to $(M + O - H)^-$ at m/z 208 was found to be linked to O^-. This was confirmed using $^{18}O_2$ as the CI reagent gas, with the formation of an anion at m/z 210, corresponding to $(M + {}^{18}O - H)^-$.

The anion at m/z 205 was found to correspond to $(M + O - 4H)^-$. However, the species responsible for the formation of this anion could not be determined using double resonance experiments. Using $^{18}O_2$ and $H_2{}^{18}O$ as CI reagents, no anion indicative of the incorporation of ^{18}O was observed. The anion at m/z 207, corresponding to $(M + O - 2H)^-$, was linked to OH^- by double resonance experiments; however, no incorporation of ^{18}O was observed when $^{18}O_2$ and $H_2{}^{18}O$ were used as CI reagents. The anions at m/z 205 and 207 were difficult to produce on the FTMS and required operating the cell temperature at 200° C. The inability to incorporate ^{18}O and the temperature dependence of these reactions suggested that the formation of these anions may not occur in the gas phase.

Further, experiments were performed on the quadrupole instrument in which oxygen and water were doped in to the methane reagent gas. Addition of water, which yields OH^-, enhanced the production of $(M - H)^-$, which supports the previous FTMS experiments. The abundances of m/z 205 (M + O - 4H) and 207 (M + O - 2H) were not significantly affected in this experiment. When oxygen was added to the reagent gas, producing primarily O_2^-, formation of the m/z 207 anion was enhanced the greatest in both 1- and 2-aminoanthracene, with the abundances of the anions at m/z 192 and 205 affected to a lesser extent. Using $^{18}O_2$ (53 atom %) doped into the reagent, an anion at m/z 209 was observed, indicating addition of ^{18}O to the anion normally observed at m/z 207. However, the intensity of the m/z 209 anion was much lower than expected, supporting the evidence obtained using the FTMS that the formation of (M + O - 2H) may not be a gas phase reaction. Upon closer inspection of the gas chromatographic profiles of the compounds as they eluted into the mass spectrometer, it was noticed that the profiles of m/z 205 and 207 anions lagged behind the profile of the $(M - H)^-$ at m/z 192. This suggested that these two anions might be formed through a surface mediated reaction. As the products of these reactions desorbed off the surface, skewed chromatographic peaks would result.

The results of these studies show that the general 0.5 eV threshold for molecular anion formation holds for azaarenes and amino-PAH as well as the parent PAH. Trace oxygen-containing impurities have been found to participate in the NICI reactions of aromatic amines with EA values less than 0.5 eV, and some of this reactions do not seem to occur in the gas phase. In addition, doping the CI reagent with oxygen was found to enhance the formation of the m/z 207 over m/z 205, with a concomitant increase in sensitivity and reproducibility of the resulting spectra. However, isomer specific information was lost.

*Research sponsored by the Office of Health and Environmental Research, U.S. Department of Energy under contract DE-AC05-84OR21400 with Martin Marietta Energy Systems, Inc.

Presented at the 35th ASMS Conference on Mass Spectrometry and Allied Topics
May 24-29, 1987, Denver, CO

Surface Ionization Organic Mass Spectrometry; II. Nitrogen-containing Cyclic Organics

Toshihiro Fujii and Hitoshi Jimba
National Institute for Environmental Studies
Tsukuba, Ibaraki 305, Japan

Four years ago we began the study of surface ionization organic mass spectrometry (SIOMS) under experimental conditions in which organic molecules were supplied from the gas phase onto a heated emitter SI ion source. Interaction of organic molecules with the hot emitter surface leads to thermionic emission. The principal mechanism of ion formation and energetic considerations are studied mass spectrometrically at the initial phase (Ref.1,2). Because, as yet, no clear rules predict which mode of surface ionization will occur for a certain compound, we decided to puesue systematic and serial research on the SIOMS by looking at all types of organic compounds separated into families on the basis of structure. The wealth of information available in the ionization energy literature is useful in predicting surface ionized species and its sensitivity, however there is not yet a body of literature relevant to many molecules of chemical and physical interest. We believe a comprehensive study is important for the interpretation of SI mass spectra and for the further development of SIOMS.

This presentation is the second of a series on the SIOMS and reports the SI mass spectra of 37 nitrogen-containing cyclic organic compounds. In this study we discovered that in the SI of diphenylamine (DPA) the ion in the form of $[(C_6H_5)_2N{=}CH_2]^+$ may be formed. We believe surface ionization involving the nucleophilic reaction between adsorbed species on the surface is responsible for this ion.

Full experimental details have been reported previously (Ref. 1,2).

The surface ionization of 37 kinds of N-containing cyclic organic compounds was investigated. Table I presents the formulas of the studied compounds with the numbering, molecular weight and ionization energy, the SI spectrum for the Re-oxide emitter (composed of an intense peak having more than 1 % base peak intensity), the postulated structures of the ions, the current densities referenced to pressure of 1 torr (determined from the heights of the lines in the mass spectrum, relative sensitivity), the temperatures corresponding to those currents, and SI/EI (the ratio of the highest intensity in the SI mode to that in the EI mode). SI spectra obtained are discussed along with the substances classified by their functional group in the following paragraphs.

Arylamines The SIOMS of five arylamines of the type $C_6H_5NR_1R_2$ was done with substituents (R_1, R_2 = H, CH_3, C_6H_5) possessing different electronic-chemical properties. As can be seen from Table I, the SI spectra of arylamines are characterized by ions of $(M+H)^+$, M^+ , $(M-H)^+$ ions, which are directly characteristic of the molecular weight and other relatively strong ion peaks. Comparison of the $(M-H)^+$ ions of these amines with varying substituents tells us that the substitution of hydrogen in the compound by a methyl or phenyl group gives rise to an increase in the ionization efficiency. This would indicate the electron-release properties of the CH_3 or C_6H_5 radicals can be easily predicted by the substituent constant (σ, sigma) in the Hammett equation.

Diphenylamine (DPA) proved to be an interesting compound for SIOMS. The SI mass spectrum of DPA showed there are ions formulated with $[(C_6H_5)_2N{=}CH_2]^+$ ions. We speculate that DPA may act as a nucleophile in reaction with the CH_3 radicals on the emitter surface. The radicals are probably produced due to a thermal decomposition on the hot emitter surface which leads to the formation of ammonim ions according to the following proposed scheme:

$$(C_6H_5)_2NH \quad + \quad CH_3 \longrightarrow (C_6H_5)_2N{=}CH_2 \quad + \quad H_2$$

Aniline Derivatives The influence of substituents in the aniline molecule on the composition of their SI mass spectra and on the ionization efficiency, is demonstrated for the SI of aniline derivatives. The SI spectra of these substances except o-nitroaniline consist of lines due to the ions $(M-H)^+$ or M^+. The efficiency of the formation of the $(M-H)^+$ ions depends significantly on the electronegativity of the substituents.

N-alkylamines N-alkylamines provided a good application for SIOMS. Their spectra were characterized by a single peak of very intense $(M-H)^+$ ions.

Azo, nitriles, azoles These compounds seem not to be amenable to SI analysis.

N,N-heterocyclic amines (5ring) Several 5-membered ring N,N-heterocyclic amine compounds were studied. Pyrrole, indole and carbazole which are a pyrrole ring fused with one and two benzene rings respectively, exclusively provide the intense molecular ion while skatole which has a structure of indole with the methyl radical as a side chain does the $(M-H)^+$ ions.

N,N-heterocyclic amines (6ring) In the ionization of pyridine, quinoline and acridine, all invariably exhibit $(M+H)^+$ ions with great efficiency. Comparison with the spectra of the corresponding 5-membered heterocyclic amines, pyrrole, indole, and carbazole reveals an interesting difference; as mentioned before, the 5-ring compounds give a single molecular ions, instead of $(M+H)^+$ ions.

Presented at the 35th ASMS Conference on Mass Spectrometry and Allied Topics
May 24-29, 1987, Denver, CO

Table I. Surface ionization mass spectrum and relative sensitivity of N-containing aromatic or cyclic organic compounds

Compound (m/z, IE)	Intense Peak (m/z)	Emitter Temp.(C)	Relative Sens(A/torr)	SI/EI (n)*	Remarks
ARYLAMINES					
1 aniline (93, 7.7)	93, M+	650	3.2x10(-3)	0.02 (93)	AP(7.8eV)
2 diphenylamine (169,)	182,(M+CH)+	400			Tc=160***
	169, M+	550	100**	2.8	
	168,(M-H)+	550	2.7	(169)	
	167,(M-2H)+	550	4.1		
3 triphenylamine (245,)	260,(M+CH3)+	400			Tc=200
	246,(M+H)+	550	100	1.3	
	245, M+	550	6.2	(245)	
	244,(M-H)+	550	28.5		
4 N-methyl-aniline (107, 7.3)	107, M+	620	0.1		
	106,(M-H)+	620	0.8	3.8 (107)	
5 N,N-dimethyl-aniline (121,)	120,(M-H)+	620	17.9	85.7 (121)	
ANILINE DERIVATIVES					
6 o-toluidine (107, 7.68)	107, M+	550	0.36		
	106,(M-H)+	550	3.4	7.5	
	79, ?	690	1.6x10(-3)	(106)	
7 o-chloroaniline (127, 7.9)	127, M+	690	6.7x10(-3)	3.6x10(-2) (127)	
8 o-nitroaniline (138,)	no peak				Tc=160
9 o-phenylene-diamine (108,)	108, M+	550	100	1.1	Tc=160
	107,(M-H)+	550	64.3	(108)	
N-ALKYLAMINE					
10 benzylamine (107, 8.64)	106,(M-H)+	550	0.53	2.9	
	79, ?	690	1.6x10(-2)	(106)	
11 phenethylamine (121,)	120,(M-H)+	550	100	4.0 (121)	Tc=130
AZO COMPOUNDS					
12 azobenzene (182,)	no peak				Tc=220
13 p-aminoazo-benzene (197,)	no peak				Tc=220
14 diazoamino-benzene (197,)	93, ?	550	100	0.48 (93)	Tc=135
BENZONITRIL					
15 benzonitril (103,)	no peak				Tc=130
16 m-tolunitrile (117,)	91,(M-CH)+	620	2.4x10(-2)	0.3 (117)	
17 benzylcyanide (117,)	no peak				Tc=150
N,N-HETEROCYCLICAMINES (5-ring)					
18 pyrrole (67, 8.2)	67, M+	690	5.8x10(-3)	0.086 (67)	
19 pyrroline (69,)	70,(M+H)+	550	3.54	28	
	68,(M-H)+	620	2.45	(68)	
	43, ?	620	3.2x10(-2)		
	42, ?	620	7.4x10(-3)		
20 pyrrolidine (71, 8.41)	72,(M+H)+	325	6.8x10(-2)		
	70,(M-H)+	550	1.36	9.1	
	68,(M-3H)+	620	1.5x10(-2)	(70)	
	43, ?	760	8.2x10(-3)		
	42, ?	620	4.1x10(-3)		
21 indole (117,)	117, M+	550	100	0.11 (117)	Tc=190
22 skatole (131,)	130,(M-H)+	550	100	1.08 (130)	Tc=190
23 carbazole (167,)	167, M+	550	100	0.33 (167)	Tc=225
AZOLE					
24 pyrazole (68,)	no peak				
25 thiazole (85,)	no peak				
26 imidazole (68,)	no peak				
HETEROCYCLICAMINES (6-ring)					
27 pyridine (79,)	80,(M+H)+	550	3.2x10(-3)	0.046	
28 2-picoline (93, 9.02)	94,(M+H)+	325	0.203	1.31 (93)	AP=7.96
29 2-picolinic acid (123,)	no peak				Tc=85
30 piperidine (85, 8.7)	86,(M+H)+	400	3.3x10(-2)		AP(8.0eV)
	84,(M-H)+	475	45.8	366.7	
	82,(M-3H)+	690	7.37	(84)	
	80,(M-5H)+	690	6.23		
31 morpholine (87,)	85,(M-H)+	400	1.3	14.8	
	56, ?	475	0.24	(87)	
32 pyrimidine (80,)	no peak				
33 pyrazine (80,)	no peak				
34 quinoline (129,)	130,(M+H)+	255	100	4.8 (129)	Tc=130
35 acridine (179,)	180,(M+H)+	550	100	0.15 (179)	Tc=250
36 phenothiazine (199,)	198,(M-H)+	550	100	0.28 (199)	Tc=275
37 purine (120,)	no peak				Tc=230

*) (n) in the SI/EI column indicates the mass number, n, of the base peak in the EI spectrum for comparison.
**) The spectrum of the compound marked by ** is epressed in the pattern coefficient in the column of Relative Sensitivity.
The percent content of (M+H)+ ions is not given because at the optimum temperature for ions of other chemical compositions the current of (M+H)+ became very small.
***) Tc is the GC column temperature.

References
1) T. Fujii and T. Kitai; Int. J. Mass Spectrom. Ion Proc., 1986, 71, 129 & 1984, 57, 63.
2) T. Fujii, H. Suzuki and M. Obuchi; J. Phys. Chem., 1985, 89, 4687.

Presented at the 35th ASMS Conference on Mass Spectrometry and Allied Topics
May 24-29, 1987, Denver, CO

CHARACTERIZATION OF MIXTURES OF ORGANIC ACIDS BY GLOW-DISCHARGE IONIZATION THERMOSPRAY LC-MS

F.A. Bencsath and F.H. Field
The Rockefeller University
New York, N.Y. 10021

The analysis of the low molecular weight organic acids has a high biomedical importance. Its field of application extends to identifying anaerobic bacteria in cultures, monitoring fermentation processes, studying metabolic disorders like diabetes mellitus and diagnostizing inborn error diseases in infants and children. Capillary GC-MS is currently the method of choice for mass spectrometric analysis of organic acids in biological fluids. This technique requires careful sample cleaning-up, concentrating and derivatizing steps. In the last years, the development of the HPLC column technology and separation methodology has shown the feasibility of the use of liquid chromatography (1) as an alternative to gas chromatography (2) to cope with such a task, promising an easier sample preparation and thereby faster analysis.

Thermospray-MS can serve as a detector in the LC-MS analysis. Until now, however, only one TS-LC-MS work was published dealing with organic acids (3) which utilized the positive ions obtained by discharge ionization. The method worked well with C_1-C_4 aliphatic acids and glycolic acid, but failed with dicarboxylic acids and even with lactic acid. The fact that organic acids easily provide stable anions upon ionization suggests that the negative ion detection mode should be more useful. Interestingly, no such investigations are known, and in general, the total bibliography of the negative TS seems to consist of 7 publications.

Our objective was to investigate the feasibility of organic acid determination by TS-MS with negative ion detection.

The first experiments showed that the addition of glow-discharge ionization to the TS ionization meaningfully (about 40-100 times) enhanced the intensity of the spectra which consisted mostly of one major peak, the $(M-H)^-$ molecular ion. All the following experiments were made by discharge ionization.

Solutions of 10 different acids were prepared with a conc. of 250 Ng/µl using pure water and 0.05 N aqueous ammonium acetate as solvent. With some acids, similar solutions were prepared using also $(NH_4)_2SO_4$, NH_4ClO_4, NH_4HCO_3 and NH_4SCN buffers (0.05N). A VG 70-250 magnetic sector MS equipped with Vestec TS source and interface was used. The source was kept at 3 kV potential and pure water was used as a liquid phase supplied by a Rainin HPLC with a flow of 0.6 ml/min. The organic acid sample solutions were injected via direct loop injections of 50µl aliquots. This size of sample plug provided continuous spectra of several seconds long which were recorded and served as a basis for comparing the MS responses of the different acids in different solutions. We found the following.

1. In the spectrum of pure water, no disturbing background ions are present. Only hydroxyl anion and its water clusters appear at m/z 17, 35, 53 and 71.
2. The lowest MW acids show a strong tendency to form clusters with water and with another acid molecule lowering thereby the upper limit of the practical range of the linear and dynamic concentrations. At 250 ppm, the formic acid dimer ion's intensity is about 60%, and the water cluster's intensity is about 35% of the formate ion's (Fig. 1a). The clusters of the acetate anion are less intense (25% water cluster, 17% dimer anion, Fig. 1b).
3. Some fragmentation is observable in the spectra of acids of more complex structure, e.g., α-keto-glutaric acid. The most prominent fragment ion is the $(M-H-H_2O)^-$ ion at m/z 99 (20%, Fig. 1c).
4. The aromatic monocarboxyl acids show hardly any decomposition. However, the increase of the retarding electrode potential results in a marked collision induced dissociation (= in-source CID) (4), which can be used e.g. to differentiate between p-hydroxylphenyllactic and homovanillic acids both having a molecular ion of the same mass (m/z 181). The mass of the fragment ions are fully compatible with the structure of the parent acids (see e.g., HVA spectrum, at 50 and 250 V, Fig. 2).
5. The injection of 250 ppm citric acid solution resulted only in spectra with low mass fragments. By injecting a solution 20 times more concentrated (5µg/µl), good quality spectra could be produced (Fig. 3) with a dominant molecular anion in it.
6. The different acids show quite different molar responses. If comparing the molecular ion intensities obtained of the several acids to that of the formate, and taking into account the differing molecular weights of these acids, one finds that the acetic, lactic and oxalic acids molar responses are somewhat lower (0.6, 0.8, 0.6) while pyruvic,

α-keto glutaric and succinic acids' are about 3x higher. The molar responses of the aromatic acids (benzoic and HVA) are about 3.0.

Since the different HPLC separations of short chain organic acids require the presence of inorganic acids and/or buffers of different ionic strengths (1-200 mM), we investigated the influence of the buffers on the spectra. We found that

1. Using 25 mM ammonium acetate buffers, the relative response of the aliphatic monocarboxylic acids did not change noticably, but that of the dicarboxylic acids decreased meaningfully; in case of oxalic and succinic acid even near to 0. The same time, the response of the organic acids increased by a factor of 3-4.
2. The different buffers show different effects on the ionization. Acetic acid's response in 0.05 N ammonium sulphate solution is 1.3 times higher, but in NH_4ClO_4, NH_4HCO_3, and NH_4SCN solutions, it is markedly lower (0.5, 0.9 and 0.4 times, respectively) than in water.

We conclude, that thermospray ionization with negative discharge ionization (TS/CI^-) is a useful detection method for aliphatic and aromatic mono and dibasic, hydroxyl and oxo carboxylic acids, but only in pure water. Buffers at a concentration of 50 mM decrease the detectability of the dibasic acids, in some instances down to 0. The TS/CI^- response of the difference acids is dependent on the acid's structure and the ionic milieu. Polycarboxylic acids exhibit 2-3 orders of magnitudes less sensitivity.

References.
1. R.F. Adams, R.L. Jones, P.L. Conway, J. Chrom. 336, 125 (1984)
2. M.L. Holland, G.R. Rhodes, D. Wiesler, M. Novotny, J. Chrom. 306, 23 (1984).
3. F. Pacholec, D.R. Eaton, D.T. Rossi, Anal. Chem. 58, 2581 (1986).
4. F.A. Bencsath, F.H. Field, ASMS 34th Conference p. 5, Cincinnati, OH. 1986.

Fig. 1

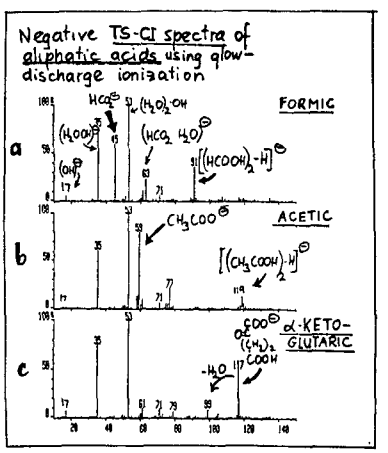

Fig. 2

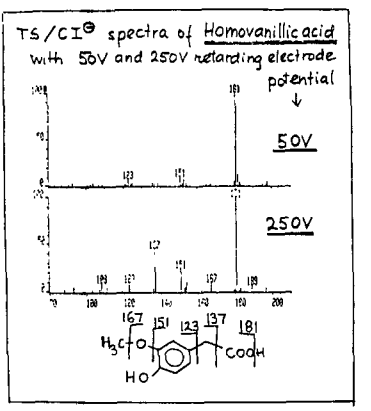

Fig. 3

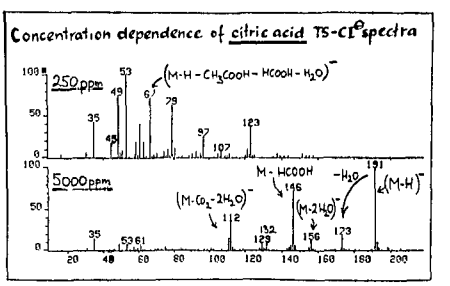

Presented at the 35th ASMS Conference on Mass Spectrometry and Allied Topics
May 24-29, 1987, Denver, CO.

DOES THE CHARGING OF A DROPLET ALTER ITS VAPOR PRESSURE? APPLICATIONS TO THERMOSPRAY.

Alan L. Rockwood and Viswanatham Katta
Dept. of Chemistry, University of Houston, Houston, Texas 77004

Theoretical understanding of thermospray is still being developed. Therefore, it is important to identify the physical factors which may be important in thermospray. According to current thought, ion production in thermospray depends on field assisted ion evaporation from charged droplets. The electric field at the droplet surface is proportional to charge and inversely proportional to the radius squared. Presumably, the required large fields at the surface are developed as the solvent evaporates and the droplet becomes smaller. We wondered whether charge on a thermospray droplet would inhibit solvent evaporation. If so this may prevent the droplet from becoming small enough to develop the large electric field required for field assisted ion evaporation. This could be a factor in determining the efficiency of thermospray ion sources.

We investigated this question using electrostatic theory combined with thermodynamics. (In addition some kinetic arguements were included for part of the analysis.) For neutral molecules evaporating from a charged sphere, the vapor pressure is given by the equation

$$\ln(P_c/P_u) = -Q^2M/32\pi r^2\epsilon_0 r^4 RTD + (QM/4r^2RTD\pi)\,dA/dr$$

Pc and Pu are the vapor pressure of the charged and uncharged spheres, Q is charge, M is molecular mass, ϵ_0 is permitivity, r is radius, R is the gas constant, T is temperature, D is density, and A is the energy to transport charge carriers across the liquid/gas interface. The term containing A is not normally included in the equation, but is included here for completeness. The quantity A could depend on the identity of the charge carriers as well as (possibly) the radius. This term is probably negligible and is not considered further. The other term is the one of interest and comes from including the electrostatic energy in the free energy of the droplet. A derivation of the equation was included to illustrate how this effect arises.

Charging of a droplet reduces the vapor pressure, regardless of the sign of the charge. Application of the equation to thermospray is difficult because not much is known about the properties of thermospray droplets. If we assume that droplets are initially formed at about one micron radius with a net charge of ten thousand to one hundred thousand elementary charges, evaporation is strongly suppressed when the droplet reaches about 0.1 micron radius. The vapor equation can be put in terms of the electric field at the surface. In this form the equation shows that the vapor pressure is suppressed by a factor of 1/e when the electric field reaches 6.3 thousand million Volts/meter at T = 373 K. (It is shown that under these conditions vaporization is kinetically inhibited, even for a droplet in vacuum.) If solvent vapor is present, a rigorous thermodynamic limit for the maximum field achievable for an evaporating drop can be given. The limit is given by the expression

$$E_* = (-2RTD\ \ln(S)/\epsilon_0 M)^{1/2}$$

where S is the saturation ratio. For a saturation ratio of 0.9, evaporation of solvent ceases when the field reaches 2.0 thousand million Volts/meter, and for a saturation ratio of 0.99 the corresponding field is 0.6 thousand million Volts/meter. If, under a given set of ambient conditions, the limiting field is less than the field required for field assisted ion evaporation of a particular ionic species, it is unlikely that the ion will be detected in thermospray.

Preliminary work in our laboratory indicates that some ions may require about 0.8 thousand million V/m for field assisted ion evaporation to be favorable. This is within the range discussed above. Thus it may be necessary to take into account the effect of charging on droplet vapor pressure in order to understand thermospray under certain operating conditions. However, the saturation ratios discussed above are quite high, and it would be unusual to operate a thermospray ion source under such nearly saturated conditions. On the other hand, some ions might require higher fields to evaporate, in which case the effect discussed here might be significant.

There are other applications of these ideas. For example, it can be shown that the thermodynamic activity of an electrochemical electrode is not significantly altered by shifts in voltage. Also, some of the thermodynamics of cluster ion formation might be analysed with these methods, although quantum effects might become important for such small systems.

Acknowledgements: Much of this work was done in the laboratory of Prof. M.L. Vestal. Partial support by NSF grant CHE-831154 is gratefully acknowledged.

References: A form of the vapor pressure equation can be found in B.J. Mason, Disc. Far. Soc., 1960, 30, 20., and in A.E. Alexander and P. Johnson "Colloid Science"; Clarendon Press: London 1949.

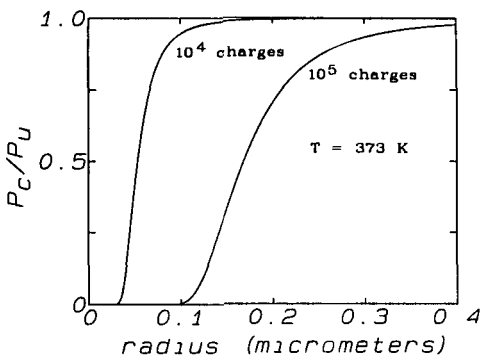

figure 1. Pc/Pu as a function of droplet size.

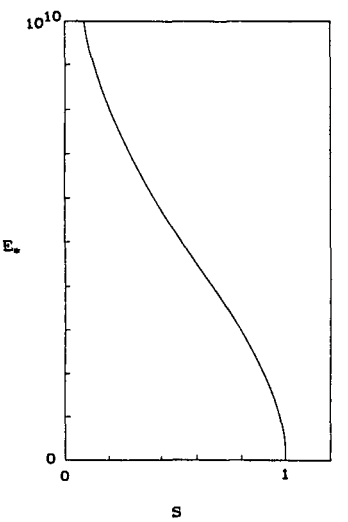

figure 2. Limiting electric field as a function of saturation ratio, T = 373 K.

Presented at the 35th ASMS Conference on Mass Spectrometry and Allied Topics
May 24-29, 1987, Denver, CO

MULTIPLE CHARGING IN ELECTROSPRAY IONIZATION OF OF POLYETHYLENE GLYCOLS

S. F. Wong, C. K. Meng and J. B. Fenn
Department of Chemical Engineering
Yale University, New Haven, CT 06520-2159

Mass spectra for polyethylene glycols (PEGS) have previously been obtained with several other soft ionization methods including Fast Atom Bombardment (FAB), Thermospray (TS), Electrohydrodynamic (EH) and Field Desorption (FD). (1-4) Reported results have indicated up to four charges per molecule with EH but no appreciable multiple charging with TS, FAB or FD. Up to three charges per molecule have occasionally been observed for other species with these methods as well as with Secondary Ionization Mass Spectrometry (SIMS), Laser Desorption (LD) and Plasma Desorption. As many as five charges per molecule of porcine trypsin have been obtained with PD. (5) Here we present experimental results indicating that Electrospray Ionization (ESPI) can deposit as many as 23 Na+ ions on PEG oligomers with molecular weights in the range from 15,000 to 20,000. A simple model assumes that the charges are bound to oxygen atom sites. It predicts that the maximum possible number of charges is reached when the binding energy of the centermost charge to such a site is equal to its electrostatic potential energy which results from coulomb repulsion by all other charges on the molecule.

The PEG samples having nominal (mean) molecular weights of 200, 600, 1000, 1450, 3350, 8000 and 17,500 were Carbowaxes obtained at no charge from Union Carbide. The PEG 400 sample came from Baker. At concentrations of 0.05 mg/ml in 50:50 methanol water they were injected into our previously described ESPI Mass Spectrometer at flow rates of 7 ul/min. (6) Figure 1 shows a spectrum obtained with PEG 400. The labelled peaks are due to quarternary ammonium ions added as mass markers. The major peaks are identified with PEG oligomers to each of which is attached a single Na+. The small satellite peaks, 5 daltons higher, are due to NH_4+. The band of peaks tagged with small circles are oligomers with K+ adducts. Those with x's have 2 Na+ ions attached. These cation adducts seem to be present in the PEG samples as received. For PEG 3350 shown in Fig. 2 bands containing 4, 5 and 6 Na+ can be resolved with an expanded m/z scale. Figure 3 shows the spectrum for "PEG Compound 20 M" which has a mean molecular weight of 17,500. We cannot resolve individual peaks because of the large multiplicity of nmer-charge combinations having nearly identical m/z values. We conclude from the position of the band maximum that the average number of Na+ per oligomer is about 23. Figure 4 shows the maximum number of Na+ per oligomer as predicted by our model (solid curve) and thus far observed (square points).

Presented at the 35th ASMS Conference on Mass Spectrometry and Allied Topics
May 24-29, 1987, Denver, CO

References.

1. R. P. Lattimer, Int. J. Mass. Spect. Ion Proc., 55,221 (1984)
2. R. H. Robins and F. W. Crow, Proc. 34th Ann.Conf.Mass. Allied Top. 570 (June 1986); R. Willoughby, T. Poppel, J. Buchner, V. Pizzitola, ibid. 596.
3. S. T. F. Lai, K. W. Chan and K. D. Cook, Macromols. 13, 953 (1980); K. W. Chan and K. D. Cook, Org. M.S. 18, 423 (1983)
4. R. P. Lattimer and G. E. Hansen, Anal.Chem. 14, 776 (1981); S. D. Maleknia and C. E. Costello, Proc. 34th Ann. Conf. Mass Spect. Allied Topics, 829 (June 1986)
5. I. Kamensky and A. G. Craig, Anal.Inst. 16, 71 (1987)
6. C. M. Whitehouse, R. N. Dreyer, M. Yamashita and J. B. Fenn, Anal. Chem. 57, 675 (1985)

Acknowledgement: This research was supported by NIH under Grant 5 R01 GM31660-03 with some help from the American Chemical Society under PRF Grant 16284-ACS.

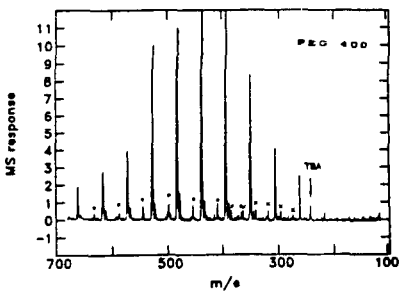

Figure 1. Electrospray mass spectrum for PEG 400. Ions are Na+ adducts except for o's which are for K+. x's are doubly charged Na+ adducts.

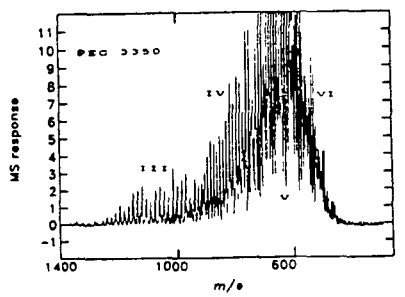

Figure 2. ESPI mass spectrum for PEG 3350. Roman numerals identify ions with that number of Na+ attached.

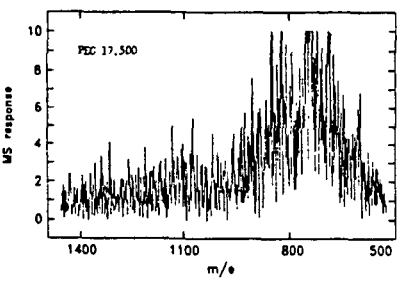

Figure 3. ESPI mass spectrum for PEG Compound 20 M (Mean Mol. Wt = 17,500.

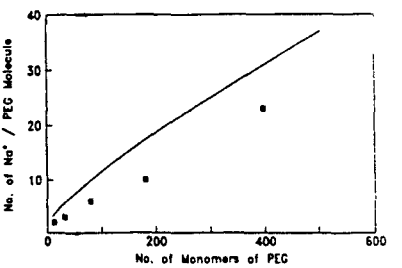

Figure 4. Maximum number of Na+ per PEG oligomer. Curve is theoretical, points are experimental.

Presented at the 35th ASMS Conference on Mass Spectrometry and Allied Topics
May 24-29, 1987, Denver, CO

HIGH MASS ION PRODUCTION USING ELECTROHYDRODYNAMIC MASS SPECTROMETRY

Terry D. Lee and Kassu Legesse
Division of Immunology
Beckman Research Institute of the City of Hope
Duarte, CA 91010

John F. Mahoney and Julius Perel
Phrasor Scientific, Inc.
Duarte, Ca 91010

Electrohydrodynamic (EHD) mass spectrometry utilizes a strong electric field to assist the desorption of sample ions directly from a liquid matrix. It is one of the most gentle of ionization techniques providing molecular ions of polar nonvolatile molecules with little or no fragmentation. While various aspects of EHD have been explored over the past two decades, little has been done to apply this ionization method to the analysis of high molecular weight compounds. To explore the possibility of using EHD to produce high mass ions, we have interfaced an EHD ion source with a JEOL HX100HF double focusing mass spectrometer. Evidence for the ability of EHD to generate large ions is found in the spectrum of 1.3 M NaI in glycerol (Fig. 1a) taken in the "fast metastable" mode (1). In addition to the peaks due to ions and small clusters at low mass is a continuum which increases in intensity with increasing mass. We call this portion the "droplet" spectrum. The droplet spectrum extends to the effective mass range limit of the instrument (m/z = 11,000). The "fast metastable" spectrum is acquired by setting the source voltage at a value higher than the energy value that the electric sector is set to accept. Ions observed in the spectrum are what remains of larger ions that have lost mass (and possibly charge) prior to reaching the electric sector. Normal (full energy) spectra (Fig. 1b) consists of ions extracted directly from solution and do not contain the droplet spectrum.

A model for evaporative loss of mass from solvent ion clusters has been developed which allows estimates to be made of % mass loss, initial and residual cluster temperatures, and evaporation times vs. ion flight times in the mass spectrometer. A number of conclusions have been reached that are relevant to the analysis of macromolecules by EHD. Residual temperatures for glycerol clusters (14 - 100 Å radius) range from 250 to 320 ^{o}K for residence times of 1ms to 1us respectively. Initial cluster temperatures range up to 540°K for 50% evaporation (Fig. 2). As would be expected, the model predicts that for a given initial temperature, larger clusters require longer times to reach the same residual temperature (Fig. 3). A less obvious conclusion is that clusters formed at higher temperatures reach their residual temperature more quickly than clusters of the same size that are formed at a lower temperature (Fig. 3). The source of cluster heating is attributed to Joule heating of the jet-like protrusions on the end of Taylor cone structures formed in the liquid during application of high electric fields. Because direct extraction of molecular ions without a solvent sheath is unlikely for large molecules, the formation of "hot" droplets is essential for desolvation. It can be argued that total desolvation is increasingly more probable as sample molecule size increases because a greater portion of a given cluster mass is sample.

It is unlikely that total desolvation of large molecules can occur during EHD analysis because the spectra of even small peptides exhibit glycerol adduct ions (Fig. 4). More encouraging results have been obtained using a methanol-water system (Fig. 5).

---

1. K.D. Cook, Mass Spectrom. Rev., 5 (1986) 467.

Presented at the 35th ASMS Conference on Mass Spectrometry and Allied Topics
May 24-29, 1987, Denver, CO

Fig. 1
1.3 M NaI in Glycerol Ves = 2.0 kV Vs = 2.1 kV

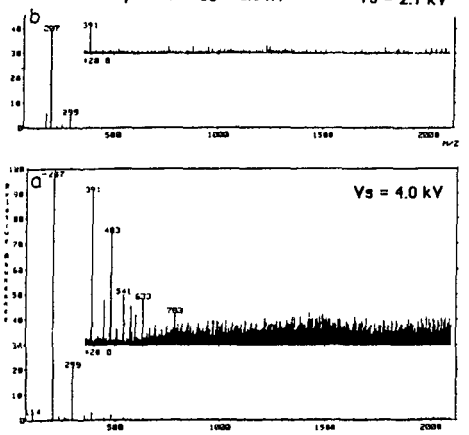

Fig. 2

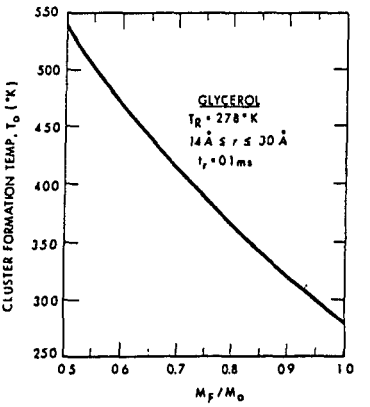

Fig 3

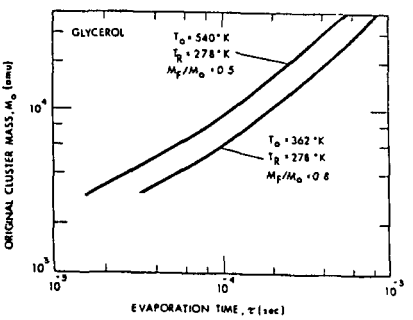

Fig 4

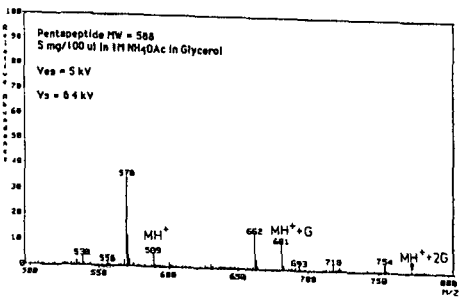

Fig. 5
Pentapeptide MW = 588
3.6 mg/100 ul in 0.1 M NH_4OAc in $MeOH \cdot H_2O$ (50:50)

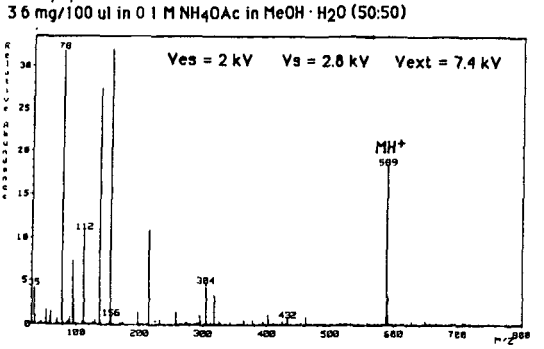

Presented at the 35th ASMS Conference on Mass Spectrometry and Allied Topics
May 24-29, 1987, Denver, CO

THERMODYNAMIC AND KINETIC CONTROL OF ION INTENSITIES IN ATMOSPHERIC PRESSURE IONIZATION MASS SPECTROMETRY. Sunner, J.; Ikonomou, M.; Kebarle, P.; University of Alberta; Edmonton, Alberta; Canada T6G 2G2.

The sensitivity of Atmospheric Pressure Ionization Mass Spectrometry (APIMS) in positive ion mode for compounds M with a wide range of gas-phase basicities (GB's) was determined. The reagent gas was air at 25°C and with ca 5 torr partial water pressure. The results are explained in terms of the kinetics and thermodynamics of ions solvated in the gas phase by a number of water molecules[1].

When moist air is ionized, a sequence of ion-molecule reactions is initiated which results, within microseconds, in the formation of $H_3O^+(H_2O)_n$ clusters[2]. These clusters are the main reagent ions in API. They protonate analytes M by the reaction:

$$H_3O^+(H_2O)_n + M = MH^+(H_2O)_m + (n+1-m)\ H_2O \qquad (1)$$

The instrument used in the present investigation was a Sciex TAGA 6000E. In the Sciex instrument the ions created in the ion source pass through an inert and moisture-free "interface" gas (N_2) before beeing sampled by a 100 µm orifice. In the dry interface gas the cluster ions undergo thermal declustering. The $H_3O^+(H_2O)_n$ reagent ions decluster down to n=2 to 4, whereas most $MH^+(H_2O)_m$ ions decluster all the way to the bare MH^+-ions.

The experimentally determined sensitivities (relative to pyridine) for compounds M are plotted in Figure 1 versus the gas-phase basicities (GB(M)). The compound shown in Figure 1 can be divided into the following groups:

A) The majority of compounds M with GB > ca.200 kcal/mol (nitrogen bases) was found to have a high and relatively uniform sensitivity with no apparent correlation with GB.

B) The majority of compound M with GB < ca.200 kcal/mol (mostly oxygen bases) was found to have a sensitivity that showed a rough positive correlation with GB. Thus, sensitivity tend to increase with increasing GB.

C) A number of compounds M had a much lower sensitivity than expected solely from their respective GB's. These compounds were mostly sulfur and carbon bases.

Figure 2 shows the same sensitivity values as Figure 1 but now plotted against the aqueous basicity ($pK_{BH^+}(M)$). For the range of compounds investigated it is seen that all compounds with a higher aqueous basicity than water itself have a high and uniform sensitivity in the API source. For compounds with an aqueous basicity lower than that of water there does not seem to be any correlation between sensitivity and pK_{BH^+}.

The sensitivities for the compounds in group A above was found to be determined by the kinetics for the proton transfer reaction (1), "kinetic control". For these high-GB compounds reaction (1) is usually close to collision-limited. The residence time of the reagent ions in the API source could be increase by increasing the distance between the corona discharge needle and the sampling orifice. For "kinetically controlled" ions this results in an increase in the ratio:

$$\sum_m I(MH^+(H_2O)_m) \ / \ \sum_n I(H_3O^+(H_2O)_n) \qquad (2)$$

This is illustrated in Figure 3 for M=pyridine.

The sensitivities for the compounds in group B above was found to be determined by reaction (1) approaching equilibrium, "thermodynamic control". This conclusion is supported by the following two observations:

a) As the residence time for the ions in the ion source is varied the ratio (2) does not change. This is illustrated in Figure 3 for M=acetone. b) The ratio (2) at equilibrium was determined by Pulsed High Pressure Mass Spectrometry, PHPMS[3]. Good agreement was found with the API source ratio.

The majority of compounds M in group C above has low sensitivities in API because the gas-phase hydration of MH^+ is particularly unfavourable[3]. The sensitivities for these compounds are under thermodynamic control. The sensitivities for many of the compounds in this group can be increased dramatically by heating the ion source[4]. This is exemplified in Figure 1 by the arrows for $(CH_3)_2S$ and furan.

Presented at the 35th ASMS Conference on Mass Spectrometry and Allied Topics
May 24-29, 1987, Denver, CO.

1) Sunner, J.; Kebarle, P. Anal. Chem., submitted.
2) Good, A.; Durden, D.A.; Kebarle, P. J. Chem. Phys. 1970, 52, 222.
3) Nicol, G.; Kebarle, P. J. Am. Chem. Soc. submitted.
4) Sunner, J.; Ikonomou, M.; Kebarle, P. Anal. Chem. submitted.

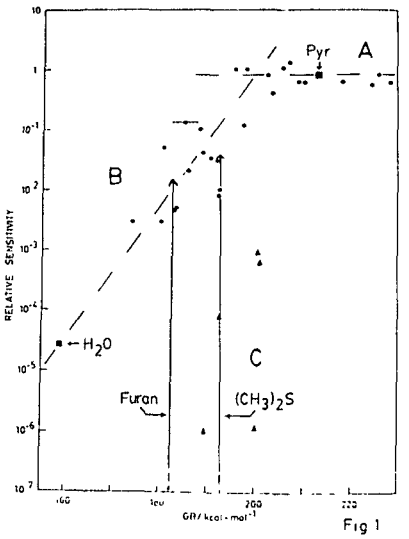

Fig 1

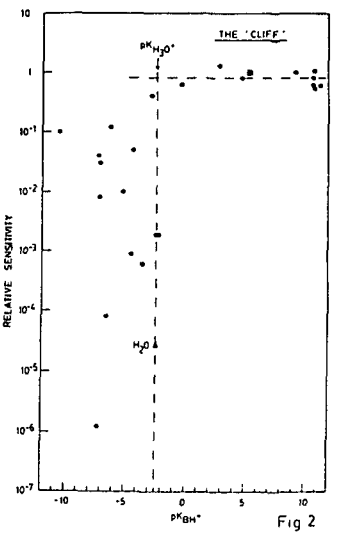

Fig 2

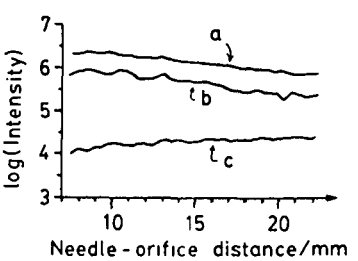

Fig 3

Figure 1. Sensitivities in API, positive ion mode, for a range of compounds plotted vs the respective gas-phase basicities. Reagent gas was air at 25°C and with ca. 5 torr water pressure. All sensitivities were measured relative to that of pyridine (Pyr). Arrows indicate increase in sensitivity obtained by heating.

Figure 2. Sensitivity data in Figure 1 plotted vs the aqueous basicities(pK_{BH^+}).

Figure 3. Intensities of (a) $H_3O^+(H_2O)$: (b) protonated acetone; and (c) protonated pyridine, versus distance between discharge needle tip and interface gas orifice. Residence time for ions in the source increases from left to right.

Presented at the 35th ASMS Conference on Mass Spectrometry and Allied Topics
May 24-29, 1987, Denver, CO

A STUDY OF INVOLATILE AND THERMALLY LABILE MOLECULES BY SPONTANEOUS DESORPTION MASS SPECTROMETRY (SDMS)*

M Salehpour and J E Hunt, Argonne National Laboratory, Chemistry Division, 9700 S. Cass Ave., Argonne, Illinois 60439, U.S.A.

This paper describes the latest findings in Spontaneous Desorption Mass Spectrometry (SDMS). SDMS, first discovered by Delle Negra et al (1), utilizes the instrumentation of 252-Californium time-of-flight Plasma Desorption Mass Spectrometery (PDMS). The main differences between PDMS and SDMS are the absence of ^{252}Cf in the latter and the fact that only one detector is used. Molecular weights are determined on the basis of relative time measurements between emitted electrons in coincidence with the spontaneously desorbed negatively charged molecules in the presence of an applied electric field.

Negative ion SD-time-of-flight mass spectra for a number of involatile and thermally labile molecules from a range of organic materials have been obtained. Fig 1 shows the high mass region of a negative ion time-of-flight mass spectrum for chlorophyll a (MW=893). The spectrum is strikingly similar to that obtained using PDMS (2). Although different apparent desorption-ionization mechanisms are responsible, it seems that the amount of internal energy transfered to the chlorophyll a molecule is about the same in both cases.

FIGURE 1

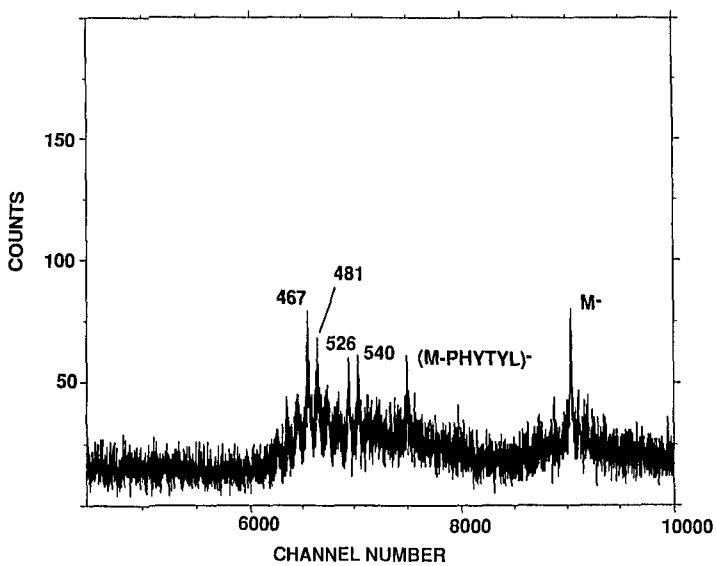

Other classes of compounds such as polymers and polypeptides have been mass analyzed. Fig 2 shows the negative ion time-of-flight mass spectrum for Luteinizing Hormone Releasing Hormone (LHRH, MW=1182) in the mass range 300-3000 u. The molecular ion is represented by M^-.

In addition, results indicate that the mechanism responsible for spontaneous desorption is unlikely to be back-sputtering due to positive ions emitted from the acceleration grid, suggested in ref 1. The conclusion is based on the following; 1) Studies of the multiplicities of the emitted molecular ions show that the average multiplicity is too high to account for incident keV atomic ions, 2) The acceration grid can be replaced with a ring and SDMS spectra can be readily obtained and 3) The rate of desorption of electrons and ion are strongly dependent on the applied field, indicating the effect being the low field tail of the field desorption effect.

(1)S Della Negra, Y LeBeyec and P Håkansson
Nucl Instr Meth B9 (1985) 103-106

*Work performed under the auspices of the Office of Basic Energy Sciences, U.S.Dept of Energy under contract number W-31-109-ENG-38.

FIGURE 2

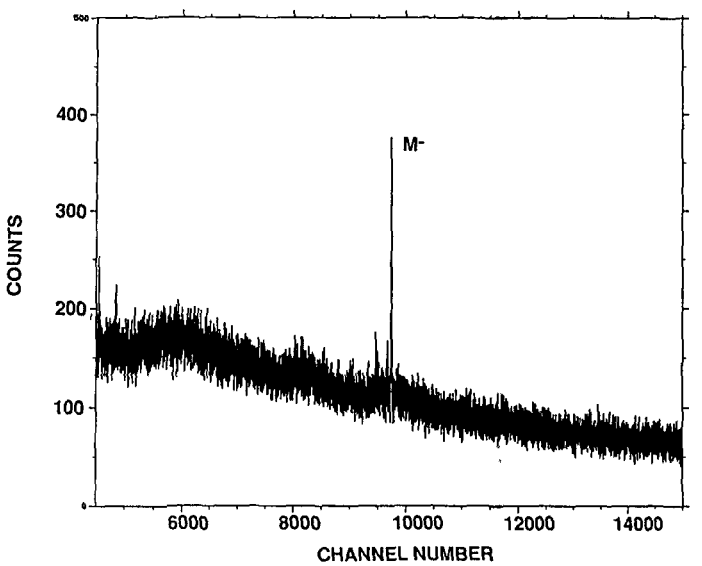

Presented at the 35th ASMS Conference on Mass Spectrometry and Allied Topics
May 24-29, 1987, Denver, CO

A FAST HEAVY ION INDUCED DESORPTION MASS SPECTROMETRY STUDY OF LANGMUIR-BLODGETT FILMS

G Säve, P Håkansson, B U R Sundqvist, E Söderström[1], S-E Lindquist[1], J Berg[2] and R E Johnson[3]

Dep. of Radiation Sciences, Division of Ion Physics,
Uppsala University, Box 533, S-751 21 Uppsala, Sweden.
(1) Institute of Physical Chemistry, Uppsala University S-751 21 Uppsala, Sweden.
(2) Institute for Surface Science, Stockholm, S-114 80 Stockholm, Sweden.
(3) Dep. of Nuclear Engineering and Engineering Physics, University of Virginia, Charlottesville, Virginia 22901, U.S.A.

Langmuir-Blodgett (LB) films [1] of fatty acids have been prepared on Si and Au backings as samples for fast heavy ion induced desorption mass spectrometry. The well ordered structure of such films has shown to be favourable in order to study the molecular ion yield as a function of the sample film thickness and the depth of which biomolecular ions may originate from.

Experimental data [2] on the molecular ion yield as a function of sample film thickness is presented in fig. 1 for Cd-stabilized arachidic acid films on Si-backings. Yield is here defined as number of detected secondary ions per incident primary ion. Primary ions of 78.2 MeV $^{127}I^{16+}$ in charge state equilibrium were used. The curve shows that the yield increases almost linearly with the film thickness from about zero for one monolayer up to 30 % for a thickness of 150 Å, where it saturates. By changing the substrate to Au-backings and repeating the above experiment, a similar thickness dependence was found except that the first monolayer on an Au-backing gave a significantly higher yield (5.5 %) and that the yield peaks around the saturation thickness, see fig. 2a. Primary ions of different energy were also used to check if the thickness dependence was influenced by the amount of energy deposited in the track of the fast ion [2]. The energies were selected so as to keep the primary ion velocity constant, which means that the radial extent of the energized track was held constant and that the energy density within the track thus scales with the energy of the primary ion. From fig. 2 it can be seen that the curves change in shape and the peak around the saturation thickness is more pronounced for the lower ionization densities. The above results indicate that the cause of the thickness dependence may be that sample material is sputtered from a volume in the sample, ranging down to a depth corresponding to the saturation thickness, about 125-150 Å. The enhanced yield found around the saturation thickness is regarded as an effect due to a weak Au/molecule bonding.

The crater formation effect was confirmed in an experiment [3] using samples of LB films consisting of marked layers. In fig. 3, spectra of negative ions for a sample of 2 monolayers of (A) arachidic acid (MW 312.5) on top of two monolayers of (B) behenic acid (MW 340.6) on 13 layers of (C) stearic acid (284.5) is shown for four different primary ion energies, i.e. electronic stopping powers dE/dx_e. The striking observation is that molecular ions originating from molecules from several layers below the surface can be observed in the spectra. The change of the relative fraction of the yields of the three fatty acids with energy density clearly indicate that a crater is formed which apparently is less voluminous and less deep for lighter primary ions, consistent with the overall decreas in neutral and ion yield with lower dE/dx_e. A nonuniform film cannot explain such a result.

Presented at the 35th ASMS Conference on Mass Spectrometry and Allied Topics
May 24-29, 1987, Denver, CO

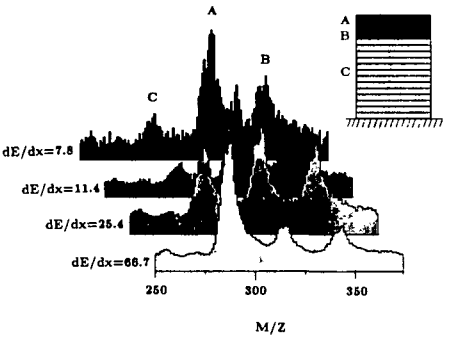

Fig. 3. Negative ion mass spectra of a mixed sample film, consisting of molecule A, B and C, for four different primary ions, i.e. electronic stopping powers. The mass spectra are normalized with respect to the total yield of A, B and C.

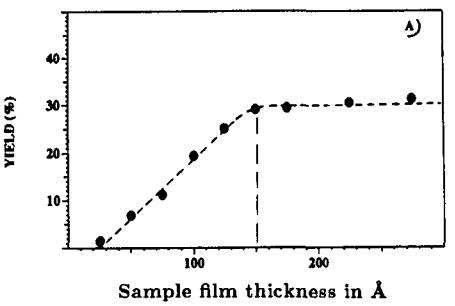

Fig. 1. Yield in percent of $(M\text{-}H)^-$ vs sample film thickness for arachidic acid on a Si backing.

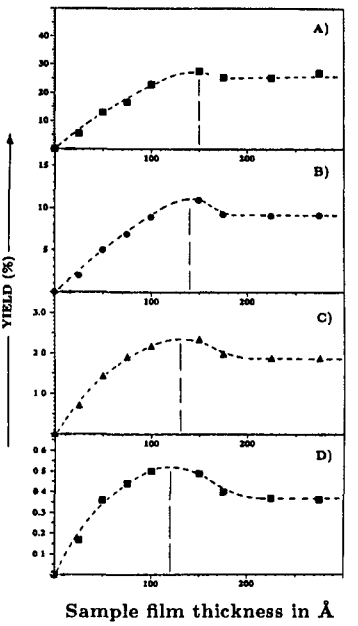

Fig. 2. Yield in percent of the negative quasi molecular ion, $[M\text{-}H]^-$, peak vs sample film thickness for four different values on the electronic stopping power, i.e. a) 66.7, b) 25.4, c) 11.4 and d) 7.8 MeV/mg/cm^2, respectively. The sample thickness was varied from 1 to 11 layers of arachidic acid on Au backings.

REFERENCES

1. H Kuhn, D Möbius and H Bucher. *Phys Meth of Chem* **1** (1972)

2. G Säve, P Håkansson, B U R Sundqvist, E Söderström, S-E Lindquist and J Berg *Accepted for publication Int J of Mass Spec and Ion Proc* (1987)

3. G Säve, P Håkansson, B U R Sundqvist, R E Johnson, E Söderström, S-E Lindquist and J Berg. Submitted for publication in *Appl Phys Lett* (1987)

Presented at the 35th ASMS Conference on Mass Spectrometry and Allied Topics
May 24-29, 1987, Denver, CO

Infrared Multiphoton Dissociation of Gaseous Ions

John R. Eyler
Department of Chemistry
University of Florida
Gainesville, FL 32611

Infrared multiphoton dissociation of gaseous ions has been carried out in a variety of ion traps using both pulsed and continuous wave CO_2 lasers. Studies in at least seven different laboratories have shed considerable light on the essential features of the technique, on the pathways and dynamics of dissociation of excited ions, on vibrational quenching mechanisms, and on the differentiation of isomeric ion structures. Recent publications from most of the active research groups are given below.

1. L.R. Thorne and J.L. Beauchamp in "Gas Phase Ion Chemistry", Vol. 3, M.T. Bowers, Ed. (Academic Press, New York, 1984), Ch. 18.

2. M.A. Hanratty, C.M. Paulsen, and J.L. Beauchamp, J. Am. Chem. Soc., 107, 5075(1985).

3. W. Tumas, Robert F. Foster, and J.I. Brauman, Israel J. Chem., 24, 223(1984).

4. C.R. Moylan, J.M. Jasinski, and J.I. Brauman, J. Am. Chem. Soc., 107, 1934(1985).

5. W.Tumas, R.F. Foster, M.J. Pellerite, and J.I. Brauman, J. Am. Chem. Soc., 109, 961(1987).

6. N.B. Lev and R.C. Dunbar, Chem. Phys., 80, 367(1983).

7. G. Baykut, C.H. Watson, R.R. Weller, and J.R. Eyler, J. Am. Chem. Soc., 107, 8036(1985).

8. C.H. Watson, G. Baykut, and J.R. Eyler, Anal. Chem., 59, 1133(1987).

9. M. Bensimon, J. Rapin, and T. Gaumann, Int. J. Mass Spectrom. Ion Proc., 72, 125(1986).

10. A.Kamar, A.B. Young, and R.E. March, Can. J. Chem., 64, 1979(1986).

11. J.H. Catanzarite, Y. Haas, H. Reisler, and C. Wittig, J. Chem. Phys., 78, 5506(1983).

Presented at the 35th ASMS Conference on Mass Spectrometry and Allied Topics
May 24-29, 1987, Denver, CO

PHOTODISSOCIATION STUDIES OF ION SPECTROSCOPY AND STRUCTURE

Robert C. Dunbar; Case Western Reserve University, Cleveland, Ohio 44106

A number of approaches are described for obtaining ion structural information by photodissociation with varying optical wavelength, (which is known as photodissociation spectroscopy, or PDS), emphasizing results with laser sources.

I. Representative photodissociation spectra.

A classical photodissociation spectrum is that of 1,3,5-hexatriene ion, reported from 540-650 nm at 1 nm resolution.[1] The prominent vibrational structure, showing vibrations at 1060 cm^{-1} and 350 cm^{-1}, suggests the spectroscopic capabilities of laser photodissociation at good optical resolution in favorable cases.

Spectra of small transition-metal-containing ions, of which $CoCH_2^+$ is an example, show very well defined photodissociation spectral peaks, which are characteristic and useful for thermochemical information, but are still poorly understood.[2]

The two-photon photodissociation spectrum of $Fe(C_5H_5)_2^+$ shows a distinct charge-transfer feature, with prominent structure (presumably vibrational) in the 580-640 nm region.[3]

II. Interpretation of Photodissociation Spectra.

Three modes of thinking have proven useful in relating the observed photodissociation peaks to the electronic structure and excited state features of radical ions:

- The correlation between PDS peak positions and the peaks corresponding to hole-promotion states in the photoelectron (PES) spectrum of the neutral molecule.[4]
- Higher energy peaks typically observed in aromatic and conjugated cations are electron-promotion peaks normally invisible in PES.[5]
- Radical ions have chromophoric groups which may not be familiar from neutral-molecule spectroscopy, such as the distinct visible and UV peaks of the conjugated diene chromophore, and the strong visible-region dissociation characteristic of alkanes.[6]

III. Substituent Effects.

The visible photodissociation peak of a number of methyl-substituted butadiene ions shows substituent shifts which are well understood in terms of molecular orbitals of the Π system, and which correlate well with the PES spectrum.[7]

The photodissociation of the "proton-labelled" α,β-unsaturated ketones, $H\overset{\oplus}{O}{=}CR_1{-}CR_2{=}CR_3R_4$, are similar to the UV absorption spectra of the corresponding unprotonated neutrals, but shifted, by the presence of the proton, to longer wavelength. The substituent effects in these spectra are well described and correlated by a set of parameters analogous to the "Woodward-Fieser" parameters for the neutrals.[8]

IV. Isomeric Ions.

Five isomers of C_5H_6 give electron-impact parent ions which are clearly distinct and distinguishable by their photodissociation spectra, even using only the limited number of wavelengths available from the argon-ion laser.[9] Agreement with PES spectra is excellent. Fragment $C_5H_6^+$ ions formed by low-energy collision-induced dissociation of parent ions of aniline, phenol and thiophenol were characterized by their photodissociation spectra, and found to have predominantly the cyclopentadiene structure.

Distinctive vibrational structure appears in the high-resolution spectra of isomeric chloropropene ions, and was used to characterize the differing structures of $C_3H_5Cl^+$ ions formed by ion-molecule reactions of 1-chloropropane and 2-chloropropane ions.[10]

Low-resolution spectra of various isomeric $C_6H_6^+$ ions are very different.[11] However,

several of the neutral molecules undergo partial rearrangement to the benzene ion structure upon ionization, as signalled by the presence of a non-dissociating fraction of the ion population.

V. Structural Implications of Dissociation Thermochemistry; Two-Photon Dissociation.

For small ions, clear photodissociation thresholds are observed, and the threshold photon energy leads to accurate ion thermochemistry. However, larger ions often have the threshold obscured by the onset of two-photon dissociation, which can be identified by pressure dependence of the extent of photodissociation. Using this idea,[12] the cleavage of Br from m-$CH_3C_6H_4Br^+$ was found to proceed with a single photon even at photon energies below 2 eV, while cleavage of I from m-$CH_3C_6H_4I^+$ is a two-photon process and 2 eV. This indicates that the bromotoluene dissociation proceeds via rearrangement to a benzyl or tropylium structure of the $C_7H_7^+$ product, while the iodotoluene case does not involve rearrangement.

Slow ion dissociation can also obscure thresholds. The photodissociation of $C_6H_5CN^+$ was time resolved by observing the extent of dissociation at varying times after the 308 nm excimer laser pulse, and showed a dissociation time constant of the order of 200 μs.[13]

VI. Infrared Spectra

In addition to straightforward infrared multiphoton dissociation, infrared spectroscopic information is available from two less obvious approaches:

- Infrared one-photon spectroscopy has been done in a a fast ion-beam spectrometer, in which most of the dissociation energy is supplied by electron impact, with only the final increment of energy being added by the lined-tuned CO_2 laser photon.[14]
- Visible-infrared two-laser dissociation uses the energy of the tunable infrared photons to assist an endothermic visible-photon dissociation process.[15]

References

1. R. C. Dunbar and H. H. Teng, J. Am. Chem. Soc. 100, 2279 (1978).
2. R. L. Hettich and B. S. Freiser, J. Am. Chem. Soc. 108, 2537 (1986).
3. J. Faulk and R. C. Dunbar, to be published.
4. P. P. Dymerski, E. Fu and R. C. Dunbar, J. Am .Chem. Soc., 96, 4109 (1974).
5. R. C. Dunbar, Chem. Phys. Lett. 32, 508 (1975).
6. R. C. Dunbar, Anal. Chem. 48, 723 (1976).
7. H. Y. So and R. C. Dunbar, to be published; H. Y. So, Ph.D. Thesis, CWRU, 1986.
8. J. P. Honovich and R. C. Dunbar, J. Phys. Chem. 85, 1558 (1981).
9. B. Asamoto and R. C. Dunbar, to be published; B. Asamoto, Ph.D. Thesis, CWRU, 1986.
10. R. G. Orth and R. C. Dunbar, J. Am. Chem. Soc. 100, 5949 (1978).
11. W. J. Van der Hart, L. J. De Koning, N. M. M. Nibbering and M. L. Gross, Int. J. Mass Spectrom. Ion Proc. 72, 99 (1986).
12. J. P. Honovich, B. Asamoto and R. C. Dunbar, to be published.
13. H. Y. So and R. C. Dunbar, to be published.
14. M. J. Coggiola, P. C. Cosby, H. Helm, J R. Peterson and R. C. Dunbar, J Phys. Chem., In press.
15. J. P. Honovich and R. C. Dunbar, J. Phys. Chem. 87, 3755 (1983).

Presented at the 35th ASMS Conference on Mass Spectrometry and Allied Topics
May 24-29, 1987, Denver, CO

High-resolution Laser Photofragment Spectroscopy of Small Molecular Ions

P J Sarre, Department of Chemistry, University of Nottingham, University Park, Nottingham NG7 2RD, United Kingdom

High-resolution laser photofragment spectroscopy is based on a combination of laser spectroscopy and ion-beam mass spectrometry. It is a powerful tool for the study of the spectroscopy, structure and dissociation dynamics of molecular ions and provides insight into ion-atom and ion-molecule collisions and some astrophysical processes. In most current work a mass-selected fast-ion-beam is irradiated coaxially with a tunable dye laser (or an infrared laser) which induces transitions to predissociated levels of the ion [1]. A laser photofragment spectrum is recorded by detection of the photofragment ion intensity as a function of laser frequency. Measurement of the translational energy of the photofragment ion is achieved with an electrostatic energy analyser. Information on the molecular geometry, electronic structure and bonding is obtained from a spectroscopic analysis of the laser photofragment spectrum. The fragmentation dynamics are probed principally through measurement of predissociation linewidths (lifetimes), photofragment kinetic energies and fragment angular distributions. The principal aim of our work is to study the energy level structure and dynamics of molecular ions in the region between the 'molecular' and 'atomic' limits. This region can be examined by the spectroscopic study of energy levels either just above or just below the dissociation limit. Laser photofragment spectroscopy can be applied in both of these situations by detection of transitions to predissociated levels (resonances) or by laser excitation followed by fluorescence and dissociation, respectively.

In the case of CH^+ [2,3,4], laser excitation from the $X^1\Sigma^+$ ground state to quasibound rotational levels (shape resonances) of the $A^1\Pi$ state results in the formation of C^+ ions which are detected. In addition to quantum mechanical tunnelling through the centrifugal barrier, non-adiabatic interactions also make an important contribution to the predissociation rate. It is found that the 'e' lambda-doublet component is predissociated to a lesser degree than the 'f' component. This is due to the difference in tunnelling rates through the centrifugal barriers in the rotationally adiabatic potential energy curves.

The photofragment spectrum of the SiH^+ ion [4,5] is markedly different from CH^+ and is dominated by Feshbach resonances, i.e. transitions to predissociated energy levels which lie beween the two fine structure

dissociation limits, $Si^+(^2P_{3/2})$ + H and $Si^+(^2P_{1/2})$ + H. In this case tunnelling cannot occur and the dissociation occurs exclusively due to non-adiabatic interactions which are strong near to the dissociation threshold. The assignment of the spectrum is achieved by combining experimental data (transition frequencies, line intensities, linewidths and nucler hyperfine splittings) and theoretical predictions of the energy level structure based on numerical solution of the radial Schrodinger equation. Additional lines are found in the spectrum which provide the first experimental evidence for 'multichannel' resonances in the photofragment spectrum of a diatomic molecule.

Rotationally resolved competitive predissociation is observed in the photodissociation of SiH_2^+ [6] which dissociates to form both Si^+ + H_2 and SiH^+ + H. The principal dissociation mechanism is the coupling of laser-pumped excited state levels with levels of the ground electronic state which lie above both of the chemically distinct dissociation limits.

The origin of additional lines [2,7] in photodissociation spectra of CH^+ near 350 nm and 530 nm is identified [4]. The lines arise from the excitation of CH^+ from energy levels just below the $C^+(^2P)$ + $H(^2S)$ dissociation limit to energy levels lying just below the $C(^1D)$ + H^+ and $C(^3P)$ + H^+ dissociation limits respectively. The transitions are observed in the photofragment spectrum because fluorescence of the laser excited levels occurs to the continuum just above the $C^+(^2P)$ + $H(^2S)$ dissociation threshold, resulting in the formation of C^+ ions. The process may be considered to be Laser Induced Fluorescence followed by Dissociation (LIFD). This is the first example of this process to be observed in a molecular ion.

References

1. J T Moseley, Adv.Chem.Phys., 1985, LX, 245.
2. H Helm, P C Cosby, M M Graff and J T Moseley, Phys.Rev.A, 1982, 25, 304.
3. P J Sarre, J M Walmsley and C J Whitham, J.Chem.Soc.Farad.Trans 2, 1986, 82, 1243.
4. P J Sarre, J M Walmsley and C J Whitham, Farad.Discuss.Chem.Soc.82 (in the press)
5. P J Sarre, J M Walmsley and C J Whitham, Phil.Trans.Roy.Soc.Lond. (in the press)
6. M C Curtis, P A Jackson, P J Sarre and C J Whitham, Molec.Phys., 1984, 52, 1453.
7. P C Cosby, H Helm and J T Moseley, Astrophys.J., 1980, 235, 52.

Presented at the 35th ASMS Conference on Mass Spectrometry and Allied Topics
May 24-29, 1987, Denver, CO

The Time Evolution of the Mass Spectra and the Dynamics of Picosecond-Laser Multiphoton Ionization-Dissociation

M. A. El-Sayed
Department of Chemistry and Biochemistry
University of California
Los Angeles, California 90024

According to the quasiequilibrium theory of mass spectrometry,[1] molecular ionization takes place immediately following electronic excitation, by the energy source used (75 eV electrons in conventional mass spectrometry). This leaves the ion electronically excited. Electronic-to-vibration energy redistribution then takes place in the subpico-to-nanosecond time scale. This leads to a statistical distribution of the vibrational degrees of freedom of the ground electronic state of the ion. Ionic dissociation occurs last and depending on the barriers involved, this can take place on the submicro-to-second time scale. The daughter ions observed in mass spectrometry must be formed in a time shorter than microsecond (the acceleration time in the analyzer).

The use of short laser pulses as ionization sources in mass spectrometry has made it possible to observe these dynamic processes in real time for the first time.[2,3] Two techniques have been described to determine the rates of energy redistribution and of daughter ions formation in laser multiphoton absorption. In addition, the average speed of the different daughter ions is also determined.

The rates of the energy redistribution in the ionic excited electronic states (formed by the multiphoton absorption of the laser light) that are precursors for the different daughter ions are determined as follows. Two picosecond lasers, the 266-nm fourth harmonic and 532-nm second harmonic of a passively mode-locked Nd:YAG laser, serve as the ionization source in a time-of-flight mass spectrometer. By monitoring each ionic species as a function of a continuously variable (0-10000 ps) delay between the two pump lasers, one may extract dynamic information concerning energy redistribution in the different electronic states responsible for the formation of the different daughter ions. If a mass peak shows more than one characteristic dynamic time, this could suggest that either it belongs to a daughter formed from two different excited electronic states or it belongs to more than one chemical ionic species. The interrelation between the signal intensity and relative delay between the two pump lasers for several ions is examined for 2,4-hexadiyne in terms of a ladder-climbing mechanism of dissociation for the parent ion and the breakdown curves of the different daughter ions. The good agreement between the predictions of the breakdown curves and our results for 2,4-hexadiyne strongly suggests that the daughter ions produced from the lower energy channels are, for the most part, produced by an ionic ladder-climbing mechanism at the laser power, wavelength, and pulse width (20 ps) used. The $C_6H_4^+$, $C_5H_3^+$, $C_4H_4^+$, $C_3H_3^+$, and a fraction of the $C_6H_5^+$ ions seem to have as a precursor an electronic excited state of the molecular ion at 13.6-14.0 eV above the ground state of the neutral molecule. The results also suggest that fragmentation of the parent ion to form the $C_4H_3^+$, C_4H^+, C_4^+, and $C_2H_3^+$ ions can occur from an excited electronic state of the molecular ion at an energy of 15.93-16.33 eV above the ground state of the neutral molecule. The results also suggest that the $C_6H_2^+$ and some of the $C_6H_5^+$ ions are formed from an excited state of the parent ion at 18.26-18.66 eV above the ground state of the neutral molecule.

The study of fragment-ion signals as a function of the delay time between the laser pulse and the pulsed extraction electric field in a linear reflectron offers a new technique for the determination of the formation rates of some of the daughter fragments. It is shown that this technique has better time resolution, higher sensitivity, and more versatility than previous methods. The formation rates of seven daughter ions resulting from laser multiphoton ionization dissociation (MPID) of 1,4-dichlorobenzene

are determined. The formation rate of $C_6H_4Cl^+$ at high laser intensities is comparable to that determined using one 14 eV photon. This suggests that its formation by MPID at high UV intensity involves the three-UV photon level (at 14.0 eV) via a ladder mechanism.

When the current signals of the parent and the different daughter ions formed by the laser multiphoton ionization fragmentation techniques are studied at longer delay between the laser pulse and the pulsed accelerating voltage of the reflectron time-of-flight mass spectrometer, a decay of the different signals is observed. The decay of most of the current signals is found to be exponential and is described in terms of ion escape rate from the collection volume of the mass spectrometer. From the square of the observed decay constants, the kinetic energies of the different daughter ions relative to that of the parent ion can be determined. Since during the ionization process via a two photon absorption, the electron carries most of the kinetic energy leaving the parent ion thermally, the relative kinetic energies of the daughter with respect to the parent are then converted into absolute kinetic energies of the daughter ions. Both of the small values of the observed average kinetic energy release and the small spread observed in these values for most of the fragment ions formed from 1,4-dichlorobenzene and 2,4-hexadiyne are discussed in terms of the statistical theory of dissociation as well as the nature of the UV multiphoton ionization dissociation process.

(1) H. M. Rosenstock, M. B. Wallenstein, A. L. Wahrhaftig and H. Eyring, Proc. Natl. Acad. Sci. 38, 667 (1952).

(2) a. D. A. Gobeli and M. A. El-Sayed, J. Phys. Chem. 89, 1722 (1985).
b. D. A. Gobeli, J. D. Simon, D. K. Sensharma and M. A. El-Sayed, Int. J. Mass. Spectrom. Ion Processes 63, 149 (1985).

(3) a. T-L. Tai and M. A. El-Sayed, J. Phys. Chem. 90, 4477 (1986).
b. T-L. Tai and M. A. El-Sayed, Chem. Phys. Lett. 130, 224 (1986).

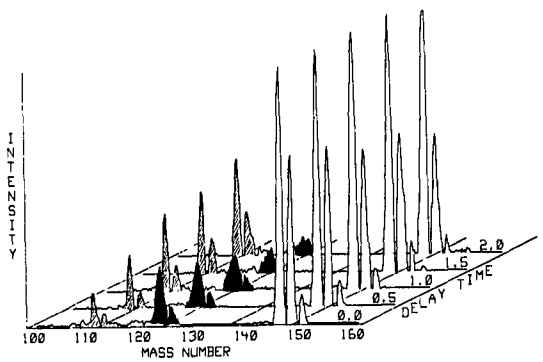

Fig. 1. The effect of the delay between the pulsed laser and the pulsed electric field on the fraction of $C_6H_4Cl^+$ formed in the ionization region (the sharp shaded mass peak at 111 amu) and that formed outside the ionization region (the broad solid peaks at 122 amu). As the delay time increases, more of the daughter ion is formed in the ionization region before pulsing the extraction field. This leads to an increase in the sharp peak intensity on the expense of the broad one. The rate of the change of both types of peaks is controlled by the rate of the formation of $C_6H_4Cl^+$.

Presented at the 35th ASMS Conference on Mass Spectrometry and Allied Topics
May 24-29, 1987, Denver, CO

NON-RESONANT MULTIPHOTON IONIZATION AND FRAGMENTATION PATTERNS OF SELECTED LOW-MASS HYDROCARBONS

William B. Martin and Rebecca M. O'Malley
Chemistry Department, University of South Florida
Tampa, Florida 33620

One aspect of the overall non-resonant multiphoton ionization (NRMPI) mechanism that remains unresolved is the identification of the possible origins of the low mass ions that have been observed in NRMPI fragmentation patterns of benzene and other substituted aromatic hydrocarbons. There has been debate as to whether these ions are formed from ionic and/or neutral precursors. It is important to a fundamental understanding of overall MPI processes that sources of these low mass ions are experimentally characterized.

This work was undertaken to characterize the NRMPI behavior of acetylene under moderate to high laser pulse energies - conditions similar to those used in studies completed on other systems. Acetylene was initially chosen by virtue of its extensive involvement in the fragmentation processes of benzene; however, since it is involved in photolytic processes of many other molecules, the study expanded to include ethylene, ethane, propylene, propane, isobutylene and cis-2-butene - systems for which little or no NRMPI data previously existed. Details of the experimental apparatus have been reported previously (1).

Electron impact (EI) and NRMPI spectra are shown in Figures 1 and 2 for acetylene and ethylene. Clearly, the NRMPI process is different from that initiated by EI. For acetylene, the $C_2H_2^{+\cdot}$ ion is the base peak in all spectra. In the EI spectrum there is minimal fragmentation; in contrast, both NRMPI spectra show extensive fragmentation. At 532 nm, relatively more $C^{+\cdot}$ and CH^+ is produced than at 355 nm. For ethylene, relatively more $C^{+\cdot}$ and $C_2^{+\cdot}$ is formed at 355 nm than at 532 nm. Results for other compounds studied are summarized in Table I. With few exceptions, ionization at 355 nm gives rise to greater proportions of the lower mass ions (those in the 12 - 25 mass range) than does ionization at 532 nm which yields relatively more higher mass ions. The results for acetylene demonstrate explicitly that neutral acetylene can and does undergo multiphoton absorption to ultimately produce the low mass ions of concern and suggest strongly that it may play a role in the overall NRMPI pathways operative in other systems. However, based on these experiments alone, for the other compounds studied it is not possible to determine whether the low mass ionic fragments are formed via ionic and/or neutral intermediates - just that they were produced along the overall pathways operative.

The laser pulse energy dependencies were investigated and the results are summarized in Table II for the low-energy region behavior and Table III for the high energy region behavior. Table I shows that in the low energy region the relative ion currents due to the low mass ions generally increase while those in the higher mass range generally decrease. However, Table III generally shows that the ion currents due to all ions remain relatively constant at high laser pulse energies. This behavior is similar to that reported earlier ([1]) for benzene, phenylacetylene and benzonitrile and can be rationalized in a similar manner. However, it is also possible that these ionic fragments are being formed by NRMPI of small neutral fragments produced as a result of the systems exhibiting class B-type behavior as defined by Gedanken et al. ([2]).

1. Martin, W. B.; O'Malley, R. M.; Int. J. Mass Spectrom. Ion Proc.; 59 (1984), 277.

2. Gedanken, A.; Robin. M. B.; Kuebler, N. A.; J. Phys. Chem.; 87 (1982), 4096.

Presented at the 35th ASMS Conference on Mass Spectrometry and Allied Topics
May 24-29, 1987, Denver, CO

Figure 1.

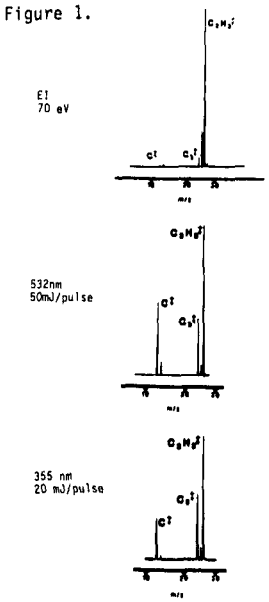

Figure 2.

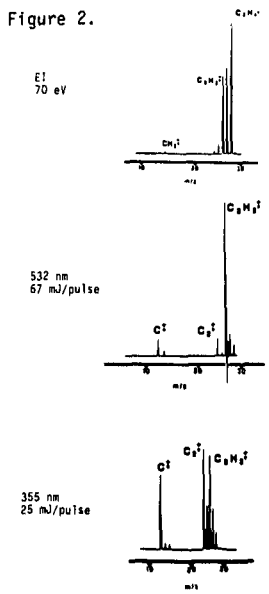

Table I. Semi-quantitative differences noted in the multiphoton ionization fragmentation patterns for each hydrocarbon studied at the two wavelengths used.

m/z	C_2H_2	C_2H_4	C_3H_6	C_3H_6	C_3H_8	iso-C_4H_8	cis-C_4H_8
	Compound						
12	G	B	G	B	B	B	B
13	G	B	B	G	B	-	B
14		B	B	B	B	-	B
15			G	B	B	B	B
24	B	B	B	B	B	B	B
25	B	B	B	B	B	B	B
26	-	G	B	G	G	G	G
27		G	G	G	G	G	G
28		-					G
29			G			G	G
37						G	G
38						G	G
39				B		G	G
41						G	G
53					G		G
56						G	G

G: Percent total ion current greater at 532 nm
B: Percent total ion current greater at 355 nm
-: Ion currents essentially the same at both wavelengths

Table II. Relative changes in ion currents noted at lower laser pulse energies

m/z	C_2H_2	C_2H_4	C_3H_6	C_3H_6	C_3H_8	iso-C_4H_8	cis-C_4H_8
	Compound						
				532 nm			
12	I	I	D	C	I	D	I
13	I		I	I	I	I	I
14			C	I	C	I	
15			I	I	D	I	I
24	D	I	C	C	C	I	I
25	I	I	D	C	C	C	I
26	D	D	C	D	C	I	C
27		D	C	D	D	C	D
28		I					
29					D		
39				C		I	C
41						C	C
56						D	D
				355 nm			
12	C	D	I	I	I	D	I
13	I	C	I	I	I	I	I
14		C	I	I	I	I	C
15			I	I	I	I	I
24	C	I	D	D	D	D	D
25	C	I	D	C	D	I	D
26	D	D	D	D	D	C	D
27		C	D	C	D	C	D
28		D					
29			C				
39				D		C	

I: Ion current increases as laser pulse energy is increased
D: Ion current decreases as laser pulse energy is increased.
C: Ion current remains constant as laser pulse energy is increased

Table III. Relative changes in ion currents noted at higher laser pulse energies

m/z	C_2H_2	C_2H_4	C_3H_6	C_3H_6	C_3H_8	iso-C_4H_8	cis-C_4H_8
	Compound						
				532 nm			
12	I	C	D	C	C	C	C
13	C	I	C	C	C	C	C
14			C	C	C	C	
15			C	C	C	C	C
24	C	C	C	C	C	C	C
25	C	C	C	C	C	C	C
26	D	D	C	C	C	C	C
27		D	C	C	C	C	C
28		C					
29					C		
39						C	C
41						C	C
56						C	C
				355 nm			
12	I	C	C	C	C	C	C
13	C	C	C	C	C	C	C
14		C	C	C	C	C	C
15			C	C	C	C	C
24	C	C	C	C	C	C	C
25	C	C	C	C	C	C	C
26	D	C	C	C	C	I	C
27		C	C	C	C	C	C
28		C					
29			C			C	
39				C		D	

I: Ion current increases as laser pulse energy is increased
D: Ion current decreases as laser pulse energy is increased
C: Ion current remains constant as laser pulse energy is increased

Presented at the 35th ASMS Conference on Mass Spectrometry and Allied Topics
May 24-29, 1987, Denver, CO

QUANTIFICATION OF PULSED ION CURRENTS PRODUCED IN RESONANCE IONIZATION MASS SPECTROMETRY (RIMS)

J.D. Fassett, R.J. Walker, J.C. Travis, and F.C. Ruegg

National Measurement Laboratory
National Bureau of Standards
Gaithersburg, MD 20899.

The use of pulsed lasers as ion sources in inorganic mass spectrometry creates a new challenge for analysts trying to make precise and accurate isotope ratio measurements. Although pulsed laser ionization processes can be much more sensitive than traditional, continuous ionization techniques, the quantification of pulsed ion signals has not been adequately addressed. Furthermore, the measurement of ratios over relatively large dynamic ranges is a nontrivial problem in pulsed ionization. Issues of detector response linearity, between and among differing species at widely different intensities, must be faced in order to demonstrate quantitative isotope ratio measurement.

We have recently developed a quantitative measurement system around time array detection with a transient digitizer which we apply to our resonance ionization mass spectrometer [1] ion signals. This RIMS system uses a Nd:YAG pumped, tunable dye laser which pulses at 10 Hz. The photoions formed are focussed through a magnetic sector mass spectrometer, and thus have a combined time-of-flight and momentum filtering. Isotope ratio measurements are made by alternating the magnetic field between two mass channels. The gains of the transient digitizer and electron multiplier can both be altered to match the signal levels of the two isotopes to the response characteristics of the electronics. Thus, the linear dynamic range of the overall measurement system is maximized. The fact that vaporization from resistively heated filaments is the source of the gas phase sample reservoir is also an important aspect of the analytical system. Relatively stable, long-lived atomic beams can be produced from analytes dried on suitably-prepared filament substrate materials. These stable atomic beams allow the extensive signal averaging necessary to achieve both precise and accurate atomic ratio measurement.

A microcomputer controlling the transient digitizer allows the processing of waveforms faster than the 10 Hz frequency of the laser. Thus, no ionization data is sacrificed. This microcomputer is a 8086/8087, 16-bit, IEEE 696 (S100)-based microcomputer with a 33 megabyte hard disk. A master (mini-)computer is connected to the 8086 microcomputer using RS-232 interfaces. The master computer controls the data acquisition programs of the microcomputer and exchanges data with it. The master computer also maintains the isotope ratio program, which controls both the laser wavelength and the magnetic field of the mass spectrometer.

Several routines were developed for processing data acquired by the transient digitizer in real time. The most general routine signal averages the waveforms acquired by the transient digitizer. In addition to averaging, a pulse-counting routine has also been incorporated into the general signal processing program. A counter is incremented if the signal is above a preset threshold in a preset window of each waveform. This routine is used for the lowest level signals. At high signal levels this routine is not useful for quantitative ion counting, but it can be used to detect pulses that saturate the transient digitizer. Thus, the routine aids in choosing the optimum scale of the transient digitizer for quantitative analog measurement.

A routine was also developed for creating a pulse height distribution for the signal processed by the transient digitizer. This routine was specifically used for the evaluation of the overall measurement system. For every laser pulse, the maximum signal was determined in the preset window of the digitized waveform. The corresponding channel in a 256-channel array, each channel of which is an allowable level of the 8-bit transient digitizer, was then incremented.

The pulse height distribution is built up by integration of a large number of laser pulses. Pulse height distributions for various average ion signal levels (187-Re^+ desorbed from a Re filament) are illustrated in the accompanying figure. The input laser was blocked for 180 laser pulses in each distribution to indicate the zero level. The electron multiplier voltage was 2000 V for the lowest signal level distribution and 1800 V for the other three distributions. Full scale for the digitizer was 0.4, 0.4, 0.8, and 4.0 V for the lowest to highest signal level distributions, respectively.

The overall goal of this work was to verify that quantitative measurements could be made for extremely low signals (ion-counting) as well as for moderate and large signals (analog detection). A further goal was to combine the two modes of operation to increase the effective dynamic range of the overall measurement system. The marriage of the pulse counting analog modes of measurement is made possible by the fact that low ion count rates are capable of being quantified by both pulse counting and analog detection.

Measurement precision and accuracy are best demonstrated by repetitive measurements of known isotopic standards. We have applied the measurement system described here to determination of numerous elemental isotopic ratios and have consistently demonstrated 1-3 % accuracies and precisions for relatively high levels of signal. Low level signals have consistently been Poisson statistics limited. Data for high and low level measurements of Os are illustrative [2].

[1] J.D. Fassett, J.C. Travis, L.J. Moore and F.E. Lytle, Anal. Chem., 55, 765 (1984).
[2] R.J. Walker and J.D. Fassett, Anal. Chem., 58, 2923 (1986).

PULSE HEIGHT ANALYSIS

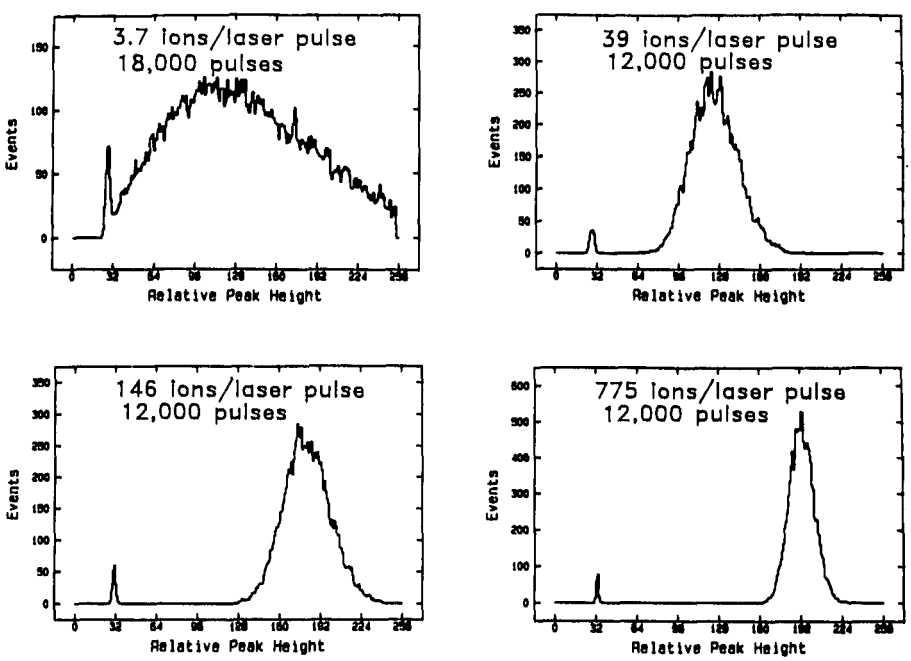

Presented at the 35th ASMS Conference on Mass Spectrometry and Allied Topics
May 24-29, 1987, Denver, CO

LASER PHOTODISSOCIATION IN A TANDEM QUADRUPOLE FOURIER TRANSFORM MASS SPECTROMETER: J. Shabanowitz, D. F. Hunt, C. R. Hauer and C. Brinegar; Department of Chemistry, University of Virginia, Charlottesville, Virginia 22901

Molecular weight analysis of oligopeptides and small proteins in the mass range, 1-13 kDa by liquid secondary ion mass spectrometry on a tandem quadrupole Fourier transform mass spectrometer has been described in an earlier publication from this laboratory (1). To obtain structural information on the desorbed sample ions we have recently initiated studies to explore the utility of laser photodissociation. Experiments have been conducted with both a carbon dioxide infrared laser and an argon fluoride excimer laser. Shown in Fig. 1 are spectra of protonated glycerol oligomers taken with and without the aid of the infrared laser. Complete fragmentation of the oligomeric ions requires exposure to approximately 10 x 10 nsec pulses of the laser. The same experimental conditions can be employed to promote extensive fragmentation of the model sugar, stachyose (Fig 2.).

Irradiation of oligopeptide (M+H)+ ions stored in the FTMS instrument with light from an argon fluoride excimer laser has allowed us to solve a number of structural problems on samples in the 10-30 pmol range. Complete sequence analysis of a tryptic peptide from purple acid phosphatase via this approach has been described previously (2). Shown in Fig. 3 is the laser photodissociation mass spectrum taken on a 10 pmol of photoaffinity labelled peptide derived from the cytokinin binding factor protein. A single 10 nsec pulse from the laser was sufficient to produce the fragmentation shown in Fig. 3. All mass measurements were found to be accurate to within 0.2 amu. The assigned sequence plus location of the labelled residue was deduced from the observed B and Y type fragment ions.

Successful sequence analysis of an N-terminally blocked phosphorylated peptide from the light harvesting chlorophyl protein complex has also been achieved using laser photodissociation of stored (M+H)+ ions in our tandem quadrupole FTMS instrument. The spectrum shown in Fig. 4 was obtained on less than 30 pmol of sample with a single pulse of light at 193 nm from the argon fluoride excimer laser. Present in the spectrum is a complete series of Y type fragment ions that define the sequence of amino acids in the sample, allow placement of the phosphate ester group on the N-terminal Thr residue, and specify the nature of the N-terminal blocking group as an acetyl moiety.

1) D. F. Hunt, J. Shabanowitz, J. R. Yates, III, N. Z. Zhu, D. H. Russell and M. E. Castro, Proc. Natl. Acad. Sci., USA (1987) 87, 620-623.

2) D. F. Hunt, J. Shabanowitz, and J. R. Yates, III, J. Chem. Soc., Chem. Commun., (1987) In Press.

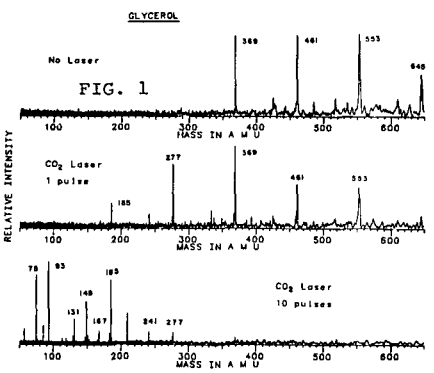

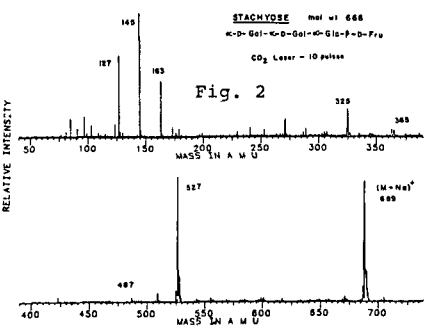

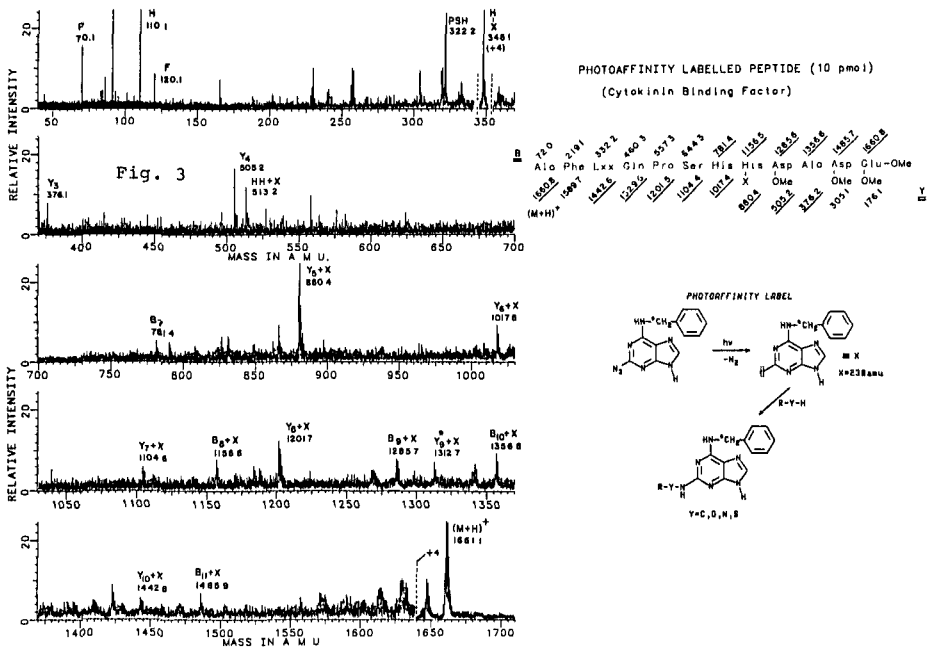
Fig. 3
PHOTOAFFINITY LABELLED PEPTIDE (10 pmol)
(Cytokinin Binding Factor)
Ala Phe Lxx Gln Pro Ser His His Asp Ala Asp Glu-OMe
PHOTOAFFINITY LABEL
X=238amu
Y=C,O,H,S
RELATIVE INTENSITY
MASS IN A M U.

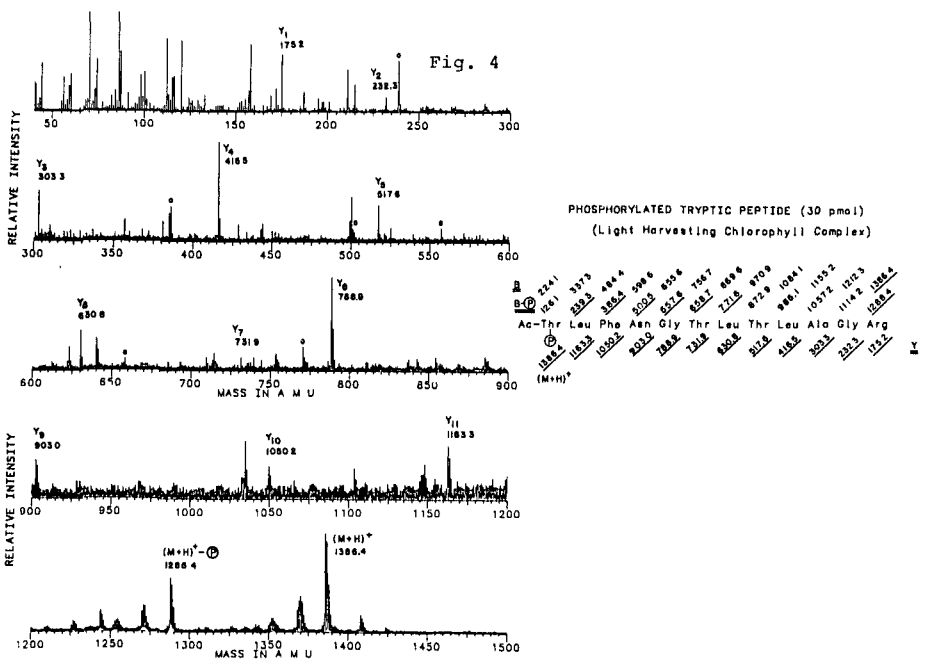
Fig. 4
PHOSPHORYLATED TRYPTIC PEPTIDE (30 pmol)
(Light Harvesting Chlorophyll Complex)
Ac-Thr Leu Phe Asn Gly Thr Leu Thr Leu Ala Gly Arg
RELATIVE INTENSITY
MASS IN A M U

Presented at the 35th ASMS Conference on Mass Spectrometry and Allied Topics
May 24 29, 1987, Denver, CO

Supercritical Fluid Injection of Small Polar Molecules Using Derivatization with Detection by Resonant Two-Photon Ionization in Supersonic Beam-MS

D. M. Lubman, C. H. Sin and H. M. Pang
Department of Chemistry
The University of Michigan
Ann Arbor, MI 48109

In this work supercritical fluids are used as a means of volatilizing nonvolatile and thermally labile molecules for supersonic jet expansion into a mass spectrometer The detection method used here is resonant two-photon ionization (R2PI). R2PI involves the absorption of two photons in the presence of an intense light source where the first photon excites the molecule to a real electronic state and the second photon causes ionization. The ionization cross-section depends on the absorption spectrum of the $S_0 \rightarrow S_1$ transition so that wavelength selectivity can be achieved in the ionization process. This can be combined with the ultracooling of the rovibronic modes obtained in supersonic jets so that sharp spectral features can be observed as a function of wavelength for unique identification. In past work (1,2) this method has been utilized with expansions of supercritical fluids of CO_2, N_2O and NH_3 and spectral cooling was obtained for the organic trace species seeded into the jet. These expansions have been performed with a reservoir pressure of up to almost 400 atm. in order to enhance the solubility of aromatic materials in these fluids while using low temperatures, i.e. ~ 35-45°C. Thus, pressure rather than temperature is used to solubilize organics into the fluids for jet expansions so that decomposition at elevated temperatures can be minimized. These experiments have been performed with a novel supersonic beam-time of flight mass spectrometer specially designed for high pressure injection and is described elsewhere (2). It consists of a differentially pumped vacuum system with a TOF mass spectrometer sitting vertically on top of the chamber The UV laser beam enters the chamber through quartz windows and R2PI is produced in the acceleration region of the TOFMS. The novel feature here is the use of a custom designed high pressure pulsed injection source synchronized with our pulsed laser ionization source so that a 200 µm orifice can be used for the jet injection into the TOFMS with a resulting high on-axis density. This valve has now been modified to operate with corrosive gases such as NH_3 and SO_2. Using this valve in conjunction with efficient LN_2 cryopumping a pressure of ~ 5×10^{-6} torr can be maintained. The supercritical fluid pressure of CO_2 and N_2O is provided by a Varian 8500 syringe pump.

Our most recent work utilizes derivatization as a means of increasing the solubility of polar biological species in supercritical CO_2 or N_2O by decreasing the polarity of the -COOH group. Aromatic carboxylic acids have been shown to have low solubility in these supercritical fluids (3); however, we have been able to solubilize various catecholamine and tyrosine metabolites (see figure 1) by converting the -COOH to a $-COOCH_3$ group. These derivatized compounds readily dissolve in the fluid at 200 atm and ~ 40° C. They absorb 280 nm radiation and ionize in R2PI as one might expect since the derivatization does not strongly change the absorption or ionization properties of the original molecule. Using R2PI spectroscopy we have been able to obtain a wavelength ionization spectrum of the methyl ester derivative of indole-3-acetic acid using a supercritical CO_2 expansion and its spectrum compares favorably with that of the underivatized compound.

A second method used to solubilize polar compounds is the use of polar solvents such as supercritical NH_3 and SO_2 and hot liquid injection from CH_3OH and H_2O. Supersonic jet cooling has been obtained for acenaphthene in NH_3 as shown in figure 2. In addition, by using polar solvents such as CH_3OH and H_2O dopamine and tyramine have been expanded in supersonic jets with detection by R2PI in our mass spectrometer. As shown in figure 3 for aniline significant jet cooling has been achieved using these hot liquids. In addition, little clustering is observed probably due to minor shock waves produced in this pulsed high density expansion.

Presented at the 35th ASMS *Conference on Mass Spectrometry and Allied Topics*
May 24-29, 1987, Denver, CO

References

(1) Sin, C.H.; Pang, H.M.; Lubman, D.M.; Zorn, J.C. Anal. Chem. 1986, 58, 487.

(2) Pang, H.M.; Sin, C.H.; Lubman, D.M.; Zorn, J.C. Anal. Chem. 1986, 58, 1581.

(3) McHugh, M.; Krukonis, V. "Supercritical Fluid Extraction: Principles and Practice", Butterworth, Stoneham, Mass., 1986.

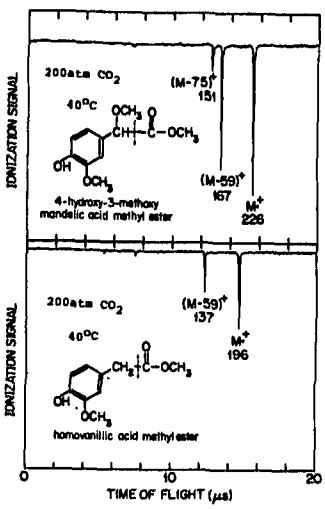

Figure 1: Mass spectra of carboxylic acid derivatives.

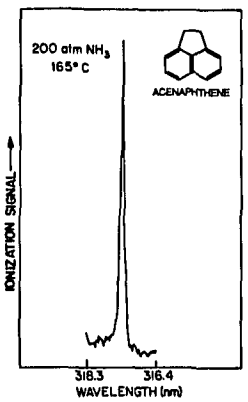

Figure 2: R2PI wavelength spectrum of acenaphthene 0-0 band with using ammonia as the solvent.

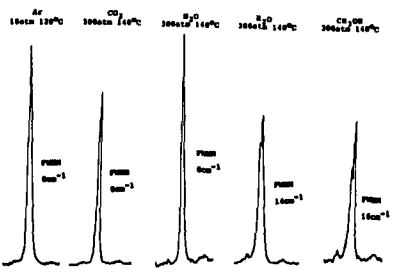

Figure 3: R2PI wavelength spectra of aniline 0-0 band with different mobile phases.

Presented at the 35th ASMS Conference on Mass Spectrometry and Allied Topics
May 24-29, 1987, Denver, CO

FUNDAMENTALS--MOLECULAR DYNAMICS

Jean H. Futrell
Department of Chemistry, University of Delaware, Newark, DE 19716

In today's lecture I should like to discuss three techniques which relate to the investigation of charge transfer reaction mechanisms. These techniques have been chosen to illustrate the kinds of detailed information which can be obtained using current instrumental techniques to investigate state-to-state reaction dynamics for simple systems. Using this information I shall demonstrate that results for a few examples may be directly related to the potential energy surfaces which are explored in the aiabatic, diabatic, or mixed transition pathways traversed by the reactants and products. The results also provide details on the ways energy transfer occurs simultaneously with charge exchange.

The first technique which I will discuss briefly has been developed in several laboratories--notably by Bowers and co-workers (1) also discussed elsewhere at this Conference. His group utilizes a conventional double focussing mass spectrometer with a tunable laser crossing the focal plane between the magnetic and electric sectors of the instrument. A drift tube ion source is used to generate relaxed cluster ions chosen for study and the laser is used to investigate the energetics of the dissociation process. Relating the information obtained from this study to potential energy curves of the relevant systems provides the information needed for interpreting thecoupling of ground state and dissociation surfaces. The experiments themselves are generally taken with three different configurations of the polarized laser beam. A critical experiment is at the so called "magic-angle" of 54.7° (1) for which the dissociation process produces an isotropic distribution of the products. Kinetic energy analysis of the products provides information on the dissociation process which is independent of details of the reaction dynamics. When compared to the energy levels of the dissociated reaction products, this technique identifies (in favorable cases) both the products and the electronic and vibrational states which are involved in the transition. It is convenient to think of the laser photodissociation experiment as a "half-collision" in which the starting point of the experiment is a molecular complex involving fixed internuclear distances between the nuclei. The other cluster photodissociation experiments which relate to dynamics are those carried out with polarization vector of the laser parallel and perpendicular to the direction of the ion beam. The analysis of the results of this experiment gives information on the antisaltropy parameter, β, and provides a direct indication of whether the dissociation proceeds immediately from a repulsive surface or involves rotations of the excited species prior to dissociation-i.e., a predissociation process.

This process corresponds exactly to the inverse experiment done with crossed molecular beams in which a single impact parameter and single configuration are explored. However, in molecular beam studies a much larger region of phase space is explored and there is no selection of impact parameter. Therefore the laser photodissociation process samples a particular subset of the total reaction mechanism; a comparison of the results of the laser photodissociation experiment therefore provides special insights into the detailed mechanism of reaction. In most cases it will demonstrate whether adiabatic pathways are followed.

The second class of advanced experimental techniques is the investigation of the state-to-state total charge transfer cross sections. A new apparatus has been developed for this purpose by Ng and collaborators (2). This triple quadrupole mass filter, double octupole ion pipe apparatus has demonstrated this capability for several simple atomic and molecular ions. It consists of a charge-transfer detector, which includes an RF octopole reaction gas cell and an enclosed inside a cylindrical cell allows the collection of > 80% of the electron transfer product ions.

In a state-to-state experiment, product ions of a state-selected reaction formed at the collision region are collected by the ion lenses and mass-

selected by the front horizontal QMF before entering the RF octopole ion guide reaction gas cell in which the product ions further react with a probing gas. The probe gas is chosen for its state-selective reactivity (2,3) using the same general approach developed for drift tube studies (4,5). The reactivity or the cross section for the electron transfer reaction between the product ions and the probing gas measured by the back horizontal QMF contains information about the internal state distribution the product ions.

Our experiments are carried out with a crossed molecular beam apparatus (3). We generate state-selected reactants in a high pressure ion source using ion molecular and plasma processes which are relatively well understood for simple systems. The mass selected ion beam is decelerated to energies as low as one electron volt (laboratory frame) and crossed by a supersonic jet which produces a very well collimnated beam of neutral particles at translational and internal temperatures of the order of 7 K. The detector is an energy analyzer and quadrupole mass filter which swings through approximately 110° in the laboratory reference frame. This explores slightly more than one quadrant of a sphere and allows us to measure differential cross sections (the probability of scattering a product in a particular quantum state into a particular solid angle at a particular collision energy) in all the reaction space in which products are observed. The details of both reactive and non-reactive scattering are governed by the potential surface or surfaces along which the collision occurs. The experimental information derived from our experiments correlates mostly directly with the detailed theory of these reactions. When combined with total cross section measurements and with "half-collision" data sufficient information now exists for us to infer the couplings which may be important in determining the detailed reaction dynamics of a few systems.

The charge transfer reaction N_2^+ with N_2 neutrals provides a nice example. The half-collision dissociation study of Bowers et al. (1) demonstrated that the dissociation occurs from the lowest energy linear configuration of N_4^+ with the properties given by the theoretical calculation of DeCastro, Schaeffer and Pitzer (4). Our low energy (0.7 eV) crossed beam study (7) demonstrates that this reaction path is also traced in the reverse direction in the sense that low kinetic energy collision proceed exclusively via a statistical complex model.

At higher energies the crossed beam experiments indicate a smooth transition from the complex mechanism to a direct mechanism which populates specific vibrational states. At the highest energies (shortest reaction times) investigated (ca. 100 eV) it appears the trapezoidal rather than the linear configuration of N_4^+ which contributes primarily to the charge transfer mechanism. Quadrupole coupling terms are responsible for the selected excitation of vibrational modes which involve two quanta of vibration being transferred in each collision. At intermediate energies such that the nuclei do not remain essentially fixed in their relative orientations during the collision, the coupling of energy into the orthogonal modes of the N_4^+ complex leads to extensive mixing of angular momentum.

In summary the technologies for carrying out experiments and the advances in quantum theory which allow the calculation of potential energy surfaces of sufficient accuracy for describing the details of these processes have permitted significant advances in our understanding of the simplest processes of ion molecule reactions. A control of kinetic energy in collisions provides a "stopwatch" with a timing accuracy of fractions of picoseconds which allows us to determine the rates at which energy is transferred into the various internal modes which are available in the collision partners. A comparison with theoretical calculations sometimes allows a determination of the internuclear distances at which charge transfer takes place with near spectroscopic precision.

1. M.F. Jarrold, A.J. Illes and M.T. Bowers, J. Chem. Phys. 81, 214 (1984).
2. C.-L. Liao, J.D. Shao, R. Xu, G.D. Flesch, Y.-G. Li and C.Y. Ng, J. Chem. Phys. 85, 3874 (1986).
3. J.H. Futrell, Int. J. Quantum Chem. 31, 133 (1987).

Presented at the 35th ASMS Conference on Mass Spectrometry and Allied Topics
May 24-29, 1987, Denver, CO

MASS SPECTROMETRY AND THE LIPID MEDIATOR NETWORK HYPOTHESIS

Robert C. Murphy
Department of Pharmacology
University of Colorado Health Sciences Center
Denver, Colorado 80262

Over the past two decades, an explosion of information has expanded our understanding of the biochemistry involved in cell-cell communications. In many instances, including acute hypersensitivity reactions which occur within the proinflammatory polymorphonuclear leukocytes, eosinophils, basophils, and mast cells, these biochemical reactions involve the synthesis of small lipid molecules derived from arachidonic acid. Arachidonic acid (5,8,11,14-eicosatetraenoic acid) is an essential polyunsaturated fatty acid found in high abundance esterified in phospholipids found within membranes of all mammalian cells. Much of the data gathered to date suggest that deesterification of arachidonic acid to its free acid form following the action of a phospholipase enzyme such as calcium dependent phospholipase A_2 (PLA_2) is necessary for the initiation of the oxidative pathways leading to the synthesis of prostaglandins and leukotrienes which possess potent biological properties. Mass spectrometry has played a central role in the structure elucidation of these eicosanoids (1,2). Furthermore, the development of quantitative mass spectrometry with stable isotope dilution was initiated in studies involving the need to measure these molecules at very small levels typically found in tissues and cell extracts. Quantitative mass spectrometry continues to be employed by numerous individuals for quantitative studies of eicosanoids only now in the picomolar and subpicomolar levels in physiological fluids (3,4).

Another class of lipid substances thought to mediate inflammatory reactions within the body, as well as serving a role as a chemical communicator between cells, is platelet activating factor (PAF), a glycerophospholipid characterized as 1-O-alkyl-2-acetyl-glycerophosphatidylcholine. This molecule is synthesized from an ether phosphatidylcholine following the action of PLA_2 followed by acetylation of the lysophosphatidylcholine using the enzyme acetyl transferase and acetyl CoA. While there is little apparent biochemical relationship between PAF and metabolites of arachidonate due to their chemical dissimilarities, we have recently suggested that a single phospholipid molecular species, 1-O-alkyl-2-arachidonyl-sn-glycerophosphatidylcholine, could serve as the requisite precursor for both lipid classes of mediators following the action of a single enzyme phospholipase A_2

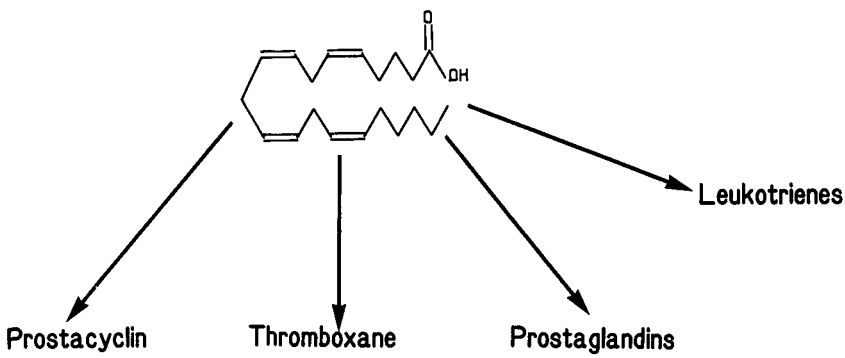

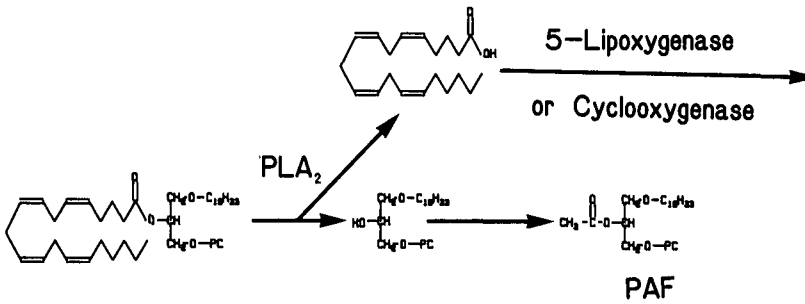

In order to test this lipid mediator network hypothesis it has been necessary to develop techniques to analyze molecular species of phospholipids which contain arachidonic acid esterified at the sn-2 position. Two general approaches have been developed. The first is essentially a nondegradative strategy where a complex mixture of phospholipids which have been extracted from cells are first separated by TLC and HPLC techniques into their individual molecular species. FAB/MS can be used to provide qualitative data necessary to characterize the total fatty acyl chain and degree of unsaturation found in each of the molecular species. Fortunately, these molecules are surface active substances and the fast atom bombardment experiment is quite sensitive. Such data can then be combined with the fatty acid analysis of the separated molecular species to characterize fully the two fatty acyl groups which are found in diacyl glycerophospholipids, or single fatty acyl groups found in ether glycerophospholipids including plasmalogens. These techniques have been used to characterize the 18 molecular species of glycerophosphatidylcholine found in the human polymorphonuclear leukocyte (5,6).

The second approach involves partial degradation of molecular species and analysis of the resultant diglycerides by HPLC and negative ion chemical ionization of the dinitrobenzoate derivative (7). This technique was employed in the identification of 1-O-hexadecyl-2-arachidonyl-glycerophosphatidylcholine as a major metabolite of platelet activating factor when instilled into the isolated perfused rat lung (8). Mass spectrometry in a negative ion chemical ionization mode was used to obtain this data, illustrating that mass spectrometry continues to be an important tool in the structure elucidation of these complex glycerophosphatidylcholines.

Acknowledgement. This work was supported in part by grants from the National Institutes of Health (HL34303 and AI20774).

REFERENCES

1. B. Samuelsson, M. Goldyne, E. Granstrom, M. Hamberg, S. Hammarstrom, and C. Malmsten. A. Rev. Biochem. 47:997-1029 (1978).
2. M. Hamberg, J. Svensson, and B. Samuelsson. Proc. Natl. Acad. Sci. USA. 72:2994-2998 (1975).
3. R.J. Strife and R.C. Murphy. J. Chromat. 305:3-12 (1984).
4. K. Green, M Hamberg, B. Samuelsson, M. Smigel, and J.C. Frolich. Adv. Prostaglandin Thromboxane Res. 5.39-94 (1978).
5. F.H. Chilton and R.C. Murphy. J. Biol. Chem. 261:7771-7777 (1986).
6. F.H. Chilton and R.C. Murphy. Prostaglan., Leukotr., and Med 23:141-148 (1986).
7. P.E. Haroldsen, N.F. Voelkel, J.E. Henson, P.M. Henson, and R.C. Murphy. J. Clin. Invest., in press.

Presented at the 35th ASMS Conference on Mass Spectrometry and Allied Topics
May 24-29, 1987, Denver, CO

ISOTOPE RATIO MASS SPECTROMETRY AND DIET

D.A. Schoeller, C.A. Leitch and P.B. Taylor
Clinical Nutrition Research Unit, University of Chicago
Chicago, IL 60637

Isotope ratio mass spectrometry for the light elements was developed by Nier (1) and by McKinney et al (2). This technique has been used extensively by geochemists for the study of hydrogen, carbon, nitrogen, and oxygen biogeochemistry. The technique has an equally long, but lesser known, history of use in human and animal metabolic studies. These mass spectrometers have been designed to maximize the precision of measuring isotope ratios such that they can detect changes in relative abundance of minor to major isotopes on the order of 1 part in 10^4 to 10^5.

The extreme precision of isotope ratio mass spectrometry makes it possible to measure natural variations in stable isotope abundances. These variations results from kinetic and equilibrium isotope effects in the geosphere and the biosphere. The extreme precision is also invaluable for tracing small quantities of stable isotope labeled compounds during biologic metabolism, an important economic consideration due to cost of stable isotope labeled compounds.

The application of isotope ratio mass spectrometry is of particular interest in nutrition. A number of investigators have taken advantage of the unique natural isotopic abundances of several of the light elements in particular foods to help quantitate their contribution to the diet of historic populations. For example, van der Merwe and Vogel (3) measured the $^{13}C/^{12}C$ of bone collagen of fossils from prehistoric inhabitants of woodland North America to estimate the percentage of corn in the diet. This is possible because corn is unusually abundant in ^{13}C compared to most other foods. Using this approach, these authors concluded that corn was not a significant part of the diet until ca. 1000 AD. Thereafter it became a staple of the woodland tribes and more than 50% of dietary carbon appears to have been derived from corn.

As indicated above, precision of isotope ratio mass spectrometry is also valuable for measuring tracer doses of stable isotope labeled compounds that have been administered as metabolic tracers. The use of water labeled with deuterium and ^{18}O to calculate carbon dioxide production and energy expenditure in free-living individuals is a prime example. The doubly labeled water method was developed by Lifson (4) over 25 years ago. It is based on the observation that after a loading dose of doubly labeled water, deuterium is eliminated as water while ^{18}O is eliminated as water and carbon dioxide. The difference between the elimination rates is therefore proportional to carbon dioxide production and this in turn can be used to calculate energy expenditure.

The doubly labeled water method has been validated in a number of small animal studies (4), but was slow to be used in humans because of the high cost of $H_2{}^{18}O$. If the doses used in the animal studies were scaled up for use in humans, the isotope costs alone would exceed $4,000. It is only through the use of isotope ratio mass spectrometry that the isotope cost can be reduced to less than $300.

Our group and others have validated the doubly labeled water method in humans at these lower doses (Table 1). Although there is still some debate about the fine points of the mathematical model to be used in the calculation of carbon dioxide production (5,6), the method has been shown to be quite accurate and to have a precision of 5 to 10%. The major advantage of the method is that it can be used in free-living subjects because elimination rates can be calculated from the isotopic abundances of the tracer relative to predose baseline in urines collected periodically after the loading dose. The subjects are therefore free to participate in their normal activities. This is the first method that is accurate, precise and that gives a subjective measure of energy expenditure in humans.

In summary, the precision of isotope ratio mass spectrometry is valuable in the study of human nutrition. Foods and nutrients that have either a natural or synthetic stable isotopic label can be detected and quantified at much greater dilutions than would be possible with most other mass spectrometric techniques.

Table 1. Validation of the doubly labeled water method in humans.

subject description	n	standard method	error	model	reference
healthy adults	5	RGE	1±8	S	7*
healthy adults	9	RGE	1±8	S	6
healthy adults	4	I/B	0±5	S	8*
hospitalized adults	5	I/B	3±6	S	9
hospitalized infants	10	RGE	-1±6	S	10
healthy adult	1	RGE	-5	L	11
healthy adults	2	RGE	-2±5	L	12
healthy adults	4	RGE	2±2	C	5
premature infants	4	RGE	-1±5	C	13

*recalculated using the S model
RGE = respiratory gas analysis; I/B = caloric intake plus change in body energy stores.
S = model described by Schoeller et al (6), equation A6; L = model described by Lifson and McClintock (4), equation 35; C = model described by Coward and Prentice (5).

References

1. Nier AOC. Rev Sci Instrum 18:398 (1947).
2. McKinney CR, et al. Rev Sci Instrum 21:724 (1950).
3. van der Merwe NJ and Vogel JC. Nature 276:815 (1978).
4. Lifson N and McClintock R. J Theor Biol 12:46 (1966).
5. Coward WA and Prentice AM. Am J Clin Nutr 41:659 (1985) (Letter).
6. Schoeller DA, Ravussen E, Schutz Y, et al. Am J Physiol 250:R823 (1986).
7. Schoeller DA and Webb P. Am J Clin Nutr 40:153(1984).
8. Schoeller DA and van Santen E. J Appl Physiol 53:955 (1982).
9. Schoeller DA, Kushner RF and Jones PJH. Am J Clin Nutr 44:291 (1986).
10. Jones PJH, Winthrop AL, Schoeller DA et al. Ped Res 21:242 (1987).
11. Klein PD, James WPT, Wong WW et al. Hum Nutr:Clin Nutr 38C:95 (1984).
12. Westerterp KR, deBoer JO, Saris WH et al. Int J Sports Med 5:74 (1984).
13. Roberts SB, Coward WA, Norhia V et al. Am J Clin Nutr 44:315 (1986).

Presented at the 35th ASMS Conference on Mass Spectrometry and Allied Topics
May 24-29, 1987, Denver, CO

MECHANISM FOR DESORPTION OF INTACT LARGE BIOMOLECULES BY FAST (MEV/NUCLEON) ION IMPACT -- THE "POPCORN" MODEL

Peter Williams[1] and Bo Sundqvist[2]
[1]Department of Chemistry,Arizona State University, Tempe, AZ 85287 and
[2]Tandem Accelerator Laboratory, University of Uppsala, Sweden

Models for the ejection of large biomolecular ions (molecular weights up to 33,000 u) by fast (~ 1 MeV/nucleon) heavy ion impact /1/ must address many features of the desorption process:

a) *intact* large ions are ejected, despite intense ionization and excitation in the 1-2 nm diameter "infratrack" around the primary ion track (energy deposition rates typically ~ 10^4 eV/nm).

b) surface binding energies for large proteins ~ 4-6 eV (20-30 hydrogen bonds) must be overcome, or the surface bonds *selectively* broken (i.e. without breaking intramolecular bonds)

c) to set a large ion, say mass 10,000 u, into motion with 1 eV kinetic energy requires an enormous momentum -- equivalent to 40 C atoms or 200 H atoms each with 50 eV kinetic energy; where does this momentum come from?

d) sputtering yields for fast ion impact are very high -- over 1000 amino acid and over 500 LHRH molecules per ion impact /2/

Points (a) and (d) require that the observed intact ions come from an extended region, the 5-10 nm diameter "ultratrack" surrounding the infratrack. The ultratrack is irradiated with low-energy secondary electrons emanating from the ionized infratrack. At distances of 1-2 nm from the infratrack boundary, most, if not all, of the secondary electrons have energies too low to induce electronic excitation. These "subexcitation" electrons do not break structural bonds, but can excite *vibrational* motion with very high efficiencies -- cross-sections are $\geq 10^{-16}$ cm^2. Some 25% of the incident ion energy loss (~ 2.5 keV/nm) appears in the ultratrack as low-energy secondary electrons. This intense electron flux excites most bonds in a molecule it traverses to at least the (v=1) vibrational level. The "hot" molecule expands rapidly, on a sub-picosecond time scale and literally pushes itself off the surface; the process is analogous to the motion of an exploding grain of popcorn /3/.

For a spherical molecule of radius r, the expansion rate is limited by the frequency of the fundamental "breathing" mode of the sphere, given by /3/

$$\nu = 1/2r(E/\rho)^{1/2}$$

where E is Young's modulus for the molecule and ρ is the density. The expansion time, Δt is 1/4 the vibrational period:

$$\Delta t = r/2(\rho/E)^{1/2}$$

For $E = 10^{10}$ N/m^2, $\rho = 10^3$ kg/m^3, r = 2 nm, $\Delta t \sim 1.5 \times 10^{-13}$s the degree of expansion can be estimated as 3-5%, either from bond anharmonicities or from macroscopic thermal expansion coefficients. Thus we have a displacement of the center of mass, $\Delta x \sim 0.03 - 0.05$ nm for a 2 nm diameter molecule, giving a velocity ~ 200-300 m/s. For a molecular weight of 10^4 this gives a kinetic energy of 2-6 eV, just sufficient to overcome a surface binding energy ~ 4-6 eV.

The vibrational excitation not only sets the molecule into motion, but also provides a microscopic hydrogen bond-breaking mechanism. The atoms comprising each hydrogen bond each have some 0.3 eV energy after excitation; under these circumstances the hydrogen bond cannot exist. Thus kinetic energies of a few eV resulting from the "popcorn" expansion are easily sufficient for desorption.

Sputtering yields can be estimated in the following way. Over the 0.7 nm thickness of a single molecular layer of LHRH molecules, secondary electrons

carry some 1.8 keV into the ultratrack. Assuming that all of this energy is efficiently converted to vibrational excitation, ~ 0.1 eV/normal mode for the 150-atom LHRH molecule requires 45 eV/molecule. Thus some 40 LHRH molecules can be sputtered from a single layer. Ion yields for LHRH saturate at a sample thickness of 7-8 nm; taking this to be an ejection depth we calculate a sputtering yield of 400-460 molecules/ion, in reasonable agreement with the experimental value of 580.

King et al /5/ and Chait /6/ have estimated internal energies for the bovine insulin molecule from the degree of fragmentation into the A and B chains. They conclude that the desorbed ions have internal energies of a few hundred eV. This molecule contains ~ 800 atoms; exciting all 2400 vibrational modes of the molecule by ~ 0.1 eV would give an internal energy ~ 240 eV, in good agreement with the experimental estimates.

Neither the popcorn model, nor others, treat ionization directly. Any of the arguments advanced for other models -- involving preformed ions, for example -- may be applied here. We suggest one additional possibility, which is that just as the ultratrack is the source of desorbed intact molecules, the infratrack must be a rich source of electrons and small positive and negative ion fragments. Ionization of the large, slow molecules desorbed from the ultratrack may proceed by attachment of a small ion or electron from the infratrack. The overlap in space and time between the particles from the two regions is small, and this may account for the low degree of ionization (~ 10^{-4}) observed for these fast ion processes.

In summary, the popcorn model appears to account for all features of the fast ion desorption process. It explains the observation of intact large ions, despite the intense excitation and ionization accompanying the primary ion passage, and accounts for the kinetic energy, the internal energy, and the momentum, of the desorbed ions. It is the first model to allow the calculation of sputtering yields which agree closely with experimental values. Finally, we can discuss extension of the process to even heavier molecules. Because, for a given degree of vibrational excitation, both the absolute expansion Δx and the expansion time Δt scale linearly with the molecule diameter, the kinetic energy arising from the expansion increases with the molecular mass. Thus, the limit of large molecule desorption seems to lie only in the extent to which very large molecules can be completely excited. It seems clear that molecules as large as perhaps 5-6 nm diameter -- molecular weights up to ~ 250,000 -- should be capable of desorption by fast ion impact.

REFERENCES

1. R.D. MacFarlane and D.F. Torgerson, Science, 191 (1976) 920

2. B. Sundqvist et al, Nucl. Instrum. Methods Phys. Res. B14 (1986) 429

3. P. Williams and B. Sundqvist, Phys. Rev. Lett. 58 (1987) 1031

4. B. Sundqvist et al, in "Ion Formation from Organic Solids 3", edited by A. Benninghoven, Springer, NY 1986, p. 6.

5. B.V. King et al, J. Chem. Phys., 82 (1985) 3641

6. B.T. Chait, Int. J. Mass Spectrom. Ion Phys., 53 (1983) 227

Presented at the 35th ASMS Conference on Mass Spectrometry and Allied Topics
May 24-29, 1987, Denver, CO

LSIMS of Rabbit and Bovine Trypsinized Cytochrome b_5 (M_r 10,000) Using An Array Detector

Bradford W. Gibson[1], Fred Walls[1], Arnold M. Falick[1], James J. Lipka[2], Lucy A. Waskell[2] and John Cottrell[3]
Department of Pharmaceutical Chemistry[1], University of California,San Francisco, CA 94143
Department of Anesthesia, Veterans Administration Medical Center[2], San Francisco, CA
and Kratos Analytical Instruments[3], Manchester, England

The analysis of polypeptides and small proteins (MW>5000) by liquid secondary ion mass spectrometry (LSIMS) on a magnetic instrument can be complicated by several factors including low ion yields, high magnetic fields and the problems of inefficient ion abstraction and detection. Recently, an array detector has been developed for the Kratos MS50 RF mass spectrometer that gives significant improved sensitivity (50-100 fold) [1]. The detector consisits of a one inch microchannel plate backed by a phosphor screen and a 1024-channel photodiode array. The detector is capable of simultaneous detection of ions over a 4% mass window with sufficient gain to detect single ions. We have used this device to analyze several high mass cytochrome b_5 fragments and methyl glucose polymer (MGP).

Cytochrome b_5 is a microsomal membrane-bound enzyme that catalyzes one-electron redox reactions and is involved in the desaturation reactions of fatty acids [2]. When treated with trypsin, the enzyme is split into two parts- a membrane associated domain and a functionally active soluble domain that contains the heme. This latter trypsin soluble domain has been the subject of many biological and mechanistic studies. However, there remain several structural questions concerning the actual C-terminal site of cleavage (Lys-86 or Arg-84) and the nature of the N-terminal blocking group on the N-extended forms. In order to resolve these questions, we analyzed both bovine and rabbit trypsin-soluble cytochrome b_5.

Trypsin soluble cytochrome b_5 from rabbit and cow were dissolved in DMSO and mixed with thioglycerol or dissolved directly in thioglycerol containing 2% TFA. The acid or DMSO was necessary to dissolve the protein but resulted in displacement of the heme group. A Kratos MS50 RF mass spectrometer fitted with an IonTech FAB gun and an array detector was used for all experiments [1]. In order to increase the longevity of the sample, a cooled probe was used [3]. Spectra were acquired in the static mode for approximately 60 sec at full accelerating voltage with a resolution of ca. 3,000 (50% valley) and calibrated with CsI.

The spectrum of approx. 300 pmole of bovine trypsin-solubilized cytochrome b_5 is shown in Fig. 1. The centroid for the MH^+ ion was 9462.4 d with repeat analyses giving values to within 0.3 mu of this measurement. This value agrees very well with the expected product with the C-terminal cleavage site at Arg-84 (predicted mass of 9462.7 d for the most abundant peak or 9463.3 d for the average mass). A similar case was found for the rabbit form which gave a centroid mass of 9502.5 d versus a predicted mass for the C-terminal Arg-84 form of 9502.4 d. The N-extended form of rabbit cytochrome b_5 containing the blocking group gave a mass centroid of 10144.7 d. Suprisingly, this meant that the N-terminal glutamine residue was not cyclized to form the pyroglutamic blocking group as expected, but was acetylated (predicted average mass for the acetylated N-terminus was 10,144.7 d compared to a predicted mass of 10,085.7 d for the N-terminal pyroglutamic acid blocked protein).

One of the problems in the LSIMS analysis of small proteins or high mass peptides is the matrix solubility of these materials. While 100 picomoles of a MW 10,000 protein may seem like a small amount of material, its actual matrix concentration is quite high. In cases where solubility is a limiting factor, the need for a highly sensitive detection system such as the array detector becomes even more critical. In addition, it remains to be seen how samples can be prepared in a suitable form at these low levels (picomoles) to take advantage of this increased sensitivity. Great care will be needed to insure the samples are free of salts and other contaminants. The fact that we were able to analyze 35 femtomole of methyl glucose polymer (MW 3515) with this array detector (Fig. 2) should not be confused with isolating and analyzing at this level, since this material was isolated in mg quantities. Nonetheless, the increased sensitivity and mass precision of high mass biopolymer detection using an array detector will certainly have a major impact on the structural analysis of proteins and carbohydrates.

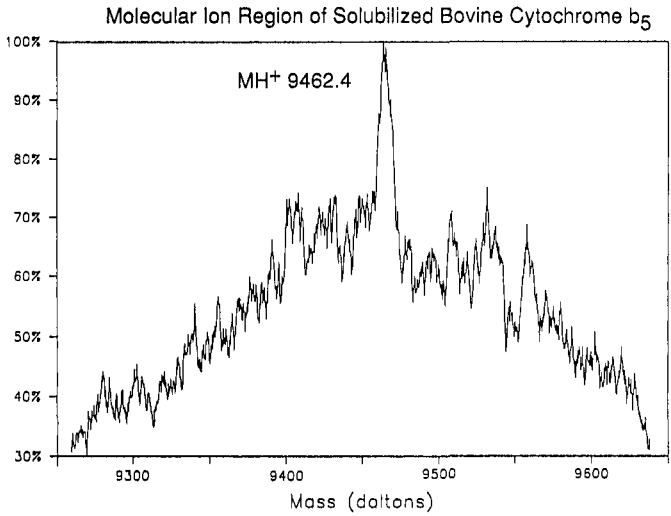

Fig. 1. LSIMS molecular ion region of bovine cytochrome b_5

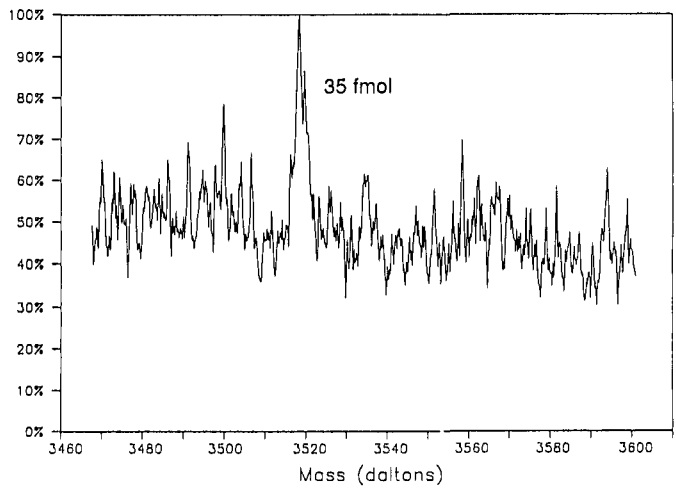

Fig. 2. LSIMS molecular ion region of 35 femtomoles of methyl glucose polymer

(1) J. Cottrell and S. Evans (1987) *Anal. Chem.*, in press
(2) B. Hagihara and E. Furuya (1978) *Pharmac. Ther. A.*, **2**, 537-550
(3) A.M. Falick, F. Walls and R. Laine (1986) *Anal. Biochem.*, **159**, 132-137

Acknowledgement: This work was supported by the NIH Division of Research Resources, Grant RR01614 (to A.L. Burlingame).

Presented at the 35th ASMS Conference on Mass Spectrometry and Allied Topics
May 24-29, 1987, Denver, CO

CLOSING THE GAP BETWEEN keV AND FISSION FRAGMENT SECONDARY ION YIELDS WITH NITROCELLULOSE

F.Lafortune[A], R.Beavis, W.Ens, X.Tang and K.G.Standing,
Chemistry and Physics Departments, [A]Collège Universitaire de Saint-Boniface and University of Manitoba, Winnipeg, Canada R3T 2N2
and
B.T.Chait,
The Rockefeller University, New York, N.Y. 10021

The use of polymers as sample matrices for mass spectrometric studies of high molecular weight peptides has grown in importance recently. For instance, plasma desorption mass spectrometry (PD-MS) studies by Macfarlane *et al* [1] and Jonsson *et al* [2] have revealed remarkable enhancements in quasimolecular ion yields for small proteins, eg insulin, desorbed from nitrocellulose. These results encouraged us to determine whether this new application technique would lead to similar improvements with low energy time-of-flight SIMS.

In general, molecular ion yields decrease as the sample molecular weight increases. In a previous comparative analysis of a series of peptides [3], we showed that quasimolecular ion yields dropped off more steeply for keV Cs+ ions than for 252-Cf fission fragments. Insulin (5733u) for example, deposited on Ag or Al-polyester substrates, could barely be detected in keV ion spectra, even with post-acceleration. We now report that differences in relative yields between these two bombardment techniques have been reduced significantly by the use of a nitrocellulose (NC) matrix.

Peptides used for these comparative studies include leu-enkephalin-arginine (712u), substance P (1346u), renin substrate (1759u), bovine insulin B-chain (3493u), bovine insulin (5733u) and aprotinin (6512u).Targets were prepared by first electrospraying an acetone solution of NC onto an aluminized mylar film to yield a ~20 μg/cm2 NC coverage. ~500 pmole of peptide mixed with leucine-enkephalin-arginine (LEA) in trifluoroacetic acid were then deposited on the NC layer. LEA was used for normalization. After drying, targets were placed in the ion source.

keV positive ion spectra were recorded on the Manitoba II time-of-flight mass spectrometer, After target bombardment by a pulsed beam of 12 keV Cs+ ions, the secondary ions produced were accelerated to 10 keV and detected by microchannel plates, with no post-acceleration. The sample foils analyzed at Manitoba were then sent by courier to Rockefeller, where the fission fragment (FF) spectra were taken. For FF analysis, 10 keV ion acceleration was also used, with no post-acceleration.

As was the case in our previous comparison, we found a remarkable similarity between spectra. Figure 1 shows the quasimolecular region for substance P, renin substrate and Bovine insulin-B chain, whereas figure 2 illustrates comparative spectra obtained with bovine insulin. Figure 3 demonstrates the dramatic improvement in molecular ion yield of insulin observed in keV spectra with NC.

To calculate the relative yield dependance on molecular weight, the same background subtraction procedure and integration limits were used. In figure 4 the keV/MeV ratios vs. mass are compared, with and without NC, and normalized to leu-enkephalin-arg and leu-enkephalin, respectively. It shows that relative molecular ion yields between fission fragment and keV spectra decrease much less rapidly with nitrocellulose, than without it. For example,the normalized yield of insulin without NC is about 20 times lower for keV ion bombardment than for fission fragment bombardment. It becomes only 4 times lower when desorbed from nitrocellulose. These results suggest that factors such as target preparation and acceleration potential may have as much influence on ion yields than the energy of bombarding particules.

Presented at the 35th ASMS Conference on Mass Spectrometry and Allied Topics
May 24-29, 1987, Denver, CO

REFERENCES
1. Macfarlane,R.D. *et al* Anal.Chem. 1986,58 1091
2. Jonsson,G.P. *et al* Anal.Chem., 1986, 58 1084
3. Ens,W. *et* al,submitted to Anal.Chem.

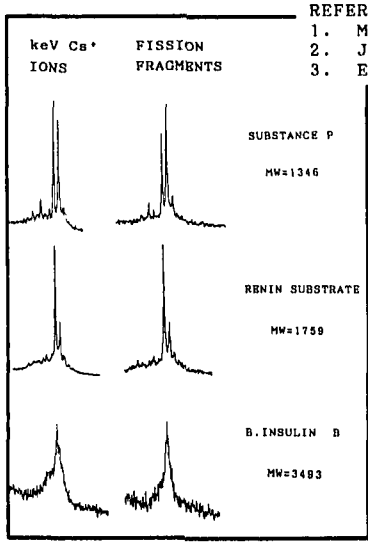

FIGURE 1 Comparison between keV and MeV quasimolecular regions for selected peptides

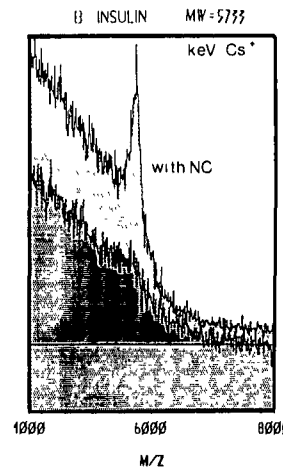

FIGURE 2 Comparison between keV and MeV +ve ion spectra of bov.insulin obtained by bombardment of the same target

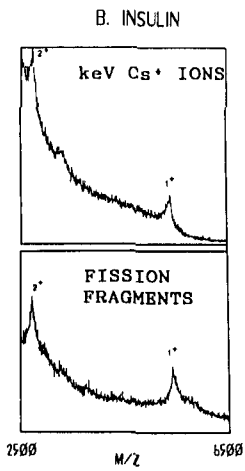

FIGURE 3 Improvement in molecular ion yield of insulin (keV spectrum) when desorbed from NC

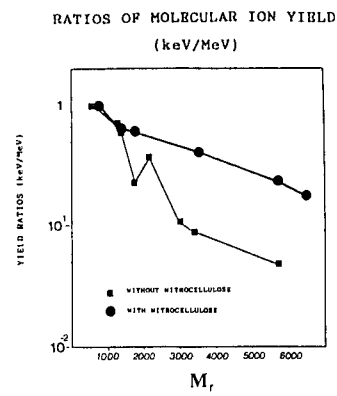

FIGURE 4 (keV/MeV) yield dependance on molecular weight with and without nitrocellulose

Presented at the 35th ASMS Conference on Mass Spectrometry and Allied Topics
May 24-29, 1987, Denver, CO

THE IDENTIFICATION AND CHARACTERIZATION OF NUCLEOTIDES BY LASER IONIZATION FOURIER TRANSFORM MASS SPECTROMETRY*

R. L. Hettich and M. V. Buchanan
Analytical Chemistry Division
Oak Ridge National Laboratory
Oak Ridge, TN 37831-6120

The examination of DNA modification by carcinogenic and mutagenic compounds is an important aspect of research in molecular dosimetry. The ability to detect and unambiguously identify both normal and modified nucleotides at the isomeric level is a vital part of these investigations. The low detection limits and experimental flexibility of mass spectrometry enable this technique to be a useful method of characterizing nucleotides. Since oligonucleotides are high molecular weight, non-volatile compounds, laser ionization mass spectrometry provides a method for the generation and structural examination of ions from these compounds.

This report illustrates the characterization of nucleotides using a Nd:YAG pulsed laser interfaced to a Nicolet FTMS-2000 mass spectrometer. The 1064 nm line of the laser was used to ionize the nucleotide samples placed on the tip of the solids probe. Laser impact generates both ions and neutrals in the source cell of the mass spectrometer. Various structural techniques, including collision-induced dissociation and ion-molecule reactions, were used to probe the structure of the ions.

Ionization of nucleotides and oligonucleotides by the Nd:YAG laser produces extensive fragmentation, generating both positive and negative ions. Laser ionization of a sample containing 5 nanograms of adenosine monophosphate yielded an appreciable ion signal, indicating that the detection limit is probably below 1 nanogram; however, difficulties in sample handling require slightly more material. Low laser energy (used to avoid formation of metal ions from the stainless steel probe tip) was found in some cases to enhance formation of both molecular and pseudo-molecular ions for the mononucleotides. The negative ion spectra were found to be the most reproducible and yielded structural information about the nucleotide via fragment ions which corresponded to the nucleic bases, sugars, and phosphates present in the original molecule. The identity of the nucleic bases, whether they are normal or modified, can be determined by inspection of the negative ion spectrum. For example, laser ionization of methyl-adenosine and glyoxal deoxyguanosine indicated ions representative of the modified bases. Figure 1 illustrates the negative ion spectrum obtained by laser ionization of deoxy (adenosine-guanosine-cytidine-thymidine) or d(AGCT). The principal fragmentation pathway appears to be cleavage of the nucleic base-sugar bonds, resulting in the generation of all the individual nucleic base ions. Collisional activation of a specific ion can also provide information necessary to identify a particular component. Figure 2 illustrates the isolation and collision-induced dissociation of m/z 134 obtained by laser ionization of d(AGCT). Exact mass measurement and observation of a daughter ion corresponding to loss of HCN from m/z 134 indicates that this ion is adenosine.

Molecular ions for oligonucleotides are difficult to generate by laser ionization, possibly due to the ease of fragmentation of the nucleic base-sugar bond. However, at low laser energy, the negative molecular ion of deoxy (cytidine-adenosine-adenosine) at m/z 1021 amu has been observed. In addition, fragment ions indicated cleavage at the phosphate ester bonds and gave structural information for this trimeric nucleotide. Further studies are underway to ionize and characterize larger oligonucleotides.

*Research sponsored by the Office of Health and Environmental Research, U.S. Department of Energy under contract DE-AC05-84OR21400 with Martin Marietta Energy Systems, Inc.

Presented at the 35th ASMS Conference on Mass Spectrometry and Allied Topics
May 24-29, 1987, Denver, CO

Figure 1

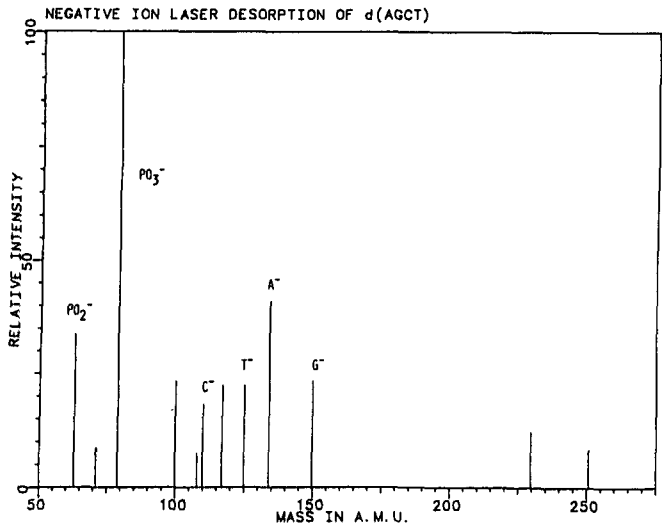

Figure 2

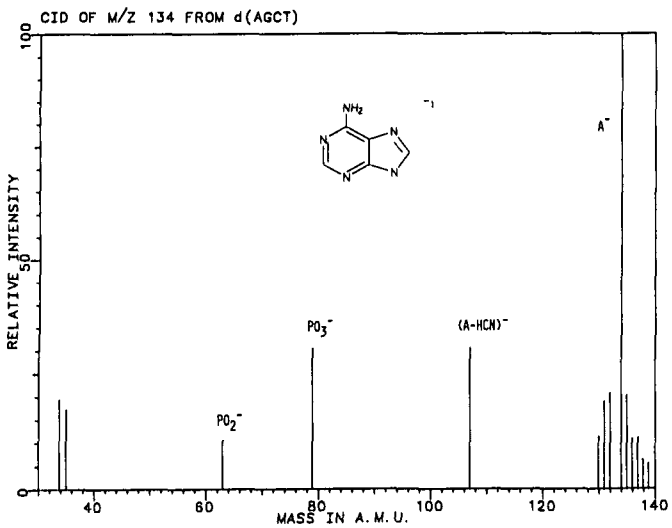

Presented at the 35th ASMS Conference on Mass Spectrometry and Allied Topics
May 24-29, 1987, Denver, CO

ANALYSIS OF OLIGOSACCHARIDES BY PLASMA DESORPTION MASS SPECTROMETRY

I. Jardine, G. S. Scanlan, Dept. of Pharmacology, Mayo Clinic, Rochester, MN 55905; M. McNeil, P. J. Brennan, Dept. of Microbiology, Colorado State Univ., Fort Collins, CO 80523; R. J. Linhardt, Dept. of Medicinal Chemistry, Univ. of Iowa, Iowa City, IA 52242

Recently, we reported on the application of Californium-252 plasma desorption mass spectrometry (PDMS) to the analysis of oligosaccharides,[1] lipooligosaccharides[1] and polysulfated aminoglycans.[2] For the examples examined, it was found that even although these compounds could not be analyzed successfully by fast atom bombardment mass spectrometry (FABMS), molecular weight and some structural information could always be obtained using PDMS. In particular, the positive ion PDMS spectrum of lipooligosaccharides electrosprayed onto PDMS targets provided definitive molecular weight information while the negative ion spectrum defined the fatty acid heterogeneity in the molecule. An entirely different approach was necessary for the PDMS analysis of polysulfated aminoglycans such as heparin fragments. The sodium salt form of the sulfated oligosaccharide was adsorbed onto an immobilized cationic surfactant film on the PDMS target. After washing, the heparin fragment was desorbed and analyzed as a surfactant-oligosaccharide complex.

Following these initial successes we have now analyzed a number of other more complex bacterial antigenic oligosaccharides, lipooligosaccharides, and glycoproteolipids as well as larger heparin fragments. These analyses have generally provided useful molecular weight and structural information. Examples of these analyses are presented below.

In general, we have found that analysis of complex oligosaccharides and their peracetylated derivatives is readily accomplished from nitrocellulose coated PDMS targets at the 1-10 µg level. Both the underivatized and derivatized species provide molecular weight information but, in general, the peracetylated derivative also provides significant oligosaccharide sequence information. The negative ion spectrum provides the fatty acid composition. The heparin analysis technique continues to provide essential molecular weight information and hence sulfate content of heparin fragments.

References

1. I. Jardine, S. W. Hunter, P. J. Brennan, C. J. McNeal, and R. D. Macfarlane, Biomed. Environ. Mass Spectrom. 13, 273-276 (1986).

2. C. J. McNeal, R. D. Macfarlane, and I. Jardine, Biochem. Biophys. Res. Commun. 139, 18-24 (1986).

Acknowledgements

This research was supported by NIH grants GM32928 and RR02682 and by the Mayo Foundation.

PHENOLIC GLYCOLIPIDS (PGL)

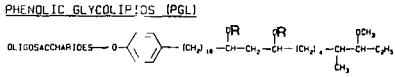

LIPOOLIGOSACCHARIDES (LOS)

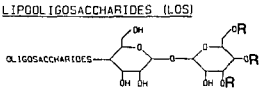

GLYCOPEPTIDOLIPIDS (GPL)

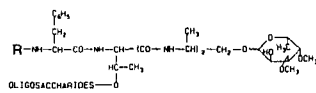

R = LONG CHAIN FATTY ACYL

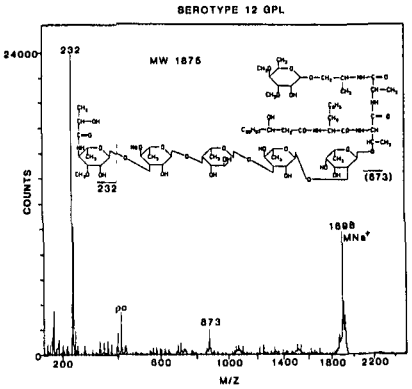
SEROTYPE 12 GPL
MW 1875
232
(673)
1898
MNa+
873
COUNTS
M/Z

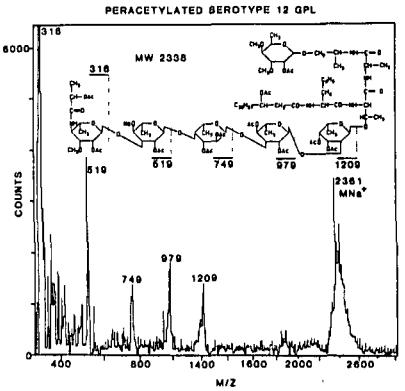
PERACETYLATED SEROTYPE 12 GPL
MW 2338
316
519
749
979
1209
2361
MNa+
COUNTS
M/Z

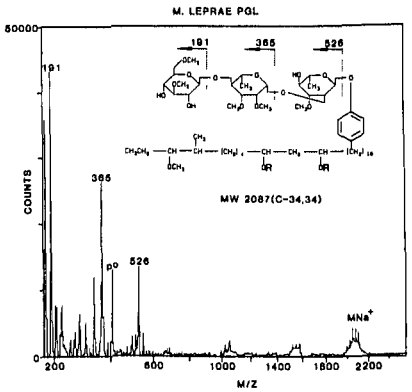
M. LEPRAE PGL
191
365
526
MW 2087(C-34,34)
MNa+
COUNTS
M/Z

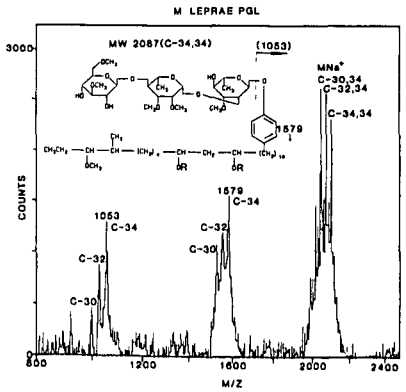
M LEPRAE PGL
MW 2087(C-34,34)
(1053)
MNa+
C-30,34
C-32,34
C-34,34
1579
1053
C-34
C-32
C-30
COUNTS
M/Z

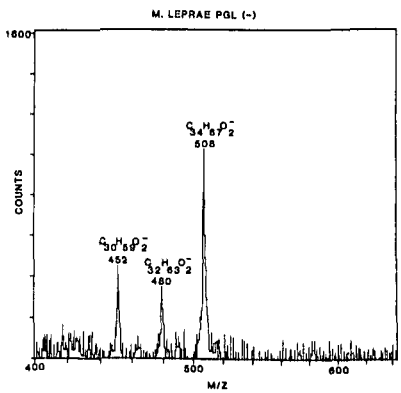
M. LEPRAE PGL (-)
508
452
480
COUNTS
M/Z

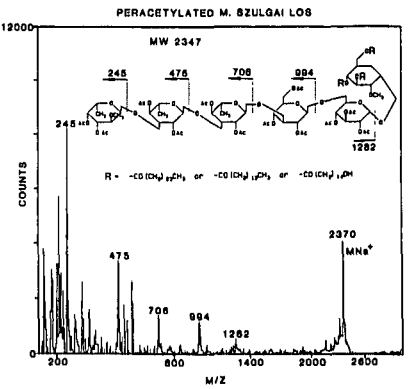
PERACETYLATED M. SZULGAI LOS
MW 2347
245
475
706
994
1282
2370
MNa+
COUNTS
M/Z

Presented at the 35th ASMS Conference on Mass Spectrometry and Allied Topics
May 24-29, 1987, Denver, CO

PLASMA DESORPTION ANALYSIS OF PROTEOLYTIC GLYCOPEPTIDES FROM BOVINE FETUIN TO ELUCIDATE GLYCOSYLATION SITE MICROHETEROGENEITY

M.ALAI, C.FENSEALU, M.HARDY, Y.C.LEE and R.R.TOWNSEND.

Johns Hopkins University, Baltimore, MD.

Oligosaccharide heterogeneity at a single glycosylation site on the peptide backbone is known to occur in most glycoproteins. This phenomenon is highly regluated and reflects the phenotype, the metabolic state and the developmental stage of the cell. Understanding the biological significance of glycoprotein heterogeneity resultng from a multipilicity of oligosaccharide structures will require studies to ascertain the carbohydrate structures at each oligosaccharide attachment site.

Plasma desorption mass spectrometry has been successfully used to determine the molecular weights of peptides and small proteins. We now show that plasma desorption mass spectrometry (PDMS) gives molecular ions of desialylated glycosylation-site specific tryptic glycopeptides up to a mass 4000 am.u. with 1-5 ug of sample. Fragmentation is not observed under the conditions employed thus providing a detection method for molecular weight heterogenity both for glycopeptide purification as well as for structural characterization of carbohydrate microheterogenity at each glycosylation site.

Tryptic asialo-glycopeptides of bovine fetuin were purified by a combination of anion exchange chromatography and reverse-phase HPLC. PDMS was implemented in the purification protocol for these glycopeptides and proved to be useful in assessing purity of glycopeptide fractions which were mixtures containing glycopeptides with different masses. Heterogenity at each of the three N-linked glycosylation sites of bovine fetuin (Spiro, R.G. (1962), J. Biol. Chem., 237: 382-389), Asn-Cys, Asn-Asp and Asn-Gly sites, was assessed by a combination of PDMS, amino acid composition and amino acid sequence data. Two ion groups differing in mass by one lactosamine unit were observed in glycopeptides from the Asn-Cys and Asn-Asp site, indicating the presence of biantennary in addition to triantennary oligosaccharides at these sites. Agreement within 3 to 5 a.m.u. was found between the mass determined by PDMS and amino acid analysis, peptide sequence and the recently reported biantennary and triantennary oligosaccharide structures on the bovine fetuin (Townsend, R.R. et al. (1986), Biochem., 25: 5716-5725; Takasaki, S. and Kobata, A. (1986), Biochem., 25: 5709-5715). Apparently of the three N-glycosylation sites of bovine fetuin, only the Asn-Gly site has exculsively triantennary oligosaccharides.

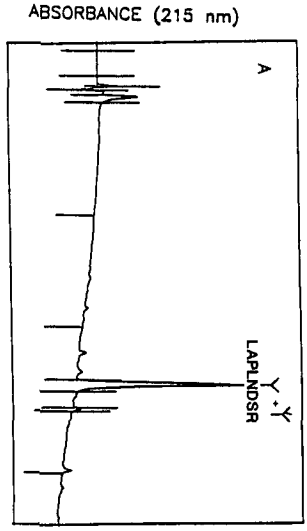

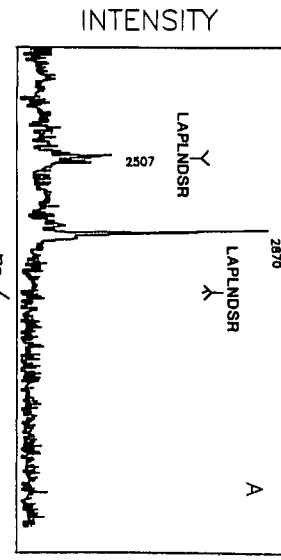

Figure 1. Glycosylation-site microheterogenity at the Asn-Asp site demonstrated by FDMS.

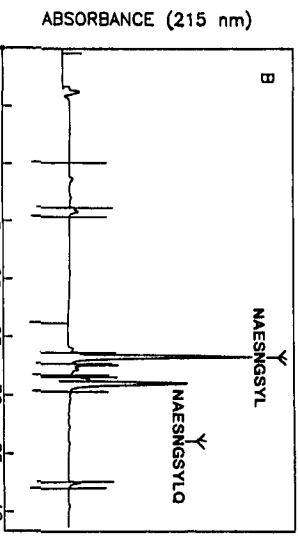

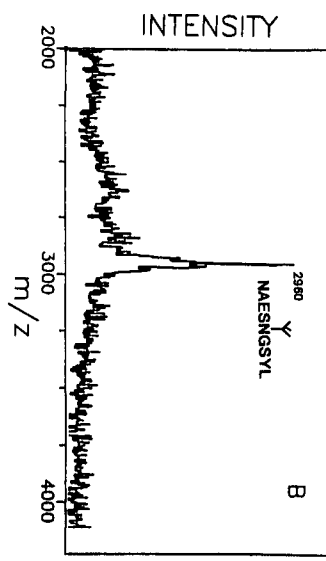

Figure 2. Absence of oligosaccharide heterogeneity at the Asn-Gly site demonstrated by FDMS.

Presented at the 35th ASMS Conference on Mass Spectrometry and Allied Topics
May 24-29, 1987, Denver, CO

PROTEIN SEQUENCING BY TANDEM MASS SPECTROMETRY

J. R. Yates III, D. F. Hunt, J. Shabanowitz; Dept. of Chemistry,
University of Virginia, Charlottesville, Virginia, 22901

Methodology for the sequence analysis of proteins based on tandem mass spectrometry and tandem quadrupole Fourier transform mass spectrometry (QFTMS) has been developed. Proteins are converted to a complex mixture of oligopeptides at the 10 nmole level using site specific enzymes or chemical reagents. An aliquot containing 100 pmoles of digested protein is removed from the digest and separated by reverse phase microbore HPLC, collecting fractions for mass analysis. The molecular weight of the peptides in each fraction are then determined by LSIMS and QFTMS using 10-50 pmoles of peptide. If the majority of peptides are below 1800 daltons the digest is separated by microbore HPLC and each peak collected as a separate fraction. The molecular weight of the peptides in each of the fractions is then determined by LSIMS using thioglycerol as the matrix and 8 keV Cs^+ ions as the projectiles on a triple quadrupole mass spectrometer. Fractions containing peptides larger than 1800 daltons (as previously determined by QFTMS) are subdigested and the molecular weights of the smaller peptides determined without prior separation.

Peptides are then sequenced by tandem mass spectrometry. Peptide $(M+H)^+$ ions in a particular HPLC fraction are selected one after another by quadrupole 1 of a triple quadrupole mass spectrometer/data system and transmitted to quadrupole 2 where they impact on argon atoms and undergo collision activated dissociation. Fragmentation occurs predominately at the amide linkages during this process. The resulting collection of fragment ions is analyzed in quadrupole 3 to produce a mass spectrum.

Basic amino acid residues in a peptide create preferential cleavage points along the amide backbone. When the basic residue is located at the N-terminus of a peptide a complete and easily interpretable B-ion series is produced. To investigate the utility of N-terminal derivatization to improve the fragmentation of peptides several basic derivatives were tried. Peptides were derivatized with methyl acetimidate, proline and histidine and their fragmentation patterns in low energy collisions (10-30 eV) studied. Methyl acetimidate derivatized peptides produced a strong series of B-17 ions with very little B-ion present. Proline and histidine were added to the N-terminus of peptides using standard peptide synthesis chemistry using the N-blocked active ester of the amino acids. Addition of proline was almost quantitative and produced a good series of B-ions in collision experiments. The effect was most dramatic when the B-ions were very weak in the underivatized peptide. If a good series of B-ions was already present in the underivatized peptide addition of proline did not improve it further. Addition of histidine was similar to proline in its effect on the fragmentation of peptides. N-terminal derivatization has promise as a method by which to control fragmentation.

Sequence analysis of the major intestinal calcium binding protein isolated from mouse has been accomplished using a combination of QFTMS and tandem mass spectrometry. The protein is N-terminally acetylated with a molecular weight of 8,898 daltons. Results of the sequence analysis show the amino acid sequence of the calcium binding protein to be highly conserved among mammals as well as to be part of the multi-gene family of proteins that includes calmodulin, troponin C and

parvalbumin.

Purple acid phosphatase and uteroferrin belong to a growing class of metalloproteins that exhibit phosphoprotein phosphatase activity. Purple acid phosphatase, a 35 kDa intracellular glycoprotein containing a bimetallic iron cluster, is isolated from beef spleen and consists of 15 kDa and 20 kDa subunits. Uteroferrin, also a 35 kDa glycoprotein, is synthesized in response to progesterone and is secreted by the glandular endometrium of the pig uterus. This extracellular protein is isolated as a single chain species, and also contains two iron atoms as well as a single asparagine-linked oligosaccaharide chain. Both enzymes exhibit distinctly similar optical and EPR spectra and magnetic behavior. Phosphatase was sequenced by tandem mass spectrometry. Uteroferrin was partially sequenced by tandem mass spectrometry and QFTMS. Independent of this effort, work on the sequence of uteroferrin was carried out in the laboratories of R. M. Roberts and K. Brew by classical Edman methodology. Information on the two proteins was pooled when sequence analysis of uteroferrin by tandem mass spectrometry showed a high degree of homology with purple acid phosphatase. Sequences of the two proteins are shown in fig 1 and 2. Particularly striking is the high degree of homology (>90%) exhibited by these two molecules that are presumed to have very different functions, that are found in greatly different quantities in diferent organs, in disparate pH environments, and in different animals. Tandem mass spectrometry was able to establish very quickly that a close structural relationship existed between these two proteins.

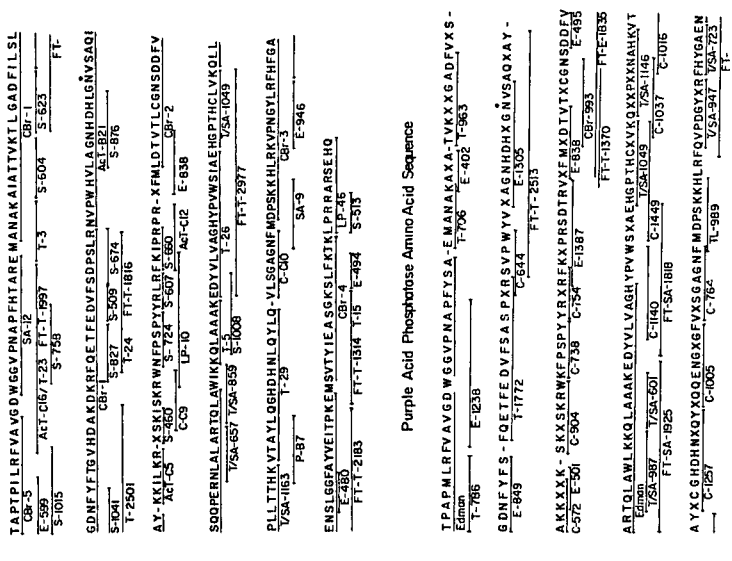

Presented at the 35th ASMS Conference on Mass Spectrometry and Allied Topics
May 24-29, 1987, Denver, CO

RESOLUTION REQUIREMENTS IN THE OPERATION OF A HIGH PERFORMANCE TANDEM MASS SPECTROMETER

S.A. Martin, H.A. Scoble, C.E. Costello, and K. Biemann
Dept. of Chemistry, MIT, Cambridge, MA 02139

The proper settings of the resolution of MS-1 and MS-2 in a tandem mass spectrometer are important parameters for the generation of product ion spectra of high quality. Maximum transmission of only the monoisotopic precursor ion in MS-1 is important to generate a product ion spectrum in which peaks are abundant singlets (rather than isotope clusters). When scanning a magnetic mass spectrometer (we use a JEOL HX110/HX110), the collector slit width has to match beam width and dispersion in such a manner that the slit width is no larger than the space between one ion beam and the next to achieve a completely resolved spectrum (Fig. 1, top). In a tandem experiment, however, MS-1 is set to transmit only the selected precursor beam (*e.g.*, the ^{12}C-only $(M+H)^+$ ion) and one can thus keep the collector slit of MS-1 twice as wide (*i.e.*, half the resolution necessary as in a scanning experiment). Scanning MS-2 across its collector slit shows a uniformly shaped single peak (Fig. 1, bottom) (because the adjacent masses do not enter MS-2) while scanning MS-1 under these conditions would give a completely unresolved envelope (Fig. 1, center). While it is desirable to scan MS-2 at a resolution that corresponds to the mass of the precursor ion, one may trade resolution for sensitivity to a certain extent without loss of information. This is demonstrated in Fig. 2 which shows a scan of the CID-fragment ion of m/z 1000.54 (the a_8-ion which contains 49 C-atoms and 13 N-atoms) from a precursor (^{12}C-only) ion of m/z 1758.93 (renin substrate tetradecapeptide). By decreasing the resolution of MS-2 from 2500 to 1000 to 500, the mass assignment is practically unchanged, while the intensity increases by a factor of 4-5. At higher mass (between 2000 and 3000 for peptides) the $^{13}C_1$-species of the $(M+H)^+$ ion is more abundant than the corresponding monoisotopic ion. Selecting the $^{13}C_1$-species by MS-1 would give a somewhat higher precursor ion current but this slight advantage is offset by the fact that the CID fragment ions now continuously change from singlets at high mass to a doublet of equal intensity in the middle of the spectrum for the fragments containing only half the carbon atoms (and/or nitrogens) to near singlets at very low mass where only a few carbon atoms are left which are most likely all ^{12}C. For this to be observed the resolution of MS-2 has to be sufficiently high (Fig. 3; the sample is still the same as used for Figs. 1 and 2 where the $^{13}C_1$-species is of about equal intensity as the ^{12}C-species). Decreasing the resolution to increase ion signal finally reaches a point where these doublets are no longer resolved and the measured mass becomes the weighted average of the two components (but not the mass corresponding to that calculated from average atomic weights of C, H, N, etc., as is the case with unresolved isotopic multiplets in MS-1!). Transmitting both ions (^{12}C + $^{13}C_1$) simultaneously through MS-1 increases the total precursor ion current entering the collision cell but further complicates the product ion spectrum. Now the CID-fragment ion spectrum is a complex set of doublets of different ratios which become near singlets at very low mass. Figure 4 displays the doublet, including the mass measured for the ^{12}C ion. At a resolution of 1000, it is still resolved and gives good mass accuracy but at 500 the experimental value is high (mass values determined by centroid rather than peak top are shown in parentheses).

These factors have to be taken into account when optimizing the instrument parameters of a four-sector tandem mass spectrometer to obtain the highest quality product ion spectra, particularly from precursor ions of high mass. Of the complex matrix made up of the mass and abundance of the precursor ion, resolution, abundance of product ions and accuracy of mass assignment, a range of useful settings for the resolution of MS-1 and MS-2 emerges, depending upon the mass and abundance of the precursor ion (Table I). In general, the signal intensity in the product ion spectrum is inversely proportional to the resolution setting of MS-2. A thorough understanding of the multiplet patterns expected from ^{13}C-containing precursor ions is particularly important in the interpretation of product ion spectra of mixtures of compounds differing by one or two mass units, such as peptides differing by COOH/$CONH_2$ or oxidized and reduced forms of peptides containing two cysteines. Figure 5 shows the fragment ion of m/z 803 from the ^{12}C-species of $(M+H)^+$ of LH-RH (I) (left), the doublet observed when the ^{13}C-species is the precursor ion (center), and (right) the doublet generated when m/z 1183.6 from a mixture of (I) and the corresponding C-terminal free acid (II) is the precursor ion (m/z 1183.6). Clearly, the doublet pattern is <u>not</u> the one expected for a product ion derived from a pure $^{13}C_1$-species (Fig. 5, center), indicating that the precursor is a mixture of a $^{13}C_1$-species and a ^{12}C-species that is one mass unit heavier.

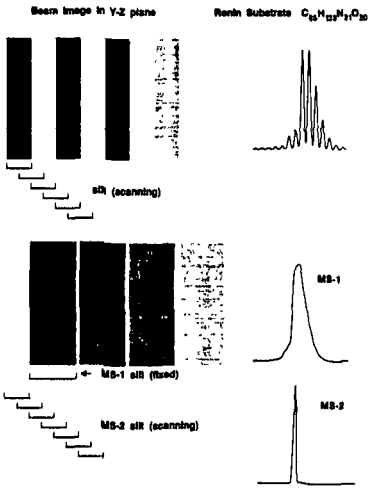

Figure 1.

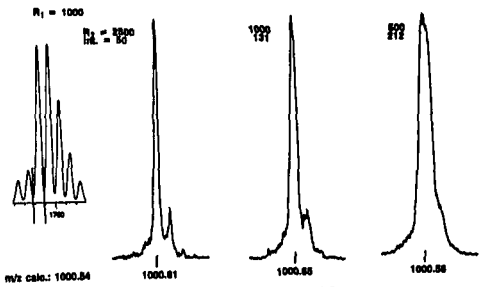

Figure 2. Precursor ^{12}C

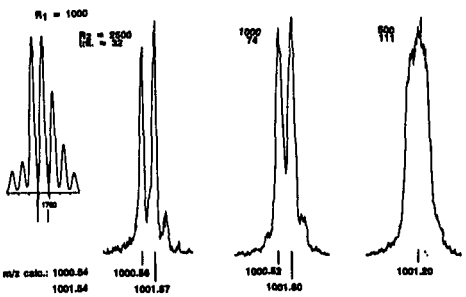

Figure 3. Precursor $^{13}C_1$

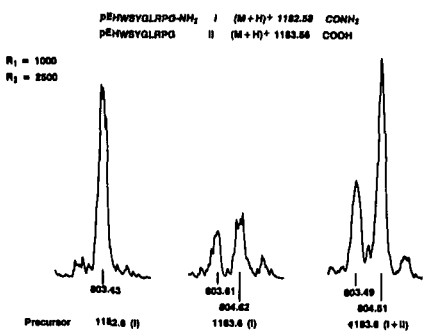

Figure 5. Mixture of amide and free acid (see text)

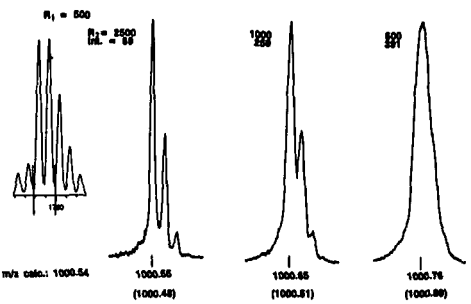

Figure 4. Precursor $^{12}C + {}^{13}C_1$

Precursor	Resolution Setting MS-1	MS-2
(M+H)+= 1000 (^{12}C)	(500-) 1000	1000
(M+H)+= 2000 (^{12}C)	1000	(500-) 1500
(M+H)+= 3000 (^{12}C)	1500	(500-) 2000
(M+H)+= 3000 ($^{12}C + {}^{13}C$)	750	500*-3000

*requires correction of product ion masses to ^{12}C only value

Presented at the 35th ASMS Conference on Mass Spectrometry and Allied Topics
May 24-29, 1987, Denver, CO

PEPTIDE AND PROTEIN MAPPING BY ^{252}Cf-PLASMA DESORPTION MASS SPECTROMETRY

A. Tsarbopoulos*, D. J. Liberatot and I. Jardine*

*Department of Pharmacology, Mayo Clinic, Rochester, MN 55905
and
†Department of Drug Metabolism, Hoffmann-LaRoche, Nutley, NJ 07110

In recent years, mass spectrometry has played an increasingly important role in the determination of the primary structure of peptides and proteins. With the advent of particle induced desorption techniques, mass spectrometry has emerged as the method of choice to solve structural problems to which conventional techniques are not applicable. An example of such a problem is the structure and nature of blocked NH_2-termini of proteins which are inaccessible to Edman degradation.

^{252}Cf-plasma desorption time-of-flight mass spectrometry (PDMS), a well-established method for the determination of the molecular weight (MW) of large molecules, is an efficient method of solving such structural problems. We have examined a "PD mapping" approach to rapidly screen proteins and recombinant-DNA protein products for sequence changes, mutations, and post-translational modifications.

In the "PD mapping" experiment, the protein is cleaved either chemically or enzymatically followed by MW determination of the resulting peptides by PDMS. The experimentally determined MW's are compared with those predicted based upon the proposed amino acid sequence. Further confirmation of the sequence assignments of individual peptides is made by additional steps of enzymatic or chemical modification of the nitrocellulose (NC)-bound peptides.

In the mapping of recombinant interleukin-2 (IL-2), the MW was first determined by PDMS on 200 pmol of material (Figure 1). Then the protein was cleaved with CNBr. followed by direct PDMS analysis of the CNBr-digest mixture. Initially, signals corresponding to only three CNBr-peptide fragments were observed (Figure 2). Further dithiothreitol reduction directly on the PDMS target generated signals corresponding to all five CNBr-peptide fragments anticipated from the DNA-derived sequence (Figure 2). Similar PDMS analysis of the tryptic digest of IL-2 did not give signals due to all tryptic peptides of the digest mixture. The tryptic fragments from the C-terminus of the protein were not observed, probably due to selective desorption from the NC-coated target. Nevertheless, PDMS analysis of the V8 digest of IL-2 and of the reduced and carboxymethylated-IL-2 provided the missing information on the IL-2 C-terminus.

Similar selective desorption patterns were observed in the PDMS analysis of other peptide mixtures (e.g., tryptic and CNBr digest of myoglobin and cytochrome c, CNBr digest of growth hormone releasing factor, tryptic digest of glucagon). In order to minimize this problem, a modified approach was followed for the analysis of the tryptic digest of recombinant human growth hormone. The digest mixture was separated by RP-HPLC into two fractions. PDMS analysis of each fraction generated ions due to almost all the peptides in the mixture. Hence, partial fractionation of the protein digest followed by PDMS analysis of the LC fractions, seems to be the preferred procedure for "PD mapping" of proteins.

In the mapping of a 28-kDa calcium-binding protein (CaBP), a similar approach was employed. The protein was cleaved with CNBr and the resulting mixture was separated by RP-HPLC. The isolated CNBr fragments of CaBP were checked in order to confirm the DNA predicted sequence, including the N- and C-terminus and any post-translational modifications. One of the isolated CNBr fragments was inaccessible to Edman degradation. When subjected to PDMS analysis, this peptide gave a signal which could be interpreted in terms of an acetylated threonine blocked N-terminus. A V8 protease enzyme digest carried out directly on the NC-bound peptide, resulted in valuable sequence information on the N-terminal fragment, as well as indirect confirmation of the acetylated-threonine structure assignment (Figure 3).

Presented at the 35th ASMS Conference on Mass Spectrometry and Allied Topics
May 24-29, 1987, Denver, CO

In conclusion, ^{252}Cf-PDMS has a number of advantageous features (high mass range, high sensitivity and nondestructive analysis) which offers a rapid and convenient way to check the sequence of native and recombinant proteins.

Acknowledgements: This work was supported by grants from the National Institutes of Health (GM 32928 and RR 02682).

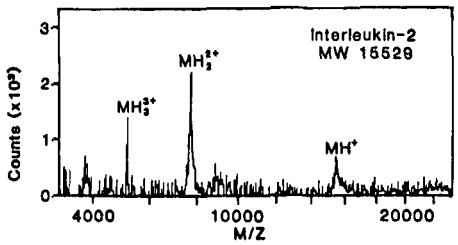

Figure 1

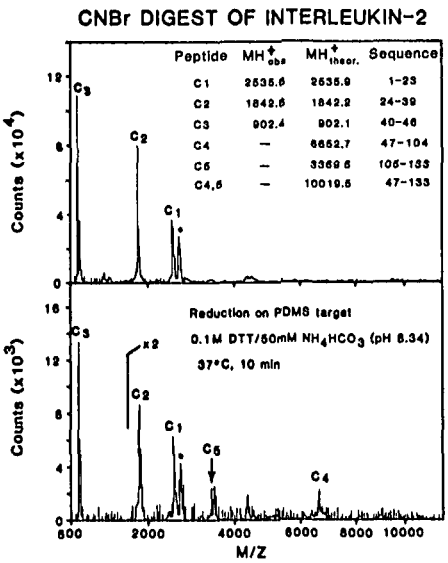

Figure 2

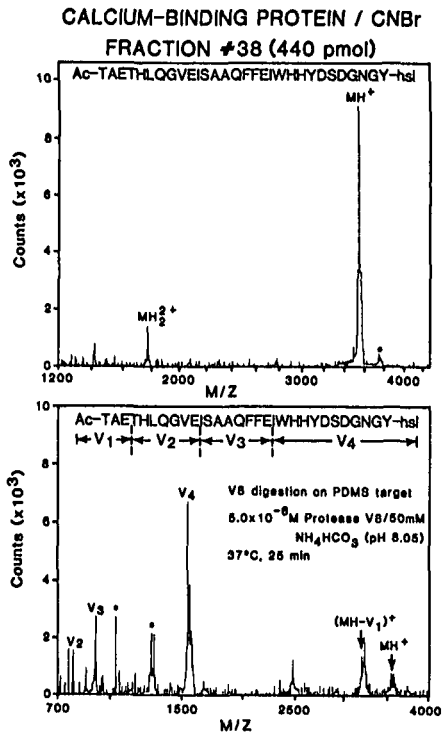

Figure 3

Presented at the 35th ASMS Conference on Mass Spectrometry and Allied Topics
May 24-29, 1987, Denver, CO.

ADVANTAGES FOR COLLISIONALLY ACTIVATING METAL ION CATIONIZED OLIGONUCLEOTIDES AND PEPTIDES,

R.L. Cerny and M.L. Gross, Midwest Center for Mass Spectrometry, Dept. of Chemistry, University of Nebraska, Lincoln, NE 68588

Fast atom bombardment (FAB) combined with tandem mass spectrometry (MS-MS) has been shown to be a useful tool in structural determination of biomolecules. Most studies have concentrated on collisional activation of $(M + H)^+$ species. One point often overlooked is that no matter how high the resolution of MS-I, a mixture of species (protonated at different sites) will be collisionally activated. The resultant MS-MS spectrum is actually a composite of the spectra of the individual species. This is particularly true for biomolecules such as peptides and oligonucleotides where a repeating structural pattern provides numerous, nearly identical sites for protonation. As an example, the FAB MS-MS spectrum of $(M + H)^+$ ions of methionine enkephalin is shown in Figure 1. Fragments related to both the N-terminus and C-terminus are observed. The most abundant ions are of the B and Y types. These result from protonation of an amide nitrogen followed by cleavage of the C-N bond.

Here the MS-MS spectrum of $(M + H)^+$ species provides ample information and facilitates sequencing from both terminii. One can imagine, however, situations where confusion may arise with a larger peptide in the assignment of ions. It would perhaps be advantageous to direct the fragmentation so that one specific type of ion is formed upon CA. One approach might be to localize the charge via derivatization. An example would be the formation of a quaternary amine at the N-terminus of the peptide (1). Problems can arise, however, when dealing with small amounts of material if the derivatization is not quantitative.

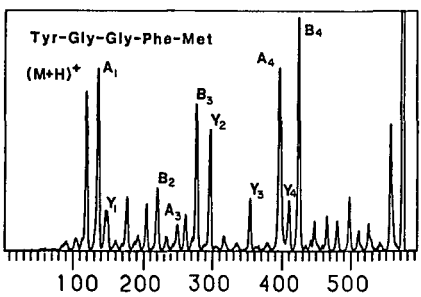

Figure 1

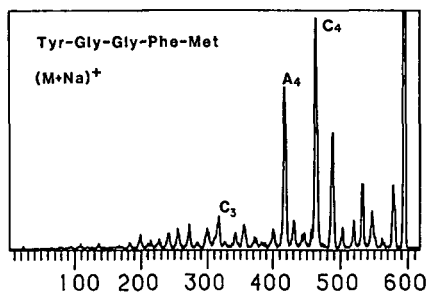

Figure 2

Another approach is to activate cationized species. Cationization may be thought of as a simple, on probe derivatization. The cationization process may be more selective or at least occur at different locations within a molecule than does protonation. The fragmentation of the cationized species may also be quite different than that of a protonated molecule and, thus, provide complementary information. We have acquired the FAB MS-MS spectra of cationized species of several peptides. The cations employed included most of the alkaline earths, Ca^{++}, Mg^{++}, and Ba^{++}, several first row transition metals in their +2 states, and Cu^+ and Ag^+.

The FAB MS-MS spectrum of $(M + Na)^+$ for methionine enkephalin is representative of CAD spectra obtained from peptides cationized by alkali metals (see Figure 2). All fragment ions appear to retain Na. Different fragmentation processes from those observed in the $(M + H)^+$ spectrum are now favored. Only N-terminus fragments are produced; the A and C type ions are now the most abundant species. The major ions arise from loss of portions of one peptide unit.

Similar processes are observed upon collisional activation of methionine enkephalin cationized by Ag^+ (see Figure 3). Again, only N-terminus ions are observed, mainly of the A and C types and Ag is retained in all the fragment ions. There is, however, a much higher abundance of fragment ions produced, with more information available in the low mass region.

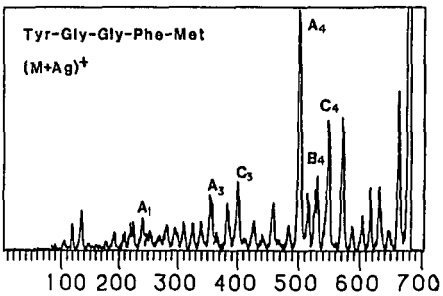

Figure 3

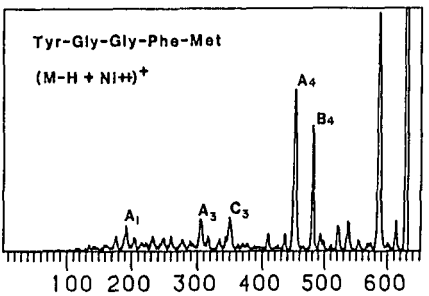

Figure 4

Collisional activation of ions formed by cationization with Ni^{++} yields a rather unique spectrum (see Figure 4). Even though the hydrogen loss is likely from the acid terminus, all fragment ions are N-terminus in nature. Also, loss of CO_2 results in the most abundant fragment ion. These two observations provide evidence that $(M - H + Ni^{++})^+$ exists as a zwitterion, with complexation of Ni^{++} within the peptide chain.

All of the cationized species of methionine enkephaline fragment, upon CA, to preferentially eliminate only one amino acid. This may indicate that the cation is in some way chelated by the remaining four amino acids, possibly through the amide nitrogens. If this model is correct, as the peptide molecule "wraps around" the cation, any extra amino acid units would be "sidechains" in a sense, and would be preferentially eliminated.

The MS-MS spectra of dinucleotides cationized by Ca^{++} (see Figure 5) are quite different from those obtained from their $(M - H)^-$ species. BH elimination, the most abundant processes for the $(M - H)^-$ ions is suppressed for $(M - H + Ca^{++})^+$. Instead, the most abundant ions arise from cleavages in the phosphate linkage, forming the so-called "sequence ions".

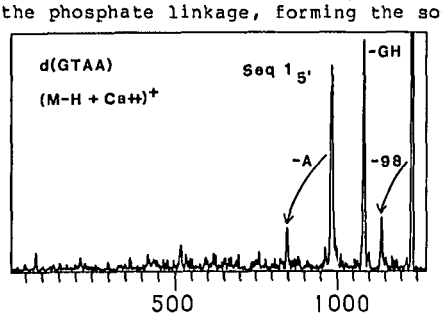

Figure 5

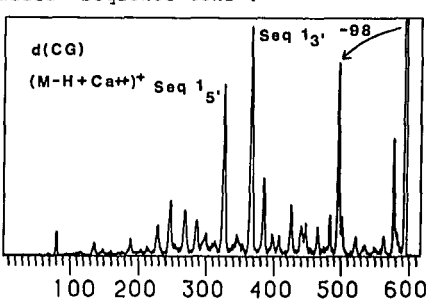

Figure 6

It appears that Ca^{++} is complexed in the dinucleotide either between the two sugar units or the two bases. This provides a second linkage between the two subunits. The cationized species then apparently eliminates H_3PO_4, (98 u). Such a rearrangement/elimination would be a quite novel process, and may hold promise for sequencing larger oligonucleotides (see Figure 6).

1. D.A. Kidwell, M.M. Ross, and R.J. Colton J. Am. Chem. Soc., 106, 2219 (1984).

Presented at the 35th ASMS Conference on Mass Spectrometry and Allied Topics
May 24-29, 1987, Denver, CO

Neutralization Reionization Studies of the Rare Gas Hydrides

Susan F. Selgren and Gregory I. Gellene

Department of Chemistry, University of Notre Dame

Notre Dame, IN 46556

The neturalization reionization mass spectrum of NeD^+ has been obtained using K as a neutralization target and NO_2 as a collisional reionization target (Fig. 1). The appearance of the parent NeD^+ peak in the mass spectrum unambiguously indicates that the netural radical survived the transit time (~0.5μs) from the point of neutralization to that of reionization. Information on the electronic state of the NeD responsible for the observed metastability is provided by the observation of the netural species directly without reionization (Fig. 2). The results of these experiments verify the existance of a long lived state of NeD (central intensity spike in the profiles obtained with K targets) as well as indicate that a substantial fraction of the NeD radicals in the beam undergo unimolecular dissociation producing ground state neon and deuterium atoms. From an analysis of the angular distribution of the netural fragments, a value of 1.4 eV is determined for the kinetic energy released in the dissociation process observed for NeD with K targets. These results can be explained by the existance of a shallow well and dissociation barrier in the ground potential energy curve lying 1.4 eV above the energy of the separated atoms. Such barriers are known to exist for the isoelectronic NH_4, H_3O, and H_2F radicals.

Analagous experiments were performed with the other rare gas hydrides (HeH, ArH, KrH, and XeH) where no evidence for metastability was observed (Fig. 3). The kinetic energy released in the dissociation of these radicals following formation by electron transfer from various target metals were determined from measurements of the angular distribution of the netural fragments. The results, which are summarized in Fig. 4, are readily interpreted in terms of the known states of these radicals.

This work was suppored by the Donors of the Petroleum Research Fund, administered by the American Chemical Society (Grant 16836-G6), the Reserch Corporation, the Notre Dame Jesse H. Jones Research Fund, and the Finnigan MAT Corporation through the American Society for Mass Spectrometry Research Award Program.

Presented at the 35th ASMS Conference on Mass Spectrometry and Allied Topics
May 24-29, 1987, Denver, CO

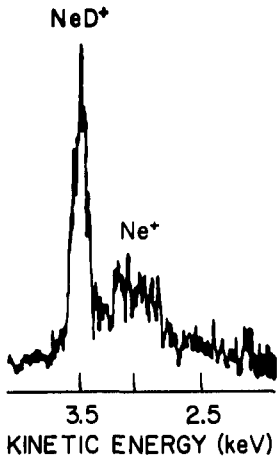

Fig. 1 Neutralization - reionization mass spectrum of NeD^+ using K as a neutralization target and NO_2 as a collisional reionization target.

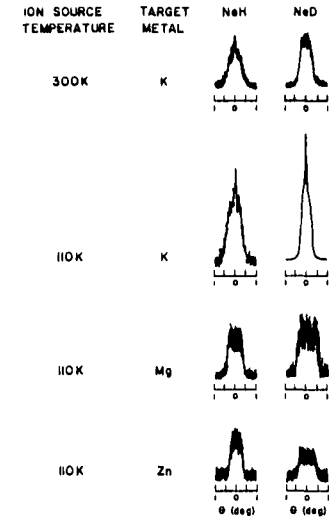

Fig. 2 Angular distribution of neutral dissociation fragments following neutralization of $NeH^+(NeD^+)$ ion beams with various target metals.

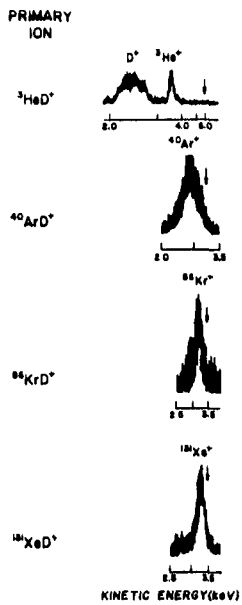

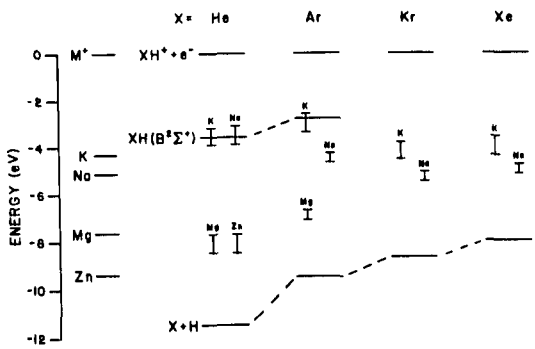

Fig. 4 Energy level diagram showing the relationship between the known states of the indicated rare gas hydrides and the fragmentation energies measured for these radicals produced by neutralization with various target metals.

Fig. 3 Neutralization - reionization mass spectra of the rare gas deuterides obtained using K as a neutralization target and NO_2 as a collisional reionization target. The arrows indicate the position in the mass spectra where the parent ion would be expected if the neutral radicals had survived the transit time between neutralization and reionization.

Presented at the 35th ASMS Conference on Mass Spectrometry and Allied Topics
May 24-29, 1987, Denver, CO

FORMATION OF LARGE CLUSTER IONS IN FTMS BY DIRECT LASER VAPORIZATION

S.W. McElvany, H.H. Nelson, M.M. Ross, and A.P. Baronavski

Code 6110/Chemistry Division
Naval Research Laboratory
Washington, D.C. 20375-5000

The main advantages of Fourier transform ion cyclotron mass spectrometry (FTMS) in studying cluster ion chemistry include the long ion residence times and the MS/MS capabilities which allow the study of ion/molecule reaction chemistry, collision induced dissociation, and photodissociation of mass-selected cluster ions.[1] Direct laser vaporization of solid samples has been utilized extensively as the source of cluster ions in the majority of FTMS studies since it is both a pulsed source of cluster ions and also maintains the low pressures required in the ion cell. Until recently, the range of cluster ion sizes formed by direct laser vaporization has been quite limited when compared to those produced in molecular beam sources. For example, carbon cluster ions, C_n^+, up to n=28 are typically observed by direct laser vaporization of graphite, but a bimodal distribution is observed (1<n<30 and 40<n<150) in the corresponding molecular beam/time-of-flight studies. Also, metal clusters are easily formed in a molecular beam source, whereas direct laser vaporization of the metal usually produces only the monomer ion. The use of a molecular beam cluster source in FTMS, however, is quite difficult and typically requires ionization external to the magnetic field followed by injection of the cluster ions into the ion trap.

In this study, we report the application of a novel, yet simple technique for the formation of large cluster ions (typically observed using molecular beam sources) by direct laser vaporization in the FTMS cell. In a related time-of-flight (TOF) experiment[2], it was observed that under certain experimental conditions in which a small laser-generated hole is formed in the stationary sample, large carbon cluster ions (50<n<180) are formed which are typically not observed by direct laser vaporization. These large cluster ions apparently result from reactions (possibly ion/molecule) which occur in the laser-generated plasma formed in this hole.

This technique for large cluster ion formation appears to be ideally suited for FTMS studies. Under nearly identical experimental conditions, however, the large carbon cluster ions were not observed in the FTMS. The inability to detect these ions apparently results from the presence of the magnetic field in the FTMS (1.0T electromagnet) in which the plasma formation and expansion of both ions and neutrals occurs perpendicular to the magnetic field. In a similar experiment in which the plasma is free to expand along the field lines, as in a superconducting magnet configuration, the large carbon cluster ions are observed as shown in Figure 1.

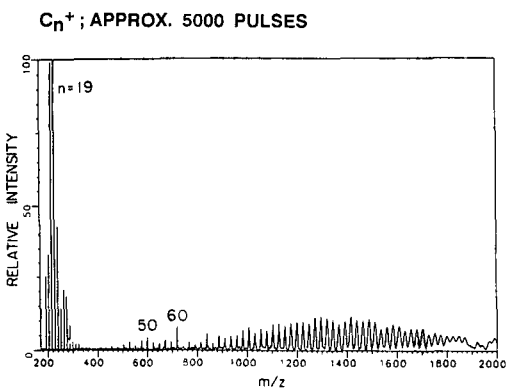

Figure 1.

Several preliminary studies of these large carbon cluster ions (n>50) were performed in the FTMS in attempt to obtain both reactivity and structural information. No ion/molecule reactions were observed between these carbon cluster ions and C_4H_2, although smaller carbon cluster ions (n<20) react quite readily. No fragment ions were observed by either collision induced dissociation (up to 50 eV,lab with Xe) or from infrared multiphoton excitation (cw CO_2 laser ; 10.6um) of these larger carbon cluster ions. These results are consistent with these cluster ions being both unreactive and quite stable.

This technique for cluster ion formation has also been extended to metal and mixed-metal systems. If a pellet consisting of a metal powder and a suitable matrix (e.g. boron nitride, in which a laser-generated hole may be formed) undergoes direct laser vaporization under similar conditions as the carbon cluster formation, it is possible to form metal cluster ions which are not typically observed by direct laser vaporization. An example of this is shown in Figure 2 in which the sample contains both bismuth and antimony powders. Mixed-metal cluster ions, $Bi_xSb_y^+$, are produced which contain up to five metal atoms, and are quite similar in size and distribution to those observed using a molecular beam cluster source.

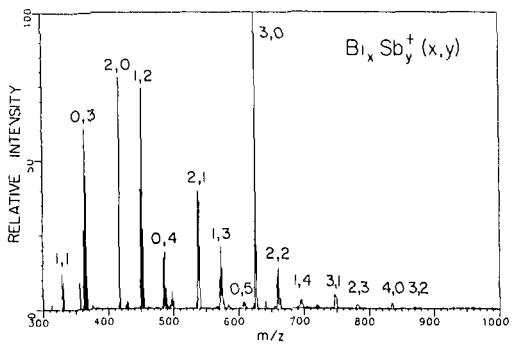

Figure 2.

REFERENCES

1) S.W. McElvany, B.I. Dunlap, and A. O'Keefe, J. Chem. Phys. A6, 715(1987).

2) A. O'Keefe, M.M. Ross, and A.P. Baronavski, Chem. Phys. Lett. 130, 17(1986).

Presented at the 35th ASMS Conference on Mass Spectrometry and Allied Topics
May 24-29, 1987, Denver, CO

THE PHYSICS AND CHEMISTRY OF LASER DESORPTION AND ITS APPLICATION TO MASS SPECTROMETRIC ANALYSIS

F. Hillenkamp, M. Karas. U. Bahr and B. Spengler
Institut fur Medizinische Physik,Universität Münster
Hüfferstr. 68,D-4400 Munster, FRG

Recent progress has been made and interesting results have been reported for two different modes of laser desorption:CO_2-laser desorption at a wavelength in the infrared without spatial resolution, followed by ICR- or time-of-flight (TOF) mass-spectrometers and UV-laser desorption with a few µm resolution, combined with TOF mass spectrometers. For CO_2-laser desorption a thermal process is usually assumed, but very few systematic studies have been reported to ascertain this assumption.This paper reports results, obtained with instruments, which use UV-wavelengths of 266 nm (LAMMA) and 248 nm and 193 nm (MULI). The beams are focused to 3 - 30 µm spots on the sample; ions are detected with a TOF spectrometer, equiped with an ion reflector to improve mass resolution.The MULI-instrument is equiped with a second excimer-dye laser combination for the postionization of laser-desorbed neutrals.

Resonant electronic absorption of molecules to be analyzed has been shown to strongly influence the threshold irradiance for ion generation, aswell as the preferably generated ion species, particularly cationized - and fragment-ions (1). In continuation of these observations the influence of a resonantly absorbing matrix on the desorption of molecules has been investigated. It was shown that molecules in the mid- mass range up to app. 3000 dalton, which, due to lack of absorption could not be desorbed directly without strong fragmentation, will readily desorb when dissolved in absorbing liquid or solid matrices such as tryptophane, nicotinic acid, NPOE or NOBA (2).

In a recent series of experiments the 193 nm wavelenght of an ArF excimer laser was used for desorption studies. In a limited irradiance range near threshold a qualitative difference in the spectra was observed as compared to spectra taken at higher irradiances or at longer wavelenghts. These differences seem to indicate that under such conditions a so far not observed photodesorption process of individual molecules takes place (3).

Fig. 1 shows schematically the instrument used for the postionization of laser desorbed neutrals. The 248 nm line of the first excimer laser was used for desorption in all these experiments, the frequency doubled dye laser, pumped by the second excimer laser was tuned to resonantly excite and ionize the neutrals in the gas phase in front of the sample. In a first series of experiments it has been established that for a selected

Presented at the 35th ASMS Conference on Mass Spectrometry and Allied Topics
May 24-29, 1987, Denver, CO

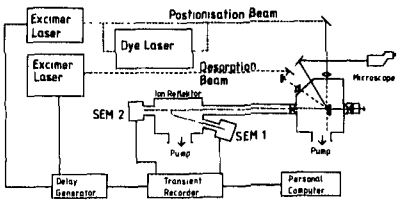

Fig.1 Schematic diagram of the MULI-instrument

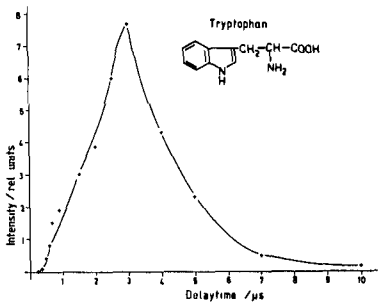

Fig.3 Photoion intensity as a function of delay between the two lasers

group of molecules parent ions with little fragmentation could be obtained; their intensity exceeds that of directly desorbed ions by 1 - 2 orders of magnitude. A variation of the desorption irradiance revealed that the desorption of neutrals begins at irradiances significantly below those for ion emission (Fig. 2). In the extended plateau region, which is reached after a sharp increase in intensity over several orders of magnitude, the intensity of the parent ion and the fragmentation pattern are relatively independent of the desorption irradiance. A variation of the delay time between the two laser pulses yields information about the translational kinetic energy of the neutrals in the fixed space between the sample surface and the postionization beam. In Fig. 3 the intensity of the photoions of tryptophane is plotted as a function of this delay time. The delay of app. 3 µs at peak intensity corresponds to a mean kinetic energy of only 40 meV or desorption at room temperatur. This must be seen in contrast to desorbed ions, which typically have energies of several 10 eV.

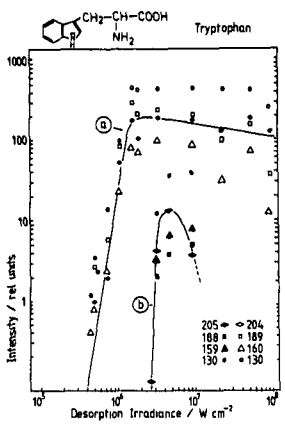

Fig.2 Intensity of photo- (open symbols) and desorbed -ions (filled symbols)

(1) M. Karas, D. Bachmann, F. Hillenkamp: Anal. Chem. 1985,57,2935
(2) M. Karas, D. Bachmann, U. Bahr F. Hillenkamp: Int. J. Mass Spectrom. Ion Proc., in print
(3) U. Bahr, M. Karas, B. Spengler, F. Hillenkamp J. Phys. Chem. submitted

Presented at the 35th ASMS Conference on Mass Spectrometry and Allied Topics
May 24-29, 1987, Denver, CO

APPLICATIONS OF LASER DESORPTION MASS SPECTROMETRY: THE STRUCTURAL ANALYSIS OF BACTERIAL CELL WALL COMPONENTS

Hisako Hara, Plamen Demirev and Robert J. Cotter
The Johns Hopkins University Baltimore MD 21205

Laser desorption mass spectrometry (LDMS) has been employed in our laboratory for the analysis of the polar lipids and lipopolysaccharides found in the cell walls of bacteria. Heller, et.al. (1) have analyzed phospholipids from intact bacterial cells. Takayama, et. al. (2,3) have used laser desorption to establish the structures of lipid-A from the lipopolysaccharides of Salmonella minnesota and Niesseria gonnorhoeae. Lipopolysaccharides are found on the outer wall of the outer membrane of gram-negative bacteria, and are anchored in the membrane by the lipid-A portion, a phosphorylated glucosamine disaccharide with from four to seven fatty acids connected by acyl or amide linkages at the 3,3' and 2,2' positions respectively. Laser desorption fragmentation patterns provide information on the location of the fatty acids (4). Direct losses of the acyl-linked fatty acids are observed, and two-bond cleavages of the reducing sugar ring can be used to establish the identity of the fatty acids attached to the 2 and 3 positions as well as the combined weight of the distal portion of the molecule. In the present study, the method has been extended to the analysis of the non-toxic lipid-A obtained from the LPS of Rhodopseudomonas sphaeroides. In addition, laser desorption has been used to study the effects of growth temperature on the composition of other lipids, primarily serratamolide and ornithine-containing lipid, in the bacteria Serratia marcescens.

The lipid-A from R. sphaeroides consists primarily of the pentaacyl structure:

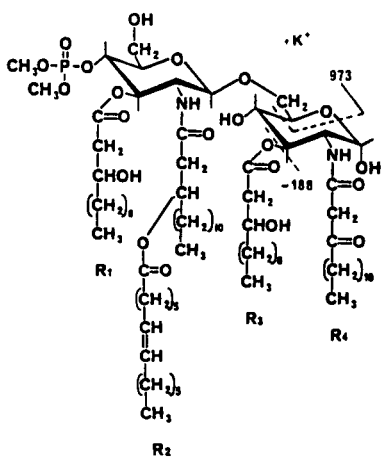

for which the LD mass spectrum is shown in Fig. 1.a. A hexaacyl component was also isolated and is shown in Figure 1.b. The loss of 242 mass units in the latter indicates that the fatty acid (3-hydroxydecanoic acid) at the 3 position has been replaced by a 3-hydroxytetradecanoic acid, and the shift in the peak at 973 amu (Fig. 1.a.) to 1214 amu (Fig. 1.b.) suggests the addition of 3-hydroxytetradecanoic acid, acyl-linked to the 3-hydroxydecanoic acid at position 3'.

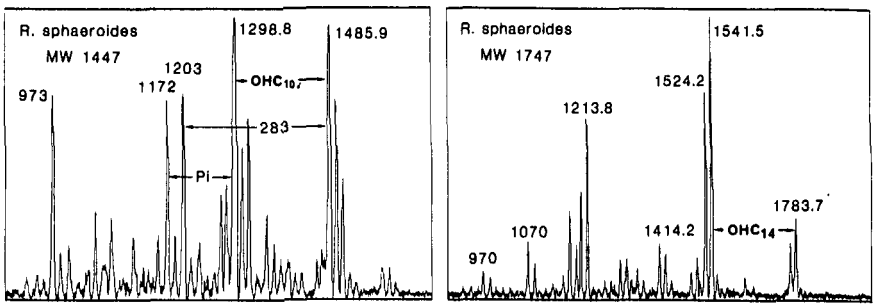

Figure 1.

Fig 2. shows the LD mass spectra of the total lipid extract from Serratia marcescens at growth temperatures of 30° and 37°C. At the higher temperature, longer chain fatty acids are incorporated into the serratamolide, and the concentration of ornithine lipid and phosphatidyl ethanolamines is increased.

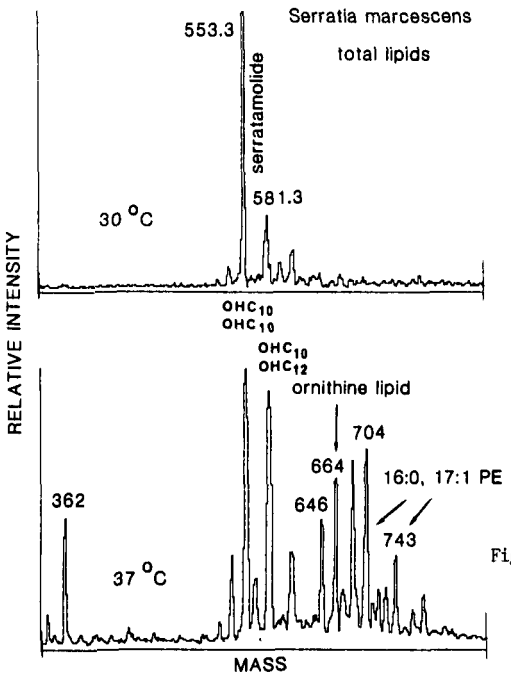

Figure 2.

(1) Heller, D.N., Fenselau,C., Cotter, R.J., Demirev, P., Olthoff, J.K., Honovich, J., Uy, M., Tanaka, T. and Kishimoto, Y.; Biochem. Biophys. Res. Commun., 142 (1987) 194.
(2) Qureshi, N., Cotter, R.J. and Takayama, K.; J. Microbiol. Meth., 5 (1986) 65-77.
(3) Takayama, K., Qureshi, N., Hyver, K., Honovich, J.,Cotter, R.J., Mascagni, P. and Schneider, H.; J. Biol. Chem., 261 (1986) 10624-10631.
(4) Honovich, J., Cotter, R.J., Qureshi, N. and Takayama, K.; Biomed. Environ. Mass Spectrom. (in press).

Presented at the 35th ASMS Conference on Mass Spectrometry and Allied Topics
May 24-29, 1987, Denver, CO

Detection of Nonvolatiles Using Laser Desorption in Atmospheric Pressure Ionization Mass Spectrometry

D. M. Lubman and S. D. Huang
Department of Chemistry
The University of Michigan
Ann Arbor, MI 48109

In this work laser desorption is used to volatilize thermally labile molecules for detection in atmospheric pressure mass spectrometry. In particular, a currently relevant problem is the detection and identification of trace amounts of explosives. One aspect of this problem requires detection of explosive residues in bombing investigations for forensic purposes. This task requires not only sensitive detection on the submicrogram level but very specific identification of the explosive component in a real sample. A limitation though in the application of mass spectrometry to explosives is the volatilization process since these compounds are thermally labile. A means of analyzing these compounds at the lowest possible temperature is preferable to minimize thermally induced fragmentation, thus enhancing mass spectra containing molecular ions. We thus use a combination of ion mobility spectrometry and atmospheric pressure mass spectrometry to explore the detection of explosives with volatilization by laser desorption (1). The mass spectra are obtained in both air and pure N_2 and compared to those obtained by a direct in-beam heated probe. The spectra are obtained generally in the negative ionization mode which appears to be preferable for these compounds. Either molecular ion peaks or fairly simple mass spectra are observed which can be used for identification with detection limits in the 200 pg range for compounds that might otherwise display extensive fragmentation.

The experimental apparatus consists of an ion mobility spectrometer (IMS) interfaced to a Spectra-El Extranuclear Quadrupole mass spectrometer and has been described previously (1,2). The ionization is produced by a ^{63}Ni β foil atmospheric pressure ionization source. Laser desorption was performed using the 532 nm second harmonic of a Nd:YAG laser. The typical laser energy was ~50 mJ or a corresponding power density of 1.5 x 10^6 W/cm^2 at a laser repetition rate of 10 Hz. This may be as much as two orders of magnitude below the power densities used in typical laser desorption (LD) experiments where desorption and ionization is performed in one step. In this work, however, the low-powered laser pulse desorbs mainly neutral species from the Macor ceramic surface probe. The desorbed neutrals are subsequently ionized by the API source with either positive or negative ions analyzed in the IMS or APIMS (see Fig. 1). Vaporization may also be achieved by raising the temperature of the cell so that the bath gas directly heats the sample on the ceramic probe. This in essence is a form of direct in-beam heating probe which minimizes decomposition that might occur upon extensive contact with glass or metal surfaces.

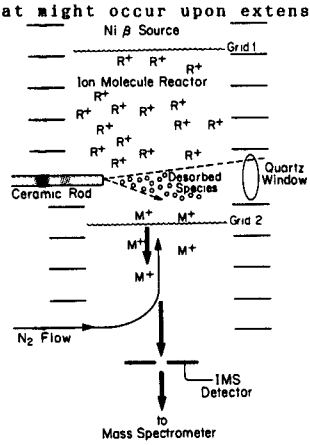

Figure 1: Laser Desorption APIMS Set-Up

In figure 2 is shown the API mass spectrum for both the positive and negative mode of a sample of zone-refined TNT. This mass spectrum was obtained using laser desorption at a temperature of 40°C or by using the heating probe technique at 90°C and the spectra obtained were found to be identical in both cases. In pure N_2 background gas a strong M^- molecular ion is observed along with a second smaller peak at mass 209 which corresponds to loss of 18 mass units and is probably due to elimination of an H_2O molecule. In air the $(M-H)^-$ peak is observed at m/z=226 rather than M^- due to abstraction of H by O_2. The ions obtained in the APIMS of TNT as well as the other compounds studied are generally also observed in chemical ionization MS (3). However, the positive mode appears to be very sensitive to the conditions present in the cell including background contamination and the temperature. The negative mode is the preferable means of detection since it appears to be less subject to the conditions used. The appearance of the M^- or $(M-H)^-$ peaks are a strong indication of the presence of TNT. The IMS of TNT in N_2 has been studied and the M^- peak corresponds to a characteristic reduced mobility of k_o=1.49 cm^2/Vsec in the negative mode. Detection of TNT in the picogram range has been demonstrated in the negative IMS mode (4). In this work detection of TNT in air using LD-APIMS and LD-IMS has been accomplished in the negative mode for an impure military block sample with the presence of a strong IMS peak at k_o= 1.53 cm^2/Vsec which corresponds to the $(M-H)^-$ peak.

RDX and HMX have significantly higher melting points than TNT or DNT and thus laser desorption is a particularly valuable means of volatilizing these compounds at relatively low temperature. This is demonstrated in Fig. 3 for RDX which compares the signal observed at 100°C in N_2 (500 counts) obtained by (a) heating and (b) laser desorption. It is apparent in this case that laser desorption enhances the volitilization process at relatively low temperature.

ACKNOLWEDGMENTS

We acknowledge support of this work from the Army Research Office under Grant #DAAG29-85-K-1005 and also the Department of Defense through the U. S. Army Research Office under Grant #DAAG29-85-G-008 for purchase of the equipment used in this work.

REFERENCES

1. Kolaitis, L.; Lubman, D.M. Anal. Chem. 1986, 58, 2137.
2. Kolaitis, L.; Lubman, D.M. Anal. Chem. 1986, 58, 1993.
3. Yinon, J. Mass. Spec. Reviews 1982, 1, 257.
4. Karasek, F.W.; Denney, D.W. J. Chrom. 1974, 93, 141.

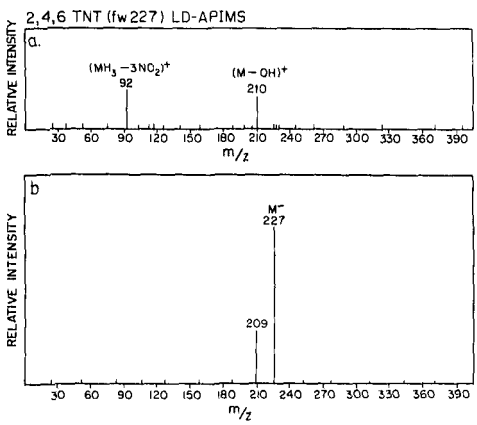

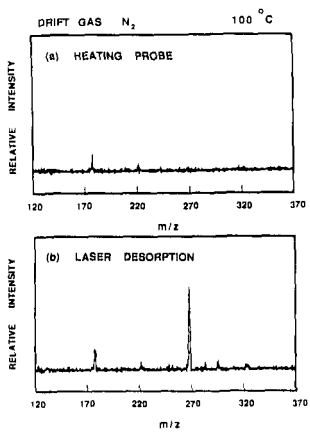

Presented at the 35th ASMS Conference on Mass Spectrometry and Allied Topics
May 24-29, 1987, Denver, CO

POST IONIZATION OF NEUTRALS ABLATED IN LASER MICROPROBE MASS SPECTROMETRY

B. Schueler, R.W. Odom, and C.A. Evans Jr.
Charles Evans & Associates, 301 Chesapeake Drive, Redwood City, CA 94063

Introduction: Laser microprobe mass spectrometry is a microanalytical materials characterization technique in which the surface composition is determined by measuring the mass and intensity of elemental and/or molecular ions created by the interaction of a high-power laser pulse with the target surface. It is well known, however, that most of the laser ablated material is not ionized. At laser irradiances on the order of 10^9 W/cm^2, charge-to-neutral ratios (y^+/y°) are typically $\leq 10^{-4}$. These ionization efficiencies can be significantly smaller for elements such as As, Hg, Zn which have a relatively high ionization potential. One method of increasing the ionization efficiency for these elements is to irradiate the plume of ablated neutrals with a second high irradiance laser pulse and to record the mass spectra of these post-ionized neutrals.

Experimental: The post-ionizing laser is a high power Q-switched (τ~5ns), frequency quadrupled (λ = 266 nm) Nd:YAG laser which has been coupled to a LIMA 2A laser microprobe system together with focusing optics. The ablating laser pulse (τ~5ns, λ = 266 nm) irradiates a ~2 μm diameter spot on the target causing the emission of charged and neutral particles. At a time interval Δt (adjustable between 0 and 2700 ns) later, the ionizing laser is fired parallel to the target surface and focused to a ~100 μm diameter spot 0.6 μm above the target. The photon flux densities in this region are $\geq 7\cdot 10^{28}$ cm^{-2}s^{-1} ($\geq 5\cdot 10^{10}$ W/cm^2) which is sufficient to achieve unit probability for nonresonant two photon ionization of all atoms and molecules having ionization potentials $\leq$9.32 eV. The spectrometer can be tuned by adjustment of the sample accelerating potential so that the ablated ions are transmitted through the ion mirror (and hit the spectrometer housing) and only post-ionized (PI) neutrals are detected.

Results

a) Sensitivity: A variety of targets such as GaAs, HgCdTe, steels etc. have been studied using this non-resonant PI of the ablated neutrals.[1] Post-ionized neutrals are generally detected at ablating laser irradiances which produce no observable ablated ion signals. At moderate ablating laser irradiances (in the vicinity of the detection threshold for ablated ions), the PI ion intensities are typically factors of 10 larger than the primary ablated ion signal. In some cases, e.g. Hg^+, from HgCdTe, the increase in ion yield for the PI mode is 10^4 times larger. Under typical ablating laser irradiances, the laser craters are usually smaller than the light microscopical resolution limit of ~0.5 μm. The increased sensitivity of the PI analysis reduces the ablation volume required to produce useful ion signal intensities and therefore the PI analysis is significantly more surface sensitive than the conventional laser microprobe. An example comparing the analysis of $Hg_{0.78}Cd_{0.22}Te$ by laser ablation and laser ablation - post ionization using identical ablating laser irradiances is illustrated in Fig. 1a and b. The most pronounced differences between the two mass spectra is the high intensity Hg^+ signal observed in the PI mode as well as the significant reduction in the $CdTe^+$ and Te_2^+ signals. The PI spectrum also gives a better qualitative picture of the actual target composition.

b) Quantitation: The single PI analysis (one ablating and one ionizing laser shot at a selected delay time Δt) appears to provide better quantitative information on the target composition than the conventional laser microprobe analysis. Cluster ions and organic background signals are generally much less intense in the PI spectra, and this greatly reduces the potential for mass spectral interferences. The PI analysis does generate some interference peaks including H^+, C^+, C_2^+, C_2H^+ produced from the ionization of residual gases in the vacuum system and from doubly charged metal ions (Fe^{++}, W^{++}, Mo^{++}).

If more quantitative information on the target stochiometry is required, a more detailed knowledge of the neutral emission dynamics is often necessary. This information can be obtained by measuring the PI ion intensities as a function of Δt for fixed ablating and ionizing laser irradiances. Fig. 2 illustrates the results of such a measurement for the $Hg_{0.78}Cd_{0.22}Te$ target. Each data point in this figure is the average of seven PI analyses. Ideally, the ion intensity ratios measured in a PI analysis of a multielement target would correctly measure the sample stoichiometry. The PI intensity ratios can be evaluated in several ways:

(1) integrating the ion intensities over the measured delay time range

(2) transforming these time distributions into velocity distributions and integrating over velocity or

(3) ratioing the intensities observed at the Δt value corresponding to the maximum intensity for elemental emission.

The delay time integration and Δt maximum (Δt = 500 ns, corresponding to the first peak in the elemental Hg emission) yield Cd^+/Te^+ ratios of 0.218 ±0.009 and 0.218 ±0.007, respectively, which are in excellent agreement with the true Cd/Te elemental ratio of 0.22 ±0.01. Both Cd and Te can be ionized via 2-photon processes under the experimental conditions employed and satisfactory quantitative results are obtained. The ionization of Hg, however, requires a 3-photon ionization process. Since the three photon ionization efficiency is greatly reduced in comparison to the two photon process, the Hg^+ PI intensity is under represented in this analysis by a factor of ~ 10.

1. B. Schueler and R.W. Odom, J. Appl. Phys. 61 (9), 4652 (1987)

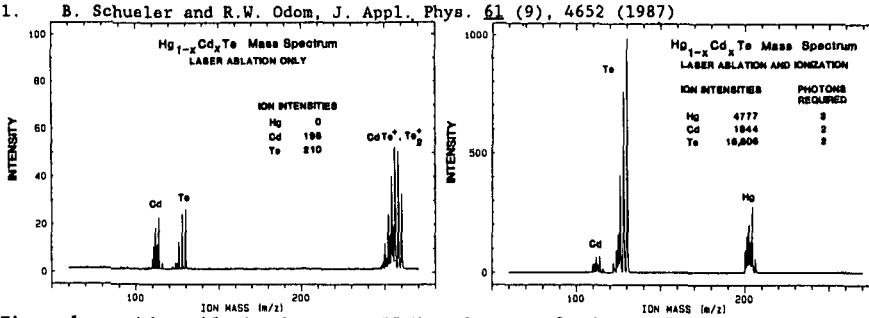

Figure 1a. and b. Ablating Laser and PI Mass Spectra of a HgCdTe Target

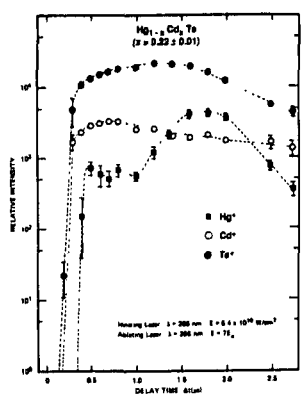

Figure 2. Delay Time Intensities from PI Analysis of a HgCdTe Target

Presented at the 35th ASMS Conference on Mass Spectrometry and Allied Topics
May 24-29, 1987, Denver, CO

GAS PHASE STUDIES OF LASER DESORBED PYRIDINIUM CATIONS

Clifford H. Watson, Gökhan Baykut,* Alan R. Katritzky

University of Florida, Department of Chemistry, Gainesville, FL 32611

* Ion Spec, Skypark Circle, Suite K, Irvine, California 92714

The use of pulsed lasers to desorb involatile species has been quite successful in recent years,[1] particularly in conjunction with Fourier transform ion cyclotron resonance (FTICR) mass spectrometry. Initial success in our laboratory with pyridinium ions suggested that this class of charged species could be produced and studied in the gas phase by laser desorption FTICR mass spectrometry. Comparing results from collisionally activated dissociation (CAD) studies of laser-desorbed N-alkylpyridinium cations has shed considerable light on their behavior.

All mass spectrometric studies were carried out in a Nicolet FT/MS-1000 FTICR mass spectrometer. The instrument was operated in a broad band mode, which corresponds to a mass range of 17-3000 daltons. Ions were detected by the standard frequency-chirp excitation method. Because of the high ionization efficiency of laser desorption 5-10 formation/detection cycles were usually sufficient to obtain a spectrum with a high signal-to-noise ratio. Laser desorption was accomplished by the use of the Lumonics pulsed carbon dioxide laser and the standard Nicolet laser interface.

Collisionally activated dissociation of the laser desorbed ions was carried out using a novel event sequence (Figure 1) in order to obtain more accurate information about the extent of fragmentation. The number of ions generated by successive laser desorption pulses often differed substantially, mostly because of sample depletion and heterogeneities of sample distribution on the surface of the probe tip. Therefore, it was necessary to acquire both pre-CAD and post-CAD mass spectra in the same event sequence without quenching and re-forming the ions. After the laser pulse and a delay time, the ions were excited to higher kinetic energy, detected, allowed to collide with an argon or xenon buffer gas, and detected a second time.

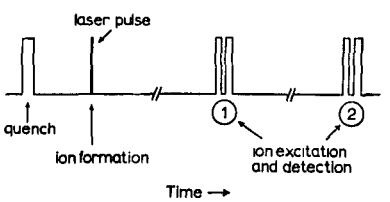

Figure 1.

We found two distinct pathways for CAD: compounds (1) in which R is an adamantyl, benzyl, p-methoxybenzyl, or triphenylmethyl group yield pyridine (3) and the corresponding carbocation (4) (see scheme 1). However, those compounds (5) in which R is ethyl, i-propyl, or t-butyl apparently dissociate by beta-elimination to yield a strain-free olefin (9) together with the pyridinium cation (see scheme 2).

Presented at the 35th ASMS Conference on Mass Spectrometry and Allied Topics
May 24-29, 1987, Denver, CO.

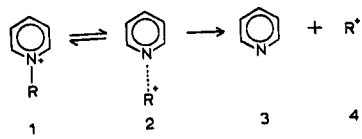

1 2 3 4

Scheme 1.

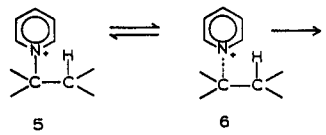

5 6

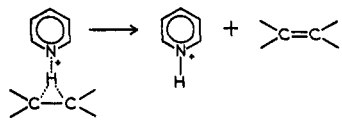

7 8 9

Scheme 2.

There is considerable evidence that alkylammonium cations undergo gas phase unimolecular fragmentation,[2] and we believe that such complexes are involved in both pathways mentioned. These complexes correspond to ion/molecule pairs for which evidence has been obtained in solution.[3]

A novel feature of this work is the determination of relative dissociation rates by simultaneous generation of two species of ions and observation of their subsequent fragmentation. Ions formed by laser desorption of a binary mixture of two pyridinium salts were allowed to collide with a buffer gas. By increasing either the buffer gas pressure or the total collision time relative changes in ion abundance were measured.

Among the ions which are constrained to decompose by the pathway of Scheme 1, there is a clear stability order:

1-adamantyl > benzyl > p-methoxy-benzyl > triphenylmethyl.

This is the order expected if the stability of the carbocation formed is the dominant factor influencing dissociation.

Also, for the ions which decompose by the pathway of Scheme 2, there is a stability order:

methyl > ethyl > i-propyl > t-butyl.

Acknowledgement

This work was supported in part by the Office of Naval Research.

References

1. F. Hillenkamp in Ion Formation from Organic Solids, A. Benninghoven, Ed., Springer-Verlag (Berlin, 1983).
2. a) R. D. Bowen, J. Chem. Soc. Perkin II, 1982, 409; 1980, 1219.
   b) C. R. Moylan and J. Brauman J. Am. Chem. Soc. 1985, 107, 761.
3. A. R. Katritzky and G. Musumarra, Chem. Soc. Reviews, 1984, 13, 47.

Presented at the 35th ASMS Conference on Mass Spectrometry and Allied Topics
May 24-29, 1987, Denver, CO

Fast Pulse Measurement in Resonance Ionization Mass Spectrometry with Time-of-Flight Detection

L.W. Green, R.G. Macdonald, F.C. Sopchyshyn
Chalk River Nuclear Laboratories, Chalk River, Ont., Canada, K0J 1J0

Time-of-flight mass spectrometers (TOFMS) are well suited for detection of resonance ionization signals from pulsed lasers because of their high sensitivity, simple structure, and ability to record the entire spectrum from each pulse. However, application of the TOFMS to isotope ratio measurements has been hindered by the difficulty of measurement of fast pulse signals with high precision. In this work several fast pulse detection systems were evaluated, and the precision controlling factors were identified.

A one meter linear TOFMS, equipped with a low-noise microchannel plate detector, was fabricated to test the pulse measurement techniques. Barium was used as the sample metal, because of the wide range in abundance and multiplicity of its isotopes. Barium was ionized by a resonant two-colour, three-photon process for which λ_1 was 5535.48 A° and λ_2 was 5784.1 A°. The mass resolution was ~400 ($M/\Delta M$, ΔM at 5% of peak height). Two detection methods were used in this laboratory; transient recording with signal averaging and gated pulse counting, and a third, time-to-digital conversion and counting, in other laboratories (1,2).

Single ion pulses were characterized by a full width half maximum of 5 ηs and amplitudes between 10 and 200 mV, depending on the detector gain setting. Multiple ion bunches were up to 40 ηs wide and 600 mV in amplitude. For accurate transient recording of these pulses, a digitizer with at least 8 bits vertical resolution, .5 ηs/pt horizontal resolution, and 300 MHz bandwidth was required. Several digitizers with specifications close to these are available, but their data processing rates are such that laser pulse rates of only 1 Hz may be used, which results in excessively long data collection times and large duty cycle losses. A digitizer was used that featured 6 bits vertical resolution, 2 ηs/pt horizontal resolution, and repetition rates of up to 200 Hz. Signal averaging of many spectra (256 K) and integration of the counts under each peak showed that relative standard deviations of isotope ratios were ~5% for the major isotopes and larger for the minor isotopes. The major precision controlling factor was the 6 bit resolution of the digitizer, especially since its full range could not be used to avoid overshoot problems from the odd large ^{138}Ba spikes.

With the gated pulse counting technique, analog to digital conversions were not required and the limitations of digitizers were avoided. The system assembled for gated pulse counting is shown in Figure 1. The signal was amplified and connected to a discriminator with four fold fan-out. Each of the four discriminator outputs were AND'ed with delayed gate pulses in a 4-channel AND logic unit; each of the delayed gate pulses were centered on a selected isotope of Ba. Gate pulse widths were set to ~60 ηs, sufficient to capture all ions of the selected mass but narrow enough to avoid ions of the adjacent mass. The outputs of the AND logic unit were counted in four separate channels of a 125 MHz scaler and isotope ratios were read directly from the accumulated counts in each channel. With more modules, any reasonable number of isotopes could be measured. With this system laser repetition rates of up to 10 kHz could be used, the upper limit is due to overlap of successive time-of-flight mass spectra.

Replicate analyses, in each of which 10,000 counts were accumulated for ^{138}Ba and 1000-2000 counts for masses 135 to 137, yielded relative standard deviations of ~2.5% for isotope ratios of the major isotopes. These results are as expected from counting statistics; accumulation of significantly more counts would have been too lengthy with the excimer pump laser which lost power rapidly at rates > 50 Hz, but could be achieved readily with a copper vapour laser. Signal strengths were kept low to avoid pulse pile-up errors.

In the time-to-digital conversion method, which is being developed by the authors of references 1 and 2 and not by us, the signal was connected through an amplifier and discriminator, to a time-to-digital converter (TDC) that precisely recorded the arrival times of up to 8 pulses. Signal strengths were set sufficiently low that less than 8 ions were formed per laser pulse, and the arrival time data were rapidly read and stored before the next laser pulse. With a high speed computer interfaced directly to the TDC, pulse repetition rates of up to 4 kHz could be used. The resultant data formed a histogram of accumulated pulse counts, and isotopic abundance data could be readily extracted. This technique is relatively new, and although well resolved mass spectra have been reported (1,2), isotopic abundance data have not. The recorded data are essentially pulse counting data, and should be comparable to those obtained by the gated pulse counting technique. The TDC method avoids the gate pre-selection requirement of the latter, but requires relatively expensive computers to rapidly read and store the TDC data.

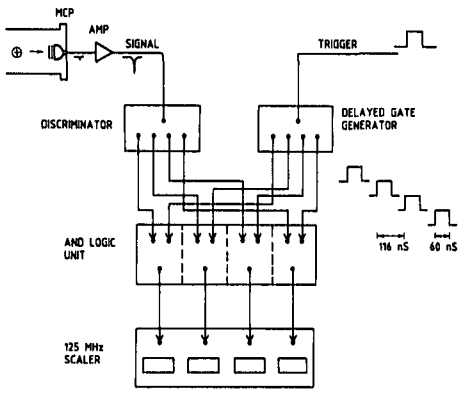

Figure 1. Four channel gated pulse counter.

1. Ens, W.; Beavis, R.; Bolbach, G.; Main, D.; Schnelter, B.; Standing, K.G. Nucl. Instr. Methods Phys. Res. A245 (1986) 146-154.

2. Rimke, H.; Penser, P.; Sattelberger, P.; Trautmann N.; Hermann, G.; Ruster, W.; Ames, F.; Kluge, H-J.; Otten, E.W. Inst. Phys. Conf. Ser. No. 84: Section 6 (1986) 235-238.

Presented at the 35th ASMS Conference on Mass Spectrometry and Allied Topics
May 24-29, 1987, Denver, CO

APPLICATION OF SEMI-VOST METHODOLOGY TO THE MEASUREMENT OF ORGANIC EMISSIONS FROM HAZARDOUS WASTE INCINERATORS

J. T. Bursey, J. L. Steger, M. A. Palazzolo, D. J. Benson,
R. L. Porch, J. A. Rice, J. B. Homolya, R. A. McAllister,
J. F. McGaughey, D. E. Wagoner
Radian Corporation
Research Triangle Park, NC 2779

J. N. Margeson, J. E. Knoll, M. R. Midgett
U.S. Environmental Protection Agency
Research Triangle Park, NC 27711

The Solid Waste Disposal Act, amended by the Resource Conservation and Recovery Act of 1975 (RCRA), requires that EPA establish a national regulatory program to ensure that hazardous wastes are managed in a manner which does not endanger human health or the environment. The statute requires EPA to promulgate performance standards for hazardous waste management. Included in the regulations are provisions for waste disposal by incineration and requirements that hazardous waste incinerators be so operated that principal organic hazardous constituents (POHCs) are destroyed and/or removed with a minimum efficiency of 99.99%. To determine Destruction and removal Efficiency, EPA has designated the Semi-VOST Method to measure flue gas concentrations of POHCs with boiling points greater than 100°C. The Quality Assurance Division of the EPA Environmental Monitoring Systems Laboratory has the responsibility to evaluate and standardize EPA source test methods. In applying Semi-VOST methodology, gaseous and particulate components are isokinetically withdrawn from an emission source and collected in a multicomponent sampling train. Under contract to EPA, Radian Corporation is providing technical assistance to evaluate the Semi-VOST Method: to provide the data necessary to determine bias, precision, applicability, and limitations of the method by a multi-task effort involving literature, laboratory, and field studies. An initial field test,utilizing a quad-train approach, provided preliminary data on method bias and precision.

After collection of the samples in the field, train components were extracted with methylene chloride, the extracts concentrated, and compounds of interest were quantified using high resolution gas chromatography coupled with low resolution mass spectrometry. The first field test showed that: 1) method precision and bias are compound-specific; 2) the distribution and recovery of POHCs in the various components of the sampling train are related to compound boiling point, compound water solubility, and chemical functionality. Subsequent to the first field test, an extensive series of laboratory experiments was performed to modify the dynamic spiking apparatus and procedures used in the first field test. Since previous experiments had shown that recoveries of certain compounds were poor or variable, laboratory experiments were performed to determine the extent and nature of compound interactions with components of the sampling train. Water soluble compounds may form salts by reaction with the wet and acidic environment normally encountered in stack emissions. These water soluble compounds are also collected in the aqueous portions of the sampling train and are poorly recovered by solvent extraction. The Semi-VOST analytical procedure was revised by pH adjustment to improve the recovery of basic and water soluble compounds. A screening procedure was also developed to determine the optimal extraction solvent and to estimate the recovery of test compounds from acidic water condensates using the present Semi-VOST methodology. In the second field test, five deuterium labeled gaseous compounds were dynamically spiked into four simultaneously operating Semi-VOST trains at a a hazardous waste incinerator equipped with a wet scrubber. Results from the laboratory experiments and the second field test provided precision and bias estimates for the test compounds (see Table 1), and provided an evaluation of laboratory-determined compound retention volumes on the solid sorbent through a series of distributive volume experiments. Data were evaluated from gaseous dynamic spiking and

liquid spiking of the test compounds on XAD-2^R resin, and the effects of sample storage time on sample stability were investigated. The use of surrogate standards during sample preparation and analysis is necessary to obtain the best representation of test compound recoveries. Deuterated *analogs, when available, are the best possible surrogates because they* behave exactly the same as the compounds of interest and will be truly representative of compound recoveries. A comparison was made between observed and spiked levels of five compounds spiked onto resin as quality control samples provided by the Research Triangle Institute. Average bias for all the compounds was -4.7%, an excellent agreement between spiked and observed values. Experimental results support the selection of the Semi-VOST method as the method of choice for sampling flue gas emissions for organic compounds with boiling points greater than 100°C.

This work was supported by the Environmental Monitoring Systems Laboratory, *Office of Research and Development U.S. Environmental Protection Agency,* under EPA Contract No. 68-02-4119.

DISCLAIMER

Although the research described in this abstract has been funded wholly or in part by the U.S. Environmental Protection Agency by contract to Radian Corporation, it has not been subjected to Agency review and, therefore, does not necessarily reflect the views of the Agency and no official endorsement should be inferred.

Table 1. BIAS AND PRECISION

Compound	Number of Valid Samples	Mean % Recovery	Percent Bias	Precision: Standard Deviation	Precision: Percent Coefficient of Variation
D_5-Pyridine	16	71.0	-29.0	12.6	17.7
D_8-Toluene	13	85.1	-14.9	12.4	14.6
D_5-Chlorobenzene	13	86.2	-13.8	11.8	13.7
D_{10}-o-Xylene	13	99.1	-0.9	8.0	8.1
D_2-Tetrachloroethane	13	81.5	-18.5	26.8	32.9

Table 2. RESULTS OF ANALYSIS OF RTI CONTROL SAMPLES

Compound	Expected Level, ug	Determined Levels, ug[1] (1)	(2)	(3)	Mean Observed Level (ug/module)	% Bias
Pyridine	1,963.8	1924	1942	1905	1,923.7	-2.04
Toluene	866.9	850	822	824	832.0	-4.03
Chlorobenzene	221.1	216	214	221	217.0	-1.84
1, 1, 2, 2-Tetrachloroethane	159.5	146	147	143	145.3	-8.90
o-Xylene	880.2	818	829	820	822.3	-6.50
Dodecane	748.8	.	.	.	.	.
				Overall Average % Bias		-4.68

[1] Values corrected for Surrogate Recovery

[2] $\% \text{ Bias} = \frac{\text{Mean Observed-Expected Level}}{\text{Expected Level}} \times 100$

Presented at the 35th ASMS Conference on Mass Spectrometry and Allied Topics
May 24-29, 1987, Denver, CO

FAB MS/MS TECHNIQUE FOR CERTIFICATION OF PESTICIDE STANDARDS

Y. Tondeur**, G.W. Sovocool, W.J. Niederhut**, and J.R. Donnelly*
U.S. Environmental Protection Agency and *Lockheed-EMSCO P.O. Box 15027,
Las Vegas, Nevada 89114 and **Environmental Research Center (ERC),
University of Nevada, Las Vegas, NV 89119

The U.S. Environmental Protection Agency maintains a quality assurance repository of pesticide standards for environmental monitoring studies. While many standards can be certified as to identity and purity by conventional chromatographic and mass spectrometric techniques, certain standards such as the heterocyclic amine cation herbicides paraquat(1) diquat dibromide(2), and difenzoquat(3) are nonroutine to analyze. Therefore, the applicability of fast atom bombardment (FAB) MS and MS/MS for certification was investigated using a VG Model ZAB-3F (8kV, Xe FAB reagent gas, He CAD reagent gas). This technique was found to provide useful structural information for the certification of these herbicides. Paraquat and related compounds are known to have high toxicity and to be unsuitable for gas chromatographic analytical techniques. Immunoassay systems have also been developed for these intractable environmental contaminants.

FAB MS was tested using a variety of matrices including glycerol, d_8-glycerol, thioglycerol, and glycerol/dimethylformamide (DMF). Singly charged ions were found in the cases of diquat dibromide and paraquat representing the dication plus one chloride or bromide anion, resulting in a monocation. In the case of paraquat (m/z 221 see Fig. 1), this assignment was confirmed by loss of 35 Daltons under collisionally activated decomposition (CAD) MS/MS conditions. This fragment (m/z 186, $C_{12}H_{14}N_2$) was the base peak in the FAB mass spectrum of paraquat, corresponding to a one-electron reduction of the di-(quarternary pyridinium) ion. This paraquat ion yielded an intense loss of methyl in both thioglycerol and glycerol/DMF matrices. Other daughter ions, assigned losses, and ion compositions in the CAD MS/MS (EB_2 scan) of paraquat are: 185, 184, 171($-CH_3$), 170, 169, 158($-C_2H_4$ or $-H_2CN$), 157, 156, 155($-H_2CNH-2H$), 154, 153, 144($-CH_3-HCN$), 143, 142, 132, 131, 130($-CH_3NCHCH_2$), 129, 128, 118($-CH_3NCHCHCH$), 117, 116, 115, 93 (see Fig. 2). The ion at m/z 93 could be rationalized as (1) a fragment whose composition corresponds to exactly one-half of the parent ion (C_6H_7N), resulting from fission of the bond between the two pyridine rings, or (2) the doubly charged dication appearing at 1/2 (m/z). This interpretation was supported by the presence of ions at m/z 92.5, 91.5, and 79.5, corresponding to the doubly charged ions 185^{+2} $[(M-H)^{+2}]$, $183^{+2}(M-2H)^{+2}$, and 159^{+2} $[(M-29)^{+2}]$ respectively, resulting from loss of an electron from the radical cation species. Since the $^{13}C_1$ isotopic glycerol matrix ion at m/z 186 $[(C_3H_8O_3)_2+H]^+$ loses $C_3H_8O_3$ to form ions of m/z 93 and 94 in 1:1 ratio, matrix contribution to m/z 93 intensity should not exceed that at m/z 94. In glycerol, 93/94 was observed to be 4/1; the assignment of m/z 93 intensity to the analyte was confirmed by use of thioglycerol matrix. A study of paraquat in d_8-glycerol matrix did not give evidence of any exchangeable hydrogens in the analyte.

Results obtained on diquat dibromide (see Fig. 3) were analogous to those of paraquat. The dication plus one bromide anion (yielding a monocation) was observed at m/z 263 (with Br_1 isotope cluster). The dication had undergone one-electron reduction to the radical cation and was observed at m/z 184 ($C_{12}H_{12}N_2$). MS/MS experiments on diquat dibromide m/z 184 ion showed the following daughter ions: 169($-CH_3$), 157(-HCN), 156(-HCNH or $-C_2H_4$), 129($-HCN-C_2H_4$), 128(-2HCNH or $-C_2H_4$-HCNH) and 106($C_5H_5NCHCH_2$; $-C_5H_4N$); see Fig. 4.

Difenzoquat is the methanesulfate salt of a pyrazolium monocation. Under FAB conditions in a glycerol/DMF matrix the higher mass cluster ion consisting of two pyrazolium cations and one counter ion was observed at m/z 609. A minor intensity adduct ion was also found corresponding to the addition of one thioglycerol to the above cation (m/z 717; see Fig. 5). The cluster ion at m/z 609 yielded on CAD-MS/MS the ion corresponding to the difenzoquat pyrazolium cation ($C_{17}H_{17}N_2$) at m/z 249. The cation at m/z 249 under CAD (EB_2 mode) resulted in the formation of the following fragments: 248, 247, 234($-CH_3$), 219($-2CH_3$ or CH_3NH), 208, 206, 193($-C_2H_4N_2$), 131[$C_6H_5C(CH)NCH_3$], 118($C_6H_5CNCH_3$), 104($C_6H_5CHCH_2$), 103, 102, 91(C_7H_7), 77(C_6H_5), 51(C_4H_3); see Fig. 6. Under negative ion FAB in glycerol/DMF, difenzoquat yielded ions of m/z: 111($CH_3OSO_3^-$, with sulfur isotopes at 112, 113), 97($HOSO_3^-$), 96(OSO_3^-), 80(OSO_2^-), 65($HOSO^-$) and 64(OSO^-); see Fig. 7.

Presented at the 35th ASMS Conference on Mass Spectrometry and Allied Topics
May 24-29, 1987, Denver, CO

PARAQUAT

(1)

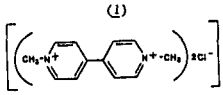

DIQUAT DIBROMIDE

(2)

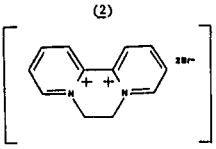

DIFENZOQUAT

(3)

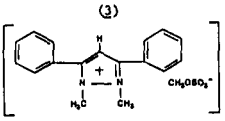

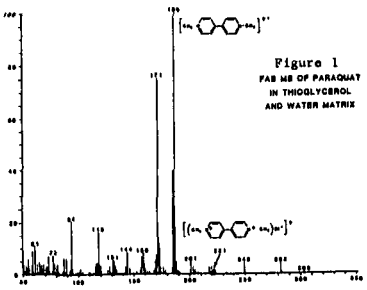

Figure 1
FAB MS OF PARAQUAT IN THIOGLYCEROL AND WATER MATRIX

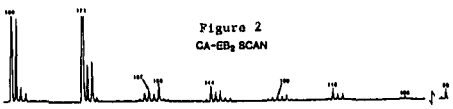

Figure 2
CA-EB$_2$ SCAN

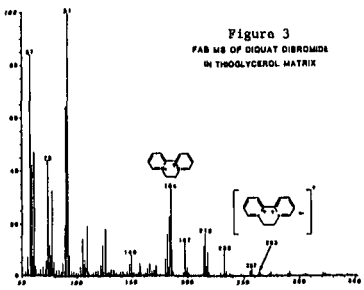

Figure 3
FAB MS OF DIQUAT DIBROMIDE IN THIOGLYCEROL MATRIX

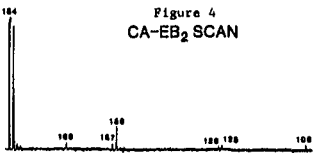

Figure 4
CA-EB$_2$ SCAN

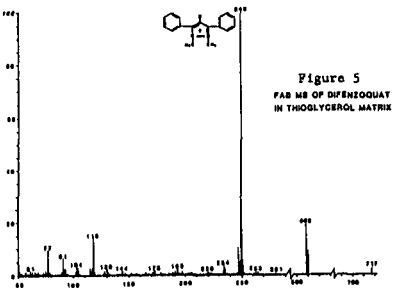

Figure 5
FAB MS OF DIFENZOQUAT IN THIOGLYCEROL MATRIX

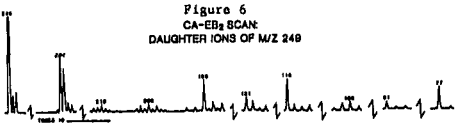

Figure 6
CA-EB$_2$ SCAN:
DAUGHTER IONS OF M/Z 249

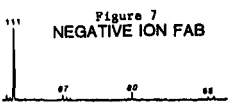

Figure 7
NEGATIVE ION FAB

NOTICE: Although the research described in this article has been funded wholly or in part by the Environmental Protection Agency contract 68-03-3249 to Lockheed-EMSCO and contract 68-01-7159 to ERC, it has not been subject to the Agency's review and therefore does not necessarily reflect the views of the Agency, and no official endorsement should be inferred.

Presented at the 35th ASMS Conference on Mass Spectrometry and Allied Topics
May 24-29, 1987, Denver, CO

A DETAILED MASS SPECTROMETRIC STUDY OF DFTPP

CODY, R.B.; KINSINGER, J.A., and WEIL, D.A.
Nicolet Instrument Corporation
Madison, WI 53711

Decafluorotriphenylphosphine (DFTPP) has been employed as an abundance calibrant for GCMS. Extensive studies of the fragmentation of DFTPP have been conducted using quadrupole and sector mass spectrometers [1-4]; in all of these studies, the ion at m/z 69 has been identified as CF_3^+. However, using Fourier transform mass spectrometry, we have noticed that this ion is, in fact, PF_2^+. The identity of this ion has been verified by accurate mass measurements, high resolution mass spectrometry, and collisional activation of the molecular ion with accurate mass measurements on the daughter ion in the electron impact spectrum of DFTPP have confirmed the assignments previously reported.

We have also examined the relative ion abundances for the electron impact spectrum of DFTPP, as obtained by a Nicolet FTMS-2000 Fourier transform mass spectrometer. These abundances are found to fall within the recently proposed revision to the EPA peak height criteria [2], provided that excitation and trapping conditions are employed that accurately reflect ion abundances in the FTMS trapping cell.

EI Spectrum of DFTPP Showing Relative Peak Heights Obtained by FTMS

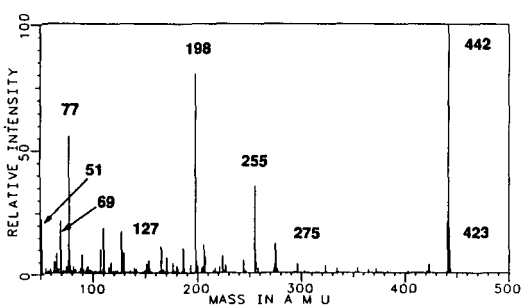

Peak Heights for Abundance Criteria Ions

m/z	Rel. Abundance
51	22.7
68	Not observed
69	21.5
70	Not observed
127	17.4
197	Not observed
198	80.3
199	4.9
275	12.3
365	1.6
441	21.4
442	Base peak (100%)
443	18.5

References:

1. Eichelberger, J.W., Harris, L.E., Budde, W.L.; Anal. Chem., 1975, 47, 995

2. Donnely, J.R., Tondeur, Y., Sovocool, G.W., Mitchem, R.K. presented at the 34th Annual Conference on Mass Spectrometry and Allied Topics, Cincinnati, OH, June 8-13, 1986

3. Federal Register, Volume 44, No. 233, p. 69532, Dec. 3, 1979

4. McGuire, J., Craig, J., Thornton, C. presented at the 31st Annual Conference on Mass Spectrometry and Allied Topics, 1983

Presented at the 35th ASMS Conference on Mass Spectrometry and Allied Topics
May 24-29, 1987, Denver, CO

ENVIRONMENTAL MONITORING PROCEDURES FOR BROMINATED DIBENZO-P-DIOXINS AND DIBENZOFURANS

R.K. Mitchum, G.W. Sovocool, W.D. Munslow*, T.L. Vonnahme*,
N.J. Nunn*, C.M. Hedin*, and J.R. Donnelly*
U.S. Environmental Protection Agency and *Lockheed-EMSCO
P.O. Box 15027, Las Vegas, NV 89114

Polychlorinated dibenzo-p-dioxins (PCDDs) and dibenzofurans (PCDFs) are considered highly toxic and have been the subject of long and intensive investigation. In contrast, very little has been reported concerning the potential environmental impact of brominated dioxins and dibenzofurans (PBDDs and PBDFs), although their analogous precursors are well known and are dispersed widely in the environment. Polybrominated biphenyl (PBB) and polybrominated diphenylether (PBDPE) fire retardants are commonly added to plastics, textiles, carpets, adhesives, coatings, and similar products. The formation of significant quantities of PBDDs from thermolysis of commercial PBDPE and PBB fire retardants has been reported; soot samples from a bowling hall fire were found to contain PBDFs and PBDDs. Mixtures of PBDDs and PBDFs were synthesized by electrophilic bromination of dibenzo-p-dioxin and of dibenzofuran. Products were characterized by mass spectrometry, gas chromatographic retention index (RI) correlations with the PCDDs and PCDFs, and the consideration of traditional electrophilic bromination substitution patterns. GC/MS data were obtained under electron ionization conditions. Significant features of these spectra include the sequential losses of $Br^{\cdot}$, $COBr^{\cdot}$, ($Br^{\cdot}$+ $COBr^{\cdot}$), and ($2Br^{\cdot}$+ $COBr^{\cdot}$). Additionally, doubly charged ions were found: M^{2+}, $(M-Br^{\cdot})^{2+}$, $(M-2Br^{\cdot})^{2+}$.

PBDPEs may interfere in the determination of PBDFs as has been reported for analysis of PCDFS in the presence of PCDPEs. Specifically, the $(M-2Br^{\cdot})^{+}$ fragment possesses the same m/z composition cluster as that of a PBDF with two fewer bromines. Further, additional fragmentation mimics the PBDF containing two fewer bromines. This report presents methane negative ion chemical ionization (NCI) mass spectra for certain PBDDs, PBDFs, and potentiallyinterfering PBDPEs. In all cases studied, dissociative electron capture leading to Br predominated, facilitating 'screening' determinations for thes e analytes by monitoring Br^{-}. NCI spectra showed losses of $Br^{\cdot}$ as well as $(M-Br+H)^{-}$ and (HBr) fragments. Under PPINICI, positive ion responses (see Figure 3) were at least a factor of one hundred lower than negative ion responses, as would be expected for these analytes. Some PCI spectra showed H_2Br^{+} fragments, $(M+H)^{+}$, alkyl adduct ions and loss of $Br^{\cdot}$ from those adducts.

Standard solutions of PBDDs and PBDFs were used to develop a method for sample preparation. Each step of a typical environmental monitoring method (US EPA Resource Conservation and Recovery Act [RCRA] Method 8280, Revised) was checked for applicability to these brominated compounds. The efficiency of each step in this method was measured for both PBDFs and PBDDs; the behavior of suspected analytical interferences (PBBs and PBDPEs) in this method was also investigated.

The preparation of environmental sample extracts under Method 8280 involves four major steps: extraction from a matrix, acid/base washing, alumina column chromatography to remove the bulk of interferences and carbon column chromatography to remove residual interferences. The recoveries of di- through hepta-BDFs and di-through hepta-BDDs after extraction from sand and after acid/base washing were greater than 80% except for the higher brominated congeners of dibenzofuran where 65-75% recoveries were observed. The behavior of the PBDFs and PBDDs in the chromatography steps of Method 8280 was studied by measuring recovery from the same fraction in which the PCDDs and PCDFs elute. These studies demonstrated that greater than 90% of the PBDDs and PBDFs elute from the alumina column in the same fraction as the PCDDs and PCDFs.

The evaluation of the carbon column demonstrated that both the PBDDs and PBDFs elute in the same faction as the PCDDs and PCDFs. The recoveries of PBDDs were about 80 percent for all congeners except HpBDD (40%). The recoveries of the PBDFs also were observed to vary between experiments. Slight variations in the preparation of the gravity flow type column used in this study may affect column capacity for the analytes and hence the amount of material recovered.

After each step of Method 8280 had been evaluated, overall recovery of PBDDs and PBDFs using Method 8280 was determined. A sand matrix was employed to mimic an environmental sample. Two experiments were conducted, one with PBDDs and one with PBDFs, each in duplicate. The extracts were prepared as described in the revised Method 8280 for analysis of PCDDs and PCDFs. These experiments resulted in recoveries of over 70%.

Chlorinated biphenyls and chlorinated diphenylethers may interfere with the analysis of PCDDs and PCDFs by this technique. Therefore, brominated biphenyls and brominated diphenylethers were tested to determine if they would provide chromatographic interference in the analysis of PBDFs and PBDDs. A standard containing two hexabromobiphenyls (71% and 10%) and one heptabromobiphenyl (19%) was eluted from an alumina column as described in the revised Method 8280. The three PBBs were found to elute in the same fraction as the PBDDs and PBDFs; about 80% of the material was recovered. The same standard mixture was used to test a gravity flow carbon column; the PBB standard mixture eluted in the methylene chloride/cyclohexane, and methylene chloride/methanol/benzene washes prior to reversing the column. Actual separation was demonstrated with a mixture containing the three PBBs and di-through heptabromodibenzofuran which had been eluted from the alumina column. Excellent recoveries of both PBBs and PBDFs in their respective fractions were obtained and no cross-contamination was observed.

The behavior of brominated diphenylethers was studied in a similar manner. A sample of PBDPEs available commercially as a fire retardant was obtained and analysed. Seven HxBDPEs (two major components) six HpBDPEs (four major components) and two NBDPEs comprised the mixture. A standard was prepared and eluted from an alumina column. The PBDPEs were found to elute in the same fraction as the PBDFs and PBDDs. The eluate was next eluted from the carbon column. Significant amounts of the brominated diphenylethers eluted in the PBDF and PBDD fraction (in the reverse-direction eluate); these compounds may present interferences in the analysis of the PBDFs using Method 8280.

The monitoring of PBDDs and PBDFs is similar in concept to that for PCDDs and PCDFs but differs in some specifics: the former pair in general have higher molecular weights, longer GC retention times, different MS isotopic cluster patterns, and possibly fewer classes of potential interferences. Whereas PCBs present chromatographic and mass interferences in the monitoring of PCDDs, PBBs do not present a mass resolution problem: unlike chlorine, bromine has an atomic weight very different from two oxygens and the m/z clusters of PBBs do not overlap those of PBDDs. Analogous to chlorinated xanthenes and diphenylethers (interferences in PCDD and PCDF determinations respectively), the brominated xanthenes and diphenylethers must be carefully considered (see Table 5). While chlorinated pyrenes can interfere in PCDF analysis and chlorinated naphthalenes can interfere with $^{13}C_{12}$-PCDDs, the brominated pyrenes and naphthalenes are not mass interferences in PBDD and PBDF analyses.

Confirmation criteria for the detection and quantification of PCDDs and PCDFs are well established. Analogous criteria for the brominated compounds are proposed: (a) Retention time/retention index must be correct for that analyte. (b) Recovery of surrogate' standard, such as $^{13}C_{12}$-TCDD or some PBDD or PBDF surrogate, must be in the 40-120% range. (c) All m/z monitored for a given analyte must maximize simultaneously $\pm$ 1s, with signal to noise ratio > 2.5 for each. Previously summarized mass spectra of PBDDs and PBDFs show that the $M^{+\cdot}$ cluster is relatively intense for all congeners. For confirmation two additional ions (m/z) should be monitored in EI-SIM-MS. A second member of the molecular ion cluster, having approximately 30-60% intensity relative to the first, provides both reasonable sensitivity and a theoretical isotopic abundance criterion. The third ion selected could be $(M-COBr)^+$ or $(M-2Br)^{+\cdot}$. The most intense member for one of these two ion clusters was found to have at least 15-20% abundance relative to the most intense $[M^{+\cdot}]$ cluster member for almost all PBDDs and PBDFs studied. These relative intensities compare favorably with the choice of $[M^{+\cdot}]$, $[M+2]^{+\cdot}$, and $[M-COBr]^+$ for TCDD confirmation. The ions selected for PBDDs and PBDFs do not generally represent the first member of an isotopic cluster due to its low abundance in the ion clusters of most congeners. SIM descriptors should be centered at the accurate mass which is significantly below nominal mass due to the large negative mass defect of bromine. (d) The ratio between the two ions of the $M^{+\cdot}$ cluster must be within 20% of theoretical (e.g. 0.30$\pm$0.06). (e) When monitoring for PBDFs, demonstrate the absence of PBDPEs (i.e., monitor for the largest component of their isotopic molecular ion cluster). (f) Brominated xanthene interference can be detected by monitoring for their $(M-H)^+$, unique and intense for that class of analytes.

NOTICE: Although the research described in this article has been funded wholly or in part by the Environmental Protection Agency contract 68-03-3249 to Lockheed Engineering and Management Services Company, Inc., it has not been subject to the Agency's review and therefore does not necessarily reflect the views of the Agency, and no official endorsement should be inferred.

Presented at the 35th ASMS Conference on Mass Spectrometry and Allied Topics
May 24-29, 1987, Denver, CO

'UNUSUAL' ENVIRONMENTAL CONTAMINANTS

G.J. Feistner[1], K.F. Faull[1] and D.B. Goldstein[2]
Departments of Psychiatry[1] and Pharmacology[2]
Stanford Medical Center, Stanford, CA 94305

Recently we encountered a cocktail of plasticizers in commercial ethanol, of which, initially, we could only identify dioctylphthalate (I in Fig. 1). Attention was drawn to these contaminants because they gave rise to an unusually strong disordering effect on mouse synaptosomal plasma membranes [1]. The 'unknown' contaminants were studied by GC-EI/CI-MS, FAB-MS, FAB-MS/MS, and FAB-B/E=const. linked scan methods. They were identified as fatty acid triethylene glycol (TEG) esters (see Fig. 3 for an example) and aryl phosphates (Fig. 2). Aryl phosphates are known for their neurotoxic activity [2] and elsewhere [1] we have shown that the observed membrane disordering can be induced by authentic TEG decanoate octanoate. Occurence of these hazardous compounds in the environment should therefore be monitored. The methods which we used for their identification may be suitable/expandable for such a purpose.

Fig. 1

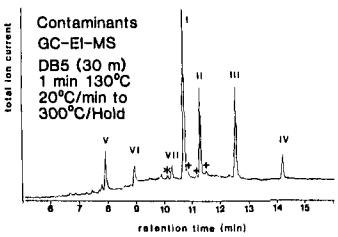

Fig. 2 General structure of encountered triarylphosphates

MWT 326 $R_1=R_2=R_3=H$
MWT 368 $R_1=i\text{-}Pr$ $R_2=R_3=H$
MWT 410 $R_1=R_2=i\text{-}Pr$ $R_3=H$
MWT 452 $R_1=R_2=R_3=i\text{-}Pr$

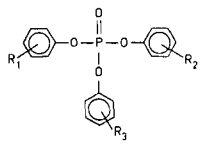

Fig. 3 Structure and fragmentation of TEG decanoate octanoate

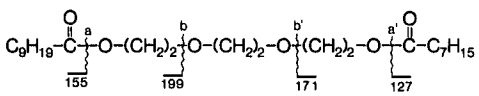

Fig. 4

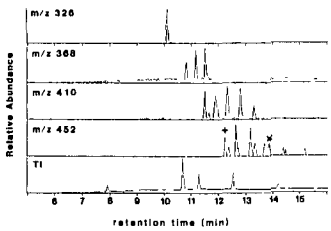

Table 1: Major fragment ions of identified TEG esters

GC-peak/Compound Name		a	b	a'	b'	$[M+H]^+$
II	TEG dioctanoate	127	171	127	171	403
III	TEG decanoate/octanoate	127	171	155	199	431
IV	TEG didecanoate	155	199	155	199	459
V	TEG monooctanoate	127	171	-	-	277
VI	TEG monodecanoate	155	199	-	-	305
VII	TEG hexanoate/decanoate	99	143	127	171	375

The total ion GC-EI(CI)-MS chromatogram (Fig. 1, reprinted from [1]) for the contaminated ethanol is dominated by dioctylphthalate and the TEG esters. The characteristic fragmentation of the latter is exemplified in Fig. 3 and summarized for the observed contaminants in Table 1. No molecular ions were seen for the TEG esters in the EI mode, but $[M+H]^+$ ions were seen in either CI or FAB mode. The structure assignment was confirmed by comparison with an authentic sample of TEG decanoate octanoate (PlastHall^R, kindly provided by the C. P. Hall Company, Torrance, CA). Similar oligoethylene glycol esters have been isolated from the Delaware river [3]. In contrast to the GC chromatogram, the FAB spectrum of the contaminated ethanol (Fig. 5) indicated a major presence of the aryl phosphates. Once aware of the aryl phosphates, we could also detect them in the GC-MS runs by selected ion chromatography (Fig. 4). The ion chromatograms also revealed that most of the aryl phosphates were present as isomeric mixtures, except triphenylphosphate (MWT 326, * in Fig. 1) which was identified by comparison with Ref. [4]. The vast differences in molecular ion abundance for the aryl phosphates in FAB-MS versus GC-EI/CI-MS are thus explained, in part, by the fact that in the latter mode the isomers are measured individually whereas in FAB mode the isomers are measured as a group.

That we were dealing with a series of homologous phosphates was apparent from the corresponding MS/MS spectra aquired for m/z 327, 369, 411, and 453 (for the MS/MS spectrum of the latter see Fig. 6). The dominant peaks in the spectrum of the lower homologues were also always present in the spectrum of the higher homologues suggesting that the four compounds differed by an increasing number of the same additional side chain. The mass increment was consistent with additional propyl groups. After

consulting [5], we considered that we might be dealing with a mixture of isopropylphenyl/phenyl phosphates. To confirm this assumption, we synthesized the corresponding triarylphosphates of 2-, 3-, and 4-isopropylphenol according to Ref. [2]. FAB-B/E=const.-MS of the molecular ions of the synthetic triarylphosphates (for the 3-isomer see Fig. 7) resulted in a fragmentation pattern similar to that observed by MS/MS of m/z 453 of the contaminated ethanol. We further found that we can differentiate the synthetic isomeric triarylphosphates both by their GC retention times as well as on grounds of differences in their EI spectra (Fig. 8). For example, the ratio of the ion abundances for M^+ (m/z 452) and M^+-CH_3 (m/z 437) seems to be characteristic for a particular isomer (Table 2). Based on these characteristics we could subsequently identify tri-(2-isopropylphenyl)phosphate (+ in Fig. 4) and tri-(3-isopropylphenyl)phosphate (x in Fig. 4) in the contaminated ethanol sample. GC-MS thus seems to provide a 'fingerprint' specific enough to pin-point a possible source of contamination, whereas FAB-MS may be the method of choice to rapidly screen for such contaminants in the first place.

Fig. 5

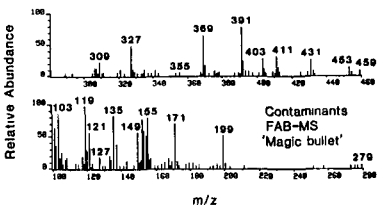

Table 2: Relative intensities M/M-15 for triisopropylphenylphosphates (two independent measurements)

	m/z 452	m/z 437	452/437
2-isomer	16.4	0.3	54.6
	14.7	0.6	24.5
3-isomer	67.4	15.7	4.3
	56.3	15.5	3.6
4-isomer	34.0	69.1	0.49
	27.1	62.8	0.43

Fig. 6

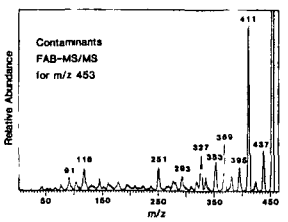

Fig. 7

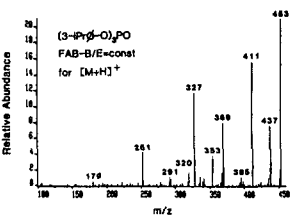

Fig. 8

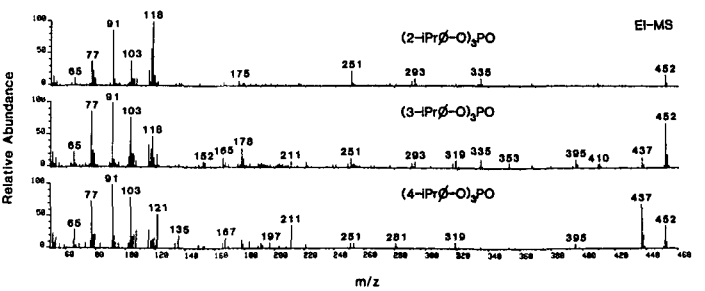

Acknowledgments: The authors wish to thank K. Tomer (NIEHS, Research Triangle Park NC) for the MS/MS spectra of the contaminated ethanol. This work was supported in part by grants AA01066, AA05972, MH23861, CHE821164, and the Alcoholic Beverage Medical Research Foundation.

References: [1] D.B. Goldstein, G.J. Feistner, K.F. Faull, K.B. Tomer, Alcohol. Clin. Exp. Res. (N.Y.) (in press); [2] P.G. Deo and P.H. Howard, J. Assoc. Off. Anal. Chem. 61, 266-271 (1978); [3] L.S. Sheldon and R.A. Hites, Environm. Sci. Technol. 12, 1188-1194 (1978); [4] M. Ende and G. Spiteller, Mass Spectrom. Rev. 1, 29-62 (1982); [5] J.K. Sears and J.R. Darby, The technology of plasticizers, John Wiley and Sons, New York, 1982.

Presented at the 35th ASMS Conference on Mass Spectrometry and Allied Topics
May 24-29, 1987, Denver, CO

IDENTIFICATION OF CIS-DIHYDRODIOLS OF THE CARCINOGEN BENZO[a]PYRENE AND ESTIMATION OF $^{18}O_2$ INCORPORATION IN THE GREEN ALGAE SELENASTRUM CAPRICORNUTUM

David Warshawsky, Koka Jayasimhulu, and Martha Radike
Department of Environmental Health, College of Medicine
University of Cincinnati, Cincinnati, OH 45267-0056

Introduction

Polycyclic aromatic hydrocarbons (PAHs) are by-products of incomplete combustion of organic substances and may reach substantial concentrations in aquatic systems bordered by areas of intense industrial activity. Deleterious effects of PAHs on aquatic organisms may have an impact on the productivity of the aquatic system and human health. The PAH, benzo[a]pyrene (BaP), is metabolized by various organisms. In mammals, BAP is metabolized to epoxides by a cytochrome P-450 monooxygenase. These epoxides can then be enzymatically hydrated to trans-dihydrodiols, nonenzymatically rearranged to phenols, or conjugated to polar molecules, such as glutathione. Trans-dihydrodiols may be further oxidized to diolepoxides. The mutagen 7,8-diol-9,10-epoxide-BP is considered to be the ultimate carcinogenic metabolite of BaP.

In bacteria, PAHs are metabolized to cis-dihydrodiols. We have shown in this laboratory that BaP is metabolized to cis-4,5- and cis-7,8-diols of BaP by the green alga, Selenastrum capricornutum.

Methods

$^{18}O_2$ Incubations and HPLC Analysis: Cultures of S. capricornutum, 5 x 10^5 cells/ml in 25 ml medium per Delong flask, were incubated with 10 µg BaP on a New Brunswick Scientific gyrotory shaker at 100 rpm in a Percival incubator at 23°C. Before adding BaP and $^{18}O_2$, four cultures were incubated for 24 hours (16 hrs light/8 hrs dark) under cool-white fluorescent lamps (General Electric F20T12/CW). Flasks were purged with N_2 (2500 ml in 5 min), $^{18}O_2$ added (40 ml in 1 min) and valves closed to maintain the atmosphere. Sterile conditions were maintained throughout. Solutions of BaP and subsequent algal incubations were carried out under gold fluorescent lamps (General Electric F20T12/GO) to avoid photooxidation of BaP. Cultures were incubated for 24 hours (16 hrs light/8 hrs dark). Algal suspensions were centrifuged at 1500 rpm, five min at 5°C. BaP and its metabolites were recovered by extraction of the supernatant with ethyl acetate (3 x 12.5 ml). Extracts were pooled, evaporated to dryness under nitrogen and stored at -20°C. Samples were brought to room temperature just prior to HPLC analysis.

Samples were reconstituted in chloroform prior to injection onto the HPLC. Separations were performed at room temperature on a Waters liquid chromatographic system equipped with a Whatman Partisil 10 ODS-2 reversed-phase column with a flow of 1 ml/min. Eluant was monitored at 254 nm with a Waters Model 440 ultraviolet absorbance detector. Fractions were collected with an ISCO Model 2111 automatic fraction collector for mass spectral analysis and for quantitation of radioactivity by scintillation counting using a Packard Tri Carb liquid scintillation counter Model 460 CD.

Mass Spectral Analysis: Metabolites of BaP, the 4,5-/11,12-diol and the 7,8-diol, separated by HPLC, were analyzed by mass spectrometry. The sample in solution was placed in a capillary tube used in the direct probe. The solvent was gently evaporated and the capillary was then placed at the tip of the direct inlet probe and inserted into the mass spectrometer source through a vacuum lock. The Kratos MS-80 high performance mass spectrometer was operated in the high resolution mode. The source temperature was maintained at 150°C and the electron voltage and the beam current were 50 eV and 100 uA, respectively. The temperature of the probe was increased slowly while a number of spectra were obtained by repeated scanning.

Presented at the 35th ASMS Conference on Mass Spectrometry and Allied Topics
May 24-29, 1987, Denver, CO.

Results

The molecular ion region showed two distinct peaks, separated by 4 amu at m/e 286 and m/e 290. The exact masses 286.0986 with a deviation of -0.8 mmu, and 290.1069 with a deviation of -0.9 mmu gave the molecular formula of $C_{20}H_{14}O_2$ and $C_{20}H_{14}{}^{18}O_2$, respectively. The (^{18}O) incorporation was calculated by peak averaging many scans in the molecular ion mass range. The percentage of the $(M + 2)^{+\cdot}$ ion compared to the $M^{+\cdot}$ ion was determined. The percentage of the ^{18}O containing molecular ion compared to the ^{16}O ion of the metabolite was found to be 13%. The positional isomers were identified by comparing the spectra with that of authentic samples and also by their chromatographic characteristics by HPLC.

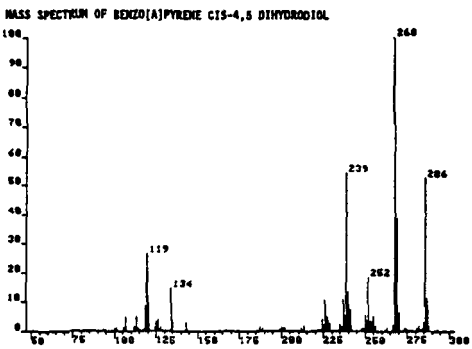

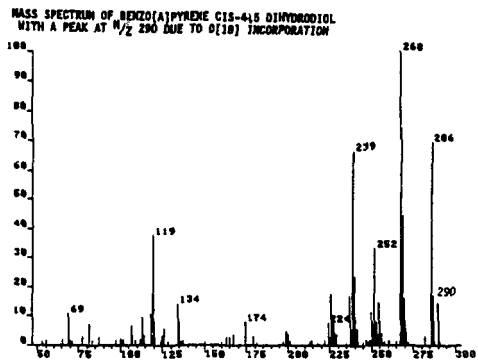

Presented at the 35th ASMS Conference on Mass Spectrometry and Allied Topics
May 24-29, 1987, Denver, CO

ANALYSIS OF VOST SAMPLES USING MEGABORE CAPILLARY GC/MS/DS

R. L. Porch, T. A. Buedel, J. T. Bursey, J. B. Homolya
Analytical Chemistry Division, Radian Corporation
Research Triangle Park, NC 27709

R. G. Fuerst, T. J. Logan, M. R. Midgett
U.S. Environmental Protection Agency (EMSL)
Research Triangle Park, NC 27711

In the current methodology for analysis of samples taken by the Volatile Organic Sampling Train (VOST)[1], samples of stack gas are collected on a Tenax®/charcoal adsorbent cartridge. The cartridges are thermally desorbed and volatilized compounds are purged through water, concentrated on a sorbent trap, and introduced into a GC/MS/DS where the separation takes place on a 3.0 mm x 2 m glass column, 1% SP-1000 on Carbopack B. If the sample matrix is not complex and the level of principal organic hazardous compounds (POHCs) does not saturate the column or the MS, quantitative analysis of target compounds will be straightforward. Qualitative analysis may also be performed on other chromatographically-resolved peaks to obtain acceptable confidence in their identification. If the sample is complex and POHCs and products of incomplete combustion (PICs) are at or near saturation of the analytical system, then the high background will interfere with identification of compounds. Because peaks eluting from a packed column may be broad (20-45 sec duration is typical), a PIC may coelute with a POHC making confident identification of either very difficult. Extensive use of background subtraction or other deconvolution techniques to obtain interpretable mass spectra of PICs or POHCs is a time-consuming process which requires a considerable level of expertise.

A method of analyzing VOST samples using a megabore fused silica capillary column was developed to improve overall chromatographic resolution and results associated with the VOST analytical method. Improvement of chromatographic resolution decreases chances of coelution to yield mass spectra of better quality and decrease overall sample analysis time. Although the current VOST method is restricted to compounds boiling between 30°C to 100°C, there is widespread interest in CH_3Cl, CH_3Br, C_2H_5Cl, and vinyl chloride as POHCs and PICs. Therefore, a goal of this program was to obtain analytical data for gases. The experimental configuration used a purge and trap concentrator with a DB-624 0.53 mm x 30 m megabore fused silica capillary interfaced directly to the ion source of a Finnigan-MAT 4500 or 5100 GC/MS/DS. A clamshell oven using He carrier gas was used to desorb volatile organic contents of a spiked VOST Tenax®/charcoal cartridge into a Purge and Trap Concentrator trap consisting of 90% Carbotrap®/10% charcoal, a composition derived through a sequence of experiments in which analytical reproducibility was studied as a function of trap composition. After desorption of the cartridge, the trap was pulse-heated to 190°C and backflushed with helium to sweep volatile organic compounds onto the head of the subambient (5°C) megabore column at a helium flow rate of 2.3 mL/min.

Analytes, surrogates, and quantitation standards were spiked onto the VOST sampling tubes at concentrations of 25, 50, 100, and 150 ng. The standards were analyzed in triplicate at each concentration to create a response factor database using d_6-benzene as the quantitation standard. Bromofluorobenzene and d_4-dichloroethane were spiked onto the cartridges as surrogates. Reproducibility of these response factors was used to evaluate the acceptability of the method. All selected VOST target compounds had coefficients of variation (CV) less than or equal to 18%. The CVs for the gases and 1,1,2,2-tetrachloroethane were higher (20-65%) but all of the gases were observed (see Table 1).

[1]E. M. Hansen, "Protocol for the Collection and Anaylsis of Volatiile POHCs Using VOST", EPA Report 600/8-84-007, March, 1984.

As an additional test of the modified method, a blind quality control sample was prepared and analyzed in triplicate, using the VOST target compounds. Reproducibility was acceptable and all values obtained for target compounds were within 14% of the spiked value. Another benefit of the modified methodology is that compounds such as naphthalene can be spiked on cartridges and desorbed and analyzed reproducibly using the megabore column. All three of the dichlorobenzene isomers are resolved completely. The range of compounds accessible to the analysis is now expanded to compounds which can be reproducibly loaded onto and desorbed from the sampling cartridges and purged through water with reproducible recoveries: naphthalene and trichlorobenzenes, for example, can be analyzed by the modified VOST method.

DISCLAIMER

Although the research described in this article has been funded wholly or in part by the United States Environmental Protection Agency to Radian Corporation, it has not been subjected to Agency review and, therefore, does not necessarily reflect the views of the Agency and no official endorsement should be inferred.

ACKNOWLEDGEMENTS

Contributions by D. Wagoner, N. Hooper, and T. Moody (Radian Corporation and E. Johnson (Finnigan-MAT Corporation) are gratefully acknowledged.

This work was supported by the Environmental Monitoring Systems Laboratory, Office of Research and Development, U. S. Environmental Protection Agency, Under EPA Contract No. 68-02-4119.

Table 1. RESPONSE FACTOR CALIBRATION CURVE FOR SELECTED METHOD 624 COMPOUNDS DESORBED FROM TENAX®/CHARCOAL CARTRIDGES

		Finnigan-MAT 4500			Finnigan-MAT 5100		
Compound	Ion	Mean Response Factor[1]	Standard Deviation	Coefficient of Variation (%)[2]	Mean Response Factor	Standard Deviation	Coefficient of Variation (%)[2]
VOST Target Compounds							
Methylene chloride	84	1 074	0 182	17	1.178	0.215	18
Chloroform	83	0 644	0.096	15	0.565	0.106	19
1,1,1-Trichloroethane	97	0 412	0 059	14	0 382	0.075	20
Carbon tetrachloride	117	0 314	0.045	14	0.220	0.040	19
Trichloroethene	130	0 278	0.026	9	0.283	0.049	17
Benzene	78	1 598	0.237	15	2.046	0.472	23
Tetrachloroethylene	164	0 801	0.089	11	0.284	0.050	18
Toluene	92	0 394	0.071	18	0.740	0.126	17
Chlorobenzene	112	2 261	0.317	14	0 684	0.101	15
Ethylbenzene	106	1 240	0.179	14	0.359	0.063	18
m,-p-Xylene	106	3 603	0.506	14	1.080	0.179	16
o-Xylene	106	1 747	0.278	16	0.440	0.083	19
Other Compounds							
Chloromethane	50	0 393	0 256	65	5.020	2.346	47
Bromomethane	94	0 077	0.031	40	0.597	0.289	48
Vinyl chloride	62	0 254	0 052	20	0.448	0 082	18
Chloroethane	64	0 097	0.020	20	0.247	0.054	22
1,1,2,2-Tetrachloroethane	83	0 087	0.277	26	0.166	0.048	29
Surrogates/Internal Standard							
d_4-1,2-Dichloroethane	65	0 273	0.017	6	0.216	0 037	17
Bromofluorobenzene	95	0.910	0.101	11	0.318	0 074	23
d_6-Benzene (IS)	84	1 000	----	----	1.000	---	---

[1] Triplicate analyses at four concentrations: 25, 50, 100, 150 ng.

[2] Coefficient of variation = $\frac{\text{Standard Deviation}}{\text{Mean}} \times 100$

Presented at the 35th ASMS Conference on Mass Spectrometry and Allied Topics
May 24-29, 1987, Denver, CO

REAL TIME ENVIRONMENTAL ANALYSES OF VOLATILE ORGANICS IN AIR BY TANDEM MASS SPECTROMETRY

by

Nicholas Kurlick
Enviresponse, Inc.
Edison, NJ 08837

and

Thomas Pritchett
EPA Environmental Response Branch
Edison, NJ 08837

The objective of this survey was to demonstrate the Mobile Low Pressure Chemical Ionization (LPCI) Tandem Mass Spectrometer Sciex 6000E's usefulness in monitoring indoor ambient air for volatile organic compounds. This device draws air samples at a rate of 90 l/minute, which provides a 10-ml/minute flow into the source. The 6000E's LPCI source has a Townsend Discharge Electrode that emits energetic electrons by ionizing ambient air (nitrogen, oxygen, water vapor, etc.), which then forms reagent ions N_2^+, O_2^+, H_3O^+, $[H_2O]^n$, $[H_3O \cdot nH_2O]^+$, etc.). These ions, in turn, ionize trace organic molecules by one of the following ionization processes: charge exchange by NO^+ or N_2^+; protonation by H_3O^+, $[H_3O \cdot nH_2O]^+$, or adduct formation by NO^+ or H_3O^+. Parent/daughter ion pairs are monitored to quantitate volatile organic compounds and to locate their possible source.

The ambient air of eight single-family houses near an Ohio Superfund waste site was monitored for the target contaminants. The monitoring was done to determine whether any target compounds were emanating from the waste site or from stored commercial products. Monitoring began with a 2-minute interval at each room's center and proceeded around the perimeter. Vents, storage areas, and furniture were checked as possible sources. When target compounds were indicated during a location change or around a certain item, the operator programmed the computer to identify the source.

Monitored Target Compounds'
Parent/Daughter Ion Pairs

Compound	Charge/Mass Ratio
Toluene	92/39, 92/51, 92/65
Methy Ethyl Ketone	73/43, 73/31, 72/43
Ethyl Benzene/Xylenes	106/65, 106/91, 107/79
1,1-Dichloroethane	63/27, 65/27
Pentane + C_5 Hydrocarbons	71/29, 71/43, 72/29, 72/43

Basement air monitored at House 12550 displayed a toluene concentration change at different locations. This might well indicate that storage shelves found there contained products with toluene, such as car wax and cleaning solutions. Despite other products containing toluene (paint, thinner) in storage areas at House 12550, the highest concentrations were in the living room and bedroom. Because high toluene concentrations were also found around the vents, the compound may have been transported to the living and sleeping areas by the ventilation system. There may have been other toluene sources that were not observed in these rooms.

The monitoring process indicated that most residents stored or used commercial products containing the target contaminants. High toluene levels were evident in Houses 12550 and 12430 where residents had stored paint and thinner, both of which contain toluene. Toluene is also found in such common household items as gasoline, paint, varnish, and adhesive solvents, gums, resins, rubber, lacquer thinner, and plastic toys and models.

Conclusions

The LPCI Tandem Mass Spectrometer has been shown in this study to be useful for monitoring low levels of volatile organic compounds in indoor ambient air and to determine their potential sources. Its advantages are:

- Sensitivity to volatile organic compounds, which are detected in the low parts per billion range;
- No sample preparation;
- Analysis time of 10 minutes per room for 39 selected ion pairs;
- Response factors relative standard deviation percentages below the accepted value of 45 percent;
- Unit mobility.

There is the possibility that other compounds or fragments that produce the same parent/daughter ion pairs as the analyte can interfere with the quantitation. This is overcome by selecting a few parent/daughter ion pairs that are characteristic of the compound, which are then used for quantitation of the analyte.

Presented at the 35th ASMS Conference on Mass Spectrometry and Allied Topics
May 24-29, 1987, Denver, CO

LC/MS AND MS/MS ANALYSIS OF CARBAMATE PESTICIDES

Kin S. Chiu (a), Calvin Tanaka (b), and Agnes VanLangenhove (a)

(a) ENSECO/ERCO Division, 205 Alewife Brook Pkwy, Cambridge, MA 02138
(b) ENSECO/California Analytical Laboratories, 2544 Industrial Blvd, West Sacramento, CA 95691

The development of thermospray technology has enabled the direct mass spectrometric analysis of eluents from high performance liquid chromatographs (HPLC). In an attempt to take advantage of the detector's specificity and definitiveness, many polar and/or thermally labile compounds hitherto analyzed using ultraviolet and fluorescence detection are being evaluated using thermospray ionization. One such class of compounds is the carbamate pesticides, which are currently analyzed using HPLC coupled with post-column hydrolysis and fluorescence detection.

The direct mass spectrometric detection of eight of the carbamate pesticides is reported in this study. Their chemical structures are shown in Fig. 1. Using the conditions in Table 1, these carbamates were resolved and analyzed as shown in Fig. 2. Because thermospray ionization is relatively "soft", there is minimal fragmentation of the carbamates (either in the filament-on or filament-off modes), as illustrated by the mass spectra of carbofuran (Fig. 3), where the M+1 ($[M+H]^+$) and M+18 ($[M+NH_4]^+$) adduct ions predominated. With the minimized fragmentation, detection limits in the nanogram levels were readily attained, even with a full mass range scan.

However, the lack of diagnostic bond cleavages limited the extent to which structural information could be inferred from the mass spectrometric data. In order to achieve more detailed characterization of the carbamates, tandem mass spectrometry (MS/MS) using triple stage quadrupole was used. Operating in the daughter ion scanning mode, the MS/MS was used to choose the molecular adduct ions for further dissociation using argon. The additional collisional energy (-25eV) introduced resulted in distinctive bond cleavages and generated daughter ion spectra which exhibited fragmentations similar to the mass spectra obtained under electron impact ionization conditions. This is illustrated in Fig. 4. Due to the ease with which the MS/MS can be used to selectively choose the adduct ions for induced fragmentation, and the structural specificity of the resultant daughter ion, tandem mass spectrometry can be directly used to analyze the carbamates without the need for prior chromatography. This could be advantageously used to provide a rapid screening method for the compounds of interest.

Table 1 HPLC/MS conditions used for the analysis of carbamate pesticides

HPLC Conditions	
Column	: 25 cm x 4.6 mm i.d. C_{18} adsorbosphere
Flow Rate	: 1.4 ml/min
Solvent System	: 0- 4 min : 30% MeOH and 70% H_2O
	4-14 min : linear ramp to 80% MeOH and 20% H_2O (all solvents in .1M NH_4Ac)
MS Conditions	
Filament	: off
Source Block	: 200°C
Vaporizer	: 110°C to 105°C in 10 min, starting at 4th min
Mass Range	: 100-300 amu scanned every 2 sec
Repeller Voltage	: 30 V

Presented at the 35th ASMS Conference on Mass Spectrometry and Allied Topics
May 24-29, 1987, Denver, CO

Carbamate Pesticides

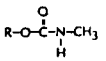

	R	Peak #
• Aldicarb		6
• Aldicarb Sulfone		2
• Aldicarb Sulfoxide		1
• Carbaryl		8
• Carbofuran		7
• 3-Hydroxycarbofuran		5
• Methomyl		4
• Oxamyl		3

Fig 1

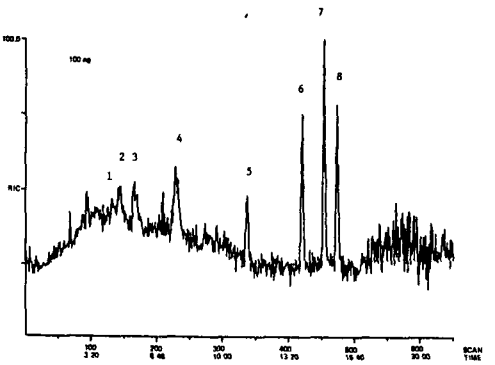

Fig 2

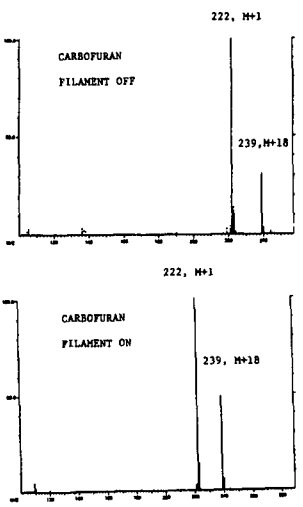

Fig 3

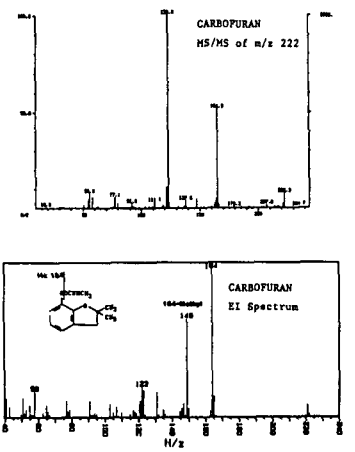

Fig 4

Presented at the 35th ASMS Conference on Mass Spectrometry and Allied Topics
May 24-29, 1987, Denver, CO

CHARACTERIZATION OF HALOGENATED ORGANIC COMPOUNDS IN ESTUARINE BIOTA AND SEDIMENTS BY CHEMICAL IONIZATION TANDEM MASS SPECTROMETRY

Colleen E. Rostad and Wilfred E. Pereira
U.S. Geological Survey
P.O. Box 25046, Denver Federal Center
Denver, Colorado 80225

Determination of trace levels of environmentally important organic compounds in the presence of overwhelming coeluting interferences is a common problem in gas chromatography/mass spectrometry (GC/MS) analysis. Additional sample preparation to remove interferences from the sample while keeping trace organic compounds of interest intact is laborious and not always successful. In preparation for an intensive field study involving an estuarine area contaminated by chlorinated compounds, a method was developed for rapid determination of selected chorinated compounds in a variety of sample matrices by gas chromatography/tandem mass spectrometry (GC/MS/MS). With minimal sample preparation, use of tandem mass spectrometry (MS/MS) enabled analysis for specific compounds in the midst of many coeluting compounds. The selected chlorinated compounds included chlorobenzene; 1,2-, 1,3-, and 1,4-dichlorobenzene; 1,2,3-, 1,2,4-, and 1,3,5-trichlorobenzene; 1,2,3,4-, 1,2,3,5-, and 1,2,4,5-tetrachlorobenzene; pentachlorobenzene; hexachlorobenzene; hexachloro-1,3-butadiene; octachlorostyrene; and octachloronaphthalene.

Analysis by MS/MS in the daughter-ion mode involves selecting only one mass through the first quadrupole, fragmenting it in the second quadrupole, and analyzing the resulting ions in the third quadrupole. In order to achieve maximum sensitivity for a compound using MS/MS, the maximum number of ions should pass through the first quadrupole. Because only one mass is allowed through at one time, the maximum number of ions of that mass is needed. For most compounds, the molecular ion is the obvious choice. Among the ionization choices of electron impact (EI), positive ion chemical ionization (+CI), and negative ion chemical ionization (-CI), the technique with effective ionization and the least intense fragmentation is needed. Application of MS/MS to analysis of estuarine biota and bed sediments was investigated.

Biota and sediment extracts were initially analyzed using GC/EI MS for a general screening tool. The samples contained fatty acids, aliphatic hydrocarbons, polycyclic aromatic hydrocarbons, and sterols that interfered with determination of the halogenated compounds of interest. EI is an excellent universal technique which generates unique fragmentation patterns that can be compared to libraries of 38,000 reference-compound spectra. Although EI is capable of ionizing most organic compounds, it is not an asset in MS/MS. The ionization is too intense, which results in excessive fragmentation. For many compounds, only a small portion, if any, of the compound remains as the molecular ion, using this ionization technique. Analysis of the molecular ion by MS/MS after ionization by EI would not be very sensitive.

When the ionization process involves CI, rather than EI, a softer ionization occurs and less fragmentation results. A variety of reagent gases can be used, allowing chemical specificity in the ionization process. Some types of compounds do not ionize well under less intense conditions. The CI process is, then, a bit more selective.

Under electron capture conditions, -CI produces very intense response for polychlorinated compounds, similar to electron capture detection (ECD) in GC. Because chlorinated compounds were the focus of this study, -CI seemed ideal. Some large, highly chlorinated compounds, such as biphenyls and biphenyl ethers, were detected in the biota and sediment samples using -CI, that were not seen at all by EI or +CI. The -CI RIC was much simpler. The -CI process generated primarily molecular ions, ideal for further MS/MS analysis. Ionization conditions were optimized for maximum generation of negative molecular ions. However, of the chlorinated compounds selected for study, only pentachlorobenzene, hexachlorobenzene, octachlorosytrene, and octachloronaphthalene produced any ions at all.

For the -CI MS/MS studies, octachloronaphthalene was used as a model compound. The negative molecular ion was analyzed under a variety of conditions for generation of negative daughter ions using argon. Under gentle fragmentation conditions, only the original molecular ion was detected. Under more intense fragmentation conditions, the molecular ion disappeared but no daughter ions were observed. If daughter ions of Cl^- at mass 35 were produced, they would not have been observed due to instrument constraints. Based on the lack of daughter ions of octachloronaphthalene and lack of molecular ions for most of the compounds under study (chlorobenzene through tetrachlorobenzenes), -CI was eliminated as an ionization method of choice.

The +CI technique primarily produced molecular ions, depending on the conditions used. When the biota and sediment samples were analyzed using methane +CI, the RIC appeared similar to the RIC generated using EI; however, the resulting spectra were quite different. Conditions for +CI were optimized for generation of molecular ions only, with no adduct or fragmentation ions. Using these molecular ions, daughter ions were generated using argon under a variety of fragmentation conditions. For each compound, conditions were optimized to generate the most daughter ions resulting from neutral loss of one chlorine. In addition to observing the ratio of daughter ions to molecular ions in the spectra, absolute ion counts also were compared, to check the efficiency of ion transmission. As the fragmentation conditions were intensified, more and more daughter ions were produced. After a certain point, the ion transmission decreased with a loss in sensitivity, even though an increased percentage of daughter ions was observed.

The scan range used to detect the resulting daughter ions was then limited to just the loss of chlorine from the molecular ion. This was essentially a neutral loss scan. However, since the neutral loss varied between Cl at mass 35 and HCl at mass 36, the daughter ion range was set over 2 amu. The sensitivity increased because the acquisition time was spent scanning a very small mass range. Response was linear over a range of 5 orders of magnitude. The detection limit (with signal-to-noise ratio of at least 5:1) for octachlorostyrene and octachloronaphthalene was 2 nanograms. The detection limit for the remaining compounds studied was 20 picograms.

Under the optimum conditions for ionization and fragmentation, extracts of contaminated bed sediment and biota tissue were analyzed. The overwhelming interferences present under the more common GC/EI MS conditions were eliminated, and sensitivity was enhanced. The +CI MS/MS technique was applied to heavily contaminated (with chlorinated compounds) bed sediment extracts to check for daughter ions from the set molecular ion mass that may result from other compounds. No evidence of this was observed.

Presented at the 35th ASMS Conference on Mass Spectrometry and Allied Topics
May 24-29, 1987, Denver, CO

GC-MS PROCEDURES FOR DETERMINATION OF BROMINATED AND BROMINATED/CHLORINATED DIBENZODIOXINS AND DIBENZOFURANS IN FIRE RETARDANT CHEMICALS

T. O. Tiernan, M. L. Taylor*, D. Wagel, G. F. VanNess, L. Harden,
J. H. Garrett and J. G. Solch
Departments of Chemistry and Pharmacology/Toxicology*,
Wright State University, Dayton, Ohio 45435

INTRODUCTION

Many of the brominated fire retardant chemicals which are currently in widespread use contain brominated phenols or similar compounds as major components. In addition, trace concentrations of chlorinated phenols and related compounds may also be present in brominated fire retardants as a result of side-reactions occurring during large-scale commercial syntheses. Therefore, since it is well known that halogenated phenol condensation reactions can give rise to dibenzo-p-dioxins and related compounds and it is well-recognized that certain of these compounds are highly toxic, a research project was undertaken in which analytical methodology for quantitating trace concentrations of toxic halogenated aromatics in brominated fire retardant chemicals was developed, validated and applied. The development and validation studies are described herein and concentrations of halogenated dibenzodioxins and dibenzofurans present in actual flame retardant chemicals and materials containing these, which were subsequently determined using the procedures developed, are reported.

METHODOLOGY DEVELOPED

Initially, the analytical procedures previously applied to quantitate chlorinated dibenzodioxins and dibenzofurans in various sample matrices were evaluated to determine their efficacy for determining the corresponding brominated and mixed bromo-/chloro-compounds (1). Prior to the present studies, it had not yet been conclusively demonstrated that small quantities (nanograms or less) of the latter compounds can survive the caustic chemical extractions and liquid chromatographic cleanup procedures which are usually applied in analyses for the analogous chlorinated compounds. Moreover, some of the sample matrices of interest in connection with the brominated compounds are polymeric in nature and appropriate extraction procedures for these had not yet been determined.

The analytical procedures which were ultimately demonstrated to be applicable for analyses of the brominated dibenzodioxins (BDD) and dibenzofurans (BDF) are outlined in the following.

1. Using methylene chloride, Soxhlet-extract A 1 g aliquot of the sample (spiked with internal standards) for 48 hours.
2. Concentrate the extract to 20 mL using a Kuderna-Danish apparatus and transfer residue to 125 mL bottle.
3. To the concentrated extract:
   a) Add 15 mL KOH (20%), shake 15 min., discard
   b) Add 15 mL distilled H_2O, shake 5 min., discard
   c) Add 15 mL conc. H_2SO_4, shake 10 min., discard.
   d) Add 15 mL distilled H_2O, shake 5 min., discard.
   e) Dry samples over Na_2SO_4.
4. Concentrate to 10 mL using Kuderna-Danish apparatus.
5. Chromatograph residue using a silica column containing, from the bottom: 1 g of neutral, 4 g of acidic, 1 g of neutral, 2 g of basic, and 1 g of neutral purified silica.
6. Using a Kuderna-Danish apparatus and a micro Snyder column, reduce the volume of the silica column eluate to approximately 2 mL.
7. Chromatograph the residue using an activated alumina column and collect the following fractions:
   a) 15 mL of hexane
   b) 10 mL of 8% methylene chloride in hexane
   c) 15 mL of 50% methylene chloride in hexane

8. Concentrate each of the three fractions to a volume less than 1 mL using a micro Synder column. Discard fractions 7a and 7b. Transfer fraction 7c to a PX-21 carbon/celite column and following chromatography, concentrate the fraction again to 0.5-1.0 mL.
9. Analyze the fractions from the carbon column by GC-MS. The GC-MS instrument utilized for the analyses consists of a Carlo Erba Model 5300 Gas Chromatograph coupled to a Kratos MS-25 Mass Spectrometer equipped with a Data General SR-120/DS-90 Data System, for data acquisition and instrument control. The gas chromatograph was configured with a capillary injector configured for splitless/split operation (split flow on at 60 seconds after injection). A 60M, 0.25 mm fused silica column coated with a 0.25 μ film of DB-5 was utilized, with hydrogen (30 PSIG head) as the carrier gas. Typically 0.2 μL of each sample was injected. The GC column was temperature-programmed, starting at an initial temperature of 190° for 1 minute post-injection, then increasing the temperature to 300°C at 5°C/minute. A single-stage Kratos glass jet separator was used as the interface between the GC and MS. The mass spectrometer was operated in Electron-Impact SIM mode, at a resolution of 1:600, with a source temperature of 250°C. The ion-masses monitored for the chlorinated dibenzodioxins (CDD) and dibenzofurans ((CDF) have been shown previously (1). Ion-masses monitored for the BDD and BDF include: DiClDiBDD, 409 $(M+2)^+$, 411 $(M+4)^+$; TriBDD, 419 $(M+2)^+$, 421 $(M+4)^+$; TetraBDF, 481 $(M+2)^+$,484 $(M+4)^+$; TetraBDD, 498 $(M+2)^+$, 500 $(M+4)^+$; PentaBDF, 562 $(M+4)^+$, 564 $(M+6)^+$; PentaBDD, 578 $(M+4)^+$, 580 $(M+6)^+$; HexaBDF, 642 $(M+6)^+$, 644 $(M+8)^+$; HexaBDD, 658 $(M+6)^+$, 660 $(M+8)^+$; HeptaBDF, 719 $(M+6)^+$, 721 $(M+8)^+$; HeptaBDD, 735 $(M+6)^+$, 737$(M+8)^+$; OctaBDF, 797 $(M+6)^+$, 799 $(M+8)^+$; OctaBDD, 813 $(M+6)^+$, 815 $(M+8)^+$.
10. $^{13}C_{12}$-TCDD and $^{13}C_{12}$-HpCDD were used as internal standards in these analyses and were added in known amounts to the samples prior to extraction.

In developing and validating the analytical procedures, representative BDD, BDF, and BCDD and BCDF were spiked into typical flame retardant chemicals and formulations in known quantities and recoveries of these were determined. The representative brominated compounds which were added in these experiments included 2,3,7,8-TBDD; 1,3,6,8-TBDD; 1,3,7,8-TBDD; 1,3,7,9-TBDD; 2,3,7-TBDD; 2,3,8-TBDD; 2,3,7,8-TBDF; 1,2,7,8-TBDF; 1,3-DC-7,8-DBDD; and 2,3-DB-7.8-DCDD. Recoveries of these various compounds which were achieved using the methodology ultimately applied ranged from 71% to 100%, thereby demonstrating that this methodology is quite acceptable.

RESULTS AND CONCLUSIONS

Following the methodology development phase of this study, several actual flame retardant compounds and formulations containing these were analyzed for BDD, BDF and mixed Br-, Cl-compounds of this type. Various BDD and BDF, including some of the tetra- isomers were detected in these flame retardant materials. Further work is in progress to validate this methodology for still other BDD and BDF isomers.

REFERENCES

1. T. O. Tiernan, "Analytical Chemistry of Polychlorinated Dibenzo-p-dioxins and Dibenzofurans: A Review of the Current Status," Chapter 13 in *Chlorinated Dioxins and Dibenzofurans in the Total Environment*, G. Choudhary et.al., Editors, Butterworth Publishers, Boston, 1983.

Presented at the 35th ASMS Conference on Mass Spectrometry and Allied Topics
May 24-29, 1987, Denver, CO

DEVELOPMENT AND APPLICATION OF A GC-MS TECHNIQUE FOR ACCOMPLISHING RIGOROUS ISOMER-SPECIFIC QUANTITATION OF 2,3,7,8-TETRA CHLORODIBENZOFURAN IN EXTRACTS OF ENVIRONMENTAL SAMPLES

T. O. Tiernan, M.L. Taylor*, L. H. Harden, D. J. Wagel, J. H. Garrett, J. G. Solch and G. F. VanNess
Departments of Chemistry and Pharmacology/Toxicology*,
Wright State University, Dayton, Ohio 45435

INTRODUCTION

There is no existing analytical procedure which is applicable for quantitatively measuring 2,3,7,8-TCDF uniquely in environmental and manufacturing process and waste sample matrices. The biological activity and toxicity of this TCDF isomer dictate the need for such a method. There has been no rigorous evaluation of the recoveries of all 38 TCDF isomers which can be achieved from such sample matrices when the elaborate extraction and liquid chromatographic cleanup procedures usually applied in such analyses are employed. Moreover, the capillary GC columns (SP-2330, DB-5) currently in general use to separate 2,3,7,8-tetrachlorodibenzo-p-dioxin (TCDD) from the other 21 TCDD isomers do not uniquely resolve 2,3,7,8-TCDF from all of the other 37 TCDF isomers.

The objectives of the present study were to develop and validate a GC-MS analytical procedure for quantitatively measuring 2,3,7,8-tetrachlorodibenzofuran (TCDF) present at parts-per-trillion to parts-per-quadrillion concentrations in various manufacturing process and wastewater samples containing all 38 TCDF isomers.

ANALYTICAL PROCEDURES DEVELOPED AND APPLIED

A. Extraction
   1. Water and wastewater (1 liter) - add $^{13}C_{12}$-2,3,7,8-TCDF internal standard. Filter and remove solids; extract filtrate with methylene chloride; Soxhlet extract solids with benzene-acetone; concentrate and combine extracts.
   2. Sludges and other solids (5 grams) - dry sample if necessary to remove water; add $^{13}C_{12}$-2,3,7,8-TCDF internal standard; Soxhlet extract with benzene-acetone; concentrate extract.

B. Cleanup (Enhanced Procedure):
   1. Rinse concentrated extracts sequentially with aqueous KOH, water, concentrated sulfuric acid and water.
   2. Pass extract through combination silica column having base-modified, acid-modified and neutral silica sections, eluting with hexane.
   3. Pass extract through two alumina columns, eluting with various mixtures of methylene chloride-in-hexane.
   4. Pass extract through a carbon-celite column, eluting with methylene chloride-in-cyclohexane and benzene-ethyl acetate, followed by reverse elution with toluene.
   5. Repeat the alumina column cleanup.
   6. Concentrate extract and redilute with a standard mix in tridecane.

C. Analysis of Extracts:
   1. Analyze Extracts using GC-MS. The instrumentation and parameters employed are as follows.
      a. Gas Chromatograph (GC):Carlo-Erba 5300
         1) Capillary Column: Various columns were evaluated, all 60 meter; SP-2330, DB-5, DB-225, DB-5/DB-225 hybrid (column of choice)
         2) Temperature Program: Isothermal at 180°C, increase to desired maximum at 1-5°C/min.
      b. Mass Spectrometer (MS):Kratos MS-25
         1) Electron impact, computer-controlled selected-ion-monitoring mode

2) Monitor m/z 241, 304, 306 (TCDF); 316, 318 ($^{13}C_{12}$-TCDF); 374 (HCDE)

In the course of the method development work, the recoveries of all 38 TCDF isomers which were obtained, when samples spiked with these were subjected to the various extraction, cleanup and GC-MS procedures utilized here, were evaluated. It was found that recoveries of the TCDF isomers from the alumina column cleanup step were markedly dependent upon the eluting solvent mixtures used. With a solvent elution sequence which yielded optimum recoveries of all 38 TCDF isomers, the extracts of "dirty" process and effluent samples retained relatively large quantities of extraneous compounds which interfered with the detection of 2,3,7,8-TCDF at very low concentrations (parts-per-trillion to parts-per-quadrillion). However, since the focus of the present study was on developing a procedure specific for only the 2,3,7,8-TCDF isomer and which would yield the lowest possible detection limits, an elution sequence was sought which would retain 2,3,7,8-TCDF, but not necessarily the other TCDF isomers, while eliminating most of the interfering compounds from the final extract which is subjected to GC-MS. It was determined that the optimum alumina column elution procedure to achieve this objective involved sequential elution with 10 mL of 3% methylene chloride-in-hexane, followed by elution with 15 mL of 20% methylene chloride-in-hexane, and finally by elution with 15 mL of 50% methylene chloride-in-hexane, collecting only the last eluate fraction.

Extensive GC column development studies were also undertaken in this study. The retention times of all 38 TCDF isomers on 60M SP-2330, 60M DB-5, 30M DB-225, and a hybrid DB-5/DB-225 column were determined. It was found that only the hybrid DB-5/DB-225 column yielded complete resolution of 2,3,7,8-TCDF from all of the other 37 TCDF isomers. On all of the other columns evaluated, 2,3,7,8-TCDF coelutes with one or more other TCDF isomers.

RESULTS AND CONCLUSION

The optimum cleanup procedures which were developed in this study, as described above, were utilized in conjunction with the newly developed hybrid DB-5/DB-225 GC column to accomplish quantitation of 2,3,7,8-TCDF uniquely, in a series of manufacturing process and waste samples. These data indiated that, for samples which were primarily aqueous (wastewater), for which a larger sample (typically 1000 grams) could be analyzed, the detection limits achieved for 2,3,7,8-TCDF were in the low parts-per-quadrillion range. For samples which were essentially solids (ash, sludges, slurries), the method yielded low parts-per-trillion detection limits. The data obtained in this study using the procedures developed also satisfy all of the quality assurance criteria usually applied to such analyses, including correct m/z 304:m/z 306 ratio, and acceptable recovery of the $^{13}C_{12}$-2,3,7,8-TCDF internal standard. It is concluded that this method facilitates reliable and accurate determinations of the 2,3,7,8-TCDF isomer uniquely, in complex manufacturing process and waste samples.

Presented at the 35th ASMS Conference on Mass Spectrometry and Allied Topics
May 24-29, 1987, Denver, CO

NOVEL MASS SPECTROMETRIC METHODS FOR MORE RELIABLE DETERMINATION OF POLYCYCLIC AROMATIC HYDROCARBONS *

W.D. Jamieson, R.K. Boyd and P.G. Sim
Marine Analytical Chemistry Standards Program
Atlantic Research Laboratory, National Research Council
1411 Oxford St., Halifax, N.S., Canada B3H 3Z1

A major problem in the determination of polycyclic aromatic hydrocarbons (PAH) in environmental samples is correct identification of the analytes of interest in the presence of random chemical interferences in the usual chromatographic separations. Though such interferences can often be avoided by mass spectrometric measurement, isomeric or isobaric co-elutants can reduce the reliability of data from selected ion monitoring mass spectrometry (1). Recent developments in our laboratory offer improvements in detector specificity with little loss in sensitivity (2).

With a VG Analytical ZAB-EQ "hybrid" instrument (BEQQ; double focussing "reversed" geometry stages, then quadrupole stages), use of the first two stages (B, E) at lowest possible resolution (ca. 1200 RP) to monitor the ^{13}C satellite peak of lowest m/z of the doubly charged molecular ions of the compounds of interest can produce large improvements in signal/noise (Figure). These peaks appear at a "half mass" and are free of interferences due to "metastable" ions and ions not multiply charged.

This strategy has been compared with analogous use of a Finnigan MAT 4500 quadrupole instrument, using an INCOS (IDOS 3) data system for which the 'MID' (Figure) and 'GAIN' software were modified to support better such a novel multiple ion detection strategy. Previously modified IDOS I software (3) ('STAB', 'PROF') aided. With a peak width of 300 mmu, it was effective to use 8 sequenced MID descriptors of 2 to 4 ions each (Figure) to aid determinations of the 16 PAH compounds for which reliable values were determined in marine sediment reference materials released recently (4). Stability of ion selection was typically as shown in the Figure.

As expected, results show either of the above approaches is useful. The BE approach is more sensitive. With the quadrupole, MID techniques recover sensitivity lost by use of a narrow peak width.

We have also used tandem mass spectrometry (ZAB-EQ) to help distinguish isomers by monitoring collisionally induced dissociations (CID) of the doubly charged molecular ions (Figure). Application of the "2E" method of detection of singly-charged ions formed at high energy from dication precursors ($M^{2+} + Xe^0 \rightarrow M^+ + Xe^+$) has been compared with the same process occurring at low energy in the Q stage. Conditions used yielded furan molecular dication CID spectra similar to those reported previously (5). Surprisingly, low energy CID yielding doubly-charged ions is an important process, though yields of these or singly-charged ions may be too low to be useful for quantitative analysis.

REFERENCES.

1. P.G. Sim, R.K. Boyd, R.M. Gershey, R. Guevremont, W.D. Jamieson, M.A. Quilliam and R.J. Gergely. Biomed. Env. Mass Spectrom., (in press).
2. P.G. Sim, W.D. Jamieson and R.K. Boyd. Rapid Comm. Mass Spectrom., (in press).
3. W.D. Jamieson, R.M. Gershey, R. Guevremont and F.G. Mason. Spectra, 10, No. 1, 15 (1984).
4. Reference Materials HS-3, HS-4, HS-5, HS-6, SES-1 available from MACSP, NRCC, address as above.
5. H.I. Kenttamaa, K.V. Wood, K.L. Busch and R.G. Cooks. Org. Mass Spectrom. 18, 561 (1983).

* NRCC No. 27780

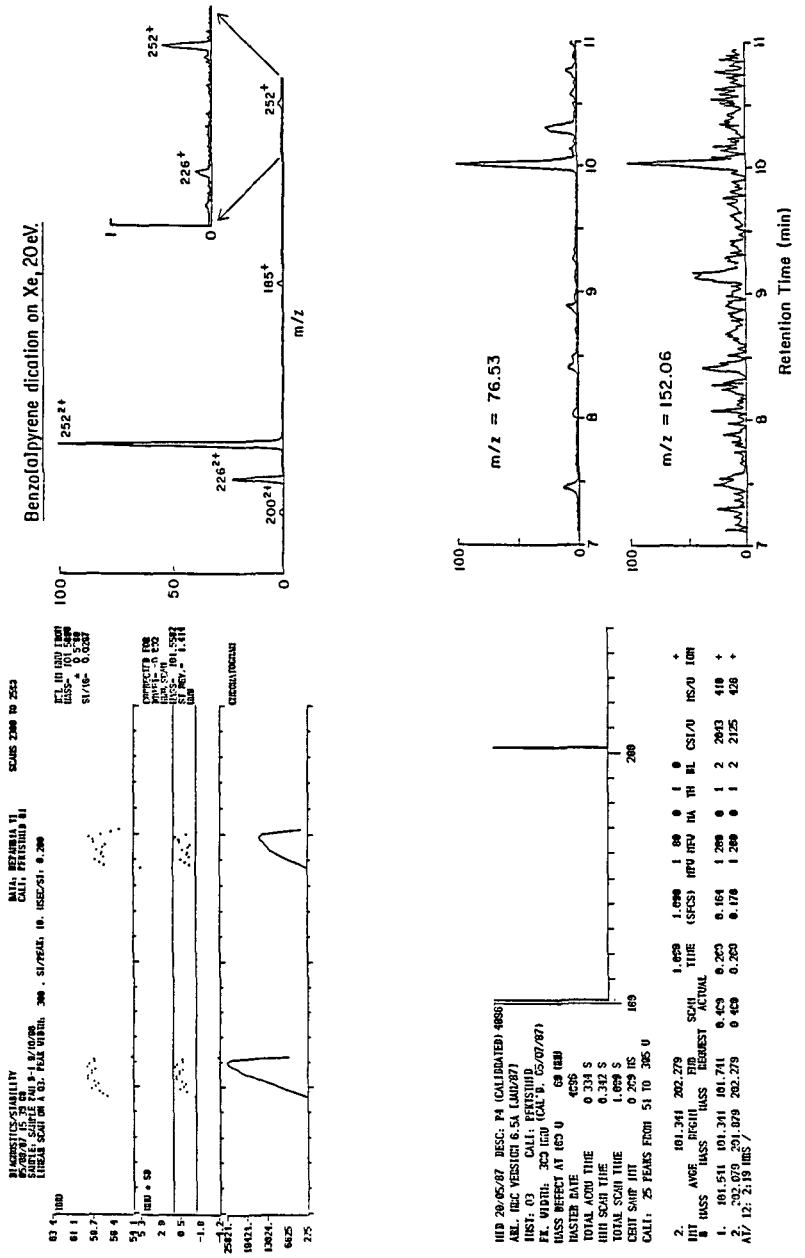
Benzo[a]pyrene dication on Xe, 20eV.
m/z
m/z = 76.53
m/z = 152.06
Retention Time (min)

Presented at the 35th ASMS Conference on Mass Spectrometry and Allied Topics
May 24-29, 1987, Denver, CO

FAB AND FAB-CID-MIKE ANALYSIS OF SULPHONATED DYES. APPLICATION ON ENVIRONMENTAL WATER SAMPLES.

J. Rivera (1), D. Fraisse (2), F. Ventura (3), A. Figueras (1), J. Caixach (1)
1.- Centre d'Investigació i Desenvolupament. J. Girona Salgado, 18-26. 034 Barcelona. Spain.
2.- CNRS. S.C.A. BP 22. 6930 Vernaison. France.
3.- Aigües de Barcelona. P. S. Joan, 39. 08009 Barcelona, Spain.

The analysis of organic pollutants in water is usually limited to those compounds amenable to GC/MS. However the development of new ionization techniques such as FD, DCI or FAB and their combination which.. tandem mass spectrometry has opened a promissing way to the analysis of polar, nonvolatile or thermally labile compounds.
Drinking water of Barcelona (N.E. Spain) is supplied by a heavy polluted river due to the presence of many factories placed at the banks of the river. Surfactant and textile industries are the most important among them. We have successfully characterized individual surfactants in raw and drinking water by FAB and FAB-CID-MIKE spectrometry (1). Organic dyes are among those productes used in textile, tannery,leather industries. Waste dumping products of these industries have been recognized as major pollutants in water, and toxicologic effects of some dyes and their metabolites has been established.
A wide range of dyes have been analyzed either by FAB mass spectrometry (2,3), 252 Cf PDMS or thermospray ionization-tandem mass spectrometry (5,6). The present work reports the FAB-CID-MIKE spectra of selected dyes after quests put forward to local manufacturers in an attempt to study the most representative ones in this area.
Several commercial dyes (nitro, azo, disazo, trisazo, oxazine and anthraquinone) ranging from mono to trisulphonated compounds were analyzed. Bests results were obtained by using glycerol as a matrix. The use of dithioerythritol + di thiothreitol (1: 1) allowed the identification of organic additives present in dye formulations. Tributil phosphate and a wide range of surfactants, used as dispersants, have been identified.
Positive FAB spectra gives $M+Na^+$ peaks with, in some cases, significant ions characteristic of the samples. A major disadvantage is the formation of glycerol clusters that could mask dye related peaks. For some compounds it was not possible to obtain the FAB spectrum either because of the nature of its molecular structure or due to the presence of glycerol clusters. (See fig. 1 as example).
Negative FAB spectra was superior in the molecular ion region and less abundant glycerol clusters (fig. 2). Nevertheless, the compounds which failed in the positive mode did also in the negative. (Spectra for all studied compounds are available upon request). In general, observed fragments arise from either azo or disazo groups of sulphonated portions of the molecules, being possible to elucidate the structure of the dye with the combination of both positive and negative modes and CID-MIKE.
As for environmental water samples or unknown commercial dyes, their identification depend on dye chemical structure and its response under FAB conditions. We were able to identify selected dyes by FAB in spiked real water extracts by combination of both modes and different matrices. The detection limit is different for each compound and sample background. Mordant Yellow 8 (500 ng) (fig. 3) in the spiked sample and positive mode give a S/N 5, whereas for Acid Blue 25 (500 ng) (fig. 4) in the negative mode is 10. Other compounds such as Acid Red 151 (500 ng), Acid Red 73 (1 ug) and Acid Blue 113 (1 ug) could be successfully identified. In real cases, CID-MIKE allows an univocal identification with other compounds at the same nominal mass.

REFERENCES

1. J. Rivera, D. Fraisse, F. Ventura, J. Caixach & A. Figueras. Presented at 10th Int. Mass Spectrometry Conference. Swansea (U.K.) 1985.
2. Monaghan, M. Barber, R.S. Bardoli, R.D. Sedgwick, A.N. Tayler. Organic Mass Spectrometry 17,10 (1982) 529; 17,11 (1982) 569; 18,2 (1983) 75
3. R.M. Brown, C.S. Creaser, H.J. Wright. Organic Mass Spectrometry 19,7 (1984) 31.

4. L.K. Pannell, E.A. Sokolaski, H.M. Fales, R. Tate. Anal Chem 57 (1985) 1060.
5. T.L. Youngless, J.T. Swasinger, D.A. Danner, M. Greco. Anal Chem 57 (1985) 1894.
6. J.M. Ballard, L.D. Betowski Organic Mass Spectrometry 21 (1986) 575.

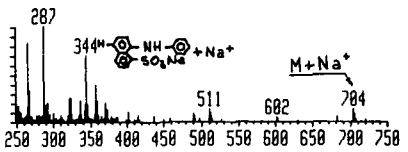

Fig 1 FAB(+) spectrum of Acid Blue 113

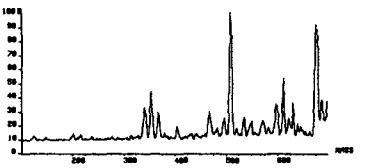

CID-MIKE spectrum of m/z 704,($M+H^+$) from Acid Blue 113.

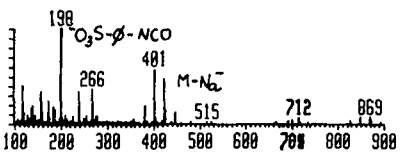

Fig 2· FAB(-) spectrum of Mordant Yellow 8

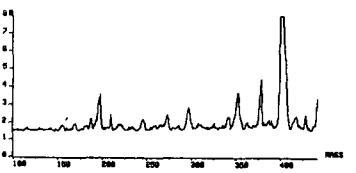

CID-MIKE spectrum of m/z 445 ($M-Na^-$) from Mordant Yellow 8.

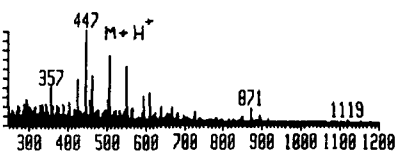

Fig 3: FAB (+) of an HPLC fraction spiked with Mordant Yellow 8 (500 ng).

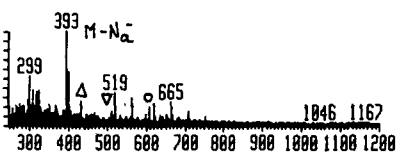

Fig 4: FAB(-) of an HPLC fraction spiked with Acid Blue 25(500ng), A.Red 151$^{\Delta}$(1µg),A.Red 73$^{\nabla}$(1µg) and A Blue 113^{o}(1µg)

Correlation of PCB to PCDF/PCDD in Combustion Accidents

D.G. Aichele, C.V. Sueper, M.L. Zimmerman, M.R. Bauer;
Battelle Columbus Division, 505 King Ave., Columbus, OH 43201

With the increased incidences of transformer accidents/fires, is it possible to predict pyrolysis products of polychlorinated biphenyls? If the Aroclor present in a transformer is known, can its PCDD/PCDF fingerprint, and levels of each pyrolysis product be predicted?

One hundred seventy of the possible 209 mono through decachlorobiphenyls (PCBs) may form tetra- through octachlorinated dibenzofurans (PCDFs) and tetra- through octachlorinated dibenzo-p-dioxins (PCDDs) during a fire. Four commercially available mixtures of a tetra- through nonachlorobiphenyls which are commonly used as heat insulators in transformers. The four Aroclors: 1242, 1248, 1254 and 1260, may show consistent PCDD/PCDF formation during transformer fires.

During the past six years, Battelle has measured PCDD/PCDF and PCB in a variety of samples from transformer fires and transformer ruptures. For some samples the Aroclor content was known (as a single Aroclor or a mixture); for others, the Aroclor content was unknown.

All PCDD/PCDF analyses were performed on a VG 7070 high resolution double focusing mass spectrometer. PCB analyses were performed on a Varian 3700 gas chromatograph.

The PCB content found in Aroclor 1260 consists of penta-, hexa- and hepta-chlorobipehnyls. These chlorinated biphenyls should act as precursors for the formation of tri- (loss of 2 ortho chlorines), tetra- (loss of 1 ortho HCl or loss of HCl involving a chloride shift), penta-, hexa-, hepta, and octa-chlorinated dibenzofurans and dioxins via all four synthesis routes. Due to the chlorine concentration of Aroclor 1260, the hexa- and heptachloro isomers should be the major constituents in this pyrolysis reaction. By taking the PCDF/PCDD isomer class of highest concentration, and normalizing all quantitive data to that class, a fingerprint of a typical PCDF/PCDD isomer distribution can be attained. The PCDD concentrations, while often higher than the PCDFs, were too inconsistent to establish a fingerprint. The concentration of PCDFs found are 5100-37,500 times less than the amount of Aroclor 1260 detected.

Aroclor 1254, which consists primarily of tetra-, penta- and hexachlorobiphenyl, should yield tetra-, and pentachlorodibenzo-p-dioxins and furans. The analyses of four wipe samples, normalized with respect to the largest quantified congener class, again gives a very reproducible fingerprint pattern. Pyrolysis of this Aroclor yielded a greater amount of tetrachlorodibenzofuran than any other congener class. A sample representing concentrations 5 times higher was compared to the average, and its fingerprint looked comparable.

Air samples were also collected and analyzed from the same transformer fire. Its fingerprint when plotted with respect to the largest chlorinated furan congener class compares well to the wipe fingerprint pattern. Fingerprints of air and wipe samples with 4-5 times higher furan concentration were also the same as the low level fingerprints.

The two Aroclors investigated, 1254 and 1260, showed a fingerprint pattern for the formation of PCDF in transformer accidents. Aroclor 1254 is of most interest due to the predominance of the formation of tetra- and pentachloro dibenzofurans, which are the most toxic PCDF classes. Aroclor 1260 demonstrated predominately hepta- and octachloro-dibenzofuran formation. From a toxicological point of view an accidental fire involving this Aroclor would be less significant as it forms appreciably less of the toxic PCDF isomers. Polychlorinated dibenzo-p-dioxin data acquired during these studies showed the formation of hepta- and octachlorodibenzo-p-dioxin, but not in a reproducible manner. Due to the variability of data, it was not used as a reference for PCDF/PCDD formation in PCB fires. In the data used for this study, dioxin concentrations ranged from 178 to 600,000 times less than the Aroclor concentrations, some extremely high quantities of OCDD were detected. PCDF data from non-cleaned buildings ranged from 4000 to 37,500 times less than the corresponding Aroclor. This allows a rough approximation of PCDF concentrations to be obtained, provided Aroclor information is available. The difference in concentration relative to the Aroclor may be attributed to the heat generated by the fire and its duration, contributions from other chlorinated aromatics, sample location with respect to the fire, and perhaps other variables. A larger data base of fires, and a greater variety of starting materials are needed to more precisely predict pyrolysis products and estimate PCDF formation.

Presented at the 35th ASMS Conference on Mass Spectrometry and Allied Topics
May 24-29, 1987, Denver, CO

ANALYSES OF ORGANIC COMPONENTS IN DRILLING FLUIDS, EXPOSURE WATER, FISH AND PLANTS

Paul H. Peterman, Ted R. Schwartz, Jon A. Lebo and J.L. Johnson
National Fisheries Contaminant Research Center
US Fish & Wildlife Service, Route 1
Columbia, MO 65201

Dan Woodward
NFCRC, Field Research Station; US Fish & Wildlife Service,
P. O. Box 1089, Jackson, WY 83001

Millions of tons of oil drilling fluids (or muds) are used annually in the US. The drilling fluids circulated from the drilling hole to spent reserve pits have adversely impacted aquatic and terrestrial organisms. Reserve pits can overflow, leak or be drained, releasing contaminants into the nearby environment. Drilling fluids vary considerably in composition according to the application, but can be loosely classified as water-based, water/oil-based or oil-based. Diesel fuel is a common lubricant additive.

Samples of three spent drilling fluids from reserve disposal pits in Wyoming were collected. Exposure studies were conducted to assess the biological effects of these wastes on fish and plants. A major objective was to characterize the semi-volatile organic compounds (especially the more toxic aromatics) in the drilling fluids, exposure water, fish and plants by GC/MS.

EXPERIMENTAL:

Groups of 10 cutthroat trout were exposed both statically and dynamically to serial dilutions (1/2 to 1/32) of the drilling fluids for 96 hours. Acute toxicity was measured. Surviving fish in the highest survivable concentration of each drilling fluid were collected for organic analyses. Water samples from the most concentrated exposure (1/2 dilution) of each fluid were also collected for organic analyses. Concentrated drilling fluid was applied to soil once before sweetclover seeds were planted. Success of germination and growth were assessed. Soil and sweetclover samples were also collected for organic analyses.

Organic constituents in aqueous samples were isolated with C_{18} sorbent cartridges and subsequently eluted with 10 mL hexanes and 10 mL dichloromethane. Fish, soil and plant samples were column extracted with dichloromethane and cleaned up using gel permeation chromatography (SX-3). Plant extracts only were further enriched with potassium silicate.

Capillary GC (30 m or 60 m DB-5) with a photoionization detector (9.5 eV) selectively screened for aromatic compounds but often was unable to differentiate target aromatic compounds from other interfering aromatic compounds in the complex drilling fluid extracts. Internal standard mixtures containing deuterated aromatic compounds were added for quantitation. Capillary GC/MS (EI) was used to detect, identify and quantitate contaminants. Mass spectra (35-550 d./sec) were acquired.

RESULTS AND DISCUSSION:

All three spent drilling fluids were acutely toxic to the fish, but the water/oil-based fluid was most toxic. Fish survived only in the 1/32 dilution of this fluid. The undiluted fluid prevented germination of sweetclover seeds that were planted nine days after the fluid was applied to the soil. The high concentration of several inorganic elements (giving a high conductivity) could have caused the lack of germination. The water/oil- and oil-based drilling fluids apparently did not mix well with control spring water. The organic compound concentrations in the water were much lower than expected.

The concentrations and variety of aromatic hydrocarbons present in the drilling fluids likely contributed to the fish toxicity (SEE TABLE BELOW). Alkane hydrocarbons and a few hydrogenated aromatics such as tetralins were also detected.

All samples (drilling fluids, water, fish and plants) contained alkylated aromatics which are common constituents of petroleum and diesel fuel. The concentrations of aromatic compounds in the Wyoming drilling fluids were 15-1000 times less than that in the EPA study of 11 Gulf of Mexico offshore (water-based) drilling fluids.[1]

Quinoline and alkyl quinolines were major organic constituents in the water/oil-based drilling fluid. These compounds are reported to be present at trace levels in crude oil but at higher levels in unrefined shale oil.[2] They were not reported in the EPA study.[1] It is not known how environmentally significant the quinoline compounds are. The quinolines were apparently metabolized by the fish, a result previously reported for quinoline.[3] Although most fish are eventually capable of metabolizing many aromatic hydrocarbons, the fish studied here demonstrated the capability to bioaccumulate aromatic hydrocarbons, especially alkyl aromatics, during a four-day exposure.

CONCLUSIONS:

The spent drilling fluids from Wyoming contained relatively high concentrations of quinoline and alkyl quinolines, but these compounds would systematically be ignored by a routine analysis for target diesel fuel components as proposed by EPA.

Since many drilling fluids may also contain relatively high concentrations of inorganic elements, we recommend that researchers adequately assess both organic and inorganic contamination.

RESULTS:

Aromatic Compounds in Drilling Fluids, Exposure Water, Fish and Plants *

Compound or Class	Drilling Fluid (µg/L) GP	BC	RK	Exposure Water (µg/L) (Nominal 1/2 Dilution) GP	BC	RK	Surviving Fish (ng/g) (1/8 Dil.) GP	(1/32 Dil.) BC	(1/4 Dil.) RK
Naphthalene	< 0.4	32	0.7	ND< 0 5	1	< 0.1	25	50	25
Alkyl Naphthalenes (C_1-C_4)	59	310	40	39	23	1 2	7,230	4,080	460
Biphenyl	0.6	4	1	ND< 1	< 0.5	< 0.1	< 10	50	15
Alkyl Biphenyls	6 4	20	2	2	< 0.5	0.1	1,405	930	145
Fluorene	ND< 0.4	12	1 5	2	< 0.5	0.3	190	215	60
Alkyl Fluorenes	ND< 1	ND< 1	ND< 1	ND	ND	ND	1,030	560	ND
Dibenzothiophenes	0.8	32	1.5	0.5	0.5	0.2	500	530	30
Alkyl Dibenzothiophenes	5.2	98	4 2	1	1	< 0.1	1,130	890	15
Phenanthrene/Anthracenes	0.8	48	3	1	0.7	0.4	975	800	75
Alkyl Phenanthrenes/Anthr.	6.4	96	7.5	3	3	0.2	970	840	75
AZARENES:									
Quinoline	ND< 0.4	200	ND< 0.2	ND< 0.5	45	< 0 2	ND< 15	90	ND< 15
Alkyl Quinolines (C_1-C_3)	6	438	ND< 0.2	< 0 5	230	< 0.2	ND< 15	470	ND< 15
TOTAL	85	1300	64	50	300	3	14,200	9,500	900
[NO. OF COMPONENTS]	[51]	[56]	[30]	[27]	[42]	[33]	[78]	[65]	[35]

* Residues are not listed above because the plants (as seeds) were only exposed to one application of drilling fluids. Most of the residues present were similar to control plants except: Alkyl Naphthalenes (330-390 ng/g), Fluorene and Dibenzothiophene (10-20 ng/g) and Phenanthrene (55 ng/g, BC type only).

ND < 1 Denotes Not Detected at Specified Limit of Detection
NQ Denotes Not Quantitated

---

1 Science Applications, Inc. Drilling Mud Assessment. Chemical Analysis Reference Volume. PB84-170000, NTIS, Washington, D.C. (1984).

2 Clark, R.C. and D.W. Brown, "Petroleum: Properties and Analyses in Biotic and Abiotic System," Chapter 1 in Effects of Petroleum on Arctic and Subarctic Marine Environments and Organisms, ed. by D.C. Malins, pp. 1-89, Academic Press: NY (1977).

3 Bean, R.M., D.D. Dauble, B.L. Thomas, R.W. Hanf, Jr. and E.K. Chess, "Uptake and Biotransformation of Quinoline by Rainbow Trout," Aq. Toxicol. 7, 221-239 (1985).

Presented at the 35th ASMS Conference on Mass Spectrometry and Allied Topics
May 24-29, 1987, Denver, CO

ANALYSIS OF INSECTICIDES BY THERMOSPRAY LIQUID CHROMATOGRAPHY-MASS SPECTROMETRY

Lily Yang and Christina Hsieh Vestal
Vestec Corporation, 9299 Kirby Drive, Houston, Texas 77054

Synthetic pyrethroid and carbamate insecticides have high usage in the United States by virtue of their high effectiveness and low mammalian toxicity. The ability to separate and identify these insecticides and their degradation and metabolic products is important because of their increasing presence in the environment. Analytical procedures for determination of these insecticides are rather limited. The insecticides in this study are thermally labile and/or non-volatile which make them poor candidates for routine GC-MS analyses. However, liquid chromatography (LC) of these compounds is applicable, but retention time is often insufficient for identification, particularly when the sample matrix may contribute materials that interfer with the detection. Thermospray LC-MS provides both mass specific and sensitive detection for these thermally labile classes of compounds.

A Vestec model 201 Dedicated Thermospray LC-MS system was used to analyze these insecticides. Samples were obtained from the USEPA Repository. The stated purities of these compounds ranged from 80 to 99%. The flow rate in all analyses was 1.0 mL/min.

Figure 1 shows the total ion chromatogram of 7 pyrethroid insecticides, 1 µg each injected on a 4.6 mm x 25 cm (5 µm) Altex Ultrasphere-ODS column while scanning m/z 200-550 in 3.2 seconds and using filament-on ionization. The separation of these compounds was accomplished using water/methanol 10/90 for 2 minutes, then an 8 minute gradient from water/methanol 10/90 to 1/99. Both solvents had 0.1 M ammonium acetate present. Resmethrin and permethrin coelute at 9.7 minutes. Apparently there is partial separation of these compounds, even though they are not resolved in the TIC. It also shows many peaks of the impurities and isomers of these standards. The thermospray mass spectra consisted of the base peak at MH^+ for trans-, cis-tetramethrin (MW 331), and resmethrin (MW 338), and at MNH_4^+ for deltamethrin (MW 503), fenvalerate (MW 419), trans- and cis-permethrin (MW 390) with chlorine and bromine isotope peaks with approximately the expected intensities. Typical examples are shown in Figure 2.

Figure 3 shows the total ion chromatograms of 4 carbamate insecticides with and without ammonium acetate present, 1 µg per compound injected on a 4.6 mm x 15 cm (5 µm) Altex Ultrasphere-ODS column under full scan conditions (scanning m/z 150-300 in 1.4 seconds). The separation of a mixture of carbofuran and its derivatives was done using a ten minute gradient from water/methanol 50/50 to 20/80. All of the compounds elute between 2 and 8 minutes. The full scan mass spectra show only the base peak at MH^+ for carbofuran (MW 221) and 3-ketocarbofuran phenol (MW 178) with and without buffer. For carbofuran phenol (MW 164) the spectrum shows the base peak at MNH_4^+ (m/z 182) with buffer and at MH^+ (m/z 165) without buffer. The mass spectrum of 3-hydroxycarbofuran (MW 237) consisted of the base peak at m/z 255 (MNH_4^+) with buffer, and at m/z 220 (loss of H_2O from MH^+) without buffer. It may result from ion-ion and ion-molecule processes in the gas phase rather than thermal effect.

Presented at the 35th ASMS Conference on Mass Spectrometry and Allied Topics
May 24-29, 1987, Denver, CO

Results for carbofuran and its derivatives obtained using the thermospray discharge mode of ionization and positive ion detection are summarized in Table I. All of these compounds showed an excellent signal-to-noise ratio at low nanogram/subnanogram levels using selected ion monitoring.

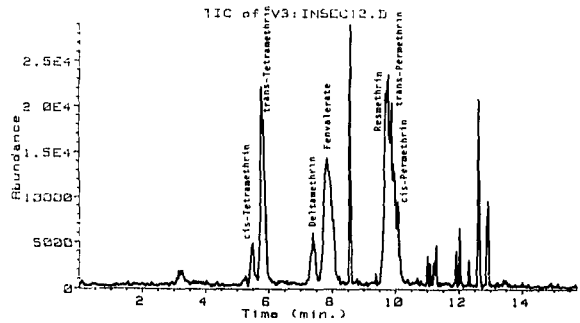

Figure 1. Total ion chromatogram of 7 pyrethroid insecticides.

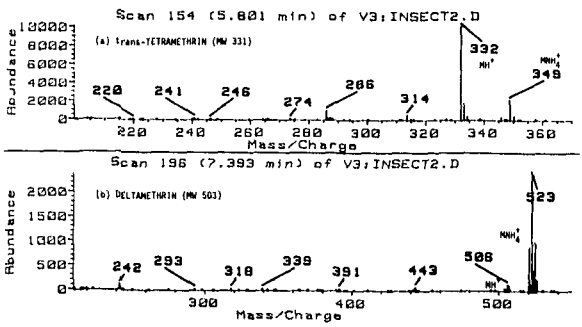

Figure 2. Thermospray mass spectra of (a) trans-tetramethrin, and (b) deltamethrin.

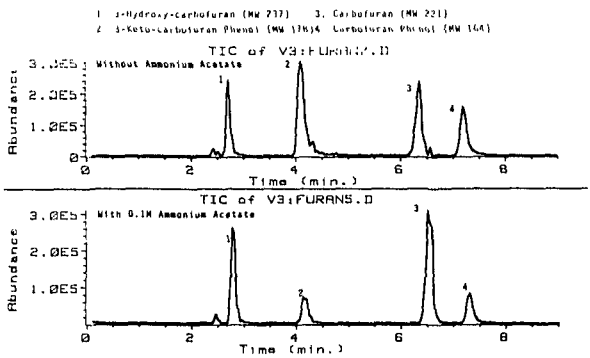

Figure 3. Total ion chromatograms of carbofuran and its derivatives without and with 0.1M ammonium acetate present in the mobile phase.

COMPOUND	MW	RT(min.)	SIM Detection Limits (ng)
3-Hydroxycarbofuran	237	2.7	2.0
3-Ketocarbofuran Phenol	178	4.1	0.6
Carbofuran	221	6.3	1.0
Carbofuran Phenol	164	7.1	1.0

Table I. Summary of 4 carbamate insecticides. No buffer present in the mobile phase.

Presented at the 35th ASMS Conference on Mass Spectrometry and Allied Topics
May 24-29, 1987, Denver, CO

NCI MASS SPECTROMETRIC ANALYSIS OF HUMAN ADIPOSE TISSUE FOR PCDDS AND PCDFS

C. C. Alley, D. G. Patterson, Jr., S. G. Isaacs; Division of Environmental Health Laboratory Sciences, Center for Environmental Health, Centers for Disease Control, Public Health Service, U.S. Department of Health and Human Services, Atlanta, Georgia 30333

INTRODUCTION

Adipose samples from residents of different industrialized countries have been shown to contain polychlorinated dibenzo-p-dioxins (PCDDs) and dibenzofurans (PCDFs). If these compounds are distributed uniformly in adipose tissue without preference for a particular site, samples might be more easily obtained. Also, results from various studies could be compared without regard to the site from which it was taken.

All of these PCDDs and PCDFs have chlorine at the 2, 3, 7, and 8 positions. As reported by Albro et al.(1), many extraction, clean-up, and gas chromatography/mass spectrometry (GC/MS) procedures have been used to quantify these compounds in adipose tissue, but Negative Chemical Ionization (NCI) appeared to provide greater sensitivity for the higher chlorinated compounds.

EXPERIMENTAL

Sample preparation: Adipose tissue samples were taken from selected sites at autopsy: heart, omentum, abdomen, kidney, buttock, and breast. They were extracted and cleaned-up by an automated column chromatography method described in (2). PCDDs/PCDFs are quantitated by isotope dilution mass spectrometry, with 13C-labeled 2378-containing congeners.

GC/MS Conditions: The Finnigan 4500 mass spectrometer was operated in the NCI mode with 5 multiple-ion descriptors containing 2 ions each for the native and the labeled dioxins and furans in each chlorination group. A 60 m DB-5, 0.25 mm, 0.25 µm fused silica capillary column was used and all PCDDs and PCDFs eluted in less than 1 hour. The column was temperature programmed as follows: 100°C (2 min) to 260°C at 20°C/min, then to 300C at 1°C/min and held at 300°C for 5 min. The ionizer temperature was 100°C, the injector temperature was 300°C, the electron energy was 70 eV, and the filament was 0.25 mA. Data was processed semiautomatically by using the INCOS data system under procedural control.

Criteria for identification and quantitation: 1) S/N > 3:1 on all native and labeled ions. 2) Observed RTs within ± 1 sec of each other for the native and labeled ions. 3) Isotope ratios of the native and the labeled congeners must be within ± 10% of the theoretical value (Figure 1).

Calibration curves for 14 congeners were established using 3 concentration levels (Figure 2). Calibration curves were verified by analysis of an analytical standard during an 8 hr shift. Instrument tuning, resolution and other parameters were checked daily to insure optimum sensitivity and selectivity. Data was processed semiautomatically using the INCOS data system under procedural control.

RESULTS

The advantage of this NCI method is increased sensitivity for penta-octa CDFs. The disadvantages are lack of selectivity and isomer specificity for tetra CDDs and CDFs.

We have applied this method in studying the anatomical distribution of PCDDs and PCDFs within human tissues. PCDDs and PCDFs were present at similar concentrations in the various adipose tissues within a given individual (Figures 3 and 4).

REFERENCES

1) Albro, et al., Anal. Chem., 57, 2717-2725 (1985).
2) Anal. Chem., 58, 713-716 (1986).

This study was supported by the Agency for Toxic Substances and Disease Registry, Public Health Service, U.S. Department of Health and Human Services, Atlanta, Georgia 30333.

Presented at the 35th ASMS Conference on Mass Spectrometry and Allied Topics
May 24-29, 1987, Denver, CO

FIGURE 1

ISOTOPE RATIOS FOR 123678-HCDD

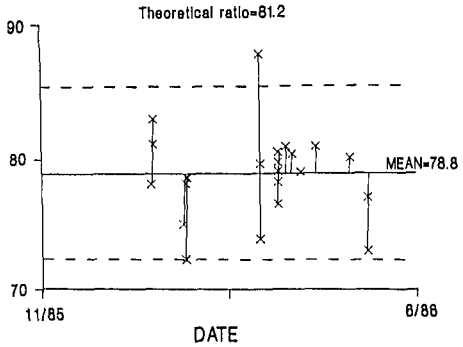

FIGURE 2

STANDARD CURVE FOR 123678-HCDD

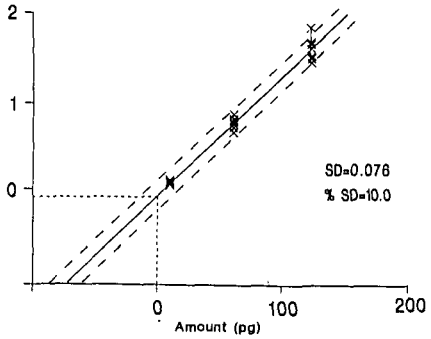

FIGURE 3

PCDFs and PCDDs in Human Adipose Tissues
(Male)

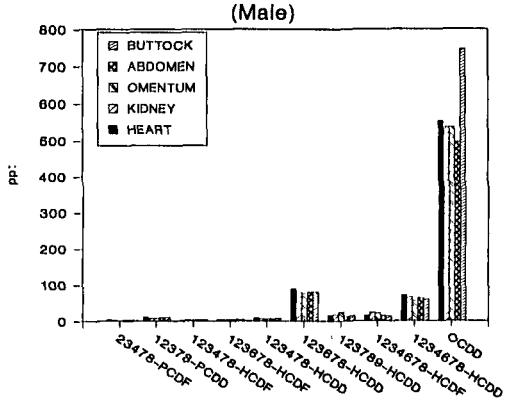

FIGURE 4

PCDFs and PCDDs in Human Adipose Tissues
(Female)

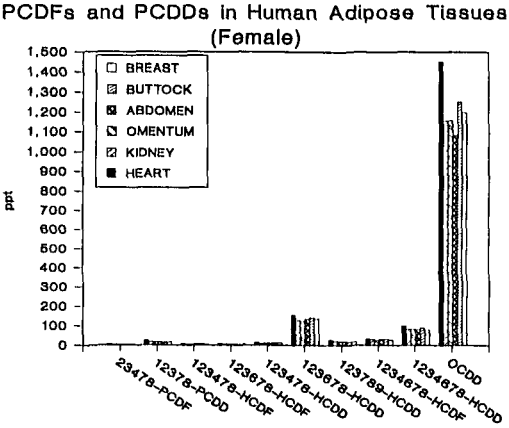

Presented at the 35th ASMS Conference on Mass Spectrometry and Allied Topics
May 24-29, 1987, Denver, CO

Screening for Polychlorinated Diphenyl Ethers and Polychlorinated Biphenylenes While Quantifying Polychlorinated Dioxins and Furans

J.M. Czucwa, F.L.DeRoos, D.G. Aichele, V.R. Katona, and M.R. Bauer
Battelle Columbus Division, Columbus, Ohio 43201

Polychlorinated dibenzo-p-dioxins (PCDDs) and dibenzofurans (PCDFs) are compounds of environmental significance due to the high toxicity of certain isomers. A proven technique for the determination of PCDD/PCDF in complex matrices is combined capillary column gas chromatography/high resolution mass spectrometry (HRGC/HRMS) analysis with selected ion monitoring. Yet, even at a mass resolution of 10,000-12,000 (M/ΔM, 10 % valley), HRGC/HRMS is not able to resolve some interferences to PCDD/PCDF.

Several classes of compounds can potentially interfere with the identification of PCDD/PCDF isomers and can cause erroneous results. Polychlorinated biphenylenes (PCBPs) produce molecular ion clusters which overlap with the molecular ion cluster of PCDDs containing one less chlorine and therefore, PCBP isomers can be inadvertently identified as PCDD isomers. For example, hexachloro-biphenelyene ions of m/z 357.8517 may be present in the m/z 357.8258 selected ion monitoring chromatogram used for the detection of pentachloro-dibenzo-p-dioxins. The resolution needed to resolve these species is 13,800.

Polychlorinated diphenyl ethers (PCDEs) can lose two chlorines, two hydrogens, or a chlorine and a hydrogen after EI ionization to produce ion masses identical to PCDF isomers. For example, the spectra of heptachloro-, hexachloro- and pentachlorodiphenyl ethers all show fragment ions at the same mass as the pentachlorodibenzofuran molecular ions. Because the exact masses are correct, these compounds will be detected as PCDF isomers. In cases where PCBP/PCDE interferences are suspected, the samples can be reanalyzed for the presence of the interfering compounds, but such analyses are time consuming and expensive.

In order to resolve this problem, we have developed a mass spectrometric data acquisition program which allows us to monitor selected ion masses for the PCDD/PCDF isomers and the interfering PCBP/PCDE compounds. The PCDD/PCDF quantification and PCBP/PCDE screening are achieved in a single HRGC/HRMS analysis. A different set of interferant ion masses is monitored during each PCDD/PCDF elution window as shown in table 1. The ion masses used to monitor for the presence of PCBPs and PCDEs were chosen for maximum sensitivity and selectivity. We also established criteria, similar to those already in use for PCDD/PCDF determinations, for the positive identification of PCBP/PCDE peaks (table 2). The program results in fewer errors in PCDD/PCDF determinations and increases the certainty of the analytical results. The addition of PCBP/PCDE ion masses to the acquisition program, however, decreases the sensitivity of PCDD/PCDF determinations and is best applied to samples for which sensitivity is not a problem. PCDD/PCDF determinations at femtogram levels may require separate quantification and screening analyses.

The mass spectrometric data acquisition program has been successfully used to identify PCBP and PCDE interferences in determinations of PCDDs/PCDFs in several environmental matrices. Data from a PCDD/PCDF determination on a building wipe sample is shown in figure 1. The two shaded peaks in the mass chromatogram of the hetachlorodibenzofurans are actually due to the presence of nonachlorodiphenyl ethers as shown in the m/z 477.7194 mass chromatogram. In this case only the four unshaded peaks in the hepta-CDF chromatogram would be included in the final quantification of PCDF concentration.

Presented at the 35th ASMS Conference on Mass Spectrometry and Allied Topics
May 24-29, 1987, Denver, CO

Table 1: MASSES USED TO SCREEN FOR INTERFERENCES

BIPHENYLENES			DIPHENYL ETHERS		
PCDD Window	Masses	Theoretical Ratio	PCDF Window	Masses	Theoretical Ratio
Tetra	321.8677 323.8648	0.62	Tetra	375.8364 377.8334	1.23
Penta	357.8258 359.8229	1.23	Penta	409.7974 411.7844	1.03
Hexa	391.7868 393.7839	1.03	Hexa	443.7584 445.7555	0.88
Hepta	425.7479 427.7449	0.88	Hepta	477.7194 479.7163	0.77
Octa	no interfering Biphenylenes		Octa	511.6805 513.6775	0.69

Table 2: CRITERIA FOR THE IDENTIFICATION OF BIPHENELENES AND DIPHENYL ETHER INTERFERENCES

* The PCBP or PCDE chlorine isotope ratios are with in 15% of the theoretical values.
* The PCBPs or PCDEs elute simultaneously with a PCDD or PCDF peak.
* The PCBP or PCDE areas must be at least 5-10% of that for the corresponding PCDD or PCDF.
* The signal to noise ratios must be at least 5:1.

Figure 1: SAMPLE MASS CHROMATOGRAMS

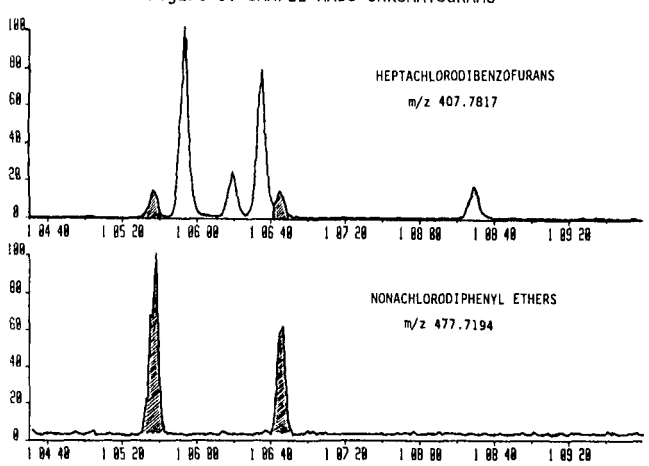

Presented at the 35th ASMS Conference on Mass Spectrometry and Allied Topics
May 24-29, 1987, Denver, CO

LIQUID CHROMATOGRAPHY-MASS SPECTROMETRY ANALYSES OF NON-VOLATILE ORGANIC ENVIRONMENTAL POLLUTANTS:

Ross C. Willoughby, S. Mitrovich, J.G. Dulak and F. Poeppel, Extrel Corporation, Pittsburgh, PA 15238; D. Sauter, ADS Consulting, Henderson, NV 89015.

INTRODUCTION

The analyses of non-volatile environmental pollutants is a considerable problem. The Solid Waste Disposal Act and later Amendments cited within the Resource Conservation and Recovery Act (RCRA) of 1976 require the analysis of such compounds. SW-846 is an EPA publication which outlines the analysis methods for compounds under compliance monitoring.

SW-846 uses at least seven different methods to analyze for compounds in wastes and ground water. There are significant technical difficulties in SW-846. In addition, there are many Appendix VIII compounds for which no analytical method is currently available.

There are many problems associated with such broad-based analytical testing. One significant problem could be overcome if the existing GC/MS based procedures could be augmented with sufficiently easy-to-use and analytically-significant LC/MS methods.

OBJECTIVES

A newly developed LC/MS interface based on particle-beam solute introduction has shown analytical capabilities for allowing augmentation of GC/MS-based method protocols. This study evaluates the analytical performance of this new interface, ThermaBeam™, for the analysis of Appendix VIII and other environmentally significant compounds. A comparison is made of the analytical figures-of-merit between LC- and GC/MS procedures.

EXPERIMENTAL

The LC/MS used in this study was a ThermaBeam™ system coupled to an EXTREL ELQ 400 mass spectrometer. Twenty-two Appendix VIII compounds were studied for both quantitative and qualitative aspects of ThermaBeam.

RESULTS

Figure 1 shows a spectrum of DFTPP acquired with ThermaBeam under 70 eV electron impact ionization conditions. The spectrum meets the required abundance criteria designated in EPA method 625. Library searchable EI spectra were obtained for 19 out of 22 of the observed analytes. Figure 2 shows a library comparison of a ThermaBeam acquired spectrum with the library spectrum and a difference plot at the bottom.

Quantitatively, this study demonstrated that method detection limits, using sample concentration factors similar to EPA GC/MS methods, were in the order of 2-15 ppb for nine components tested. Minimum detectable response has been observed between 5-50 ng for all respondents. The technique also demonstrated linear response over several orders of magnitude.

CONCLUSIONS

ThermaBeam LC/MS is a viable analytical approach to augmentation of the existing GC/MS protocols to include Appendix VIII and other environmentally significant compounds.

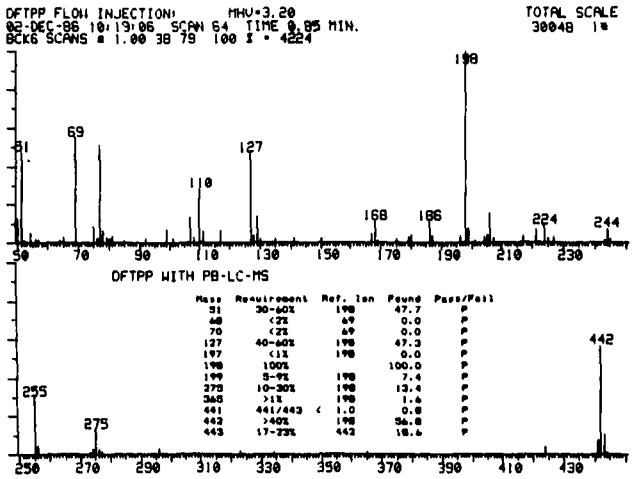

Mass	Requirement	Ref. Ion	Found	Pass/Fail
51	30-60%	198	47.7	P
68	<2%	69	0.0	P
70	<2%	69	0.0	P
127	40-60%	198	47.3	P
197	<1%	198	0.0	P
198	100%		100.0	P
199	5-9%	198	7.4	P
275	10-30%	198	13.4	P
365	>1%	198	1.6	P
441	441/443 <	1.0	0.8	P
442	>40%	198	56.8	P
443	17-23%	442	18.6	P

Figure 1. The inset table shows the found fragmentation data versus the standard EPA requirement. No deviations from criteria are observed.

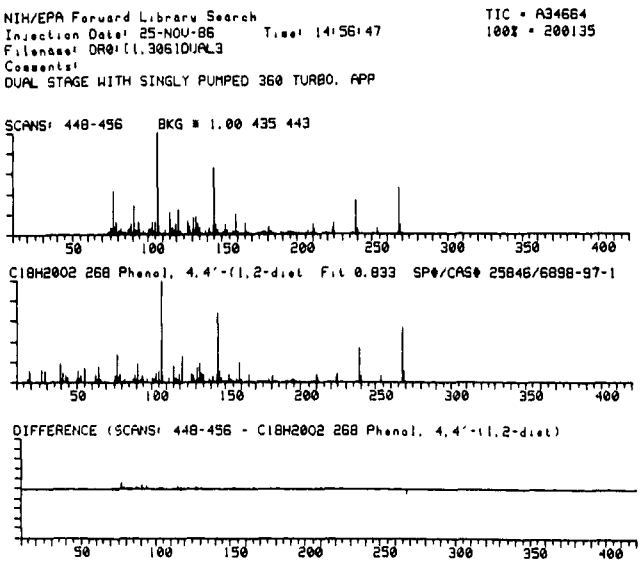

Figure 2. 42,000 compound NIH/EPA library search on DES delivered through the ThermaBeam™ LC/MS interface.

Presented at the 35th ASMS Conference on Mass Spectrometry and Allied Topics
May 24-29, 1987, Denver, CO

AMBIENT AIR MONITORING FOR TOXIC CONTAMINANTS BY PROCESS MASS SPECTROMETRY;
*CESSNA, G, BARTMAN, C, AND PATTERSON, T; EXTREL CORPORATION, PITTSBURGH, PA.

INTRODUCTION

Users and producers of toxic gases must monitor multiple plant locations to insure that the levels of toxic chemicals in environmental air are below the threshold limit values (TLV) mandated by the Environmental Protection Agency and the Occupational Safety and Health Agency (OSHA).

In order to satisfy this requirement, the air monitor must have

- O Fast response time
- O PPB detection limits
- O Stable operation
- O Component selectivity
- O A wide dynamic range.

Traditional techniques for ambient air monitoring such as specific component probes or sorption techniques followed by gas chromatography fail to meet all of the requirements for ambient air monitoring of toxic materials.

This abstract reports on a real time technique for accurate quantitation of toxic chemicals typically monitored for potentially hazardous conditions. The technique is demonstrated with laboratory data including the rare gas isotopes in air, benzene and toluene. Additionally, specific sample introduction techniques are discussed to minimize the lag time associated with inlet clearing and maximize the total cycle time of the analysis.

The monitor used in this study was a Questor Process Analyzer manufactured by EXTREL CORPORATION in Pittsburgh, Pa. The Questor is a quadrupole mass spectrometer designed for process monitoring. It is coupled with a 16-port rotary valve and is data system controlled to allow for very flexible operation.

RESPONSE TIME

Provided that fresh sample is constantly pumped to the Questor inlet, the analyzer valve can be cleared in less than 2.0 seconds and as many as 5 components can be reported in less than 1.0 second. The Questor was set-up to monitor the major components in air and the 650 ppb Kr-84 isotope. A variety of analysis times were evaluated and reported between 4 and 200 seconds. There was no degradation in the data as the analysis time was reduced to 4 seconds. The percent relative standard deviation reported for the Kr-84 isotope throughout the range of analysis times was less than 6%. This means that as few as 6 seconds per location are required to both clear the Questor inlet and report the average of 4 scans for as many as 5 components. As a result, as many as 10 locations can be reported in less than one minute of cycle time.

DETECTION LIMIT

Using the rare gases in ambient air to demonstrate the Questor's lower detection limit, data is reported for the 8 ppb Xe-136 isotope at a signal

to noise ratio of 3 to 1 and a percent relative standard deviation of less than 10% for 250 scans. This performance indicates that the signal to noise ratio at the typical TLV levels, nearly 100 times larger than the detection limit, is excellent.

STABILITY

The stability of the Questor analyzer was demonstrated by analyzing low level impurities in helium. A ten hour stability test was performed with statistics reported for each set of 5000 scans (approximately 1 hour). The percent relative standard deviation for 2 ppm oxygen, 8 ppm argon and 5 ppm carbon dioxide was less than 3% in all cases.

DYNAMIC RANGE

The dynamic range of the Questor analyzer was demonstrated by analyzing a variety of standards over a range of 50 ppb to 100 ppm. The linear regression yielded a correlation coefficient of 0.9992 (99.92% fit) and a y-intercept of -1.4 ppb. This indicates that the analyzer is capable of accurately reporting the concentration of the toxic component at both high and low concentrations relative to the TLV.

RESULTS

Data was presented for the measurement of the exponential decay of benzene and toluene in the contaminanted headspace of a glass container as the two components were washed out of the headspace with air. The toluene levels decayed from 1.0 ppm to 200 ppb in a period of 10 minutes and signal levels were well above baseline. The benzene levels decayed from 1.0 ppm to 150 ppb in a period of 6 minutes and were also still well above the baseline. The calculated detection limits for both components was approximately 20 ppb with a signal to noise ratio of 3 to 1.

CONCLUSIONS

The application of quadrupole mass spectrometers for ambient air monitoring of highly toxic chemicals offers several significant advantages over the more traditional techniques. Quadrupole mass spectrometers optimize the total cycle time for analyzing multiple plant locations with one analyzer and can report as many as 10 locations for up to 5 components in less than 1 minute. The long term stability, dynamic range and low levels of detection ensure no false alarms are sounded and that accurate quantitation is made at concentrations above and below the TLV. The repeatability is better than 10% at concentrations 10 times lower than typical threshold limit values for most toxic chemicals.

Presented at the 35th ASMS Conference on Mass Spectrometry and Allied Topics
May 24-29, 1987, Denver, CO

ENVIRONMENTAL AND BIOCHEMICAL APPLICATIONS OF TRACE ANALYSIS BY MS/MS

S.T. KROLIK AND C.J. PORTER.
VG ANALYTICAL LTD., FLOATS ROAD, WYTHENSHAWE M23 9LE. UK.

Recent developments in MS-MS instrumentation have facilitated ion beam tuning and optimisation procedures. It is the objective of this work to ascertain quantitatively the sensitivity of the technique on a hybrid mass spectrometer. The instrument chosen for this study was a VG 70-250SEQ.

ENVIRONMENTAL APPLICATIONS.

Collision - induced dissociation at low collision energy results in fragmentation which is often dependent upon the collision energy. For environmental samples where ultimate levels of ion detection are often necessary the method of multiple reaction monitoring MRM is the preferred GC-MS-MS analysis technique. It is important that for such an analysis a specific collision energy value is associated with each of the chosen reactions. This may be seen from the first figure which shows a series of mass chromatograms for each of the daughter ions generated from m/z 247 as parent ion from 1-nitropyrene as a function of collision energy. The capability for fast and precise switching of the voltages of the mass spectrometer is also a prerequisite for any such analysis. These requirements in total can most easily be achieved using full computer control.

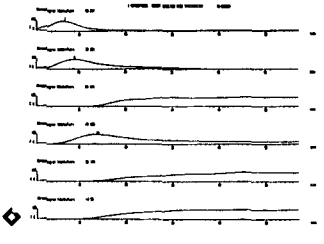

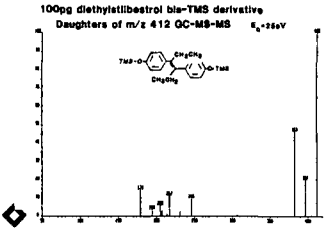

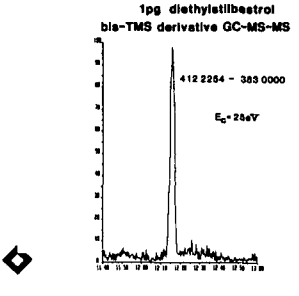

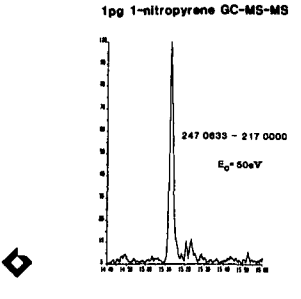

Presented at the 35th ASMS Conference on Mass Spectrometry and Allied Topics
May 24-29, 1987, Denver, CO

BIOCHEMICAL APPLICATIONS.

The ionisation of the matrix material together with the sample in FAB significantly limits the ultimate level of ion detection. This has serious implications when only low sample quantities are available resulting in the sample being unobserved in the matrix.

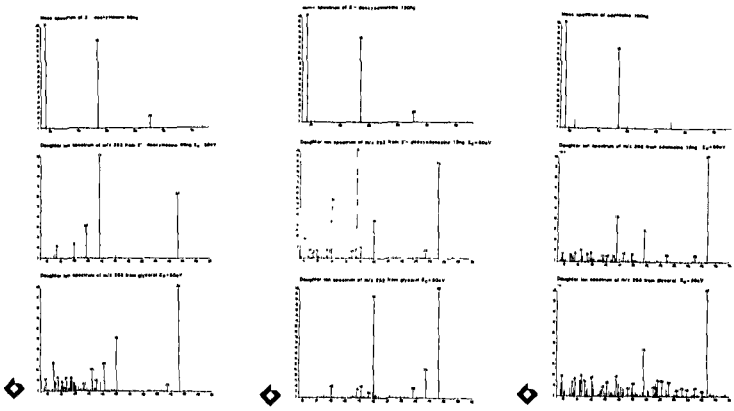

Full daughter ion spectra from a series of nucleosides have been obtained with computer aided collision energy optimisation using the multichannel analysis mode of acquisition. These spectra show improved signal to noise compared with the normal mass spectra in which relevant sample ions are unobserved.

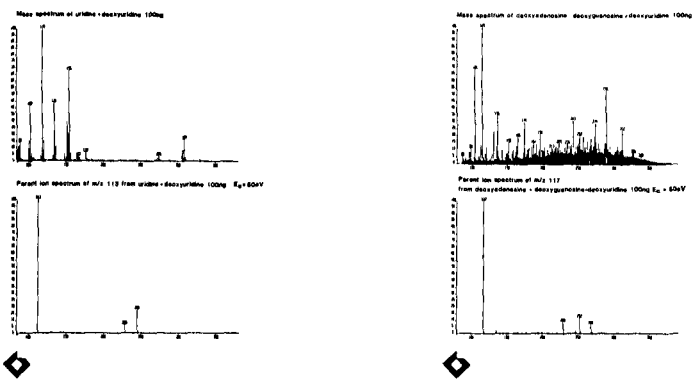

Full parent ion spectra of characteristic sugar and base moieties are shown from which molecular weight information from a multi-component mixture of nucleosides may be obtained. The normal mass spectrum of the mixture does not readily yield this information at comparable levels of sample concentration.

Presented at the 35th ASMS Conference on Mass Spectrometry and Allied Topics
May 24-29, 1987, Denver, CO

ADVANCES IN GC-HRMS DATA ACQUISITION TECHNIQUES FOR THE QUANTITATIVE ANALYSIS OF POLYCHLORINATED DIBENZODIOXINS AND DIBENZOFURANS.

J.C. Bill, B.W. Gray, B.N. Green, J.A.Yoffe; VG Analytical Ltd., Floats Road, Manchester M23 9LE, UK.

INTRODUCTION

High resolution SIR is the most sensitive and specific technique for the analysis of PCDDs and PCDFs in complex mixtures. With a total of 136 isomers in the tetra to octa CDFs and CDDs, it is clearly advantageous to use automated data acquisition and analysis techniques. However, automatic analyses of these compounds require careful monitoring, at all stages, to ensure data integrity. With this in mind, we have developed a method of computerised SIR data acquisition and processing, the principal features of which are described.

SENSITIVITY

The lower line in Figure 1) illustrates the relative sensitivity change which would result from voltage switching over the whole mass range. Under these conditions the relative sensitivity for the octa CDFs and CDDs would be appproximately 56% of the sensitivity for the tetra CDFs and CDDs.

This reduction in sensitivity can be substantially lessened by separating the masses to be monitored into 5 groups, corresponding to each CDF and CDD homologue, in each of which the mass range is no more than 10% for these compounds. Between each group the magnet is switched to a higher mass position, thus enabling the voltage for each group to remain close to the maximum. The upper line in Figure 1) shows that when this technique is used the relative sensitivity is maintained to within 10% for the complete analysis.

DATA ACQUISITION PARAMETERS

The parameters used to control the acquisition of data from the penta CDF and CDD group of masses are shown in Figure 2).

Note that 2 ions are monitored for each Analyte and its respective Internal Standard. These are used to provide isotopic ratio checks during the data processing operations.

Newly introduced parameters provide full control of the 'lock mass' span, and the amount of correction to be applied during each cycle through the group of masses. Such control is necessary to avoid the 'hunting' which could otherwise occur. However, an option is provided to enable much larger lock mass corrections to be applied during the first few seconds of each group during the magnet settling period.

MASS SCALE CALIBRATION

A display of the voltage/mass calibration for the penta CDF and CDD mass range is shown in Figure 3). The ppm error of the actual voltage from the theoretical voltage is graphically illustrated in the upper display. The PFK reference compound used for this operation is left in the system to provide the peaks for the Lock Mass channels.

RESOLUTION CHECK

Confirmation of instrumental resolution, over the mass range of operation, is provided in the display illustrated in Figure 4). A clearly marked and calibrated grid enables the resolution, at the extremities of the mass range of any group, to be recorded.

LOCK MASS OPERATION

A Lock Mass is used primarily to correct for short or long term drifts. This is achieved by making a scan over this peak and comparing its actual centroid position with the required position. By also recording the intensity of the Lock Mass the integrity of the data is continuously monitored, and this information is used for corrections in the event of a disturbance affecting sensitivity. Figure 5) shows a typical sequence through a group of masses containing a lock mass.

FAST LOCK ON

Whenever magnet switching is used there is a small, but possibly significant, time for the magnet to settle at its new position. The Fast Lock On procedure overrides the Lock Mass step size, and provides a full corrective step during this period. After achieving a stable Lock On the Lock Mass step size is restored to its controlled value. Figure 6) shows the comparative performance of a sytem with, and without, Fast Lock On.

RESULTS

A typical trace from one of the ions monitored for the PeCDFs (m/z 339.8597), together with the 13C labelled internal standard, is shown in Figure 7). The peak detection process uses first and second differentials to define peak start, end, valley, and shoulder points, and has parameters to control the degree of baseline tracking across groups of un-resolved peaks.

QUANTITATION

A new Data Base Editor facility allows simple construction of targetting information for the quantitation routines. Figure 8) shows a segment of such a data base containing information for the identification of the PeCDFs and PeCDDs.

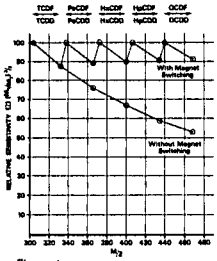

Figure 1

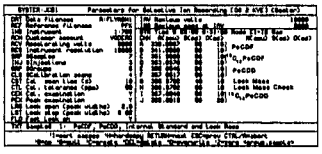

Figure 2.

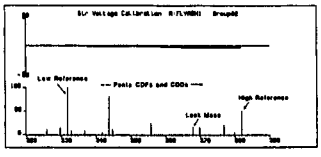

Figure 3.

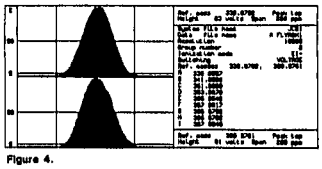

Figure 4.

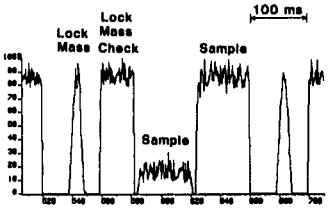

Figure 5.

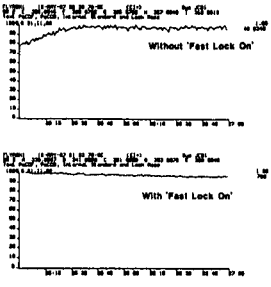

Figure 6.

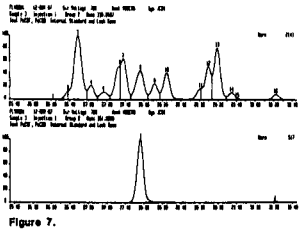

Figure 7.

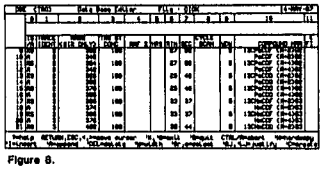

Figure 8.

Presented at the 35th ASMS Conference on Mass Spectrometry and Allied Topics
May 24-29, 1987, Denver, CO

SPECIFICITY AND SENSITIVITY IN TRACE ANALYSIS BY GC/MS

Frank M. Benoit, Health and Welfare Canada, Ottawa, Ontario, Canada.

In trace analysis for environmental contaminants by GC/MS the analyst often faces the difficult problems of concurrent unequivocal identification and accurate quantitation of an analyte contained in a complex matrix extracted from the environment. This requires the production of a mass spectrum that is highly characteristic of the analyte while at the same time retaining sufficient instrument sensitivity to be able to detect the analyte at the low levels usually found in environmental media. High quality results are obtained when these two dichotomous requirements - specificity vs sensitivity - can be reconciled.

The amount of information that must be available in a mass spectrum in order to be considered sufficiently specific for unequivocal compound identification is difficult to establish absolutely. In our experience, a mass spectrum should contain, as a minimum, information on the molecular weight of the analyte and at least one abundant fragment ion peak, preferably in the mass region of the molecular ion, in order to be considered specific for purposes of analyte identification.

In recent years considerable progress has been achieved in the development of alternate modes of ionization in mass spectrometry. In our laboratory, the mass spectrometer is equipped with four modes of ionization : electron impact (EI), methane chemical ionization (CI), methane electron capture (EC) and oxygen negative chemical ionization (ONCI). By varying the mode of ionization it is possible to select the mode that best fits the needs of the analysis. As an example, we have examined the behaviour of methyl chloroacetates under the four modes of ionization.

On an arbitrary scale of 1 to 4 the specificity of each methyl chloroacetate was estimated on the basis of the heights of the molecular ion and fragment ion peaks. Electron impact exhibited poor specificity with weak or absent molecular ions and a strong peak at m/z 59 characteristic of the ester function but not of the original molecule. Both methane chemical ionization and oxygen negative chemical ionization showed high specificity with strong molecular ion and fragment ion peaks. Methane electron capture showed average specificity with abundant molecular ions but weak fragmentation.

The sensitivity for each methyl chloroacetate and each ionization mode was measured on a scale of 1 to 100 based on the height of the base peak per unit of quantity injected. Methane chemical ionization (100) was the most sensitive mode followed by electron impact (40), oxygen negative chemical ionization (10) and methane electron capture (<5).

Fortuitously, methane chemical ionization produced mass spectra with the highest specificity and provided the highest sensitivity for all three of the methyl chloroacetates examined in the present study and would be the method of choice for the analysis for these compounds in environmental media. In other cases, where one mode of ionization is not both the most specific and the most sensitive, the analyst would have to seek additional modes of ionization or would have to select the mode of ionization most appropriate to the requirements of the analysis.

Presented at the 35th ASMS Conference on Mass Spectrometry and Allied Topics
May 24-29, 1987, Denver, CO.

COMPOSITION AND SIZE DISTRIBUTION OF THE ORGANIC CONSTITUENTS OF ATMOSPHERIC PARTICULATE MATTER IN THE PONCE, PR AREA

Rafael Infante, Nidia Santiago, and Arnaldo Carrasquillo
Biomedical Research Program
Catholic University of Puerto Rico
Ponce, P.R. 00732.

In recent years particulate elemental composition in the atmosphere has received an increasing amount of attention. Studies by a number of research groups has produced a large amount of information concerning the composition and distribution of organic compounds in the atmosphere. However, there is less information available for urban areas located on tropical islands where the pollutants are assumed to be rapidly dispersed by ocean breezes. The purpose of this study is to establish the presence of the most important organic compounds in airborne particulate matter collected in a residential town area located on a tropical island as well as to determine their size distribution.

Ambient levels of organic compound, especially polycyclic aromatic hydrocarbons (PAH's), are of concern because their potential for adverse biological effect, including transformation of some of these substances to mutagens and carcinogens. Since the majority of PAH compounds are adsorbed on airborne particulate matter, their potential carcinogenic effect on human health depends largely on the extend to which these compounds are distributed in the respirable size range below about 7 um diameter. Only particles smaller than this size can be transported through the upper respiratory tract into the bronchioles and alveoli of the lungs.

Samples of airborne particulate matter were collected at five residential zones in the Ponce area. The sites were selected taking into account predominant wind patterns and known sources of air pollution. Airborne particulate samples were collected on glass fiber filters mounted in a high volume sampler. The samplers were run simultaneously for 24-hours periods at least once every six days. For the aerosol size fractionation study a cascade impactor mounted on a high volume sampler was used. The cascade impactor separates the airborne particulate into five distinct fractions based on their aerodynamic diameter: >7 um; 3.3-7.0 um; 2.0-3.3 um; 1.1-2.0 um and < 1.1 um. The cascade impactor was run for 72-hours in order to get enough sample.

A monthly composite sample from each of the sampling stations was ultrasonically extracted using methylene chloride for 20 minutes. The extracts were concentrated using Kuderna-Danish under a nitrogen atmosphere. The organic fraction was analyzed using capillary gas chromatography-mass spectrometry. The major peaks in each of the fractions analyzed were identified by comparison of their mass spectra with an on line library of over 20,000 spectra; comparison with the spectrum of reference compounds; comparison of retention times with that of standard compounds for an homologous series; manual interpretation of the mass spectrum and selective ion monitoring and retention time data.

The organic fraction of the Ponce aerosol consisted mainly of normal paraffins, polycyclic aromatic hydrocarbons were also observed but in smaller concentration. The polycyclic aromatic hydrocarbons (PAH's) were observed mainly in the Ponce center and the Ponce east stations. In the Ponce center station the major sources of PAH's were the approximately 50,000 motor vehicles

commuting within the city limits, while in the Ponce east station PAH's were associated with the agricultural burning activities in this area.

The results obtained from the methylene chloride extractable organic matter in each of the five fraction size analyzed suggests that most of the organic matter is associated with the particles having the smallest aerodynamic diameter (< 1.1 um), even though the airborne particles that predominates in the Ponce area are in the 1.1-2.0 um size range. Particles with an aerodynamic diameter < 1.1 um comprise only the 13.4 % of the airborne particulate for the city of Ponce. The organic compounds that were identified in the < 1.1 um size are presented in Table 1. For all cases the PAH's were observed in the < 1.1 um particle size. This fact suggest the anthropogenic nature for this compounds class.

In summary, the concentration of saturated hydrocarbons relative to PAH's observed indicate that contributions from natural sources rather than anthropogenic dominates the particulate organic matter in this area. It was also observed that an increase in the levels of benzo(a)pyrene and benzo(e)pyrene was related to the agricultural burning activities in this area. Regarding their size distribution the PAH's were mainly observed in the < 1.1 um particle size range.

Table 1. Individual Compounds Identified in the Extractable Organic Matter (< 1.1 um)

1. Normal alkanes

$C_{10}H_{22}$ - $C_{37}H_{56}$

2. Aromatic hydrocarbons

Naphthalene	Phenanthrene
Acenaphthene	Pyrene
Acenaphthylene	Chrysene
Flourene	Benzo[a]pyrene
Anthracene	Benzo[e]pyrene

Acknowledgement
Support of this work from MBRS-DRR-NIH Grant No. 0867 and GM-NIH Grant No. 07732 is acknowledge.

Presented at the 35th ASMS Conference on Mass Spectrometry and Allied Topics
May 24-29, 1987, Denver, CO

ANALYSIS OF SULFUR VESICANTS BY CAPILLARY COLUMN ISOBUTANE CHEMICAL IONIZATION MASS SPECTROMETRY, Paul A. D'Agostino and Lionel R. Provost, Defence Research Establishment Suffield, Ralston, Alberta, Canada, TOJ 2NO.

The vesicant bis(2-chloroethyl)sulfide (mustard or H), first used as a chemical warfare agent during the battle of Ypres in 1917, has recently been identified on the Iran/Iraq battlefield by a United Nations team of experts (1). Electron-impact (EI) ionization may be used for the identification of mustard, other vesicants and related compounds provided the mass spectra exhibit significant molecular and higher molecular weight fragmentation ions (2-4). An alternative ionization technique, such as chemical ionization (CI) (5), may be required for the identification of compounds that do not provide sufficient EI information. CI mass spectrometry has been applied to the analysis of organophosphorus chemical warfare agents (6-8). However, reports of CI applications to sulfur vesicants appear to be limited to only mustard and sesquimustard (Q) (3). We report the application of capillary column isobutane chemical ionization mass spectrometry to mustard containing samples. Pseudo-molecular $(M+H)^+$ and structurally significant CI fragmentation ions were observed for mustard, other sulfur vesicants and related compounds.

Capillary column GC-MS (isobutane CI) analyses were performed with a VG 70/70 E mass spectrometer equipped with a Varian 3700 gas chromatograph under the following conditions: (GC column: 15 m x 0.32 mm ID J+W DB-1; Temperature program: 50°C (2 min) 10°/min 280°C (5 min); Injector: cold on-column at 50°C; Source pressure: 2 x 10^{-4} torr; Source temperature: 120-140°C; Emission current: 500 µA; Electron energy: 150 eV; Scan function and rate: 450 to 20 u, 1 s/dec.).

Figure 1 illustrates a typical capillary column GC-MS (isobutane CI) total-ion-current chromatogram of about 2 µg of HT. Ten sample components, listed in Table 1, were identified (or tentatively identified) in the HT mustard. The sulfur vesicant, bis[(2-chloroethylthio)ethyl]ether (T), was typical of the longer chain compounds characterized. Molecular ion information was absent under EI conditions. However, pseudo-molecular $(M+H)^+$ and structurally significant CI fragmentation ions were observed during isobutane CIMS (Figure 2).

Figure 3 illustrates the capillary column GC-MS (isobutane CI) total-ion-current chromatogram of an Iran/Iraq battlefield soil sample extract. Mustard and seventeen other related compounds, listed in Table 2, were identified (or tentatively identified) in the soil sample extract based on the acquired mass spectral data. Figure 4 illustrates the isobutane CI mass spectra of two previously uncharacterized dehydrochlorination products identified in the soil sample extract. Both compounds exhibited intense $(M+H)^+$ and $(M+H-H(S \text{ or } O)CH{=}CH_2)^+$ ions under isobutane CI conditions.

Capillary column isobutane chemical ionization mass spectrometry was found to be an excellent method for the mass spectral characterization of mustard, other vesicants and related compounds. Interpretation of the pseudo-molecular and CI fragmentation information afforded by this technique enabled the indentification of many previously unreported mustard impurities. This data may prove useful for future chemical warfare agent verification exercises as the identities of trace sample components may provide analysts with information on munitions type, origin or synthetic procedures.

References

1. "Report of the Mission Dispatched by the Secretary-General to Investigate Allegations by the Islamic Republic of Iran Concerning the Use of Chemical Weapons", United Nations Security Council S/16433, 26 March 1986.
2. E.R.J. Wils and A.G. Hulst, Fresenius Z. Anal. Chem., 321, 471, 1985.
3. E. Ali-Mattila et. al., Intern. J. Mass Spectrom. Ion Phys., 47, 371, 1983.
4. D.N. Tripathi et. al., Can. Soc. Forens. Sci. J., 17, 55, 1984.
5. M.S.B. Munson and F.H. Field, JACS, 88, 2661, 1966.
6. S. Sass and T.L. Fisher, Org. Mass Spectrom., 14, 257, 1979.
7. P.A. D'Agostino et. al., J. Chromatogr., 347, 257, 1985.
8. P.A. D'Agostino and L.R. Provost, Biomed. Environ. Mass Spectrom., 13, 231, 1986.

Presented at the 35th ASMS Conference on Mass Spectrometry and Allied Topics
May 24-29, 1987, Denver, CO

Fig 1

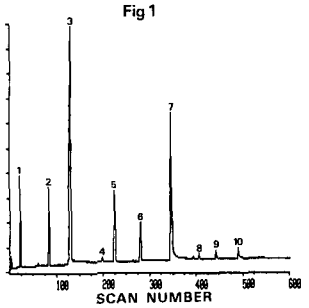

CAPILLARY COLUMN GC-MS (ISOBUTANE CI)
TOTAL-ION CURRENT CHROMATOGRAM (100 - 450 u)
OF ABOUT 2 μg OF HT

Fig 3

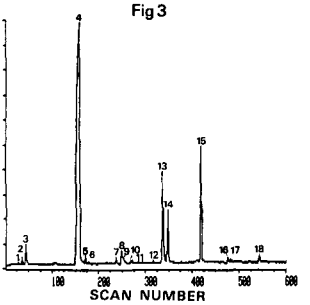

CAPILLARY COLUMN GC MS (ISOBUTANE CI)
TOTAL-ION-CURRENT CHROMATOGRAM (100 - 450 u) OF
THE EQUIVALENT OF 0.36 mg OF IRAN/IRAQ SOIL SAMPLE

Table 1

COMPOUNDS IDENTIFIED IN
HT MUSTARD SAMPLE

PEAK NO	MOL WT	STRUCTURE
1	104	
2	120	
3	158	$(ClC_2H_4)_2S$ (MUSTARD H)
4	190	$(ClC_2H_4)_2S_2$
5	202	$ClC_2H_4-S-C_2H_4-O-C_2H_4Cl$
6	218	$ClC_2H_4-S-C_2H_4-S-C_2H_4Cl$ (Q)
7	262	$(ClC_2H_4SC_2H_4)_2O$ (T)
8	306	$ClC_2H_4-S-C_2H_4-O-C_2H_4-S-C_2H_4-O-C_2H_4Cl$
9	322	$ClC_2H_4-S-C_2H_4-S-C_2H_4-O-C_2H_4-S-C_2H_4Cl$
10	368	$(ClC_2H_4-S-C_2H_4-O-C_2H_4)_2S$

Table 2

COMPOUNDS IDENTIFIED IN IRAN/IRAQ SOIL EXTRACT

PEAK NO	MOL WT	STRUCTURE
1	104	
2	122	$CH_2=CH-S-C_2H_4Cl$
3	104	$CH_2=CH-S-C_2H_4OH$
4	158	$(ClC_2H_4)_2S$ (H)
5	168	$ClC_2H_4-S-C_2H_4-O-C_2H_5$
6	166	$ClC_2H_4-S-C_2H_4-O-CH=CH_2$
7	190	$(ClC_2H_4)_2S_2$
8	182	$ClC_2H_4-S-C_2H_4-S-CH=CH_2$
9	174	$(ClC_2H_4)_2S=O$
10	202	$ClC_2H_4-S-C_2H_4-O-C_2H_4Cl$
11	190	$(CH_2=CH-S-C_2H_4)_2O$
12	222	$(ClC_2H_4)_2S_2$
13	218	$ClC_2H_4-S-C_2H_4-S-C_2H_4Cl$ (Q)
14	226	$CH_2=CH-S-C_2H_4-O-C_2H_4-S-C_2H_4Cl$
15	262	$(ClC_2H_4-S-C_2H_4)_2O$ (T)
16	278	$(ClC_2H_4-S-C_2H_4)_2S$
17	286	$CH_2=CH-S-C_2H_4-O-C_2H_4-S-C_2H_4-S-C_2H_4Cl$
18	322	$ClC_2H_4-S-C_2H_4-O-C_2H_4-S-C_2H_4-S-C_2H_4Cl$

Fig 2

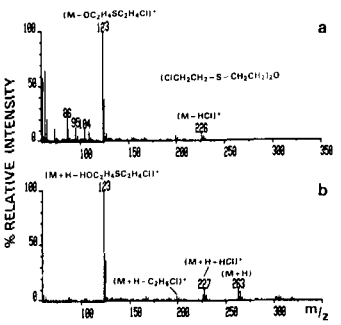

a) EI AND b) ISOBUTANE CI MASS SPECTRA OF
BIS[(2 CHLOROETHYL)THIO]ETHER (T) OBTAINED
DURING GC MS ANALYSIS

Fig 4

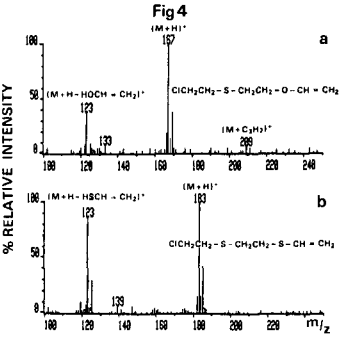

ISOBUTANE CI MASS SPECTRA OF
a) (2 CHLOROETHYLTHIO)ETHYL VINYL ETHER AND
b) (2 CHLOROETHYLTHIO)ETHYL VINYL SULFIDE
TENTATIVELY IDENTIFIED IN SOIL SAMPLE

Presented at the 35th ASMS Conference on Mass Spectrometry and Allied Topics
May 24-29, 1987, Denver, CO

MS/MS ANALYSES OF NITROFLUORANTHENES AND NITROPYRENES

Andrea M. Dietrich, Christian R. Guenat*, Louise M. Ball
University of North Carolina, Chapel Hill, NC 27514
*National Institute of Environmental Health Sciences, RTP, NC 27709

Nitropyrenes (NP) and nitrofluoranthenes (NF) are environmental mutagens produced from combustion processes and present in the ambient air. The mutagenicity of these compounds is thought to be mediated by their ability to interact with DNA and form adducts (Howard et al., 1983). Since mutagenicity varies for different isomers (Klopman and Rosenkranz, 1984), it is important to be able to characterize which isomer is present in an environmental sample.

In this research, 1-Nitropyrene and 1, 2, 3, and 7 -mononitrofluoranthene were investigated for isomer specific fragmentation patterns with respect to loss of NO• and $NO_2^{\bullet}$. Nitroarenes can exhibit varying fragmentation patterns, depending on internal hydrogen atom transfers (Meyerson et al., 1966; Beynon et al., 1973; Bursey et al., 1973).

Synthesis of nitrofluoranthene isomers was acheived by nitration of fluoranthene with nitric acid in acetic acid, or by synthesis from 3-aminofluoranthene (Kloetzel et al., 1955). Isomers were purified by silica gel chromatography, recrystallization, and normal phase HPLC fractionation. Specific identification was by NMR spectroscopy. High purity, 99.9+%, 1-Nitropyrene was from Midwest Research.

The individual nitroarenes were analyzed by direct probe +EI MS and MS/MS on a VG-ZAB 4F of B1E1-E2B2 configuration, operated in +EI mode. The probe was heated to 50-70°C. MS/MS was utilized to eliminate ^{13}C isotopic interferences, and to reduce thermal effects resulting from the slight differences in nitroarene volatilities. For MS/MS experiments, He gas was introduced into the grounded collision cell to reduce the intensity of the main beam by 50%. Daughter ion scans were produced from B/E linked scans of MS2.

Differences in ion abundances are readily apparent in the spectra presented , particularly for m/z 217 $(M-NO\bullet)^+$ relative to m/z 201 $(M-NO_2^{\bullet})^+$ (see Figures; data are normalized to m/z 201). Three categories of isomers can be distinguished; 1) Isomers with a hydrogen atom peri to the nitro group (3-NF and 1-NP) readily lose NO•; 2) Isomers with the nitro group in the pseudo bay region (1-NF and 7-NF) which lose NO• less readily (similar to the ortho effect); and 3) Isomers with neither a peri or pseudo bay region hydrogen (2-NF), which exhibit loss of NO• as a minor fragment. Mechanisms for these fragmentation pathways are shown with the spectra. These pathways can be rationalized by intramolecular rearrangements, as has been done previously for nitroarenes. A peri or pseudo bay region hydrogen is capable of transferring to the nitro group, and subsequently can rearrange to a hydroxy-nitrosoarene, followed by loss of NO•. Any nitro group, particularly in the absence of a transferrable hydrogen, can rearrange to the nitrite form, followed by loss of NO•.

The relative abundances of m/z 217/201 are presented below.

Ratio, m/z 217/201

PERI		PSEUDO BAY		REMAINING POSITIONS	
3-NF	2.3	1-NF	10.6	2-NF	28.5
1-NP	2.3	7-NF	8.35		

Reproducibility measurement for MS/MS analyses of 3-NF on three separate occasions yielded a value of 2.3 ± 0.064.

These results demonstrate that EI-MS/MS data can be reliably utilized to indicate which nitroarene isomer may be present.

Beynon, J.H., M. Bertrand, R.G. Cooks; JACS, 95, #6 (1973) 1739-1745.
Bursey, J.T., M.M. Bursey, D.G. Kingston; Chem Revs, 73, #7 (1973) 191-234.
Howard, P.C., R.H. Heflich, F.E. Evans, F.A. Beland; Cancer Res, 43 (1983) 2052-2058.
Kloetzel, M.C., W. King, J.M. Menkes; JACS, 78 (1955) 1165-1169.
Klopman, G., and H.S. Rosenkranz; Mutation Research, 126 (1984) 227-238.
Meyerson, S., I. Puskas, E.K. Fields; JACS, 88, #21 (1966) 4974-4980.

Peri Hydrogen Transfer

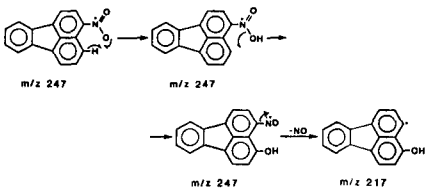

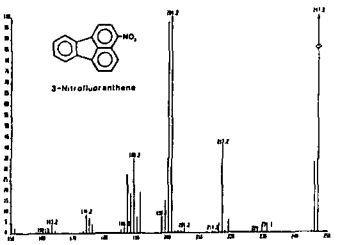

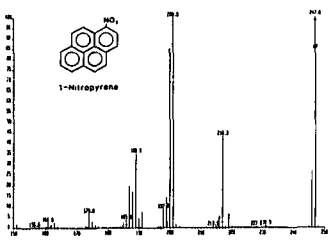

Pseudo Bay Hydrogen Transfer

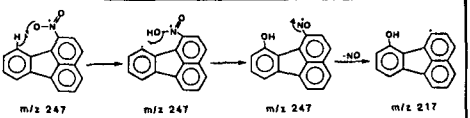

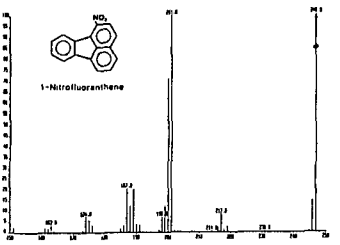

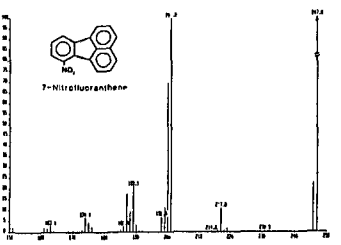

No Hydrogen Transfer, Nitrite Rearrangement

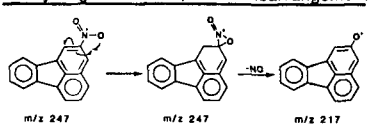

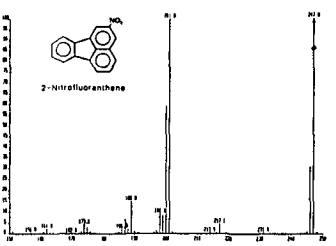

Presented at the 35th ASMS Conference on Mass Spectrometry and Allied Topics
May 24-29, 1987, Denver, CO

APPLICATIONS OF FOMBLIN L AS A HIGH RESOLUTION NCI REFERENCE COMPOUND

John de Kanel[1], Bih-Hsiung Hsu[2], Sharon Kelly[3] and Sheng-Yuh Tang[3]
Florida Dept. of Business Regulation, 1350 NW 12th Ave, Miami, FL 33136
College of Pharmacy, University of Florida, Gainesville, FL 32610
Rorer Central Research, 800 Business Center Drive, Horsham, PA 19044

NCI mass spectrometry is a sensitive method which, for many compounds, exhibits advantages over EI. Intense molecular ion clusters with less fragments result in high sensitivity in the most diagnostic region of the spectrum. Many problems associated with GC/EI analysis of TCDD isomers which result from chromatographic and mass spectral interferences with other ubiquitous compounds may be eliminated in NCI mode.

The primary difficulties with routine use of NCI mass spectrometry results from irreproducibility of results from different instruments and instrumental conditions. In addition, calibration is done in EI mode. This results in mass measurement errors when the instrument is placed in NCI mode and limits its use to low resolution mass spectrometry. Numerous reference compounds were tested for their effectiveness as an NCI calibration material. Fomblin L (poly(perfluoropropylene oxide) (sold by PCR, Inc.) which was suggested by Ligon (1978) and Bruin (1980) as a mass spectral reference material, met all the criteria necessary to serve this purpose. It produces similar spectra on instruments of different design; has strong, evenly spaced ions over the mass range 100 to 1000 and is not sensitive to minor changes in ion source conditions such as temperature or reagent gas pressure.

In Figure 1 the NCI mass spectrum obtained from the VG 7070SE mass spectrometer is shown. Similar spectra were obtained from Kratos MS80 RFA and Finnigan 4510 mass spectrometers. In Table 1 the formulas, theoretical masses and intensities used in calibration tables for the different instruments tested are given. Changes in conditions did not change the ions produced but did affect the relative intensities somewhat. This did not affect the ability to calibrate the instruments. Isobutane was used as the moderator gas, initially.

In Figures 2, 3 and 4 and Tables 2 and 3 information is presented on high resolution (3500) GC/MS using a Kratos MS80 RFA mass spectrometer. TCDD and a PCB were injected on a 12 meter capilary column. Methane at 1 X 10^{-4} torr was used as the moderator gas. The calibration table did not have to be changed from that used with isobutane. Fomblin was introduced on the DIP at ambient source temperature of 150°C. The probe was inserted to block the openning in the source. Sufficient sensitivity was exhibited to obtain full scan spectra at 3500 resolution down to less than 500 pg per component.. SIM should permit sensitivities of 20pg. In Figures 3 and 4 mass spectra of chromatographic peaks are presented with accurate mass measurements. Note the presence of Fomblin calibration peaks in these spectra to permit high resolution mass measurement. In Tables 2 and 3 the high resolution mass measurements are presented with elemental composition. NCI mass spectrometry eliminates the interferences found between TCDD and compounds such as PCB's and PCN's commonly found at higher levels in environmental samples. These interferences have been discussed in detail by Tondeur et al (1986) and Orth et al (1986).

In Figure 5 the NCI low resolution mass spectrum of a macrocyclic lactone extracted from the plant Inula cappa is shown. The EI spectrum of this compound produces no molecular ion at 70 EV. This makes it impossible to obtain a high resolution spectrum, including the molecular ion, without reducing the electron energy and sensitivity. Using Fomlin L as the reference material, isobutane reagent gas and a VG 7070 SE mass spectrometer at 7200 resolution the high resolution mass measurement shown was produced. High resolution mass measurement of samples introduced by Direct Insertion Probe may be obtained routinely.

NCI mass spectrometry, with the use of Fomblin L as a reference material has been shown to enable high resolution mass measurement using both DIP and GC for sample introduction. This is a useful technique to obtain elemental compositions for compounds which do not yield molecular ions in EI mode. In addition, GC/high resolution mass spectrometery in NCI mode eliminates many of the interferences commonly found in the analysis of environmental and biological samples for TCDD.

Ligon, Woodfin V., Jr (1978) Analytical Chemistry 50,8:1228.
Bruins, A.P. (1980) Biomedical Mass Spec. 7,10:454.
Donnely, J; et al. (1986) ASMS 34th Annual Conference, p488.
Orth, R.; et al. (1986) ASMS 34th Annual Conference, p484.

Presented at the 35th ASMS Conference on Mass Spectrometry and Allied Topics
May 24-29, 1987, Denver, CO

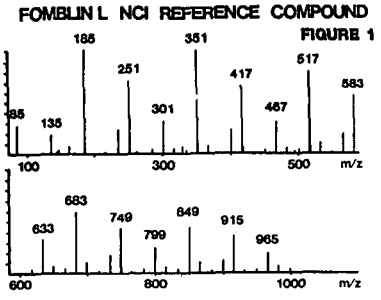

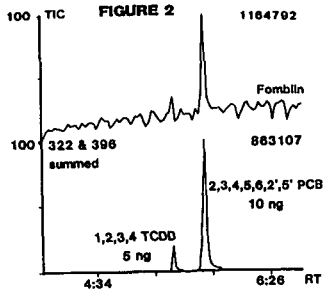

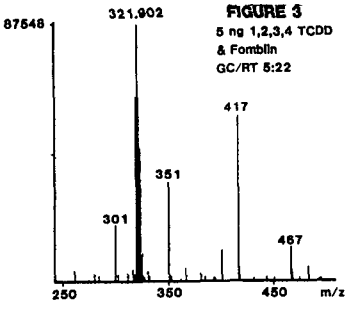

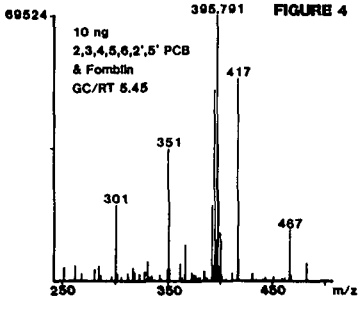

REFERENCE FILES USED FOR NCI CALIBRATION **TABLE 1**

FORMULA	MASS	HEIGHT % FINNIGAN 4510	VG TOTOSE	KRATOS MS80 RFA
CF_3O	84.99012	25	27	58
C_3F_4O	127.98853	7	1	40
C_2F_5O	134.98693	9	18	32
$C_3F_5O_2$	162.98180	3	—	—
C_3F_6O	165.98533	—	1	9
C_3F_7O	184.98374	16	95	100
C_4F_9O	234.98054	10	21	43
$C_4F_9O_2$	250.97546	55	67	69
$C_5F_{11}O_2$	300.97227	17	31	38
$C_5F_{11}O_3$	316.96718	3	3	3
$C_5F_{12}O_2$	319.97067	3	—	—
$C_6F_{13}O_2$	350.96907	38	100	73
$C_6F_{13}O_3$	366.96399	11	6	5
$C_7F_{15}O$	384.97096	4	1	1
$C_7F_{15}O_2$	400.96588	18	21	19
$C_7F_{15}O_3$	416.96079	98	71	59
$C_8F_{17}O_2$	450.96268	3	3	4
$C_8F_{17}O_3$	466.95760	28	32	35
$C_8F_{17}O_4$	482.95251	10	5	4
$C_9F_{19}O_4$	500.95949	4	4	4
$C_9F_{19}O_3$	516.95441	49	78	56
$C_9F_{19}O_4$	532.94932	21	8	7
$C_{10}F_{21}O_2$	550.95630	7	2	4
$C_{10}F_{21}O_3$	566.95121	22	18	15
$C_{10}F_{21}O_4$	582.94613	100	56	44
$C_{11}F_{23}O_4$	632.94293	26	29	28
$C_{11}F_{23}O_5$	648.93785	11	6	4
$C_{12}F_{25}O_4$	682.93974	32	66	39
$C_{12}F_{25}O_5$	698.93465	19	9	8
$C_{13}F_{27}O_4$	732.93655	16	15	9
$C_{13}F_{27}O_5$	748.93146	70	48	29
$C_{14}F_{29}O_5$	798.92827	19	25	17
$C_{14}F_{29}O_6$	814.92318	12	6	3
$C_{15}F_{31}O_5$	848.92507	30	43	19
$C_{15}F_{31}O_6$	864.91999	21	10	5
$C_{16}F_{33}O_5$	898.92188	16	13	5
$C_{16}F_{33}O_6$	914.91680	57	36	13
$C_{17}F_{35}O_6$	964.91360	20	19	6
$C_{17}F_{35}O_7$	980.90852	14	6	2

—Not used for this instrument.

MASS LIST OF 1,2,3,4 TCDD GC PEAK **TABLE 2**

MEASURED MASS	INTENSITY	% INT BASE
482.9510	4571	5.2
466.9576	11337	12.9
416.9606	56339	64.2
400.9657	10238	11.7
366.9793	4077	4.7
350.9849	33644	38.4
327.8908	1182	1.4
326.8929	1566	1.8
325.8917	9355	10.6
324.8949	7983	9.1
323.8980	45353	51.7
322.9002	9034	10.3
321.9018	87548	100.0
320.9027	8517	9.7
319.9035	62801	71.7
316.9670	3832	4.4
305.9721	19084	21.7

ATOMIC COMPOSITION REPORT: MASS 321.9018

^{12}C	^{16}O	^{1}H	^{35}Cl	^{37}Cl	Deviation mmu
12	1	6	2	2	-9.6
12	1	4	1	3	9.8
12	2	6	4	0	-18.3
12	2	4	3	1	6.2

MASS LIST OF 1,2,3,4,5,6,2',5' PCB GC PEAK **TABLE 3**

MEASURED MASS	INTENSITY	% INT BASE
482.9527	4648	6.7
466.9576	13331	19.3
416.9606	52872	76.1
401.7884	1438	2.1
400.9657	10356	14.9
399.7839	12711	18.3
398.7853	3609	5.3
397.7863	35478	51.2
396.7963	9805	14.1
395.7970	69534	100.0
394.7992	8171	11.8
393.7937	50015	71.9
392.8030	3816	5.5
391.8036	19707	28.3
366.9439	9223	13.3
350.9489	34730	50.0
316.9670	3193	4.6
305.9721	19594	28.2

ATOMIC COMPOSITION REPORT: MASS 395.7937

^{12}C	^{1}H	^{35}Cl	^{37}Cl	Deviation mmu
12	3	6	1	-8.8
13	1	5	3	9.8
11	5	1	6	-9.7
11	3	0	7	6.9

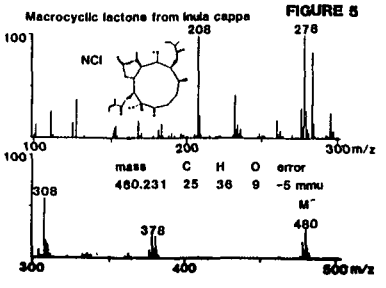

Presented at the 35th ASMS Conference on Mass Spectrometry and Allied Topics
May 24-29, 1987, Denver, CO

Mass Spectrometry of Polybrominated-dibenzodioxins Using Negative Chemical Ionization

Marbury, G.D., Turlington, J.M., and Tuschall, J.R., Chemical Quality Assurance and Standards Program, Northrop Services, Inc.; 2 Triangle Dr., Research Triangle Park, N.C. 27709

As part of ongoing efforts to develop methods for the analysis of dioxin reference materials for the U.S. EPA, selected Polybromodibenzo-p-dioxins (PBDD) were analyzed using EI, methane positive CI (PCI), and methane- and oxygen- negative chemical ionization (NCI, ONCI)[1-3] to identify relationships between spectral characteristics of specific PBDD isomers and ionization mode. Samples of several individual isomers (tetra- through octa-brominated) were characterized by direct probe (DP), desorption chemical ionization (DCI) and GC/MS. It was found that for NCI, the principal ions above m/z 150 were the $[M]^-$ and $[M-Br_n]^-$ series (Fig 1.), with no significant changes found in relative intensities over a 10 fold change in reagent gas (RG) pressure. However, spectra obtained by ONCI were pressure dependent (Fig. 2,3). with $[M]^-$, $[M-Br_n+O]^-$, and ether cleavage fragments $[Br_xC_6O_2H_{4-x}]^-$ and $[Br_yC_6O_2H_{4-y}]^-$ being major ions (x,y = number of Br atoms on each ring). Relative intensities varied over 100 fold depending on RG pressure, increased pressure ($3x10^{-4}$ torr vs. 5x10Pt-3Pt torr) favoring the ether fragment having the lower bromine content.

For example, 1,2,3,4,7,8-hexabromodibenzo-p-dioxin (mw = 652, Fig. 3), fragments at m/z 420 $[Br_4C_6O_2]^-$, and m/z 264 $[Br_2C_6O_2H_2]^-$, were found in the ONCI spectra but not in PCI or EI spectra, structural information thus being obtained that was unavailable by conventional EI MS.

It was found that the high melting points of PBDD's (280-365 °C) prevented the use of conventional capillary columns (upper limit= ca. 320 °C), but that commercially available aluminum-clad bonded fused silica capillary columns (Quadrex Corp., temp. limit = 450 °C) provided a facile means of analyzing tetra- through octa-brominated dibenzodioxins (Fig. 4). For our GC system, the temperature limits of the injector and GC/MS transfer lines caused poor peak shape for octa-BrDD, but was an improvement over conventional capillary techniques.

Experimental:

EXTREL 400-1 GC/MS, operated in negative ion mode, with either filament on (methane, air) or Townsend discharge (pure oxygen).

GC/MS studies used Varian 3400 GC with 10M, 0.1uM, aluminum clad capillary column, 75 °C to 385 °C at 25 °C/min, splitless injection

References

1. Hunt, D.F, Harvey, T.M., and Russel, J.W., J. Chem. Soc., Chem. Commun. No. 5, p. 151 (1975).
2. Hass, J.R., Friesen, M.D., and Hoffman, M.K., Org. Mass. Spectrom. 14 (1), 9 (1979)
3. Miles W.F., Gurprasad, N.P., and Malis, G.P. Anal. Chem., 57, 1133-1138 (1985).

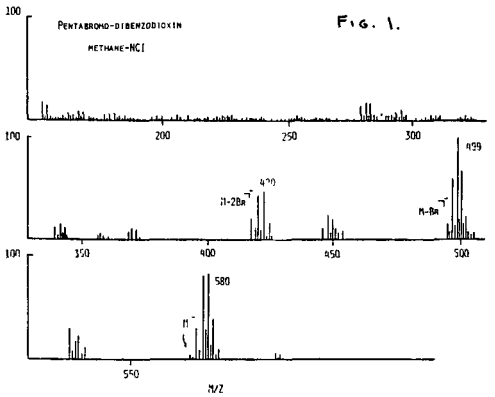
PENTABROMO-DIBENZODIOXIN
METHANE-NCI
FIG. 1.
100
200
250
300
100
350
400
450
500
M-2Br⁻
M-Br⁻
499
100
550
580
M⁻
M/Z

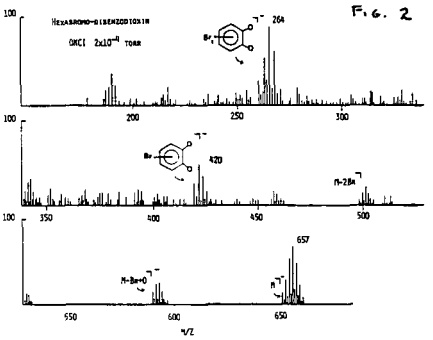
HEXABROMO-DIBENZODIOXIN
NCI
FIG. 2
100
200
250
264
300
100
350
400
420
450
M-2Br⁻
500
100
550
600
M-Br+O⁻
657
M⁻
650
M/Z

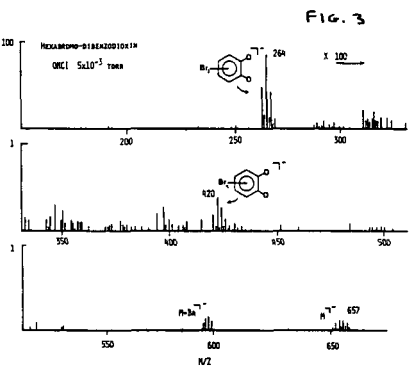
FIG. 3
HEXABROMO-DIBENZODIOXIN
NCI
100
264
X 100
200
250
300
1
420
350
400
450
500
1
M-Br⁻
M⁻
657
550
600
650
M/Z

Presented at the 35th ASMS Conference on Mass Spectrometry and Allied Topics
May 24-29, 1987, Denver, CO

DETERMINATION OF THE PHOTODEGRADATION PRODUCTS OF BASIC YELLOW 2 BY THERMOSPRAY HPLC/MS AND GC/MS:

R. D. Voyksner and T. W. Pack, Analytical and Chemical Sciences, Research Triangle Institute, P. O. Box 12194, Research Triangle Park, NC 27709, H. S. Freeman, W. N. Hsu, and C. A. Haney, North Carolina State Univ., P. O. Box 7003, Raleigh, NC., 27695

Most dyes used for coloration are plagued with fading upon exposure to light. The fading of a dye is a complex process which is dependent on temperature, heat, and light. In order to inhibit the fading of dyed fabrics, the main mechanisms of the degradation process must be determined. In this study the degradation chemistry of a cationic dye, basic yellow 2, $[(CH_3)_2NC_6H_4]_2C{=}NH_2^+\ Cl^-$ was studied by HPLC/MS and GC/MS. The most abundant degradation product formed was identified as Michler's ketone $[(CH_3)_2NC_6H_4]_2C{=}O$ which is formed so rapidly that it appears in the control samples as well as the faded samples, however, the amount increases with exposure.

The first experiment performed involved a solution of Basic Yellow 2 in acetonitrile which was exposed to light for periods of 0, 24, 48, 72, and 96 hours. The photodegradation products identified from the solution fading experiment appear in Figure 1. Two of these compounds are also found in the fabric fading experiments described below.

The second experiment involved cloth strips dyed with Basic Yellow 2 which were subjected to fading caused by alternating cycles of darkness (1 hour per cycle) and light (3.7 hours per cycle) over a 48 hour period, or by backside fading (87°C, no light). An unmodified fabric sample was used as a control. The fabrics were powdered and extracted with methanol in a soxhlet apparatus. The degradation products identified are shown in Figure 2. Structures for several additional degradation products, observed by thermospray HPLC/MS analysis of backside faded sample only, are proposed (Figure 3) and experiments to confirm these structures are in progress. Due to the absence of fragmentation in the thermospray spectra (only $[M+H]^+$ ions were observed) the dye extracts were analyzed by gas chromatography/mass spectrometry (GC/MS) to confirm the identity of the degradation products. Many of the degradation products were sufficiently volatile to analyze by GC/MS or to give molecular ions and structurally important fragment ions to compliment the thermospray data. Also, it was observed that increasing the repeller voltage while operating the thermospray source with discharge chemical ionization resulted in structurally important fragment ion formation. Only "ketone" degradation products were observed in the fabric extracts due to the rapid nucleophilic displacement of the iminium ion with trace amounts of water in the methanol solvent.

This research was supported by the National Science Foundation grant number RII-8511734

Figure 1. Photodegradation products identified by GC/MS and HPLC/MS in the solution fading of Basic Yellow 2.

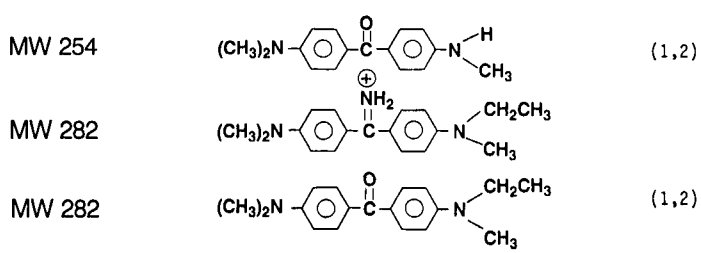

Figure 2. Degradation products identified from fabric fading experiment.

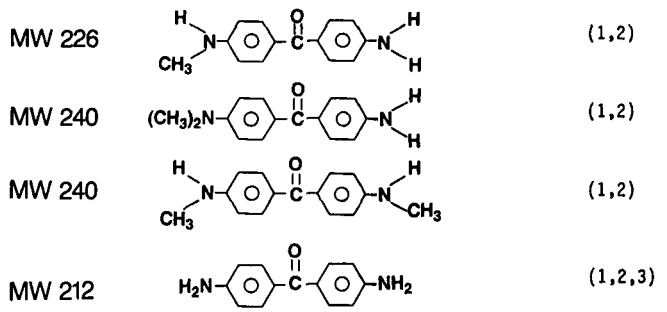

1 - present in dark/light faded fabric

2 - present in backside faded fabric

3 - detected by HPLC/MS only

Figure 3. Degradation products proposed from thermospray HPLC/MS analysis of backside fading experiments.

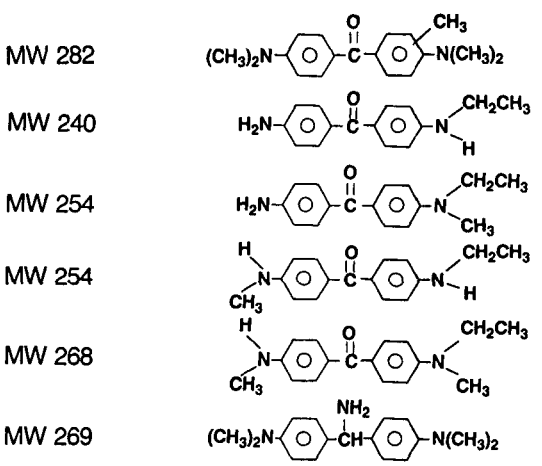

Presented at the 35th ASMS Conference on Mass Spectrometry and Allied Topics
May 24-29, 1987, Denver, CO

ENVIRONMENTAL APPLICATIONS OF THERMOSPRAY LCMS: QUALITATIVE ANALYSIS OF SULFONATED AZO DYES

Donald A.Flory, Matthew M. McLean and Marvin L. Vestal:
University of Houston-University Park, Houston TX 77004
Leon D. Betowski: USEPA-EMSL,Las Vegas, NV

INTRODUCTION

The proposed USEPA regulatory program for the dye industry (1) requires the development of mass spectrometric methods for the qualitatative confirmation of sulfonated azo dyes that are easily adaptable to inexpensive routine analytical procedures. Three ionization techniques; Thermospray(2), FAB(3,4,5) and API(6) offer potential for development into relatively simple on-line LC/MS methods for the analysis of environmentally significant compounds, Although these soft ionization techniques all share the limitation of providing limited structural information, they should be entirely suitable for routine monitoring of dye wastes that have been thoroughly characterized by soft ionization MS/MS methods. We have,therefore, begun conducting an investigation of thermospray parameters so that optimized conditions for sulfonated azo dye analysis can be determined.

EXPERIMENTAL

Spectra were obtained with a Thermospray MS assembled in our laboratory. A Model 5988A Hewlett-Packard mass spectrometer was connected to a Scientific Systems,Inc Model GS400 HPLC gradient system via a Vestec Thermospray interface. A Rheodyne sample injection valve was installed in the Thermospray inlet line for injection of dye solutions into flowing mobile phases. Full scanning (1 sec) in negative ion mode was used to obtain reference spectra and single ion monitoring (SIM) data were recorded to investigate Thermospray ionization parameters and estimate ultimate detection limits.All studies were conducted on aqueous solutions of commercial dye preparations supplied by EPA-EMSL, Las Vegas, NV and the NCTR, Jefferson, AR. The dye solutions were introduced into the MS with the injection valve to obtain SIM data for sensitivity estimates and by direct flow to obtain the reference spectra. The mobile phase flow rate was 1.0 ml/min in all cases. The effect of varying several parameters known to affect Thermospray ionization were investigated for Direct Red 81. These included source temperatures, mobile phase pH, mobile phase composition and dye concentration. Mobile phases examined were pure water, varying concentrations of ammonium acetate and varying concentrations of ammonium sulfate.

RESULTS AND DISCUSSION

1) pH and Ion Source Parameters

The best results were obtained at neutral pH in the negative ion mode. The thermospray source temperatures were optimized to give maximum response for each dye and mobile phase investigated but were esssentially identical for all experiments as follows:

Control: 124-126 C; Tip: 200-225 C; Vapor: 230-255 C;Block: 290-292 C

2) Reference Spectra

Spectra obtained for direct flow of 10^{-3}M pure water solutions of the dyes listed above are given in the table below. The spectra represent dye amounts ranging from 1-5 micrograms depending on the actual dye concentrations

DYE	MAJOR IONS(RELATIVE ABUNDANCE)[COMPOSITION]
Direct Red 81	314.5(100)$[M-2Na]^{2-}$;652(80)$[M-Na]^{-}$; 427(45)$[2M-3Na]^{3-}$
Direct Red 2	339(100)$[M-2Na]^{2-}$;701(42)$[M-Na]^{-}$
Direct Yellow 4	289(100)$[M-2Na]^{2-}$;601(57)$[M-Na]^{-}$;
Direct Violet 32	356(100)$[M-2Na]^{2-}$;735(91)$[M-Na]^{-}$ 482(65)$[2M-3Na]^{3-}$; 1493(33)$[2M-Na]^{-}$; 988(31)$[3M-3Na]^{3-}$;
Direct Blue 8	356(100)$[M-2Na]^{2-}$;490(88)[???]; 735(60)$[M-Na]^{-}$;484(45)[???]
Acid Blue 113	317.5(100)$[M-2Na]^{2-}$;658(33)$[M-Na]^{-}$;
Acid Red 114	392(100)$[M-2Na]^{2-}$;807(21)$[M-Na]^{-}$
Direct Blue 10	474(100)$[M-2Na]^{2-}$;971(41)$[M-Na]^{-}$; 503(24)[???]; 308(15)[$[M-3Na]^{3-}$;
Direct Blue 14	937(25)$[M-Na]^{-}$

[???]= Composition not known, probably a contaminant

The following mass spectral characteristics were observed:

1. $[M-2Na]^{2-}$ formed by loss of sodium from the salt is the base peak in eight dyes, $[M-Na]^{-}$ is the base peak in Direct Blue 14.
2. Doubly and triply charged ions are formed by additional losses of sodium atoms up to x-1 where x is the number of sodium atoms in the monomer or cluster ion.
3. Dimer and trimer clusters were formed by some of the dyes.

3) Effect of Dye Concentration and Buffer Composition

The table below gives the results of varying dye concentration on Thermospray response for Direct Red 81 in pure water. The response values listed were obtained from full scan data over the range m/z 200 to m/z 700 and are the average of five 20 microliter injections. SIM data for the major DR81 ion at mz 314.5 gave an average response of 100,000 for 20 microliter injections of 10^{-6} M dye (14 nanograms) indicating low nanogram detection limits should be easily obtainable.

DYE CONC.(M)	10^{-6}	10^{-5}	10^{-4}	10^{-3}	10^{-2}
RESPONSE ($x10^{-3}$)	45	170	780	1700	3100

The table below gives Thermospray response for DR81 dye as a function of ammonium acetate concentration. The data were obtained in full scanning mode over the m/z range 200-700 using direct flow . The dye concentration was 10^{-4} M. The spectra are averages of 80 scans(1 sec/scan) and represent 1 microgram of dye. The reconstructed ion current values (RIC) are the sum of the five major ions found that can be attributed to DR81 plus their carbon isotopes. Several other contaminant ions appeared and increased in intensity as the buffer concentration increased.

		MASS SPECTRAL RELATIVE ABUNDANCES (m/z)				
NH_4OAc	RICx10^{-3}	314.5	427	630	641.5	652
1.0x10^{-5}M	8.8	100	7	ND	ND	29
5.0x10^{-4}	11	100	9	ND	ND	37
1.0x10^{-3}	8.5	100	6	ND	ND	54
2.5x10-3	11	100	7	10	6	31
5.0x10^{-3}	18	100	9	14	11	48
1.0x10^{-2}	17	100	6	30	16	50
5.0x10^{-2}	6.8	100	ND	35	9	36
1.0x10-1	3.5	100	ND	27	5	19

ND= not detected m/z 314.5 = $(M-2Na)^{2-}$; m/z 427 = $(2m-3Na)^{3-}$
m/z 630 = $(M-2Na+H)^{-}$; m/z 641.5 = $(2M-3Na+2H)^{-}$ m/z 652 = $(M-2Na)^{-}$

The m/z 630 and 641.5 columns column indicate that protonation by the ammonium acetate begins to occur at concentrations between 10^{-3} and 2.5x10^{-3}M. There is some enhancement of DR-81 ionization from this point to 10^{-2}M concentrations , but larger amounts of ammonium acetate actually suppress the response. These results indicate that anion ejection directly from the droplet is the major ionization process. Suppression of ionization at higher salt concentrations is due to ejection of the more volatile salt anion (relative to the dye) before the field strength is sufficient to eject dye anions from the evaporating droplets. The increase in dye response expected by increased droplet field strength is being negated by the preferential ejection of the more volatile buffer ions. We then investigated the effect of ammonium sulfate on Thermospray ionization to determine if sulfate anions are less volatile than acetate anions. Results for ammonium sulfate were similar to those for ammonium acetate giving no significant enhancement at low buffer concentrations (10^{-4} to 10^{-3} M) and a definite suppression of dye TIC at buffer concentrations above 10^{-2} M.

REFERENCES

1.Federal Register,40-CFR,1986, Parts 261 and 271(proposed)
2.Blakley,C.R.;Vestal,M.L.*Anal.Chem.*1983,55,750-54.
3.Monaghan,J.J.;Barber,M.;Bordoli,R.S.;Sedgwick,R.D.;Tyler,A.N.*Org. Mass. Spectrom.* 1983,18,75-82.
4.Caprioli,R.M.,Fan,.T, and Cottrell,J.S. *Anal.Chem. 1986, 58, 2949-2954*
5.Itoh,Y.,Takeuchi,T.,Ishii,D.,Goto,M.*J.Chrom.*1985,346,161-166
6.Henion,J.; Bruins,A. 34th Annual Conference on Mass Spectrometry and Allied Topics.1986, 371-2

DISCLAIMER AND ACKNOWLEDGEMENT

Although the research described in this report has been partially supported by USEPA Grant CR 812877 , it has not been subjected to Agency review and does not, therefore, necessarily reflect the views of the Agency and no official endorsement should be inferred. Mention of trade names or commercial products does not constitute endorsement or recommendation for use.

Presented at the 35th ASMS Conference on Mass Spectrometry and Allied Topics
May 24-29, 1987, Denver, CO

DIRECT EQUILIBRIUM HEAD-SPACE ANALYSIS OF ENVIRONMENTALLY IMPORTANT PURGABLE COMPOUNDS USING GAS CHROMATOGRAPHY WITH ION TRAP DETECTION

A.J. Patkin and J.V. Hinshaw, Jr.
North American Instrument Division
The Perkin-Elmer Corporation, Norwalk, CT 06859-0090

Head-space gas chromatography (HSGC) has found many uses in the analysis of volatile components in liquids, solids, and complex mixtures. HSGC is limited, however, in its ability to provide positive compound identification without extensive use of standards and multiple columns or detectors. Combining capillary HSGC retention time information with mass spectral data from an ion trap detector can provide positive and rapid compound identification.

Direct equilibrium head-space is easy and straightforward. It avoids tedious sample preconcentration, clean-up procedures, and wet chemistry. The Equilibrium head-space procedure consists of placing the sample in a vial and hermetically sealing it The vial is then thermostated for a predetermined time to equilibrate the sample. At the end of this period the vial is pressurized with the GC carrier gas and equilibrated. The normal carrier flow to the GC column is temporarily replaced with that from the vial for a pre-set sample injection time. All stages and conditions of the head-space procedure are controlled for precise reproducibility, and automated analysis of up to 100 samples is possible.

The ion trap detector (ITD) is a mass spectrometric detector based on the principle of ion trapping. The ion trap creates ions by conventional electron ionization, stores them within a toroidal radio-frequency field, and then selectively extracts the ions for detection by increasing the field potential. Mass resolution is similar to that of quadrapole mass spectrometers Full-scan sensitivity and detection limits are superior. The mass spectra produced by the ITD can be computer searched against conventional mass spectral libraries for compound identification.

This presentation will demonstrate the analysis of sludge and water samples for several compounds of environmental interest, including some EPA priority pollutants. Sensitivities achieved are at or below the typical EPA method detection limits required for dynamic head-space (purge and trap).

Experimental

A standard solution of nine components was prepared in quartz distilled water. A 2 ml portion of this solution was transferred to a head-space vial and then sealed. A second 2 ml portion of the solution was transferred to a vial which contained 5 gm of rocky-sandy soil, and then sealed.

Chromatographic conditions are shown in Table 1. Both this and the following analysis use a Perkin-Elmer 8500 gas chromatograph with a P-E HS-6 head-space injector and a P-E Ion Trap Detector.

Results

Figure 1a shows the chromatogram for the standard. Note that two peaks contain chromatographically unresolved components. Figure 2 shows the extracted ion current profiles (EICP) used for analyzing each of the components Using the EICP, each component can be detected and quantitated selectively, without interference from a co-eluting peak. This selectivity is one of the major advantages of ion trap detection.

Figure 1b shows the chromatogram of the spiked soil sample. Note that the two chromatograms are nearly identical, showing excellent recovery of the components. Very good matches are obtained searching the mass spectra of these components against the 42,000 compound NBS/EPA/NIH library.

Table 2 summarizes the results.

Discussion

In all cases, the estimated detection limits (EDL, three times noise) are better than the method detection limits (MDL) required for the EPA 624 purge-and-trap procedure.

The poor EDL for Freon-113 is probably due to vaporization and component loss during sample preparation. All EDL's and recoveries are preliminary. More work must be done to fully characterize the system. Various "salting out" techniques are known for increasing component recovery from water. Analysis of soils and sludges is known to suffer from matrix-effect problems which often depend on the nature of the soil or sludge analyzed (rocky, sandy, clay, organic, etc.). Detection limits may be improved by one to three orders-of-magnitude by optimization of the chromatographic conditions, using larger head-space vials and samples, and employing Automatic Gain Controll (AGC) detection on the Ion Trap

Presented at the 35th ASMS Conference on Mass Spectrometry and Allied Topics
May 24-29, 1987, Denver, CO

Conclusions

Equilibrium head-space analysis with ion trap detection has been shown to have the sensitivity and specificity required to analyze volatile trace-level components in water and soil. Head-space analysis of EPA Priority Pollutants appears promising.

In contrast to the complex sample preparation procedure for purge-and-trap analysis, equilibrium head-space requires minimal sample preparation - the sample is sealed in a disposable vial. This can be done at the sampling site, minimizing potential for sample loss. Also, cross-contamination is eliminated.

Sample throughput is limited only by the time required for the GC run and oven cool-down. Four or more samples per hour are possible, and quantitative reports can be generated automatically at the end of each analysis.

Up to 100 samples can be run, completely automatically, with the HS-101 version of the equilibrium head-space sampler.

In summary, equilibrium head-space analysis shows great promise for the analysis of environmentally important trace-level volatile materials in water or complex matrices

Figure 1a. Standard Chromatogram

Figure 1b. Soil Chromatogram

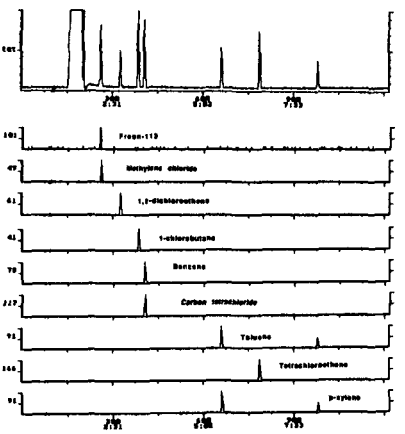

Figure 2 Extracted Ion Current Profiles

Table 1

Experimental Conditions

Head Space Analysis of Priority Pollutants

Gas Chromatography

Column:	25m x 0.25 mm ID fused silica df = 0.25 µm Methyl phenyl (5%) silicone *Open/Split interface to ITD*
Temperature Column	3 min isothermal at 35°C, programmed at 8 °C/min from 35°C to 75°C, programmed from 75°C to 135°C at 15°C/min
Injector	180°C
Transfer line	200 °C
Carrier Gas	Helium, u = 30 cm/sec
Injection	Thermostat vial at 60°C for 15 min Pressurize for 30 sec Inject for 6 sec *Capillary split flow at 10 ml/min*

Ion Trap Detector

ITD Scan Mode.	Full Scan 30 to 275 µ 2 scans/sec

Table 2. Summary of Results

Compound	EICP Ion	EDL (µg/ml)	MDL EPA (µg/ml)	Recovery (%)
Freon-113	101	1.13	na	104
Methylene Chloride	49	0.049	2.8	105
1,2-dichloromethane	61	0.10	1.6	104
1-chlorobutane	41	0.036	na	98
Benzene	78	0.41	4.4	101
Carbon tetrachloride	117	0.93	1.6	92
Toluene	91	0.16	6.0	92
Tetrachloroethene	166	0.23	4.1	85
p-xylene	91	0.24	na	82

Presented at the 35th ASMS Conference on Mass Spectrometry and Allied Topics
May 24-29, 1987, Denver, CO

THE APPLICATION OF ICPMS TO ENVIRONMENTAL SAMPLES

J.R. Donnelly, D. Cardenas, J.M. Henshaw, D.E. Dobb, D.C. Hillman,
*L.C. Butler, *R.F. Smiecinski, *E.M. Heithmar, *R.K. Mitchum,
**C.N. Rowland, **A.N. Eaton
Lockheed-EMSCO and *U.S. Environmental Protection Agency
P.O. Box 15027, Las Vegas, Nevada 89114, and
**V.G. Instruments Inc., Stamford, CT 06901

ABSTRACT

The U.S. Environmental Protection Agency (EPA) has an interest in applying Inductively Coupled Plasma-Mass Spectrometry (ICPMS) for the routine analysis of environmental samples. The analytes of interest include the Superfund Contract Laboratory Program (CLP) elements: Al, Sb, As, Ba, Be, Cd, Ca, Cr, Co, Cu, Fe, Pb, Mg, Mn, Hg, Ni, K, Se, Ag, Na, Tl, V, and Zn. To date, the work has centered on the optimization of the plasma operating conditions (gas flow rates, RF power, and distance from the MS sampler), the determination of the analytical characteristics (eg, detection limits, analysis rates, and linear dynamic ranges), and comparison of ICPMS to ICPAES and AAS for the analysis of real samples. This presentation compares analytical and performance characteristics of ICPMS to ICPAES and AAS.

The EPA Las Vegas laboratory has access to two different manufacturer's ICPMS instruments. The data presented herein is representative of the performance of both instruments. The ICPMS instruments can be operated in a selective ion monitoring mode (SIM) or a scan mode (entire mass range scanned). The CLP required detection limits (CRDL's) are met using either mode, as shown in Table One. The instrument detection limits (IDL's) for the SIM mode are generally 0.1 to 0.5 ppb, while those for the scan mode are 1 to 5 ppb. In addition to increased sensitivity, the SIM mode also provides a faster analysis (for the CLP elements, the SIM mode is about 3 times faster than the scan mode, taking ca. 2 hours for determining 22 elements in 10 samples, along with all the CLP required quality control analyses). The scan mode is useful when it may be necessary to review the data for elements not originally determined. A drawback of the high sensitivity for analysis of typical environmental samples is a limited upper concentration range. For best results, analytes must be less than 1 ppm. Consequently, large dilutions are often required to determine high concentration sample constituents. Several types of environmental samples (fish, soil, water, and Method 1310 EP extracts) have been analyzed by ICPMS following CLP protocols (IFB 784). Preliminary analyses indicate good agreement with AAS and ICPAES results, although the EP extract matrix (3.5% acetic acid) presents an interference for some isotopes. As shown in Figure One, samples containing appreciable levels of carbon (EP extracts and fish) will give poor results for the normally used isotopes Mg^{24}, Ca^{44}, and Cr^{52}, presumably due to formation of a carbon dimer, CO_2, and Ar-C species, respectively. Use of other isotopes such as Mg^{26}, Ca^{43}, and Cr^{53} will avoid the carbon interferences. Other problems with samples containing high dissolved solids (>2%) have been seen. Clogging of the sampler orifice that interfaces the plasma to the Mass Spectrometer is common with high solids samples. Dilution of the sample will eliminate the problem without jeopardizing the instrument's ability to meet CRDL's. In summary, from our initial work, ICPMS appears to be a promising technique for environmental analysis, possessing required sensitivity, speed, and multielement capability.

Notice: Although the research described in this article has been funded wholly or in part by the Environmental Protection Agency contract 68-03-3249 to Lockheed Engineering and Management Services Company, Inc., it has not been subjected to the Agency's review and therefore does not necessarily reflect the views of the Agency and no official endorsement should be inferred.

Presented at the 35th ASMS Conference on Mass Spectrometry and Allied Topics
May 24-29, 1987, Denver, CO.

Table One. Detection Limit Comparison

INSTRUMENT DETECTION LIMITS - PPB

Element	CRDL	ICPAES	GFAA	ICP-MS SIM	ICP-MS Scan
Al	200	45		0.3	0.8
Sb	60	50	5.0	0.1	2.0
As	10	80	1.0	0.09	1.0
Ba	200	20		0.1	0.9
Be	5	2		0.1	0.9
Cd	5	6	0.3	0.2	1.0
Ca	5000	700		5.0	6.0
Cr	10	5		0.1	0.8
Co	50	15		0.05	0.8
Cu	25	8		0.1	0.8
Fe	100	30		10.0	4.0
Pb	5	35	1.0	0.4	2.0
Mg	5000	20		0.1	1.0
Mn	15	9		0.08	0.8
Hg	0.2		0.2 cv		0.1
Ni	40	30		0.07	1.0
K	5000	1500			
Se	5	200	1.0	0.5	3.0
Ag	10	5		0.1	0.9
Na	5000	500		0.3	3.0
Tl	10	160	5.0	0.2	0.7
V	50	17		0.06	0.6
Zn	20	17		0.3	2.0

ICP-MS SIM Mode determined at 3 X S.D. with 1 ppb std.
ICP-MS Scan Mode determined at 3 X S.D. with 20 ppb std.

Figure One. Analysis Comparisons of Selected Sample Types

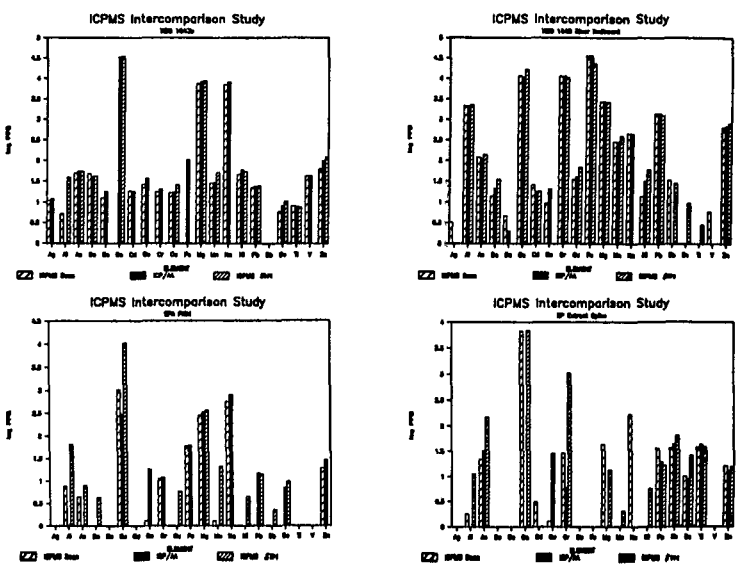

Presented at the 35th ASMS Conference on Mass Spectrometry and Allied Topics
May 24-29, 1987, Denver, CO

ROUTINE ON-SITE GC-MS ANALYSIS
A FULLY MOBILE SYSTEM WITH PRACTICAL APPLICATIONS

G. Matz, Technical University of Hamburg Harburg, Harburger Schloßstraße 2o
2loo Hamburg 9o, W. Germany
B. Forbes, Bruker Instruments, Manning Park, Billerica, Mass o1821
A.G. Loudon, Bruker-Franzen Analytik, Kattenturmer Heerstr. 122, 28 Bremen
W. Germany

Introduction

This mobile mass spectrometer was designed for the fast semiquantitative identification of trace amounts of organic contaminants in the environment or work place. The instrument was specially designed for use under extreme conditions e.g. high humidity, temperatures from -2o°C to +5o° and to survive the vibrations ocurring during transport, e.g. mounted in a four wheel drive car. It is fully microprocessor controlled and easily operated by non-expert personel. It has been shown to be very suitable for environmental problems such as looking for chlorinated hydrocarbons, hidden in waste dumps and in the detection of pesticides on surfaces, in water or after an explosion or fire in a chemical plant. This work has been helped by the newly developed GC Sampler described here. This gives better separation than the normal sampler, which is necessary for the identification of individual compounds of interest in a complex mixture.

Apparatus (The MM-1)

The apparatus consists (fig. 1) of a combined sampling and detection system, control electronics and the operators control console. The detector consists of a quadrupole (1-4oou) with an electron impact source both mounted in a heated UHV system with an automatic main valve pumped by an ion getter pump. The gas inlet system is a membrane separator. The combined air/surface sampler allows the determination of substances in the air down to the low ppb level in a few seconds. Solid components with melting point up to ca. 24o°C on the surface in concentrations down to a few mg/m² can be detected, using the sampler. The sampler is equipped with 3.5 m of chemically bond SE54 capillary column, which can be temperature programmed, but the separation is often not good enough for complex mixtures.

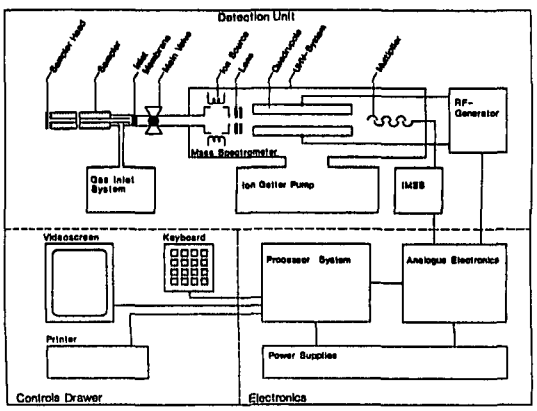

Fig. 1: Principle diagramm of the MM-1

GC Sampler

The GC Sampler can be quickly attached to the instrument and gives much better separation. It is designed for on column injection of thermally desorbed samples (fig. 2). The samples in solution can be injected onto glass wool in a tube, or contaminated air can be sucked through a tenax tube. The tube is placed in the injector (T = 25o°C) and the substances are thermally desorbed for ca. 1 min in a stop flow mode. The flow then starts and the samples are sucked onto the cold gc capillary (here 12.5 m long), which is mounted in the gc oven. After a further 15 s clean air is pumped through the T junction between tube and capillary which stops the injection and cleans the tube. The compounds are separated by a temperature program. The whole process and analysis is automatically controlled by the MM-1's electronics.

Results

The MM-1 can operate either in the selected ion monitor mode using four ions per compound or can acquire a series of complete spectra. The results (fig. 3, 4) for a pesticide mixture were obtained using the latter mode. Here a hexane solution containing ca. 1 µg of each of the pesticides was injected

Presented at the 35th ASMS Conference on Mass Spectrometry and Allied Topics
May 24-29, 1987, Denver, CO

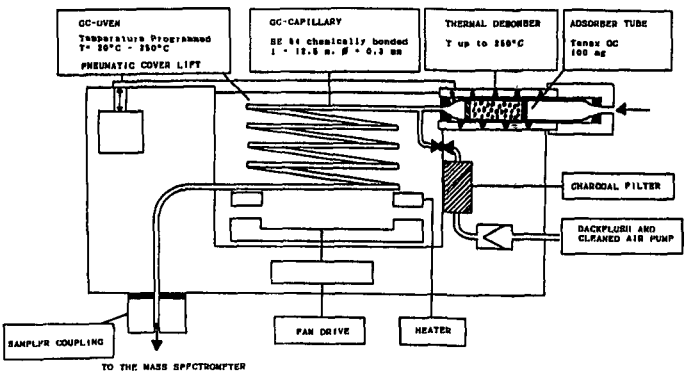

Fig. 2: Principle diagramm of the GC-Sampler

into a Tenax filled tube and the compounds separated with a temperature program running from 5o - 25o°C. The scan time was 6s, the mass range 8o to 3oo u and 12o spectra (fig. 3) were obtained. Each spectrum is characterized by three lines corresponding to the log (counts/s) of the most intense ions in the mass ranges 6o - 12o, 12o - 18o and over 18o u. This allows the identification of overlapping compounds (see peaks 3 and 4). The gc peak widths were ca. 6s. the spectra (fig. 4) allowed the identification of the four compounds via the 4 characteristic ions stored in the MM-1 for the SIM detection mode. The signal/minimum detection limit ratio was ca. 1oo:1.

Conclusions

These results show that the MM-1 with gc sampler can be a powerful tool for the investigation of pollutants in the environment, in this case present due

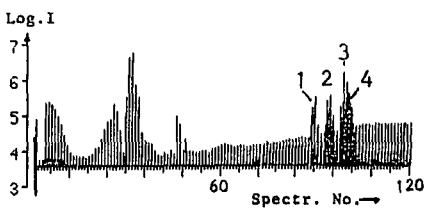

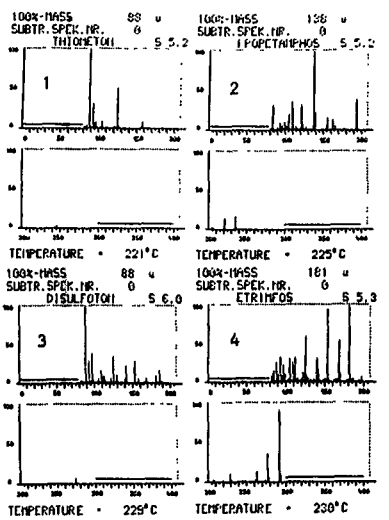

Fig. 3: Spectra series, 8o-3oo u, scan time 6s of a mixture of 4 pesticides, "TIC"-display

Fig. 4: Mass spectra 1-4 out of spectra series, automatically identified in the four peak library

a fire in a chemical store. These investigations, started in 1987 in Hamburg Harburg are designed to produce standard procedures for sampling air, using this system to provide high enrichment factors, analysing water and contaminated soil e. g. from the rubbish dump in Hamburg Georgswerder.

Presented at the 35th ASMS Conference on Mass Spectrometry and Allied Topics
May 24-29, 1987, Denver, CO

LOW LEVEL IMPURITY DETECTION FOR "PURE" GASES:

V.Pizzitola and R.Schaeffer, EXTREL CORPORATION, Pittsburgh, Pa. 15238

Trace impurities in semiconductor grade "PURE" gases are of vital importance and concern to all workers and researches involved in the production and processing of semiconductor chips. Impurities at part per million and sub-part per million levels can have high rates of reaction relative to the bulk gas reaction and so can cause significant chemical and electronic distortion of materials being processed.

Attempts have been made to assess the purity of "PURE" bulk gases using a mass spectrometer (MS) involving clean, low-background UHV chambers and similiar inlet systems. Some successes can be achieved on particular gases but many common impurity gases such as Oxygen, Nitrogen, Argon, Carbon Dioxide are already present as significant background peaks in the inlet and UHV chambers, thus making it difficult to analyze low levels.

GC/MS is shown to be a highly sensitive technique for the detection of sub-ppm impurity gases in semiconductor grade "bulk" gases. Detection limits as low as 3 ppb (fig.1) have been demonstrated utilizing single ion monitoring (SIM) in conjunction with GC/MS. Data are presented showing impurity gases in UHP Helium containing 12 ppm Nitrogen (fig.3) and impurities in UHP Methane (fig.4).

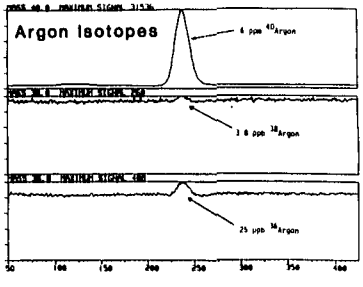

fig 1

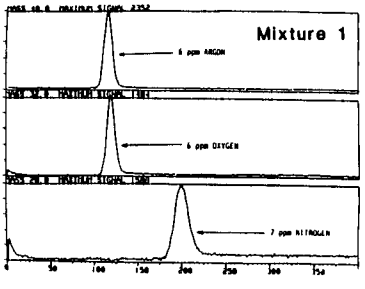

fig 2

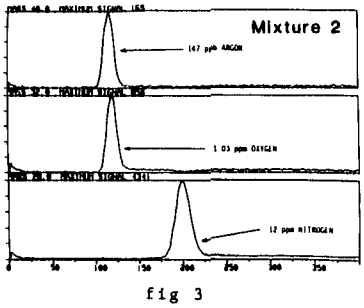

fig 3

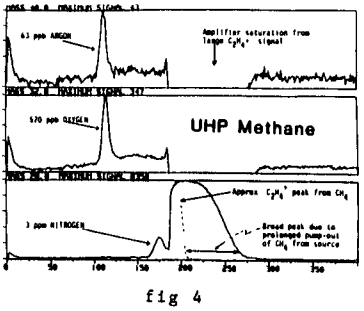

fig 4

The analysis of the other more reactive semiconductor grade gases are also important. The use of GC/MS for the analysis of trace reactive contaminants in silicon precursor gases, dopants, and reactant gases requires an extremely inert chromatography system. However in some applications where more inert trace contaminants are presented in reactive gases, one may choose to employ a "stripper" column to remove the reactive gas from the stream prior to the analytical separation. Alternatively, backflush and cut techniques can achieve the same result of protecting the analytical separation column and the mass spectrometer ion source. With these applications, a direct inlet approach is often easier. Substantial improvements in detection limits are observed with background peak effects becoming almost insignificant thus improving the signal to noise ratio.

Shown below is a schematic of the direct inlet system equipped with a flow by tee incorporating a fixed leak into the mass spectrometer (fig.5).

Direct Inlet System

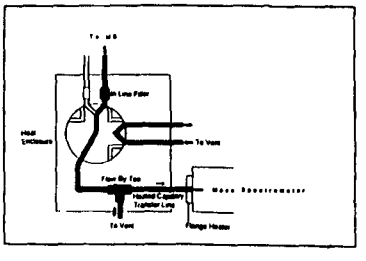

fig 5

Data are presented detecting Argon, Oxygen, and Nitrogen impurities in UHP Helium (fig.6). Detection limits as low as 8 ppb of Xe-136 and 26 ppb of Kr-80 in ambient air vs a pure Nitrogen stream.

DIRECT INLET MS

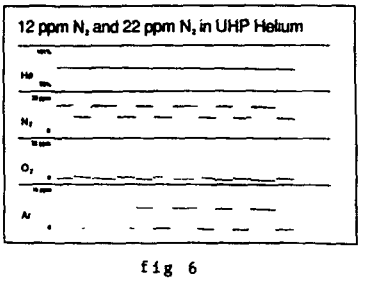

fig 6

DIRECT INLET MS

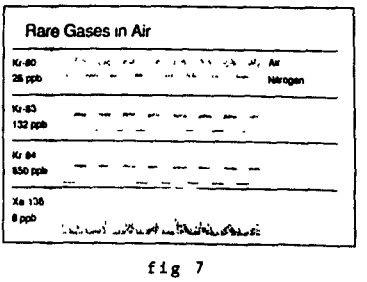

fig 7

While the direct inlet approach is often easier than the hyphenated technique, the decision is often dependent upon the chemical nature of the gases and the complexity of the matrix. In short, both GC/MS and direct inlet MS prove to be valuable tools in the detection and monitoring of low level impurities in semiconductor grade "PURE" gases.

Presented at the 35th ASMS Conference on Mass Spectrometry and Allied Topics
May 24-29, 1987, Denver, CO

DETERMINATION OF MOLECULAR WEIGHT DISTRIBUTIONS OF LOW MOLECULAR WEIGHT POLYMERS USING TIME-OF-FLIGHT SECONDARY ION MASS SPECTROMETRY

Ioannis V. Bletsos and David M. Hercules
Department of Chemistry
University of Pittsburgh
Pittsburgh, PA 15260
U.S.A.

and

Dieter vanLeyen and Alfred Benninghoven
Physikalisches Institut der Universitat Munster
D-4400 Munster
FRG

Time-of-flight secondary ion mass spectrometry (TOF-SIMS) has been used for structural characterization of polymers (1,2). Polymer fragments correspond to well-defined fragmentation series from which they can be easily identified. Polymers can be identified also from the spacing between consecutive peaks of the same series; this spacing is equal to the mass of the repeat unit. Molecular weight distributions of low molecular weight polymers can be obtained from TOF-SIMS spectra by direct measurement of the masses of intact cationized oligomers. Number average molecular weights (Mn) are calculated from TOF-SIMS spectra by measuring the masses and intensities of cationized oligomers.

Molecular weight distributions for various low molecular weight polymers (Mn < 10,000) obtained from TOF-SIMS spectra were evaluated by using polystyrene (PS) standards having known molecular weight distributions. The PS standards (Polymer Laboratories Inc., Amherst, MA) were dissolved in toluene. The concentrations of the solutions were approximately 1×10^{-3} M with respect to the repeat unit. A 1-5 µl quantity of the solution was deposited on 100 mm^2 of a Ag substrate which had been cleaned by etching with HNO_3 (20% vol.). The spectra were obtained using a TOF-SIMS equipped with a mass selected primary ion source, an angle and time focusing TOF analyzer, and a single ion counting detector (3).

A TOF-SIMS spectrum of a PS standard with Mn = 2964 determined by gel permeation chromatography (GPC) is shown in Figure 1. In the range m/z = 1750-4700 intact oligomers are detected giving rise to the $[nR + C_4H_9 + H + Ag]^+$ series, where R is the repeat unit for PS. These peaks are the most intense in this mass range, and their intensity distribution reflects the number average molecular weight distribution of the PS standard. Loss of a terminal $-C_4H_9$ group results in the $[nR + Ag]^+$ series having lower intensity than $[nR + C_4H_9 + H + Ag]^+$. The higher intensity of the $[nR + C_4H_9 + H + Ag]^+$ series indicates that even if some fragmentation occurs, the dominant process in the m/z = 1750-4700 range is the desorption of intact polymer molecules cationized with Ag^+. The value Mn = 2780 was calculated from peak intensities. The calculated value Mn = 2780 is within 6% of Mn = 2964 determined by GPC.

Two important questions to consider are whether fragmentation and ionization/desorption processes affect molecular weight distributions determined by TOF-SIMS and how instrumental parameters influence oligomer detection. Fragmentation and ionization/desorption will interfere with ion quantitation if the fragmentation and ionization/desorption probabilities of individual oligomers vary significantly with size of oligomer. To evaluate this the sputtering cross sections of oligomers and fragments were determined from:

$$N_d(t) = N_d(t=0)\exp(-\sigma It/Aq_e) \qquad [1]$$

Where N_d is the number of secondary ions detected, σ is the sputtering cross section, I is the primary ion current, A is the area bombarded by primary ions, q_e is the charge of an electron, and t is the time of sputtering. According to [1], a plot of ln (signal intensity) vs. time of sputtering is linear, and $\sigma I/Aq_e$ is given by the slope of the curve. From the slope of the curve we found that σ varies beween $\sigma = 2 \times 10^{-17}$ m^2 to $\sigma = 5 \times 10^{-17}$ m^2 for PS oligomers having molecular weights between 1000 and 5000.

Instrumental factors which influence the determination of Mn include the resolution of the TOF-SIMS and the postacceleration. In the lower part of the distribution range fragments having a terminal $-C_4H_9$ and whole polymer molecules with a $-C_4H_9$ terminal group intact will give rise to peaks which are not resolved. Consequently, the $[nR + C_4H_9 + H + Ag]^+$ series may appear to be more intense in the lower part of the distribution region due to contribution from fragmentation. Such an effect will cause the distribution to be weighed toward lower molecular weight oligomers. Also, it has been established that the TOF-SIMS detection efficiency decreases with increasing mass. The fragmentation and ionization/desorption processes combined with the TOF-SIMS detection bias for small masses appear to shift the molecular weight distributions toward lower masses, but this does not seem to affect significantly the value of Mn.

In conclusion, TOF-SIMS is a useful technique for the structural characterization of polymers and the determination of molecular weight distributions of low molecular weight polymers (Mn < 10,000).

1. Bletsos, I. V.; Hercules, D. M.; Greifendorf, D.; and Benninghoven, A., Anal. Chem., 1985, 57, 2384.

2. Bletsos, I. V.; Hercules, D. M.; vanLeyen, D.; and Benninghoven, A., Macromolecules 1987, 20, 407.

3. Steffens, P.; Niehuis, E.; Friese, T.; Greifendorf, D.; and Benninghoven, A., J. Vac. Sci. Technol., A 1985, 3, 1322.

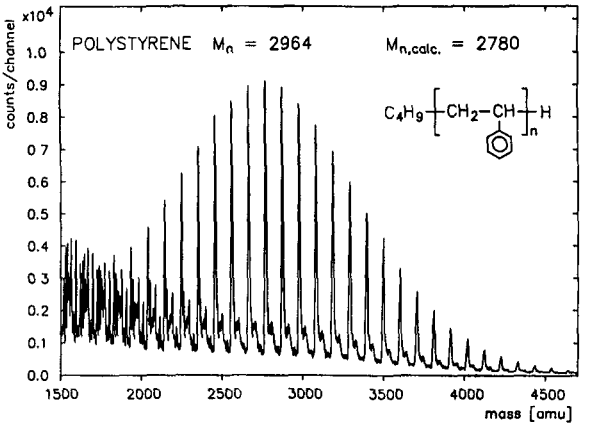

Figure 1: TOF-SIMS Spectrum of PS Standard in the Range m/z = 1500-4700 Showing the Distribution of PS Oligomers Cationized with Ag^+

Presented at the 35th ASMS Conference on Mass Spectrometry and Allied Topics
May 24-29, 1987, Denver, CO.

TIME-OF-FLIGHT SECONDARY ION MASS SPECTROMETRY: COPOLYMER SPECTRA FROM THIN FILMS TO POLYMER SPECTRA FROM THICK SAMPLES

Ioannis V. Bletsos and David M. Hercules
Department of Chemistry
University of Pittsburgh
Pittsburgh, PA 15260
U.S.A.

and

Dieter vanLeyen and Alfred Benninghoven
Physikalisches Institut der Universitat Munster
D-4400 Munster
FRG

Time-of-flight secondary ion mass spectrometry (TOF-SIMS) has been used for structural characterization and determination of molecular weight distributions of various polymers (1). TOF-SIMS spectra of random copolymers (e.g., styrene/acrylic acid) having known composition have also been obtained. The fragmentation pattern is consistent throughout the detectable mass range for a given composition studied. Spacings between peaks correspond to the mass of the repeat unit of polystyrene or polyacrylic acid components. Peaks could be assigned to fragments which contain a number of polystyrene or polyacrylic acid repeat units.

Polymers are typical insulators; to avoid charging of the polymer surface during ion bombardment the polymers are dissolved and cast as thin films on a Ag substrate. Dissolving a polymer can often be time consuming or very difficult (e.g., in cross-linked polymers); in addition, it prohibits surface characterization of intact polymer films. Charge accumulation on insulator surfaces causes serious problems ranging from signal instability to complete loss of signal in a period of a few seconds (2). In SIMS studies of thick polymer samples to date, charging has been compensated by flooding the insulating surface with electrons. Spectra obtained this way are still restricted to the low mass range.

TOF-SIMS spectra of thick polymer samples (e.g., 1 mm cross-linked polydimethylsiloxane (PDMSO); 200 μm Teflon) were obtained in the mass range m/z $\leq$ 4500. Difficulties arising from charging of the polymers were overcome by placing a Ni grid on the polymer surface. The primary ion dosage was kept low to minimize charge accumulation, and the energy range of the electrostatic deflector of the TOF-SIMS instrument (3) was adjusted to match the energy of the secondary ions, which was increased due to charging. The spectra were similar to those otained from thin polymer films, and fragments containing a large number of repeat units up to m/z 4500 were detected.

A TOF-SIMS spectrum of a thick film (i.e., 1 mm) of a cross-linked (PDMSO) sample is shown in the range m/z 590-4010 in Figure 1. The range m/z 1200-4300 is characteristic of the PDMSO sample, while the range m/z 600-1200 is dominated by peaks characteristic of Teflon which is a contaminant on the PDMSO surface. In the mass range dominated by PDMSO (m/z 1200-4300) there appear two series of peaks. The most intense peaks correspond to $[nR + Ni]^+$, where n = 15, . . . , 57 and R is the repeat unit of PDMSO (R = 74 amu). Peaks of lower intensity appearing on the low mass side of the $(nR + Ni)^+$ series (Δm/z 15) correspond to the $[nR - CH_3 + Ni]^+$ series. Every peak in both series corresponds to an integral number of repeat units; the spacing between consecutive peaks in each series is equal to the mass of one repeat unit of PDMSO. The PDMSO fragments of both series are cationized with Ni. Ni ions are produced from sputtering the Ni grid used for charge compensation.

The peaks in the range m/z 600-1200 have spacing of 50 amu (i.e., the mass of CF_2) and are attributed to Teflon. Cleavage of Teflon chains produces four series of peaks which in order of decreasing intensity are:

$$(CF_2)_nCF^+ > (CF_2)_nC_2F^+ > (CF_2)_nC^+ > (CF_2)_nC_3F^+.$$

Teflon appears as contamination on the sample surface because PDMSO was stored between two thin Teflon films. While unpeeling the Teflon films to obtain the PDMSO sample, some Teflon remained on the PDMSO surface thus was detected by TOF-SIMS.

Meaningful TOF-SIMS spectra were obtained from thick polymer samples without prior sample preparation. Therefore, TOF-SIMS can be used to characterize polymers difficult or impossible to dissolve, as well as for surface analysis of polymers or other insulating materials. Detection of fragments in the medium mass range provides unambiguous structural information about polymers and their surface contaminants.

1. Bletsos, I. V.; Hercules, D. M.; vanLeyen, D.; and Benninghoven, A., Macromolecules 1987, 20, 407.

2. Werner, H. W. and Morgan, A. E., J. Appl. Phys. 1976, 47, 1232.

3. Steffens, P.; Niehuis, E.; Friese, T.; Greifendorf, D.; and Benninghoven, A., J. Vac. Sci. Technol. A 1985, 3, 1322.

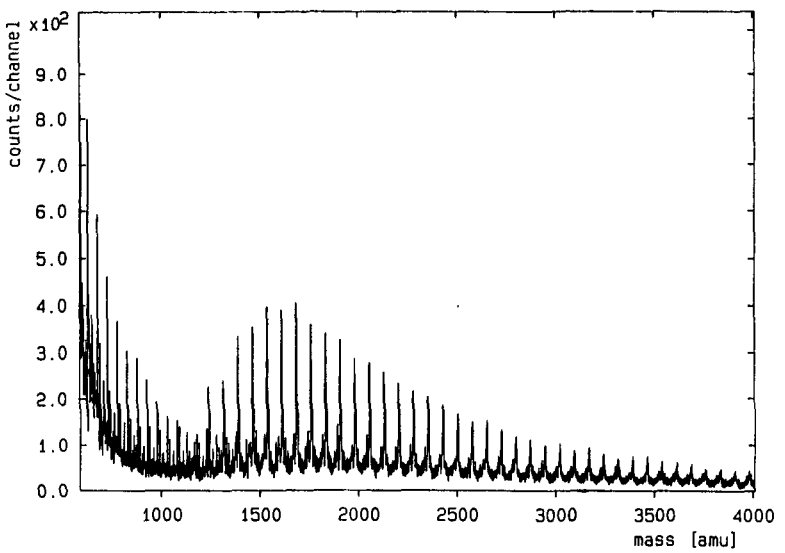

Figure 1: TOF-SIMS Spectrum of 1 mm Thick Polydimethylsiloxane Sample in the Range m/z = 590-4010

Presented at the 35th ASMS Conference on Mass Spectrometry and Allied Topics
May 24-29, 1987, Denver, CO

Identification of Organic Additives in Uncured Rubber Compounds Using Mass Spectrometry

R. P. Lattimer and R. E. Harris
The BFGoodrich Research and Development Center
Brecksville, Ohio 44141 (USA)

C. K. Rhee
The Uniroyal Goodrich Tire Company
Brecksville, Ohio 44141 (USA)

H.-R. Schulten
Fachhochschule Fresenius
D-6200 Wiesbaden (FRG)

The identification of the ingredients in a compounded polymer is often a complex task for the analytical chemist. A wide variety of components is involved--polymers, fillers, solvents, and organic and inorganic additives. This report considers the identification of organic additives in uncured rubber compounds by various mass spectrometric methods. The general subject of the mass spectral characterization of additives in compounded polymers has recently been reviewed.[1] Three uncured, carbon black-filled rubber compounds of known composition were analyzed in the present study. In an earlier study, we examined the same rubber compounds in their vulcanized (cured) states.[2]

The three uncured stocks were analyzed by direct thermal desorption with three different methods of ionization (EI, CI, FI). In addition the three rubbers were examined by FAB-MS (without liquid matrix) as a means for surface desorption/ionization. Extracts of the rubbers were also examined using two different solvents (acetone and acetonitrile). Each extract was examined directly by five methods of ionization (EI, CI, FI, FD, FAB). Analyses were carried out using either a Finnigan MAT 311A/Incos 2400 mass spectrometer system (Brecksville) or else a Finnigan MAT 731/SS-200 system (Wiesbaden).

Of the various vaporization/ionization methods, it appears that FI/FD is the most efficient for identifying typical organic additives in rubber stocks. The analysis can be carried out using either the untreated rubber (FI mode) or else a solvent extract (FI or FD mode). Molecular ions are dominant, which facilitates the characterization of the complex organic additive mixtures that are present in typical compounded rubbers. For samples in which the identity of FD/FI molecular ions is unclear, further analysis using other methods (EI, CI, FAB, MS/MS, GC-MS, LC-MS, high resolution) can be carried out to gain additional information. We conclude that FD and FI yield the most useful information in the shortest period of time.

The various classes of additives studied can be discussed individually in terms of their ability to be detected in the rubbers by mass spectrometry. Antioxidants and antiozonants used in the recipes include aromatic amines and a hindered bisphenol. These compounds could be detected quite readily by either extraction or direct analysis and by use of any vaporization/ionization method. Stearic acid could be identified only by direct analysis of the rubber, using any vaporization/ionization method. Stearic acid was not observed in any of the extracts; this indicates that it remains in the rubber bulk during the extraction process.

In our experience tackifier resins are difficult to detect in rubbers by mass spectral analysis. While ions due to the t-octylphenol/formaldehyde resin could be observed in several spectra, their relative intensities were always quite low. The principal difficulty seems to be interference from other species, particularly processing oil and paraffin wax. We have generally found that the best way to detect these resins in rubbers is by EI-MS, either by direct analysis of the rubber or else by use of an extract. FI/FD may also be successful, provided that the oil/wax level is not excessively high. A particularly effective means for detecting tackifier resins by direct rubber analysis is MS/MS; this approach is considered in a separate paper.[3]

Processing oil and paraffin wax are characterized well in rubber only by FD- and FI-MS. Other methods of ionization (EI, CI, FAB) tend to give mostly lower mass fragment ions for the oil and wax components. The general molecular weight distribution of the processing oil can be estimated by either FI or FD analysis of the extract or else by direct FI analysis of the rubber. One interesting effect is that wax oligomers (C_nH_{2n+2}) are quite prominent in the FD mass spectrum of the extracts, while these species are masked by oil oligomers in the FI spectra of the heated rubbers. The reason for this effect is that the wax molecular ions are desorbed more efficiently from the emitter (FD mode) than are the oil components. In FI mode, the ionization efficiencies are apparently similar for the oil as compared to the wax components.

Since accelerators and other curatives decompose during the crosslinking process, one does not usually find the original (intact) accelerator in the vulcanizate.[1-2] In this study of uncured rubbers, we found that the curatives could be detected intact. The best method to observe accelerator molecular ions ($M^{+\cdot}$ or MH^+) was CI-MS, although FI/FD-MS could also be used. In EI-MS, sulfur (S_8) is readily observed, but most accelerators tend to fragment extensively so that molecular ions are not distinctive in the mixture of additives. There was some indication in this study that accelerators might be easier to detect via direct analysis as compared to extract analysis.

The relative merits of extraction versus direct analysis methods have been discussed in detail elsewhere.[1-2] In this study, there was no clear advantage for direct analysis as compared to analysis of the extract. Both approaches gave generally comparable results. The two solvents used in this study (acetone and acetonitrile) were also compared in the earlier study.[2] The main difference between them is that acetonitrile is less efficient at extracting oil and wax components than is acetone. (This can be either an advantage or a disadvantage.) It might be noted that the identification of the ingredients in the cure system is most readily accomplished by direct analysis of the rubber.

[1] R. P. Lattimer and R. E. Harris, Mass Spectrom. Rev. 4, 369 (1985).

[2] R. P. Lattimer, R. E. Harris, C. K. Rhee and H.-R. Schulten, Anal. Chem. 58, 3188 (1986).

[3] R. P. Lattimer, 35th ASMS Conf. Mass Spectrom. Allied Topics, Denver, May 24-29, 1987, paper MPA44.

/gg
8.27-87

Presented at the 35th ASMS Conference on Mass Spectrometry and Allied Topics
May 24-29, 1987, Denver, CO

Tandem Mass Spectrometry (MS/MS) for Analysis of Additives in a Rubber Vulcanizate

Robert P. Lattimer
The BFGoodrich Research and Development Center
Brecksville, Ohio 44141

Commercial rubber and plastic formulations are composites of many different types of materials--polymers, fillers, and organic and inorganic additives. MS/MS applications involving polymer analysis have not been extensive to date. In this report we describe the direct MS/MS analysis of organic additives in a rubber compound. We show how daughter ion, parent ion and neutral loss MS/MS scans can be used to reduce the chemical noise and provide added specificity for component identification. All data were acquired with a Finnigan MAT HS-Q 30 mass spectrometer (Finnigan MAT GmbH, Bremen, F.R.G.). This is a hybrid instrument (BEQQ). CID was carried out in Q-1 with air as the collision gas. The rubber sample was analyzed via heated direct probe introduction with 70 eV electron impact ionization.

Daughter ion scan. This technique is useful for gaining chemical structure information on a particular ion of interest. In mixture analysis, one can select a molecular ion and get its fragmentation pattern without doing any physical or chemical separation of the various components. Figures 1 and 2 are both daughter ion spectra of m/z 256 from the rubber sample. The spectrum in Figure 1 was obtained early in the run (with little sample heating), while the spectrum in Figure 2 was obtained later on at a sample temperature ~150°C. Figure 1 is clearly the spectrum of sulfur (S_8, MW 256), while Figure 2 is that of palmitic acid (MW 256), a fatty acid component in the recipe. This nicely illustrates how MS/MS can help to distinguish ions arising from different chemical species that have the same nominal mass.

Parent ion scan. This allows one to select a particular fragment ion in a "normal" mass spectrum and search for precursors that yield that fragment. Parent ion scans are useful for screening a sample for specific functional groups or substructures that yield characteristic fragment ions. Figure 3 is a parent ion scan for m/z 353, which is a known fragment ion from the t-octylphenol/formaldehyde tackifier resin used in the recipe. The main precursors to m/z 353 turn out to be m/z 424 and 465, which clearly arise from tackifier components. Thus the parent ion scan can be used to confirm the presence of the tackifier in the sample. In earlier work[1] it was shown that tackifier resins are very difficult to identify by direct analysis of rubber vulcanizates using conventional (single-stage) mass spectral methods. Figure 3 illustrates how easily MS/MS can reduce the chemical noise to produce an unequivocal confirmation for the presence of the tackifier.

Neutral loss scan. This technique is useful for searching for a particular class of compounds whose mass spectra are distinguished by a specific neutral loss. Figure 4 shows the neutral loss spectrum for m/z 71 (C_5H_{11}). This is an easily lost fragment from aromatic compounds containing a t-octyl group. Thus, several ions in Figure 4 can be attributed to DODPA (m/z 322 and 393), TODPA (m/z 434 and 505), and tackifier oligomers (m/z 424 and 536). Stearic acid (M^+. 284) also shows a loss of C_5H_{11} from the aliphatic chain.

In summary, MS/MS has considerable potential as a means for improved direct mass spectral characterization of rubber compounds. MS/MS reduces the chemical noise to improve the specificity for identification of organic additive components in complex polymer matrices.

[1] R. P. Lattimer, R. E. Harris, C. K. Rhee and H.-R. Schulten, Anal. Chem. 58, 3188 (1986).

Presented at the 35th ASMS Conference on Mass Spectrometry and Allied Topics
May 24-29, 1987, Denver, CO

FIGURE 1. DAUGHTER ION SCAN (m/z 256 - SULFUR).

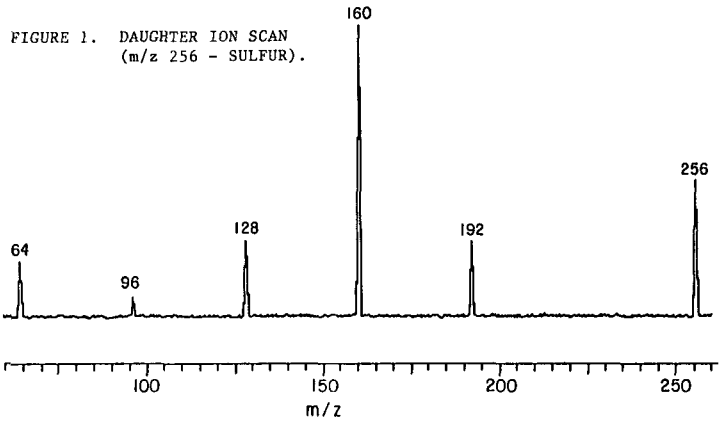

FIGURE 2. DAUGHTER ION SCAN (m/z 256 - PALMITIC ACID).

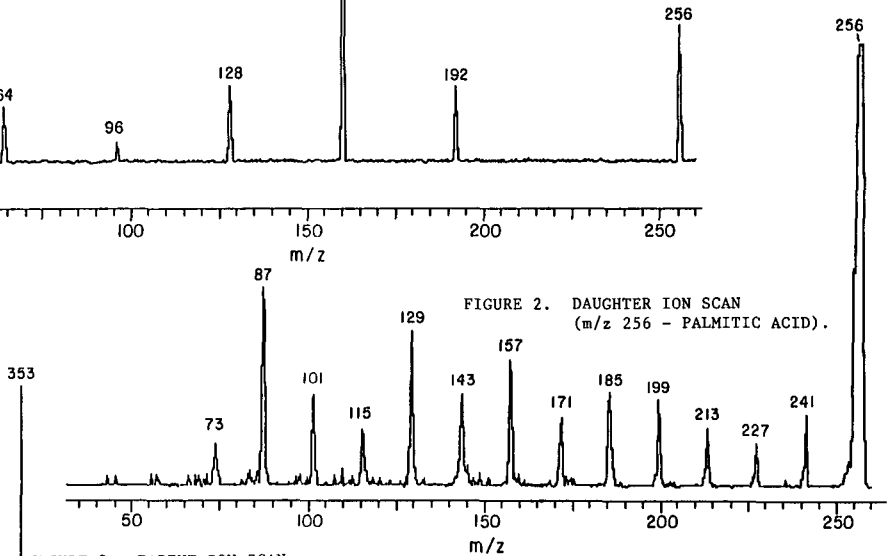

FIGURE 3. PARENT ION SCAN (m/z 353).

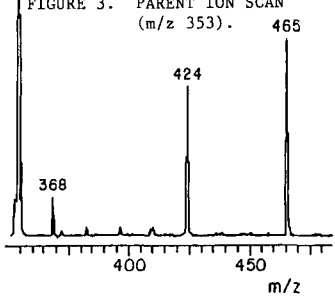

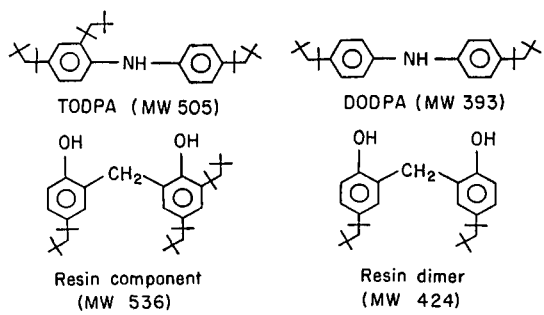

FIGURE 4 - NEUTRAL LOSS SCAN (m/z 71).

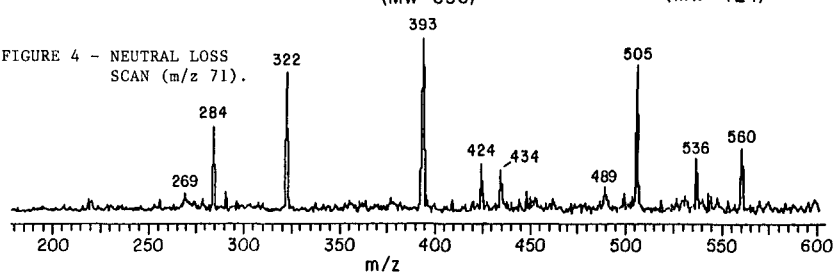

Presented at the 35th ASMS Conference on Mass Spectrometry and Allied Topics
May 24-29, 1987, Denver, CO

PYROLYSIS GAS CHROMATOGRAPHY/NEGATIVE CHEMICAL IONIZATION MASS SPECTROMETRY OF MALEIC ANHYDRIDE FUNCTIONALIZED POLYETHYLENES (MAFP)

Timothy A. Snow, Conoco Inc., Petroleum R & D,
Ponca City, Oklahoma 74603

Poly(olefins) functionalized with reactive maleic anhydride graft sites lead to many exciting combinations of very different grafted polymers. These graft copolymers often display the favorable properties (such as heat resistance, flexibility, tensile strength, etc.) characteristic of each of the homopolymers. Critical in the synthesis and design of these new polymers are structure-property relationships. The determination of microstructure of polymers is invaluable in helping to better understand these relationships. Pyrolysis gas chromatography/negative chemical ionization mass spectrometry (PyGC/NCIMS) has been found to be a useful tool in the analysis of this new class of polymer.

Earlier work in the pyrolysis GC/MS of MAFP with electron impact ionization showed pyrolysates of the poly(ethylene) interfered with the detection of the small amount of pyrolysates resulting from the functional sites. Negative ions formed by methane chemical ionization allows specific mass spectrometric detection of pyrolysates related to the maleic anhydride functional sites. Anhydrides yield true molecular anions and appear to be formed by electron attachment.

Pyrolysis temperatures were determined by comparison of thermal gravimetric analyses (TGA) of the samples. A temperature of 200°C was found to completely drive off any unreacted material and 800°C was found to be the temperature at which most of the sample was volatilized.

Three specific questions to be determined in the analysis of maleic anhydride functionalized poly(ethylene) (MAFP) were: 1) how efficient has the functionalization been?, 2) how has the polyethylene been effected by the functionalization?, and 3) what is the nature of the functional site? Four possible functional site types are thought to exist in the functionalized poly(olefin):

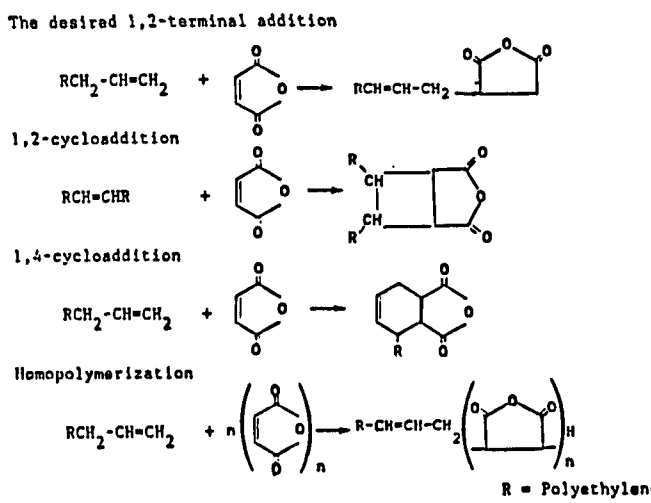

The low temperature pyrolysis primarily showed the unreacted maleic anhydride and low molecular weight reacted material. The maleic anhydride is assumed to be the unreacted residual anhydride. The total area of the m/e = -98 (molecular anion) single ion chromatogram was used with the calculated pyrolytic activity to yield a semiquantitative value for free maleic anhydride. A MAFP standard with free maleic anhydride in a high enough concentration to be measured by FTIR was used to calibrate the method.

The sensitivity of the method for maleic and phthalic anhydrides was determined by injecting standard solutions. A signal to noise of 9 to 1 for the m/e = -98 single ion chromatogram was achieved for a microliter injection of a 178 ppb maleic anhydride solution and a 3 to 1 signal to noise on the m/e = -148 single ion chromatogram for a 3.0 ppt solution of phthalic anhydride (~2 picograms). This sensitivity could be improved by single ion monitoring or increasing the sample size.

The low temperature pyrolysis also exhibits small amounts of substituted maleic anhydride and substituted phthalic anhydride. Both of which suggest some cracking of the polymer must occur during the functionalization process. The higher sensitivity of this method for phthalic anhydrides relative to maleic anhydride does indicate this cracking occurs at a much lower extent than the 1,2-terminal addition. The large amount of alkyl maleic anhydrides generated by the 800°C pyrolysis, indicates that the 1,2-terminal addition is the predominant type of functional site.

The MAFP samples studied were all found to be primarily functionalized with 1,2-terminal addition graft sites with a minor amount of 1,4-cycloaddition graft sites also present. High temperature pyrolysis GC/NCIMS was found to be a useful tool for qualitatively assessing the nature of the bulk functional site. However substantiation or denial of the existence of some of the less prevalent functional site types is difficult when one type of addition dominates the polymer.

Presented at the 35th ASMS Conference on Mass Spectrometry and Allied Topics
May 24-29, 1987, Denver, CO.

POLYMERIZATION OF CYCLOPENTADIENE STUDIED BY FIELD DESORPTION MASS SPECTROMETRY AND PYROLYSIS GC/MS

C. S. Hsu and A. Malatesta
Exxon Research and Engineering Co., Annandale, NJ 08801
Exxon Chemical International, B-1920 Machelen, Belgium

Thermal polymerization of cyclopentadiene (CPD) generally proceeds via Diels-Alder cycloadditions. These are second order reactions and generally fast even at moderate temperatures. The products formed have a condensed multi-ring structure with only two double bonds. Higher reaction temperatures (>200°C), however, yield mixtures of 2+4 pi Diels-Alder adducts and amorphous low molecular weight polymers.

We have synthesized polymers from several CPD oligomers (CPD dimers, trimers, tetramers, and mixtures of dimers/trimers and dimers/tetramers) to study their structures. Multistage pyrolysis with a single sample load was used to analyze these polymers to differentiate the CPD polymers (monomer through tetramers) from the volatiles and from the pyrolysates. This technique provides more accurate, quantitative information for the pyrolysates. In the pyrolysates of high-temperature low-molecular-weight CPD polymers, we found a new class of compounds. Figure 1 shows a typical mass spectrum of a tetramer belonging to this class. The spectrum shows fragments from simple bond cleavage from the molecular ion; they are different from fragments in the mass spectra of tetramers derived from Diels-Alder cycloaddition, shown in Figure 2, where retro-Diels-Alder processes predominate. We also found that amounts of this new class of compounds decrease with increasing size of the oligomers used as starting materials for polymerization. The presence of this new class of compounds gives us a clue of the polymer enchainment resulting from the linkage of CPD cycloadducts.

The linked structure in the high-temperature thermal CPD polymers was confirmed by comparing the field desorption mass spectrum (FDMS) of a thermal polymer with that of its corresponding hydrogenated products, shown in Figure 3. The oligomers derived from the Diels-Alder reaction of CPD are in a condensed form (A) with only two double bonds available for hydrogenation. The presence of 4+H products in the hydrogenated CPD polymers confirms the linked structure (B) in the high-temperature thermal CPD polymers. The degree of hydrogenation increased with the number of CPD units in the hydrogenated oligomers. For example, the most predominant tetramer is the tetrahydro (4H) products; in heptamers, octahydro (8H) products predominate. FDMS also shows that most of oligomers in the CPD polymers contain 3 to 10 CPD units. Tsuchiya, et al. (1), reported similar results.

In conclusion, pyrolysis GC/MS and FDMS analyses of thermal and hydrogenated CPD polymers revealed the presence of copolymers formed from a free-radical mechanism through norborneno and cyclopenteno double bonds. Copolymerization may occur during or after the Diels-Alder additions. Pyrolysis of hydrogenated CPD polymers also indicated that hydrogenating the residual double bonds stabilizes the unsaturated copolymers due to the release of strains on these double bonds.

---

(1) Tsuchiya, S., Imai, I.; Ohshima, A.; Hayashi, H., J. Japan Petrol. Inst., 27, 26-30 (1984)

Presented at the 35th ASMS Conference on Mass Spectrometry and Allied Topics
May 24-29, 1987, Denver, CO

A

(a Condensed Structure)

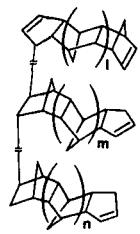

B

(A Linked Structure)

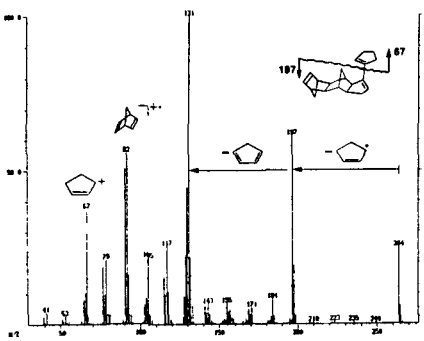

FIGURE 1

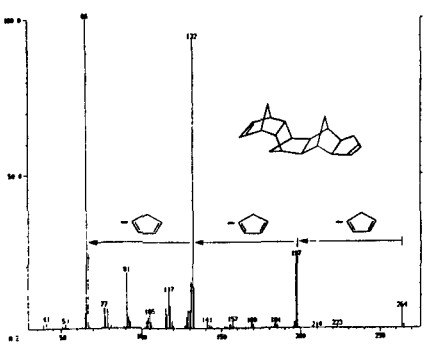

FIGURE 2

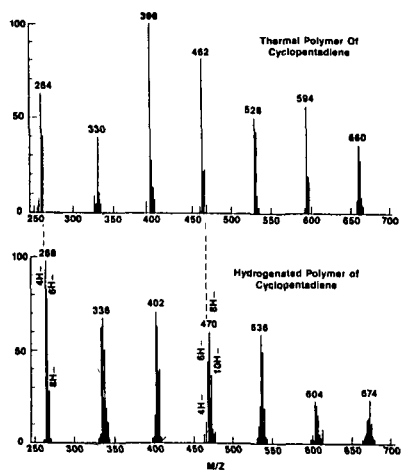

FIGURE 3

Presented at the 35th ASMS Conference on Mass Spectrometry and Allied Topics
May 24-29, 1987, Denver, CO

APPLICATIONS OF MS-MS TO THE ANALYSIS OF UNCURED EPOXY RESIN MIXTURES

T G BLEASE, D A CATLOW, E CLAYTON, JOHN J MONAGHAN AND J H SCRIVENS
IMPERIAL CHEMICAL INDUSTRIES PLC, RUNCORN HEATH, CHESHIRE, UK, WA7 4QD

As part of our investigation into the application of MS-MS to the analysis of mixtures of industrial significance, we have examined an uncured epoxy resin mixture of current commercial interest.

The alternative analytical method (chromatographic separation followed by spectroscopic identification of individual components) is time consuming and it was hoped that MS-MS would provide a rapid, reliable method of analysis for this type of sample.

The study was carried out using a VG ZAB-HSQ hybrid spectrometer of BEQQ geometry. Samples were introduced using the heated probe. Daughter ion spectra of selected precursor ions in the EI and isobutane CI spectra of the mixture using argon as the collision gas at a pressure of 1 mtorr. The collision energy was typically 25ev.

The EI spectrum of the resin mixture (fig 1) was complex making direct identification of individual compounds difficult.

Fig 1 EI of Resin Mixture

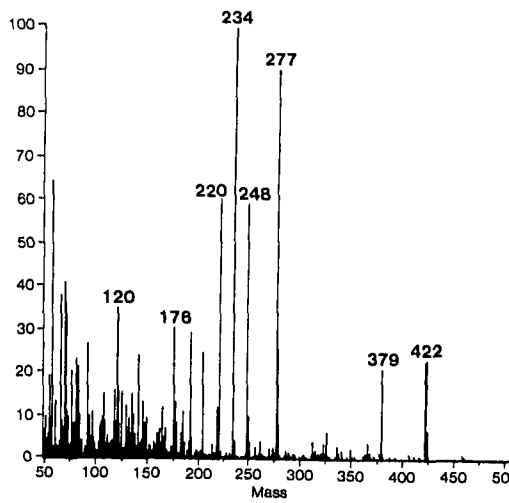

A daughter ion scan of the ion at m/z 422 suggested that the species was TGDDM,

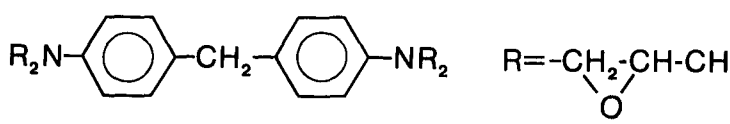

By running a sample of TGDDM under identical conditions, this suggestion was confirmed. With the structure of one component established, a daughter ion spectrum of the highest unattributed ion ($m/_z$277) was obtained. The spectrum indicated that the species was GDA,

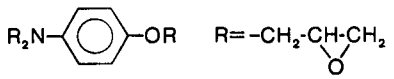

and this was confirmed by examining a reference sample of GDA.

Of the prominent higher mass ions in fig 1, only $m/_z$ 248 cannot now be accounted for by either TGDDM or GDA. Fig 2 shows the daughter ion spectrum of this ion.

Fig 2 Daughters of m/z 248 in Mixture

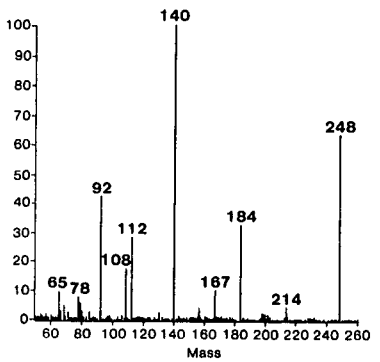

Whilst this spectrum is clearly suggestive of a diaminodiphenylsulphone (DADPS), a common curing agent in epoxy resins, several isomeric structures are possible. Daughter ion spectra of the molecular ions of several isomers showed that isomeric distinction could be achieved and that the species present in the mixture was 3,3′-DADPS.

An investigation of the CAD spectra of the CI-generated $(M+H)^+$ ion of 4,4′-DADPS showed a structurally significant ion, $m/_z$ 156, not prominent under EI conditions. In the EI case, rearrangement of the molecular ion occurs to yield prominent daughter ion at $m/_z$ 140 and $m/_z$ 108.

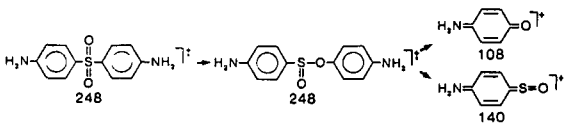

The presence of the $m/_z$ 156 ion, H_2N-Ar-SO_2 moiety, shows that under CI conditions structural information more closely related to the intact molecule is produced.

CONCLUSIONS

1 MS-MS is of value in the analysis of industrially important mixtures.

2 The method has given reproducible CAD spectra with excellent agreement between standards and mixture components.

3 Use has been made of the isomer discrimination provided by the technique and the complementary structural information obtained from soft ionisation methods.

Presented at the 35th ASMS Conference on Mass Spectrometry and Allied Topics
May 24-29, 1987, Denver, CO

ANALYTE DETECTION IN SOLID POLYMER MATRICES BY PYROLYSIS-ATMOSPHERIC PRESSURE CHEMICAL IONIZATION-MS/MS

A. Peter Snyder and Johannes H. Kremer
Chemical Research, Development and Engineering Center
Aberdeen Proving Ground, MD 21010-5423

Shirley A. Liebman
GEO-CENTERS, INC., Chemical Research, Development and Engineering Center, Aberdeen Proving Ground, MD 21010-5423

Richard A. Yost
Department of Chemistry, University of Florida, Gainesville, FL 32611

Pyrolysis and thermolysis are well-established methods for the introduction of a solid sample to the ion source of a mass spectrometer. Extraction of information from pyrolyzate fragments has been investigated under 1 torr or lower pressure conditions with CI and EI, respectively. However, only a handful of investigations have been reported under CI conditions at atmospheric pressure (1,2).

A CDS Pyroprobe was interfaced to the APCI source of a Sciex TAGA™ 6000 mass spectrometer (Figure 1). The presence of specific analytes in various commercial product, solid polymer matrices was investigated under pulsed and linear programmed (LP; 60°C/min) heating modes to a final temperature of 500°C. Oxidative and nonoxidative (nitrogen) conditions were used and 0.5 mg amounts were used. Unlike EI, APCI is selective in the ionization of neutrals introduced to the ion source and primarily ionizes oxygen and nitrogen functional groups.

HTPB-2 is composed of a multi-polymer formulation (HTPB-1, 60% by weight) that acts as a binder for the propellant cyclotrimethylenetrinitramine (RDX) (40% by weight). Figure 2 presents HTPB-1, RDX and HTPB-2 Py-APCI mass spectra under different conditions. The m/z 44, 60, 75 and 85 RDX features dominate in the pulsed vs LP mode in HTPB-2 thermal processing, and under nonoxidative conditions, only the RDX features are present. Figure 3 presents an LP, air oxidation mass spectrum of the Shell No-Pest Strip®. The pesticide dichlorvos $(CH_3O)_2P(O)OCH{=}CCl_2$, is indicated by the dichlorvos MH^+ ion cluster at m/z 221, m/z 223, and 225.

The decongestant Contac was investigated for pharmaceutical content in the white, pink and yellow pigmented beads. The active ingredients in Contac are phenylpropanolamine, (vasoconstrictor) and chlorpheniramine maleate (antihistamine) (Figure 4). Figure 4 shows the Py-APCI mass spectra of each crushed bead and MS/MS patterns of m/z 135, 127 and 111. Phenylpropanolamine loses an hydroxyl group in the thermolysis process and is protonated (m/z 135) while the maleate compound produces various pyrolyzate fragments (m/z 85, 97, 99, 111 and 127). The white and pink beads contain different amounts of the two compounds, based upon the m/z 111/135 ratio while the yellow bead contains essentially only the maleate. This produces a clear, qualitative account of the beads' differential substance content and therefore time-release phenomenon. The alkaloid matrices responsible for the time-release properties produce a negligible effect on the mass spectral detection and characterization of the pharmaceutical compounds.

The rapid, convenient and selective technique of APCI-MS/MS has been shown to be promising in the analysis of solid material pyrolyzate/thermolyzate. The selectivity of APCI greatly enhances the presence of low molecular weight compounds with oxygen/nitrogen functional groups in complex polymer matrices.

(1) Shushan, B., Davidson, B. and Prime, R.B. In "Analytical Calorimetry"; Vol. 5, Johnson, J.F., Gill, P.S., Eds.; Plenum Press:New York, 1984; 105-111.
(2) Lawrence, A.H., Anal. Chem., 1986, 58, 1269-1272.

Presented at the 35th ASMS Conference on Mass Spectrometry and Allied Topics
May 24-29, 1987, Denver, CO

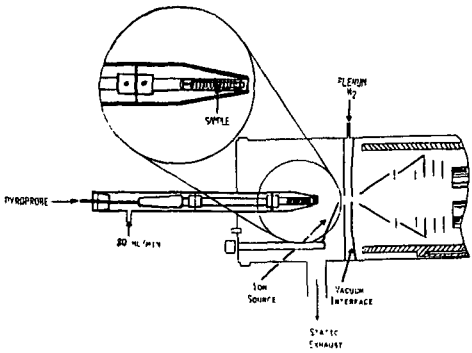

FIGURE 1

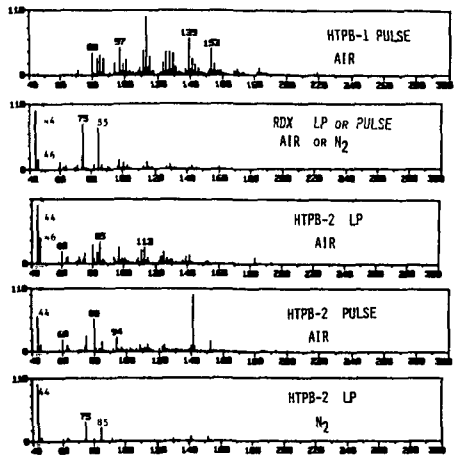

FIGURE 2

FIGURE 3

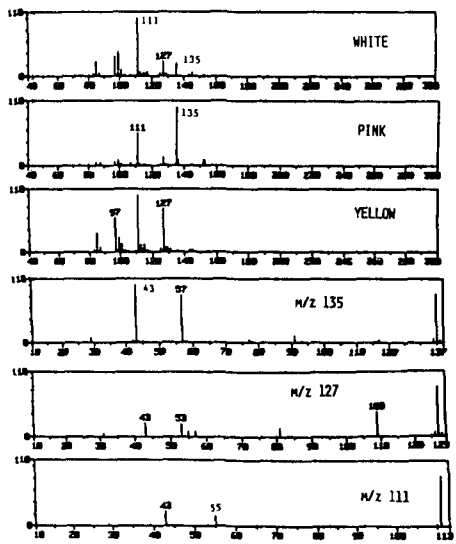

FIGURE 5

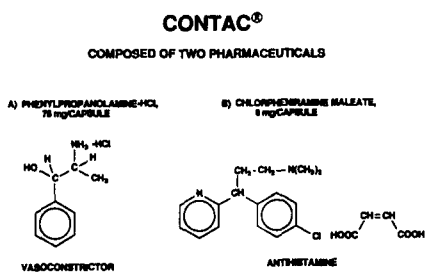

FIGURE 4

Presented at the 35th ASMS Conference on Mass Spectrometry and Allied Topics
May 24-29, 1987, Denver, CO

Laser-Ion Beam Photodissociation Studies: The $Mn_2(CO)_y^+$, $Fe_3(CO)_y^+$ and $Co_4(CO)_y^+$ Systems.

R.E. Tecklenburg, Jr., and D.H. Russell

Texas A&M University
Department of Chemistry
College Station, TX 77843

Understanding of the reactive and intrinsic properties of transition metal clusters has been the focus of a large number of research groups.[a,b] Theoretical and experimental understanding of small ligated and bare metal clusters is an essential first step to the understanding of bulk metal catalytic properties. Photodissociation methods are potentially quite useful for characterization of ionic transition metal clusters, especially for measurements of metal-metal and metal-ligand bond energies and electron affinities.[c,d] To date most of the photodissociation work on transition metal systems has been performed by ion cyclotron resonance (ICR). A problem with ICR based methods is that the ions are trapped for long periods of time in the presence of neutral atoms or molecules. Thus, ion-molecule reactions can occur while photodissociation is being performed.

Laser-ion beam photodissociation techniques provide an alternative to ICR photodissociation. Specifically, ions can be produced and probed without interference from neutrals (collisionless conditions), or if desired the ions can be collisionally stabilized within the ion source prior to photodissociation in the field-free region of the mass spectrometer. Studies on the photodissociation reactions of transition metal cluster carbonyl fragments provides structural information on these systems, as well as estimates of bond dissociation energies, $\bar{D}$(M-CO), and $\bar{D}$(M-M), derived from photodissociation thresholds. The present study presents the results of photodissociation studies of ionic cluster fragments formed by the 70 eV direct electron impact and chemical ionization of stable transition metal carbonyls of manganese, iron, and cobalt, i.e., $Mn_2(CO)_{10}$, $Fe_3(CO)_{12}$, and $Co_4(CO)_{12}$.

The photodissociation apparatus has been described elsewhere.[e] The photodissociation cross-sections are normalized for variations in laser power at each wavelength, ion current at the collector, photofragment peak intensities, and signal averager gain. Metal-metal and metal-ligand binding energies can be estimated for those ions whose photodissociation cross-sections tend toward zero above some critical threshold wavelength.

Table I compares the average metal-metal and metal-carbonyl bond dissociation energies (measured from the first field free region coaxial photodissociation experiment) to available literature values. Many of the measured bond dissociation energies are found to lie substantially below the average bond energies taken from the literature. To explain these results one must assume electron impact ionization produces ions with substantial amounts of internal energy. To test the validity of the coaxial photodissociation results, a third field free region photodissociation cross-beam experiment was performed, whereby the same ions were formed in a chemical ionization source. Many of the fragment ions of manganese, iron, and cobalt carbonyls were found to produce lower energy fragment ions both with and without Ar bath gas present in the source. This result suggests the some ions have a mechanism for energy loss between the first and third field free regions. This result discounts the accuracy of the bond energies measured by the first field free region coaxial experiment.

Variations in the photofragment ion yields for many of the $Mn_2(CO)_y^+$ ions were examined when a dual coaxial cross-beam experiment was performed. Both $Mn_2(CO)_5^+$, and $Mn_2(CO)_4^+$ ions were found to exhibit substantial increases in the yield for high energy fragment ions when the laser beam was aligned simultaneously with the ion beam in the first and third field free regions. For example Figure 1 a-c show the photofragment ion yields for $Mn_2(CO)_4^+$ in the first, third, and simultaneous first-third field free regions respectively. Note the ion energy distribution is substantially "cooler" in the third field free region experiment as compared to the first field free region photodissociation experiment. The dual coaxial cross-beam experiment yields an increase in the Mn_2^+ and $Mn(CO)^+$ intensities at the expense of lower energy fragment ions ($Mn_2(CO)_2^+$, and

---

a Armentrout, P. B.; Beauchamp, J. L. *J. Am. Chem. Soc.* 1981, *103*, 6628.
b Anderson Fredeen, D. J.; Russell, D. H. *J. Am. Chem. Soc.* 1985, *107*, 3762.
c Dunbar, R. C. "Gas Phase Ion Chemistry", Volume 2; Bowers M. T. Ed.; Academic Press: New York, 1979; p 181.
d Hettich, R. L.; Jackson, T. C.; Stanko, E. M.; Freiser, B. S. *J. Am. Chem. Soc.* 1986, *108*, 5086.
e Krailler, R. E.; Russell, D. H.; Jarrold, M. F.; Bowers, M. T. *J. Am. Chem. Soc.* 1985, *107*, 2346.

$Mn_2(CO)^+$). These results suggest that the $Mn_2(CO)_5^+$ and $Mn_2(CO)_4^+$ ions are capable of carrying the energy of the first field free region photon for tens of microseconds to the third field free region before absorbing a *second photon* and *photodissociating*.

Improvements in the accuracy of bond dissociation measured using the laser ion-beam technique can be obtained by performing the photodissociation experiment in the third field free region, since most of the transition metal ions studied are substantially "cooler" after they live for several microseconds. Special precautions (e.g. collisional stabilization prior to third field free region photoactivation), may still be required for ions such as $Mn_2(CO)_5^+$ and $Mn_2(CO)_4^+$ which yield extremely low measured bond dissociation energies in the first field free region coaxial experiment, and can retain excess internal energy very effectively.

Table 1. Comparison of D(M-M) and D(M-CO) obtained from the literature and those obtained by the laser-ion beam photodissociation technique. All values are reported in kcal/mole.

M=	Mn		Fe		Co	
	Liter.	This Work	Liter.	This Work	Liter.	This Work
D(M-CO)	24[a]	<25.0	27.7[b]	23.9	34[c]	22.6
D(M-M)	32[d,e]	>43.9	27-50[f]	----	22[h]	15.8

[a] Connor, J. A.; Skinner, H. A.; Virmani, Y. *Faraday Symp. Chem. Soc.*, 1984, *8*, 18.

[b] Lineberger, W. C. *J. Am. Chem. Soc.* 1979, *101*, 5569.

[c] Baev, A. K. *Russian J. Phys. Chem.* 1980, *54*, 1.

[d] Jarrold, M. F.; Illies, A. J.; Bowers, M. T. *J. Am. Chem. Soc.* 1985, *107*, 7339.

[e] Connor, J. A.; Zafarani-Moattar, M. T.; Bickerton, J.; El Saied, N. I.; Suradi, S.; Carson, R.; Al Takhin, G.; Skinner, H. A. *Organometallics* 1983, *1*, 1166.

[f] Brucat, P. J.; Zheng, L. S.; Pettiette, C. L.; Yang, S.; Smalley, R. E. *J. Chem. Phys.* 1986, *84*, 3078.

Figure 1 a

Photofragment Ion Yield for $Mn_2(CO)_4^+$:
λ = 488 nm, First Field Free Region

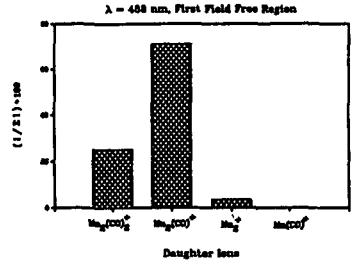

Figure 1 b

Photofragment Ion Yield for $Mn_2(CO)_4^+$:
λ = 488 nm, Third Field Free Region

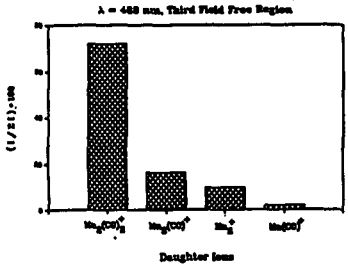

Figure 1 c

Photofragment Ion Yield for $Mn_2(CO)_4^+$:
λ = 488 nm, First and Third Field Free Regions

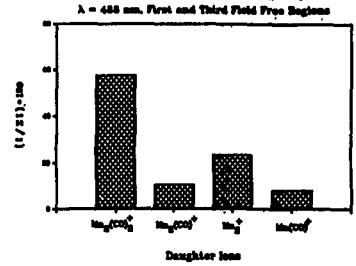

Presented at the 35th ASMS Conference on Mass Spectrometry and Allied Topics
May 24-29, 1987, Denver, CO

PHOTODISSOCIATION/TANDEM MASS SPECTROMETRY OF MANGANESE CARBONYL IONS

John H. Callahan, Mark M. Ross, Andrew P. Baronavski, and Royal B. Freas[1]
Chemistry Division/Code 6112/Naval Research Laboratory
Washington, D.C. 20375-5000

INTRODUCTION

Tandem mass spectrometry has been used to study the photodissociation of a variety of ions, including metal carbonyls (2). Metal carbonyl systems are amenable to study by photodissociation because many of their ions absorb light in the uv-visible wavelength regions and the energetics of their formation and dissociation have been studied. We have been interested in using metal carbonyl systems to study the photodissociation of ions by tandem mass spectrometry, to determine whether this technique can be used to probe the structures of larger systems, and to study the energetics of dissociation processes. This report will focus on manganese carbonyl and cluster ions formed from reactions between manganese carbonyl and electron ionization-induced fragments. These processes were studied by focusing (coaxial with the ion beam) an argon ion laser or a tunable dye laser in the second field-free region of a double focusing, reverse geometry mass spectrometer.

RESULTS

The photodissociation spectra of manganese carbonyls are characterized by two major processes: the cleavage of an Mn-Mn bond to yield $[MnCO_5]^+$, or the cleavage of Mn-CO bonds to yield products of the form $[Mn_x(CO)_y]^+$ (where x=2-4, and y=2-15). For example, both processes are observed in the photodissociation of $[Mn_2(CO)_{10}]^+$ (figure 1) at 514 nm.

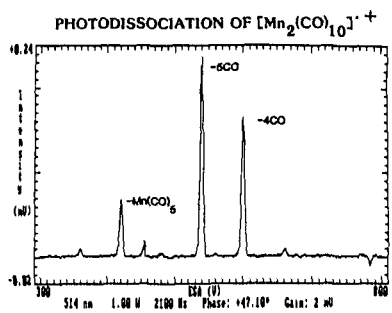

Figure 1

$[Mn(CO)_5]^+$ is observed, as well as the products of the loss of 4 and 5 CO from $[Mn_2(CO)_{10}]^+$. The cleavage of the Mn-Mn bond requires roughly 0.8 eV of energy (3), and is consistent with the amount of energy available from the absorption of a 2.5 eV (514 nm) photon. The loss of 4 or 5 CO is more difficult to reconcile, however, as the average Mn-CO bond energy has been estimated at 0.7-1.0 eV (3,4). This indicates that the ion possesses significant internal energy (on the order of 1.5 eV) initially. However, the unimolecular dissociation spectrum of $[Mn_2(CO)_{10}]^+$ suggests that the internal energy content of the ion is less than 1.5 eV. Thus, the results of the photodissociation studies indicate that Mn-CO bond energies may be less than estimated, or that they decrease as more CO is lost from the ion.

The photodissociation of manganese carbonyls is dependent on ion structure. When cluster ions formed by the reactions of $Mn_2(CO)_{10}$ and fragments induced by the electron ionization process were studied, it was found that as the cluster ion increased in size, photodissociation became less extensive. For example, photodissociation of $[Mn_3(CO)_{10}]^+$ at 514 nm was characterized by loss of $Mn(CO)_5$ or loss of three CO, while the spectrum of $[Mn_4(CO)_{10}]^+$ showed only the loss of a single CO. This behavior may result from changes in the absorption spectra of the ions as they increase in size. It is also likely that the less extensive dissociation, particularly the absence of Mn-Mn bond cleavage, reflects an increase in metal-metal bonding as the cluster increases in

size, which in turn prevents dissociation by 2.5 eV photons. Similar effects have been observed in the CID of manganese carbonyl cluster ions (5).

Photodissociation was compared with other types of dissociation in $[Mn_2(CO)_{10}]^+$. The photodissociation spectrum reflects deposition of a limited range of energies, involving electronic excitation followed by radiationless decay to a vibrationally excited ground state. That a range of dissociation processes is observed reflects the initial internal energy distribution of the ion. A limited range of dissociation processes (mainly loss of $Mn(CO)_5$) is also observed in low energy collision-induced dissociation (10 eV, under single collision conditions in a triple quadrupole). The fact that Mn-Mn cleavage is the primary loss mechanism shows that a narrow range of low internal energies is deposited in low energy CID. Additionally, the fact that only channels involving Mn-Mn bond cleavage (and subsequent CO loss from $Mn(CO)_5$) suggests that excitation occurs through a different mechanism (i.e. vibrational) in low energy CID. By contrast, the high energy CID spectrum (8 keV, single collision conditions) exhibits not only Mn-Mn bond cleavage, but also successive loss of up to 8 CO from the parent (to give ions of the form $[Mn_2(CO)_y]^+$). This is consistent with deposition of a broad range of energies in high energy CID; the loss of successive CO in a manner similar to photodissociation indicates that both electronic excitation and vibrational excitation play a role.

The photodissociation behavior of the manganese carbonyls is also wavelength dependent. For example, the ratio of $[Mn_2(CO)_5]^+$ (-5CO) to $[Mn_2(CO)_6]^+$ (-4CO) increases with increasing photon energy. Figure 2 shows a plot of the ratios of relative intensities vs. photon energy for three different fragmentation channels for $[Mn_2(CO)_{10}]^+$, showing that higher energy dissociation processes are favored with increasing photon energy.

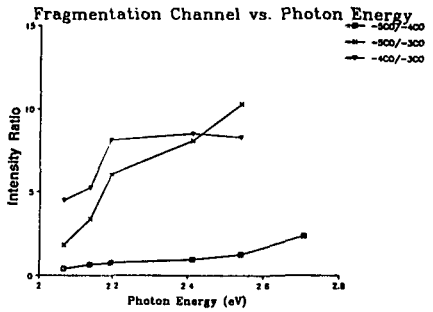

Figure 2.

The photodissociation of $[Mn_2(CO)_{10}]^+$ is also dependent on the initial internal energy of the ion. As the source temperature increased, the ratio of $[Mn_2(CO)_5]^+$ to $[Mn_2(CO)_6]^+$ also increased, reflecting the rising internal energy content of the parent ion. However, not all ions were similarly sensitive to temperature. For example, $[Mn_2(CO)_5]^+$ formed in the EI source photodissociates with the loss of 1, 2 and 3 CO. While the relative intensities are sensitive to wavelength in the expected fashion, the relative intensities of the products are not very sensitive to source temperature, indicating that much of the internal energy of the parent is carried off by the loss of CO. Furthermore, the internal energy of parent ions can be lowered by collisional cooling with a buffer gas in the source region. This shifts the relative ratios of the fragmentation channels toward lower energy processes. The extent of this collisional cooling increases in the order He < CO_2 < isobutane < SF_6, consistent with the expected collisional cross sections for the buffer gases. Finally, the energy of the electrons used to ionize the parent also has an effect on the photodissociation spectrum. Lower energy fragmentation channels are favored as the electron ionization energy decreases, again reflecting the smaller amount of internal energy deposited into the parent with decreasing ionization energy. The results suggest that photodissociation may provide a method by which the internal energies of ions can be monitored in a controlled fashion.

1). Present address: Dept. of Chemistry, University of Houston.
2). Tecklenburg, R.E.; Russell, D.H. 1986, 34th ASMS Conference, 677.
3). Connor,, J.A. Topics Current Chem. 1977 , 71, 22.
4). Svec, H.J.; Junk,G.A. J. Am. Chem. Soc. 1967, 89, 2836.
5). Freas, R.B.; Campana,J.E.; Ridge,D.P., manuscript in preparation.

Presented at the 35th ASMS Conference on Mass Spectrometry and Allied Topics
May 24-29, 1987, Denver, CO

DISSOCIATION PROCESSES OF METHANOL CLUSTERS FOLLOWING MULTIPHOTON IONIZATION

S. Morgan, R. G. Keesee, and A. W. Castleman, Jr.

Department of Chemistry
The Pennsylvania State University
University Park, PA 16802

Studies on neutral clusters commonly involve an ionization step for mass spectrometric detection. Consequently, an understanding of the effect of ionization in regard to the extent and time-scale of fragmentation is important in relating the cluster size distribution observed in mass spectra to the original neutral cluster size distribution. This paper presents results on the dynamics of dissociation of methanol clusters following multiphoton ionization at 266 nm as obtained with a time-of-flight mass spectrometer (TOFMS).

The apparatus employed in these studies has been described in detail elsewhere (1) and only a brief description is given here. Clusters are formed via adiabatic cooling of a gas exiting a pulsed nozzle. The clusters are intercepted by a laser beam and undergo multiphoton ionization (MPI) in an electrostatic field of the TOFMS. The resulting ions are accelerated, typically to 1 or 2 keV, into a field-free region. At the end of this region, another electric field (the reflectron) reflects the ions before they are finally detected whereupon a time-of-flight (TOF) spectrum is obtained.

The reflectron is used to investigate dissociation in the field-free region. The separation of nondissociating parent ions and dissociated daughter ions occurs as a result of the loss of kinetic energy (due to mass loss) with essentially no change in the velocity of the ion upon dissociation. Species with greater kinetic energy penetrate deeper into the reflectron and hence arrive later at the detector. In addition to affording TOF separation, the reflectron may also be used as an energy analyzer whereby only daughter ions below a specified kinetic energy are reflected and other ions pass through the reflectron. Typically, ions enter the field-free region about a microsecond after ionization and reach the reflectron 10 to 100 μsec later, so that dissociation processes on the order of 10^4 to 10^6 sec^{-1} lead to the direct observation of daughter ions.

Figure 1 shows a conventional time-of-flight mass spectrum of methanol clusters obtained by multiphoton ionization. A sequence of ions (labelled A) of the form $H^+(CH_3OH)_n$ are observed. Another sequence (labelled B) of the form $H^+(H_2O)(CH_3OH)_n$ also begins to appear at about seven methanol units. In Figure 2, the spectrum of only daughter ions is shown (parent ions were not reflected). Several series of peaks are apparent. The mass loss is determined by the time-of-flight and also by the threshold potential required for reflection. The A labelled series represents the loss of one methanol molecule (32 daltons) from an ion that enters the field-free region as $H^+(CH_3OH)_n$. Series B results from the loss of one methanol molecule from the species $H^+(H_2O)(CH_3OH)_n$. Series C derives from a mass loss of 78 daltons from $H^+(CH_3OH)_n$ where the mass loss corresponds to the loss of both a methanol and dimethyl ether molecule. Peak D corresponds to the loss of a mass of 18 daltons (H_2O) from $H^+(CH_3OH)_2$. Series E results from the reflection of a small portion of the undissociated ions on the low energy side of the birth potential distribution. By further reduction of the reflecting potentials, the shoulders on the early arrival side can be resolved and reveal more extensive methanol evaporation, e.g., the loss of up to five methanol molecules from the protonated octamer.

The spectra suggest several dissociative processes. First, ionization leads to a rapid internal (intracluster) proton transfer reaction to produce $H^+(CH_3OH)_n$ followed by the slower evaporative processes, as has been observed earlier for ammonia clusters (1). In addition, intracluster reactions are observed. The protonated dimer is seen to eliminate water to produce protonated dimethyl ether. This process requires at least several tenths of a microsecond since little or no $(CH_3)_2OH^+$ is observed in the conventional TOF spectrum. The gas-phase analogue of this reaction is also known (2). For the larger clusters, however, C_2H_6O elimination occurs and leads to the production of $H^+(H_2O)(CH_3OH)_n$. As opposed to the protonated methanol dimer, water evidently is retained in the cluster ion since H_3O^+ is more strongly solvated by methanol than is $(CH_3)_2OH^+$. Furthermore, this process occurs on the order of one to twenty microseconds for clusters of less than 8 molecules (as suggested by series C in Figure 2), but requires less than two microseconds for larger clusters (as suggested by the appearance of series B in Figure 1).

Presented at the 35th ASMS Conference on Mass Spectrometry and Allied Topics
May 24-29, 1987, Denver, CO

REFERENCES

1. O. Echt, P. D. Dao, S. Morgan, and A. W. Castleman, Jr., J. Chem. Phys. 82, 4076 (1985).
2. L. M. Bass, R. D. Cates, M. F. Jarrold, N. J. Kirchner, and M. T. Bowers, J. Am. Chem. Soc. 105, 7024 (1983).

ACKNOWLEDGMENTS

Financial support by the Department of Energy, Grant, No. DE-AC02-ER-60055, and the Department of the Army, Grant No. DAAG29-85-K-0215, is gratefully acknolwedged.

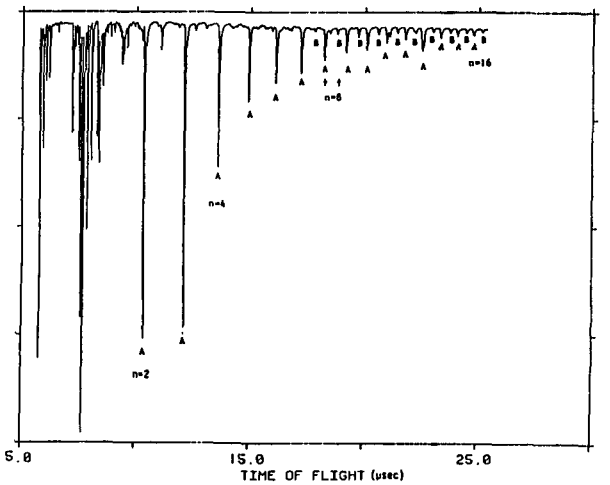

Figure 1. Conventional time-of-flight mass spectrum of methanol clusters by multiphoton ionization at 266 nm. Series A = $H^+(CH_3OH)_n$; Series B = $H^+(H_2O)$-$(CH_3OH)_n$.

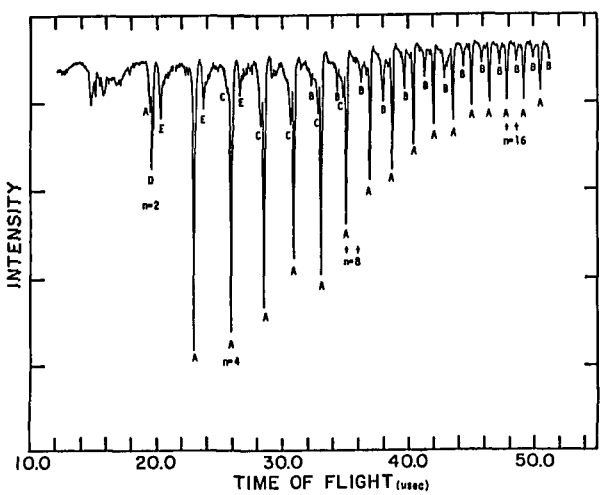

Figure 2. Spectrum of dissociation product ions. Series labels described in text. The sizes of the precursor ion $H^+(CH_3OH)_n$ (for Series A, C, D, and E) and $H^+(H_2O)(CH_3OH)_n$ (for Series B) are indicated.

Presented at the 35th ASMS Conference on Mass Spectrometry and Allied Topics
May 24-29, 1987, Denver, CO

CID STUDIES OF CLUSTER IONS CONTAINING TETRA-ALKYLAMMONIUM CATIONS

Emirgul Tolun* and John F.J. Todd
Chemical Lab. University of Kent at Canterbury, U.K.
*University of Tennessee, Stout Neuroscience Mass Spectrometry Lab
Memphis, TN 38163

INTRODUCTION

It has been shown that NR_4X salts (where NR_4 = NMe_4, NEt_4 and X = Cl, Br, I) form high mass cluster ions under FAB ionization from solution (1). Also, the stability and dissociation of the positive and negative cluster ions of NR_4X salts are found to strongly depend on the concentration of the salt in the matrix solvent (2-4). Following these observations we have studied the FAB-MS of mixtures of two different NR_4X salts in solution and observed the formation of all combinations of mixed cluster ions.

The objective of this study is to investigate the main factors influencing the stabilities and fragmentation pathways of certain mixed anion and cation cluster ions.

EXPERIMENTAL

Both positive and negative ion FAB mass spectra were recorded from equimolar concentrated mixed salt solutions in glycerol. The FAB mass spectra were obtained on an AEI-MS9 double-focusing mass spectrometer updated by VG-Analytical Ltd., using fast Xenon atoms (2mA-8Kv). The CID spectra were obtained with Argon as the target gas, using B/E linked scanning.

RESULTS

Positive and negative mixed halide cluster ions of the type $[(NR_4)_{n+1}X_{n-1}Y]^+$ and $[(NR_4X)_nY]^-$ (n=1-13) exhibit increased stability at n=4, 7, or at n=6, 12 depending on the nature of the cation. These ion intensity enhancements are related to the formation of clusters with certain stable structures, which is favored when the size of the ionic constituents is small (1,3).

The CID studies have shown that the mixed cluster ions preferentially decay to the mixed or pure species having a smaller (n) value, through loss of a neutral entity containing a smaller anion or cation (Table 1).

Table 1 Preferential elimination of the NEt_4X molecules containing smaller halide, from corresponding n=2 mixed halide cluster ions

Precursor ions (n=2)	Relative abundances of product ions		
	$(P-NEt_4Cl)^-$	$(P-NEt_4Br)^-$	$(P-NEt_4I)^-$
$[(NEt_4Cl)_2Br]^-$	10	2	-
$[(NEt_4Br)_2Cl]^-$	8	2	-
$[(NEt_4Cl)_2I]^-$	4.3	-	1
$[(NEt_4I)_2Cl]^-$	5	-	1
$[(NEt_4Br)_2I]^-$	-	2.6	0.2
$[(NEt_4I)_2Br]^-$	-	1	0.2

Mixed cluster ions also show the elimination of the two or three neutral molecules with both of the anions or cations which are presumably neutral clusters (4). For example, the fragmentation pathway of the mixed halide cluster ions of the formula $[(NMe_4)_{n+1}X_{n-1}Y]^+$ for n=3, 4 involve two routes:

a) formation of pure cluster ions through loss of two and/or three molecules with both of the halogens

$$[(NMe_4)_{n+1}X_{n-1}Y]^+ \xrightarrow[n=3-4 \quad m=2-3]{-(NMe_4)_mX_{m-1}Y} [(NMe_4)_{(n-m)+1}X_{n-m}]^+$$

b) fragmentation leading to the preceeding mixed cluster ions having smaller (n) values

$$[(NMe_4)_{n+1}X_{n-1}Y]^+ \xrightarrow[n=2-4]{-NMe_4X} [(NMe_4)_nX_{n-2}Y]^+$$

CONCLUSIONS

1) Anion and cation size plays an important role in determining the higher mass cluster ion formation and stabilities.

2) The preferential fragmentation of the mixed cluster ions usually involving the elimination of a smaller neutral molecule, suggest that the stability of the neutral molecules and/or clusters lost is the important factor influencing the fragmentation route.

3) CID pathway may reflect the reverse of the clustering processes. With this assumption, the attachment of the cation/anion and/or n = 1 species to the $[(NR_4)_{n+1}X_nY]$ mixed neutral clusters become a more likely process for the formation of mixed cluster ions. CID studies also confirm the existence of mixed neutral clusters.

REFERENCES

1. E. Tolun and J.F.J. Todd, Org. Mass Spectrom. 21, 751, 1986.
2. E. Tolun and J.F.J. Todd, presented at the 34th Annual Conf. on Mass Spectrom and Allied Topics (ASMS), Cincinnati, OH, 1986.
3. E. Tolun and J.F.J. Todd, submitted Org. Mass Spectrom.
4. E. Tolun and J.F.J. Todd, submitted Int. J. Mass Spectrom. Ion Phys.

ACKNOWLEDGMENTS

One of us (E.T.) wishes to thank the ASMS committee for the award of a travel stipend to attend the meeting.

Presented at the 35th ASMS Conference on Mass Spectrometry and Allied Topics
May 24-29, 1987, Denver, CO

Ionization and Fragmentation of Biomolecules investigated by Laser Mass Spectrometry.

J. Grotemeyer, U. Boesl, K. Walter, E.W. Schlag

Institut für Physikalische und Theoretische Chemie, TU München
Lichtenbergstr. 4, D-8046 Garching, Germany.

Multiphoton Ionization (MUPI) has been established in recent years as a general ionization method for the different fields of mass spectrometry. Especially for analytical purposes and for the mass spectrometric investigations MUPI can have several advantages over other mass spectrometric methods such as a real soft ionization and the possibility of tuneable fragmentation.
The focal points of our mass spectrometric technique are : 1. Separation of the vaporization and ionization process 2. Laser evaporization of intact neutral molecules (LEIM) 3. Cooling of the evaporated neutral molecules 4. Ionization by multiphoton ionization (MUPI) 5. Detection by a high mass resolution Reflectron-Time-of-Flight mass spectrometer (RETOF-MS).
The multiphoton ionization can occur in different modes. One possibilty for ionization is the resonance enhanced absorption of photons via an intermediate state (REMPI), the other is a non resonant multiphoton process.

As an example for a non resonant multiphoton ionization the mass spectrum of the amino acid L-arginine is shown in figure 1. This is the first time, that the free molecular ion of free arginine is dectected with mass spectrometric techniques. The electron impact as well as chemical ionization mass spectra of the intact sample are unknown, since this compound decomposes upon heating./2/

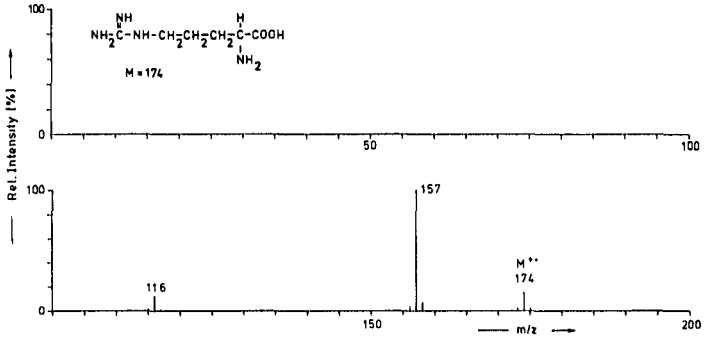

Figure 1. The non-resonant multiphoton ionization mass spectrum of L-arginine.

Only in Field Desorption it is possible to measure the protonated compound. MUPI shows the molecular ion of L-Arginine at 2450 Å with an intensity of strong 15%. The base peak is produced by the loss of ammonia from the molecular ion, yielding the signal at m/z 157. The signal at mass 116 is due to the loss of the guanidino group from the molecular ion.
As an example for the soft ionization possibility as well as the tuneable fragmentation the MUPI mass spectra of some dipeptides are listed in table 1.
In every entry soft ionization leads to the molecular ion. This is in contrast to some results discussed in the literature/3/.
The fragmentation reactions occuring in the partial hard ionization mode are mostly due to the loss of the aromatic side chains and to the bond rupture of the peptide bond. This demonstrates clearly the possibility of detecting the sequence of peptide chains by multiphoton ionization, as noted previously/5/.

Presented at the 35th ASMS Conference on Mass Spectrometry and Allied Topics
May 24-29, 1987, Denver, CO

Table : Main Ions in MUPI-mass spectra of some dipeptides

Compound	MW	Soft ionization	Hard ionization
Phe-Gly	222	222 (100)	222(20),221(100),147(28),131(10)
Tyr-Gly	238	238 (100)	238(15),221(100),147(15),132(70),107(16)
His-Gly	212	212 (100)	212(10),195(21),137(100),109(25)
Lys-Tyr	332	332 (100)	332(100),314(17),291(52),187(7),101(20)
Trp-Glu	333	333 (100)	333(100),316(16),315(81),146(15),130(95)
Tyr-Glu	310	310 (100)	310(36),293(44),292(61),185(60),107(100)
Trp-Phe	351	351 (100)	351(16),333(58),187(10),130(100)
Phe-Trp	351	351 (100)	351(81),333(31),187(14),130(100)
Phe-Tyr	328	328 (100)	328(44),311(46),310(100),204(44),107(66)
Tyr-Phe	328	328 (100)	328(17),310(100),204(22),120(17),107(26)
Trp-Tyr	367	367 (100)	367(84),350(40),204(6),130(10)
Tyr-Trp	367	367 (100)	367(21),349(55),187(13),130(100)

Figure 2 displays a mass spectrum of insuline obtained by laser desorption-multiphoton ionization/4/. Again this mass spectrum shows as prominent signal the molecular ion of the protein at mass 5927. Besides this signal group peaks for the A-chain at mass 2334 and for the B-chain at mass 3895 appear. Focusing on this mass spectrum, it should be noted, that this spectrum is drawn as measured. Neither a background correction nor a mass cut off in the lower mass range has been done. Therefore even product ions of low intensity as from the loss of a methyl group can be detected in this mass spectrum.

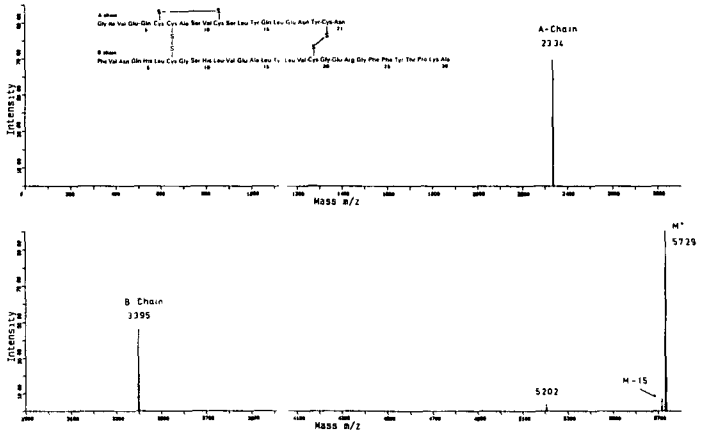

Figure 2. LEIM-MUPI mass spectrum of insuline.

These results demonstrate, that MUPI combined with laser desorption in a RETOF-instrument can be used to investigate delicate small as well as large molecules.

References :
/1/ U.Boesl,J.Grotemeyer,K.Walter and E.W.Schlag; Anal.Instrum. 16, 151 (1987).
/2/ J.Grotemeyer,U.Boesl,K.Walter and E.W.Schlag; Int.J.Mass Spectrom.Ion Proc., in press.
/3/ R.Trembreull and D.Lubman; Anal.Chem. 59, 1003 (1987).
/4/ J.Grotemeyer and E.W.Schlag; NATO-ASI series in press.
/5/ J.Grotemeyer,U.Boesl,K.Walter,E.W.Schlag; Org.Mass Spectrom. 21, 595 (1986).

Acknoledgment: This work has been supported by a grant from the Bundesministerium für Forschung und Technologie (13N5307) in collaboration with Bruker-Franzen Analytik, Bremen.

Presented at the 35th ASMS Conference on Mass Spectrometry and Allied Topics
May 24-29, 1987, Denver, CO

UNIMOLECULAR DECAY RATES FROM METASTABLE BROADENING IN A TIME-OF-FLIGHT MASS SPECTROMETER

G.R.KINSEL AND M.V.JOHNSTON, DEPARTMENT OF CHEMISTRY AND BIOCHEMISTRY & COOPERATIVE INSTITUTE FOR RESEARCH IN ENVIRONMENTAL SCIENCE, UNIVERSITY OF COLORADO, BOULDER, CO 80309-0215.

Resonance enhanced multiphoton ionization / fragmentation (REMPI/F) allows one to view ion fragmentation processes at selected ion internal energies. In a one-color REMPI/F experiment the uncertainty in the parent ion internal energy typically ranges from 0 to 1.5 eV depending on the molecular ionization energy and the energy of the photons absorbed. This uncertainty is quite narrow when compared to other ion activation methods such as collisionally induced dissociation (CID) or low energy electron impact. As a result the fragmentation processes observed can vary dramatically as the wavelength used for ionization / fragmentation is changed.

In our studies of the wavelength dependent behavior of the mass spectrum of p-chloroaniline significant metastable broadening of the fragment ions at m/z 92 (M^+-Cl) and m/z 100 (M^+-HCN) was observed (Fig. 1).[1] These results were obtained using a time-of-flight mass spectrometer (TOFMS) with a continuous drawout voltage. The fragment ion at m/z 91 (M^+-HCl) was also shown to be metastably broadened by performing time-lag pulsed drawout voltage experiments. Because of the extensive overlap in the metastable ion region conventional methods for determining the unimolecular decay rates by fitting the exponential tail of the broadened peak could not be employed. In order to overcome this barrier a program was developed which, upon input of the appropriate instrumental parameters and initial rates for the competing fragmentation pathways, generates a mass spectrum of the metastably broadened ions. The program also allows for convolution of the intrinsic instrumental resolution by creating a Gaussian distribution at each calculated ion flight time and then numerically integrating these distributions. The program varies the individual competing fragmentation rates until a best fit with the experimental data is obtained (Fig. 2).

The calculated rates for the four competing processes in the 266 nm spectrum are shown in Fig. 3 for four different spectra. The uncertainty in the parent ion internal energy is 1.14 eV as determined by subtracting the ionization energy of p-chloroaniline from the energy of two 266 nm photons. This is undoubtedly much larger than the actual parent ion internal energy distribution as suggested by recent work performed by Reilly and Zare on aniline and chlorobenzene respectively.[2,3]

We believe that the program developed provides several advantages for the calculation of unimolecular decay rates in a TOFMS. First, it allows for the deconvolution of overlapping metastable peaks. Second, a better rate value is obtained by requiring a fit to both the total and individual rates of decay. Third, direct visual comparison of the experimental and best fit mass spectra can be performed. This type of analysis is important when looking for unusual metastable behavior resulting from competing state selected unimolecular decay. Finally, systematic errors are reduced by correcting for instrumental resolution in the appropriate mass range.

REFERENCES

1. Kinsel, G.R. and Johston, M.V., ORG. MASS SPEC., (In Press).

2. Reilly, J.P. et. al., J. CHEM. PHYS., 82 (4) 1985.

3. Zare, R.N. et. al., J. CHEM. PHYS., 80 (5) 1984.

Presented at the 35th ASMS Conference on Mass Spectrometry and Allied Topics
May 24-29, 1987, Denver, CO

METASTABLE IONS AT 266 NM

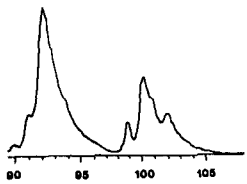

Fig. 1 The metastably broadened fragment ions in the 266 nm REMPI\F mass spectrum of p-chloroaniline at m/z 91, 92, 100 and the ^{37}Cl isotope at m/z 102. The peaks at m/z 90 and 99 are non-metastably fragments created upon the 2 photon fragmentation of the parent ion.

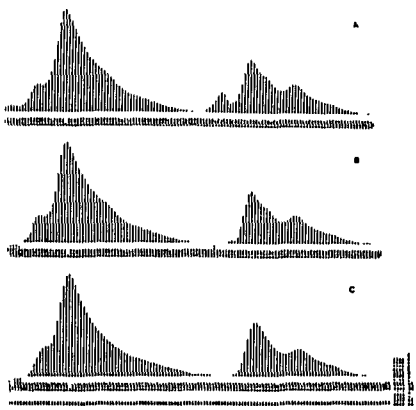

Fig. 2 A. The above data transferred to a personal computer and normalized to a scale of 100.
B. Same as A. after the 2 photon processes have been subtracted.
C. The computer generated best fit mass spectrum.

CALCULATED RATES AT 266 NM

	m/z 91	m/z 92	m/z 100	m/z 102
SPEC 1	2.80	5.18	4.94	5.76
SPEC 2	3.00	6.00	5.63	5.94
SPEC 3	2.67	5.91	5.46	5.87
SPEC 4	2.38	5.41	5.13	5.81
AVE	2.7±.3	5.6±.4	5.3±.4	5.8±.2

ALL RATES x 10^5 sec^{-1}

Fig. 3 Rates of formation for the 4 metastably broadened processes calculate by the described program.

Presented at the 35th ASMS Conference on Mass Spectrometry and Allied Topics
May 24-29, 1987, Denver, CO

UNIMOLECULAR DECAY MEASUREMENTS WITH AN ION MIRROR.

X. Tang, R. Beavis, W. Ens, F. Lafortune[a], B. Schueler, K. G. Standing & J. B. Westmore[a];
Departments of Physics and Chemistry(a), University of Manitoba, Winnipeg, Canada R3T 2N2

A reflecting time-of-flight (TOF) mass spectrometer (illustrated schematically in fig. 1) has been used to obtain daughter ion mass spectra of metastable cationized molecules of several small peptides. The cationized molecules were produced by Cs^+ ion bombardment of thin solid layers deposited on etched silver foils or electro-sprayed onto aluminized mylar films.

The secondary ions produced by a pulsed 13 keV Cs^+ beam are accelerated through 5 keV, then traverse a flight tube into an ion mirror. After reflection by 180°, the ions again traverse the flight tube and are detected by a microchannel plate detector beside the target. The total effective path length is ~2 m. Neutral fragments resulting from the decay of parent ions in the first section of free flight are detected by a second detector behind the mirror.

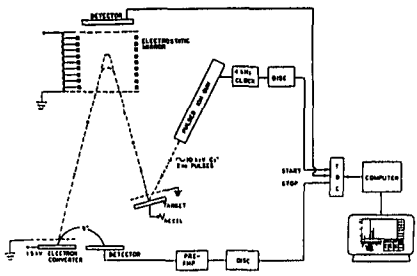

Figure 1. MANITOBA II. A reflecting TOF mass spectrometer with an ion mirror.

Analysis of metastable ions.

The instrument can be operated in two modes:

Ion mirror off: All charged and neutral fragments are recorded by the top detector. In this way a "normal" or "direct" mass spectrum is obtained.

Ion mirror on: A retarding potential greater than the ion acceleration potential reflects charged particles back towards the detector located near the ion source, while neutral particles are recorded in the top detector. The "neutral species" spectrum corresponds to the flight times of parent ions that decompose during the upward leg of field-free flight. The "reflected ion" spectrum recorded by the lower detector actually contains two overlapping mass spectra with differing time calibrations, i.e. daughter ions and parent ions. By opening a time window corresponding to detection of a given neutral species it is possible to select from the reflected ion spectra only those ions that correspond to the event leading to production of the neutral species, i.e. a daughter ion spectrum corresponding to decomposition of a selected parent ion.

Mass calibration and resolution.

Mass calibration of the instrument was achieved by measuring flight times for parent and daughter ions of the metastable decompositions of cesium iodide cluster ions under the same accelerating and mirror potentials that are used for the peptide studies:

$$Cs(CsI)^+_{n+p} \text{ ----> } Cs(CsI)^+_n + (CsI)_p \qquad (n \geq 2)$$

The mass m' of a daughter ion is $m' = m[2(t'/t) - 1]$ (t' is the daughter ion flight time).

Instrument performance: daughter ion spectra of cationized molecules of peptides.

To illustrate the performance of the instrument for daughter ion analysis experimental and calculated masses of some daughter ions of cationized molecules of leucine and methionine enkephalins are compared in the Tables. It can be seen that the experimental masses are reliable to within a few tenths of a mass unit. Figure 2 illustrates, for leucine enkephalin, the several types of mass spectra that can be obtained.

The daughter ion spectra of $[M + H]^+$, $[M + K]^+$ and $[M + 2Na - 1]^+$ give, for the most part, known sequence ions or their alkali atom analogs, although the sequences observed do differ. The daughter ion spectra of $[M + Na]^+$ and $[M + Ag]^+$ are quite different and exhibit daughter ions that have no analogs among the daughter ions from the other cationized molecules, while "normal" sequence ions are suppressed. This implies that the metal ions are bound to the peptide in such a way that peptide bond fission is prevented. Chelation of the peptide to the metal ions provides an attractive mechanism for reducing the number of decomposition channels and directing fragmentation along alternative pathways [1].

1. X. Tang, et al, in preparation.

Presented at the 35th ASMS Conference on Mass Spectrometry and Allied Topics
May 24-29, 1987, Denver, CO

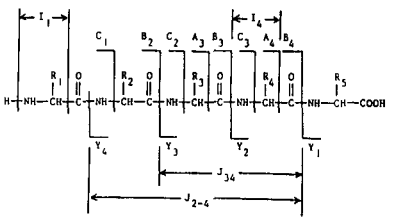

R_1 = $CH_2C_6H_4OH$; R_2 = R_3 = H; R_4 = $CH_2C_6H_5$

R_5 = $CH_2CH(CH_3)_2$ (leu); R_5 = $CH_2CH_2SCH_3$ (met)

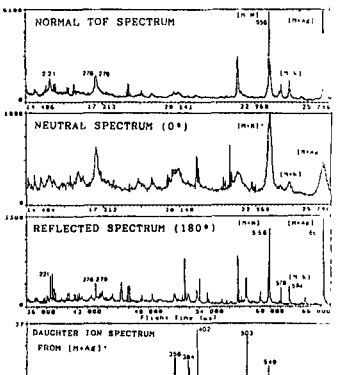

Fig. 2. TOF mass spectra of leucine enkephalin.

TABLE 1 Leucine Enkephalin

ION PARENT	DAUGHTER	MASS EXP.	CALC.	DIFF EXPL-CALC
[M+H]+		556 29	556 28	0.01
	B_4+17+H	443.05	443.19	-0.14
	B_4	425.08	425.18	-0.10
	A_4	397 05	397.19	-0 14
	Y_3+2	336.14	336 19	-0.05
	Y_3+2	279.42	279.17	0.25
	B_3	278.20	278.11	0.09
	J_{2-4}+1	262 13	262 12	0.01
	B_2	220.71*	221.09	-0.38
	J_{34}+1	205 18	205.10	0.08
	J_{34}+1-CO?	176 43	177.10	-0 67
	I_1+1	135.77	136.07	-0.30
	I_4+1	120.51	120 08	0.43
[M+Na]+		578.20	578.26	-0.06
	B_4+17+Na	465.08	465.17	-0.09
	?	406 01		
	?	349.55		
	B_3+17+Na	317 97	318 11	-0 14
[M+K]+		594.20	594.23	-0.03
	A_4-1+K	435 03	435 11	-0.11
	C_3+1+K[b]	332.95	333.10	-0 15
	C_3+1+K-NH_3[b]	316.43	316.07	0 36
	C_2+1+K	276 21	276 07	0.11
[M+^{109}Ag]+		662 17	662.17	
	B_4+17+Ag	549 13	549 09	0.04
	B_4-1+Ag	531 10	531.08	0 02
	A_4-1+Ag	503 02	503 08	0.06
	B_3+17+Ag	401 99	402 02	-0 03
	B_3-1+Ag	381 13	384 01	0.12
	A_3-1+Ag	355.97	356.02	-0 05
	B_2-1+Ag	326.81	326 99	-0 18
[M+2Na-1]+		600.22	600.24	-0.02
	Q-$CH_2C_6H_4OH$	493 01	493 19	-0.18
	?	162 64		
	Y_4+2Na	436.85	437 18	-0 33
	?	418.82		
	Y_3+2Na	379.75	380.16	-0 41
	C_3+2Na[b]	338.70	339.10	-0 40
	Y_2+2Na	322.73	323.13	-0 40
	?	312.76		
	C_2+2NA	281.60	282.08	-0.18
	C_1+2Na	221.66	225 06	-0 40
	?	175.62		

TABLE 2 Methionine Enkephalin

ION PARENT	DAUGHTER	MASS EXP.	CALC.	DIFF EXPL-CALC
[M+H]+		574 19	574.23	
	B_4	425.17	425.18	-0.01
	Y_4+2	410.94	411 17	-0.23
	A_4	397 02	397.19	-0.17
	Y_3+2	354 32	354.15	0.17
	Y_2+2	297.08	297 13	0.05
	B_3	278.21	278 11	0.10
	J_{2-4}+1	262 43	262.12	0.31
	B_2	221 28	221.09	0.19
	J_{34}+1	205.19	205 10	0.09
	J_{34}+1-CO	177.03	177.10	-0.07
	V_1+2	150.12	150.06	0.06
	I_1+1	136 19	136.08	0.11
	I_4+1	120 10	120.08	0 02
[M+Na]+		596.19	596.23	-0 04
	B_4+17+Na	465.03	465.17	-0.14
	A_4-1+Na	419.29	419.17	0.12
	?	396 26		
	B_3+17+Na	318.33	318.11	0.22
[M+K]+		612.20	612.19	0.01
	A_4-1+K	434.98	435.14	-0.16
	?	348.09		
	C_3+1+K[b]	332.76	333.10	-0.34
	C_3+1+K-NH_3	314 55	316.07	-0.52
	A_3+1+K?	290.28		
	C_2+1+K	276 22	276 07	0.15
[M+^{109}Ag]+		680.06	680.13	-0 07
		610.46		
	B_4+17+Ag	548 92	518.08	-0.16
	B_4-1+Ag	531.08	531.08	0 00
	Y_4+1+Ag	516 93	517.07	-0.14
	A_4-1+Ag	502 79	503 80	-0.29
	Y_3+1+Ag	159 69	160.05	-0.36
	B_3+17+Ag	401 77	402 02	-0.25
	B_3-1+Ag	383.92	384.01	-0.09
	A_3-1+Ag	356.31	356.02	0.29
	B_2-1+Ag	326.68	326.99	-0.31

Presented at the 35th ASMS Conference on Mass Spectrometry and Allied Topics
May 24-29, 1987, Denver, CO

MS/MS/MS/MS ON A FOUR-SECTOR (BE-EB) MASS SPECTROMETER (AND ONE STEP BEYOND)

K.B. TOMER, C. GUENAT AND J. DINO, JR.
LABORATORY OF MOLECULAR BIOPHYSICS, NIEHS PO 12233 RES.TRI.PK,NC 27709

An advantage of multisector mass spectrometers is their capability to determine the fragment ions arising from a specific precursor ion. This capability (MS/MS) has been used extensively in structure elucidation and mechanistic studies. As the number of sectors has increased, the number of consecutive reactions that can be examined has also been increased. Thus, the capability of performing MS/MS/MS experiments developed with the development of three-sector mass spectrometers (1). FT-MS instrumentation has also made available the capability of investigating sequential reactions (MS4 has been reported) (2).

With the advent of four sector instruments (3), we undertook a program to study the feasibility of obtaining MS/MS/MS/MS (MS4) and MS/MS/MS/MS/MS (MS5) data. This study was performed on a VG-ZAB 4F of BE-EB geometry (3). (Fig. 1).

In the MS4 experiment (Fig 1) the metastable ion formed in FFR1 for the A+->B+ transition is passed through B1. This ion is activated in FFR2 and the resulting C+ ion is focussed through E1. The C+ ions are activated in FFR3 and the daughter ion spectrum obtained by a B2/E2 linked scan of MS-II. For MS5 studies, the D+ ion formed by activation of the C+ ion in FFR3 is focussed through E2. The metastable decompositions occurring in FFR4 are then analyzed by scanning B2. The lack of a collision cell between E2 and B2 inhibited the use of CA.

An example of a study of a reaction sequence by MS4 is the study of the m/z 105 ion in the EI spectrum of butyrophenone. The MS/MS spectrum of the source formed 105 ions (Fig. 2a) is distinguishable from the 105 ions formed from the following sequence (Fig. 2b).

m/z 148 -> m/z 120 -> m/z 105 -> fragments
MS1 MS2 MS3 MS4

No loss of 18 amu is observed from source formed 105 ions while 18 loss is observed from the 105 ion arising from m/z 120. Presumably, the loss of 18 arises from an m/z 105 ion in which the original H transferred in the McLafferty rearrangement is still attached to the carbonyl oxygen.

ONE STEP BEYOND: If only the m/z 77 ion formed in the 3rd FFR is permitted to pass through E2 and B2 is then scanned, the unimolecular MS/MS spectrum of the m/z 77 ion can be obtained. The resulting spectrum (Fig 3) is and example of MS5!

MS/MS is increasingly used to elucidate the structure of small peptides. We have successfully applied MS4 to the sequencing of several small peptides. In the illustrated examples (Fig. 4a,b), the sequential loss of amino acid residues from two tripeptides containing either leucine or isoleucine as the C-terminus is followed. MS/MS of the m/z 86 ion (MS4) arising from the x-Leu residue readily differentiates the two residues.

Conclusion: MS4 and MS5 experiments are readily performed on the four-sector tandem instrument and applications to reaction sequencing and structure elucidation have been made.

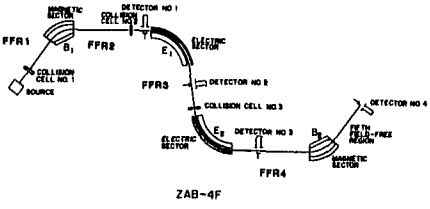

Fig. 1. VG-ZAB-4F

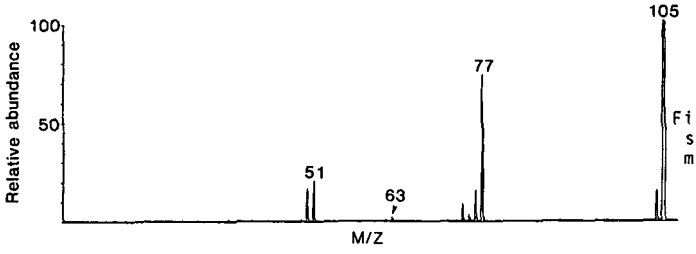

Fig. 2a) MS/MS of source-formed m/z 105.

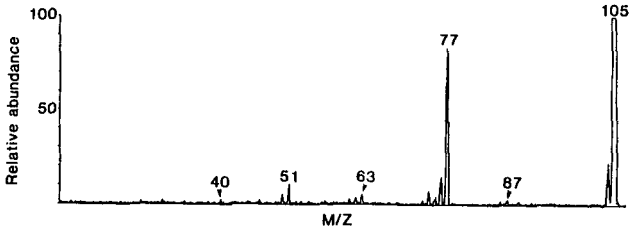

Fig. 2b) MS4 spectrum of m/z 105.

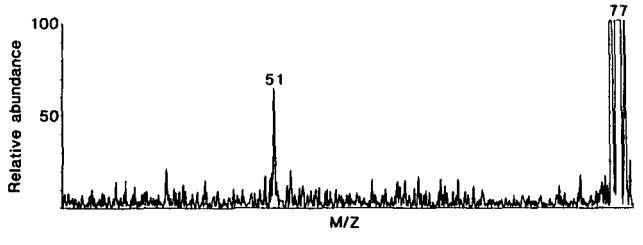

Fig. 3. MS5 spectrum of m/z 77.

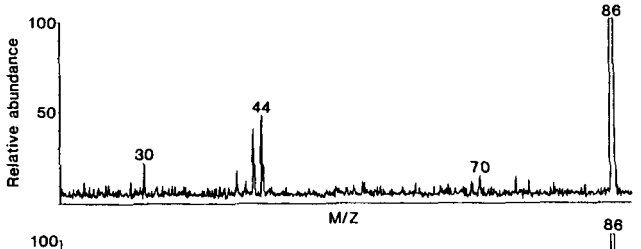

Fig. 4a) MS4 spectrum of m/z 86 from Gly-Gly-Leu.

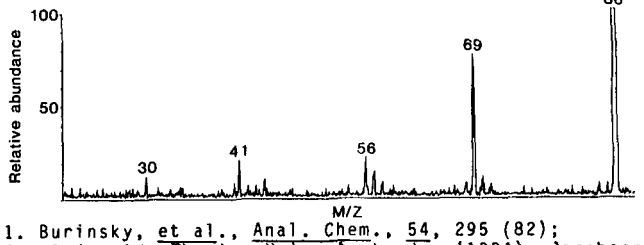

Fig. 4b) MS4 spectrum of m/z 86 from Gly-Gly-Ile.

1. Burinsky, et al., Anal. Chem., 54, 295 (82);
2. Kleingeld, Thesis, Univ. Amsterdam (1984); Jacobson & Freiser, JACS, 106, 4623 (1984).
3. Hass, et al., Proc. 32nd ASMS, San Antonio, TX 1984 p380.

Presented at the 35th ASMS Conference on Mass Spectrometry and Allied Topics
May 24-29, 1987, Denver, CO

CHARGE SEPARATION PROCESSES OF POLYCYCLIC AROMATIC HYDROCARBON TRICATIONS: Gregory K. Koyanagi and Raymond E. March, Department of Chemistry, Trent University, Peterborough, Ontario Canada, K9J 7B8

There is now a considerable body of reliable mass spectrometric evidence for the existence of molecules, both large and small, from which three bonding electrons have been removed. Thus the lifetimes of these trication species exceed 10^{-6}s. An excellent though brief review has been published [1], to which should be added the first account of charge separation of trications [2]. Two recent studies of trications derived from polycyclic aromatic hydrocarbons (PAHs) have been reported [3,4].

We report here a study of dications and trications which are produced by 100eV electron impact of six selected PAHs; 2,3-Benzanthracene, chrysene, triphenylene, triptycene, perylene and benzo[a]pyrene.

Initially, it was convenient to identify separately all of the multiply-charged species produced from each PAH. For each compound, a triply-charged ion mass spectrum and a doubly-charged ion mass spectrum were obtained following the technique of Appling and Moran [5], modified for a mass spectrometer of reverse geometry. Benzyl chloride was employed as the collision gas in the first field-free region of the mass spectrometer. Trications, $M^{3+\cdot}$, accelerated through a potential of 8kV and collided with molecules of benzyl chloride in the first field-free region of the mass spectrometer undergo charge exchange.

$$M^{3+\cdot} + C_6H_5CH_2Cl \rightarrow M^{2+} + C_6H_5CH_2Cl^+ \qquad (1)$$

The dicationic products of reaction 1 possess virtually the same kinetic energy as their tricationic precursors and are transmitted by the magnetic sector at an apparent mass of $M^* = 3M/4$ so that, in the resulting mass spectrum, adjacent masses are separated by 3/4 amu. Separation of product dications was achieved by setting the electric sector at 3E/2, where E is the required potential difference across the electric sector plates in order to transmit unreacted ions. The resulting spectrum is known as a 3E/2 mass spectrum analogous to the 2E mass spectrum which consists solely of cations derived from dication precursors. Thus the incidence of dications and trications from each PAH was obtained directly from the 2E and 3E/2 mass spectra, respectively.

Mass-analyzed ion kinetic energy spectra (MIKES) have been observed for trications derived from five PAHs; those for trications from benzo [a] pyrene were reported earlier [4]. Specifically, the ion kinetic energy releases, T, upon charge separation of cations.

$$M^{3+\cdot *} \rightarrow M_2^{2+} + M_3^{+} + T \qquad (2)$$

derived from the five PAHs have been measured. From these spectra attempt have been made to determine the mechanisms of charge separations [3] which the trications undergo. Low order molecular orbital calculations have been performed for triphenylene and triptycene in order to obtain the localized π-charge density and the resulting coulombic repulsion within the molecular ion framework. The results of the theoretical calculation agree well with experimental observations.

The instrument used in this work was a hybrid mass spectrometer of BEQQ geometry (B, magnetic sector; E, electric sector; QQ, quadrupole collision cell and mass filter) and is described elsewhere [6]. The electric sector permits measurement of ion kinetic energy to 14keV, thus the full range of acceleration voltage, 1-8kV, could be employed for charge separation studies of trications, while that of dications was limited to 1-6kV. PAHs and benzyl chloride were obtained from Aldrich Chemical Co. and were used without further purification. The ion source block was maintained at 250°C while the direct insertion probe temperature was adjusted to 20-50°C below the melting point of each compound.

For the compounds studied, 2E mass spectra exhibited intense peaks corresponding to production in the source of dications with the general formula $[M-X(C_2H_2)-y(H_2)]$, where X=0,1 and 2 and y is any integer such that all hydrogens could be lost. 3E/2 mass spectra exhibited similar patterns for the production of trications in the ion source. However trication fragments from which all hydrogen atoms had been stripped were not as intense as their dication counterparts. This is most evident from a comparison of 3E/2 spectra for 4 ring compounds with those of Kata-annellated 5 ring Peri-condensed compounds. Kata-annellated compounds which had lost a C_2H_2 fragment exhibit intense peaks at [M-26] and [M-28] but not at [M-30,32,or34]. This is most probably due to the production of stable 4-member ring systems from terminal 6 member rings which have lost 2 carbon atoms.

In both 3E/2 and 2E mass spectra, peaks of approximately 1% relative intensity were observed corresponding to the production of multiply charged [M-15] ions; triptycene, being an exception as it has two aliphatic carbon centres, displayed a peak of 34% relative intensity [M-15] in the 2E mass spectrum.

Charge separation energies were measured for triply charged molecular and [M-2] ions which underwent charge separation leading to singly charged fragments with 1 through 5 carbon atoms. The corresponding doubly charged fragment ion was recorded in each case and the charge separation energy determined from the width of the kinetic energy release peak at 5% height. Charge separation energies ranged from 3.6 eV to 5.6 eV, and were in fair agreement with earlier work [3].

Structure of Triphenylene[3] Figure 1
() = bond length in pm.

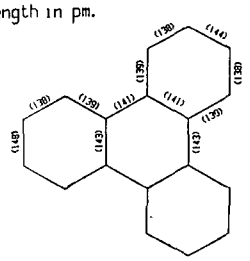

References

1. T.D. Mark, Int, J. Mass Spectrom. Ion Processes, 55(1983/1984) 325.
2. J.H. Beynon, R.M. Caprioli, W.E. Baitinger and J.W. Amy, Org. Mass Spectrom., 3(1970) 661.
3. R. Kingston, M. Guilhaus, A.G. Brenton and J.H. Beynon, Org. Mass Spectrom 20(1985) 406.
4. R.E. March and R.J. Hughes, Int. J. Mass Spectrom. Ion Processes, 68(1986) 167.
5. J.R. Appling and T.F. Moran, Org. Mass Spectrom., 20(1985) 534.

Presented at the 35th ASMS Conference on Mass Spectrometry and Allied Topics
May 24-29, 1987, Denver, CO

NEUTRAL DISSOCIATION/REIONIZATION TECHNIQUES AND POSITIVE/NEGATIVE ION CONVERSION IN TANDEM MASS SPECTROMETRY

R.Feng, C. Wesdemiotis, M.-Y. Zhang, D.E. Drinkwater, and F. W. McLafferty

Department of Chemistry, Cornell University, Ithaca, NY 14853-1301

In conventional mass spectrometric methods, structural information is derived from ionic fragmentations. However, the extensive isomerization of ions before dissociation has often made these methods structurally insensitive to several types of isomers. Neutralization-reionization mass spectrometry (NRMS)[1] offers, along with many other capabilities for studying gas phase ion and neutral chemistry[2,3], improved sensitivity for differentiating between isomers. Neutralization provides a convenient means to "freeze" isomeric ions into their original structures, as the isomerization barriers in neutral species are often much higher than in their ionic counterparts. These "frozen" neutrals can then be dissociated by collisions with a target gas to generate structurally characteristic fragments which, upon collisions with reionization target gas, yield structural information characteristic of the original molecular structures[4].

Collision of fast neutrals with a target gas produces both positive and negative ions, depending on whether an electron is removed from or attached to the projectile. For both processes, the reionization efficiency is heavily dependent on the target as well as the projectile. These dependencies make selective reionization of neutrals possible and thus greatly enhance the sensitivity for structural analysis of a mixture of neutral fragments produced by collisional dissociation of a neutral precursor.

Among the six targets tested for the positive reionization (cationization), NO_2 gives the highest yield for molecular species such as propene. NO, on the other hand, outperforms other targets for the cationization of radical species such as the allyl radical.

The electron affinity of the neutral projectile plays an important role in negative reionization (anionization). In general, neutrals with positive electron affinities, such as many radicals and molecules with strong electronegativity or high degree of unsaturation, can be converted into anions upon collision with a target gas. Molecules with large size and polarizability are good choices as anionization targets. Among fifteen targets tested, Xe and C_6H_6 are two of the best for reionizing the two neutral projectiles $CH_3O^{\cdot}$ and $C_5H_5^{\cdot}$ into anions.

Cations and anions often have reversed stability orders, e.g. $HOCH_2^+ >> CH_3O^+$, yet $HOCH_2^- << CH_3O^-$. Thus, combination of anionization with cationization is particularly useful for selectively detecting one of the neutral isomers in the presence of the other with no or little

interference, or vice versa. Although, in general, anionization is less efficient than cationization, its high selectivity and distinctive fragmentation patterns give it an edge over cationization in some cases. For example, anionization distinguishes between HCOH and H_2CO neutral isomers, whereas cationization provides less structural information for these two neutral isomers.

Upon collisions with a neutral target, cations can be directly converted to anions, via either a one step $2e^-$ transfer or stepwise electron transfer. This direct charge conversion is termed charge reversal (CR). Fragmentation pathways of anions are sometimes more structurally significant and, in general, different from those of the corresponding cations, so that complementary structural information can be obtained by charge reversal. For example, charge reversal of $Cl_2C{=}CH_2^{+\cdot}$ and $ClHC{=}CHCl^{+\cdot}$ easily differentiates the two isomers by yielding Cl_2C^- for the former and $ClHC^-$ for the latter, although the corresponding EI spectra of the two are very similar. The charge reversal spectrum of m/z 30 in the EI spectrum of cyclopropanol indicates the presence of the isobars $HCOH^{+\cdot}$ and $CH_3CH_2^{+\cdot}$, in line with high resolution measurements; positive NRMS and CAD fail to reveal the presence of 30% $HCOH^{+\cdot}$ due to the overlap of the fragmentation patterns of the two isobaric cations.

References:

1. Danis, P.O.; Wesdemiotis, C.; McLafferty, F.W. J. Am. Chem. Soc., 1983, 105, 7454-7456. Danis, P.O.; Feng, R.; McLafferty, F.W. Anal. Chem., 1986, 58, 348-354. Ibid., 355-358.

2. Wesdemiotis, C.; Feng, R.; Williams, E.R.; McLafferty, F.W. Org. Mass Spectrom., 1986, 21, 689-695. Wesdemiotis, C.; Feng, R.; Danis, P.O.; Williams, E.R.; McLafferty, F.W. J. Am. Chem. Soc., 1986, 108, 5847-5853. Wesdemiotis, C.; Feng, R.; Tso, J.; McLafferty, F.W. J. Am. Chem. Soc., 1985, 107, 8059-8066.

3. Terlouw, J.K.; Keiskamp, W.M.; Holmes, J.L.; Mommers, A.A.; Burgers, P.C. Int. J. Mass Spectrom. Ion Proc., 1985, 64, 245-250. Holmes, J.L.; Mommers, A.A.; Terlouw, J.K.; Hop, C.E.C.A. Int. J. Mass Spectrom. Ion Proc., 1986, 68, 249-264.

4. Feng, R.; Wesdemiotis, C.; McLafferty, F.W., 34th Annual Conference on Mass Spectrometry and Allied Topics, Cincinnati, OH, June 8-13, 1986, p. 433.

Presented at the 35th ASMS Conference on Mass Spectrometry and Allied Topics
May 24-29, 1987, Denver, CO

DISSOCIATION OF ENERGY-SELECTED ETHYL FORMATE ION: "Is the fragmentation controlled by an intermediate isomer or by an isolated state ?"

Q. Zha, T. Nishimura and G. G. Meisels* Department of Chemistry, University of Nebraska-Lincoln, Lincoln, Nebraska 68588-0312

Our recent threshold photoelectron-photoion coincidence (TPEPICO) mass spectrometric study of methyl formate[1] suggested that the dissociation of this molecular ion can not be reconciled with the statistical theory of mass spectra (RRKM/QET)[2] assuming only one isomer or one state. We have here studied the dissociation of ethyl formate ion using TPEPICO mass spectrometry in order to elucidate its reaction dynamics, and report its breakdown curves, kinetic energy release accompnaying fragmentation, and decay rate constants as a function of internal energy of the ethyl formate molecular ion.

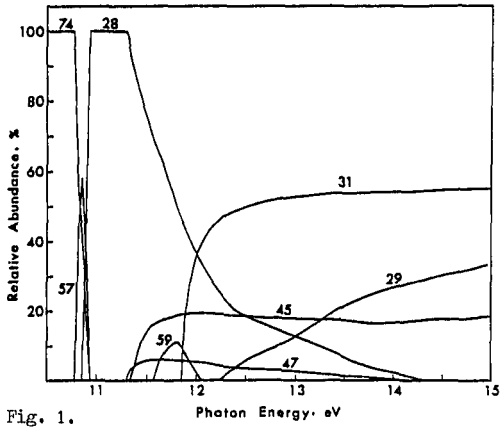

Fig. 1.

Major fragment ions detected are CH_2OCHO^+ (m/z 59), $C_2H_5CO^+$ (m/z 57), $HCO_2H_2^+$ (m/z 47), $C_2H_5O^+$ (m/z 45), CH_2OH^+(m/z 31), $C_2H_5^+$ or HCO^+ (m/z 29), and $C_2H_4^+$ (m/z 28). Fig. 1 presents the TPEPICO breakdown diagram constructed from ion abundances obtained from peak areas in coincidence TOF mass spectra.

This TPEPICO breakdown graph shows the production of two fragment ions $C_2H_4^+$ and $C_2H_5CO^+$ at lower energies. The $C_2H_4^+$ ion may result from a transfer of a H atom from the beta carbon to the carbonyl oxygen: the transition state may be a six-membered ring.[3] The appearance potential of $C_2H_5CO^+$ (10.79 $\pm$ 0.05 eV) indicates that this ion is formed via isomerization of ethyl formate ion to propionic acid ion before dissociation. The protonated formic acid $HCO_2H_2^+$ also results from a significant rearrangement involving a transfer of two H atoms.[3]

The formation sequence for CH_2OH^+ was directly determined from the TPEPICO breakdown curves: the first step is loss of the CH_3 radical from the molecular ion, the second is loss of CO. The precursor ion spectra measured on a Kratos MS-50-TA also showed that the CH_2OCHO^+ (m/z 59) is the precursor of the CH_2OH^+ ion (m/z 31).

Average kinetic energy releases for the formation of $C_2H_5O^+$ (m/z 45) and $C_2H_5^+$ or HCO^+ (m/z 29) were extracted from their TOF distributions and were compared with the RRKM/QET calculations. The formation of $C_2H_5O^+$ indicated a large conversion rate, 13 %, of internal excess energy to translation while the statistical theory predicts about 4 %. The kinetic energy release observed for m/z 29 ions was found to be statistical.

Asymmetric TOF distributions due to metastable dissociation were observed

for the formation of both $C_2H_4^+$ and $C_2H_5CO^+$, and were well fitted with a single component decay rate. However, decay rate constants observed for the formation of $C_2H_4^+$ were found to be different from those of $C_2H_5CO^+$ (Fig. 2): in a simple direct fragmentation mechanism decay rates should be identical for both processes because only the total decay rate constant reflects itself in TOF distributions of fragment ions.

This observation of different decay rate constants may suggest involvement of an intermediate isomer. One possibility is isomerization of the molecular ion in competition with direct fragmentation.[4] This model expects a two-component decay rate for direct product. For the $C_2H_5CO^+$ formation, the rate constant measurable from its flight-time distributions will be basically equal to the fragmentation rate from isomer. However, this possibility can be discarded because RRKM/QET predicts no metastable dissociation even for the $C_2H_5CO^+$ formation.

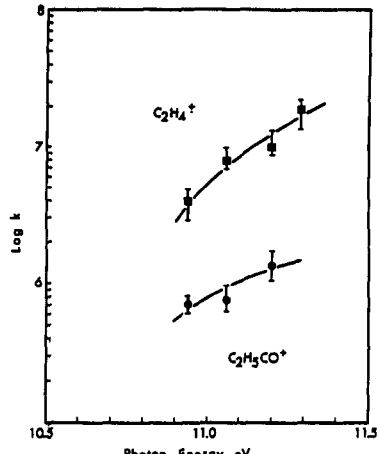

Fig. 2.

Secondly, dissociation may occur from intermediate isomers specific to respective fragment ions. In this case the isomer involved in the formation of $C_2H_5CO^+$ should be much more stable than the propionic acid ion.

Another interpretation may be given by state-specific dissociation. Two ionic states overlap in the energy regime of interest. If the first excited ionic state is not interconverted to the ionic ground state, the formation of $C_2H_4^+$ and $C_2H_5CO^+$ can take place with different decay rates corresponding to different precursors: one is the molecular ion in the ionic ground state, the other is that in the first excited state. Slow dissociation can be caused by state-crossing from one to another along the reaction coordinate.

While we conclude that the ionic dissociation of this molecule to the fragments $C_2H_4^+$ and $C_2H_5CO^+$ may involve two intermediates, both different intermediate isomers and/or at least one noninterconverting state offer plausible explanations of our observation.

ACKNOWLEDGMENTS: We gratefully acknowledge the Department of Energy for support of this work under Contract No. DE-AC02-76-ER02567 and the Regional Facility in Mass Spectrometry at the University of Nebraska.

(1) T. Nishimura, Q. Zha, and G. G. Meisels, J. Chem. Phys. (accepted). (2) (a)H. M. Rosenstock, M. B. Wallenstein, A. L. Wahrhaftig, and H. Eyring, Proc. Natl. Acad. Sci. USA 38, 667 (1952); (b)P. J. Robinson and K. A. Holbrook, Unimolecular Reactions (Wiley, New York, 1972). (3) (a)A. B. King and F. A. Long, J. Chem. Phys. 29, 374 (1958); (b)D. Van Raalte and A. G. Harrison, Can. J. Chem. 41, 2054 (1963); (c)M. S. Munson and J. L. Franklin, J. Phys. Chem. 68, 3191 (1963). (4) T. Baer, W. A. Brand, T. L. Bunn, and J. J. Butler, Faraday Discuss. Chem. Soc. 75, 45 (1983).

Presented at the 35th ASMS Conference on Mass Spectrometry and Allied Topics
May 24-29, 1987, Denver, CO

FRAGMENTATION OF ACETIC ACID IONS WITH SELECTED INTERNAL ENERGY

Qingmei Zha, Toshihide Nishimura and G. G. Meisels
Department of Chemistry University of Nebraska, Lincoln NE 68588-0304

The unimolecular dissociation of acetic acid ions has been studied using threshold photoelectron photoion coincidence (TPEPICO) mass spectrometry in the photon energy range of 10.5-17.0 eV. The detailed breakdown graph was obtained (Fig. 1) and the fragmentation pathways were elucidated. The major fragment ions observed are $COOH^+$ (m/z 45), CH_3CO^+ (m/z 43), CH_2OH^+ (m/z 31), HCO^+ (m/z 29), CH_4^+ (m/z 16) and CH_3^+ (m/z 15).

Early work[1] based on electron impact studies and QET calculations reported that CH_2CO^+ and CH_2^+ ions dominate the breakdown graph in the internal energy range of 1-3 eV. A later study[2] also reported the H_2O loss from ionized acetic acid but concluded that it was unable to compete significantly with OH loss. The remarkable low intensity of m/z 42 ion (H_2O loss) observed could be due to H_2O loss requiring an "ordered transition state".

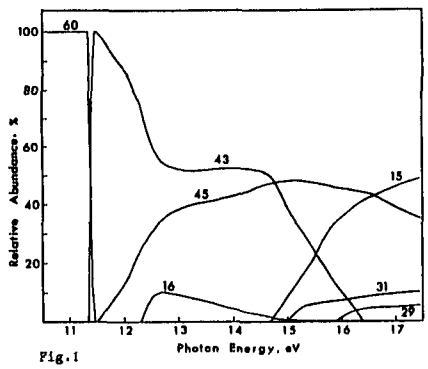

Fig. 1

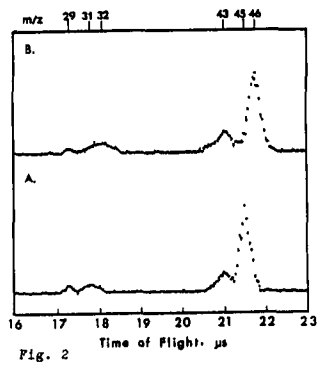

Fig. 2

There are two possible structures of m/z 31 and m/z 29 ions formed by two different channels:

$$CH_3COOH^+ \longrightarrow CH_2OH^+ + {}^{\cdot}COH \quad (1)$$
$$CH_3COOH^+ \longrightarrow CH_3O^+ + {}^{\cdot}COH \quad (2)$$

and

$$CH_3COOH^+ \longrightarrow CH_2OH^+ + {}^{\cdot}COH \longrightarrow HCO^+ + {}^{\cdot}COH + H_2 \quad (3)$$
$$CH_3COOH^+ \longrightarrow COOH^+ + {}^{\cdot}CH_3 \longrightarrow COH^+ + {}^{\cdot}CH_3 + O \quad (4)$$

Fig. 2 shows the TOF spectra of acetic acid (2a) and CH_3COOD (2b). The fact that m/z 31 ion was obtained in 2a while both m/z 31 and 32 ions were obtained in 2b indicates the structure of m/z 31 from acetic acid is CH_2OH^+ formed via process (1) by a two-step rearrangement-dissociation. Fig. 2 also shows that m/z 30 ion was not observed from CH_3COOD. This result indicates that the m/z 29 is HCO^+ formed from acetic acid via process (3) by 1,2-elimination from CH_2OH^+.

The experimental breakdown graph was fitted with a theoritically calculated one based on RRKM-QET. The activation energy Ea and factor F (reflecting loose or tight for the transition state) were used as the adjustable parameters until the calculated and experimental breakdown grephs matched. The best values of E_a and F were then adopted in the determination of rate constants and kinetic energy releases. The calculated brekdown graph and corrected experimental data points are shown in Fig. 3. Very good fit to the

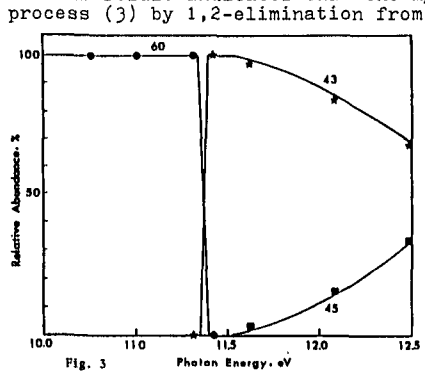

Fig. 3

experimental data points was obtained up to a photon energy of ca. 12.5 eV. The discrepancies at higher internal energies may be the result of the appearance of CH_4^+ ion which may be formed via an unusual fragmentation channel.

The best values of F factor for the formation of $COOH^+$ and CH_3CO^+ are 0.8 and 1.1, respectively. These values (F<1) indicate loose transition states while dissociation undergoing through a rearrangement is associated with a tight transition state (F>1). A plausible explanation for a slightly tight transition state (F=1.1) involved in the CH_3CO^+ formation could be given by an intramolecular hydrogen bonding between the hydroxyl hydrogen and the carbonyl oxygen although a direct cleavage of the C-O bond should result in this fragmentation due to loss of OH.

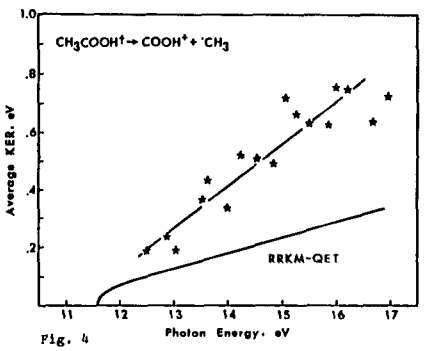

Fig. 4

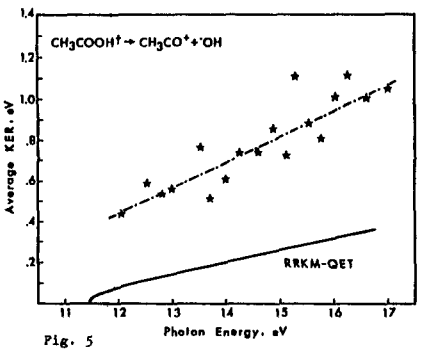

Fig. 5

Average kinetic energy releases for the formation of $COOH^+$ ion are shown in Fig. 4. At the vicinity of threshold, the slope of average KER observed was consistent with that calculated by RRKM-QET suggesting that kinetic energies released in this dissociation may arise mainly from the excess internal energy of the activated complex and that there is no reverse activation energy. At higher energies almost 14 % of the internal excess energy was found to be converted to translation while RRKM-QET predicts only about 7%.

The formation of CH_3CO^+ demonstrated average KER much higher than that of $COOH^+$ (Fig. 5). The average KER observed for this ion near onset showed KER much higher than the RRKM-QET prediction while the conversion rate derived from the slope of the KER curve was statistical. This result may indicate a considerable contribution to KER from reverse activation energy. Average KER (E_t) for the formation of CH_3CO^+ could be expressed by

$$E_t = E_e + 0.35 \text{ (eV)},$$

where E_e is the contribution from excess internal energy. The value 0.35 eV is the kinetic energy release originated from the reverse activation energy.

ACKNOWLEDGMENTS: The authers are grateful to the Department of Energy for support of this study under Contract No. DE-AS02-76-ER02567.

References:

1. Fueki,K. and Hirota, K. J. Chem. Soc. Japan, Pure Chem. Sec. (Nippon Kagaku Zasshi), 81 (1960) 356.
2. Schwarz, H.; Williams, D. H. and Wesdemiotis, C. J. Am. Chem. Soc. 100 (1978) 7052.

Presented at the 35th ASMS Conference on Mass Spectrometry and Allied Topics
May 24-29, 1987, Denver, CO

ELECTRON-CAPTURE (CHARGE-EXCHANGE) REACTIONS OF MULTIPLY CHARGED POLYCYCLIC AROMATIC IONS.

R.G.Kingston, A.G.Brenton, F.M.Harris and J.H.Beynon.

Mass Spectrometry Research Unit, University College of Swansea,
Swansea SA2 8PP, U.K.

Condensed-ring aromatics are important constituents in many chemical systems. Their mass spectra show that multiply charged molecular and fragment ions are formed in the gas phase often in high abundance [1]. The structures of multiply charged ions have been studied by various mass spectrometric techniques, for example, 2E mass spectra [2] and unimolecular charge separations [3]. There have been relatively few studies, however, on triply charged organic ions, due to their scarcity.

In the present study, rather than examining doubly or triply charged ion mass spectra, or charge separation reactions electron capture (charge exchange) reactions have been employed to investigate these of multiply charged ions. In addition, the method of translational spectroscopy that we have employed allows us to characterise and assign the likely states of the reacting ions providing basic data on the energetics and rates of these reactions. The reactions which we have examined are

$$M^{2+} + N \longrightarrow M^{+\cdot} + N^{+\cdot} \qquad (1)$$

and

$$M^{3+\cdot} + N \longrightarrow M^{2+\cdot} + N^{+\cdot} \qquad (2)$$

where N is a neutral target gas and M is either benzene, naphthalene, anthracene or 2,3-benzanthracene.

Experimental

Experiments were performed on a ZAB-2F mass spectrometer. Doubly and triply charged ions were formed in an electron impact source and were mass selected at m/z M/2 and M/3, where M is the molecular ion mass. The electron capture process takes place in the collision cell on rare gas targets, in the second field free region (2FFR). Energy loss spectra were recorded by scanning the electric sector voltages around values of either 2E or 3E/2, for reactions (1) and (2), respectively. An energy resolution of 10,000 (10% definition) was employed, at an accelerating voltage of 3 kV.

Results and Discussion.

Calibrating the energy scale.

To accurately assign the states involved in reaction the translational energy scale has to be calibrated with a known system. We used the reactions

$$Ar^{2+} + X \longrightarrow Ar^{+\cdot} + X^{+\cdot}$$

and

$$Ar^{3+\cdot} + X \longrightarrow Ar^{2+} + X^{+\cdot}$$

where X = He, Ne, Ar, Kr and Xe which have been studied in detail and give a reliable energy scale for subsequent use with unknown systems.

Energy loss spectra for doubly charged ions.

Examples of the spectra obtained are shown in Figure 1. The labelling of reaction channels shown is as follows :

(i) *Roman numerals I, II, III ... represent ground state, first excited state and second excited states of the incident multiply charged ion.*

(ii) The Greek symbols α, β, γ ... represent the ground and successively higher excited states of the product ion.

(iii) Roman capitals X, A, B ... represent the ground and higher excited states of the target after capture.

It can be seen from the energy loss spectra that both exothermic and endothermic processes occur. The main reaction channel is generally IβX which shows that excitation of the product ion is favoured. Another general feature of the spectra is that electron capture proceeds from a range of vibrational states, of the ground electronic states. This is shown clearly for $C_6H_6^{2+}$ on Xe where the peak top is located midway between IαX and IβX (which represent the v = o thresholds for these two reactions).

Energy loss spectra for triply charged ions.

For most of the systems examined these showed that IαX was the dominant reaction. However, contributions from vibrationally excited states seemed less likely which is difficult to reconcile with doubly charged ions. This may reflect a greater uncertainty in our calibration in the energy scale which we are currently investigating.

Cross section (rate) measurements.

These were measured for all observable reactions and are shown in Figure 2. Doubly and triply charged rare gas ions were used to calibrate this data. It is fairly well established that electron capture collisions occur most effectively in moderately exothermic reactions through crossings of the diabatic potential energy curves at internuclear separations, R_c, given by

$$R_c = \frac{14.4\ (q - 1)}{\Delta E}$$

where q is the charge number of the projectile and ΔE is the asymptotic energy defect. Analysis of a large number of monatomic systems reveals the existence of a maximum in the electron-capture cross section at $3\text{Å} < R_c < 7\text{Å}$ and has led to the concept of a reaction window. However, the results shown here show a breakdown of this picture for the systems we have studied.

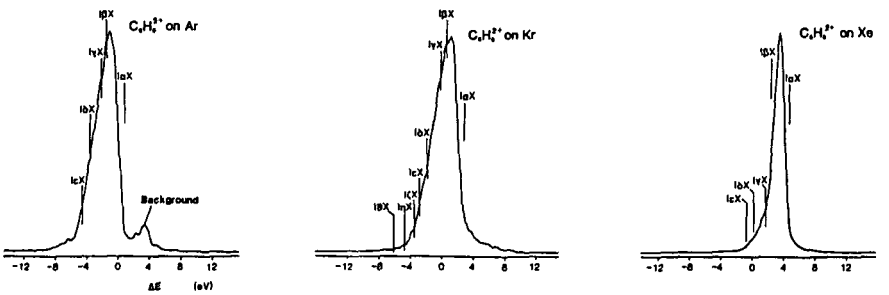

Figure 1 $C_6H_6^{2+} + R \rightarrow C_6H_6^{+} + R^{+}$, where R = Ar, Kr and Xe.

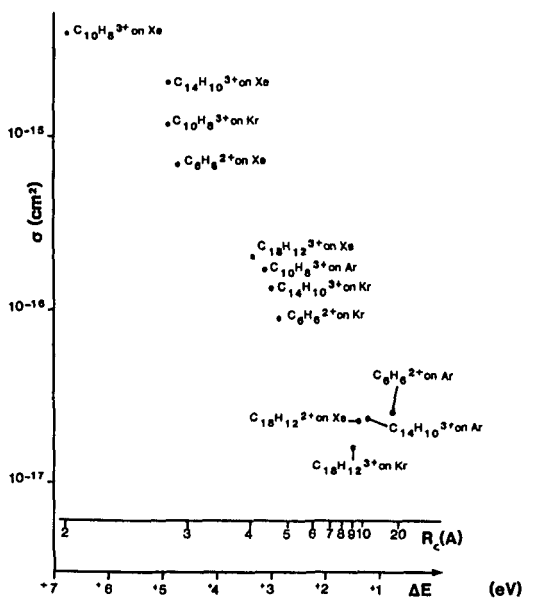

Figure 2

Cross sections (σ) plotted against ΔE (exothermicity) and R_c (Å), the classical crossing radius.

References

1. M.E.Wacks and V.H.Dibeler, J.Chem.Phys., 31, 1557 (1959).
2. B.P.Mathur, E.M.Burgess, D.E.Bastwick and T.F.Moran, Org.Mass Spectrom. 16, 92 (1981).
3. M.Rabrenović and J.H.Beynon, Int.J.Mass Spectrom.Ion Phys., 54, 87 (1983).

Presented at the 35th ASMS Conference on Mass Spectrometry and Allied Topics
May 24-29, 1987, Denver, CO

ION KINETIC ENERGY MEASUREMENT IN A TANDEM QUADRUPOLE MASS SPECTROMETER

Claude BEAUGRAND and Gérard DEVANT, S.N.NERMAG, 49 quai du Halage, F 92500 RUEIL-MALMAISON, Daniel JAOUEN, Hélène MESTDAGH and Christian ROLANDO, Ecole Normale Supérieure, Département de Chimie, 24 rue Lhomond, F 75231 PARIS CEDEX 05

The RF only collision cell of a tandem quadrupole mass spectrometer was modified in order to measure kinetic energy of parent and fragment ions in a CAD process : the quadrupole of this cell was split in two independant quadrupoles C1 and C2 (figures 1, 2). Recording of the ionic current due to a given ion as a function of C2 potential (C1 potential being fixed) gives a stopping curve, from which average kinetic energy E and energy dispersion W of the considered ion are easily deduced. The tensions C1 and C2 are furnished by two fast rise power supplies drived by an auxiliary micro computer which is synchronised by the main data system. Families of stopping curves could thus be recorded in a single experiment. In the case of a CAD two processes are taking place (2,3) :

first activation $M^+ + N \rightarrow (M^+)^* + N$ then dissociation $(M^+)^* \rightarrow M1^+ + M2$

which are characterised by two energetic parameters Q (internal energy transferred to the parent ion M^+ through collision with the neutral gas N) and T (kinetic energy released through fragmentation of $(M^+)^*$). These parameters could be estimated from comparison of measured Ef, Wf (fragment ion) and Ep, Wp (parent ion) by fitting experimental data with curves calculated assuming a model of the CAD processes. The main assumptions are :(i) no scattering during the activation step, (ii) isotropic dissociation. This method was applied to CAD fragmentation of n-butylbenzene radical cation:

$$\underset{m/z\ 134}{(C_6H_5\text{-}C_4H_9)^{+\cdot}} \rightarrow \underset{m/z\ 91}{C_7H_7^+} + C_3H_7 \quad \text{and} \quad \underset{m/z\ 92}{C_7H_8^{+\cdot}} + C_3H_6$$

In the case of $C_7H_7^+$ (m/z 91) formation, kinetic energy Ef of the fragment is close to its lower limit, especially at low Ep (figure 3) : this limit corresponds to maximum available internal energy transfer, i.e. Q = Ecm (kinetic energy of the M^+ + N system in the center of mass frame). Q values obtained for $C_7H_7^+$ formation are about 3-4 eV, slightly below the corresponding reported plateau value (3). In contrast kinetic energy of $C_7H_8^{+\cdot}$ (m/z 92) is close to its upper limit, corresponding to very low Q values. Energy dispersions Wf found for $C_7H_8^{+\cdot}$ fragment ion are larger than corresponding dispersions of $C_7H_7^+$ fragment ion, indicating larger T values.

A remarkable difference thus appears between energetic characteristics of the two fragmentation channels of m/z 134 parent ion.

REFERENCES :

(1) P.H. DAWSON and D.J. DOUGLAS, "Collisionally Activated Dissociation of Low Kinetic Energy Ions" in Tandem Mass Spectrometry, F.W. Mc Lafferty, edr., John Willey, 1983.
(2) D.J. DOUGLAS, J. Phys. Chem., 86, 185 (1982).
(3) S.NACSON and A.G.HARRISON, Int.J.Mass Spectrom.Ion Proc.,63,325 (1985).

DOUBLE QUADRUPOLE COLLISION CHAMBER

Figure 1

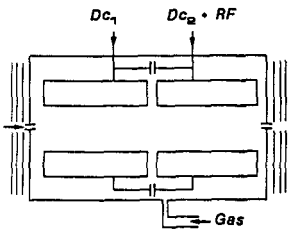

- *12 cm pathway*
- *Baratron gauge*
- *gas flow regulated with Mass Flow meter*

- *PRESSURE UP TO 20 millitorr*
- *KINETIC ENERGY ANALYSIS OF CAD*

INSTRUMENT POTENTIAL

Figure 2

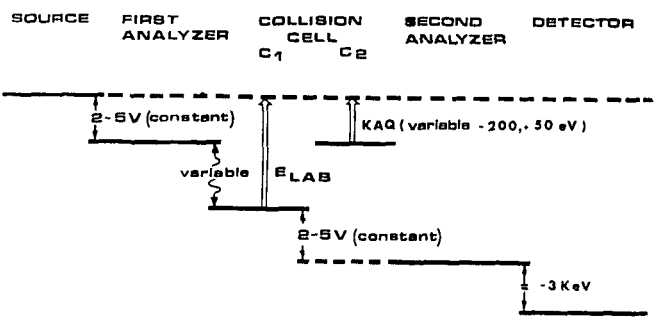

DEPENDANCE OF MEASURED FRAGMENT ION ENERGY WITH PARENT ION ENERGY

Figure 3

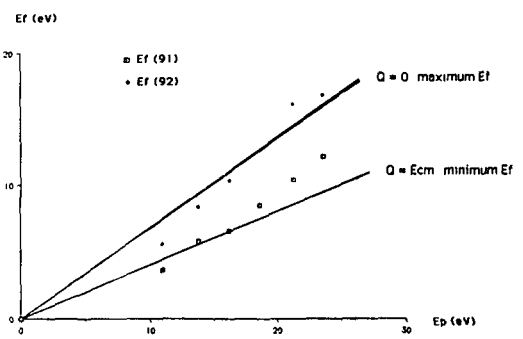

Presented at the 35th ASMS Conference on Mass Spectrometry and Allied Topics
May 24-29, 1987, Denver, CO

Evaluation of Deuterium Isotope Fractionation in Protonated Water Clusters with a Flowing Afterglow - Triple Quadrupole

Mark D. Brickhouse, Susan T. Graul, Robert R. Squires; Department of Chemistry, Purdue University, West Lafayette, IN 47907

Collisional activation experiments with partially deuterated $H_3O(H_2O)^+_{n=1-3}$ ions have been carried out with a flowing afterglow - triple quadrupole instrument. As shown in eq. 1, the clusters can be made by electron impact on H_2O or D_2O to form the unmixed hydronium ion clusters. Clustering up to the proton bound tetramer occurs readily in the 0.4 torr of helium buffer gas in the flow tube. Addition of the appropriate isotopomer downstream in the flow tube forms the mixed clusters by H/D exchange.

$$(1)\quad \begin{array}{l} H_3O^+(H_2O)_n \xrightarrow{D_2O} \\ D_3O^+(D_2O)_n \xrightarrow{H_2O} \end{array} \underset{\text{"M"}}{H_xD_yO^+_{n+1}} \xrightarrow{\text{CID}} \begin{bmatrix} M-H_2O \\ M-HOD \\ M-D_2O \end{bmatrix}^+$$

A small portion of the plasma is sampled and focused into the quadrupoles; the clusters are then subjected to collisionally induced dissociation (CID) in the second quadrupole. Daughters corresponding to the loss of H_2O, HOD and D_2O are observed, and for all clusters studied, loss of the deuterium containing water molecules was in excess of the statistical loss percentages.

To minimize mass discrimination effects, all experiments were preceeded by a calibration experiment. Electron impact on CH_3Cl readily produces the $ClCH_2^+$-$ClCH_3$ cluster. The isotopomer containing one ^{35}Cl and one ^{37}Cl, m/z 101, is subjected to CID and conditions are adjusted until the $^{35}ClCH_2^+$ and $^{37}ClCH_2^+$ daughter ions are of equal intensity. Chlorine isotope effects in the thermalized ions obtained from the flowtube are expected to be minimal. For the hydrate cluster ions, it was found that collision energy, collision gas pressure, D_2O and H_2O flow rates and the order of cluster formation (eq. 1) had no effect on the deviation of solvent loss percentages from their statistical values. As shown in Fig. 1, HOD loss from the mixed tetramer was greater than statistical for the D - poor clusters while D_2O loss was always in excess of the statistical values. (Dashed lines) The experimental data (solid lines) represent the average of six runs from six

different days by two operators. The standard deviation was ±1% while the observed losses were consistently 2-5% from the calculated loss percentages.

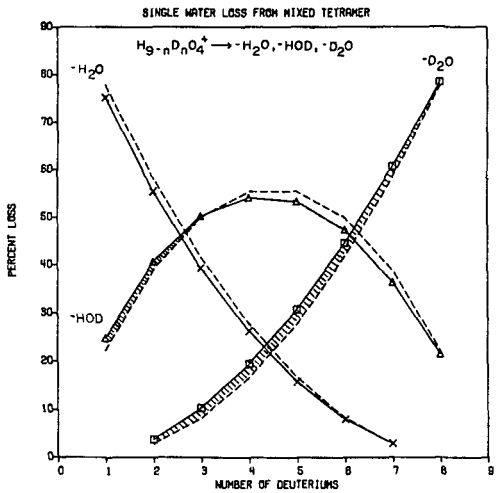

Figure 1

A plausible explanation for the observed results is that hydrogen and deuterium completely scramble in the clusters, but that deuterium preferentially occupies the peripheral (water) positions rather than the bridging (hydronium) positions in the clusters. These results are in accord with zero point energy differences of the hydronium ions calculated by Henchman, Smith and Adams.[1] Substitution of deuterium for hydrogen in H_3O^+ is shown to be mildly endothermic. Larson and McMahon also determined in ICR equilibrium studies that deuterium preferentially resides in the water molecules rather than on the lyonium ions (L_3O^+,L=H,D).[2] Our results indicate that this type of fractionation is also occuring within the solvated hydronium ion clusters themselves.

1) Henchman,M.J.; Smith,D.; Adams,N.G. Int. J. Mass Spec. Ion Phys. 1982, 42, 25.
2) Larson,J.W.; McMahon,T.B. J. Am. Chem. Soc. 1986, 108, 1719

Presented at the 35th ASMS Conference on Mass Spectrometry and Allied Topics
May 24-29, 1987, Denver, CO

THE GAS PHASE REACTIONS OF Fe^+ AND Cr^+ WITH ALIPHATIC ALCOHOLS: A HIGH ENERGY CAD STUDY.

S.K. Huang, Adamantech Inc., Linwood, PA 19061; R.W. Holman, Department of Chemistry, Univ. of Nebraska-Lincoln, Lincoln, NE 68588.

In a previous study, we have reported that gas-phase atomic transion metal ions, Fe^+ and Cr^+ undergo C-O, C-H, and C-C insertion reactions with aliphatic alcohols in the ion trap of an FTMS[1]. The present report then, is a high energy collisional activation (CA) study aimed at the structure determination of the same M^+/alcohol adducts.

The M^+/alcohol adducts were collisionally stabilized in the high pressure chemical ionization source of a tandem mass spectrometer. The adducts were then collisionally activated and their MIKES spectra were aquired for the structure determination.

The high energy CAD spectra for the Fe^+- and Cr^+-alcohol complexes are tabulated in Tables 1 and 2 respectively. Several salient features for these tables shall be highlighted.

Firstly, it is clear that the Cr^+/alcohol complexes, upon collisional activation, dissociate to Cr^+ much more readily than the Fe^+/alcohols dissociate to Fe^+. Secondly, the product distribution in the high energy CA-decomposition of these metal-ion/alcohol complexes include $FeOH^+$, $CrOH^+$, and FeH^+. These species are not present in the thermal FTMS decomposition of the same complexes.

Because the Cr^+/alcohol complexes dissociate to Cr^+ so readily under high energy CAD conditions it is likely that Cr^+ has not inserted into any of the bonds of the alcohol prior to the collisional activation process. The Cr^+, then, may be best described as being only loosely coordinated to the alcohol prior to CAD. That the Fe^+/alcohol complexes do not dissociate to Fe^+ very readily make it reasonable that Fe^+ has already inserted into a C-O, C-C, or C-H bond of the alcohol prior to the CAD process. These insertions lead to dehydration, reductive elimination, and dehydrogenation products, respectively. As such, the Fe^+ ion may be thought of as being more reactive towards alcohols than is Cr^+.

The ions observed in the high energy CA-dissociation of these M^+/alcohol adducts, which are not seen in the thermal FTMS dissociation, must be high energy processes. Hence, $FeOH^+$, $CrOH^+$, and FeH^+ are high energy processes which must be induced by the collisional activation process.

In conclusion, the high energy CAD analysis of metal ion/organic complexes can be employed to probe the degree of bond insertion that takes place between the metal ion and the organic species. The high energy CAD technique is best used for structure determination of organometallics in conjunction with thermal FTMS results. The combination allows for assigning the high energy fragments that are induced by the CAD process.

1) Huang, S.K.; Holman, R.W.; Gross, M.L. Organometallics, 5, 1857 (1986).

Presented at the 35th ASMS Conference on Mass Spectrometry and Allied Topics
May 24-29, 1987, Denver, CO

TABLE 1 CAD Spectra of Fe^+/Alcohol

Alcohols	Fe^+	FeH^+	$FeCH_3^+$	$FeOH^+$	FeH_2O^+	$FeC_2H_4^+$	$FeC_2H_5^+$	$FeC_2H_5O^+$	$FeC_2H_6O^+$	$FeC_4H_8^+$	$FeC_4H_8^+$	$FeC_3H_6O^+$	$FeC_3H_8O^+$	$Fe(M-H_2O-H_2)^+$	$Fe(M-H_2O)^+$	$Fe(M-CH_3)^+$	$Fe(M-CH_4)^+$	$Fe(M-C_2H_4)^+$	$Fe(M-C_2H_6$
Methyl	100.0	17.0		46.0															
Ethyl	76.0	14.0		40.0	19.0	100.0									100.0			19.0	
Propyl	12.0	3.0		9.0	4.0		100.0	17.0							100.0				
Isopropyl	16.0	5.2		12.0	18.0		100.0								100.0				
Butyl	1.5	<1.0	<1.0	2.2	<1.0	1.0		<1.0	<1.0	2.5		<1.0		2.5	1.2	1.0	<1.0		
sec-Butyl	3.0	1.0		7.0	4.0					11.0				11.0	100.0	6.0			
t-Butyl	5.0	2.0	2.0	2.0	3.0										100.0				
Pentyl	8.3	3.8	1.4	9.9		8.3	14.5	6.4				4.5		10.1	3.9	1.2		45.0	
3-Pentyl	2.5	1.0		2.5	2.5	2.1	10.0			8.3				18.3	100.0	9.2	7.1	14.2	
Neopentyl	2.1	3.0	5.3	7.6	2.3	1.5	9.1			2.0				33.3	100.0	69.7	31.8	2.3	
t-Pentyl	4.5	1.0	2.0		2.7	1.2	5.4			10.3				6.9	100.0				
3-Methyl-2-Butyl	7.1	2.6		6.5	6.5	2.6	12.3			8.1				16.2	100.0	21.4	13.0		
2-Pentyl	1.2	<1.0	1.2	2.1	<1.0	<1.0	1.9			2.0				6.4	7.2	1.5	<1.0		
2-Methyl-Butyl	1.0		<1.0	<1.0			<1.0		<1.0	1.0				2.9	1.6	1.2	<1.0		
1-Hexyl	4.4	3.0		5.7		6.3	17.0		6.4	3.4			15.2		<1			23.0	33.8
2-Hexyl	2.1	2.4		3.6	2.4	3.0			7.3	4.5	10.3	2.4			27.5			11.2	
3-Methyl-3-Pentyl	6.2		6.2	6.2			8.9				8.9			8.9	100.0				13.3

TABLE 2 CAD Spectra of Cr^+/Alcohol

Alcohols	Cr^+	$CrOH^+$	CrH_2O^+	$CrCH_2O^+$	$CrCH_3OH^+$	$CrC_2H_5^+$	$CrC_2H_6^+$	$CrC_2H_6O^+$	$CrC_2H_8O^+$	$CrC_3H_6^+$	$CrC_3H_7^+$	$CrC_3H_8^+$	$CrC_3H_8O^+$	$CrC_3H_9O^+$	$CrC_4H_8^+$	$CrC_4H_8O^+$	$Cr(M-C_2H_4)^+$	$Cr(M-H_2O-H_2)^+$	$Cr(M-H_2O)^+$	$Cr(M-$
Ethyl	100	26		3				3												
Propyl	100	28			5									31						
Isopropyl	100	33	20				14							27					14	
Butyl	100	28		4	4	5			4	3						21				
2-Butyl	100	37	33							8		48				7			48	
t-Butyl	36	17	33									100				5			100	
Pentyl	100	39		4	8	10					3			19		3	4			3
2-Pentyl	100	51	47			16								7			8	66		
3-Pentyl	100	47	46			11				6				8			9	81		
t-Pentyl	29	17	26			4												100		
Neopentyl	100	27	25	4	6	4					4						4	29	7	
2-Methyl-Butyl	100	66	43			15					21			14			14	30		
3-Methyl-2-Butyl	100	47	64			12					7			5			12	96		
Cyclopentyl	82	28	34												22	6		100		
Hexyl	100	37			6	11			6	6				9		11				
2,3-Dimethyl-2-Butyl	21	10	12			3												100	25	
3-Methyl-3-Pentyl	16	7	9								3							100		

Presented at the 35th ASMS Conference on Mass Spectrometry and Allied Topics
May 24-29, 1987, Denver, CO

INVESTIGATION OF ALKOXYPERFLUOROPRORIONATE SALTS: NOVEL DISSOCIATIONS OF FAB GENERATED CARBANIONS.

S. L. Hunt, P. A. Lyon, and M. J. Pellerite,
3M, St. Paul, MN. 55144.

The pyrolysis of perfluoroalkoxypropionate salts with loss of CO_2 and NaF is a standard literature route to the formation of perfluoroalkyl trifluorovinyl ether prepolymers. However, when hydrocarbon alkyl groups are incorporated the trifluorovinyl ethers are no longer formed (1). Fast atom bombardment and tandem mass spectrometry were used to investigate the differences between the hydrocarbon and fluorocarbon compounds.

A series of alkoxyperfluoropropionate salts were studied using a Kratos MS50 HMTA. The alkyl groups included fluorocarbons, hydrocarbons, and partially fluorinated hydrocarbons. Survey mass spectra of FAB-generated positive and negative ions were aquired. In addition to stable molecular ions, significant clustering of the form $(LM)_nL^-$ was observed up to n = 9. These compounds also form association complexes with several NaF ion pairs. The perfluoroinated propionate anions desorbed with as many as six NaF adducts. Association complexes were also observed with the hydrogen containing compounds but to a lesser extent. Collision induced dissociation (CID) was used to study the ion chemistry of major carbanions observed in the normal FAB spectra.

All of the propionate anions undergo homolytic cleavage and loss of neutral CO_2 upon collision activation. However, an additional significant fragment ion (m/z 97) occurs only in the spectra of the hydrocarbon alkoxides (see figure 2a and b). This fragment is a rearrangement product of the M - CO_2 ion (m/z 131), confirmed by a parent scan (figure 3b) and has a composition of C_2F_3O by exact mass measurements. Molecular mechanics (MMPI) was used to calculate the stability of three possible structures for the rearrangement ion (figure 1). Structures B and C have the lowest total energy but the actual structure of the ion may be a stable transition state between these two structures. The proposed transition state is supported by the CID spectrum of the rearrangement ion (figure 3a) which contains both the CF_3 anion (m/z 69) and the COF anion (m/z 47).

Collision activation of the propionate anions of two isomers, $C_2F_5OCF_2CF_2CO_2$ (I) and $C_2F_5OCF(CF_3)CO_2$ (II), illustrate the destabilizing effect of alpha fluorines on carbanions. The ether carbanion is the most abundant anion in the CID spectrum of (II). The addition of an alpha fluorine and the subtraction of a beta fluorine in (I) result in a decreased abundance of the ether carbanion in the CID spectrum of (I). The alpha fluorine destabilization and beta fluorines stabilization of carbanions is in agreement with earlier work on perfluoroalkylsulfonates.(2)

1. M. J. Pellerite, Presented at 8th Winter Fluorine Conference, St. Petersburg, FL, Jan. 1987.
2. S. Hunt, P. Lyon, F. Behr, L. Winter, 3M; R. Cerny, K. Tomer, and M. Gross, MCMS; submitted to Analytical Chemistry.
3. MMPI calculations provided by M. L. Brostrom, 3M; Transition state theory by M. L. Gross; Parent scan by R. L. Cerny.

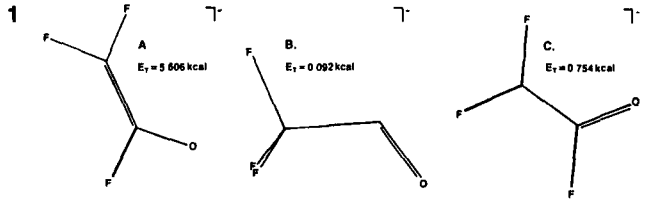

Figure 1. MMPI calculations for three possible structures for the *rearrangement* anion, C_2F_3O.

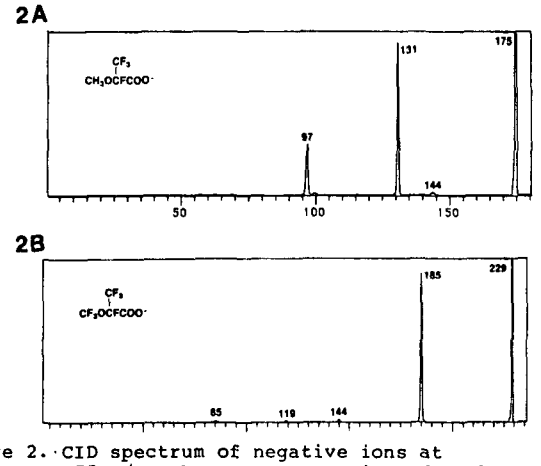

Figure 2. CID spectrum of negative ions at
A. 175 m/z, the molecular anion of methoxyperfluoropropionate.
B. 229 m/z, the molecular anion of perfluoromethoxyprorionate.

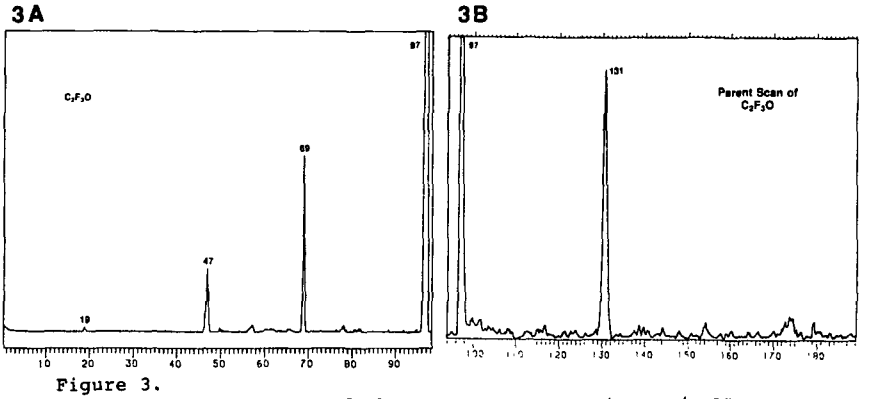

Figure 3.
A. CID spectrum of the rearrangement anion, m/z 97.
B. Parent scan of the rearrangement anion, m/z 97.

Presented at the 35th ASMS Conference on Mass Spectrometry and Allied Topics
May 24-29, 1987, Denver, CO

Chemical Ionization Mass Spectrometry of K-Region Arene Oxide Methanolysis Products

L.K. Pannell, N. Nashed and S. Grossman
Laboratory of Bioorganic Chemistry, NIDDK, National Institutes of Health
Bethesda, MD 20892

In a study to elucidate the mechanism of action of xenobiotic microsomal epoxide hydrolase from rat liver, thirteen arene oxides (polycyclic aromatic hydrocarbon epoxides) were reacted with methanol and under base catalysed conditions to give adducts resulting from the trans-addition of methanol. While symmetrical arene oxides give a single methanol addition product, unsymetrical ones give two products. The adducts from each arene oxide in the study were separated/purified by preparative liquid chromatography and the two

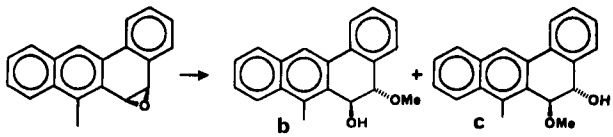

structures differentiated using extensive/time consuming NMR coupling experiments. The ammonia chemical ionization mass spectra were run to further confirm their identity. The main fragments in the CI spectra are accounted for by loss of either methanol or water from the MNH_4^+ or MH^+ ions. These losses are quite predictable, especially considering the stability afforded to the resultant product ions by delocalization in the adjacent aromatic ring systems. The ratio of formation of the $-H_2O$ and -MeOH ions for a particular adduct can be called the "preference" of the molecule.

While obtaining the spectra of the unsymmetrical adducts (e.g. B and C above), it was noticed that the "preference" of the two molecules was different, that is, one had a larger water loss than methanol loss compared with the other adduct. For instance, in the case of 7-methylbenzanthracene (shown above) the change in the "preference" for B to C was 18.8 for the MNH_4^+ ion and 29.4 for the MH^+ ion. Spectra readily show this change:

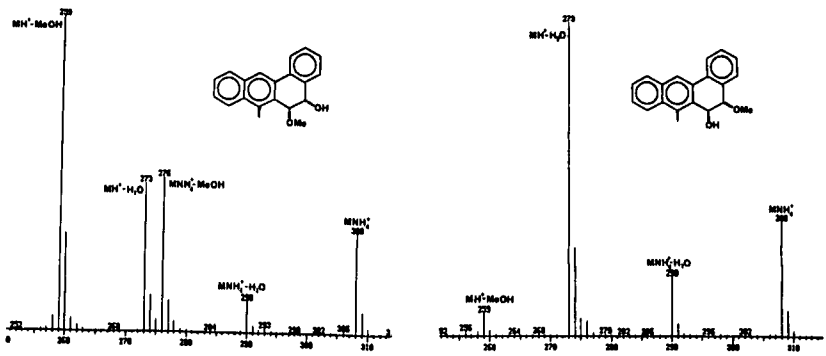

When comparing the NMR assignments of the methanol adducts for a series of unsymmetrical arene oxides to the chemical ionization "preferences," it was found that the adduct with the -OH closest to the larges aromatic piece (e.g. B) had a preference to lose water, while the converse was true for the isomer with the -OMe closest to the largest aromatic piece. This ratio of "preferences (i.e., "preference" of B isomer to C isomer) shows a consistent trend and is diagramatically shown for some adducts below (value for MH^+ ion; arrows show increased ratio):

It can be expected that a neutral loss leading to the ring carbocation with more delocalization will have a lower transition state than one leading to a less stabilized ion. This fact is consistent with all the structures above. Furthermore, the addition of another aromatic ring increases the "preference ratio." Do the two aromatic systems at

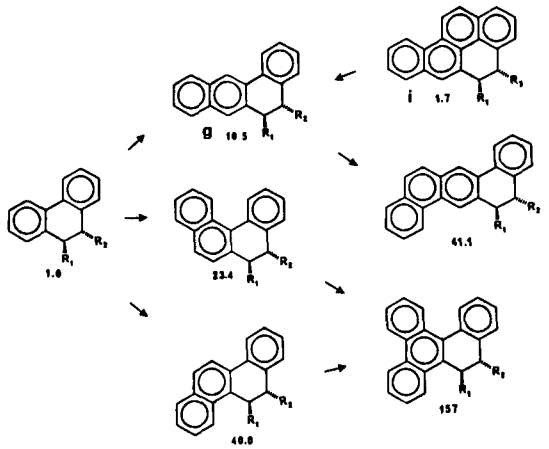

each end of the molecule interact and assist each other? Adducts "I" show a low "preference ratio" compared with "G" as here there is a definite link in the aromatic systems. In other cases, calculations of the degree of twist of the two aromatic systems (XIRIS Molecular Modeling System) shows an angle of about 15°, reducing the overlap between ends. This angle can be increased by adding methyl groups to the benzanthracene structure, reducing the overlap even further. This change is reflected in the "preference ratio":

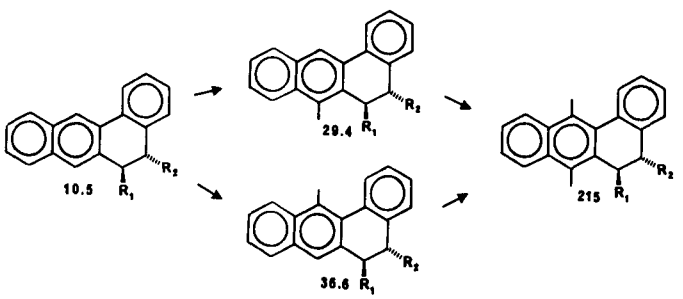

The angle between the two ring systems in these structures is approximately 37°. Further support of the delocalization giving lower transition state energy can be obtained by comparing the methane CI spectra with the ammonia CI spectra. When methane forms MH^+ ions, it imparts far more energy to the molecule than in the case of ammonia. Therefore in methane, the transition state energy will have a less directing effect in the fragmentation. This is reflected in the "preference ratio" which is a lot less in methane CI (for 12-methylbenzanthracene this goes from 36.6 in ammonia to 1.53 in methane) although the same trend is observed.

Further work is continuing on a series of cis-methanol adducts formed form acid catalyzed methanolysis. These show a similar trend to the trans-adducts and structures are also assignable from their ammonia CI spectra.

CONCLUSION

The regiochemistry of the methanol addition adducts of K-Region arene oxides may be readily assigned by a comaprision of the ammonia chemical ionization spectra of the resultant products.

Presented at the 35th ASMS Conference on Mass Spectrometry and Allied Topics
May 24-29, 1987, Denver, CO

NOVEL MASS SPECTRAL FRAGMENTATION OF SOME CHLOROACETANILIDES.

Hideji Fujiwara and Joseph M. Malik

Monsanto Agricultural Company
An Operating Unit of Monsanto Company
700 Chesterfield Village Parkway,
St. Louis, Missouri 63198

The chloroacetoanilide family of herbicides contains a number of very selective grass herbicides which are in wide use today. Among these are alachlor (2-chloro-2',6'-diethyl-N-methoxymethylacetanilide) the active ingredient in LASSO® herbicide and butachlor (N-butoxymethyl-2-chloro-2',6'-diethylacetanilide) the active ingredient in the rice herbicide MACHETE®[1]. During the course of the studies of environmental fate of these compounds, detailed mass spectral studies of a number of the degradation products indicated an unexpected mass fragentation pattern. An unusal EI/MS alkyl radical cleavage of the alkoxy-methyl moiety was observed for norchloroalachlor and norchlorobutachlor derivatives, (4) and (5) (see Scheme 1).

Scheme 1

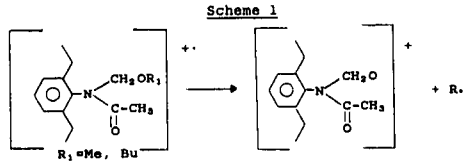

In order to accurately established mass fragmetational schemes of chloroacetanilides and related compounds to aid in the structural elucidation of unknown metabolites, various deuterium and carbon-13 labeled compounds were synthesized and examined by mass spectrometry.

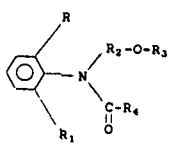

Compound	CP No.	Substituents R	R_1	R_2	R_3	R_4	
(1)	50144	Et	Et	CH_2	CH_3	CH_2Cl	alachlor
(2)	79756	Et	H	CH_2	CH_3	CH_2Cl	
(3)	53619	Et	Et	CH_2	n-Bu	CH_2Cl	butachlor
(4)	73905	Et	Et	CH_2	CH_3	CH_3	norchloroalachlor
(5)	^{13}C-73904	Et	Et	CH_2	n-Bu	$^{13}CH_3$	norchlorobutachlor
(6)	-	Et	H	CH_2	CH_3	CH_3	
(7)	d_3-50144	Et	Et	CH_2	CD_3	CH_2Cl	
(8)	d_2-50144	Et	Et	CD_2	CH_3	CH_2Cl	
(9)	d_2-79756	CH_3CD_2	H	CH_2	CH_3	CH_2Cl	
(10)	d_3-73905	Et	Et	CH_2	CD_3	CH_3	
(11)	d_2-73905	Et	Et	CD_2	CH_3	CH_3	
(12)	-	CH_3CD_2	H	CH_2	CH_3	CH_3	
(13)	d_3-73905	Et	Et	CH_2	CH_3	CD_3	
(14)	^{13}C-50144	Et	Et	CH_2	CH_3	$^{13}CH_2Cl$	

In addition, high resolution EI/MS as well as metastable ion analysis using the Direct Analysis of Daughter Ion (DADI) technique were applied to the fragmentational analysis of some compounds, (1) and (4).

The mechanism of the alkyl cleavage seems to involve a 1,5 hydrogen rearrangement (see Scheme 2), which was deduced from analysis of the fragmentations of the deuterium analogs (10), (11), and (13).

Scheme 2

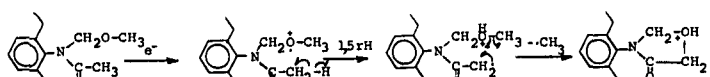

1. J. F. Olin, USP 3442945, 3547620.

The overall EI mass fragmentational scheme of chloroacetanilides and norchloroacetanilides is shown in Scheme 3.

Scheme 3.

EI-MS Fragmentation Scheme for Alachlor and Related Acetanilides as Defined by HR-MS, Isotopic Labelling and Metastable Ion Analysis

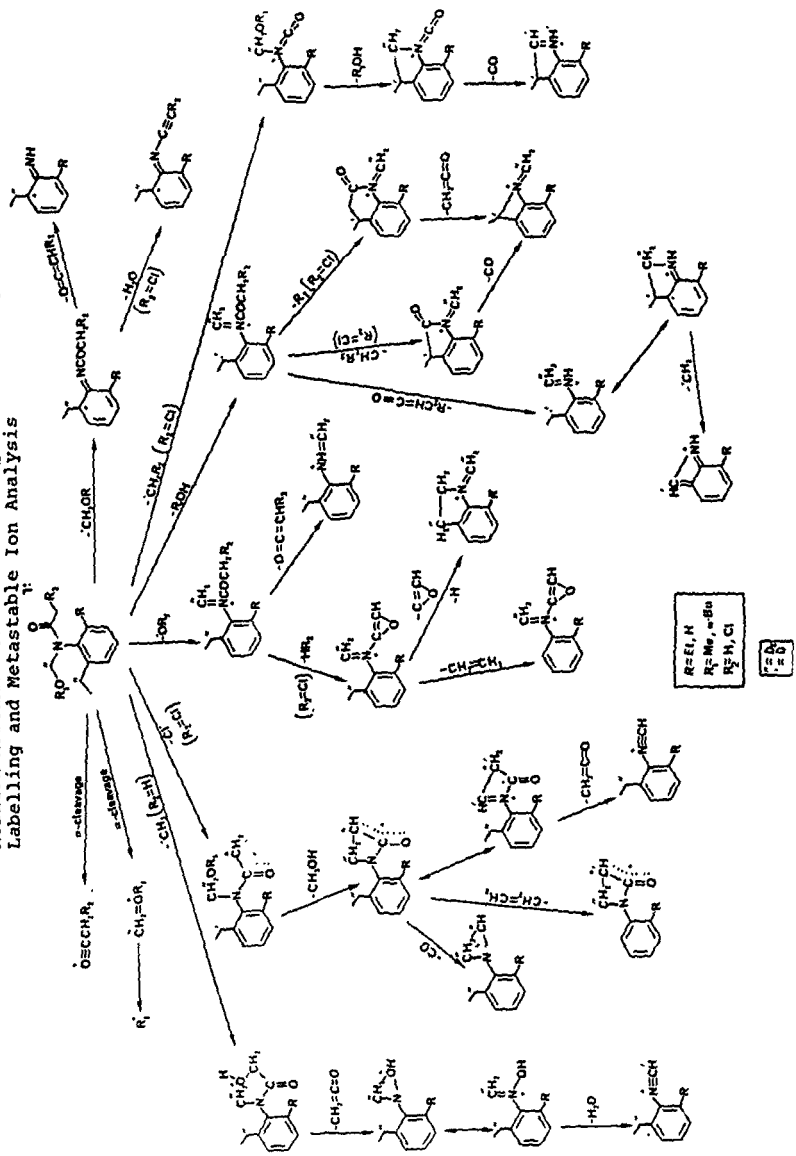

Presented at the 35th ASMS Conference on Mass Spectrometry and Allied Topics
May 24-29, 1987, Denver, CO

STUDY OF NON-AQUEOUS COLOR INDICATORS BY ELECTRON IMPACT, LIQUID SECONDARY ION, AND COLLISION-INDUCED DISSOCIATION MASS SPECTROMETRY

P. Jane Gale and Bryan L. Bentz

David Sarnoff Research Center

Princeton, New Jersey 08543-5300

We have characterized several chelated metal salts by electron impact (EI) and Liquid SIMS mass spectrometry. For some species of this type, the spectra obtained by both techniques give information on structure and molecular weight. Other compounds are thermally labile and decompose and/or exchange ligands during volatilization in the mass spectrometer ion source, rendering the EI spectra not very informative. Depending on the liquid matrix employed, sputtering need not induce decomposition. The Liquid SIMS spectra acquired by this technique using glycerol as a solvent/matrix in general contain strong signals for the preformed ions. Representative EI and Liquid SIMS spectra for tetramethylethylene acetoacetonate nickel (II) nitrate ($Ni^{II}TMENAcAcNO_3$) are shown in Figure 1. Structures assigned to the ions were confirmed by collisional dissociation of selected parent ions.

FIGURE 1. MASS SPECTRA OF $Ni^{II}TMENAcAcNO_3$

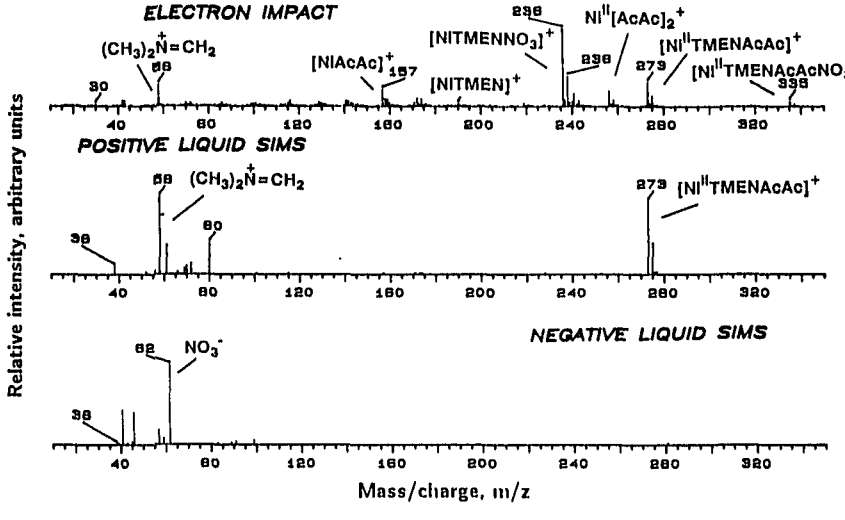

Because of their unusual solvation properties, several compounds of this type were synthesized in our laboratory for use as indicators of solvent nucleophilicity. They exist as brightly colored solids and retain that color in solvents with which they interact weakly or not at all (e.g., glycerol). In strongly electron-donating solvents they change color, owing to changes in the geometry of the complexes induced by incorporation of solvent molecules within the coordination sphere. Such changes were reflected in the Liquid SIMS spectra in which solvents other than glycerol were employed as the sputtering matrix. An example of such behavior is shown in Figure 2. $Cu^{II}TMENAcAcNO_3$ is a blue solid. It dissolves in glycerol to form a blue solution and yields the Liquid SIMS spectrum shown in 2a, in which the principal species observed is the intact cation, C^+. Dissolved in sulfolane, the complex retains its blue color, and a strong signal corresponding to C^+ is observed. Also present in the spectra, however, are complexes in which the solvent has been incorporated. When the compound is dissolved in thioglycerol, the solution turns yellow and gives the Liquid SIMS spectrum shown in 2c. The spectrum is dominated by a signal from the TMEN ligand ($TMENH^+$ at m/z 117). At much smaller intensities are ions related to solvated species. The dramatic changes in the ions observed in the Liquid SIMS spectrum are the analytical corollary of the visual cues to strong solvent/chelate interaction given by solution color changes. Such data provide a direct means for probing changes in chelate bond strengths following solvation.

FIGURE 2. LIQUID SIMS SPECTRA OF $Cu^{II}TMENAcAcNO_3$ OBTAINED IN THREE SOLVENT MATRICES

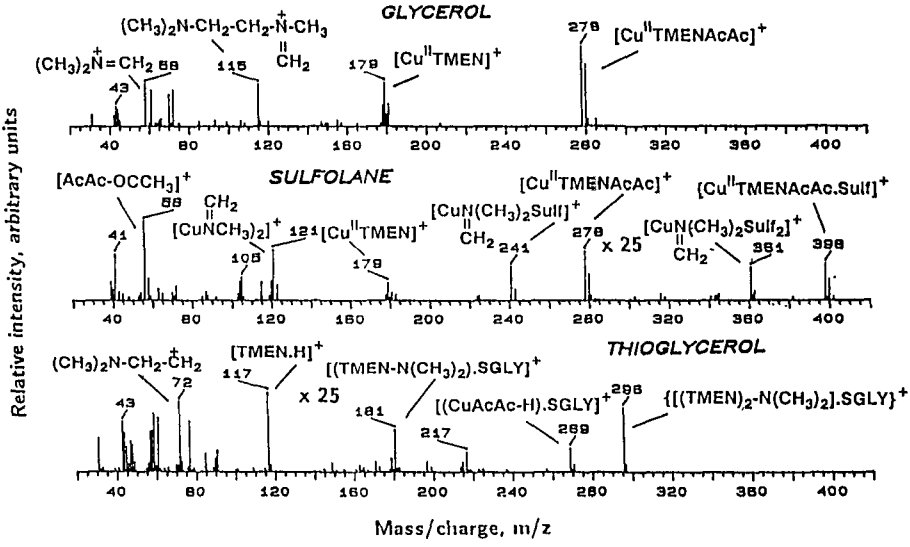

Presented at the 35th ASMS Conference on Mass Spectrometry and Allied Topics
May 24-29, 1987, Denver, CO

ENERGETICS OF CHARGE REMOTE FRAGMENTATION

V.H. Wysocki, M.E. Bier, and R.G. Cooks
Purdue University, West Lafayette, IN 47905

Recently, in a series of papers, Gross and coworkers have reported their investigations of a general type of fragmentation which they term remote site, or charge remote, fragmentation [1]. Either name conveys the principle characteristic of the process, namely the fact that bond cleavage is unaffected by the charge site, which does not participate in the reaction. It is explicit in the publications on this topic that the nature of the ionic group has no influence on the mechanism of remote site fragmentation and it follows that it should have no influence on its energetics.

Many of the reports of charge remote fragmentation have suggested that high (keV) translational energies are required to promote this type of fragmentation. Our interest in the energetics of ionic dissociation prompted the present study. Results of recent attempts to induce charge remote fragmentation by using low-energy collisional activation with neutral target gas or with a metal surface (surface-induced dissociation) are reported. Remote site fragmentation occurs in n-dodecylbenzenesulfonate upon activation by 30 eV collisions with argon atoms under multiple collision conditions. Stearyl sulfate shows a minor amount of remote site fragmentation under these conditions and requires much more vigorous conditions, 70 eV collisional activation with a surface, to produce a series of remote site fragment ions of 5-20% relative abundance (Figure 1). The stearate anion and protonated octadecylamine (Figure 2) show no detectable remote site fragmentation upon activation by collisions with argon (30 eV, multiple collisions) or a surface (30-100 eV). These data, in conjunction with information on internal energy deposition associated with these methods of activation [2], indicate the amount of internal energy needed to promote charge remote fragmentation. An internal energy deposition of more than 5 eV is required to observe charge remote fragmentation of n-dodecylbenzenesulfonate anion and stearylsulfate anion while more than 10 eV is required for charge remote fragmentation of both the stearate anion and protonated octadecylamine.

The results suggest that the internal energy required for remote site fragmentation is compound dependent. This implies in turn that the mechanism may be more complex than previously thought. Activation energies which are consistent with the high internal energy requirements described are either high or associated with large kinetic shifts. Additional mechanistic and thermochemical studies of charge remote fragmentation are highly desirable not only for linear compounds such as those investigated here, but also for biological compounds.

Presented at the 35th ASMS Conference on Mass Spectrometry and Allied Topics
May 24-29, 1987, Denver, CO

1. N.J. Jensen, K.B. Tomer, M.L. Gross J. Am. Chem. Soc. 1985, 107, 1863.

2. (a) V.H. Wysocki, H.I. Kenttämaa, R.G. Cooks Int. J. Mass Spectrom. Ion Processes 1987, 75, 181; (b) M.E. Bier, J.W. Amy, R.G. Cooks, J.E.P. Syka, P. Céja, G. Stafford Int. J. Mass Spectrom. Ion Processes 1987, in press.

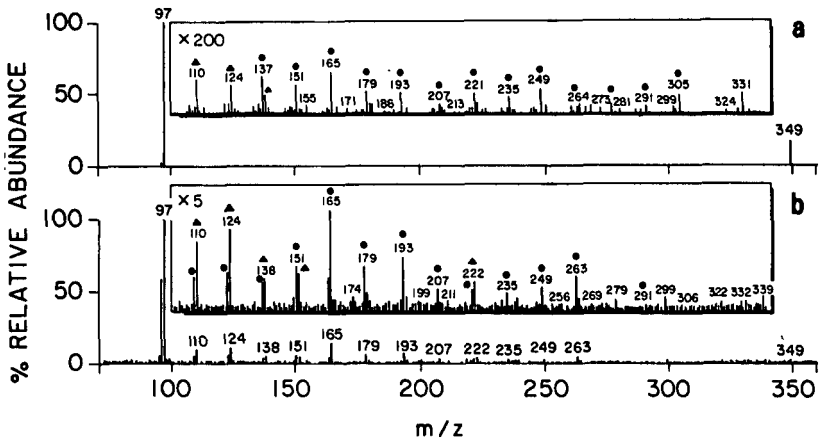

Figure 1. Daughter spectra of stearylsulfate anion (349^-) obtained by (a) collisional activation at 30 eV, multiple collision conditions and (b) surface-induced dissociation at 70 eV. (● indicates loss of C_nH_{2n+2}; ▲ indicates loss of C_nH_{2n+1})

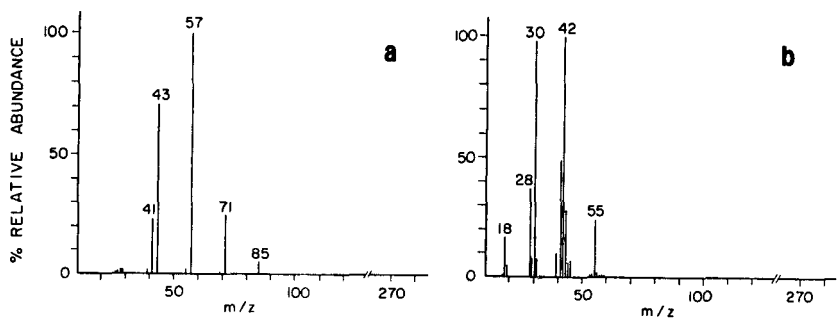

Figure 2. Daughter spectra of octadecylammonium cation (270^+) obtained by (a) collisional activation at 30 eV, multiple collision conditions and (b) surface-induced dissociation at 100 eV.

Presented at the 35th ASMS Conference on Mass Spectrometry and Allied Topics
May 24-29, 1987, Denver, CO.

WHAT FATTY ACID FUNCTIONAL DERIVATIVES UNDERGO CHARGE-REMOTE DECOMPOSITIONS?

L. J. Deterding
MCMS, Department of Chemistry,
University of Nebraska
Lincoln, NE 68588.

Fast atom bombardment (FAB) in conjunction with tandem mass spectrometry has become a useful approach for analyzing and characterizing a wide variety of fatty acids. In previous work (1), we showed that picolinyl ester derivatives of common fatty acids can be readily desorbed by FAB as positive ions and then collisionally activated. CA spectra of the $(M + H)^+$ ion of the derivatized fatty acids reveal that structurally informative remote-charge-site fragmentations occur. The probable mechanism is a process which involves 1,4-hydrogen eliminations with subsequent formation of terminally unsaturated picolinyl esters and neutral alkenes.

The $(M + H)^+$ ions desorbed from a variety of fatty acids, esters, amides, and other related compounds are collisionally activated and their decomposition spectra are compared. Protonated fatty acids (Fig. 1) fragment upon collisional activation to give abundant acylium ions $(M + H - H_2O)^+$ which then lose CO to give alkyl ( ) and alkenyl ( ) ions. Also formed is a series of $(C_nH_{2n-1}O_2)^+$ ions ( ) by losses of olefins. Protonated esters (Fig. 2) lose alcohols instead of water to give acylium ions, and ultimately the alkyl and alkenyl ( ) ions. In addition, fatty acid ethyl, propyl, and iso-propyl esters undergo the losses of the elements of C_nH_{2n} to give the abundant ion of m/z 229. This daughter ion may be regarded as arising from a McLafferty rearrangement. It should be noted that no remote-site fragmentation occurs.

The $(M + H)^+$ ions of primary, secondary, and tertiary amides fragment upon CA to undergo both charge-initiated fragmentations and remote-site decompositions ( ) (Fig. 3). The low mass ions can be assigned to the alkyl and alkenyl ion series. High mass fragment ions are produced by the losses of the elements of C_nH_{2n+2} from the $(M + H)^+$ ion. As substitution on the nitrogen on the amide group is changed from H to CH_3 to $(CH_3)_2$ or CH_2CH_3, the abundance of remote-site fragmentation increases from 16% to 22% to 27% or 25%. Because the N-ethyl amide can also undergo rearrangement to lose C_2H_4, this isomer can be distinguished from the N,N-dimethyl isomer. Stearanilide and stearic diethanolamide (Fig. 4) $(M + H)^+$ ions fragment upon CA to give ions corresponding to protonated aniline and protonated diethanolamide, respectively, as the most abundant ions. Remote-site fragmentation ( ) does occur, but these ions are of relatively lower abundance than the proximate-charge decompositions.

It appears that the proton affinity of the fatty acid functional derivative has a bearing on the decomposition of the $(M + H)^+$ ions of these derivatives. The increase of the proton affinity of the amide group (202-210 kcal/mol) over the ester group (187-193 kcal/mol) apparently results in an increase in the remote-site decompositions. Because the amides have a higher proton affinity, the charge is more tightly localized than on the ester derivatives, and losses of NH_3 or substituted amines are not favored because these losses shift the positive charge to a carbonyl group.

A variety of other fatty acid related compounds were also FAB-desorbed and collisionally activated. Fatty amines (Fig. 5) undergo the losses of the elements of C_nH_{2n+2}. These remote-site fragmentations ( ) continue until those daughter ions merge with the $(C_nH_{2n+1})^+$ and $(C_nH_{2n-1})^+$ ion series. $(M + H)^+$ ions of fatty alcohols (Fig. 5) give no remote-site fragmentations, but rather lose water to form $(C_nH_{2n+1})^+$ and $(C_nH_{2n-1})^+$ ions ( ). Also formed is a series of $(C_nH_{2n+1}O)^+$ ions ( ).

Since protonated amines give abundant remote-site fragment ions and protonated alcohols give none, these derivatives are used to bracket the internal energy requirements for charge-remote decompositions based on their proton affinities and various heats-of-formation. n-Butanol and n-butylamine are the model compounds used to estimate the energy requirements. The amount of energy required for n-butanol to fragment into $1\text{-}Bu^+$ and H_2O is 1.4 eV, and the energy requirement for n-butylamine to fragment into $1\text{-}Bu^+$ and NH_3

is calculated to be 2.7 eV. Because a protonated alcohol readily loses H_2O and a protonated amine does not lose NH_3 but rather undergoes charge-remote decompositions, the estimate for the internal energy required for remote-charge-site decompositions to occur is greater than 1.4 eV but less than 2.7 eV.

Acknowledgment: This research was conducted under the direction of Professor M. L. Gross.

Reference:

(1) L. J. Deterding and M. L. Gross, Anal. Chim. Acta, in press.

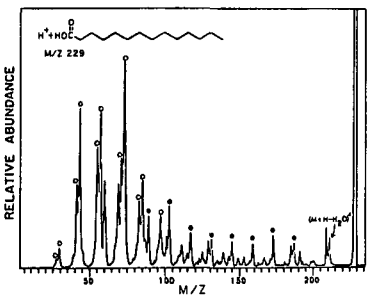

Figure 1

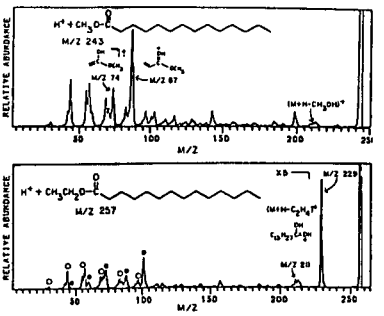

Figure 2

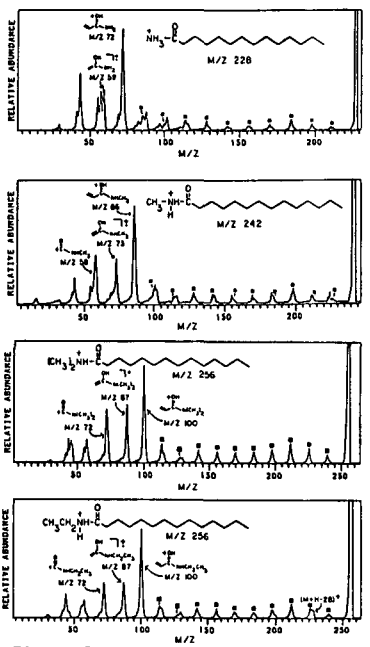

Figure 3

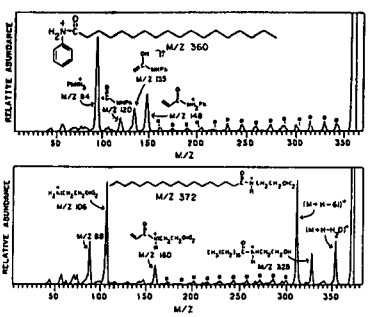

Figure 4

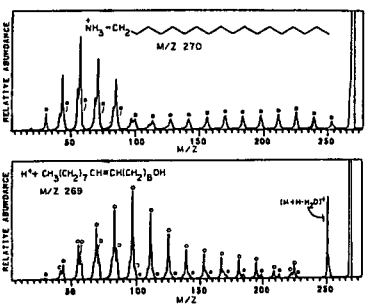

Figure 5

Presented at the 35th ASMS Conference on Mass Spectrometry and Allied Topics
May 24-29, 1987, Denver, CO

Collisional Activation of Li^+-Cationized Prostaglandins, Fatty Acid Esters, Sterols, and Vitamins

Jeanette Adams, Midwest Center for Mass Spectrometry, Department of Chemistry, University of Nebraska, Lincoln, NE 68588-0362

The $(M + 2Li - H)^+$ ions of prostaglandins and the $(M + Li)^+$ ions of fatty acid esters, sterols, and vitamins decompose by collisional activation (CA) to give structurally informative remote-charge-site fragmentations. The analytes are desorbed from the matrix 3-nitrobenzyl alcohol saturated with LiI, by using fast atom bombardment (FAB). A MS-50 Triple Analyzer (E_1B/E_2) is used for performing MS/CA-MS and CA-MS/CA-MS experiments.

For MS/CA-MS, FAB-desorbed parent ions are mass-selected by using E_1B and collisionally activated with helium in the 3rd field-free region between E_1B and E_2. Fragment ions are energy-analyzed by using E_2. For CA-MS/CA-MS, parent ions are collisionally activated in the 1st field-free region between the ion source and E_1, and fragment ions of interest are energy-selected by using E_1 and mass-selected by using B. The selected fragment ions are then collisionally activated in the 3rd field-free region, and decomposition ions are energy-analyzed by using E_2.

Prostaglandins. MS/CA-MS of $(M + 2Li - H)^+$ ions of prostaglandins produces decompositions unique for each prostaglandin. Two examples are shown in Figures 1 and 2. Low-mass ions **a-c** are formed by remote-charge-site cleavages of the carboxylate-containing hydrocarbon chain, and high-mass ions **1-9** are formed by losses of H_2O, LiOH, and either C_2H_4O or C_3H_8. MS/CA-MS of deuterium-labelled prostaglandins shows that the ions **5** (Figure 2) and **8** (Figure 1) arise primarily by cleavages through the ring (loss of C_2H_4O and losses of H_2O and C_2H_4O, respectively).

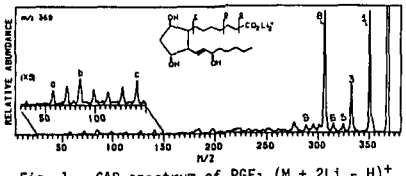

Fig. 1. CAD spectrum of PGF_1 $(M + 2Li - H)^+$ ions.

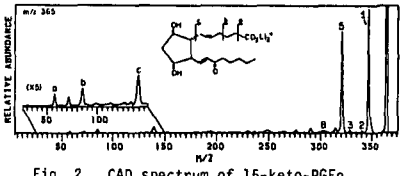

Fig. 2. CAD spectrum of 15-keto-PGF_2 $(M + 2Li - H)^+$ ions.

CA-MS/CA-MS of the high-mass fragment ions shows that the multiple neutral losses occur sequentially. In addition, CA-MS/CA-MS in conjunction with deuterium labelling also provides information for discerning the structures of and the mechanisms responsible for the fragment ions. For loss of C_3H_4O from 15-keto-PGF_2 (to give ion **5** in Figure 2), a mechanism that is consistent with deuterium labelling (loss of C_2H_3DO) and the CA decomposition spectrum of the fragment ion is shown in eq. 1.

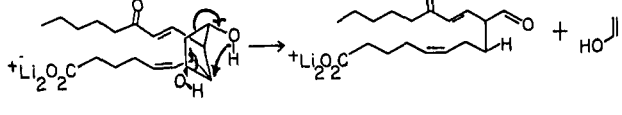

eq. 1

The decompositions shown here for prostaglandin $(M + 2Li - H)^+$ ions contrast with decompositions of $(M - H)^-$, $(M + Li)^+$, and $(M - H + Ca)^+$ ions. The latter three parent ions decompose to give less structural information, and no abundant low-mass ions analogous to those from the $(M + 2Li - H)^+$ ions are formed.

Presented at the 35th ASMS Conference on Mass Spectrometry and Allied Topics
May 24-29, 1987, Denver, CO

Fatty Acid Esters. MS/CA-MS of $(M + Li)^+$ ions of fatty acid esters produces remote-charge-site fragmentations analogous to those of $(M + Li)^+$ and $(M + 2Li - H)^+$ ions of fatty alcohols and acids, respectively (1-3). The examples shown in Figures 3-4 illustrate the usefulness of the technique for determining highly unsaturated and 2-hydroxy esters. This strategy is also useful for determining iso- and anteiso-branched, mono- and other polyunsaturated, 3-hydroxy and mid-chain hydroxy, and cyclopropane- and cyclopropene-containing esters.

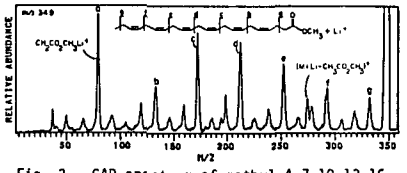

Fig. 3. CAD spectrum of methyl 4,7,10,13,16, 19-docosahexaenoate $(M + Li)^+$ ions.

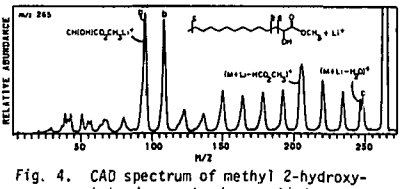

Fig. 4. CAD spectrum of methyl 2-hydroxy-tetradecanoate $(M + Li)^+$ ions.

Sterols. MS/CA-MS of $(M + Li)^+$ ions of sterols results in remote-charge-site decompositions that indicate structure of the alkyl side chain and, to a limited extent, structure of the cholestanol ring system (Figure 5). The $(M + Li)^+$ ions of cholestanones undergo decompositions that are similar to decompositions of the cholestanols.

Vitamins. MS/CA-MS of $(M + Li)^+$ ions of vitamins that contain a long alkyl chain produces remote-charge-site decompositions that provide structural information concerning the alkyl chain (Figure 6 shows vitamin K_1). Decompositions involving the highly conjugated ring system are not facile, however, and the most abundant low-mass ion (h) contains the intact conjugated ring.

The $(M + Li)^+$ ions of vitamins D_2 and D_3 undergo CA to give decompositions similar to decompositions of the cholestanols.

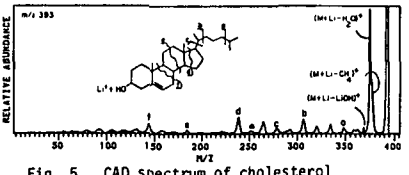

Fig. 5. CAD spectrum of cholesterol $(M + Li)^+$ ions.

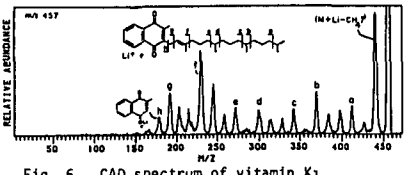

Fig. 6. CAD spectrum of vitamin K_1 $(M + Li)^+$ ions.

Acknowledgment. Thanks go to Drs. Rod Matthews and John Pike of Upjohn for supplying some of the prostaglandins, and to Michael L. Gross for invaluable suggestions.

Literature Cited

1. Adams, J.; Gross, M.L. J. Am. Chem. Soc. 1986, 108, 6915-6921.
2. Adams, J.; Gross, M.L. Anal. Chem. (in press).
3. Adams, J.; Gross, M.L. (submitted).

Presented at the 35th ASMS Conference on Mass Spectrometry and Allied Topics
May 24-29, 1987, Denver, CO

KINETIC ENERGY SPECTROSCOPY OF THE IODOMETHANE DICATION*

R.K.Boyd
Atlantic Research Laboratory, National Research Council,
1411 Oxford Street, Halifax, N.S., Canada B3H 3Z1

J.M.Curtis, A.G.Brenton and J.H.Beynon
University College, Swansea SA2 8PP, Wales, U.K.

Recent experimental and theoretical work (1)(2) has shown that monocations $(CH_3{-}{-}X)^{+\cdot}$, with C_{3v} symmetry, are of similar energies to those of the isomeric ylide forms, $(CH_2{-}{-}X)^{+\cdot}$. Similar theoretical treatments of the corresponding dications (3)(4), for cases where X involves first-row elements (OH or F), suggests that in this case the ylide forms may be more stable.

As part of our continuing investigations of small symmetrical dications, we have investigated the molecular dication of iodomethane using techniques of ion kinetic energy spectroscopy (MIKES, VG Analytical ZAB-2F spectrometer). The dications were generated by electron ionization (70 eV, 200 C) in a conventional Nier-type source, accelerated through 8kV, mass-selected by the magnet, and their spontaneous and collision-induced dissociations studied in a time-window some 5-10 microsec. after formation.

Apart from losses of H atoms, the only reactions observed were: (i) charge-separation reaction to $(CH_3^+ + I^+)$; two channels, separated by 0.9 eV in the respective k.e. release values, were observed (Fig.1); (ii) formation of I^{2+} dication (plus presumably $CH_3\cdot$) in a process again involving two channels (Fig.2), one with large values for both collisional energy loss and k.e. release and the other with much smaller values for both parameters.

It seems appropriate, at least for these dissociation channels, to attempt an interpretation in terms of the C_{3v} structure, since neither reaction of these long-lived ions suggests an ylide structure for those ions observed to dissociate. This conclusion is not necessarily valid for the much shorter-lived ions studied previously (5) using synchrotron radiation to form the ions, with photoion-photoion coincidence (PIPICO) detection (charge separation reactions only). Also, the theoretical results (3)(4) for X = F, for example, may not be valid for the X = I case.

Accordingly we have attempted an interpretation in terms of electron configurations established by photoelectron spectroscopy, within the C_{3v} point group. The strong spin-orbit coupling approximation appropriate to the I atom required that the extended C_{3v}* point group be employed. It is not useful to attempt a summary of this discussion in the space available, and this will be published in full elsewhere. Note that the composite peak shape observed for the I^{2+} channel (Fig.2) is similar to that observed previously (6)(7)(8) for the analogous reaction of the iodomethane monocation, and suggests a similar interpretation; this will also be discussed more fully in the complete account of this work.

(1) Bouma et al., J.Am.Chem.Soc. 104 (1982) 2930.
(2) Holmes et al., Can.J.Chem. 61 (1983) 2305.
(3) Bouma and Radom, J.Am.Chem.Soc. 105 (1983) 5484.
(4) Maquin et al., J.Chem.Soc.Chem.Commun. (1984) 504.
(5) Dujardin et al., Chem.Phys. (in press).
(6) Weber et al., Org.Mass Spectrom. 16 (1981) 514.
(7) Mukhtar et al., Int.J.Mass Spectrom.Ion Phys. 42 (1982) 77.
(8) Appling et al., Org.Mass Spectrom. 17 (1982) 644.

* NRCC NO. 27659

Presented at the 35th ASMS Conference on Mass Spectrometry and Allied Topics
May 24-29, 1987, Denver, CO

FIGURE 1

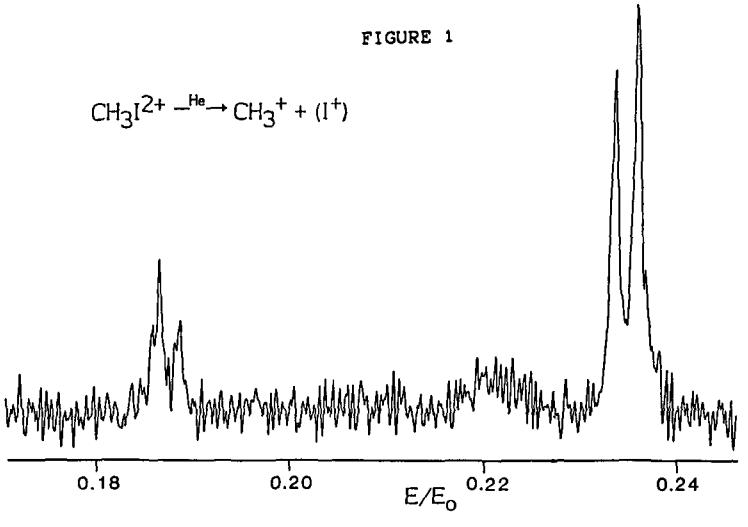

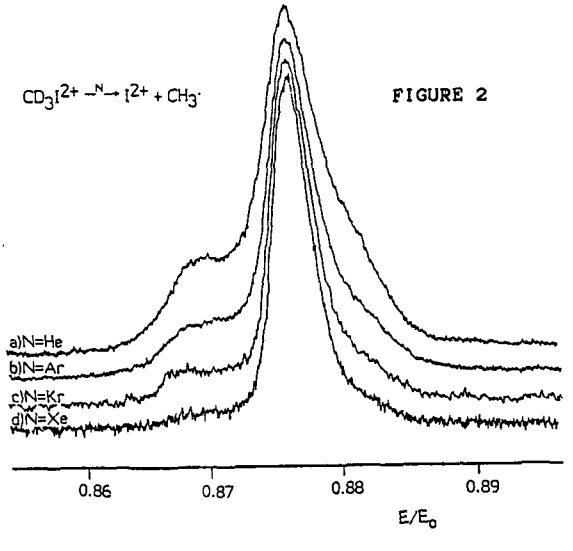

FIGURE 2

Presented at the 35th ASMS Conference on Mass Spectrometry and Allied Topics
May 24-29, 1987, Denver, CO

REACTION-INTERMEDIATE MASS SPECTROMETRY

D.E. Giblin and R.W. Holman
Midwest Center for Mass Spectrometry
Dept. of Chemistry, University of Nebraska,
Lincoln, NE 68588-0304.

INTRODUCTION

Reaction-intermediate mass spectrometry (RIMS) is a form of MS-MS-MS in which are analyzed the intermediate daughter ionic species between a parent and a second-generation mass-selected ionic species[1]. The technique thus provides a tool for elucidating ionic structures and decomposition pathways. RIMS is capable of providing high-resolution spectra of the intermediate ionic masses but it provides only low selectivity of the parent and final product masses[2].

INSTRUMENTATION

RIMS has been implemented on a modified Kratos MS-50TA. Both collision cells are employed for high-energy (8kV) collisional activation or unimolecular decompositions. Daughter ions formed from a mass-selected parent ionic species at the first collision cell are mass analyzed by a linked B/E_1 scan. From those daughter ions are formed a second generation of daughter ions at the second collision cell. Only ions of a specific mass are then passed through the second ESA, which is held at a constant potential, the value of which depends on the ratio of the masses of the final product to parent ionic species. This is possible because the accelerating potential is held constant.

To make RIMS possible on the Kratos MS-50TA required modifications not only to allow that mode of operation but also to improve the instrumental performance in the linked B/E_1 scan which is an integral part of the RIMS mode of operation.

RIMS is invoked as a variant of the regular B/E_1 linked scan. To decouple ESA_2 from ESA_1, the MIKES Manual mode is engaged simultaneously with the B/E_1 linked scan on the Metastable Control Unit. The potential of ESA then is set by the Width control to the value $E_2 = (m_3/m_1)E_{2,0}$ where m_3 and m_1 the masses of the final product and parent ionic species and $E_{2,0}$ is the normal potential on ESA_2. The selection of the parent mass and operation of the linked B/E_1 scan are standard. Since the simultaneous operation of MIKES Manual with B/E_1 linked scan decouples ESA_1 from the magnetic field tracking circuitry, a switch was added to restore tracking between ESA_1 and the magnetic field.

The improvement of instrumental performance of the B/E_1 linked scan required several modifications of the MS-50TA to correct for design deficiencies.

The first problem involved the compromise of the accuracy of the tracking of the magnetic field by the first ESA because of significant offset voltages generated by the operational amplifiers used in the tracking circuitry. Those amplifiers were replaced by precision units which have ultra-low offset voltages about three orders of magnitude less than the original units.

A second significant problem involved the potentials on the Y and Z deflectors, which are located after the first collision cell. The deflection potentials for these deflectors and for the source focus plates, which are located before the collision cell, were driven from a common inverter supply. This supply and the inverter supply for the Y focussing potential were keyed to follow the source accelerating potential. If these potentials as adjusted by their various source controls were not near electrical neutrality, severe and progressive loss of the beam of daughter ions occurred during a linked B/E_1 scan because the kinetic energy of the daughter ions decreases with decreasing fragment mass. To correct the problem, separate inverter supplies for the Y and Z deflection and Y focussing potentials were built. To key these supplies to follow the potential of the first ESA, modifications were made to the Source Reference

board and control wiring in the Source Control Unit.

A third problem was that the potentials on the hexapoles also were keyed to follow the source accelerating potential. This tracking problem could cause resolution degradation during a linked B/E_1 scan. The problem was corrected by changing cables such that the Hexapole Control Unit was keyed into the reference chain of the first ESA.

A further improvement of instrumental performance involved the adapting of the current-regulated supply of the magnet to field control by using the output of the Hall probe of the Mass Marker along with modifications of the current regulator control board. As a result, the tracking of the magnetic field to an exponential scan law was improved hence mass assignment was made easier.

EXPERIMENTAL RESULTS

RIMS was employed to examine sequential decompositions resulting from CAD of several systems.

The first system involved CAD of 1-heptanol. The CAD spectra of the molecular ion, m/z 116, is dominated by the m/z 98 peak which results from a facile H_2O loss by a modified McLafferty rearrangement. Analysis by RIMS of the decomposition pathways between the molecular ion and species of m/z ratios of 70, 69, and 56 indicates that each of the product ions results from the fragmentation of m/z 98 species. The final fragments correspond respectively to losses of C_2H_4, $C_2H_5\cdot$, and C_3H_6 from the m/z 98 species.

Sequential decompositions resulting from CAD of 1-tetralol were studied. The CAD spectra of the molecular ion, m/z 148, shows major fragments at m/z 130, 120, 105, and 91. RIMS was performed for intermediate species between the molecular ion and the fragments with m/z ratios of 115, 105, and 91. The results show that the m/z 130 fragment ion is the major intermediate between the m/z 148 and m/z 115 species. The sequential decompositions are a H_2O loss followed by a $CH_3\cdot$ loss. The m/z 120 fragment is the major intermediate between the molecular ion and both the m/z 105 and m/z 91 fragments. It is derived from the molecular ion by cycloreversion and decomposes further by $CH_3\cdot$ loss or by H· and CO loss. The m/z 147 fragment that is formed from the molecular ion by H· loss appears to be an intermediate on minor routes to the m/z 115 and m/z 105 fragments and on a major route to the m/z 91 species. In addition, ions of m/z 130, 119, and 92 appear as intermediates on minor routes to m/z 91. These decomposition pathways for 1-tetralol are consistent with previous data[3], but RIMS has allowed much easier access to this information.

RIMS was used to examine a decomposition pathway of the benzene 2-iodopropane binary adduct, m/z 248, formed in a CI source. That route was from m/z 248 to m/z 121 by reductive elimination of I· to produce a likely arenium ion, which can lose C_3H_6 to form m/z 79.

These few studies have shown the utility of RIMS in elucidating the decomposition pathways of ions resulting from CAD. The technique would also be useful in determining ionic structures.

REFERENCES

[1]R.G. Cooks, L.G. Wright and J.R. O'Lear, 34th Annual Conference ASMS, Cincinnati, 17 (1986).

[2]A. Fraefel and J. Seibl, Mass Spectrom. Rev., 4(2), 151 (1985).

[3]M.L. Gross, E. Chiu, D. Pokorny and F.L. DeRoos, Org. Mass Spectrom., 12(2), 55 (1977).

Presented at the 35th ASMS Conference on Mass Spectrometry and Allied Topics
May 24-29, 1987, Denver, CO

A TRIPLE QUADRUPOLE MASS SPECTROMETER WITH FACILITIES FOR CONSECUTIVE RECORDING OF NORMAL AND METASTABLE SCANS

D. Charles Smith, and Derek Swain V.G. MassLab., Manchester, England

David M. Hindenlang and R. Donald Sedgwick, Allied-Signal Inc.
Morristown, NJ 07960

The VG Mass Lab 30.250T triple quadrupole mass spectrometer described here was recently installed at Allied-Signal in Morristown, NJ. This machine acted as the prototype for the Trio 3 range of spectrometers. Two 3000 mass range quadrupole filters with pre- and post-filters, act as the mass resolving elements Q1 and Q3 as shown in the figure below. Q2 is an RF-only collision gas cell for inducing ionic dissociations at energies up to 200eV. The instrument provides a choice of EI, CI FAB and thermospray ionization modes and a variety of inlet systems including GC and LC. Both positive and negative ion operations are available under data system control The 30-250T also has a novel arrangement of two off-axis collectors located at the exits of Q1 and Q3 respectively. Use of collector #1 permits recording of normal single quadrupole mass spectra. Use of collector #2 permits recording of single quadrupole mass spectra resolved in either Q1 or Q3 with the other two elements operating in the RF only mode. The two ion detectors are of a new design utilizing an off-axis conversion dynode, an electron activated phosphor and a sealed photomultiplier tube.

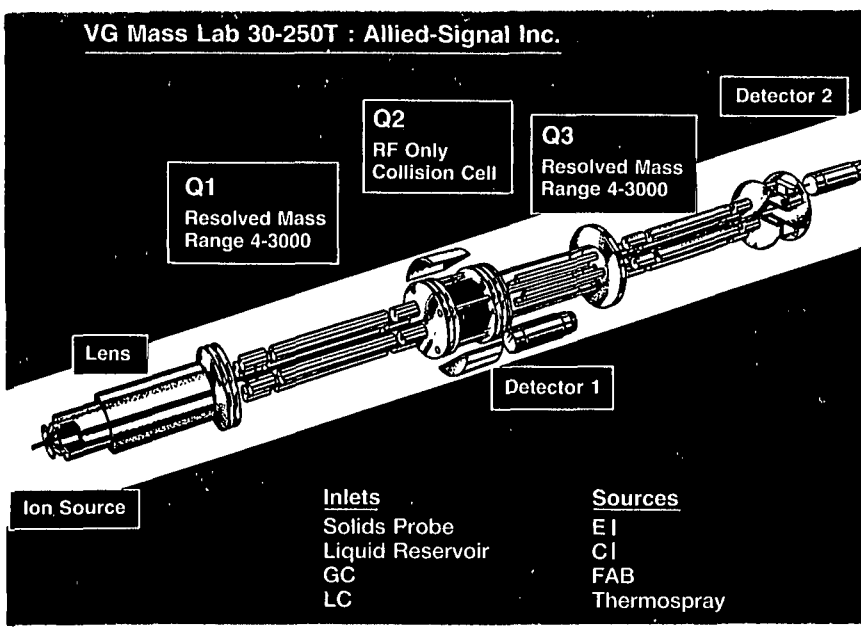

Integrated computer control of both scanning elements permits operation of the instrument in three metastable detection modes with collision energies up to 200ev with variable gas pressures in Q2, the RF only element. Daughters of a single parent ion, parents of a single daughter and common neutral loss scans all rely on signal detection at collector #2. Normal single quadrupole spectra can be detected at collector #1 independent of the pressure of gas in the collision cell (Q2). The instrument is thus capable of being scanned in six modes as shown in the following table.

MS	Q1	Det. 1	Q3	Det. 2
1. Normal MS	Scan DC/RF	On	–	Off
2. Single MS	RF	Off	Scan DC/RF	On
3. Single MS	Scan DC/RF	Off	Scan DC/RF	On
MS-MS	**Q1**	**Det. 1**	**Q3**	**Det. 2**
4. Daughters	Fix DC/RF	Off	Scan DC/RF	On
5. Parents	Scan DC/RF	Off	Fix DC/RF	On
6. Neutral Loss	Scan DC/RF	Off	Scan DC/RF	On

Combination of computer control of scanning functions and collector switching permits sequential recording of unperturbed normal spectra detected at collector #1 followed by a change to any metastable mode with detection at collector #2 without the need to change the conditions in the collision cell. Facilities are available to set up a repetitive cycle of up to twenty different scans consisting of normal or metastable modes with varying parameters in any order. This allows, for example, recording of normal spectra in both positive and negative ion modes together with a variety of associated MS-MS scans in a repetitive sequence limited only by the scan repetition rate. Computer acquired scans are labelled according to the relevant scan functions and can be displayed in isolation or combination with other scan functions.

We have found that operations of Q1 with detector 1 is independent of the conditions of Q2 and Q3 including the gas pressure in Q2. Spectra are identical with those from similar single quadrupole instruments. The off-axis detectors eliminate neutral particle noise.

Instrument tuning is under computer control with a split screen analogue display of up to four scan ranges for monitoring of peak shape, mass resolution and ion intensities. This feature allows observation of performance of both quadrupole filters in isolation for MS operations or in combination for MS-MS operations. The software system is menu driven and includes graphic displays of instrument status.

We have used these facilities to record, for example, a normal EI+ scan of the pesticide DDE followed by a daughter ion scan of the molecular ion, a parent ion scan of the $(M-Cl_2)^+$ ion and a neutral loss scan for elimination of Cl_2 in a repetitive cycle lasting 4 seconds. Alternatively longer scan times (10 sec) are appropriate for FAB ionization and we have found a combination of normal scans in both positive and negative ionization modes followed by daughter ion scans from $(M+H)^+$ and $(M-H)^-$, repetitively, to be an efficient use of peptide samples for structural determination.

Presented at the 35th ASMS Conference on Mass Spectrometry and Allied Topics
May 24-29, 1987, Denver, CO

ANALYSIS OF NITROGEN COMPOUNDS IN REFINERY PROCESS STREAMS BY THE USE OF AMMONIA CHEMICAL IONIZATION GC/MS.

I.DZIDIC, M.D.BALICKI AND H.V. HART
SHELL DEVELOPMENT COMPANY, HOUSTON, TX.

There is a continuing demand for improved methods for the analysis of nitrogen compounds in refinery process streams since the knowledge about nitrogen compounds is useful for the further treatment and use of these refinery stocks. The analysis of nitrogen compounds in a highly complex hydrocarbon matrices is not an easy task and generally requires extensive separation and isolation procedures prior to the identification by various spectroscopic techniques.

In order to minimize sample preparation and improve quantification, we have recently applied an ammonia chemical ionization method which is selective for the analysis of nitrogen compounds in hydrocarbons samples. The selective detection of protonated nitrogen containing molecular ions, MH^+, in combination with the use of an internal standard allows for quantification by this technique.

Figures 1A and 1B show the electron impact and NH_3/CI total ion chromatograms of catalytically cracked clarified slurry oil. While a peak due to the internal standard, 9-phenylcarbazole is observed in both chromatograms it is clear that the higher selectivity of detection for this compound is observed in the NH_3/CI chromatogram. For example, paraffinic hydrocarbons exhibited in the electron impact chromatogram (C_{19}-C_{29}) are not ionized and detected in the NH_3/CI chromatogram, and therefore, do not interfere with the detection of nitrogen compounds. The selective detection of carbazole and its alkyl homologues in the slurry oil sample by NH_3/CI is shown in Figure 2. The observation of the MH^+ ions at m/z 168,182,196,210, and 224 is an indication that carbazole and its C_1-, C_2-, C_3-, and C_4- alkyl homologues are present in this sample. The identity of carbazole was confirmed by the use of a standard.

The detection of C_2-alkyltetrahydroquinolines and/or C_3-dihydroindoles, and alkyl anilines in the polar kerosine fraction is shown by the NH_3/CI spectrum in Figure 3. Relative concentrations of the major nitrogen compound types in hydrocarbon samples can be obtained from the relative intensities of the corresponding MH^+ ions. Table 1 shows the relative percent concentrations of the major nitrogen compound types identified in two kerosines produced under different catalytic conditions. The difference in the hydrotreating conditions is evident from the relative concentrations of different nitrogen compound types in the two fuels.

The above examples illustrate that it is possible to obtain a detailed analysis of nitrogen compounds in refinery process streams by the use of the NH_3/CI GC-MS technique.

GC/MS Chromatograms of Slurry Oil from a West Coast Refinery

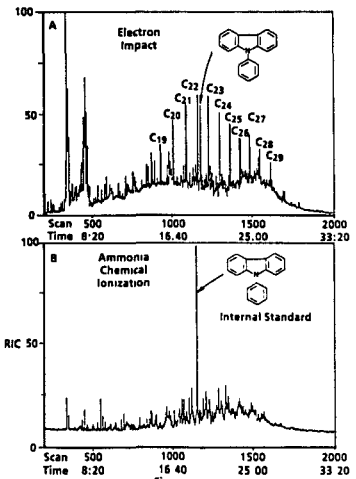

Figure 1

Detection of Nitrogen Compounds in the West Coast Slurry Oil by Selected Ion Monitoring of MH+ Ions

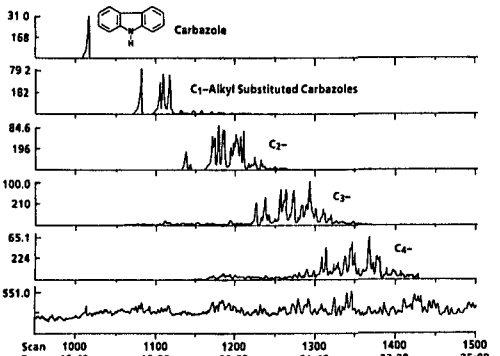

Figure 2.

Ammonia Chemical Ionization Mass Spectrum of the Kerosine Fuel Polar Fraction Exhibits the MH+ Ions of the Nitrogen Compounds

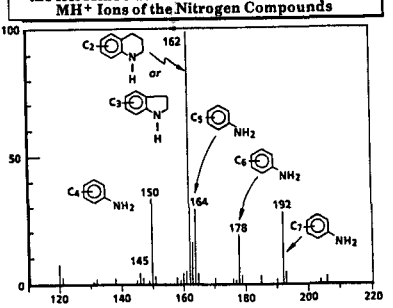

Figure 3.

Relative Concentrations of Nitrogen Compound Types in Two Kerosine Fuels*

Mol Wt.	Atomic Composition	Identity	% of Total	
			Kerosine-A	Kerosine-B
170	C_2H_8N	C_2 Pyridines	0 8	-
121	$C_8H_{11}N$	C_1-Pyridines	3 1	-
135	$C_9H_{13}N$	C_2-Pyridines	6 0	-
149	$C_{10}H_{15}N$	C_3-Pyridines	1 9	-
163	$C_{11}H_{17}N$	C_4-Pyridines	1,7	-
177	$C_{12}H_{19}N$	C_5 Pyridines	1 7	-
191	$C_{13}H_{21}N$	C_6 Pyridines	1 4	-
		Total	15 6	0 0
203	$C_{14}H_{21}N$	C_1 Cyclohexyl Pyridines	0 7	-
217	$C_{15}H_{23}N$	C_2 Cyclohexyl Pyridines	2 3	-
231	$C_{16}H_{25}N$	C_3-Cyclohexyl Pyridines	12 1	0 5
245	$C_{17}H_{27}N$	C_4-Cyclohexyl Pyridines	4 5	2 5
259	$C_{18}H_{29}N$	C_5-Cyclohexyl Pyridines	2 8	1 6
273	$C_{19}H_{31}N$	C_6 Cyclohexyl Pyridines	1 2	1 1
287	$C_{20}H_{33}N$	C_7 Cyclohexyl-Pyridines	0 2	0 5
		Total	23 9	6 2
121	$C_8H_{11}N$	C_1 Anilines	0 1	0 4
135	$C_9H_{13}N$	C_2 Anilines	2 1	2 6
149	$C_{10}H_{15}N$	C_3 Anilines	1 0	7 6
163	$C_{11}H_{17}N$	C_4 Anilines	5 0	7 9
177	$C_{12}H_{19}N$	C_5-Anilines	4 3	5 8
191	$C_{13}H_{21}N$	C_6-Anilines	2 7	3 1
205	$C_{14}H_{23}N$	C_7 Anilines	1 7	1 5
		Total	16 9	28 9
143	$C_{10}H_9N$	C_1-Quinolines	0 5	-
157	$C_{11}H_{11}N$	C_2-Quinolines	4 0	-
171	$C_{12}H_{13}N$	C_3Quinolines	8 0	0 6
185	$C_{13}H_{15}N$	C_4-Quinolines	7 4	1 9
199	$C_{14}H_{17}N$	C_5 Quinolines	5 6	2 0
213	$C_{15}H_{19}N$	C_6 Quinolines	3 1	2 4
227	$C_{16}H_{21}N$	C_7-Quinolines	1 5	1 8
241	$C_{17}H_{23}N$	C_8 Quinolines	0 4	1 3
		Total	30 5	10 0
147	$C_{10}H_{13}N$	C_2 Dihydroindoles/ C_1 tetrahydroquinolines	1 3	-
161	$C_{11}H_{15}N$	C_3-Dihydroindoles/ C_2 tetrahydroquinolines	3 8	5 9
175	$C_{12}H_{17}N$	C_4-Dihydroindoles/ C_3 tetrahydroquinolines	3 8	12 8
189	$C_{13}H_{19}N$	C_5-Dihydroindoles/ C_4 tetrahydroquinolines	2 1	13 7
203	$C_{14}H_{21}N$	C_6-Dihydroindoles/ C_5 tetrahydroquinolines	1 0	12 4
217	$C_{15}H_{23}N$	C_7-Dihydroindoles/ C_6 tetrahydroquinolines	-	7 8
231	$C_{16}H_{25}N$	C_8-Dihydroindoles/ C_7-tetrahydroquinolines	-	2 4
		Total	12 0	55 0

Presented at the 35th ASMS Conference on Mass Spectrometry and Allied Topics
May 24-29, 1987, Denver, CO

AN IMPROVED HYBRID MASS SPECTROMETER FOR COLLISIONALLY ACTIVATED DISSOCIATION STUDIES:

J.E. Curtis, A. Kamar and R.E. March, Department of Chemistry, Trent University, Peterborough, Ontario, Canada and U.P. Schlunegger, Department of Chemistry, University of Bern, Switzerland.

In 1984, a novel hybrid mass spectrometer (EBQiQa) was described [1] as being composed of an AEI MS-30 mass spectrometer with electrostatic analyzer, ESA1, and magnet, B, (EB) to which had been appended a QUISTOR (quadrupole ion store, Qi) and a quadrupole mass filter (Qa). While the MS-30 mass spectrometer was a single beam version of the usual double beam instrument, the spacious detector housing was unchanged and could accommodate a QUISTOR mounted in place of the normal source of a quadrupole mass filter. The QUISTOR was oriented so as to allow the ion beam to pass diagonally through the ion trap. The axis of cylindrical symmetry of the QUISTOR-quadrupole combination was directed at an angle of 125° to the incoming ion beam. Ions produced by electron impact were selected sequentially in the MS-30 operated at 4kV and directed into the QUISTOR. A pulsed gas valve was employed to created pressure pulses of collision gas with which the ions suffered multiple collisions. The subsequent loss in momentum permitted a fraction of the ions to be stored in the QUISTOR.

Described here is an improved hybrid mass spectrometer in which the following changes have been made: the collision gas flow is now constant rather than pulsed and is directed into a collision cell of length 10cm; and a spectrum selector has been incorporated into the detector housing. The spectrum selector is a standard stationary feature of a normal double beam MS-30 instrument. One beam is directed through a hole drilled lengthwise through the main block of the selector; the second beam is directed through a small electrostatic analyzer (ESA 2) across the plates of which a fixed potential is applied so as to deflect the ion beam onto the second detector. The entire selector has been separated from its normal mounting flange and remounted in a movable seating as shown in Fig.1, so that the single ion beam may be deflected through ESA 1 and onto a standard detector. External adjustment brings about a lateral displacement of the selector such that the ion beam is now directed through the cylindrical channel in the selector block. Collision gas is fed to the mid-point of the channel so as to pressurize the collision cell.

Mass spectra observed conventionally as a result of collision induced dissociation (CID) are highly discriminatory in that fragment ions produced only in glancing dissociative collisions, and retaining an appropriate fraction of parent ion energy, are detected and contribute to CID spectra. Observation of high energy processes is favoured in angle resolved (0.5-1°) spectra [2-4], and detectable changes in fragmentation patterns have been observed in such spectra in comparison to those of conventional CID spectra. In the hybrid instrument described here, a collisionally thick helium target gas is used to interface the high kinetic energy components of the MS-30 instrument to the low kinetic energy quadrupole components. Ions mass-selected in the MS-30 suffer multiple collisions in rapid succession and are scattered over a wide range of angles though not displaced appreciably from the path of the collision-free ion beam. Dissociation and deceleration of projectile ions produce thermalized fragment ions. When the thermalization step which reduces fragment ion kinetic energy to less than 10eV occurs within the QUISTOR, the fragment ion is stored. Stored ions may be accumulated selectively, for ion monitoring, or non-selectively. Similarly, both the ejection of stored ions and external detection of stored ions my be accomplished non-selectively or mass-selectively.

A Monte-Carlo simulation model, used previously to investigate the effect of charge exchange collisions on the motion of ions (single-ion model [5,6] and two-ion model [7] in a QUISTOR, was extended [1] to simulate high kinetic energy ion/neutral collisions which may result in ion fragmentation. The study indicated that some 2% of 4keV projectile ions may be stored. Under optimum trapping conditions, it is estimated that from 0.5-3% of the incident projectile ions are stored.

There are several possible modes of operation of the hybrid instrument depending on the position of the spectrum selector; thus the ion beam is either deflected or directed. EI mass spectra can be obtained with a magnet scan when the ion beam is deflected onto the detector. Similarly, and somewhat surprisingly, ions directed into the QUISTOR can be deflected by a large negative DC potential on the bottom endcap; the ions pass through the quadrupole mass filter operating in the total ion mode to yield an EI mass spectrum. A psendo-EI mass spectrum can be obtained when collisionally thermalized projectile and fragment ions are intermittently ejected from the QUISTOR with the mass filter operating in the total ion mode. When the MS-30 is operated in mass-selective mode, pulsed ejection of stored ions into the quadrupole mass filter operating in the scanning mode yields a CID mass spectrum of the mass-selected ion. It was observed that a fraction of some mass-selected molecular ions survive collisional thermalization intact.

The location of ESA 2 after the magnet permits the observation of unimolecular fragmentation occurring between these sectors [8,9]. The potential across the plates of ESA 2 was scanned manually to yield a mass-selected ion kinetic energy spectrum in fair agreement with that reported by Beynon et al. [10].

Fig. 1

Detector Housing

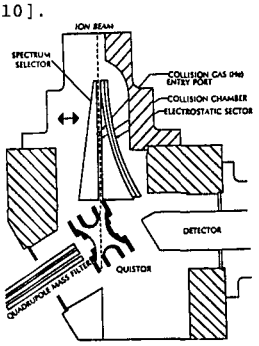

Acknowledgement

The authors gratefully acknowledge the assistance of David W. Priddle (University of Toronto) in obtaining the spectrum selector, the financial assistance of the Natural Sciences and Engineering Research Council of Canada, and the Canada-Switzerland Exchange Program of the National Research Council of Canada.

References

1. M.Ho, R.J.Hughes, E.M.Kazdan, P.J.Matthews,A.B.Young and R.E.March. Proceedings of the 32nd Annual Conference of the American Society for Mass Spectrometry, San Antonio, Texas, U.S.A., pp. 513-4 .
2. P.H.Hemberger, J.A.Laramee, A.R.Hubik and R.G.Cooks J.Phys. Chem.85(1981) 2355
3. E.E. Kingston,A.G.Brenton,R.K.Boyd, and J.H. Beynon, Int. J. Mass Spectrom, Ion Phys., 47 (1983)117.
4. S.A. McLuckey, S.Verma, R.G. Cooks, J.J. Farncombe, R.S. Mason and K.R. Jennings, Int. J. Mass Spectrom. Ion Phys., 48 (1983) 423.
5. R.F. Bonner, R.E.March, J.Durup, Int. J. Mass Spectrom Ion Phys.,22(1976)17
6. R.F. Boner, R.E.March, Int. J. Mass Spectrom Ion Phys., 25(1977) 411
7. M.C.Doran, J.E.Fulford, R.J.Hughes, Y.Morita and R.E.March, Int.J. Mass Spectrom. Ion Phys., 33 (1980) 139.
8. J.M. Miller and G.L. Wilson, Int. J. Mass Spectrom.Ion Phys., 12(1973)225.
9. J.M. Miller, J. Ross, J. Rustenberg, G.L. Wilson, Anal.Chem.,45(1973) 627
10. C.J.Porter, J.H. Beynon and T.Ast, Org. Mass Spectrom 16(1981) 101.

Presented at the 35th ASMS Conference on Mass Spectrometry and Allied Topics
May 24-29, 1987, Denver, CO

IMPROVED SCANNING MODES USING A MULTIQUADRUPOLE MS/MS/MS INSTRUMENT

Claude BEAUGRAND and Gérard DEVANT, S.N.NERMAG, 49 quai du Halage, F 92500 RUEIL-MALMAISON, Daniel JAOUEN, Nicole MORIN and Christian ROLANDO, Ecole Normale Supérieure, Département de Chimie, 24 rue Lhomond, F 75231 PARIS CEDEX 05

With an MS/MS/MS spectrometer seven scanning modes are available as described by R.G.Cooks (1). Preliminary results reported last year at ASMS have shown the potentialities of an MS/MS/MS instrument (2) using three quadrupole analysers and two RF-only quadrupolar collision cells (2) . All the results were obtained using the most classical mode of scanning : first analyser fixed, second fixed and the third scanned. Our main investigations were the different possibilities opened by the various uses of the RF-only collision chambers (dissociation, reaction, non dissociative collision). A very specific use of this instrument is the study of reactive collisions. We report here the possibilities opened to this approach by the various scanning modes.

The reaction of $Fe(CO)^+$ with isobutane was chosen in order to examplify the scanning modes. All the following spectra are displayed with full resolution of the interfaces (about 22 points per mass unit) and are not tabulated in order to show the exact resolution of the instrument. The observed results are in agreement with literature data (ref 3).

Q_1 FIXED Q_2 SCAN Q_3 NON-RESOLVING or Q_1 FIXED Q_2 NON-RESOLVING Q_3 SCAN

Main use : obtention of classical MS/MS spectrum from the triple quadrupole analyser MS/MS/MS instrument

Example : reaction of $Fe(CO)^+$ with isobutane

Experiment :

SOURCE	FIRST ANALYSER	FIRST CELL	SECOND ANALYSER	SECOND CELL	THIRD ANALYSER
$Fe(CO)_5$	m/z 84 $Fe(CO)^+$	isobutane REACTION	SCAN m/z 50,200		RF-only

or

SOURCE	FIRST ANALYSER	FIRST CELL	SECOND ANALYSER	SECOND CELL	THIRD ANALYSER
$Fe(CO)_5$	m/z 84 $Fe(CO)^+$	isobutane REACTION	RF-only		Scan m/z 50-200

Remark : the two analysers give identical spectra and have the same unitary resolution .

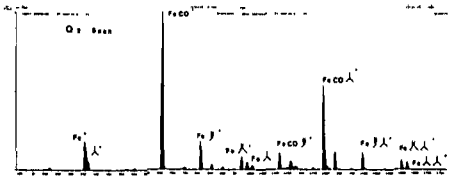

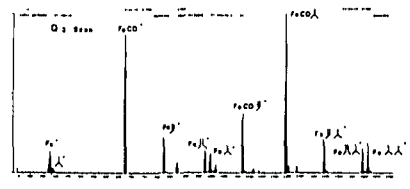

Q_1 FIXED Q_2 FIXED Q_3 SCAN

Main use : determination of the structure of a product from reactive collision

Example : structure of ion m/z 142

Experiment :

SOURCE	FIRST ANALYSER	FIRST CELL	SECOND ANALYSER	SECOND CELL	THIRD ANALYSER
$Fe(CO)_5$	m/z 84 $Fe(CO)^+$	isobutane REACTION	m/z 142	Argon CAD	Scan m/z 50-200

Conclusion : From the CAD spectrum showing mainly one fragment at m/z 84 attributed to $FeCO^+$, the structure of ion m/z 142 is likely : $Fe(CO)isobutane^+$.

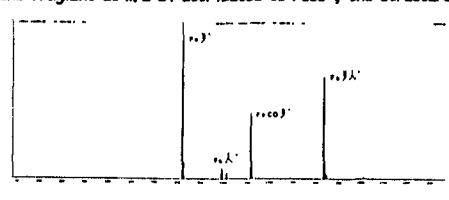

Q_1 FIXED Q_2 SCAN Q_3 FIXED

Main use : determination of all the reaction products containing a stable ligand

Example : determination of all the ions liganded to propene

Experiment :

SOURCE	FIRST ANALYSER	FIRST CELL	SECOND ANALYSER	SECOND CELL	THIRD ANALYSER
$Fe(CO)_5$	m/z 84 $Fe(CO)^+$	isobutane REACTION	SCAN	Argon CAD	m/z 98 $Fe(propene)^+$

Conclusion : The ligand researched is present principally in the ions m/z 126 and m/z 156. The most probable structures for these ions are $Fe(CO)propene^+$ and $Fe(propene)isobutane^+$ respectively.

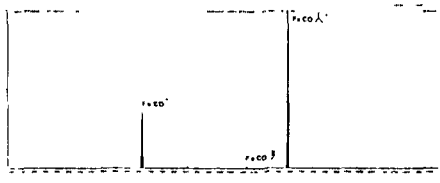

Q_1 SCAN Q_2 FIXED Q_3 FIXED

Main use : determination of all the reactive ions in source leading to a specific product ; this can be applied to understanding of processes involved in chemical ionisation.

Example : determination of all the ions in source reacting whith isobutane to give $Fe(CO)isobutane^+$. The product is characterised by the transition from m/z 142 to m/z 84 during CAD.

Experiment :

SOURCE	FIRST ANALYSER	FIRST CELL	SECOND ANALYSER	SECOND CELL	THIRD ANALYSER
$Fe(CO)_5$	SCAN	isobutane REACTION	m/z 142 $Fe(CO)isobutane^+$	Argon CAD	m/z 84 $Fe(CO)^+$

Conclusion : All the carbonylated iron species $Fe(CO)_n^+$ (n=1 to 5) present in the source are reactive. We can notice also the reactivity of doubly charged ions.

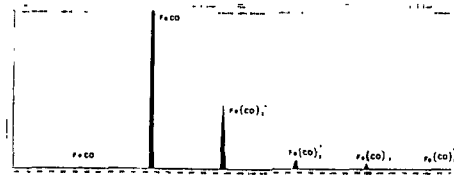

Q_1 FIXED Q_2 SCAN linked Q_3 SCAN

Main use : determination of all the reaction products containing a labile ligand

Example : determination of all the ions liganded to isobutane

Experiment :

SOURCE	FIRST ANALYSER	FIRST CELL	SECOND ANALYSER	SECOND CELL	THIRD ANALYSER
$Fe(CO)_5$	m/z 84 $Fe(CO)^+$	isobutane REACTION	SCAN	Argon(CAD) linked(-m/z 58)	SCAN

Conclusion : Among the ions containing the investigated ligand we can notice ions m/z 114, 142, 156, 170 and 172. The most probable structures for these ions are $Fe(isobutane)^+$, $Fe(CO)isobutane^+$, $Fe(propene)isobutane^+$, $Fe(isobutene)isobutane^+$ and $Fe(isobutane)_2^+$ respectively.

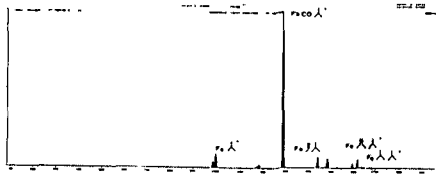

References : (1) J.N.Louris, L.G.Wright, R.G.Cooks and A.E. Schoen, Anal.Chem., 57, 2918(1985).
(2)C. Beaugrand, G. Devant, D. Jaouen and C.Rolando, Int. J. Mass Spectrom. Ion Processes, in press.
(3) B.S. Larsen and D.P. Ridge, J.Amer.Chem.Soc, 106, 1912 (1984).

Presented at the 35th ASMS Conference on Mass Spectrometry and Allied Topics
May 24-29, 1987, Denver, CO

POST-SECTOR BEAM DEFLECTION IN TIME-RESOLVED ION MOMENTUM SPECTROMETRY (TRIMS) AND ITS USE WITH TIME ARRAY DETECTION (TAD) FOR MS/MS MAP ACQUISITION

B.A. Eckenrode, B.H. Newcome, J.F. Holland, C.G. Enke
Departments of Chemistry and Biochemistry,
Michigan State University, East Lansing, MI 48824

Time-resolved ion momentum spectrometry (TRIMS) is achieved by measuring flight times of ions through a modified magnetic sector mass spectrometer (1). For a particular apparent mass (m*), ions that have undergone collisionally activated dissociation or those that have metastably dissociated in the first field-free region of a single sector mass spectrometer have a slower velocity than stable ions that might appear at the same mass setting. Employing only a magnetic sector instrument, the spectra of stable ions and metastable ions are superimposed. By time encoding the ion beam of a modified LKB-9000 magnetic sector mass spectrometer, separate observation of stable ions and daughter ions at a particular magnetic field value (ion momentum) is possible. The daughter ions will have the flight time of their parent (m_1) and a mass determined by $(m_1 m^*)^{1/2}$. TRIMS, therefore, can provide the complete MS/MS data field in one sweep of the magnet.

Two techniques have been explored for time encoding the ion beam; source pulsing and post-sector beam deflection. The method of source pulsing utilizes ion source trapping with pulsed extraction (2). Unfortunately, it was observed that to achieve good time resolution, a high extraction voltage is necessary, but this results in poor magnetic field resolution. Conversely, to achieve good momentum resolution, a low extraction voltage is needed, but the time resolution suffers.

In the present configuration post-sector beam deflection is employed to allow good resolution in both momentum and time. An LKB-9000 mass spectrometer was modified by adding a deflection assembly and a flight tube for time-of-flight analysis of the ions (see Fig. 1). With post-sector beam deflection the resolution along both axes (B and T) improved as well (both ~500 m/Δm). As shown in Fig. 2, accurate ion intensity profiles from which energy distributions can be obtained are now produced by this instrument.

Source pulse mode yielded a detection limit for the molecular ion of n-decane of 2μg (S/N = 5). Under similar conditions, post-sector beam deflection yielded a detection limit of 13ng (S/N = 5).

TRIMS WITH TIME-ARRAY DETECTION

The real advantage of TRIMS is now realized because of the high data acquisition rate of the integrating transient recorder (ITR) (3). With the ITR attached to the TRIMS instrument a complete MS/MS map on the time scale of a chromatographic peak can now be achieved.

In time-of-flight, each ion pulse produces a complete arrival time spectrum (transient). Since the ITR "monitors" the ion current in each transient with 5ns resolution over an 80usec range, the flight time spectrum from each pulse is recorded. A variable number of transients can be summed at each magnetic field setting.

Fig. 3 shows a plot of the total ion current versus scan number for n-decane. In order to collect the complete MS/MS data field, 1280 scans were taken for n-decane at regular intervals along the magnetic field axis. The ITR summed 200 transients at each momentum setting to improve the signal-to-noise ratio for each scan. The three scans shown were selected from among the 1280 scans collected in only 30 seconds.

Future work will involve both developing algorithms for post-processing the full data field and further reducing the time required for a complete map.

Presented at the 35th ASMS Conference on Mass Spectrometry and Allied Topics
May 24-29, 1987, Denver, CO

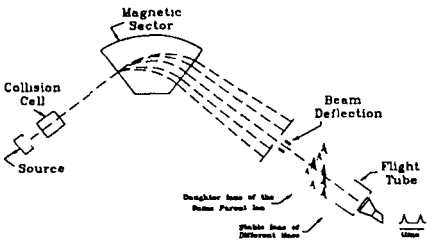

Fig. 1. Schematic diagram of the TRIMS instrument showing the post-sector deflection and flight tube modifications.

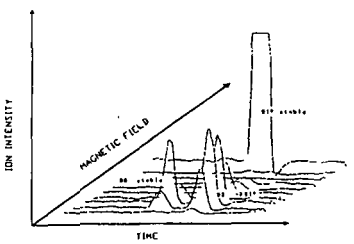

Fig. 2. TRIMS data field for the molecular ion region of toluene. Successive time sweeps along the momentum axis showing the 90 and 91 stable ions separated from the 91 daughter of the molecular ion of toluene.

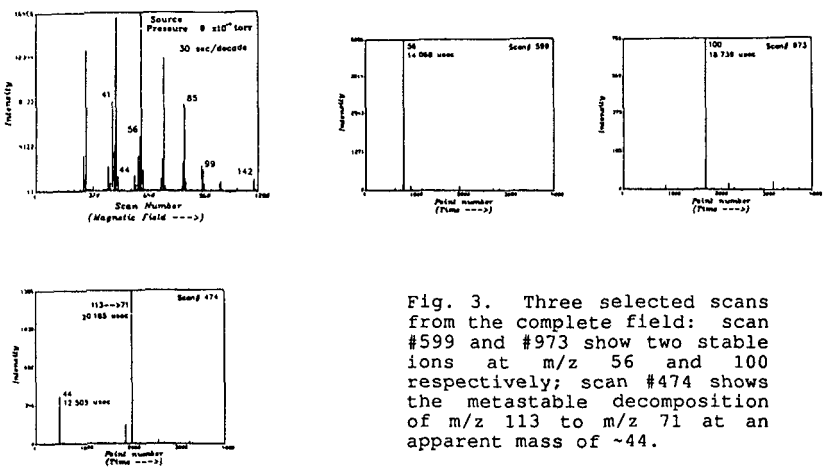

Fig. 3. Three selected scans from the complete field: scan #599 and #973 show two stable ions at m/z 56 and 100 respectively; scan #474 shows the metastable decomposition of m/z 113 to m/z 71 at an apparent mass of ~44.

REFERENCES
(1) Stults, J.,Enke,C. ,Holland,J. Anal. Chem., 55, 1983.
(2) Stults, J.,Holland,J.,Watson, J.T.,Enke,C. Int. Jour. Mass Spec. Ion Proc., 71, (1986).
(3) Newcome B.,Erickson,E.,Yefchak,G.,Davenport,M.,Holland, J. ASMS Cincinnati, June 8-13, 1986.

Presented at the 35th ASMS Conference on Mass Spectrometry and Allied Topics
May 24-29, 1987, Denver, CO.

Resonant Two-Photon Ionization of Leu- and Met-Enkephalin Using Pulsed Laser Desorption in Supersonic Beam Mass Spectrometry

Liang Li and David M. Lubman

Department of Chemistry
The University of Michigan
Ann Arbor, MI 48109

Resonant two-photon ionization (R2PI) has been used as an ionization source with several unique features for mass spectrometry. R2PI has generally been shown to be a soft ionization tool where the parent ion can be produced with efficiencies that may range up to several percent or higher within the laser beam during the pulse. In addition, as the laser beam power density is increased, extensive fragmentation is produced which can be varried as a function of the laser power thus affording greater control over fragmentation as compared to CI, EI and other ionization methods. The truly unique property of R2PI is the potential for wavelength selectivity. In R2PI molecules can be selectively ionized in a mass spectrometer based upon their broad absorption in the near UV or visible. Supersonic jet expansions have been used to increase selectivity by ultracooling of the internal modes of large molecules to produce sharp spectral features. Previous R2PI studies have generally been limited to reasonably volatile systems, but has been recently applied to nonvolatile and thermally labile molecules using pulsed laser desorption.

In this work we have studied the laser induced MPI of leu- and met-enkephalin which are two important neurotransmitters in the brain. The experimental apparatus consists of a supersonic beam time-of-flight mass spectrometer (1,2). Laser desorption is performed using a CO_2 laser mildly focussed onto a ceramic surface on which the sample is coated. The sample is situated on a Macor machinable ceramic rod located about 4 mm downstream of the jet orifice and 4 mm from the molecular beam axis. Upon desorption, the plume of organic neutral molecules is entrained into a pulsed supersonic jet pulse of CO_2 carrier gas. The actual sequence of events is controlled by several delay generators where the pulsed CO_2 laser fires first to produce desorption followed by the pulsing of the jet injection valve. The two events are synchronized in time so that the desorbed plume is entrapped in the jet and carried into the acceleration region of the TOFMS. Another delay generator is timed to pulse the UV ionization laser as the jet reaches the mass spectrometer. Laser R2PI is produced and the mass spectrum is recorded by a Lecroy 9400 digital oscilloscope. In this work the ionization frequency is the 4th harmonic of the Nd:YAG laser which generates 266 nm radiation. The typical laser energy is 10-15 mJ which is required to induce fragmentation.

The fragmentation patterns obtained for leu- and met-enkephalin by using laser desorption/R2PI technique are shown in figure a and b with the corresponding structural assignments. There are several salient common fragmentation characteristics observed in these compounds and also the smaller di-, tri- and tetra-peptides examined in our work. In each case a molecular ion M^+ is observed without any apparent cationization in the mass spectrum. The molecular ion (M^+) can further absorb UV photons to produce a fragmentation pattern which can be related to the structure of the peptide These characteristic fragments include the various sequence of acylium and aldimine-type ions as well as β-cleavage at the tyrosine and phenylalanine side chains. The results obtained by LD/MPI complement the data obtained by other techniques such as FAB/CAD and LD for assignment of the structure of these peptides. Moreover, LD/MPI has the potential to provide a degree of spectroscopic selectivity based upon the gas-phase wavelength absorption of radiation. In addition, it does not have the background problems of FAB at low mass since it does not require a glycerol matrix nor does it have the sample preparation difficulties of FD.

Presented at the 35th ASMS Conference on Mass Spectrometry and Allied Topics
May 24-29, 1987, Denver, CO

References

1. Tembreull, R.; Lubman, D.M Anal. Chem. 1987, 59. 1082

2. Lubman, D.M.; Tembreull, R. Anal. Instrum (Advances in Time-of-Flight Mass Spectrometry, Campana, J., Ed.), 1987, 16, 117.

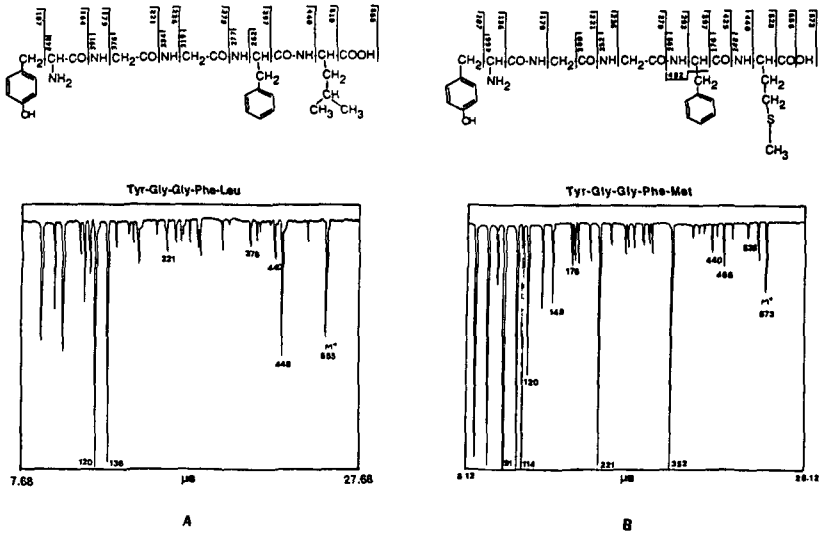

Figure a LD/MPI ionization-fragmentation pattern at λ = 266 nm of leu-enkephalin.

Figure b LD/MPI ionization-fragmentation pattern at λ = 266 nm of met-enkephalin.

Presented at the 35th ASMS Conference on Mass Spectrometry and Allied Topics
May 24-29, 1987, Denver, CO

Ion Source Design for Thermospray™ LC/MS

J.D.Buchner, R.C.Willoughby, S.N.Ketkar, R.J.Madden, Extrel Corporation, Pittsburgh, PA. 15238

Considerable debate has occurred recently concerning the benefits of electrostatic elements in the ion source region of Thermospray™ ionizers. Although it is not possible to focus an individual ion in a point to point fashion within the viscous flow region of the TSP ionizer, electrostatics can be used to increase the density of ions at the sampling point and therefore increase ion sampling yield. A source was designed and evaluated which incorporates isolated and independently variable retarding grid, repeller, concentric transfer tube (CTT) and sampling aperture (figure 1).

A solution of Polypropylene glycol (PPG), 70 ppm in 50 % MeOH and 50 % 0.1 M NH_4OAc was thermally nebulized into the ion source at a flow rate of 2 ml/min. It was observed that ion energy with respect to the mass filter was determined by the voltage applied to the sampler. The axial ion energy chosen for this study was 16.4 volts. The repeller, retarding grid, and CTT could be varied to direct and stop ions without effecting peak shape and resolution.

With the retarding grid, CTT, and sampler all fixed at 16.4 V, the repeller exhibited a singular maximum across all masses at 16 - 17 volts. This maximum represents the best overall tune with respect to total ion sampling within this study.

When the voltage applied to the retarding grid is tracked independently or together with the repeller, keeping the CTT and the sampler at 16.4 V, a bimodal optimization is observed. The maximum current is still derived when both the repeller and repeller and retarding grid is 16 - 17 V, however the retarding grid when floated independently has a secondary maximum at 160 Volts (figure 2). When these voltage profiles for both optima are subjected to ion trajectory modeling, we find that indeed a convergent situation exists, at the sampler, when a singular energy for the ions is assumed.

The CTT also exhibits bimodal optimization with respect to higher mass ions within the glycol series. When the CTT and retarding grid are both fixed at voltages corresponding to their individual secondary maximum, and then the repeller varied from -100 to +200 volts, we observe the total ion current is only 50 % of the previous maximum yield tune but that high mass yield increases approximately 70 % at 600 m/z.

Therefore, we conclude that the repeller in this geometry of the source appears to have only limited utility relative to total ion sampling, when other source electrodes are optimized. However, tuning conditions may be derived, which favor mass ion sampling. Depending upon the fractional ion abundance distribution of the compounds of interest, this effect may be desirable or undesirable.

Thermospray is a trademark of Vestec Corp.

Presented at the 35th ASMS Conference on Mass Spectrometry and Allied Topics
May 24-29, 1987, Denver, CO

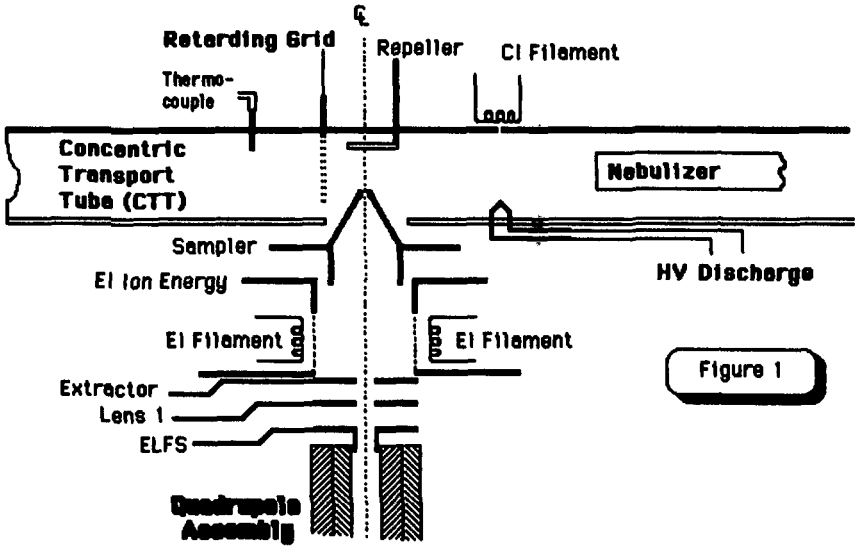

Figure 1

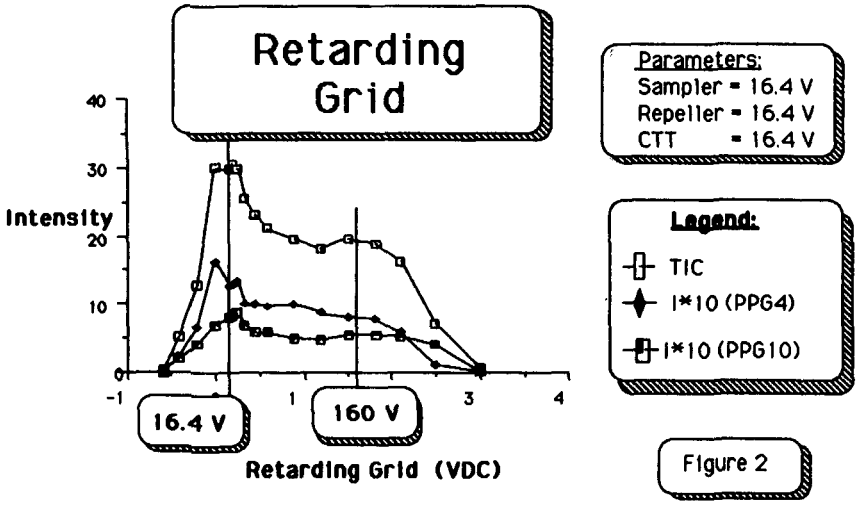

Figure 2

Presented at the 35th ASMS Conference on Mass Spectrometry and Allied Topics
May 24-29, 1987, Denver, CO

ION-ION RECOMBINATION REACTIONS INVOLVING SF_6 AND C_7F_{14}; EFFECTS ON ELECTRON CAPTURE MASS SPECTROMETRY RESPONSES

C.A. Valkenburg, L.J. Sears and E.P. Grimsrud
Department of Chemistry, Montana State University 59717

In the ion source of a high pressure (1 Torr) electron capture mass spectrometer (HPECMS), the rate of an electron capture reaction, Reaction 1, can be sufficiently fast as to destroy most of the analyte molecule, M, as it passes through the ion source. Neutralization of the negative ion M^- also occurs very rapidly by either contact with the ion source walls or by recombination with positive ions, Reaction 2. For a strongly responding compound, the steady-state concentration of M in the ion source will depend significantly on whether the molecule M is regenerated by neutralization, as shown in Reaction 2a, or is not, as shown in Reaction 2b. While the rate coefficients for ion-ion recombination reactions are well-known, no evidence concerning the products formed in ion-ion recombination reactions of polyatomic ions exists, to our knowledge.

The objective of this study was to develop a method by which the extent of molecular regeneration caused by positive ion recombination as shown in Reaction 2a could be determined. The molecular anions of SF_6 and C_7F_{14} (perfluoromethylcyclohexane) were chosen for this study due to several desireable characteristics of these well-studied negative ions. An additional objective was to demonstrate that the details of Reactions 2a and 2b for a given compound and its molecular anion can directly affect that compound's sensitivity of detection by HPECMS.

Measurements of electron capture and ion-ion recombination events for SF_6 and C_7F_{14} were performed using the specialized pair of identical, tandem Electron Capture Detectors (ECDs) shown in Figure 1. The atmospheric pressure effluent ($Ar/10\%CH_4$) from a packed-column gas chromatograph is passed through the two detectors. Low concentration samples of SF_6 and C_7F_{14} in nitrogen were introduced to the GC by a gas sampling loop. The responses of the two detectors to C_7F_{14} and SF_6 were monitored on a 2-pen recorder as shown in Figure 2. The dynamics occurring within these well-characterized, fixed-frequency, pulsed ECDs is adequately understood as to allow the average electron population, $\overline{N}_e$, existing within them to be deduced from the measured standing current, I. As shown in Figure 3, $\overline{N}_e$ can be varied at will by changing the frequency of electron-collecting pulses applied to the ECDs.

As can be seen in Figure 2, both SF_6 and C_7F_{14} are at least partially destroyed as they pass through the tandem ECDs. It can be shown that the expected ratio of peak area responses obtained from ECD 1 and ECD 2 for any molecule which undergoes Reactions 1, 2a and 2b will be given by: $(1-X)\cdot B = F/\overline{N}_e\ (Q_1/Q_2 - 1)$, where B is the electron capture rate constant, X is the tendency for molecular regeneration by Reaction 2a (X = 0 to 1), F is the carrier gas flow rate, $\overline{N}_e$ is the average electron population, and Q_1/Q_2 is the ratio of ECD 1 to ECD 2 peak area responses. Predictions of Q_1/Q_2 for any $(1-X)\cdot B$ product can be made for any magnitude of $\overline{N}_e$ selected by choice of pulsing frequency. Four predictions of this type are shown in Figure 4.

Typical measurements of Q_1, Q_2 and Q_2/Q_1 as a function of pulse period for SF_6 and C_7F_{14} are shown in Figure 5. It is seen that the SF_6 data in Figure 5 is most closely matched by the first prediction shown in Figure 4 where $(1-X)\cdot B = 3.0 \times 10^{-7}$ cc/sec. For C_7F_{14} the third prediction shown in Figure 4 where $(1-X)\cdot B = 3.0 \times 10^{-8}$ cc/sec most closely matches the experimental result in Figure 5. More detailed analyses of numerous experiments of the type shown in Figure 5 lead to the results summarized in Table 1. Also shown in Table 1 are independently measured[1] values of B for SF_6 and C_7F_{14} at 150 deg. C. With knowledge of B the magnitude of X for SF_6 and C_7F_{14} can be deduced. These are also listed in Table 1. It is seen that SF_6 tends to follow pathway 2b (X = 0.1) and is largely destroyed in the ion-ion recombination event while C_7F_{14} tends to proceed by way of pathway 2a (X = 0.75) and is largely regenerated by ion-ion recombination.

The sensitivity of HPECMS to strongly responding compounds is expected to depend significantly on the fate of a molecular anion upon neutralization. We would also expect this dependence to be amplified with use of higher filament emission currents and higher electron/positive ion densities. In Figure 6 the ratio of molecular ion intensities observed for a low-concentration, equimolar mixture of SF_6 and C_7F_{14} in methane is shown. It is seen that the intensity of the $C_7F_{14}^-$ signal relative to that of SF_6^- increases strongly as emission current is increased from very low levels to those normally used in HPECMS. It is noted that the response to C_7F_{14} can then exceed that of SF_6, inspite of the fact that the electron capture rate coefficient of SF_6 is 3 times greater. Also shown as the solid curve in Figure 6 is a prediction of this experiment based on a recently developed model[2] of HPECMS. In this model the values, $B = 1.2 \times 10^{-7}$ cc/s and X

= 0.75, were used for C_7F_{14} and B = 4.2 x 10^{-7} cc/s and X = 0.1 were used for SF_6. The predictions of this model are in good qualitative agreement with the experimental results.

1. D. Smith, N.G. Adams, and E. E. Alge, J. Phys., B17, 461 (1984), and E. Alge, N.G. Adams and D. Smith, J. Phys., B17, 3827 (1984). 2. L.J. Sears, J.A. Campbell and E.P. Grimsrud, Biomed. and Environ. Mass Spectrom., (to appear 1987).

$$e + M \longrightarrow M^- \quad (1)$$

$$M^- + P^+ \rightarrow M + \text{neutrals} \quad (2a)$$

$$M^- + P^+ \rightarrow \text{altered neutrals} \quad (2b)$$

X = fraction of M^- ions which react by pathway 2a to regenerate molecular species M

Figure 1. Tandem Electron Capture Detectors

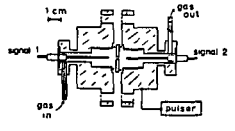

Figure 2. Typical Tandem ECD Responses

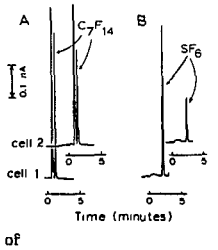

Figure 3. Selection of Electron Population by choice of ECD Pulse Frequency

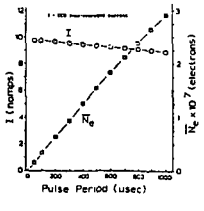

Figure 4. Predictions of Tandem Cell Responses

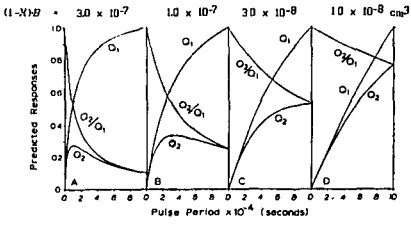

Figure 5. Typical Tandem Cell Results

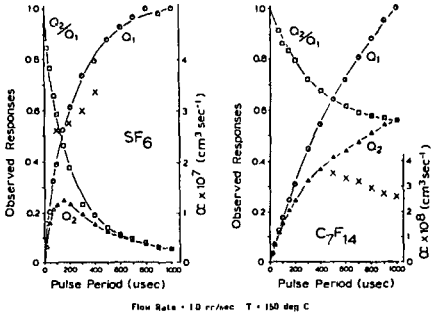

Figure 6. Relative HPECMS Responses to Equimolar Mixture of C_7F_{14} and SF_6 in Methane

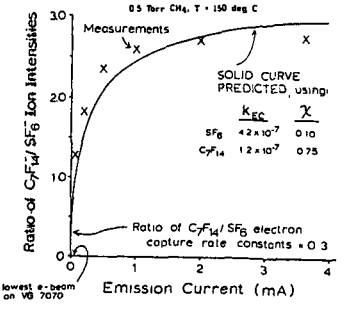

Table I. Summary of Results

	$(1-X)\cdot B$ (cc/s)	B $(cc/s)^1$	X
SF_6	3.7 (±1.1) x 10^{-7}	4.2 (±0.8) x 10^{-7}	0.1 (±0.3)
C_7F_{14}	3.0 (±0.8) x 10^{-8}	1.2 (±0.3) x 10^{-7}	0.75 (±0.10)

Presented at the 35th ASMS Conference on Mass Spectrometry and Allied Topics
May 24-29, 1987, Denver, CO

MASS DISCRIMINATION IN QUADRUPOLE MASS SPECTROMETERS USED AS MOLECULAR BEAM DETECTORS

Frank T. Greene, J. Eugene O'Donnell, and David Robaugh
Midwest Research Institute
425 Volker Boulevard
Kansas City, MO 64110

Molecular beam mass spectrometric (MBMS) measurements are often made of unstable, condensable, or highly reactive species for which direct calibration is not possible. Concentrations of these species must be calculated from measured intensities using first principles. Many of the errors which may occur and the corrections needed have been previously discussed by Greene.[1] In this study an additional error, which is attributed to inefficient extraction of ions resulting from momenta retained from the molecular beam, was observed.

Measurements were made of the apparent nitrogen to argon ratio along the axis of a methane/air flame using a molecular beam mass spectrometric system with an EAI quadrupole fitted with a simple electrostatic focusing ion source aligned with the analyzer axis both perpendicular to and coaxial with the molecular beam. Typical results are shown in Figure 1. The nitrogen argon ratios obtained in the cross beam mode show a dramatic drop with increasing gas temperature and hence beam velocity even though this ratio should be virtually constant. When the quadrupole was aligned in the axial mode, only a relatively small change in this ratio was observed which could be attributed to differential scattering or other effects for which no calibration was attempted. Approximately a factor of 10 increase in beam intensity for the hot gas was obtained using the axial mode. This effect was attributed to ion velocities transferred from the supersonic molecular beam.

Additional measurements were made using a calibration gas mixture which contained equal quantities of Ne, Ar, Kr, and Xe. This mixture was introduced into the burned gas region of a methane/air flame and the quadrupole adjusted to produce maximum sensitivity for the higher mass species in the hot gas beams. The combined ion extraction efficiency, ion transmission, and multiplier efficiency curves are shown in Figure 2. Significant discrimination is clearly present even with optimized focusing.

These data show that ion extraction efficiencies in quadrupole mass spectrometers used as molecular beam detectors can be affected by beam velocity. Calibration measurements should therefore be made using beams having comparable velocities as those encountered in the experimental measurements. The data also show that higher efficiencies can be obtained with quadrupole mass spectrometers oriented coaxially with the molecular beam, particularly when making measurements in high velocity beams.

[1] Greene, F. T., Twenty-Fifth Annual Conference on Mass Spectrometry and Allied Topics, p. 92, 1977.

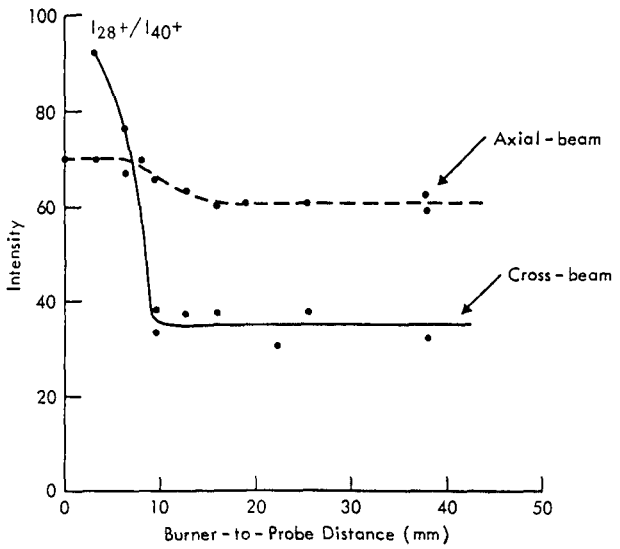

Figure 1 - Combined CO and N_2 Intensities Relative to Argon Obtained Along the Axis of a Premixed Methane-Air Flame Using a Quadrupole Mass Spectrometer in the Axial and Crossed Beam Modes

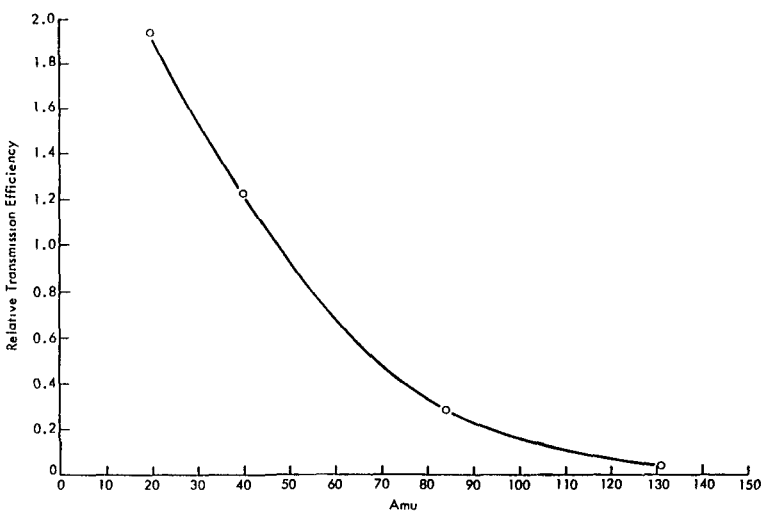

Figure 2 - Calibration Curve for Mass Discrimination of Quadrupole in Crossed Beam Mode

Presented at the 35th ASMS Conference on Mass Spectrometry and Allied Topics
May 24-29, 1987, Denver, CO

The Characteristics of a Multichannel Electro-optical Detection System and its Application to the Analysis of Large Molecules by Fast Atom Bombardment Mass Spectrometry.

John S. Cottrell* and Syd Evans
Kratos Analytical Instruments, Barton Dock Rd., Manchester M31 2LD, UK.

Scanning mass analysers, such as magnetic sectors or quadrupole filters, reject all but a small fraction of the ion current leaving the source region. This may be unimportant for specific experiments in which only a single mass or a limited number of mass channels needs to be monitored. But in the majority of cases, this inefficiency has a direct impact on detection limits, and parallel detection of a substantial portion of the mass spectrum would provide a very significant increase in sensitivity.

Studies of large molecules using FAB-MS would seem to be an ideal application for parallel detection, because many samples of biological importance are only available in minute quantities, and the detection limits for analysis by mass spectrometry compare unfavourably with those for competing techniques. Even when large amounts of sample are available, molecules in the mass range above 5000u generally produce only feeble molecular ion currents. An additional problem, unique to high mass work, is the necessity to scan very wide mass ranges, either because the molecular weight is not known, or in order to observe fragment ions.

We have designed and built an electro-optical "array" detector suitable for fitting to a Kratos MS50RF mass spectrometer. This detector provides simultaneous detection over a 4% mass window with sufficient gain to register the arrival of single ions. For high resolution work, a conventional detector with adjustable resolving slit may be exchanged for the array detector without breaking the vacuum.

Figure 1 is a schematic representation of the new detector. A pair of microchannel plates mounted in a chevron configuration is aligned with the mass spectrometer focal plane. Secondary electrons leaving the rear face of the MCP assembly are accelerated towards a phosphor screen coated onto the front of an extended fibre-optic faceplate. The fibre optic faceplate is sealed into the wall of the detector vacuum envelope so as to minimise the number of components inside the vacuum system. Butted against the output face of the fibre-optic faceplate is a model RL1024SF photodiode array (EG&G Reticon, Sunnyvale, CA.).

Using a narrow source slit, the detector limited resolution is greater than 5000 fwhm. Figure 2 shows the molecular ion region of the peptide substance P, $[MH]^+$=1348.7u, which is almost fully resolved. A limited region of this spectrum is also plotted with a scale expansion of X100 to illustrate the dynamic range of the detector, which can be seen to be well in excess of 1000. The useful working range of the detector is very much greater than the dynamic range because the exposure time can be varied from 10mS up to 10S or more.

The spectra in Figure 3 show the molecular ion region of bovine insulin, $[MH]^+$=5730.6u, obtained from a total sample loading of 1 picomole. The data in Figure 3a were taken from the array detector, while those in Figure 3b were taken from a standard post-acceleration detector, using an identical procedure. In both cases, the signal was integrated for 60 seconds, and the data have not been smoothed or processed in any way apart

from subtraction of the fixed pattern photodiode array noise. The width of the resolving slit on the single channel detector was approximately 600ppm against the array detector width of 40,000ppm. This would indicate a sensitivity advantage for the array detector of 40,000/600 = 67, resulting in an 8 fold improvement in ion statistical noise.

When large amounts of sample are available, the sensitivity advantage of an array detector may be used to reduce acquisition time. Using a single channel detector, a signal accumulation time of some 10 minutes was required to attain a reasonable signal to noise ratio in the molecular ion region of bovine proinsulin I. With the array detector, it was possible to obtain a similar spectrum in only 7 seconds (Figure 4). The measured centroid of the molecular ion cluster is 8681.83u, which is identical to the calculated value.

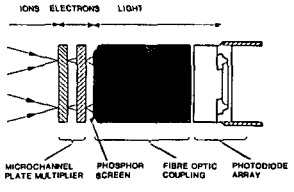

Figure 1

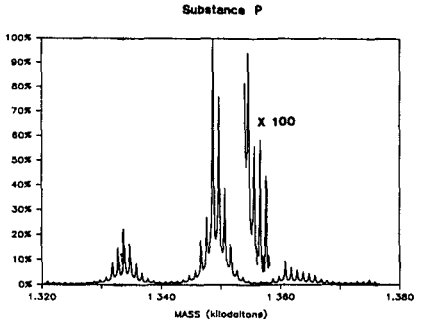

Figure 2

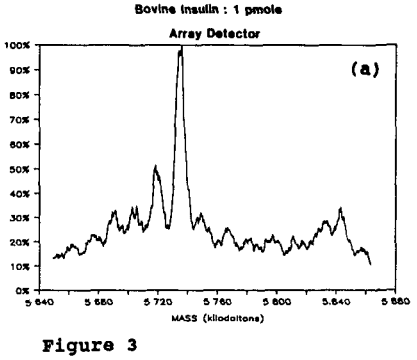

Figure 3

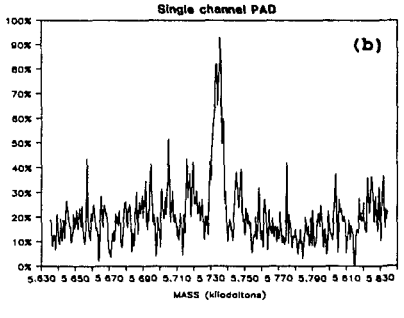

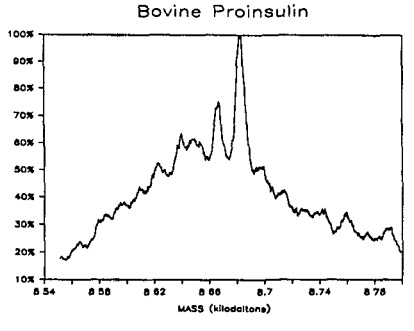

Figure 4

Presented at the 35th ASMS Conference on Mass Spectrometry and Allied Topics
May 24-29, 1987, Denver, CO

A NEW HIGH EFFICIENCY HIGH MASS ION DETECTOR

R.H. BATEMAN AND P.A. BOTT, VG ANALYTICAL LTD. MANCHESTER M23 9LE. UK

Beuler et al (1) showed that there is a threshold velocity of about 18000 m/second for ions impinging on a copper surface to produce secondary electrons. This corresponds to ion energies of 1.7keV at mass 1000, and 17keV at mass 10,000. Although lower velocity ions have commonly been detected, possibly through the use of different surface materials, it is generally accepted that post acceleration is desirable for good detection efficiencies of high mass ions.

A typical off-axis ion detection arrangement employing post acceleration is shown in Figures 1 and 2. For positive ions (Fig. 1), the conversion dynode is negatively charged to accelerate the ions on to its surface, and secondary electrons are conveniently accelerated away towards the electron multiplier, giving an overall ion detection efficiency of near 100%. For negative ions (Fig. 2), applying a positive charge to the conversion dynode accelerates the ions on to its surface, but does not allow secondary electrons to escape. Consequently, it has become common practice to merely detect the secondary positive ions sputtered from the dynode surface (2). This, however, has a typical ion detection efficiency of about 30%, and less than 5% for certain types of ions.

A new ion detector has been constructed which incorporates two conversion dynodes, a phosphor and a photomultiplier (Fig. 3). The two dynodes are arranged off-axis to allow the ion beam to pass through when the dynodes are grounded, and to intercept and detect the ion beam when the dynodes are charged. In operation, the solid positive ion conversion dynode voltage may be varied between -10 and -20kV, the phosphor voltage may be varied between +10 and +20kV, and the hollow negative ion conversion dynode is maintained at half the phosphor voltage.

Positive ions are accelerated towards the negatively charged solid dynode and secondary electrons are accelerated away towards the positively charged phosphor. Negative ions are accelerated towards the positively charged hollow dynode, impinge on its inner surface, and secondary electrons are again accelerated towards the positively charged phosphor. Both positive and negative ions are detected without need to switch or reverse any of the high voltages.

Figure 4 shows the negative ion spectra of pentafluroidobenzene obtained using electron capture ionisation with the source at -8kV. The spectra were recorded using a negative to positive ion aluminium conversion dynode, a negative ion to electron conversion dynode as described above, and a Faraday collector. For the two detectors employing conversion dynodes, the ion detection efficiencies for $C_6F_5^-$ ions were 30% and 55%, and for I^- ions were 2% and 35% respectively.

The ion detection efficiency for this new detector was determined up to mass 3500 by measuring the detected ion current for each of the positive and negative Cesium Iodide cluster ions of the form $(C_sI)_nC_s^+$ and $(C_sI)_nI^-$, (n=1 to 13), and comparing to the ion currents measured on a Faraday collector. The source voltage was $\pm$ 5kV. The detected ion current was measured by using an ion statistical analysis method (3) with a probable error of $\pm$23%. The mean ion detection efficiency for positive ions was 95% and for negative ions was 71%.

The new ion detector described above has been shown to have a similar high ion detection efficiency for positive ions, improved ion detection efficiency for negative ions, and reduced discrimination against certain negative ion species when compared to previous ion detection systems.

By virtue of using a photomultiplier rather than an open electron multiplier, it also has the advantage of having greatly increased immunity to vacuum failure and a substantially increased life time.

(1) Beuler R.S, and Friedmann L. (1980). Nucl. Instru. Methods, 1709, 309-315.

(2) Wang G.H, Aberth W, and Falick A.M. 34 ASMS, Cincinnati, Ohio. 1986.

(3) Schiff L.I, and Evans R.D, (1936) Rev. Sci. Inst. Vol 7, No. 12. 456-462.

Presented at the 35th ASMS Conference on Mass Spectrometry and Allied Topics
May 24-29, 1987, Denver, CO

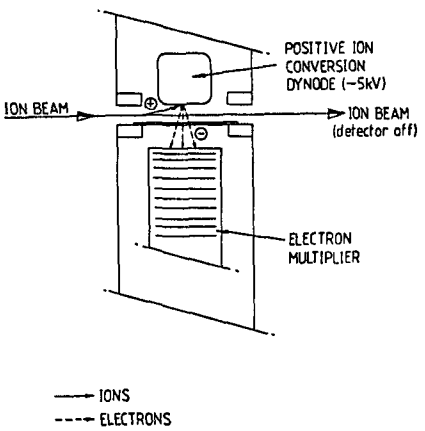

FIGURE 1.

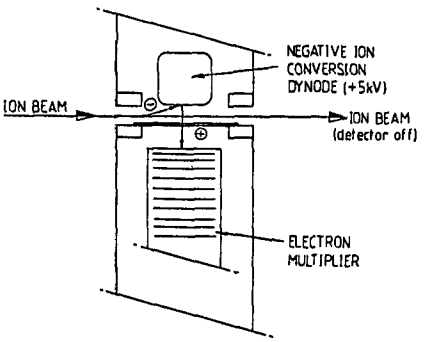

FIGURE 2.

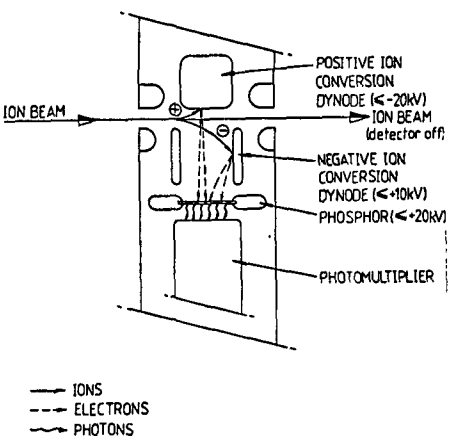

FIGURE 3.

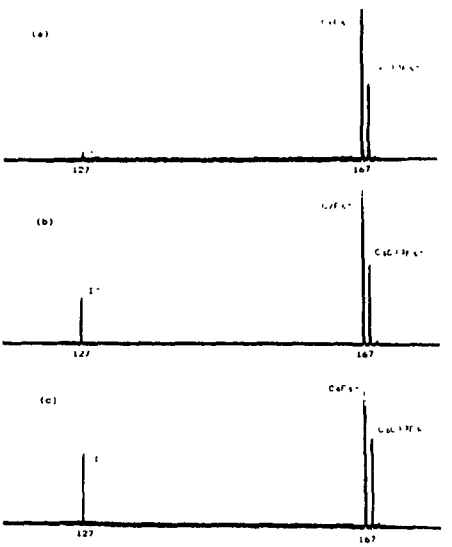

Negative ion spectra of Pentafluorobodobenzene
(a) Negative ion to positive ion conversion dynode
(b) Negative ion to electron conversion dynode
(c) Faraday cup

FIGURE 4.

Presented at the 35th ASMS Conference on Mass Spectrometry and Allied Topics
May 24-29, 1987, Denver, CO

A SIMPLE ANALOG CIRCUIT FOR IMPROVED PERFORMANCE IN DAC SCANNED MAGNETIC MASS SPECTROMETERS

By JAMES P. FREEMAN, REGGI HALL AND JACKSON O. LAY, Jr.

The National Center for Toxicological Research, Jefferson, AR 72079

INTRODUCTION

In low resolution magnetic sector mass spectroscopy where the computer controls magnet scans as well as data acquisition, the computer may employ a 16 bit digital to analog converter (DAC) to convert the computer signal to an analog voltage that controls the magnetic field strength. With higher resolution or higher m/z range magnets, more precise magnet control may require a larger DAC (20 bit DAC). Such requirement may involve costly and time consuming replacement of the instrument interface and/or the entire data system.

This paper presents an inexpensive analog circuit consisting of three operational amplifiers, resistors and switches that provide extended range to the present DAC as well as rapid control of low and high m/z scan limits for improved ease of magnet calibration. The operational amplifiers are used to yield less-than-unity gain and low-end offset, thus allowing the entire DAC range to be employed over a relatively small m/z scan. The low-end offset allows the starting m/z to be set while the less-than-unity gain control sets the ending m/z.

EXPERIMENTAL

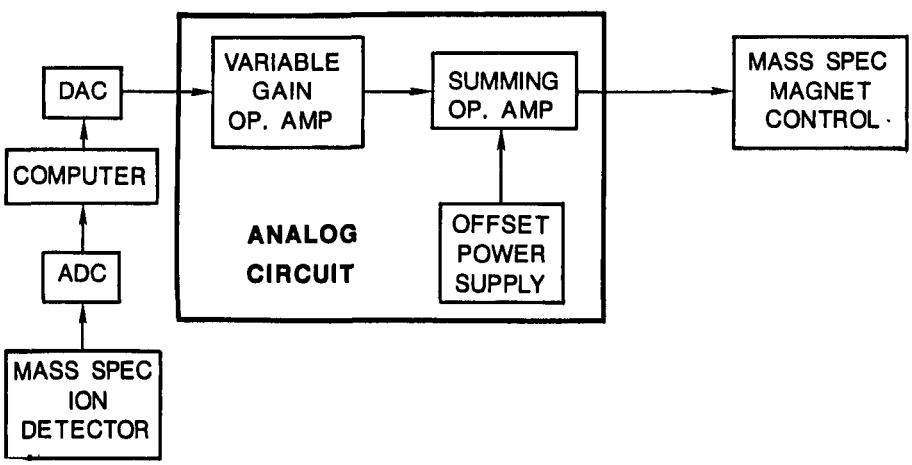

FIGURE 1. Block Diagram of Analog Circuit Installed

The circuit is easy to build, connect and use. The circuit is stable and provides improved ease of calibration for both quadratic and exponential scan functions. For scans over a full m/z decade, a two fold increase in high mass signal was observed compared to exponential scanning. The circuit may be quickly removed from the instrument to allow the original configuration to be restored. Power for the circuit may be obtained from the mass spectrometer or from the instrument interface, thus reducing the costs of construction.

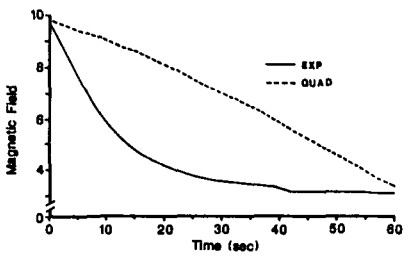

FIGURE 2. Magnetic Field strength in Exponential and Quadratic Magnetic Scan Modes

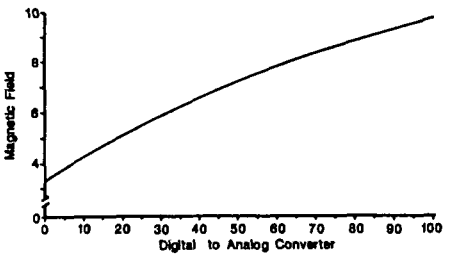

FIGURE 3. Magnetic Field Strength vs. DAC Output in Quadratic Scan Mode

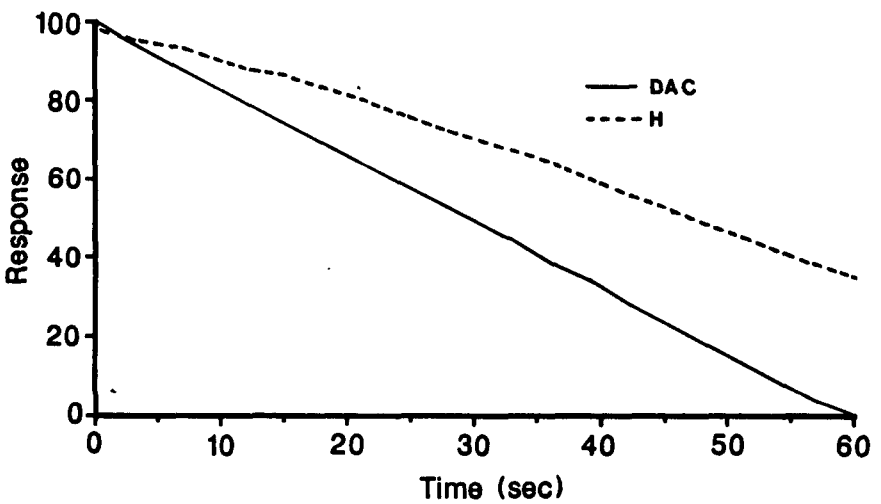

FIGURE 4. Magnetic Field vs. Time (Quadratic Scan & 100 Dalton offset.

CONCLUSION

I. The circuit is stable and does not degrade the normal scanning parameters of the mass spectrometer interface.

II. The circuit improves the ease of calibration because of the ability to easily set the low and high scan limits.

III. The circuit allows the use of the full DAC range over any selected m/z scan limits thereby increasing the computer's resolution for controlling the magnet.

IV. Although the circuit was not tested with a high field magnet because of delays in installation of the magnet, it is expected that the circuit will also function in the same manner with such a magnet.

Presented at the 35th ASMS Conference on Mass Spectrometry and Allied Topics
May 24-29, 1987, Denver, CO

DESIGN EXPERIENCE WITH AND RECENT ENHANCEMENTS TO THE SIMION PC/AT ELECTROSTATIC LENS DESIGN PROGRAM

David A. Dahl and James E. Delmore
Idaho National Engineering Laboratory
EG&G Idaho, POB 1625 Idaho Falls, ID 83415 (208) 526-9915

Introduction

The SIMION PC/AT program is the authors' extensively modified IBM PC version of the original SIMION electrostatic lens design program developed by D. C. McGilvery[1]. SIMION PC/AT has been used to design experimentally verified primary and secondary optics for an SF_6 neutral beam SIMS[2]. Moreover, SIMION PC/AT has been further enhanced by improved trajectory algorithms, fast electrode voltage adjustment, and a general code speedup.

Experience with Primary Optics

The SF_6 neutral beam SIMS employs the auto-neutralization characteristics of certain SF_6 anions The use of the auto-neutralization process requires a drift tube between the primary optics and the SIMS target area to allow a fraction of the SF_6 anions to neutralize before they impact the target. Therefore all acceleration and focusing of the SF_6 anions must be completed before they enter the drift tube. The specific design objective involved fitting an existing instrument having a 2.75 m drift tube with short residence time cylindrical primary optics capable of focusing a 0.5 mm diameter beam of neutral SF_6 molecules on the target.

SIMION PC/AT was used to evaluate various lens options. This analysis process resulted in a five element lens design that was predicted to have the less than 0.01 degree divergence required. The characteristics of the as built lens agreed quite well with SIMION predictions. Further testing of the primary lens uncovered a new collection of voltage settings that appeared to dramatically improve the lens characteristics. Analysis with SIMION verified the existence of this tuning region and ability of the lens to sharply focus a zoomable image of the ion source aperture on the multi-channel plate target. SIMION's predicted voltages for focusing were within 2% of those observed. This error is well within measurement and lens geometry uncertainties and is surprisingly small when one considers the 2.75 m drift tube and the very small ion angles involved.

Experience With Secondary Optics

A field immersion asymmetric lens design was developed for secondary ion extraction and focusing into a quadrupole mass spectrometer. The design incorporated an ion collimation and deceleration region designed to introduce a small hollow tube of ions having low divergence angles and adjustable energies into the quadrupole Preliminary analysis of results with SIMION indicated that actual secondary ion energies were different from design criteria. SIMION was used to design an additional lens element for the system that helped preserve collimation of a wider energy range of ions during deceleration. The modification improved secondary ion sensitivity by a factor of 20.

In addition, tests were run to measure initial secondary ion energies by blocking lower energy ions with a reversed voltage exit electrode. This allowed a comparison with the SIMION predicted ion pass energy spectrum at given tuning points. While the natural divergence characteristics of decelerating ions make quantitative comparisons difficult, the ion energies passed at a given tuning point were in basic agreement with those predicted by SIMION Moreover, SIMION was very useful in predicting the secondary optics tuning behavior and determining the root cause of specific lens characteristics.

Recent SIMION PC/AT Enhanceme-

SIMION PC/AT has been extensively enhanced The new version 3.0 of SIMION PC/AT now takes advantage of the additive solution property of the Laplace equation. This property allows electrode voltages to be quickly adjusted through the scaled additive combination of previous solutions for individual electrodes. Electrode voltage adjustments of large arrays that once took 20 minutes to refine are now accomplished in a few seconds.

A new program called REFINEPA has been created to assist the user in creating the individual electrode solution arrays needed by the fast voltage adjustment feature. The user creates a master potential array file with all adjustable electrodes set to special voltages. For example, all electrode points corresponding to electrode number one are set to one volt. Likewise electrode number two's points are set to two volts. REFINEPA recognizes the adjustable electrodes and automatically makes and refines each required potential array file. The user can also create several master potential array files representing various lens geometry options and have REFINEPA create all the required supporting files in an unattended batch mode at night.

The ion trajectory algorithms have been extensively revised. A new interpolation algorithm gives smoother voltage gradients while properly handling voltage gradients near electrodes. Numerical integration uses a fourth order Runge-Kutta technique. A more powerful variable time step technique, using the notion of ion stop length, is employed to maximize accuracy while minimizing the number of integration steps required. With this technique plotting and computational accuracy are varied automatically to compensate for high ion curvature regions. The new trajectory algorithms also conserve energy better in ion trapping regions.

The magnetic field capability has been expanded to model symmetrical lenses in magnetic fields. Ions can now start at negative y locations and magnetic fields can be applied without any magnetic symmetry assumptions. Moreover, version 3.0 is two to ten times faster in functions like file IO, contouring, and graphics display.

Conclusions

SIMION PC/AT has proven itself to be a valuable verified tool for the design and analysis of ion optics systems used in our investigations. Furthermore, the new version 3.0 of SIMION PC/AT represents a significant step toward a more productive environment for analysis and design of these electrostatic optics systems.

References

(1) McGilvery, D.C., Ph.D. Dissertation, LaTrobe University, 1978.
(2) Appelhans, A.D., Delmore, J.E., and Dahl, D.A., Anal. Chem., in press.

Acknowledgement

Work supported by the U.S. Department of Energy INEL internal research funds and by the Division of Chemical Sciences, Basic Energy Sciences, Office of Energy Research, Department of Energy under Contract 3ED102.

Presented at the 35th ASMS Conference on Mass Spectrometry and Allied Topics
May 24-29, 1987, Denver, CO

APPLICATION OF STORED-WAVEFORM, INVERSE FOURIER TRANSFORM EXCITATION TO FTMS

CODY, R.E., HEIN, R.E., HANNA, D.A.
Nicolet Instrument Corporation
Madison, WI 53711

Stored-waveform, inverse Fourier transform ("SWIFT") excitation [1,2] offers a convenient approach for designing excitation waveforms for Fourier transform mass spectrometry (FTMS). SWIFT waveforms can be "tailored" to a given experiment, providing well-behaved, uniform and selective ion excitation and ejection.

Figure 1 shows the use of SWIFT to select one ionic species in the center of an isobaric multiplet.

A comparison of signal strength vs. RF attenuation for SWIFT and swept-frequency ("chirp") excitation, Figure 2, [3] leads to the following observations:

1. Chirp excitation provides well-behaved relative ion abundances, provided that the trap voltage, sweep rate, and RF level are selected to avoid z-axis ejection of ions [4].

2. The maximum orbital radius achieved with a chirp is about 1/4 to 1/10 of that achieved by SWIFT "multiple ion monitoring". Therefore, SWIFT may be used to improve sensitivity and detection limits.

3. The RF levels required to obtain maximum signal strength, or to eject ions, are mass-independent for SWIFT multiple ion monitoring.

Figure 3a shows a PFTBA spectrum taken under standard chirp excitation conditions. Figure 3b is an enlarged view of this spectrum, showing some very small peaks in the background, which are barely distinguishable above the noise level. Figure 3c shows the enhancement in signal-to-noise that results from SWIFT multiple ion monitoring for the four indicated background ions.

These advantages claimed for SWIFT result from the fact that the frequency range covered for the SWIFT excitation is different from that for the chirp excitation. However, it is very convenient to use SWIFT to design a well-behaved excitation waveform that only excites the frequencies of interest. Hence, we believe that SWIFT will ultimately become the method of choice for FTMS excitation.

References:

1. Marshall, A.G., Wang, T.-C. L., Ricca, T.L.; JACS 1985, 107, 7893-7897

2. Wang, T.-C. L., Ricca, T.L., Marshall, A.G.; Anal. Chem. 1986, 58, 2935-2938

3. Comisarow, M.B., Marshall, A.G.; Chem. Phys. Lett. 1974, 26, 489-490

4. Rempel, D.L., Gross, M.L.; Int. J. Mass Spec. Ion Proc. 1986, 72, 15-31

Presented at the 35th ASMS Conference on Mass Spectrometry and Allied Topics
May 24-29, 1987, Denver, CO

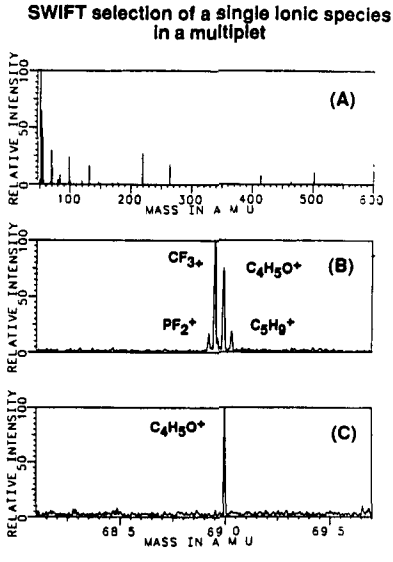

FIGURE 1

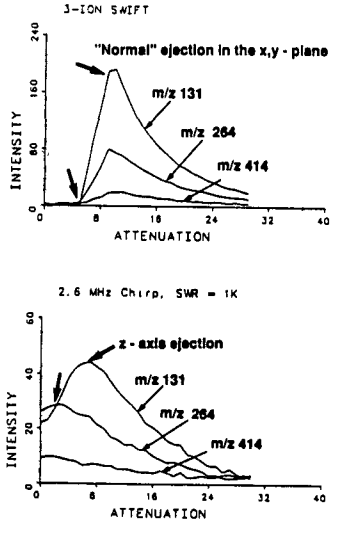

FIGURE 2

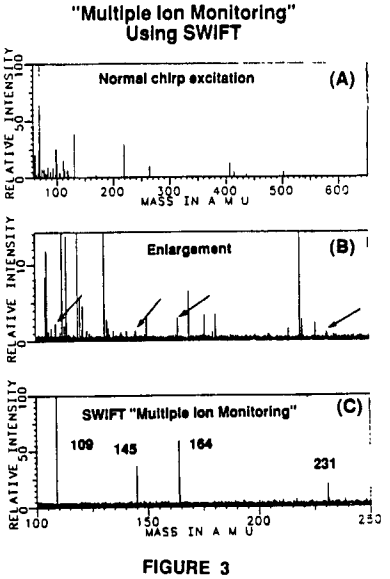

FIGURE 3

Presented at the 35th ASMS Conference on Mass Spectrometry and Allied Topics
May 24-29, 1987, Denver, CO

APPLICATIONS OF MULTIDIMENSIONAL GAS CHROMATOGRAPHY/ HIGH RESOLUTION MASS SPECTROMETRY (GC/GC/HRMS) TO TRACE ANALYSIS

Sydell Lewis and Ray Clothier
Rohm and Haas Co.
727 Norristown Road
Spring House, PA 19477

Numerous systems have been described that couple dual gas chromatographs to quadrupole mass spectrometers and the utility of this technique is well known for resolving very complex mixtures. The work presented describes the coupling of Siemens Sichromat double oven capillary gas chromatograph that incorporates a valveless ('live') column switching system to a Kratos MS80RF double focusing high resolution mass spectrometer. This unique instrumentation can be used to obtain accurate mass data on unknown components which are present at trace concentrations without the need for conventional extraction techniques.

The difficult problem of coupling a high voltage MS system to an unconventional pneumatic system was solved with the use of flexible glass end metal tubing with a quarter inch cuff (Swagelok), which was blown onto a quartz reentrant. This was coupled to a modified Siemen's mass spectrometry interface.

The analysis of impurities present in the monomer methyl methacrylate illustrates the utility of the GC/GC/HRMS system. Fig. 1 is a gas chromatogram obtained with a flame ionization detector (GC/FID) of 1 ul of MMA introduced with a split injection of 1/100. The labelled peaks were unknown impurities present at 15, 5 and 4 ppm, respectively, which were determined with an internal standard. In order to obtain low resolution mass spectrum of these components 1 to 2 ul of MMA must be analyzed. Fig. 2 is the GC trace of 1.5 ul of MMA injected on-column to a J&W DB1-30W (1u film thickness) capillary column. Impurity A eluted under the tail of the overloaded MMA peak. However, if column switching is used the major portion of MMA can be directed from the pre-column to the GC detector and the remainder of the sample can be directed to the main column (J&W DB1-30W,.25u film thickness) and into the mass spectrometer. This technique is called 'heart-cutting'.

The results are shown in Fig. 3, the total ion current chromatogram (TIC), obtained from GC/GC/LRMS analysis. Peak A has been totally separated from the MMA tail and was identified as butyl acrylate from analysis with electron impact and chemical ionization mass spectrometry. The structure was confirmed by analysis of an authentic standard. Peaks B and C were isomers with molecular weight 218. In order to elucidate their structures, high resolution mass spectral analysis was performed on a 10-fold concentrated sample of MMA using column switching. Fig. 4 is the mass spectrum of peak B, which includes accurate mass data obtained at 6500 resolution. From this information the structure of dimethyl-2-methylol-5-methyladipate (DMMA) was proposed (Fig. 5). Support was obtained for the structure by the analysis of a trimethylsilyl derivative.

Four samples of MMA obtained from various manufacturers were analyzed for BA and DMMA. All samples contained DMMA and only two contained BA.

In addition trace analysis GC/GC/MS is extremely useful for analysis of samples present in problematic solvents such as water and BSTFA. An example of this application is the analysis of benzoquinone in water in a mixture which was derived from a process development experiment. Two ul of sample was injected in splitless mode onto a DB1-30W (1u film thickness) column. The water was heart-cut to the pre-column FID detector. The remainder of the sample was transferred to the main column and analyzed by low resolution mass spectrometry. In order to search for benzoquinone, nominal mass chromatography (NMC) was performed on the molecular ion at m/z 108. Benzoquinone was found to be present at approximately one ppm.

In summary GC/GC/HRMS has been shown to be useful in elucidating the structures of components present in complex mixtures at concentrations below 5 ppm. An additional utility of a GC/GC/MS was demonstrated in analyzing samples in problematic solvents.

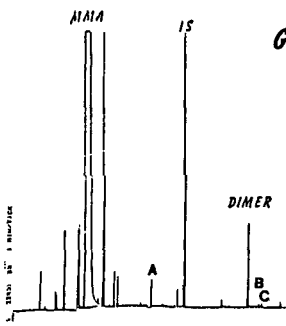

Fig 1

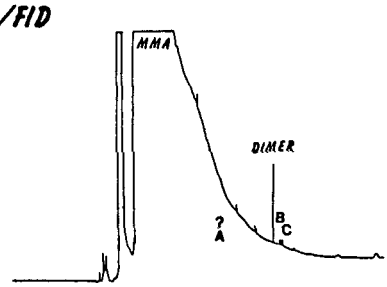

Fig 2

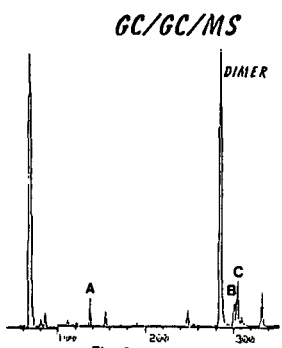

Fig 3

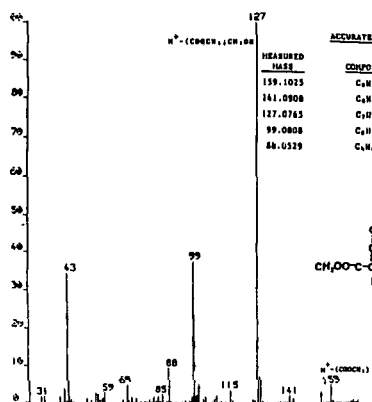

ACCURATE MASS DATA

MEASURED MASS	COMPOSITION	MASS DEVIATION PPM
159.1025	$C_8H_{15}O_3$	4.47
141.0908	$C_8H_{13}O_2$	-5.13
127.0765	$C_7H_{11}O_2$	4.97
99.0808	$C_6H_{11}O$	-2.20
88.0529	$C_4H_8O_2$	5.20

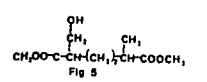

Fig 5

Fig 4

Presented at the 35th ASMS Conference on Mass Spectrometry and Allied Topics
May 24-29, 1987, Denver, CO

MASS RANGE EXTENSION OF THE ION TRAP MASS SPECTROMETER THROUGH THE APPLICATION OF DC ELECTRIC FIELDS

J.F.J. Todd and J.J. Bexon, Chemical Laboratory, University of Kent, Canterbury, Kent, CT2 7NH, U.K., M. Weber-Grabau, P.E. Kelley and G.C. Stafford, Jr., Finnigan MAT, San Jose, CA 95134, and R.D. Smith, Finnigan MAT, Hemel Hempstead, HP2 4TG, U.K.

Recent research on the quadrupole ion storage trap (QUISTOR) has led to mass analysis being effected by mass selective instability[1], and subsequent applications have included the use of extended trapping times to promote chemical ionization[2] and the acquisition of collision-induced MS/MS data through the super-position of an rf field in resonance with the secular oscillations of the parent ions[2].

One of the present limitations of ion trap performance is the upper mass limit of m/z 650, resulting from the combination of trap dimensions and the frequency and maximum amplitude of the drive potential currently employed. The purpose of this contribution is to explore a number of ways in which the application of a dc potential to the ring electrode combined with alternative forms of rf scan allows mass selective instability to be achieved at different operating points on the boundaries of the (a,q) stability diagram. In the conventional mass selective instability mode, the high mass limit of the spectrum is given by $(m/z) = 4V' (r_o^2\Omega^2 q_{eject})$, where V' is the maximum rf amplitude (zero-peak), r_o is the radius of the ring electrode, Ω is the drive frequency and q_{eject} is the point at which the scan line intersects the $\beta_z = 1$ boundary of the (a,q) stability diagram. Figure 1 shows a stability diagram upon which are marked the normal rf-only scan line (1) and two dc/rf scan lines (2, 3). For each of these scans, ionization occurs under optimised rf-only conditions. With scan line (2), the first (low mass) portion of the spectrum is acquired along scan line (1), but after a pre-set time a gated negative dc potential is applied to the ring electrode, superimposed upon the rf drive potential, such that the two potentials are ramped together. As a result the scan line intersects the $\beta_z = 1$ boundary at a $q_z = 0.814$, extending the mass range up to m/z 725. For scan line (3), the trap is first operated with a rising 'forward' rf-only scan along line (1) until m/z 650 is reached, after which a positive dc potential is gated to the ring electrode and the dc/rf amplitudes then ramped down ('reverse' scan) so as to cause ions to become unstable at $q_{eject} = 0.27$ along the $\beta_z = 0$ boundary. The scanning sequence is shown in Figure 2, which also contains a standard forward 'analytical' scan as part of the duty cycle. Using this method m/z 1466 from tris(perfluorononyl)-S-triazine has been recorded. For the recording of low mass spectra it appears that the application of dc potential improves both resolution and sensitivity.

References

1. G.C. Stafford, Jr., P.E. Kelley, J.E.P. Syka, W.E. Reynolds and J.F.J. Todd, Int. J. Mass Spectrom., Ion Proc. 60, 85 (1984).
2. P.E.Kelley, G.C. Stafford, Jr., J.E.P. Syka, W.E. Reynolds, J.N. Louris and J.F.J. Todd, Advances in Mass Spectrometry 1985 (ed. J.F.J. Todd), John Wiley & Sons, Chichester (1986) p. 869.

Presented at the 35th ASMS Conference on Mass Spectrometry and Allied Topics
May 24-29, 1987, Denver, CO

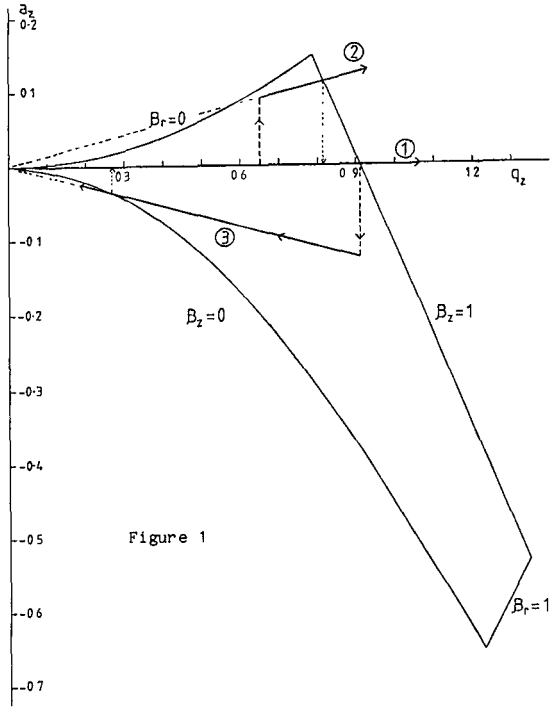

Figure 1

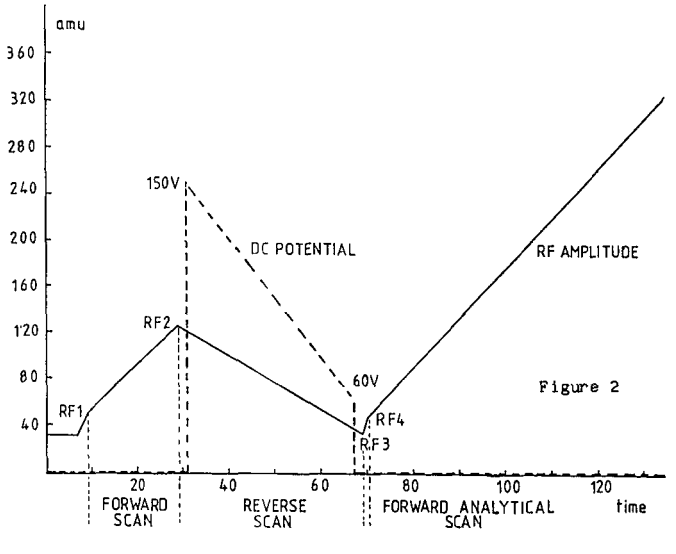

Figure 2

Presented at the 35th ASMS Conference on Mass Spectrometry and Allied Topics
May 24-29, 1987, Denver, CO

ENERGETIC CONSIDERATIONS FOR FRAGMENTATION PATHWAYS OBSERVED FOR COLLISIONALLY ACTIVATED MODEL PEPTIDES FORMED BY FAB IONIZATION

L. M. Mallis[1] and D. H. Russell

Department of Chemistry
Texas A & M University
College Station, TX 77843

A major factor influencing the dissociation reactions energetically accessible to $[M+A]^+$ type ions is the binding energy of A^+ to the sample molecule (i.e., $D^o(M--A^+)$) and the energetics for dissociation of the $[M+A]^+$ ion complex. The $[M+A]^+$ complex can dissociate to give the alkali metal ion or a fragment ion containing A^+ (e.g., F_i+A^+), reactions 1 and 2, respectively.

The branching ratio for reactions 1 and 2 will depend upon the absolute values for $D^o(M--A^+)$ and the appearance energy for the $[F_i + A]^+$ ($AE(F_i + A^+)$) fragment ions. Assuming that $D^o(M--A^+)$ is greater than $AE(F_i+A^+)$, if the average internal energy of a molecular ion species is greater than the $D^o(M--A^+)$, the molecular ion can dissociate to form the alkali metal ion and the neutral molecule (reaction 1) or $[F_i+A]^+$ (reaction 2). The branching ratio between reactions 1 and 2 will depend upon the shapes of the k(E) curves for the two reaction channels. If, however, the average internal energy of the molecular ion species is greater than the $AE(F_i+A^+)$ energy but less than $D^o(M--A^+)$, the molecular ion will dissociate to form exclusively alkali attached fragments ions, e.g., $[F_i+A]^+$. Since the relative $D^o(M--A^+)$ values are in the order $Li^+ > Na^+ > K^+ > Rb^+ > Cs^+$ it follows that by choosing a specific alkali metal cation one can bracket the internal energy of the $[M+A]^+$ ion fragmenting to give a specific $[F_i+A]^+$ ion. That is, the appearance energy for formation of $[F_i+A]^+$ will not be very sensitive to the nature of A^+ (e.g., Li^+ or Na^+). However, the binding energies for A^+ to the organic molecule cover a range of ca. 10-50 kcal/mole. This bracketing method allows us to determine the relative energetics for cleavage of specific bonds.

$$[M + A]^+ \longrightarrow \begin{cases} M + A^+ & (1) \\ [F_i + A]^+ + N & (2) \end{cases}$$

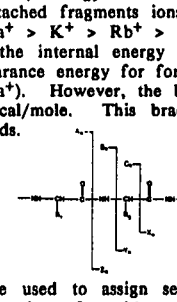

Figure 1. Scheme used to assign sequence fragment ions of peptides

There are three sequence fragment ions observed for collisionally activated $[M+A]^+$ ions of small peptides (see Figure 1). These fragment ions correspond to cleavage of the amide bond (*A* type), cleavage of the NH-CH bond (*B* type) and cleavage of the CH-CO bond (*C* type) all with retention of charge by the N-terminus fragment of the peptide. By using the bracketing method described above, we can impose an upper limit on the internal energy of the $[M+A]^+$ ion undergoing dissociation, and it is possible to determine the relative bond strength for the three different sequence fragment ions. That is, by calculating the percent total fragment ion yield for *A*, *B* and *C* type fragment ions for a series of $[M+A]^+$ ions of peptides the relative energetics for the three types of cleavage reactions observed for collisionally activated peptides can be determined.

In these studies, the CID spectra for a series of $[M+A]^+$ (A = H, Li, Na, K, Rb, Cs) ions of hippuryl-histidyl-leucine (HHL) and leucine enkephalin are investigated to determine the relative bond strengths for the sequence fragment ions (see Figures 2 and 3).[2] We propose that the average internal energy of the collisionally activated $[M+A]^+$ ion of a peptide is proportional to the ionization energy of the alkali metal atom. In addition, by imposing an upper limit on the average internal energy of the molecular ion an estimate of the relative binding energy for the sequence fragment ions observed in a CID spectrum of small peptides can be determined.

Breakdown graphs based on the CID spectra of the $[M+A]^+$ ions of HHL and leucine enkephalin are derived for the *A*, *B*, and *C* type sequence ions as a function of the ionization energy of the alkali metal atom (see Figure 4 and 5). A general trend in the breakdown graph is evident. That is, at low energies *C type* fragment ions are observed almost exclusively, whereas at high energies *A*, *B*, and *C* type fragmentation channels are competitive.

Having established that the lowest energy dissociation reactions for $[M+Na]^+$ ions of peptides correspond to *C type* cleavage reactions we can now begin to discuss in a general nature CID as a structural characterization tool for large biomolecules. In a recent paper from our laboratory we

reported that the amount of translational energy of the incident ion (m_1^+) partitioned as internal energy of m_1^+ upon collision with a neutral target gas atom represents a fundamental limit for the analytical utility of CID. That is, we proposed that the analytical utility of CID is limited by the dynamics of energy partitioning accompanying collisional activation rather than the dissociation dynamics of large polyatomic ions.[2] The data reported in this paper provides additional information for this hypothesis. For example, if we plot the relative abundance of *C type* fragment ions versus the total number of degrees-of-freedom of the $[M+H]^+$ ions we obtain a monotonically increasing function (see Figure 6). That is, as the size of $[M+H]^+$ ion increases the relative abundance of the *C type* fragment ions in the CID spectrum increases. We propose that the relative abundance of the C type fragment ions icnreases due to the fact that the average internal energies of the collisionally activated ions decreases with increasing mass, i.e., energy partitioning, translational ⟶ internal energy, decreases as mass increases.

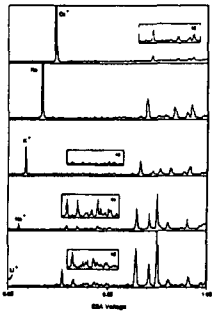

Figure 2. CID spectra of the $[M+A]^+$ ions of hippuryl-histidyl-leucine (HHL).

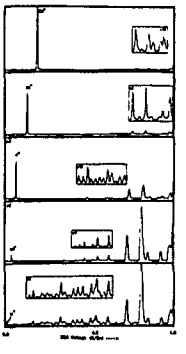

Figure 3. CID spectra of the $[M+A]^+$ ions of leucine enkephalin.

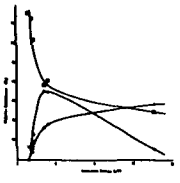

Figure 4. Breakdown graphs for sequence fragment ions observed for HHL (□ - C type, ● - B type, ▲ - A type.

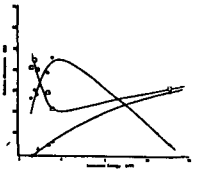

Figure 5. Breakdown graphs for sequence fragment ions observed for leucine enkephalin (□ - C type, ○ - B type, ▲ - A type.

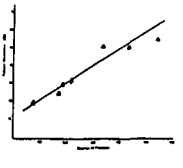

Figure 6. Plot of percent relative abundance of C type fragment ions versus the degrees of freedom for some model peptides.

(1) Present Address: Department of Chemistry, The University of Iowa, Iowa City, Iowa 52242
(2) Bricker, D. L.; Russell, D. H. *J. Am. Chem. Soc.* 1986, *108*, 6174.

Presented at the 35th ASMS Conference on Mass Spectrometry and Allied Topics
May 24-29, 1987, Denver, CO

A MASS BALANCE OF PCBS IN SISKIWIT LAKE, ISLE ROYALE

Deborah L. Swackhamer and Ronald A. Hites

Environmental Health, University of Minnesota, Minneapolis, MN
and
School of Public and Environmental Affairs and Department of Chemistry
Indiana University, Bloomington, IN

This study evaluated the transport processes and fluxes of polychlorinated biphenyls (PCBs) in and out of an aquatic system using a steady state five-compartment box model. The objectives were to determine the relative importance of the major transport pathways and to calculate a dry deposition velocity (V_d) and overall liquid mass transfer coefficient (K_{ol}) for PCBs by using a mass balance approach. Neither of these mass transfer coefficients can be measured directly. This study was unique because it was the first time that a mass balance has been constructed for PCBs using an entirely self-consistent data set.

Transport pathways of PCBs to lakes in the absence of point sources, include dry deposition of aerosols containing PCBs, removal of aerosols and gas-phase PCBs by precipitation events, and vapor transfer across the air-water interface. PCBs are removed by sedimentation and volatilization from water to air. If we assume that the lake is in steady state (1) then

$$F_{dry} + F_{wet} + F_{gas} = F_{sed} + F_{evap}$$

where F stands for PCB flux to or from the lake. The expanded form of this equation is the following:

$$(10^3 L/m^3)(C_r J_r + C_s J_s) + (3.16\times10^5 m\cdot sec/cm\cdot yr) C_a V_d = (10^4 cm^2/m^2) C_{sec} pd/@$$
$$+ (365 d/yr)\, K_{ol}\, [C_g RT/H - (10^3 L/m^3) C_l]$$

where C_r = concentration of contaminant in rain, ng/L; J_r = annual precipitation rate of rain, m/yr; C_s = concentration of contaminant in snow, ng/L; J_s = annual precipitation rate of snow, m/yr; C_a = surface level concentration of contaminant in aerosol, ng/m^3; V_d = deposition velocity, cm/sec; C_{sed} = concentration of contaminant in surficial sediments, ng/g; p = *in situ* density, g/cm^3; d = sedimentation rate, cm/yr; @ = sediment focusing factor, dimensionless; K_{ol} = overall liquid mass transfer coefficient, m/d; C_g = surface level concentration of contaminant in gas phase, ng/m^3; R = universal gas constant, 8.21×10^{-5} m^{3}atm/deg-K mol; T = temperature at air-water interface, deg K; H = Henry's Law constant, atm m^3/mol; C_l = concentration of contaminant in surface water dissolved phase, ng/L.

Siskiwit Lake, located on Isle Royale in Lake Superior, was chosen as our study site. Its remote location ensures that the only source of PCBs is by atmospheric deposition. Its location within Lake Superior makes it an ideal laboratory in the field for studying the Great Lakes, long a region of concern regarding PCB contamination. The lake is approximately 11 km long with a mean width and depth of 1.4 km and 21 m.

Samples were collected over a four month period in summer 1983 and a one month period in January, 1984. Air samples, both particulate and vapor, were collected weekly during these times. Rain samples were collected after every rain event, and one integral snow core was obtained. Water samples were collected weekly during the summer, and sediment cores from two depositional areas were obtained. All samples were Soxhlet extracted, cleaned using alumina and silica gel column chromatography, and analyzed by a Hewlett Packard 5890 GC-ECD using a 30 m DB-5 column. Confirmation of PCBs in each compartmental matrix was done by an HP 5985B GC-MS operated in the negative ion mode. Samples were quantitated for 17 PCB congeners having from 2 to 8 chlorines. Concentrations from each compartmental matrix were time-averaged to obtain yearly, integrated values.

Concentrations of PCB congeners in air are shown below. Air vapor concentrations ranged from 0.3 to 0.002 ng/m^3 (ranges reported are arranged by increasing chlorination). Winter air vapor concentrations were lower than summer values. Less chlorinated congeners were enriched in the vapor phase, and several of the higher chlorinated congeners were not detected in the vapor phase, which is expected due to the decrease in vapor pressure with increasing chlorination. Winter and summer particulate air concentrations were comparable to one another and ranged from 4 x 10^{-3} to 10^{-4} ng/m^3. Water concentrations ranged from 0.14 to 0.01 ng/L.

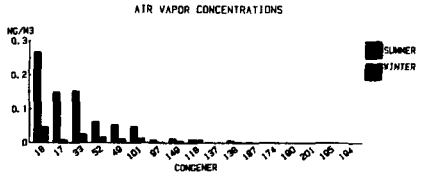

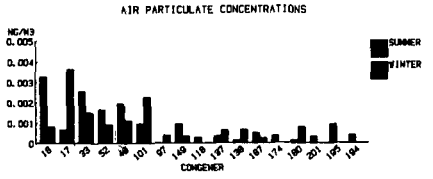

Concentrations of PCBs were similar between rain and snow, with values ranging from 0.07 to 1.5 ng/L. Congener distributions were similar to air samples. The PCB fluxes for rain and snow (see below) were calculated from the measured concentrations and the rate of annual precipitation. Inputs of PCBs were greater from rainfall than snow. Sediment concentrations ranged from 0.03 to 1.6 ng/g and were used to calculate sediment fluxes (shown below).

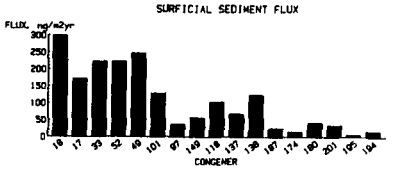

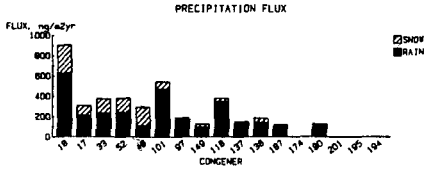

Thus the only terms needed to complete the mass balance are V_d and K_{ol}, which are used to calculate PCB flux due to dry deposition and vapor exchange. For non-volatile compounds, the vapor exchange term drops out of the above equation and the mass balance can be solved for V_d. Congeners #174, 194, 195, and 201 were not present in the vapor phase, and were used to calculate a mean V_d of 0.3 m/sec. The dry deposition flux was then calculated for all PCB congeners using this value. The mass balance equation was then solved for K_{ol}, for all congeners, yielding a mean value of 0.11 m/day. These mass transfer coefficients are consistent with previously modeled estimates from the literature.

The total mass balance of PCB congeners in and out of Siskiwit Lake is shown below. Wet deposition is the dominant input pathway. The ratio of wet-to-dry input had a mean value of 3.3. Removal of PCBs from the lake by volatilization is of equal or greater importance than sedimentation. Thus the mass balance approach serves as a useful approximation for understanding PCB congener transport in and out of lakes.

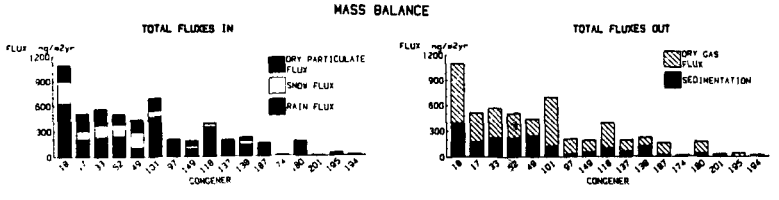

(1) Swackhamer, D.L. and D.E. Armstrong. Environ. Sci. Technol. 20: 879-883.

Presented at the 35th ASMS Conference on Mass Spectrometry and Allied Topics
May 24-29, 1987, Denver, CO

LONG-TERM MEASUREMENT OF AMINO ACID TURNOVER AND THE SYNTHESIS OF PLASMA APOLIPOPROTEINS

D.L. Hachey, B.W. Patterson, G. Ghiselli,* L. Marks,
J. Boriack, G. Cook, L. Brown-Booth, A.M. Gotto,* and P.D. Klein

USDA/ARS Children's Nutrition Research Center, Department of Pediatrics and
*Department of Medicine, Baylor College of Medicine
Houston, TX 77030

Lipoproteins are large aggregates whose primary function is to transport dietary lipids in response to a fat-containing meal. Lipoproteins occur as discrete particles in blood, distinguished by their ultracentrifugation characteristics. The very-low-density lipoprotein (VLDL) is a triglyceride-rich particle that contains ApoB-100, ApoC-I, ApoC-II, ApoC-III, and ApoE. The low-density lipoprotein (LDL) transports cholesterol esters and phospholipids; it contains only ApoB-100. The high-density lipoprotein (HDL) transports phospholipids, cholesterol esters, and cholesterol. The major HDL proteins are ApoA-I and ApoA-II. Mathematical models which describe lipoprotein kinetics have been developed by several investigators (1-2). These models were developed using radioactive tracers, which are unsuitable for studies in women or in children. Therefore, we developed stable isotopic tracer techniques to study lipoprotein metabolism in these populations.

Seven adult subjects have been studied. Each subject received a 5 - 10 mg/kg i.v. bolus dose of L-lysine-4,4,5,5,-$^2H_4$. Fifteen blood samples were collected during the first 12-h period, followed by blood collections at 24-h intervals during the next 7 - 21 days. Lipoproteins were isolated by preparative ultracentrifugation and the individual proteins were separated by polyacrylamide gel electrophoresis. Individual protein bands, which contained 5 - 20 µg of a single protein, were excised from the gel, dried and hydrolyzed in 12N HCl. Free amino acids (AA) were isolated from the protein hydrolysate by cation exchange chromatography. AA were converted to the n-propyl ester, N-heptafluorobutyrate derivative for analysis by negative chemical ionization GC/MS. Approximately 200 - 500 pg of derivatized lysine was injected into the capillary column for isotopic analysis. Careful preparation, storage, and handling of reagents resulted in less than 1 - 2% contamination of a 5-µg protein sample. These techniques can measure isotopic enrichments from 0.01 to 30 mole % excess with 5% precision.

Figure 1 shows L-lysine-$^2H_4$ clearance from the plasma of two subjects who had received a 5 mg/kg dose. These curves illustrate the rapid initial clearance of the tracer from plasma (inset figure). The plasma isotopic enrichment beyond 24 h reflects the reappearance of lysine previously incorporated into whole-body protein which was subsequently degraded. The isotopic enrichment of plasma lysine is used as an input function during the modeling process to drive the intracellular apparatus that is responsible for protein synthesis. Figure 2 shows the incorporation of L-lysine-$^2H_4$ into VLDL, intermediate density lipoprotein (IDL), and LDL ApoB-100. These data demonstrate the rapid synthesis of ApoB, its secretion into VLDL particles, and its delipidation and conversion to IDL and LDL particles. Although a detailed compartmental analysis has not been performed, these data are consistent with the ApoB model published by Fisher and co-workers (3). We have measured the synthesis of ApoA-I and ApoA-II and their incorporation into HDL_2 and HDL_3 particles in these same subjects.

In summary, we have developed stable isotopic tracer methods which enable us to measure the synthesis of several proteins involved in the lipoprotein transport system. These methods offer several technical advantages over radiotracer techniques, including the ability to study several proteins simultaneously without requiring excessive volumes of blood.

References

1.) J.B. Marsh. In: Liver and Lipid Metabolism, S. Calandra, N. Carulli, and G. Salvioli (Eds). Elsevier Science Publishers, New York, 1984, pp 13-26.
2.) W.R. Fisher and B.W. Patterson. Mathematical Biosciences 72:387-405 (1984).
3.) W.R. Fisher, L.A. Zech, P. Bardalaye, G. Warmke, and M. Berman. J. Lipid Res. 21:760-774 (1980).

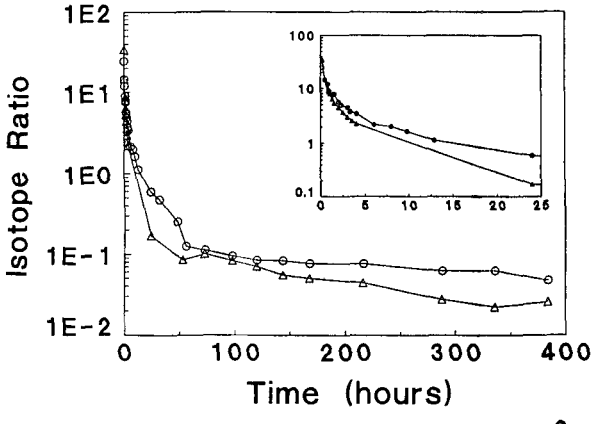

Figure 1. Plasma disappearance of L-lysine-4,4,5,5-$^2H_4$.

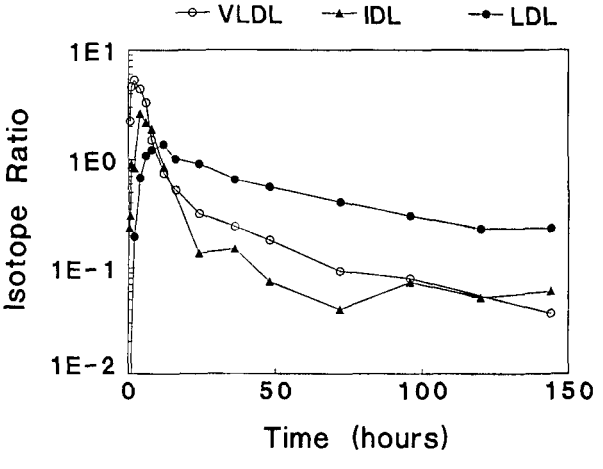

Figure 2. Incorporation of L-lysine-4,4,5,5-$^2H_4$ into VLDL, IDL, and LDL ApoB-100.

Presented at the 35th ASMS Conference on Mass Spectrometry and Allied Topics
May 24-29, 1987, Denver, CO.

MECHANISTIC STUDIES OF DRUG-DRUG INTERACTIONS USING STABLE ISOTOPES. KETAMINE-DIAZEPAM.

Thomas A. Baillie and Louis Y. Leung
Department of Medicinal Chemistry, University of Washington, Seattle, WA 98195

Stable isotope techniques are being adopted increasingly for studies on the dynamics of biological systems, and recently have been applied to the investigation of pharmacokinetic drug-drug interactions (1). In this communication, we report on the application of stable isotope methodology to elucidate the mechanism of the interaction between ketamine, an intravenous anesthetic agent, and the benzodiazepine derivative, diazepam.

Although ketamine possesses a number of desirable therapeutic features, it is of limited value clinically because of the high incidence of emergence delirium experienced by patients. Premedication with diazepam, however, suppresses these adverse reactions, possibly by inhibiting the metabolism of ketamine to psychoactive products. In order to test this hypothesis, we examined the effect of diazepam on the major route of ketamine metabolism, viz N-demethylation, using the rat as an animal model. Specifically, we sought to determine the influence of diazepam on the fraction of an i.v. dose of ketamine which is metabolized to the primary amine, norketamine.

The classical approach to determining the fraction of a drug metabolized to a specific product (f_m) requires that two separate studies be performed, in which drug and metabolite are given on separate occasions, and the areas under the respective plasma concentrations vs time curves (AUCs) are determined in each case (2). Implicit in this experimental design is the assumption that metabolite clearance remains constant between the two studies, an assumption which, if not strictly valid, can lead to serious errors in calculations of f_m. On the other hand, the novel stable isotope approach employed in the present work obviates this assumption, in that parent drug and metabolite-of-interest (one of which is labeled) are given simultaneously. AUC data for biologically-derived and preformed metabolite are thus obtained under identical physiological conditions, and calculated f_m values are inherently more accurate than those obtained from the classical approach.

A group of four rats was given a bolus i.v. injection of a mixture of [$^2H_2$]ketamine (labeled in the aromatic ring) and unlabeled norketamine (20 mg kg^{-1} of each). Plasma concentration of [$^2H_2$]ketamine, [$^2H_2$]norketamine and unlabeled norketamine were then followed by GC-MS analysis of their respective PFP derivatives. Quantitative determinations of these analytes were carried out by SIM at m/z values corresponding to their $[M-Cl]^+$ or $[M-Cl-CO]^+$ ions, and employed unlabeled ketamine as internal standard. Plasma concentration vs time data were fitted to a two-compartment linear open model, and the ratios of AUCs for metabolically-generated and preformed norketamine obtained to give values for f_m. This procedure was then repeated 3 days later, using a cross-over design and employing the same rats, in the presence of diazepam (2 mg kg^{-1} i.v., given 15 min before drug administration).

The results of this interaction study demonstrated that in control rats, approximately one-third of an i.v. bolus dose of ketamine underwent N-demethylation to norketamine in the first 2 hours (f_m = 36.8 ± 2.4%), while in diazepam-pretreated animals, the fraction metabolized was not significantly altered (f_m = 35.3 ± 4.3%). Furthermore, diazepam did not exert a statistically-significant effect on the half-lives, plasma clearances or volumes of distribution of either ketamine or norketamine. It may be concluded, therefore, that diazepam (under the above dosing regimen) has no discernible effects on the pharmacokinetics or metabolic N-demethylation of ketamine in the rat. Based upon these findings, it would appear that the clinically-valuable interaction between ketamine and diazepam most likely has a pharmacodynamic basis, rather than a metabolic or pharmacokinetic origin.

Stable isotope techniques, such as the method outlined in this communication, offer a number of significant advantages over alternative methods for the study of metabolic and pharmacokinetic processes, notably with regard to the accuracy and precision with which parameters such as f_m can be determined experimentally. Moreover, by using each rat as its own control, the number of animals in the present study was reduced to a minimum, and statistical treatment of the data by the paired t-test allowed conclusions to be drawn about intra-animal changes, free from the influence of inter-animal variability in ketamine disposition.

This work was supported by NIH grant NS 17956

(1) M. Eichelbaum, J. Clin. Pharmacol., 26, 469 (1986).

(2) J. B. Houston, in Pharmacokinetics: Theory and Methodology ed. by M. Rowland and G. T. Tucker, Pergamon, New York, 1986, pp. 131-162.

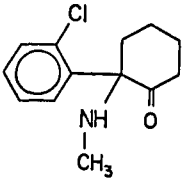

KETAMINE

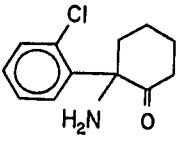

NORKETAMINE

Presented at the 35th ASMS Conference on Mass Spectrometry and Allied Topics
May 24-29, 1987, Denver, CO

FOLLOWING DYNAMIC BIOCHEMICAL SYSTEMS ON-LINE USING FABMS

Richard M. Caprioli
Department of Biochemistry and Molecular Biology, and
The Analytical Chemistry Center, University of Texas
Medical School, Houston, Texas, USA

Fast atom bombardment mass spectrometry (FABMS) has been utilized for the on-line analysis of biochemical reactions. The analyses are performed directly using the aqueous reaction mixture for real-time mass specific detection of the products of the reaction. The systems which have been studied thus far include enzyme reactions involving proteases and glycosidases. Applications tend to fall into one of two general classes. The first are those in which the enzymic reaction is being used as a tool for obtaining information about a particular substrate as, for example, in the use of trypsin for cleaving proteins to give peptides for sequence analysis. The second are those applications where the enzyme reaction itself is of prime interest as, for example, in the determination of reaction kinetics, specificity, etc.

The samples are introduced into the mass spectrometer using the continuous flow FAB probe (1). This device allows aqueous reaction samples to be introduced directly into the mass spectrometer and provides several advantages. Data obtained using this probe for sample introduction generally show significantly higher sensitivity due to the decrease in the chemical background characteristic of high glycerol containing solutions and increased ion yields due to the lower viscosity of aqueous sample solution being bombarded (2). In addition, a significantly decreased ion suppression effect has been observed (3), i.e., the tendancy for hydrophobic ions to populate the surface of the sample and suppress ion from more hydrophilic compounds.

The continuous flow FAB probe can be used in either the continuous flow mode where sample is constantly leaked into the source (Figure 1) or the flow injection mode where individual injections are made automatically at specified intervals (Figure 2). Each mode has certain advantages and may be of choice depending on the application. For example, continuous flow techniques are advantageous when systems are in a rapid state of flux and changes may occur over a period of seconds. Flow injection, on the other hand, may be of choice where the enzyme reaction conditions are not the same as that required, for example, for maximum sensitivity on the probe tip.

Several applications of these methods of reaction monitoring have been evaluated. First, the determination of enzymic reaction rates and kinetics for trypsin and subtilisin were made using relatively large natural substrates. These data provide the nature of the specific clips, the time-order release of the fragments, and kinetic parameters for some specific clips. Using the automated apparatus shown in Figure 2, a complete kinetic analysis can be completed in a few hours. Second, the use of exopeptidases, alone and in combination with endopeptidases, were used for the determination of sequences for polypeptides. In this case, the time-course data provides peptide maps which enable the fragments produced by endopeptidases to be linked and aligned more easily. Third, the monitoring of batch reactions in real-time were done where the evolution of a particular product or fragment of a reactant was of particular interest.

In all of these applications, use of the continuous flow probe has specific advantages which allows the mass spectrometer to be used as a mass specific detector for on-going biochemical reactions. These include the ability to analyze aqueous samples directly, increased detection limits due to the reduction of the background normally observed with FAB, detection of many ions normally 'suppressed' with standard FAB techniques, and the ease of repetitive and serial introductions of samples.

Presented at the 35th ASMS Conference on Mass Spectrometry and Allied Topics
May 24-29, 1987, Denver, CO

REFERENCES

1. Caprioli, R. M., Fan, T. and Cottrell, J. S. (1986) Anal. Chem. 58, 2949-2954.

2. Caprioli, R. M., and Fan, T. (1986) Biochem. Biophys. Res. Comm. 141, 1058-1065.

3. Caprioli, R. M., Fan, T. and Moore, W. T. (1987) Rapid Comm. Mass Spectrom. 1, 1-8.

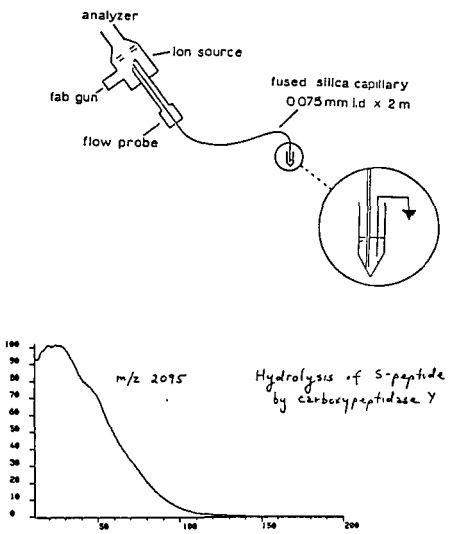

Figure 1. Continuous flow reaction monitoring.

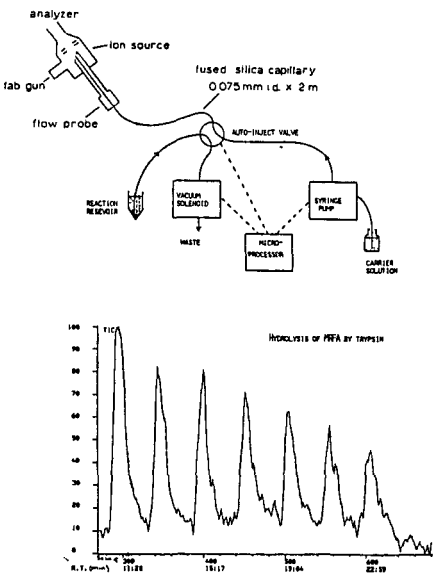

Figure 2. Reaction monitoring using flow-injection methods.

Presented at the 35th ASMS Conference on Mass Spectrometry and Allied Topics
May 24-29, 1987, Denver, CO

FIRST RESULTS FROM A TIME-OF-FLIGHT MASS SPECTROMETER USING HIGHLY ENERGETIC IONS FROM ARGONNE TANDEM-LINEAR ACCELERATOR SYSTEM (ATLAS)*

J E Hunt, M Salehpour, E Kanter, W Kutschera, B Zabransky, R Pardo and R Dunford
Argonne National Laboratory, Chemistry Division, 9700 S. Cass Ave, Argonne, IL 60439.

Studies have shown that an accelerator can be of great use in studies of mechanisms of desorption/-ionization processes in mass spectrometry. A time-of-flight mass spectrometer was designed and constructed at Argonne National Laboratory to be attached to the ATLAS (Argonne Tandem-Linear Accelerator System) accelerator. The ATLAS consists of a 9-MV FN tandem Van De Graff injector and a superconducting linac accelerator. This system accelerates ions up to mass 130 at energies up to 5 MeV/amu. The major elements of ATLAS for use in mechanistic studies on ion-induced desorption mass spectrometry are its high energy, excellent time resolution and the ability to vary the beam duty cycle.

The design parameters of the mass spectrometer include: the insertion of up to five large area targets (2 inch diameter), interchangeable sample and grid positions, easily modifiable acceleration distance, a 45° angle of incidence for the primary ion and the capability for incident ions to impact the target from the front or from behind. A cryopump is used to achieve the typical operating pressure of 1×10^{-8} torr. A schematic of the mass spectrometer is shown in Figure 1. Accelerated ion impact on a thin aluminized mylar film which supports the sample produces secondary ions which are accelerated and then drift to a channel electron multiplier assembly. The incident ions, which pass through the sample/film, are detected in a solid state detector, to provide both energy and start timing information. Each signal is amplifed, discrimnated and connected to a multi-event time digitizer. The corresponding start and stop signals are acquired in a LeCroy (Model 4208) 8-stop time digitizer, processed through a multibus-based front end processor and are recorded both as event mode data on tape and as mass spectral histograms directly to disk. Since the LeCroy 4208 is a multi-stop digiitzer, we can record each of the eight individual stop events, as well as the total mass spectrum composed of all eight events. Each of the eight individual stops and the sum of eight hits, can be presented as a mass spectral histogram. The same mass spectrometer and data acquisition system, without an ion source is used to perform spontaneous desorption experiments.[1]

A typical mass spectrum is shown in figure 2. A portion of the mass spectrum of octylethyl porphine at a resolution of 1ns/ch is shown in this figure. The incident ion is 300 MeV $^{58}Ni^{22+}$. The total acquistion time for the spectrum was 58 minutes with approximately 200 incident ions/sec. The molecular ion region shown contains several peaks separated by one mass unit. These are the molecularl ion at m/z 534, a protonated molecular ion at m/z 535, a $(M-H)^+$ ion at m/z 533 and ions at m/z 536 and 537. An estimation of the resolution of the mass spectrometer for this orgainc ion is 1200. The yield of the molecular ion (i.e., the number of molecular ions divided by the number of incident ions) is approximatedly 12%. Several other compounds have been analyzed including valine, luteinizing hormone releasing hormone (LHRH), polyethylene glycol, and cesium iodide.

Investigations continue in mass spectrometry of high molecular compounds using highly energetic beams from ATLAS. The accelerator/mass spectrometer will also continue to be used to characterize the desorption/ionization process.

[1] M Salehpour and J Hunt, these proceedings.

*Work performed under the auspices of the Office of Basic Energy Sciences, U.S. Department of Energy, under contract number W-31-109-ENG-38.

Presented at the 35th ASMS Conference on Mass Spectrometry and Allied Topics
May 24-29, 1987, Denver, CO

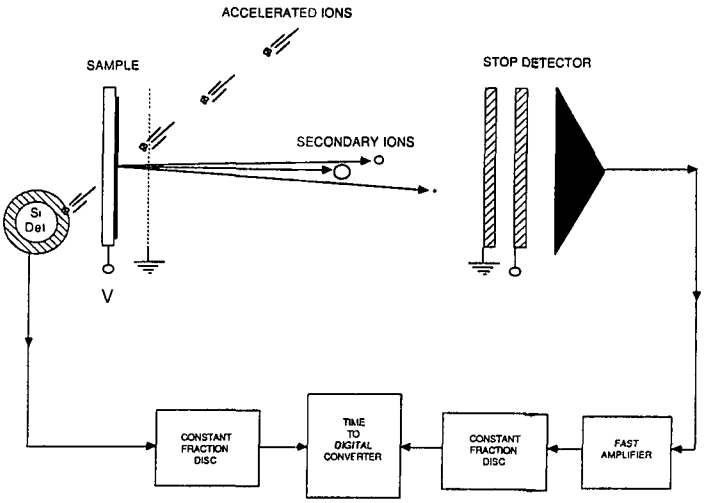

Figure 1

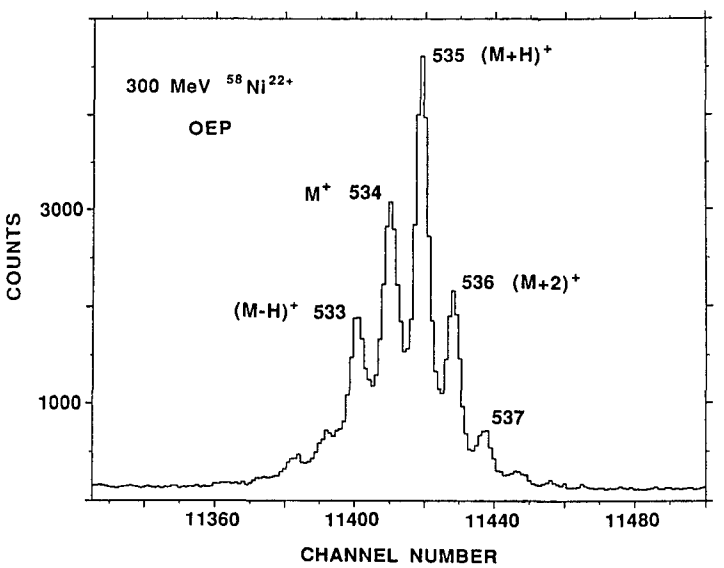

Figure 2

Presented at the 35th ASMS Conference on Mass Spectrometry and Allied Topics
May 24-29, 1987, Denver, CO

TIME ARRAY DETECTION: MASS SPECTROMETRY'S ANSWER TO HIGH RESOLUTION CHROMATOGRAPHY. J. F. Holland[1], E. D. Erickson[2], B. A Eckenrode[2], and J. T. Watson[1,2], Departments of [1]Biochemistry and [2]Chemistry, Michigan State University, East Lansing, MI, 48824.

The mass spectrometer has become an elegant and wide-spread detector for many types of gas and liquid chromatography. The continuing improvements in column performance leading to higher resolution are placing stringent requirements on the mass spectrometers for faster and faster production of scan files. In fact, many of the columns in common use today require up to 20 scan files a second in order to preserve the chromatographic information. The quadrupole and magnetic sector instruments commonly used today simply are not capable of producing complete spectra at these rates. Of the options available to solve this problem, TOFMS appears to have the greatest potential. Each transient waveform produced at the detector after extraction from the ion source contains the information needed for the complete mass spectrum. Since the ion source may be extracted at rates up to 10,000 times a second, the potential for the generation of scan files at high speed is clearly obvious. In addition to the potential for rapid spectrum generation, TOFMS offers the following advantages: simple, and relative low cost; all ions follow the same optical path, hence the mass range is limited only by the ion detection means and the mass axis calibration can be based on exact mathematical definition.

For the rapid production of complete mass spectra in TOFMS, techniques involving time-slice detection (TSD) are universally employed. In TSD, after the extraction pulse a programmed delay occurs after which the time-sampling window is opened and the data are taken for a short burst in time Hence, from each source extraction, information at only one spot along the mass axis is acquired. To gain information for a full spectrum, the delay between the extraction pulse and the sampling window is linearly ramped. In TSD methods, less than 1% of the data striking the detector after each pulse of the source are actually used in the creation of the scan files. Under ideal conditions, scans can be produced in one to two seconds. These rates are comparable with those of the quadrupole and magnetic sector instruments, but are still far below the needed rates for chromatographic resolution.

To utilize more efficiently the information striking the detector, and facilitate faster scan file generation, a technique called time array detection (TAD) can be employed. In TAD, all of the information in each transient waveform after every source extraction is captured and utilized. Fundamental to this technique, however, is the availability of an electronic system capable of bandpasses in excess of 100 MHz. An integrating transient recorder (ITR) designed to meet this need (1) records a burst of data for 80 microseconds during each transient, encompassing information in the mass range from 14-800 m/z. A 200 megasamples per second analog to digital converter establishes the time resolution, or time bin, at 5 nanoseconds. For each transient, up to 16,000 sequential time bins may be recorded. The information from each transient is stored in one of two emitter-coupled logic (ECL) summing registers (16 x 1,000 x 24 bits). While incoming information is being stored in one bank of the ECL, the other bank is being read out into the transfer and processing circuits of the ITR. The information from successive transients is summed (integrated) in order to improve the ion statistics while also accommodating the shift in time domain from the transient to the mass chromatogram.

Another major requirement for TAD is that the ion packets of every mass throughout each transient be in focus at the detector. Quite simply, the space and energy variations of the ions created in the three-dimensional ion source must be corrected in order for TAD to reach its full potential. Several approaches have been used in this laboratory for this correction. A magnetic sector is used prior to the time-of-flight measurement to focus the ions by their momentum (2). Immediate, full-range scanning is obviously sacrificed by this momentum filtering, however, with the use of TAD the entire two-dimensional data field necessary for the information (parent, daughter, and neutrals) of an MS/MS analysis can be obtained with a single scan of the magnetic sector. This can presently be done within the time frame of a single chromatographic peak obtained by standard packed column chromatography. Another approach uses an electric sector to energy-filter the ions from the source prior to their being analyzed by time-of-flight (3). While this technique enables full mass range scanning with all of the ions in adequate focus, it does so at a sacrifice in sensitivity due to the attenuation in the energy filter. Much of this loss can be recovered by the integration used in TAD. Applications of the TAD technique directly to the linear TOF tube is an area of active investigation at the present time.

The advantages of TAD can be summarized as the following:

1. Integrity of the fragmentation pattern. Since the ions are being extracted from the source in a time frame that does not permit variations in source pressure, the fragmentation pattern of a single compound will be consistent whether taken at the apex of the peak, or the rapidly changing sides of the chromatographic profile. Successive summation produces summed spectra with the same fragmentation pattern. In the case of a single

component, successive spectra can be summed over an entire chromatographic peak to increase the sensitivity and precision of the measurement. In the case of compounds that are not separated by chromatography, the unambiguous identification of a single m/z as being attributed to a single molecule will allow a linear subtraction, removing the contribution of fragment ions arising from that molecule from the total sum. Indeed, exotic deconvolution methods may be reduced to simple linear subtractions.

2. Speed of scan file generation. With the present ITR, ten transients must be summed before the data can be transferred and processed. This results in the potential for a thousand scan files to be generated each second. This is far in excess of the rate necessary to represent chromatographic profiles at the present time.

3. Improved statistics. The summation of successive transients allows background noise to be ameliorated and signals to be enhanced with the resulting improvements in signal-to-noise, total range, dynamic range, and sensitivity. Figure 1 illustrates some simple benchmarks on signal-to-noise as a result of successive summations from ten sums to 10,000 sums. (the RMS of the background and the total range were used for the S/N calculations and represent the maximum attainable precision under the current instrumental conditions.)

4. The ability to adjust the time required for scan file generation with the time base needed for optimal reproduction of the chromatographic resolution. Figure 2 illustrates the representations of two peaks striking the detector in less than five seconds as obtained by scan file generation in periods from 2.0 to 0.0170 seconds. In this example, 40 scan files generated per second reproduce the original peaks with good fidelity. Faster generation of scan files simply reduces the signal-to-noise. Slower generation of scan files sacrifices chromatographic information. The ability of TAD to optimize these parameters is one of its strongest assets in its application to a GC-TOF-MS.

References

1. Newcome, B., Erickson, E., Yefchak, G., Davenport, M., and Holland, J. *Proc. 34th Ann. Conf. on Mass Spectrom. and Allied Topics*, p. 158, Cincinnati, OH, 1986.

2. Stults, J. T., Enke, C. G., and Holland, J. F. *Anal. Chem.*, **55**, 1323 (1983).

3. Pinkston, J. D., Rabb, M., Watson, J. T., and Allison, J. *Rev. Sci. Instr.*, **57**, 583 (1986).

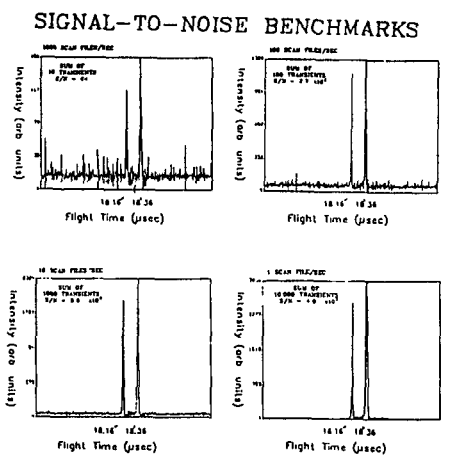

Figure 1

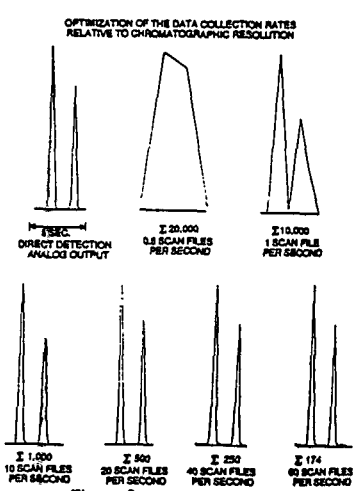

Figure 2

Presented at the 35th ASMS Conference on Mass Spectrometry and Allied Topics
May 24-29, 1987, Denver, CO

SURFACE INDUCED DISSOCIATION IN A NEW TANDEM QUADRUPOLE MASS SPECTROMETER

M. E. Bier, R. G. Cooks, J. Amy
Dept. of Chemistry, Purdue University, West Lafayette, IN 47907

G. Stafford, P. C. Ceja, J. E. P. Syka
Finnigan MAT, 355 River Oaks Pkwy., San Jose, CA 95134

A tandem quadrupole mass spectrometer (Figure 1) was built to study polyatomic ion/surface collision phenomena at translational energies of 10 - 100 eV[1]. The instrument consists of two mass analyzing quadrupoles, Q1 and Q3, and a rf-only quadrupole, Q2. The source has electron, chemical, and Cs^+ gun ionization capabilities. The mass spectrometer can be operated in two distinct modes: (a) deflection mode and (b) ion/surface collision mode. In the deflection mode, the ion beam is turned through a 90° arc without colliding with the target surface. In the ion/surface collision mode, the ion beam collides with the surface producing secondary ions (surface-induced dissociation (SID)). The secondary ions resulting from the intimate ion/surface collisions are extracted at an angle of 90° to the incoming beam and are mass analyzed by Q3. The SID daughter spectra obtained using this instrument compare well with spectra taken using a BQ hybrid instrument[2].

Studies with tetraethylsilane molecular ion show striking results. Activation of this ion occurs with an average 16 % of the laboratory ion kinetic energy being converted to internal energy in the collision range of 10 - 100 eV (Figure 2).

Larger molecules, such as the refractory polynuclear aromatic hydrocarbon ion pyrene and the peptide Met-Arg-Phe-Ala fragment extensively as shown in Figures 3 and 4, respectively. The high fragmentation efficiency for these molecules suggests that SID might be a superior method for dissociating large biomolecules when compared to CAD. The SID efficiency of ca. 15 - 20 % for Met-Arg-Phe-Ala was determined by comparison of the total fragment ion current to the intensity of the deflected parent ion beam. Typical SID efficiencies for small organic ions are ca. 5 %. In addition to fragmentation, low kinetic energy charge inversions have been shown to occur for ions from hexafluoropropylene (+ to -) (Figure 5) and for benzoic acid (- to +) without the need for a special target as in CAD[3] (e.g. SF_6).

Reactive additions and chemical sputtering have also been observed for specific molecular ions. For example, ionized pyrazine (m/z = 80) abstracts a hydrogen atom producing $(M+1)^+$ (m/z = 81) as the base peak. Reactive additions have been shown to be useful for distinguishing isomers[4]. Chemical sputtering has been observed for positive fluorinated ions which are typically neutralized at kinetic energies of ca. 100 eV producing a charge exchange spectrum of even electron hydrocarbon ions. The sputtered hydrocarbon ions are attributed to adsorbates on the surface at a pressure of 10^{-6} torr.

1. M. E. Bier, et. al., Int. J. Mass Spectrom. Ion Processes, (1987) in press.

2. Md. A. Mabud and R. G. Cooks, Int. J. Mass Spectrom. Ion. Processes, 67, (1985), 285.

3. D. J. Douglas and B. Shushan, Org. Mass Spectrom., 17, (1982), 188.

4. Md. A. Mabud and R. G. Cooks, 34th ASMS, (1986), 669.

Presented at the 35th ASMS Conference on Mass Spectrometry and Allied Topics
May 24-29, 1987, Denver, CO

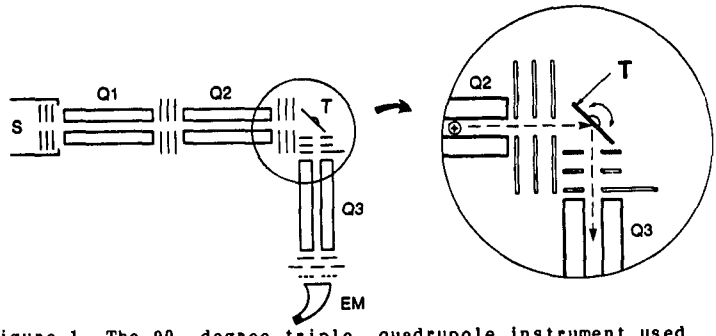

Figure 1. The 90 degree triple quadrupole instrument used for SID and an enlargement of the target region.

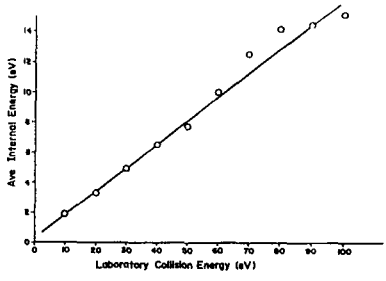

Figure 2. Average internal energy deposited into the molecular ion of tetraethylsilane versus the laboratory collision energy.

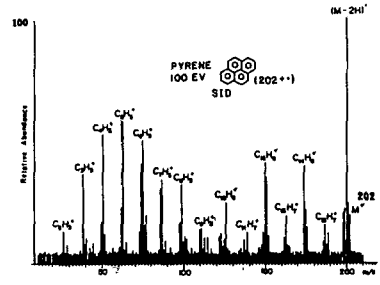

Figure 3. SID daughter spectrum of the pyrene molecular ion, $M^{+}\cdot$, m/z = 202, at a collision energy of 100 eV indicates high energy deposition.

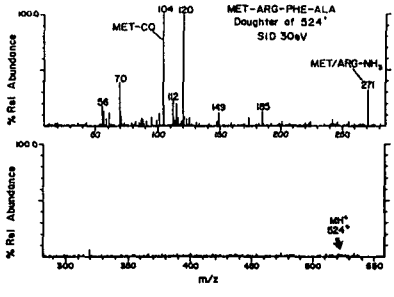

Figure 4. SID daughter spectrum of Met-Arg-Phe-Ala, MH^{+}, m/z = 524, at a collision energy of 30 eV.

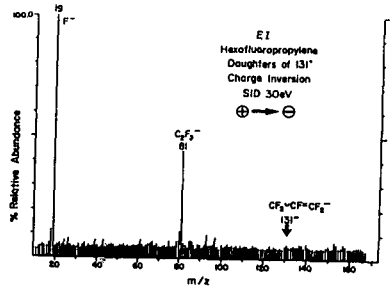

Figure 5. SID charge inversion daughter spectrum of m/z = 131^{+} from hexafluoropropylene.

Presented at the 35th ASMS Conference on Mass Spectrometry and Allied Topics
May 24-29, 1987, Denver, CO

MOLECULAR IMAGING SECONDARY ION MASS SPECTROMETRY

Greg Gillen and Peter Williams
Department of Chemistry
Arizona State University
Tempe, AZ 85287.

Secondary Ion Mass Spectrometry (SIMS) has become widely used for studies of fragile organic compounds. Imaging SIMS systems have long allowed ion microscopy of sample surfaces using atomic species, and it has been suggested that molecular ion microscopy of biological tissue samples may be possible (1). That no such capability has yet been demonstrated is due to the destructive nature of keV ion bombardment. We have taken a new look at the damage problem in molecular SIMS, and have been able to show that a high sputter yield matrix can serve as a damage "buffer", allowing intact molecular ion signals to be generated as sputtering proceeds well beyond the outermost monolayer. We have used a secondary ion microscope instrument(Cameca IMS-3f) to image the distribution of a variety of molecular species on surfaces with um lateral resolution. In particular, images of neuroactive compounds in water ice at physiological concentration levels have been obtained. Such a capability demonstrates that molecular ion microscopy of frozen hydrated biological tissue should now be possible.

Ion beam sputtering is inherently a destructive technique, and would seem especially so in the case of molecular desorption. It is conventionally believed that an incoming ion destroys roughly ten surface molecules for each molecule desorbed intact(2). Each primary ion penetrates several hundred angstroms below the sample surface, rupturing intramolecular bonds in subsurface layers. Subsequent primary ions would therefore be expected to sample only fragments. If this is true, then a simple calculation shows that molecular imaging in biological tissue should be impossible. A useful lateral resolution in biological tissue would be ~ 1um. For an analyte concentration of $2x10^{-3}$ (molar), some 10^3 molecules are in a 10 A thick surface layer 1x1 um square. Given an instrument transmission of 10^{-3}, and assuming that the ion yield is as high as 10%, a molecular ion signal of no more that 0.1 counts/um^2 can be expected if only the outermost monolayer is sampled, clearly below the threshold for imaging.

Our experimental results indicate that this damage problem may not be as severe as expected. Monitoring of the intensity of the molecular ion peak vs. primary ion dose for several of the compounds studied (quaternary ammonium salts) indicates that intact molecular ion emission is still detectable at primary ion doses of $>10^{15}$ ions/cm^2, exceeding the monolayer destruction dose of 10^{13} by 2 orders of magnitude. Additional evidence for damage resistance comes from the work of Cooks (3) who found that compounds mixed with ammonium chloride exhibited unusual resistance to primary beam damage. We have measured the sputter yield for ammonium chloride and determined that ~100 molecules are desorbed per incident ion (8 keV Ar+ primary ions). This suggests a damage removal process in which the damaged material is removed in the same sputtering event that creates it, leaving a fresh undamaged surface to be sampled by the next primary ion. Such a mechanism allows us to predict that other high sputter yield matrices may also be useful for reducing primary beam damage. In particular, this process would be expected to occur in the water ice matrix, which has a sputter yield similar to that of ammonium chloride. If this is the case, water ice should be the ideal matrix from which to sputter sufficient molecular ions to form a useful image from biological tissue. To adapt the ion microscope for biomolecular imaging, we have increased the mass range of our instrument from 300 u to 1100 u by lowering the secondary ion acceleration voltage. Small (factors of 3-5) degradations in instrument transmission and detector sensitivity resulted from this change. Additional modifications have included the implementation of microprobe imaging capability and the installation of a high gain curved channel plate for imaging of low intensity molecular ion signals.

Molecular ion images have been obtained for a number of organic compounds including organic dyes, neurotransmitters, tetraalkyl quaternary ammonium salts, alkaloids, and neurotoxins. Figure 1 shows a molecular image and mass spectrum of the compound neostigmine evaporated from aqueous solution onto silver foil (~1 ng in 400 um^2 analysis area). In most cases, images were obtained from nanogram quantities of analyte.

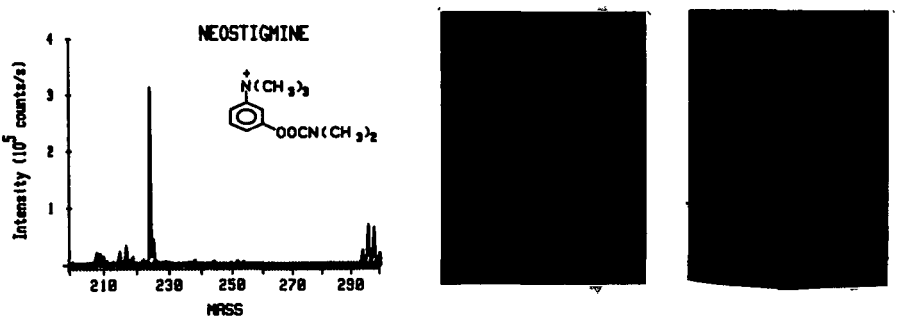

Figure 1. Molecular ion image of neostigmine (field of view 400 um) Silver ion image included for comparison.

Images have successfully been obtained from samples frozen in water ice. Figure 2 is a molecular ion image of the alkaloid muscarine in frozen aqueous solution. The presence of water ice was verified by imaging of mass 19 and from the presence of water clusters observed in the mass spectrum. Similar results have been obtained for several organic dyes in frozen aqueous solution. The total number of muscarine molecules available to be sampled was ~10^6 molecules um^3 (~30 ppm molar). Such concentrations are typical of those found in biological tissue. The ability to image such low concentrations confirms that molecular ions can be sampled undamaged from deep within the water ice matrix.

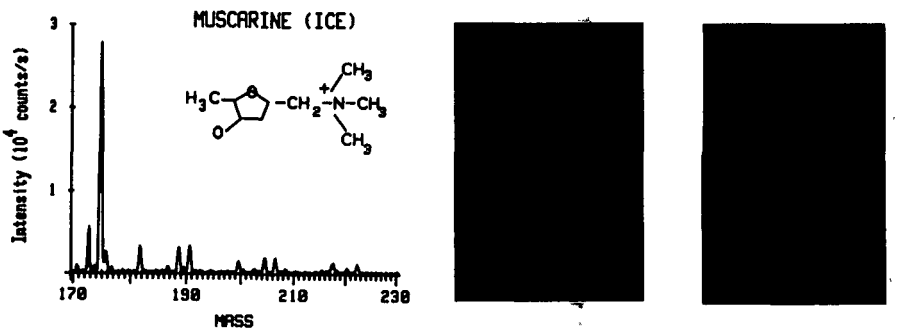

Figure 2. Molecular ion image of muscarine (400 um field of view) Water ice (mass 19) ion image shown for comparison.

(1) Magee, C.W. Int. J. Mass Spec. Ion Phys. 1983, 49, 211.

(2) Day, R.J.; Unger, S.E.; Cooks R.G. Anal. Chem. 1980, 52, 557A.

(3) Hsu, B.H.; Busch, K.L.; Xie, Y.X.; Cooks, R.G. Int. J. Mass Spec. Ion Phys. 1983, 51, 225.

Presented at the 35th ASMS Conference on Mass Spectrometry and Allied Topics
May 24-29, 1987, Denver, CO

CAPILLARY ZONE ELECTROPHORESIS WITH ON-LINE MASS SPECTROMETRIC DETECTION,

R. D. Smith, J. A. Olivares and N. T. Nguyen, Chemical Methods and Separations Group, Chemical Sciences Department, Pacific Northwest Laboratories (Operated by Battelle Memorial Institute), Richland, Washington 99352

We have recently developed and demonstrated the first on-line combination of capillary zone electrophoresis and mass spectrometry (CZE-MS). Mikkers, Jorgenson, and co-workers (1, 2) have reported on the use of capillary zone electrophoresis (CZE) for high-resolution separations of amino acids, peptides, proteins, and complex salt mixtures. This technique has been shown to provide separation efficiencies of up to 10^6 theoretical plates, often in less than 20 min (3). Capillary zone electrophoresis is particularly useful in the separation of ionized and partially ionized species in aqueous solvents, although nonaqueous solvents have also been used (4). In CZE separation occurs in a capillary tube filled with a buffer and immersed in buffer reservoirs at each end. The sample is typically introduced as a sample plug by electromigration from a separate sample reservoir (2). Electroosmotic flow in the capillary is caused by the migration of ions from the diffusive layer of the electrical double layer at the capillary surface, under the influence of an electrical field imposed tangentially to the surface, causing the ions to migrate toward the oppositely charged electrode (5). The resulting bulk electroosmotic flow can be sufficiently fast so that positively charged ions, neutral species, and negatively charged ions elute in short times, with the separation due to differences in the electrophoretic mobilities of the analytes.

The CZE-MS combination would appear to provide an attractive complement for GC-MS and SFC -MS methods, allowing highly polar and nonvolatile analysis to be addressed. Our evaluation of the requirements for a mass spectrometer interface suggested an approach that incorporates the electrospray ionization technique developed by Dole et al. (6) and the more recent work reported by Fenn and co-workers (7).

EXPERIMENTAL SECTION

Electrospray ionization was carried out at atmospheric pressure in a 2.54 cm long by 2.3 cm i.d. stainless steel cylinder. The ion sampling nozzle (0.5 mm i.d. orifice) was made from copper, at ground potential. This cylinder surrounds the electrospray assembly and was heated to 60°C by a system of cartridge heaters. The electrospray needle, focusing ring, and ion sampling nozzle are concentric with the mass analyzer. These components can be positioned independently relative to the fixed skimmer (with the aid of linear motion drives), even while high voltage is on, in order to maximize ion formation and transmission. A curtain of N_2, at a flow rate of 2.5 L/min, is fed between the focusing ring and the nozzle and allowed to flow counter to the electrospray to aid in the desolvation processes.

The vacuum system consists of a three-stage differentially pumped chamber. The first stage allows for a supersonic beam expansion through the ion sampling nozzle. This region is pumped to 0.85 torr by a 150 L/s roots blower. A portion of the supersonic beam is sampled by a 1.2 mm i.d. beam skimmer. The second differentially pumped stage houses a 22 cm long, 0.95 cm diameter quadrupole filter. The pressure in this region is maintained at 8×10^{-4} torr with a 1500 L/s turbomolecular pump. An electrically isolated stainless steel plate (-28 V dc), with an 0.635 cm i.d. orifice, allows the mass spectrometer chamber to be maintained at $<2 \times 10^{-6}$ torr, using a 550 L/s turbomolecular pump.

RESULTS AND DISCUSSION

In our initial work with CZE-MS we have used (50/50) water-methanol with 10^{-4} M KCl as the separation and electrospray medium (7). We have observed that water-methanol provides a considerable electroosmotic mobility (3.6×10^{-4} $cm^2/(Vs)$). Thus, positively ionized compounds should (with $V_{CZE} = 37000$ V). As our initial test mixture we chose five ammonium salts: tetramethylammonium bromide, tetraethylammonium perchlorate, tetrapropylammonium hydroxide, tetrabutylammonium hydroxide, and trimethylphenylammonium iodide. These quaternary ammonium salts all gave good electrospray signals with the dominant peak in the mass spectrum being the quaternary ammonium cation (8). Initial results of this study have been reported (8).

The ability to combine CZE with mass spectrometry is based on the fact that the cathode need not be in a buffer reservoir, but only biased negative with respect to the anode. Thus, a metalized segment of capillary tubing or other electrical contact with the buffer provides the essential control of the electric field. This approach (necessary for mass spectrometric interfacing) does not alter the electroosmotic flow, at least to an extent that is detectable with fluorescence detection just prior to the electrospray. The success of this approach is further supported by the high efficiency separations presented in this communication. Electrospray ionization of various compound classes has been demonstrated, and a better understanding of this technique (including the role of pH, buffer concentration, and chemical nature) should allow broad application of CZE-MS. On the basis of these initial results, electrospray ionization appears to provide an ideal interface for the marriage of a highly efficient separation technique, capillary zone electrophoresis, with the sensitive and highly specific detector provided in the mass spectrometer.

REFERENCES:

(1) Mikkers, D. W. P.; Everaerts, F. M.; Verhegge, Th. P. E. *J. Chromatogr.* **1979**, *169*, 11.
(2) Jorgenson, J. W.; Lukacs, K. D. *Science* **1984**, *222*, 266.
(3) Lauer, H. H.; McManigill, D. *Anal. Chem.* **1986**, *58*, 166.
(4) David, P. A.; Pellechia, P. J.; Manning, D. L.; Maskarisha, M. P. Report ORNL/TM-9141, April 1984.
(5) Pretorius, V.; Hopkins, B. J.; Schieke, J. D. *J. Chromatogr.* **1974**, *99*, 23.
(6) Mack, L. L.; Kralik, P.; Rhonde, A.; Dole, M. *J. Chem. Phys.* **1970**, *52*, 4977.
(7) Whitehouse, C. M.; Dreyer, R. N.; Yamashita, M.; Fenn, J. B. *Anal. Chem.* **1985**, *57*, 675.
(8) Olivares, J. A., Nguyen, N. T.; Yonker, C. R.; Smith, R. D. *Anal. Chem.* **1987**, *59*, 1230.

Presented at the 35th ASMS Conference on Mass Spectrometry and Allied Topics
May 24-29, 1987, Denver, CO

INFRARED SPECTROSCOPY/MASS SPECTROMETRY

David Presser and Rob Robinson
Mattson Instruments, Inc.
1001 Fourier Court, Madison, WI 53717, (608) 831-5515

Infrared spectroscopy and mass spectrometry are used in tandem in analyses which would be difficult to solve by either of the techniques alone. By combining infrared with mass spectrometry, the strengths from one technique can support the other. The result is a method of identification which is more powerful than either of the individual techniques.

The sensitivity of conventional lightpipe GC/FT-IR techniques has lagged behind the sensitivity of GC/MS creating a difficulty in successfully combining mass spectrometry with infrared spectroscopy. Thus, the Cryolect^{tm} 4800 uses matrix isolation as its sampling technique for GC/FT-IR with a concomitant increase in sensitivity equivalent to that of GC/MS. The Cryolect 4800 employs a triple splitter in the gas chromatograph which diverts approximately 40% of the effluent to the matrix isolation infrared interface, 40% to the mass spectrometer and 20% to a flame ionization detector on the gas chromatograph. Mass spectra, infrared spectra and a FID trace are all obtained from a single sample injection.

At the infrared interface, argon gas is mixed in with the GC effluent and the mixture is sprayed onto a gold coated disk held near 12 Kelvin. The argon freezes on the disk trapping the sample molecules in a cage of argon. Since each sample molecule is surrounded by argon atoms, intermolecular interactions are minimal. As a result, infrared absorption bandwidths become very narrow. The cage of argon atoms prevents all but the smallest of molecules from rotating, thus the vibrational spectrum is free from rotational perturbations as well. The result is an infrared spectrum which consists of narrow intense peaks.

The key to the enhanced sensitivity of the infrared lies in the intrinsically narrow absorption bandwidths of a matrix-isolated compound. As peak width decreases, there is an accompanying increase in peak height or absorption which in turn means an increase in sensitivity. An example of the sensitivity can be seen in figure 1 which is a spectrum of approximately 200 pg of ethyl vanillin.

The focus of analyses has been on those where the interpretation of fragmentation patterns is complicated by the presence of isomeric compounds. The mass spectra of 6-methylbenz(a)pyrene and 7-methylbenz(a)pyrene are essentially identical. However, figure 2 shows how the complementary information from infrared spectra enables one to differentiate 6-methylbenz(a)pyrene and 7-methylbenz(a)pyrene. In order to determine if a rat metabolized benz(a)pyrene to 6-methyl B[a]P or 7-methyl B[a]P, an extract from a rat injected with benz(a)pyrene was run on the Cryolect. The isomers coelute so the pyrene peak was scanned and no trace of the 7-methyl B[a] was detected. Only the 6-methyl B[a] P was present.

Similarly, infrared can easily differentiate the isomers of the tetrachlorodibenzodioxins which is a difficult task for mass spectrometry. Figure 3 is an overlay of the dioxin isomers 1,2,4,7-tcdd and 1,2,4,8-tcdd. The marker dioxin 1,2,3,4-tcdd has been detected by the Cryolect with an approximately 150 pg injection. (M. Mossoba, Food and Drug Administration, Cryolect Users' Meeting, November, 1986). The tetrachlorodibenzodioxin compounds exemplify the sensitivity of the IR/MS Cryolect and its specificity by differentiating all 22 isomers.

Presented at the 35th ASMS Conference on Mass Spectrometry and Allied Topics
May 24-29, 1987, Denver, CO.

Figure 1.

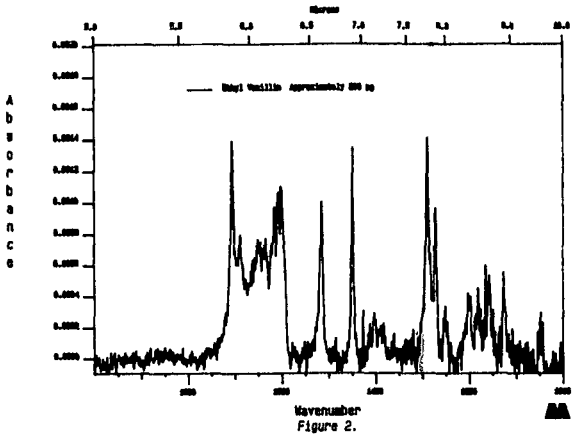

Figure 2.

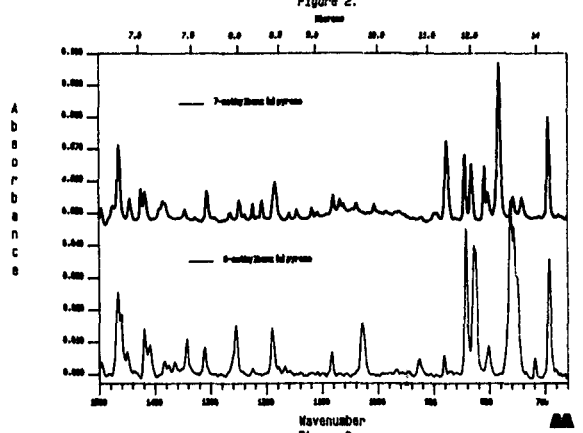

Figure 3.

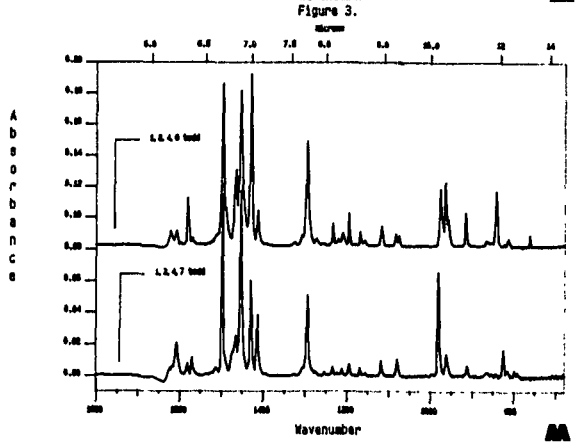

Presented at the 35th ASMS Conference on Mass Spectrometry and Allied Topics
May 24-29, 1987, Denver, CO

A LIQUID SAMPLING SYSTEM FOR MASS SPECTROMETRIC STUDY OF CONDENSED-PHASE CHEMICAL REACTIONS

James C. Tou and Damoder Reddy
Analytical Laboratories, B-574
Dow Chemical Company
Midland, Michigan 48640

Mass spectrometry is well recognized to be a very powerful and versatile spectroscopic technique for direct analysis of a gas phase reaction. The reaction system can be interfaced with a mass spectrometer by either using a flow restrictor such as a molecular leak[1], a capillary tubing or employing a semi-permeable membrane[2]. For sampling reaction species such as radicals, gaseous ions, a molecular beam interface has to be used in order to minimize the collisions of the reactive species with the walls of the interface system. For on-line mass spectrometric analysis of a condensed phase chemical reaction, semi-permeable membrane interfaces have been utilized[4,5] However, the technique is limited only to permeable and volatile organics.

In this paper, a more general sampling system is reported. The system as shown in Figure 1 involves injection of 1-2 μl of a liquid stream flowing through a Bendix liquid injection valve into a preheated inert gas stream such as helium at atmospheric pressure. Upon injection, the liquid is flashly vaporized. The vapor is carried by the inert gas stream into a series of chambers of equal volume and then mixed with a second helium stream for further dilution before exiting to vent. At the conclusion of the sample flow path, a molecular leak or a membrane inlet is used for the introduction of a small amount of the gas stream into a mass spectrometer.

An equation was derived to describe the concentration-time profile at the exit of the last chamber,

$$C_n = \frac{nC_o}{(n-1)} \left(\frac{ft}{v}\right)^{n-1} e^{-ft/v} \qquad \ldots\ldots(1)$$

where C_n is the concentration at the exit of the last chamber at time t after the injection, C_o the initial concentration in the first chamber with volume v, and f the helium flow rate.

The maximum concentration and the time at the maximum concentration are therefore

$$C_{max} = \frac{nC_o}{(n-1)} (n-1)^{n-1} e^{-(n-1)} \qquad \ldots\ldots(2)$$

and $$t_{max} = (n-1) \frac{v}{f} \qquad \ldots\ldots(3)$$

The concentration-time profiles are calculated as functions of the number of chambers, n, and also of flow rates, f. The results are shown in Figures 2 and 3. When n = 10, the profile becomes symmetric in shape and also exhibits a faster decay of the concentration than the case when a single exponential dilution chamber is used. This benefits the sampling turn-around time. The theoretical calculation has also been confirmed with experimental data as demonstrated in Figure 4.

The technique has been applied to the study of the hydrolysis rates of methyl acetate in an open reactor. Both the valve and the mass spectrometer are controlled by a data system developed in this laboratory. The specific ion plot is shown in Figure 5 for ions at m/z 31 methanol and 74 methyl acetate. The initial decrease of the intensity of ion at m/z 74 is attributed to the evaporation and the following decay to the evaporation and the hydrolysis reaction taking place when 1M HCl was added. Accompanying the above decrease is the increase of the intensity of ions at m/z 31 due to the formation of the hydrolysis product, methanol. The rate plots are shown in Figure 6. The rates of evaporation and reaction at several different conditions are shown in Table 1. The rate of reaction is in good agreement with the literature value, 2.2 x 10^{-4} sec at 25°C[6].

In conclusion, the on-line liquid sampling system presented in this paper can be used for mechanistic and kinetic study as well as process monitoring of a condensed phase reaction.

Presented at the 35th ASMS Conference on Mass Spectrometry and Allied Topics
May 24-29, 1987, Denver, CO

REFERENCES
1. B. Kasemo, Rev. Sci. Instrum., 1979, 50, 1602.
2. L. B. Westover, J. C. Tou and J. H. Mark, Anal. Chem. 1974, 46, 569.
3. C. A. Stens, F. J. Kohl and R. A. Miller, Ind. Res. & Devel., 1980, 116.
4. J. C. Tou, L. B. Westover and L. F. Sonnabend, J. Phys. Chem., 1974, 78, 1096.
5. Brodbelt, J. S. and Cooks, R. G., Anal. Chem. 1985, 57, 1153.
6. Moelwyn-Hughes, E. A., "The Kinetics of Reactions in Solution", Oxford Univ. Press, 1974, p. 321.

TABLE 1

THE RATES OF HYDROLYSIS OF METHYL ACETATE AT 20°C

solution	C_{H^+}	k_e	k_{er}	k_r	$k^*(k_r/C_{H^+})$
				10^{-4} sec^{-1}	
HCl	1M	0.52	2.7	2.2	2.2
HCl	2M	0 58	3.5	2 9	1.5
HCl-	2M	0.54	3.4	2.8	1.4
0.5 KCl					

*literature value = 2 2x10^{-4} sec^{-1} at 25° C

FIGURE 1

AN ON-LINE LIQUID SAMPLING SYSTEM FOR A MASS SPECTROMETER

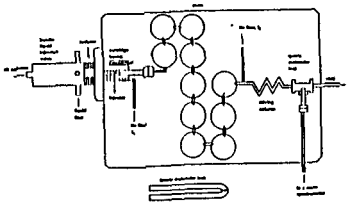

FIGURE 3

THE CONCENTRATION-TIME PROFILE AS FUNCTION OF FLOW RATE, f

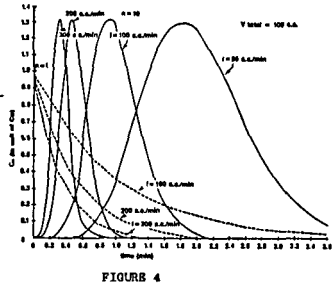

FIGURE 5

THE SPECIFIC ION PLOTS FOR THE HYDROLYSIS REACTION OF METHYL ACETATE

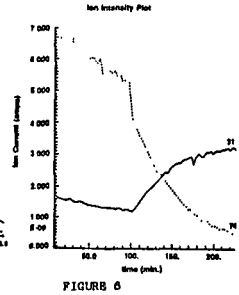

FIGURE 2

THE CONCENTRATION-TIME PROFILE AS FUNCTION OF NUMBER OF CHAMBERS, n

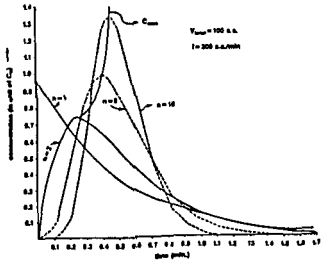

FIGURE 4

THE THEORETICAL AND EXPERIMENTAL CONCENTRATION-TIME PROFILE AT A FLOW RATE, 44 C.C./MIN

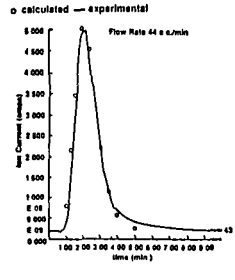

FIGURE 6

THE RATE PLOTS FOR EVAPORATION AND THE REACTION OF METHYLACETATE HYDROLYSIS IN 1M HCl

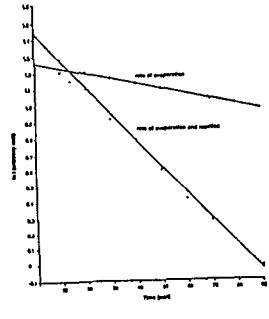

Presented at the 35th ASMS Conference on Mass Spectrometry and Allied Topics
May 24-29, 1987, Denver, CO

PARTICLE BEAM-LIQUID CHROMATOGRAPHY-MASS SPECTROMETRY (PB-LC-MS): ADVANTAGES AND APPLICATIONS.

R. C. Willoughby and F. Poeppel, EXTREL Corporation, Pittsburgh, PA 15238.

Particle beam sample introduction into the mass spectrometer can be described as any technique where sample in the form of an aerosol is accelerated through a small aperture forming a high velocity aerosol beam. The gaseous components of the aerosol beam radially expand about the axis of the aerosol beam more rapidly than the aerosol particulates when expanded into a vacuum. Consequently, a highly enriched particle beam can be produced by sampling or skimming only the core of the aerosol beam.

This technique of sample introduction has been used with real time aerosol monitoring and with LC/MS. Early developments with particle beam LC/MS were performed with Particle Impact Mass Spectrometry (PIMS)[1] and MAGIC-LC-MS[2]. This early work demonstated both EI and CI capabilities, as well as little chromatographic degradation. Preliminary results demonstrated significant analytical potential.

The present studies have focussed on developing particle beam liquid chromatographic interfaces with improved solute transport efficiencies as well as enhanced control over the aerosol generation processes. The present interface has significant improvements in solute transport efficiency over a prototype-MAGIC interface. In addition, design problems with beam alignment and particle dispersion have been resolved.

Analysis with the present particle beam interface yields spectra for low volatility analytes under EI, CI, FAB and discharge ionization conditions. Both normal and reversed phase chromatographic separations have been performed under isocratic and gradient conditions. Universal response characteristics are associated with this technique.

1. F. T. Greene, "Further Development of Particle Impact Mass Spectrometry," presented at the 29th Annual Meeting of the ASMS, New York, N.Y. (1980).

2. R. C. Willoughby and R. F. Browner. Anal. Chem. 56(14), 2626 (1984).

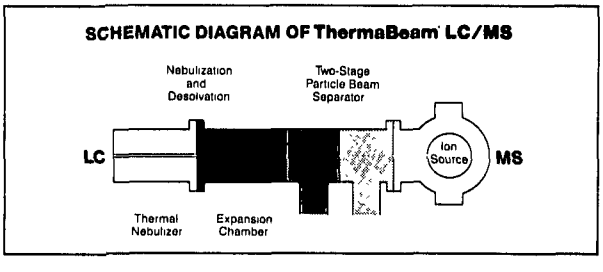

Presented at the 35th ASMS Conference on Mass Spectrometry and Allied Topics
May 24-29, 1987, Denver, CO.

A NEW ATMOSPHERE SAMPLING ION SOURCE*

Scott A. McLuckey and Gary L. Glish
Analytical Chemistry Division
Oak Ridge National Laboratory
Oak Ridge, TN 37831

There are many applications where mass spectrometry could make important contributions given an ion source that can sample directly from air, have high sensitivity with minimal ionization discrimination, run continuously without maintenance, and keep the gas flow into the mass spectrometer to a level that does not require a very large pumping system. While the β-emitter and corona discharge atmospheric pressure ionization sources can sample directly from air, the former has a limited sensitivity, while the latter, as commercially available, requires frequent maintenance and a very large pumping system. This paper reports a new design for an atmospheric sampling ion source that overcomes these problems.

Our atmospheric sampling ion source samples directly from ambient air; however, the ionization is done at sub-atmospheric pressure. The air is inlet into the ionization source through a 200 micron aperture. This allows a sampling rate of approximately 6 ml of air a second. The region in which the ionization takes place is typically held between 0.1 and 1 torr by pumping with a mechanical pump. An 800 micron aperture, parallel to the inlet aperture plate, interfaces the ion source to the mass spectrometer. A 1000 l/s turbo pump keeps the pressure in the analyzer region at $5x10^{-5}$ torr. The atmosphere side aperture plate is attached to the outside face of a 6 inch conflat flange while the other aperture plate is attached to the inside face of this flange. Both are attached with nylon screws with the vacuum seal being provided with an o-ring, which also provides electrical isolation. Holes drilled through the side of the flange (normal to the axis between the aperture plates) provide the pumpout ports. Figure 1 shows a schematic of the ion source.

The ionization occurs in a glow discharge that can be established either between the two aperture plates or between two parallel plates perpendicular to the axis between the aperture plates. Generally a discharge current of 1-10 milliamps is used. This is obtained, at the normal source pressures, with a voltage difference between the electrodes (plates) of about 400 volts. For negative ion analyses, the discharge is struck between the two aperture plates, while for positive ion analyses, the other two plates are used to establish the discharge.

The pressure and discharge voltage/current can be used to affect the appearance of the mass spectrum in the positive ion mode of operation. At high pressures and minimum discharge voltage/current, the mass spectra have the appearance of a combination of EI and CI spectra. This is shown in Figure 2 which is the mass spectrum obtained from the head space vapor of drinking water with 150 ppm trichloroethylene. In the molecular ion region both $M^{+\cdot}$ and MH^{+} are present and fragment ions from $Cl\cdot$ loss from each can also be seen. At lower pressures or high discharge voltages/currents the spectra show more fragmentation, indicating that greater amounts of internal energy are being deposited into the molecule when it is ionized at lower pressures or higher discharge voltages/currents. This is demonstrated in Figure 3 in which the upper portion of the mass spectrum of n-butylbenzene is shown as a function of discharge voltage. Here the molecular ion abundance is drastically decreased as the discharge voltage is changed from 376 to 392 volts. A further increase then drastically changes the m/z 91/92 ratio, in favor of the higher energy fragment, m/z 91. In the negative ion mode, these parameters do not affect the appearance of the mass spectrum very much, for the compounds we have studies. However, they do affect the absolute ion signal.

Because of the lower pressures used in this ion source, clustering is greatly reduced. In the negative ion mode, hardly any cluster ions have been observed. In the positive ion mode, water clustering with the sample molecules is sometimes observed. The clustering is a function of the parameters discussed above as well as the chemical composition of the sample; however, a molecular ion of equal or greater intensity than the cluster ion(s) is usually observed.

As an example of the sensitivity of the ion source, a signal of 400,000 cts/s has been obtained from sampling the head space vapor over trinitrotoluene. The saturated head space vapor pressure of trinitrotoluene is 6 ppb.

A disadvantage of this ion source is that the ions can be formed at various points along the discharge. Since the electric field potential changes, this leads to a wide energy spread in the ions being emitted from the source. However, this has been a minimal problem since we are using a quadrupole mass filter as the mass spectrometer.

In summary, some of the major feature of this ion source are its simplicity, ruggedness (it has operated for over a year without maintenance), and sensitivity. The preliminary results suggest that this source could be useful for a wide range of applications where continuous monitoring of the atmosphere is desired.

*Research sponsored by the U. S. Department of Energy, Office of Basic Energy Sciences, and Office of Safeguards and Security, under Contract DE-AC05-840R21400 with Martin Marietta Energy Systems, Inc.

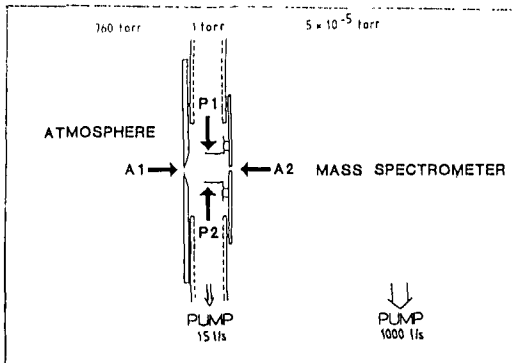

Fig. 1

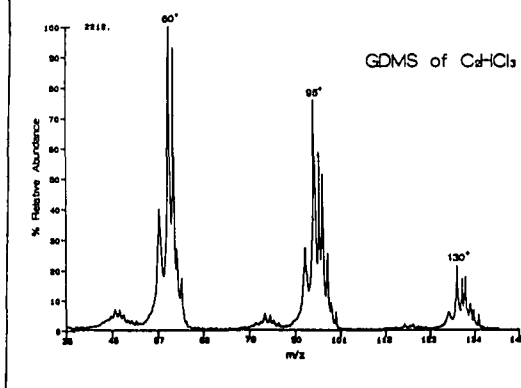

Fig. 2

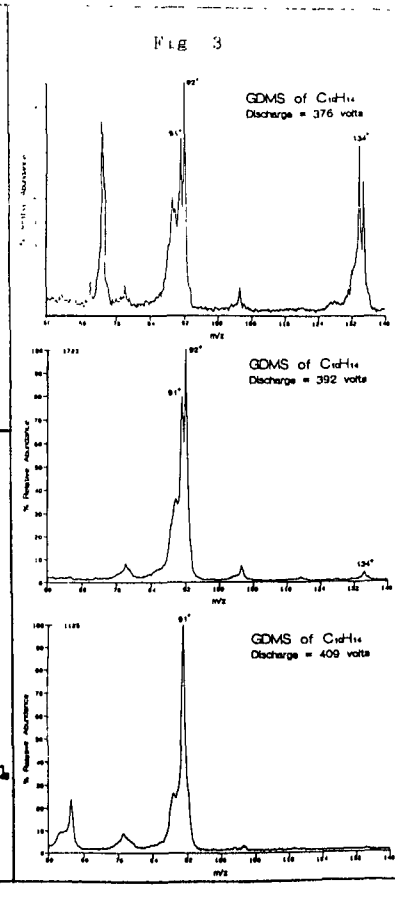

Fig 3

Presented at the 35th ASMS Conference on Mass Spectrometry and Allied Topics
May 24-29, 1987, Denver, CO

A MEDIUM RESOLUTION ATMOSPHERIC PRESSURE IONIZATION MASS SPECTROMETER

Andrew H. Grange
Department of Environmental Science and Engineering
Oregon Graduate Center, Beaverton, Oregon 97006

Robert J. O'Brien
Department of Chemistry and Environmental Science Doctoral Program
Portland State University, Portland, Oregon 97207

Douglas F. Barofsky
Department of Agricultural Chemistry
Oregon State University, Corvallis, Oregon 97331

Atmospheric pressure ionization (API) mass spectrometry is sufficiently sensitive to identify and quantify organic analytes in the gas phase at ppb to ppt levels; dynamic ranges of three or more decades are observable for many organic compounds.[1] Mixtures of trace components can be studied over a wide range of concentrations without the time consuming and the potentially sample-altering prerequisites of concentration and separation necessary with less sensitive ionization methods. Unfortunately, resolutions for existing quadrupole (unit resolution)[1] or single focusing magnetic sector instruments (300, 10% valley)[2] are very limited.

We built an API source for a VG 7070E-HF mass spectrometer (Figure 1) to study oxidized hydrocarbons in simulated atmospheres.[3] A major problem in coupling an API source to a double focusing magnetic sector instrument is the arcing which occurs as a result of the high accelerating potential used in the ion source. We designed and built an arc suppression device (Figure 2) which solves this problem by separating the pressure and potential gradients in the pumping line (Figure 3). The source operates stably at a corona discharge current of 0.2 μA (less than 0.03 μA of drift) over periods exceeding 1 h.

Disaggregation of hydronium ion water clusters, $H_3O(H_2O)_n^+$, and fragmentation of molecular ions through collsionally induced dissociation within the API source is controlled via an acceleration potential across a dissociation region. Relative humidity of the sample gas, adjusted through dilution with dry zero air, and the corona region pressure are used to limit cluster formation. Cluster, parent, and fragment ions can be differentiated by observing the trends in their abundances as functions of any or all of the three aforementioned variables.[4]

We achieved a resolving power sufficient to separate oxidized hydrocarbons with molecular weights as great as 150 daltons from other molecules having the same nominal masses. Figure 4a is a mass spectrum of the fully resolved (R=2,778) protonated molecular ions of pinacolone (m/z 101.09664) and 2,4-pentanedione (m/z 101.06025) recorded at one-sixth of their maximum signal strengths, and Figure 4b is a mass spectrum of the fully resolved (R=3,354) protonated benzaldehyde ion (m/z 107.04969) and the ^{13}C-xylene radical ion (m/z 107.08161) recorded at one-tenth of their maximum signal strengths. We estimated the maximum resolving power of the VG 7070E-HF operating in the API mode to be on the order of 4,600 (1% valley).

Acknowledgement. This work was supported by EPA Grant No. R811876-01-0.

References.

1. N.M. Reid, J.B. French, J.A. Buckley, D.A. Lane, A.M. Lovett, and G. Rosenblatt, 4th Joint Conference on Sensing Environmental Pollutants; American Chemical Society: Washington, D.C., 1978; p. 594.
2. M. Sakairi and H. Kambara, Mass Spectroscopy, 31, 87 (1983).
3. A.H. Grange, R.J. O'Brien, and D.F. Barofsky, submitted to Rev. Sci. Instrum. (1987).
4. A.H. Grange, R.J. O'Brien, and D.F. Barofsky, submitted to Anal. Chem. (1987).

Presented at the 35th ASMS Conference on Mass Spectrometry and Allied Topics
May 24-29, 1987, Denver, CO

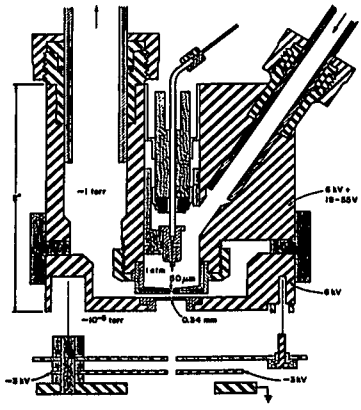

Figure 1. Construction details of the API source.

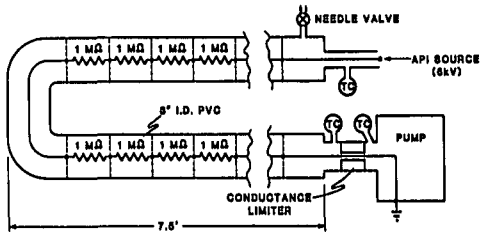

Figure 2. Arc suppression system.

Figure 3. Potential (dash) and pressure (solid) gradients along the pumping line from the collisionally induced dissociation (CID) region.

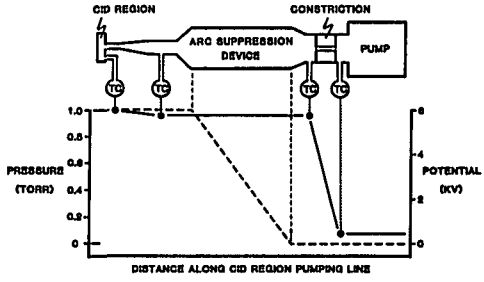

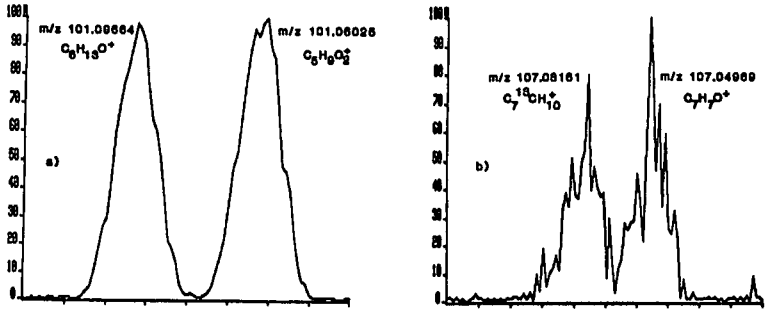

Figure 4. Molecular ion mass spectra a) for pinacolone and 2,4-pentanedione and b) for benzaldehyde and ^{13}C-xylene.

Presented at the 35th ASMS Conference on Mass Spectrometry and Allied Topics
May 24-29, 1987, Denver, CO

DESIGN AND PERFORMANCE OF A NEW API SOURCE COMPATIBLE WITH A COMMERCIAL TANDEM MASS SPECTROMETER

K.P. Matuszak, M.E. Hail, and J.V. Johnson
University of Florida, Gainesville, Florida, 32611

Atmospheric pressure ionization (API) has proven to be very useful for direct atmospheric monitoring in a variety of environmental situations. Here we describe the design, development, and preliminary characterization of a new API source for direct atmospheric analysis which has been developed to be compatible with a commercially available, turbomolecularly pumped, tandem mass spectrometer, specifically the Finnigan-MAT TSQ-70. While atmospheric pressure ionization is not new, most of the previously developed API sources have had limited use as direct atmospheric analyzers due to the problems of clustering of ions and orifice clogging that are associated with sampling moist, particulate-loaded air. The one API source that has performed direct atmospheric analysis effectively is attached to a liquid helium cryogenically pumped tandem mass spectrometer. This instrument is essentially limited to performing exclusively API and lacks the interchangeability with standard EI/CI sources which have proven to be the standard for MS/MS analysis of complex solid and liquid samples.

The API source (Figure 1) has been designed and constructed so that it is interchangeable with a standard EI/CI source. A modified lens assembly is substituted for the normal ion source block with the removal of two screws. A normal, blank, instrument flange has been modified to contain a replaceable diaphragm with a laser-drilled orifice. On the atmospheric side of this flange, one can mount either the API source itself or a blank metal plate to close the leak from the atmospheric region to the vacuum region. Because the instrument is turbomolecularly pumped, the instrument can be vented, the sources switched, and once again pumped-down and running in 20-30 minutes.

Air is drawn through concentric glass tubes, past the discharge region, and out through a side port of the source by means of a 10 mL/s blower fan. The source utilizes a corona discharge for the primary ionization of atmospheric species. Sample molecules are ionized by interaction with the ionized atmospheric species undergoing proton transfer and charge transfer reactions, and are pulled through the orifice into the vacuum region of the mass spectrometer by electric fields.

In the development of this source, the SIMION ion optics program has been used to model our lens design for the region between the orifice and the quadrupoles. We have compared the modeled electrical potentials with those which have been experimentally determined to provide the best results. One example of the use of the SIMION program to solve an ion optics problem was the need to direct the ions through a grounded source mounting plate. With the help of SIMION we have implemented a cylindrical lens that effectively shields the ions from the ground potential field and helps focus the ion trajectories toward the pre-quadrupole lenses.

Design work has also included the characterization of gas dynamics to minimize cluster ion formation and to prevent orifice clogging. We have utilized a small tube to provide a "jet" of nitrogen gas streaming past the orifice. This provides a "dry" region before the orifice which minimizes the number of non-ionized atmospheric species which make it into the vacuum region of the mass spectrometer. In the post-orifice region the ions and molecules undergo a free-jet expansion; and the associated cooling which the they undergo can cause clustering reactions for species which readily undergo gas-phase hydrogen bonding. Figure 2 shows the difference in the background ions detected with (a) the nitrogen jet off and (b) the nitrogen jet on. The number of water molecules clustered together is drastically reduced and the intensity of the peaks significantly increased with the nitrogen jet on. The cluster ions can also be declustered by increasing the potential difference between the conical lens and the orifice (Figure 2c). The combination of these effects provides molecular ions, pseudo-molecular ions, and small sample cluster ions.

Preliminary characterization of the source has been performed using pure solvents and aromatics injected into a gas stream flowing through the source, and in direct ambient air monitoring of vapors from the caps of solvent bottles. Figures 3 shows the (a) benzene, (b) acetone, and (c) methanol ions that have been generated through charge exchange and proton transfer reactions when performing direct atmospheric analysis. Preliminary studies have demon-strated the importance of the corona discharge needle position, current, and voltage on the ions produced and their relative intensities.

ACKNOWLEDGEMENTS

We would like to thank the Air Force Engineering and Services Center at Tyndall AFB who funded this research, the University of Florida Chemistry Department Machine Shop who constructed the API source, Finnigan-MAT for their cooperation and technical advice, and D.J. Dahl and J.E. Elmore of the Idaho National Engineering Laboratory who modified the SIMION program and allowed us to use it.

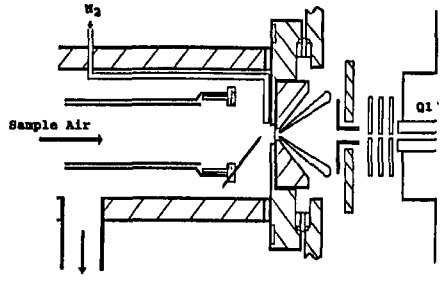

Figure 1. Schematic representation of the new API source.

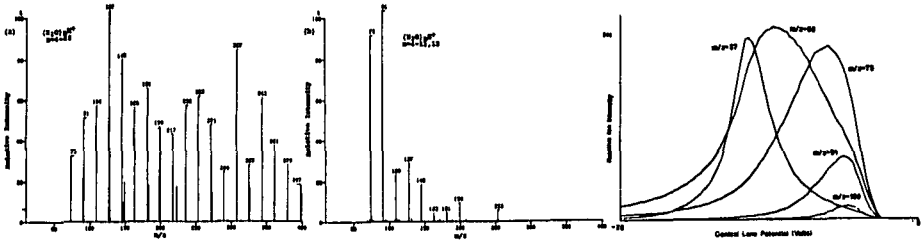

Figure 2. Background cluster ions produced with (a) no nitrogen jet, (b) nitrogen jet, and (c) varying potential difference between the conical lens and the orifice.

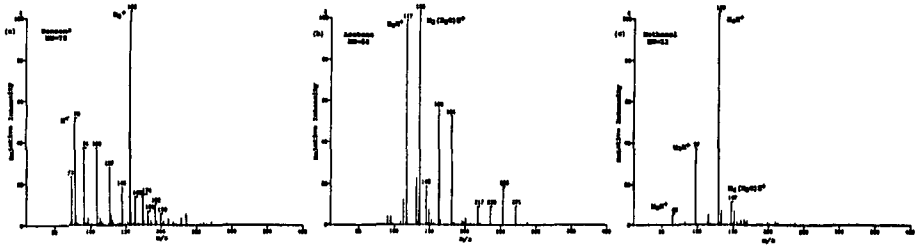

Figure 3. Sample ions produced by direct atmospheric sampling for (a) benzene, (b) acetone, and (c) methanol.

Presented at the 35th ASMS Conference on Mass Spectrometry and Allied Topics
May 24-29, 1987, Denver, CO

A NEW HIGH RESOLUTION TIME-OF-FLIGHT SECONDARY ION MASS SPECTROMETER

E. Niehuis, T Heller, H. Feld and A. Benninghoven
Physikalisches Institut Universität Münster, Wilhelm-Klemm-Str. 10, D-4400 Münster, FRG

We have developed a time-of-flight SIMS instrument which combines the extremely high sensitivity of the TOF analyzer with high mass resolution [1]. The primary beam system, based on a pulsed 90° deflection, produces mass separated Ar ion pulses with a duration of less than 1 ns at an intensity of up to 5000 ions per pulse. A reflectron type time-of-flight analyzer has been optimized for the specific requirements of the secondary ion source. Calculations of the energy dispersion of the analyzer including the acceleration gap show that a mass resolution of 15000 is possible for a relative energy spread of 0.4 %.

Two instruments of this type were built for biochemical and biomedical applications. Some features of these instruments are important for routine analysis:

1. The sample transfer system provides the introduction of eight samples at a time
2. Due to the quasisimultaneous detection of all masses the time for the accumulation of a complete spectrum is a few seconds.
3. The polarity of the spectra can be changed within ms without recalibration of the mass scale.
4. Differential pumping provides the analysis of samples with high vapour pressure (glycerol).

The mass resolution of these instruments was limited by the registration system (100 MHz signal averager).

Now a new registration system was implemented that consists of a time-to-digital converter (TDC), a fast buffer memory and an accumulating memory board It is capable of accumulating spectra in ion counting mode up to a total flight time of 160 μs with a time resolution of 1.25 ns. The maximum number of stop events per pulse can be higher than 256 and the maximum average count rate is 2.5×10^6 c/s. The spectrum is accumulated in a RAM array with 128k channels and a word length of 24 bits.

The time base for the TDC is a triggerable 400 MHz clock, which is phase locked to a crystal controlled reference oscillator by a special type of phase locked loop (PLL). This PLL, although it maintains the frequency extremely constant, does not destroy the phase information which is introduced by the trigger pulse. The trigger pulse is driven by the high voltage pulse generator for the primary beam deflection. The clock frequency is doubled to 800 MHz and divided to 100 MHz. For each time slot of 10 ns the incoming events are shifted with 800 MHz into a fast 8-stage shift register. If one or more stop events are in the shift register after these 10 ns, then its content is stored in the fast buffer memory together with the content of a 16 bit time slot counter, which is advanced every 10 ns. All these operations of shifting and storing occur simultaneously and no additional dead time is introduced. The overall dead time for the registration system is equal to the channel width of 1.25 ns.

The buffer memory contains 8 bits of time information from the shift register in an 'n out of 8' code (n=1-8) plus 16 bit of binary coded coarse time information from the 100 MHz counter. Up to 256 of these words can be stored in the buffer memory. The memory is capable of quasisimultaneous write/read operations, so again no dead time is needed to read the content. After reading a word of flight time information the first 8 bits are converted to one or more words of 3 bit binary code, depending on the number of bits set. Together with the last 16 bits these form 19 bit words of binary coded flight time.

The accumulating memory board takes these words (actually only the first 17 bits are used) as the address for one of its 128k channels. The content of the addressed channel is incremented and in that way the

spectrum is accumulated. The total number of counts per channel can be as high as 1.6×10^7 corresponding to a 24 bit word. The incrementing cycle takes about 400 ns, therefore up to 2.5×10^6 events/s can be processed.

A 16 bit microcomputer is used for spectra processing, storing and graphic display. It is connected to the accumulating memory board by a SCSI interface, which allows transfer rates of 1 Mbyte/s.

The width of the H^+-peak reflects the overall time resolution of a TOF-SIMS which is determined by the primary pulse width, the timing properties of the secondary ion detector and the registration system. With the new registration system this peak width (10%) is one channel (1.25 ns). Taking into account the channel profile of the TDC, the time dispersion of the analyzer for M=1 and the accuracy of the constant-fraction discriminator this results in a primary pulse width of about 800 ps. We have measured the peak center of various masses in the low mass range for different delays (125 steps) to get an estimate of the accuracy of the flight time in the low mass range. The standard deviation was less than 5 ps. Therefore an exact mass calibration is possible with a precision in the ppm range.

First tests of mass resolution were made with Crystal Violet (M.W. 372.24). At an acceleration voltage of 2 kV a resolution of 13000 has been achieved (FWHM).

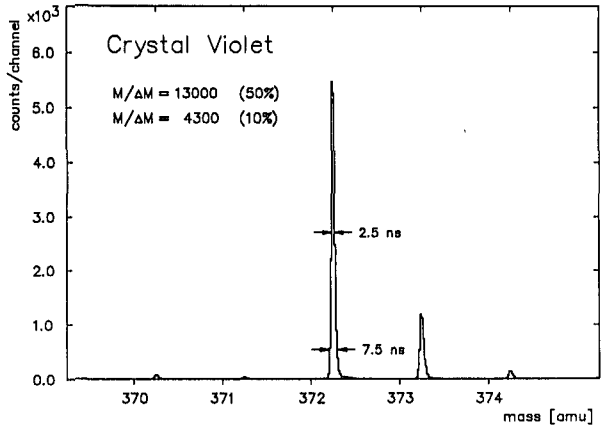

[1] E. Niehuis, T. Heller, H. Feld and A. Benninghoven
Springer Proceedings in Physics, edited by A. Benninghoven
(Springer, Berlin 1986), Vol. 9, p.198

Presented at the 35th ASMS Conference on Mass Spectrometry and Allied Topics
May 24-29, 1987, Denver, CO

EFFECTS OF SAMPLE PREPARATION ON MOLECULAR ION FORMATION IN PLASMA DESORPTION MASS SPECTROMETRY OF PEPTIDES AND PROTEINS.

P. Roepstorff, P.F. Nielsen and K. Klarskov
Department of Molecular Biology, Odense University
DK 5230 Odense M, Denmark.

B.U.R. Sundqvist, P. Håkansson and G. Jonsson
Tandem Accelerator Laboratory, Uppsala University,
S-751 21 Uppsala, Sweden.

Plasma desorption mass spectrometry (PDMS) has been demonstrated to be a very useful technique for molecular weight determination of peptides and proteins. A major improvement in spectrum quality has been obtained by adsorption of the sample to nitrocellulose followed by washing of the surface in order to remove low molecular weight contaminants (1). The major differences observed compared to the electrospray technique traditionally used for sample preparation are increased abundance of multiply charged molecular ions, narrower peaks indicating lower internal energy of the ions and increased sensitivity. A similar effect has been observed by cospraying the sample with reduced glutathione (GSH) (2). We have recently observed the same improvement in spectrum quality by simply drying peptide samples on nitrocellulose surfaces without subsequent washing, provided that the absolute amount of sodium is low. Somewhat higher sodium contents can be handled if a protein or peptide sample is dried on a spinning nitrocellulose surface. The latter technique has resulted in approximately one order of magnitude increase in sensitivity for proteins like insulin (mw 5778)(Fig. 1) and trypsin (mw 23,463).

By using the above mentioned sample preparation techniques we have been able to study the yield of molecular ions, expressed as number of molecular ions formed per 100 primary ions as function of different parameters:

- Increasing the abundance of alkalimetal ions in the sample estimated by the abundance ratio of Na^+/H^+, reduces the molecular ion yield. For the peptide antibiotic Nisin it is further demonstrated that increasing the sodium content causes extensive fragmentation.
- Molecular ion yield shows a sample specific dependency of the pH of the sample solution. This effect is seen when the sample is adsorbed to nitrocellulose and subsequently rinsed, and is most probably related to adsorption of the sample to nitrocellulose.
- For samples dried on nitrocellulose either directly or by spin drying a sensitivity optimum is observed at rather low sample quantities. Increasing the sample amount reduces the molecular ion yield. (Fig. 1).
- By addition of the spray solution, an increase in molecular ion yield and a decrease in Na^+/H^+ ratio is observed. The effect of GSH, therefore, seems to be related to the removal of sodium.
- Energy density scaling experiments using the Uppsala tandem accelerator showed similar results for samples sprayed with or without glutathione but differing from samples adsorbed on nitrocellulose, indicating that lower energy is required for desorption/ionization of molecular ions for molecules bound to nitrocellulose (3).

The observations described here lead to the conclusion that molecules exposed directly on the surface give much higher molecular ion yields, and molecular ions desorbed from the surface have lower internal energy. The effect of alkalimetals is believed mainly to be related to solubility properties of sample versus alkalimetal ions. In the solvent evaporation proces the more soluble alkalimetal salts tend to migrate to the surface and thus form the outer layer of the dry particle/layer. Furthermore, it seems as if sample molecules adsorbed directly on nitrocellulose are more easily desorbed/ionized than when interacting with other sample molecules in multilayers.

References:

1. G. Jonsson, P. Håkansson, B. Sundqvist, P. Roepstorff, P.F. Nielsen, K.E. Johansson, I. Kamensky and M. Lindberg. Anal. Chem. 58 1084 (1986).

2. M. Alai, P. Demirev, C. Fenselau and R.J. Colter. Anal. Chem. 58 1303 (1986).

3. P. Roepstorff, P.F. Nielsen, B.U.R. Sundqvist, P. Håkansson and G. Jonsson, Int. J. Mass Spectrom. Ion Proc. in press.

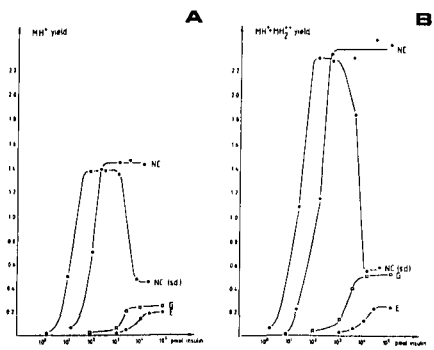

Fig. 1. Molecular ion yields for porcine insulin, expressed as the number of molecular ions per 100 fission fragments as a function of the sample amount applied. The four different sample preparation methods were electrosprayed with (G) and without (E) glutathione, adsorbed (with subsequent rinsing) to nitrocellulose (NC) and spindried on nitrocellulose (NC(sd)). A: Yields of MH^+ only, B: Sum of yields of MH_2^{++} and MH^+.

Presented at the 35th ASMS Conference on Mass Spectrometry and Allied Topics
May 24-29, 1987, Denver, CO

KINETIC MODELLING OF FAB SPECTRA OF DIETHANOLAMINE SOLUTIONS IN GLYCEROL AND MODELS OF DESORPTION IONIZATION.

Sunner, J., Morales, A., Kebarle, P.; Department of Chemistry; University of Alberta; Edmonton, AB; Canada T6G 2G2.

The intensities of molecular ions, fragment ions and cluster ions in Fast Atom Bombardment (FAB) mass spectra of diethanolamine, DEA, solutions in glycerol were measured at different DEA concentrations, from neat glycerol to neat DEA. A gas-phase kinetic scheme based on the "gas collision model" (GCM) was shown to successfully reproduce the experimental results[1]. The formation of a "gas" is explained[2] as a result of a "phase explosion" from liquid to gas that occurs as a result of the liquid matrix approaching the limit of "absolute stability" or the "spinodal"[3].

The intensities of the major ions in the FAB spectra of the DEA/glycerol solutions are shown in Figure 1 as a function of DEA concentration. It is seen that the concentration dependence of the intensities is quite regular. The DEA peaks increase very rapidly as the DEA concentration increases from zero, whereas glycerol-derived ions decrease. This observation is in accordance with the high preference observed earlier[4] for analytes with high gas-phase basicitie

The experimental result was modelled by the kinetic scheme in Table I, R1- . The result is shown in Figure 2. The kinetic scheme is based on the GCM model for FAB ionization[1]. The central idea in the GCM model is that extensive ion-molecule chemistry occurs during the FAB desorption process in what is best described as a gas[2]. The collision cascade causes extensive ionization in the matrix, R1-2. The resulting ions as well as ions preformed in the liquid engage in ion-molecule reactions and also undergo extensive recombination in the expanding matrix.

It is seen in Figure 1 that the glycerol ions decrease approximately exponentially with increasing DEA concentration. A gradual increase in the exponential decay of the glycerol ions occurs in the following order: fragments, F_G^+ GlH^+ $(Gl)_2H^+$ $(Gl)_3H^+$ (Fig. 1). This behaviour can be explained if it is assumed that the emitted ions have a distribution of residence times in the "gas". Glycerol ions emitted very shortly after the atom impact are detected mainly as glycerol fragment ions. Glycerol ions with longer residence times are detected mainly as molecular ions followed by cluster ions. This behaviour can have two different explanations. Either successive clustering occurs in the "gas" or the extent of declustering and fragmentation in the vacuum of emitted glycerol clusters change with the residence time ("the gas cools down").

The glycerol ions detected as clusters have a longer exposure to the high-gas-phase basicity analyte and are thus attenuated more strongly by the analyte. This behaviour is modelled by R3-7 in Table I. The calculated ion intensities are shown in Figure 2 and the residence time distribution in Figure 3.

The behaviour of the DEA ions and of the mixed cluster shown in Figure 1 was modelled by Reactions R8-13 in Table I.

The formation of the "gas" assumed in the GCM model is explained[2] by a "phase explosion" model. As a liquid in vacuum undergoes rapid heating, it will at a temperature close to the critical temperature approach the limit of "absolute stability"[3]. A liquid that reaches this limit undergoes a transition to a gas without the formation of vapor bubbles, a "phase explosion". For water this occurs, in a thermalized system, at ca. 300°C. The enthalpy content of the water phase at the onset of the explosion is, however, not sufficient for complete vaporization. Thus, the extensive clustering observed in SIMS spectra of water ice is explained as a direct consequence of the energetics of the phase explosion. The same argument also explains the extensive clustering observed in SIMS spectra of solid N_2[5] as well as the gradual decrease in clustering observed in SIMS spectra for a series of n-alkyl alcohols with increasing alkyl chain length[2].

1. Sunner, J.; Morales, A.; Kebarle, P. Anal. Chem.- submitted.
2. Sunner, J.; Ikonomou, M.; Kebarle, P. Int.J. Mass Spectrom. Ion Proc., submitted.
3. Gibbs, W. The Scientific Papers, Vol. 1, Dover Publ. Inc.: New York, 1961.
4. Sunner, J.; Kulatunga, R.; Kebarle, P. Anal. Chem. 1986, 58, 1312.
5. Jonkman, H.T.; Michl, J. J. Am. Chem. Soc. 1981, 103, 1007.

Presented at the 35th ASMS Conference on Mass Spectrometry and Allied Topics
May 24-29, 1987, Denver, CO

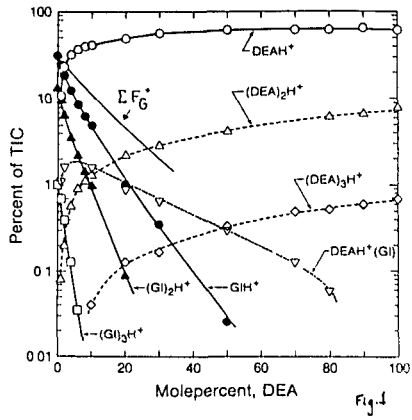

Fig. 1

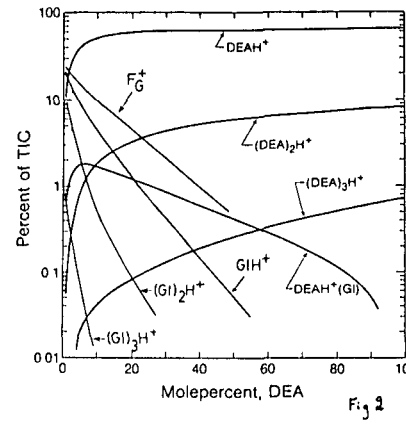

Fig 2

Table I. Reactions and rate constants used in "full" kinetic model for glycerol/DEA mixtures

No	Reaction	$k/10^9\ M^{-1}\cdot s^{-1}$
R1)	$Xe + Gl = F_G^+ + C^-$ (or e^-) $+ Xe$	
R2)	$Xe + DEA = F_D^+ + C^-$ (or e^-) $+ Xe$	
R3)	$F_G^+ + Gl = GlH^+ + (F_G\text{-}H)$	0 42
R4)	$GlH^+ + Gl = (Gl)_2H^+$	0 175
R5)	$(Gl)_2H^+ + Gl = (Gl)_3H^+$	0 035
R6)	$\{F_G^+, GlH^+, (Gl)_nH_+\} + DEA = F_D^+ + N_i$	1.3
R7)	$\{F_G^+, GlH^+, (Gl)_nH_+\} + DEA = DEAH^+ + N_i$	8 7
R8)	$F_D^+ + DEA = DEAH^+ + N_i$	1.95
R9)	$DEAH^+ + DEA = (DEA)_2H^+$	0 054
R10)	$(DEA)_2H^+ + DEA = (DEA)_3H^+$	0 039
R11)	$DEAH^+ + Gl = DEAH^+(Gl)$	0.025
R12)	$DEAH^+(Gl) + Gl = DEAH^+(Gl)_2$	0.020
R13)	$DEAH^+(Gl) + DEA = (DEA)_2H^+ + Gl$	3 0
R14)	$DEAH^+(Gl)_n + DEA = DEAH^+(DEA)(Gl)_{n-1} + Gl$	3 0

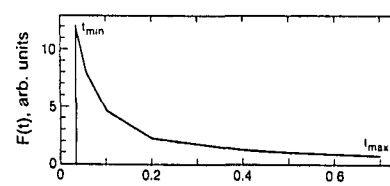

Fig 3.

Figure 1. Intensities in percent of total ion current, TIC, of the main ions in FAB spectra of solutions of DEA in glycerol (Gl); F_G^+, glycerol fragment ions.

Figure 2. Result of kinetic model (Table I) calculation of FAB spectra of DEA/glycerol solutions, c.f. Figure 1 for the experimental results.

Figure 3. Fitted residence time distribution for ions in the FAB "gas". Ions with short residence time are detected mainly as fragments and ions with longer residence time as protonated molecular ions and as cluster ions.

Presented at the 35th ASMS Conference on Mass Spectrometry and Allied Topics
May 24-29, 1987, Denver, CO

DIFFERENTIAL APPEARANCE OF ANALYTE AND MATRIX DURING THE FIRST SECONDS OF SPUTTERING BY FAST ATOM BOMBARDMENT: B. D. Musselman, J. T. Stults, and J. F. Holland, Department of Biochemistry, Michigan State University, East Lansing, MI, 48824-1319.

During FAB analysis, the observed ion currents normally stabilize approximately one second after desorption has been initiated. However, different behavior of analyte and matrix ions has been observed to occur during the first few seconds of fast atom bombardment. An enhanced level of analyte ion $(M+H)^+$ is observed during the initial period of sputtering and is followed by a reduction to its steady state level. This temporary enhancement can be observed repeatedly by turning the fast atom beam on and off. The desorption of matrix related ions such as the m/z 93 $(M+H)^+$ ion of glycerol produces a different ion current profile, a monotonic increase in ion current to the steady state.

A number of peptide molecules have been examined using this method. The typical desorption profile of a protonated peptide is shown in Figure 1. After a short delay or approximately 700 msec,, there is desorption in the abundant ion current at the $(M+H)^+$ which can be monitored by selected ion monitoring (SIM). The glycerol desorption profile, on the other hand, is more gradual as shown. During this time period, enhancement of signal to background is apparent. Fragment ions from the analyte behave in the same manner as the intact molecular ion species. This suggests that the appearance of this type of desorption profile is analytically useful as a means of identifying unknown components in the sample and discriminating them from matrix components.

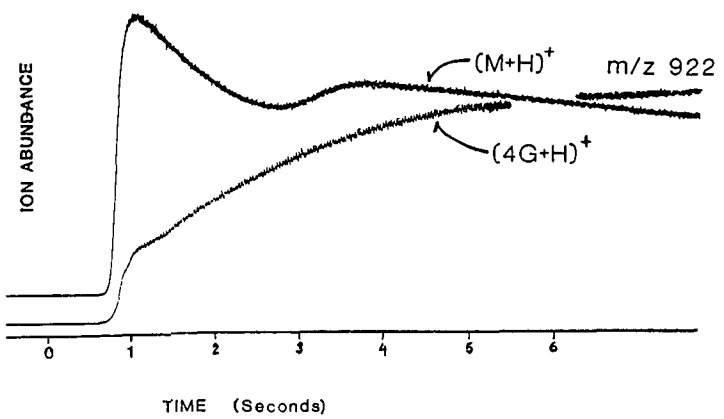

Figure 1: Desorption profile for protonated octapeptide (VHLTPVEK) *vs* proponated glycerol cluster ion.

Through analyses of a series of compounds with different chemical properties, the cause of these differential observations are being investigated. The initial desorption profile of protonated sucrose was similar to the ion abundance profile for protonated glycerol. This result was expected since, in this case, both the analyte and matrix were polyhydroxylated molecules. Desorption of the surfactant Triton X-100 showed a rapid increase in production of $(M+H)^+$, followed by an equally rapid drop in the abundance of the ion. During desorption of the Triton X-100, the appearance of protonated glycerol species from the matrix is negligible. These results indicate that surface activity plays a key role in desorption of the analyte during this early time period.

Figure 2: Differential desorption of analyte *vs* matrix as monitored by selected ion monitoring for the octapeptide from Figure 1.

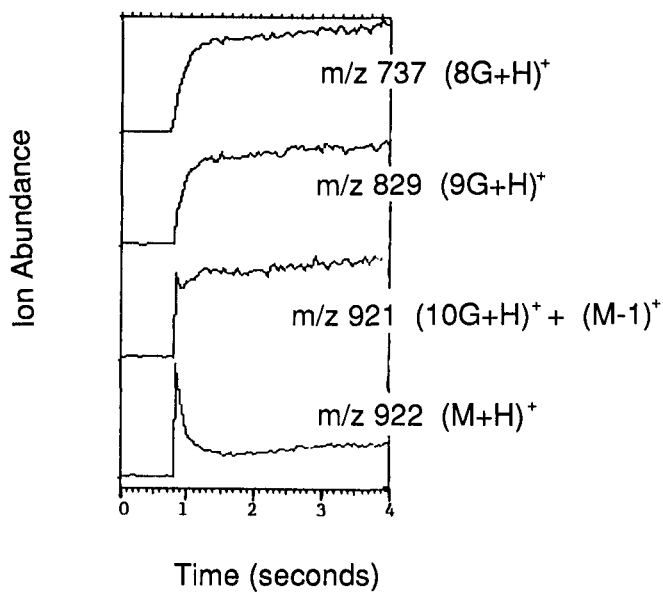

The authors wish to acknowledge the NIH and DOE for their funding of this work.

Presented at the 35th ASMS Conference on Mass Spectrometry and Allied Topics
May 24-29, 1987, Denver, CO

SURFACE CONCENTRATION IN LIQUID SIMS*

Peter J. Todd
Analytical Chemistry Division
Oak Ridge National Laboratory
Oak Ridge, TN 37831

The relationship between the analyte concentration, primary particle flux and the relative intensity of analyte characteristic peaks in the secondary ion mass spectrum is reported. Measurement of primary and mass-resolved secondary ion currents were done by Faraday cup and particle multiplier, respectively; surface concentration was determined indirectly. To do this, octylamine was introduced onto the surface of glycerol under 5 keV Ar^+ bombardment. From Henry's Law, and the relationship between analyte surface activity and analyte partial pressure, surface concentration in the limiting case of zero primary ion current was determined as a function of amine partial pressure. To extrapolate to conditions of zero primary ion current density, the relationship between protonated octylamine secondary ion intensity, octylamine partial pressure, and primary ion current density were determined by experiment.

At any primary ion current density between 0.05 and 2 $\mu A/cm^2$, protonated octylamine secondary ion intensity, $[130^+]$, showed the same functional dependence with pressure, P. In short, an asymptotic value of [130+] was reached as pressure was increased linearly. From these data, equation (1) was determined.

$$[130^+] = [130]_\infty\{1-\exp(-k_1P)\} \quad (1)$$

where k_1 is a function of primary ion current density.

Keeping octylamine pressure constant, an exponential relationship was determined between [130+] and primary ion current density. Secondly, it was found that as primary ion current was reduced to zero - the limit at which surface concentration is unambiguously linearly related to octylamine partial pressure, $\log[130^+]$ approached a finite value for each pressure at which the experiment was conducted. In the limit of zero primary ion current density, the behavior of $[130^+]$ as a function of pressure is identical to that of equation (1), but with a different value for k_1. From these data, it was determined that the relationship between primary ion current density, φ, octylamine mole fraction, X, and relative intensity of protonated octylamine in SIMS spectra of octylamine/glycerol solutions is given by equation (2),

$$[130^+] = 0.35\{1-\exp(-k_2X + k_3\varphi X)\} \quad (2)$$

where $k_2 = 1.75 \times 10^5$ and $k_3 = 0.52\ cm^2/\mu A$.

To show that a similar relationship holds for involatile solutes dissolved in liquids, spectra taken of a 1 mole % anthraquinone/sulfuric acid solution at two different primary ion current densities are shown in Figure 1. This solution was used because sulfuric acid is unequivocally acidic with respect to anthraquinone in both the gas and condensed phases, and does not suffer from cumulative radiation damage. What is clear from the spectra is that the relative intensity of any analyte characteristic ion depends not only on its concentration to a limited extent, but to the primary particle flux density to a major extent.

*Research sponsored by the U. S. Department of Energy, Office of Basic Energy Sciences, under Contract DE-AC05-84OR21400 with Martin Marietta Energy Systems, Inc.

"The submitted manuscript has been authored by a contractor of the U.S. Government under Contract No. DE-AC05-84OR21400. Accordingly, the U.S. Government retains a nonexclusive, royalty-free license to publish or reproduce the published form of this contribution, or allow others to do so, for U.S. Government purposes."

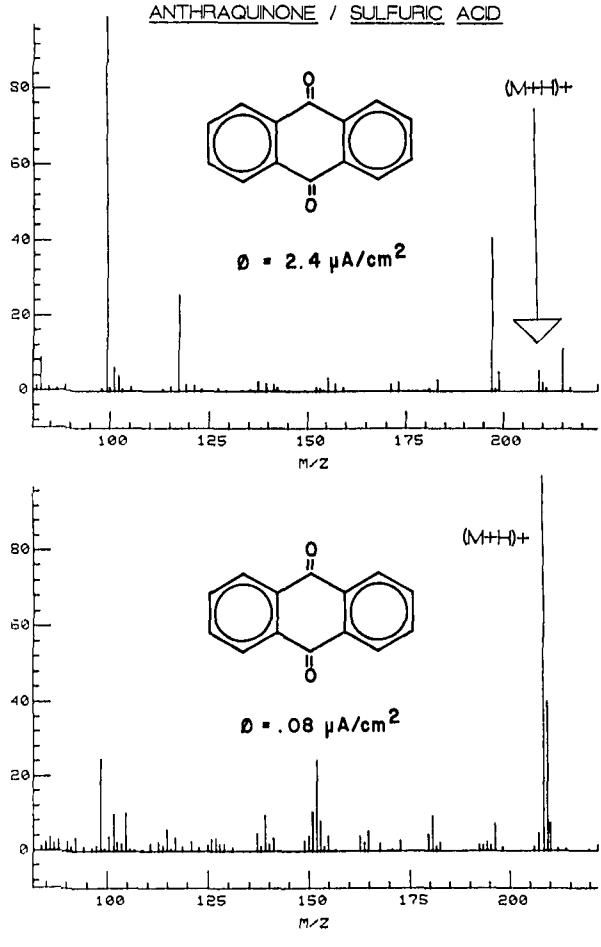

Figure 1. SIMS spectra of the same sample of a 1 mole % anthraquinone/sulfuric acid solution at two different primary ion current densities.

Presented at the 35th ASMS Conference on Mass Spectrometry and Allied Topics
May 24-29, 1987, Denver, CO

Paper TOC 915-----STUDIES OF THE SPUTTERING OF MULTIPLY CHARGED IONS FROM THE LIQUID PHASE: Woodfin V. Ligon, Jr. and Steven B. Dorn, General Electric Company, Corporate Research and Development, Schenectady, N.Y. 12301

It is well known that multiply-charged ions are not very abundant in the Liquid SIMS spectra of small molecules and that when they are observed it is usually as cluster ions whose net charge is unity. This has been explained by the suggestion that sputtering of multiply-charged ions is energetically unfavorable (1,2). Examination of the ion yield (singly-charged M+ or M-) versus charge state for some tetraacids (- ion mode) and tetraamines (+ ion mode) has revealed that, by itself, this interpretation is incomplete. In order for a molecule to be detected in the SIMS experiment, that molecule must approach the surface of the solution. We report here that, for relatively small molecules (m/z < 1000), as little as 2 charges are sufficient to almost completely remove the molecules from the surface. We conclude, therefore, that the lack of surface activity contributes to the difficulties encountered in observing multiply-charged ions.

The evidence for this conclusion is as follows: SIMS spectra from glycerol of 1,4,8,11-tetramethyl-1,4,8,11-tetraazacyclotetradecane, and a proprietary tetraacid with a molecular weight 556 were obtained using varying amounts of acid in the former case and varying amounts of base in the latter. For the amine, positive ion spectra were examined and for the acid, negative ion spectra were obtained. Solutions with a concentration of 0.01 M were used in each case. Figures 1 and 2 provide the results of these experiments.

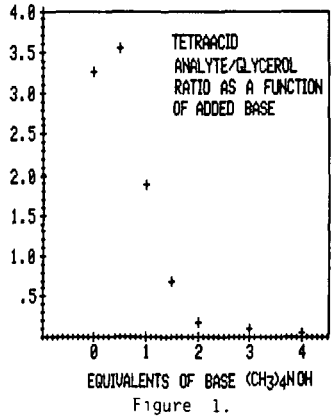

Figure 1.

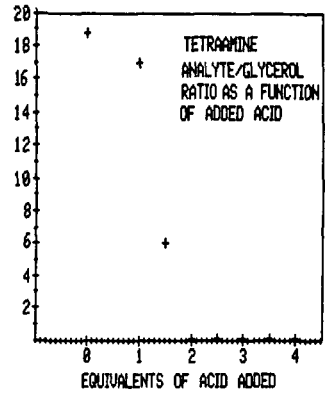

Figure 2

In both cases the SIMS signal for the analyte as measured by its ratio to the glycerol matrix signal was at its greatest for the neutral molecule. The signals diminished in a linear fashion approaching zero after addition of 2 equivalents of acid or base. In each case a relatively strong glycerol-free mass spectrum was progressively replaced with a spectrum which was dominated by glycerol matrix ions. Further addition of acid or base, respectively, beyond two equivalents did not substantially alter the spectra.

Since two equivalents of acid or base presumably converts all of the analyte to doubly-charged ions in each case and because it is considered energetically unfavorable to sputter doubly-charged ions, one might be inclined to argue that it is not necessary to propose that the analyte species has been removed from the surface but rather one need only propose that relative to glycerol the doubly-charged ions are not the most favored charge carriers. We submit that this argument is unlikely. Consider that, in the case of the acid, this argument requires us to propose that the anion of glycerol is more stable than both the doubly- and singly-charged anions of the acid. The singly-charged species must be included here because the glycerol/analyte signal ratio does not approach one but rather approaches zero. If the analyte were actually at the surface in an abundance equal to the situation without addition of base and its di-anion served as a base to ionize

glycerol during the bombardment then each of these processes should produce a singly-charged acid species which we should observe with good intensity. Instead, the singly-charged intensity approaches zero in both a relative and an absolute sense. This could only happen if glycerol also neutralized the singly-charged ions--a very unlikely occurrence. It should also be noted that none of these spectra exhibit cluster ions of the type (M--X+)- or (M++X-)+. Furthermore, even the addition of one equivalent of base dramatically reduces the analyte signal--an effect which cannot possibly involve the unfavorable energetics of doubly-charged ions. We propose that the doubly-charged ions do indeed serve as either an acid or base respectively toward glycerol producing the singly-charged ions which are observed but that the small abundance of these ions does not reflect unfavorable energetics but rather accurately reflects surface composition.

In addition to this rather strong evidence based on the spectra themselves, we have sought independent confirmation of changes in surface composition. Figure 3. shows the results of an experiment in which the drop weight was obtained for each of the solutions used to obtain the curve in figure 2. Drop weight is a classical method to quickly and easily determine relative surface tensions. The plot clearly demonstrates that, as base is added, the surface tension rises and that after two equivalents of base have been added little additional change occurs. This correlates exceedingly well with the SIMS data and suggests that a largely hydrocarbon-like low energy surface is replaced with a largely glycerol high-energy surface after addition of two equivalents of base.

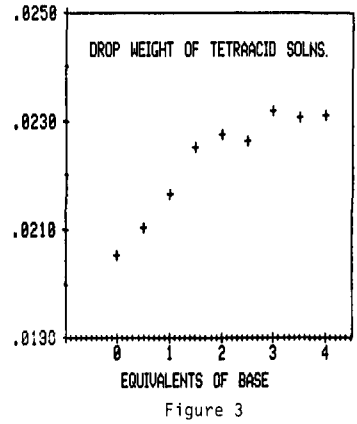

Figure 3

These data suggest, therefore, that the routine addition of acid or base in SIMS experiments will not always provide the best sensitivity. It also indicates that although the presence of precharged ions or the ready formation of an ion under the bombardment conditions are important criteria in determining sensitivity, surface activity remains the major controlling parameter in determining the ultimate sensitivity obtained. It is important to note that these experiments provide evidence that even a single formal charge reduces sensitivity significantly. We suggest, therefore, that derivatization schemes which introduce a full positive or full negative charge will probably provide less sensitivity than will schemes that introduce an uncharged functionality, such as a carboxylic acid, which combines both ready formation of ions and high surface activity. In our view, the concept of "reverse derivatization" (3) as practiced in liquid-SIMS may need to be revised slightly in light of these new findings.

References:

1) D. N. Heller, J. Yergey and R. J. Cotter, Anal. Chem., 55, 1310 (1983).
2) L. R. Schronk and R. J. Cotter, Biomed. Environ.Mass Spectrom., 13, 395 (1986).
3) K. L. Busch, S. E. Unger, A Vincze, R. G. Cooks and T. Keough, J. Am. Chem. Soc., 104, 1507 (1982).

Presented at the 35th ASMS Conference on Mass Spectrometry and Allied Topics
May 24-29, 1987, Denver, CO

FAB without a Liquid Matrix Using a Magnetic Sector Analyser and Parallel Detection : A Technique for Reducing Chemical Noise.

L.C.E.Taylor, Burroughs Wellcome Co., Research Triangle Park, NC 27709.
J.S.Cottrell, Kratos Analytical Instruments, Manchester M31 2LD, UK.

No liquid matrix is used in static SIMS experiments, nor was any used in the early days of FAB. Running samples dry reduces the chemical background to a few isolated peaks originating from the probe tip material. The penalties of this approach are lower signal levels, and difficulty in ionising very large molecules with kilovolt primary beams. Also, the use of a high intensity FAB gun causes extensive radiation damage, so that useful signals appear only briefly after the primary beam has been switched on. For these reasons, the preferred apparatus for sputtering dry samples is a pulsed primary ion beam and a time-of-flight analyser.

Many of the difficulties of performing static organic SIMS on a sector instrument could be alleviated by using a multichannel detection system. We have investigated the quality of data obtainable from a combination of a standard FAB source, a magnetic sector mass analyser (Kratos MS50RF), and a new electro-optical detector which provides parallel detection of a 4% mass window. (This detector is described elsewhere in these proceedings).

Thyrotropin Releasing Hormone, (TRH), is a blocked tripeptide of molecular weight 362u with a relatively poor detection limit for analysis by FAB. Figure 1 shows the appearance of the molecular ion region for a sample loading of 1µg of TRH in acidified glycerol. The detection limit may be reduced to 100ng by monitoring daughter ions in an MS/MS experiment.

To investigate the FAB spectrum of TRH without a liquid matrix, weighed samples of TRH were taken up in methanol and diluted with Analar water. Measured aliquots of sample solution were deposited onto a gold plated probe tip and evaporated to dryness under a rough vacuum. Our standard procedure for cleaning the probe tip using nitric acid followed by rinsing in Analar water proved to be inadequate for dry FAB experiments. The signal from the peptide was masked by intense background peaks which presumably originate from residues left by the cleaning procedure. To eliminate this problem, the cleaned probe tip was exposed to the FAB beam at full intensity until the initial burst of secondary ion emission had fallen to a stable level, (typically 10 to 30 seconds).

The saddle field FAB gun was operated at a beam energy of 4keV and a current of 8µA, which was the minimum level at which a stable discharge could be obtained. Even so, useful ion current from a monolayer sample was observed only during the initial one or two seconds of irradiation, making some form of parallel detection essential. Initial experiments showed a dramatic decrease in ion current when sample loading dropped below the equivalent of a monolayer. For the $1mm^2$ probe tip used in this work, a monolayer of TRH was calculated to be approximately 1ng.

Figure 2 shows the molecular ion region of the matrix free FAB spectrum of TRH at a total loading of 500pg. The spectrum of a solvent blank is included for comparison.

One advantage of using a magnetic sector instrument for this work was the facility for making accurate mass measurements. The upper spectrum in Figure 3 shows a peak observed in the spectrum of a tissue extract believed to contain TRH. Although the nominal mass, 385u, corresponds to the sodium

adduct ion of TRH, it was possible to determine by accurate mass measurement that this was not the case. (Mass measurement accuracy for a narrow peak on the array detector was generally better than +/- 20ppm).

Similar reductions in detection limit were not observed at higher mass. For Dynorphin(6-17), molecular weight 1609u, the detection limit for the dry material was identical to that for a glycerol solution, (2ng). However, the most reproducible results were obtained from co-depositing the sample with a thin film of glycerol by adding 1% glycerol to the aqueous sample solution, (Figure 4).

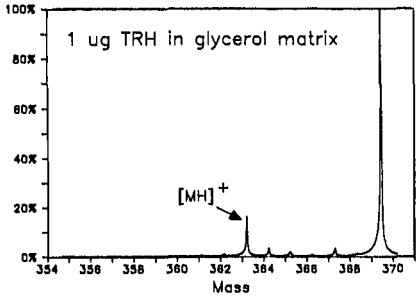

Figure 1

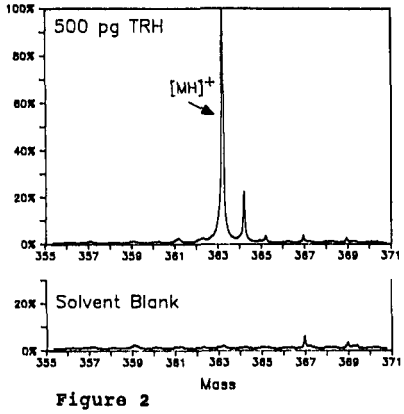

Figure 2

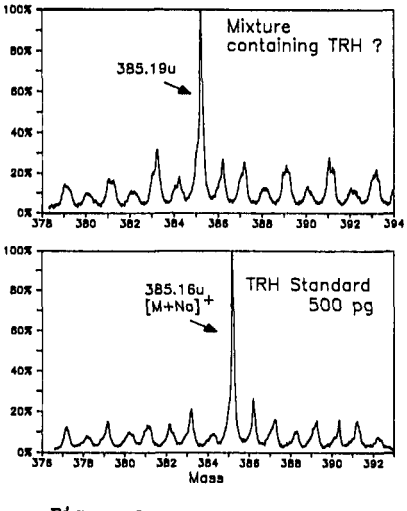

Figure 3

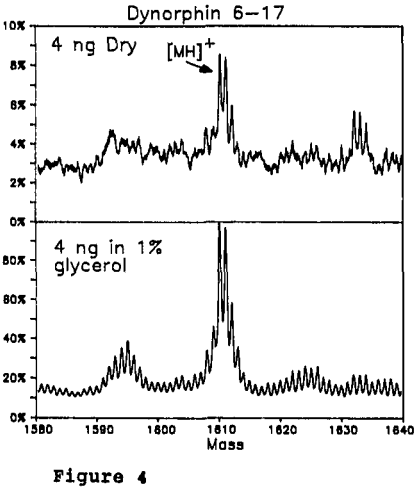

Figure 4

Presented at the 35th ASMS Conference on Mass Spectrometry and Allied Topics
May 24-29, 1987, Denver, CO.

LIQUID ASSISTED SIMS WITH A HIGH CURRENT DENSITY - HIGH ENERGY LIQUID METAL ION PRIMARY BEAM

Lon-fei Jiang, Elisabeth Barofsky, and Douglas F. Barofsky
Department of Agricultural Chemistry
Oregon State University, Corvallis, Oregon 97331

We have attached a commercial (FEI Corporation), focusing liquid metal ion (LMI) column to a single focusing magnetic sector instrument (Hitachi RMU-6E) in part to study the possibilities of achieving greater sensitivity in the liquid assisted secondary ionization mode. The experimental arrangement is depicted schematically in Figure 1. The LMI column delivers a 0.1-0.4 nA positive ion beam into a spot on the target less than 10 μm in diameter; this corresponds to current densities on the order of 0.1 mA cm^{-2}. The column can be operated at 25 kV; using a bismuth source, which emits primarily doubly charged ions, a sample can be bombarded with heavy ions (209 daltons) at energies up to 50 keV. The full impact of the beam can be concentrated into a microspot on the target, or the octupole/stigmator can be used to raster the beam over a relatively large area of the target providing effective current densities as low as 1 nA cm^{-2} (the static SIMS limit). With the aid of a small electron multiplier located in the vicinity of the sample and a display monitor, the system can be operated in a scanning ion microscope or microprobe mode in which the sample can be simultaneously or alternately imaged and mass analyzed.

In order to make the most efficient use of available analyte, it is necessary to deposit it on as small an area as practicable and to position this small patch of blob of sample both under the radiation umbrella of the primary beam and precisely within the acceptance zone of the mass analyzer (Figure 2). We utilize wire sample holders and take advantage of our LMI column's microscopic imaging capability to accomplish these tasks. A small amount of analyte (0.1-50 ng) in 1-10 nL of glycerol is suspended on a 10 μm diameter tungsten wire like a pearl on a string; the analyte is either premixed in the glycerol or deposited from an aqueous or organic solution, allowed to dry, and subsequently redissolved in a glycerol droplet that is placed over its residue. The wire, which is mounted on a conventional field desorption emitter holder, is inserted into the ion source with a standard field desorption probe, and the tiny sample droplet is located and positioned with the aid of the scanning ion microscope. The sample wire, even with its axis only approximately perpendicular to the finely focused primary beam, always presents the latter with a relatively large zone that falls within the range of incidence angles (55°-85°) that produce maximum sputtering yields.

We attain the greatest absolute signals and the greatest signal-to-noise ratios from our microsamples when the bulk of the glycerol is gone and a warmed, highly viscous, gel like, matrix remains on the wire; signal-to-noise ratios for very small amounts of analyte are strongly dependent on the degree to which the glycerol has been concentrated on the sample wire. This finding is similar to the recent observation by Ackermann et al. that certain saturated matrices, when heated, simulate the desired properties of glycerol without creating as much unwanted background and that detection limits in the submicrogram range might be achievable by this thermally assisted desorption ionization technique.[1] Also interesting is the statement by Röllgen that field-induced extraction of desolvated ions from a matrix that bears some qualitative resemblance to the one we observe is the most important mechanism by which gaseous molecular ions are formed from thermally labile or nonvolatile compounds during field desorption.[2] It seems plausible that these three independent observations might, in fact, reflect a common ionization mechanism.

We have obtained usable mass spectra from subnanogram amounts of glutathione (L-Glu-Cys-Gly), thyrotropin releasing hormone (TRH: pGlu-His-Pro-NH_2), and thyrotropin releasing hormone - free acid (TRH-FA: pGlu-His-Pro). Figure 3a shows a positive ion mass spectrum produced from ~80 ng of TRH-FA ~5 min after the sample was introduced into the mass spectrometer; the spec-

trum is qualitatively very similar to spectra produced from ~50 μg of TRH-FA on a KRATOS MS50-TC. In either case the mass peak corresponding to the molecular ion (m/z 364) is easily identifiable, but structurally significant mass peaks are lost in chemical noise. Figure 3b shows a positive ion mass spectrum of ~50 ng of TRH-FA recorded ~20 min after sample introduction while the sample is being warmed with a heating current of 6 mA and when nearly all of the glycerol has been evaporated; the matrix conditions are nearly ideal as evidenced by the marked absence of interfering glycerol peaks, the excellent signal to noise ratio, and the presence of easily discernable mass peaks corresponding to cleavages of the two peptidic bonds.

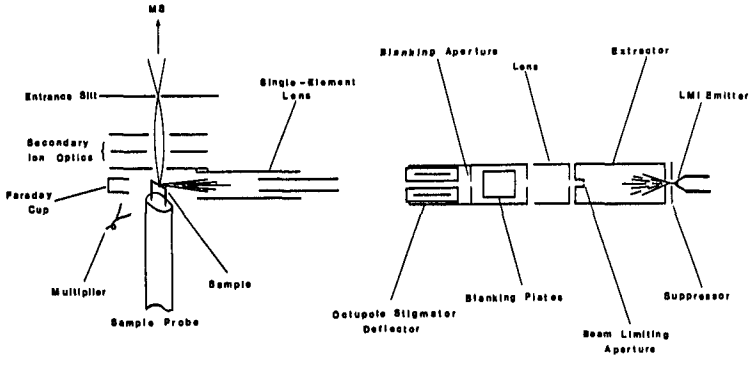

Figure 1.

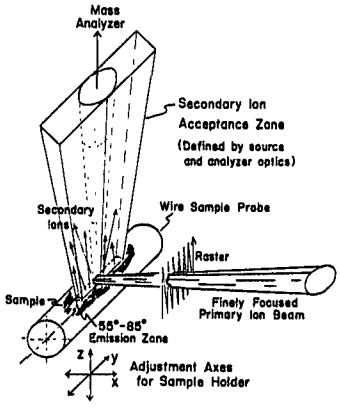

Figure 2.

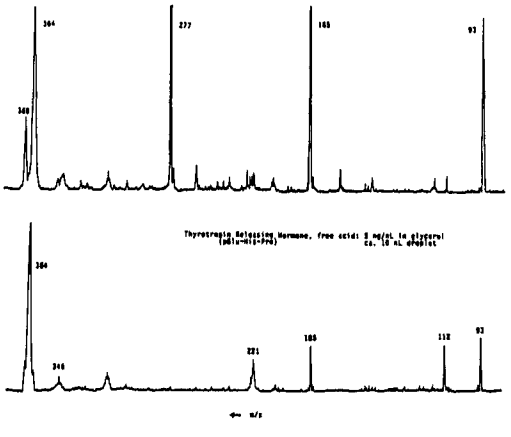

Figure 3.

Acknowledgement. Support for this work was provided by NIADDK Grant AM36050.

References.

1. B.L. Ackermann et al., Anal. Chem. 57, 2656 (1985).
2. F.W. Röllgen, In Ion Formation from Organic Solids; A. Benninghoven, Ed.; Springer-Verlag: Berlin, 1983; p 2.

Presented at the 35th ASMS Conference on Mass Spectrometry and Allied Topics
May 24-29, 1987, Denver, CO.

STUDIES OF SPUTTERED IONS IN A HIGH-PRESSURE FAST-ATOM BOMBARDMENT ION SOURCE

Mark M. Ross and John H. Callahan
Chemistry Division/Code 6112
Naval Research Laboratory
Washington, D.C. 20375-5000

INTRODUCTION

It has been shown that a variety of ion/molecule reactions can be implemented in a special high-pressure fast-atom bombardment ion source to affect significantly the observed mass spectra [1]. The processes that have been observed to occur between sputtered species and the buffer gas include charge exchange, chemical ionization, and collisional stabilization. The purpose of this work is to extend the utility of this source through a better understanding of these processes. The approach is to work with samples with well-characterized secondary ion mass spectra and to study only selected processes. Therefore, the focus of this report is on collisional stabilization of sputtered species and reactions that occur between sample and buffer gas species.

RESULTS

Collisional Stabilization

The secondary ion mass spectra of alkali halides are well-known and the "magic numbers" of cluster ions appear because of relative stabilities of different ion structures. Figure 1 shows a plot of log of CsI cluster ion, $[Cs(CsI)_n]^+$, abundance versus the cluster number, n, for two sets of experimental conditions. The first is the normal FAB experiment and the anomalous regions are apparent, especially between n=13 and n=16. The second plot shows the data obtained when 0.25 Torr of isobutane was admitted into the high-pressure FAB source. The anomalous regions have been "smoothed out" and the overall distribution has become an exponential curve. The cluster ions with excess internal energy that normally dissociate to more stable structures (e.g., n=14 to n=13) are stabilized by collisions with buffer gas molecules and are observed with significantly greater abundances.

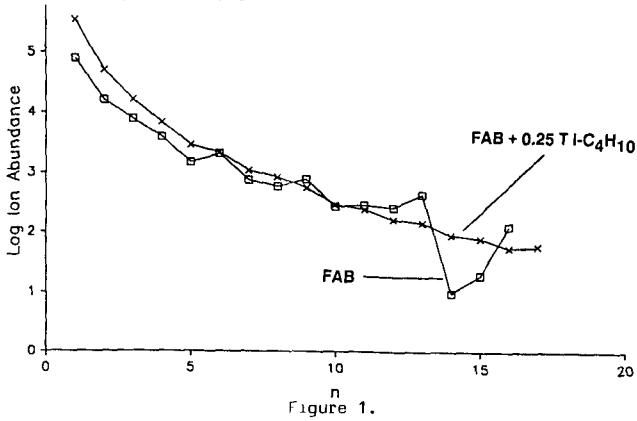

Figure 1.

The extent of collisional stabilization depends on the pressure of the buffer gas, the identity of the gas, and the repeller voltage. As the pressure of isobutane is increased from 0 to 0.25 Torr there is a corresponding decrease in the abundances of the "magic" cluster numbers relative to those of the adjacent clusters. Similarly, as the buffer gas is changed from a poor collisional stabilization gas to a good one ($He<CO<CO_2<i\text{-}C_4H_{10}$), at a constant pressure, the cluster ion abundance distribution becomes more smooth. Finally, it was discovered that the potential on the FAB probe tip had a large effect on the spectra when a gas was present in the source. For instance, as the repeller voltage was increased from 0 to +20 volts, with 0.1 Torr of isobutane, there

was a decrease in collisional stabilization and an increase in collision-induced dissociation, which resulted in a reappearance of the anomalous regions. Confirmation of the collisional stabilization effect was obtained by measuring a significant decrease in the abundances of fragment ions in the mass-analyzed ion kinetic energy spectra (MIKES) of cluster ions produced under the high-pressure conditions relative to normal FAB.

Collisional stabilization effects have been observed with organic samples as well. When olive oil (a mixture of triglycerides) is sputtered only diglyceride ions, corresponding to the loss of one acid moiety, and $[M+H-H_2O]^+$ species are observed above m/z 500. With SF_6 buffer gas, the $[M+H-H_2O]^+$ species disappear and $[M+H]^+$ ions are observed. If isobutane is used, isobutane reagent ions are produced by collisional ionization with the fast-atom beam and the abundances of the $[M+H]^+$ species increase significantly. This is an example of both collisonal stabilization of energetic sputtered ions and chemical ionization of desorbed neutrals occurring simultaneously.

Reactions

In an attempt to increase further the collisional stabilization of sputtered alkali halide cluster ions SF_6 was tested as a buffer gas. Instead of the expected collisional stabilization of CsI species, new cluster ions containing Cs, I, and F were observed. Figure 2 shows the ion abundance distributions for three types of cluster ions observed with 0.05 Torr of SF_6 in the source. In addition to the CsI cluster ions, which have been reduced in abundance, $[Cs(CsF)_n]^+$ and $[Cs(Cs_nI_{n-1}F)]^+$ are shown. All of the other possible cluster ions resulting from exchange of one F for one I are observed and the abundances of these species depend on the pressure of SF_6. At approximately 0.7 to 0.8 Torr of SF_6 the only ions observed are $[Cs(CsF)_n]^+$ species.

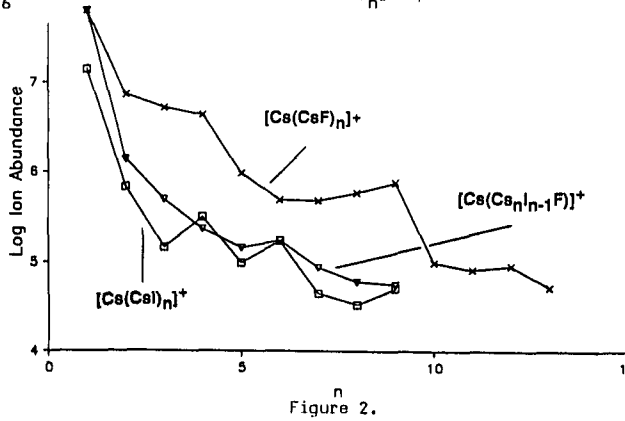

Figure 2.

We have observed in a triple quadrupole instrument that Cs_2^+, when mass-selected and passed through Q2 containing SF_6, will yield $[Cs_2F]^+$. However, no large CsF cluster ions have been formed in this way and it is unlikely that a gas-phase process can account for the formation of large CsF cluster ions. Therefore, these species can be formed either by unassisted reactions between SF_6 and the CsI surface or by fast-atom beam-induced reactions.

The first possibility was ruled out because no CsF cluster ions are observed when CsI is exposed to SF_6 (neutral or ionized), evacuated, and then sputtered. X-ray photoelectron spectroscopic (XPS) analysis of a CsI sample that had been exposed to a high pressure of SF_6 (yielding only CsF cluster ions by FAB) showed more I than F on the surface. A reduced fluence sputtering of a similar sample confirmed these results. At this point the mechanism of formation of these CsF cluster ions seems to be a beam-induced mixing of CsI and F (or F^-) to yield the observed reactions product cluster ions. This phenomenon may be similar to reactive ion etching [2].

1. R.B. Freas, M.M. Ross, J.E. Campana, JACS, 107, 6195 (1985).
2. H.F. Winters, J.W. Coburn, J. Vac. Sci. Tech. B 3(5), 1376 (1985).

Presented at the 35th ASMS Conference on Mass Spectrometry and Allied Topics
May 24-29, 1987, Denver, CO

SIMS AND CHEMISTRY OF SUBSTITUTED AROMATIC/SULFURIC ACID SOLUTIONS*

C.P. Leibman‡, P.J. Todd, and G. Mamantov‡

Oak Ridge National Laboratory, Oak Ridge, TN. 37831

and

University of Tennessee, Knoxville, TN. 37966‡

SIMS spectra of substituted polynuclear aromatic hydrocarbons dissolved in concentrated sulfuric acid show abundant molecular and protonated molecular ions. The base organic-characteristic peak in SIMS spectra of aromatic compounds which are known to be extensively protonated in concentrated sulfuric acid (1) corresponds to the protonated molecular ion ($M+H^+$). The molecular ($M^{+\cdot}$) secondary ion is generally more abundant than the protonated molecular secondary ion in SIMS spectra of compounds which are weakly basic in concentrated sulfuric acid (1). Frequently associated with abundant molecular ($M^{+\cdot}$) ions were ions indicative of sulfonation. This is apparent in Figure 1, the SIMS spectrum of weakly basic 9-anthracenecarbonitrile dissolved in concentrated H_2SO_4. The molecular ion does not arise from gas phase ionization of the sputtered aromatic because the kinetic energy distribution for protonated sulfuric acid ions and the kinetic energy distribution of 9-anthracenecarbonitrile molecular ions were essentially identical. The 10 Volt kinetic energy distribution width observed corresponds to a 100 micron thick region in our secondary ion source. Gas phase ionization of sputtered neutrals would occur in a region wider than 100 microns because the primary ion beam used is diffuse.

Sulfonation of substituted aromatic compounds in concentrated sulfuric acid is believed to proceed through a sigma complex of the aromatic with SO_3 (or solvated SO_3) (2). The final step to sulfonation is aromatic to sulfonic group proton transfer. Equilibrium between protonated, complexed, and sulfonated forms is summarized by reaction scheme 1. We hypothesized that the protonated analyte was the precursor to the protonated secondary molecular ion and that the sigma complex was the precursor to the secondary molecular ion. Addition of ammonium bisulfate to aromatic sulfuric acid solutions decreases the concentration of protonated and complexed aromatic the same extent (2). SIMS spectra of substituted aromatic/H_2SO_4 solutions to which we had added NH_4HSO_4 revealed a pronounced change in the mass spectrum associated with the matrix but no change in $[M^{+\cdot}]/([M+H)^+]$. We did observe a decrease in the fraction of the total ion current associated with analyte characteristic ions, consistent with the expected decrease in condensed phase concentrations of complexed and protonated forms of the analyte.

SIMS spectra were obtained for three nitrogen containing heterocycles dissolved in both polyphosphoric acid (PPA) and H_2SO_4. The characteristic $[M^{+\cdot}]/[M+H]^+$ ratio observed for each compound was the same in either matrix. This was surprising because the constituents of polyphosphoric acid, H_3PO_4 and P_2O_5, and various oligomers thereof, do not form sigma complexes with aromatic compounds. Consequently, it appears that molecular and protonated molecular ion intensities observed in SIMS spectra of substituted aromatic/mineral acids are principally determined by the aromatic compound.

1) Stewart, R. The Proton: Applications to Organic Chemistry; Academic Press: New York, 1985.

2) Cerfontain, H. Mechanistic Aspects of Aromatic Sulfonation and Sulfonation; Wiley Interscience: New York, 1968.

Presented at the 35th ASMS Conference on Mass Spectrometry and Allied Topics
May 24-29, 1987, Denver, CO

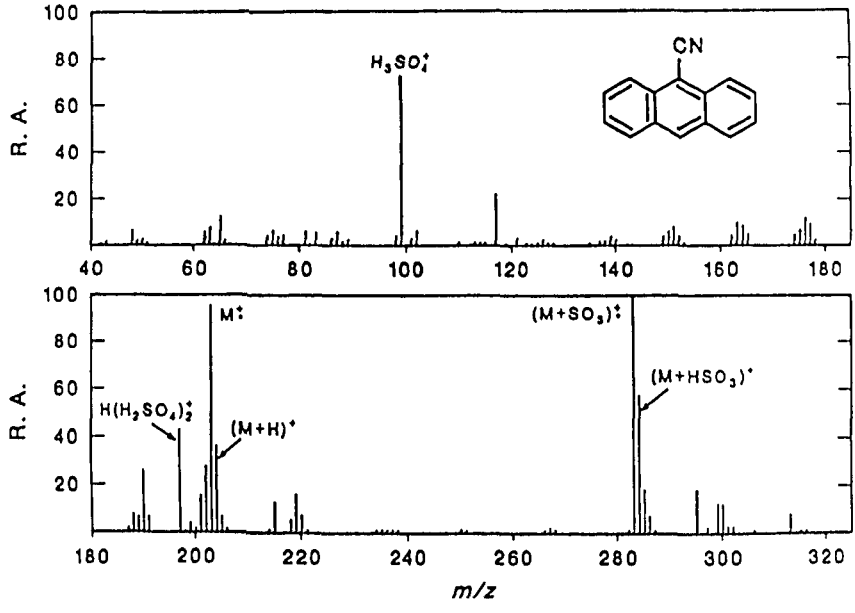

Figure 1. SIMS spectrum of a 5 weight % 9-anthracenecarbonitrile/H_2SO_4 solution.

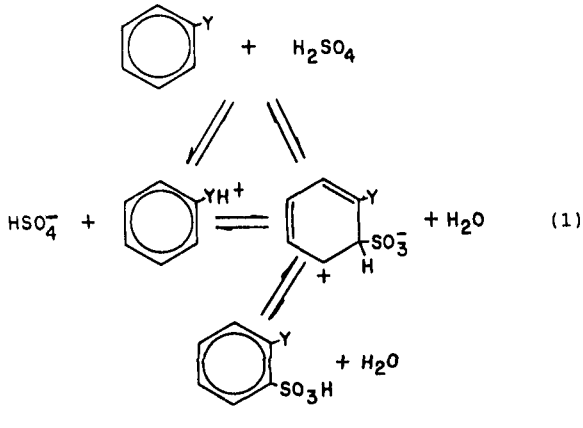

*Research sponsored by the U. S. Department of Energy, Office of Basic Energy Sciences, under Contract DE-AC05-84OR21400 with Martin Marietta Energy Systems, Inc.

"The submitted manuscript has been authored by a contractor of the U.S Government un it No DE-AC05-84OR214C gly, the U.S Government n honexclusive, royalty-free license to pupesh or reproduce the published form of this contribution, or allow others to do so, for U.S Government purposes."

Presented at the 35th ASMS Conference on Mass Spectrometry and Allied Topics
May 24-29, 1987, Denver, CO

A STUDY OF THE FAB-INDUCED ADDUCT FORMATION BETWEEN PEPTIDES AND GLYCEROL

Chhabil Dass and Dominic M. Desiderio
University of Tennessee, Memphis
800 Madison Avenue, Memphis, TN 38163

Previous studies have reported occurrence of ion adducts between glycerol and analytes comprising of primary and secondary amines during FAB irradiation of the sample (1). We also made similar observation during investigation of FAB-induced fragmentation of several opioid peptides (2). The positive ion FAB mass spectra contained several ions having mass numbers greater than the MH^+ ions of the peptides (Figure 1). In this study, we report a detailed investigation of the phenomenon of the adduct ion formation. The research was accomplished by acquiring normal magnet scan FAB mass spectra and collisionally-activated dissociation (CAD) linked-field scan spectra, and use of isotopic labelling. The CAD experiments were conducted in the first field-free region of the VG 7070E-HF forward geometry (E=ESA precedes, B=magnet) MS using He as the collision gas. Pressure of He was adjusted so as to reduce the main beam by 40-50%. The set of compounds studied included hydrophobic, basic amino acid containing peptides, and N-terminus-blocked peptides.

Figure 1 shows the FAB-MS of Pro-Phe-Gly-Lys and proctolin (Arg-Tyr-Leu-Pro-Thr). Several ions above the MH^+ ions are prominently seen in these spectra. The most dominant ion corresponded to the addition of 12 amu. This ion was selected for further studies. By monitoring the $(MH+12)^+$, it was observed that the main requirement for the adduct ion formation was the presence of free N-terminus group and/or a basic amino acid group in the peptide sequence (Table 1). The intensity of $(MH+12)^+$ increased with the time of FAB irradiation (Figure 2). It was also observed that the adduct formation was influenced by relative concentration of the peptide and glycerol; the more dilute solutions showed increased abundance of the $(MH+12)^+$ ion (Figure 3). Addition of HCl (2 µL of 0.1N) to the probe reduced the adduct formation considerably, whereas addition of NH_4OH (1µL of 20% solution) either helped or decreased the intensity of $(MH+12)^+$ ion (Table 2).

The comparison of the daughter ion spectra of MH^+ and $(MH+12)^+$ ions acquired using the CAD-B/E-linked-field scan technique showed that the site of glycerol attachment to the peptide is preferentially the terminal NH_2 group and the NH_2 group of the basic amino acids Arg and Lys (Figure 4). The use of d_5-glycerol and the B^2/E linked-field scan revealed that initially-formed adduct between the peptide and glycerol (monomer) is thermodynamically unstable and dissociates by the loss of water. The $(MH+12)^+$ ion is formed from thiS latter ion by the successive losses of CH_3OH and CHOH (Scheme 1). Multiple addition of glycerol is also observed to the peptide (Figure 1).

REFERENCES

1. H. Pang, C.E. Costello, and K. Biemann (1984) in 32nd Annual Conference on Mass Spectrometry and Allied Topics, Extended Abstract, pp. 751-752.
2. C. Dass and D.M. Desiderio, Analyt. Biochem., in press.

Presented at the 35th ASMS Conference on Mass Spectrometry and Allied Topics
May 24-29, 1987, Denver, CO.

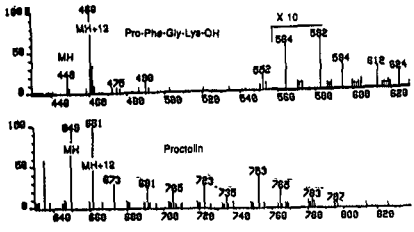

Fig. 1

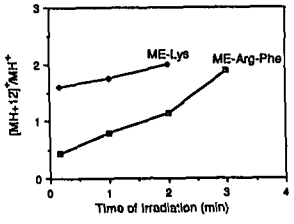

Fig. 2

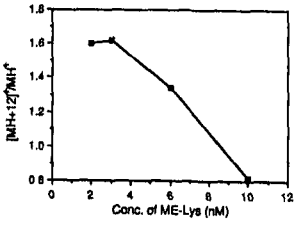

Fig. 3

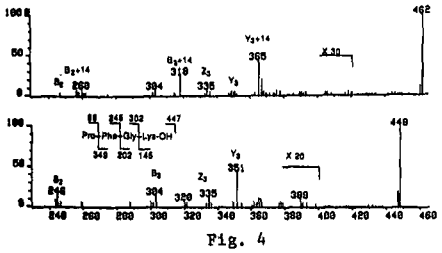

Fig. 4

Table 1

Peptide	$MH^+/(MH + 12)^+$
p-Glu-His-Gly-OH	—
Tyr-Gly-Gly-Phe-Leu-OH	11.7
Tyr-Gly-Gly-Phe-Met-OH	12.4
Tyr-Pro-Phe-Pro-Gly-Pro-Ile-OH	8.7
Tyr-Gly-Gly-Phe-Leu-Arg-OH	1.2
Tyr-Gly-Gly-Phe-Leu-NH_2	1.8
Tyr-Gly-Gly-Phe-Met-Lys-OH	0.5
Pro-Phe-Gly-Lys-OH	0.3

Table 2

	$MH^+/(MH+12)^+$		
Peptide	Neat	NH_4OH	HCl
Leucine Enkephalin	11.7	3.5	89
Methionine Enkephalin	12.4	3.3	79
Pro-Phe-Gly-Lys-OH	0.3	0.7	61
Proctolin	1.5	1.5	65
Kentsin	1.8	2.7	13
ME-Arg-Gly-Leu-OH	1.1	2.8	39

Scheme 1

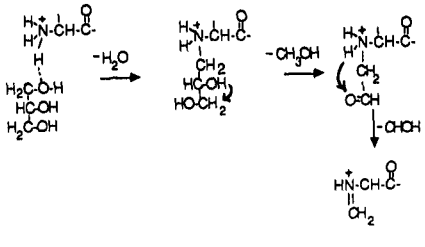

Presented at the 35th ASMS Conference on Mass Spectrometry and Allied Topics
May 24-29, 1987, Denver, CO

FACTORS INFLUENCING RELATIVE SENSITIVITY FOR SMALL PEPTIDES IN LIQUID SIMS

A.M. Falick, Ke Jiang, B.W. Gibson and F.C. Walls
Mass Spectrometry Facility, Department of Pharmaceutical Chemistry
University of California, San Francisco, California 94143-0446

The process by which secondary ions are formed and the precise role of the matrix in liquid secondary ionization mass spectrometry (LSIMS) are not yet fully understood. Several researchers have pointed out the importance of variables such as surface activity, molecular charge in solution, diffusion rate and gas phase basicities. Yet, there is no adequate theory at present to describe the processes that occur between the initial primary particle impact and the appearance of the secondary ions that are mass-analyzed and detected.

In order to better understand these phenomena, we have begun to explore the positive and negative liquid SIMS spectra of a series of small peptides. The qualitative correlation between surface activity, hydrophobicity and relative abundance of the protonated molecule has been noted by several investigators. Hydrophobic solutes in hydrophilic solvents are highly surface active. Naylor et al. (1) and Findeis et al. (2) have pointed out that, in certain peptide digests, the appearance or non-appearance of a particular component in the FAB mass spectrum was very well correlated with a hydrophobicity index derived from the measurements of Bull and Breese (3). Bull and Breese measured the free energy of transfer of various amino acids from the bulk of a solution to the surface. The value for glycine was then set to zero and the other values adjusted accordingly, to give a set of relative values, Δf. By summing these values for the individual amino acids making up a particular peptide, one obtains an overall Δf value (1,2).

We measured the MH^+ and $(M-H)^-$ abundances of a number of di-, tri- and tetrapeptides and plotted these values as a function of Δf. A correlation was clearly evident but with a great deal of scatter. There are several possible reasons why such plots might have excessive scatter. The Bull and Breese values were measured for individual amino acids in 10% aqueous NaCl solution at a pH adjusted to the isoelectric point for each acid. Clearly, no account of interactions between residues is included in the summing procedure. Furthermore, at pH values far from the isoelectric point one would expect the hydrophobicity, and therefore the surface activity, to differ from their isoelectric values. However, one would expect some of these variables to cancel out in a plot of relative abundances of MH^+ vs. $(M-H)^-$ for the same series of peptides. Such a plot is shown in Figure 1. The correlation is satisfying in that it supports the idea that surface concentrations are quantitatively related to observed signal strengths.

Another aspect of the problem was addressed in some preliminary measurements of the time dependence of the MH^+ ion abundances in a sample containing both a relatively hydrophilic (Gly-Gly-Tyr-Arg) and a more hydrophobic peptide (Glu-Val-Phe). The data at shorter times (Fig. 2) show the expected dominance of the more surface-active component. However, at longer times, the signal from Gly-Gly-Tyr-Arg becomes increasingly important. We hypothesize that this behavior is due to two competing processes: matrix evaporation and stripping of surface layers by sputtering. The former can account for the increase with time of the hydrophilic MH^+ signal due to concentration of the non-volatile analytes as the matrix evaporates. The latter process could account for increased loss of the surface-active analyte with time as the more concentrated surface layers are stripped away. Further experiments to test this hypothesis are underway.

Acknowledgement

This work was supported by the NIH Division of Research Resources, Grant RR01614 (to A.L. Burlingame).

References

1. Naylor, S., Findeis, A.F., Gibson, B.W. and Williams, D.H., J. Am. Chem. Soc. (1986) 108, 6359-6363.
2. Findeis, A.F., Naylor, S., Gibson, B.W. and Williams, D.H., manuscript in preparation.
3. Bull, H.B. and Breese, K., Arch. Biochem. Biophys. (1974) 161, 665-671.

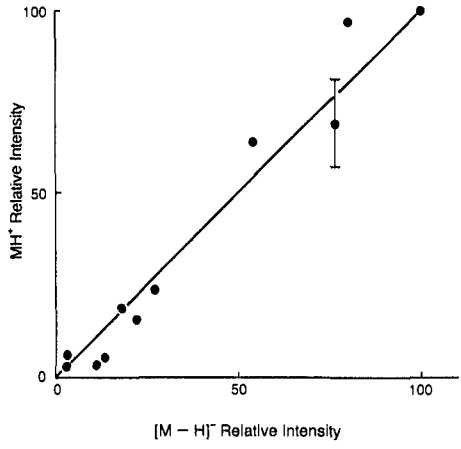

Figure 1. Relative intensities of quasi-molecular ions for a series of peptides: positive mode vs. negative mode correlation.

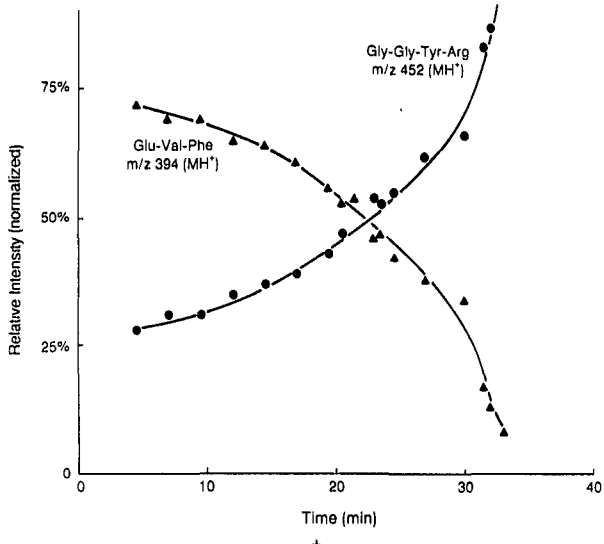

Figure 2. Relative intensities of MH^+ ions for two small peptides (Glu-Val-Phe and Gly-Gly-Tyr-Arg) as a function of time. Intensities are plotted as a percent of the sum of both MH^+ intensities.

Presented at the 35th ASMS Conference on Mass Spectrometry and Allied Topics
May 24-29, 1987, Denver, CO

FAB-MS OF LOW MOLECULAR WEIGHT SLIGHTLY POLAR MOLECULES.

Robert T. Rosen[1], Thomas G. Hartman[1], Chi-Tang Ho[2], and Joseph D. Rosen.
Center for Advanced Food Technology[1] and Food Science Department[2], Cook College, Rutgers University, New Brunswick, New Jersey 08903.

FAB-MS has been successfully used for the determination of high molecular weight compounds such as polypeptides and oligosaccharides. Little attention has been paid to the determination of low molecular weight materials because such compounds are often best analyzed by traditional ionization methods. FAB, however, being a desorption technique, has a definite advantage with thermally labile species that would decompose rapidly, and is often so selective that interfering compounds are "invisible" under normal operating conditions.

Examples that were shown included aliphatic and aromatic alcohols, carbamates, organophosphates, primary, secondary and teritary amines. Analogs of catechol, pyrogallol and some aliphatic alcohols, give molecular ions rather than protonated molecular ions that result from charge exchange. The fragmentation patterns obtained by fast atom bombardment of many small molecules are similar to the fragmentation patterns obtained by chemical ionization mass spectrometry, indicating that similar processes are occurring. This technique has been particularly useful in the identification of species in complex mixtures. This includes identification of a carbamate fungicide in a polyethylene glycol dispersant, flavor compounds from ginger, natural antioxidants from herbs, and organophosphate plasticizers and aromatic phosphite antioxidants from polymers.

The close similarity of the fragmentation patterns of the CI and FAB mass spectra of these compounds indicates that ionization probably occurs in the gas phase at close distance to the solution interface. The use of isobutane CI at low pressure (0.3 Torr) gave similar M^{+}/MH^{+} ratios for the hydroxybenzene analogs as did FAB-MS. Also, simple solution chemistry does not account for the formation of pseudomolecular ions (MH^{+}) of relatively non-polar organics such as triphenyl phosphate and triphenyl phosphite by FAB-MS, especially in such high yields as was observed. NJAES #J-10542-1-87.

Presented at the 35th ASMS Conference on Mass Spectrometry and Allied Topics
May 24-29, 1987, Denver, CO

Temperature Effects in the Bombardment Mass Spectrometry of DC704

R.N. Katz and F.H. Field
The Rockefeller University
New York, N.Y. 10021

FAB mass spectra of Dow Corning diffusion pump fluid DC704, a tetramethyltetraphenyltrisiloxane, 1, have been obtained in the gaseous and condensed states as a function of temperature and bombardment beam intensity. The bombardment beam used is Ar^+/Ar° or Ar° accelerated by 8 keV. The spectrum of liquid DC704 at 25C (Figure 1a) has a characteristic fragmentation pattern devoid of the $(M-CH_3)^+$ ion (m/z 469) which dominates the EI spectrum (Figure 1b). At temperatures warmer than 70C, the bombardment spectrum of DC704 vapor (Figure 1c) is very similar to the EI spectrum. The difference between the spectra of gaseous and condensed DC704 indicates that 5 keV Ar^+/Ar° transfers to DC704 vapor approximately the same energy as do 70 eV electrons. The higher degree of fragmentation observed in condensed DC704 probably results from transfer of translational energy from the Ar^+/Ar° to the sample during the collision cascade following impact.

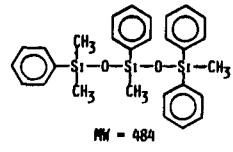

1

In a series of experiments similar to those reported for methanol[1], ethylene glycol[2], and glycerol[2] it was found that the typical spectrum of condensed phase DC704 remained sensibly constant at temperatures ranging from 25C to -45C. The sample was bombarded at successively lower temperatures using argon atoms, and at -61C the spectrum changed, showing extensive fragmentation and none of the features of the warmer temperature spectra. In these experiments Ar^+ was deflected out of the bombardment beam because surface charging by Ar^+ caused complete suppression of the DC704 spectrum at ca. -20C. The behavior of DC704 as a function of temperature is analogous to that of the hydroxylated compounds studied previously[1,2]. It was found however, that the characteristic DC704 spectrum could be obtained at T<-100C using a low intensity ($\leq$5μA) Ar° beam. Continuous bombardment at low intensity of the sample maintained at -100C or bombardment of a fresh sample with a 50 μA Ar° beam produced a damage spectrum (Figure 2). In contrast the spectrum of liquid DC704 at 25C was unaffected by one hour's bombardment. It was subsequently shown that a single sample of DC704 could be cycled from 18C to T<-100C and back, and the spectra to be anticipated based upon the temperature and duration of bombardment were observed. It is concluded from these data that the extensive fragmentation associated with the low temperature spectra reported here and elsewhere[1,2] is the result of sputtering accumulated radiation damage products from the surface of the sample immobilized by the low temperature.

Acknowledgement

This work was supported in part by the Division of Research Resource, National Institutes of Health.

1. R.N. Katz, T. Chaudhary and F.H. Field, J. Am. Chem. Soc. 1986, 108, 3897.
2. R.N. Katz, T. Chaudhary and F.H. Field, Int. J. Mass Spec. Ion Proc. In press.

1a.

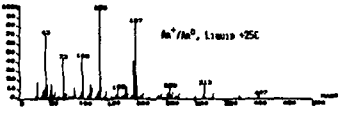

1b.

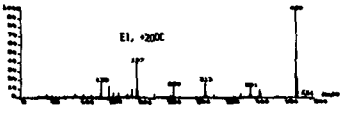

1c.

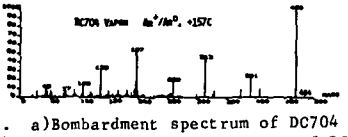

Figure 1. a)Bombardment spectrum of DC704 liquid, b)electron ionization spectrum of DC704 vapor, and c)bombardment spectrum of DC704 vapor.

2a.

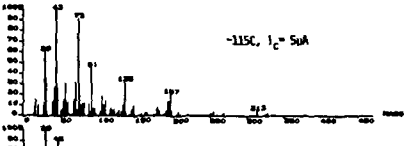

2b.

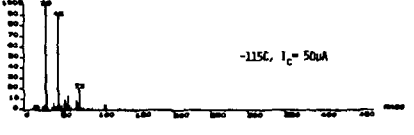

Figure 2. Bombardment spectrum of condensed phase DC704 at differing bombardment beam intensities; a) Ar°, 8.0 keV, 5μA discharge current, b) Ar°, 8.0 keV, 50μA discharge current.

Presented at the 35th ASMS Conference on Mass Spectrometry and Allied Topics
May 24-29, 1987, Denver, CO

FOURIER TRANSFORM ION CYCLOTRON RESONANCE STUDIES OF NEGATIVE IONS

Nico M.M. Nibbering

Laboratory of Organic Chemistry, University of Amsterdam,
Nieuwe Achtergracht 129, 1018 WS Amsterdam, The Netherlands

Fourier transform ion cyclotron resonance (FT-ICR) mass spectrometry, first developed by Comisarow and Marshall in 1974 (1), has become in recent years a well-established and blossoming branch in the field of mass spectrometry (2).

A highly attractive and powerful feature of this exciting method is that in its operation a programmable sequence of pulses can be applied to meet the requirements for solving an analytical problem or studying in detail the chemistry involved in ion/molecule reactions. In this way it is possible, for example, to isolate ions with a particular m/z value selectively in the cell of the instrument by application of either a series of ion ejection pulses (3) or the so-called notch ejection pulse (4). With the former method of ion ejection it has been shown possible very recently to isolate selectively in the cell of our Bruker CMS 47 instrument either $C_9H_{10}^{+\cdot}$ or $C_7H_{14}S^{+\cdot}$ ions generated from a 1:1 mixture of the corresponding neutral precursors which requires a so-called front-end resolution of mass selection in excess of 35000 (5). It will be clear, that this is important not only for analytical studies, but also for detailed studies of the chemistry and mechanisms associated with ion/molecule reactions.
Such studies in their turn can contribute to a further insight in organic reactions where ions frequently play an important role, but now in the absence of solvent molecules or counter ions.

A variety of organic reaction types including hydrogen/deuterium exchange reactions, nucleophilic aromatic substitutions, S_N2 versus addition-eliminations, cycloadditions and hydride transfer reactions has been studied by FT-ICR over the past few years in the author's group (6). Here the results of some recently performed studies will be presented.

The first concerns the reaction between a base and diethyl ether which proceeds by elimination. For NH_2^-, CH_3NH^- and $C_2H_5NH^-$ as bases only unsolvated or free ethoxide anions are formed, but with the weaker base OH^- both free and water solvated ethoxide anions are generated (7). Using various ^2H-labelled diethyl ethers the kinetic isotope and leaving group effects have been determined for these reaction channels as function of the base strength (8). It is found that going from NH_2^- to OH^- the β-hydrogen isotope effect varies from 5.6 tot 2.2, respectively, for the free ethoxide anion formation which values differ only slightly from the corresponding values of 5.5 and 2.1 obtained via flowing afterglow and based on overall reaction rates (9). Interestingly, the β-hydrogen isotope effect for the water solvated ethoxide formation is essentially lower, i.e. 1.55, indicating that the free and water solvated ethoxide anions are generated most probably via different elimination mechanisms.
Taking into account the theories of isotope effects (10) and the small, but notable leaving group effects observed, the free ethoxide formation has been interpreted to correspond to an anti elimination and the water solvated ethoxide formation to a syn elimination (8), their transition states being visualized below.

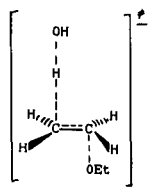

ANTI

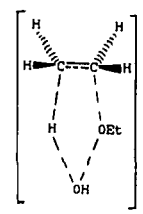

SYN

Within this picture the relatively large isotope effect of 5.6 in the case of NH_2^- for the free ethoxide anion formation has been interpreted to correspond to a symmetric linear arrangement for the base, β-hydrogen and β-carbon in the transition state of anti elimination, while the smaller isotope effect of 2.2 in the case of the weaker base OH^- of this channel is believed to be due to a

product-like transition state in which the β-proton is more than half-transferred.

A similar approach has been applied to study the mechanism of the base induced gas phase elimination reaction of diethyl sulfide (11). It is found that reaction of this molecule with the nitrogen bases NH_2^-, $C_2H_5NH^-$ and $(CH_3)_2NH^-$ preferentially proceeds via an α',β-elimination mechanism, where α' proton abstraction from the sulfide results in the formation of an α'-thio carbanion, which undergoes an intramolecular syn elimination to generate the ethyl thiolate anion. Reaction with OH^-, CH_3O^- and F^- exclusively proceeds via an E2 mechanism. However, for the reaction with OH^-, rapid exchange is observed within the reaction complex between the α-hydrogens of the sulfide and the hydroxide hydrogen prior to E2 elimination. With the bases OH^- and CH_3O^- only free ethyl thiolate anions are formed, but with F^- as base both free and HF solvated ethyl thiolate anions are generated. As for diethyl ether discussed above, the kinetic isotope and leaving group effects have been determined for these reaction channels as function of the base strength using various ^2H-labelled diethyl sulfides. The results obtained for OH^- and CH_3O^- can be interpreted with an anti elimination with the transition state for the weaker base CH_3O^- more product-like than for OH^-, while for the HF solvated ethyl thiolate anion formation a syn elimination can be advanced similar to that for the water solvated ethoxide anion formation (vide supra). Interestingly, for the free ethyl thiolate anion formation with F^- as base, a relatively low β-hydrogen isotope effect of 1.68, but a large α-hydrogen isotope effect of 1.30 has been measured. These observations have been interpreted (11) to indicate that in this case an E2C-like mechanism is operative, involving a bent β-proton transfer and covalent interaction of F^- with the α-carbon as visualized in eq. 2.

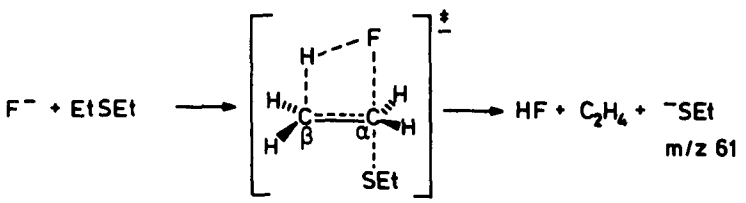

E2C

Acknowledgements

The author gratefully acknowledges the former and present members of his group listed in the references for their contributions to this work and the Netherlands Organization for Pure Research (SON/ZWO) for continuous support.

References

1. (a) M.B. Comisarow and A.G. Marshall, Chem. Phys. Lett. 25, 282 (1974); (b) M.B. Comisarow and A.G. Marshall, Can. J. Chem. 52, 1997 (1974).
2. D.A. Laude, Jr., C.L. Johlman, R.S. Brown, D.A. Weil and C.L. Wilkins, Mass Spectrom. Rev. 5, 107 (1986).
3. J.C. Kleingeld and N.M.M. Nibbering, Org. Mass Spectrom. 17, 136 (1982).
4. (a) A.G. Marshall, T.C. Lin Wang and T. Lebatuan Ricca, Chem. Phys. Lett. 105, 233 (1984); (b) A.J. Noest and C.W.F. Kort, Comput. Chem. 7, 81 (1983); (c) J.C. Kleingeld and N.M.M. Nibbering, Tetrahedron 39, 4193 (1983).
5. L.J. de Koning, R.H. Fokkens. F.A. Pinkse and N.M.M. Nibbering, Int. J. Mass Spectrom. Ion Proc., in press.
6. N.M.M. Nibbering, Recl. Trav. Chim. Pays-Bas 105, 245 (1986).
7. R. van Doorn and K.R. Jennings, Org. Mass Spectrom. 16, 397 (1981).
8. L.J. de Koning and N.M.M. Nibbering, J. Am. Chem. Soc. 109, 1715 (1987).
9. V.M. Bierbaum, J. Filley, C.H. DePuy, M.F. Jarrold and M.T. Bowers, J. Am. Chem. Soc. 107, 2818 (1985).
10. L. Melander and W.H. Saunders, Jr., "Reaction Rates of Isotopic Molecules", Wiley-Interscience, New York, 1980.
11. W.W. van Berkel, L.J. de Koning and N.M.M. Nibbering, J. Am. Chem. Soc., submitted.

Presented at the 35th ASMS Conference on Mass Spectrometry and Allied Topics
May 24-29, 1987, Denver, CO

CHEMICAL REACTIONS OF NEGATIVE IONS AS A PROBE OF STRUCTURE

Charles H. DePuy and Veronica M. Bierbaum
Department of Chemistry and Biochemistry
University of Colorado
Boulder, CO 80309-0215

In a flowing afterglow (FA) ions are created at the beginning of the flow tube, usually by electron impact, cooled by many collisions with the helium buffer gas which is present at approximately 0.5 torr, and carried out of the ionizing region by the fast helium flow (8000 cm/sec). As the ions are carried down the meter-long flow tube several sequential reactions can be carried out. In our studies of negative ions we generally produce initially a strongly basic and reactive ion like HO^-, NH_2^- or F^- by direct ionization. Then an organic ion is produced by proton transfer or other chemical reaction. For example electron impact on ammonia produces amide ion, which in turn reacts with 1-methylpyrrole to produce an anion by protron transfer.

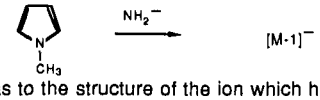

The problem then arises as to the structure of the ion which has been produced. We have developed a number of chemical probes which are useful in helping to determine the structure of organic negative ions. One of the most versatile reagents for this purpose is nitrous oxide, N_2O. This reagent reacts with an anion in a wide variety of ways depending upon its structure. In particular it reacts with primary, secondary and tertiary carbanions in quite different ways to give new ions which can usually be identified in the spectrum. For example primary carbanions, which have two remaining hydrogens on the carbanionic center, react to form diazoanions , $[M+25]^-$.

The mechanism of this transformation has been shown to involve addition, proton transfer and loss of HO^- to form a complex of the neutral diazocompound and hydroxide ion. Before separation of the complex the hydroxide ion abstracts the acidic proton on the diazo carbon, forming the stable diazoanion.

When a secondary carbanion, with only one remaining hydrogen on the carbanionic carbon, is allowed to react with N_2O, addition, proton transfer and loss of hydroxide ion can still occur, but no hydrogen remains on the resulting diazo carbon. Instead a proton on an adjacent carbon is removed leading, after loss of nitrogen, to the formation of a vinyl carbanion, $[M-3]^-$

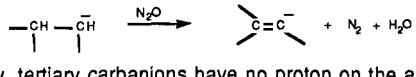

Finally, tertiary carbanions have no proton on the anionic carbon and cannot form diazo compounds. Instead they may undergo other types of reactions including addition or oxygen transfer.

Using reaction with N_2O as a probe we were able to deduce that proton abstraction from 1-methylpyrrole occurs from the methyl group because of the formation of a $[M+25]^-$ peak.

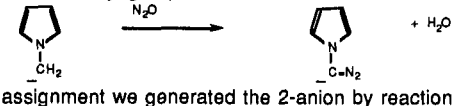

In order to confirm this assignment we generated the 2-anion by reaction of the 2-trimethylsilyl derivative of 1-methylpyrrole with fluoride ion. As expected, this tertiary anion reacts with N_2O by addition. No pyrrole anion is formed by reaction of the 3-trimethylsilyl derivative with F^-,

indicating that it is too basic to be formed this way. We can therefore postulate that the relative acidity of the protons in 1-methylpyrrole is methyl > alpha >beta.

We have also found that carbonyl sulfide, COS, and carbon disulfide, CS_2, are useful if less versitale reagents for gaining insight into ion structure. With highly basic anions sulfur atom transfer is a common reaction. This reaction does not distinguish among isomeric anions. However highly unsaturated anions often undergo unusual reactions which can be diagnostic. For example reaction of the allenyl anion with CS_2 gives cleavage into two fragments, and in substituted cases can be used to deduce the site of deprotonation.

$$CH_2{=}C{=}CH^- + S{=}C{=}S \longrightarrow CH_2{=}C{=}S + {}^-CH{=}C{=}S$$

By far the most generally useful reaction we have developed, however, is that of hydrogen/deuterium exchange. Properly used, this reaction can reveal a great deal about not only the carbanionic site but also about other sites within the molecule. For example proton abstraction from 2-, 3-, or 4-methylpyridine leads to M-1 anions which exchange two protons when CH_3OD is added downstream. These results are only consistent with proton abstraction from the methyl group, leading to a benzyl-type anion. A deuterated alcohol can bring about exchange of protons with identical or nearly identical acidity. For example reaction of the anion derived by proton abstraction from thiophene with CH_3OD results in a single exchange.

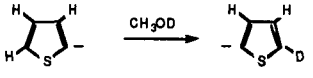

In contrast, D_2O and ND_3, because they bring two or three exchangable deuterons into the reaction complex at the same time, are capable of exchanging not only hydrogens of the same acidity but less acidic hydrogens as well. This same thiophene anion, for example, exchanges all three of its hydrogens for deuterium when D_2O is used as the exchange reagent.

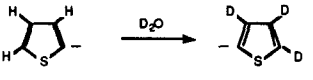

We noted above that in 1-methylpyrrole the alpha hydrogens appear to be more acidic than the beta. This result is confirmed by the observation that in the M-1 anion four deuterium atoms are introduced upon reaction with ND_3, while in the anion from 1-methyl 2-deuteriopyrrol the deuterium atom is removed upon reaction with NH_3.

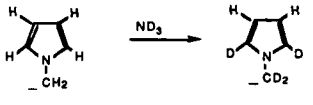

As these examples are meant to indicate, chemical reactions are as useful in determining ion structures in the gas phase as they have been for over a century for determining structures in solution. Gas phase anions undergo in general the same types of reactions in either phase, and the same strategies for structure determination can be used.

Presented at the 35th ASMS Conference on Mass Spectrometry and Allied Topics
May 24-29, 1987, Denver, CO

THE FRAGMENTATION OF NEGATIVE IONS FORMED BY ELECTRON CAPTURE NEGATIVE ION MASS SPECTROMETRY.

E. A. Stemmler* and R. A. Hites, School of Public and Environmental Affairs and Department of Chemistry, Indiana University, Bloomington, IN 47405

Electron capture negative ion mass spectrometry (ECNIMS) is particularly useful for the sensitive detection of electrophilic compounds in complex samples; however, little is know regarding the use of this technique for compound identification. This question was addressed by measuring the spectra of over 350 compounds, emphasizing compounds of environmental interest. As ECNI mass spectra are influenced by instrumental conditions such as ion source temperature, pressure, tuning parameters and sample concentration, the spectra were acquired at two set ion source temperatures (100° and 250° C) under similar conditions of ion source pressure and sample concentration. The instrument was tuned to meet relative ion abundance criteria using decafluorotriphenylphosphine as a calibration standard.

Under methane ECNI conditions, negative ions formed by electron capture may fragment via simple cleavage or rearrangement reactions. The energy available for these fragmentations is determined by the internal energy of the neutral molecule, the energy of the captured electron and the electron affinity of the negative ion that is formed. Under ECNI conditions, the mean electron energy is thought to be near 0 eV. This factor, in conjunction with most electron affinity values (less than 4 eV) and the collisional stabilization which occurs in the CI source results in formation of low energy negative ions. Fragmentations observed under ECNI conditions reflect this low energy.

Types of ions observed under ECNI conditions can be divided into those formed by simple bond cleavages, those formed by loss of two atoms producing a double bond, and those formed by other rearrangement reactions. In addition, unconventional ions are observed where species, such as hydrogen or a methyl radicals, are incorporated into a fragment or molecular ion.

Simple cleavage reactions that are observed involve cleavage of weak bonds such as carbon-halogen, -oxygen, -sulfur, -sulfone, and -tertiary nitrogen and phosphorous bonds and give ions capable of stabilizing the negative charge. Simple cleavages that are not generally observed involve stronger bonds, such as carbon-carbon or carbon hydrogen bond cleavages.

Often compounds lose two atoms to produce a double bond and enhance the resonance stabilization of the resulting fragment. Examples of these fragmentations are shown below. Product ion stability influences the fragmentation. For example, the meta isomer of compound 3 gives a weak $[M-2Cl]^-$ ion because resonance stabilization cannot occur in that negative ion structure.

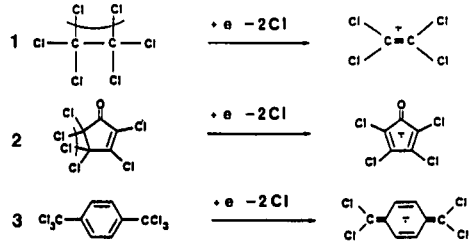

Many rearrangement reactions are observed under ECNI conditions. For example, hexachlorocyclopentadiene derivatives 4 undergo retro-Diels Alder rearrangements with loss of Cl to give $C_5Cl_5^-$ anions. Kepone 5 also gives a $C_5Cl_4O^-$ ion by a retro [2+2] cycloaddition reaction.

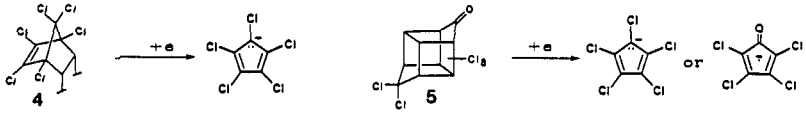

*Present Address: Oak Ridge National Laboratory, Oak Ridge, TN 37831-6120

Presented at the 35th ASMS Conference on Mass Spectrometry and Allied Topics
May 24-29, 1987, Denver, CO

Rearrangements are frequently seen in the spectra of nitroaromatics. Some of these reactions are quite complex. For example, dialkyl substituted dinitroanilines such as 6 and 7, undergo a loss of the nitro group, followed by a loss of C_nH_{2n}.

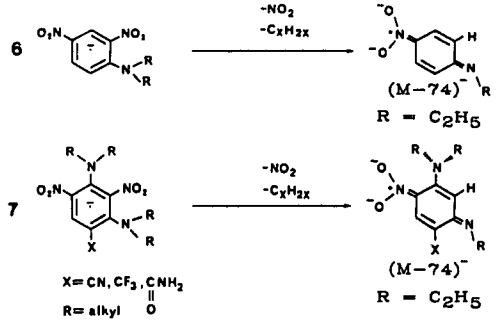

ECNI spectra of isomeric compounds frequently show ions specific to a particular isomer. For example, 2- and 4-chlorobenzophenone can be easily identified because the 2- isomer gives a unique ion at $[M-HCl]^-$. Other isomeric pairs, such as the o,p- and p,p- isomers of DDE, DDD and DDT can be differentiated by a unique ion at m/z 246 found in the spectra of the o,p- isomers. Other isomers show differences in relative ion abundance.

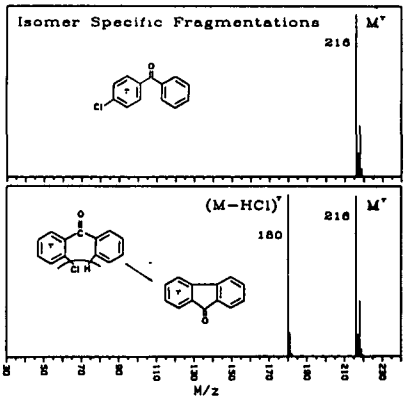

Unconventional ions, which show incorporation of species originating from the reagent gas, are also observed. For example, highly halogenated benzenes, naphthalenes, biphenyls and furans show $[M+xH-xCl]$ ions.

In summary, ECNI generally provides less structural information than spectra acquired under electron impact conditions. The number of simple cleavage reactions are reduced and make identification of certain substituents, such as alkyl groups, impossible. While the number of simple cleavages are reduced, some appear in the spectra and can be helpful in assigning structures. Ions resulting from rearrangement reactions are often observed. If the rearrangement is characterized such ions can be used to distinguish classes of compounds. ECNI mass spectra are often more sensitive towards isomeric structures than EI spectra.

Presented at the 35th ASMS Conference on Mass Spectrometry and Allied Topics
May 24-29, 1987, Denver, CO

IONIZATION DYNAMICS WITHIN THE HIGH PRESSURE ELECTRON CAPTURE MASS SPECTROMETER

L.J. Sears and E.P. Grimsrud
Department of Chemistry, Montana State University, 59717

The High Pressure (1 Torr) Electron Capture Mass Spectrometer (HPECMS), when used in conjunction with gas chromatography, is presently one of the most powerful tools available for the trace analysis of numerous organic molecules. One reason for this success is that rate constants for favorable electron capture reactions can be up to two orders of magnitude greater than those of ion-molecule reactions. In theory, the ionic products formed by electron capture should be quite simple. Molecular anions would be expected if the process is Resonance EC, and simple fragment ions would be expected if the process in Dissociative EC. In practice, however, using standard Chemical Ionization (CI) conditions, EC spectra are often observed which can not be explained in terms of simple EC processes. In order to understand these and other observations made by HPECMS, we have developed a detailed model of the HPECMS ion source. The model is briefly explained below and then is applied to several cases where unexpected EC spectra have been observed.

The model is shown in Figure 1. In it, four different pathways to unusual ions are described. Pathway A is initiated by EC, followed by neutralization of M^- by wall contact or by recombination with positive ions to form the neutral species Z, which undergoes EC to form Z^-. Pathway B is initiated by an ion-molecule reaction, followed by a neutralization step and an EC reaction to form unusual ion X^-. Pathway C is initiated by the reaction of a free radical (which are abundant is the normal CI ion source), followed by EC to form MR^-. Pathway D involves the alteration of M by a wall reaction which then leads to unusual ion W^-. Considerable knowledge concerning all of the elementary steps involved in this model is available. Using it, we have constructed a simulation of the HPECMS ion source which has aided us in understanding several observations of unexpected EC mass spectra. A few of these are discussed below.

In Figure 2 is shown the HPECMS spectra (0.5 Torr CH_4, 150°C) observed for tetracyanomethane. This spectra provides an example of Pathway C in which reactions of free radicals with TCNE occur prior to EC. Our model calculations concerning such systems indicate that the spectra shown in Figure 2 is possible only for compounds which react extraordinarily rapidly with free radicals, but have only modest EC coefficients.

In Figure 3A is shown the EC spectra of the trifluoracetic derivative of 9-aminophenanthrene. For this compound and also for the related isomers of aminoanthracene and aminophenanthrene, a major ion in the EC spectrum is the unexpected $(M-O)^-$ ion. In spectrum 3B, triethylamine was added to the CH_4 buffer gas and the selective dimunition of the $(M-O)^-$ ion was caused. We believe that this ion is produced by Pathway B in which the initiating step, a positive ion-molecule reaction, is suppressed by the presence of TEA. Our model calculations for this system indicate that the observance of major ions by Pathway B is possible only for cases where the EC coefficient of the original molecule is not ultra-fast. Indeed, no such unusual ions are observed for these compounds when a larger perfluorinated group is used in the preparation of the derivatives.

In Figure 4 is shown the HPECMS spectra of fluoranil and chloranil. In both cases the most intense ion corresponds to the species $(M+H-X)^-$, where X = F or Cl. Model calculations show that Pathway D involving wall reactions can be competitive with even fast EC. By parallel electron impact analysis of these molecules in an ion source just recently used for CI, we have shown that the species (M+2H) is formed from chloranil and fluoranil upon contact with the CI-activated ion source wall. Furthermore, reconstructed single ion chromatograms using a cool ion source, such as shown in Figure, 5 provide additional evidence that the spectra of fluoranil and chloranil are explained by:

$$M \xrightarrow{\text{wall}} (M+2H)^{\cdot} \xrightarrow{e} \begin{cases} (M+H-X)^- + HX \\ (M-2X)^- + 2HX \end{cases}$$

The EC spectra of related, but more complex molecules such as that shown for Pentac in Figure 6, can be explained as shown in Figure 7 by a combination of Pathway D, in which wall reactions add 2 H atoms to a neutral species, and Pathway A, in which repeated electron attachment to intermediate neutrals leads to the numerous fragment ions differing by 34 mass units in the mass range 400 to 264 amu. Model calculations clearly show that there is ample time for all of the processes shown in Figure 7 to occur as Pentac passes through the ion source.

The pathways to unusual ions described here are likely to occur under the typical conditions of HPECMS. In fact, they have been used for analysis for some time, without

knowledge of their causes. In the future, continued and expanded uses of these processes are expected because of the unsurpassed sensitivity offered by HPECMS. Greater knowledge of the dynamics involved in these secondary processes will be of significant assistance in these developments.

Figure 1. Model of HPECMS Events Leading to Unusual Ions

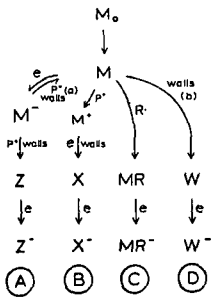

Figure 2. HPECMS Spectrum of Tetracyanoethylene

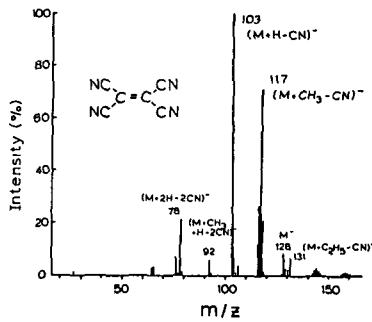

Figure 3. Effect of Triethylamine on Spectrum of 9-AP

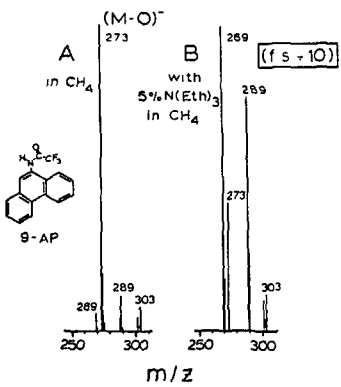

Figure 4. HPECMS Spectrum of Fluoranil and Chloranil

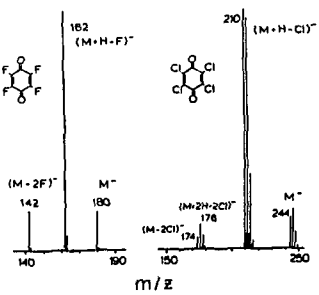

Figure 5.

Single Ion Reconstructed Chromatogram of Fluoranil

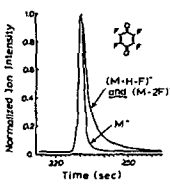

Figure 6. HPECMS Spectrum of Pentac

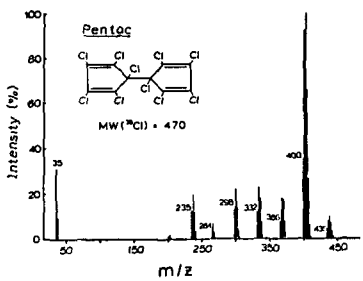

Figure 7. Proposed Mechanism for Pentac

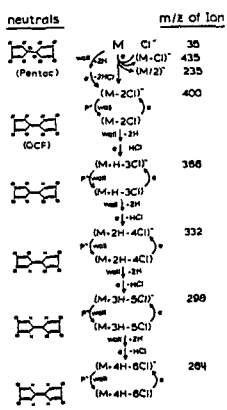

Presented at the 35th ASMS Conference on Mass Spectrometry and Allied Topics
May 24-29, 1987, Denver, CO

THE USE OF REACTIVE COLLISIONS OCCURRING IN A TRIPLE QUADRUPOLE MASS SPECTROMETER IN DIFFERENTIATION OF ISOMERIC IONS WHICH PRODUCE IDENTICAL CAD SPECTRA

H.I. Kenttämaa and R.R. Pachuta
Department of Chemistry, Purdue University, West Lafayette, IN 47907

Some isomeric ions produce dissociation product distributions that are so similar that it is difficult if not impossible to differentiate the ions on the basis of their fragmentation reactions. Often, the ions isomerize to a common structure or mixture of structures at the internal energies necessary for fragmentation. In the present study, ion-molecule reactions occurring in the middle quadrupole of a triple quadrupole mass spectrometer are used to differentiate isomer pairs which produce similar dissociation products upon activation through collisions with a gas-phase target (CAD) and a surface [1] (surface-induced dissociation, SID). The attractive characteristics of a triple quadrupole instrument in studies of ion-molecule reactions [2] include: (i) information is available from both endo- and exothermic reactions, (ii) reaction conditions can be easily varied, providing a means to control the type of reactions occurring, and (iii) thermochemical data (e.g., proton affinities) are available through variation of the parent ion kinetic energy (Figure 1).

Protonated cyclohexene oxide and cyclohexanone produce identical high-energy [3] and low-energy (5-30 eV) CAD spectra as well as SID spectra, which is explained on the basis of the small barrier for isomerization for the epoxide ion (Figure 2). The lowest-energy product, m/z 81 formed by H_2O loss from protonated cyclohexene oxide and cyclohexanone, is cyclohexenyl cation (low-energy CAD: $41^+:53^+=100:21$) and not a methylcyclopentenyl cation ($41^+:53^+=100:13$) as suggested [4] earlier. The isomeric parent ions, protonated cyclohexene oxide and cyclohexanone, can be differentiated only by avoiding activation, by generating the epoxide ion in the ion source with a very small amount of internal energy, and by using ion-molecule reactions occurring in the middle quadrupole to examine the structures of the isomeric ions. The ions yield different product distributions with various reactive collision gases, including 1,3-pentadiene, dimethoxymethane, crotonaldehyde and methyl formate. Ethyl vinyl ether forms a stable adduct (m/z 171) with the epoxide ion (Figure 3), while protonated cyclohexanone, gamma- and delta-valerolactones and cyclohexanol fail to produce an adduct.

Isomeric protonated delta- and gamma-valerolactones give identical CAD spectra, while their product distributions obtained in reactions with ethyl vinyl ether are different. The same applies to the protonated natural products shown in Figure 4: only the ion with the hydroxy group in 3-position produces an abundant vinylated molecule (m/z 375) by loss of ethanol from the complex with ethyl vinyl ether (Figure 4a).

The use of a reactive collision gas instead of argon in the middle quadrupole proved to be useful in identification of compounds by providing information in addition to CAD data. This is especially important in cases where low-energy collisional activation does not deposit large enough energies to induce fragmentation.

[1] Md. A. Mabud, M.J. DeKrey and R.G. Cooks, Int. J. Mass Spectrom. Ion Processes 67 (1985) 285.

[2] M.T. Kinter and M.M. Bursey, J. Am. Chem. Soc. 108 (1986) 1797.

[3] R. Wolfschutz, H. Schwarz, W. Blum and W.J. Richter, Org. Mass Spectrom. 8 (1979) 462.

[4] T. Gaumann, R. Houriet, D. Stahl, J.-C. Tabet, N. Heinrich and H. Schwarz, Org. Mass Spectrom. 18 (1983) 215.

Presented at the 35th ASMS Conference on Mass Spectrometry and Allied Topics
May 24-29, 1987, Denver, CO

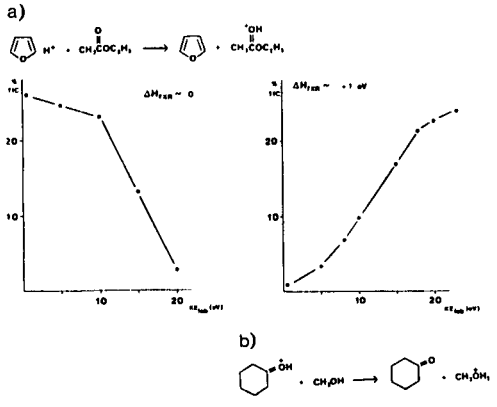

Figure 1. Ion kinetic energy dependence of (a) an exothermic and (b) an endothermic proton transfer reaction (multiple-collision conditions).

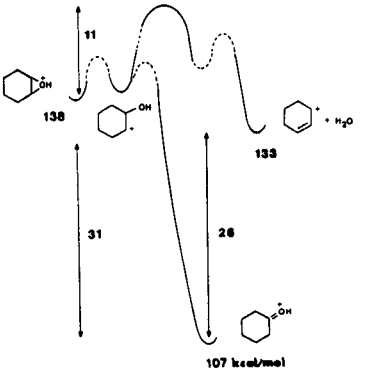

Figure 2. Potential energy diagram for protonated cyclohexanone and cyclohexene oxide (PA estimated to be 200-202 kcal/mol by energy-resolved ion-molecule reactions).

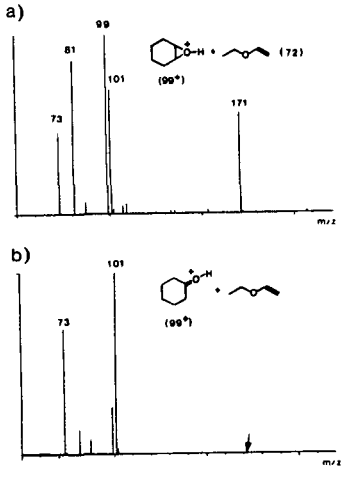

Figure 3. Ionic products obtained from reactions of ethyl vinyl ether with (a) protonated cyclohexene oxide and (b) protonated cyclohexanone (multiple-collision conditions).

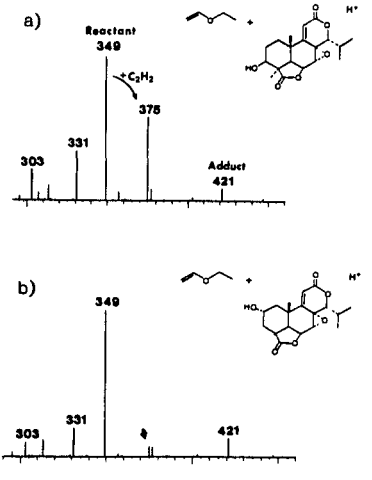

Figure 4. Ionic products obtained from reactions of ethyl vinyl ether with isomeric protonated diterpene dilactones (multiple-collision conditions).

Presented at the 35th ASMS Conference on Mass Spectrometry and Allied Topics
May 24-29, 1987, Denver, CO

AN INVESTIGATION OF ISOMERIC IONS DERIVED FROM ACETONE, DIACETONE ALCOHOL AND MESITYL OXIDE.

Alex Young and Raymond March; ORICL, Department of Chemistry, University of Toronto, Toronto, Canada. M5S 1A1.

The Aldol type condensation followed by dehydration reactions are well known in solution chemistry; an investigation of these reactions was performed in the gas phase. In solution, 2-propanone (acetone) produces 4-hydroxy-4-methyl-2-pentanone (diacetone alcohol). Dehydration of the condensation product affords 4-methyl-3-penten-2-one (mesityl oxide), viz.

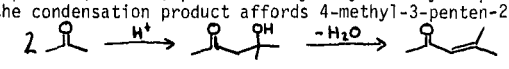

(1)

This reaction was studied in the gas phase and the structure of the protonated dimer formed from acetone was compared to protonated diacetone alcohol, produced under similar conditions. Furthermore, the dehydration product, m/z 99 was investigated in both the above cases and compared to protonated mesityl oxide.

A reverse geometry mass spectrometer (ZAB.2FQ)[1] was employed to investigate the structures of ions generated in the source either via methane or isobutane CI. Mass selected ions were analyzed by high energy collisional dissociation (CID) and MIKES. A deflector electrode may be employed to allow only fast neutrals to enter the collision cell and collisional dissociative reionization afforded the identification of same.

It had been demonstrated in an earlier study[2] that the protonated dimer species of m/z 117 formed by acetone differed from protonated diacetone alcohol. This finding was confirmed via high energy CID of the isomeric adduct ions (fig. 1); the structure of m/z 117 formed from acetone was rationalized as a proton bound dimer, producing predominantly protonated acetone, m/z 59 and not readily dehydrating to m/z 99; in contrast protonated diacetone alcohol readily dehydrated, but formed very little m/z 59.

The dehydration products of the isomeric m/z 117's as well as protonated mesityl oxide were investigated as these species had proved unamenable to analysis in the earlier study. The ions of m/z 99 formed from the three distinct precursors afforded unique CID spectra (fig. 2). In acetone, the dominant pathway of m/z 99 was loss of neutral acetone to produce the alkyl cation m/z 41. This result suggested an ion-dipole complex for the structure of of this ion;

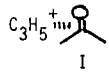

; m/z 99 (2)

I

which was verified by the similar CID spectrum produced from the partially deuterated analogue of I, formed in the source by clustering $C_3H_5^+$ with perdeutero acetone.

That m/z 99 produced via dehydration of protonated diacetone alcohol differed from protonated mesityl oxide upon CID was further investigated by the measurement of the kinetic energy release (KER) of the metastable decomposition of the isomeric ions in the second field free region (2FFR). The process measured was m/z 99 producing CH_3CO^+ plus neutral isobutene. In diacetone alcohol, the KER at half height (To.5) was 10.4 meV, whereas the isomeric m/z 99 from mesityl oxide had To.5 of 32.1 meV, suggesting a greater reaction endothermicity for the process.

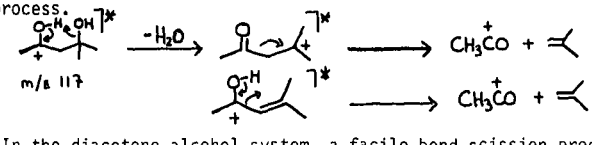

(3)

(4)

In the diacetone alcohol system, a facile bond scission produces m/z 43 (reaction 3), whereas the process from protonated mesityl oxide (reaction 4) involves a proton transfer via a 4-centre rearrangement.

Both the m/z 99's formed from diacetone alcohol and mesityl oxide eliminate methane, affording m/z 83. The CID spectra of these m/z 83 ions were very similar, with small differences in the abundances of ionic products of m/z 39,41,42 and 43 (fig. 3). These results may be rationalized by proposing two structures for m/z 83 in diacetone alcohol, one of which is identical to m/z 83 from mesityl oxide. The dominant metastable decomposition of both m/z 83's was the loss of 28 amu to produce m/z 55. That the neutral lost was CO was demonstrated by dissociate collisional reionization.

REFERENCES

1. A.G. Harrison, R.S. Mercer, E.J. Reiner, A.B. Young, R.K. Boyd, R.E. March and C.J. Porter; Int. J. Mass Spec. Ion Proc., 74, 13 (1986).

2. R.E. March, A. Kamar and A.B. Young; Can. J. Chem., 64, 1979 (1986)

Presented at the 35th ASMS Conference on Mass Spectrometry and Allied Topics
May 24-29, 1987, Denver, CO.

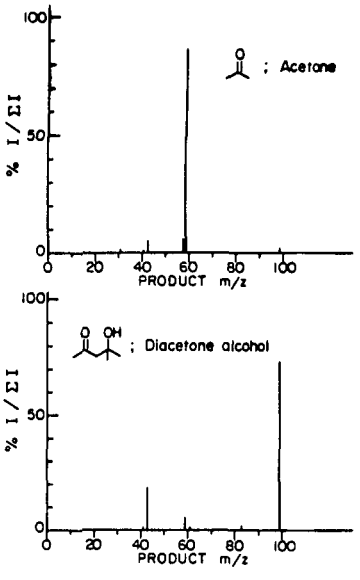

FIG. 1

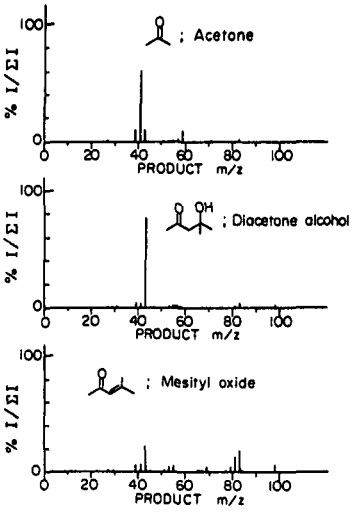

FIG. 2

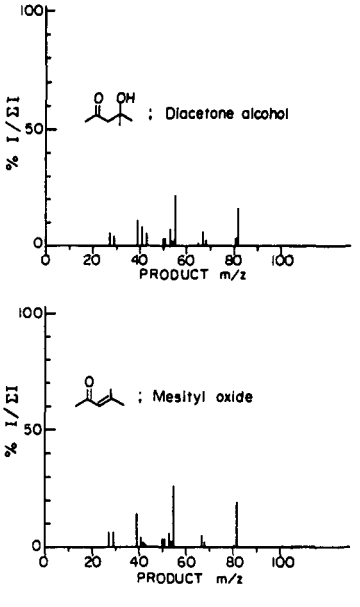

FIG. 3

Presented at the 35th ASMS Conference on Mass Spectrometry and Allied Topics
May 24-29, 1987, Denver, CO

IRON ION CHEMISTRY AND ISOMER DISCRIMINATION USING FTMS.

Asgeir Bjarnason and James W. Taylor.
Department of Chemistry, University of Wisconsin,
Madison, Wi 53706.

Gas-phase reactions of various metal ions with organic molecules have been investigated by several researchers. The selectivity of metal ions as chemical ionization agents has been recognized, but the potential for analytical applications remains largely unexplored. In an attempt to evaluate the method for analytical purposes, a study of the reactions of iron(I) ions with the isomers of several disubstituted benzene derivatives was performed. The goal of the research was to determine if reactions of iron ions, generated by laser/metal interaction in a FTMS, with the isomers of aromatic compounds could be made diagnostic for the isomers. Electron impact spectra for this class of compounds are generally too similar for isomer identification.

The iron ions were produced by the interaction of a focused CO_2 laser pulse with the stainless steel tip of the direct insertion probe in a Nicolet FTMS-2000. The iron ions were allowed to react with the neutral isomer under study (in the gas phase) for times varying from 0.003 to 12.8 s at pressures ranging from $1*10^{-7}$ to $1*10^{-6}$ torr.

The samples investigated were the ortho, meta and para isomers of: xylene, methylanisole, fluoroanisole, bromoanisole, fluorotoluene, chlorotoluene, fluorobenzaldehyde, fluoronitrobenzene, bromofluorobenzene and chlorofluorobenzene. The results can be categorized in three classes. The first class exhibited high discrimination. As an example, the iron ions reacted with fluoronitrobenzene to produce spectra, obtained after 0.4 s or more, where all three isomers can be easily identified by glancing at the spectra. These spectra are shown in figure 1. The reactions are complex and numerous reaction channels are observed which can, in part, be attributed to the number of different stable leaving groups in fluoronitrobenzene. The second class, with fluorobenzaldehyde as an example, also exhibited complex reactions but less obvious differences between the isomers. The ortho isomer can be easily distinguished as its spectrum, obtained at the same reaction time, is significantly different from the others. Distinction between meta and para isomers do, however, require greater attention to realize consistent spectral differences. The third class contains only xylene whose reactions with the iron ions

were too simple to reveal any significant differences between the isomers. Production of $Fe(M)^+$ was observed, followed by generation of $Fe(M)_2{}^+$, where M stands for the neutral xylene molecule.

The study reported here is a preliminary effort with instrument access provided through the courtesy of the Nicolet Instrument Corporation and the cooperation of Drs. James A. Kinsinger and David Weil. Studies are continuing to search for better discrimination conditions and to explore the generality of the method.

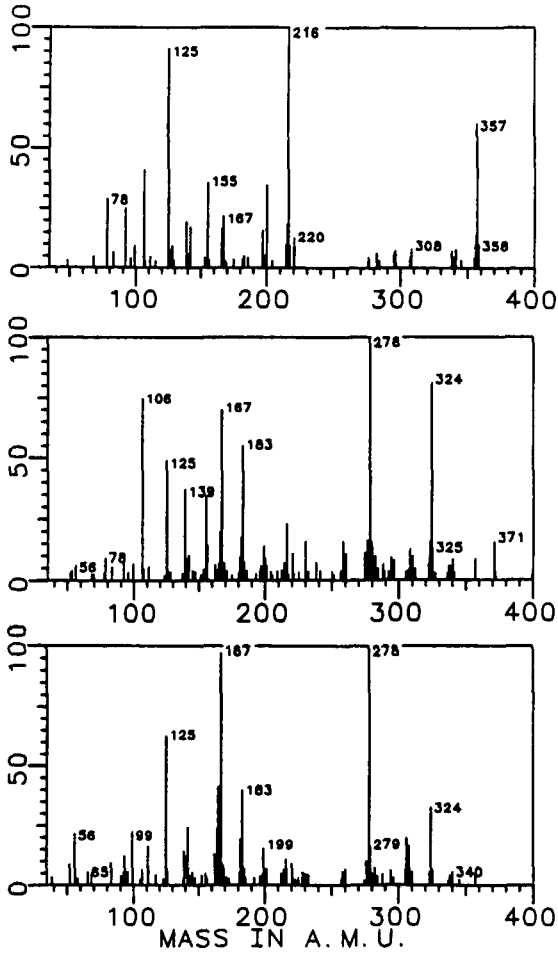

Figure 1.

Spectra produced after 0.4 s reaction time of iron ions with floronitrobenzene at $3*10^{-7}$ torr. The ortho isomer spectrum is at top, then meta, and the para spectrum at the bottom.

Presented at the 35th ASMS Conference on Mass Spectrometry and Allied Topics
May 24-29, 1987, Denver, CO

Collision Induced Dissociation of Metal Cluster Ions

Martin F. Jarrold and J. Eric Bower
AT&T Bell Laboratories, Murray Hill, NJ 07974

Metal clusters are interesting for several reasons. There is considerable fundamental interest in how their physical and chemical properties change with cluster size and approach bulk behavior. From a more practical point of view there is reason to believe that these studies may be relevant as catalysis and that clusters could provide a route to generating novel materials with tailored properties. Studying cluster ions rather than their neutral analogs offers several advantages, the most significant being that it is very easy to select out a particular cluster size for detailed study.

We have investigated the collision induced dissociation of size selected aluminum cluster ions with up to twenty-six atoms. We have studied both the bare metal clusters, Al_n^+, and aluminum clusters with chemisorbed oxygen, $Al_nO_m^+$. These studies provide information on the lowest energy dissociation pathways of the clusters and on their relative stability. It should be stressed that these studies provide no real structural information about the clusters.

The clusters for these studies were generated by pulsed laser vaporization [1] of an aluminum rod in a continuous flow of helium buffer gas. Just before exiting the source the clusters are ionized by a high energy electron beam. Details are given elsewhere [2]. After exiting the source the cluster ions are focussed into a quadrupole mass spectrometer where a specific cluster size is selected. The cluster ion of interest is then focussed into a low energy ion beam and passed through a gas cell where the collision gas (argon) is introduced. The products and undissociated ions are then focussed into a second quadrupole where they are analyzed. At the end of this quadrupole the ions are detected by a high voltage collision dynode and off-axis electron multiplier.

The main products observed from the collision induced dissociation of the bare clusters are Al^+ for the small clusters and Al_{n-1}^+ for the larger ones. The shift from mainly Al^+ to mainly Al_{n-1}^+ occurs at Al_{14}^+. this change in the product distribution probably occurs at the point where the ionization potential of the Al_{n-1} species drops below the ionization potential of the atom as it beads down towards the bulk work function.

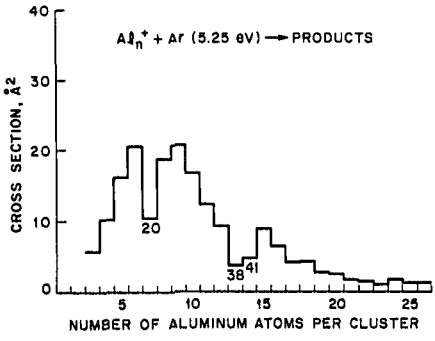

Figure 1. Cross sections for collision induced dissociation of bare aluminum cluster ions, Al_n^+. The numbers on the histogram give the number of valence electrons around the shell closings with 20 and 40 valence electrons.

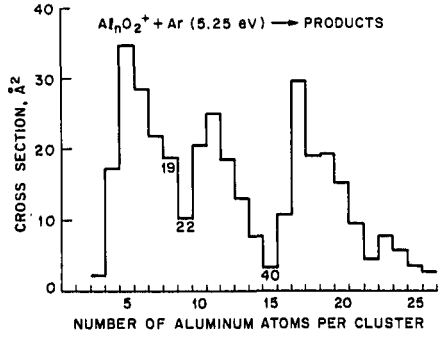

Figure 2. Cross sections for collision induced dissociation of aluminum clusters with two chemisorbed oxygen atoms.

Cross sections for collision induced dissociation of the bare clusters are shown in Figure 1. There are clear minima in the cross sections at Al_7^+ and Al_{13}^+, Al_{14}^+. We interpret these results as indicating that these clusters are particularly stable. The enhanced stability of these species can be accounted for by the electronic shell model [3]. There are prominent shell closings for 20 and 40 valence electrons. Aluminum is trivalent, so Al_7^+ has exactly 20 valence electrons and Al_{13}^+ (38 valence electrons) and Al_{14}^+ (41) are close to the shell closing with 40 valence electrons.

Chemisorption of oxygen onto the clusters dramatically changes the products observed from collision induced dissociation. Instead of Al_{n-1}^+ or Al^+ as observed for the bare clusters the products observed from $Al_nO_m^+$ (n=3-26, m=1,2) arise from loss of Al_2O molecules from the clusters [4]. Loss of Al_2O dominates because of the stability of the Al_2O molecule. Cross sections for collision induced dissociation of $Al_nO_2^+$ are shown in Figure 2. The minima observed in the cross sections for the bare clusters at n=7 and n=13,14 have shifted over and are now at n=9 and n=15 for $Al_{15}O_2^+$. The shift in the minima can be accounted for by the removal of valence electrons from the cluster orbitals by oxygen. Binding an oxygen atom to the cluster (either ionically or covalently) would be expected to result in the withdrawal of two valence electrons from the cluster orbitals. So $Al_9O_2^+$ has 22 valence electrons (close to the shell closing with 20) and $Al_{15}O_2^+$ has 40 valence electrons (which is a closed shell configuration). These results provide strong evidence that electronic properties rather than geometric symmetries control the stabilities of these metal clusters.

References

[1] T. G. Dietz, M. A. Duncan, D. E. Powers and R. E. Smalley, J. Chem. Phys. 74, 6511 (1981); V. E. Bondybey and J. H. English, J. Chem. Phys., 74, 6978 (1981).

[2] M. F. Jarrold, J. E. Bower and J. S. Kraus, J. Chem. Phys., 86, 3876 (1987).

[3] M. Y. Chou and M. L. Cohen, Phys. Lett., 113A, 420 (1986).

[4] M. F. Jarrold and J. E. Bower, J. Chem. Phys., (in press).

Presented at the 35th ASMS Conference on Mass Spectrometry and Allied Topics
May 24-29, 1987, Denver, CO

Studies of the Chemistry of Metal Cluster Ions

Martin F. Jarrold and J. Eric Bower
AT&T Bell Laboratories, Murray Hill, NJ 07974

In the preceding article we described our experimental studies of the collision induced dissociation of size selected metal cluster ions. Here we describe our investigations of the chemistry of these species. Metal clusters are a whole new class of chemical compound and some of the questions we would like to answer are how do the chemical properties change with cluster size and how do they correlate with processes observed on well defined surfaces? The work we describe here concerns the reactions of aluminum cluster ions with simple molecules, specifically oxygen [1] and deuterium [2]. It is well known that a clean aluminum surface is rapidly oxidized in air, however, chemisorption of hydrogen into polycrystalline aluminum has not been observed [3]. As we will see the reactivity of the clusters towards oxygen and deuterium is also dramatically different.

1. Reactions with Oxygen

The reactions between aluminum cluster ions and oxygen is very exothermic and results in extensive cluster fragmentation. The main products observed are Al^+_{n-m}, only a small proportion of product ions contain oxygen. For a center of mass collision energy of 1.2 eV the main products observed for the smaller clusters (n=3-7) are Al^+ and Al_2O^+. For clusters in the size range n=8-13 the main products are Al^+_{n-5} and Al^+. For clusters with n=14 and larger the main product is Al^+_{n-4}, except for Al^+_{19} which produced mainly Al^+_{n-5}. Loss of five aluminum atoms from Al^+_{19} results in Al^+_{14} which is a particularly stable cluster [4]. Collision induced dissociation of $Al_nO^+_2$ species shows products arising from the loss of one and two Al_2O molecules. It seems likely that the Al^+_{n-4} product observed in the chemical reactions of the clusters with oxygen results from the formation of two Al_2O molecules. Thus the reaction between the clusters

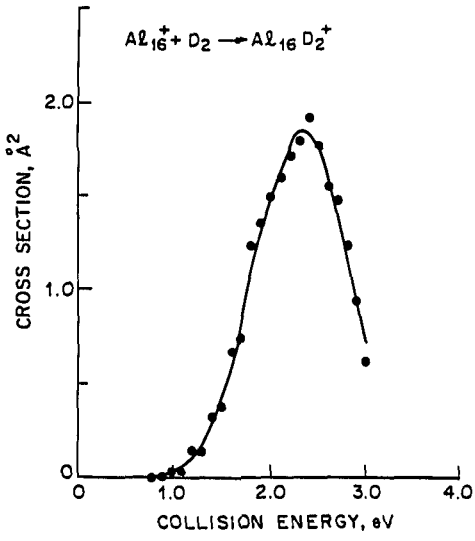

Figure 1. Plot of the cross section for adduct formation against collision energy for Al^+_{16}. The points are the experimental data and the line is the result of a least squares fit to determine the true threshold.

and oxygen probably first involves chemisorption of oxygen onto the cluster followed by loss of two Al_2O molecules. If the Al^+_{n-4} fragment contains sufficient internal energy it will further dissociate resulting in Al^+_{n-5} and Al^+ which are observed for the smaller clusters. Estimates of the available energy suggest that there should be sufficient to further fragment the Al^+_{n-4} species for the larger clusters as well. That this is not observed suggests that the Al_2O species carry away a substantial fraction of the heat of chemisorption of the oxygen onto the cluster, which implies very rapid loss of the Al_2O species after chemisorption. Total reaction cross sections for the reactions between the clusters and oxygen increase with cluster size. The increase in the cross sections roughly correlates with the increase in the physical size of the clusters. This behavior is expected for exothermic reactions at relatively high collision energies.

2. Reactions with deuterium

In contrast to the reactions with oxygen the reactions with deuterium show substantial kinetic energy thresholds which suggests that either the reactions are endothermic or there is an activation barrier to surmount. Two processes are observed for the interaction between aluminum cluster ions and deuterium. First, chemical reactions which are observed for all cluster sizes if the collision energy is raised sufficiently high; and second $Al_nD_2^+$ adduct formation which is observed for clusters with n=8-12, 14-27.

The chemical reactions result in several products, $Al_{n-1}D^+$ (+AlD) and Al^+ are the main products observed at a collision energy of 3.0 eV for clusters with n=3-11. For clusters with n=12-27 the main product is Al_nD^+. Adduct formation is the main process observed for the larger clusters (n>16). Studies of the gas cell pressure dependence of adduct formation demonstrate that the adduct arises from a single collision process (i.e. there are no stabilizing collisions). Thus the adduct contains sufficient energy to dissociate but is metastable due to the large number of internal degrees of freedom in the cluster. In the same way that thresholds were observed for the chemical reactions with deuterium, collision energy thresholds are also observed for metastable adduct formation. An example is shown in Figure 1 where the cross section for adduct formation is plotted against collision energy. The points are the experimental data and the line is the result of a least squares fit to the data to determine the true threshold. The fall-off in the cross section at the higher collision energies results from unimolecular dissociation of the adduct before it is detected. It seems reasonable to relate the thresholds determined from these studies to the activation barriers for clusters with an even number of atoms are smaller than those with an odd number. These oscillations presumably reflect the role of the unpaired electron in the HOMO in activating the deuterium molecule. We are currently investigating the influence of chemisorbed oxygen atoms on the height of the activation barrier.

References

[1] M. F. Jarrold and J. E. Bower, J. Chem. Phys. (in press).

[2] M. F. Jarrold and J. E. Bower, to be published.

[3] F. Pellerin, C. LeGressus and D. Massigron, Surf. Sci., 111, L705 (1981).

[4] M. F. Jarrold, J. E. Bower and J. S. Kraus, J. Chem. Phys., 86, 3876 (1987).

Presented at the 35th ASMS Conference on Mass Spectrometry and Allied Topics
May 24-29, 1987, Denver, CO

PROTONATION OF HEXAMETHYLDISILOXANE (HMDS) IN PARTICULAR AND ORGANOSILICON COMPOUNDS IN GENERAL

John A. Stone and Xiaoping Li

Chemistry Department, Queen's University, Kingston, Ontario, Canada K7L 3N6

The proton affinity of a compound is best measured by the equilibrium method using a reference base of well documented proton affinity. The few published proton affinities of silicon compounds have generally been obtained by the bracketing method which is subject to considerably more uncertainty than is the equilibrium method. The latter is usually found to be inappropriate for silicon compounds because of complications engendered by the tendency of protonated organosilicon compounds to transfer a silicon containing group rather than the proton. This is well illustrated by the mass spectral patterns of organosilicon compounds in which silicon group migrations can be significant, especially when migration is to oxygen. In previous work (1) we have shown that alkylbenzenes have relatively low affinities for $(CH_3)_3Si^+$ compared with oxygen bases and do take part in proton rather than $(CH_3)_3Si^+$ transfer in certain cases. We have employed this property to determine the proton affinity of HMDS and triethylsilanol by the equilibrium method using pulsed electron beam, high pressure mass spectrometry. In all cases equilibrium constants have been measured over as wide a temperature range as possible (maximum 300 - 600 K) and proton affinity differences (ΔH° values) have been obtained from van't Hoff plots.

Highly exothermic protonation in methane chemical ionization leads mainly to $(CH_3)_5Si_2O^+$ by dissociative proton transfer and to a small yield of $HMDSH^+$

$$(CH_3)_3SiOSi(CH_3)_3 + CH_5^+ \longrightarrow (CH_3)_3SiOSi(CH_3)_2^+ + 2CH_4$$
$$\longrightarrow HMDSH^+ + CH_4$$

Protonation by $t\text{-}C_4H_9^+$ in $i\text{-}C_4H_{10}/CH_4$ mixtures yields only $HMDSH^+$. The results of equilibrium measurements are independent of the reagent gas employed but $i\text{-}C_4H_{10}/CH_4$ is preferable because of the much simpler spectra. The data obtained are detailed in the following thermodynamic ladders ($-\Delta H^\circ$ values (kcal mol^{-1}) for the process $B_1H^+ + B_2 \quad B_1 + B_2H^+$; basicity increases upward in each table).

Presented at the 35th ASMS Conference on Mass Spectrometry and Allied Topics
May 24-29, 1987, Denver, CO

Table 1

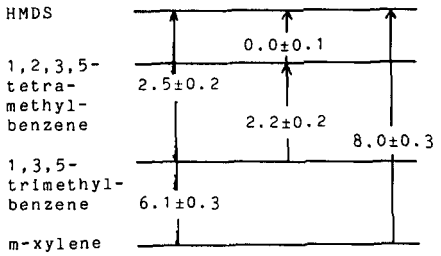

Table 2

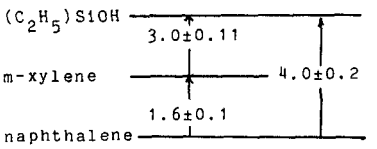

Table 3

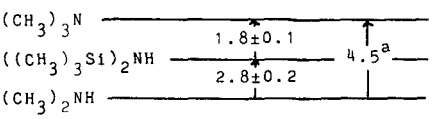

[a] Reference 2

The data lead to PA(HMDS) = 203.4±0.4 kcal mol^{-1} which is in excellent agreement with an earlier estimate of ~ 203 kcal mol^{-1} (3); $PA((CH_3)_3SiN(H)Si(CH_3)_3)$ = 222.4±0.3 kcal mol^{-1}; $PA((C_2H_5)_2SiOH)$ = 197.8±0.4 kcal mol^{-1}.

The equilibrium results in Table 3 for hexamethyldisilazane suggest that equilibrium studies might also be possible with a variety of non-oxygen containing bases as references and that it is the strength of the Si-O interaction that precludes the use of the more common oxygen bases.

References

1. A.C.M. Wojtyniak and J.A. Stone. Int. J. Mass Spec. Ion Proc. 74, 49 (1986).

2. S.G. Lias, J.F. Liebman and R.D. Levin, J. Phys. Chem. Ref. Data 13, 695 (1984).

3. C.G. Pitt, M.M. Bursey and D.A. Chatfield, J.C.S. Perkin 2, 434 (1976).

Presented at the 35th ASMS Conference on Mass Spectrometry and Allied Topics
May 24-29, 1987, Denver, CO

ION/MOLECULE REACTIONS IN A QUADRUPOLE ION TRAP

Jennifer S. Brodbelt and R. Graham Cooks, Department of Chemistry, Purdue University, West Lafayette, IN 47907

The capabilities of the quadrupole ion trap for investigations of ion/molecule reactions are demonstrated through studies of chemical ionization, proton transfer equilibria, and methylations and halomethylations of aromatic compounds. The recently-developed ion trap operated in the mass-selective instability mode (1) has several features which make it a promising device for the study of ion/molecule reactions, viz., the ability to store ions for long periods, mass-selective storage, access to time- and pressure-resolved data, and MS/MS capabilities. Two ion traps were utilized for the study of ion/molecule reactions: a Finnigan 700 Ion Trap Detector (ITD) modified to allow measurement of pressure and introduction of multiple compounds through metering valves, and a prototype Finnigan Ion Trap Mass Spectrometer (ITMS) which has collision-activated dissocation (CAD) capabilities (2). In either case, the software allowed implementation of a multi-step radio frequency scanning scheme. A sequence of intervals for ion storage, ion/molecule reactions, and ion ejection could be designated. These capabilities permit exploration of ion/molecule reactions either for analytical applications, as in chemical ionization, or for more fundamental studies such as for the investigation of thermodynamics and kinetics of gas phase reactions, examination of reaction mechanisms, and the characterization of ion structures.

Chemical ionization has recently been developed in the ion trap (3), and it is similar to the ICR chemical ionization method in that low reagent gas pressures (10^{-6} to 10^{-5} torr) and long reaction times (> 10 msec) are used. Because of its mass-selective trapping capabilities, the trap affords an additional degree of selectivity not possible with conventional high pressure chemical ionization. For example, in methane chemical ionization, the reagent ion can be specified for subsequent reactions with the sample molecules by setting the radio frequency voltage appropriately to store only $C_2H_5^+$ or both $C_2H_5^+$ and CH_5^+. This selection affects the extent of fragmentation of the sample molecules due to the different relative exothermicities of the proton transfer reactions using the two different reagent ions. Both charge exchange and proton transfer types of chemical ionization have been demonstrated in the ion trap (3), and these new ionization capabilities extend the versatility of the ion trap for analytical applications.

The energetics of proton transfer reactions are widely studied by ion/molecule reaction equilibria techniques such as in high pressure ion sources and flowing afterglow spectrometers. The ion trap is also suitable for such measurements. After allowing two chosen bases to attain equilibrium in the ion trap (0.5 - 1.0 sec) by undergoing hundreds of collisions, one can estimate the difference in the proton affinities of the two bases from their equilibrium constant. As shown in Figure 1, the intensities of protonated 3-methylpyridine and 2-methoxypyridine reach a constant ratio of 6.1 after 500 msec. The proton affinity difference calculated from this ratio is 1.6 kcal/mole, compared with the accepted difference in proton affinity of 2.2 kcal/mole. The method of introducing known partial pressures of the chosen bases into the trap is currently being optimized, so results are expected to improve.

The capabilities of an ion trap mass spectrometer for the study of ion/molecule reactions in conjunction with tandem mass spectrometry is demonstrated for the gas phase methylation and halomethylation of aromatic compounds. For instance, the reaction of dimethylchloronium ion, $CH_3ClCH_3^+$, produced from methyl chloride with phenol yields an ion of m/z 109 in the ion trap. This ion may be isolated and then

collisionally activated by applying a supplementary AC voltage of 1.5 volts at 218305 Hz across the end-cap electrodes of the trap. The ions undergo collision-activated dissociation, and the resulting spectrum (shown in Figure 2) closely resembles the daughter spectrum of methylated phenol obtained using a triple quadrupole mass spectrometer (20 eV collision energy, 2 mtorr argon collision gas). The reactivity of a series of substituted aromatic compounds towards electrophilic addition was also studied as a function of substituent. The ion/molecule reaction of interest involved an addition of CH_2Cl^+, followed by elimination of HCl, resulting in net addition of methyne. As predicted, the relative extent of the reaction was indicative of the electron-withdrawing and electron-releasing properties of the substituent. The daughter spectra of the product ions were compared to those obtained from model compounds. For example, the daughter spectra of m/z 141 from the methyne addition product of naphthalene matched that obtained from the ion of m/z 141 obtained from 1-chloromethylnaphthalene. Both produced only m/z 115 through loss of C_2H_2 and m/z 89 via a second loss of acetylene.

The ion trap is a versatile instrument for the study of ion/molecule reactions. In the future, it should become increasingly popular for investigations of thermochemistry and kinetics of gas phase ions, for mechanistic studies and ion structural elucidations.

References
1) G. Stafford, P. Kelley, J. Syka, W. Reynolds, J. Todd, Int. J. Mass Spectrom. Ion Processes, 60 (1984) 85.
2) J.Brodbelt, J. Louris. R.G. Cooks, Anal. Chem., 59 (1987) 1278.
3) J. Louris, R.G. Cooks, J. Syka, P. Kelley, G. Stafford, J. Todd, Anal. Chem., in press.

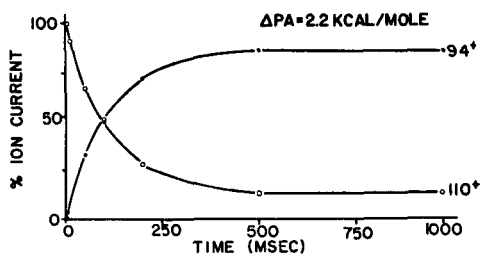

Figure 1. Proton transfer equilibrium for 3-methyl- and 2-methoxypyridine.

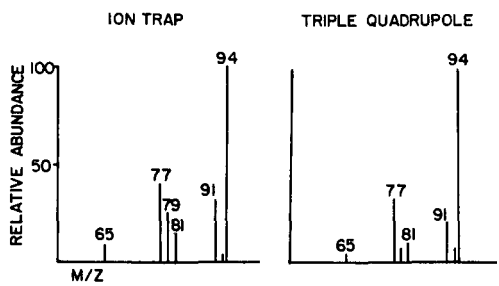

Figure 2. Daughter spectra of methylated phenol (m/z 109).

Presented at the 35th ASMS Conference on Mass Spectrometry and Allied Topics
May 24-29, 1987, Denver, CO

ION KINETIC ENERGY MEASUREMENT ON TANDEM QUADRUPOLE MASS SPECTROMETERS

Claude BEAUGRAND, Gérard DEVANT,
S.N. NERMAG, 49 Quai du Halage, F 92500 RUEIL-MALMAISON
Daniel JAOUEN, Hélène MESTDAGH, Christian ROLANDO,
Ecole Normale Supérieure, Département de Chimie, 24 rue Lhomond, F 75231 PARIS

Allowing a long and variable interaction time for an ion-molecule reaction is a way of improving its efficiency and of getting kinetic and/or thermodynamic information about the processes involved. In order to achieve this goal, ions were trapped in the RF only collision cell of a tandem quadrupole mass spectrometer. The successive steps of the confinement process were obtained by varying the entrance and exit potentials of the collision cell according to the sequence described in the figure 1.

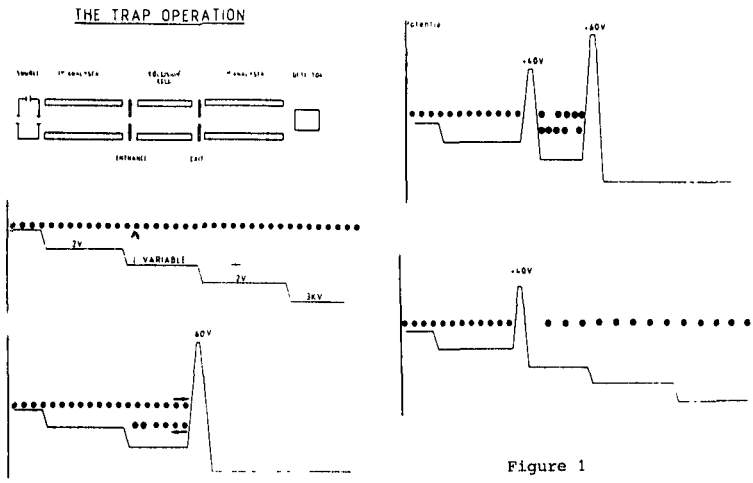

Figure 1

In all the experiments performed, the total ionic current detected remained fairly independent of the storage time, which shows that no ion loss occured during the storage step.

The ion confinement procedure was applied to the following processes :

- <u>Collision - induced fragmentation of $FeCO^{\pm}$</u> :

$$FE(CO)_5 \xrightarrow{Q1} FeCO^+ \xrightarrow[\text{confinement}]{\text{CAD Ar}} \begin{matrix} Fe^+ \\ FeCO^+ \end{matrix} \quad \begin{matrix} (m/z\ 56) \\ (m/z\ 84) \end{matrix} \xrightarrow{Q3}$$

The ammount of fragmentation increases with storage time Ts (figure 2)

as expected from theory, $\ln \dfrac{(FeCO^+)}{(FeCO^+) + (Fe^+)}$ is linearly decreasing

with Ts, and the absolute value of the corresponding slope increases with argon pressure (figure 3).

Presented at the 35th ASMS Conference on Mass Spectrometry and Allied Topics
May 24-29, 1987, Denver, CO

Figure 2

EVOLUTION OF Fe^+ AND $FeCO^+$ WITH Ts

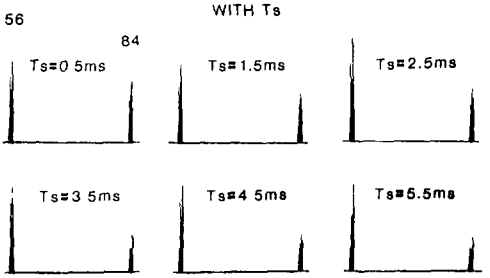

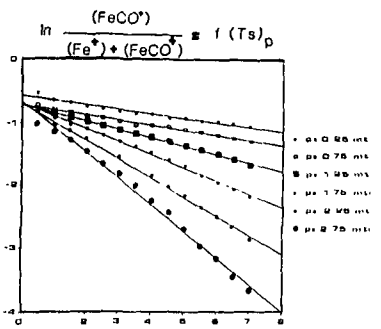

Figure 3

- Decomposition of a "metastable" ion

$$(Ph\ (CH_2)_3\ CH_3)^+ \longrightarrow \begin{cases} C_7H_7^+ \text{ (m/z 91)} \\ C_7H_8^+ \text{ (m/z 92) "metastable"} \end{cases} \xrightarrow{\text{confinement}} \xrightarrow{Q3}$$

The ion mixture (m/z 91) and (m/z 92) was trapped in the empty cell (no collision gas). The relative intensity ratio 91/92 increased with storage time, which shows that $C_7H_8^+$ ion has a short lifetime compared to $C_7H_7^+$ ion.

- Ion molecule reaction

$$Fe(CO)_5 \xrightarrow{Q1} FeCO^+ \xrightarrow[NH_3,\ Ar\ \text{confinement}]{CAR} Fe^+,\ FeNH_3^+,\ FeCO^+,\ Fe(NH_3)_2^+,\ Fe(NH_3)_3^{2+},\ Fe(NH_3)_4^{3+}$$

The reaction mixture composition is strongly dependent of storage time (figure 4). The observed dependence is consistent with the following scheme :

$$FeCO^+ + NH_3 \xrightarrow[\text{rapid}]{\text{very}} \begin{matrix} FeNH_3^+ \\ Fe^+ \end{matrix} + NH_3 \xrightarrow{\text{slow}} Fe(NH_3)_2^+ + NH_3 \xrightarrow[\text{slow}]{\text{very}} Fe(NH_3)_n^+$$

EVOLUTION OF REACTION PRODUCTS WITH Ts

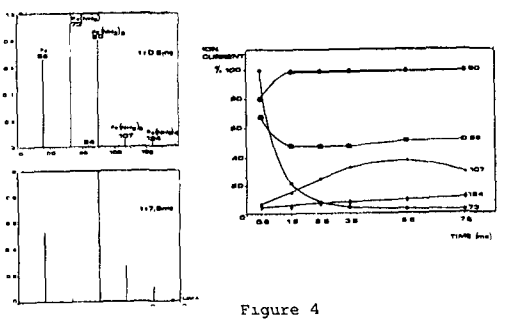

Figure 4

The results obtained on these three examples, which will be further studied, show the efficiency of the ion trapping procedure.

Presented at the 35th ASMS Conference on Mass Spectrometry and Allied Topics
May 24-29, 1987, Denver, CO

ANOMALOUS EFFECTS IN FRAGMENTATION PATTERNS

J.C. Lorquet, B. Leyh-Nihant, F. Remacle, D. Dehareng, and C. Krier
Département de Chimie, Université de Liège, Sart-Tilman, B-4000 Liège 1, Belgium.

Anomalous behavior does not necessarily indicate a breakdown of all of the basic assumptions of QET. In many cases, the simple QET-RRKM equation may not be directly applicable although the molecular ion reacts in a state of microcanonical equilibrium, because the conventional picture of the transition state is inadequate. This is the case, e.g., when a crossing between potential energy surfaces takes place. The reaction is then called non-adiabatic. However, it is then sometimes possible to recover the structure of QET at the expense of a further elaboration of the concept of transition state. It is thus much more adequate to classify unimolecular reactions using a double criterion : statistical or not, adiabatic or not. This leads to the following classification scheme.

1) Statistical, adiabatic reactions.
   QET is directly applicable, although it is preferable for careful work to adopt the variational transition state version of the theory [1]. (Many molecules fall into this category).

2) Statistical, non-adiabatic reactions.
   A state of microcanonical equilibrium is obtained in a time scale much shorter than the dissociation lifetime, but the bottleneck results from a surface crossing. Several expressions of the rate constant have been developed [2] which have basically the same form as in QET. The simplest one reads :

$$k^{nadia}(E) = [1/h\ N(E)] \int_0^E dE_u\ N_u^*(E_u)\ P(E-E_c-E_u)$$

   where N(E) is the total density of states of a system with n degrees of freedom, E_c is the energy of the crossing point, E_u is that fraction of the internal energy which is stored in the system of (n-1) degrees of freedom other than the reaction coordinate, and $N_u^*(E_u)$ is the corresponding density of states. The star indicates that the relevant frequencies have to be calculated at the crossing point. Each exit channel (each state of the activated complex) is weighted by a variable transmission coefficient P of quantum origin, which represents the probability of hopping from one electronic surface to the other. Peculiar effects are commonly observed in such reactions. It has been possible to account [3] for a strong isotope effect on the released kinetic energy and hence upon the metastable peak shape observed in the dissociation of the $HOCO^+$ ion [4]. A model has been designed [5] to account

for the peculiar behavior observed in the case of CH_3ONO^+ [6]. The unusually large isotope effect on the rate constant results from a tunneling effect due to the fact that the equilibrium geometries differ greatly for each electronic state. Secondly, it is observed that, in this particular case, the transmission coefficient P decreases when the internal energy increases. As a result, the rate constant does not significantly increase when E rises, at least above a certain threshold.

3) Non-statistical, adiabatic reactions.
These are the intriguing "non-ergodic reactions" detected in the case of acetone [7] and formaldehyde [8]. The reactive trajectories do not extend over the entire phase space. Two circumstances seem to be required to bring about this kind of specific behavior [9] :
(i) Nonlinear resonances determine a selective energy transfer when energy-dependent frequencies are in a simple ratio [e.g., $\nu^{str}(E)/\nu^{bend}(E) \simeq 2 : 1$].
(ii) There exists an approximate "specular relationship" between the structure of the initial conditions and that of the exist transition state.

4) Non-statistical, non-adiabatic reactions.
In some cases, narrowly avoided crossings can lead to a very specific energy deposition, i.e., to very well defined initial conditions. It has been speculated [10] in the case of CH_3OH^+ that this might lead to a branching between the reactive trajectories : one path leading to the usual randomized mass spectrum, and the other to a specific production fo CH_3^+ ions which would then appear to result from an "isolated state decay".

[1] D.G. Truhlar and B.C. Garrett, Acc. Chem. Res., 13, 440 (1980) ; W.L. Hase, ibid, 16, 258 (1983).
[2] J.C. Lorquet and B. Leyh-Nihant, to be submitted.
[3] F. Remacle, D. Dehareng, and J.C. Lorquet, to be submitted.
[4] P.C. Burgers, J.L. Holmes, and J.E. Szulejko, Int. J. Mass Spectr. Ion Proc., 57, 159 (1984).
[5] B. Leyh-Nihant and J.C. Lorquet, to be submitted.
[6] J.P. Gilman, T. Hsieh, and G.G. Meisels, J. Chem. Phys. 78, 3767 (1983).
[7] G. Depke, C. Lifshitz, H. Schwarz, and E. Tzidony, Angew. Chem., Int. Ed. Engl., 20, 792 (1981).
[8] W.J. Bouma, P.C. Burgers, J.L. Holmes, and L. Radom, J. Am. Chem. Soc., 108, 1767 (1986).
[9] C. Krier and J.C. Lorquet, work in progress.
[10] C. Galloy, C. Lecomte, and J.C. Lorquet, J. Chem. Phys., 77, 4522 (1982).

Presented at the 35th ASMS Conference on Mass Spectrometry and Allied Topics
May 24-29, 1987, Denver, CO

The Dissociation Rates of Ion-Dipole Complexes - Are they Non-Statistical?

Tomas Baer, Jian-Dong Shao, J.C. Morrow, M. Fraser-Monteiro
Chemistry Department
University of North Carolina
Chapel Hill, NC 27514

The dissociation rates of numerous energy selected metastable ions have been investigated by the technique of photoelectron photoion coincidence (PEPICO) during the past 10 years. In virtually all cases, the measured rates have been consistent with the predictions of the statistical theory of unimolecular reactions (RRKM/QET). This is not surprising since metastable ions are, by definition, slowly dissociating so that there should be sufficient time for total randomization of the internal energy.

There are many examples of slowly dissociating ions that have small phenomenological activation energies (appearance energy - ionization energy). An example is 1,5 hexadiyne, which is a higher energy isomer of the benzene ion. Its IE lies above the dissociation energy for H atom loss. Yet, this ion dissociates with the same slow rate as the benzene ion. Evidently, direct H atom loss from 1,5 hexadidyne is not energetically favorable compared to isomerization to the benzene ion structure. Once the ion has rearranged to benzene, its rate is slow and it appears as a metastable ion. Lifshitz has verified this process by a time resolved photoionzation experiment in which ions are trapped for up to milliseconds prior to mass analysis.

There is a class of slowly dissociating ions that are characterized by small activation energies, but that do not appear to have any isomer structures sufficiently low in energy to account for the slow rates. The common feature among these reactions is the loss of dipolar neutral species such as HCl loss from the ethylchloride and 1,2 diethylchloride ions, HBr loss from the 2-bromobutane ion, and H_2O loss from the n-propanol ion.

We have investigated the energetics and dissociation dynamics of the n-propanol ion in detail by PEPICO and a combination of PEPICO with photodissociation.[1] The latter experimental set-up is shown in Figure 1. The idea is to energy select the ions by PEPICO and then to photodissociate these energy selected ions with a pulsed laser. The photodissociation behavior can then be used to probe the ion structure as a function of its internal energy. Holmes <u>et al</u>.[2] have shown that n-propanol ions rearrange to an ion dipole complex prior to dissociation, and that the product ion has the cyclopropane ion structure, as opposed to the lower energy propene ion structure. The dissociation energy for H_2O loss lies, however, 0.2 eV above the thermochemical dissociation limit to cyclopropane ion and H_2O. Since the n-propanol ion dissociates to CH_2OH^+ (m/z 31) + CH_3 while the ion-dipole complex produces $C_3H_6^+$ (m/z 41) + H_2O, the two structures can be distinguished by either CA or by photodissociation. As the data in Figure 2 show, only CH_3OH^+ ions are produced by photodissociation. This indicates that the barrier for dissociation is actually an isomerization barrier, and that there is probably no barrier between the ion-dipole complex and the final dissociation products. The resulting potential energy curve is shown in Figure 3.

The well depth for the ion-dipole complex has been reported by Holmes <u>et al</u>.[2] In addition, we calculated its energy relative to the dissociation products by <u>ab initio</u> methods. This well depth does not

account for our measured slow dissociation rate. However, we note that the ion-dipole complex has a long range interaction potential which goes as $-r^{-2}$. We have shown that such a potential has an infinite number of vibrational energy levels, some of which are shown in Figure 4. This infinity of levels is moderated by the rotational motion of the H_2O molecule. However, the vestigial remains of this large number of states evidently results in the slow dissociation rate. Further work on the details of this dissociation are in progress.

---

1. T.L. Bunn and T. Baer, J. Chem. Phys. 85 6361 (1986)
2. J.L. Holmes, A.A. Mommers, J.E. Szulejko, and J.K., Terlouw, J. Chem. Soc. Commun. 165 (1984)

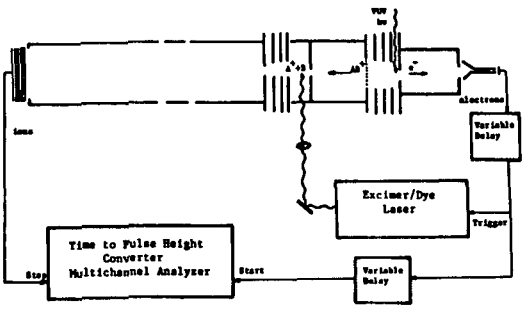

Fig. 1. The PEPICO-PD apparatus. Ions are formed in the VUV source and photodissociated by the excimer pumped dye laser.

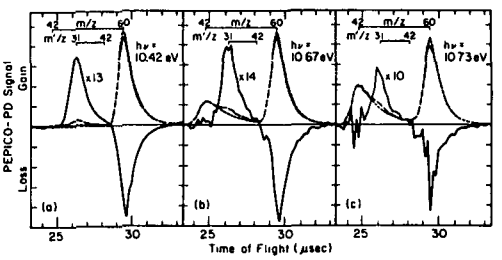

Fig. 2 The PEPICO-PD signal of energy selected propanol ions at three ion internal energies. The two sets of dashed lines are the PEPICO (no laser) and the PEPICO-PD signals, while the solid line is the difference spectrum. Metastable ion products (m/z 41) from the source are also observed.

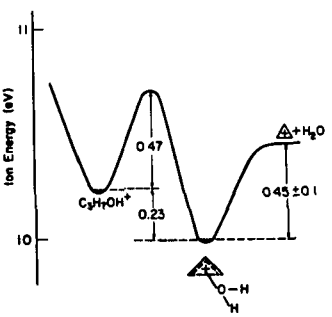

Fig. 3. The 0 K ion energetics, based on neutral propanol.

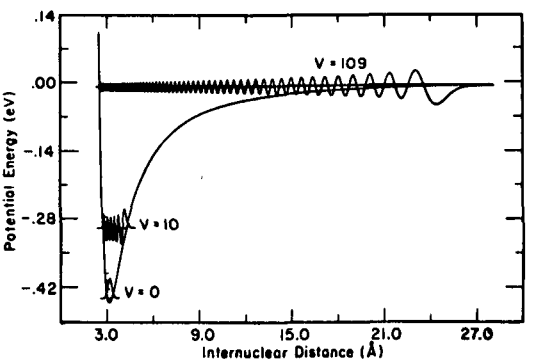

Fig. 4. Some vibrational wavefunctions for the $E[(\sigma/r)^{10} - (\sigma/r)^2]$ potential function. There are an infinite number of vibrational levels.

Presented at the 35th ASMS Conference on Mass Spectrometry and Allied Topics
May 24-29, 1987, Denver, CO

THE ATOMIC OXYGEN ANION AS A CHEMICAL IONIZATION AGENT: MECHANISTIC DETAILS

Joseph J. Grabowski and Steven J. Melly
Department of Chemistry, Harvard University
Cambridge, MA 02138

Negative chemical ionization is an established technique in the field of analytical mass spectrometry. The atomic oxygen anion is of special interest because it easily formed by dissociative electron attachment and because it is highly reactive. The atomic oxygen anion is a strong base, ΔH^{o}_{acid} = 382.2 ± 0.4 kcal/mole, able to abstract a proton from many organic molecules. There is an unique aspect to O^-; it is an open shell anion. The atomic oxygen anion thus has the possibility of abstracting H_2^+ from suitable molecules, generating in turn, other radical anions. A variety of such reactions have been observed for organic molecules. Here, we report the details of mechanistic studies of the reaction of O^- with a series of substituted methanes. The results reported were obtained utilizing the flowing afterglow technique, in 0.3 torr of helium buffer gas.

A sample branching ratio plot for the reaction of O^- with CD_3CN is shown in the first figure below, while the next figure summarizes the data from repeated measurements.

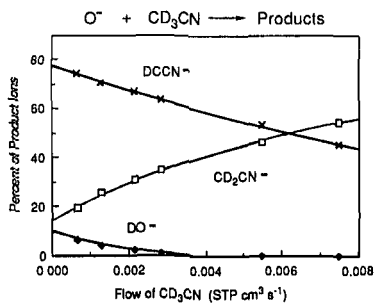

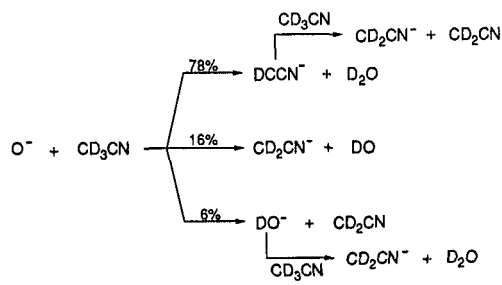

Thus we find that the carbene radical anion, $DCCN^-$, is the principle initial product ion. In addition, $DCCN^-$ undergoes a rapid reaction with an additional molecule of CD_3CN to give CD_2CN^-. The initially formed DO^- likewise undergoes a proton transfer with a second molecule of the nitrile. Thus with moderate additions of acetonitrile, one can convert a signal of only O^- into a signal of only CD_2CN^-, but this requires sequential reactions!

The reactions of O^- with CH_3Cl, CH_2Cl_2, CH_3NO_2 and CH_3CHO were examined and are summarized in the following figures.

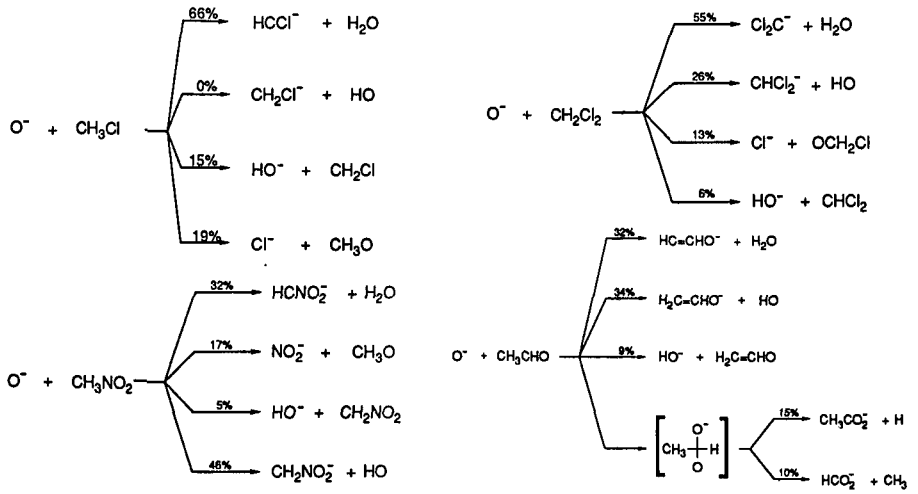

In the CH_3Cl system, both the HO^- and $HCCl^-$ initial product ions react with a second molecule of CH_3Cl by nucleophilic displacement. Likewise, in the CH_2Cl_2 system, both the $CHCl_2^-$ and the HO^- initial product ions react by displacement with CH_2Cl_2. However in this system, Cl_2C^- is stable to further reaction. In the CH_3NO_2 system, $HCNO_2^-$ reacts with a second CH_3NO_2 molecule by displacement while HO^- abstracts a proton from CH_3NO_2. Finally, in the CH_3CHO system, HO^- abstracts a proton from a second molecule of CH_3CHO, while $HCCHO^-$ undergoes an addition/radical displacment reaction. The products from this latter secondary reaction are $HC(O^-)=CHCHO$ and $CH_3C(O^-)=CHCHO$.

In general, the reaction of O^- with any of the substituted methanes examined are fast. For such systems, the pathways can be summarized as follows:

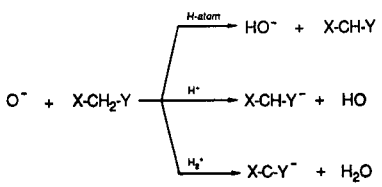

In addition, if X or Y is a good leaving group, displacement will be observed. If X or Y contains a carbonyl group, then addition to the carbonyl, followed by radical loss from the tetrahedral intermediate will also be observed. When the substituted methane is non-acidic (e.g., methane, dimethyl ether, dimethyl sulfide), the H-atom pathway is the only product channel observed. When the molecule is very acidic (e.g., $CH_2(CN)_2$ or $CH_2(CO_2CH_3)_2$) the predominant if not exclusive pathway is proton transfer. Only in the intermediate acidity range are all three channels observed. The greatest yield of radical anion found to date is in the acetonitrile system.

Presented at the 35th ASMS Conference on Mass Spectrometry and Allied Topics
May 24-29, 1987, Denver, CO

ISOTOPE EXCHANGE REACTIONS AS A PROBE OF REACTION DYNAMICS

Veronica M. Bierbaum, Charles H. DePuy, Jane M. Van Doren
and Stephan E. Barlow

Department of Chemistry and Biochemistry, University of Colorado,
Boulder, CO 80309-0215

A new tandem flowing afterglow-SIFT-drift instrument has been developed which provides high sensitivity, resolution and chemical versatility. With this instrument we have mass-selected and injected a variety of isotopically labelled ions, including $^{18}O^-$ and $^{37}Cl^-$, from unenriched precursors. Studies of the isotope exchange reactions of these ions serve as a sensitive probe of the reaction dynamics.

At thermal energy, unlabelled O^- appears to react with H_2O, CO_2 and O_2 only by slow three-body association. In contrast, $^{18}O^-$ reacts by facile bimolecular exchange:

$$^{18}O^- + H_2O \longrightarrow O^- + H_2{}^{18}O \qquad \text{efficiency} = 50\%$$

$$^{18}O^- + CO_2 \longrightarrow O^- + {}^{18}OCO \qquad \text{efficiency} = 67\%$$

$$^{18}O^- + O_2 \longrightarrow O^- + {}^{18}OO \qquad \text{efficiency} = 17\%$$

For H_2O and CO_2, the exchange efficiencies equal the statistical limit; for O_2, where the intermediate ion-dipole complex is expected to have a shorter lifetime, the oxygen atoms have not become equivalent.

The reactions of O^- with NO, CO and SO_2, proceed by rapid associative detachment. Studies of the reactions of $^{18}O^-$ with these reagents indicates that isotope exchange competes with detachment. This suggests that the intermediate molecular negative ion has comparable lifetimes toward dissociation and electron detachment.

The thermoneutral exchange reactions of $^{37}Cl^-$ have been studied for two mechanistically distinct processes: proton/deuteron transfer and nucleophilic substitution. The reactions:

$$^{37}Cl^- + H^{35}Cl \longrightarrow {}^{35}Cl^- + H^{37}Cl$$

$$^{37}Cl^- + D^{35}Cl \longrightarrow {}^{35}Cl^- + D^{37}Cl$$

both proceed with 50% efficiency, indicating that a long-lived complex is formed and that the barrier to proton/deuteron transfer is small. In contrast, the S_N2 reaction:

$$^{37}Cl^- + CH_3{}^{35}Cl \longrightarrow {}^{35}Cl^- + CH_3{}^{37}Cl$$

is immeasurably slow at thermal energy ($k < 2 \times 10^{-13}$ cm^3 s^{-1}) indicating a barrier which protrudes above the energy of the reactants. The kinetic energy dependence of the rate constant for this reaction has been studied in the drift tube from thermal energy to 1.4 eV; at this highest energy the rate coefficient approaches 1×10^{-11} cm^3 s^{-1}.

ACKNOWLEDGMENT--We gratefully acknowledge support of this work by the National Science Foundation, the U.S. Army Research Office and the Petroleum Research Fund, administered by the American Chemical Society.

Presented at the 35th ASMS Conference on Mass Spectrometry and Allied Topics
May 24-29, 1987, Denver, CO.

TIME-RESOLVED AND COLLISIONALLY INDUCED DISSOCIATION STUDIES OF GAS PHASE IONS

Nico M.M. Nibbering

Laboratory of Organic Chemistry, University of Amsterdam,
Nieuwe Achtergracht 129, 1018 WS Amsterdam, The Netherlands

Although the method of field ionization kinetics (FIK) dates back to the beginning of the seventies (1) and is used by only a few research groups nowadays, it still continues to be the most direct method in mass spectrometry to study in a time-resolved way the chemistry of molecular ions as a function of their lifetime ranging from approximately 10^{-11} to 10^{-6} s following ionization. The strength of the FIK method in such reaction mechanistic studies is frequently shown to full advantage when it is used in combination with stable isotopic labelling (2). Collisionally induced dissociation experiments performed on ions with lifetimes in excess of 10^{-6} s following ionization, sometimes again in combination with stable isotopic labelling, can further provide information on the structures of the ions involved which is invaluable to complement the mechanistic picture.

Three recently performed FIK studies in the author's group may illustrate the statements made above.

The first study concerns the elimination of C_5H_8 from the molecular ions of the endo, but not exo, isomers of 8,9-disubstituted tricyclo [5.2.1.$0^{2,6}$] decenes via a retro-Diels-Alder reaction. This highly stereospecific fragmentation observed upon electron impact (3) requires a double hydrogen transfer in the molecular ions as shown in Scheme 1, which could take place in either a concerted or stepwise fashion.

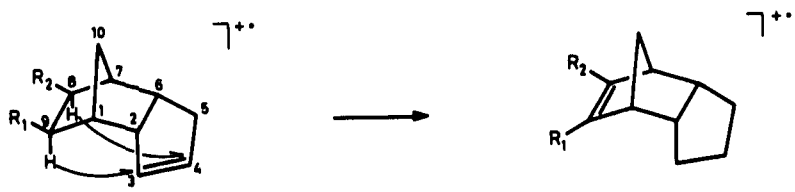

If the hydrogen atoms would migrate in a concerted fashion, then it is an example of a dyotropic reaction being defined as an uncatalyzed process in which two σ-bonds simultaneously, but not necessarily via a fully symmetrical mode, migrate intramolecularly (4). Such a suprafacial dyotropic transfer of hydrogen is a thermally "allowed" [$_{8s}+_{2s}+_{2s}$] pericyclic reaction (5). FIK experiments performed for the compound with $R_1 = R_2 = OCH_3$ show losses of C_5H_6 and C_5H_8, the former occurring at ion lifetimes < 10^{-10} s and the latter at ion lifetimes > 10^{-10} s. Loss of $C_5H_7^{\cdot}$, however, is not observed in this case over the whole time range studied (6). For the compounds with $R_1 = R_2 =$ OH and R_1 = OH, $R_2 = OCH_3$, $C_5H_7^{\cdot}$ loss is observed in addition to the losses of C_5H_6 and C_5H_8, but the shapes of the normalized rate curves of these competing channels have shown that the $C_5H_7^{\cdot}$ loss is related to the loss of C_5H_6, but not to that of C_5H_8 (6). In other words, FIK has provided strong support for the concerted character of the double hydrogen transfer, i.e. the above mentioned dyotropic hydrogen rearrangement, in the molecular ions studied prior to the retro-Diels-Alder reaction.

The second study concerns the elimination of methyl from ionized homoadamantane:

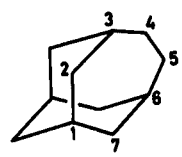

1

In this case a previous electron impact study combined with collisionally induced dissociation and ^2H- and ^{13}C-labelling experiments has demonstrated that

the molecular ion of homoadamantane exclusively rearranges to that of 1--methyladamantane prior to methyl loss to give exclusively the 1-adamantyl cation as product ion (7). Nevertheless, FIK experiments in combination with specific ^2H- and ^{13}C-labelling have shown that the molecular ions of homoadamantane eliminate a methyl radical via at least three different channels (8). In two of these channels, the methyl group lost contains one of the methylene groups of positions 4 and 5 and one of the bridgehead hydrogen atoms of positions 3 and 6 (see for numbering structure 1), while in the other channel the methyl group originates from other positions. The two first-mentioned channels have been interpreted as being due to a competition between a 1,2- and a 1,6--hydrogen shift in the C_4-C_5 bond cleaved molecular ions of homoadamantane, the former taking place at short ion lifetimes and the latter at long ion lifetimes (8).

The third study concerns the elimination of an ethyl radical from ionized 2--ethylbutanoic acid. In this case FIK experiments have indicated that the ethyl loss is a delayed process with respect to the ethylene loss, while ^2H- and ^{13}C-labelling have shown that the former reaction exclusively involves one of the original ethyl groups (9). Collisionally induced dissociation experiments on the resulting $[M-C_2H_5]^+$ ions have shown further that the major part has the structure of protonated crotonic acid, whereas the minor part has the structure of protonated methacrylic acid (9). These observations can be explained by an initial 1,4-hydrogen shift in the molecular ion from one of the methylene groups to the carbonyl oxygen atom. The protonated crotonic acid can then be formed by cleavage of the C_2-$C_{3'}$ bond in this rearranged molecular ion, while successive shifts of the protonated carboxyl group from C_2 to C_3 and of hydrogen from C_3 to C_2 in the rearranged molecular ion followed by cleavage of the C_2-$C_{3'}$ bond would generate the protonated methacrylic acid species. The latter sequence of reactions is well documented in the literature (10).

Acknowledgements

The author gratefully acknowledges his co-workers and colleagues listed in the references for their cooperation and the Netherlands Organizazion of Pure Research (SON/ZWO) for continuous support.

References

1. P.J. Derrick, A.M. Falick and A.L. Burlingame, 20th Annual Conference on Mass Spectrometry and Allied Topics, Dallas, Texas, June 1972, Paper No. H4.
2. N.M.M. Nibbering, Mass Spectrom. Rev. 3, 445 (1984).
3. R. Herzschuh, R.M. Rabbih, H. Kühn and M. Mühlstädt, Int. J. Mass Spectrom. Ion Phys. 47, 387 (1983).
4. M.T. Reetz, Tetrahedron 29, 2189 (1973).
5. R.B. Woodward and R. Hoffmann, "The Conservation of Orbital Symmetry", Verlag Chemie, GmbH, Weinheim/Bergstr., 1970, p. 141.
6. E. Kluft, N.M.M. Nibbering, H. Kühn and R. Herzschuh, J. Am. Chem. Soc. 108, 7201 (1986).
7. H. Schwarz, C. Wesdemiotis, T. Weiske, K.-P. Zeller and R. Müller, Z. Naturforsch. Teil B, 35, 207 (1980).
8. E. Kluft, N.M.M. Nibbering, H. Schwarz, R. Müller and K.-P. Zeller, Int. J. Mass Spectrom. Ion Proc. 73, 167 (1986).
9. E. Kluft, N.M.M. Nibbering and J.H. Bowie, manuscript in preparation.
10. H. Schwarz, Advan. Mass Spectrom. 10, 13 (1985) and references cited therein.

Presented at the 35th ASMS Conference on Mass Spectrometry and Allied Topics
May 24-29, 1987, Denver, CO

ANALYSIS OF A DIVERSE SET OF BACTERIA BY PYROLYSIS-MASS SPECTROMETRY WITH PATTERN RECOGNITION TECHNIQUES:

*Voorhees, K.J., Durfee, S.L. and Updegraff, D.
Colorado School of Mines, Golden, Colorado

Most of the published work involving pyrolysis of micro-organisms has focused on specific biopolymers or whole bacteria grown under carefully controlled conditions (1,2). The present investigation had as its major goal, the assessment of growth conditions, age and diversity on the ability to use Py-MS with pattern recognition to identify bacteria. A total of 40 bacteria were studied as individual species and as components in mixtures.

Pyrolysis of the bacteria was done on an Extrel Curie-point pyrolysis mass spectrometer using 510°C wires. Fifty spectra were summed together to generate a spectrum for pattern recognition. Each bacterium was run in at least triplicate. The data was subjected to principal components/factor analysis analysis with graphical rotation procedures (3).

Experiments in which a set of bacteria was grown to different stages of growth showed that the age of the culture had little or no effect on the ability of a linear classifier (using Py-MS data) to model the bacteria within the range of viability. In an experiment to investigate the effect of different methods of killing, all of the bacteria were correctly identified without regard to the method (if any) used to kill them.

A large Py-MS data set consisting of 28 species of bacteria, 2 yeasts and 2 fungi, with several different strains for some of the species, was examined. The individual species of bacteria could be discriminated for about a third of these bacteria, indicating that the uniqueness of the bacterium and the complexity of the data space modeled affect the efficiency of the data analysis. Comparison of the results from the large data set to the results from the age and killing study indicated that the number of bacteria which could be done without seriously affecting the capabilities of the factor analysis was about 20 different samples. The species that were identified in all three studies had similar factor spectra. Figure 1 represents the factor spectra from the three studies for E. Coli.

Pyrolysis-MS mixture experiments were performed using a simplex model for a set of four species of bacteria in the presence of varying contributions from pollen and atmospheric particles. A factor-factor plot for the data is shown in Figure 2 (note the similarity of the position of the various samples to the simplex model). The presence of bacteria was readily detected, and, once found, the species of bacteria present was be determined. Mixture experiments involving a more complex background (seven completely different components with lower concentrations of seven different species of bacteria) could not be classified reliably.

The results from this study shows that Py-MS with pattern recognition can be used to identify bacteria grown under varible conditions provided that the number samples do not overwhelm the software capabilities. In future studies where large numbers of bacteria are included in a data set, pyrolysis with tandem mass spectrometry will be used to reduce the complexity of the data set.

Presented at the 35th ASMS Conference on Mass Spectrometry and Allied Topics
May 24-29, 1987, Denver, CO

References

1. Meuzelaar, H.L.C., J. Haverkamp and F.D. Hileman, "Pyrolysis Mass Spectrometry of Recent and Fossil Biomaterials", Elsevier, Amsterdam, 1982.

2. Irwin, W.J., "Analytical Pyrolysis: a Comprehensive Guide", Marcel Dekker, New York 1982.

3. Voorhees, K.J. and Tsao, R., Anal. Chem., 1985, 57, 1630.

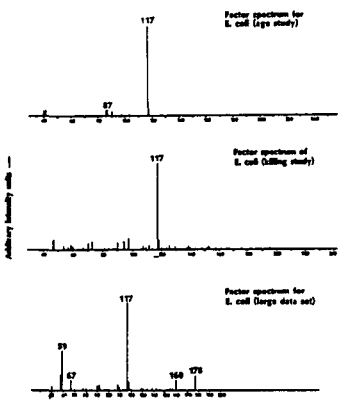

Figure 1. Factor spectra for E. Coli from three different studies.

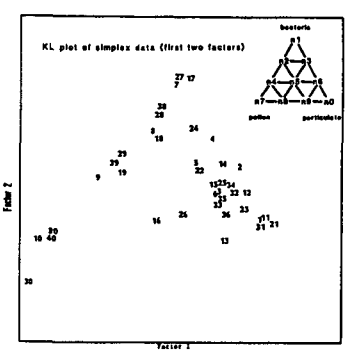

Figure 2. KL Plot of Factor 1 and Factor 2 for Simplex Data.

Presented at the 35th ASMS Conference on Mass Spectrometry and Allied Topics
May 24-29, 1987, Denver, CO

SMALL COMPUTER-DATA SYSTEM FOR RESEARCH APPLICATIONS IN MASS SPECTROMETRY. William F. Haddon, Masahiro Handa, Robert Lundin and Ronald Nachman, Western Regional Research Center, USDA, 800 Buchanan St., Albany, CA 94939.

Introduction. An interactive instrument control, graphics display computer system can be a significant asset in a mass spectrometry laboratory where frequent adaption to new samples and projects is necessary. As may be the case generally, we felt removed from the current revolution in scientific software and personal computing through reliance on a mini-computer based data system that, while excellent for routine samples, adapted poorly or not at all to changing research needs in our laboratory. A number of recent new projects, including the measurement of LSIMS spectra of insect neuropeptides (1) prompted us to investigate a more flexible approach to data acquisition and computing than was available to us through the vendor supplied system. The most important objective of the work was to construct a data system that will allow research applications involving the mass spectrometer to be rapidly "breadboard" designed to test their feasibility and then polished, as time permits, into functional tools for day-to-day sample analysis.

Approach. Our approach to achieving such a system involves four concepts: 1) In order to make maximum use of the mass spectrometer and existing data system, the supplemental data system is built around the use of trigger signals originating from analog or digital electronic units already available. For example, trigger signals from the existing digital scan unit provide start and stop magnetic scan signals for synchronizing the two computer systems. This concept avoided the need to re-program an already perfectly adequate magnet scan generator. 2) As a front end to the supplemental data system we use a data acquisition and control unit with its own microprocessor, operating system and considerable memory, backed up by an AT compatible "personal" computer. The first two figures show the overall configuration that results, and some additional details of the data acquisition unit (MDAS-7000, Trans-Era Corp., Provo, UT). 3) To make the system expandable and adaptable to future computing developments, we use a standard IEEE-488 interface bus to connect the data acquisition box with its host computer (Equity III, Epson Co. of America). Thus while we use an AT computer currently, addition of a Macintosh computer, for example, can be carried out easily. 4) For programming simplicity, we use an interpreted BASIC. The particular BASIC language set must be chosen very carefully to meet the grahics, calculation and data transfer speed requirements of real time mass spectrometry. In addition, we use a comprehensive scientific software system to provide statistical, curve fitting and additional graphics capability (the ASYST program from Macmillan Software)

Results. The alternative data system, assembled as described above, has produced spectacular results within six months in the analysis of peptides in the 1000-1800 mw. range using a VG 70/70 HS mass spectrometer. The exising data system had serious shortcomings because of inability to separate partially resolved peaks, difficulty with changing baseline, and frustrating sensitivity to minor high voltage discharges on the Cs^+ primary ion source that we use for LSIMS. Mass assignments were frequently in error by a mass unit above mass 1000 due to use of an inappropriate mass assignment procedure. Our approach to resolving these difficulties was to use the magnetic scan capabilities of the existing data system (VG DS-2000), but to record analog data into the MDAS-7000.

Two examples are shown The first is a mass resolved spectrum of a synthetic peptide that was thought to be the amide of the indicated structure. The mass of MH^+ indicated the C-terminal OH was present, and revealed the presence of an impurity containing 1 less aspartic acid residue, 115 amu lower The second example shows a case where resolution has been lowered to increase sensitivity. This sample was run prior to LC separation of products to check for the possible presence of the sulfated target peptide LSK-II (1). Its molecular ion cluster and the sodiated adduct are present, thus indicating the desirability of additional purification effort. For about 50 samples examined with the new data system, mass assignments have been within 0.15 amu for 80 per cent of the samples, but slightly poorer, as expected, for unresolved clusters.

1. R. J. Nachman, G. M. Holman, W. F. Haddon and N. Ling, *Science*, 1986, **234**, 71-73.

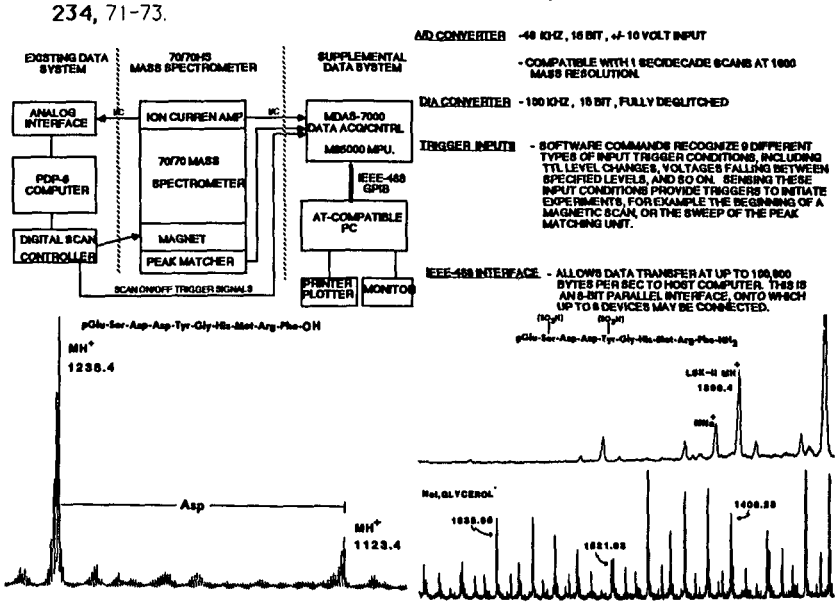

Presented at the 35th ASMS Conference on Mass Spectrometry and Allied Topics
May 24-29, 1987, Denver, CO

A HIGH SPEED DATA SYSTEM/TIMESHARING SYSTEM LINK.

H.A. Bondarovich, C. Cone, S. Patel and S. Stoddart
IFF R&D, Union Beach, N.J., 07735

INTRODUCTION

For approximately six years we have been transferring data for complete gcms analyses of complex samples from our data systems to a VAX/VMS timesharing system using 9 track magnetic tape. Automatically selected scans from each gcms run are searched against both the NBS(NIH/EPA) library and our own in-house libraries. Our chemists can also compare any spectrum in their gcms run with any spectrum in the libraries at graphics terminals in their laboratories.

AIM

Avoid transferring data on magnetic tapes and make data available more rapidly to our chemists by installing a high speed link to directly transfer complete gcms runs from complex samples with typically 3000 to 5000 individual mass spectra. The amounts of data make the use of an RS232C link running at 9600 or even 19,200 baud barely practical. When this link was initially planned the only higher speed link for which both hardware and software drivers were available for both DG and DEC computers was the IEEE 488-1975 data bus. This bus is byte parallel and can run at a maximum data rate of 40 Kbytes/sec .

DATA SYSTEMS

Three data systems are presently connected to the link. They are Kratos DS55 systems based on DG minicomputers and have the following configurations.

A. DG Nova 3 with 256 Kbytes of RAM/DG 6050 (Phoenix) disk drive/DG 6060A 96 Mbyte disk drive/Kratos preprocessor interface (MS9)/Versatec V1110A printer-plotter/DG 800bpi 9 track magnetic tape drive

B. DG Nova 4X with 128 KBytes of RAM/DG 73 Mbyte Winchester disk drive/Kratos preprocessor interface (MS25)/Versatec V80 printer-plotter/DG 800bpi 9 track magnetic tape drive

C. DG Eclipse S120 with 256 KBytes of RAM/DG 6050 (Phoenix) disk drive/DG 96 Mbyte disk drive/Kratos preprocessor interface (MS50L)/Versatec V1110A printer-plotter/DG 800bpi 9 track magnetic tape drive (shared)

The terminals are a mix of older Tektronix 4010's and newer Tektronix 4105's and 4107's.

LINK HARDWARE

1. RBI Systems (Silver Spring, MD) interface boards, one in each DG minicomputer. 2. A Black Box ABCDE switch.
3. A HP 37203A fibre optic link between the DG minicomputers and the VAX.
4. A DEC IEC11 UNIBUS interface.

The RBI systems boards are each set to device number 0 on the IEEE 488 bus; the IEC11 is set to device number 30 (decimal). The fibre optic cable not only allows us to exceed the standard distance limit of the IEEE 488 bus (our data systems are approximately 500 feet from our VAX) but also ensures complete electrical isolation between our mass spectrometers and our timesharing system.

TIME SHARING SYSTEM

This is a DEC VAX 11/785 with 32 Mbytes of RAM and a disk capacity of 2.95 Gigabytes. On the Unibus of this system are an Ethernet with ca. 175 ports on terminal servers, DZ11 and VMZ controllers for ca. 50 ports, the controller for the RA81 disk drives, and the DEC IEC11 IEEE 488 controller. The IEEE 488 interface is physically 2 Unibus boards; the first (IEC11A) implements the basic functions of the bus; the second (IEC11B) makes possible DMA transfer of data blocks.

THE DATA TRANSFER SOFTWARE

The code for transmission of DS55 data from the DG computers is imbedded in

a modified version of an earlier program for archiving DS55 data to magnetic tape in a compact data format (supplied to IFF by Terwilliger Software). An additional switch has been added to indicate whether the data is to be written to tape in 4096 byte blocks or transmitted to the VAX via the link in 512 byte blocks. Data transmission, and control of the link mode is via the assembly language drivers for the IEEE 488 bus provided by RBI systems.

The VAX code is written in VAX Fortran (Fortran 77 with extensions) and uses the drivers and simplified interface supplied by DEC with the IEC11 for reading data which is written to a scratch file as received. When transmission of the file is complete the VAX command procedure starts another program to reformat the data for the search and related programs.

LINK PERFORMANCE
The link is in daily routine use with both Nova computers. The board for the Eclipse system has been reconfigured for DG device number 42(octal) and we hope to have it in use shortly.

Over the approximately 9 months that the link has been in routine use data transfer has been generally, but not completely, reliable. We have transmitted many complete gcms runs without any errors but have encountered data errors approximately 6 different times during this 9 month period and are not sure whether minor changes in the programs or reseating boards in the various computers overcame some of these problems.

It presently takes approximately 1 hour to transmit a gcms run of 0.7 Mbytes when our VAX is lightly used (2-4 users). This means that we are now only sending data over the link at a thruput of approximately 400 bytes/sec. When our VAX is fairly heavily used during the week (30-40 users) data transfer is not significantly slowed. However if there is another program running in the foreground of the Nova sending data to the VAX data transfer is significantly slowed. This indicates that the major bottle neck is at the DG end and that we should be able to significantly speed up data transfer with the new program for reading and archiving DS90 data described in the next section.

FUTURE DEVELOPMENTS We plan the following :-
1. Try to discover the causes of the occasional unreliablity of data transfer referred to above in the section on the performance of the link.
2. Modify the drivers supplied by RBI systems so that they can be linked to code written in DG Fortran V, in which most of the programs of the newer Kratos DS90 system are written. A recently written Fortran V program to archive DS90 data to magnetic tape is considerably faster than the corresponding Fortran IV program for archiving DS55 data.
3. Make changes to increase the efficiency of the data transfer. These include calculating at the DG end the same CRC value for a data block that the VAX microcode would calculate. We would then not transmit each block twice. Also experiment with the data block sizes.
4. Use the IEEE 488 bus for transfer of data between our data systems and for more effective sharing of peripherals between these systems. One problem is that while the DEC bus interface was designed to be used as either a controller or not, the RBI Systems interface was designed to always be the bus controller. C. Webster believes that he can overcome this limitation with modifications to the relevant driver routines. We will be testing these in the next few months.
5. Add an interface for our newest data system which is based on a DG30 desktop system. RBI systems does not make a board for this system.

ACKNOWLEDGEMENTS
The assistance of T.E. Lindsay (DSE Inc., Matawan, NJ) with the help in the selection of the hardware used to implement this link, C. Webster (Webster Research Corporation, Mount Airy, MD) with help in the programming at the DG end and S. Brown (IFF) in testing this link is gratefully acknowledged.

Presented at the 35th ASMS Conference on Mass Spectrometry and Allied Topics
May 24-29, 1987, Denver, CO

IMPLEMENTATION OF A NON-AUTOCONSOLE KRATOS MS-25/DS-90 SYSTEM TO PERFORM SELECTED ION MONITORING QUANTITATION OF PARTS-PER-TRILLION CONCENTRATIONS OF MULTIPLE ANALYTES DURING A SINGLE ANALYSIS

J. H. Garrett, J. G. Solch, C. D. Miller, T. O. Tiernan and M. L. Taylor*
Departments of Chemistry and Pharmacology/Toxicology*
Wright State University, Dayton, Ohio 45435

INTRODUCTION

Recent regulatory requirements relating to the measurement of polychlorinated dibenzo-p-dioxins (PCDD) and polychlorinated dibenzofurans (PCDF) in hazardous chemical wastes and environmental samples have dictated the need to accurately determine multiple isomers of these compounds in a single GC-MS analysis. While the capability to analyze for the entire chlorinated spectrum of PCDD and PCDF using GC-MS-SIM (Selected-Ion-Monitoring) has been established for some time in our laboratory and others, no simple method has been previously available to demonstrate that all isomers of each chlorinated congener group can indeed be detected. Such a calibration procedure which can be implemented on a regular basis during a series of analyses is essential for accurate analyses of this type. Another problem which has been encountered in the past in accomplishing such analyses is that the hardware and software previously used with the Kratos sector mass spectrometers in our laboratory to determine multiple PCDD and PCDF isomers in a single analysis have somewhat restricted the number of ions which can be monitored for each congener group under conditions which rapidly switch the mass spectrometer between these groups.

The objectives of the present work were: a) to develop an improved analytical technique for accomplishing quantitation of parts-per-trillion levels of multiple PCDD and PCDF isomers in extracts of complex environmental samples by making the needed changes in existing Kratos MS-25 hardware and implementing new software to accomplish more rapid switching between pre-programmed groups of ion masses. This would permit monitoring of a larger number of ions for each chlorinated congener group, and enhanced sensitivity; b) to devise a simplified calibration procedure to demonstrate that all PCDD/PCDF isomers of each chlorinated group are detected and quantitated during the GC-MS analysis; and c) to demonstrate the efficacy of the improved analytical technique through the analysis of extracts of actual samples.

INSTRUMENTATION UTILIZED IN THE PRESENT STUDIES

The instrumentation and parameters utilized for the present studies are summarized below.

A. Gas Chromatograph

A Carlo-Erba Model 5300 Gas Chromatograph with capillary injector configured for splitless/split operation (split flow on at 60 seconds after injection) was employed. A 60M, 0.25 mm fused silica column coated with a 0.25 μ film of DB-5 was utilized, with hydrogen (30 PSIG) as the carrier gas. Typically, 0.2 μL of each sample was injected. The column temperature program implemented entailed isothermal operation at 190° for 1 minute post-injection, then the temperature was increased to 300°C at 5°C/minute. A single stage Kratos glass jet separator was used as the interface between the GC and MS.

B. Mass Spectrometer

A Kratos MS-25/Data General SR-120/DS-90 mas spectrometer system was employed. The operating parameters were: Resolution, 1:600; Ionizing Voltage, 70 eV; Source Temperature, 250°C. The mass spectrometer was operated in the SIM mode with appropriate masses monitored for each chlorinated congener group of PCDD and PCDF.

MODIFICATIONS REQUIRED TO ENABLE NON-AUTO CONSOLE MS-25 TO RUN SELECTED ION MONITORING (SIM) UNDER DS-90 SOFTWARE CONTROL

The modifications made to the mass spectrometer and computer data acquisition system in the course of the present work included the following:

1. A new ERMPM board (extended range multiple peak monitoring board) was installed in the MS-25 chassis. This board controls ESA scans and contains the computer controlled magnet reference. Extensive wiring changes were required to install this board.

2. A new selected-ion-monitoring data acquisition board (SIM DAC board) was installed iin the preprocessor interface.

3. The DS-90 software package was installed on the Data General SR-120 Computer.

GAS CHROMATOGRAPHIC RETENTION TIME STUDIES--PREPARATION OF GC WINDOW-DEFINING CALIBRATION MIXTURES

The gas chromatographic retention times for a large number of PCDD and PCDF isomers were determined on the 60M DB-5 capillary GC column under typical operating conditions. From these measurements, it was determined that the retention time differences between the last eluting isomer of a given chlorinated congener group and the first eluting isomer of the next higher chlorinated congener group under typical GC operating conditions were as follows: Cl_4-Cl_5, 25 seconds; Cl_5-Cl_6, 63 seconds; Cl_6-Cl_7, 231 seconds; Cl_7-Cl_8, 415 seconds. These times correspond to the maximum allowable switching and settling times during which the mass spectrometer must be retuned by the computer to monitor a new set of ions indicative of the following chlorinated congener group. Accordingly, the modified computer control system was adjusted to achieve these switching times.

The GC retention data were also used as the basis for preparing a set of PCDD and PCDF isomers which can be used to demonstrate at regular intervals during a series of GC-MS analytical runs that the first and last eluting isomers of each chlorinated congener group are indeed being detected. For the DB-5 GC column, these mixtures include the following: PCDD: 1,3,6,8-TCDD; 1,2,8,9-TCDD; 1,2,3,6,7-PeCDD; 1,2,3,8,9-PeCDD; 1,2,4,6,7,9-/1,2,4,6,8,9-HxCDD; 1,2,3,4,6,7-HxCDD; 1,2,3,4,6,7,8-HpCDD; 1,2,3,4,6,7,9-HpCDD; OCDD. PCDF: 1,2,6,8-TCDF; 1,2,8,9-TCDF; 1,3,4,6,8-PeCDF; 1,2,3,8,9-PeCDF; 1,2,3,4,6,8-HxCDF; 1,2,3,4,8,9-HxCDF; 1,2,3,4,6,7,8-HpCDF; 1,2,3,4,7,8,9-HpCDF; and OCDF. Mass chromatograms showing analyses and display of data from these mixtures, as well as corresponding data for actual samples analyzed were presented.

Presented at the 35th ASMS Conference on Mass Spectrometry and Allied Topics
May 24-29, 1987, Denver, CO

AUTOMATED QUANTITATION OF MULTIPLE ANALYTES IN A LARGE STUDY

D.M. Fast, F.L. Cardinali, G.D. Todd, and J.S. Holler

Toxicology Branch
Environmental Health Laboratory Sciences Division
Center for Environmental Health
Centers for Disease Control
Public Health Service
U.S. Department of Health and Human Services
Atlanta, Georgia 30333

To assess the possibility that children were exposed to chlorinated phenols or phenoxy acid herbicides, we were responsible for quantifying up to 12 analytes at the 1-10 ppb level in each of approximately 300 samples. The raw data were acquired in a single data file on a Finnigan MAT TSQ-46 mass spectrometer as +CI-daughter-ion-MID spectra for 2,4-dichlorophenoxyacetic acid (2,4-D), 2,6-dichlorophenol, 3,5-dichlorophenol, 2,5-dichlorophenol, 2,4-dichlorophenol, 3,4-dichlorophenol, 2,4,6-trichlorophenol, and 2,4,5-trichlorophenol (DCP and TCP), and as NCI-MID spectra for pentachlorophenol (PCP), 2-(2,4,5-trichlorophenoxy)propionic acid, 2,4,5-trichlorophenoxyacetic acid (2,4,5-T), and 2,4-dichlorophenoxybutyric acid. We used ^{13}C labelled 3,4-DCP, 2,4,5-TCP, and PCP as internal standards for the phenols and the phenoxyacids and unlabelled 2,3-D as the internal standard for 2,4-D. All internal standards concentrations were 50 ppb except for PCP, which was 20 ppb.

Monitoring two ions per compound allowed us to compute the chlorine isotope ratios. We wrote a series of INCOS procedures to separate the raw data files and recombine individual ions into two single-ion chromatograms (arbitrarily putting the first ion monitored into the first chromatogram and the second ion monitored into the second chromatogram). We then selected peaks in the chromatograms for each analyte of interest, wrote those scans to a scan list, and automatically computed the height and area for each peak. Automatic processing of data in this step decreased the operator time required for each sample from about 1 hour to 20 minutes. To remove redundant or misassigned peaks, the operator edited heights and areas for each ion chromatogram, and the data for both ion chromatograms of a sample were combined into a single quantitation list.

We included two standards in the range 1-12 ppb (1-100 ppb for PCP) in each daily run, along with two quality control samples and at least eight case or control samples. We analyzed all samples in the study and then computed height and area response factors from the mean for all standards run during the study after eliminating outliers. Standards outliers were eliminated in an iterative procedure by discarding all points outside $\pm$ 2 SD of the mean and then recomputing the mean and the SD. This procedure was repeated until no more values were deleted. Typically, less than 25% of the 105 standards values were deleted; for 2,5-DCP and 2,4,5-T, about 50% of the values were deleted.

We computed analyte amounts for each height and area in the quantitation list and transferred the results from INCOS to our PC-based local area network We then computed ion ratios for heights and areas by using a BASIC program that printed out the ratios for comparison with theoretical values derived from the expected chlorine substitution of each compound. We considered results acceptable if the ion ratios fell within a ±20% limit, which we had previously established by using quality control material. Analyte concentrations for those results were reported on the basis of peak area. If ion ratios were not within the previously established limits, we used a decision tree to select an ion and height or area for quantitation

After final manual verification of retention times, ion ratios, and quantitation ion, the concentrations were passed to a data base which printed the final report and stored the complete results with operator comments

We obtained the final statistical reports for the 3,600 possible analytical values from the data base by using PC-SAS. This procedure is being refined for a larger followup study of 12 analytes in at least 1,000 samples. Except for verification of peak selection, all data validation, transfer, and reporting will be done without operator intervention.

This study was supported by the Agency for Toxic Substances and Disease Registry, Public Health Service, U.S. Department of Health and Human Services, Atlanta, Georgia 30333.

Use of trade names is for identification only and does not constitute endorsement by the Public Health Service or the U.S. Department of Health and Human Services.

Presented at the 35th ASMS Conference on Mass Spectrometry and Allied Topics
May 24-29, 1987, Denver, CO

A NEW DATA SYSTEM FOR THE PROCESSING OF ENVIRONMENTAL DATA.

S.Kennerley, P.A.Ryan, D.J.Milton and D.A.Shiel

Kratos Analytical, Barton Dock Road, Urmston, Manchester M31 2LD UK

Introduction

A suite of software programs has been designed for use in environmental GC-MS applications. The software runs on the Data General systems as supplied on Kratos Analytical's instruments such as the MS25E dedicated environmental GC-MS.

DS90E is based on Kratos's DS90 menu driven data system. For environmental GC-MS analysis the presentation has been simplified to provide a quick and easy to use system. Full data processing capabilities are provided via a standard DS90 processing option.

Acquiring Data

Data acquisition is performed through standard DS90 acquisition menus. One additional feature of the system is the incorporation of a *TUNING REPORT*. This allows instant confirmation that DFTPP or BFB intensity criteria have been met. A typical report is presented in figure 1 and the corresponding DFTPP spectrum shown in figure 2.

Data Processing

A library of target compounds can be specified containing up to 4 masses for identification and/or quantitation. Standard target libraries are already provided, additional ones may be added by the user. A peak detection routine matches these target compounds from the acquired data. Any unmatched peaks are entered into an unknowns scan list for library searching at a later stage. The results of peak detection can be displayed on chromatogram reports, as is illustrated in figure 3. Internal standards are searched for first, followed by target samples.

Detected peaks can be processed in one of several ways depending on the status of the data:

1. The initial requirement is to perform a calibration on target library compounds. Peak detected data from a dilution series is collated and average response factors calculated. The calibration reports are generated from the Public Domain software written and supplied by the EPA and incorporated into DS90E software.
2. For sample analysis, concentrations per component are calculated using the response factors produced at the calibration stage. Figure 4 shows a typical report produced by this part of the EPA software package. The header gives information about each injection to allow sample tracking and quality control to take place.
3. Any unidentified peaks in a sample that have been recorded in the identify peaks routine are recorded and fed through to library search routines. After library searching, possible matches are reported and can be displayed graphically using the spectrum plotting facility.

Conclusions

DS90E is an easy to use system that enables quick analysis of priority pollutants and provides for other environmental applications. By incorporating the EPA's Public Domain software, it provides standard EPA report formats and sample tracking information.

SPECTRUM: DFTPP8014 2/17/87
INSTRUMENT: MS25RF
SAMPLE: TEST OF DFTX
CONDITIONS:
308

SPECTRUM FIT TO DFTPP CRITERIA

M/Z	INTEN	LIMITS	FOUND RA	
51	783480.	30-60% OF 198	32.47	OK
68	14144.	< 2% OF 69	1.38	OK
69	1026850.	NOT SPECIFIED	47.35	OK
70	0.	< 2% OF 69	0.00	OK
127	1128450.	40-60% OF 198	52 00	OK
197	7376.	< 1% OF 198	0.34	OK
198	2164700.	100% (BASE PK)	100.00	OK
199	154112.	5-9% OF 198	7.11	OK
275	621560.	10-30% OF 198	28.69	OK
365	44608.	> 1% OF 198	2.06	OK
441	174592.	< 100% OF 443	73 18	OK
442	1134590.	> 40% OF 198	52.36	OK
443	238592.	17-23% OF 442	21.03	OK

Figure 1

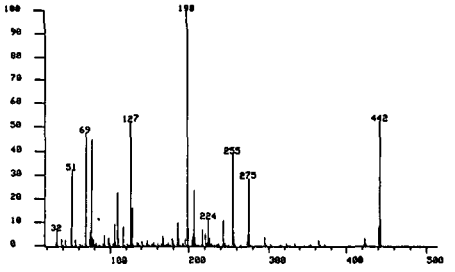

Figure 2

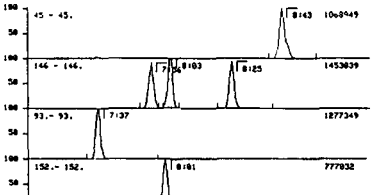

Figure 3

SAMPLE #(1) METHOD(6) 8625 PROD RUN(1) 625
QC CODE(1) MATRIX CODE(1) 101 OPT CLEANUP(1)
REGION #(1) CASE #(1) BATCH #(1)
QC REPORT #(1) ANALYST INIT(1) WCD
DATE RECVD(1) 2/12/87 CONCENTRA LEVEL(1) M PH(1) 7 0
DATE EXTR(1) 2/12/87 SHIFT EXTR(1) EXTRACTION CODE(1)
DATE ANALYZ(S) 4/12/87 SHIFT ANALYZ(S) 8 TIME ANALYZ(S) 16:18
EXTRACT VOL(1) *1000 SAMPLE SZ(1) 1 0000L % WATER(1) 0
INJECTION VOL(1) 1000 DILUTION FACT 0 1 % WATER DECANT(1) 0

RESPONSE FACTORS USED FROM AVERAGE (DATE 2/27/87 TIME 12 18)

QC CASE(2)	CONCENTRATION/AMT(1-3) (UG/L) MEASURED	ADDED	DET LM	NAME(2)
111444	10 3303			BIS 2 CHLOROETHYLETHER
541731	10 0126			M DICHLOROBENZENE
106467	10 9613			P DICHLOROBENZENE
95501	10 3453			O DICHLOROBENZENE
108601	9 9040			BIS 2CHLOROISOPROPYLETHER
621647	10 0443			N NITROSODIPROPYLAMINE
67721	10 2469			HEXACHLOROETHANE
98953	9 8936			NITROBENZENE
78591	10 5338			ISOPHORONE
111911	10 1836			BIS 2CHLOROETHOXYMETHANE
120821	10 3403			1,2,4 TRICHLOROBENZENE
91203	11 2287			NAPHTHALENE
77474	10 6310			HEXACHLOROBUTADIENE

Figure 4

Presented at the 35th ASMS Conference on Mass Spectrometry and Allied Topics
May 24-29, 1987, Denver, CO

DEVELOPMENT OF ON-LINE QC/QA TECHNIQUES FOR STATISTICAL EVALUATION OF GC/MS ENVIRONMENTAL DATA

G.E. PRILL and J.V. Headley,
Alberta Environmental Centre, Bag 4000 VEGREVILLE, Alberta, TOB 4LO

Laboratories equipped for high sample throughput and environmental analyses face the constant challenge of maintaining high quality of their data while sustaining high productivity. Failure to meet this challenge satisfactorily can result in serious consequences such as poor efficiency or even loss of credibility.

To be cost effective, modern laboratories have become well equipped, using automation of environmental analyses where appropriate. For example, hard copies of GC/MS analytical reports in a format suitable for a client, may be generated using autosamplers for data acquisition and subsequent automated data processing techniques. However, manual validation of the enormous volume of data generated by these processes is slow and tedious.

The objectives of this study was to develop on-line quality control and quality assurance (QC/QA) procedures to expedite the monitoring and evaluation of (a) sample extractions, (b) instrumental data acquisition, and (c) computerized data reduction. Procedure files were developed for environmental analyses employing Hewlett Packard GC/MS systems, experimental parameters of which are described elsewhere[1]. The files are complex sequences of executable commands which access on-line computed data[2] of: (1) the recoveries of surrogate standards; (2) the instrumental responses for multi-internal standards; (3) integration profiles of quantification ions; and (4) the laboratory performance for standard reference materials.

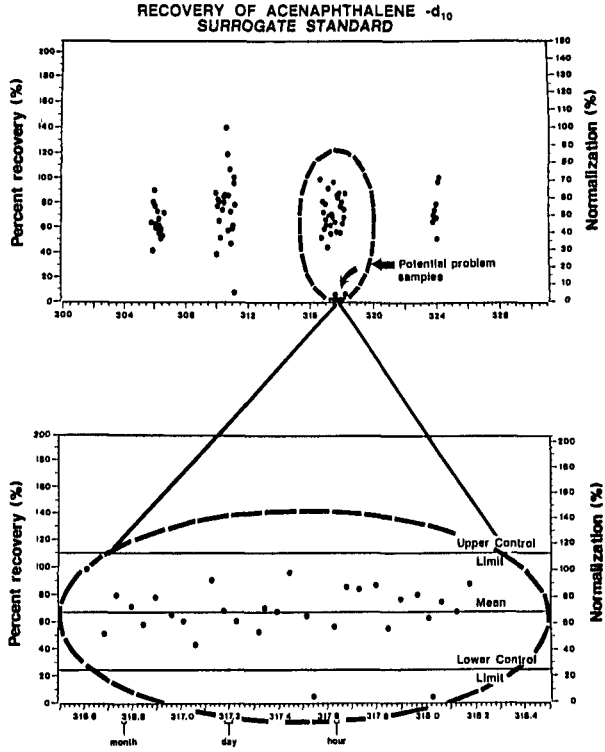

Figure 1

Applications of the procedures are illustrated in Figures 1-4. Recovery data for a surrogate standard are shown in Figure 1. The "moving window" concept is supported permitting x-bar charts to be plotted for evaluation of variable periods of a data set or

composite data sets.

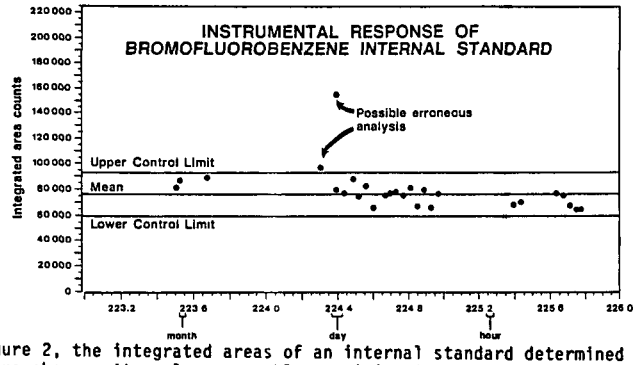

Figure 2

In Figure 2, the integrated areas of an internal standard determined for sequential analyses are shown. At a glance, problems arising from matrix effects or poorly spiked standards can be flagged.

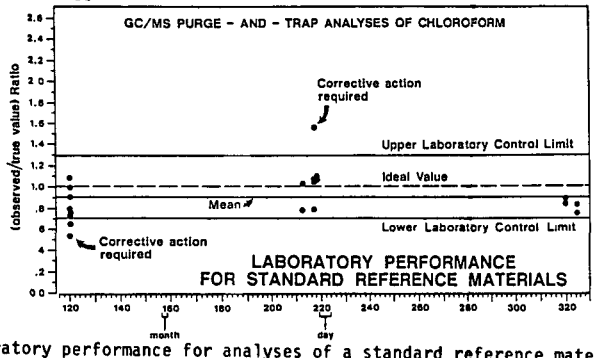

Figure 3

The laboratory performance for analyses of a standard reference material is shown in Figure 3. This chart facilitates the evaluation of the quality of data and implementation of corrective action, if required.

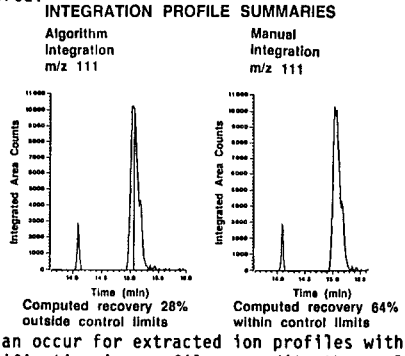

Figure 4

Erroneous integration can occur for extracted ion profiles with poor peak shape. Hard copy summaries of the quantification ion-profiles expedite the evaluation of this problem, an example of which is illustrated in Figure 4.

The applications of the on-line QC/QA techniques facilitate the rapid diagnosis of problems arising in GC/MS environmental analyses and permit the statistical evaluation of condensed summaries of large volumes of data.

References

1. J. V. Headley, Biomed. Environ. mass spectrum (1987) in press.
2. A. G. Dexter, E.T.C. Aquarius reference manual (1984).

Presented at the 35th ASMS Conference on Mass Spectrometry and Allied Topics
May 24-29, 1987, Denver, CO

QUALITY CONTROL VERIFICATION AND REPORTING OF RESULTS FROM ENVIRONMENTAL ANALYSES

D. Thomas Terwilliger and Ann L. Behbehani
Computer Science Corporation

and

William L. Budde
U.S. Environmental Protection Agency

Cincinnati, Ohio 45268

Laboratories using gas chromatography/mass spectrometry (GC/MS) or other methods to identify and measure toxic organic pollutants in environmental samples for the U.S. Environmental Protection Agency (EPA) are required to maintain a rigorous quality control (QC) program. This intense level of QC is not generally practiced in analytical programs because of the substantial additional cost factor, which may amount to as much as 40% of the total analytical cost.

The objective of this work is to automate as much as possible of the QC data gathering and reporting processes in order to lower the cost of QC, and to provide rapid feedback of accurate QC information to scientists and managers to ensure that problems in the analytical method are recognized in real time, and appropriate corrections are made on a timely basis. Automation, shown below, includes the capture, in machine readable form, of all reportable data from individual GC/MS data systems, calculations to produce data needed for QC checks, tracking of samples analyzed to determine if proper procedures were used, generation of reports containing QC information, and, as a result, removal of most QC decision making and responsibility from the instrument technician.

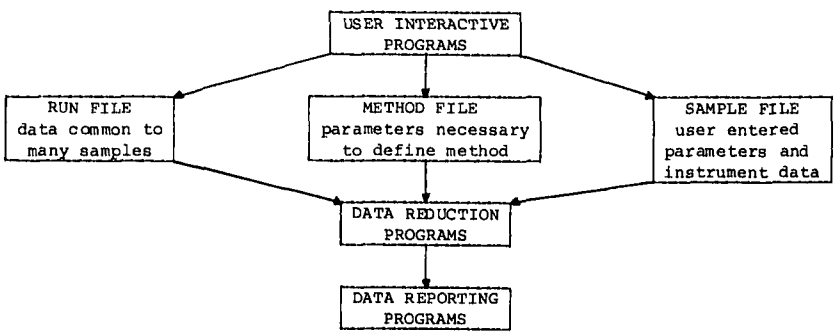

Required QC for EPA samples includes measurement of blanks, sample duplicates, matrix spikes, spiked blanks, and surrogate compounds. Real time information is needed on the results of these measurements, and on the results of required continuing calibration checks, regular instrument calibration and performance checks, and internal standard signal changes. Also required are checks on sample holding times, concentrations outside the calibration range, deviations from retention time windows, and the required sequence and timing of various QC checks.

Computer software that currently operates on several GC/MS systems and personal computers was developed to gather raw quantitation data, library search results, and

spectra of performance check compounds and place this information in a data file common to all systems. Modules were developed to allow the user to enter from a keyboard a variety of additional information including spiking levels, detection limits, sample matrices, holding time requirements, types and frequency of QC samples, calibration requirements, recovery limits, precision requirements, blank limits, and time and peak area requirements. Also included is administrative information such as Chemical Abstracts Service Registry Numbers, sample numbers, reporting requirements, units of measure, sample preparation codes, etc. Data entry modules were also developed to allow the user to enter data from non-GC/MS methods, for example gas chromatography or liquid chromatography systems, that use similar calculations and require similar QC checks.

All programs in this package are driven by a "Method File" which is defined separately for each analytical method. This file contains all required checks to be performed along with the control limits to be observed. A series of data reduction and processing programs, shown below as DFTPP, BFB, EPARED, EPAAVG, EPASNG, EPAURF, EPAQCR, and TCDD, were developed to generate the needed information, including quantitative calculations of concentrations, and to perform many of the required QC checks on the data automatically as it is generated. Central to this process is the program EPARED. It consolidates all data from a single sample, performing all QC checks that only require data from that sample, and creates files used by the other programs. These files contain processed data as well as QC flags indicating which conditions were not met. All reduced data may be printed in a series of reports using EPADMP and other programs, or placed into a standard format designed for transmission of the results on magnetic or telecommunications media to another computer or a data base management system. Printed reports flag all errors so the responsible laboratory scientist can take appropriate corrective action in a timely manner.

All of the file management and data reduction software currently operates on five commercial GC/MS data systems and in a stand-alone version for MS-DOS personal computers.

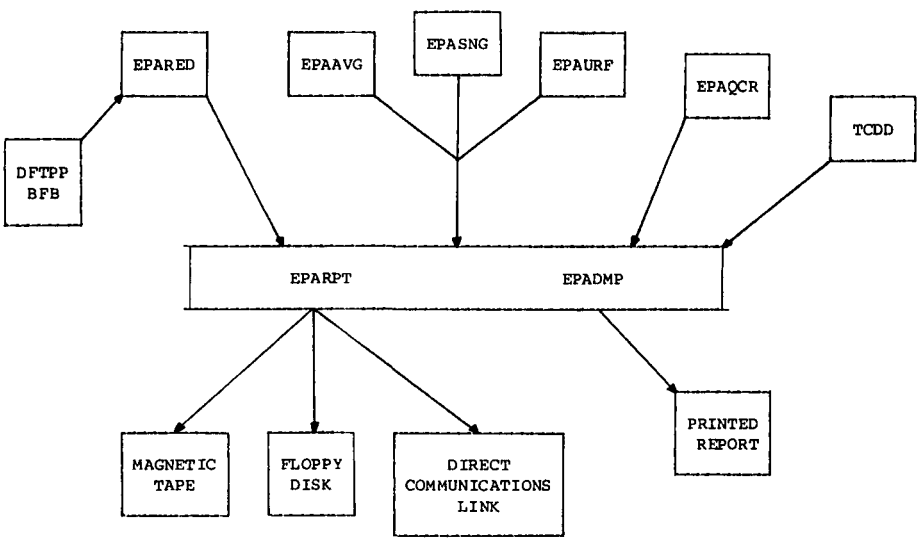

Presented at the 35th ASMS Conference on Mass Spectrometry and Allied Topics
May 24-29, 1987, Denver, CO

CHEMICAL INTERPRETATION OF EMPIRICALLY DERIVED SUBSTRUCTURE IDENTIFICATION RULES

K.J. Hart, A.P. Wade, P.T. Palmer, B. Nourse and C.G. Enke,

The Chemistry Department, Michigan State University, East Lansing, MI 48824.

Interpretive approaches to structure elucidation, as used here, require that a set of interpretation rules be applied to the spectra of unknown compounds. It has been shown that empirical rules for MS/MS spectra can be automatically generated by software tools such as MAPS. These make use of the complete MS/MS fragmentation map.

MAPS is a collection of LISP functions for the identification of spectral feature / substructure correlations present in MS/MS spectra. These correlations are expressed as rules of the form: "IF (spectral feature A) AND (spectral feature B)... THEN (substructure X) is present". A training set of known compounds and a library of recognized substructures are used to generate these rules as shown by the dashed line in Figure 1. The rules generation process has been described elsewhere (1). MAPS includes several diagnostic functions to evaluate the quality of the rules and the modes of application (2). The rules must accurately represent the relationships present in the database and be amenable to logical chemical interpretation. The MAPS software is currently written in InterLISP-D and runs on a Xerox 1108 AI Workstation. A Common LISP version is under consideration. This will run on a DEC AI VAXstation, along with other software tools developed for this project.

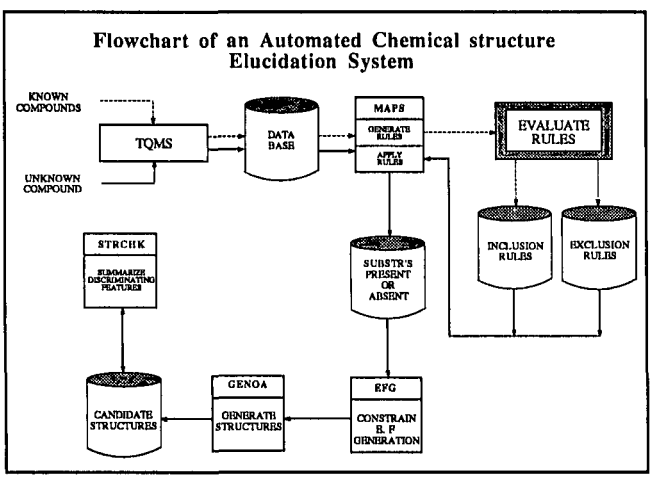

Figure 1

Current results show that the MAPS rules yield primary scan correlations that compare favorably with well established MS correlation tables (3), as well as providing

correlations such as daughter ions and specific parent to daughter transitions that can only be observed by MS/MS. These provide an extra dimension of characterization to the structure elucidation process.

A limited manual study indicated the absence of certain expected features from the MS/MS spectra of some oxygen-containing aromatic compounds. This led to the investigation of two new substructures, "BENZYLOXY" (Ph-(CH_2)-O-) and "BENZYL ESTER" (Ph-CH_2-OOC-R). The application of MAPS produced a rule for "BENZYLOXY", but it was unable to do the same for "BENZYL ESTER" since there were insufficient occurrences of that substructure within the current training set. When considering the MAPS rules for the "BENZYL", "BENZYLOXY", "1,4-PHENYL" and "XPHENYL" substructures using a RULE-DIFFERENCE function, it became obvious that the clauses the rules share are due to the break-up of the aromatic ring, and that the differences can be quite specific to the individual substructures. Ideally, the rules should be able to distinguish the occurrence of one substructure from another, and indicate when in fact several similar substructures are present. The RULE-DIFFERENCE function can also be used in mixture analysis applications where one desires to ascertain which spectral features are diagnostic for species of interest. This may lead to improved experimental design.

Findings from the application of the MAPS rules are also used by other software tools. These include a constrained empirical formula generation program (EFG), which is written in Fortran and currently runs on a DEC PDP-11 and a DEC AI VAXstation in our laboratory. Constraints for this program can be derived from MAPS analysis of the MS/MS data space for a compound, by passing the program the the empirical formulae of the substructures found. For example, if the "PHTHALATE" substructure were recognized by MAPS, then any empirical formulae for the unknown should contain at least 8 carbon and 4 oxygen atoms. Also used is the GENOA structure generation program originally developed at Stanford University as part of the DENDRAL project. The commercial version of the software is written in VAX C and is also currently running on our AI VAXstation. As part of the current work, GENOA is being modified to interact more readily with other software tools. The program requires an empirical formula and will accept as constraints the presence or absence of particular substructures. It also includes a structure checking facility (STRCHK) which can be used to identify the recognized substructures present in a larger structure.

Conclusions:

Evaluation of the MAPS rules has led to verification of the pattern recognition/ AI approach used by this software. Examination of the spectra for absent or unique rule clauses can lead to new rules (e.g. "BENZYLOXY"). In the course of evaluation of the rules a new MAPS function, RULE-DIFFERENCE, was developed. The demand for software tools for computer-aided interpretation of MS/MS spectra will become increasingly important as new methods are developed which can rapidly acquire full fragmentation maps (e.g. B-TAD (4)), and as commercial tandem MS instruments proliferate.

1. A.P. Wade, P.T. Palmer, K.J. Hart and C.G. Enke, pp. 426-7, Proc. 34th ASMS Conference, Cincinnati, OH, June 1986.
2. P.T. Palmer, A.P. Wade, K.J. Hart and C.G. Enke, poster TPA12, 35th ASMS Conference, Denver, CO, May 1987.
3. F. McLafferty, "Interpretation of Mass Spectra", 3rd Edn., University Science Books, Mill Valley, CA, (1980)
4. B.A. Eckenrode, B.H. Newcome, J.F. Holland and C.G. Enke, Poster MPB35, 35th ASMS Conference, Denver, CO, May 1987.

This work was supported by NIH grant #GM28254.

Presented at the 35th ASMS Conference on Mass Spectrometry and Allied Topics
May 24-29, 1987, Denver, CO

EVALUATION OF AN AUTOMATED METHOD FOR GENERATING SUBSTRUCTURE IDENTIFICATION RULES FROM MS/MS DATA

P.T. Palmer, A.P. Wade+, K.J. Hart and C.G. Enke*,
The Chemistry Department, Michigan State University,
East Lansing, Michigan 48824

+ also of BP Research Centre, Sunbury-on-Thames, UK

A pattern recognition / artificial intelligence program, known as MAPS (Method for Analyzing Patterns in Spectra) has been developed in this laboratory to predict the presence or absence of defined substructures in unknown compounds using substructure identification rules which are automatically generated from MS and MS/MS data (1,2).

The rules generation procedure is outlined in Figure 1. Two types of mass spectral features are considered for inclusion in these rules: features which correlate strongly with substructures and features which are specific to substructures. In this generation, the user specifies the value of the CG variable (Correlation factor for rule Generation), which sets the minimum degree of correlation for a feature to appear in a rule. As the CG value decreases, the length of each rule usually increases.

Figure 1. Generation of Substructure Identification Rules via MAPS.

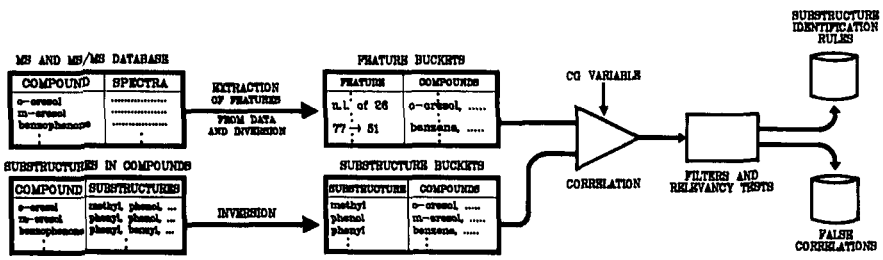

In the rules application, the user specifies the value of the CA variable (Correlation factor for rule Application), which sets the minimum fraction of features present in a rule which must be present (or absent) in the mass spectral data of an unknown for that substructure to be recognized in (or excluded from) the unknown.

MAPS now includes functions for analyzing the predictive capabilities of the rules. These apply the rules to a set of known compounds; the results are then tabulated into four categories - correct and incorrect predictions of the presence of substructures (inclusions), and correct and incorrect predictions of the absence of substructures (exclusions). These are shown in Figure 2 for two substructures at three different CA values.

Figure 2. Performance of XPHENYL and PHTHALATE-ESTER rules at several CA values.

XPHENYL 33 clauses in rule

CA	% CORRECT INCLUSIONS	% INCORRECT INCLUSIONS	% CORRECT EXCLUSIONS	% INCORRECT EXCLUSIONS
100%	0	0	0	0
75%	49	0	11	0
50%	95	16	84	5

PHTHALATE-ESTER 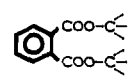 61 clauses in rule

CA	% CORRECT INCLUSIONS	% INCORRECT INCLUSIONS	% CORRECT EXCLUSIONS	% INCORRECT EXCLUSIONS
100%	0	0	0	0
75%	75	9	10	0
50%	88	51	49	12

There are certain substructures whose identification is unavoidably ambiguous from MS and MS/MS data. One example of this is the carbonyl substructure, whose rule is given below:

IF neutral loss of 28 amu (CO)
THEN substructure indicated is CARBONYL

Thus, any compound which undergoes a neutral loss of ethylene would be erroneously flagged as containing the carbonyl substructure. MAPS automatically recognizes "ambiguous" substructures and can remove them from consideration. Thus, the number of incorrect predictions is substantially decreased. The predictive capabilities of the rules are described by a "merit factor", which is calculated as shown below:.

$$\text{Merit Factor for inclusions} = \frac{(\%\ \text{correct inclusions} \times 100\%)}{(\%\ \text{correct inclusions} + \%\ \text{incorrect inclusions})}$$

$$\text{Merit Factor for exclusions} = \frac{(\%\ \text{correct exclusions} \times 100\%)}{(\%\ \text{correct exclusions} + \%\ \text{incorrect exclusions})}$$

Figure 3 plots the merit factor for inclusions and exclusions versus the CA variable when "ambiguous" substructures are not considered.

FIGURE 3. MERIT FACTOR FOR INCLUSIONS AND EXCLUSIONS VERSUS CA OMITTING AMBIGUOUS SUBSTRUCTURES

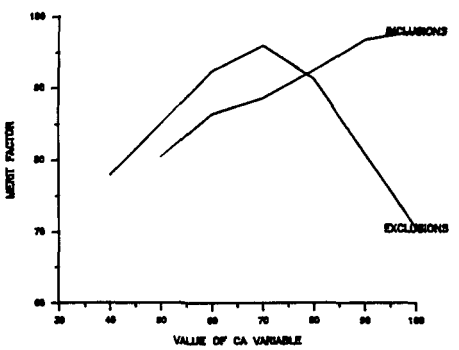

Currently, the MAPS database comprises 45 rules, 76 compounds, 67 different substructures, 2509 mass spectral features and 2048 clauses in the rules. Different criteria exist for predicting the presence and absence of substructures, and thus two different types of rules should be independently formulated for inclusion and exclusion of substructures. From the results, it is evident that expansion of the database along with optimization of the CG and CA variables for each rule will improve the predictive capabilities of the rules.

Acknowledgements: This work was supported by NIH grant GM-28254. The authors thank Finnigan MAT for the loan of and support for a Xerox 1108 AI workstation.

References:
1) A.P. Wade, P.T. Palmer, K.J. Hart, and C.G. Enke, 34th Annual ASMS Conference, Cincinnati, June, 1986, p. 426.
2) A.P. Wade, P.T. Palmer, K.J. Hart, and C.G. Enke, manuscript in preparation.

Presented at the 35th ASMS Conference on Mass Spectrometry and Allied Topics
May 24-29, 1987, Denver, CO

Expert Program for the Interpretation of GC/MS Data on Fossil Fuels

Thomas Aczel, S.G. Colgrove
Exxon Research and Engineering Co.
and
Lan Le, University of Houston

We have developed an expert program for the automatic interpretation of GC/MS data on fossil fuel distillates. The program is designed to reduce professional time spent in interpretation and quantitation. It mimics decisions made by human experts when examining the output from Manufacturers' data systems.

Need for such a program stems from the following facts:

- Each of up to 1000 components must be determined
- Many components are unresolved; some GC/MS peaks contain as many as 5 or 6 different compounds
- There are no pure compound spectra for most components likely to be present in fossil fuels
- Replicate identifications are frequent
- Library identifications are based on spectral matching, not on spectra/structure correlations; they are often misleading
- Quantitation, sorting, is extremely time consuming

The main principles of the program are the following:

- Each GC/MS peak is treated as a mixture and is deconvoluted using classical MS type analyses
- A carbon number range (2 to 3) is assigned to each deconvoluted component, based on its elution time relative to that of n-paraffin calibrants
- Molecular ions are searched for within the boundaries defined above. In this step, the program distinguishes between true molecular ions, isotopes, fragment ions and rearrangement ions
- Library identifications are accepted only if "fit" is higher than an a-priori set value and if they are within the boundaries set above.
- Library identifications are further checked against the molecular ions found, as shown below:

SUMMARY OF RULES FOR ASSIGNMENT OF SPECIFIC STRUCTURES

FOUND		
MOLECULAR ION(S)	ACCEPTABLE STRUCTURE	DECISION
NO	NO	ASSIGN TYPE, "MOST PROBABLE" CARBON NUMBER FOR EACH TYPE
NO	YES	ASSIGN STRUCTURE, CORRESPONDING CARBON NUMBER, TYPE
YES	NO	ASSIGN TYPE, CARBON NO. TO MOLECULAR IONS FOUND
YES	YES	MATCH: ASSIGN STRUCTURE; SELECT BEST "FIT" IF MORE THAN ONE MATCH NO MATCH: ASSIGN TYPE, CARBON NO. OF MOLECULAR ION FOUND; DECLARE CONFLICT

This approach assures that all components are assigned either a specific structure or at least a generic structure (carbon number, type).

The program is executed "on line", and it yields a detailed diagnostic output and a condensed summary (1 line per component that lists retention time, generic identification, specific identification if available, calculated boiling point, and concentration). Components are also sorted according to type and carbon number. Additional calculations yield average carbon number, average MW, elemental C, elemental H, etc. for each type and for the total sample.

Evaluation of the program with several complex petroleum distillates showed that it yields the same interpretation as a "human" expert in 95 percent plus cases. In addition, it detects minor and trace components not easily seen by "human" experts.

Future work planned includes expanded evaluation, addition of more type analyses, the use of retention time indexes to better identify isomers, and the use of "DENDRAL" type spectra/structure correlations.

Development of the program was greatly aided by the advise and efforts of Professor S. Deming of the University of Houston, Dr. D.L. Larsen and Dr. R.S. Stepelman of Exxon Research, Corporate Laboratories, Clinton, N.J., and Debra Richards and Pat Sharp of Exxon Research, Baytown, who carried out the experimental work on the GC/MS instrument.

Presented at the 35th ASMS Conference on Mass Spectrometry and Allied Topics
May 24-29, 1987, Denver, CO

Hugh Gregg, Lawrence Livermore National Laboratory
PO Box 808 L-310, Livermore, CA 94550
Carla Wong, NASA Ames Research Center
M/S 244-7, Moffett Field, CA 94035

The TQMSTUNE knowledge based system was designed to optimize the triple quadrupole mass spectrometer (TQMS) built at LLNL. The goals and associated rules for TQMSTUNE have evolved over several years and are presented in their "final" form (no program is ever really finished!).

The TQMSTUNE system is based on obtaining goals (e.g. TUNE.FOR.MSMS). Each goal has its own set of rules that determine what actions are to be performed. The goals and actions are shown in figure 1, and the actions are summarized below:

DO.SUBGOAL	perform a subgoal
SET	set value of an instrument parameter
SWITCH	switch a parameter (e.g. Q1DC on/off)
REMEMBER	save a value for later comparison
SET.TWEAK.PARAM	modify default tweak parameters
MAKE.LINKED.KNOB	create virtual LinkedKnob and record offsets
UNIPLEX	single parameter optimization
SIMPLEX	multiple parameter optimization

Rules are used to select the tweak (optimization) parameters, such as the tweak limits and the data function to use. By default, signal intensity at the center of a peak is used by the tweak functions, unless a rule similar to that shown in figure 2 selects signal "goodness". "Goodness" includes a measure of peak shape as well as intensity, but because more data is required to compute the goodness factor, intensity only data is preferred so that the tuning process takes as little time as possible.

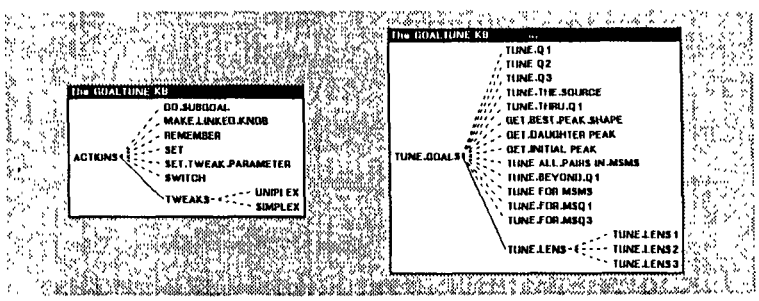

Figure 1: Goals and Actions

```
The EXTERNAL.FORM slot
OwnSlot: EXTERNAL.FORM from GOODNESSFA1
   Inheritance: SAME
   ValueClass: LIST
   AVUNITS: RULEPARSE
     Facet Inheritance: UNION
   Values: (IF [AND (THE Position OF Q1DC IS ON)
                    (OR (Q1FieldAxis IS IN KNOBS.TO.TWEAK)
                        (AND (LinkedKnobs IS IN KNOBS.TO.TWEAK)
                             (OR (THE PrimaryKnob OF LinkedKnobs IS Q1FieldAxis)
                                 (A SecondaryKnobs OF LinkedKnobs IS Q1FieldAxis]
               THEN
               (THE DATAFXN OF ?TWEAKACTION IS FFTGOODNESS))
```

Figure 2: One of the goodness rules

The goals and rules are presented here in FORTRAN style (indeed, the tuning system could be written in any language) rather than the original LISP for brevity and clarity.

Goal: TUNE.FOR.MSMS

```
    SWITCH              Q1DC ON
    SWITCH              Q3DC OFF
    SET                 CAD.GAS.PRESSURE 0
    DO.SUBGOAL          GET.INITIAL.PEAK
    REMEMBER            starting intensity
    DO. SUBGOAL         TUNE.THRU.Q1
if intensity > 2 x starting intensity, then
        DO. SUBGOAL         TUNE.THRU.Q1
endif
    SWITCH              Q3DC ON
    SET                 CAD.GAS.PRESSURE to initial
    DO.SUBGOAL          GET.DAUGHTER.PEAK
    REMEMBER            daughter intensity
    DO.SUBGOAL          TUNE.BEYOND.Q1
    MAKE LINKED.KNOB    Q2FA L3A L3B L3C Q3FA
    SIMPLEX             LinkedKnobs Q2Mass
if intensity > 2 x daughter intensity, then
        DO SUBGOAL          TUNE.BEYOND.Q1
        MAKE.LINKED.KNOB    Q2FA L3A L3B L3C Q3FA
        SIMPLEX             LinkedKnobs Q2Mass
endif
```

Subgoal: GET.INITIAL.PEAK

```
if a peak shape cannot be measured then
   SET              defaults for all elements
endif
if a peak shape still cannot be measured, then
   SET              SEMVoltage + 100 up to 2000 Volts
endif
if a peak exists (i.e. shape can be measured), then
   DO.SUBGOAL       GET.BEST.PEAK.SHAPE
else
   warn operator and skip to the next tune
endif
```

Subgoal: GET.DAUGHTER.PEAK

```
if a peak shape cannot be measured, then
   SET              default for Q2FA L3A L3B L3C Q3FA
endif
if a peak shape still cannot be measured, then
   SET              SEMVoltage + 100 up to 2000 Volts
endif
if a peak exists (i.e. shape can be measured), then
   DO.SUBGOAL       GET.BEST.PEAK.SHAPE
else
   warn operator and skip to the next tune
endif
```

Subgoal: GET.BEST.PEAK.SHAPE

```
if shape is OK, then
    Subgoal is done
endif
if (tuning for MSQ1) or
  (tuning for MSMS and CAD gas is off), then
    UNIPLEX         Q1FA
else
    UNIPLEX         Q3FA
endif
```

Goal: TUNE.FOR.MSQ1 and TUNE.FOR.MSQ3

```
    SWITCH              QnDC on/off as needed
    SET                 CAD.GAS.PRESSURE 0
    DO.SUBGOAL          GET.INITIAL.PEAK
    REMEMBER            starting intensity
    DO.SUBGOAL          TUNE.THRU.Q1
    DO.SUBGOAL          TUNE.BEYOND.Q1
if intensity > 2 x starting intensity, then
        DO.SUBGOAL          TUNE.THRU.Q1
        DO.SUBGOAL          TUNE.BEYOND.Q1
endif
```

Subgoal: TUNE.THRU.Q1

```
DO.SUBGOAL    TUNE.THE.SOURCE
DO.SUBGOAL    TUNE.LENS1
DO.SUBGOAL    TUNE.Q1
DO.SUBGOAL    TUNE.LENS2
```

Subgoal: TUNE.BEYOND.Q1

```
DO.SUBGOAL    TUNE.Q2
DO.SUBGOAL    TUNE.LENS3
DO.SUBGOAL    TUNE.Q3
```

Subgoal: TUNE.THE.SOURCE

```
SIMPLEX       Repeller Drawout Focus
```

Subgoal: TUNE.LENSn

```
SIMPLEX       LnA LnB LnC
```

Subgoal: TUNE.Q1

```
if tuning for MSQ3,  then
   SIMPLEX              Q1FA Q1MASS
else
   UNIPLEX              Q1FA
endif
```

Subgoal: TUNE.Q2

```
if tuning for MSMS, then
    SET                 CAD.GAS.PRESSURE initial
    MAKE.LINKED.KNOB    Q2FA L3A L3B L3C Q3FA
    SET.TWEAK.PARAM     to use intensity, not goodness
    SIMPLEX             LinkedKnobs Q2mass
else
    SIMPLEX             Q2FA Q2Mass
endif
```

Subgoal: TUNE.Q3

```
if tuning for MSQ1,  then
   SIMPLEX              Q3FA Q3MASS
else
   UNIPLEX              Q3FA
endif
```

Work performed under the auspices of the U.S. Department of Energy by the Lawrence Livermore National Laboratory under contract number W-7405-ENG-48.

Presented at the 35th ASMS Conference on Mass Spectrometry and Allied Topics
May 24-29, 1987, Denver, CO

DETERMINATION OF AROCLOR COMPOSITION FROM PCB LEVEL OF CHLORINATION DATA

L.E.Slivon and P.M.Schumacher
Battelle Columbus Division, Columbus, Ohio 43201

INTRODUCTION

The conventional GC/MS approach to the identification of Aroclors is an extension of well known GC/ECD techniques (1) which rely heavily on precise retention time and high resolution chromatographic separation in order to identify as many as 40 specific PCB isomers as a prelude to identification of Aroclors (2).

The classification and quantification of PCB by summed level of chlorination has been described (3-5). This approach eliminates the need for rigorous retention time and separation control as well as the time consuming and sometimes uncertain process of specific isomer identification. This approach, which yields results in terms of the total PCB at each of the 10 possible chlorination levels has been automated (6). Despite the advantages of the level of chlorination approach, the lack of Aroclor content information represents a serious drawback to those analysts who require identification and quantification of PCB in terms of Aroclors.

APPROACH

During the development of the level of chlorination technique, it was observed that individual pure aroclors exhibited level of chlorination patterns analogous to their specific isomer patterns. This paper describes the results obtained from a computer program which utilizes only the level of chlorination data to estimate Aroclor content.

The program AROCLOR is yet another permutation of a stepwise multivariate regression technique that has been adapted to the isomer specific Aroclor and related mixture problems by others (1,2,7,8). The heart of the algorithm is a 90 element matrix (3) containing relative amounts at each of the 10 possible levels of chlorination for 9 pure Aroclors.

The algorithm consists of two competing processes. One process selects an Aroclor which, with previously selected Aroclors, is regressed onto the "unknown" to provide the best reduction in variance. The competing process attempts to eliminate an Aroclor from the solution set on the basis of quantitative significance. The program continues in an iterative fashion until a user defined boundary condition is reached.

RESULTS

In order to verify the accuracy of the program, several laboratory prepared Aroclor mixtures and matrix spikes were analyzed. Qualitative and quantitative agreement was obtained in approximately 80 percent of the laboratory test cases, even when as many a 6 Aroclors were present.

CONCLUSIONS

Software is available for at least two commercial GC/MS data systems (Finnigan, HP) that provides automated data reduction of PCB GC/MS data to summed level of chlorination. Despite the fact that specific isomer information is lacking in this approach, the Aroclor content information is retained and may be extracted by multivariate regression techniques.

The program AROCLOR is interactive since correct identifications were not obtained by "blind" application in all test cases. Strong similarity between Aroclors 1016 and 1242 as well as the lack of level of chlorination distribution for Aroclor 1221 at times resulted in misidentification when these Aroclors were present in significant quantities. The program provides for analyst direction when necessary to resolve such cases.

The authors wish to acknowledge the work of Ms. Ann Alford-Stevens, USEPA, who provided much of the GC/MS data that led to the development of this work.

LITERATURE CITED

(1) Dunn,W.J.;Stalling,D.L.;Schwartz,T.R.;Hogan,J.W.;Petty,J.D.; Johansson,E.;Wold,S. Anal.Chem.1984,56,1308-1313.

(2) Liu,R.H.;Ramesh,S.;Liu,J.Y.;Kim,S.Anal.Chem.1984,56,1808-1812.

(3) Alford-Stevens,A.L.;Bellar,T.A.;Eichelberger,J.W.;Budde,W.L.Anal.Chem. 1986,58,2014-2022.

(4) Alford-Stevens,A.L.;Bellar,T.A.;Eichelberger,J.W.;Budde,W.L.Anal.Chem. 1986,58,2022-2029.

(5) Gebhart,J.E.;Hayes,T.L.;Alford-Stevens,A.L.;Budde,W.L.Anal.Chem.1985, 57,2548-2463.

(6) Slivon,L.E.;Gebhart,J.E.;Hayes,T.L.;Alford-Stevens,A.L.;Budde,W.L. Anal.Chem.1985,57,2464-2469.

(7) Tunicliff,D.D.;Wadsworth,P.A.Anal.Chem.1965,37,1082-1085.

(8) Burkhard,L.P.;Weininger,D.Anal.Chem.1987,59,1187-1190.

Presented at the 35th ASMS Conference on Mass Spectrometry and Allied Topics
May 24-29, 1987, Denver, CO

PROCESSING OF HIGH RESOLUTION MASS SPECTRAL DATA BY USE OF KENDRICK MASSES IN A RECTANGULAR ARRAY

by

Ronald D. Grigsby

IIT Research Institute
National Institute for Petroleum and Energy Research
P.O. Box 2128, Bartlesville, OK 74005

Because high resolution mass spectrometry (HRMS) can provide elemental compositions on molecules in complex mixtures, it is one of the most useful methods available for analyzing petroleum and other sources of hydrocarbon fuels.

To reduce the time required to process and interpret high resolution data, methods for automatic formula assignment are being investigated in our laboratory. This work has led to the development of a computer program that can partially assign formulas to the ions and produce output that is easily edited to complete the assignments. The program is based on the concepts of Kendrick mass and nominal mass z series, both of which have been used for many years by petroleum mass spectrometrists.

According to the Kendrick scale, masses of the ions are based on CH(2) instead of carbon-12. This concept allows ions to be classified into homologous series whose members have masses differing by exactly 14 amu, i.e, each member has the same mass defect. By nominal mass z series, ions are classified according to integer mass, irrespective of elemental composition. Fourteen homologous series are specified by the numbers +2 through -11, which are the remainders obtained from dividing the integer mass of an ion by 14.

Combination of the Kendrick mass scale with nominal mass z series results in a method for displaying high resolution spectra in a rectangular array having 14 columns and a variable number of rows, depending on the number of peaks in the spectrum. A computer program generates separate arrays for different elemental combinations, such as CH or CHO, and the intensity of an ion is placed at the proper location in the array only if the ion's experimental mass is within a specified ppm error of the theoretical mass calculated for a specific elemental composition.

An array with partial CH assignments from the mass spectrum of a fraction containing one-ring aromatic neutrals is shown below. This fraction was separated from the 200-425 deg C distillate of the Cerro Negro (Venezuela) heavy petroleum by methods described in the literature. Only columns with z numbers +2 through -5 are given. The number of carbons, N, is constant for a row, and the number of hydrogens is specified for the right-hand column (z = +2) by 2N+2. The theoretical mass for any ion is easily obtained by subtracting one from the mass number and adding the value of the Kendrick mass defect plus one given at the top of the column. For example, the theoretical mass of C(8)H(12) is 108.0000 - 1.0000 + 0.9732 = 107.9732.

All ions whose experimental masses are not within the specified ppm error of the theoretical masses are placed in nominal mass z series at the end of the output. This display of unassigned peaks allows the array output to be easily edited to complete any missing assignments and to remove any that are misplaced. Once this editing is complete, changes can be made in the data

RSPCNM. 8/12/86. CN 200-425 DEG C 1-RING COMPDS. RUN 1. SCAN 1
MAX. PPM ERR. = 6.0 TIC = 0.3152E+07 ELEM. COMP.: C(N)H(2N+Z)

NOMINAL MASS Z NUMBERS									
-5	-4	-3	-2	-1	0	1	2		
KENDRICK MASS DEFECT + 1.0000									
0.9665	0.9732	0.9799	0.9866	0.9933	1.0000	1.0067	1.0134		
SPECIFIC Z NUMBERS									
-5	-4	-3	-2	-1	0	1	2	N	2N+2
MASS/INTENSITY/PPM ERROR									
.....	.....	.....	.....	.....	.....	.....	.....	...	....
107.0	108.0	109.0	110.0	111.0	112.0	113.0	114.0	8	18
	46.9	182.5		211.9		29.2			
	1.0	-0.2		5.8		-4.7			
121.0	122.0	123.0	124.0	125.0	126.0	127.0	128.0	9	20
						29.0			
						0.1			
135.0	136.0	137.0	138.0	139.0	140.0	141.0	142.0	10	22
	45.2	115.0		54.1					
	-1.5	-3.2		-3.4					
.....	.....	.....	.....	.....	.....	.....	.....	...	....

file and the program run again to force the incorrect assignments into their proper locations, i.e., into the array itself or into the unassigned list at the end of the output. For example, the ion of mass 124.994 and intensity 183.1 given below in the NMZ = -1 column, should be placed at mass number 125.0 in the above array. The ppm error calculated by the program is greater than the maximum specifed (6.0 ppm).

NOMINAL MASS Z NUMBERS							
-5	-4	-3	-2	-1	0	1	2
MASS/INTENSITY							
.....	.....	.....	.....	.....	.....	.....	.....
134.956	135.962	122.981	137.897	96.994	111.910	126.916	127.923
213.4	1384.2	226.1	24.2	255.6	58.4	37.4	37.1
134.962	135.975	150.889	151.896	124.904	125.910	140.916	141.924
62.4	8.5	11.6	17.1	103.0	79.8	39.8	21.1
134.964	177.883	164.890	179.895	124.994	125.911	140.917	155.922
43.8	14.5	21.8	22.4	183.1	33.5	21.5	13.9
.....	.....	.....	.....	.....	.....	.....	.....

By testing the data with arrays for CH, CHO, CHN, and CHS, the Cerro Negro fraction was found to consist predominantly of C(n)H(2n+z) hydrocarbons with z numbers of -8 and -10. Only traces of oxygen and nitrogen compounds were found, but sulfur compounds having the formulas C(n)H(2n+z)S with z numbers less than or equal to -4 were found in significant quantities. These types of compounds are in agreement with those anticipated from the HPLC method used in the fractionation of the distillate.

ACKNOWLDGMENT

Appreciation is expressed to the U.S. Department of Energy for support of this work under Cooperative Agreement DE-FC22-83FE60149.

Presented at the 35th ASMS Conference on Mass Spectrometry and Allied Topics
May 24-29, 1987, Denver, CO

An Efficient Algorithm for Sequencing Peptides Using Fast Atom Bombardment Mass Spectral Data

Marshall M. Siegel*, Norman Bauman

American Cyanamid Company, Medical Research Division
Lederle Laboratories, Pearl River, N.Y. 10965

INTRODUCTION

An efficient algorithm is described for sequencing peptides from sequence ions appearing in FAB and FAB MS/MS mass spectra. The peptide structure is built up stepwise from the mass differences in neighboring sequence ions appearing in the spectrum. In this way, the peptide is built up from low mass subsequences and therefore peptides up to 3,000 daltons can be sequenced. The minimum input data necessary for this algorithm are: the molecular weight of the peptide, its N- and C-"terminating groups", probable amino acid residues present in the peptide, FAB fragmentation rules of peptides and the sequence ions appearing in the mass spectrum. "Terminating groups" are those structural units which when removed from the ends of a linear peptide leave only a series of amino acid residues.

PEPTIDE SEQUENCING ALGORITHM

The peptide sequencing algorithm involves two procedures. The first consists of generating tables of all possible fragment ion residues from the amino acid residues possibly present in the peptide. The second involves the sequencing of the peptide by matching the fragment ion entries in the tables with the mass differences of neighboring sequence ions appearing in the "reconstructed" mass spectrum.

A) GENERATION OF FRAGMENT ION TABLES FROM AMINO ACID RESIDUES

Two tables of fragment ions are compiled. One table consists of N-terminal fragment ions and the other C-terminal fragment ions which are mathematically re-expressed as N-terminal fragment ions. The tables are generated from all combinations of amino acid residues expected to be present in a peptide. The tables contain the masses of all the amino acid subsequences, their masses after undergoing fragmentation and the probability for each fragmentation ion occuring. (The fragmentation probabilities are based upon the intensity and mass of the sequence ions observed in model peptides.) Tables of fragment ions up to 450 daltons suffice for obtaining the correct sequences of peptides having molecular weights greater than 3,000 daltons.

B) STEPWISE SEQUENCING ALGORITHM

Main features of the sequencing algorithm are: (1) each member of the observed sequence ions is considered to arise from all possible combinations of N- and C-terminal fragment ions, (2) all N- and C-terminal ions as well as the molecular weight of the peptide are mathematically re-expressed as N-terminal residue ions (These re-expressed ions constitute the "reconstructed" FAB mass spectrum.), and, (3) the peptide is sequenced by starting from the N-terminal and working towards the C-terminal, ignoring the N- and C-terminating groups.

The stepwise analysis is initialized by taking the lowest re-expressed sequence ion mass and finding its corresponding mass enteries in the respective N- or C-Terminal Residue Fragment Ion Table. In the stepwise iteration proceedure, mass differences between the subsequent re-expressed sequence ions and all the amino acid residues making up the previous subsequences are computed. The mass differences are also looked up in the appropriate N- or C-Terminal Residue Fragment Ion Table. In this way, the peptide is built-up systematically from sequence ion information available from the lowest residue mass to the residue mass of the molecular weight.

Since there are a number of possible degenerate subsequence solutions for each ion, all combinations of the computed subsequences for each ion is analyzed using a Backtrack Subroutine. In the peptides studied to date, the most probable peptide sequence has been found to be the sequence having the fewest amino acid residues present and the highest fragmentation probability per amino acid residue.

APPLICATIONS OF THE PEPTIDE SEQUENCING ALGORITHM

Applications of the peptide sequencing algorithm are illustrated for two peptides each having a molecular weight greater than 1,000 daltons. Decapeptyl (M.W. 1310), (pyro)Glu-H-W-S-Y-W-L-R-P-G-NH2, is sequenced from its FAB mass spectrum and an "unknown" peptide (M.W. 1485), H-L-K-N-L-D-L-K-H-L-A-G-K [1], is sequenced from its FAB MS/MS daughter ion spectrum generated from the proton- adduct molecular ion. Some of the sequences computed by the peptide sequencing algorithm for each of the peptides are listed in the Tables below. Note that the sequence with the fewest numbers of amino acid residues and highest fragmentation probability per amino acid is the correct peptide sequence.

[1] D. H. Hunt, Y. R. Yates, J. Shabanowitz, S. Winston, C. R. Hauer Proc. Natl. Acad. Sci. U.S.A. 83, 6233 (1986).

Computed Peptide Sequences for Decapeptyl	#	FPA
H-W -S-Y-W -L-R -GP	9	22.22
H-W -S-Y-W -L-GV-GP	10	20.00
H-W -S-Y-SV-L-R -GP	10	20.00
H-W -S-Y-AD-L-R -GP	10	20.00
H-W -S-Y-GE-L-R -GP	10	20.00
H-SV-S-Y-W -L-R -GP	10	20.00
H-AD-S-Y-W -L-R -GP	10	20.00
H-GE-S-Y-W -L-R -GP	10	20.00
H-W -S-Y-GN-K-R -GP	10	19.80
H-W -S-Y-VL-S-R -GP	10	19.70
H-W -S-Y-PD-S-R -GP	10	19.70

Computed Sequences for "Unknown" Peptide	#	FPA
H-L-K -N -L-D-L-K -H-L-A-G-K	13	13.85
Y-S-K -N -L-D-L-K -H-L-A-G-K	13	13.62
H-L-GA-N -L-D-L-K -H-L-A-G-K	14	12.86
H-L-K -2G-L-D-L-K -H-L-A-G-K	14	12.86
H-L-K -N -L-D-L-GA-H-L-A-G-K	14	12.86
H-L-K -N -L-D-L-K -H-L-A-G-GA	14	12.86
Y-S-GA-N -L-D-L-K -H-L-A-G-K	14	12.64
Y-S-K -2G-L-D-L-K -H-L-A-G-K	14	12.64
Y-S-K -N -L-D-L-GA-H-L-A-G-K	14	12.64
Y-S-K -N -L-D-L-K -H-L-A-G-GA	14	12.64

# = Number of amino acid residues.
FPA = Fragmentation probability per amino acid residue.

Presented at the 35th ASMS Conference on Mass Spectrometry and Allied Topics
May 24-29, 1987, Denver, CO

PHASE CONSIDERATIONS IN THE EXCITATION OF IONS IN FOURIER TRANSFORM ION CYCLOTRON MASS SPECTROMETRY

G. Baykut, C.H. Watson, J.R. Eyler, Department of Chemistry, University of Florida, Gainesville, Florida 32611

The purpose of this work was to characterize and understand the effect of frequency chirp excitation on ions constrained to move in cyclotron orbits by an external magnetic field. In order to do this the equations of motion for an ion of mass m, charge q, and velocity v in a magnetic field of induction B and an oscillating electric field of frequency w_1 were derived considering the electric field phase.

$$\vec{\mathcal{F}} = m\frac{d\vec{v}}{dt} = q(\vec{E} + \vec{v} \times \vec{B})$$

$$\vec{E} : (E_0 \sin(\omega_1 t + \varphi), 0, 0) \; ; \; \vec{B} : (0, 0, B)$$

$$\frac{dv_x}{dt} = \frac{qE_0}{m}\sin(\omega_1 t + \varphi) + \omega_c v_y$$

$$\frac{dv_y}{dt} = -\omega_c v_x \quad ; \quad \omega_c = \frac{qB}{m}$$

The solutions of the differential equation with the initial position coordinates x_0 and y_0 and initial velocity v_0 (thermal) were obtained for both off resonance ($w_1 \neq w_c$) and resonance cases.

$\omega_1 = \omega_c$: Resonance

$$x(t) = x_0 + \frac{v_0}{\omega_c}\left\{\sin(\omega_c t - \delta) + \sin\delta\right\} + \frac{qE_0}{2m\omega_c^2}\cos\varphi \sin\omega_c t - \frac{qE_0 t}{2m\omega_c}\cos(\omega_c t + \varphi)$$

$$y(t) = y_0 + \frac{v_0}{\omega_c}\left\{\cos(\omega_c t - \delta) - \cos\delta\right\} - \frac{qE_0}{m\omega_c^2}\cos\varphi + \frac{qE_0}{2m\omega_c^2}\left\{\cos\varphi\cos\omega_c t + \cos(\omega_c t + \varphi)\right\} + \frac{qE_0 t}{2m\omega_c}\sin(\omega_c t + \varphi)$$

$\omega_1 \neq \omega_c$: Off Resonance

$$x(t) = x_0 + \frac{v_0}{\omega_c}\left\{\sin(\omega_c t - \delta) + \sin\delta\right\} - \frac{qE_0}{m(\omega_c^2 - \omega_1^2)}\left\{\cos\omega_c t \sin\varphi + \frac{\omega_1}{\omega_c}\sin\omega_c t\cos\varphi - \sin(\omega_1 t + \varphi)\right\}$$

$$y(t) = y_0 + \frac{v_0}{\omega_c}\left\{\cos(\omega_c t - \delta) - \cos\delta\right\} - \frac{qE_0}{m(\omega_c^2 - \omega_1^2)}\left\{\sin\omega_c t \sin\varphi - \frac{\omega_1}{\omega_c}\cos\omega_c t\cos\varphi + \frac{\omega_c}{\omega_1}\cos(\omega_1 t + \varphi)\right\} - \frac{qE_0\cos\varphi}{m\omega_1\omega_c}$$

Computer simulations of the ion motion before, during and after a swept frequency excitation chirp were performed using the above solutions for x(t), y(t), $v_x(t)$ and $v_y(t)$.

The ion position was calculated after a delay time or a suitable irradiation time t at frequency w_1. The calculated position and velocity were then used as new initial conditions for the next time period. The time and frequency were incremented and this procedure was repeated to cover the swept frequency range.

As expected, an initial packet of randomly moving ions was excited to form a coherently moving ion "clump". From the final position of the ions one can calculate a coherent radius for the ion motion. The length of this vector is directly related to the ion signal. By varying parameters associated with the sweep one can study the factors that affect the signal strength in FTICR mass spectrometry.

In the excitation of an ion at its resonant frequency two special cases can be considered:

a) when the electric field vector is pointing in the direction of the ion's velocity vector (on phase)

b) when the electric field vector is pointing opposite to the ion's velocity vector (off phase)

As indicated by the following equations, the excitation has a certain delay time in case (b) since the first term in the square root goes to zero and then increases again.

$\omega_i = \omega_c$

Special cases :

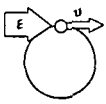

$\varphi = 90^\circ \; ; \; \delta = 0$

$$r \approx \left\{ \left(\frac{v_0}{\omega_c} + \frac{E_0 t}{2B} \right)^2 - \frac{q^2 E_0^2 t}{2 m^2 \omega_c^3} \sin^2 \omega_c t \right\}^{1/2}$$

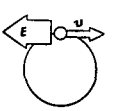

$\varphi = -90^\circ \; ; \; \delta = 0$

$$r \approx \left\{ \left(\frac{v_0}{\omega_c} - \frac{E_0 t}{2B} \right)^2 + \frac{q^2 E_0^2 t}{2 m^2 \omega_c^3} \sin^2 \omega_c t \right\}^{1/2}$$

In Figure 1 these equations are plotted for an ion m/z 40, at a magnetic field of 0.5 Tesla and excitation voltage of 5.0 volts.

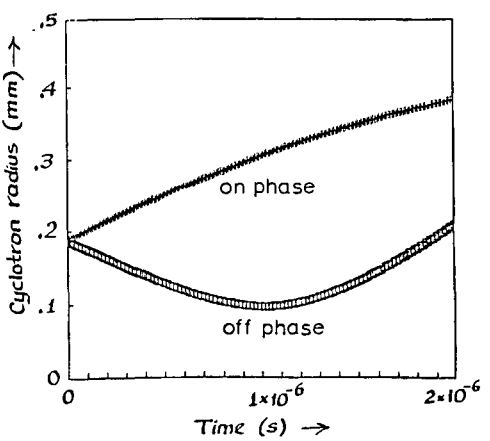

Note that the off-phase resonance results in an initial deceleration, but at longer times the radius increases again. Although at longer irradiation time this initial "phase shift" in the excitation becomes unimportant, at short frequency steps of the chirp excitation it may lead to some loss of the ion signal.

Presented at the 35th ASMS Conference on Mass Spectrometry and Allied Topics
May 24-29, 1987, Denver, CO

COMPARISON STUDY OF SEARCH ALGORITHMS AND DATA BASE LIBRARIES FOR COMPOUND IDENTIFICATION FROM MASS SPECTRAL DATA*

Frank B. Burns and Philip J. Rodacy
Sandia National Laboratories
Albuquerque, New Mexico 87185

Objective.

The objective of this study is to determine if there are significant differences in compound identification when using different mass spectral libraries and search algorithms.

Introduction.

The most ubiquitous method employed for compound identification from mass spectral fragmentation patterns is the computer-based comparison of the unknown spectrum with each member of a library of reference spectra. The effectiveness of this method is dependent upon having access to a library that is large enough to contain reference spectra relevant to the unknown as well as a search algorithm that is effective at retrieving those spectra.

We recently gained access to two commercial data bases, Chemical Information Services (CIS)[1] and Cornell University Computer Services.[2] It was of interest to determine if these larger libraries and the use of different search algorithms would improve our identification capabilities significantly. The CIS data base contains two separate libraries, each of which can be searched by either Biemann (KB) or Probability Based Matching (PBM) algorithms. The Cornell data base consists of one library and PBM search.

Experimental.

Mass spectral (m/z vs. abundance) data were obtained for forty-eight organic compounds using a Finnigan MAT 112S/SS200P GC-Mass Spectrometer and data system. Sample introduction was by direct insertion probe or by gas chromatography, depending upon whether the sample was a pure standard or mixture. 70 eV (nominal) electron ionization was used for all analyses. Tabulations of the resulting spectra were abridged to intensities ≥ 1%. The compounds examined contained a wide variety of functional groups such as aldehydes, ketones, carboxylic acids, amines, ethers, and aromatics. Also included were multifunctional organics such as indicator dyes, plasticizers, UV stabilizers and antioxidants. Library searches were performed on the collected mass/intensity data using seven different combinations of data base libraries and search algorithms (Table 1).

Results and Discussion.

The results of the library searches (based on 48 samples) are shown (Fig. 1). All of the sample compounds had CAS registry numbers, but spectra of three were not contained in any of the libraries. The total number of unmatched compounds per search ranged from eight (Finnigan Incos) to twenty (CIS MSSS PBM). Only two of the unmatched compounds were common to all libraries/searches. Statistically combining the results of more than one library/search significantly improved the number of correct identifications. (Fig. 2).

A comparison of the data acquired by the Finnigan MAT for many of the unmatched compounds with library data for those same compounds shows that there is often markedly different, or even incorrect, data in different libraries. Additional conclusions that were derived from the study are:

1. No functional group discrimination was detected in the library search results.
2. Spectra contained in small libraries are not always present in large libraries.
3. Because m/z-abundance intensities are instrument dependent, spectral redundancy within a library can be beneficial.
4. Identification failures can be related to differences in library and experimental m/z-abundance data as well as the search algorithm used.

*This work performed at Sandia National Laboratories supported by the U. S. Department of Energy under Contract No. DE-AC04-76DP00789.

Presented at the 35th ASMS Conference on Mass Spectrometry and Allied Topics
May 24-29, 1987, Denver, CO

Table 1. Libraries and Search Algorithms

Library	Spectral Entries (No.)	Search Routine	Comments
Finnigan Incos	38,791	Forward	GC-MS Library
Finnigan MAT	33,898	Biemann	GC-MS Library
CIS MSSS	42,229	Biemann (KB)	Commercial Data Base
CIS MSSS	42,229	PBM	Commercial Data Base
CIS Wiley	72,919	Biemann (KB)	Commercial Data Base
CIS Wiley	72,919	PBM	Commercial Data Base
Cornell Univ	79,560	PBM	Commercial Data Base

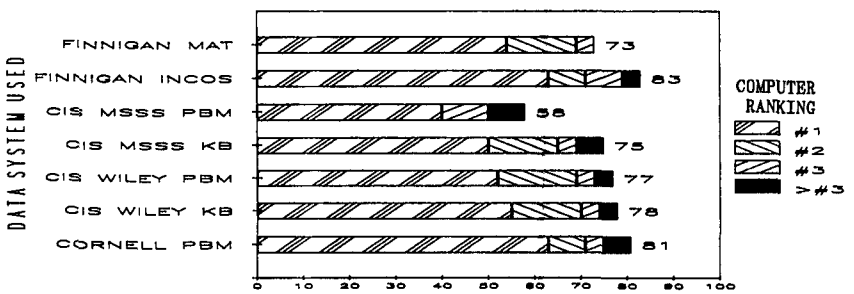

Fig. 1. Compound identification using mass spectral searches. Each search lists several possible matches in rank order; the rank of the correct identification is shown.

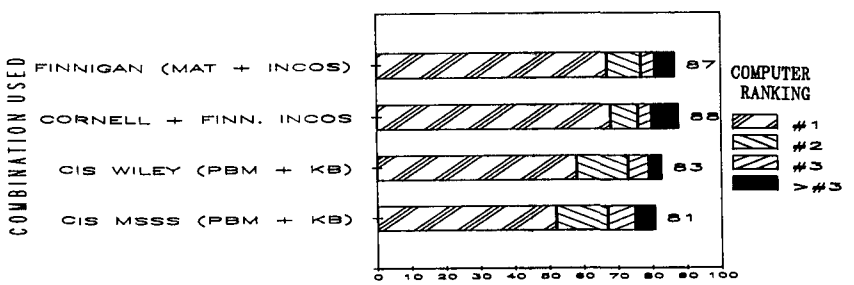

Fig. 2. Compound identification by combining mass spectral searches.

References.
1. Chemical Information Services, 7215 York Road, Baltimore, MD 21212.
2. Cornell University Computer Services, 440 Day Hall, Ithaca, NY 14853.

Presented at the 35th ASMS Conference on Mass Spectrometry and Allied Topics
May 24-29, 1987, Denver, CO

COMPUTER ENHANCEMENT OF MS DATA: MS/MS SPECTRA FROM HADAMARD TRANSFORMS AND COMPOUND IDENTIFICATION USING 130,000 REFERENCE SPECTRA:

D. B. Stauffer, S. Y. Loh, K. D. Henry, A. B. Twiss-Brooks, and Fred W. McLafferty

Chemistry Department, Cornell University, Ithaca, NY, 14853-1301

For tandem mass spectrometry with Fourier-transform or ion trap instruments, any combination of parent ions can be dissociated to produce a collective daughter ion spectrum. This makes it possible to achieve the Hadamard transform advantage of 0.5 $n^{0.5}$ in signal/noise or 4/n in required time for measuring individual daughter ion spectra of n parent ions. Thus measuring MS-II spectra of 100 MS-I peaks would require only 1/25 of the time of individual measurement, encouraging routine use of this extra dimension of information. We have tested this idea with computer-simulated spectra, adding random noise at a specified average level to each of the scans. As expected, performance depends on the proportion of daughter ion peaks common to the parent ion spectra. The Hadamard method appeared to be increasingly effective in improving signal/noise as the amount of noise was increased.

The number of required scans can be reduced further in MS/MS monitoring for many target compounds of infrequent occurrence by utilizing "no-peak" information. If a significant peak in the MS-II spectrum of a target parent ion is of negligible abundance in the collective MS-II specrum of all parent ions, this shows that the corresponding target compound is not present in the sample.

Our enlarged data base of electron-ionization mass spectra contains 130,544 different spectra of 113,587 different compounds (5414 uniquely from the National Bureau of Standards collection), requiring 90 Mbytes of storage. This has been reduced to 27 Mbytes by eliminating data calculable from other data, and compressing the remainder using minimum bit designators assigned using Huffman code. A printed version containing bar graph spectra of all different compounds, sorted by structural type as well as elemental compositon and molecular weight, is in preparation.

The probability of incorrect matches using the enlarged data base has increased much less than its increase in size, showing that the diversity of spectral information has been substantially increased. Using exact mass data with probability based matching (PBM) of unknown mass spectra eliminates 50% of incorrect matches.

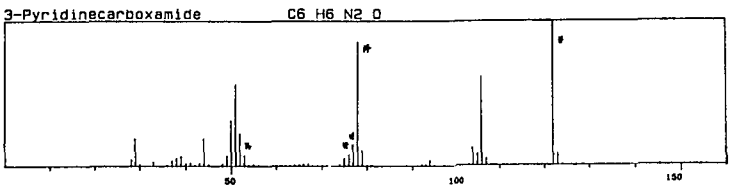

Fig. 1. "Unknown" spectrum randomly selected from the Wiley/NBS database of 130544 mass spectra, with exact mass measurements made at masses 53, 76, 77, 78, 122.

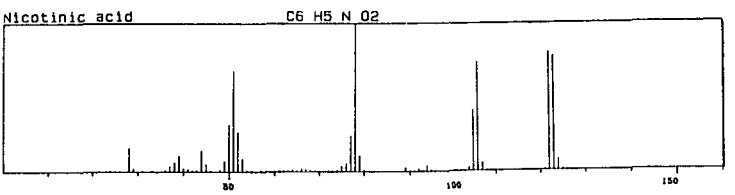

Fig. 2. Spectrum of nicotinic acid, previously retrieved at a reliability of 64% is no longer retrieved by PBM.

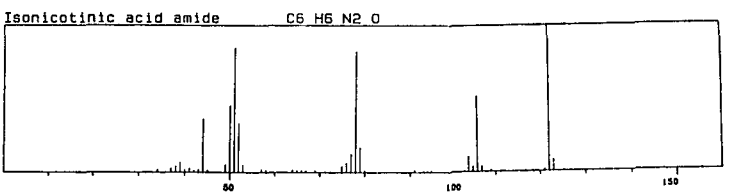

Fig. 3. Isonicotinic acid, a class 4 match for 3-pyridine-carboxamide, is retrieved at 97% reliability.

Presented at the 35th ASMS Conference on Mass Spectrometry and Allied Topics
May 24-29, 1987, Denver, CO

AN INTERACTIVE APL PROGRAM TO CALCULATE ISOTOPIC PATTERNS IN DAUGHTER IONS

J. A. G. Roach, R. H. Albert and W.C. Brumley
Food and Drug Administration, 200 C St, SW, Washington, DC 20204

The isotope patterns observed for daughter ions aid in the interpretation of MS/MS spectra, but differ from those observed in MS spectra. Isotope patterns are dependent upon the natural isotopic abundances of elements and upon an appropriate probability distribution. To predict isotope distributions in daughter ion spectra, the correct distribution must first be explicitly calculated for the particular selected parent ion.

An interactive program was written to compute the isotopic patterns of the daughter ions of parent combinations of chlorine, bromine,oxygen, carbon, nitrogen, sulfur and silicon. The program enumerates all combinations of the seven elements in a selected parent ion and computes the parent ion isotopic distribution. It then calculates isotope patterns for specified daughter ions. The program will run on any computer that supports the APL programming language.

In the case of sulfur dichloride, assuming 2 abundant isotopes of sulfur and 2 abundant isotopes of chlorine, there are 8 parent ion compositions:

PARENT MASS	ATOM TYPE S	Cl	Cl	PRODUCT OF NATURAL ABUNDANCES	PROBABILITY PRODUCT	DAUGHTER OF MASS 104 LESS CHLORINE
102	32	35	35	(0.95)(0.7553)(0.7553)	= 0.5419542	
104	32	35	37	(0.95)(0.7553)(0.2447)	= 0.1755808	67
104	32	37	35	(0.95)(0.2447)(0.7553)	= 0.1755808	69
104	34	35	35	(0.0422)(0.7553)(0.7553)	= 0.0240742	69
106	34	35	37	(0.0422)(0.7553)(0.2447)	= 0.0077995	
106	34	37	35	(0.0422)(0.7553)(0.2447)	= 0.0077995	
106	32	37	37	(0.95)(0.2447)(0.2447)	= 0.0568842	
108	34	37	37	(0.0422)(0.2447)(0.2447)	= 0.0025269	

There are 3 [P+2] parent ions (104, 104, 104) and 3 daughter ions (67, 69, 69) for the process: $SCl_2^{-\bullet}$ --> SCl^- + $Cl^\bullet$

The calculated relative abundances of the daughter ions (m/z 67 and 69) are the normalized sums of their probability products: 0.175581:0.19965 or 88:100.

The daughter ion isotope patterns arising from the [P+2] ion of ethion, O,O,O',O'-tetraethyl S,S'-methylene bisphosphorodithioate, are primarily due to the effect of sulfur. The methane CI MS/MS [P+2] daughter ion data for the $[M+H]^+$ ion show evenly distributed isotopic doublets at m/z 143, 171, 199 and 215 arising from the loss of 2 of the 4 sulfur atoms that are present in the parent ion. The [P+2] ion contains one sulfur atom of mass 34. There is an equal probability that this atom of sulfur will be one of the atoms in a daughter ion containing 2 of the original 4 atoms, so the daughter ion pattern is a 1:1 ratio. The doublets at m/z 97, 125, 153 and 231 are not even distributions because they contain either 1 or 3 of the original 4 atoms of sulfur. The probability of an uneven distribution of this type produces abundance ratios of 3:1 or 1:3. In each case, the [P+2] daughter data provide information about the elemental composition of the daughter ions.

Daughter ion data can be used to identify fragment ions containing polyisotopic elements by noting the differences between [P] and [P+2] spectra. Methane CI MS/MS data for carbophenothion, O,O-diethyl S-(p-chlorophenyl)thiomethyl phosphorodithioate demonstrate that care should be taken so that the data reliably record the abundances of small isotope peaks. The ions with a mass of 125, 143, 171 and 199 daltons are present in both the [P] and [P+2] data. Does this mean that they contain neither sulfur nor chlorine? Hardly. Comparison of the [P+2] carbophenothion data with calculated daughter ion isotope patterns in the table on the next page suggests possible elemental compositions for these daughter ions which include sulfur and chlorine.

The [P] data of carbophenothion contain ions of 125 and 127 daltons. The observed value for m/z 127 in the [P+2] data suggests the presence of an isobaric species at m/z 127 such as CH_4OPS_2. The isotope pattern for this daughter ion would include an ion of 129 daltons with a 127-129 ratio of 100:25. There is an ion at m/z 129 in the [P+2] data with a 127-129 ratio of 100:8.6. Use of the abundance of m/z 129 to adjust the 125-127 ratio does give a ratio for 125-127 that matches the calculated value. However, other modes of analysis are required to identify isobaric contributions.

DAUGHTER MASSES	OBSERVED RATIO	CALCULATED RATIO	SUGGESTED DAUGHTER IONS	
125-127	100:18.3	100:11.7	$C_2H_6O_2PS$	
127-129	100:8.6	100:25.2		CH_4OPS_2
143-145	100:26.6	100:25.2	$CH_4O_2S_2$	
157-159	24.9:100	25.2:100		C_7H_6SCl
171-173	100:25.5	100:25.2	$C_3H_8O_2PS_2$	
199-201	100:23.4	100:25.2		$C_5H_{12}O_2PS_2$

(carbophenothion [P+2] data - values calculated using O, S, Cl abundances)

Phenkapton, O,O-diethyl S-(2,5-dichlorophenyl)thiomethyl phosphorodithioate, contains 3 sulfur atoms, 2 oxygen atoms and 2 chlorine atoms. The EI MS/MS spectra of phenkapton contain many of the ions observed with carbophenothion and ethion as well as several that are unique to phenkapton. Calculation of the isotope patterns for daughter ions containing various combinations of sulfur, oxygen and chlorine can be used to suggest the elemental compositons of the observed daughter ions. When none of the probable combinations fit the observed data, isobaric ions may be present.

The isotope cluster at m/z 295 is consistent with a loss of 35 and 46. Loss of 35 is observed at m/z 341. The loss of 46 could be loss of the elements of C_2H_5OH or CH_2S. The observed isotope data are consistent with values calculated for the loss of CH_2S (100:88.4) rather than the loss of C_2H_5OH (100:71.0).

The isotope pattern at m/z 153-155 (100:19.2) does not match the value calculated (100:6.6) for its likely composition. These ions are also found in the normal MS spectrum of phenkapton. Examination of this portion of the normal spectrum with a ZAB-2F set at a resolution of 10,000 determined that m/z 153 had an exact mass consistent with the suggested composition of $C_4H_{10}O_2PS$ (6 ppm) and that m/z 155 consisted of at least 4 isobaric ions.

[P+2] daughter spectrum for the $[M]^{+\cdot}$ ion of phenkapton

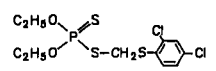

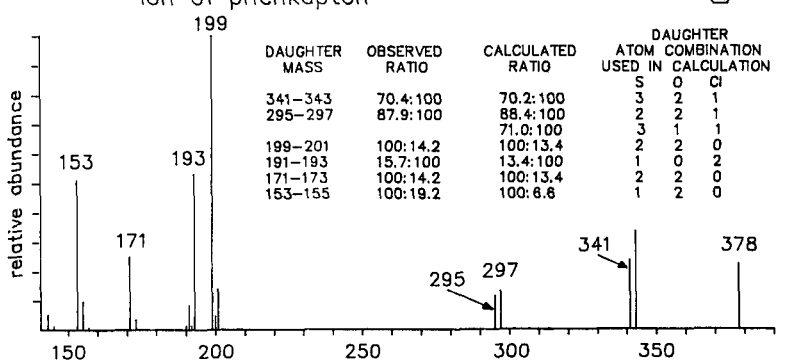

DAUGHTER MASS	OBSERVED RATIO	CALCULATED RATIO	DAUGHTER ATOM COMBINATION USED IN CALCULATION S	O	Cl
341–343	70.4:100	70.2:100	3	2	1
295–297	87.9:100	88.4:100	2	2	1
		71.0:100	3	1	1
199–201	100:14.2	100:13.4	2	2	0
191–193	15.7:100	13.4:100	1	0	2
171–173	100:14.2	100:13.4	2	2	0
153–155	100:19.2	100:6.6	1	2	0

Presented at the 35th ASMS Conference on Mass Spectrometry and Allied Topics
May 24-29, 1987, Denver, CO

ADDITIONAL ADVANTAGES FOR COMPARING THE MS/MS DAUGHTER ION SPECTRA OF M AND M+1 IONS.

M. H. Bozorgzadeh
Midwest Center for Mass Spectrometry
University of Nebraska
Lincoln, NE 68588

The method of using the MIKE or MIKE/CAD spectra of the most naturally abundant isotopes of an ion or a molecule M with that of containing the isotope of one mass unit heavier M+1, to determine the elemental compositions of its fragments has been described previously[1]. The method is based on obtaining an experimental value for the "isotope ratios" of the parent, and each daughter ion. By knowing the "isotope ratio" of the parent, the daughter's "isotope ratio" can be found, and its elemental composition also can be determined.

In this approach, two additional applications of this ratio are discovered and introduced here.

The ratio R of the "isotope ratios" of the parent and each selected daughter ion is equal to:

$$R = X / T$$

where X and T are the "isotope ratio" of the daughter and parent, respectively.

By substituting the quantity X from the general equation[1] into the above equation, the quantity R can be obtained:

$$R = \left(\sum_{j=1}^{i} I_j \sum_{j=i+1}^{n+1} I'_j - \sum_{j=1}^{i} I'_j \sum_{j=i+1}^{n} I_j\right) / I_i \sum_{j=1}^{n+1} I'_j$$

where I_x and I'_x are the abundances of the daughter ions under study in the two spectra of M and M+1; $I_1, I_2, \ldots I_n$, $I'_1, I'_2, \ldots I'_{n+1}$ are the abundances of the other daughters of adjoining masses in a series, respectively.

The ratio R may be used in the two following ways:

1- Determining the distribution of an atom at a specific position in the daughters of labeled.

When a labeled parent ion is selected in an MS/MS experiment, that parent has an "isotope ratio" of 100, the daughters that contain the labeled element also have the "isotope ratio" 100, and those which do not have an "isotope ratio" of 0. If a daughter ion from the labeled parent is formed as a mixture of labeled and unlabeled, the "isotope ratio" will be between 0-100, and the ratio indicates the percentage of the labeled position that is involved in daughter ion formation.

The percentages of the daughters containing the 1-C obtained by comparing the CAD spectra of the molecular ion of propionic acid with that of the 1-^{13}C are shown in Table 1. As Table 1 shows, the ion CH_3O^+ contains %61 1-C, and %39 a carbon atom other than 1-C. This confirms the rearrangement of the hydroxyl group during the fragmentation.

2- Finding the formula of parent and its daughters.

Since the number of proposed formulae for an ion or a molecule of a certain mass is limited because of the rules of chemistry, the value of R may characterize a specific only certain parent and daughter ion. This means that the formulae of the parent and its daughter can be found simultaneously. For this purpose, a formula for the parent is assumed, and then formulae for a daughter ion are possible. The calculated value of R can be found in each case and be compared with the experimental value, and the relative error can be calculated. The correct choice of parent and daughter should give the smallest average value error.

The results of comparing the cal. and exp. values of R of three major daughters of the molecular ion of mass 82 of cyclohexene are shown in Table 2. As Table 2 shows, the average error of R of the parent formula C_6H_{10} is the smallest value compared to the values of the other parent formulae.

1- M. H. Bozorgzadeh, and R. L. Lapp; ASMS 34th. Ann. Con. 1986.

Presented at the 35th ASMS Conference on Mass Spectrometry and Allied Topics
May 24-29, 1987, Denver, CO

Table 1. The distribution of 1-C in the CAD spectrum of the molecular ion of propionic acid .

ion fragment			neutral fragment		% of the ion fragment containing 1-C
mass	intensity	formula	mass	formula	
73	1520	$C_3H_5O_2$	1	H	100.1
56	19	C_3H_4O	18	H_2O	95.9
45	16	C_2H_5O CHO_2	29	CHO C_2H_5	97.1
55	13	C_3H_3O	19	H_3O	100.0
27	12	C_2H_3	47	CH_3O_2	4.5
28	8	C_2H_4 CO	46	CH_2O_2 C_2H_6O	4.9
29	7	C_2H_5 CHO	45	CHO_2 C_2H_5O	48.1
30	5	C_2H_6 CH_2O	44	CO_2 C_2H_4O	7.2
31	2	CH_3O	43	C_2H_3O	61.3

Table 2. Comparing the calculated and experimental "ratio" between the isotope ratio of the parent mass 82 of cyclohexene and its three major daughters .

parent 82		daughter 67, $R_{exp.}$ = 0.835				daughter 54, $R_{exp.}$ = 0.668				daughter 39, $R_{exp.}$ =0.497				aver.
formula	$T_{cal.}$	formula	$X_{cal.}$	$R_{cal.}$	error	formula	$X_{cal.}$	$R_{cal.}$	error	formula	$X_{cal.}$	$R_{cal.}$	error	
$C_2H_2N_4$	3.73	C_2HN_3	3.345	0.897	7.4%	CN_3 $C_2H_2N_2$	2.22 2.99	0.595 0.802	10.9% 20.0%	C_2HN	2.605	0.698	40.5%	19.6%
$C_3H_2N_2O$	4.137	C_3HNO	3.752	0.907	8.6%	CN_3 $C_2H_2N_2$ C_2NO C_3H_2O	2.22 2.99 2.627 3.397	0.537 0.723 0.635 0.821	19.7% 13.4% 4.9% 22.9%	C_2HN	2.605	0.630	26.7%	13.4%
$C_3H_4N_3$	4.5	$C_3H_3N_2$ C_2HN_3	4.115 3.345	0.914 0.743	9.5% 11.0%	CN_3 $C_2H_2N_2$	2.22 2.99	0.493 0.664	26.1% 0.5%	C_3H_3 C_2HN	3.375 2.605	0.750 0.579	50.9% 16.5%	8.8%
C_4H_4NO	4.907	C_4H_3O C_3HNO	4.522 3.752	0.921 0.765	10.4% 8.4%	C_2NO C_3H_2O C_3H_4N	2.627 3.397 3.76	0.535 0.692 0.766	19.9% 3.6% 14.7%	C_3H_3 C_2HN	3.375 2.605	0.668 0.531	38.4% 6.8%	6.3%
$C_4H_6N_2$	5.27	C_4H_5N $C_3H_3N_2$	4.805 4.115	0.927 0.781	11.0% 6.5%	$C_2H_2N_2$ C_3H_4N C_4H_6	2.99 3.76 4.53	0.567 0.713 0.860	15.1% 6.8% 28.7%	C_3H_3 C_2HN	3.375 2.605	0.641 0.494	28.9% 0.5%	4.6%
C_5H_6O	5.677	C_4H_3O	4.522	0.796	3.8%	C_3H_2O C_4H_6	3.397 4.53	0.598 0.798	10.4% 19.4%	C_3H_3	3.375	0.594	19.6%	11.3%
C_5H_8N	6.04	C_5H_7 C_4H_5N	5.655 4.805	0.936 0.809	12.1% 3.1%	C_3H_4N C_4H_6	3.76 4.53	0.622 0.750	6.0% 12.3%	C_3H_3 C_2HN	3.375 2.605	0.559 0.431	12.4% 13.2%	7.4%
C_6H_{10}	6.81	C_5H_7	5.655	0.830	0.5%	C_4H_6	4.53	0.665	0.4%	C_3H_3	3.375	0.496	0.3%	0.4%

Presented at the 35th ASMS Conference on Mass Spectrometry and Allied Topics
May 24-29, 1987, Denver, CO

Applications of Collision Induced Dissociation (CID) Mass Spectra in the Analysis of Antibiotics,

L. Baczynskyj and D.J. Duchamp,
Physical and Analytical Chemistry Research,
The Upjohn Company, Kalamazoo, MI 49001

The objectives of this study were the automation of acquiring and processing scans of metastable ions and the application of such scans to fragmentation studies of pseudo-molecular ions of some antibiotics. We also compared the daughter ion scans and CID scans of various ions using several collision gases.

Experimental.

The FAB mass spectra were obtained on the V.G. ZAB 2F instrument fitted with an Ion Tech gun operated at 9 kV and using Xenon as the bombarding gas. Daughter and CID scans were obtained on the same instrument. The collision cell is located in the second field free region and the gas pressure was adjusted until the main beam ion was reduced by a factor of 5. Daughter ion (MIKES) and CID scans were recorded at 10 sec./dec. using a linear scan function. All programs were written in Fortran and developed on the Harris 800 dual CPU computer and are integrated in the UPACS II (Upjohn Physical and Analytical Chemistry System). The processing programs can average, smooth, print a report and plot any or all the scans stored in temporary file. Any scan in the temporary file can be displayed on the Tektronix 4014 CRT screen. Two scans can be displayed side by side for comparison purposes. In addition library functions for permanently storing and recalling daughter or CID scans have been implemented. These scans are correlated to regular low resolution mass spectra and to the structure libraries using an eight character identification code.

Results and Discussion.

The implemented software was tested on three antibiotics: lincomycin hydrochloride, erythromycin A and paulomycin. The positive ion FAB mass spectrum of lincomycin hydrochloride shows a strong pseudo-molecular ion at m/z 407. The daughter ion scan performed on this ion shows major peaks corresponding to losses of water, methyl thiol and the formation of the ion at m/z 126. This last ion corresponds to the imminium ion of hygric acid, i.e., N-methyl-3-propyl pyrrolidinium ion. Minor peaks were observed for the formation of ions at m/z 317, 271, and 112. CID spectra of the (M+H) ion were recorded using three different collision gases (Helium, Argon and CO_2). All looked very similar to the daughter ion scans with the exception of some intensity changes. Thus the intensity of the peak corresponding to the loss of methylthiol decreased while the peak at m/z 126 increased. Comparing the daughter ion scans and CID scans with normal low resolution FAB mass spectrum shows little additional structural information. Similar experiments performed in the negative ion mode on the (M+Cl) ion showed only one peak in daughter ion and CID scan. It corresponds to the loss of Cl.

Similar experiments were performed for erythromycin. The low resolution positive ion FAB mass spectrum of erythromycin A shows a (M+H) ion at m/z 734 (25% of the base peak at m/z 158). Major fragment ions appear at m/z 158, 116, 83 and 72. Minor ions are present at m/z 576, 558, 231, 174, 127 and 98. The daughter ion and CID scans of the (M+H) ion were very similar. They show two prominent peaks corresponding to the loss of water and the loss of one of the sugars. Note that since both sugars differ only by 1 dalton it is not possible to determine which sugar is lost, since hydrogen rearrangements are common in FAB mass spectra. Minor peaks correspond to the loss of OMe radical and the appearance of the ions at m/z 558, 540, 522 (three losses of water from 576) and ions at m/z 317 and 158. All these ions, with the exception of that at m/z 317 have a corresponding ion in the regular low resolution FAB mass spectrum.

Finally paulomcyin, the major components of a new class of antibiotics, was investigated in the same manner. Since this class of antibiotics do not yield molecular ion information in the positive ion FAB mode, but give very strong $M^{-\cdot}$ in the negative ion FAB mode, the daughter ion and CID scans were recorded on the $M^{-\cdot}$. In both cases only one major ion corresponding to the loss of water from the molecular ion is observed. However when two fragment ions obtained in the positive ion mode were investigated by the same methods several structural deductions could be made. Thus the MIKES and CID spectra of the ion at m/z 515 show the loss of water, ketene and acetic acid. This indicates the presence of hydroxy and acetoxy functions in this part of the molecule. On the other hand the same type of experiments performed on the ion at m/z 259 corresponding to the other part of paulomycin B shows an intense loss of 32 daltons indicating the presence of a methoxy function.

Conclusions.

The automation of acquiring and processing metastable ion scans on a double focusing instrument with reversed geometry has allowed us to investigate the fragmentation of three antibiotics. In all cases the MIKES and CID scans were compared. Several collision gases (He, Argon, NH_3, isobutane, CO_2) were used. No large differences could be observed. In general both MIKES and CID spectra were comparable and reflected processes observed in a regular low resolution FAB mass spectrum.

Presented at the 35th ASMS Conference on Mass Spectrometry and Allied Topics
May 24-29, 1987, Denver, CO

A PROGRAM FOR THE DETERMINATION OF THE AMINO ACID COMPOSITION AND SEQUENCE OF SMALL PEPTIDES FROM THEIR FAST ATOM BOMBARDMENT SPECTRA.

M.J. BERTRAND, P.THIBAULT, M.J.EVANS AND D.ZIDAROV
Regional Center for Mass Spectrometry, Department of Chemistry,
Université de Montréal
P.O. Box 6128, Stn A, Montreal, Quebec, CANADA, H3C 3J7

In recent years, the use of desorption ionization techniques has enhanced the potential of mass spectrometry in the analysis of polar and high molecular weight compounds. The mass spectrometric identification of peptides using desorption ionization techniques has been the object of numerous studies and even if disparities, due to experimental conditions, exist in the literature common features in the mass spectra of peptides can be identified. These are the presence of the molecular ion cluster, of fragment ions related to the sequence and of ions observed at the lower mass end of the spectrum arising from the cleavage of the side chains of the amino acid moieties present in the peptide. Since these types of ion reflect the primary structure of the peptide, an algorithm can be designed in order to analyze the mass spectral data and obtain the identification of the compound.

The algorithm that has been developped in our laboratory to analyze the FAB spectra of peptides comprises three steps that are related to the information content of the three different types of ions observed in the spectrum. These steps include i) the generation of peptide selective empirical formulae, ii) the generation of possible amino acid compositions and iii) the generation of the most probable sequences in accordance with the ions observed in the mass spectrum.

The generation of peptide selective empirical formulae is done using data on the accurate mass and isotopic peak ratios obtained from the molecular ion cluster (1). The empirical formulae generated in the procedure are mathematically analyzed to ensure that they correspond to peptides. The generation of the possible amino acid compositions for the compound under study is done by decomposing the empirical formulae into amino acid compositions taking into account the amino acids that can be included or excluded from the peptide. These are indicated by the presence or absence of diagnostic ions found in the mass spectrum below m/z 160. This information is then used to solve equation [1] that will yield all the possible

$$C_xH_yO_nN_zS_w = N_L\ (C_2H_2NO) + TERM + \sum_{i=1}^{SAA} X_iR_i + \sum_{j=SAA+1}^{AA} Y_jR_j \qquad [1]$$

acid compositions for the peptide. R_i and R_j represent the atomic compositions of the residues of saturated and unsaturated amino acids present in the peptide and X_i and Y_j the number of each residue in the composition. This second step yields a list of amino acid compositions that are consistent with the accurate mass of the compound, the isotopic peak ratios of the molecular ion cluster and ions observed at the lower mass end of the spectrum.

The amino acid sequences can be generated from each amino acid composition. This is done by substracting repetitively the masses of five fragments that correspond to the five fragmentation schemes known for peptides (2) and verifying if the predicted sequence ions are present in the mass spectrum of the compound. Whenever a match is found, the intensity of the ion is used as a subscore, the amino acid is positioned in the sequence and discarded from the composition. The process is repeated until all the amino acids have been positioned and for all amino acid compositions. If during the course of establishing the position of each amino acid none of the five ionspredicted for a partial sequence are observed in the spectrum, the sequence is discarded. During this process the ten sequences with the highest scores are retained. At the end of the analysis the remaining sequences are ranked using a scoring system which is based on the presence of consecutive sequence ions observed in the spectrum for each fragmentation scheme. The highest score indicates the most probable sequence.

In order to demonstrate the working of the approach for peptide identification the FAB spectrum of Angiotensin I is shown on Figure 1 and the inputs and outputs of the algorithm are shown in Table I. The inputs include the measured mass and isotopic

peak ratios with their experimental tolerances, the amino acids which are included or excluded based on the presence of diagnostic ions below m/z 160 and all the ions above m/z 200 in the corrected mass spectrum. As can be seen from the table the algorithm outputs the most probable sequences with their respective scores. The elements that are underlined represent elements of the true sequence. In this particular case the algorithm has determined the true sequence to be the most probable one. Similar analyses have been conducted on typical peptides and the results, presented in table II indicate that the approach is useful for the identification of peptides since the true composition and sequence appear in the output for all the compounds studied.

1) M.J. Bertrand, P. Thibault, M.J. Evans and D. Zidarov, Biomed & Env. Mass Spectrom (in press).
2) P. Roepstorff, J. Fohlman, Biomed. Mass Spectrom, 11, 601 (1984)
3) M.J. Bertrand and P. Thibault, Biomed. Mass Spectrom. 13, 347 (1986).

FIGURE 1

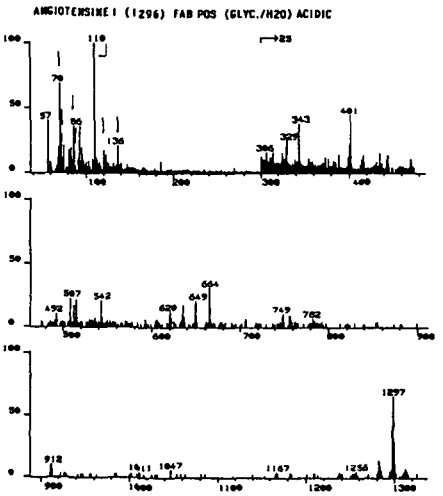

TABLE 1

SEQUENCE ANALYSIS OF ANGIOTENSINE I

INPUT

Exact mass	1295.676	Δ M : 15 ppm
M+1/M:	74.3	Δ R1 10 %
M+2/M:	39.6	Δ R2: 40 %
M+3/M	16.1	Δ R3. 40 %

A.A. includes. P, R, V, H, F, Y, L
A A. excludes: K, M, W

Sequence ions; Mass spectrum m/z > 200 Daltons

OUTPUT

SEQUENCES	TERM	SCORE
DRVYLHPFHL	OH	354
DRVYLHPFGPP	NH_2	273
VHPRDYLFHL	OH	253
VHPRDYLFGPP	NH_2	212
DRVLYHPFHL	OH	209
VYRYEHPFHL	OH	178
VHYPDRLFHL	OH	166
DRVLYHPFGPP	NH_2	165
VYEYRHPFHL	OH	158
VHYPDRLFGPP	NH_2	150

TABLE 2

COMPOSITION AND SEQUENCE ANALYSIS

PEPTIDES	MASS	RANKING	SCORE
1 YGGFL -OH	555	YGGFL-OH YWFL-OH	282 91
2 YGGFM -OH	573	YGGFF-OH YGGFM-OH	221 221
3 WHDF -NH2	596	WHDF-NH2 DFHW-NH2	298 128
4 YLGFQ -NH2	625	YLGFQ-NH2 LYGFQ-NH2	334 291
5 DRVYLHPF -OH	1045	DRVYLHPF-OH DHVYLHPP-OH	265 182
6 RPPGFSPFR -OH	1059	RPPGFSPFR-OH RPPGFSPRF-OH	342 326
7 WRVFVHPF -OH	1086	WRVFVHPF-OH WRVFVHHF-OH	364 223
8 WRVFVHPY -OH	1102	WRVFVHPY-OH WRVFVPHY-OH	307 289
9 DRVYLHPFHL-OH	1295	DRVYLHPFHL-OH DHVYLHPFGPP-OH	354 273
10 RPKPQQFFGLM -NH2	1346	RPKPQQFFGLM-NH2 RPQPKQFFGLM-NH2 RPQPQKFFGLM-NH2	110 110 110

Presented at the 35th ASMS Conference on Mass Spectrometry and Allied Topics
May 24-29, 1987, Denver, CO

THE ANALYSIS OF MICROBIAL NATURAL PRODUCTS BY THERMOSPRAY LC-MS

G S King, L P Gordon and N Runnalls
ICI PLC, Plant Protection Division, Jealott's Hill Research Station,
Bracknell, Berkshire, RG12 6EY, UK

The Problem

We had obtained a complex (11 component) mixture of natural products by fractionation of a microbial fermentation broth. This fraction was relatively non-polar and showed interesting insecticidal activity. We suspected the presence of Piericidins (Structure 1) because of the type of organism and the ultra-violet absorption spectra we saw using an lc-diode array system. Sixteen Piericidins have been reported to date.

Structure 1

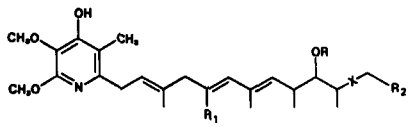

Piericidin	C_2	C_3	D_1	(X = double bond or epoxy)
R	H	H	CH_3	
R_1	CH_3	H	H	
R_2	CH_3	isopropyl	CH_3	
X	epoxy	epoxy	epoxy	

Equipment

A Finnigan 4600 quadrupole mass spectrometer with the Finnigan thermospray source, coupled to a Spectra-Physics HPLC pump and automatic injector system.

Methods

The mobile phase was 80% methanol, 20% water with 0.01M ammonium acetate. An S5ODS2 HPLC column was used with a flow rate of 1ml min^{-1}. The thermospray source was tuned for maximum stability on the methanol-water-ammonium adduct ions.

Ten microlites of the samples were injected by way of the automated injection system. The positive ion spectra were recorded.

Results

We found protonated molecular ions which corresponded to the correct molecular weights for a number of Piericidins. We found that we could correlate the peaks from the selected ion traces almost exactly with the peaks seen on the diode-array detector. This process was made easier by the fact that we used exactly the same column and mobile phase on both systems: this is now standard practice for us, columns are imported from the chemist and used on the lc-ms equipment.

We found that we could distinguish between compounds with the same molecular weight, by using the u.v. spectra. Those piericidins with $R_1 = CH_3$ had an absorption maximum at 225nm and those where R_1 = H had a maximum at 235nm. An example of this are the Piericidins C_2 and D_1:-

Piericidin C_2	R=H	$R_1=CH_3$	$R_2=CH_3$	max=225	MH+ 446
Piericidin D_1	$R=CH_3$	$R_1=H$	$R_2=CH_3$	max=235	MH+ 446

We found by thermospray lc-ms some previously unsuspected isomers, these can be seen as small peaks before C_3 and D_1 in trace 2.

Later we isolated several of the major Piericidins and ran their electron impact spectra using direct insertion. We found very good agreement with the spectra published by Yoshida and co-workers (Agric. Biol. Chem., 41, 855 (1977)).

Presented at the 35th ASMS Conference on Mass Spectrometry and Allied Topics
May 24-29, 1987, Denver, CO.

Conclusions

* Thermospray lc-ms is a valuable technique in the identification of natural products.
* Useful complementary data are obtained from thermospray mass spectra and lc-diode-array equipment.
* Even quite lipophilic compounds give good thermospray results and sensitivity.

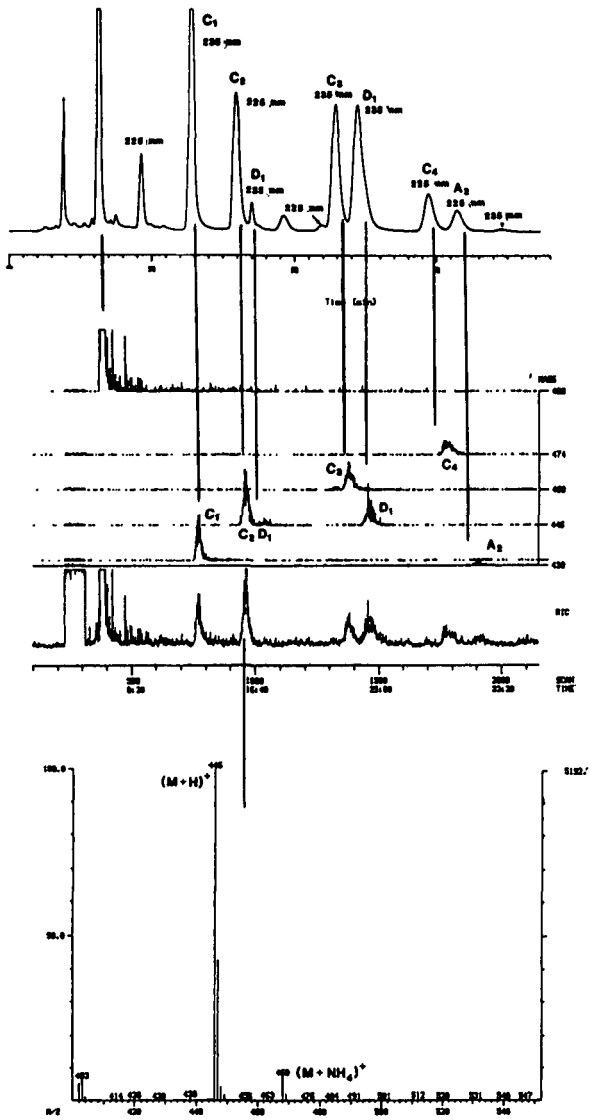

Presented at the 35th ASMS Conference on Mass Spectrometry and Allied Topics
May 24-29, 1987, Denver, CO

THE IDENTIFICATION OF A SULPHATE CONJUGATE OF A PYRETHROID METABOLITE BY NEGATIVE ION SOFT IONISATION TECHNIQUES

G S King, J Heath, N Runnalls and I Hammond
ICI Plc, Plant Protection Division, Jealott's Hill Research Station, Bracknell, Berkshire, RG12 6EY, UK

The Problem

A metabolite of the aromatic portion of Compound 1 had been isolated using radiotracer techniques. Using both proton and fluorine n.m.r. it was established that the structure corresponded to Compound 2 and that X and Y were different. A sulphate conjugate was suspected because of its hydrolysis and chromatographic properties.

Mass spectrometry were asked to establish the identity of the compound.

Compound 1 (Tefluthrin, PP993)

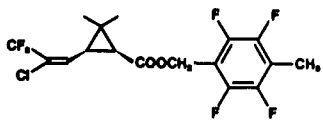

Compound 2

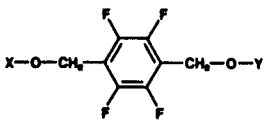

Equipment

FAB analysis: Finnigan 8200 double focussing mass spectrometer, using an Ion-Tech FAB gun.

Thermospray: Finnigan 4600 quadrupole mass spectrometer, using a Finnigan thermospray source and HPLC injector. The pump was a Spectra-Physics 8100 unit.

Method

FAB analysis: The FAB gun was adjusted to produce the maximum ion current of Xenon atoms, when an accelerating voltage of 8KV was applied. The accelerating voltage of the source was 3KV. A background FAB spectrum of the glycerol matrix was recorded for later subtraction. The sample was dissolved in the glycerol matrix and the FAB spectrum recorded in either positive or negative ion mode.

Thermospray: The mobile phase was 100% water with 0.05M ammonium acetate. The flow rate was 1ml min^{-1}. The thermospray source was tuned for maximum stability and sensitivity using the solvent ion clusters. Ten microlitres of the sample was injected into the mobile phase using a loop injector. Both positive and negative spectra were recorded.

Results

We first examined the material by positive ion Fast Atom Bombardment in a glycerol matrix, even after the addition of oxalic acid we could not identify any meaningful ions. In the negative ion FAB spectrum we saw a number of minor ions in addition to the matrix signal, but the results were not very conclusive (Spectrum 1). We examined the sample by negative ion thermospray using "loop" injection: there was a clear signal showing the presence of a molecular anion at m/z 289 (Spectrum 2). This signal agreed with one of the minor ions in the negative FAB spectrum (Spectrum 1).

Presented at the 35th ASMS Conference on Mass Spectrometry and Allied Topics
May 24-29, 1987, Denver, CO

Spectrum 1 Fast atom bombardment mass spectrum of the conjugate (negative ions)

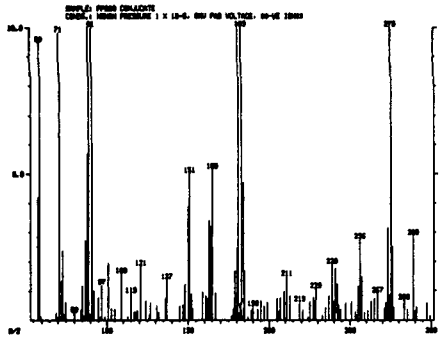

We decided that the structure was Compound 3, from a prior knowledge of a partial structure and consideration of the possible groups which would give rise to a molecular anion at m/z 289.

We were able to confirm this later by comparison with a synthesised sample of the conjugate which we looked at using negative FAB (Spectrum 3).

Spectrum 2 Thermospray mass spectrum of the conjugate

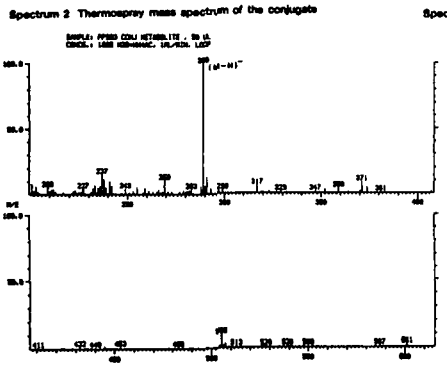

Spectrum 3 Fast atom bombardment spectrum of a synthesised standard (negative ions)

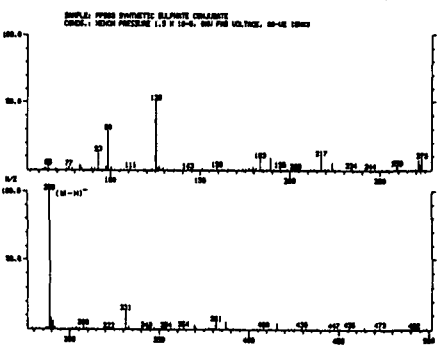

Compound 3

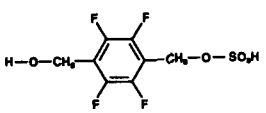

Conclusions

* We were able to determine the identity of the sulphate conjugate; this could not have been done in our laboratories using any other techniques.
* Negative ionisation is very useful for investigating sulphate conjugates.
* We found it easier to get molecular ion information with a limited amount of sample, by using thermospray rather than FAB.

Presented at the 35th ASMS Conference on Mass Spectrometry and Allied Topics
May 24-29, 1987, Denver, CO

A DIRECT LIQUID INLET FOR TIME-OF-FLIGHT MASS SPECTROMETRY USING RESONANCE ENHANCED MUTIPHOTON IONIZATION/FRAGMENTATION

K.R. SEGAR, G.R.KINSEL & M.V. JOHNSTON DEPT. OF CHEMISTRY AND BIOCHEMISTRY
UNIVERSITY OF COLORADO, BOULDER, CO. 80309-0215

Much interest and effort has gone into the development of LC/MS interfaces. One of the major advantages of uniting these two techniques is being able to obtain molecular, and with some ionization methods, structural information about relatively nonvolatile and/or thermally labile compounds. The goal of our research in this area is to develop a direct liquid inlet for use in a time-of-flight mass spectrometer with resonance enhanced multiphoton ionization / fragmentation (REMPI/F). The advantages of this method include the extended mass range of the TOF obtainable after each laser pulse and the ability to obtain both molecular weight (soft ionization) and structural (hard ionization) information by simply varying the laser power and/or wavelength.

The original design of the inlet was patterned after the one reported by Frei and coworkers.[1] Since then, several modifications have been made in arriving at the current design shown in Figure 1. The liquid is pumped through a 100 um capillary transfer line, then through a restricting capillary and nebulized into a stream of heated helium gas. The addition of this gas inlet was prompted by other work done in our lab on gas dynamic focusing. The entire mixture is expanded directly into the ionization region of the mass spectrometer through a 300-700 um orifice. The metal restrictor guide helps to center the restrictor and facillitates heat transfer. A brass plug with a 1/4 " swage thread soldered into the center of a 1 5/16" stainless steel conflat and three 1/8" diameter brass plugs placed equidistant around the circumference of the conflat helps us to attain better and more uniform heating of the inlet. During operation, the end of the inlet is heated by a 1" heating collar while the upper portion is maintained around room temperature by a flow of air (see Figure 2). Ion source pressure is maintained at around 4 E-5 torr by differential pumping.

Preliminary experiments designed to determine the optimum working conditions have shown that one of the most critical variables is the temperature of the inlet. Ideally, one would like to work at a temperature which provides sufficient heat to vaporize the liquid at the end of the restrictor, thereby achieving a constant source pressure. The optimum temperature ranges for methanol, dichloromethane, and 50/50 methanol/water are 160-200°C, 100-175°C, and 170-225°C respectively. At temperatures below this range iceballs form, above it, vaporization occurs up inside the restrictor instead of only at the end. Another experimental variable is the position of the restrictor with respect to the nozzle orifice. The data from experiments pertaining to this variable have shown the optimum position to be 1 mm from the orifice inside the nozzle. This position allows for efficient nebulization with minimum loss of analyte due to coating onto the walls of the nozzle. In addition, instead of expanding in all directions as would be expected, a "focusing" effect of the vaporized effluent was observed. We believe this characteristic will enhance sensitivity. Other experimental variables are currently under investigation.

Figure 3 shows two spectra of tryptophan, one taken before the optimization experiments (Fig. 3a), the other after (3b). The peaks at m/z 204 and 130, which appear in both spectra, are due to the parent ion and its primary daughter ion caused by photofragmentation. However, in the spectrum in Fig. 3a, peaks due to the thermal decomposition of tryptophan at m/z 160 (tryptamine) and 117 (indole) are also observed. No such peaks are present in Fig. 3b, a spectrum which was taken at a significantly lower nozzle temperature than that in Fig. 3a.

From the preliminary experiments we have determined the optimum restictor position and learned that there is an optimum working temperature which is solvent dependent. The tryptophan spectrum suggests that this inlet can be used to obtain molecular weight and structural information about thermally labile compounds without complications from thermal degradation. The fact that we are using a pulsed ionization source means that the inlet can be operated in the

continuous flow mode making a pulsed valve unecessary. Also, with a laser, we can ionize the molecule at a wavelength which the solvent does not absorb thus reducing solvent cluster peaks. Other advantages of this inlet system include its simple and inexpensive design and its ability to operate at flow rates (30-50 ul/min) compatible with microbore LC.

1. J.A. APffel, U.A.Th. Brinkman, R.W. Frei, and E.A.I.M. Evers, Anal. Chem. (1983) *55*, 2280

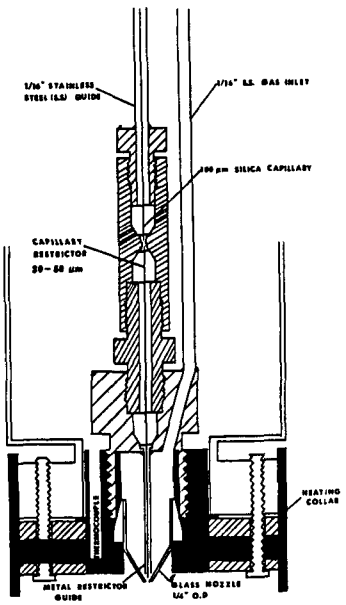

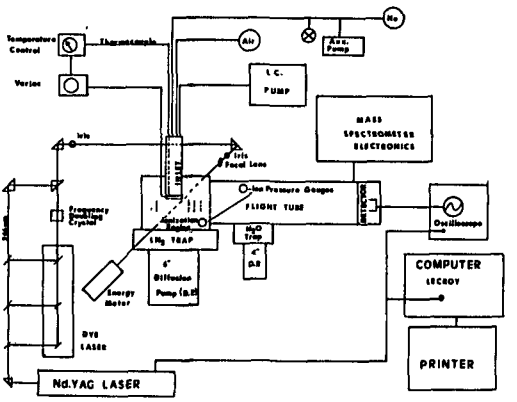

Figure 1: Left is a drawing of the inlet. The blackened area in the bottom conflat represents the brass plugs.
Figure 2: Above is a schematic of the total instrument setup.

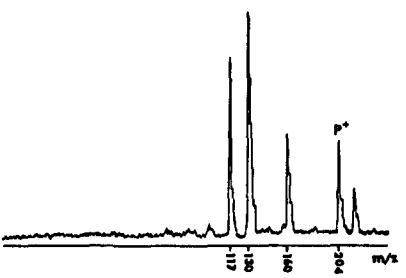

Figure 3a: Tryptophan in methanol
Flow rate: 30ul/min
Nozzle temp: 275°C
Laser power: 25.4 uJ Wavelength:266nm

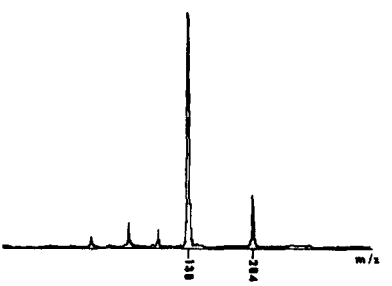

Figure 3b: Tryptophan in methanol
Flow rate: 40 ul/min
Nozzle temp.: 165°C
Laser power: 5.7 uJ Wavelength: 266nm

Presented at the 35th ASMS Conference on Mass Spectrometry and Allied Topics
May 24-29, 1987, Denver, CO

CHARACTERISTICS OF LIQUID CHROMATOGRAPH/ATMOSPHERIC PRESSURE IONIZATION MASS SPECTROMETER (LC/API-MS)

Minoru Sakairi and Hideki Kambara
Advanced Research Laboratory, HITACHI Ltd., Kokubunji, Tokyo, Japan

Recently, for mixture analysis of nonvolatile compounds, an LC/MS has shown promise as a new analysis method in various fields. Many groups have reported various LC/MS systems including a thermospray method, a moving belt method and more (1). However, these methods do not satisfy all of the requirements of an ideal LC/MS system such as no restriction to LC operations, no deterioration of LC separations, feasibility of ionization of nonvolatile compounds, high sensitivity and wide dynamic range for quantitative analysis.

The authors have developed an LC/API-MS using a double focusing mass spectrometer based on the successful ionization of many nonvolatile compounds (2-4). Therefore, the authors investigated the extent to which this system satisfies the requirements of the ideal LC/MS system.

The principle of sample detection in the LC/API-MS system is as follows. Small droplets are produced from LC effluents with a nebulizer which is composed of a heated stainless pipe. These droplets are introduced into a vaporizer which is composed of a heated stainless block for further heating. Produced sample and solvent molecules are ionized by a corona discharge followed by ion-molecule reactions under atmospheric pressure. The resultant ions are introduced into a vacuum through two apertures and mass-analyzed with a double focusing mass spectrometer.

As a result of investigating the performance of this system, it has become apparent that this system has characteristics, as follows. First, this system has no severe restriction to LC operations such as kinds of mobile phase, flow rates and gradient elutions. As for kinds of mobile phase, organic solvents, water, their mixtures and buffer solutions containing volatile salts are available in this system. The flow rates ranging from 0.5 to 1.4 ml/min for water and from 0.5 to 2.0 ml/min for methanol can be accomodated in this system. In addition, both gradient and isocratic elutions are available. Second, this system has little deterioration of LC separations because broadening and tailing of mass chromatograms are almost negligible. Third, this system can successfully be applied to many nonvolatile compounds including amino acids, PTH-amino acids, peptides, antibiotics, nucleosides, nucleotide, lipids, steroids, alkaloids, sugars, vitamins and conjugates. Fourth, it has high sensitivity. For example, the present detection limit is 5pg for Theophylline and 10pg for Thiolutin. The fifth is wide dynamic range for quantitative analysis , usually 4-5 orders. Consequently, this system was proven to be promising in terms of the performance, as shown above.

Mass chromatograms for a mixture of Spiramycin I, II and III are shown in figure 1. This spiramycin mixture can be separated with an LC using a buffer solution (0.1 M ammonium acetate solution/ acetonitrile/methanol, 55/40/5). The mass spectra of these spiramycins are shown in figure 2. The intent quasi-molecular ions are obtained for all spiramycins.

1)S. Tsuge, K.Matsumoto, PROTEIN, NUCLEIC ACID AND ENZYME,30,1138 (1985).
2)H.Kambara, Anal.Chem., 54,145(1982).
3)M.Sakairi and H.Kambara, Mass Spectrometry, 31,87(1983).
4)M.Sakairi and H.Kambara, Anal. Chem., to be published.

Presented at the 35th ASMS Conference on Mass Spectrometry and Allied Topics
May 24-29, 1987, Denver, CO

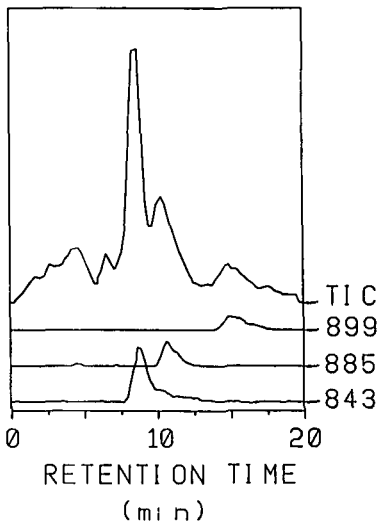

Fig.1 Mass chromatograms for spiramycins

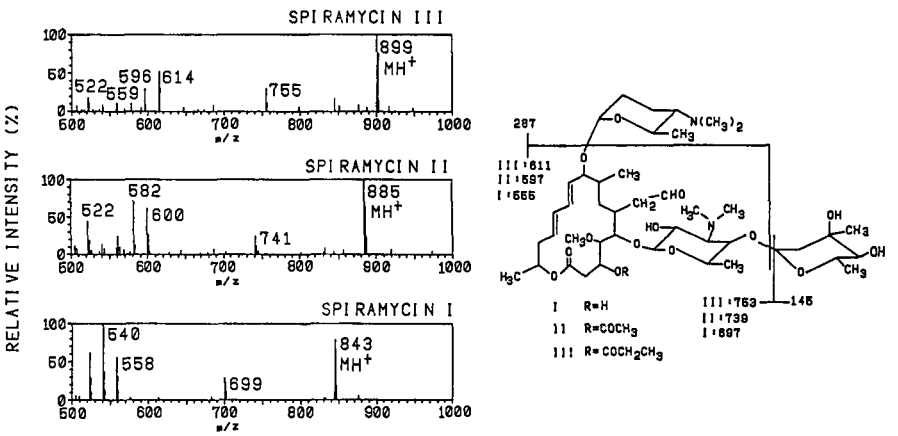

Fig.2 Mass spectra of spiramycins

Presented at the 35th ASMS Conference on Mass Spectrometry and Allied Topics
May 24-29, 1987, Denver, CO

TRANSPORT PROCESSES, LOSS MECHANISMS AND SIGNALS IN MAGIC-LC/MS

Richard F. Browner, J. Daniel Kirk, Debbie A. Garrett and Deborah D. Perkins
School of Chemistry
Georgia Institute of Technology
Atlanta, Georgia 30332-0400

The Monodisperse Aerosol Generation Interface for Combining Liquid Chromatography with Mass Spectrometry (MAGIC-LC/MS) involves a particle-beam approach to LC/MS interfacing that is quite distinct from other common techniques. In MAGIC-LC/MS, the total column effluent is used to form a uniform aerosol. The aerosol is desolvated at near atmospheric pressure and ambient temperature. The two-stage supersonic flow separator is used to remove solvent vapor and helium dispersion gas form the particle beam. Finally, the analyte is introduced into the mass spectrometer through a line-of-sight. Because the source pressure is low, electrom impact ionization can be performed in addition to chemical ionization with choice of CI gas. This study involved three areas of investigation: transport efficiency, loss mechanisms, and signals.

For the transport efficiency and loss mechanism studies a device was constructed for easy collection of analyte at the point of the ion source. The MAGIC-LC/MS interface was joined to a chamber evacuated by a turbomolecular pump. A sidearm of the chamber held an easily removeable probe upon which the analyte was deposited. Barium was injected and the resulting deposit on the probe tip washed into volumetric flasks with 1% nitric acid solution. The solutions were subsequently analyzed by ICP/MS for their barium content. Signals and transport effeciencies were studied while varying the flow rates and helium pressures.

Loss mechanisms in the interface were studied in both a quantitative and qualitative way. The transport efficiency device was utilized for quantitative studies. Barium was injected into the interface. The interface was then taken apart and each section carefully washed with 1% nitric acid into volumetric flasks. The solutions were then analyzed by ICP/MS. A comparison of results obtained for the previous interface, MAGIC III, with the current interface, MAGIC IV, is given in the figures below. Considerable improvement of transport to the source has been achieved with the new design, from 5% to 17%. Qualitative studies were performed by observing the accumulation of methyl red on surfaces within the interface. Primary areas of loss are the first half of the desolvation chamber, the first skimmer's orifice, and the backside of the first skimmer.

Finally, the magnitudes of analytical signals for selected compounds were studied. In these experiments, the MAGIC interface was attached to an HP5988 quadrupole. All compounds of interest were compared relative to a standard compound, methyl stearate. It was found that most compounds exhibit near equal response. Very volatile analytes as well as extremely involatile analytes, however, gave lower responses.

Presented at the 35th ASMS Conference on Mass Spectrometry and Allied Topics
May 24-29, 1987, Denver, CO

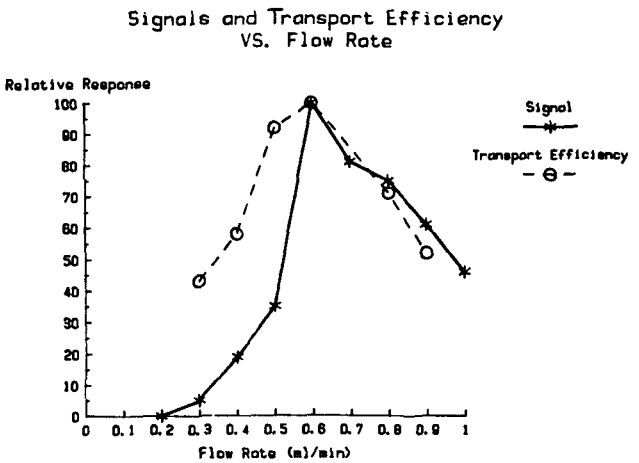

MAGIC III

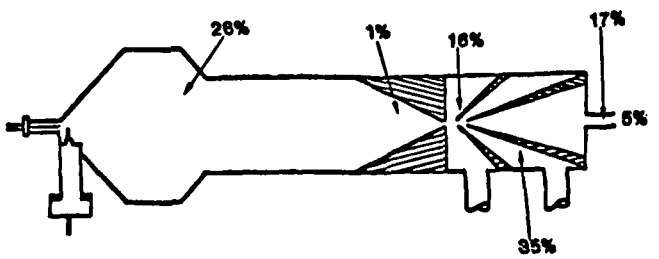

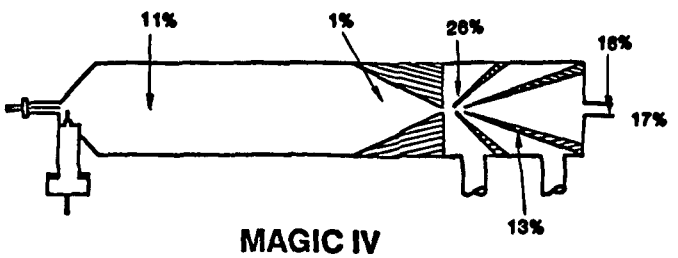

MAGIC IV

16% Lost to roughing pumps

Presented at the 35th ASMS Conference on Mass Spectrometry and Allied Topics
May 24-29, 1987, Denver, CO

Heat-Induced Dissociation in LC/MS Analyses

J. L. Crawford, J. L. Little, D. R. Wilder
Building 150, Eastman Chemicals Division
Kingsport, Tennessee 37662

Heat-induced dissociation (HID) and diversion of the major component employing a thermospray LC/MS (liquid chromatography/mass spectrometry) interface has proven to be very useful in the identification of low-level impurities in various chemicals in our laboratory. HID is employed to generate very useful fragmentation data which can easily be correlated with structure. HID is performed by increasing the vaporizer exit temperature of the thermospray interface from 40 to 300°C above the temperature required to vaporize 100% of the LC eluent (takeoff temperature). Normally the vaporizer exit temperature of the thermospray interface cannot be operated more than 20 to 30°C above the takeoff temperature due to a significant loss in sensitivity when no source of external ionization is employed. However, the use of an external ionization source such as a discharge electrode with the thermospray interface places no theoretical upper limit on the vaporizer exit temperature.

The lack of fragmentation data is often noted as one of the major limitations to the use of a thermospray interface in characterization of organic compounds. This is demonstrated in the spectrum of Compound I in Figure 1. The spectrum was obtained at the takeoff temperature employing a 90% acetonitrile/10% acetate buffer LC eluent and a discharge electrode for external ionization. By increasing the vaporizer exit temperature over 300°C above the takeoff temperature, the HID spectrum in Figure 2 was obtained. The fragmentation information obtained is easily correlated with the structure of the compound and is very similar to the collision-induced spectrum obtained with a triple quadrupole mass spectrometer.

The fragmentation data and increased sensitivity obtained with HID was initially thought to be a result of pyrolysis of compounds in the capillary of the thermospray interface. However, holding the vaporizer exit temperature (~500°C) at high temperature and varying the source temperature indicated that the fragmentation for Compound I was not occurring as a result of pyrolysis in the hot thermospray vaporizer. A reasonable explanation for the increased fragmentation in molecules such as Compound I is that the additional vibrational energy imparted to the molecules by the elevated vapor temperatures causes additional fragmentation after they are ionized.

The thermospray interface is routinely employed to identify low-level impurities (0.03 to 7% by area) in various chemicals in our laboratory. Detection of such components often entails the injection of 400-800 micrograms of sample on conventional (150 x 4.6 mm) analytical columns. To minimize source contamination, probe plugging and "ghosting" of the major component, the bulk of the major component is diverted to waste. This is done with the aid of a UV detector and a standard high-pressure switching valve in series with the thermospray interface. Despite the high sample loading and the cosolvents employed to dissolve large sample concentrations, reasonable column efficiency and resolution are maintained.

In conclusion, HID and diversion of the major component with a thermospray interface with external ionization are very powerful techniques for identifying low-level unknowns in organic compounds. A supplementary text available from the authors includes additional examples, experimental details, and applications to problem solving.

Presented at the 35th ASMS Conference on Mass Spectrometry and Allied Topics
May 24-29, 1987, Denver, CO

Figure 1: **Spectrum of Compound I Near Takeoff Temperature**

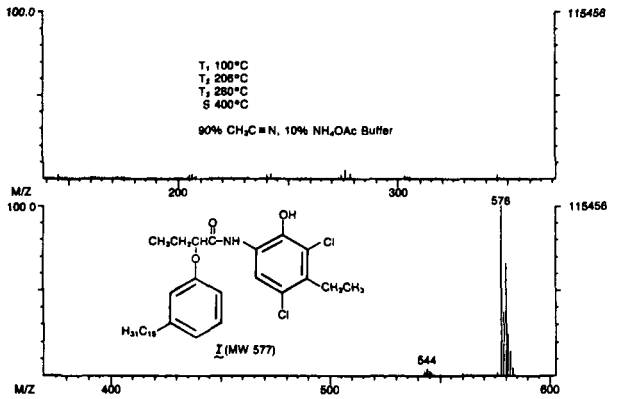

Figure 2: **HID Spectrum of Compound I**

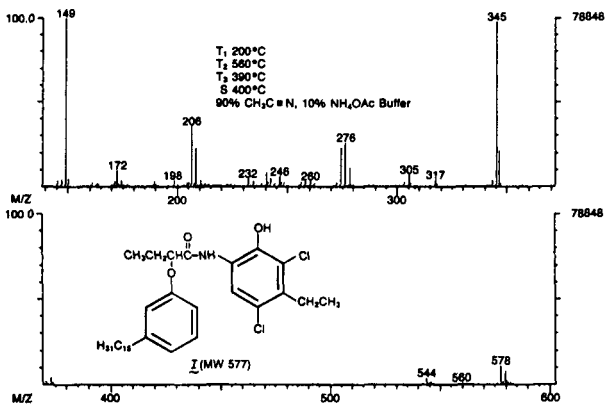

Presented at the 35th ASMS Conference on Mass Spectrometry and Allied Topics
May 24-29, 1987, Denver, CO

PACKED CAPILLARY LC/MS USING A MOVING BELT INTERFACE

Robert W. Reiser* and Aldos C. Barefoot
Agricultural Products Department
Experimental Station
Wilmington, Delaware 19898

The objective of this work is to develop an LC/MS technique that allows us to obtain good quality EI and CI mass spectra with high sensitivity for identification of unknowns that are too polar and/or thermally unstable for GC/MS analysis. We are using packed fused silica capillary LC columns (0.25mm ID) to obtain increased mass sensitivity (two orders of magnitude higher than with conventional 4.6mm ID columns). This is very important when the sample is limited, such as in many environmental and biomedical analyses. The low flow rate (1-2 μL/min.) simplifies interfacing to a mass spectrometer. Packed capillary LC columns offer a practical alternative to wall-coated open tubular columns, whic h require extremely small volumes (6-10 μ ID columns). A comparison of the relative ID's of packed capillary, microbore and conventional LC columns is shown on Figure 1.

Our first approach (Reference 1) was direct coupling of packed capillary columns to a quadrupole mass spectrometer, since we thought that the best interface is no interface. However, with direct coupling, the EI sensitivity was poor due to the presence of the mobile phase in the ion source, and thermally labile compounds decomposed in the capillary interface line.

Use of a moving belt interface with a magnetic mass spectrometer (Finnigan MAT Model 8230) allowed us to routinely obtain good quality EI and CI spectra on injection of a 0.1 μg sample into the LC. The mass spectra obtained are very similar to those obtained using a direct exposure probe. Figure 2 shows a separation obtained on a mixture of glucose and two glucosides using ammonia CI. Strong $M+NH_4^+$ ions were obtained in the mass spectra of each component.

Presented at the 35th ASMS Conference on Mass Spectrometry and Allied Topics
May 24-29, 1987, Denver, CO

We are using this technique daily to identify unknown metabolites obtained in environmental studies of agricultural chemicals, as well as to identify impurities in our products and intermediates. We are also continuing research with this technique to make further improvements in the liquid chromatography and moving belt interface.

REFERENCE

1. Barefoot, A. C. and Reiser, R. W., J. Chromatogr., in press (1987).

FIGURE 1

Relative Sizes of LC Columns (Blown-up 10 X)

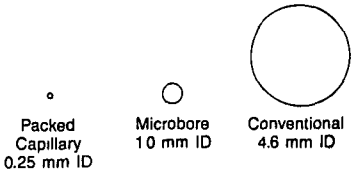

FIGURE 2

Separation of Glucose and Glucosides - CI/NH_3

Column: 30 cm Nucleosil ODS
Mobile Phase: 40% CH_3CN/60% H_2O (PH3)

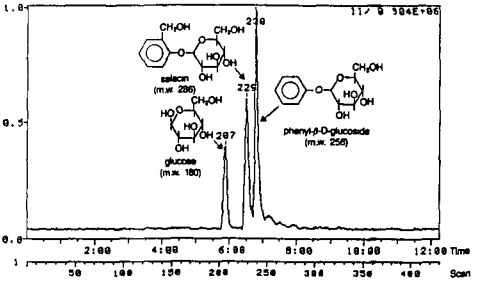

Presented at the 35th ASMS Conference on Mass Spectrometry and Allied Topics
May 24-29, 1987, Denver, CO

LC-MS ACCURATE MASS MEASUREMENT USING PLASMASPRAY

Bateman, R H., Krolik, S T., *Jones, D J and Major, H J.
VG Analytical Ltd, Floats Rd, Wythenshawe, M23 9LE, UK

Plasmaspray HPLC-MS uses a basic interface consisting of a directly heated steel capillary inlet system to vaporise the mobile phase. Plasmaspray ionisation is achieved by initiating a glow discharge inside the ion source using the probe tip as an electrode. This aspect is a unique feature of the VG design which differentiates Plasmaspray from related forms of filament assisted thermospray. A fundamental consequence of this geometry is that all sample and solvent entering the ion source must pass through the cathode dark space which surrounds the probe tip. The cathode dark space is the region within the discharge which is particularly rich in energetic ions, neutrals and metastable species responsible for ionisation of the sample entering through the cathode.

The main benefits of Plasmaspray HPLC-MS are:

Spectra can be obtained from buffered or non-buffered, aqueous or non-aqueous media (Figures 1&2).
Accurate mass measurement is now possible as a result of stabilising mass spectral peak profiles (Figure3)
Spectra yield more structural information (Figure 4).
Probe temperature does not have to be stringently monitored and can be used to control the degree of fragmentation (Figures 5&6).

Six compounds, representing a broad range of chemical classes, were investigated using PEG as a reference. Elemental compositions were assigned to each of the molecular ions. The results are summarised in Table 1. All data was obtained on a VG 70 SE mass spectrometer operating at 8kV accelerating voltage and 5000 resolution.

Users of conventional thermospray have previously been limited to molecular ion information without the ability to unambiguously identify compound of interest. The elemental composition of ions generated by Plasmaspray on a magnetic sector mass spectrometer can be determined with ease. The accuracy of the technique is such that elemental compositions of molecular ions and fragments can be assigned with a high degree of confidence a valuable aid to compound identification in routine HPLC-MS analyses. The increased sensitivity and reproducibility afforded by Plasmaspray (Figure 7) further enhances its utility for HPLC-MS analyses on sector mass spectrometers.

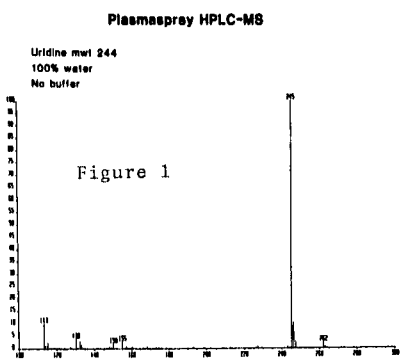

Figure 1

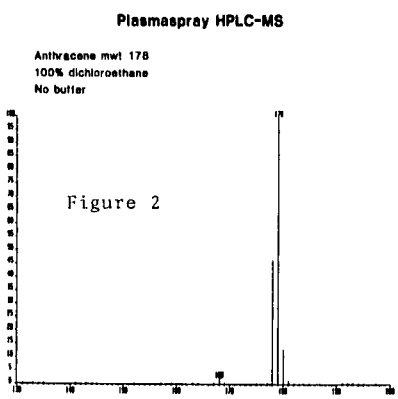

Figure 2

Peak profiles from the protonated molecular ion of adenosine MH 268 using both thermospray and plasmaspray

Figure 3

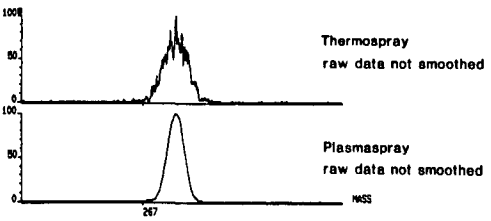

Compound	Formula	Pseudo Molecular Ion			Error mmu	Std Dev	Method	No of Scans
		Ion	Calc	Obs				
Glucose	$C_6H_{12}O_6$	MNH_4^+	198 0978	198.0986	+0 8	1 1	CRcSc	10
Phenylbutazone	$C_{17}C_{19}H_2ON_2O_2$	MH^+	309 1603	309 1603	0	1 1	CRcSc	10
			309 1603	309 1606	+0 3	--	MRcSc	10
Chlorpromazine	$C_{17}H_{19}O_9N_2S$	MH^+	319 1036	319 1027	-0 9	1 4	CRcSi	6
Beclomethasone Dipropionate	$C_{28}H_{37}O^{37}Cl$	MH^+ (^{35}Cl)	521.2306	521 2318	+1 2	2 0	CRcSc	10
			521 2306	521 2311	+0 5	--	MRcSc	10
			521 2306	521 2313	+0 7	1 8	CRcScm	9
Organometallic	$C_{40}H_{54}S_2N_2{}^{65}Zn$	MH^+ (^{64}Zn)	771 2844	771 2838	-0 6	--	MiSi	6
Lorazepam	$C_{15}H_{10}Cl_2N_2O_2$	MH^+ (^{35}Cl)	321 0198	321 0187	-1.1	4 0	CRcSi	6

M - Simple Accurate Mass Voltage Scanning Sc - Continuous Sample Feed C - Real Time Centroiding
Si - Injected Sample Rc - Continuous Reference Feed Scm - Sample Injected Through Column
Ri - Injected Reference Scm - Sample Injected Through Column

Table 1 Mass Measured Molecular Ions of Compounds Studied

Beclomethasone dipropionate Thermospray Mode

Figure 4

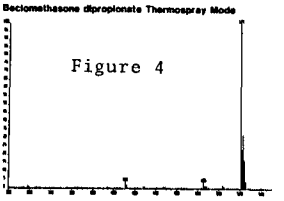

Beclomethasone dipropionate Plasmaspray

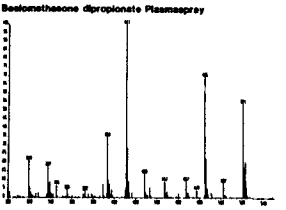

Influence of Probe Temperature on Degree of Fragmentation

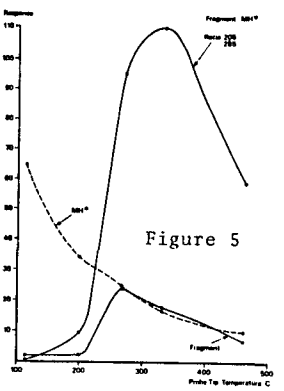

Figure 5

Variation of Response with Probe Tip Temperature for M/Z 78 (NH_4OAc) H^+ of Ammonium Acetate

Figure 6

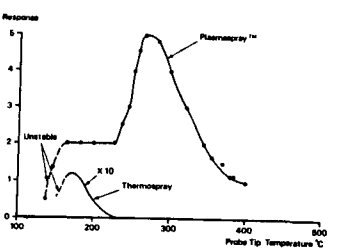

Comparative Sensitivity Between Thermospray and Plasmaspray using Caffeine

Figure 7

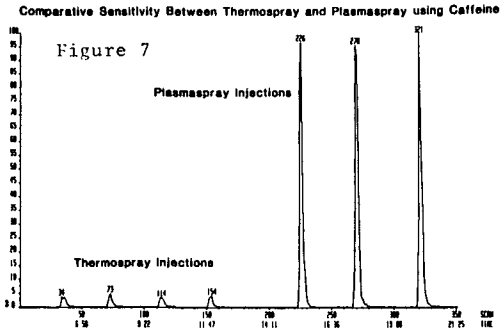

Presented at the 35th ASMS Conference on Mass Spectrometry and Allied Topics
May 24-29, 1987, Denver, CO

EFFECTS OF SOURCE DESIGN ON THE NATURE OF THERMOSPRAY MASS SPECTRA

John E. Coutant[1], Bradley L. Ackermann[1], and Marvin L. Vestal[2]

[1] Merrell Dow Research Institute, 2110 E. Galbraith, Cincinnati,OH 45215
[2] Department of Chemistry, University of Houston, Houston,TX 77004

The increased use of liquid chromatography-mass spectrometry, especially using the thermospray interface, has generated a large number of reports on various applications. One outcome of this large amount of data being produced is a concern about the differences observed in the mass spectra of certain compounds obtained from ion sources of different design. Although several parameters which affect the nature of the observed mass spectra in thermospray have been reported(1,2), these studies usually have dealt with the optimization of a single source design. This study was undertaken to look at the effect of the physical size and shape of the desolvation chamber and the placement and use of repellers on the thermospray mass spectra. Three very different source designs, as shown in Figure 1, were investigated including a Finnigan thermospray source, a standard Vestec thermospray source, and a prototype Vestec thermospray source in two different configurations. A Finnigan TSQ-46 MS/MS was used to obtain data from all the above sources. In addition, a Vestec/ HP MSD system was also used to acquire some of the repeller data. Liquid chromatography was done with a Waters gradient system.

Higher molecular weight peptides are difficult compounds to analyze by thermospray MS. Robbins and Crow(2) have shown that a smaller vaporizer diameter and higher repeller settings help in getting good spectra of peptides. In addition, it appears that an auxillary heater on the thermospray probe tip and a more open desolvation chamber are helpful. These changes appear to be important because peptide ions are believed to be formed by ion desolvation as opposed to chemical ionization, which is often the dominant mechanism of ionization for smaller molecules (MW<500). This is demonstrated in the mass spectrum of bradykinin, shown in Figure 2, from a Finnigan source (repeller but no additional vaporizor heater and a smaller desolvation chamber) and, in Figure 3, from a Vestec prototype source (no repeller but auxillary vaporizor heater and a larger desolvation geometry).

The effects of a repeller on the response to the protonated molecular ion of adenosine (m/z 268) for three different source designs is shown in Figure 4. For a closed geometry, such as the Finnigan source, the maximum response is observed at 150 volts. On the other hand, the maximum response is close to 0 volts for a source with open geometry such as the Vestec prototype. When the volume of the Vestec prototype is reduced with an insert, the voltage of maximum response is shifted to higher voltages (100V) similiar to the Finnigan source. This effect is mass dependent and appears to be greater in source designs like the Finnigan source.

When a filament or discharge is used to produce ions in a thermospray source and high repeller voltages are present, fragmentation of the compound is observed. First reported by Zakett et al.(1), this phenomenon has been attributed to CID processes occurring in the ion source(1,3). When 2-aminochrysene is run in acetonitrile with discharge and a repeller of 120V the spectrum shown in Figure 5 is observed. When compared to the daughter ion of the protonated molecular ion of 2-aminochrysene (m/z 244) as shown in Figure 6, there are more fragment ions in the discharge spectra than can be explained by CID processess alone. When the effect of repeller voltage on reagent ion intensity of an acetonitrile/water/acetic acid mobile phase produced by filament ionization was examined, the curves as shown in Figure 7 were observed. At higher repeller voltages (the actual value depends on ion density) few positive ions reach the ion exit regardless of the inital mode of ionization. This occurs because negative ions and electrons are accelerated to the repeller causing the plasma in front of the sampling region to be charged positive. As the repeller voltage is increased further, electrons accelerated toward the repeller reach high enough energy to ionize vapor components present. These ions produced may be the same as initially observed but some ions may also be formed by electron impact dissociation of the ions present rather than the neutrals (such as m/z 56). These processes are probably responsible for the observed fragmentation of 2-aminochrysene.

In conclusion, a major factor in the "differences" observed in the spectra from thermospray ion sources of different manufacture is related to desolvation chamber geometries. Chamber design also has a large effect on the magnitude of a positive repeller response. In addition, the dissociation produced by high repeller voltages in combination with filament or discharge ionization appears to have a strong electronic contribution in addition to the CID component.

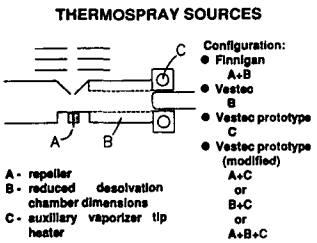

Figure 1

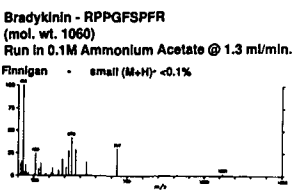

Figure 2

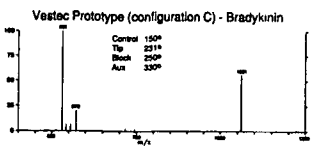

Figure 3

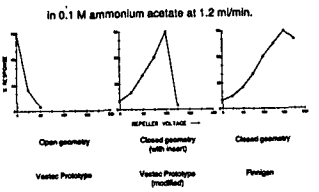

Figure 4

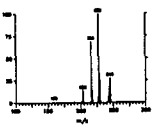

Figure 5

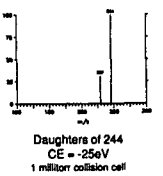

Figure 6

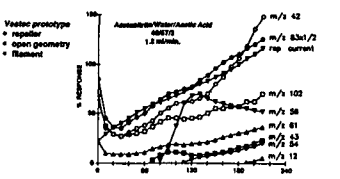

Figure 7

References

1. D. Zakett, G.J. Kallos, and P.J. Savickas presented at 34th Annual Conf. on Mass Spec., Cincinnati, OH, June 1986.

2. R.H. Robbins and F.W. Crow, presented at 34th Annual Conf. on Mass Spec., Cincinnati, OH, June 1986.

3. W.F. McFadden and S. Lammert, J. Chrom., 385:201 (1987) .

Presented at the 35th ASMS Conference on Mass Spectrometry and Allied Topics
May 24-29, 1987, Denver, CO

DEVELOPMENT OF A NEW INTERFACE FOR COMBINED OPEN-TUBULAR LIQUID CHROMATOGRAPHY WITH MASS SPECTROMETRY.

Jos S.M. de Wit[1,2], Carol C. Parker[1], James W. Jorgenson[2] and Kenneth B. Tomer[1].

[1]Laboratory of Molecular Biophysics, National Institute of Environmental Health Sciences, PO Box 12233, Research Triangle Park, NC 27709.

[2]Department of Chemistry, University of North Carolina at Chapel Hill, Chapel Hill, NC 27514.

The design and performance of a probe that allows direct liquid introduction of the total effluent of an open-tubular liquid chromatography column into a quadrupole mass spectrometer is presented (Fig. 1). The probe can be introduced into the mass spectrometer through the standard vacuum lock normally used for the solid probe, without breaking vacuum. The mass spectrometers in use are a Finnigan 3300 electron impact mass spectrometer and a Finnigan 3300 chemical ionization mass spectrometer previously modified for negative ion detection. No modifications to the mass spectrometer are necessary.

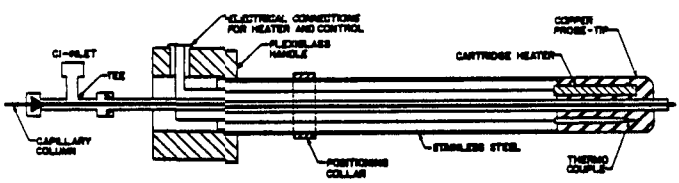

Figure I. OTLC-MS Interface Probe.

Two kinds of OTLC columns are employed: 15 um i.d. etched borosilicate glass capillaries with chemically bonded stationary phases, and 10 um i.d. fused silica columns coated with OV-17-V. Flow rates for these columns are lower than 0.1 ul/min, allowing direct introduction of the entire effluent into the ion source. The amount of vapor generated is so low that both CI mass spectra, with a choice of reagent gases, and EI mass spectra can be obtained.

The actual OTLC column makes up part of the interface, since the column end has to be tapered in order to successfully detect compounds of low volatility. The column end passes through a copper probe tip which has to be heated to obtain good results. Tapering the column creates an exit orifice of sub-micron dimensions. The actual process at the column tip has similarities to both thermospray and direct liquid introduction.

In Figure 2 the total ion current chromatogram of a synthetic mixture of 5 pesticides is shown. This chromatogram was obtained under methane negative chemical ionization conditions, and acquired in the full scan mode over the mass range from 60 to 350 amu. The column used was a 1 meter by 10 um i.d. fused silica column coated with OV-17-V stationary phase. The mobile phase was 75:25 methanol:water (v:v). The copper probe tip was maintained at 320°C. Excellent negative chemical ionization mass spectra were obtained, on only 1 ng of solute for each peak. Figure 3 shows the mass spectrum obtained for the first eluting peak, metribuzin.

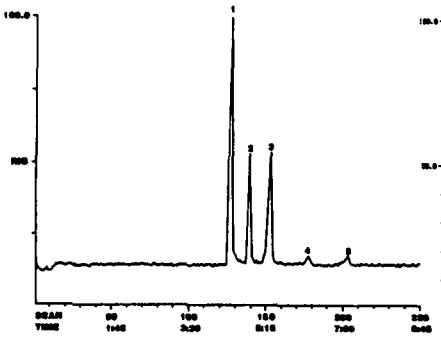

Fig. 2. I=metribuzin;2=methyl parathion; 3=ethyl parathion;4=merphos;5=treflon.

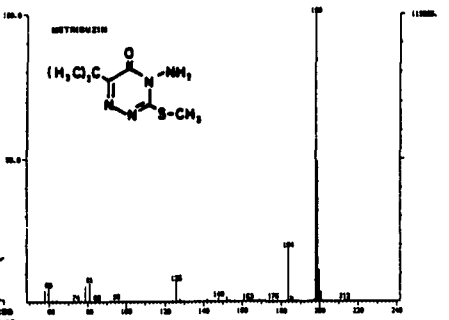

Fig. 3. Neg. CI spectrum of metribuzin.

One outstanding quality of this OTLC/MS system is that EI spectra can be obtained under standard operating conditions. Figure 4 shows the TIC trace and the trace of two characteristic ions of the separation of propazine and trietazine, two isomeric herbicides, under similar chromatographic conditions as the separation mentioned above. These isomers have very distinguishable EI mass spectra. In Figure 5 EI mass spectra for trietazine are shown; the upper spectrum was obtained from several milligrams using the solid probe, the lower one was obtained from the chromatogram on only 1.6 ng of material. The ^{13}C and ^{37}Cl isotope clusters observed for the major high mass ions in the OTLC mass spectrum compare favorably with those observed in the solid probe mass spectrum.

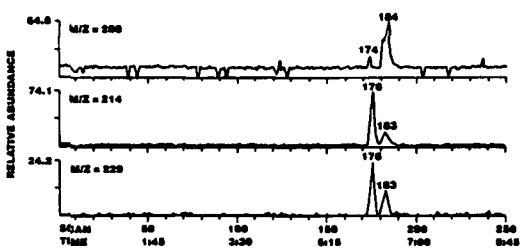

Fig.4. Propazine; Trietazine.

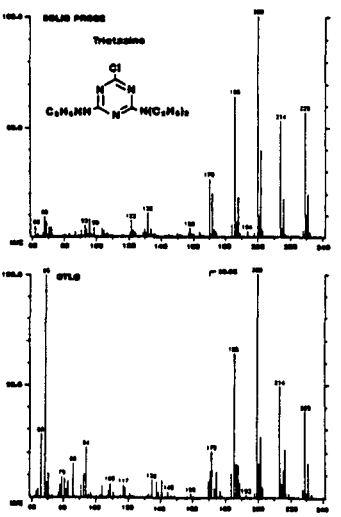

Fig 5. Solid probe (mg's) vs OTLC (ng's) EI mass spectra.

Presented at the 35th ASMS Conference on Mass Spectrometry and Allied Topics
May 24-29, 1987, Denver, CO

Fundamental Studies of Thermospray Ionization: Investigation of the Thermospray Plume

Mike S. Lee and Richard A. Yost; Department of Chemistry, University of Florida, Gainesville, FL 32611.

With the increasing number of applications of thermospray LC/MS there is only limited understanding of the physical and chemical processes involved in the formation of molecular and fragment ions by thermospray ionization. Vaporization, droplet charging, droplet evaporation, and ion evaporation all appear to play important roles in the thermospray ionization mechanism. The study of these processes is difficult due to the complexity of the thermospray plume (large number of droplets and non-uniform droplet sizes). We have constructed an observation chamber which permits sampling of the plume under vacuum conditions so that temperature, pressure, and current characteristics of the plume can be investigated. Temperature measurements of the thermospray plumes yielded information on vaporization and droplet evaporation while the current measurements yielded information on droplet charging and ion evaporation.

The vacuum chamber consisted of a modified Finnigan 1015 vacuum console designed with entrance ports for the vaporizer probe, temperature, pressure, and current probes, a six inch diameter observation window, and a pump out line connected to a 300 L/min mechanical pump. The pump out line was situated 180# from the vaporizer probe. Temperature and pressure measurements of the plumes were obtained by placing the thermocouple (1 mm o.d.) and pressure sampling tube (2 mm i.d.) directly into the center of the plume, perpendicular to the direction of the vapor and droplet flow from the vaporizer probe. Current measurements were obtained in the same manner with a 2" X 2" wire mesh screen placed into the center of the plume. Sampling distances were varied by adjusting the distance of the vaporizer probe from the sampling probes. Preliminary plume measurements under vacuum conditions were performed with distilled water.

Three plume types were studied in vacuum: wet, nearly dry, and dry. Wet plumes correspond to <95% vaporization of the mobile phase and consists of both droplets and vapor. Nearly dry plumes correspond to >95% vaporization of the mobile phase and also consists of both droplets and vapor. Dry plumes correspond to 100% vaporization and consists of only vapor. Wet and dry plumes typically yield poor thermospray performance while nearly dry plumes yield optimum thermospray performance.

At atmospheric conditions, thermospray plumes are characterized by a dense cloud of droplets and vapor. Under vacuum conditions, thermospray plumes are less visible. Droplets were observed to exit the nozzle at wider angles than plumes produced at atmospheric pressure. With wet plumes, crystals of ice were observed striking the glass observation window. At even lower tip temperatures (<90% vaporization) ice particles would form at the tip, often clumping together and eventually falling off.

Plume pressures remained constant for all distances measured within the plume at constant flow rate. Pressures of 2.4, 2.6, and 2.8 torr were obtained with flow rates of 1.5, 1.75, 2.0 mL/min, respectively. Other instrumental parameters had no effect on pressure measurements.

The effects of flow rate and tip temperature on plume temperature measurements are shown in Figure 1. Plume temperatures for water are dependent on the distance at which the plume is sampled. The greatest fluctuations in plume temperature were observed at distances <1.5 cm from the vaporizer probe tip. Temperatures remain constant at distances of 2-5 cm from the probe. High flow rates, tip temperatures, and source temperatures, combined with low source pressure produce higher plume temperatures.

The effects of flow rate and tip temperature on plume current measurements are shown in Figure 2. Plume currents for water are also very dependent on the distance at which the plume is sampled. The greatest fluctuations in plume current were observed at distances <1.5 cm from the vaporizer probe tip. Results from the tip temperature experiments show that dry plumes do not transport as much current as nearly dry and wet plumes. Higher flow rates, tip temperatures, source temperatures, and source pressures produce a larger range of currents.

With the use of a single piston LC pump, the effects of pump pulsing on ion current was also determined. To demonstrate this effect, a selected ion monitoring (SIM) experiment was performed on a Finnigan TSQ-45 selecting the 77^+ ion of ammonium acetate $(CH_3COONH_4)^+$ with 0.013 second scans as the three plume types were sprayed into a Vestec thermospray source. The ion current obtained versus the pumping cycle (pumping stroke and refill) is shown in Figure 3. With wet plume types, ion current was observed to increase with the refill cycle. Due to interruption of flow during the refill cycle, ion intensity was expected to decrease. However, a wet plume contains a droplet rich environment. As the flow is interrupted, heat is still provided to the vaporizer probe resulting in greater vaporization of the remaining mobile phase. Plume conditions similar to a nearly dry plume are obtained, therefore, ion intensity increases. The opposite effect with pump pulsing was observed with dry plume types. During the refill cycle ion intensity decreased due to the interruption of flow to the probe tip. As a result, less vapor exits the probe and a decrease in ion intensity is observed. Nearly dry plume types are relatively stable to pump pulsing, as the pumping cycle had little effect on ion intensity. The same experiment was performed on the 119^- ion of ammonium acetate $(CH_3COOH \cdot CH_3COO)^-$ and identical results were obtained for each plume type.

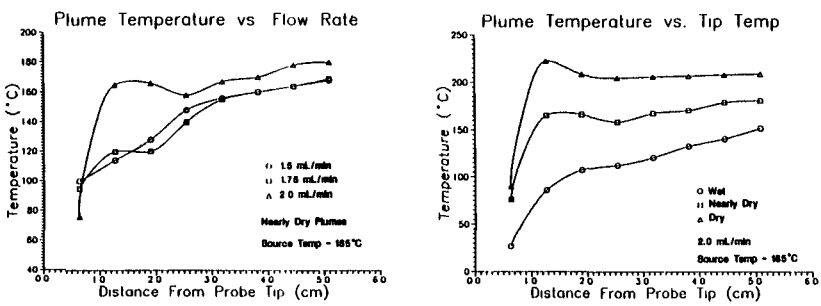

Figure 1. Plume temperature measurements of water.

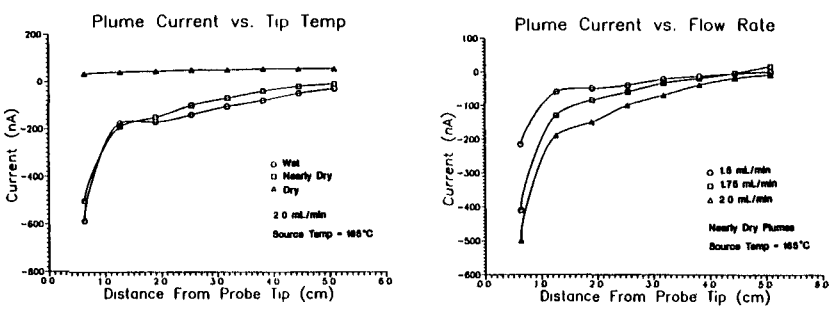

Figure 2. Plume current measurements of water.

Presented at the 35th ASMS Conference on Mass Spectrometry and Allied Topics
May 24-29, 1987, Denver, CO

EVALUATION OF A DISPOSABLE MOVING RIBBON LIQUID CHROMATOGRAPHY-MASS SPECTROMETRY INTERFACE

William DeMaio
University of Houston, Department of Chemistry
Houston, Texas 77004

This presentation covered some of work done with the disposable moving ribbon liquid chromatography-mass spectrometry (LC-MS) interface, which I first introduced at the 1986 ASMS Conference. This interface utilizes a single pass concept where the transport medium is used only once. The main advantages of this approach are (1) no memory effects whatsoever, (2) increased sample deposition efficiency because sample deposition takes place at atmospheric pressure, and (3) this inter ce is ideal for mass spectrometers utilizing particle induced (SIMS, FAB) and laser desorption (LD) ionization. The main advantage of being able to interface LC to SIMS and LD mass spectrometers is the ability to analyze mixtures containing high molecular weight, polar biomolecules.

Seven ribbon materials were tested with the disposable ribbon LC-MS interface. They were: polyimide film, polyester film, audio recording tape, black polyester (the reverse side of audio recording tape), stainless steel, aluminum, and darkened aluminum. Darkened aluminum was the only material that worked well in the interface. Darkened aluminum ribbon appreciably absorbs laser radiation and is oil-free. A ribbon must be oil-free for use with SIMS because SIMS is especially sensitive to oils. Darkened aluminum was manufactured in our laboratory by treating aluminum ribbon in a hot aqueous solution containing sodium carbonate and sodium chromate. The sodium salts used in the treatment process enhance sodium adduct ion formation in LDMS,

which makes possible the observation of molecular ions of thermally labile molecules such as raffinose.

The interface was used to produce LC/LDMS chromatograms of test mixtures of nucleosides and analgesics. The LC/LDMS chromatogram of the analgesic mixture also demonstrated that LD from darkened aluminum ribbon is more sensitive to non-acidic compounds than for organic acids.

Laser desorption mass spectra of four aminoglycoside antibiotics, gentamycin, kanamycin, sisomycin, and netilmycin were also presented. An intense sodium adduct molecular ion was easliy observed for each of the antibiotics. In addition, each antibiotic LD mass spectrum exhibited sodium adducts of structurally significant fragments.

This system, which consists of the disposable moving ribbon LC-MS interface to a laser desorption mass spectrometer, is almost ready for widespread application. Sensitivities and limits of detection could be improved by employing a mass spectrometer capable of recording an entire mass spectrum from a single laser pulse, such as a time-of-flight instrument. The interface portion of the system works well and is ready for routine LC-MS.

Presented at the 35th ASMS Conference on Mass Spectrometry and Allied Topics
May 24-29, 1987, Denver, CO

STUDIES OF THE KINETICS OF CALCIUM METABOLISM

A.L. Yergey, D.G. Covell, N.E. Vieira
NIH, Bethesda, MD 20892.

The metabolism of calium is of great importance in the growth and development of humans. The age dependence of skeletal growth and development is perhaps the most obvious example, but age dependent variations in absorption rates may also be an extreemly important aspect of public health issues. The use of tracer kinetic methodologies in the study of this element's metabolism leads to insights that are simply not available from studies employing metabolic balance, i.e. the summing of inputs and outputs over several week of carefully controlled dietary intake. Over the last several years we have developed methodologies using two isotopic tracers simultaneously coupled with thermal ionization mass spectrometric measurement of Ca ratios to determine various aspects of Ca metabolism[1]. The use of two tracers permits the direct measurement of absorption and endogenous fecal excretion that cannot be determined by balance methods. In addition, the more apparent quantities of urinary and total fecal excretion can be determined by this methodology. Perhaps of more interest however, is the fact that internal distribution into several metabolic pools can be deduced from following the time course of tracer dilution in plasma, urine and stool. Results from our studies that illustrate measurements of different aspects of Ca metabolism, and the kinetic principles behind them were discussed. The treatment of absorption of dietary Ca presented previously[1], has been expanded to include intestinal resorption. The major conclusion from the earlier treatment, that is a plateau for fractional absorption, determined from urinary measurements, is reached after a sufficent time has passed, holds. The absorption plateau is illustrated in Fig. 1 from a data set obtained from a subject studied over a six week period. Fractional absorption results are shown only for an 11 day period. A second aspect of Ca kinetics that is of interest, but illustrates an interesting aspect of Ca metabolism in infants is determined from fitting a sum of exponentials to the isotope dilution in the rapidly turning over internal compartment (likely associated with plasma and extracellular fluid). The zero time intercept of the ordinate corresponds to the i.v. tracer's dilution at the "instant" of injection. in fact this instaneous dilution is a direct measure of the size of that rapidly turing over pool. Fig. 2 summarizes these determinations for 6 subjects, numbers 1-3 are adults and 4-6 are premature infants. The third column of the Table is an calculations of this pool size based on estimate of plasma and exracellular fluid volumes based on body weight. For the adults, the agreement is good, but for the infants, the pool size determined from isotope dilution is 2-3 times bigger than that determined from body weight estimates. This latter is consistant with the expected very rapid turnover of bones in infants. Finally, Figure 3 shows a six week i.v. isotope dilution study done in a normal adult woman. A four compartment model for internal Ca distribution has been fit to these data. The estimated errors associated with the internal exchange rate constants are all less than 10%. We have found, as predicted from earlier simulations done in conjunction with 3 week studies, that 4 internal compartments could be identified if 6 week studies were done. We were able to distinguish between 3 and 4 internal compartment models, and, using the F statistic to test the improvement in total variance by the increased complexity, were able to show the 4th compartment to exist with a significance at the P=0.001 level.

1. A.L.Yergey, D.G.Covell, N.E.Vieira, J.Muenzer, Proceedings of the 34th Annual Meeting on Mass Spectrometry and Allied Topics, Cincinnatti, OH, June 8-13,1986, p 262-3.

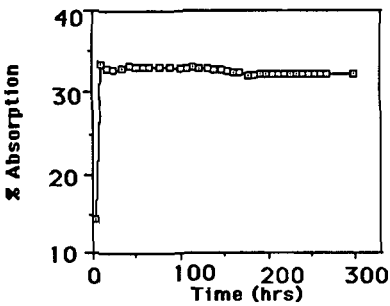

Figure 1.

Intravenous Tracer Dilution
at
Time Zero

Figure 2.

Subject	Exponential Fit	Physiological Estimate
1	915	1112
2	712	1348
3	265	320
4	1346	3704
5	800	1856
6	695	1854

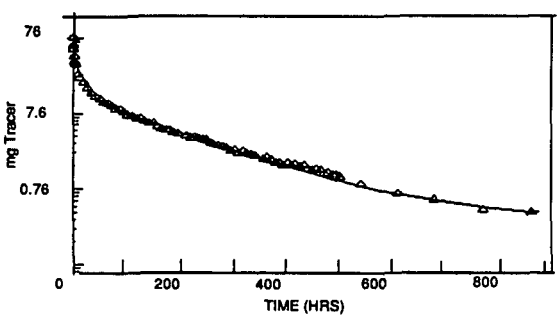

Figure 3.

Presented at the 35th ASMS Conference on Mass Spectrometry and Allied Topics
May 24-29, 1987, Denver, CO

THERMOSPRAY SPECTRA OF QUATERNARY AMMONIUM SALTS

David S. Mitchell, Keith R. Jennings, Department of Chemistry, University of Warwick, Coventry, U.K. and James H. Scrivens, I.C.I. C and P, Wilton, Cleveland, U.K.

Cationic surfactants are used in fabric conditioner formulations and bind to hydrophyllic surfaces thereby protecting the fibres. A commonly-used group of cationic surfactants comprises quaternary ammonium salts of the type $(R_1R_2R_3R_4)N^+Cl^-$ in which R_1 and R_2 are typically methyl groups and R_3 and R_4 are typically C_{12}-C_{20} alkyl groups. Standard methods for the quantitative analysis of mixtures of these salts are time-consuming and the objective of this work was to investigate the suitability of LC/MS and thermospray ionisation for the quantitative analysis of cationic surfactants.

All spectra were obtained on a Kratos MS80RF mass spectrometer fitted with a Kratos Thermospray source. Typical operating conditions were as follows:-

Flow rate	1 cm^3 min^{-1}	Vaporiser Temperature	543 K
Mass Range	4-600 amu	Scan Speed	3 s $decade^{-1}$
Solvent	Water or Methanol	Source Temperature	513 K
Resolving Power	1000	Ammonium Acetate Conc.	0.1 M

The thermospray spectrum given by Softlan JGE 930 is shown in Figure 1 together with the fast atom bombardment spectrum in Figure 2. In the FAB spectrum, peaks at m/z = 550, 522 and 494 were assigned to $(CH_3)_2(C_{18}H_{37})_2N^+$, $(CH_3)_2(C_{16}H_{33})(C_{18}H_{37})N^+$ and $(CH_3)_2(C_{16}H_{33})_2N^+$ ions respectively. These peaks were absent in the thermospray spectrum in which peaks at m/z = 536, 508 and 480 are assigned to $(CH_3)(C_{18}H_{37})_2NH^+$, $(CH_3)(C_{16}H_{33})(C_{18}H_{37})NH^+$ and $(CH_3)(C_{16}H_{33})NH^+$ ions respectively, due to the replacement of a methyl group by a hydrogen atom. Much more intense peaks at m/z = 298 and 280 arise from the ions $(CH_3)_2(C_{18}H_{37})NH^+$ and $(CH_3)_2(C_{16}H_{33})NH^+$ respectively, in which a larger alkyl group has been replaced by a hydrogen atom. It is therefore concluded that no quaternary ammonium ions are found in thermospray spectra and that all ions arise from protonated tertiary amines.

Possible routes to these ions are as follows:

1) Thermal decomposition of molecules or ion-pairs in the vaporiser followed by protonation of the tertiary amine. (This is a well-known reaction of the solid).

2) Intramolecular rearrangement in which a quaternary ammonium ion eliminates an alkene, although this obviously cannot explain the replacement of methyl by a hydrogen atom.

Several experimental factors were varied in order to investigate the mechanism by which the R_3NH^+ ions were formed. In each case, the intensity ratio $I(R_4N^+)/I(R_3NH^+)$ was monitored as conditions were varied and the results are summarised below:

1. The ratio was insensitive to changes in solvent, counter ion or ammonium acetate concentration.
2. The ratio falls from ~ 1.2 for $(CH_3)_4N^+X^-$ to essentially zero for alkyl groups of C_{10} or above, using a vaporiser temperature of 543 K.
3. For tetrapropylammonium bromide, the ratio falls from approximately 3.5 at a vaporiser temperature of ~ 470 K to unity at ~ 570 K.
4. In the case of Tetrapentylammonium bromide, the ratio fell from ~ 1.5 at a concentration of 5×10^{-3} mol dm^{-3} to ~ 0.2 at 5×10^{-2} mol dm^{-3}.

The above evidence supports the view that thermal decomposition is the main source of R_3NH^+ ions. Thermal desorption spectra show the same dependence as thermospray spectra and alkyl group size. The fall in intensity ratio as the concentration rises is ascribed to an increase in concentration of molecules or ion pairs which undergo thermal decomposition.

It is concluded that thermospray ionisation is unsuitable for the quantitative analysis of mixtures of quaternary ammonium salts owing to the thermal decomposition of the salts at normal vaporiser temperatures.

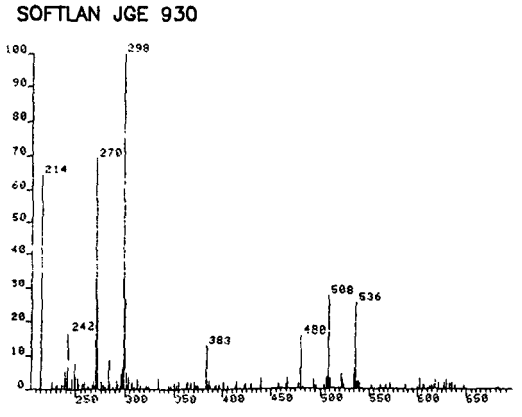

Figure 1. Thermospray spectrum of Softlan JGE 930

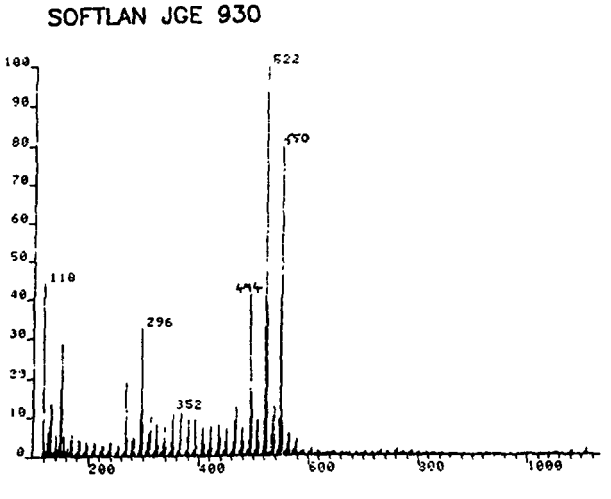

Figure 2. FAB spectrum of Softlan JGE 930

Presented at the 35th ASMS Conference on Mass Spectrometry and Allied Topics
May 24-29, 1987, Denver, CO

THE APPLICATION OF FAB AND THERMOSPRAY TO THE STRUCTURE DETERMINATION OF ω-CARBOXY-α-AMINO ACIDS.

R.T. APLIN, R.R. DIXON AND G.W.J. FLEET,
THE DYSON PERRINS LABORATORY, OXFORD UNIVERSITY,
OXFORD, OX1 3QY.

Mass spectral analysis of simple ω-carboxy-α-amino acids (I-V) using either IBEI or NH_3DCI fails to provide unambiguous molecular weight information.

I $HO_2C(CH_2)_2\text{-}CH(NH_2)CO_2H$

II $HO_2C(CH_2)_3CH(NH_2)CO_2H$

III $HO_2CH(CH_2)_4CH(NH_2)CO_2H$

IV $HO_2C\text{-}CH(CH_3)\text{-}CH_2CH(NH_2)CO_2H$

V $HO_2C\text{-}C(=CH_2)\text{-}CH_2CH(NH_2)CO_2H$

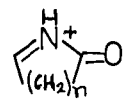

c, n=2,3,4.

Their mass spectra are dominated by thermal degration products, usually the lactam ion (c) being the only significant ion above m/z 50, its mass m/z 84,98 or 112 reflecting the relationship between the ω-carboxyl group and the amino group. Their NH_3 DCI mass spectra showed abundant ions corresponding to $[M-H_2O]+H^+$ and $[M-H_2O]+NH_4^+$, together with the lactam ions observed in their IBEI spectra (Fig.1). The hydroxylated compounds (VI-VIII) decomposed even more readily on IBEI analysis and their NH_3DCI spectra afforded a series of $[M-_nH_2O]+H^+$ and $[M-_nH_2O]+NH_4^+$ ions of the value of n depending on both the number and position of the hydroxyl groups.

$HO_2C\text{-}CH(CH_3)\text{-}CH(OH)\text{-}CH(NH_2)CO_2H$

VI

$HO_2C(CH_2)_2\text{-}CH(OH)\text{-}CH_2CH(NH_2)CO_2H$

VII

$HO_2C(CH_2)_2CH(OH)\text{-}CH(OH)\text{-}CH_2\text{-}CH_2CH(NH_2)CO_2H$

VIII

Presented at the 35th ASMS Conference on Mass Spectrometry and Allied Topics
May 24-29, 1987, Denver, CO.

In marked contrast the + ve ion FAB spectra run from glycerol following protonation with 5 µl of 5% oxalic acid in methanol, or as Dynamic FAB spectra from 10% glycerol in water; methanol, 1:2 containing 2% oxalic acid, afford unambiguous molecular weight information, MH^+ being the base peak in the majority of cases, the only significant, >10% fragment ion being the loss of water. Thermospray (TSP) spectra run from 0.1M aqueous ammonium acetate solution at low retarding electrode potential (150v) gave results very similar to those obtained by FAB. At high retarding electrode potential (325v) TSP afforded spectra containing abundant structurally useful fragment ions similar to those observed in their NH_3DCI spectra.

Fig.1.

Major ions in the NH_3 DCI, +ve FAB and +ve TSP Mass Spectra of ω-Carboxy-α-aminoacids.

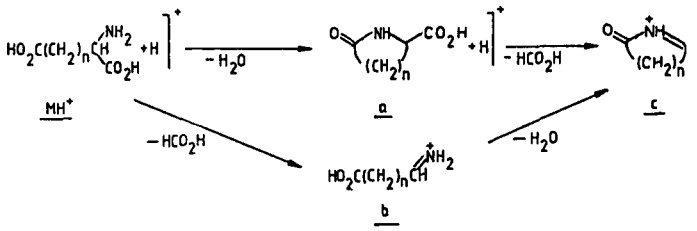

Presented at the 35th ASMS Conference on Mass Spectrometry and Allied Topics
May 24-29, 1987, Denver, CO

THE APPLICATION OF THERMOSPRAY TO CYANOGENIC GLYCOSIDES.

R.T. APLIN, THE DYSON PERRINS LABORATORY, OXFORD UNIVERSITY, OXFORD, OX1 3QY, U.K., S.G. ERRINGTON, SCHOOL OF APPLIED CHEMISTRY, WESTERN AUSTRALIAN INSTITUTE OF TECHNOLOGY, BENTLEY, WESTERN AUSTRALIA.

Cyanogenic glycosides are currently isolated and purified by HPLC[1], but have as yet not been the subject of HPLC-MS analysis, although they have been shown to afford good characteristic CI[2], FAB[3] and FD[4] mass spectra.

+ve Ion thermospray analysis of the glycosides (I-IV) from 0.01M aqueous ammonium acetate solution affords NMH_4^+ as the base peak in their mass spectra. At high retarding electrode potential (275 volts) two abundant fragment ions are formed corresponding to the loss of the cyanhydrin moiety: MH^+-HOCRR'CN and MNH_4^+-HOCRR'CN.

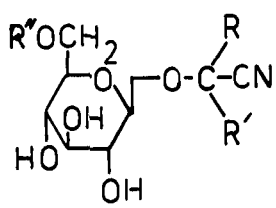

I $R = R' = CH_3$; $R'' = H$.

II $R = CH_3CHCH_3$; $R' = R'' = H$.

III $R = R'' = H$, $R' = Ph$.

IV $R = H$; $R' = Ph$; $R'' = 1,6$-linked glucose.

Combined HPLC-TSP using a C_{18} reverse phase column and MeOH: aq., 0.01MNH_4OAc; 15:85 provides both structural data and separation of mixed cyanogenic glycosides and the free sugars with which they are isolated.

References:

1. A. Nahostedt, Cyanide in Biology, Ed., B. Vennegland, E.E. Conn, C.J. Knowles, J. Westley and F. Wissing, (1981), Academic Press, p. 145.
2. T. Cairns and E.G. Siegmund, (1982), Biomed. Mass Spectrom., 9, 307.
3. F.A. Mellonand and G.R. Fenwick, (1984), ibid., 11, 375.
4. P.A. Driefuss, G.E. Wood, J.A.G. Roach, W.C. Bromley, D. Andozejewski and J.A. Sphon, (1980), 7, 201.

Presented at the 35th ASMS Conference on Mass Spectrometry and Allied Topics
May 24-29, 1987, Denver, CO

ION SPRAY API LC/MS AND LC/MS/MS DETERMINATION OF SULFOCONJUGATED ANABOLIC STEROIDS IN THE HORSE

Tina M. Pawlowski, Lars Weidolf, Edgar Lee, and Jack Henion, Drug Testing and Toxicology, New York State College of Veterinary Medicine, Cornell University, 925 Warren Drive, Ithaca, New York 14850

Steroids are frequently abused to affect the outcome of sports events, such as horse racing. It is necessary to monitor these compounds and their metabolites in biological fluids. This is complicated by metabolites that are usually polar and involatile. Conjugates of glucuronic or sulphuric acid, for example, pose unique analytical problems which are difficult to solve by established methods. It is advantageous to preferentially isolate, detect, and confirm intact conjugates. This has been demonstrated for the intact sulfoconjugates of the anabolic steroids of boldenone (BOS), testosterone (TS), 19-nortestosterone (NTS), and related steroids in horse urine using a selective solid phase extraction (SPE) procedure (1) and subsequent analysis by micro-bore LC/MS and LC/MS/MS via an unheated ion spray interface (2).

Micro-bore HPLC separation of the conjugates is done on a Shandon ODS-Hypersil (5um, 1mm x 100mm) column. The mobile phase is methanol/2.5 mM ammonium acetate (40/60) and the flow rate is 40uL/min. The eluent is transferred directly from the column to the ion spray interface designed for micro-bore HPLC. To monitor the negative ions of intact sulfoconjugates, the interface electrode voltage is -3 kV. Ions are focussed from the API source of a triple quadrupole mass spectrometer (Sciex TAGA 6000E) into the mass analyzer. Argon is used for collision induced dissociation (CID) and the collision energy is 70eV.

By API LC/MS SIM, the molecular weights of the intact sulfoconjugates $[M-1]^-$ were determined (4lng on-column). CID spectra of the $[M-1]^-$ ions of monosulfates are quite simple. The aliphatic 17β-sulfates, of BOS, TS, and NTS, in addition to the $[M-1]^-$ ion, give a base peak at m/z 97 ($[HSO_4]^-$) with an accompanying m/z 96 fragment (possibly $[SO_4^-]$). The m/z 80 is a prominent fragment as well ($[SO_3^-]$). BOS and TS produce an abundant m/z 177 fragment, possibly due to the D-ring with an intact sulfate moiety ($[C_6H_9O_4S]^-$). The aliphatic 3β-sulfate dehydroepiandrosterone is unique because of its simple CID spectrum which consists of the $[M-1]^-$ and a base peak of m/z 97.

Estradiol 3-sulfate, an aromatic 3-sulfate, does not give an m/z 97 fragment, but a base peak at m/z 80 ($[SO_3^-]$). The neutral loss of m/z 80 with charge retention on the parent ion produces a "phenolate" fragment m/z 271 and subsequently a m/z 145 fragment ($[C_{10}H_9O]^-$) (3). The lack of m/z 97 for this aromatic sulfate clearly distinguishes it from an aliphatic sulfate.

The unheated ion spray system proves to be advantageous in determining disulfates such as 17β-estradiol disulfate which produces only the $[M-2]^{2-}$ ion at m/z 215 in the LC/MS SIM mode. CID of m/z 215 produces a complex spectrum with characteristic fragments of aromatic 3-sulfates and aliphatic 17B-sulfates. A low abundance fragment at m/z 350 is observed and is probably due to $[M-2-SO_3]^-$ (Figure 1).

The LOD for LC/MS SIM is 10-12 pg on-column. For SRM the LOD is 110-370pg on-column. Full-scan daughter ion spectra of the molecular ions were obtained from 5-10 ng of compound on-column. The dynamic range of aromatic and aliphatic sulfates was found to be linear (R=0.998) over 2.4 orders of magnitude with the response for both being equal.

Confirmation of boldenone sulfate is obtained from 2mL of 10-408 hour post-administration horse urine samples with full-scan daughter ion spectra (Figure 2). The levels of Boldenone sulfate in the 10 and 408 hour urine samples had previously been determined to be 0.76 and 0.4 ug/mL.

Presented at the 35th ASMS Conference on Mass Spectrometry and Allied Topics
May 24-29, 1987, Denver, CO

REFERENCES
1. Weidolf, L,; Henion, J.D. Manuscript in preparation.
2. Bruins, A.; Covey, T.; Henion, J. 34th Annual Conference on Mass Spectrometry and Allied Topics, June 8-13, 1986, Cincinnati, OH. Abstracts, p. 585-586.
3. Rudewicz, P.; Straub, K.M. Anal. Chem. 1986, 58, 2928-2934.

Figure 1

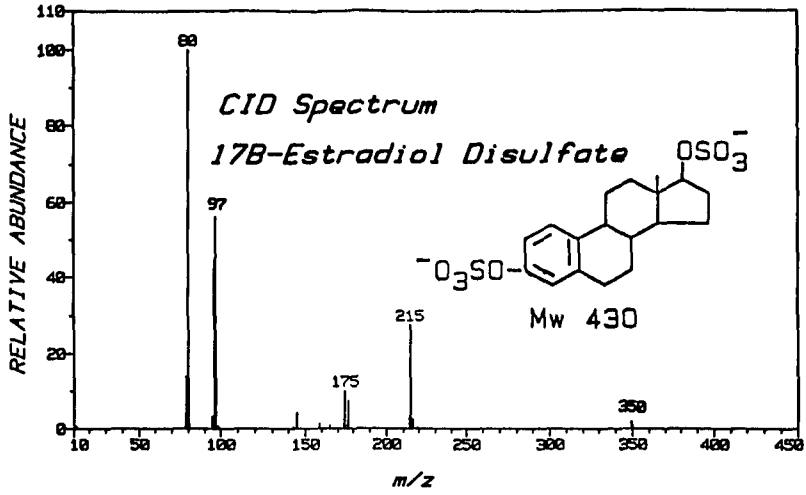

Figure 2

TOTAL ION CHROMATOGRAM
10-Hour Post-Dose Horse Urine Extract
(0.76ug/mL)

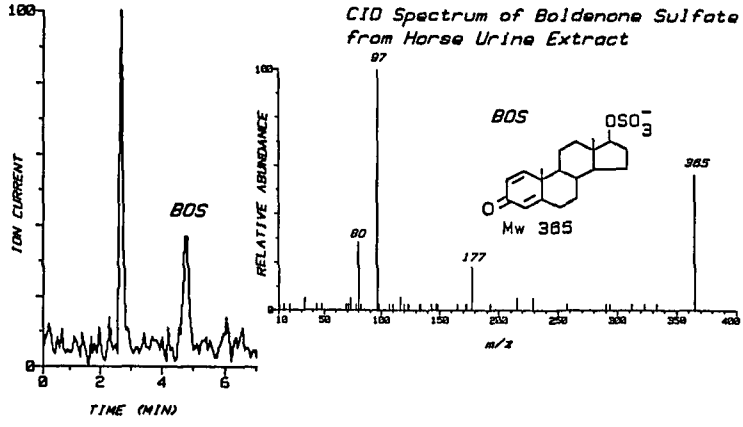

Presented at the 35th ASMS Conference on Mass Spectrometry and Allied Topics
May 24-29, 1987, Denver, CO

DIRECT INTERFACING OF CAPILLARY SUPERCRITICAL FLUID CHROMATOGRAPHY WITH MASS SPECTROMETRY UNDER ELECTRON AND CHEMICAL IONIZATION

Shih Hsein Hsu, Edgar D. Lee and Jack D. Henion, Drug Testing and Toxicology, New York State College of Veterinary Medicine, Cornell University, 925 Warren Drive, Ithaca, New York 14850

INTRODUCTION

Capillary SFC/MS provides the potential for a highly selective and sensitive chromatographic technique utilizing the distinct chromatographic properties of a supercritical fluid. This study describes an investigation of capillary supercritical fluid chromatography and its combination with mass spectrometry for the separation and confirmation with electron ionization (EI) and chemical ionization (CI) mass spectrometry (1-3).

EXPERIMENTAL

The mass spectrometer used was a Hewlett-Packard model 5985B GC/MS equipped with a dual EI/CI ion source. The chromatographic system consisted of a Brownlee dual-syringe micropump combined with a Hewlett--Packard model 5840 GC oven, Valco micro-loop injector, and 50 um id. x 10 m fused-silica capillary column. The capillary column was directly interfaced to the HP5985 ion source. A stainless steel 100 mesh (screen) was placed in between the interface line and ion source for declustering the N_2O adduct ions. Sample injection was made in the split mode with a different diameter of capillary column as split controller. The separations were achieved by programmed pressure gradient elution of the Brownlee pump.

RESULTS AND DISCUSSION

The effect of varying the electron energy and emission current of the filament were investigated. It was observed that higher emission current provides higher sensitivity and that EI spectra were best obtained at lower electron energy (40 ev). The effect of the source conditions on fluid phase clustering was studied by varying the source pressure at different ion source temperatures. It appears that increased ion source temperature lowers the amount of cluster ions of the mobile phase. By applying a stainless steel mesh in between the interface line and ion source, cluster ions (m/z 88, 132, 176, 220...) of N_2O can be efficiently broken up which enables the mass scan range to begin at 45 Daltons (Fig. 1). When ion clustering was reduced, increased sensitivity was observed. Sensitivity achievable by EI (low pressure) conditions on this system appears less for most compounds than that by CI (high pressure) conditions. Under CI conditions, EI-like spectrum can be obtained by a charge exchange ionization process with helium as make-up gas (Fig. 2). The disadvantage of the charge exchange ionization process is that EI/CI mixed spectra are often obtained.

REFERENCES

1. S.C. Subba Rao and C. Fenselau, Anal. Chem. 50, 1978 (511-15).
2. D.F. Hunt and P.J. Gale, Anal. Chem., 56, 1984, (1111-1114).
3. R.D. Smith, J.L. Fulton, R.C. Petersen, A.J. Kopriva and B.W. Wright, Anal. Chem., 58, 1986 (2057-64).

Presented at the 35th ASMS Conference on Mass Spectrometry and Allied Topics
May 24-29, 1987, Denver, CO

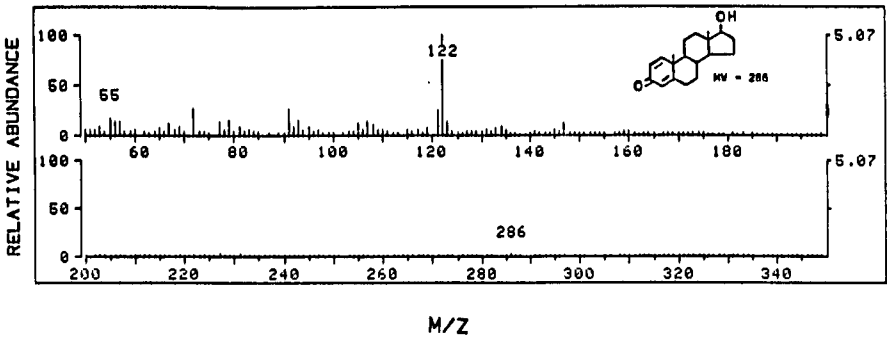

FIGURE 1. EI SFC/MS MASS SPECTRUM OF BOLDENONE

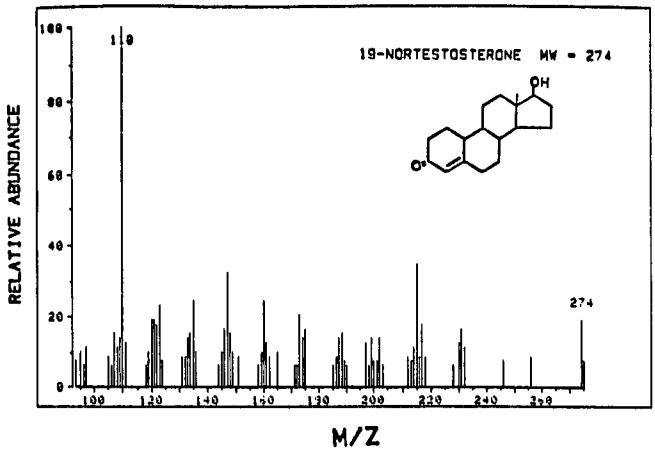

FIGURE 2. CHARGE EXCHANGE/HELIUM SFC/MS
MASS SPECTRUM OF 19-NORTESTOSTERONE

Presented at the 35th ASMS Conference on Mass Spectrometry and Allied Topics
May 24-29, 1987, Denver, CO

THE FORMATION OF IONS IN THERMOSPRAY LC/MS

David A. Kidwell, John H. Callahan, and Mark M. Ross
Chemistry Division, Naval Research Laboratory, Washington, DC 20375

We have an interest in analyzing polar toxins and drugs of abuse at the low nanogram levels. Due to their polar nature, thermospray LC/MS was the only viable method of analysis. However, the required sensitivity is often difficult to achieve. To achieve optimum sensitivity, we have investigated some of the methods by which ions are produced and detected by thermospray.

Our inability to observe tetrodotoxin prompted us to examine other zwitterionic and highly-polar salts with our thermospray interface (see Table 1). The thermospray mass spectrum of an equal molar mixture of tetraalkyl ammonium salts shows almost a complete absence of tetramethyl ammonium ion at m/z 74 in both the discharge-on and discharge-off modes of ionization. Likewise, several of the salts listed in Table 1 are not observed. However, all of the compounds listed in Table 1 are observed with a Finnigan TSP 46 instrument. The reason for this difference is not readily apparent but could be related to how the vaporizer is heated.

A diagram of the Vestec thermospray source is shown in Figure 1. Ion trajectories were modeled with the program SIMION in an effort to improve its performance. Various modifications, as listed in Table 2, were then made to the ion source, guided by the program SIMION. No increase in sensitivity could be achieved with these modifications. We believe that electrostatic fields have little effect due to the high pressure in the ion source. Ions escape the source by mass flow which is governed by the exit hole diameter versus the source pumping. The exit hole cannot be increased significantly without increasing the analyzer pressure.

Regardless of the mechanism for ion formation, due to the many collisions with neutral solvent molecules in the high pressure source, the ions must have a higher proton affinity to survive without neutralization. This gives thermospray its CI-like character.

A Vestec thermospray source can be operated in two ionization modes: discharge-off and discharge-on. The spectrum obtained with the discharge on has significantly higher background than with the discharge off. This increase in background effectively limits the sensitivity of the discharge-on mode of ionization in thermospray. We have observed this increase in noise at every mass with many compounds and have attributed it to fast neutrals striking the electron multiplier. With the discharge on, many more solvent ions are created allowing more fast neutrals to be formed in the high pressure region of the ion source.

Initial Vestec ion sources did not have a repeller. Claims were made that a repeller would not work with this source design. Our results substantiate these claims. The effects of a repeller on the mass spectra of morphine are shown in Figure 2. The ratio of the protonated molecular ion to the solvated ion does not change with the repeller voltage. Also, there is a strong decrease in sensitivity with increasing repeller voltage. This is always observed. Some molecules fragment with moderate repeller voltages, but the decrease in sensitivity outweighs the additional information that fragments provide.

CONCLUSIONS

The sensitivity of thermospray is highly dependent on source design and operating conditions. The factors that affect sensitivity still must be delineated. The ions produced by thermospray are not affected by electric fields due to the high source pressures. Ions escape from the source primarily by mass transfer with the solvent molecules. A repeller, with the Vestec source design, has little affect on fragmentation for many compounds and when fragmentation does occur sensitivity decreases significantly.

Presented at the 35th ASMS Conference on Mass Spectrometry and Allied Topics
May 24-29, 1987, Denver CO

Table 1- Relative Intensities of Ammonium Ions by Thermospray in the Discharge-on Mode

Compound	Ion Structure	Relative Intensity
Tetramethylammonium Bromide	$(CH_3)_4N^+$	0.03
Tetraethylammonium Bromide	$(CH_3CH_2)_4N^+$	0.64
Tetrapropylammonium Bromide	$(CH_3CH_2CH_2)_4N^+$	0.85[a]
Tetrabutylammonium Bromide	$(CH_3CH_2CH_2CH_2)_4N^+$	0.98
Tetrapentylammonium Bromide	$(CH_3CH_2CH_2CH_2CH_2)_4N^+$	1.00
Taurine	$\overset{+}{N}H_3CH_2CH_2SO_3H$	----
Betaine	$(CH_3)_3\overset{+}{N}CH_2CO_2H$	----
Choline Chloride	$HOCH_2CH_2\overset{+}{N}(CH_3)_3$	----

[a]The contribution to m/z 186 from the tetrapropylammonium ion and from the tetrabutylammonium fragment were calculated from spectra of individual compounds.

FIGURE 1

SCHEMATIC DIAGRAM OF THE MODIFIED THERMOSPRAY SOURCE

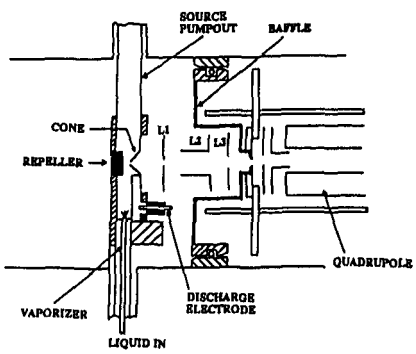

FIGURE 2

DISCHARGE-ON THERMOSPRAY MASS SPECTRA OF MORPHINE

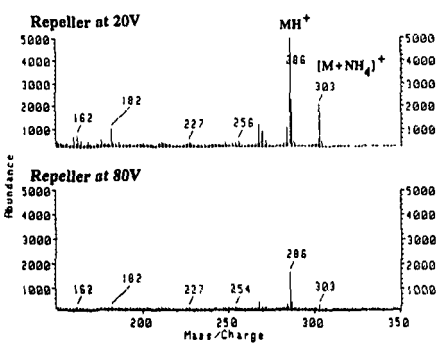

TABLE 2

Modification	Results
Replaced cone with flat plate	No change in spectra
Increased exit hole in ion source	Analyzer pressure increase - No increase in sensitivity
Installed repeller	Sensitivity decrease if repeller on
Increased hole in lens 1	No change in spectra
Installed high-voltage extraction grid between cone and lens 1	No increase in sensitivity
Increased voltage on lens 2	No change in spectra
Removed lens 3	No change in spectra
Decreased exit hole in baffle	Small decrease in sensitivity

m/z 286 and m/z 303 versus Repeller Voltage

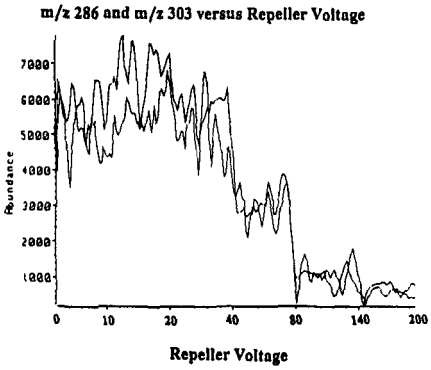

Presented at the 35th ASMS Conference on Mass Spectrometry and Allied Topics
May 24-29, 1987, Denver, CO

Mass Spectrometry Analysis of Esperamicins

George R. Dubay,[1] Gary S. Groenewold,[2] Jerzy Golik
Bristol-Myers Pharm. Res. and Dev. Div.
Wallingford, CT 06492

Structure elucidation of Esperamicin A1 (Figure 1), a novel extremely potent antibiotic, presented a challenge in which mass spectrometry played a vital role. The esperamicins were isolated from Actinomadura verrucosaspora and they were determined to be high molecular weight (MW > 1000 μ) and chemically labile as well as highly toxic. Esperamicins are produced in small amounts by the organism so samples of only 50 mg were initially available for full characterization. The compounds were not analyzable by x-ray diffraction and the amorphous solid contained some residual solvents. Thus, mass spectrometry was required to establish the molecular weight and elemental composition of these compounds.

The initial low resolution FAB-MS experiments were performed in several matrices and the results varied depending on the matrix and the solvent used for the analysis. This was an indication that the compound was chemically labile under FAB experimental conditions. Attempts at chemical manipulation of the molecule at times resulted in uncontrolled degradation. Thus, esperamicins were found to be chemically labile within and outside of the mass spectrometer.

A definitive assignment of the molecular ion was needed by a technique other than FAB-MS. Once the molecular ion was known then other experiments could be designed to improve spectral quality. The development of thermospray ionization (TSP) for mass spectrometers which could scan to mass 1500 μ or greater allowed us to determine the pseudomolcular ion at low resolution. TSP-MS was performed with and without buffers and with and without organic modifiers. Here, the results were reproducible. The $(M + H)^+$ ion for Esperamicin A1 was observed at M/Z = 1325. The degradation products, Esperamicins C & D, were found to have $(M + H)^+$ ions at M/Z = 932 and 772, respectively. This was consistent with sugar losses observed. Thus, TSP-MS provided crucial information.

Immediately, FAB-MS was performed in as many matrices as possible. The most useful results were obtained when m-nitrobenzyl alcohol was used. High resolution peak matching gave extremely accurate results for the pseudomolecular ions (less than 3 ppm for all compounds - Table 1). It was possible to limit the possible elemental compositions from our knowledge of the number of nitrogens and sulfurs, the NMR and other analytical data. In this way the elemental composition was confirmed despite the high mass of the compounds.

These mass spectrometry experiments and others not described were used with NMR, IR and other data to solve this structural riddle. The high resolution FAB and TSP-MS were used in a complimentary way to help solve this difficult problem.

1. current address; Dept. of Chemistry, P.M. Gross Chem. Lab., Duke University, Durham, NC 27706
2. current address; Idaho Natl. Eng. Lab., P.O. Box 1625, Idaho Falls, ID 83415

Presented at the 35th ASMS Conference on Mass Spectrometry and Allied Topics
May 24-29, 1987, Denver, CO

Esperamicin A1

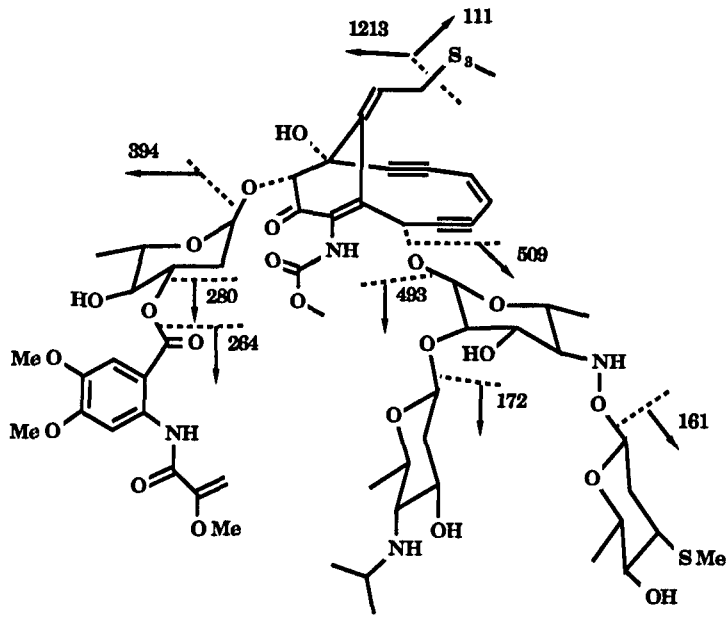

M+H ion = 1325.4229
measured +0.3 ppm

Figure 1

Table 1

FAB-MS in NOBA

Nominal Mass	HRMS FAB	Elementals	ppm (from calc)
1325	1325.4229	C59H81N4O22S4	+0.3
1213	1213.4746	C58H77N4O22S	-0.3
932	932.2799	C40H58N3O12S4	-0.3
772	772.2240	C33H46N3O12S3	-0.5
601	TSP/MS only		
509	509.2534	C22H41N2O9S	+0.3
493	493.2599	C22H41N2O8S	+3.2
333	333.2020	C15H29N2O6	-1.8
Sugars by EIMS			
192	192.0826	C8H16O3S	+3.1
203	203.1522	C10H21N1O3	+0.5

Presented at the 35th ASMS Conference on Mass Spectrometry and Allied Topics
May 24-29, 1987, Denver, CO

DEVELOPMENT OF A MAGIC LC/MS SYSTEM

A. APFEEL AND B. NORDMAN, HEWLETT-PACKARD CO., PALO ALTO, CA.

Monodispersed Aerosol Generation Interface Combining Liquid Chromatography and Mass Spectroscopy (MAGIC) is a technique which provides a viable approach for generating Electron Impact (EI) spectra from samples separated by High Performance Liquid Chromatography (HPLC) without compromising either technique. This exciting possiblility has lead to increased interest in the possibilities and limitaitons of the approach.

MAGIC LC/MS operates by initially generating an aerosol from the HPLC effluent which consists of a narrow range of droplet sizes of approximately 10um diameter. These droplets pass through a dissolvation chamber inwhich the volatile solvent is evaporated leaving a particle of non-volatile analyte. The mixture of vapor and particle enters a two stage momentum separator in which the relatively low (and consequently momentum) solvent molecules are pumped away. The greatly enriched stream of particles continues into the mass spectrometer source chamber where the particles colide with a heated surface and are flash vaporized. The resulting free molecules are then available for ionization by standard techniques (EI or CI). The spectra which are generated in this manner are identical to standard EI spectra and are library-searchable.

The critical parameters in the operation of the system are involved in the nebulization process, the desolvation temperature and pressure, and the source temperature, which all exhibit optimum conditions. The system can be run with all standard mobile phases used in HPLC with the restriction that buffer systems must consist of volatile low molecular weight buffers. Flow rates in the HPLC can be varied from 0.1 to 1.0 mL/min.

The performance of the system appears to be comparable to GC/MS for a variety of compounds, in terms of both sensitivity and selectivity (spectral quality). Using caffeine as a test probe, minimum detectable quantities have been found to be 50pg for single ion monitoring and 2ng for full scan (50-300amu). A wide range of compounds have been screened for applicability, including steroids, amino acids, various drugs, azo-dyes, carbamate pesticides, triazine pesticides, phenylurea herbicides and EPA Appendix IX compounds. The latter three compound groups are shown as complete applications.

In conclusion, MAGIC LC/MS offers unique possibilities for combining two otherwise poorly compatible techniques in a straight-forward manner. The great potential of this approach suggests the potential for the growth of LC/MS in a manner analogous to that of GC/MS.

Presented at the 35th ASMS Conference on Mass Spectrometry and Allied Topics
May 24-29, 1987, Denver, CO

FIELD LIMIT FOR ION EVAPORATION FROM MOBILITIES OF CHARGED THERMOSPRAY DROPLETS

Viswanatham Katta and Alan L. Rockwood
Department of Chemistry, University of Houston,
Houston, Texas-77004.

OBJECTIVE: In thermospray interface for LC\MS ion evaporation occurs from charged droplets. The research objective is to determine the electric field required for ion emission, at the surface of the charged droplet, from the mobilities of the droplets measured in a time-of-flight, flow-type drift tube equipped with a mechanical chopper to pulse the droplets.

INTRODUCTION: Ion evaporation or emission from charged droplets becomes energetically favorable, when the electric field at the surface reach a sufficient level E_i. Once this field is reached, further evaporation of ions and neutrals take place, so as to maintain the field strength constant. By experimentally measuring the mobilities [1] of such droplets, the field strength at the surface could be determined.

EXPERIMENTAL APPROACH: An indirectly heated vaporizer was used in the present experiments. As the droplets exiting the vaporizer have high masses (m/z $\sim 10^6$-10^7) and high momenta, a mechanical chopper was used to pulse them into the drift tube (Figure 1). As the initial droplets have a distribution of sizes and charges, they were sampled away from the vaporizer (5.5 cm), such that they evaporate and reach final state before reaching the chopper (at least an order of decrease in radius). As the spray divergence increases at such distances, a beam of droplets with a small cross sectional area was obtained by use of skimmers. A combination of LED-photodiode, mounted inside the chamber, provided a 'start time' signal for drift time measurements. Observed peak times were corrected for timelag between gating pulse and photodiode signal. Figure 2 is ablock diagram showing the relation between various components in the drift tube. All the experiments were done with the vaporizer temperature 197-200 °C and a flow rate of 1.5 mL/min. Collector voltage (drift field) was varied to change the drift times.

RESULTS AND DISCUSSION: The resolution of the drift tube was reasonably good with a peak width (FWHM) of 1.03 ms for a gating pulse width of 0.53 ms. Mobilities were determined from the slope of a straight line, obtained by plotting $1/t_{obs}$ versus collector voltage (drift field), where t_{obs} is the observed peak time (Figure 3). Highest mobility (reduced) observed was 0.5 $cm^2\ V^{-1}\ s^{-1}$, which is smaller than the mobilities reported for cluster ions. Assuming the droplet to be a hard sphere, and using a molecular ion limit for the droplet, the reduced mobilities were directly correlated with surface charge densities and field strengths.

Interestingly, surface field strengths determined for ammonium acetate, sulfonated azo dyes and other electrolytes fall in a narrow range (7.3×10^8 to 9.1×10^8 V/m), even with a large variation in concentrations of solutions used (Tables 1 and 2). This indicates that the sampled droplets have reached a final stage, and the field remained constant. The observed fields fall in the same range of the critical fields required for creating surface instabilities [2]. Such instabilities produce microprotrusions at the surface with a field enhancement of an order of magnitude or more. As the fields required for extracting an ion from condensed phase were

expected to be lower than 10^{10} V/m [3], ion emission from such protrusions becomes energetically favoured and even may occur spontaneously.

CONCLUSIONS: Suface field strengths determined for various electrolytes appear to be constant (7.3×10^8 V/m to 9.1×10^8 V/m), and thus might actually correspond to a rate limiting step of creating instabilities at the droplet surface. Once the fields reach this limit, microprotrusions are formed, and ion emission occurs from such protrusions as a natural process.

ACKNOWLEDGEMENTS: We thank Dr. Marvin L Vestal for helpful discussions. This work is funded by National Science Foundation and Robert A. Welch Foundation.

REFERENCES: 1. Mason E. A., in PLASMA CHROMATOGRAPHY, Carr T. W. Ed, Plenum (1984).
2. Geissmann U. and Rollgen F. W., *Int. J. Mass Spectrom. Ion Proc.*, 1981, *38*, 267.
3. Vestal M. L., *Mass Spectrom. Rev.*, 1983, *2*, 447.

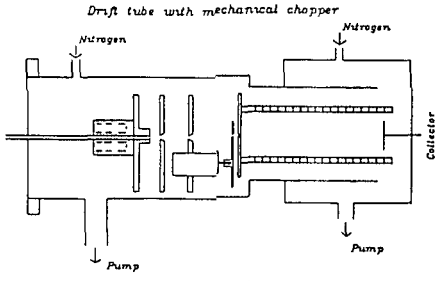

Figure 1

Block diagram showing the relation between various components

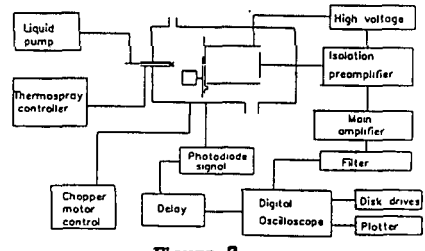

Figure 2

Figure 3

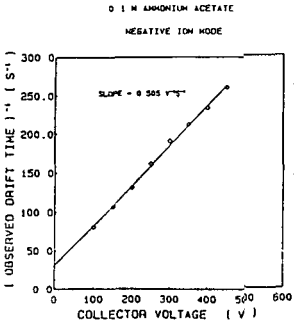

Table 1

MOBILITIES AND FIELD STRENGTHS OBTAINED FOR AMMONIUM ACETATE

Conc M	Reduced mobility cm²V⁻¹s⁻¹	Surface field strength 10^8 V/m	Ion type
0.6	0.48	8.33	−
0.1	0.49	8.48	−
0.06	0.50	8.69	−
0.01	0.49	8.47	−
0.001	0.49	8.37	−
0.5	0.53	9.00	+
0.1	0.53	9.00	+
0.06	0.50	8.69	+
0.01	0.48	8.19	+

Table 2

MOBILITIES AND SURFACE FIELD STRENGTHS OBTAINED FOR ELECTROLYTES (POSITIVE ION MODE)

Electrolyte	Conc. (M)	Reduced mobility cm²V⁻¹s⁻¹	Surface field strength 10^8 V/m
Direct red 2	10^{-5}	0.47	7.99
	10^{-4}	0.45	7.70
Direct blue 33	10^{-3}	0.44	7.44
	10^{-4}	0.49	8.34
MPEG-1900*	10^{-2}	0.49	8.34
NaOAc	10^{-3}	0.47	7.99
	10^{-2}	0.46	7.80
NH_4Cl	0.1	no definite peak	

* Methoxy polyethylene glycol-1900 in 0.05 M NH_4OAc

Presented at the 35th ASMS Conference on Mass Spectrometry and Allied Topics
May 24-29, 1987, Denver, CO

The Utility of Solution Electrochemistry MS for Enhancing Thermospray Spectra and Elucidating Electrochemical Redox Processes

T.A. Getek, Department of Chemistry
University of Houston, Houston, TX 77004

Overview

The ability of Thermospray mass spectrometry (TSMS) to examine solutes of interest in aqueous solutions with 0.1 M ammonium acetate makes it ideal for interfacing to an electrochemical flow cell. A block diagram for this method of solution electrochemistry mass spectrometry (SECYMS) is displayed in Fig. 1. It is important to note that the coulometric cell is external to the Thermospray (TS) source; that is at atmospheric pressure. The criteria for a coulometric cell have been discussed (1). An additional feature of the cell was that segregation of the auxiliary and working electrode chambers. This was accomplished in the newly constructed coulometric cell by Nafion film.

Advantages of Utilizing SECYMS

The technique of SECYMS may be useful for identifying compounds which normally exhibit a single parent molecular peak ($[M+H]^+$) by fragmenting or dimerizing the solute of interest electrochemically in the SECYMS cell. The compound *o*-aminophenol (OAP), MW=109, produces a spectral peak at m/z 110. After oxidation at varying anodic potentials, the m/z 110 decreases and spectral peaks indicating the oxidation products grow in (Fig. 2). The selective ion monitoring (SIM) of these products may act as an additional fingerprint in identifying OAP.

As reported earlier (1), SECYMS may be utilized to enhance spectra in TSMS. The example of hydroquinone (HQU) was chosen to examine the feasibility of SECYMS to assay intractible compounds in TSMS. This assay was performed by oxidizing HQU (MW=110) to quinone (QU), MW=108, and integrating the peak area for m/z 124 after direct injection with 0.1 M ammonium acetate. Normally HQU gives no TS spectral peaks either in the positive or negative ion modes. The spectral peak at m/z 124 is indicative of QU which may have undergone a reaction with ammonium acetate. It is speculated the m/z 124 is the protonated form of a amine attachment to QU. The peak area vs. HQU injected gave a correlation coefficient (R) of 0.997 over a range of 6.23 to 0.25 μg injected. The corresponding coulometric response (μA, peak height) gave a R of 0.994.

The oxidation products of acetaminophen (APAP), MW=151, were studied by SECYMS at varying pH and electrochemical potential. The TS spectra tracked the Faradaic current produced by the coulometric cell exactly. An example is given for pH 6.5 in Fig. 3. The products observed included m/z 150 and 108 for the N-acetyl-*p*-quinoneimine and peaks at m/z 124 were indicative of quinone. Other reported examples of electrochemical-TSMS of solutes of interest include N,N-dimethylaniline (2) and biological samples by tandem MS (3).

1. Getek, T. *34th ASMS Conference on Mass Spectrometry and Allied Topics*, Cincinatti, June, 1986, 756.

2. Hambitzer, G.; Heitbaum, J. *Anal. Chem.* 1986, *58*, 1067.

3. Brajter-Toth, A.; Volk, K. *The 1987 International Electroanalytical Symposium*, Schaumburg, IL, 1987.

Presented at the 35th ASMS Conference on Mass Spectrometry and Allied Topics
May 24-29, 1987, Denver, CO

Fig. 1

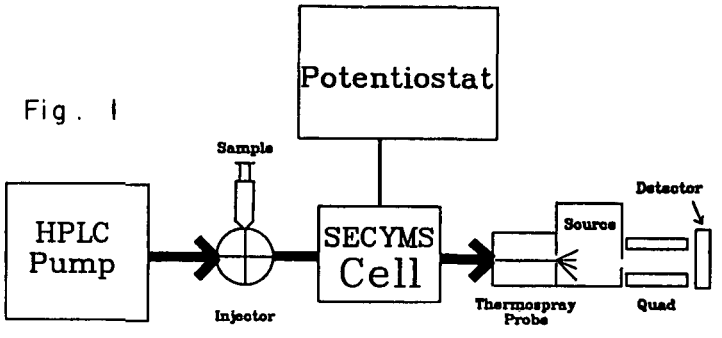

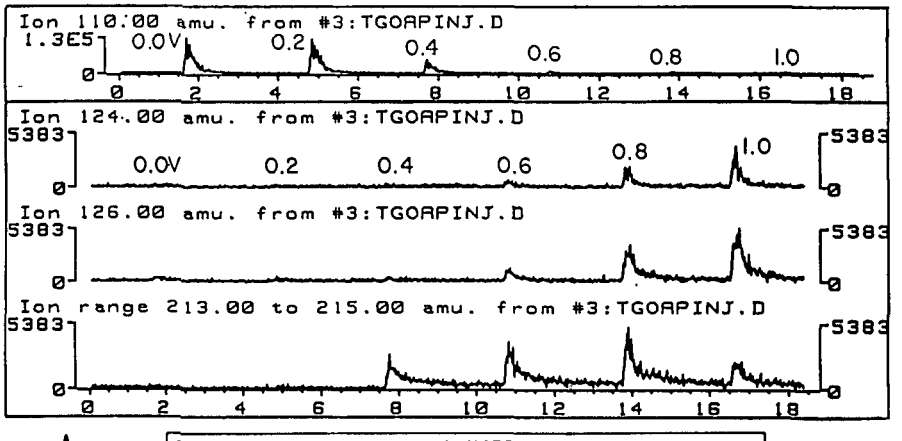

Fig. 2

Fig. 3

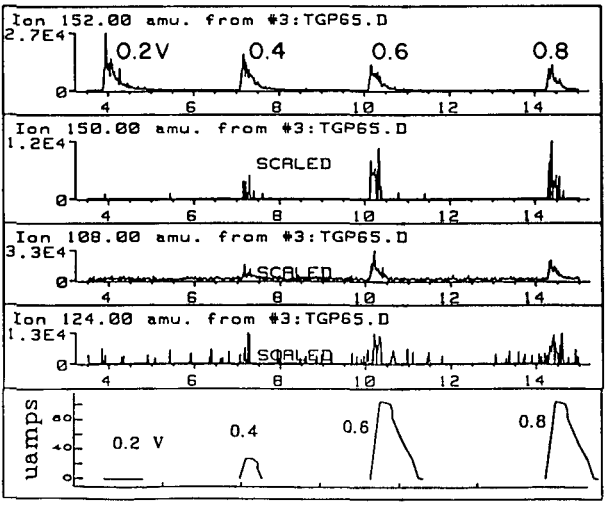

pH
6.5

Presented at the 35th ASMS Conference on Mass Spectrometry and Allied Topics
May 24-29, 1987, Denver, CO

VANILLOID METABOLITE IDENTIFICATION BY STABLE-ISOTOPE-CLUSTERS (SIC)-MS

R. J. Strife, J. H. Gardner, W. K. Sietsema, R. D. Stratton
Procter & Gamble Miami Valley Labs, Cincinnati, OH 45239-8707

Introduction -- The vanilloid capsaicin has long been known as the primary pungent component of chile peppers. It stimulates unmyelinated nerve fibers which release substance P. The fibers then become refractory to further stimulus[1]. Olvanil (fig. 1), also a vanilloid, shows favorable analgesic and anti-inflammatory activity. It is slowly absorbed from an oral dose and extensively metabolized. Metabolites of olvanil were identified in order to design stable analogs and to find hypothesized active metabolites.

EI Mass Spectra of Vanilloids -- Previous work in the vanilloids field showed that GC/MS of TMS derivatives was a viable approach to this analysis[2]. The mass spectra of several vanilloid-TMS derivatives were examined and it was found in general they: 1) produce molecular ions of 10-100% relative intensity, with higher $M^{+\cdot}$ intensities for shorter N-alkyl chains, or N-alkyl chains with unsaturations; 2) cleave at the benzyl carbon (m/z 209 benzyl carbonium ion, often the base peak) and nitrogen (m/z 224); 3) undergo double methyl losses from the molecular ion, from m/z 209 and from m/z 224. These latter fragmentations violate even-odd electron rules. They are driven energetically by formation of the dimethyl siloxane ring with resonance stabilzation of the formed oxonium ion.

Stable Isotope Clusters (SIC) Approach -- This method, described formally for drugs in the early 1970's, consists of dosing a 1:1 mole ratio of a drug with a stable-isotope-labelled (SIL) analog. Metabolites retaining the label(s) will have characteristic doublets in the molecular ion, and hopefully other regions, of their mass spectra. Other advantages are conferred as well, and this topic was recently reviewed[3].

SIL-olvanil was synthesized by condensing 1-[^{13}C]-vanillin with [^{15}N]-hydroxyl amine, followed by catalytic reduction to labelled vanillamine. The amine was condensed selectively with 9,10-[^{2}H]$_2$ oleic acid via the unsymmetric anhydride, generated in situ from isobutylchloroformate, to give SIL-olvanil (fig. 1). After dosing, (including a small amount of benzyl [^{14}C]-labelled tracer), urine was collected at -70°, lyophilized, and methanol extracted. Fractions from crude, semi-prep RP-HPLC runs, and then analytical runs, were lyophilized and derivatized (BSTFA). Four advantages of SIC-MS were found in this single study.

CASE 1 -- Figure 2 demonstrates how metabolites are easily differentiated from urine matrix materials which dominate the gas chromatogram. The capillary GC peak for the metabolite N-vanillyl-adipamide was less than 0.5% of the total chromatogram. The odd molecular weight (nitrogen rule) and 2 dalton spacing of the molecular ion, doublets at m/z 209-210 (40%) and m/z 224-226 (55%), gave evidence for a [^{13}C,^{15}N]-labelled compound, missing the deuterium atoms. A conspicuously high ratio of m/z 75/73 (C_2H_7OSi, 38%, and C_3H_9Si, 100%) suggested aliphatic or carboxylic OTMS. The compound was identified as a product of omega-, beta-oxidation. Also identified was the metabolite N-vanillyl-succinamide, produced by an additional cycle of beta-oxidation.

CASE 2 -- Identification of products of extensive metabolism can sometimes be problematic. The mass spectral behavior of such components may be vastly different than the parent drug or its analogs. The metabolite N-vanillyl-succinimide (fig. 3) is an example of this, and SIC-MS simplified its identification. The odd molecular weight (307 daltons), 2 dalton spacing of the cluster, and double methyl loss all suggested a vanilloid derivative but the weak m/z 209 ion seemed inconsistent with that partial structure.

The final structure was arrived at by careful study of the spectrum of another metabolite, at a different GC t_R, N-vanillyl-succinamide (methyl ester, TMS derivative, $M^{+\cdot}$ m/z 339). This compound fragments by specific loss of methanol, to form a proposed cyclic succinimide ion at m/z 307 (fig.4). It shows no loss of methoxyl. Comparison of this m/z 307's daughter ions, between m/z 240-300, to the mass spectrum of the succinimide metabolite, showed simlarities (fig. 3). Subsequent synthesis of both metabolites proved the structures. The cyclic metabolite has not been previously reported for any vanilloid. Further experiments showed it did not arrive artifactually by dehydration of the succinamide.

Two other advantages were realized in this study as well. Several matrix components, probably products of catecholamine metabolism, had vanilloid-like spectra. They were ruled out as putative metabolites because of the absence of clusters in their spectra. Finally, vanillamine and N-acetyl vanillamine were shown to arise strictly from olvanil as the N-acetyl vanillamine contained clusters in its spectrum. A few scattered reports in the literature suggest vanillamine as an endogenous compound.

The metabolism found for Olvanil was consistent with previous reports from in-vitro systems (amide hydrolysis, omega-, beta-oxidation, vanillamine metabolism). The cyclic metabolite is a new finding. SIC-MS will continue to be useful, especially in the last three cases cited. MS-MS techniques are not useful in these circumstances.

1. S. H. Buck, T. F. Burks, P'col. Rev.,38(1986), 180-226.
2. S. Lee, Haksurwon Nonmunjip Cha'yon Kwahak P'yon, 22(1983), 139-181.
3. T. A. Baillee, A. W. Rettenmeier, J. Clin. P'col., 26(1986), 481-483.

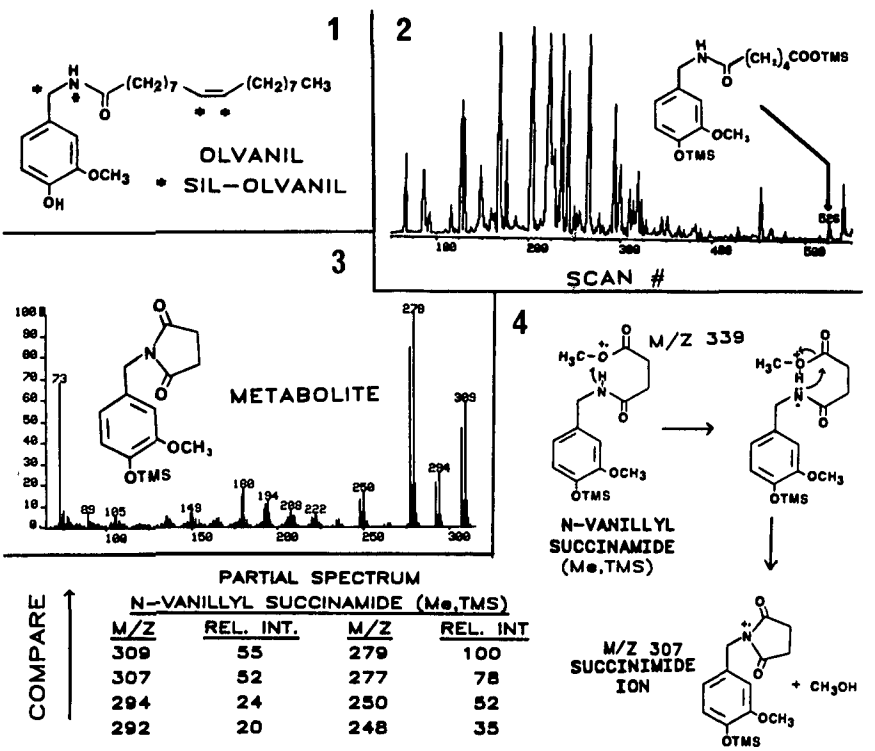

N-VANILLYL SUCCINAMIDE (Me,TMS)

M/Z	REL. INT.	M/Z	REL. INT
309	55	279	100
307	52	277	78
294	24	250	52
292	20	248	35

Presented at the 35th ASMS Conference on Mass Spectrometry and Allied Topics
May 24-29, 1987, Denver, CO

COMPARISON OF EC-NCI AND EI METHODS FOR THE DETERMINATION OF DEXAMETHASONE IN PLASMA. K. A. Kayganich, J. T. Watson, Departments of Chemistry and Biochemistry, East Lansing, MI, 48824, and J. J. Vrbanac, Department of Pharmacology, Medical University of South Carolina, SC, 29403

This paper compares preliminary results obtained by an EI method and an EC-NCI method for the quantitation of dexamethasone in plasma.

The dexamethasone suppression test, which has been used for years to identify patients with Cushing's syndrome, has also been proposed for the diagnosis of endogenous depression in patients. Following a 1 mg dose of dexamethasone, the cortisol levels in normal subjects are suppressed for the subsequent 24-hour period. The cortisol levels in depressed patients may be initially suppressed, but return to normal levels within a few hours. This behavior serves as the basis for the diagnosis of endogenous depression. A controversy exists, however, as to whether the pharmacokinetics of dexamethasone differ between normal and endogenously depressed patients. Radioimmunoassay (RIA) methodology has been used to monitor the dexamethasone concentrations in the plasma of patients over time. RIA, however, is subject to cross-reactivity with endogenous steroids and thus may give dubious results. Mass spectrometric methods are inherently more specific than RIA. Present GC/MS methods consist of the preparation of a derivative of dexamethasone followed by either EI, CI, or EC-NCI mass spectrometry. Another approach is to oxidize, rather than derivatize dexamethasone, to obtain a highly electrophilic analog of the compound which is then analyzed by GC/EC-NCI/MS.

Two different procedures were used to extract dexamethasone from plasma samples. The first procedure outlined below has the advantage of greater selectivity for dexamethasone, while the second procedure has the advantage of greater recovery of dexamethasone from the plasma.

A. Highly Selective Procedure: a plasma sample diluted to twice its original volume with distilled water is passed through a silica Bond-Elut column in series with a Waters C18 Sep-pak. Prior to addition of the diluted plasma the extraction cartridges are conditioned with 3ml of methanol followed by 4ml of distilled water. The silica phase is then removed and the C18 Sep-pak washed with 3ml of 5% methanol in water and 4ml of chloroform. Dexamethasone is then eluted with 2.5ml of chloroform/methanol (3:1).

B. Highly Efficient Procedure: the plasma sample is passed through a Waters C18 Sep-pak cartridge which has been preconditioned with 3ml of methanol and 4 ml of water, followed by a 5ml distilled water wash. Three ml of hexane is passed through the cartridge to remove the water. The steroid fraction is then eluted with 3ml of methanol.

The conversion of dexamethasone to an electrophilic compound by oxidation is the basis for the EC-NCI/MS method. Oxidation of dexamethasone extracted from a plasma sample is accomplished by reconstituting the dried plasma extract in 1 ml of dry CH_2Cl_2 and adding excess pyridinium chlorochromate (PCC) finely ground up with celite. To buffer the acid liberated during oxidation anhydrous sodium acetate is added. The reaction is stirred at room temperature for 3 hours. A Bond-Elut silica column is used to remove the excess reagent. The oxidized product of dexamethasone is eluted with 3.5 ml of ethylacetate, while the excess PCC remains on the column.

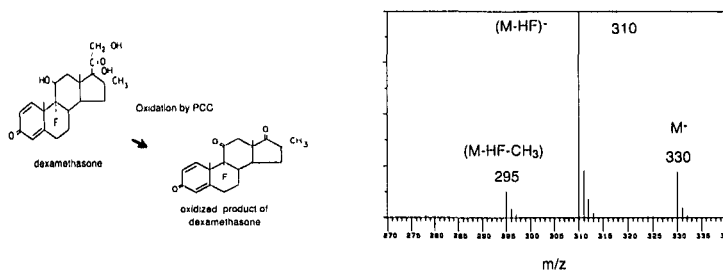

figure 1. (left) oxidative conversion of dexamethasone (right) EC-NCI mass spectrum of oxidized dexamethasone. MS conditions: 150°C, methane ca. 0.3 torr, 230 eV, 300 uA, multiplier 3000v, dwell time 250 ms/ion

The EC-NCI detection limit of oxidized dexamethasone on the HP5985 GC/MS is 30pg injected on-column with S/N=13

Presented at the 35th ASMS Conference on Mass Spectrometry and Allied Topics
May 24-29, 1987, Denver, CO.

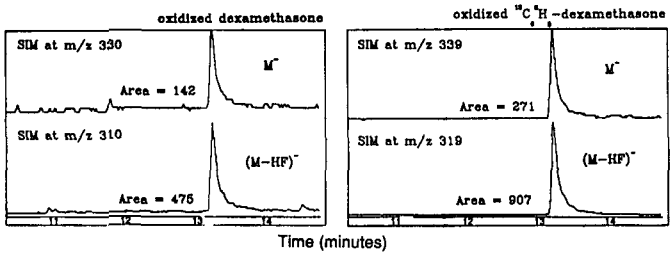

figure 2. Shown here is a SIM profile at m/z 330 and m/z 310 from the analysis of the oxidized plasma extract from a patient to whom dexamethasone had been administered. Prior to extraction by method A above, 40ng of the internal standard, $^{13}C_6$ - $^2H_3$ - dexamethasone, was added to the plasma sample. These data represent a plasma concentration of .61 ng/ml. On the order of 100 pg of oxidized dexamethasone was injected.

Derivatization of dexamethasone prior to GC/MS analysis is a common approach to prevent thermal decomposition of the side chain and to ensure good chromatographic properties. The derivative which gave the most satisfactory results from the standpoint of ease of preparation and completeness of formation was 3,20 - methoxime - 21 - trimethyl silyl (MO_2 -TMS) dexamethasone. To prepare the MO_2 - TMS derivative of dexamethasone which has been extracted from a plasma sample, the dried residue is reacted at 60°C in 20 ul of 100 ug/ul methoxyamine-HCl in dry pyridine. After four hours, the sample is dried under nitrogen and extracted from water into ethylacetate. After evaporation of the ethylacetate, 20 ul of BSTFA with 1% TMCS (Regisil) is added to the residue and heated to 80°C for one hour.

Only one chromatographic peak is obtained following derivatization of a dexamethasone standard by this procedure. Derivatization of the internal standard, $^{13}C_6$-$^2H_3$-dexamethasone, also resulted in only one peak.

The EI/MS detection limit of MO_2 - TMS dexamethasone as a pure standard is 100 pg with S/N = 5. The detection limit of the derivative in plasma is about 1 ng.

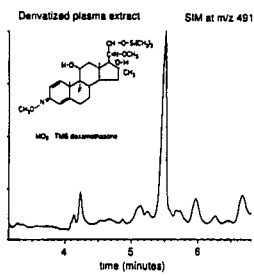

figure 3. The SIM profile above, which represents ca. 2 ng of dexamethasone, was obtained by extracting, according to procedure B, 20 ml of plasma spiked with dexamethasone to a concentration of 2 ng/ml, and derivatizing the extract to form the MO_2 - TMS of dexamethasone. HP5970B MSD conditions: 70eV, 2400v multiplier, m/z 491.25, dwell time 250 ms/ion

The EC-NCI method shows promise for detecting low levels of dexamethasone in plasma. Selectivity against the matrix components is provided by the ionization technique. The high sensitivity results from the oxidation of dexamethasone to an electrophilic product. Quantitation at the 1 ng/ml level in ca. 1ml plasma sample size has been achieved. In order to quantitate lower concentrations of dexamethasone in plasma, improvements in the oxidation yield and the extraction recovery of dexamethasone from plasma must be made.

Due to the matrix interferences and the small volumes of plasma samples, the sensitivity of the EI method is not adequate to quantitate real samples. An HPLC step will be incorporated to remove matrix interferences. This should lower the detection limit of MO_2-TMS dexamethasone in plasma.

Presented at the 35th ASMS Conference on Mass Spectrometry and Allied Topics
May 24-29, 1987, Denver, CO

DETERMINATION OF 3-QUINUCLIDINYL BENZILATE IN URINE, G. D. Byrd, L. T. Sniegoski, and E. White V, Center for Analytical Chemistry, National Bureau of Standards, Gaithersburg, MD 20899.

The compound 3-quinuclidinyl benzilate (BZ) is a potent muscarinic cholinergic antagonist. The effect of this agent on the brain and nervous system can produce incapacitation at very small doses (1-5 μg/kg) which makes BZ a serious hazard. In response to the scheduled destruction of U. S. military stockpiles of BZ and the increased potential for worker exposure, our laboratory has been working to develop a specific confirmatory test for human exposure to BZ. Since the exact relationship between BZ dose and levels of BZ and its metabolites in urine is not well known, it is desirable for the test to determine the amount of the parent compound in the urine as well as the two major metabolites quinuclidinol (Q) and benzilic acid (BA). Previous work in our laboratory demonstrated that BA and Q could be determined in urine at their target concentration of 5 ng/mL as based on a proposed maximum acceptable exposure level. The work described here demonstrates the recovery of the parent compound from urine at its target level and describes the results of a test for BZ exposure on several spiked and blank urine samples.

Only a small percentage of unmetabolized BZ is expected to be found in the urine of exposed persons. Estimates based on a proposed maximum acceptable exposure level have set a target concentration for BZ in urine of 0.5 ng/mL, ten times lower than that for the metabolites BA and Q. In the method developed to determine BZ, the urine sample is spiked with isotopically labeled BZ (3-quinuclidinyl-^{18}O-benzilate-d_5) and adjusted to pH 9-10. The BZ is removed by solid phase extraction using a C_{18}-packed cartridge. A water-acetonitrile solution is used to clean-up the sample and BZ is eluted with methanol. The eluent is dried and the residue is dissolved in a derivatizing agent to form the trimethylsilyl derivative for analysis by GC/MS. Quantitation is performed by monitoring the fragment ion $(C_6H_5)_2CO\text{-}TMS^+$ at m/z 255 and the analogous ion from the isotopically labeled internal standard at m/z 260. Figure 1 shows a chromatogram of an extract from a urine sample containing BZ at 0.5 ng/mL.

This method for the quantitation of BZ in urine has been incorporated into an analytical method for determining exposure to BZ that quantitates both the metabolites BA and Q in addition to the BZ for a 60 mL urine sample. Figure 2 shows a diagram that summarizes this method. The analytical method was tested on 8 different urines which were subdivided into various samples. Some of the subsamples were spiked with known amounts of the analytes near the target levels, others were spiked at ten times the target levels (which might be the amounts measured in case of an actual exposure), and other subsamples were blank. The test was designed to evaluate the analytical method with regard to variability of sample preparation, variability of GC/MS measurements, and variability from urine-to-urine. The validation test data showed that the sample preparation, GC/MS measurement, and urine-to-urine variabilities are approximately equal. The imprecision of a single measurement is approximately 15% at and above the target level. The validation test gave no false positives based on the target concentration limits and no false negatives were apparent.

Presented at the 35th ASMS Conference on Mass Spectrometry and Allied Topics
May 24-29, 1987, Denver, CO

Figure 1: SIM chromatogram of m/z 255 and m/z 260 from an extract of urine spiked with 0.5 ng/mL BZ.

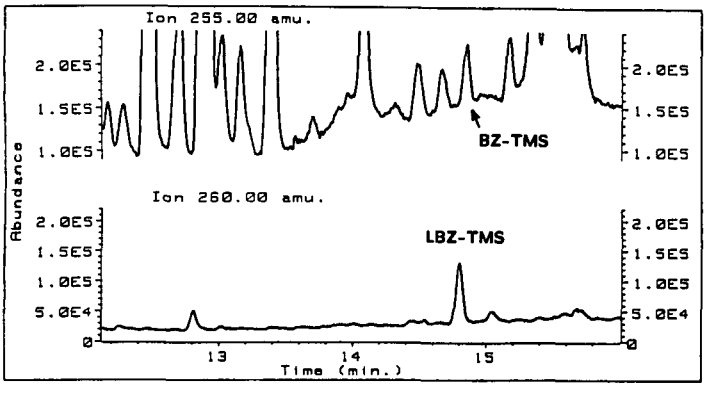

Figure 2: Summary of analytical method.

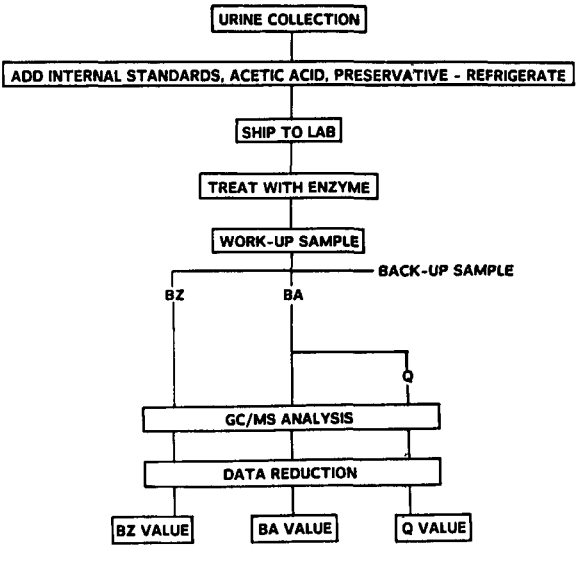

POSITIVE TEST DEFINED AS MEASURING EITHER:

1. **BZ AT A LEVEL OF 0.5 ng/mL OR HIGHER**
   OR
2. **BA AND Q AT LEVELS OF 5 ng/mL OR HIGHER**

Presented at the 35th ASMS Conference on Mass Spectrometry and Allied Topics
May 24-29, 1987, Denver, CO

THERMOSPRAY HPLC/MS STUDIES OF A PROSTAGLANDIN DERIVATIVE LUPROSTIOL AND ITS METABOLITES

C. A. WEERASINGHE, L. A. LOCKE AND R. WANG
SmithKline Beckman Animal Health Products
1600 Paoli Pike, West Chester, PA 19380

The use of mass spectrometry in the analysis of prostaglandins have been extensive and fruitful. GC/MS have been the technique very commonly used for both qualitative and quantitative analysis of this class of compounds. [1,2] However, elaborate sample preparation and derivatization are essential requirements prior to analysis and the latter may preclude the investigation of certain metabolic pathways in biological systems. Thermospray HPLC/MS can be an alternative technique, although lacks the sensitivity of the GC/MS, provide the advantage of an ease of operation, and the specificity, especially with the HPLC which maintains integrity of the chromatographic resolution. Thermospray HPLC/MS have been successfully applied in the analysis of compounds belonging to this class. [3,4]

In this presentation, we describe the application of on-line thermospray HPLC/MS technique in the analysis of Luprostiol and its metabolites in urine after the intramuscular administration of the drug to a dairy cow.

The urine sample was collected 0-12 hrs. following the administration of the drug. A 200 mL aliquot of the urine was utilized for the analysis. The pH of the sample was adjusted to 4.5 with 0.1N HCl, and the subsequent sample preparation involved: 1) solid-phase extraction (C-18 Bond Elut), 2) derivatization with CH_2N_2, 3) silica chromatography followed by 4) alumina chromatography. Both silica and alumina chromatography were performed on columns made in disposable pasteur pipets.

Thermospray HPLC/MS was done on a Finnigan 4600 coupled with a Vestec thermospray interface. The aerosol thermocouple of the interface was replaced with a repeller which was connected to an external power supply. This modification enabled us to monitor the effect of repeller voltage on the fragmentation. A mobile phase consisting of acetonitrile/0.1 ammonium acetate with a linear gradient of 9% to 65% over 30 minutes was used in the analysis. The samples were analyzed under following conditions: 1) thermospray ionization followed by +/- ion detection 2) thermospray/filament chemical ionization with +/- ion detection and 3) discharge ionization/repeller at 0, 80, 100 and 140 volts.

Negative ion detection with thermospray, filament on, was the most sensitive mode of analysis for Luprostiol and its metabolites. $(M + CH_3COO)^-$ was the major ion seen for the majority of the compounds analyzed. $(M-H)^-$ and some characteristic fragments (weak) were seen for some metabolites. In the positive ion mode, $(M+NH_4)^+$, $(M+NH_4-H_2O)^+$ and $(M+NH_4-H_2O)^+$ were seen for some compounds. Spectra of Luprostiol in negative and positive ion modes are given in Figures 1 and 2 respectively. Several metabolites of Luprostiol were identified with this procedure. The technique provides the following advantages:1) simplicity of operation, 2) provide molecular ion data, molecular ion (acetate adduct) being the base peak for the majority of compounds, 3) simplicity of spectra which can be helpful in thermospray HPLC/MS/MS of unknowns for their structure determination, 4) +/- ve ion detection during the same run and 5) do not require elaborate sample preparation. The increase of repeller voltage did not provide any useful molecular ion information. The enhancement of the lower mass fragments were evident with the incerase of the voltage which may probably due to the thermolability of the Luprostiol and its metabolites.

Presented at the 35th ASMS Conference on Mass Spectrometry and Allied Topics
May 24-29, 1987, Denver, CO.

REFERENCES:

1. M. Clays, C. Van Hove, A. Duchateau and G. A. Herman, Biomed. Mass Spectrom., 7, 544, 1980.

2. D. Roberts, R. Strife, J. Gerber, R. Murphy, and A Nies, Am. J. Physiol., 248, 830, 1985.

3. R. D. Voyksner, E.D. Bush, 34th. ASMS, Cincinnati, OH, pp 114-115, 1986.

4. J. A. Yergey, H. -Y, Kim, N. Salem, In 'Advances in Mass Spectrometry', Vol 10, J.F. J. Todd, Ed., Wiley, Chichester, 1986.

ACKNOWLEDGEMENT:

The authors wish to acknowledge R. D. Voyksner of the Research Triangle Institute, RTP, NC for the thermospray/HPLC/MS analysis. Thanks are also due to E. Warrakah, L. Geschwindt and S. Shuman for their help in sample preparation.

Figure 1

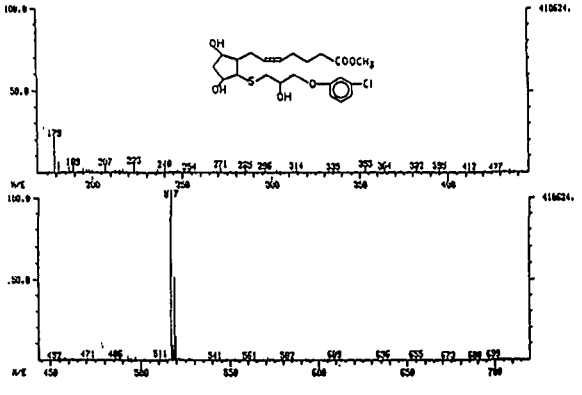

Figure 2

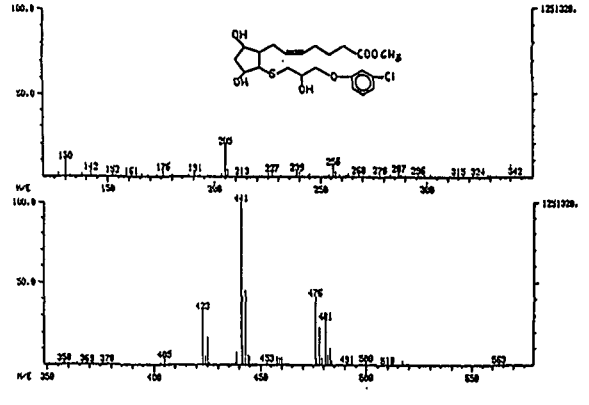

Presented at the 35th ASMS Conference on Mass Spectrometry and Allied Topics
May 24-29, 1987, Denver, CO

THE UTILITY OF THERMOSPRAY LIQUID CHROMATOGRAPHY/MASS SPECTROMETRY FOR THE DIRECT ANALYSIS OF RAT BILE FOR ACETAMINOPHEN AND TWO OF ITS CONJUGATES

L. D. Betowski*, W. A. Korfmacher, J. O. Lay, Jr., D. W. Potter, and J. A. Hinson, *U.S. Environmental Protection Agency, Las Vegas, NV 89114 and National Center for Toxicological Research, Jefferson, AR 72079

INTRODUCTION

Acetaminophen (4'-hydroxyacetanilide) is a widely used nonprescription analgesic and antipyretic drug. It is believed to be safe when therapeutic doses are administered; however, large doses of acetaminophen may cause hepatic damage and renal damage has been reported in some overdose victims.[1] The toxicities are not a result of the parent drug but a consequence of metabolism involving the conversion of acetaminophen to the reactive metabolite N-acetyl-p-benzoquinoneimine (NAPQI).[2] At therapeutic doses this metabolite is efficiently detoxified by conjugation with glutathione to produce 3-(glutathion-s-yl) acetaminophen (GS-A).[3] Following toxic doses, the glutathione pathway is overwhelmed and the reactive metabolite interacts with macromolecules.[3]

Thermospray (TSP) ionization LC/MS has been successfully applied to the analysis of various thermally labile biologically important compounds. In this work we describe the use of thermospray LC/MS for the direct analysis of an untreated bile sample from rats dosed with acetaminophen. For comparison, the results of the analysis of the same bile sample by fast atom bombardment mass spectrometry (FAB/MS) are also reported.

EXPERIMENTAL

The GS-A standard was synthesized by reacting glutathione (GSH) with synthetic NAPQI as described by Potter et al.[4] The acetaminophen glucuronide (GLU-A) standard was a generous gift from Dr. T. L. Gates (Mc Neil Pharmaceutical Co., Springhouse, PA). The acetaminophen was obtained from commercial sources.

Male CD rats from the NCTR breeding colony were administered acetaminophen (500 mg/kg, ip) in 3 mL of saline after their hepatic bile ducts were cannulated with 0.28 mm id PE-10 tubing. Bile was collected from rats for 5 hours.

Theromspray LC/MS was performed with a Finnigan MAT 4500 Triple Stage Quadrupole (TSQ) interface with a Vestec Corp. thermospray system and a Spectra Physics SP8700-XR solvent delivery system. The HPLC flow rate was set to 1.4 mL/min with aqueous 0.1 M ammonium acetate/methanol (87.5:12.5/v:v) as the eluant through a Brownlee 5-um RP-18 (10 cm x 4.6 cm) column.

Positive and negative ion FAB mass spectra were obtained with a Kratos MS-50 high resolution mass spectrometer equipped with an M-Scan fast atom gun.

RESULTS AND DISCUSSION

A bile sample from acetaminophen-dosed rats was injected onto the analytical column without any pretreatment and the LC/mass chromatograms

showed the MH^+ ions of acetaminophen, GLU-A, and GS-A at m/z 152, 328, and 457, respectively. Injection of standard compounds on the system verified both the retention order and retention times of these compounds in the bile sample. The mass spectra for the standards were also in excellent agreement with the separate compounds that eluted from the bile sample.

An analysis of the bile sample by FAB/MS was also attempted. Direct FAB/MS analysis of the bile samples from the acetaminophen-dosed and untreated animals showed very small peaks at all masses corresponding to acetaminophen and its two conjugated metabolites, but no significant identifiable differences were observed in these spectra. To explore the possibility that the ions of interest were being obscured under low resolution MS conditions by the high noise level generated during FAB ionization, the mass of the MH^+ ion of GS-A was mass selected ($\pm$150 ppm) and examined in the single ion monitoring mode at 10,000 resolution. No signal was observed corresponding to protonated GS-A.

CONCLUSION

These results demonstrate the utility of TSP LC/MS for the analysis of bile samples. The method was shown to be useful for the direct analysis of a bile sample without any preextraction or purification step.

On the other hand, FAB/MS did not give signals for any of the three compounds observed with TSP LC/MS. Although similar amounts of purified GS-A have shown intense FAB mass spectra, the GS-A adduct could not be identified directly from bile by FAB/MS. This appears to be a powerful demonstration that even the highest mass resolution cannot substitute for chromatographic separation when the ionization method suffers from limitations imposed by selective ionization.

NOTICE: This article has not been subjected to Agency policy review and therefore does not necessarily reflect the views of the Agency. Mention of trade names or commercial products does not constitute endorsement or recommendation for use.

REFERENCES:

1. E. M. Boyd and G. M. Bereczky, Br. J. Biochem. 26, 606 (1966)

2. D. C. Dahlin, G. T. Miwa, A. Y. H. Lu, and S. D. Nelson, Proc. Natl. Acad. Sci. USA 81, 1327 (1984).

3. J. R. Mitchell, D. J. Jollow, W. Z. Potter, J. R. Gillete, and B. B. Brodie, J. Pharmacol. Exp. Ther. 187, 211 (1973)

4. D. W. Potter, D. W. Miller, and J. A. Hinson, Mol. Pharmacol. 29, 155 (1986).

Presented at the 35th ASMS Conference on Mass Spectrometry and Allied Topics
May 24-29, 1987, Denver, CO.

NEGATIVE ION CHEMICAL IONIZATION GCMS ANALYSIS OF VALPROIC ACID IN SALIVA AND SERUM AND ITS METABOLITES IN SALIVA. Abbott, F.S., Kassahun, K., and Panesar, S. Faculty of Pharmaceutical Sciences, University of British Columbia, Vancouver, Canada, V6T 1W5.

The antiepileptic drug valproic acid (VPA) is extensively metabolized in humans. We recently reported the identification of a new VPA metabolite in human urine[1]. There is a great deal of interest in studying VPA metabolism because several VPA metabolites possess anticonvulsant properties and other metabolites are thought to be involved with rare but fatal cases of hepatotoxicity. We were interested in developing a highly sensitive method of analysis for the detection and quantitation of trace metabolites and to study the pharmacokinetics of metabolites in small animals.

The objectives of this study were to evaluate the suitability of negative ion chemical ionization (NICI) GCMS for the detection and assay of trace level VPA and its metabolites, to apply the method to the determination of VPA in saliva and serum and to identify VPA metabolites in saliva. This work was part of a drug interaction study between VPA and carbamazepine which involved five healthy volunteers who were on VPA steady-state for a month. One volunteer also received six doses of hexadeuterated VPA on selected days. Blood was collected on days 7 and 23 at hourly intervals after the morning dose. Saliva samples were collected following stimulation with 5% citric acid solution and were taken simultaneous to blood samples. Free serum concentrations were measured after ultrafiltration. Serum samples were extracted according to a previously published method[2]. Saliva samples were acidified to a pH of 2, extracted with ethyl acetate and concentrated to 200 µL under N_2.

The concentrated serum or saliva extract was derivatized to give the pentafluorobenzyl (PFB) ester by treating with 10 µL of PFBB (30% in ethyl acetate), 10 µL of diisopropylethylamine (neat) and heating at 40°C for 45 minutes[3]. The 3,5-bis(trifluoromethyl)benzyl (bis-TFMB) derivative of VPA was formed in a similar manner to that of the PFB derivative. The instrument used was a Hewlett-Packard 5987A GCMS. Ionization energy was 120 eV with a source pressure of 1.0 torr. Methane was used as the reagent gas.

In the NICI mode, both fluorinated derivatives gave the same base anion, m/z 143, corresponding to the $[M-181]^-$ of the PFB derivative and $[M-227]^-$ of the bis-TFMB derivative. The PFB derivative was about 5 times as sensitive as the bis-TFMB derivative of VPA when the m/z 143 ion was monitored. In the NICI mode, the PFB derivative also proved to be 30 - 50 times more sensitive than the t-BDMS ($[M-57]^+$) derivative by EI.

With the PFB derivative and using $[^2H_6]$-VPA as the internal standard, the intra- and inter- assay variations were less than 10% at serum VPA concentrations of 10 to 800 ng/mL. When the m/z 143 ion was monitored, the lower limit of detection of VPA extracted from serum was 10 pg. Linearity was observed over the concentration range of 10 ng/mL to 20 µg/mL. A good correlation was found between saliva and both serum total ($r = 0.9058$, $n=30$) and free ($r = 0.9035$, $n=27$) VPA concentrations. This suggests that measuring VPA in saliva by this method would be suitable for pharmacokinetic and drug interaction studies.

The NICI method using the PFB derivative was sensitive enough to detect trace salivary metabolites of VPA. Seven VPA metabolites were detected and identified in saliva both by SIM and linear scan. The SIM chromatograms of these metabolites along with their deuterated analogs are shown in figure 1. Interestingly, none of the more polar hydroxy VPA metabolites were detected in saliva.

In summary, the PFB derivatives of VPA and its metabolites produced intense $[M-181]^-$ ions ($[M-181-CO_2]^-$ for 3-keto VPA) which are suitable for SIM analysis as well as identification of VPA metabolites. The analytical method is adequate for the analysis of trace VPA and its metabolites as demonstrated by quantitation of VPA in saliva and the detection of trace salivary metabolites of VPA.

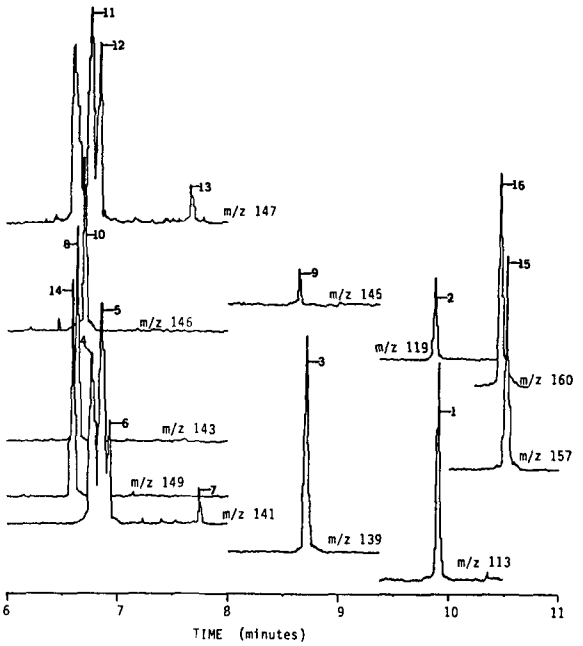

FIGURE 1. SIM CHROMATOGRAMS OF THE PFB DERIVATIVES OF VPA AND $[^2H_6]$-VPA METABOLITES IN SALIVA EXTRACT. PEAKS: 1 = 3-KETO VPA, 2 = $[^2H_6]$-3-KETO VPA, 3 = (E,E)-2,3'-DIENE VPA, 4 = 4-ENE VPA, 5 = 3-ENE VPA, 6 = (Z)-2-ENE VPA, 7 = (E)-2-ENE VPA, 8 = VPA, 9 = (E,E)-$[^2H_6]$-2,3'-DIENE VPA, 10 = $[^2H_5]$-4-ENE VPA, 11 = $[^2H_6]$-3-ENE VPA, 12 = (Z)-$[^2H_6]$-2-ENE VPA, 13 = (E)-$[^2H_6]$-2-ENE VPA, 14 = $[^2H_6]$-VPA, 15 = 4-KETO VPA, 16 = $[^2H_3]$-4-KETO VPA

References
1. F.S. Abbott, K. Kassahun and R. Burton, Pharmaceutical Research, 3, 163S (1986).
2. F.S. Abbott, J. Kassam, A. Acheampong, S. Ferguson, S. Panesar, R. Burton, K. Farrell and J. Orr, J.Chromatogr., 375, 285 (1986).
3. B.H. Min, J. Pao, W.A. Garland, J.A.F. de Silva and M. Parsonnet, J.Chromatogr., 183, 411 (1980).

Presented at the 35th ASMS Conference on Mass Spectrometry and Allied Topics
May 24-29, 1987, Denver, CO

GC/MS ASSAY OF PROSTAGLANDINS IN CEREBROSPINAL FLUID. James A. Yergey, Norman Salem, Jr., John W. Karanian, Markku Linnoila; Laboratory of Clinical Studies, National Institute on Alcohol Abuse and Alcoholism, DICBR, Room 3C-218, Building 10, NIH, Bethesda, MD 20892.

A relationship between the central nervous system effects of ethanol and the production of prostaglandins is suggested by the results of several workers. In humans and in animal models, treatment with prostaglandin sythesis inhibitors has been shown to attenuate the central effects of ethanol, such as cognative impairment and withdrawal symptoms. With these reports in mind, the principal objective of this study was to develop a sensitive and specific assay for prostaglandins in human cerebrospinal fluid (CSF) collected from patients with alcoholism and appropriate controls, using gas chromatography/mass spectromety.

Cerebrospinal fluid samples (2 mL) were drawn on ice into tubes containing indomethacin, transfered to tubes containing tetradeuterated internal standards, and frozen at -70°C. Thawed samples were acidified to pH 3.5, and extracted using a 1 mL C-18 reverse-phase cartridge. Samples were then derivatized to the methoxime, pentaflurobenzyl ester, trimethysilyl ether and analyzed by on-column capillary gas chromatography / negative chemical ionization mass spectrometry. Limits of quantification were 3 pg/mL for PGE_2, PGE_1, PGF_{2a}, PGF_{1a}, and 6-keto-PGF_{1a} using tetradeuterated PGE_2, PGF_{2a}, and 6-keto-PGF_{1a} as internal standards.

Samples assayed since completing methodological improvements (n=49) contained no quantifiable concentration of prostaglandins PGE_2, PGE_1, PGF_{2a}, or PGF_{1a} (Figure 1). The concentration of 6-keto-PGF_{1a} was measureable in many of the samples, but was never more than twice the limit of quantification. Internal standards were recovered in good yield (at least >75%), indicating that sample extraction and derivatization were proceeding reliably.

Comparisons of GC/MS and radioimmunoassay determinations of prostaglandin levels in CSF were undertaken to further corroberate these data. Reasonable agreement was obtained between the two techniques for phosphate-buffered saline which was spiked with PGE_2 and 6-keto-PGF_{1a} (levels ranged from 10 to 1000 pg/mL). In a more representative experiment, CSF samples which had been stored without prior addition of tetradeuterated internal standards were extracted, and assayed by both methods for PGE_2 and 6-keto-PGF_{1a}. Duplicate CSF samples, collected at the same time, were spiked with 13 pg/mL each of PGE_2 and 6-keto-PGF_{1a}, extracted, and again assayed by both methods. Both methods were unable to detect either prostaglandin in the unspiked samples and in the spiked samples detected 14 ± 2 pg/mL (RIA) and 12 ± 3 pg/mL (GC/MS).

A positive control was found upon examining several CSF samples which had been collected from Rhesus monkeys. At the present time only samples which were collected during withdrawal from anesthesia were available. Several of the measured prostaglandins were present in each of the monkey samples (n=4), and were easily quantifiable (Figure 2). More complete examination of monkey CSF, including normals and 24 hour profiles might provide interesting information that could be of great value in understanding the levels found to date in humans.

In conclusion, the levels of the five measured prostaglandins in human cerebrospinal fluid from normal individuals and alcoholics following three weeks of abstinence are near or below the 3 pg/mL level. Literature reports of much higher levels in normal controls, i.e. tens to hundreds of pg/mL appear to be incorrect. Further studies, including examining samples from drinking alcoholics and alcoholics during acute withdrawal are in progress.

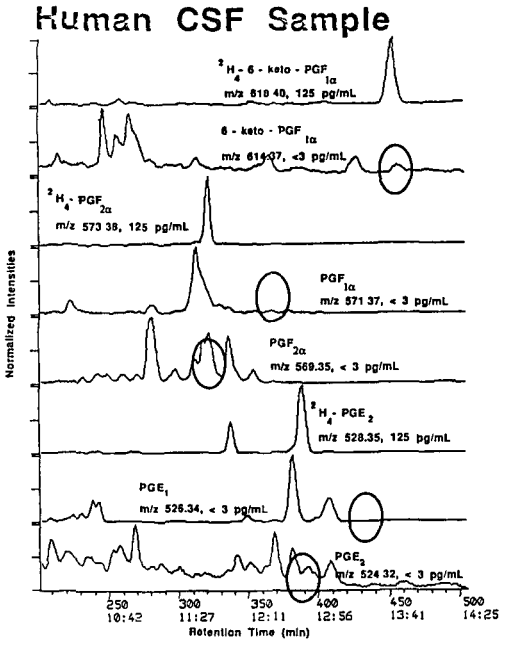
Human CSF Sample
$^2H_4$ - 6 - keto - PGF$_{1\alpha}$
m/z 618.40, 125 pg/mL
6 - keto - PGF$_{1\alpha}$
m/z 614.37, <3 pg/mL
$^2H_4$ - PGF$_{2\alpha}$
m/z 573.38, 125 pg/mL
PGF$_{1\alpha}$
m/z 571.37, < 3 pg/mL
PGF$_{2\alpha}$
m/z 569.35, < 3 pg/mL
$^2H_4$ - PGE$_2$
m/z 528.35, 125 pg/mL
PGE$_1$
m/z 526.34, < 3 pg/mL
PGE$_2$
m/z 524.32, < 3 pg/mL
Normalized Intensities
250 10:42
300 11:27
350 12:11
400 12:56
450 13:41
500 14:25
Retention Time (min)

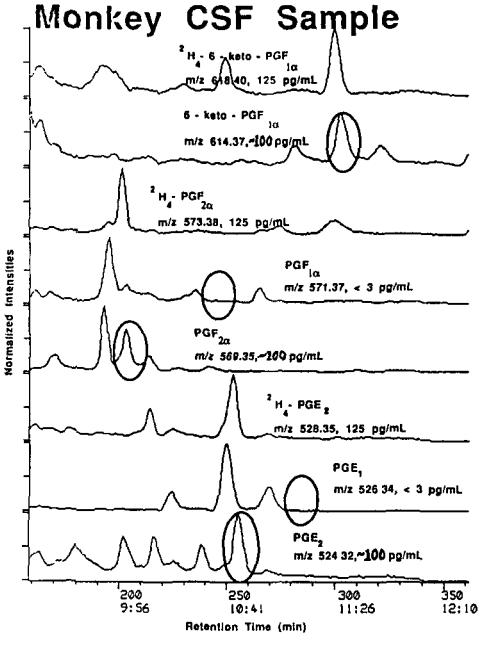
Monkey CSF Sample
$^2H_4$ - 6 - keto - PGF$_{1\alpha}$
m/z 618.40, 125 pg/mL
6 - keto - PGF$_{1\alpha}$
m/z 614.37, ~100 pg/mL
$^2H_4$ - PGF$_{2\alpha}$
m/z 573.38, 125 pg/mL
PGF$_{1\alpha}$
m/z 571.37, < 3 pg/mL
PGF$_{2\alpha}$
m/z 569.35, ~100 pg/mL
$^2H_4$ - PGE$_2$
m/z 528.35, 125 pg/mL
PGE$_1$
m/z 526.34, < 3 pg/mL
PGE$_2$
m/z 524.32, ~100 pg/mL
Normalized Intensities
200 9:56
250 10:41
300 11:26
350 12:10
Retention Time (min)

Presented at the 35th ASMS Conference on Mass Spectrometry and Allied Topics
May 24-29, 1987, Denver, CO

A CANDIDATE REFERENCE METHOD FOR THE MEASUREMENT OF SERUM CHOLESTEROL

Michael Kinter, Judy Hundley, David A. Herold, Michael R. Wills and John Savory
Departments of Pathology, Biochemistry and Internal Medicine
University of Virginia Medical Center, Charlottesville, VA 22908

Introduction

Recent studies on the use of serum cholesterol as a risk factor in atherosclerosis indicate a need for improved analytical performance in routine assays. The Laboratory Standardization Panel of the NIH National Cholesterol Education Program has set goals of 0±3% for both bias and precision. Towards this end, the Panel has also established a definitive method, which uses isotope dilution mass spectrometry, and a reference method, which uses a colorimetric assay. There is, however, a continued need for the wide spread availability of reference and pseudo-definitive methods with physical methods being preferred.

We have developed a GC/MS procedure for the measurement of serum cholesterol using a structural isomer, 7,(5a)-cholesten-3b-ol, as the internal standard. The cost of a stable isotope labeled internal standard based assay is prohibitive because of the high concentration of endogenous cholesterol. In addition, the GC/MS measurement is made at a moderately high mass resolution (R = 5000) to enhance the selectivity and ensure an interference-free assay.

Materials and Methods

Reagent and Standards. The cholesterol Standard Reference Material (SRM 911a) and Certified Human Serum (SRM 909) were obtained from the National Bureau of Standards (Gaithersburg, MD 20899). 7,(5a)-cholesten-3b-ol was obtained from Steraloids, Inc. (Wilton, NH 03086). Reagents used in the hydrolysis, extraction and derivatization are as follows: Absolute ethyl alcohol, HPLC grade hexane, methanol and acetonitrile, reagent grade potassium hydroxide and N,O-bis(trimethylsilyl)trifluoroacetamide with 1% trimethylchlorosilane (BSTFA with 1% TMCS).

Preparation of Certified Serum. The lyophilized Certified Human Serum was reconstituted according to NBS procedure A. Pools used had concentrations of 143.1 mg/dl (sets 1-8) and 142.6 mg/dl (sets 9-10).

Sample Preparation. A 0.5 ml aliquot of serum and a 0.5 ml aliquot of the internal standard solution was pipetted into a centrifuge tube using an automatic pipettor and the sample hydrolyzed in alcoholic KOH at 37 °C for 3 hrs. The sample was then extracted with 10 ml of hexane, the hexane evaporated and the residue reconstituted in 5 ml of methanol. A 100 ul portion of the methanol solution was transferred to a reaction vial and evaporated to dryness. 100 ul of BSTFA and 100 ul of acetonitrile was added and the sample derivatized for 0.5 hr at 60 °C. The samples was then evaporated to dryness and reconstituted in 500 ul of tetradecane for analysis. A 211.4 mg/dl standard was also prepared by pipetting 0.5 ml of a standard cholesterol solution and 0.5 ml of the internal standard solution in a centrifuge tube, evaporating to dryness, and reconstituting the standard in 5 ml of methanol from which a 100 ul portion was transferred for derivatization.

Gas Chromatography/Mass Spectrometry. The mass spectrometer used was a double focusing, reverse geometry instrument (Model 8230, Finnigan Mat) with a SpectroSystem 300 data system. The instrument was operated in the electron ionization mode using 100 ev electrons. Data were acquired in a selected ion monitoring experiment, monitoring m/z 458,394, at a rate of 4 hz yielding approximately 25 data points per chromatographic peak. A DB-1 bonded phase fused silica capillary column, 30 m x 0.32 mm, was used. Samples were injected on column at a temperature of 200 °C followed by a 20 °C/min ramp to 300 °C. Duplicate preparations of the Certified Human Serum and a 211.4 standard were run in triplicate.

Results and Discussion

The 100 eV EI mass spectra of cholesterol and 7,(5a)-cholesten-3b-ol are shown in Figure 1. As can be seen, a molecular ion is observed for each compound and was, therefore, chosen as the ion to be monitored. The chormatographic separation of these compounds is shown in Figure 2 which contains a typical chromatogram obtained for the analysis of the Certified Human Serum. This figure also shows that the intensity of the signal obtained under these conditions is large enough to provide good counting statistics, and that no additional chromatographic peaks are observed, indicating good selectivity. As shown in Figure 3, the analysis in linear over a wide range (0 - 1000 mg/dl). This linearity allows the calculation of sample concentration using a responce factor obtained form a single standard.

Presented at the 35th ASMS Conference on Mass Spectrometry and Allied Topics
May 24-29, 1987, Denver, CO

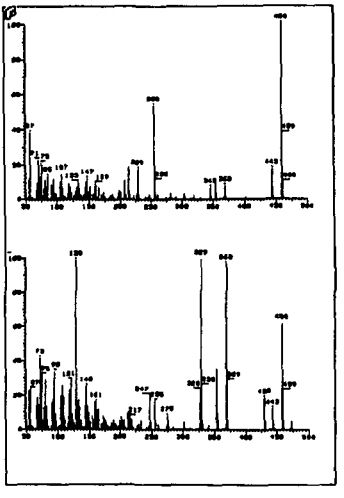

FIGURE 1. 100 eV EI MASS SPECTRA OF A) CHOLESTEROL AND B) 7,(5α)-CHOLESTEN-3β-OL.

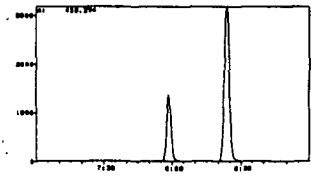

FIGURE 2. SELECTED ION MONITORING ANALYSIS OF NBS CEPTIFIED HUMAN SERUM.

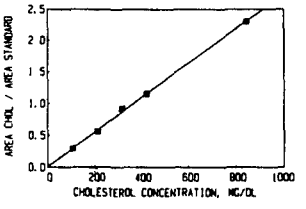

FIGURE 3. CALIBRATION CURVE FOR THE ANALYSIS OF A SERIES OF CHOLESTEROL STANDARDS.

Concentration values for the Certified Human Serum determined by this method in 10 consecutive analysis sets are shown in Table 1. From these data the accuracy appears to be excellent with a bias of -0.5%. The relative standard deviation of this data set, 2.6%, is approaching the target precision of a reference method. The exclusion of set #9 as an outlier would improve this precision to 1.7% with a mean of 142.9 mg/dl.

Table 1. Cholesterol Concentrations for NBS Certified Human Serum.

Analysis Set	Cholesterol Concentration, mg.dl #1	#2	ave
1	143.2	not run	143.2
2	146.8	not run	146.8
3	144.2	144.1	144.2
4	140.4	146.7	143.6
5	142.0	138.4	140.2
6	138.0	141.9	140.0
7	146.0	145.2	145.6
8	142.9	141.8	142.4
9	130.0	137.3	133.7
10	142.1	138.6	140.4
			x = 142.0 mg/dl
			s = 3.7 mg/dl
			cv = 2.6%

Conclusion

A GC/MS reference method for the measurement of serum cholesterol using a structural isomer as an internal standard has been developed. The advantages of this method are the cost effectiveness of using an unlabeled internal standard and the specificity of using gas chromatography/high resolution mass spectrometry. This assay will allow the establishment of reference serum cholesterol assays in laboratories with high resolution mass spectrometry capabilities and, therefore, lead to the wider availability of serum cholesterol reference methods in the future.

Presented at the 35th ASMS Conference on Mass Spectrometry and Allied Topics
May 24-29, 1987, Denver, CO

QUANTITATION OF CLENBUTEROL IN BIOLOGICAL FLUIDS USING AMMONIA CI AND AUTOMATED CAPILLARY GCMS

E.M. Ecker, H.J. Förster, A. Wittrock and K.L. Rominger
Division of Research, Boehringer Ingelheim KG,
6507 Ingelheim am Rhein, FRG

Clenbuterol (I) is a potent sympathomimetic drug used in treatment of humans and mammalian animals. Pharmacokinetic studies in man necessitate assaying I x HCl in concentrations $\geq$ 10 pg/ml since the oral therapeutic dose is only 20 µg. This represents a considerable challenge even by today's standard. Our assay is based on capillary GCMS of the O-TMS ethers of I and the deuterated internal standard and selected ion recording of the $(M+H)^+$ ions formed by ammonia CI. Starting with 2 ml of alcaline plasma and 2.5 ng/ml of D9-I x HCl an extract of I in methyl-tert.-butylether (MTB) was prepared which was purified by an additional acid/base distribution. The overall yield of the extraction was 67 % as checked by radioactive I. Removal of impurities of the solvent which could react with the analyte proved crucial for the successful application of the assay. The solvent cleansing procedure involved washing MTB with an aqueous solution of the structurally related ß-blocking agent bunitrolol x HCl followed by distillation. Extracts were derivatized with hexamethyldisilazane (HMDS) / MeCN (1:1) and after removal of the reagents reconstituted in 20 µl CH_2Cl_2/HMDS (95:5) and transferred to autosampler vials. 1 - 2 µl of this solution was injected by a DANI autosampler at 60°C (splitless) into a 25m x 0.31mm i.d. CPSIL5CB-capillary (film thickness 0.12 µm) which was then heated ballistically to 250°C. The O-TMS-ethers of I and the internal standard elute under these conditions from the column at 230°C as symmetrical peaks of less than 1 sec peak width at half height.

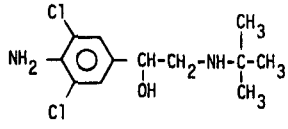

I

Hardware required for the automatic injection and data acquisition is similar to those previously described (1). The automated system permitted threefold injection of 40 plasma samples in a 20 h - period without operator intervention. The Finnigan 4021 GCMS-system distributed the total scan time of 0.25 sec between the signals m/z 349 und 358 at a ratio of 8:1. I x HCl-supplemented plasma samples containing 15 - 200 pg/ml and 2.5 ng/ml of D_9 - I x HCl were used for calibration purposes.

Calibration curves were computed by linear regression of measured peak height ratios on concentrations of I x HCl. Calibration curves were linear (r=0.999) and passed through the origin. I x HCl concentrations of 15 pg/ml could still be measured with a signal/background ratio of 3. The coefficient of variation was 11 % at the 25 pg/ml - and 4 % at the 100 pg/ml - level. Analysis of variance done on data at the 100 pg/ml - level showed that the sample workup contributed $\leq$ 20 % to the total variance, 80 % of the total variance were due to the GCMS analysis. Accuracy checks were performed with I - supplemented plasma samples in concentrations (0 - 150 pg/ml) unknown to the analyst. Measured concentrations deviated from "true" concentrations by 3.8 %.
The assay was used for measuring plasma levels of I after oral administration of 20 µg I x HCl to man (0 - 24 h). Plasma levels in humans after intravenous injection of 40 µg I x HCl were measurable over a 0 - 96 h period.
The assay was also used in order to assess the homogeneity and stability of medicated feeds containing 0.04 ppm of I x HCl (160 mg of active ingredient in 4 tons of pig rearing feed!).

References: 1. J. Lauber and P. Waldmeier, 15th International Symposium on Chromatography, October 1 - 5, 1984, Nuremberg, FRG, abstract 4PF-41.

Presented at the 35th ASMS Conference on Mass Spectrometry and Allied Topics
May 24-29, 1987, Denver, CO

ANALYTICAL METHODOLOGY TO STUDY THE EFFECTS OF DIETARY METHYLXANTHINES ON THEOPHYLLINE METABOLISM

E.D. Bush, C.M. Loi, S.G. Jue, and R.E. Vestal
Clin. Pharmacol. and Gerontology Res. Unit VA Medical Center, Boise, ID; College of Pharm., ISU, Pocatello, ID; and Univ. of Wash., Sch. of Med., Seattle, WA.

Theophylline (1,3-dimethylxanthine) and caffeine (1,3,7-trimethylxanthine) are two chemically closely related compounds. Both drugs are metabolized by N-demethylation and aromatic hydroxylation mediated by the cytochrome P-450 isozymes. When given concomitantly, caffeine prolongs the elimination half-life of theophylline. This results from direct competition for the same drug metabolizing enzyme(s) between these two compounds. Since caffeine competitively inhibits the elimination of theophylline, the dose of caffeine administered or ingested may significantly influence the extent of this interaction. A study was designed to investigate whether the inhibition of theophylline metabolism by caffeine is a dose-related phenomenon. In order to conduct the study an analytical method was needed to quantitate the plasma levels of unlabeled theophylline, caffeine and a stable isotope labeled theophylline analog. The method needed to be simple, rapid, reliable and highly automated in order to efficiently handle the 700-1000 samples eventually expected for the study.

The quantitative method developed is as follows: 1) Plasma samples were separated from whole blood immediately after collection and stored at -20C until analysis. 2) 100ul of an ethanol stock solution of internal standards containing $^{13}C_3$-caffeine and $^{2}H_6$-theophylline was added to 1ml of the thawed plasma. 3) The samples were extracted with 10ml of isopropanol/chloroform (5/95), the organic phase separated and evaporated with dry N_2. 4) The samples were resuspended with 100ul of MeOH, transferred to microvials suitable for the GC/MS autosampler and analysed immediately. The analyses were performed on a HP 5988A GC/MS system fitted with a 5890 GC and a 7673A autosampler with tray. The instrument was operated in EI mode, and the source, injector and transfer line temperatures were 200, 250 and 280C respectively. A 12 meter fused silica HP-1 capillary column was used with He as the carrier gas at a head pressure of 5 psi. The oven temperature was held constant at 135C for 1min then ramped at 25C/min to 300C. Total program time was 8min. All MS, GC and autosampler parameters were under the control of the HP MSD-Chemstation data system. Each set of samples (75-80 vials including standard curve samples) were injected, integrated, plotted and quantitated under computer direction utilizing the sequencing software from HP. The retention time for caffeine was 3.7min and the calibration curves were linear from 0.5 to 10ug/ml. Retention time for theophylline and $^{13}C_1,^{15}N_2$-theophylline were 4.5min and the calibration curves were linear from 0.25 to 5.0ug/ml for the unlabeled theophylline and 0.025 to 0.5ug/ml for the labeled theophylline. The r^2 values for the calibration curves were usually greater than 0.99.

In order to determine the methods reproducibility and stability a series of spiked quality control samples were prepared and analyzed over a period of five weeks. Two stock solutions of QC samples were generated, one with high analyte concentrations (8.0, 4.0, and 0.4ug/ml of caffeine, theophylline, and labeled theophylline respectively) and one with low analyte concentrations (0.8, 0.4, and 0.04ug/ml respectively). After thorough mixing the stock solutions were divided into 1ml aliquots and frozen until analysis. On the day of each GC analysis 3 high and 3 low samples were thawed and analysed with the normal subject samples. Care was taken to keep the three vials of each set in order (labeled A, B and C) such that all manipulations were performed on sample A first, then B, etc to avoid a nested ANOVA design. Each sample was analyzed in triplicate thus making the design a standard two-way model II ANOVA with replicate measures. All statistical calculations were performed utilizing SPSS/PC+ on an IBM XT computer. The ANOVA results are listed below as a percent of the overall variance attributable to each factor.

ANOVA DATA

ANOVA Factors	Analyte Variables: Caffeine high	Caffeine low	Theophylline high	Theophylline low	Labeled-Theophylline high	Labeled-Theophylline low
inter day	22	71	10	16	80	84
inter sample	0	0	0	0	0	0
day x sample	67	19	50	35	1	5
replication	11	10	40	49	19	11
CV (%)	0.5	0.9	6	8	8	11

In summary, the method is rapid, reliable and reproducible. The sources of error in the analysis vary with the specific analyte and its concentration. The replication error which represents the error due to the instrument and the data system analysis accounts for less than 50% of the variance of the data in the worst case. And finally, the readily available ANOVA procedure gives the analyst useful information about the sources of error in a new method.

Utilizing this method a pilot clinical study was performed on six healthy male nonsmokers (age 25-33 yr). In random order each subject received placebo, low dose caffeine (8mg/kg/day), and high dose caffine (16mg/kg/day) orally for six days. On the fifth day of each regimen, subjects were given $^{13}C_1$, $^{15}N_2$-theophylline 10mg i.v. and theophylline 160mg orally simultaneously. Serial blood samples were drawn over 24hr for GC/MS assay of caffeine, theophylline and labeled theophylline. Protein binding was determined by equilibrium dialysis. The effect of caffeine dose on the pharmacokinetic parameters of labeled theophylline are given below with standard errors in parentheses.

PHARMACOKINETIC DATA

Dose	Half-life (hr)	Vd (L/kg)	Clearance (ml/kg/hr)	Free Fraction (%)
Placebo	6.6(0.6)	0.41(0.02)	44(3)	56(2)
Caffeine				
8mg/kg/day	8.0(0.4)[a]	0.41(0.02)	36(2)[b]	55(3)
16mg/kg/day	9.5(0.3)[b,c]	0.43(0.02)	32(2)[b,d]	53(1)

[a] $p<0.05$ statistical comparisons between placebo and caffeine treatment.
[b] $p<0.01$ statistical comparisons between placebo and caffeine treatment.
[c] $p<0.05$ statistical comparisons between the two caffeine treatments.
[d] $0.05<p<0.10$ statistical comparisons between the two caffeine treatments.

In conclusion, the mean plasma clearance of labeled theophylline decreased 18% with low dose caffeine and 27% with high dose caffeine. The difference in clearance values of labeled theophylline between low dose and high dose caffeine treatments showed a trend, but was not as significant as expected. The mean half-life of labeled theophylline was prolonged 21% with low dose caffeine and 44% with high dose caffeine. Neither caffeine treatment had an effect on the volume of distribution or protein binding measurements.

Thus the results suggest that dietary consumption of caffeine may significantly influence the plasma concentration of theophylline given for therapeutic indications. Further studies in this area will investigate how this interaction is influenced by age and smoking habits of the subjects.

Presented at the 35th ASMS Conference on Mass Spectrometry and Allied Topics
May 24-29, 1987, Denver, CO

QUANTITATIVE METABOLIC PROFILING OF DRUGS BY AUTOMATED GC/MS. APPLICATIONS TO STUDIES ON THE BIODISPOSITION OF VALPROIC ACID IN HUMANS

A. W. Rettenmeier, R. H. Levy, D. J. Witek, T. A. Baillie* and W. N. Howald*
Departments of Pharmaceutics and *Medicinal Chemistry, University of Washington, Seattle, WA 98195

Introduction

Valproic acid (VPA; fig.1) is a short branched-chain carboxylic acid with anticonvulsant activity which is used clinically in the treatment of multiple forms of epilepsy. Numerous studies have shown that VPA undergoes extensive metabolism and a large number of oxidation and conjugation products have been identified in plasma and urine. Due to the complexity and the wide concentration range of endogeneous organic acids in biological fluids, identification and (in particular) quantitation of VPA and its metabolites represent a major analytical problem. We describe here a fully-automated GC/MS procedure to determine 14 metabolites of VPA in the presence of the parent compound. This procedure has been used in expanded clinical studies on the biodisposition of VPA in adults and has proven useful for identifying metabolic alterations occurring in suspected cases of VPA-induced hepatotoxicity.

Experimental

Valproic acid was obtained as the free acid from Abbott Laboratories (North Chicago, Ill.). Synthetic samples of VPA metabolites used were prepared as described elsewhere (1,2,3,4) PSA was a kind gift from Dr. F. S. Abbott (Univ. of British Columbia, Vancouver, B.C. Canada). 2-n-propyl- and 2-[3-OH-propyl] hexanoic acid, analogs of VPA and 5-OH-VPA, respectively, were employed as internal standards. The 2-n-propyl hexanoic acid was prepared, via its ethyl ester, by the reaction of ethyl caproate and propyl bromide according to the general ester alpha alkylation method reported by Gregge. The 2-[3-OH-propyl]-hexanoic acid was synthesized in a two-step sequence which involved alkylation of ethyl caproate with allyl bromide to yield the intermediate, 2-allyl-caproate, followed by hydroboration to the acid products as described by Rettenmeier.(1) The derivatization reagent, BSTFA, was purchased from Supelco Inc. (Bellefonte, PA.) and all solvents used were analytical grade obtained from commercial sources. Plasma and urine samples were prepared in a similar fashion for GC/MS analysis. GC screening of a specimen from each patient was performed to establish a suitable sample volume necessary for quantitation. As a result, a predetermined aliquot (50-500µl) of the biological fluid was transferred into a screw-capped glass tube and distilled water added to yield a final volume of 500µl. The two internal standards were then added with through mixing. After heating for 30min. at 60° with 3N NaOH, the hydrolyzed samples were acidified with 4N HCL and extracted with ethyl acetate (2 x 3ml). 150µl of the derivatizing reagent was then added and the mixture heated at 90°C for 30min. The derivatized samples were transferred to and sealed in auto sampler vials for subsequent analysis. In addition to the calibration samples prepared by the admixture of appropriate amounts of VPA, VPA metabolites and the two internal standards, plasma and urine, obtained by the pooling of in-study patient samples were used to evaluate the methodology.

Fig. 1 Proposed Scheme for Phase I metabolism of VPA in humans and analytes quantified.

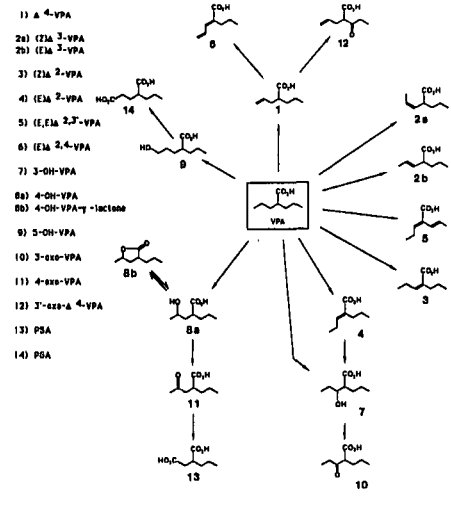

Presented at the 35th ASMS Conference on Mass Spectrometry and Allied Topics
May 24-29, 1987, Denver, CO

The analysis of the derivatized extracts was carried out by capillary GC/MS on an HP 5970B MSD quadrupole mass spectrometer operated in the EI mode at 70eV electron energy, 220μA emission current, 200°C source temp. and CG interface temp of 280°C. The instrument was equipped with a 60m fused silica column (0.32mm I.D.- 0.25 micron thickness) coated with the bonded phase DB-1 (J&W Scientific). Helium was employed as carrier gas (head pressure 10 p.s.i.). Samples were injected in the splitless mode (injector temp., 250°C) and "cold trapped" on the column at 40°C. The column oven temperature was then raised rapidly to 80°C and programmed linearly as follows: 2°C min^{-1} to 120°C, then 4°C min^{-1} to 180°C, and finally stepped to 250°C. Under these conditions, the parent drug, metabolites and internal standards exhibited baseline separation (Table 1). Detection was performed by SIM of the $[M-CH_3]^+$ ion of each component of interest, with the exception of 3-oxo-VPA and 4-OH-VPA-γ-lactone for which the M+ and $[M-C_3H_6]^+$ respectively, are monitored.

The analysis is fully-automated with injection, data acquisition, integration, calibration and quantitative report functions being carried out during unattended operation by an HP 59979C ChemStation computer system.

Results and Conclusions

The method demonstrated good linearity (corr. coeff. >0.990 for all analytes), precision and reproducibility with the high dynamic range of the instrument allowing quantitation of VPA and its Δ^4-metabolite at 250 μg and 14ng ml^{-1} respectively, in a single 38min. chromatographic run. The intra-day reproducibility of the assay as determined by replicate analyses of pooled plasma samples yielded coefficients of variation of <7% for all but one metabolite (PSA), whose mean concentration was found to be significantly below its calibration range. The inter-day reproducibility of the assay, measured by the analysis of a pooled plasma sample with each of the patient studies (30) over a 4-month period, resulted in coefficients of variation of <12% for all of the mono TMS derivatives with significantly higher values for those analytes which gave multiple peaks on GC analysis.

The stability and sensitivity of the assay, combined with the fully automated features of the instrument, make the method most useful for expanded clinical studies and the routine monitoring of high risk patients on VPA therapy.

Supported by NIH grants NS 17111 and GM 32165.

1. K. S. Prickett and T. A. Baillie, Biochem. Biophys. Res. Comm., 122:1166-1173 (1984).
2. A. W. Rettenmeier et. al., Drug Metab. Disp., 13:81-96 (1985).
3. A. W. Rettenmeier et al., Drug Metab. Dispos., 14:443-453 (1986).
4. A. W. Rettenmeier et al., Drug Metab. Dispos., 14: 454-464 (1986).

Table 1 Chromatographic Retention and Selected Ions Monitored for the TMS derivatives of the Analytes

Ion Monitored m/z	Compound	Retention Index MU
100	4-OH-VPA-γ-lactone	11.25 & 11.32
201	VPA TMS	11.41
199	Δ^4 - VPA TMS	11.31
	Δ^3 - VPA TMS	11.46
	(Z)Δ^2 - VPA TMS	11.59
	(E)Δ^2 - VPA TMS	12.03
197	(E)$\Delta^{2,4}$ - VPA TMS	12.20
	(E,E)$\Delta^{2,3'}$ - VPA TMS	12.63
215	4-exo-VPA TMS	12.91
	Internal Standard I	12.40
302	3-oxo-VPA diTMS	14.15 & 14.29
289	3-OH-VPA diTMS	13.94
	4-OH-VPA diTMS	13.86 & 14.05
	PSA diTMS	14.48
	5-OH-VPA diTMS	14.62
285	3'-exo-Δ^4-VPA diTMS	14.11 & 14.35
303	PGA diTMS	15.07
	Internal Standard II	15.22

Table 2

Characteristics of Standard Curves for Quantification of Plasma Concentrations of VPA and VPA Metabolites

Compound	Range of Calibration [μg ml^{-1}]	y Intercept	Slope	Correlation Coefficient
VPA	7.9—250	3.44	0.348	0.995
4-Ene-VPA	0.014—0.59	$-1.27 \cdot 10^{-3}$	0.443	>0.999
3-Ene-VPA	0.059—2.8	$1.50 \cdot 10^{-5}$	0.182	>0.999
2(Z)-Ene-VPA	0.020—1.0	$-6.37 \cdot 10^{-4}$	0.519	>0.999
2(E)-Ene-VPA	0.20—10.2	$7.40 \cdot 10^{-5}$	0.798	>0.999
2(E),4-Diene-VPA	0.060—2.0	$-9.14 \cdot 10^{-3}$	0.509	>0.999
2,3'(E,E)-Diene-VPA	0.25—14.3	$-2.28 \cdot 10^{-2}$	0.318	0.999
3-OH-VPA	0.14—3.5	$-1.58 \cdot 10^{-2}$	1.005	>0.999
4-OH-VPA	0.10—.85	$-7.30 \cdot 10^{-2}$	3.12	0.993
5-OH-VPA	0.035—1.1	$-6.66 \cdot 10^{-3}$	6.10	>0.999
3-Oxo-VPA	0.28—14.3	$9.78 \cdot 10^{-2}$	0.882	0.998
4-Oxo-VPA	0.019—1.6	$-6.48 \cdot 10^{-3}$	0.252	0.992
3'-Oxo-4-ene-VPA	0.0083—0.091	5.93 10^{-2}	42.1	>0.999
PSA	0.016—0.33	$1.42 \cdot 10^{-2}$	5.33	>0.999
PGA	0.0017—0.47	$4.90 \cdot 10^{-3}$	4.38	0.999

Presented at the 35th ASMS Conference on Mass Spectrometry and Allied Topics
May 24-29, 1987, Denver, CO

IDENTIFICATION OF MORPHINE AND CODEINE IN EXTRACTS OF MAMMALIAN BRAIN

K.F. Faull[1], G.F. Feistner[1] and C.J. Weitz[2]

[1]Laboratory of Behavioral Neurochemistry, Department of Psychiatry and Behavioral Sciences, Stanford University School of Medicine, Stanford, CA 94305 and [2]Addiction Research Foundation, Palo Alto, CA 94305

Opium has long been known for its addictive and analgesic qualities. Morphine is the chief active ingredient in opium and codeine its immediate biosynthetic precursor. Previously it had been thought that these alkaloids only occurred naturally in a few species of plants, most notably members of the Asian poppy genus Papaver. However, reports dating back to the mid-1970s have suggested that these compounds may be more widespread as trace constituents of mammalian tissues and foods than had hitherto been suspected, although the identity of these compounds has never been convincingly resolved. Members of the Addiction Research Foundation have been characterizing the compounds in mammalian brain extracts which are recognized by antisera raised against morphine[1,2]. These antisera do not recognize opioid peptides. Using solvent extraction, phase partitioning and reverse- phase HPLC, 3 non-peptide peaks of morphinan immunoreactivity (ir) have been reliably detected in extracts of bovine hypothalamus and adrenal and rat brain; the morphinan ir (in morphine equivalents) accounted for by the total of these 3 peaks in the 3 different sources amounts to 5-25, 0.001-0.10 and 0.001-0.20 pmol/g of wet weight, respectively. The predominant ir peak (peak A) in the extracts behaved in a manner identical with morphine in all the analytical procedures: peak B behaved in a manner indistinguishable from codeine: the chromatographic characteristics of the remaining ir peak were not consistent with either morphine, codeine, codeinone, salutaridine, reticuline, thebaine or oripavine.

To establish unequivocably the identity of these morphinans, a large-scale purification from 1200 frozen bovine hypothalami (wet weight ≈20kg) was carried out. Strict precautions were taken to eliminate artifacts. Glassware, reagents and columns were sequestered exclusively for this work. A tissue-less extraction was performed using the same volumes of solvents, etc., as were used for the tissue extraction. This blank sample was carried through all subsequent steps of the purification. Chronologically, the tissue extracts followed immediately after the tissue-less blank using the same glassware and columns etc. The final step in the purification involved HPLC with acetonitrile/trifluoroacetic acid eluant in the order described in Figure 1's legend. Appropriate fractions from the final HPLCs were pooled, lyophilized, redissolved, transferred to glass capillary tubes and dried again. Trifluoroacetyl (TFA) derivatives were prepared with N-methylbis(trifluoroacetamide). Samples were analyzed by GC/MS (HP 5985B, EI, 70 eV) in the order listed in Figure 1. GC components and conditions were as follows: column-fused silica capillary, bonded phase, medium polarity, 30m x 0.255mm, film thickness 0.25 μm; injection port and transfer line } 250°C; column conditions } 180°C for 1 min, increasing to a plateau at 250°C; carrier gas } He. The elemental composition of the peak A derivative was determined using a Varian 3700 gas chromatograph (column specifications and GC conditions as described above) coupled with a VG ZAB-SE mass spectrometer (static resolution 8000; scan rate 2 sec/decade; mass range 500-300; reference PFK).

Figure 1A shows the reconstructed total ion chromatograms (RTIC) for the samples obtained from the purification of peak A. The solvent blank and tissue-less blank samples (Figure 1A, a and b) each revealed a single GC peak with the same retention times (≈ 11.5min) and similar mass spectra suggesting probable identity as a phthalate. The tissue and authentic morphine samples (Figures 1A, c and d) both revealed an earlier eluting GC peak with identical retention times (≈ 9min) and mass spectra (Figure 2A). Confirming the identity of peak A as morphine, GC/high-resolution MS studies of the TFA derivative of peak A yielded a molecular ion of m/z 477.1009 ± 0.0016 (SEM) [calculated value for bis(trifluoroacetyl)morphine ($C_{21}H_{17}F_6NO_5$): 477.1011, M^+] and a major fragment ion of m/z 364.1173 ± 0.0011 (SEM) (calculated value for $C_{19}H_{17}F_3NO_3$; 364.1161, $[M-O_2CCF_3]^+$.

Figure 1B shows the RTIC for the samples obtained from the purification of peak B. This series of chromatograms revealed several GC peaks although the solvent blank and sequential blank (Figures 1B, a and b) were free of peaks corresponding in m/z values to the major ions in the spectra of derivatized morphine (m/z 477 and 364) and codeine (m/z 395 and 282). One of the peaks in the chromatogram from the derivatized tissue sample (Figures 1B, c) had a retention time (≈10min) and mass spectrum identical to that of authentic codeine (Figure 2B), confirming the identity of peak B as codeine.

Future experiments are aimed at determining the structure of the remaining peak of morphinan ir found in bovine hypothalami extracts. The biosynthetic origin and physiological significance of these morphinans in mammals is still uncertain.

ACKNOWLEDGMENTS: Supported by grants from NIMH and NIDA (MH 23861 and DA 01207 to Jack D. Barchas and DA 1199 to Avram Goldstein).

REFERENCES: [1]Goldstein, A., Barrett, R.W., James, I.F., Lowney, L.I., Weitz, C.J., Knipmeyer L.L. and Rappaport, H. Proc. Natl. Acad. Sci. (USA) 82:5203-5207, 1985. [2] Weitz, C.J., Lowney, L.I., Faull, K.F., Feistner, G. and Goldstein A. Proc. Natl. Acad. Sci. (USA) 83:9784-9788, 1986.

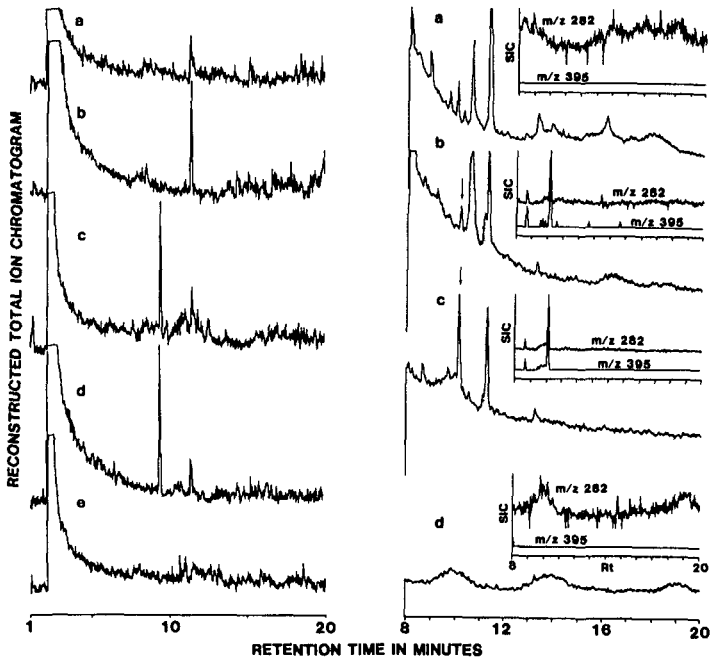

Figure 1A (left): RTIC from the analysis of Peak A samples: a) HPLC solvent blank, 500µl water; b) tissue-less blank; c) ir peak from tissue extract; d) external standard of morphine at the estimated concentration of the ir peak from tissue; e) GC solvent blank (5µl heptane). B (right): RTIC from the analysis of Peak B samples: a) tissue-less blank; b) ir peak from tissue extract; c) external standard of codeine at the estimated concentration of the ir peak from tissue; d) GC solvent blank (5µl heptane) [selected ion current (SIC)].

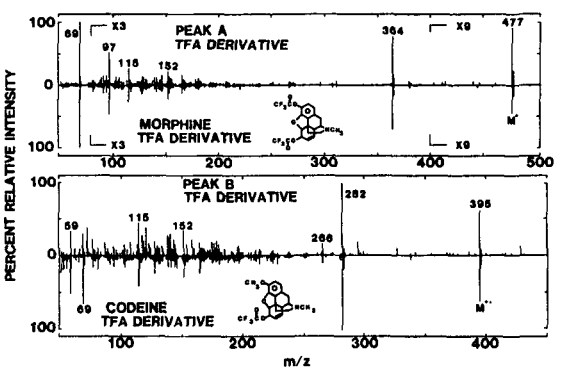

Figure 2A (top): Comparison of the mass spectra of the GC/MS peaks from Figure 1A(c) and (d). B (bottom): Comparison of the mass spectra of the peaks designated with arrows in Fig. 2A(b) and (c).

Presented at the 35th ASMS Conference on Mass Spectrometry and Allied Topics
May 24-29, 1987, Denver, CO

DIFFERENTIATION OF ISOMERIC IONS IN MASS SPECTRA OF PYRROLIZIDINE ALKALOIDS USING COLLISIONAL ACTIVATION

A. Daniel Jones,[1] Ronald B. Kelley,[2] Carl K. Winter,[3]
H. J. Segall, [3] and James N. Seiber[2]

(1) Facility for Advanced Instrumentation
(2) Department of Environmental Toxicology
(3) Department of Veterinary Pharmacology and Toxicology
University of California, Davis, CA 95616

Pyrrolizidine alkaloids (PAs) occur in numerous plant species worldwide and have been responsible for poisonings of livestock and humans. The polarity of these compounds often causes tailing during gas chromatographic analyses, and resolution of isomers is difficult even with capillary columns. One solution to this problem is to use direct probe introduction and tandem mass spectrometry to identify PAs as Haddon and Molyneux[1] have demonstrated. Here we extend their work to demonstrate that isomeric ions can be differentiated using collisional activation MS/MS.

Numerous problems must be addressed in order to conduct a thorough analysis of PAs. In the first place, PAs and their metabolites usually occur in nature as mixtures of amine and N-oxide forms, and the identification and quantitation of N-oxides is hampered by their polarity and low volatility. The susceptibility of PAs toward hydrolysis is an incentive to minimize sample handling. PA pyrroles (dihydropyrrolizines) are particularly unstable. In addition, PAs often exist in several isomeric or isobaric forms which coelute during chromatographic separations.

Our experimental approach has been to minimize sample treatment and chromatographic isolation steps in order to reduce the formation of artifacts. In the course of this investigation, we observed the production of small amounts of $[M - H]^+$ ions from many PAs under both FAB and chemical ionization conditions. Senecionine, for example, gives a weak $[M - H]^+$ ion at m/z 334 which is isomeric with ions produced from seneciphylline, 19-hydroxysenecionine, and senecionine pyrrole.

CAD MIKE spectra of the daughters of m/z 334 were acquired to assess the similarities among these isomeric ions, and these spectra appear in Figure 1. Seneciphylline and 19-hydroxysenecionine gave virtually identical daughter spectra, exhibiting a prominent daughter at m/z 120. However, both senecionine and senecionine pyrrole produced daughters at m/z 118, suggesting that hydride abstraction of senecionine occurs on the pyrrolizidine ring.

Examination of spectra of the daughters of m/z 154 from retronecine and retronecine pyrrole gave similar results, and provide additional evidence of hydride abstraction from the pyrrolizidine ring. However, these two ions produced distinctly

different daughter spectra, with additional decomposition pathways being accessible to the $[M + H]^+$ from retronecine pyrrole that are not accessible to the $[M - H]^-$ from retronecine.

From the observed differences in the CAD MIKE spectra, it is often possible to differentiate isomeric ions. However, the similarities in some of the spectra serve as a reminder that hydride abstraction must be taken into account as a potential source of artifacts when natural products are identified in mixtures by direct probe MS/MS.

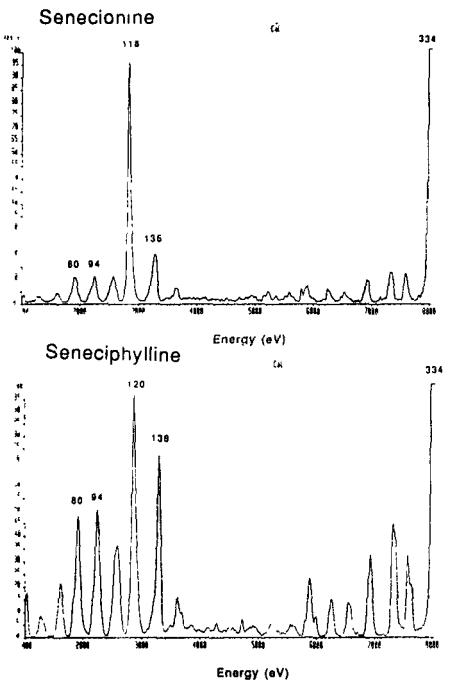

Figure 1. CAD MIKE Spectra of Daughters of m/z 334 from Senecionine and Seneciphylline.

REFERENCES

1. W. F. Haddon and R. J. Molyneux, in Tandem Mass Spectrometry, F. W. McLafferty, Ed., Wiley, New York, 1983, pp. 451-464.

Presented at the 35th ASMS Conference on Mass Spectrometry and Allied Topics
May 24-29, 1987, Denver, CO

THE IDENTIFICATION OF AMPICILLIN AND ITS METABOLITES USING THERMOSPRAY LC/MS

Somchai Suwanrumpha, Donald A. Flory, Royal B. Freas
Department of Chemistry, University of Houston, Houston, TX 77004

INTRODUCTION

An advantage of coupling liquid chromatography and mass spectrometry (LC/MS) is that structural information for each chromatographic peak can be obtained from mass spectra. We illustrate this advantage using thermospray ionization LC/MS for the identification of penicillin and its metabolites. The metabolites normally contain the main structure of the parent drug. It should be possible to deduce the metabolic structure from the mass spectra, although thermospray ionization mass spectra often contain little structural information. Tandem mass spectrometry (MS/MS) was also used to confirm these identifications.

EXPERIMENTAL

Ampicillin, a β-lactam antibiotic, and two known metabolites {1}, ampicillin penicilloate and ampicillin piperazine-2,5-dione, were studied. Ampicillin was purchased from Sigma Chemical Co. and used without purification. Penicilloic acid and piperazine-2,5-dione were synthesized from ampicillin, as described in the literature {1}.

The urine samples were frozen to precipitate proteins, melted, and filtered through a 0.5 μm membrane filter. Twenty microliters of these samples were used for LC analysis. A chromatographic procedure for cleaning-up the urine samples utilized a column switching technique {2}. The following LC conditions were used:

Stationary Phase		Mobile Phase
Pre-Column:	3 cm x 0.21 cm, C-18, 5 μm	0.2 M NH_4COOH + 0.2 M CH_3COOH (pH 4.75)
Analytical Column:	25 cm x 0.46 cm, C-18, 5 μm	0.2 M NH_4COOH + 0.2 M CH_3COOH:CH_3CN = 88:12
		Flow Rate: 1 mL/min

A quadrupole mass spectrometer (HP 5988A) was used with a thermospray interface. The thermospray vaporizer temperature was adjusted to maximize the intensity of protonated ampicillin (m/z 350). The temperatures were: inlet temperature = 109°C, vaporizer exit temperature = 224°C, downstream vapor temperature = 232°C , and block temperature = 260°C. The mass spectrometer was scanned from m/z 100 to m/z 500.

RESULTS AND DISCUSSION

Figure 1 shows the total ion chromatogram of (A) a urine sample after orally administering 500 mg of ampicillin, (B) a blank urine sample, and (C) a blank urine sample spiked with 8 μg of ampicillin. Figure 2 shows the mass spectra of ampicillin from urine samples in Figs. 1A and 1C. The mass spectra show the fragment ions that characterize the structure of ampicillin at m/z 350, 324, 232, 218, 191, 175, 160, and 150.

Figure 3 shows the mass chromatograms from Fig. 1A for selected fragment ions that arise from ampicillin. These figures reveal 5 separated peaks. Peaks #1, #2, and #5 are identified as ampicillin penicilloate, ampicillin, and ampicillin piperazine-2,5-dione. These identifications are assigned using retention times and mass spectral data of urine samples spiked with these compounds

Figure 4 shows the mass chromatograms at m/z 192 and 175, obtained by subtracting the spectrum in Fig. 1A from that in Fig. 1B. This figure reveals more clearly two other possible metabolites of ampicillin, peaks #3 and #4. The mass spectra of these two peaks are shown in Fig. 5. The identifications of these two components are still under investigation.

A hybrid tandem mass spectrometer (VG 70-SEQ) was used to confirm the identification of ampicillin and piperazine-2,4-dione in the chromatograms using low-energy CID with Ar in the collision quadrupole. The protonated molecules were formed by fast-atom bombardment (8 keV Xe; glycerol matrix) of a urine extract. Figure 6 compares the FAB/CID spectra of protonated ampicillin (m/z 350) and m/z 350 from peak #2 of the urine sample. Figure 7 compares the FAB/CID spectra of protonated piperazine-2,5-dione (m/z 350) and m/z 350 from peak #5 of the urine sample.

CONCLUSIONS

- Mass chromatograms of the urine samples indicate the presence of two possibly new metabolites.
- The LC/MS procedure permits the unambiguous identification of ampicillin metabolites in urine samples.
- The CID spectra can be used to confirm the assignments of ampicillin and piperazine-2,5-dione in the chromatographic peaks.
- The CID spectra can be used to distinguish ampicillin from its isomeric metabolite piperazine-2,5-dione.

Presented at the 35th ASMS Conference on Mass Spectrometry and Allied Topics
May 24-29, 1987, Denver, CO.

ACKNOWLEDGEMENTS

We thank Dr. Marvin Vestal for valuable assistance, and the Texas Advanced Technology Research Program for partial support of this work.

REFERENCES

1. (a) Uno, T.; Masada, M.; Yamaoka, K.; Nakawa, T. *Chem. Pharm. Bull.* **1981**, *29*, 1957. (b) Everett, J.R.; Jennings, K.R.; Buckingham, M.J.; Woodnutt, G. *J. Chem. Soc. Chem. Comm.* **1984**, 894.

2. Nazareth, A.; Jaramillo, L.; Karger, B.L.; Giese, R.W. *J. Chromatogr.* **1984**, *309*, 357.

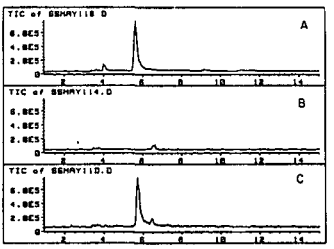

FIGURE 1

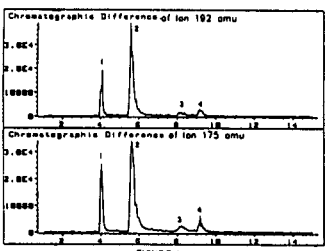

FIGURE 4

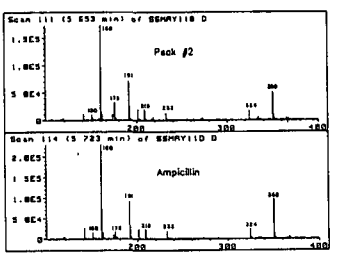

FIGURE 2

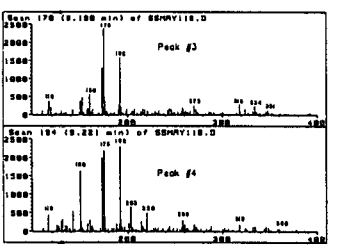

FIGURE 5

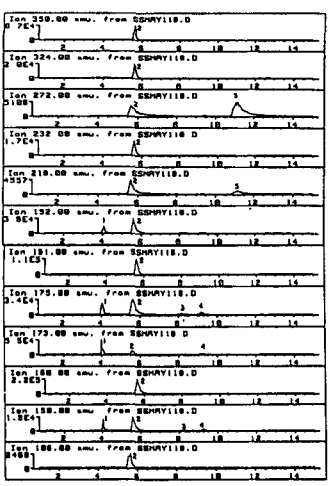

FIGURE 3

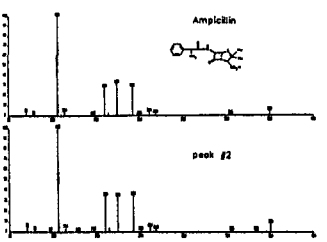

FIGURE 6

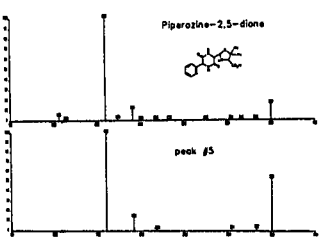

FIGURE 7

Presented at the 35th ASMS Conference on Mass Spectrometry and Allied Topics
May 24-29, 1987, Denver, CO

ISOLATION AND CHARACTERIZATION OF THE URINARY METABOLITES OF ARBAPROSTIL IN THE FEMALE DOG AFTER INTRAVENOUS ADMINISTRATION

L.A. O'LEARY, J C. GREENFIELD, K J. COOK AND H. HARPOOTLIAN

Drug Metabolism Research
The Upjohn Company, Kalamazoo, MI 49001

Arbaprostil (15-[R]-15 methyl PGE_2) is a prostaglandin drug being evaluated for the treatment of duodenal ulcers Arbaprostil differs from the naturally occurring prostaglandin E_2 by the substitution of a methyl group at C-15. This substitution is to block the metabolic oxidation of the C-15 carbon which readily occurs in the metabolism of PGE_2.

An earlier study using arbaprostil-^{3}H administered intravenously to female dogs resulted in 75% of the total excreted radioactivity being recovered in the urine, thereby establishing the major route of elimination.

Two female dogs were dosed with arbaprostil-^{3}H twice daily for two days at 400 µg/kg. Each dog received 20 mg (200 µCi) over the duration of the study Urine was collected by catheterization, pooled, frozen and stored at-20 C.

Initial isolation was performed using a column slurry packed with Amberlite XAD-4 resin which had been extensively washed. Radioactive prostaglandin-related materials were eluted from the column with acetone:water (90·10 v/v). The urine extract (97% recovery; 23 4 mg-eq) was methylated with ethereal diazomethane to enhance the stability and chromatographic properties of the metabolites.

Countercurrent chromatography (CCC) using an Ito multilayer coil separator-extractor (P.C. Inc.) was used to further purify and fractionate the crude methylated urine extract. A portion of the extract was almost equally partitioned within the biphasic layers of an ethyl acetate:95% ethanol: cyclohexane: water (1:1:1:1 v/v) solvent system The upper (organic) layer showed enrichment of less polar components and was used as the mobile phase while the lower (aqueous) layer contained an enrichment of more polar components.

Four fractions were recovered from CCC. Each fraction was further purified by semipreparative HPLC using a RP-C_{18} Nucleosil-10 (Machery-Nagel) column. Arbaprostil-^{3}H and its major metabolites were separated using a linear gradient and a water/methanol mobile phase system Detection was performed using a radioactivity monitor equipped with a solid scintillator flow cell A total of eleven isolates were collected and each was assayed for radioactivity to determine its yield.

Prior to GC/MS, each isolate was further derivatized to its methyl ester-methoxime-trimethylsilyl ether[1]. The derivatives were chromatographed on a 6ft x 3mm glass column packed with 3% OV-101 on Gas-Chrom Q (Alltech). Positive ions were detected by chemical ionization using methane as the reagent gas. In nine of the isolates recovered from semipreparative HPLC, the principal components were identified by their GC retention indices[2] (carbon number) and by peak matching to library reference standards which had been synthetically prepared. Components found in the two remaining isolates were tentatively identified by their molecular ions.

The results confirm the proposed mechanism that β-oxidation of the carboxy side-chain to the 15-[R,S]-2,3,4,5-tetranor-15 methyl-PGE_2 metabolite is the most significant pathway of biotransformation. The identification of the 2,3-dinor-15-[R,S]-15methyl PGE_2 intermediate presumably results from initial β-oxidation of the parent drug which rapidly undergoes further β-oxidation to the tetranor moiety which is the major metabolite. Since arbaprostil-^{3}H was administered intravenously, the 15-[R,S]-2,3,4,5-tetranor-15-methyl-PGA_2 and the 15-[R,S]-2,3,4,5-tetranor-15-methyl-PGB_2 were most probably derived enzymatically from the major metabolite. However, it was observed with arbaprostil that some chemical dehydration can also occur to a limited extent during the methylation process.

References

1. C.J. Hartzell and N.H Anderson, Biomed. Mass Spectrom, 12, 303 (1985).
2. S Bergström, R. Ryhage, B. Samuelsson, and J. Sjövall, J. Biol. Chem. 238, 3555 (1963).

Presented at the 35th ASMS Conference on Mass Spectrometry and Allied Topics
May 24-29, 1987, Denver, CO

PROBABLE PATHWAY IN THE METABOLISM OF ARBAPROSTIL IN FEMALE DOGS

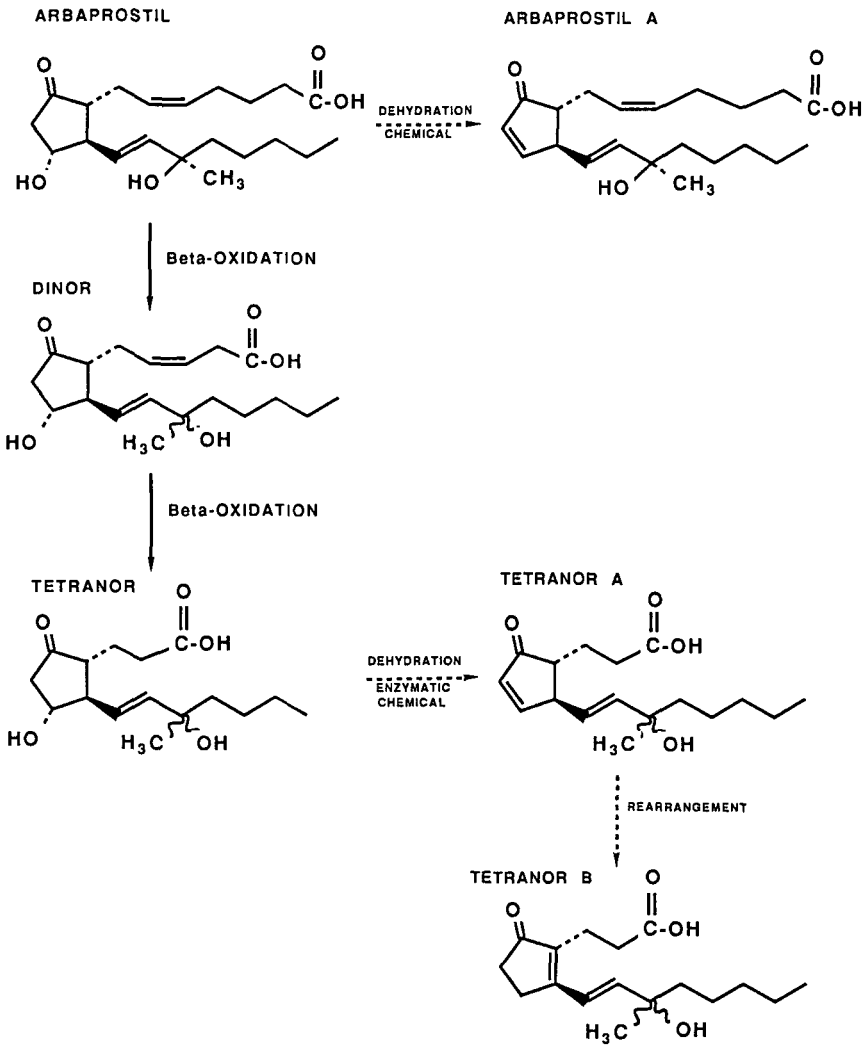

Presented at the 35th ASMS Conference on Mass Spectrometry and Allied Topics
May 24-29, 1987, Denver, CO

GC-NICI-MS ANALYSIS OF MACROCYCLIC TRICHOTHECENES

JOSEPH D. ROSEN[1], ROBERT T. ROSEN[2] and THOMAS G. HARTMAN[2], Department of Food Science[1], Center for Advanced Food Technology[2], Cook College, Rutgers University, New Brunswick, New Jersey 08903

Macrocyclic trichothecene mycotoxins are produced by Stachybotrys and Myrothecium fungal species. These mycotoxins have caused serious outbreaks of disease among farm animals (1) and recently were implicated as possible factors in chronic human disease (2) caused by S. atra infestation of a cold air return duct in a heating system. Analytical techniques for these polar non-volatile mycotoxins have been based on TLC (3) and HPLC (4). Recently, an analytical method based on hydrolysis of the macrocyclic trichothecenes to verrucarol followed by derivatization and quantification by GC-NICI-MS has been proposed (5) but the hydrolysis step causes severe loss of material. We have demonstrated that verrucarin J and the trimethylsilyl ethers of verrucarin A, roridin A, and roridin E, satratoxin G, satratoxin H and baccharin B_5 can be chromatographed on a short (7-8 m) GB1 fused-silica capillary column (6) using on-column injection. With EI selected ion monitoring, nanogram quantities of the macrocyclic trichothecenes could be detected. Sensitivity of the method is greatly enhanced in NICI because of the presence of a butadienyl lactone moiety common to all the macrocyclic trichothecenes. For example, the limit of detection of a verrucarin J standard is estimated to be 1 pg (2 fmole). The limit of detection for veruccarrin A is 10-20 pg. We will present our method for detection of macrocyclic trichothecenes in a fungal extract. Because of the selectivity of the method, no clean-up is required, although a simple clean-up based on first passing the extract through a reverse phase HPLC column may be used.

1. B. Harrach, A. Bata, E. Bajmocy and M. Benko, Appl. Environ. Microbiol. 45 (1983) 1419.
2. W.A. Croft, B.B. Jarvis and C.S. Yatawara, Atmos. Environ. 20 (1986) 549.
3. R.M. Eppley and W.J. Bailey Science 181 (1973) 758.
4. T. Fernando and G. Bean, Food Chem. 20 (1986) 235.
5. T. Krishnamurthy, E.W. Sarver, S.L. Greene and B.B. Jarvis, JAOAC 70 (1987) 132.
6. J.D. Rosen, R.T. Rosen and T.G. Hartman, J. Chromatog. 355 (1986) 241.

NJAES Publication #J-10201-87-1

Compound	-R-
Verrucarin A	$-CHOHCHCH_2CH_2CH_2OC(=O)-$
Verrucarin J	$-CH=CCH_2CH_2CH_2OC(=O)-$
Roridin A	$-CHOHCHCH_2CH_2CH_2OCHCHOHCH_3$
Roridin E	$-CH=CCH_2CH_2CH_2OCHCHOHCH_3$
Satratoxin G	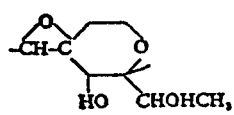
Satratoxin H	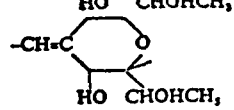

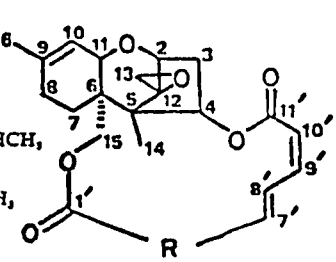

Presented at the 35th ASMS Conference on Mass Spectrometry and Allied Topics
May 24-29, 1987, Denver, CO

GC/MS ANALYSIS OF N-NITROSODIISOPROPANOLAMINE AT THE ng/g LEVEL IN A GEL FORMULATION CONTAINING A NON-STEROIDAL ANTI-INFLAMMATORY AGENT

J.C. James, M.J. Pastel, K.A. Ledoux, and J.M. Baldoni
American Cyanamid Company
Medical Research Division
Pearl River, NY 10965

INTRODUCTION:

The nitrosamine N-nitrosodiisopropanolamine (NDIPA), CAS 53609-64-6, is a suspected carcinogen and occurs as a trace impurity in diisopropanolamine (DIPA), CAS 110-97-4.[1] DIPA is an excipient in a topical gel formulation. The objective of our laboratory was to develop and validate a method to analyze the gel for NDIPA with a detection level below 10ng/g. Trace analysis of nitrosamines in complex matrices is accomplished by isolating and concentrating the analyte, and then quantitating it using one of several techniques.

In this work, two preparative chromatographic systems were used to isolate NDIPA from the gel matrix. The two hydroxyl groups on the isolated NDIPA were converted to t-butyldimethylsilyl (tBDMS) ethers. Quantitation at the ppb level was achieved with a capillary GC interfaced to a benchtop mass spectrometer. Selective ion monitoring used for m/z 333, the $(M-57)^+$ fragment ion (loss of one t-butyl). The resolution of the capillary GC together with SIM made the method highly specific for NDIPA analysis.

EXPERIMENTAL:

Sample Preparation (Fig 1)- 1g of gel was mixed with silica gel and sulfamic acid (to scavange nitrite) and dried in a vacuum desiccator. The dry powder was transferred to a small polyethylene column and eluted with ethyl acetate. DIPA remained on the column. The eluent was evaporated to dryness, the residue loaded onto a silica gel flash column, and the column eluted with acetonitrile. The first 20mL was discarded. NDIPA eluted in the next 40mL, which was collected and brought to dryness. The residue was derivatized using t-butyldimethylchlorosilane/imidazole/dimethylformamide and acetonitrile to form the bis(tBDMS)ether of NDIPA.

Instrumental- The derivatized sample was analyzed by GC/MS using a Hewlett Packard 5890 GC interfaced to a FinniganMAT 710 ITD. The column was 30m x 0.25mmID fused silica with 0.25um DB5 with He carrier at 30cm/sec. The injection was 3.7uL splitless at 180 C. The oven was held at 60 C for 0.5min, ramped at 30 /min to 200 C, held for 10min, and ramped again at 30 /min to 250 C. Total run time was 22min. The open split interface was maintained at 200 C. The ITD was set to monitor m/z 333 at 2 scans/sec. The solvent delay was 10min, and the acquisition time 16min.

RESULTS:

Concentrations of NDIPA in three batches of the gel formulation ranged from 2.4 to 4.1 ng/g, corrected for recovery.

DISCUSSION:

Instrument response was linear (r=0.9986) from 5 to 60 ng/g. The limit of detection was 1 ng/g (S/N=3:1) or 40 pg. The method precision was c.v. 11.6% with a recovery of 76%+/-9% at the 95% confidence level. The method of standard additions (Fig 2) was used to compensate for matrix effects and to correct for recovery.

NDIPA is thermally unstable and must be derivatized for GC. The bis(trimethylsilyl) ether is more volatile, but its $(M-15)^+$ ion at m/z 291 is not unique in the chromatogram at the ng/g level. The tBDMS derivative provides a more intense unique ion, and so was chosen for this work.

REFERENCE:

1. Issenberg, P., Conrad, E.E., Nielsen, J.W., Klein, D.A., and Miller, S.E. "Determination of N-nitrosobis(2-hydroxypropyl)amine in enviromental samples." in N-NITROSO COMPOUNDS: OCCURANCE, BIOLOGICAL EFFECTS AND RELEVANCE TO HUMAN CANCER, Proceedings of the VIIIth International

Presented at the 35th ASMS Conference on Mass Spectrometry and Allied Topics
May 24-29, 1987, Denver, CO

Symposium on N-Nitroso Compounds. I.K. O'Neill et al., eds. 1984. IARC Scientific Publication No. 57, pp 43-50.

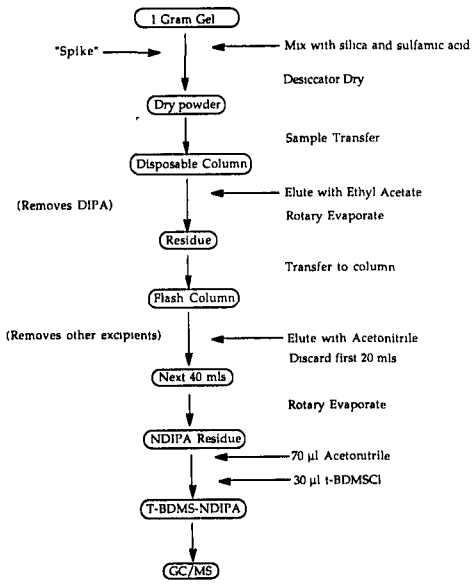

Fig 1

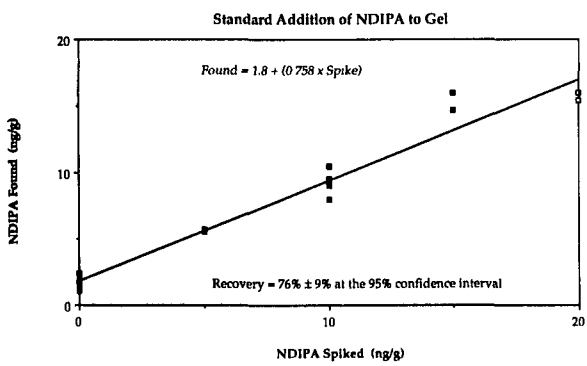

Fig 2

Presented at the 35th ASMS Conference on Mass Spectrometry and Allied Topics
May 24-29, 1987, Denver, CO.

OFF-LINE SEARCHING OF THE NIH BERDY DATABASE USING MASS SPECTRAL DATA

Mark S. Bolgar, B.M. Warrack, S.E. Unger, W.C. Lui
The Squibb Institute for Medical Research
P.O. Box 4000
Princeton, NJ 08540

The antibiotic database established by the National Institute of Health is an invaluable aid for the rapid screening of new lead antibiotics. In combination with mass spectral data, screening against over 12,000 known antibiotics can be accomplished in minutes.

Using this screening procedure the presence of a novel compound is often immediately apparent. This procedure eliminates the extensive isolation and characterization necessary for other analytical spectroscopic techniques.

Often, this screening method involves searching the database against molecular weight or formula established by low or high resolution analysis. Therefore, emphasis is placed upon the rapid generation and identification of the intact molecular or pseudomolecular ion.

Four common techniques employed at Squibb include fast-heating chemical ionization, fast atom bombardment, thermospray ionization and field desorption. The presence of confirming positive and negative parent ions, the use of multiple matrices for desorption, and the combined use of several ionization methods affords an accurate molecular weight and formula for searching.

In combination with other physical and chemical properties such as color, solubility, biological activity and UV spectrum, proposed antibiotic candidates can be identified or established as novel compounds. A proposed structure is often confirmed from fragmentation seen in the MS/MS spectrum of the desorbed parent ion.

The NIH Berdy Database resides on a Digital Equipment Corporation VAX computer. Once logged onto the VAX computer and connected to the Berdy account the search is initiated by selecting the query editor. The search type is selected and parameters entered from this screen (shown below). A search can be executed using one type of data or any combination of the types listed.

QUERY EDITOR

IDENTIFIERS	TESTS	ISOLATION
Chemical Type	Elemental Analysis	Isolation
Name	Optical Rotation	Extraction
Molecular Formula	UV Spectra	Filtration
Producing Organism	Stability	Ion Exchange
Molecular Weight	Qualitative Analysis	Absorption
Equivalent Weight	Chromatography	Chromatography
Physical Characteristics	Stability	Crystallization
	Test Organism	
	Toxicity	

After a biologically active material has been isolated and purified, two or more desorption ionization techniques are used to generate the positive and negative molecular ions. Multiple ionization techniques are used to insure that the molecular ion is correctly identified. The next step in the screening procedure is to search the database on the basis of the compound's nominal mass or to perform an accurate mass measurement to generate a formula by which to search the database. The magnitude of the molecular weight determines whether a molecular weight or formula search is more useful.

DISTRIBUTION OF NIH DATABASE CANDIDATES BY MOLECULAR WEIGHT

Total Candidates:	12,842
Candidates w/Molecular Weight < 1000:	6,740
Candidates w/Molecular Weight > 1000:	1,335
Candidates not listed by M.W.:	4,767

There are two categories of entries not listed by molecular weight. The first type are entries whose molecular weight is unknown or poorly defined. The second type are those that have a known molecular formula but whose molecular weight was not entered into the database.

Presented at the 35th ASMS Conference on Mass Spectrometry and Allied Topics
May 24-29, 1987, Denver, CO

NATIONAL INSTITUTE OF HEALTH DATABASE

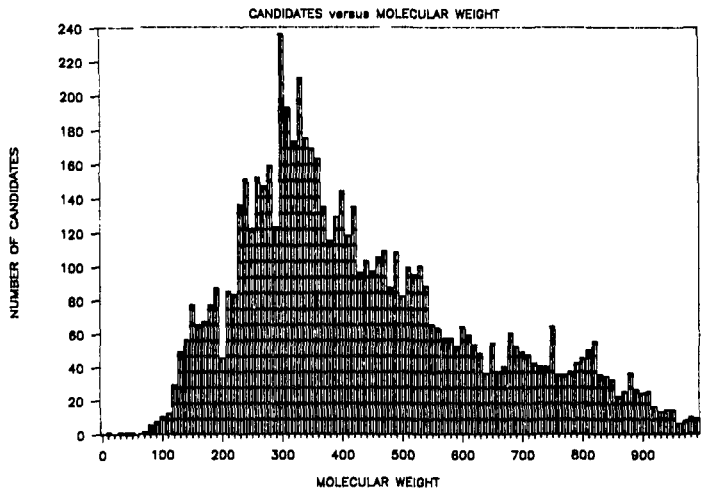

HIGH MOLECULAR WEIGHT CASE

If the compound of interest has a high molecular weight (>500) the database is searched only on the basis of the molecular weight. A molecular formula search is usually not performed due the difficulty associated with formula determination at high masses. This difficulty arises from the increase in the number of formulas that correspond to an accurate mass number as mass increases.

EM5603 = MONACTIN

The FAB mass spectral analysis of a new antibiotic, EM5603, yielded possible molecular weights of 750 and 767. A metastable scan of the 768$^+$ ion indicated that it was an NH_3 adduct of the 751$^+$ ion. A search of the Berdy Database on a molecular weight of 750 yielded 14 candidates. Monactin and three of its isomers were among the candidates. The final identification of EM5603 was based on infrared and UV data.

NIH ANTIBIOTIC DATABASE LISTING

BCN: 23410000887
Name: MONACTIN
Chemical Type: CYCLOPOLYACTONE
Formula: $C_{41}H_{66}O_{12}$
Producing Organism: ACT. CHRYSOMALLUS-
CARTENOIDES, S.FLAVEOLUS
S.ROSEOCHROMOGENES
Physical Characteristics: WHITE CRYSTALS
Molecular Weight: 750

LOW MOLECULAR WEIGHT CASE

At lower masses (< 500) molecular weight and formula searchs are performed. Usually the formula search is more useful than the molecular weight search due to the large number of low mass candidates listed in the database. A nominal mass search could yield more than 30 candidates. A formula search generally gives only one candidate.

EM5607 = FRAGIN

From CI and FAB mass spectral analyses EM5607 was determined to have a molecular weight of 273. A molecular weight search yielded seven candidates, but their physical properties did not match those of EM5607. An accurate mass measurement of the molecular ion yielded a molecular weight of 273.2047. The only formula found within 10 ppm of the exact mass was $C_{15}H_{27}N_3O_3$. On the basis of this formula, another search of the NIH Database was performed. Only one candidate was found. A portion of the database listing is shown.

NIH ANTIBIOTIC DATABASE LISTING

BCN: 9225003778
Name: FRAGIN
Chemical Type: FATTY ACID DERIVATIVE
Formula: $C_{15}H_{27}N_3O_3$
Producing Organism: PS. FRAGI
Physical Characteristics: WHITE CRYSTALS
Elemental Analysis: N: 15%
Optical Rotation: Value: -122 Solvent: ETOH
UV Spectra: λ: 248 ε: 8000 Solvent: ETOH

Presented at the 35th ASMS Conference on Mass Spectrometry and Allied Topics
May 24-29, 1987, Denver, CO

DCI MASS SPECTRA OF PEPTIDYL AMINOSTEROIDS

Lan K. Wong[1] Michael Mokotoff[1] Ming Zhao[2] Qing-jiang Liao[2] and Emil W. Fu[3] School of Pharmacy University of Pittsburgh[1] Pittsburgh, PA 15261, Pharmaceutical University of China[2] Nanjing, PR China, Sandoz Research Institute[3] East Hanover, NJ 07936.

INTRODUCTION

Several peptidyl derivatives of Amefalone, an aminosteroid, have been synthesized by a collaborative effort of the University of Pittsburgh School of Pharmacy and the Pharmaceutical University of China. These peptidyl steroids represent a new class of compounds which are being evaluated as potential antiarrhythmic agents. Experiments carried out in China revealed that some amide and N-alkyl derivatives of Amefalone retained the antiarrhythmic activity of Amefalone, but possessed lower toxicity. At the University of Pittsburgh, peptidyl derivatives of Amefalone have been synthesized using the novel polymeric reagent method of Mokotoff and Patchornik [Int. J. Peptide Res. 21, 145 (1983)]. In this report, the mass spectra of these novel compounds are described. These results are useful for future metabolism and pharmacological studies of this new class of drug.

EXPERIMENTAL

The DCI mass spectra of the synthetic peptidyl aminosteroid samples were obtained on a Finnigan-Mat 4600 mass spectrometer with the superincos data system. The CI reagent gas was isobutane. The synthetic samples included Pro-Pro-Amefalone, D-Ala-Pro-Amefalone, D-Ala-Gly-Amefalone, Ala-Gly-Amefalone and their corresponding t-boc precursor derivatives. During the mass spectrometric analyses, the ion source was set at 110°C and the pressure was adjusted to about 0.3 torr. Electron energy was at 100 eV and filament emission current was at 0.3 mA. These source conditions generally yielded a ratio of m/z 57 intensity to m/z 43 intensity close to 10 for isobutane. Sample introduction was via a direct exposure probe. The power supply of the probe was set to deliver current to the probe tip at 50 mA/SEC to effect rapid heating of the sample. The scan cycle time was 1 second.

RESULTS

The isobutane DCI mass spectra of all peptidyl aminosteriods examined exhibited M + H ions as the base peaks in their mass spectra. It should be noted that the EI mass spectra of these compounds did not show any molecular ions. In the DCI mass spectra, fragment ions which are indicative of the peptide skeleton are discernible in all cases. The fragment ions are more intense in the t-boc derivatives. The key features in these DCI mass spectra are tabulated in the accompanying table. In almost all cases, the fragment ions A, B, C, X involve double hydrogen transfers. Fragment ion C is absent in Pro-Pro-Amefalone and D-Ala-Pro-Amefalone because of the cyclic nature of proline. The ions at m/z 289 and m/z 306 are very good verification of the presence of the Amefalone moiety while the fragment ion D gives information on the peptidyl portion of the molecules.

CONCLUSION

DCI mass spectrometry using isobutane as the reagent is suitable for the characterization of peptidyl aminosteriods. These DCI mass spectra give good molecular ion information. In future metabolism studies of peptidyl Amefalone, any metabolic modification of the aminosteroid can be detected by inspecting the fragment ions at m/z 289 and m/z 306. Information on the metabolic modification of the peptide portion can be obtained from fragment ions A, B, C, and D.

Presented at the 35th ASMS Conference on Mass Spectrometry and Allied Topics
May 24-29, 1987, Denver, CO

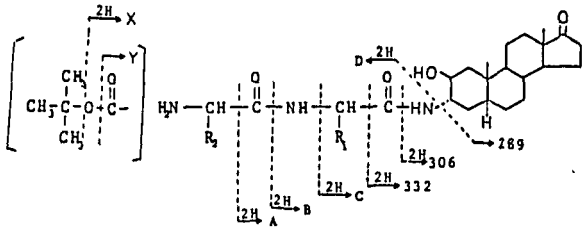

	M+H	(M+H) $-H_2O$	A	B	C	D	X	Y
PRO-PRO-AMEFALONE	500	482	431	403		212		
T-BOC-PRO-PRO-AMEFALONE	600	582	431	403		312	544	526
D-ALA-PRO-AMEFALONE	474	456	430	403		186		
T-BOC-ALA-PRO-AMEFALONE	574	556	431	403		286	518	500
D-ALA-GLY-AMEFALONE	434	416	391	363	348	146		
T-BOC-ALA-GLY-AMEFALONE	534	516	391	363	348	246	478	460
ALA-GLY-AMEFALONE	434	416	391	363	348	146		

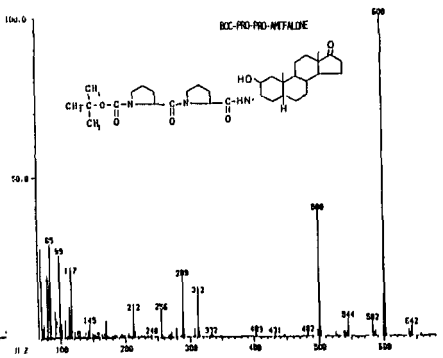

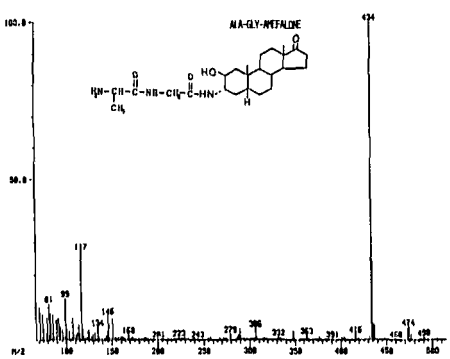

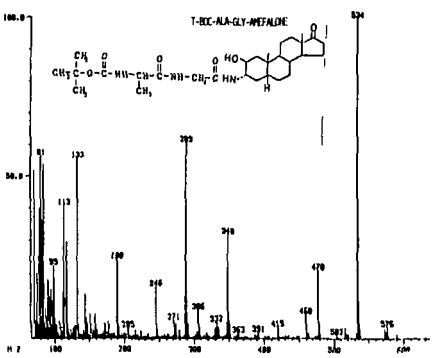

Presented at the 35th ASMS Conference on Mass Spectrometry and Allied Topics
May 24-29, 1987, Denver, CO

DETERMINATION OF THE ACTIVE PHOTOSENSITIZER IN THE PHOTODYNAMIC CANCER THERAPY (PDT) DRUG HEMATOPORPHYRIN DERIVATIVE (HPD): B. D. Musselman[1], C. K. Chang[2], and J. T. Watson[1,2], Departments of Biochemistry[1] and Chemistry[2], Michigan State University, East Lansing, MI, 48824.

Photodynamic therapy (PDT) has been applied in the clinical setting for both delineation and eradication of tumors in humans. The predominant drug used in this therapy is Hematoporphyrin derivative (HPD), or Photofrin II supplied by Ortho Diagnostics Systems of Raritan, NJ.

HPD is the product of the reaction of hematoporphyrin (HP) with glacial acetic acid and H_2SO_4 (20:1) which is subsequently treated with base to effect hydrolysis of the acetate functional groups from the HP. During the base hydrolysis step it has been shown that porphyrin oligomers are formed. FAB-MS was used to determine the molecular weight of these oligomers. Oligomers containing up to five HP sub-units were observed in the fraction oh HPD which is known to localize in tumors *in situ*.

Determination of the type of bond associating these oligomers was completed by applying chemical reduction with $LiAlH_4$ to the components of the tumor-localizing fraction. FAB-MS of reduced HPD showed that, while some porphyrin dimer was present in the drug, most of the polymers were reduced to porphyrin monomers with a mass of 570u. This mass is consistent for the reduction product of HP.

FAB-MS of the reduction product of the commercial PDT drug, Photofrin II, produced different results. Ions representative of reduced HP-oligomers were identified at m/z 1123, 1675, 2227, and 2779u. The m/z values of these ions correspond to the mass of protonated HP-dimers, -trimers, -tetramers, and -pentamers. These data confirm that HPD contains HP based polymers, however, the structure of these polymers may vary with ether and ester linkages being the primary covalent bonds associating the molecules.

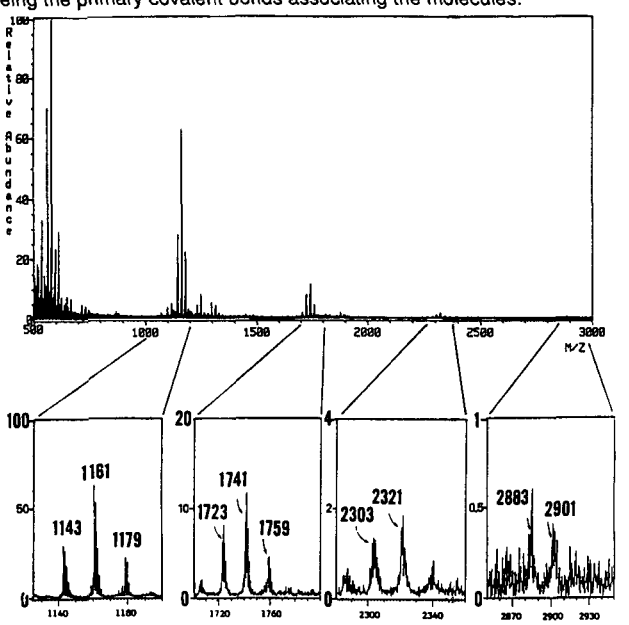

Figure 1: FAB mass spectrum of the high molecular weight fraction of HPD. Mass ranges for HP-dimer, trimer, tetramer and pentamers expanded to allow for mass assignment of individual ions.

Figure 2: FAB mass spectrum of the high molecular weight fraction of (A) HPD and (B) Photofrin II reduced with $LiAlH_4$ prior to analysis. Dimer, trimer, and tetramer mass ranges expanded to provide for mass assignment of individual ion species.

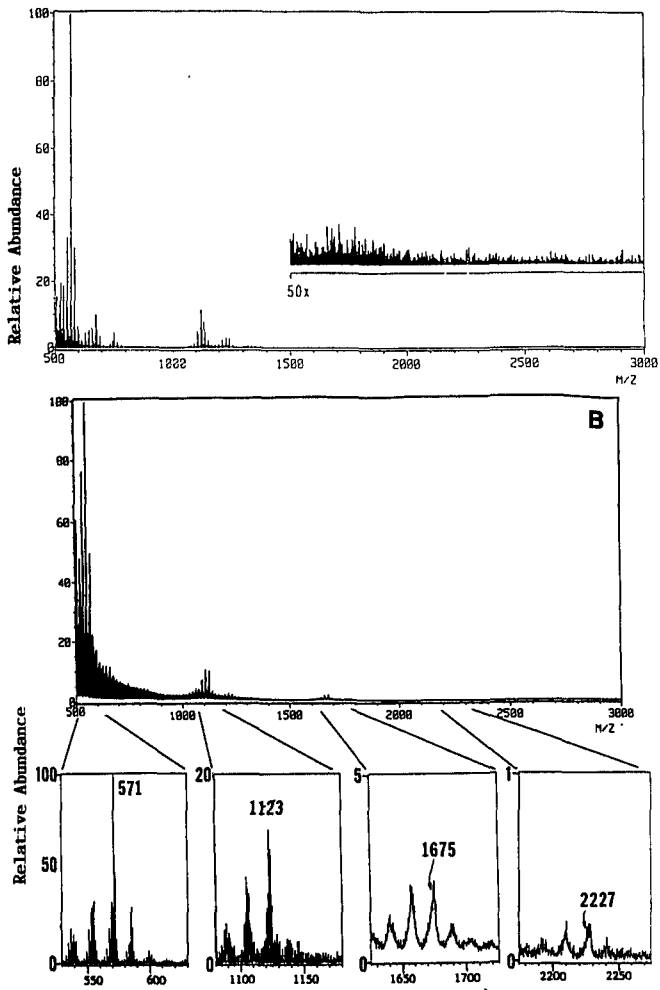

Reduction of model compounds including dimethyl HP and permethyl HP served to provide standards for FAB-MS analysis. The dimethyl ester of HP reduced readily to a HP-tetra alcohol with mass of 570u. Permethyl-HP showed the loss of 56u from its protonated molecule mass of 655u to 599u, consistent with reduction of the ester to alcohols, however, as expected for the reaction conditions employed, the methyl ether structures remained intact.

Acknowledgement: The authors wish to thank the NIH for their generous support of this research.

Presented at the 35th ASMS Conference on Mass Spectrometry and Allied Topics
May 24-29, 1987, Denver, CO

INVESTIGATION OF ETHYLENEDIAMINE ANTIHISTAMINES AND THEIR N-OXIDES BY DCI/MS, FAB/MS, AND FAB/MS/MS;

J. O. Lay Jr., C. L. Holder, W. M. Cooper, and W. A. Korfmacher, National Center for Toxicological Research, Jefferson, AR 72079

ABSTRACT

We have examined the N-oxides of five ethylenediamine-type antihistamines by DCI/MS, FAB/MS, and FAB/MS/MS. Typically, a weak protonated molecule and numerous fragment ions, including a prominent peak corresponding to loss of the oxygen atom from the N-oxide moiety, were observed using DCI/MS. With FAB/MS, no protonated N-oxide molecules were observed using thioglycerol as a liquid matrix. With glycerol however, intense protonated molecules were observed. Collisional activation of the FAB produced protonated molecules, which were mass selected using a three sector magnetic MS/MS instrument, produced fragment ions via characteristic cleavages adjacent to either nitrogen atom of the ethylenediamine moiety. The FAB/MS/MS spectra of a few other classes of antihistamines and their N-oxides were also examined for comparison. The same neutral losses were often observed from compounds having common functional groups, for example, a dimethylamine moiety.

INTRODUCTION

Most antihistamines can be grouped into three structurally similar classes, namely ethylenediamine, ethanolamine, or propylamine derivatives (1). The ethylenediamines are the most frequently used (1). Unfortunately, two ethylenediamine antihistamines have been shown to have unwanted properties. Methapyrilene appears to be a significant rat hepatocarcinogen (2), while pyrilamine induces unscheduled DNA synthesis (3). For this reason, several mass spectral methods have been applied to the analysis of antihistamine metabolites (ref. 4 for example). In this work, we compare the fragmentation behavior of seven antihistamines, and their N-oxides by DCI/MS, FAB/MS, and FAB/MS/MS. We report specific fragmentations which appear to be class specific for these three classes of related antihistamines, and their corresponding N-oxides.

EXPERIMENTAL

The antihistamines are the commercially available materials. The N-oxides were synthesized using standard methods which give dimethylamine N-oxides (5). DCI/MS: Samples were introduced into a Finnigan-MAT 4023 via a platinum filament. The reagent gas (methane or 10% ammonia in nitrogen) was set to an uncorrected nominal source pressure of 0.25 torr. FAB/MS: Spectra were obtained with a Kratos MS-50 equipped with an M-scan fast atom source and gun. Because thioglycerol reduced the N-oxides to their parent antihistamines, glycerol was used as a liquid matrix. FAB/MS/MS: Spectra were obtained using an MS-50 triple analyzer instrument equipped with an Ion Tech fast atom gun. MIKES scans were obtained by mass selecting the protonated molecule for collision activation.

figure 1

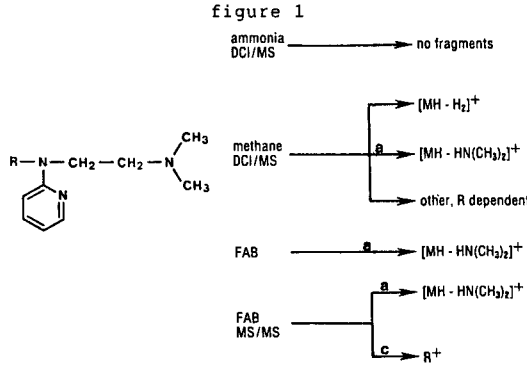

RESULTS AND DISCUSSION

For the ethylenediamine antihistamines, ammonia DCI/MS gave an intense protonated molecule and no fragments. Methane DCI/MS and FAB/MS both gave a protonated molecule, and a fragment corresponding to loss of dimethylamine (cleavage a in figure 1). With FAB/MS/MS an additional fragment was also observed corresponding to loss of the ethylenediamine moiety to give an ion whose mass was indicative of the mass of the unique group characteristic of each different antihistamine (cleavage c in figure 1). Some additional compound dependent fragments as well as loss of molecular hydrogen were also observed using methane DCI/MS.

For the N-oxides of the ethylenediamine antihistamines, ammonia DCI/MS, methane DCI/MS and FAB/MS (with glycerol) all gave protonated molecules and a fragment (a in figure 2) corresponding to loss of dimethylamine-N-oxide. DCI/MS also showed signals corresponding to loss of 16 and 30 daltons. With methane DCI/MS however the protonated molecule was quite weak, and the loss of 16 daltons was quite intense. This same ion, corresponding to loss of O from the protonated molecule was also observed with FAB using thioglycerol and is attributed to reduction of the N-oxide by the matrix thio group. Fragmentation at c, (figure 2) was also observed with the N-oxide using FAB/MS/MS.

CONCLUSION

Ammonia DCI/MS and FAB/MS provided intense protonated molecules and little or no fragmentation for the antihistamines and their N-oxides. Methane DCI/MS gave considerably weaker protonated molecules and more fragmentation, including a large and possibly misleading fragment due to loss of oxygen from the N-oxide moiety. Collisional activation of FAB produced protonated molecules gave class specific fragment ions for the antihistamines and their N-oxides. These fragments appear to be class specific rather than compound specific, with the members of a class of antihistamines showing the same neutral losses.

REFERENCES

(1) R. F. Doerge, in 'Textbook of Organic Medicinal and Pharmaceutical Chemistry' C. O. Wilson, O. Gisvold, and R. F. Doerge, eds. J. B. Lippincott, Philadelphia, PA, p. 648 (1977).

(2) W. Lijinsky, M. D. Reuber, and B. N. Blackwell, Science 209, 817 (1980).

(3) G. S. Probst, and J. B. Neal, Cancer Lett. 10, 67 (1980).

(4) J. O. Lay Jr., W. A. Korfmacher, D. W. Miller, P. Siitonen, C. L. Holder, and A. B. Gosnell, Biomed. Environ. Mass Spectrom. 13, 627 (1986).

(5) N. K. Chaudhuri, O. A. Servando, M. J. Manniello, R. C. Luders, D. K. Chao and M. F. Bartlett, Drug Metab. Dispos. 4,373 (1976).

figure 2

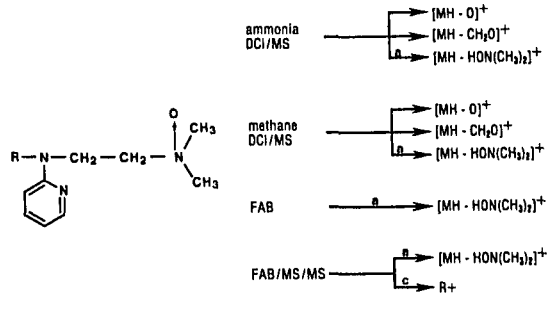

Presented at the 35th ASMS Conference on Mass Spectrometry and Allied Topics
May 24-29, 1987, Denver, CO

DETERMINATION OF MDL 19,744A AND STABLE ISOTOPE LABELED MDL 19,744A IN PLASMA BY CAPILLARY GAS CHROMATOGRAPHY/MASS SPECTROMETRY.

Edward L. Olberding and John D. Stuhler

Merrell Dow Research Institute, Indianapolis, IN 46268

MDL 19,744A (1α,2α,3β)-6,7-dihydro-5-(((2-hydroxy-3-phenoxycyclopentyl)-amino)-methyl)-2-methylbenzo)b)thiophen-4(5H)-one hydrochloride), is currently being evaluated as an antihypertensive agent.

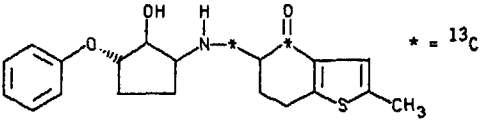

In order to support stable isotope MDL 19,744A pharmacokinetic studies, a capillary GC/MS method was developed for the determination of unlabeled MDL 19,744A and C-13 MDL 19,744A, labeled in the carbonyl position and in the carbon of the amino methyl bridge.

Blood samples were obtained by jugular venipuncture. The samples were collected in heparinized glass tubes, centrifuged, and the plasma isolated. After addition of the internal standard, a methyl analogue of MDL 19,744A, the plasma samples were basified and the MDL 19,744A extracted with toluene. Following evaporation of the toluene, the residues were derivatized with pentafluoropropionic anhydride.

Capillary gas chromatography/negative chemical ionization mass spectrometry employing selected ion monitoring (GC/NCI-SIM) was used for quantitation. A splitless injection onto a J&W Scientific 10 m x 0.25 mm Durabond-5® column was used for chromatographic resolution of the MDL 19,744A and internal standard. m/z 623 (C-12 MDL 19,744A), m/z 625 (C-13 MDL 19,744A), and m/z 637 (internal standard) were monitored for quantitation (Figure 1). The method was validated over a concentration range of 0.5-50 ng/mL for each compound.

The method has proven reliable for the analysis of several hundred plasma samples from pharmacokinetic and bioavailability studies. These studies have shown that the use of a stable isotope form of MDL 19,744A as an "internal standard" allows simultaneous administration of two different formulations of the drug, minimizing intra-subject variability in bio-availability studies.

Presented at the 35th ASMS Conference on Mass Spectrometry and Allied Topics
May 24-29, 1987, Denver, CO

SIM MASS CHROMATOGRAM OF DOG PLASMA

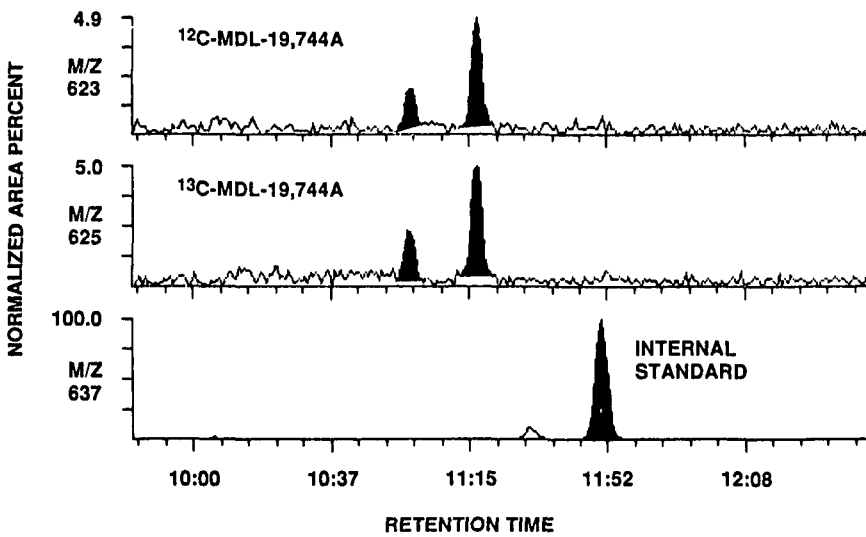

Presented at the 35th ASMS Conference on Mass Spectrometry and Allied Topics
May 24-29, 1987, Denver, CO

IDENTIFICATION OF BUSPIRONE METABOLITES BY GC/MS:

H.K. Jajoo, R.F. Mayol*, J.Labudde* and I.A. Blair.
Department of Pharmacology, Vanderbilt University, Nashville, Tenn. 37232
*Pharmaceutical Research and Development Division, Bristol-Meyers Company, Evansville, IN 47221

INTRODUCTION

Buspirone [8-(4-(4-(2-pyrimidinyl)-1)-1-piperazinyl)-butyl)-8-azaspiro-[4.5]-decane-7,9-dione] is a potent anti-anxiety drug that has recently been introduced into clinical practice. It is equipotent as an anti-anxiety agent with the benzodiazepines. However, it lacks the hypnotic, anti-convulsant and muscle relaxant side effects which are quite commonly observed with benzodiazepines (1). Buspirone is known to undergo extensive metabolism in vivo and only 1% of the drug is excreted unchanged. The two known major metabolites are 5- hydroxy-buspirone (5-OH-Bu) and 1-pyrimidinyl-piperazine (1PP). Buspirone also forms two more metabolites which are hydroxy derivatives of 5-OH-Bu whose structures have yet to be assigned completely (2).

As part of a program to fully elucidate the in vivo metabolism of buspirone, a metabolic study in the rat has been carried out. The structural characterization of the four major metabolites obtained from the bile of rats treated with buspirone is presented.

EXPERIMENTAL

The ^{14}C labeled drug was administered orally to a group of Sprague-Dawley rats, the bile was collected, pooled and lyophylized. Lyophylized bile (33ml) was deconjugated using a large excess of glucuronidase/sulphatase (750mg) by incubation at 37°C in 6ml water and 2ml 2M ammonium acetate (pH 5.2), for 3 hours. The deconjugated bile was applied to prewashed C_{18} Sep-Paks. The metabolites were eluted from the Sep-Paks with 4ml methanol and dried under a stream of nitrogen. They were then dissolved in 2ml 50% methanol: water and filtered through a 4.5 µm disposable filter to remove suspended matter. The mixture of metabolites was separated using high performance liquid chromatography (HPLC). A semi-preparative ODS column (10 µm; 10mm x 250mm) was used. A gradient from 25% methanol: 0.01M ammonium acetate to 65% methanol: 0.01M ammonium acetate was used over a period of 25 minutes. The flow rate was 3ml/min. Four major peaks of radioactivity were collected. They had retention times 4.5 min, 15 min, 17 min and 21 min. The major constituent of each peak was purified to homogeneity using a similar HPLC system. The metabolites are referred to as I, II, III and IV respectively. The metabolites were converted to their corresponding trimethylsilyl (TMS) derivatives in order to improve their GC characteristics. They were analyzed by capillary column GC/MS on a Nermag R1010C quadrupole mass spectrometer in the electron impact (EI) mode. The metabolites were dissolved in 99.96% acetonitrile-d_3 and NMR spectra obtained on a Bruker NR-300 Fourier transform NMR spectrometer.

RESULTS AND DISCUSSION

Metabolite I co-eluted on HPLC with an authentic sample of 5-hydroxy-1PP (5-OH-1PP). The mass spectrum of I showed an ion at m/z 196 which confirmed the presence of an OTMS group on the aromatic ring. The molecular ion at m/z 324 arose through formation of a bis-TMS derivative. The NMR spectrum was identical with an authentic sample of 5-OH-1PP.

Metabolites II and III had identical mass spectra. The mass spectrum of II is shown in Figure 1. Ions at m/z 196 and 265 indicated the presence of an OTMS group on the aromatic ring. Ions at m/z 353 and 365 indicated the presence of another OTMS group on the spiro end of the molecule. The molecular ion at m/z 561 was consistent with a bis-TMS derivative of a dihydroxy compound. It was impossible to distinguish II and III based on mass spectra alone. Fast atom bombardment and accurate mass EI also failed to distinguish II and III.

The NMR Spectrum of II showed a low field 1-H singlet at δ 4.6 ppm which was 0.4 ppm downfield from the methine proton observed in metabolite III. A 2-H AB quartet centered at δ 2.5 ppm was 0.1 ppm to higher field than was observed for metabolite III. The aromatic region appeared as a sharp singlet. This confirmed the presence of a hydroxyl group at the 5 position on the aromatic ring. The aliphatic region of II was identical to that of synthetic 3-oxo-N-(4-(4-(2-pyrimidinyl)-1-piperazinyl)-butyl)-2-oxaspiro-[4.4]-nonane-1-carboxamide (oxa-Bu) and hence II was identified as 5-OH-oxa-Bu. The NMR spectrum of III showed a sharp singlet at δ 4.2 ppm and an AB type quartet centered at δ 2.6 ppm. This suggested that the site of hydroxylation was at the 6' position next to the spiro carbon atom. The

aromatic region appeared as a sharp singlet, indicating that the other hydroxy group was at the 5 position on the aromatic ring. Based on this data III was identified as 6',5-dihydroxy-buspirone. It was further shown that II and III could be interconverted under basic conditions. This observation suggested the possibility that metabolite III was formed as a consequence of the isolation procedure.

Metabolite IV co-eluted on HPLC with an authentic sample of 5-hydroxy buspirone (5-OH-Bu). The mass spectrum of IV showed a molecular ion at m/z 473. This indicated the presence of an OTMS group in the molecule. Ions at m/z 265 and 196 indicated the presence of an OTMS group on the aromatic ring. Ions at m/z 277 indicated that there was no hydroxylation at the spiro end of the molecule and suggested that IV was a hydroxy derivative of Bu. The NMR spectra of IV was identical with authentic 5-OH-Bu.

CONCLUSIONS

1. Four major metabolites of buspirone present in rat bile have been identified as 5-OH-1PP, 6',5-dihydroxy Bu, 5-OH-oxo-Bu and 5-OH-Bu.

2. Metabolite II and metabolite III interconvert under basic conditions.

3. The identification of minor metabolites from rat bile and metabolites from rat urine is in progress.

REFERENCES

1. K.L. Goa and A. Ward, Drugs, 32:(1986),114.

2. R.E. Gammans, R.F. Mayol and J.A. Labudde, Am. J. Medicine, 80:(1986),41.

ACKNOWLEDGEMENTS

This work was supported by NIH Grant RR01688, USHPS Grant EHS 521085 and Bristol-Myers.

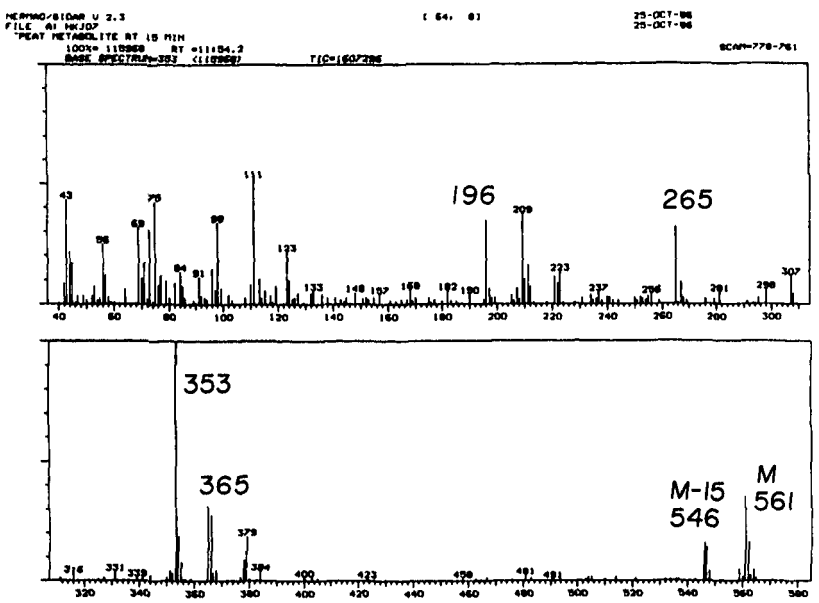

Figure 1 - EI/MS spectrum of metabolite II as a TMS derivative.

Presented at the 35th ASMS Conference on Mass Spectrometry and Allied Topics
May 24-29, 1987, Denver, CO

GC-MS Method for the Quantitation of Enantiomers of Rimantadine in Human Plasma and Urine.

B.J. Miwa, N. Choma, N. Keigher, W.A. Garland and E.K. Fukuda
Hoffmann-La Roche Inc., Nutley, New Jersey 07110

Most drugs having chiral centers are given as racemates with no consideration given to potential differences in the therapeutic action, kinetics, metabolism or toxicity of the enantiomers. In this presentation, a method is described for the analysis in plasma and urine of the enantiomers of rimantadine, an antiviral drug having a chiral center. The method involves extracting rimantadine from plasma onto a Bond-Elute® column at pH 9.1, and derivatizing the residue from a methanol column eluate with an optically active reagent, (+)α-methyl-α-methoxy (pentafluorophenyl) acetic acid[1,2]. Catalysts in the reaction are dicyclohexyl carbodiimide and 1-hydroxy benzotriazole, well-known coupling reagents in peptide chemistry. The reaction solvent is dichloromethane.

In order to verify that the derivatization reactions did not cause racemization, optically pure α-methyl-benzylamines were each derivatized with the optically active reagent. GC-MS analysis verified that a single diastereomer was generated in each case.

The rimantadine diastereomers are analyzed by methane NCI on a Kratos MS-50 GC/MS using the following chromatographic conditions: a 30m DB-1 capillary column, H_2 as carrier gas, a 164°C to 264°C temperature program (10°C/minute). The diastereomers are detected by methane NCI, monitoring the $[M-HF-CH_3OH]^-$ ion (m/z 379). Quantitation was achieved using tetradeuterated rimantadine as the reference standard, and measuring the m/z 379:m/z 383 ion ratio. Plasma and urine concentrations of each stereoisomer were measured over a range from 250-2.5 ng/ml and 1250-12.5 ng/ml, respectively. The overall inter-assay precision for plasma was 5.48% and 4.50% for the first and second eluting diastereomer, respectively.

Figure 1 shows a typical selected ion current profile of the rimantadine stereoisomers from the plasma of a healthy male subject administered a 200 mg dose of rimantadine. Different rates of reaction for

the formation of each diastereomer commonly occur in reactions involving chiral centers [1,3] and is apparent by the different SIM heights of peaks A and B.

Figure 2 shows the plasma concentration vs. time profile of the two rimantadine stereoisomers in one individual. Analysis of plasma and urine samples from four patients administered a 200 mg oral solution of rimantadine showed no significant differences in concentration vs. time profile of the two stereoisomers.

1. Pohl, L.R. and Trager, W.F. J. Med. Chem. 16, 475 (1973).
2. Valente, E.J., Pohl, L.R. and Trager, W.F. J. Org. Chem. 45, 543 (1980).
3. Morrison, J.D. and Mosher, H.S. "Asymmetric Organic Reactions", Prentice-Hall, Englewood Cliffs, NJ. pp. 50-83, 1971.

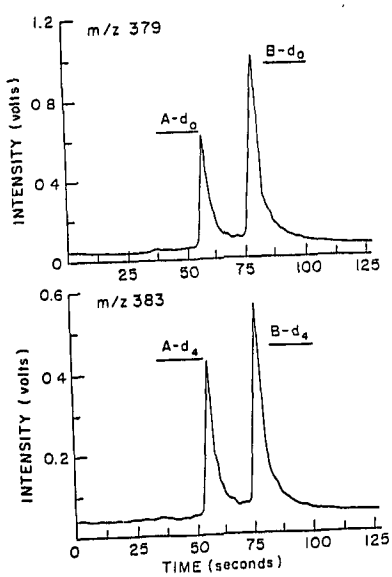

Figure 1

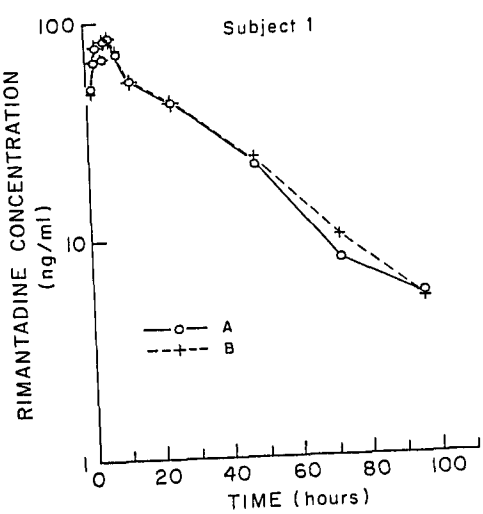

Figure 2

Presented at the 35th ASMS Conference on Mass Spectrometry and Allied Topics
May 24-29, 1987, Denver, CO.

MEASUREMENT OF RIMANTADINE IN PLASMA BY CAPILLARY GAS CHROMATOGRAPHY-MASS SPECTROMETRY

D.A. Herold, P.K. Anonick, M. Kinter and F.G. Hayden
Departments of Pathology and Internal Medicine
University of Virginia Medical Center
Charlottesville, VA 22908

INTRODUCTION

Rimantadine has well documented prophylactic and therapeutic efficacy in influenza A virus infection. We were involved in a study to measure plasma levels of Rimantadine in a large group of elderly patients treated with Rimantadine. Previously reported methods include electron capture gas chromatography and gas chromatography/mass spectrometry, utilizing methane chemical ionization and stable isotope dilution. We have simplified the mass spectrometry procedure previously reported by Fukuda et al. by using a more readily synthesized deuterium labeled Rimantadine as an internal standard and a simplified derivatization procedure for preparing the t-butyldimethylsilyl derivative. These modifications provide an efficient, accurate and precise analysis of Rimantadine in human plasma.

MATERIAL AND METHODS

A. PREPARATION OF d_3-RIMANTADINE.

Chemicals

Absolute Ethanol (Warner-Graham Co., Cockeysville, MD 21030); Ethyl Acetate, Toluene, Certified (Fisher Scientific Co., Fair Lawn, NJ 07410); Anhydrous Ether, Purified (J.T. Baker Chemical Co., Phillipsburg, NJ 08865); Hydrogen Chloride Gas, Tech. (Matheson Gas Products, Inc., Baltimore, MD 21227); Sodium Borohydride (Fisher Scientific Co., Fair Lawn, NJ 08865); 1-Adamantane Carbonitrile, 97%, Methyl-d_3-Magnesium Iodide, 99+ atom % D, 1.0 M Solution in Diethyl Ether (Aldrich Chemical Co., Milwaukee, WI 53233).

Synthesis

CD_3MgI in diethyl ether (0.1 L, 0.1 M) was added slowly to a solution of 1-Adamantane carbonitrile (8.0 g, 0.05 M) in toluene (100 ml) and boiled gently until 60 ml of the ether had been distilled. The heat was removed and the solution was stirred for 72 hours. A solution of $NaBH_4$ (1.87 g, 0.055 M) in absolute ethanol (20 ml) was added slowly to the reaction mixture and stirred for 1 hour. The mixture was then quenched with 95% ethanol and the d_3-Rimantadine extracted into ether. The hydrochloride salt was obtained by bubbling HCl gas through the ether. The white crystals were recrystalized from absolute ethanol and ethyl acetate.

Yield - 2.07 g d_3-Rimantadine; 23.3% of Theoretical.

B. SEPARATION, EXTRACTION, DERIVATIZATION OF PLASMA SAMPLES

Chemicals

Methanol, HPLC grade (J.T. Baker Chemical Co., Phillipsburg, NJ 08865); Sodium Phosphate Dibasic, Anhydrous (Fisher Scientific Co., Fair Lawn, NJ 07410); EDTA Disodium Salt, Dihydrate (Sigma Chemical Co., St. Louis, MO 63178); Bond Elect CN Solid Phase Extraction Columns, 3 ml (Analytichem International, Harbor City, CA 90710); Argon (Roberts Oxygen Co., Rockville, MD 20855); Acetonitrile UV (American Scientific Products, McGaw Park, IL 60085); N-Methyl-N-tert-butyldimethylsilyl)-trifluoroacetamide (MTBSTFA) (Pierce Chemical Co., Rockford, IL 61105).

Extraction and Derivatization

For this analysis, 200 ng of d_3-Rimantadine was added to 1.00 ml of plasma, previously pH adjusted to pH 9.1 by the addition of 1 ml of a 0.1 M HNa_2PO_4 buffer. The sample was then applied to a Bond-Elute CN column which had been activated by 2 x 1 ml methanol washes and 2 x 1 ml H_2O washes. Following application of the sample, the column was washed with 2 x 1 ml portions of H_2O and the analyte eluted using 2 x 1 ml portions of methanol. The methanol fraction was then quantitatively transferred to a 5 ml Reacti-vial for derivatization.

Prior to derivatization, the sample was dried under a stream of dry argon at 40°C. The residue was then dissolved in 50 ul of CH_3CN and 50 ul of MTBSTFA added. The reaction mixture was then vortexed and reacted at 40°C for 30 minutes.

C. GC/MS ANALYSIS

Rimantadine levels were determined by GC/MS analysis in a selected ion monitoring (SIM) experiment. A mass resolution of 3000 (M/dM, 10% valley) was used with the ions at m/z 236.183 and m/z 239.202 being monitored. These ions correspond to the loss of C_4H_9 from the

t-butyldimethylsilyl derivative of d_0- and d_3-Rimantadine, respectively. Data were acquired at a rate of 1.5 cycles per second, providing approximately 10 data points across the chromatographic peak, with a dwell time of 284 msec per channel per cycle. A 30 meter x 0.25 meter DB-1 capillary column with a film thickness of 0.25 microns was used. Samples were injected on-column at an oven temperature of 50°C which was immediately ramped to 300°C at 15 C/min. Under these conditions, Rimantadine eluted at approximately 11 minutes with the d_3-Rimantadine having a peak centroid slightly ahead of the d_0-Rimantadine.

D. CALCULATIONS

For each set of samples three standards were run: an assay blank and two calibrators 33 ng/ml and 330 ng/ml.

Linear regression of the experimental ratio yielded an equation

X (ng/ml) = A + BY
where A = X-intercept
B = slope
Y = experimental ratio A236/A239

RESULTS

A. INTERNAL STANDARD

Figure 1 is a scanned EI spectra of the derivatization Rimantadine d_3. Figure 2, a SIM chromatogram of the d_3-Rimantadine, is also shown to demonstrated the contribution of the internal standard to the analyte peak (m/z 236).

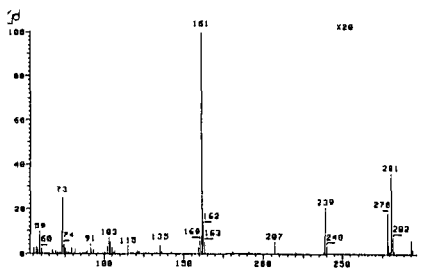

Figure 1

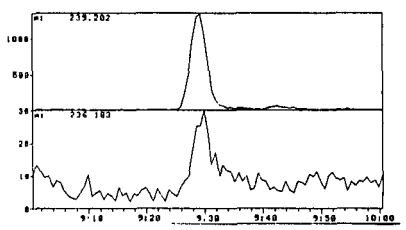

Figure 2

B. LINEARITY

A standard addition study demonstrated linearity over the range from 30-1500 ng/ml.

C. PRECISION

	Within Run			Run-to-Run		
	n	X + s.d.	c.v.	n	X + s.d.	c.v.
Low Control	11	29 + 2.6	8.9%	11	29 + 1.6	5.4%
High Control	11	302 + 9	3.0%	11	302 + 11	3.6%

D. RANGE

Treated volunteers (n=86) provided plasma samples with a range of 153-1035 ng/ml.

E. LIMIT OF DETECTION

Limit of detection was 10 ng/ml.

F. INTERFERENCES

Under the conditions of the assay, no interferences were noted.

CONCLUSIONS

1. The use of the t-butyldimethylsilyl derivative simplified the sample preparation and provides interference-free high intensity peaks.
2. The d_3-Rimantadine was synthesized by an easy method that allowed excellent isotope incorporation.
3. This GC/MS method offers a rapid and precise analysis of Rimantadine in plasma.

Presented at the 35th ASMS Conference on Mass Spectrometry and Allied Topics
May 24-29, 1987, Denver, CO

CHARACTERIZATION OF BILIARY METABOLITES OF A SYNTHETIC VASOPRESSIN ANALOGUE BY FABMS:

K. Straub, C. Garvie, M. Davis and R.K. Lynn
Department of Drug Metabolism, Smith Kline & French Laboratories, Swedeland, PA 19479

SK&F 101926 ([PMP^1-(D)Tyr(Et)^2-Val^4-desGly^9]-AVP; structure 1) is a synthetic octapeptide analogue of the antidiuretic hormone, arginine vasopressin (AVP)[1]. This structure incorporates a number of novel features, including replacement of the N-terminal cysteine of AVP by a cyclopentamethylenepropionate (PMP) moiety and substitution of an O-ethyl-D-tyrosine for the tyrosine residue at position 2. This agent blocks the direct renal (V2 receptor) effects of endogenous and exogenous vasopressin, resulting in a reduction in urine osmolality and increased water clearance. Following intravenous administration to rats, SK&F 101926 undergoes rapid disappearance from the circulation and is excreted primarily via extraction into bile Approximately 80% of the administered dose (10 µg/kg) is excreted into bile over a 48 hr time period, with over 75% appearing in the first twelve hours. HPLC analysis of bile obtained after administration of radiolabeled SK&F 101926 showed that extensive degradation of the drug had taken place to a series of metabolites. The present study was undertaken to isolate and characterize these biliary metabolites, and to thereby identify the major routes of biotransformation that SK&F 101926 undergoes.

Because of the low therapeutic dose of this agent (10-100 µg/kg) and its relatively high molecular weight, mass spectrometry was the principal technique used for the structural characterization of isolated metabolites. In general, quantities of metabolites ranging from 100 ng- several µg could be isolated in a relatively pure state from bile samples using reverse phase HPLC. FABMS analysis then provided molecular weight information, but sequence ions were either of very low relative intensity, or were absent altogether. Additional information on these structures was therefore provided *by amino acid analyses of acid hydrolysates, using either HPLC or GCMS methodologies.*

SK&F 101926 labeled with ^{3}H in the 3-position of the D-Tyr residue (s.a. 4.35 Ci/mmol) was employed in these studies. The common bile duct of male Sprague-Dawley rats weighing 250-260 gm was cannulated with PE-50 tubing, and ^{3}H-SK&F 101926 was administered as a single bolus (10 µg/kg, as 2.5 µg/200 µl of saline) or as three separate 333 µg doses at 3 hr intervals (cumulative dose 4 mg/kg) through a jugular vein cannula. Bile samples were collected into polypropylene test tubes over dry ice and stored at -70°. These samples were then analyzed by HPLC on an Aquapore RP300 column (C-8 packing with a 300 Å pore size; 4.2mm or 7mm x 25cm), using linear gradients of 0.25% (v/v) trifluoroacetic acid (TFA) in water and acetonitrile. For preparative isolation, bile samples were first subjected to a preliminary cleanup step by applying the sample to a C18 solid phase extraction cartridge, and eluting with solvent containing various percentages of acetonitrile-water containing 0.25% TFA (v/v).

FAB mass spectra were recorded on a VG7070-EHF mass spectrometer, using glycerol (containing ~ 1% TFA) or thioglycerol as the matrix. Metabolites were analyzed for amino acid content by hydrolysis with 6N HCl-TFA (2:1 v/v, 150°, 2 hr, under an argon atmosphere), followed by reaction with phenyl isothiocyanate (PITC). The resulting amino acid derivatives were then separated by HPLC and detected by absorbance at 254 nm (Waters 'Picotag' methodology). Typically 0.05-1.0 µg of metabolite was used for this analysis; the yield of D-tyrosine under these conditions ranged from 70-80%, while the yields of other 'standard' amino acids ranged from 90-98%. Alternatively, hydrolysates were analyzed by GCMS after conversion to N-pentafluoropropionyl, n-butyl esters.

An HPLC/LSC profile of a bile sample obtained after administration of ^{3}H-SK&F 101926 at a dose of 10 µg/kg is shown in figure 1. Fraction 4, marked with an asterisk, had a retention time equal to that of the parent drug, and FABMS analysis confirmed that it had a molecular weight of 1078.5 [$(M+H)^+$ m/z 1079.5; $(M+Na)^+$ m/z 1101.5; $(M-H)^-$ m/z 1077.5); figure **2A**]. In addition, the amino acid analysis of this fraction was shown to be identical to that of the parent drug. The major component present in bile, fraction 5, was found to have an amino acid composition identical to that of parent drug, but FABMS analysis showed a mass shift of 1 amu (m/z 1080.5 and 1102.5 in positive ion mode; figure **2B**). This corresponds to the conversion of an -NH_2 group to an -OH, via hydrolysis of the C-terminal amide. Confirmation of the identity of this metabolite as structure 2 ([PMP^1-(D)Tyr(Et)^2-Val^4-desGly^9-OH]-AVP) was obtained by a comparison of the HPLC retention time and FAB mass spectrum of the isolated metabolite with a standard, prepared by treatment of SK&F 101926 with trypsin.

Fraction 9 was observed to yield m/z 924, 946 and 968 in positive ion mode and m/z 922 in negative ion mode. This corresponds to a molecular weight of 923, and a mass difference of 156u from the parent drug This is equivalent to a single arginine residue, confirmed by amino acid analysis. The identity of peak 9 was therefore established as [PMP^1-(D)Tyr(Et)^2-Val^4-desArg^8-desGly^9-OH]-AVP, (structure 3). Peak 8 gave a FAB mass spectrum with ions at m/z 849 and 871 (positive mode) and m/z 825 and 847 (negative ion mode). This is consistent with a molecular weight of 826, corresponding to a difference in mass of 252 amu from SK&F 101926. This difference is accounted for by hydrolysis of the terminal amide and the loss of the two C-terminal residues, arginine and proline. This conclusion was supported by amino acid analysis, leading to the assignment of structure 4 to peak 8.

Attempts at increasing the relative abundance of sequence ions or at using MS/MS techniques to enhance the amount of structural information in the FAB mass spectra were hampered by the presence of alkali metal contamination in the samples. This appears to be a general problem with samples that are isolated from bile, and poor recovery of analytes from HPLC procedures limits the number of repetitive chromatographic steps that can be carried out. Conversion of the cyclic hexapeptide moiety to a linear sequence by reduction of the disulfide bond (with dithiothreitol or other reducing agents) and derivatiztion of the resulting sulfhydryls yielded products that gave enhanced fragmentation when ionized by FAB, but this procedure is difficult to carry out on a picomole scale. For these types of samples, then, FABMS appears to be most useful for obtaining molecular weight information only.

Presented at the 35th ASMS Conference on Mass Spectrometry and Allied Topics
May 24-29, 1987, Denver, CO

The observation that peptidase-mediated hydrolysis of C-terminus residues was a major route of biotransformation prompted an investigation of the utility of using FABMS to monitor this hydrolysis reaction. Because of the complex, multifunctional nature of these structures, chromatographic resolution of the parent drug and its hydrolysis products may not be readily achievable in all cases. In contrast, such enzyme mediated reactions can be readily monitored by FABMS, as first outlined in a series of papers by Caprioli and coworkers[2]. Using this approach, the conversion of an Arg-NH2 terminus to an Arg-COOH, corresponding to an increase in mass of 1 u, could be monitored directly by mass spectrometry (*eg*, figure 3, for the hydrolysis of SK&F 101926 by a tissue (rat jejunum) homogenate, as m/z 1079.5 → 1080.5). This methodology can be used to screen for the presence of specific hydrolytic activities in a tissue homogenate towards a given peptide drug, or to evaluate the relative sensitivity of a series of analogues towards a given enzymatic activity. These techniques should be generally applicable to the study of the metabolism of other modified peptides.

1. Huffman, W.F. *et. al.*, J. Med. Chem. 28, 1759-1760 (1985).
2. R.M. Caprioli and L. Smith, Anal Chem. 58, 1080-1083 (1986).

	X	Y	Z
1	Pro	Arg	NH_2
2	Pro	Arg	OH
3	Pro	OH	-
4	OH	-	-

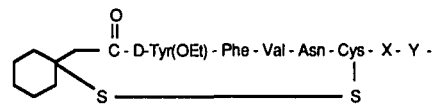

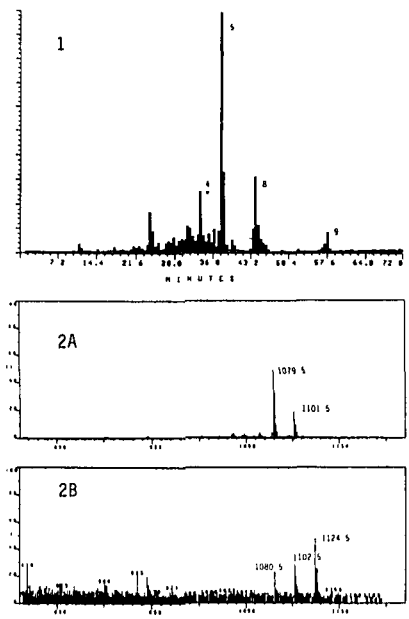

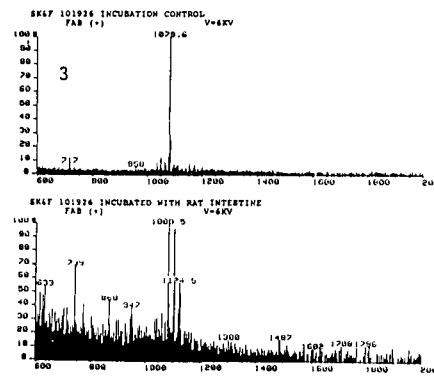

Presented at the 35th ASMS Conference on Mass Spectrometry and Allied Topics
May 24-29, 1987, Denver, CO

THERMOSPRAY LC/MS IDENTIFICATION OF MITOMYCIN C AND PORFIROMYCIN DNA ADDUCTS

Steven M. Musser[1], Patrick S. Callery[1] and Su-Shu Pan[2]

1. Department of Medicinal Chemistry and Pharmacognosy, Univ. of Maryland, Baltimore, MD. 21201
2. Univ. of Maryland Cancer Center, Baltimore, MD. 21201

Mitomycin C (MC) and its N-aziridinyl methyl analog porfiromycin (PFM) are both effective anticancer drugs. The proposed mechanism of action of both drugs is alkylation of DNA either by forming crosslinks or monofunctional adducts. The structure of the major product of monofunctional alkylation has recently been identified by NMR and FTIR as N^2-(2-"β,7"-diaminomitosen-1"-α-yl), 2'-deoxyguanosine (1). The objective of this work was to determine the usefulness of thermospray mass spectrometry for identifying and assaying drug-DNA adducts. Since the mitomycin C-DNA adduct was well defined and of clinical importance we decided it would be a good candidate for study by thermospray LC/MS.

The mitomycin C or porfiromycin DNA adducts were prepared by enzymatically reducing the drug in the presence of calf thymus DNA and then enzymatically digesting the DNA to single nucleosides (2). Separation of the digested DNA was carried out on a reverse phase C18 column, with a mobile phase consisting of 0.1 M ammonium formate. The LC effluent was introduced directly into a Finnigan 4500 mass spectrometer via a Vestec thermospray interface. The entire procedure from alkylation of the DNA to the MS analysis of the DNA adduct takes less than 24 hours.

The total ion chromatogram shows peaks corresponding to the four DNA bases along with a smaller peak corresponding to the drug-DNA adduct. The mass spectrum of the MC or PFM DNA adducts displays a protonated molecular ion of approximately 2% relative abundance. The structurally informative fragments include, loss of the deoxyribosyl moiety from the nucleoside and cleavage of the drug-nucleoside bond. The base peak in the spectrum corresponds to the nucleic acid to which the drug is attached providing additional proof that the drug is covalently bound to a deoxyguanosine nucleoside. It is important to note that the thermospray conditions must first be optimized for deoxyguanosine, such that the molecular ion (m/z 268) is at least 10% of the base peak (m/z 152) or a molecular ion will not be observed for the drug-DNA adduct.

REFERENCES

1. M. Tomasz, R. Lipman, G. Verdine, and K. Nakanishi, Biochemistry., 1986, 25, 4337.

2. S. Pan, T. Iracki, and N. Bachur, Molecular Pharmacology., 1986, 29, 622.

Presented at the 35th ASMS Conference on Mass Spectrometry and Allied Topics
May 24-29, 1987, Denver, CO

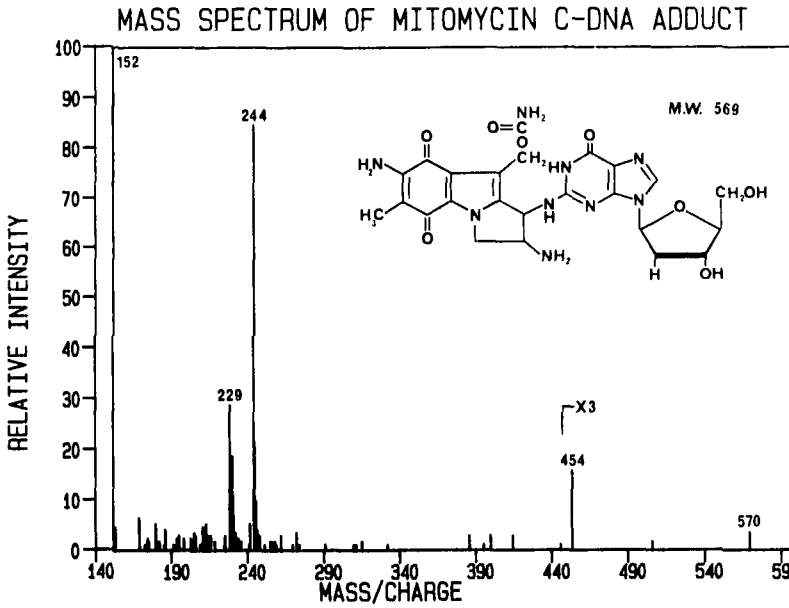

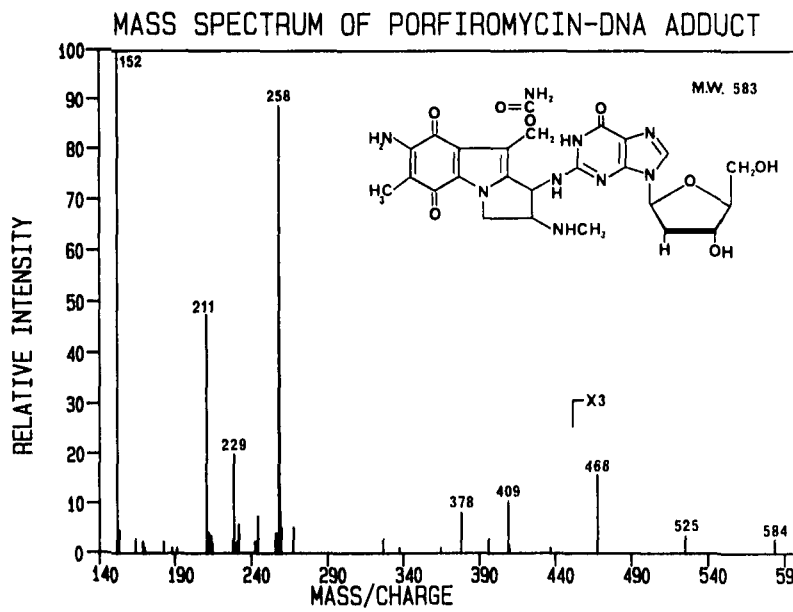

Presented at the 35th ASMS Conference on Mass Spectrometry and Allied Topics
May 24-29, 1987, Denver, CO

DIMETHYLFORMAMIDE DIMETHYLACETAL AS A DERIVATIZING AGENT FOR GC-MS DETERMINATION OF UNSTABLE SECONDARY AMINES. Mary F. Kaiser and Patrick S. Callery, Department of Medicinal Chemistry and Pharmacognosy, School of Pharmacy, University of Maryland at Baltimore, Baltimore, MD.

A problem inherent in the GC-MS analysis of a probable nicotine metabolite[1], 4-(3-pyridyl)-4-methylaminobutanoic acid, is its on-column conversion to the corresponding lactam, cotinine, a verified nicotine metabolite.

In order to distinguish between the two, derivatization of the amino acid was necessary. Various reagents, alone or in combination, were used in an attempt to derivatize both the carboxylic acid and secondary amine moieties. Because PMGABA is not stable at room temperature, a more stable analog, 4-methylaminobutanoic acid (NMGABA), was used as a model compound in tests of the reagents.

Several acylating agents, among them trifluroacetic anhydride and BSTFA, as well as silylating agents such as TMS failed to react with the amine group first, resulting in a carboxyl group activated to cyclization. Dimethylformamide dimethylacetal (DMFDMA) successfully derivatized both NMGABA and PMGABA.

Experimental

An Extrel Simulscan Model Mass Spectrometer used in the EI mode interfaced with a Carlo-Erba Model 4130 capillary gas chromatograph or a HP Model 5970 MSD interfaced with a HP Model 5980 capillary gas chromatograph were used. Spectra were obtained at the rate of 500 amu/s over the range 40-500 amu. Chromatography was carried out over 80-180° C at 15° C/min.

An excess of DMFDMA was heated with the amino acid at 100°C for 15 minutes. Water was added to the cooled mixture, and the derivative was extracted with methylene chloride.

Results

The N-formyl methyl ester derivative of NMGABA was formed in two steps upon reaction with DMFDMA. In the first, a methyl ester formamide acetal intermediate is formed. In the second, the acetal is hydrolyzed to yield the N-formyl product.

The ester is produced via either of two possible mechanisms, the formamide acetal by transamination.[2] PMGABA is derivatized similarly.

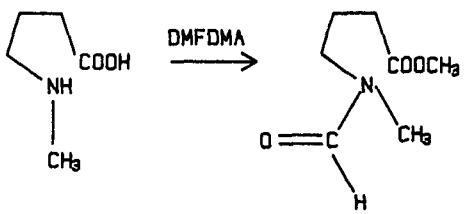

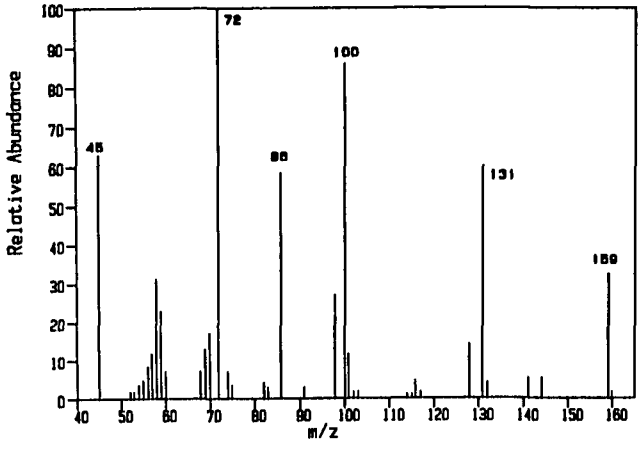

References

1. H. McKennis, Jr., L. B. Turnbull and E. R. Bowman, J. Am. Chem. Soc., **80** 6597-600 (1958).
2. M. S. B. Nayar and Patrick S. Callery, Anal. Lett., **13(A7)** 625-34 (1980).

Presented at the 35th ASMS Conference on Mass Spectrometry and Allied Topics
May 24-29, 1987, Denver, CO

LASER DESORPTION-FOURIER TRANSFORM MASS SPECTROMETRY OF ANTIBIOTICS

Mildred L. Coates
Department of Chemistry
University of California
Riverside, CA 92521

Development of desorption/ionization methods has allowed mass spectral examination of many biologically significant molecules. The group of compounds exhibiting antibiotic activity consists of molecules of a variety of structural types. The objective of this work is to compare the mass spectral behavior of different types of antibiotics using laser desorption-Fourier transform mass spectrometry (LD-FTMS) (1) and to evaluate the use of this technique for their characterization.

The LD-FTMS system used for this study has been described previously (2). Antibiotic samples are prepared either by affixing undoped powdered samples to the probe tip with double-sided-adhesive tape or by dissolving samples in appropriate solvents (water, methanol, or chloroform) and depositing an aliquot onto a layer of tape on the probe tip. Dopant can be added by depositing an aliquot of a methanol/water solution of KCl onto the sample surface.

Seventeen antibiotics have been examined using LD-FTMS. All have approximately cyclic structures, whether simple or branched, except for the aromatic systems whose "core" structures are fused-ring systems. Simple cyclic systems tend to give predominantly $(M+Cat)^+$ ion peaks with little or no fragmentation observed. Branching, either with sugar or peptide moieties, increases the likelihood of fragment ions appearing in the spectrum. The more complex the branching, the more fragmentation observed. Aromatic or conjugated ions are favored. For example, the most intense peak in the spectrum of tetracycline corresponds to the loss of two water molecules from $(M+H)^+$, which should yield a completely conjugated system.

Negative ion spectra have only been obtained for valinomycin and bacitracin, both peptide antibiotics. Experimental conditions are similar for negative and positive ion spectra, the only difference being the trapping potential (+0.7 V for positive ions, -1.2 V for negative ions), yet the spectra are quite different. While the positive ion spectrum of valinomycin (Figure 1) consists solely of peaks corresponding to $(M+Na)^+$ and $(M+K)^+$, the major peaks in the negative ion spectrum (Figure 2) correspond to losses of carboxylic and amino acid moieties from $(M-H)^-$. Conversely, while the major peaks in the positive ion spectrum of bacitracin correspond to the loss of 3/4 of the peptide branch from $(M+Na)^+$ and $(M+K)^+$, a major peak in the negative ion spectrum corresponds to $(M-H)^-$, with other peaks corresponding to sequential losses of amino acid residues from the branch. These differences between positive and negative ion spectra are attributable to different structural stabilization of the charges.

Antibiotics of different structural types behave differently under LD-FTMS conditions. Of the compounds examined, molecular weight information is most easily obtained for macrolide and simple cyclic peptide antibiotics. Molecular weight and some structural information can be obtained for polyene, aromatic system, and branched cyclic peptide antibiotics. Molecular weights cannot be obtained for either of the glycopeptides examined (vancomycin and ristocetin) due to the high degree of fragmentation.

1. Laude, D.A., Jr.; Johlman, C.L.; Brown, R.S.; Weil, D.A.; Wilkins, C.L. Mass Spectrom. Rev. 1986, 5, 107-166.

2. Coates, M.L.; Wilkins, C.L. Anal. Chem. 1987, 59, 197-200.

The author gratefully acknowledges the support of the National Institutes of Health, Grant GM-30604.

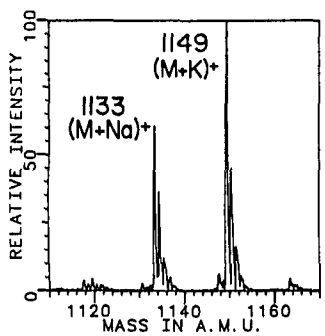

Figure 1. Positive ion LD-FT mass spectrum of undoped valinomycin.

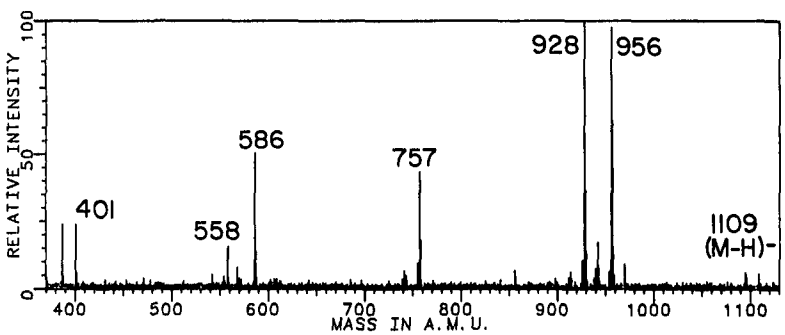

Figure 2. Negative ion LD-FT mass spectrum of valinomycin.

Presented at the 35th ASMS Conference on Mass Spectrometry and Allied Topics
May 24-29, 1987, Denver, CO

IDENTIFICATION OF URINARY RAT METABOLITES OF CGS 15855A UTILIZING LC/MS, GC/MS AND A STABLE ISOTOPE LABEL TRACER

M. HAYES, D. GAUDRY, H, EGGER, J. MIOTTO, M. BAX,
R. IANNUCCI, D. ALKALAY
DEVELOPMENT DEPARTMENT, PHARMACEUTICALS DIVISION,
CIBA-GEIGY CORPORATION, 444 SAW MILL RIVER ROAD,
ARDSLEY, NEW YORK 10502

CGS 15855A is an experimental drug showing selective dopamine autoreceptor agonist properties. It is readily absorbed and extensively metabolized when administered to the rat.

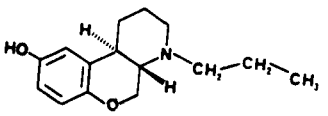

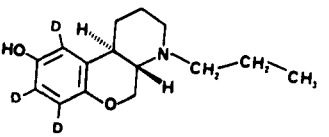

When dosed with a mixture of unlabelled and tri-deuterated CGS 15855A, the rat gave nine metabolites, five of which were glucuronide conjugates. These were identified by characteristic isotope clusters in the excreted urinary components. Table 1 lists the metabolites found by each experimental technique. The metabolites found, resulted from oxidative biotransformations.

Thermospray LC/MS allowed the direct identification of conjugated as well as nonconjugated metabolites. GC/MS required derivatization, but provided EI spectra useful in obtaining structural information on the primary metabolites. GC/MS afforded greater sensitivity compared to LC/MS. An additional technique utilized in the GC/MS work was the use of labelled derivatizing agent. By using both acetic anhydride and d6-acetic anhydride, it was possible to determine the number of labile hydrogens on each metabolite (see Table 1).

For the two primary drug related urine components, the stable isotope label results were confirmed using traditional isolation and identification methods utilizing the radiolabel. The two species were isolated and high resolution mass spectra and NMR were obtained. The results indicated parent drug and the despropyl metabolite, which agree with the stable label data.

TABLE 1

METABOLITES IDENTIFIED USING LC/MS AND/OR GC/MS
(ISOTOPE PATTERN SEARCH)

METAB. NO.	METABOLITE ID	MW	LC/MS PATTERN	GC/MS PATTERN (active H)
	CGS-15855A	247	248/251	290/293
1	CGS-15855A glucuronide	437	438/441	
2	N-despropyl	205	206/209	290/293
3	N-despropyl glucuronide	395	396/399	
4	[methoxy] (intermediate)	277		320/322
5	methoxy glucuronide	467	468/470	
6	[catechol] (intermediate)	263		348/350
7	catechol glucuronide	453	454/456	
8	methoxy, N-despropyl	235	236/238	320/322
9	methoxy, N-despropyl gluc.	425	426/428	

Presented at the 35th ASMS Conference on Mass Spectrometry and Allied Topics
May 24-29, 1987, Denver, CO

CHARACTERIZATION OF GLUTATHIONYL CONJUGATES BY FAB/TANDEM MS.

Helen Hughes, Marc H. Reilly, Peter E. Haroldsen, Simon J. Gaskell
Center for Experimental Therapeutics, Baylor College of Medicine, Houston, Texas 77030
Christopher J. Porter
VG Analytical Ltd., Wythenshawe, Greater Manchester M23 9LE, U.K.

The formation and excretion of glutathione (GS) conjugates during the metabolism of drugs and chemicals represents a major detoxification pathway for potentially harmful reactive intermediates. The identification of these conjugates is therefore of great importance in pharmacology and medicine. FAB-MS has been used successfully to analyze glutathione conjugates, and abundant molecular species have been observed for synthetic standards (e.g., reference 1). Structurally significant fragmentation is often lacking or obscured in FAB spectra, however, and this is particularly the case when biological extracts are analyzed. A few studies have demonstrated the potential of tandem MS in studies on synthetic GS conjugates (2,3,4). Here we report the results of low energy (25-50 eV) CAD analyses of both standards and biologically derived conjugates using a hybrid instrument of BEQQ design (VG ZAB SEQ).

CAD analyses were carried out on $[M+H]^+$ ions with argon as collision gas in the first quadrupole, with daughter spectra recorded using the second quadrupole filter. Analyses of authentic standards indicated that abundant daughter ions were formed principally via fragmentation of the glutathionyl moiety (fragments a, b, c, d, Figure 1). The nature of the glutathione substituent was found to strongly influence the daughter ion spectrum, where prominent ions corresponding to an additional loss of H_2O (particularly following d fragmentation) were often observed. This influence of the substituent on daughter ion spectra was clearly demonstrated in the case of two isomeric GS conjugates of styrene oxide; S-(2-phenyl-2-hydroxy)ethylglutathione yielded a base peak of m/z 281 in the daughter ion spectrum of its MH^+ ion corresponding to d fragmentation followed by loss of H_2O. However the S-(1-phenyl-2-hydroxy)ethylglutathione isomer yielded a base peak at m/z 299 with only a relatively minor ion at m/z 281.

The application of this methodology to biological samples has been demonstrated for the analysis of the GS conjugate of acetaminophen. Acetaminophen (250 mg/kg, i.p.) was administered to rats and the bile collected for a two-hour period (open fistula model). Following a C_{18} Sep-Pak extraction and HPLC isolation, the extract was subjected to FAB and FAB-CAD analysis. In normal FAB analyses, only low intensity $[M+H]^+$ ions were observed with little fragmentation discernible. The CAD spectra however indicated prominent daughter ions were formed via fragmentations analogous to those observed for the authentic standards (Figure 2). In conclusion, FAB-CAD mass spectrometry of glutathione conjugates using a hybrid tandem instrument yields excellent diagnostic daughter ion spectra enabling these metabolites to be clearly identified in complex biological extracts.

1. Pallante SL, Lisek CA, Dulik DM, and Fenselau C. Drug Metab Disp 14: 31, 1986.
2. Lay O Jr, Potter DW, and Hinson JA. In Proceedings of the 34th Annual Conference on Mass Spectrometry and Allied Topics, 1986, p 1038.
3. Stock BH, Bend JR, and Eling TE. J Biol Chem 261: 5959, 1986.
4. Straub KS. In Mass Spectrometry in Biomedical Research, Gaskell SJ, ed, John Wiley, Chichester, U.K., 1986, p 125.

Presented at the 35th ASMS Conference on Mass Spectrometry and Allied Topics
May 24-29, 1987, Denver, CO.

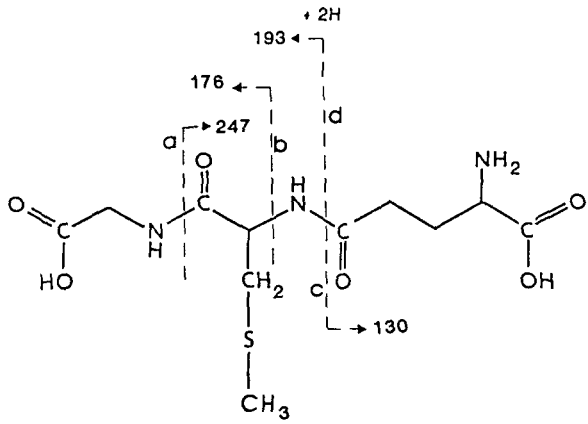

FIGURE 1: CAD fragmentation of S-methyl-glutathione.

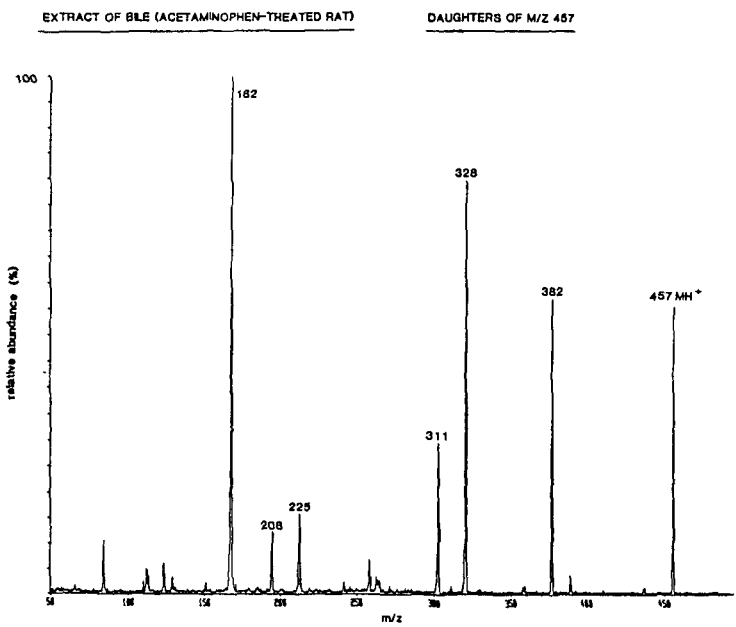

FIGURE 2: CAD daughter ion spectrum of MH^+ of S-glutathionyl-acetaminophen isolated from rat bile.

Presented at the 35th ASMS Conference on Mass Spectrometry and Allied Topics
May 24-29, 1987, Denver, CO

QUANTIFICATION OF CGS 16617 IN PLASMA BY COMBINED CAPILLARY GAS CHROMATOGRAPHY/NEGATIVE IONIZATION MASS SPECTROMETRY.

D. Gaudry, L. Khemani, J. Miotto, and D. Alkalay
Development Department, Pharmaceuticals Division
CIBA-GEIGY Corporation, Ardsley, New York 10502.

CGS 16617 (Fig. 1) is a novel long acting angiotensin-convering enzyme (ACE) inhibitor. Compounds inhibiting the ACE activity can be expected to offer an important contribution to the treatment of hypertension and congestive heart failure. Early clinical studies indicated ACE inhibition and blood pressure lowering effects at low plasma concentrations.
A highly sensitive capillary gas chromatographic/mass spectrometric method was developed for the quantification in plasma of CGS 16617.

We used tetradeuterated CGS 16617 as an internal standard. The work-up procedure involved purification by ion exchange and a two-step derivatization with pentafluoropropionic anhydride and pentafluoropropanol.
The high sensitivity was achieved by negative chemical ionization and selected ion monitoring with nitrous oxide as reagent gas, utilizing a Nermag R10-10 GC/MS system and splitless injection. We monitored selectively the ions at m/z 619 for the drug and m/z 623 for the deuterated internal standard.

The method allows a 73 ± 10% extraction recovery (tested with radioactive drug). It is suitable for drug concentrations in plasma ranging from 0.1 to 50 ng/ml. A representative test run involved 22 spiked human plasma samples with concentrations unknown to the two analysts. Accuracy was achieved over the entire tested range. The precision was associated with standard deviations of 10.6% for the 11 subnanogram concentrations, and 5.9% for the 11 samples having concentrations exceeding 1.00 ng/ml.

The usefulness of the method was tested in both animal and human single dose pharmacokinetic studies.

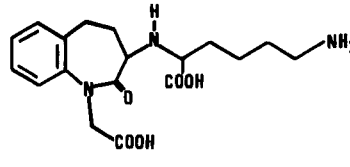

Figure 1

Presented at the 35th ASMS Conference on Mass Spectrometry and Allied Topics
May 24-29, 1987, Denver, CO

THE USE OF A HEATABLE-COOLABLE FAB PROBE FOR IMPROVED PERFORMANCE IN FAB MS:

T. D. McClure, P. F. Baker, and K. H. Schram; Department of Pharmaceutical Sciences, College of Pharmacy, University of Arizona, Tucson Arizona 85721

INTRODUCTION

The technique of Fast Atom Bombardment (FAB) is limited by the requirement tat the sample be soluble in a matrix. The matrix generally contributes a significant background to the mas spectrum which can mask important information, especially at lower masses. Recently work has been reported using a heated[1] and cooled[2-3] probe to expand the range of materials that can be analyzed by FABMS. The results of several apsects of the use of a heatable-coolable probe will be presented.

OBJECTIVE

To explore the use of heating and/or cooling of the FAB probe to:

1. expand the range of matrix materials to permit the use of commonly used organic solvents possessing a wide range of dissolving powers.
2. use these matricies to expand the application of FAB to new classes of compounds.
3. to explore the use of "matrix-less FAB" for the analysis of thermally stable pure compounds.

EQUIPMENT

This work was done using a Varian MAT 311A mass spectrometer with an SS-300 data system (using version 6 software). The heatable-coolable probe was purchased from AMD Intecra Inc. The mass spectrometer was equiped with a post acceleration dector and negative ion option, also purchased from AMD Intectra. The fast atom/ion source was an Ion Tech FAB11N gun.

MATRIX LIFETIME VS. TEMPERATURE

The following graph shows the relationship between temperature and time to matrix evaporation for a constant 2 microliters of materials. The relationship appears to be nonlinear. Further work is forth comming in hopes of establishing a predictive collection of information.

Reproducibility is a function of vacuum conditions and beam current, but is within 20 percent if these are held constant.

COOLING EXPERIMENTS USING DMSO AT THE MATRIX

Results have been published to date using DMSO as a matrix material.[2-3] While using DMSO for nucleosides, we saw a sample related ion enhancement vs. temperature analogous to that reported with thermally assisted FAB[1], however materials analyzed in this fashion need not be thermally stable at temperatures above ambient.

THERMALLY ASSISTED FAB - NO MATRIX

Both diaminonaphthalene [DAN] and adenosine were melted onto the FAB target outside of the instrument and inserted into the mass spectrometer. Until the tip was heated, only source background was seen. Once the sample melted, a FAB spectrum was obtained indicating that the melted sample could function as its own matrix. Subtraction of background ions (which were few) was easily performed. The result was a FAB spectrum of the compound of interest without the use of any additional matrix.

Presented at the 35th ASMS Conference on Mass Spectrometry and Allied Topics
May 24-29, 1987, Denver, CO

CONCLUSION

Heating and cooling of the FAB target expands the capabilities of FABMS through:

1. Use of matrix materials which have inappropriate vapor pressures at ambient temperatures but highly desireable solvent characteristics.
2. Ion enhancement at low temperatures is possible by ramping the target temperature starting at subambient temperatures.
3. One can generate FAB spectra of compounds that are thermally stable by melting them on the target and without the use of additional matrix materials.

REFERENCES

1. B.L. Ackermann, J.T. Watson, and J.F. Holland, Anal.Chem., 1985, 57, 2656.
2. A.M. Falick, F.C. Walls, and R.A. Laine, 34th Ann. Conf. Mass Spectrom. Allied Topics, 1986, 377.
3. K. Heckles, R.A.W. Johnstone, and A.H. wilby, Tetrahedron Lett., 1987, 28,103.

This work supported by NIH grant CA42309.

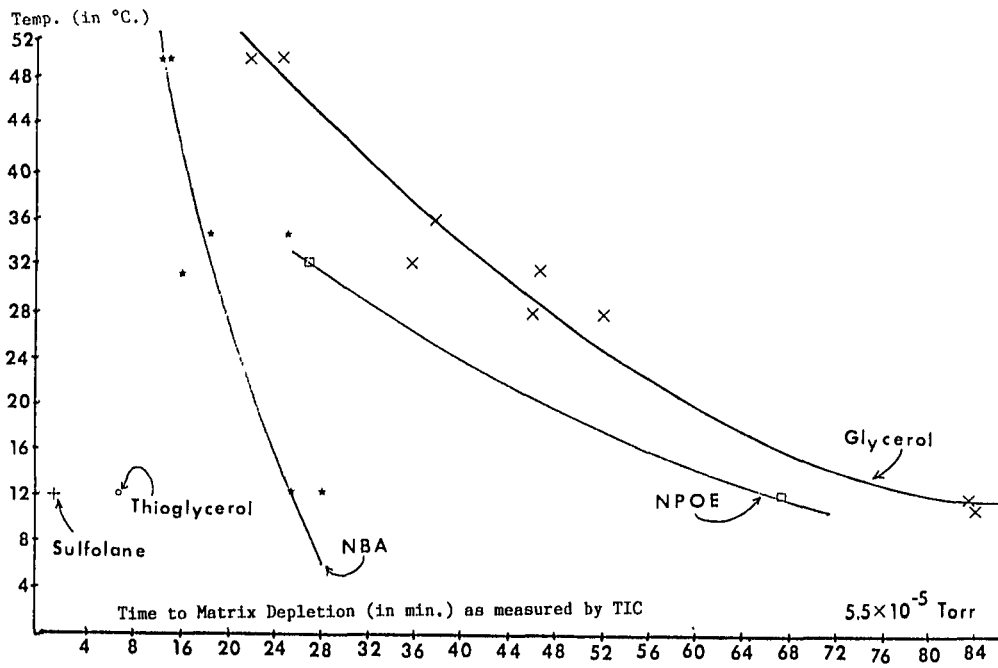

Presented at the 35th ASMS Conference on Mass Spectrometry and Allied Topics
May 24-29, 1987, Denver, CO

CHARACTERIZATION OF LYSOPHOSPHATIDYL CHOLINES USING POSITIVE ION AND NEGATIVE ION FAST ATOM BOMBARDMENT MASS SPECTROMETRY:

B.J. Sweetman, M. Tamura*, K. Higashimori*, T. Inagami* and I.A. Blair
Departments of Pharmacology and Biochemistry*, Vanderbilt University
Nashville, Tenn. 37232

Membrane-bound $Na^+.K^+$-activated adenosine triphosphatase ($Na^+.K^+$-ATPase) contains a receptor for cardiac glycosides such as ouabain and digitalis, which has prompted speculation as to the existence of a humoral factor which may modulate the properties of $Na^+.K^+$-ATPase. The presence of such inhibitors have been implicated in the pathogenesis of hypertension, and volume-dependent types of essential hypertension. Using the acutely saline infused hog as a model, we have shown that infusion releases into plasma oleic and linoleic acids, which do show activity. The current work addresses the problem of isolation and characterization of other compounds in plasma having inhibitory activity. An anesthetized hog was infused with isotonic saline and blood was collected and centrifuged to produce plasma (600ml) which was suspended in water (600ml), applied to an Amberlite XAD-2 column, washed with 3 volumes of water and inhibitory activity eluted using 3 volumes of methanol. Methanol was removed in vacuo and the residue in methanol was subjected to HPLC as shown below. Columns and conditions used were: (i) Aminopropyl (AP) column; decreasing linear concentration gradient of acetonitrile at a flow-rate of 1ml/min. (ii) Reverse phase chromatography using a Zorbax octadecylsilane (ODS) column or a SynChropak octylsilane (OS) column and linear gradients of acetonitrile or 2-propanol in 0.1% trifluoroacetic acid at a flow rate of 1ml/min or a Zorbax cyanopropyl (CP) column with a gradient of acetonitrile (0-100%) in 0.1% trifluoroacetic acid over 60 min. at a flow rate of 1ml/min. Fast atom bombardment (FB) spectra were obtained using a VG 70/250 instrument using a standard gun of the saddle field type operated at 8kV and 1mA using xenon gas. The instrument was set to switch on alternate scans between positive and negative ion detection. Samples containing 1-4 micrograms of compound in methanol (1-1.5 microliter) were mixed on a stainless steel target with thin films of glycerol or a 5:1 mixture of dithiothreitol: dithioerythritol as matrices. FB spectra of Fr 1-8, obtained initially using DTE-DTT matrix were confusing showing peaks due to multiple attachments of matrix to double bonds and apparently reactions of double bonds with S and H_2S. The spectra in glycerol however were clearly recognizable as being those of a family of lysophosphatidyl cholines having various alkoyl chain lengths and degree of unsaturation. The FB^+ and FB^- spectra of FR3, shown below, established the presence of γ-arachidoyl LPC.

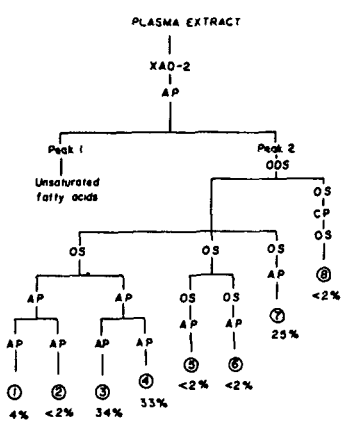

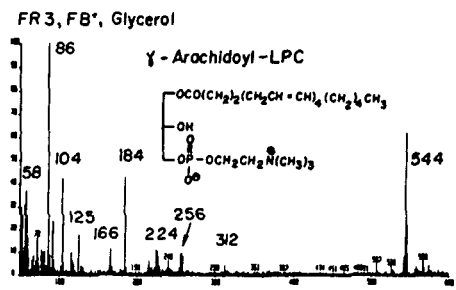

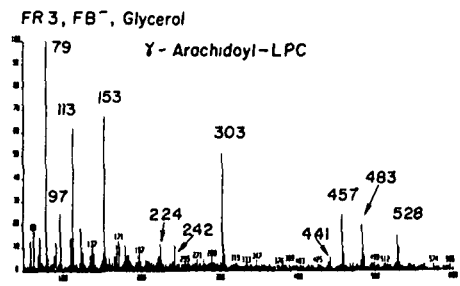

The fraction, name and structure of the specific alkoyl chains found in the various fractions are tabulated below.

Name	Fraction	Structure
β-arachidoyl	1	$CH_3\ (CH_2)_4\ (CH{=}CH\ CH_2)_4\ (CH_2)_2\ COO-$
γ-arachidoyl	2+3	$CH_3\ (CH_2)_4\ (CH{=}CH\ CH_2)_4\ (CH_2)_2\ COO-$
γ - oleoyl	7	$CH_3\ (CH_2)_7\ (CH{=}CH)\ (CH_2)_7\ COO-$
γ - stearoyl	8	$CH_3\ (CH_2)_{16}\ COO-$
γ - palmitoyl	5+6	$CH_3\ (CH_2)_{14}\ COO-$
γ - linoleoyl	4	$CH_3\ (CH_2)_4\ (CH{=}CH{-}CH_2{-}CH{=}CH)\ (CH_2)_7\ COO-$
γ - docosapentaenoyl	5	$CH_3\ (CH_2)_2\ (CH{=}CHCH_2)_5\ (CH_2)_3\ COO-$
γ - eicosatrienoyl	5	$CH_3\ (CH_2)_4\ (CH{=}CH{-}CH_2)_3\ (CH_2)_5\ COO-$

These LPC's proposed do have significant $Na^+.K^+$-ATPase activity. They are structurally unusual in the high percentage of unsaturated fatty acids found - γ-arachidoyl (34%), γ-linoleoyl (33%), and γ-oleoyl (25%), since most naturally occurring LPC's found previously have a fully saturated alkoyl chain in the γ-position. Phospholipids having unsaturated chains tend to have them in the β-position. This appears to be the first isolation, identification and characterization of a γ-arachidoyl LPC.

Both positive and negative ion FB spectra of LPC's show extensive structural information. Positive ions which arise from the phosphatidylcholine (m/z 58, 86, 104, 125, 166, 184) or glycero-phosphatidylcholine (m/z 224, 256, 258, 312) moieties are common to all LPC's. In addition, all positive ion spectra show an abundant MH^+. Information from the FB^- spectra is complementary to the positive ion spectra showing ions at m/z 79, 97 and 153 arising from the phosphatidylcholine and at m/z 224 and 242 from the glycero-phosphatidyl choline moiety. Negative ion spectra show no $(M-H)^-$ but do show peaks at M-15, due to the loss of $CH_3^{\bullet}$, together with peaks at M-60, M-86 and M-102, attributable to cleavages along the phosphatidylcholine chain. These various fragmentation pathways can be rationalized by considering the LPC as a zwitterion where protonation of $P\text{-}O^-$ leads to a series of positive fragment ions and loss of the CH_3 from $^+N(CH_3)_3$ leads to a series of negative fragment ions.

To further study the fragmentation mechanisms of the lysophosphatidylcholines, first field free region (metastable) daughter ion scans of ions in the spectrum of oleoyl-LPC (Sigma) were obtained using argon as collision gas, glycerol as matrix and the instrument was set to detect positive ions. These revealed a number of daughter ions arising in unimolecular (neutral hydrocarbon losses) processes from MH^+ by fragmentations along the hydrocarbon chain and several by losses from the glycerophosphatidyl choline moiety.

The spectrum of arachidoyl-LPC was complicated greatly by the use of the DTE:DTT matrix. We examined the FAB spectra of a number of other unsaturated aliphatic compounds to test the generality of this effect. It does appear that all unsaturated compounds will show peaks in the spectrum due to attachment ions between matrix and some or all of the double or triple bonds in the molecule. The double bonds are implicated because saturated acids or LPC's containing saturated chains show no attachment ions. The effect is not specific to DTE:DTT, since thioglycerol behaves in an analogous manner. In addition, the spectra shows series of ions corresponding to addition of S and/or H_2S to MH^+ or to MH^+.Matrix attachment ions. Two series of peaks are also seen at m/z values 18 and 36 m.u. lower than these. These observations may suggest the occurrence of some free-radical processes on the FAB target when using thiol matrices. Therefore, thiol matrices should generally be avoided for obtaining the FAB spectra of unsaturated compounds. However, comparison of FAB spectra run in glycerol and in thiol matrix could be used to evaluate the number of double bonds present in an unsaturated unknown.

In conclusion, a series of unusual lysophosphatidylcholines containing long chain fatty acids has been isolated from the plasma of acutely saline infused hog and characterized using positive ion and negative ion fast atom bombardment mass spectrometry. These represent a new class of $Na^+.K^+$-ATPase inhibitors. Evaluation of the pathophysiological significance of these interesting compounds is continuing. This work was supported by HL14192, HL35323, GM15431, RR01688 and RR05424.

Presented at the 35th ASMS Conference on Mass Spectrometry and Allied Topics
May 24-29, 1987, Denver, CO

THE USE OF DIMETHYL ETHER CI/MS TO DIFFERENTIATE STRAIGHT FROM BRANCHED CHAIN FATTY ACID METHYL ESTERS (FAMES)

LEW KILLMER, JR., PHYSICAL AND STRUCTURAL CHEMISTRY, SK&F LABS SWEDELAND, PA 19479

Fatty acids are an integral part of many biologically important compounds. Just as simple amino acids represent the building blocks for more complex peptides and proteins, fatty acids are the building blocks for most of the lipids. Fatty acids can also be found in pharmacologically active compounds derived from natural sources. Determining whether the fatty acid is straight or branched chain is a difficult but frequently required analytical task.

Direct ionization of dimethyl ether (DME) at a source pressure of ~0.1 torr generates $C_2H_5O^+$ and $C_2H_7O^+$ as the major reactant ions (1). In the presence of branched fatty acid methyl esters (FAMES) the $C_2H_5O^+$ ion acts as a hydride extractor and is essentially unreactive toward straight chain or normal FAMES. With DME, the base peak for both branched and normal FAMES is always the $(M+H)^+$ ion. For normal FAMES, the $(M-H)^+$ ion varies from 0.5 to 5% of the base peak. In contrast, for branched FAMES the $(M-H)^+$ ion varies from 12 to 49% of the $(M+H)^+$ ion intensity.

All of the data was generated on Finnigan models 3600 and 4610 quadrupole mass spectrometers. The DME was obtained from Matheson Gas Products Inc., East Rutherford NJ. All of the fatty acids and esters were obtained from Analabs Norwalk, Conn. and were used without purification. High source temperatures (>200°C) are used to minimize the $(M+C_2H_5O)^+$ and the $(M+C_2H_7O)^+$ adduct ions, thereby increasing the relative abundances of the $(M+H)^+$ and $(M-H)^+$ ions as well as greatly simplifying the mass spectra.

A synthetic mix of branched and normal FAMES (concentration per component-0.5mg/ml of CH_2Cl_2) was evaluated using DME as the CI reagent gas and chromatographed using a 30m x 0.25mm DB-1 fused silica capillary column. Table #1 is the summary of the results.

TABLE #1

Normal FAMES		Branched FAMES	
Chain Length	$\frac{(M-H)^+}{(M+H)^+} \times 100$	Chain Length	$\frac{(M-H)^+}{(M+H)^+} \times 100$
C_6	0.6%	aC_9	12.9%
C_8	1.5%	iC_{10}	15.4%
C_{10}	2.3%	aC_{11}	16.3%
C_{12}	3.7%	iC_{12}	30.9%
C_{14}	4.5%	aC_{13}	34.7%
		iC_{14}	49.3%

a= ante
i= iso

Note that in the case of the branched FAMES the $(M-H)^+$ ion was 10 to 20 times more intense then the $(M-H)^+$ ion response for the straight chain analogs. The following DME/CI mass spectra are typical examples of the spectra that are obtained for normal and branched FAMES.

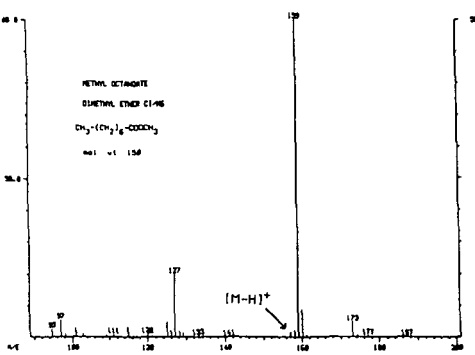

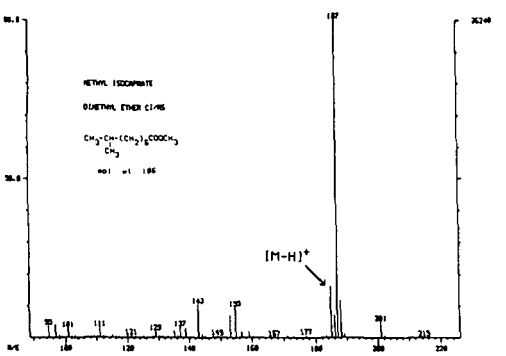

1. Keough, T. Anal. Chem. (1982) 54,2540-2547.

DME has the potential to differentiate between branched and normal unsaturated FAMES. Unfortunately we have not yet been able to demonstrate this potential due to the lack of availability of suitable reference standards. In the case of normal unsaturated FAMES, DME again generates very little $(M-H)^+$ ion (<5%) while methane CI generates a sizeable $(M-H)^+$ ion (15-75%).

DME can also be used to distinguish branched from straight chain fatty acids, but the differences in the $(M-H)^+$ ion intensities are not as dramatic as are observed for the methyl esters. Table #2 is a summary of the fatty acid data.

TABLE #2

Fatty Acids via DME/CI/MS

Normal Acids		Branched Acids	
Chain Length	$\frac{(M-H)^+}{(M+H)^+}$ X100	Chain Length	$\frac{(M-H)^+}{(M+H)^+}$ X100
C_{12}	8.9%	iC_{12}	22.4%
C_{15}	10.3%	aC_{15}	27.6%
C_{16}	11.7%	iC_{16}	23.6%
C_{19}	13.7%	aC_{19}	26.4%

i= iso
a= anto

Note that the relative $(M-H)^+$ ion intensities for the branched fatty acids are at least double those of the normal fatty acid responses. DME/CI will also differentiate branched from normal fatty acids with chain lengths of at least twelve carbons based on the ratio of the $(M+H)^+/(M+H-H_2O)^+$ ion intensities. See Table #3.

TABLE #3

$(M+H)^+/(M+H-H_2O)^+$ Ratios

Normal Acids		Branched Acids	
Chain Length	$\frac{(M+H)^+}{(M+H-H_2O)^+}$ X100	Chain Length	$\frac{(M+H)^+}{(M+H-H_2O)^+}$ X100
C_{12}	21.4%	iC_{12}	27.7%
C_{15}	22.4%	aC_{15}	51.9%
C_{16}	25.8%	iC_{16}	56.2%
C_{19}	26.3%	aC_{19}	87.6%

i=iso
a=anto

Trimethylsilyl derivatives of branched and straight chain fatty acids generate identical CI mass spectra using DME as the CI reagent gas.

In summary, the use of DME/CI for determining branching in FAMES has the following advantages over carbon NMR, capillary GC, and capillary GC/MS using other CI reagent gases:

1. The results are unequivocal
2. Requires no reference compounds
3. Can be used with nanogram amounts of sample
4. The technique is simple and the results can be obtained in minutes.

Unfortunately DME/CI does not yield characteristic fragment ions to establish the branch site.

Presented at the 35th ASMS Conference on Mass Spectrometry and Allied Topics
May 24-29, 1987, Denver, CO

ANALYSIS OF GLUTATHIONE CONJUGATES AND RELATED COMPOUNDS BY TSP MS

J.S.M. de Wit, C.E. Parker, R.W. Smith, M.B. Gopinathan, O. Hernandez, J.R. Bend, and K.B. Tomer

Laboratory of Molecular Biophysics, NIEHS,
Research Triangle Park, NC 27709

Conjugation with glutathione is an important mechanism for the metabolism and excretion of many drugs, pesticides, steroids, and other environmental chemicals. The reaction of glutathione (GSH) with electrophilic compounds involves a family of enzymes (the glutathione transferases) which are responsible for the initial conjugation of the molecules with the tripeptide glutathione (GSH = γ-GLU-CYS-GLY), bonding with the -SH group of the cysteine, followed by loss of the glutamic acid residue, removal of the glycine residue, and N-acetylation of the remaining S-substituted cysteine to give a mercapturic acid. For arene oxides and epoxides, generally only the N-acetylcysteine derivatives are found in urine. Bile and feces often contain GSH, cysteinyl glycine, and cysteine conjugates.

Recent work in our laboratories has involved the development of glutathione conjugate derivatives which are amenable to separation by HPLC. In addition, methods for the separation of diastereomers of these conjugates has also been developed as part of a research program on the stereospecificity of glutathione transferase enzymes from different tissues. Thus it was of interest to develop an LC/MS method which could be used for the study of glutathione conjugates.

Sixteen cysteine, glutathione, and derivatized cysteine and glutathione conjugates were prepared from a series of compounds (Table 1). These conjugates were analyzed by TSP LC/MS on a VG 12-250 quadrupole mass spectrometer, using either a VG or a Vestec TSP interface. The solvent used was 0.1 N ammonium acetate, at a flow rate of 0.8 to 1 ml/min.

In general, although sensitivities varied widely from compound to compound, positive ion TSP was more sensitive than negative ion TSP for these compounds. While some of the smaller molecules showed (M-1)- ions (Figure 1), most of the larger conjugates did not give useful negative ion TSP mass spectra (Table 1). In positive ion TSP, many of the cysteine, substituted cysteine, and TFAG conjugates showed (M+1)+ or (M+Na)+ ions (Table 1, Figures 2-4). Common fragmention pathways included breakage of the bonds to the sulfur (with proton transfer), as well as loss of portions of the conjugating group. Positive ion TSP spectra from underivatized glutathione conjugates of the larger molecules did not contain much structural information.

It is interesting to note that the TFAG conjugates, originally developed to allow the HPLC separation of arene oxide diastereomers, also yield positive ion TSP mass spectra with more sensitivity and structural information content than the underivatized glutathione conjugates.

In conclusion, positive ion TSP LC/MS should prove useful for the analysis of glutathione and related conjugates of arene oxides and other compounds, provided that the conjugates studied are of the cysteine, derivatized cysteine, or the TFAG type. Thermospray LC/MS for underivatized glutathione conjugates was less successful than for the other conjugates, but showed some promise for the smaller molecules studied.

Presented at the 35th ASMS Conference on Mass Spectrometry and Allied Topics
May 24-29, 1987, Denver, CO

Table 1. Molecular ion information from TSP spectra of compounds studied.

Compound	Chemical Name	Pos.	Neg.
I	Styrene oxide-CYS	x	x
II	Benzo(a)pyrene oxide-CYS	x	
III	Styrene oxide-CYS, N-acetyl	x	x
IV	Styrene oxide-CYS, N-acetyl, methyl ester		
V	Tetrahydronaphthyloxide, 2-CYS,-1-O-benzoyl, N-acetyl methyl ester	x	
VI	Tetrahydronaphthyloxide-1-CYS-2-O-benzoyl-N-acetyl methyl ester	x	
VII	Butyl acrylate-GSH	x	
VIII	Styrene oxide-GSH		
IX	α-Methyl styrene oxide-GSH		
X	9,10-Phenanthrene oxide-GSH		
XI	Benzo(a)pyrene oxide-GSH		
XII	N-TFA-GSH, dimethyl ester (TFAG)	x	x
XIII	β-Methyl styrene oxide-TFAG	x	
XIV	Pyrene oxide-TFAG,4-O-benzoate		
XV	Benzo(a)pyrene-TFAG-4-O-benzoate	x	
XVI	BPDE-TFAG-peracetate	x	

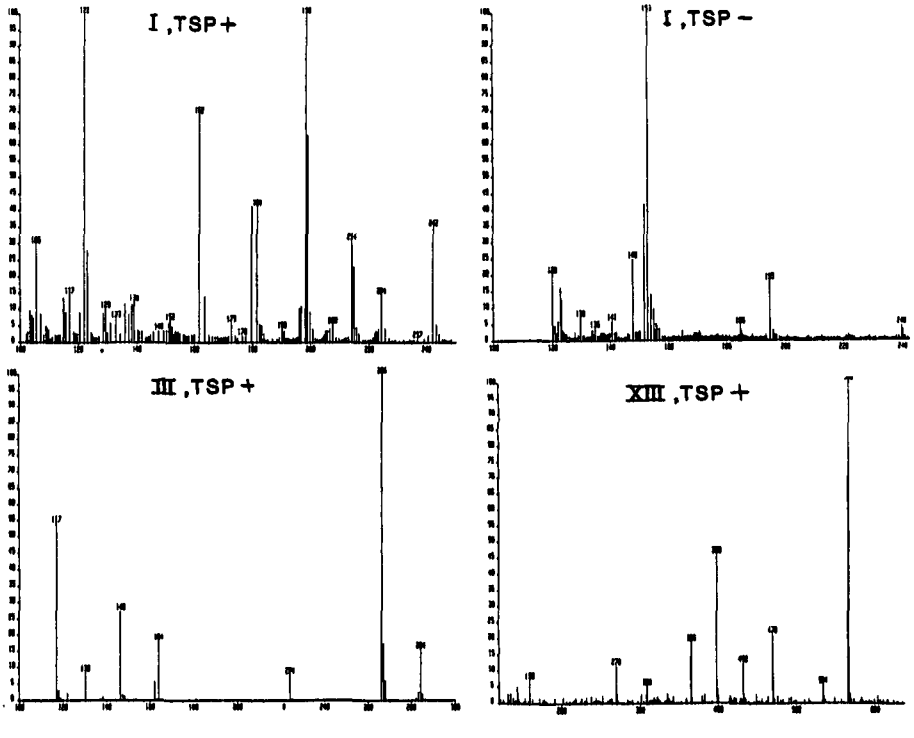

Presented at the 35th ASMS Conference on Mass Spectrometry and Allied Topics
May 24-29, 1987, Denver, CO

EVALUATION OF FAB/MS AND FAB/MS/MS FOR THE STRUCTURAL ELUCIDATION OF BISBENZYLISOQUINOLINE ALKALOIDS.

J. A. Masucci[1], G. W. Caldwell[1], W. N. Wu[1], R. K. Isensee[2] and J. R. B. Slayback[2]; McNeil Pharmaceutical, Spring House, PA[1]; Oneida Research Services, Inc., Whitesboro, NY[2].

INTRODUCTION: The families Berberidaceae, Menispermaceae, Monimiaceae and Ranunculaceae are rich sources of bisbenzylisoquinoline (BBI) alkaloids (1). Their diverse pharmacological effects include hypotensive, antimicrobial, muscle relaxant and antitumor activities (2). The BBI alkaloids consist of two benzylisoquinoline units linked by ether bridges.

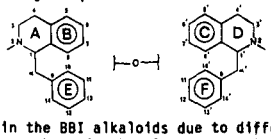

A variety of compounds arise in the BBI alkaloids due to differences in the number of aromatic oxygen substituents and the number of ether linkages. These are classified as Type A, (e.g., Compounds 10-12) containing one ether linkage, and Type B, (e.g., Compounds 3-9) containing two ether linkages. The aporphine-benzylisoquinolines (ABI) differ only due to an additional carbon-carbon bond between C-8' and 10' of rings C and F (e.g., Compounds 1-2). The ether linkage is between C-13' of the F ring and the E ring. The electron ionization (EI) spectra for these alkaloids have been studied (3). In the case of Type A BBI and ABI alkaloids, these exhibit weak molecular ions (ca. 0.1%) and intense ions due to the highly favored benzylic cleavage to rings A and B, and/or C and D. For the ABI alkaloids only the benzylic cleavage to the A and B ring is observed. Most of the structurally significant ions for the Type A BBI and ABI are typically <0.2% of the base peak. Thus, elucidation of molecular structure is difficult. In contrast, Type B BBI alkaloids give rich EI spectra with cations arising from the molecular ion (45-100%), from double heterolytic benzylic cleavage (loss of rings E and F), from loss of rings C and D, from loss of ring E and ions due to rings A and B or C and D.

The twelve isoquinoline alkaloids investigated were: (ABI) 1-thalicarpine, 2-thalicarpine dimethodiiodide; (Type B, BBI) 3-thalrugosine, 4-thalrugosine dimethodiiodide, 5-homoaromoline, 6-homoaromoline dimethodiiodide, 7-thalrugosidine, 8-thalrugosidine dimethodiiodide, 9-thalidasine; (Type A, BBI) 10-northalistyline, 11-thalistyline, 12-methothalistyline.

Our goal was to aid in the structural elucidation of ABI and Type A BBI alkaloids utilizing FAB/MS and FAB/MS/MS.

EXPERIMENTAL: The FAB/MS data was obtained using a VG7070E spectrometer utilizing an Ion Tech saddefield gun which generated a primary beam of argon atoms at 8 keV and 2 mA. The FAB/MS/MS data was collected with a Finnigan TSQ46 triple-sector instrument which utilized a Phrasor capillaritron gun which generated a primary beam of krypton atoms at 8 keV and 4μA. The collision cell was filled with argon at 2×10^{-3} torr and collision energies of -17 to -30 volts were applied. Samples of alkaloids (100-300 μg) were predissolved in the liquid matrix thioglycerol (2 μL). Alkaloids were isolated and purified by published methods (4).

RESULTS AND DISCUSSION: The free base alkaloids (1,3,5,7,9 and 10) produced protonated molecular ions (MH^+), while the di-quaternary ammonium salts (2,4,6,8 and 12) produced cations including $(M-I)^+$, $(M-I-HI)^+$ and $(M-I-CH_3I)^+$ (Table 1). Compound 11 produced $(M-Cl)^+$. Thus, molecular weight information can be obtained for all alkaloids. It is interesting to note that the counter-anion can be determined for the di-quaternary salts and there is an increase in fragmentation for the Type A BBI and ABI salts when compared with the free bases. Compound 10 produced structurally significant fragments at m/z 220, 236 and 464 while Compounds 11 and 12 produced fragments at m/z 220, 236, 272 and 478 in relatively high abundance (Scheme 1). The aromatic oxygen substituents ($-OCH_3$) of rings A and B can be assigned from m/z 236 while the m/z 220 can be used to assign rings C and D. The fragment m/z 464 (or m/z 478 from Compounds 11 and 12) is useful for determining the substitution of rings E and F. The total number of aromatic oxygen substituents of ring E can be assigned. It is difficult to use EI data to assign substituents on rings E and F for Type A BBI alkaloids and the FAB/MS data is clearly more useful in these cases. The ABI alkaloids (Compounds 1-2) also produced structurally significant fragments (m/z 388 and 340, Table 1) which can be used to determine the $-OCH_3$ substituents of the benzylisoquinoline and aporphine units. Additionally, individual substitution of rings B and E can be determined.

In addition to the protonated molecular ion (MH^+) at m/z 609, there is a significant abundance of molecular ion ($M^{+\cdot}$) for Compound 3, as well as 5,7 and 9 (Table 1). The FAB/MS spectra for these Type B BBI alkaloids exhibit few structurally significant fragments, unlike the EI studies (3). None of the observed fragments contain rings E or F, in contrast to both the EI studies and FAB/MS of Type A BBI and ABI alkaloid data.

The fragments, from the double benzylic cleavage, (m/z 381 and 367) of Compound 3, are observed under FAB/MS conditions as in EI (3) (Scheme 2). Similar results were obtained for Compounds 5,7 and 9. Thus, the total number of oxygen substituents can be identified for rings A and B or C and D. The tentative structure of the m/z 381 fragment is consistent with the CAD spectrum (i.e., m/z 381→m/z 174), and comparison with Compounds 7 and 9, which only differ in the ether linkage position and addition of $-OCH_3$ substituents.

Note that the fragment at m/z 381 does not originate directly from MH^+ (m/z 609) - the MS/MS data indicates that m/z 367 and 192 are produced. The m/z 192 allows the total number of $-OCH_3$ substituents on rings A and B or C and D to be determined. The fragment m/z 367 is presumed to rise from the loss of a $CH_3\cdot$ and $H\cdot$, but further MS/MS studies are required to substantiate this. It appears that FAB/MS is a less useful technique for the structural elucidation of Type B (Compounds 3-9) BBI alkaloids.

Presented at the 35th ASMS Conference on Mass Spectrometry and Allied Topics
May 24-29, 1987, Denver, CO

TABLE 1. Summary of FAB/MS Data

Compound #	(MW)	m/z of Observed Ions (Relative Abundance)
1	696	(MH+) 697(11), (M+) 696(4), 206(100), 204(14)
2	980	(M-I)+ 853(21), 725(100), 711(38), 695(11), 388(14), 340(20), 206(87)
3	608	(MH+) 609(100), (M+) 608(21), 593(5), 563(7), 381(13), 367(16)
4	892	(M-I)+ 765(11), 637(45), 623(100), 607(8)
5	608	(MH+) 609(100), 593(8), 381(17), 367(13)
6	892	(M-I)+ 765 (33), 637(93), 623(100), 607(14)
7	638	(MH+) 639(100), (M+) 638(19), 623(8), 411(9)
8	922	(M-I)+ 795(20), 667(83), 653(100), 637(8), 622(6)
9	652	(MH+) 653(100), (M+) 652(23), 637(7), 425(8), 411(23)
10	682	(MH+) 683(19), 464(10), 236(100), 220(87), 252(21)
11	824	(M-Cl)+ 697(40), 478(48), 236(17), 220(100)
12	966	(M-I)+ 839(56), 711(62), 697(76), 478(26), 372(70), 236(78), 220(100)

TABLE 2. Summary Of FAB/MS/MS Data.

Compound	m/z of Parent Ion [Collision Energy, Volts]	Daughter Ions (Relative Abundance)
1	697 206	206 (100), 189 (10), 165 (43) 190 (100), 174 (7), 162 (53), 145 (49)
2	711 [29.7] 388	502 (7), 457 (5), 427 (3), 206 (60), 58 (100) 189 (42), 167 (53), 151 (10), 58 (100)
3	609 381	367 (72), 192 (100), 174 (58), 148 (41) 335 (13), 190 (21), 174 (100), 162 (11), 146 (24)
4	623 [29.5]	580 (2), 227 (3), 208 (10), 191 (10), 174 (9), 58 (100)
5	609 381	367 (66), 192 (67), 176 (100), 174 (77), 146 (48) 335 (22), 190 (21), 174 (100), 162 (17), 146 (38)
6	623 [23.6]	580 (9), 227 (3), 208 (2), 191 (9), 174 (9), 159 (6), 58 (100)
7	639 411	397 (54), 227 (25), 206 (79) 192 (100), 174 (57) 204 (100), 188 (24), 178 (40), 160 (18)
8	653 [-18.4]	608 (18), 576 (6), 206 (12), 190 (10), 174 (5), 58 (100)
9	653 425	411 (73), 365 (28), 206 (100), 204 (77), 190 (54), 174 (33) 379 (66), 363 (55), 335 (58), 204 (100), 190 (60), 174 (37), 161 (37)
10	683 [17.2] 236 220	652 (3), 236 (100), 220 (18), 195 (3) 220 (100), 206 (97), 202 (87), 192 (37), 175 (67), 174 (89), 148 (50) 204 (100), 176 (15), 159 (13), 147 (15), 131 (13), 118 (8)
	464	236 (100), 227 (26), 188 (13)
11	697 220 478	652 (17), 477 (9), 220 (38), 58 (100) 204 (100), 176 (10), 148 (12), 146 (13), 131 (8), 118 (9) 325 (2), 311 (3), 267 (4), 227 (16), 220 (7), 219 (9), 204 (5), 195 (7), 188 (6), 181 (4), 58 (100)
12	839 697 372	712 (31), 698 (100), 697 (20) 652 (25), 477 (4), 234 (20), 216 (12), 58 (14) 371 (56), 327 (19), 121 (9), 58 (11)

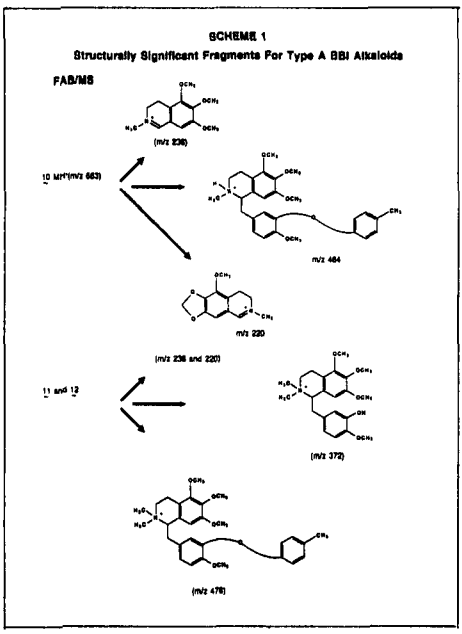

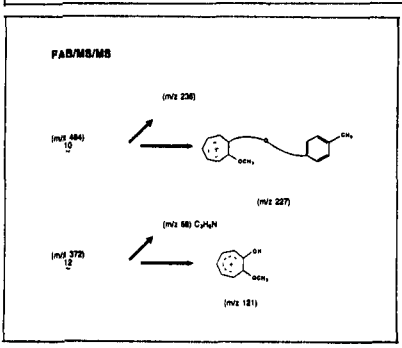

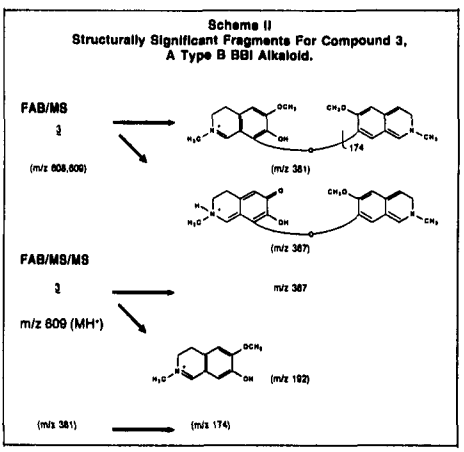

REFERENCES

1 K P. Guha, B. Mukherjee and R. Mukherjee, J. Nat. Prod., *42*, 1 (1979)

2. P.L. Schiff, Jr., J Nat, Prod , *46*, 1 (1983).

3 J. Baldas, I.R.C. Bick, T Ibuka, R.S. Kapil and Q.N. Porter, J.C.S. Perkin I, 592-97 (1972)

4 W.N. Wu, J.L. Beal and R W. Doskotch, Tetrahedron Lett., 3687 (1976); W N. Wu, J.L. Beal and R W. Doskotch, J. Nat. Prod., 40, 508 (1977); L.A. Mitcher, W.N. Wu, R.W. Doskotch and J.L. Beal, J. Chem. Soc., Chem. Comm., 589 (1977).

Presented at the 35th ASMS Conference on Mass Spectrometry and Allied Topics
May 24-29, 1987, Denver, CO

SELECTIVE AND SENSITIVE DETERMINATION OF AMINES IN URINE

Michael J. Avery and Gregor A. Junk
U.S.D.O.E., Ames Laboratory, Ames, Iowa 50011

Methyl amine present in urine at trace levels can be determined accurately and with high sensitivity by using a bonded phase column clean up, direct derivatization with pentafluorobenzaldehyde (PFB), imine extraction with a second bonded phase column and measurement by HRGC/MS. Test data are presented to show that the procedure is almost certainly applicable to ethyl and n-propyl amines and is probably suitable for the clinically significant putrescine and cadaverine.

EXPERIMENTAL

Methodology.-- A 0.5 mL sample of undiluted urine was spiked with 5 μg of D_3-methylamine internal standard, mixed, and passed through a 1 mL cartridge containing 100 mg of octadecyl (C_{18}) bonded porous silica. This step removed non-polar interferences present in the urine by adsorption onto the C_{18} bonded silica.

The urine eluate containing the polar constituents was combined with a 200 μL 0.1 N borate wash of the cartridge and this mixture was transferred to a 5 mL vial. One-half mL of acetonitrile containing 5 mg PFB was added, the mixture heated to 80°C and held at that temperature for 30 min. This step converted the primary amines present in the eluate to PFB-imines [1].

After the reaction mixture had cooled to ambient, 0.5 mL of water was added to the vial and the imine derivatives were adsorbed from the reaction mixture by passing this solution through a second C_{18} cartridge. The cartridge was washed with 1 mL water to remove any remaining water-soluble interferences, and dried by aspirating room air through the cartridge for 5 min. The imine derivatives were eluted with 200 μL of ethyl acetate.

RESULTS AND DISCUSSION

A typical GC/MS/RIC resulting from application of the method to a sample of urine fortified with three primary alkyl amines is shown in Fig. 1. The responses for each imine derivative are cleanly separated from the unreacted PFB. Common urine constituents such as ammonia, di- and trimethylamine do not interfere since they will not react with PFB.

The best quantitative data are obtained with isotope-labelled internal standards so that similar partitioning, derivatization efficiency and GC retention behavior can be realized. The PFB derivative of D_3-methylamine is measured, free of interference from the unlabeled analyte, at m/z 211. The simultaneous detection of three analytes and the deuterated internal standard is shown in Fig. 2. Response relative to concentration was determined by analyzing pure water containing 10 μg/mL of D_3-methylamine and 50 ng/mL to 10 μg/mL of methylamine.

The accuracy of the method was tested by spiking 0.5 mL aliquots of a urine sample from a 38- year-old male with 10 to 30 μg/mL of methylamine. The average error was found to be 9%. The reproducibility of the method was determined by analyzing four aliquots of this same sample. At the native methylamine level of about 1 μg/mL, a 4% coefficient of variation was obtained. Comparable accuracy and precsion were obtained for sample volumes as low as 0.1 mL. The applicability of the method to these small sample sizes is a necessary feature for some clinical applications and a requirement for potential application to blood and serum studies.

Other primary amines can almost certainly be determined based on interpretation of additional test data. The chromatograms shown in figures 1 and 2 illustrate the wide separation between the three amine derivatives, allowing easy measurement. The equivalent responses suggest that the same high sensitivity could also be obtained. Quantitation could be achieved by standard additions or by using additional labelled amines.

The possible selective and sensitive determination of the diamines putrescine and cadaverine is indicated by the data shown in Fig. 3. This chromatogram was obtained from an extract of urine fortified with 10μg/mL of the two diamines. The low background and high sensitivity are typical for primary aliphatic amines analyzed by this method.

---

1. M. J. Avery and G. A. Junk, Anal. Chem., 57 (1985) 790.

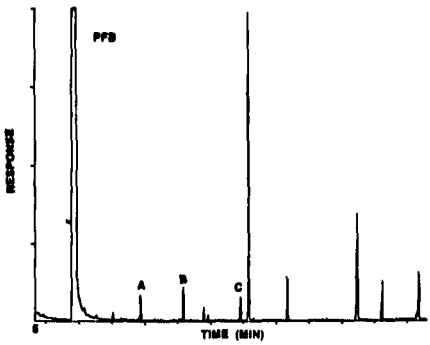

Fig. 1 GC/MS/RIC of an extract from treated urine sample fortified with 10 μg/mL of A) methyl-, B) ethyl- and C) propylamines

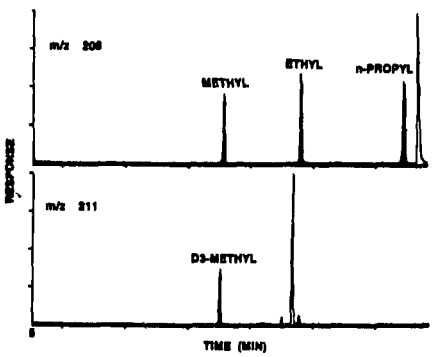

Fig. 2 GC/MS/MIM of an extract from treated urine sample fortified with 10 μg/mL of aliphatic amines.

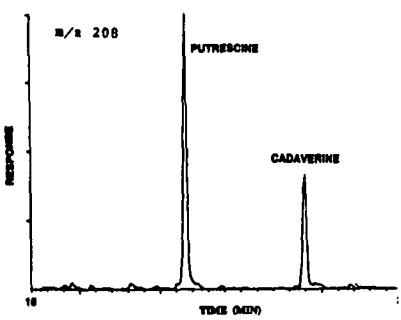

Fig. 3 GC/MS/SIM of an extract from treated urine sample fortified with 10 μg/mL of aliphatic diamines.

Presented at the 35th ASMS Conference on Mass Spectrometry and Allied Topics
May 24-29, 1987, Denver, CO

MS STUDIES OF ISOMERIC PHENYLPROPANOIDS

Ronald D. Plattner and Robert Kleiman

ARS-USDA, Northern Regional Research Center
Peoria, IL 61604

During the course of a search for new allelochemicals, we discovered that seed extracts of several species of the genus Pimpinella had significant activity in a seed germination bioassay. A series of related esters with substituted phenylpropanoid skeletons isolated from the seed extracts were found to account for most of the biological activity. This class of secondary metabolites had previously been reported as constituents of the roots and seeds of several Pimpinella species, but no biological significance had been attached to them.

Furthermore, early literature reports for the structure of some compounds were apparently incorrect. The assignment of the correct substitution pattern for the aromatic ring between trisubstituted phenylpropanoids of type 1 and 2 generally made by NMR can be a difficult analytical problem. The proton NMR coupling pattern for both structures is the same; and the chemical shifts of the aromatic protons are not sufficiently unique to allow unambiguous assignment of structure based on proton chemical shifts alone. Recently, two groups demonstrated that sophisticated NMR experiments can be used to establish the correct structure (1,2).

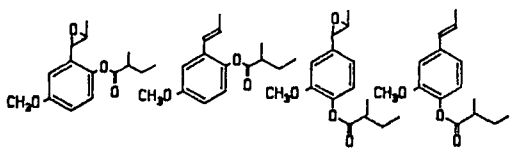

1a 1b 2a 2b

Because these NMR experiments can require about 50 mg of pure material, mass spectrometry is a desirable alternate means to distinguish the substitution pattern requiring much less sample. We have analyzed a series of fourteen synthetic and naturally occurring di- and trisubstituted phenylpropanoids by EI- and CI-MS. No CI spectra for phenylpropanoids have been reported.

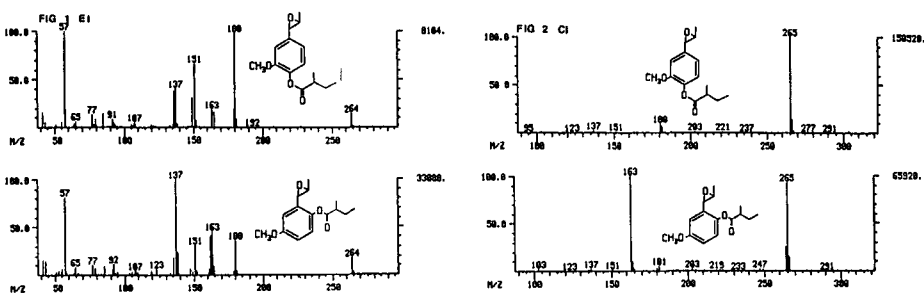

Isomers with epoxypropenyl groups (like 1a and 2a) can be distinguished by EI. (fig 1). The most significant difference in the EI spectra is that 1a has an intense fragment at m/z 162 while this fragment is absent in 2a. This fragment is likely from rearrangement of the 1,2 substituted isomer to form 2-methyl-5-methoxy-benzofuran. 2a cannot undergo this rearrangement. This benzofuran has previously been reported as a natural constituent in Pimpinella roots, and Martin et al. (1) obtained it by steam distillation of compound 1a in 0.1 N HCl. In isobutane CI, an acidic gas phase system, we observe intense signals for protonated benzofurans in the mass spectra of all the 1,2 substituted isomers, but not the 1,4 substituted ones (fig 2).

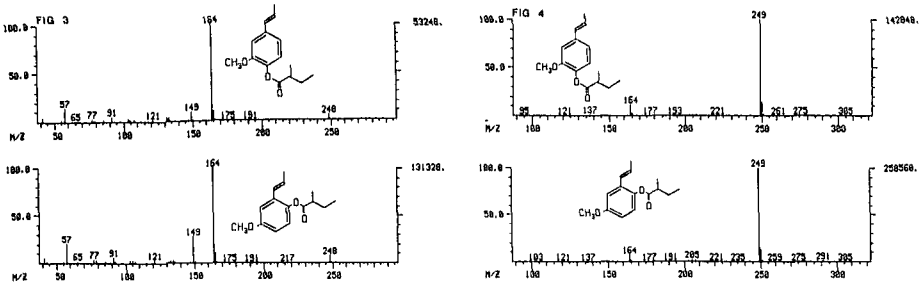

The isomers with unsubstituted propenyl groups (like 1b and 2b) have virtually identical spectra in both EI and CI (fig 3,4). Compounds 1b and 2b can be distinguished by the collisionally activated decomposition daughter spectra of the protonated molecule from CI (fig 5) which have markedly different intensities for their daughter fragments.

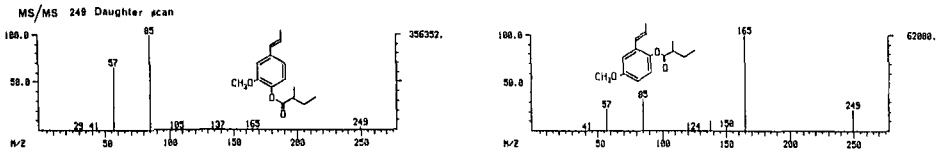

References

1) R. Martin, J. Reichling and H. Becker, Planta Medica (1985), p. 198.
2) A. Bottini, V. Dev, D. Garfagnoli, C. Mathela, A. Melkani, A. Miller and N. Sturm, Phytochemistry (1986) 25, p. 207.

Presented at the 35th ASMS Conference on Mass Spectrometry and Allied Topics
May 24-29, 1987, Denver, CO.

IDENTIFICATION OF PLATELET-ACTIVATING FACTOR BY TANDEM MASS SPECTROMETRY

Ronald D. Plattner and Robert J. Stack, ARS-USDA, Northern Regional Research Center, Peoria, IL 61604; and Brent Sommers and Richard S. Criddle, University of California, Davis, CA 95616

Platelet-activating factor (PAF), a phospholipid [1-O-alkyl-2-O-acetyl-sn glyceryl-3-phosphorylcholine (AGEPC)], is a potent mediator of inflammation and acute hypersensitivity reactions. PAF action is not yet fully understood, but appears to follow from its interaction with specific receptor sites on cell membranes and the induction of multiple effects including platelet aggregation and changes in cell metabolism. PAF is produced following specific stimulation of various cells, and is active at very low concentrations *in vivo*, generally 10^{-10} to 10^{-11} M. Therefore indigenous levels of PAF are generally determined by activity measurements (such as serotonin release), which are compared to the response generated by known levels of authentic PAF.

Recently PAF activity was detected in a novel source, the fright-induced secretions from the unicellular epidermal gland cells, termed "club cells", of the saltwater catfish *Arius thalassinus*. In this paper we report chemical ionization MS and MS/MS spectra of AGEPC standards and the confirmation of the chemical presence of AGEPC in these catfish secretions.

Experimental

The AGEPC standards were purchased from Sigma Chemical Company, St. Louis, MO, and Calbiochem, LaJolla, CA. *A. thalassinus* epidermal cell secretion (21 ml) was extracted by homogenation with methanol (399 ml) and centrifuged to remove precipitated solids (10,000 g, 15 min). Chloroform (399 ml) and water (336 ml) were added to promote phase separation. The PAF activity-containing lower phase was separated, dried under nitrogen, redissolved in chloroform-methanol (2:1), and purified by four successive thin layer chromatographic (tlc) steps. Following each step, fractions were eluted from the plate and assayed for PAF activity. Active fractions were pooled and applied to the next tlc step. The four solvent systems employed for the tlc steps were: (1) chloroform-methanol-water, 65:35:6; (2) methanol-dimethylsulfoxide, 82:18; (3) same as 1; and (4) methanol-water, 2:1. After four steps, the recovered PAF fraction had activity corresponding to less than 1 microgram of AGEPC as measured by serotonin release bioassay.

All spectra were recorded with a Finnigan TSQ 46 triple quadrupole mass spectrometer. For CI mass spectra, gas (isobutane) pressure in the source was 0.3 torr. The sample (5 ng-10 μg) was placed on the loop of the direct exposure probe, inserted into the CI plasma and electrically heated. Liquid secondary ion spectra (liquid SIMS) were obtained using the discharge ionization/secondary ionization mass spectrometry accessory. The AGEPC standard (2 μg) in 1 microliter of chloroform was added to a small drop of glycerol on the probe tip and bombarded with 5 kV xenon atoms. Collisionally activated decomposition (CAD) experiments were done with argon (1 millitorr) at 20 v.

Results and Discussion

A chemical ionization mass spectrum was obtained from an aliquot of the tlc purified catfish extract with activity equivalent to about 50 ng of AGEPC (fig 1a). The relevant signals for AGEPC are present in the spectrum, but even after four successful preparative tlc steps the sample is not pure. This high level of "chemical noise" makes positive identification of AGEPC by comparison to the mass spectrum of the standard (fig 1b) impossible. Therefore we investigated the use of MS/MS experiments as a means to lower the chemical noise.

The authentic AGEPC samples are mixtures of phospholipids with various chain lengths for the 1-O-alkyl group, predominately C16 and C18. The protonated molecules for the C16 and C18 ether homologs, m/z 524 and 552, were selected

by quadrupole 1 for CAD. In each case, two intense daughter fragments, (MH-183) and m/z 184 were observed. The daughter ion at m/z 184, which *arises from fragmentation with protonation of the choline phosphoester*, was not observed in the CI spectrum. Selecting this daughter for a parent experiment gives a mass spectrum which shows the protonated molecule for all the homologs in the AGEPC in a single scan. When this parent experiment was run for an aliquot of the tlc-purified catfish extract chemical, noise is effectively removed; and the spectrum looks like the standard (fig 2), allowing a more positive chemical confirmation of the presence of AGEPC.

The liquid SIMS spectrum of the authentic AGEPC shows intense protonated molecules. A similar parent experiment for m/z 184 showed these parents as well. However, our quadrupole instrument does not efficiently remove neutral particles which are also sputtered from the source and detected as random noise by the detector. Therefore with this instrument, we do not see improvement in signal-to-noise in the MS/MS experiment when ions are generated by liquid SIMS rather than CI. Successful analysis of the catfish extract was not feasible.

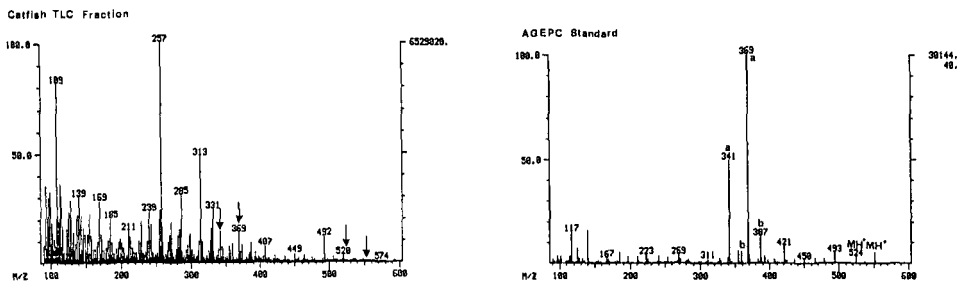

Fig 1. Isobutane CI spectra of catfish extract (a) and authentic AGEPC sample (b).

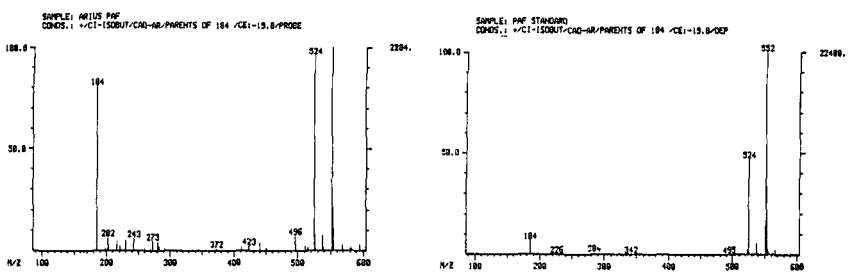

Fig 2. MS/MS parent scan for catfish extract (a) and AGEPC sample (b).

Presented at the 35th ASMS Conference on Mass Spectrometry and Allied Topics
May 24-29, 1987, Denver, CO

SEPARATION AND IDENTIFICATION OF GLUCOSINOLATES FROM BRASSICA VEGETABLES USING HIGH PERFORMANCE CAPILLARY GC-MS.

G. John Shaw and Denis Andrzejewski; Food and Drug Administration,
200 C Street, S.W., Washington,D.C. 20204.

Introduction

The recent interest in monitoring endogenous levels of glucosinolates (1) in Brassica vegetables stems from the important physiological activities of the associated aglycone products following endogenous enzyme mediated hydrolysis in disrupted unheated plant tissue and the relatively high human and domestic animal consumption of these crops. Numerous studies(1) have collectively demonstrated that the aglycone products are not only responsible for the characteristic pungent volatile flavour of these crops but are also associated with food taints, cyto- and phytoplasmic toxicity, anticarcinogenic effects, and various nutritive and antinutritive effects.

The currently preferred analytical method for chemical characterization and quantitation of intact glucosinolates from crucifers relies on desulfation of resin-bound glucosinolates and then chromatography of the resulting desulfoglucosinolate (2) mixture. Direct HPLC analysis or packed column GC (and sometimes GC-MS) analysis of the corresponding pertrimethylsilyl-desulfoglucosinolate (3) analogues is now used extensively. Recently, the application of capillary GC has been reported using different liquid phases and temperature programming conditions(2,3). Data presented in this paper demonstrate the utility of high performance capillary GC and show how this technique, together with methane positive ion chemical ionization (PICI) MS, can be used to distinquish individual glucosinolates in Brassica vegetables.

Experimental

Mass spectra were collected using a Finnigan-Mat TSQ46 operating under standard methane PICI conditions. Glucosinolate samples were prepared by slight modification of the method described by Heaney et al.(4). Individual components were separated on a 25m x 0.2mm(id) x 0.33um WCOT fused silica HP1 column which was temperature programmed from 210°C(3 min.) to 300°C(20 min.) at 10°/min. Helium linear velocity was 27cm/sec.

Results and Discussion

Figure 1 shows a typical total ion current profile from the high performance capillary separation of glucosinolates from rutabaga, analysed as their pertrimethylsilyldesulfoglucosinolate analogues. Table 1 tabulates the glucosinolates identified in both brussels sprout and rutabaga, together GC retention times, natural occurrence and main MS diagnostic ions.

Examination of the chromatographic data shows that despite their similar side chain structures, major glucosinolates in each extract were completely separated by capillary GC using a non-polar WCOT column. The enhanced resolving power of the capillary column facilitates separation of a wider range of glucosinolates compared to packed column GC analysis. In addition, use of a bonded liquid phase WCOT capillary together with a higher column temperature programme allowed a more detailed glucosinolate analysis of each vegetable extract compared to previous reports.

The mass spectrum of each pertrimethylsilyldesulfoglucosinolate is primarily distinquished by a major fragmentation pathway involving thioglycosidic cleavage at the S-C(oxime) bond and loss of the oxime TMS group giving the oximium sidechain ion $[R_3\text{-C}\equiv\text{NH}]^+$. For the alkyl, alkenyl and aryl glucosinolates, this fragment or its corresponding daughter ion, $[R_3]^+$, as demonstrated by MS/MS studies, is the main decomposition process of diagnostic significance. In contrast the hydroxyalkenyl glucosinolates, represented by progoitrin (9) and gluconapoleiferin (10), give diagnostic ions again corresponding to $[R_3\text{-C}\equiv\text{NH}]^+$ but now shifted to m/z 170 and 184, respectively. The main fragment ions, however occur at m/z 129 and m/z 143 and arise from a further cleavage of the side chain moiety to give $[CH_2\text{=CH-CH=OTMS}]^+$ and $[CH_2\text{=CH-CH}_2\text{-CH=OTMS}]^+$. Other appreciable fragmentation is also observed under the conditions described and appears due to the formation of other structurally relevant ions such as $[R_3\text{-C}\equiv\text{NOTMS}]^+$ and $[R_3\text{-C(S)=NOTMS}]^+$ and from extensive fragmentation of the pertrimethylsilyl β-D-glucose moiety.

The value of methane PICI MS is further extended in establishing the presence of co-eluting compounds. For example under the chromatographic conditions described, the pertrimethylsilyldesulfo analogues of sinigrin (5) and glucocochlerain (6) are not resolved. Nevertheless, in the appropriate mixed mass spectra, both compounds are readily identified and could be quantitated by single ion monitoring or mass chromatography of the diagnostic ions m/z 68 and m/z 84.

Conclusion

High performance capillary GC-PICIMS extends current analytical procedures designed for the routine monitoring of intact glucosinolates in *Brassica* vegetables. Results show that the combination of high performance capillary separation of complex mixtures of pertrimethyldesulfoglucosinolates together with the relatively intense diagnostic mass spectral fragment ions that these compounds produce under the chemical ionization conditions described gives a greater opportunity for more detailed studies on the distribution of glucosinolates in *Brassica* than currently exist.

References

(1) Fenwick, G.R., Heaney, R.K. and Mullin, W.J., CRC Crit. Rev. Food Sci., 18,123 (1983).
(2) Sosulski, F.W. and Dabrowski, K.J. J. Agric. Food Chem., 32, 1172 (1984).
(3) Hiltunen, R. et al., Acta Pharm. Fenn., 89, 31 (1980).
(4) Heaney, R.K. and Fenwick, G.R., J. Agric. Food Chem., 31593 (1980).

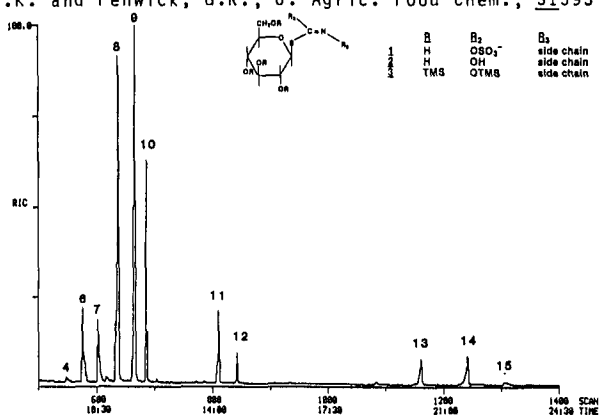

FIGURE 1. Capillary GC of glucosinolates from rutabaga.

TABLE 1

GLUCOSINOLATES IDENTIFIED IN BRUSSELS SPROUT AND RUTABAGA.

Analysed as their corresponding per trimethylsilyldesulfoglucosinolates

GLUCOSINOLATE	SIDE CHAIN(R_3)	R.T.(m:s)	OCCURRENCE BS[b]	OCCURRENCE S[c]	MAIN MS DIAGNOSTIC IONS[d] [R_3-CHNH]	[R_3]	[R'CH=OTMS]$^+$
glucoputranjivin(4)[a]	Isopropyl	9 39	-	+	70(100)	ND	
sinigrin(5)	2-Propenyl	10:06	+	-	68(100)	ND	
glucocochlearin(6)	1-Methylpropyl	10:06	-	+	84(100)	ND	
gluconapin(7)	3-Butenyl	10:36	+	+	82(100)	ND	
glucobrassicanapin(8)	4-Pentenyl	11:09	-	+	96(100)	69(31)	
progoitrin(9)	2-Hydroxy-3-butenyl	11:42	+	+	170(20)	143(8)	129(98)
gluconapoleiferin(10)	2-Hydroxy-4-pentenyl	12:04	-	+	184(60)	157(7)	143(100)
gluconasturtiin (11)	2-Phenylethyl	14:16	-	+	132(100)	105(9)	
glucoberteroin(12)	5-Methylthiopentyl	14:51	-	+	144(85)	117(10)	
glucobrassicin(13)	3-Indolylmethyl	20:50	+	+	229(10)	202(100)	
4-hydroxyglucobrassicin(14)	4-Hydroxy-3-indolmethyl	22 12	+	+	317(17)	290(98)	
4-methoxyglucobrassicin(15)	4-Methoxy-3-indolylmethyl	23:46	+	+	259(10)	232(100)	

a = corresponding compound numbering in Figures 1 and 2; b = Brussels sprout; c = Rutabaga; d = positive ion CI(CH_4).

ND = not determined because of interference from methane reagent ion signals.

Presented at the 35th ASMS Conference on Mass Spectrometry and Allied Topics
May 24-29, 1987, Denver, CO

FRAGRANCE ANALYSIS BY CAPILLARY GAS CHROMATOGRAPHY/ MASS SPECTROMETRY.

Jia-shen Wang, Avelina Qua, and Ira E. Rosenberg
Clairol Inc., Stamford, Connecticut 06922

Fragrances are some of the most expensive raw materials in the cosmetic industry. Developoing analytical methodolog for characterization of essential oils, therefore, is always a very interesting topic in this industry. The potential for applying an integrated capillary GC/MS system for the analysis of fragrance materials is very obvious. The unique features are that the resolving power of a capillary column is adequate to study complicated mixtures such as essential oils, and that identification can be obtained simultaneously.

In this investigation, all analyses were carried out using a Finnigan 4000 GC/MS/DS system. We have set up an in-house library of fragrance materials to increase the identification capability of this system. To date, this library contains 339 mass spectra of pure fragrance components. All these spectra were obtained from pure standards or from known compounts of mixtures which have been used commonly in industry or have been approved by RIFM. With the addition of this library, at least 90% of the essential oils and fragrance raw materials encountered in our samples have been characterized. Many essential oils such as lemon, bay, rose, clove, eucalyptus, and peppermint oils have been characterized successfully.

The software of the data system was improved with additional in-house written procedures which perform rapid analysis of multiple similar type mixtures. The program (AUTOFN) shown here is a procedure which has the following features: defines the peaks in an RIC, performs an FR library search and an NB library search (if FR search fail), and provides a quantitative report. The marks "-->" in the program indicate that the subsequent sections should be defined as subprograms which enable a user to change criteria easily.

The detection limit for a component will vary with the nature of the compound. In general, if the concentration of a compound of interest is less than 0.01%, it requires special attention. This is a weak point of this analytical method since it is possible to have a component at high odor value but at a much lower concentration. With this system, the analysis of fragrance materials in a finished product is possible, however, a preseparation process is also required. The example given here is the result of using a CO_2 extractor (Kontes) to study the fragrance materials in the product Condition Shampoo.

COMPOUND	FOUND	RAW MATERIAL*
Linalool	7	40
Linallyl Acetate	6	31
Eugenol	19	60
C-11 Alcohol		15
Caryophyllene Acetate	10	4
Lilial	3	4
Isoamyl Salicyclate	6	10
Rossacetal	4	11
Diethyl Phthalate	100	100
Amyl Cinnamic Aldehyde	51	76
Cedryl Acetate	10	22
Benzyl Salicylate	65	42

*Not a complete list

In this experiment, we have found that most fragrance components in the product can be extracted with this device, however, the efficiency for each component is not identical. In general, the efficiency of esters are better than those of alcohols.

PROGRAM: AUTOFN

```
        ERASE
        SETS $
        EDSL (-;W;E)
        --> MAP (I;50,400;N-3,6,5>;U50;F1;T;D;E)
        --> SETQ TEMP
            SETL TEMP
            EDQL ,$ (-;W;E)
            --> ERASE
                --> SET4 FR
                GETS
                --> ENLB (I;T900;X;X2;D;J1,;E)
                ERASE
(A)             -->
                    --> IF #1, !26
                        --> SET4 NB
                        ENLB (I; T850;X2; D;J1,E)
                        --> IF #1,!26
                            LIBR (ED;R20;#TP;I!1;Z)
                            SET4 TP#1
                            RETURN ---     :To (A)
                        EDLB (#TP;G;R20;I!1;E)
                        RETURN ---         :To (A)
                    --> CHRO (I;R/TP,1;#;T;G-5,5;U2,3;0;N-2,4;
                              A-5,1<;D-20,20;E)
                    --> IF #1,!28
                        EDQL (N;W;E)
                    EDQL ,$ (A;E)
                    LOOP
                --> LIBR (ED;$TT;#TP;G1;I!1;Z)
                QUAN $ (D;H;E)
```

Presented at the 35th ASMS Conference on Mass Spectrometry and Allied Topics
May 24-29, 1987, Denver, CO.

FAST-ATOM BOMBARDMENT MASS SPECTROMETRY: AN ALTERNATIVE METHODOLOGY FOR THE CHARACTERIZATION OF AMILORIDE ANALOGUES

Y. Tondeur[1,3], W. Niederhut[1,4], and E.J. Cragoe, Jr.[2]

1) ERC, University of Nevada, Las Vegas, NV 89119
2) Merck Sharp and Dohme Laboratories, West Point, PA 19486
3) Current address: Triangle Labs, Research Triangle Park, NC 27713
4) Current address: ITAS, Export, PA 15632

INTRODUCTION

Amiloride analogues consist of a series of substituted pyrazines (Fig. 1), some of which exhibit unique ion-transport inhibiting properties. The importance of these compounds resides primarily in their ability to probe ion translocation mechanisms in biological systems. Although an extensive amount of physiological and conformational (by NMR) studies have been conducted on amiloride analogues, no mass spectrometric characterization of these diuretic substances were reported thus far.

In an effort to provide additional analytical support to metabolic and photoactivation studies involving these promising drugs, fast-atom mass spectrometry (FAB/MS) was evaluated in conjunction with collisionally activated dissociation (CAD) MS/MS on selected amiloride analogues.

The structure of **amiloride** is shown in Fig. 1. Its pKa of 8.7 implies that amiloride exists predominantly as an acylguanidinium ion in the physiologic pH range. Thus, amiloride analogues should constitute a class of compounds easily amenable to FAB/MS.

RESULTS AND DISCUSSION

A representative FAB mass spectrum of an amiloride analogue (compound IV) is shown in Fig. 2. The spectrum is characterized by the presence of an easily recognizable chlorine-containing hydrated molecular ion along with a few fragment ions such as the 3-amino-5-ethylisopropylamino-6-chloropyrazine acylium ion at m/z 241 and other fragments reminiscent of the lateral guanidinic chain (m/z 86, 60). The $[M + H]^+$ relative abundances range from 20% for compound V to 100% for amiloride itself. In general, the hydrated species constitute the base peak if the guanidine chain possesses at least two amino groups. The possibility of charge delocalization on the terminal amidinium moiety may be responsible for that observation.

Occasionally, as it is observed for compound III, a glycerol adduct ion ($[M + G + H]^+$) can be detected. The signal at m/z 372 corresponds to a non-chlorine-containing impurity that can be removed by chromatography. (The CAD-EB_2 mass spectrum - recorded on a magnetic triple-sector instrument [VG Analytical, ZAB-3F] - supports the presence of an acylguanidine moiety in the structure of the impurity.) A FAB-induced dehalogenation reaction (m/z 266, Fig. 2) is detected for all the amiloride analogues presenting a pyrazinyl chlorine group in position 6.

Losses of ammonia and hydrochloric acid are commonly found in the CAD MS/MS spectra (a set of examples is summarized in Table 1) of the hydrated molecular ion species of amiloride analogues. The former is particularly preponderant for the amiloride analogues presenting a substitution on the guanidinic chain. Other decomposition reactions leading to fragment ions reminiscent of the pyrazine nucleus are also apparent and can be effectively used during metabolic investigations. With a few exceptions, the base daughter ion signal generally corresponds to the formation of the acylium ion.

Presented at the 35th ASMS Conference on Mass Spectrometry and Allied Topics
May 24-29, 1987, Denver, CO

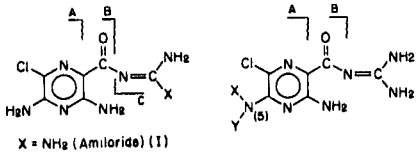

X = NH_2 (Amiloride) (I)
$NH(CH_2)_{11}CH_3$
$NHCH_2C_6H_5$
$NHCH_2(C_6H_3Cl_2-3,4)$
$NHCH(CH_3)$ (1-naphthyl)
NHC_6H_5 (II)
$NHCONH_2$

X = CH_3 Y = CH_3 (III)
X = C_6H_5 Y = $CH(CH_3)_2$ (IV)
X = C_2H_5 Y = $CH_2(C_6H_3-2-OCH_3-4-NO_2)$
X = CH_3 Y = (CH_2) $CON=C(NH_2)_2$

Figure 1. Structures of amiloride analogues

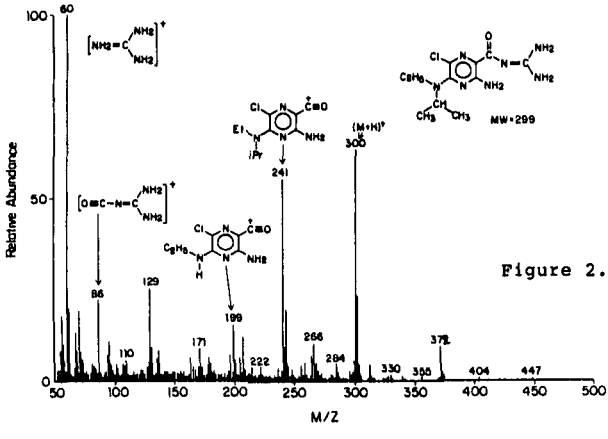

Figure 2. Positive ion FAB mass spectrum of IV

TABLE 1

Collisionally Activated Daughter Ion MS/MS Spectra: Amiloride Analogues with Guanidino Nitrogen Substitution

(Ion abundances are expressed as a percentage of the total daughter ion current)

Daughter Ion \ X	NH_2	$NH(CH_2)_{11}CH_3$	$NHCH_2(C_6H_5)$	$NHCH_2(C_6H_3Cl_2)$	$NHCH(CH_3)(C_{10}H_7)$ [a]	$NH(C_6H_5)$	$NHCONH_2$
$[M+H-NH_3]^+$	5.62	4.63	16.0	4.97	0.65	14.9	50.7
$[M+H-Cl]^+$	0.77	0.44	0.85	3.02	—	0.36	0.73
$[M+H-HCl]^+$	1.04	0.88	0.93	1.18	0.82	0.39	0.70
$[M+H-XH]^+$	5.82	0.44	0.79	0.46	0.80	1.58	0.98
$[BNH_2]^+$	2.08	0.74	7.08	1.29	—	2.27	0.82
$[M+H-HC]^+$	46.6	18.2	29.4	24.5	4.01	32.1	11.6
$[A]^+$	5.24	0.79	2.97	2.57	—	3.57	1.97
$[H_2C]^+$	1.88	34.3	2.80	22.3	0.91	16.2	1.10
$[H_2C-NH_2]^+$	—	—	0.46	0.55	—	1.62	1.21
$[XH_2]^+$	—	0.52	0.51	—	—	1.37	0.72

(a) Base daughter ion is at m/z 230 (amiloride)

Presented at the 35th ASMS Conference on Mass Spectrometry and Allied Topics
May 24-29, 1987, Denver, CO

ENHANCEMENT OF MOLECULE ION YIELDS IN PLASMA DESORPTION MASS SPECTROMETRY.

A.G. Craig[1], A. Engström[1], H. Bennich[1] and I. Kamensky[2]

[1] Department of Immunology, University of Uppsala, Box 582, S-751 23 Uppsala Sweden.
[2] Bio-Ion Nordic AB, Box 15045, S-750 15 Uppsala, Sweden.

A simple variation of the *nitrocellulose sample preparation* technique[1] used with plasma desorption mass spectrometry (PDMS) increases the yield of molecule ions. Experiments to determine the dependence of molecule ion yield on the salt concentrations using this method are presented.

The protein dissolved in an aqueous 0.1 % trifluroacetic acid solution is diluted with alcohol before applying to the nitrocellulose. After 1 minute the nitrocellulose surface is rinsed with water. The water is blown off the nitrocellulose with nitrogen.

An increased yield of *singly and multiply charged molecule ion peaks* is observed over the corresponding measuerement without the addition of alcohol. This method has been used to measure several protein samples (such as interferon-B, bovine carbonic anhydrase and porcine pepsin) which had not previously been measured. Figures 1 and 2 show the intense spectra observed for porcine pepsin and bovine carbonic anhydrase using this method.

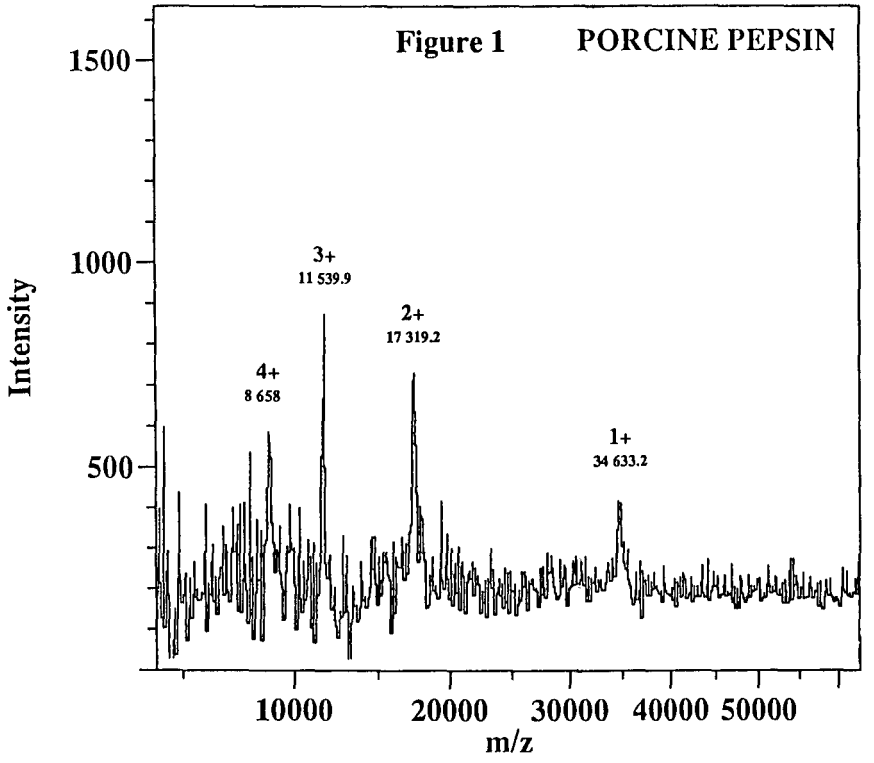

The measured average mass for pepsin (34630 u) can be compared with the mass based on the reported sequence[2] of the active enzyme, where the activation peptide includes residues 1-42 or 1-44, is either 34688 or 34504 daltons respectively.

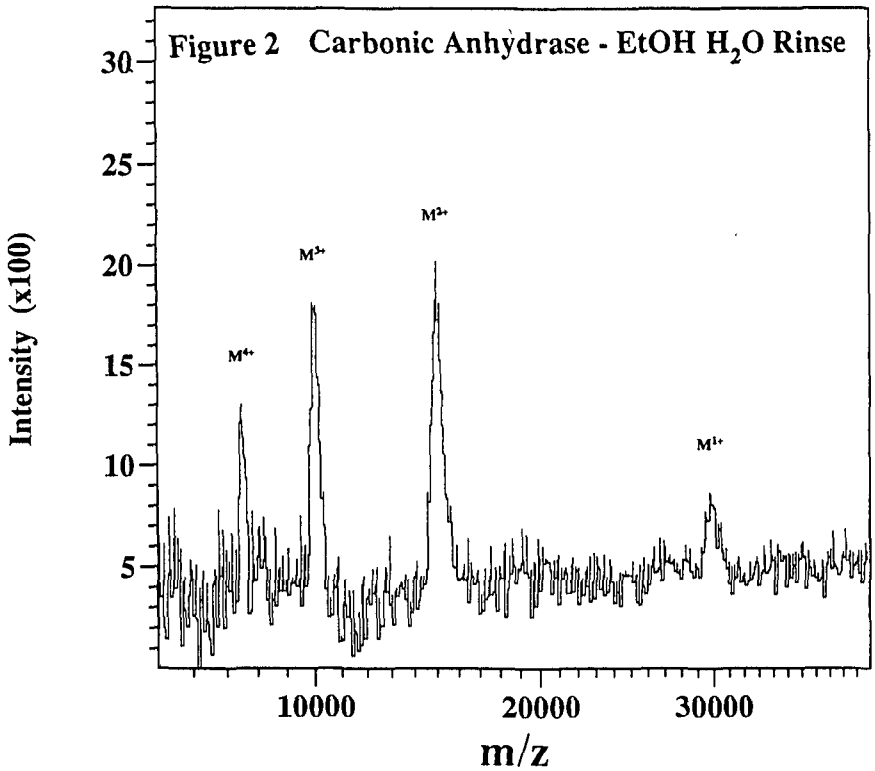

The enhancement is not observed from an aqueous solution applied to nitrocellulose which has been wet with alcohol. Similarly no enhancement is observed if an aqueous solution is simply washed from the nitrocellulose surface with alcohol.

If the sample is not rinsed the resulting spectrum contains no indication of the intact molecule ion peaks. If this sample is withdrawn from the mass spectrometer rinsed and remeasured, intense peaks commensurate with a sample prepared and rinsed immediately are observed. The Na_+ peak is absent in spectra which are rinsed, but present in the unrinsed sample.

Solutions of sodium citrate, sodium acetate, sodium sulphite and sodium dihydrogen phoshate when applied to rinsed samples inhibited molecule ion formation. Subsequent rinsing and remeasurement verified that the effect of these salts can be reversed.

In conclusion by using a simple variation to an established technique the range of samples amenable to the PDMS ionisation technique is extended. As a result more questions concerning the size of biomolecules may be addressed using PDMS. The imporatnt role salt concentrations play in the ionisation process has been verified although we observe that alkali cationisation 'per se' does not prohibit ionisation.

1 G. Jonsson et. al., Anal. Chem., 58, (1986) 1084.
2(a) L. Moravek and V. Kostka, F.E.B.S. Lett., 43, (1974) 207.
2(b) P. Sepulveda et. al., J. Biol. Chem., 250, (1975) 5082.

Presented at the 35th ASMS Conference on Mass Spectrometry and Allied Topics
May 24-29, 1987, Denver, CO

METABOLISM OF HOMOLOGUES OF DELTA-8- AND DELTA-9-TETRAHYDROCANNABINOL IN MICE

D.J. Harvey and N.K. Brown

University Department of Pharmacology, South Parks Road, Oxford, OX1 3QT, UK.

Introduction

Delta-9-tetrahydrocannabinol (delta-9-THC, I), the major psychoactive constituent of marihuana, has a C_5 side-chain and is often accompanied, in the source plant (Cannabis sativa L.) by variable concentrations of propyl, methyl and butyl homologues (listed in order of decreasing abundance). The metabolism of delta-9-THC has been well studied (1) but little is known about the metabolism of the other homologues other than a report of the metabolism of the propyl homologues at the 1986 ASMS meeting. We have now synthesised homologues of delta-9- and the related delta-8-THC (II) with side-chains of one to six carbon atoms and studied their in vivo metabolism in mice in order to investigate the effect of chain-length and, hence, lipophilicity, on the ratio of acid and hydroxy metabolites. Metabolism of the heptyl homologue has been reported in an earlier publication (2).

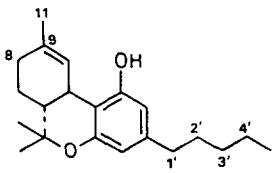

delta-9-THC

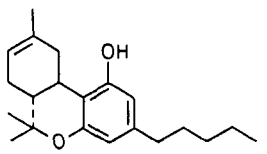

delta-8-THC

Methods

Methyl, ethyl, propyl, butyl and hexyl homologues of delta-8-THC were synthesized by condensation of (1S)-cis-verbenol with the appropriate 5-alkyl-1,3-dihydroxy-benzene and these compounds were converted into the delta-9-isomers by a hydrochlorination, dehydrochlorination reaction. The heptyl homologue of delta-9-THC was a gift from Dr. E.W. Gill (Oxford). Metabolism of all of these compounds was studied in male Charles River CD-1 mice after intraperitoneal injection. Hepatic metabolites were extracted with ethyl acetate, purified by chromatography on Sephadex LH-20 and converted into TMS, [$^2H_9$]TMS, or methyl ester/TMS derivatives. In addition, they were reduced with lithium aluminium deuteride prior to TMS ether formation. These derivatives were examined by GC/MS (25 eV) using a VG 12B mass spectrometer interfaced to a Varian 2440 gas chromatograph (2m x 2mm, 3% SE-30) and to a VG 2050 data system. The acceleration voltage was 2.4 kV and the trap current 100 uA. Data were acquired and processed with a VG 2050 data system. Octanol:water partition coefficients of the homologues were estimated by a gas chromatographic method (3).

Metabolites were identified by comparison of their GC/MS data with those of reference samples of the pentyl homologues and with published spectra (4). Fig. 1 shows the 25 eV mass spectrum of the TMS derivative of methyl-delta-9-THC-11-oic acid.

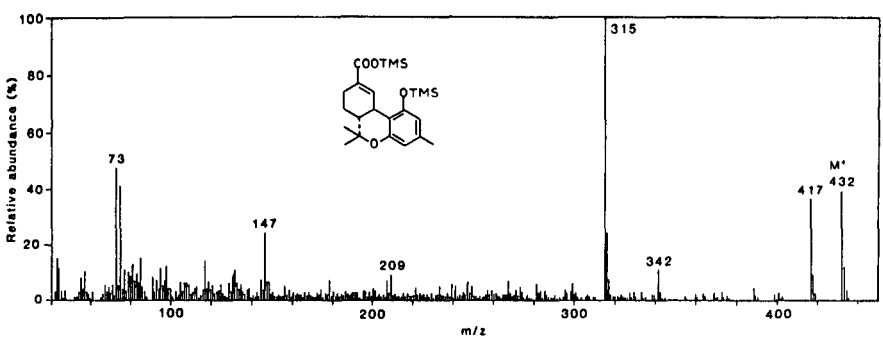

Fig. 1. 25 eV Mass spectrum of the TMS derivative of methyl-delta-9-THC-11-oic acid.

Results

All of the compounds showed similar routes of metabolism namely hydroxylation on the terpene ring and side-chain and oxidation of primary alcohols, mainly the 11-hydroxy metabolite, to carboxylic acids. Metabolism of the lower homologues was simple (Fig. 2) with, for example, 95% of the metabolic fraction from the methyl homologues consisting of the 11-oic acid. As the side-chain length increased, more metabolites were produced with the acid being much less prominent (Fig. 3). Hydroxy and polyhydroxy metabolites were much more abundant from the higher homologues.

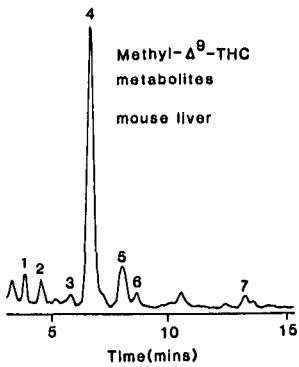

Fig. 2. Ion chromatogram (m/z 240 - 700) of the metabolites of methyl-delta-9-THC extracted from mouse liver. Peak 4 is the methyl homologue of delta-9-THC-11-oic acid and peaks 5 - 7 are hydroxylated derivatives of this compound.

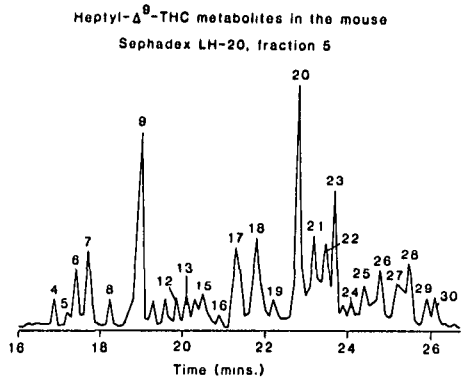

Fig. 3. Ion chromatogram (m/z 300 - 700) of the metabolites of heptyl-delta-9-THC extracted from mouse liver. The 11-oic acid metabolite is peak 13. Peak 9 is the heptyl derivative of 8-alpha,11-dihydroxy-delta-9-THC and peak 20 is the 2',3',11-trihydroxy metabolite. Other peaks are mainly di- and tri-hydroxy metabolites.

The ratio of the 11-hydroxy and 11-oic acid metabolites was found to be linearly correlated to the octanol:water partition coefficient which, in turn, was linearly related to the alkyl chain length (Fig. 4).

Conclusion

These results suggest that the greater lipophilicity of the higher homologues made them more accessible to the membrane-bound cytochrome P-450 enzymes and restricted access to cytosolic alcohol dehydrogenases.

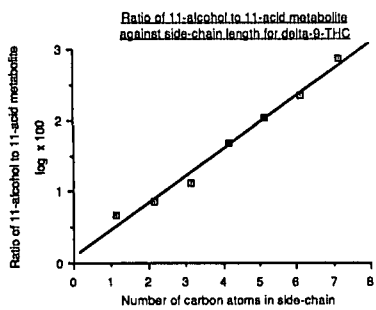

Fig. 4. Plot of the ratio of the 11-hydroxy to 11-oic acid metabolites of delta-9-THC to the alkyl chain length.

References

1. D.J. Harvey and W.D.M. Paton, Rev. Biochem. Toxicol., 1984, 6, 221.
2. D.J. Harvey, Xenobiotica, 1985, 15, 187.
3. K. Valko, O. Papp and F. Darvas, J. Chromatogr., 1984, 301, 355.
4. D.J. Harvey, Mass Spectrom. Rev., 1987, 6, 135.

Acknowledgements

This work was supported by grants from the Wellcome Trust and NIDA.

Presented at the 35th ASMS Conference on Mass Spectrometry and Allied Topics
May 24-29, 1987, Denver, CO.

THE IN VITRO ANALYSIS OF DELTA-9 TETRAHYDROCANNABINOL BY NICI AND DEP MASS SECTROMETRIC TECHNIQUES,

Vincent M. Papa, Patrick S. Ng, Eugene F. Robbins, David W. Ou, Research Resources Center, and West Side Veterans Hospital, University of Illinois at Chicago

ABSTRACT

Although a wide variety of methods have been published to detect and quantitate the presence of delta-9 tetrahydrocannabinol (D-9THC) ,these methods require varying degrees of sample preparation which lowers recovery. Also, a number of these methods are based on electron impact techniques which can cause confusion in identifying the molecular ion. A number of investigators have demonstrated that negative ion chemical ionization (NICI) using Gas Chromatography (GC) and Direct Exposure Probe (DEP) MS methods generated simplified spectra without the need for elaborate sample preaparation (1,2,3,4). A tissue culture system was adapted from the literature to isolate and maintain lymphocytes and monocytes (5) that were used in evaluating the potential of NICI and DEP methods to monitor the presence of D-9 THC in vitro. While the GCMS method resulted in a sensitivity of 2 ng/ml with prominent ions at m/e 309,313,326, the DEP techniques resulted in subnanogram sensitivity for the same compound.Recovery studies show that the recovery of D-9THC from tissue culture supernatants had a range from 64-85% (n=10,Mean=71,sd=4). In conclusion, both DEP and NICIGC methods offer important advantages and disadvantages in vitro cannabinoid analysis and a multi-method approach is recommended.

METHODS

A Finnigan 4510 GCMS with Incos data system was operated in NICI mode using methane (0.55 Torr) and ammonia (0.35 Torr) as reagent gases employing J+W (15M , 0.25 uM) DB-1,5,225 columns programmed from 160(2)-270(3) , 20D/M. Electronics were set at 1300 kV for the electron multiplier, electron energy 100 eV and 0.25 microamps filament current. Mass scanning was from m/e 100-650, 3 sec/scan GC (1sec/scan DEP) at 120 DC souce temperature. Underivitized, derivitized, (n-methyl tributyl silyl fluoroacetamide (MTSBFA) and trifluoroacetic anhydride (TFA) (Pierce, Rockford, Ill.)) (6) ,extracts from tissue culture supernatants from lymphocytes and monocytes (5% CO2,37 DC, 1hr incubation with varying concs. of D9 -THC) were injected onto the DB-1,5,225 columns. In a parallel series of experiments, 1 uL of underivitized tissue culture fluid (D-9 THC treated and 1 hr incubation) was placed on a rhenium loop with the voltage programmed from 0.015-1.335 mA at 20 mA /sec. In the final series of experiments, a 200 ng / ml ampule of D-9 THC (Applied Sciences, State College, PA.) was diluted to 50 ng/ml with ethanol and was added to isolated lymphocyte and monocyte (7). The samples were incubated for 1 hr at the above conditions. Finally, the cells were seperated by centrifugation and 1uL was placed on a DEP rhenium loop for analysis.

RESULTS AND DISCUSSION

NICI using ammonia gas at 0.35 torr resulted in a 2ng/ml sensitivity of 2 ng/ml for D-9 THC with prominent ions at m/e 309, 313,326 when using the DB-1 column and subnanogram sensitivity using the DEP probe. In our study, all of the columns used (DB-1,5,225) detected D9THC in both directly injected standards and extracted specimens. This is in agreement with the literature studies indicating that SE-30 like columns are most suited for cannabinoid analyses. Also, a number of investigators have shown that DEP is ideal for the analyses of compounds with minimal sample preparation. Foltz et al. (1) reported that MTBSTFA and TFA derivatives of D9THC were detected by NICI techniques with sensitivity and specificity in biological fluids. However, in our studies we found that derivitization of lymphocyte and monocyte supernatants resulted in no significant increase in sensitivity and specificity. Finally, in our studies recovery of THC ranges from 64-85 % (mean=71, n=10, sd=4).

In conclusion, we believe that a multimethod approach including DEP and NICI to the analyses of cannabinoids offers numerous advantages : (1) subnanogram sensitivity, (2) consistent recovery, (3) minimal sample preparation and (4) analysis time of under 4 minutes for the DEP method. Studies are actively being carried out to apply these techniques to the analysis of other cannabinoids in a variety of cell systems.

REFERENCES

1.Foltz, R.M., McGinnis, K.M. and Chinn, C.M.,"Negative Ion Assay for delta-tetrahydrocannabinol and its metabolites," Biomedical Mass Spectrometry ,vol. 10, no. 5, pg. 316-323, 1983.

2.Schilling, A.B., Zulak, I.M., Puttemans, M.L., Hall, E.R.,and Venton, D.L.," Ammonia and Direct Chemical Ionization Mass Spectrometry of Underivitized Prostaglandin H2 and other selected Prostaglandins," Biomedical and Environmental Mass Spectrometry , vol. 13, pg 545-551, 1986.

3.Houriet, R., Stahl, D. and Winkler, F.J.,"Negative Chemical Ionization of Alcohols," Environmental Mass Spectrometry, vol.36, pg 63-68, 1980.

4.Cotter, R. and Fenseleau, C.," The effects of Heating Rate and Sampling Size on the Direct Exposure/Chemical Ionization of Biological Conjugates, " Biomedical Mass Spectrometry, vol. 6, no. 7, pg. 287-293, 1979.

5.Zlak, A., Discontinuous Density Gradient of Human Mononuclear Leukocytes using a Percoll density media, J. Immunol. Methods 30, pg 1-10, 1979.

6.Knapp, D., "Handbook of Analytical Derivitization Reactions," John Wiley and Sons, 179, pg 87, 1979.

7.Papa, V.M., Wiederhold, M.D. Javaid, J.I. and Ou, D. W., "Immunological and Metabolic Consequences of Delta-9 Tetrahydrocannabinol Administration to Lymphoid Cells in Culture," Spectros. Int. J. pg 431-438, 1984.

Presented at the 35th ASMS Conference on Mass Spectrometry and Allied Topics
May 24-29, 1987, Denver, CO

CHARACTERIZATION OF PROPYLENE OXIDE-DNA ADDUCTS BY MASS SPECTROMETRY. ALKYLATION AT N-3 OF CYTOSINE RESULTS IN DEAMINATION TO A URACIL ADDUCT.

Jerome J. Solomon, F. Mukai, K. Decker and A. Segal

Institute of Environmental Medicine, New York University Medical Center, New York, NY 10016

Propylene oxide (PO) is a direct acting mutagen and rodent carcinogen. It is used in the manufacture of polyurethane foams and in the preparation of polyester resins. Production in the USA in 1986 was $2.5X10^9$ pounds. We have used spectroscopic methods (UV and MS) to characterize how PO modifies model 2'-deoxynucleosides at pH 7 and 37°C for 10 hours. PO forms the following 2-hydroxypropyl (HP) adducts: N^6-HP-dAdo (7% yield), 7-HP-Gua (37%), and 3-HP-dThd (4%). Alkylation at the N-3 of dCyd resulted in the conversion of the adjacent exocyclic imino group at C-4 to an oxygen (hydrolytic deamination) with the formation of a dUrd adduct, 3-HP-dUrd (14%).

The structure of the adducts are given in Figure 1 and their isobutane CI mass spectra are shown in Figure 2. CI results in MH which fragments by loss of H_2O and CH_3CHOH which establishes the configuration of the hydroxypropyl side chain. The protonated molecular ion of the nucleosides further decomposes with hydrogen transfer to base plus two hydrogens, bH_2, which also loses H_2O and CH_3CHOH from the side chain.

The reaction of PO with dCyd resulted unexpectedly in the isolation of 3-HP-dUrd instead of the expected 3-HP-dCyd. To check our structural assignment we determined the accurate mass of diagnostic ions in the CI and EI mass spectra of this adduct. Spectra were recorded with a VG 70SE at 4500-6000 resolution using a linear voltage scan which included three PFK peaks and the unknown whose accurate mass was to be determined. Two of the PFK peaks were used to establish the mass scale and the third reference peak was used to verify the accuracy of mass measurement. In all experiments, accuracy was better than 0.0006 amu. Data was collected for at least 10 scans of the reference plus unknown in the multichannel analysis mode. Table 1 lists the results which confirm our structural assignment as 3-HP-dUrd. As a further proof of structure, PO was reacted with dUrd and the product we obtained had identical chromatographic and spectral properties to our dCyd reaction product, 3-HP-dUrd.

PO was reacted with calf thymus DNA (pH 7, 37°C, 10 hours) and yielded N^6-HP-dAdo (1 nmol/mg DNA), 7-HP-Gua (19 nmol/mg DNA) and 3-HP-dUrd (13 nmol/mg DNA). The dCyd adduct in DNA underwent a hydrolytic deamination to yield 3-HP-dUrd which accounted for 39% of the total DNA adducts. Deamination of C to U by other mutagens is well known. Nitrous acid, the classical oxidative deamination reagent, converts C to U and results in a predictable basepairing change. The mutations of bisulfite are likely to result from the hydrolytic deamination of C to U. A specific enzyme, uracil glycosylase, is available to remove the U which results from this deamination. Repair of alkyl-dUrd by a specific glycosylase is unknown. We postulate that the hydrolytic deamination is catalyzed by the OH on the hydroxypropyl side chain which polarizes the adjacent imine bond. Water then adds across this bond to form a carbinolamine which subsequently loses NH_3 to form 3-HP-dUrd, Figure 3. This reaction should occur with other aliphatic epoxides after initial reaction at N-3 of cytosine. Preliminary results in our laboratory indicate that both epichlorohydrin and glycidol react with dCyd to form similar 3-alkyl-dUrd adducts. This cytosine to uracil conversion may be a common phenomenon with epoxides and may play a role in their mutagenic and carcinogenic activity.

Supported by NCI grant CA 13343 and NIEHS grants ES 00260 and ES 03563.

Figure 1

HYDROXYPROPYL (HP) ADDUCTS OF PROPYLENE OXIDE WITH 2'- DEOXYNUCLEOSIDES

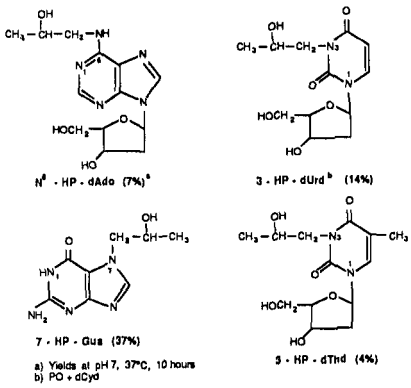

Figure 3

POSTULATED MECHANISM FOR HYDROLYTIC DEAMINATION OF 3 - HP - dCyd TO 3 - HP - dUrd

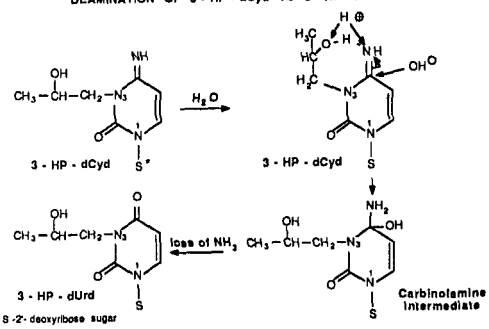

Figure 2

CHEMICAL IONIZATION (i-C_4H_{10}) MASS SPECTRUM OF HYDROXYPROPYL (HP) ADDUCTS OF PROPYLENE OXIDE WITH 2'- DEOXYNUCLEOSIDES

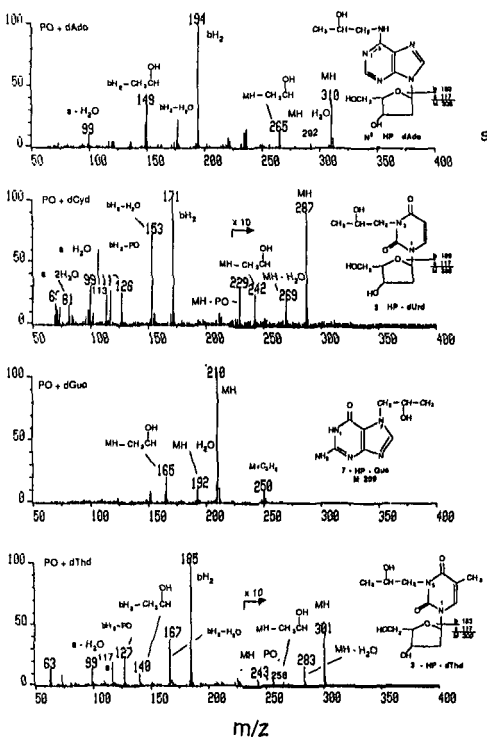

Table 1

ACCURATE MASS MEASUREMENT OF DIAGNOSTIC IONS IN THE EI ANG CI MASS SPECTRA OF 3-HP-dUrd

Ionic Species	Elemental Composition	Calculated Mass	Observed Mass
EI[a]			
M⁺	$C_{10}H_{14}O_5N_2$	242.0903	242 0908
b'H	$C_5H_8O_2N_2$	126.0429	126.0433
S	$C_5H_9O_3$	117.0552	117 0549
CI			
MH	$C_{12}H_{19}O_6N_2$	287 1243	287.1242
MH-H_2O	$C_{12}H_{17}O_5N_2$	269 1137	269 1141
bH_2	$C_7H_{11}O_3N_2$	171 0770	171 0767
bH_2-H_2O	$C_7H_9O_2N_2$	153.0664	153 0664

[a] The EI mass spectrm of 3-HP-dUrd (M 286) results in pyrolysis with loss of acetaldehyde to form 3-Me-dUrd (M⁺ 242).

Analysis of Ethylene Oxide/Propylene Oxide Bis-Phenol A Adducts by Thermospray LC/MS/MS

Patrick J. Rudewicz, Thomas R. Covey and William H. McFadden
Finnigan MAT, 355 River Oaks Parkway, San Jose, CA 95134

Introduction

Nonionic surfactants are second only to the anionic class in annual production, being produced in more than 1×10^9 lb quantities annually. They are generally formed by the condensation of ethylene and/or propylene oxide with fatty alcohols or alkylphenols to form a product mixture of ethers. Their widespread use as industrial and household detergents and emulsifiers has prompted concern over their metabolic fate in the environment as well as their toxicity. Analytical methodologies for their detection in wastewater effluents, sewage sludges, and natural waters generally include an enrichment step followed by effective separation and detection. For lower molecular weight nonionics, the latter two steps are generally carried out using high resolution gas chromatography with either FID or MS detection. The higher molecular weight compounds, however, generally require HPLC separation followed by appropriate detection.

The use of thermospray LC/MS for the separation and identification of nonionic surfactants is a viable alternative to current methodology for a number of reasons. First, because nonionics are polyfunctional oxygenated compounds, they tend to display a high affinity for the ammonium ion in the gas phase and, therefore, their TSP sensitivities with an ammonmium acetate buffer system is good. Secondly, with mass spectrometric detection, one can obtain both molecular weight information and structural information. This can be accomplished with either a single stage quadrupole LC/MS system using a repeller electrode to induce fragmentation or by the combination of LC and tandem quadrupole MS. In this paper, the application of thermospray (TSP) LC/MS and TSP LC/MS/MS for the analysis of the reaction products of ethylene oxide (EO) and propylene oxide (PO) with bis-phenol A (BPA) is described.

Experimental

The TSP LC/MS experiments were done using a Finnigan MAT 4600 single stage quadrupole mass spectrometer equipped with a Finnigan MAT TSP™ interface. The LC conditions were: Beckman C-8 column (.42 by 25 cm), isocratic mode, 60% methanol/40% 0.05M ammonium acetate, flow rate 1.0 ml/min. A discharge electrode was used for ionization at a potential of 1 kV.

The LC/MS/MS experiments were done with a Finnigan MAT TSQ® 70 triple stage quadrupole mass spectrometer equipped with a Finnigan MAT TSP interface. For these experiments, the mixtures were introduced directly into the ion source via the injection loop (no column separation). The TSP source conditions were: vaporizer 120°C, source block 250°C, repeller voltage 50 V, mobile phase 20% acetonitrile/80% 0.05M ammonium acetate. In the MS/MS experiments, argon was used as the collision gas at a pressure of 1.0 millitorr. The collision energy (Q2 offset) was 50 eV.

Discussion

TSP LC/MS. The compounds of interest are formed by the condensation of ethylene oxide (EO) and propylene oxide (PO) with bis-phenol A to form a product mixture of oligomers having the general formula:

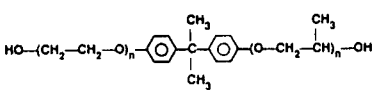

Under typical thermospray source conditions using a low repeller voltage (40 V) each component in the mixture forms an $(M+NH_4)^+$ ion with essentially no fragmentation. Figure 1 shows the $(M+NH_4)^+$ ion profiles obtained using reverse-phase HPLC separation with TSP detection at low repeller voltage (40 V). Prominent $(M+NH_4)^+$ ions are observed for the major components in the mixture. At higher repeller settings (80 V), high pressure collisional activation of these molecular adduct ions occurs inside the TSP source resulting in significant fragmentation (Figure 2). This repeller-induced CID has been reported previously and is more efficient under discharge ionization conditions (1,2). Hence, with LC/MS, the reaction products may be fully characterized by an appropriate selection of repeller voltage.

TSP LC/MS/MS. For the LC/MS/MS analysis of the reaction mixture, a molecular ion profile was obtained by scanning Q1 only. This was followed by daughter ion scans on the molecular ions of the major components in the mixture. The daughter ion spectra obtained were very similar to the repeller-induced CID spectra and reveal characteristic CID fragment ions for the EO/BPA substructure (m/z 179) and the PO/BPA substructure (m/z 193). Parent ion scans for these ions provide a rapid characterization of the mixture according to adduct type (EO,PO, or mixed EO/PO). In contrast to the single stage quadrupole LC/MS experiments, with the use of data-dependent instrument control language (ICL) available on the Finnigan MAT TSQ 70, all of these scans can be made sequentially during one loop injection (no column separation) and complete structural characterization of the oligomers can be achieved within 30 seconds.

Literature Cited

1. Bencsath, F.A.; Field, F.H. Paper presented at the 34th Annual Conference on Mass Spectrometry and Allied Topics, Cincinnati, OH, 1986.

2. Zakett, D.; Kallos, G.J.; Savickas, P.J. Paper presented at the 34th Annual Conference on Mass Spectrometry and Allied Topics, Cincinnati, OH, 1986.

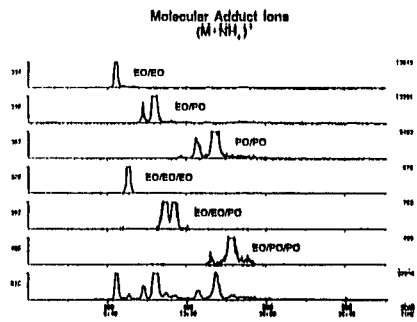

Figure 1. **$(M+NH_4)^+$ ion profiles obtained with a low repeller setting (40 V)**

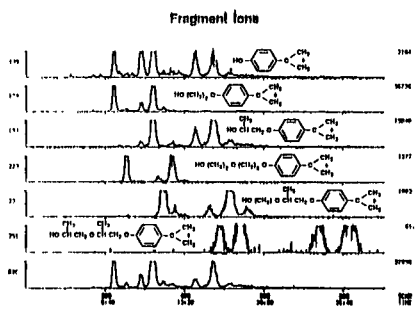

Figure 2. **Selected ion profiles of fragment ions obtained for the individual oligomers using repeller-induced CID**

Presented at the 35th ASMS Conference on Mass Spectrometry and Allied Topics
May 24-29, 1987, Denver, CO

ANALYSIS OF LABILE BIOMOLECULES USING A HIGH-RESOLUTION TIME-OF-FLIGHT MASS SPECTROMETER WITH LASER DESORPTION AND RESONANCE ENHANCED MULTIPHOTON IONISATION

R. Frey, G. Weiss, and H. Kaminski
Bruker-Franzen Analytik GmbH,
D-2800 Bremen, Kattenturmer Heerstrasse 122, W.-Germany
Bruker Analyt. Meßtechnik GmbH,
D-7512 Rheinstetten 4, Silberstreifen, W.-Germany

U.Boesl, H.Grotemeier, K.Walter and E.W.Schlag
Institut f. Physikal. u. Theoret. Chemie, TU München,
D-8046 Garching, Lichtenbergstrasse 4, W.-Germany.

The combination of a time-of-flight mass spectrometer with an ion source based on resonance-enhanced multiphoton ionization shows features which are especially valuable for the analysis of large and labile molecules such as biomolecules.

In principle a time-of-flight mass spectrometer has an unbounded mass range, in practice it is limited only by the efficiency of the ion detector. The interesting properties of the ion source which includes a tunable laser system are the capability to soft or hard ionization and to selective ionization. Soft ionization generating almost only parent molecular ions or hard ionization yielding more fragments can be set up by controlling the laser power. Thus molecular weight determination and structure analysis is very much simplified. Selective ionization of one component of a mixture is achieved by tuning the laser wavelength to spectral regions where efficient absorption and thus ionization only of this component occurs. This capability may be especially valuable for the analysis of biological mixtures

The system we have developed (1) is called TOF1 photon resonance mass spectrometer specifying the analyzer system and the ion source. A mass resolution of 10 000 at mass 106 has been achieved (2), using very short laser pulse duration. Typically using 5 nsec laser pulses the system has a mass resolution of higher than 5000 (1) which also holds for higher masses (3).

In order to apply the system on biomolecules which are normally nonvolatile and thermally labile these have to be vaporized as intact molecules before ionization. For this a new vaporization unit has been incorporated, based on a recently developed method (3)(4):
The sample molecules are desorbed by short IR-laser pulses into the expansion region of a supersonic jet. They are cooled by the supersonic jet and transferred to the ionization region where they are ionized by resonant laser light.

In this way the particular features of the photon resonance ion source are maintained for the analysis of nonvolatile , labile molecules. Due to the separation of desorption and ionization the latter can be controlled from soft to hard ionization. No other mass spectrometric method has this capability.

As an example the mass spectrum of erythromycin is shown in fig.1. In the soft ionization mode at low laser power almost only the molecular mass is generated. By enhancing the laser power several specific fragments are observed.

Another example is seen in fig.2. It is the soft ionization mass spectrum of the polypeptide try-met-asp-phe-amide. Mainly the molecular mass is generated. Again several specific fragment masses appear if the laser power is increased. This can be seen for the example of the octapeptide angiotensin II (fig.3), where the molecular mass and some specific fragments are generated in the partial hard ionization mass spectrum.

Presented at the 35th ASMS Conference on Mass Spectrometry and Allied Topics
May 24-29, 1987, Denver, CO

Erythromycin

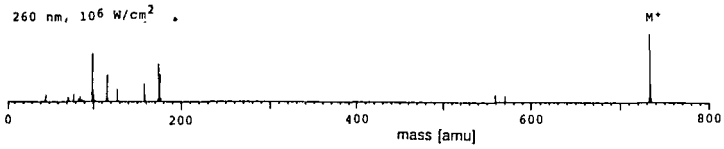

fig.1

Try-met-asp-phe-amide

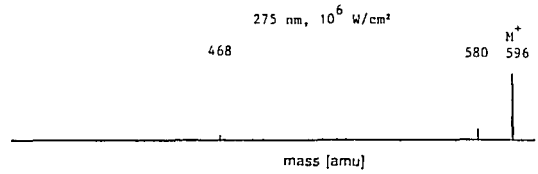

fig.2

Angiotensin II

Asp-Arg-Val-Tyr-Ile-His-Pro-Phe, m1045

275 nm, 10^7 W/cm^2

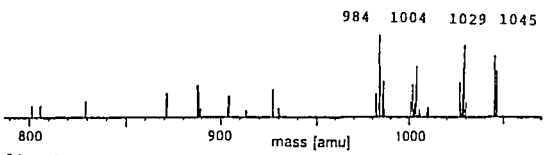

fig.3

All these mass spectra are taken with only three laser pulses each. The summing up of more mass spectra would still improve the intensity and statistics in the mass spectra.

From these and other results obtained with this method the following aspects can be deduced which promise to simplify very much the analysis of biomolecules:

- The mass spectra can be taken from the simple extract of a natural sample without lengthy sample preparation. This is due to the selective ionization of a single compound in a mixture.

- The mass spectra are easy to interprete. In the soft ionization mode mainly the molecular mass M is generated. In particular no H, Na or K adduct ions are observed which is the case in other mass spectrometric methods.

- The degree of fragmentation can be controlled by the laser power. Thus the amino acid sequence information of polypeptides can be easily obtained.

1. R.Frey, G.Weiss, H.Kaminski and E.W.Schlag, Z. Naturforsch. 40a, 1349 (1985)
2. K.Walter, U.Boesl and E.W.Schlag, Int.J.Mass Spectrom.Ion Proc. 71,309 (1986)
3. J.Grotemeyer, U.Boesl, K.Walter and E.W.Schlag, Org.Mass Spectrom. 21,645(1986)
4. H.v.Weissenhoff, H.Selzle and E.W.Schlag, Z.Naturforsch. 40a, 674 (1985)

Presented at the 35th ASMS Conference on Mass Spectrometry and Allied Topics
May 24-29, 1987, Denver, CO

ALTERNATIVE PRIMARY ION SOURCES FOR HIGH MASS FAB APPLICATIONS;

BELL, D and GREEN, B.N, VG ANALYTICAL LTD, FLOATS ROAD, WYTHENSHAWE, MANCHESTER, UK.

INTRODUCTION.

Fast Atom Bombardment using xenon atoms of about 8keV energy as the primary particles has shown that molecules up to about 10kDa can be ionised, but with poor sensitivity. Primary particles of higher bombarding energy offer improved sensitivity at the higher masses[1], but data on compounds above 10kDA molecular weight is sparse. To assess the utility in analysing small proteins with molecular weights over 10kDA, we have fitted a 35keV cesium ion gun to one of our mass spectrometers. In addition to giving the improved sensitivity expected up to 10kDA, this new gun allowed us to obtain measurable spectra on small proteins up to 24kDa molecular weight. In this paper, are shown spectra from small proteins in the molecular weight range 10-24kDa. 17 known small proteins were analysed and the accuracy in determining their molecular weights assessed.

EXPERIMENTAL

The mass spectra were obtained on a VG ZAB-SE (mass range 15kDa at 8keV ion energy) fitted with a cesium ion gun delivering about 2 microamps of cesium ion current with about 30keV energy at the sample. All the proteins were analysed as received, generally by dissolving them directly into 2-3 microlitres of thioglycerol containing 1% of trifluoroacetic acid.

In most cases, two types of scan were produced. The first of these were wide or survey scans made at an instrumental resolution of 300-500 and covering about a factor of 4 in mass. The second covered a narrower mass range, generally 1-1.5kDa in width, at 700-1000 resolution. Scans were exponentially down in mass and the scan rate chosen so that each scan took about 15 seconds. Several scans were summed to produce the final spectrum, in most cases over a total time of 1.5-2 minutes. Mass scale calibration was by means of cesium iodide clusters ($(CsI)nCs^+$) produced from solid cesium iodide introduced within 10 minutes of analysing the samples.

Data was recorded by a VG 11-250 data system operating as a multi-channel analyser. The number of data points collected was roughly 2 per dalton. Thus the survey scans contained 20,000-25,000 data channels and the narrower scans 2000-3000 channels depending on the mass range scanned. Up to molecular weights of about 16kDa, where a relatively sharp peak indicative of molecular weight was obtained, the data was smoothed and the position of the peak tops determined by an automatic procedure supplied with the data system. Calibration and mass measurement were then carried out by the same programmes used for these procedures at the lower masses. Above 16kDa molecular weight, where only a very broad peak was produced, the point of maximum intensity was estimated from the spectrum print out and used to calculate the mass.

RESULTS.

All 17 proteins analysed produced a detectable peak associated with the singly charged molecule. The majority also showed peaks associated with the doubly and triply charged molecule, a notable exception being the cytochrome C's. Common to all the spectra was a broad (several hundred daltons wide) asymmetrical peak extending above and below the expected molecular weight. The point of maximum intensity indicated the approximate molecular weight. These features are illustrated by the spectra of bovine lactalbumin (Figure 1) and bovine and porcine trypsins (Figure 2).

For the 10 proteins analysed with molecular weights less than 16kDa, a narrower (20-30Da wide) peak was superimposed on the broad peak. This narrow peak (MH^+) allowed the molecular weight to be determined to better than 2Da (0.02%) in 7 of the cases and to better than 6Da (0.04%) in the remaining 3. In the 7 cases analysed between 16 and 24kDa molecular weight, only the broad peak was evident. Nevertheless, the point of maximum intensity indicated the molecular weight to about 0.5%. (See Table).

Ref. 1. A Comparison of 8keV and 30keV Cesium Ion Bombardment for the Desorption of Large Biomolecules; Elliott, G.; Cottrell J.S. and Evans, S.; presented at the 34th Annual Conference on Mass Spectrometry and Allied Topics, Cincinnati, Ohio, June 8 - 13, 1986.

Figure 1

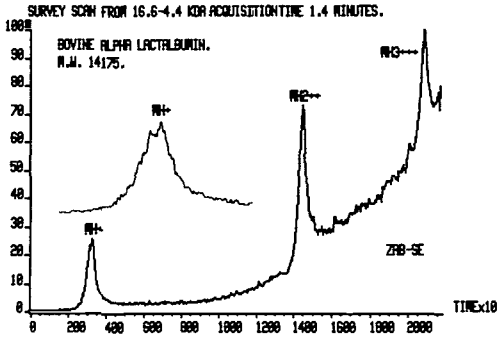

Figure 2

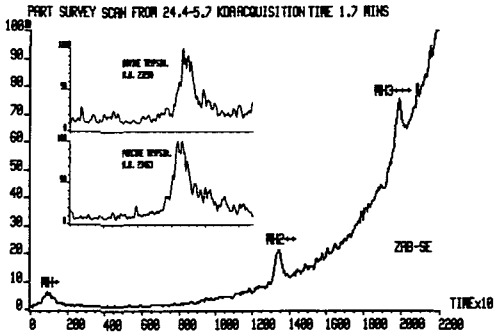

ACCURACY OF MOLECULAR WEIGHT DETERMINATION OF SMALL PROTEINS

	MOLECULAR WEIGHT MEASURED	MOLECULAR WEIGHT EXPECTED	ERROR	
A. 10-16 kDa M.W				
Peptide	10833.6±2.1	10832.5	1.1	(4)
Thioredoxin E.c.	11672.2±1.3	11673.4	-1.2	(4)
Cytochrome C				
a) Tuna Heart	12028.7±1.6	12028.6	0.1	(5)
b) Rat Heart	12131.5±3.3	12132.8	-1.3	(2)
c) Pigeon Breast	12191.9±5.4	12190.9	1.0	(2)
d) Horse Heart	12359.4±0.7	12360.1	-0.7	(4)
Peptide	13112.8	13110.9	1.9	(1)
Lactalbumin (bovine)	14177.3±0.9	14175.0	2.3	(2)
Lysozyme (hen egg)	14301.8±2.2	14306.1	-4.3	(6)
Superoxide dismutase	15585.8±4.6	15591.4	-5.6	(4)
B. 16-24 kDa M.W.				
Calmodulin (bovine brain)	16769	16749	20	
Lactoglobulin (bovine milk)	18300	18277	-23	
		18363	63	
Interferon 1.	19419	19315	104	
Interferon 2.	19531	19484	47	
Bovine Trypsin	23445	23290	155	
Porcine Trypsin	23540	23463	77	
Trypsinogen	24063	23978	85	

Note The figures in brackets refer to the number of measurements.

Presented at the 35th ASMS Conference on Mass Spectrometry and Allied Topics
May 24-29, 1987, Denver, CO

Presented at the 35th ASMS Conference on Mass Spectrometry and Allied Topics
May 24-29, 1987, Denver, CO

PROTEIN SEQUENCE ANALYSIS BY TANDEM MAGNETIC DEFLECTION MASS SPECTROMETRY

Steven A. Carr, [1]Robert J Anderegg, Mark E. Hemling, and Gerald D. Roberts
Dept of Physical and Structural Chemistry
Smith Kline and French Laboratories, L-940, King of Prussia, PA 19406
and [1]Dept. of Chemistry, University of Maine, Orono, ME 04469.

Tandem mass spectrometry, particularly in conjunction with FAB ionization, holds great promise for providing detailed structural information on polar, involatile compounds which may yield only MW information in their "normal" FAB mass spectra. Stable molecular entities (such as $(MH)^+$ ions of peptides) may be induced to fragment by collision with a neutral gas such as He or Ar, a process referred to as collision-induced decomposition. In these studies, we use a VG ZAB-SE 4F tandem double-focusing high resolution mass spectrometer. Peptide and carbohydrate sequence analysis is best performed using instruments of this type, which a) allow selection and analysis of both parent and daughter ions at unit resolution or higher, greatly reducing the potential for interferences and incorrect assignment of fragment structure, and b) employ high energy (keV) collisions to fragment the selected parent, yielding simpler, more reproducible and more easily interpreted tandem mass spectra of peptides than can be obtained with low energy (eV) collisions.

In practice, the first of two coupled, double-focusing mass analyzers is used to select the monoisotopic molecular ion. Daughter fragments produced by collision in a cell located between the two instruments are analyzed by the second double-focusing combination. These ions provide new sequence information not observed in direct FABMS analysis. Peptides to thirty amino acids in length may be analyzed by this approach using a few nanomoles or less of material; peptides this large may require selection of the unresolved molecular ion cluster in order to obtain analytically useful daughter ion spectra. In contrast to conventional Edman technology, sequence information can be obtained for peptides in simple mixtures and for blocked or otherwise posttranslationally modified peptides

Our collaborative studies on the cellular retinaldehyde binding protein (CRALBP), a visual system-specific protein (M_r = 33,000), are illustrative of the principles involved (1). The blocked protein was reduced and Cys residues pyridylethylated. After Lys residues were acylated with succinic anhydride, the protein (ca. 150 μg, 4 nmol) was cleaved specifically at Arg residues with trypsin. An HPLC fraction of this digest containing a peptide resistant to Edman degradation was then identified. The FAB mass spectrum of 400 pmol of the blocked peptide fraction exhibited $(MH)^+$ peaks at m/z 743 and 866 (Fig. 1). No sequence informative fragments were observed.

Tandem MS of the ion at m/z 866 produced the daughter ion spectrum shown in Fig. 2. A complete series of fragments derived from the carboxyl-terminus are present (W_n, X_n, Y_n and Z_n), with the Y_n+2H and W_n+0,1H dominating. The latter series corresponds to Y fragments from which the side chain of the new amino terminal residue is lost with or without the transfer of a hydrogen (S. Martin, unpublished observation). The W series fragments are formed with particular ease when the side chains of Glu, Thr and Phe are involved. In addition, a complete series of acylium fragments (B_n) from the amino-terminus are also present. These fragments establish the sequence of this peptide as Acetyl-Ser-Glu-Gly-Ala-Gly-Thr-Phe-Arg.

Tandem MS is also useful in locating errors in protein sequences predicted from DNA sequences Spermine-binding protein is an androgen-dependent secretory glycoprotein isolated from rat prostrate and characterized by an extremely high affinity for spermine. The cDNA has been recently sequenced and a protein sequence predicted (2). The amino-terminus of the protein is blocked, and we were asked to use mass spectrometry to investigate the nature of the blocking group. Tryptic digestion of the protein followed by FAB-mapping gave the molecular weights of numerous peptides consistent with the predicted sequence. However, three signals could not be assigned based on the gene sequence: $(MH)^+$ = 586, 1174, and 2565. Only the 2565 fragment did not change mass upon Edman degradation, suggesting that it was the blocked amino-terminus. Following reversed-phase HPLC, the 586 and 1174 fragments were analyzed by MS/MS; and the sequences Gly-xLeu-Gln-xLeu-Arg and xLeu-Phe-xLeu-Thr-xLeu-xLeu-Thr-xLeu-xLeu-Lys were proposed. These results allowed us to pinpoint an error in the gene sequence and propose that an omission of a series of bases had occurred. Work is in progress to identify the blocking group and to more fully explain the discrepancy between the gene sequence and the observed protein sequence.

References:

1. S.A. Carr, J.C. Saari, and J.W. Crabb, FEBS Lett in press 1987.

2 C. Chang, A.G. Saltzman, R.A. Hiipakka, I.Y. Huang, and S. Liao, J. Biol. Chem. **262**, 2826 (1987).

Presented at the 35th ASMS Conference on Mass Spectrometry and Allied Topics
May 24-29, 1987, Denver, CO

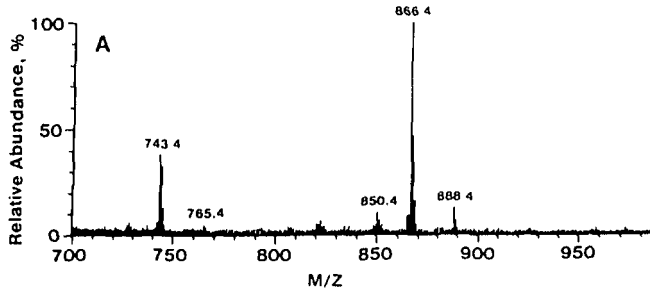

Figure 1. Normal FAB mass spectrum of the HPLC fraction containing the blocked octapeptide

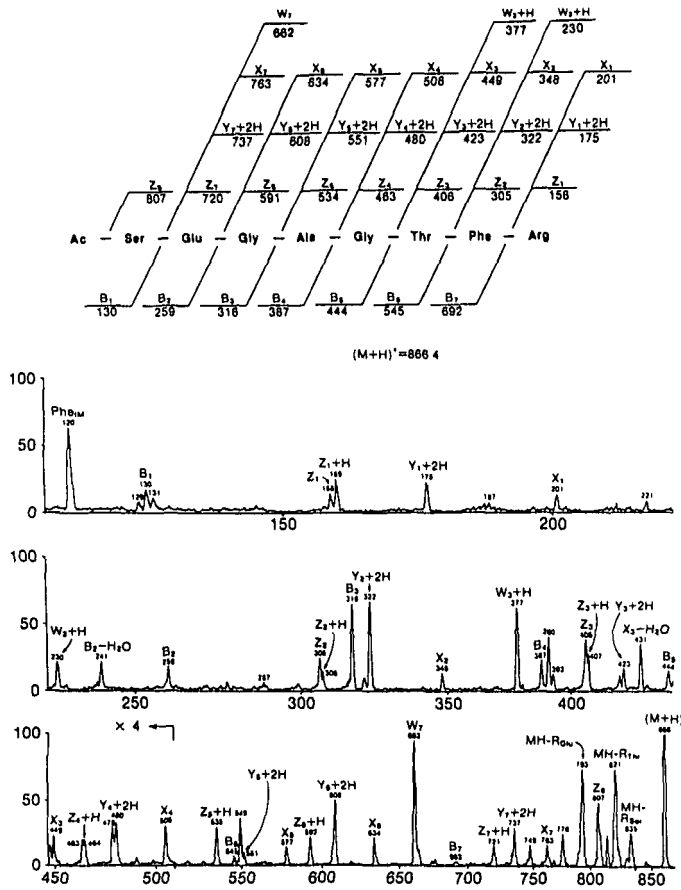

Figure 2 Daughter ion mass spectrum of the protonated molecular ion of the blocked octapeptide with $(M+H)^+$ = 866 4 Data was obtained on 500 pmol; six 30s/dec scans were summed. Fragment ions observed are shown in the Scheme

Presented at the 35th ASMS Conference on Mass Spectrometry and Allied Topics
May 24-29, 1987, Denver, CO.

MATRICES FOR PEPTIDE SEQUENCING BY MONITORED ENZYMATIC HYDROLYSIS

Peter Bel[1] and Kelsey D. Cook*
Department of Chemistry, University of Tennessee, Knoxville, TN 37996-1600
([1]Permanent address: Israel Institute for Biological Research, 70450 Ness Ziona, Israel)

Electrohydrodynamic (EH) mass spectrometry can be applied as an alternative to FAB for acquisition of primary structure and kinetic data by monitoring enzymatic peptide hydrolysis proceeding within the ion source. EH avoids problems due to enzyme deactivation resulting from rapid evaporation of water and/or damage induced by the fast atom beam (1,2). However, in studies described at the last ASMS meeting, a glycerol- water matrix was found to provide low sampling efficiency for EHMS of the intact peptide. Therefore, subsequent efforts have been directed at identifying a better matrix. Ideally, such a matrix should provide: retention of enzyme activity; vacuum compatibility with EH source pressures ($<10^{-5}$ torr); good solubility for the enzyme, substrate, and hydrolysis products; and high sampling efficiency for peptides and amino acids. With these goals in mind, several matrices were tested (Table I):

TABLE I: MATRIX EFFICACY

Matrix	Amino acids	Di-,tri- peptides	Higher peptides	Enzyme activity
Glycerol (G)	+	+	N/A	-
Triethanolamine (TEA)	+	N/A	N/A	-
Thiodiethanol (TDE)	+	+	N/A	-
G + 30% H_2O	+	-	+[a]	+[b]
TDE + 20-50% H_2O	+	+	+	+[c]
TEA + 30% H_2O	+	-	N/A	+[d]
Thioglycerol + 30% H_2O	+	+	N/A	-

+ Analyte was detected as protonated and/or sodiated adduct.

- Analyte peaks were not detected, or enzyme was not active.

[a] Detected only after 8 hrs of observation.
[b] Caprioli et al. (1)
[c] 21% of activity retained in 20% H_2O; 34% in 30% H_2O; 45% in 40% H_2O.
[d] 15% of activity retained.

Of the matrices tested, the most promising was thiodiethanol/water, which apparently retains some of the desirable "acidic" properties of thioglycerol, while not inhibiting enzyme activity. Sampling efficiencies for amino acids increased somewhat as water concentration increased beyond 40 vol%, but emission was not stable. Representatives of the anticipated products of enzymatic peptide hydrolysis could be sampled with good efficiency from TDE with 30-40 vol% water (Table II):

TABLE II: COMPONENTS SAMPLED FROM TDE/H_2O

A. Amino acids: Alanine (Ala); Arginine (Arg); Aspartic acid (Asp); Glycine (Gly); Glutamic acid (Glu); Glutamine (Glu); Histidine (His); Leucine (Leu); Lysine (Lys); Methionine (Met); Phenylalanine (Phe); Proline (Pro); Threonine (Thr); Tryptophane (Trp); Valine (Val).
B. Dipeptides: AlaMet; LeuGly; ProAla; ProTrp.
C. Tripeptides: TyrGlyGly; AlaGlyGly.
D. Oligopeptides: PheGlyGlyPhe; AlaGlyGlyGly.

Presented at the 35th ASMS Conference on Mass Spectrometry and Allied Topics
May 24-29, 1987, Denver, CO

The biologically active peptide leucine enkephalin (TyrGlyGlyPheLeu) was chosen to test the feasibility of monitoring the progress of carboxypeptidase Y-induced hydrolysis in 60/40 vol% TDE/water. 5 mg of the peptide were dissolved with 22 units of the enzyme and 37.5 mg NaI (supporting electrolyte) in 0.5 ml of solvent. The EHMS results are summarized in Figure 1:

FIGURE 1: EHMS MONITORING OF ENZYMATIC HYDROLYSIS

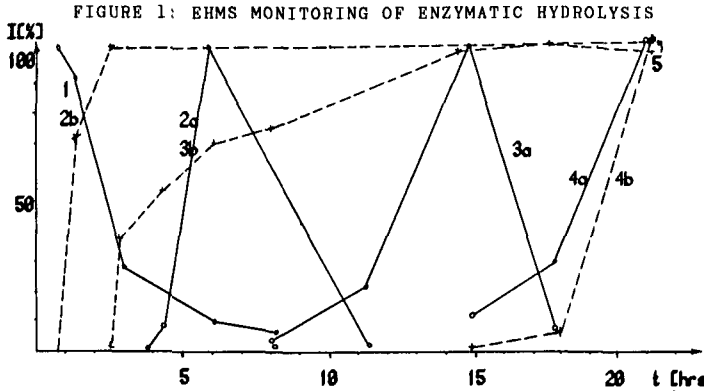

Intensity (relative to Leu) of each major species detected:
1 - TyrGlyGlyPheLeu; 2a - TyrGlyGlyPhe; 2b - Leu (relative to matrix peaks); 3a - TyrGlyGly; 3b - Phe; 4a - TyrGly; 4b - Gly; 5 - Tyr

Hydrolysis is observed only in the presence of the enzyme, the activity of which was retained for >20 hrs. However, the time dependence of EH mass spectra indicated partial deactivation; maximum EHMS intensity of tripeptide (TyrGlyGly) ions was observed after 15 hr, vs only 6 hr required to match the absorbance expected for complete hydrolytic removal of Leu and Phe. If water content was reduced to 20%, hydrolysis was slowed; expected absorbance was reached in 15 hr. Enzyme activity in the EHMS experiment was evidently reduced by evaporation of water.

Molecular ions of the intact peptide and all hydrolysis products were detected, confirming the primary structure of the substrate. Sensitivity was better for the amino acids than for oligopeptides; the amino acids appeared before the corresponding co-products.

In summary, 60/40 vol% TDE/water is the best solvent of those tested for peptide sequencing by monitored enzymatic hydrolysis in situ in EHMS. It provides better sensitivity than the more common glycerol/water solvent for both amino acids and peptides. Despite evidence of slow water evaporation, enzyme activity retained over a long (>20 hr) run period. This suggests that TDE/water should be a good FAB matrix, as well.

References

(1) Smith, L. A. and Caprioli, R. M., Biomed. Mass Spectrom. 11, 392-5 (1985); Smith, L. A. and Caprioli, R. M., Biomed. Mass Spectrom. 10, 98-102 (1984); Caprioli, R.M., Mass Spectrom. Rev. 6, 237-287 (1987).
(2) Przybylski, M., Fresenius Z. Anal. Chem. 315, 402-421 (1983).

Acknowledgement

This work was supported in part by a grant from the National Science Foundation (grant # DMR-84-06825, funded jointly by the U.S. Army Research Office).

Presented at the 35th ASMS Conference on Mass Spectrometry and Allied Topics
May 24-29, 1987, Denver, CO

MAPPING OF PEPTIDES FROM HUMAN SERUM ALBUMIN BY FAB MASS SPECTROMETRY

Richard B. van Breemen and Johnny Creech
Department of Chemistry, North Carolina State University,
Raleigh, N.C. 27695-8204

Human serum albumin, weighing approximately 66,439 daltons (1), is the most abundant protein of the blood plasma and functions as a carrier protein for many drugs, drug metabolites and endogenous compounds. These properties help make albumin a frequent target molecule for alkylation by activated drug metabolites and other electrophilic compounds. As part of a project to characterize modified albumin by mass spectrometry in this laboratory, peptide mapping studies were carried out beginning with human serum albumin.

Because of the high molecular weight of albumin, cleavage by a combination of cyanogen bromide and trypsin was used to produce peptide fragments weighing less than 5,000 daltons for mass spectrometric analysis. First, serum albumin was reduced and carboxymethylated and then digested with cyanogen bromide to form seven peptides, ranging in size from approximately 3,400 to 21,000 daltons. These were purified by reversed-phase HPLC as described by Iadorola and coworkers (2). (See Figure 1.) Next, the CNBr peptide fragments were trypsinized in 0.2 M ammonium acetate at pH 8.0 (3).

Positive ion FAB mass spectra were obtained using a JEOL HX110 double-focussing mass spectrometer equipped with a high field magnet, DA 5000 data system and post acceleration detection. The resolution was 5,000, and the accelerating voltage was 10 KeV. The sample was dissolved in a thioglycerol/glycerol matrix (2:1,v/v) containing 0.01 M HCl and was bombarded with xenon fast atoms at 3 KeV.

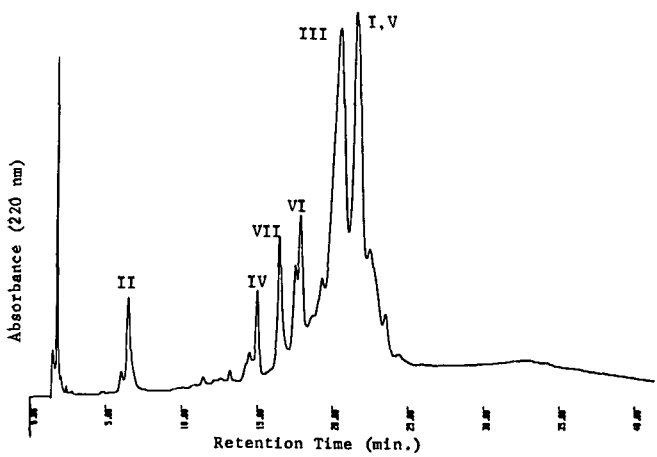

Figure 1. HPLC chromatogram of CNBr fragments from human serum albumin.

The lowest molecular weight CNBr peptides fragments (MW < 5,000) were measured by FAB mass spectrometry both before and after trypsinization, otherwise only tryptic digests were analyzed. Results of these measurements are summarized in Tables I and II and Figure 2. Protonated molecular ions were observed for the smallest CNBr fragments without trypsinization (Figure and Table I). Tryptic digests of each CNBr fragment were analyzed as a mixture, and the theoretical and measured masses of the largest of these peptides are compared in Table II.

Analytical procedures have been developed for peptide mapping of human serum albumin. The peptide map will be completed following HPLC purification of those tryptic peptides, which could not be detected by mass spectrometry while in the tryptic digest mixture. FAB mass spectrometry has partially confirmed the amino acid sequence determined by other techniques (1). This mapping procedure will be applied to the analysis of covalently modified human serum albumin in subsequent investigations.

Presented at the 35th ASMS Conference on Mass Spectrometry and Allied Topics
May 24-29, 1987, Denver, CO

Table I. Analysis of CNBr Fragments (MW < 5,000) from Human Serum Albumin by Positive Ion FAB Mass Spectrometry.

Fragment	Theoretical $[M+H]^+$	Measured $[M+H]^+$ (m/z)
CNBr II	4353.0	-
CNBr IV	3353.6	3353.1
CNBr VII	4096.9	4097.0

Table II. Analysis of Tryptic Digests of Purified CNBr Peptides by Positive Ion FAB Mass Spectrometry.

Fragment	Theoretical $[M+H]^+$	Measured $[M+H]^+$ (m/z)
CNBr I	2490.3	-
CNBr II	1076.5	-
CNBr III	2089.8	-
CNBr IV	1559.8	1559.7
	633.3	633.2
CNBr V	1658.7	-
	1555.5	-
	1511.8	-
	1279.7	-
	960.9	960.8
CNBr VI	2389.1	-
	2260.9	2260.9
	1755.8	-
	1000.6	1000.9
CNBr VII	1071.4	-
	1041.5	-
	1013.6	1013.4

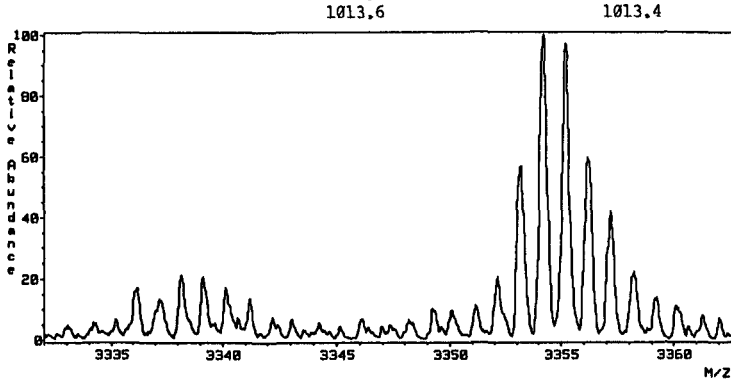

Figure 2. Positive ion FAB mass spectrum of CNBr IV from serum albumin.

References.

(1) T. Peters, Jr., Adv. Protein Chem., 37, 161 (1985).

(2) P. Iadorola, G. Ferri, M. Galliano, L. Minchiotti and M.C. Zapponi, J. Chromatogr., 298, 336 (1984).

(3) P. Tempst, M. HunkaPillar and L. Hood, Anal. Biochem., 137, 188 (1984).

Presented at the 35th ASMS Conference on Mass Spectrometry and Allied Topics
May 24-29, 1987, Denver, CO

THE DETERMINATION OF THE PRIMARY STRUCTURE OF A SERINE PROTEASE INHIBITOR BY HIGH PERFORMANCE TANDEM MASS SPECTROMETRY

I.A. Papayannopoulos and K. Biemann
Department of Chemistry, M.I.T., Cambridge, MA 02139

The primary structure of a serine protease inhibitor, isolated from *Sarcophaga bullata* (1), and exhibiting homology with other protease inhibitors containing six cysteines, was determined by high performance tandem mass spectrometry of peptides produced by specific chemical or enzymatic digests of the protein. Such peptides were sequenced by collisionally-induced dissociation (CID) of their precursor ions in a four-sector mass spectrometer (JEOL HX110/HX110). Specific cleavage at cysteine (2) produced a set of degradation peptides, in which the N-terminal cysteine cyclizes during the cleavage reaction to a 2-iminothiazolidine-4-carboxylic acid. These peptides, having blocked amino termini, gave predominantly a- and b-type fragment ions upon collisionally-induced dissociation (CID) of their precursor ions (Figures 1 and 2). Their CID mass spectra as well as those from tryptic peptides of the protease inhibitor provided overlapping sequence information, confirmed by the molecular weights of peptides produced by digestion with *S. aureus* V8 protease (Figure 3). The molecualr weight of this protein was also determined mass spectrometrically (Figure 4) and was found to be in agreement with the proposed structure.

(1) The protease inhibitor was isolated by Professor M. Sugumaran and coworkers (UMass/Boston) who provided us with a sample.
(2) Stark, G.R., *Methods in Enzymology 47 Enzyme Structure*, Hirs, C.H.W., and Timasheff, S.N., Eds., Academic Press Inc., New York, 1977, 129-132.

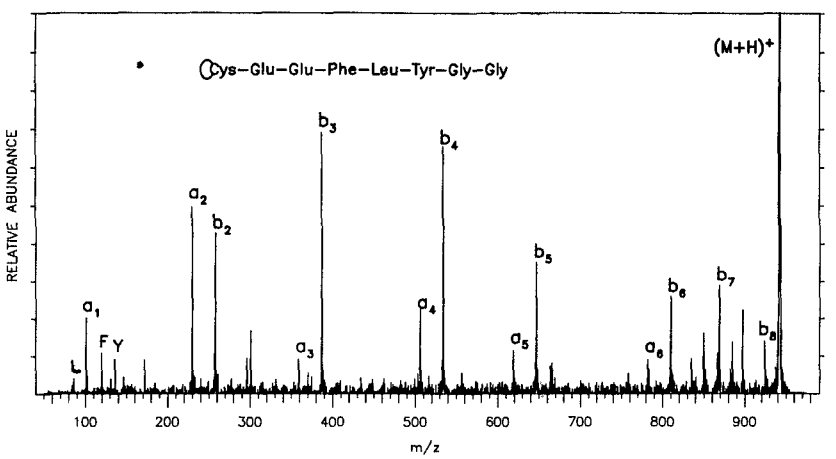

Figure 1 The CID mass spectrum of the NTCB–produced peptide of $(M+H)^+$=942.

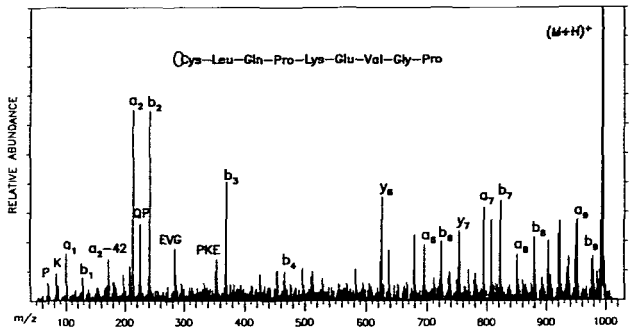

Figure 2 The CID mass spectrum of the NTCB-produced peptide of $(M+H)^+$=995.

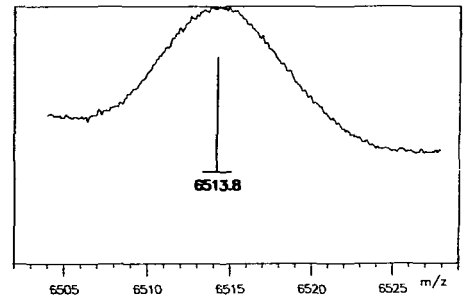

Figure 4 The protonated molecular ion region of SBPI; sum of eight 9 sec scans over 25 u at 1000 resolution.

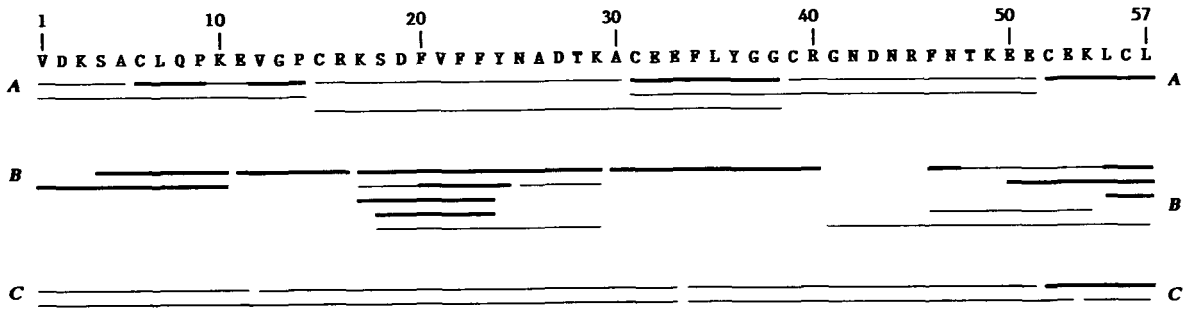

Figure 3 The amino acid sequence of *Sarcophaga bullata* protease inhibitor (SBPI); the peptides produced from enzymatic and chemical cleavages are underlined: (A: NTCB, B: trypsin, C: *S. aureus* V8 protease). Bold (—) underlining indicates that this sequence (or regions thereof) was derived from the CID mass spectrum of the peptide, while simple (—) underlining indicates peptides detected by FABMS and identified by their protonated molecular ions.

Presented at the 35th ASMS Conference on Mass Spectrometry and Allied Topics
May 24-29, 1987, Denver, CO

STRUCTURAL STUDIES ON ALDOSE REDUCTASE, MITE ALLERGENS, AND PHOSPHOPEPTIDES BY TANDEM MASS SPECTROMETRY

P. R. Griffin, D. F. Hunt, J. Shabanowitz, and N-Z. Zhu;
Department of Chemistry, University of Virginia, Charlottesville, Virginia 22901

Extensive structural information on aldose reductase and two mite allergens has been obtained and new methodology for the sequence analysis of phosphorylated peptides has been developed. Protein sequencing by tandem mass spectrometry involves enzymatic or chemical cleavage of the protein into a mixture of oligopeptides which are then fractionated by HPLC. Peptides in each fraction are sequenced by employing either collision activated dissociation on a triple quadrupole instrument (1) or laser photodissociation on a tandem quadrupole Fourier transform mass spectrometer.

Aldose reductase is a 40 kDa glycoprotein that catalyzes the reduction of aldo sugars and hydrophobic aldehydes to the corresponding alcohols (2). Over production of sugar polyols in the lens of the eye results in cellular swelling and formation of cataracts. A great deal of interest has been evoked recently in aldose reductase because of its suspected involvement in the etiology of some of the complications associated with diabetes mellitus. Experiments in rats clearly show that diabetic cataract can be prevented, and even reversed, by specific aldose reductase inhibitors. Primary sequence information will help in the development of a specific aldose reductase inhibitor or even in the development of a substrate based suicide inhibitor. Partial sequence information has been obtained and from this an oligonucleotide probe has been constructed.

Synthetic oligonucleotide probes deduced from protein sequence data are widely used to screen cognate coding sequences in libraries of cloned DNA segments (3). However, due to the degeneracy of amino acid codons, the deduced nucleotide sequences will almost inevitably include elements of ambiguity. One way to overcome this problem is to use an appropriate base analog that "pairs" with any of the four natural bases at the ambiguous positions. Deoxyinosine-containing oligonucleotides have been shown to be powerful tools for cloning genes whose amino acid sequences are known but whose corresponding base sequences can not be determined precisely due to codon degeneracy (4). Using partial sequence information obtained on aldose reductase a deoxyinosine-containing oligonucleotide was designed and constructed. This probe was used to screen a bovine lens cDNA library.

The association between house dust allergy and asthma has long been recognized, and it has been demonstrated that the major allergens in house dust are related to the presence of mites of the genus Dermatophagoides. Two of the major allergens are 24 kDa glycoproteins found in mite feces. Structural information on Der f1 and Der p1 has been obtained and is shown in table 1.

Presented at the 35th ASMS Conference on Mass Spectrometry and Allied Topics
May 24-29, 1987, Denver, CO

Phosphorylation of serine, threonine, and tyrosine residues plays an important role in the regulation of many enzymes. Until recently, identification of phosphorylated amino acids by the classical Edman sequencing procedure proved to be difficult (5). Described here are the result of experiments to determine the location of phosphorylated residues in peptides with and without chemical derivatization by collision activated dissociation. Some phosphorylated peptides can be sequenced directly by MSMS (see figure 1) while others suffer loss of phosphoric acid, a step that prevents unambiguous assignment of the phosphorylated residue (see figure 2). Derivatization to replace the phosphate by less labile groups can be used to overcome this problem (see figure 3).

1) D. F. Hunt et. al., Proc. Natl. Acad. Sci. USA, (1986), 83, 6233-6237.
2) J. A. Cromlish and T. G. Flynn, J. Biol. Chem., (1983), 258, 3416-3424.
3) R. Lathe, J. Mol. Biol., (1985), 183, 1-12.
4) E. Ohtsuka et. al., J. Biol. Chem., (1985), 260, 2605-2608.
5) H. E. Meyer et. al., FEBS Letters, (1986), 204, 61-66.

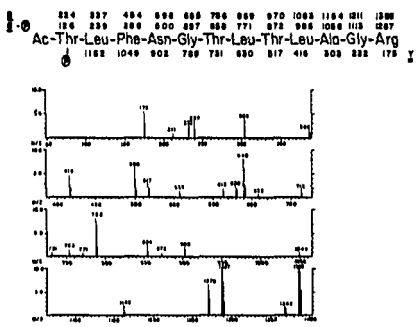

Figure 1

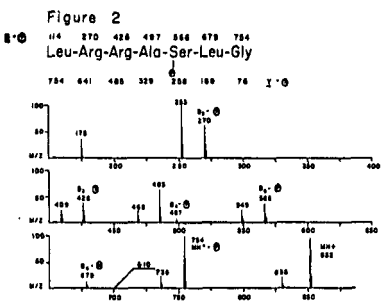

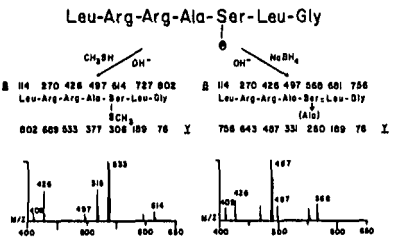

Figure 3

Table 1

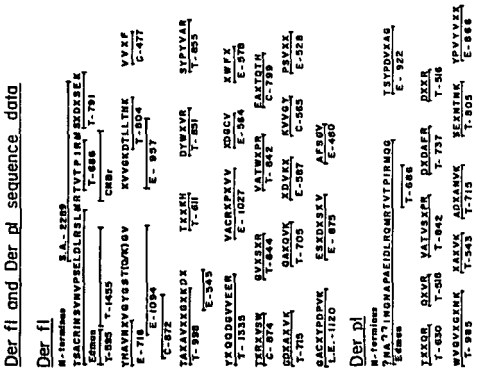

Presented at the 35th ASMS Conference on Mass Spectrometry and Allied Topics
May 24-29, 1987, Denver, CO

FAST ATOM BOMBARDMENT AND LOW ENERGY COLLISIONALLY-ACTIVATED DECOMPOSITION OF PEPTIDES USING A HYBRID INSTRUMENT.

Simon J. Gaskell and Marc H. Reilly
Center for Experimental Therapeutics, Baylor College of Medicine, Houston, Texas 77030
Christopher J. Porter
VG Analytical Ltd., Floats Road, Wythenshawe, Greater Manchester M23 9LE, U.K.

Fast atom bombardment (FAB) mass spectra are readily obtained for small peptides; $[M+H]^+$ and $[M-H]^-$ ions are generally prominent and fragment ions characteristic of structure may be observed. Detailed structural analysis, however, may be restricted by three factors:

1) a high background attributable, in part, to the matrix;
2) a reduction in the relative abundances of fragment ions when the peptide of interest is present as a component of a mixture;
3) the association of fragment ions with a particular parent ($[M+H]^+$ or $[M-H]^-$) is inferential.

Tandem MS with collisionally-activated decomposition (CAD) addresses each of these issues. CAD of peptides, using a variety of instrument configurations, has been recently reviewed.[1] Hybrid instruments (particularly of BEQQ configuration) may be uniquely well-suited to the analysis of small peptides; in providing facilities for both low and high energy CAD. We describe systematic studies of the CAD of the enkephalin pentapeptides using insruments of BEQQ and EBQQ design (the VG ZAB SEQ and VG 70SEQ, respectively). $[M+H]^+$ ions were selected as parents using the sector portion of the instrument and subjected to CAD in the first quadrupole, using argon as the collision gas and collision energies of 30-50 eV.

Figure 1 shows the CAD daughter ion spectrum of $[M+H]^+$ ions derived from leu-enkephalin (Tyr-Gly-Gly-Phe-Leu). The spectrum was obtained using the continuum mode of acquisition, with accumulation of ca. 15 scans. Each member of the Y" fragmentation series (Roepstorff and Fohlman nomenclature[2]) is observed, together with prominent A_1, B_2, B_3, and B_4 fragments. The importance of unit resolution of daughter ions is illustrated by the separation of m/z 278 and 279, corresponding to B_3 and Y_2" fragments, respectively. Ions of m/z 262 and 205 are attributed to mid-chain fragments incorporating the (Gly-Gly-Phe) and (Gly-Phe) residues, respectively. Ions of m/z 234 and 177 are associated with additional CO losses.

The above assignments were confirmed by comparison of data for the leu- and met-enkephalins, N-acetyl derivatives, N-acetyl methyl esters, $[^{18}O]$-labeled analogues and the enkephalinamides. Thus, for example, the CAD spectrum of $[M+H]^+$ from $[^{18}O_2]$-enkephalin, obtained by $[^{18}O]$-exchange of carboxyl oxygens, showed a shift of 4 u for all the Y" fragments. In addition to "labeling" N-terminal fragment ions, N-acetylation also had the effect of introducing significant differences in CAD. Relative abundances of A_1 and B_2 fragments, for example, were reduced, with a corresponding increase in the importance of the Y_4" fragmentation. These trends presumably reflect a decreased tendency for initial charge localization on the N-terminus following acylation.

Presented at the 35th ASMS Conference on Mass Spectrometry and Allied Topics
May 24-29, 1987, Denver, CO

The importance to spectral interpretation of N-acetylation is even more apparent in the study of larger peptides such as angiotensin I. The CAD daughter ion spectrum of $[M+H]^+$ ions shows a prominent series of A-type ions which are shifted 42 u upon acetylation.

1. Sheil M, Derrick PJ, in Mass Spectrometry in Biomedical Research; Gaskell SJ, ed; Wiley; Chichester, U.K.; 1986, p 251.
2. Roepstorff P, Fohlman J, Biomed Mass Spectrom 1984; 11: 601.

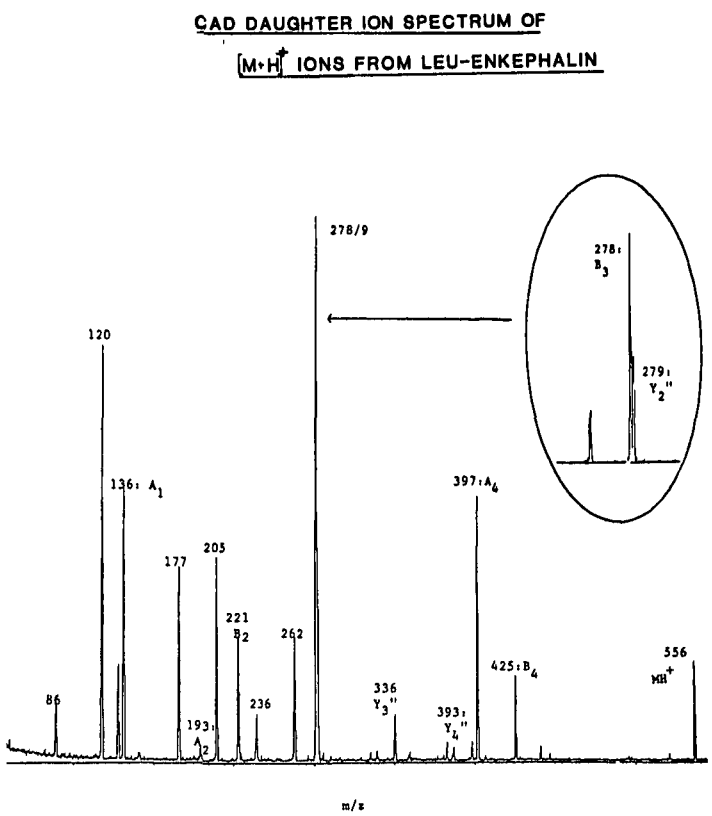

FIGURE 1. CAD daughter ion spectrum of $[M+H]^+$ ions derived from leu-enkephalin. The resolution of the full plot is less than the actual mass resolution; the inset (taken from the same accumulated scan) shows that unit daughter ion resolution was achieved.

Presented at the 35th ASMS Conference on Mass Spectrometry and Allied Topics
May 24-29, 1987, Denver, CO.

EFFECT OF STRUCTURAL VARIATIONS AND CATIONIZATION ON THE COLLISIONALLY ACTIVATED MS/MS SPECTRA OF PEPTIDES

C.Guenat*, J.Dino,Jr.*, K.B.Tomer*#,
*Laboratory of Molecular Biophysics NIEHS P.O.Box 12233 Research Triangle Park, NC 27709 and #Midwest Center for Mass Spectrometry, Univ. Nebraska, Lincoln, NE 68588

The increasing number of reports of the use of the combination of FAB with MS-MS for structure determination of biomolecules attests to its utility. The combination of MS-MS and tryptic digestion is becoming the method of choice for the determination of complex peptides as exemplified by the work of Biemann (1) and Richter (2).

To optimize employment of MS-MS for structure elucidation, an understanding of the factors that can affect MS-MS data and how these factors affect that data is useful. As part of our effort in this area we have investigated several factors: 1) the influence of various amino acid residues on the MS-MS spectra and; 2) the effect on peptide sequence information of changing the cationizing species from H+ to an alkali metal.

MS-MS spectra were obtained on either a VG ZAB-4F tandem double focussing mass spectrometer (BE-EB) (NIEHS) or on an MS-50 triple analyzer (EBE) (MCMS). Sufficient collision gas (He) was introduced so as to reduce the intensity of the parent ion by 50%. The ratio of N-terminal to C-terminal sequence ions obtained for a peptide on both instruments varied by less than 5%.

From an investigation of 21 peptides several conclusions could be reached.

1) In the absence of a strongly basic C-terminal residue, N-terminal sequence ions dominate [as observed by others (3)].
2) A strongly basic C-terminal amino acid enhances C-terminal sequence ions, especially Z-series ions (4). Arg enhances C-terminal sequence ions to a greater extent than does Lys (Fig 1).
3) N-terminal Arg enhances N-terminal sequence ions but also leads to enhanced Arg loss - formally a Y-series ion (Fig 2).
4) N-terminal Pro is readily lost to form a Y-series ion (Fig 3).
5) Internal Pro is often protonated leading to a Y-series ion (Fig 4).

Cationization: alkali metal salts are "often" present in biochemical mixtures and sometimes lead to the presence of (M+metal)+ cations rather than (M+H)+ ions. Russell has investigated the interaction of alkali metal with amino acid residues in peptides by examining the MS-MS spectra of (M+Na)+ ion (5). As part of our project we have examined the utility of the MS-MS data obtained from (M+metal)+ ions for sequencing peptides.

The MS-MS data for the (M+Na)+ ion of small peptides (Methionine enkephalin, Fig.5) yields very little sequence information compared to that of the (M+H)+ ion. Cleavage between the amine-N and carbon of the C-terminal amino acid with transfer of two hydrogens yields the major daughter ion (m/z 465). Loss of the C-terminal amino acid and the adjacent CO with H-transfer yields the second most abundant daughter ion.

As the peptide becomes larger, sequence ions begin to become important again (Hepta substance P, Fig. 6). The sequence ions observed are predominantly the A-series ions.

1) K.Biemann and S. Martin, Mass Spectrom. Rev., 6, 1 (1987).
2) F.Raschdorf, et al., in 'Mass Spectrometry in the Analysis of Large Large Molecules', C.McNeal, ed., Wiley & Sons, NY, 1986, p.131.
3) D.Lippstreu-Fisher and M.L.Gross, Anal. Chem., 57, 1174 (1985).
4. S.Seki and H.Kambara, Mass Spectrosc., (Japan), 33, 371 (1985).
5. L.Mallis and D.Russell, Anal. Chem., 58, 1076 (1986).
6. K.Tomer, F.Crow, M.Gross and K.Kopple, Anal. Chem., 56, 880 (84).

Presented at the 35th ASMS Conference on Mass Spectrometry and Allied Topics
May 24-29, 1987, Denver, CO

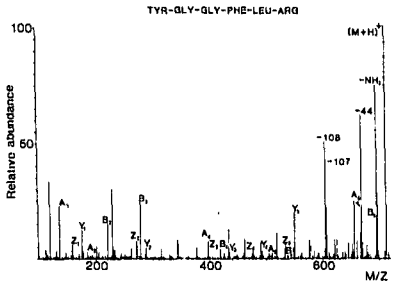

Fig. 1a. MS/MS spectrum of the (M+H)+ of Leu-enkephalin-Arg.

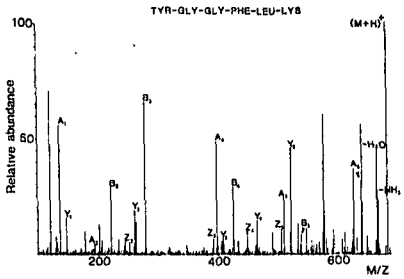

Fig. 1b. MS/MS spectrum of the (M+H)+ of Leu-enkephalin-Lys.

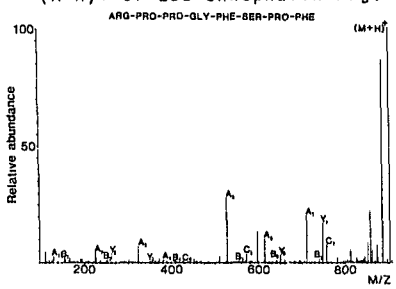

Fig. 2. MS/MS spectrum of (M+H)+ of [Des-Arg9]-Bradykinin. Y7 = loss of N-terminal arginine.

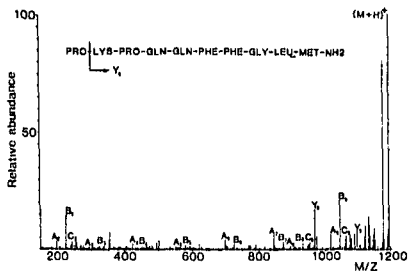

Fig. 3. MS/MS spectrum of the (M+H)+ Substance P 2-11. Y9 = loss Of N-terminal proline.

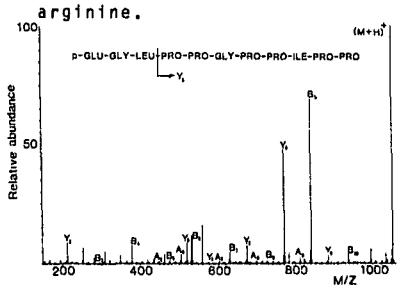

Fig. 4. MS/MS spectrum of (M+H)+ of Bradykinin potentiator C. Y8 = internal cleavage at proline to form a Y-series ion.

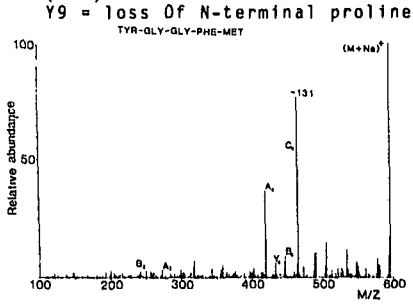

Fig. 5. MS/MS spectrum to the (M + Na)+ ion of Met-enkephalin.

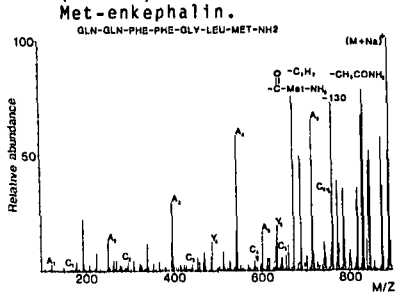

Fig. 6. MS/MS spectrum of the (M+Na)+ ion of Substance P 5-11.

Presented at the 35th ASMS Conference on Mass Spectrometry and Allied Topics
May 24-29, 1987, Denver, CO.

Modification of the Fragmentation of Peptides in a Tandem Mass Spectrometer by Derivatization

R. S. Johnson and K. Biemann
Dept. of Chemistry, MIT, Cambridge, MA 02139

Under certain conditions, CID spectra of peptides may lack complete sequence information. For instance, if the peptide does not contain a basic amino acid a_n+1H (Scheme I) or z_n+1H (1) radical cations may not be formed. These are important because subsequent β,γ-bond cleavage result in fragment ions which permit the differentiation of leucine and isoleucine. To promote these fragmentation processes we have investigated the CID spectra of peptide derivatives in which a stable positive charge or a strongly basic group has been introduced.

One such derivative involves the conversion of the ε-NH_2 group of lysine to a 2,4,6-trimethylpyridinium cation under conditions where α-NH_2 groups do not react. The CID spectrum of the peptide cation, when compared with that of the $(M+H)^+$ ion of the underivatized peptide, exhibited reduced abundances of the amino acid immonium ions, the internal fragment ions, and the b_n ions. Perhaps the most significant aspect of this data is that the derivatized peptides undergo remote site fragmentations (2) both in the CID spectra and the normal FABMS spectra. Thus, the fragmentation mechanisms seem to involve a fixed charge, rather than a mobile proton.

For specifically directing fragmentation it would be desirable to make a derivative that places a positive charge, or a highly basic group, at either the amino or carboxy terminus of a peptide independent of the prescence of a particular amino acid. One such derivative was found to be the β-guanidinopropionyl group, which would always be the most basic moiety in any peptide (unless it contains arginine) and thus the most likely site of protonation. The ε-NH_2 group of lysine (if present) does not react to a significant extent under the conditions used (0.4 M 1-ethyl-3-(3-dimethylaminopropyl)carbodiimide, 1 M β-guanidinopropionic acid, 1.5 hr at room temperature and pH 4-5), presumably because of the difference in pKa between α-NH_2 (pKa = 8) and ε-NH_2 (pKa = 10.5). The process that permits differentiation of leucine and isoleucine from N-terminal fragments is depicted in Scheme I. Figures 1 and 2 show the CID spectra of underivatized and derivatized Val-His-Leu-Thr-Pro-Val-Glu-Lys. In the latter spectrum abundant ions resulting from β-γ cleavage of a_n+1H ions are indicated by asterisks. For example, the peak 42 u below a_3 (and the absence of one 28 u below a_3) clearly shows that amino acid 3 is leucine and not isoleucine. The normal FABMS spectrum of this derivatized peptide resulted in the same a_n ions and their associated β-γ bond cleavage ions. Since this derivatization significantly alters the fragmentation observed upon collisional activation, it may also be of use for the relatively few cases where the CID spectrum of an underivatized peptide gives ambiguous results.

The CID spectra were obtained with a JEOL HX110/HX110 tandem mass spectrometer of EBEB configuration. The collision cell was located in the third field free region and He was the collision gas. A neutral Xe beam of 6 keV energy was used for ionization of the samples, which were dissolved in glycerol at a concentration of 2 μg/μl.

1. Johnson, R. S., Martin, S. A., Biemann, K., Stults, J. T., Watson, J. T., submitted for publication to *Anal. Chem.* (see also, Stults, J. T. and Watson, J. T., ASMS 1987)

2. Jensen, N. J., Tomer, K. B., Gross, M. L. *J. Amer. Chem. Soc.* **1985**, 107,, 1863-1868

Presented at the 35th ASMS Conference on Mass Spectrometry and Allied Topics
May 24-29, 1987, Denver, CO

Scheme I

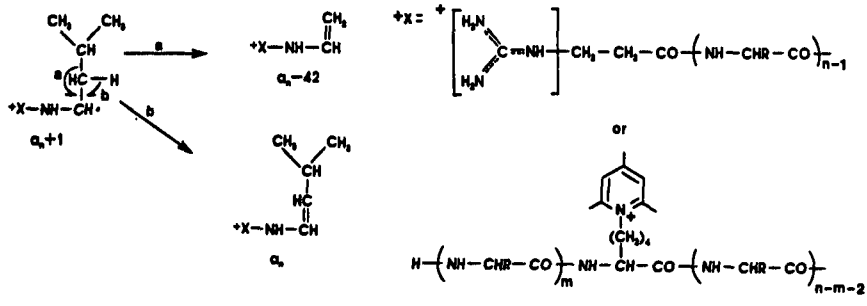

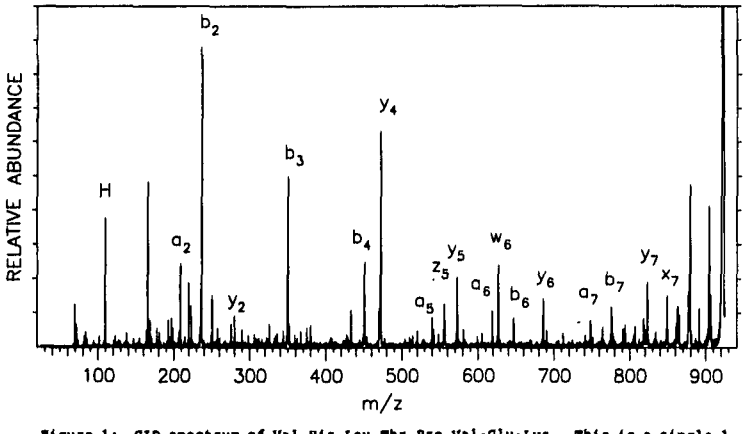

Figure 1: CID spectrum of Val-His-Leu-Thr-Pro-Val-Glu-Lys. This is a single 1 min scan at 100 Hz filtering with the resolution of MS1 sufficient to select only the ^{13}C-species, and a resolution of 1000 for MS2. The ion nomenclature is a modification of that described by Roepstorff and Fohlman.

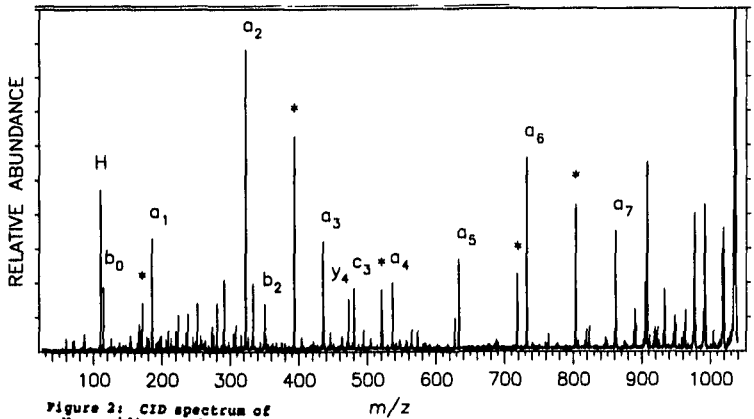

Figure 2: CID spectrum of α-N-guanidinopropionyl-Val-His-Leu-Thr-Pro-Val-Glu-Lys. The instrument parameters were as described for Fig. 1. Asterisks indicate fragment ions produced according to Scheme I, path a.

Presented at the 35th ASMS Conference on Mass Spectrometry and Allied Topics
May 24-29, 1987, Denver, CO.

COLLISIONALLY-ACTIVATED DISSOCIATION SPECTROSCOPY OF NEUROPEPTIDES

Chhabil Dass and Dominic M. Desiderio
University of Tennessee, Memphis
800 Madison Avenue, Memphis, TN 38163

The analysis of samples of biological origin is a challenging task because of the presence of unwanted contaminants, even after best possible HPLC purification step. Fast atom bombardment, a "soft ionization" technique is the most suitable mode of ionization for these highly polar and thermally labile compounds. However, the major drawback of the technique is the presence in the spectrum of chemical noise generated from the matrix ions and the ions formed by its interaction with the sample (1). These difficulties may pose problems in the unambiguous structural characterization of compounds of biological interest. To overcome these potential pitfalls of FAB-MS, one needs to use MS/MS techniques. In a typical MS/MS experiment, a unique ion of interest can be mass-selected and its daughter ion spectrum acquired, thereby increasing the molecular specificity of the analytical measurement. In a forward geometry instrument (E=ESA precedes B=magnet), a daughter ion spectrum can be acquired by using the B/E linked-field scan. We are actively involved in identification and quantitation of a variety of neuropeptides in biological tissues with the ultimate aim of understanding the peptidergic pathways involved in their physiological action. Towards that end, one needs to understand the mass spectrometric fragmentation behavior of each peptide of interest so that highly specific quantitation methods can be developed based on monitoring the selected daughter ions. In this study, we report on the fragmentation characteristics of the collisionally-activated FAB-desorbed MH^+ ions of several neuropeptides. Furthermore, we also wish to evaluate the potential of the B/E linked-field technique for sequencing peptides. CAD was performed in the first field-free region of EB (VG 7070E-HF) mass spectrometer using He as a collision gas.

The peptide studied (C-terminal extended methionine enkephalin and leucine enkephalin peptides, peptides belonging to dynorphin and endorphin families, β-casomorphin, etc.) follows the general fragmentation pattern (Figs. 1 and 2) shown in Scheme 1. The most important fragmentation is cleavage of the peptide bond (-CO-NH-) yielding B- and Y-type ions. This observation is in contrast with the data obtained in the normal FAB mass spectrum, where it was observed that cleavage of the amino-alkyl (-NH-CHR-) bond was the dominant reaction of this class of compounds (2), suggesting that the collisionally-activated and the FAB-desorbed MH^+ ions differ energetically.

The presence of basic amino acid residues influence the yield of the N- or C-terminus ions. The loss of tyrosine side chain is energetically-favored reaction. This ion along with the Y-type ions can be used as candidates for quantitation of these peptides using selected reaction monitoring technique. The CAD-B/E linked-field scan, in most cases, yields useful data for sequencing the peptides. The low mass ions are not seen in the spectra because of their low translational energy. This is a limitation of B/E linked-field technique. However, in most cases, sequencing of the peptides studied here can be accomplished by considering both C- and N-terminus ion series.

REFERENCES

1. C. Dass and D.M. Desiderio, Extended Abstract #TOC11:30, in this issue.
2. C. Dass and D.M. Desiderio, Analyt. Biochem., in press.

Presented at the 35th ASMS Conference on Mass Spectrometry and Allied Topics
May 24-29, 1987, Denver, CO.

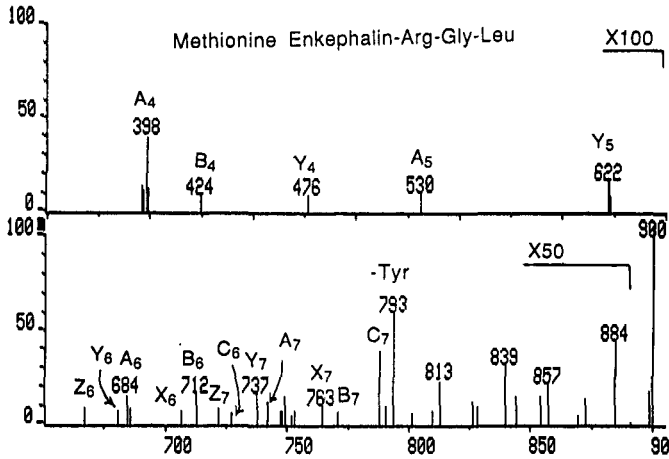

Fig. 1

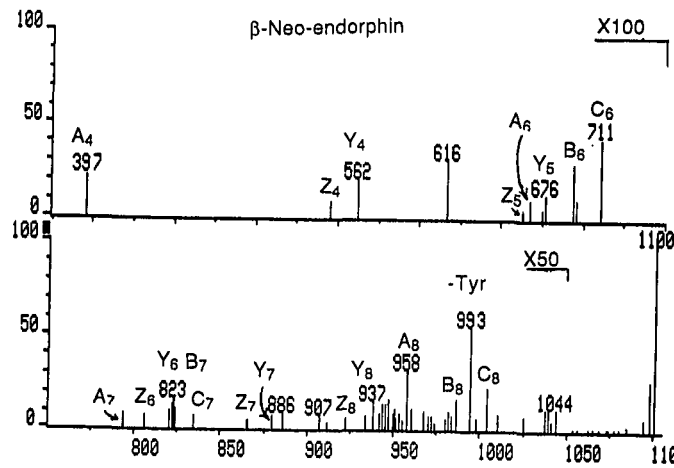

Fig. 2

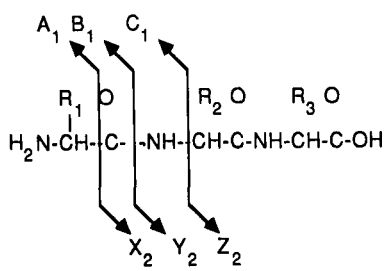

SCHEME 1

Presented at the 35th ASMS Conference on Mass Spectrometry and Allied Topics
May 24-29, 1987, Denver, CO.

MATRIX SELECTION IN THE FAB-MS ANALYSIS OF PEPTIDES

Bradley L. Ackermann and John E. Coutant
Merrell Dow Research Institute, Cincinnati, OH 45215

Matrix selection is probably the most important variable influencing the success of a FAB analysis. This is especially true for peptides where several matrices have been reported. In many instances, statistically different results, with respect to sensitivity, can be attributed to the matrix employed. For example, Lehmann and coworkers reported that thioglycerol is superior to glycerol for observing the $(M+H)^+$ ion of angiotensin II (1). Unfortunately, while several matrices are currently used, an understanding of which matrix is best suited for a particular analysis is an area of concern that has not been sufficiently addressed.

In this study, the four matrices most commonly used for peptide analysis: glycerol (G), 1:1 glycerol/thioglycerol (G/TG), thioglycerol (TG), and 5:1 (w/w) dithiothreitol/dithioerythritol ("magic bullet", MB) were compared for their respective sensitivity towards a series of 25 peptides. The peptides were selected to emphasize various characteristics including charge, size, hydrophobicity, and the presence of disulfide bonds.

Data were collected by repetitive scanning over the region of the protonated molecule $(M+H)^+$, at or near the 1 nmol level, where sensitivity was simply defined as the fraction of the total ion current attributed to the $(M+H)^+$ cluster. Relative standard deviations for repetitive determinations of each peptide-matrix pair were typically <5% (n= 3 to 7). This enabled the matrices to be statistically resolved for most of the peptides investigated and allowed the matrices to be ranked according to sensitivity for each peptide. Ranking was done by assigning points based on performance (4=best, 1=worst). Four points were only awarded when a matrix was found to be superior to all others for a particular peptide. In cases where matrices were statistically equivalent, each received the same number of points.

Table 1 displays selected results from the study. The rows correspond to different peptide classifications which are defined in the table or in the legend below. The columns list the total points awarded to each matrix for a given peptide class following normalization of the largest total to 100. The number of peptides included in each class is also listed. The results are of course limited by the number of peptides studied, and by the mass range of our current instrument (Finnigan TSQ-46, 1900u).

Several conclusions may be drawn from the data in Table 1. First, magic bullet displayed the best results overall and for most of the classes listed. Hence, it is the logical choice for many applications including unknowns. Thioglycerol also performed well overall, although not as consistently. It may, however, be the best choice for hydrophobic peptides. While glycerol performed the worst overall, it does function relatively well for acidic peptides. Finally, because magic bullet was the least susceptible to differences in charge, size, and polarity, it should be the most suitable matrix for peptide mapping. This hypothesis shall be tested subsequently.

Presented at the 35th ASMS Conference on Mass Spectrometry and Allied Topics
May 24-29, 1987, Denver, CO

Table 1: SELECTED RESULTS FROM PEPTIDE MATRIX STUDY

Class	G	G/TG	TG	MB	# Peptides
Overall	58	76	82	100	25
Acidic (pI<6)	92	85	81	100	9
Neutral (pI 6-9)	53	89	89	100	6
Basic (pI>9)	36	64	78	100	10
Small (MW<1000)	73	80	87	100	10
Medium (MW>1000)	49	74	78	100	15
Hydrophilic (ΔF>160)	44	64	80	100	7
Amphipathic (-51<ΔF<160)	63	77	63	100	9
Hydrophobic (ΔF<-51)	63	85	100	96	9

ΔF values (cal/mol) were calculated from the hydrophobicity scale developed by Bull and Breese (2), and applied recently to FAB mapping by Williams et al. (3).

References

(1) W.D. Lehmann, M. Kessler, and W.A. Konig, Biomed. Mass. Spectrom. 11, 217 (1984).

(2) H.B. Bull and K. Breese, Arch. Biochem. Biophys. 161, 665 (1974).

(3) S. Naylor, A.F. Findeis, B.W. Gibson, and D.H. Williams, J. Am. Chem. Soc. 108, 6359 (1986).

Presented at the 35th ASMS Conference on Mass Spectrometry and Allied Topics
May 24-29, 1987, Denver, CO

FAB/MS FOR THE DETERMINATION OF ENDORPHINS:

R. D. Voyksner and F. P. Williams, Analytical and Chemical Sciences, Research Triangle Institute, P. O. Box 12194, Research Triangle Park, NC 27709

Progress in neuropeptide research will rely on the existence of specific, sensitive, and accurate methodology for the detection and quantification of peptides in various biological matrices. Soft ionization techniques such as fast atom bombardment (FAB) together with advances in expanding instrumental mass range allows mass spectrometry (MS) to analyze higher molecular weight neuropeptides such as endorphins.

α-Endorphin (mw 1745), β-endorphin (mw 3463), and γ-endorphin (mw 1858) are two important neuropeptides chosen to evaluate FAB/MS analysis. The main goals of the research were: 1) optimization of FAB/MS conditions to achieve best sensitivity, 2) understanding of fragmentation patterns in order to sequence the peptide, 3) evaluation of collisional induced dissociation-mass analyzed ion kinetic energy spectrometry (CID-MIKES) and high resolution/MS for the detection of endorphins, 4) determination of detection limits, and 5) determination of matrix effects on the spectra and detection limits of the endorphins.

The results from this evaluation are summarized below, respectively:

(1) A variety of liquid matrices and chemical modifiers for FAB have been evaluated to determine their effect on the $[M+H]^+$ ion intensity for β-endorphin and γ-endorphin. Thioglycerol with the addition of trifluoroacetic acid (TFA) produced the most intense $[M+H]^+$ ion current for the endorphins. Increasing the molarity of TFA in the matrix did not significantly change the ion current, but increased the formation of the $[M+H]^{+2}$ ions. Negative ion MS detection proved slightly more sensitive than positive ion detection. The addition of inorganic salts suppressed sample ionization and resulted in the formation of alkali metal adduct ions (i.e. $[M+Na]^+$, $[M-H]+2Na]^+$, etc.). This loss in ion current indicates that biological extracts must be void of salt interferences, stressing the need for on-line HPLC/MS techniques for sensitive detection of the endorphins.

(2) The full scan FAB/MS spectra contained sequence information for the analysis of only 2-5 μg of γ-endorphin (Figure 1) or β-endorphin. The spectra exhibited a base peak corresponding to the $[M+H]^+$ ion cluster with fragmentation enabling the verification of the amino acid sequence.

(3) The use of tandem MS and high resolution MS has not been shown to increase specificity or sensitivity for the analysis of some opioid peptides. Both of these techniques were evaluated for the analysis of endorphins. Tandem MS proved inadequate for the analysis of endorphin due to low daughter ion yield. As the molecular weight of a compound increased there were more degrees of freedom available to distribute the energy gained in a collision without fragmentation. The usefulness of high resolution mass measurements also decreases with molecular weight. For example, β-endorphin requires a resolution of about 4000 to resolve (10% valley) the molecular ion cluster. At higher resolution (i.e., 40,000) transmission is greatly decreased reducing sensitivity. A few ppm measurement error will still result in hundreds of empirical formulas for the elements composing β-endorphin.

(4) Estimated detection limits were determined for several endorphins spiked in plasma. The plasma samples (2 mL) were acidified using 1 M HCl and extracted using a SepPak® C_{18} cartridge. The cartridge was washed with 1 mL H_2O and the endorphins were eluted with three washes of 80% acetonitrile, 19.5% water and 0.5% TFA solution. The extraction procedure proved to be 59 ± 16% efficient. The FAB/MS analysis of the extracts demonstrated α-endorphin could be detected down to 400-500 ng under full scan conditions (Figure 2). In cases where target peptides are sought, the estimated detection limits, for solvent standards monitoring the $[M+H]^+$ ion were determined to be about 20 ng for α-endorphin (12 pM) and 80 ng for β-endorphin (23 pM).

(5) The SepPak® extraction procedure did not remove all inorganic or organic interferences. These matrix components could interfere with direct probe MS type of analysis by suppressing ionization, producing false positives, and increasing the chemical noise resulting in poorer detection limits. The presence of inorganic salts were demonstrated to greatly suppress ion formation for the endorphins as well as favor $[M+ \text{alkali metal}]^+$ ions over $[M+H]^+$ ions. The FAB/MS analysis of the plasma extract for α-endorphin exhibited an $[M+H]^+$ ion current 2.2 times less intense than an equivalent amount in solvent. Chemical noise observed in the plasma extract was minimal. No ions were detected above mass 1500 that were not observed in the solvent standard. Samples primarily exhibited a greater background in the low mass portion of the spectrum.

This research was supported by the National Institute on Drug Abuse, grant number 1R01 DAC 4202-01.

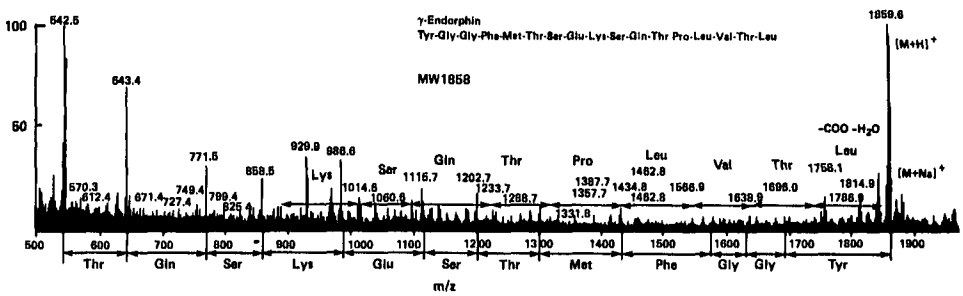

Figure 1. FAB/MS of γ-endorphin showing peptide sequence ions.

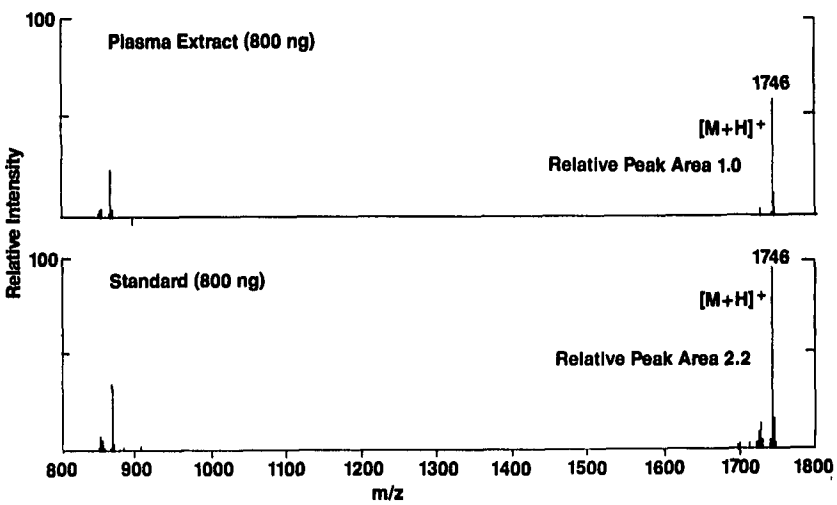

Figure 2. FAB/MS analysis for α-endorphin (460 pM) extracted from plasma and the same quantity of α-endorphin in solvent.

THE USE OF FAST ATOM BOMBARDMENT MASS SPECTROMETRY FOR EVALUATION OF SOLID PHASE PEPTIDE SYNTHESIS

S.T. Weintraub and R.J. Klebe, Departments of Pathology and Cellular and Structural Biology
The University of Texas Health Science Center, San Antonio, Texas 78284

P. Kanda and R.E. Lanford, Department of Virology and Immunology
Southwest Foundation for Biomedical Research, San Antonio, Texas 78284

The use of a solid phase technique for peptide synthesis was proposed by Bruce Merrifield in 1959, and formally introduced by him in 1963 (1), in order to overcome the numerous problems of peptide synthesis in solution. This innovation revolutionized the entire peptide field, and has permitted the synthesis of peptides up to about 200 residues long. As in any synthetic procedure, there is an absolute requirement for precise characterization of the final product. In many cases, the traditional approach of amino acid analysis is sufficient to confirm the composition of the peptide. Not infrequently, however, small unexpected problems in the synthesis, minor alterations in side chains and even residual blocking groups often go undetected by amino acid analysis. Fast atom bombardment mass spectrometry, on the other hand, is capable of revealing minute differences in peptide composition, with the added benefit of providing sequence verification in many instances.

The power of FAB-MS to correctly characterize synthetic peptides can clearly be seen in the examples described below. In each case, the nature of the difficulty encountered in the synthesis was not able to be completely ascertained by amino acid analysis. FAB mass spectra were acquired on a Finnigan-MAT 212 mass spectrometer in combination with an INCOS 2200 data system. An Ion Tech saddle field atom gun, operating at 8 kV, was used with xenon gas. During an automated peptide synthesis procedure, it was suspected that a problem had occurred when the seventh amino acid was coupled to the chain. A portion of the resin was removed, cleaved with HF and purified. The resulting HPLC analysis revealed the presence of 3 components: r.t. 20.7 min, $[MH]^+$ m/z 731; r.t. 21.6 min, $[MH]^+$ m/z 830; r.t. 25.2 min, $[MH]^+$ m/z 645. Since the desired heptamer, Lys-Val-Gly-Gly-Leu-Glu-Glu has a molecular weight of 730, peak 1 contained the correct product. The $[MH]^+$ of the compound in peak 2 was 99 a.m.u. higher than 731, suggesting the presence of an additional valine in the peptide. This was confirmed by subsequent amino acid analysis. Since the peptide in peak 3 had a lower molecular weight than 730, it was apparent that omission of at least one amino acid had occurred. An $[MH]^+$ at m/z 645, as seen in the peptide eluting in peak 3, would be observed if the amino-terminal lysine had not been coupled to the peptide and, instead, an acetyl group were present. Amino acid analysis of the compound in peak 3 was able to confirm the absence of the lysine, but could give no information about the presence of the acetyl group. From the FAB-MS it was possible to deduce that incomplete deblocking of the precursor hexamer prevented quantitative formation of the heptamer.

An investigation into the mechanism of fibronectin-mediated cell adhesion is currently in progress. A hexapeptide (Gly-Arg-Gly-Asp-Ser-Pro, M.W. 587) which is part of the cell attachment region of fibronectin has been shown to inhibit cell adhesion. We have synthesized this hexapeptide by a manual method using trifluoromethane sulfonic acid (TFMSA) for cleavage. Initially, the cleavage reaction was run at 27 °C. In addition to an intense $[MH]^+$ at m/z 588, a significant unexpected peak was seen at m/z 570. A similar spectrum was obtained after HF cleavage at 0 °C. When the TFMSA cleavage reaction was run at 4 °C, however, the ion at m/z 570 was reduced by over 90%. It has previously been reported that problems can occur during synthesis of peptides which contain aspartic acid, particularly when this residue is adjacent to either a glycine, an alanine or a serine (2). During HF or other acid cleavage, the carboxyl group on the side chain of aspartic acid can react with a nearby amide nitrogen to form a succinimide ring. The existence of the imide ring cannot be ascertained by amino acid analysis because of the hydrolysis required prior to measurement. The formation of the imide presents several serious problems. First, it is an undesired side product which, to date, has not been separated from the main product by HPLC. More serious, however, are the implications derived from its presence - that isomerization and/or racemization of the M.W. 587 peptide might have occurred. Use of FAB-MS to monitor the cleaved peptide enabled choice of proper conditions to minimize imide formation, thus, lessening the chances for modification of the main product.

Currently, efforts are underway to elucidate the mechanism of protein transport in mammalian cells. Recent experiments with SV40 have demonstrated that a localized region of the T-antigen is responsible for nuclear transport. If this seven amino acid core segment is attached to another protein, even up to molecular weights of 400,000, the complex is carried into the nucleus, following microinjection into the cytoplasm (3). The sequence of the core peptide is: Pro-Lys-Lys-Lys-Arg-Lys-Val. This core segment has now been

synthesized as part of a peptide which has a spacer added to the carboxy terminus, a tyrosine included to aid in UV visualization and an amino-terminal cysteine which permits attachment to other proteins. This hexadecamer was produced by means of an automated synthesizer (Cys-Gly-Tyr-Gly-Pro-Lys-Lys-Lys-Arg-Lys-Val-Gly-Gly-Leu-Glu-Glu, M.W. 1747.9). Following addition of each residue, starting with the trimer (Leu-Glu-Glu, M.W. 389.2), an aliquot of the peptidyl-resin was removed from the reaction vessel. Cleavage and deprotection were accomplished with HF, followed by isolation and purification. On a qualitative basis, the resulting spectra were clearly different for the group consisting of the 3-mer to the 7-mer as compared to the group of the 8-mer to the 15-mer, with the 16-mer exhibiting further differences. Most notably, $[MH]^+$ was the base peak for the first group, but this ion exhibited decreasing intensity as the number of amino acids increased above 7. Furthermore, it appeared that ions at m/z 112 and m/z 129 were extremely intense in the spectra in which $[MH]^+$ was low. When expressed as percent of total ionization, after background subtraction, the intensities of these ions clearly varied with the number of amino acids in the chain, as shown below: It was observed that the C'' series was consistently found for all peptides up through the 14-mer, and that the C'' fragment which was formed by cleavage between Arg-Lys was strikingly intense. For the 16-mer, however, neither the $[MH_2]^{++}$ nor C_9'' were observed. In addition, starting with the 14-mer the sequence ions were only marginally detectable, with mainly the C-terminus series observed as opposed to the predominant N-terminus series ions seen in the spectra of the smaller peptides in this study. From the overall appearance of the spectra, in combination with the intensity data it seems that the addition of the arginine residue next to a lysine produced a profound effect on the fragmentation pattern. Experiments are in progress to elucidate the origin of the m/z 112 ion, which is not a predicted sequence ion for any of the peptides.

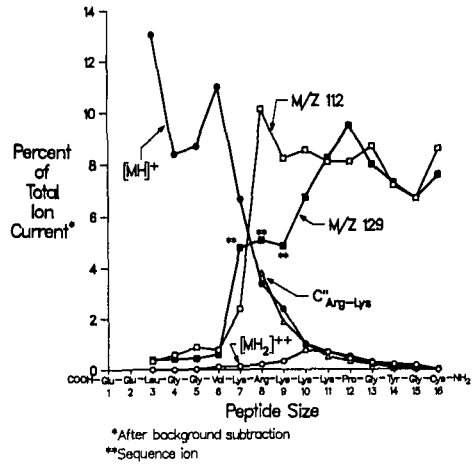

At the present time it is felt that the m/z 129 ion is derived from the arginine residue, as a result of immonium ion formation (4). The ion at m/z 112 might be formed by loss of ammonia from m/z 129. The proposed structures of these ions are:

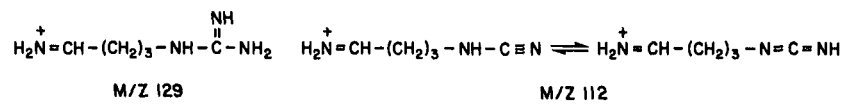

M/Z 129 M/Z 112

Fast atom bombardment mass spectrometry is clearly superior to amino acid analysis for evaluation of synthetic peptides by providing information about: 1) molecular weight; 2) differentiation between aspartic acid/asparagine, glutamic acid/glutamine, free carboxy terminus/C-terminal amide and free amino terminus/N-acetylated peptide; 3) detection of blocked amino acids; 4) identification of side chain rearrangements; 5) sequence verification/elucidation. Finally, FAB-MS can be performed in a matter of minutes, as compared to approximately 4 hours for amino acid analysis. FAB-MS, therefore, is essential for accurate characterization of synthetic peptides.

References

1. Merrifield, R.B. J. Am. Chem. Soc. 85:2149-2154, 1963.
2. Stewart, J.M. and Young, J.D. in Solid Phase Peptide Synthesis, 2nd edition. Pierce Chemical Company, Rockford, Illinois. pp. 1-50, 1984.
3. Lanford, R.E., Kanda, P. and Kennedy, R.C. Cell 46:575-582, 1986.
4. Barber, M., Bordoli, R.S., Sedgwick, R.D. and Tyler, A.N. Biomed. Mass Spectrom. 9:208-214, 1982.

Acknowledgements - supported in part by NIH grant AG06872 to R.J.K.

Presented at the 35th ASMS Conference on Mass Spectrometry and Allied Topics
May 24-29, 1987, Denver, CO.

Determination of Enzymic Reaction Parameters by On-Line FABMS

William T. Moore, Terry Fan, and Richard M. Caprioli
Department of Biochemistry and Molecular Biology
and the Analytical Chemistry Center
The University of Texas Medical School at Houston
Houston, Texas 77225

Endoproteases are hydrolytic enzymes that cleave peptide bonds by catalyzing an acyl-transfer reaction. An acyl moiety involved in the peptide bond of a polypeptide substrate is transferred to an acceptor water molecule resulting in the fragmentation of the polypeptide substrate into smaller peptides. Biologically, the proteases are important in extensively degrading polypeptides for digestive and nutritional purposes. In addition the enzymes are important and exquisitely specific regulators in biological control processes whereby they often act to cause a more limited fragmentation of polypeptide chains thereby subtly modifying structure and function: hormone production, defense mechanisms - blood clotting and dissolution, and macromolecular assembly. Furthermore the proteases are extensively used by the protein chemist in the fine detail analysis of protein structure - generation of peptide maps for identification purposes and as a prelude to primary structure determination of a polypeptide chain.

Before FABMS, protease action was only conveniently assayed and studied with light spectroscopy employing colorimetric, chemically modified peptides that only approximate the condition of a natural substrate. Studies involving natural substrates were involved and entailed extensive structural determination of generated fragments.

Our laboratory has previously shown that FABMS can be used to determine the relative rates of trypsin catalyzed hydrolysis of small and large polypeptides and the pertinent kinetic parameters for these reactions (1,2). These experiments were performed by removing timed aliquots and stopping the reaction with oxalic acid and freezing the aliquot for future (off-line) FABMS analysis using the standard FAB sample probe with its associated shortcomings. The objective of this study is to demonstrate the use of the Continuous-Flow sample probe that was developed in our laboratory (3) to monitor the progress of protease catalyzed reactions on-line.

Two basic methods of continuous-flow probe operation were examined. Firstly, continuous flow reaction monitoring was investigated when the pH and reaction conditions were suitable for FABMS analysis as is the pepsin hydrolysis of alpha-MSH. The progress of this reaction was directly monitored by flowing the reaction solution into the source at 1 µL/min, the flow being created by the pressure differential between the atmosphere and the source vacuum. Figure 1 indicates the reaction progress profile - the disappearance of substrate and the appearance of products for the pepsin catalyzed reaction as deduced from the acquired data generated as specific ion chromatograms. Apparent initial rates of substrate disappearance and product appearance may be estimated from directly examining the slopes of the chromatograms. Secondly, a flow injection reaction monitoring system was devised for peptide hydrolysis studies involving trypsin and subtilisin Carlsberg since the reaction conditions in these cases is not conducive to FAB analysis by direct flow of reaction solution into the source. This approach involves the timed injection of reaction solution into a stream of acidic and glycerol containing aqueous carrier pumped through the flow probe at 5µL/min. Injection of timed aliquots and, sample loading, and flow rate were microprocessor controlled by incorporating the use of an Applied Biosystems Model 130A Separation system (HPLC unit). With this method we examined the hydrolysis of the simple tetrapeptide M-R-F-A by trypsin and estimated the kinetic constants so that we could compare the values obtained for the continuous flow probe with those previously obtained with the standard flow probe. Table 1 presents the values for comparison and indicates that the values of pertinent kinetic parameters are in close agreement. Results for the hydrolysis of a three substrate mixture by subtilisin Carlsberg are presented in Fig 2 to further illustrate the use of the continuous flow probe and the flow injection method to monitor on-line enzymic reactions in real time. The progress of the respective hydrolyses can be directly observed from following the disappearance of each substrate in the mixture and the appearance of the related products when this

data is processed into specific ion chromatograms, each peak representing an injection of an aliquot of the reaction solution.

FAB mass spectrometry was performed with a Kratos MS50RF equipped with an Ion Tech b11NF saddle field ion gun using Xe to create fast atoms. The spectrometer was generally operated at a resolving power of 1500 and an accelerating potential of 4KV. The magnet was scanned at 10 or 30 sec/decade. Data was acquired and processed using the DS90 raw data programs.

We conclude that on-line FABMS analysis using the continuous flow probe systems described is a powerful tool for studying protease action in relation to protein structure in both enzyme and substrate.

(1) Caprioli and Smith, Anal. Chem., 1986, 58 1080.
(2) Seifert and Caprioli, abstr. 34th annual ASMS meeting, 1986 p.844.
(3) Caprioli, Fan, and Cottrell, Anal. Chem., 1986, 58, 2949.

Table 1 Kinetic Constants for the Tryptic Hydrolysis of Met-Arg-Phe-Ala (M-R↓F-A)

Method	Km, nM	k_{cat}, S^{-1}	k_{cat} / Km, $M^{-1}S^{-1}$
Standard Probe (1)	1.90	7 1	3622
Continuous Flow Probe	1 85	9.1	4927

(1) Caprioli and Smith. Anal Chem.. 1986. 58. 1080-1083.

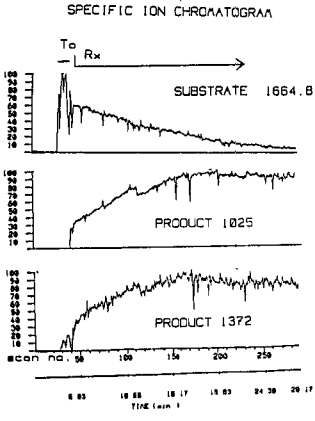

Figure 1 On-line monitoring of the hydrolysis of alpha-MSH by pepsin using the continuous flow method.

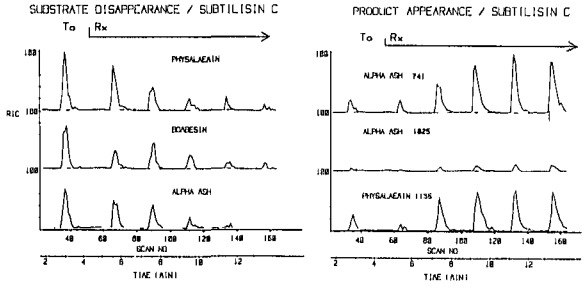

Figure 2 On-line monitoring of the hydrolysis of a three peptide mixture by subtilisin Carlsberg using the flow injection method.

Presented at the 35th ASMS Conference on Mass Spectrometry and Allied Topics
May 24-29, 1987, Denver, CO.

A NOVEL C-TERMINUS SPECIFIC PEPTIDE DERIVATIZATION DESIGNED TO ENHANCE FAB-MS SENSITIVITY: CHEMICAL INTRODUCTION OF QUATERNARY AMINE FUNCTIONALITY SPECIFICALLY TO C-TERMINUS VIA AZLACTONE INTERMEDIATE

BRIAN D. BENNETT and RICHARD A. DAY
Department of Chemistry
University of Cincinnati
Cincinnati, OH 45221

The introduction of a formal charge into molecules has been shown to increase the effective sensitivity in FAB-MS. In light of these observations we developed a method which attaches a positively charged quaternary amine specifically to the C-terminal carboxy group of peptides. The selective C-term carboxy activation is afforded by azlactone formation which can occur only at this site. The activated carbonyl reacts readily with a N-protected aminoalcohol to give the ester. This tertiary amino-ester is readily methylated with iodomethane to give the positively charged quaternary ammonium ester of the peptide.

Quaternization of Peptides : C-Terminus Labelling

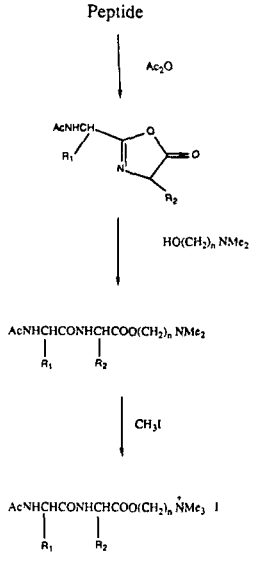

To effect this derivatization the peptide is vortexed in 1 ml 50:50 10% acetic acid/H_2O:Monomethylformamide solution for several minutes. Then 1 ml acetic anhydride is added and the mixture is vortexed for 2 hours at room temperature. Excess acetic anhydride is added (1-2 ml) and samples are placed in a vacuum oven. The solvents are removed in vacuo at 40°C. To the residual peptide monomethylformamide solution 2 ml 3-dimethylamino-propanol or 2-dimethylaminoethanol is added. After mixing leave overnight at room temperature then remove all excess aminoalcohol in vacuo at 40°C. Cool sample with a stream of N_2 then add 0.5 ml iodomethane and vortex. To form a homogeneous mixture add 0.5 ml ETOH, 0.1 ml H_2O, and 0.2 ml DMF.

After sonication remove the iodomethane with a stream of N_2. Add an appropriate volume of glycerol and condition the sample for FAB in vacuo at 60°C.

A series of dipeptides were derivatized in this fashion. These peptide derivatives gave FAB-MS spectra with intense molecular ions. For example, derivatives of LV, GY, and LY at the 0.1 M level (theoretical) gave intense molecular ions and the spectra contained no chemical noise due to glycerol. Clench et al. (1985) ran a series of peptides noting the glycerol trimer to molecular ion ratio. For comparison, the above derivatization of LY yields an intense molecular ion without detection of glycerol trimer when theoretical yield is set to 0.01 M. Clench et al. found the ratio of m/z 277/M+1 for YL to be 0.83 at the 0.01 M level. More rigorous quantitative comparison between derivatized and underivatized peptides are now being made in our laboratory. From this study we have ascertained that it is possible to selectively place a positive formal charge on the C-terminus of peptides. This reverse derivatization procedure for FAB-MS of peptide may prove to be useful in increasing effective sensitivity via stable preformed ion generation.

Improvements in the Sequencing of Peptides By Gas Chromatographic Mass Spectrometry

J.E. Vath and K. Biemann
Department of Chemistry
MIT, Cambridge, MA 02139

Mass spectrometry has proven to be a very powerful tool in the determination of the amino acid sequences of polypeptides and proteins. Although present efforts in mass spectrometric peptide sequencing focus primarily on FABMS/MS techniques, there remain advantages in the improvement of earlier approaches involving chemical conversion followed by GCMS. These advantages include low cost and high efficiency in instrument use and the ability to provide complementary sequence information from regions randomly located within a polypeptide or protein.

The GCMS sequencing technique developed over time in our laboratory involves the conversion of mixtures of small peptides to their corresponding polyamino alcohol-O-trimethylsilyl ethers (PATSE)[1]. One major drawback was the relatively large amount of sample required (50-100 nmols per component) which was due to the derivatization rather than the sensitivity of GCMS. In an effort to greatly increase the sensitivity of the reductive sequencing method, we developed methodology that minimized the surface area of the reaction vessel and eliminated solvents and liquid reagents first by using gaseous reagents and an inert carrier gas[2]. In a further development described here all of the reactions are carried out by contact of reagent vapor with the solid peptides deposited in a thin layer.

The trifluoroacetylation, reduction, solvolysis and silylation reactions are all carried out using the reaction vessel depicted in Figure 1. A 1-2 μL sample containing 0.1-1.0 nmol per peptide component is placed into a capillary tube (~9 cm x 1.2 mm i.d.). The solvent is evaporated <u>in vacuo</u> creating a solid film on the inner wall of the sample tube (more dilute solutions are evaporated in consecutive batches). Up to three sample tubes are placed horizontally in the reaction vessel as shown. The well containing ~200μL of the appropriate reagent mixture is chilled with dry ice and the apparatus evacuated to 0.05 torr. The stopcock is closed and the vessel is subjected to the temperature for the time specified in Scheme I. At the end of each reaction dry ice is again applied to the reagent well and the vessel is evacuated to remove any residual reagents and volatile by-products. The sample tubes are then transferred to another identical vessel containing the appropriate reagents to bring about the next reaction. The resulting PATSE poly-hydrochlorides contained on the sample tube are introduced directly into the GCMS (Finnigan MAT 212) via a Caplan and Cronin solid sample GC injector[3].

The process of reacting solid sample films with condensed reagent vapors eliminates sample losses due to transfers and extractions and also reduces the sample contamination from involatile components in the reagents. The resulting improvements reduce the amount of peptide required for the derivatization by a factor of 100-1000 and allow the use of the full sensitivity of GCMS.

The procedure was optimized and tested at the 100 pmol level on a ten component mixture of di- to hexapeptides representing all twenty common amino acids.

The technique was also applied to a peptide of known sequence. The total ion plot in Figure 2 displays the results of the derivatization of 1.0 nmol of a 20 min. acid hydrolysate of glucagon. The peptides identified by GCMS are listed in Table I and correlated with the structure in Figure 4.

The results indicate that the derivatization involved in the reductive peptide sequencing method can be carried out with reagent vapor on peptides containing all twenty common amino acids. At the same time the sample requirement is reduced 100-1000 fold over that of the earlier liquid phase procedure. Further experiments that are planned include applying this technique to proteins of known and unknown primary structure.

1) Carr, S.A.;Herlihy, W.C.;Biemann, K. *Biomed. Mass Spectrom.* 1981, 8, 51.
2) Zollinger, M.;Biemann, K. Proceedings of the 33rd Annual Conference on Mass Spectrometry and Allied Topics, 1985, 508.
3) Caplan, P.J.;Cronin, D.A. *J. Chromatogr.* 1983, 267, 19.

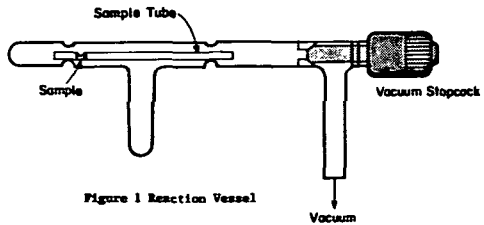

Figure 1 Reaction Vessel

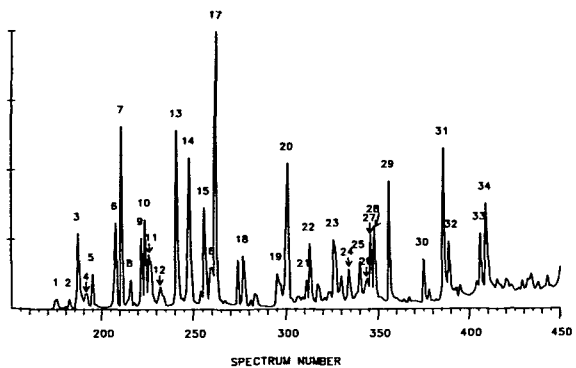

Figure 2 Total ion plot of the PATSEs obtained by acid hydrolysis of glucagon (see Table I).

H S Q G T F T S D Y S K Y L D S R R A Q D F V Q W L M N T

Figure 3 Amino acid sequence of glucagon, the peptides identified in the acid hydrolysate are underlined.

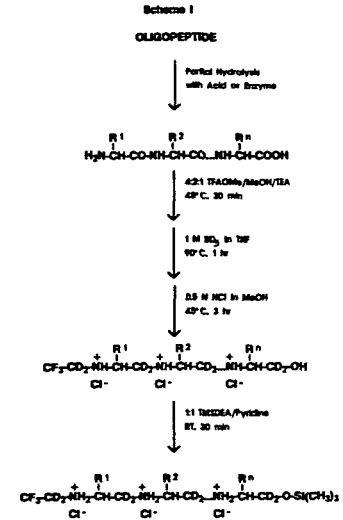

Table I Peak identification for Figure 2

Number in fig. 2	Derivative of:	Number in fig. 2	Derivative of:
1	Orn-Ala	18	Asp-Phe
2	Arg-Ala	19	Ser-Glu(5)
3	His	20	Tyr-Leu
4	Ala-Glu	21	Tyr-Ser
5	Glu-Gly	22	Thr-Ser-Asp
6	Leu-Asp	23	Asp-Tyr
7	Tyr	24	Leu-Met-Asp
8	Val-Glu	25	Trp-Leu
9	Ser-Asp	26	Asp-Phe-Val
10	Leu-Met	27	Lys-Tyr
11	Ser-Orn	28	Thr-Phe-Thr
12	Ser-Arg	29	Phe-Val-Glu
13	Ser-Glu	30	Glu(5)-Asp-Phe
14	Ser-Lys	31	Asp-Tyr-Ser
15	Met-Asp	32	Tyr-Leu-Asp
16	Glu-Asp	33	Lys-Tyr-Leu
17	Phe-Thr, Thr-Phe	34	Ser-Lys-Tyr

Presented at the 35th ASMS Conference on Mass Spectrometry and Allied Topics
May 24-29, 1987, Denver, CO

ANALYSIS OF ARGINYL PEPTIDES AT THE 20-200 PICOMOLE LEVEL BY CAPILLARY GAS CHROMATOGRAPHY-MASS SPECTROMETRY. Kevin D. Ballard and Daniel R. Knapp, Department of Molecular and Cellular Pharmacology and Experimental Therapeutics, Medical University of South Carolina, Charleston, SC 29425.

In the application of gas chromatography-mass spectrometry (GC-MS) of small peptides for generating amino acid sequence information, arginine residues have presented a particular problem because of the high basicity and polarity of the guanidino group. In previous work, these residues have been volatilized either through their conversion to N^{δ}-2-(4,6-dimethyl)pyrimidylornithine (DMPO) derivatives in the permethylation derivatization scheme for peptides[1], or by the conversion of arginine to ornithine through hydrazinolysis in the polyaminoalcohol derivatization scheme[2]. Because hydrazinolysis involves a high risk of peptide bond cleavage, we have explored the possibility of incorporating the formation of DMPO derivatives of arginine residues into two modified forms of the polyaminoalcohol scheme, to form N-trifluoroethyl-O-TBDMS-N^{δ}-2-(4,6-dimethyl)pyrimidylornithyl polyaminoalcohols (N-TFE-O-TBDMS-DMPO polyaminoalcohols), and N,O-di-TBDMS-N^{δ}-2-(4,6-dimethyl)pyrimidylornithyl polyaminoalcohols (N,O-di-TBDMS-DMPO polyaminoalcohols). The TBDMS group was employed because of the enhanced hydrolytic stability of these derivatives over their TMS counterparts, and because of the molecular weight information afforded by the M-15, M-57 diad characteristic of TBDMS derivatives.

Using several model arginine-containing di- through tetra-peptides, and checking each step by fast atom bombardment mass spectrometry, we have optimized the derivatization chemistry to permit sucessful formation and detection of the N-TFE-O-TBDMS polyaminoalcohol derivatives at the 20-200 picomole level for selected ion monitoring applications with minimal formation of reaction by-products. Briefly, arginyl peptides are first allowed to react with 2,4-pentanedione under basic conditions with heating at 100 °C for 4 hours, to form the DMPO derivatives of arginyl residues[3]. After hydrolyzing Schiff's bases with with aqueous acetic acid and extracting excess pentanedione with diethyl ether, the samples were esterified with 3 M methanolic HCl at room temperature for 30 minutes, then N-trifluoroacetylated with MBTFA/tetrahydrofuran with heating at 80 °C for 1 hour. The dried samples were then reduced with 1 M diborane/tetrahydrofuran, heating at 90 °C for 30 minutes. The boroamine complexes were decomposed by heating at 90 °C for 1 hour with 1 M methanolic HCl. The resulting N-TFE-DMPO polyaminoalcohol HCL salts were then converted to the free amines by extraction from aqueous 25% and saturated potassium carbonate with methylene chloride. The samples were finally O-silylated with MTBSTFA/pyridine, heating at 80 °C for 1 hour. This reaction mixture was either used directly for GC-MS analysis or dried and redissolved in pyridine.

The N,O-di-TBDMS-DMPO polyaminoalcohol derivatives of arginyl peptides were prepared by first allowing the peptides to condense with 2,4-pentanedione in the manner described above. The samples were then reduced with 1 M diborane/tetrahydrofuran, treated with 1 M methanolic HCl, and extracted from 25% and saturated potassium carbonate to yield DMPO polyaminoalcohols. The samples were then N,O-silylated with MTBSTFA/acetonitrile, heating at 60-80 °C for 1 hour (note: MTBSTFA reacts much more rapidly with primary amines than with secondary amines). This reaction mixture was used for GC-MS analysis.

Capillary GC-MS analyses were performed using a Varian 3700 GC interfaced to a Finnigan MAT 212 mass spectrometer equipped with a Spectrosystem SS200 data system. Columns used were a 15 m and a 4 m narrow bore DB-1 (J&W Scientific) fused silica capillary column interfaced directly into the ion source of the mass spectrometer. For a typical analysis, a sample was injected on-column with the GC oven at 170 °C (130 °C for samples redissolved in pyridine). The oven temperature was rapidly ramped to 220 °C, then programmed to 325 °C at 10 °C/minute.

Both types of derivatives of arginyl peptides used in this study exhibited excellent gas chromatographic properties on DB-1 fused silica capillary columns. Under the GC conditions employed, the pentapeptide RPPGF eluted at 320 °C as the N-TFE-O-TBDMS-DMPO polyaminoalcohol derivative on a 15 m column, and the tetrapeptide RPPG eluted eluted at 270 °C as the N,O-di-TBDMS-DMPO polyaminoalcohol derivative on a 4 m column. Typical peak widths were 6-8 seconds baseline to baseline.

The mass spectral properties of these types of derivatives are quite similar. Both give rise to complete amino acid sequence information in a fashion directly analogous to the well known N-trifluoroethyl-O-TMS polyaminoalcohols[2], with the molecular weight information imparted by the easily recognizable M-15, M-57 diad characteristic of TBDMS derivatives. The DMPO moiety gives rise to several ions diagnostic for arginine residues, namely m/z 124, 136, 176, and 190. The m/z 176 rearrangement ion is very intense (frequently the base peak) in the mass spectra of all of the model compounds studied.

Under GC-MS selected ion monitoring conditions, 20 pmoles of the tripeptide RPP and 200 pmoles of RPPG derivatized as N-TFE-O-TBDMS-DMPO polyaminoalcohols gave signal to noise ratios of 80:1 and 12:1, respectively, monitoring the m/z 358 A_2 ion common to both compounds. The entire derivatized sample was injected for both of these analyses. Although overall sensitivity studies have not been performed with the N,O-di-TBDMS polyaminoalcohol derivatives, preliminary studies indicate that these derivatives may enable the detection of sub-nanogram amounts of arginyl peptides. A 30 ng (60 pmoles) injection of RPP as the N,O-di-TBDMS-DMPO derivative gave a signal to noise ratio of 2000:1, monitoring the m/z 390 A_2 ion, and 300 pg (1 pmole) of RF gave a signal to noise ratio of 35:1, monitoring the m/z 176 ion. One problem encountered with the N-TFE-O-TBDMS-DMPO polyaminoalcohol derivatives was deterioration of column performance with repeated injections of low level samples. It is believed that the use of the N,O-di-TBDMS-DMPO polyaminoalcohol derivatives will obviate this problemas well as eliminate two derivatization steps with their inherent losses and reaction by-products.

Further studies with arginyl peptides have focussed on the development of an arginyl peptide selective extraction procedure. An initial crude peptide extract is formed using a C_{18} cartridge column with heptafluorobutyric acid (HFBA) as an ion-pairing reagent. The extract is then allowed to react with 1,2-cyclohexanedione under basic conditions in the presence of borate to form borate-complexed dihydroxycyclohexyl (DHCH) derivatives of guanidino groups[1]. The sample is acidified with HFBA to hydrolyze the borate complexes, and desalted with a C_{18} cartridge column. The sample is dissolved in a basic buffer and chemisorbed onto a column of immobilized phenylboronic acid[1]. The column is washed with basic buffer, and the DHCH derivatives are eluted with aqueous HFBA directly onto a C_{18} cartridge column, which is then washed, and the desalted DHCH derivatives are eluted from the C_{18} cartridge column. The dried sample is treated with 2,4-pentanedione under basic conditions, during which reaction the pentanedione exchanges with the DHCH group to form the highly stable DMPO derivative. The remaining derivatization steps are then performed to generate the N,O-di-TBDMS-DMPO polyaminoalcohol derivatives. The isolation of several arginyl peptides with this procedure has been verified by fast atom bombardment mass spectrometry, and a sample of RF in phosphate buffered saline extracted with this procedure has been successfully analyzed by GC-MS as, the N,O-di-TBDMS-DMPO polyaminoalcohol derivative.

In conjunction with the arginyl peptide selective extraction procedure, the new derivatives should be useful for sequencing and ultimately quantitating arginyl peptides at low levels.

This work was supported in part by NIH grants HL29566 and RR01239.

REFERENCES

1. K. Rose, J.D. Priddle and R.E. Offord, J. Chromatogr. 210, 301 (1981).

2. S.A. Carr, W.C. Herlihy and K. Biemann, Biomed. Mass Spectrom. 8, 51 (1981).

3. H.R. Morris, R.J. Dickinson and D.H. Williams, Biochem. Biophys. Res. Commun. 51, 247 (1973).

Presented at the 35th ASMS Conference on Mass Spectrometry and Allied Topics
May 24-29, 1987, Denver, CO.

NEGATIVE ION CHEMICAL IONIZATION MASS SPECTROMETRY OF AMINO ACID THIOHYDANTOINS

Todd D. Williams, David S. Morison, and Robert J. Anderegg

Department of Chemistry
University of Maine, Orono, Maine 04469

The Edman degradation continues to be an important tool in protein sequencing. Improvements in methodology and instrumentation, particularly gas/liquid and solid phase sequencers, have made microsequencing of subnanomolar quantities of protein possible. The limit of sensitivity is determined by the detection method used for the released amino acid phenylthiohydantoins (PTH). Quantitation is usually by HPLC with UV detection, although a variety of mass spectrometric techniques have been proposed including the use of electron impact, chemical ionization, and secondary ion mass spectrometry. Mass spectrometric methods have the advantage of identification of PTH-amino acids without chromatographic separation and comparable or greater detection limits than HPLC. The relatively complex and expensive instrumentation of mass spectrometry, however, has not been widely accepted by workers routinely using the Edman degradation.

Because negative ion chemical ionization mass spectrometry (NICI MS) has been demonstrated to have extreme sensitivity for electrophiles, we sought to explore whether the PTH-amino acids from Edman degradation of proteins could be analyzed by NICI MS. Such an approach would require a relatively modest investment in a quadrupole mass spectrometer. As a first step, we investigated the positive chemical ionization (PCI) and NICI mass spectrometry of PTH-amino acids using methane as the reagent gas. The PCI spectra we obtained were similar to those reported in the literature (1). We found that use of a desorptive chemical ionization (DCI) probe improved the sensitivity (more ion current in the MH^+ ion) and decreased fragmentation. With few exceptions, NICI spectra of PTH amino acids exhibited 2-50 times as much ion current in diagnostic ions as did PCI spectra. Although the $(M-H)^-$ was the base peak for a number of simple amino acids (Gly, Ala, Val, Leu, Ile, Met, Phe, His), considerable fragmentation was observed for the others. In addition, all ions were often part of a cluster due to hydrogen losses, complicating the assignments of, for example, Asp vs Asn and Glu vs Gln. For the PTH amino acids, PCI is recommended in spite of poorer sensitivity, since identification is less ambiguous.

By using a modified isothiocyanate, we hoped to produce a more electrophilic derivative that would respond better in NICI-MS. A variety of isothiocyanates have been proposed in the literature as alternatives to phenylisothiocyanate (PITC). One of these, dimethylaminoazobenzene isothiocyanate (DABITC) (2), is commercially available, and has a structure that would be predicted to produce a more electrophilic derivative than PITC. We again compared PCI and NICI-MS of the DABTH-amino acids. The PCI sensitivity for the DABTH-amino acid was significantly worse than the PCI sensitivity of PTH-amino acids. In NICI-MS, the responses of DABTH-amino acids were very good, about a factor of 100 better than the PCI response of an equivalent amount of the corresponding PTH-amino acid. In nearly every case, the molecular anion was the base peak of the spectrum, providing a diagnostic ion for quantitation.

The DABITC reagent may not be the best choice for the proposed NICI-MS methodology. The coupling to peptides is difficult, requiring a second coupling step with PITC (3); and the low volatility makes NICI of the DABTH derivatives of the largest amino acids a problem. Other electrophilic isothiocyanates are currently under investigation.

References

1. T. Fairwell, Methods Enzymol. 91, 502-511, (1983),
2. J.Y. Chang, Biochem. J. 163, 514-520, (1977).
3. J.Y. Chang, D. Brauer, and B. Wittman-Liebold, FEBS Lett., 93, 295, (1978).

Acknowledgement

This work was supported by the National Institutes of Health Grant #GM 32602

Presented at the 35th ASMS Conference on Mass Spectrometry and Allied Topics
May 24-29, 1987, Denver, CO

STRUCTURE DETERMINATION OF TRITERPENES FROM LICHENS BY TANDEM MS

P. Allemand, G. Tsoupras, R. Tabacchi
Chemical Institute of Neuchâtel University
Avenue de Bellevaux 51

CH-2000 Neuchâtel

INTRODUCTION

Triterpenes have always been considered as rare compounds in lichens. This is probably due to the fact that no analytical method was accurate enough to deal with the small quantities of products present in a complex matrix. Analysis of some lichen species extracts allowed the identification of several triterpenoids and steroids.

METHODS

Using chromatographic methods (essentially HPLC) we isolated 5 triterpenes from extracts of *Evernia Prunastri* (Oak moss). The structures were established on the basis of CI, EI and MS-MS spectra on a triple quadrupole system. (NERMAG R30-10 at 70 Ev, collision energy 25-40 eV; P 10^{-1} Torr).

Structures of the compounds identified :

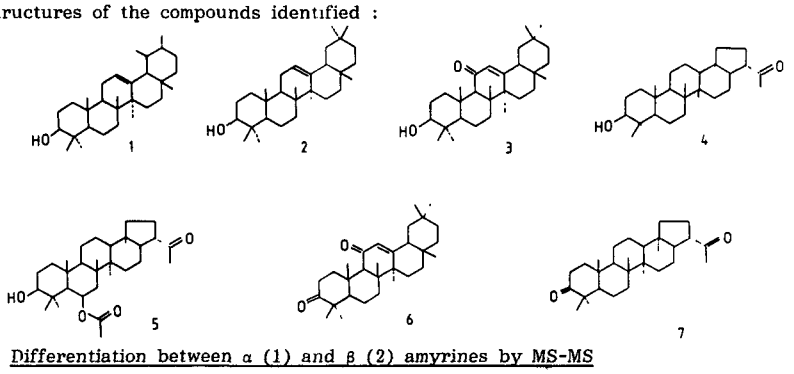

1. Differentiation between α (1) and β (2) amyrines by MS-MS

It is well known that α and β amyrine give very similar spectra when studied by MS and that it is difficult to identify them especially if the sample contains other compounds. Relying on the fact that differents ions should lead to different collision spectra, we studied the MS spectra of m/z 218 for both compounds. It appeared that α-amyrine's spectra contained an important signal at m/z 122, while β-amyrine led to a signal at m/z 94. Mechanisms have been proposed for both fragmentations.

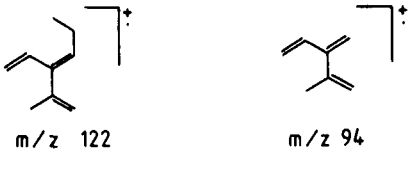

2. Hopane derivatives identification

As part of our research, we isolated a compound whose H^1NMR spectrum suggested a structure partly similar to that of lupeol, and partly similar to that of 30-nor-hopan-3,22-dione (7). We postulated the structure of the 30-nor-hopan-3β- ol-22-one (4), but no references of this product were available. A closer study of the MS spectra of compound and of 7 showed the following :

- Both the product and 7 led to a signal at m/z 191 corresponding to cycles D and E of the molecules. Collision spectra (daughter ions) of m/z 191 confirmed this hypothesis.
- The study of daughter ions of both M^+, showed that our product led to ion m/z 207, by a mechanism similar to the one for the m/z 205 of the 30-nor-hopan-3,22-dione. The two unit difference could be explained by the presence of an -OH group in our structure instead of the keto group of 30-nor-hopan-3,22-dione.

In the same way we identified a product as 30-nor-hopan-6-acetoxa-3β-ol-22-one (5) through different experiments of tandem MS. In this case, we were able to show the structural difference between the two fragments of m/z 205 obtained from our product and from 30-nor-hopan-3,22-dione. Both fragments corresponded to cycles A and B of the products.

3. Confirmation of the fragmentation mechanism by MS-MS

In the MS spectrum of 4 , we noted an impurity at m/z 440. MS-MS analysis of it's daughter ions showed some spectral's similarities with the spectrum of olean-12-ene-3,11-dione(6). Further MS-MS analysis demonstrated that it was olean-12-ene-3β-ol-11-one.(3). The basic skeleton was established as oleane, and not ursane by comparison with the collision spectra of α and β amyrines. The mechanism of fragmentation was confirmed by the synthesis of a product leading to the same ion structure as the fragment m/z 135 proposed for our product. MS-MS of both ions confirmed the similitude of the fragments. *

CONCLUSION

Using low energy collisionally activated MS spectra, we established the structures of five oleane ursane and hopane derivatives.

Fragmentation mechanism of the differents basic structures leading to key characteristic ions, were established.

This method allows the identification of trace compounds without prior chromatographic separation.

*

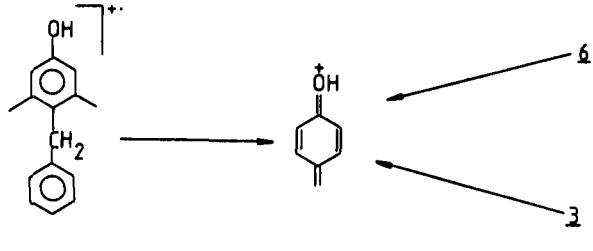

Synthetised product m/z 135

Presented at the 35th ASMS Conference on Mass Spectrometry and Allied Topics
May 24-29, 1987, Denver, CO

PLASMA DESORPTION MASS SPECTROMETRY OF HIGH MASS AND LABILE COMPOUNDS.

A.G. Craig[1] ,B.U.R. Sundqvist[2] and I. Kamensky[3]

[1] Department of Immunology, University of Uppsala, Box 582, S-751 23 Uppsala, Sweden.
[2] Tandem Accelerator Laboratory, University of Uppsala.
[3] Bio-Ion Nordic AB, Box 15045, S-750 15, Uppsala, Sweden.

Plasma desorption mass spectrometry (PDMS) utilises high energy (100 MeV) primary particles to bombard the sample. Using this technique it has been possible to analyse biological samples which intuitively would be expected to decompose. Protein and large peptide samples are adsorbed to a nitrocellulose film[1] which assists in the desorption of these intact molecule ions.

Recent advances in PDMS sample preparation techniques have allowed measurement of high mass compounds upto 35,000 dalton[2] . Using these techniques it has been possible to measure recombinant DNA synthesis products such as Interferon-B and Interleukin-2 (Figures 1 and 2).

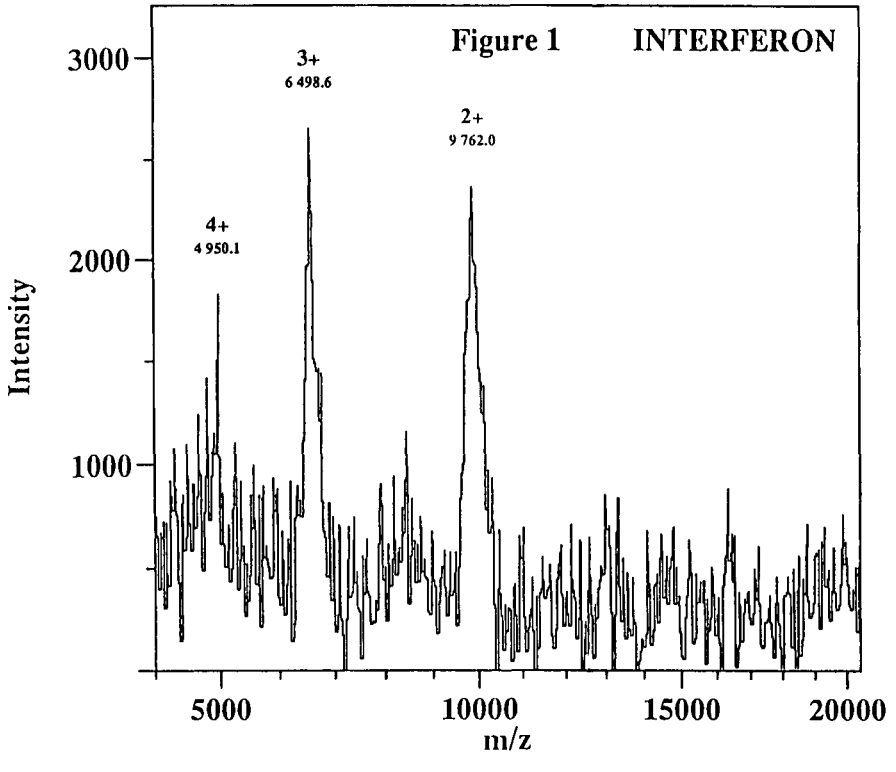

The mass measured for Interferon-B (19510 u) verified the expected sequence (19484 u) within error limits. In contrast, the mass measurement of Interleukin-2 (15570 u) is considerably above the expected theoretical mass (15418 u). The mass spectrometric measurement is however consistent with the expected mass of recombinant Interleukin-2

(when expressed in E.coli) containing an additional N-ter methionine (15549 u).

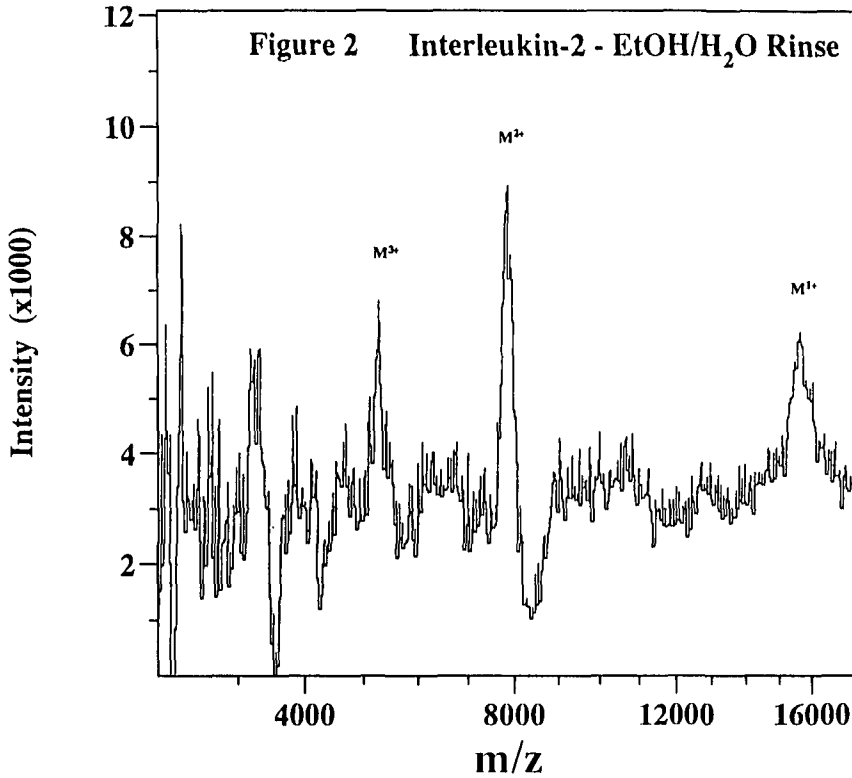

A nitrocellulose film can also be used as a support matrix for the measurement of intact and cationised molecule ions of labile[3] organic dyes. The spectrum of Cibakron blue measured by depositing an aqueous solution and then evaporating contains prominent peaks in the molecular ion region. These peaks are assigned as (M-Na+2H), (M+H) and (M+Na).

Previously a limitation in the mass determination of medium size peptides has been the inability to resolve the protonated and sodium cationised species. Spectra measured using an extended flight path plasma desorption mass spectrometer show the increased resolution is able to distinguish between components present in the antibiotic peptide nisin[4] . The mass determination of insulin-like growth factor exemplifies how the extended flight path instrument also enables significant improvement in mass accuracy.

1 G. Jonsson et al, Anal. Chem. 58, (1986) 1084.
2 A. Craig et. al. presented at 35th ASMS Denver 1987 (TPB45).
3(a) J.M.E. Quirk in Comprehensive Heterocyclic Chemistry, 3, (1984) 465
Edt. A.J. Boulton and A. McKillop, Pergamon Press, Oxford.
3(b) J.A. Ross and B.G. Tweedy, Org. Mass Spectrom., 3, (1970) 219.
4 P. Roepstorff et. al. (manuscript in preparation).

Presented at the 35th ASMS Conference on Mass Spectrometry and Allied Topics
May 24-29, 1987, Denver, CO

FAB MS DETECTION OF A PEPTIDE BOND REARRANGEMENT OCCURRING DURING CNBr TREATMENT OF LIPOXYGENASE

Yazdanparast, R.; Steczko, J.; Shibata, D.; Dixon, J.; Axelrod, B.
Department of Biochemistry, Purdue University, West Lafayette, Indiana 47907

The FAB MS analysis of a CNBr fragment of a soybean lipoxygenase isoenzyme (LOX-1) facilitated the characterization of a chemical bond rearrangement using pmol quantities of the sample. It has been observed that the treatment of a polypeptide with CNBr sometimes fails to cause complete cleavage at Met-Thr and Met-Ser bonds. Our data indicates that this failure may be due to a rearrangement process resulting in formation of a homoseryl-threonyl peptide bond or a homoseryl -β-O-threonyl ester bond.

The mass spectrometry analysis was achieved using a Kratos MS-50 mass spectrometer with xenon atom bombardment (8kv, 0.1mA) and 8kv accelerating voltage. The resolution of the mass spectrometer was set at approximately 1000. Mass assignments were made with reference to CsCl solution and the M.W. determinations were done on the unresolved centroid ion clusters with an accuracy of $\pm$ 1 mu. A mixture of DTT and DTE (3 to 1 ratio) has been used as the matrix throughout this investigation.

The mass spectrometric analysis of the tryptic digestion of a purified CNBr fragment (peak I corresponds to residues 104 to 350) revealed a number of ions which were consistent with the deduced primary structure of LOX-1 and the amino acid composition data (1). However, an ion cluster was observed at M/z 2787 which was shifted by 22 and/or 38 mu to higher masses after addition of sodium and/or potassium ion solutions, respectively. A computer search of the complete amino acid sequence of LOX-1 failed to locate any region compatible with this ion.

Incomplete cleavage of the peptide bond between Met341 and Thr342 (Fig. 1) inferred from amino acid composition and Edman degradation data suggested the assignment of the ion at M/z 2787 to a fragment of peak I corresponding to amino acid residues 327 to 350 after undergoing a peptide bond rearrangement. The details of this chemical process are shown in scheme 1. According to this scheme, the peptide bond in a Met-Thr arrangement might either undergo a normal cleavage as shown in pathway A resulting in the formation of III and IV or a rearrangement reaction will occur as indicated in pathway B. This rearrangement process could result from nucleophilic attack of the hydroxyl group of the adjacent Thr 342 on the oxazolinium ring of intermediate II. This process will result in the formation of intermediate V. Hydrolysis of V could then result in the formation of an amide bond (VI) and/or ester (VII). In either case, both compound VI and VII will have the same M.W. Based on this hypothesis, we expected to observe an ion cluster at M/z 2787 corresponding to amino acid residues 327 to 350, taking into account the above mentioned peptide bond rearrangement and the hydrolysis of the β-lactone ring of the C-terminal homoserine residue resulting from the cleavage of the peptide bond between Met 350 and Ile 351 by CNBr. These modifications will collectively account for a 12 mu shift in M.W. of the peptide (residues 327 to 350) from M/z 2799 to 2787.

These results indicate the value of FAB mass spectrometry in accounting for unusual chemical rearrangements that may occur during CNBr treatment of polypeptides prior to sequencing studies.

Presented at the 35th ASMS Conference on Mass Spectrometry and Allied Topics
May 24-29, 1987, Denver, CO

Phe-Pro-Gln-Pro-His-Val-Val-Gln-Val-Ser-Gln-Ser-Ala-Trp-Met-Thr-Asp-Glu-Glu-Phe-Ala-Arg-Glu-Met
330 340 350

Figure 1. Partial Amino Acid sequence of Soybean Lipoxygenase-1 Showing Residues 327 to 350.

SCHEME I

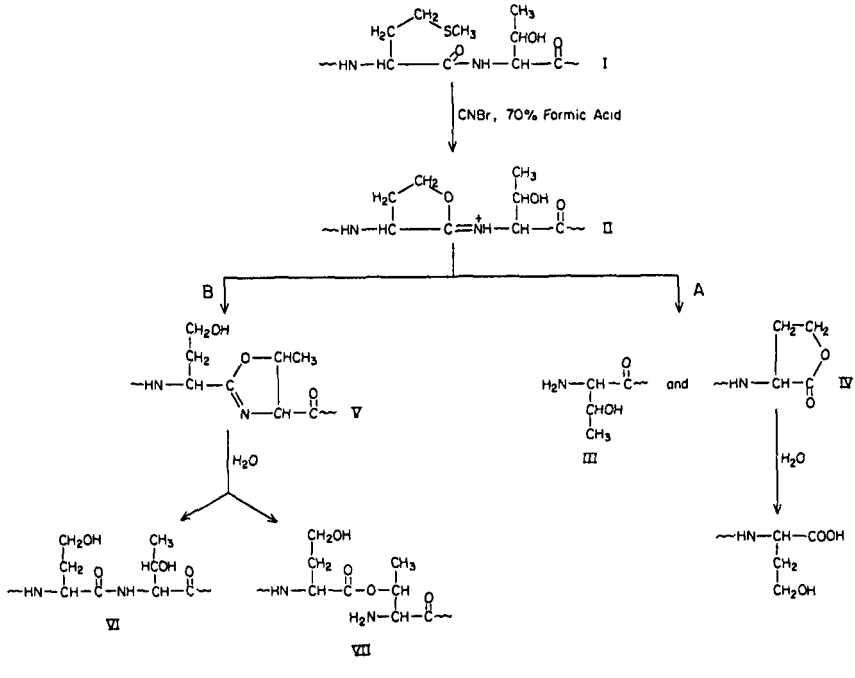

Reference 1. Shibata, D., Steczko, J., Dixon, J.E., Hermodson, M.A., Yazdanparast, R. and Axelrod, B.; J. Biol. Chem., in press

Presented at the 35th ASMS Conference on Mass Spectrometry and Allied Topics
May 24-29, 1987, Denver, CO

A Study of the Halide Ion Addition to a Selected Group of Lewis Acids Using a Variable Temperature Selected-Ion Flow Tube

Charles R. Herd and Lucia M. Babcock
Louisiana State University
Baton Rouge, LA. 70803

The basic ion-molecule association mechanism is given below:

$$BX_3 + X^- \underset{k_d}{\overset{k_a}{\rightleftharpoons}} (BX_4^-)^*$$

$$(BX_4^-)^* \xrightarrow{k_s(M)} BF_4^- \qquad (BX_4^-)^* \xrightarrow{k_r} BF_4^- + h\nu$$

$$k_{obs} = \frac{k_a k_s(M) + k_a k_r}{k_d + k_s(M) + k_r}$$

where k_a is the rate coefficient for association, k_d is the rate coefficient for unimolecular decay, k_s is the rate coefficient for collisional stabilization, k_r is the rate coefficient for radiative stabilization, and k_{obs} is the apparent overall bimolecular rate coefficient. This mechanism assumes that an excited complex is first formed by an amount of energy released from formation of the bond and then stabilized by collision with an inert third body or by emmission of a photon, i.e. radiative stabilization. A previous study[1] along with recent evidence[2] has shown the halide ion addition of F^- to BF_3 to possess both collisional and radiative stabilization pathways even at the "high" pressures of a flowing afterglow (FA) or selected ion flow tube (SIFT), 0.2 to 2.0 torr. Other halide ion-boron trihalide systems $BF_3 + Cl^-$ and $BCl_3 + Cl^-$ studied previously[1] were shown to behave similarly to the $BF_3 + F^-$ system. We have chosen to investigate the temperature dependence (TD) of the above systems as well as the systems of $BF_3 + Br^-$, $BCl_3 + Br^-$, $SiF_4 + F^-$, Cl^-, and Br^-, and $SF_4 + F^-$, Cl^-, and Br^-, with the following goals in mind:

(1) to study the TD of these systems since ion-molecule association reactions often display an inverse dependence upon temperature (opposite that of most neutral-neutral reactions) thus, this area is one of much theoretical and experimental investigation;

(2) to study different halide ion-Lewis acid systems to evaluate the properties of a system, such as bond strength and number of internal degrees of freedom which must be present for radiative stabilization to occur;

(3) lastly, to obtain information about the individual rate coefficients characterizing the basic ion-molecule mechanism to learn more about the type of radiative transition occurring.

Each system was studied using a variable temperature SIFT over the pressure range 0.2 to 0.9 torr and over the temperature range 220 to 410 K, typically at 50 K intervals. Naturally the ability to study each system over the entire pressure and temperature range depended upon its particular characteristics. Each system displayed a positive dependence upon the number density of the third-body (M), and a negative dependence upon temperature. A typical example of this behavior is shown below for the $BF_3 + F^-$ system. The symbols are actual experimental data points while the lines are values of k_{obs} at various (M) generated using our method of data analysis described previously.[2]

The magnitude of the temperature dependence, n, of all systems was

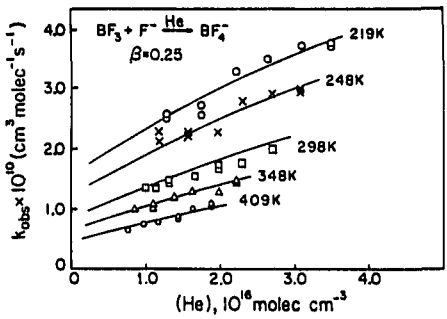

evaluated using experimental data and theory. The value of k_d at each temperature for each system was determined using the method of data analysis mentioned above. Using the relation, $k_d = AT^n$ (from RRK theory) and constructing log/log plots, the value of n can be determined from the slope. The value determined theoretically was done using the low pressure thermal model modified to include vibrational contributions of the reactants.[3] The agreement between experiment and theory is excellent as the value of n increases from system to system as the number of lower lying vibrations increases, in accord with theory. This is shown below.

SYSTEM	$n_{exp.}$	n_{theory}
$BF_3 + X^-$	2.1 (Avg.)	1.79 to 2.77
$BCl_3 + X^-$	2.4 (Avg).	2.33 to 3.87
$SiF_4 + X^-$	3.3 (Avg).	2.25 to 4.69
$SF_4 + F^-$	3.4	2.05 to 4.93

The boron systems with the exception of $BF_3 + Br^-$ all possess radiative stabilization pathways. The magnitude of the radiative rate coefficient k_r, indicates the possibility of an electronic transition, or for a small collisional efficiency factor of 0.01, an infrared transition. The silicon tetrafluoride or sulfur tetrafluoride systems appear not to radiate at the experimental conditions of this study.

In conclusion, in addressing the first goal, the study of the TD, it was shown that there was excellent agreement between experiment and theory indicating that low lying vibrational modes are important in determining the magnitude of the TD, n, for these systems. In addressing the second goal, evaluation of the properties necessary for radiative stabilization, we conclude that a large well depth and possible proper placement of an excited electronic state are at least two properties needed for radiative stabilization to occurr. Finally in addressing the last goal, determination of the rate coefficients characterizing the basic ion-molecule association mechanism, we were able to successfully evaluate k_d and k_r by our method of data analysis, and conclude that both k_d and k_r for the boron trihalide systems can compete with collisional stabilization even at the "high" pressures of a FA or SIFT.

1. L. M. Babcock and G. E. Streit, J. Phys. Chem., 88, 5025 (1984).
2. C. R. Herd and L. M. BAbcock, J. Phys. Chem., 91, 2372 (1987).
3. A. A. Viggiano, J. Chem. Phys., 84, 244 (1986).

Presented at the 35th ASMS Conference on Mass Spectrometry and Allied Topics
May 24-29, 1987, Denver, CO

DIFFERENTIAL CROSS-SECTIONS FOR FINE-STRUCTURE TRANSITIONS IN $Kr^+[Kr,Kr]Kr^+$ AND $Ar^+[Ar,Ar]Ar^+$

S. Howard, A. Rockwood, W. Trafton, B. Friedrich, S. Anderson, and J. Futrell
Department of Chemistry
University of Delaware
Newark, DE 19716

The cross-beam method was used to investigate the charge-transfer reactions of Ar, Kr, and Xe. A weak plasma source was used to generate a nearly pure $^2P_{3/2}$ state ion beam. The charge-exchange reaction of state-selected krypton atoms proceeding via the homonuclear Kr_2^+ diatomic intermediate is an especially favorable case in that the spacing between the two levels of the ground electronic state of Kr^+ are sufficiently large that the complete resolution of the fine-structure transition in our apparatus is straightforward. Calculations by Johnson[1,2] have shown that the ratio of the cross-section from Reaction 1 to that of Reaction 2 has an onset, a maximum, and then reduces at higher energy.

$$Kr^+(^2P_{3/2}) + Kr(^1S_0) \text{ -- } Kr(^1S_0) + Kr^+(^2P_{3/2}) \qquad (1)$$

and

$$Kr^+(^2P_{3/2}) + Kr(^1S_0) \text{ -- } Kr(^1S_0) + Kr^+(^2P_{1/2}). \qquad (2)$$

His thoeretical discussion presents a detailed discussion for these reactions as well as the equivalent reactions for argon and xenon. Two thoeretical curves are shown representing the calculations with and without the inclusion of rotational coupling. As shown for argon, the inclusion of rotational coupling increases the ratio by approximately a factor of 2. Figure 1 displays such results for argon and for krypton. Also shown is a series of points deduced from the experimental study of Ng et al.[3] which appear to show that the onset energy and the shape of the curve are shifted to higher energy than indicated by theory in the case of argon.

Since the problem as formulated by Johnson is identical for all rare gases, the curves scale in a straightforward way with the magnitude of the spin-orbit splitting. Curves shown in Figure 1 indicate that the onset energy for krypton should have an observable threshold of about 700 eV collision energy and that the maximum should occur in the neighborhood of 10,000 eV. The curves labelled CT and D label those reactions in which this fine-structure transition is and is not accompanied by charge transfer respectively. The indicated energy is approximately 3 orders of magnitude higher than the collision energy investigated

in our laboratory. Clearly the mechanism for the fine-structure transition is not that described by Johnson. We speculate that Johnson's principal transition moment involves relatively long range interaction and that the subtleties of the shapes of the six spin-orbit state potential curves may be responsible for a charge-transfer reaction occurring at significantly lower energy.

The angular scattering associated with our observations suggest that the crossing may occur in the repulsive region of the II(½)u and the I(½)u curves of the Kr system. This crossing would occur at about 6 eV collision energy.

No evidence for such a low energy process was found by Ng et al.[3], however, angular capability enhances the probability of detection. We have detected such cross-sections for Ar at energies as low as 2 eV. Our higher energy data for Ar follow the theoretical curves.

REFERENCES:

1. Johnson, R., J. Phys. Soc. Jpn., 32, 1612 (1972).

2. Johnson, R., J. Phys. B, 3, 539 (1970).

3. Liao, C.-L., Liao, C.-X, and Ng, C., J. Chem. Phys., 82, 5489 (1985).

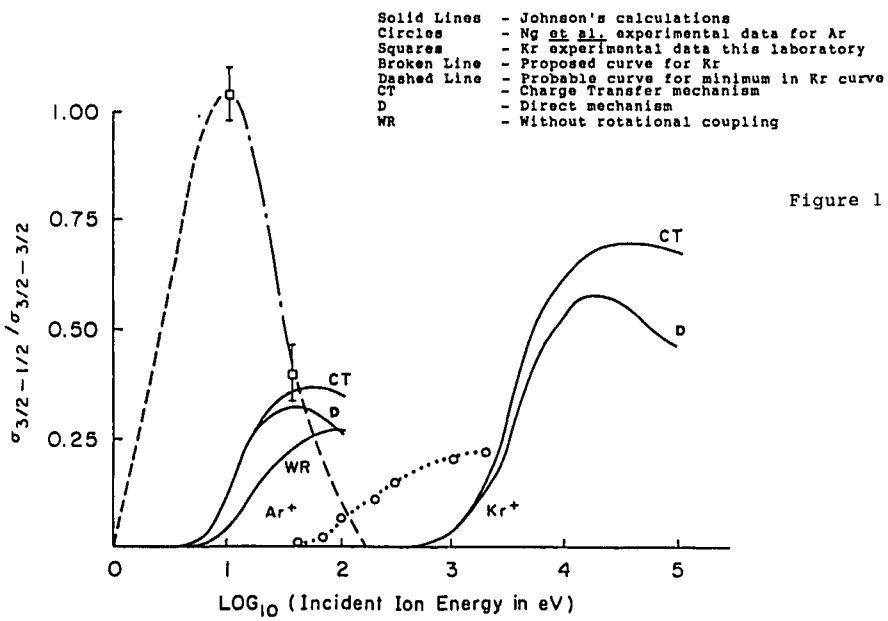

Figure 1

Presented at the 35th ASMS Conference on Mass Spectrometry and Allied Topics
May 24-29, 1987, Denver, CO

ABSOLUTE CROSS-SECTION MEASUREMENTS IN QQQ INSTRUMENTS: $Ar^+(Ar,Ar)Ar^+$ for Ar TARGETS.

Richard I. Martinez
Center for Chemical Physics
National Bureau of Standards
Gaithersburg, MD 20899

and

Seksan Dheandhanoo
Department of Chemistry
Georgetown University
Washington, DC 20057

ABSTRACT

The symmetric (resonant) charge transfer cross sections $\sigma(E)$ for $Ar^+(Ar,Ar)Ar^+$ were measured in our triple quadrupole (QQQ) tandem mass spectrometer. Our $\sigma(E)$, for P=0.04-0.43 mtorr and E= 5-60 eV (LAB) [the range of collision energies used for collisionally activated dissociation (CAD)], agree to within 10% with the Rapp-Francis theory (impact parameter method in the two-state approximation), as corrected by Dewangan.[1] We measured identical $\sigma(E)$ from both the rate of reactant decay and the rate of product formation; i.e., our instrument is kinetically well behaved.[1,2] The measurement of these $\sigma(E)$ in other QQQ instruments can be used to validate whether or not a QQQ instrument has been properly designed to be kinetically well behaved. This is essential if generic, instrument-independent CAD spectral databases are to be developed on the basis of the absolute cross-sections for the CAD of known ionic substructures.[1] That is, since tandem mass spectrometry (MS/MS) exploits the ion fragmentation patterns characteristic of ionic substructures, the characteristic profiles ["breakdown curves"] of ion abundance vs. target thickness (or collision energy) correspond uniquely to the sequence:

$$(\text{parent})_i \xrightarrow{\sigma_{ij}} (\text{daughter})_j \xrightarrow{\sigma_{jk}} (\text{granddaughter})_k, \text{ etc.}$$

Hence, computer simulation of experimentally observed breakdown curves enables the structure of an unknown species to be assigned on the basis of the absolute cross-sections σ_{ij}, σ_{jk}, etc. for CAD of known ionic substructures i, j, k, etc. Thus, if the calculated and experimental breakdown curves agree, the structure would be characterized.

INTRODUCTION

The generation and interchange of reference libraries of CID spectra necessitates standardized, instrument-INDEPENDENT operating conditions for the various types of QQQ instruments. A recent international round robin evaluation of the reproducibility of standard operating conditions indicated that CID gas target thickness was not a well-controlled parameter.[3]

To provide a generic standard for in-situ calibration of Ar target thickness in Type A [3] (molecular beam target) and Type B [3] (collision chamber) QQQ instruments, we measured the $\sigma(E)$ for $Ar^+(Ar,Ar)Ar^+$ by using the kinetic method we had previously validated in our kinetically well behaved instrument.[2]

EXPERIMENTAL

Measurements were made in a specially designed QQQ instrument which can be configured as both a Type A or Type B MS/MS. The Type B configuration was used for the measurements reported here. Mass filters Q1 and Q3 are completely nude (no housing); a collision chamber enclosure surrounds Q2.

Ar^+ ions were generated by 70 eV electron impact, and the Ar^+ projectiles were selected by Q1. The energy spread of the projectiles entering Q2 was determined to be $\lesssim$1.8 eV for 90% of the ions [$\lesssim$3 eV for 99% of the ions] when measured by using the Q2 pole bias (rod offset) to generate a stopping potential curve. $E_{90\%}$ is the Q2 potential required to stop 90% of the ions. The collision energy E_{coll} was selected by setting the Q2 pole bias = $E_{90\%} - E_{coll}$.

The $\sigma(E)$ shown as (•) in Fig 2 for E_{coll}=5-60 eV [⇔ ion velocities v=0.5-1.8 (x10^6) cm s^{-1}] were derived from the rate of decay of the projectile when measured as a function of the target pressure P_{Ar} [see Fig 1]. For E_{coll}= 10 and 40 eV, the $\sigma(E)$ determined from the rate of production of $^{40}Ar^+$ in $^{36}Ar^+(^{40}Ar,^{36}Ar)^{40}Ar^+$ are shown in Fig. 2 as (o) and were the same as the $\sigma(E)$ (• in Fig. 2) determined from the rate of decay of the $^{40}Ar^+$ projectile in $Ar^+(Ar,Ar)Ar^+$.

Presented at the 35th ASMS Conference on Mass Spectrometry and Allied Topics
May 24-29, 1987, Denver, CO

RESULTS

Fig. 1 - Projectile decay experiments. Plots of Ln Y vs. P_{Ar} at fixed values of E_{coll}.
$Y = [^{40}Ar^+]_0/[^{40}Ar^+]$ and
$\ln Y = k_E L_{eff}(m/2E_{coll})^{1/2}\,[Ar]$
$= \sigma L_{eff}\,[Ar]$
$\equiv \beta P_{Ar}$
L_{eff} = actual path length traversed by ion within Q2 collision chamber (corrected for rf effects).
m = mass of $^{40}Ar^+$ projectile.

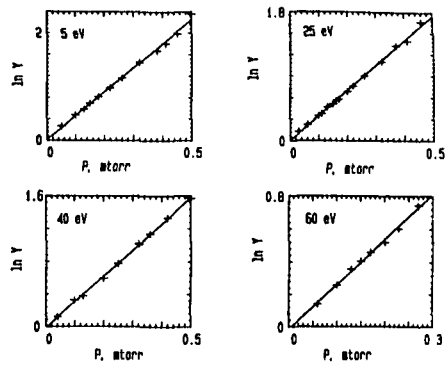

Fig. 2 - Plot of $\sigma^{1/2}$ vs. v.
Comparison of our results with other workers and with the Rapp-Francis theory.
● - projectile decay experiments
o - product growth experiments

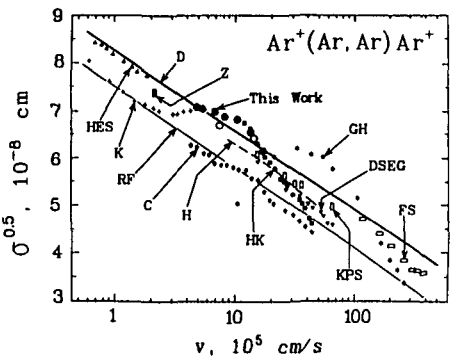

DISCUSSION

Our $\sigma(E)$ measurements (see Fig. 2) agree to within ±10% with other workers and with theory, and can be used for in-situ calibration of Ar target thickness in other kinetically well-behaved instruments. Hence, absolute cross-sections for the CAD of known ionic substructures can be measured in such instruments.

REFERENCES

1. R.I. Martinez and S. Dheandhanoo, J. Res. Natl. Bur. Stand. (US) 92, 229 (1987), and references therein.
2. R.I. Martinez and S. Dheandhanoo, Int. J. Mass Spectrom. Ion Processes 74, 241 (1986).
3. P.H. Dawson and W.-F. Sun, Int. J. Mass Spectrom. Ion Processes 55, 155 (1983/1984).

Presented at the 35th ASMS Conference on Mass Spectrometry and Allied Topics
May 24-29, 1987, Denver, CO

REACTIONS OF GROUND STATE AND EXCITED STATE ATOMIC METAL IONS WITH HALOGEN MOLECULES. A TANDEM ICR STUDY.

F. Strobel and D. P. Ridge
Chemistry Dept. and Center for Catalytic Science
and Technology, University of Delaware, Newark Delaware 19716

In order to study the effects of the electronic state of the metal on simple, exothermic, oxidative reactions, we have built a tandem ICR. This allows us to use higher pressures in the source which allows us to obtain ground state metal ions by thermal surface ionization.

The principle that our tandem ICR is based on is that an ion in perpendicular electric and magnetic fields will move along the equipotential lines. In the present experiment, the equipotential lines go through a slit between two differentially pumped regions. Ionization occurs in the first region and reactions and mass analysis occurs in the second.

Our interest is in the use of thermal surface ionization to produce ground state atomic metal ions. Thermal surface ionization is accomplished by heating a wire in the presence of the vapor of a metal compound. Electron impact on the same metal compounds to give atomic metal ions is carried out in the same apparatus under identical conditions.

Experiments were done in drift mode with a balanced bridge detection and signal averaging on a Nicolet 1080 computer.

Thermal surface ionization produces ground state Cr^+ from $Cr(CO)_6$. Electron impact on Cr(CO)6 produces Cr^+ in both the ground state and an excited state.[1] By comparison of the reactions of Cr+ formed by the two methods, it is therefore possible to study the effects of the electronic excitation on the chemistry of Cr^+.

The reactant chosen was ICl. It is a strong oxidant that should react exothermically with most metal ions. It is a diatomic, simplifying dynamical interpretation of the results. It can give two distinct products so that the effect of excited states can be detected in an easily measured branching ratio.

Cr^+ was formed by electron impact and thermal surface ionization. The Cr^+ reacts with ICl to form ICr^+ and $CrCl^+$. Electron impact gives 74.3±3.9% excited Cr^{+*}[1]. An analysis of plots(figures 1 and 2) of the intensity of the products over the initial Cr^+ intensity as a function of nominal pressure of the ICl allows us to calculate ratios of rate constants. Using the mechanism shown;

$$Cr^+ + ICl \xrightarrow{k_1} CrI^+ + Cl$$
$$\xrightarrow{k_2} CrCl^+ + I$$
$$Cr+ + ICl \xrightarrow{k_1^*} CrI^+ + Cl$$
$$\xrightarrow{k_2^*} CrCl^+ + I$$

We calculate k_1/k_2 =.085±.045, k_1^*/k_2^* =.61±.13 and $(k_1^*+k_2^*)/(k_1+k_2)$=1.30±.20

Mn^+ will also react with ICl to produce $MnCl^+$ and MnI^+. The two types of Mn^+ studied were formed by electron impact on $Mn_2(CO)_{10}$ and thermal surface ionization of $Mn(CH_3(C_5H4)(CO)_3$. The percentage of MnI^+ formed in the reactions were 38.2±1.6% for electron impact and 19.8±3.0% for thermal surface ionization. The difference in the branching ratios clearly shows the effects of excited Mn^+ formed by electron impact. There has been previous evidence for an excited Mn^+ ion formed by electron impact on $Mn_2(CO)_{10}$.[2] Ground and excited states form both products. This suggests the branching ratios are determined by dynamical rather then thermochemical considerations.

In conclusion, Electron impact on $Cr(CO)_6$ and $Mn_2(CO)_10$ produce some excited state metal ions. A difference in the reactivity of the excited metal ions is evident in the branching ratios for their reactions with ICl, which

are determined by dynamical considerations as well as thermochemical considerations.

1.William D. Reents, F. Strobel, R.B. Freas,III, John Wronka and D. P. Ridge, The Journal of Physical Chemistry, 1985, 89,pp. 5666-5670.
2.J. L. Elkind and P. B. Armentrout, Journal of Chemical Physics, 1986, 84, pp.4862-4871.

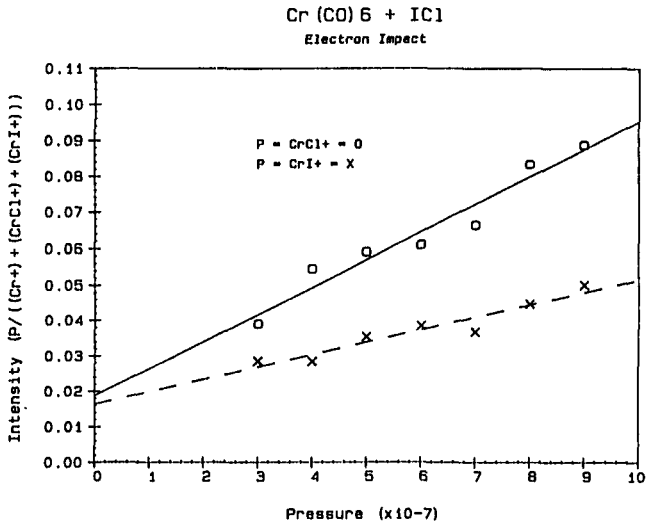

Figure 1

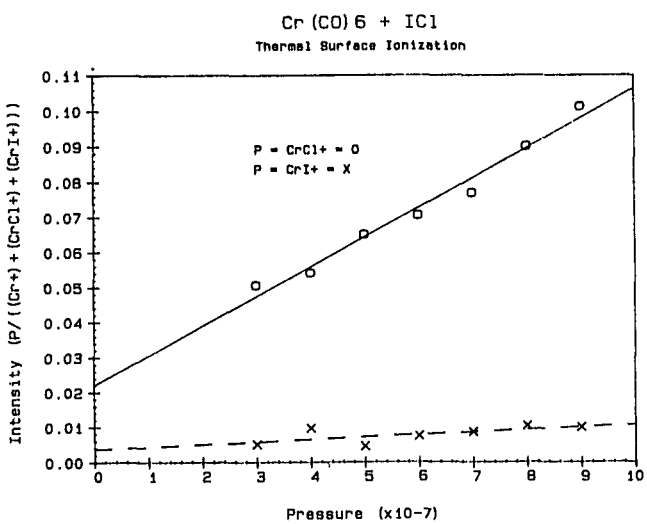

Figure 2

Presented at the 35th ASMS Conference on Mass Spectrometry and Allied Topics
May 24-29, 1987, Denver, CO

Ion Molecule Reactions of Gold Ions with Aliphatic and Aromatic Hydrocarbons

A. Kasem Chowdhury, Department of Chemistry
University of California, Riverside, CA 92521

Introduction - In recent years there has been a growing interest in the study of gas phase reactions of transition metal ions with hydrocarbons. Fundamental interest in such work stems from the possibility of studying ion-molecule interactions in the absence of complicating solvent effects. Here, the gas phase reactions of gold cation with aliphatic and aromatic hydrocarbons and alkyl halides are examined. In addition, reactions of the relatively inert anion, Au^-, are reported.

Experimental - All experiments were carried out using a Nicolet FTMS-1000 mass spectrometer. The instrument is equipped with a 1-7/8 x 2.54 cm cubic trapping cell and a 3.0T superconducting solenoid magnet. Positive and negative metal ions were generated by focusing the beam of Tachisto 215G pulsed TEA CO_2 laser onto a probe tip coated with either metallic films or salts of interest.

Results and Discussion - Two types of reaction products, hydride abstraction and dehydrogenation, predominate in the ion-molecule reactions of Au^+ with both linear and cyclic alkanes. Reactions of Au^+ ions with higher alkanes occurs almost exclusively by hydride transfer and hydride transfer induced fragmentation. For example, Au^+ reacts with n-hexane according to reaction (1).

$$Au^+ + n\text{-}C_6H_{14} \xrightarrow{0.99} [C_6H_{13}^+]^* \xrightarrow{-C_3H_6} C_3H_7^+$$
$$[C_6H_{13}^+]^* \xrightarrow{M} C_6H_{13}^+ \quad M = C_6H_{14} \text{ and Ar}$$
$$[C_6H_{13}^+]^* \xrightarrow{-C_2H_4} C_4H_9^+ \qquad (1)$$
$$Au^+ + n\text{-}C_6H_{14} \xrightarrow{0.01} AuC_6H_{12}^+ + H_2$$

No fragmentation products ($C_3H_7^+$ and $C_4H_{19}^+$) are observed when the pressure of the system increased from 1×10^{-7} torr to 2×10^{-6} torr with argon. This significant pressure quenching might indicate the presence of internally excited $C_6H_{13}^+$ ions which fragments in competition with collisional stabilization. Collision induced dissociation of stabilized hexyl cation ($C_6H_{13}^+$) yielded the same two products $C_3H_7^+$ (major) and $C_4H_9^+$ (minor) observed in reaction (1).

With aromatic hydrocarbons, Au^+ undergoes both charge transfer and complexation. One additional product ion corresponding to hydride transfer was observed with alkyl benzene.

Au^+ reacts with CH_3Cl and CH_3Br according to reaction (2).

$$Au^+ + CH_3X \quad (X = Cl,Br) \xrightarrow{major} AuCH_2^+ + HCl \qquad (2)$$
$$Au^+ + CH_3X \quad (X = Cl,Br) \xrightarrow{minor} Au(CH_3X)^+$$

With CH_3I, Au^+ reaction yields predominately AuI^+, $AuCH_3^+$, and $Au(CH_3I)^+$ along with lesser amounts of $AuCH_2^+$ and H_2CI^+. Assuming that only exothermic reactions occur, CH_3Br and CH_3I reactions with Au^+ give lower limits for the bond dissociation energies, $D(Au^+-CH_2) > 92.4$ kcal/mol and ≥ 95 kcal/mol, respectively.

Ion-molecule reactions of Au^- - Gold anions are unreactive with CH_3Cl, but undergo slow S_N2 displacement reactions with CH_3Br and CH_3I forming Br^- and I^- anions, respectively suggesting Au^- is kinetically a poor nucleophile. The lower and upper limits of bond dissociation energies of gold methide $D°(Au-CH_3) > 39.1$ kcal/mol and > 45.8 kcal/ mol, and < 53.1 kcal/mol, are estimated from CH_3I, CH_3Br, and CH_3Cl reactions respectively. Au^- reacts slowly with $CHCl_3$ and very rapidly with CCl_4 to yield $AuCl_2^-$ ion.

Presented at the 35th ASMS Conference on Mass Spectrometry and Allied Topics
May 24-29, 1987, Denver, CO

ION/MOLECULE REACTIONS OF SILICON CATION CLUSTERS, Si_n^+, n=1 TO 6

William R. Creasy[a], Anthony O'Keefe[b], and J. R. McDonald
Chemistry Division, Naval Research Laboratory
Washington, D. C. 20375

The reactivity of gas phase silicon cation clusters, Si_n^+, for n=1 to 6, is studied with the small molecules H_2O, CH_3OH, NH_3, C_2H_2, O_2, and N_2O. Rate constants and branching ratios are measured for each cluster ion. The results provide information about the relative reactivity as a function of cluster size, and show the preferred reaction mechanisms. The results are interpreted in terms of the cluster structures and energetics, and are also compared to silicon surface reactions. Similar studies on other reagents have published by Reents, Mandich, and Bondybey.[1]

The measurements are done using Fourier Transform Mass Spectrometry (Nicolet FTMS/1000). The ions are produced by laser vaporization of single crystal silicon using the frequency-doubled output of a Nd:YAG laser (532 nm, 5-10 mJ/pulse), which is focussed to a 0.5 mm spot size. The silicon sample is located flush with the bottom plate of a cubic ion cyclotron resonance cell. The ions are trapped by a 1.0 T magnetic field and 2.0 V trapping potential. One cluster ion is isolated by resonant frequency ejection of the other ions, and it is allowed to react for a variable delay time of 0.1 to 5 sec, at pressures of 1 to 5 X 10^{-7} torr. Rate constants and branching ratios to the observed products are obtained.

Figure 1 shows the relative rates of the cluster ion reactions as a function of cluster size, for the neutral molecules shown. The rate constants are normalized to the maximum rate constant for each reagent, and plotted on a log scale. The rate constants decrease sharply between n=3 and n=4. For n>3, reactions are not observed for N_2O, H_2O, C_2H_2, and NH_3, and the rate constant for CH_3OH decreases by a factor of twenty. This decrease shows that the larger ions have very different reactivity from the small ions. The small species may be more reactive due to the presence of terminal Si atoms on a chain. Theoretical calculations predict that neutral Si_3 has a ring structure, but has a very low energy for ring opening. By analogy, Si_3^+ should readily form a linear species during reaction, and therefore have reactivity similar to that of Si^+ and Si_2^+. For n>3, the ions are calculated to form strongly-bound ring structures, which lack the reactive terminal sites.

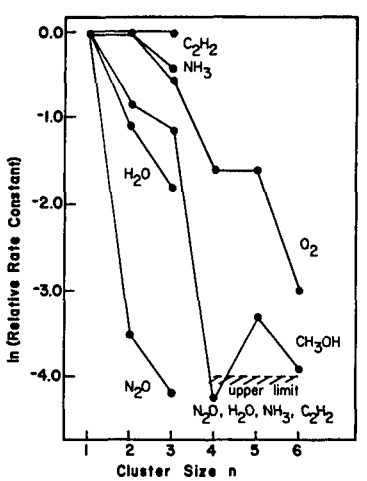

Figure 1

The products observed for the reactions with CH_3OH, H_2O, C_2H_2, and NH_3 suggest that the reaction mechanism begins with insertion of the ion into an OH, NH, or CH bond. The rapid rates for n=1 to 3 suggest that the bond insertion is very facile. For n>3, the decrease in reactivity may be due to a less favorable insertion step, or to energetically unfavorable fragmentation of the collision complex following the insertion step.

Figure 2 shows the pathway for the reactions of the ions with O_2. For Si_4^+ and larger ions, the reaction involves loss of a unit of Si_2. From energetic considerations, the neutral products are probably two SiO molecules. On the other hand, for n=2 and 3, the reactions form a variety of products, which reflects the greater reactivity of these species. For Si^+, no exothermic channels are available. The observed reactions are exothermic by at least 40 kcal/mol, due to the formation of strong SiO bonds. However, the reaction rates are very small. The largest rate constant, for the loss of Si_2^+, is 4×10^{-11} cm^3/s. The slow rates show that a large barrier is associated with the bond insertion step. This may be attributed to the insertion of the Si_n^+ ions into an O_2 bond being forbidden by orbital symmetry, according to Frontier Orbital Theory, so that the insertion has an energy barrier associated with it. Alternately, the reactions may involve a restricted four-center transition state.

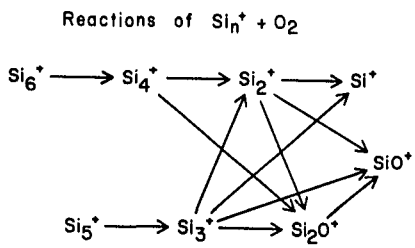

Figure 2

Several comparisons can be made to the surface reactions of silicon. For example, the reaction of Si_6^+ with CH_3OH produces the product ion $Si_6OCH_3^+$. This ion is reminiscent of previous observations of the reaction of CH_3OH with silicon surfaces, in which a methoxy group binds to the surface. Silicon surfaces react with O_2 with relatively slow rates, which is analogous to the cluster ion reactions. However, reactions are not observed for the cluster ions of n>3 with H_2O, NH_3, and C_2H_2, although surface reactions have been observed for these reagents. In general, theoretical calculations indicate that small clusters are very different in structure from surfaces, with more dangling bonds and more surface area. Therefore, species larger than n=6 are necessary to extrapolate to surface chemistry.

REFERENCES

a) NRC/NRL Cooperative Research Associate.

b) Current address: Western Research Corp., San Diego, CA.

1. M. L. Mandich, W. D. Reents, Jr., and V. E. Bondybey, J. Phys. Chem. 1986, 90, 2315; W. D. Reents, Jr., M. L. Mandich, and V. E. Bondybey, Chem. Phys. Lett. 1986, 131, 1; M. L. Mandich, V. E. Bondybey, and W. D. Reents, Jr., J. Chem. Phys. 1987, 86, 4245.

2. K. Raghavachari and V. Logovinsky, Phys. Rev. Lett., 1985, 55, 2353; K. Raghavachari, J. Chem. Phys. 1986, 84, 5672; J. Chem. Phys. 1985, 83, 3520.

Presented at the 35th ASMS Conference on Mass Spectrometry and Allied Topics
May 24-29, 1987, Denver, CO

THE REACTIONS OF TRIALKYLGERMYLIUM (R_3Ge^+)

John A. Stone and Wilhelmus J. Wytenburg

Chemistry Department Queen's University, Kingston, Ontario, Canada, K7L 3N6

Methane chemical ionization of R_4Ge (R = CH_3, C_2H_5, C_3H_7 and C_4H_9) leads to dissociative protonation, the only product being R_3Ge^+

(1) $R_4Ge + CH_5^+ \dashrightarrow R_3Ge^+ + CH_4 + RH$.

R_3Ge^+ is a gas phase Lewis acid which readily and reversibly forms complexes with bases.

(2) $R_3Ge^+ + B \rightleftharpoons R_3GeB^+$

A mass spectrometer fitted with a high pressure source (2-5 torr, 300-600 K) and pulsed electron beam has been used to investigate the thermodynamics of reaction 2 for B = H_2O. The results are shown in Table 1 as are similar data for $(CH_3)_3Si^+$, $(CH_3)_3Sn^+$ and $(CH_3)_3)C^+$.

Table 1

	$-\Delta H_2^\circ$ (kcal mol^{-1})	$-\Delta S_2^\circ$ (kcal mol^{-1})
$(CH_3)_3Ge^+$	28.6 ± 0.5	34.4 ± 0.9
$(C_2H_5)_3Ge^+$	24.9 ± 0.15	31.6 ± 1.0
$(n\text{-}C_3H_7)_3Ge^+$	23.4 ± 1.3	31.8 ± 2.7
$(C_4H_9)_3Ge^+$	20.6 ± 1.2	30.3 ± 2.8
$(CH_3)_3Si$ (1)	30.1 ± 1.9	27.0 ± 3.2
$(CH_3)_3Sn^+$ (2)	25.7 ± 2.0	31.7 ± 3.0
$(CH_3)_3C^+$ (3)	11.7	

The larger the alkyl group R the lower the binding energy of R_3Ge^+ to H_2O. The stability of R_3Ge^+ increases with increasing size of R by a combination of charge-induced dipole interaction and electron delocalization from R into the vacant P_z orbital on Ge. The extra stabilization afforded by H_2O then decreases inversely with the stability of R_3Ge^+. The hydration energy of $(CH_3)_3M^+$ decreases in the order M = Si > Ge > Sn, presumably reflecting the size of M. The very low $-\Delta H_2^\circ$ value for $(CH_3)_3C^+$ shows that much more extensive charge delocalization occurs for M = C.

Presented at the 35th ASMS Conference on Mass Spectrometry and Allied Topics
May 24-29, 1987, Denver, CO

$(CH_3)_3Ge^+$ reacts with $(CH_3)_4Ge$ to form $(CH_3)_7Ge_2^+$. Similar $(CH_3)_7M_2^+$ complexes have been observed for M = Si (1) and Sn (2). No mixed complexes such as for example $(CH_3)_7SiGe^+$ in $CH_4/(CH_3)_4Si/(CH_3)_4Ge$ mixtures are observed, instead CH_3^- transfer occurs (reactions 3 and 4).

		$-\Delta H^\circ$ kcal mol^{-1}
(3) $(CH_3)_3Si^+ + (CH_3)_4Ge$	$(CH_3)_4Si + (CH_3)_3Ge^+$	8.1 ± 0.5
(4) $(CH_3)_3Ge^+ + (CH_3)_4Sn$	$(CH_3)_4Ge + (CH_3)_3Sn^+$	10.2 ± 0.6

No equilibria could be set up in mixtures containing $(CH_3)_4C$ and $(CH_3)_4X$ (X = Si, Ge, Sn). The thermodynamic data for 3 and 4 are in excellent agreement with measured differences in appearance potentials for $(CH_3)_3X^+$ from $(CH_3)X_4$ (4).

References

1. J.A. Stone, A.C.M. Wojtyniak and W.J. Wytenburg. Can. J. Chem. 64, 575 (1986).

2. J.A. Stone and D.E. Splinter. Int. J. Mass. Spec. Ion Proc. 59, 169 (1984).

3. K. Hiraoka and P. Kebarle. J. Am. Chem. Soc. 99, 360 (1977).

4. M.F. Lappert, J.B. Pedley, J. Simpson and T.R. Spalding. J. Organometal Chem. 29, 195 (1971).

Presented at the 35th ASMS Conference on Mass Spectrometry and Allied Topics
May 24-29, 1987, Denver, CO

REACTIVITY OF $Fe(CO)_5$ NEGATIVE IONS WITH ACTIVATED OLEFINS, KETONES, AND ALCOHOLS

Gary H. Weddle, John Wronka, Wilma K. Meckstroth, and Douglas P. Ridge
Department of Chemistry, University of Delaware, Newark, DE 19716

We have investigated the reactivity of radical anions formed from $Fe(CO)_5$ in the gas phase with activated olefins, ketones, and alcohols. The reactivity data show distinctive trends and suggest that radical anions of this kind effectively coordinate with various types of organic molecules and may be useful for facilitating various kinds of organic transformations. Particularly striking selectivity is shown by maleic anhydride. $Fe(CO)_4^-$ is unreactive with all examined compounds except maleic anhydride. In addition, the decarbonylation of maleic anhydride occurs in subsequent reactions.

The dominant ions formed from $Fe(CO)_5$ by low energy electron capture processes are $Fe(CO)_3^-$ and $Fe(CO)_4^-$. The reactions of these ions were followed using ion cyclotron resonance techniques. The reactions most commonly observed with an organic molecule (ligand), L, are shown in eqs. 1 and 2.

$$Fe(CO)_3^- + L \text{ ----> } Fe(CO)_2L^- + CO \quad (1a)$$
$$\text{----> } Fe(CO)L^- + 2CO \quad (1b)$$

$$Fe(CO)_4^- + L \text{ ----> } Fe(CO)_3L^- + CO \quad (2a)$$
$$\text{----> } Fe(CO)_2L^- + 2CO \quad (2b)$$
$$\text{----> } Fe(CO)L^- + 3CO \quad (2c)$$

Table I lists the number of carbonyls displaced by various organic ligands, L, from $Fe(CO)_3^-$ and $Fe(CO)_4^-$. Ligands which react with only $Fe(CO)_3^-$ have a polar unsaturation (ketone) or two double bonds in conjugation (butadiene and α, β-unsaturated ketones). Only maleic anhydride and derivatives react with both $Fe(CO)_3^-$ and $Fe(CO)_4$. Ligands which do not react at all are saturated (alcohols) or have a single nonpolar unsaturation (olefin). Assuming that the number of carbonyls displaced by a ligand reflects the energy of the metal-ligand bond, then the metal-ligand bond energies increase in the order:

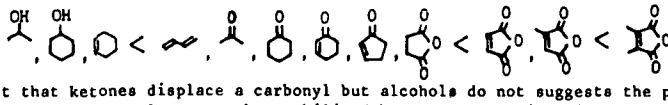

The fact that ketones displace a carbonyl but alcohols do not suggests the possibility that the metal-ketone complexes may be stabilized by a structure in which the metal coordinates through the oxygen atom of the carbonyl. The stability of the metal-butadiene complex may be understood in terms of delocalization of charge through the conjugated system. The unusual reactivity of maleic anhydride and its methyl substituted derivatives may also be the result of delocalization of charge as discussed below.

It is interesting to consider the following observed reaction 3 of maleic anhydride, MAH, with $Fe(CO)(MAH)^-$, which is formed by reaction 1b.

$$Fe(CO)(MAH)^- + MAH \text{ ----> } Fe(MAH)(MAHD)^- + 2CO \quad (3)$$

(MAHD represents a molecule of MAH which has lost one CO.) The reaction involves elimination of a carbonyl from maleic anhydride attached to the metal in the reactant ion. If M^- attacks MAH at the carbon of a CO group, the rearrangements shown in I to III with subsequent CO transfer onto a metal bonding site as in IV would facilitate charge delocalization and elimination of CO in reaction 3.

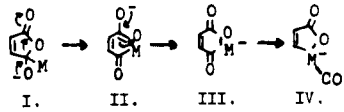

I. II. III. IV.

The observation of the decarbonylation reaction 3 raises the question as to whether the carbonyl displacement reactions observed were simple substitution reactions or whether they also involve decarbonylation of maleic anhydride. For example, in a reaction between $Fe(CO)_4^-$ and MAH, the CO lost could come from either species:

$$Fe(CO)_4^- + C_3{}^{13}CH_2O_3 \text{ ----> } Fe(CO)_3(C_3{}^{13}CH_2O_3)^- + CO \quad (4)$$
$$m/z\ 239$$
$$\text{----> } Fe(CO)_4(C_3H_2O_2)^- + {}^{13}CO \quad (5)$$
$$m/z\ 238$$

Reaction 4 shows substitution of maleic anhydride for a CO resulting in the loss of carbon from $Fe(CO)_4^-$. Reaction 5 shows the decarbonylation of maleic anhydride resulting in the loss of carbon from MAH. Analysis of the sources of m/z 239 by ICR double resonance, using compounds with a natural abundance of ^{13}C, suggests that the reaction is substitution.

Presented at the 35th ASMS Conference on Mass Spectrometry and Allied Topics
May 24-29, 1987, Denver, CO

The results of a more extensive investigation of the reactivity of $Fe(CO)_4^-$ and $Fe(CO)_3^-$ as well as $Fe(CO)_2^-$ with maleic anhydride, MAH, is shown in Table II. All reactions were verified by double resonance. (MAHD is decarbonylated MAH.) The horizontal arrows show reactions where one CO in the anion is substituted by MAH. The arrows at 45° show reactions where two CO's are substituted by MAH. The perpendicular arrows show the loss of CO, which is a collision-induced decomposition process observed only when the reactant is heated to its cyclotron frequency. The numbers above the arrows are relative rate constants for the reactions. Decarbonylation is clearly general and facile in this system. This suggests that anion attack at the carbonyl carbon of MAH is quite general and facile. Note also that $Fe(CO)_3(MAH)^-$ is less reactive than $Fe(CO)_4^-$ by three orders of magnitude.

Summary

1) $Fe(CO)_3^-$ reacts readily by ligand substitution with a variety of organic ligands. Ligand reactivity increases with polarity and unsaturation.
2) $Fe(CO)_4^-$ reacts only with maleic anhydride (MAH) and its derivatives. The reaction observed is ligand substitution.
3) Decarbonylation of the MAH occurs readily in reactions of $Fe(CO)_n(MAH)_m^-$ species. Decarbonylation of MAH also occurs in the CID of such species.

Table I. Reactions of Radical Anions Formed from $Fe(CO)_5$ with Organic Molecules

Organic Molecule	Number of CO's Displaced: $Fe(CO)_3^-$	Number of CO's Displaced: $Fe(CO)_4^-$
	1	0
	1	0
	1	0
	1	0
	1	0
	0	0
	0	0
	0	0
	1	0
	2	1
	2	1
	2	3

Table II. Reactions of Radical Anions Formed from $Fe(CO)_5$ with Maleic Anhydride, MAH (MAHD = Decarbonylated MAH)

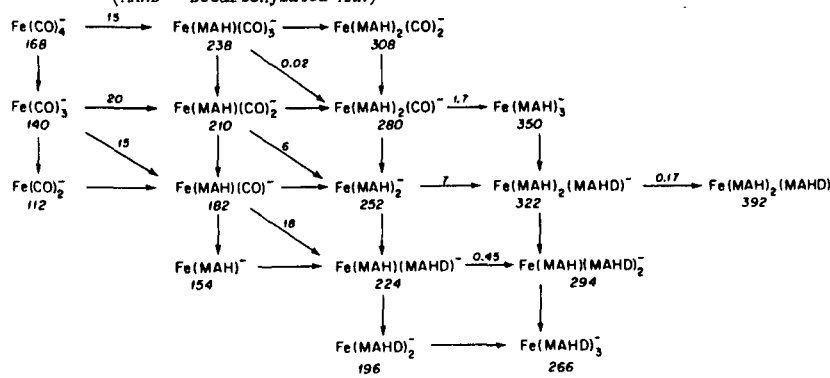

Presented at the 35th ASMS Conference on Mass Spectrometry and Allied Topics
May 24-29, 1987, Denver, CO

REACTIONS OF $C_3H_3^+$ WITH ACETYLENE AND DIACETYLENE IN THE GAS PHASE

F. Ozturk, G. Baykut, M. Moini, and J. R. Eyler
Department of Chemistry
University of Florida
Gainesville, Florida 32611

Introduction:

The $C_3H_3^+$ ion has received considerable attention in recent years as a possible soot precursor because it is found in quite high abundance in fuel-rich and sooting flames.[1-3] The ion is postulated[4,5] to react with neutrals such as acetylene, diacetylene, and C_2H in rapid, sequential condensation and condensation/elimination reactions, forming successively larger ions, which can rearrange to cyclic species during the ion/molecule reaction chain. Two isomeric structures of $C_3H_3^+$ are important in discussing its role in ion/molecule reaction mechanisms. The fist is the cyclopropenylium ion, recognized as the most stable isomer; the second and potentially more important is the linear propargylium ion. It was demonstrated[6] that the cyclopropenylium ion was relatively unreactive toward simple hydrocarbon fuels whereas the linear propargylium ion was quite reactive.

Experimental:

A Nicolet FTMS-1000 Fourier transform ion cyclotron resonance (FTICR) mass spectrometer with a superconducting magnet was used. Reaction pathways were delineated using the ejection capabilities of FTICR which make it possible to eject one ion from a complicated reaction mixture to determine its contribution to the mass spectrum of all the other ions. Reaction rate coefficients were determined by monitoring the intensity of the $C_3H_3^+$ ions as a function of time after ejection of all other ions from the analyzer cell. $C_3H_3^+$ ions produced by charge transfer reactions of propargyl iodide with Xe^+ were used in studies of the reactions of this ion with acetylene and diacetylene. $C_5H_5^+$ ions produced from different precursors (norbornadiene, 1-penten-3-yne, cyclopentadiene, dicyclopentadiene, and cycloheptatriene) with different charge transfer gases (Xe, N_2, Ar) were used in the corresponding studies of $C_5H_5^+$ ion.

Results:

$C_3H_3^+$ reactions with acetylene: Despite an earlier report[6] that linear $C_3H_3^+$ is quite reactive with acetylene, we found no significant $C_5H_5^+$ or $C_5H_3^+$ formation by reaction of linear $C_3H_3^+$ with C_2H_2. It was also observed that C_2H_2 led to the isomerization of linear $C_3H_3^+$ ions to their cyclic form, thus rendering them unreactive toward their parent neutral (C_3H_3I) as well as toward C_2H_2. This isomerization was followed as a function of C_2H_2 pressure and a direct pressure dependence was found, as can be seen in Figure 1.

$C_3H_3^+$ reactions with C_2D_2: To achieve a better understanding of the isomerization of linear $C_3H_3^+$, C_2D_2 instead of C_2H_2 was used as the neutral reactant. Isotope exchange reactions which produced $C_3H_2D^+$, $C_3HD_2^+$, and $C_3D_3^+$ were observed. Ion intensity vs. time curves for the $C_3H_3^+ + C_2D_2$ reaction are shown in Figure 2.

$C_5H_5^+$ reactions with acetylene: $C_5H_5^+$ ions reacted slowly with acetylene producing very small amounts of $C_7H_7^+$. Depending on the precursor used to form the $C_5H_5^+$ ion, rate coefficients for the disappearance of $C_5H_5^+$ were found in the range of (2-8) * 10^{-11} cm^3/s.

$C_3H_3^+$ reactions with diacetylene: Consecutive C_2 and C_4H_2 addition reactions were observed forming $C_5H_3^+$, $C_7H_3^+$, $C_7H_5^+$, $C_9H_5^+$, $C_{11}H_5^+$, and $C_{13}H_7^+$. Ion intensity vs. time curves for the $C_3H_3^+ + C_4H_2$ reaction are

shown in Figure 3. A value of (1.4 ± 0.7) * 10^{-9} cm^3/s was calculated for the rate coefficient of disappearance of $C_3H_3^+$.

$C_5H_5^+$ reactions with diacetylene produced $C_7H_5^+$, $C_9H_7^+$, and $C_{13}H_9^+$. Depending on the precursor used to form the $C_5H_5^+$ ion, rate coefficients for disappearance of $C_5H_5^+$ were found in the range of (1-8) * 10^{-10} cm^3/s.

Discussion:

Although the results of this work are not in agreement with the earlier report[6] of $C_3H_3^+/C_2H_2$ reactivity, the discrepancy is most likely due to limitations of the older pulsed ICR instrumentation for studying ion/molecule reaction pathways in complicated systems when compared to newer FTICR capabilities. The most likely mechanism of the observed isomerization of $C_3H_3^+$ ions by collisions with acetylene is a "reactive" rather than a "non-reactive" one. That is, it results from an intimate encounter of the ion and neutral in the $C_5H_5^+$ collision complex. This hypothesis is confirmed by the fact that deuterated forms of $C_3H_3^+$ were produced when C_2D_2 was the neutral reactant (see Figure 2). The extensive ion/molecule condensation reaction sequences observed when $C_3H_3^+$ reacts with C_4H_2 suggest that this aspect of the proposed[4,5] ionic path to soot formation is quite credible. some of the product ions formed have been seen to be abundant in both nonsooting and sooting flames[2].

References:

1. Goodings, J. M.; Bohme, D. K.; Comb. and Flame 1979, 36, 27.
2. Olson, D. B.; Calcote, H. F. Eighteenth Symposium (Int.) on Combustion, 1981, 453.
3. Michaud, P.; Delfau, J. L.; Barrasin, A. Eighteenth Symposium (Int.) on Combustion, 1981, 443.
4. Calcote, H. F.; Comb. and Flame 1981, 42, 215.
5. Olson, D. B.; Calcote, H. F. in Particulate Carbon Formation during Combustion, Siegla, D. C.; Smith, G. W., Eds., Plenum Press (New York, 1981), 177-205.
6. Smyth, K. C.; Lias, S. G.; Ausloos, P. Combust. Sci. and Tech., 1982, 28,147.

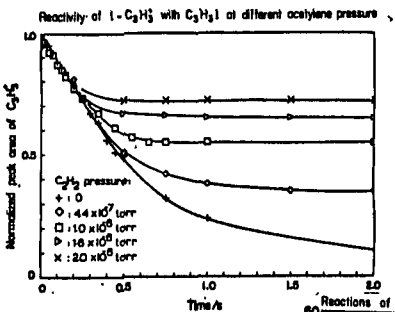

Figure 1. Isomerization of linear $C_3H_3^+$ ions at different pressures of C_2H_2.

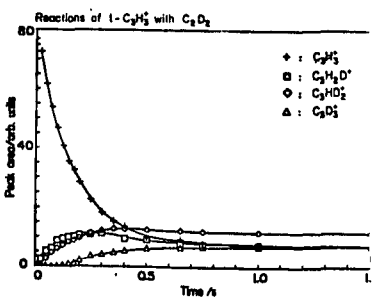

Figure 2. Isotope exchange reactions of $C_3H_3^+$ with C_2D_2

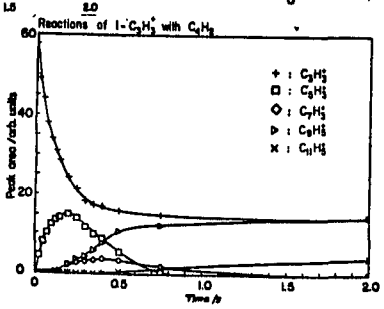

Figure 3. Reactions of $C_3H_3^+$ with C_4H_2.

Presented at the 35th ASMS Conference on Mass Spectrometry and Allied Topics
May 24-29, 1987, Denver, CO

Reactions of Catecholate and Resorcinolate Anions with Selected Lewis Acids

William S. Taylor and Lucia M. Babcock
Louisiana State University
Baton Rouge, LA 70803

We have been interested in examining gas phase reactions between Lewis acids and dihydroxy ligand anions. These ligands can often be either mono- or bidentate, coordinating to the central atom of the Lewis acid through either one or both oxygen donor atoms. The Lewis acids are ideal neutral partners for such kinetic, mechanistic studies because they can undergo ion-molecule association reactions to add the ligand anion, and then, if geometry and energetics are favorable, an intramolecular substitution/elimination involving the second oxygen donor atom can occur. The particular ligands we focus on in the work presented here are 1,2-dihydroxybenzene (catechol) and 1,3-dihydroxybenzene (resorcinol). The reactions of the dihydroxybenzene anions are particularly interesting because the aromatic ring keeps the anion fairly rigid and defines the relative orientation of the two hydroxyl groups. This lack of flexibility has been shown to be important in solution reactions of catechol with boron acids,[1] where coordination of the first oxygen orients the second hydroxyl group in a manner which facilitates ring closure. In fact, in solution coordination of the first oxygen atom is rate determining, and is followed by rapid ring closure; the only products observed in solution are those in which catechol is bidentate.[1-3]

In the gas phase, trigonal boron trihalides and tetrahedral silicon tetrafluoride can add anions to become tetracoordinate and pentacoordinate respectively, and we have examined the reactions of these with catecholate (I) and resorcinolate (II) anions:

I

II

In the flowing afterglow, these ions can be generated in small quantities by direct electron impact, but this process is slow and provides a downstream source of reactant ion. It is preferable to generate the desired ion via an acid-base reaction in which methoxide anion, CH_3O^-, abstracts a proton from the neutral to produce $C_6H_5O_2^-$. Products of reaction are the same for both methods of reactant ion generation, but accurate rate coefficients are obtained in the latter case. For catecholate, one can envision formation of both monodenate and bidentate products as shown below for BX_3; (a similar scheme can be drawn for SiF_4):

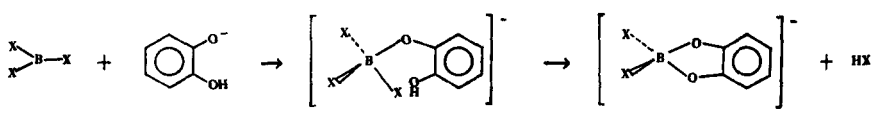

For reactions with the resorcinolate anion, one would suspect ring closure and formation of the bidentate product to be prohibited on geometric grounds.

Using our room temperature flowing afterglow apparatus, we have examined reactions of resorcinolate anion (II) with BF_3 and SiF_4. Both reactions occur essentially at the collision rate. In both cases the only products observed are the addition product and a fluoride transfer product which is formed from further reaction of the addition product as shown below for BF_3:

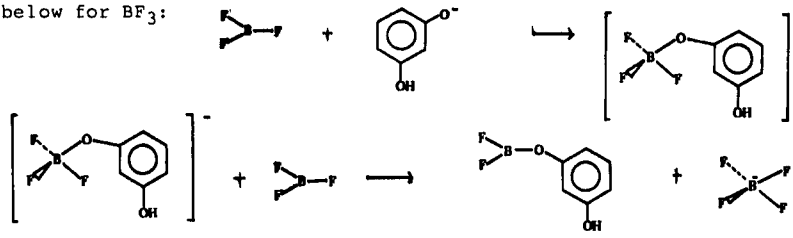

Again, an analogous reaction can be written for SiF_4. Reactions of BF_3, BCl_3, and SiF_4 with the catecholate anion (I) are much more varied. Again, $C_6H_5O_2^-$ reacts with the Lewis acid at essentially the collision rate. For the reactions with BCl_3 and SiF_4, both the monodentate and bidentate products are observed as is the fluoride transfer product. Product ratios indicate that both the F^- transfer and bidentate products are formed from the monodentate via subsequent reaction with the neutral as shown below for SiF_4:

$$C_6H_5O_2^- + SiF_4 \text{ -----> } SiF_4O_2C_6H_5^-$$

$$SiF_4O_2C_6H_5^- + SiF_4 \text{ -----> } SiF_5^- + SiF_3O_2C_6H_5$$

$$\text{-----> } SiF_3O_2C_6H_4^- + HF \ .$$

In the case of BF_3, however, no bidentate product is observed - only the addition product and subsequent F^- transfer product are formed. Furthermore, it is interesting to note that in both SiF_4 and BF_3 reactions with catecholate, there is preliminary evidence for existence of two kinetically distinct forms of the addition product: one which undergoes further reaction to the bidentate and/or F^- transfer products, and one which is unreactive toward further addition of neutral. In both cases, we examined the reaction of the addition product with neutral, and were able to deplete the reactant ion only to a certain point beyond which no further reaction occurred. It is interesting that in both cases the ratio of reactive to unreactive ion is 10 to 1. The postulate of two different forms is also supported by the observation that there is a dramatic change in the product ratios as a function of pressure for the BF_3 reaction.

We are currently continuing our studies in order to determine whether there are indeed two distinct forms of the addition product for catecholate reactions with these Lewis acids, and, if so, to characterize them. Perhaps the two are structural isomers corresponding to different coordination numbers for the central atom. We are also exploring reasons for the absence of ring closure in the reaction of BF_3 with catecholate.

1. R. Pizer and L. Babcock, Inorg. Chem., 16, 1677 (1977).
2. L. Babcock and R. Pizer, Inorg. Chem., 19, 56 (1980).
3. L. Babcock and R. Pizer, Inorg. Chem., 22, 174 (1983).

Presented at the 35th ASMS Conference on Mass Spectrometry and Allied Topics
May 24-29, 1987, Denver, CO

ION-MOLECULE REACTIONS IN Di-i-PROPYL ETHER

Regina Barry and Burnaby Munson

Department of Chemistry, University of Delaware, Newark DE 19716

The use of dilute di-i-propyl ether mixtures as a reagent system for chemical ionization mass spectrometry has recently been reported.[1] In order to control the distribution of reagent ions and to interpret the CI spectra, it is important to know how the reagent ions are formed and the extent to which they react with di-i-propyl ether and the samples. The major reagent ion in mixtures of di-i-propyl ether under CI conditions is 103^+, with a smaller amount of 61^+ which also reacts with a variety of samples. The $61^+/103^+$ ratio decreases with increasing pressure of ether and with decreasing temperature.

Double-resonance spectra of 103^+ under ICR conditions indicate that this ion is formed from ion/molecule reactions with di-i-propyl ether, 102, of all EI fragment ions except the unreactive fragment ion, $(M-CH_3)^+$, 87^+. The other product ion, 61^+, presumably protonated isopropanol, is formed from ion/molecule reactions of 45^+ and 43^+ with di-i-propyl ether. These experiments also showed that 61^+ could be formed by collisionally induced dissociation of 103^+.

The reactions of 43^+ and 45^+ to produce 61^+ are particularly interesting as they may be examples of rapid, endothermic, dissociative proton transfer reactions.

$$s\text{-}C_3H_7^+ + 102 \rightarrow 61^+ + 2CH_3CH{=}CH_2 \qquad (1)$$

The dissociative proton transfer from 43^+ to neutral di-i-propyl ether to produce 61^+ in reaction (1) is calculated to be +4 kcal/mole endothermic.[2] Although this is a small endothermicity, the heats of formation of the products and reactants are relatively well known and this reaction may be endothermic.

$$CH_3CHOH^+ + 102 \rightarrow CH_3CHO + 61^+ + CH_3CH{=}CH_2 \qquad (2)$$

Formation of 61^+ by dissociative proton transfer from 45^+ to di-i-propyl ether is +11 kcal/mol if 45^+ is protonated acetaldehyde. Formation of 61^+ from 45^+ by dissociative proton transfer is +12 kcal/mol endothermic if 45^+ is protonated ethylene oxide. The endothermicity of the reaction appears to be greater than the likely uncertainties in the thermochemical data.

Using entropies calculated using Benson's group additivities[3] and the assumption that the difference in entropies of two ions is the same as the difference in entropies of their conjugate bases, we estimate that $G^o(1)$ is - 7 kcal/mol and $G^o(2)$ is about 0 kcal/mol.

Trapped-drift (or time dependence) experiments were performed on the major ions in di-i-propyl ether under ICR conditions (Fig. 1). The 43^+ and 45^+ ions reacted rapidly to form 61^+, which reacted rapidly to produce 103^+. The overall scheme appears to be the consecutive reactions,

$$\begin{matrix} 43^+ \\ 45^+ \end{matrix} + 102 \rightarrow [103^{+*}] \rightarrow 61^+ \xrightarrow{102} 103^+$$

This mechanism of dissociative proton transfer from the reagent ions to form 61^+ followed by proton transfer from 61^+ to give 103^+ is consistent with

observations under the high pressure conditions of CI experiments which showed that the $103^+/61^+$ ratio was directly proportional to sample size. That is, there was no evidence for collisional stabilization of the excited complex, 103^{+*} by the reagent gas.

Plots of log (I) vs. t at a constant pressure under ICR conditions were used to obtain second order rate constants for the reactions of 43^+ and 45^+ with di-i-propyl ether. The data for for 61^+ and 103^+ were fitted using a simplex non-linear least squares routine.[4] The pressure used to calculate the rate c onstants is the corrected ion gauge pressure. The actual pressure is probably lower and the rate constant probably higher.[5] Theoretical capture collision rate constants were calculated for comparison[6] and are included in Table I. The rate constants are large and nearly the theoretical limits, despite the calculated endothermicity of the reactions.

Table I

Experimental and Theoretical Rate Constants
for Reactions in Di-i-propyl Ether

	k(theo)	k(exp)
45^+ + 102	1.81 x 10-9 cm^3/mol-s	1.27 x 10^{-9} cm^3/mol-s
43^+ + 102	1.84 x 10-9 cm^3/mol-s	9.0 x 10-10 cm^3/mol-s
61^+ + 102	7.3 x 10-10 cm^3/mol-s	6.4 x 10-10 cm^3/mol-s

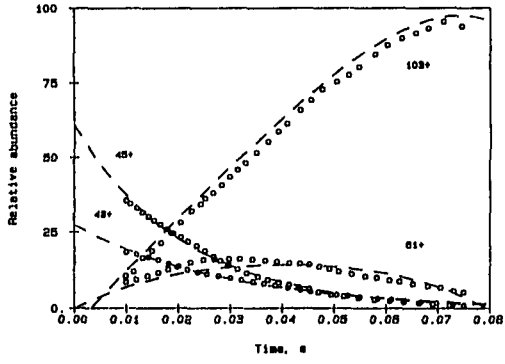

1. Barry, R. and Munson, B. Anal. Chem. 1987, 59, 466.

2. Lias, S. G.; Liebman, J.F., and Levin,R. D. J. Phys. Chem. Ref. Data (1984). 13, no. 3, pp. 695-808.

3. Benson, S. W. and O'Neal, H. Kinetic Data on Gas Phase Unimolecular Reactions 1970, pp. 40-44.

4. Noggle, J.H. "Physical Chemistry on a Microcomputer"; Little, Brown: New York, 1985: p. 148.

5. Reents, Jr.W. D.; Strobel, F.; Freas III, R. B.; Wronka, J. and Ridge, D. P. J. Phys. Chem. (1985), 89 (26) 5666-5670.

6. Su, T. and Chesnavich, W. J. J. Chem. Phys.(1982), 76, 5183.

Presented at the 35th ASMS Conference on Mass Spectrometry and Allied Topics
May 24-29, 1987, Denver, CO

SELECTIVE DETERMINATIONS BY LOW ENERGY ION-MOLECULE REACTIONS

S. R. Missler[1], R. B. Freas[2], and P. E. Kelley[3]

1. EPTD, Texaco, Inc. P. O. Box 425, Bellaire, TX 77401
2. Department of Chemistry, University of Houston, Houston, TX 77004
3. Finnigan MAT, 355 River Oaks Parkway, San Jose, CA 95134

Low energy ion-molecule reactions were examined as a method for differentiating isomeric olefins and cycloalkanes (naphthenes) in gasolines by tandem mass spectrometry. In this study, both a hybrid (EBQQ) MS/MS and an ion trap configured for MS/MS were used to evaluate the effects of collision cross section and target thickness on product ion formation. In a model system, the molecular ion of vinylethyl ether was found to react with butadiene collision gas to form an addition product at m/z 126, indicative of a Diels-Alder condensation (Figure 1). Variation of instrumental parameters enabled optimization of selected product ion fragments, while controlling secondary reactions.

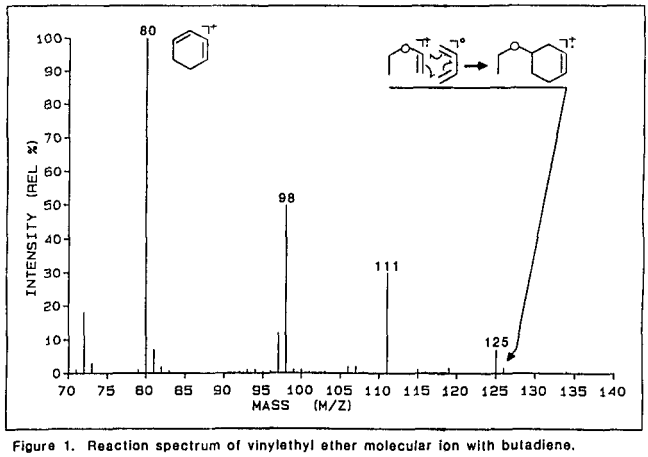

Figure 1. Reaction spectrum of vinylethyl ether molecular ion with butadiene.

Reaction of 1-hexene molecular ion with isoprene produced the expected addition product at m/z 152 along with associated fragment ions (Figure 2). Collisional activation of a reaction with cyclohexane molecular ion and isoprene also resulted in addition products, although they occurred at masses different than those for the 1-hexene--isoprene system (Figure 3). The reaction pathway is not understood, but is believed to involve collision induced dissociation of the parent cyclohexane or isoprene to yield a reactive daughter ion which forms an addition product with isoprene.

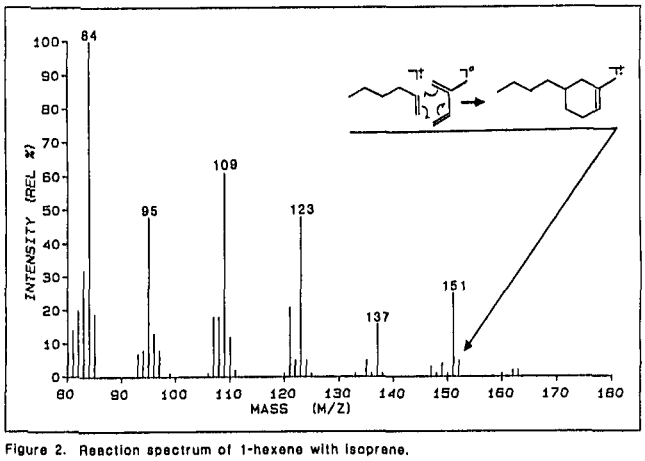

Figure 2. Reaction spectrum of 1-hexene with isoprene.

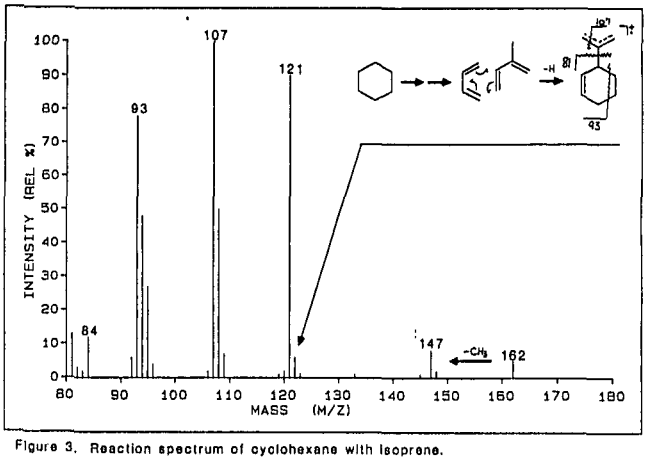

Figure 3. Reaction spectrum of cyclohexane with isoprene.

These results indicate that selective low energy ion-molecule reactions can be used to differentiate isomeric compounds in complex mixtures. Future efforts will attempt to provide practical application of this technique for the determination of olefins in refined petroleum products using a similar scheme.

Presented at the 35th ASMS Conference on Mass Spectrometry and Allied Topics
May 24-29, 1987, Denver, CO

ION-MOLECULE REACTIONS FOR DISTINGUISHING STRUCTURAL ISOMERS OF ORGANIC IONS IN THE GAS PHASE.

M. H. Bozorgzadeh
Midwest Center for Mass Spectrometry,
University of Nebraska, Lincoln,
NE 68588.

Comparing the mass spectra of unknown and known isomers of a desired compound is used as a traditional method for structural elucidation of unknowns. The method is also applied by using the CAD spectra of a fragment ion instead of the mass spectrum of the whole molecule. This method has the disadvantage that sometimes the isomers have the same CAD spectra and cannot be distinguished. In the ion-molecule reaction approach, this disadvantage can be overcome by reacting the desired ion with a suitable reagent prior to obtaining its CAD spectrum. Indeed, those isomeric fragent ions that have the same CAD spectra will be converted in part to larger ions that give different CAD spectra[1].

The isomers of $C_4H_9^+$ ions of butyl bromides have the exact same CAD spectra, but if they are reacted with a suitable nucleophile, the product adducts have different CAD spectra by which they can be distinguished. The nucleophiles that were tested are; ROH (R = H, CH_3, C_2H_5, n-C_3H_7, iso-C_3H_7, and n-C_4H_9); RNH_2 (R = H, CH_3, and C_2H_5); and pyridine. The results show that the best nucleophile for this purpose is n-C_3H_7OH. Further experiments were done by reacting n-C_3H_7OH with the isomers of C_4H_9-X (X = Cl, I, and C_6H_5). As the results show, with the exception of the isomers of C_4H_9-C_6H_5, the other isomers give adducts that have distinctive CAD spectra, showing that the butyl group is not isomerized. Also, the CAD spectra of likely adducts that were prepared by protonating appropriate alcohols, ethers, or amines have been investigated and compared with those obtained from their corresponding unknown ions.

The results show that, n-$C_4H_9^+$ ion will isomerize to tert-$C_4H_9^+$ if the source pressure is increased. It can be explained that a portion of n-$C_4H_9^+$ is isomerized to sec-$C_4H_9^+$ and tert-$C_4H_9^+$. These two product isomers have more internal energy than what the n-$C_4H_9^+$ ion had before reaction (because of the differences of the heat of formations of the isomers of butyl ions). If the two product isomers of so high internal energy collide with n-C_3H_7OH the adducts may not be formed, or if they are formed, their internal energies are too high to let them being stable to reach the region where the collisional activation decomposition will happen. When the source pressure increases the gases in the source can collisionaly stabilize the excited ions of sec-$C_4H_9^+$, tert-$C_4H_9^+$ and their adducts. Therefore, the adducts are enough stable that their CAD spectra can be taken. The CAD spectra of the isomers of the adducts of $C_4H_9^+$ ions and n-C_3H_7OH, and their protonated appropriate ethers are shown in Figure 1. As Fig. 1 shows, at low source pressure the CAD spectra of the isomers of $C_4H_9^+$ are distinguished by the differences of the ratio of the abundances of the two major daughter ions of M/Z 57 ($C_4H_9^+$) and 61 ($C_3H_7\overset{+}{O}H_2$).

The method is summerized as follows:

1 - React the unknown isomer with a reagent and obtain the CAD spectrum of the product.
2 - React all probable isomers with the same reagent under the same conditions and obtain their CAD spectra.
3 - Compare the obtained spectra to choose the correct isomer.
4 - Choose another reagent if the CAD spectra of the products are still the same.

1 - P. P. Dymerski, and W. F. McLafferty; J. Amer. Chem. Soc., 1976 98, pp. 6070.

Fig. 1

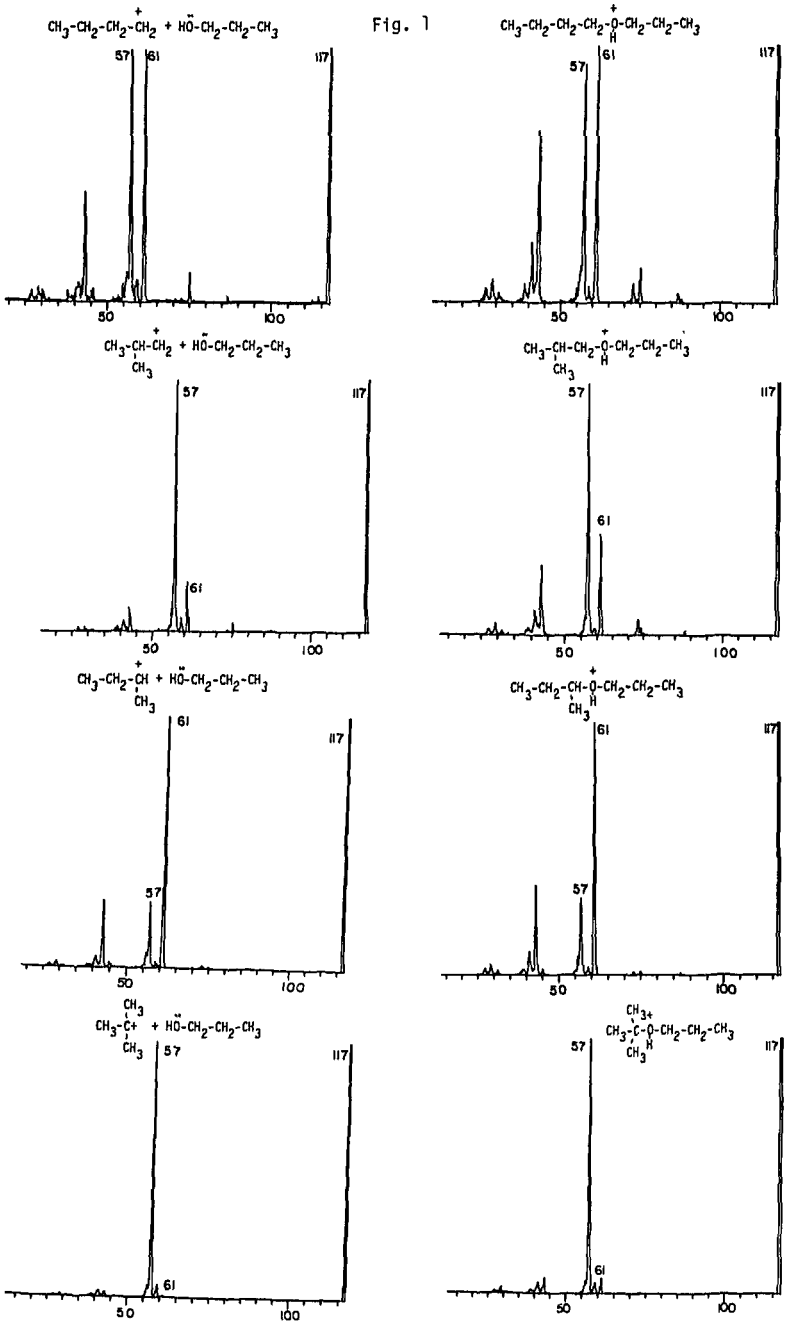
CH3-CH2-CH2-CH2+ + HÖ-CH2-CH2-CH3
CH3-CH2-CH2-CH2-O(+)H-CH2-CH2-CH3
CH3-CH(CH3)-CH2+ + HÖ-CH2-CH2-CH3
CH3-CH(CH3)-CH2-O(+)H-CH2-CH2-CH3
CH3-CH2-CH(+)-CH3 + HÖ-CH2-CH2-CH3
CH3-CH2-CH(CH3)-O(+)H-CH2-CH2-CH3
CH3-C(+)(CH3)-CH3 + HÖ-CH2-CH2-CH3
CH3-C(+)(CH3)-O(+)H-CH2-CH2-CH3
57
61
117
50
100

Presented at the 35th ASMS Conference on Mass Spectrometry and Allied Topics
May 24-29, 1987, Denver, CO

HYDROGEN FLUORIDE ELIMINATION FROM 2-FLUORO-2-PROPYL CATION

T.A. Shaler, J. Moenig, D.A. Stams, R. Kondrat, and T.H. Morton
Department of Chemistry, University of California, Riverside, CA 92521

The mechanism of HF elimination from the 2-fluoro-2-propyl cation has been investigated using MIKES. Four different routes to the cation were examined (Scheme I). The metastable peak shape for $(CH_3)_2CF^+ + C_3H_5^+$ is independent of the method of production of the parent ion, with $T_{0.5}$ = 0.88±0.02 eV.

The deuterium isotope effect for loss of HF <u>versus</u> loss of DF was studied for various deuterated analogues of the cation (Scheme II). There was no significant effect of deuterium substitution on the kinetic energy release. The value of k_{HF}/k_{DF} is 4 for $CH_3(CD_3)CF^+$, shown by the metastable peaks shown in Figure 1, and 11±3 for $CH_3(CHD_2)CF^+$.

<u>Scheme I</u>

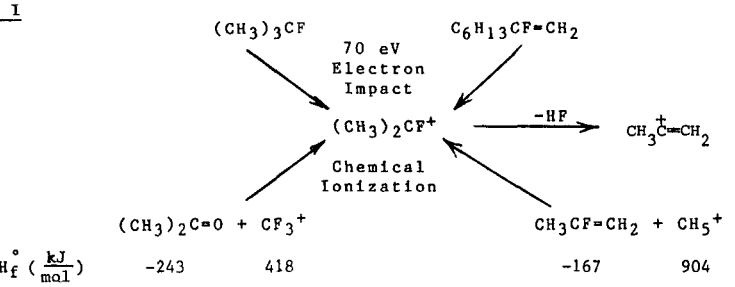

Large kinetic energy releases such as those observed here have been postulated as being evidence of a number of different types of fragmentation mechanisms. The most obvious fragmentation giving a large kinetic energy release is the separation of two charged daughters from a doubly charged parent ion. This possibility was eliminated by examining the normal EI mass spectrum of t-butyl fluoride which showed no traces of a peak at m/z 122, so that the probability that our m/z 61 parent ion is really 122^{2+} is very low.

Another type of fragmentation that is believed to result in a large kinetic energy release is a fragmentation with a very large reverse activation energy, such as fragmentation from an excited electronic state. This is also believed not to be the case in our system. First of all semi-empirical MO calculations suggest that the first excited singlet electronic state of the 2-fluoro-2-propyl cation is $\geq$5 eV above the ground state. If we assume that the fragmentation is occurring by the same pathway in each method by which the cation is produced (and it is highly unlikely that the electronically excited state is accessed in the CI methods) then the fragmentation could not be occurring from an excited electronic state. The fragmentation of interest is endothermic by about 26 kcal/mole. The activation barrier must therefore be at least as high as this ΔH plus the kinetic energy release (47 kcal/mol) but must be less than the combined heats of formation of the CI reactants minus ΔH_f° [$(CH_3)_2CF^+$]. The average kinetic energy release $T_{0.5}$ is therefore at least two-thirds of the activation barrier.

A third type of fragmentation pathway that partitions a large proportion of excess energy into kinetic energy release is one which has a very late transition state for separation of the fragments. We believe this to be case here. <u>Ab initio</u> calculations predict a local potential energy minimum corresponding to $CH_2{=}C(FH^+)CH_3$, which is related to $(CH_3)_2CF^+$ by an orbital symmetry-forbidden [1,3]-sigmatropic shift. The reverse energy barrier may result from concerted conversion to this intermediate.

Presented at the 35th ASMS Conference on Mass Spectrometry and Allied Topics
May 24-29, 1987, Denver, CO.

Scheme II

analogue	precursor	method
D1	n-$C_6H_{13}CF{=}CHD$	EI
D1	$CH_3CF{=}CH_2$	CI/CD_4
D2	n-$C_6H_{13}CF{=}CD_2$	EI
D3	$CH_3(CD_3)_2CF$	EI
D6	$CD_3\overset{O}{\overset{\|}{C}}CD_3$	CI/CF_4

FIGURE 1 Metastable peaks corresponding to DF and HF loss from $CD_3\overset{+}{C}FCH_3$ (8 kV main beam)

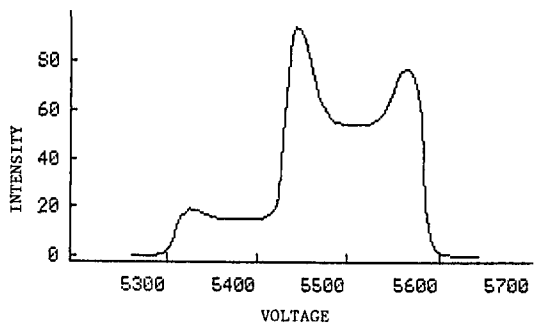

The table to the right compares the HF elimination with expulsion of molecular hydrogen from $C_3H_7^+$, an analogous reaction that has been extensively studied.[1] $C_3H_7^+$ is a rapidly interconverting set of isomers

$$CH_3\overset{+}{C}HCH_3 \rightleftarrows CH_3CH_2CH_2^+ \rightleftarrows H_3\overset{+}{C}\triangleleft$$

while $(CH_3)_2CF^+$ does not appear to adopt any structure besides the classical 2-fluoro-2-propyl prior to passage over the energy barrier. The variety of structures available for $C_3H_7^+$ admits both orbital symmetry-allowed and forbidden pathways for H_2 expulsion.

Acknowledgment. This work was supported by the NSF. Ab initio calculations were performed on the Cray XMP/48 at the San Diego Supercomputing Center at the University of California, San Diego.

Comparison with H_2 loss from $C_3H_7^+$ (1)

	$C_3H_7^+ \rightarrow C_3H_5^+ + H_2$	$C_3H_6F^+ \rightarrow C_3H_5^+ + HF$
Parent ion:	configurationally labile	configurationally stable
Intermediates:	no	yes
Structure of product:	allylic cation	vinylic cation
$T_{0.5}$:	37kJ	88kJ
k_H/k_D:	2-2.5	4.1
Isotope effect on T:	no	no
Orbital symmetry prediction:	allowed or forbidden pathways	only forbidden pathways

1. G. Hvistendahl and E. Uggerud, Org. Mass Spectrom. 1986, 21, 347-350.

Presented at the 35th ASMS Conference on Mass Spectrometry and Allied Topics
May 24-29, 1987, Denver, CO

Kinetics & Equilibria of Ion Molecule Reactions

Richard J. Gallagher, Rod S. Mason, Keith R. Jennings & Anthony J. Wickham,
Department of Chemistry, University of Warwick, Coventry, U.K.

Three body association reactions are of importance in the chemistry of planetary atmospheres, gas-cooled nuclear reactors and in the formation of gas-phase cluster ions. There is therefore interest in knowing the rate constants of such reactions as a function of temperature and as a function of the third body M in reactions of the type

$$X^{+\cdot} + X + M \rightarrow X_2^{+\cdot} + M \qquad (1)$$

The variation of k with T is usually expressed as $k = CT^{-n}$ where C and n are constants for a given reaction, but both are found to depend on the nature of M. Although there is now a general measure of agreement on values of C and n for several reactions in which M = X, inconsistent values have been reported for systems in which M = He, for example, and this paper describes a study of the two systems in which $X = N_2$, CO and M = the reactant or a rare gas.

Experiments were carried out using a rebuilt Kratos MS9 mass spectrometer fitted with either a pulsed high pressure source as previously described[1] or a pulsed drift source, modelled on the source described by van Koppen *et al*[2]. Operating conditions for the two cources were as follows;

	Pulsed High Pressure Source	Pulsed Drift Source
Electron energy/eV	400	17
Pulse width/μs	10-50	5-10
Pressure/Torr	0.5-3.5	0.3-1.5
Temperature/K	350-650	320-610

The reaction is assumed to proceed <u>via</u> the energy-transfer mechanism:

$$X^{+\cdot} + X \rightarrow X_2^{+\cdot *} \qquad k_f \qquad (2)$$

$$X_2^{+\cdot *} \rightarrow X^{+\cdot} + X \qquad k_b \qquad (3)$$

$$X_2^{+\cdot *} + M \rightarrow X_2^{+\cdot} + M \qquad k_s \qquad (4)$$

in which k_f and k_b are assumed to be given by the ADO theory,

$$k_{ADO} = (2\pi q/\mu^{\frac{1}{2}})[\alpha^{\frac{1}{2}} + C\mu_D(2/\pi kT)^{\frac{1}{2}}] \qquad (5)$$

where q = charge on the ion, μ = reduced mass, μ_D = dipole moment of the molecule, α = polarisability of the molecule, C = dipole locking constant. The stabilisation rate constant k_s is equated to the collisional rate constant k_c multiplied by the stabilisation efficiency β. The limiting low pressure third-order rate constant is given by

$$k_3 = \frac{k_f k_c \beta}{k_b + k_f k_c \beta [M]} = CT^{-n} \qquad (6)$$

The stabilisation efficiency β has a value between 0 and 1 and might be expected to vary with the nature of M. In general, β is not considered to vary significantly with temperature, although for some systems, such a variation has been suggested.[3]

In the pulsed high pressure source,[1] the intensity I of $X^{+\cdot}$ is followed as a function of time after the onset of free diffusion and a plot of ln[I] v. time gives a straight line of slope S. By measuring S as a function of the partial pressure of M, a plot of S[M] v. $[X][M]^2$ when [M]>>[X] gives a straight line of slope k_3 where k_3 is the overall third order rate constant defined in eqn. (6).

In the pulsed, drift source,[2] the concentrations of $X^{+\cdot}$ and $X_2^{+\cdot}$ are followed as a function of time and a plot of $\ln\{I_t(X^+)/(I_t(X^+)+I_t(X_2^{+\cdot}))\}$ against t gives a straight line of slope $k_3[X]^2$.

Results for $X = N_2$

Previous work from this laboratory[1] on the nitrogen system, $M = N_2$, had suggested that n in the expression $k_3 = CT^{-n}$ had a value of approximately 3.8, much higher than the commonly accepted value of 1.8±0.1. This value is now known to be incorrect due to saturation effects in the detector system and as

the results in Table 1 indicate, results obtained from the high pressure pulsed source and the drift source are in good agreement with literature values. When M = He, there is a serious discrepancy in the literature between results of Bowers *et al*[3] using a pulsed drift source and Smith *et al*[4], using a SIFT apparatus. The drift source results suggested that for M = He, n is lower than that found for M = N_2, whereas the SIFT results suggest that the opposite is the case. Our results obtained using the high pressure pulsed source are in much better agreement with those of Bowers *et al* rather than those of Smith *et al*, both for the room temperature rate constant and for the temperature dependence. For M = Ar, on the other hand, the temperature dependence is very similar to that found for M = N_2.

Results for X = CO

Table 2 summarises results obtained for the CO system in which M = CO, He, Ar. Where comparison with the literature is possible, the agreement between our results and those in the literature is good. Once again, the temperature dependence for M = He is much less than that for the one-component system, M = CO, but the results for M = Ar are very similar to those for M = CO.

In general, for both N_2 and CO systems, He is less efficient than the parent molecule as a third body at 300 K and the temperature dependence of k_3 is markedly lower. In contrast, Ar behaves very similarly to the parent molecule in both systems. For the CO system, however, although there is reasonably good agreement on the temperature dependence of k_3 with M = CO or He, there is still an uncertainty of about a factor of 2 in room temperature values of k_3.

References

1. J.V. Headley, R.S. Mason & K.R. Jennings, J. Chem. Soc. Faraday Trans.I, 78 (1982), 933.
2. P.A.M. van Koppen, P.R. Kemper, A.J. Illies & M.T. Bowers, Int. J. Mass Spectrom. Ion Processes, 54 (1983), 263.
3. P.A.M. van Koppen, R. Devai, P. Kemper, S. Liu and M.T. Bowers, Int. J. Mass Spectrom. Ion Processes, 73, (1986), 41.
4. D. Smith, N. Adams & E. Alge, Chem. Phys. Letters, 105, (1984), 317.

TABLE 1 X = N_2

METHOD	M	$10^{30} \times k_3$ (300K)/ MOLECULE^{-2} CM^6 S^{-1}	n IN $k_3 = CT^{-n}$	SOURCE
DRIFT	N_2	5.3	1.75	THIS WORK
H.P.P.S.		7.6	1.95	THIS WORK
DRIFT, H.P.P.S.		4.5 – 7.9	1.64 – 3.8	LITERATURE
H.P.P.S.	He	1.1	1.67	THIS WORK
DRIFT		0.9	1.54	BOWERS ET AL
SIFT		1.6	2.4	SMITH ET AL
DRIFT	Ne	1.4	1.54	BOWERS ET AL
H.P.P.S.	Ar	8.4	1.85	THIS WORK

TABLE 2 X = CO

METHOD	M	$10^{30} \times k_3$ (300K)/ MOLECULE^{-2} CM^6 S^{-1}	n IN $k_3 = CT^{-n}$	SOURCE
DRIFT	CO	20.5	1.54	THIS WORK
H.P.P.S.		14.3	1.50	THIS WORK
DRIFT H.P.P.S.		11.4,19.7	1.50,1.60	LITERATURE
H.P.P.S.	He	8.8	1.17	THIS WORK
H.P.P.S. DRIFT		4.78,14.2	1.22,1.5	LITERATURE
DRIFT	Ne	5.47	1.20	BOWERS ET AL
H.P.P.S.	Ar	19.5	1.53	THIS WORK

Presented at the 35th ASMS Conference on Mass Spectrometry and Allied Topics
May 24-29, 1987, Denver, CO

THE ENERGY DEPENDENCE OF THE REACTIONS OF Ar^+ AND Ar_2^+ WITH METHANE AND CARBON DISULFIDE

R. J. Shul, R. Passarella, X. L. Yang, R. G. Keesee,* and A. W. Castleman, Jr.

Department of Chemistry
The Pennsylvania State University
University Park, PA 16802

The rate coefficients for the reactions of Ar^+ and Ar_2^+ with CH_4 and CS_2 are obtained as a function of energy by using a selected ion flow tube with an electric drift field. The reactant ions (Ar^+ and Ar_2^+) are produced by electron impact on a free jet expansion of neutral Ar into vacuum. The ions are focused into the quadrupole mass filter, where the desired ionic species is mass selected and injected into the flow tube. A homogeneous electric field is established along the flow tube axis by a series of electrostatic rings that are inserted in the flow tube. The reactant ions injected into the flow tube are transported into the drift region by the carrier gas. Varying either the electric field intensity or flow tube pressure changes the drift velocity, which is directly related to the center-of-mass kinetic energy of the reactants (1). Neutral reactant gas is added through an inlet that is located in the drift field. Rate coefficients are obtained by monitoring the decay of the reactant ion as a function of the concentration of the neutral reactant gas in the flow tube. The product distributions are determined by extrapolation to zero neutral reactant in order to remove the influence of secondary reactions.

Measurements of the dependence of the overall rate coefficient for the reaction of Ar^+ with methane on the center-of-mass kinetic energy are in good agreement with previous studies (2,3). As opposed to an earlier study where C^+ and CH^+ were reported (3), the observed products in this study, namely CH_2^+, CH_3^+, and CH_4^+, are in accord with thermochemical expectations. The charge transfer channel CH_4^+ disappears at higher energy (see Figure 1). The reaction of Ar_2^+ with methane (Figure 2) exhibits only a slight increase with increasing energy. The charge transfer product CH_4^+ is dominant but the CH_3^+ channel, which is thermoneutral, increases in importance as the field energy increases. An exception to this trend at a center-of-mass kinetic energy of 0.06 eV suggests that the total reaction energy becomes resonant with a charge transfer process. In the reaction of Ar^+ with carbon disulfide (refer to Figure 3), the energy dependence of the rate coefficient exhibits a pronounced minimum which is typical of slow reactions which proceed via complex formation (4). The onset of the appearance of CS^+ at a center-of-mass kinetic energy of 0.4 eV is consistent with the appearance potential for CS^+ from CS_2 of 16.1 eV (5) and the recombination energy of Ar^+ of 15.7 eV. The behavior of the branching ratios for S^+ and CS_2^+ with energy suggest curve crossings of the $A^2\Pi_u$, $B^2\Sigma_u^+$, and $C^2\Sigma_g$ states of CS_2^+ with a repulsive state as shown in Figure 4. In the reaction of Ar_2^+ with CS_2, the reaction energy is insufficient to reach these curve crossings and CS_2^+ is the only observed product except at center-of-mass kinetic energies greater than 0.4 eV where reaction energies are sufficient to produce S^+ directly from CS_2, although with low probability.

REFERENCES

1. G. H. Wannier, Bell Syst. Tech. J. 32, 170 (1953).
2. H. Stori, E. Alge, H. Villinger, F. Egger, and A. Lindinger, Int. J. Mass Spectrom. Ion Phys. 30, 263 (1979).
3. H. Chatham, D. Hils, R. Robertson, and A. G. Gallagher, J. Chem. Phys. 79, 1301 (1983).
4. E. E. Ferguson, in Swarms of Ions and Electrons in Gases, (W. Lindinger, T. D. Mark, and F. Howorka, eds.), Springer-Verlag, New York, p. 126 (1984).
5. V. H. Dibeler and J. A. Walker, J. Opt. Soc. Am. 57, 1007 (1967).

ACKNOWLEDGMENTS

Support by the National Science Foundation, Grant No. ATM-82-04010, is gratefully acknowledged.

Presented at the 35th ASMS Conference on Mass Spectrometry and Allied Topics
May 24-29, 1987, Denver, CO

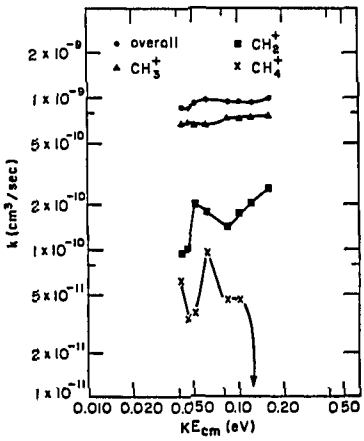

Figure 1. The rate coefficients for the overall reaction and for the product ions are plotted as a function of the center-of-mass kinetic energy for the reaction of Ar^+ with CH_4.

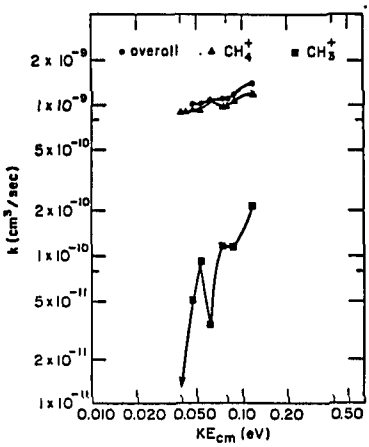

Figure 2. The rate coefficients for the overall reaction and for the product ions are plotted as a function of the center-of-mass kinetic energy for the reaction of Ar_2^+ with CH_4.

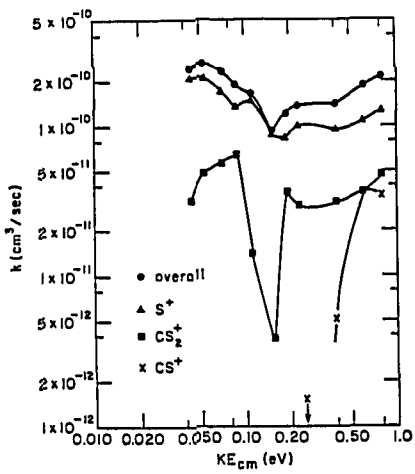

Figure 3. The rate coefficients for the overall reaction and for the product ions are plotted as a function of the center-of-mass kinetic energy for the reaction of Ar^+ with CS_2.

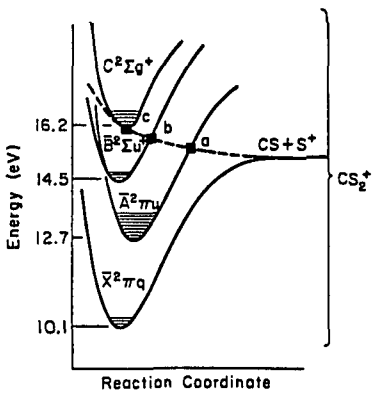

Figure 4. The electronic states of CS_2^+ illustrated in this diagram are referenced to the ground state neutral. The dashed line represents the postulated repulsive curve of S^+. The curve crossings of the S^+ repulsive state and the electronic wells of CS_2^+ are evaluated in this study; a = 15.7 eV, b = 15.8 eV, and c = 16.0 eV.

Presented at the 35th ASMS Conference on Mass Spectrometry and Allied Topics
May 24-29, 1987, Denver, CO

SUBSTITUENT EFFECTS ON THE FRAGMENTATIONS OF METHOXYMETHYLBENZENES

Gary R. Chipman
Amoco Corporation, Naperville, IL 60566

A series of para substituted methoxymethylbenzenes (methyl benzyl ethers) were synthesized and their mass spectra collected and studied. The objective was to determine the effect of remote substituents (X) on the fragmentations of the methoxymethyl group under electron impact. Spectra were obtained by GC/MS (packed 3% OV-17 column) to insure pure components were being studied while probe spectra at 10K resolution were also acquired to verify elemental compositions. Linked scanning techniques (B/E and B^2/E) were employed to study metastable transitions. Comparative partial spectra are presented in Table I.

Substituents included in this study were X = CH_3, F, Cl, Br, CN, CO_2H, CO_2CH_3 and NO_2. These fall into two groups based on the spectral data. The first four listed were inactive and their spectra closely resemble that of the unsubstituted parent compound. The major difference is a larger $(M - X)^+$ peak in some cases. However, the last four substituents are active and cause major unique changes in the fragmentation of the methoxymethyl group.

The major features of the mass spectrum of the unsubstituted parent compound are large peaks for $M^{+\cdot}$, $(M - H)^+$ and $(M - CH_3O)^+$ and minor peaks for $(M - CH3)^+$ and $(M - CH_2O)^{+\cdot}$. The largest peak is $(M - CH_3O)^+$ which is not surprising since this should have a stable benzyl or tropylium structure and arises from cleavage of a single benzylic bond. However, metastable transitions indicate that a two-step process involving consecutive loss of hydrogen and formaldehyde is also operative.

The $(M - CH_3)^+$ peak is greatly enhanced when X = CO_2CH_3 as reported earlier[1] and also when X = CO_2H as revealed by the present study. Deuterium labelling showed the ether methoxyl to be the source of the lost methyl radical with some scrambling also occurring. An intermediate ion-neutral complex allowing interaction of the methoxymethyl and acid/ester groups offers a possible explanation for these observations. When X = CH_3, the $(M - CH_3)^+$ peak is also large, but labelling here revealed predominant loss of the ring methyl group.

When X = CN, the largest peak in the spectrum is $(M - CH_2O)^{+\cdot}$ although $(M - CH_3O)^+$ is almost as large. The particular property of the cyano group responsible for this is not obvious, but formation of a conjugated quinoid structure may help stabilize the $(M - CH_2O)^{+\cdot}$ ion.

The most unusual fragmentation of the methoxymethyl group occurs when X = NO_2. Here the largest peak in the spectrum is $(M - C_2H_4O_2)^{+\cdot}$. Metastable transitions reveal that at least part of this ion arises from consecutive losses of formaldehyde from the molecular ion. High resolution data verified that the composition of this ion is C_6H_5NO and not C_7H_7O which could arise from the more plausible loss of formaldehyde and nitric oxide. A possible mechanism involving interaction of the methoxymethyl and nitro groups as an ion-neutral complex is proposed in Scheme 1.

1. R. Herrmann and H. Schwarz, Z. Naturforsch., 31, 870 (1976).

Presented at the 35th ASMS Conference on Mass Spectrometry and Allied Topics
May 24-29, 1987, Denver, CO

TABLE I

Comparative Mass Spectra of Para Substituted Methoxymethylbenzenes

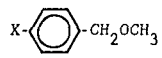

X =	H	CH_3	F	Cl	Br	NO_2	CN	CO_2CH_3	COOH
$M^{+\cdot}$	67.2	41.3	33.9	27.9	16.2	0.3	5.4	13.1	15.1
$(M - H)^+$	59.2	26.4	33.9	25.0	10.3	2.9	28.5	21 9	32.0
$(M - CH_3)^+$	2.2	74.0	1.6	0.8	0.3	--	6.5	58.1	79 8
$(M - CH_3 - H_2)^+$	3.9	7.2	4.5	2.6	4.5	1.4	4.2	--	5.3
$(M - CH_2O)^{+\cdot}$	15.9	7.7	13.0	2.1	1.1	0.2	100.0	3.3	5 3
$(M - CH_3O)^+$	100.0	100.0	100.0	80.9	34.3	3.8	72.5	93.8	62.5
$(M - CH_3OH)^+$	3.4	28.1	2.7	0.5	0.1	1.0	2.8	4.0	2.1
$(M - CH_2OCH_3)^+$	23.1	44.3	8.1	4.3	2.8	1.2	17.1	3.9	2.4
$(M - X)^+$	(59.2)	(74.0)	1.1	100.0	100.0	11.0	1.3	100.0	100.0
$(M - C_2H_4O_2)^{+\cdot}$	--	--	--	--	--	100.0	--	--	--

Relative intensities shown have been corrected for ^{13}C isotopic peaks.

SCHEME 1

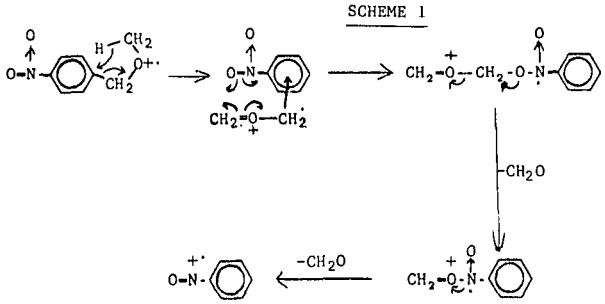

Presented at the 35th ASMS Conference on Mass Spectrometry and Allied Topics
May 24-29, 1987, Denver, CO

ON THE LOSS OF SEVENTEEN MASS UNITS FROM METHYLARYLSULFIDES.

M. T. Cheng, Stauffer Chemical Company, Richmond, CA

In a paper published in 1966 by Bowie & et al on the mass spectra of aromatic thioethers[1], the authors noted fairly abundant (6%-10%) of M-17 ions from the mass spectra of the methylthioanisoles. An accurate mass measurement confirmed the only reasonable composition ($M-CH_5$), this loss however is not observed in the spectra of the methylanisoles. The goal of this study is to investigate the source of the CH_5 group and the structure of the $M-CH_5$ ion.

The mass spectrum of the following compounds synthesized by regular routes were

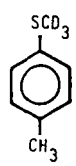

(I)

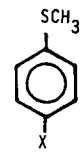

X=Br (II)
X=t-C_4H_9 (III)
X=CD_3 (IV)

obtained[2]. The mass spectrum of compound I shows losses of 18 amu, 19 amu and 20 amu, the loss of 18 amu is consistent with the observation by Bowie and et al that S-methyl is lost resulting in the formation of a benzyl (or tropylium) cation. However, compounds II and III show only the loss of methyl and no loss of 17 amu.

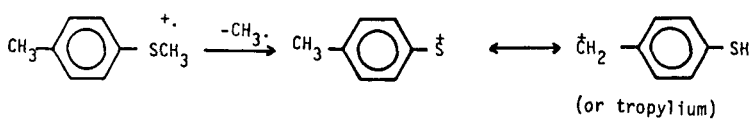

It is possible that because compounds II and III (Figure 1) do not form the stable benzyl (or tropylium) ion therefore they do not show a loss of H_2 after methyl loss. The mass spectrum from compound IV shows losses of 16 (CH_4, 3.2% of base peak), 17 (CH_5 or CH_3D, 2.2%), 18 (CH_4D, 3.5%), 19 (CH_3D_2, 1.9%) (Figure 2). In the mass spectrum of p-methylthioanisole there is a peak due to $M-CH_4$ at 2% of the base peak. This same amount of contribution is subtracted from the intensity of the M-17 ($M-CH_5$ or $M-CH_3D$) peak from compound IV. After this correction the ratio of H_2:HD:D_2 losses is 3:63:34. However, assuming complete scrambling of the seven atoms (H_4D_3) in the $M-CH_3$ ion of compound IV, the loss of H_2:HD:D_2 will have the ratio 29:57:14, which is distinctly different from the ratio 3:63:34 for compound IV. The above information is consistent with the following mechanism: after the initial loss of methyl group attached to sulfur, a deuterium is transferred to the sulfur atom with the formation of tropylium ion, followed by the elimination of the deuterium on sulfur and a hydrogen or deuterium to form the M-18 or the M-19 ion, respectively. The ratio of HD:D_2 losses of approximately 2:1 (63:34) is consistent with the complete scrambling of H_4D_2 on the ring. This fragmentation is not found in the methylanisoles perhaps due to the smaller and less polarizable oxygen atom compared to sulfur atom.

References

(1) Bowie, J. H.; Lawesson, S. -O; Madson, J. O; Scholl, G; Williams, D. H. J. Chem. Soc. (B), 1966, 951.

(2) All mass spectra were obtained on a VG7070E-HF mass spectrometer with 70 eV electrons, 50 µA trap current, 6KeV accelerating voltage, and source temperature of 150°C.

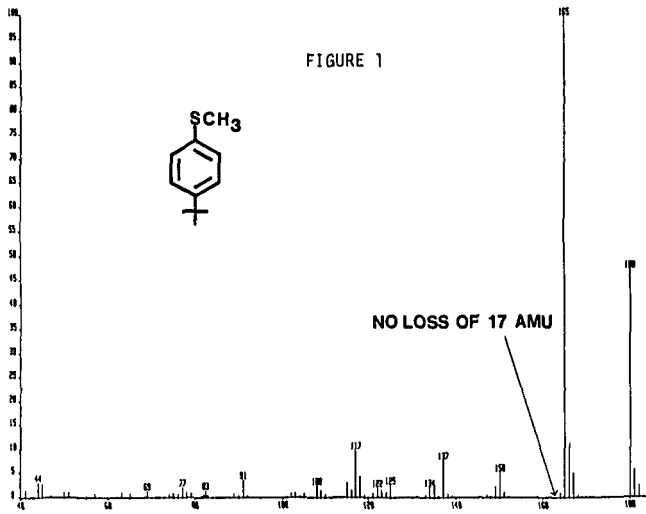

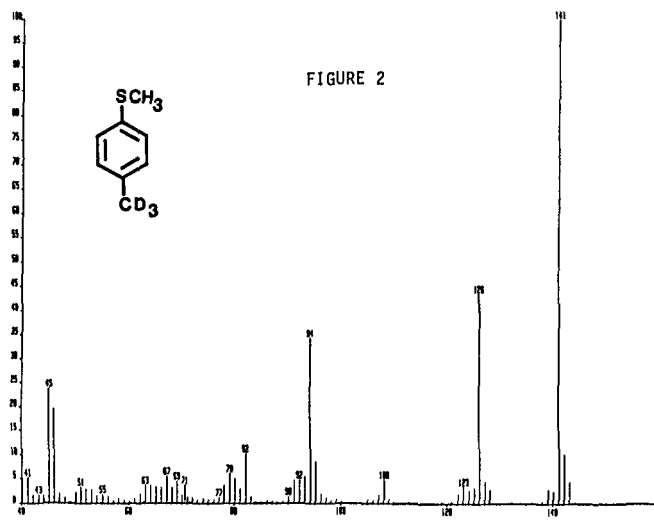

Presented at the 35th ASMS Conference on Mass Spectrometry and Allied Topics
May 24-29, 1987, Denver, CO

A STUDY OF ADDUCT ION FORMATION: REACTIONS OF THE TRIMETHYLSILYL ION WITH OXYGENATED COMPOUNDS

Ron Orlando and Burnaby Munson

Department of Chemistry, University of Delaware, Newark, DE 19716

Tetramethylsilane (TMS) was introduced as a chemical ionization reagent gas for two reasons.[1] The reagent ion spectrum is a simple one, containing mostly trimethylsilyl ions at m/z 73; and the CI spectra for many nucleophilic compounds contain abundant adduct ions, $(M+73)^+$.

The mechanism for the formation of these adduct ions has generally been assumed to be the formation of an excited collision complex which is collisionally stabilized with the sample or TMS, reactions (1) and (2).

$$73^+ + M \rightleftharpoons (M+73)^{+*} \qquad (1)$$

$$(M+73)^{+*} + X \rightarrow (M+73)^+ + X^* \qquad (2)$$

However, a detailed study and verification of this mechanism has not been previously reported.

It was found by a variety of techniques under ICR and CI conditions that the trimethylsilyl ion reacts with aliphatic alcohols to form the hydrated trimethylsilyl ion at m/z = 91, (3). This ion then reacts by a displacement of water with another molecule of the alcohol to form the adduct ion, $(M+73)^+$ (4).[2]

$$(CH_3)_3Si^+ + C_nH_{2n+1}OH \rightarrow (CH_3)_3SiOH_2^+ + C_nH_{2n} \qquad (3)$$

$$(CH_3)_3SiOH_2^+ + C_nH_{2n+1}OH \rightarrow (CH_3)_3SiOHC_nH_{2n+1} + H_2O \qquad (4)$$

When the trimethylsilyl ions react with di-alkyl ethers, $C_nH_{2n+1}OC_nH_{2n+1}$, the major ionic products are alkyl ions, (5a); fragment ions from the loss of one or two C_nH_{2n} groups from the excited intermediate, (5b) and (5c); and adduct ions. Both ICR and CI experiments showed that the fragment ions react by displacement of water or alcohol by the ether to form adduct ions in reactions analogous to those found for the alcohols, (6) and (7).

$$(CH_3)_3Si^+ + C_nH_{2n+1}OC_nH_{2n+1} \rightarrow \begin{cases} C_nH_{2n+1}^+ & (5a) \\ (CH_3)_3SiOHC_nH_{2n+1}^+ & (5b) \\ (CH_3)_3SiOH_2^+ & (5c) \end{cases}$$

$$(CH_3)_3SiOH_2^+ + ROR \rightarrow (M+73)^+ \qquad (6)$$

$$(CH_3)_3SiOHC_nH_{2n+1} + ROR \rightarrow (M+73)^+ \qquad (7)$$

The occurrence of these displacement reactions is consistent with the suggestion that the trimethylsilyl ion affinity of water is less than the trimethylsilyl ion affinity of an alcohol which is less than that of an ether.

For both the alcohols and the ethers, there was no evidence for any formation of adduct ions by direct addition followed by collisional stabilization, reactions (1) and (2). Therefore, the lifetimes of the collision complexes must be less than 0.1 us, a rough upper limit obtained by using a collision rate of 10^{-9} cm^3/molecule-s.

The TMS CI spectra of some simple aromatic ethers, aldehydes, ketones, and phenols contain essentially only adduct ions, $(M+73)^+$. "Trapped drift" experiments under ICR conditions showed that the adduct ions were formed by a bi-molecular addition of the trimethylsilyl ions to these molecules, (8).

$$(CH_3)_3Si^+ + M \rightarrow (M+73)^+ \qquad (8)$$

Both the shapes of the curves in Figure 1 and the pressure independence of the rate constant for this reaction demonstrate that the adduct ions are formed by "sticky collisions", direct bi-molecular addition reactions which do not require collisional stabilization.

We have found two mechanisms for the formation of the trimethylsilyl adduct ion for several oxygenated compounds. The first, for aliphatic alcohols and di-alkyl ethers, is by formation of an intermediated which then reacts with another sample molecule. The excited collision complex exothermically decomposes before sufficient energy can be lost. In the second case, there are no favorable irreversible decomposition pathways and the adduct ions are formed by simple addition.

REFERENCES

1. T. J. Odiorne, D. J. Harvey, and P. Vouros, J. Phys. Chem. **76**, 3217 (1972).

2. R. Orlando, F. Strobel, D. P. Ridge, and B. Munson, Org. Mass Spectrom., in press.

Figure 1

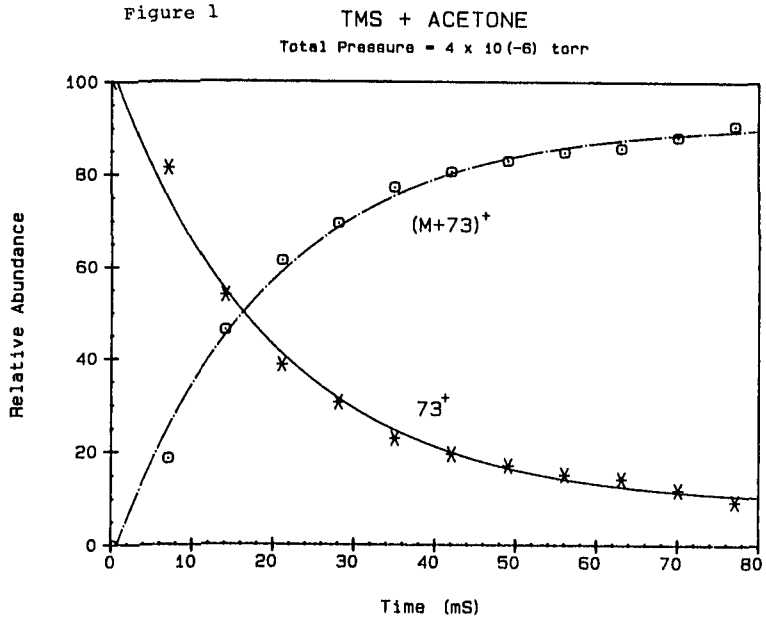

Presented at the 35th ASMS Conference on Mass Spectrometry and Allied Topics
May 24-29, 1987, Denver, CO

MASS SPECTROMETRIC STUDY OF BORONTRIHALIDE MONOAMINES

Kenneth Ng, B. Piatek, C. Shimanskas
CIBA-GEIGY Corporation, Analytical Research Department,
Ardsley, NY 10502

Borontrihalide monoamines are a class of compounds generally found at low concentrations in one component epoxy resin systems as curing agents or even at a lower amount as latent accelerators. No previous mass spectrometric analysis has been reported on this class of compounds.

Detection and identification of such complexes in the sample matrix by direct analysis are usually non-specific and insensitive. Isolation is often cumbersome and non straight-forward since the complex is very reactive with the epoxy system.

A series of these Lewis acids complexes was examined by mass spectrometry using EI and DCI modes. Both modes gave an abundant fragment ion corresponding to the loss of a halide atom from the molecular ion. In addition other ions indicative of both the Lewis acids and the amine structures were also observed. Fig. I, II and Table I.

Figure III is a direct mass spectrometric analysis of a commercial epoxy resin system. Compound I was identified as the specific complex used. This method was shown to be simple and fast without the need for prior separation or isolation. DCI mode was preferred over EI because it generated a much simpler spectrum. This is especially true when an epoxy resin system was being analyzed.

TABLE I

DCI DATA OF BORONTRIHALIDE MONOAMINE $BX_3.A$

COMPOUND		MW	(M-X)+	AH+	(A-H)+	ADDUCT	IONS
(I)	X = Cl A = C_4H_{12}-N-$(CH_3)_2$	273	238	158	156	395	(M-X)A+
(II)	X = F A = HN⟨⟩	153	134	86	84	287	(M-X)M+
(III)	X = F A = $CH_3CH_2NH_2$	113	94	--	--	207 159	(M-X)M+ (M+A)H+
(IV)	X = Cl A = H⟨⟩N	228	193	113	--	----------	
(IVa)	X = F A = H⟨⟩N	180	161	113	--	----------	

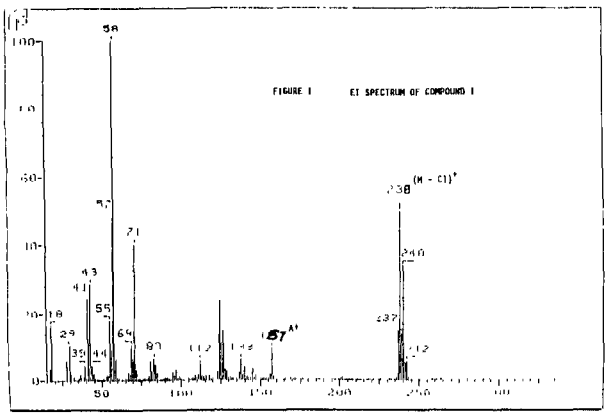
FIGURE I
EI SPECTRUM OF COMPOUND I
58
71
43
55
57
238 (M - Cl)+
240
237

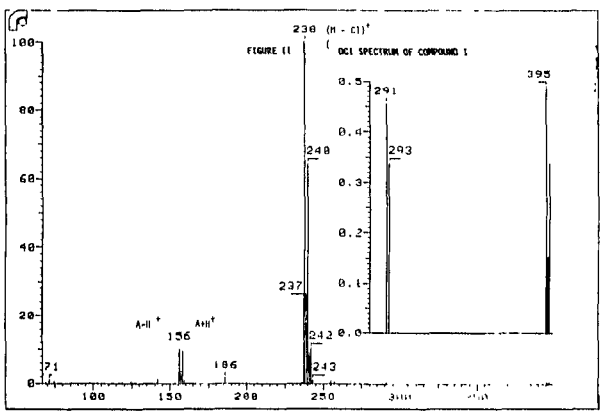
FIGURE II
CCI SPECTRUM OF COMPOUND I
238 (M - Cl)+
240
237
242
243
156
186
71
291
293
395

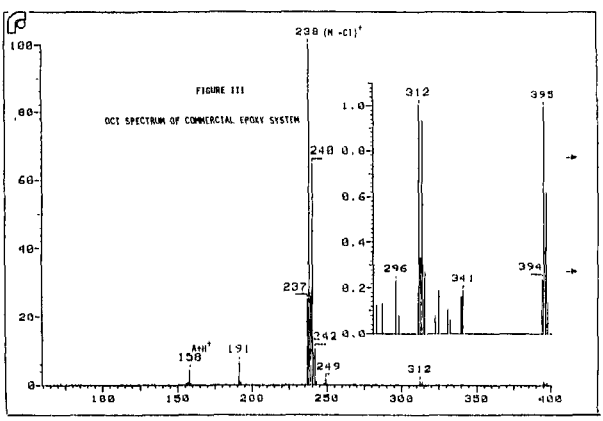
FIGURE III
CCI SPECTRUM OF COMMERCIAL EPOXY SYSTEM
238 (M -Cl)+
240
237
242
249
156
191
312
296
341
394
395

Presented at the 35th ASMS Conference on Mass Spectrometry and Allied Topics
May 24-29, 1987, Denver, CO

FORMATION OF THE MH^- ION IN THE NCI SPECTRUM OF CHLORPROTHIXENE

Patrick S. Callery, William A. Garland and Elaine K. Fukuda, Department of Medicinal Chemistry, University of Maryland, Baltimore 21201 and the Drug Metabolism Department, Hoffmann-La Roche, Inc., Nutley, NJ 07110

The negative ion chemical ionization mass spectrum of chlorprothixene shows an unusual MH^- ion. This ion can be accounted for by hydrogen radical attachment followed by electron capture. The MH^- ion recorded with methane as reagent gas was shifted to MD^- when tetradeuteromethane was used in place of methane. Bleeding a small amount of air into the source region decreased the relative proportion of MH^-, perhaps by radical scavenging by oxygen. The most probable site of radical attachment was concluded to be related to the sulfur atom of the thiothixene ring based on the observation of analogous ions for structurally related compounds, all containing a heterocyclic sulfur. Dihydrochlorprothixene, synthesized by reduction of the exocyclic double bond of chlorprothixene with lithium aluminum hydride, also displayed a measurable MH^- ion as did deschlorochlorprothixene and chlorpromazine. SIMS spectra of sulfur containing heterocycles have been shown to contain MH^- ions (1). Amitriptyline, which is similar in structure to chlorprothixene but does not contain sulfur, showed no MH^-. The ratio of $(M-H)^-$ to MH^- did not change with increasing emission current suggesting that the process is independent of radical concentration in the CI plasma. This is in contrast to findings by McEwen and Rudat (2) and Blom and Munson (3) who also observed $(M+15)^-$ and $(M+29)^-$ radical attachment ions. No $(M+15)^-$ or $(M+29)^-$ ions were observed for chlorprothixene. These results suggest that hydrogen radical attachment to chlorprothixene may occur at a source wall surface. Further evidence that the origin of the hydrogen radical may be from surfaces within the CI source was gained in a preliminary experiment in which sputtering of gold into the source reduced the relative proportion of the MH^- ion.

1. D.E. Main, W. Ens, R. Beavis, B. Schueler, K.G. Standing, J.B. Westmore and C.-M. Wong, Biomed. Mass Spectrom., **14**, 91 (1987).

2. C.N. McEwen and M.A. Rudat, J. Am. Chem. Soc., **101**, 6470 (1979).

3. K. Blom and B. Munson, Int. J. Mass Spectrom. Ion Phys., **43**, 17 (1982).

Presented at the 35th ASMS Conference on Mass Spectrometry and Allied Topics
May 24-29, 1987, Denver, CO

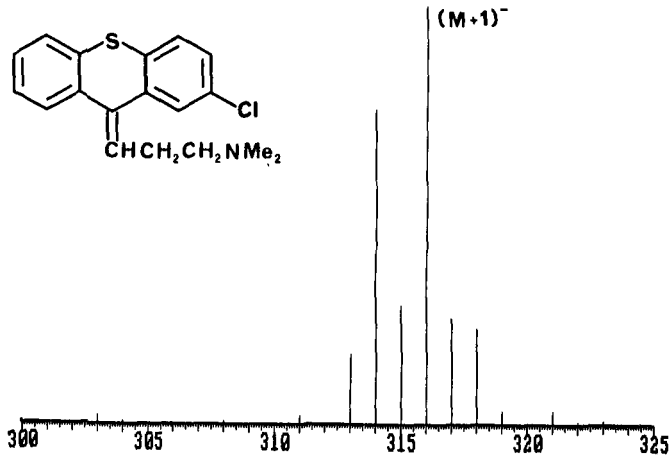

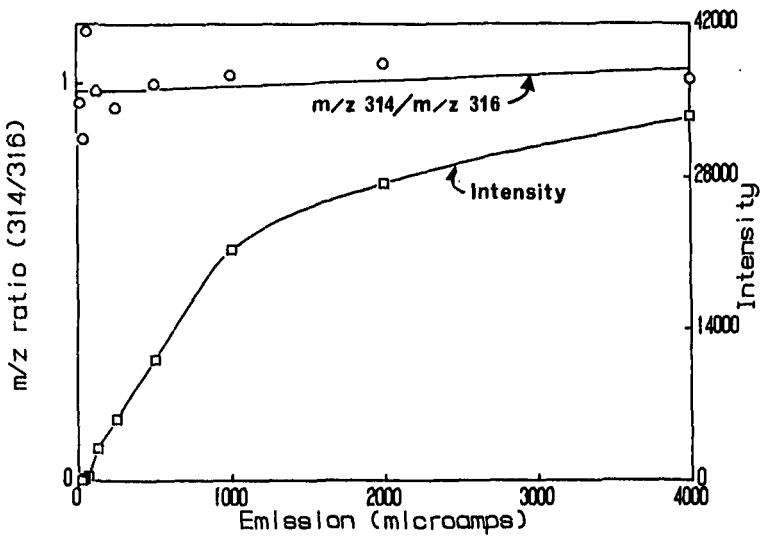

Presented at the 35th ASMS Conference on Mass Spectrometry and Allied Topics
May 24-29, 1987, Denver, CO

Lithiated Polypropyleneglycols for Calibration of Tandem Mass Spectrometers

J. M. Gilliam and J. L. Occolowitz*, Lilly Research Laboratories, Indianapolis, IN 46285

The aim of the work described was to find a substance having a collision induced dissociation (CID) spectrum sufficiently rich, regular, and reproducible that it could be used to calibrate and test the performance of MS2 of tandem mass spectrometers. Such a substance is especially useful if no auxilliary ion source, situated in the field-free region between MS1 and MS2, is available for the direct calibration of MS2.

Spectra shown were obtained using a VG ZAB-3F mass spectrometer. Precursor ions were selected by B_1, daughter ions were generated by He collision in the 2nd FFR and they were separated by link scanning E and B_2. For precursors of less than 1000d. a 50" decade^{-1} scan rate was used, for higher mass precursors a scan rate of 100" decade^{-1}. Data were acquired using a MAT SS-200 data system using an attenuated E potential for mass calibration. Commercially available polypropyleneglycols (PPG) fractions were dispersed in "magic bullet" containing an alkali-metal halide and ionized using a cooled FAB target.

The extensive FAB induced fragmentation of cationized PPGs reported by Cook[1] suggested that individual components of these mixtures might yield rich CID spectra. The CID spectrum of m/z 1243 from lithiated PPG 1200 bears a close resemblance to the FAB spectrum of lithiated PPG 1750 in the mass range where the latter contains only fragment ions (Fig. 1). Consequently the CID fragmentation was rationalized as shown in Fig. 2.

Figs. 3 and 4 show CID spectra of m/z 779 from lithiated PPG 725 and of m/z 1243 from lithiated PPG 1200. A similar spectrum was obtained from m/z 1765 from lithiated PPG 1750. Relatively intense precursor ions can be generated from higher MW PPG fractions, e,g, PPG 2000, however, the loss of sensitivity resulting from obtaining adequate precursor ion resolution in our MS1, which is single focusing, precluded examining these higher MW precursors.

Similar CID spectra were obtainable by cationizing PPGs with other alkali metals, however, the low atomic weight of lithium resulted in calibration ions at lower masses than for other alkali metal cations.

The accuracy obtainable using E for mass calibration of the linked B_2/E scans was investigated using these calibration compounds. For example, a calibration using m/z 1243 from PPG1200 was used to check the accuracy of mass assignments for fragments of m/z 1185 derived from the same source. This was accomplished by attenuating the E signal until the data system acquisition processor read the correct mass for m/z 1185 when the mass spectrometer was focused on this precursor. Measurements of this type showed that the E signal gave acceptable (0.5d<) errors for fragments derived from precursors up to approximately 1000d.

[1] J. C. Cook, University of Illinois, private communication, 1984.

Presented at the 35th ASMS Conference on Mass Spectrometry and Allied Topics
May 24-29, 1987, Denver, CO

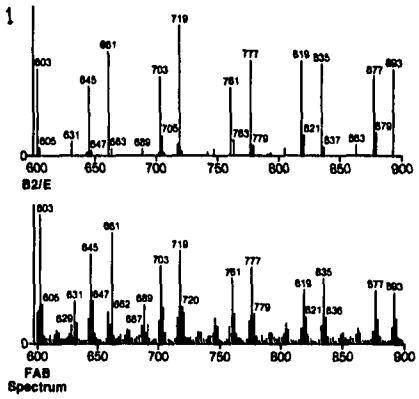

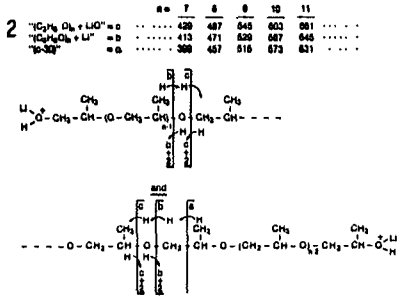

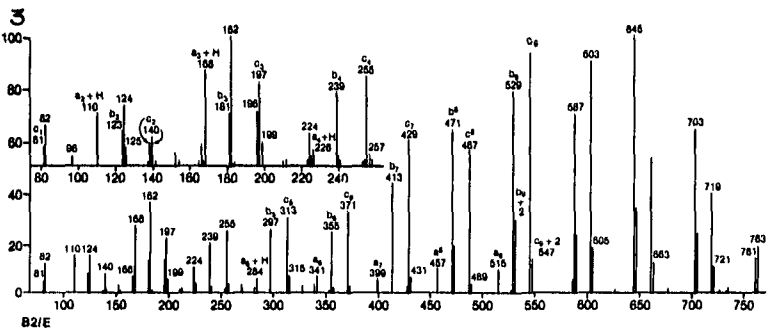

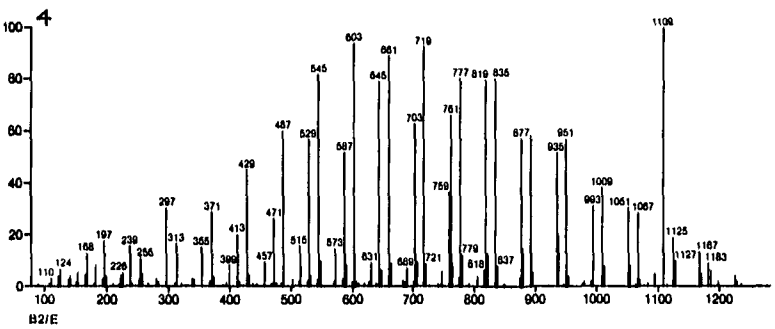

Fig. 1. Top: CID spectrum of m/z 1243 from lithiated PPG 1200
Bottom: FAB spectrum of lithiated PPG 1750
Fig. 2. Origin of major fragments in CID spectra of lithiated PPGs
Fig. 3. CID spectrum of m/z 779 from lithiated PPG 725
Fig. 4. CID spectrum of m/z 1243 from lithiated PPG 1200

Presented at the 35th ASMS Conference on Mass Spectrometry and Allied Topics
May 24-29, 1987, Denver, CO

Decomposition Reactions of Alkylbenzene Molecular Ions revealed by Multiphoton Ionization Mass Spectrometry: Propylbenzene Molecular Ions.

J. Grotemeyer, U. Boesl, K. Walter, E.W. Schlag

Institut für Physikalische und Theoretische Chemie, TU München
Lichtenbergstr. 4, D-8046 Garching, Germany.

Multiphoton Ionization (MUPI) is an excellent method for the investigation of polyatomic molecules, due to its intrinsic features. One of the features is the sharp energy distribution of the produced ions/1/. This behaviour and the possibility of soft ionization with an exclusive production of molecular ions makes this method perfect for the investigation of isomerization and fragmentation reactions.
In this paper the isomerization and fragmentation reactions of the n-propylbenzene molecular ion and its labelled derivatives are investigated in a two color pump-pump experiment/2/. The molecular ion is produced in soft two photon ionization at 2773Å. Some 4.5 ns later a second laser is fired producing photons of a wavelength of 4800 Å. These photons induce in a controlled way fragment ions from the n-propylbenzene molecular ion. The time lag between both lasers guarantees that photons from the second laser pulse are only used for the fragmentation processes and not for the ionization of the resonant excited state as well/2/. The mass spectrometer used in these investigation is a Refectron-Time-of-Flight mass spectrometer/1/. For the investigation of the metastable decomposition the instrument is running in the partial corrected mode. The decomposition of the n-propylbenzene molecular ion is dominated in the metastable region by three different fragmentation channels : loss of a methyl-radical (m/z 105), loss of a ethyl radical as well as ethylene (m/z 91,92) and the loss of propene (m/z 78). In contrast to EI metastable decomposition as well as to the EI mass spectrum the loss of propene occurs in MUPI with higher intensity. One question arising from this behavior is the mechanism of this fragmentation reaction.
The scheme below shows the metastable peak pattern for the loss of propene from different labelled n-propylbenzene molecular ions investigated by MUPI and EI/3/ respectively.

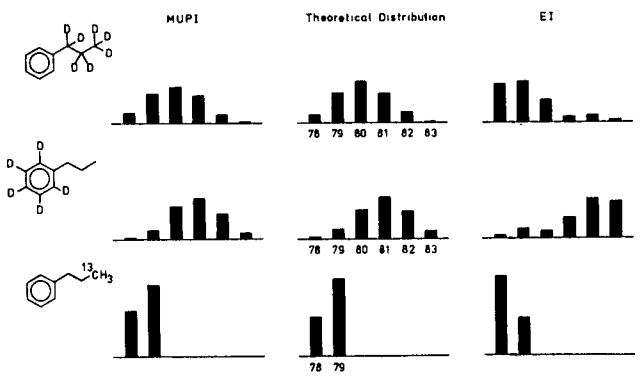

Scheme 1. Peak pattern for the metastable loss of propene from n-propylbenzene.

This scheme demonstrates, that prior to the decomposition into propene and benzene the propylbenzene molecular ion undergoes a extensive rearrangement reaction leading in MUPI mass spectrometry to a nearly complete statistical distribution of all carbon and hydrogen atoms. Under EI conditions this scrambling process ist not complete as also seen from scheme 1. This behavior is due to the fact, that by using the feature of 2+1 photon excitation the energy

necessary for the fragmentation reaction is controlled. Scheme 2 shows some results of MNDO-calculation for the interconversion and fragmentation reaction of n-propylbenzene.

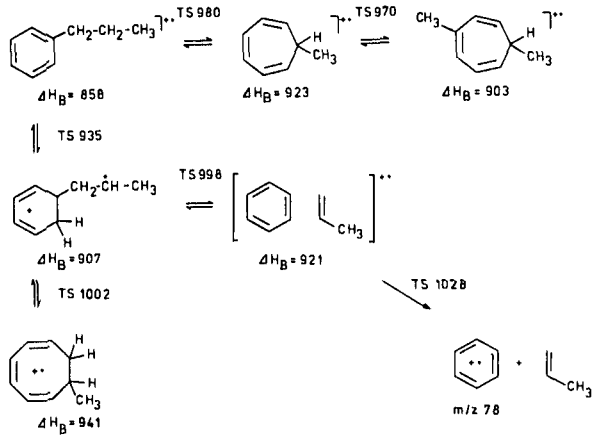

Scheme 2. MNDO calculations of the interconversion and fragmentation reactions in n-propylbenzene. (all values in kJ/mol).

The calculation as well as the high intensity of the propene loss in the metastable mass spectra lead to the conclusion that one of the key steps in the isomerization of propylbenzene is the formation of an ion-molecule complex. To prove the possibility of such a complex, we succeeded in producing a neutral complex of benzene and propene. The mass spectrum of this complex is dominated by the loss of propene and the formation of the benzene radical ion. The results of the metastable investigation of this complex formed by propene and ^{13}C labelled benzene are shown below. Again a statistical behavior is seen for the metastable loss of propene.

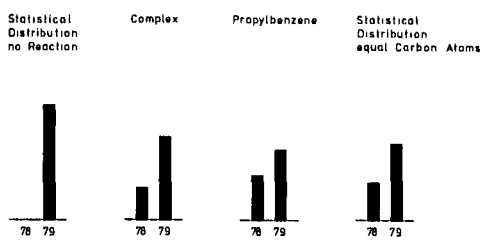

Scheme 3. Metastable peak pattern for the loss of propene from the propene-^{13}C-benzene.

These results demonstrate, that this ion-molecule complex is stable in the gas phase. Further it is shown by the scrambling of the carbons, that this complex participate in the isomerization reaction of propylbenzene.

/1/ U.Boesl, J.Grotemeyer, K.Walter and E.W.Schlag; Anal.Instrum. 16, 151 (1987).
/2/ J.Grotemeyer, U.Boesl, K.Walter and E.W.Schlag; Adv.Mass Spectrom. 10b, 945 (1985).
/3/ J.Grotemeyer, R.Uphoff and H.Fr.Grützmacher; unpublished results.

Presented at the 35th ASMS Conference on Mass Spectrometry and Allied Topics
May 24-29, 1987, Denver, CO

BRANCHING RATIOS AND MECHANISMS OF TWO COMPETING HYDROGEN REARRANGEMENTS IN THE ELECTRON IMPACT FRAGMENTATION OF SUBSTITUTED ACETOACETANILIDES

Thomas R. Sharp
Mass Spectrometry Applications Laboratory
Center for Chemical Characterization and Analysis
Department of Chemistry, Texas A&M University, College Station, Texas 77843, U.S.A.

Electron impact-induced fragmentation of a series of ring-substituted acetoacetanilides (Structure I) has been examined. The majority of the total ion current in the spectra of these compounds resides in three ions -- $[M]^{+\cdot}$ and two hydrogen rearrangement ions, $[M-58]^{+\cdot}$ and $[M-84]^{+\cdot}$, resulting from loss of neutral acetone and diketene, respectively. Mechanisms proposed for these two rearrangements are given in equations 1 and 2. The spectrum of p-methylacetoacetanilide is given in Figure 1 as representative of this series of compounds.

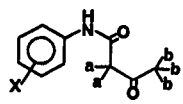

X = H, p-CH_3, m-CH_3, p-Cl, o-OCH_3, p-OCH_3, m-Cl

Structure I

Correlation of the relative abundances of the $[M-58]^{+\cdot}$ and $[M-84]^{+\cdot}$ ions with the electron-donating nature of the remote ring substituent gave Hammett linear free energy correlations[1]. Donation of electron density, by such as a methoxy substituent, to the aromatic system stabilizes the $[M-58]^{+\cdot}$ substituted isocyanate radical cation, while withdrawal of electron density by such as a chloro substituent destabilizes $[M-58]^{+\cdot}$. The nature of the ring substituent has little effect on the overall stability of the $[M-84]^{+\cdot}$ substituted aniline radical cation[1].

Deuterium labeling experiments were conducted to identify the source of the rearranging hydrogen. The methylene hydrogens (position a of Structure I) and the amido hydrogen are readily exchanged with saturated Na_2CO_3 in D_2O. Exchange of the terminal methyl hydrogens (position b, Structure I) requires incubation of the compound in 0.5 M KOD/D_2O at appx. 80°C for 30-45 minutes. Recovery from KOD/D_2O was achieved by neutralization and extraction into Et_2O, followed by washing with saturated $NaHCO_3/H_2O$ to remove deuterium from the amido and methylene positions.

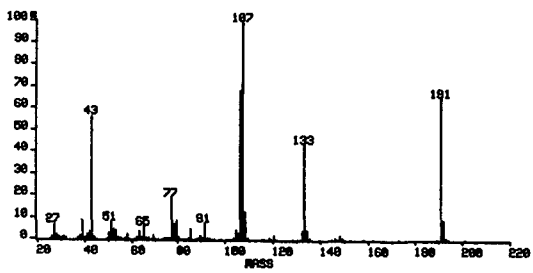

Figure 1: 70 eV spectrum of p-methylacetoacetanilide

Migration of the amido hydrogen onto the methylene carbon, shown in Eq. 1, results in neutral loss of acetone to give the $[M-58]^{+\cdot}$ isocyanate radical cation. Deuterium from neither site a nor site b should be retained in $[M-58]^{+\cdot}$. The experimental observations are completely consistent with Equation 1.

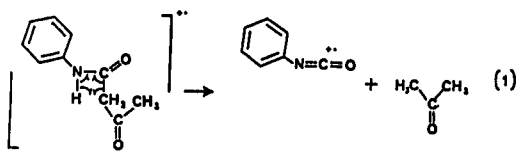

(1)

A hydrogen migrating from the sidechain to the nitrogen, in order to form the anilinium radical cation, could come from either position a, via a four-membered cyclic intermediate (equation 2a), or position b, via a six-membered cyclic intermediate (equation 2b).

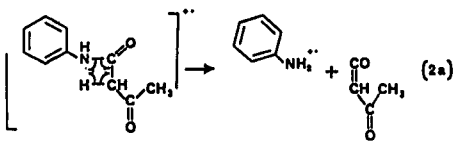

(2a)

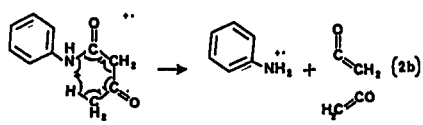

(2b)

Deuterium labeling experiments suggested that, for the p-methoxy compound, only the methylene hydrogens (position a) were migrating. Upon examining other labeled compounds, normal mass spectral scan data suggested that mechanism 2b began to contribute as the electron-withdrawing nature of the substituent varied (Table I). For compounds labeled in position b, the $[M-84]^{+\cdot}$ ion showed higher than expected deuterium content if only mechanism 2a were operating.

Presented at the 35th ASMS Conference on Mass Spectrometry and Allied Topics
May 24-29, 1987, Denver, CO.

Difficulties in preparing fully labeled compounds in a specific position, and of evaluating the isotope patterns prompted using B/E linked scans to investigate this problem.

Table I: Evaluation of deuterium content from normal scan mass spectra

Cmpd	labeling in position b	labeling in $[M-84]^{+\cdot}$
p-OCH_3	73% d_3	10% d_1
H	83% d_3	33% d_1
p-Cl	68% d_3	17% d_1

Table II: B/E daughter ion relative intensities

Cmpd	Transition	w/out collision gas	with collision gas
p-OCH_3	$M^{+\cdot}$ --> $[M-58]^{+\cdot}$	45 %	73 %
	$M^{+\cdot}$ --> $[M-84]^{+\cdot}$	55 %	27 %
H	$M^{+\cdot}$ --> $[M-58]^{+\cdot}$	8 %	26 %
	$M^{+\cdot}$ --> $[M-84]^{+\cdot}$	92 %	74 %
p-Cl	$M^{+\cdot}$ --> $[M-58]^{+\cdot}$	33 %	64 %
	$M^{+\cdot}$ --> $[M-84]^{+\cdot}$	67 %	36 %

Relative intensities of the two daughter ions for unlabeled compounds are given in Table II, and were found to differ, depending upon whether collision gas was present or absent in the collision cell. The two ions constituted > 90% of the total ion current in the B/E scans.

B/E scans of $M^{+\cdot}$ of o-methoxy aceto-acetanilide, labeled in position a, are shown in Figure 2. The m/z 208 $M^{+\cdot}$, labeled with a single deuterium, shows approximately equal intensity $[M-84]^{+\cdot}$ daughter ion peaks at m/z 123 and m/z 124, while the m/z 209 $M^{+\cdot}$, containing two deuterium labels in position a, shows exclusively a m/z 124 $[M-84]^{+\cdot}$ daughter ion -- results consistent with rearrangement occurring via mechanism 2a. B/E scans of the selected molecular ions of unsubstituted (Figure 3), p-methoxy- and p-chloro-acetoacetanilides with labels in position b generated predominantly the unlabeled $[M-84]^{+\cdot}$ daughter ion. The minor, but reproducible, intensities corresponding to label-carrying $[M-84]^{+\cdot}$ ions can be readily attributed to extraneous methylene labeling in the samples used. Results regarding the operative rearrangement mechanism do not change for observations made with or without collision gas.

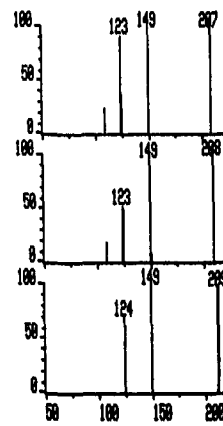

<---- Figure 2: ----
B/E scans of molecular ions of o-methoxy acetoacetanilide, labeled in position a.

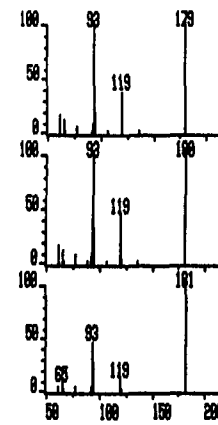

---- Figure 3: ---->
B/E scans of molecular ions of aceto-acetanilide, labeled in position b.

In conclusion, the isotope patterns presented in the normal scan mass spectra, which suggested a multiplicity of rearrangement mechanisms, have been shown to be misleading. B/E linked scans of deuterated compounds labeled in a specific position have demonstrated that a single hydrogen rearrangement mechanism, via a four-membered cyclic intermediate (equation 2a), is the predominant, if not exclusive mechanism operating in this entire series of compounds.

Observations were made with a VG Analytical 70-S double focusing instrument with DS-11/250J datasystem[2]. Samples were introduced on the direct insertion probe, which was heated to 80-140°C, depending upon the compound. B/E linked scan experiments were performed using helium as the collision gas, in a first field-free region collision cell, to reduce the $[M]^{+\cdot}$ intensity by 50%. Comparisons were made in the presence and absence of collision gas.

---

1. G. El-Taliawi, T.R. Sharp, C. Walling (1983). 30th Ann. Conf. Spectroscopy Society of Canada, Vancouver, B.C., Canada, 6-8 October 1983.
2. Mass Spectrometry Applications Laboratory, Center for Chemical Characterization and Analysis, Dept. of Chemistry, Texas A&M University. Established in part with funds from NSF grant CHE-8705697

Presented at the 35th ASMS Conference on Mass Spectrometry and Allied Topics
May 24-29, 1987, Denver, CO

NEW CONSIDERATIONS FOR CHOOSING A LIQUID MATRIX FOR FAST ATOM BOMBARDMENT

E. Schroeder, R. Pesch, and G. Dielmann
Finnigan MAT GmbH, Barkhausenstr. 2, D-2800 Bremen, FRG

Introduction

Fast Atom Bombardment (FAB) has greatly facilitated the study of large and polar biomolecules. However, its ionization mechanism was unknown. In recent publications, it has been shown that ion/molecule reactions in the gas phase above the liquid matrix are the most important processes which yield high ion currents of protonated molecules and cluster ions (1,2). The significant dependence of ion yield on FAB beam cross section has demonstrated the validity of this theory (2,3).
On the basis of this theory, we have investigated theoretically "designed" FAB matrices. The data show that it is possible to predict results of FAB experiments. The data indicate that there is a correlation between the matrix and the substrate polarity.

Results and discussion

Ammonia chemical ionization of carbohydrates is most suitable for molecular weight determination since intense $[M+NH_4]^+$ ions are formed in most cases. These spectra show a significant loss of water from $[M+NH_4]^+$. In contrast, the isobutane chemical ionization mass spectra show no $[M+H]^+$ ion, but only fragment ions corresponding to sequential loss of one, two and three water molecules from $[M+H]^+$.
Applying the gas phase theory to FAB, one would expect that FAB of aqueous ammonium acetate would produce a mixture of $CH_3COOH_2^+$ and NH_4^+ ions in the gas phase. The mass spectrum confirms this assumption (4,5).
So, the FAB spectra of carbohydrates in aqueous ammonium acetate show characteristics of both chemical ionization with ammonia and with isobutane (Fig. 1).

The solubility of the substrates in the liquid FAB matrix and the transport efficiency significantly affect the ion yield from the matrix surface. We have acquired FAB mass spectra of 5-leucine-enkephalin in various solvents. All solvents produce the same spectrum of the peptide. Differences lie in the ratio of substrate ions to solvent ions. The higher the polarity of the solvent, the smaller is the yield of solvent ions (Fig. 2).
5-leucine-enkephalin has a polar (non ionic) N-terminus and a non-polar C-terminus. So, there is a high probability that the non-polar part of these peptides results in a high concentration at the surface in highly polar solvents.

Experimental

FAB mass spectra were produced with a Finnigan MAT 8430 mass spectrometer. The FAB gun (Ion Tech FAB 11NF) was run with xenon at about 0.4 mA and 8 kV. The xenon gas pressure in the ion source housing was 2×10^{-3} Pa (2×10^{-5} mbar).
A 10 molar aqueous ammonium acetate solution was used as matrix for the mass spectra of the monosaccharides.
Solutions of 5-leucine-enkephalin (1 µg/µl) in methanol, dioxane, 3-nitrobenzylalcohol, glycerol and melted fructose were used to measure ratios of substrate-to-solvent ion yields.
The highly volatile matrices (methanol, acetic acid, dioxane) were absorbed on methylcellulose, resulting in a viscous droplet on the FAB target. A FAB target cooled to -30 °C was used instead of the methylcellulose.

Conclusion

The data demonstrate that the gas phase model of ion formation from non ionic substrates under FAB offers new ways to find a liquid FAB matrix. A complete interpretation of the results and a correlation between matrix and substrate polarity are still in process at this time.

1) E. Schroeder, H. Muenster, and H. Budzikiewicz
Org. Mass Spectrom. 21, 707 (1986)
2) H. Muenster, F. Theobald, H. Budzikiewicz, and E. Schroeder
Int. J. Mass Spectrom. Ion Proc. in press
3) H. Budzikiewicz, H. Muenster, F. Theobald, and E. Schroeder
"The Formation of a Matrix Plasma in the Gas Phase under Fast Atom Bombardment (FAB) Conditions." presented at the 35th ASMS Conference on Mass Spectrometry and Allied Topics,
May 24-29, 1987, Denver, CO.
4) A.M. Hogg, T.L. Nagabhusan, Tetrahedron Lett., 4827 (1972)
5) D.B. Horton, J.D. Wander, R.L. Foltz
Carbohyd. Res. 36, 75 (1974)

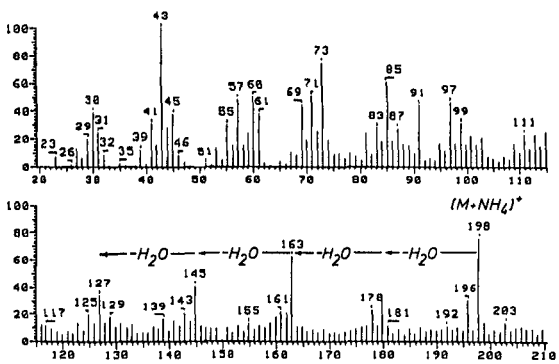

FIG. 1 D-(+)-Galaktose in NH4OAc/H2O

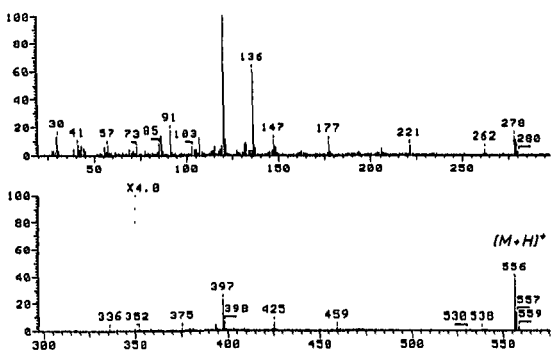

FIG. 2 Enkephalin in Fructose

Presented at the 35th ASMS Conference on Mass Spectrometry and Allied Topics
May 24-29, 1987, Denver, CO

SIMULTANEOUS MASS-SELECTIVE EJECT/EXCITE FOR FT/ICR MASS SPECTROMETRY

Ling Chen and Alan G. Marshall

Department of Chemistry
(and Dept. of Biochemistry)
The Ohio State University
120 West 18th Avenue
Columbus, OH 43210

Compared to prior-art pulse [1] or frequency-sweep [2] excitation, the recently demonstrated Stored Waveform Inverse Fourier Transform (SWIFT) technique [3-5] can produce frequency-domain excitation/ejection power with higher mass resolution and with arbitrary magnitude profile for both FT/ICR and ion-trap mass spectrometry. In particular, SWIFT can produce a power spectrum with multiple steps, to achieve simultaneous (high-power) ejection of ions of a given m/z-range(s) and (low-power) excitation of ions of other m/z-range(s).[6]

Figure 1 shows the simultaneous ejection of ions of two selected m/z-values and excitation (for subsequent detection) of all other ions in the detected mass range. Note that the relative intensities of the peaks remaining after selection ion ejection (d) are the same as in the normal mass spectrum (b).

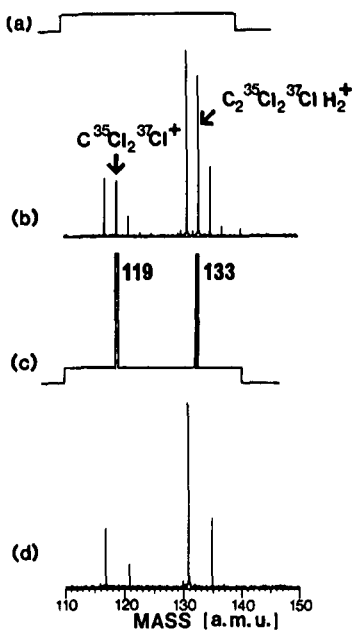

Figure 1. Magnitude spectra of the SWIFT excitations (a) and (c) used to generate FT/ICR mass spectra (b) and (d) of electron-ionized 1,1,1,2-tetrachloroethane. Uniform SWIFT excitation (a) gives the normal mass spectrum (b), whereas SWIFT ejection/excitation (c) ejects ions of nominal masses 119 and 133 with simultaneous undistorted detection (d) of the rest of the mass spectrum. This experiment was performed in direct-mode.

SWIFT excitation thus effectively compresses a multiple excitation event sequence by combining the ejection and excitation periods. By eliminating the time delay between ejection and excitation, we can make the total excitation period either longer (for higher mass selectivity) or shorter (to reduce the extent of ion-molecule reactions during the excitation period). Simultaneous eject/excite at a mass resolution >20,000 at m/z 92 is demonstrated in Figure 2.

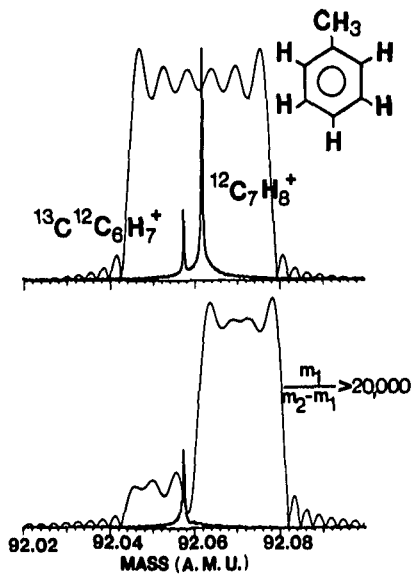

Figure 2. Heterodyne-mode simultaneous FT/ICR excitation/ejection of two ions of very similar mass-to-charge ratio, produced via electron ionization of toluene. In each plot, the broad line represents the experimental FT/ICR mass spectrum, and the thin line represents the magnitude-mode excitation spectrum used to produce that ICR signal. Although the originally specified excitation magnitude spectrum is flat, the finite excitation period introduces the ripple seen in the Figure.

Top: $^{12}C_6H_8^+$ (92.062 amu) and $^{13}C^{12}C_6H_7^+$ (92.058 amu) excited with uniformly-tailored SWIFT excitation extending from 92.04-92.08 amu.

Bottom: FT/ICR mass spectrum obtained via SWIFT simultaneous ejection/excitation, at a ratio of 5:1, demonstrating ultrahigh mass selectivity ($(m_2/(m_2 - m_1) > 20,000$) in a single excitation event.

[This work was supported by N.I.H. GM-31683, N.S.F. CHE-8218998, and The Ohio State University.]

1. Comisarow, M. B.; Marshall, A. G. (1974) Chem. Phys. Lett. 25, 282-283.
2. Comisarow, M. B.; Marshall, A. G. (1974) Chem. Phys. Lett. 26, 489-490.
3. Marshall, A. G.; Wang, T.-C. L.; Ricca, T. L. (1985), J. Am. Chem. Soc. 107, 7893-7897.
4. Wang, T.-C. L.; Ricca, T. L.; Marshall, A. G. (1986), Anal. Chem. 58, 2935-2938.
5. Chen, L.; Wang, T.-C. L.; Ricca, T. L.; Marshall, A. G. (1987) Anal. Chem. 59, 449-454.
6. Chen, L.; Marshall, A. G. (1987) Rapid Commun. Mass Spectrom., in press.

Presented at the 35th ASMS Conference on Mass Spectrometry and Allied Topics
May 24-29, 1987, Denver, CO

ADAPTION OF THERMOSPRAY LC-MS FOR MICRO LC.

R.A. OSTERMAN, C. R. BLAKLEY, G. J. FERGUSSON, AND M. L. VESTAL
Vestec Corporation, Houston, TX 77054.

Thermospray has become accepted as a practical technique for interfacing liquid chromatography with mass spectrometry, but performance has generally been unacceptable at LC flow rates below 0.5 mL/min. The rapid development of smaller bore LC columns over the past few years has aroused considerable interst in LC-MS at lower flow rates, particularly since the lower solvent flows and higher relative sample concentrations should correspond to more favorable conditions, at least in principle, for interfacing to mass spectrometry.

One of the major problems with thermospray at low flows is that the liquid velocity in the vaporizer capillary determines the maximum temperature at which vaporization can occur without causing premature vaporization within the capillary. Thus, low flow rates require smaller diameter vaporizer nozzles for acceptable performance. The initial studies accomplished during the present work employed smaller diameter stainless steel hypodermic needle tubing instead of the drawn SS tubing used previously. Results with the hypodermic needle tubing were initially quite disappointing in that the exit temperatures observed with ca. 50 micron ID tubing were substantially below those calculated from an approximate theoretical model described earlier. (1) This model accounted satisfactorly for results obtained using ca. 150 micron ID tubing at flow rates on the order of 1 mL/min, but predicted much higher exit temperatures than were observed using the 50 micron ID tubing at all flow rates between 0.1 and 1.0 mL/min.

Some additional experiments were conducted which have signficantly clarified the effect of capillary diameter on the properties of thermospray. In this work a series of thermocouples were attached at intervals along the capillary as shown in Figure 1, and these temperatures were monitored as functions of the control temperature for several different flow rates. As has been discussed previously (1), the thermospray controller used in this work provides a constant power per unit flow at a given value of the control temperature, T1. Results obtained for several different flows of water through a 50 micron ID stainless steel capillary are summarized in Figure 2. From these data approximate profiles of the tube temperatures along the heated portion can be constructed as shown in Figure 3. The calculated exit temperature for each flow is also indicated on the figure. From these results it appears that the calculated temperatures are more closely related to the average temperature along the capillary in the region where vaporization is ocurring rather than to the temperature at the exit.

After considering this discrepancy, we conclude that the model used in calculating exit temperatures at complete vaporization as a function of liquid velocity contains and unstated approximation which becomes poorer at smaller capillary diameters. In our earlier treatment (1) we calculated the exit temperature at complete vaporization by setting the liquid velocity equal to the vaporization velocity at the exit. By numerically inverting the resulting equation the exit temperature can be calculated as a function of liquid velocity. After considering our recent results, it is clear that this equation should use the average vaporization velocity over the heated length rather than that at the exit. Because of the large pressure drops due to high velocity vapor flows through narrow bore capillaries, this approximation is very poor for even 0.2 mL/min through a 50 micron capillary, even though it is reasonably satisfactory for flow of ca. 1 mL/min through a 150 micron capillary.

Reference: M. L. Vestal and G. J. Fergusson, Anal. Chem. 57, 2373 (1985)

Acknowledgement: This work was supported in part by NIH grant 1R43 GM 37313-01.

Presented at the 35th ASMS Conference on Mass Spectrometry and Allied Topics
May 24-29, 1987, Denver, CO

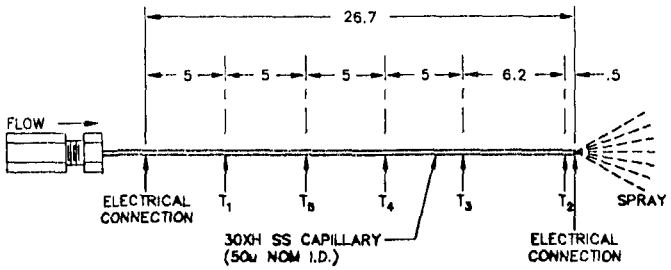

Figure 1. Schematic diagram of experiment for determining temperature along vaporizer capillary.

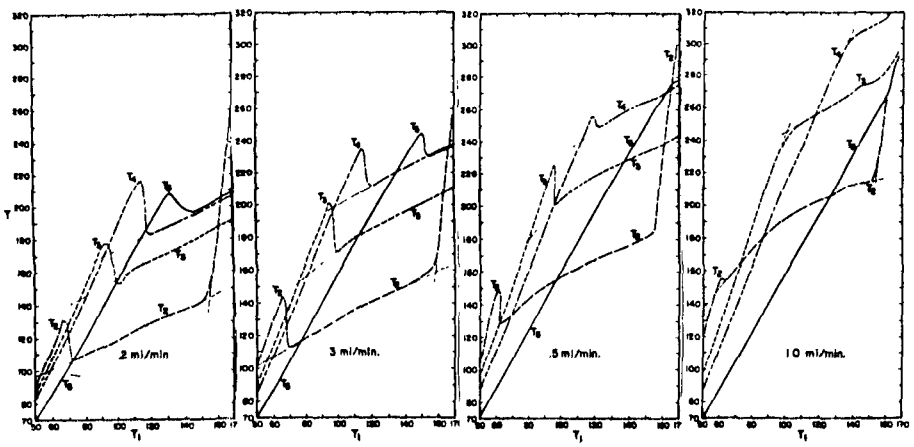

Figure 2. Measurement of temperatures at selected points along the thermospray capillary for water through a 50 micron ID capillary. The initial rise corresponds to heating liquid, the flatter portion to vaporization, and the sharp upward break in T_2 to completion of vaporization

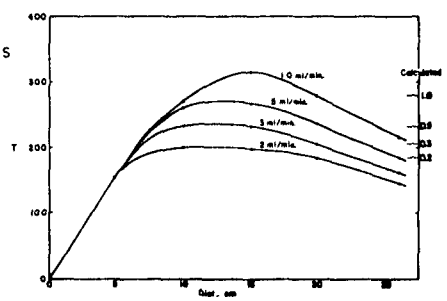

Figure 3. Temperature vs. distance along the capillary at f=1 at the exit, taken from the data shown in Fig. 2.

Presented at the 35th ASMS Conference on Mass Spectrometry and Allied Topics
May 24-29, 1987, Denver, CO

THERMOSPRAY ANALYSIS: STRUCTURAL IDENTIFICATION USING REPELLER CID WITH A TRIPLE STAGE QUADRUPOLE TO OBTAIN CID/MS/MS DATA

W.H. McFadden, P.J. Rudewicz, and D.A. Garteiz, Finnigan MAT, San Jose, CA 95134

Introduction

Increased use of soft ionization methods has provided the mass spectrometrist with tools that give mass analysis of labile or low volatility samples but which often give no fragmentation for structural analysis or increased specificity in target analysis. To obtain such fragmentation often necessitates the use of multiple mass or energy analyzers to give MS/CID/MS data but it is also possible to obtain CID fragmentation without extra stages of mass separation. Last year, Zackett et.al. (1) reported the observation that controlled CID could be obtained from a thermospray discharge ionization source by increasing the repeller voltage; CID fragmentation generally occurs in the voltage range 80-100 volts. This phenomenon is closely related to similar acceleration processes that have been used to break ionic clusters but the thermospray process, termed repeller CID, is easy to implement and greatly extends the capability of thermospray ionization.

Expermimental Results

Figure 1 presents a typical thermospray spectrum at low repeller voltage. The spectrum of this compound (nabilone) is characterized by the MH^+ ion with minimal fragmentation of limited utility. Figure 2 presents the spectrum of the same compound obtained at higher repeller voltages. Extensive fragmentation is observed thus providing ample information for structural studies or target specificity.

The spectra shown in Figures 1 and 2 were obtained with a single quadrupole mass spectrometer (Finnigan Model 4600) but give information that is closely related to data obtained from a triple quadrupole in MS/MS mode. It follows that with a triple quadrupole mass spectrometer, repeller CID will extend the system capability to give data that is closely related to MS/MS/MS data. More generally, repeller CID provides an additional stage of fragmentation for any specified mass analysis system.

The ability to obtain a second stage of CID with a triple quadrupole can be of significant value when working in a molecular weight range of 300 daltons or higher. As is seen in Figure 2, many important fragment ions are in a mass range of 200-300 daltons but unless a great deal of background information is available on the sample, it is difficult to make any reasonable suggestions regarding the structure of those ions. However, if these fragment ions from repeller CID are now selected for MS/MS analysis, the daughter spectra of the primary fragments are in a lower mass range that can often permit logical suggestions of structure. As a brief illustration Figures 3 and 4 present the spectra obtained from the repeller CID daughter ions at masses 247 and 249. It is immediately apparent that these two fragment ions have significantly different structures. The 247 ion (which was formed by loss of C_9H_{18} from the MH^+ ion) shows fragment ions characteristic of rings or unsaturation and some heteroatom(s) to give mass losses of 46, 58, and 86. In contrast, the 249 ion shows fragmentation characteristic of the aliphatic side chain and a peak suggesting aromaticity. The CID/MS/CID/MS experiments on the other primary daughter ions provided similar information.

The additional stage of CID fragmentation can also be used for increased target specificity. MS/MS analysis has been used for some samples by selecting a target MH^+ ion and mass analyzing the CID fragment ions. However, there is always a danger that an isomer or isobar is present that will contribute to the CID spectrum, but use of repeller CID to give a second stage of fragmentation greatly reduces the probability of interfering mass peaks. Figure 5 shows the spectrum obtained at low repeller voltage on a crude extract of cannabis sativa. The spectrum is dominated by the MH^+ ion of tetrahydrocannabinol at mass 315, but it is also known that cannabidiol would be present and contribute at mass 315. From authenic sample studies, it is known that tetrahydrocannabinol gives a strong repeller CID peak at mass 193 which is absent in the repeller CID spectrum of cannabidiol. By selecting the mass 193 ion of the extract for MS/MS CID analysis, a spectrum is obtained that is essentially identical to that obtained from authenic tetrahydrocannabinol (Figure 6).

Repeller CID spectra have been shown to be almost qualitatively identical to MS/MS CID spectra for 30 to 40 compounds. The nabilone repeller CID spectrum (Figure 2) is a notable exception to this generality. Figure 7 compares the MS/MS CID spectrum of nabilone-D6 with the 80V repeller CID spectrum. (The ring gem-dimethyls are deuterated). It is apparent that several prominent peaks are absent from the conventional MS/MS spectrum. By comparing the deuterated and undeuterated spectra (Figure 7 and Figure 2), it is noted that only fragmentation involving the C9 chain occurs in the MS/MS spectrum. This unexpected phenomenon should be studied further to determine which of the many different features of the collision cell cause this difference.

References

1. D. Zackett, G.J. Kallos, and P.J. Savickas, 34th Annual Conference on Mass Spectrometry and Allied Topics, June 1986, Cincinnati, OH, Paper MOB3

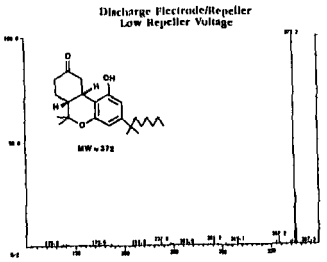

Figure 1

Figure 2

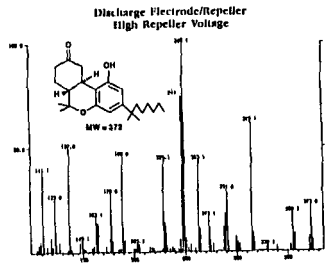

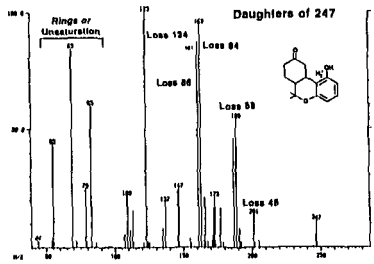

Figure 3

Figure 4

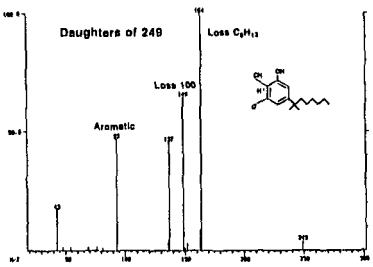

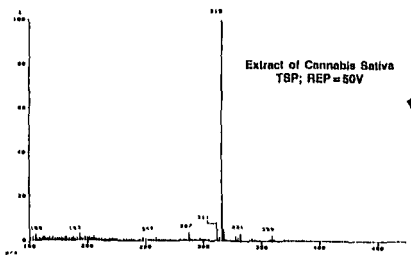

Figure 5

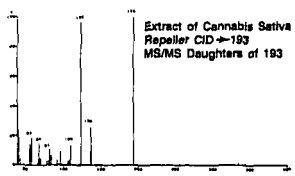

Figure 6

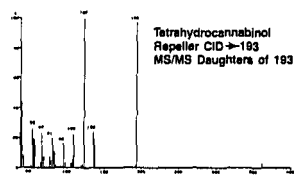

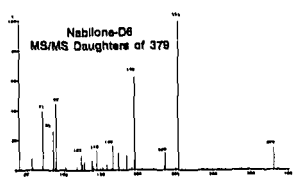

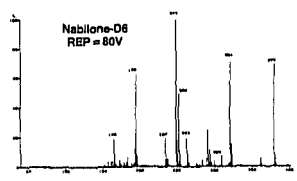

Figure 7

Presented at the 35th ASMS Conference on Mass Spectrometry and Allied Topics
May 24-29, 1987, Denver, CO

Continuous Flow FAB-MS Analysis of Peptide Digests

David W. Hutchinson, Adrian R. Woolfitt, Keith R. Jennings and Alison E. Ashcroft, Department of Chemistry, University of Warwick, Coventry, England.

The conventional FAB-MS method of analysing mixtures of peptides and dipeptides suffers from a number of difficulties which make it unsuitable for quantitative studies. Competition effects resulting in differing sensitivity for different components coupled with the high matrix background can lead to the complete suppression of peaks from one or more components. This paper describes the use of continuous flow FAB-MS methods for peptide sequencing using enzymes to cleave dipeptides. A Kratos probe was used on an MS50 mass spectrometer with flow rates of 2-10 µl/min, a source block temperature of 40-70°C, and CH_3OH/H_2O or CH_3CN/H_2O solvents containing 5% glycerol or m-nitrobenzyl alcohol.

Dipeptidyl peptidase I (DPPI) cleaves dipeptides sequentially from the N-terminal end of unblocked peptides and proteins. It has a broad specificity but no cleavage occurs if proline is in position 2 or 3 from the N-terminus. Digestion takes place at pH 5.6 in the presence of ammonium acetate and mercaptoethylamine hydrochloride. Dipeptidyl peptidase IV (DPP IV) behaves similarly but will cleave dipeptides if proline is in position 2 but not if it is in position 3 from the N-terminus. Digestion takes place at the somewhat higher pH of 7.0-7.8 so a compromise of pH = 6.5 -7.0 was chosen for work with the two enzymes.

The following peptides were chosen for study:

β-Casomorphin	Tyr-Pro-Phe-Pro-Gly	(MH^+ = 580)
Angiotensin	Asp-Arg-Val-Tyr-Ile-His-Pro-Phe-His-Leu	(MH^+ = 1297)
Octapeptide	Val-His-Leu-Thr-Pro-Val-Glu-Lys	(MH^+ = 922)

When β-casomorphin is treated with DPP IV, two dipeptides are cleaved successively giving Tyr-Pro (MH^+ = 279) and Phe-Pro-Gly (MH^+ = 320) followed by Phe-Pro (MH^+ = 263) and Gly (MH^+ = 76). Three individual injections of 0.8 nmol peptide equivalent were made (i) in the absence of DPP IV, (ii) after 40 min. digestion and (iii) after 150 min. digestion. No peaks corresponding to the above fragment ions were observed in the absence of DPP IV but after 40 min. the only significant peaks above m/z = 250 were m/z = 263, 279, 320 and 580. After 150 min., when digestion was essentially complete, equal amounts of Tyr-Pro and Phe-Pro should be present in the digest but the relative intensities of the MH^+ peaks associated with these dipeptides were in the approximate ratio 1:10, the spectrum being dominated by the peak m/z = 263 together with low intensity peaks due to glycerol adducts at m/z = 355 and 447 and the proton bound dimer at m/z = 525. This result indicates that discrimination effects are still present in the spectra of mixtures obtained using the continuous flow FAB probe. Continuous monitoring of the course of the digestion using a flow-rate of 6-7 µl min^{-1} required a total volume of sample of ~ 200 µl. The variation of relative peak heights with time could readily be followed but discrimination effects and spikes due to unstable operation of the probe limit the usefulness of the technique for quantitation.

Digestion of human angiotension with DPPI has a slow first stage due to the presence of argenine in the 2-position and is followed by a much faster second stage after which the presence of proline in the 3-position prevents further digestion. As a result of the different rates of the two steps, the MH^+ ion of the intermediate octapeptide at m/z = 1025 is not observed and MH^+ of the hexapeptide at m/z = 763 dominates the spectrum after 10 min. digestion. Peaks corresponding to MH^+ of the two dipeptides at m/z = 290 and 281 were not observed above background either because of discrimination effects or because of the relatively low peptide loadings of ~ 0.12 nmol. Despite the above-mentioned problems, good semiquantitative chromatographic peak areas were obtained with short analysis times and negligible probe memory effects.

A reverse-phase HPLC-continuous flow FAB experiment was performed using a 0.46 cm i.d. 3 cm long Pecosphere 3CR C18 column with flow rates of 0.4 - 0.5 ml min^{-1} and a 1:100 splitter giving a probe flow rate of 4 - 5 µl min^{-1} of

the aqueous CH_3CN solvent containing 5% glycerol and 0.1% TFA. Although the HPLC broadens peaks so reducing overall sensitivity, elution conditions suitable for reverse phase columns are fully compatable with the continuous flow FAB probe and, in addition, a UV detector can be used. For similar solvent flow rates, the smaller HPLC column gives superior resolution and is three times faster than the standard column.

Digestion of the octapeptide by DPPI gives only one dipeptide, Val-His (MH^+ = 255) and a hexapeptide, (MH^+ = 686). The octapeptide and the two products were readily separated by the column so avoiding discrimination effects and quantitation would be possible with appropriate isotopically-labelled compounds. Detection limits of 10 pmol and 50 pmol were estimated for the hexapeptide and dipeptide respectively and although the octapeptide was not detectable by HPLC alone, the much wider dynamic range of FAB-MS compared with that of the UV detector allowed MH^+ at m/z = 922 to be detected and possibly quantified so that, in principle, the equilibrium could be calculated.

Finally, the method was applied to the analysis of an "unknown" peptide, M.Wt. = 941. When digested with DPPI, using 33% CH_3CN/H_2O with 10 nmol injected to give 0.1 nmol. on the probe tip, the peptide yielded three partly-separated peptides giving peaks at m/z = 935, 662 and 442, indicating the loss of dipeptides of molecular weight 291 and 238 the MH^+ ions of which were not detectable above background. No additional digestion was obtained using DPP IV so that the partial sequence suggested is:

$$\begin{Bmatrix}\text{Ser-Trp}\\ \text{Trp-Ser}\end{Bmatrix} - \begin{Bmatrix}\text{Gly-Tyr}\\ \text{Tyr-Gly}\end{Bmatrix} - \text{X} - \text{Y} - \text{Pro} -$$

After adjusting the HPLC conditions to resolve the dipeptides, known samples of Gly-Tyr and Tyr-Gly were injected and from comparison of retention times, the second dipeptide produced in the digest was identified as Tyr-Gly. The actual structure of the starting material was Trp-Ser-Tyr-Gly-Leu-Arg-Pro-Gly-$CONH_2$.

From these preliminary experiments, continuous flow FAB-MS is a promising method of following the time-course of enzymic digests of peptides and when used with a micro HPLC column, components in the digest can be separated, thereby minimising discrimination effects.

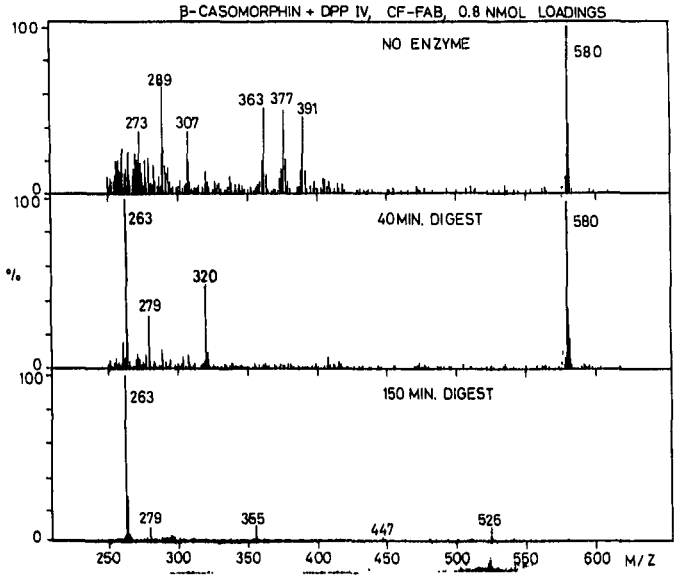

Presented at the 35th ASMS Conference on Mass Spectrometry and Allied Topics
May 24-29, 1987, Denver, CO

MICROBORE HPLC / MS USING A CONTINUOUS FLOW FAB PROBE INTERFACE

Richard M. Caprioli, Beverly DaGue, Terry Fan, and William T. Moore
Department of Biochemistry and Molecular Biology
and the Analytical Chemistry Center
The University of Texas Medical School at Houston
Houston, Texas 77030

High performance liquid chromatography has become the method of choice for the separation and isolation of a wide variety of biological compounds, particularly for peptides and proteins. Sample detection of peptides is usually accomplished by spectrophotometric means at a wavelength of approximately 210 nm where absorption of the peptide bond is monitored. Although this can be done simply and with high sensitivity, it is far from the ideal detector for these compounds because of its lack of specificity. Mass spectrometry offers some unique advantages as a detector for HPLC because it is able to perform a mass specific analysis of the compounds eluting from the column.

Fast atom bombardment mass spectrometry (FABMS), as well as a number of other desorption ionization techniques, has provided a means for the direct analysis of peptides and other biological compounds without the need for chemical derivatization. Although FABMS analyses are usually done in solutions containing 95% or more glycerol, it has recently been shown (1,2) that, using a continuous flow sample interface, analysis of aqueous solutions can be accomplished effectively and offers particular advantages. The HPLC/MS interface used in this work utilizes a fused silica capillary to transport the eluate from the column to the tip of the sample probe in the ionization chamber of the mass spectrometer.

We report on the use of this interface for the HPLC/MS analysis of a number of mixtures of peptides in the molecular weight range of 1000-6000 daltons, including the separation and molecular identification of several species of intact insulins. In addition, data are presented which show the HPLC/MS identification of sixteen specific molecular fragments from the tryptic digestion of sperm whale myoglobin.

MATERIALS AND METHODS

Apparatus: An Applied Biosystems model 130A microbore HPLC system fitted with a 0.1 x 25 cm Brownlee RP-300 column was used for the chromatographic separations. The end of the column was connected directly to the continuous flow FAB probe by a one meter length of 0.075 mm (i.d.) fused silica capillary. The HPLC was operated at a flow of 5 µL/min. Gradient elutions were accomplished using a mixture of 5% glycerol in water with 0.1% TFA as solvent A, and %5 glycerol, 60% acetonitrile, and 0.1 % TFA as solvent B.

A Kratos MS50RF high resolution mass spectrometer equipped with a DS90 (S/280) data system was used. The instrument was operated at 4 keV accelerating voltage and a resolution of about 1200. The probe tip was maintained at 40 C. The Ion Tech B11NF saddle field gun was operated at 8 keV and 40 µa current using xenon gas.

RESULTS AND DISCUSSION

LOW MOLECULAR WEIGHT PEPTIDE MIXTURES:

A mixture of 125 pmol each of angiotensin II (MW 1045), angiotensin III (MW 930), substance P (MW 1347), and bombesin (MW 1618) was injected onto the microbore RP300 column. The mass spectrometer was continuously scanned from m/z 1700 - 900 at a rate of 10 sec/scan. The peptides were well separated except for Angiotensins II and III which were not separated from each other. The eluted peaks, at 10% peak height, were approximately of two minutes duration.

ANALYSIS OF TRYPTIC DIGEST OF MYOGLOBIN:

Figure 1 shows the total ion chromatogram produced from the analysis of 100 pmol of tryptic digest of sperm whale myoglobin. The mass spectrometer

was continuously scanned from m/z 2300-250 at a rate of about 20 sec/scan. Figure 1 also shows the selected ion chromatograms for the higher molecular weight peptide fragments. The complete digestion of this protein would be expected to give 19 peptides ranging from 2 to 17 residues in length. A total of 16 peptides were identified in the HPLC/MS analysis. Only two dipeptides and one tripeptide were missed in the analysis, this presumably the result of these signals being obscured by the high chemical background common to the FAB process at low masses.

HIGH MOLECULAR WEIGHT PEPTIDES:

A mixture containing 1 nmol each of ribonuclease S peptide (MW 2165), glucagon (avg MW 3482), and oxidized insulin B chain (avg MW 3497) were analyzed with the mass spectrometer scanned from m/z 3510 - 1950 at a rate of about 11 sec/scan. Elution times were; S peptide, 9.4 min; B-chain, 37.8 min; glucagon, 41.8 min. The mass spectra of the molecular ion region for the two higher molecular weight compounds are shown in Figure 2 with the measured value of $(M+H)^+$ indicated.

ANALYSIS OF INSULINS:

In order to evaluate the high mass capability of the microbore HPLC/FABMS system, a mixture of 400 pmol each of bovine, ovine, equine, and porcine insulins were analyzed using the gradient system described above. The mass spectrometer was scanned from m/z 6100 - 5500 at a rate of 3.2 sec/scan. The four proteins were reasonably well separated and eluted between 22 and 50 min. Since the resolution of the mass spectrometer was set to about 1200, molecular ion species were not resolved from their isotopes. Average mass values, calculated from the mass peaks using centroiding software available with the data system, gave mass assignments to an accuracy of about ± 0.4 mass units.

CONCLUSION

Data presented here has shown that microbore HPLC and fast atom bombardment mass spectrometry can be effectively coupled using a continuous flow interface. The mass detection system operates with high sensitivity up to about m/z 6000, and appears to have no high mass limitations other than that normally imposed by the FAB process itself. Microbore HPLC is an ideal separation technique for this application because it operates at relatively low flow rates and is compatible with the normal pumping capacities of most mass spectrometers. Peaks are eluted in relatively small volumes, typically about 10 µL, and therefore can be detected at high sensitivity.

REFERENCES

1. Caprioli, R. M., Fan, T. and Cottrell, J. S. (1986) Anal. Chem. 58, 2949-2954.
2. Caprioli, R. M., and Fan, T. (1986) Biochem. Biophys. Res. Comm. 141, 1058-1065.

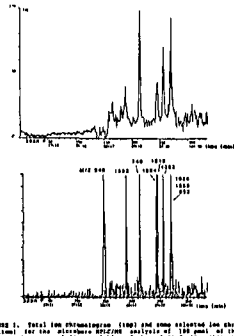

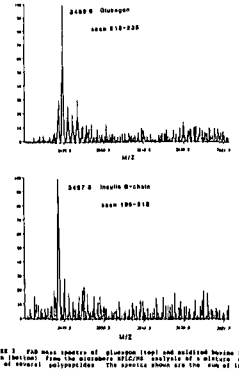

Presented at the 35th ASMS Conference on Mass Spectrometry and Allied Topics
May 24-29, 1987, Denver, CO

APPLICATIONS OF CONTINUOUS FLOW FAB MASS SPECTROMETRY FOR THE STUDY OF NON-POLAR, THERMALLY LABILE MOLECULES.

M.Barber, D.J.Bell and L.W.Tetler
UMIST, Manchester, M60 1QD, UK
D.B.Gordon
Manchester Polytechnic, Manchester, M1 5GD, UK
A.E.Ashcroft, R.S.Brown and G.Elliot
Kratos Analytical, Barton Dock Road, Urmston, Manchester, M31 2LD, UK

Since its advent in 1981[1] FAB has been widely applied to many previously intractable mass spectrometric problems. Sample preparation, although relatively simple, suffers from the problem of solvent/matrix selectivity. Furthermore in order to obtain the best mass spectrum the judicious addition of other materials may be required leading to complex solvent/matrix "cocktails". Other problems may arise owing to sample interactions with the matrix and mass spectral interpretation is often complicated by the presence of an intense background associated with the solvent/matrix system.

Recently the development of continuous flow probes[2][3] has been described and we have undertaken an investigation into such a system in order to assess its applicability for obtaining FAB mass spectra.

A commercially available (Kratos Analytical) continuous flow probe (figure 1) was employed in conjunction with an MS50FS (Kratos Analytical) mass spectrometer. The instrument was standard except that the FAB source was fitted with a heater and temperature sensor and maintained at 40°-60°C. Gentle heating is required to balance the cooling effect due to constant evaporation of the aqueous/organic solvent systems continually flowing into the source. Constant flow rates were obtained using a Brownlee HPLC micropump, those were of the order 1-10 ul min^{-1}. Sample introduction may be effected in one of three ways:- a) injecting a solution of the sample into a flowing "mobile phase". b) continuous introduction of the sample solution directly into the source. c) employment of an HPLC column inserted prior to source entry.

Samples to be injected were dissolved in a suitable solvent (1ug ul^{-1}) then introduced into the mobile phase via a standard LC Rheodyne 7520 injection valve (20ul loop).

The following mobile phases have been employed:-

[1] H_2O:CH_3OH (1:1) with either 5% glycerol or thioglycerol
[2] H_2O:CH_3CN (1:1) with either 5% glycerol, thioglycerol or m-nitrobenzyl alcohol (m-NBA)
[3] CH_3CN with either 5% thioglycerol or m-NBA.
[4] Toluene with 5% m-NBA.

Totally non-polar materials eg. fats, lipids and glycerides often prove difficult to run under standard FAB conditions. Employing the mobile phase described in [3], CF-FAB mass spectra were routinely obtained (eg. figure 2).

Many organometallic compounds, especially phosphines are air and/or moisture sensitive and therefore present great difficulty for standard FAB. Preliminary studies on organometallics using [4] have shown that such materials will afford mass spectral information with CF-FAB. Initial work employed toluene solutions of air/moisture sensitive samples with little success, however the subsequent addition of m-NBA allowed spectra to be obtained. We believe that the presence of such viscous matrices is necessary for the production of CF-FAB mass spectra. Amongst other materials investigated have been sugars (in both +ve and -ve ion mode) and vitamin B_{12} co-enzyme. The CF-FAB mass spectra (using [1]) exhibits a much increased $(M+H)^+$ intensity compared to standard FAB. (Figure 3).

An area of particular interest is the mass spectral analysis of peptide mixtures generated by trypsin digests of protein/peptides. Analysis by standard FAB does not always allow the observation of each individual component.[4] Figure 4 shows the CF-FAB mass spectrum of a tryptic digest of glucagon (sample introduction (b)). Not all the expected fragments are seen indicating a similar process as to that for standard FAB. We have shown that

the combination of HPLC and CF-FAB has proved successful with model peptide mixtures and we therefore suggest that a similar procedure applied to tryptic digests will also be required to produce unambiguous results. We are at present continuing these investigations.

Continuous flow-FAB offers advantages over probe FAB in that mass spectra of "difficult" materials may be more routinely obtained. The much lower sample:matrix ratio employed in CF-FAB results in a much enhanced signal:chemical noise and reduces any matrix/sample interactions that may be taking place. The technique also allows acheivement of rapid sample throughput if desired. The combination of LC and CF-FAB would appear ideally suited to the analysis of peptide mixtures.

References

(1) M.Barber, R.S.Bordoli, R.D.Sedgwick and A.N.Tyler: *J.Chem.Soc.Chem.Commun.* 936 (1982)

(2) Y.Ito, T.Takeuchi, D.Ishi and M.J.Goto: *J.Chromatogr.* 346, 161 (1985)

(3) R.M.Caprioli, T.Fan and J.S.Cottrell: *Anal.Chem.* 58, 2949 (1986)

(4) M.R.Clench, G.V.Garner, D.B.Gordon and M.Barber: *Biomed.Mass Spectrum.* 12, 355 (1985)

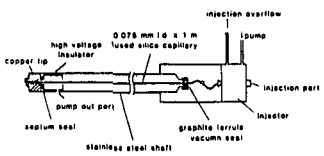

Figure 1

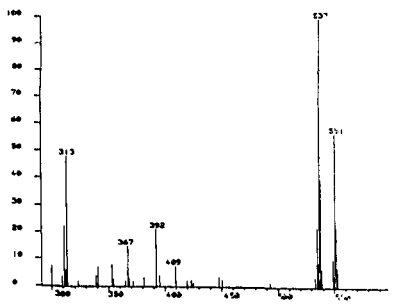

Figure 2

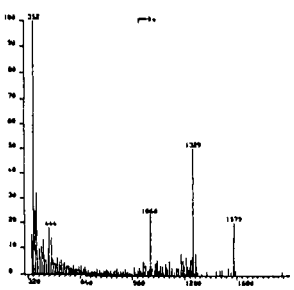

Figure 3

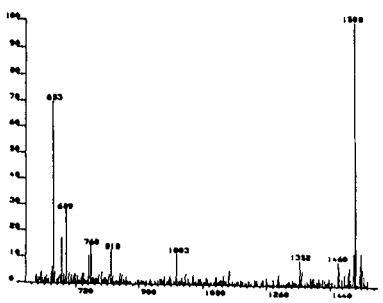

Figure 4

Presented at the 35th ASMS Conference on Mass Spectrometry and Allied Topics
May 24-29, 1987, Denver, CO

RECENT DEVELOPMENTS OF FRIT-FAB LC/MS INTERFACE

Y. Itagaki, T. Kobayashi, T. Mizuno, and E. Kubota,
JEOL LTD. Akishima Tokyo Japan,
D. Ishii, Nagoya Univ., Nagoya, Japan

We have developed the FRIT-FAB LC/MS interface.[1] In this system, the total effluent is directly introduced into the FAB ion source through a fused silica capillary tube and then dispersed on the frit. Samples on the frit surface are bombarded with a neutral beam. Although it was found that this interface is particularly useful for the measurement of nonvolatile, high molecular weight compounds, the flow rate was limited to 0.5~5μℓ/min. and the effects of the ion source and the interface temperature were not examined precisely. We have improved the structure of the FRIT-FAB target to be able to use a much higher LC solvent flow rate and examined the mass spectroscopic behaviors under different ion source temperatures, solvents and flow rates. The FRIT-target modifed for this work consists of a 100μm I.D. 560μm O.D. fused silica capillary tube, a 600μm I.D. 3mm O.D. stainless steel tube, a stainless steel mesh(3μm)FRIT and 5mm I.D. 6mm O.D. stainless steel cap which transfers the temperature from the ion source chamber to the mesh FRIT. Fig. 1 shows the details of the basic structure of the FRIT-target.

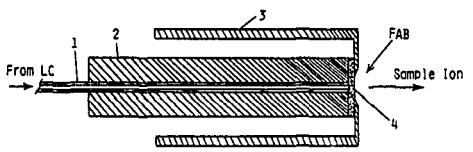

Fig.1
Basic structure of FRIT-target
1: Fused silica capillary tube;
100μm I.D.x 560μm O.D.
2: Stainless-steel tube;
600μm I.D.x 3mm O.D.
3: Stainless-steel cap; 5mmI.D.x6mm O.D.
4; Stainless-steel Frit(3μm)

The maximum amount of mobile phase introduced was 30μℓ/min. and the optimum introduction amount was 10~20μℓ/min. An excess of sample and matrix flows along the circumference of the stainless steel tube. The required ion source temperature varies with the used solvents and flow rate.

MH^+ ion intensity of erythromycin (50ng dissolved in 2% glycerol H_2O solution) was measured as a function of the ion source temperature and the flow rate of the mobile phase(Fig. 2). At a flow rate of 10μℓ/min., the most suitable ion source block temperature was 80~100°C, and higher flow rates require higher temperature. But at any flow rate, suitable ion source block temperature range was over 20°C wider and required no strict temperature control. The sample was also measured with different

solvents; MeOH, H_2O/MeOH=1:1, H_2O/MeCN=1:1, H_2O (to all solvents 2% glycerol was added; flow rate 10μℓ/min.) Again, the ion source block temperature conditions were not critical and suitable temperature range was about 20°C. The linearity of response of this interface was determined. A mass spectrum and a selected ion monitor chromatogram of ampicillin are shown in Fig. 3. A linear calibration curve from 10pg-500ng was observed by monitoring $(M+H)^+$ ions of ampicillin (Fig. 4) at a flow rate of 20μℓ/min.

It was proved that the improved FRIT-FAB has a wider availability of flow rate, temperature and solvent composition range.

1) Y. Ito, T. Takeuchi, D. Ishii, M. Goto and T. Mizuno
J. Chromatogr. 358, 201 (1986)

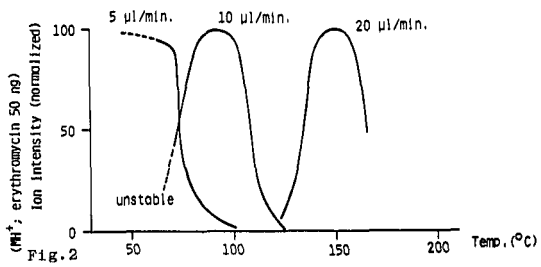

Fig.2 Ion intensity as a function of the ion source temperature and the flow rate of mobile phase (H_2O; 2% glycerol)

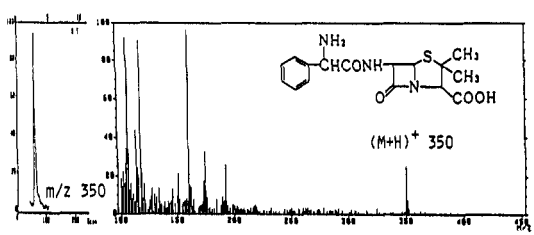

Fig.3 Mass chromatogram and mass spectrum of ampicillin : 100 ng
Mobile phase; H_2O
Flow rate; 20μl/min.

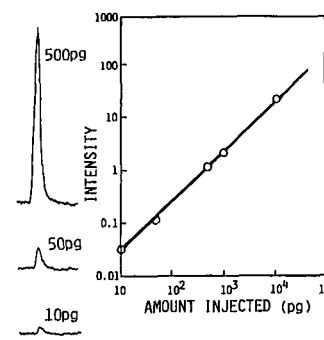

Fig.4 CALIBRATION CURVE FOR AMPICILLIN m/z350(MH^+)

Presented at the 35th ASMS Conference on Mass Spectrometry and Allied Topics
May 24-29, 1987, Denver, CO

NEW APPROACHES TO THE SUPERCRITICAL FLUID CHROMATOGRAPHY-MASS SPECTROMETRY INTERFACE FOR THE ANALYSIS OF NONVOLATILE MATERIALS*,

H. T. Kalinoski, H. R. Udseth, J. A. Olivares and R. D. Smith, Pacific Northwest Laboratory (Operated by Battelle Memorial Institute), Richland, Washington 99352

A primary application of supercritical fluid chromatography-mass spectrometry (SFC-MS) is the analysis of mixtures not amenable to GC-MS due to insufficient compound volatility. Recently acquired information on the nature of the supercritical fluid expansion process has indicated limitations in current SFC-MS interface designs for nonvolatile materials. These limitations result from the rapid ($<10^{-6}$ sec.) nucleation of nonvolatile materials during fluid expansion into the ionization region, particularly for higher molecular weight compounds. For moderately polar or less volatile compounds, the major interface difficulty typically results from precipitation in the restrictor. This can be addressed by proper restrictor design (1) and/or operation at elevated flow rates. Further development of practical SFC-MS applications is also facilitated by improvements in injection methods for SFC, which can result in increased sample loading and greater dynamic range (sensitivity).

One interface design, the high flow rate (HFR) interface, has been developed to meet many of the requirements for improved performance (2). The interface allows operation at much higher gas flow rates than previous capillary direct fluid injection interfaces which permits use of both capillary and microbore chromatographic columns. Further benefits of this design include splitless injection for improved quantitation, increased sample capacity and dynamic range, and extended application to compounds having very low volatility.

The relative advantages of packed and capillary columns can be studied using the high flow rate interface. For analyses requiring better detection limits, broader dynamic range, greater sample loading or retention but lower chromatographic efficiency, microbore packed columns are advantageous. This preference results from the higher phase ratio in a typical (HPLC) packed column, 10^2 to 10^3 times greater than a typical SFC capillary column. Analyses of higher molecular weight materials, or those requiring a higher number of effective plates, are more appropriately performed with currently available capillary columns since at a given instrument pressure limit substantially lower retention is obtained.

The advantages of the use of polar fluid modifiers and pressure programming on packed microbore columns are illustrated in Figure 1. An eight component mixture of organophosphorus pesticides was analyzed under a variety of conditions on a 1.0 x 100 mm column packed with 5 μm silica particles coated with an amino-modified phase. The upper chromatograms show reasonable separation of most of the components, with easy identification

from the mass spectra, but with significant tailing observed for the most polar compounds. Addition of a small amount of isopropanol resulted in dramatic improvement in the separation, as evidenced by the improved peak shape and reduced tailing. This is largely due to coverage of highly adsorptive stationary phase sites; such small modifier concentrations do not appreciably increase the fluid phase solubilities or affect retention on well-deactivated capillary columns. The advantages of pressure programming are already well-established for separations on capillary columns (3). The separation with a 25 bar/min pressure program and 2% (v/v) isopropanol in CO_2 shows in Figure 1 improved peak shape, nearly equivalent peak widths for all components.

New interface designs are being utilized to broaden the range of analytical problems that can be addressed by SFC-MS. Both capillary and microbore packed columns are being utilized, with fluid pressure programming, to fully exploit the properties of supercritical fluids. Further efforts to more completely address the truly nonvolatile analytes are required before the promise of the technique is fully realized.

*This work supported by the U. S. Department of Energy, Office of Health and Environmental Research, under Contract DE-AC06-76RLO-1830.

(1) R. D. Smith, J. L. Fulton, R. C. Petersen, A. J. Kopriva and B. W. Wright. Anal. Chem., 1986, 58, 2057-2064.

(2) R. D. Smith and H. R. Udseth. Anal. Chem., 1987, 59, 13-22.

(3) R. D. Smith, E. G. Chapman and B. W. Wright. Anal. Chem., 1985, 57, 2829- 2836.

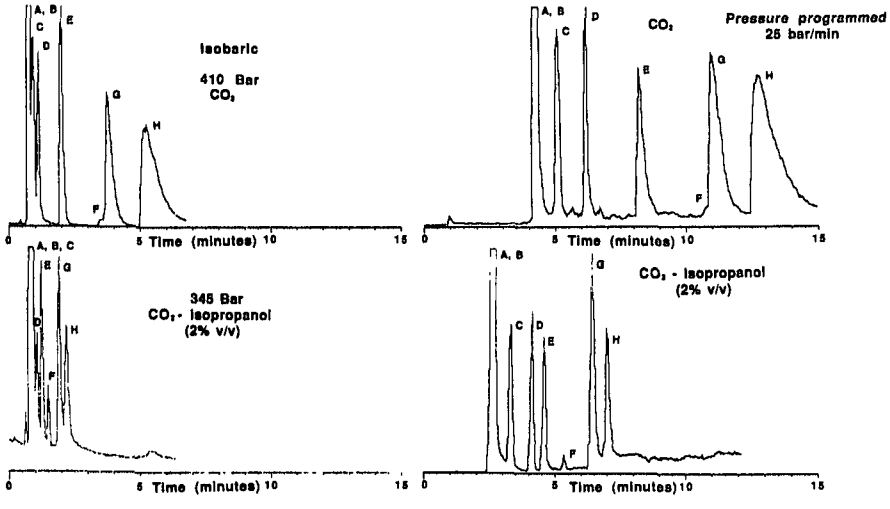

Presented at the 35th ASMS Conference on Mass Spectrometry and Allied Topics
May 24-29, 1987, Denver, CO

INTERFACES FOR PACKED AND CAPILLARY COLUMN SFC/MS

A.J. Berry, D.E. Games, I.C. Mylchreest, J.R. Perkins and S. Pleasance
Department of Chemistry, University College, P.O. Box 78, Cardiff CF1 1XL, Wales

The usefulness of a supercritical fluid as a chromatographic mobile phase lies in its combination of physical properties, which in some cases are gas-like and in others liquid-like. This results in favourable behaviour for the transport of solutes through a chromatographic column, without the need for vaporization. Supercritical fluid chromatography (SFC) thus is complementary to both high-performance liquid chromatography (LC) and gas chromatography (GC). Interfacing of SFC to a mass spectrometer is easier to effect than LC/MS, because the gas volumes generated from the mobile phase are lower and the various approaches have recently been reviewed [1-3]. We report here on our development of interfaces for both capillary and packed column SFC/MS.

Capillary SFC is the method of choice for the study of complex mixtures, since chromatographic efficiencies approaching those obtainable by GC can be obtained and the technique does not have the volatility requirement inherent in GC. Our initial studies [2,3] utilized a Brownlee dual syringe pump which was interfaced to a Finnigan 4500 GC/MS system using a 60nl Valco valve loop injector which had a splitter attached. Interfacing to the mass spectrometer was via the capillary GC/MS inlet line and a 5μm fused silica restrictor was connected to the end of the SFC column using a low dead volume connector. The system worked well, but because the restrictor could not be heated to above 300°C, difficulty was experienced in handling involatile compounds. Considerable improvements have been effected by construction of a direct introduction probe system to replace the normal GC/MS interface. In this system we have replaced the 5μm fused silica restrictor by a 50μm fused silica restrictor containing an integral frit and a tip heater has been incorporated, which enables heating of the restrictor to temperatures in excess of 500°C. Studies with this interface have utilized a Lee Scientific 501 supercritical fluid syringe pump together with a 100nl Valco valve loop injector. We have found this system can be used without post injector splitting. EI sensitivity is considerably improved over our previous interface, though still not as good as when the system is used in the CI mode. In addition, lower volatility compounds can be readily handled. The system has been used in studies of high boiling point petroleum fractions and coal tar fractions and TIC traces compare favourably with those obtained using a flame ionization detector.

Packed column SFC has the advantages over LC of faster analysis time and method development and better chromatographic efficiencies. It is also an extemely effective method for the isolation of compounds in a pure form. With this approach much higher mobile phase gas volumes are generated making SFC/MS interfacing more problematic. We have developed two packed column SFC/MS interfaces. Our first approach was to use moving belt LC/MS interfaces [4,5]. A Hewlett-Packard 1084B liquid chromatograph which had been modified for SFC was interfaced to the moving belt interfaces on a Finnigan MAT 4500 mass spectrometer and a VG Analytical 70/70E mass spectrometer using a modified Finnigan MAT spray deposition device. The spray deposition device was connected in-line using a 60cm length of 1/16" o.d. x 0.006" i.d. stainless steel transfer line via a 'T' piece between the UV detector exit and the outlet back-pressure regulator of the chromatograph. In order to maintain SFC conditions to the point at which the eluent leaves the system, the end of the stainless steel tubing used in the spray deposition device was slightly crimped. The tubing was heated to prevent solute precipitation and freezing of the eluent at the tip. Use of this approach enabled good chromatographic integrity to be maintained and EI and CI mass spectra can be obtained. Detection limits were better than with LC/MS.

Problems can be encountered with thermal decomposition of thermally labile molecules when moving belt interfaces are used. In order to extend the range of compounds amenable to packed column SFC/MS and further improve detection limits, SFC/MS has been effected using a Finnigan MAT thermospray source in the filament-on mode [6]. Interfacing to the thermospray source was effected as described for the moving belt system. The ion source was modified in that the coiled hypodermic stainless steel vaporizer was replaced by a straight piece of the same material which was slightly crimped at the end to maintain SFC conditions to the point at which the eluent leaves the vaporizer. The system was used in the filament-on mode and excellent retention of chromatographic integrity was observed. When methanol was used as a modifier for SFC solvent moderated full scan CI spectra were obtained at the low ng injected on column level. If carbon dioxide alone was used as mobile phase, then charge exchange spectra closely resembling EI mass spectra were obtained.

Both the packed column SFC/MS systems have been used for studies of a wide range of polar compounds which include sulphonamides, indole alkaloids, PTH-amino acids, veterinary drugs, carbanate, triazine and organophosphorous pesticides and milbemycin antibiotics.

1. B.W. Wright, H.T. Kalinoski, H.R. Udseth and R.D. Smith, J. High Resolut. Chromatog. Chromatog. Commun., 1986, 9, 137.
2. D.E. Games, A.J. Berry, I.C. Mylchreest, J.R. Perkins and S. Pleasance, Laboratory Practice, 1987, 36, 45.
3. D.E. Games, A.J. Berry, I.C. Mylchreest, J.R. Perkins and S. Pleasance, European Chromatography News, 1987, 1, 10.
4. A.J. Berry, D.E. Games and J.R. Perkins, J. Chromatogr., 1986, 363, 147.
5. A.J. Berry, D.E. Games and J.R. Perkins, Anal. Proc., 1986, 23, 451.
6. A.J. Berry, D.E. Games and J.R. Perkins, Biomed. Environ. Mass Spectrom., 1987 in press.

Presented at the 35th ASMS Conference on Mass Spectrometry and Allied Topics
May 24-29, 1987, Denver, CO

SUPERCRITICAL FLUID CHROMATOGRAPHY-MASS SPECTROMETRY USING A "HIGH MASS" QUADRUPOLE MASS SPECTROMETER AND SPLITLESS INJECTION

J. David Pinkston[1], Grover D. Owens[1], David S. Millington[2], David A. Maltby[2], Leisa J. Burkes[1], Thomas E. Delaney[1]

1. The Procter & Gamble Company, Miami Valley Labs, P.O. Box 39175, Cincinnati, OH 45247
2. Duke University Medical Center, Division of Pediatric Genetics and Metabolism, Box 3028, Durham, NC 27710

Capillary supercritical fluid chromatography-mass spectrometry (SFC-MS) is an important tool for complex mixture analysis. It combines the power of traditional chromatographic-mass spectrometric techniques with unique advantages of its own. This work focusses on two problems that hamper the wider application of SFC-MS:

1) Solutes ranging into the thousands of daltons in molecular mass may be eluted in SFC (1). However, most SFC-MS has been done using quadrupole mass analyzers of upper mass limit of 1500 Da or less. Progress in SFC-MS using sector and Fourier transform instruments with greater mass ranges has been slow (2,3).

2) Most capillary SFC uses splitting injection. Split ratios vary with temperature, pressure, and molecular weight, making quantitation difficult.

To counter the first problem, we've designed and built SFC-MS interface probes (see Figure 1) for a VG 30-253 quadrupole instrument of upper mass range limit of 3000 Da. We hoped to establish whether solutes of mass greater than 1500 Da could be transported intact through our interface probe (probe tip temperature typically 300 to 350°C) and efficiently ionized. Concerning the second problem, we wanted to determine a limit of detection (LOD) for this SFC-MS combination. This was facilitated by using <u>splitless</u> injection. We linked a 50 um i.d. x 50 cm retention gap directly to a nominal 0.06 ul Valco injection valve. The retention gap was coupled to the 50 um i.d. column with a zero-dead-volume union. Using a typical robot-pulled tapered capillary restrictor (3 um aperture, 4 cm taper length) the retention times of standards were near those expected. We scanned above any ions produced by the broad solvent front. The elution and detection of early eluting peaks did not appear to be hampered by this mode of splitless injection. All the work described here was performed in this manner without any obvious ill effects.

Tuning and mass calibration were performed by injecting a mixture of polydimethylsiloxane in supercritical CO_2 directly into the chemical ionization (CI) source volume through our interface probe. This manner of supercritical fluid injection (SFI) was useful in tuning the instrument. It also shows promise for rapid characterization of oligomeric mixtures. Figure 2 is a typical NH_3 CI spectrum collected during a tuning session. The mass axis was not calibrated when this spectrum was collected. Most of this work was performed at less than "unit" resolving power (FWHM definition) above mass-to-charge ratio (m/z) 1000 for improved sensitivity.

Figure 3 is an SFC-MS reconstructed-total-ion-current (RTIC) chromatogram of the polydimethylsiloxane used in the tuning mix. All oligomers gave simple NH_3 CI spectra: virtually all the ion current was concentrated in the ammonium adduct ion. Adduct ions up to m/z 2998 (centroid) were observed, corresponding to 39 dimethylsiloxane groups incorporated in the oligomer. Adduct ions of subsequent oligomers were above the mass range of the instrument. The stronger spectra contain weak (less than 10 % relative abundance) ions related to the oligomeric structure. The ions correspond in mass to structures such as:

$$CH_3 - \underset{CH_3}{\overset{CH_3}{Si}} - (O - \underset{CH_3}{\overset{CH_3}{Si}})_n - NH_3^+$$

with n = 6 through 11 (scanning from m/z 500 to 3000).

Figure 4 illustrates the RTIC chromatogram and NH_3 CI spectra from an SFC-MS run of silylated oligosaccharides (a commercial corn syrup solid, Maltrin 100). In previous SFC work with flame ionization detection, it was postulated that the doublets were due to the anomeric forms of the terminal glucose unit. Some doubt was cast on this hypothesis because of the irregular spacing between the members of the doublets. Our SFC-MS work quickly demonstrated that the two species forming each doublet had the same molecular weight, thus lending support to the original hypothesis. The oligomers again show simple spectra dominated by the ammonium adduct ion. Ions at m/z 773 and 1152 are ions related to the oligosaccharide structure containing two and three glucose units.

An LOD of 0.8 ng was determined for methyl arachidate, with a signal-to-noise ratio of roughly 4 for the ammonium adduct ion at m/z 344. The instrument was tuned to "unit" resolution (10 % valley definition) when this measurement was performed. The instrument was scanned from m/z 100 to 500 with a 1 s cycle time.

This work demonstrates that species of molecular mass up to 3000 Da can be introduced to the CI volume through a simple interface probe, ionized, and detected using a "high mass" quadrupole instrument. The only limit to the analysis of higher molecular weight species in this work appeared to be the upper mass limit of the analyzer. Splitless injection in SFC-MS can be performed using conventional 50 um i.d. capillary technology.

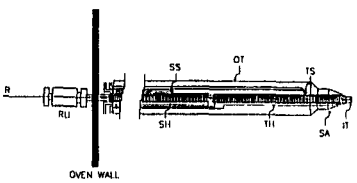

Figure 1: SFC-MS interface probe (R - restrictor, RU - reducing union, SH - stem heater, SS - stem sensor, OT - outer tube, TH - tip heater, TS - tip sensor, SA - source adaptor, IT - inner tube).

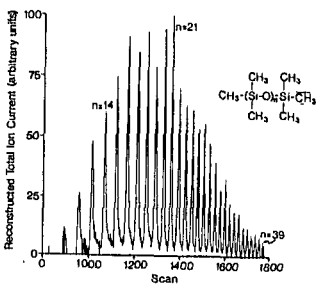

Figure 3: SFC-MS RTIC chromatogram of polydimethylsiloxane.

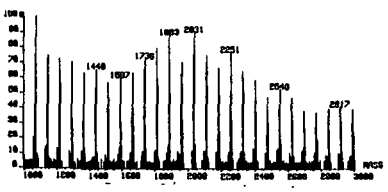

Figure 2: SFI-MS of 3 %. polydimethylsiloxane in CO_2.

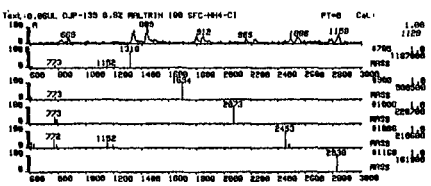

Figure 4: SFC-MS RTIC chromatogram and spectra of oligosaccharides.

1. T.L. Chester, D.P. Innis, J. High Resol. Chromatog. Chromatog. Comm. 1986, 9, 209-212.
2. R.D. Smith, presented at the 1987 Pittsburgh Conference & Exposition on Analytical Chemistry and Applied Spectroscopy, Atlantic City, NJ, March 9-13, 1987.
3. J. Henion, E. Lee, presented at the 34th Annual Conference on Mass Spectrometry and Allied Topics, Cincinnati, OH, June 8-13, 1986.

Presented at the 35th ASMS Conference on Mass Spectrometry and Allied Topics
May 24-29, 1987, Denver, CO

AUTOMATED OFF-LINE LC/MS OF PEPTIDE DIGESTS USING TIME-OF-FLIGHT, SOLID PHASE SIMS

R.C. Beavis, D.E. Main, X. Tang, F. Lafortune and K.G. Standing, Department of Physics, University of Manitoba, Winnipeg, Manitoba CANADA R3T 2N2.

We have developed an off-line LC/MS interface for the Manitoba I time-of-flight (TOF) MS. The interface developed exploited the advantages of TOF SIMS for organic analysis, such as: solid phase samples; high sensitivity; and little beam induced sample damage. The spectrometer has been described before(1). It used a 10 keV Cs primary ion beam with a beam current density of approximately 1 pA/mm^2. The samples used in this instrument were deposits on a conductive (metallic) substrate. Several deposition methods were used, but the method used for the LC/MS interface was electrospray of solutions.

To adapt the MS for use with HPLC eluent, it was desirable to make as few changes as possible to the instrument. Therefore, it was decided to decouple the MS from the HPLC, i.e. an off-line interface. The system was shown in Figures 1 and 2. Figure 1 showed the eluent deposition apparatus. The total eluent of a special microbore HPLC system (0.5 mm i.d., reversed phase) was deposited by electrospraying the liquid from the tip of the outlet needle onto the substrate strip. Using a focussing electrode, the spray plume was deposited onto a small area (1 mm dia.), increasing the surface density of sample on the substrate and matching the size of the deposit to the size of the primary ion beam. The strip bearing the chromatogram (the involatile portion) was then mounted and loaded into the MS (Note: The sample introduction system of the Manitoba I MS was not of the probe type.). Each of the collected fractions was then examined to determine the materials present in the deposit (Figure 2).

Initial application of the LC/MS system to peptide mixtures produced promising results (2). However, the spectra produced were dominated by sodium adduct ions and had very few structurally related fragments. To improve the spectra, modification of the substrate material was tried. The substrate initially used was bare aluminium foil: a hydrophobic Al_2O_3 layer. The surface was altered by thickening the oxide layer and making it porous by anodizing the strip in dilute sulfuric acid. The resulting layer was made hydrophillic by boiling the strip in water for ten minutes, converting the Al_2O_3 to (AlO)OH (also called boehmite). The boehmite layer was very effective in suppressing the effects of sodium contamination, although the mechanism producing this suppression has not been confirmed. Possible explainations for the effect were:

i) The porous layer allowed the sodium to diffuse into the hydroxide layer;

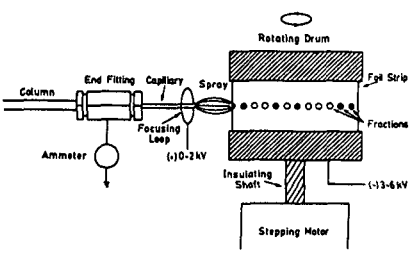

Figure 1. Microbore HPLC fraction collection apparatus; eluent deposition by electrospray.

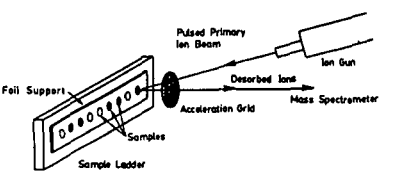

Figure 2. Manitoba I TOFMS sample introduction system, modified to use HPLC fractions as samples (fraction bearing strip was moved horizontally).

2) the hydroxide layer strongly binds the sodium anions to the surface;
3) the hydrophillic surface caused the individual sprayed droplets to spread out on impact with the surface, increasing the surface area of each individual deposit, reducing the surface concentration of sodium.

Evidence for each of these three possibilities has been found.

The main reason for setting up the LC/MS system was to be able to analyse mixtures of peptides and determine the structure of the peptides from the fragentation patterns in the mass spectra. An application of this was the separation of enzyme digest mixtures. To obtain good sequence information, a peptide should be relatively small (less than 1500 u). Smaller peptides can be made from larger ones by enzyme digestion and if the cleavage is specific enough, only a small amount of sequence information is lost by the cleavage. Trypsin was chosen by us because of its highly specific cleavage at basic residues. Neuropeptides in the range 1000 - 2000 u were cleaved and the mixture of products analysed by the LC/MS system.

The results obtained for one peptide, neurotensin, were shown in Figure 3. Some of the peptides were found to fragment at only one specific type of bond on the amino linkage backbone (e.g. the first spectrum), producing sequence ions of the type described by Roepstorff, et al. (3). Other peptide molecules produced fragments by breaking two bonds (e.g. the second spectrum). In general, the fragmentation patterns were dominated by one type of bond breaking (single or double), but the bonds broken and the end of the ion retaining the charge (N- or C- terminal) depended on the amino acid residue sequence. Some peptides did not produce any significant fragmentation, particularly those peptides containing a C-terminal basic residue. Measurements of the metastable decomposition of the quasimolecular ions in the mass spectrum demonstrated that the gas phase anions of these molecules were particularly stable. This stability was thought to imply an unusual stability for molecules with this residue sequence.

1) B.T. Chait and K.G. Standing, Int. J. Mass Spectrom. Ion Phys., 40(1981) 185.
2) R.C. Beavis, G. Bolbach, W. Ens, D.E. Main, B. Schueler and K.G. Standing, J. Chromatogr., 359(1986)489.
3) P. Roepstorff, P. Horjup and J. Moler, Biomed. Mass Spectrom., 12 (1985) 181.

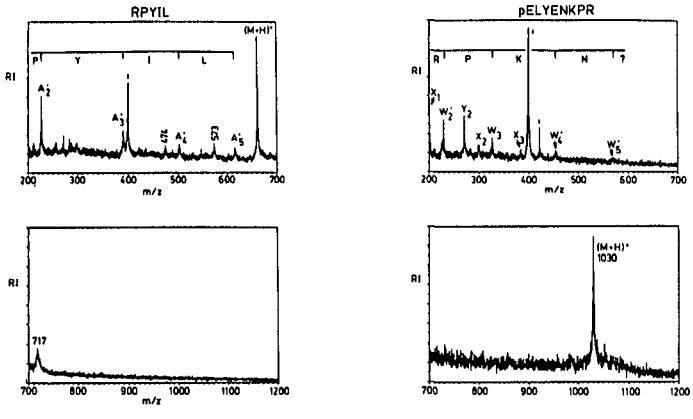

Figure 3. TOF SIMS spectra of the two trypsin cleavage products of neurotensin. The chromatographic conditions were: mobile phase 60:40 2-PrOH:H_2O + 0.05% pH=3.0 TFA/TEA buffer; flowrate = 3.0 µl/min; stationary phase 3 µm, C8 silica; column diameter 0.5 mm i.d.; column length 20 cm.

Presented at the 35th ASMS Conference on Mass Spectrometry and Allied Topics
May 24-29, 1987, Denver, CO

ION SPRAY LIQUID CHROMATOGRAPHY/API TANDEM MASS SPECTROMETRY DETERMINATION OF PEPTIDES

Edgar D. Lee, Lars O.G. Weidolf, and Jack D. Henion, Drug Testing and Toxicology, New York State College of Veterinary Medicine, Cornell University, 925 Warren Drive, Ithaca, NY 14850

The Ion Spray (pneumatic nebulizer-assisted electrospray) interface for combined liquid chromatography/mass spectrometry reported by Bruins et al. (1) produces a mild form of liquid ionization at atmospheric pressure and ambient temperature. Ion spray usually produces abundant $[M+H]^+$ $[M+2H]^{2+}$, and $[M+3H]^{3+}$ positive ions or $[M-H]^-$, $[M-2H]^{2-}$, and $[M-3H]^{3-}$ negative ions and is particularly well suited for the determination of species which exist as ions in aqueous solution. Mild ionization coupled with the absence of heat, which could produce thermal decomposition, make ion spray a potential method for the determination of peptides by liquid chromatography/mass spectrometry (LC/MS).

A Sciex TAGA 6000E triple quadrupole mass spectrometer equipped with an atmospheric pressure ion source was used to sample ions generated from the ion spray LC/MS interface. This interface (Figure 1) was constructed of two concentric stainless steel capillaries held at a high potential of +3KV. The applied potential and the assistance of nitrogen nebulizing gas which flows through the annular space between the two capillaries forms charged droplets from which the ions are emitted. The inner capillary, through which the chromatographic eluent flows is 100 um i.d. x 225 um o.d. and the outer capillary, with an inside diameter of 500 um was tapered at the end to a diameter of 300 um. The linear velocity of the nebulizing gas was measured to 216 m/sec at the exit of the capillaries. The ion spray interface was positioned 5 mm off-axis of the orifice to the mass analyzer to prevent the vapor jet from penetrating the nitrogen curtain which passes over the sampling orifice.

The chromatographic system consisted of a Brownlee Labs Micropump for solvent delivery. A Rheodyne 7410 injector was equipped with a 0.5 ul sample loop. The column used was a 1 mm i.d. x 10 cm Vydac C_{18}, 5 um packing, packed by Keystone Scientific. The mobile phase flow rate used was 40 ul/min. The solvent composition was 18/82 acetonitrile/water with the pH adjusted to 2.8 with trifloroacetic acid, for isocratic runs and programmed from 14/82 to 40/60 over a 20 min time period for gradient elution.

Ion spray mass spectrometry determination of the peptides exhibited primarily the diprotonated doubly charged molecular ion and/or protonated singly charged molecular ion. The more acidic the eluent the more dominant the diprotonated species. When high aqueous eluents were used, the mass spectra also exhibited some minor adduct peaks with H_3O^+. LC/MS/MS (Figure 2) of the protonated molecular ion or the diprotonated molecular ion contained daughter ions which are consistent with the sequence of the peptide.

The detection limit and linearity for leucine enhephalin was determined by selected ion monitoring of the protonated molecular ion. Triplicate injections of the peptide, after three solvent blank injections, were made over the range of 56 amole to 90 pmole were made. The response was found to be linear over the range of 30 fmole to 90 pmole and the minimum detected quantity was 65 amole by SIM LC/MS.

REFERENCE

1. Bruins, A.P.; Covey, T.R.; Henion, J.D. 34th Annual Conference on Mass Spectrometry and Allied Topics, June 8-13, 1986, Cincinnati, OH. Abstract p. 585-586.

Presented at the 35th ASMS Conference on Mass Spectrometry and Allied Topics
May 24-29, 1987, Denver, CO

ION SPRAY LIQUID CHROMATOGRAPHY/ MASS SPECTROMETRY

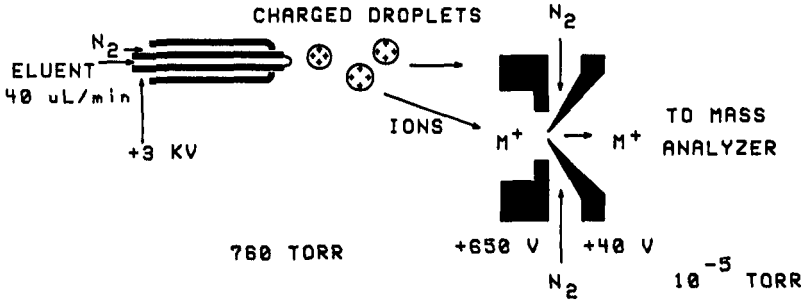

Figure 1. Schematic diagram of the ion spray LC/MS interface

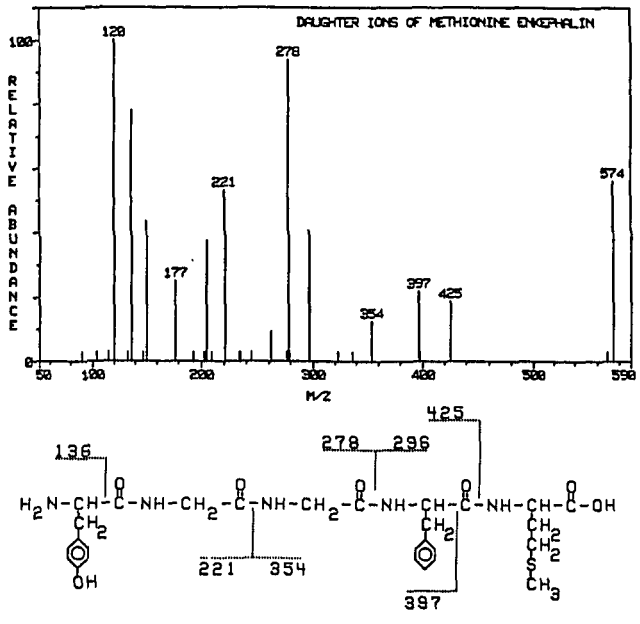

Figure 2. Ion spray LC/MS/MS daughter ion spectrum of methionine enkephalin at 50 eV collision energy.

Presented at the 35th ASMS Conference on Mass Spectrometry and Allied Topics
May 24-29, 1987, Denver, CO

ADVANTAGES AND DIFFICULTIES OF FT/ICR FOR ANALYTICAL MASS SPECTROMETRIC APPLICATIONS

Alan G. Marshall

Department of Chemistry
(and Dept. of Biochemistry)
The Ohio State University
120 West 18th Avenue
Columbus, OH 43210

Apart from its uses for investigating ion-molecule reaction paths, kinetics, and equilibria, FT/ICR mass spectrometry [1] is particularly suited to solve several kinds of mass spectrometric problems. First, low-pressure capability (10^{-6}-10^{-10} Torr) makes possible the direct probe analysis of heat-sensitive samples of low volatility (e.g., metal complexes and organometallics). Second, thermal ions may be trapped for extended periods (1-100 s) to produce ion-molecule reaction products of mechanistic or analytical value. These two features are nicely illustrated in Figure 1, which shows a series of triosmium dimer cations generated in the mass spectrometer by self-reaction of electron-ionized triosmium monomer cations with $H_2Os_3(CO)_{10}$ neutral parent molecules.

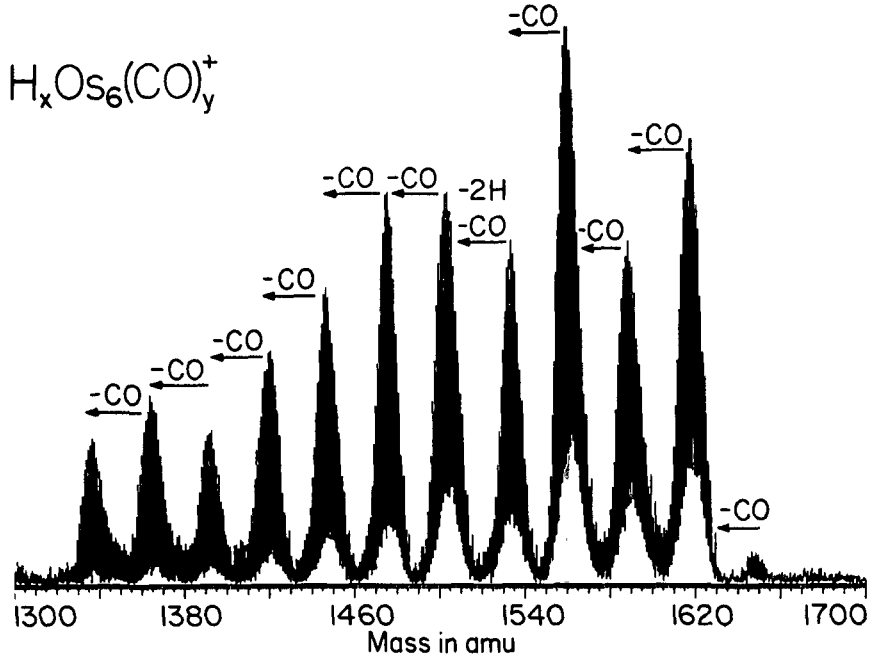

Figure 1. FT/ICR mass spectrum of positive ions formed from the 0.5 s self-reaction of $H_2Os_3(CO)_{10}$ (1x10-9 Torr) with its molecular and daughter ions to give species ranging from $Os_6(CO)_7^+$ to $H_2Os_6(CO)_{18}^+$. By detecting only the products produced after selective ejection of all but one $H_xOs_3(CO)_y^+$ (x = 0,2; y = 0-10) species, it is possible to determine which triosmium dimer product ions are formed from which triosmium monomer reactant ions.[2]

Third, FT/ICR is inherently a pulsed experiment, and is thus ideally matched to pulsed laser desorption for analysis of involatile species (e.g., drugs; polymers). Furthermore, because LD/FT/ICR experimental conditions can be very similar for observation of chemically different compounds, the technique is uniquely valuable for simultaneous detection of chemically different components of a mixture, at mass resolution sufficient for accurate determination of the chemical formula of each component. These features are illustrated by the laser desorption mass spectrum of Figure 2, in which characteristic ions from both components of a solid polymer/dye material are detected together.

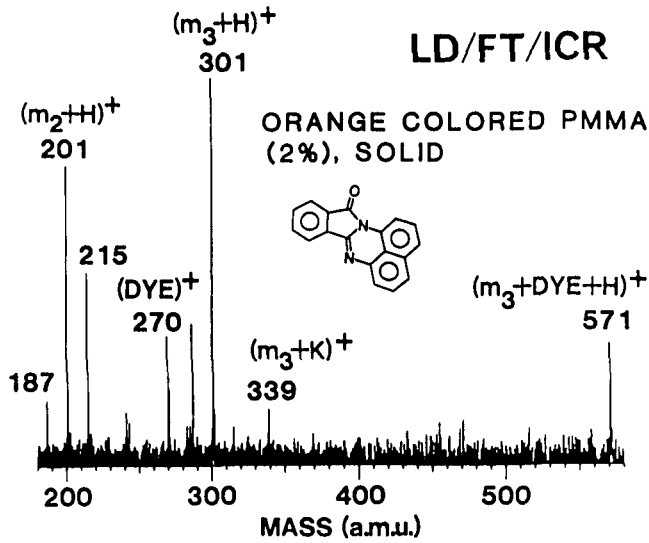

Figure 2. Laser desorption FT/ICR mass spectrum for unadulterated solid polymethylmethacrylate (MW > 10^6) into which a red dye had been incorporated before the polymer was formed. Both the dye and the characteristic fragments of the polymer can be identified from accurate-mass determination of their chemical formulas. In this case, mass spectrometric sensitivity (~0.2%) for dye identification is about 10 times higher than by means of conventional infrared spectrometry (~2%). We have detected as many as three different dyes in a single PMMA sample.

Fourth, FT/ICR offers unsurpassed ultrahigh mass resolution, both for directly ionized species and for daughter ions in MS/MS experiments. For example, M. B. Wise has recently identified numerous components of tar collected from environmental tobacco smoke, including as many as three different chemical formulas at the same nominal mass.[4]

The principal practical difficulties with FT/ICR are its limited analog dynamic range (about 1000:1) and its inherently digital data. Remedies for those problems are becoming available (e.g., ref. 5).

[This work was supported by grants (to A.G.M.) from N.I.H. GM-31683 and The Ohio State University.]

1. Marshall, A. G.; Acc. Chem. Res. 18, 316-322 (1985).
2. Mullen, S. L.; Marshall, A. G.; submitted for publication.
3. Hsu, A. T.; Marshall, A. G.; submitted for publication.
4. Wise, M. B.; 1987 Pittsburgh Conference on Analytical Chemistry and Applied Spectroscopy, Atlantic City, NJ, March, 1987), Paper #527.
5. Wang, T.-C. L.; Ricca, T. L.; Marshall, A. G. Anal. Chem. 58, 2935-2938 (1986).

Presented at the 35th ASMS Conference on Mass Spectrometry and Allied Topics
May 24-29, 1987, Denver, CO

Application of Fourier Transform Mass Spectrometry To Study Transition Metal Cluster Chemistry

D. B. Jacobson and J. R. Diers

Department of Chemistry
North Dakota State University
Fargo, North Dakota 58105

Using Fourier transfer mass spectrometry (FTMS) a variety of transition metal cluster ions, both bare and specifically ligated, can be generated and studied. For example the iron cluster ions, $Fe_3(CO)_{10}^+$, $Fe_4(CO)_{12}^+$, and $Fe_6(CO)_{18}^+$, can be generated directly from the condensation reactions of ionized $Fe(CO)_5$. Collisional activation (CA) of $Fe_3(CO)_{10}^+$ and $Fe_4(CO)_{12}^+$ yields facile elimination of the carbonyls resulting in formation of the naked cluster ions Fe_3^+ and Fe_4^+. CA of $Fe_6(CO)_{18}^+$ yields an initial facile elimination of $Fe(CO)_5$ followed by sequential loss of all the carbonyls yielding Fe_5^+, process 1.

$$Fe_6(CO)_{18}^+ \xrightarrow[-Fe(CO)_5]{CID} Fe_5(CO)_{13}^+ \longrightarrow Fe_5^+ + 13(CO) \qquad (1)$$

These clusters (Fe_2^+, Fe_4^+, Fe_5^+) are much less reactive towards alkanes than the corresponding atomic cation Fe^+. For example Fe_3^+ is unreactive with propane whereas Fe^+ reacts readily with propane by both dehydrogenation as well as methane elimination. The corresponding dioxide, $Fe_3O_2^+$, is much more reactive towards alkanes than Fe_3^+ as exemplified by the rapid dehydrogenation of propane, process 2.

$$Fe_3O_2^+ + C_3H_8 \dashrightarrow Fe_3O_2C_3H_6^+ + H_2 \qquad (2)$$

$Fe_3O_2^+$ was generated by reaction 3

$$Fe_5^+ + O_2 \dashrightarrow Fe_3O_2^+ + Fe_2 \qquad (3)$$

Larger clusters of iron are also formed by allowing Fe_4^+ to condense with $Fe(CO)_5$ resulting in formation of the inert cluster $Fe_{10}(CO)_{16}^+$. CA of $Fe_{10}(CO)_{16}^+$ yields sequential elimination of the carbonyls from which Fe_{10}^+ can be isolated and studied.

Decomposition of metal clusters containing nitrosyl ligands yield a much richer chemistry than the binary carbonyl species. For example CA of $Co_2(CO)NO^+$ (formed from $Co(CO)_3NO$) yields both elimination of CO and CO_2

as the primary fragmentation processes, reactions 4 and 5. The elimination of

$$Co_2(CO)NO^+ \xrightarrow{CID} \begin{cases} Co_2NO^+ + CO & (4) \\ Co_2N^+ + CO_2 & (5) \end{cases}$$

carbon dioxide, process 5, was confirmed over the sequential CO and O eliminations by observing that Co_2NO^+ eliminates NO exclusively upon CA with <u>no</u> Co_2N^+ observed. In addition, Co_2NO^+ reacts with CO yielding Co_2N^+, process 6, further confirming

$$Co_2NO^+ + CO \dashrightarrow Co_2N^+ + CO_2 \qquad (6)$$

the elimination of CO_2 for process 5. CA of $Co(CO)_2NO^+$ yields initial elimination of CO followed by the competitive elimination of CO and CO_2, vide supra. Finally, CA of $Co_3(CO)NO^+$ yields exclusively initial elimination of CO forming Co_3NO^+ with <u>no</u> Co_3N^+ observed. These results show that both the degree of saturation as well as cluster size are critical for observing oxide transfer to CO.

Presented at the 35th ASMS Conference on Mass Spectrometry and Allied Topics
May 24-29, 1987, Denver, CO

FOURIER TRANSFORM MASS SPECTROMETRY IN THE STRUCTURAL CHARACTERIZATION OF OLIGOPEPTIDES AND PROTEINS: D. F. Hunt and J. Shabanowitz; Department of Chemistry, University of Virginia, Charlottesville, Virginia 22901

Methodology for the sequence analysis of proteins using a combination of enzymatic or chemical degradation steps, HPLC of oligopeptide fragments, and sequence analysis of peptides in mixtures by collision activated dissociation mass spectrometry on a triple quadrupole instrument has been described previously (1). Starting with 10 nmol of a 50 kDa protein, it is usually possible to obtain sequence information covering 25 - 60% of the sample in 4-5 days required to perform the above biochemical and instrumental manipulations. Presently this approach is limited by the 1800 Da mass range of our instrument and by the sample quantity 0.1 - 1.0 nmol of peptide, required for sequence analysis.

To reduce the sample size by an order of magnitude and to extend the methodology to mixtures of larger oligopeptides, new instrumentation, a tandem quadrupole Fourier transform mass spectrometer (Fig. 1) has been constructed and is now employed routinely for characterizing the molecular weights of peptides in protein digests at the 10-50 pmol level in the mass range up to m/z 6,000. Horse cytochrome-C at m/z 12,385 is the largest biological molecule observed to date on the new instrument (2).

To obtain molecular weight information, sample at the 10-50 pmol level in 0.5 ul of glycerol-thioglycerol (1/1) is exposed to a beam of 10 keV Cs+ ions for 4 ms. Sample ions sputtered from the matrix under these conditions are transferred through the fringing fields of a 7-T superconducting magnet with the aid of two sets of rf only quadrupole rods and are then trapped in an elongated ion cyclotron resonance cell. Once trapped, the ions are excited by an rf pulse containing a range of frequencies that causes them to move coherently in large orbits at cyclotron frequencies characteristic of their individual masses. Image currents on two of the cell plates produced by this motion are amplified, digitized, and Fourier transformed to generate a mass spectrum. Data from 50-200 such experiments on the same sample are acquired and summed in less than 20-60 s to produce the desired mass spectrum. Structural information on oligopeptide samples is presently being generated by the technique of laser photodissociation. Fragmentation of trapped (M+H)+ ions is induced with a single 10 nsec pulse of irradiation t 193 nm from an argon fluoride excimer laser. Generation of complete sequence information from a number of samples at the 10-30 pmol level has been achieved by this approach (3).

Examples of the utility of the Fourier transform instrument in our research on protein structure are described below. One very important role involves monitoring enzyme digests on trace amounts of protein to determine the experimental conditions, choice of enzyme and time of digestion, to generate an optimal set oligopeptide fragments for sequence analysis by either CAD on the triple quadrupole instrument or laser photodissociation on the FT instrument. Trial digests are conducted at the 100 - 500 pmol level. Aliquots corresponding to 50-100 pmol of peptide are withdrawn at various time intervals, fractionated by HPLC and the peptide content of each fraction is then monitored by FTMS. Each mass spectrum covering the mass range 200-8000 is generated in seconds and requires only 10-50 pmol of peptide.

FTMS is also employed to confirm the proper placement of small oligopeptides in the sequence when the final protein structure is being assembled. Sequence information on purple acid phosphatase, a 35 kDa glycoprotein from beef spleen, is shown in Fig. 2. Molecular weights of amino acid sequences underlined and labelled FT- were confirmed by measurements made on the tandem quadrupole FTMS instrument.

Use of laser photodissociation on the FTMS instrument to obtain structural information on oligopeptide samples is illustrated here with data from a study to determine which amino acid residues in the protein, cytochrome-C, were involved in the binding to a monoclonal antibody prepared against this protein.

Presented at the 35th ASMS Conference on Mass Spectrometry and Allied Topics
May 24-29, 1987, Denver, CO

Treatment of the protein with diethylpyrocarbonate was expected to label the protein at a single His residue. This modification inhibited the binding of cytochrome-C to the antibody. Location of the modified residue was accomplished by digesting the labelled protein with a combination of S. aureus protease and chymotrypsin. Peptide fragments were fractionated by HPLC and then examined by mass spectrometry. Only one peptide, KGGKHKTGPNLHGLF, showed an (M+H)+ ion at a mass value 72 amu above that predicted from the known sequence of the protein. This mass shift was consistent with that expected for incorporation of a single label onto the above peptide. Shown in Figure 3 is the laser photodissociation mass spectrum of this labelled peptide. Mass assignments are accurate to within 0.2 amu. Observed fragment ions are of type Y and therefore contain the C-terminus of the peptide. Fragment ions Y8-Y10 are not shifted to higher mass by 72 amu and therefore do not contain the label. Fragment Y11 containing His 26 is shifted by 72 amu. Accordingly, His 26 is assigned as the labelled residue. Support for this assignment was obtained by acetylating the labelled peptide. Introduction of acetyl groups occurred at the N-terminus and on the side chains of all three Lys residues. Treatment of the acetylated peptide with trypsin failed to cleave the sample. The above observations ruled out the possibility that one of the Lys residues contained the ethoxycarbonyl label. All of the above experiments were carried out on less than 100 pmol of labelled peptide.

1) D. F. Hunt, J. R. Yates, III, J. Shabanowitz, S. Winston, and C. R. Hauer, Proc. Natl. Acad. Sci., USA, (1986) 83, 6233-6237.

2) D. F. Hunt, J. Shabanowitz, J. R. Yates, III, N. Z. Zhou, D. H. Russell, and M. E. Castro, Proc. Natl. Acad. Sci., USA, (1987) 84, 620-623.

3) D. F. Hunt, J. Shabanowitz, and J. R. Yates, III, J. Chem. Soc., Chem. Commun., (1987) In Press.

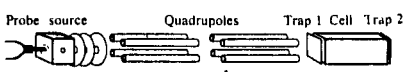

FIG. 1. Diagram of the tandem quadrupole Fourier-transform mass spectrometer.

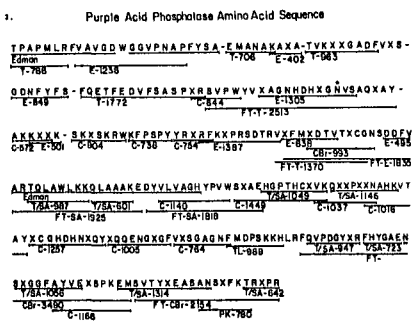

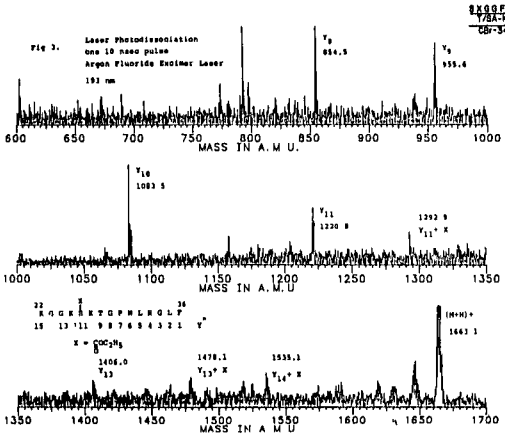

Presented at the 35th ASMS Conference on Mass Spectrometry and Allied Topics
May 24-29, 1987, Denver, CO

KINETIC CHARACTERIZATION OF IONS DERIVED FROM METAL CARBONYLS

W. Reents, Jr., AT&T Bell Labs;

F. Strobel, J. Wronka and D. P. Ridge,

Chemistry Department and Center for Catalytic Science and

Technology, University of Delaware, Newark, Delaware 19716

It has long been known that ionic fragments of metal carbonyls react with neutral metal carbonyls to produce metal carbonyl cluster ions retaining all the metal atoms from both reactants. Sequential reactions of this kind produce metal cluster ions with as many as ten or more metal atoms and varying numbers of carbonyls. The ability to generate and study these species represents a unique opportunity. A variety of techniques have been used to produce bare metal clusters. Coordinatively saturated metal clusters can be prepared in condensed phase. The clusters produced in the ion molecule reactions vary from coordinately saturated to highly unsaturated but not completely without ligands. In $Re_2(CO)_{10}$, for example, ions of stoichiometries $Re_6(CO)_n^+$ with n=14-20 and 22 are observe. This is an important range of coordinative unsaturation not generally available for study. The first objective of studying these ions is to provide a structural characterization. Examination of the kinetics of the clustering reactions provides a key to doing that. In many instances, a simple relationship between structure and reactivity appears to obtain. The relationship is based on the notions that (1) reactivity should increase with coordinative unsaturation and (2) coordinative unsaturation depends not only on stoichiometry but also on the number of metal-metal bonds and hence on the structure. Examples involving groups 7 and 8 metal carbonyls have been discussed in the literature[1]. FTMS and ICR techniques provide the critical kinetic data for this analysis.

Recently FT-ICR techniques have been used to extend the range of the size of clusters observed as a result of clustering reactions of metal caronyls. Heating unreactive clusters at their cyclotron frequency so that they decompose on collisions prduces reactive clusters that react with the neutral metal carbonyl to form even larger clusters. Species containing 16 or more metal atoms have been observed in decacarbonyl dirhenium[2].

The reactions of some of the rhenium clusters with cyclohexane have been examined[2,3]. Clusters with three and four rhenium atoms dehydrogenate the cyclohexane. In general $Re_n(CO)_m^+$ reacts with cyclohexane to give $Re_nC_6H_{2(6-x)}(CO)_{m-y} + xH_2 + yCO$. The number of H_2 molecules eliminated, x, is generally one or two. The yield of H_2 per mole of reaction for n=3 and 4 clusters is plotted verses electron deficiency D in Fig 1. The electron deficiency of a cluster is the difference between 18 and the average number of valence electrons per metal atom in the cluster. For the rhenium clusters it is given by $18-((7n+2m+2b-1/n)$ where b is the number of metal-metal bonds in the cluster. b is taken to 3 for n=3 and 6 for n=4. Plotted in Fig. 2 is the yield of CO relative to the H_2 yield for the n=3 and4 cluster ions. Note that a yield of 1 corresponds to a cyclohexene containing product, a yield of 2 corresponds to a cyclohexadiene product and a yield of 3 corresponds to a benzene product. Nonintegral yields indicate more than one kind of product. Zero yields are plotted where no product was observed. n=3 clusters give higher H_2 yields than n=4 clusters. The reactivity of both n=3 and n=4 clusters disappears when D decreases below 2.5-3. The H_2 yields for the n=4 clusters increase as D increases. That effect is less dramatic in the n=3 clusters. The relative CO yields decrease with increasing electron deficiency in the n=4 clusters but not in the n=3 clusters. Thus the reactivity depends on the number of metal atoms in the cluster and on the number of ligands.

1. Meckstroth, W.K.; Freas, R. B.; Reents, Jr., W. D.; Ridge, D. P. Inorg. Chem., 1985, 24, 3137 and references therein.

2. Forbes, R. A.; Laukien, F. H. and Wronka, J. submitted for publication.

3. Forbes, R. A.; Laukien, F. H.; Wronka, J. ; Ridge, D. P. to be published.

Presented at the 35th ASMS Conference on Mass Spectrometry and Allied Topics
May 24-29, 1987, Denver, CO

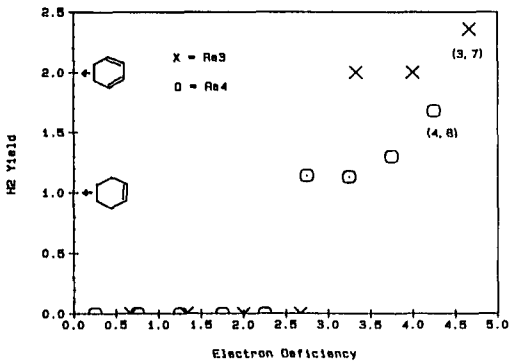

Figure 1

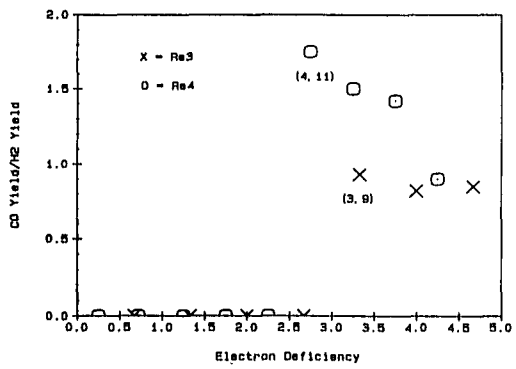

Figure 2

Presented at the 35th ASMS Conference on Mass Spectrometry and Allied Topics
May 24-29, 1987, Denver, CO

PROBLEM-SOLVING APPLICATIONS OF FTMS

CODY, R.B., Nicolet Analytical Instruments
5225-1 Verona Road; Madison, WI 53711

In addition to its well-known uses in physical chemistry, FTMS has been applied to a surprising diversity of "real world" problems. Among the demonstrated applications of FTMS are quantitative gas analysis, determination of the moisture content of integrated circuits, analysis of surface contaminants, industrial waste, and drugs in human body fluids, geological dating, drug characterization, tobacco smoke analysis, analysis of unstable compounds, and studies of peptides, polymers, and saccharides.

If "real problems" are defined as problems for which the answer is not known in advance, then there can be no doubt that FTMS is being applied to "real" problems. It may be instructive to consider how FTMS has been used to solve several specific problems, in order to understand the analytical approaches that may be employed for FTMS analyses.

The insecticide chlorpyrifos undergoes complex rearrangements and direct bond cleavages under low energy collisional activation. Due to the large number of heteroatoms, it is a difficult task to determine the nature of each of the fragment ions observed. Accurate mass measurements on the daughter ions facilitate this task by allowing us to calculate a number of elemental compositions for each fragment (Table I). Where assignments cannot be made on the basis of mass measurements alone, one can obtain additional information by performing MS/MS/MS experiments [1]. For example, the identity of the m/z 214 peak was determined from the fact that the daughter ion at m/z 214 undergoes further fragmentation to produce the granddaughter ion at m/z 178. This loss of 37 amu is indicative of HC_1 loss, and a pair of elemental compositions may be found from the mass measurements for both 214 and 178 which support HC_1 loss. These compositions are marked with an arrow in Table I.

A similar approach has been used to identify a trace contaminant in the mass spectrometer, which is only occasionally evident under soft ionization conditions such as laser desorption, or chemical ionization. Accurate mass measurements on the [M+H]+ ion which appears at m/z 214 for self-CI with long reaction times (>5 seconds), suggest the elemental composition $C_{10}H_{15}NO_2S$. Support for this assignment comes from the presence of an 11% M+1 peak, an M+2 peak with an isotopic abundance consistent with the presence of one sulfur, and from the odd molecular weight, which indicates the presence of an odd number of nitrogens. Collisional activation at 30eV produces fragments which are easily identified by their accurate mass measurements (Table II). From this information, the contaminant is readily identified as N-butyl benzene sulfonamide. This compound is found to be a trace contaminant in mechanical pump oil, which may be eliminated if the mechanical pump traps are baked out on a regular basis.

Other analytical approaches have been applied to the solution of very different problems. In the analysis of particulates from the effluent from a steel mill, accurate mass measurements assisted in the GC-MS identification of components whose EI spectra might lead to ambiguous assignments, or where different components were not completely separated by the gas chromatograph [2]. Analysis of "intractable" polymers by laser desorption/FTMS has identified differences in the polymer composition resulting from different synthetic methods [3]. The highly-reactive and thermolabile organoiodine compounds CH_3OI_2 and CH_3OI_3 have been identified in nuclear reactor waste by direct probe introduction into the FTMS at subzero temperatures [4].

It should be evident from these examples that the "unconventional" nature of FTMS makes it well-suited to solving problems that are difficult to attack by conventional methods. The additional information available from accurate mass measurements, MS/MS, and even MS/MS/MS methods are valuable in solving complex problems requiring as much chemical information as possible.

Presented at the 35th ASMS Conference on Mass Spectrometry and Allied Topics
May 24-29, 1987, Denver, CO

References:

1. R. Cody, Analytical Chemistry, submitted.
2. J.F. Muller, F. Verdun, J. Kinsinger, unpublished results.
3. C.E. Brown, et al, Analytica Chimica Acta, 178 (1985) 43-66
4. M. Kabat, R. Cody, unpublished results.

TABLE I

50 eV CAD of Chlorpyrifos $[M+H]^+$

Accurate Mass Measurements on Daughter Ions

Measured Mass	Formula	Calculated Mass	Difference (ppm)
46.96838	PO	46.96813	5.39
	C Cl	46.96831	1.67
96.95058	C O ^{37}Cl	96.95010	4.97
	$H_2 O_2$ P S	96.95077	-1.90
	C H_2 O Cl S	96.95049	-3.71
177.92703	$C_3 H_6$ Cl P	177.92672	1.70
	$C_4 O_3$ N ^{37}Cl P	177.92694	0.50
	$C_5 O_2$ N ^{35}Cl ^{37}Cl	177.92711	-0.48
→	$C_4 H_2$ O N Cl S P	177.92776	-4.23
	$C_2 H_4$ O3 Cl_2 S	177.92527	9.84
	$C_5 H_2$ N Cl_2 S	177.92795	-5.22
197.92699	$C_7 O_3$ Cl P	197.92681	0.90
	$C_8 O_2 Cl_2$	197.92699	0.01
	$C_4 H_3 O_2$ N Cl_2 P	197.92730	-1.57
	$C_5 H_3$ O N Cl_3	197.92747	-2.45
	$C_8 H_2$ ^{37}Cl S P	197.92684	0.76
199.92344	C_7 H N Cl_2 P	199.92182	8.11
	$C_7 O_3$ ^{37}Cl P	199.92366	-2.11
	$C_8 O_2$ ^{35}Cl ^{37}Cl	199.92404	-2.99
	$C_4 H_3 O_2$ N ^{35}Cl ^{37}Cl P	199.92435	-4.55
	$C_5 H_3$ O N $^{35}Cl_2$ ^{37}Cl	199.92452	-5.42
	$C_7 H_2$ O Cl S P	199.92470	-6.33
	$C_8 H_2 Cl_2$ S	199.92488	-7.20
213.90311	C_4 H O_3 N ^{35}Cl ^{37}Cl P	213.90361	-2.35
	$C_7 O_2$ Cl S P	213.90397	-4.01
→	$C_4 H_3$ O N Cl_2 S P	213.90446	-6.29
275.86040	$C_5 H_2 O_2$ N Cl_3 S P	275.86040	0.01
293.86973	$C_8 O_3$ N Cl_3 P	293.86759	7.27
	$C_5 H_4 O_3$ N Cl_3 S P	293.87096	-4.20
	$C_9 H_2$ N $^{35}Cl_2$ ^{37}Cl S P	293.86762	7.18
295.86743	$C_8 O_3$ N ^{35}Cl2 ^{37}Cl P	295.86464	9.42
	$C_8 H_2$ O N Cl_3 S P	295.86548	6.57
	$C_5 H_4 O_3$ N Cl_2 ^{37}Cl S P	295.86801	-1.98
323.89742	$C_7 H_8$ N $^{35}Cl_2$ ^{37}Cl S P	323.89931	-5.86
324.93265	$C_9 H_{12} O_3$ N Cl_3 S P	349.93357	-2.62

Presented at the 35th ASMS Conference on Mass Spectrometry and Allied Topics
May 24-29, 1987, Denver, CO.

Reactions of molecular ions in association with inert gas clusters.

A.J. Stace and D.M. Bernard, School of Molecular Sciences, University of Sussex, Falmer, Brighton BN1 9QJ, U.K.

Ion clusters of the type $Ar_n.X^+$ and $(CO_2)_n.X^+$ can be formed by electron impact following the adiabatic expansion of an inert gas/X mixture. In all cases it is observed that X^+ is able to undergo quite extensive unimolecular fragmentation without significantly disrupting the inert gas component[1-4]. Examples of some of the observed reactions are:

$$(CO_2)_n.CH_3COCH_3^+ \rightarrow (CO_2)_n.CH_3CO^+ + CH_3$$

$$Ar_n.(CH_3)_2O^+ \rightarrow Ar_n.CH_3OCH_2^+ + H$$

$$\rightarrow Ar_n.CHO^+ + H_2 + CH_3$$

$$Ar_n.CH_3COC_3H_7^+ \rightarrow Ar_n.C_3H_7CO^+ + CH_3$$

$$\rightarrow Ar_n.CH_3CO^+ + C_3H_7$$

$$(CO_2)_n.CH_3COC_2H_5^+ \rightarrow (CO_2)_n.CH_3CO^+ + C_2H_5$$

$$\rightarrow (CO_2)_n.C_2H_5CO^+ + CH_3$$

In the reactions studied so far, the observed fragmentation pattern of the cluster-bound ion has always differed significantly from that found for the corresponding isolated ion. From these experiments we have concluded that reactive ions occupy sites that are on, or close to, the surface of the cluster. Two facts support this conclusion. Firstly, many of the observed reactions involve extensive fragmentation of the polyatomic ion concerned and these processes would shatter the cluster if the reactant ion was completely solvated by the inert gas. Secondly, the relative product ion intensities for large values of n appear to be independent of cluster size. Therefore, we would suggest that the inert gas clusters influence the fragmentation patterns through steric and, possibly, caging interactions.

Another aspect of the previous experiments[1-4] has been concerned with establishing the mechanism responsible for exciting reactant ions above their dissociation limits. Existing chemical evidence[1-4] suggests that some form of charge transfer mechanism is in operation, where the molecular ion receives the energy difference between I_p(inert gas) - I_p(molecule). Recent photoionization experiments provide strong support for the charge transfer conclusion[5-7]. Once molecular ions have acquired the above energy difference, there exists a competition within the cluster between the breaking of covalent bonds and vibrational predissociation of the inert gas component. Approximate calculations suggest that in order for the molecular ion to decompose the reaction timescale must be less than 10^{-12} s.[1-4]

Table 1 displays the results for the reactions of butan-2-one and pentan-2-one in association with argon and carbon dioxide. The presence of the inert gas cluster has clearly altered the fragmentation patterns of the molecular ion when compared with mass spectroscopic and charge transfer data for the isolated ion. If the exact role of the inert gas component can be established then it may be possible to consider some of the cluster reactions as models for surface processes.

This work has recently been extended to consider argon and carbon dioxide in association with 2-methylhexan-3-one. This molecule contains sufficient α, β, and γ hydrogens adjacent to the carbonyl group that the parent ion can undertake two well established rearrangement processes. These rearrangements give rise to a ketene and an enolate ion. Preliminary results on 2-methylhexan-3-one with inert gas clusters indicate that no enolate ions or ketene ions are observed. This observation would suggest that the inert gas component prohibits all rearrangement processes and not just those involving an oxygen atom.

1. A.J. Stace, J. Am. Chem. Soc., **106**, 4380 (1985).
2. A.J. Stace, J. Am. Chem. Soc., **107**, 755 (1985).
3. A.J. Stace, J. Phys. Chem., **91**, 1509 (1987).
4. D.M. Bernard and A.J. Stace, J. Chem. Soc., Faraday Trans. 2, **83**, 29 (1987).
5. A. Ding, J.H. Futrell, R.A. Cassidy, L. Cordis, and J. Hesslich, Surf. Sci., **156**, 282 (1985).
6. W. Kamke, B. Kamke, H.U. Kiefl, and I.V. Hertel, Chem. Phys. Lett., **122**, 356 (1985).
7. P.D. Dao and A.W. Castleman Jr., J. Chem. Phys., **84**, 1435 (1986).

Table 1. Normalised data for butan-2-one and pentan-2-one

	this work		charge-transfer data				70 eV mass spec.
	$(Ar)_{13}$	$(CO_2)_{13}$	Ar^+	CO_2^+	CO^+	H_2O^+	
			butan-2-one				
$CH_3COC_2H_5^+$	100	58	8	3	0	3	16
$C_2H_5CO^+$	75	16	5	5	5	15	7
CH_3CO^+	81	100	100	100	100	100	100
$C_2H_5^+$	—	—	35	17	24	15	24
$C_2H_3^+$	—	—	18	4	20	0	20
			pentan-2-one				
$CH_3COC_3H_7^+$	100	100	17	2	0	3	25
$C_3H_7CO^+$	96	25	12	4	4	13	9
$CH_3C(OH)=CH_2^+$	—	—	12	4	4	15	9
CH_3CO^+	55	83	100	100	100	100	100
$C_2H_5^+$	—	—	10	2	4	1	16
$C_2H_3^+$	—	—	19	7	20	1	10

Presented at the 35th ASMS Conference on Mass Spectrometry and Allied Topics
May 24-29, 1987, Denver, CO

ION-DIPOLE AND ELECTRON-DIPOLE REACTIONS

David C. Clary
University Chemical Laboratory
Lensfield Rd
Cambridge CB2 1EW
UK

We have been developing a quantum based theory for calculating cross sections and rate coefficients for chemical reactions dominated by long-range intermolecular forces. In particular, we have been applying the theory to the reactions of ions and electrons with dipolar molecules. The method involves calculating rotationally adiabatic potential curves on which it is assumed the charged particle moves. The theory yields rate coefficients that agree well with experiment for temperatures as low as 27 K for the reactions of ions such as N^+ and C^+ with H_2O, H_2S, SO_2 and HCl.

We have extended the theory to derive an analytical rate coefficient formula for the reactions of electrons with dipolar molecules. The theory includes the rotational levels of the molecule explicitly and also accounts for quantum mechanical reflection from an attractive potential. The theory predicts that, for the exothermic or thermoneutral reactions of electrons with strongly polar molecules, the rate coefficient is

$$k(T)= [\, 2\pi/(kT)\,]^{1/2} \quad + B^{1/2}\, \pi\; 2^{1/2}\, [2\mu_D{}^2 / \; (2\mu_D{}^2 + 3)] \,/\, [\, kT]$$

where B is the rotor constant of the molecule, μ_D is the dipole moment and atomic units have been used. This is a very different formula to that obtained for ion-dipole reactions where, to a good approximation, the rate coefficient depends on $\mu_D/T^{1/2}$ and does not depend on B for $kT>B$.

We have also adapted the same theory to the spectroscopy of the photodetachment of electrons from dipolar anions. Systems examined include

Presented at the 35th ASMS Conference on Mass Spectrometry and Allied Topics
May 24-29, 1987, Denver, CO

$CH_2CN^- \xrightarrow{h\nu} CH_2CN + e^-$ and $CH_2CHO^- \xrightarrow{h\nu} CH_2CHO + e^-$

for which rotationally resolved experimental spectra have been reported previously. The technique involves the calculation of the rotationally adiabatic potentials by diagonalising a hamiltonian containing a simple potential constructed from an electron-dipole interaction plus a damped polarisation term. Calculations of the energies and widths of the Shape and Feshbach resonances for these potentials are identified with the positions and widths of the lines in the photodetachment spectra. A novel analysis of the hamiltonian for the electron-dipole interaction leads to simple formulae relating to the resonance energies and widths. This theoretical analysis also provides a clear explanation of several experimental results including the regular rotational structure observed for the line positions in the photodetachment spectrum, the independence of the line widths on the symmetric top projection quantum number k for CH_2CN^- and the sharp increase of the line width with increasing k for CH_2CHO^-.

In the figure below we show an example of the rotationally adiabatic curves for CH_2CHO+e^-. These curves support the Shape resonances that give the lines in the photodetachment spectrum. The arrow shows the Feshbach resonance that involves jumping from the curve with symmetric top projection quantum number k=2 to that for k=1. For this type of molecule, the line-widths are predicted to scale roughly as $(2k-1)^2$.

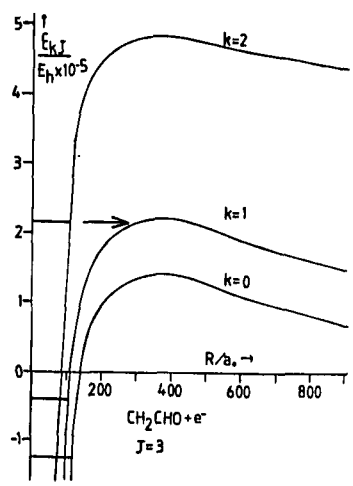

Presented at the 35th ASMS Conference on Mass Spectrometry and Allied Topics
May 24-29, 1987, Denver, CO

NON-ADIABATIC EFFECTS IN ION-MOLECULE PROCESSES

P. B. Armentrout
Chemistry Department, University of Utah, Salt Lake City, UT 84112

One of the truly powerful features available in the study of ion-molecule chemistry is the ease with which the kinetic energy of the reactants can be altered over a very wide range. A comparable ability in neutral chemistry is achieved with great difficulty over much narrower energy regions. This ability is a very useful tool for probing the potential energy surfaces of reaction systems, but in practice, it has seen surprisingly limited use. One of the key aspects of our recent research has been detailed investigations of the kinetic energy dependence of ion-molecule reaction cross sections and the extent to which these investigations provide useful kinetic, dynamic and thermochemical information. Coupled with this is the concomitant need to control the extent of internal energy in the reactants. This has led to the development of techniques for producing state-specific information on ion-molecule reactions. The combined ability to examine the effects of electronic and translational energy provide a tremendously valuable view of chemistry. In this talk, several examples in which non-adiabatic behavior has been identified will be discussed.

The experimental technique used in our work is that of guided ion beam tandem mass spectrometry. The apparatus has been described in detail.[1] Briefly, ions formed in one of several sources are focused into a magnetic sector for mass analysis before being decelerated to the desired kinetic energy and focused into an rf octopole ion beam guide which passes through a collision cell. There the ions react under single collision conditions with the neutral reactant. The product and remaining reactant ions are analyzed with a quadrupole mass filter, and detected with an ion counter. Ion intensities are converted to absolute reaction cross sections having uncertainties of ±20%.[1]

The octopole ion beam guide, first developed by Teloy and Gerlich,[2] is the key to the capabilities of this apparatus when compared with more conventional tandem mass spectrometers. The device acts as a trap for charged particles in the radial direction while not affecting the axial energy of the ions. This means that product ions are collected with near 100% efficiency regardless of the dynamics of the reaction but the kinetic energy of the ions is still well defined. Further, the octopole can be used as a retarding field energy analyzer to calibrate the absolute energy of the interaction to within 0.1 eV.[1] Finally, very low ion kinetic energies (~0.05 eV) can be achieved.[1,3]

Control over the extent of electronic excitation of the ions is obtained by varying the ion source conditions. Three types of sources are used: conventional electron impact (EI), surface ionization (SI), and electron impact combined with a high pressure drift cell (DC). The EI source produces ions with a range of excitations dependent on the electron energy. The SI source yields ions having a Maxwell-Boltzmann distribution of states characteristic of the SI filament temperature, typically 2200 K. The DC source is a versatile source where ions produced by EI can be thermalized via collisions with an inert gas or where chemical reactions can produce (or deplete) a particular electronic state of the ion of interest.

One interesting example of the type of information which can be obtained from these studies is given by studies of reactions 1 and 2. Reaction 1 is an exothermic and highly efficient process

$$Ar^+ + D_2 \rightarrow ArD^+ + D \qquad (1)$$

$$Kr^+ + D_2 \rightarrow KrD^+ + D \qquad (2)$$

which proceeds at two-thirds the collision cross section at thermal energies.[1] As the kinetic energy increases, the reaction efficiency increases to 90% before falling off precipitously.[1] Reaction of Ar^+ with H_2 and HD show identical behavior. In contrast, reaction 2, also exothermic, is rather inefficient, exhibits an unusual feature at high energies, and shows a strong intermolecular isotope effect for reaction with H_2 and HD.[4] These results are obtained for ion beams with statistical mixtures of the two spin-orbit states of the rare gas ions: twice as much $^2P_{3/2}$ ground state as $^2P_{1/2}$ excited state. Insight into the cross section behavior is obtained by examining the state specific reactions of Kr^+ in the J = 3/2 ground state and J = 1/2 state, 0.67 eV higher, where we find that the ground state reaction is much more efficient than the excited state reaction and the high energy feature is associated exclusively with the ground state.

The observed behavior for both reactions 1 and 2 can be explained by noting that the products correlate directly (diabatically) with the $Rg + H_2^+$ surface. Therefore, reactions 1 and 2 occur by interaction of the $[Rg^+ + H_2]$ and $[Rg + H_2^+]$ surfaces in the entrance channel. In the Ar system, these surfaces cross near the bottom of the H_2 well such that the mixing is efficient and no

intermolecular isotope effects are observed. In the Kr system, the crossing point is well above the bottom of the H_2 well such that the mixing and thus reaction is less efficient and there are strong isotope effects. The differences among the various spin-orbit states comes about because only the Rg^+ states with mJ = ±1/2 have the right symmetry ($^2A'$ in C_s symmetry) to correlate with products and only the J = 3/2, mJ = ±1/2 components correlate adiabatically. Thus, the J = 1/2, mJ = ±1/2 components can react only via non-adiabatic transitions to the adiabatic surface. In the Ar^+ system, these transitions are apparently much more efficient due to the smaller spin-orbit splitting, 0.17 eV. This leads to the observed two-thirds reaction efficiency at low energies since only the J = 3/2, mJ = ±3/2 components are unreactive. In the Kr^+ system, we believe it is this component that is responsible for the high energy feature since it is observed only for reaction of the J = 3/2 state. Since this surface has the wrong symmetry ($^2A''$) to mix with the reactive $^2A'$ surface, we hypothesize that rotationally non-adiabatic (coriolis) coupling is the mechanism which allows this state to react. Further, we postulate that the comparable state in the Ar^+ system explains the increased reaction efficiency as the kinetic energy is increased to 1 eV.

Other types of systems which can usefully be explored using these methods include transition metal reactions. Studies of the state-specific reactions of ground state $Fe^+(^6D)$ and the first excited state $Fe^+(^4F)$, 0.25 eV higher in energy, have been especially fruitful.[5,6] Results for the endothermic reaction 3 show that the ground state is much less reactive than the excited state.[5]

$$Fe^+ + D_2 \rightarrow FeD^+ + D \qquad (3)$$

This is a result of the different electron configurations for $Fe^+(^6D,\ 4s3d^6)$ and $Fe^+(^4F,\ 3d^7)$ and can be explained using fairly simple molecular orbital ideas. Complementary results for many other atomic transition metal ions support these ideas.[7,8] For Fe^+, the most important difference between these two states is the occupancy of the 4s orbital. The occupied 4s orbital of the ground state leads to repulsive interactions with the filled σ_g orbital of D_2. Thus, reaction of this state is inefficient. The ^4F state avoids this repulsion and therefore reacts much more efficiently.

When the reactions of $Fe^+(^6D,\ ^4F)$ with alkanes are examined, the ground state remains relatively unreactive for the methane and ethane systems.[9] For propane, however, only the endothermic channels behave in this manner. For the exothermic reactions, processes 4 and 5, it is the $Fe^+(^6D)$ ground state which is most reactive but only at low kinetic energies.[6] We believe this change in behavior

$$Fe^+ + C_3H_8 \rightarrow FeC_3H_6^+ + H_2 \qquad (4)$$

$$\rightarrow FeC_2H_4^+ + CH_4 \qquad (5)$$

with kinetic energy is a result of non-adiabatic behavior due to interaction of the potential energy surfaces evolving from the two iron ion states. Namely, at low energies, the system behaves adiabatically, i.e., ground state reactants form ground state products. At higher energies, the reactions proceed along the diabatically allowed pathways, i.e., $Fe^+(^4F)$ is most reactive. Thus, at low energies, spin-orbit mixing of the potential energy surfaces must be occurring. At higher energies, the electrons can no longer adjust rapidly enough to the faster nuclear motion and this mixing begins to break down.

[1] K. M. Ervin and P. B. Armentrout, J. Chem. Phys. 83, 166 (1983).

[2] E. Teloy and D. Gerlich, Chem. Phys., 4, 417 (1974).

[3] K. M. Ervin and P. B. Armentrout, J. Chem. Phys. 86, 2659 (1987).

[4] K. M. Ervin and P. B. Armentrout, J. Chem. Phys. 85, 6380 (1986).

[5] J. L. Elkind and P. B. Armentrout, J. Am. Chem. Soc. 108, 2765 (1986); J. Phys. Chem. 90, 5736 (1986).

[6] R. H. Schultz and P. B. Armentrout, J. Phys. Chem. submitted.

[7] J. L. Elkind and P. B. Armentrout, J. Phys. Chem. 89, 5626 (1985); 90, 6576 (1986); J. Chem. Phys. 84, 4862 (1986); 86, 1868 (1987).

[8] J. L. Elkind and P. B. Armentrout, J. Phys. Chem. 91, 2037 (1987).

[9] R. H. Schultz, J. L. Elkind, and P. B. Armentrout, work in progress.

Presented at the 35th ASMS Conference on Mass Spectrometry and Allied Topics
May 24-29, 1987, Denver, CO

CROSSED BEAM STUDIES OF ION-MOLECULE REACTION DYNAMICS

James M. Farrar
University of Rochester
Rochester, NY 14627

The method of crossed ion and molecular beams in the study of elementary reaction dynamics has a number of advantages, including precise definition of the initial relative kinetic energy, single collision conditions, and the ability to use kinetic energy release as a probe of energy disposal in simple reactions. In addition, product angular distributions often allow one to distinguish between "direct" processes and "complex" collisions proceeding through a transient intermediate living a fraction of a rotational period. In this regime, the time resolution of a crossed beam experiment is approximately 0.1 picoseconds.

The reaction of vibrationally energy selected NH_3^+ cations with D_2 provides an example of the power of crossed beam techniques. This system is unusual because it represents one in which the reactions are exothermic but slow. By preparing NH_3^+ cations by charge exchange between Kr^+, Ar^+, or N_2^+ with NH_3, the vibrational energy content of the ions may be controlled between 3.3 and 5.0 eV, and the competitive effects of vibration and translation may be probed in this system. Product flux distributions may be used to sort out the mechanistic details of the exchange reaction to produce NH_2D^+ + HD and the abstraction reaction yielding NH_3D^+ + D. In the latter reaction, center of mass flux distributions indicate that the reaction proceeds with "rebound" dynamics in which NH_3^+ approaches D_2 with its C_3 axis aligned collinearly with the D_2 bond axis. The NH_3D^+ product then recoils in the backward direction relative to the incoming reagent ion. A small barrier in the entrance channel can be overcome by translational energy, with only a small coupling of reagent vibration to the product translational energy. In contrast, reagent vibration plays an important role in the rate of the exchange reaction. Product flux distributions indicate that the reaction proceeds through a transient collision complex living approximately one rotational period. Center of mass angular distributions show flux peaks of nearly equal size at 0° and 180°, suggestive of a prolate complex decaying along its symmetry axis. Increasing vibrational energy leads to increasing asymmetry in the flux distributions, indicative of a reduced lifetime for the complex. The reaction coordinate for this system appears to have a shallow well for the $NH_3^+ \cdot D_2$ complex, and vibrational energy surmounts a barrier of height < 1 eV to an isotopically exchanged $NH_2D^+ \cdot HD$ electrostatic complex which then decomposes to products.

In the past several years, a number of workers[1] have suggested that many low energy ion- molecule reactions may proceed on a potential energy surface with two minima separated by an intermediate isomerization barrier, as shown in Figure 1.

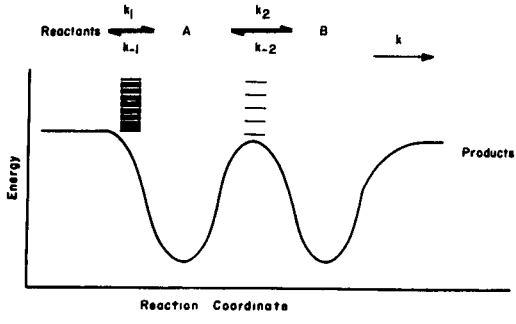

The encounter complex A produced by the approaching reagents must cross the isomerization barrier to complex B in order to yield reaction products. Because reversion of the encounter complex A to reagents is energetically unfavorable but entropically favorable as indicated by the high density of states for k_{-1} in Figure 1, whereas passage over the isomerization barrier is an entropy bottleneck as evidenced by the sparse density of states for k_2, the probability for chemical reaction from the encounter complex can be significantly less than unity because of nonreactive decay to reagents. Previous studies have assumed that the decay rates for complexes A and B on Figure 1 are governed by statistical factors, but experimental tests have been lacking.

We have examined the elimination reactions of Li^+ with tert-butyl alcohol (TBA), isopropyl chloride (IPC), n-propyl chloride (NPC), and isopropyl bromide (IPB), forming an olefin + HX, with X= a halogen or OH. These systems are hypothesized to react on double minimum surfaces, and we have examined them over the collision energy range from 0.6 eV to 2.5 eV, in order to probe the underlying dynamics of intramolecular energy redistribution. Full differential cross sections at collision energies up to 1.2 eV show increasing asymmetry in the angular distributions as a function of initial collision energy and suggest that the reactions take place on a timescale of 0.2 to 0.5 picoseconds. The observation of Li^+ nonreactively ejected from the initial encounter complex formed by approaching reactants is consistent with a double minimum reaction coordinate and a comparison of the nonreactive flux with the flux for elimination products allows an estimate of the heights of intermediate isomerization barriers separating the wells on the potential surface. The barrier heights are in the order IPC < IPB < NPC < TBA. For the alkyl halides, this ordering is what one expects from a transition state at the isomerization barrier in which M^+ has begun to remove X^- from carbon, generating a partial positive charge on carbon. The anomalously high barrier for TBA indicates that other factors, including hydrogen atom transfer and rehybridization of carbon as the incipient double bond forms also play a role at the barrier.

Nonreactive energy loss, computed as the difference between the incident translational energy and the mean kinetic energy of Li^+ ejected from the complex is typically at least 80% of the statistical value, suggesting a high degree of intramolecular vibrational energy redistribution in the complex. The kinetic energy distributions for Li^+(HX) and Li^+(olefin) products and nonreactively scattered Li^+ are in reasonable agreement with phase space theory calculations which include all product vibrational modes.

The energy dependence of the Li^+(HX)/Li^+(olefin) branching ratios can be accounted for with statistical calculations which include product dissociation. The higher density of states of the products containing the olefin channels more of the total energy into these products, and thus the Li^+(olefin) product dissociates preferentially.

The discrepancy between the statistical recoil energy distributions and apparent complex lifetimes several orders of magnitude shorter than the predictions of RRKM theory can be understood in terms of incomplete transfer of energy from the incident Li^+ to the internal degrees of freedom of the initial encounter complex. The experimental data suggest that the dynamics of these reactions are governed by an underlying statistical behavior, but that specific features of the dynamics control angular distributions and lifetimes in this energy regime. We expect that experiments at lower collision energies will reveal consistency among product state energy distributions, complex lifetimes, and product branching ratios.

REFERENCES

1. W.N. Olmstead and J.I. Brauman, J. Am. Chem. Soc. 99, 4219 (1977).

Presented at the 35th ASMS Conference on Mass Spectrometry and Allied Topics
May 24-29, 1987, Denver, CO

Urinary Steroid Profiles of Athletes

Caroline K. Hatton and Don H. Catlin
Paul Ziffren Olympic Analytical Laboratory
Departments of Pharmacology and Medicine
University of California, Los Angeles, Ca. 90024

Virtually all professional and amateur athletic organizations forbid the use of androgenic anabolic steroids (AAS). The International Olympic Committee, United States Olympic Committee and more recently the National Collegiate Athletic Association enforce the regulations by conducting urine testing. Since 1983 we have screened several thousand urines for AAS by GC-MS in the selected ion monitoring mode (1).

In addition our screening procedure includes estimating the peak heights of androsterone (A, 3α-hydroxy-5α-androstan-17-one), etiocholanone (Ae, 3α(hydroxy-5β-androstan-17-one), testosterone (T, 17β-hydroxy-4-androsten-3-one), and epitestosterone (Epit, 17α-hydroxy-4-androsten-3-one) relative to d_2T ([1,2-$^2H_2$]testosterone). These data together with the gender and sport of the athletes who submitted the urines exist in a large data base resident on an IBM 3090 mainframe computer. Herein we describe the frequency distribution of A, Ae, T, A/Ae and T/Epit for female (N=388) and male (N=1113) olympic athletes representing 18 different sports.

It is generally acknowledged that AAS are commonly abused in sports that require great strength or weight (2). To determine if male athletes competing in one of these sports differ from all other male athletes, we selected one such sport and refer to it as a "high risk sport" (HRS). A HRS is one in which previous aggregate testing experience reveals that a relatively large number of competitors (>2%) test positive for AAS. We compared the frequency distributions of 94 males representing one HRS with those of all other males (N=1019).

METHODS

During the 1984 Olympic Games in Los Angeles 1510 athletes provided a urine sample under observation between about 30 minutes and 3 hours after competing. Most samples were collected between 15:00 and 21:00 hours, and the analysis was initiated within about 12 hours of collection. Sample preparation included the addition of 200 ng of d_2T internal standard to 4 mL of urine, XAD-2 column chromatography, enzymatic deconjugation, diethyl ether extraction, and derivatization of the dried extract to trimethylsilyl derivatives. In the GC-MS analysis we monitored 20 ions at a time. Computerized data reduction started with location of the internal standard, followed by location of endogenous steroids and search for exogenous banned steroids.

The data for the 94 athletes were deleted from the data base leaving 1019 athletes in the category "all other males" (AOM). Next each variable was sorted in order of ascending values and a rank transformation was performed such that each rank contained 20% of the cases and rank 1 contained the lowest values and rank 5 the highest values. The HRS cases were assigned to class 1-5 where the class is defined by the boundaries established in the rank transformation of AOM and counted in each class. Finally the relative percent deviation from zero was calculated for each variable and rank as: (observed - expected/ expected)(100) where observed = the number of cases in the class and expected=(N/number of ranks, ie 94/5).

RESULTS

The 5 variables are not normally distributed (table 1). Accordingly Gaussian based statistical procedures are not appropriate. As expected from previous work(3) males differ from females by the distribution of A, Ae, T, and A/Ae. A comparison of the frequency distributions of T/Epit

Presented at the 35th ASMS Conference on Mass Spectrometry and Allied Topics
May 24-29, 1987, Denver, CO

for males and females shows no apparent differences.

Table 1 Frequency distributions of A, Ae, A/Ae, and T/Epit

	A/d_2T		Ae/d_2T			A/Ae			T/Epit	
Interval	%M	%F	%M	%F	Interval	%M	%F	interval	%M	%F
0-10	5.0	12.0	6.0	7.0	0 -0.62	8	33	0-0.5	18.5	25.5
21-20	13.0	27.5	17.0	17.5	to 0.87	19	31	to 1.0	18.0	20.5
21-30	19.0	19.0	21.0	17.5	to 1.12	30	18.5	to 1.5	21.5	15.5
31-40	21.0	15.0	20.0	13.0	to 1.37	17.5	10.5	to 2.0	16.5	17.5
41-50	16.0	9.5	15.0	14.0	to 1.62	12	4	to 2.5	9.5	9.0
51-60	12.0	6.0	9.0	9.0	to 1.87	7	1	to 3.0	6.0	6.0
61-70	5.0	4.0	5.5	7.0	to 2.12	4	1	to 3.5	3.5	0.5
71-80	3.5	2.5	3.0	6.0	to 2.37	2	1	to 4.0	1.5	0.5
81-90	2.5	3.0	2.0	4.0	> 2.37	0.5	0	> 4.0	5.0	3.0
>91	3.5	1.5	1.5	3.5						

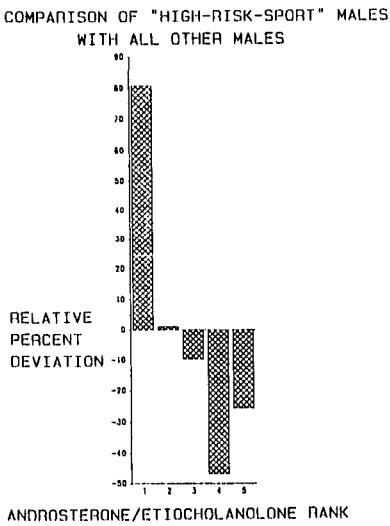

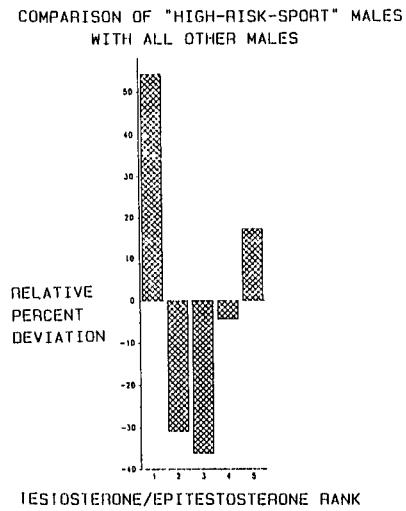

Compared to all 1019 other males, the 94 males in the high risk sport have less urinary A and Ae and a smaller A/Ae ratio. The low concentrations of A and Ae could be correlated with low specific gravity. Together the three findings show a shift of A and Ae concentrations toward lower values, with a greater shift for A than Ae. Low A/Ae ratios have been interpreted to mean decreased activity of 5α-reductase, which converts androstenedione to androsterone (3). These findings are consistent with the hypotheses that: a) they differ from other males due to factos such as heredity, training, diet, or drugs b) their decreased A/Ae ratio is due to decreased activity of hepatic 5α-reductase.

(1) Catlin, D. H., Kammerer, R. C., Hatton, C. K. et al, Clin. Chem., 33, 319-327 (1987).
(2) Wade, N., Sci., 176:1399-1403 (1972)
(3) Deslypere, J. P., et al, Acta Endocrinologica, 96, 265-272 (1981).

Presented at the 35th ASMS Conference on Mass Spectrometry and Allied Topics
May 24-29, 1987, Denver, CO

MEASUREMENTS OF URINARY ORGANIC ACIDS IN SMALL SAMPLES USING AN ION TRAP DETECTOR

Shen-Nan Lin, P-S Cheng, and R. M. Caprioli, The University of Texas Medical School, Houston, Texas 77025

In this study we investigate the linear response of the Finnigan-Mat ITD for organic acid analysis. The new variable ionization control (VIC) software program for the ITD allows optimal performance. This program improves the quality of the mass spectra and the linear dynamic range of the detector for quantitative measurements. A new sample preparation procedure was developed which not only allows quantitative recovery in high yields of water soluble urinary compounds but also limits the amount of sample entering the detector. This helps ensure that quantitative measurements are made within the linear dynamic range of the instrument. Quantitative urinary metabolic profiles obtained both by the Finnigan-Mat 1020 and the ITD GC/MS are compared.

Standard mixtures of TMS derivatives of mesaconic, 3-methyl glutaric, o-hydroxy phenylacetic and adipic acids at various concentrations were prepared so that each injection of 2 ul contained from 1 to 500 ng of the compounds. The results show that linear relationships for the ITD GC/MS can easily be achieved over the 1 to 300 ng range. The detector is also sensitive for organic acid analysis. A reconstructed total ion current chromatographic peak of 1 ng mesaconic acid TMS shows a signal to noise ratio of 10.8. Since our standard procedure for urinary organic acid analysis starts with 1 ml urine and ends with a final volume of 150 ul, of which 2 ul are used for injection, then, a quantitative linear range is estimated to be from 75 ng to 22.5 ug per ml urine. As a comparison, 3-hydroxy butyric acid was added to normal urine at levels of 100, 500, and 1000 ug/ml. Analyses of these samples by the 1020 give the results of 96.5, 530.9 and 628.3 ug/ml, respectively. Thus, good quantitative value are obtained up to concentration of about 500 ug/ml by the 1020 GC/MS.

The non-linear response of the ITD detector is thought to be the consequence of ion-molecular reactions taking place at high sample concentrations. Since the rate of ion-molecular reaction is dependent on the concentration of neutrals in the detector, a small volume sample preparative method is developed to limit amounts of samples entering the detector.

Urine samples less than or equal to 100 ul were used. The sample was added 50 ul 1N NaOH and 250 ul pyridine containing 25 mg EO reagents. After heating at 60 C for 30 min, 1 ml ethyl acetate and 10 ug 4-Cl benzoic acid in 10 ul methanol were added. After vigorous mixing, the whole sample was evaporated to dryness by a nitrogen stream and the residue was then TMS derivatized with 50 ul pyridine and 100 ul BSTFA at 60 C for 30 min.

Figure 1 compares chromatograms obtained with samples prepared by the small sample volume procedure (A) and the more conventional ethyl acetate extraction method (B). The GC/MS used was the ITD GC/MS system. The most distinctive difference between the two is that the GC peak sizes of #21, 25, and 38 (glycerol, glyceric and 3-hydroxy, 3-methyl glutaric acid TMS derivatives respectively) are greater in A panel than in B panel. These compounds are highly water soluble and therefore, are poorly recovered by the ethyl acetate extraction procedure. The small sample volume procedure allows recoveries in high yields of these urinary organic compounds.

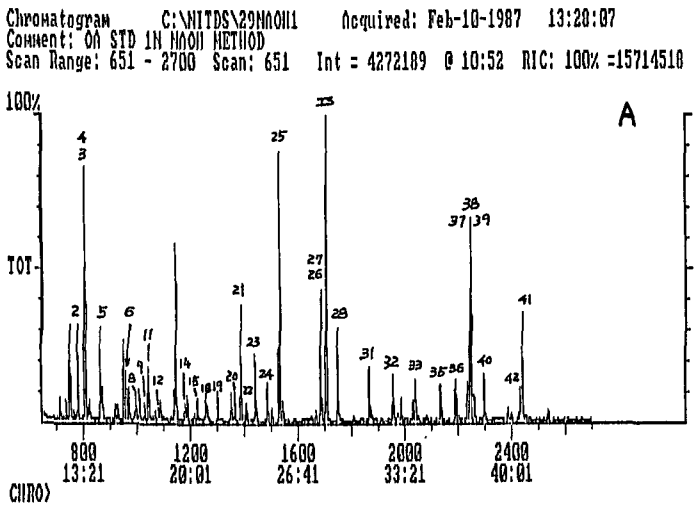

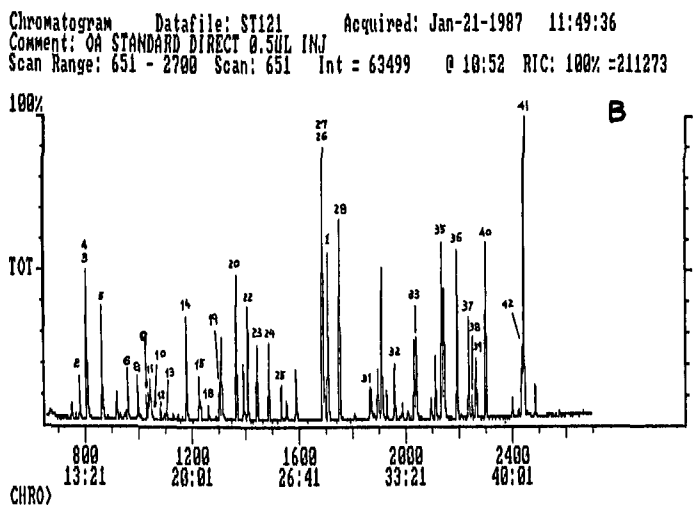

Our conclusion is that the ITD GC/MS can be used effectively to detect human metabolic disorders of various acidurias. However, quantitative measurements must be carried out within the linear dynamic range of the detector in order to monitor the therapeutic progress of patients. The small sample volume method for sample preparations is quantitative and is effective in recovery of highly water soluble urinary compounds.

Presented at the 35th ASMS Conference on Mass Spectrometry and Allied Topics
May 24-29, 1987, Denver, CO

REAL TIME RESPIRATORY GAS MONITORING WITH QUADRUPOLE MASS SPECTROMETRY:

M. Winsborough, G. Cessna, C. Bartman, and T. Patterson, ARE/PL, Alverstoke, Hampshire, England, presently attached to Naval Medical Research Institute, Bethesda, MD.

Pulmonary functions tests are used to study the respiratory affects of increased gas density and cold associated with deep sea diving, aerospace travel and a variety of medical problems. By measuring parameters such as lung volume, oxygen consumption, cardiac output and stroke volume under a variety of stressful conditions, researchers can better understand respiratory problems and suggest solutions.

The objective of this study is to demonstrate the capabilities of a quadrupole mass spectrometer as a non-invasive technique to monitor respiratory gases for use in pulmonary function tests.

Subjects were placed in an environment chamber which can be both pressure and temperature controlled. Respiratory gases are monitored while breathing both normal room air or especially prepared blends. The mass spectrometer used in these studies is the Questor Gas Analyzer manufactured by Extrel Corporation of Pittsburgh, PA.

In a nitrous oxide rebreathing experiment, a bag is filled with 10% N_2O, 10% Ar and 30% O_2 in a N_2 balance. The subject breathes room air until a steady state is reached for end tidal P_{O_2} and P_{CO_2}. The subject then begins breathing the nitrous oxide mixture. The levels of N_2, O_2, Ar, CO_2 and N_2O in the mixing bag are continuously monitored at a rate of approximately 25 msec/component. Typical traces of % concentration vs. time for argon and nitrous oxide and CO_2 are shown in Figure 1.

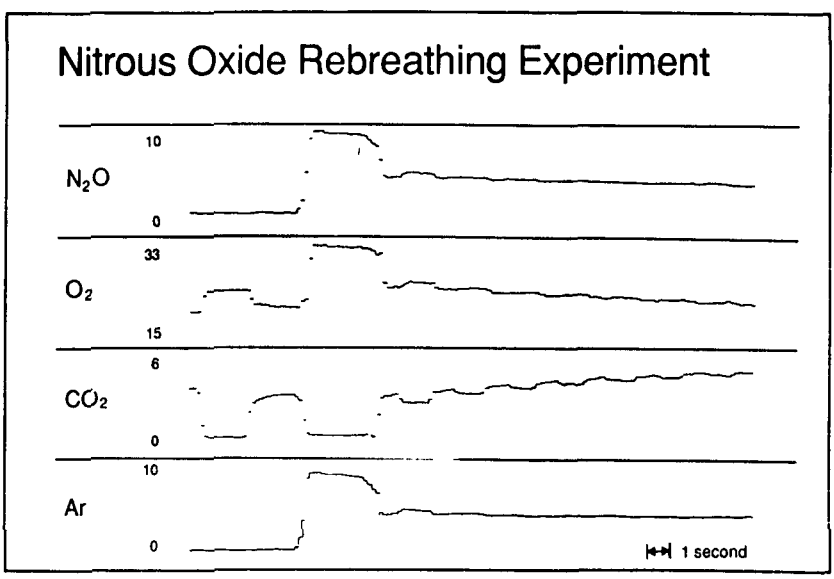

These data can be used to calculate a variety of parameters which describe pulmonary functions as follows:

$$\text{Lung volume} = V_A = V_{insp} \cdot \frac{\text{Initial argon concentration}}{\text{Final argon concentration}}$$

where V_{insp} = volume of inspired gas

$$\text{Cardiac output} = Q_C = \frac{V_A \cdot \lambda \cdot \beta}{T_{\beta H} \cdot \alpha_\beta} \ln \frac{[N_2O]T_1}{[N_2O]T_2}$$

where V_A = lung volume

λ = correction factor for solubility of N_2O in water in the lung

β = barametric pressure correction factor

$T_{\beta H}$ = time of breath holding

α_β = solubility of N_2O in whole blood

Stroke volume = Q_C/heart rate.

Questor was used to study the effects of temperature on respiration. Gas analysis was performed at periodic intervals on a subject exposed to a temperature of 4.4 degrees Celsius for 90 minutes. Data were compared to a control study performed at 22 degrees Celsius and were the average of two subjects.

The data showed that oxygen consumption and pulmonary tissue volume increase dramatically on exposure to cold. Such phenomena must be understood and controlled to avoid the potential severe bodily injury associated with hypothermia.

The results of this study show the capabilities of the Questor quadrupole MS for respiratory gas analysis. The calculations that are routinely performed indicate that the critical performance characteristics are:

- Instrument response time to square wave input must be less than 0-95% in 100 msec.
- % RSD must be better than 1% at a concentration of 1%.
- S/N must allow definition of end tidal gases.
- Stability must be better than 0.5% over 24 hours.

Presented at the 35th ASMS Conference on Mass Spectrometry and Allied Topics
May 24-29, 1987, Denver, CO

STRUCTURE CONFIRMATIONS OF INTERMEDIATES IN THE VITAMIN B_{12} BIOSYNTHETIC PATHWAY OF *Propionibacterium shermanii* BY FAB MASS SPECTROMETRY

Patricio J. Santander*, Thomas R. Sharp#, A. Ian Scott.*
*Center for Biological NMR, and #Center for Chemical Characterization and Analysis
Department of Chemistry, Texas A&M University, College Station, Texas 77843

No single instrumental or chemical technique can suffice to determine the complete molecular structure of a complex organic natural product molecule. Mass spectrometry, however, and especially with the development of the fast atom bombardment (FAB) technique, can now assume a much more active role in this task than was previously possible. Finding the specific matrix and sample preparation conditions for a particular group of natural products is the principal remaining obstacle to significant progress in structure elucidation of the target molecules.

We have investigated these questions in relation to determining the structures of intermediates along the biosynthetic pathway of vitamin B_{12} in the bacterium, *Propionibacterium shermanii.* The pathway of this organism can be manipulated by nutritional and culture conditions to accumulate various intermediates or sideproducts. Purification of these materials, chemical reactions and modifications of the molecules, refeeding of labeled compounds to the organism, etc., permit our assembling a detailed description of the chemical events leading from uroporphyrinogen III, the last intermediate at a branch point in the general porphyrin biosynthetic pathway, after which intermediates are committed to the production of vitamin B_{12}.

We have thus far examined 20 porphyrin compounds -- isolated intermediates or derivatives thereof -- with 100% success and considerable ease, using +Ve FAB-MS and a m-nitrobenzyl alcohol matrix[1] (Aldrich, 95%). Some typical spectra are shown in Figure 1. The number includes metal-free porphyrins, as well as species containing metal atoms. prominent $[M+H]^+$ is observed in all cases, and is the principal feature of the spectrum, constituting a large proportion of the total ion current ascribable to the target analyte. A relatively small amount of fragmentation is seen, consisting of losses of small functional groups from the molecular ion. These conditions, however, are ideal for conducting experiments in which the molecules are derivatized or otherwise chemically transformed, and the changes in molecular weight used to infer the presence and number of functional sites on the original molecule. We have conducted a number of experiments in the former category, and shall describe two cases in the following report.

Factor III is the last identified porphyrin ring structure on the pathway to vitamin B_{12} before contraction of the ring to the corrin structure. Preparation of Factor III with strategically placed isotopic labels is key to defining the chemical steps, presently unknown, whereby Factor III is converted, ultimately, to vitamin B_{12}. The scarcity of starting materials, and the small structural changes expected demand an accurate and sensitive way to analyze products. FAB-MS has demonstrated itself able to accomplish this task.

^{13}C-labeled Factor III was prepared by incubating whole cells of *P. shermanii* with [3-^{13}C]aminolevulinic acid and [methyl-^{13}C]methionine. According to the known labeling pattern, Factor III should contain eight labeled sites in the ring and propionate side chains (shown by the black dots in the structure of Figure 2), derived from aminolevulinic acid, and three methyl groups derived from methionine. The FAB-MS analysis, shown in Figure 2, indicates that the [^{13}C]-Factor III was, as expected, 11 mass units heavier than the unlabeled material.

[^2H]-Cobester was prepared by methanolysis, in CH_3OD/D_2SO_4, of Vitamin B_{12}. Under the esterification conditions, ^{13}C and ^1H NMR spectroscopy showed that only the proton at C-10 had been exchanged. Confirmation of this minute change was possible by analysis of he FAB-MS spectra of labeled and unlabeled material (Figure 3), showing a molecular weight difference of only one mass unit.

Observations were made a VG Analytical 70-S double focusing magnetic sector instrument with DS-11/250J datasystem[2]. Samples were dissolved in a few microliters of the matrix, and introduced on the FAB insertion probe. Neutral argon at 6-8 KeV was used as the bombarding particle, produced by an Ion Tech saddle field source operated at 1.5 - 2 mAmp. The mass spectrometer was adjusted to approximately 2000 resolving power, and scanned at 10 sec/decade over a typical mass range of 90-1500 mass units. Mass calibration was achieved using conc. H_2SO_4[3].

---

1. J. Meili, J. Seibl (1984). **Org. Mass Spectrom.** 19,581-2.
2. Mass Spectrometry Applications Laboratory, Dept. of Chemistry, Texas A&M University. Purchased in part with funds from NSF grant CHE-8705697.
3. T.R. Sharp (1987). **Org. Mass Spectrom.** 21,793-5.

Presented at the 35th ASMS Conference on Mass Spectrometry and Allied Topics
May 24-29, 1987, Denver, CO

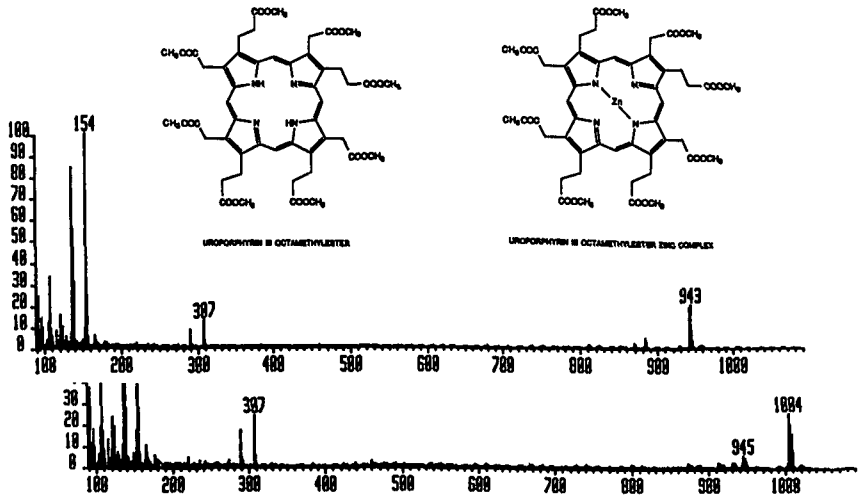

Figure 1: +Ve FAB mass spectra of uroporphyrinogen III octamethyl ester (m.w. 942, upper) and the zinc complex (m.w. 1004, lower) using m-nitrobenzyl alcohol as matrix. Major peaks below m/z 307 are from the matrix.

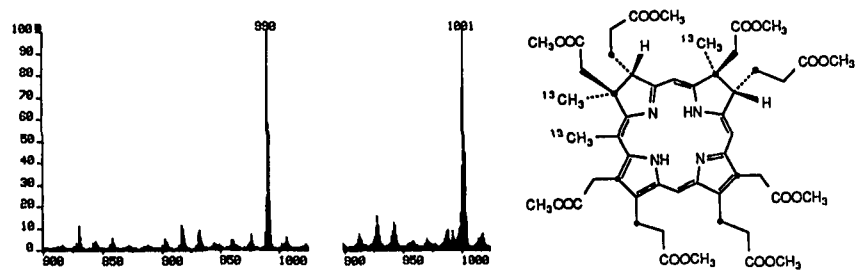

Figure 2: Molecular ion region for Factor III (left, MH^+ 990) and ^{13}C-labeled Factor III (right). Labeling is shown as black dots (from aminolevulinic acid) and $^{13}CH_3$ (from methionine)

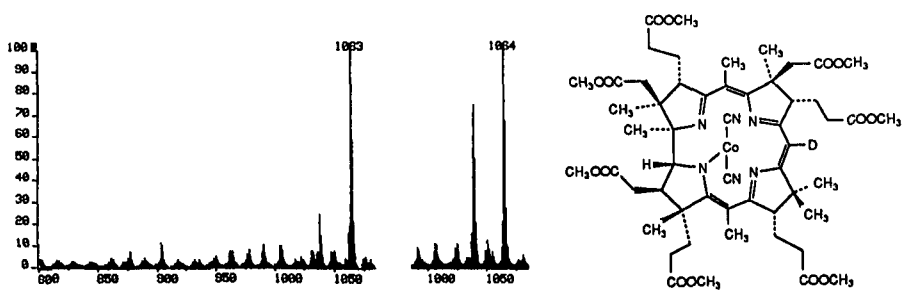

Figure 3: Molecular ion region for cobester (left, MH^+ 1063) and deuterated cobester (right, MH^+ 1064). Position of acid-exchangeable hydrogen is shown in the structure at right.

Presented at the 35th ASMS Conference on Mass Spectrometry and Allied Topics
May 24-29, 1987, Denver, CO

GC-MS DETERMINATION OF ISOTOPIC ENRICHMENT AND QUANTITATIVE ANALYSIS OF VITAMIN C: APPLICATION TO HUMAN METABOLIC STUDIES

David A. Wagner and Meg Annan
Shriners Burns Institute, Boston, MA

Introduction

There has been much controversy about the dietary requirement for vitamin C in both health and disease. Notable scientists have made claims that very high daily doses of vitamin C are beneficial in some disease conditions, while in contrast it is clear that man is able to survive on daily intakes that are a small fraction of this. Pharmacokinetic data with radiotracers indicate that normal ascorbate turnover is between 45 and 60 mg/day with a total pool size of 1500 mg. However, plasma vitamin C levels are decreased with smoking, stress, trauma, and chronic diseases, suggesting enhanced vitamin C turnover under these conditions. An accurate assessment of vitamin C pool size and turnover under pathological conditions will be essential to provide answers to delineating requirements for the vitamin.

Vitamin C plays important roles in many biochemical pathways such as hydroxylation reactions involving incorporation of molecular oxygen into the substrate. An essential role of the vitamin in the hydroxylation of proline and lysine during skin collagen synthesis has been well documented. The collagens are the major proteins of skin and connective tissue. The hydroxylated amino acids are necessary to form a stable extracellular matrix (hydroxyproline) and for glycosylation (hydroxylysine). We hypothesize that there is an increased requirement for vitamin C during wound healing in burn patients because of the tremendous amount of collagen synthesis which is occurring.

Therefore, our objective was to develop a vitamin C tracer method to measure vitamin C turnover and pool size in burned patients. Because of the dangers associated with radioactive tracers, we wanted to use stable isotope labeled vitamin C in our experients. We needed to develop a GC-MS procedure to measure not only isotopic enrichment but total vitamin C levels. We would measure the latter with an ascorbate internal standard and use isotope dilution methods. The only gas chromatographic method for vitamin C reported in the literature is a trimethylsilyl derivative of ascorbate. This derivative was unacceptable to us because of the special precautions necessary to prevent decomposition of the derivative and more importantly, the high natural isotopic abundance of MW + 1 ions of the four trimethylsilyl groups on this derivative prevented the use of a ^{13}C-vitamin C tracer. We have developed a new derivative to overcome these problems.

Methodology

One ml of fresh serum is placed in a 15 ml corex test tube and spiked with an internal standard of uniformly labeled $^{13}C_6$-ascorbic acid (99 atom % excess ^{13}C). The vitamin C is extracted from serum with addition of 1 ml 3% meta-phosphoric acid. The sample is centrifuged for 10 minutes at 10,000 x g, 4°C. Serum protein will precipitate and the decanted supernatant is transfered to another 15 ml corex test tube. The supernatant may at this time be stored at -20 °C without loss of vitamin C if desired. The analysis should be done on fresh serum because vitamin C will decompose to other products. Thus, samples are at least taken to the meta-phosphoric acid extraction. The meta-phosphoric acid is removed by addition of 3 ml absolute ethanol; the acid is insoluble in ethanol. The mixture is vortexed and then centrifuged for 10 minutes at 10,000 x g, 4°C. The supernatant is transfered to a 13 x 100 mm screw cap test tube and evaporated to dryness using a Speed Vac evaporator (Savant Instruments, Farmingdale, NY).

The methyl-2,3-O-boron-n-butane-5,6-O-ascorbic acid derivative (MBB

derivative) is used for the GC-MS analyses. The MBB derivative is made by addition of 1 ml butane boronic acid (Aldrich Chemical Co.) 40 mg/ml in pyridine. The solution reacts for 30 minutes at room temperature and then the pyridine is evaporated with nitrogen gas at 50°C. Then, excess etheral diazomethane (about 2 ml) is added and allowed to react for 15 minutes at room temperature. The diazomethane is evaporated with nitrogen gas but not to dryness. A precipitate, excess butane boronic acid, forms after addition of diazomethane and 4 ml of ethyl acetate is added to extract the MBB derivative. The solution is centrifuged for 10 minutes at 10,000 x g. The supernatant is removed and evaporated just to dryness with nitrogen gas. The residue is redissolved in 100 ul ethyl acetate.

The MBB derivative was analyzed by GC-MS on a Hewlett Packard 5985 B instrument operating in the positive chemical ionization mode with methane as the reagent gas. Selected ion monitoring (SIM) of m/z = 271 (MH + 1), 272 (^{13}C-ascorbate), and 277 (for internal standard) was used to detect the appropriate isotopic peak. Gas chromatography was performed on a 12.5 m x 0.53 mm OV-1 (methylsilane) capillary column (Hewlett Packard). Oven temperature was initially 160°C and programmed to increase immediately at a rate of 15°C/min. Injection port temperature was 250°C and the source temperature was 150°C. An isotope dilution standard curve was made to measure total vitamin C levels. Atom % excess ^{13}C-ascorbic acid was calculated from the area of m/z = 271 and 272 and subtracting naturally occurring MW + 1 isotope.

Results

The MBB-ascorbic acid derivative gave good chromatographic peaks and the derivative was stable for weeks. The electron ionization mass spectrum revealed a small molecular ion at m/z = 270 and a base peak at m/z = 144 which is loss of the butyl boronate, viscinal ethane diol. The positive chemical ionization (CI) mass spectrum showed an intense molecular ion and base peak at m/z = 271. Using positive C.I., SIM at m/z = 271 and 277, a linear standard curve was found for a range of ascorbate concentrations (0 - 20 ug/ml). The relative standard deviation for the entire range was 5%.

Application of the method to human studies revealed that the kinetics of an oral dose of L-1-^{13}C-ascorbic acid (120 mg) could be followed in blood. The maximum blood levels of the isotope (14 atom % excess) were achieved at one hour. Blood levels of the isotope showed a very slow decay at six hours (9 atom % excess). Total blood vitamin C levels were initially 1.1 mg/dl and rose to 1.35 mg/dl after 15 minutes and then returned to baseline after 90 minutes.

Summary

A new GC-MS procedure has been developed to determine ascorbic acid levels and isotopic abundance in blood. The derivative is specific only for ascorbic acid and not dehydro-ascorbic acid. Using isotopic dilution mass spectrometry, this procedure may be a candidate reference method with further validation. Human metabolic studies can be conducted to measure ascorbic acid turnover and to define nutritional requirements in health and disease.

Presented at the 35th ASMS Conference on Mass Spectrometry and Allied Topics
May 24-29, 1987, Denver, CO

INTRAMOLECULAR ISOTOPE EFFECTS IN THE DEAMINATION OF DIAMINES by DIAMINE OXIDASE

Babu Subramanyam, Linda A. Geelhaar and Patrick S. Callery, Department of Medicinal Chemistry, University of Maryland, Baltimore, MD, 21201.

Applications of stable isotopes and mass spectroscopy have yielded significant information on nature of a number of complex biological systems. Diamine oxidase is the enzyme primarily responsible for deamination of histamine and other physiologically important diamines. Since pyridoxal phosphate is regarded as a prosthetic group at the active site of diamine oxidase, a probable mechanism of deamination involves formation of an amine-pyridoxal imine. With the assistance of a base, the next step is the abstraction of a hydrogen from the alpha position of the amine in order to promote a prototropic shift and conversion into an aldehydepyridoxamine Schiff base. Hydrolysis of this imine yields deaminated substrate. With 1,4-diaminobutane (putrescine) as substrate, the product is 4-aminobutanal, which rapidly forms 1-pyrroline. Similarly 1,5-diaminopentane and 1,6-diaminohexane yield the corresponding six and seven membered cyclic imines.

Based on kinetic deuterium isotope and medium effects, Bardsley etal. , proposed that the rate limiting step in the oxidation of p-methylaminomethylbenzylamine with diamine oxidase involves breaking a carbon-hydrogen bond. Mass spectrometry is the method of choice for evaluating the influence of deuterium on enzyme reactions involving symmetrical substrates with 2 sites on the same molecule available for reaction, one deuterium labeled and the other unlabeled. With such a substrate the degree of retention of label in the product provides an estimate of the intramolecular isotope effect on the relative rates of reaction of the isotope labeled site and unlabeled site.

Diamines, 1,1-$^2H_2$-diaminoethane through 1,1-$^2H_2$-1,7-diaminoheptane were synthesized either from their corresponding aminoalkylnitrile precursors or phthalimidoalkylnitrile intermediates by catalytic reduction with $^2H_2$. The products of enzymatic oxidation of these substrates were reduced *in situ* with sodium borohydride and derivatized with pentafluorobenzoyl chloride in toluene under biphasic conditions. The pentafluorobenzoyl derivatives were analyzed by EI/GC/MS and the ratio of dideuterated to monodeuterated product determined. The proportion of dideuterated product provided a measure of the oxidation at the unlabeled methylene while the presence of monodeuterated product indicated that oxidation had occured at the labeled methylene.

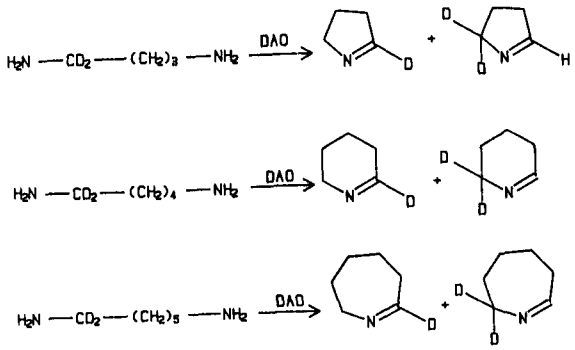

d_1 d_2

COMPOUND	INTRAMOLECULAR ISOTOPE EFFECT (d_2/d_1 Ratio)
1,1-$^2H_2$-1,4-Diaminobutane	4.28
1,1-$^2H_2$-1,5-Diaminopentane	1.47
1,1-$^2H_2$-1,6-Diaminohexane	1.80

* Mean of 3 experiments.

Analysis of intramolecular isotope data from 1,1-$^2H_2$-1,4-diaminobutane, 1,1-$^2H_2$-1,5-diaminopentane and 1,1-$^2H_2$-1,6-diaminohexane indicate that there could be a significant change in the nature of the rate limiting step for the deamination reaction with carbon chain length in the diamine series. Further work in extrapolating this data to other diamines in this series is under progress.

Presented at the 35th ASMS Conference on Mass Spectrometry and Allied Topics
May 24-29, 1987, Denver, CO

THE METABOLISM OF 2-OCTYNOIC ACID, A SUICIDE SUBSTRATE FOR GENERAL ACYL-CoA DEHYDROGENASE, AND ITS EFFECT ON ENDOGENOUS FATTY ACID METABOLISM.

J.A.Montgomery*, O.A. Mamer* and E. Colle

*The Biomedical Mass Spectrometry Unit, McGill University, 1130 Pine Ave. W., Montreal, Canada, H3A 1A3.
The Montreal Children's Hospital, 2300 Tupper, Montreal, Canada, H3H 1P3.

There are a number of human diseases associated with defective fatty acid oxidation. Some are of genetic origin like Medium Chain Acyl-CoA Dehydrogenase Deficiency (MCAD), Short Chain Acyl-CoA Dehydrogenase Deficiency and Glutaric Aciduria Type II (Multiple Acyl-CoA Dehydrogenase Deficiency). Others are of less defined origin having an environmental component influencing the disease, such as Jamaican Vomiting Sickness (plant toxin), Reye's Syndrome (pesticides or aspirin) and Sudden Infant Death Syndrome. The last two syndromes are a dilemma to physicians. Children with certain inborn errors of metabolism, especially MCAD, can be mistaken as having one of these syndromes. Their proper diagnosis will improve patient care and also will remove them from consideration when researchers try to unravel the factors precipitating these two deadly syndromes.

To better understand the underlying defects of fatty acid metabolism, an animal model is needed that can be manipulated in a controlled manner. Our approach has been the use of a suicide substrate, 2-octynoic acid, that bind covalently to pig kidney general acyl-CoA dehydrogenase in vitro(1). We injected rats with 2-octynoic acid (20 or 60 mg) and collected post-load urines to determine the metabolic fate of this acid and its effect on medium chain fatty acid metabolism.

We found that the 2-octynoic acid was extensively metabolized by microsomal (ω-1)- and ω-oxidation. All the rats treated with 2-octynoic acid excreted large quantities of 7-hydroxyoct-2-ynoic, 8-hydroxyoct-2-ynoic and 2-octynedioic acids. Figure 1 is a typical gas chromatogram of the urinary organic acids 0-3h post-load and Figure 2 is the mass spectra of the TMS derivatives of 2-octynoic acid and its metabolites. The elemental compositions of these metabolites were confirmed by high resolution GC/MS.

The 2-octynoic acid also had a dramatic effect on endogenous fatty acid metabolism. Medium chain metabolites rose 10-80 times their pre-load level 0-3 hours post injection. The major metabolites were medium chain saturated, unsaturated and 3-hydroxylated dicarboxylic acids. In addition there was a significant increase in the excretion of long chain fatty acids.

Large quantities of 3-ketooctanoic and smaller amounts of 3-ketohexanoic acids were also an unusual finding. It is difficult to determine whether these acids represent endogenous fatty acid accumulation or whether they reflect partial mitochondrial beta-oxidation of the 2-octynoic acid.

In conclusion, 2-octynoic acid undergoes microsomal oxidation to 7-hydroxyoct-2-ynoic, 8-hydroxyoct-2-ynoic and 2-octynedioic acids. There is a concomitant increase in endogenous medium chain fatty acid metabolite excretion. A large accumulation of 3-ketooctanoic acid suggests a block at the thiolase step of beta-oxidation.

1. Freund,K., Mizzer,J., Dick,W. and Thorpe, C., Biochemistry:24,5996(1985)

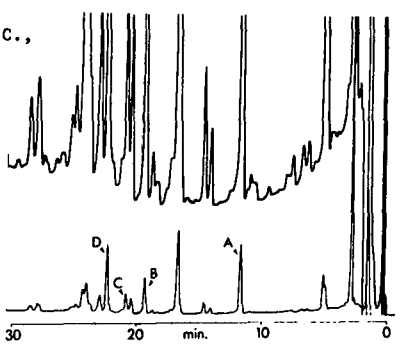

Fig. 1

Fig. 2

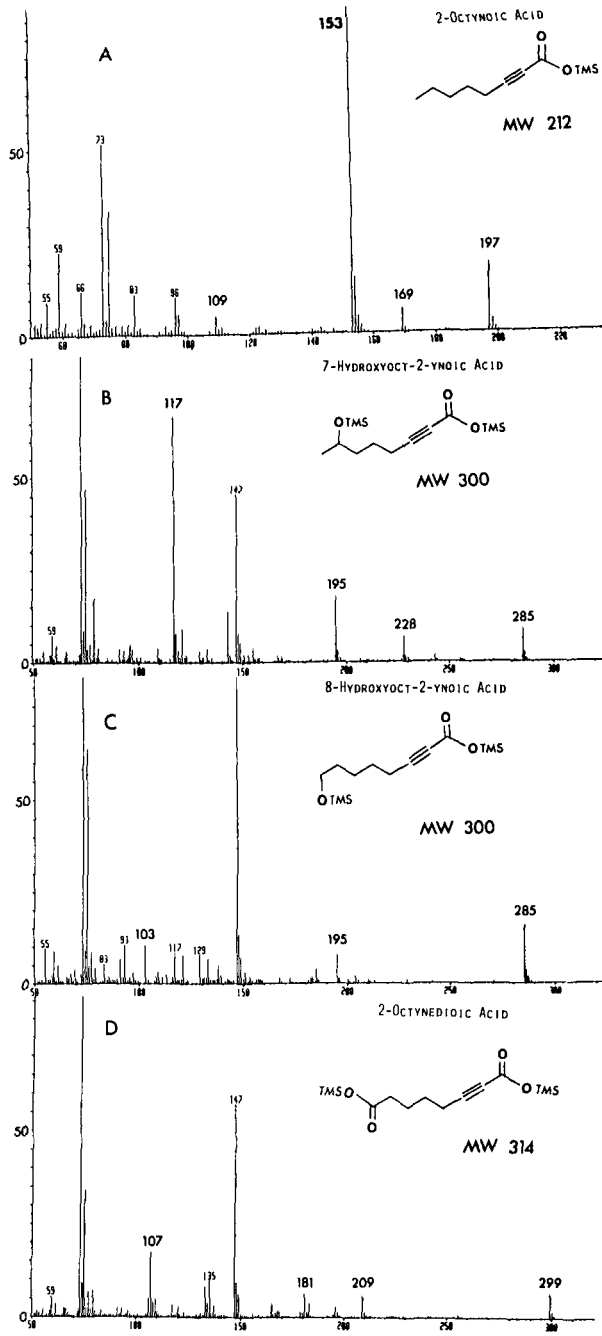
A
2-Octynoic Acid
OTMS
MW 212
153
73
59
55
66
83
95
109
169
197
7-Hydroxyoct-2-ynoic Acid
B
117
OTMS
OTMS
MW 300
147
195
228
285
8-Hydroxyoct-2-ynoic Acid
C
OTMS
OTMS
MW 300
55
83
93
103
117
129
195
285
2-Octynedioic Acid
D
TMSO
OTMS
MW 314
147
107
135
181
209
299

Presented at the 35th ASMS Conference on Mass Spectrometry and Allied Topics
May 24-29, 1987, Denver, CO

DETERMINATION OF ISOTOPIC ABUNDANCES OF CALCIUM AND MAGNESIUM BY FABMS

Ya-mei Liu, Xiangyu Jiang, Berdine Martin
Connie Weaver and David Smith
Departments of Medicinal Chemistry and Pharmacognosy,
and Foods and Nutrition,
Purdue University, West Lafayette, IN 47907

Because the exact mineral requirements of very low birth weight infants have not been established, accurate data on mineral absorption is required. Recommended intakes of calcium and magnesium are based upon the in utero rate of accumulation of minerals and limited metabolic balance data. Errors inherent in metabolic balance studies are large and lead to over estimation of intestinal absorption. Newer methodology which uses naturally occurring stable isotopic tracers provide a more accurate measure of intestinal absorption.

Calcium absorption by low birth weight infants has been determined previously (Ehrenkranz et al, Am. J. Clin. Nutr. 40:72,1984) by adding a stable isotopic tracer to formula and assuming that it is absorbed with the same efficiency as calcium endogenous to the formula. Concern that calcium from different sources,i.e., cow milk, human milk, soy milk etc., may not be absorbed equally has caused uncertainty in regard to the optimum food for infants. We have addressed this concern by determining absorption of calcium and magnesium using both intrinsic and extrinsic tracers.

Recognizing the need for analytical methods suitable for quantifying stable isotopic tracers of metals in biological materials, we have developed a method which fulfills these needs. Unique to our approach is use of a conventional high resolution mass spectrometer which is normally used for qualitative structure analyses. The method and representative results have been described previously (Jiang et al, Proceedings of the 34th Annual Conf. on Mass Spectrom. and Allied Topics, p 266). Our ability to accurately determine the enrichment of calcium isotopes with this method is illustrated in Fig 1.

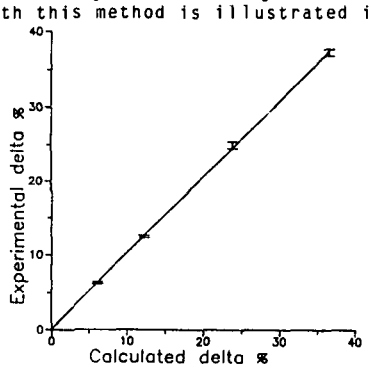

Figure 1 Plot of ^{44}Ca enrichment determined by FABMS versus ^{44}Ca enrichment in urine spiked with known quantities of ^{44}Ca. Slope 1.02, Intercept 0.11%.

Human milk intrinsically labeled with ^{42}Ca and ^{25}Mg was prepared by giving these tracers intravenously to a lactating woman and collecting her milk for the next two days. Milk obtained at the 22 hour expression had ^{42}Ca and ^{25}Mg enrichments of 278 and 201 percent, respectively. Extrinsic tracers, ^{44}Ca and ^{26}Mg, as well as a commercial mineral supplement, were added to the intrinsically labeled

milk. After stabilizing the infants on similarly enriched but nonlabelled milk for several days, they were given the labeled milk for one feeding. All stools were collected for the next 96 hours, ashed, and analyzed for tracer content. The quantity of tracer that was absorbed was determined from the difference between the administered dose and the quantity excreted.

The temporal excretion of the four tracers is illustrated for one infant in Figures 2 and 3. For one infant, 88% of both calcium tracers was absorbed, while 91% of both magnesium tracers was absorbed. These results show that the supplemental calcium and magnesium are absorbed with the same efficiency as calcium and magnesium endogenous to milk. They also demonstrate the utility of FABMS for quantifying stable isotopic tracers of metals for clinical investigations.

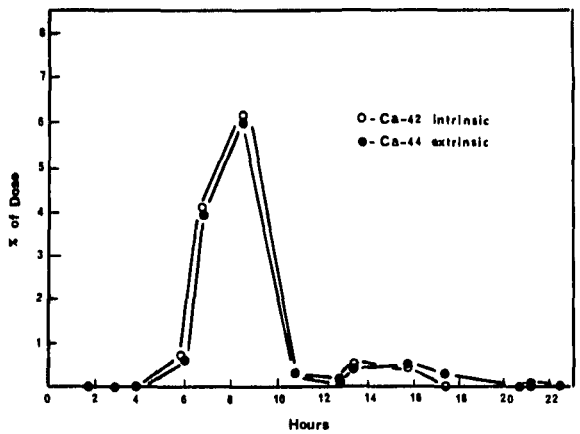

Figure 2 Fecal excretion of isotopic tracers of calcium by one infant.

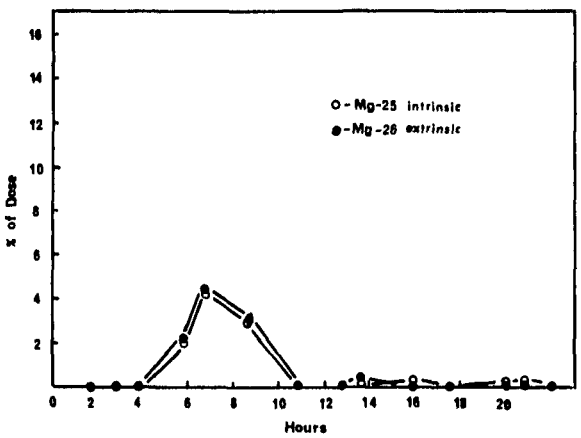

Figure 3 Fecal excretion of isotopic tracers of magnesium by one infant.

Presented at the 35th ASMS Conference on Mass Spectrometry and Allied Topics
May 24-29, 1987, Denver, CO

Determination of selected Herbicides and Chlorinated Phenols in Urine by Gas Chromatography/Mass Spectrometry

J.S. Holler, R.H. Hill, Jr., D.M. Fast, F.L. Cardinali, G.D. Todd, J.M. McCraw, S.L. Bailey, and L.L. Needham

Center for Environmental Health, Centers for Disease Control
Public Health Service
U.S. Department of Health and Human Services, Atlanta, GA 30333

Introduction. The increased awareness of inadequate disposal of waste chemicals and the widespread use of toxic organic compounds have led to considerable public concern. In particular, interest is focused on adverse health effects that might be associated with human exposure to these chemicals. In a recent investigation, residents near a manufacturing site for herbicides were concerned about risks from potential environmental exposure. Assessing risk in such a situation requires information that adequately describes human exposure. A simple, noninvasive monitor for such human exposure is the measurement of chemical residues in urine. A group of 100 children ages 2 to 6 and living within the vicinity of the manufacturing site were matched with 100 children living in another city. The analytes to be measured were those known to have been present in the manufacturing site. Other analytes previously observed in a urine-based monitoring program (1) were also measured. The goals of the study were for an analytical procedure that would measure all analytes in one determination, was sensitive to 1 ppb, and was specific for each analyte to ensure valid quantitative results.

Analytical Methodology. The process of preparing the samples including addition of the internal standards, acid hydrolysis, extraction with benzene, derivatization with diazoethane, and silica gel column chromatography. p-Cymene is added as a keeper solvent and the sample extracts are concentrated. We quantified the more volatile compounds by using capillary column gas chromatography-positive chemical ionization and mass spectrometry/mass spectrometry. Less volatile compounds are quantified by using electron capture negative chemical ionization and the single mass spectrometry mode. The instrument used is a Finnigan MAT TSQ46. The capillary column used is a DB-5 (J & W Scientific) 30 M x 0.25 mm ID with a 0.25 μ film thickness. A 1M precolumn and post-column of 0.25 mm ID deactivated fused silica capillary is employed. Methane reagent gas is used at a source pressure of 0.5 torr. The gas chromatographic program starts at 70°C for 5 minutes, programs to 220°C at 6°C/minute and holding at the final temperature for 1 minute. Details of the data system descriptors, experiments and procedures have been described (2). Details of the quantitative approach have been presented previously (3). Losses during sample preparation and analysis are compensated for by corresponding losses in the internal standard. Good analyte recovery is still desirable to facilitate maximum sensitivity and the best precision in the measurement process. Using a weighed-in standard of the previously prepared ester of 2,4-dichlorophenoxyacetic acid (2,4-D), we estimate recovery at 94% (CV=9.7% for N=9) at the 7.5 and 10.0 ppb levels.

Quality Control. Quality control (QC) must be an integral part of all analyses. Studies without QC are always subject to question and criticism. We prepared a quality control material which contained the study analytes spiked at the 10 ppb level into a base urine pool from adult donors. Quality control values and limits were established before and during the sample analyses. Samples were available to permit replication of any analytical runs found to be out of control. Little guidance is available about the best approach for using multiple values in a QC program. We have chosen to sum the square of the deviates for each of the study analytes and the resulting sum is plotted versus run number for a simple quality control chart. When this approach was used, none of the study runs were outside the 99% limits.

Results. All samples in the study were successfully analyzed by using this analytical methodology. All quantitative results were normalized on the basis of measured creatinine values for the associated urine. Review of the data indicated no significant differences between case and control groups (4).

Specificity in this analytical method was provided by monitoring two different ions in the chlorine cluster for each of the target compounds. A consistent problem was encountered in the abnormally low isotope ratios for the 2,5-dichlorophenol (2,5-DCP) measurements. This was a concern because 2,5-DCP is an indicator of human exposure to 1,4-dichlorobezene, and 2,5-DCP was observed in most of the samples in the study. The consistent observation of low isotope ratios may be explained by the presence of a coeluting interfering compound. Further study with a DB-225 (J & W Scientific) capillary column allowed this compound to be separated and its mass spectral characteristics to be observed. Under positive chemical ionization the interfering compound yields a significant ion at m/z 193, which upon collisional activation forms the daughter ion at m/z 165. Under the conditions of the analysis, the interfering compound does not contribute to the m/z 191 daughter ion used for quantitation.

We reviewed urine residue values reported previously (1) and compared them with those obtained in this study; our results demonstrated improved detection limits. An improvement of only 5 ppb in detection limits increased the frequency of observation of 2,4,5-trichlorophenol by a factor of 5. A similar improvement in the frequency of observation was obtained for 2,4-D. These results suggest that, even though the sample size in this study did not approach the number in the previous NHANES study, small incremental improvements in analytical methodology can lead to considerable improvements in exposure assessment in human populations.

Summary. The analytical goals for sensitivity, specificity, and stability have been achieved as indicated in the application to and completion of the case-control study. The results obtained by using this methodology with improved detection limits and specificity indicate the need to reexamine national norms for toxic chemical exposure. New pesticide products introduced since the last national study should also be monitored. Work is currently under way to establish target compounds and select final methodological details. The upcoming national NHANES III study scheduled to begin in 1988, will facilitate a current assessment of exposure.

This study was supported by the Agency for Toxic Substances and Disease Registry, U.S. Public Health Service.

References.

1. R.S. Murphy, F.W. Kutz, and S.C. Strassman, Environ. Health Perspect. 1983,48, 81-86.

2. D.M. Fast and J.S. Holler, "Multiple Experiments for the Quantitation of Twelve Analytes by Using Combined GC/MS/MS and GC/MS," Finnigan MAT User's Forum, 1987.

3. D.M. Fast, et al., "Automated Quantitation of Multiple Analytes in a Large Study," poster presentation TPA 5, ASMS, 1987.

4. Teresa To, "A Report on the Results of the Phenol and Herbicide Exposure Survey. Jacksonville and Conway, Arkansas." Arkansas Department of Health, February, 1987.

Presented at the 35th ASMS Conference on Mass Spectrometry and Allied Topics
May 24-29, 1987, Denver, CO

SECONDARY METABOLITES OF ERWINIA AMYLOVORA POSSIBLY INVOLVED IN NECROTIC SYMPTOMATOLOGY OF FIREBLIGHT DISEASE

G. J. Feistner

Department of Psychiatry and Behavioral Sciences
Stanford Medical Center, Stanford, CA 94305

Fireblight is a bacterial disease of rosaceous species, including apple and pear, caused by Erwinia amylovora (Burril) Winslow et al., characterized by necrotic lesions of the diseased plant, and typically accompanied by a black ("firetorched") discoloration. The underlying virulence mechanisms are unclear. However, disease symptoms may be induced in a pear cell suspension culture by fractions of the culture filtrate from E. amylovora grown in a chemically defined medium, thus indicating a possible involvement of secondary metabolites from E. amylovora in the disease process. Excretion products identified so far are 2-amino-1,7-dihydro-6H-purine-6-thione (6-thioguanine, 6-TG, (I)), valine, phenylalanine, and (S)-(-)-α-amino-1,4-cyclohexadiene-1-propanoic acid (dihydrophenylalanine, DHP, (II)) [1, 2]. Results from our in vitro bioassay suggest that DHP may be the putative necrotoxin. This tentative conclusion is supported by numerous reports in the literature describing DHP as an enzyme inhibitor (for example [3]). On the other hand, both 6-TG and DHP are reducing agents and as such, may neutralize oxygen radicals produced by the diseased plant in a defense reaction ([4] is suggested for further reading).

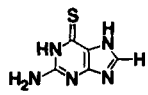

(I)

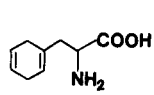

(II)

To prove any occurrence of these compounds in planta, very sensitive and specific analytical, and in particular mass spectrometric, methodology will have to be developed. Although 6-TG and DHP have been known for quite some time, their identification by MS alone was not possible, due to the lack of readily available reference spectra (not listed in the EPA/NIH mass spectral data base (38762 entries)); the present communication is intended to bridge this gap.

6-TG is easily recognized by its UV absorbance maximum of 340 nm in acidic and neutral medium, which shifts to 320 nm in base. 340 nm also happens to be the absorbance maximum of NADH, but the absorbance maximum of the latter is not pH dependent. Since even under standard EI-MS conditions, abundant molecular and characteristic fragments ions ([M-NH_3] m/z 150, [M-CH_2N] m/z 139, [M-SH] m/z 134, [M-CH_2N_2] m/z 125, and [M-CNS] m/z 109) are produced (Fig. 1), the mass spectrometric confirmation of 6-TG poses no problem.

Fig. 1 EI-MS of 6-TG

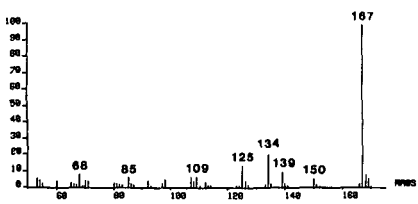

Fig. 2 EI-MS of solid DHP

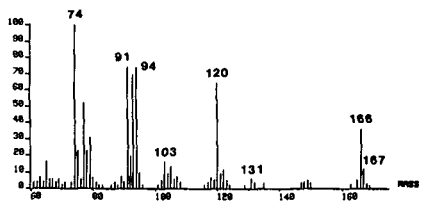

The situation is quite different for DHP because it is unstable and decomposes easily to phenylalanine. Not surprisingly, the EI mass spectrum of DHP (Fig. 2) resembles that of phenylalanine. However, it shows an abundant ion at m/z 166, which nominally corresponds to $[M+H]^+$ of phenylalanine and which may be formed from the latter under auto-CI conditions [5], but, since a control measurement with phenylalanine did not produce any molecular ions, it must be an unusually strong $[M-H]^+$ of DHP. Fortunately, DHP gives an atypical brick-orange color reaction with ninhydrin, so this characteristic can be used to quickly show the possible presence of DHP and then the proper actions can be taken to confirm this assumption by mass spectrometry. As can be seen from Fig. 3 and 4, CI and FAB create conditions suitable for the formation of $[M+H]^+$ ions from DHP. Still, these spectra also contain $[M+H]^+$ ions of phenylalanine, presumably because the sample was dried down between NMR and mass spectroscopy; this is known to facilitate the decomposition of DHP [6]. (The sample had previously been shown by ^{13}C NMR to be pure DHP. Opposite to its behavior in the solid state, DHP is quite stable in aqueous solution, as judged by ^{1}H NMR monitoring over several weeks.) Figs. 2 and 3 have been

acquired from the same sample using the alternating CI/EI mode. The same sample was also used for Fig. 4, but after a delay of several weeks. Thus, the greater abundance of $[M+H]^+$ ions for phenylalanine in FAB versus CI mode could have been indicative of further decomposition of DHP due to the longer shelf life of the sample. Alternatively, it was conceivable that FAB itself could have lead to a rapid decomposition of DHP in the ion source. To investigate the latter possibility, DHP was repurified by RP-HPLC using H_2O/20% CH_3CN/0.1% TFA as mobile phase. The fraction containing DHP was concentrated to almost dryness, but complete drying was avoided. DHP obtained in this manner gave the FAB spectrum shown in Fig. 5 at the onset of the measurement. However, after 9 min of bombardment, a large portion of DHP had been converted to phenylalanine (Fig. 6) and after 15 min the sample consisted almost entirely of phenylalanine (data not shown). Thus, it is clear that under FAB conditions rapid decomposition of DHP occurs. Note that this oxidation is not prevented by the reducing thioglycerol matrix.

Fig. 3 CI(methane)-MS of solid DHP

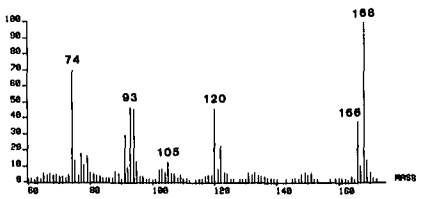

Fig. 4 FAB-MS of solid DHP in thioglycerol

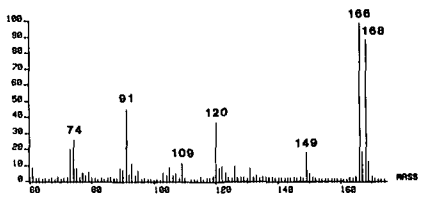

Fig. 5 Initial FAB-MS of 'wet' DHP

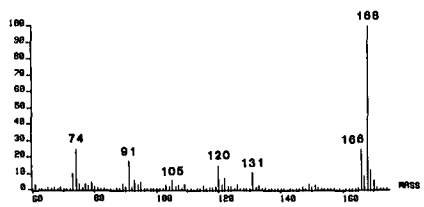

Fig. 6 FAB-MS of 'wet' DHP after 9 min

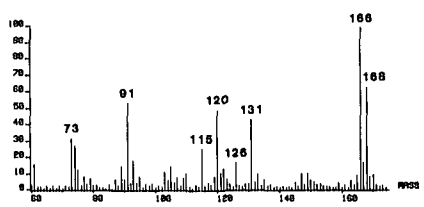

For a peptide, a strong M+3 ion is often considered to be an indication for an intramolecular cystine bridge [7]. As part of a peptide DHP would mimic such behavior, but clarity could be gained from a time course study, since with a cystine containing peptide the reduced form would increase with time, whereas with a DHP containing peptide the oxidized form would become more abundant. The formation of phenylalanine from DHP under FAB conditions may possibly be explained by dual H· abstraction initiated by radicals believed to be abundant in the FAB matrix [8]; a mechanism which is of interest also with regard to the possible biological role of DHP as scavenger of reactive oxygen radicals. Oxidation of DHP in two steps seems to be indicated by the apparent facile loss of a single hydrogen under EI conditions. With regard to optimizing the detection of DHP in biological samples, a combination of RP-HPLC with either continuous-flow FAB or thermospray MS seems to be most promising.

Acknowledgments: The author gratefully acknowledges a Feodor-Lynen fellowship of the Alexander-von-Humboldt Foundation as well as mass spectrometric assistance by H. Budzikiewicz (University of Koeln, FRG), D. Jones (University of California, Davis) and S. Ogden (University of California, Berkeley) while he was working on this project at the Department of Bacteriology, University of California at Davis.

References: [1] G. Feistner and C. Staub, Current Microbiol. 13, 95-101 (1986); [2] G. Feistner in: E.L. Civerolo et al. (eds)., Plant Pathogenic Bacteria, p. 509-519, Martinus Nijhoff Publishers, Boston, 1987; [3] Y. Watanabe et al., Biochem. Biophys. Res. Commun. 85, 273-279 (1978); [4] B. Halliwell and J. M. C. Gutteridge, Free radicals in biology and medicine, Clarendon Press, Oxford, 1985; [5] K. Heyns and H.-F. Gruetzmacher, Justus Liebigs Ann. Chem. 677, 194-204 (1963); [6] C. Ressler, J. Org. Chem. 37, 2933-2936 (1972); [7] K. Biemann and S. A. Martin, Mass Spectrom. Rev. 6, 1-76 (1987); [8] C. N. McEwen, Mass Spectrom. Rev. 5, 521-547 (1986).

Presented at the 35th ASMS Conference on Mass Spectrometry and Allied Topics
May 24-29, 1987, Denver, CO

ANALYSIS OF QUINOLIZIDINE ALKALOIDS IN BIOLOGICAL FLUIDS BY TANDEM MASS SPECTROMETRY

A. Daniel Jones[1], James E. Meeker[2], and Wendell W. Kilgore[2]

(1) Facility for Advanced Instrumentation
(2) Department of Environmental Toxicology
University of California, Davis, CA 95616

Ingestion of various species of lupine has resulted in acute poisoning of sheep and cattle, and this toxicity is largely due to the quinolizidine alkaloids. The quinolizidine alkaloid anagyrine has been implicated as a probable teratogen in cattle, and a human deformity has been associated with *in utero* exposure to anagyrine as a result of maternal ingestion of milk from goats which had foraged on lupines.

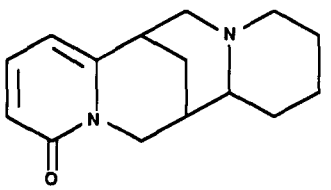

Anagyrine

This work has been concerned with studying the toxicokinetics of anagyrine in the blood and milk of goats. To minimize analysis time, our objective has been to use the MS/MS capabilities of a VG ZAB-HS-2F mass spectrometer for the detection and quantitation of the quinolizidine alkaloids anagyrine and lupanine in goat milk and blood. The polarity of anagyrine and its poor chromatographic behavior provided an additional incentive to develop a non-chromatographic method for its detection.

Toxicokinetic studies were conducted by feeding lupine extracts to goats and collecting milk and blood samples over a 24-hour period. These samples were extracted with 1-chlorobutane followed by acid-base fractionation.

Anagyrine and lupanine were quantified by monitoring two metastable decompositions for the molecular ion of each alkaloid (m/z 244—>98 and 244—>136 for anagyrine and m/z 248—>149 and 248—>136 for lupanine). Aliquots of 1.0 μL of each extract was applied to the desorption chemical ionization probe, and the sample was ballistically heated upon introduction to the ion source by passing a current of 1 Ampere through the probe wire. Amounts of both alkaloids were quantified relative to external standards.

Calibration curves were generated for each of the two decompositions for both alkaloids and an example is shown in Figure 1. Linear response was obtained for sample loadings of 0-

500 ng.

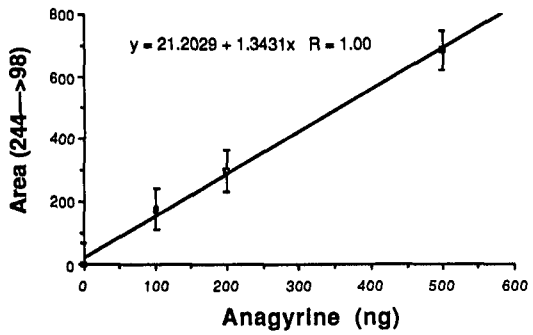

Figure 1. Calibration curve for the Metastable Decomposition m/z 244—>98 for Anagyrine

The following conclusions could be drawn from these experiments:

1) quantitative determinations of anagyrine and lupanine in goat milk and blood were accomplished in 10% of the time required for GC/MS analysis. The time required to analyze ten samples in duplicate, including generation of a calibration curve, was less than three hours;

2) the toxicokinetic data obtained were in good agreement with results obtained by gas chromatography with flame ionization detection;

3) limits of detection of less than 5 ng applied to the probe were established for both anagyrine and lupanine; and

4) memory effects were insignificant when the probe was introduced into a flame between samples.

Presented at the 35th ASMS Conference on Mass Spectrometry and Allied Topics
May 24-29, 1987, Denver, CO

TOXICOLOGICAL APPLICATIONS OF THE ION TRAP DETECTOR™

H. K. Lim, C. O. Sakashita, and R. L. Foltz
Center for Human Toxicology, University of Utah, Salt Lake City, UT, 84112

The Ion Trap Detector (ITD) has capabilities that are very useful in analytical toxicology: 1) good quality full-scan mass spectra can be obtained on low levels of analyte, and 2) either electron ionization or chemical ionization mass spectra can be generated by software controlled switching between modes of operation.

Using the pentafluorobenzamide derivatives of seven amphetamine analogs, we evaluated the sensitivity of the ITD under both EI and CI conditions, looking at 1) the level at which a good quality mass spectrum can be obtained by scanning from m/z 100-450 (TABLE 1); and 2) the limit of detection using a signal to noise ratio ≥ 5 for the peaks at m/z 252 under EI conditions and at m/z 388 under CI conditions (TABLE 2).

The ion trap operates best when it contains an certain number of ions. Automatic gain control software used in the EI mode optimizes the quantity of ions generated in the trap. However, if the analyte accounts for only a small percentage of the molecules entering the trap, as can happen with biological extracts, the sensitivity of an assay may be lower than that achieved with organic solutions of pure analyte.

Use of a relatively selective chemical ionization reagent gas is one method of limiting the number of ions generated. Optimum operating conditions were determined for the analysis of the amphetamine analog derivatives with acetone, acetonitrile, ammonia, isobutane, and tetramethylsilane reagent gases (TABLE 3). We then evaluated the gases in terms of sensitivity and selectivity, and obtained the best sensitivities (on organic standards) with isobutane. However, set-up of the CI conditions for isobutane is difficult. Acetonitrile is easier to work with than isobutane, and we felt that selectivity with acetonitrile as the reagent gas was as good as, and in some cases better than, that obtained with isobutane. Therefore, we used acetonitrile for the second (limit of detection) sensitivity comparison.

Sensitivity is often increased by monitoring a very limited number of ions. Currently, operation of the ion trap in the single-ion monitoring (SIM) mode does not give the improvement in sensitivity usually seen with conventional SIM. However, application of a supplemental DC voltage to the ring electrode, which causes trapping of a selected number of ions, does improve sensitivity.

The values listed in Table 1 and 2 reflect our results for the pentafluorobenzamide derivative of methylenedioxymethamphetamine (MDMA). Similar results were obtained for the other six amphetamine analogs.

Table 1. ITD FULL SCAN SENSITIVITY

	ELECTRON IONIZATION	ISOBUTANE CHEMICAL IONIZATION
ORGANIC STANDARD SOLUTION (amount injected on column)	50 pg	1 pg
SPIKED URINE EXTRACT (2 milliliters urine extracted)	5 ng/mL	1 ng/mL

Table 2. LIMIT OF DETECTION COMPARISON

ION TRAP			QUADRUPOLE
Electron Ionization		Acetonitrile Chemical Ionization	Acetonitrile Chemical Ionization
Full Scan*	DC**	Scanning m/z 310-440	Single Ion Monitoring Mode
1 ng/mL	50 pg/mL	50 pg/mL	25 pg/mL

Based on signal/noise of ≥ 5 as measured for m/z 252 in EI mode and for m/z 388 in CI mode for analysis of urine containing known quantities of MDMA

*Full scan range m/z 150-450

**Application of DC voltage to ring electrode to selectively trap m/z 251-254 ions

Table 3. CHEMICAL IONIZATION REAGENT GASES INVESTIGATED WITH THE ITD

Reagent Gas	Reaction level (dacs)	Reaction Time (msec)	Ionization Time (μsec)	Seg. 1 Tune setting (dacs)	Predominant Analyte Ions Formed ITD	Quadrupole (Finn. 4500)
Acetonitrile	200	240	480	65	MH^+	MH^+
Acetone	200	240	480	75	MH^+	
Ammonia	90	220	450	30	MH^+	$M+NH_4^+$
Isobutane	150	240	500	60	MH^+	
Tetramethylsilane	200	220	480	70	$M+(CH_3)_3Si^+$	

Presented at the 35th ASMS Conference on Mass Spectrometry and Allied Topics
May 24-29, 1987, Denver, CO

QUANTIFICATION OF LSD AND NOR-LSD IN URINE BY CAPILLARY GAS CHROMATOGRAPHY/NEGATIVE CHEMICAL IONIZATION MASS SPECTROMETRY

H.K. Lim, P. Francom and R.L. Foltz: Center for Human Toxicology, University of Utah, Salt Lake City, UT 84112.
R.T. Jones: Langley Porter Neuropsychiatric Institute, University of California-San Francisco, San Francisco, CA 94143.

Lysergic acid diethylamide (LSD), a potent hallucinogen, has been listed recently among the 20 controlled substances most commonly responsible for overdose cases encountered in emergency rooms nationwide, reflecting continuing street trafficking in LSD. Despite a long history of abuse associated with LSD, little information is available regarding disposition of the drug in humans. However, the disposition and toxicology of LSD have been well studied in animals. These experiments have identified N-demethylation, N-deethylation, aromatic hydroxylation, and oxidation at position 2 as metabolic pathways for LSD. Until now, no metabolites derived from these routes have been reported in humans.

An investigation of metabolism of LSD by human liver was undertaken, according to the in vitro method of Jurima et al, (1985). The NCI mass spectrum of NOR-LSD isolated from the human liver incubate (Figure 1) is identical to that of synthetic NOR-LSD, confirming that N-6-demethylation is one of the metabolic pathways of LSD in humans.

The electron-capturing properties of various N-perfluoroacyl derivatives of LSD and NOR-LSD were investigated by NCI mass spectrometry. Only N-trifluoroacetyl derivatives formed stable molecular anions upon capturing thermal electrons. Considerable fragmentation of N-trifluoroacetyl LSD occurred above 120°C, suggesting conversion from a nondissociative to a dissociative electron-capture mechanism with increasing ionizer temperature.

A capillary GC/EC-NCI-MS assay for LSD and NOR-LSD in urine was developed. The assay involves selected ion monitoring of the molecular anions of the N-trifluoroacetyl derivatives of LSD, its demethylated metabolite, and an internal standard (the decadeuterated analog of LSD). Calibration curves for LSD and NOR-LSD were linear from 0.05 to 5.0, and from 0.03 to 5.0 ng/mL urine, respectively. In each case, the correlation coefficient was at least 0.99. Recoveries of LSD and NOR-LSD from urine were 82% and 61%, respectively. The mean coefficient of variation, both intra and inter-assays, was less than 10%.

The assay was applied to a pilot disposition study of LSD in a healthy adult volunteer. Figure 2 shows ion current profiles of human urine 6-8 hours after oral administration of 1 μg/kg LSD. The assay permitted monitoring of LSD for 18 hours, and of NOR-LSD for 72 hours post administration. Pharmacokinetic parameters calculated from the urinary excretion data appear in Table 1.

Acknowledgement: This work was supported by the Office of Naval Research, contract No. N00014 85-C-0336.

REFERENCES

1. Tox. Talk 10(4), 1986
2. Niwaguchi T., Inoue T., Sakai T., and Nakahara Y., Iyo Masu Kenkyushi Koenshu, 4, 75, 1979.
3. Siddik Z.H., Barnes R.D., Dring L.G., Smioth R.L. and Williams R.T., Biochem. Pharmacol. 28, 3081, 1979.
4. Siddik Z.H., Barnes R.D., Dring L.G., Smith R.L. and Williams R.T., Biochem. Pharmacol. 28, 3093, 1979.
5. Jurima M., Inaba T., and Kalow W., Drug Metab. Dispos. 13, 151, 1985.

Presented at the 35th ASMS Conference on Mass Spectrometry and Allied Topics
May 24-29, 1987, Denver, CO

FIGURE 1

NCI MASS SPECTRA OF NOR-LSD ISOLATED FROM HUMAN LIVER INCUBATE

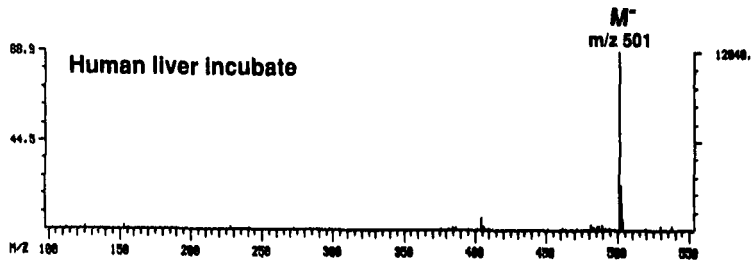

FIGURE 2 SELECTED-ION-MONITORING PROFILES OF DERIVATIZED EXTRACT OF URINE (6-8 h) FROM A HEALTHY ADULT VOLUNTEER GIVEN 1 μg/kg LSD

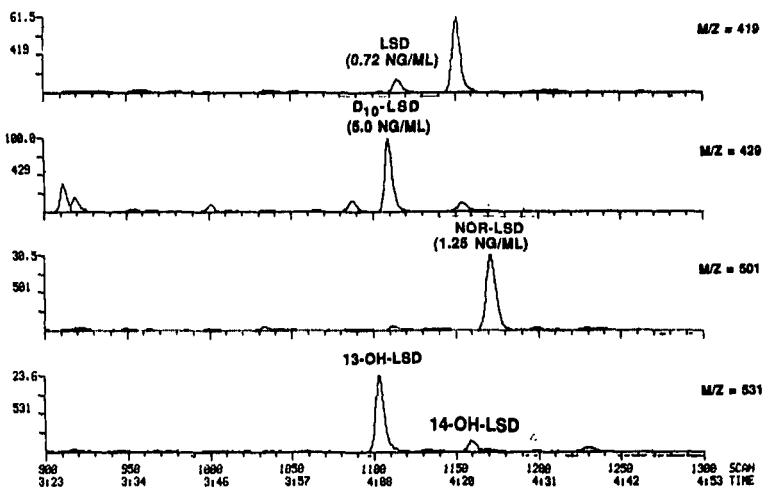

TABLE 1 PHARMACOKINETIC PARAMETERS

PARAMETERS	LSD	NOR-LSD
Elimination half-life	3.6 hours	10.0 hours
Elimination rate constant	0.2 $hours^{-1}$	0.1 $hours^{-1}$
Percent of dose excreted in urine	0.9 %	1.2 %

Presented at the 35th ASMS Conference on Mass Spectrometry and Allied Topics
May 24-29, 1987, Denver, CO

INVESTIGATION OF GUANINE ADDUCTS BY POSITIVE AND NEGATIVE THERMOSPRAY MASS SPECTROMETRY

Jan Crowley, S. O'Hara, P. Valladier, K. Stone, R. Hood and L.J. Marnett
Department of Chemistry,Wayne State University,Detroit Michigan 48202

Malondialdehyde (MDA) is a known product of lipid peroxidation and is produced in the biosynthesis of prostaglandins. Acrolein is a major intermediate in the chemical industry. Both MDA and acrolein substituted with good leaving groups at the β-position will induce frame shift mutations in *Salmonella typhimurium*. The adducts these compounds form with deoxyguanosine are believed to play a role in their mutagenicity. The ability to identify the adducts is important for the verification of standards and in vivo quantitation.

The mass spectrometer used in the study is a Finnegan 4000 with a Vestec Thermospray Ionizer. The four adducts are shown below. Thermospray results were obtained with .1M NH_4OAC directly into the probe. When the discharge electrode was turned on the signal was enhanced. However, the base peak was a fragment of guanine and M+1 was less than 1% of the base peak. Slight fluctuations in the flow seemed to be a more critical factor with these adducts than slight variations in the vaporizer temperature. A flow of 1.5 ml/min seemed to minimize the flow affects. Operating with the vaporizer in a range of 220-260 degrees showed little change in the spectra.

Because future work will involve studies carried out with a dCpGpC trinucleotide that contains the MDA adduct it would be very useful to be able to identify this molecule. Thermospray was run on a commercially available dinucleotide 5'dGpC. The positive spectra of pdA, pdC, pdG, and pdT were in agreement with previously reported data[1] but the dinucleotide spectra showed only the BH2+ ions of the cytosine and guanine. The M+1 of the dinucleotide 3'5'ApC has been observed.[2]

The negative spectra of the nucleoside adducts had strong ions at B-1, and $(M+OAC)^-$. Adduct A which contains the side chain off the ring system also has ions at $(Guanine+OAC)^-$,$(B+OAC)^-$,M-1,$(M-H_2O)$, B-H_2O, and $(M-(CH_2)_3OH)^-$. The adduct D which has no sugar showed no M-1 or $(M+OAC)^-$ ions. The only ion is an (M-MDA)-1. The nucleotide bases all had strong $B+(OAC)^-$ and $(Nucleoside+OAC)^-$ ions . All except pdC had a strong B-1. The M-1 and $(M+OAC)^-$ ions were not always detected. The M-1 for pdG was .2% of the base peak and the $(M+OAC)^-$ for pdC (.8%) and pdT(.1%) were also small. The dinucleotide gave no signal in any of three buffers tried ammonium acetate, acetic acid and trifluoacetic acid, where it should exist as a negative, neutral and positively charged species repectively.

In conclusion, TSP/MS gave good results with this series of adducts. One adduct, D, is not identifiable by other means of ionization. Initial work done with a dinucleotide indicated that identification of the adduct incorporated into a trinucleotide would not be possible.The most informative data was obtained with positive ions and no external means of ionization.

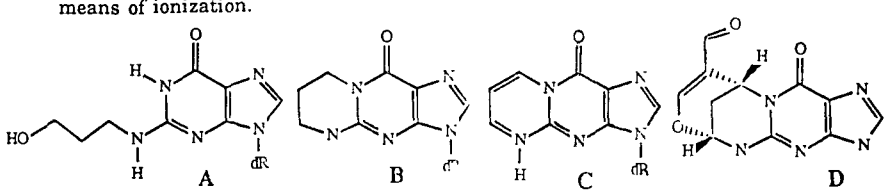

[1] C.G. Edmonds, F.F.Hsu and J.A. McCloskey, 33rd Annual Conference on Mass Spectrometry and Allied Topics 1985 pp.516-517
[2] R. Voyksner, 34th Annual Conference on Mass Spectrometry and Allied Topics 1986 pp. 758-759

Presented at the 35th ASMS Conference on Mass Spectrometry and Allied Topics
May 24-29, 1987, Denver, CO.

DETECTION AND IDENTIFICATION OF TETRACHLORODIBENZOFURAN METABOLITES BY GC/MS

C.E. Parker and K.B. Tomer, Laboratory of Molecular Biophysics, NIEHS, Research Triangle Park, NC 27709

L.T. Burka and L.S. Birnbaum, Toxicology Research and Testing Program, NIEHS, Research Triangle Park, NC 27709

The 2,3,7,8 isomer of tetrachlorodibenzofuran is a highly toxic contaminant found in polychlorinated biphenyls and chlorinated phenol mixtures. In both structure and toxicity, 2,3,7,8-tetrachlorodibenzofuran (TCDF) is closely related to 2,3,7,8-tetrachlorodibenzo-p-dioxin (TCDD). In rats,TCDF, unlike TCDD, is readily metabolized and excreted via the bile into the feces. Preliminary investigation of the biliary metabolites by other researchers has revealed, after methylation of glucuronidase/ sulfatase-treated bile, tetrachloromethoxy-, trichloromethoxy-, and trichlorodimethoxy-dibenzofuran isomers, and a possible ring-opened product, a tetrachlorodimethoxybiphenyl.

In order to confirm the structure of the biliary TCDF metabolites, a program of rational synthesis and GC/MS analysis of possible metabolites has been initiated.

Four compounds are currently under investigation: 2,2'-dimethoxy-4,5,4',5'-tetrachlorobiphenyl (DMTCB), 1-methoxy-2,3,7,8-tetrachlorodibenzofuran (1-MTCDF), 3-methoxy-2,3,7,8-tetrachlorodibenzofuran (3-MTCDF), and 4-methoxy-2,3,7,8-tetrachlorodibenzofuran (4-MTCDF). TCDF metabolites were synthesized by adapting the method of Safe and Safe (J. Agr. Food Chem. 34 (1984) 66-71). For 4-MTCDF, this synthesis resulted in a ~50:50 mixture of 3- and 4-MTCDF (by proton NMR).

Analysis by HRGC/MS has allowed the separation of DMTCB, 1-MTCDF, 3-MTCDF, and 4-TCMDF, and spectra of these standards have been obtained in EI, PCI, and NCI ionization modes. The EI mass specta of DMTCB (peak A) shows an intense molecular ion and (M-CH3)+. The EI mass spectra of 1-MTCDF (peak B) and 4-MTCDF (peak D) show intense molecular ions and (M-43)+ ions. The assignment of the 3-MTCDF structure to peak C is based on comparison with the EI mass spectra of 2,6- and 2,3-dichloroanisole. The EI spectrum of peak C (Figure 1) shows mainly (M-CH3)+. DMTCB did not give a useable NCI mass spectrum, while the MTCDF isomers gave (M-CH3)- ions by dissociative electron capture. Of the three MTCDF isomers, the 1-MTCDF isomer was the most sensitive. DMTCB and 1-MTCDF were of comparable sensitivities by PCI.

HRCG/FID analysis of bile from a rat which had been treated with TCDF shows a very small peak which coelutes with DMTCB, and a larger peak which coelutes with 1-MTCDF. No TCDF was found in the rat bile. The presence of 1-MTCDF was confirmed by HRGC/NCI/MS. Due to the low levels in the bile sample studied, the presence of DMTCB has not yet been confirmed.

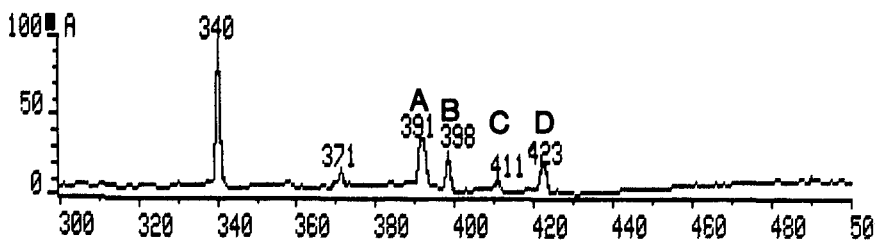

A

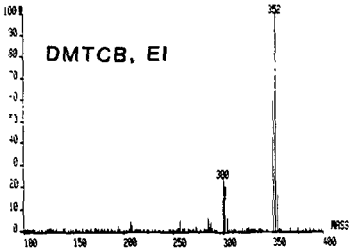
DMTCB, EI

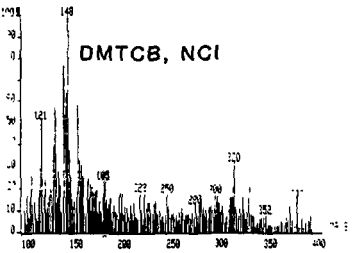
DMTCB, NCI

B

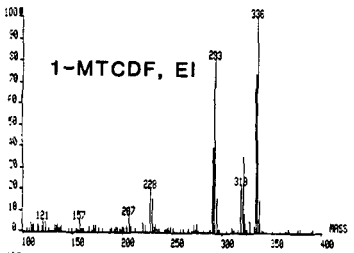
1-MTCDF, EI

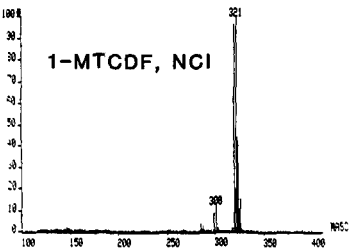
1-MTCDF, NCI

C

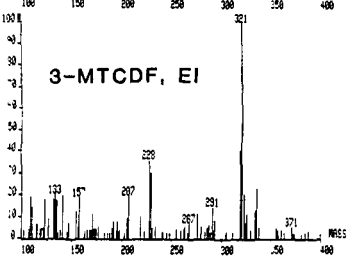
3-MTCDF, EI

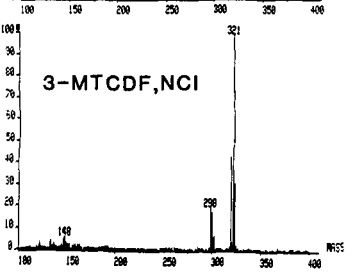
3-MTCDF,NCI

D

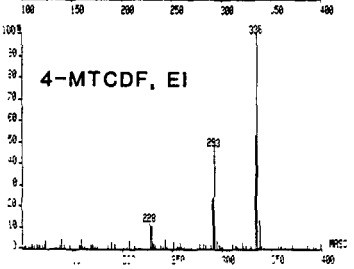
4-MTCDF, EI

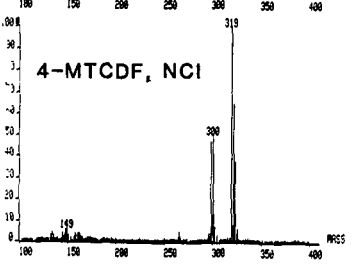
4-MTCDF, NCI

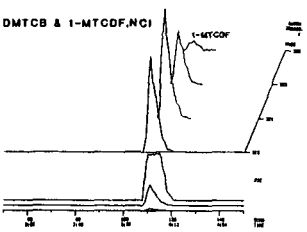
DMTCB & 1-MTCDF,NCI
1-MTCDF

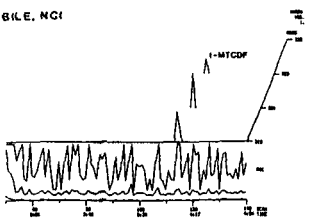
BILE, NCI
1-MTCDF

Presented at the 35th ASMS Conference on Mass Spectrometry and Allied Topics
May 24-29, 1987, Denver, CO

METHODS FOR QUANTITATIVE DETERMINATION OF THE DNA ADDUCT O^4-ETHYLTHYMIDINE BY ELECTRON CAPTURE NEGATIVE ION CHEMICAL IONIZATION MASS SPECTROMETRY.

Max J. Turner, Jr, Suzanne A.M. Koch,
Joyce A. Boucheron, James A. Swenberg.
Chemical Industry Institute of Toxicology
P.O. Box 12137
Research Triangle Park, NC 27709

Exposure to the strong alkylating agent diethylnitrosamine (DEN) produces the DNA adduct O^4-ethylthymidine (I). Quantitative determination of such adducts in dosimetry studies may lead to a better understanding of the relationship between these adducts and the initiation of carcinogenesis or mutagenesis. A radioimmunoassay (RIA) has been developed to quantify this adduct down to 0.3 picomoles, however more sensitivity is necessary to measure adduct concentrations of environmental concern.

The addition of strong electrophore-containing functional groups with subsequent detection by electron capture GC (GC-ECD) or negative ion chemical ionization mass spectrometry (NICI-MS) can enhance detection by several orders of magnitude for many compounds. We have developed methodology using pentafluorobenzyl (PFB) derivatives of O^4-ethylthymidine (II) and thymine (III) with detection by GC-ECD and NICI-MS for potential use in quantitation of this adduct in biological samples.

Figure 1 shows the procedures used for preparation of the various PFB derivatives of O^4EtdT used in this study. In addition, a stable isotope labelled derivative (methyl-D_3) was prepared for use as an internal standard. Isolated DNA was enzymatically hydrolyzed and O^4-EtdT was separated from the normal nucleosides by reversed phase HPLC.

Electron capture NICI mass spectra were produced using a Finnigan 4500 GCMS system with methane (0.6 torr) as the moderating gas. Samples were chromatographed on a Finnigan 9610 GC fitted with a J & W on-column injector and a DB-5 bonded phase capillary column inserted directly into the ion source. Single ion monitoring (m/z 305 for O^4-EtdT and m/z 308 for internal standard) was used to enhance sensitivity and specificity. Virtually all the ion current in the negative ion spectra is produced by the m/z 305 (loss of one PFB residue) ion which greatly enhances sensitivity. A typical SIM chromatogram showing ion currents from m/z 305 and m/z 308 is shown in Figure 2. Detection limits for this derivative are less that 0.05 x 10^{-15} moles per microliter injected. Standards were prepared at concentrations from 0.05 fm to 100 fm, each containing 2.0 fm of the internal standard. The calibration curve prepared from the analysis of these standards is shown in Figure 3.

While the described method appears adequate, several problems persist. Due to the large amount of normal thymidine present (10^5 to 10^6 times as much) in the DNA hydrolysates, some thymidine appears to tail into the retention window (HPLC) where O^4-EtdT elutes. Since acid hydrolysis of (I) removes the O-ethyl group as well as the ribosyl group, both normal thymidine and O^4-EtdT produce the same product, thymine. This residual thymidine appears as a positive response in this assay. We are attempting to remedy this situation by using a second HPLC step to separate excess thymidine. Pentafluorobenzyl derivatives adhere or absorb onto teflon surfaces. This is especially a problem in the syringes used for on-column injection. Extreme care must be taken not to draw sample into the syringe barrel and to thoroughly rinse the syringe between injections.

A procedure has been developed to remove the ribosyl group without removing the O-ethyl group, producing O^4-ethylthymine (Figure 1, Scheme C), which can be derivatized with PFB-Br to afford (IV). This derivative would avoid the problem of residual thymidine since (III) and (IV) are easily distinguished by GC and MS. This method is currently being evaluated in our laboratory. It would also be desirable to produce a stable isotope labelled derivative to allow accurate recoveries to be determined for each step in this procedure.

A very sensitive method for detecting and quantitating O^4-EtdT has been described. It should be noted that the highest concentration considered here is less than the lower limit of detection afforded by the RIA method we currently use. When fully implemented, this method should allow accurate quantitation of this adduct produced from exposures of much lower levels of DEN than previously employed in dosimetry studies. Such data should prove useful in accessing risk to humans exposed to this and other carcinogens. It is hoped that techniques learned with this adduct can be applied to other adducts of interest.

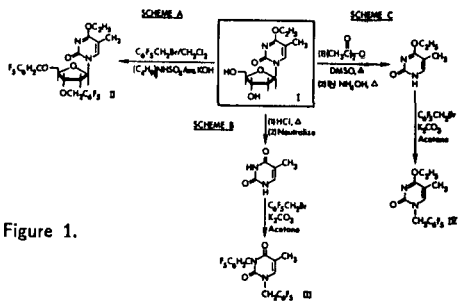

Figure 1.

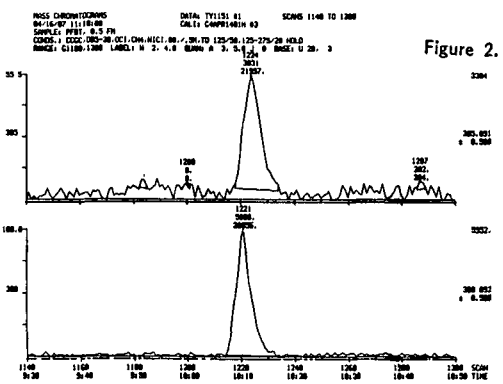

Figure 2.

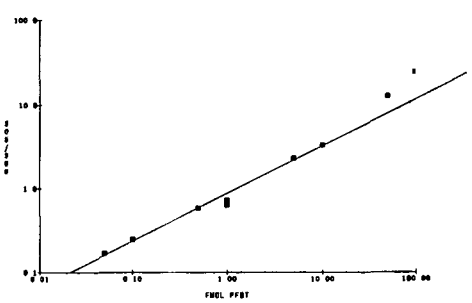

Figure 3.

Presented at the 35th ASMS Conference on Mass Spectrometry and Allied Topics
May 24-29, 1987, Denver, CO

METHANE NEGATIVE ION MASS SPECTROMETRY OF NITRO-POLYCYCLIC AROMATIC HYDROCARBON METABOLITES

W.A. Korfmacher, Z. Djurić, E.K. Fifer and F.A. Beland

National Center for Toxicological Research, Jefferson, AR 72079

INTRODUCTION

Nitro-polycyclic aromatic hydrocarbons (nitro-PAHs) are environmental contaminants that have been detected in diesel exhaust, urban air particulates, and coal fly ash. Certain of these compounds are mutagenic in bacteria and eukaryotes, and tumorigenic in laboratory animals; therefore, they pose a potential human health concern. A major nitro-PAH detected in environmental samples is 1-nitropyrene, which contributes up to 30% of the bacterial mutagenicity associated with diesel emission. Also found in diesel emission are 1,3- 1,6-, and 1,8-dinitropyrene. Although these dinitropyrenes are found in substantially lower quantities than 1-nitropyrene, they are among the most mutagenic compounds ever tested in bacterial mutagenesis assays.

A number of analytical techniques have been used to detect nitro-PAHs. These include high performance liquid chromatography (HPLC), gas chromatography (GC), gas chromatography/mass spectrometry (GC/MS) operated in the positive ion electron impact (EI) mode and the electron capture negative ion chemical ionization (ECNICI) mode, high resolution MS, MS/MS, negative ion atmospheric pressure ionization (NIAPI) MS and NIAPI-MS/MS. Of the mass spectral techniques, ECNICI and NIAPI offer the advantage of greater selectivity and sensitivity than EI.

Recently, Stemmler and Hites (1) reported the negative ion mass spectrometric analysis of hexachlorocyclopentadiene derivatives using methane reagent gas in the chemical ionization mode and referred to this technique as "methane enhanced negative ion MS". This terminology is useful because it avoids the confusion that can occur when the term ECNICIMS is used to describe experiments in which ion-molecule reactions are not the major mechanism for the production of the molecular anions. We have adopted the simpler terminology of "methane negative ion mass spectrometry" (MNIMS) to describe the methodology used for the MS experiments described in this work.

In order to be able to monitor environmental exposure to nitro-PAHs, and to be able to identify the metabolic products of nitro-PAHs in laboratory studies, sensitive methods must be developed to detect their metabolites. Toward this goal, we have examined the utility of MNIMS for the detection of various metabolites of nitro-PAHs. This work describes the utility of MNIMS for the analysis of metabolites of 1-nitropyrene and 1,3-, 1,6-, and 1,8-dinitropyrene.

EXPERIMENTAL

Metabolites

All nitro-PAH metabolites were obtained from microsomal incubations as described by Djurić et al. (2-4). The metabolites were separated from the substrate using HPLC. The metabolites were identified by comparing their retention times and MNI mass spectra to the HPLC retention times and MNI mass spectra of the synthesized standards.

Instrumentation

Mass spectra were obtained with a Finnigan-MAT 4023 (San Jose, CA) mass spectrometer incorporating the standard pulsed positive ion negative ion chemical ionization electronics and EI/CI source. Samples were analyzed via a Vacumetrics (Ventura, CA) direct-exposure probe incorporating a platinum filament and a 60-sec heating ramp with a rate of 0.05 A/sec. All analyses were conducted in the negative ion CI mode. The methane was adjusted to an uncorrected nominal source pressure of 0.25 torr (33 Pa) and the source temperature was set to 270°C. Typically, ions were monitored using a two-sec scan from m/z 100 to 750. For increased sensitivity, some analyses were performed using a two-sec scan from m/z 100 to 500. The electron energy was set to 70 eV with an emission current of 0.25 mA. The electron multiplier was adjusted to 1200 V and the conversion dynode voltage was 3 KV.

Nitro-PAH metabolites were available in only limited quantities.

Typically, 10-20 µl of methanol was added to 0.5 to 5 µg of a metabolite and 1-2 µl was applied to the direct-exposure probe (sometimes called a desorption chemical ionization probe) for MS analysis.

RESULTS AND DISCUSSION

MNI mass spectra were obtained for the following compounds: 1-nitropyrene, 3-hydroxy-1-nitropyrene, 6-hydroxy-1-nitropyrene, 8-hydroxy-1-nitropyrene, 1-nitropyrene 4,5-oxide, 1-nitropyrene 9,10-oxide, 1-nitropyrene trans-4,5-dihydrodiol, 1-nitropyrene cis-4,5-dihydrodiol, 1-nitropyrene trans-9,10-dihydrodiol, 1,3-dinitropyrene, 1-amino-3-nitropyrene, N-acetyl-1-amino-3-nitropyrene, 1,6-dinitropyrene, 1-amino-6-nitropyrene, N-acetyl-1-amino-6-nitropyrene, 1,8-dinitropyrene, 1-amino-8-nitropyrene, and N-acetyl-1-amino-8-nitropyrene. In all cases, except for 1-nitropyrene 9,10-oxide, the M^- ion was the base peak. For 1-nitropyrene 9,10-oxide the M^- ion had a relative intensity of 68% of the base peak. For most of the compounds, no significant fragmentation was observed. The exceptions to this were 1-nitropyrene 4,5-oxide, 1-nitropyrene 9,10-oxide and 1-nitropyrene cis-4,5-dihydrodiol, which each displayed two or more significant fragment ion peaks. Figure 1 shows the MNI mass spectra of: (a) synthetic 1-nitropyrene cis-4,5-dihydrodiol; (b) synthetic 1-nitropyrene trans-4,5-dihydrodiol; and (c) the microsomal metabolite, 1-nitropyrene trans-4,5-dihydrodiol.

MNIMS analysis of the corresponding metabolites produced mass spectra that agreed well with the mass spectra of the standards. Thus, by using these results in combination with the HPLC retention times, identification of the metabolites was accomplished. Typically, 1-3 µg of metabolite was available for MS analysis and 5-10% of the total was used for each mass spectrum. Thus, for some of the metabolites, full mass spectra were obtained with 50 ng of the compound actually applied to the direct exposure probe.

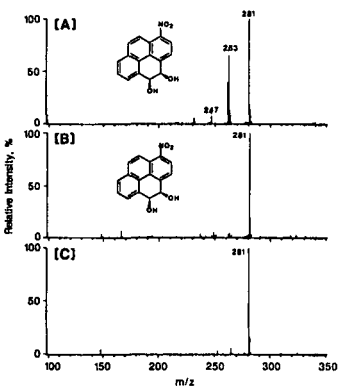

Figure 1.

CONCLUSION

The results shown in this study demonstrate that for these nitro-PAHs and their metabolites, MNIMS provides an M^- as the major ion, typically the base peak. In some instances, spectra were obtained with only 50-100 ng of sample applied to the direct-exposure probe. Therefore, these experiments demonstrate that MNIMS provides a sensitive method for the characterization of nitro-PAH metabolites that still contain a nitro group function.

REFERENCES

1. E.A. Stemmler and R.A. Hites, Anal. Chem. 57, 684 (1985).
2. Z. Djurić, E.K. Fifer, P.C. Howard and F.A. Beland, Carcinogenesis 7, 1073 (1986).
3. Z. Djurić, E.K. Fifer and F.A. Beland, Carcinogenesis 6, 941 (1985).
4. Z. Djurić, D.W. Potter, R.H. Heflich and F.A. Beland, Chem.-Biol. Interact. 59, 309 (1986).

Presented at the 35th ASMS Conference on Mass Spectrometry and Allied Topics
May 24-29, 1987, Denver, CO

TRICYCLIC AROMATIC IONS FROM CI FRAGMENTATION OF ANTIDEPRESSANT AMINES

Robert M. Geidner and Steven M. Schildcrout
Dept. of Chemistry, Youngstown State Univ.,Youngstown, OH 44555

Tricyclic antidepressant amines are a widely used class of drugs, and there has been interest in their analytical characterization by mass spectrometry, including CIMS. Nevertheless previously reported CI spectra show inconsistencies, and mechanistic interpretations and comparisons of CI mass spectra among these drugs have not been given. The compounds used in this study are shown below.

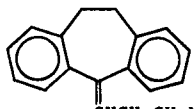

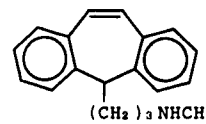

Amitriptyline (AMI), R = CH_3
Nortriptyline (NOR), R = H or D

Protriptyline (PRO)

The purposes of this work are to report a methane CI spectrum for PRO, which has not been previously done, to compare it with spectra of AMI and NOR measured under similar conditions, and to rationalize the CI spectra, especially the fragmentation, of the three compounds in terms of substituent effects (secondary vs. tertiary amine, location of the double bond) and possible interactions or competition among the functional groups at which protonation or ethylation may occur and which may direct fragmentation.

Drugs were obtained commercially. NOR was deuterated at N with D_2O. A Finnigan MAT 1020B GC/MS was used. GC analysis assured purity of the materials. The results are tabulated below.

Methane CI Mass Spectra (m/z>150)

	Rel. abundance (m/z)		
ion	AMI	NOR	PRO
$[M+C_3H_5]^+$	2.8 (318)	4.4 (304*)	4.0 (304)
$[M+C_2H_5]^+$	17.9 (306)	19.2 (292*)	17.5 (292)
$[M+H]^+$	100 (278)	100 (264*)	100 (264)
$[M]^{+\cdot}$		3.0 (263*)	
$[M-H]^+$	43.8 (276)	20.1 (262*)	15.7 (262)
$C_{20}H_{21}^+$		1.8 (261)	
$C_{19}H_{21}^+$		1.1 (249*)	
$C_{18}H_{17}^+$	4.5 (233)	8.9 (233)	
$C_{17}H_{17}^+$	0.6 (221)	3.9 (221*)	
$C_{15}H_{11}^+$	1.3 (191)		4.4 (191)

*Increases one unit for deuterated NOR.

All three compounds show similar relative abundances of the molecular adducts with $C_2H_5^+$ and $C_3H_5^+$. Although abundances are relative to 100% for $[M+H]^+$, the base peak in each case arises from an iminium ion $[CH_2{=}NRCH_3]^+$. Evidence from simpler amines indicates that this ion arises primarily by alkide abstraction under CI conditions[1], so its formation should not compete with that of other fragments whose precursors are $[M+H]^+$ or adduct ions.

Hydride abstraction occurs most readily for AMI, indicating that the tertiary amine function is advantageous, but the ring system also affects this process since NOR > PRO, and an analogous trend is seen in data previously reported[2] where AMI > doxepin > imipramine for the $[M-H]^+$ peak, and where each of these drugs has the same side chain as AMI. For AMI and NOR we postulate loss of the allylic hydride as energetically favored and enhanced by the electron-donating R=CH_3 of AMI. Resonance structures of the resulting ion show charge delocalization over the rings as well as the side chain (Fig. 1).

$C_{18}H_{17}^+$ (m/z 233) would result from protonation at N followed by heterolytic cleavage of the C-N bond to expel neutral CH_3NHR. Such cleavage

should be favored when R is more electron-withdrawing (H rather than CH_3), as observed with NOR > AMI. The resulting ion would not be especially stable, but an allylic H^- shift will permit extensive charge delocalization as for $[M-H]^+$. This is not possible for PRO.

An analogous loss of neutral CH_3NH_2 from ethylated NOR might seem to explain m/z 261, which has the same abundance ratio to $[M+C_2H_5]^+$ that m/z 233 does to $[M+H]^+$; however if ethylation occured at the N atom, a complex skeletal rearrangement would be needed. For aniline, protonation occurs mainly at the N atom, but ethylation occurs on the ring.[3] The present observations for NOR are explained if ethylation similarly occurs on the ring system, followed by intramolecular proton transfer to N. Reaction would then proceed as for loss of CH_3NH_2 from $[M+H]^+$.

Loss of a neutral imine from $[M+H]^+$ and $[M+C_2H_5]^+$ accounts for m/z 221 and 249, with similar abundances relative to their respective parent ions for NOR. For deuterated NOR these fragments retain D. Markovnikovian addition of the electrophile E^+ (H^+ or $C_2H_5^+$) to the double bond gives an ion (Fig. 2) whose resonance structures show charge delocalization over its ring system. Such a mechanism is not available to AMI or PRO.

The only skeletal fragmentation observed for PRO, with charge retention on the ring system, gives $C_{15}H_{11}^+$ at m/z 191. After protonation at N, heterolytic benzylic-like cleavage with intramolecular proton transfer gives methylpropylamine and the dibenzotropylium ion, whose charge is delocalized over all of its 15 carbon atoms. PRO's 10,11 double bond favors this process.

Summary: The ions observed in the methane CI spectra do not involve fragmentation of the tricyclic ring skeleton. Hydride abstraction gives abundant ions with charge delocalized on the rings and side chain, but not at N. Protonation at N gives loss of neutral amine with charge delocalized on rings (dibenzotropylium ion from PRO) or on rings and chain (AMI and NOR). A similar situation results if ethylation (on rings) leads to intramolecular protonation at N. Protonation or ethylation at the exocyclic double bond (NOR) gives loss of a neutral imine with H rearrangement and charge delocalization on the rings.

Conclusions: The fragmentation of these compounds is directed by both the amine function and the aromatic ring system, which are not chemically separate. Mechanisms involving their interaction account for the ions and their relative abundances observed for these compounds. Although protonation, ethylation, and hydride abstraction tend to occur on the amine side chain, the resulting fragment ions achieve stability by unusually extensive charge delocalization over the tricyclic aromatic ring system or over both the ring system and the side chain conjugated to it. Skeletal fragmentation involves loss of neutral amines or imines with hydrogen rearrangement.

1. Reiner, E.J.; Poirier, R.A.; Peterson, M.R.; Csizmadia, I.G.; Harrison, A.G. Can. J. Chem. 1986, 64, 1652-1660.
2. Jenkins, R.G.; Friedel, R.O. J. Pharm. Sci. 1978, 67, 17-23.
3. Maquestiau, A.; Van Haverbeke, Y.; Mispreuve, H.; Flammang, R.; Harris, J.A.; Howe, I.; Beynon, J.H. Org. Mass Spectrom. 1980, 15, 144-148.

Fig. 1

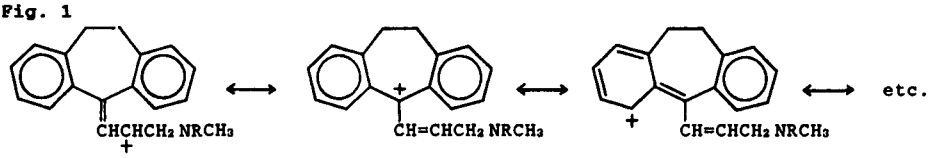

Fig. 2

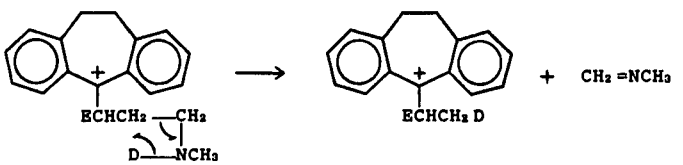

Presented at the 35th ASMS Conference on Mass Spectrometry and Allied Topics
May 24-29, 1987, Denver, CO

STIMULATED SURFACE IONIZATION OF ALKALI METALS FROM ALKALI ALUMINUM SILICATES IN THE PRESENCE OF F_2 OR Cl_2

Toshihiro Fujii
National Institute for Environmental Studies
Tsukuba, Ibaraki 305, Japan

In experiments aimed at a search for emitters which surface-ionize organics efficiently, based on the understanding that work function of the surface is greatly increased by the chemisorption of electronegative gases, a considerable increase in potassium and sodium ion currents is always observed when chlorine is introduced into a mass spectrometer with a thermal ionization source.

Many studies of an analogous phenomenon have been reported. Helbing et al. have found so-called "stimulated surface ionization", showing that any superthermal neutral atom of an energy between 20 and 200 eV can stimulate any species of alkali atoms intentionally coated on the W substrate to be surface-ionized. Hershbach's group has also reported some analogous observations on the reaction of hot hydrogen atom beams on an alkali-coated filament. From their observations, they have speculated that the incident H atoms react individually with the surface coat to form alkali hydride molecules and the energy release per molecule formed is used to eject alkali ions. According to this mechanism, they suggest that other species such as halogen atoms which form stronger bonds to alkali atoms should be detectable by stimulated surface ionization at lower kinetic energies.

In the present study the surface-involved ionization reaction of halogen gases (F_2 or Cl_2) and alkali oxides (A_2O, A:alkali atom) contained in aluminum silicate (Al_2O_3:SiO_2) has been studied systematically under static conditions, in order to determine what is the principal mechanism of this phenomenon and where the reactive interaction takes place.

MECHANISM MODEL As a possible process involved in ionization of A_2O on the surface in the presence of chlorine, one can propose that shown in equations (1), in which alkali halide is produced:

$$2A_2O(s) + Cl_2(g) \longrightarrow 2ACl(s) + A^+(g) + AO(s) + O(g) + e(F) \quad (1)$$

Indexes (g), (s) mean a gas-phase molecule and a molecule on the surface respectively while F indicates the Fermi level in the surface. For the calculation of the reaction exoergicity, E, needed for the production of alkali ion, we assume the following reaction channel for equation (1).

$$A_2O(s) + Cl_2(g) \longrightarrow 2ACl(s) + O(g) \quad (2)$$

$$E = 2\Delta Hf(ACl) + \Delta Hf(O) - \Delta Hf(A_2O) \quad (3)$$

$$A_2O(s) \rightarrow A^+(g) + AO(s) + e(F) \quad (4)$$

where Hf(X) is the standard heat of formation of a given substance, X. The calculated E is summarized in Table I.

Table I. Energetic considerations for stimulated surface ionization of alkali atoms from alkali aluminum silicate surface in the presence of halogen gases.

alkali ions	evaporation energy (eV)	reaction exoergicity (E) surface reaction equation	E
Li	53.9	$Li_2O(s) + F_2(g) \longrightarrow 2LiF(s) + O(g)$	90.0
		$Li_2O(s) + Cl_2(g) \longrightarrow 2LiCl(s) + O(g)$	-7.2
Na	44.8	$Na_2O(s) + F_2(g) \longrightarrow 2NaF(s) + O(g)$	112.6
		$Na_2O(s) + Cl_2(g) \longrightarrow 2NaCl(s) + O(g)$	37.2
K	35.3	$K_2O(s) + F_2(g) \longrightarrow 2KF(s) + O(g)$	122.6
		$K_2O(s) + Cl_2(g) \longrightarrow 2KCl(s) + O(g)$	61.9
Rb	28.5	$Rb_2O(s) + F_2(g) \longrightarrow 2RbF(s) + O(g)$	121.7
		$Rb_2O(s) + Cl_2(g) \longrightarrow 2RbCl(s) + O(g)$	65.2

EXPERIMENTAL Figure 1 shows an experimental set-up schematically. The vacuum manifold contains a NEVA NBA-515 quadrupole mass filter with a thermionic ionizer in the ion chamber of a conventional electron impact source.

The thermionic ionizer is a small mineral bead (about 2 mm diameter) fused to 0.25 mm diameter Pt filament wire. The bead is prepared with a thoroughly grounded mixture of Li_2O:Al_2O_3:Si_2O in a 1:1:1 molar ratio for Li alkali ions. For other alkali ions (Na^+,K^+,Rb^+), we can prepare the analogous mixture of its alkali oxide.

The experimental runs were performed after proceeding through surface temperature determination to degassing. The emitter temperature was varied with the heating dc current. The admitted gas could strike the bead surface in the mass spectrometer when the bellows metering valve was open. The fluorine and chlorine were studied. The ion signal was measured as a function of temperature starting at low temperature for two different settings of the gas admission; 1) in vacuum condition, 2) the admission gas on.

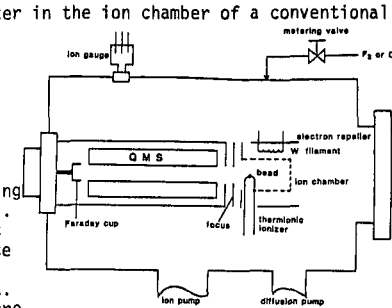

Fig.1

The time variation in the ion current was always observed to have a complicated form. However, the alkali jon current, i, from the mass spectrometer finally reached a constant value.

Presented at the 35th ASMS Conference on Mass Spectrometry and Allied Topics
May 24-29, 1987, Denver, CO

RESULTS AND DISCUSSION

1. Energy required to eject an alkali ion We may probably identify $\psi+$ with the energy required to remove an alkali ion from the bulk material.

$$i(T) = A\, f(T) \exp(-\psi+/kT) \qquad (5)$$

where i(T) is the positive ion current density at T(K).

Fig.2 shows the result of plotting the data for Li, Na or Rb ion emission according to Eq (5). The $\psi+$ value for four alkali ion species (Li, Na, K, Rb) was measured in a systematic heating manner in which the filament temperature was varied from low to high (Table I).

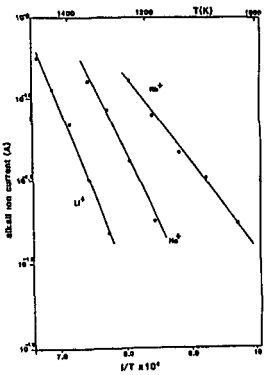

Figure 2.

2. Stimulated surface ionization (SSI) ions Strong alkali ion currents from the thermionic ionizer of the alkali aluminum silicate bead (A_2O bead) were detected in the presence of chlorine or fluorine, which decreased drastically when these gases were stopped. Apparently stimulated surface ionization takes place; large yields of alkali ions are emitted from the emitter with the bead except for the experimental combination of Li_2O or Na_2O bead and the Cl_2 environment.

2.1 Temperature dependence of SSI ions. A typical plot of the alkali ion currents vs emitter temperature (1/T) is shown in Fig.3 for the case of Li_2O and Rb_2O at 2.2 x 10^{-7} torr Cl_2. A threshold temperature (T_t) of SSI Rb ions was observed around 910 K. This value is less than temperature with the appearance of Rb^+ ions under the vacuum conditions.

2.2 Dependency of SSI ions on different gases. The ion signal was measured as a function of temperature, starting at low temperature for two different admissions of the halogen gases, viz., (1) F_2 in He and (2) Cl_2. The results are shown in Fig. 4 for the Rb_2O bead emitter.

2.3 Dependency of SSI on the pressure of halogen gases. The SSI ions were measured as a function of the partial pressure of chlorine (or fluorine) at a given temperature (Fig.5).

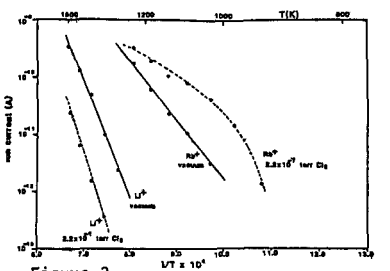

Figure 3.

3. The postulated mechanism of SSI The surface reaction

$$A_2O + Cl_2 \rightarrow 2ACl + O + e(F) \qquad (6)$$

may take place in the low temperature region, where the chemisorbed Cl_2 presumably diffuse on the surface. This postulated mechanism is consistent with the experimental results of stimulated surface ionization. For KCl production from Cl_2 with reaction exoergicity, E, higher than the ion evaporation energy, SSI was observed at considerably higher levels; while SSI was not observed for the NaCl or LiCl production from Cl_2 gases with E lower than the ion evaporation energy. Comparison of the alkali ion intensity in the F_2 environment with that in the Cl_2 environment showed that F_2 molecules enhanced surface ionization more than Cl_2 did. These observations imply that the SSI efficiency strongly depends on the difference between E and $\psi+$.

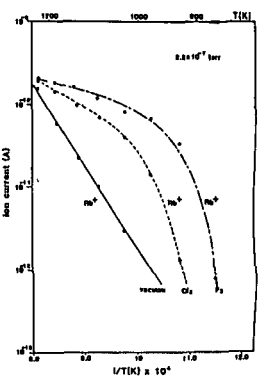

Figure 4.

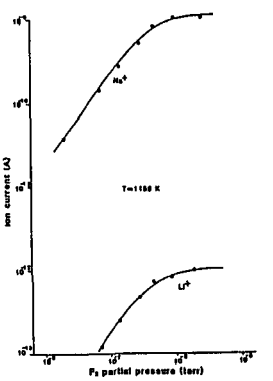

Figure 5.

In conclusion, the exothermic reaction on the surface is responsible for the SSI phenomenon. This mechanism explains the dependence on gas type and pressure from the reaction rate of the particular halogen molecular species with the bead material. It also provides a concrete support of Herschbach's suggestion that the halogen atoms should be detectable by stimulated surface ionization at lower kinetic energies.

Presented at the 35th ASMS Conference on Mass Spectrometry and Allied Topics
May 24-29, 1987, Denver, CO

APPLICATIONS OF METHANOL THERMOSPRAY IONIZATION TO COMPOUNDS OF PHARMACEUTICAL INTEREST.

Pradip R. Das, Birendra N. Pramanik and Rodney D. Malchow
Schering-Plough Corporation, Bloomfield, N.J. 07003

INTRODUCTION

Thermospray ionization has been generally regarded as a soft ionization technique for the characterization of nonvolatile, polar molecules and is most sensitive in higher percentage aqueous phases. However, under these conditions, many relatively less polar compounds fail to be detected or perhaps be weakly detected. Moreover, many thermolabile compounds degrade thermally at the higher temperatures required for optimum sensitivity for direct thermospray.

During the course of our efforts to develop an analytical technique for analyzing various classes of compounds of pharmaceutical interest using thermospray, we have found that methanol thermospray (filament or discharge ionization) using 100% methanol as the mobile phase is a convenient method for the rapid analyses of such compounds in either positive or negative ion modes. For most compounds studied (e.g. sugars, aminoglycoside, vitamin K_1, penem β-lactams and steroids) predominant pseudomolecular ions were observed in the mass spectra with the filament on; whereas the discharge electrode produced, in addition to strong pseudomolecular ions, many structurally characteristic fragments in many cases.

EXPERIMENTAL

An Extranuclear ELQ400-1 quadrupole mass spectrometer was used in these studies with a modified thermospray ion source from Vestec.

The methanol flow rate was 0.8 ml/min and all samples were introduced into the ion source by direct flow injection.

Ammonium acetate crystals were added to the sample solution (5-10μg sample in approximately 10-20μl of methanol) instead of mixing with the mobile phase.

A Vestec thermospray interface was used with typical operating temperatures as follows:

Tip (°C)	Vapor (°C)	Block (°C)	Compound
125	290	310	Steroids
160	200	220	Penems
125	200	220	Sugars
125	250	270	Aminoglycoside
125	270	300	Vitamin K_1

The emission current with the filament on was typically 200μA.

RESULTS & DISCUSSIONS

A disaccharide sample, derivatized lactose, displayed $(M+NH_4)^+$ as the only ion in the mass spectrum by filament ionization whereas it produced fragments corresponding to the individual pyranose units with the discharge.

The semi-synthetic aminoglycoside antibiotic, netlimicin, gave intense $(M+H)^+$ ion at m/z 451 with the filament whereas, many structurally informative fragments were generated with the discharge on. Vitamin K_1 behaved similarly although fewer fragments were observed in the mass spectrum.

The penem β-lactam antibiotics are polar, nonvolatile, thermolabile compounds. Initial attempts to apply direct thermospray with higher percent age aqueous phases failed to provide molecular/pseudomolecular ions; since this required higher temperatures (tip and vapor) for optimum sensitivity (with respect to solvent and electrolyte ions) and the penems degraded thermally. Methanol thermospray with filament on provided a simple solution to this since lower temperatures could be used for optimum sensitivity. Many penem β-lactam antibiotics, both free acids and their sodium salts, provided strong $(M+H)^+$, $(M+Na)^+$ and/or $(M+2Na-H)^+$ ions. However, sensitivity for this class of compounds was relatively poor.

Negative ion specta of these β-lactam antibiotics, Figure 1, using ammonium chloride as electrolyte, instead of ammonium acetate, showed $(M+Cl)^-$ adduct ions which were easy to recognize due to the presence of chlorine isotope in the spectrum. The discharge again produced several structurally important fragment ions; Figure 2.

Biologically active steroids displayed $(M+H)^+$ and/or $(M+NH_4)^+$ as the pseudomolecular ion depending on the proton affinity of the sample relative to ammonia and its polarity. Addition of pyridine in the pulsed mode, instead of ammonium acetate, showed selectivity in forming $(M+C_5H_5NH)^+$, Figures 3&4, depending on the extent of conjugation in the ring. Formation of π complexes appears to be the controlling factor behind this selectivity[1].

CONCLUSION

1. Compounds of a wide range of polarity can be analyzed by filament/discharge methanol thermospray.
2. Many thermolabile compounds are better suited for filament/discharge thermospray with methanol at lower operating temperatures.
3. Addition of buffer/electrolyte in "pulsed mode" enables different ones to be tested as reagent ions without changing the mobile phase. This also keeps the system cleaner and reduces capillary blockage.
4. Both the filament and the discharge electrode operate relatively trouble free in methanol.

REFERENCES

1. P.R. Das, B.N. Pramanik, R.D. Malchow and K.J. Ng
Biomed. Env. Mass Spectrom., (Submitted)

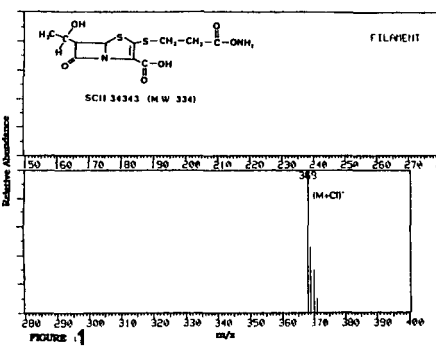

FIGURE 1

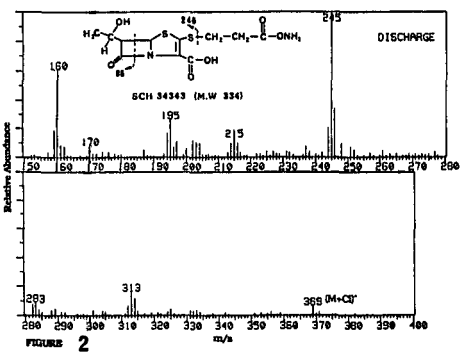

FIGURE 2

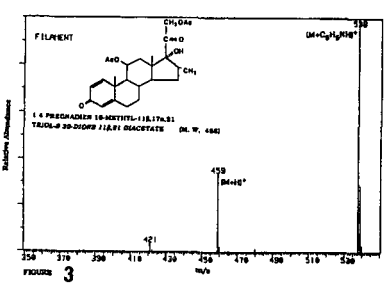

FIGURE 3

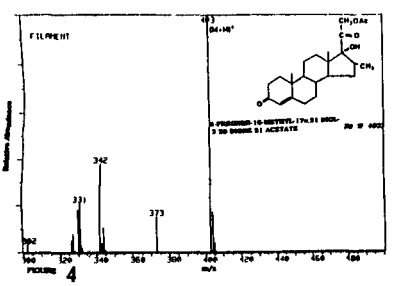

FIGURE 4

Presented at the 35th ASMS Conference on Mass Spectrometry and Allied Topics
May 24-29, 1987, Denver, CO

NEGATIVE ION MASS SPECTROMETRY OF POLYCHLORODIBENZO-P-DIOXIN AND POLYCHLORODIBENZOFURANS: CORRELATIONS BETWEEN OBSERVED FRAGMENTATIONS AND CALCULATED TOTAL INTERNAL ENERGIES

J. Laramee, B. Arbogast, Y-S. Chang, M. Deinzer
Oregon State University, Corvallis, Oregon 97331

Methods developed allow ionic abundance predictions of $M^{\pm}$, $(M-Cl)^-$ and Cl-anions using closed shell CNDO and MNDO calculations. Mechanisms of ion production in electron capture negative ion chemical ionization (ECNICI) include resonance and dissociative electron capture (Scheme I). Competitive dissociative electron capture pathways are accessed via an activation energy which is required during electron reorganization. Difference in total internal energies of products obtained by the two dissociative pathways, which should be related to the difference in activation energies, is given by isodesmic equation 1:

Scheme I

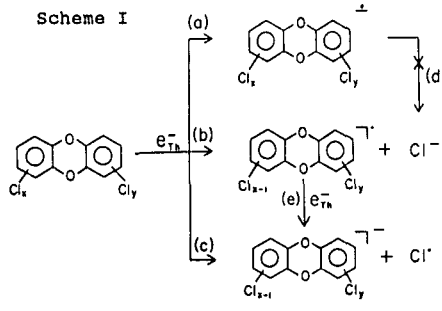

$$\Delta E = E(M-Cl)^- + E(Cl^{\cdot}) - [E(M-Cl)^{\cdot} + E(Cl^-)] \quad (1)$$

Dependence of the dissociative capture cross-section upon ΔE and ion structure has a theoretical basis (1) and is shown experimentally (Fig. 1 & 2) (2). For dioxin substrate, isomers were chosen that would yield unique product species irrespective of the chlorine lost and avoid complications associated with the regiochemistry of the departing chlorine. These isomers (1-MCDD, 2-MCDD, 2,3-DCDD, 2,7-DCDD, 2,8-DCDD, 2,3,7,8-TCDD, and 1,4,6,9-TCDD) were used to calibrate $\log[(M-Cl)^-/(Cl^-)]$ vs. ΔE relationship (Fig. 1). Chlorine loss which relieves steric crowding or provide efficient stabilization of the aromatic product species correlates with data points neighboring near to the calibration line. The loss of chlorine 7 yields increased interannular charge polarization or smaller steric relief--a worse relationship between $\log[(M-Cl)^-/(Cl^-)]$ vs. ΔE. For the dibenzofuran substrate (Fig. 2) greater ion stability is expected when regiospecific chlorine loss will result in steric relief and/or charge stabilization. Thus, loss of an epichlorine (chlorine 4 or 6) may be the lower energy pathway as illustrated by the congeners: 2,4-DCDBF, 2,3,8-TrCDBF, 1,2,-3,7,9-PcDBF, 1,2,3,6,7,9-HcDBF, 1,2,3,4,6,7,8-HpCDBF, and OCDBF. Results are clearly affected by regiospecific chlorine loss. This approach could ultimately be used to predict isomer identification on the basis of ion ratio measurements.

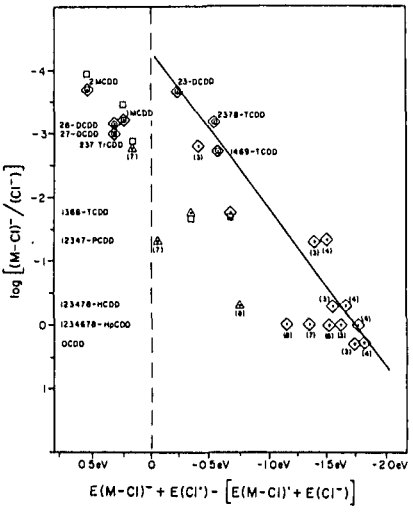

Figures 1 & 2

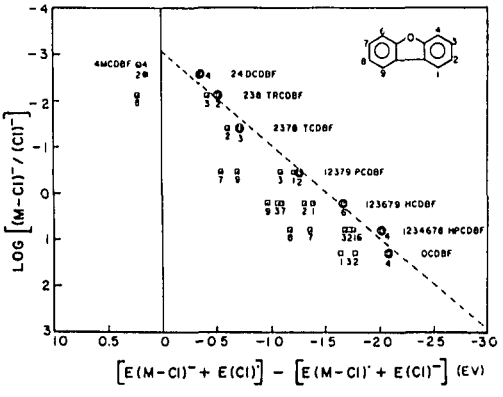

Presented at the 35th ASMS Conference on Mass Spectrometry and Allied Topics
May 24-29, 1987, Denver, CO

Molecular anion abundances from polychlorodibenzofurans and polychlorodibenzo-p-dioxins correlated with calculated lowest unoccupied molecular orbital (LUMO) energies (Fig. 3). Anion abundances were measured under ECNICI conditions; LUMO energies, calculated by the closed-shell CNDO method. By utilizing Koopmans' theorem, a correspon-dence is assumed between electron affinity (EA) and orbital energy of the LUMO. Relative molecular radical anion abundances were measured to be zero when LUMO energies are above 1.6 eV for polychlorodibenzofurans. LUMO energies below 1.4 eV gave $M^{\cdot-}$ abundances of $\geq$ 80% (Fig. 3). Polychlorodibenzo-p-dioxin isomers with LUMO energies above 2.0 eV yield no molecular anion current. Threshold energy for molecular radical anion formation is thus similar, and the mechanisms for electron capture and stabilization of anion must be similar. However, chlorodioxins with LUMO energies below 0.8 eV show less predictable $M^{\cdot-}$ abundances by this model.

Differences in electron capturing ability between chlorinated dibenzofurans and dibenzo-p-dioxins may be related to their structural differences (flat vs. bent ring systems, respectively). Resonance structures of chlorodibenzofurans congeners allow charge delocalization through the whole molecular system. The extra oxygen atom in the dioxin substrate insulates the two rings, and the π-electron system of each seems to act independently. Polarization results as the captured electron in one ring causes a net charge depletion in the other. This condition is exacerbated by electron-withdrawing effects of the local chlorine atoms. Such a system may raise total energy of the ion, and thus its electron affinity (3). Alternatively, the barrier for Cl^- dissociation might be changing. Increase in electron affinity, with greater chlorination, increases the internal energy in $M^{\cdot-}$ available for dissociation. When EA exceeds DE $[M^{\cdot-} \rightarrow (M\text{-}Cl)^{\cdot} + Cl^-]$, a new reaction channel opens, and a decreasing $M^{\cdot-}$ radical anion abundance is expected with decreasing LUMO energy.

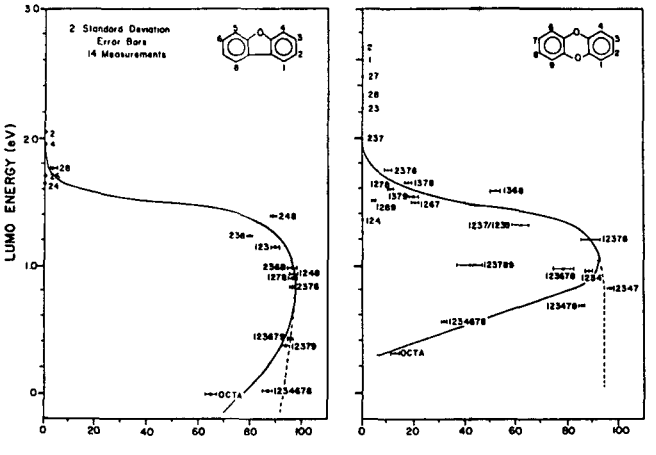

References

1. Christophoru, L.G. Environ. Health Pers. 36 3 (1980).
2. Laramée, J.A.; Arbogast, B.C.; Deinzer, M.L. Anal. Chem., 58 2907 (1986).
3. Naff, W.T.; Compton, R.N.; Cooper, C.D. J. Chem. Phys. 54 212 (1971).

Presented at the 35th ASMS Conference on Mass Spectrometry and Allied Topics
May 24-29, 1987, Denver, CO

STRUCTURAL ANALYSIS OF UNDERIVATIZED LIPID-A USING LASER DESORPTION (LDMS) AND PLASMA DESORPTION (PDMS) MASS SPECTROMETRY

R. Wang and Robert J. Cotter, Johns Hopkins University, Baltimore, MD 21205
N. Qureshi and K. Takayama, Veterans Administration Hospital, Madison, WI 53705

Lipid-A are portions of the lipopolysaccharides found in the outer wall of the outer membrane of gram-negative bacteria. They are mono- or diphosphorylated glucosamine disaccharides, with four to seven fatty acids connected to the sugar ring by amide or acyl linkages. Laser desorption mass spectrometry has been an important analytical tool for elucidating the structures of lipid-A from several bacteria (1,2). Because the ions produced by laser desorption are generally formed by gas-phase cationization of neutral molecules (3), lipid-A structures have been analyzed following dephosphorylation (1) or as the methyl derivatives (2). The latter approach has proven advantageous as well because HPLC separations of heterogeneous mixtures can be carried out, based upon the number of hydroxy fatty acids (2).

The lipid-A of E. coli have much less heterogeneity than that of S. minnesota or N. gonnorhoeae analyzed previously (2), so that highly purified and homogenous samples of the free acid may be obtained without HPLC separation. Therefore we have undertaken a comparison of the desorption of free acid and derivatized samples using laser desorption (LD) and plasma desorption (PDMS) mass spectrometry.

Positive ion LD and both positive and negative ion PDMS spectra were obtained for the (underivatized) monophosphoryl lipid-A (MLA) of E. coli and a dimethyl derivative of a MLA component of R. sphaeroides.

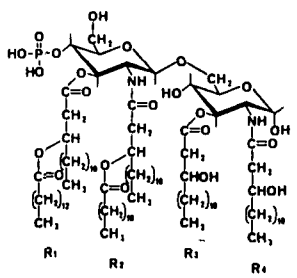

MLA of E. coli

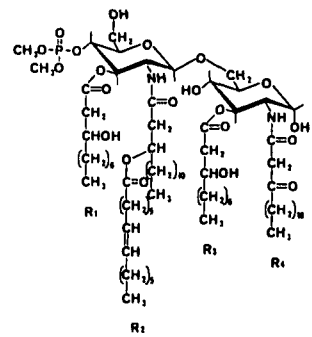

Dimethyl MLA of R. sphaeroides

The laser desorption mass spectrum of the dimethyl derivative produced an abundant molecular ion peak $(M+K)^+$, with a major fragment peak due to the loss of the acyl-linked fatty acid at the 3 position (R3). In contrast, the underivatized sample produced primarily ions resulting from loss of the anionic phosphate group (Figure 1). Plasma desorption produced similar spectra from both the derivatized and free acid samples. The positive ion spectra produced protonated species from underivatized lipid-A as well as from the dimethyl derivative (Figure 2). The negative ion PDMS spectra produced $(M-H)^-$ ion from the free acid form and $(M-CH3)^-$ ions from the derivatized sample.

While both LDMS and PDMS techniques are useful for the structural analysis of lipid-A, the spectra provide a probe of the differences between the techniques, resulting the differences in the mechanisms of ion formation. Laser desorption shows a clear preference for the more neutral species, from which ions may be formed by alkali ion attachment. Protonation in PDMS appears to be equally facile for both samples, while negative ion PDMS takes advantage of the anionic phosphate group. Structural information is different in the two positive ion techniques. The PDMS method results in fragmentation at the glycosidic bond to produce an oxonium ion, while fragmentation of the reducing sugar ring is observed in LD spectra (4).

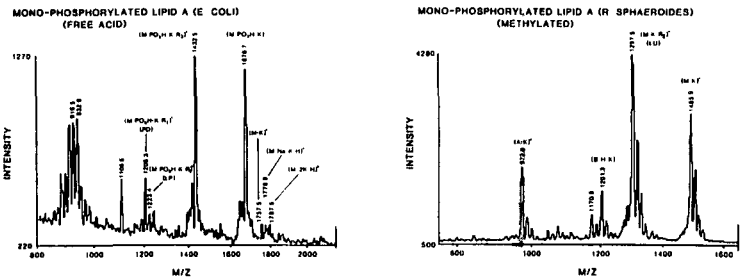

Figure 1. Laser desorption positive ion spectra of monophosphoryl lipid-A of E. coli and dimethyl-monophosphoryl lipid-A of R. Sphaeroides

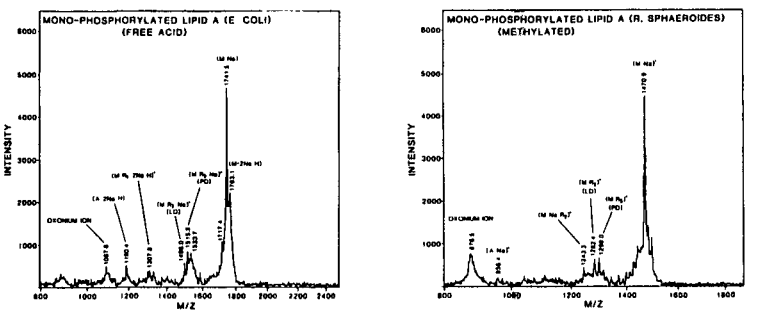

Figure 2. Plasma desorption positive ion spectra of monophosphoryl lipid-A of E. coli and dimethyl-monophosphoryl lipid-A of R. Sphaeroides

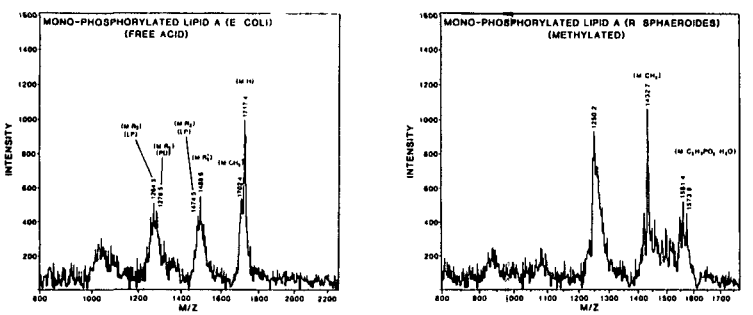

Figure 3. Plasma desorption negative ion spectra of monophosphoryl lipid-A of E. coli and dimethyl-monophosphoryl lipid-A of R. Sphaeroides

Reference:

(1) Seydel, U., Lindner, B., Wollenweber, H.-W. and Rietschel, E. Th.; Eur. J. Biochem., 145 (1984) 505-509.
(2) Takayama, K., Qureshi, N., Hyver, K., Honovich, J.,Cotter, R.J., Mascagni, P. and Schneider, H.; J. Biol. Chem., 261 (1986) 10624-10631.
(3) Tabet, J.-C. and Cotter, R.J.; Anal. Cham., 56 (1984) 1662-1667.
(4) Honovich, J., Cotter, R.J., Qureshi, N. and Takayama, K.; Biomed. Environ. Mass Spectrm. (in press).

Presented at the 35th ASMS Conference on Mass Spectrometry and Allied Topics
May 24-29, 1987, Denver, CO

EFFECT OF PRIMARY BEAM ENERGY ON SECONDARY ION SAMPLE EFFICIENCY IN THE 5-30KEV ENERGY RANGE

William Aberth and A.L. Burlingame
Mass Spectrometry Facility
Department of Pharmaceutical Chemistry
University of California, San Francisco, CA 94143-0446

Typical primary beam energies used for LSIMS are between 5 and 10 keV. Higher energies are usually preferred since secondary efficiency tends to increase with increasing energy in this range. Recently, a spectrum of human lysozyme at 14,701d was obtained using a Cs^+ beam of 30 keV energy [1]. We have employed a cesium ion gun similar to that used in reference [1] to perform a study of secondary ion efficiency of two high mass biocompounds as a function of primary Cs^+ beam energy between 5 and 30 keV. The small size of the cesium ion gun permitted mounting the gun on a 10mm dia alumina rod inside the source housing and electrically floating it to obtain primary energies above 10 keV (see Figure 1). Analyses were performed using 10 picomoles of bovine insulin (5733d) in the positive mode and 2.5 picomoles of methylglucose polysaccaharide, MGP (3514d) in both negative and positive ion modes. Small amounts of these samples were used to maintain a low signal so as not to saturate the microchannel plate pulse counting system. The pulses from a portion of the spectrum which included the molecular ion were accumulated on a 512 channel MCA [2,3] until the molecular ion signal became insignificant (15-20 minutes). The probe tip was freon cooled when throglycerol matrix was used to reduce loss of matrix by evaporation. Figure 2 is a plot of integrated positive ion bovine insulin signal as a function of primary cesium ion energy and Figure 3 is a similar plot for negative ion MGP. Both plots show a similar behavior of increasing rapidly with energy, reaching a maximum at about 15keV and then decreasing at higher energies. This behavior can be qualitatively explained by noting that most secondary ions are emitted from a depth of only a few angstroms in the collision region. Increasing primary energy initially increases the size of the impact area. If the primary particle energy, however, becomes too large it will penetrate deep below the target surface where its energy deposition cannot contribute substantially to surface excitation resulting in a decrease in conversion efficiency. Figure 4 shows a spectrum of MGP taken in the negative mode using a primary Cs^+ of 15 keV which represents the maximum conversion efficiency indicated in Figure 3.

Acknowledgements. This work was supported in part by NIH Grant GM 32315.

References:

1. G.J. Elliott, J.S. Cottrell and S. Evans, 34th Annual Conf. on Mass Spectrom. and Allied Topics, Cincinnati, OH, 1986, p. 880.

2. W. Aberth, Int. J. Mass Spectrom, Ion Phys. (1981) 37, 379.

3. W. Aberth, Advances in Mass Spectrom. Vol. 10, John Wiley and Sons, N.Y., J.F.J. Todd, ed., (1986), p. 1469.

Presented at the 35th ASMS Conference on Mass Spectrometry and Allied Topics
May 24-29, 1987, Denver, CO.

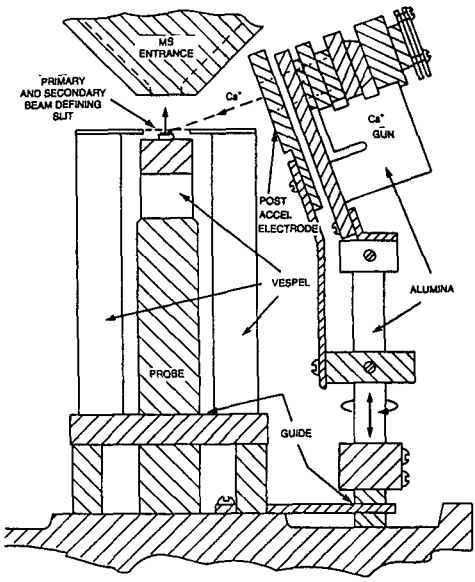

Figure 1. Cesium ion gun arrangement for obtaining 30keV primary beam. Cesium gun can produce up to 10keV ions at gun exit. Additional 20keV is obtained by floating gun 20kV above post-accel voltage

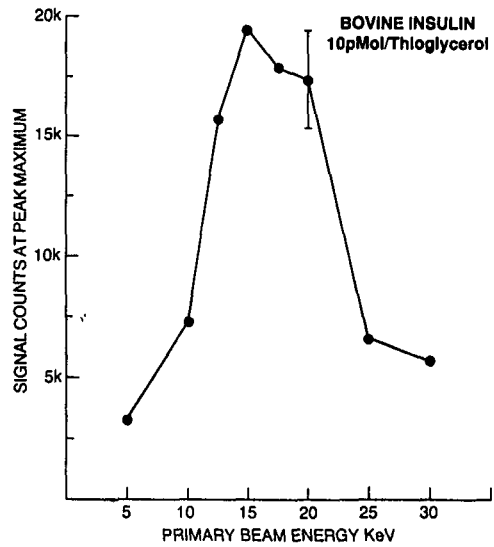

Figure 2. Plot of integrated bovine insulin positive molecular ion signal vs energy. Each point represents at least three measurements.

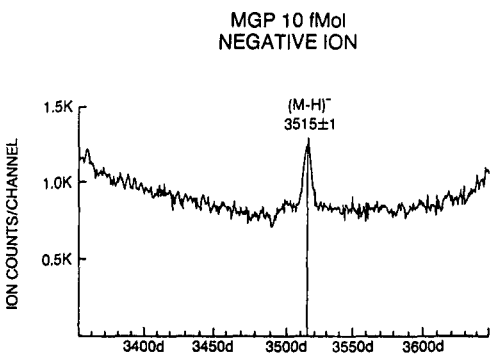

Figure 4. Integrated negative ion spectrum of MGP obtained using 15keV Cs^+ primary beam on 10 femtomoles of sample in 0.5ul of thioglycerol.

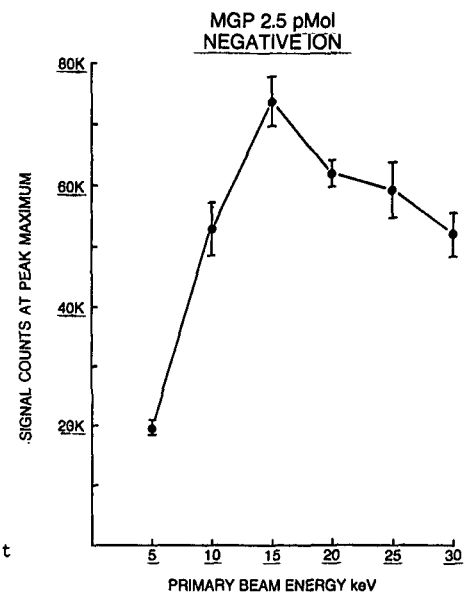

Figure 3. Plot of integrated MGP negative molecular ion signal vs primary ion energy. Each point represents an average of at least 3 measurements.

Presented at the 35th ASMS Conference on Mass Spectrometry and Allied Topics
May 24-29, 1987, Denver, CO

POSITIVE AND NEGATIVE ION FABMS OF p-TERT-BUTYLCALIX-8-ARENE TETRAALKYL AMMONIUM SALTS

J.A. Leary, L.E. Zebre, G.E. Hofmeister, S.F. Pedersen
College of Chemistry, University of California, Berkeley

Air sensitive tetraalkylammonium and sodium salts of p-tert-butylcalix-8-arenes are being examined as starting materials for the synthesis of metallacalixarenes (1). Mass spectrometric characterization of these starting materials is intended to help with future characterization of the metal containing compounds such as the di-titanium compound shown in Figure 1. These moisture sensitive salts have been analyzed by both positive and negative FAB using nitrophenyl octyl ether as the matrix. Samples were mixed and mounted on the probe tip using standard glove box techniques and the probe tip covered before removing from the box. The entrance port to the source was covered with a glove bag and constantly purged with Argon. With the probe in the bag, the protective covering was removed from the probe tip without disturbing the sample, and the probe introduced into the source. Both the tetraethyl and the triethyl benzyl ammonium salts of the di-anionic calix-8-arene show predominate (M+H) and (M-H) in the positive and negative FABMS spectra respectively. Table 1 lists the positive and negative fragment ions for both tetraalkyl ammonium salts. These salts show successive loss of cations followed by protonation to give either the corresponding positive or negative ion fragment. This process continues until the molecule has been stripped of both cations and only the fully hydroxylated compound remains. However, the relative abundance of the completely hydroxylated molecule depends to a large extent on how the sample is handled i.e.; the more the samples comes in contact with moisture, the greater the abundance of the hydroxylated calixarene. Handling of moisture sensitive compounds becomes more paramount when analyzing metallacalixarenes such as the di-titanium sodium salt. This compound not only gives cluster ions at higher mass, but it also rearranges to give a completely different spectrum.

Refs.

1. G.E. Hofmeister, S.F. Pedersen; unpublished results
2. S.S.J. Ho, M.E. Coddens, C.F. Poole,; Org. Mass Spec., 1985, 20(5), 377-379.
3. H.J. Veith; Org. Mass Spec., 1983, 18(4), 154-158.

Presented at the 35th ASMS Conference on Mass Spectrometry and Allied Topics
May 24-29, 1987, Denver, CO

Figure 1.

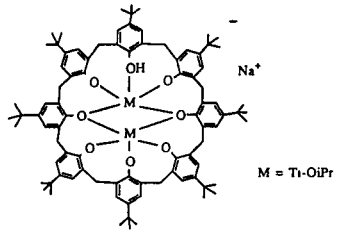

[p-tert-butylcalix[8]arene(TiOiPr)]$^-$[Na]$^+$

Table 1.

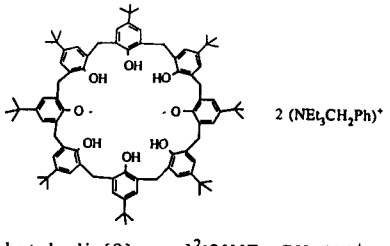

[p-tert-butylcalix[8]arene]$^{2-}$2[NEt_3CH_2Ph]$^+$

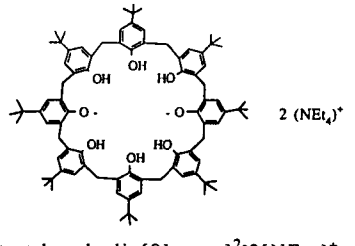

[p-tert-butylcalix[8]arene]$^{2-}$2[NEt_4]$^+$

positive ions		negative ions		positive ions		negative ions	
1872	$(MC)^+$	1679	$(M-H)^-$	1686	$(MC)^+$	1555	$(M-H)^-$
1681	$(MH)^+$	1488	$(M-C)^-$	1557	$(MH)^+$	1426	$(M-C)^-$
1490	$(MH-C+H)^+$	1296	$(M-2C+H)^-$	1428	$(MH-C+H)^+$	1296	$(M-2C+H)^+$
1298	$(MH-2C+2H)^+$						

Presented at the 35th ASMS Conference on Mass Spectrometry and Allied Topics
May 24-29, 1987, Denver, CO

MASS SPECTROMETRIC STUDIES OF MULTIPLY-CHARGED DIATOMIC SPECIES

Kevin L. Harbol and Robert W. Kiser
Department of Chemistry
University of Kentucky
Lexington, KY 40506-0055

The occurrence of multiply-charged positive ions of aromatic hydrocarbons and hydrocarbon derivatives by electron impact ionization has been well documented, but there have been few reports of triply-charged ions of small molecules. A. S. Newton[1] first reported the occurrence of the small, triply-ionized molecular species CS_2^{3+}, COS^{3+}, and $C_2N_2^{3+}$. More recently, M. P. Sampson,[2] reported in her electrom impact studies, the existence of $CSSe^{3+}$, CSe_2^{3+}, $AlCl_2^{3+}$, S_2Cl^{3+}, and the triply-charged diatomic species S_2^{3+} and Se_2^{3+}. Mórvay and Cornides[3] also reported the observation of CSe_2^{3+} and S_2^{3+}[2] ions in their spark source studies.

The present work reports the first observation and characterization of the triply-charged diatomic halogen species of chlorine, bromine, iodine, and iodine monobromide, as well as diatomic tellurium. Previous investigations in our laboratory of the Group VA homonuclear diatomic species provided no evidence for the existence of triply-charged species of N_2, P_2, or As_2. A probable explanation of these observations is that the removal of three electrons from the anti-bonding orbital of the Group VIA and Group VIIA diatomics substantially increases the bond order between the atoms of the triply-charged species. Removal of three electrons from the Group VA diatomics results in loss of bonding electrons, reducing the bond order, and assists the Coulombic repulsion in the dissociation of the ion.

The experimental work was carried out using a VG ZAB-2F reverse geometry mass spectrometer and a Hitachi RMU-7 double focusing mass spectrometer. All ionization efficiency curves for the species of study and reference ion were recorded on both instruments. Agreement of ionization energy determinations between the two sets of data was within two electron volts. Identification of the triply-charged ions was accomplished by the observation of those ionic species appearing at non-integral M/z values, the measurement of isotopic abundance ratios of the ionic species observed, peak matching to provide precise mass information, and some collision-induced dissociation studies of the multiply-charged ions.

Ion intensities of the triply-charged ions were simultaneously measured at various electron energies and compared to a well documented triply-charged reference species, usually Xe^{3+} or CS_2^{3+}. Relative ion intensity and Kth root ion intensity (K = 3 for triply-charged ions) of both reference and the studied triply-charged species were plotted as a function of electron energy. The extrapolated voltage technique was also utilized in determining the appearance energies of the triply-charged species. The energy compensation technique was also used to determine the appearance energy of related singly- and doubly-charged ion species.

Relative ion abundances for the singly- to doubly- to triply-charged ions are found to be in the general ratios of 100 to 1 to 0.005. Appearance and ionization energies, in electron volts, for the ions are:

Te_2^+	8.6	8.6	Br_2^+	10.5	10.5
Te_2^{2+}	23 ± 2	17	Br_2^{2+}	30 ± 1	19
Te_2^{3+}	60 ± 5	37	Br_2^{3+}	54 ± 2	24

IBr^{+}	10.5	10.5	I_2^{+}	9.5	9.5
IBr^{2+}	29 ± 3	18.5	I_2^{2+}	28 ± 2	18
IBr^{3+}	53 ± 4	24	I_2^{3+}	50 ± 5	22
Cl_2^{+}	11.7	11.7			
Cl_2^{2+}	33 ± 2	21			
Cl_2^{3+}	62 ± 2	29			

This study provides the first observation and characterization of triply-charged diatomic halogen species. The first, second and third ionization energies for these simple diatomic systems are found to be lower than those of noble gas atomic systems of similar charge. Increasing the bond order of an ion by removal of anti-bonding electrons apparently partially balances the Coulombic repusion of charges within the triply-charged ion. Lifetimes of the order of > 10 microseconds for these triply-charged diatomic ions permits their detection mass spectrometrically. This study leads us to predict the existence of the Group VI-VII heteronuclear triply-charged diatomic ions.

References

1. A. S. Newton, J. Chem. Phys. **40**, 607 (1964).

2. M. P. Sampson, "Electron Impact Investigation of Multiply-Charged Ionic Species Formed in Di- and Tri-atomic Systems," M. S. Thesis, University of Kentucky, 1984.

3. L. Morvay and I. Cornides, Int. J. Mass Spectrom. Ion Processes **62**, 263 (1984).

Presented at the 35th ASMS Conference on Mass Spectrometry and Allied Topics
May 24-29, 1987, Denver, CO

SOLUTE AGGREGATION IN ELECTROSPRAY IONIZATION OF ARGININE SOLUTIONS

C. K. Meng and J. B. Fenn
Department of Chemical Engineering
Yale University, New Haven, CT 06520

Into our previously described Electrospray Mass Spectrometer solutions of arginine at modest concentrations in 50:50 methanol water were injected. (1) The resulting spectra show appreciable currents of both singly and doubly charged clusters containing in some cases up to at least 11 molecules of solute arginine. Solute concentrations ranged from 10 ng/ul to 1.0 ug/ul. Over a range of sample flow rates from 5 to 15 ul/min the extent of clustering did not change very much but seemed to be greatest at about 9 ul/min, the rate used for all results reported here. Figure 1(a-d) shows a sequence of spectra obtained at increasing arginine concentrations. Ion currents for dimers and trimers are barely distinguishable at 10 ng/ul but become larger and are joined by currents due to higher clusters as the concentration goes up. At the highest concentration of 1.0 ug/ul there are significant ion currents attributable to singly charged clusters containing 6 monomers and doubly charged clusters containing up to at least 11 monomers. It seems intuitive reasonable that the extent of clustering should increase with increasing solute concentration and that the charges should be preferentially attracted to the larger clusters as they become more numerous. It should be remembered that because of extensive evaporation, when an ion is desorbed from a droplet the actual solute concentration will be much higher than the initial value.

Figure 2(a-d) illustrate the pronounced effects of decreasing pH by addition of acetic and hydrochloric acid. Entirely similar results were obtained with additions of ammonium, sodium and potassium chloride. Of the other co-solutes tried, sodium hydroxide as well as sodium and ammonium acetates had very little effect on the cluster ion currents. We as yet have no unifying rational for this behaviour and plan further experiments with additional co-solute species over a wider range of conditions.

Reference: (1) C. M. Whitehouse, R. N. Dreyer, M. Yamashita and J. B. Fenn, Anal. Chem. 57, 675, (1985)

Acknowledgement: This work was supported by the National Institutes of Health under Grant 5 R01 GM31660-03.

Presented at the 35th ASMS Conference on Mass Spectrometry and Allied Topics
May 24-29, 1987, Denver, CO

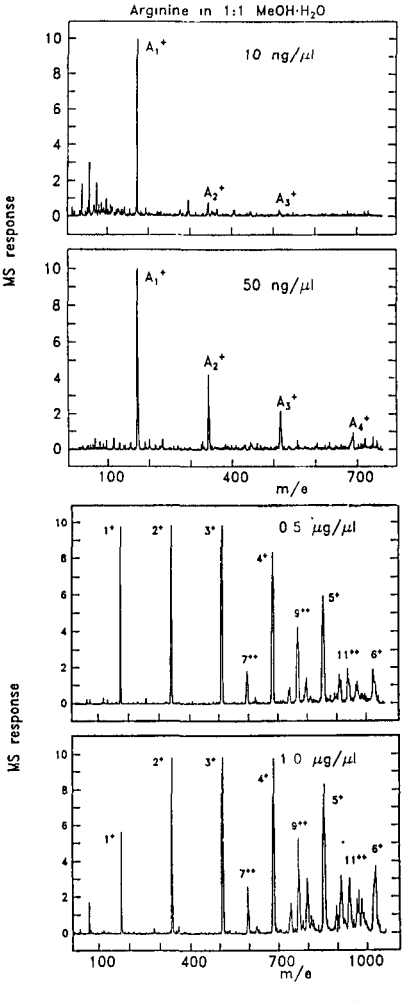

Figure 1 a - d (top to bottom). Dependence of clustering on concentration of arginine in solution.

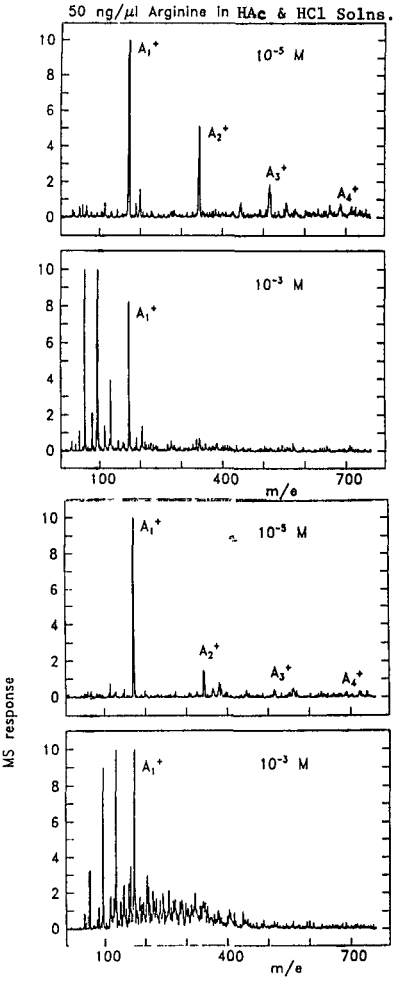

Figure 2, a - d (top to Bottom) Dependence of arginine clustering on solution acidity. The upper frames, a and b, are for acetic acid, the lower frames, c and d, are for HCl.

Presented at the 35th ASMS Conference on Mass Spectrometry and Allied Topics
May 24-29, 1987, Denver, CO

Multiphoton Ionization of Cyclic Ketones: Conformational Studies of Ground State Structures

Timothy J. Cornish and Tomas Baer
University of North Carolina
Chapel Hill, N. Carolina

The 2-photon excitation of the 3s Rydberg state of cyclic ketones and their methylated isomers have been investigated by resonance enhanced multiphoton ionization (REMPI). A pulsed and seeded molecular beam of cold sample gas is crossed with a pulsed laser beam from an excimer pumped dye laser. As the laser is scanned, the total ionization signal is monitored at constant intensity as a function of wavelength. Spectra in the region of 380 to 420 nm were obtained at sufficient resolution (< 1 cm^{-1}) to allow identification of some rotational contours.

Figure 1 plots the n->3s Rydberg spectra of the 8 to 5 membered unsubstituted cyclic ketones along with bicyclic norcamphor. The transition energy of the 3s transition gradually decreases with decreasing ring size. This trend is reversed from the corresponding ordering of the ionization potentials and is found to relate closely to the decreasing carbonyl C-CO-C bond angle of the smaller rings. It is also interesting to note that the n->3s transition of acetone (though not pictured here) occurs at approximately the same energy as that of cycloheptanone which suggests that these 2 chromophores are equivalent while the other transition energies are perturbed by ring strain.

Methylation at various ring positions of cyclohexanone (Figures 2 and 3) shift the electronic transition energy depending upon the location and orientation of the methyl group. This n->3s transition energy is highly sensitive to alkyl substitution apparently because of extensive delocalization of the lone-pair wavefunction throughout the ring. While equatorial substitution at C4 has little effect on the transition energy, C3 substitution affects the energy substantially. Equatorial substitution at this position lowers the ground state energy while axial substitution raises it. This results in a shift of the transition to higher and lower energy respectively. Dimethyl isomers oriented cis and trans to each other relative to the ring plane are therefore separated in energy corresponding to the extent of ground state non-bonded interactions. While the 3- and 4- methyl isomers exhibit a strong origin peak indicating little geometric rearrangement in the excited state, the 2-methyl (and 2-ethyl) isomers show extensive splitting in the 3s spectrum. We conclude that repulsions between the carbonyl oxygen and the adjacent equatorial methyl cause the ring to flip upon electronic excitation. This reorientation excites the lowest energy ring bending mode (100 cm^{-1}) and produces a large Franck-Condon envelope. The repulsive potential is also evident from the shift of the 3s transition to lower energy indicating a destablization of the ground state.

The same trends are observed in the methyl substituted cyclopentanone isomers (Figure 4). That is, 3-methyl substitution shifts the transition origin to higher energy while 2-methyl substitution lowers the energy though the magnitudes of the displacements are different than those in the 6 membered rings. Cis and trans isomers are again separated in energy according to conformational interactions.

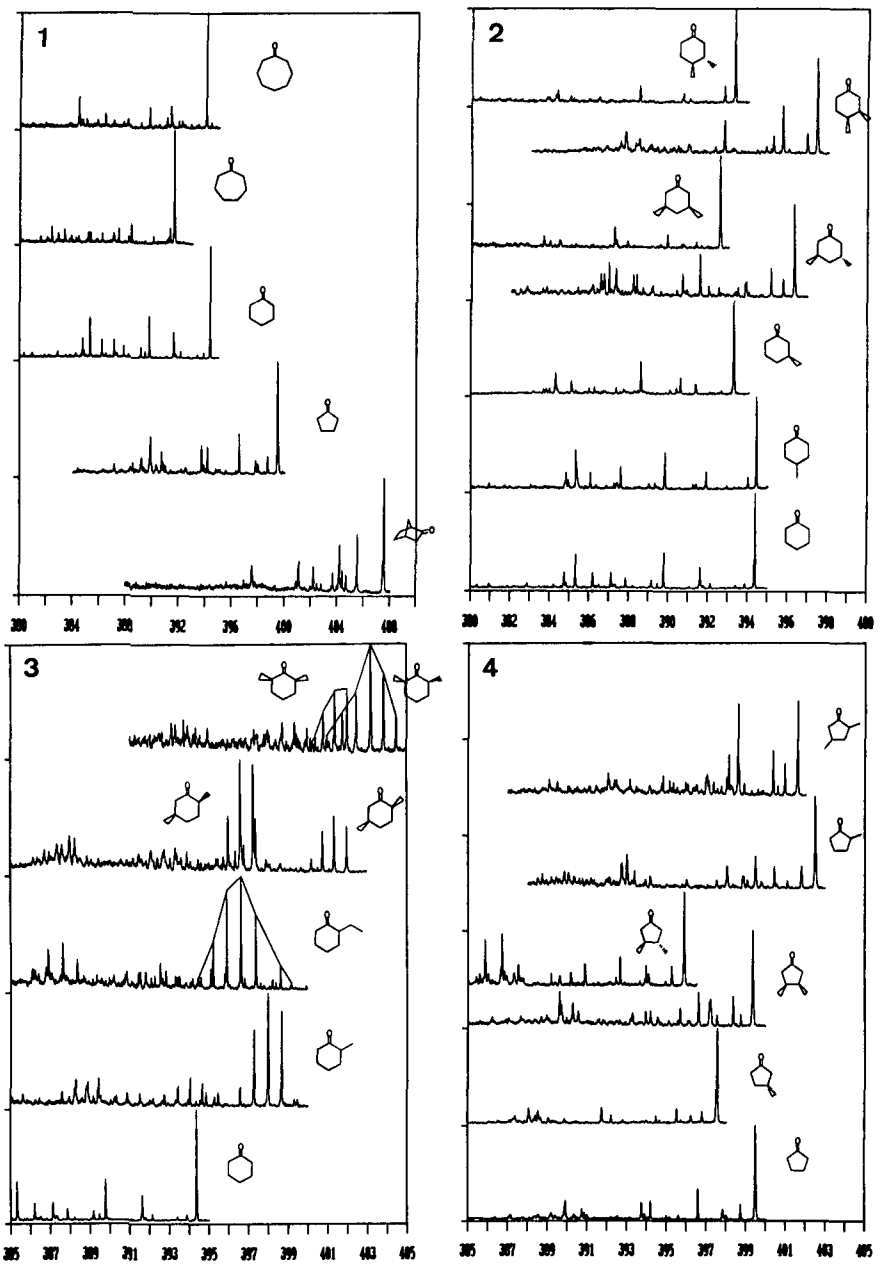

2+1 REMPI n-3s spectra of cyclic ketones and their methylated isomers

Presented at the 35th ASMS Conference on Mass Spectrometry and Allied Topics
May 24-29, 1987, Denver, CO

DESORPTION AND IONIZATION METHODS FOR FOURIER TRANSFORM MASS SPECTROMETRY

J. A. Loo, E. R. Williams, J. J. P. Furlong, B. H. Wang, and F. W. McLafferty
Chemistry Department, Cornell University, Ithaca, NY 14853-1301

Fourier transform mass spectrometry (FTMS) enjoys several advantages for the analysis of high molecular weight compounds, which include simultaneous ion detection over a wide mass range, relatively high mass resolution, and MS/MS capabilities. Plasma desorption (PD) induced by the 100 MeV fission fragments of Cf-252 has produced molecular ion species from trypsin, MW 23,463, on time-of-flight instruments [1]. As shown by Tabet et al. [2], an obvious marriage with high potential is the PD/FTMS system. Sample foils placed over a 50 μCi Cf-252 source on the end of a direct probe are inserted into the prototype Nicolet dual-cell FTMS-2000 with a 2.86 T superconducting magnet. Samples are either mixed with glutathione and electrosprayed directly onto the aluminized mylar foil or adsorbed onto a nitrocellulose layer on the foil. Ion collection times of 1-2 minutes and the elimination of the cell ion quenching event dramatically increase the sensitivity as well as the molecular ion relative abundance. Repeated measurement cycles up to a total time of 14 hours predictably improve the S/N but also enhance the relative abundance of the molecular ion. Internal mounting of the source perpendicular to the magnetic field lines allows for both front-side and back-side sample desorption. A variety of biological compounds (bradykinin, substance P, vitamin B_{12}, angiotensin I, neurotensin, gramicidin D, alamethicin) and a microlithography electron-beam resist (poly(butene-1 sulfone)) yield spectra with useful structural information. Gramicidin S (Fig. 1) and chlorophyll a produced dimer as well as molecular ion species under certain sample preparation conditions.

Another useful desorption/ionization technique is ion bombardment SIMS. Previous results from Cs^+ SIMS/FTMS [3] suggest the use of a higher energy primary ion beam to increase molecular ion yields. To produce a higher kinetic energy beam, 40 keV Ta^{4+} ions can be generated by a MicroMEVVA (Metal-vapor Vacuum Arc) ion source [4]. Preliminary data show the production of $(TaH_n)^{m+}$ (n=1-3,5; m=1-4) and larger ion-molecule products and desorption of CsI.

UV (ArF 193 nm) laser desorption, photoionization, and photodissociation studies were performed using a Lambda Physik EMG 101 excimer laser. Back-side desorption is done with a 14 ns single pulse through a hollow direct probe and power density of 5×10^{-7} W/cm^2. Samples are electrosprayed onto thin stainless steel or nickel mesh (transmittance ~40%) and secured on the end of the hollow probe. Spectra of a variety of peptides have been obtained, resulting in both soft ionization and good S/N. CAD (Fig. 2) and photodissociation of laser desorbed and PD produced ions are possible with our experimental setup. Thus, the UV excimer laser appears to be a much more versatile replacement for the IR CO_2 laser conventionally used with FTMS.

Because electronic-vibrational transition energies are highly sensitive to small changes in molecular structure, many compounds whose EI spectra are similar can be differentiated by photodissociation/photoionization. Even without the selectivity of a tunable laser and the increased spectral resolution obtained in a supersonic expansion, isomers such as toluene/cycloheptatriene and alpha-fluorotoluene/p-fluorotoluene show very different MPI spectra. Selectivity is observed in both the fragmentation pathways, as well as the relative ionization efficiencies. Results obtained with photodissociation of EI generated ions [5] demonstrate the selective fragmentation expected from high internal energy deposited into an ion in a narrow range. Figure 3 shows the selective and complementary fragmentation of photoionization and photodissociation of acetophenone.

Presented at the 35th ASMS Conference on Mass Spectrometry and Allied Topics
May 24-29, 1987, Denver, CO

[1] Sundqvist, B.; Roepstorff, P.; Fohlman, J.; Hedin, A.; Hakansson, P.; Kamensky, I.; Lindberg, M.; Salehpour, M.; Sawe, G. Science 1984, 226, 696-698.
[2] Tabet, J.-C.; Rapin, J.; Poretti, M.; Gaumann, T. Chimia 1986, 40, 169-171.
[3] Amster, I.J.; Loo, J.A.; Furlong, J.J.P.; McLafferty, F.W. Anal. Chem. 1987, 59, 313-317.
[4] Brown, I.G.; Galvin, J.E.; MacGill, R.A.; Wright, R.T. Appl Phys. Lett. 1986, 49, 1019-1021.
[5] Bowers, W.D.; Delbert, S.-S.; McIver, R.T., Jr. Anal. Chem. 1986, 54, 969-972.

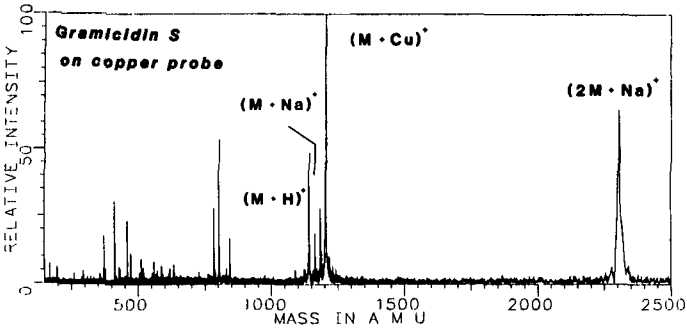

Figure 1

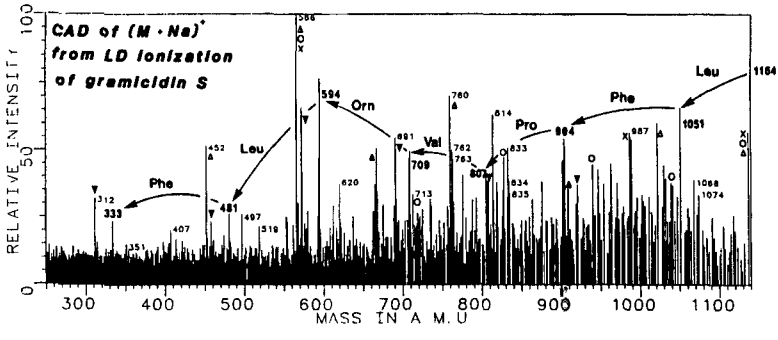

Figure 2

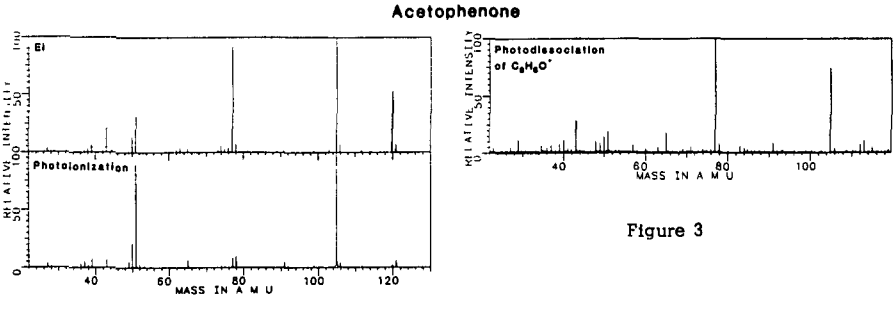

Figure 3

Presented at the 35th ASMS Conference on Mass Spectrometry and Allied Topics
May 24-29, 1987, Denver, CO

DERIVATIZATION OF PEPTIDES FOR MULTIPHOTON IONIZATION-FOURIER TRANSFORM MASS SPECTROMETRY

R. P. Grese
MCMS-Dept. of Chemistry
University of Nebraska
Lincoln, NE 68588

Multiphoton ionization and negative ion mass spectrometry of derivatized peptides offer strategies for improving detection limits making mass spectrometry more compatible with other biochemical techniques. Two derivatization methods have been investigated to improve the sensitivity of FTMS analysis of amino acids and peptides.

Derivatization methods that incorporate naphthalene moieties into amino acids or peptides are attractive because picomolar detection limits were previously achieved with MPI-FTMS naphthalene (1). Protection of the N-terminus by a naphthoyl group may be one method to permit MPI-FTMS analysis of a peptide. This method suffers from the involatility and thermal instability of the derivatives. The M+H ion in the spectrum of naphthoyl isoleucine methyl ester may be caused by the increased cell pressure from the heating this derivative required for volatilization. A two step laser desorption/multiphoton ionization method similar to Engelke (2) and Grotemeyer (3) may be advantageous for these derivatives.

An alternative method for the FTMS analysis of small peptides is the sequential chemical degradation by reaction with 1,2-naphthoquinone (4). The reaction is similar to the Edman degradation and sequentially cleaves off the N-terminal amino acid giving a naphthoxazoline, I, with the side chain of the amino acid in the 3-position. The reaction with the C-terminus or free amino acids gives a naphthoxazole, II.

The positive ion MPI spectrum of "leucine-naphthoxazole" consists principally of the molecular ion, however fragment ions resulting from cleavages of the alkyl side chain are also observed. The positive ion MPI spectrum of "leucine-naphthoxazoline" indicates that the cross-section for absorption at 266nm is lower than the corresponding naphthoxazole. No molecular ion is observed, and the largest ion is the loss of CO to give the naphthoxazole (5). In the negative ion mode a large increase in sensitivity is observed for I. The mechanism of negative ion formation is proposed to be electron capture of photoelectrons emitted from the metal surface of the FTMS cell. The naphthoxazoles give no negative ions with these conditions.

A strategy for sequencing small peptides can be devised using this method. The method is illustrated using the tripeptide Ala-Leu-Gly. 1) The peptide is degraded using a reagent ratio of 2:1, which gives the N-terminal residue in the negative ion mode. 2) The peptide is further degraded using a 20:1 reagent ratio. The negative ion spectrum now gives both the N-terminus and the second amino acid residues. 3) The C-terminus is deduced from the positive ion spectrum. The capability of rapidly switching between positive and negative ion modes in FTMS is crucial for this method.

The FTMS cell can be used to store electrons (6). Several experiments were performed to investigate the optimum conditions for producing negative ions by laser produced photoelectrons. The issues addressed were the relationship of ion intensity versus laser wavelength, laser energy, delay time between laser and excitation, and trap voltage. These results are given in Figures 1-3. No signal was observed when 532nm light was used.

The relationship of ion intensity versus electron energy is plotted in Figure 4. This plot resembles the study of hexafluorobenzene by charge exchange with I- (7).

Future work will include determination of detection limits of I and II by positive and negative ion modes, application of this method to other amino acids, application to GC/MS, and further study of negative ion formation.

Acknowledgment: This research was conducted under the direction of M.L. Gross.

Presented at the 35th ASMS Conference on Mass Spectrometry and Allied Topics
May 24-29, 1987, Denver, CO

References:

(1) T.M. Sack, D.A. McCrery, and M.L. Gross, Anal. Chem., 57, 1291 (1985).
(2) F. Engelke, J.H. Hahn, W. Henke, and R.N. Zare, Anal. Chem., 59, 909 (1987).
(3) J. Grotemeyer, U. Boesl, K. Walter, and E.W. Schlag, Org. Mass Spectrom., 21, 645 (1986).
(4) K. Jayasimhulu and R.A. Day, Biomed. Mass Spectrom., 7, 7 (1980).
(5) W. Reichen, Helv. Chim. Acta, 60, 186 (1977).
(6) E.B. Ledford, Jr., D.L. Rempel, and M.L. Gross, Int. J. of Mass Spectrom. and Ion Proc., 55, 143 (1983).
(7) C. Lifshitz, T.O. Tiernan, and B.M. Hughes, J. Chem. Phys., 59, 3182 (1973).

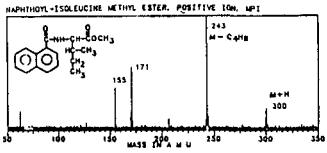

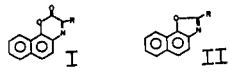

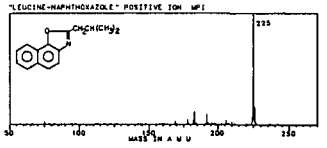

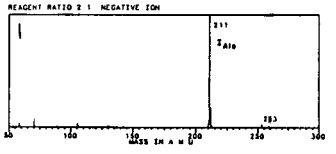

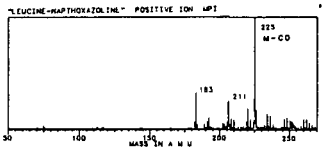

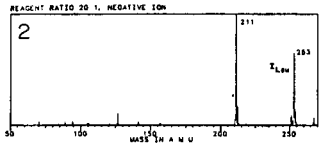

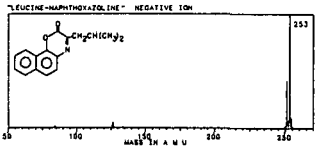

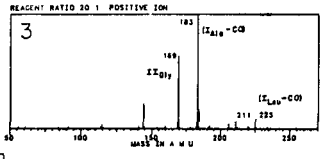

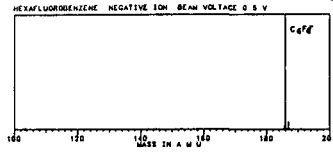

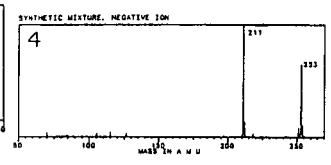

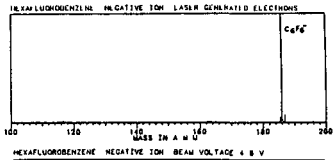

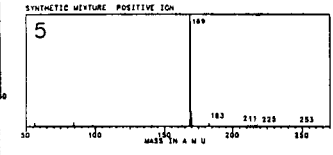

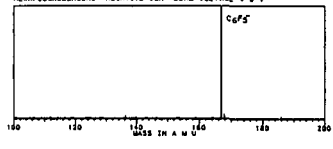

Figure 1 - Intensity of $C_6F_6^-$ versus Laser Energy

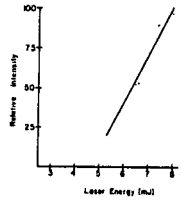

Figure 2 - Intensity of $C_6F_6^-$ versus Delay time

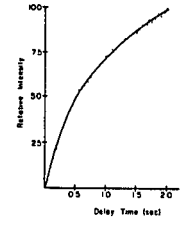

Figure 3 - Intensity of $C_6F_6^-$ versus Trap voltage

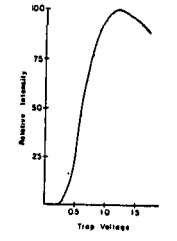

Figure 4 - Intensity of $C_6F_6^-$ and $C_6F_5^-$ versus Beam Voltage

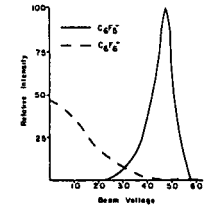

Presented at the 35th ASMS Conference on Mass Spectrometry and Allied Topics
May 24-29, 1987, Denver, CO

BIASED ELECTRON ATTACHMENT MASS SPECTROMETRY (BEAMS): ANALYSIS OF PERFLUOROCARBONS

Ripudaman Malhotra, Gilbert A. St.John, and Michael J. Coggiola
Mass Spectrometry Program, SRI International, Menlo Park, CA 94025.

INTRODUCTION

We routinely use field ionization mass spectrometry (FIMS) for the analysis of complex mixtures of hydrocarbons such as fossil fuels. For most hydrocarbons the technique produces the molecular ions only, thereby simplifying the analysis.[1] However, materials containing strong electron-withdrawing groups do not field ionize efficiently and often field ionization results in extensive fragmentation of such molecules. For example, we have not been successful in obtaining strong signals from PCBs and other polychlorinated aromatics or nitroaliphatics. On the other hand, these materials are prone to accepting electrons to give negative ions. Anbar and St.John have shown the feasibility of inverting the polarity of field desorption and field ionization source to produce negative ions from a variety of inorganic and organic materials.[2,3] For organic molecules, they also noted substantial amount of fragment ion peaks as well as the parent ion.[3] The objective of the present study was to further explore the production of negative ions by attaching electrons to the molecules while minimizing dissociations and use the technique for analyzing a complex mixture of perfluorocarbons in much the same way as we analyze hydrocarbons, that is, in terms of z-series.

DESCRIPTION OF THE MASS SPECTROMETER

The mass spectrometer used for this study consists of an activated metal foil field ionizer interfaced with a 60° magnetic sector mass analyzer, ion-counting electronics, and a PDP 11/23 computer for data acquisition and analysis. We reversed the polarity of the field ionization source and made the activated metal foil the cathode and the counter electrode, which is placed 80 µm downstream, the anode. We also reversed the polarity of the magnetic sector analyzer and in order to detect negative ions the slit and the entry cone of the multiplier were set at ground potential. The electron collector of the multiplier was set +2500 V. The signal was capacitatively coupled to the ion-counting electronics.

We have been able to analyze the negative ions from several different kinds of materials such as perfluorocarbons and nitroaromatics. Dissociative attachment is minimized by biasing the cathode, and hence the name of the technique: Biased Electron Attachment Mass Spectrometry or BEAMS. Typically, we applied a potential difference of 800 to 1200 V between the cathode and the anode, corresponding to field strengths on the order of 10^7 V/m. However, due to the curvature of the emitters, the local field strengths were probably a few orders of magnitude greater.

RESULTS

A mixture of perfluorocycloalkanes[4] was analyzed by BEAMS and also by negative CI on a Ribermag 1010C spectrometer using NH_3 as reagent gas. The nominal molecular masses were used to calculate possible elemental compositions (C_nF_{2n+z}). With hydrocarbons, only 14 series (z = +2 to -11) can be identified at nominal masss; more highly unsaturated series overlap with one of these series. With fluorocarbons, nominal mass information can be used to identify 50 series (CF_2 = 50 daltons).

The BEA-mass spectrum of the particular sample we analyzed shows two series of peaks separated by 19 daltons (Figure 1). The more prominent series is of even molar masses and is probably due to parent ions. The peak

intensities follow a gaussian distribution and they all correspond to fluorocarbons with 28 carbons and varying degress of unsaturation. The odd-mass peaks correspond to $[M - F]^-$ ions. The intensity of the [M + 1] peaks is largely due to ^{13}C. The negative CI mass spectrum of the sample shows the odd-mass ions ([M ± F]) to be more intense (Figure 2). Furthermore, there is substantial amount of fragmentation, as judged by ions at lower molecual weights, including an intense signal at m/z 605 (not shown in Figure 2). We also attempted analysis of a similar mixture under field ionization (positive) conditions. Over 60% of the signal was formed due to CF_3^+, $C_2F_5^+$, and $C_3F_7^+$ fragment ions.

Acknowledgement. We wish to express our thanks to Dr. David W. Thomas of SRI International for his help in obtaining the negative CI-spectra.

REFERENCES

1. G. A. St.John, S. E. Buttrill, Jr., and M. Anbar, in "Organic Chemistry of Coal," Editor, J. Larsen, Am. Chem. Soc. Symposium Series 71, Washington D.C., 1978, p. 223.
2. M. Anbar and G. A. St.John, J. Am Chem. Soc., 1975, 97, 7195.
3. M. Anbar and G. A. St.John, Science, 1975, 190, 781.

4. The sample is a propietary material known to contain perfluorinated cycloalkanes.

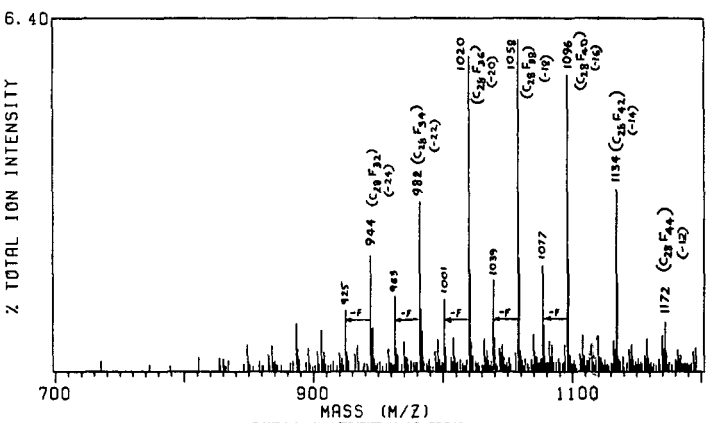

FIGURE 1. BIASED ELECTRON ATTACHMENT MASS SPECTRUM OF A MIXTURE OF PERFLUOROCYCLOALKANES.

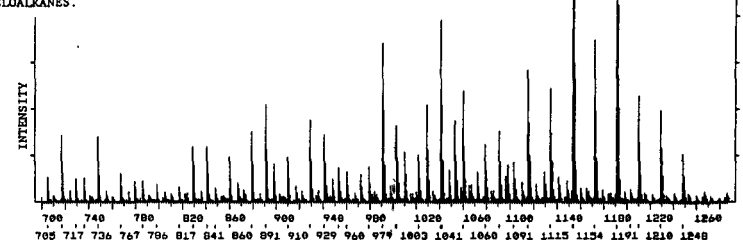

FIGURE 2. NEGATIVE CI MASS SPECTRUM OF A MIXTURE OF THE SAME SAMPLE

Presented at the 35th ASMS Conference on Mass Spectrometry and Allied Topics
May 24-29, 1987, Denver, CO

K^+ IONIZATION OF DESORBED SPECIES (K^+IDS) - THE DEPENDENCE OF STRUCTURAL AND MOLECULAR WEIGHT INFORMATION OBTAINED ON THE TEMPERATURE VARIABLE,

Karen J. Light, Daniel B. Kassel, John Allison, Department of Chemistry, Michigan State University, East Lansing, MI 48824

Recently, a new desorption/ionization (DI) technique called K^+IDS (K^+ Ionization of Desorbed Species) has been described (1,2). This technique utilizes thermionic emitters composed of an alkali-aluminosilicate which, when heated, emits metal ions such as K^+. Such an emitter, built onto the end of a simple probe, can be inserted into the ion source of a mass spectrometer. If a nonvolatile analyte is deposited onto the emitter surface, and the temperature is rapidly increased, molecules can desorb intact into the gas phase, where they form adducts with K^+, which is emitted from the surface as well. Recently, a "two filament" design has been employed, in which the analyte is placed on a separate support that is in close proximity to the K^+ source. This separation provides a better overlap between the analyte desorption and K^+ emission profiles, such that K^+ ions are available at the same time that desorbed species are abundant in the gas phase.

We believe that K^+IDS offers advantages over other DI methods. No matrix is required. It is simple to implement; no instrument modifications are required. The technique is essentially "universal", yielding spectra for all compounds studied to date. One feature that we are currently pursuing is the temperature/time dependent nature of the observed spectra. Two types of behavior have been investigated. The first concerns the final temperature to which the emitter is stepped (in the 800-1200°C range). If the final temperature is below that at which desorption rates exceed decomposition rates, only K^+ adducts of thermal degradation products are observed. Higher temperatures may lead to desorption of the intact molecules. Thus, depending on whether molecular weight or structural information is required, the experiment may be designed to produce the desired spectra. While this expected behavior is observed for some molecules, our general observation is that the probability of observing desorption-only for the intact analyte decreases as the size, structural complexity and number of functional groups present increases.

A second feature that we have found more useful is the mass spectral variations within a run. If a thermally labile organic sample is rapidly heated, and the gases above the sample are being monitored, one might expect the following: as the temperature rises, thermal degradation products are first formed. A temperature may be achieved at which degradation <u>and</u> intact analyte desorption may occur. At long times, degradation of molecules may again dominate for long-lived surface-bound molecules. Typically a smooth transition is observed between these phases, in which various types of decomposition products exhibit unique temporal profiles. We believe that this is an aspect of the experiment that can be exploited to yield further structural information. Work is currently underway to determine why the temporal trends in thermal degradation pathways occur. These variations appear to be due to a combination of temperature-dependent processes including the energetics of the degradation and desorption processes.

In-run variations are presented for the cardiac glycosides ouabain, digitonin, digoxin and digoxigenin. These compounds contain a saccharide chain and a steroid moiety. The K^+IDS spectra contain K^+ adducts of thermal degradation products resulting from 1,2-eliminations about the various glycosidic linkages. At certain times within the run, ions due to the steroid are also observed. Thus, the observation of these ions, coupled to their unique temporal behavior, becomes a useful indicator of the various structural features. Work is underway to determine how these variations can be further exploited. Below are two K^+IDS spectra

of digoxigenin, ($C_{23}H_{34}O_5$) showing within-run variations. The K^+ adduct of the molecule is seen at m/z 429. In Figure b, the low mass ions all come from the steroid group in the molecule.

1. D. Bombick, J.D. Pinkston, J. Allison, Anal. Chem., 1984, 56, 396.
2. D. Bombick, J. Allison, Anal. Chem., 1987, 59, 458.

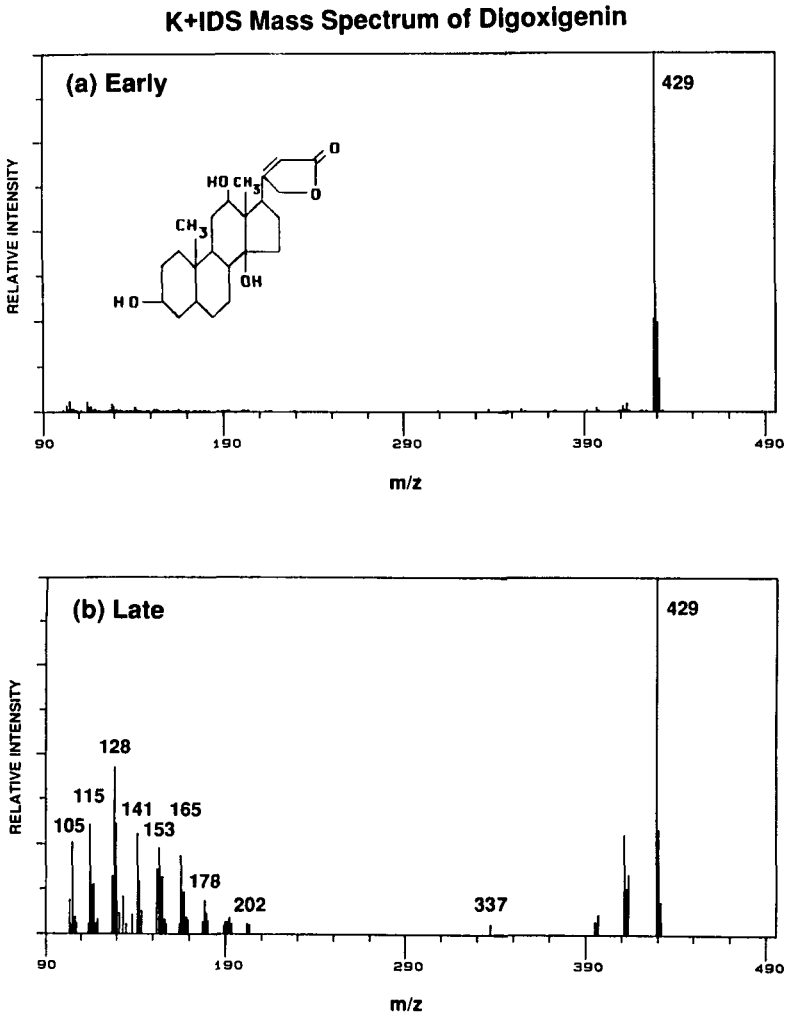

Presented at the 35th ASMS Conference on Mass Spectrometry and Allied Topics
May 24-29, 1987, Denver, CO

DESORPTION MECHANISMS USING A NEW LIQUID-SIMS-TOF MASS SPECTROMETER

James K. Olthoff, Ihor Lys, and Robert J. Cotter
Johns Hopkins University, Baltimore, MD 21205

A time-of-flight mass spectrometer has been constructed which utilizes time-lag focusing techniques introduced by Wiley and McLaren. The flight tube is short (approx. 60 cm) for improved sensitivity. New pulse electronics have been developed which produce fast (<20 ns rise times) ion extraction pulses for improved resolution. Ion detection is performed using a dual channel plate with 12 kV postacceleration. Pulsed deflection plates, which selectively deflect low mass ions, have been installed to prevent detector saturation.

Desorption ionization from solid or liquid samples is induced by keV Xenon ions from a Kratos Minibeam I ion gun. The ion gun electronics have been modified to produce either a high flux (>1 ua) continuous beam, or primary ion pulses with widths varying from 0 to 10 usec. Following the primary ion pulse, secondary ions are extracted into the flight tube by a combination of pulses on the backing plate and the drawout and acceleration grids. The time delay between the ionization and extraction pulses is variable from 0 to 50 usec to allow "time-lag focusing" or additional fragmentation time.

Data is collected, digitized, summed and averaged by a LeCroy 3500 SA signal averaging system. Generally, 1000 to 10000 spectra are summed.

A schematic diagram of the instrument is shown below.

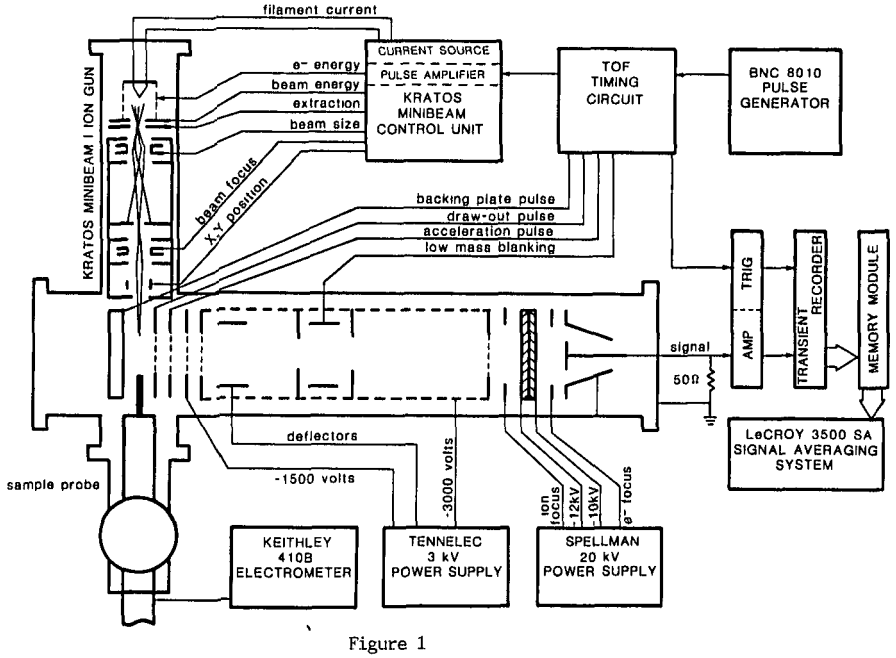

Figure 1

We have used the capability of the instrument to vary the frequency of the primary ion pulses to study the repair mechanisms of the liquid matrix. In most instances, the intensity of secondary ions decreases with increasing primary ion frequency (Figures 2 and 3). This "memory effect" implies that sample repair from one pulse may not be complete before the next primary ion pulse strikes the sample. The rate of sample repair may be effected by convection, migration, diffusion, or chemical damage of the sample. However, note that for pure glycerol (where sample and matrix are the same) no frequency dependence is observed (Figure 4).

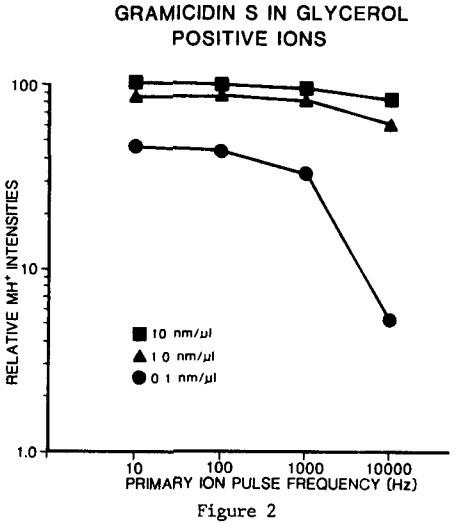

Figure 2

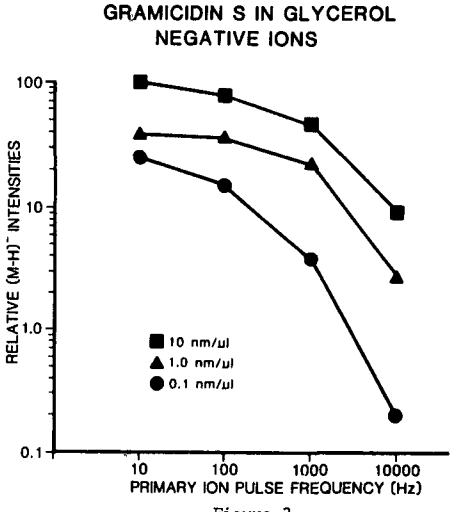

Figure 3

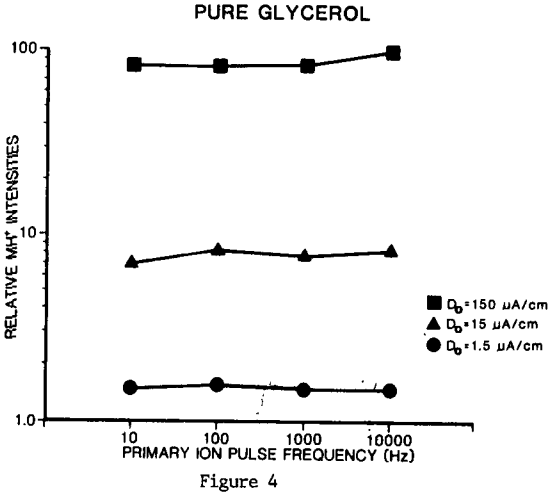

Figure 4

Presented at the 35th ASMS Conference on Mass Spectrometry and Allied Topics
May 24-29, 1987, Denver, CO

FOCUSED, RASTERABLE, HIGH ENERGY NEUTRAL MOLECULAR BEAM PROBE FOR SIMS

Anthony D. Appelhans, James E. Delmore, and David A. Dahl
Idaho National Engineering Laboratory
EG&G Idaho, POB 1625 Idaho Falls, ID 83415 (208) 526-2820

A variety of ion and neutral atom sources have been developed for Secondary Ion Mass Spectrometry (SIMS) and Fast Atom Bombardment Mass Spectrometry (FABMS) ranging from micrometer-dimensioned ion beams capable of imaging to a variety of schemes for producing broad, unfocused beams of neutral atoms. However, one area that has seen little development is that of focused (as opposed to collimated), rasterable neutral atom/molecule beams.

We have produced such a beam by applying a unique neutralization mechanism: autoneutralization, the spontaneous ejection of an electron from an anion leaving a neutral molecule. Earlier studies have shown that there are several autoneutralizing excited states of SF_6^- that undergo the second step of the following sequence:

$$SF_6 + e^- \text{ ----> } SF_6^{-*} \text{ --}^{k}\text{--> } SF_6 + e^- \qquad [1$$

where 1/k, the mean lifetime, is 10-20 microseconds. This makes it possible to focus and accelerate the SF_6^- ions prior to autoneutralization and still achieve adequate neutralization within a reasonable length flight tube (~18 cm). The small mass of the ejected electron relative to SF_6 permits the molecules to maintain focus as neutralization occurs.

We have produced a cylindrically focused near-parallel beam of ~0.5 mm diameter (at 2.5 m from the source) with a divergence angle of ~0.01 degrees, rasterable in the y and z directions. This beam has been used to sputter secondary ions from bulk samples (~1 cm square by 0.5-2 mm thick) of Teflon, Mylar and Acrylic polymers (all highly insulating) that historically have been difficult to analyze via SIMS [1]. While previous SIMS measurements [2-4] of these types of insulating materials have employed some type of sample-surface charge neutralization (e.g. electron flood guns or conductive grids) to overcome surface charging problems we found this unnecessary with the SF_6 neutral beam. The secondary ion quadrupole mass spectrometer was operated with a channeltron multiplier in the analog mode that was calibrated against an integral Faraday cup. Typical primary neutral beam currents were 10^{-12} to 10^{-11} (amp-equivalent) and the quadrupole signals were 10^{-15} to 10^{-14} amps. Source housing pressure was 2 X 10^{-6} Torr or lower resulting in sample housing pressures in the low 10^{-7} Torr range.

Figures 1 and 2 show spectra of Teflon, and Mylar produced with the neutral SF_6 beam. The only change necessary to acquire the spectra from one sample type to another was to slightly refocus the SIMS extractor lens. The spectra agree qualitatively with previously published spectra [2], showing no obvious influence of the SF_6 components on the spectra. Comparing the results of Figures 1 and 2 with previously published data [2-4] it appears the SF_6 beam is doing an excellent job of producing secondary ions at very low primary beam fluxes. Typical primary beam currents employed in the previous studies [2-4] with atomic ion beams were 10^{-9} amps/cm^2 or higher, and the secondary ion yields, defined as the ratio of secondary ion peak intensity (ions/s) to the primary beam intensity (ions or neutrals/s), were in the 10^{-7} to 10^{-6} range. The SF_6 primary beam secondary ion yields (at a flux of ~10^{-11}) were in the 10^{-3} range for the major peaks of equivalent materials. The SF_6 beam appears to produce three to four orders of magnitude more intense secondary ion yields than equivalent-energy atomic (charged or neutral) beams. This comparison is hampered somewhat by the differences in experimental apparatus and procedures applied by the various groups, and we plan to directly compare the performance of an atomic beam with the SF_6 beam in our apparatus in the future. However, the current evidence strongly suggests that the SF_6 beam, although composed of 7-atom molecules with lower per-atom-momenta than commonly used atomic (Ar, Xe) beams, is unexpectedly efficient at sputtering secondary ions from these polymer surfaces.

A reasonable length neutralization distance (~18 cm) is sufficient to achieve adequate neutral beam intensity, making it straight forward to add the source to existing systems with only minor modifications (if a suitable vacuum port is available). The source imposes low gas loads on the sample chamber and is simple to operate. In addition to the

obvious applications of a focused neutral beam for conventional SIMS and FABMS, such a beam has significant potential application in Fourier Transform Ion Cyclotron Resonance (FTICR) SIMS. Current commercial FAB sources do not have sufficiently fine focusing for such applications and the high gas load imposed by charge-exchange neutralization cells is unacceptable. We are currently designing a SF_6 source to operate on a double focusing magnetic mass spectrometer and also plan to install and test a source on an FTICR.

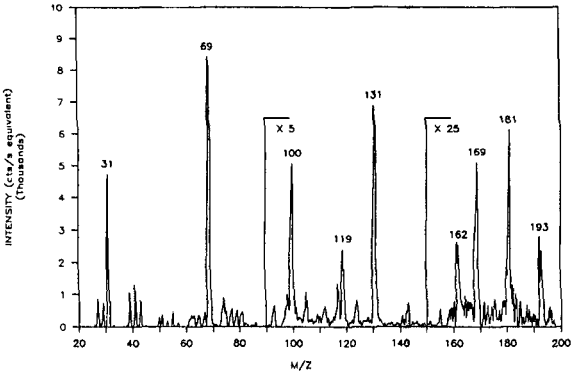

Figure 1. SIMS spectrum of bulk Teflon, 3 keV neutral SF_6 beam, ~1 picoamp neutral equivalent current.

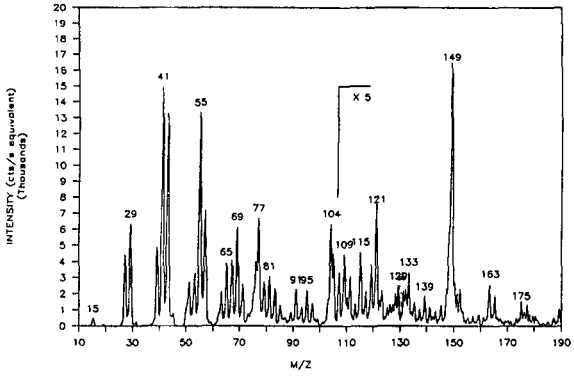

Figure 2. SIMS spectra of bulk Mylar sheet, 17 keV neutral SF_6, 5 X 10^{-11} amp-equivalent/cm^2, 0.02 cm^2 beam.

(1) Appelhans,A.D., Delmore, J.E., and Dahl,D.A. Anal. Chem., in press.
(2) Briggs,D. Surf. Interface Anal. 1982, vol 4, 151-155.
(3) Briggs,D., Hearn, M.J., Ratner, B D. Surf. Int. Anal. 1984, vol 6, 184-192.
(4) Brown,A., van den Berg,J.A., Vickerman,J.C. Spectr. Acta., 1985, vol 40B, 871-877.

Work supported by the U.S. Department of Energy INEL internal research funds and by the Office of Health and Environmental Research, Office of Energy Research, DOE under contract 4AA901.

Presented at the 35th ASMS Conference on Mass Spectrometry and Allied Topics
May 24-29, 1987, Denver, CO

Stereochemical Effects in the Ammonia Chemical Ionization Spectra of Isomeric Allylic Alcohols

Marbury, G.D., Northrop Services, Inc. and Guenat, C., NIEHS, Res. Triangle Pk., N.C. 27709;
Zoretic P.A., Dept. of Chemistry, ECU, Greenville, N.C. 27834
Chambers, R.J., Pfizer Inc., Groton, Ct.; and Tabet, J.C., Service Central d'Analyse, Vernaison, France

Four diastereomer pairs of secondary allylic alcohols were synthesized to allow study of relationships between conformation and chemical ionization spectra using well characterized reference materials. The ammonia chemical ionization (CI) spectra of isomers of octahydro-8a,b-carbomethoxy-7, 7-ethylenedioxy-hydroxynapthal-enes (M.Wt.=268) were compared at 0.4E-5 mbar and 3E-4 mbar reagent gas pressure. Relative intensities of $[M+NH4]^+$ (m/z 286), $[M+NH4-H2O]^+$ (MsH^+,m/z 268), $[M+NH4-NH3]^+$ (MH^+, m/z 269), and $[M+NH4-H2O-NH3]^+$ (m/z 251) were found to be a function of conformation and reagent gas pressure. Cis- and trans-isomers in which carbomethoxy and hydroxy groups were positioned two carbons apart on the same side of the hydronapthyl ring favored stabilization of the $[M+NH4]^+$ and $[MH]^+$ ions via intramolecular hydrogen bonding (Fig. 1), whereas epimers having the two groups positioned across the bridgehead carbons favored formation of the MsH^+ ion with subsequent loss of NH3 to form m/z 251 (Fig. 2). When the functional groups were separated by four carbon atoms, stabilization of $[M+NH4]^+$ was found to be greater in the cis- isomers. Higher reagent pressure favored greater $[M+NH4]^+$ formation in cis- isomers than in trans- isomers.

In the case of 3-hydroxy isomers, systems having a delta-4, 4a double bond produced a substitution product (MsH^+), whereas a delta 1, 2 configuration did not (Fig. 3). We hypothesize that the ability to form an allylic stabilized carbocation at or hear a tertiary center favors substitution to form the MsH^+ ion in these compounds.

The spectra were acquired on a V.G 7070, with source temperature at 150°C and 200 mA emission current, using direct probe introduction.

1.

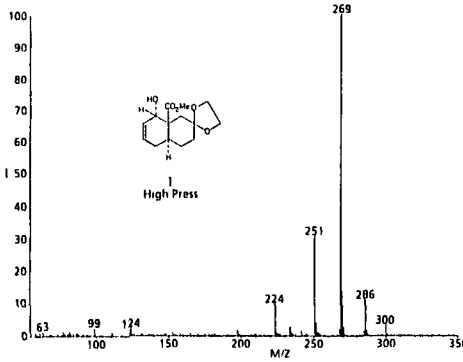

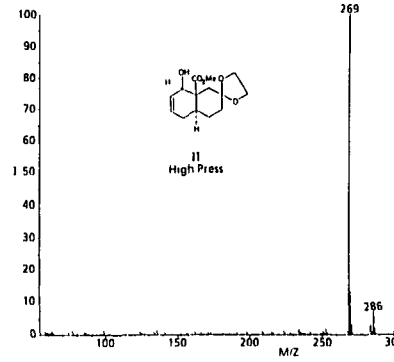

2.

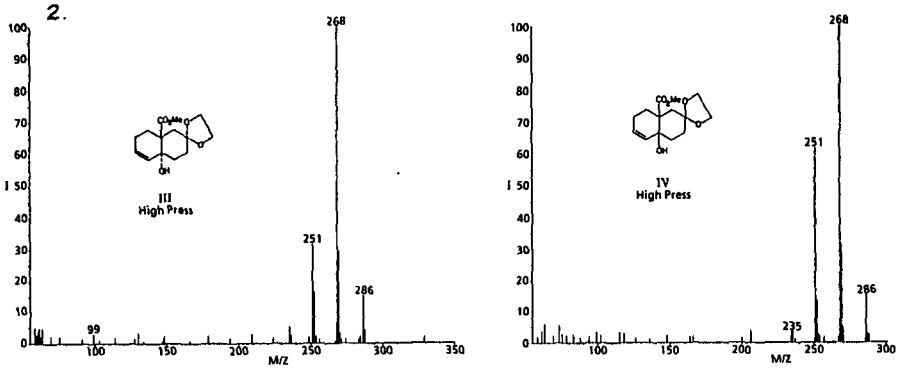
III
High Press
IV
High Press
M/Z

3.

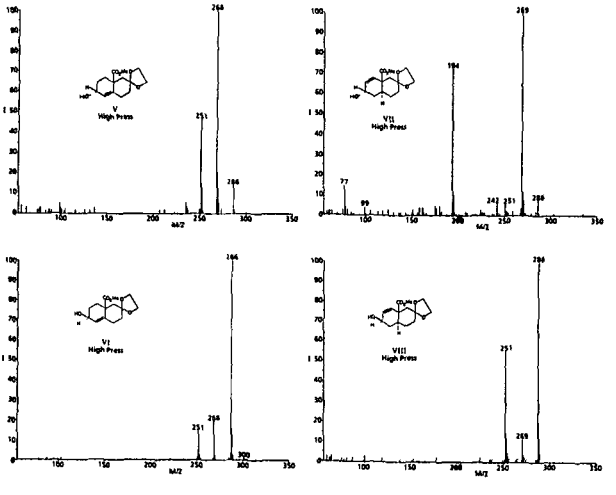
V
High Press
VII
High Press
VI
High Press
VIII
High Press
M/Z

Presented at the 35th ASMS Conference on Mass Spectrometry and Allied Topics
May 24-29, 1987, Denver, CO

USE OF LEAKY DIELECTRIC END PLATES ON COLLISION CELLS IN TRIPLE QUAD MS/MS:

Wade L. Fite and S. N. Ketkar, Extrel Corporation, Pittsburgh, PA 15238.

In triple quadrupole MS/MS, the fringe fields between the first and third quads and metal end plates on the collision cell containing the second quad cause instabilities of trajectories in these regions, rejection of ions, and reduced transmission and sensitivity.

If one uses end plates made of leaky dielectric materials, which act as dielectrics to the rf fields and as conductors to dc fields, and makes the phases of the rf fields on all three quads coincide, one gets superposition of the rf fringe fields from the quads, which tends to keep the ions on stable trajectories in the intermediate regions.

From Maxwell's equations we have

$$\bar{\nabla} \times \bar{H} = \frac{\varepsilon}{c} \frac{\sigma \bar{E}}{\sigma t} + \frac{4\pi}{c} \sigma \bar{E}$$

for a sinusoidal electric field

$$\bar{E}(\bar{r},t) = \bar{E}(\bar{r}) e^{iwt}$$

$$\Rightarrow \quad \bar{\nabla} \times \bar{H} = \frac{iw}{c} \varepsilon_c \bar{E}(\bar{r}) e^{iwt}$$

where $\varepsilon_c = \varepsilon(1 - \alpha)$ is the complex dielectric constant

with $\alpha = \frac{4\Pi\sigma}{\varepsilon w} = \frac{2\sigma}{\varepsilon f}$ where σ is the conductivity and f is the frequency.

If $\frac{2\sigma}{\varepsilon f} >> 1$ the material will act as a conductor whereas if $\frac{2\sigma}{\varepsilon f} << 1$ the material will act as a dielectric.

For normal quadrupole operating frequencies of about 1 MHz and dielectric constants of about 3-7 the material will act as a dielectric if its resistivity $= \frac{1}{\sigma} >> 10^5$ ohm-cm. Figure 1 shows schematically the shielding effects of a leaky dielectric placed between the first and second quadrupole of a triple quadrupole MS/MS system.

Experiments were performed to compare the transmission of a triple quadrupole MS/MS system using metal end plates with one using end plates made of leaky dielectric material. The results are summarized in Table 1.

Experiments show that an improvement of at least a factor of three occurs at each end of the collision cell when using the leaky dielectric end plates rather than metal end plates of the same geometry. Experiments further show that one can reduce the aperture diameter when using leaky dielectric plates without appreciable loss of transmission, and thereby reduce the requirements of pumping of the gas emerging from the collision cell containing the middle quad.

Presented at the 35th ASMS Conference on Mass Spectrometry and Allied Topics
May 24-29, 1987, Denver, CO

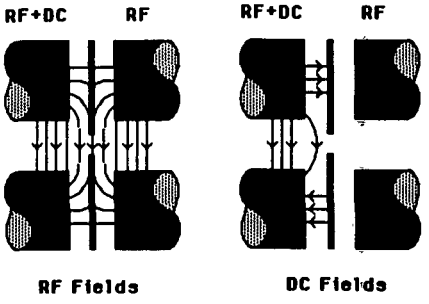

Figure 1

Transmission %

m/z	Metal	Leaky Dielectric
69	18.8	44.4
131	12	36.6
219	8	21
414	5	16
502	4	12

$$\text{Transmission} = \frac{\text{Intensity in neutral loss mode with a loss of 0}}{\text{Intensity in the Q1}^{+}\text{MS mode}}$$

Table 1

Presented at the 35th ASMS Conference on Mass Spectrometry and Allied Topics
May 24-29, 1987, Denver, CO

ADVANTAGES OF PERFLUORINATED POLYETHERS AS FAB CALIBRATION MATERIALS; A STUDY OF CALIBRATION MATERIALS: T.D. McClure, P.F. Baker, K.H. Schram, Department of Pharmaceutical Sciences, College of Pharmacy, University of Arizona, Tucson, Arizona 85721

Considerable research effort continues to be spent searching for information which will extend the usefulness of FABMS for the analysis of important classes of compounds which remain elusive to analysis by mass spectrometry. One practical difficulty of concern which remains is the selection of reference standards for mass-time calibration. The criterion for selection of an ideal reference standard includes the following: 1. The reference standard should leave little background in the ion source of the mass spectrometer and/or be easily removed by baking the ion source. 2.The reference standard should remain on the FAB target (at ambient target temp.) long enough to allow time for instrument tunning and adjustment and permit the acquisition of a number of scans at a slow scan rate, e.g. 40 sec. per decade from m/e=100 to m/e=2500, 3. the reference standard should have a wiede mass range (50 to 2500 amu) with regularly and closely spaced ions through out the spectrum. A_1spacing of between 12 and 44 amu has been mentioned as workable for calibration[1], 4. the high mass ions in the reference standard (above m/e=1000) should have intensities large enough for unambigious recognition by computer software. In our laboratory this requires intensities of greater than 0.2 percent of the base peak, and 5. the reference standard should be usable in negative and positive ion mass spectrometry.

Glycerol (G) is one of the most widely used sample matrix materials. G has been extensively studied using FAB mass spectrometry, and is known to generate clusters of ions at $m/e=[93+(92)_x]^+$ for postive ion and $m/e=[91+(92)_x]^-$ for negative ion mass spectrometry. G can be used for mass-time calibration, however the spacing between ion clusters is on the order of 91 amu apart (enough to cause possible calibration errors). The ions above m/e=700 are very weak, further limiting G as a usefull reference standard.

Possibly the most common reference standard currently being used in FAB is a mixture of G and an alkyl halide. CsI + G has been used in our laboratory with the following limitations: a) many ions change in relative intensity over time, due to the changing concentration of CsI/G as a result of differing volatility of G and CsI, and b) unacceptably high background which is not reduced by baking the source, thus necessitating frequent source removal and abrasive cleaning.

Poly(ethylene-glycol) (PEG) mixtures[1] have been used for FAB calibration. The spacing of ions is approximately 44 amu throughout the mass range. Difficulties associated with using PEG mixtures include: the need to add KI to the mixture to achieve high mass range, which will contaminate the source in like fashion to CsI, the need to mix several materials together requires considerable sample handling and is a source of irreporducibility.

Presented at the 35th ASMS Conference on Mass Spectrometry and Allied Topics
May 24-29, 1987, Denver, CO

Phosphazenes and triazenes produce spectra with FAB which can be used for mass-time calibration. Disadvantages include: Phosphazenes suffer from a region (m/e=313 to m/e=766) where ion adundance is insufficient to insure accurate mass calibration. Tiazenes also suffer from limitations in high mass calibration with a maximum of approximately m/e=1500.

The use of polyfluorinated polyether (PFPE) oils for mass-time calibration have the following advantages over previously mentioned materials: a) Very little background is seen with the source at elevated temperatures (as can be the case with a cooled probe). At ambient temperatures, background is seen after using PFPE oils, but baking the source over night reduces the background to very acceptable levels; b) The spacing between the ions and the relative intensity throughout the mass range, m/e=50 to m/e=2500, allow for accurate and rapid mass-time calibration; c) Relative ion intensities do not change appreciably over time since the components of the PFPE oils do not vary widely in volatility, and d) PFPE oils function well as calibration materials for negative ion as well as postive ion FAB, PFPE iols are commercially available.[2]

In conclusion, we recommend the use of PFPE oils for mass-time calibration in FAB for negative and positive ion modes.

REFERENCES

1. K.J. Bare, Org. Mass Spectrom.,20, 693 (1985).

2. Perflourinated polyethers are available commercially as Fomblin oil, a product of Montedison Co. and from SCM/PCR of Gainsville Florida as some of the Ultramark materials.

This work supported by NIH grant CA 42309.

Presented at the 35th ASMS Conference on Mass Spectrometry and Allied Topics
May 24-29, 1987, Denver, CO

THE ROLE OF MATRIX CHEMISTRY IN "MATRIX-ASSISTED" MASS SPECTROMETRY

Johnny D. Reynolds, John H. Callahan[1], and Kelsey D. Cook*
Department of Chemistry, University of Tennessee, Knoxville, TN 37996-1600
([1]Current address: Naval Research Laboratory, Washington, DC 20375-5000)

Several workers (e.g., Refs. 1-4) have attributed reduction observed in fast atom bombardment to processes induced by the probe beam. While this is undoubtedly true in some cases, the possibility that specific systems may experience a strictly chemical reduction induced by the matrix has not been considered fully. Electrohydrodynamic mass spectrometry (EHMS) provides a means of examining this solution chemistry without the possibility of complications from beam damage.

In a previous EHMS study, evidence for chemical reduction of 1,3-bis(trimethylammonium) benzene diiodide was observed (5). In other studies, transition metal-containing ions bearing 2+ charge have been detected with good sensitivity (6), in contrast with the case usually reported in FABMS. We now report results from a series of transition metal salts and bipyridyl (bpy) complexes with varying redox chemistry. The results are consistent with a contribution from simple solution chemistry and may explain some of the difficulties reported in FABMS of multiply charged metal complexes.

CASE 1: $Ru(bpy)_3^{3+}$

The $Ru(bpy)_3$ system is unusual in that two oxidation states are reasonably stable in aqueous solution - Ru(II) and Ru(III). However, the only Ru-containing ion in the EHMS spectrum of a glycerol solution of $Ru(bpy)_3(ClO_4)_3$ was $Ru(bpy)_3^{2+}$. Use of an internal standard and comparison with spectra from a corresponding solution of the Ru(II) salt indicated that reduction of Ru(III) was quantitative. Optical spectra confirmed that the reduction occurred independent of mass spectral sampling.

CASE 2: $Cu(bpy)_2^{2+}$

The $Cu(bpy)_2^{2+}$ complex is more difficult to reduce than the Ru(III) complex (E^o = 0.12 V, vs. 1.3 V for $Ru(bpy)_3^{3+}$ and -1.0 V for $Ru(bpy)_3^{2+}$). Consistent with these values, it was possible to see ions containing Cu(II) in the EHMS spectrum of a glycerol solution of $Cu(bpy)_2(ClO_4)_2$ (Table I). However, these complex ions were paired with NO_3^- from the supporting electrolyte. Evidence of some reduction was also observed ($Cu(bpy)_2^+$).

TABLE I: $Cu(bpy)_2^{2+}$

Sample	Detected Ion	Mass	Intensity
$Cu(bpy)_2(ClO_4)_2$ (0.006 M)	$[Cu(bpy)_2NO_3]^+$	439	37.7
+ $NaNO_3$ (0.74 M)		437	69.1
+ KNO_3 (0.028 M)	$[Cu(bpy)_2]^+$	377	31.4
		375	59.5
	$[K + G_3]^+$[a]	315	19.1
	$[K + G_2]^+$	223	100.
$Cu(bpy)_2(ClO_4)_2$ (0.005 M)	$[Cu(bpy)_2Cl]^+$	414	68.5
+ NaCl (0.74 M)		412	114.8
+ KCl (0.014 M)		410	88.3
	$[Cu(bpy)_2]^+$	377	11.9
		375	17.6
	$[K + G_3]^+$	315	50.1
	$[K + G_2]^+$	223	100.
	$[Cu(bpy)_2]^{2+}$	188.5	27.0
		187.5	44.9

[a]G denotes solvating glycerol.

Cl^- has been reported to suppress reduction of simple Cu(II) salts in glycerol solution (7). As a test for the possibility that reduction of the $Cu(bpy)_2^{2+}$ complex was somehow induced by the EHMS sampling process, the spectrum was obtained from a solution with NaCl supporting electrolyte (instead of $NaNO_3$). The results (Table I) reflect the expected solution chemistry: reduction is inhibited (though not completely eliminated).

CASE 3: Cu^{2+}

As a further test of the reflection of solution chemistry in EHMS spectra, two simple Cu(II) salts were examined. Except for $CuCl_2$, such salts are reportedly reduced to the metal (Cu^o) by glycerol at slightly elevated temperatures (7). EHMS spectra were consistent with this prediction (Table II):

TABLE II: Cu^{2+}

Sample	Detected Ions	Comment
$Cu(NO_3)_2$ (0.48 M)	$[Cu + G_n]^{2+}$	n = 4-9
	$[Cu + G_n]^+$	n = 2-5
	$[CuNO_3 + G_n]^+$	n = 2-5
	Cu (s)	precipitate
$CuCl_2$ (0.62 M)	$[CuCl + G_n]^+$	n = 2-5

CASE 4: 1,3-bis(trimethylammonium) benzene diiodide

The evidence of chemical reduction of a diquaternary ammonium salt by glycerol noted above has now been confirmed by NMR. The reaction proceeds slowly in the absence of I^-; its progress can be monitored by observing the time dependence of the EHMS spectrum. The reaction does not proceed in water, as evident from both EHMS and NMR spectra.

CONCLUSIONS

These studies confirm that the glycerol matrix can induce chemical reduction of organic and inorganic ions, even in the absence of an invasive energetic particle beam. This chemistry appears to be reflected in EHMS spectra, and should be considered in interpretation of spectra obtained in other matrix-assisted mass spectrometry experiments.

REFERENCES

1. Pelzer, G.; DePauw, E.; Dung, D.V.; Marien, J. J. Phys. Chem. 1984, 88, 5065-5068.
2. Cerny, R.L.; Bursey, M.M.; Jameson, D.L.; Malachowski, M.R.; Sorrell, T.N. Inorg. Chim. Acta 1984, 89, 89-93.
3. Williams, D.H.; Findeis, A.F.; Naylor, S.; Gibson, B.W. J. Am. Chem. Soc. 1987, 109, 1980-1986.
4. Miller, J.M.; Balasanmugam, K.; Nye, J.; Deacon, G.B.; Thomas, N.C. Inorg. Chem. 1987, 26, 560-562.
5. Cook, K.D.; Chan, K.W.S. Int. J. Mass Spectrom. Ion Proc. 1983, 54, 135-149.
6. Chan, K.W.S.; Cook, K.D. J. Am. Chem. Soc. 1982, 104, 5031-5034.
7. Segur, J.B. In "Glycerol", Miner, C.S.; Dalton, N.N., Eds.; Reinhold: New York, 1953, p. 385.

ACKNOWLEDGEMENT

This work was supported in part by a grant from the National Science Foundation (grant # DMR-84-06825, funded jointly by the U.S. Army Research Office).

Presented at the 35th ASMS Conference on Mass Spectrometry and Allied Topics
May 24-29, 1987, Denver, CO

ACETONITRILE AS A SELECTIVE CHEMICAL IONIZATION REAGENT.

Jorma Jalonen
Department of Chemistry, University of Turku,
SF-20500 Turku, FINLAND.

A wide variety of chemical ionization (CI) reagent ion systems have been applied to date.[1] Exothermic proton transfer reagents are the most widely used. Thus, methane (PA = 130.5 kcal/mol) and isobutane (PA = 196.9 kcal/mol) plasmas react with almost all samples with high efficiency producing predominantly protonated product and more or less fragmentation. The third common reagent gas, ammonia (PA = 204.0 kcal/mol) is clearly softer reagent producing predominantly $(M+H)^+$ and/or $(M+NH_4)^+$ ions depending on relative PA's of the sample, with very little fragmentation. Formation of the adduct ion $(M+NH_4)^+$ is a very strong function of the pressure and temperature of the ion source as well.[2] The control of the fragmentation in these systems is thus based mainly on thermochemistry of reactive species.

Other means to utilize ion/molecule reactions in chemical ionization is to consider more specific reactions. Applications of NO, biacetyl and tetramethylsilane are examples of addition reagents as methyl vinyl ether can be used for condensation and amines for substitution reactions.[1]

With these facts in mind we started to study ion/molecule reactions of acetonitrile in CI conditions. Earlier, ion cyclotron resonance (ICR) studies[3] showed that acetonitrile can protonate lower alcohols but in higher, more branced alcohols other reaction channels do appear. Recently, Meot-Ner and Karpas[4] examined alkylation of acetonitrile by alcohols. They observed that acetonitrile can be alkylated by protonated alcohols to form nitrilium ions or in cases where PA of the nitrile is higher than that of the alcohol alkylation occurs by condensation reaction. Similarly, radiolytically formed carbenium ions react with nitriles in the gas phase yielding corresponding nitrilium ions.

The proton affinity (PA) of acetonitrile is 190.9 kcal/mol and it is thus slightly harder reagent than isobutane. The acetonitrile plasma is very simple. Protonated acetonitrile $C_2H_4N^+$ being the base peak with other ions ($C_2H_3N^+$, $C_2H_2N^+$ and $C_3H_4N^+$) of 10 - 15% relative intensity. At higher ion source pressures dimeric species, $(CH_3CN)_2H^+$, m/z 83 also appears. By slow constant introduction of the alcohol to the acetonitrile plasma gives rise to increased dimer formation, couse by the ligand-switching reaction.[5] Therefore great care should be exercised if gas chromatographic introduction is used.

The main reaction channels observed with alcohols (Table 1) are protonation, elimination, substitution, hydride loss and adduct formation. The relative importance

of these reactions seems to be a very delicate balance between relative proton affinities and steric requirements. For instance, normal-, branced-, and cyclic alcohols can be easily differentiated. However, this is not so evident in ketones and aldehydes. The main difference is that in alcohols very favorable substitution reaction occur leading to the formation of stable nitrilium ions.

TABLE 1. Main reaction channels of alcohols in $(CH_3CN)CI$ conditions.

Compounds	*Ions/%RI					
	E	M-1	M	M+1	S	A
1-propanol	-	17	12	75	100	48
2-propanol	-	12	14	13	100	7
1-pentanol	100	-	-	-	5	-
cyclopentanol	42	8	30	5	45	8
tetrahydrofurfyrol	92	-	-	100	-	-
2-propen-1-ol	-	40	18	-	100	-
2-propyn-1-ol	47	100	8	20	37	6
3-phenyl propanol	100	-	22	33	-	-
2-phenyl ethanol	100	-	50	5	13	-

*E is $(M\text{-}OH)^+$, S is $RNCCH_3^+$ and A is $MH{:}CH_3CN^+$. Intensities >5% RI are included.

All measurements were carried out using a VG-7070E - 11/250 mass spectrometer The samples were introduced through a batch inlet system. CD_3CN was used to check fragmentation reactions in all cases.

ACKNOWLEDGEMENTS: The author is indebted to Ms. Kirsti Wiinamäki for her skillful assistance and M.Sc. Pentti Oksman for his help.

REFERENCES.

1. A.G. Harrison, "Chemical Ionization Mass Spectrometry", CRC Press, Boca Raton' Florida, 1983.
2. H. Nakata, H. Konishi, N. Takeda, A. Tatematsu and M. Suzuki, Mass Spectrosc. (Tokyo) 31, 275 (1983)
3. G.A. Grey, J. Am Chem. Soc. 90, 6002 (1968).
4. M. Meot-Ner (Mautner) and Z. Karpas, J. Phys. Chem. 90, 2206 (1986).
5. P. Rudewicz and B. Munson, Anal. Chem. 58, 2903 (1986).

Presented at the 35th ASMS Conference on Mass Spectrometry and Allied Topics
May 24-29, 1987, Denver, CO

THE FORMATION OF A MATRIX PLASMA IN THE GAS PHASE UNDER FAST ATOM BOMBARDMENT (FAB) CONDITIONS.

HERBERT BUDZIKIEWICZ, HELMUT MONSTER and FRANK THEOBALD
Institut für Organische Chemie der Universität,
Greinstr. 4, D-5000 Köln 41, West Germany

ERNST SCHRÖDER
Finnigan-MAT GmbH, Barkhausenstr. 2,
D-2800 14, West Germany

Recently we have suggested [1] that under FAB conditions ion formation of organic compounds which are not present in the matrix in an ionic form takes place in the gas phase by a CI process where matrix ions act as the reagent gas plasma. This hypothesis hinges on two assumptions, *viz.* (a) that a matrix ion plasma is formed in the gas phase and (b) that the plasma ion concentration is high enough to allow reactions with plasma molecules to an appreciable extent.

(a) The FAB beam possesses a conically widening shape. The volume covered by it within the ionization chamber is determined by the entrance hole. Its diameter (8 mm) in an MAT 731 instrument is large enough so that the beam does not only hit the target but covers also a wide portion of the chamber itself. By placing shields with circular apertures in front of the entrance hole the FAB beam can be narrowed step by step until (at 2.2 mm) it essentially hits the target (loaded with 2 µl glycerol) only. From Fig. 1 it can be seen that the width of the apertures correlates with the intensity of the ion current carried by $[glycerol + H]^+$. This result cannot be rationalized if an ion formation occurs only in the condensed phase, on its surface, or in a selvage region; in these cases the ion yield should remain constant. It is, however, consistant with a gas phase reaction $[glycerol]^{+\cdot}$ + glycerol typical for a CI plasma of alcohols.

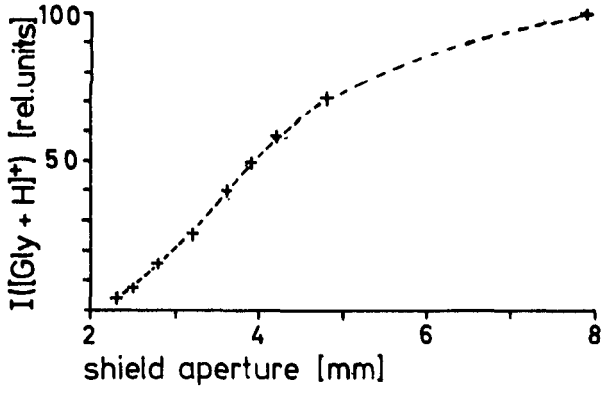

Fig. 1

(b) To demonstrate substrate matrix plasma ion reactions in the gas phase divided targets have been used where two different compounds were placed on the two halves of the latter. Eg., for the system *m*-nitro benzyl alcohol (NBA) and glycerol (GLY) ions of the type $[NBA + GLY + H]^+$ were obtained. Mixing of the two compounds in the condensed phase by "creeping" of the liquids or by back-sputtering could be excluded by recovering and reintroducing them separately into the ion source. No mutual contamination could be detected in this way.

Most convincing, however, in an experiment where the divided target loaded with NBA and GLY was turned stepwise (ca. 10° per spectrum) around its axis while spectra were recorded. Starting from the spectrum of the pure NBA successively spectra were obtained which contained increasingly abundant ions of GLY while those characteristic for NBA decreased until the spectrum of pure GLY was observed (Fig. 2, traces of *m/z* 154 from NBA and of *m/z* 93 from GLY). When both halves of the target were hit about equally by the FAB beam $[NBA + GLY + H]^+$ could be observed as mentioned before.

From results obtained by Campana with FAB-CI [2] it is known that a large amount of neutrals is sputtered into the ion source under FAB conditions. Our experiments show that neutral matrix molecules can be ionized in the gas phase and that these matrix ions can react with matrix molecules to give i.a. $[matrix + H]^+$. These ions are formed in a sufficiently high concentration to serve as a CI plasma for the ionization of other molecules as required by the hypothesis advanced by us for FAB ion formation [1].

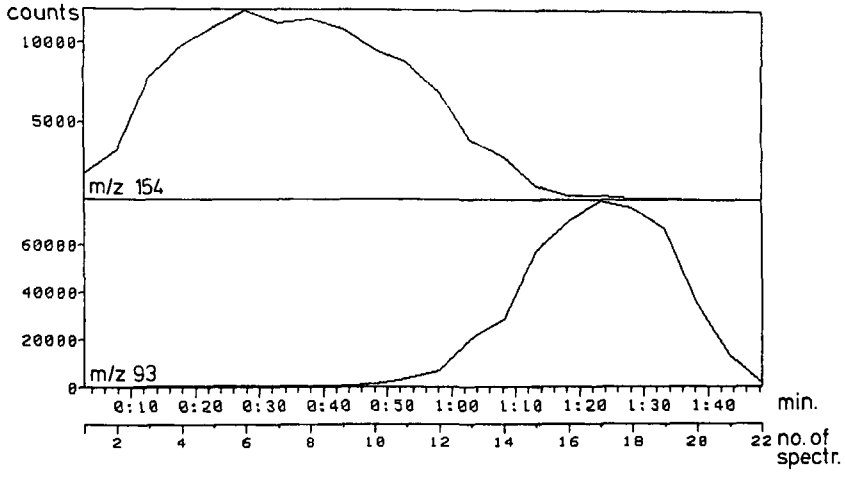

Fig. 2

[1] E. Schröder, H. Münster and H. Budzikiewicz, Org. Mass Spectrom. 21 (1986), 707.

[2] R.B. Freas, M.M. Ross and J.E. Campana, J. Am. Chem. Soc. 107 (1985), 6195.

Presented at the 35th ASMS Conference on Mass Spectrometry and Allied Topics
May 24-29, 1987, Denver, CO

BIOMOLECULAR PDMS ION YIELDS FROM SAMPLES PREPARED BY DIFFERENT TECHNIQUES VS ENERGY DENSITY IN THE FAST ION TRACK:

G Jonsson, P Håkansson, BUR Sundqvist, P Nielsen[1] and P Roepstorff[1]

Department of Radiation Sciences, Division of Ion Physics, Uppsala University, Box 535, S-751 21 Uppsala, Sweden

(1) Molecular Biology, Odense University, Campusvej 55, DK-5230 Odense M, Denmark

Sample preparation is a critical step in all types of secondary ion mass spectrometry analysis. In this work different sample preparation methods of large biomolecules have been studied by Plasma Desoption Mass Spectrometry (PDMS). Different heavy ions of the same velocity were used to bombard the samples in order to vary the energy density in the ion track.

Samples of porcine insulin and human proinsulin were prepared by three different techniques, i.e. adsorption to nitrocellulose (1) and electrospraying with and without glutathione (2). Phospholipase A2 and porcine trypsin were prepared by adsorption to nitrocellulose. Fast heavy ions of a velocity of about 1 cm/ns from the Uppsala Tandem Accelerator have been used to study yields of the biomolecular ions from these samples. The choice of fast ions of the same velocity keeps the geometry of the fast ion track constant. Four different ions (78.2 MeV ^{127}I, 35.7 MeV ^{58}Ni, 19.7 MeV ^{32}S and 9.9 MeV ^{16}O) in charge state equlibrium were chosen to change the energy density.

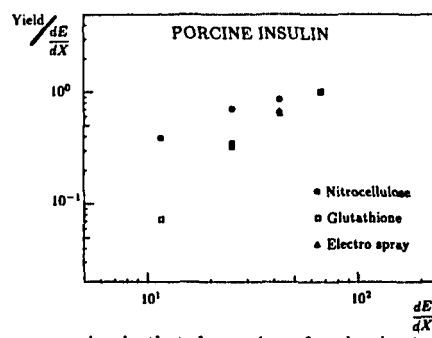

Fig. 1. Yield divided by energy deposited by the primary ion vs the deposited energy. The different curves have been normalized to be the same for the highest stopping power value.

With this technique it has been shown previously that desorption of molecular ions occurs at much lower energy densities when adsorption to nitrocellulose is used instead of electrosprayed multilayers (3). The comparison has been extended to the mentioned systems. Even though the spectra from samples electrosprayed with glutathione and adsorbed to nitrocellulose look alike, the results indicate that adsorption to nitrocellulose is the method for which desorption/ionization occurs at the lowest energy density in the fast ion track (fig 1 and 2).

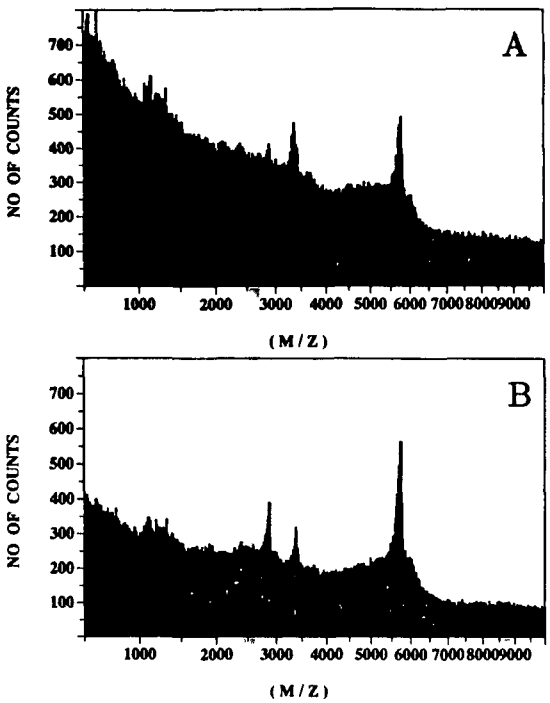

Fig. 2. Porcine insulin desorbed by 78.2 MeV ^{127}I (500000 startpulses) a) electrosprayed with glutathione b) adsorbed to nitrocellulose.

REFERENCES:

(1) G Jonsson, A Hedin, P Håkansson, B U R Sundqvist, G Säve, P Nielsen, P Roepstroff, K-E Johansson, I Kamensky, M Lindberg, Anal. Chem. 58 (1986) 1084

P Roepstorff, P Nielsen, B U R Sundqvist, P Håkansson, G Jonsson, Accepted for publication in Int J Mass Spec. Ion Proc.

(2) M Alai, P Demirev, C Fenselau, R J Cotter, Anal. Chem. 58 (1986) 1303

(3) A Hedin, P Håkansson, B U R Sundqvist, Nucl. Instr. Meth B22 (1987) 491-496.

Presented at the 35th ASMS Conference on Mass Spectrometry and Allied Topics
May 24-29, 1987, Denver, CO

THICKNESS AND VOLUME EFFECTS IN MeV ION INDUCED DESORPTION (PDMS)

G. Bolbach*, S. Della-Negra, C. Deprun, Y. Le Beyec, K.G. Standing[1)]
Institut de Physique Nucléaire, B.P. N°1, F-91406 Orsay Cedex
*Institut Curie, Section Physique et Chimie, 11 rue P.&M. Curie, F-75005 Paris

Well organized film of molecules can be prepared on silver or gold substrates through the Langmuir-Blodgett technique. The thickness of the film is known from the number of molecular layers which are deposited.

Cd stearate and arachidate molecules have been used to prepare various kinds of targets. The objective was to investigate the origin of the ion emission in MeV ion induced desorption : are the ions emitted from the surface only or from a certain distance underneath the surface ? Experiments have been performed with fission fragments from a ^{252}Cf source and ions of 1.16 MeV/u accelerated by the linear accelerator at Orsay. Time of flight mass spectrometry techniques were used to identify the secondary ions.

The dependence of the Secondary ions yield on the target thickness is known and has already been studied. Targets were prepared through different techniques [1,2,3]. With homogeneous Langmuir-Blodgett layers of Cd stearate or Cd arachidate it has been shown that the ion yield increases with the number of deposited layers and saturates above 8-10 ML [4]. Fig. 1 from ref. [3] shows the experimental observed dependence. With Kr ions at 1.16 MeV/u and various incident charge states (therefore different dE/dx in the first layers) the same dependence is observed. Fig. 2 shows the ion yield of $(M-H)^-$ (stearic acid) for three targets : 2 ML, 6 ML and 12 ML as a function of the incident charge state. For a given charge state the ion yield increases rapidly from 2 and 6 ML and remains almost constant between 6 and 12 ML. These experiments do not provide complete evidence for ion emission from layers underneath the surface. It was argued that a relatively thick layer (> 4

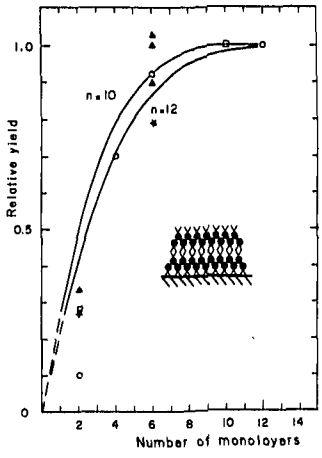

Figure 1

1) Permanent address : University of Manitoba, Winnipeg, Canada

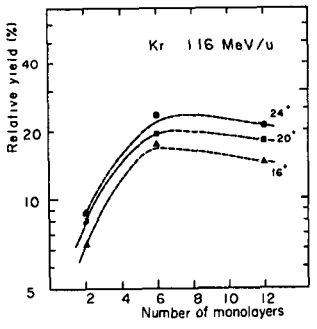

Figure 2

ML) of homogeneous material could be responsible for a coherent energy transfer from inside material to the surface layers.

It appeared therefore necessary to be able to distinguish between molecular ions emitted from the surface and from the "bulk". For that purpose, composite films of superposed Langmuir-Blodgett layers have been prepared. Two monolayers of cadmium arachidate have been covered by 2, 4, 6, 8 layers of Cd stearate. The negative molecular ion yield $(M-H)^-$ of arachidic acid has been measured as a function of the number n of layers covering the first two layers. It is found that the intensity of the molecular in peak $(M-H)^-$ decreases when n increases but intact ions are still visible in the mass spectra although they originate from a distance larger than 150 A (6 monolayers).

The variation of the ion yield as a function of the LB film thickness of the same molecule (as seen in Fig. 1) as well as the decrease of the yield for ions from layers under the surface are compatible with an emission from a conical volume having a depth of ∿ 200 A.

It is likely that other types of organic solid films exhibit the same behaviour and that ion emission from a certain volume should be considered in MeV ion desorption. There is not only a transfer of energy from inside the material to the surface but also a volume emission. Further experiments with LB films are under progress at our Laboratory.

[1] H. Danigel, H. Jungclas and L. Schmidt, Int. J. Mass Spectr. and Ion Phys. 52 (1983) 223.
[2] B.U.R. Sundqvist, A. Hedin, P. Häkansson, M. Salehpour, G. Save and R.E. Johnson, Nucl. Instr. and Meth. B14 (1986) 429 ;
G. Save, P. Häkansson, B.U.R. Sundqvist and U. Jonsson, submitted to Nucl. Instr. and Meth. B.
[3] G. Bolbach, R. Beavis, S. Della-negra, C. Deprun, W. Ens, Y. Le Beyec, D.E. Main, B. Schueler and K. Standing, in preparation.
[4] G. Bolbach, S. Della-Negra, C. Deprun, Y. Le Beyec and K. Standing, in press Rapid Communication in Mass Spectrometry.

Presented at the 35th ASMS Conference on Mass Spectrometry and Allied Topics
May 24-29, 1987, Denver, CO

SPONTANEOUS DESORPTION AND PLASMA DESORPTION MASS SPECTROMETRY : A SIMPLE WAY TO COMPARE keV AND MeV ION INDUCED DESORPTION

G. Bolbach*, S. Della-Negra, C. Deprun, Y. Le Beyec
Institut de Physique Nucléaire, BP N°1, F-91406 Orsay Cedex
*Institut Curie, Section Physique et Chimie, 11 rue P.&M. Curie, F-75005 Paris

The observation of spontaneous and simultaneous emission of negative ions and electrons in a time-of-flight mass spectrometer has already been reported [1]. After traversing the field free region of the TOF instrument both particles are detected by a set of microchannel plates. The time-of-flight differences between electrons and negative ions are measured by a multistop time digitizer and mass spectra of various compounds can be recorded rapidly. A constant electrostatic field is maintained between the target (at a potential of 5 to 12 keV) and a grid (at ground). Virtually no ion sources needed for the generation of the incident particle. The method is therefore extremely simple. It has been recently proved [2] that the secondary ion emission is induced by charged particles coming from the accelerating grid and hitting the target or from the target causing secondary emission from the grid. In any case the analogy with SIMS has been established. In the same TOF apparatus a ^{252}Cf source can be completely retracted so that direct comparison between keV and MeV primary particle can be studied. The same targets can therefore be investigated. Following the work made in collaboration with the Winnipeg group [3] we have used targets prepared through the Langmuir-Blodgett technique. It has been observed that in SD the maximum yield is observed with two monolayers of Cd arachidate on a gold substrate and that the SI yield decreases with the augmentation of the film thickness. In contrast, with MeV particles (fission fragments) bombarding the same target the SI yield saturates beyond 6 ML. Fig. 1 shows the results obtained with composite films of superposed layers of Cd arachidate (2 ML) superposed by 2, 4, 6, 12 monolayers of Cd stearate. The molecular ion yield of the top layer (stearic acid $(M_2-H)^-$ increases with the number of layers of the same compound in the ^{252}Cf mode but decreases rapidly in the SD mode. A strong difference between ^{252}Cf and SD is also observed in the molecular ion yield of

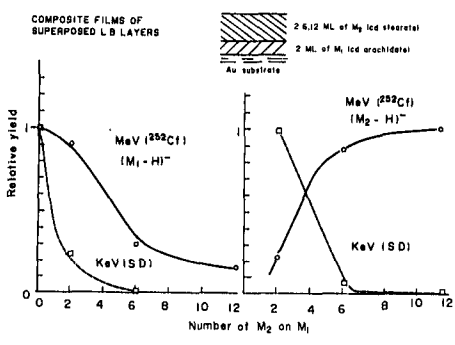

Figure 1

arachidic acid $(M_1-H)^-$ (underneath layer). The yield decreases slowly with ^{252}Cf. This means that ion emission is also taking place from underneath layers (see G. Bolbach et al, this conference). In SD the ion yield decreases very rapidly after coverage of the first 2 monolayers.

Mass spectra are shown in Fig. 2 for two targets consisting of 2 ML of Cd stearate on 2 ML of Cd arachidate and on 12 ML of Cd arachidate. The two peaks at mass M/Z = 283 and M/Z = 311 corresponds to the molecular ion (stearic and arachidic acid). It is observed that the width of the peaks in SDMS are smaller than PDMS. Since the measurements are made under the same conditions this difference indicates that there are more in flight fragmentations in fission fragments induced desorption than in keV ion induced desorption. The same observation has been made with other targets. It is therefore assumed that more internal energy is on the average transferred to the molecular ions when they are emitted from layers bombarded by MeV ion. Further experiments using the coincidence method [4] will be performed soon in order to investigate differences between keV and MeV ion induced desorption.

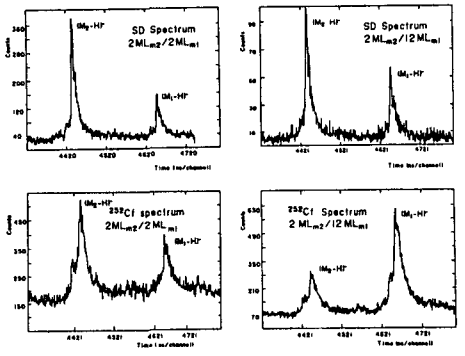

Figure 2

[1] S. Della-Negra, Y. Le Beyec, P. Häkansson, Nucl. Instr. and Meth. Phys. B9 (1985) 103.
[2] S. Della-Negra, C. Deprun, Y. Le Beyec, F. Röllgen, K.G. Standing, B. Monart, G. Bolbach, Int. J. of Mass Spectr. and Ion Processes, in press.
[3] G. Bolbach, R. Beavis, S. Della-Negra, C. Deprun, W. Ens, Y. Le Beyec, D.E. Main, B. Schuler and K.G. Standing, in preparation,
[4] S. Della-Negra and Y. Le Beyec, Analytical Chemistry 57 (1985) 2035.

Presented at the 35th ASMS Conference on Mass Spectrometry and Allied Topics
May 24-29, 1987, Denver, CO

QUANTITATIVE ANALYSIS OF MODIFIED NUCLEOSIDES USING FAST ATOM BOMBARDMENT COMBINED WITH TANDEM MASS SPECTROMETRY

R.L. Cerny, Midwest Center for Mass Spectrometry, Dept. of Chemistry, University of Nebraska, Lincoln, NE 68588

There is increasing interest in the use of modified nucleosides to combat diseases associated with viruses. One of the better known examples is the use of 3'-azidothymidine (AZT) in the treatment of AIDS. Currently treatment involves ingestion of large doses of the modified nucleoside in an effort to block replication of the virus. Problematic side effects, however, will force investigators to determine the effective blood levels for these types of drugs. In anticipation of this, it is important to develop analytical methodology capable of detecting and monitoring low levels of these types of compounds.

Modified nucleosides are quite amenable to analysis using FAB because the basic functionalities are readily protonated in the matrix to produce ultimately gas-phase $(M + H)^+$ ions. This eliminates the problems associated with derivativization which may be necessary to form intact ions of many modified nucleosides by either EI or CI. However, matrix interference can be a major problem in the analysis of small quantities of material by FAB MS, particularly for substances of low molecular weight. The "peak-at-every-mass" phenomenon limits detection (see Figure 1).

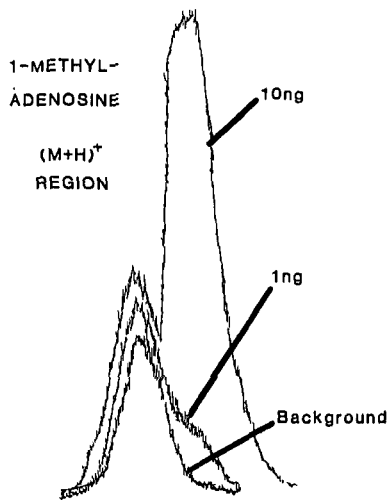

Figure 1

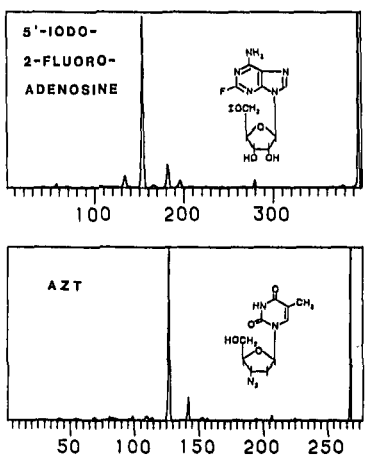

Figure 2

The $(M + H)^+$ ions of nucleosides readily fragment upon collisional activation to form BH_2^+ (B = base) (see Figure 2). By taking advantage of the specificity of this reaction, detection limits can be greatly improved. This is achieved by selected reaction monitoring (SRM) in the FAB MS/MS analysis. The Kratos MS-50 TA used in these experiments has an electrostatic analyzer as MS-II. SRM is performed by scanning over a narrow voltage range around $E_{daughter}$ = (m daughter/m parent) x E parent. Scanning over a narrow range is preferred to peak-top monitoring as it produces a peak profile. Evaluation of this peak profile offers enhanced specificity when determining if a true positive response has been acquired.

Presented at the 35th ASMS Conference on Mass Spectrometry and Allied Topics
May 24-29, 1987, Denver, CO

FAB often suffers from problems in reproducibility due to the dynamic nature of the sputtering process. To minimize this source of error in quantitation, a species which undergoes similar fragmentation can be introduced to each sample as an internal standard. A scan controller designed and built in our laboratory allows monitoring of two different parent ions and two distinct transitions in the same acquisition. For these experiments, thymidine was used as the internal standard at a constant level of 1 g. This amount was selected to minimize background interference in the standard channel. SRM was of m/z 243 127 (TH_2^+). The amount of AZT was varied from 1 g to 100 pg. Again TH_2^+ formation was measured by SRM of 268 127. Acquisition was alternated between the two channels with a dwell time of 0.3 sec for thymidine and 3 sec for AZT. The data were signal averaged with the total acquisition time held constant at 2 min. (For typical data, see Figure 3).

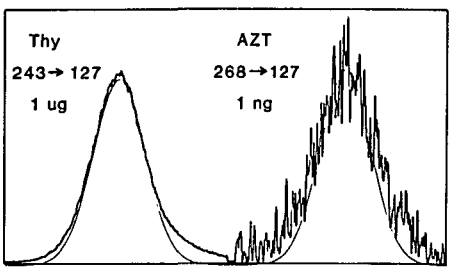

Figure 3

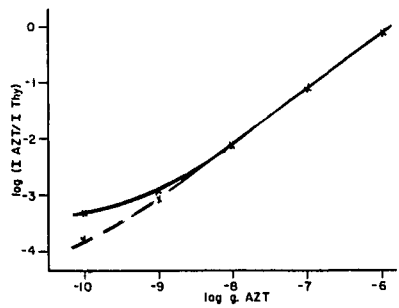

Figure 4

The calibration plot shown in Figure 4 provides a good linear relationship over the four orders of magnitude from 1 µg to 100 pg of AZT. The leveling effect observed for the lower amounts of AZT is the result of the sample signal intensity approaching that of the chemical noise in the monitored region. The linearity of the plot is improved by subtraction of the chemical background arising from the glycerol matrix.

Limitations to the technique likely lie in the FAB process itself. As was mentioned earlier, background interference can be a major problem when analyzing small amounts of low molecular weight material. Careful consideration must be given to the matrix used to minimize this interference. Operation of MS-I at higher resolution may prove advantageous. Although some abundance of $(M + H)^+$ may be sacrificed, the increased specificity may enhance the S/N. This holds promise because in test experiments the noise was found to be chemical in nature rather than electronic.

Another problem may lie in the preferential sputtering often encountered in FAB. This is more acute when a large difference between the concentrations of two analytes occurs. This effect can be minimized by carefully adjusting the level of the internal standard to match that of the species being determined.

Presented at the 35th ASMS Conference on Mass Spectrometry and Allied Topics
May 24-29, 1987, Denver, CO.

Assessment of the Risk of Environmental Pollutants

Vernon N. Houk, M.D., Assistant Surgeon General
Director
Center for Environmental Health, Centers for Disease Control
and
Assistant Administrator
Agency for Toxic Substances and Disease Registry
Public Health Service, U.S. Department of Health and Human Services
Atlanta, Georgia 30333

Today, people often think of risk assessment in terms of complicated computer models of exposure, sophisticated statistical analyses of laboratory data, and rows and rows of rat cages. This view is somewhat misleading, for, in a sense, we all assess and manage risk without such exotic paraphernalia. Situations involving risk are a part of everyday life, and therefore, assessments of risk and actions in response that is, risk management are activities in which we all routinely engage. Institutions have also evolved within our society to determine risk in specific situations and to provide the individual a means for responding in an appropriate manner. With such established activities and experience in risk management, why is it that we as a society have such a difficult time dealing with questions and issues concerning artificial sweeteners, nuclear power, dioxin, the 55-mile-per-hour speed limit, leaded gasoline, and seat belts? Society finds these issues difficult to resolve because of the changes in contemporary ways of thinking about risk, the problems of personal perceptions of risk, and the conflict between individual versus governmental responsibility for risk management.

In 1985, the Department of Health and Human Services (HHS), in a task force report, described a general philosophy of risk.

> Individuals have always lived with risk, presently live with risk, and will continue to live with risk in the future. Some degree of risk of adverse health effects from toxic substances is inevitable, as a consequence of exposure to both naturally occurring and man-made toxicants. The public should be made aware of the nature of the risk. Public health risks that are not acceptable should be reduced or eliminated when feasible. Means to accomplish this goal should not pose additional significant risks.

The task force took into account the laws administered by the Department, the acceptability of risk, the voluntary aspects of risk, the public's perception of risk, and the processes of risk assessment and risk management. Concerning the last item-both the government and the public should understand that uncertainties are associated with risk assessment and risk management and that educating the public about these processes is of the utmost importance. Agencies can, of course, amend this general statement as needed, as, for example, when laws dictate otherwise. The task force outlined specific ways to put this philosophy into practice. A risk assessor should clearly define the elements that go into the process as science policy, fact, consensus, or assumption. By "science policy," we mean the agency decision on how it is going to handle controversial issues. Scientific fact is, in most instances, the least available element. In any risk assessment, an attempt should be made to clearly identify all of the main assumptions made and to indicate their probable effect on the risk assessment.

Most of the carcinogens, both man-made and naturally occurring, that have been identified have been shown to be carcinogenic for animals, not humans, and, they have shown their cancer-causing effects in tests with dose levels far higher than will ever be found in the environment. Therefore, if we use animal data to estimate the risk of environmental exposure for humans, we must extrapolate these laboratory findings across species and from high to low doses. We do not have enough scientific data on which to base these extrapolations, so, as an alternative to fact-based hypothesis, we must make assumptions. This is not objectionable, as long as we keep in mind that we are dealing with assumptions, not facts. Unfortunately, in discussions, scientific reviews, rule making, and cleanup activities, this has rarely been emphasized. When assumptions are the basis for our actions, research aimed at validating the assumptions is of the highest priority.

Six assumptions are most critical in making a quantitative assessment of cancer risk. The first is that regardless of how low the carcinogen level is--it may even be below the detection limit--there is still a finite risk. The second assumption is that experience

with animals can be transposed to humans by using a dose scale of milligrams of carcinogen per kilogram of body weight per day. The third assumption is that the dose-response relationship observed at the very high dose levels used in bioassays is the same as the relationship at the very low dose levels found in the environment. Number four is that the observed concentration of a carcinogen in water is not altered by any treatment at the water plant, by boiling at home, or by any other treatment. The fifth assumption is that the exposure is for a lifetime--that is, that the level of exposure will not change in a full life span or, if it does change, that the changes will balance each other out. The sixth assumption is that the real dose-response relationship in animal and human carcinogenesis equals the relationship in the mathematical model used to determine the dose-response relationship from test results.

It is important to understand that risk assessments and risk estimates are based on assumptions and that these assumptions need to be validated. So-called conservative assumptions will not suffice. We must strive to learn how far and in what direction these assumptions differ from the truth. In considering the data base underlying the proposed rule making and in communicating risk estimates to the public or to anyone using the estimates, we should be acutely aware of the great impact that errors in these assumptions may have on the estimates.

Cancer risk estimates, as presented by the Environmental Protection Agency (EPA), are the 95% upper bound of the point estimates, and they address risks to individuals, not populations. Thus, a risk of 1 in 100,000 indicates that the best risk estimate, accepting all assumptions to be valid and correct, is much lower or may even be zero. Let me make a conservative choice by translating a 1 in 100,000 upper bound risk to a 1 in 200,000 point estimate of a lifetime risk. In more understandable terms, this is a risk, over a century, of an average of 1 cancer case a year in a population of 1.4 million people. To put this estimate in perspective--in the United States, 10,000 cases of new cancers have been observed, with high accuracy, to occur in the same 1.4 million people because of the risks we are already taking, knowingly or unknowingly. In considering these risks, we should keep in mind that the estimated 1 case a year per 1.4 million people is obtained with a risk model based on very conservative assumptions--that is, they err on the side of caution. The real risk may be far lower than the estimated risk.

The major challenge in risk management is to enhance public welfare by effectively managing the risks of substances that have toxic effects under practical conditions of use and exposure. The problem-solving approach to risk management provides a framework for overcoming difficulties by analyzing the risk assessment, analyzing options, promoting understanding and acceptance of risk-management decisions, and evaluating the effectiveness of the option chosen. This is a framework through which policy makers can assess information, determine risks faced by the public, and allow for the democratic process to decide the acceptability of each risk on an incremental basis.

Our challenge is to improve each of these estimated determinations and thus reduce the overall uncertainty. As this is done, our assessments of risk and our management of risks should continue to improve. Improvement in risk assessment requires better exposure assessment, better hazard evaluation for health effects in humans, and better dose-response assessment based upon human data. These improvements will demand continued advances in analytical chemistry, toxicology, and epidemiology.

The role of laboratory measurements, and in particular, mass spectrometry, should be clear. The better the picture of the environmental situation--toxicants present, distribution, and migratory pathway--the better the risk assessment. Efforts to improve valid sampling, laboratory quality control, and interlaboratory standardization are important. As is always the case, improved lower limits of detection and quantification are needed to measure many of the toxic substances present at trace levels.

In summary, it seems that the wisest role for public health in the environmental field is to prevent exposure. Even in the absence of conclusive evidence that harm to humans has occurred, if the data and evidence from laboratory animal studies are sufficiently strong that harm may occur, then preventing future populations from being exposed is a reasonable action. The policy maker must address what the potential harm is, what the potential remedial action is, what the cost of that remedial action is, and whether it is warranted? In an era of diminishing resources, remedial action must be weighed against proven public health measures of beneficial intervention.

Presented at the 35th ASMS Conference on Mass Spectrometry and Allied Topics
May 24-29, 1987, Denver, CO

MOLECULAR DOSIMETRY

John S. Wishnok

Department of Applied Biological Sciences
Massachusetts Institute of Technology
Cambridge, MA 02139

There is now little doubt that environmental factors contribute to human cancer risk. The evidence for this includes epidemiological data showing that people who move, for example, from Japan to the United States, begin to show cancer risk profiles which more closely resemble those of the general U.S. population than those of Japan. Despite such evidence, however, it has generally proved difficult to show firm correlations between specific carcinogens and specific site tumors in humans. Additionally, it has generally been impossible to identify those individuals within a population who are at either higher or lower risk than the average for that group. The first of these problems arises directly from the limitations of classical epidemiology, i.e., success typically requires a marked elevation in risk within a well-defined group along with a measurably higher exposure to an identifiable agent. Systematic observations of occupationally-related disorders have been documented for over 500 years, and occupationally-related cancer, the well-known description of scrotal cancer in English chimney sweeps by Percival Pott, has been known since at least the 1700's. Virtually all human carcinogens were in fact first detected in the workplace and were associated with unusually high risks toward certain tumor types. Workers exposed to 2-naphthylamine or asbestos, for example, were found to have relative risks of 87 for bladder cancer and greater than 100 for mesothelioma, respectively. It is well known from animal studies, however, that tumors can be initiated by chronic exposure to very low concentrations of carcinogens, i.e., it is possible if not probable that people can be at risk from an agent present at virtually undetectable levels. Cancer epidemiology in the broader sense is then typically faced with highly subtle situations. Two countries, for example, may have very similar overall cancer rates while one has a higher rate of a given tumor type. The question of variations of individual risk within a given group is also complex, and, in the case of chemically initiated cancer, probably reflects the net effects of factors such as individual exposure and differences in distribution and metabolism which may in turn arise from or be superimposed on genetic differences and differences in, for example, lifestyle. In the face of such considerations, it is becoming increasingly apparent that classical epidemiological techniques in which exposure is based on measurement of ambient levels of potentially toxic substances, on estimations of dietary intake, or on answers in questionnaires, is inadequate.

Most chemical carcinogens are metabolically activated to strong electrophiles which then presumably react with biological macromolecules, such as DNA, in what is generally believed to be the first of a long series of events that eventually results in cancer. The concentration of an electrophile in a given body compartment is the net result of at least three factors: exposure to the original carcinogen, distribution of the carcinogen within the body, and metabolism. This implies that ambient concentrations of a carcinogen may bear little relationship to an ultimate biological response. The level of DNA damage in an individual would then in principle be better than, say, dietary levels of a presumed carcinogen, as an index of cancer risk for that person. This would be especially true if it were possible to quantitate the interaction with DNA of the active metabolites via substances of known structures. These ideas were put forward in the 1970's most notably by Lars Ehrenberg and his co-workers at the University of Stockholm. Because of the impracticality of obtaining workable amounts of DNA from humans and because of the analytical sensitivity which would have in addition been required, analysis of proteins such as albumin or hemoglobin was proposed at the time as an

alternative. The major assumption, which has now been borne out in several systems, was that the electrophilic metabolite would react proportionately with DNA and protein, i.e., that relative levels of protein adducts would reflect relative levels of DNA adducts. Despite the appeal of these concepts, however, experimental realization of them has not been trivial. Several factors have contributed to this. Even with the relatively large amounts of hemoglobin or albumin which can be obtained from people, the total amount of adduct available for analysis is often in the femtomole range and is typically present, even after extensive cleanup, in a complex mixture. The most appropriate protein and adduct product for a given carcinogen must each be determined empirically, i.e., no universal method is becoming apparent. During the past five years or so, however, and due to a major extent to developments in mass spectrometry, it has become possible not only to quantitate protein adducts for several carcinogens but also under some circumstances to quantitate nucleic acid adducts. The ability to measure both of these is proving especially useful because of their complementary natures. DNA adducts, for example, are short-lived. The levels of these adducts then reflect recent exposure to the carcinogens. Proteins on the other hand have lifetimes on the order of months; protein adduct levels thus can give an 'integrated' measure of exposure over such time intervals.

In addition to chromatography-based methods, a number of researchers are developing immunological methods to screen for protein or nucleic acid adducts. These methods potentially have sensitivities equal to or greater than the instrumental methods along with the advantages of greater speed and lower cost, and are thus probably better suited to large-scale screening. The specificity of the immunological methods, however, is lower, especially in comparison to MS methods.

As noted earlier, the sequence leading to a clinical tumor in an individual is long and probably complex, requiring in many cases more than 20 years. A numerical index of relative risk is therefore at the moment impossible. The more modest, but nonetheless important, goal of developing an index of exposure to active carcinogen metabolites, however, appears practical in some specific cases, and may prove practical in a more general sense, leading ultimately to more power and more insight in cancer epidemiology. The following papers in this symposium will cover developments in several aspects of this area and should serve both as an introduction to molecular dosimetry and as a stimulus for additional scientists to enter and contribute to this field.

This work was supported by Grants from N.I.E.H.S. (No. 2-P01-ES00597-13), The American Cancer Society (No. SIG-10-I), and the D.H.H.S. Shared Instrument Program (No. S10-RR01901).

Presented at the 35th ASMS Conference on Mass Spectrometry and Allied Topics
May 24-29, 1987, Denver, CO

DO DNA ADDUCT MEASUREMENTS IN HUMAN URINE PROVIDE ACCURATE DATA FOR CANCER RISK ASSESSMENT?

John D. Groopman
Boston University School of Public Health,
Boston, MA 02118.

Risk assessment procedures for individuals exposed to carcinogens will be facilitated by rapid, accurate methods to quantify metabolites of carcinogens in urine. The development of these methodologies will also benefit from the use of complementary methodologies to confirm the identity of DNA adducts. We have been refining these methods by determining the relationship between dose and excretion of aflatoxin B1 and its excretion of aflatoxin B1 and its adducts in chronically exposed people. The aflatoxins are among the few chemically identified environmental carcinogens for which quantitative estimates of human exposure have been systematically sought. The motivation for these studies is the presumed role of aflatoxins in the causation of primary liver cancer in man. Several epidemiological studies have been designed to obtain information on the relationship of estimated dietary intake of aflatoxin to the incidence of primary human liver cancer. There was a positive association between the two parameters in that high intakes of aflatoxin were consistently associated with high incidence rates for cancer. The incidence of liver cancer is found to be a linear function of the log of dietary aflatoxin intake has been found.

Our laboratory has produced various monoclonal antibodies which recognize aflatoxins, using antigens ranging from aflatoxin-modified DNA to aflatoxin-adducted proteins. These antibodies are now being used in conjunction with other analytical techniques as reagents for the non-invasive screening of humans to monitor for exposure to these naturally-occurring mycotoxins. These methods depend upon the ability to quantify aflatoxin and its metabolites, including DNA adducts, in readily accessible compartments, such as serum and urine. Therefore, we have combined procedures of analytical chemistry such as HPLC with a preparative monoclonal antibody-affinity chromatography column to both purify the aflatoxin adducts and metabolites from urine from interfering compounds and to confirm their identities.

People exposed to AFB1 from dietary sources were identified for pilot studies by collaborators at the Institute of Health in Beijing, China. Urine was obtained in two 12 hour fractions for three consecutive days during a one week period. These urine samples were obtained only after dietary aflatoxin levels had been measured for at least three consecutive days. The average male intake of AFB1 was 48.4 ug per day for a total exposure over the 7 day period of 276.8 ug. The average female daily intake was 92.4 ug per day. Immunoassays were performed on aliquots of the 12 hour urines following clean-up of the samples by C18 Sep-Pak and monoclonal antibody affinity chromatography. Total AFB excretion for the 12 hour period by multiplying the urine volume by the concentration of AFB determined in the aliquot of urine. These data reveal that the urinary excretion of AFB is a saturable process and an inverse relationship exists between

increasing dose and the percentage of excreted AFB. We also performed HPLC analysis of the urine samples for AFM1, AFP1 and the major AFB-DNA adducts. Taken together, it appears that urine is a valid compartment to sample people for aflatoxin exposure, but more data must be collected for developing a risk model for people.

Primary hepatocellular carcinoma is one of the most lethal and common cancers in the world. It is particularly prevalent on the continents of Africa and Asia. A number of epidemiological studies have associated the exposure status of people to aflatoxin B1 as being important in the etiology of liver cancer. However, to date these studies have relied upon the criteria of presumptive intake data, rather than relying upon quantitative analyses of aflatoxin DNA adduct and metabolite content obtained by monitoring biological fluids from exposed people. Information obtained by monitoring exposed individuals for specific DNA adducts and metabolites will define the pharmacokinetics of aflatoxin B1 in people, thereby facilitating risk assessments.

We have developed monoclonal antibodies specific for aflatoxin metabolites, especially the DNA adducts. These monoclonal antibodies are used in solid phase immunoassays for the preparative purification of these aflatoxin derivatives from biological fluids. These methods in conjunction with other analytical procedures have resulted in the development of rapid protocols used to quantitatively measure aflatoxins in urine obtained from people dietarily exposed to this carcinogen. The people examined live in the Gambia and high liver cancer regions in the People's Republic of China. We have recently completed a pilot study in China where we have now begun to identify the pharmacokinetic parameters associated with chronic exposure of aflatoxin B1 in the diet.

Despite the development of these new technologies, we must continue to define animal model systems which can be used to interpret the human data. Our work using animal models based on the differential effects of ethoxyquin on the kinetics of aflatoxin-DNA adduct and gamma glutamyl transpeptidase-positive foci formation indicate that the direct linear extrapolation of total adduct content in target tissues to dose may be inappropriate to assign risk to people (or rats). However, our findings do support the concept that measurement of the major, rapidly excised AFB-N7-Gua adduct in tissues and fluids is an appropriate dosimeter for estimating exposure status and risk in individuals consuming this mycotoxin. Further studies employing different classes of modifiers of aflatoxin carcinogenesis in rodent models should better define the relationships between hepatic and urinary levels of AFB-N7-Gua and susceptibility to neoplasia.

Presented at the 35th ASMS Conference on Mass Spectrometry and Allied Topics
May 24-29, 1987, Denver, CO

NUCLEIC ACID-CARCINOGEN ADDUCTS IN HUMAN DOSIMETRY

Peter B. Farmer
MRC Toxicology Unit, Carshalton, Surrey, SM5 4EF, U.K.

The initial event in carcinogenesis by alkylating agents is presumed to be a modification of the bases or phosphate esters in DNA. A close representation of the biologically significant dose received by an individual of an alkylating carcinogen would thus be a determination of the extent of its binding at its target site of action in DNA. A wide variety of analytical approaches is currently being developed to determine such adduct formation although the application of these to human samples has not so far been extensive. Exposure to benzo(a)pyrene[1] and aflatoxin B_1[2,3] has been detected by immunoassay, or by HPLC coupled with fluorescence measurements, of their DNA adducts. Immunoassay has also been used to monitor exposure to the anti-cancer drug cis-platin[4]. The [^{32}P]-post labelling technique, which is capable of detecting one adduct in 10^9 - 10^{10} nucleotides has shown the presence of carcinogen adducts in placental samples from smokers[5].

GC-MS approaches have been developed in our laboratories for monitoring human exposure to methylating agents. Amongst the major modified bases resulting from methylating agent exposure are 7-methylguanine (7-MeG) and 3-methyladenine (3-MeA). Both bases are removed from the DNA by spontaneous chemical or enzymic reactions and are excreted completely in urine. Measurement of these thus provides a convenient non-invasive method for monitoring human methylating agent exposure. 7-MeG was extracted from urine on a heptanesulphonic acid treated C_{18} Sep Pak cartridge and determined by EI GC selected ion monitoring (SIM) of its N-heptafluorobutyryl O-pentafluorobenzyl derivative (M^+ 541)[6]. [$^2H_3$]-7-MeG, synthesised by the reaction of guanosine with di [$^2H_3$]-methyl sulphate, was used as internal standard (M^+ 544). As rather high levels of 7-MeG exist naturally in urine, due to turn-over of t-RNA, the assessment of the exposure-monitoring method was made using stable isotope labelled methylating agents, i.e. [$^2H_3$]-labelled methylating agents were administered and the excretion of [$^2H_3$]-7-MeG was monitored using unlabelled 7-MeG as internal standard. Dose-response relationships were observed for animals treated with directly or indirectly acting methylating agents[7]. Studies on humans administered deuterium-labelled drugs are currently in progress.

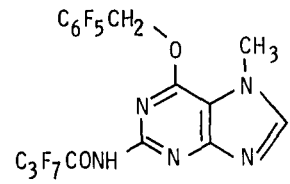

As high background levels of 7-MeG in human urine limited the value of its determination for exposure monitoring, we have now developed an assay method for 3-MeA, whose urinary background levels were unknown. 3-MeA is purified from urine by XAD-2 chromatography followed by HPLC, and quantified by EI GC SIM using the $(M-C_4H_9)^+$ ion of its TBDMS derivative, (m/z 206). [$^2H_3$]-3-MeA, synthesised by the reaction of 5-formyl-4,5,6-triaminopyrimidine with [$^2H_3$]methyl iodide, was used as internal standard [$(M-C_4H_9)^+$, 209]. The background levels of 3-MeA found in the urine of rat (ca. 0.2 µg/day) and human (9.7 ± 4.1 µg/day) (n = 21) were at least 500-fold lower than the 7-MeG concentrations. The 3-MeA concentration in the urine of cigarette smokers was significantly higher than controls at 14.8 ± 5.9 µg/day (n = 10). The source of the methyl group is unknown although several methylating agents such as tobacco-specific nitrosamines are known to be present in cigarette smoke. The effect of dietary intake of nitrate, which may enhance the production of nitroso-compounds, on urinary excretion of 3-MeA is also being studied in human volunteers.

Presented at the 35th ASMS Conference on Mass Spectrometry and Allied Topics
May 24-29, 1987, Denver, CO

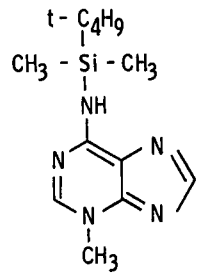

We are now exploring the potential of MS-MS using collision-induced fragmentation for the identification of alkylating agents in unknown or complex exposures (e.g. carcinogens derived from dietary sources or from environmental pollution). Analyses are carried out on a VG 70 SEQ (EBQQ) mass spectrometer using EI for sample ionisation and air as the gas in the quadrupole collision cell, preceding the quadrupole analyser. It is possible to identify 7-MeG directly in a sample of urine by the collision induced decomposition spectrum of its molecular ion (165); identical spectra are obtained to those of an authentic sample. For the higher alkylated guanines 7-ethylguanine and 7-(2-hydroxyethyl)guanine the collision spectra from the molecular ions (179 and 195 respectively) contain the common fragment m/z 151 ($guanine^+$) and we are now investigating the possibility that this ion might be a useful marker for detecting other alkylated guanines. Parent ion scans for the ion at m/z 151 from purines isolated from a 25 ml aliquot of human urine revealed several ions, including predominantly m/z 179, 180 and 195. The identity of the 179 and 195 peaks is under further study but the peak at m/z 180 appears to be due to theophylline as the CID spectrum of the molecular ion of theophylline (M^+ 180) compares well with the analogous spectrum from urine.

References

1. Harris, C.C., Vahakangas, K., Newman, M.J., Trivers, G.E., Shamsuddin, A., Sinopoli, N., Mann, D.L. and Wright, W.E. (1985) Proc. Natl. Acad. Sci. USA 82, 6672-6676.

2. Groopman, J.D., Donahue, P.R., Zhu, J., Chen, J. and Wogan, G.N. (1985) Proc. Natl. Acad. Sci. USA 82, 6492-6496.

3. Autrup, H., Wakhisi, J., Vahakangas, K., Wasunna, A. and Harris, C.C. (1985) Environ. Health Perspec. 62, 105-108.

4. Poirier, M.C., Reed, E., Zwelling, L.A.., Ozols, R.F., Litterst, C.L. and Yuspa, S.H. (1985) Environ. Health Perspec. 62, 89-94.

5. Everson, B.B., Randerath, E., Santella, R.M., Cefalo, R.C., Avitts, T.A.and Randerath, K. (1986) Science 231, 54-57.

6. Shuker, D.E.G., Bailey, E., Gorf, S.M., Lamb, J.and Farmer, P.B. (1984) Anal. Biochem. 140, 270-275.

7. Farmer, P.B., Shuker, D.E.G. and Bird, I. (1986) Carcinogenesis 7, 49-52.

8. Shuker, D.E.G., Bailey, E., Parry, A., Lamb, J. and Farmer, P.B. (1987) Carcinogenesis, in press.

Presented at the 35th ASMS Conference on Mass Spectrometry and Allied Topics
May 24-29, 1987, Denver, CO

A FOURIER TRANSFORM QUADRUPOLE ION TRAP MASS SPECTROMETER

J. E. P. Syka and W. J. Fies, Jr.
Finnigan MAT, San Jose, CA 95134

Mass selective detection is the oldest mode of operation of the RF quadrupole ion trap having first been described in the original RF quadrupole patent of Paul and Stienwedel[1] and then demonstrated by Fischer[2] and Rettinghaus[3]. This technique is akin to ICR as mass analysis is accomplished by detecting the natural frequency of ions held in a trapping field. The experiment described herein involves the application of Fourier transform methodology to the mass selective detection technique.

The apparatus is constructed so as to excite and then detect trapped ion oscillations along the axis of the quadrupole trap structure. The natural oscillation of an ion within the quadrupole field is composed of a series of distinct frequencies. Excitation at any of these frequencies results in a resonant condition. The sequence of resonant frequencies for an ion is $(\beta/2)f$, $(1-\beta/2)f$, $(1+\beta/2)f$, $(2-\beta/2)f$, $2+\beta/2)f$. . .; where f is the applied RF field frequency and the parameter β is determined by the mass-to-charge ratio, m/z, of the ion and the quadrupole field parameters f, U, V, and r_0. For trapped ions, β is restricted to values between 0 and 1. For ions of a single polarity in a defined trapping field, m/z uniquely defines the resonant frequencies of any ion. Calculations based on approximate expressions for β indicate that ion frequencies and dispersions comparable to those produced in high field FT-ICR instruments can be obtained with RF quadrupole ion traps having reasonable field parameters. Transient excitation of ions can be shown to impart a coherent component of motion to all ions having the same m/z. A conceptual diagram of the Fourier transform ion trap apparatus is shown in Fig. #1. Excitation was accomplished by applying a sinusoidal voltage pulse between end caps of the electrode structure. The resultant ion image current signal transient induced between the end caps was amplified and fed into a Fourier transform spectrum analyzer. Fig. #2 shows an ion image current signal transient from m/z 91 u and 92 u ions of Toluene. Fig. #3 shows the frequency spectrum of this transient signal. It is believed that space charge interaction of the two trapped ion species resulted in coupled motion and hence, a single common spectral line was produced. Similar effects are observed in FT-ICR instruments at high ion concentration.

Presently, other mass analysis techniques using the RF quadrupole ion trap have superseded the mass selective detection technique. The demonstrated feasibility of applying Fourier transform techniques to this method warrants renewed interest in this technology.

1. W. Paul and H. Stienwedel, U.S. Patent 2,939,952 (1960)
2. E. Fischer, Z. Phys., 156 (1959) 26
3 G. Rettinghaus, Z. Agnew Phys. 22 (1967) 321

FIGURE 1

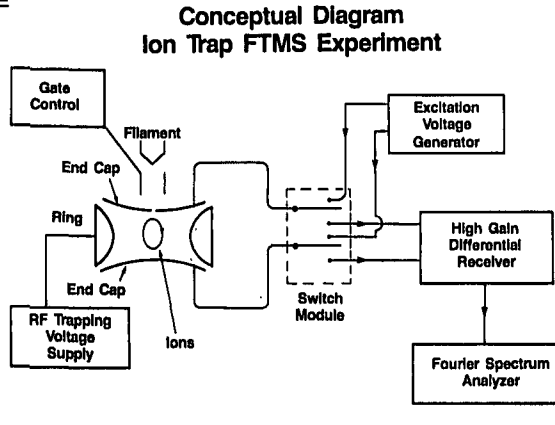

FIGURE 2

Ion Transient Signals from Toluene *m/z* 91, 92

Toluene Pressure:
4.7×10^{-7} torr (Corrected)

Amplifier Gain: 2×10^4

Amplifier Bandwidth: 2.3 KHz

Excitation: 973 KHz for 8 ms

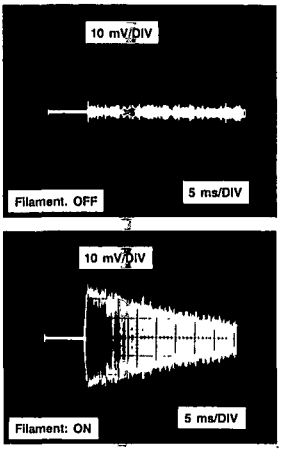

FIGURE 3

Toluene *m/z* 91, 92

Excitation: 973 KHz for 8 ms

Amplifier Bandwidth: 2.3 KHz

Transients RMS Averaged 32 Times

Transform Resolution: 73 Hz

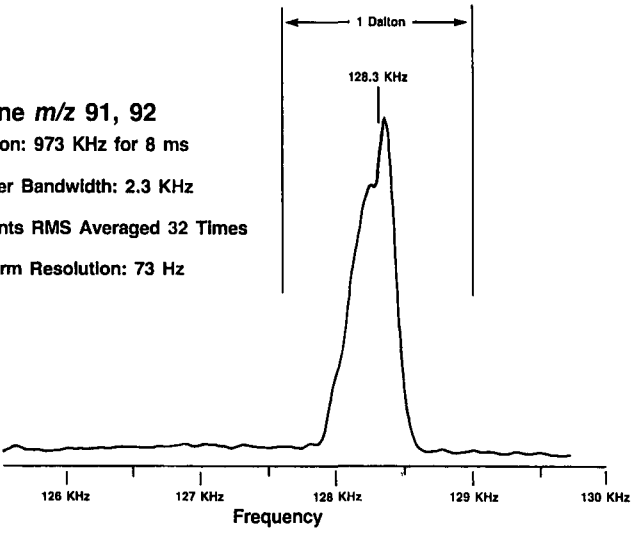

THE QUADRUPOLE ION TRAP AS A TANDEM MASS SPECTROMETER - INSTRUMENTATION AND APPLICATIONS

J.N. Louris, J. Amy, T. Ridley, C. Kascheres, R.G. Cooks, Purdue University, West Lafayette, IN 47907; M. Weber-Grabau and G. Stafford, Jr, Finnigan MAT, San Jose, CA 95134.

The quadrupole ion trap mass spectrometer may be used to generate daughter spectra of mass-selected parent ions. Ions are created within the trap by electron impact, undesired ions are ejected from the trap, and the selected parent ion undergoes collisionally activated dissociation (CAD). The CAD efficiency can be greatly increased by applying a small supplementary AC voltage of appropriate frequency across the end cap electrodes. Very high efficiency is often achieved, although the internal energy deposited is small (less than 2eV).

To provide an alternative to CAD for producing a daughter spectrum in the ion trap, a simple fiber optic interface which allows photodissociation has been developed. The apparatus consists of a Finnigan ion trap mounted on an optical rail in a vacuum manifold [1]. A probe consisting of a stainless steel tube encloses the fiber optic. The probe enters the vacuum cradle via a vacuum port, and the fiber is sealed to the probe with an O-ring seal. An aperture (1.3 mm diameter) in the trap's ring electrode allows insertion of the fiber so that light can irradiate the trap. The beam from a pulsed Nd:YAG laser equipped with harmonic generating crystals is focussed 1 cm before the end of the fiber optic so that the entire face of the fiber is illuminated. The laser is triggered by the same computer that controls all scan functions of the trap and a variety of experiments are possible by triggering the laser at the appropriate place in the scan. For example, if the laser is triggered instead of applying the supplementary AC voltage in a ms/ms scan, then the products of photodissociation may be observed. If the laser is triggered instead opening the electron gate, then a photoionization experiment is performed. Of course, photoionization products may also be produced in the photodissociation experiment, depending on the wavelength of light used and the nature of the compound.

Figure 3 illustrates two such experiments performed with the fiber optic. Both spectra were obtained by using a pulse of 266 nm light in place of electron impact ionization. The second spectrum differs from the first in that a 100 ms pause was inserted between the laser ionization pulse and the mass analysis scan. The first spectrum closely resembles an electron impact spectrum, but the second spectrum shows the products of an ion/molecule reaction. The ion of m/z 137 was further investigated by coupling photoionization, a reaction period, and an ms/ms scan using the supplementary AC voltage. CAD of this ion yielded m/z 81 and m/z 95, and not the monomeric ion, indicating that m/z 137 results from a dimerization with a covalent bond and not from a proton-bound dimer.

Previously, ions were always generated within the cavity of the trap rather than being generated outside of the trap and injected into the trap. In theory, ions injected into the trap must eventually strike a wall because of the excess kinetic energy which allowed them to enter the trap from the outside. This requirement severely restricts the use of modern ionization methods such as FAB, SIMS, and laser desorption because of the poor access to the cavity of the trap. Since it is known that about 1 millitorr of helium improves the performance of the trap, it seemed likely that this gas would permit the trapping of injected ions by removing kinetic energy through collisions. An ion injection source was constructed to inject ions through the aperture in the end cap through which electrons were usually admitted (along the axis of the trap). Figure 1 shows the three elements of the einzel lens which focuses the ions from an electron impact source (constructed from the lenses of a Finnigan 3200 source) onto this aperture. Figure 2 shows a cross section of the ion injection source (including the parts from the 3200 source which are affixed to the first element of the einzel lens which also serves as a support flange).

Figures 4 and 5 show preliminary results with this source indicating that spectra can be readily obtained. Both spectra in figure 4 were obtained with an electron energy of 20 V, which produced much less noise from stray ions than 70 V, because of the high helium pressure. The rising baseline in figure 5 is evidently due to an RF voltage dependence of the movement of stray ions around the trap.

Figure 6 shows the photodissociation of an ion which has been injected into the trap with a single pulse of the laser.

1. J.N.Louris, R.G.Cooks, J.E.P.Syka, P.E.Kelley, G.C. Stafford and J.F.J Todd, Anal. Chem., in press

Presented at the 35th ASMS Conference on Mass Spectrometry and Allied Topics
May 24-29, 1987, Denver, CO

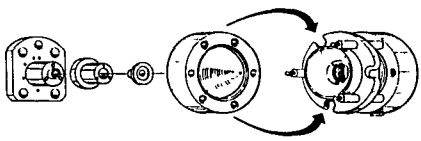

Figure 1 (Above)

Figure 2 (Right)

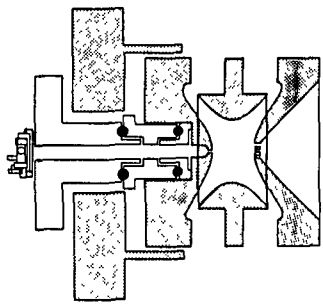

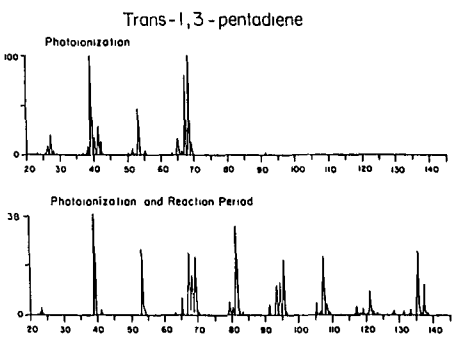

Figure 3

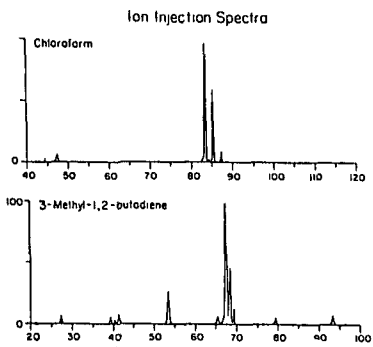

Figure 4

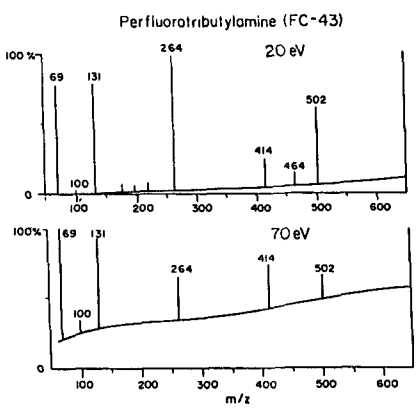

Figure 5

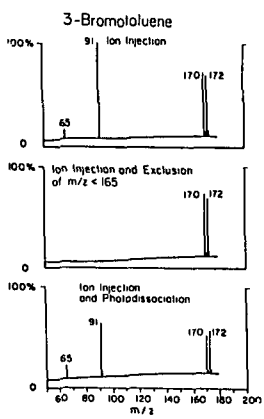

Figure 6

Presented at the 35th ASMS Conference on Mass Spectrometry and Allied Topics
May 24-29, 1987, Denver, CO

COLLISION ACTIVATED DECOMPOSITION OF NEGATIVE IONS IN AN ION TRAP MASS SPECTROMETER

Scott A. McLuckey and Gary L. Glish
Analytical Chemistry Division, Oak Ridge National Laboratory
Oak Ridge, TN

Paul E. Kelley
Finnigan MAT
San Jose, CA

Recent developments in the operation of three-dimensional quadrupoles have made these instruments useful analytical tools. In particular, the Finnigan Ion Trap Mass Spectrometer (ITMS) has been shown to be capable of routinely obtaining positive chemical ionization mass spectra and electron-impact mass spectra as well as MS/MS data. We are faced with analytical problems that are best approached by analyzing negative ions. The usefulness of negative chemical ionization (NCI) in the analysis of compounds that form stable negative ions is firmly established. Negative ions, however, had not been studied using the ITMS under the conditions in which it is normally operated. The objectives of this study were to establish if negative ions could be readily formed by NCI under conditions similar for positive ion CI, to determine if MS/MS spectra could be obtained for the anions, and, if MS/MS data could be obtained, to compare the spectra with MS/MS data acquired using other types of instruments.

Water was chosen as the reagent gas since it is usually present in the ion trap and it gives OH^- and $O^{-\cdot}$ reagent ions. Several organic nitro compounds were tested since these compounds are known to form stable negative ions and MS/MS data from other types of MS/MS instruments are available. The reagent ions expected for water were formed in the ratio $OH^-/O^{-\cdot} \approx 3$ under the conditions usually used to form reagent ions in positive CI. Electrons were pulsed into the trap and the ring electrode was held at a radio-frequency amplitude sufficiently low to allow the reagent ions to build up from ion/molecule and electron/molecule reactions. Helium is always present at a pressure of about 1 mtorr. Figure 1 compares the H_2O NCI mass spectrum of 2,4-dinitrotoluene obtained using the ITMS with an NCI mass spectrum obtained using a sector mass spectrometer and isobutane as a moderating gas. The major difference expected from the use of different reagent gases is that very few ions that serve as Bronsted bases are present with isobutane and, therefore, very little signal due to $(M-H)^-$ is observed for this reagent gas. The major reagent ion from water, on the other hand, is OH^- which tends to ionize by proton abstraction. Except for the $(M-H)^-$ ion, which is the base peak with water NCI but is largely absent with isobutane NCI, the mass spectra are very similar. Characteristic fragment ions are observed in both spectra that correspond to $(M-OH)^-$, $(M-NO)^-$, and NO_2^-. NCI mass spectra were also obtained for other dinitrotoluene isomers using the ion trap. The isomers could be readily distinguished based on the mass spectra.

MS/MS spectra were obtained for most of the major high mass anions formed in this study. Figure 2 compares the daughter ion MS/MS spectra of the molecular anions of three dinitrotoluenes. The major fragment ions are characteristic of nitroaromatic compounds and the isomeric ions can be distinguished based on their MS/MS spectra. The most noteworthy observation for the MS/MS spectra of the anions is the wide variation in the efficiency with which they can be converted to daughter ions. MS/MS efficiency is defined as the percentage of parent ions, present prior to collisional activation, converted to daughter ions. For the nitroaromatic anions, all molecular anions showed high MS/MS efficiencies (>55 %) whereas the $(M-H)^-$ ions all showed MS/MS efficiencies less than 25 %. The MS/MS efficiency for the $(M-H)^-$ anion derived from 2,4,6-trinitrotoluene was found to be <1 %. The variation in efficiencies is due to competition between electron detachment and fragmentation.

Presented at the 35th ASMS Conference on Mass Spectrometry and Allied Topics
May 24-29, 1987, Denver, CO

The MS/MS spectra obtained using the ITMS for anions derived from nitroaromatic compounds were similar to those acquired using a VG ZAB instrument. That is, the same mass daughter ions were observed in both sets of data. Rather different behavior, however, was observed for anions derived from 1,3,5-trinitro-1,3,5-triazacyclohexane. Some of the MS/MS spectra acquired with the ITMS and the VG ZAB instruments were similar for the same nominal mass parent ions but others were not. When more experience is gained with the ITMS in analyzing negative ions, the reason(s) for the observed differences may become apparent.

The conclusions of this work are that negative ions can be readily formed in the ITMS and analyzed by MS/MS. The sensitivity of MS/MS can, however, be affected by the relative propensities for electron detachment and fragmentation. For the most part, NCIMS and MS/MS data obtained with the ITMS are similar to the data obtained from other mass spectrometers. However, some exceptions were found that may implicate the relatively reactive environment in the ITMS.[1]

1. S.A. McLuckey, G.L. Glish and P.E. Kelley, Anal. Chem., In Press.

This work was supported by the U.S. Department of Energy, Office of Basic Energy Sciences, through Contract DE-AC05-840R21400 with Martin Marietta Energy Systems, Inc.

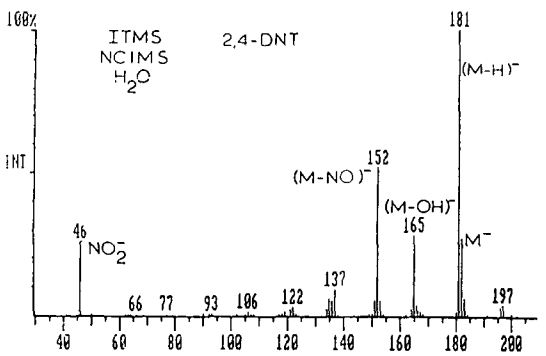

NEGATIVE ION MASS SPECTRA OF 2,4-DNT

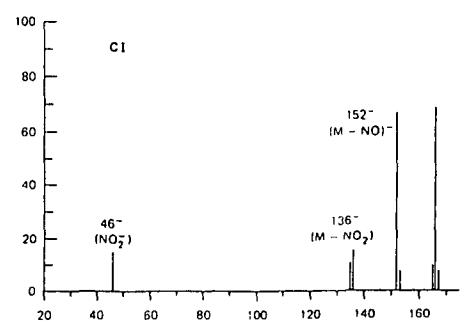

Figure1

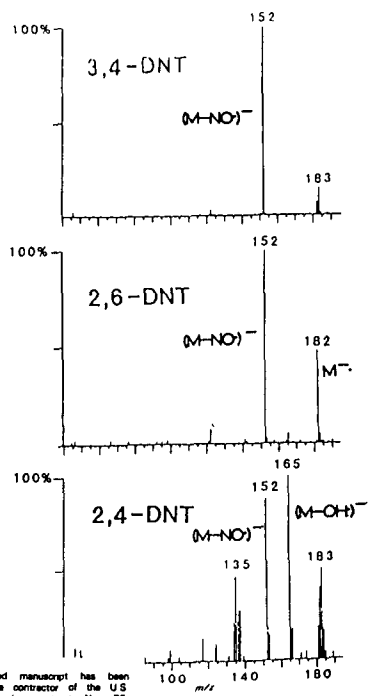

Figure 2

"The submitted manuscript has been authored by a contractor of the U.S. Government under contract No. DE-AC05-84OR21400. Accordingly, the U.S. Government retains a nonexclusive, royalty-free license to publish or reproduce the published form of this contribution, or allow others to do so, for U.S. Government purposes."

Presented at the 35th ASMS Conference on Mass Spectrometry and Allied Topics
May 24-29, 1987, Denver, CO

COMPARISON OF MS/MS WITH TRIPLE QUADRUPOLE AND ION TRAP TANDEM MASS SPECTROMETERS

J.V. Johnson and R.A. Yost
Chemistry Dept., Univ. of Florida, FL 32611
D. Bradford and P. Kelly
Finnigan MAT, San Jose, CA 95134

The ion trap mass spectrometer (ITMS) represents a new approach to instrumentation for tandem mass spectrometry (MS/MS). With the ITMS, ionization of molecules, selection of parent ions, collisionally activated dissociation (CAD) of the parent ions, and mass analysis of their daughter ions all occur sequentially in the same physical space, and thus, MS/MS is tandem in time. This is in direct contrast to tandem mass spectrometry with triple quadrupole instruments, where these processes occur in discrete regions and MS/MS is tandem in space. Here we report the results of our comparison of an ITMS and a triple quadrupole instrument (QQQ) with respect to fragmentation efficiency, collection efficiency, overall sensitivity, limit of detection, and linear dynamic range.

The performance of the two types of MS/MS instruments was evaluated for the methane PCI-CAD of the $(M+H)^+$ ions of diethylethylphosphonate (DEEP) and diisopropylmethylphosphonate (DIMP). The preliminary triple quadrupole characterization of these compounds was performed on a Finnigan MAT TSQ45 and the quantitation reported below was done on a Finnigan TSQ70. All ion trap data was obtained on a Finnigan ITMS instrument. For the quantitative comparisons, DIMP was introduced via a GC (Varian 3300 with a 28 m DB-5 FSOT capillary column and a Varian 3400 with a 30 m SE-54 FSOT column for the ITMS and TSQ, respectively: injection ports and GC/MS interfaces were set to 250 C: 1.5 uL splitless injections; column at 50 C for 1 min and then heated to 160 C @ 30 C/min). Samples for quantitation were prepared by serial dilution from a DIMP in methanol stock solution of ca. 1 ppthousand.

The relative abundances of the daughter ions are ca. the same for PCI-CAD daughter spectra of the $(M+H)^+$ ion of DEEP obtained on the triple quadrupole and ITMS. However, the abundances of the daughter ions relative to that of the parent ion in the daughter spectra indicate that the ITMS gives a higher fragmentation efficiency. This fragmentation efficiency can be varied on both instruments by changing the CAD energy (i.e. the Q2 quad offset voltage for QQQ and the tickle voltage for the ITMS). For the QQQ, there is significant CAD occuring even at an indicated Q2 quad offset of zero as the ions must have some axial energy in order to transverse the quadrupoles and be detected (Figure 1a). However, in the ITMS the ions are already in the CAD region and only need to be energized to have sufficient kinetic energy to allow CAD to occur. Thus, one obtains relatively sharp rises in the daughter ion intensities once a sufficient appearance energy has been reached (Figure 1b). As the relative abundances of the daughter ions are ca. the same, the amount of internal energy added to the parent ion during CAD is similar in the two systems. The greater fragmentation efficiency observed with the ion trap is due largely to the time scale and nature of the CAD process. Whereas with the QQQ, a parent ion must undergo CAD during its single pass through the collision chamber, the ITMS is able to contain the parent ion and keep energizing it to undergo multiple collisions until CAD does occur. This control of the CAD reaction time, allows one to increase significantly the yield of daughter ions. Also because of the more effective containment or trapping of the daughter ions in the ion trap, the subsequent collection and mass analysis of the daughter ions was ca. 27 times more efficient in the ITMS than in the QQQ system.

Due to this increased efficiency of fragmentation, collection, and mass analysis, higher MS/MS sensitivity was expected with the ITMS than for the QQQ. Calibration curves obtained from the quantification of DIMP in methanol standards are shown in Figure 2 for the ITMS with full scan (50 -> 225 u in 1 sec, 7 microscans) and for the TSQ 70 with selected reaction monitoring (SRM, 181^+ -> 97^+) and full scan (50 -> 225 u in 1 sec). The limits of detection are ca. 2 pg of DIMP injected onto the GC column for both the QQQ SRM and for the ITMS. Whereas the TSQ 70 was only able to obtain good, qualitative spectra (without background subtraction) on ca. 1.5 ng DIMP injected (Figure 3), the ITMS was able obtain very good daughter spectra on only 15 pg (Figure 4). Although the

triple quadrupole yielded a linear dynamic range of 4 orders of magnitude with SRM, the QQQ full scan and ITMS full scan only exhibited a linear dynamic range of 3 orders of magnitude. The linear dynamic range is limited at the upper range in the ITMS by space charge effects which lead to the broadening of the ion peak and apparent shifts in the secular frequencies of the parent ions. Although not investigated here, various approaches to overcoming this limitation are available, including automatic variation of the ionization time and mass-selectively filling of the trap.

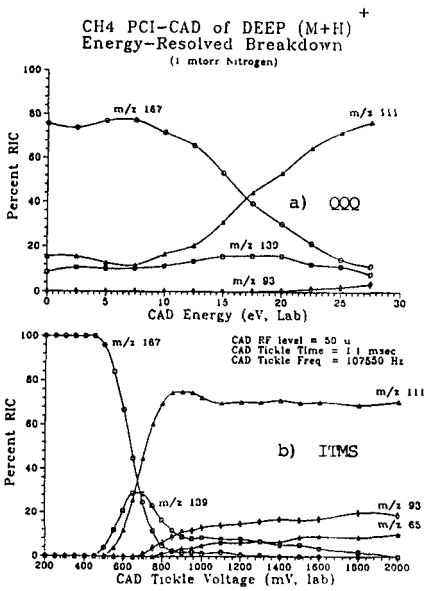

Figure 1.

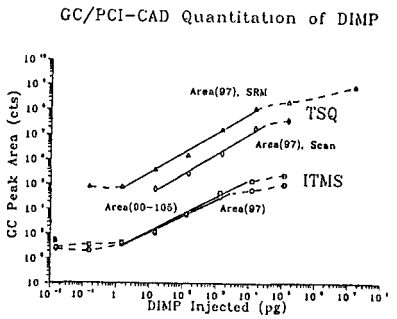

Figure 2.

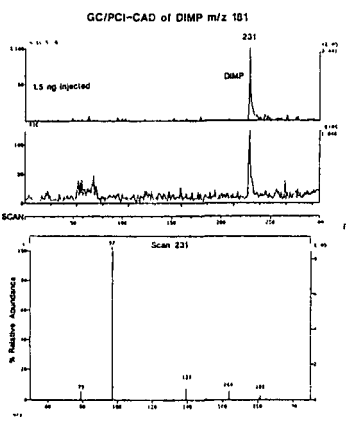

Figure 3. QQQ

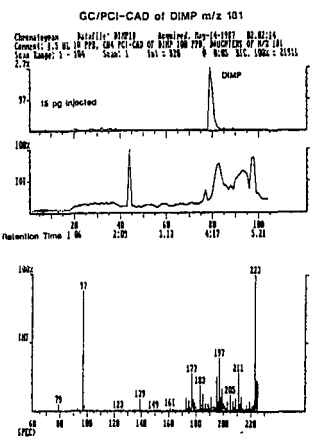

Figure 4. ITMS

Presented at the 35th ASMS Conference on Mass Spectrometry and Allied Topics
May 24-29, 1987, Denver, CO

ENHANCED SENSITIVITY & DYNAMIC RANGE ON AN ION TRAP MASS SPECTROMETER WITH AUTOMATIC GAIN CONTROL (AGC)

George C. Stafford, Dennis M. Taylor, Steve C. Bradshaw, John E. P. Syka &
Mark Uhrich, Finnigan MAT, San Jose, California

The working sample dynamic range of any ion trap mass spectrometer is limited by the onset of space charge. As the analyte sample pressure increases inside a working ion trap, the number of stored ions will increase proportionally. If a high enough concentration of stored ions is reached, the resulting space charge can partially cancel the quadrupole field causing stability limits to change. This effect will appear as a shift in mass peak position. Secondly, space charge can cause inhomogeneity in the quadrupole field thus smearing the ion stability limits. This second effect will appear as a loss in mass resolution. Figure I illustrates this space charge effect on mass peak 131.

A new scan function (AGC) has been developed for ion trap instruments that automatically under computer control measures the total amount of stored ions, and then adjusts the ionization time to maximize sensitivity while preventing unwanted effects from space charge. The rf ion trapping voltage level for the AGC scan function is shown in figure 2.

Ion trap sample response in the non AGC mode is shown in figure 3. The units for sample amount are not labeled as they are dependent on sample characteristics and filament emission current. Typical response lines are shown for a long ionization time of 10 msec and a short ionization time of 0.1 msec. Low level sample detection limit is set by the minimum number of detectable trapped ions (approximately 100). High sample concentration is limited by sample charge and, as shown in figure 3, occurs around 100 K stored ions. This non AGC method gives a working sample concentration dynamic range of approximately 1000.
The ion trap response with AGC is illustrated in figure 4. Sensitivity is increased at low sample concentrations by automatically ionizing at the maximum time of 25 msec. Space charge is avoided and the integrity of the mass spectrum is maintained at high sample concentrations by ionizing at the minimum time of 78 usec. With this AGC method, up to 6 orders of linear dynamic response can be achieved.

A GC/ion trap response curve for a volatile organic analysis via liquid sample concentrator is shown in figure 5. In this example, m/z 112 is plotted for chlorobenzene under full scan operation with and without AGC. Under AGC operation, these response data were automatically normalized for the actual ionization time used when the individual spectra were acquired.

In summary, automatic gain control of ion trap ionization time provides: (1.) Increased sensitivity at low sample concentrations allowing full scan spectra, (2.) reduced sensitivity at high sample concentration to maintain spectral line shapes, (3.) improved range of linear sample response.

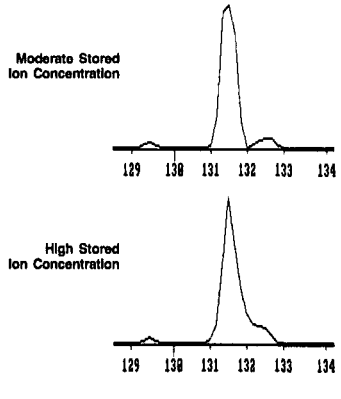

Figure 1. Effects of ion trap space charge on spectral line shapes

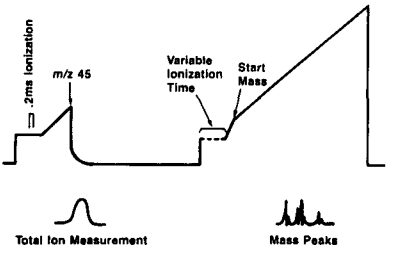

Figure 2. Ion Trap Automatic Gain Control (AGC)

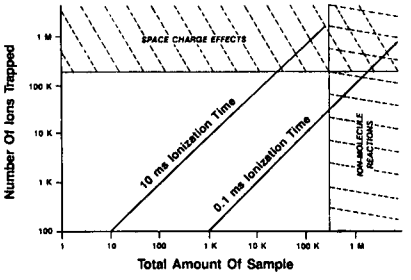

Figure 3. Ion trap response non AGC

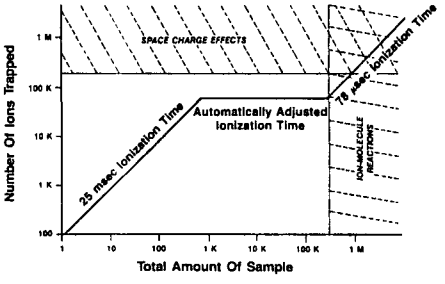

Figure 4. Ion trap response in AGC operation

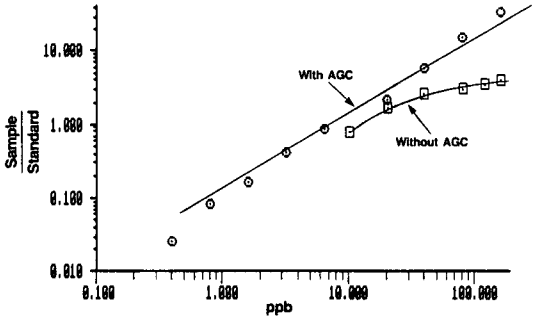

Figure 5. Chlorobenzene response curve via liquid sample concentrator

Presented at the 35th ASMS Conference on Mass Spectrometry and Allied Topics
May 24-29, 1987, Denver, CO

Bimolecular Reactions of Carbon Dioxide Microcluster Ions with Water, Investigated with a Tandem Molecular Beam Quistor Quadrupole Instrument

G. Romanowski*, R.-H. Gabling** and K. P. Wanczek
Inorganic Chemistry, NW 2, University, D-28 Breen 33, West Gemany

The properties of van der Waals clusters have been of great interest in recent years. They are of fundamental importance in the understanding of nucleation and condensation phenomena. Weak molecular interactions can be studied. Clusters link the properties of the isolated molecules in the gas phase to the bulk properties in the condensed phase.
Cold microclusters of carbon dioxide were generated by supersonic expansion with a molecular beam instrument, which has been described in detail elsewhere (1). The apparatus consists of three stages which are differentially pumped, the nozzle, skimmer, and collimator chambers. Stagnation pressures of up to 3 bars can be used with a nozzle of 0.3 mm diameter. Mass analysis of the clusters ionized by 90 eV electron impact is performed by a quadrupole mass spectrometer. For the study of the reactions with monomeric molecules and of collision-induced dissociation and slow unimolecular decomposition the cluster ions are trapped in a Quistor ion trap between 0 and 50 ms. Mass analysis is carried out with the quadrupole mass spectrometer after ejection of the ions from the Quistor. The pressure of the neutral gas can be varied between 10^{-5} and 10^{-6} mbar. It can be determined only outside the Quistor. Therefore the values are only lower limits. The mass range which can be trapped with the Quistor is limited by the amplitude of the rf radiation, which is generated with a homebuilt generator (2). m/z 20 - 230 is covered. Therefore the reactions of the cluster ions $(CO_2)_2^+$, $(CO_2)_3^+$, $(CO_2)_4^+$, and $(CO_2)_5^+$ can be studied. These clusters have lifetimes of more than 50 ms and are stable enough to undergo ion-molecule reactions under single collision conditions.
Three kinds of reactions of cluster ions have been studied:
- slow unimolecular decompositions,
- bimolecular reactions of ionized clusters with neutral molecules (cluster ion-molecule reactions), and
- bimolecular reactions in the cluster ions (intracluster ion-molecule reactions) (1).

Here only the cluster ion-molecule reactions of carbon dioxide cluster ions with water will be discussed.
The reactions start already at water pressures as low as 10^{-6} mbar. Two product ions are observed, $CO_2H_2O^+$, m/z = 62, and $(CO_2)_2H_2O^+$, m/z = 106. No further product ions are detected in the pressure range up to 10^{-5} mbar. With mass-selective trapping experiments the formation reactions 1 and 2 are determined:

$$(CO_2)^+_{x+1} + H_2O \rightarrow CO_2H_2O^+ + x\,CO_2 \quad , x \geq 2 \qquad 1$$

$$(CO_2)^+_{y+2} + H_2O \rightarrow (CO_2)_2H_2O^+ + y\,CO_2 \quad , y \geq 3 \qquad 2$$

*Present address: Philips Research Laboratories, D-51 Aachen, F.R.G.
**Present Address: Bruker Franzen Analytik, D-28 Bremen, F.R.G.

The binding energy of the mixed cluster ions formed in reactions 1 and 2 is large enough to yield dissociation of at least two neutral carbon dioxide molecules (reaction 1) or three carbon dioxide molecules (reaction 2).
The bond dissociation energies of the dimer, trimer and tetramer ions are 0.51±0.04 eV, 0.14±0.06 eV and 0.12±0.02 eV (3). From the known bond dissociation energies limits for the heat of formation of $CO_2H_2O^+$ can be deduced from equations 1 and 2. From eq. 1

$$(0.14 + 0.12)\ \text{eV} = 0.26\ \text{eV} \gtrsim -\Delta H(1) \gtrsim 0.65\ \text{eV} = (0.51 + 0.14)\ \text{eV}$$

is obtained and from eq. 2

$$(0.14 + 2 \times 0.12)\ \text{eV} = 0.38\ \text{eV} \gtrsim -\Delta H(2) \gtrsim 0.77\ \text{eV} = (0.51 + 0.14 + 0.12)\ \text{eV}.$$

If one assumes that the adduct formation in both reactions occurs by association of H_2O to a CO_2^+ ion:

$$H_2O + CO_2^+ \rightarrow CO_2H_2O^+ \qquad 3$$

one gets for the heat of formation of $CO_2H_2O^+$ (4)

$$0.38\ \text{eV} \gtrsim -\Delta H(f) \gtrsim 0.65\ \text{eV}.$$

1. G. Romanowski and K. P. Wanczek, Int. J. Mass Spectrom. Ion Processes 62 (1984) 227.
2. R.-H. Gabling, G. Romanowski and K. P. Wanczek, Int. J. Mass Spectrom. Ion Processes, 69 (1985) 153.
3. S. H. Linn and C. Y. Ng, J. Chem. Phys., 85 (1981) 4921. (1981) 4446.
4. G. Romanowski and K. P. Wanczek, Int. J. Mass Spectrom. Ion Processes, in press.

Presented at the 35th ASMS Conference on Mass Spectrometry and Allied Topics
May 24-29, 1987, Denver, CO

SELECTION OF PARAMETERS FOR ION EXCITATION AND EJECTION IN FOURIER TRANSFORM MASS SPECTROMETRY

CODY, R.B., GOODMAN, S.D , GHADERI, S.
Nicolet Analytical Instruments
Madison, WI 53711

SHOHET, J.L.
University of Wisconsin
Madison, WI 53705

Two excitation methods are commonly employed in Fourier transform mass spectrometry (FTMS). These are pulsed, single-frequency ("burst") excitation and swept frequency "chirp" excitation. Stored waveform, inverse Fourier transform ("SWIFT") excitation is a recently-developed method which is extremely promising [1,2].

We have examined the characteristics of these excitation methods by monitoring ion abundance for different masses as a function of excitation amplitude. Burst excitation is well-behaved, and may be used as a model for comparison with chirp and SWIFT excitation.

Chirp excitation is found to have several idiosyncracies. Ion trajectory models show that ions excited by a chirp are drifted off-center slightly (approximately one orbital radius), and have a smaller final orbital radius than expected (0.5 cm.). If very slow sweep rates, high excitation amplitudes, or low trapping voltages are used, then z-axis ejection may occur, starting with low masses. However, if the excitation parameters are kept within recommended bounds, then FTMS spectra with chirp excitation accurately reflect relative ion abundances in the cell. Three-dimensional ion trajectory models for standard chirp excitation conditions confirm these statements.

Constant-phase SWIFT excitation is found to have many characteristics in common with burst excitation. Ions may be excited to the maximum possible orbital radius at a predictable excitation amplitude, and all ions may be ejected at the same amplitude, regardless of mass. Ejection of ions along the z-axis is not found to present a problem for constant-phase SWIFT excitation. Both burst and SWIFT excitation may be used to excite ions to the maximum possible orbital radius thus obtaining greater sensitivity than is possible with chirp excitation.

References:

1. Marshall, A.G.; T.-C. L. Wang; Ricca, T.L. - J. Am. Chem. Soc. 1985, 107, 7893-7897

2. Wang, T.-C. L.; Ricca, T.L.; Marshall, A.G. - Anal, Chem. 1986 58, 2935-2938

Presented at the 35th ASMS Conference on Mass Spectrometry and Allied Topics
May 24-29, 1987, Denver, CO

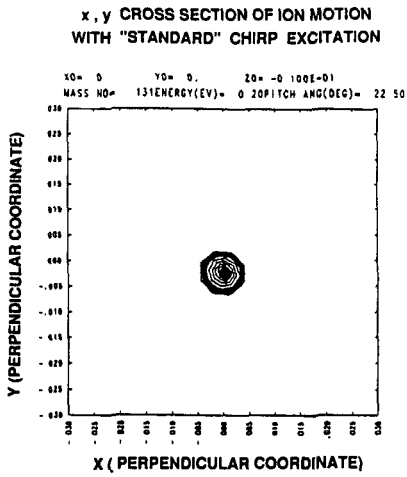

FIGURE 1: x,y cross section trajectory for an ion undergoing chirp excitation

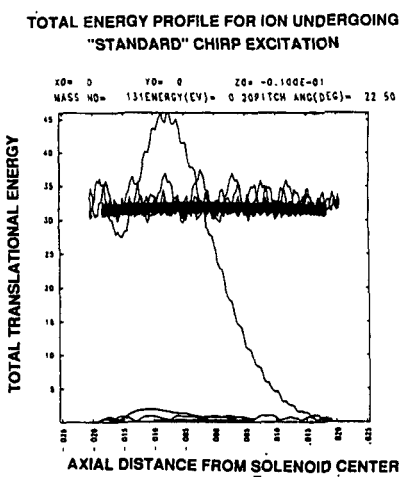

FIGURE 2: total ion energy vs. z-axis position for an ion undergoing chirp excitation

Presented at the 35th ASMS Conference on Mass Spectrometry and Allied Topics
May 24-29, 1987, Denver, CO

COLLISIONAL SIGNAL DECAY AND ULTRA-HIGH RESOLUTION FTICR

F.H.Laukien; Chemical Physics, Harvard U., Cambridge, MA 02138.

I. COLLISIONAL SIGNAL DECAY

The Langevin [1] cross section σ^L for gas-phase ion-neutral collisions is inversely proportional to the relative velocity v. As v increases, the Langevin approximation ceases to be valid. Figure 1 demonstrates that σ^L is realistic only for near-thermal collisions with energies up to about 0.4 eV.

In ICR at 4.7 Tesla this corresponds to cyclotron radii ρ_c up to about 0.2 mm. Since the radii of accelerated ions are 10-100 times larger, we conclude that collisional signal decay has to be analyzed using hard-sphere models.

Fig.1

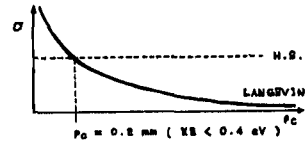

Hard-sphere collision cross sections frequently scale with mass according to models A or B:

Model A: σ^A = constant

Model B: $\sigma^B \propto m^{2/3}$

Model A is useful for atomic ions and isotope patterns, whereas model B is applicable for organics and clusters. Using σ^A and σ^B instead of σ^L has a profound impact on the expressions for the mean-free time τ, the mass resolving power $m/\Delta m$, the peak height H, and the signal-to-noise ratio S/N of FTICR in the collisional broadening domain. The mean-free times depend on mass m and ρ_c according to

Langevin: $\tau^L \propto \mu^{1/2}$

Model A: $\tau^A \propto m / \rho_c(t)$

Model B: $\tau^B \propto m^{1/3} / \rho_c(t)$

The expressions for the FTICR resolution in the collisional broadening domain aregiven by

Langevin: $(m/\Delta m)^L \propto \mu^{1/2} / m$

Model A: $(m/\Delta m)^A \propto 1 / \rho_c(0)$

Model B: $(m/\Delta m)^B \propto 1 / m^{2/3}\rho_c(0)$

The expressions for $m/\Delta m$ are valid only for effective ion-removal collisions [2].

In the time-domain, both the initial signal intensity s(0) and the initial S/N are proportional to $\rho_c(0)$ [3]. In FTICR, however, we measure the frequency (mass) domain signal height H and S/N. Both are proportional to the area under the signal-decay envelope, which is approximately given by $s(0)\tau$. Although in the Langevin approximation both H and S/N are proportional to $\rho_c(0)$, an analysis using hard-sphere cross sections shows that both H and S/N are independent of $\rho(0)$. Experiments corroborate these theoretical results:

Fig. 2a

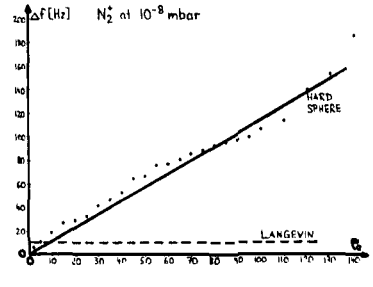

Fig. 2b

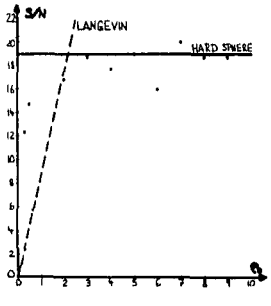

Consequently, as far as ρ_c is concerned, there is no trade-off between resolution and S/N in FTICR: However, while the Langevin model suggests that large ρ_c should be chosen in order to maximize S/N without loss of resolution, the correct hard-sphere model, on the contrary, predicts that small cyclotron radii maximize the resolution without any penalty in sensitivity. Experimentally, this fact often is obscured by space-charge broadening for small ρ_c.

Moreover, H and S/N depend on how exactly the hard-sphere cross sections scale with mass [2]. Hence, if relative peak heights are to be measured very precisely in FTICR, appropriate corrections factors, which have to be calculated from detailed prior knowledge of σ, should be applied. A final conclusion is that the pressure broadening domain extends to much lower pressures than previously assumed.

II. ULTRA-HIGH RESOLUTION FTICR: THEORETICAL PREDICTIONS

Using the combination of a titanium-sublimation pump and a 60l/sec ion pump shown in Fig.3 we reach vacua below 10^{-11} mbar. On a Bruker CMS 47, we have observed signal decays which last over 40 seconds. Our best mass resolution at 18 amu was 4 x 10^8 with a FWHM of .009 Hz, and S/N = 10.

Fig.3

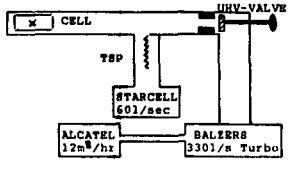

In supercon magnets the long-term field decay, due to the residual resistance of about 10^{-14} Ω, limits the maximum mass resolution to $m/\Delta m = 10^{11}/T_{obs}$. Obviously, as T_{obs} approaches 100 seconds, the FTICR resolution will ultimately be limited to about 10^9. If higher resolution is desired, it will become mandatory to counter this field decay by applying a voltage ramp to the B_0-coil of a room-temperature shim system. For short-term random drifts a feedback loop may have to be utilized in addition. While the use of NMR locks is conceivable, the most promising solution seems to be a heteromolecular ICR field-frequency lock, which monitors a reference ion in dispersion mode while observing the ion of interest in absorbtion mode.

Previous theoretical calculations [4] have shown that radial magnetic field gradients g_ρ will limit the resolution; the same holds true for radial terms in the electrostatic field E. We suggest here a method for overcoming this limitation by modulating the radial magnetic and electrostatic terms by a sine wave. If g_ρ determines the resolution, then a 10-100 Hz modulation, which is symmetric about zero, should increase $m/\Delta m$ considerably.

A corollary of this technique is the theoretical prediction that a sudden reversal of the sign of g_ρ during the signal decay will refocus ions which have become dephased due to a spread in the cyclotron radii [4]: if the sign reversal occurs at time t, then an ICR echo will appear at time 2t. Whether the ICR echoes predicted here are useful like NMR echoes remains to be seen.

REFERENCES

[1] P.Langevin, Ann. Chim. Phys., 5 (1905) 245.
[2] F.H.Laukien, to be submitted to Int.J. Mass Spec. Ion Proc.
[3] M.B.Comisarow, J. Chem. Phys. 69 (1978) 4097.
[4] F.H.Laukien, Int.J. Mass Spec. Ion Processes., 73 (1986) 81.

Presented at the 35th ASMS Conference on Mass Spectrometry and Allied Topics
May 24-29, 1987, Denver, CO

Laser Desorption Fourier-Transform Mass Spectrometry Using a Dual-Cell Configuration: Evaluation and Applications

David A. Weil and Richard Hein
Nicolet Instrument Corporation, 5225-1 Verona Road, Madison, Wi 53711

Previously reported laser desorption-Fourier transform mass spectrometry (LD/FTMS) studies by several research groups used a Nicolet FTMS-1000. In the single-cell configuration of the FTMS-1000, ion formation and ion detection are done in the same cell. In FTMS, mass resolution is proportional to pressure,so lower pressures yield better resolution. Two problems are encountered with laser desorption: **A)** sample pump-down delay caused by solvent evaporation from the sample (up to 30 minutes for the system to reach 1 - 2 x 10^{-8} torr); and **B)** no separation of ion formation (pressure burst accompanies laser desorption event) from excitation and detection, so a delay up to several seconds is added. In general, the dual-cell configuration of the FTMS-2000 is employed to separate the high-pressure ion formation region from a low-pressure excitation and detection region. For laser desorption, this allows faster sample turn-around times, and minimal delays between ion formation and detection. The dual-cell configuration has these advantages:

- **Improved sample throughput** from reduced pump-down time (source pressure in low 10^{-8} torr range after 5 minutes).
- **More efficient parabolic reflective optics used** (less susceptible to damage from ablated sample material compared to ZnSe focussing lens of the FTMS-1000.
- **Improved focussing ability gives smaller spot size diameter** (~150 microns) and thus higher power-density at sample surface.
- **Fewer unimolecular and ion-molecule reactions** by minimizing delay between ion formation and detection.
- **High resolution measurements made more simple** by separating ion formation from ion detection.

Some important applications of LD/FTMS is for surface and bulk analysis of silicon wafers, polymer films, and impurities on metals. In the analysis of silicon wafers, a negative ion LD/FTMS spectrum of a "control" wafers produces carbon cluster ions C_n+, with **n** from 4 to 12, indicating the presence of carbon on the wafer surface. The positive ion spectrum of the control wafer, Figure 1A, shows primarily Si^+ and $SiOH^+$ on the surface. Positive ion LD/FTMS of an impure wafer shows, in addition, P^+ and PO^+, indicating the presence of a phosphorus-containing impurity. Accurate mass analyses are also possible using LD/FTMS. The 55 - 57 Dalton region of the spectrum is shown in Figure 2, revealing that there are 5 major peaks at m/e 56. This is a resolution of better than 7000, sufficient to fully resolve Fe^+ from Si_2^+, if present . Depth profiling is also possible, showing, for example, a decrease in PO^+ and an increase in P^+ with number of laser events at the same site.

A recent analytical problem was the analysis of a green deposit found on the inside of a section of water pipe which had been in use for some time. The positive ion LD/FTMS spectrum of the deposit is shown in Figure 3A, showing significant Pb^+ and $PbOH^+$ ions. $PbOH^+$ was identified by accurate mass measurement to better than 0.3 ppm relative error. The negative ion spectrum in Figure 3B shows a strong peak at m/e 79, arising from the PO_3^+ ion. The green deposit is probably a combination of copper and lead phosphate or phosphite.

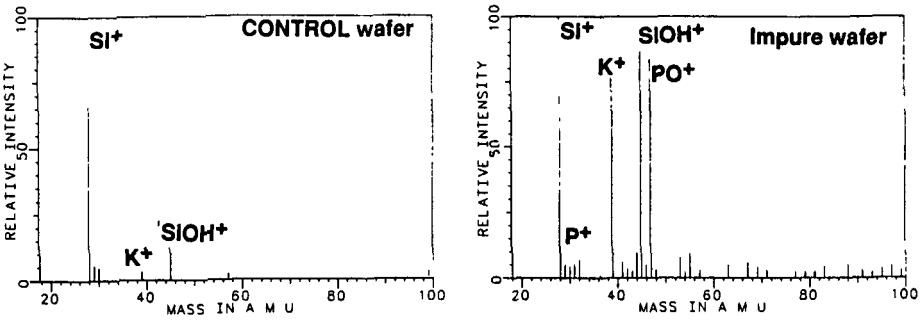

Figure 1. A: Control wafer, positive ion spectrum; B: Impure wafer, positive ion spectrum.

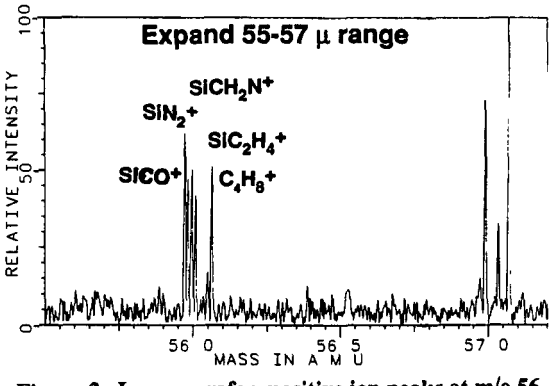

Figure 2. Impure wafer, positive ion peaks at m/e 56.

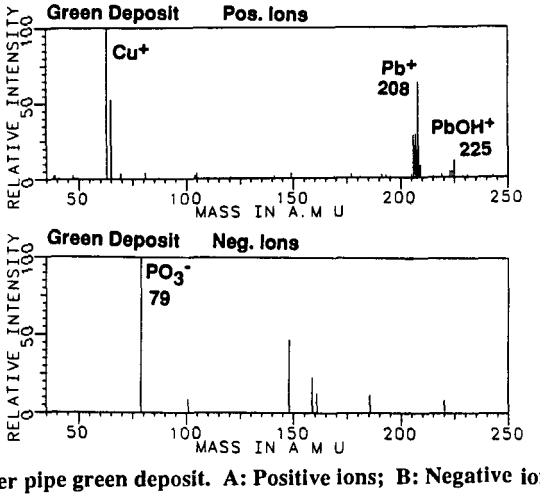

Figure 3. Water pipe green deposit. A: Positive ions; B: Negative ions.

Presented at the 35th ASMS Conference on Mass Spectrometry and Allied Topics
May 24-29, 1987, Denver, CO

Laser Desorption/Fourier Transform Mass Spectrometry for the Analysis of Polymer Additives

Carolyn L. Johlman and C.L. Wilkins, Department of Chemistry, University of California, Riverside, CA 92521 and M. Youssefi, Union Carbide Corporation, Bound Brook, NJ 08805

Mass spectrometry offers several advantages over other analytical techniques for the identification of polymer additives in that only a small amount of sample is required, and by using soft ionization techniques the molecular weight of the additives can usually be obtained directly from the mass spectrum. This paper presents a comparison of the application of laser desorption Fourier transform mass spectrometry (LDFTMS), and fast atom bombardment (FAB) to the analysis of polymer additives.

The LD/FTMS system used here couples a Tachisto 215G pulsed TEA CO_2 laser with a Nicolet FTMS-1000 mass spectrometer equipped with a 3.0-T superconducting magnet. For the measurements reported here, the laser delivered between 300 and 1000 mJ per 40-ns pulse at 10.6 μm. The maximum repetition rate was 1.0 Hz. The laser beam enters the vacuum system through a zinc selenide window and travels parallel to the magnetic field, striking the sample probe. A 2-in. cubic analyzer cell made of 80% transmissive etched stainless steel was used. The laser beam was focused by a 3-in. focal length zinc selenide lens to a diameter of approximately 500 μm on the stainless-steel probe tip. Power density at the probe tip was in the range of 10^8 to 10^9 W/cm^2. The laser was triggered as part of the FTMS experimental sequence. To increase mass resolution, a delay of 3-10 s between the laser pulse and detection was used. A bandwidth of 100 MHz and 64 K data were sufficient to provide at least 10000 mass resolution at m/z 1000 for all spectra. Samples were prepared by dissolving polymer additives in suitable solvent (CH_2Cl_2 or methanol) and depositing the mixture on a stainless steel probe tip. A salt, usually KBr or NaCl, was present in the sample as dopant.

Table I presents a compilation of the polymer additives for which spectra were obtained by LD/FTMS. In general it was found that the technique provided predominately molecular weight information although diagnostic fragment ions were also observed. A comparison of LD/FTMS and FAB spectra was conducted and demonstrated the superiority of LD/FTMS for all additives. Either no FAB spectrum could be obtained or extensive fragmentation severely limited the utility of the method for analysis. For example, Figure 1 contrasts FAB and LD/FTMS spectra for the additive Seenox 4125.

Irganox 1010, which is an antioxidant in polymers such as polyethylene glycol, served as a model additive in the development of analytical procedures which utilized LD/FTMS to make direct measurements. In contrast to more traditional analysis procedures which require extraction and concentration of the Irganox, the positive ion LD/FTMS spectrum of the additive in dry mixes and films with polyethylene exhibits an intense $(M+K)^+$ when KBr is present. The polyethylene substrate does not interfere with detection of the molecular species because it yields no background ions above 300 amu. Even at levels below 0.1% in dry mixes with polyethylene, the predominate $(M+K)^+$ for Irganox permits identification and suggests the superiority of LD/FMTS for rapid direct analysis of additives. As an alternative, polymer additives extracted from the polymer matrix may also be examined. Figure 2 presents an LD/FTMS Irganox 1010 spectrum obtained by extracting the additive (present at 100 ppm) from a commercial resin with cyclohexane.

Presented at the 35th ASMS Conference on Mass Spectrometry and Allied Topics
May 24-29, 1987, Denver, CO.

name	M.W.	fragmentation LD/FTMS	fragmentation FAB
distearyl thiodipropionate	683	$(M+K)^+$; m/z 722	--
dilauryl thiodipropionate	514	$(M+K)^+$; m/z 553	--
spinuvex	1800-2000	envelope from m/z 800 to 3800	--
Goodrite 3114	784	$(M+K)^+$; m/z 822	$(CH_2C_6H_3(C_4H_9)_2OH)^+$; m/z 219
Seenox 4125	1161	$(M+Na)^+$; m/z 1184	$(H_2SC_{12}SCH_2)^+$; m/z 215
Sandostab PEPQ	1035	M^+; m/z 1035	$P[OC_6H_3(C_4H_9)_2]_2^+$; m/z 441
Irganox 1010	1177	$(M+Na)^+$,$(M+K)^+$; m/z 1200,1215	$(HOC_6H_2(C_4H_9)CH_2)^+$; m/z 219

Table 1. Compilation of LD/FTMS and FAB data for polymer additives. The predominant ions from each spectrum is listed.

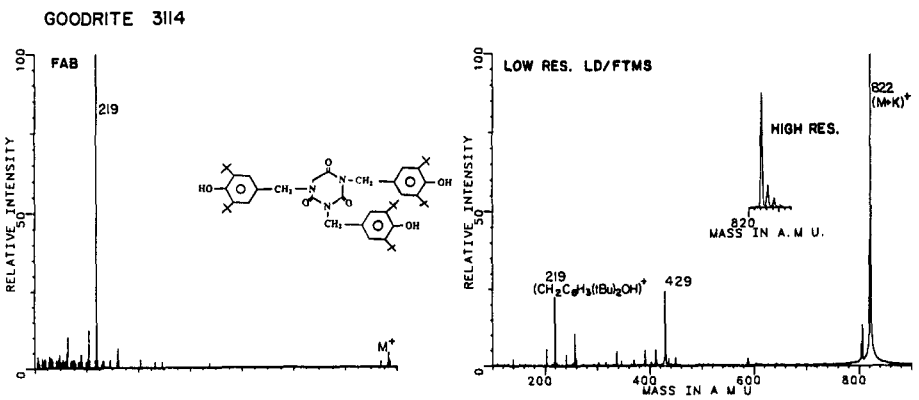

Figure 1. Comparison FAB and LD/FTMS spectra of the polymer additive Goodrite 3114 (MW = 783.5). The FAB spectrum was obtained on a VG-ZABHF at an 8 kV accelerating voltage with an instrument resolution of 1000. The additive was prepared in a matrix of 3-nitrobenzyl alcohol.

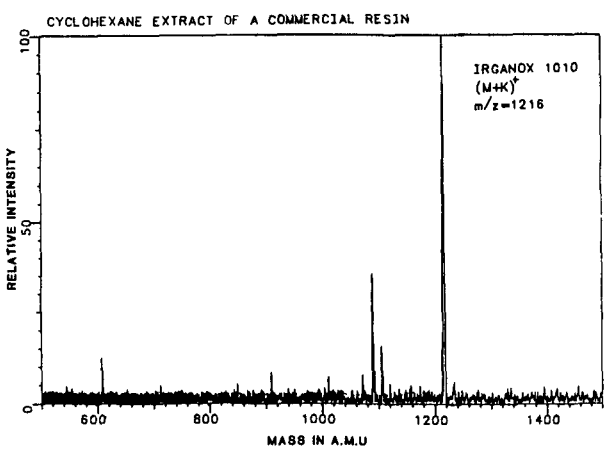

Figure 2. LD/FTMS spectrum of Irganox 1010 present at 100 ppm in a commercial resin, extracted with cyclohexane.

Presented at the 35th ASMS Conference on Mass Spectrometry and Allied Topics
May 24-29, 1987, Denver, CO

STABILITY DIAGRAM DETERMINATION AND ION TRAJECTORY MODELLING FOR THE ION TRAP MASS SPECTROMETER

J.F.J. Todd and J.J. Bexon, Chemical Laboratory, University of Kent, Canterbury, CT2 7NH, UK, and R.D. Smith, Finnigan MAT, Hemel Hempstead, HP2 4TG, U.K.

Earlier extensive work on the quadrupole ion storage trap (QUISTOR) demonstrated how device performance could be characterised in terms of the observed Mathieu stability diagram[1]. A recent development of this device has been the Ion Trap Mass Spectrometer, which affords a means of analysis using mass selective instability combined with light-gas moderation[2]. Relatively little information on the physical characteristics of this instrument has been published, and the purpose of this paper is to examine the ways in which observed performance relates to the theory of operation.[3]

Trajectory Modelling

Using the 'ultra simple' model for calculating the one-dimensional trajectories of Ar^+ ions in a scanning rf quadrupole field[4] it has been possible to determine the value of the parameter q_{eject} at which the ions become mass selectively unstable. The values obtained indicate a critical dependence upon the initial displacement and the phase-angle of the drive potential at the point of ion creation, which in turn affects the resolution. Introducing into the model the effect of moderating collisions with He atoms dramatically reduces the spread in values of q_{eject}, as shown in Figure 1.

Stability Diagrams

Experimental determinations of partial stability diagrams for the trap have been made by observing the apparent masses on the Ion Trap Detector at which ions of m/z 40 just become unstable as a dc potential is applied to the ring electrode. Figure 2 suggests that the $\beta_z = 1.0$ boundary moves to lower apparent mass, i.e. reduced q_z, as the helium is introduced, in contradiction to the predictions of the model.

References

1. J.F.J. Todd, Dynamic Mass Spectrometery Vol. 6 (Ed. D. Price and J.F.J. Todd), Heyden & Son, London (1981),p.44.
2. G.C. Stafford, Jr., P.E. Kelley, J.E.P. Syka, W.E. Reynolds and J.F.J. Todd, Int. J. Mass Spectrom. Ion Proc. 60, 85, (1984).
3. P.E. Kelley, G.C. Stafford, Jr., W.J. Fies, Jr., J.E.P. Syka, R.T. McIver, Jr., J.J. Bexon and J.F.J. Todd, 32nd Annual Conference on Mass Spectrometry and Allied Topics, San Antonio, Texas, 1984, p. 505.
4. R.B. Turner, G. Lawson and J.F.J. Todd, Dynamic Mass Spectrometry Vol 4 (Ed. D. Price and J.F.J. Todd), Heyden & Son, London (1976), p.79

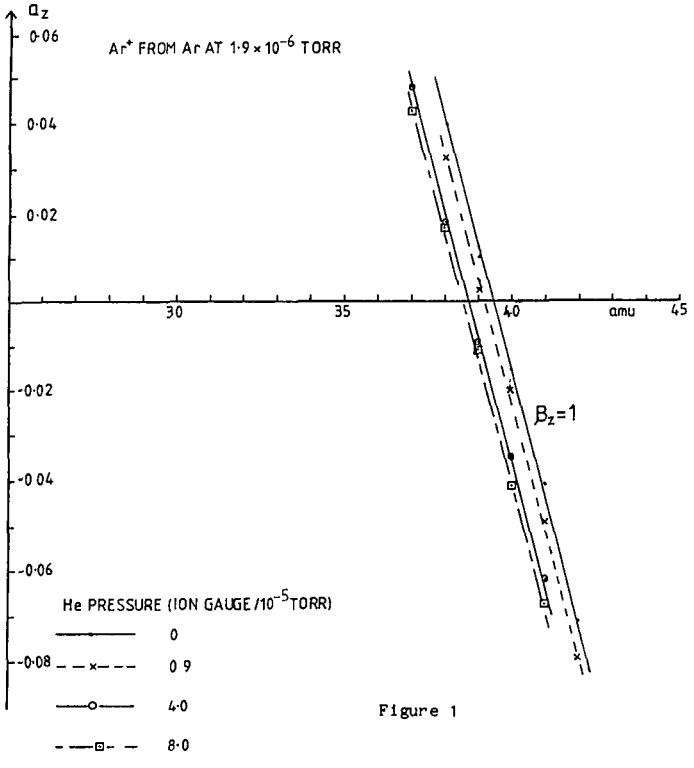

Figure 1

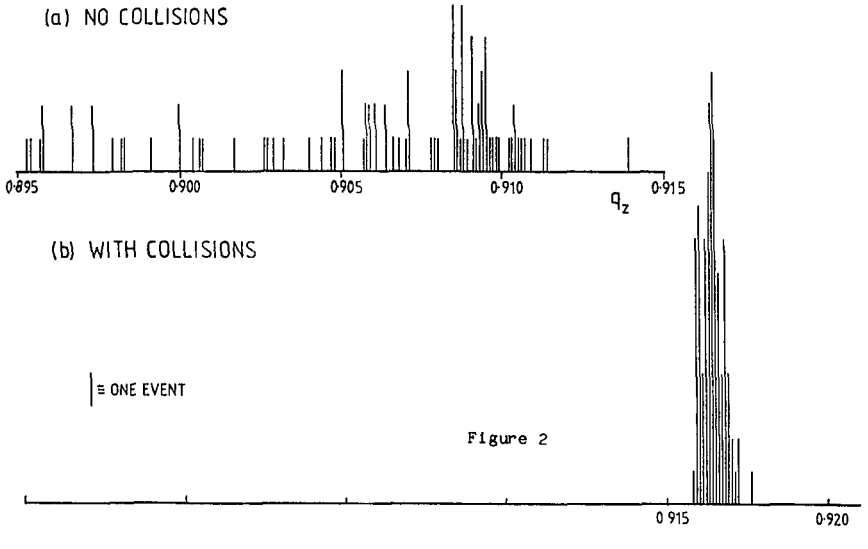

Figure 2

Presented at the 35th ASMS Conference on Mass Spectrometry and Allied Topics
May 24-29, 1987, Denver, CO

PICOGRAM TO MICROGRAM ANALYSIS BY GAS CHROMATOGRAPHY/ION TRAP MASS SPECTROMETRY

Richard A. Yost, Chemistry Dept., Univ. of Florida, Gainesville, FL
William McClennen, Biomaterials Profiling Center, Univ. of Utah, Salt Lake City, UT
A. Peter Snyder, U.S. Army CRDEC, Aberdeen Proving Grounds, MD

The dynamic range of any device which converts analytes into charged particles (e.g., flame ionization detectors or mass spectrometers) will be limited by the onset of space charge. These space-charge effects lead to saturation of instrument response when the density of charged particles (ions) rises so high that ion-ion repulsions become significant. These effects are especially evident in devices which trap or store ions. In the ion trap, these effects are manifest when too large an analyte concentration leads to loss of mass resolution and degradation of mass-spectral quality (e.g., self-chemical ionization to form $(M + 1)^+$ ions).

We have recently evaluated the new Automatic Gain Control (AGC) ITD which provides automatic variation of ionization time. This approach maximizes sensitivity for low levels of analyte, and prevents saturation of the ion trap at high levels of analyte. The results are impressive, with full scan EI mass spectra easily obtained at low picogram levels injected, while linear response is maintained up to low microgram levels.

Whereas the operation of the ion trap has traditionally used a fixed (1 ms) ionization time, the new approach automatically selects an ionization time from 0.078 ms to 25 ms (a range of 320) for each microscan, depending on the amount of analyte in the trap. For low levels (e.g., for baseline or small GC peaks) a maximum ionization time of 25 ms is selected, offering an improvement of approximately 25 times in sensitivity. As the amount of analyte increases, the ionization time is automatically decreased in order to prevent overfilling the trap with ions. The ion signals in each microscan are automatically scaled to correct for the variation in ionization time. The new scan function is compared with the normal scan function in Figure 1. A short "prescan", consisting of a 0.2 ms ionization provides an estimate of the number of ions formed in the trap. This value is then used to calculate the optimum ionization time for the actual mass scan which follows.

In order to evaluate this new approach, solutions of JP-10 jet fuel (tricyclodecane), methyl salicylate, n-decanol, dipropyleneglycol monomethyl ether, and bis-methoxy-ethyl ether were analyzed by GC/EIMS (full scan) with the ion trap. Samples were analyzed with a 15 m x 0.32 mm ID, 0.25 µm film thickness, DB-5 open tubular column (programmed from 30°C to 130°C at 20°C min^{-1}, 4.4 psig inlet pressure, 1 µl on-column injections), scanning from m/z 40 to 160. Standard solutions ranged from 150 fg μl^{-1} to 1.5 µg μl^{-1}. The chromatograms for a solvent blank and 15 pg of tricyclodecane are compared in Figure 2. The tricyclodecane peak at a retention time of 4:20 is clear at the 15 pg level in the reconstructed ion chromatogram (RIC), as well as in the mass chromatograms for the molecular ion (m/z 136) and the most abundant fragment ion (m/z 67). The background-subtracted mass spectrum for the 15 pg GC peak is shown in Figure 3a. This spectrum compares favorably with that obtained for 150 ng (10,000 times more analyte), shown in Figure 3b.

The clearest indication of the performance of this new approach is the linear dynamic range indicated in the calibration curves for tricyclodecane shown in Figure 4. Over 6 decades of concentration, the calibration curves for the RIC, m/z 67, and m/z 136 (M^+) show excellent agreement and linearity (slope of the log-log plots = 1.0). Similar results were observed for the other compounds studied.

In conclusion, this new operational mode provides the ITD with sensitivity and dynamic range which equal if not exceed those of any other GC/MS system. The use of relatively long ionization times offers extremely high full-scan sensitivity for trace-level components in the low picogram range, while the automatic variation of ionization time provides linear response into the low microgram range, well above the upper limit of open-tubular-column GC capability.

Presented at the 35th ASMS Conference on Mass Spectrometry and Allied Topics
May 24-29, 1987, Denver, CO

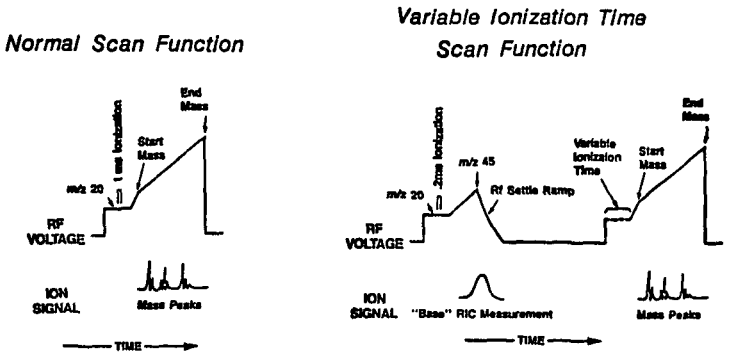

Figure 1.

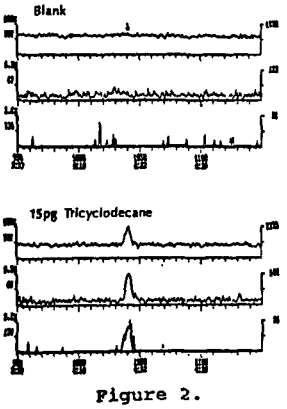

Figure 2.

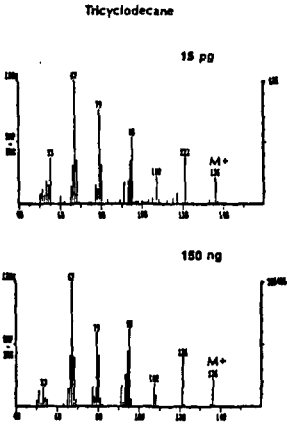

Figure 3.

Figure 4.

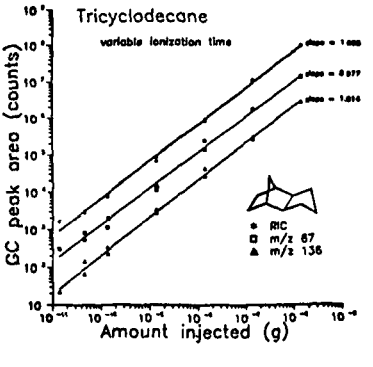

Presented at the 35th ASMS Conference on Mass Spectrometry and Allied Topics
May 24-29, 1987, Denver, CO

SLOW UNIMOLECULAR DISSOCIATIONS OF RADICAL CATIONS; ANISOLE AND C_6H_6 ISOMERS

C. Lifshitz, N. Ohmichi, J.-P. Ziesel and V. Aviyente
Department of Physical Chemistry and
The Fritz Haber Center for Molecular Dynamics
The Hebrew University of Jerusalem, Jerusalem 91904, Israel

Time-resolved photoionization efficiency (PIE) curves have been determined by the technique of TPIMS (Time-resolved Photoionization Mass Spectrometry)[1] for $C_6H_6^+$ from anisole and for $C_6H_5^+$, $C_4H_4^+$ and $C_3H_3^+$ from two C_6H_6 isomers - 2,4-hexadiyne and 1,5-hexadiyne. PIE's and breakdown curves were modelled by RRKM/QET calculations. The results have been compared to previous PEPICO (photo-electron photoion coincidence)[2,3] and photodissociation[4] data. Anisole cation radical loses formaldehyde in a reaction which demonstrates a large kinetic shift. It has been studied in order to determine the activation parameters - activation energy and activation entropy of the reaction. The appearance energy (AE) as a function of storage time is as follows: time: AE = 6 μs: 11.30±0.05 eV; 32 μs: 11.10±0.05 eV; 46 μs: 11.07±0.05 eV; 500 μs: 10.85±0.05 eV; 2000 μs: 10.85±0.05 eV. Modelling of PIE curves at 6 μs and 2 ms storage times, as well as performance of a sensitivity analysis of the breakdown curve parameters - crossover energy and crossover shift - yielded a critical energy of activation, for the anisole reaction, of E_0 = 59.6±0.6 kcal/mol (2.585±0.025 eV) and an equivalent activation entropy based on the frequencies of the transition state, $\Delta S^{\ddagger}$ (1000 K) = +7.25±2.2 eu. The rather loose transition state is in keeping with a four-membered or five-membered cyclic hydrogen transfer state proposed for the reaction, and should be compared with the tighter transition state for the decarbonilation of phenole cation.[1] The activation parameters obtained from TPEPICO experiments[2] for anisole correspond to E_0 = 1.68 eV and $\Delta S^{\ddagger}$ (1000 K) = -11.42 eu.

There is disagreement between PEPICO[3] and photodissociation[4] data regarding the question whether 2,4-hexadiyne cation radical isomerizes to benzene prior to dissociation. The previously known AE's for fragment ions are all in excess of calculated ones. We have determined AE's for $C_3H_3^+$, $C_4H_4^+$ and $C_6H_5^+$ at t = 2 ms and found all three values to coincide with the n = 4 member of a Rydberg series which converges to the $\tilde{A}$ state of the ion. It is thus conceivable that the autoionizing Rydberg states isomerize to benzene while the $\tilde{A}$ state does not.[4] On the other hand, the AE's are easily reconcileable with the energetics of the reactions provided cyclic $C_4H_4^+$ and $C_3H_3^+$ cations are formed while linear $C_6H_5^+$ is formed at threshold. This is in agreement with the photodissociation experiments which indicate that the $\tilde{A}$ state undergoes internal convertion, that the $\tilde{X}$ state forms cyclic $C_4H_4^+$ and $C_3H_3^+$ but that it does not isomerize to benzene. The linear ground state cation does not form phenyl. The situation is quite different for 1,5-hexadiyne where the looser molecular frame allows isomerization to benzene. The parent cation is unstable with respect to dissociation to phenyl$^+$ + H· and the AE for $C_6H_5^+$ shifts down to the ionization energy for long storage times.

The PIE curve for $C_4H_4^+$ from 2,4-hexadiyne at t = 2 ms is shown in Figure 1. The arrows show the (vertical) energies for the n = 4 state of the Rydberg series converging to the $\tilde{A}$ state[3] and the $\tilde{A}$ state itself. Calculated 0 K AE's for $C_4H_4^+$ are: AE (cyclic) = 10.675 eV, AE (linear) = 11.08 eV while the previous literature value is 11.27±0.2 eV.[5]

Presented at the 35th ASMS Conference on Mass Spectrometry and Allied Topics
May 24-29, 1987, Denver, CO

[1] Y. Malinovich and C. Lifshitz, J. Phys. Chem. 90 (1986) 4311.
[2] P.R. Das, J P. Gilman and G.G. Meisels, Int. J. Mass Spectrom Ion Processes, 68 (1986) 155.
[3] T. Baer, G.D. Willett, D. Smith and J.S. Phillips, J. Chem. Phys. 70 (1979) 4076.
[4] R.E Krailler, D.H. Russell, M F. Jarrold and M.T. Bowers, J. Am. Chem. Soc. 107 (1985) 2346.
[5] H.M. Rosenstock, K.E. McCulloh and F P. Lossing, Int. J. Mass Spectrom. Ion Phys. 25 (1977) 327.

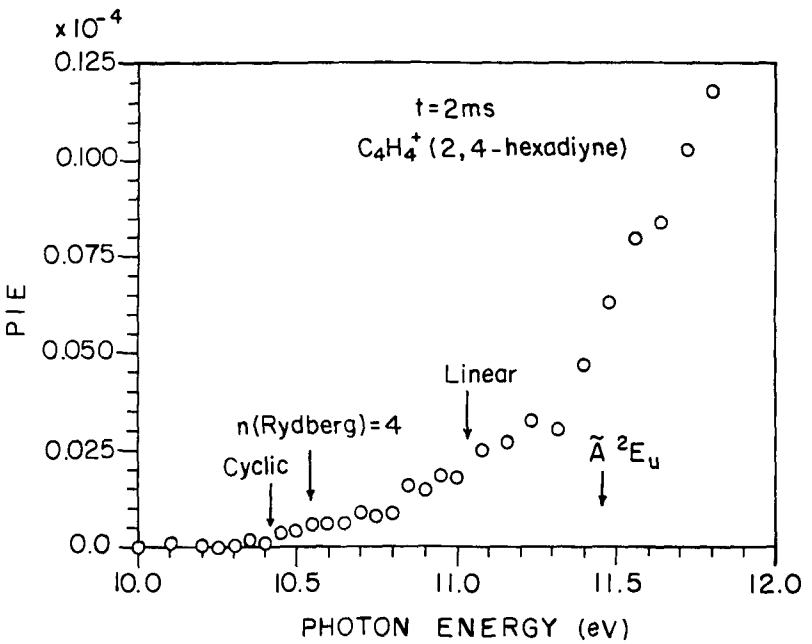

Figure 1

Presented at the 35th ASMS Conference on Mass Spectrometry and Allied Topics
May 24-29, 1987, Denver, CO

VIBRATIONAL AND ELECTRONIC STATES IN $H_2^{+\cdot}$ STUDIED BY FIELD IONIZATION OF RYDBERG H ATOMS

J.Bordas-Nagy and J.L. Holmes; Chemistry Department, University of Ottawa, Ottawa, Ontario, Canada, K1N 9B4

Collisions between high velocity (KeV energies) diatomic ions such as H_2^+, D_2^+, N_2^+, O_2^+ and noble gas target atoms (Xe, He) produce high Rydberg (HR) molecules, ions and atoms. In a previous study [1] it has been shown that these processes can be studied in a double focussing mass spectrometer by field ionizing the neutral HR species and then measuring their ion kinetic energy spectra. The reactions involved were

$$M_2^+ \xrightarrow{\text{Xe or He}} M_2(HR)^* \longrightarrow M + M(HR) \xrightarrow{FI} M^+ \qquad (1)$$

$$M_2^+ \xrightarrow{\text{He}} M_2^+(HR)^* \longrightarrow M^+ + M(HR) \xrightarrow{FI} M^+ \qquad (2)$$

where $M_2(HR)^*$ indicates a HR M_2 molecule with a vibrationally excited core, FI indicates field ionization. (The dissociative HR molecule ($M_2(HR)^*$) or molecular ion ($M_2^+(HR)$) are only intermediate species, their lifetimes being of the order of a molecular vibrational period.) The ion core model [2] of HR molecules and ions was applied to the observations to separately identify reactions (1) and (2). The principle of the ion core model is that the HR fragments in the dissociative ionization of molecules, originate from the dissociation of HR molecular states. These states can be described as a singly charged molecular ion core surrounded by an electron in a distant orbit. It is the repulsive states of the molecular core ion which determine the dissociative processes. This model has been extended to the HR states of singly charged molecular ions, which are described as a Rydberg electron bound to a doubly charged core. In our previous study [1] of H_2^+ ions with Xe as collision gas, one single-collision event produced HR fragments, (process 1). This is capture of an electron by the projectile H_2^+ ion from the target gas atom into a HR orbit, accompanied by a simultaneous vibrational excitation of the ion core into the dissociative continuum. The excited ion core dissociates, the HR electron joins the ionic fragment, H^+, and the resulting HR $H^\cdot$ atom can readily be field ionized. This produces a single, narrow peak in the ion kinetic energy spectra. (See central peaks in the Fig.) With He as collision gas, the above also took place but in addition, another process of comparable importance was observed. This, (process 2), is the vertical electronic excitation of the H_2^+ projectile ion upon collision, into a HR state of H_2^+ which converges to a dissociative electronic state of the doubly charged ionic core. The doubly charged core dissociates into two H^+ ions and the HR electron joins one of them. The kinetic energy spectrum for this field ionized $H^\cdot$ atom shows a kinetic energy release of the order of 5-10 eV in the centre of mass system, giving rise to the dished peak, i.e. a pair of

Presentea at the 35th ASMS Conference on Mass Spectrometry and Allied Topics
May 24-29, 1987, Denver, CO

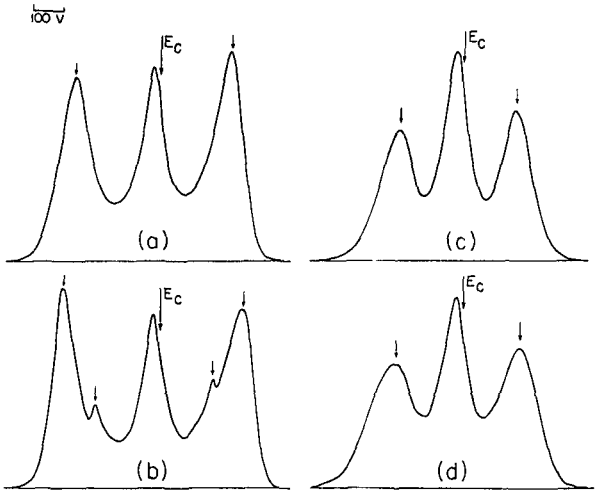

Ion kinetic energy spectra of field ionized HR(H$^{\cdot}$) atoms for (He) collisionally activated H_2^+ produced from (a) H_2, (b) H_2O, (c) CH_4, (d) H_2S.

peaks separated by hundreds of volts due to the amplification when the centre of mass framework is transformed to the laboratory framework. The observed kinetic energy release reflected the vibrational energy of the original, H_2^+ molecular ion. The potential curve for the doubly charged electronic state to which the H_2^+ was excited by collision is known, and so the internuclear distance for the dissociating species can be determined from the kinetic energy release for process 2, provided the excitation occurs to a repulsive part of the potential curve. The transition to that state will be a vertical process because the collision time is much shorter than a vibrational or rotational period of the molecule. Consequently, this calculated internuclear distance is that at the outer turning point of the most highly populated vibrational state in the molecular ion beam, and so the vibrational energy distribution in the projectile ion beam can be characterized. The results are summarised in the Table.

Excitations of H_2^+ Yielding Fragments with a Large Kinetic Energy Release (KER)

Precursor	*Designated Transition*	*KER(eV)*
H_2	$H_2^+(1s\sigma_g, v'=3) \rightarrow H_2^+(HR)$	8.1 ± 0.2
H_2O	$H_2^+(1s\sigma_g, v'=1) \rightarrow H_2^{2+}(HR)$	10.8 ± 0.2
	$H_2^+(1s\sigma_g, v'=1) \rightarrow H_2^+(2p\sigma_u)(HR)$	4.4 ± 0.2
CH_4	$H_2^+(1s\sigma_g, v'=11) \rightarrow H_2^{2+}(HR)$	5.2 ± 0.2
H_2S	$H_2^+(1s\sigma_g, v'=13) \rightarrow H_2^{2+}(HR)$	4.5 ± 0.2

1. J. Bordas-Nagy and J.L. Holmes, Chem. Phys. Lett. 132 (1986) 200.
2. R.S. Freund, in: Rydberg States of Atoms and Molecules, ed. R.F. Stebbings and F.B. Dunning (Cambridge Univ. Press, 1983).

Presented at the 35th ASMS Conference on Mass Spectrometry and Allied Topics
May 24-29, 1987, Denver, CO.

Absolute State-to-State Cross Sections for the Charge Transfer Reactions H_2^+ + Ar and Ar^+ + H_2

J.D. Shao, R. Xu, C.L. Liao, G.D. Flesch, Y.G. Li, and C.Y. Ng

Ames National Laboratory, Iowa State University, Ames, IA 50011

Recently a tandem photoionization mass spectrometer[1] (TPIMS) and a crossed ion-neutral beam apparatus[2] (CINBMS) have been combined to measure the absolute state-to-state cross sections for the charge transfer reactions :

$$H_2^+(X^2\Sigma_g^+, v'=0\text{-}4) + Ar(^1S_0) \rightarrow Ar^+(^2P_J) + H_2(X^1\Sigma_g^+, v) \quad (1)$$

$$Ar^+(^2P_{1/2,3/2}) + H_2(X^1\Sigma_g^+, v=0) \rightarrow H_2^+(X^2\Sigma_g^+, v') + Ar(^1S_0) \quad (2)$$

With the TPIMS, the absolute state-selected cross sections were measured for the reactions (1) and (2) in the collision energy range from Ec.m.=0.48 to 95.2 eV and Ec.m.=0.24-11.90 eV respectively. The results are shown in Fig.1(a) and (b). At low collision energies, reaction (1) is favored with the reactants in v=2 vibrational state, as is also reaction (2) when the Ar ion is in the J=1/2 spin-orbit state. However, as the collision energy increases, the internal state dependence of both reactions are diminished.

The CINBMS was used to measure the product state distributions. Reaction (1) was used as the probing reaction for reaction (2) and vice versa. The experimental product state distributions are shown in Fig.2(a), (b) and (c). Reaction (1) at low collision energies and low vibrational energies in H_2+ produces predominantly Ar ions in the 3/2 spin-orbit state. However, for v larger than 1, most Ar ions are produced in the 1/2 state. As collision energy increases, the difference between the population in the two spin-orbit states becomes smaller and approaches the statistical value of 0.67 shown as the dash line in Fig.2(a). For reaction (2), v=2 is the most favored state for product population at low collision energies. At higher collision energies, it tends to populate evenly in v=0-4 states.

According to the energy level diagram shown in Fig.3, the small energy gap of 25 meV between the states of $Ar^+(^2P_{1/2})$ + $H_2(v=0)$ and $H_2^+(v'=2)$ + $Ar(^1S_0)$ leads to a strong resonance effect at low collision energy. At high collision energies, the diminution of internal state dependence of the absolute cross section and the product state distribution indicates that energy is transfered from the collision energy to internal energy. Therefore, the degeneracy of the product states become dominant and the product state distribution reaches the statistical limit at high collision energies as the data shown in Fig.2.

The absolute state-to-state cross sections for reactions (1) and (2) are calculated with the following equations:

$$\sigma_{i\rightarrow f} = \sigma_i * X_{i\rightarrow f}$$

where $\sigma_{i\rightarrow f}$ is the absolute state-to-state cross section, σ_i the state-selected cross section and $X_{i\rightarrow f}$ the product state distribution. Part of the results are shown in Fig.4.

Microscopic reversibility was used without considering the rotational states in this system. The calculated values and the experimental data in Fig.2(b) and (c) are in good agreement.

REFERENCES

1. J.D. Shao and C.Y. Ng, J. Chem. Phys. 84, 4317(1986).
2. C.L. Liao, J.D. Shao, R. Xu, G.D. Flesch, Y.G. Li and C.Y. Ng, J. Chem. Phys. 85, 3874(1986).

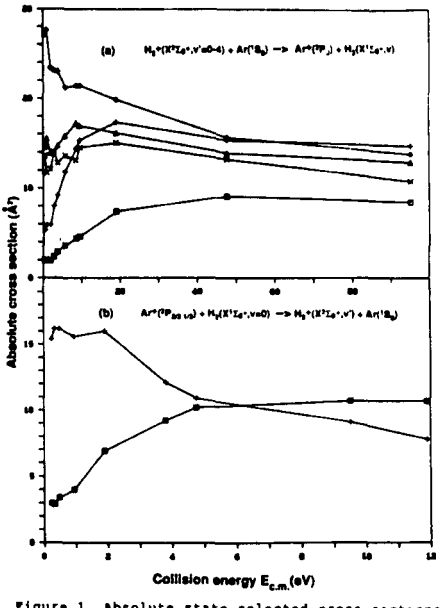

Figure 1. Absolute state-selected cross sections for reaction (1) and (2). (a) □: v=0, +: v=1, ◊: v=2, Δ: v=3, x: v=4. (b) +: J=1/2, □: J=3/2.

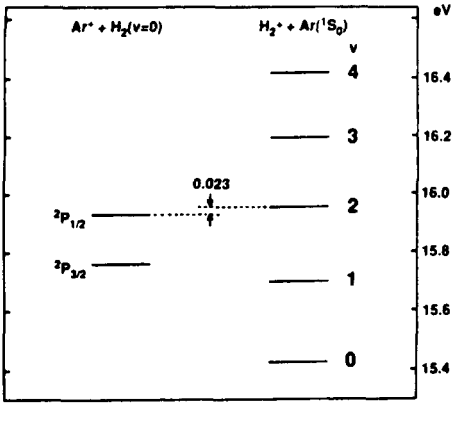

Figure 3. Energy level diagram for the Ar+ + H2 <-> H2+ + Ar reaction.

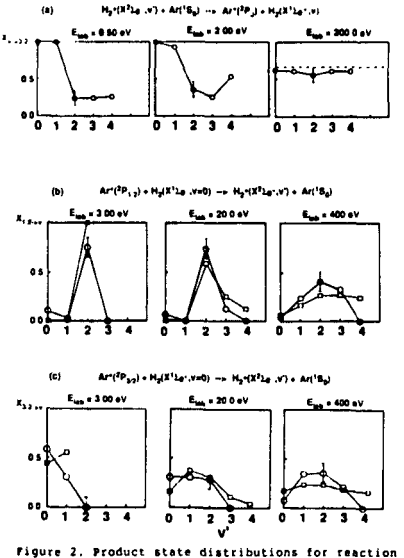

Figure 2. Product state distributions for reaction (1) and (2). □: experimental data. o: calculated values in terms of microscopic reversibility. --: statistical limit.

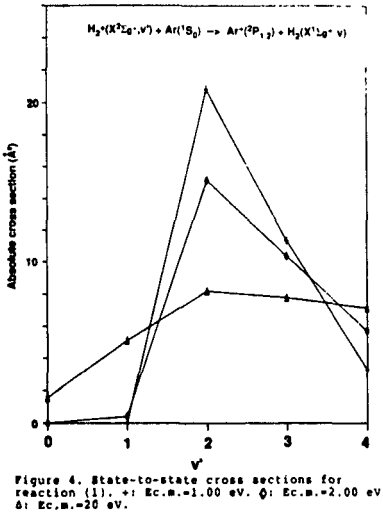

Figure 4. State-to-state cross sections for reaction (1). +: Ec.m.=1.00 eV. ◊: Ec.m.=2.00 eV. Δ: Ec.m.=20 eV.

Presented at the 35th ASMS Conference on Mass Spectrometry and Allied Topics
May 24-29, 1987, Denver, CO

PRODUCT SELECTION IN GAS PHASE ACID-BASE REACTIONS. LEWIS vs. BRONSTED AND BRONSTED vs. BRONSTED PATHWAYS.

Thomas Hellman Morton, Eric W. Redman, and Dion A. Stams
Department of Chemistry, University of California, Riverside, CA 92521

Two pathways can be envisaged for a Brønsted acid-base reaction between an alkyl cation and an n-donor base: a Lewis pathway (called a "condensation" elsewhere[1]) and an Eigen pathway (called a "proton transfer" elsewhere[1]). The Lewis pathway, represented by the reaction $R^+ + NX_3 \rightarrow [R{-}NX_3^+] \rightarrow NX_3H^+$, has been shown by Ausloos and Lias[1] and by us[2] to account for only a small proportion of the reaction. The predominant mechanism must therefore correspond to the intermediacy of hydrogen bonded structures, i.e. the Eigen pathway.

Both pathways operate in competition with one another. The choice between them could, in principle, represent two competing transition states for ion-molecule capture, but this is not consistent with current models involving orbiting transition states. The other alternative stipulates subsequent bottlenecks, for which the flux corresponding to the Lewis pathway is less than for the Eigen pathway. If this be a correct interpretation, as depicted by the scheme below (where the broad arrow stands for the n-donor base, with its permanent dipole moment, and the solid arrow represents the acidic cation, with both Brønsted and Lewis acidic positions), then there must be an intermediate of nonzero lifetime between the transition state for capture and the critical configurations for pathway selection.

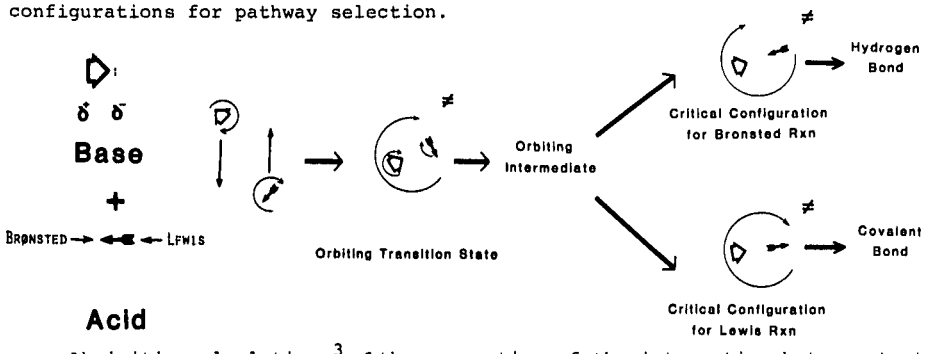

Ab initio calculations[3] of the energetics of the interaction between tert-butyl cation, $(CH_3)_3C^+$, and trimethylamine, $N(CH_3)_3$ at a large nitrogen-sp^2 carbon separation (10 a.u. = 5.29 Å; the center of charge of trimethylamine is displaced 0.13 Å from the nitrogen) show that the ion-permanent dipole potential is greater than estimated on the basis of a point charge/point dipole interaction. With the $N(CH_3)_3$ dipole pointed towards the sp^2 carbon and the vacant carbon 2p orbital pointed towards the nitrogen, the STO-3G interaction energy is -13.9 kJ/mol, not greatly different from the classical calculation of -12.3 kJ/mol using the experimental dipole moment of $N(CH_3)_3$, 0.612 D, and an induced dipole corresponding to the mean molecular polarizability of $N(CH_3)_3$, 8.0 $Å^3$. With the amine rotated 90° the STO-3G interaction energy is -1.9 ± 0.4 kJ/mol (average of three rotational orientations of tert-butyl that maintain the p-orbital pointed towards nitrogen).

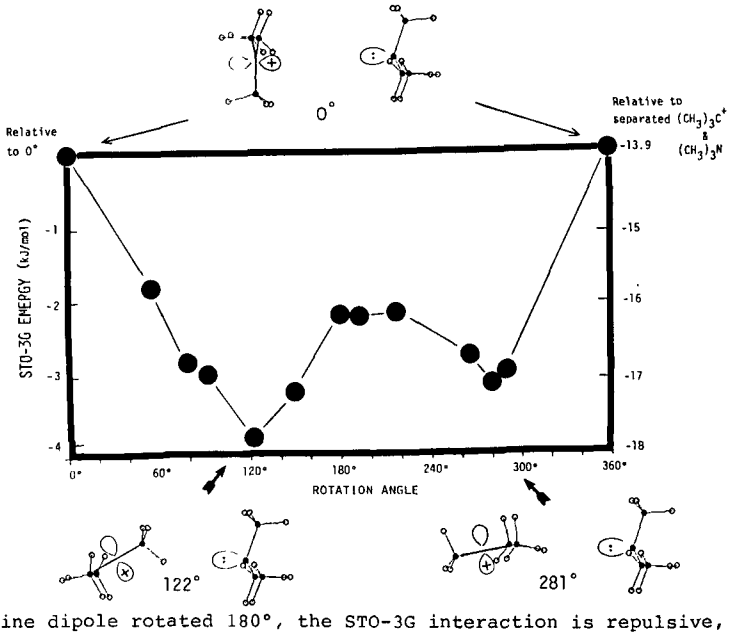

With the amine dipole rotated 180°, the STO-3G interaction is repulsive, +6.0 kJ/mol, contrary to the classical calculation, which predicts -1.3 kJ/mol.

With the amine dipole fixed towards the cation, rotation of the cation gives STO-3G energies that are least attractive at the geometry (0°) corresponding to a Lewis pathway and that are most attractive at geometries (122° and 281°) corresponding to Eigen pathways, as shown above.

One way to probe the orbiting transition state experimentally is to examine the partition between two different Eigen pathways, for instance the Hoffmann and Saytzeff product channels from 1-methylcyclopentyl cation, shown to the right.

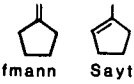

	Hoffmann	Saytzeff
$\Delta H^\circ_{f,300}$(kJ/mol)	11	-4
S°_{300}(J/mol-K)	313	327

For a series of tertiary amines, variation of proton affinity and of steric bulk exhibit the effects on product ratio that are expected on the basis of there being negligible contribution from Lewis pathways. $N(CH_3)_3$ gives a "random" distribution (Saytzeff/Hoffman = 4/3). Decreasing the proton affinity increases the product ratio, while increasing the steric bulk of the base decreases the product ratio. Therefore the critical configurations for the competing Eigen channels must have acid-base separation distances short enough for proton abstraction from methyl to be sterically more accessible than proton abstraction from an acidic CH_2.

Acknowledgment. Ab initio calculations were performed on the Cray XMP/48 at the San Diego Supercomputing Center at UCSD, time provided by the UC Riverside Block Grant.

1. P. Ausloos and S. Lias, J. Am. Chem. Soc. 1986, 108, 1792-1796.
2. E.W. Redman and T.H. Morton, J. Am. Chem. Soc. 1986, 108, 5701 - 5708.
3. J.S. Binkley, M.J. Frisch, D.J. DeFrees, K. Rahgavchari, R.A. Whiteside, H.B. Schlegel, E.M. Fluder, and J.A. Pople, GAUSSIAN 82, Department of Chemistry, Carnegie-Mellon University, Pittsburgh, PA.

Presented at the 35th ASMS Conference on Mass Spectrometry and Allied Topics
May 24-29, 1987, Denver, CO

MODELING THE ELECTROSTATIC INTERACTIONS BETWEEN TRANSITION METAL IONS AND POLAR MOLECULES: THE RELATIONSHIP BETWEEN PREFERRED COMPLEX GEOMETRIES AND PRODUCT DISTRIBUTIONS: Deborah J. Hankinson, Eric J. Hooper, John Allison, Department of Chemistry, Michigan State University, East Lansing, MI 48824

In the exothermic reactions of transition metal ions with organic molecules, we propose that four fundamental steps are involved. First, an electrostatic ion/molecule complex is formed. Second, the metal ion inserts into a bond. Third, a group that is β- to the metal, usually an H-, shifts across the metal, resulting in the formation of two stable molecules bound to the metal. Finally, there is a competitive ligand loss, in which the more strongly bound ligand is preferentially retained. While mechanisms by which reaction products are formed have been proposed, it is still unclear as to what aspects of the chemistry dominate in controlling the distribution of products, or more precisely, the extent to which insertion into the various bonds occurs.

At last year's ASMS meeting, we presented a simple model for calculating ion/molecule electrostatic interaction energies. The calculations include: 1) ion-induced dipole interactions, using a bond-polarizability description of the molecule; 2) ion-atom interactions which take two forms - the first is that due to the ion interacting with charges placed on the atoms; the second is a repulsive term approximated from potential curves for diatomics such as CrH^+ and CrC^+. Calculations of this type for the interaction of the spherically symmetric chromium ion (d^5 ground state) with butane suggested that the electrostatic Cr^+-butane complex in which the Cr^+ is in close proximity to the interior C-C bond is more strongly bound than that in which Cr^+ is close to a terminal C-C bond. We suggest that this correlates with the observed chemistry for first row transition metal ions with butane, in which insertion into the interior C-C bond occurs to a greater extent than that for the terminal C-C bond. That is, we suggest that a distribution of metal ion/butane complexes are formed which determine the sites of insertion.

We have performed similar studies into the chemistry of metal ions with polar compounds such as n-butyl chloride. Significant differences exist when comparing butane and butyl chloride at this level due to a number of factors. First, butyl chloride is obviously a polar molecule; the chlorine atom carries a charge of approximately two-tenths of an electron, with an equal, positive charge distributed throughout the butyl group. Second, the C-Cl bond is much more polarizable than C-H and C-C bonds, both along the bond axis, and perpendicular to the bond.

In comparing the potential surfaces about butyl chloride to those for butane, there is a general skewing of the alkane-like potentials in response to these factors. While one may expect that a geometry in which the C-Cl-Cr^+ atoms are colinear may be very favorable, this is not necessarily the case. The most strongly bound complex places the metal ion "atop" the C-Cl bond, due to the dominant contribution of the ion-induced dipole terms involving parts of the alkyl group. Thus, the metal ion is attracted to a greatest extent towards the C-Cl bond. Regions in the potential surface about the various C-C bonds bear some resemblence to that observed for butane, altered by the net positive charge deposited throughout the alkyl chain.

At the extended Hückel level, we have investigated the extent to which the charge is distributed among the atoms of the alkyl group, since this charge distribution is what differs among various polar molecules. In the case of butyl choride, most of the positive charge on the alkyl group is located on the C bound to the Cl, as would be expected. C atoms carry most of the charge; the charge on H atoms vary little as a function

of the charge on the C atom to which they are attached. For alkyl chlorides, chainlengths larger than butyl- are required to yield a charge on the end methyl group that is the same as that on the methyl group of the corresponding alkane. Thus, the ion does not interact with parts of the alkyl group as it does with those parts in the corresponding alkanes, unless the chain is fairly long.

Exemplary of the results of these calculations, the figure below shows lines of constant potential in one plane about a selected configuration of butyl chloride. Note that the most attractive interaction (labeled -64 kcal/mol) occurs in close proximity to the C-Cl bond.

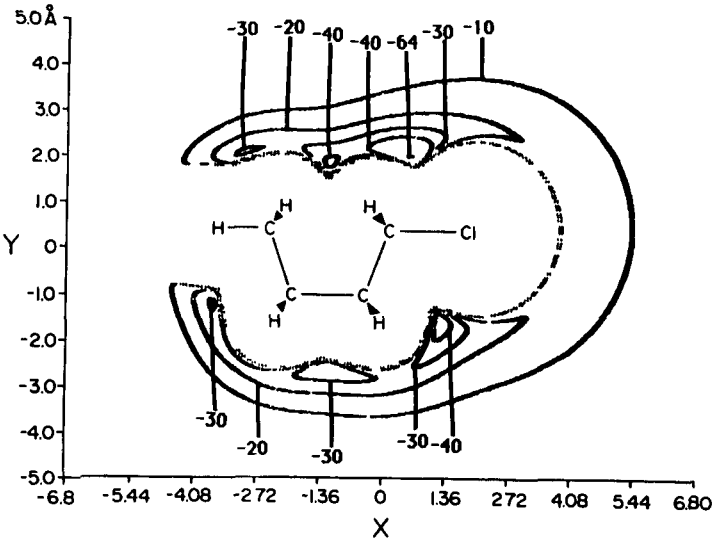

Presented at the 35th ASMS Conference on Mass Spectrometry and Allied Topics
May 24-29, 1987, Denver, CO

GAS -PHASE CHEMISTRY OF THE BENZENE RADICAL CATION: REACTION WITH CYCLIC ALKANES

CHARLES D. WARNER, HASTINGS COLLEGE, HASTINGS NE 68901;
MICHAEL L. GROSS AND ROBERT W. HOLMAN, MIDWEST CENTER FOR MASS SPECTROMETRY, LINCOLN, NE 68501

Earlier work[1, 2] showed that benzene radical cation reacted with a variety of electron rich compounds to form a distonic adduct. This paper extends our study of distonic radical cations to include bimolecular adducts formed when benzene radical cation reacts with either cyclopropane or cyclobutane. In comparison to 1,3-butadiene and ethylene, cyclopropane is less reactive than the former and more reactive than the latter. The distonic adducts were studied using both Fourier Transform Mass Spectromertry (FTMS) and tandem mass spectrometry.

When cyclopropane was admitted to the FTMS cell containing the benzene radical cation a m/z 91 ion was observed which is characteristic of the bimolecular adduct. When neutral benzene was admitted to the cell containing the cyclopropane radical cation the ions observed were those from reaction of cyclopropane radical cation with cyclopropane.

A 1:1 mixture of benzene and cyclopropane was ionized in the source of the tandem mass spectrometer. A third body, CS_2, was admitted into the source for collisional damping of adduct internal energy. Varying the CS_2 partial pressure allows the study of the adduct as a function of internal energy. The collisionally activated decomposition spectrum (CAD) of the m/z 120 adduct of benzene radical cation and cyclopropane (I) had many ions in it, but only the abundances of the

$$1)\ [C_6H_6]^{+\cdot} + C_3H_6 \longrightarrow \underset{\mathrm{I}}{[C_9H_{12}]^{+\cdot}}\ (m/z\ 120)$$

m/z 105, 92, and 91 ions were more than 5% of the total ion current. If the adduct is the distonic ion, **II**, (n=1) a possible reaction path might be a 1,4-hydrogen shift to give an ion like n-propylbenzene, **III** (n=1). However, the distonic ion might also cyclize to an ion like 8,9-dihydroindan, **IV** (n=1). Support for this 1,5-cyclization of the distonic is evident in the work of Beckwith and coworkers [3,4], who have shown that 5-hexenyl radicals undergo facile 1,5-cyclization to cyclopentenyl methyl radicals. Comparison of the CAD spectra of the adduct and of the model, n-propylbenzene,

Scheme 1:

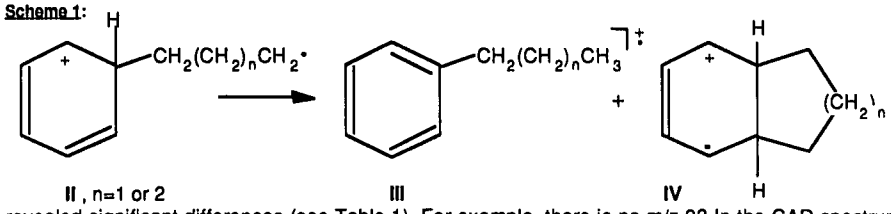

revealed significant differences (see Table 1). For example, there is no m/z 92 In the CAD spectrum of n-propylbenzene and there is a significantly lower abundance of m/z 105 than in the CAD of the adduct. Thus, the adduct and n-propylbenzene do not appear to have the same structure.

TABLE 1: PARTIAL CAD SPECTRA OF M/Z 120 IONS

	M/Z:105	92	91
ADDUCT (4X10-4 torr)	5.2%	7.5%	46%
N-PROPYL BENZENE (280 EV)	3.5%	-	68%
4,7-DIHYDROINDAN (280 EV)	8.1%	16%	28%
COMBINATION	6%	8.7%	46%

The 8,9-dihydroindan model compound was not available for use, so the CAD spectrum of a related model, 4,7-dihydroindan, was obtained. The m/z 92 Ion which was absent in the n-propylbenzene model CAD spectrum was quite abundant in the CAD spectrum of 4,7-dihydroindan. Because neither model compound completely accounted for the relative abundance of the ions formed by collisional activation of the adduct, various linear combinations of the model compound CAD spectra were compared with the CAD of the adduct. The linear combination of 55% dihydroindan

and 43% n-propylbenzene matched the CAD of the adduct with less than 5% error. This result suggests that after the distonic adduct forms, two reaction paths are available to the ion: 1,4-hydrogen migration to give n-propylbenzene or 1,5-cyclization.

Collisional activation of the m/z 134 adduct from the reaction of benzene radical cation and cyclobutane produced many ions, but the structurally significant ones were m/z 119, 105, 92, and 91. One reaction pathway for the distonic **II**, (n=2) would be a hydrogen migration to the terminal carbon on the chain. The CAD spectrum of the n-butylbenzene model is dominated by the m/z 92 and 91 ions while the m/z 119 ion is much less abundant. Cyclization of the distonic adduct would give an ion like 9,10-dihydrotetralin (**IV**, n=2). The CAD spectrum of 5,8-dihydrotetralin (the 9, 10-

TABLE 2: PARTIAL CAD SPECTRA OF M/Z 134 IONS

	M/Z:119	105	92	91
ADDUCT (4X10-4 torr)	8.6%	5.2%	20%	28
N-BUTYLBENZENE (280 EV)	1 9%	4.9%	32%	41
5,8-DIHYDROTETRALIN (280 EV)	15%	8.4%	21.%	23.2

isomer was not available) was similar to the CAD of the adduct, but it was not identical. When various ratios of the CAD spectra of the models were combined, no combination matched the CAD of the adduct as well as the combination did in the benzene radical cation-cyclopropane case. One possible explanation for the lack of an accurate match between the various combinations and the CAD of the adduct is that the CAD spectrum of the 5,8- isomer is quite different from the CAD spectrum of the 8,9- isomer. The second is that the distonic forms an ion with an entirely different structure that contributes to the CAD spectrum of the adduct. The hydrogen migration and the obvious 1,6-cyclization can be accompanied by a 1,7-cyclization. This second cyclization product is possible because the reactive site in the distonic is on the terminal carbon of a four (rather than three) carbon chain. Beckwith[3,4] measured the rates of 1,6- and 1,7-cyclizations in 6-heptenyl radicals and found the 1,6- to be only 6.3 times greater than the 1,7-cyclization. If these three pathways are competitive for this distonic, the CAD spectra of three models would be necessary to match the CAD of the benzene radical cation-cyclobutane adduct. Therefore, the question of the structure of the ions contributing to the fragment ions observed in the CAD spectrum of the adduct is not completely answered.

In the case of the benzene radical cation-cyclopropane adduct the closer match between the CAD of the adduct and the combination of the CAD spectra of only two model CAD spectra is due to the absence of a second cyclization pathway for this distonic. Beckwith and coworkers [3,4] found that with 5-hexenyl radical the 1,5-cyclization is 56 times faster than the 1,6. With this difference in rates it is not surprising that combination of the CAD spectra of two models provides a good match with the CAD of the adduct.

The FTMS results and the CAD of the adducts from the reaction of benzene radical cation and cyclopropane or cyclobutane support a two step mechanism. The initially formed distonic adduct undergoes either cyclization or hydrogen migration to the terminal carbon of the chain. In the case of cyclopropane only one cyclization product predominates and thus the CAD of the adduct i s accounted for by a combination of the CAD spectra of the two models. With cyclobutane the longer carbon chain in the distonic adduct allows the reactive terminal carbon to react on the ring at two locations in addition to the hydrogen migration. Thus a more accurate match between the CAD of the adduct spectrum and combinations of model CAD spectra would require the CAD spectrum of a third model compound. These reactions further illustrate the unique chemistry of the distonic ions formed when the electrophilic benzene radical cation reacts with various neutral species.

[1] R. W. Holman, M. D. Rozeboom, M. L. Gross, and C. D. Warner, Tetrahedron, 1986, **42**, 6235-6244.
[2] C D. Warner, R. W. Holman, and M. L Gross, 34th Annual Conf. of ASMS, Cincinnati, O, 1986, p.616-617.
[3] A. L. J. Beckwith , C H Schiesser, Tetrahedron Lett., 1985, **26**, 373-376.
[4] A. L. J. Beckwith, C. J. Easton, T. Lawrence, A K. Serelis, Aust. J. Chem., 1983, **36**, 545-56.

Presented at the 35th ASMS Conference on Mass Spectrometry and Allied Topics
May 24-29, 1987, Denver, CO.

CHARACTERIZATION AND REACTIVITY OF CARBON CLUSTER IONS USING FTMS

Stephen W. McElvany and Herbert H. Nelson

Code 6110/Chemistry Division
Naval Research Laboratory
Washington, D.C. 20375-5000

INTRODUCTION

The study of neutral and ionized molecular clusters formed by laser vaporization of solid samples has received considerable theoretical and experimental attention. Most techniques used to study clusters employ molecular beam sources with time-of-flight mass analysis which does not allow for the detailed study of the ion/molecule chemistry of specific ionic clusters. This study utilizes the MS/MS capability and the long ion residence times available with FTMS to characterize mass selected carbon cluster ions. Specifically, changes in reactivity and structures as a function of cluster size can be determined from ion/molecule reactions and collision induced dissociation studies.

ION/MOLECULE REACTIONS

Positive carbon cluster ions (C_n^+; n=3-25) are formed by direct laser vaporization of a graphite sample located within the low pressure FTMS cell. The use of frequency swept ejection techniques allows the study of mass-selected cluster ions (MS/MS). The ion/molecule reactions of the mass selected carbon cluster ions have been studied with the neutral reagents D_2, O_2, CH_4, C_2H_m (m=2,4,6). A general mechanism for reaction of the cluster ions has been proposed and is easily illustrated with the reactions with D_2. Two ion/molecule reaction channels are observed with D_2 as shown in reaction 1.

$$C_n^+ + D_2 \longrightarrow C_nD^+ + D \quad (n=3\text{-}9) \quad (1a)$$

$$\longrightarrow C_{n-3}D_2^+ + C_3 \quad (n=6,8) \quad (1b)$$

Although the structures of these carbon cluster ions are not known, MNDO calculations suggest that the smaller cluster ions (n<10) are linear in structure with two carbene ends $(:C\text{-}C_{n-2}\text{-}C:)^+$ while the clusters with $n \geq 10$ are monocyclic rings. The reaction of the carbon cluster ions can be considered to proceed by a general mechanism which involves bond insertion by the carbene end of the cluster ion (i.e. formation of two C-D bonds). The excess energy resulting from complexation is then lost through cleavage of one of the C-D bonds (Rxn 1a) or C-C bond cleavage by loss of C_3 (Rxn 1b). At longer reaction times, the primary product ion C_nD^+ reacts further as seen in reaction 2.

$$C_nD^+ + D_2 \longrightarrow C_nD_2^+ + D \quad (2)$$

This reaction presumably proceeds at the remaining terminal carbene site of the linear cluster ion as in reaction 1a. No further ion/molecule reactions were observed suggesting that there exist only two reactive sites which supports the predicted structure (i.e. linear with two reactive carbene ends).

A dramatic change in reactivity was observed between n=9 and 10. Although the smaller carbon cluster ions react near the collision rate, no ion/molecule reaction products were observed for C_n^+ with $n \geq 10$ ($k < 10^{-13}$ cm^3/sec). This decrease in reactivity is consistent with the MNDO calculations which suggests that a structural change from linear to cyclic forms occurs between n=9 and 10 (i.e. there are no reactive carbene sites in the monocyclic rings).

Structural Isomers of C_7^+

While performing the reaction rate studies of C_7^+, only approximately 33% of the initial C_7^+ reacted to yield C_7D^+ as shown in reaction 3.

$$C_7^+ + D_2 \longrightarrow C_7D^+ + D \quad (33\%) \qquad (3)$$

$$\longrightarrow \text{No Reaction} \quad (67\%)$$

This suggests that two different forms of C_7^+ exist, i.e. both a reactive and unreactive fraction. Experimental tests to probe for internal or translational energy differences to explain this difference were unsuccessful. Therefore, the difference in the reactivity of C_7^+ must be due to the presence of two structural isomers - a linear form (33%) that reacts with D_2 similar to the smaller C_n^+ ($n<10$) and a cyclic form (67%) that is unreactive as are the larger cyclic carbon cluster ions ($n \geq 10$).

The ion/molecule reactions of the carbon cluster ions with other neutrals (O_2, CH_4, C_2H_2, C_2H_4, and C_2H_6) yield similar results and are consistent with the conclusions made for the D_2 reactions.

COLLISION INDUCED DISSOCIATION

The low energy collision induced dissociation of the carbon cluster ions was also studied in an attempt to obtain structural information. The major fragment ion (80-100%) observed for n=6-15 is C_{n-3}^+ with the corresponding loss of C_3. The loss of C, C_2, and C_4 neutrals constitute the other minor fragmentation channels. The C_3 loss is not surprising due to its relative stability to the other fragmentation channels. In comparison to the ion/molecule reaction results in which changes in structure and evidence for isomers was observed, no dramatic changes in the collision induced dissociation process were observed from n=9 to 10 or for n=7.

Presented at the 35th ASMS Conference on Mass Spectrometry and Allied Topics
May 24-29, 1987, Denver, CO

DO ALKYL CARBANIONS EXIST IN THE GAS PHASE?

Susan T. Graul, Robert R. Squires
Department of Chemistry, Purdue University
West Lafayette, Indiana, 47907

Although the chemistry of organic anions has been the subject of study for many years, relatively little is known about the important class of aliphatic, alicyclic, and vinylic carbanions, a class which includes the prototypical carbanion, CH_3^-. Such anions are not produced efficiently by electron impact ionization. Furthermore, due to the weak acidity of the neutral hydrocarbon precursors, common chemical ionization methods also fail to generate these anions.

We recently demonstrated that collision-induced dissociation (CID) of carboxylate ions in an FTMS provides an excellent method for producing carbanions in the gas phase with complete regiospecificity (eq. 1). We have now

$$(1) \qquad R\text{-}CO_2^- \xrightarrow{CID} R^- + CO_2$$

extended this approach to our new flowing afterglow-triple quadrupole instrument, and are exploring the scope of this ion synthesis method in the context of the title question. A key observation is that acetate ion can be collisionally decarboxylated to yield the methyl anion (eq. 2). Since the

$$(2) \qquad CH_3CO_2^- \xrightarrow{CID} CH_3^- + CO_2$$

electron affinity of methyl is extremely low ($EA(CH_3) = 1.8$ kcal/mole) and yet we can observe CH_3^- as a CID fragment, we conclude that any carbanion which is comparably bound will appear from CID of the appropriate carboxylate ion precursor. We have examined some forty or fifty carboxylate anions to date and conclude that collision-induced decarboxylation is a fragmentation process common to all these ions, allowing us to determine which carbanions are capable of existence on the post-microsecond timescale. Listed below are some representative carbanions examined by this method as well as examples of interesting new carbanions that cannot be generated by proton transfer reactions. We expect that decarboxylation of carboxylate ion precursors that

Observed		Not Observed
CH_3^-	$CH_3CH_2CH{=}CH^-$	$CH_3CH_2^-$
CD_3^-	$CH_2{=}CHCH_2CH_2^-$	$(CH_3)_2CH^-$
	$CF_3CH_2CH_2^-$	$(CH_3)_3C^-$
	$CH_3\bar{C}{=}O$	$(CH_3)_2CHCH_2^-$
$CH_2{=}CH^-$	CH_3CHCl^-	
$CH_3\bar{C}{=}CH_2$		$CH_3OCH_2^-$

would lead to carbanions such as the ethyl anion $CH_3CH_2^-$ is accompanied by rapid electron detachment, such that for practical purposes these unobserved anions do not exist in the gas phase (that is, their lifetimes are much less than the microsecond required for detection in our instrument). In general,

we find that most all of the simple alkyl carbanions fail to appear under conditions that readily yield CH_3^-. Preliminary studies indicate that accurate heats of formation for carbanions formed by collision-induced decarboxylation can be determined from threshold decarboxylation measurements.

We have also examined the ion-molecule reactions of several carbanions produced by decarboxylation, by using a reactive gas such as N_2O as the Q2 collision gas in place of the inert collision gas argon. In these experiments, the reactive gas serves as both the target for CID and as a reactive partner in the subsequent ion-molecule reactions of the daughter carbanions. Using this technique, we have been able to examine for the first time the reactions of the methyl anion. The methyl anion can be seen to abstract protons from ethylene and butadiene to produce $C_2H_3^-$ and $C_4H_5^-$, respectively. However, when using the labeled ion CD_3^-, no proton transfer with CH_4 can be detected on the timescale of our experiment. Reactions corresponding to addition of methyl and elimination of H_2 could also be observed with ethylene and butadiene, leading to product ions at m/z 41 and 67. Reaction of CH_3^- with OCS resulted in formation of CH_3S^- and HS^-, as well as several ions which may be products of reactions with the parent acetate ion. In general, such ambiguities could be resolved by observing the energy dependence of the product ions, and relating it to the energy dependence of the methyl daughter ion. A novel reaction corresponding to methyl exchange could be observed when using $(CH_3)_4Si$ as the collision gas and $CD_3CO_2^-$ as the parent carboxylate. At energies high enough to form the CD_3^- daughter, CH_3^- could also be detected at much lower intensities, with no evidence of CHD_2^- or CH_2D^- from possible H/D exchange reactions. The product ion CH_3^- probably results from addition and elimination of methyl to the silane, proceeding through a pentavalent silicon intermediate in which the methyl substituents are equivalent. Further investigations are underway of the chemistry of the methyl anion, as well as some of the other carbanions that can be produced by this decarboxylation method.

Presented at the 35th ASMS Conference on Mass Spectrometry and Allied Topics
May 24-29, 1987, Denver, CO

CHARACTERIZATION OF CONSTITUENTS IN TOBACCO SMOKE USING FOURIER TRANSFORM MASS SPECTROMETRY

M. B. Wise
Analytical Chemistry Division
Oak Ridge National Laboratory
Oak Ridge, TN 37831-6120

The use of differentially pumped dual cells has greatly improved the analytical capabilities of Fourier transform mass spectrometry (FTMS). Using this configuration, ions formed in the source cell under relatively high pressures can be transferred into the analyzer cell where they may be detected at much lower pressures. This allows a wide range of experiments to be routinely performed including gas chromatography/mass spectrometry, chemical ionization, mass spectrometry/mass spectrometry, and direct probe vaporization of samples without sacrificing the outstanding mass spectrometric performance of FTMS. The extended mass range, high mass resolution, rapid data acquisition, and exact mass capabilities are particularly well suited for the study of complex mixtures.

Dual cell FTMS is currently being evaluated in our laboratory as a new technique for the characterization of tobacco smoke tars. Tobacco smoke is a highly complex mixture containing thousands of polar and nonpolar compounds. The ultimate goal of this research will be to characterize the composition of tobacco smoke particulates in the environment. Initial studies however, have focused on the analysis of concentrated smoke tars generated from well characterized standard 2R1 Kentucky reference cigarettes. This has allowed the analytical utility of FTMS to be compared with that of conventional methods used for smoke characterization including gas chromatography and combined gas chromatography/mass spectrometry.

The approach that is presently being employed involves the collection of smoke tar on filter pads, extraction with hexane, and deposition of the extract on the direct insertion probe. Low energy electron impact and chemical ionization techniques are used to generate molecular and pseudomolecular ions. Separation of the components in the tar is achieved by acquiring medium to high resolution mass spectra, allowing isobaric ions to be well separated. Internal mass calibrants further enable the exact mass of these ions to be accurately determined. An example low energy electron impact spectrum is shown in Figure 1 with the regions around m/z 124 and m/z 176 expanded in Figure 2.

Although exact mass measurements are extremely valuable for determining empirical molecular formulae, structural information of these ions is also desirable. For direct probe samples, this is most easily achieved by utilizing the collisionally activated dissociation (CAD) capability of the FTMS. Taking full advantage of the dual cell design of the FTMS-2000, it is possible to collisionally dissociate ions under a high pressure of argon in the source cell and detect the daughter ions in the analyzer under conditions that enable high resolution spectra to be obtained. This is particularly important for complex mixture analysis where isobaric parent ions may be simultaneously dissociated to form isobaric daughter ions. The combined information of exact mass and the CAD spectra provides a much higher degree of confidence in the identification of constituents.

An important feature of the direct probe FTMS analysis is the ability to observe both polar and nonpolar compounds in a single experiment. This is in contrast to most methods involving chromatographic separation of components. Additionally, it has been demonstrated that it is possible to obtain quantitative information on various constituents by the addition of internal standards into the sample. Using the internal standard method, a linear calibration curve for nicotine was generated over a concentration range of 2 orders of magnitude. Determination of the amount of nicotine in a standard reference cigarette using direct probe quantification compared favorably to the results obtained by established chromatographic methods.

Presented at the 35th ASMS Conference on Mass Spectrometry and Allied Topics
May 24-29, 1987, Denver, CO

Figure 1

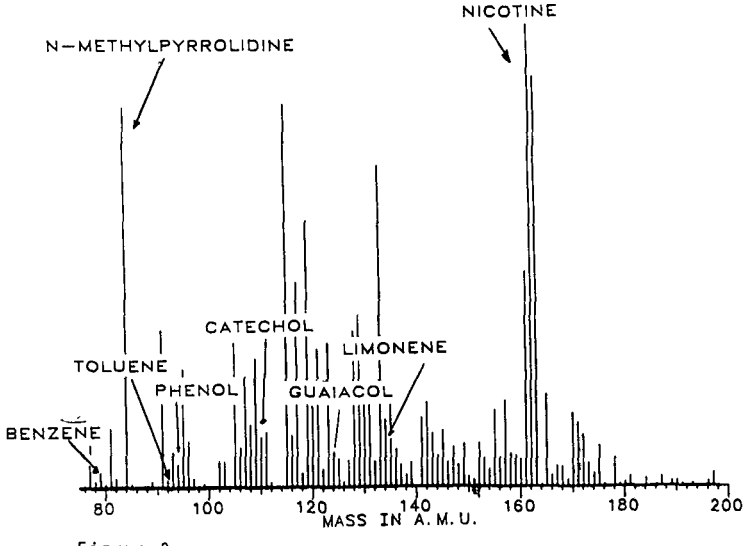

Figure 2

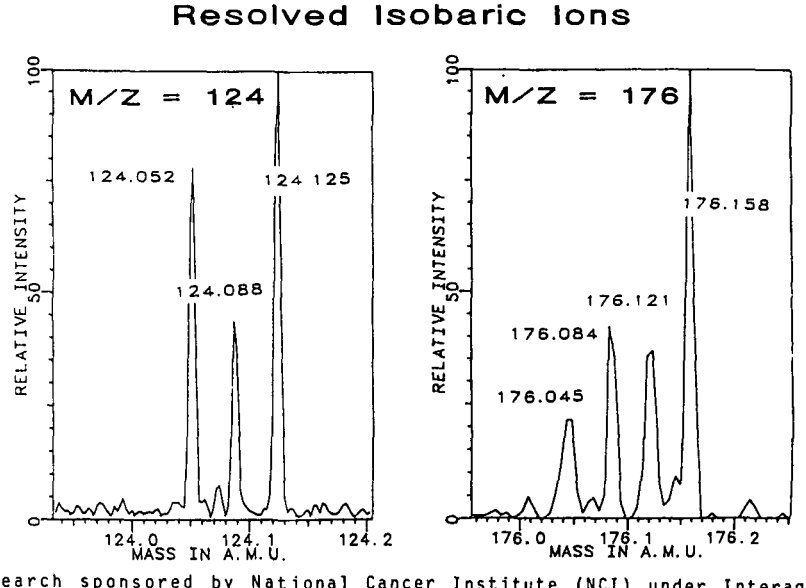

*Research sponsored by National Cancer Institute (NCI) under Interagency Agreement No. Y01-CP-30508 under Martin Marietta Energy Systems, Inc., contract DE-AC05-84OR21400 with the U.S. Department of Energy.

Presented at the 35th ASMS Conference on Mass Spectrometry and Allied Topics
May 24-29, 1987, Denver, CO

DETECTION AND QUANTIFICATION OF OH-NO_2-PAH, OH-NO_2-PAK AND OH-NO_2-AROMATIC COMPOUNDS BY NCI GC/MS

M. G. Nishioka and D. A. Contos

BATTELLE
Columbus Division

Atmospheric transformation of PAHs is proposed as a mechanism to account for increased percentages of mass and mutagenicity in polar compound class fractions of urban air particulate extracts relative to point source emission particulate extracts. Atmospheric hydroxylation followed by nitration should result in production of both nitrated-PAH (NO_2-PAH) and hydroxylated NO_2-PAH (OH-NO_2-PAH). The presence of atmospheric NO_2-PAH is documented[1]; OH-NO_2-PAH have not been identified to date.

The simplest analogs of OH-NO_2-PAH, NO_2-phenols and NO_2-cresols, have been produced via atmospheric exposure of benzene and toluene in smog chambers[2]. Several NO_2-phenols and NO_2-cresols are identified here from EI and NCI GC/MS analyses of an urban air particulate extract. Quantification (see Table 1) was performed without derivatization using cold, on-column injection NCI GC/MS with methane reagent gas. The NCI spectra of compounds capable of intramolecular hydrogen bonding have the M^- as base peak. However, the NCI spectra for which such bonding of -OH and -NO_2 functional groups is not possible have a base peak of $(M-1)^-$ and M^- intensity of 9-15 relative percent. The EI spectra of NO_2-cresols in which -CH_3 and -NO_2 groups are ortho to each other have a base peak at $(M-17)^+$, apparently due to loss of an oxygen from the nitro group and a methyl proton.

Bioassay-directed fractionation through four sequential separation steps and EI and NCI GC/MS analyses has led to the proposed identification of OH-NO_2-PAH and OH-NO_2-polycyclic aromatic ketones (PAK) reported here. The EI and NCI mass spectra of reference 6-OH-1-NO_2-pyrene and a tentatively identified OH-NO_2-fluorenone (OH-NO_2-PAK) are shown in Figure 1. Primary interest, however, is focussed on the isomer identification of a OH-NO_2-fluoranthene, thought to be mutagenic on the basis of the mutagenicity of NO_2-fluoranthene isomers and isomeric OH-NO_2-pyrene isomers. Quantification is included in Table 1.

(1) T. Randahl, et al. Nature 321, 425-427 (1986).

(2) D. Grosjean, Atmos. Environ. 18, 1641-1652 (1984).

Presented at the 35th ASMS Conference on Mass Spectrometry and Allied Topics
May 24-29, 1987, Denver, CO

TABLE 1. QUANTIFICATION OF OH-NO_2-AROMATIC COMPOUNDS

Compound	Conc., µg/g Acid Fraction	Conc., µg/g Extract
2-NO_2-phenol	630	43
3/4-NO_2-phenol	520	36
3-CH_3-2-NO_2-phenol	20	1
3-CH_3-4-NO_2-phenol	30	2
X-CH_3-3/4-NO_2-phenol	75	5
OH-NO_2-fluoranthene	70	5

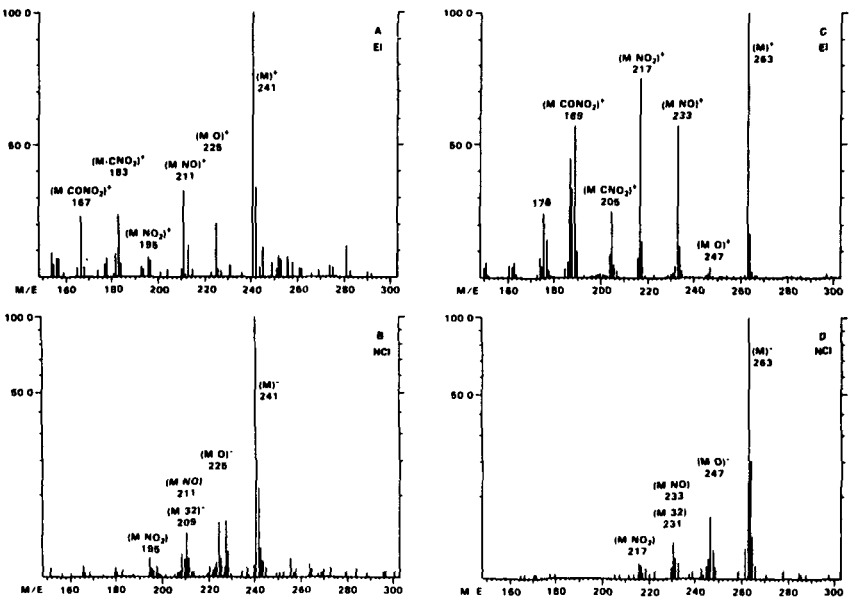

FIGURE 1. EI (A) AND NCI (B) SPECTRA OF ATMOSPHERIC OH-NO_2-FLUORENONE
EI (C) AND NCI (D) SPECTRA OF REFERENCE 6-OH-1-NO_2-PYRENE

Presented at the 35th ASMS Conference on Mass Spectrometry and Allied Topics
May 24-29, 1987, Denver, CO

FORMATION OF POLYCYCLIC AROMATIC HYDROCARBON ADDUCT IONS IN NEGATIVE ION CHEMICAL IONIZATION

L.R. Hilpert and E. White V
Center for Analytical Chemistry, National Bureau of Standards,
Gaithersburg, MD 20899

The methane negative ion chemical ionization (NICI) mass spectra of polycyclic aromatic hydrocarbons (PAH) are dominated by the molecular anion for species which show high NICI sensitivity, and by the molecular anion and adduct ions for NICI-insensitive species. Adduct ions are observed in the NICI mass spectra of all PAH examined when hydrocarbon reagent gases are used. They are useful analytically in differentiating isomeric PAH and they are helpful in elucidating processes occurring in the ion source under NICI conditions.

The NICI spectra of thirty-nine PAH were obtained using methane and deuteromethane as the reagent gases. The ion source pressure and temperature, both known to affect adduct ion abundance, were set at 0.3 Torr and 200 °C respectively. The adduct ions observed indicate that at least two mechanisms, involving reactions of the PAH with radical species present in the reagent gas plasma, are responsible for the adduct ion formation. The reactions are similar to those postulated by Dillow and Gregor in 1986 (1). The first reaction proceeds through a substitution mechanism and the second pathway through an insertion mechanism.

Benzo(e)pyrene is a five condensed ring PAH which shows low NICI sensitivity and a correspondingly high adduct ion abundance (the adduct ion at m/z 266 is the base peak in the spectrum). The reactions leading to the formation of the m/z 266 adduct ion in the CH_4 NICI mass spectrum of benzo(e)pyrene are shown in Figure 1.

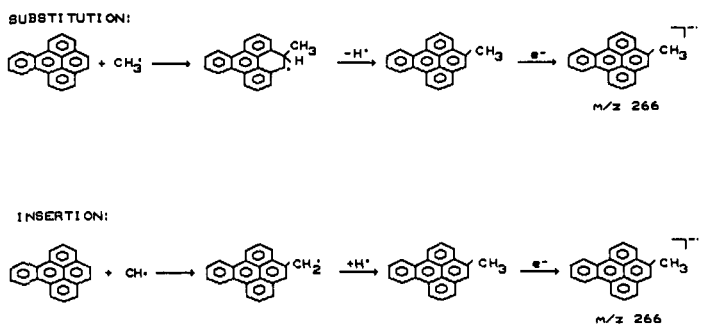

Figure 1
Formation of Benzo(e)pyrene Adduct Ions with CH_4 Reagent Gas

In the first step of the substitution reaction, the neutral PAH reacts with a radical of the form $C_nH_{2n+1}\cdot$ to yield a radical adduct of the form $(M + C_nH_{2n+1})^{\cdot\cdot}$. The actual position of C-alkylation is not known at this time, and is depicted as shown for illustrative purposes only. The radical adduct subsequently loses H· in a reaction presumably driven by the restoration of aromaticity. The neutral adduct is ionized via resonance electron capture in the final step. In the insertion mechanism, the neutral PAH reacts with a CH· radical to yield a radical adduct in the first step. The radical adduct reacts with another radical present in the reactant gas plasma, R· (where R = H or alkyl), to form the neutral adduct which is subsequently ionized in the final step. It should be noted that in both cases, formation of the benzo(e)pyrene adduct occurs prior to ionization by resonance electron capture.

It is impossible to separate the contributions of the substitution and insertion reactions to the adduct ion abundance when CH_4 is the reagent gas, as both yield an adduct ion at m/z 266. When CD_4 is the reagent gas, however, the adducts formed by the two pathways can be isolated, as they appear at different masses as shown in Figure 2.

Presented at the 35th ASMS Conference on Mass Spectrometry and Allied Topics
May 24-29, 1987, Denver, CO

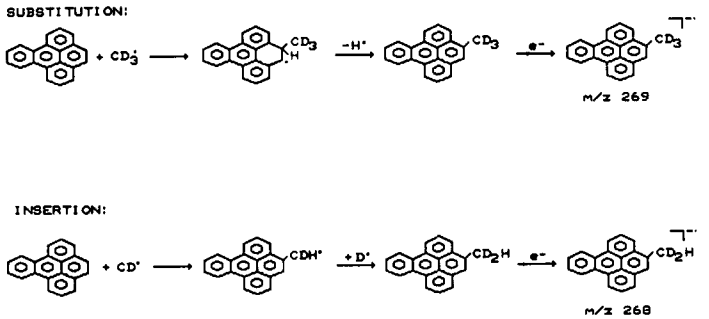

Figure 2
Formation of Benzo(e)pyrene Adduct Ions with CD_4 Reagent Gas

The CD_4 data indicate that at least two reaction pathways are involved in the formation of the $(M + C_nH_{2n})^{-\cdot}$ ion, as each ion is replaced by two ions of the form $(M + C_nD_{2n})^{-\cdot}$ and $(M + C_nD_{2n+1} - H)^{-\cdot}$. The adduct ion resulting from the substitution mechanism $(M + CD_3 - H)^{-\cdot}$ appears at m/z 269, and the adduct ion formed by the insertion mechanism $(M + CD_2)^{-\cdot}$ appears at m/z 268. Table 1 shows the contributions of the two reactions to the adduct ion abundances observed in the NICI mass spectra of PAH.

TABLE 1

CONTRIBUTIONS OF TWO REACTIONS TO THE ADDUCT ION ABUNDANCES OBSERVED IN THE NICI MASS SPECTRA OF PAH

	Relative Abundance			
	Substitution	Insertion		Observed
Compound	$(M+CD_3-H)^{-\cdot}$	$(M+CD_2)^{-\cdot}$	Total	$(M+CH_2)^{-\cdot}$
Fluoranthene	1.7%	5.3%	7.0%	6.0%
Pyrene	11.3	15.2	26.5	35.6
Benz(a)anthracene	2.2	5.5	7.7	7.3
Chrysene	5.1	16.1	21.2	19.6
Benzo(b)fluoranthene	0.8	1.1	1.9	2.0
Benzo(k)fluoranthene	1.2	2.0	3.2	3.8
Benzo(e)pyrene	25.6	100.0	125.6	100.0
Benzo(a)pyrene	0.9	0.7	1.6	2.2
Perylene	19.0	39.3	58.3	56.9
Indeno(1,2,3-cd)pyrene	1.2	1.1	2.3	2.9
Benzo(ghi)perylene	1.1	1.3	2.4	2.9

As is seen from the data in Table 1, there is generally good agreement between the total abundance of adduct ions from the substitution and insertion mechanisms when CD_4 is used as the reagent gas and the abundance of the $(M + CH_2)^{-\cdot}$ adduct when CH_4 is the reagent gas.

It is noteworthy that although the $(M + CH_2)^{-\cdot}$ species is the most abundant adduct ion observed in the NICI spectra of PAH, adducts as large as $(M + C_4H_8)^{-\cdot}$ have been observed in the methane NICI spectrum of fluoranthene, indicating the presence of radicals as large as $C_4H_9\cdot$ in the NICI ion source.

The ratio of the $(M + CH_2)^{-\cdot}$ adduct ion abundance to the molecular anion $(M^{-\cdot})$ abundance varied over more than two orders of magnitude for the thirty-nine PAH which were examined, and relative adduct ion abundance is a good predictor of NICI sensitivity for PAH. Those compounds which show high adduct ion abundance show low NICI sensitivity and those PAH which show low adduct ion abundance show high NICI sensitivities. Indeed, the relative adduct ion abundance shows the best correlation with NICI sensitivity ($r^2 = 0.7212$) of all factors (including electron affinity, ionization potential, and length-to-breadth ratio) examined to date.

References

1. Dillow, G.W., and Gregor, I.K., Org. Mass Spectrom. 21, 386 (1986).

Presented at the 35th ASMS Conference on Mass Spectrometry and Allied Topics
May 24-29, 1987, Denver, CO

A HYBRID HRGC/MS/MS METHOD FOR THE CHARACTERIZATION OF TETRACHLORINATED-p-DIOXINS IN ENVIRONMENTAL SAMPLES

Yves Tondeur, Warren N. Niederhut, and Joseph E. Campana
Environmental Research Center, University of Nevada
Las Vegas, Nevada 89119-9970

and

Steven R. Missler
Texaco USA, P.O. Box 425
Bellaire, Texas 77401

Polychlorinated dibenzo-p-dioxins (PCDDs) have been the subject of concern in the biomedical and environmental sciences because of their pronounced toxicological effects in laboratory animals. The most hazardous of the possible 75 congeners is presently thought to be the 2,3,7,8-tetrachlorodibenzo-p-dioxin (TCDD) isomer.

A new instrumental method for the characterization of the analyte 2,3,7,8-TCDD by using selected-reaction monitoring (SRM) was investigated [1]. This method used high-resolution gas chromatography (HRGC) coupled to a hybrid tandem mass spectrometer. The technique was evaluated with regard to four performance parameters: sensitivity, linearity, repeatability, and selectivity. The method was found to compare favorably with the traditional selected-ion monitoring (SIM) technique as used with HRGC/high-resolution mass spectrometry (HRMS). Furthermore, the HRGC/(hybrid)MS/MS SRM method showed selectivity that surpassed the HRGC/HRMS SIM method.

A VG 7070-EQ mass spectrometer of EBQ_1Q_2 geometry was used for the HRMS/MS/MS SRM investigations. Three TCDD compounds were used: the analyte -- 2,3,7,8-TCDD, an internal standard -- ^{13}C-labeled 2,3,7,8-TCDD, and a recovery standard -- ^{13}C-labeled 1,2,3,4-TCDD. Two parent (isotopic) ions from each TCDD compound were of interest: m/z 320 and m/z 322 for the analyte and m/z 332 and m/z 334 for the two ^{13}C-labeled standards. The loss of native or ^{13}C-substituted $CO^{35}Cl$ from the three TCDDs were monitored in the MS/MS experiments. In addition, the m/z 331 ion from PFK was used as a lock mass in the HRMS experiments, and its daughter ion at m/z 243, formed by the loss of CF_4, was used to monitor the instrument stability in the MS/MS experiments.

The SRM experiments were performed as follows; the five parent ions of interest were sequentially mass-selected with a 1-s cycle time by using the EB portion of the hybrid mass spectrometer, which was operated at a resolving power of about 1000. Each of these ions were sequentially transmitted into the collision region region (Q_1) of the hybrid mass spectrometer where they underwent collision-induced dissociation with argon at a collision energy of 0.5 eV (center-of-mass). Each daughter ion of interest, formed by collisional activation of each parent, was analyzed by synchronously stepping the quadrupole mass analyzer Q_2 with the parent-selecting EB spectrometer. By using this technique, it was found that 2 pg of 2,3,7,8-TCDD could provide a response with a signal-to-noise of 4:1 under unoptimized conditions.

The repeatability of the technique was evaluated by measuring the isotopic ratios of the daughter ions (257/259 and 268/270) from calibration solutions that varied form 2.0 to 100.0 pg/uL of 2,3,7,8-TCDD. The experimental ion abundance ratios, 1.09+05, compare favorably with the theoretical value 1.03. These repeatabilities are similar to those obtained by the HRGC/HRMS SRM technique. The linearity was determined by comparing the relative response factors of the TCDD analyte and internal standards over the concentration range of the calibration solutions. The coefficients of variation of the data relating to linearity ranged from 3.2% to 17.3%, which again is comparable to linearity results obtained using the HRGC/HRMS SIM method.

Presented at the 35th ASMS Conference on Mass Spectrometry and Allied Topics
May 24-29, 1987, Denver, CO

The selectivity of the HRGC/MS/MS SRM and the HRGC/HRMS method was challenged through the analysis of synthetic performance check solutions. The selected-ion monitoring profiles from HRGC/HRMS, shown in Figure 1, were obtained by the injection of 10 ng of a PCB mixture (Aroclor™ 1260) onto a capillary GC column with the mass spectrometer operating at a resolving power of 10,000. The ion current profiles are similar to those that are recorded during the analysis of TCDDs; however, in this case there were no TCDDs present in the PCB mixture. The corresponding TCDD ion signals arise only from PCB interferences (daughter ions of hexa- and heptachlorobiphenyls). The top SIM profile in Figure 1 indicates the interfering effect of the PCBs by showing where the relevant TCDDs coelute.

The HRGC/(hybrid)MS/MS method can be extremely selective; the first mass spectrometer can act as a prefilter such that the critical PCB interferences such as the ones exemplified in Figure 1 can be filtered out. A solution containing a low level (10 pg) of 2,3,7,8-TCDD in the presence of a 100,000 fold excess of PCBs (Aroclor™ 1260) was used to demonstrate this capability. Figure 2 shows the SRM profiles obtained by HRGC/MS/MS following the injection of a mixture containing 10 pg of 2,3,7,8-TCDD, 10 pg of $^{13}C_{12}$-2,3,7,8-TCDD, 10 pg of $^{13}C_{12}$-1,2,3,4-TCDD, and 1 ug of Aroclor™ 1260. This figure shows that the detection, characterization, and identification of 2,3,7,8-TCDD is relatively invarient to large quantities of interfering PCB isomers in a sample. The traces (A, B, D, and E) in Figure 2 indicate that 2,3,7,8-TCDD can be quantified at the low picogram level in the presence of high concentrations of interfering PCBs. However, the Inset B_1, shown in Figure 2, was obtained from the analysis of the PCB mixture without any TCDDs, and it indicates that high levels of PCBs cause potential interference problems. (This inset can be compared with the bottom trace in Figure 1.) The various ion peaks that appear in the inset can interfer with the determination of the other TCDD isomers. In addition, Trace C of Figure 2 shows that the elution of the large quantities of the PCBs into the ion source results in an instability of the ion signal. When the interfering PCBs are reduced to a 1000-fold excess, these limiting phenomena are not observed.

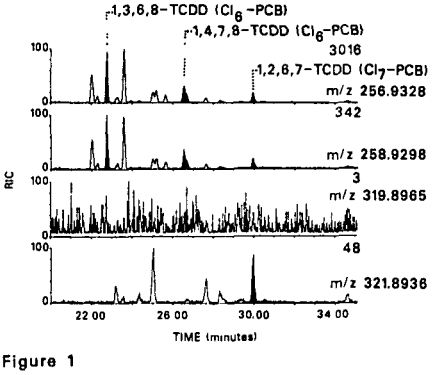

Figure 1

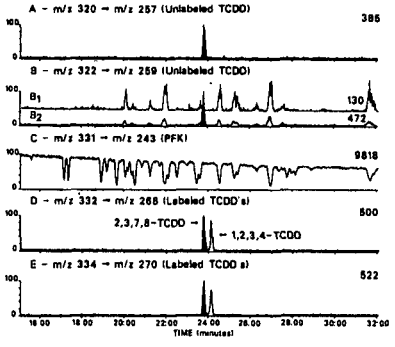

Figure 2

The SRM method adds an additional dimension of selectivity, making possible the analysis of partially cleaned-up samples. Nevertheless, selectivity of the detection scheme should not alone be a substitute for judicious sample cleanup. The multitude of interferences encountered in real matrices can ultimately cause unforseen problems because of the high-sensitivity of the SIM and SRM mass spectrometric methods.

REFERENCE

1. Y. Tondeur, W. N. Niederhut, J. E. Campana, and S. R. Missler, Biomed. Environ. Mass Spectrom., in press.

Presented at the 35th ASMS Conference on Mass Spectrometry and Allied Topics
May 24-29, 1987, Denver, CO

Measurement of Photoinduced Loss of Low Vapor Pressure Molecules by Mass Spectrometry.

Robert Orth, Cheryl Ritchie, and Fred Hileman

Environmental Sciences Center, Monsanto Company, 800 N. Lindbergh Blvd., St. Louis, Missouri 63167.

Many molecules which enter the environment are found to be stable towards biodegradation as well as chemical degradation. This means that a major loss mechanism would be through reactions in the vapor phase. This would be true for low vapor pressure molecules such as 2,3,7,8- tetrachlorodibenzo-p-dioxin, TCDD, which has a vapor pressure of 1 x 10^{-9} torr at 25 degrees C. Thus it is of interest to determine what the rates of degradation are for such low vapor pressure molecules. The degradation pathways that are possible are reactions with O_3, OH^-, and photoinduced degradation. The pathway examined in this study was the photoinduced degradation which required the construction of an apparatus with the ability to detect low vapor pressure molecules, be specific, and allow real time acquisition.

Figure 1 shows a diagram of the apparatus used. A carrier gas such as He flows over a glass tube which is coated with 2,3,7,8-TCDD at a temperature of 140 degrees C. The He transports the TCDD into a Quartz bulb which is thermally controlled at 150 degrees C. The quartz cell can be irradiated with a wavelength of light selected from a 1 KW Hg-Xe arc lamp. The TCDD then flows directly into a mass spectrometer where it is detected by use of selected ion monitoring. The mass spectrometer offers the sensitivity, less than a picogram per second, specificity, and real time data. The procedure involves transporting an initial amount of TCDD into the quartz cell and then diverting the flow of the He so that the carrier gas bypasses the TCDD generator while maintaining He flow into the quartz cell and into the mass spectrometer. The TCDD flows into the mass spectrometer following a first order rate loss when no light is present in the cell. When the light is turned on the loss from the cell as measured by the mass spectrometer is increased due to photoinduced loss mechanism.

As can be seen in figure 2 the light does induce a loss of TCDD in the cell vs. the no light loss. Using the two measure rates the rate constant for photoinduced loss can be calculated. This rate when combined with the rate determined from a reference compound such as acetone yields a quantum yield for the process. This resulted in a measured quantum yield of 0.033 with a precision of 70% when He was the carrier gas.

Other carrier gases can be used since the mass spectrometer is a specific detector. Therefore, the rate of photoinduced loss with air as the carrier was found to be the same within experimental error as that for He. The rate was also examined with a carrier of He with 10% isobutane and found to increase by a factor of 1.7.

It is important to note that at low vapor pressures the amount of sample on the surface of the cell can be larger than that in the gas phase. Thus the induced loss observed in the system can be photoinduced loss on the surface not the gas phase . For this system the surface problem is addressed by being sure that after the TCDD is picked up by the carrier gas the carrier plus the TCDD always experiences an increase in temperature. Since this does not eliminate the possibility the loss is due to photoinduced loss at the surface, experiments involving different surface areas are presently being investigated.

In conclusion an apparatus was constructed which can examine the photodegradation of low vapor pressure molecules using a mass spectrometer as the detector. The apparatus was used to measure a quantum yield of 0.033 for 2,3,7,8-TCDD with a precision of 70%. Considering the absorption curve of TCDD vs. sunlight, 2,3,7,8-TCDD has a finite life in the vapor phase.

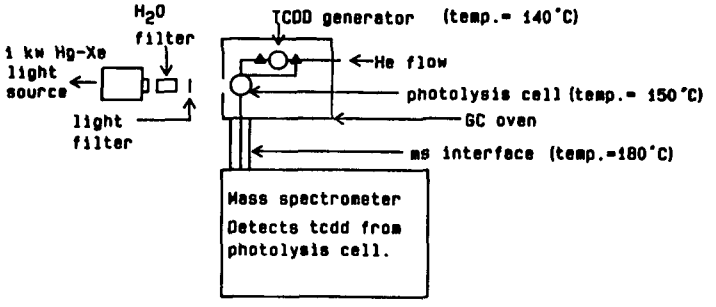

FIG 1

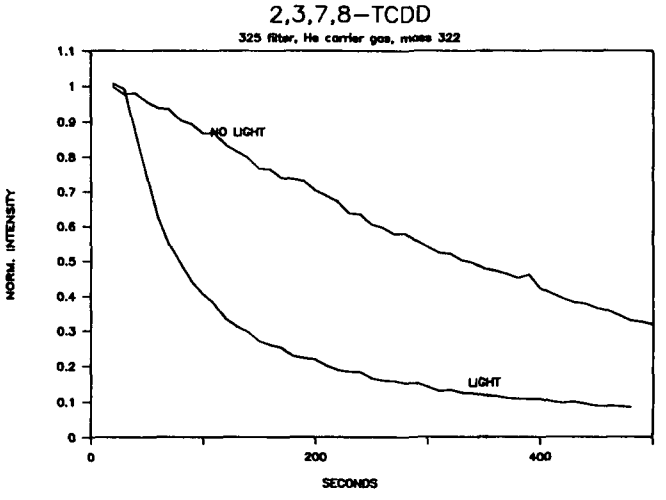

FIG. 2

Presented at the 35th ASMS Conference on Mass Spectrometry and Allied Topics
May 24-29, 1987, Denver, CO

EVALUATION OF MULTIPLE CARBON-13 LABELED INTERNAL STANDARDS FOR THE GC/MS DETERMINATION OF CHLORINATED DIBENZO-P-DIOXINS AND DIBENZOFURANS

L.M. Sack and J.S. Stanley
Midwest Research Institute
425 Volker Boulevard
Kansas City, MO 64110

Analytical methods which employ GC/MS for the determination of polychlorinated dibenzo-p-dioxins (PCDD) and dibenzofurans (PCDF) must rely on the availability of isotopically-labeled internal standards for accurate quantitative measurements. However, until recently only a minimum number of labeled PCDD and PCDF standards have been available to the analytical community. In many methods, for example Method 8280 (1), as few as 1 or 2 isotopically-labeled internal standards, typically ^{13}C labeled TCDD and OCDD, are used to quantify all 136 of the tetra-octa CDD and CDF's. Since the chromatographic and mass spectrometric behavior of the PCDD and PCDF's, such as retention times and relative ionization cross-sections, can vary considerably, the use of such a small number of internal standards limits the accuracy and precision of the overall analysis. This is particularly true for the precision of the relative response factors (RRF) derived from the standard curve and the accuracy of both the recovery measurements and the actual quantification of native PCDD and PCDF's.

Recently, a new analytical method for the ultra-trace determination of PCDD and PCDF's in adipose tissue was developed and validated in this laboratory (2). As the method was designed to employ isotope dilution techniques to quantify 17 specific 2,3,7,8 substituted PCDD's and PCDF's, a large number of isotopically-labeled internal standards were used (see Table 1). The validation study and on-going sample analyses have yielded a large amount of experimental data on which a thorough assessment of the use of multiple internal standards was based. This set of data was quantified in two ways. First, relative to the large set of 8 internal standards, in which each of the native PCDD and PCDF's were quantified versus their labeled homologs. The second quantification method was based upon Method 8280, in which ^{13}C-2,3,7,8-TCDD was used to quantify the tetra and penta CDD and CDF's and ^{13}C-OCDD was used to quantify hexa through octa CDD and CDF's. Specifically, the quality of the analytical data as a function of the number of internal standards was addressed in terms of the precision of the standard curve and consistency of the daily RRF's, as well as the accuracy and precision of the analyses of a set of real samples for the 2,3,7,8-substituted PCDD and PCDF congeners.

TABLE 1. Labeled internal standards

$^{13}C_{12}$-1,2,3,4-TCDD
$^{13}C_{12}$-2,3,7,8-TCDD
$^{13}C_{12}$-2,3,7,8-TCDF
$^{13}C_{12}$-1,2,3,7,8-PeCDD
$^{13}C_{12}$-1,2,3,7,8-PeCDF
$^{13}C_{12}$-1,2,3,6,7,8-HxCDD
$^{13}C_{12}$-1,2,3,4,7,8-HxCDF
$^{13}C_{12}$-1,2,3,4,6,7,8-HpCDD
$^{13}C_{12}$-OCDD

The initial standard curve calibration was established by the triplicate analyses of six concentration calibration solutions. The results demonstrate the marked improvement in the RRF precision (Figure 1) for nearly all of the native compounds when 8 internal standards are used. Those compounds which have retention times that are significantly different from those of TCDD or OCDD show the most improvement by the use of isotope dilution methods. This is due to the fact that the homologous internal standards experience most nearly the same chromatographic and mass spectrometric conditions as their respective native compounds. This improvement in precision is carried over into the sample analyses in which the initial calibration curve must be verified daily. In this case, the use of a larger number of internal standards increases the reproducibility of the RRF's and the probability of successful validation of the calibration curve on a daily basis. In fact, using this improved method, there has not been a need to repeat the initial calibration for up to six months (see Figure 2).

During the validation study, a set of adipose samples were spiked with known levels of the PCDD and PCDF's and analyzed in triplicate to assess the accuracy of the method. When the whole set of internal standards was used to compute the results of this standard addition experiment, it was observed that the accuracy of the analysis was improved significantly over that resulting from the use of only the labeled TCDD and OCDD. Figure 3 shows a comparision of the two computational methods in terms of the slope of the regression lines for the standard addition curve, which is a measure of the linearity of response of the analytical system to a known amount of analyte. A value of 1.0 for the slope is ideal, with deviations from that value indicating significant departure from linearity of response. Values derived from the use of 8 internal standards tend to cluster much more closely to 1.0 than for the set of 2 internal standards, especially for those analytes, such as the PeCDF's, which exhibit method recoveries which are significantly different from TCDD. In fact, the improvement in accuracy due to the use of the expanded set of internal

standards can for the most part be attributed to the improved measurement of recoveries made possible by the inclusion of more stable, isotopically labeled analogs.

Drawbacks related to the use of a larger number of labeled internal standards include increased cost and complexity of the analysis. However, the most problematic disadvantage is that PCDF's labeled with ^{13}C have isobaric ions with native PCDD's having the same number of chlorine atoms. This is illustrated in Figure 4, where the quantitation ions for OCDD, m/z 458 and 460, have significant contributions from the labeled OCDF, which is a real problem when a DB5 column is used due to the similar retention times of OCDD and OCDF. A possible solution to this problem is the use of resolving powers in excess of 10,000 (10% valley definition), which is sufficient to eliminate the contribution of the labeled PCDF's from the native PCDD channels.

In conclusion, the use of multiple ^{13}C labeled PCDD and PCDF internal standards can improve the accuracy and precision associated with the ultra-trace determination of PCDD and PCDF's due to the improvement in the precision of the initial calibration curve, improvement of the long term reproducibility of RRF measurements, increased accuracy in the recovery measurements for the surrogate compounds, and increased linearity of response for the quantification of native analytes.

REFERENCES

1. EPA Method 8280, "The Analysis of Polychlorinated Dibenzo-p-dioxins and Polychlorinated Dibenzofurans."

2. Stanley, J.S.; Ayling, R.E.; Bauer, K.M.; McGrath, M.J.; Sack, T.M.; and Thornburg, K.R. "*Analysis for Polychlorinated Dibenzo-p-Dioxins and Dibenzofurans in Human Adipose Tissue:* Method Evaluation Study," EPA Publication No. EPA-560/5-86-026, 1986.

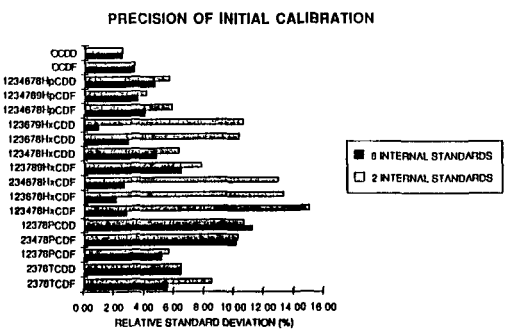

FIGURE 1

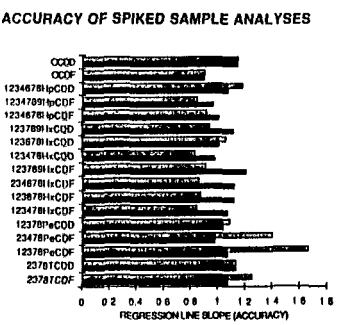

FIGURE 3

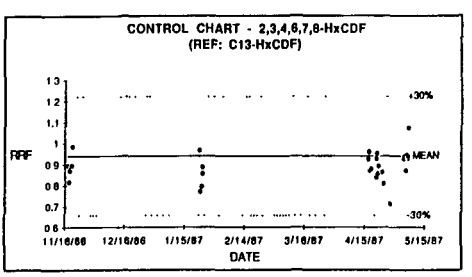

FIGURE 2

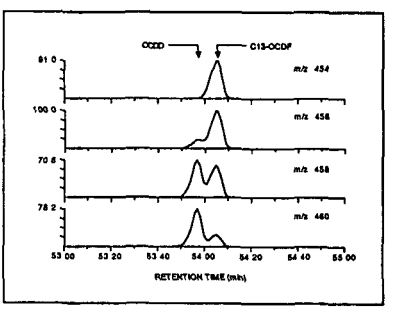

FIGURE 4

Presented at the 35th ASMS Conference on Mass Spectrometry and Allied Topics
May 24-29, 1987, Denver, CO

HIGH RESOLUTION SELECTED ION MONITORING OF POLYCHLORINATED DIBENZO-P-DIOXINS AND DIBENZOFURANS USING NON-PFK LOCKMASSES

Taguchi, V.Y., Reiner, E.J., Hallas, B., and Wang, D.T.

ONTARIO MINISTRY OF THE ENVIRONMENT, REXDALE, ONTARIO, CANADA

Recent studies (1) have shown that the bioaccumulation of polychlorinated dibenzo-p-dioxins (PCDD) and polychlorinated dibenzofurans (PCDF) increase with increasing chlorine substitution. Also, the acute lethality of some Cl_5 and Cl_6 DD and DF congeners have LD_{50} values only an order of magnitude higher than that of 2,3,7,8-Cl_4DD, the most toxic congener. These two observations indicate that the monitoring of all PCDD and PCDF is important. Sensitivity and mass resolution are also important considerations. A high resolution mass spectrometric - selected ion monitoring (HRMS-SIM) methodology has been developed at the Ministry of the Environment (MOE) utilizing a VG ZAB-2F mass spectrometer at 12,000 RP and employing non-PFK lockmasses.

To determine exact masses in the HRMS-SIM mode, simultaneous introduction of a reference compound (lockmass), typically PFK, is required. The lockmass level must be set as low as practically possible because of contamination and suppression of the sample ion current. For PFK, control of the lockmass level is quite difficult with the conventional VG heated liquid inlet system. Also, the majority of the ion current in the PFK mass spectrum, as shown in Figure 1, is carried by ions below M/Z=300 (the range of interest in PCDD and PCDF analysis is M/Z=300 to 450) causing suppression of the sample ion current. By using a mixture of solid unsaturated hydrocarbons such as coronene, tetraphenylcyclopentadiene and decacyclene, where the majority of the ion current is carried by the molecular ions in the range of interest (as shown by Figure 2), suppression is greatly reduced and a corresponding enhancement in sensitivity by approximately a factor of 3 in all five groups monitored (see Table 3) is achieved. Because the lockmasses are solids, their levels in the ion source are easily controlled using the solid probe heater. Also, these compounds being mass sufficient give greater resolution between the lockmasses and the mass deficient PCDD and PCDF than between PFK and PCDD and PCDF.

The MOE method includes the monitoring of the isotopic ratios of the three most intense ions of the molecular ion cluster; in addition, COCl loss from the molecular ion may also be monitored at 12,000 RP. Internal standards labelled with ^{13}C and/or ^{37}Cl are used to determine recoveries and injection standards such as $^{13}C_{12}Cl_6DF$ are used to monitor instrument performance. External standards are used to determine response factors for the various congeners. An external standard is injected initially and every third injection thereafter. Concentrations are determined using the standards injected immediately before or after the sample. This type of "correction" is necessary because of possible drift in instrument sensitivity. The data used for the standard curve shown in Figure 3 were processed in this manner. This curve is linear over 4 orders of magnitude and has a correlation coefficient of 1.0000.

In conclusion, the advantages of the MOE lockmass system over the conventional PFK System are: a sensitivity enhancement by a factor of three for all PCDD and PCDF monitored, easier control of the lockmass levels in the ion source, and greater resolution between the lockmass and sample ion signals.

(1) D.E. Laycock, Canadian Chemical News, November, 1986, Pg. 7.

Presented at the 35th ASMS Conference on Mass Spectrometry and Allied Topics
May 24-29, 1987, Denver, CO

Figure 1 : PFK Lockmasses

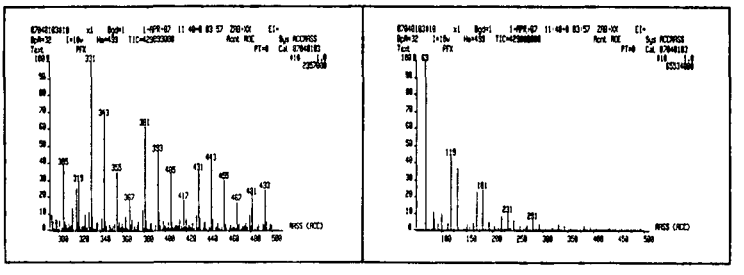

Figure 2 : MOE Lockmasses

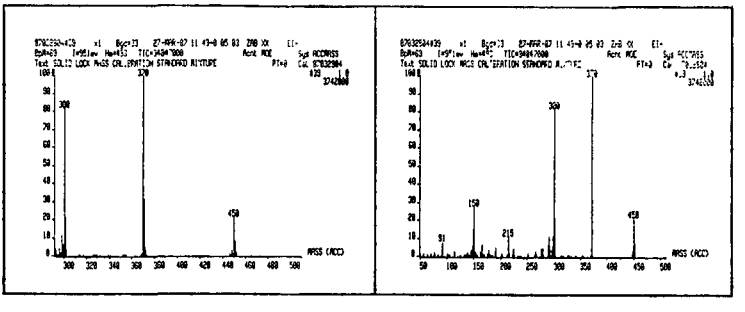

Table 3 :

	MOE Lockmass Area/Pg	PFK Lockmass Area/Pg	Enhancement A(MOE)/A(PFK)
C_4gDF	3.90	1.55	2.6
C_4gDD	2.92	0.99	3.0
$^{13}C_{12}C_4gDD$	2.02	0.59	3.4
C_5gDF	3.89	1.49	2.6
C_5gDD	2.28	0.75	2.9
C_6gDF	4.35	1.42	3.1
C_6gDD	2.56	0.77	3.3
C_7gDF	3.52	1.07	3.3
C_7gDD	3.11	0.80	3.9
C_8gDF	3.45	1.06	3.3
C_8gDD	2.30	0.66	3.5
$^{13}C_{12}C_8gDD$	2.02	0.59	3.4
			X = 3.19
			S = 0.38

Comparison of PFK and MOE Lockmass Systems

Figure 3 :

Linear Dynamic Range Using MOE Lockmasses

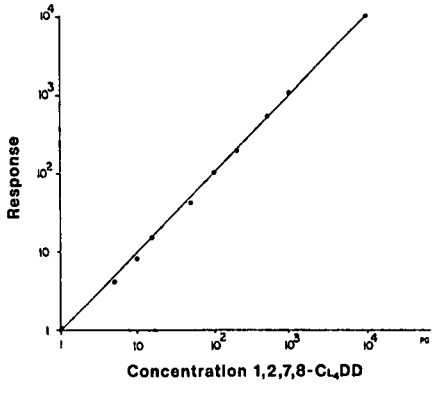

Presented at the 35th ASMS Conference on Mass Spectrometry and Allied Topics
May 24-29, 1987, Denver, CO

ISOMER SPECIFIC GC/MS DETERMINATION OF CHLORINATED DIBENZO-P-DIOXINS

G.W. Sovocool, J.R. Donnelly*, W.D. Munslow*, and R.K. Mitchum
U.S. Environmental Protection Agency and *Lockheed-EMSCO
P.O. Box 15027, Las Vegas, Nevada 89114

Chlorinated dibenzo-p-dioxins (PCDDs) are compounds of great concern. The U.S. Environmental Protection Agency (U.S. EPA) conducts monitoring of PCDDs and related compounds in the environment. The gas chromatographic retention index (RI) has been used to identify individual isomers within a closely related series. Chlorinated biphenyls and chlorinated dibenzofurans are two examples of series identified by GC RI combined with MS.[1,2]

To calculate the RIs for PCDDs we assume that the RI for each isomer is a sum of two halves (see Figure 1). Because of the symmetry of the dioxin molecule, there are only 10 possible "halves," or "single rings" (see Figure 2). This model also requires a term for ring-to-ring interaction when chlorine atoms occupy both the 1 and 9 positions or the 1, 4, 6, and 9 positions. The RIs for twelve PCDDs are used to determine these values. It is then possible to calculate the retention indices for the remaining PCDDs (see Table 1). A plot of calculated values against experimental data yielded a linear correlation coefficient of .999.

The proposed assignments by different research groups for 1,2,7,8-, 1,2,7,9-, and 1,2,6,8-TCDDs (which were not in agreement) were tested. Plots of assignments versus the calculated RI values revealed that each data set was internally consistent (showed a linear correlation) only if one choice of structural assignments was used (see Figure 3). The RI of a standard of 1,2,7,8-TCDD, which was prepared by unambiguous synthesis, agreed with the isomer assignment predicted by the model. Agreement with our assignments for the three TCDDs in question was reached in a conversation with a representative of the research group which had proposed the alternate set of assignments.

Published RT or RRT data for penta- through octachlorodibenzo-p-dioxins were checked for linearity (internal consistency) with excellent agreement of assigned structures and RI model predictions. When combined with mass spectrometry, this GC technique can result in accurate structural assignments during environmental monitoring by GC/MS. Most PCDDs can be identified isomer specifically. This method has been extended to brominated dioxins and dibenzofurans through correlation with the retention indices predicted (and experimentally verified) by the chlorinated models (see Figures 4 and 5).

REFERENCES

1. P.W. Albro, J.K. Haseman, T.A. Clemmer, and B.J. Corbett, J. Chromatogr., 136, 147 (1977).

2. F.D. Hileman, M.D. Hale, T. Mazer and R.W. Noble, Chemosphere, 14, 601 (1985).

NOTICE: Although the research described in this article has been funded wholly or in part by the Environmental Protection Agency contract 68-03-3249 to Lockheed Engineering and Management Services Company, Inc., it has not been subject to the Agency's review and therefore does not necessarily reflect the views of the Agency, and no official endorsement should be inferred.

Presented at the 35th ASMS Conference on Mass Spectrometry and Allied Topics
May 24-29, 1987, Denver, CO

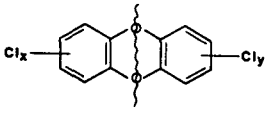

FIGURE 1.

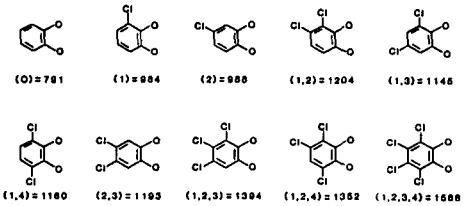

FIGURE 2.

Figure 3

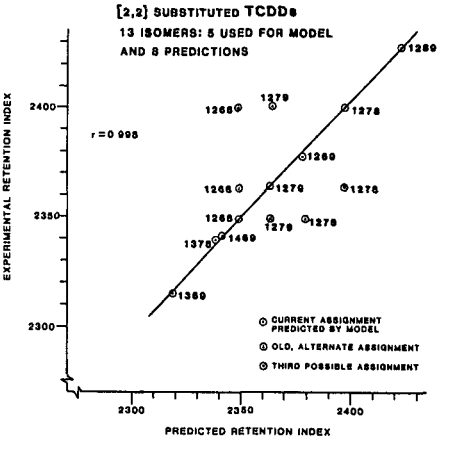

Figure 4

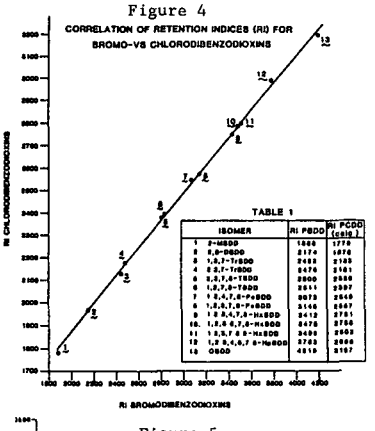

Figure 5

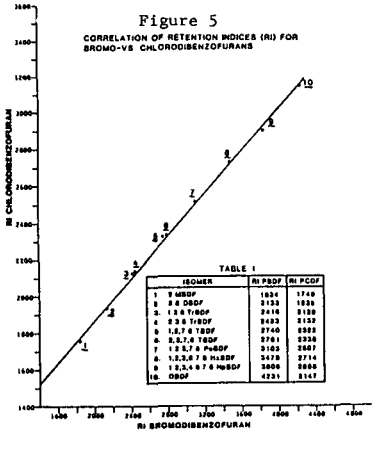

TABLE I.
THE 75 CONGENERS OF PCDDs LISTED BY INCREASING RI (CALCULATED)

ISOMER	CALCULATED RI	MEASURED RI	Δ	ISOMER	CALCULATED RI	MEASURED RI	Δ
1,3	1936			1,2,6,9	2378	2378	0
1,4	1951			1,2,3,4	2379	2379*	0
1,6	1968			1,2,3,7	2382	2382*	0
1,7	1972			1,2,3,8	2382	2382	0
1,8	1972			2,3,7,8	2386	2386*	0
2,7	1976	1985	−9	1,2,3,9	2392	2392	0
2,8	1976	1985	−9	1,2,7,8	2397	2400†	−3
1,9	1982			1,2,6,7	2408	2408*	0
2,3	1984	1993	−9	1,2,8,9	2422	2428	−6
1,2	1995			1,2,4,7,9	2511	2501	+10
1,3,6	2129			1,2,4,6,8	2511	2501	+10
1,3,7	2133			1,2,4,6,9	2533		
1,3,8	2133			1,2,3,6,8	2539		
1,3,9	2143			1,2,4,7,8	2545		
1,2,4	2143	2152	−9	1,2,3,7,9	2553		
1,4,8	2148			1,2,3,6,9	2568		
1,4,9	2158			1,2,4,6,7	2570		
1,7,8	2177			1,2,4,8,9	2570		
2,3,7	2181			1,2,3,4,7	2576	2573	+3
1,2,3	2185			1,2,3,4,6	2586		
1,2,6	2188			1,2,3,7,8	2587	2587	0
1,2,7	2192			1,2,3,6,7	2598	2604	−6
1,2,8	2192			1,2,3,8,9	2612	2623	−11
1,2,9	2202			1,2,4,6,8,9	2725	2713	+12
1,3,6,8	2290	2290*	0	1,2,4,6,7,9	2725	2713	+12
1,3,7,9	2304	2304*	0	1,2,3,4,6,8	2747	2742	+5
1,3,6,9	2319	2315	+4	1,2,3,6,8,9	2760		
1,3,7,8	2338	2340	−2	1,2,3,6,7,9	2760		
1,2,4,7	2340	2340	0	1,2,3,4,6,9	2769		
1,2,4,8	2340	2340*	0	1,2,3,4,7,8	2781	2781*	0
1,4,6,9	2341	2341	0	1,2,3,6,7,8	2788	2788*	0
1,2,6,8	2349	2349†	0	1,2,3,7,8,9	2802		
1,2,4,6	2350	2346	+4	1,2,3,4,6,7	2806	2812	−6
1,2,4,9	2350	2346	+4	1,2,3,4,6,7,9	2961	2949	+12
1,4,7,8	2353	2353*	0	1,2,3,4,6,7,8	2996	2994	+2
1,2,7,9	2363	2364†	−1	1,2,3,4,6,7,8,9	3197	3196	+1
1,2,3,6	2378	2378*	0				

*Used to develop the model
†See text for basis of assignment.

Presented at the 35th ASMS Conference on Mass Spectrometry and Allied Topics
May 24-29, 1987, Denver, CO

A GAS CHROMATOGRAPHY-MASS SPECTROMETRY METHOD FOR SELECTED HERBICIDES IN SURFACE WATER

R. G. Smith, F. M. Triebe, L. M. Horner, R. Lauer,
S. R. Baszis, and A. J. Klein; Monsanto Company, St. Louis, MO 63198

A method has been developed to determine five herbicides in water using capillary gas chromatography-mass spectrometry with selected ion monitoring. The method was developed and used to estimate the presence of these chemicals in surface water from agricultural watersheds.

The method has been validated in the range 0.20–25 ppb for alachlor, atrazine, cyanazine, metolachlor, and simazine in raw and finished surface water. Isotopically labeled analogs of each analyte were purchased or synthesized.

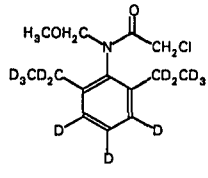

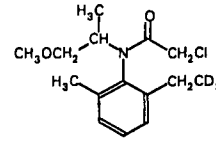

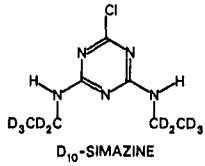

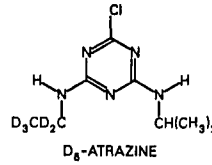

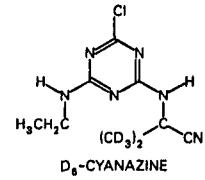

The isotopically labeled analog of each analyte is first added to 1.0 liter samples of water, followed by solid phase extraction, and concentration of the extracts to 1 mL. The analysis has been automated by data system procedures and an autosampler.

The quality assurance program for this study included the analysis of field fortified samples and storage stability samples. Other QA samples were run with each 20-sample set, including a deionized water blank, fortified deionized water, a sample duplicate, and a fortified sample. Two samples were fortified at each site where weekly samples were collected. All herbicides were shown to be stable in water for at least eight weeks under refrigeration and for at least one week at 37–39°C. Recovery and precision of alachlor, atrazine and metolachlor were excellent, 98–101% overall recoveries and 6–8% RSD. Less satisfactory were the recoveries and precision of cyanazine and simazine, 91–95% overall recoveries with 11–25% RSD.

Presented at the 35th ASMS Conference on Mass Spectrometry and Allied Topics
May 24-29, 1987, Denver, CO.

Percent Recoveries of Herbicides from Laboratory-Fortified Field Samples

Fortification Level (PPB)	n	Statistic	Herbicide				
			Alachlor	Atrazine	Cyanazine	Metolachlor	Simazine
0.2	7	Mean	96	99	91	102	93
		St. Dev.	9	12	45	7	13
0.5	9	Mean	98	96	72	102	94
		St. Dev.	6	6	20	5	8
1.0	9	Mean	101	98	91	98	93
		St. Dev.	5	7	21	5	11
5.0	8	Mean	103	97	96	98	91
		St. Dev.	9	8	27	5	16
10.0	8	Mean	105	100	96	96	100
		St. Dev.	8	5	12	9	6
25.0	6	Mean	101	94	101	98	104
		St. Dev.	13	6	15	4	11

Each compound and its deuterated analog were quantified at two m/z values. The agreement between these two values was determined for each sample by calculation of the relative difference (equation 1):

$$Rel.\ Diff. = \frac{(A_\alpha - A_\beta)(100\%)}{\frac{A_\alpha + A_\beta}{2}} \tag{1}$$

where A is the quantified value at masses α and β. The accompanying figure shows the relative difference of alachlor plotted against the mean concentration of the two values, $(A_\alpha + B_\beta)/2$. The increased variability of relative difference as the mean concentration approaches zero reflects increased uncertainty at these levels.

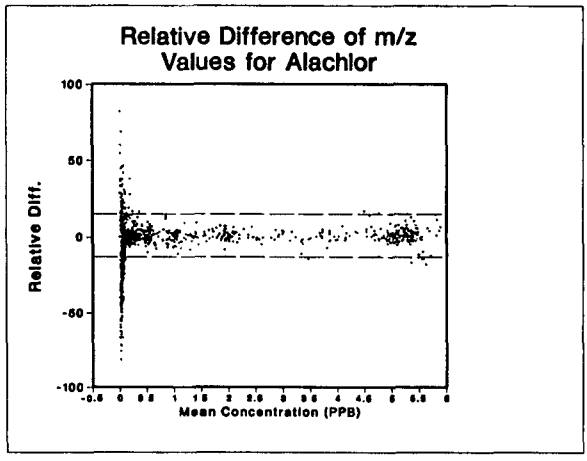

This figure represents nearly a thousand data points comprised of checks, fortified checks, field samples, and fortified field samples. The dashed lines represent ±3 standard deviations about the mean of data points above 1.0 ppb. Data outside these limits are considered potential outliers and may not be reliable.

Presented at the 35th ASMS Conference on Mass Spectrometry and Allied Topics
May 24-29, 1987, Denver, CO

Determination of Trace Levels of Surfactants In Environmental Matrices Using FAB/MS

S. R. Ward, J. R. Simms, B. L. Moore, M. M. Bandurraga and T. Keough
The Procter & Gamble Company, Miami Valley Laboratories and Ivorydale Technical Center, P.O. Box 398707, Cincinnati, OH 45239-8707

Fast atom bombardment (FAB) mass spectrometry has been evaluated for the quantitative measurement of both cationic and anionic surfactants, at low parts-per-billion levels, in river waters, effluents, and sewage influents. The purpose of the study was two-fold: (1) to compare the utility of FAB/MS, with our well-established HPLC methods, for the routine quantitative analysis of surfactants in complex environmental matrices. (2) to determine the effect of instrumental parameters such as scan range, scan speed, and mass resolution on the accuracy, precision, and limits of quantitation that can be achieved with FAB/MS. We felt that this information would guide us in selecting appropriate instrumentation dedicated to this application, if the FAB technique compared favorably with the competing HPLC methods.

The sample preparation scheme used for quantitation of the cationics,

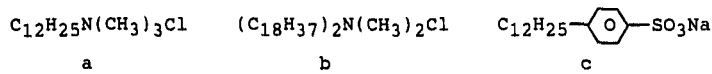

C_{12}TMAC (a) and DTDMAC (b), is summarized in Figure 1. N-[^{2}H]$_3$-methyl analogs were used as the internal standards. Sample preparation for quantitation of the anionic surfactant, LAS (principally c), was similar to that used for the cationics, but a [^{2}H]$_7$-analog was employed as its internal standard. All sample preparations, including that of appropriate blanks and spikes, were performed at a location remote from the MS facility. Furthermore, all MS analyses were conducted "blind" and most of these results were compared to independent results obtained by HPLC.

For the cationics, quantitative data were obtained in two ways. First, several low resolution (M/ΔM ~1000) mass spectra, generated by scanning the magnet over the range of 50-1000 Da at 10 sec/decade, were averaged (Figure 2, upper). The intensities of the $(M-Cl)^+$ molecular cations of the analytes and standards were determined from the averaged mass spectrum. This approach allows simultaneous quantitative multicomponent analysis of targeted analytes. Second, higher resolution (M/ΔM ~2-3,000) mass spectra, generated by scanning the magnet at 700 sec/decade over a 10-20 Da window centered on the ions of interest, were obtained by signal averaging techniques (Figure 2, lower). Again, the relative intensities of the analyte and standard were determined from the averaged spectrum. With our current commercial data system software, the signal averaging technique allows quantitation of only a single analyte at a time. With this method, we analyzed all submitted samples for one surfactant, reset the magnet, and then reanalyzed all of the samples for the next surfactant.

The precision and accuracy of the FAB/MS methods were judged to be acceptable based on the analysis of over seventy samples, with the cationics spiked at concentrations ranging from 5-500 ppb. Furthermore, FAB results were compared with independent results obtained by HPLC. The average recovery of theoretical spike, which varied from 86-107%, compared favorably with that from HPLC (~95%). We did note that below the 20 ppb level, the C_{12}TMAC results obtained with the low resolution scanning method were consistently 10-30% higher than results obtained with the higher resolution signal averaging method. This results, at least in part, because of a slight interference at the same nominal mass as that of the C_{12}TMAC molecular cation. The interference is clearly evident in the higher resolution spectra, Figure 3. No such interference was noted for DTDMAC. The precision of the FAB methods is also quite reasonable. The average coefficient of variation was ~15 ± 11% with the scanning method and only about 7 ± 3% with the signal averaging approach. With HPLC below the 20 ppb level, the average coefficient of variation was ~20 ± 10%.

Presented at the 35th ASMS Conference on Mass Spectrometry and Allied Topics
May 24-29, 1987, Denver, CO

The limits of quantitation achieved with FAB/MS depend upon the method used. With the low resolution technique, the limit of quantitation is ~1 ppb because of chemical interference. With higher resolution and signal averaging, 100 parts-per-trillion can be readily obtained for the two cationics studied. The HPLC limit of quantitation is 10 ppb.

Speed is the principal advantage of the FAB/MS method relative to HPLC. When considering sample preparation and analysis time, FAB is conservatively five times faster than our HPLC methods. This is even true for the signal averaging approach which currently allows quantitation of only one component at a time. In general, we anticipate that development of accurate FAB/MS methods will be considerably faster than development of HPLC approaches. This results because of the high sensitivity and specificity that FAB exhibits for ionic surfactants and because of the use of ideal (stable-isotope-labeled) internal standards. Furthermore, it may be possible to develop a single FAB/MS method that allows accurate, trace quantitative analysis of both cationic and anionic surfactants. Preliminary results from river water, Figure 4, indicate that cationics (+FAB) and anionics (-FAB) can be observed with high sensitivity without interference.

Sample Preparation for HPLC (and FAB/MS)

Add FAB/MS internal standards to 200mL of sample
Evaporate to dryness on steam bath
Extract ionics with chloroform/methanol
Separate ionics on Alumina "B" Sep-pak.

FIGURE 1

(River Water)

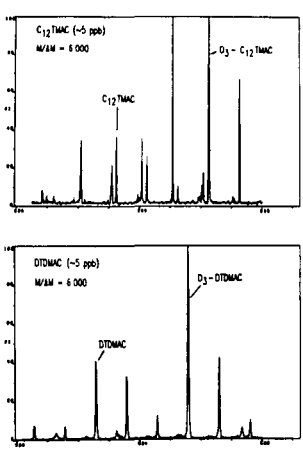

FIGURE 3

(River Water)

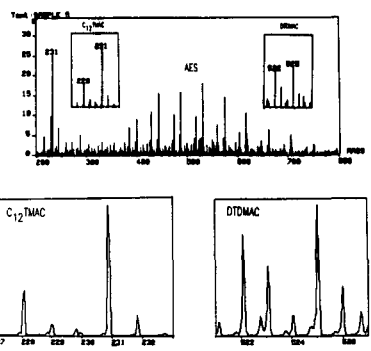

FIGURE 2

(River Water)

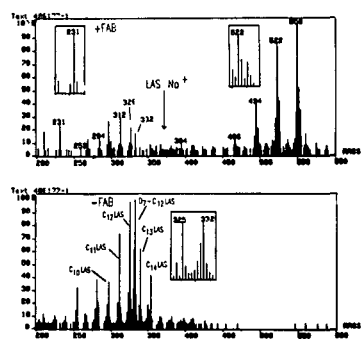

FIGURE 4

Presented at the 35th ASMS Conference on Mass Spectrometry and Allied Topics
May 24-29, 1987, Denver, CO

TIME AND MASS STUDIES OF UNIMOLECULAR FRAGMENTATION OF LARGE IONS

Robert J. Cotter

The Johns Hopkins University, Baltimore MD 21205

There has been considerable concern about the lack of fragmentation of large molecules ionized by desorption techniques. However, Barber et.al. (1) have recorded B-chain daughter ions in the MIKES spectrum of bovine insulin, noting a large contribution from unimolecular decomposition. Chait and Field (2) have noted the continued unimolecular fragmentation of bovine insulin for up to 200 µS in the flight tube of a time-of-flight mass spectrometer, contributing in this case to the incoherent ion signal at low mass. In contrast, Hunt has recorded FTMS spectra of bovine insulin, noting the requirement for ion stability over several milliseconds in that technique (3). We have reported low resolution FAB spectra of epidermal growth factor (4) and note the abundance of non-specific low mass ions and small peripheral group losses, consistent with quasi-equilibrium theory predictions of Bunker and Wang (5) for preferrential end-chain fragmentation.

While these observations are consistent with prolonged fragmentation (into the microsecond, but not the millisecond time frame) of molecules with many degrees of freedom, we have attempted in this study to demonstrate a direct relationship between extended fragmentation and molecular weight, and to show that such fragmentation does lead to structurally useful ions (i.e. middle chain fragmentation). In the first case we have varied the accelerating potential in a plasma desorption mass spectrometer to control the residence time of ions in the source and measured the changing ratio of molecular ion to incoherent signal for three peptides of different mass (6). This "fragmentation slope" above 200 ns is small for leu enkephalin (MW 556), larger for melittin (MW 2846) and largest for bovine insulin (MW 5733), indicating the prolongation of fragmentation for ions with increasing mass. That such prolonged fragmentation leads to structurally significant ions is demonstrated using a "pulsed TOF" configuration, in which the ion residence time is maintained in a field-free source. Figure 1 compares the spectra obtained from PDMS (immediate acceleration), liquid SIMS (after 20 µS) and laser desorption (after 60 µS). The spectra obtained several microseconds after ion desorption show structurally useful ions.

On the other hand, molecular ion measurements of large molecules are clearly very useful. We have used such measurements to assess sugar heterogeneity of high mannose oligosaccharides, phosphate heterogeneity in riboflavin-binding peptide, to survey peptides in crude extracts from pancreas and to measure covalent dimerization of insulins. Primary sequences and x-ray crystallographic structures of ovomucoids have been reported (7), and the glycosylated structure of the third domain ovomucoid from Japanese quail has been crystallized by this same group. We have measured (in Figure 2) the molecular weights of the glycosylated and unglycosylated peptide. The ability to "count" the number of sugars is intended to aid the interpretation of the crystallographic data.

We believe that there is a promising future for high mass measurements. Techniques which provide primarily (but reliably) molecular weight measurements will generate chemical and enzymatic methods (rather than fragmentation) for structure elucidation. On the other hand, developments in ion trapping and control of internal energy in the desorbed ions will improve our ability to record fragment ions.

(1) Barber, M., Bordoli, R.S., Elliott, G.J., Tyler, A.N., Bill, J.C. and Green, B.N.; Biomed Mass Spectrom., 11 (1984) 186.
(2) Chait, B.T. and Field, F.H.; Int. J. Mass Spectrom. Ion Processes, 65 (1985) 169-180.
(3) Hunt, et.al., Proc. Natl. Acad. Sci. USA, 84 (1987) 622.
(4) Hyver, K.J., Campana, J.E., Cotter, R.J. and Fenselau, C.; Biochem. Biophys. Res. Commun., 130 (1985) 1287-1293.
(5) Bunker, D.L. and Wang, F.-M.; J. Am. Chem. Soc., 99 (1977) 7457.
(6) Demirev, P., Olthoff, J.K. Fenselau, C. and Cotter, R.J.; Anal. Chem. (in press).
(7) Weber, E., Papamakos, E., Bode, W., Uber, R., Kato, I. and Laskowski, M. Jr.; J. Mol. Biol. 149 (1981) 109-123.

Presented at the 35th ASMS Conference on Mass Spectrometry and Allied Topics
May 24-29, 1987, Denver, CO

Figure 1.

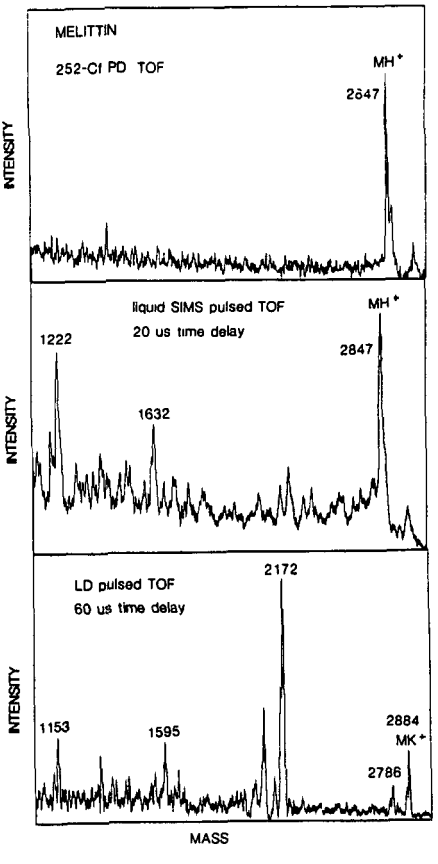

Figure 2.

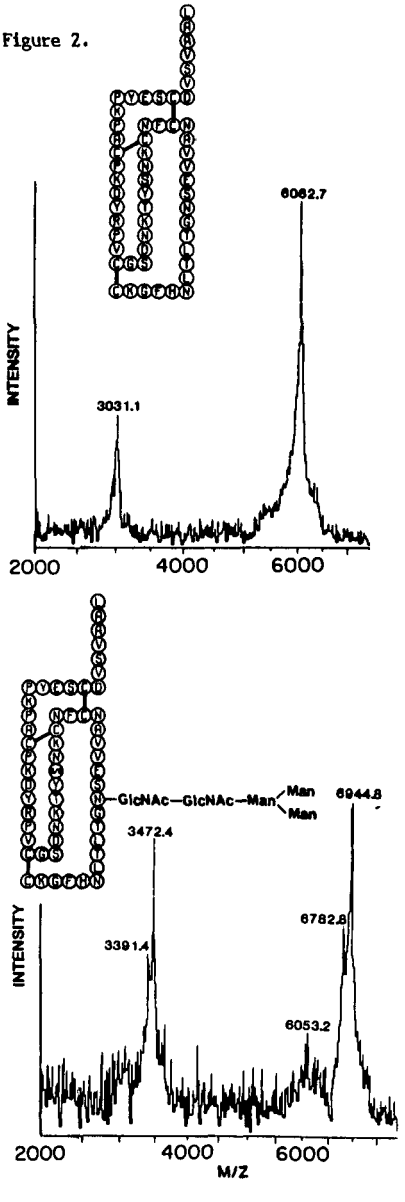

The author acknowledges contributions from Catherine Fenselau, Mershid Alai, Jeffrey Honovich, Plamen Demirev, James Olthoff and Rong Wang (Johns Hopkins), Steve Unger (Squibb; for covalent insulin dimers), Phil Andrews (Purdue; for pancreatic peptide mixtures), Michael Laskowski (Purdue; for ovomucoids) and Hal White (University of Delaware; for riboflavin-binding peptide).

Presented at the 35th ASMS Conference on Mass Spectrometry and Allied Topics
May 24-29, 1987, Denver, CO

DESORPTION AND FRAGMENTATION MECHANISMS OF LARGE MOLECULES AND CLUSTERS:

I.S.T. Tsong, Department of Physics, Arizona State University, Tempe, Arizona 85287

In the desorption of very large molecules and clusters from surfaces undergoing energetic particle bombardment, fragmentation can be considered to occur in two ways: (1) fragmentation as part of the desorption process, and (2) fragmentation after desorption has taken place. A good illustration of these two types of fragmentation process is given by the study of mass distribution of $(CsI)_n Cs^+$ cluster ions conducted by the Naval Research Laboratory group using a sector-field mass spectrometer [1] and by the University of Manitoba group using a time-of-flight (TOF) mass spectrometer [2]. In the TOF experiment where an ion needs to survive only long enough (~0.17 μs) to be fully accelerated in order to appear at its orignial mass number, only type (1) fragmentation is observed where the cluster ion yield decreases steadily with increasing cluster size n. In sector-field experiment, however, an ion takes 750 μs to traverse the instrument and type (2) fragmentation occurs during this time resulting in discrete peaks in the mass distribution reflecting certain stable geometric structures of the cluster ions. In the desoprtion of large molecules, e.g. bovine insulin (MW5733), the α and β chains are considered to be the result of type (1) fragmentation while the unresolved baseline signal are due to type (2) fragmentation. The question of course remains as to how short a time scale for type (1) fragmentation to occur. The answer to this question will have to wait for picosecond time-resolved experiments.

Type (2) fragmentation can be treated by conventional RRKM theory of unimolecular decomposition. Bunker and Wang [3] have studied the limiting behavior of RRKM rate constants for very large molecules. They arrive at the interesting result that the rates of molecular chain breaking approach zero for bonds near the center of chains, but remain finite for end-atom fragmentation. Their conclusion agrees with experimental observations of unimolecular fragmentation within the flight tube. Type (1) fragmentation have been treated theoretically by Tsong and co-workers [4-6] using RRK theory in which desorption/fragmentation is considered to occur via vibrational excitation. The energy deposited by the incident particle is absorbed in the form of vibrational motion of the molecules. If a molecule is sufficiently energized to reach an excited vibrational level of the transition state, bonds can be broken and the molecule can be desorbed in given configurations. The mass distribution is predicted by calculating the various rate constants for individual molecules or clusters. From the results, the energy deposited per normal mode for the desorption/fragmentation process agrees closely with that estimated from energy loss by nuclear stopping or electronic stopping as governed by the scheme of bombardment.

Our latest experimental and theoretical studies of desorption of water clusters, $(H_2O)_n H^+$, from ice by keV ion bombardment [7] shows the applicability of RRK theory to describe the type (1) fragmentation. The observed magic number cluster ion, $(H_2O)_4 H^+$, is thought to be due to subsequent dissociation, although the entire question of magic numbers of water clusters still awaits the results of proper time-resolved experiments.

REFERENCES

[1] J.E. Campana, T.M. Barlak, R.J. Colton, J.J. DeCorpo, J.R. Wyatt and B.I. Dunlap, Phys. Rev. Lett. 47, 1046 (1981).
[2] W. Ens, R. Beavis and K.G. Standing, Phys. Rev. Lett. 50, 27 (1983).
[3] D.L. Bunker and F.M. Wang, J. Am. Chem. Soc. 99, 7457 (1977).
[4] B.V. King, A.R. Ziv, S.H. Lin and I.S.T. Tsong, J. Chem. Phys. 82, 3641 (1985).
[5] B.V. King, A.R. Ziv, S.H. Lin and I.S.T. Tsong, Surface Sci. 167, 18 (1986).
[6] I.S.T. Tsong, J.W. Christiansen, S.H. Lin and B.V. King, in "Mass Spectrometry in the Analysis of Large Molecules", ed. C.J. McNeal, (Wiley, 1986), p. 67.
[7] J.W. Christiansen, I.S.T. Tsong and S.H. Lin, J. Chem. Phys. 86, 4701 (1987).

Presented at the 35th ASMS Conference on Mass Spectrometry and Allied Topics
May 24-29, 1987, Denver, CO

SEQUENCE ANALYSIS OF MACROMOLECULES BY TANDEM MAGNETIC DEFLECTION MASS SPECTROMETRY

Steven A. Carr, [1]Brian N Green, Mark E. Hemling, Gerald D Roberts, [2]Robert J. Anderegg and Richard Vickers, Dept. of Physical and Structural Chemistry, L-940, SmithKline and French Laboratories, King of Prussia, PA 19479, [1]VG Analytical, Ltd., Manchester, UK and [2]Dept. of Chemistry, University of Maine, Orono, ME 04469

Our laboratory is interested in practical application of MS/MS to protein and glycoconjugate structure problems that are not amenable to solution by conventional methodologies. In the present study we have tried to define the operational parameters that are important in producing analytically useful tandem mass spectra of peptides and glycoconjugates in order to make MS/MS more routinely applicable to macromolecules. The instrument used for these studies is the VG ZAB-SE 4F tandem double focusing mass spectrometer located at SKF We focused on the effects of gas pressure, gas type (Ar vs. He) and collision energy (via use of an electrically floated collision cell) on the fragmentation efficiency (FE) and the yield of structurally informative ions in the daughter ion spectra of peptides and glycoconjugates in two size regimes: under 2000 daltons and 2000 to 4200 daltons These results were compared to data obtained on CsI (1692 and 3510), a more ideally behaved model, and are summarized below.

1. Fragmentation Efficiency: For CsI parents up to mass 4000 measured FE's were essentially independent of the mass of the selected precursor; FE = 20-25% for He, 12-15% for Ar. However, Ar produces easily detectable daughters to far lower mass than He. Observation of lower mass daughters in the Ar data is consistent with the heavier gas producing more effective collisions and inducing less translational energy (TE) loss than He (vide infra). The lower FE for Ar is probably due to scattering which increases with the mass of the target gas. In contrast, the maximum FE observed for organics was 5-8% for carbohydrates and 4-6% for glycopeptide antibiotics (primarily sugar losses); peptides to 2000 daltons gave significantly lower FE values of 1-4%.

2 Gas Pressure: Collision gas is absolutely essential to observe a significant population of daughters for either CsI or organics Although massive organic ions (>2000 daltons) undergo spontaneous decomposition during their flight from source to final detector, intensities of daughters in the "no gas" spectra are much lower and certain fragments are missing or selectively attenuated compared to the collision-induced (CID) spectra. The overall intensity of the daughter ion spectra of peptides up to 2000 daltons increases with pressure to ca. 70% attenuation of the parent. Between 70% and 90% attenuation the intensities of low mass daughters increase (X2-4) at the expense of more structurally informative high mass daughters For peptides with masses above ca. 2000 daltons use of parent attenuations >70% is in fact deleterious resulting in extensive loss of higher mass daughters These losses are due to scattering, loss of TE, etc. which together outweigh potential gains from increased uptake of collisional energy via multiple collisions

3. Gas Type: As noted above, use of Ar permits the detection of lower mass daughters from a given CsI parent even though the FE is lower than for He. The measured fractional TE losses increase with gas pressure (>3% for 1692 → 133 at 90% atten. (He)) and increase with decreasing daughter ion mass; TE losses are significantly lower (>X5) with Ar Use of Ar should also result in more effective collisions due to its increased mass vs He Unique fragment ions are observed in the Ar-CID spectra of peptides and glycopeptides; the differences are mainly in the intensities of fragments which require multiple bond cleavages in order to form. For example, partial side-chain losses from the A-series peptide backbone cleavages ("D" ions, Fig 1) are enhanced in the Ar vs. He spectra Fragments D4, D8, D9 and A2 are absent or insignificant in the He data but are pronounced when Ar is used. These effects are even more pronounced when the collision cell is floated. For peptides with masses above 2000 daltons Ar can no longer be used since ion loss processes now outweigh the positive attributes of the heavier gas. However, He still provides useful MS/MS spectra (Fig. 2).

4 Collision Energy. When the coll. cell is floated (typically to 1/2 of the source potential (CE = 0.5)), the lowest KE that a fragment may possess is 5keV. This has several beneficial effects: fractional energy spread is decreased, higher daughter ion resolution is achieved without further closing slits and MS-2 is more easily calibrated. Below 2000 daltons there are interesting and analytically useful differences between the daughter ion spectra acquired at C E = 1 (grounded cell) and C.E = 0.5. In addition to the differences noted in #3, above, low mass daughters are significantly enhanced in the floated cell spectra. With the floated cell the Ar data is qualitatively superior to the He data for organics up to 2000 daltons. Unfortunately, at present the floated cell is not useful for molecules of significantly higher mass because the percentage of daughters actually forming in the cell drops off with increasing mass.

We have demonstrated that when operational parameters are properly adjusted, massive organic ions approaching 4000 daltons may be successfully collisionally dissociated and structurally useful data obtained using a tandem double focusing mass spectrometer. The major limitation at high mass is not transmission of the instrument, but rather the fundamental problems of decreasing parent ion yield with increasing mass and low FE for organics. Improvements in these areas will greatly improve the applicability of MS/MS to macromolecules.

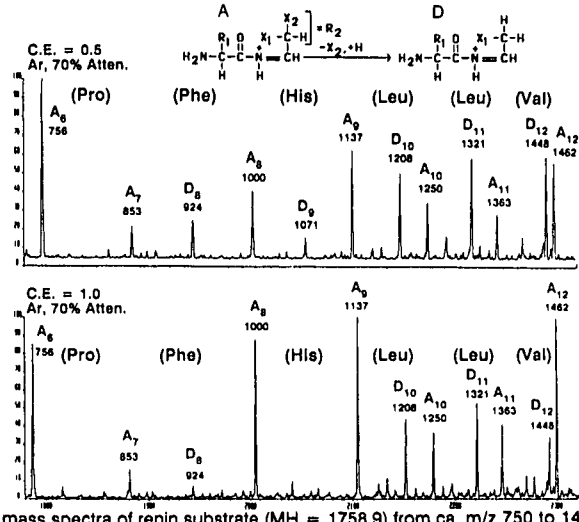

Figure 1 Daughter ion mass spectra of renin substrate (MH = 1758 9) from ca m/z 750 to 1480 The data obtained using Ar (70% atten of parent) at C E. = 0.5 (top) and 1 0 (bottom) are compared Inset illustrates relationship between the A and D ion series.

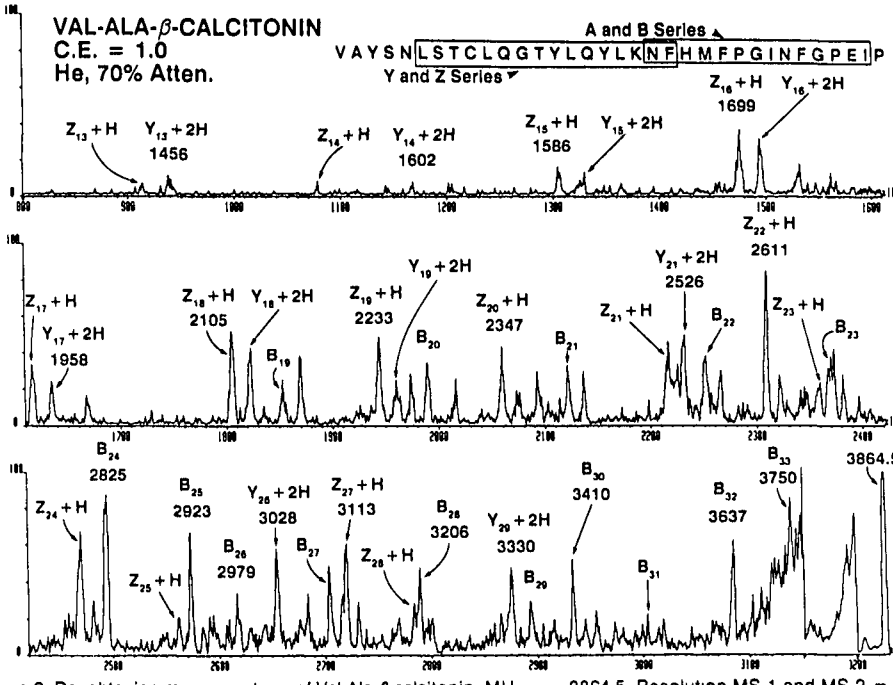

Figure 2. Daughter ion mass spectrum of Val-Ala-β-calcitonin, MH_{ave} = 3864.5. Resolution MS-1 and MS-2 = 600 Sequence ions observed cover the boxed region of the sequence

Presented at the 35th ASMS Conference on Mass Spectrometry and Allied Topics
May 24-29, 1987, Denver, CO

TWO COLOR LASER DESORPTION-PHOTOIONIZATION STUDY BY FOURIER TRANSFORM MASS SPECTROMETRY

Lydia M. Nuwaysir, Robert S. Brown, and Charles L. Wilkins
Department of Chemistry, University of California,
Riverside, California 92521

Laser desorption Fourier transform mass spectrometry (LD-FTMS) has shown considerable promise as a tool for structural analysis of molecules with masses in excess of 1,000 daltons. In a great many cases, fragmentation resulting from CO_2 laser desorption is limited and, accordingly, methods such as collision induced dissociation (CID) must be employed in order to obtain structural information. In our experience, low energy CID under conditions which are suitable for FTMS analysis is of limited value, particularly for species with masses above 1000 amu. Thus, the use of an excimer laser, operating at 308 nm, has been examined as a means of photodissociating selected trapped ions formed by pulsed carbon dioxide laser desorption. In addition, photodissociation offers several advantages over other fragmentation methods. The laser wavelength can be chosen for excitation of specific chromophores leading to more selective fragmentation. Also, the laser energy can be varied to allow for single or multiphoton events.

Samples were applied as solutions to the tip of a hollow direct introduction probe and the solvent was evaporated. Experiments were performed using a Nicolet FT-1000 Mass Spectrometer and a Tachisto pulsed CO_2 laser to desorb the sample. Ejection sweeps were performed to isolate the ion(s) of interest. A Lambda Physik EMG 201 MSC excimer laser was then fired through a lens in the probe to photofragment the isolated ion(s). No signal averaging was performed.

Rhodamine B (M.W. 479) and reserpine (M.W. 609) were chosen for study, in part, due to the convenient UV-visible absorption characteristics. Using 308 nm photodissociation, both Rhodamine B and reserpine yield primarily the same photofragment ions as those derived from infrared multiphotonionization. An FTMS spectrum of reserpine ionized by (carbon dioxide) laser desorption is shown in Figure 1 with ejection of ions below the molecular ion. The photodissociation experiment yields the spectrum of reserpine shown in Figure 2. This experiment was performed by firing the excimer laser after the ejection sweeps.

The initial probe design, in which the excimer beam traversed a hollow probe and lens, lead to some anomalous results. Large intensity metal ions, such as cesium and potassium, and impurities from previously run samples were observed after firing the excimer laser. These contaminants are due presumably from desorption of neutrals from the cell trap plates. Multiphoton events occurring at the focus of the excimer beam as well as single photon events in the expanded region of the beam were also possible. With these problems in mind, the FTMS system was redesigned to direct the excimer laser adjacent to the probe and into the analyzer cell perpendicular to the previous path. The design allowed for more consistent interaction between laser beam and ions in the cell.

Further studies using a different excimer gas (ArF), 193 nm excitation and the new optical design are currently underway. McIver et al. (1) have previously shown that use of this wavelength can lead to efficient photodissociation of oligopeptides formed by chemical ionization with observation by FTMS. Our studies will include samples such as oligopeptides and antibiotics.

1) William D. Bowers, Sherri-Sue Delbert, Richard L. Hunter, Robert T. McIver, Jr., J. Am. Chem. Soc., 106, pp. 7279-7288 (1984).

Presented at the 35th ASMS Conference on Mass Spectrometry and Allied Topics
May 24-29, 1987, Denver, CO

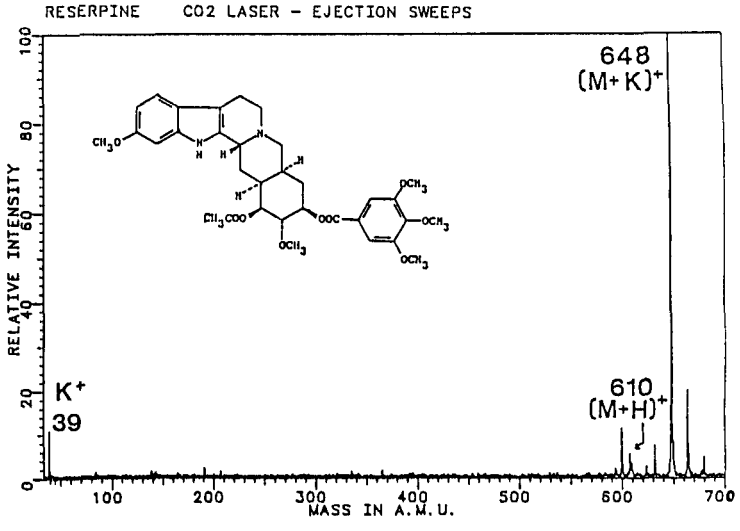

FIGURE 1

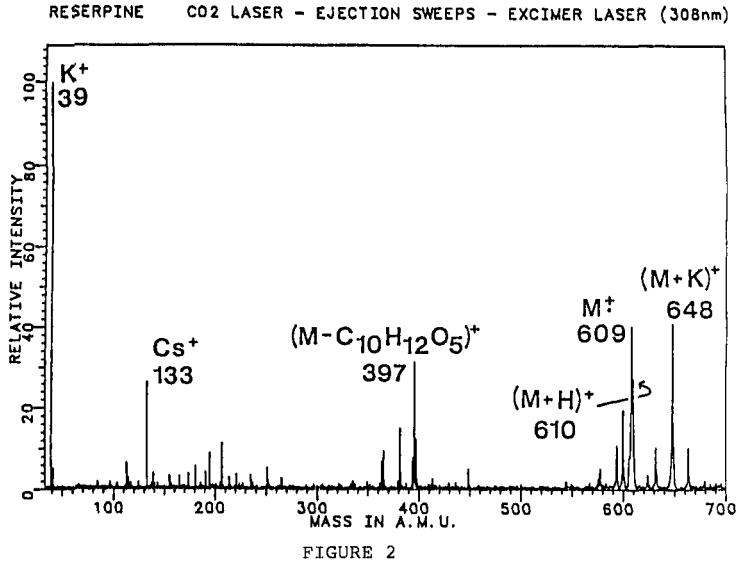

FIGURE 2

Presented at the 35th ASMS Conference on Mass Spectrometry and Allied Topics
May 24-29, 1987, Denver, CO

STUDIES OF THE ACTIVATION AND DISSOCIATION OF LARGE POLYATOMIC IONS.

David H. Russell, Department of Chemistry, Texas A&M University, College Station, Texas 77843

The use of tandem mass spectrometry for structural characterization of large polyatomic systems is an active research area, and the activity in this area has increased considerably since the introduction of fast-atom bombardment (FAB) ionization. Our activities in this area emphasize the fundamental aspects of the activation and dissociation processes, and include fundamental studies of collisional activation, the use of photodissociation as an alternative/complementary method for ion activation, and the use of organo-alkali metal ion complexes to enhance specific, structurally informative dissociation reaction channels.

Although collision-induced dissociation has been used extensively for structural characterization of relatively small systems, the sensitivity (conversion of incident ions to fragment ions) for larger systems imposes a practical limit on the method. Our studies led us to conclude that the limited efficiency for fragment ion production arises because collisional activation of the incident ion is in direct competition with excitation of the target neutral. In fact, these studies show that ionization of the target gas is a much more favorable process. Such an interpretation of the data is consistent with other studies. For example, Derrick (Org. Mass Spectrom. *1984*, *19*, *165*) *showed that the amount of translational energy lost by the incident ion* upon collision with the target atom increased with increasing mass of the incident ion. Assuming that excitation of the target gas can be neglected, this result suggest that the activation energy imparted to the incident ion increases with increasing mass of the incident ion. That is, the limited efficiency for the collision-induced dissociation of large ionic systems is a "kinetic shift" effect. On the other hand, our studies on the chlorophyll *a* and related systems (J. Am. Chem. Soc. 1986, *108*, 6174) suggest that the increased energy loss with increasing mass arises as a direct result of excitation (including ionization) of the target gas. The evidence for target gas excitation is derived from energy loss measurements using different target gases (e.g., He, Ne, Ar, Kr, and Xe), measurements performed at different incident ion energies, and direct measurements of the production of the ionized target.

The studies on photodissociation of large polyatomic systems are directed toward understanding the dissociation dynamics. The photoexcitation is performed using the uv (ca. 365 nm; 3.4 eV) and visible (454-514 nm; 2.73-2.41 eV) lines of a CW Ar ion laser. The model peptides used for these studies do not absorb in the low-energy uv or blue-green visible wavelength range, therefore suitable chromophores (either the dansyl or dinitrophenyl group) are attached to the N-terminus of the peptide. This approach permits the portion of the ion which receives the initial excitation to be specified, and by changing the structure (amino acid sequence) of the ion the dynamics of energy randomization and the structural features which influence energy randomization can be probed. As an extension of this data set, by examining the photodissociation of the $[M+Na]^+$ ion both the position of the charge and point of initial photoexcitation can be specified (see below). The preliminary resutls from these studies can be generalized as follows: (i) excitation of the dansyl chromophore with low-energy uv radiation favors dissociation of the dansyl group or cleavage of bonds in the peptide located adjacent to the dansyl group, (ii) excitation of the dinitrophenyl chromophore with blue-green radiation favors cleavage of bonds within the peptide and very little fragmentation of the chromophore. Although data is available on only a limited number (10-12) of derivatized peptides and the size of the peptides studied is also limited (up to a heptapeptide), the data can be summarized in the following manner. The utility of photodissociation for structural characterization of peptides and related molecules will be dependent upon the relative rates for energy randomization and dissociation (implicit assumption regarding non-occurrence of photoinduced isomerization). That is, if the energy of the photon is high, relative to the bond dissociation energies, and energy randomization is slow with respect to the rate of dissociation, cleavage of bonds near the site of activation will be favored. On the other hand, if the activated ion is sufficiently long-lived, cleavage of bonds remote to the activation site become more probable. We are presently working on expanding the available data base and exploring the use of additional chromophores in order to test further these ideas.

The last category of studies deals with enhancing the structural information obtained by forming an ionic organo-alkali metal ion complex such as $[M+xNa-(x-1)H]^+$, where x=1-3. Again, the model systems used for these studies are peptides and specific nucleosides. The basic idea involved is that the more basic amino acid residues (e.g., arginine, lysine, histidine, etc.) comprising a peptide have specific alkali metal ion affinities. Thus, the site of attachment of the alkali metal ion to the peptide will depend upon the relative alkali metal ion affinities of the amino acids, and this preference will be further enhanced by secondary factors (e.g., steric effects) which enhance the stability of the ionic complex. Such ideas were initially invoked to explan the dramatic differences in the collision-induced dissociation spectra of the $[M+H]^+$ and $[M+Na]^+$ ions of hippuryl-histidyl-leucine (Mallis, Anal. Chem. **1986**, *58*, 1076) and several nucleosides (Mallis, Anal. Chem. **1987**, *59*, 980). These ideas have since been expanded to a series of peptides containing multiple basic amino acid residues (Mallis, Int. Mass Spectrom. Ion Proc., in press). In all cases studied to date, a strong preference for dissociation near the most basic amino acids is observed for the $[M+xNa-(x-1)H]^+$ ions, i.e., fragmentation near the charge site is preferred. Related studies are underway on additional systems and synthetic peptides having specific amino acid residues. The final objective of this work is to design methods for disecting large peptides at specific amino acid residues and then sequence these individual fragments using tandem mass spectrometry methods.

Presented at the 35th ASMS Conference on Mass Spectrometry and Allied Topics
May 24-29, 1987, Denver, CO.

Tracing Reaction Pathways by Collisionally Activated Dissociation: $CH_3\overset{+}{O}{=}CHCH_3$ and $CH_2{=}\overset{+}{O}CH_2CH_3$. D.J. McAdoo and C.E. Hudson, Marine Biomedical Institute, University of Texas Medical Branch, Galveston, Texas 77550

Studies of $C_3H_7O^+$ ions have contributed significantly to two concepts in gas phase ion chemistry: (1) rate determining isomerizations over substantial barriers,[1] and (2) the intermediacy of ion-neutral complexes in unimolecular decompositions.[2] The first idea was supported by the conclusion that $CH_3\overset{+}{O}{=}CHCH_3$ (1) isomerizes to $CH_2{=}\overset{+}{O}CH_2CH_3$ (2) over a high barrier prior to decomposing.

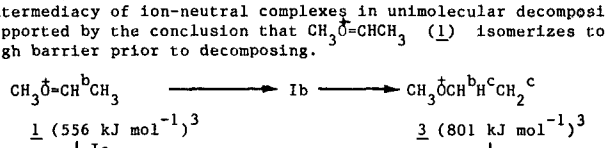

Hvistendahl and Williams[1] suggested symmetry forbidden 1→2a occurs, although 1→3→2b seemed equally plausible. 1→2a might dominate because at least 245 kJ mol^{-1} is needed for 1 to isomerize to 3.

Hydrogen/deuterium exchange patterns in labeled forms of 2 led to the proposal that 2 decomposes through a proton-bound complex of ethylene and formaldehyde, with the proton usually going with the species of higher proton affinity upon decomposition. Intermediacy of this complex also accounted for the isomerization of 2 to 4.

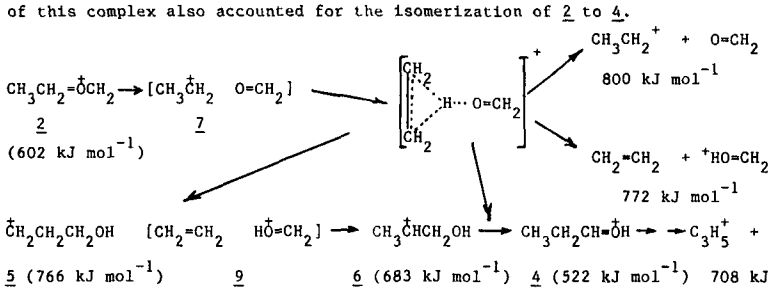

However, the conclusions derived from the isotopic distribution are not compelling, and the statement that the species of higher proton affinity will get the proton is equivalent to saying the most stable products will be prefered and does not indicate a specific mechanism. Therefore we sought more definitive information regarding the decompositions of 1 and 2.

We obtained additional information on the hydrogen exchange processes in 1 and 2 from CAD spectra of the products of the decompositions of 1 and 2. The CAD spectra in Table 1 demonstrate that $CH_2{=}OH^+$ fragments to OH^+ and CH_2 without appreciable hydrogen exchange upon collision with He, enabling correlation of the positions of hydrogens in products to their positions in precursors.

Table 1. Partial CAD Spectra of $CH_2{=}OD^+$ and $CD_2{=}OH^+$.

m/z	13	14	15	16	17	18	19
$CH_2{=}OD^+$	59	100	5	6		53	23
$CHD{=}OH^+$	16	38	100	-	28	10	8

Table II gives metastable decompositions and products of $C_3(H,D)_7O^+$ ions.

Table II. Metastable $C_3(H,D)_7O^+$ Decomposition Patterns

Ion	CH_3O^+	CH_2DO^+	CHD_2O^+	CD_3O^+
$CH_3CH{=}\overset{+}{O}CD_3$		4	100[e]	20 (25)[a]
$CH_3CD{=}\overset{+}{O}CH_3$	100	22 (25)[a,d]		
$CD_3CD{=}\overset{+}{O}CH_3$	23 (25)[a]	100		
$CD_3CH\overset{+}{O}CH_3$	54	100 (100)[a,b,c]		
$CH_3CH_3\overset{+}{O}{=}CD_2$	43 (51)[b]	100 (100)[b,f]	53 (25)[b,g]	
$CH_3CD_2\overset{+}{O}CH_2$	67 (51)[b]	100 (100)[b,f]	25[b,g]	
$CH_3CD_2\overset{+}{O}{=}CD_2$	15 (22)[b]	48 (100)[b,h]	100 (67)[b,g]	231 (6)[b]
$CD_3CH_2\overset{+}{O}{=}CH_2$	21 (22)[b]	100 (100)[b,f]	63 (67)[b,i]	6 (6)[b]

a. Expected based on H and D transfer from the methoxy followed by random return from the ethyl so formed to oxygen. b. Expected for a random distribution of all H + D atoms. CAD spectra of products indicated the following identities.

c. $CD_2{=}OH^+$
d. $CH_2{=}OD^+$
e. Contains some $C_2HD_4^+$
f. $CHD{=}OH^+$, CH_2OD^+
g. $CD_2{=}OH^+$, $CHD{=}OD^+$
h. Predominantly $CHD{=}OH^+$
i. Predominantly $CHD{=}OD^+$

Underlining - composition expected for b-H transfer to $CH_2{=}O$. ^{13}C labeling indicated no presence of ethyl carbons in $CH_2{=}OH^+$ formed from 2.

From Table II it is apparent that 1 decomposes largely by transfer of a methoxy hydrogen to form an ethyl followed by the ethyl to oxygen with only a slight discrimination against the abstraction of the transfered H or D.

There is a slight preference for β-H transfer in the formation of $CH_2{=}\overset{+}{O}H$ from 2. This preference is more prominent in the ion source and in collision-induced dissociations of 2. Data in Table II demonstrate extensive exchange of hydrogens between all of the carbons of 2, in contrast to 1. This and its strong water loss demonstrate almost complete isomerization of 2 to 4, 5 and 6. Some preference for β-H transfer to oxygen also apparent in water losses from 2 (Table III).

Table III. $(H,D)_2O$ Losses from $C_3(H,D)_7O^+$ Ions

Ion	$-H_2O$	-HDO	$-D_2O$
$CH_3CH_2\overset{+}{O}{=}CD_2$	100 (100)	33 (100)	1 (10)
$CH_3CD_2\overset{+}{O}{=}CH_2$	100 (100)	46 (100)	1 (10)
$CH_3CD_2\overset{+}{O}{=}CD_2$	73 (25)	100 (100)	18 (51)
$CD_3CH_2\overset{+}{O}{=}CH_2$	13 (51)	100 (100)	44 (25)

Parenthesis = random

This suggests that the decomposition and skeletal isomerization of 2 are both initiated by the same transfer of a β-hydrogen.

We speculate that the different behaviors of 1 and 2 are due to a) abstraction near threshold of the bridging H in a complex resembling 8 without full H exchange in the proton bridged ethylene (probably the most stable $C_2H_5^+$ structure). b) Near hydrogen randomization within $C_2H_5^+$ before H-transfer to oxygen at the higher energies at which 2 is formed by isomerization from 1; the latter decomposition being too rapid for the C-C bond formation producing 5 to occur. c) H transfer prior to C-O bond cleavage in the decomposition of 2 at even higher energies. The last may reflect a general tendency for complex-mediated reactions to diminish in importance with increasing excess energy.

Acknowledgements. We thank the Midwest Center for Mass Spectrometry for use of the MS 50TA mass spectrometer.

1. G. Hvistendahl and D.H. Williams, J. Am. Chem. Soc., 97, 3097-3101 (1975).
2. R.D. Bowen, D.H. Williams and G. Hvistendahl, Org. Mass Spectrom., 13, 721-728.
3a. R.H. Nobes and L. Radom, Org. Mass Spectrom., 19, 385-393 (1984). b. J.C. Traeger, Int. J. Mass Spectrom. Ion Proc., 58, 259-271 (1984).
4. C.E. Hudson and D.J.McAdoo, Int. J. Mass Spectrom. Ion Proc., 59, 325-332 (1984).

Presented at the 35th ASMS Conference on Mass Spectrometry and Allied Topics
May 24-29, 1987, Denver, CO

THE METHOXY LOSS FROM IONIZED METHYL ACETATE AND THE KETO/ENOL TAUTOMERIZATION OF VINYL ALCOHOL IN THE GAS PHASE

C. Wesdemiotis, R. Feng, M.-Y. Zhang, and F. W. McLafferty

Chemistry Department, Cornell University, Ithaca, NY 14853-1301

Neutralization-reionization mass spectrometry (NRMS) has successfully been used for the generation and characterization of unconventional neutral molecules in the gas phase.[1] The structure and unimolecular reactions of these molecules can be elucidated by collisionally activated dissociation (CAD) of the neutrals before reionization, and by their complementary reionization to either positive or negative ions.

CAD of neutral acetaldehyde (CH_3-CH=O) mainly breaks the C-C and C-H bonds at the carbonyl group yielding weakly bound ·CHO and CH_3CO· radicals, respectively, that easily dissociate further to CO. CO can be detected with high sensitivity because of its relatively good reionization cross-section to positive ions.

Vinyl alcohol (CH_2=CH-OH), that is inaccessible in pure form in condensed phases, can be prepared in the gas phase by vertical neutralization from the corresponding radical cation; it survives neutralization without any appreciable isomerization to more stable acetaldehyde. Upon collisional activation neutral vinyl alcohol dissociates directly to CH_2=CH-O· + ·H and CH_2=CH· + ·OH, but also produces CO whose formation requires rearrangement of CH_2=CH-OH to a structure that contains a carbonyl moiety (vide supra). Investigation of CH_2=CH-OD, CH_2=CD-OH and CH_3-CD=O reveals that the mentioned rearrangement starts with the 1,2-H migration CH_2=CH-OH → CH_3-C-OH yielding hydroxymethylcarbene molecules that fragment further to CH_3CO· + ·H.

CH_3-C-OH molecules prepared independently by CH_3-C-OH·$^+$ neutralization isomerize partly to non-dissociating CH_3-CH=O. Thus, the transition state energy for CH_3-C-OH → CH_3-CH=O must be located below the dissociation threshold of acetaldehyde; it is estimated to lie ~15-20 kcal/mol above the energy of CH_3-C-OH. This value is also a lower limit for the transition state of CH_3-C-OH → CH_2=CH-OH, as CH_3-C-OH forms a negligible amount of CH_2=CH-OH (Figure 1). The direct 1,3-H rearrangement of vinyl alcohol to acetaldehyde is not observed.

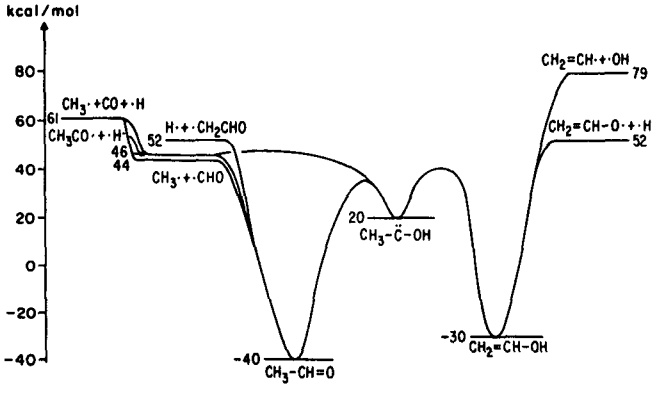

Figure 1. Proposed energy profile for the C_2H_4O neutral tautomers.

Presented at the 35th ASMS Conference on Mass Spectrometry and Allied Topics
May 24-29, 1987, Denver, CO

The reionization efficiencies of neutral molecules strongly depend on their structures.[2] Neutrals with a very poor reionization cross-section to positive ions can often be detected with higher sensitivity and specificity as negative ions. E.g., $CH_3O^{\cdot}$ radicals can be transferred easily to stable CH_3O^- but not to stable CH_3O^+. For the isomeric $^{\cdot}CH_2OH$ radical the situation is reversed: now, $^{\cdot}CH_2OH^-$ is unstable but $^{\cdot}CH_2OH^+$ can be formed with good yield (Figure 2). Such positive and negative reionization spectra can be used to determine the structure of the $COH_3^{\cdot}$ radical from the dissociation of ionized methyl acetate. Our data are consistent with predominant (>90%) loss of $CH_3O^{\cdot}$ from collisionally activated $CH_3CO_2CH_3^{\cdot +}$, with metastable ions losing ~70% $CH_3O^{\cdot}$ and ~30% $^{\cdot}CH_2OH^{\cdot}$

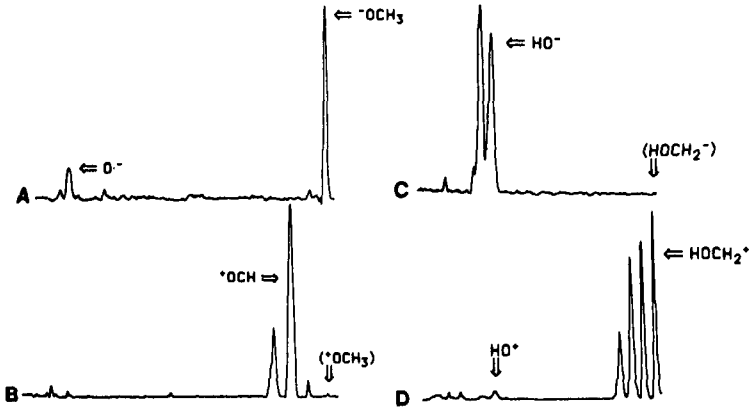

Figure 2. (A) He/Xe, (B) He/O_2, (C) Hg/Xe, and (D) Hg/O_2 neutralization-reionization spectra of mass-selected CH_3O^- anions (A,B) and CH_2OH^+ cations (C,D). He and Hg (90% transmittance) are used for the neutralization of CH_3O^- and CH_2OH^+ to the respective radicals. Xe and O_2 (70% transmittance) reionize the radicals to negative and positive ions, respectively.

Collisional reionization by electron attachment provides a novel route for the formation of anions from mass-selected fast neutrals. Direct charge reversal of positive into negative ions is also possible. The best targets for these processes are C_6H_6 or Xe. Radicals generally show better yields for electron attachment than do molecules. However, highly unsaturated hydrocarbons, like C_3H_2, and carbon clusters, like C_3, exhibit high cross-sections for reionization to negative ions.

1. Wesdemiotis, C.; McLafferty, F. W. Chem. Rev. 1987, 87, June.
2. Danis, P. O.; Feng, R.; McLafferty, F. W. Anal. Chem. 1986, 58, 355-358.

Presented at the 35th ASMS Conference on Mass Spectrometry and Allied Topics
May 24-29, 1987, Denver, CO

THE STRUCTURE AND GAS PHASE ENERGETICS OF $C_7H_7^+$ IONS: TOLYL, BENZYL, AND TROPYLIUM IONS

S. Olesik(1), T. Baer, J. C. Morrow

Department of Chemistry, University of North Carolina, Chapel Hill, N. C. 27514

J. Ridal, J. Holmes

Department of Chemistry, University of Ottawa, Ottawa, Ontario, Canada K1N 6N5

Mass spectrometry(2), collisional activation(CA)(3), ion cyclotron resonance(4), photoionization(5,6) photoelectron photoion coincidence(PEPICO)(7), and molecular orbital calculations(8) have been used to provide information on gas phase $C_7H_7^+$ ions. The $C_7H_7^+$ isomers formed by dissociative ionization are, in order of increasing energy, tropylium ion, benzyl ion, and tolyl ion. Little agreement concerning the energetics of these ions exists. In the present study, $C_7H_7^+$ ions were obtained by dissociative photoionization of nine monohalotoluenes (o-, m-, p-; chloro-, bromo-, iodo-) and ethylbenzene and subjected to PEPICO experiments which provided rate and energetic data. CA experiments provided structural information.

Ionization potentials of the subject molecules were determined from the photoionization efficiency as a function of photon wavelength. The PEPICO experiments, designed to measure only those ions in coincidence with electrons with zero initial energy, gave the time of flight(TOF) distribution for all daughter ions formed from the parent ion at a selected internal energy. Dissociation rate, in the range 10^4 to $10^7 s^{-1}$, and kinetic energy(KE) released to the products can be determined from the TOF distribution (Fig. 1)(9). KE release and CA measurements were carried out with a VG Analytical ZAB-2F double focusing mass spectrometer.

Fragmentation onsets were determined by extrapolating the dissociation rates obtained in the PEPICO experiments to the onset using the RRKM/QET model. However, the PEPICO data contain no information about the product ion structure. The CA data show that most of the dissociations produce mixtures of $C_7H_7^+$ product ion structures. Methyl loss from ethylbenzene produces a mixture of benzyl and tropyl ions in a proportion that changes slowly with ion internal energy. This indicates that direct dissociation and isomerization to a different structure have nearly the same energy barrier. The ion prepared from o-iodotoluene produces the tolyl ion with little KE release. The other halotoluenes in this study dissociated into a mixture of benzyl and tropylium ions with the release of considerable KE. Since all of the reactions which produced tropylium ion did so with considerable release of KE, it was possible only to set the upper limit of 860 kJ/mol for ΔH^o_{f298} of the tropylium ion. PEPICO data gave the following values for the other two ions: ΔH^o_{f298}(tolyl)= 1034±10 kJ/mol and ΔH^o_{f298} (benzyl) = 890±10 kJ/mol. These differ considerably from previously reported values.

The observed two component decay rates of the iodotoluene ions reveal the participation of a lower energy $C_7H_7^+$ isomer in the dissociation process. The identity of this isomer is not known. However, it probably does not have the tropylium ion structure because there is considerable kinetic energy released in this dissociation.

Acknowledgement: The National Science Foundation and the Department of Energy provided financial support for this work.

(1) present address: Department of Chemistry, Ohio State University, Columbus, OH.
(2) Leung, H.W., Ichikawa, H., Li, Y.H., Harrison, A.G. J.Am.Chem.Soc. 1978, 100, 2479.
(3) Dymerski, P.P., McLafferty, F.W. J.Am.Chem.Soc. 1976, 98, 6070.
(4) Honovich, J.P., Dunbar, R.C., Int.J.Mass Spectrom.Ion Proc. 1982, 42, 33.
(5) McLoughlin, R.G., Morrison, J.D., Traeger, J.C., Org.Mass Spectrom.1979,14,104.
(6) Lifshitz,C., Goldenberg,M.,Malinovich,Y.,Peres,M.,Org.Mass Spectrom.1982,17,453.
(7) Bombach,R.,Dannacher,J.,Stadelmann,J.P., Chem.Phys.Lett. 1983,95,259.
(8) Abboud,J.L.M.,Hehre,W.J.,Taft,R.W. J.Am.Chem.Soc. 1976,98,6072.
(9) Baer,T., Adv.Chem.Phys. 1986,64,111.

Fig. 1

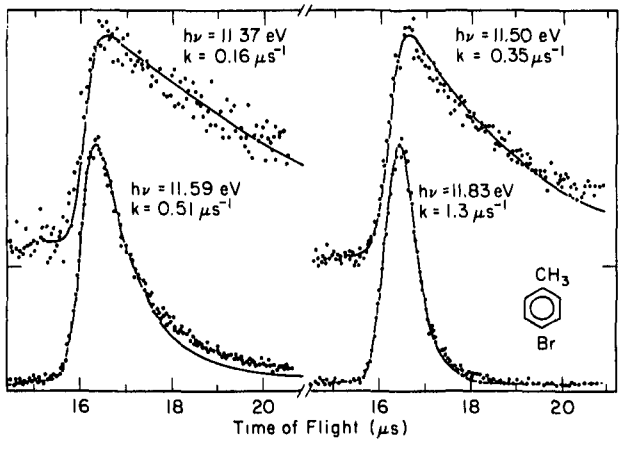

Fig. 2

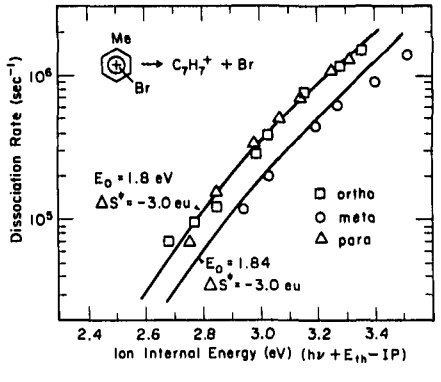

Fig. 3

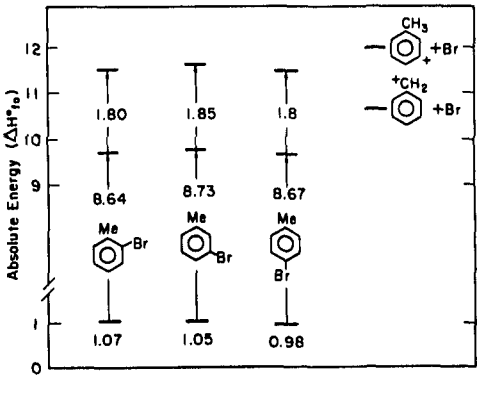

Presented at the 35th ASMS Conference on Mass Spectrometry and Allied Topics
May 24-29, 1987, Denver, CO

SECONDARY DEUTERIUM KINETIC ISOTOPE EFFECT ON THE CYCLOREVERSION OF 2,2,3-TRIPHENYLCYCLOBUTANONE

Grant Gill Smith and Sudhakar G. Reddy
Department of Chemistry and Biochemistry, Utah State University
Logan, UT 84322-0300

The secondary deuterium kinetic isotope effect has been studied with EI fragmentation of 3-deuterio and 4,4-dideuterio 2,2,3-triphenylcyclobutanones. The two most significant fragmentations were the two retrograde 2 + 2 cycloaddition reactions The cyclobutanone rings opened by two pathways, one forming ketene and triphenylethene, pathway **A**, and the other, pathway **B**, diphenylketene and styrene. Deuterium substitution at the **3**-position had a major effect on the mode of fragmentation. Substitution by two deuteriums at the **4**-position had very little effect. These results strongly suggest a KIE is occurring with the fragmentation of the **3**-deuterioated compound and may shed light on the nature of the transition state of fragmenation. These results may assist in a better understanding of the mechanism of 2 + 2 cycloaddition of ketenes to alkenes. Although 2 + 2 reactions are known to be highly periselective (only 2 + 2 with no 2 + 4 cycloaddition), supraselective on the diene (only cis-fused products), regioselective (always adding to attach the sp carbon at the least hindered position), these findings strongly suggest the reaction is concerted. From a KIE study, Baldwin and Kapecki (1) proposed a concerted mechanism while Collins, *et al* (2) and Holder, *et al* (3) proposed a stepwise mechanism also from a deuterium KIE study. The model suggested by Collins, *et al* appears to best describe the nature of the transition state in the 2 + 2 cycloaddition of diphenylketene to styrene. Theory predicts that an inverse KIE, $k_H/k_D < 1$, for sp^2 going to sp^3 (4).

The most recent study of the deuterium KIE study of this 2 + 2 reaction was carried out by Holder, *et al.* In contrast to the two already mentioned which were intermolecular studies, it was an intramolecular study. Intramolecular studies are thought to be more accurate than intermolecular ones (5). They also showed an inverse KIE when deuterium was at the ß-position of styrene. They concluded that the cycloaddition takes place *via* a two step mechanism.

In the EI fragmentation of cycloreversion of 2,2,3-triphenylcyclbutanone and the 3-deuterio and, 4,4-dideuteriotriphenylcyclobutanone an opposite KIE would be expected as this is the reverse of the 2 + 2 cycloaddition reaction. In this EI study of the two cycloreversal reaction which occurred, only path **B** is the reverse of the 2 + 2 cyclo- addition reaction already discussed. There are two major observations to be noted. Substitution by deuterium at the **4,4**-position had no significant effect on the ion abundance. However, substitution by deuterium at the **3**-position had a marked effect. Deuterium at this position increased the ion from styrene to appear as the base peak.

Deuterioation at the **C-3** position caused a marked change in the ion abundance as shown in pathway **A**. In the non-deuterioated and in the 4,4-dideuterioated triphenylcyclo- butanone fragmentation formed *m/z* 256 as the base peak. The intensity of the corresponding ion, *m/z* 257, dropped to 42 with the **3**-deuterioated triphenylcyclobutanone. What conclusions can be drawn from these results? Substitution at the 3-position is in agreement with the previously reported findings of both Baldwin and Kapecki, Collins, *et al* and Holder, *et al.* They reported a $k_H/k_D > 1$ for the 2 + 2 reaction and proposed a weakening of the C-H in the transition state to explain this KIE. If a similar mechanism occurs in the reverse reaction as studied with mass spectroscopy the converse would be true, k_H/k_D would be **< 1.** This was observed. The **3**-deuteriotriphenyl- cyclobutanone reacted faster by pathway **B** than the undeuterioated compound. Presumably the C-H bond at **C-3** is weakened in the activated complex causing the isotope effect. The lack of an isotope effect for the 4,4-dideuteriotriphenylcyclobutanone was surprising as it was expected from the 2 + 2 KIE studies. We have concluded that the reaction studied with mass spectrometric fragmentation was not a concerted one and the rate determining step involved cleavage at **C-3** carbon. It is questionable if the mechanism in the fragmentation of the cyclobutanone ring initiated by electron impact occurs simply as a reverse of the mechanism of the 2 + 2 cycloaddition. Abundance ratios in mass spectrometry are significant in a study of KIE only when the internal energy of

the two remain constant (5). Intramolecular KIE in mass spectrometry are more reliable than are intermolecular studies. The KIE studies in this work, and the earlier work referred to (1,2) are intermolecular studies. Abundance of ions, not rate constants, *k*, are measured in mass spectrometry. Kinetic isotope effects are concerned with rate constants, *k*, and it is essential to realize that effects of isotope substitution upon abundance and isotope effects upon rate constants are not the same thing (5).

Cycloreversion of 2,2,3 - Triphenylcyclobutanone
Effect of Deuterium Substitution
Pathway A and B

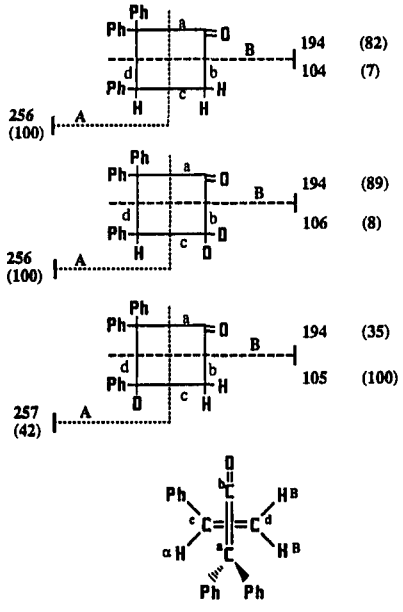

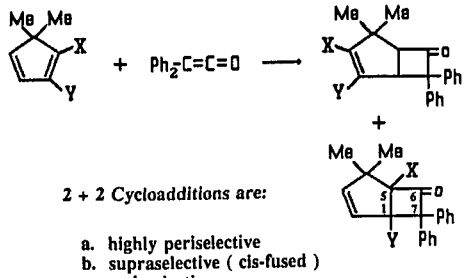

2 + 2 Cycloadditions are:

a. highly periselective
b. supraselective (cis-fused)
c. regioselective

This reaction has been widely interpreted as concerted

k_H/k_D = 0.82 (New bond $C_5 - C_6$)

k_H/k_D = 1.06 (New bond $C_1 - C_7$)

KIE studies strongly suggest a ***nonconcerted*** mechanism. $sp^2 \longrightarrow sp^3$ in forming $C_5 - C_6$ *in the rate determining step. No KIE in forming* $C_1 - C_7$.

Holder, *J. Am. Chem. Soc.*, 1983, *105*, 2928.

Collins, Benjamin and Kagalka, *J. Am. Chem. Soc.*, 1978, *100*, 2570.

1. Balwin, J E. and Kapecki, *J. A. J. Am. Chem. Soc.*, **1969**, *91*, 3106; *ibid.*, **1970**, *92*, 4874.
2. Collins, C. J., Benjamin, B. M.; Kabalka, G. W. *J. Am. Chem. Soc.* **1978**, *100*, 2570.
3. Holder, R. W.; Graf, N. A.; Moss, J. C. *J. Am. Chem. Soc.* **1983**, *105*, 2929.
4. (a) Streitwieser, J. E., Jr.; Jagow, R. H.; Fahey, R. C.; Suzzuki, S.; *J. Am. Chem. Soc.* **1958**, *80*, 2326. (b) Wolfsberg, M.; Stern, M. J. *Pure and Appl. Chem.* **1964**, *8*, 225, 323. *J. Chem. Phys.* **1966**, *45*, 2618.
5. Derrick, P. J. *Mass Spectrometry Reviews*, **1983**, *2*, 285.

Presented at the 35th ASMS Conference on Mass Spectrometry and Allied Topics
May 24-29, 1987, Denver, CO

GAS PHASE RADICAL CATION ANALOGUES OF [4+2] CYCLOADDITIONS

L.W. Castle, and M.L.Gross, Midwest Center for Mass Spectrometry, U. of Nebraska, Lincoln, NE 68588.

The ability of tandem mass spectrometry (MS/MS) to monitor a single ion for collisional activation (CAD) makes it a very effective tool for studying bimolecular gas-phase reactions. Using the CI source as a reaction vessel allows for the study of these reactions as a function of internal energy. Because the reaction is conducted in the presence of a bath gas in a CI source, its reaction adduct is collisionally stabilized and observed. In order to take spectra without any collisional stabilization we also do the reaction in the ion cyclotron resonance mass speactrometer. With these two complimentary tools we are able to take spectra at various different pressures and obtain structural information about the reaction products and intermediates.

We have used this strategy to study a series of radical cation analogues of [4+2] cycloadditions. The specific reactions studied are those of butadiene radical cation plus neutral methyl vinyl ketone, methyl acrylate and vinyl acetate. Assignment of adduct structure were based on the comparison of adduct CAD spectra with those of likely intermediates.

Through ejection studies conducted in the ICR we were able to determine that ionized butadiene is reacting with the neutral olefin. This information makes it clear that a [3+2] cycloaddition is taking place.

The ability to study the adduct as a function of internal energy allows us to intercept the reaction intermediate and take its spectrum. In the ICR, where the adduct is completely isolated, we have taken our lowest stabilized spectrum. We see from this spectrum the key fragments of the adduct are in qualitative agreement with the key fragments of the cyclic model compounds CAD spectrum. The next experiment was done in the CI source and monitored by tandem mass spectrometry. The adduct was formed in the CI source where a combined pressure of reactants plus products was equal to 5 X 10^{-8} torr. The adduct which was formed at low stabilization shows the key fragments of both our cyclic and our acyclic model compounds. The spectrum of the cyclic and acyclic adduct, at low stabilization, are superimposed on the same spectrum making it very complicated to interpret. In the next experiment the adduct was formed in the CI source with a bath gas added to a pressure of 9 X 10^{-4}. The spectrum of the adduct then was at its highest stabilization, and showed a fragmentation pattern very similar to that of our acyclic model compound.

We interpret these results to be a two-step cycloaddition in which an acyclic intermediate is formed. The fact that we were able to intercept the acyclic intermediate and take its spectra makes it clear that these reactions do not go by a concerted mechanism. The acyclic model compound spectra cannot model our intermediate completely because the acyclic adduct is a distonic ion. We are comparing a conventional molecular ion with a

distonic intermediate thus an exact correlation cannot be expected.

Analogues of [4+2] radical cation cycloadditions also take place in the condensed-phase as well as the gas-phase. The results of the gas-phase studies may be applicable to predicting the outcome of condensed-phase chemistry.

References:
1. Groenewold G.S.; Gross M.L., J. Am. Chem. Soc. 1984, 106, 6575
2. Groenewold G.S.; Gross M.L., J. Am. Chem. Soc. 1984, 106, 6569

TWO STEP CYCLOADDITION

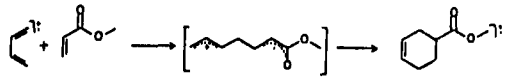

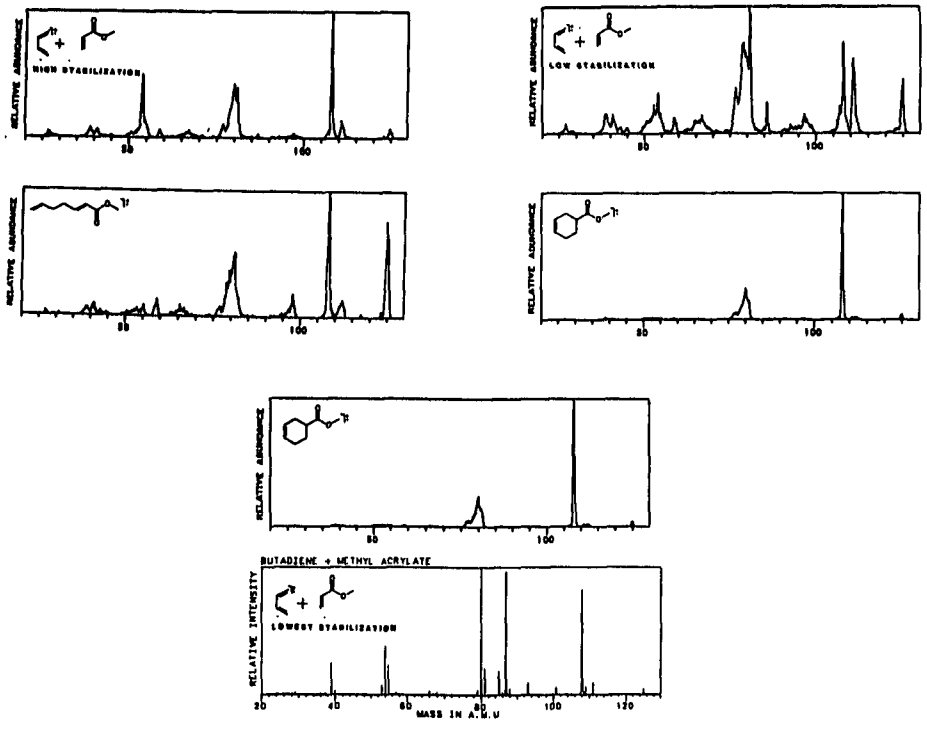

Presented at the 35th ASMS Conference on Mass Spectrometry and Allied Topics
May 24-29, 1987, Denver, CO

HYDROGEN INTERCHANGE PRIOR TO THE FRAGMENTATION OF PROTONATED MOLECULES

A.G. HARRISON, Department of Chemistry, University of Toronto, Toronto, Canada.

Various protonated ethanol species specifically labelled with deuterium have been subjected to collision-induced dissociation at 10 eV collision energy. As the results in the table show both the hydronium ion and ethyl ion products contain various numbers of deuteriums irrespective of the original position of deuteration. Also shown in the table are the relative abundances expected if complete randomization of all H/D occurred. Clearly extensive hydrogen interchange between carbon and oxygen has occurred although complete randomization is not achieved. By contrast, protonated isopropanol shows very little interchange of hydrogens between carbon and oxygen prior to fragmentation (to $C_3H_7^+$) while protonated butyl amines show practically no interchange of hydrogens between carbon and nitrogen prior to fragmentation (to NH_4^+). Recently, it has been reported (1) that there is interchange of hydrogens between oxygen and carbon prior to fragmentation of protonated methyl isopropyl ether.

A mechanism for fragmentation of the protonated species $RHXH^+$ (RH=alkyl, X=OH, OCH_3NH_2) is shown in the Scheme. It is proposed that initially an ion-dipole complex 1 is formed. This complex may fragment to RH^+ + XH or, by way of the proton-bound complex 2 and the ion-induced dipole complex 3, may fragment to XH_2^+ + R. The complex 3 is sufficiently loosely bound that rotation may occur and, on reversion to 1, any of the hydrogens bonded to the heteratom may transfer to carbon. Thus, interchange of hydrogens will occur if 3 can revert to 1. This will be possible if 1 is not higher in energy than the products XH_2^++R. The ion-dipole complex 1 is 50 kJ mol^{-1} more stable than RH^+ + XH. This leads to the conclusion that 1 will be more stable than XH_2^+ + R provided PA(XH) - PA (R) $\leq$ 50 kJ mol^{-1}. This argument rationalizes the experimental results and leads to the conclusion that hydrogen interchange is not likely for protonated alkyl amines or alcohols, except for ethanol. However, interchange should be observed for a number of alkyl ethers and esters.

Full details of this work will appear in Org. Mass Spectrom.

1. J.K. Terlouw et al. Org. Mass Spectrom. 21, 665 (1986)

Presented at the 35th ASMS Conference on Mass Spectrometry and Allied Topics
May 24-29, 1987, Denver, CO

TABLE
FRAGMENTATION OF PROTONATED ETHANOLS
RELATIVE ABUNDANCE

	$C_2H_5OD_2^+$		$C_2D_5OH_2^+$		$CH_3CD_2OH_2^+$	
	expt	calcd*	expt	calcd*	expt	calcd*
H_3O^+	21	29			35	29
H_2DO^+	48	57	28	14	52	57
HD_2O^+	32	14	48	57	12	14
D_3O^+			24	29		
$C_2H_5^+$	48	5			4	5
$C_2H_4D^+$	29	48			27	48
$C_2H_3D_2^+$	23	48			70	48
$C_2H_2D_3^+$			19	48		
$C_2HD_4^+$			27	48		
$C_2D_5^+$			55	5		

* on basis of complete H/D randomization.

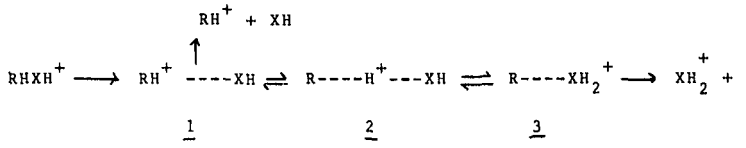

SCHEME

Presented at the 35th ASMS Conference on Mass Spectrometry and Allied Topics
May 24-29, 1987, Denver, CO

ON THE INTRINSIC PROPERTIES OF ALKYL-SUBSTITUTED ARENIUM IONS: A STUDY IN THE GAS PHASE.

R.W. Holman, Dept. of Chemistry, Univ. of Nebraska, Lincoln, NE 68588

The vast majority of electrophilic aromatic substitutions (EAS) proceed via a single mechanism, known generally as the arenium ion mechanism. This mechanism involves an electrophilic attack on a benzenoid π-system giving rise to a protonated intermediate known as an arenium ion (see scheme 1). Much of the detail regarding the nature of the arenium ion is unknown, or is a present, under debate.

We have employed tandem mass spectrometry (MS/MS) techniques to isolate and characterize a series of alkyl substituted benzene arenium ions produced by chemical ionization (CIMS). Mass spectrometry provides an ideal way to study such systems as it overcomes the problem of forming and isolating such transient species, while providing for analysis free of solvent effects.

The main fragmentation process seen in the collisionally activated (CA) decomposition of alkylated benzene arenium ions is the formation of C_6H_6 and the alkyl carbenium ion (i.e., propyl benzenium ion $\rightarrow C_6H_6 + C_3H_7^+$, butyl benzenium ion $\rightarrow C_6H_6 + C_4H_9^+$). It is of interest to note that in the CA decomposition of the non-protonated parent molecular ions of the same alkyl benzenes, little or no formation of the alkyl carbenium ion is seen (see figure 1). The extent of alkyl carbenium ion formation in the decomposition of these arenium ions was found to increase with increasing thermodynamic stability of the alkyl carbenium ion (see Table 1).

The above observations suggest that π-complex character may exist in the bonding of alkylated benzene arenium ions. However, if π-complex characater does exist then one would expect that alkyl side-chain isomerizations would be observed.

All propyl-, butyl-, and pentyl-arenium ions were found to possess unique CAD spectra with the exception of the 2- and 3- pentyl benzenium ions, which shared a common spectra. That the CAD spectra of the 2- and 3-pentyl arenium ions are identical indicates that a $2^\circ \rightleftarrows 2^\circ$ isomerization to a like structure has taken place (see figure 2). As such it was surprising that no other isomeric arenium ions shared common CAD spectra. One would expect that if the near thermal-neutral $2^\circ \rightleftarrows 2^\circ$ isomerizations take place then clearly, $1^\circ \rightarrow 2^\circ$ and $2^\circ \rightarrow 3^\circ$ isomerizations should take place even more readily.

If alkyl rearangements arise only from the π-complex form of arenium ions and $2^\circ \rightleftarrows 2^\circ$ isomerizations are observed, but $1^\circ \rightarrow 2^\circ$ are not, then it is plausible that the π-complex form of 1° arenium ions may be energetically inaccessible.

To test this premise three experiments were conducted. Firstly, para-n-butyl-sec-butyl benzene, C_6H_5-C_6H_4-$CH(CH_3)_2$, was protonated to its corresponding arenium ion and collisionally activated to see whether its predominant alkyl loss would be $^+C_3H_7$ or $C_4H_9^+$ (if the 1° alkyl benzenium π-complex is inaccessible then only $^+C_3H_7$ should form). Secondly, deuterated sec-butyl benzene, C_6H_5-$CH(CD_3)CH_2CH_3$, was protonated to its arenium ion and studied to see if it would undergo a degenerate $2^\circ \rightleftarrows 2^\circ$ isomerization. Finally, the 1,2-dimethyl-1-phenyl propane and the 2-methyl-2-phenyl butane arenium ions were collisionally activated to see if they rearranged to a common structure via a $2^\circ \rightleftarrows 3^\circ$ isomerization.

The para-n-butyl-sec-propyl benzenium ion was found to yield C_4H_9-C_6H_6 + $C_3H_7^+$, and C_3H_7-C_6H_6 + $C_4H_9^+$ with equal facility even though the former process is 14 Kcal/mol favored over the latter (see figure 3). This result rules out the possibility that the π-complex form of 1° alkyl benzenium ions is energetically inaccessible. This experiment also proves to be insightful in that if one assumes the n-butyl moiety of the para-n-butyl-sec-propyl benzenium ion undergoes isomerization in the π-complex to sec-butyl moiety then the formation of sec-$C_4H_9^+$ would be 3 Kcal/mol favored over $C_3H_7^+$ formation, which experimentally is bore out in a 1.2/1.0 ratio for $C_4H_9^+/C_3H_7^+$ (see figure 4).

The deuterated sec-butyl benzenium ion was found to readily undergo a degenerate $2^\circ \rightleftarrows 2^\circ$ isomerization, as expected. However, the arenium ions of 1,2-dimethyl-1-phenyl propane and 2-methyl-2-phenyl butane were found to be unique.

The conclusion then, is that all these arenium ions undergo isomerization.

However, only those that are energetically degenerate or near-degenerate will be reflected by the isomerized species sharing a common CAD spectra (i.e., 2- and 3-phenyl benzenium ions, and the labeled sec-butyl isomerizations). All those that release energy upon isomerization (i.e., n- to sec-butyl benzenium ion etc.) will deposit that energy into the cleavage of the benzene-alkyl bond in the formation of $C_6H_6 + R^+$. As such, the exothermic rearrangements between $1^\circ \rightarrow 2^\circ$ and $2^\circ \rightarrow 3^\circ$ isomeric alkyl benzenium ions do take place but are transparent to us in that the CAD spectra of the isomeric species will be unique, with all evidence of rearrangement lost with the cleavage of the rearranged alkyl carbenium ion.

That alkyl rearrangements do take place is strong evidence for π-complex formation preceding σ-complex arenium ion formation in the reaction coordinate for electrophilic aromatic substitution (see scheme 2).

scheme 1

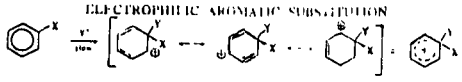

Table 1

ARENIUM ION	ALKYL CARBONIUM (TIC)
Toluene arenium ion	--
Ethyl benzenium ion	--
sec-propyl benzenium ion	23
sec-butyl benzenium ion	50
sec-pentyl benzenium ion	62

figure 1

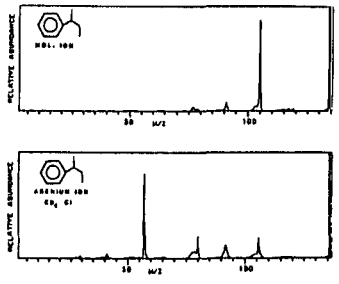

figure 2

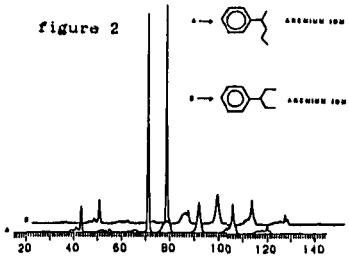

figure 3

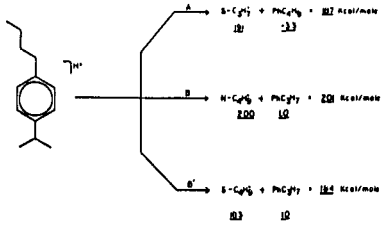

figure 4

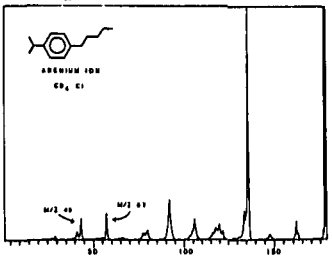

scheme 2

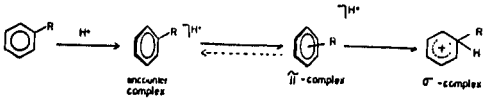

Presented at the 35th ASMS Conference on Mass Spectrometry and Allied Topics
May 24-29, 1987, Denver, CO

Mass Spectra of 3-Nitrochromenes and 3-Nitrochromans

David S. Mitchell, Richard D. Bowen and Keith R. Jennings,
Department of Chemistry, University of Warwick, Coventry, U.K.,
and Rajender S. Varma and George W. Kabalka, Department of Chemistry,
University of Tennessee, Knoxville, Tennessee, U.S.A.

Interest in 3-nitrochromenes, A, reflects the reported radioprotective properties of chromenes which contain electron-attracting substituents at the 3-position. The corresponding saturated analogues, 3-nitrochromans, B, have only recently been prepared by reduction of 3-nitrochromenes with sodium borohydride in methanol/tetrahydrofuran. A study of the mass spectra of these two groups of heterocyclic compounds is therefore timely.

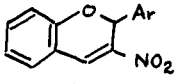

A

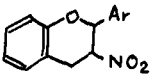

B

The 70 eV electron ionisation spectra of eight 2-aryl-3-nitrochromenes and ten 2-aryl-3-nitrochromans were obtained. All the compounds give a significant abundance of molecular ions but the spectra of the chromenes and chromans differ in a number of important respects. The spectra of 2-phenyl-3-nitrochromene and 2-phenyl-3-nitrochroman are illustrated in Figure 1.

The relative abundance of molecular ions is greater for the chromenes (3-8% total ion current) than for the corresponding chromans (1-5% total ion current) and for each class of compound, the relative abundance of the molecular ion is increased by the presence of electron-rich alkoxy substituents in the 2-aryl group or at the 8-position, but it is reduced if the 2-phenyl is replaced by the 2-naphthyl group.

A major difference in the spectra of the two classes of compounds is the relative abundances of the three ions $[M-NO_2]^+$, $[M-HNO_2]^{+\cdot}$ and $[M-NO_2-H_2]^+$. The base peak in each of the eight nitrochromenes was that due to the $[M-NO_2]^+$ ion, together with a peak due to $[M-NO_2-H_2]^+$ which is often of appreciable intensity. In contrast, in the spectra of nitrochromans, the peak due to $[M-HNO_2]^{+\cdot}$ ions is the most important of the three ions, although it is never the base peak. Substituents at the 6- or 8- position or the replacement of 2-phenyl by 2-naphthyl very much reduce the abundance of the $[M-HNO_2]^{+\cdot}$ ions. Hydrogen transfer from the 2-position to the oxygen of the nitro group leads to the expulsion of HONO and the formation of a stable ion. This is supported by the observation that HONO is specifically eliminated in metastable transitions of the 3,4-dideutero-2-phenyl-3-nitrochroman.

The base peak of the nitrochroman spectra is the structurally informative ion of nominal structure $[ArCH_2]^+$ which defines the composition of the 2-aryl substituent in each case. This ion is believed to arise by loss of NO_2 by the molecular ion followed by the elimination of benzofuran. Plausible mechanisms for the formation of other ions of lower relative abundance are also suggested.

A brief study of the negative ion spectra of the two classes of compound, using ammonia as buffer gas, indicated that $[M-NO_2]^-$ is the base peak in each case with $[M]^{-\cdot}$ giving peaks of 10-20% of the intensity of this peak. The nitrochromans also gave a significant peak at m/z = 46 due to the NO_2^- ion.

A full account of this work has been accepted for publication in J. Chem. Soc. Perkin II.

Presented at the 35th ASMS Conference on Mass Spectrometry and Allied Topics
May 24-29, 1987, Denver, CO.

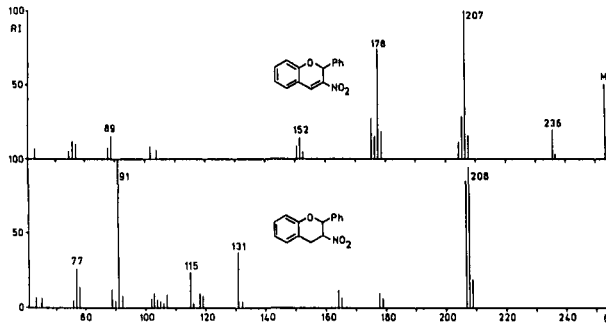

Presented at the 35th ASMS Conference on Mass Spectrometry and Allied Topics
May 24-29, 1987, Denver, CO

EFFECTS OF SITE OF PROTONATION ON LOW AND HIGH ENERGY DAUGHTER ION MS/MS SPECTRA OF PHENOTHIAZINES

Scott A. McLuckey and Gary L. Glish
Analytical Chemistry Division, Oak Ridge National Laboratory
Oak Ridge, TN

Gerald C. DiDonato and Kenneth L. Busch
Indiana University
Bloomington, IN

Phenothiazines are a class of drugs consisting of derivatives of the phenothiazine ring system shown below as structure I. We have noted that positive chemical ionization mass spectra of many of these derivatives are very sensitive to the nature of the reagent gas. This is not particularly surprising since the exothermicities of the proton transfer reactions differ greatly. However we have also observed that the daughter ion MS/MS spectra, in some cases, vary dramatically with the reagent gas. This is a curious result in light of the fact that MS/MS spectra, unlike CI mass spectra, are generally insensitive to differences in parent ion internal energy.

For simplicity, results for one phenothiazine, promethazine, are presented. CI mass spectra and MS/MS spectra have been obtained using methane (proton affinity = 128 kcal/mol) and ammonia (proton affinity = 205 kcal/mol) as the reagent gases. Spectra were collected on each of three instruments: viz., a hybrid EBQQ mass spectrometer, a BE geometry mass spectrometer, and an Ion Trap mass spectrometer (ITMS). The structure of promethazine is shown as structure II:

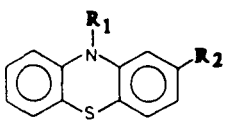

I

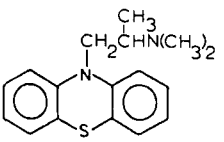

II

Note that there are three potential sites of protonation including the two nitrogen sites and the sulfur site. The sulfur site is considerably less basic than the two nitrogen sites. The major fragmentation pathways are not easily rationalized by protonation on the sulfur for either reagent gas. The two major ion structures are therefore deemed to result from either protonation on the ring nitrogen or on the side chain nitrogen.

Figure 1 shows the CI mass spectra of promethazine obtained using the EBQQ instrument. These mass spectra are similar to those obtained with the other instruments. All ammonia CI mass spectra show the fragment at m/z 72 to be the base peak with relatively few fragment ions at m/z 86. The methane CI mass spectra show both fragment ions to be abundant. Figure 2 shows the MS/MS spectra of the $(M+H^+)$ ions obtained using the EBQQ instrument. The MS/MS spectra obtained with the other instruments are qualitatively similar with respect to the major daughter ions. All MS/MS spectra obtained using ammonia CI show the most intense daughter ion to appear at m/z 86 (not m/z 72 as in the CIMS!). The MS/MS spectra obtained using methane CI show abundant daughter ions at both m/z 72 and m/z 86.

The results can be rationalized if it is assumed that the ion at m/z 72 is formed from the side chain-protonated species and that the ion at m/z 86 arises from the ring-protonated structure. These assumptions are based on what appears to be the most likely mechanisms for their formation as shown below:

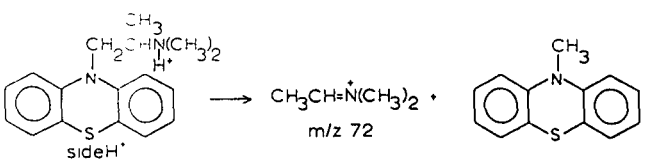

Presented at the 35th ASMS Conference on Mass Spectrometry and Allied Topics
May 24-29, 1987, Denver, CO

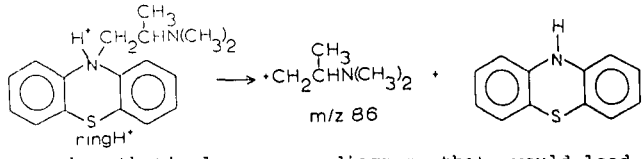

Figure 3 shows a hypothetical energy diagram that would lead to the observed results. We conclude that there is little interconversion between the two structures since the MS/MS spectra differ so dramatically even when the data are obtained using instruments with widely different time-scales.

In ammonia CI, enough internal energy is deposited into the side chain-protonated form upon ionization to cause a large fraction of ions of this structure to fragment in the ion source. Too little energy is imparted upon ionization, however, to significantly deplete the ring-protonated form. The ions that survive the first stage of mass analysis are largely of the ring-protonated form, which give m/z 86 in the MS/MS spectrum. In methane CI, both forms can fragment in the ions source. Therefore, the mixture of structures that survives for MS/MS analysis is not as heavily weighted in one structure. Both daughter ions at m/z 72 and m/z 86 are therefore observed. This situation is shown schematically in Figure 4 where r represents the ring-protonated form and s is the side chain-protonated form.

This work was supported by the U.S. Department of Energy, Office of Basic Energy Sciences, through Contract DE-AC05-840R21400 with Martin Marietta Energy Systems, Inc.

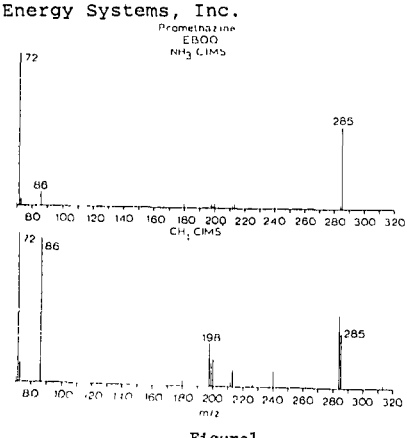

Figure1

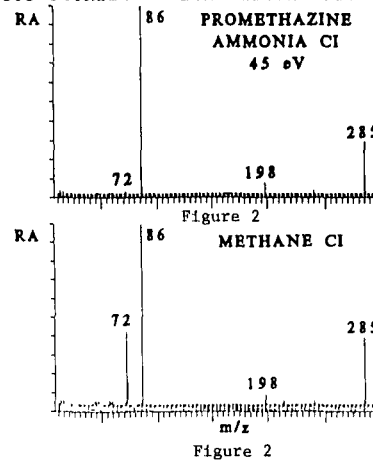

Figure 2

Figure 2

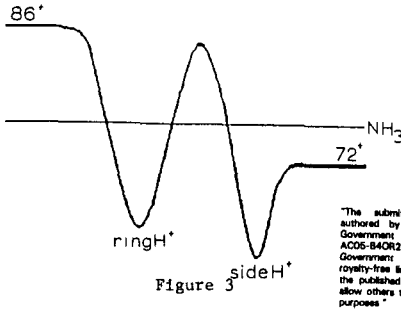

Figure 3

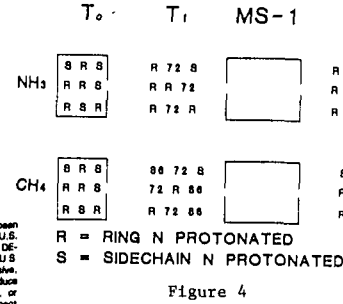

Figure 4

"The submitted manuscript has been authored by a contractor of the U.S. Government under contract No. DE-AC05-84OR21400. Accordingly, the U.S. Government retains a nonexclusive, royalty-free license to publish or reproduce the published form of this contribution, or allow others to do so, for U.S. Government purposes."

Presented at the 35th ASMS Conference on Mass Spectrometry and Allied Topics
May 24-29, 1987, Denver, CO

DIFFERENT FRAGMENTATION OF ISOMERIC METHYL ETHYL AND ETHYL METHYL CITRACONATES UNDER ELECTRON IMPACT.

A. Mandelbaum[a], D. Bornstein[a], T. Tamiri[b] and S. Zitrin[b]
[a]Department of Chemistry, Technion-Israel Institute of Technology, Haifa, Israel
[b]Mass Spectrometry Laboratory, Israel Police Headquarters, Jerusalem, Israel

The isomeric methyl ethyl and ethyl methyl citraconates 1 and 2 give rise as expected to almost identical IR and NMR spectra. These closely similar isomers afford different electron impact mass spectra which enable their clear distinction. The major differences in the fragmentation pattern of 1 and 2 are shown in Scheme 1.

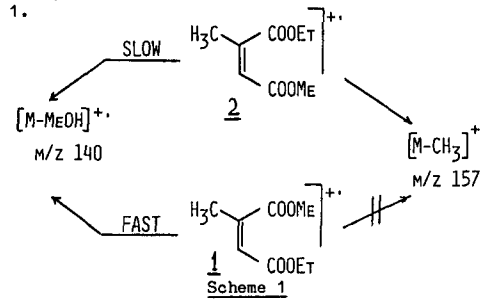

Scheme 1

$[M-CH_3]^+$

Loss of CH_3 from the molecular ion occurs only in isomer 2. Analogs 2a and 2b labeled with deuterium at the ester methyl and ethyl groups retain all the deuterium in the $[M-CH_3]^+$ ions indicating involvement of the methyl group from

2a 2b

the citraconic moiety in this process. A mechanism for this highly specific elimination of CH_3 is suggested in Scheme 2.

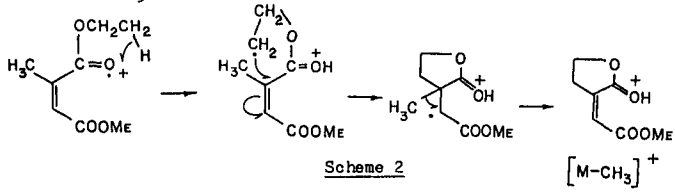

Scheme 2

A CID study aimed at the determination of structure of the $[M-CH_3]^+$ ion is under way. The absence of $[M-CH_3]^+$ ion in the mass spectrum of 1 may be explained by steric hindrance in the cyclization step.

$[M-CH_3OH]^{+\cdot}$

Methanol elimination takes place in diester 1 to a greater extent than in isomer 2. Deuteromethanol (CH_3OD) is eliminated in 1b and 2b but unlabeled methanol is lost in 1c and 2c. These results clearly indicate involvement of a hydrogen

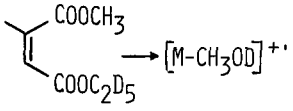

1b

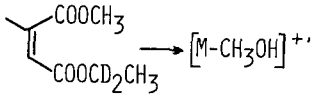

1c

atom from position 2 of the ethyl group by mechanism shown in Scheme 3.

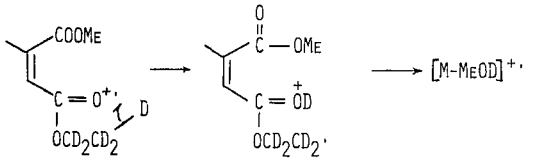

Scheme 3

The lower abundance of the $[M-CH_3OH]^{+\cdot}$ ion in 2 may be attributed to competition with the loss of CH_3 radical from the same intermediate.

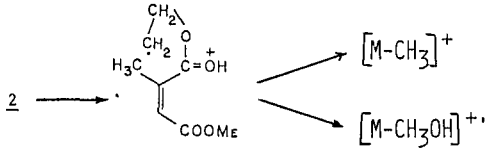

We have previously reported on a different behavior of the closely similar ethyl methyl and methyl ethyl halosuccinates under electron impact.[1] N.m.r and i.r. spectra of these isomers are also almost identical, and mass spectrometry is the best technique for their differention and structure determination. It seems that pronounced differences in mass spectra may be expected in isomeric mixed diesters in various systems, providing an efficient way for their analysis. The different behavior of these isomers under electron impact opens a new way for mechanistic studies of fragmentation processes in gas phase ions.

Reference

1. D. Bornstein, B. Domon, A. Mandelbaum, D. Mueller and W.J. Richter; presented at the 34th Annual Conference on Mass Spectrometry and Allied Topics, Cincinnati, June 8-13, 1986; Proceedings p. 95.

Presented at the 35th ASMS Conference on Mass Spectrometry and Allied Topics
May 24-29, 1987, Denver, CO.

MASS SPECTROMETRY OF L-β-ASPARTAMIDO-CARBOHYDRATES ISOLATED FROM OVALBUMIN

Tsong-hui Wang, Tse-fang Chen, and Douglas F. Barofsky
Department of Agricultural Chemistry
Oregon State University, Corvallis, Oregon 97331.

Ovalbumin is an abundant, carbohydrate rich protein contained in the whites of chicken eggs. There have been a large number of studies aimed at characterizing the carbohydrate structures of this important biological system. Because of this large wealth of information, we considered ovalbumin to be a good source of known glycopeptides and polysaccharides and set out to isolate and purify relatively large stocks of these compounds to use as models in investigating and developing mass spectrometric procedures. In the process, we performed what we believe to be the most complete characterization to date of the L-β-aspartamido-carbohydrate fraction of ovalbumin.

Following established methods for exhaustive pronase digestion and gel permeation chromatography[1], we isolated 0.42 g of material testing positive for mannose[2] from 8 g of hen ovalbumin (Sigma Grade V). We collected several L-β-aspartamido-carbohydrates and some additional glycopeptides containing two or more amino acids by fractionating the hexose containing mixture on a Dowex column at 4°C (Figure 1). Each of the glycopeptides fractions obtained off the Dowex column were fractionated further by high performance liquid chromatography (HPLC); we improved the resolution of our HPLC by using a water jacket around the column. In total we isolated 28 glycopeptides; we attribute seven of these compounds to ovamucoid[3] and two of them to ovatransferrin[4-6], both of which are likely impurities in our starting material. At least six of the isolated components, appearing in fractions B2, C3, D1, E2, and H, have never appeared in previously published chromatograms.

Each of the isolated and purified chromatographic components was examined by FAB mass spectrometry on a KRATOS MS50-TC. Monothioglycerol was used as the liquid matrix; both positive and negative mass spectra were recorded. The mass spectra of the six, unknown, chromatographic components confirm that they indeed correspond to unidentified compounds. The structures of the known glycoasparagines have been determined by combinations of enzymatic, chemical, and instrumental methods to be of the following general form:

$$\begin{matrix} R\ (1\rightarrow 6) \\ R'\ (1\rightarrow 4) \\ R''(1\rightarrow 3) \end{matrix} \!\!\!\

Presented at the 35th ASMS Conference on Mass Spectrometry and Allied Topics
May 24-29, 1987, Denver, CO

FAB spectra of the unknown compounds suggest the following structures:

Dowex Fraction	Molecular Weight (daltons)	R	R′	R″
B2	1916	Man-O, Man-O > Man-	GlcNAc-	Man-O, GlcNAc-O > Man-
C3	1713	?	?	?
D1	1551	Man-O, Man-O > Man-	-	GlcNAc-O-Man-
E2	1389	GlcNAc-O-Man-	-	Man-O-Man-
H	1227	GlcNAc-O-Man-	-	Man-
H	1227	Man-	-	GlcNAc-O-Man-

The proposed structure for the compound in fraction B2 is supported only weakly by the mass spectrometric evidence. The proposed structures for the compounds in fractions D1 and E2 were predicted on the basis of a hypothesized biogenetic sequence[6] and are well supported by their mass spectra. The two isomers in fraction H were differentiated on the basis of the preference in negative ion spectra for cleavage of the (1→6) glycosidic bond, over the (1→3) bond, to the core mannose as stated in rule 1). We are presently augmenting our mass spectrometric analysis of these compounds with derivatization (e.g. permethylation) and chemical degradation procedures.

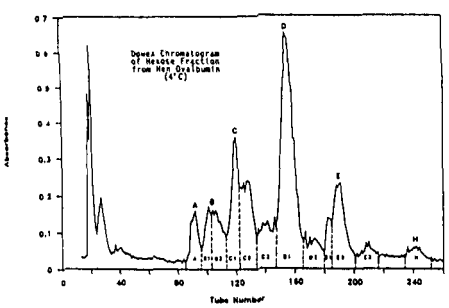

Figure 1.

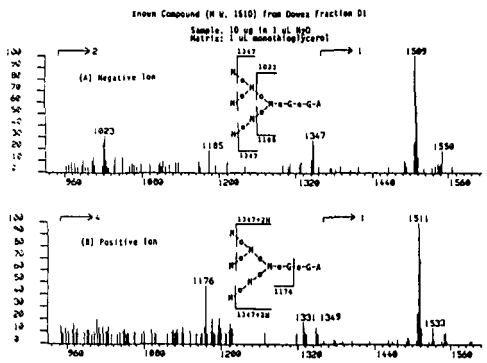

Figure 2.

Acknowledgement. Support for this work was provided by NIEHS Grant ES00210.

References.

1. C.C. Huang et al., Carbohydr. Res. 13, 127 (1970).
2. M. Dubois et al., Anal. Chem. 28, 350 (1956).
3. K. Yamashita et al., J. Biol. Chem. 257, 12809 (1982); Ibid. 258, 3099 (1983).
4. T. Tai et al., J. Biol. Chem. 250, 8569 (1975); Ibid. 252, 6687 (1977).
5. G.D. Longmore and H. Schachter, Carbohydr. Res. 100, 365 (1982).
6. H. Nomoto and Y. Inoue, Eur. J. Biochem. 135, 243 (1983).

Presented at the 35th ASMS Conference on Mass Spectrometry and Allied Topics
May 24-29, 1987, Denver, CO

LSIMS SPECTRA AND DAUGHTER ION STUDIES OF LACTOSAMINE SERIES OLIGOSACCHARIDES

K. M. Pamidi*, R.K. Jain+, S.A. Abbas+, K.L. Matta+, and R.A. Laine*

*Dept. of Biochemistry, Louisiana State University, Baton Rouge, LA 70803
+Roswell Park Memorial Institute, State of New York, Dept. of Health, Buffalo, NY 14263

EXTENDED ABSTRACT

Liquid secondary ionization mass spectra (LSIMS) and collision activation daughter ion (CADI) studies of a series of linkage-isomeric fucosyl-lactosamine compounds were obtained to assess the available chemical structural information. CADI spectra were obtained for the molecular ions as well as the major fragments. The following three compounds were synthesized and tested: Fuc(1->3)-; Fuc(1->4)-; and Fuc(1->6)-linked to GlcNAc(1->3)Gal, possible terminal saccharides on polylactosamines. Objectives were to distinguish among the different fucose to N-acetylglucosamine linkages in the otherwise identical trisaccharides.

The reducing end was synthesized as the beta-O-methyl glycoside to distinguish its mass from the non-reducing end hexose. The molecular [MH]+ ion was at m/z 544 for this compound with major fragments at lower masses corresponding to the monosaccharides. Ions were also observed at [2M + H]+ (m/z 1087), and MH + one and 2 glycerol moieties. Ions seen in the LSIMS spectra included m/z 398 representing loss of Fucose, m/z 350 and 366 representing loss of Galactose-O-Me, and m/z 204 representing the remnant N-acetyl glucosamine fragment which apparently carries the charge.

Daughters of 544 included m/z 398 for loss of fucose, 350 for loss of O-methyl galactoside, and 204 for the remaining GlcNAc. For the 3-linked compound, loss of fucose gave a 17% m/z 398 ion whereas 398 was held to below 5% in the 3-, and 6-linked compounds. The m/z 544 ion yielded 8% under 30eV of collision energy, while the ion was more stable for the 4-, and 6-linked compounds at 20% relative intensity. Stability of the m/z 350 ion was again highest at 80% for the 6-linked species where it was 65% for the 4-linked compound, and only 20% in the 3-linked form. The m/z 366 ion from cleavage on the galactose side of the GlcNac glycosidic oxygen was below 1% in the 6-linked compound, 6% in the 4-linked and 4% in the 3-linked. Facile loss of water from the m/z 204 of the 4-linked version was apparent with the appearance of high m/z 168 and 186 ions.

CADI spectra show that m/z 204 arises through either m/z 398 or 350, and indicates the presence of an internal N-acetylhexosamine.

Since the m/z 350 ion contains the Fucose and GlcNAc residues, linkage information arising from differences in stability of positional isomers was examined in CADI of m/z 350. Collision energy was held at 30eV and 4 scans were averaged for CADI of m/z 350. For the alpha(1->3) and alpha(1->4) linkages, m/z 350 was 35% relative intensity, whereas the alpha(1->6) linkage was 60% relative intensity. The m/z 350 ion formed from the 6-linked compound appears more stable under these conditions. Comparing the 3-substituted GlcNAc with the 4-substitution, m/z 204 was lower in intensity in the 3-linked fucose->GlcNac, relative to the daughters of 204 including m/z 186 and 168 signifying loss of water. The m/z 138 fragment putatively resulting from loss of water and formaldehyde from 204, was the base peak in the 3-linked compound, while it was 80% in the 4-linkage. Since loss of water from the hydroxyl on the 3-position of GlcNAc and the proton from the 2-position could result in an unsaturation which would stabilize the charge retained on the nitrogen, m/z 204

should be less stable in the 4-linked compound than the 3-linked compound. This seems to be true since m/z 204 is only 58% relative intensity in CADI of 350 from the 4 linked compound while it is base peak in the 3-linked compound. However, the 6-linked form also shows m/z 204 as base peak. This may be partially due to the more stable m/z 350 ion. For a comparative result on the 204 fragmentation, we may need to repeat the experiment with enough collision energy to bring the m/z 350 to 30% in the 6-linked compound. The ion at m/z 126, resulting from loss of water and acetic acid from 204, was 25% in the 4-linkage and 68% in the 3 linkage. Again, if the change were stabilized in the 4-linked daughter at m/z 186, loss of acetic acid might be less likely. For the 6-linkage, m/z 126 occurs at 95% of m/z 204, indicating that loss of acetate is more facile in the 6-linked compound than in either the 3-, or 4-linked forms. Interestingly, in the CADI of 350, fragments were not seen between 350 and 204 in the 3-, and 4-linked species showing a real lack of ions resulting from splitting the ring of fucose under the experimental conditions. In the 6-linked compound, ions of low intensity were seen at 260 and 292, as yet unidentified.

Thus, some features of the LSIMS tandem mass spectra of oligosaccharides may give inferences that could lead to direct linkage determination based on stability of the ions in collisional activation daughter ion experiments.

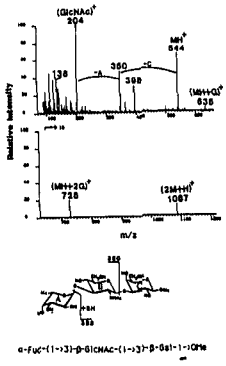

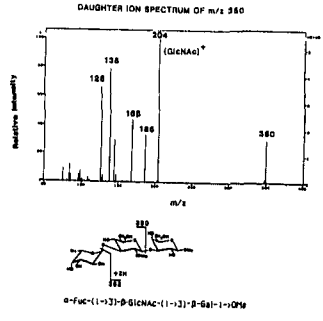

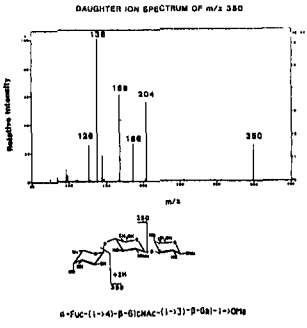

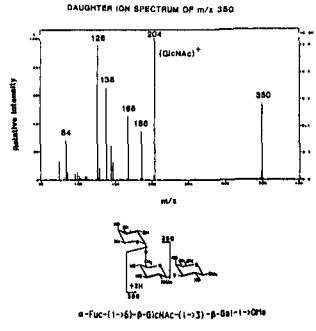

ACKNOWLEDGEMENT: We would like to thank Dr. Alan Schoen, Finnigan MAT Corp., San Jose, CA for help with the CADI experiments. This work was supported, in part by an NIH Shared Instrumentation grant, and Grants #R01AM33755 and R01GM32594 to R.A.L.

Presented at the 35th ASMS Conference on Mass Spectrometry and Allied Topics
May 24-29, 1987, Denver, CO

Liquid Secondary Ion Mass Spectrometry of Complex Carbohydrates from Glycoproteins

Beth Gillece-Castro, William Aberth, Ke Jiang and A.L. Burlingame
Dept. of Pharmaceutical Chemistry, University of California, San Francisco, CA 94143-0446

Work is underway to develop liquid secondary ion mass spectrometry (LSIMS) for the analysis of complex carbohydrates isolated from glycoproteins by enzymatic cleavage. In this report the branched high mannose classes of oligosaccharides were analyzed following cleavage from yeast or human glycoproteins using Endo-H type enzymes. The liberated oligosaccharide reducing terminus was derivatized with p-aminobenzoic acid ethyl ester (ABEE) to form a secondary amine derivative (1) which contains a UV absorbing chromophore, as well as a preferred site of protonation and deprotonation. Unlike the underivatized carbohydrates where the use of less polar matrices such as monothioglycerol or tetraethylene glycol result in enhanced sensitivity, the ABEE derivative enhances sensitivity (~250 pmol in negative ion mode) when run in glycerol with a favorable signal to chemical noise. A primary cesium ion beam (2) was used for the majority of these sputtering experiments. The effect of the primary beam voltage (kinetic energy) on the spectrum of the ABEE derivative of maltoheptaose (MW 1301) was studied using a Wien mass spectrometer (3) which uses a microchannel plate detector. The molecular ion region was detected and summed over the lifetime of the sample at each primary beam energy point (see Figure 1). Although the total secondary beam increased with increasing energy, the glycerol clusters (matrix) increased much more than the sample $(M-H)^-$ ion. Decreasing the volume of glycerol by applying 0.5 µl of a 20% solution of glycerol in water increased both the ratio of sample to matrix ions as well as the total $(M-H)^-$ ions detected.

A mixture of $(Man)_n$ Man_{10}-GlcNAc was analyzed as the ABEE derivative to determine the total number of mannose residues present. After HPLC chromatography using an Alltech "carbohydrate" column, a fraction was analyzed by FAB ionization on a Kratos MS-50 equipped with an array detector (4). Molecular ions were detected in + and - ion modes for n = 8,9 and 10 (average MW 3271, 3433 and 3595) (see Figure 2). Negative ion mode gives both enhanced sensitivity and enhanced fragmentation. However, since the major fragmentation pathway involves glycosidic bond cleavage with a hydrogen rearrangement, the product has the same mass as a molecule containing one less residue. Therefore, in mixture analysis positive ion mode is used to verify molecular weights. A second fragmentation pathway resulting in low mass ions was found to originate from the non-reducing terminus by accurate mass measurement and comparison of the spectra of the deuterated ABEE derivative of maltoheptaose (Glc_7) (see Figure 3). These spectra were obtained in negative ion mode using a primary cesium beam of 10 KeV. The fragment has the structure R-O-C$\underline{H}$=CH-O$^-$ where R is any number of sugar residues (ie. mass 221 = Glc_1 + 58 amu[5] and so on for m/e 383, 545, 707, 869). In straight chain compounds such as maltoheptaose the intensities of the fragments follow a smooth envelope. Interestingly branched high mannose oligosacchrides show varying intensity according to the branching pattern. For the structure:

```
Man-Man-Man-Man-GlcNAc-ABEE
          |   |
        Man Man
              |
             Man
              |
             Man
```

losses of 1,2,3,4 or 8 mannose containing fragments can occur by single bond cleavages as can Man 1,2,3 or 4 + 58 ion production. All of these ions were much more intense than the 5,6 or 7 Man fragments.

In conclusion, the strategy proposed using the p-aminobenzoic acid ethyl ester derivative of oligosaccharides is extremely useful in determining the structure of branched and straight chain oligosaccharides (6). Proper selection of analytical conditions, such as the use of a Cs^+ primary beam with a kinetic energy suited to the sample and matrix as well as detection of positive or negative secondary ions results in greater sensitivity.

References

1. Wang, W.T., LeDonne, N.C., Jr., Ackerman, B. and Sweeley, C.C. (1984) Anal. Biochem., 141, 366-381.
2. Aberth, W., Straub, K.M. and Burlingame, A.L. (1982) Anal. Chem., 54, 2029-2034.
3. Aberth, W. (1986) Anal. Chem., 58, 1221-1225.
4. Cottrell, J. and Evans, S. (1987) Rapid Comm. in Mass Spectrom., 1, 1; Anal. Chem., in press.
5. Dell, A. and Ballou, C.E. (1983) Biomed. Mass Spectrom., 10, 50-56.
6. Gillece-Castro, B.L., Fisher, S.J., Tarentino, A.L., Peterson, D.L. and Burlingame, A.L. (1987) Arch. Biochem. Biophys., in press.

Acknowledgement

This work was supported by the NIH Division of Research Resources, Grant RR01614 (to A.L. Burlingame).

FIGURE 1

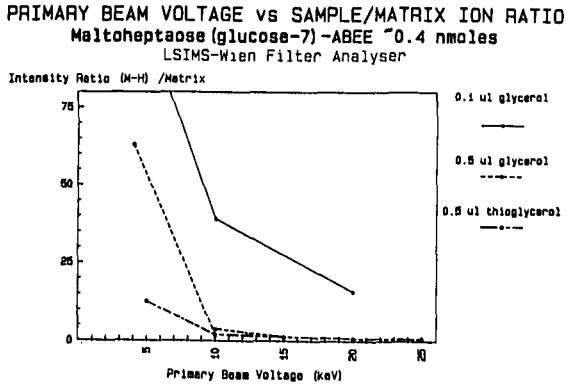

FIGURE 2

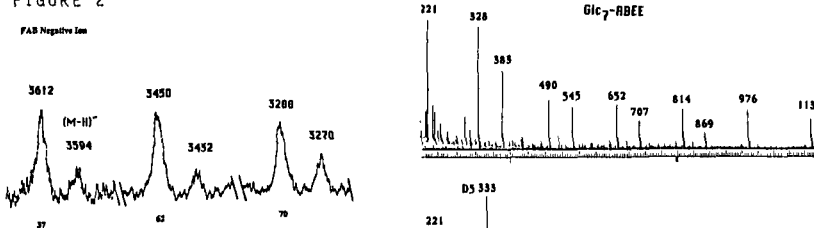

FIGURE 3

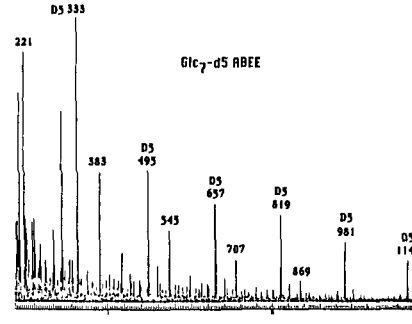

Presented at the 35th ASMS Conference on Mass Spectrometry and Allied Topics
May 24-29, 1987, Denver, CO.

FAB AND SEQUENTIAL (MS/MS/MS) MASS SPECTROMETRY WITH A VG ZAB-EQ: HEXOSE AND 2-AMINO-2-DEOXY-HEXOSE STEREOISOMERS

J.L.C.Wright and R.Guevremont, National Research Council of Canada, Halifax, Nova Scotia, Canada B3H 3Z1.

Several methods for the identification of stereoisomeric saccharides in oligosaccharides and in glycoconjugates by MS and MS/MS have been described (1-3). We have extended the approach of Richter and Blum (1) using collision induced dissociation (CID) of saccharide-derived ions for identification of the stereoisomeric hexoses and amino hexoses in complex molecules. In addition we have used MS/MS/MS experiments (sequential mass spectrometry) to determine if the daughter ions have structural differences which are characteristic of the saccharide stereoisomers from which they were formed. Details of the instrumentation, a hybrid MS/MS system (VG Analytical ZAB-EQ) have been described elsewhere(4). The modifications to this system which were necessary for the MS/MS/MS experiment have been reported (5).

Peracetylated sugars and peracetylated 2-amino-2-deoxy sugars have been found to be more easily differentiated by CID MS/MS than the corresponding underivatized sugars. The acetate (or other aglycone) at the anomeric position (carbon 1) of these peracetylated sugars is easily lost during FAB ionization to produce an abundant ion of m/z 331, M+H-HOAc, (330 for amino sugars). The hexoses, including glucose, galactose, and mannose, can be distinguished on the basis of the pattern of ion abundances, or 'fingerprints', of daughter ions resulting from the CID reactions of ions of m/z 331. Allose cannot easily be distinguished from galactose in this experiment. The peracetylated amino sugars glucosamine, galactosamine and mannosamine can also be distinguished on the basis of the ion abundance 'fingerprint' of the daughter ion spectra of ions of m/z 330.

The granddaughter spectra of ions of m/z 271, 211 and 169 are shown in Figure 1. These spectra are the result of two sequential CID reactions: the first was a high energy (8kV,He) CID reaction of ions of m/z 331 (M+H-HOAc) in the 2nd field free region, and the second was a low energy (50eV,Xe) collision in the rf-only quadrupole. Isotope labeling experiments (6) have suggested pathways for the CID reactions of peracetylated glucose. Our investigation of the decomposition pathway using MS/MS/MS has shown that the daughter ions having m/z 271 (331-HOAc) from acetylated glucose and galactose retain isomeric information, and the granddaughter spectra display differences. However, the decomposition of ions of m/z 211 from glucose and galactose results in spectra which cannot be distinguished.

Granddaughter spectra of ions of m/z 270, 210, and 168 from acetylated glucosamine and galactosamine are illustrated in Figure 2. The granddaughter spectra of m/z 270 of glucosamine and galactosamine are easily distinguished on the basis of the ratio of m/z 210 to 228. The granddaughter spectra of ions of m/z 168 and 150 (not shown here) cannot be distinguished in the experiments conducted by us. Structural information related to the original amino sugar molecule is retained through ions of m/z 330 to m/z 270 to m/z 210.

These ion intensity 'fingerprints' suggest that pathways taken during CID reactions are determined by the geometry of the parent ion. The structure of predominant daughter ions from glucose may not be the same as those from galactose, even though their masses are identical. The sequential dissociation of these daughter ions to granddaughter ions also results in 'fingerprint' patterns which are unique to the molecular structure of the daughter ions. The isotopic labeling experiments of Hogg (6) suggest that in the case of peracetylated glucose several competing, parallel CID

NRCC No.27657

reactions lead to ions of the same mass. The ion intensity 'fingerprints' in daughter and granddaughter spectra should be interpreted as the results of changes in the relative abundances of ions formed through such competing pathways.

The sequential collision experiments are a useful tool for probing the molecular structures of ions formed by collision induced dissociation. A more detailed report describing the application of sequential collision experiments to other hexoses and 2-deoxy-2-amino hexoses is in preparation.

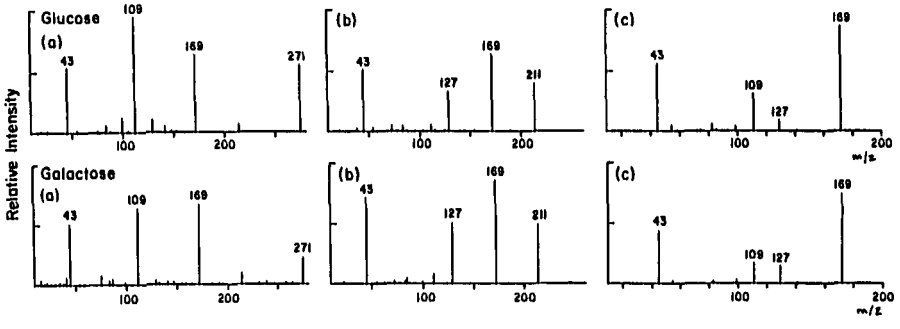

Figure 1. Granddaughter spectra of ions of (a) m/z 271, (b) m/z 211, and (c) m/z 169, daughters of m/z 331 from peracetylated glucose and galactose.

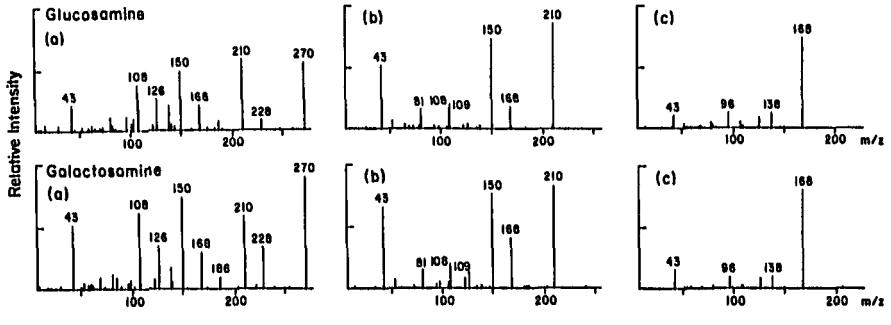

Figure 2. Granddaughter spectra of ions of (a) m/z 270, (b) m/z 210, and (c) m/z 168, daughters of m/z 330 from peracetylated glucosamine and galactosamine.

(1) Richter, W.J., and Blum, W., In Tandem Mass Spectrometry ed. F.W.McLafferty, pg.424-6, Wiley N.Y. (1983).
(2) Samuelsson, B.E., In Advances in Mass Spectrometry, ed. J.F.J.Todd, 10,225, Wiley (1986).
(3) Carr, S.A., Reinhold, V.N., In Advances in Mass Spectrometry, ed. J.F.J.Todd, 10,1431, Wiley (1986).
(4) Harrison, A.G., Mercer, R.S., Reiner, E.J., Young, A.B., Boyd R.K., March, R.E., Porter, C.J., Int. J. Mass Spectrom. Ion Processes 74, 13 (1986).
(5) Guevremont, R., Wright, J.L.C., Rapid Comm. Mass Spectrom., 1 (1987) in press.
(6) Hogg, A.M., Nagabhushan, T.L., Tetrahedron Letters 47,4827(1972).

Presented at the 35th ASMS Conference on Mass Spectrometry and Allied Topics
May 24-29, 1987, Denver, CO

CHARACTERIZATION OF GLYCOCONJUGATES BY TANDEM FOUR SECTOR MASS SPECTROMETRY

B. Domon and C.E. Costello,
Dept. of Chemistry, MIT, Cambridge, MA 02139.

High performance tandem mass spectrometry in conjunction with fast atom bombardment is a technique of imminent interest for structural elucidation of biomolecules. A detailed study has been undertaken in order to explore the utility of this new tool for the characterization of glycoconjugates. The preliminary results obtained for underivatized glycosphingolipids and gangliosides are presented here.

METHODS

This study was performed on a four sector instrument of EB-EB configuration (JEOL HX110/HX110). Product ion spectra of the molecular species, selected by MS-1 and decomposed by collision with helium in a cell located between MS-1 and MS-2, were obtained by linked scans of MS-2 at constant B/E ratio. Samples were dissolved in DMSO (5 μg/μl) and this solution was mixed 1:1 with the matrix (glycerol or triethanolamine). Spectra were recorded using 0.3 μl of the resulting solution (ca. 1 μg of sample). In some cases, the glycoconjugate mixtures were separated by HPLC. Neutral and anionic glycosphingolipids were chromatographed on a reversed phase column using methanol/water and acetonitrile/ammonium acetate buffer (pH 7.0) systems respectively.

RESULTS

Glycolipids containing simple carbohydrate moieties (one or two sugar units) have been investigated in the positive and negative ion modes. In both cases, collision spectra of the FAB generated molecular species (protonated and deprotonated molecular ions respectively) contain pertinent fragments informative about the ceramide constitution (i.e. long chain base and N-acyl residue). The positive ion CID spectrum of a lacto-ceramide is shown in Fig. 1.

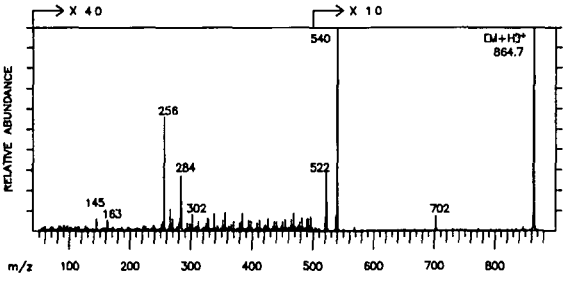

Fig. 1: FAB MS/MS spectra of N-palmitoyl-dihydro-lacto-cerebroside (positive ion mode).

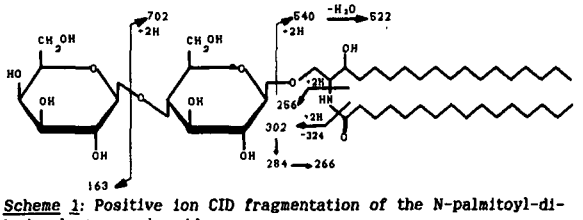

Scheme 1: Positive ion CID fragmentation of the N-palmitoyl-dihydro-lacto-cerebroside.

An investigation of homologous compounds containing various N-acyl groups was carried out in order to ascertain fragmentation pathways. Product ions still containing the N-acyl residue undergo a shift, whereas the fragments resulting from the base remain unchanged.

Information regarding the glycosidic portion can mainly be obtained from the negative ion collision spectra. The ions arising from the carbohydrate moiety involve cleavages of the glycosidic bond with or without retention of the oxygen atom, as well as fragmentation of the sugar rings.

The samples investigated usually contained mixtures of homologous compounds (heterogeneity located in the ceramide moiety). However, by taking full advantage of tandem mass spectrometry, the CID spectra of each component could be recorded.

Gangliosides carrying one or two N-acetyl-neuraminic acid moieties have also been investigated by CID MS/MS. Very different patterns have been observed in these cases due to the fact that the negative charge is preferentially located on the carboxyl group. Most of the fragments observed contain sialic acid as exemplified in Fig. 2 with the CID spectrum of one of the GM_1 homologs (precursor: $[M-H]^-$ ion).

Surprisingly, even sodium adduct ions $[M-2H+Na]^-$ give very informative collision spectra and thus allowed an immediate differentiation of the two isomeric GD_1 gangliosides.

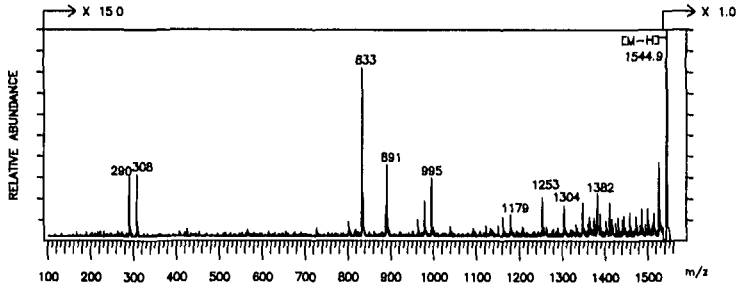

Figure 2: FAB MS/MS spectrum of one of the homologous GM_1 gangliosides (negative ion mode).

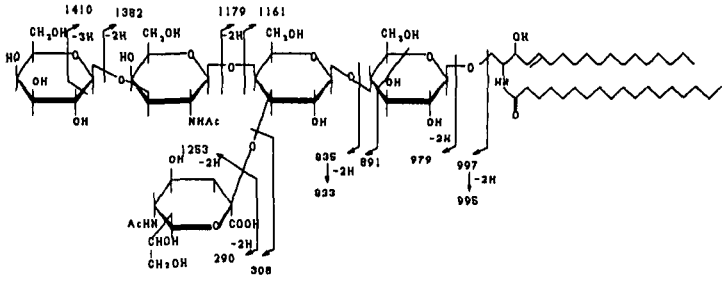

Scheme 2: CID fragmentation of one of the GM_1-gangliosides (precursor ion at m/z 1544.9).

CONCLUSION

This study demonstrates the potential of high performance tandem mass spectrometry for the characterization of glycosphingolipids and gangliosides. This highly sensitive technique is of particular interest for the investigation of such biological samples, often limited in supply and usually containing mixtures of homologous compounds. Information on each of the components can be gained by recording the CID spectra of the different molecular species and selected fragments.

Positive ion collision spectra yield mainly structural information on the lipophilic part of glycosphingolipids. For compounds containing larger oligosaccharide moieties, the negative ion mode shows a higher sensitivity, and appears to be more suitable. Such CID spectra allow the determination of the sugar sequence and the degree of branching of the carbohydrate.

A further advantage of high performance tandem mass spectrometry over conventional FAB-MS is the elimination of most interfering signals from the matrix, thus making possible the identification of fragments at low mass.

Acknowledgments: Presentation of this work was furthered by data reduction and spectra plotting programs written by J.E. Biller. The M.I.T. Mass Spectrometry Facility is supported by Grant No. RR00317 from N.I.H Division of Research Resources (to K. Biemann). B.D. expresses his gratitude to the Swiss Science Foundation.

Presented at the 35th ASMS Conference on Mass Spectrometry and Allied Topics
May 24-29, 1987, Denver, CO

CHARACTERIZATION OF LIPIDS IN BACTERIA BY CONSTANT NEUTRAL LOSS SCANS

D. Heller, W. Martin, C. Murphy, M. Uy, and C. Fenselau
Johns Hopkins University, Baltimore, MD 21205

Membrane lipids are important biomarkers that can be used to differentiate bacteria from one another (Ref. 1). Phospholipids, a major part of the lipid composition, are formed by combination of two fatty acids and a polar head group with a glycerol molecule. The head group determines the phospholipid class.

Fast atom bombardment mass spectrometry can produce membrane lipid molecular ions from mixtures of the entire cell contents (Ref. 2).

The nature of phospholipid classes occuring in bacteria is a function of taxonomic grouping. The fatty acid constituents, and thus the molecular weights, of phospholipids vary with culture conditions. If fragmentation pathways can be discerned which are unique to each class of phospholipid, then scanning for a constant neutral loss (CNL) might permit characterization of these biomarkers despite variations in their molecular and fragment masses.

Linked scanning or tandem mass spectrometry techniques are well suited to the analysis of targeted components in mixtures such as lysed bacteria.

The CNL protocol was evaluated on a two-sector mass spectrometer of EB geometry, tuned to 2500 static resolution and scanned at 30 s/dec. Normal magnet scans, B/E linked scans for daughter ions of selected ions, and CNL linked scans for loss of a selected mass were applied to lysed bacteria samples, to detect metastable decompostions occuring in the first field free region.

Two simple bond cleavages can result in neutral losses characteristic of polar head group. In positive FAB, loss of the phosphate and head group was consistently observed in magnet scans of lysed bacteria cells. In negative FAB, cleavage between the head group and phosphate was also observed, but with smaller relative intensity.

Figure 1 shows an oscillograph tracing of protonated phosphatidylethanolamines (PE) from P. fluorescens which decompose with loss of the phosphoethanolamine head group, as detected by CNL scanning for loss of 141 daltons. This type of cleavage was found to occur only from MH+ ions, and not from MNH4+ or MNa+ ions generated in positive FAB.

A comparison of the CNL scans for PE applied to various E. coli preps and strains (Fig. 2, 3, and 4) shows that PE ions can be detected cleanly and reliably regardless of fatty acid heterogeneity. The difference in strain and culture condition are evident in the different fatty acid distributions.

1. LeChevalier, M.P.; CRC Crit. Rev. Microbiol. 1977, 5, 109-210.

2. Heller, D.N.; Fenselau, C.; Cotter, R.J.; Demirev, P.; Olthoff, J.K.; Honovich, J.; Uy, M.; Tanaka, T.; Kishimoto, Y.; Biochem. Biophys. Res. Comm. 1987, 142, 194-199.

Presented at the 35th ASMS Conference on Mass Spectrometry and Allied Topics
May 24-29, 1987, Denver, CO

POSITIVE FAB, LYSED CELLS, NO COLLISION GAS
Thioglycerol matrix

Constant neutral loss scan: loss of 141, phosphoethanolamine from protonated phosphatidylethanolamines

Figure 1

P. fluorescens, 3 uG lysed cells

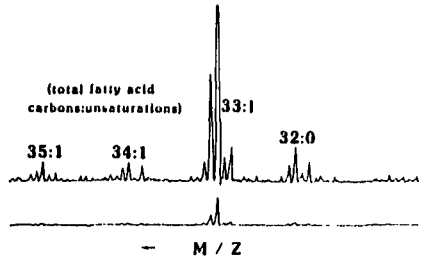

Constant neutral loss scans (precursor ions); average of 3 scans.
(protonated phosphatidylethanolamines)

Figure 2 E. coli, C-600, prep 1

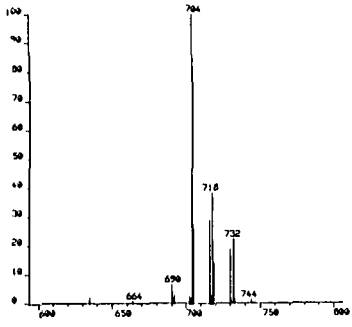

Figure 3 E. coli, C-600, prep 2

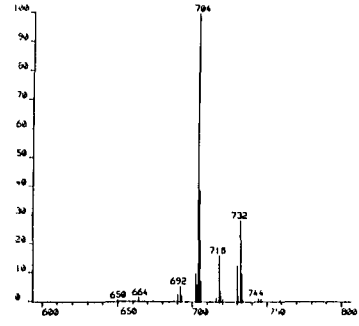

Figure 4 E. coli, B (ATCC 11303)

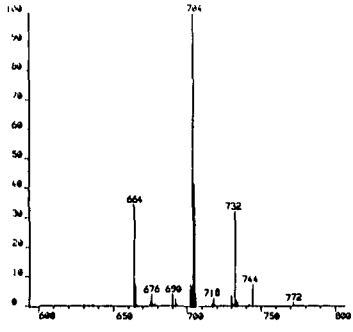

MH+ PRECURSOR	TOTAL FATTY ACID CARBONS: UNSATURATIONS
664	30:0
676	31:1
690	32:1
692	32:0
704	33:1
718	34:1
732	35:1
744	36:2

Presented at the 35th ASMS Conference on Mass Spectrometry and Allied Topics
May 24-29, 1987, Denver, CO

Direct Chemical Ionization Mass Spectrometry of Underivatized Arachidonic Acid Metabolites: Application to Leukotriene Biosynthesis

Gene C. Jamieson *, Joseph Gut **, James R. Trudell**
* Zoecon Research Institute, Sandoz Crop Protection, Palo Alto, CA, 94304
** Dept. of Anesthesia, Stanford University School of Medicine, Stanford, CA, 94305

Introduction: Leukotrienes are a group of endogenous compounds active in hypersensitivity reactions and inflammation. Several key intermediates in leukotriene biosynthesis are highly unstable and not amenable to derivatization or GC/MS.(i.e. prostaglandin H_2 and leukotriene A_4 could not successfully be analyzed by these techniques). Soft ionization techniques such as FAB and Thermospray LC/MS have been applied to the analysis of these compounds. In addition, Direct Chemical Ionization (DCI) Mass Spectrometry of underivatized prostaglandins has been reported[1].

Direct chemical ionization mass spectra of leukotriene metabolites were obtained using ammonia as a reagent gas and a direct chemical ionization probe previously described[2]. The technique involves rapid sample heating by depositing sample on an extended probe constructed of polyimide coated fused silica and direct insertion into an ammonia chemical ionization plasma.

Extensive use of HPLC is made to isolate metabolites in the biosynthetic route of arachidonic acid through to leukotriene LTB_4. The immediate precursor to LTB_4 is the highly unstable allylic epoxide leukotriene LTA_4. This metabolite is derived from 5-hydroperoxyeicosatetraenoic acid (5-HPETE), a lipooxygenase product of arachidonic acid (see Figure 1 for a representative spectrum.) Enzymic hydrolysis of LTA_4 by LTA_4-hydrolases leads to the formation of LTB_4.

Off-line direct chemical ionization mass spectrometry is used to identify the HPLC isolated products. There is significant advantage in this approach. HPLC and mass spectrometry conditions can be optimized individually to control the environment of unstable molecules and allow low nanogram detection limits in the full scan mode.

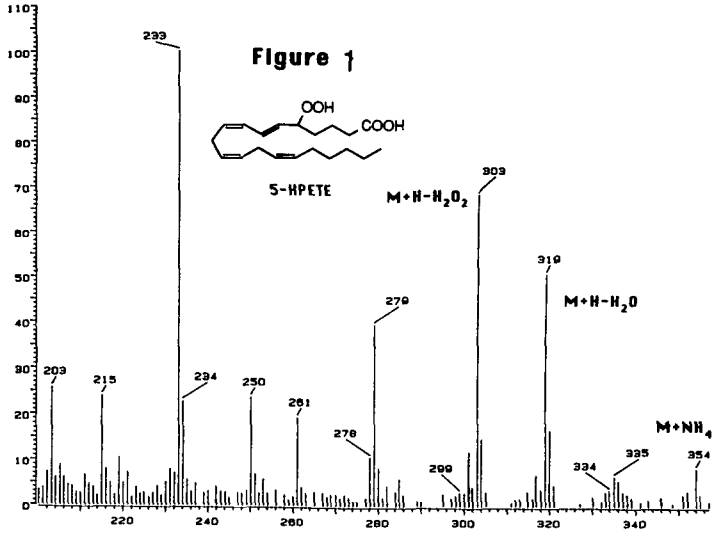

Application: 5- and 15-HPETE's were quantified by selected ion monitoring of major ions, integration of vaporization peak profiles and external standard calibration. 100 pg could easily be detected (see Figure 2).

Application of this technique to biological systems is demonstrated by confirming the formation of leukotriene LTB_4 isolated from a human liver microsomal preparation following a 2 min. incubation of LTA_4. Excellent agreement of the m/z values of the peaks in the reference and the biological sample, as well as the close similarity of their intensity ratios, substantiate the assignment of LTB_4 to the biological product.

Conclusion: High performance liquid chromatography followed by Direct Chemical Ionization Mass Spectrometry is a useful tool for the identification and quantification of oxygenated arachidonic acid metabolites. Derivatization is not required for analysis as with GC/MS. HPLC chromatography and mass spectrometry conditions can be optimized individually without the compromise necessary in interfaced systems. A higher concentration of analyte per unit time is introduced into the mass spectrometer resulting in improved signal to noise and sensitivity. There is very little background interference such as the chemical noise seen in FAB/MS.

We were able to produce spectra on difficult samples such as LTA_4 and the hydroperoxides. We were unsuccessful in the analysis of sulphidopeptide leukotrienes C_4,D_4 and E_4. Ions from the peptide and leukotriene moieties were observed, but not intact product.

Quantification of sub-nanogram amounts of HPETEs is possible with the addition of heavy isotope-labeled internal standards.

1)A.B.Schilling, I.M.Zulak, M.L.Puttemans, E.R.Hall, D.L.Venton
Biomed. and Envir. Mass Spectrom. 13, 545 (1986)

2)G.C.Jamieson, C.C.Reuter, W.L.Fitch
Anal. Chem. 57(1), 121 (1985)

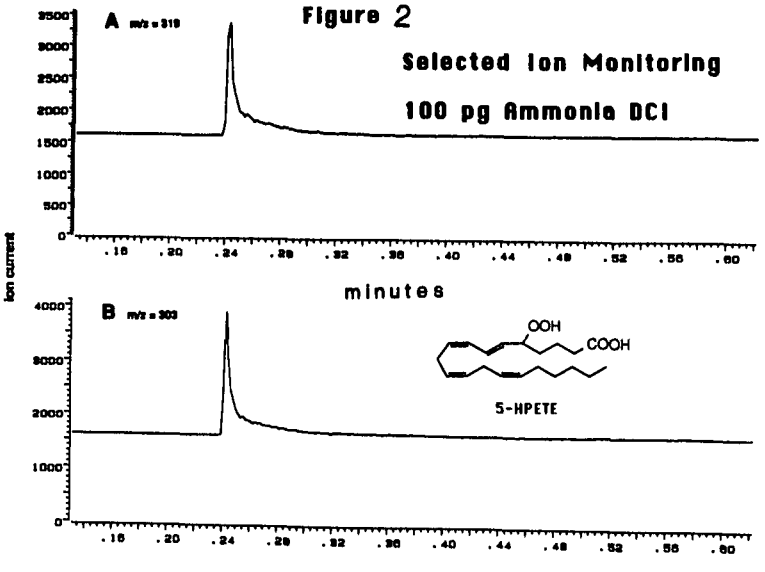

Presented at the 35th ASMS Conference on Mass Spectrometry and Allied Topics
May 24-29, 1987, Denver, CO.

DETERMINATION OF OLIGOSACCHARIDE ISOMERIC BRANCHING BY CID-MS

S.Santikarn, V.N. Reinhold, C.E. Costello, and C. Warren.

Department of Nutrition, Harvard School of Public Health,
665 Huntington Avenue, Boston, MA 02115, USA.
Massachusetts Institute of Technology, Cambridge, MA 02139.
and
Massachusetts General Hospital, Boston, MA 02114.

Oligosaccharide structural analyses are generally tedious and time consuming. At present there is not one general method that can reliably provide the primary sequence of a typical unknown oligosaccharide. When sufficient material (tens to hundreds of micrograms) and appropriate standards are available, branching and linkage information can usually be obtained by using a combination of methylation analysis and nuclear magnetic resonance (NMR) spectroscopy. The results are not always unambiguous, and a sensitive direct method for the determination of oligomer branch positions remains elusive.

Our FAB-MS studies of single and double-branched isomeric oligosaccharides showed that useful branching information could be obtained. However the results were difficult to reproduce due to uncontrollable factors such as the presence and the level of sample contaminants which are normally encountered in most biological isolates.

Tandem mass spectrometry offers four advantages that are important for oligosaccharide structural characterization:
a) it is a relatively sensitive technique, requiring typically less than a microgram per analysis;
b) it is fast, each analysis usually takes less than half an hour to complete;
c) it can provide useful structural information; and
d) it does not have a very strict sample purity requirement, each component in a simple mixture can be independently analysed by this technique.

High energy (kilovolts) tandem mass spectrometry has not yet been extensively employed for the structural studies of many oligosaccharides, although increasing availability of tandem magnetic mass spectrometers and increasing demands for oligosaccharide structural characterization could change this situation in the near future.

In this report we compare product ion spectra of two isomeric tetrasaccharides and three isomeric pentasaccharides recorded on a two sector and a four sector instruments. The resulting FAB-CID mass spectra of these oligosaccharides show abundant product ions that appear to have been produced by simple glycosidic cleavages which are diminished in abundance at the branch points.

The CID mass spectra of the branched and linear oligosaccharide isomers reflect their structural difference. The relative abundances of the product ions at m/z = 366, and 384 (assigned as MG in fig. 1 and 2) are greatly diminished in the spectrum of the branched isomer (M3GIa) in comparison with those of the linear M3GIb isomer. These results can be rationalized in terms of the numbers of glycosidic bond cleavages required for the production of the MG daughter ions : the linear M3GIb isomer requires one glycosidic bond cleavage, while the branched M3GIa requires two glycosidic bond cleavages therefore showing diminished MG daughter ions.

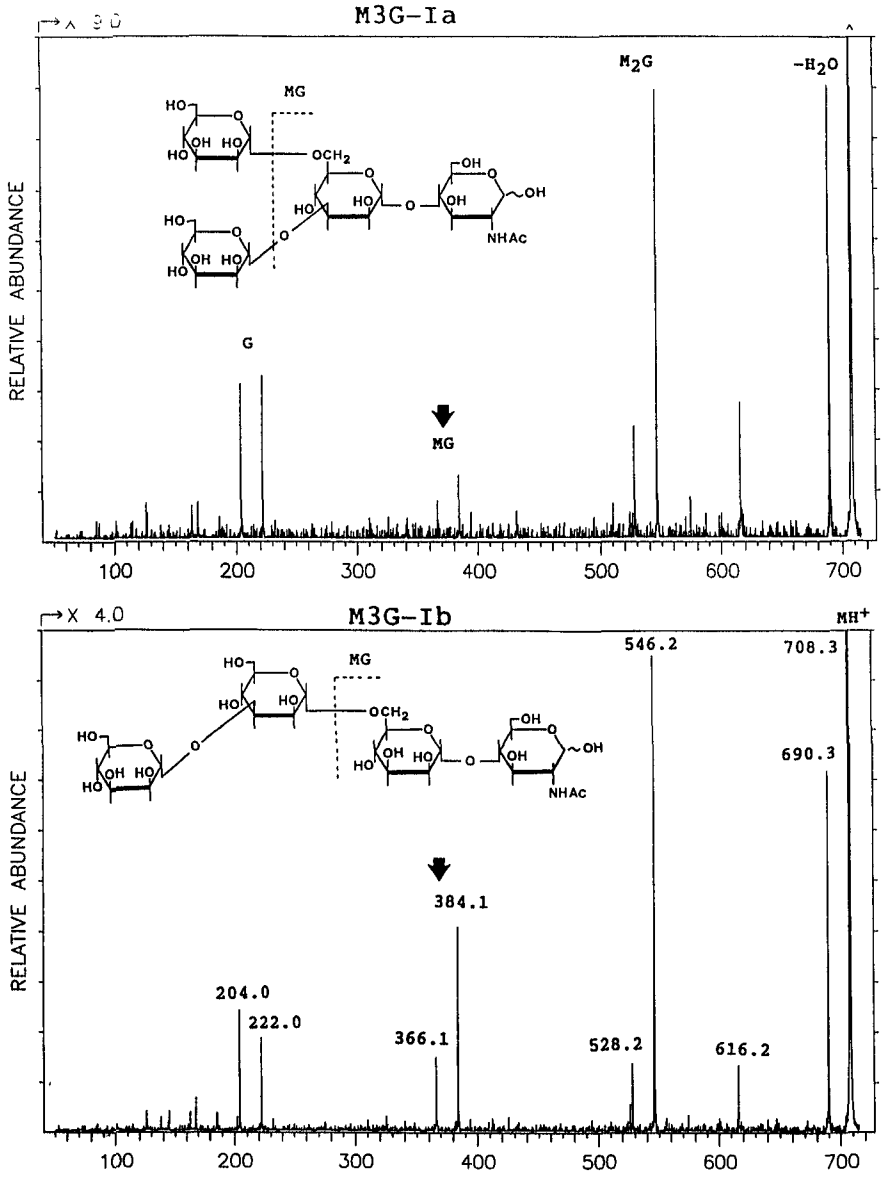

fig.1 positive ion FAB-CID mass spectra of 1 μg of the tetra - saccharide isomers (M3GIa, and M3GIb) recorded on a four sector tandem mass spectrometer.

Presented at the 35th ASMS Conference on Mass Spectrometry and Allied Topics
May 24-29, 1987, Denver, CO

CHARACTERIZATION OF THE GLYCOLIPID MEMBRANE ANCHOR OF HUMAN ERYTHROCYTE ACETYLCHOLINESTERASE

S. Santikarn, V. Reinhold, W. Roberts, and T. Rosenberry

Department of Nutrition, Harvard School of Public Health,
665 Huntington Avenue, Boston, MA 02115, USA.

and
Case Western Reserve University, Cleveland, Ohio 44106, USA.

Proteins vary considerably in the nature and extent of their interactions with the cell surface. The enzyme acetylcholinesterase (AChE) occurs in a variety of molecular forms which are anchored to the cell surface by different attachment structures. Globular, dimeric (G_2) AChE's isolated from drosophilia heads, torpedo electric organs, and mamalian erythrocytes by extraction with non-ionic detergents belong to a unique group of membrane proteins. These proteins have diverse functions but are attached to cell surface by a common glycolipid anchor which contains phosphatidylinositol (PI) glycosylated with glucosamine (GlcN, not N-acylated), an oligosaccharide of variable size, and an ethanolamine bridge that is covalently linked to the C-terminus of the protein.

One important characteristic of the glycolipid anchors of most of these proteins is their susceptibility to enzymatic cleavage by PI-specific phospholipase C (PIPLC). Human erythrocyte (E^{hu}) AChE is known to have an inositol containing glycolipid anchor which is resistant to cleavage by PIPLC. The glycolipid anchor is released from the protein by proteolysis and composition analysis showed that it contains inositol, one ethanolamine bridge, one ethanolamine with free amino group, 2-3 hexose residues, 2-3 phosphate residues, and two fatty acid residues.

Various chemical and enzymatic methods were used to break down the glycolipid anchor and the composition analysis of the purified fragments enabled a partial structure to be proposed. FAB mass spectra of the fragment generated by pronase cleavage followed by base hydrolysis and several steps of purification are shown in figure 1.

fig.1a: negative FAB mass spectrum of the pronase fragment in triethanolamine (peak at m/z = 446 represents the matrix trimer).

fig.1b: positive ion FAB mass spectrum of the pronase fragment in thioglycerol. Approximately 1 μg of sample was used for each of the spectrum.

fig.1c: the results from the above spectra, and other mass spectra of deuterium labeled fragments (not shown here) allows the partial structure to be constructed. The nominal masses (calculated from the structure) of some of the relevant fragment ions are indicated in the diagram.

The partial structure of E^{hu}AChE glycolipid anchor is:

```
..His.Gly.ethanolamine-phosphate.Man.Man.Man.GlcN.Inositol.lipid
                                         |
                                         phosphoethanolamine
```

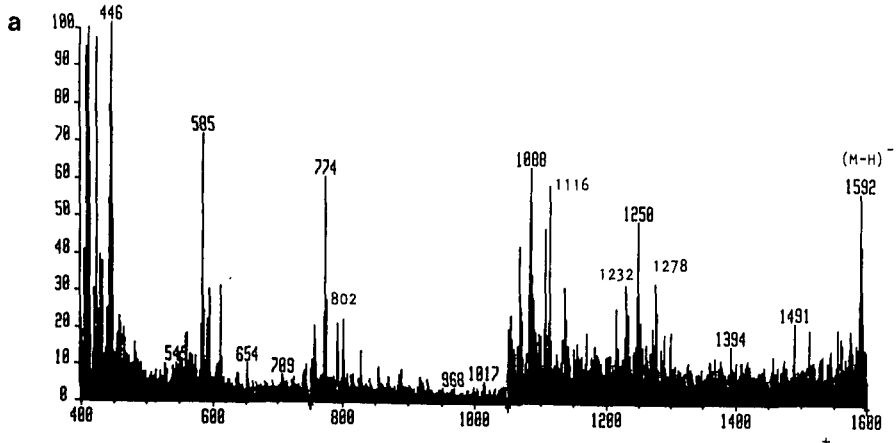
a
446
585
774
802
1088
1116
1250
1232
1278
1394
1491
(M-H)⁻
1592
544
654
709
968
1017

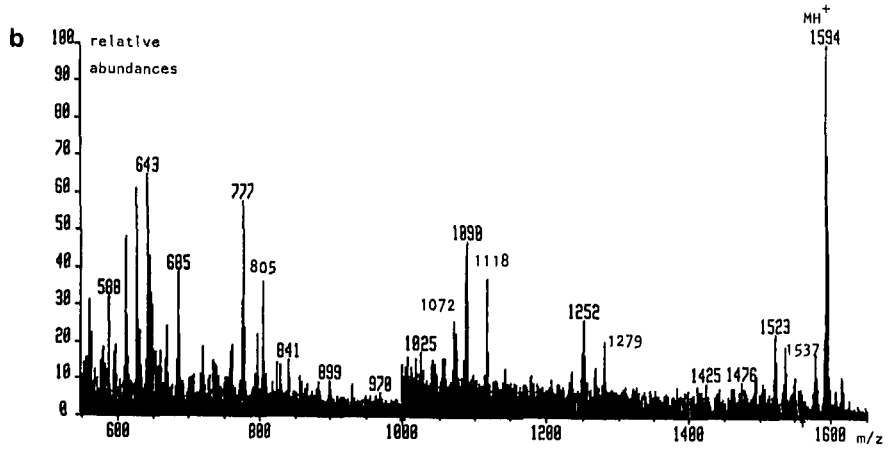
b
relative
abundances
MH⁺
1594
643
777
805
685
588
841
899
970
1025
1072
1090
1118
1252
1279
1425
1476
1523
1537
m/z

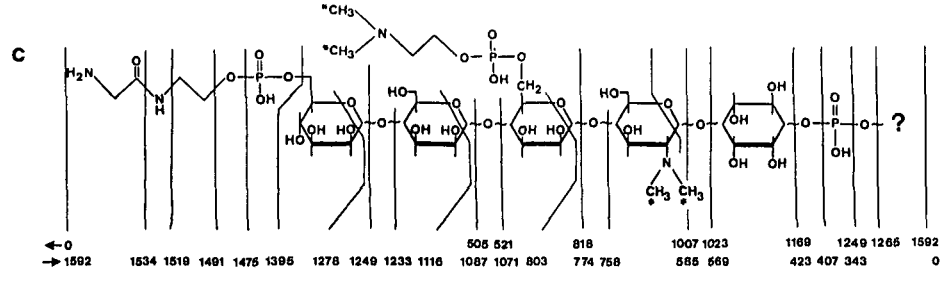
c
?
←0
→1592
1534 1519 1491 1475 1395 1278 1249 1233 1116 1087 1071 803 774 758 585 569 423 407 343 0

Presented at the 35th ASMS Conference on Mass Spectrometry and Allied Topics
May 24-29, 1987, Denver, CO

STRUCTURE ELUCIDATION OF THE LIPOPOLYSACCHARIDE FROM COXIELLA BURNETII

G.R. Her, S. Santikarn, V.N. Reinhold, and J.C. William.

Harvard School of Public Health, Boston, MA 02115
and
USAMRIID Fort Detrick, Frederick MD 21701

Coxiella burnetii is an obligate intracellular pathogen of eukaryotic cells and is recognized as the etiologic agent of Q fever. This organism is a Gram-negative bacterium that undergoes a distinct phase variation. The naturally occurring phase I changes to avirulent phase II during serial passage in nonimmunologically competent hosts such as embryonated eggs or tissue culture. Lipopolysaccharides is a class of macromolecules in the outer membrane of Gram-negative bacteria. They are made up of two chemically distinct portions: a heteropolysaccharide and a covalently bounded lipid. A comparison of Coxiella burnetii lipopolysaccharides by gel electrophoresis along with the sugar composition analysis showed that the complexity and the size of lipopolysaccharides increased according to the phase (phases II,514, and I in that order). The phase I LPS has much higher molecular weight than phase II LPS(18K daltons vs 3K daltons) and has many more different kind of sugars than phase II LPS(8 vs 2).

The phase II LPS was permethylated before FAB-MS analysis(Fig 1). The FAB mass spectrum showed multiple peaks in the molecular ion region, most likely due to the heterogeneity of fatty acid composition. In order to determine the molecular weight of underivatized LPS II, the number of methyl groups incorporated into the phase II LPS during permethylation has to be determined. Therefore, the phase II LPS was perdeuteromethylated and analyzed by FAB-MS(Fig 2). Forty methyl groups accounted for the mass difference between the molecular weights of permethylated and perdeuteromethylated LPS II, therefore, the molecular weight of underivatized LPS II is calculated to be ~2800 daltons.

The O-antigen and lipid A were prepared from LPS II by mild acid hydrolysis. The O-antigen was peracetylated and then analyzed by DCI- and FAB-MS. The LPS II has been shown to consist of only two sugars; mannose(M) and mannoheptose(H). With this understanding, the major ions can be assigned as a disaccharide-MH, a trisaccharide-MH_2 and a tetrasaccharide-M_2H_2. To determine the sequence, CID-MIKE spectra were obtained for the major ions observed in the normal FAB spectrum. The MIKE spectrum of the tetrasaccharide $(M_2H_2-60)^+$ is shown in Fig 3. These data provided the evidence that the structure of the major component of the O-antigen is shown in Figure 4. This is consistent with the fact that only terminal mannose is observed in the linkage analysis.

Lipid A of many Gram-negative bacteria can be easily studied by FAB-MS. Surprisingly, no FAB spectrum cab be recorded with the Coxiella burnetii counterpart. A DCI-MS spectrum, however, proved successful and indicated this lipid entity to be unusual. The molecular weight is exceptionally low, 600-700 Da range, as compared to over 1000 daltons for Salmonella lipid A.

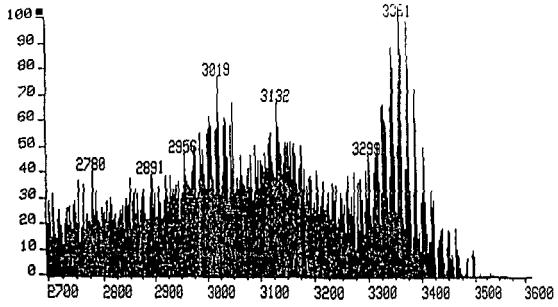

Figure 1. FAB mass spectrum of permethylated LPS II.

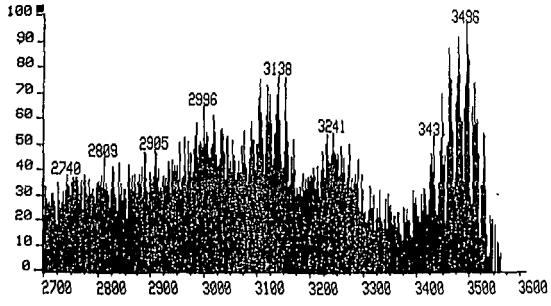

Figure 2. FAB mass spectrum of perdeuteromethylated LPS II.

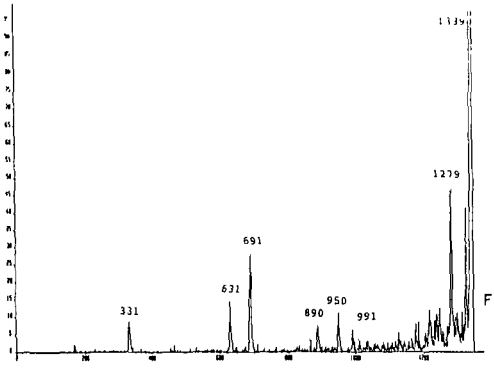

Figure 3. CID-MIKE spectrum of the tetrasaccharide (precursor ion at m/z 1339)

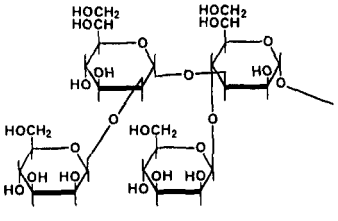

Figure 4. The structure of LPS II O-antigen.

Presented at the 35th ASMS Conference on Mass Spectrometry and Allied Topics
May 24-29, 1987, Denver, CO.

The Structure Determination of *Neisseria Gonoccocal* Lipid Oligosaccharides by LSIMS

Bradford W. Gibson, Jim Webb, Susan A. Fisher, A.L. Burlingame, Ryohei Yamasaki and J. MacLeod Griffiss
Departments of Pharmaceutical Chemistry, Laboratory Medicine and Medicine, University of California, San Francisco, CA 94143

Gonoccocal disease is a major cause of morbidity world-wide, particularly in less developed countries where the disease often goes undetected or medical treatment is scarce. Clearly, a vaccine against this disease would offer considerable advantages. The lipidoligosaccharides (LOS) of the outer membrane of *Neisseria Gonorrhoeae* are one of the major cell surface antigens, and thus represents one of the main targets for the development of a vaccine. In order to understand the immunological response to gonoccocal infection at the molecular level, we have partially determined the structure of the oligosaccharide portion of one gonoccocal strain (JW31R) using a combination of liquid secondary ion mass spectrometry (LSIMS) and GC/MS methods.

The oligosaccharide portion of JW 31R LOS was released by acid hydrolysis (1% acetic acid, 2h, 100°C) and separated directly by Bio-Gel P-4 chromatography with or without prior purification on Sephadex G-50. These oligosaccharides were found to be heterogeneous after Bio-Gel P-4 chromatography on the basis of refractive index detection (see Table1). When various fraction were analyzed by negative ion LSIMS as the free oligisaccharides (2-10 ug), abundant $(M-H)^-$ ions were observed that allowed for the molecular weights to be readily determined. The most prominent species ranged from MW 1838 to 2222. The molecular basis for this heterogeneity was subsequently determined by exact mass measurements and GC/MS to be largely due the presence of an additional hexose (Gal), phosphoethanolamine and /or a $C_4H_4O_3$ moiety. For example, the oligosaccharides with $(M-H)^-$ 1960, 1999, and 2122 are different from the $(M-H)^-$ of 1837 by the addition of phosphoethanolamine (1837+<u>123</u> = 1960), hexose (1837+<u>162</u> = 1999) and hexose + phosphoethanolamine (1837+123+162= 2122), respectively. In general, we found that 5-10 ug of OS was sufficient to give an abundant $(M-H)^-$ with some limited fragment ion data also present in the spectra. More recently, we have used the new Kratos array detector on a MS 50RF for screening Bio-Gel P-4 LC fractions (1% aliquots, 0.05-1 ug) and have found that our sensitivity has increased by a factor of 10 or more (Fig. 1).

Alditol acetate analysis by GC/MS showed the presence of two terminal hexoseamines (GalNAc and GlcNAc), a terminal hexose (Gal), one to two 1,4-Gal, two 1,4-Glc, 1,3-Gal, 1,2,3-Heptose and a 1,3,4-Heptose. Previous silylation analysis also indicated the presence of a KDO in addition to phosphorous and ethanolamine. Given these data, the exact compositions of these oligosaccharides could be easily fitted to the molecular weights determined by LSIMS. This demonstrates the importance of first determining the molecular weights of the underivatized oligosaccharides. Subsequent LSIMS analyses of the permethylated and perdeuteromethylated derivatives provided additional sequence information, often complementary to that observed from the spectra of the free material. For example, the LSIMS spectra of the free oligosaccharides gave fragment ions resulting from cleavages at all ends of the structure with charge retention at both the reducing terminus and the non-reducing termini (Fig. 2) while the permethylated derivatives produced predominantly ions with charge retention at the non-reducing termini.

From these data a core structure could be proposed that was consistent both the fragmentation of free and permethylated OS. The structures we have determined for *Neisseria gonorrhoeae* JW31R OS are similar in many respects, but not identical, to that of *meningococcal* OS reported by Jennings *et al.* [2].

1. J. S. Cottrell and S. Evans (1987) *Anal. Chem.*, in press
2. H. Jennings, K. Johnson, and L. Kenne (1983)*Carbohy. Res.* **121**, 233-241
3. H. Shneider *et al.* (1984) *Infect. Immun.*, **45**, 455-549
4. M.A. Apicella and N.C. Gagliardi (1979) *Infect. Immun.*, **26**, 870-874
5. J.M. Griffiss *et al.* (1987) *Rev. Infect. Dis.*, in press

Presented at the 35th ASMS Conference on Mass Spectrometry and Allied Topics
May 24-29, 1987, Denver, CO

TABLE 1

Fraction	$(M-H)^-$ of Free Oligosaccharides
1	**2122**, 2222
2	**2122**, 2222
3	**1960**, 2060, 2122, 2222
4	1942, **1960**, 1982
5	1960, 1982, **1999**
6	1756, **1937**, **1999**, 2099
7	**1837**, **1937**, 2099
8	**1595**, **1837**, 1937
9	**1595**, **1837**, 1937

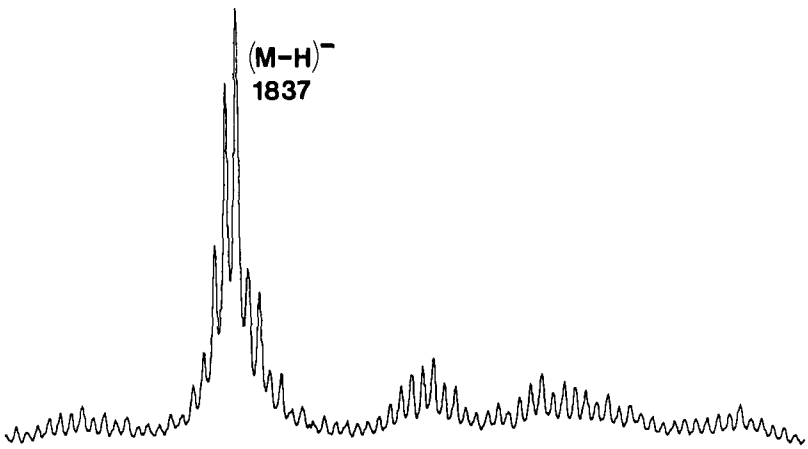

Fig. 1 LSIMS of oligosacchaides after P-4 chromatography on MS50 RF with array detector.

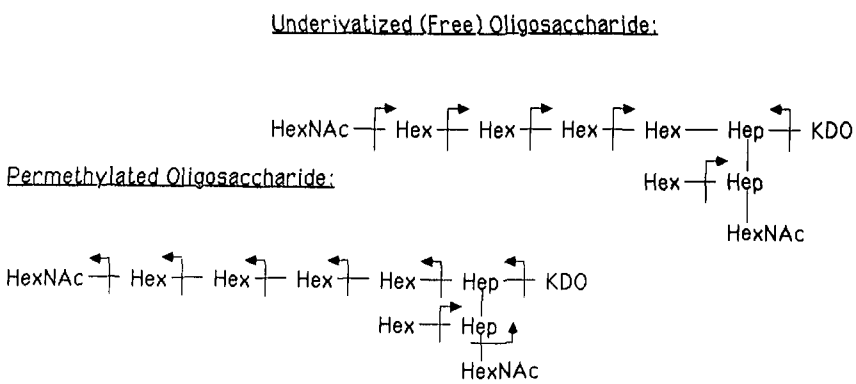

Fig. 2. *Fragmentaion of free and permethylated forms of JW31 R oligosaccharides.*

Acknowledgement: This work was supported by the NIH Division of Research Resources, Grant RR01614 (to A.L. B game).

Presented at the 35th ASMS Conference on Mass Spectrometry and Allied Topics
May 24-29, 1987, Denver, CO.

ISOLATION AND CHARACTERIZATION OF 3-(3-AMINO-3-CARBOXYPROPYL)URIDINE, A NEW NUCLEOSIDE FROM HUMAN URINE

G.B. Chheda*, H.A. Tworek*, A.K. Bhargava[a], J.A. McCloskey[†§], E. Rachlin[†], S.P. Dutta* and H.B. Patrzyc*
Depts. of Biophysics* and Laboratory Medicine[a], Roswell Park Memorial Institute, Buffalo, NY, and Depts. of Medicinal Chemistry[†] and Biochemistry[§], University of Utah, Salt Lake City, Utah

Of the 60 modified nucleosides known to be present in mammalian tRNA, nineteen have been isolated from human urine (1). Included among these are the anticodon adjacent modified nucleosides N-[N-9-β-D-ribofuranosylpurine-6-ylcarbamoyl)]-L-threonine (t^6A) and 1-methylinosine. Modified nucleosides are biosynthesized by alteration of the common nucleosides present within the tRNA precursor polynucleotide chains. Reported here is the isolation and characterization of a new hypermodified nucleoside identified as 3-(3-amino-3-carboxypropyl)uridine (I) (acp3U) (Fig. 1) isolated from the 24 hr urine collection of a normal male volunteer (160 μg) and 24 hr urine collections of a chronic myelogenous leukemia patient (42 μg) and a lung carcinoma patient (38 μg). This study constitutes the first report of the presence of 3-(3-amino-3-carboxypropyl)uridine in urine. The acp3U is known to occur in $tRNA^{Phe}$ (2).

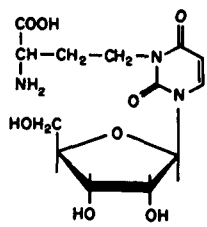

I

Fig. 1

The 24 hr urine (1490 ml) was processed according to the previously described procedure (3). The unknown nucleoside (I) present in the cis-diol fraction was purified by reversed phase high performance liquid chromatography. The ultraviolet spectra of nucleoside I exhibited a λ_{max} 263 nm in neutral (pH 6.0), acidic (pH 1.0) and alkaline (pH 11.0) media. These maxima coupled with similar molecular extinction coefficients at all pH's is suggestive of a N3 substituted uridine.

The NMR spectrum of the unknown nucleoside I in D_2O exhibited a pair of doublets centered at 7.89 ppm (J=8.0 Hz) and 5.97 ppm (J=8.1 Hz) which can be assigned to C6 and C5 protons of uridine. The anomeric doublet at 5.94 ppm (J=4.3 Hz) and the multiplet in the 3.6-4.5 ppm region are consistent with the ribose proton splitting patterns in uridine nucleosides. The multiplet centered at 2.25 ppm is in good agreement with the expected signal for the $>CH-CH_2-CH_2$ side chain of the N-3 substituent group. On the whole, the NMR spectrum agrees very well with the NMR spectrum of the authentic (acp3U) in D_2O.

Trimethylsilyl (tms) derivative of the urinary unknown (I) gave a molecular ion at m/z 633 with M-15 ion at m/z 618 (Fig. 2). Based on the mass spectra obtained by McCloskey and his associates (2) this is a spectrum of the tetra tms derivative of the 3-(3-amino-3-carboxypropyl)uridine. High resolution mass measurement for the M-15 ion at 618.2543 (calcd. 618.2519), provided the molecular composition of $C_{25}H_{51}N_3O_8Si_4$ for the molecular ion leading to the composition of $C_{13}H_{19}N_3O_8$ for the free nucleoside. The ions at masses 516 and 461 are unique to this urinary nucleoside and arise from the modified base (Fig. 3), while the ions at m/z 349, 259, 243 and 217 correspond to the unmodified sugar. High resolution mass measurement of the 516.2378 (calcd. 516.2381) ion further supported the molecular composition of $C_{13}H_{19}N_3O_8$ with a molecular weight of 345 for underivatized nucleoside I. The mass spectra of the (tms)4 derivative of authentic sample are identical to those of the urinary unknown (I). In addition to the tetrasilyl derivative, a pentasilyl derivative of this nucleoside was observed for both the unknown (I) and the synthetic nucleoside, giving molecular ion at m/z 705 and M-15 at m/z 690.

The retention time on HPLC of the naturally occurring nucleoside and authentic 3-(3-amino-3-carboxypropyl)uridine are very similar in 4 solvent systems. Comparison of the UV NMR and GC/MS spectral data and HPLC mobility

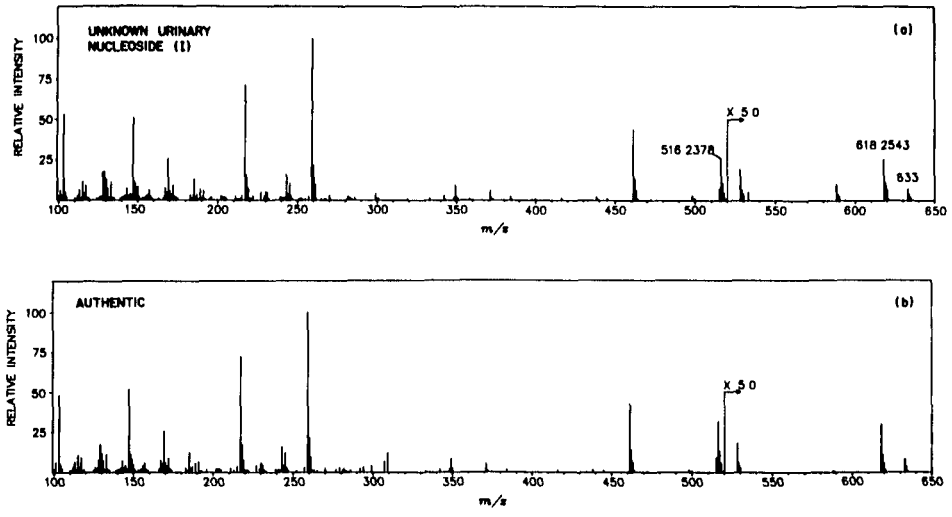

Fig. 2. Mass spectrum of (a) urinary nucleoside I and (b) of authentic 3-(3-amino-3-carboxypropyl)uridine (tms)4.

of the natural material with those of the authentic 3-(3-amino-3-carboxypropyl)uridine led to the confirmation of I as acp^{3}U.

This hypermodified nucleoside was originally isolated from the extra region (loop III) of tRNA^{Phe} of Escherichia coli. The ubiquitous presence of acp^{3}U in tRNA in various other sources suggests its conservation in evolution but with a relocation to the dihydrouridine loop (loop I) in the higher eucaryotes. It has been demonstrated that growth regulation and tRNA turnover rates influence the hypermodification phenomenon. Thus the detection of decreased levels of excretion of acp3U in the urines of the two cancer patients may suggest a perturbation of this hypermodification mechanism in the neoplastic state. Even though the functions of the hypermodified nucleosides are not well understood, the complexity and ubiquitous presence of (I) in a wide range of organisms invites speculation as to its importance in tRNA biomechanisms. The urinary excretion level of this metabolite may, therefore, be a valuable indicator for monitoring alterations in normal cellular processes and specific enzyme mechanisms.

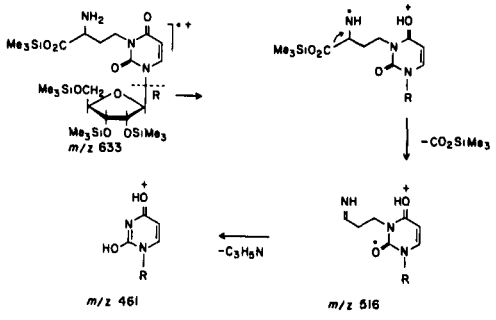

Fig. 3. Fragmentation scheme (2).

1. G.B. Chheda, In: Fasman, G., Ed., Handbook of Biochemistry, Vol. 1, Chemical Rubber Co., Cleveland, Ohio, 251 (1975).
2. Z. Ohashi, M. Maeda, J.A. McCloskey and S. Nishimura, Biochemistry 13, 2620 (1974).
3. H.A. Tworek, W. Bolanowska, A.K., Bhargava, E.M. Rachlin and G.B. Chheda, Nucleosides and Nucleotides 5. 253 (1986).

Presented at the 35th ASMS Conference on Mass Spectrometry and Allied Topics
May 24-29, 1987, Denver, CO.

CAPILLARY GC AND GCMS OF TRIMETHYLSILYL DERIVATIVES OF URIDINE, CYTIDINE AND SELECTED ANALOGS.

K.H. Schram and G. Sudhakar Reddy
Department of Pharmaceutical Sciences,
University of Arizona, Tucson, AZ 85721.

The high polarity and polyfunctional nature of nucleosides necessitates chemical derivatization in order to analyze by GC or GCMS.[1] Although a number of derivatives have been investigated for a variety of nucleosides, trimethylsilyl (TMS) derivatives have been shown to exhibit the best overall chromatographic characteristics.[2] Most of the previously reported work employed packed columns which exhibited strong tendency to form broad peaks in case of cytidine and its analogs.[3]

In an attempt to study the pharmacokinetics of the antitumor pyrimidine nucleosides by selected ion monitoring GCMS, we have investigated the capillary GC and GCMS of TMS derivatives of uridine, cytidine and their arabinosyl analogs.[4] Figure 1 shows the RIC of a mixture of these compounds. A base line separation was obtained for all the compounds including the cytidine and its analog. A 15m OV-1 capillary column was employed in this work.

It is interesting to note that a mixture of derivatized uridine, dihydrouridine (DHU) and tetrahydrouridine (THU) showed only two peaks (Figure 2) indicating the fact that the two of the above three components were being coeluted. Ion chromatograms plotted for ions m/z 593 (THU), 517 (URI) and 519 (DHU) clearly established that uridine and THU coeluted on the OV-1 capillary column. In contrast, these three nucleoside derivatives were well resolved on a 25m OV-101 capillary column, along with a minor impurity associated with THU (Figure 3). Interestingly, chromatography of uridine, DHU and THU TMS derivatives gave a single peak at 16.17 minutes on a 60m Carbowax capillary column, pointing out their decomposition to a single product. Results from this study indicate that column selection is very important in preventing the coelution and decomposition of some

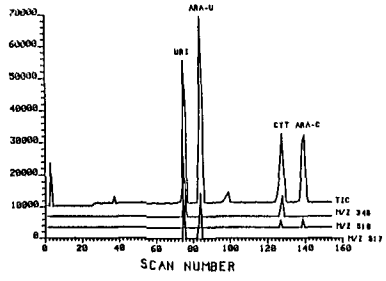

Figure 1. RIC trace of a mixture of four nucleoside TMS derivatives.

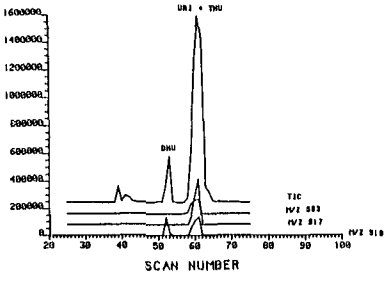

Figure 2. RIC trace showing coelution of URI and THU TMS derivatives on OV-1 Capillary Column.

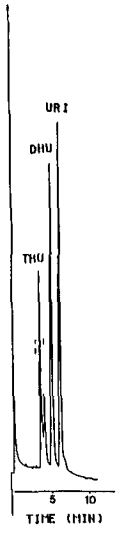

Figure 3. Separation of URI, THU and DHU derivatives on an OV-101 Capillary Column.

of these nucleosides.

The EI spectra of these nucleoside derivatives were examined which showed less abundant M^+ ions with diagnostic $(M-15)^+$, $(B+H)^+$ and $(B+2H)^+$ ions, consistent with previous data.[4] The CI spectra of DHU and THU exhibited strong $(M+H)^+$ along with other characteristic fragment ions.

One of the authors (GSR) acknowledges Shrader Analytical Laboratories, Detroit, Michigan for their generous support.

References

1. K. H. Schram and J. A. McCloskey, in GLC and HPLC Determination of Therapeutic Agents' part 3, ed. K. Tsuji, Marcel Dekkar, 1979. Pp. 1149-1189.
2. E. Csato, P. Keresztes, L. D. Szabo and D. Knausz, J. Chromatogr., 348, 280 (1985).
3. M. Jacobson, J. R. O'Brien, and C. Hedgcoth, Anal. Biochem., 25, 363 (1968).
4. For the preparation of TMS derivatives of these nucleosides see: H. Pang, K. H. Schram, D. L. Smith, S. P. Gupta, L. B. Townsend and J. McCloskey, J. Org. Chem., 47, 3923 (1982).

Presented at the 35th ASMS Conference on Mass Spectrometry and Allied Topics
May 24-29, 1987, Denver, CO

IMPROVED MATRIX FOR THE DETECTION OF NUCLEOTIDES BY FAB/MS

Hanspeter Moser and Gordon W. Wood
Department of Chemistry and Biochemistry
University of Windsor, Windsor, Ontario, Canada N9B 3P4

INTRODUCTION

FAB/MS is a well-suited method for detection and identification of nucleotides. However, use of pure glycerol as matrix produces a multiplicity of peaks in the molecular ion region, arising from a series of adduct ions. This complicates the spectra and increases the detection threshold.

Both positive and negative FAB spectra were improved by the addition of p-toluenesulfonic acid (pTSA) to the glycerol matrix. This study explores the effect of the matrix glycerol/pTSA to several nucleotides.

EXPERIMENTAL

Six different di(adenosine-5') nucleotides and P^1,P^4-di-(guanosine-5') tetraphosphate (=Gp_4G) were used as samples. All nucleotides were in the form of Na, Li, or NH_4 salts. Structure of the adenosine compounds as free phosphoric acids:

n =	2	3	4	5
Comp =	Ap_2A	Ap_3A	Ap_4A	Ap_5A

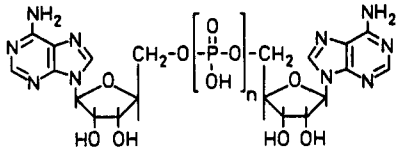

A Varian Mat CH5 DF mass spectrometer was used together with an Incos data system. The saddle field type ion gun was operated at 0.45 mA and 3.1 kV with xenon as ionizing gas.

The samples were deposited on the FAB probe tip as solutions in deionized water. The water was then evaporated and 1 µl of the matrix was added with a micropipet. The mass spectrometer was scanned at 12s/decade.

RESULTS AND DISCUSSION

With glycerol/pTSA as matrix, we usually have just one peak in the molecular ion region, corresponding to the molecular ion as free phosphoric acid plus or minus a proton ($^{\pm}$FAB), see Fig. 1a) and 1b). The formation of these ions may be rationalized in terms of exchange of Na/Li ions and protons between sample and pTSA according to their relative acidities:

$$pKa = pH + \log \frac{[\text{acid}]}{[\text{salt of acid}]}$$

From experiments with benzenesulfonic acid and 4-hydroxybenzene-sulfonic acid as additives to glycerol, it could be seen that the surfactant effect of pTSA also helped to improve the detection of nucleotides, at least by suppressing the glycerol cluster formation. The best results for the detection of the high molecular weight samples, like Ap_4A, Ap_5A, and Gp_4G, were obtained after the prepared FAB probe was sitting in the mass spectrometer for about 20 minutes.

The fact that we have not found this effect with samples like Ap_2A or Ap_3A raises the possibility of slow transport of these molecules to the surface. The detection limits were determined in positive FAB mode, with a 0.2 molar solution of pTSA in glycerol as matrix and a S/N ratio between 2 and 3. In Fig. 2, the positive FAB spectrum of 250 ng of Ap_5A is presented.

	Sample	Det. limit	Mol. weight (free acid)
Ap_2A	Na salt	200 ng	676
Ap_3A	NH_4 salt	200 ng	756
Ap_4A	NH_4/Li salt	250 ng	836
Ap_5A	NH_4/Li salt	250 ng	916
Gp_4G	Na salt	250 ng	868

CONCLUSIONS

A 0.2 molar solution of pTSA in glycerol is a useful matrix for the detection of nucleotides by FAB/MS. Compared to pure glycerol as matrix, the spectra are simpler and the detection limits are improved by a factor of ten. The following three properties of pTSA contribute to this result: 1) Solubility in glycerol; 2) High acidity; 3) Surfactant properties.

Fig. 1a): Positive FAB spectrum of 10 µg of Ap_2A in glycerol

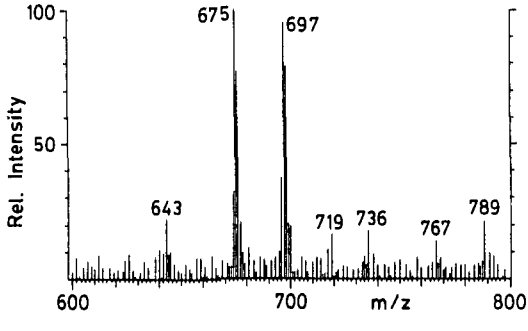

Fig. 2:

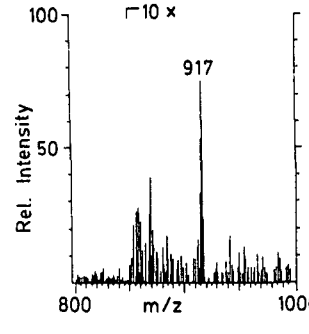

Fig. 1b): Positive FAB spectrum of 10 µg of Ap_2A in pTSA/glycerol

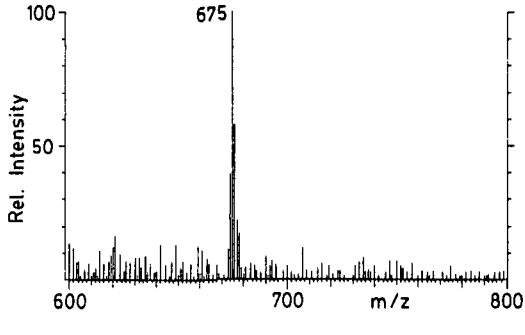

Presented at the 35th ASMS Conference on Mass Spectrometry and Allied Topics
May 24-29, 1987, Denver, CO.

DISCRIMINATION OF POSITIONAL ISOMERS OF NUCLEOSIDE MONOPHOSPHATES BY CAD/MIKES: M. Suzuki, N. Takeda, K. Masuda, K. Harada, A. Tatematsu, T. Takeda* and K. Shiratsuchi*; Faculty of Pharmacy, Meijo University, Nagoya 468 Japan and *Shimadzu Co. Scientific Equipment Division, Kyoto 604, Japan

The successful application of fast atom bombardment (FAB) mass spectrometry to the anlysis of a variety of underivatized nucleosides, nuceotides and modified nucleoside and nucleotides has been reviewed recently (1). However, the applications reported so far are mainly discussed from the viewpoint of structural characterization of constituents of nucleic acids and sequence determination of oligonucleotides. No systematic study concerning the determination of the location of the phosphoryl residue on the constituent sugar of nucleotides have been presented. The use of collisionally activated dissociation/mass analysed ion kinetic energy (CAD/MIKE) spectra can be of greart values in the analysis of isomeric compounds, even if their mass spectra are nearly identical; Kingston et al. recently described the use of CAD/MIKE spectra of $[MH]^+$ generated by FAB ionization to identify some isomeric cyclic nucleotides extracted from animal and plant tissues (2).

The purpose of the study is to evaluate the possibility and limitations of FAB in combination with CAD/MIKE spectrometry for the determination of positioal isomers (2'-, 3'- and 5'-phosphate) of nucleoside monophosphate.

A set of three positional isomers of uridine monophosphate (UMP), cytidine monophosphate (CMP), adenosine monophosphate (AMP), and guanosine monophosphate (GMP) was used as model nucleotides. All samples were obtained from Sigma Chemical Co. Nucleotides free acid forms were prepared from the commercial salts by ion exchange chromatography on TSKgel SP-Toyopearl 650M (H^+). FAB mass spectra were obtained using a reversed geometry Shimadzu GCMS 9020-DF mass spectrometer and GCMS PAC 1100 Data System. The source accelerating voltage was 3 kV. Xenon beam from the FAB gun had an energy of 6 kV. Glycerol was used as a FAB liquid matrix.

CAD/MIKE spectra of the $[MH]^+$, whose ion intensity was reduced to 20% of its original values by using helium, showed the reproducible differences among the positional isomers of all the mononucleotides examined; the ratios of diagnostic daughter ions (a_1-d) for each nucleotide were characteristic of the positional isomers (Fig. 1). The relative intensities of the main peaks are listed in Table 1. General spectral features in terms of their positional isomers are given as follows:

i) 2'-Phosphate, except for 2'-UMP (1), is easily recognized by the presence of a_3 ion; the m/z values occurred at $+\Delta 80$ mass unit compared with the corresponding a_3 ion from 3'- and 5'-phosphates.

ii) The most characteristic feature of the 3'-phosphate is the fairly abundant b ion compared with the spectra of the other phosphates.

iii) Differentiation of 5'-phosphate from 2'- and 3'-phosphates is possible; 5'-phosphate is recognized by the presence of d_2 and almost absence of d_1, while 2'- and 3'-phosphates are recognized from intense d_1 ion.

1) A. L. Burlingame, T. A. Baillie and P. J. Derrick, Anal. Chem., 58, 165R-211R (1986).
2) E. E. Kingston, J. H. Beynon and R. R. Newton, Biomed. Mass Spectrom., 11, 367-374 (1984).

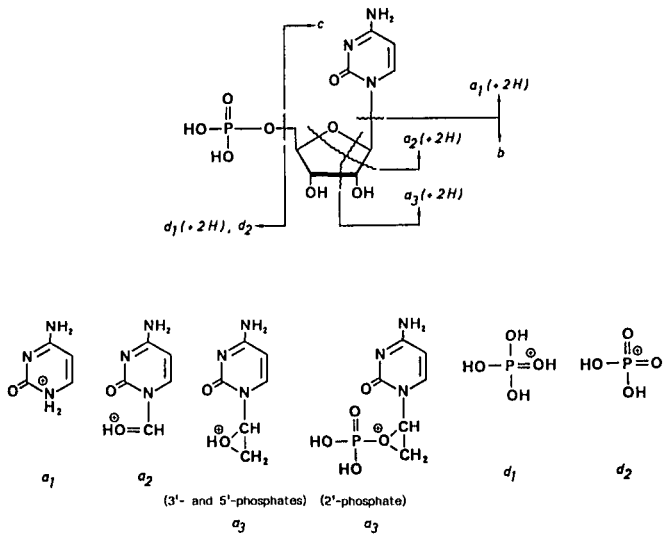

Fig. 1. Diagnostic daughter ions (a_1-d_2) for nucleoside monophosphates.

Table 1. CAD/MIKE Spectra of Protonated Nucleotide Monophosphates (1 - 12) Obtained with FAB Ionization[a]

nucleotide	$[MH]^+$	a_1	a_2	a_3	b	c	d_1	d_2	other		
2'-UMP (1)	325	113 (25)	141 (-)	235 (-)	213 (100)	227 (61)	99 (25)	97 (-)[b]	165 (10)		
3'-UMP (2)	325	113 (25)	141 (2)	155 (3)	213 (100)	227 (45)	99 (27)	97 (-)[b]	165 (12)	195[d] (3)	177[e] (4)
5'-UMP (3)	325	113 (19)	141 (2)	155 (5)	213 (33)	227 (6)	99 (-)[c]	97 (100)	165 (3)	195[d] (2)	
2'-CMP (4)	324	112 (100)	140 (-)	234 (3)	213 (3)	226 (2)	99 (7)	97 (-)[b]	164 (8)		
3'-CMP (5)	324	112 (100)	140 (2)	154 (3)	213 (6)	226 (2)	99 (11)	97 (-)[b]			
5'-CMP (6)	324	112 (100)	140 (2)	154 (3)	213 (-)	226 (4)	99 (-)[c]	97 (12)			
2'-AMP (7)	348	136 (100)	164 (13)	258 (8)	213 (2)	250 (4)	99 (8)	97 (-)[b]	119[f] (6)	178 (4)	190 (4)
3'-AMP (8)	348	136 (100)	164 (12)	178 (4)	213 (4)	250 (-)	99 (14)	97 (-)[b]	119[f] (4)		
5'-AMP (9)	348	136 (100)	164 (22)	178 (7)	213 (1)	250 (4)	99 (-)[c]	97 (25)	119[f] (6)		
2'-GMP (10)	364	152 (100)	180 (1)	274 (4)	213 (2)	266 (1)	99 (5)	97 (-)[b]	135[f] (6)	165 (10)	
3'-GMP (11)	364	152 (100)	180 (2)	194 (4)	213 (4)	266 (3)	99 (9)	97 (-)[b]	135[f] (7)		
5'-GMP (12)	364	152 (100)	180 (2)	194 (2)	213 (-)	266 (-)	99 (-)[c]	97 (12)	135[f] (4)		

[a]Relative intensities are given in parenthese. [b]Overlaps d_1. [c]Overlaps d_2. [d]$[b-H_2O]^+$. [e]$[b-2H_2O]^+$. [f]$[a_1-NH_3]^+$.

Presented at the 35th ASMS Conference on Mass Spectrometry and Allied Topics
May 24-29, 1987, Denver, CO.

BI-DIRECTIONAL SEQUENCING OF OLIGODEOXYNUCLEOTIDE ANALOGS

D. Griffin[1], E. Stirchak[3], J.E. Summerton[3], D. Weller[2], and M. Deinzer[1]
Departments of Agricultural Chemistry[1] and Chemistry[2], Oregon State University, Corvallis, Oregon 97331 and Antivirals Inc.[3], Corvallis, Oregon 97333

Oligodeoxynucleotide analogs with carbamate linkages between the sugars, instead of the usual phosphate linkages, have been synthesized. There are no nucleases to digest these biopolymers and, therefore, there are no standard sequencing protocols available. Fast atom bombardment mass spectrometry (FABMS) in the negative ion mode was used to confirm structures of these molecules, which ranged in length from dimers to eleven-mers (Table 1).

Typically (figure 1) amino groups on adenine and cytidine were blocked with the benzoyl (Bz) group and guanine was blocked by the phenylacetyl group. The 3' hydroxyl group of the terminal cytosine in one dimer was blocked also with a nitrobenzoyloxy group, and all 5' amino groups were blocked with the monomethoxytrityl group.

Negative ion fast atom bombardment mass spectra were obtained on a KRATOS MS-50-TC-RF mass spectrometer. Crystalline samples were added to a thin film of monothioglycerol or "magic bullet" on a copper target, which was cooled with freon to prolong sample lifetime. A saddle field neutral beam gun was used to generate a beam of xenon atoms with beam voltage of +8 KV. Post acceleration detection was used at +25-30 KV.

Protected oligodeoxynucleotide analogs with carbamate linkages yield fairly intense $(M-H)^-$ ions when analyzed by negative ion FABMS (figure 2). Under these conditions they also fragment to yield ion series which can be used to determine the sequence of shorter chain oligodeoxynucleotides. Cleavage of the 3'-oxygen-carbonyl carbon bond occurs regularly up to five monomer units. Cleavage of the 5'-nitrogen-carbonyl carbon bond also occurs, but not as readily, and the ion series from this cleavage is less reliable.

Unprotected oligodeoxynucleotides show intense $(M-H)^-$ ions, but fragmentation occurs at the 3'-carbon-oxygen bond and at the 5'-carbon-oxygen bond of the phosphodiester group (Grotjahn, et al., 1982), yielding a predictable ion series for sequencing in both directions.

Acknowledgement

This work is supported in part by Public Health Service Grant ES03874.

Reference

1. Grotjahn, L.; Frank, R.; Blöcker, H. Nucleic acids Res. 10, 4671 (1982)

Presented at the 35th ASMS Conference on Mass Spectrometry and Allied Topics
May 24-29, 1987, Denver, CO.

Figure 1.

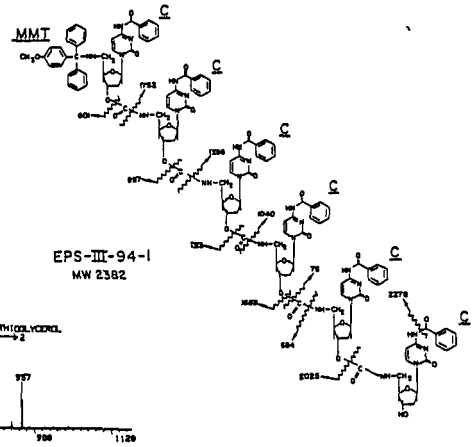

Figure 2.

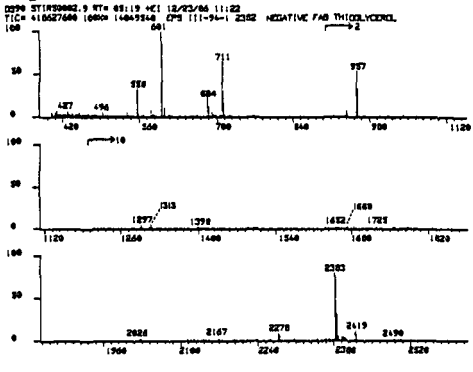

Table 1.

Oligonucleotides STUDIED

Number	Oligodeoxynucleotide analog	Calculated (M-H)⁻	Measured (M-H)⁻	Confirmed Fragments A	Confirmed Fragments B
OV-II-27-1 ($C_{28}H_{31}O_{19}N_{10}$)	5' 3' mmT HN-C-G-OH	1011.37893	1011.36	601	
OV-II-29-1 ($C_{24}H_{29}O_{19}N_{10}$)	5' 3' mmT HN-C-A-OH	981 38637	981 35	601	
EPS-III-69-1 ($C_{60}H_{52}O_{14}N_6$)	5' mmT HN-C-C-O-C-O-(⟨⟩)-NO_2	1122 36334	1122.31	601	(494)
EPS-III-73-1 ($C_{87}H_{81}O_{20}N_{16}$)	5' 3' mmT HN-C-C-C-C-OH	1669.58126	1669.53	601, 957, 1313	(328), 684, 1041
OV-II-6-1 ($C_{31}H_{31}O_{18}N_{22}$)	5' 3' mmT HN-A-A-G-C-OH	1771.62552	1771.60	625, 1005, 1415	(328) (738) (1118)
OV-II-8-1 ($C_{31}H_{32}O_{18}N_{22}$)	5' 3' mmT HN-G-C-A-A-OH	1771.62552	1771.73	655, 1011, 1391	(352) (738) (1088)
EPS-III-94-1 ($C_{121}H_{113}O_{30}N_{24}$)	5' 3' mmT HN-C-C-C-C-C-C-OH	2381 80537	2381 87	601, 957, 1313, 1669, 2025	684, 1040, 1396, 1752
OV-II-38-1 ($C_{197}H_{140}O_{38}N_{41}$)	5' 3' mmT HN-G-C-C-A-T-A-G-G-OH	3215 09080	3215.26	665, 1011, (1367), 1747	382, 792, 1172 (1439) (1819), (2175)
OV-II-39-1 ($C_{188}H_{144}O_{38}N_{39}$)	5' 3' mmT HN-G-C-C-A-T-A-C-G-OH	3161.06901	3161 35	655, 1011, (1367), (1747)	382, 738, 1118 1385 (1765)
OV-II-43-1 ($C_{211}H_{164}O_{44}N_{44}$)	5' 3' mmT HN-G-C-A-A-T-G-A-A-A-G-C-OH	4355.46068	4355	655, 1011, (1391), 1771, (2329)	2555, (3316)

Presented at the 35th ASMS Conference on Mass Spectrometry and Allied Topics
May 24-29, 1987, Denver, CO

ENHANCED SENSITIVITY OF LITHIUM-OLIGONUCLEOTIDE SALTS USING POSITIVE ION FABMS

Julie A. Leary, Sherri Ogden, Stefan Krolik, Chris Porter
College of Chemistry, University of California, Berkeley

It has been shown that repetitive scanning of concentrated oligonucleotides is often required to obtain molecular ion and sequence information using negative ion Fast Atom Bombardment Mass Spectrometry (FABMS) (1,2). The goal of this project was to determine how to render oligomers more amenable to FABMS so that less material would be needed for analysis. The attachment of Li to oligonucleotides immediately prior to mass spectral analysis has been investigated as a possible means of accomplishing this goal.The triethyl ammonium salt of a partially protected ribonucleotide, (5'C-U-A-A 3'), was dissolved in 0.07M LiCl, mixed with a 1:1 mixture of glycerol:thioglycerol, and 1 uL (corresponding to 500 ng) deposited onto the probe tip. A single scan spectrum was recorded in the positive ion mode and the resulting spectrum and fragmentation scheme shown in Figures 1 and 2 respectively. Table 1 is a list of the corresponding mass assignments. Very recently, this data has been obtained on less than 175 ng using a somewhat different procedure (3). In comparison, 1.5 ug of the original triethylammonium salt was required to obtain a similar intensity spectrum when run under the same conditions in the negative ion mode. Sequence ions were not observed at this concentration in the negative ion spectrum. The one problem arising in the lithium spectrum however, is the sometime low signal to noise ratio which is highly dependant on the concentration of LiCl used i.e.; high concentrations of Li can dominate the spectrum and obscure fragment ions. It was therefore anticipated that the MS/MS experiment would rectify this problem. Although the MS/MS data was somewhat "cleaner" and structural data was evident, the expected sequence ions arising from cleavage at the phosphate bonds was not seen (Figure 3). We have subsequently started using a lithiated Dowex column in order to exchange the triethyl ammonium ions and therefore lower the amount of excess Li present in solution.

Refs.
1. Grotjahn,L., Blocker,H., Frank,R.; Biomed. Mass. Spec., 1985, 12,(9), 514-524.
2. Grotjahn,L., Frank,R., Blocker,H.; Nucl. Acids Res., 1982, 10 (15), 4671-4679.
3. Leary,J., Ogden,S., Unpublished results

Acknowledgements
The authors wish to thank Mr. Spencer Cahill and Prof. Peter Schultz for providing us with the triethylammonium salt of CUAA and Mr. John Hanson and Prof. Paul Bartlett for the lithiated thermolysin inhibitor.

Presented at the 35th ASMS Conference on Mass Spectrometry and Allied Topics
May 24-29, 1987, Denver, CO

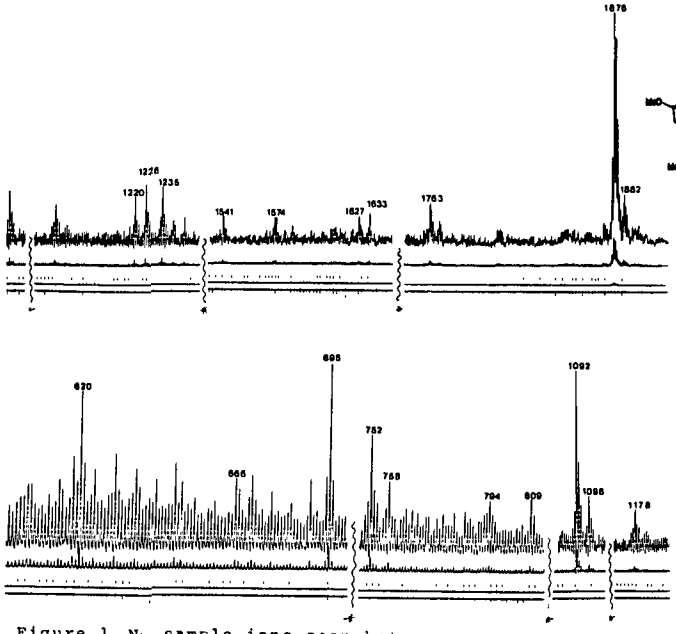

Figure 1. No sample ions seen between segments

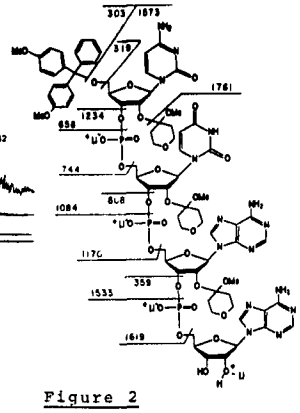

Figure 2

Table 1: FABMS MASS ASSIGNMENT

1882	[M-H + 2 Li]
1876	[MHLi]
1769	[M-MTHP + Li + H]
1763	[M-MTHP + 2 H]
1633	[1619 + 2 Li]
1627	[1619 + Li + H]
1574	[M-trityl + H]
1541	[1533 + Li + H]
1235	[1234 + H]
1184	[1170 + 2 Li]
1178	[1170 + Li + H]
1098	[1084 + 2 Li]
1092	[1084 + Li + H]
809	[808 + H]
758	[744 + 2 Li]
752	[744 + Li + H]
666	[658 + Li + H]
360	[359 + H]
303	trityl group

* MTHP = methoxy tetrahydropyran

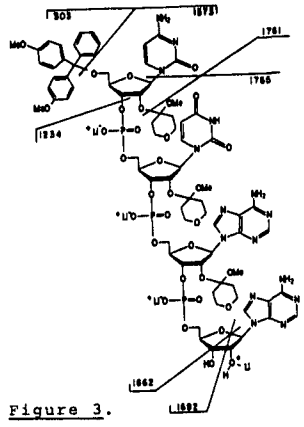

Figure 3.

Presented at the 35th ASMS Conference on Mass Spectrometry and Allied Topics
May 24-29, 1987, Denver, CO

DIFFERENTIATION BETWEEN ISOMERIC O-ALKYLTHYMIDINES BY TIME-OF-FLIGHT SIMS

F.Lafortune[A], R.Beavis, B. Schueler, X.Tang, K.G.Standing and J.B.Westmore, Chemistry and Physics Departments, [A]Collège Universitaire de Saint-Boniface and University of Manitoba, Winnipeg, Canada R3T2N2.

INTRODUCTION

Alkylation of pyrimidine oxygens in DNA has been implicated in mutagenesis and carcinogenesis. The size of the alkyl group has also been found to correlate with the carcinogenic potency of such compounds (1). We have analyzed some of these modified nucleosides [a series of O2 and O4-alkylthymidines (alkyl = Me,Et,iso-Pr, figure 1), synthesized in our chemistry department (2)] with the Manitoba II time-of-flight (TOF) mass spectrometer, which incorporates an ion mirror (3). We will demonstrate how this technique can reveal unequivocal indicators of the isomeric form.

EXPERIMENTAL

1. Sample preparation:

O-alkylthymidines were dissolved in methanol containing less than 10% water, at a concentration of ca 1 mg/ml. A few μL of each solution were then deposited on aluminum foil treated to give a boehmite, AlO(OH), surface.

2. Mass spectrometry:

Sample targets were bombarded by a pulsed beam of primary Cs+ ions (2 ns pulses full width at half-maximum, repeated at a frequency of 2 kHz). The Cs+ ions struck the target with an energy of 13 keV for positive ion studies, and 23 keV for negative ion studies, respectively. The secondary ions produced and ejected, which had a lifetime larger then ca 10^{-7} s, were then accelerated to +/- 5 keV and allowed to drift along the flight tube. When the ion mirror is off, "direct" mass spectra are obtained. When an electric field is applied on the ion mirror, reflected spectra are produced, where stable ions are separated from daughter ions and neutrals, as described in an accompanying paper (4).

DIRECT SPECTRA

In both positive and negative ion spectra, the two most important fragmentations involve dealkylation and the loss of the sugar moiety. In all instances, they are accompanied by hydrogen transfers. Both mechanisms have been interpreted by a McLafferty-type rearrangement (figure 2). In +ve spectra, quasimolecular ions are present in significant yields, whereas they are hardly detected at all in -ve spectra. Contrary to what has been observed in solution (5), dealkylation succeeds the loss of sugar in positive spectra, while in the negative mode, dealkylation can be concomitant with, or can even precede the loss of sugar. Deglycosylation,with charge retention on the base,is more favored for O4-alkylthymidines, while charge retention on the sugar (+ve mode) is more predominant with O2-isomers.

METASTABLE ION STUDIES

A reflecting TOF-mass spectrometer can help establish *genetic relationships* (metastable mapping) between secondary ions. Daughter ion spectra can be obtained (4) by extracting from reflected spectra only those ion fragments that are correlated with selected neutral fragments. Fragmentation pathways for +ve O-alkylthymidine ions spectra are illustrated in figure 3.

Half-lives and rate constants have also been measured for several metastable ions. In particular, [M+Na]+ ions of O4-alkylthymidines were found to be significantly more stable than those of O2-alkylthymidines. This difference in stability suggests that the O2-keto oxygen of O4-alkyl molecules is involved in chelation of Na+, perhaps in a complex (figure4) which involves a syn orientation about the N-glycosyl bond and simultaneous binding to the sugar O4' and O5' atoms. A similar complex would seem less likely for [M+Na]+ ions of O2-alkyl molecules

Unimolecular rate constants thus provide useful tools to differentiate isomeric compounds by TOF-SIMS. Investigations with more challenging isomeric problems such as diastereomeric oligonucleotides are currently under way.

REFERENCES

(1) B.Singer, Cancer Research 46, (1986) 4879
(2) G.Birnbaum *et al*, J.Am.Chem.Soc. 108,(1986) 1671
(3) K.G.Standing *et al*, Analytical Instrum. 16(1), (1987) 173
(4) X.Tang *et al*, these proceedings
(5) B.Singer et al, Biochemistry 17, (1978) 1246

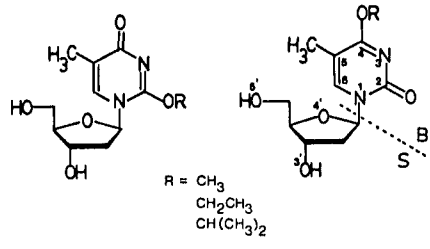

FIGURE 1 O2 and O4-alkylthymidines

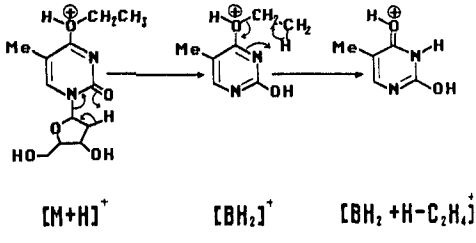

FIGURE 2 Deglycolysation and dealkylation of O4-ethylthymidine

METASTABLE MAPPING

$$[2M+Na]^{+} \rightarrow [M+Na]^{+} \rightarrow [BH+Na]^{+} \rightarrow [BH+Na\text{-alkene}]^{+}$$

$$[M+H]^{+} \rightarrow [BH_2]^{+} \rightarrow [BH_2+H\text{-alkene}]^{+}$$

$$[\text{sugar}]^{+} \rightarrow [\text{sugar}-H_2O]^{+}$$

$$\rightarrow [\text{sugar}-44]^{+}$$

FIGURE 3 Metastable mapping for positive ion spectra of O-alkylthymidines

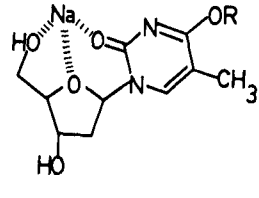

FIGURE 4 Chelation of Na by O4-alkylthymidines

Presented at the 35th ASMS Conference on Mass Spectrometry and Allied Topics
May 24-29, 1987, Denver, CO

SEQUENCING OF A PEPTIDE ISOLATED FROM HUMAN SEMEN

K. Schneider, J. Reiner, G. Spiteller,
Institut für Organische Chemie I, Universität Bayreuth,
D-8580 Bayreuth / W. Germany

INTRODUCTION

Peptide structure elucidation requires two procedures: amino acid determination and sequencing. Sequencing of peptides in minute quantities (about 0.5-1.0 nanomoles) is achieved by Edman degradation /1/. Far more material is needed for the amino acid determination. The amino acid determination can be circumvented by a molecular weight determination by soft ionisation MS /2/.

COMBINATION OF EDMAN DEGRADATION WITH MS

In principle sequencing of peptides by MS is possible, but the samples used for MS must be perfectly pure, in order to enable detection of fragment ions. Even then complete sequencing without any additional information seems to us in many cases ambiguous. Additional methods must be applied, e.g. derivatisation or an Edman degradation. We have found that the material used for MS can be recovered unchanged from the introduction rod and, after purification (without loss) by HPLC, may be used for a subsequent Edman degradation, thus avoiding amino acid determination.

STRATEGY

Purification of biologically occurring peptides is achieved by dialysis, gel filtration chromatography, ion exchange chromatography and finally reversed phase HPLC. Collected samples are subjected to lyophylisation in order to remove the solvent. The residue is dissolved in 0.11% TFA/50% MeCN and transferred to the rod, a number of spectra is run (about 30-80), and the average spectrum of these runs is recorded /3/. The sample is then removed from the rod with methanol. The solution is purified by HPLC. Then the sample is degraded according to the modified Edman procedure of Chang and Wittmann-Liebold (double derivatization with DABITC and PITC) /1/. Carboxylic and -amide groups may be determined by reacting sample with HCl/CH_3OH - after an hour at 100°C they are converted quantitavely into $COOCH_3$ /4/. The amino terminus is determined by reaction with dansyl chloride (Dns-Cl) /5/.

EXAMPLE

A previously unknown peptide was isolated from human seminal plasma by a combination of dialysis, gel-, ion exchange-, and HPLC-chromatography. At first no molecular ion could be detected in its LSIMS spectrum. The peptide was therefore subjected to enzymatic cleavage reactions with (i) trypsin, giving the fragments T1, T2 and T3 and (ii) chymotrypsin, resulting in the fragments C1 and C2. The fragments were purified by HPLC.

The LSIMS mass spectrum of C1 showed $MH^{\oplus}$ at mass 805. The spectrum allowed partial sequencing from the C-terminus (sequence: L/I-P-S-E-F till mass 231). This mass fits only with the dipeptides N-V or G-R or the reverse sequences V-N or R-G.

A distinction between these four possibilities was achieved by adding one drop CH_3OH/2N HCl to the sample C1: The shift of the $MH^{\oplus}$ in the LSIMS spectrum of the reaction product from mass 805 to mass 833 indicated the presence of two ester groups, excluding the N-terminus of either N-V or V-N.

To differentiate between G-R or R-G the sample was reacted with dansyl chloride. After hydrolysis Dns-Glycin was detected with HPLC. Distinction between I and L was possible by reacting the hydrolysate with Dns-Cl, followed by HPLC. Thus C-1 was shown to have the sequence G-R-L-P-S-E-F.

C2 had a $MH^{\oplus}$ of mass 1413, but due to the lack of fragments sequencing was not possible.

The tryptic fragments T1 and T2, had $MH^{\oplus}$ ions of mass 504 and 1501. No molecular ion could be obtained from T3. T3 was therefore subjected to a chymotryptic cleavage which provided two products, CT2 and CT1. CT1 was identical with C1, CT2 showed a $MH^{\oplus}$ of mass 928, but only a few sequence specific ions: therefore it was sequenced according to Chang and Wittmann-Liebold /1/, giving the sequence S-Q-F-P-H-G-A-G-K. In the same manner the structure of T1 was determined to be G-Q-H-Y.

Chymotryptic cleavage of T2 gave two fragments. The first (CT3) had $MH^{\oplus}$ 592 and had the same sequence as C1 except that the N-terminus of C1 (G-R) was missing. The second fragment was identical with CT2.

If the MW of the chymotryptic fragments C1 (804) and C2 (1412) are added and water (= 18 amu) is substracted one ends up with a MW of 2198. The same MW is obtained if the fragments of the tryptic cleavage products T1 (503) and T3 (combination of CT1 (804) and CT2 (927) are added and two molecules of water are substracted.

The N-terminus determination of the intact peptide showed the sequence G-R, consequently the structure of the peptide is:

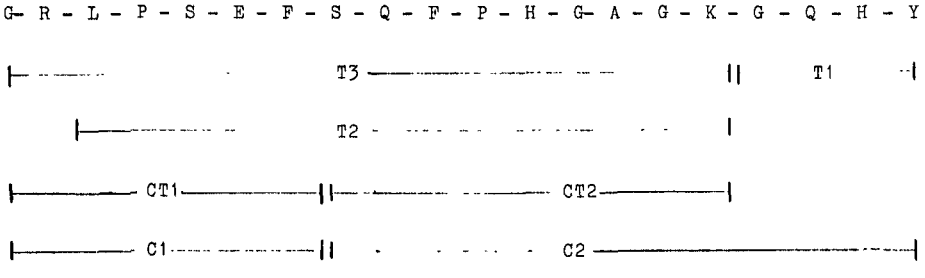

REFERENCES
1) J.Y. Chang, D. Bauer, B. Wittmann-Liebold, FEBS lett., 93, 205 (1978).
2) M. Barber, R.S. Bordoli, R.D. Sedgwick, A.N. Tyler, J. Chem. Soc. Chem. Commun., 325 (1981).
3) L. Grotjahn, L.C.E. Taylor, Org. Mass Spectrom., 20, 146 (1985).
4) M.A. Young, D.M. Desiderio, Anal. Biochem. 70, 110 (1976).
5) W.R. Gray, Methods in Enzymology, 25 121 (1972).

Presented at the 35th ASMS Conference on Mass Spectrometry and Allied Topics
May 24-29, 1987, Denver, CO

IDENTIFICATION OF MODIFIED AND UNMODIFIED BASES AND NUCLEOSIDES USING SELF-CHEMICAL IONIZATION FOURIER TRANSFORM ION CYCLOTRON RESONANCE MASS SPECTROMETRY

R.R. Weller, J.A. Mayernik, and C.S. Giam
Department of Industrial Environmental Health Sciences
Graduate School of Public Health
University of Pittsburgh
Pittsburgh, PA 15261

The reactions of active carcinogens with nucleic acids or their constituents to form adducts are believed to be the initial events leading to mutation and malignant transformation resulting from chemical exposure. The identification of specific nucleotide adducts in vivo is an essential step in assessing the potential use of nucleotide modification as an indicator of genotoxic damage. Many mass spectrometric techniques have been used for adduct identification but self-CI FT-ICR-MS is the most successful in producing a molecular ion peak.

Self-CI FT-ICR mass spectra of uracil, thymine, cytosine, adenine, guanine, uridine, thymidine, cytidine, adenosine, guanosine, O^6-methylguanine, 7-methylguanine, O^6-ethylguanine, 1,N^6-ethenoadenine, and 3,N^4-ethenocytidine were greatly improved over those obtained under EI conditions. A protonated molecular ion peak was observed for all compounds and in the majority it was a single intense peak (Figures 1, 2). Under broadband, medium resolution conditions all but one peak resulted in mass errors of less than 20 mAMU (half less than 5 mAMU).

The ability to give an excellent pseudo-molecular ion with no sample preparation, derivatization, or interfering ions makes it an excellent method for the qualitative analysis of mixtures. The spectrum of an equimolar mixture of bases and adducts (Figure 3) produced an easily identifiable $(M+H)^+$ peak for each component. Similar results were obtained for a mixture of nucleosides (Figure 4). The results indicate that the relative proton affinities are similar enough for qualitative analysis.

As shown, self-CI, a unique feature of FT-ICR, provides an excellent technique to identify nucleic acid constituents. Coupled with the other capabilities of FT-ICR and the trapping cell (e.g. MS^n and CID) self-CI may provide an excellent method to easily identify and characterize an important class of compounds.

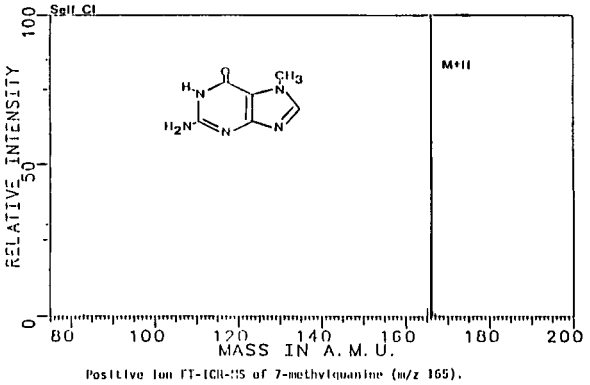

Figure 1

Positive Ion FT-ICR-MS of 7-methylguanine (m/z 165).

Presented at the 35th ASMS Conference on Mass Spectrometry and Allied Topics
May 24-29, 1987, Denver, CO

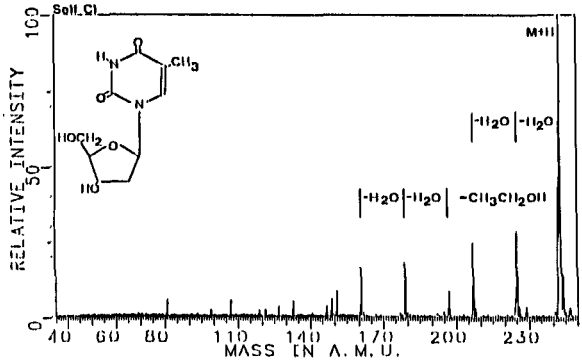

Positive Ion FT-ICR-MS of Thymidine (m/z 242).

Figure 2

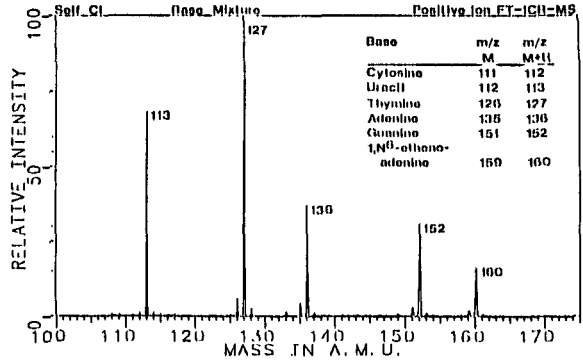

Figure 3

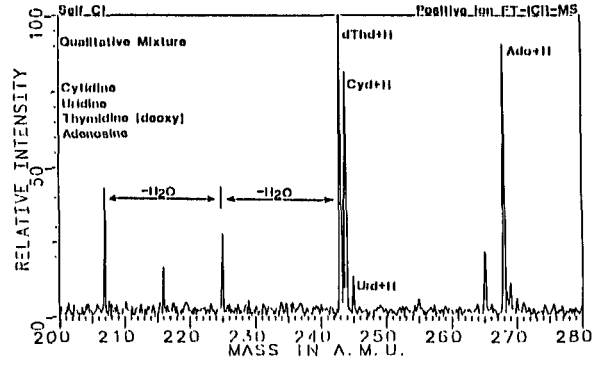

Figure 4

Presented at the 35th ASMS Conference on Mass Spectrometry and Allied Topics
May 24-29, 1987, Denver, CO

MASS SPECTROMETRY OF NEW DIDEOXYNUCLEOSIDES AND 4-THIODIDEOXYNUCLEOSIDES

Maya B. Kempff and Robin Hood, Chemistry Dept., Wayne State University, Detroit, MI, 48202
Jerome P. Horwitz and Eduardo Palomino, Michigan Cancer Foundation, Detroit, MI, 48202

INTRODUCTION

Dideoxynucleosides are currently the compounds of choice for treating serious manifestations of infections in patients with acquired inmunodeficiency syndrome (AIDS)[1]. 3-Azido-2',3'-dideoxythymidine (azidothymidine or AZT), the first compound of this kind to be approved against AIDS, causes depression of the bone marrow as a significant side effect, limiting its use to severely infected patients. Another limitation of AZT is its poor distribution in the Central Nervous System (CNS) where the AIDS virus concentrates causing dementia and other neurological disorders. In our search for compounds with better therapeutic profile against AIDS we have focused our efforts on the modeling of the framework of AZT using two basic concepts: 1) replacement of the azido moiety (N3) with groups containing multiple bonds (CN, NC, CNO, NO2, etc.) with the purpose of increasing its overall activity, and 2) replacement of one or two of the oxygen atoms in the base to improve its distribution in the CNS and reduce the severity of its side effects.
The preparation of dideoxynucleosides follows standard guidelines but some of the intermediates are prone to rearrangements and eliminations. An acceptable method to characterize intermediates and products in the synthesis of dideoxynucleosides was sought[2,3], and the results of the mass spectrometric studies of some of these compounds are presented here.

RESULTS AND DISCUSSION

4-Thiothymidine, early precursor for the formation of the thio-analogue of AZT, gives under EI conditions a predominant fragmentation pattern of the base thiothymine and the deoxysugar with a very small molecular ion (Fig Ia). Under TSP conditions $(M+H)^+$ is the most intense ion with little structural information from fragmentation (Fig Ib). When CI+ analysis is performed on this compound using isobutane as the reagent gas (Fig Ic), not only the $(M+H)^+$ ion is obtained but the fragmentation of the deoxynucleoside and its structural components can be easily assigned. These results confirm the fact that under mass spectrometry oxygenated precursors of dideoxynucleosides are relatively more stable molecules than the dideoxynucleosides themselves, and that the overall stability of the molecule is more dependent on the substitution on the sugar moiety than on variations of the base

Protection of the 5' position of 4-thiothymidine with a trityl group renders an unstable molecule under EI, CI+ and other techniques. This unstability is due predominantly to the formation of the very stable triphenylcarbonium ion (Ph_3C^+, M/Z=243). It was reasoned that a negative mode of a soft technique should override the electron-donating abilities of the trityl group, and implementation of CI- (Fig IIa) gave the molecular ion along with fragments of important structural information. Similar criteria was used for the

selection of CI+ as the method of analysis of the new dideoxynucleoside 3'-azido-4-thio-2',3'-dideoxythymidine (Fig IIb) and of the mesylated intermediate 3'-methanosulfonyl-2',3'-dideoxythymidine (Fig IIc). This approach clearly demonstrates that mass spectrometry can be suited to the chemical behaviour of the dideoxynucleoside analogue under analysis, a method that avoids chemical derivatization in some cases. Other dideoxynucleosides and intermediates that analyzed successfully by a combination of +/-CI includes fluoro and cyano analogues of AZT and some dideoxycytidines. Our research in this area continues on MS of more unstable dideoxynucleosides bearing multiple-bond substituents.

FIG I

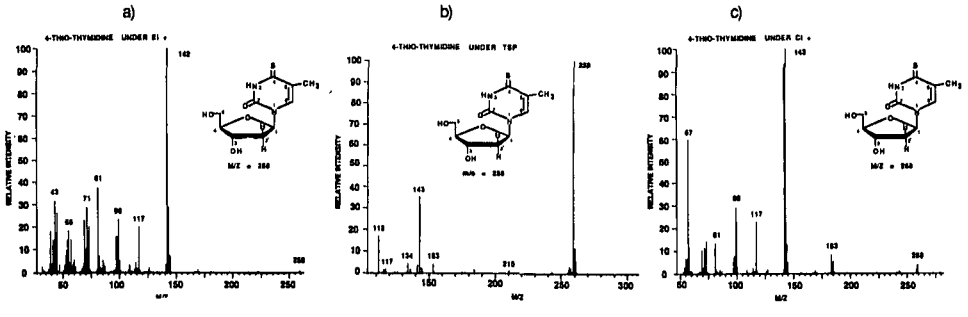

FIG II

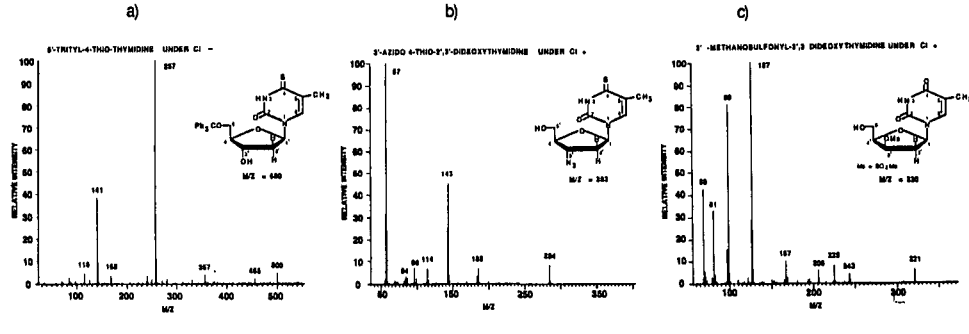

References

1. AIDS: Modern Concepts and Therapeutic Challenges; Samuel Broder, editor. Marcel Dekker, Inc. 1987, pp 303-333.

2. Puzo, G; Wieber; J.L. Nucleic Acid Res., 1981, 9(18), 4655

3. McCloskey, J.A., in Basic Principles in Nucleic Acid Chemistry Vol 1, pp 209-309, Academic Press, N.Y.

Presented at the 35th ASMS Conference on Mass Spectrometry and Allied Topics
May 24-29, 1987, Denver, CO

MASS SPECTRAL ANALYSES OF OLIGONUCLEOTIDES AND PRODUCTS OF BENZO[a]PYRENE REACTIONS WITH DNA IN VIVO AND IN VITRO

JOHN J. DINO, JR., CHRISTIAN R. GUENAT AND DAVID G. KAUFMAN*
LABORATORY OF MOLECULAR BIOPHYSICS, NIEHS, RTP, NC, 27709 and
*UNIVERSITY OF NORTH CAROLINA DEPARTMENT OF PATHOLOGY, CHAPEL HILL, NC 27514

Benzo[a]pyrene (BP) is a potent mutagen and carcinogen in a variety of in Vitro and in Vivo systems. It is a byproduct of organic combustion, and is ubiquitous in man's environment. Metabolic activation by the mixed-function oxidase enzyme system in Vivo is believed to be a key event in the initiation of neoplasia by BP. The resulting electrophilic arylalkylating agents react with cellular macromolecules such as DNA, RNA and proteins.

Adducts of BP metabolites with DNA have been measured in Vivo and in Vitro, and attempts have been made to correlate adduct levels with biological endpoints such as mutation frequencies or tumor incidences (1). In many of these studies, carcinogen-modified DNA is extracted from the organs of interest, enzymatically digested to nucleosides, and chromatographed on Sephadex LH-20 or reverse-phase HPLC columns with methanol/water gradients.

In addition to DNA adducts, a common finding in studies using tritiated BP has been the appearance of peaks bearing radioactivity in the early portion of chromatograms (1). Based on the fact that LH-20 and C-18 columns retain non-polar compounds, and the demonstration by this material of UV absorbance at 260 nm, we initially hypothesized the presence of carcinogen-modified oligonucleotides. Identical patterns of "early eluting" peaks have also been obtained with other tritiated carcinogens and in a variety of animal strains and organs (2). Many attempts to identify the components of these peaks have given equivocal results (3). It was the objective of this study to characterize these materials with chromatographic and mass spectral techniques.

Initial modelling studies examined the chromatographic and mass spectral behavior of unmodified oligonucleotides and oligonucleotides reacted in Vitro with the ultimate metabolite of BP, benzo[a]pyrene diol-epoxide (BPDE). An HPLC column, containing 5 micron silica which was coated with polyethyleneimine and cross-linked with ethylene diglycidyl ether, was developed for these compounds (4). It utilizes a potassium phosphate/ammonium sulfate binary buffer system. This column was found to be very effective for separating complex mixtures of oligonucleotides modified in Vitro with BPDE. Either UV or fluorescence detection was used.

Mass spectral analyses of unmodified oligonucleotides, utilizing negative ion FAB with CAD and MS/MS demonstrated "sequence" ions resulting from cleavage of bonds at the 3' or 5' side of the internucleotide linkage. Additional masses were observed, such as loss of water from sequence ions. Spectra were obtained in single runs, from as little as 5 micrograms of material. FAB studies done in positive ion mode gave some sequence information for particular oligonucleotides, but the spectra were complicated by many additional fragmentations. With dAGCT, for example, there were ions corresponding to losses of the bases from the phosphate/sugar backbone.

Mass spectral studies of BPDE-modified oligonucleotides, using the negative ion FAB technique mentioned above, gave sequence ions equivalent to those for unmodified oligonucleotides, with some of the ions shifted 302 mass units higher due to the presence of the BPDE moiety. A major peak for loss of BPDE was also observed. In the case of pCTCT, fragment ions indicative of both possible reaction products were observed.

In Vivo studies examined the contents of radioactive peaks from liver tissue of A/HeJ mice treated with 2 mCi of tritiated BP. Liver DNA was extracted, deproteinated and ethanol precipitated. Purified DNA was digested with DNase I, venom phosphodiesterase and alkaline phosphatase. The digest was pumped through a Waters C-18 precolumn containing 0.1 grams of sorbent. The eluent was water at 1 ml per minute, and 100 0.5 ml fractions were collected. Two major peaks were observed in the plot of DPM vs. fraction number.

When fractions comprising the first peak were chromatographed on the Polyethyleneimine-coated column, the peak patterns were indistinguishable from those for standard mixtures of RNA and DNA nucleosides. A second HPLC system was therefore developed, utilizing a Waters C-18 column and isocratic elution with ammonium formate buffer. This system had proven effective previously for separating nucleosides of DNA and RNA. When a concentrate of fractions comprising the first digest peak was run on this column, ten peaks were observed. Four coincided with the nucleosides of DNA, and four with RNA. Two peaks are currently unidentified. A concentrate of the second peak gave a peak pattern identical to the first; the peaks were merely smaller. This led to speculation that the two "peaks" in the digest chromatogram actually represent sequential elutions of the same radioactive material from the 2.5 ml sample loop. The precolumn has only 25 theoretical plates, and it is difficult to imagine it being able to achieve baseline resolution of similar compounds.

Electron impact mass spectrometry was performed on a concentrate of fractions comprising the first digest peak. The spectrum contained peaks from thymine, adenine and guanine, as well as 2' deoxyribose and phosphoric acid, which was a byproduct of the enzymatic digestion. Also observed were peaks from tris hydroxymethyl aminomethane, which is used to buffer the digestion. No peaks representative of tritiated nucleosides were observed, although this is probably due to the fact that their concentrations were below the limit of detection of the instrument. Multiple C-18 chromatogram runs of this material have been made and the peaks collected and counted for tritium activity; calculations have shown that approximately 75% of the tritium in the digest chromatogram is exchanged into nucleosides. Positive ion FAB was performed on the concentrate, due to the lack of molecular ion peaks for the DNA nucleosides in the EI spectrum. The FAB spectrum demonstrated protonated molecular ions for each of the DNA nucleosides. Again, peaks representative of tritiated nucleosides were not seen.

CONCLUSIONS

The major components of "early-eluting" material from liver tissue of A/HeJ mice are nucleosides of DNA and RNA. Also present are phosphoric acid and tris buffer from the digestion procedure.

Tritium exchange between BP and unmodified nucleosides is responsible for the majority of radioactivity in these peaks. Previous studies have shown that enzymatic activity is necessary for the exchange to occur; it does not occur in Vitro.

Both EI and FAB mass spectrometry and HPLC using UV or fluorescence detection were useful tools in examining this difficult biological question.

REFERENCES

1. Anderson, M.W., et al. Cancer Res., 41, 4309-4315 (1981).
2. Eastman, A., et al., Chem-Biol interact., 23, 345-353 (1978).
3. Pelkonen, O., et al., Mol. Pharm., 14, 306-322 (1978).
4. Pearson, J.D. and Regnier, F.E., J. Chrom., 255, 137-149 (1983).

Presented at the 35th ASMS Conference on Mass Spectrometry and Allied Topics
May 24-29, 1987, Denver, CO

HPLC-Thermospray Mass Spectrometric Analysis of DNA Bases

W.C. Davidson[1], R.J. Greathead[1], Thomas L. Walden Jr.[2], William F. Blakely[2], Eric Holwitt[2], and Miral Dizdaroglu[3].
(1)Kratos Analytical, Ramsey, NJ 07446; (2)Armed Forces Radiobiology Research Institute, Bethesda, MD 20814; (3)National Bureau of Standards, Gaithersburg, MD 20899.

Understanding of the molecular mechanisms inherent in cellular injury and its repair from oxidative damage is facilitated by characterization of damage produced in the genome (DNA). Oxidative damage is known to produce a broad spectrum of products, (1)several of which are thermally unstable. Here we describe preliminary development of thermospray LC/MS analysis of DNA damage.

Purine and Pyrimidine bases were separated by reverse phase HPLC. An eluant of 5% methanol/water was analyzed by an in line UV detector (Kratos Model 783). Post detector addition of ammonium acetate provided a final concentration of 0.1M for thermospray analysis. The eluant was admitted to a Kratos LC/MS25 via its thermospray interface. Mass spectra contained M+1 and M+18 ions. Exact mass determinations for calculation of molecular formulas and linked scan MS/MS analysis provided additional structural information. Mass spectra of thymine glycol, a predominant product from oxidation of thymine was obtained. Mass spectra of several DNA oxidative damage products were also acquired.

Figure 1 shows mass chromatograms extracted from full scan data acquired in the analysis of radiation damaged DNA bases. The four bases (as shown) and several damage products were seen. Figure 2 shows the mass spectrum and precise mass calculation for adenosine. Figure 3 shows the thermospray MS chromatogram obtained in analysis of radiation damaged thymine and the mass spectrum of the major product identified as dihydrothymine. Thymidine glycol is a frequently observed product of oxidatively damaged DNA. A thermospray spectrum obtained by analysis of an attempted synthesis is shown in Figure 4. Clearly, numerous impurities are present. MS/MS analysis (Figure 5) confirms the identity of thymidine glycol. Ions characteristic of the base (161,177) and the sugar (117) are observed.

TSP/MS is thus shown to be an excellent method for analysis of DNA bases. MS/MS and exact mass analytical capabilities demonstrate a powerful combination for qualitative identification of DNA damage products.

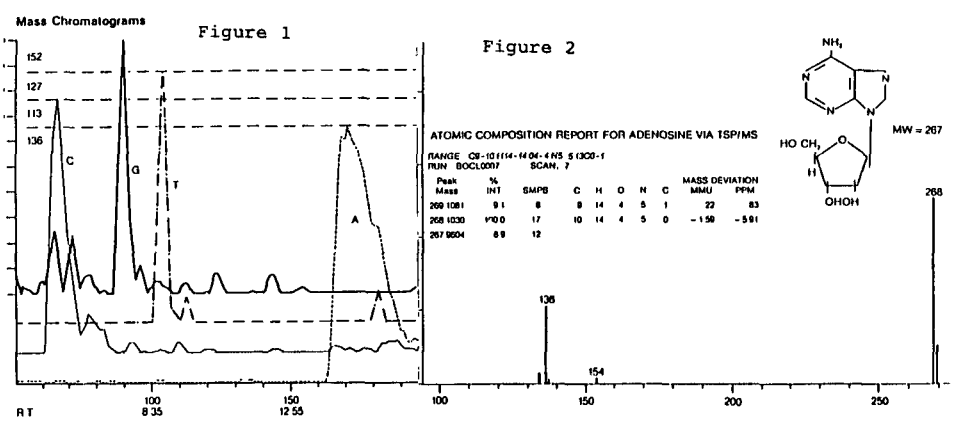

Figure 3

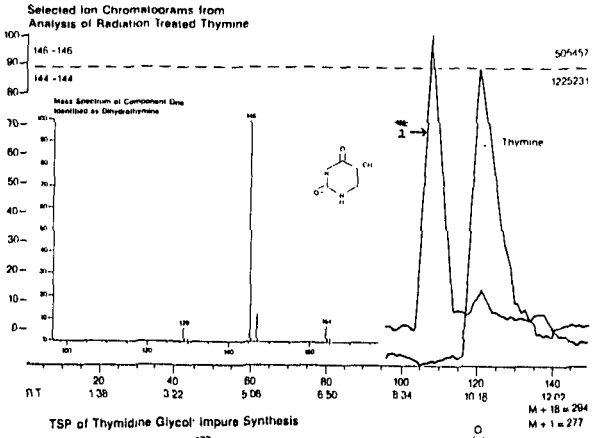

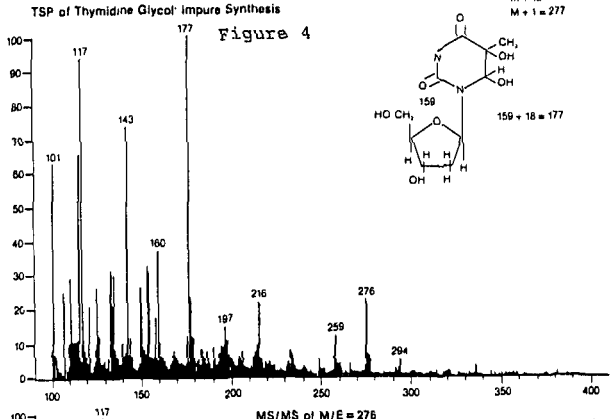

Figure 4

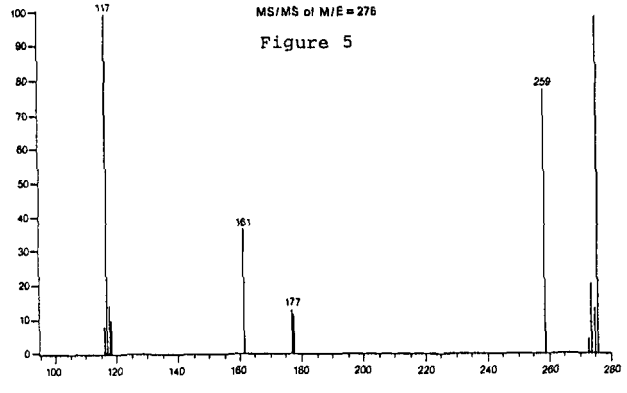

Figure 5

Presented at the 35th ASMS Conference on Mass Spectrometry and Allied Topics
May 24-29, 1987, Denver, CO

FAST ATOM BOMBARDMENT MASS SPECTROMETRY OF TETROCARCIN-A:

A. Mahender Reddy, and Karl H. Schram, Dept. of Pharmaceutical Sciences, College of Pharmacy, University of Arizona, Tucson, Arizona 85721

INTRODUCTION

The present paper describes a detailed study of the structural analysis of tetrocarcin-A, a potent antitumor antibiotic, using the FAB ionization technique under positive and negative ion conditions. Attempts to determine the molecular weight of tetrocarcin-A by EI and CI were unsuccessful.

Tetrocarcin-A consists of a novel aglycone (tetronolide), a novel nitrosugar (tetronitrose), two L-digitoxoses and two L-amicetoses.[1,2] The antibiotics know to have a similar nitrosugars are kijanimicin and antlermicin. Recently FABMS studies on kijanimicin, a closely related compound,have been reported.[3]

RESULTS AND DISCUSSION:

The positive ion FAB mass spectrum showed an intense quasi-molecular ion $[M+Na]^+$at m/z 1336 which is in agreement with a composition of $C_{67}H_{96}N_2O_{24}Na$ (1335.7574). The positive ion FAB spectrum also displayed structure specific fragment ions useful in determining the sequence of the sugars in tetrocarcin-A. A majority of the fragment ions were formed by the glycosidic bond cleavage. This occurs at either side of the glycosidic oxygen with hydrogen transfer to the sugars attached to the aglycone unit. Presence of individual sugar ions clearly establishes the sequence of the four sugars. The ions at m/z 231, 184, and 124 indicate presence of nitro sugar. These ions are important in distinguishing nitro sugars from the deoxy sugars.

The negative ion FAB spectrum showed only a very intense peak at m/z 1311 which represents [M-H] ions. (See figure 1).

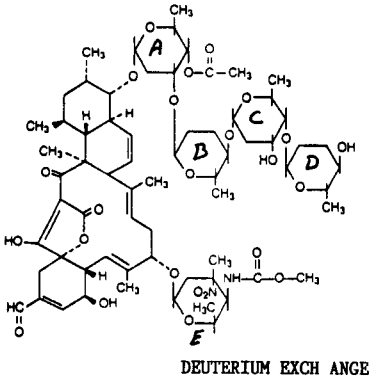

$C_{67}H_{96}N_2O_{24}$

1312.7574 (cal)

DEUTERIUM EXCH ANGE EXPERIMENTS

Under positive ion FABMS the $[M+Na]^+$peak at m/z 1336 shifted to m/z 1341, indicating the presence of five active hydrogen atoms. The negative ion FABMS spectra showed a shift from m/z 1311 to m/z 1316, also indicating the presence of five active hydrogen atoms.

CONCLUSIONS

1. The molecular weight of tetrocarcin-A is shown to be 1312 as a result of positive and negative ion FABMS experiments.
2. Nitrobenzyl alcohol is the solvent of choice for FAB analysis of tetrocarcin type compounds.
3. Positive ion FAB gives more structural information than negative ion FAB.
4. Deuterium experiments are easy to perform and reconfirmation of the above molecular weight from the ion at m/z 1341 (positive FAB) and m/z 1316 (negative FAB).

Further work is in progress to confirm the proposed fragmentation pattern by linked scan and MIKE experiments. These results will be compared with the degradation product of tetrocarcin-A.

Presented at the 35th ASMS Conference on Mass Spectrometry and Allied Topics
May 24-29, 1987, Denver, CO

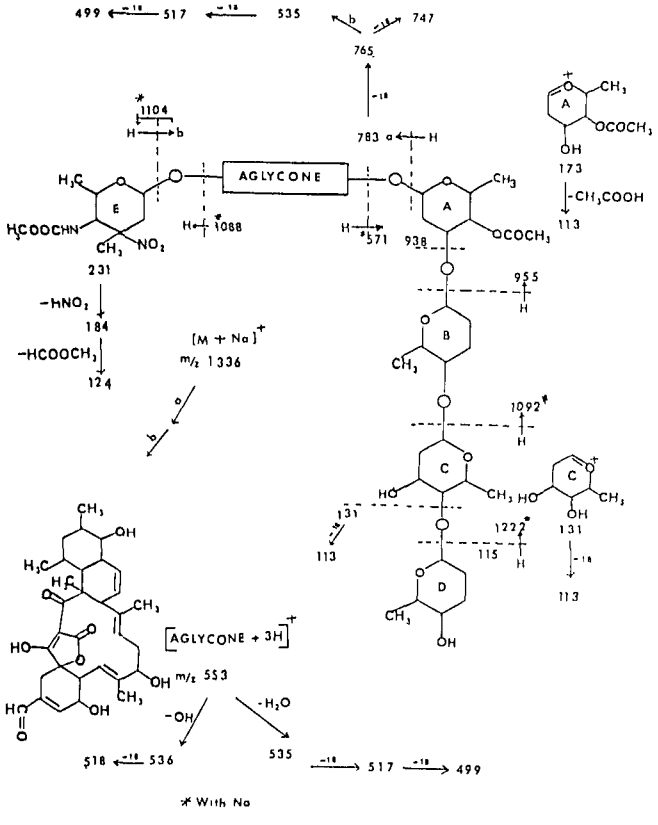

Figure 1.

REFERENCES

1. F. Tomita, T. Tamaoki, K. Shirahata, M. Kasai, M. Mo rimoto, S. Ohkubo, K. Mineura, S. Ishi; J. Antibiotics 33:(6)668(1980).

2. T. Tamaoki, F. Tomita, F. Kawamura, and H. Saito, Agric. Biol. Chem. 47(1)59(1983).

3. B. N. Pramanic, A. K. Mallams, P. L. Barnetr, R. R. Rossman, J. B. Morton, and J. H. Mcglotten, J. Antibiotics.37(7)818(1984).

ACKNOWLEDGEMENT
This work supported by NIH Grant No. CA42309.

REMOVAL OF ISOBARIC INTERFERENCES VIA PULSED LASER RESONANCE IONIZATION MASS SPECTROMETRY (RIMS) FOR LEAD AND BISMUTH MIXTURES

B. L. Fearey, J. E. Anderson, C. M. Miller, and N.S. Nogar
Los Alamos National Laboratory,Los Alamos, NM 87545

and

M. W. Rowe
Texas A&M University, College Station, Texas 77843

Abstract

Pulsed laser single color 2+1 multiphoton ionization is used to eliminate isobaric interferences for lead and bismuth mixtures detected via resonance ionization mass spectrometry.

Introduction

Interest in measuring large isotope ratios for rare isotopes with small sample sizes continues to increase (1,2). Resonance ionization mass spectrometry (RIMS) overcomes the major problems of isobaric interferences in standard thermal ionization mass spectrometry (1,3).

The particular driving force in the present studies is the need to measure large isotope ratios of neutron deficient isotopes of bismuth (Bi). Lead (Pb) isotopes are particularly ubiquitous and are the primary isobaric interference for detection of Bi isotopes in standard thermal mass spectrometry. The elementally selective technique of RIMS is the logical solution to this problem.

In addition, there is the future need to measure the small but finite quantity of the radioactive isotope ^{210}Pb in lead. Lead solder is used extensively in interconnections of computer chips, where the decay of minute amounts of ^{210}Pb can damage the integrated circuit. This problem may become acutely important for future generations of super-computers, where smaller chips lead to more intimate contact of the solder and the integrated circuit. Here, the sensitivity of RIMS may be used to advantage.

Experimental

Briefly, an excimer-pumped dye laser operating with pulse energies of 2 to 4 mJ is tuned to the two-photon frequency for either Pb ($6p7p\ ^3P_0 \longleftarrow 6p^2\ ^3P_0$ @ 44401 cm^{-1}) or Bi ($6p^27p$ J = 3/2 $\longleftarrow 6p^3\ ^4S^\circ_{3/2}$ @ 42941 cm^{-1}) transitions. The laser is focused to a 500 μm diameter ~2 to 4 mm above the sample filament in a quadrupole mass spectrometer. The spectrometer then is mass scanned to observe the isotopes of interest.

A critical component required in the performance of these analyses was the use of co-plating with platinum. Typically, 20 μg of the element(s) of interest were co-plated at 2.7 V in a 100 $\mu\ell$ drop of 1.5 *M* HCl onto a rhenium filament with 50 μg of platinum (4). This method significantly slowed the sample evolution from the filament and greatly simplified analysis. Samples could be used in excess of 2 hours at filament temperatures of ~1500 K with no significant degradation of signal.

Results

Figure 1 shows the observed mass spectra of Pb (upper) and Bi (lower) where in each case the laser is tuned to the particular atom's transition. The Bi two-photon transition at 41125 cm^{-1} ($6p^27p$ J = 1/2 $\longleftarrow 6p^3\ ^4S^\circ_{3/2}$) also was observed, although with an order of magnitude smaller ion signal. In the case of lead, all of the major isotopes are seen in good agreement with published abundances (1 to 2% deviation). Note that the ^{204}Pb peak shows a signal-to-noise ratio of >5 suggesting the capability for isotopic measurements in excess of 100:1 with the present very simple apparatus. For Bi excellent signal to noise also was observed. It should also be pointed out that in each case no isobaric interferences from the other element were observed, even in mixed samples.

Figure 2 shows the dependence of ion signal on the laser energy for Bi (a.) and Pb (b.). The dependences were modeled with a rate equations approach discussed previously (5,6). In each case, the upper state oscillator strength had to be determined to calculate a two-photon cross-section (7). In the case of Bi, the ionization cross section was estimated to be ~5 x 10^{-18}, with an estimated oscillator

strength of ~0.07. The oscillator strength of Pb was found to be 0.4 ± 0.1 where the ionization cross section has been previously measured to be 5 x 10^{-18} (8). For Pb, note that with modest pulse energies that saturation is nearly achieved, while for Bi this is not the case. These results suggest that for Pb a high efficiency of ionization can occur which leads to excellent analytical sensitivity and insensitivity to laser fluctuations. Although Bi has a higher sensitivity to laser noise, approximately 50% ionization is achieved, which still should give good sensitivity.

Conclusions

These results have demonstrated that it is possible and feasible to determine isotope ratios of Bi and Pb using a simple RIMS procedure. Further, some reasonable estimates of oscillator strength for the upper high energy states was attained. Possible improvements include a higher resolution mass spectrometer with increased averaging for more precise isotope ratio measurement. Further, the use of CW single frequency lasers, to increase the duty cycle and to optically select the isotope of interest, is presently being considered.

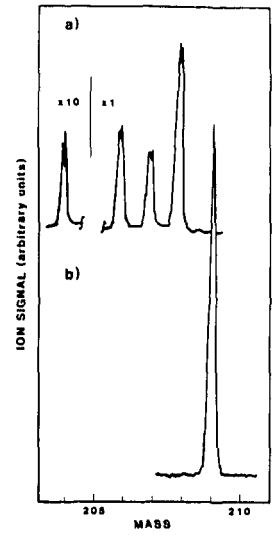

Figure 1. Mass spectra of Pb and Bi

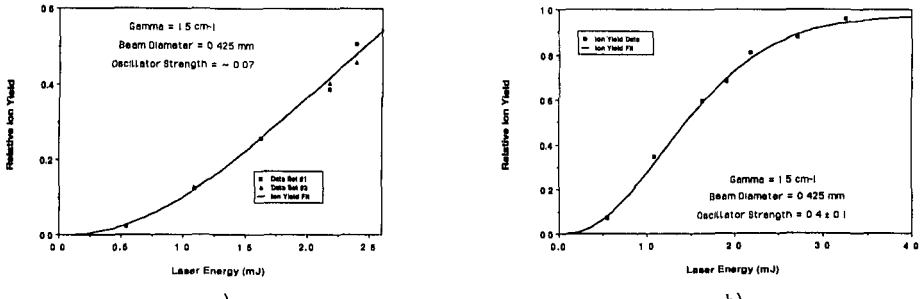

a). b).

Figure 2. Power dependences for bismuth a). and lead b).

References

1. C. M. Miller, N. S. Nogar, E. C. Apel and S. W. Downey, in *Resonance Ionization Spectroscopy 1986*, G. S. Hurst and C. G. Morgan, Eds. (Inst. of Physics, Bristol, England) (1986), 109.
2. G. S. Hurst, in *Resonance Ionization Spectroscopy 1986*, G. S. Hurst and C. G. Morgan, Eds. (Inst. of Physics, Bristol, England), (1986) 1.
3. L. J. Moore, J. D. Fassett, and J. C. Travis, *Anal. Chem.* **56** (1984), 2770.
4. D. J. Rokop, R. E. Perrin, G. W. Knobeloch, V. M. Armijo, and W. R. Shields, *Anal. Chem.* **54** (1982), 957.
5. C. M. Miller and N. S. Nogar, *Anal. Chem.* **55** (1985), 481.
6. E. C. Apel, J. E. Anderson, R. C. Estler, N. S. Nogar, and C. M. Miller, *Appl. Opt.* **26** (1987), 1045.
7. G. Grynberg and B. Cagnac, *Rep. Prog. Phys.* **40** (1977), 791.
8. M. G. Kozlov, S. A. Mileshina, and G. P. Startsev, *Opt. Spectrosc.* **35** (1973), 89.

Presented at the 35th ASMS Conference on Mass Spectrometry and Allied Topics
May 24-29, 1987, Denver, CO

ANALYSIS OF MONOSUBSTITUTED GROUP VI METAL CARBONYLS BY EI, DCI, FD AND FAB MASS SPECTROMETRY

Richard B. van Breemen, LeRoy B. Martin and Anton F. Schreiner
Department of Chemistry, North Carolina State University
Raleigh, NC 27695-8204

Transition metal carbonyls complexes are used as catalysts in organic synthesis and as precursors in the preparation of other organometallic compounds. Substituted carbonyl complexes of tungsten, chromium and molybdenum have been shown to be catalysts for cis-trans isomerization and metathesis of acyclic olefins. In this investigation, monosubstituted group VI carbonyls of the type, $M(CO)_5L$ (where M=Cr, Mo or W; and $L=P(Ph)_3$) were characaterized by mass spectrometry.

Mass spectra were obtained with a JEOL HX110 double-focussing mass spectrometer equipped with a DA5000 data system at a resolution of 1000 and an accelerating voltage of 10 KeV. Four ionization methods were used including positive ion EI, DCI, FD and FAB. Samples were introduced into the mass spectrometer using a direct insertion probe. For FAB ionization, samples were dissolved in a matrix of 18-crown-6-ether and tetramethyleneglycoldimethylether as reported by Minard and Geoffrey (1). Monosubstituted carbonyls were synthesized and purified by standard methods (2) and were more than 99% pure by normal phase HPLC with UV detection at 254 nm.

Molecular ions were detected for each of the nine substituted metal carbonyls using each of the four ionization methods (Figure 1). Fragmentation, corresponding to a sequential loss of CO groups or ligand, L, was observed with all ionization methods except FD. Intense molecular ions and essentially no fragmentation were formed by FD. Therefore, FD would be the ionization method of choice for confirmation of molecular weight. In DCI, abundant fragment ions of the ligand, L, were observed. In EI and positive ion FAB, fragment ions were formed primarily from the loss of CO molecules from the molecular ion. This was confirmed by B/E linked scanning. Compared to EI, FAB ionization produced more abundant molecular ions but also considerable fragmentation. A comparison of the positive ion EI, DCI, FD and FAB mass spectra for one of the carbonyls, tungsten pentacarbonyltriphenylphosphine, is presented in Figure 1. In this investigation, the first DCI, FD and FAB spectra for substituted group VI transition metal carbonyls have been obtained.

---

(1) R.D. Minard and G.L. Geoffrey, 30th Annual on Mass Spectrometry and Allied Topics, Honolulu, June 6-11, 1982.

(2) T.A. Magee, C.N. Matthews, T.S. Wang and J.H. Woltiz, J. Am. Chem. Soc., **83**, 3200 (1961).

(3) S.T. Bond and N.V. Duffy, J. Inorg. Nucl. Chem., **35**, 3241 (1973).

(4) O. Gambino, P. Michelin-Lausarot, G.A. Vaglio, M. Valle, P. Volpe and L. Operti, Transition Met. Chem., **7**, 330 (1982).

Presented at the 35th ASMS Conference on Mass Spectrometry and Allied Topics
May 24-29, 1987, Denver, CO

Figure 1. Comparison of EI, DCI, FD and FAB mass spectra of tungsten pentacarbonyltriphenylphosphine.

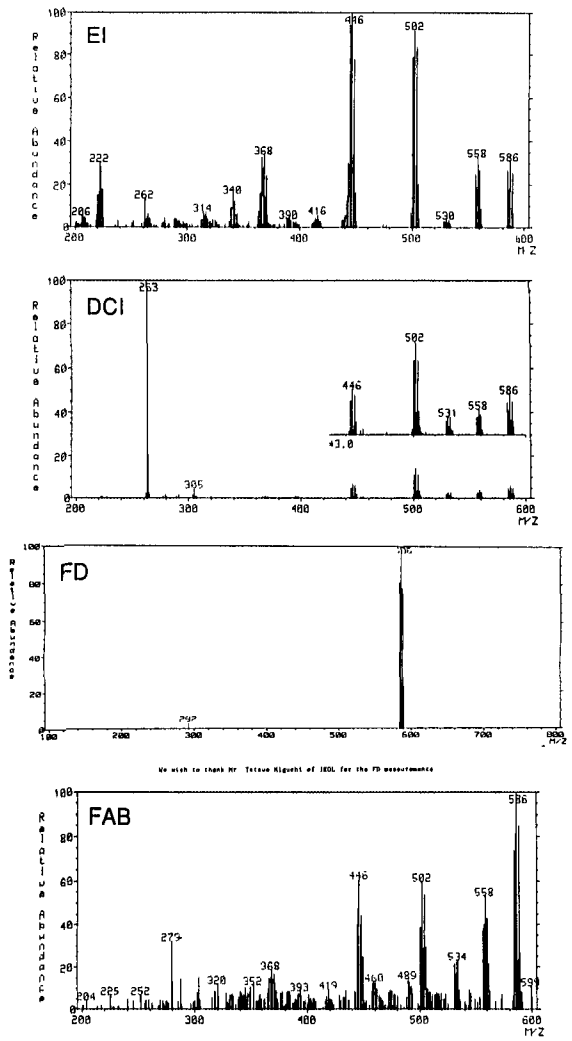

Presented at the 35th ASMS Conference on Mass Spectrometry and Allied Topics
May 24-29, 1987, Denver, CO

Mass Spectrometric Determination of Structural and Geometrical Isomers of Chromium(III)-β-diketonates

B.W. Wenclawiak and P. Schultze; Department of Chemistry, The University of Toledo, 2801 W. Bancroft St., Toledo, OH 43606

Electron impact mass spectrometric investigations of metal-β-diketonates, viz., pentane-2,4-dionates (acetylacetonates, $M(acac)_n$ were first reported by McDonald and Shannon in 1966 [1]. During the following years several papers were published on the topic. Pentane-2,4-dione, 1,1,1 trifluoro-pentane-2,4-dione (Htfa), and other fluorinated β-diketones were used as ligands. The fragmentation of trivalent metal-β-diketones (ML_3) has been rationalized very well in terms of even-electron ions and odd-electron neutral species [2]. The main fragments are $[ML_2]^+$ (basepeak) and $[ML]^+$ besides $[ML_3 - s]^+$ and $[ML_2 - s]^+$ where s denotes an α- or γ-substituent on the chelate ring.

We have studied the mass spectrometric behavior of Cr(III) chelates with β-diketones having aliphatic α-substituents such as methyl, n-butyl, isobutyl, and tert-butyl respectively.

Substituents containing γ-H atoms undergo McLafferty rearrangement. This requires a γ-H-atom on the α-substituent. Instead of a chelate structure an open chain structure is needed. Open chain chain structures have been proposed by McDonald and Shannon [1] to rationalize fragmentation. Therefore, evidence of open chain structure in the mass spectrometer is given.

All Cr-β-diketones show the typical subsequent losses of whole ligands. The main fragment is $[ML_2]^+$.

Complexes with ligands which contain either n. or s.butyl as substituents, e.g., ud or tod, show mass losses of 42 m/e, due to the rearrangement (Fig. 1). Thus $Cr(thd)_3$ can easily be distinguished from its structural isomers $Cr(tod)_3$ and $Cr(ud)_3$ (Fig. 1).

Complexes of mixed ligand Cr-β-diketones exhibit two $[ML_2]^+$ peaks and two $[ML]^+$ peaks due to losses of either ligand. This unique characteristic can be used for detection and assignment [3].

[1] G.C. McDonald, J.S. Shannon, Australian J. Chem. 19, 1545 (1966)

[2] C. Reichert, G.M. Bancroft, J.B. Westmore, Inorg. Chem. 7, 870 (1968)

[3] R.E. Sievers, K.C. Brooks, Int. J. Mass Spectrom. Ion Phys. 47, 527 (1983)

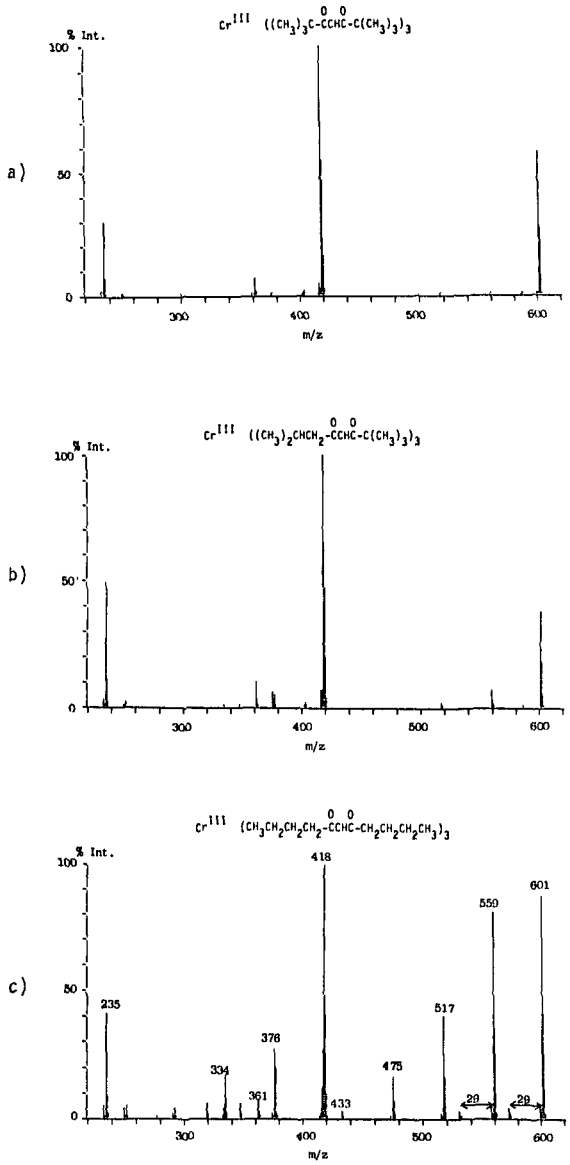

Fig. 1 Electron impact mass spectra of:
a) $Cr(thd)_3$ b) $Cr(tod)_3$ c) $Cr(ud)_3$

Presented at the 35th ASMS Conference on Mass Spectrometry and Allied Topics
May 24-29, 1987, Denver, CO.

FAST-ATOM BOMBARDMENT OF MOLTEN BORON TRIOXIDE

Robert J. Doyle, Jr.
Chemistry Division
Naval Research Laboratory
Washington, DC 20375-5000

The structure of vitreous boron trioxide (B_2O_3) has been a topic of debate for several decades. The most recently proposed structure involves a random network of boroxol (B_3O_3) rings linked together by random numbers of BO_3 triangles. The extremely low vapor pressure of B_2O_3 has, until recently, limited the utility of mass spectrometry as a structural probe. However, the advent of fast-atom bombardment-mass spectrometry (FAB-MS) now enables the desorption of potentially structurally characteristic ions from the surfaces of intractable materials.

Vitreous boron trioxide is a very hygroscopic glass that is not easily purged of water. It reacts readily with ambient water vapor to form a surface coating of boric acid ($B(OH)_3$). Even at typical FAB operating pressures (10^{-6}-10^{-5} Torr), the residual water vapor is sufficient to provide a continuously renewable source of $B(OH)_3$ to the surface of the glass sample. Elevated sample temperatures are therefore required to both purge the sample of water and to prevent the formation of $B(OH)_3$.

Fast-atom bombardment mass spectra of vitreous boron trioxide have been obtained at elevated temperatures using a ZAB-2F mass spectrometer. The experiments utilized a new high-temperature sample holder that has been described in detail elsewhere (1). Spectra were obtained over a sample temperature range of 150-700°C. Boron trioxide is thermally stable over this temperature range and its low vapor pressure and high viscosity assure a long lived sample and a consistent surface geometry.

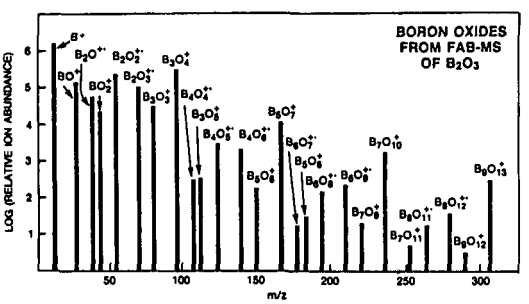

Figure 1. Boron oxide ion distribution from the FAB-MS of boron trioxide.

This technique enabled the first observation of high-molecular-weight, gas-phase boron oxides (Figure 1). The FAB-MS of vitreous B_2O_3 has yielded a complex distribution of boron oxide ions, most of which have been observed for the first time. Six groups of boron oxide ions have been identified and they may be described by six general formulae: $[B_{2n+1}O_{3n}]^+$, $[B_{2n+1}O_{3n+1}]^+$, $[B_{2n+2}O_{3n+1}]^{+\cdot}$, $[B_{2n+1}O_{3n+2}]^+$, $[B_{2n+2}O_{3n+2}]^{+\cdot}$, and

$[B_{2n+2}O_{3n+3}]^{+\cdot}$, where n=0,1,2,3,... . The maximum values of n observed are 4,6,2,3,3, and 4 respectively. Local abundance maxima are observed for $[B_{2n+1}O_{3n+1}]^{+}$ ions which implies an enhanced stability for species such as $[B_3O_4]^+$, $[B_5O_7]^+$, $[B_7O_{10}]^+$, $[B_9O_{13}]^+$, etc.

The collision-induced dissociation (CID) mass spectra of mass-selected boron oxide ions show a remarkable similarity between the dissociation products of boron oxide ions within each group. For example, $[B_{2n+1}O_{3n+1}]^+$ ions, where n>0, all show the loss of B_2O_3 as the principal dissociation pathway (Figure 2 a-c). On the other hand, $[B_{2n+2}O_{3n+3}]^{+\cdot}$ ions, where n>0, all show the loss of $^{\cdot}BO_2$ as the principal dissociation pathway. Common dissociation losses can be explained in terms of structural features that are common to each group.

Although the numerous structural isomers of boron oxide ions cannot be distinguished by CID methods, the general form of boron-oxygen bonding can be deduced. For example, boron is always found 2-or 3- coordinated with oxygen. Boron oxide ions are composed of integral BO_3 triangles and terminal -B=O units. Figure 2d shows examples for the $[B_{2n+1}O_{3n+1}]^+$ series of ions.

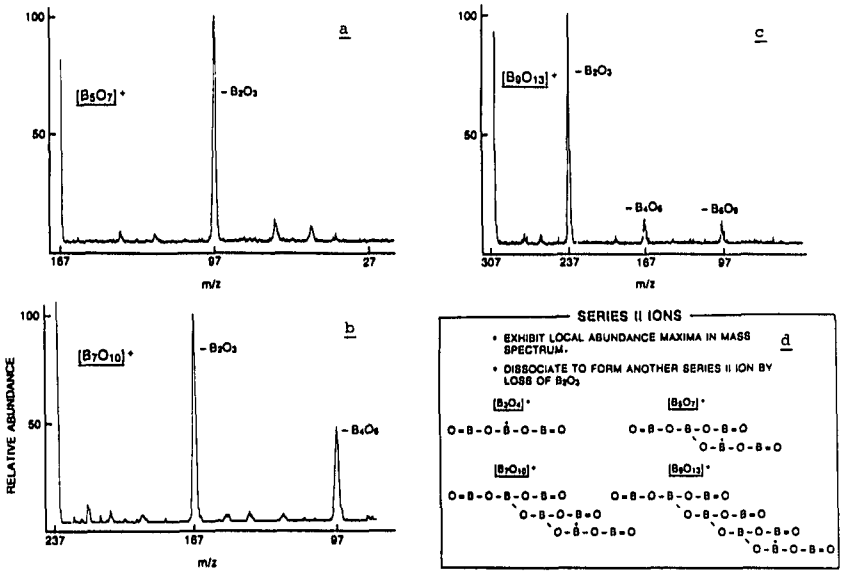

Figure 2. a-c CID spectra of $[B_{2n+1}O_{3n+1}]^+$ ions.
d Proposed structures for this series of boron oxide ions.

1. Doyle, R.J., Jr, Anal. Chem. 1987, 59, 537-539.

Presented at the 35th ASMS Conference on Mass Spectrometry and Allied Topics
May 24-29, 1987, Denver, CO.

EFFECTS OF BORON SUBSTITUENTS ON THE FRAGMENTATION OF PYRAZABOLES (AND THE USE OF SPECTRAL DATA AS A GUIDELINE TO SYNTHETIC STUDIES)

M. T. Mojesky and K. Niedenzu
Department of Chemistry
University of Kentucky
Lexington, KY 40506-0055

Introduction. This paper describes how the use of electron impact (EI) mass spectral observations can be utilized as a guideline to chemical synthesis.

Pyrazabole (Fig. 1), $H_2B(\mu\text{-pz})_2BH_2$ (Hpz = pyrazole) is a chemically and thermally stable compound containing four-coordinate boron and a central B_2N_2 ring system. This unusual stability is illustrated by the central ring skeleton remaining intact upon substitution reactions to the carbon sites. The parent pyrazabole, having been well characterized (1), features the extreme ready loss of one H atom (presumably from a BH_2) under electron impact ionization.

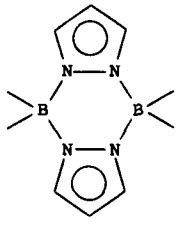

Figure 1

Experimental. The mass spectral experiments were carried out using a double focusing VG ZAB-2F instrument at an electron beam energy of 70 eV. The data was recorded by photographic stripchart (5 galvanometer Honeywell 15083 visrecorder) and computer (Digital PDP-8a) techniques. Precise mass measurements were performed on selected ions using peak meaching (perfluorokerosene as reference).

Findings. The following compounds examined fall into three categories: A) B-organo; $(C_2H_5)_2B(\mu\text{-pz})_2B(C_2H_5)_2$ where pz = pz and pz-$(CH_3)_2$, $(n\text{-}C_3H_7)_2B(\mu\text{-pz})_2B(n\text{-}C_3H_7)_2$, $(C_6H_5)_2B(\mu\text{-pz})_2B(C_6H_5)_2$ where pz = pz and pz-$(CH_3)_2$, and $(C_6H_5)_2B(\mu\text{-pz})_2BH_2$, B) B-Cl; $Cl_2B(\mu\text{-pz})_2BCl_2$ where pz = pz, pz-CH_3, pz-$(CH_3)_2$, pz-n-C_3H_7, pz-C_6H_5, pz-C_3F_7, and pz-Cl, and C) B-F; $F_2B(\mu\text{-pz})_2BF_2$ where pz = pz, pz-CH_3, and pz-$(CH_3)_2$.

The B-organo substituted pyrazaboles follow the trend set by the parent $H_2B(\mu\text{-pz})_2BH_2$ and feature an ion loss of one H atom (presumably from the boron-organo substituent). One entire boron substituent loss is also evident and observed as the base peak depicted in the example $(C_2H_5)_2B(\mu\text{-pz})_2(C_2H_5)_2$, Fig. 2. The B_2N_4 ring skeleton appears to remain intact while each of the four boron substituents are split off (M/z = 157). A common ion in the series observed at M/z = 79, corresponds to $C_2H_4BN_2$, suggesting $HB(\mu\text{-pz})$.

The B-Cl compounds also follow suit by having one boron substituent (Cl) easily lossed. An example $Cl_2B(\mu\text{-pz})_2Cl_2$ is shown in Figure 3. This chloride loss is complemented by the chemical reaction with strong Lewis acids e.g., $AlCl_3$ leading to $[X_2B(\mu\text{-pz})_2BX]^+[AlCl_3X]^-$, where X = F, Cl, Br. A second Cl atom is split off while still maintaining the B_2N_4 ring skeleton. A doubly charged ion $[Cl_2B(\mu\text{-pz})B]^{++}$ was observed and appears throughout the halogen series. Evidence for the formation of rearrangement ions containing

the well known and synthetically obtainable (through independent chemical syntheses) B_2N_4 and B_3N_4 ring systems (2) was observed at M/z = 86 corresponding to HB_2N_2Cl. Spectral data obtained on $Cl_2B(\mu\text{-pz-}CH_3)_2BCl_2$ in the presence of Br_2 suggested a ready halogen exchange $[Cl_2B(\mu\text{-pz-}CH_3)BBr]^+$. Confirmation by synthetic studies followed by producing $Cl_2B(\mu\text{-pz})_2BClBr$, $ClBrB(\mu\text{-pz})_2BBrCl/Cl_2B(\mu\text{-pz})_2BBr_2$, $BrClB(\mu\text{-pz})_2BBr_2$, and $Cl_2B(\mu\text{-pz-Br})_2BClBr$.

The B-F compounds have a slightly different pattern. They exhibit a strong molecular ion as depicted in Figure 4. An F is then split off. Unlike the above compounds, the next major fragment (M/z = 165) suggests the loss of a pz group leaving the four boron substituents intact. Also observed was a fragment corresponding to 1/2 M^+ ($C_3H_3BNF_2$) at M/z = 116. As with the B-Cl compounds the B-F appear to have the formation of rearrangement ions containing the B_2N_2 and B_2N_3 ring skeletons (HB_2N_2F).

References

(1) May, C.E., Niedenzu, K., Trofimenko, S., Z. Naturforsch., 31b, 1662 (1976).

(2) Beeker, K., Gmelin Handbuch der Anorganischen Chemie., Erg.-Werk, Vol. 22, 292 (1975).

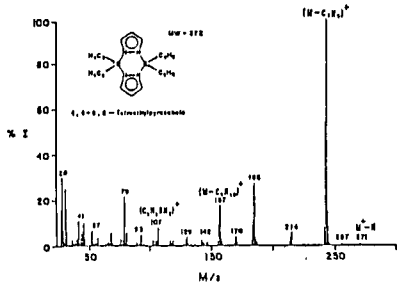

Fig. 1

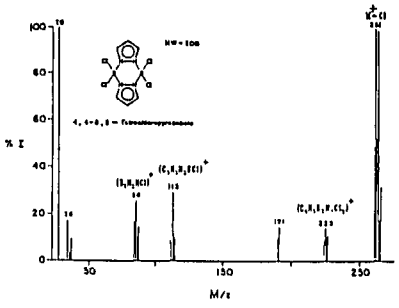

Fig. 2

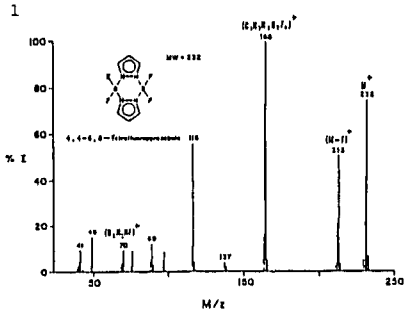

Fig. 3

Presented at the 35th ASMS Conference on Mass Spectrometry and Allied Topics
May 24-29, 1987, Denver, CO

GAS-PHASE OSMIUM CLUSTER ION STRUCTURES FROM FT/ICR MS/MS AND ION-MOLECULE REACTION KINETICS OF $H_2Os_3(CO)_{10}$ AND ITS DIMERS, TRIMERS, AND FRAGMENTS

Steven L. Mullen[1] and Alan G. Marshall

Department of Chemistry (and Department of Biochemistry)
The Ohio State University
120 West 18th Avenue
Columbus, Ohio 43210

Large metal clusters are of current interest both because of their intrinsic structure and bonding and their possible catalytic activity. We have produced large osmium carbonyl clusters containing up to fifteen osmium atoms by self-reacting electron-ionized $H_2Os_3(CO)_{10}$ in an FT/ICR mass spectrometer.[2,3] Triosmium dimer cations range from $Os_6(CO)_7^+$ to $H_2Os_6(CO)_{18}^+$, trimers (Figure 1) from $H_xOs_9(CO)_{13}^+$ to $H_xOs_9(CO)_{23}^+$, tetramers from $H_xOs_{12}(CO)_{21}^+$ to $H_xOs_{12}(CO)_{26}^+$, and pentamers from $H_xOs_{15}(CO)_{27}^+$ to $H_xOs_{15}(CO)_{32}^+$. No Os-Os bonds are broken in forming the larger clusters.

To determine the reaction pathways involved in the dimerization reactions, we isolated, by means of selective stored-waveform (SWIFT)[4] ion ejection, individual triosmium monomer isotopic multiplets, $H_xOs_3(CO)_y^+$ (x = 0 or 2; y = 0-10), and allowed them to react with the parent neutral (Fig. 2). Any product arising in such an experiment must have come from the isolated monomer. The isolation experiments showed that the dimerization reactions occur in general with the loss of two and three carbonyls. The same losses result from the condensation of triosmium dimer cations with parent neutrals to form trimers.

Ridge and coworkers[5,6] have been able to relate average metal electron deficiency with structure and reactivity of various transition metal cluster ions. For a given structure and number of bonds, a discontinuity in average osmium electron deficiency between the observed triosmium dimers, $H_2Os_6(CO)_{14}^+$ and $Os_6(CO)_{13}^+$, and between the observed trimers, $H_2Os_9(CO)_{20}^+$ and $Os_9(CO)_{19}^+$, is predicted. However, kinetics measurements show a continuous variation in reactivity with number of carbonyls for both the triosmium dimers and trimers. Therefore, the present results indicate a change in number of bonds on loss of hydrogens from the triosmium dimers and trimers.

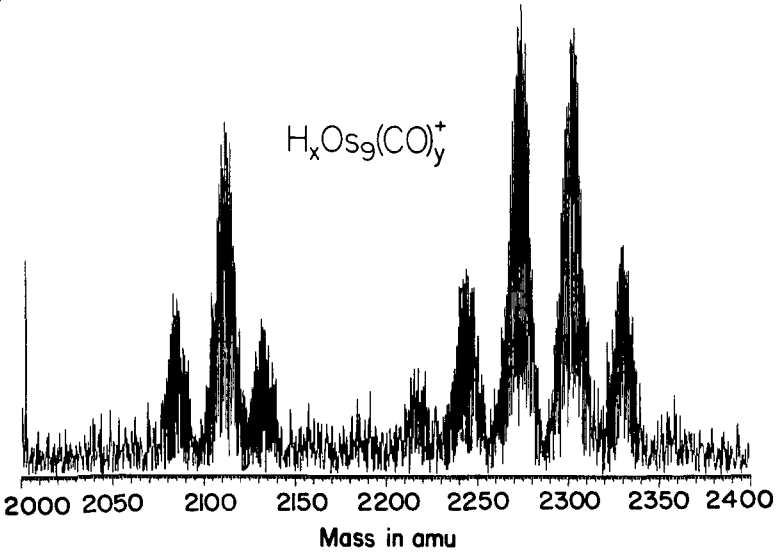

Figure 1. Triosmium trimer region of the FT/ICR mass spectrum of ionic products of the self-reaction of $H_2Os_3(CO)_{10}$ with its molecular and daughter ions for 10.0 s at 1×10^{-9} torr. The triosmium trimer ions range from $H_xOs_9(CO)_{13}^+$ to $H_xOs_9(CO)_{23}^+$.

Presented at the 35th ASMS Conference on Mass Spectrometry and Allied Topics
May 24-29, 1987, Denver, CO

By analogy to known neutral $H_2Os_6(CO)_{18}$ and $Os_6(CO)_{18}$ structures, we propose (see Figure 2) capped square pyramid and bicapped tetrahedron structures for triosmium dimers with and without hydrogens. A tricapped ($\square^3$) trigonal prism arrangement is suggested for triosmium trimers possessing $\geq$20 carbonyls, and a tricapped octahedron for trimers with $\leq$19 carbonyls. In the absence of relevant x-ray structural data for homologous triosmium trimer neutrals, the formation of Os-Os double bonds (rather than structural changes) is possible, but unlikely, since large osmium clusters do not generally contain such bonds. An electron deficiency much greater than two is avoided by the triosmium trimers, in which the electron deficiency is lowered by the addition of hydrogens.

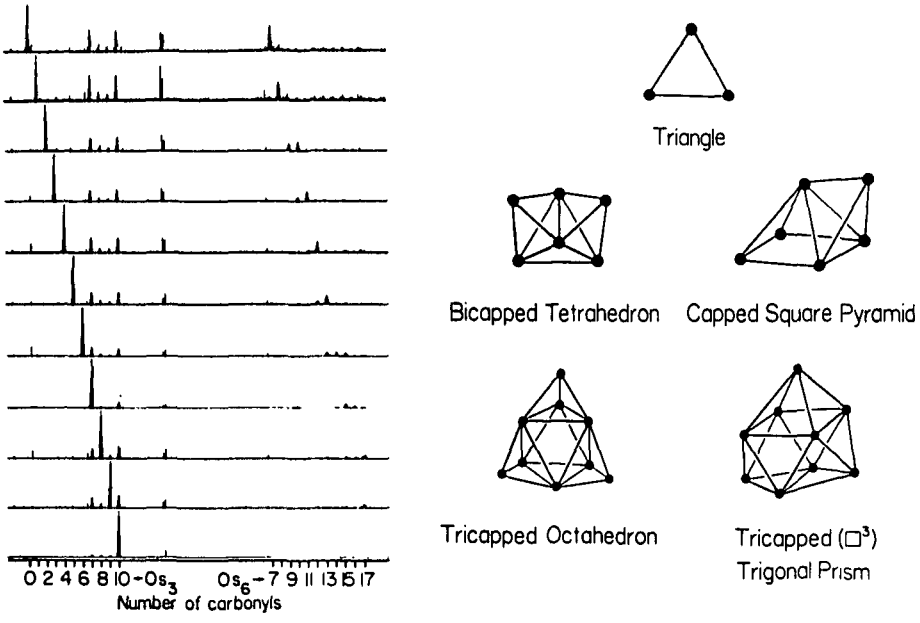

Figure 2. Left: FT/ICR mass spectra of the $H_xOs_3(CO)_y^+$ monomers and $H_aOs_6(CO)_b^+$ dimers, after each monomer has been successively isolated by means of SWIFT excitation and allowed to react with neutral $H_2Os_3(CO)_{10}$. Each mass spectrum is scaled such that the peak for the most abundant ion is at full vertical displacement.

Right: Proposed metal-metal bonds of triosmium monomers (top), dimers (middle), and trimers (bottom). Carbonyls and hydrogens are not shown.

The authors thank S. G. Shore for helpful discussions and for providing $H_2Os_3(CO)_{10}$. This work was supported by grants (to AGM) from the National Science Foundation (CHE-8617244), the U.S.A. Public Health Service (GM-31683), and The Ohio State University.

(1) Current address: NIH/MSU Mass Spectrometry Facility, Michigan State University, East Lansing, Michigan 48824
(2) Mullen, S. L. and Marshall, A. G. 34th ASMS Annual Conference on Mass Spectrometry and Allied Topics (Cincinnati, OH, June, 1986), p. 429.
(3) Mullen, S. L. Doctoral Dissertation, The Ohio State University, 1987.
(4) Marshall, A. G.; Wang, T. C. L.; Ricca, T. L. (1985) J. Am. Chem. Soc. 107, 7893.
(5) Meckstroth, W. K.; Ridge, D. P.; Reents, W. D., Jr. (1985) J. Phys. Chem. 89, 612.
(6) Meckstroth, W. K.; Freas, R. B.; Reents, W. D., Jr.; Ridge, D. P. (1985) Inorg. Chem. 24, 3139.

Presented at the 35th ASMS Conference on Mass Spectrometry and Allied Topics
May 24-29, 1987, Denver, CO

Quantitative Depth Profiling of Semiconductors

D J Hall and P M Charalambous

VG Isotopes Ltd, Ion Path, Road Three, Winsford, Cheshire, CW7 3BX, UK

Introduction

Glow Discharge Mass Spectrometry (GDMS) is becoming acknowledged as one of the most complete techniques in the field of bulk materials analysis. The prime attributes which have established this position may be summarised:

(i) complete elemental coverage across the periodic table

(ii) a small range of elemental sensitivity factors

(iii) the independence of relative ion yields from matrix effects

In addition, the use of a high resolution analyser with dual Faraday/Daly collector configuration (as on the VG 9000 GDMS) offers:

(iv) a collector dynamic range spanning eleven orders of magnitude, providing ppb detection limits in relatively short analysis times

(v) a high resolution mass analyser permitting the ready resolution of the majority of isobaric/molecular/multiple charge interferences (a prerequisite for ppb detection limits.)

Depth Profile Analysis

Recent work on the VG 9000 has shown that GDMS is also capable of making a valuable contribution to the field of depth profiling, and surface analysis in general (a field which has until now been dominated by SIMS analysis). Results presented at QSA-4 (ref 1) showed quantitative analysis of silicon profiles in gallium arsenide epitaxial layers (approx 2 um thick), at concentration levels of 1 and 10 ppm in the layers and 25 ppm in the substrate. The importance of a high resolution mass analyser for such trace analysis was clearly demonstrated, permitting the resolution of the potential interference from the CO molecular species from the Si (28) peak.

In addition, the profile definition of a thin layer (width 100 nm) of tungsten between layers of aluminium analysed by GDMS (ref 1) was such that the technique was clearly shown to be capable of resolving structures on the nanometre scale. This work did, however, demonstrate that work is required to reduce the extent of the "crater edge effect" (well documented in the SIMS literature), which leads to a degradation in depth resolution on profiling from a high to a low concentration. Such work has now been carried out successfully at VG Isotopes Ltd.

The results of the work presented may be summarised:

i. A reduction in crater edge effect has been achieved by masking the sample with a thin sheet of tantalum, permitting sample sputtering only within the mask. In this way the experimentally determined drop in concentration across a physically sharp interface has been improved by over two orders of magnitude. The effect is demonstrated on an NBS coated steel sample (SRM 1361).

ii. An investigation has been made into the crater profile obtained by prolonged sputtering of a gallium arsenide sample. Results are presented, which show a low degree of crater bottom roughness, particularly in the area of the crater edge (< 3% of the total depth sputtered).

iii. It is known that the depth resolution for sputter dependent techniques improves as the sputter rate is decreased; although this may be achieved by careful control of discharge conditions, it has been demonstrated that a change in discharge gas from argon (mass 40) to neon (mass 20) leads to a further reduction in sputter rate by a factor of two.

It may be concluded that high resolution glow discharge mass spectrometry offers a highly quantitative alternative to SIMS for depth profile analysis. Work is continuing at VG Isotopes to establish the ultimate depth resolution of the technique.

Ref 1: Presented at the Fourth International Conference on Quantitative Surface Analysis held in London (UK) 18-20 Nov 1986. Proceedings to be published in Surface and Interface Analysis, Summer 1987.

Presented at the 35th ASMS Conference on Mass Spectrometry and Allied Topics
May 24-29, 1987, Denver, CO

METAL CARBONYL CLUSTER IONS - FORMATION OF VERY LARGE CLUSTERS AND REACTIONS WITH HYDROCARBONS

J. Wronka*, Chemistry Dept., Northeastern University, Boston, MA
R. A. Forbes, Bruker Instruments Inc., Billerica, MA
F. H. Laukien, Chemical Physics, Harvard University, Cambridge MA

A comprehensive experimental methodology for the analysis of sequential ion-molecule reactions is applied to the synthesis of large metal-carbonyl clusters and their gas-phase reactions with hydrocarbons. In a large cylindrical ICR cell at 4.7 Tesla, low mass ions can undergo several hundreds of thousands of collisions before they escape from the trap. Sequential reactions consisting of over 20 consecutive reaction steps occur, and the gas-phase polymerization reactions of decacarbonyldirhenium produce large metal-cluster ions containing over 35 metal atoms. The application of selective collisional activation (CA) and collision induced decomposition (CID) to unreactive intermediates permits the synthesis of unusual and very large metal-carbonyl clusters. Rhenium-carbonyl clusters are observed up to mass 8,828 Daltons, with unit mass resolution for masses higher than 4,000 Daltons.

A novel selective ion ejection method called FERETS, for Front-End Resolution Enhancement using Taylored Sweeps, results in very high front-end resolution. FERETS consists of the application of multiple Taylored excitation sweeps. Typically, the sweeps consist of 2 high-power fast sweeps to remove most of the ions and 2 low-power slow sweeps to remove the ions close to the ion of interest. For a a 3000 Dalton wide ejection window leaving m/z 1025 the high-power sweeps take 25 milliseconds while the low power sweeps take 350 milliseconds. Using FERETS, we have obtained much better than unit mass front-end resolution (FER) at mass 1,025 Daltons. The exact FER ($m/\Delta m$ FWHM) measured at mass 895 Daltons was 5,300. If we normalize this FER to 100 Daltons according to $m/\Delta m \propto 1/m$, then the normalized FER is approximately 47,000. High FER isolation requires high-power rf amplification (400Vpp) and a wide range of attenuation (61 dB). In addition to low pressure and the proper rf amplification, software is necessary to provide control over the number, type, duration and power level of the various ejection sweeps applied.

The clusters are isolated by FERETS as a function of the number of metal atoms and carbonyls present. After single ion isolation, the metal-carbonyl clusters react with cyclohexane admitted through a pulsed-valve inlet. The reactivity of these clusters with hydrocarbons is found to vary with the number of metal atoms and carbonyl ligands present. Four and three rhenium atom positive ion clusters with an average electron deficiency greater than 3 react with cyclohexane to remove one hydrogen molecule and form a cyclohexene ligand or to remove two hydrogen molecules and form a cyclohexadiene ligand. As the electron deficiency increases a greater percentage of the reaction involves the loss of 2 hydrogen molecules. $Re_3(CO)_7^+$ is capable of removing 3 hydrogen molecules from cyclohexane.

Presented at the 35th ASMS Conference on Mass Spectrometry and Allied Topics
May 24-29, 1987, Denver, CO

REACTIONS OF RHENIUM-CARBONYL CLUSTERS WITH CYCLOHEXANE

$Rhenium_4$ Series

Ion	Products	Loss	Branch %	e- Deficiency
$Re_4(CO)_{16}^+$	No Reaction			1/4
$Re_4(CO)_{15}^+$	No Reaction			3/4
$Re_4(CO)_{14}^+$	No Reaction			1 1/4
$Re_4(CO)_{13}^+$	No Reaction			1 3/4
$Re_4(CO)_{12}^+$	No Reaction			2 1/4
$Re_4(CO)_{11}^+$	No Reaction			2 3/4
$Re_4(CO)_{10}^+$	$Re_4(CO)_8C_6H_8^+$	$2CO + 2H_2$	7	3 1/4
	$Re_4(CO)_7C_6H_8^+$	$3CO + 2H_2$	6	
	$Re_4(CO)_9C_6H_{10}^+$	$CO + H_2$	56	
	$Re_4(CO)_8C_6H_{10}^+$	$2CO + H_2$	10	
	$Re_4(CO)_7C_6H_{10}^+$	$3CO + H_2$	21	
$Re_4(CO)_9^+$	$Re_4(CO)_8C_6H_8^+$	$CO + 2H_2$	16	3 3/4
	$Re_4(CO)_7C_6H_8^+$	$2CO + 2H_2$	14	
	$Re_4(CO)_7C_6H_{10}^+$	$2CO + H_2$	70	
$Re_4(CO)_8^+$	$Re_4(CO)_6C_6H_8^+$	$2CO + 2H_2$	30	4 1/4
	$Re_4(CO)_7C_6H_8^+$	$CO + 2H_2$	38	
	$Re_4(CO)_7C_6H_{10}^+$	$CO + H_2$	11	
	$Re_4(CO)_6C_6H_{10}^+$	$2CO + H_2$	21	

$Rhenium_3$ Series

Ion	Products	Loss	Branch %	e-Deficiency
$Re_3(CO)_{13}^+$	No Reaction			2/3
$Re_3(CO)_{12}^+$	No Reaction			1 1/3
$Re_3(CO)_{11}^+$	No Reaction			2
$Re_3(CO)_{10}^+$	No Reaction			2 2/3
$Re_3(CO)_9^+$	$Re_3(CO)_8C_6H_8^+$	$CO + 2H_2$	67	3 1/3
	$Re_3(CO)_7C_6H_8^+$	$2CO + H_2$	33	
$Re_3(CO)_8^+$	$Re_3(CO)_7C_6H_8^+$	$CO + 2H_2$	59	4
	$Re_3(CO)_6C_6H_8^+$	$2CO + 2H_2$	34	
	$Re_3(CO)_5C_6H_8^+$	$3CO + 2H_2$	7	
$Re_3(CO)_7^+$	$Re_3(CO)_5C_6H_8^+$	$2CO + 2H_2$	36	4 2/3
	$Re_3(CO)_5C_6H_6^+$	$2CO + 3H_2$	64	

Presented at the 35th ASMS Conference on Mass Spectrometry and Allied Topics
May 24-29, 1987, Denver, CO

GAS PHASE PHOTODISSOCIATION OF FERROCENE ION:|

Jim Faulk and Robert C. Dunbar, Department of Chemistry,
Case Western Reserve University, Cleveland, Ohio 44106.

Photodissociation of gas phase ferricenium ion was measured from 585nm to 643nm with a dye laser and from 476nm to 515nm with an argon ion laser. In addition it was demonstrated that photodissociation in this wavelength region required 2 (or more) photons.

The photodissociation of ferricenium ion was followed by monitoring the icr signal of the parent ion, $Fe(C_5H_5)_2^+$. The signal of the product ion, $Fe(C_5H_5)^+$, appeared only with irradiation.

$$Fe(C_5H_5)_2^+ \xrightarrow{h\nu} Fe(C_5H_5)^+ + C_5H_5.$$

The photodissociation spectrum from 476nm to 515nm showed little wavelength dependence. It is compared in figure 1 with an absorption spectrum taken at room temperature in 10% HBF_4 (From reference 1).

The photodissociation spectrum from 585nm to 643nm is shown in figure 2. Also shown are 3 condensed phase absorption spectra taken from references 1 and 2. The photodissociation spectrum appears to have vibrational fine structure with a peak spacing of approximately 25nm in contrast to the 6 K spectrum with a peak spacing of approximately 10nm. This is currently under investigation.

The energy required to cleave one of the C_5H_5 ligands was calculated from tabulated values of electron impact ion formation energies as approximately 6.5 eV (which corresponds to light of 191nm). Since photo dissociation was observed at energies below 2.5 eV (or with light of wavelength longer than 496nm) a 2 (or more) photon mechanism was proposed following the usual sequential multiphoton mechanism.

$$Fe(C_5H_5)_2^+ \xrightarrow{h\nu} Fe(C_5H_5)_2^{+*} \xrightarrow{nh\nu} Fe(C_5H_5)^+ + C_5H_5.$$

To confirm the proposed mechanism we measured the dependence of the photodissociation on the chopping rate of the laser. A photodissociation requiring the sequential absorption of 2 (or more) photons is ex pected to show a marked dependence on the chopping rate. This can be qualitatively understood in the following way. The first photon promotes the ion to an excited state below the threshold for dissociation. If the ion is to dissociate it must remain in the excited state until a second photon is available to promote it above the dissociation threshold. Experimentally the best way to do this is by a single light pulse of sufficient duration to supply both photons. As the pulse rate increases the pulse duration decreases in order to maintain a constant time average intensity. Therefore the availability of the second photon during the pulse time decreases with increasing chopper rate. Since the delay between pulses is long enough to allow the ions to relax below the one photon threshold, the decrease in the availability of the second photon during the pulse time results in a decrease in photodissociation. The ferricenium ion photodissociation showed typical 2 (or more) photon dependence on the chopping rate at 515nm as shown in figure 3.

Conclusions:

We were able to obtain a photodissociation spectrum of gas phase ferricenium ion from 585nm to 643nm that showed vibrational fine structure with a peak spacing of approximately 25nm. We were also able to show that this photodissociation required 2 (or more) photons.

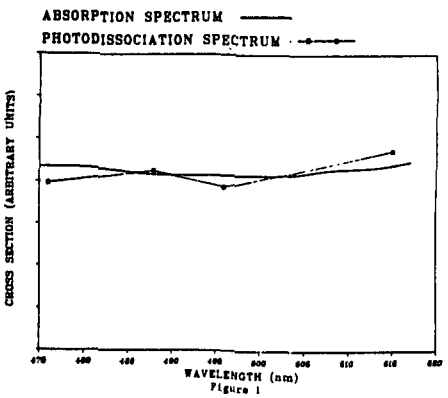

Figure 1

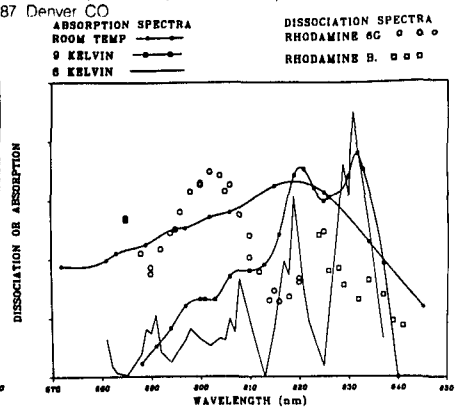

Figure 2

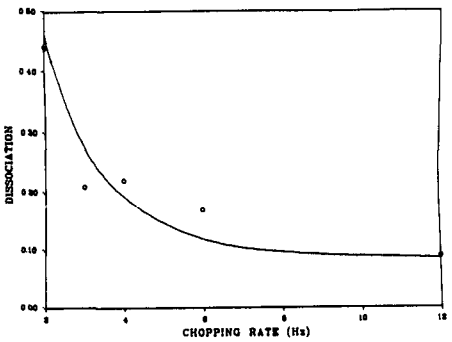

Figure 3

References:

1. Rowe, M.D.; McCaffery, A.J. J. Chem. Phys. 1972, 59(7), 3786

2. Rowe, M.D.; Gale, R.; McCaffery, A.J. Chem. Phys. Lett. 1973, 21(2), 360.

3. Ion thermochemical values were taken from Rosenstock, H.M.; Draxl, K.; Steiner, B.W.; Herron, J.T. J. Phys. Chem. Ref. Data 1977, Vol. 6, Suppl. 1.

Presented at the 35th ASMS Conference on Mass Spectrometry and Allied Topics
May 24-29, 1987, Denver, CO

ISOTOPIC ANALYSIS OF CALCIUM

J. R. Tackett and R. E. Ellefson
Monsanto Resarch Corporation-Mound, Miamisburg, OH 45342

Isotopic ratios of Ca are measured at Mound to support research on chemical isotopic enrichment. Very good external precision is required to measure enrichment profiles; thus a robust method is sought which can accomodate the variety of impurities encountered in the research. Predictable fractionation control is achieved in a low-temperature distillation mode for triple filament thermal ionization operation. Our method also addresses impurity removal and control of Ca contamination.

Production of a stable Ca beam which is necessary for precise single collector measurements requires clean samples. Common impurities which affect stability are K, Na, Si and hydrocarbons. If excessive K or Na are present, a miniature anion exchange resin column is used for cleanup. The AG-50W-X8 resin is washed with 2N-HNO_3 followed by a 0.2N-HNO_3 wash. The Ca sample is loaded onto the column in 0.2N HNO_3; impurities are washed out with more 0.2N-HNO_3. The Ca is recovered with 2N-HNO_3; evaporated to dryness and diluted to 0.1 mg-Ca/ml in 2N-HNO_3 for direct loading onto sample filaments. If Si, determined by ICP emission spectroscopy is high (>10wgt-% of sample), chemical removal of the Si is necessary and achieved by adding a drop of perchloric acid and 2 drops of HF to the sample in a TFE tube and heated to dryness. The Si leaves as SiF_4. The sample is then redissolved for loading.

Natural abundance calcium is ubiquitous so efforts must be made to minimize contamination of isotopically enriched samples. Class 100 clean work areas are present where most of the work is done. To determine the contamination blank in the research area and the analysis areas, highly-enriched ^{44}Ca is processed and analyzed. The natural abundance Ca introduced in the process area was 72 ng (10% Of a normal sample) and in the analysis area the blank was 0.8 ng.

Sample loading involves direct loading and drying 700 ng-Ca/filament as Ca in 2N-HNO_3. The 1.6 X 30 mil zone-refined Re filaments are degassed before loading the sample. The solution is evaporated with 1.2 A current flowing through the filament and further dried for 15 min at the same current. The samples are promptly loaded into the mass spectrometer source or kept dry until they are run. The heating pattern is given in Table 1. The final operating condition is a 1700°C ionizing filament and 700+/-50 °C sample filaments. At this operating condition, the measured isotope ratio is constant for over 1 hour which allows continued measurement of the ratio and no time-dependent correction model for absolute calibration. The mass discrimination that results is 0.22%/amu for all Ca isotopes. The behaviour of the ratio with time is shown in Fig. 1. Ratio measurements are taken between 40 and 90 min (+ in Fig.1).

We find that a less-stable but useful ion beam is produced when side filaments are raised to 1100°C; however the beam exhibits the normal fractionation behaviour of decrease in light-to-heavy species ratio with increasing time. Other experimentors report a reverse fractionation effect for Ca (1,2,3) for conditions of lower operating temperatures than those reported here. Models that explain reverse fractionation (2) include dual processes: The normal process is depletion of light isotopes from the sample filament which when ionized shows the normal depletion of light isotopes with time. The competing process is a deposition of sample on the ionizing filament from which surface ionization takes place. The preferential deposition of light isotope and preferential surface ionization of light isotopes gives rise to an increase in light-to-heavy ratios with time, the so-called reverse fractionation. Under conditions of low center and side filament temperatures, reverse-fractionation

dominates; for high ionizing and sample filament temperatures, normal fractionation dominates. Our case is a balance of the two effects.

A natural abundance Ca standard has been analyzed by this method for over two years as a quality control measure for the method. The overall results using the 0.22 %/amu mass discrimination gives 46.56 +/- 0.04 (95%-CL;n=14) and during the past year an average of 46.55 +/- 0.02 (95%-CL; n=9). The advantage of the method is a broad time period over which precise measurements can be made.

Table 1. Sample Heating Pattern (Input Resistor = 10^{11} Ohms)
(Ionizing Filament: 1700 °C)

Time (Min)	Sample Filaments Current(A)	^{40}Ca(V)
0	0.46 A	
2	0.72	
3	0.86	
4	0.96	
5		0.05 V
10		0.5
15		1.2
20		2.5
25		3.5
38	Measure Baseline	
40	Begin Ratio Measurement	
90	End Normal Measurement	

1. Moore and L.A. Machlan, Anal. Chem. 44, 2291 (1972).
2. L.J. Moore, E.F. Heald & J.J. Fillibin, "Advances in Mass Spectrometry", N.R. Daly,Ed., 7A, London: Heyden, p. 466-468.
3. N.E. Vieira, M.P. Schmidt and A.L. Yergey, Proc. of 33rd Annual Meeting on Mass Sectrometry and Allied Topics, San Diego, CA, May 26-31, 1985, p. 615.

Fig. 1. Ca 40/44 Ratio Vs: Time (Min)

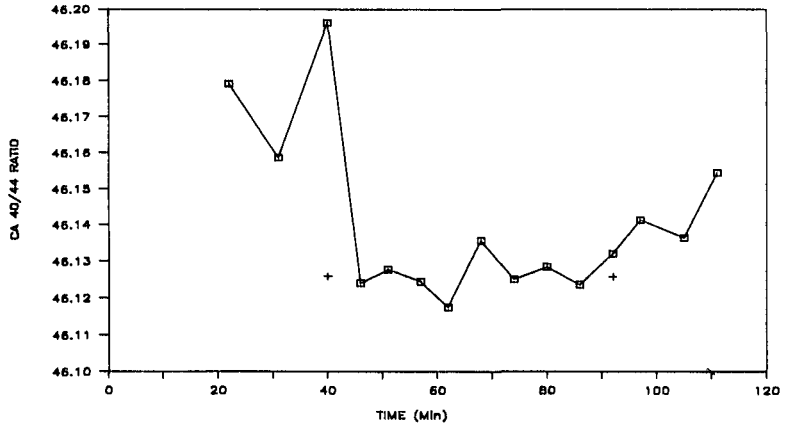

Presented at the 35th ASMS Conference on Mass Spectrometry and Allied Topics
May 24-29, 1987, Denver, CO.

MASS SPECTROMETRY OF DIMETHYLSILOXANES

P. S. EPSTEIN; CLAYTON ENVIRONMENTAL CONSULTANTS, NOVI, MI. 48050;
M. D. CURTIS; UNIVERSITY OF MICHIGAN, ANN ARBOR, MI. 48107

The mass spectra of oligomeric siloxanes of the type, $RMe_2SiO(SiMe_2O)_nSiMe_2R'$ (R, R'=Me, H, or Ph) are reported using electron impact and chemical ionization. Regardless of the ionization method, the siloxanes fragment extensively by loss of an R-group followed by loss of neutral, cyclic fragments or by forming cyclic ions.
The oligomers, $E'D_nE$ and $E'D_nE'$, fragment primarily via cyclic intermediates (Scheme I) as do the permethyl series ED_nE, investigated previously.[1] However, the presence of Si-H groups increases the number of distinct fragmentation pathways (migration of H or Me in Path B, Scheme I) and the fragment ion spectra of the $E'D_nE$ and $E'D_nE'$ series are correspondingly more complex than observed for the ED_nE.

Scheme I. Formation and Fragmentation of Cyclic Intermediates in the Mass Spectra of Oligo(dimethylsiloxanes), $E^RD_nE^R$.

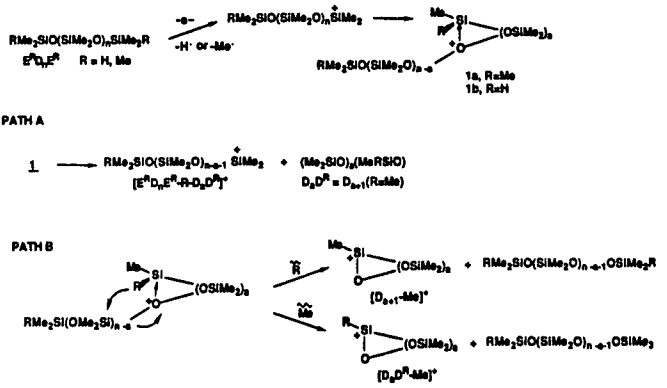

In addition to the "cyclic" fragmentation path discussed above, at least one other fragmentation pathway must be very efficient. The smallest siloxane which can form the 6-membered ring in the cyclic path is ED_2E. Thus the fragmentation of EE and EDE must proceed along a "linear" pathway. This linear pathway produces neutral silanone fragment, RR'Si=O. Note also that the Me_3Si^+ ion is either the base peak or has very high relative abundance even when the neutral siloxane has no Me_3Si groups. Therefore, methyl group mobility, via 1,3- 1,5-, etc. shifts, must be extremely efficient in siloxanes. Eqs. 1-3 illustrate these methyl shifts and the linear fragmentation to a a neutral silanone. The mechanism suggested in eq. 1 is consistent with the studies of Orlov on metastable siloxane ions.[1] The net result of these shifts is that the pendant groups appear to be highly mobile along the siloxane backbone.

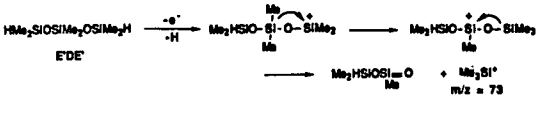

(1)

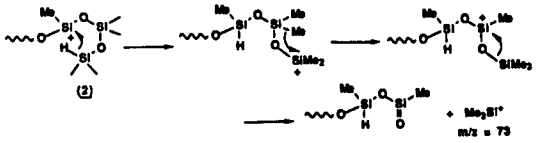

(2)

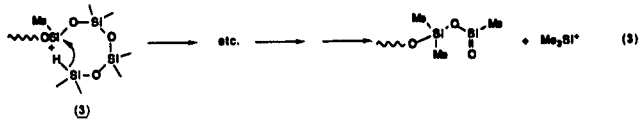

An interesting fragmentation pathway observed in the phenyl siloxanes is loss of methane following the loss of methyl. Deuterium labelling of the phenyl ring established that one of the four hydrogen atoms in the methane was supplied by the phenyl group. For example, in the EI-MS of EPhE , the $[M-CH_3]^+$ (m/z=209) ion is the base peak. This ion then loses methane and the $[M-CH_3-CH_4]^+$ ion at m/z=193 has relative abundance 64. The spectrum of the perdeuterophenyl analog is analogous: the base peak is $[M-CH_3]^+$ (m/z=214) and the next fragment has m/z=197 corresponding to $[M-CH_3-CH_3D]^+$.
As the siloxane chain gets longer, successive losses of CH_4 (or CH_3D) occurs. These observations are consistent with the fragmentation path shown in Scheme II for $E^{Ph}D_2E$. The relative abundances for the ions 341(345), 325(326) and 309(311) (Scheme II) are low - only 1-2% that of the base peak ($PhMe_2Si^+$).

Scheme II. Methane Loss Mechanism in $E^{Ph}D_2E$ as Revealed by Isotopic Labelling.

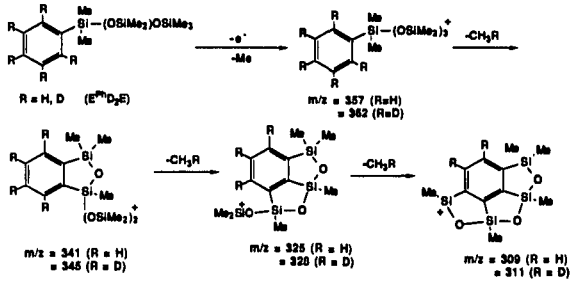

The CI-MS (NH_3 Reagent Gas) of two siloxane series $E'D_nE'$ and ED_nE have been obtained. The most striking and useful feature of these spectra is the high intensity of the peak corresponding to the attachment of NH4+ to the neutral molecule. Thus, the parent ion, $[M+18]^+$, allows an immediate identification of the MW of the oligomeric siloxane. Figures 1 and 2 show the CI-MS(NH_3) spectra of ED_5E and $E'D_5E'$, respectively.

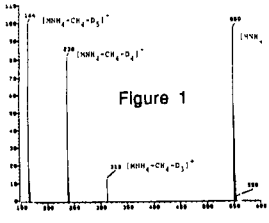

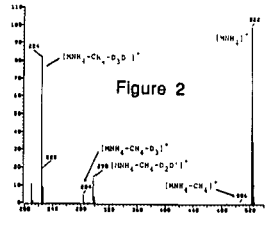

The abbreviated notation used here[2] to denote the structure of oligomeric siloxanes employs the basic symbols, E (end group)=$Me_3SiO_{1/2}$, D(difunctional)=$Me_2SiO_{2/2}$, and T (trifunctional)=$MeSiO_{3/2}$. A primed letter denotes H for Me substitution on silicon.

References

1. Yu Orlov, Zh. Obshch. Khim. 37,2300 (1967), J. Gen. Chem., U. S. S. R., 37,2188 (1967)

2. M. D. Curtis and P. S. Epstein, "Redistribution Reactions on Silicon Catalyzed by Transition Metal Complexes." in Advances in Organometallic Chemistry, Vol. 19, F. G. A. Stone and R. West, eds., Academic Press, New York, 1981, pp213-255

Presented at the 35th ASMS Conference on Mass Spectrometry and Allied Topics
May 24-29, 1987, Denver, CO.

DIRECT DETERMINATION OF TRACE ELEMENTS BY LASER MASS SPECTROMETRY

L. Q. Huang, R. J. Conzemius and R. S. Houk*
Ames Laboratory-USDOE and Dept. of Chemistry
Iowa State University, Ames, IA 50011

The application of laser mass spectrometry (LMS) to elemental characterization of solid materials has grown significantly in recent years (1). Relative sensitivity factors (RSF) are determined for impurity elements in metal samples using laser mass spectrometry in the power density range of 1 to 3 x 10^9 W cm^{-2}. Metallic impurities are found to have RSFs near unity while nonmetallic impurities are less efficiently ionized relative to iron. The results indicate uniform sensitivities for all the elements may be expected as the power density reaches 5 x 10^{10} W cm^{-2} in agreement with earlier studies. (2).

Our previous work (3) indicated that interstitial impurities could be determined in metals. In the present work, determination of trace oxygen in semiconductors such as Si-Ge has been investigated by the analysis of standards and by comparison of the results to neutron activation measurements. The resulting calibration curve is linear up to 5% atomic for oxygen in silicon. The detection limit is approximately 10 parts-per-million-atomic. The achievable precision is 10% relative when the system is carefully optimized by monitoring the Si^{+2} signal which is sensitive to laser power fluctuations (4).

Acknowledgement
The Ames Laboratory is operated for the US Department of Energy by Iowa State University under Contract No. W-7405-Eng-82. This research was supported by the Director for Energy Research, Office of Basic Energy Sciences.

References

1. R. J. Conzemius and G. Junk, DOE/NBM-7001005 (1986).
2. Yu. A. Bykovskii, G. I Zhuravlev, V. I. Belousov, and V. N. Nevolin, Sov. J. Plasma Phys. 4, 180 (1978).
3. Zhao Shankai, R. J. Conzemius, and H. J. Svec, Anal. Chem. 56, 382 (1984).
4. R. J. Conzemius, Zhao Shankai, R. S. Houk, and H. J. Svec, Int. J. Mass Spectrom. Ion Processes 61, 277 (1984).

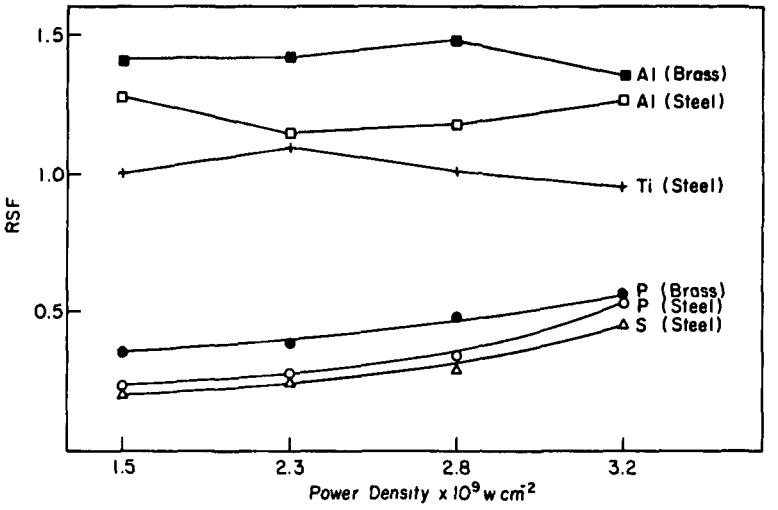

Figure 1. Plot of RSF's vs. laser power density.

Presented at the 35th ASMS Conference on Mass Spectrometry and Allied Topics
May 24-29, 1987, Denver, CO

THE USE OF A COMBINED INTERNAL STANDARD AND ASSAY SPIKE FOR THE ISOTOPE DILUTION MASS SPECTROMETRIC ASSAY OF PLUTONIUM

David W. Crawford, Margaret A. Legel, and M. Irene Spaletto

U. S. Department of Energy, New Brunswick Laboratory
Argonne, IL 60439

ABSTRACT

An evaluation of a triple-atom plutonium isotopic material for use as a combined internal isotopic standard and assay spike has been performed. The isotopic composition of this material, with its significant quantities of Pu-240, Pu-242, and Pu-244, enables an isotope dilution mass spectrometry measurement and internal normalization isotope ratio measurement for plutonium to be made on a single sample during a single analysis. Such a capability has significant safeguards applications as it allows for high precision and accuracy measurements on plutonium of a variety of concentration and impurity levels. Furthermore, the use of a combined internal standard-assay spike reduces the time spent performing separate plutonium sample and calibration measurements. Thermal ionization mass spectrometric measurements on submicrogram quantities of plutonium are reported to precisions and accuracies on the assay value of 0.01-0.02% using this combined internal standard-assay spike.

The use of an internal normalization isotope ratio (or internal standard) is recognized as a valuable tool in the improvement of precision in making isotope ratio measurements using thermal ionization mass spectrometry. The technique involves a normalization of a measured ratio in a sample which is unknown to an isotope ratio of the internal standard which is known and exists within the same analyte. This normalization allows for a precise bias correction for the isotopic fractionation occurring during the analysis to be determined and applied to the observed ratio of interest in the sample. A requisite for high accuracy application of the internal standard is the determination of the isotopic composition of the internal standard to a high degree of certainty.

The use of the internal standard for improvement in mass spectrometric isotope ratio measurements was first proposed by Dietz, et al.; utilization of the technique in nuclear isotopic measurements has been demonstrated by others (Ref. 1,2,3). The work presented here expands the use of the internal standard technique to isotope dilution mass spectrometry (IDMS) measurements for plutonium by the quantitative blending together of a plutonium-bearing material and an accurately known spike isotope, and by normalizing this sample-spike isotope ratio to a well-calibrated internal standard isotope ratio which exists within the spike material. This yields a highly precise and accurate assay value for plutonium in the sample.

The advantages of using the internal standard technique are the elimination of sample loading effects, instrumental and fractionation variation effects, and systematic errors due to chemical impurities. Therefore, using the internal standard technique in conjunction with IDMS allows for the accurate assay of plutonium in a wide variety of concentration levels and chemical matrices. This makes the use of the internal standard-assay spike technique especially useful in the assay of plutonium for safeguards purposes. The application of the internal standard technique in the IDMS assay of plutonium is demonstrated by the use of a currently available Pu-240:242:244=2:3:1, or "triple atom" internal standard-assay spike.

EXPERIMENTAL AND RESULTS

The triple-atom material was received from ORNL as a PuO_2. It was dissolved, chemically purified, and apportioned into aliquots for calibration and for use as assay spikes.

The mass spectrometer used for the isotopic measurements was a Finnigan MAT 261 solid-sample thermal ionization type with a 30-cm radius 90° magnetic sector. The ion detection system consists of six Faraday cup collectors which allowed for simultaneous isotope ratio measurements. The mass spectrometer's operation and data acquisition were controlled by a desktop minicomputer. A high-stability current source was used to calibrate the relative gains of the amplifiers in the multiple collector system. Because all ion beams were collected and integrated simultaneously, fluctuations and instabilities in ion beam did not impact on the internal precision of each measurement.

The isotopic content of the triple-atom material was measured by mass spectrometry. NBL Certified Reference Material (CRM) No. 128 Plutonium Isotopic Standard was used as the

calibration material. The chemical assay (elemental analysis) of the plutonium content was determined by control-potential coulometry (Ref. 4). The isotopic and elemental content of the triple-atom spike material is shown in Table I.

TABLE I: Isotopic and Elemental Content of the Triple-Atom Spike (Decay-corrected to 5/1/87)

Pu isotope:	238	239	240	241	242	244	Assay of Plutonium	
Atom Percent:	0.2169	2.1557	32.586	2.5348	45.287	17.220	mg/g soln.:	0.45756
±95% C.I.:	0.0008	0.0012	0.002	0.0011	0.004	0.003		0.00024

The triple-atom spike aliquots, each containing 1-2 mg plutonium, were blended with aliquots of a plutonium metal standard (NBL CRM No.126) and oxide standard (NBL CRM No. 122). These mixes were analyzed for plutonium content using the IDMS technique, with the Pu-242/Pu-239 (isotope dilution ratio) being normalized using the Pu-244/Pu-240 (internal standard ratio). A Pu-240/Pu-239 measurement was made to determine the relative concentrations of the spike and sample. Since all ratios were measured at the same point in time, corresponding to the exact points on the theoretical fractionation curve, bias corrections determined from the internal standard isotope ratio were applicable to the isotope dilution ratio.

The results of the assay of plutonium metal and oxide CRMs using the triple-atom material are given below in Table II. The table also compares the overall mean of each data set with the known value for each CRM.

TABLE II: Plutonium Assays Using the Triple-Atom Spike Material (Decay-corrected to 5/1/87)

Analysis No.	mg Pu Metal in Sample	mg Pu in Sample	%Pu/Pu Metal (Recovery)	mg Pu Oxide in Sample	mg Pu in Sample	%Pu/Pu Oxide (Recovery)
1	1.32311	1.32259	99.961	2.60008	1.31572	87.675
2	1.23674	1.23621	99.957	1.11455	0.97731	87.687
3	1.13979	1.13933	99.959	1.27196	1.11494	87.655
4	1.05223	1.05205	99.983	1.13919	0.99904	87.697
5	1.46270	1.46238	99.978	1.08056	0.94866	(87.793)
6	1.12079	1.12049	99.973	1.67780	1.47083	87.664
7	1.19123	1.19087	99.969	1.41632	1.24192	87.686
8	0.99811	0.99802	99.990	1.39705	1.22474	87.666
		$\bar{x}$:	99.971			87.676
		%RSD:	0.012			0.017
		95% C. I.,%:	±0.010			±0.016
% difference from known value :			+0.015			-0.021

CONCLUSION

This work, as well as previous studies, has demonstrated that the internal standard technique is a precise method for the determination of isotope ratios in mass spectrometry. High accuracy can be obtained if the internal standard's isotopic composition is known to a high degree of certainty. Unique to this study was the consolidation of a well-characterized internal standard with a well-characterized spike isotope within the same material to yield high precision and accuracy elemental assay values. This internal standard-assay spike technique allowed IDMS precision and accuracy improvements of at least a factor of 5 or 10 over external calibration methods to be obtained.

Since the internal standard and sample mixture has a single physiochemical characteristic, behavior anomalies between standard and sample due to impurities, matrices, and analytical conditions do not exist when using the technique. This makes the use of the triple-atom as a calibration material especially useful in IDMS and safeguards measurements.

REFERENCES

1. Dietz, L.A., et al., Anal. Chem., 34 (1972), 709-710.
2. Smith, D.H., et al., INMM Journal, XIII, No. 2 (May,1985), 44-46.
3. Callis, E.L., Anal. Chem. in Nucl. Tech, Ann Arbor: Ann Arbor Science, 1982, pp 115-123.
4. Holland, M.K., et al., NBL-299 (June, 1981).

Presented at the 35th ASMS Conference on Mass Spectrometry and Allied Topics
May 24-29, 1987, Denver, CO

MATRIX EFFECTS IN SPUTTER ATOMIZATION/RESONANCE IONIZATION MASS SPECTROMETRY OF URANIUM*

Douglas E. Goeringer, Warner H. Christie, and Robert E. Valiga
Oak Ridge National Laboratory, Analytical Chemistry Division
P.O. Box Y, Oak Ridge, Tennessee 37831

Although SIMS is without peer as a qualitative surface analytical technique, its quantitative aspects are plagued by wide variations in secondary ion yields attributed to sample matrix effects. Because the major fraction of secondary particle emission from an ion beam sputtered surface usually consists of neutral atoms and molecules, post-ionization of the desorbed neutral fraction potentially has significant advantages of enhanced sensitivity and reduction of such matrix effects. Sputter atomization/resonance ionization mass spectrometry (SA/RIMS), which combines ion beam sample bombardment, resonant multiphoton post-ionization of sputtered atoms, and mass analysis of laser-generated ions, is used in this paper to investigate matrix effects on the neutral fraction ejected from ion-bombarded, uranium-containing compounds.

The ion microprobe mass analyzer (IMMA) used in this work has been described (1). Modifications to the ion extraction lens system, which aid discrimination against secondary ions while allowing efficient collection of lower energy laser-generated ions, have also been detailed there. The laser system was a tunable dye laser (Quanta Ray PDL-2) pumped by a pulsed (10 Hz) Nd:YAG laser (Quanta Ray DCR-2A). Data acquisition and control for the experiments were performed by a DEC-LSI-11/23-Plus based microcomputer system. U has a strong resonance ionization signal at 591.5 nm corresponding to a two step, bound-bound transition followed by an ionization step. Further experiments revealed that UO^+ and UO_2^+ photoions can also be produced at all wavelengths covered by the tuning range of the Rhodamine 610 dye (580-595 nm). To demonstrate the effect of sample matrix on neutral yields, a set of depth profile measurements using cw Ar^+ sputtering was made on a thin film UO_2/U metal sample by monitoring U^+, UO^+, and UO_2^+ photoion signals produced at 591.5 nm as a function of time. In the absence of any matrix effects on neutral yields, the U^+ signal from the UO_2 film would be about 3 times smaller than that from U metal. However, as shown in Figure 1, the photoion signal for U^+ from the UO_2 layer was over 40 times less than that from the U metal suggesting that the ground-state U atom fraction was strongly influenced by a matrix effect. Additionally, the photoion signals for UO^+ and UO_2^+ photoions decreased at the transition from the UO_2 layer to the U metal surface, suggesting that those molecular ions were primarily produced by direct photoionization of neutral oxide molecules and not by the reaction of residual oxygen with laser-generated uranium ions or by combination of sputtered U atoms with residual oxygen followed by photoionization. A set of experiments demonstrating the effect of surface contamination on U neutral yields was also performed by monitoring the photoion signal for U^+ during an Ar^+ pulsed-cw-pulsed sputtering sequence on U metal. The primary beam pulse duration was varied from 5 to 200 µs for the set of experiments, with the laser fired at the end of the gating pulse in each case. Figure 2 shows the time response of the U^+ photoion signal for two of the pulse widths used, 5 and 200 µs. For all pulse widths there was an immediate increase

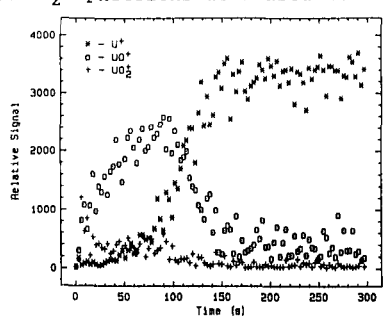

Figure 1

*Research sponsored by the U.S. Department of Energy, Office of Basic Energy Sciences, under Contract DE-AC05-84OR21400 with Martin Marietta Energy Systems, Inc.

in the photoion signal for U^+ upon switching to cw mode; in each case the signal was also observed to decay at the transition from cw to pulsed mode as the surface was again covered with chemisorbed impurities. The data suggest that monolayer coverage occurred about 60 s after the transition from cw to pulse-sputter mode (indicated elapsed time 100 s). However, the reduction in photoion signal for U^+ at that point was greater than the factor of about 3 expected from the reduced density of surface U atoms. Figure 3 shows the time response of signals for UO^+ and UO_2^+ photoions in a pulsed-cw sequence (5 µs pulse). The oxide photoion signals were quite evident during pulse-sputtering then declined rapidly under cw bombardment. These experimental results suggest that the ground-state U atom fraction from sputtered U metal is sensitive to a matrix effect due to chemisorbed surface impurities. The signals for UO^+ and UO_2^+ photoions observed in pulse-sputter mode suggest that oxide formation on U metal is responsible for this matrix effect.

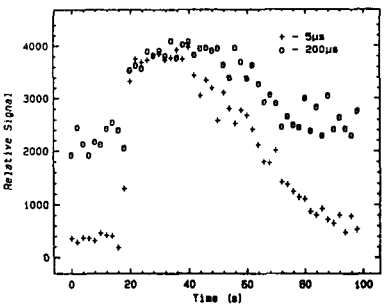

Figure 2

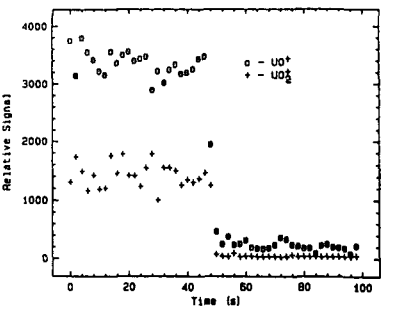

Figure 3

Results from Kimock et al. (2) indicated that the photoion signal from pulse-sputtering should equal that from cw-sputtering for pulse widths > 5 µs. Therefore, neglecting the matrix effect from chemisorbed oxygen, the photoion signal for U^+ with 5 µs pulse-sputtering is assumed equal to that with cw-sputtering. Kimock et al. also calculated the fraction of neutrals intersected by the laser beam during a 5 µs sputter pulse to be approximately 0.28. Thus, with these assumptions, the number of ground-state U atoms ejected with a 5 µs sputter-pulse can be obtained by dividing the number of laser-generated ions from cw-sputtering by the factor 0.28. The number of secondary ions generated in such a sputter-pulse can easily be calculated from secondary ion count rates by multiplication. Given these caveats, the ratios of ground-state uranium atoms to ions (U°_{Ar}/U^+_{Ar}) for cw, Ar^+ ion sputtering from U metal and UO_2 are estimated to be 3.0×10^3 and 6.2×10^1, respectively. The relative ratio of ground-state uranium atoms from U metal and oxide ($U^\circ_{metal}/U^\circ_{oxide}$) is estimated by direct division of the corresponding U^+ photoion signals to be 4.4×10^1.

Just as found in SIMS, where chemistry in the sputter region controls relative ion yields, it is also becoming clear that similar effects can control the composition of the sputtered neutrals available in the gas phase for RI or MPI. The possibility that the neutral fraction for a single element in the sputtering event may be partitioned between a matrix dependent variety of species (atoms, polyatomics, clusters, etc.) can reduce the sensitivity and quantitative capability of techniques based on post-ionization of sputtered atoms.

(1) Donohue, D.L.; Christie, W.H.; Goeringer, D.E., McKown, H.S. Anal. Chem. **1985**, 57, 1193-1197.
(2) Kimock, F.M.; Baxter, J.P.; Pappas, D.L.; Kobrin, P.H.; Winograd, N. Anal. Chem. **1984**, 56, 2782-2791.

"The submitted manuscript has been authored by a contractor of the U.S. Government under contract No. DE-AC06-84OR21400. Accordingly, the U.S. Government retains a nonexclusive, royalty-free license to publish or reproduce the published form of this contribution, or allow others to do so, for U.S. Government purposes."

Presented at the 35th ASMS Conference on Mass Spectrometry and Allied Topics
May 24-29, 1987, Denver, CO

METALS ANALYSIS BY GLOW DISCHARGE MASS SPECTROMETRY: FACTORS AFFECTING QUANTITATIVE ANALYSIS.

F. L. King and W. W. Harrison, University of Virginia, Charlottesville, VA 22901

Glow discharge mass spectrometry is a technique that provides for the direct elemental analysis of solid conducting samples. This technique has developed to the point where it is now employed in commercial and industrial applications requiring semiquantitative analysis. The extension of the technique to perform quantitative analyses requires that operating parameters be more closely controlled and attention paid to their effects on the spectra obtained. In addition, Relative Sensitivity Factors may be employed to improve the accuracy of the data obtained.

In simplest terms the glow discharge is like a neon lamp. Potential applied across a low pressure atmosphere of rare gas leads to electrical breakdown of the gas. In our case the gas is argon and the cathode is the sample of interest. The breakdown produces argon ions which impact the sample, "sputtering" material into the negative glow region, where collisions with metastable argon atoms lead to Penning ionization of sample atoms. The ion population, which reflects the composition of the sample, can then be sampled by a mass spectrometer.

EXPERIMENTAL

In the following studies the sample metal was machined into a pin, 1.7 mm in diameter with 5 mm of length exposed. This pin is mounted into a direct insertion probe that provides the cathode potential connection. The macor probe tip is constructed to shield the pinholder, exposing only the sample pin to the discharge. The probe is introduced to the source region through a .5 in. ball valve assembly. This allows sample intoduction without exposing the source region to atmosphere, and provides a means of adjusting the distance from the sample to the ion exit orifice.

The mass spectrometry system consists of the glow discharge source coupled to a quadrupole mass analyzer. The source region is simply a 1 in. stainless steel tube with a Cajon Ultra-Torr tee attached to one end and the other end welded to the ball valve assembly. This ball valve assembly is connected to the mass spectrometer housing by an adjustable bellows. The tee is modified such that an ion exit orifice is mounted to allow axial sampling of the discharge. Adjustment of the bellows permits optimization of the alignment between the ion exit orifice and the differential pumping orifice to the quadrupole chamber.

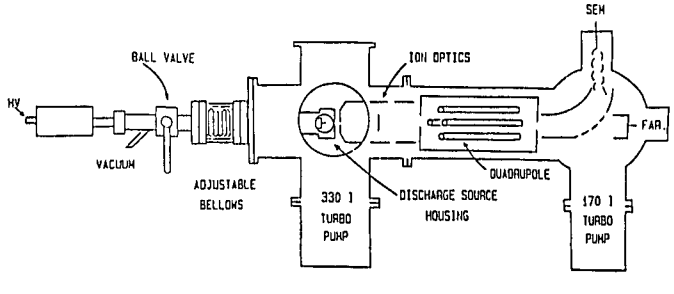

The ions pass through the differential pumping orifice to a three lens ion optic with a neutral beam stop where they are then focused into the quadrupole mass analyzer. The analyzed ions can be detected by either an on-axis Faraday cup or deflected to a 90 off-axis SEM. The SEM is operated in the ion counting mode with a Tracor Northern TN-7200 MCA to acquire spectra. The MCA is interfaced to a Hewlett-Packard 9816 computer which is used to process the data and control the quadrupole.

RESUSTLS AND DISCUSSION

With the system described, detection limits on the order of 10 ppb are routinely observed. This sensitivity has made the problem of isobaric molecular interferents a greater concern. The concentration of $FeAr^+$ in a steel sample is seen to be 400 ppm. At the current detection limits, species present at 25 ppm can contribute MAr^+ to the observed spectra. In an effort to investigate minimization of contribution from these species, studies have been conducted to ascertain the effect of sampling distance and discharge pressure on the relative magnitude of these species.

The direct insertion probe allowed the cathode to be moved relative to the ion exit orifice without terminating the discharge, allowing us to profile the plasma. The intensities of the $FeAr^+$, mass 96, and the Fe_2^+, mass 112, relative to the intensity of the Mo isotope at mass 100 was followed as a function of distance. Attributing the intensity at 96 which is beyond that expected for ^{96}Mo to contribution from $FeAr^+$, it is observed that a distance of 5 mm is optimal for reducing argides. The signal at 112 is due to Fe_2^+ and is seen to drop drastically, and then level off, as the distance is increased to 6mm. The signal at 100 is taken to profile a sputtered species without interference, the ^{100}Mo isotope. The plot shows that operation at 13 mm optimizes signal while not greatly increasing the contribution of moleculars from their minimum values.

The pressure dependence of the molecular species relative to the monoatomic species was studied with the sampling distance set at 13mm as indicated by the previous study. Again the ratios of intensities at mass 96 and mass 112 relative to mass 100 were followed. The $FeAr^+$ signal reaches a minimum at .7 Torr and the Fe_2^+ signal levels off at a minimum when the pressure is 1.2 T or greater.

Relative Sensitivity Factors (RSF) are applied to correct data for variations in sensitivity between elements. Signal to concentration ratios are calculated for the elements in a known standard; these ratios are averaged for a series of runs. RSFs are calculated from these averaged values according to the following equation: RSF = (Intensity Y/Conc. Y)/(Intensity X/Conc. X). Conc. X is known for the sample to be analyzed as well as for the standard. Conc. Y is known in the standard and not known in the sample. The advantage to be gained in using these RSFs was studied using NBS 1261a as the sample for which concentrations were to be obtained. Certified concentration values for this standard were compared with concentrations calculated with and without RSF correction. For most species the RSF correction provides more accurate results.

Ion optic optimization was shown to have a significant effect on signal intensities across the mass range. The effect of ion optic voltages is seen to lead to significant changes in RSF values across the mass range. Species close in mass to Ni exhibit smaller changes than those at higher mass.

In advancing from semiquantitative analysis to quantitative analysis, the operating conditions of a glow discharge mass spectrometry system must be chosen and reproduced with greater care. Studies of sampling distance and pressure effects indicate that there are conditions which minimize the contribution of molecular interferents to the spectra. Ion optic settings are shown to have a large effect on the observed sensitivity of species across the mass range. Employing RSFs in data analysis is seen to improve the accuracy of the concentration values obtained for a sample.

Presented at the 35th ASMS Conference on Mass Spectrometry and Allied Topics
May 24-29, 1987, Denver, CO

STRUCTURAL DETERMINATION OF GLYCOPEPTIDE ANTIBIOTICS BY TANDEM MAGNETIC DEFLECTION MASS SPECTROMETRY

Gerald D. Roberts, Steven A. Carr and [1]Siegfried B. Christensen, Dept of Physical and Structural Chemistry, L-940 and [1]Macromolecular Sciences, SmithKline and French Laboratories, King of Prussia, PA 19406

During the past few years structural determination of new glycopeptide antibiotics of the vancomycin-ristocetin family has been an important task in our laboratories. These molecules consist of a peptide core, usually made up of uncommon amino acids, with one or more carbohydrate units attached to this core through an atom of oxygen (Fig. 1). We have shown that fast atom bombardment mass spectrometry (FABMS) plays a vital role in providing essential information in solving these structural problems Information that can be obtained from the "normal" FAB spectra includes the molecular weight, the number of atoms of chlorine present, elemental composition and, in favorable cases, carbohydrate composition and sequence (Roberts et al., 1985).

Spectra obtained in the MS/MS mode of operation are now being used to extend the amount of structural information that is obtainable by FABMS. The daughter ion spectra resulting from high energy collision-induced decomposition (CID) of selected MH^+ ions provide unique structural information about functional groups appended to the cyclic peptide core. In addition, carbohydrate-related fragments are easily detected in the MS/MS spectra and substantiate assignments based on interpretation of the normal FAB spectra. The daughter ion spectra of vancomycin, parvodicin C_1 and ardacin A are discussed here in terms of the structural information present and the differences in the spectra when some of the key operating conditions are varied.

Daughter ion spectra were obtained in our laboratories on the VG ZAB-SE 4F a four sector magnetic deflection instrument of B_1E_1-E_2B_2 geometry. Daughter ions were produced in collision cell 3, located between the two instruments, by collision with a neutral gas (helium or argon) at energies of either 1.0 (grounded cell) or 0.5 (cell floated at 5 kV or 1/2 the accelerating voltage).

In general most of the significant peaks observed in the daughter ion spectra (Fig. 2) result from the cleavage of the glycosidic bonds. In the daughter ion spectrum of vancomycin major peaks are present that correspond to loss from the MH^+ of vancosamine (m/z 1305) and both vancosamine and glucose residues (m/z 1143). In addition, fragments corresponding to a) the vancosamine oxonium ion and possible fragments of this residue and b) a portion of the N-methyl leucine amino acid residue are observed

Glycolipid-containing antibiotics such as parvodicin C_1 and ardacin A (both of which contain two carbohydrate units, mannose and a glycolipid, e.g., Fig 1b) yield CID spectra (Fig. 2b) similar to that of vancomycin. Peaks are observed for the loss of the glycolipid residue and for the oxonium ion of the glycolipid itself. The loss of carbon dioxide is also indicated for both compounds. An unusual and intense fragment is observed in the CID spectra of both parvodicin C_1 and ardacin A that possibly corresponds to the combined loss of methylamine, carbon monoxide and both carbohydrate residues.

Daughter ion FAB spectra are quite different from the normal spectra. Although similar high mass fragments are observed in both the CID and normal spectra, lower mass fragments are not obvious in the latter. The only low mass fragment observed in the normal FAB spectrum of vancomycin is at m/z 100 (for comparison see Fig. 2 for the CID spectrum) Collision gas is necessary to observe a significant number of daughter ion peaks in tandem MS For example, the "no gas" MS/MS spectra of glycopeptide antibiotics show peaks corresponding to loss of the carbohydrate units but no significant peaks at lower masses

Modifying the collision energy also has a significant impact on the appearance of the daughter ion spectra. For vancomycin, the daughter ion spectrum taken at a collision energy of 0 5 is qualitiatively similar to the spectra acquired at a collision energy of 1.0; but the intensities of the low mass peaks are significantly greater in the former. A possible explanation for this observation is that at a collision energy of 1.0 low mass fragments have lower translational energies than the same fragments at a collision energy of 0.5 and thus are discriminated against more by the analyzer. The use of different collision gases can also produce differences in the daughter ion spectra. Although the He and Ar daughter ion spectra of the vancomycin MH^+ are qualitatively and quantitatively similiar at a collision energy of 0.5, minor differences are evident in the relative intensities of certain high mass peaks.

In conclusion, daughter ion mass spectra of the glycopeptide antibiotics provide structural information that both confirms and supplements the normal FAB data The most useful analytical data are obtained at a collision energy of 0.5 using either He or Ar as the target gas. Peaks resulting from the loss of carbohydrate as well as carbohydrate ion peaks themselves are observed The peptide core, especially when completely cyclized is very stable and fails to dissociate to any measurable extent. However, functional groups such as carboxylic acid groups or substituted amino groups and exocyclic amino acids pendent to the cyclic core can be determined by tandem MS

1 Roberts, G D , Carr, S. A., Rottschaefer, S. and Jeffs, P. W., (1985) J Antibiotics, 38, 713-720.

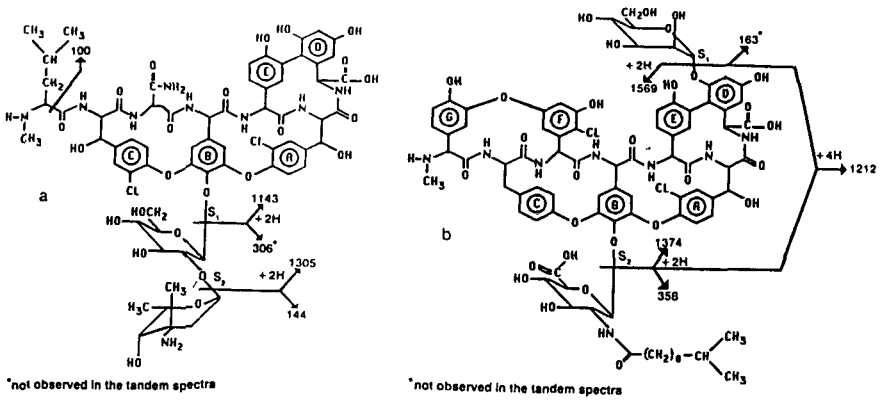

Figure 1. Structure of a) vancomycin and b) parvodicin C_1 with predicted collision induced cleavage points and anticipated daughter ions

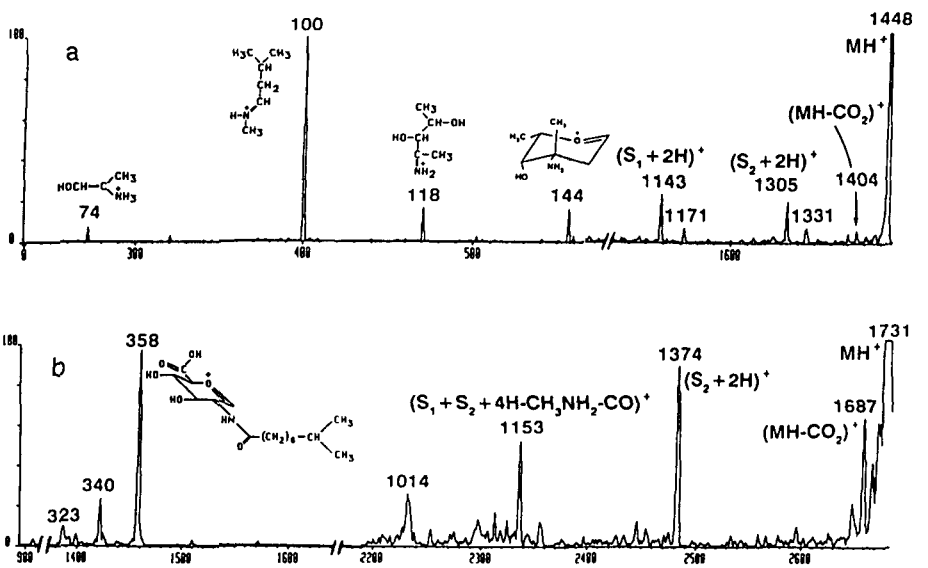

Figure 2 Daughter ion spectrum of a) vancomycin and b) parvodicin C_1. Solid sample was dispersed on the stainless steel probe in a matrix of monothioglycerol (3-mercapto-1,2-propanediol) containing oxalic acid. C. E. = 0.5, He, 50% Atten

Presented at the 35th ASMS Conference on Mass Spectrometry and Allied Topics
May 24-29, 1987, Denver, CO

STRUCTURAL ELUCIDATION OF AN UNKNOWN TRICHOTHECENE USING CAD FRAGMENTATION MAPS.

R.J. Pawlosky, C.J. Mirocha, and H.K. Abbas
The University of Minnesota
St. Paul, MN, 55108

The chemical structure of an isomer (3-15 hydroxy-4-acetoxy-8-[3-methyl butryloxy]-12,13 epoxy trichothece-9-ene) of HT-2 toxin was deduced using primary and secondary fragmentation mass spectra. The compound belongs to a group of sesquiterpenoids that have been shown to have toxic activity in humans and animals. These toxins are produced by fungi (Fusarium spp.) which infest food grains. The isomer was isolated along with other trichothecenes from a fungus culture grown in the laboratory.

The primary mass spectra of the isomer's trifluoro acetyl derivative in both CI and EI confirmed the molecular weight as 616. The mass spectra were similar to both the C3,4 HT-2 toxin and the C3 T-2 toxin (3-hydroxy 4,15 diacetoxy-8-[butryloxy] 12,13-epoxy trichothec-9-ene).

Establishing the structure of the unknown compound was undertaken using the collisional activated decomposition (CAD) spectra of various primary ions. These spectra were compared to a library of CAD spectra of other various trichothecenes. The C3,15 isomer's fragmentation was mapped from the molecular ion to mass 81. Structures corresponding to the various fragment ions were deduced from mass spectral comparison to known trichothecenes.

Collision activated decomposition was undertaken at low energy (14 eV) using a hybrid mass spectrometer (EBQQ geometry) with argon (pressure 1X10-6 torr measured remotely at the throat of the CAD chamber).

Analysis of the fragmentation maps concluded the structure to be the C3,15 isomer of HT-2 toxin (C3,4) rather than the C4,15 isomer. The proof was carried out through two separate fragmentation pathways. One pathway followed the C15 fragmentation, the other followed the C4 fragmentation. Comparisons of those CAD spectra to T-2 (C3), iso T-2 (C4), and HT-2 CAD spectra concluded the structure as the C3,15 isomer of HT-2.

ISO HT-2 TOXIN C3,15 HYDROXY TFA derivative.

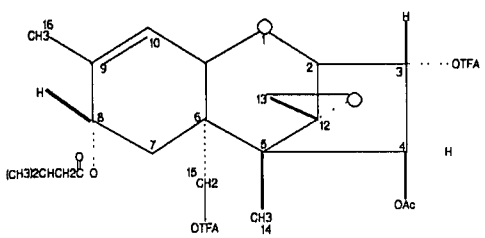

Presented at the 35th ASMS Conference on Mass Spectrometry and Allied Topics
May 24-29, 1987, Denver, CO

A NOVEL METHOD FOR DETERMINING THE ACTIVE HYDROGEN CONTENT OF TRACE QUANTITIES OF BIOLOGICAL MATERIALS

Fulton G. Kitson
Central Research & Development Department, E. I. du Pont de Nemours & Company
Wilmington, DE 19898

OBJECTIVE

To aid the identification of unknown metabolites and other materials of biological origin by using TMS and d_9-TMS derivatization to determine the number of active hydrogens in all components in a single capillary GC/HRMS run.

INTRODUCTION

Many biological identification problems involve mixtures of trace components of low volatility that will not elute from capillary GC columns without preparing volatile derivatives. Even with accurate mass measurement, a number of possible elemental compositions exist. In our laboratory, the number of possibilities are routinely reduced by determining the number of TMS groups that exchange for active hydrogens on any compound of interest in the mixture.

EXPERIMENTAL PROCEDURE

A small portion of the sample is dissolved in the minimum amount of solvent and the solution is divided into two equal portions. The usual TMS derivative is prepared using one portion. The other portion is used to prepare the deuterated TMS derivative. After the reactions are completed, the two portions are mixed and a sample is injected immediately into the capillary GC/HRMS system. In general, the first part of the GC peak contains the deuterated derivative (scan 241) while the second part of the GC peak contains the regular TMS derivative (scan 246).

REAGENTS USED:

N, O-BIS (Trimethylsilyl)acetamide
Cat. No. 38838, Pierce Chemical Company, Rockford, IL 61105

N, O-BIS (Trimethylsilyl-D9)acetamide
Cat. No. MD-1060 Merck & Company, Rahway, NJ 07065

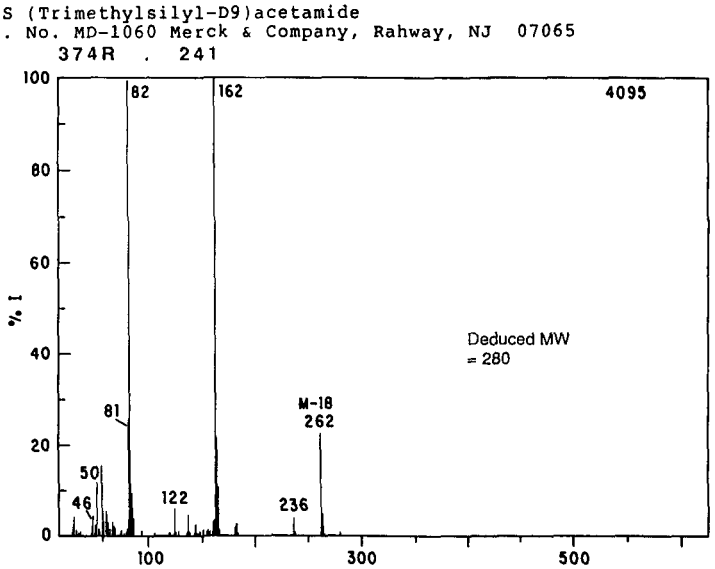

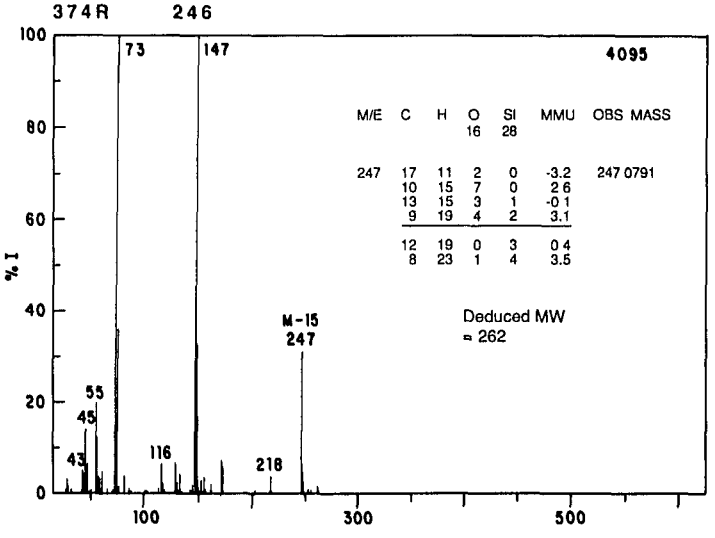

INTERPRETATION OF THE DATA FIRST GC PEAK

Mass difference between the deduced molecular weights = 18

Therefore, 2 TMS groups are present.

The elemental composition of m/z 247 is:	$C_8 H_{11} O_4 Si_1$
Adding CH_4 to deduce *the molecular formula*	CH_4
	$C_{10} H_{15} O_4 Si_1$
Subtracting $C_3 H_9 Si$ for each active hydrogen	$C_3 H_{18} Si_2$
The original molecular formula	$C_7 H_6 O_4$

This is succinic acid

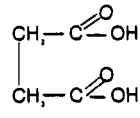

CONCLUSION

Although deuterated derivatives have been used in this and other laboratories for some time, trace levels of materials of biological origin can be efficiently identified by combining this simple derivatization procedure with capillary GC and high resolution mass spectrometry. The elemental compositions of each component in a complex mixture are available along with retention time data from the gas chromatograph and the number of active hydrogens from the derivatization procedure. This data combination significantly enhances structure assignment.

Presented at the 35th ASMS Conference on Mass Spectrometry and Allied Topics
May 24-29, 1987, Denver, CO

CATIONIZATION EFFICIENCY IN LASER DESORPTION FT/ICR MASS SPECTROMETRY

Ronald E. Shomo, II, Francis R. Verdun, and Alan G. Marshall

Department of Chemistry (and Department of Biochemistry)
The Ohio State University
120 West 18th Avenue
Columbus, OH 43210

Laser desorption Fourier transform ion cyclotron resonance mass spectrometry (LD/FT/ICR), performed with a Tachisto 215G pulsed CO_2 laser (10.6 μ), typically produces a prominent pseudomolecular $(M+K)^+$ ion for involatile organic [1,2] or polymer [3] samples previously doped with potassium bromide.

In investigating the effect of cation (as the Li, Na, K, Rb, Cs iodide salts added to the sample before laser desorption) on both the extent of fragmentation and the degree of cationization of the molecule and its fragments, for organic (e.g., sucrose) and polymer (e.g., Triton®) samples, we find that cationization of laser-desorbed neutral molecules by alkali ion attachment enhances the production of pseudomolecular ions while minimizing fragmentation.

Rollgen et al. [4] showed that among various alkali metals, the highest cationization yield of glucose was produced by attachment of Na^+ ions. The relative abundances of pseudomolecular (e.g., $(M+Na)^+$) and fragment ions appeared to depend upon the polarity of the neutral parent, the metal ion affinity, and the initial kinetic energy of the alkali metal ion.

In an attempt to separate these effects, we exposed neutrals (Triton® X100 and glucose) to various laser-generated alkali metal ions, as a function of laser energy and reaction period. For example, Figure 1 shows that glucose is most efficiently cationized by Cs^+, followed closely by Rb^+. All of the alkali metals ions except for Cs^+ form abundant metalized glucose dimer ions.

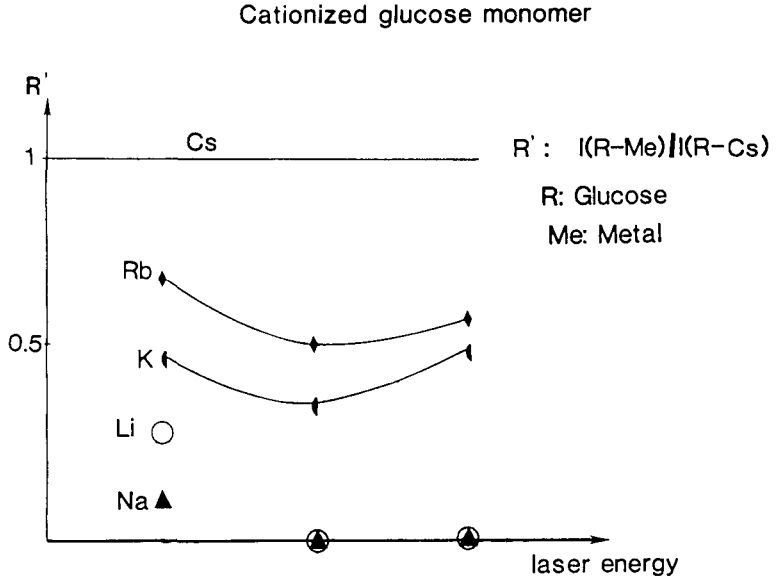

Figure 1. Cationization efficiency (measured from FT/ICR relative peak areas) vs. laser power, for reaction of alkali metal ions with glucose.

Variation of the ion-molecule reaction period (i.e., the period between the reagent ion-forming laser pulse and product ion excitation/detection) shows that non-equilibrium conditions prevail for up to ~1.5 seconds before the relative abundances of various cationized Triton® X100 species stabilize (see Figure 2).

Table 1 lists the number- and weight-average molecular weights, M_n and M_w, determined from the relative abundances of cationized Triton® oligomers, detected 1.5 sec after a single laser pulse, for various binary combinations of alkali metals. Interestingly, M_n and M_w for attachment of a given alkali metal ion to the various oligomers depend on which other alkali metal(s) is (are) present. In any case, M_n and M_w determined from attachment of alkali metal ions alone or in combination are quite similar to the values determined by chromatography. Of all the alkali metals, Rb gave M_n and M_w is closest agreement with the chromatographic values.

Based on our preliminary results, we conclude that Cs^+ appears to produce the most abundant pseudomolecular ions with minimal fragmentation, whereas Rb^+ appears to produce an ion distribution which most closely reflects the distribution of neutral oligomers in the original polymer.

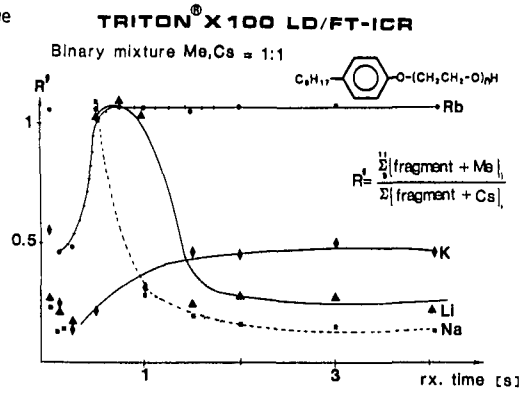

Figure 2. Triton® X100 cationization efficiency (relative to Cs^+), measured from the combined FT/ICR mass spectral peak areas for all cationized oligomers (9-11 monomeric units) containing a given alkali metal vs. time between the laser pulse and ion detection.

Table 1. Number- and weight-average molecular weights, M_n and M_w, determined from the relative FT/ICR mass spectral abundances of cationized oligomers of Triton® X100. Note the close agreement with M_w determined by chromatography.

	M_n	M_w
Li/Cs	709/616	713/686
Na/Cs	704/640	708/687
K/Cs	619/611	624/623
Rb/Cs	645/599	640/617
Σ Me/Cs	559/565	564/574

LC/MS Data: M_w = 646 amu

We thank D. G. Westmoreland (Rohm & Haas Company) for providing Triton® X100 and for valuable discussions. This work was supported by grants (to AGM) from the National Science Foundation (CHE-8617244), the U.S.A. Public Health Service (GM-31683), and The Ohio State University.

1. Shomo, R. E., II; Marshall,A. G.; Weisenberger, C. R. (1985) Anal. Chem. 57, 2940-2944.
2. Shomo, R. E., II; Marshall, A. G.; Lattimer, R. P.; (1986) Int. J. Mass Spectrom. Ion Proc. 72, 209-217.
3. Verdun, F. R.; Shomo, R. E., II; Marshall, A. G.; Westmoreland, D. G.; "Mass Spectrometry of Polymers via Laser Desorption Fourier Transform Ion Cyclotron Resonance"; 38th Pittsburgh Conference March, 1987, Atlantic City, N. J., paper #945.
4. Schmelzeisen-Redeker, G.; Giessmann, U.; Rollgen, F. W.; (1985) Org. Mass Spectrom. 20, 305-309.

Presented at the 35th ASMS Conference on Mass Spectrometry and Allied Topics
May 24-29, 1987, Denver, CO

FAB-MS AND PEPTIDE STRUCTURE DETERMINATION:

A. Van Dorsselaer , P. Lepage and D. Fraisse°

Centre de Neurochimie CNRS, UA31, 5 rue B. Pascal 67084 Strasbourg FRANCE and °Centre d'Analyse CNRS, BP22, 69390 Vernaison, FRANCE.

Peptide structure elucidation is usually performed by Edman degradation associated with amino acid analysis. We would like to illustrate that FAB-MS is able to yield informations which are not given by other methods.

Two new lipophilic proteins also named proteolipids (1) were partially sequenced with the aid of FAB-MS mass spectrometry.

These proteins were cleaved by enzymatic (trypsin) and chemical (CNBr, HBr/DMSO) reagents in peptides which were purified by reversed phase HPLC (2). Amino acid analysis, partial manual sequence and FAB-MIKES mass spectrometry were used to sequence isolated peptides. Mass spectrometry allowed sequence determination with a very high degree of confidence.

Often enzymatic or chemical cleavages of proteins produced peptides with apparently very close characteristics (same amino acid composition, same Edman degradation) which correspond to several close HPLC peaks. FAB-MS, and especially MIKES, permitted an easy identification of several of these peptides. Structure with pyroglutamic forms, methylated glutamic acid, cyclised homoserinelactone, and chymotryptic peptides were identified. An exemple is given on figure 1 two peptides from the same protein showed very close characteristics (amino acid analysis, Edman degradation) but MIKES was able to identify and localize the difference which was a methylation of the glutamic acid. This methylation is probably an artefact of the extraction procedure.

FAB-MS is also very usefull as a supplementary criteria of identification for large synthetic peptides. For exemple an impurity was isolated from synthetic Growth Hormone Releasing Hormone (chemical mass: 5040.7). Figure 2 shows that the chemical mass of this impurity was higher of 16 amu than authentic GHRH. Other methods were not able to detect this oxidation. It is worth while to note that to obtain this information a resolution of 1000 was sufficient.

In conclusion:

1°) Mass spectrometry should always be use, at least as a control, for peptide sequencing.

2°) Mass spectrometry is the best method for solving the problem of cleavage peptides with close structures. FAB-MS is able to determine subtle modifications on peptides.

3°)High molecular weight measurement of the chemical mass at low resolution could already yield important data on a peptide.

REFERENCES:
1- G. Helynck et al. Eur. J. Biochem., 133, 689-695, (1983).
2- P. Lepage et al. Biochimie, 68, 669-686 (1986).

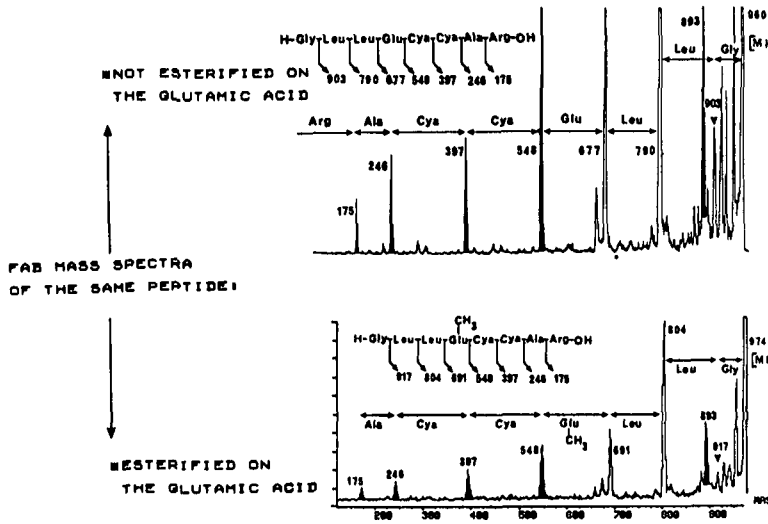

Figure 1: MIKES of two different peptides isolated from the same protein (1). The difference is clearely localized on the glutamic acid.

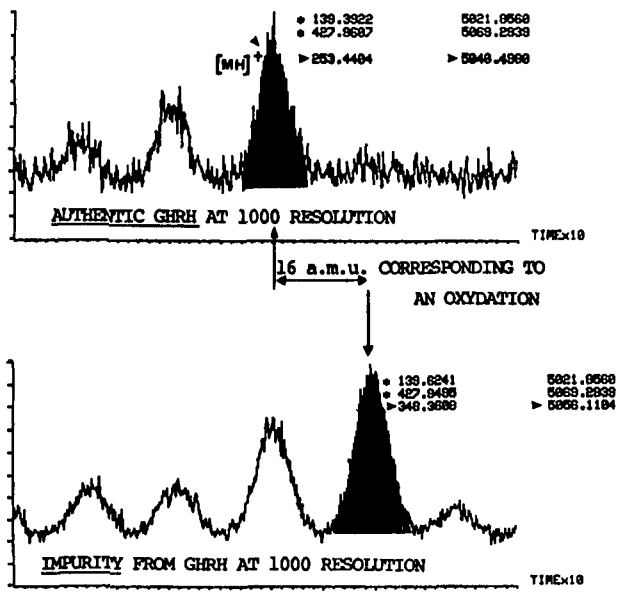

Figure 2: Chemical mass measurement of synthetic Groth Hormone Releasing Hormone and of an impurity isolated by HPLC which have the same amino acid analysis and the same Edman degradation as GHRH. FAM-MS showed that this impurity is an oxidized form of GHRH.

Presented at the 35th ASMS Conference on Mass Spectrometry and Allied Topics
May 24-29, 1987, Denver, CO

FAB MAPPING PROTEIN STRUCTURAL DETERMINATION OF RECOMBINANT HUMAN INTERFERON GAMMA

FIONA M. GREER[1], HOWARD R. MORRIS[2], TONY FALLON[3] and STEVE J. BREWER[4]

1. M-Scan Ltd. Silwood Park, Sunninghill Ascot, Berks. UK.
2. Dept. Biochemistry, Imperial College of Science and Technology , London.
3&4*. G.D. Searle & Co. Ltd. Lane End Road, High Wycombe, Bucks. UK.

Protein structural determination of recombinant human Interferon gamma (IFN-gamma) was carried out using the technique of "FAB MAPPING" (Morris, et al. 1981, 1983). The concept is to use specific enzymic or chemical digests to produce a mixture of peptide fragments followed by FAB mass spectrometry either directly or on partially purified mixtures to identify their molecular weights. Various operations may be then carried out on the peptide mixture to aid interpretation. A definite advantage of the "FAB MAPPING" procedure is that there is an equal probability of observing the C-terminal as well as the N-terminal regions of the protein.

A sample of IFN-gamma was first digested with Trypsin and the MAP produced on the unfractionated mixture of peptides. This results in 72% of the protein structure being MAPPED. A less specific enzyme, Chymotrypsin, was then chosen in an attempt to MAP those portions not covered in the Tryptic FAB MAP. This digest proved very successful with 82% of the IFN-gamma structure covered, including all the mid-portions of the molecule previously unobserved in the Tryptic MAP. Despite the success of this digest, signals for the anticipated N- and C-terminal peptides were noticeably absent and no strong unexplained signals were present to replace them. Whilst it is not uncommon for a proportion of peptides to be unobserved in the spectrum of mixtures due to surface suppression phenomena, it is unusal that these should be concentrated at the N- and C-termini. In order to study the integrity of the C-terminus, a CNBr cleavage was carried out. The results showed a clear signal at m/z 1090 for the C-terminal peptide :

LEU - PHE - ARG - GLY - ARG - ARG - ALA - SER - GLN^{146}

although the strength of the signal was low suggesting the possibility of C-terminal "ragged-ends". The overall structural confirmation achieved represents 93% of IFN-gamma.

CNBr treatment of the insoluble IFN-gamma suggested the existence of a C-terminally truncated molecule in addition to the intact C-terminus.

Evidence for this is difficult or impossible to obtain by conventional sequence analysis. An experiment was therefore carried out to separate the CNBr peptides according to molecular weight by gel permeation chromatography. Individual fractions were then screened by FAB-MS

In addition to the anticipated intact CNBr fragment $\overset{138}{\text{LEU}}$-$\overset{146}{\text{GLN}}$, m/z 1090, a second major component was observed at m/z 648. This peptide corresponds to residues 138-142.

$$\text{LEU - PHE - ARG - GLY - ARG}^{142}$$

This provides evidence for a ragged C-terminus due to the loss of residues 143-146. Carboxypeptidase digest data fully substantiate this conclusion, showing rapid liberation of two major amino-acid signals, Glutamine and Arginine.

The use of FAB MAPPING has proved to be a versatile and sensitive method of protein and glycoprotein structural analysis. In particular the ability to observe that region of the protein which is most difficult to analyse by conventional methods i.e. the C-terminus, and detect heterogeneity by the strategy described here, constitutes a powerfull new procedure for Protein Chemists.

1. Morris, H.R., Panico, M., Barber, M., Bordoli, R.S., Sedgwick, R.D. and Tyler, A. (1981) Biochem. Biophys. Res. Commun. 101, 623-631.

2. Morris H.R., Panico, M. and Taylor, W. (1983) Biochem. Biophys, Res. Commun, 117, 299-305.

3. The mass spectrometric study shown here is based on reports from M-Scan Limited to G.D. Searle in December 1983, March 1984 and May 1984 and is published with their permission.

*Present addressess

3. British Bio-technology Ltd., Brook House, Watlington Road, Cowley, UK.

4. Monsanto Co., 700 Chesterfield Village Pkwy, St. Louis, Missouri.

Presented at the 35th ASMS Conference on Mass Spectrometry and Allied Topics
May 24-29, 1987, Denver, CO

Peptide/Protein Mapping at the Subnanomole Level by LSIMS: Application to Fatty Acid Binding Protein.

Bradford W. Gibson[1], Zhonghua Yu[1], William Aberth[1], A.L. Burlingame[1] and Nathan M. Bass[2]
Department of Pharmaceutical Chemistry[1] and Medicine[2], University of California,
San Francisco, CA 94143

Mass spectrometric analysis of peptides by liquid secondary ion mass spectrometry (LSIMS) can readily detect the protonated or deprotonated molecular ions and yield accurate molecular weight information. These data become particularly useful when combined with other sequencing strategies such as DNA sequencing or Edman degradation [1]. More recently, MS/MS approaches have made it easier to determine the sequences of peptides through selective collision activation of their gas phase molecular ions [2]. However, all these approaches depend upon the high abundances of the molecular ions and when analyzing very low sample amounts (low nanomole to picomole) of protein hydrolyzates or peptides, the molecular ions are generally low or absent altogether. This is due in part to chromatographic losses, inefficient transfers and introduction of contaminants originating from the solvents and HPLC packings. In order to investigate more carefully the limitations of obtaining abundant molecular ions from peptides purified at the picomole level, we have analyzed several enzymatic digests of rat heart fatty acid-binding protein (FABP).

Fatty acid-binding proteins (FABP) are a small group of proteins (MW 15,000) which are essential for binding, transport and utilization of fatty acids [3]. We have mapped out this proteins reported sequence [4] using a combination of HPLC separations followed by LSIMS analysis on a Kratos MS 50 mass spectrometer and/or a prototype Wien mass spectrometer. For these experiments, approximately 500 pmol to 1nmol of FABP was digested with trypsin and chymotrypsin respectively and separated by reverse phase HPLC on analytical (4.6 mm i.d.), narrow bore (2 mm i.d.) and/or microbore (1 mm i.d.) columns. Samples were applied to either a Wien mass spectrometer [5] or a Kratos MS 50 mass spectrometer. At these low levels, special sample handling techniques were used that minimized drying, freezing or concentration steps prior to LSIMS analysis.

In one experiment using 500 pmol of FABP, the protein was digested with trypsin and the peptides separated on an Ultrasphere ODS column (25cm x 2.1mm) (Fig. 1). The eluting peptides were analyzed by Wien MS equipped with an array detecter using 5% aliquots (25 pmol). Figure 2 shows the molecular ion region of one peptide fraction using a total of 25 pmol of material. More material was required (100 pmol or more) on a scanning Kratos MS 50 mass spectrometer system as shown in Fig. 3, but some limited fragmentation data was also observed. Some of the smaller hydrophilic peptides required acetylation to increase their surface activity. A secondary chymotryptic digest of 1 nmole was analyzed by LSIMS after HPLC separation. Between these two experiments, almost the entire structure was covered which indicated the presence of two incorrect regions-- the N-terminus and a short region in the interior domain containing residues 47-51. We have obtained a corrected N-terminal sequence from amino acid analysis, MS and MS/MS data using a total of 1 nmole:

N-acetyl-Ala-Asp-Ala-Phe-Val-Gly-Thr-Trp-Lys

From these experiments, abundant molecular ions were easily detected at the picomole level, even in cases where two or more components co-eluted. This procedure has application to proteins where only small amounts are available (1 nmole or less). However, great care needs to be taken in sample handling to obtain satisfactory results. In particular, one should avoid drying HPLC samples down prior to deposition on the probe surface. We have found that below 500 pmoles as much as 90% can be lost in this step alone. We also recommend using either microbore or narrowbore HPLC where peptides generally elute in volumes between 20-100 ul. Subsequently, aliquots should be dried directly on the probe tip where a small amount of thioglycerol (1/4 ul) has been previously applied. Alternatively, a small amount of glycerol or thioglycerol can be added to HPLC tubes prior to concentration on a Speedvac liquid concentrator.

Acknowledgement: This work was supported by the NIH Division of Research Resources, Grant RR01614 (to A.L. Burlingame) and NIH Grant AM 27643 to the Liver Center.

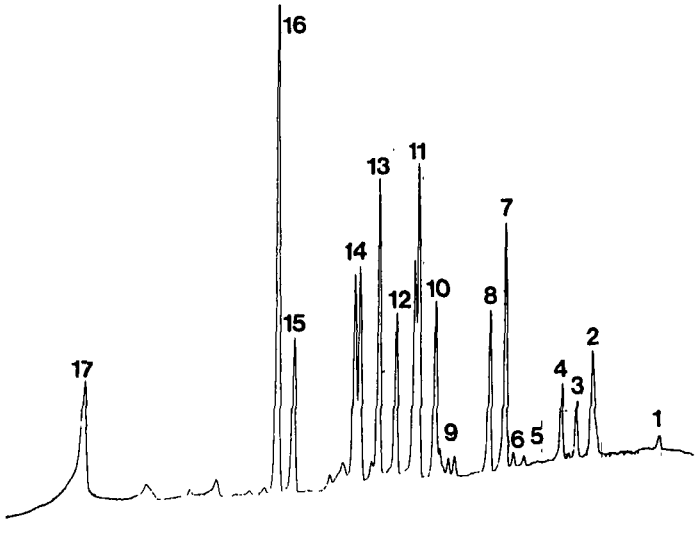

Fig. 1. HPLC separation of a FABP tryptic digest containing 500 pmole

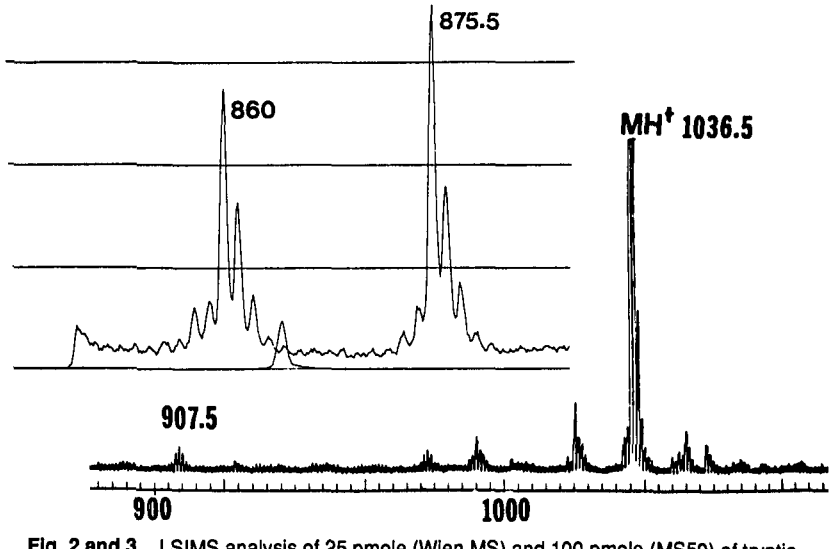

Fig. 2 and 3. LSIMS analysis of 25 pmole (Wien MS) and 100 pmole (MS50) of tryptic peptides from FABP isolated by HPLC.

(1). Gibson, B.W. and Biemann, K. (1984) *Proc. Nat. Acad. Sci.*, **81**, 1956-1960
(2). Biemann, K. (1986) *Anal. Chem.*, **58**, 1288A-1300A
(3). Bass, N. M. (1985) *Chem. Phys. Lipids*, **38**, 95-114
(4). Sacchettini, J.C. et al. (1986) *J. Biol. Chem.*, **261**, 8218-8223
(5). Aberth, W. (1986) *Int. J. Mass Spectrom. Ion Proc.*, **69**, 209-212

Presented at the 35th ASMS Conference on Mass Spectrometry and Allied Topics
May 24-29, 1987, Denver, CO

LOCATION OF CROSS-LINKAGES IN PROTEINS BY FABMS

Zhou Zhongrui, Yiping Sun and David Smith
Department of Medicinal Chemistry and Pharmacognosy
Purdue University, West Lafayette, IN, 47907

The rate at which protein sequences can be predicted from their corresponding cDNA far exceeds the rate at which protein chemists can characterize post-translational modifications using traditional biochemical methods. This dilemma has led to widespread use of FABMS to comfirm sequences and to investigate post-translational modifications. Formation of disulfide cross-linkages is one of the most frequently encountered modifications. In an earlier investigation from this laboratory (Yazdanparast et al, J. Biol. Chem., 262, 2507, 1987) we demonstrated that all of the disulfide bonds in hen egg-white lysozyme and ribonuclease A can be located using a combination of specific cleavage reactions and FABMS.

Despite the availability of many highly specific enzymes, examples frequently arise in which peptides with only one disulfide bond cannot be formed. This may be due to folding of the protein such that the enzyme is excluded from the normal cleavage point on the protein, or because a segment separating two cysteines does not have the required amino acid sequence. The latter case is particularly troublesome when cysteines which are not linked by a disulfide bond are separated by only a few amino acids.

The purpose of this investigation was to determine whether **non-specific** methods of protein cleavage, such as partial acid hydrolysis, could be used to produce peptides which may be diagnostic for disulfide bonding. The general approach is illustrated in Scheme I. Since acid hydrolysis is relatively nonspecific, cleavage occured at many points to give a large number of peptides. Hydrolysis conditions (acid concentration, temperature, and reaction time) were varied to find conditions which gave the highest yield of disulfide-bonded peptide pairs. The reversed-phase chromatogram in Fig. 1 illustrates the complexity of the hydrolysate when hen egg-white lysozyme is treated with 0.25 M oxalic acid at 100°C for 24 hrs.

Scheme I Procedure used to locate disulfide bonds in hen egg-white lysozyme.

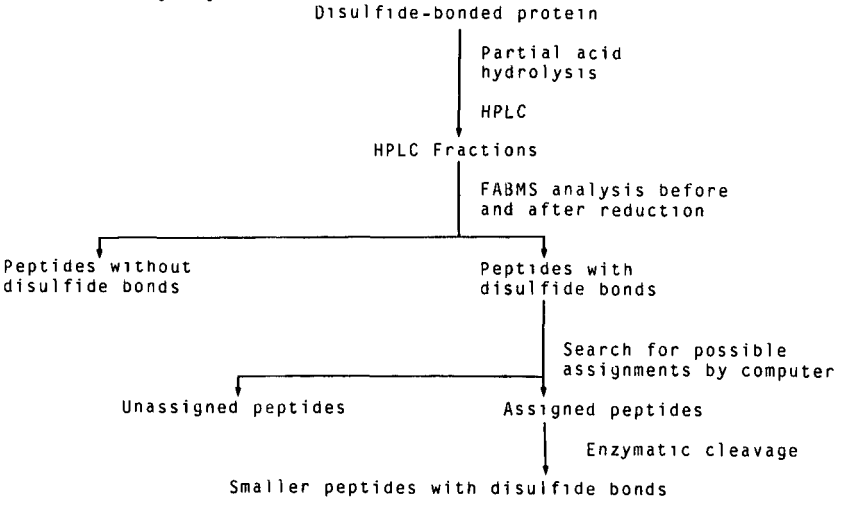

Presented at the 35th ASMS Conference on Mass Spectrometry and Allied Topics
May 24-29, 1987, Denver, CO

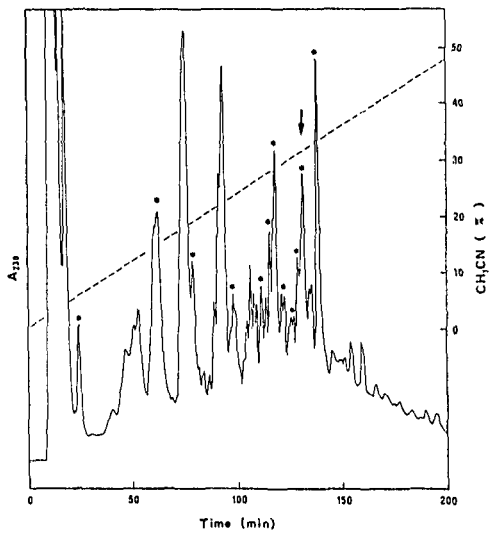

Fig 1 Reversed phase HPLC chromatogram of partial acid hydrolysate of hen egg-white lysozyme. Asterisks indicate peaks which have disulfide-bonded peptides.

To determine which fractions contained disulfide-bonded peptides, all fractions were collected and analyzed by FABMS before and after chemical reduction of disulfide bonds. These fractions are indicated with asterisks in Fig. 1. Because acid hydrolysis is not highly selective, some fractions contained several disulfide-bonded peptides. For example, the fraction indicated by the arrow had seven with molecular weights between 600 and 2700.

A computer program was used to list all disulfide-bonded segments of the parent protein which would have molecular weights equal to those indicated by the FAB mass spectrum. For example, these results showed that the fraction (Fig. 1) contained a disulfide-bonded peptide with a molecular weight of 1449. A search of the amino acid sequence of the original protein showed that there are 121 hypothetical disulfide-bonded peptides with molecular weight of 1449.

Since this analysis usually did not lead to a unique identification of the disulfide bonded-peptides, the hydrolysate was then treated with a highly specific enzyme, such as trypsin or S. aureus V8 and analyzed again by FABMS. New peaks in the mass spectrum were used along with a list of molecular weights of hypothetical disulfide-bonded peptides, which would be formed by treatment of the hydrolysate with the particular enzyme, to make final identification of the disulfide bonded peptides. Using this procedure, we were able to identify enough peptides to locate all four disulfide bonds in hen egg-white lysozyme.

Presented at the 35th ASMS Conference on Mass Spectrometry and Allied Topics
May 24-29, 1987, Denver, CO

Examination of the w-Ions in FAB-CAD Spectra of Peptides. John T. Stults and J. Throck Watson, Department of Biochemistry, Michigan State University, East Lansing, MI, 48824-1319

Introduction: Collisionally activated dissociation (CAD) of peptide $M+H^+$ ions yields a wealth of daughter ions from which considerable sequence information can be obtained. Often these daughter ions are part of a series (e.g., a_n, b_n, y_n) from which all or part of the amino acid sequence can be deduced. Many of the ions, however, are less readily identified. *For example, the products of side chain cleavages, rearrangement reactions, and* multiple cleavages are more difficult to identify. One such group of ions, the w-ions (S.A. Martin and K. Biemann, 34th ASMS Meeting, Cincinnati, OH, 1986), is formed by cleavages of both the peptide backbone and an amino acid side chain. We have collected data that support a revised structure for the w-ions. This revised structure allows one to differentiate between leucine and isoleucine in the sequence of a peptide.

The following scheme shows two possible isobaric ion structures for the w_n ion which is formed at a particular amino acid in the peptide. Structure I was initially proposed, being formed by loss of the N-terminal amino acid side chain from a type y_n ion. However, it was observed that when the β-carbon was branched, as in the case of Ile, Thr, and Val, the w_n *ion mass was shifted by the mass of one of the β-carbon substituents. Such data indicated that Structure II is more likely. We present here further evidence for Structure II:* (1) exact mass measurements from conventional FAB spectra, (2) mass shifts observed in daughter spectra of deuterium-labeled peptides.

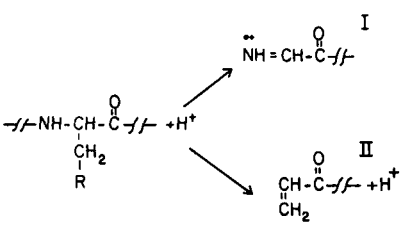

Exact Mass Measurements: Small w-ions were observed in the conventional FAB spectra of a number of peptides. Exact mass measurements were made on three of these ions and the results are listed in Table I. The underlined amino acid in each peptide is the N-terminus for each w_n ion examined. The exact mass measurements were made at a resolving power of 10,000 using the JEOL HX110 analog peak matching unit. Glycerol cluster ions were used as reference masses.

Table I. Exact Mass Measurements

	Structure I		Structure II		
peptide/ ion	*molecular formula*	*calculated mass*	*molecular formula*	*calculated mass*	*measured mass*
RPPGFSPFR	$C_{22}H_{31}N_7O_5$	473.2387	$C_{23}H_{33}N_6O_5$	473.2513	473.2510
LQQIGALK	---	---	$C_{21}H_{38}N_5O_6$	456.2822	456.2841
LQQIGALK	$C_{25}H_{45}N_7O_7$	555.3381	$C_{26}H_{47}N_6O_7$	555.3506	555.3510

Deuterium-labeling Studies: Mass shifts in the daughter spectra of deuterium-labeled peptides also were used to confirm the w_n ion structure. For two peptides which had been characterized as producing w-ions, analogs were synthesized in which a deuterium-labeled side chain was incorporated on the amino acid at the site of the putative w_n ion N-terminus. The complete sequence of each peptide is given in the next paragraph. The locus of the labeled amino acid is shown by underlining. The precursor ions were formed by fast atom bombardment using 6keV Xe atoms in a JEOL HX110 operated at 10kV accelerating voltage, resolving power = 3,000. The matrix was either glycerol or 5:1 dithiothreitol:dithioerythritol. Helium was admitted to the collision cell (first field-free region) to establish the pressure required to attenuate the abundance of the precursor ion to 30% of its original value. The JEOL DA-5000 data system generated a linked scan at constant B/E. The raw data profiles were acquired (30s/decade) with the accumulation software, summing 10-15 spectra per sample.

Figure 1 shows the shift in mass for the un-labeled and d_7-deuterated analogs of the peptide Ac<u>P</u>QTETK (M_r = 744 → 751). The w-ion for either proposed Structure I or II would appear at m/z 660; the observation of a peak at m/z 660 in Fig. 1a does not distinguish between I and II. The FAB spectrum (Fig. 1b) of the same peptide containing d_7-proline shows a 3 u shift (660 → 663) in the mass of the w_6 ion; these data are consistent with Structure II. Figure 2 shows the mass shift for the w_{5a} ion of the un-labeled and deuterated (d_3 - Ile) peptide LQQ<u>I</u>GALK (M_r = 869 → 872). (When an amino acid is branched at the β-carbon, the two possible w_n-ions are labeled w_{na} and w_{nb}.) Structure I would give a peak at m/z 442 for w_5. Figure 2a shows no peak at m/z 442 but does show two peaks at m/z 456 and 470 for w_{5a} and w_{5b}, respectively, corresponding to the retention of the methyl or ethyl group of the isoleucine side chain. Figure 2b shows mass shift of m/z 456→459; this is consistent with a methyl-d_3 substituent at the Ile β-carbon. This ion w_{5a} now appears at m/z 459 but w_{5b} has not shifted in mass.

Conclusion: The w-ions correspond to z_n ions with loss of the amino terminus side chain but retaining the β-carbon and a proton. This structure has been confirmed by: (1) observation of mass shifts of the w-ions when there is branching at the β-carbon; (2) exact mass measurements from conventional FAB spectra; (3) appropriate mass shifts when spectra from deuterium-labeled peptides were examined. Examination of the peptides studied shows that the w-ions are not observed for Gly, Ala, or those amino acids with aromatic side chains. In addition, presence of a basic amino acid at or near the C-terminus appears to be required for observation of the w-ions. These w-ions allow one to differentiate Ile and Leu because Leu is not branched at the β-carbon. Analogously, w-ions can be used to provide confirming evidence for the other β-branched amino acids, Thr and Val. The structure of the w_n ion is important for structure elucidation as it can be used to differentiate Ile and Leu and to provide confirming evidence for Thr and Val.

Acknowledgements: Discussions with R. S. Johnson, S. A. Martin, and K. Biemann of MIT are gratefully acknowledged; a collaborative manuscript on this subject has been submitted to *Anal. Chem.* The deuterated peptides were prepared by John A. Smith of Massachusetts General Hospital. The funds for the JEOL HX110 were provided by the DOE University Research Instrumentation Program 8402-0036. This work was performed in the MSU Mass Spectrometry Facility, supported in part by NIH DRR-00480.

Fig. 1

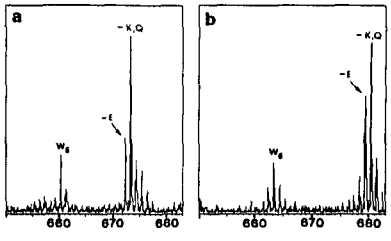

Fig. 2

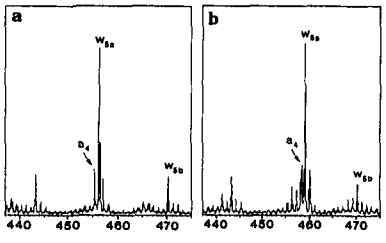

Presented at the 35th ASMS Conference on Mass Spectrometry and Allied Topics
May 24-29, 1987, Denver, CO

THE MASS SPECTROMETRIC CHARACTERISATION OF OLIGOSACCHARIDES RELEASED FROM RED CELL GLYCOPEPTIDES BY ENDO-β-GALACTOSIDASE.

A.M. Lawson, P. Scudder, R.A. Carruthers, S.B. Wilson, R. Childs, E.F. Hounsell and T. Feizi.
MRC Clinical Research Centre, Watford Road, Harrow, Middesex HA1 3UJ, UK.

Introduction. Endo-β-galactosidase enzymes have been used in sequence determination and functional studies of oligosaccharides with poly-N-acetyllactosamine [ie $(3Gal\beta1\text{-}4GlcNAc1)_n$] structures in which they hydrolyse internal β-galactosidic linkages. The branched-point β-galactosidic linkage in erythrocyte glycolipids with the sequence

```
....GlcNAcβ1↘6
            ↓
            Galβ1-4GlcNAcβ1-3Galβ1-4Glcβ1-Cer
....GlcNAcβ1↗3
```

is resistant to β-endo-galactosidase enzymes isolated from Bacteroides fragilis and from Escherichia freundii (1), although a recent study has shown that the latter enzyme can hydrolyse this bond in the oligosaccharides of band 3 glycoprotein (2).

In the present investigation, to establish if the branched-point β-galactosidic bonds in erythrocyte glycopeptides could be cleaved by endo-β-galactosidase of B. fragilis, mass spectrometry has been essential for structure characterisation.

Experimental. Oligosaccharides released by the B. fragilis enzyme from erythrocyte glycopeptides were reduced with sodium borohydride and purified by Bio-Gel P-4 chromatography. Methylation analysis of fractions was carried out and positive ion FAB-MS (glycerol/thioglycerol) on approximately 0.5 nM of permethylated purified oligosaccharides.

Results. Ten oligosaccharide alditols were identified from the digest and comprised both linear and branched chain structures. The branched structures are shown in Figure 1. GC-MS of the products of methylation analysis confirmed monosaccharide composition and linkage in each case, but no evidence for the methylated alditol acetate from a -6(3)Gal.ol residue was found in any oligosaccharide fraction. The anomeric configurations were assumed from the known poly-N-acetyllactosamine nature of erythrocyte glycopeptides and from the specificity of endo-β-galactosidase

Molecular weight information was obtained from permethylated samples by +ve FAB-MS. Mass spectra from two of the oligosaccharide fractions are shown in Figure 2 and these illustrate representative features in the spectra of all the oligosaccharides isolated. Fragmentation at the acetamido glycosidic bonds gave intense ions from non-reduced terminal branches (3), GlcNAc (m/z 260), Gal-GlcNAc (m/z 464) and Fuc-Gal-GlcNAc (m/z 638) and from elimination of the reduced terminal galactitol (eg m/z 1158.6, 1710.9). Retention of charge on the fragment arising from the combined loss of Gal.ol together with proton-rearrangement loss of a non-reduced terminal branch produced the ions m/z 695, 899 and 1073.5.

Conclusions. The structures of 90% of the oligosaccharides released by the B. fragilis enzyme have been determined by mass spectrometry and linkage and composition data obtained from the remaining material. The sequence GlcNAcβ1-3(GlcNAcβ1-6)Galβ1-4GlcNAcβ1-3Gal.ol was present in each branched structure indicating that the enzyme cannot hydrolyse branch-point linkages in erythrocyte glycopeptides. Knowledge of this specificity will be of importance to the analysis and recognition of oligosaccharide sequences from other cellular sources.

Presented at the 35th ASMS Conference on Mass Spectrometry and Allied Topics
May 24-29, 1987, Denver, CO

References
1. Scudder,P., Hanfland,P., Uemura,K. and Feizi,T. J. Biol. Chem. 259 (1984) 6586-6592.
2. Fukuda,M., Dell,A., Oates,J.E. and Fukuda,M.N. J. Biol. Chem. 259 (1984) 8260-8273.
3. Dell,A., Morris,H.R., Egge,H., von Nicolai,H. and Strecker,G., Carbohydr. Res. 115 (1983) 41-52.

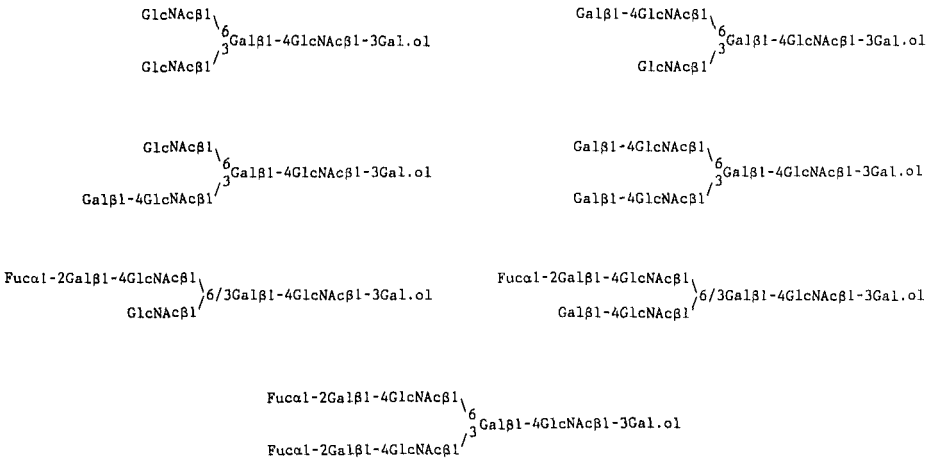

Figure 1

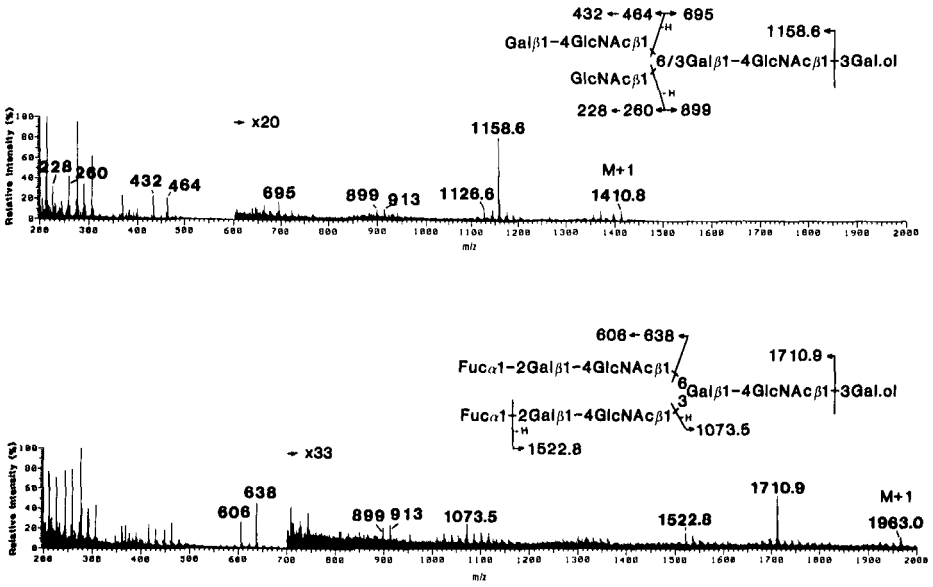

Figure 2

Presented at the 35th ASMS Conference on Mass Spectrometry and Allied Topics
May 24-29, 1987, Denver, CO

STRUCTURE ANALYSIS OF BIOLOGICALLY IMPORTANT COMPLEX NUCLEOSIDES OF BACTERIAL ORIGIN BY DIFFERENT IONIZATION MODES COMBINED WITH TANDEM MASS SPECTROMETRY

B.C. Das*, J.P. Cosson*, E. Guittet*, M. Hassani**, T. Staron**
and F. De Maack***
* Institut de Chimie des Substances Naturelles, CNRS
91190 Gif-sur-Yvette, France
** Station des Antibiotiques et des Bioconversions
INRA, 28110 Lucé, France
*** S.N. Nermag, 49 Quai du Halage, 92500 Rueil-Malmaison, France

Among the different groups of biologically important natural products (antibiotics, antifungals, etc.) of bacterial origin, the occurrence of a number of nucleoside derivatives is recorded in the literature. Many of them are thermally unstable involatile polar substances having a variety of structural features in their molecular framework. Their structural analysis by mass spectrometry (MS) required in the past, in several instances, the use of prior derivatization and degradative methods. The full range of ionization techniques currently available to the mass spectrometrists, along with tandem MS, can be a powerful tool for analyzing intact molecules, thereby widening the scope of mass spectrometry for structural elucidation. The purpose of the present investigation is to explore the possibilities offered by these newer techniques toward the structural analysis of various naturally occurring complex nucleosides.

This work is illustrated with four examples: (i) Sinefungine 1, an antifungal antibiotic having antiparasite activity[1]; (ii) anthelmycin 2, a nucleoside disaccharide antibiotic[2]; (iii) 30-(5'-adenosyl) hopane 3, a novel nucleoside triterpene and (iv) a new 5,6-dihydrouridine derivative 4 possessing antifungal properties. The latter two compounds have recently been isolated by us from a Streptomyces species.

FAB mass spectrometry was found to be ideally suited for analyzing 1 and 2, both of which are highly polar compounds. The FAB-CAD-MS/MS analysis provided excellent spectra confirming the structural features of these two compounds.

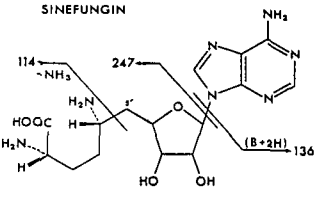

1 MH⁺ 382

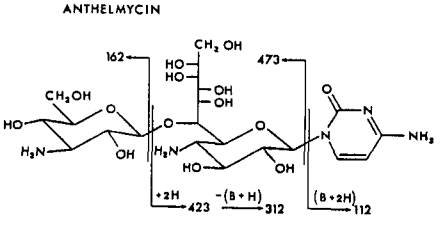

2 MH⁺ 584

30-(5'-adenosyl) hopane 3 ($M^{+\cdot}$ 661) possessing both hydrophilic and hydrophobic moieties, was not amenable to analysis by FAB MS. However, fragment ions observed in the EI spectrum (m/z 136, 191, 305, 369, 454) together with the CI-CAD-MS/MS analysis gave structural information (B + 2H daughter ions at m/z 136) facilitating its quick identification. This compound was previously isolated[3] as its triacetate from a different source.

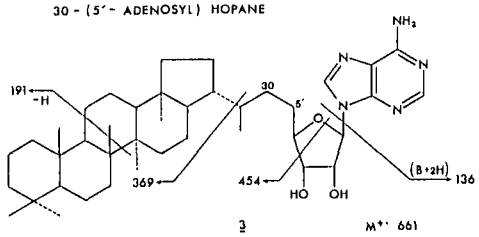

3 M+· 661

The structure of an unknown antifungal antibiotic 4 (R = H) has also been investigated by MS. Attempts to obtain a FAB spectrum of this thermally unstable compound were unsuccessful. The EI and CI spectra were obtained, although not without difficulty. High resolution EIMS established the molecular formula $C_{32}H_{43}N_3O_6$ ($M^{+\cdot}$ 565). The presence of a 5'-amino-5'-deoxy 5,6-dihydrouridine moiety was suspected from the occurrence of the peaks at m/z 115 $(B + 2H)^4$, 157 $(B + 44)^4$ and 246 in the CI spectrum. The CI mass spectrum of the corresponding isopropylidene derivative (RR = $Me_2C<$) along with the CI-CAD-MS/MS experiments* provided further support to this partial structure. Full structural details were then elaborated from an analysis of its NMR spectra as well as from selective chemical degradation.

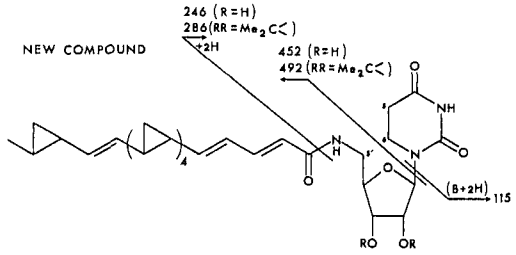

4 R = H (MH+ 566)
RR = $Me_2C<$ (MH+ 606)

In conclusion, a variety of complex nucleoside antibiotics can be efficiently characterized by the selective use of the currently available ionization techniques together with tandem mass spectrometry.

* MS-MS experiments have been performed with a NERMAG R 30-10 triple quadrupole instrument.

REFERENCES

1. M. Geze, et al., J. Am. Chem. Soc., 1983, 105, 7638-7640 and references cited.
2. S. Ennifar et al., J.C.S. Chem. Commun., 1977, 41-42.
3. S. Neunlist and M. Rohmer, Biochem. J., 1985, 228, 769-771.
4. M.S. Wilson and J.A. McCloskey, J. Am. Chem. Soc., 1975, 97, 3436-3444; D.L. Slowikowsky et al., Nucleosides and Nucleotides, 1985, 4, 347-376.

Presented at the 35th ASMS Conference on Mass Spectrometry and Allied Topics
May 24-29, 1987, Denver, CO

Structural Studies of Oligosaccharide Antibiotics, Everninomicins by Negative Ion Fast Atom Bombardment Mass Spectrometry (FABMS).

B.N. Pramanik, A.K. Ganguly and P.L. Bartner, Pharmaceutical Research and Development Division, Schering-Plough Corp., Bloomfield, New Jersey 07003, USA.

Everninomicins, a novel class of oligosaccharide antibiotics are produced by Micromonospora Carbonaceae and are highly active against Gram-Positive bacteria. These compounds possess unusual features in their structures, such as orthoester functionalities, methylene dioxy group, phenolic ester and nitrosugar moiety. The positive ion FABMS studies of everninomicins have been reported[1,2] and FABMS data provided important structural insight which lead to the structural elucidation of Sch 13384-1 & 5.[3,4]

Recently, we have investiagted the use of negative ion FABMS for the structural studies of this class of highly complex antibiotics and we wish to report the results of our studies.

In the present investigation, FABMS data were obtained on a VG ZAB-SE mass spectrometer equipped with a FAB source operating at an accelerating voltage of 8KV. The primary atom beam being comprised of Xenon, was produced using a saddle field ion source operating at a tube current of 1-1.5 mA at an energy of 8 Kev.

Negative ion FAB mass spectra of everninomicins produced very intense deprotonated molecular ions $[M-H]^-$. In Sch 13384-1 & 5, fragment ion formation was greatly influenced by the presence of the second ester group 2-methyl-4,6-dihydroxybenzoate on sugar H. A series of fragment ions corresponding to the loss of each sugar unit (from H → A) was illustrated in figures A & B. Intense fragment ions at 149 and 167 amu indicated the presence of the 2-methyl-4,6-dihydroxybenzoate moiety in (1) and (2). The prominent ions at 1478 and 1448 amu provided evidence for the second ester linkage on sugar H (1) and (2). In contrast, the absence of this second ester function in compounds (3) & (4) were clearly indicated in their FAB spectra (Figure C & D).

The compounds (1) & (3) showed an ion at m/z 251 which corresponded to $[A+NO_2]^-$ and could be important for the detection of nitrosugars.

Negative FABMS method is simple, sensitive and will be of great value in determining the structures of molecules of similar complexities.

References

1. A.K. Ganguly, B.N. Pramanik, V. Girijavallabhan, O. Sarre and P.L. Bartner, J. Antibiotics 1985, 38, 808
2. B.N. Pramanik and A.K. Ganguly, Ind. J. Chemistry, 1986, 25B, 1105.
3. B.N. Pramanik, A.K. Ganguly, J. Morton, T. Chau, O. Sarre, P. Bartner and V. Girijavallabhan, Abstract. 34th Annual Conference Mass Spectrum and Allied Topics, 1986, 903-904.
4. A.K. Ganguly, B.N. Pramanik and O. Sarre, "New Oligosaccharide Antibiotics", To be presented at the Gordon Research Conference," June, 1987.

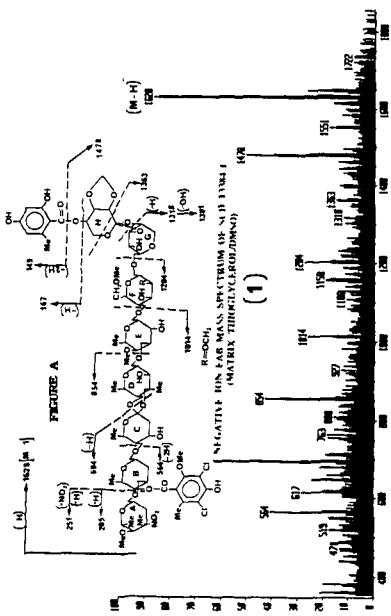
FIGURE A
NEGATIVE ION FAB MASS SPECTRUM OF SCH 13384-1
(MATRIX THIOGLYCEROL/DMSO)
(1)
R=OCH3

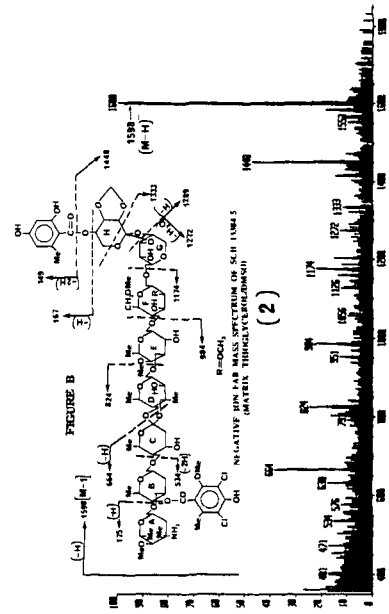
FIGURE B
NEGATIVE ION FAB MASS SPECTRUM OF SCH 13384-5
(MATRIX THIOGLYCEROL/DMSO)
(2)
R=OCH3

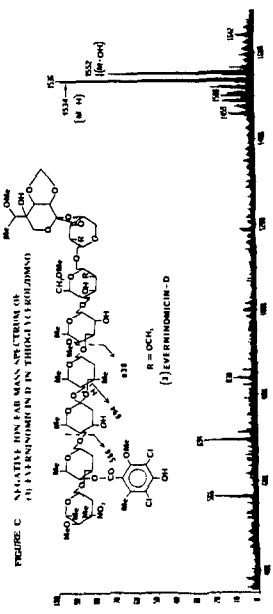
FIGURE C
NEGATIVE ION FAB MASS SPECTRUM OF
(3) EVERNINOMICIN D IN THIOGLYCEROL/DMSO
R=OCH3
(3) EVERNINOMICIN-D

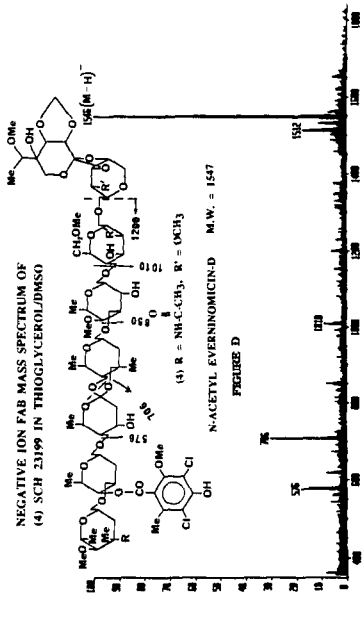
NEGATIVE ION FAB MASS SPECTRUM OF
(4) SCH 23199 IN THIOGLYCEROL/DMSO
(4) R = NH-C-CH3, R' = OCH3
N-ACETYL EVERNINOMICIN-D M.W. = 1547
FIGURE D

Presented at the 35th ASMS Conference on Mass Spectrometry and Allied Topics
May 24-29, 1987, Denver, CO

APPLICATION OF FAB MS-MS TO THE ANALYSIS OF C-GLYCOSIDIC FLAVONOIDS

D. FRAISSE, M. BECCHI

S.C.A.- C.N.R.S.- B.P. 22 - 69390 VERNAISON - FRANCE

C-Glycosidic flavonoids (figure 1) are polar compounds occuring primarily in plants. They are characterized by a large variety of isomers. This paper presents FAB conditions and results of an FAB MS-MS study for seventeen representatives of mono- and di-saccharide compounds obtained from purified extracts of plants. (1, 2,)

FAB mass spectra were obtained on a ZAB-HF (VG Analytical, Manchester) equipped with an Ion tech saddle field gun operated to provide an 8 KeV xenon atom beam. The MIKE and CAD-MIKE spectra were carried out by scanning the collision gas at a pressure required to reduce the main bean intensity factor of 3.
Samples were dissoved in DMSO (1 to 10 µg/µl) and 1 to 3 µl of the solution was added to the appropriate matrix. A careful study conducted with different matrices showed that diethanolamine in the negative mode was the most effective for this class of compounds.

RESULTS and DISCUSSION

Figure 2 is the FAB spectrum of Schaftoside (MW 564) in diethalomine. This typical spectrum of the compounds studied shows an abundant deprotonated molecular ion as well as less intense fragment ions ; a weak adduct ion involving matrix molecules can be also observed. The presence of $(M-H)^-$ ion, m/z 619 in the spectrum of vitexine-2"-O-rhamnoside-4"'-O-acetyl demonstrates the interest of the FAB. In EI ionization mode molecular weight information is lost for acylated compounds.
In addition to molecular weight information, useful structural information are obtained by FAB MS-MS. The MIKE spectra of $(M-H)^-$ ions, m/z 447 of Orientine and Isoorientine allows us to distinguish these two isomers as shown in figure 3. An intense fragment ion corresponding to the loss of water is observed when the C-sugar is in position 6. Two other abundant fragment ions $(M-H-C_3H_6O_3)$ and $(M-H-C_4H_8O_4)$ which are produced by cleavages B and/or C and A (figure 4) respectively, are also observed. Therefore the site of attachment is readily distinguished in the case of mono-C-glycosides. This was confirmed by the study of Vitexine, Isovitexine and Scoparine.

Figure 5 shows the MIKE spectra of $(M-H)^-$ ions of two di-C-glucosides, Schaftoside and Isoschaftoside. Two of the fragment ions observed, (M-H-60) and (M-H-104) produced by cleavages C and D, respectively, were enhanced when the pentose was in position 6. This result was confirmed by observing the MIKE spectra of Vicenin-2 and Corymboside. The site of attachment of a pentose is clearly distinguished for the dissymmetric di-C-glycosides.

For di-OC-glycosides there are two types of possible attachment for the O-sugar, either on the aglycone or on the first C-sugar. The MIKE spectra of the deprotonated molecular ion of Isovitexine-7-O-glucoside, Isoorientine-3'-O-glucoside and Isoorientine-4'-O-glucoside clearly demonstrated the site of attachment of the O-sugars shown in figure 6.
In addition the MIKE spectra of Isoorientine-2"-O-glucoside, Isoorientine-6"-O-glucoside, Vitexine-2"-O-rhamnoside, Vitexine-2"-O-rhamnoside-4"'-O-acetyl and Isovitexine-2"-O-glucoside allowed us to determine the position of the di-saccharide chain and the site of attachment of the O-sugar on the C-sugar (figure 6).

CONCLUSION

FAB mass spectrometry and FAB MS-MS in negative mode can provide molecular weight and very useful structural information for C-glycoside flavonoids without derivatization. Diethanolamine gave an intense deprotonated molecular ion for all the compounds studied. MIKE and CAD-MIKE spectra provide characteristic fragment ions which permit to differentiate isomers.

1 - J.B. HARBORNE and T.J. MABRY "The Flavonoïds - Advances in Research" ed. Chapman and Hall, London (1982)

2 - J. ULRICH - Internal Communication. CEA France 1984.

1

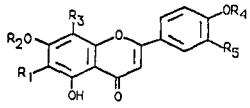

R_1, R_3 = H, C-Glycosyl
R_4 = H, O-Glycosyl
R_5 = H, OH, OCH_3, O-Glycosyl

2

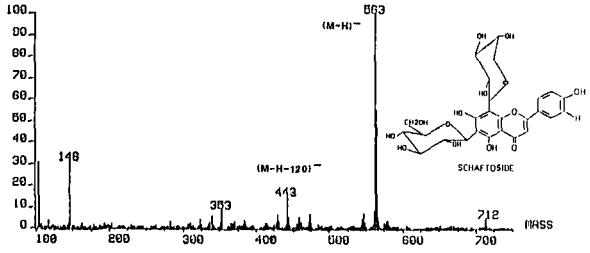

4

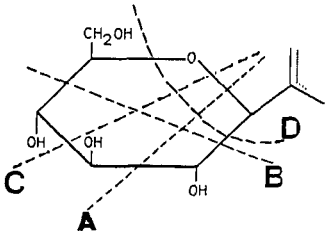

3

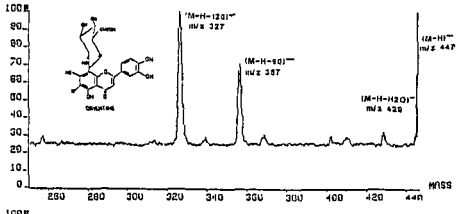

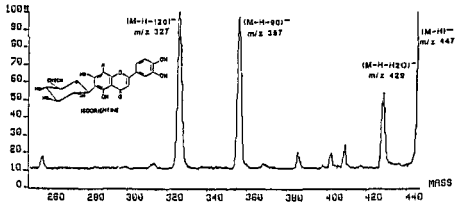

6

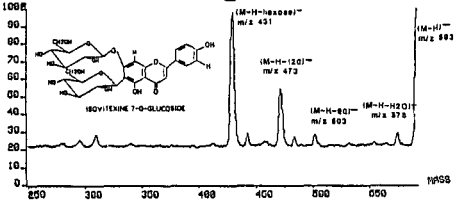

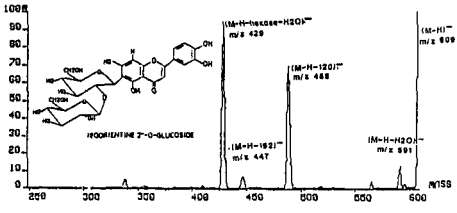

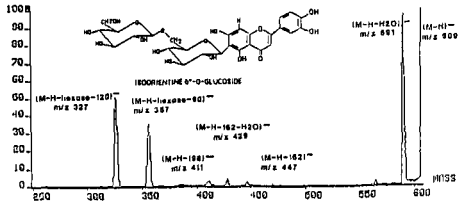

5

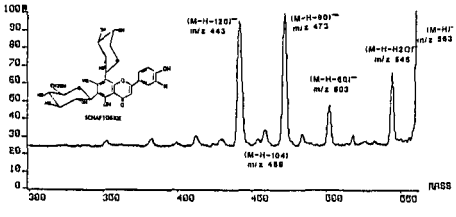

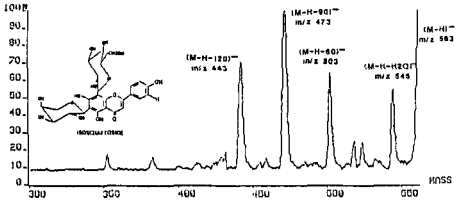

Presented at the 35th ASMS Conference on Mass Spectrometry and Allied Topics
May 24-29, 1987, Denver, CO

The Role of Serum Pentitol Concentrations in the Diagnosis of Disseminated Visceral Candidiasis.

John Roboz, Diana Kappatos, and James F. Holland
Department of Neoplastic Diseases, Mount Sinai School of Medicine, New York, N.Y.

GC and GC-MS techniques currently used for the determinationof serum "arabinitol" concentration do not provide for the separation of pentitols (arabinitol, adonitol, xylitol) and measure, in fact, total pentitol, TP,(1) concentrations. Although endogenous serum concentrations of adonitol and xylitol are small compared to that of arabinitol, we did find, on occasions, increased adonitol in patients with candidiasis. The objectives of this work were: (a)To develop techniques for the separation of the trimethylsilyl (TMS) derivatives of pentitols; (b) To eliminate false positives by the TP technique due to contributions from adonitol and xylitol; (c) To investigate the relevance of adonitol and xylitol in the diagnosis of disseminated candidiasis.

Serum pentitols were separated as TMS derivatives using two 25m long, 0.32 mm i.d. bonded methyl silicone columns by selected ion monitoring of the (M+1) ions of the pentitols (m/z = 513) and the internal standard (m/z = 520, deuterated arabinitol). The coefficients of variation for individual pentitols were: intraday 5-11% (n=10), interday 10-14 (n=7). The concentrations of endogenous pentitols in the control sera used for calibration, determined by extrapolating calibration curves to the abscissa, were not significantly different from those found using(2) pentaacetyl derivatives. The following mean concentrations (ug/mL+s.d.) and ranges (in parenthesis) were obtained for controls (n=25): arabinitol 0.38±0.12 (0.22-0.68), adonitol 0.07±0.03 (0.02-0.12) and xylitol 0.07+0.03 (0.02-0.12). Individual serum pentitol concentrations in normals and uninfected cancer patients were not significantly different. In renal failure (n=10) arabinitol increased to 2.0+0.35 but both adonitol (0.04±0.02) and xylitol (0.09+0.04) remained normal.

The population studied consisted of 173 samples from 73 patients. These were selected from a population of 1250 samples from 284 patients for whom TP data were available. Selection criteria for pentitol analyses were: (a) Blood culture confirmed candidiasis; (b) Suspected candidiasis with negative culture; (c) Unexplained increased TP during monitoring of patients undergoing chemotherapy. In candidiasis confirmed by blood culture (n=37) pentitol concentrations were: arabinitol 2.04±1.48; adonitol 0.20+0.17, xylitol 0.22+0.16. In the culture-negative group, 62% (48/77 samples) exhibited increased (≥0.75 ug/mL)arabinitol; 52% of these were from patients with renal dysfunction (creatinine ≥ 1.5 mg/dL). A thought-provoking observation is that 71% of patients in the culture-negative group with normal renal function died within 8 days after the last increased arabinitol was found. The corresponding death rate among those patients with normal arabinitol was 13%. These cases may represent the situation where the increased arabinitol was caused by disseminated candidiasis but cultures were negative, possibly because of the lack of circulating organisms.

Increased TP was found in 56 samples in the culture negative (0.9-12.8 ug/mL) and 40 samples in the no-culture (0.9-2.9 ug/mL) groups. Of these, eight (14%) and seven (17%), respectively, had normal arabinitol and were, therefore, false positives, In all cases, the increased TP could be explained by larger than normal contributions by adonitol (0.05-4.9 ug/mL), xylitol (0.02-0.36 ug/mL) or both.

Conclusions and recommendations: (a) The technique developed for the quantification of individual pentitols can be used to eliminate false positives caused by increased adonitol and/or xylitol concentrations when using the TP technique; (b) We recommend continued use of the TP method because of its simplicity and speed. When a sample with increased TP and normal creatinine is encountered, it should be analyzed for individual pentitols; conveniently, the same sample can be used for both determinations; (c) Small quantities of adonitol are produced by Candida organisms; increased adonitol occurs in one-half of confirmed candidiasis cases; adonitol does not increase in renal failure. Thus, adonitol may be a useful diagnostic aid for candidiasis in cases of renal dysfunction.

Supported by Grant CA-40050 from NCI and by the T.J. Martell Memorial Foundation for Cancer and Leukemia Research.

References:

1. Roboz, J., Suzuki, R. and Holland, J.F. J.Clin.Microbiol., 12, 594-602 (1980).
2. Roboz, J., Kappatos, D., Greaves, J. and Holland, J.F. Clin. Chem., 30, 1611-1615 (1984).

Presented at the 35th ASMS Conference on Mass Spectrometry and Allied Topics
May 24-29, 1987, Denver, CO

AMMONIA DCI OF DOLICHOLS: QUANTITATION, DETERMINATION OF MOLECULAR WEIGHT AND STRUCTURES

James E. Evans, Hamdy M. Abdel-Maksoud and Peter F. Daniel
E. K. Shriver Center, Waltham, MA.

Dolichols are long chain polyprenols containing from 16 to 23 isoprene units (C_{80} - C_{115}) and reside mainly in tissues and biological fluids as the free alcohols, phosphate esters and esters of fatty acids. Dolichols function as lipid carriers for oligosaccharide residues in the synthesis of N-glycosidically linked protein. Several methods for the determination of dolichols in tissues have been used, including HPLC with UV or fluorescence detection. However, the latter method required derivatization. Field desorption mass spectrometry, although, a complicated technique was successfully used to identify molecular ions of high molecular weight dolichols. The lack of solubility in matrices inhibited the use of FAB-MS technique. The accumulation of dolichols in aging and diseases such as Alzheimers and the Neuronal Ceroid Lipofuscinoses has prompted the necessity of measurement in biological samples. We have developed a DCI-MS method for the determination and measurement of dolichol molecular species in biological samples. Dolichols were extracted from bovine heart, porcine liver and mouse kidney and were assayed by HPLC and by ammonia DCI-MS. Quantitation of dolichol levels in these samples was undertaken, and a standard curve was created based on the use of a standard dolichol-19. A methyl ether derivative of dolichol-19 was used as the internal standard. The ammonia DCI spectrum of dolichols provides a strong $[M+NH4]^+$ ion that is the base ion above 200 amu. It also provides a M^+ ion that is 10% the intensity of the base ion. Comparison of the quantitative results obtained by this method with that of HPLC method was quite satisfactory.

Experimental

I- DCI-MS

Samples dissolved in CCL_4 were applied to the DCI probe emitter using a 10 µl syringe (5 µl of 1µg/µl concentration was applied). Slow evaporation of the solvent coated the platinum emitter with a thin film of sample material. The DCI probe was introduced via a vacuum lock to VG:70-250SE mass spectrometer ion source. The source heater was at 180°C, the trap current at 100 µA and the DCI probe tip was rapidly heated by passing a 1.5 AMP current through the DCI filament. The source pressure was maintained at 5 x 10-5 mbar with ammonia reagent gas. Acceleration voltage was at 7kv.

II- HPLC

Dolichols were analyzed isocratically on 3 micron octylsilica reversed-phase column (4.6 x 33 mm; Supelco inc., Bellefonte, PA) with methanol-isopropanol (65:35) as the mobile phase and UV detection at 210 nm.

III- Isolation of dolichols

Dolichols were extracted from tissues with chloroform-methanol, applied to a Unisil™ column and isolated in the neutral lipid fraction by elution with chloroform. Lipids were methanolized in methanolic 0.6% NaOH and neutralized with methanolic HCl. The base stable lipids were desalted and separated from other lipids by passage over a C_{18} reversed-phase bond Elut Cartridge (Analytichem International, Harbor city, CA) using a modification of the procedure of Wong and Lennarz (1982).

IV- Synthesis of O-methyl-dol-19 internal standard

Methyl sulfinyl carbanion reagent (dimsyl potassium, 1.0 ml) was added slowly to a solution of dolichol-19 (1.0 mg) in methyl iodide (0.5 ml) placed in ice-acetone bath. The mixture was kept at zero°C overnight. The reaction mixture was diluted with water (2 ml) and extracted with n-hexane (2 ml). The hexane phase was separated and washed twice with 95% methanol (2 ml). Recovery and purity of the derivative was assessed by TLC (n-hexane-benzene; 1:1)

Presented at the 35th ASMS Conference on Mass Spectrometry and Allied Topics
May 24-29, 1987, Denver, CO

Results

The molecular ion region mass spectrum of a mixture containing 2 μg each of standard dolichol-19 and O-methyl-dol-19 is shown in Figure A. The M^+ ion is shown at m/z 1315 cluster ion, whereas m/z 1333 refers to $[M + 18]^+$ ion, and m/z 1347 is the $[M + 18]^+$ ion for O-methyl-dol-19. Figure B is the mass spectrum of the molecular ion region of dolichols obtained from beef heart sample (2 μg) with 5 μg of O-methyl-dol-19 internal standard added. A calibration curve based on the response ratio of dol-19 and internal standard is shown in Figure C.

Conclusions

1. DCI has proven to be a practical technique for profiling and measuring dolichols in biological extracts. The sensitivity achieved for measurement is in the low μg range with a limit of detection (S/N = 3) of about 200 ng when the molecular ion region (m/z 1150 - 1550) is scanned.

2. DCI also produces fragment ions from both the hydroxyl and methyl ends of the molecule predominately by cleavage between the 1 and 2 carbons of each isoprene unit that would allow easy detection of structural differences.

3. Because DCI is a rapid technique, high sample throughput can be achieved with analysis times around 2 min. per sample.

Support: NIH grants NS 16447-06 and NS 24279-01.

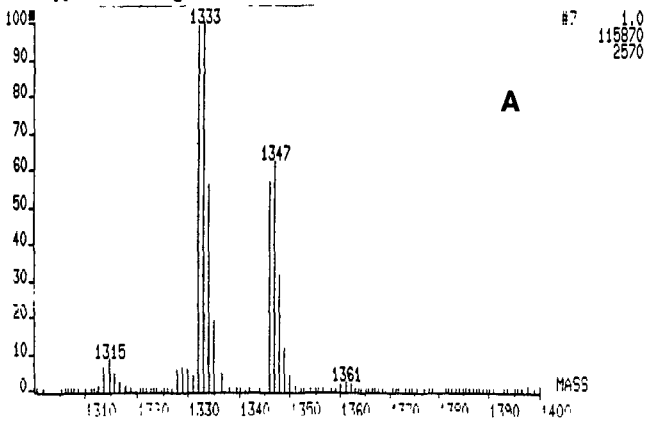

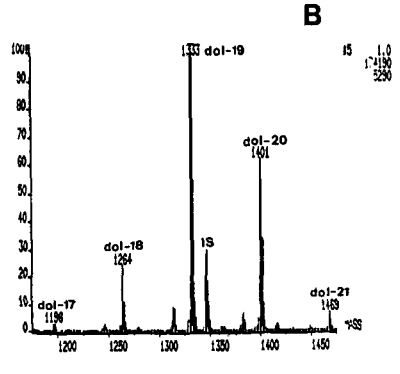

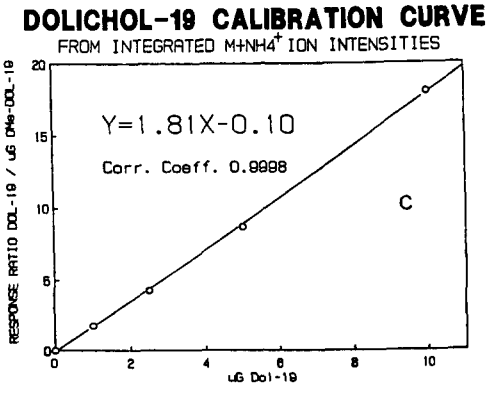

Presented at the 35th ASMS Conference on Mass Spectrometry and Allied Topics
May 24-29, 1987, Denver, CO

ON-LINE THERMOSPRAY (TSP) ANALYSIS OF THE CEPHALOSPORIN CEFTIOFUR AND RELATED COMPOUNDS IN THE BULK DRUG AND IN BIOLOGICAL FLUIDS

Russell H. Robins and Prem S. Jaglan
The Upjohn Company, Kalamazoo Michigan

New methodology is described for the analysis of cephalosporin based antibiotic agents by thermospray LC/MS. PURPOSE: To develop a sensitive mass spectral analysis for the identification of the decomposition products of Ceftiofur in the bulk drug and metabolites in biological fluids. INTRODUCTION: Ceftiofur is a non-volatile, thermally unstable cephalosporin antibiotic useful in the treatment of respiratory infection in cattle. Understanding the stability and metabolic fate of the active ingredient affords optimization of the product dosage form. CONVENTIONAL IONIZATION METHODS: Because Ceftiofur is thermally unstable, desorption electron (EI) impact and chemical mass (CI) spectra do not provide useful molecular weight or structural information due to sample decomposition. Fast atom bombardment (FAB) ionization provides molecular weight information, however, sensitivity is inadequate for trace analysis. (ca. 100mcg required). THERMOSPRAY IONIZATION: Thermospray ionization provides both molecular weight and limited structural information with adequate sensitivity for trace analysis (ca. 1 mcg). Fragmentation indicates the presence of major sub-structural moieties. EXPERIMENTAL: The LC/MS is shown schematically at right. On-line and flow injection experiments were performed using a gradient acetonitrile:water(0.1M ammonium acetate) mobile phase. An analytical Dupont Zorbax C8 column was employed for on-line analysis. SAMPLE PREPARATION: C18 and ion exchange column chromatography was used to concentrate metabolites from rat urine prior to analysis. Metabolites were traced using scintillation counting of the C14 label. RESULTS: The UV trace of thermally challenged bulk drug is shown. Two decomposition products the anti-oxime and the lactone, and their TSP mass spectra are illustrated. The metabolite, the free alcohol, isolated from rat urine is also shown at right. CONCLUSIONS: Thermospray ionization is useful for the analysis of thermally labile, non-volatile cephalosporin antibiotics. Molecular weight and useful structural information is obtained. Sensitivity is adequate for trace analysis.

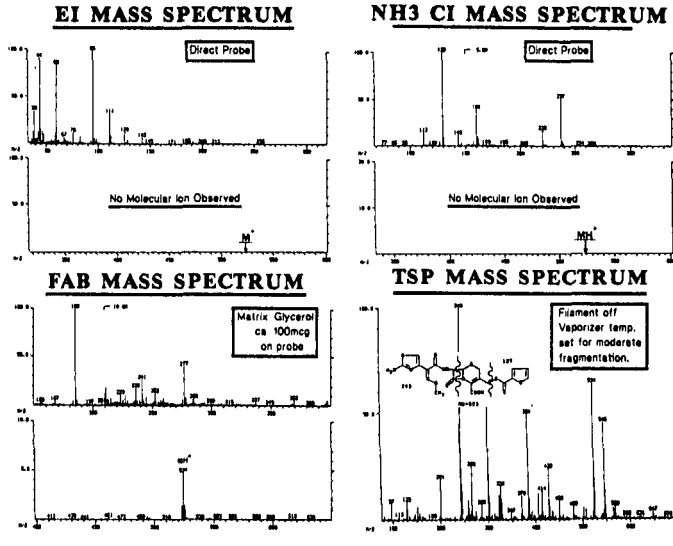

Presented at the 35th ASMS Conference on Mass Spectrometry and Allied Topics
May 24-29, 1987, Denver, CO

HPLC/TSP/MS SYSTEM

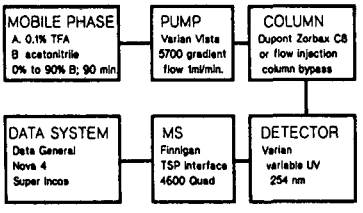

SAMPLE PREPARATION

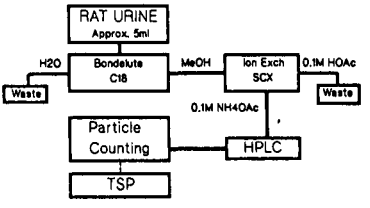

UV CHROMATOGRAM

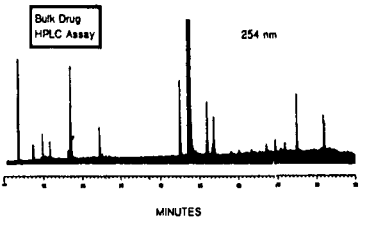

METABOLITE CHROMATOGRAM

Rat urine extract with UV and scintillation detection.

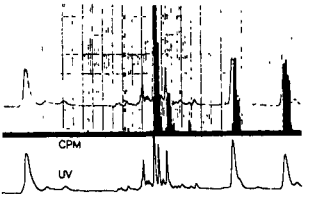

ANTI-OXIME IMPURITY

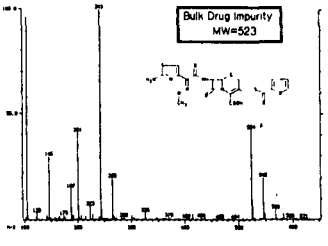

LACTONE IMPURITY

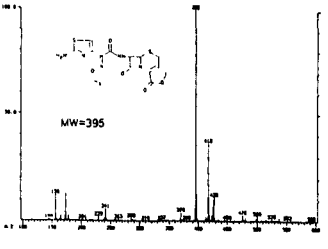

ALCOHOL METABOLITE

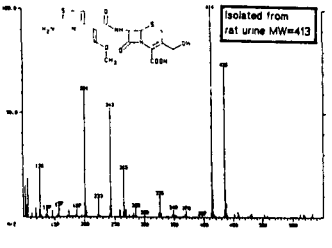

Presented at the 35th ASMS Conference on Mass Spectrometry and Allied Topics
May 24-29, 1987, Denver, CO

Developments of MS and MS/MS Methods for the Quantification of Enkephalins

Emirgul Tolun, Chhabil Dass and Dominic M. Desiderio
University of Tennessee, Memphis,
Stout Neuroscience Mass Spectrometry Laboratory
Memphis, TN 38163

INTRODUCTION

FABMS, together with MS/MS and CAD techniques has been used for the measurement of opioid peptides from biological extracts (1). Tissue extracts also contain numerous other contaminants, that may produce background in the mass spectra even after HPLC purification. Selected reaction monitoring (SRM) which is performed first by selecting a molecular ion and then monitoring the daughter ions formed by metastable transitions can overcome these background problems to some extent and provide high level of molecular specificity at the femtomole level.

OBJECTIVES

1) To determine the metastable transitions for enkephalins in which the background interference from the biological matrix is minimal.
2) To improve the detection limits for neuropeptides.

Methionine enkephalin (YGGFM) is chosen as a model compound for this study.

EXPERIMENTAL

The data were recorded on a VG-7070E-HF forward geometry-mass spectrometer. The FAB gun was operated at 7KeV with xenon as the bombarding gas. A VG 11- 250 M+ data system was used to record the data in the selected reaction monitoring (SRM) mode during 1.5 minute fast atom bombardment time. The solutions (1 ug ul^{-1}) of the synthetic enkephalins in water and in 20% NH_4OH was diluted sequentially to provide solutions in 0.5-10 ng ul-1. Glycerol (0.2 ul) was used as liquid matrix.

RESULTS

The most intense daughter ions in the positive ion FAB-B/E linked scanning spectrum of (M+H)+ m/z 574 of ME are, N-terminus ion at m/z 425, C-terminus ion at m/z 354 and an ion arising from the tyrosine side chain loss at m/z 467. Although the positive ion FAB provides more intense spectra, the matrix background interference on 574→354, 574 → 425 and 574 → 467 SRM transitions are quite high.
In order to minimize the background interferences we have utilized negative ion FABMS for quantification studies.

The most abundant fragment ions in the negative ion FAB-B/E spectrum of $(M- H)^{-m/z}$ 572 of ME are, m/z 465 corresponding to the tryrosine side chain loss of 107 mass units and m/z 481 arising from the loss of 92 mass units from phenylalanine side chain. The glycerol matrix backgoround interferences on 572 → 465 and 572 → 481 were studied for both ME and the other enkephalins such as LE and ME-RGL and in each case the negative ion [(M-H) - 107]- transition showed the lowest interference from the background.

The increase in the total ion current occurs when the peptide spectra are recorded for FAB matrices such as diethanolamine, diethanolamine + tetramethylurea and magic bullet. However, matrix background contribution to the 572 → 465 transitionis very high. As a result, among these FAB matrices only glycerol is suitable for quantitative studies using SRM of $[(M-H)- 107]^-$ transition for the enkephalins.

The level of detection sensitivity in the FAB MS/MS negative ion mode is 1 ng of synthetic ME.

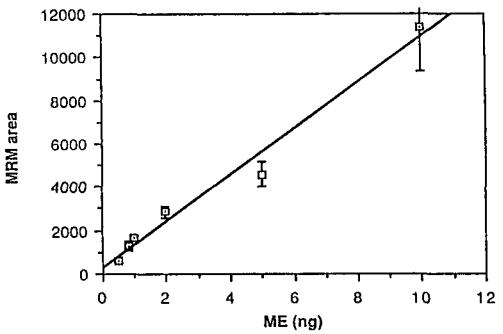

FIGURE 1. Selected ion monitoring (SRM) of 572 → 465 transition area data for series of synthetic ME solutions in 20% NH_4OH/H_2O/glycerol.

The detection limit for the enkephalins can be further lowered by adding different solvents to glycerol matrix. Dissolving the peptides in 20% NH_4OH solution enhances the preionization hence the abundances of both molecular and fragment ions observed in the negative ion spectrum.

Addition of NH_4OH improves the detection sensitivity and as low as 0.5 ng (900 fmoles) of synthetic ME can be detected, and this matrix composition can be used for the low level estimation of ME from HPLC tissue extracts Figure 1).

Effect of different FAB matrices in negative ion studies

The addition of glutathione (2) to the peptide/H_2O solution on glycerol matrix has the similar effect as the addition of NH_4OH, such that in both cases there is approximately 50% of enhancement of the molecular ion intensity.

The detection limits of the peptides are further improved by recording the spectra from glutathione/20% NH_4OH/peptide solution deposited on glycerol.

This matrix composition provides further enhancement of the ion current corresponding to the peptide while suppressing the background peaks. Further suppression of the matrix is achieved by adding a surfactant solution (such as dodecanol) to the GSH/H_2O/peptide mixture (where GSH represents reduced glutathione).

CONCLUSION

1) Matrix interferences are minimized by using [(M-H) - 107]- transition for enkephalins in the negative ion FABMS - selected reaction monitoring mode.

2) Addition of NH_4OH, glutathione or surfactants to the peptide solution improves the detection limits by a factor of 2 or 3 and also provides background suppression.

3) The methods developed in this study can be used for the low level quantification of peptides from biological tissue extracts.

REFERENCES

1) D.M. Desiderio; Analysis of Neuropeptides by Liquid Chromatography and Mass Spectrometry, Elsevier, (1984).
2) M. Alai, P. Demirev, C. Fenselau, R.J. Cotter,; Anal. Chem. 58, 1303, 1986.

ACKNOWLEDGMENTS

One of us (E.T.) wishes to thank the ASMS committee for the award of a travel stipend to attend the meeting.

Presented at the 35th ASMS Conference on Mass Spectrometry and Allied Topics
May 24-29, 1987, Denver, CO

USE OF THE GROWTH MEDIUM TO ANALYZE BACTERIA VIA MS WITH CI

D.C. Conway and Humberto Lopez, Department of Chemistry, and
J.M. Quarles, Jr., Department of Medical Microbiology and Immunology,
Texas A&M University, College Station, TX., 77843

At first the analysis of the bacteria growth medium by MS with CI seemed to be of great value in the rapid identification of the bacteria, but when a second set of samples were prepared, the very important 198/108 ratios were not reproduced.[1] The analytical method,[1] where the CI gas is CH_4 with a trace of H_2O and C_6H_6, has been studied in more detail. The microcomputer that processes the spectra from the multichannel analyzer is now a Zenith-158 PC with an 8087 microprocessor. The Zenith is more than an order of magnitude faster in processing spectra than the old IMSAI microcomputer.

The dependence of the mass spectra on growth time was studied. Growth media were inoculated with Listeria monocytogenes (1706), and aliquots, removed at various times. The bacteria were killed with ethanol and separated by centrifugation. After evaporation of the liquid, 0.50 mg samples were analyzed as previously.[1] Results for the first 11 hours are shown in Table I. The 198/108 ratio appears to be much smaller at 24 hours, but this experiment will be repeated. The effect of sample size for the 11 hour growth of the LM (1706) bacteria is shown in Table II.

The 150 and 198 intensities increase faster than the sample size increases between 0.25 and 0.50 mg. A reasonable explanation for these results is that these are cluster ions, e.g., for the 198 ion

$$2(90) = (90)_2$$

$$NH_4^+ + (90)_2 \rightarrow NH_4^+(90)_2$$

(To protect labile species, the ion source is not heated directly. In addition, the pulsed discharge provides little heat, so clustering is favored.) Similarly, the 150 ion could be $H^+(59)(90)$. The other ions in Table II could also be cluster ions, e.g., 108 could be $NH_4^+(90)$, and 125, $NH_4^+NH_3(90)$. The relatively constant 125/108 ratios in Table I could indicate that the NH_3 concentration in the ion

source is relatively independent of the age of the growth medium. However, the 90 yield is a function of the age of the growth medium at typical growth times (~ 16 - 18 hours)

It is seen that the 198/108 ratio is a function of growth time and sample size, so it must also depend on the number of bacteria used in the inoculation Such peaks can not be used to identify bacteria by analysis of the growth medium without further research.

Acknowledgement: We wish to thank Kathleen Conway for growing the samples used in this study.

Reference: 1. D.C. Conway, Humberto Lopez, and J.M. Quarles, Jr., Proc. 34th Annual Conf , Amer. Soc. for Mass Spectrom., 451.

Table I. Intensity ratios vs growth time for 0.50 mg samples.

Hours	0	2	4	11
198/108	0.14	0.29	0.22	1.9
125/108	1.7	2.1	1.6	1.8

Table II. Per cent of ions at given mass vs sample size for 11 hour growth.

Mass	108	125	150	198
Sample size (mg)				
0.125	5.0	3.7	0.5	0.9
0.25	4.5	4.3	1.0	1.6
0.50	5.2	8.4	5.5	9.0
1 00	4.7	6.8	9.5	19.5

ANALYSIS OF NAPHTHENIC ACIDS IN CRUDE OILS BY FLUORIDE ION CHEMICAL IONIZATION

I. DZIDIC, A. C. SOMERVILLE, J. C. RAIA AND H. V. HART
SHELL DEVELOPMENT COMPANY, HOUSTON, TX

Chevron scientists have found that naphthenic acids present in California crude oils are composed of a highly complex mixture of carboxylic acids[1]. Chevron's work required exhaustive sample preparation procedures prior to the identification by various spectrocsopic techniques.

In order to minimize sample preparation and improve quantification, we have recently applied a fluoride ion chemical ionization method which is selective for the analysis of naphthenic acids in a complex hydrocarbon matrix. Naphthenic acids are ionized selectively by the ion - molecule reaction : $F^- + RCOOH \longrightarrow RCOO^- + HF$. Hydrocarbons cannot be ionized by this reaction. The fluoride ion chemical ionization mass spectra even of highly branched acids exhibit only the $RCOO^-$ ions. Since fragment ions are not formed the relative distribution of different acid types within the mixture can be obtained from the relative intensities of $RCOO^-$ ions. Naphthenic acid distribution data are useful in the studies of the mechanisms involved in the biodegradation of crudes, corrosion problems at refineries, and fish toxicity in refinery wastewaters.

A Finnigan 4500 mass spectrometer equipped with a Townsend discharge in combination with the use of nitrogen trifluoride as the reagent gas were employed to generate the fluoride reagent ion and naphthenic acids mass spectra.

Figure 1 shows the total negative ion profile of $RCOO^-$ ions obtained by probe introduction of the acid extract from a California crude blend. Acids were " distilled off" from the heated probe; the starting and the final temperatures were 70°C and 300°C respectively, and the heating rate was 40°C/min. The probe was maintained at the final temperature for 10 min. Figure 1, therefore, represents the total negative ion current as a function of time and probe temperature. The area under the total ion curve contains the acids representing a molecular weight range of 150-500 which corresponds to the carbon range between C_{10}-C_{35}.

Mass spectra of a standard mixture of naphthenic acids obtained from Eastman Kodak plus the sample obtained at point A of the total ion current curve illustrated in Figure 1, are shown in Figures 2 and 3. Each peak in the spectrum corresponds to one individual acid. Since the $RCOO^-$ ions in these spectra are two masses apart, the acid types are identified by the hydrogen deficiency or the z formula $C_nH_{2n+z}O_2$ where n represents the number of carbon atoms, and z varies from 0 for the paraffinic acids, to -2 for monocyclic acids, -4 for the dicyclics, and so on. The classification of hydrocarbons by z numbers has been widely used in the mass spectrometric analysis of petroleum samples.

The quantitative determination of acids classified by the z numbers is accomplished in a two step process utilizing an INCOS data system user written procedure. The resulting report gives the relative percentages of each acid type within the total sample as shown by Table 1. Duplicate analyses data included in Table 1 indicate acceptable reproducibility.

The above results indicate that the identification and quantification of naphthenic acids in complex hydrocarbon matrices can be determined quickly and inexpensively by the use of fluoride ion chemical ionization mass spectrometry.

References:
1. W. K. Seifert, Carboxylic Acids in Petroleum and Sediments, Springer Verlag, New York (1975), Chapter 1.

Figure 1. Total Negative Ion Current (M−1)⁻, Representing the Mixture of C_{10}–C_{35} Carboxylic Acids Obtained by Direct Probe Introduction of the *California Blended Crude* Acid Extract

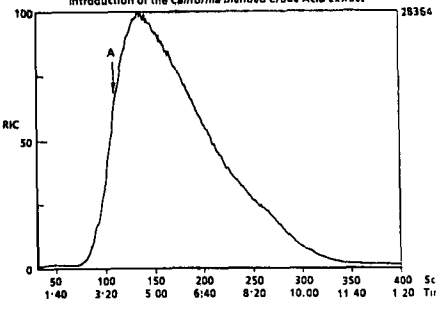

Figure 3 Fluoride Ion Chemical Ionization Mass Spectrum of the Carboxylic Acid Mixture Obtained at the Point A of the Total Ion Current Shown in Figure 1

Each odd mass (M−1) ion in the spectrum represents a specific carbon number and the acid type

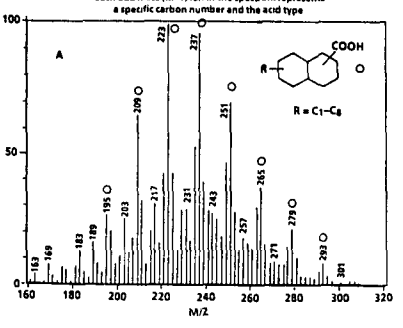

Figure 2. Fluoride Ion Chemical Ionization Mass Spectra of Kodak Naphthenic Acid Obtained at Two Different Retention Times

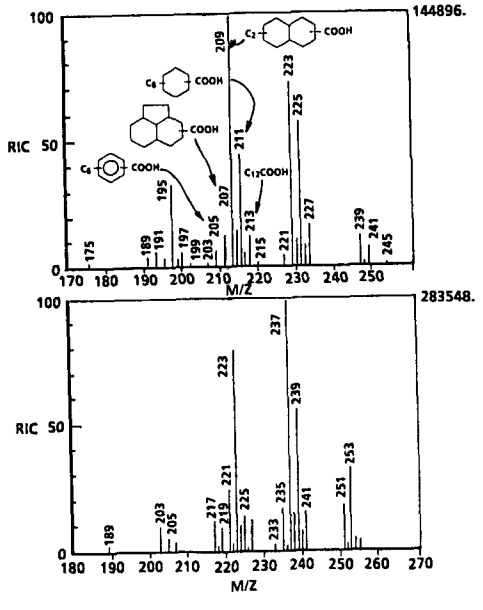

Table 1. California Blend Crude Relative Concentrations of Acid Types, $C_nH_{2n+z}O_2$ (n = 10 to 35 and z = 0 to −12) in the Total Sample Obtained from Duplicate Analysis

z	% Total	
0	9.22	9.92
−2	15.58	16.04
−4	24.35	24.56
−6	17.16	17.50
−8	10.68	10.55
−10	11.89	10.84
−12	11.12	10.58

Presented at the 35th ASMS Conference on Mass Spectrometry and Allied Topics
May 24-29, 1987, Denver, CO

The Effect of Metal Atoms on EI and CI Mass Spectra of Geoporphyrins

Brian D. Beato, Dept. of Chemistry, University of Florida, Gainesville, FL 32611
J. Martin E. Quirke, Dept. of Chemistry, Florida International University, Miami, FL 33199

Geoporphyrins are biological marker compounds which provide information on fossil fuels, such as sample maturation, depositional environment of sample, and oil-source rock correlation. Structure elucidation of metalloporphyrins by mass spectrometry is of considerable interest in fossil fuel research and exploration. A systematic characterization of the effect of the metal atoms on electron ionization (EI) and chemical ionization (CI) mass spectra of metalloporphyrins should aid structure elucidation by suggesting transmetalations (metal exchanges) to enhance or diminish fragmentation.

In this study, EI and NH_3CI mass spectral data from a series of metalloporphyrins was used to determine the effect of various metals on fragmentation. The extent of fragmentation was then correlated to a measure of stability towards demetalation by acid in solution, known as the stability index (1). Buchler defined the stability index, S_i, as

$$S_i = \frac{100(\text{Pauling electronegativity})(\text{charge on metal})}{(\text{ionic radius of metal in pm})}$$

The lower the stability index, the greater the reactivity of the metalloporphyrin in demetalation reactions. Although originally developed to describe solution chemistry, this index is shown to correlate with EI and NH_3CI mass spectral data as well.

The metalloporphyrins studied were eight derivatives of 2,3,7,8,12,13,17,18-octaethyl-21H,23H-porphine (OEP):

Fe(III)(OEP)Cl	Ni(II)(OEP)	Zn(II)(OEP)
Cr(III)(OEP)Cl	Cu(II)(OEP)	Mg(II)(OEP)
Mn(III)(OEP)Cl	Co(II)(OEP)	

These were also compared to metal-free OEP (see figure 1).

In reducing solutions, Cu(II) porphyrins have been observed to be reduced to Cu(I) (1). Under NH_3 desorption CI conditions, Cu(II) porphyrins have been observed to completely demetalate and fragment as metal-free porphyrins (2). This is due to reduction of Cu(II) to Cu(I) which is readily extruded. If Cu(II) porphyrins are reduced under NH_3CI conditions, it is likely that Fe(III) and Mn(III) porphyrins are also reduced in the NH_3 plasma, as they have higher standard reduction potentials than Cu(II) in solution:

$$Cu(II) + e^- \rightleftharpoons Cu(I) \qquad E^o = +0.153\ V$$
$$Fe(III) + e^- \rightleftharpoons Fe(II) \qquad E^o = +0.771\ V$$
$$Mn(III) + e^- \rightleftharpoons Mn(II) \qquad E^o = +1.541\ V$$

Results for both oxidation states of these metals will be discussed.

All spectra were obtained on a Finnigan MAT TSQ45 via a solids probe which heated 2 µg of sample at 99°C/min. EI results were obtained with an electron voltage of 70 eV and emission current of 0.3 mA. Under these conditions, the doubly charged β-cleavage fragments were much more intense than the singly charged fragments (see figure 2a). The metalated derivatives all showed more β-cleavage fragmentation than the metal-free OEP did. In fact, the greater the stability index of the metalloporphyrin, the greater the relative abundance of doubly charged ions compared to the singly charged molecular ion (see figure 2b). Also, the higher the stability index, the greater the relative abundance of doubly charged fragments to the doubly charged molecular ion. These observations are due to greater charge localization on the metal atom withdrawing more electron density from the periphery resulting in enhanced B-cleavage fragmentation, as noted previously (3).

The NH_3CI spectra were obtained with 0.4 torr NH_3, 100 eV electron voltage, and 0.3 mA electron energy. Besides the expected $(M+H)^+$ peaks, most of the derivatives also yielded pyrrolic fragments, as well as various NH_2^+, NH_3^+, and NH_4^+ pyrrole adducts (see figure 3a). The mass chromatograms indicate that the pyrroles do not arise simply out of NH_4^+

attack of the molecular ion, since the traces do not resemble one another (see figure 3b). The NH_3CI spectra do not show any porphyrinogen $(M+6H+H)^+$ formation as previously observed in NH_3 desorption CI, where repeated attack by NH_4^+ has been postulated to lead to pyrrole fragments (2). This indicates that the porphyrins undergo thermal decomposition to pyrroles in the ammonia plasma.

The extent of pyrrole formation is very dependent on the specific metal in the metalloporphyrin. The greater the stability index, the lower the relative abundance of pyrroles formed, compared to $(M+H)^+$ (see figure 3c).

While Cu(II)(OEP) and Ni(II)(OEP) have very similar stability indices, Cu(II)(OEP) yields significantly higher intensities of pyrroles than does Ni(II)(OEP). In fact, Cu(II)(OEP) behaves very much like metal-free OEP. This supports Cu(II)(OEP) reducing in the NH_3 plasma. The correlation of pyrrole formation with Fe(II) and Mn(II) is much better than with Fe(III) and Mn(III), indicating that these metals are also reduced under NH_3CI conditions, as expected.

In conclusion, it has been shown that the extent of metalloporphyrin fragmentation in EI and CI mass spectrometry can be correlated with the stability index of the metal. This should aid the structure determination of metalloporphyrins by suggesting transmetallations which would enhance or diminish fragmentation, as desired.

REFERENCES: (1) J.W. Buchler in "Porphyrins and Metalloporphyrins", Ed. Kevin M. Smith, Elsevier, Amsterdam (1975) p. 196-202.
(2) C. Djerassi, et. al., J. Am. Chem. Soc., 108, 1363 (1986).
(3) K.M. Smith in "Porphyrins and Metalloporphyrins", Ed. Kevin M. Smith, Elsevier, Amsterdam (1975) p. 396.

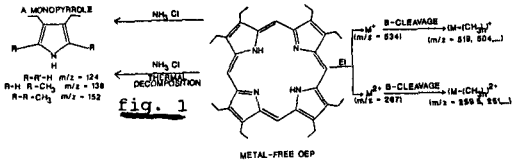

fig. 1

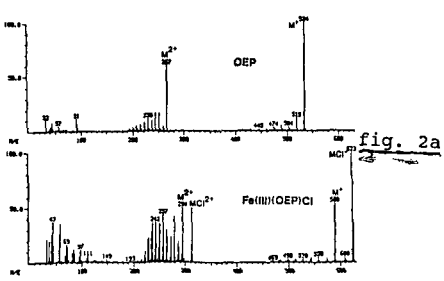

fig. 2a

fig. 3a

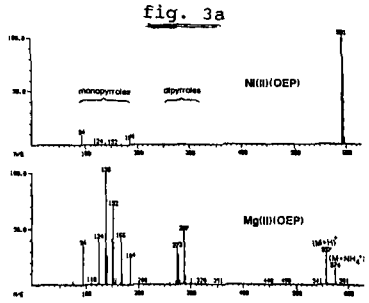

fig. 3b

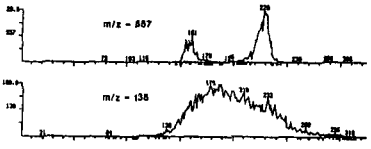

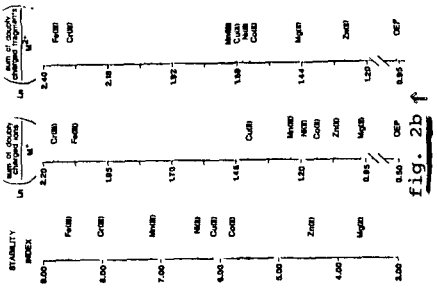

fig. 2b

fig. 3c

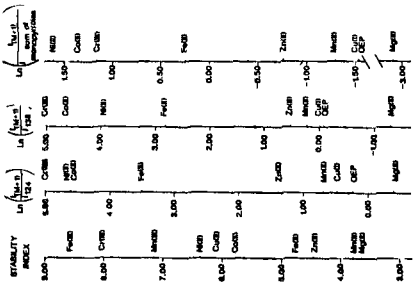

Presented at the 35th ASMS Conference on Mass Spectrometry and Allied Topics
May 24-29, 1987, Denver, CO

Tandem Mass Spectrometry for the Determination of Trace Steranes in Crude Shale Oil

J.V. Johnson, Chemistry Dept., University of Florida, Gainesville, FL 32611. C.M. Wong*, and H.R. Gregg, Lawrence Livermore National Laboratory, P.O. Box 808, Livermore, CA 94550. *Current Address: Ames Research Center, Moffett Field, CA 94035

Steranes are a class of biomarkers used in fossil fuel exploration to ascertain the origin (terrestrial or marine), maturity, migration, and chemical and biodegradation changes of the fossil fuels. Due to low levels of individual steranes in oil (ppm) and the complexity of the sterane composition, extensive clean up procedures and GC temperature programming have been required, resulting in lengthy analyses with the traditional GC/EI-MS methods of analysis. Here we report the results of our evaluation of the use of triple quadrupole tandem mass spectrometry (MS/MS) to: 1) characterize the MS/MS behavior of steranes, 2) rapidly determine the sterane content in crude shale oil without prior sample cleanup, and 3) distinguish sterane stereoisomers.

The EI (70 eV, 0.3 mA, 150 C) collisionally activated dissociation (CAD, 1.1 mtorr N_2, 25 eV) daughter mass spectra of the $M^{+\cdot}$ ions of the sterane standards (5-α-androstane, 5-α-pregnane, 5-α- and 5-β-cholestane, 5-α-ergostane, and 5-α-stigmastane) are characterized by abundant $(M-15)^+$ and 217^+ daughter ions with the daughter mass spectra becoming dominated by these two daughter ions with increasing molecular weight of the sterane (shown in Figure 1 for 5-α-stigmastane). In addition loss of a neutral fragment of 110 u from the parent molecular ion yields a characteristic daughter ion, e.g. m/z 290 for the 5-α-stigmastane. Unlike the EI-CAD of the $M^{+\cdot}$, the methane PCI (100 eV, 0.9-1.0 torr CH_4, 150 C)-CAD (25 eV, 1.1 mtorr N_2) of the $(M-H)^+$ ions yielded numerous daughter ions which consisted of four major ion series: 91 + $(CH_2)_n$, 79 + $(CH_2)_n$, 67 + $(CH_2)_n$, and 69 + $(CH_2)_n$ with the most characteristic and usually the most abundant daughter ion in each series being m/z 203, m/z 149, m/z 95, and m/z 111, respectively. It should also be noted, that although methane PCI yields a much greater relative abundance of the $(M-H)^+$ ions than does EI for the $M^{+\cdot}$ ions, the $(M-H)^+$ ions are much more stable towards CAD and are not as efficiently fragmented.

Solids probe MS/MS was evaluated for the determination of steranes in the crude oils obtained from three different shale oils by the EI-CAD parent scan of 217^+ and the PCI-CAD parent scans of 95^+, 149^+, and 203^+. Figure 2 illustrates the results of such screenings for a sterane-rich oil. In all cases, parent ions were detected which were indicative of the steranes with the EI-CAD parent scan of m/z 217 being the most characteristic and having the least interference from other compounds (note the m/z 372, m/z 386, and m/z 400 parent ions in Figure 2a which are indicative of C27, C28, and C29 steranes, respectively). Subsequent EI-CAD daughter mass spectra of the detected parent ions were only characteristic of steranes for the most abundant of the detected $M^{+\cdot}$ ions, there being too much chemical interference for the lower abundant ions (compare the EI-CAD of m/z 400 in crude oil in Figure 3 with that of the 5-α-stigmastane standard in Figure 1). Although this method permits very rapid screening of an oil for its sterane content, some type of sample pretreatment is necessary to reduce the chemical interferences and to reduce the extensive contamination of the instrument (the entire quadrupole stack and ion source had to be cleaned after only 10 oil samples).

MS/MS was evaluated for its ability to distinguish the 5-alpha and 5-beta-diastereomers of the steranes. The comparison of the EI-CAD and PCI-CAD daughter mass spectra of the $M^{+\cdot}$ and $(M-H)^+$ ions, respectively, showed the EI-CAD daughter mass spectra to be more characteristic. The daughter mass spectra obtained with less harsh CAD conditions (5 - 15 eV and 1.1 mtorr N_2) contained daughter ions diagnostic of the two diastereomers: m/z 107, m/z 136, and m/z 148 for 5-α-cholestane and m/z 108, m/z 135, and m/z 152 for 5-β-cholestane (Figure 4). As the collision energy and pressure were increased, the difference in the daughter mass spectra of the two stereoisomers became less distinct.

Presented at the 35th ASMS Conference on Mass Spectrometry and Allied Topics
May 24-29, 1987, Denver, CO

EI-CAD Daughter Spectrum of $M^{+\cdot}$

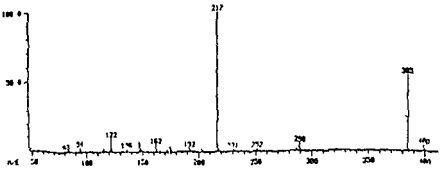

Methane PCI-CAD Daughter Spectrum of $(M-H)^{+}$

Figure 1.

EI-CAD Parents of m/z 217

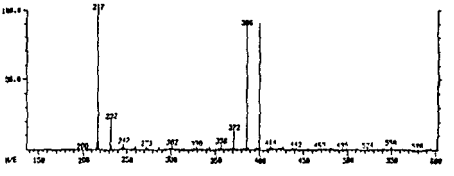

Methane PCI-CAD Parents of m/z 140

Figure 2.

EI-CAD Daughters of m/z 372

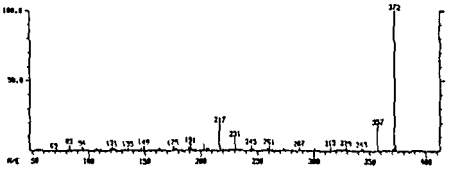

EI-CAD Daughters of m/z 400

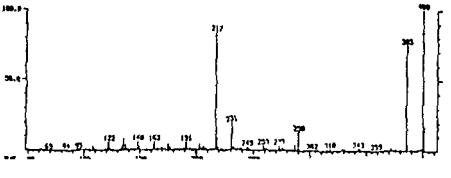

Figure 3.

EI-CAD Daughter Spectra of $M^{+\cdot}$
(15 eV, 1.1 mtorr nitrogen)

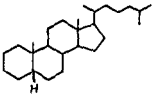

5-alpha-Cholestane

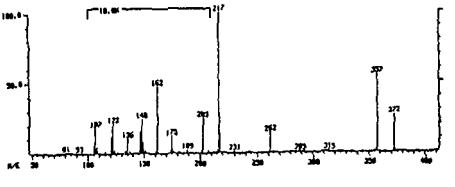

5-beta-Cholestane

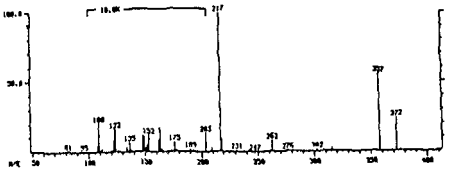

Figure 4.

Presented at the 35th ASMS Conference on Mass Spectrometry and Allied Topics
May 24-29, 1987, Denver, CO

FAB-MS and -MS/MS of PETROLEUM SULFONATES

S. R. Missler

Exploration and Production Technology Division
Texaco, Inc.
Bellaire, TX 77401

Fast atom bombardment mass spectrometry was used to characterize commercially available synthetic alkylbenzene sulfonate mixtures and petroleum sulfonates. Negative ion FAB spectra using different matrices including glycerol generated abundant ion intensities for the organic anion, and little fragmentation making this technique suitable for molecular weight profiling (Figures 1 and 2).

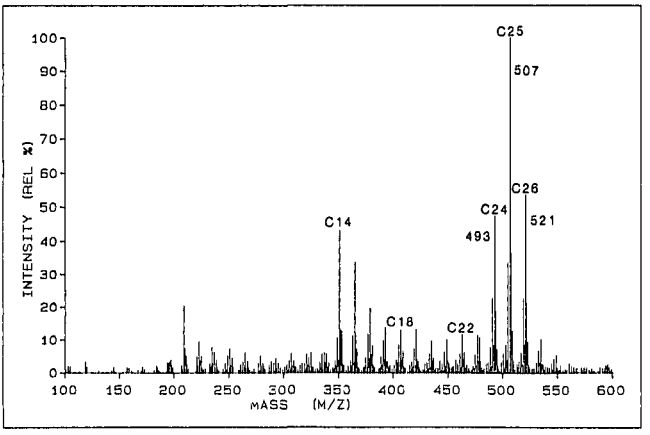

Figure 1. FAB-MS spectrum of Aristonate E (Pilot Chemical Co.)

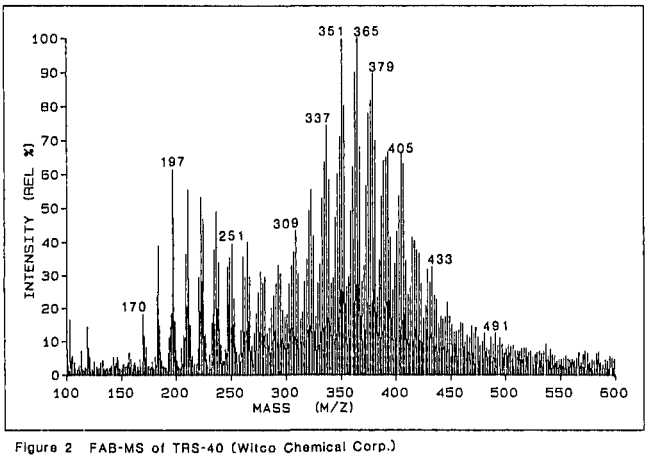

Figure 2 FAB-MS of TRS-40 (Witco Chemical Corp.)

Further characterization of components in these mixtures using low energy collision induced dissociation (CID) in a hybrid mass spectrometer (EBQQ design) gave information on aromaticity, alkyl substitution and branching. A study of low energy CID fragmentation was performed using authentic alkylaryl sulfonate standards. CID fragmentation was found to occur in a manner similar to conventional EI-MS of alkylaryl compounds. Examples of MS/MS scans used to characterize sulfonate mixtures are given in Figures 3 and 4.

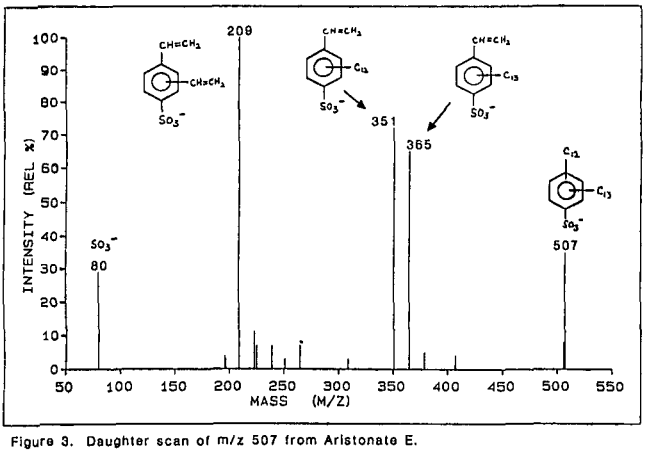

Figure 3. Daughter scan of m/z 507 from Aristonate E.

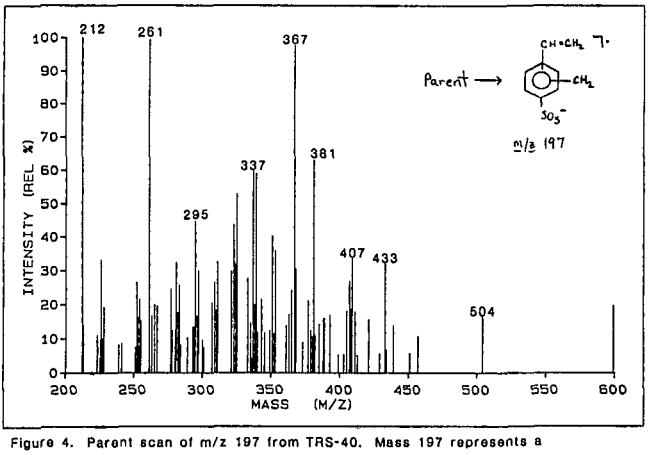

Figure 4. Parent scan of m/z 197 from TRS-40. Mass 197 represents a dialkylbenzene sulfonate having one substituent branched at the alpha carbon.

Presented at the 35th ASMS Conference on Mass Spectrometry and Allied Topics
May 24-29, 1987, Denver, CO

STRUCTURE AND DISTRIBUTION OF STRAIGHT-CHAIN FATTY ACIDS AND ESTERS IN COAL EXTRACTS STUDIED BY MS/MS AND FD-MS

Y. Niwa and K. Ishikawa
National Chemical Laboratory for Industry, Yatabe, Ibaraki 305, Japan

Fatty acids and esters frequently occur in materials of geological interest and have been proposed as a source of geochemically formed n-alkanes. In the extensive studies on geological fatty acids, their identifications have been performed on methylated samples by GC. The analyses of ester mixtures have been made by GC identification of acids and alcohols resulting from saponification of the samples. (*See* C.E. Snape, B.J. Stokes and K.D. Bartle, *Fuel* 1981, 60, 903 and references therein.) In this study, MS/MS analysis of coal extracts has been made for a detailed structural identification of these compounds and their distribution among coals of various ranks has been investigated by FD mass spectrometry to reveal their geological implications.

EXPERIMENTAL

Coals studied were two lignites (carbon content: 65.6 and 68.0 daf wt%), two subbituminous coals (carbon content: 75.3 and 76.2 daf wt%) and three bituminous coals (carbon content: 80.8, 83.5 and 85.9 daf wt%). Solvent extractions were carried out with pyridine in a Soxhlet apparatus for 24 h. The hexane-soluble fraction of each extract was treated with cold diethyl ether and its insoluble portion was subjected to mass spectrometric study. All observations were made using a JEOL HX-100 mass spectrometer. Mass spectra of daughter ions resulting from collision-induced dissociation (CID) of selected ions were measured using *B/E* linked scan method by mounting a gas cell immediately following an ion source.

RESULTS AND DISCUSSION

Fig. 1 shows a typical FD mass spectrum for extracts of lignites. As seen from the figure, they contain two series of homologues as major constituents. Their elemental compositions were found to be $C_nH_{2n}O_2$ to a precision of 4 mmu from the precise mass measurements, indicating that their possible chemical structures are either saturated fatty acids or esters. The number of carbon atoms contained in each component (n) is shown in *Fig.* 1, which shows that the components with even n predominate over those with odd n.

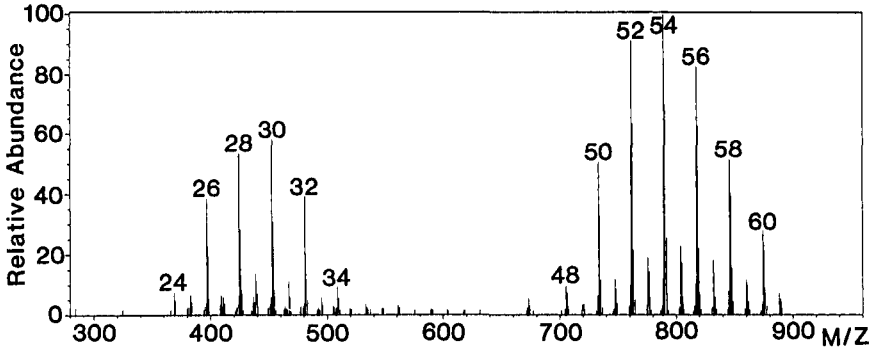

Fig. 1 FD mass spectrum of the extract of Morwell coal (carbon content 68 wt%).

CID spectra of the components in mass range between 360 and 520 ($24 \leq n \leq 34$) exhibit abundant ions belonging to the series $C_kH_{2k}COOH^+$. A periodic variation in their intensities exists and the ions of k = 6, 10, 14,···, which are separated by four methylene units, dominate in the series. Since these observations are in parallel with the fragmentations induced by EI ionization of straight-chain fatty acids, the components in a lower mass range can be identified as those with C_{24} to C_{34}. This was confirmed by the fact that CID spectra observed were in good agreement with those of corresponding authentic compounds.

Fig. 2 shows the CID spectrum of the component of molecular weight 788.9. CID spectra of the components in mass range between 700 and 930 ($48 \leq n \leq 64$) are similar each other except for the distribution of ions whose masses are represented by 369 + 28k (k = 1, 2, ···), as marked with ● in *Fig.* 2. The

distribution extends to a higher mass with an increase in mass of precursor ions. These fragmentation behaviors are obviously different from those observed for fatty acids and their esters with small alcohol, which raises the possibility of long chain fatty esters of type RCOOR' as the molecular structures of components in a higher mass range. Since a pair of peaks of $C_{15}H_{31}COOH^+$ and $C_{15}H_{31}COOH_2^+$ are observed significantly abundant in the CID spectrum of stearyl palmitate, the marked peaks in *Fig.* 2 can be assigned to type $RCOOH_2^+$. Their multiple appearances indicate that each component is a mixture of isomeric RCOOR' with different pairs of R and R'. For the components of molecular weight 788.9 ($C_{54}H_{108}O_2$), for example, the ions of mass 369, 397, 425 and 453 are assigned to $C_{23}H_{47}COOH_2^+$, $C_{25}H_{51}COOH_2^+$, $C_{27}H_{55}COOH_2^+$ and $C_{29}H_{59}COOH_2^+$, respectively, which implies that the components are mainly composed of $C_{23}H_{47}COOC_{30}H_{61}$, $C_{25}H_{51}COOC_{28}H_{57}$, $C_{27}H_{55}COOC_{26}H_{53}$ and $C_{29}H_{59}COOC_{24}H_{49}$. Thus, the relative

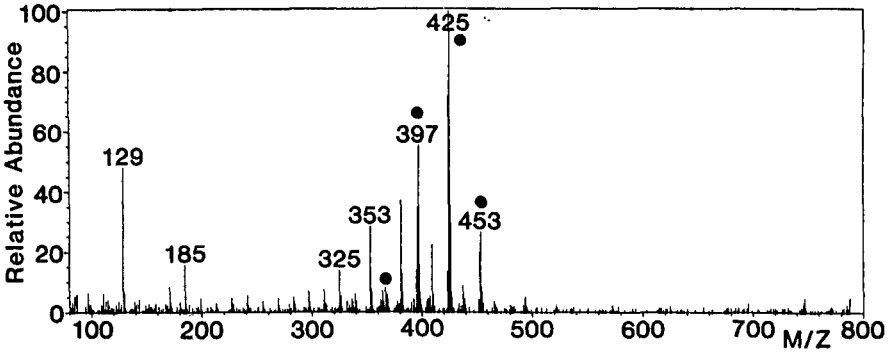

Fig. 2 CID spectrum of the component of MW 788.9 in the extract of Morwell coal.

abundances of isomeric esters can be estimated from the relative intensities of marked peaks. Overall carbon-number distributions of acyl and alkoxyl groups among the whole ester mixture were derived assuming that the relative abundances of esters of a given molecular weight were proportional to their ion intensities observed in the FD mass spectrum. The results obtained are shown in *Fig.* 3. As seen from *Figs.* 1 and 3, the free acids, and the acyl and the alkoxyl groups in esters all exhibit similar carbon-number distributions extending from C_{24} to C_{34}.

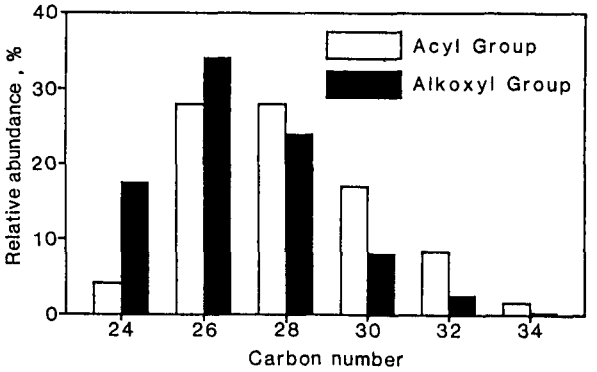

Fig. 3 Carbon-number distributions of the acyl and the alkoxyl groups of fatty esters in the extract of Morwell coal.

In contrast to lignites, esters are missing in extracts of subbituminous coals although they contain free fatty acids with C_{24} to C_{34} whose relative abundances are qualitatively similar to those observed for lignites. Extracts of bituminous coals exhibit entirely different spectra that give no indication of any significant amounts of free acids and esters. These observations lead us to the following conclusions: (a) The free acids, the acyl and alkoxyl groups in the esters have a common origin; (b) The free acids are most likely derived from hydrolysis of the esters during maturation, and the disappearance of free acids from bituminous coals may be associated with their complete chemical changes such as conversions into n-alkanes.

Presented at the 35th ASMS Conference on Mass Spectrometry and Allied Topics
May 24-29, 1987, Denver, CO

ISOBUTANE CI FOR ON-LINE DETERMINATION OF AMMONIA FROM OIL SHALE PYROLYSIS

Richard W. Crawford, Thomas T. Coburn,
Philip E. Miller and Myongsook S. Oh
Lawrence Livermore National Laboratory
Box 808, L-310, Livermore, CA 94550

Ammonia is the predominant nitrogen containing species formed during the pyrolysis of oil shale. It is important to study the factors effecting its formation as it could be a valuable by-product. In addition, its release must be controlled for environmental reasons. The major problem in developing an accurate mass spectrometric determination of ammonia is the presence of water, often in large quantities such as in steam retorting. Isobutane chemical ionization forms NH_4^+ readily and H_3O^+ only slightly. Under normal CI conditions, some H_2O^+ forms, interfering with the ammonia determination.

Initial experiments used the collision cell of the triple quadrupole mass spectrometer[1] to investigate ion-molecule reactions to remove the water interference. We found that, at high pressures, NO charge exchanged with H_2O^+ 10 times more than with NH_4^+. While carrying out these experiments we found that scattering due to the collision gas is proportional to the log of the pressure (equivalent to scattering of light as described by Beer's law).

Although the charge exchange cleanup is analytically useful, we find that by modifying CI conditions we reduce the water interference to a negligible level. The major CI condition reducing water interference is increasing the CI gas pressure going into the source to 600 mtorr as read on a Granville-Phillips Convectron 275 (probably < 30 mtorr true pressure). This reduces the percent of H_2O^+ related to H_3O^+ to <1%. In addition, carefully drying the isobutane and baking the reagent gas lines leading to the source reduces water interference to a low level. Combining these techniques lets us determine ammonia at <50 ppm in steam.

A laboratory scale retort is attached to the inlet of the TQMS allowing for on-line, real time analysis of ammonia formed (or decomposed) as the retort is heated. The heating of the retort is controlled by an HP 85 computer to give an extremely constant heating rate, and uses an outer and inner heater to maintain temperature uniformity across the sample[2]. All lines exiting the retort are heated to ~150°C to eliminate water condensation and the possible loss of ammonia as $(NH_4)_2CO_3$ or $(NH_4)_2S$. The inlet to the TQMS is a two-stage pressure-reduction system (Balzers GES 010 with 0.3 mm capillary) maintained at 200°C. Approximately 200 cc/m argon is passed through the retort, flows past the inlet to the capillary and is vented to the atmosphere.

To reduce drift during long runs (up to four hours) the isobutane pressure is maintained precisely at 600 ± 3 mtorr (as read) with a Granville-Phillips Convectron gauge driving a Datametrics valve controller We monitor the isobutane fragment at mass 37 and use this data to correct any drift measured in the ammonia signal.

We must determine the volume of ammonia created. Since the pressure at the inlet to the capillary is constant, a method was developed to measure the change in volume of the gas due to formation of pyrolysis products The pyrolysis gas is doped with a constant amount (4 cc/m) of trimethyl-

---

[1] Wong, C. M.; Crawford, R. W.; Barton, V. C.; Brand, H. R., Neufeld, K. W.; Bowman, J. E *Rev. Sci. Instrum.* 1983, *54*, 996-1004.

[2] Oh, M. S.; Taylor, R. W. American Chemical Society Petroleum Division Preprints, April 1987, *32 (1)*, 97-102

amine at the retort furnace exit. The flow is held constant by immersing the $(CH_3)_3N$ tank and five meters of 0.13 mm capillary in a constant temperature water bath at 37.2°C. The trimethylamine serves as a flow and sensitivity reference. The M+H ion at mass 60 from $(CH_3)_3N$ is monitored and the decreases in intensity are inversely proportional to the increases in gas flow. The ammonia data is corrected by this data to give volume information.

Initial experiments studied ammonia decomposition using steam, H_2, and inert sweep gas. We found that the temperature at which 50% of the ammonia decomposed was 700°C with Ar, 800°C with H_2 and close to 1000°C with 56% steam in Ar.

In western oil shale, part of the nitrogen is inorganic in the form of Buddingtonite. We have studied the formation of ammonia from this mineral and find that three times as much NH_3 is evolved with steam retorting as with Ar, with the maximum evolution at 630°C when heating at 4°C/m.

Finally, we have determined ammonia while pyrolyzing several western shales and an eastern shale. The figure below shows a western shale from Tract C-a with a yield of 35 gal/ton. We used two heating rates, the upper 12°C/m and the lower 4°C/m. The difference in the maximum can be used to calculate the kinetics of ammonia formation. The peak at 450°C is concurrent with oil production. The peak at 630°C is a combination of Buddingtonite decomposition and reactions of other nitrogen sources with hydrogen donors during charring. The drop in evolution at 700°C is due to ammonia decomposition.

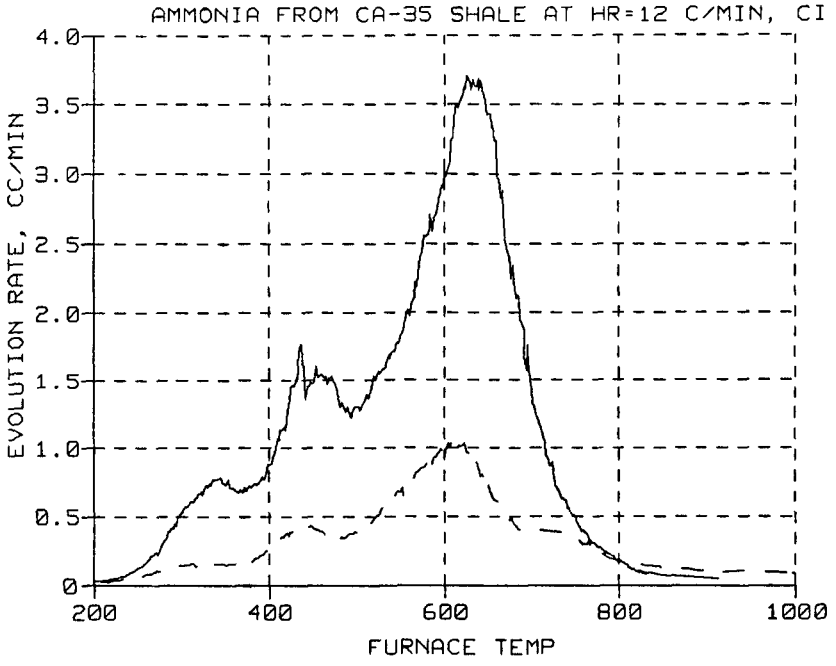

Work performed under the auspices of the U.S. Department of Energy by the Lawrence Livermore National Laboratory under contract W-7405-ENG-48

Presented at the 35th ASMS Conference on Mass Spectrometry and Allied Topics
May 24-29, 1987, Denver, CO

ENERGY RESOLVED MS/MS SPECTRA OF IONS FORMED FROM TRANSITION METAL ACETYLACETONATES

G. C. DiDonato and K. L. Busch
Department of Chemistry, Indiana University, Bloomington, IN 47405

Mass spectrometric studies of organometallic compounds have provided results directly relevant not only to inorganic and physical organic chemistry, but to catalytic and surface chemistry as well. Most work has involved the mass spectra of inorganic and organometallic compounds generated in electron and chemical ionization sources. Organometallic ions in the gas phase are very reactive species. Clustering and polymerization reactions occur in the source of the mass spectrometer as a function of the amount of sample, the rate of vaporization into the source, and the source temperature and pressure. The variety of reactions provide an opportunity to study a diversity of gas phase organometallic ions. In this work, we have used energy-resolved mass spectrometry/mass spectrometry (ERMS/MS) to study the dissociations of small ions formed from transition metal acetylacetonates (acac). Energy resolutions of 2 eV were obtained across the collision energy range of 5 to 100 eV. Similar energy-resolved data can be obtained with Fourier transform mass spectrometry; a wider number of cluster/polymeric ions are available for study, however, with the use of a high pressure electron or chemical ionization source.

Breakdown curves are plotted as a function of percent relative abundance of the daughter ion versus collision energy; here, percent relative abundance is the intensity of a given daughter ion divided by the sum of all daughter ion intensities. Daughter ion MS/MS spectra were measured for $Met(acac)_2^+$ and $Met(acac)^+$ for all of the first row transition metals. Figure 1 plots the abundance behavior of the loss of (acac) from $Met(acac)_2^+$ as a function of collision energy across the first row transition metals. The data suggest an increasing relative stability of the fragment ion in the series from Zn to Cr. Since these reactions can be considered as a formal reduction of the metal, increasing stabilities of $Met(acac)^+$ relative to $Met(acac)_2^+$ are indicated.

The general schemes of dissociation for $Met(acac)_2^+$ and $Met(acac)^+$ ions are given in Figure 2. The predominant dissociation paths are the same as those found previously in other studies. In addition to these pathways, several new reactions have been established under low energy collision conditions. These reactions include loss of carbonyl from the molecular ion of the bis acetylacetonates (previously seen only for the second and third row metal complexes), and a loss of carbonyl followed by a loss of acetylene.

The energy-resolved MS/MS data provide the most interesting data. The daughter ion MS/MS spectrum of $Co(acac)_2^+$ contains a triplet of ions at m/z 157, 158, and 159, representing $Co(acac)_2-H^+$, $Co(acac)^+$ and $Co(acac)H^+$. The relative abundance of the ions in this grouping exhibit a remarkable sensitivity to collision energy. At 13 eV, ions at m/z 157, 158, and 159 are in an abundance ratio of about 3:1:2, with the ions resulting from the two rearrangement reactions predominating. An increase in collision energy of only 10 eV to 23 eV changes the ratio to 1:2:1, with the cleavage reaction more abundant at this slightly higher energy. In the center-of-mass energy frame, the collision energy difference of 8 eV is equivalent to a 2.3 eV difference. A strong energy dependence of the dissociative rate constants must be invoked to explain these differences across such a small energy range. Figure 3 displays the daughter ion MS/MS spectra of $Zn(acac)^+$ at 5, 39, and 45 eV. The daughter ions are formed by loss of the methyl radical, loss of methane, and loss of water. The ratios of the ions at m/z 140, 142, and 143 change significantly and reproducibly, again indicating a strong dependence on the k(E) curve.

In some situations, structures in the breakdown curves were noted, with a periodicity approximating 10 eV. These have been related to the effect of the q value of the RF only quadrupole. The effect of the q value is to produce changes in the transmissions of the ions into the final mass analyzing quadrupole, which are ultimately seen as changes in the relative abundances of the daughter ions in the MS/MS spectrum. A simple test for the occurrence of a q-based mass discrimination effect is to vary the q value and chart the shift in the daughter ion abundance maxima. Although

such effects can be evaluated on each individual instrument, the compilation of libraries of MS/MS spectra is made more difficult by this instrumental effect. Furthermore, this effect cannot be eliminated by setting the q value at a constant level, which may prevent the passage of all daughter ion masses. Further, scanning the q value either as a function of daughter ion mass will change the transmissions of the parent ions, an additional complication in the determination of the true daughter ion abundances.

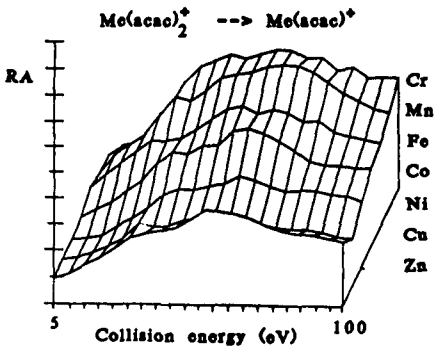

Figure 1

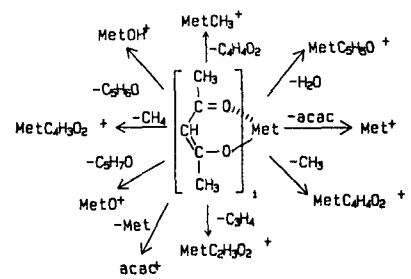

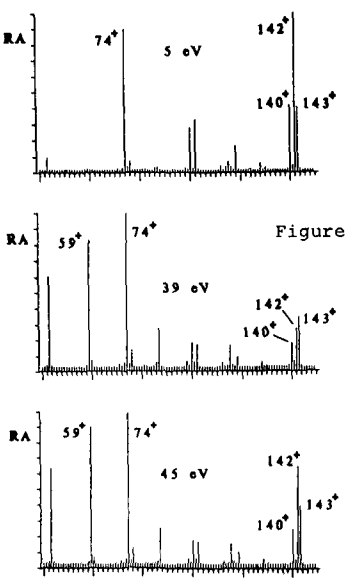

Figure 3

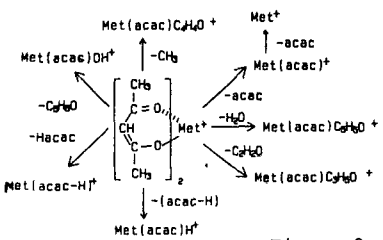

Figure 2

Presented at the 35th ASMS Conference on Mass Spectrometry and Allied Topics
May 24-29, 1987, Denver, CO

RAPID CHARACTERIZATION OF LIQUID BIOMASS PYROLYSIS PRODUCTS BY MOLECULAR BEAM, MASS SPECTROMETRY AND MULTIVARIATE ANALYSIS TECHNIQUES

Robert J. Evans and Thomas A. Milne
Solar Energy Research Institute
Golden, Colorado 80401

Introduction

Biomass pyrolysis oils produced by the flash pyrolysis of oils are difficult to analyze by conventional chromatographic techniques because of their complex, polar nature, reactivity, and thermal instability. The major information needed for the practical applications of biomass pyrolysis is the general characterization of the oil so that composition can be related to the formation chemistry and be modified to obtain the optimum composition for a particular use.

Molecular beam, mass spectrometry (MBMS) has been used to determine the major classes of solid-phase pyrolysis reactions of biomass and the subsequent secondary cracking pathways as a function of gas phase residence time (1). This mechanistic perspective of composition has been used as a basis for the development of a rapid compound class anaysis of the liquid products of applied pyrolysis systems. The low energy EI mass spectra of 70 liquid products from several conversion systems have been combined in a data base along with mass spectra from real time studies of biomass pyrolysis. Multivariate analysis (2) of this data base has allowed the relative amounts of 6 compound classes to be determined: (1) carbonyl compounds, (2) furfurals/lactones, (3) anhydrosugars, (4) monomethoxy phenols, (5) dimethoxy phenols, and (6) phenols.

Experimental

The specifics of the experimental procedure has recently been reviewed (1). In brief, the oil samples are flash volatilized in a tubular reactor into flowing 500°C helium which gives approximately 90% volatilization compared to conventional chromatographic analysis where less than 50% of the oil is typically mobilized. The effluent from the reactor is expanded across a series of two orifices and the resulting molecular beam has line-of-sight introduction into the mass spectrometer ion source (22.5 eV EI). The mass range of interest (typically 15 to 300 amu) is repetiitively scanned as the liquid is volatilized. Residence time in the gas phase was kept as short as possible (less than 75 ms) to minimize potential gas-phase secondary reactions. Direct studies of secondary cracking in real time (1) have shown only minimal changes in product distribution below 500°C and residence times of 1 second. The pyrolysis of biomass utilizing this system has also been studied and pyrolysis spectra of the components of wood have been included in the data base since they show the types of compound classes in whole wood pyrolysis.

The data was autoscaled by typical procedures (2) and factor analysis was performed using the SIGMA program developed by the Biomaterials Profiling Center at the University of Utah. Compound classes were determined by graphical rotation methods utilizing variance diagrams developed by Windig and Meuzelaar (2).

Results and Discussion

Factor analysis of the data set resulted in seven factors that contained 75% of the original variance in the data set. The factor score plot (factor 1 vs. factor 2) is shown in Fig. 1A for the seventy samples of oil and feedstocks used in this study. The variance diagram (2) in Fig. 1B shows the regions (indicated by the three maxima in variance) where correlated masses are clustered, which indicate component axes. The three major maxima in the F1 vs. F2 plot are the methoxy phenols, the phenols/aromatics and the cellulose-derived products. Each of these maxima were further resolved

utilizing the other five factors to isolate the six compound classes of interest that are listed above. The factor spectra for the monomethoxyphenols and the dimethoxyphenols are shown in Fig. 2 as an example. Factor scores for the six compound classes for each sample have been calculated and allow a comparison of the oils to be made based on composition.

This technique allows the rapid characterization of oils with six parameters that can be related to the formation chemistry. The future work in this area will include quantitation and correlation with properties important for fuel utilization or upgrading.

Acknowledgements

This work was supported by the Energy from Municipal Waste Program of DOE. The SIGMA software was provided by the Biomaterials Profiling Center of the University Of Utah.

References

1. Evans, R. J., and Milne, T. A., Energy and Fuels, 1(2), 123-137 (1987).
2. Windig, W., and Muezelaar, H. L. C., Anal. Chem., 56, 2297-2303 (1984).

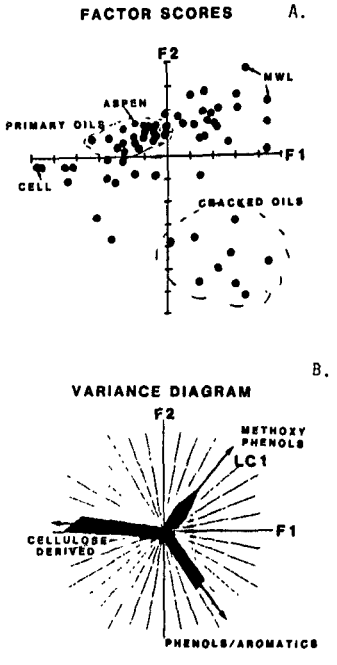

Figure 1

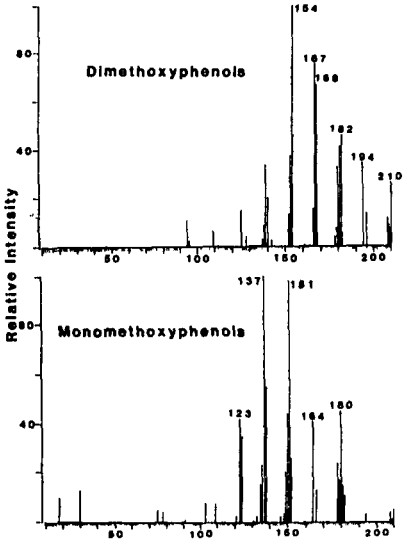

Figure 2

Presented at the 35th ASMS Conference on Mass Spectrometry and Allied Topics
May 24-29, 1987, Denver, CO

CHARACTERIZATION AND DETERMINATION OF ALKYL GROUPS OF ZINC DIALKYLDITHIOPHOSPHATES AND OTHER ANTIOXIDANTS IN MOTOR OILS BY PYROLYSIS GAS CHROMATOGRAPHY/MASS SPECTROMETRY

T. H. Wang, Pennzoil Products Company
P.O. Box 7569, The Woodlands, Texas 77387

Due to their broad range of activity, zinc dialkyldithiophosphates (ZDDPs) are one of the most important lubricant additives. They are employed as antioxidants, antiabrasion agents, corrosion inhibitors, and high pressure additives. These performance properties are largely dependent upon the structure and chain length of the alkyl groups in the ZDDP molecules. The skeletal structure of ZDDPs is as follows:

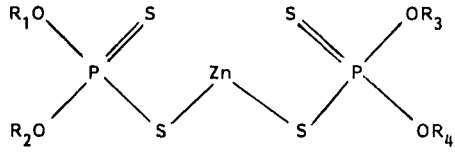

R: alkyl group

As a source of ZDDPs, we used those extracted from fully formulated motor oils. The ZDDPs were isolated by solvent extraction and column chromatography. Following separation of the ZDDPs, the alkyl groups of the various ZDDPs and other antioxidants were successfully characterized and determined by pyrolysis gas chromatography/mass spectrometry (GM/MS) with the aid of ^{13}C-NMR spectroscopy.

Several micrograms of the extract were placed on a coil probe of a CDS pyroprobe and inserted into a thermal desorption chamber at 275°C. Upon pyrolysis (300°C) of the isolated ZDDP extract, alkenes and alkanethiols were formed; pyrograms of the mixture give an indication of the various alkyl groups present in ZDDPs and other additives. Typical pyrograms are shown in Figure I. Various commercial additive packages were separated from process oils and subsequently analysed by pyrolysis GC/MS with the aid of ^{13}C-NMR spectroscopy. Butyl, hexyl, octyl, decyl, and dodecyl ZDDPs were detected in the additive packages. The results are shown in Table I.

When comparing U.S. vs. Japanese motor oils, it was found that Japanese motor oils contain lower levels of ZDDPs than those of their American counterparts. This is consistent with low phosphorous levels in Japanese oils to minimize poisoning of the catalytic converter. Although the most predominant type of additive found in the motor oil extracts were ZDDPs, quinoline, hindered phenol and diphenylamine- type additives were also found. These compounds function as antioxidants and stabilizers. The alkyl groups of ZDDPs and other antioxidants were identified in various motor oils

(Table II). The relative concentrations of ZDDP fragments and other antioxidants are characteristic for each motor oil.

This pyrolysis GC/MS method is simple, rapid, reproducible, and efficient for screening various ZDDPs and other antioxidants commonly found in motor oils.

Figure 1

Typical Pyrograms of Motor Oil Extracts

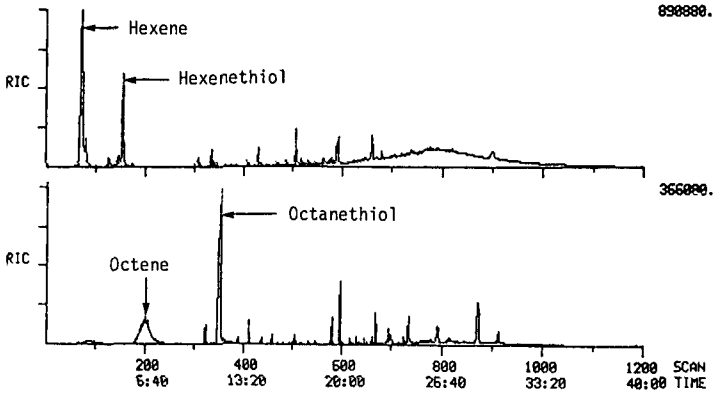

Table I Type of ZDDPs Found in Additive Packages

Company	Additive Packages	Type of ZDDPs Found
A	A-1	Decyl
A	A-2	Octyl
A	A-3	Butyl
B	B-1	Butyl & Octyl
B	B-2	Butyl & Octyl
B	B-3	Hexyl
B	B-4	Octyl
B	B-5	Dodecyl
C	C-1	Butyl & Octyl
C	C-2	Butyl & Octyl
C	C-3	Butyl & Octyl
C	C-4	Octyl
C	C-5	Butyl & Octyl
C	C-6	Butyl & Octyl
C	C-7	Octyl
C	C-8	Octyl
D	D-1	Octyl
D	D-2	Hexyl
D	D-3	Hexyl
D	D-4	Butyl & Hexyl
E	E-1	Octyl
E	E-2	Hexyl & Octyl
F	F-1	Butyl & Octyl
F	F-1	Butyl & Octyl

The butyl, hexyl, octyl, decyl, and dodecyl groups are n-butyl(or isobutyl), 4-methyl-2-pentyl, 2-ethyl-hexyl, isodecyl and n-dodecyl respectively, which have been confirmed by ^{13}C-NMR spectroscopy

Table II. Types of ZDDPs and Antioxidants Found in Motor Oils

Company	Motor Oil	Type of ZDDPs Found	Type of antioxidants found
G	5W-30 (A-1)	Butyl & Hexyl	-
G	5W-30 (A-2)	Butyl & Hexyl	-
G	5W-30 (B-1)	Butyl & Hexyl	-
G	5W-30 (B-2)	Butyl & Hexyl	-
G	10W-30 (C-1)	Butyl & Hexyl & Octyl	-
G	10W-30 (C-2)	Butyl & Hexyl & Octyl	-
G	10W-30 (D-1)	Butyl & Hexyl & Octyl	-
G	10W-30 (D-2)	Butyl & Hexyl	-
G	10W-30 (E-1)	Hexyl & Octyl	-
G	10W-30 (E-2)	Octyl	-
H	5W-30	Octyl	-
H	10W-30 (A)	Octyl	-
H	10W-30 (B)	Hexyl	-
H	10W-40	Hexyl	-
H	20W-40	Hexyl	-
I	5W-30	Hexyl	P
I	10W-30	Hexyl	-
I	10W-40	Hexyl	-
J	10W-30 (A)	Octyl	-
J	10W-30 (B)	Hexyl	-
K	10W-30	Hexyl	Q, D
L	15W-40	Octyl	-
M	10W-30	Octyl	P
N	15W-40	Hexyl & Octyl	Q

The butyl, hexyl, octyl groups are n-butyl (or isobutyl), 4-methyl-2-pentyl and 2-ethyl-hexyl respectively, which have been confirmed by ^{13}C-NMR spectroscopy

- : Non-detected at the current experimental conditions.
Q : Quinoline-type additives.
P . Hindered phenol-type additives
D Diphenylamine-type additives

Presented at the 35th ASMS Conference on Mass Spectrometry and Allied Topics
May 24-29, 1987, Denver, CO

A NEW INTERNAL STANDARD FOR PYROLYSIS-MS OF FOSSIL FUELS

Randall E. Winans, Robert G. Scott and Robert L. McBeth

Chemistry Division, Argonne National Laboratory,
9700 South Cass Avenue, Argonne, IL 60439

Pyrolysis Mass Spectrometry (PyMS) in the precise mass measurement mode has been found to be very useful for characterizing coals, coal macerals, and chemically modified coals (1,2). However, there has been a quantitation problem when comparing different samples. The purpose of this study is to develop a reliable internal standard for PyMS of coals. The standard must meet certain requirements: (1) Volatilize in the 200-500°C region, (2) Give high yields with little degradation or polymerization, (3) Yield mostly a single fragment ion or molecular ion, and (4) this ion should have a precise mass which differs from those found in coal pyrolysis products. In addition, the method should not rely on transferring a known amount of coal to the probe, since it is not unusual for solid particles to be lost in the analysis. The approach taken is to use a Diels-Alder adduct (I) synthesized from perdeuteroanthracene and maleic anhydride.

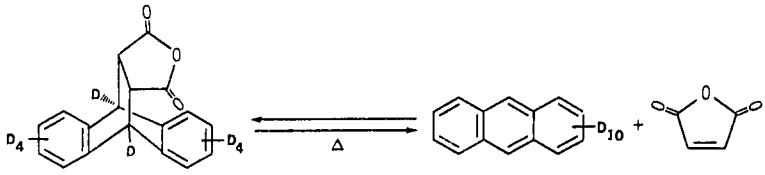

(I)

The retro Diels-Alder products d_{10}-anthracene and maleic anhydride and the adduct itself yield ions typically not found in coals. At temperatures below 400°C deuterium scrambling between antrhacene and coal is not expected.

Experimental. In a typical experiment 1 ml of a 0.1 mg/ml CH_2Cl_2 solution of (I) is added to 10 mg of the sample to be pyrolyzed. This slurry is applied to the platinum grid of an all quartz, directly heated probe designed in this laboratory. For the faster scanning, lower resolution experiments (3 sec/decade, 5,000 resolution) the probe is inserted directly into the source of a Kratos MS25 (50 eV EI). The sample is heated at 50°/min from 100-800°C by a computer controlled DC power supply. The scans are collected with a DS-55 data system and eventually the data is transferred to a DEC microVAXII for sorting and identification. For higher resolution (up to 80,000) and slower scanning experiments, the probe is inserted into an all glass heated inlet system, which was designed and built in this laboratory and attached to an MS50 mass spectrometer. The inlet system is designed so that the sample can be flash pyrolyzed into a 1 liter volume and leaked into the spectrometer or heated gradually and the products admitted directly into the source. Either a standard 70 eV or a low eV EI source is used.

Results and Discussion. When a large sample of (I) was heated from 200°C to 500°C in a vacuum, it was cleanly volatilized leaving no detectable residue. An averaged spectrum for I from a PyMS run is shown in Figure 1. As expected, even at 50 eV there is little fragmentation. The base peak is the perdeuteroanthracene, 188.1416 (+0.6 millimass error) $C_{14}D_{10}$. Also, the molecular ion for I is seen at 286.1425 (+1.1) $C_{18}H_2D_{10}O_3$ which would suggest that part of the sample is being vaporized without undergoing a retro Diels-Alder reaction. Other fragments in smaller abundance have deuterium in them such as 94.0704 (-3.2), $C_7H_4D_3$ and can be distinguished from the coal fragments. A total-ion pyrogram is shown in Figure 2 for I only, in this case the probe was heated from 200-800°C at 50°/min. The compound volatilizes at a temperature lower than coal but at a high enough temperature to be used as a standard. Also, there is less chance of deuterium exchange at these lower temperatures. The 188/187/186 ratios do not change at <400°C.

Some selected ion pyrograms for a low rank and a high rank coal are shown in Figures 3 and 4, respectively. With the standard, direct comparisons can be made between the two

samples. Note that there is significant increase in alkylnaphthalene species with the increase in rank while dihydroxybenzene species disappear in the high rank coal. Examples of the reproducibility for some selected ions are shown in Figures 5 and 6. Overall, this standard appears to meet the requirements listed in the introduction. Also, the desirability of using precise mass measurement with PyMS is demonstrated.

Acknowledgments. This work was performed under the auspices of the Office of Basic Energy Sciences, Division of Chemical Sciences, U.S. Department of Energy, under contract number W-31-109-ENG-38. The all quartz, direct heating probe and the AGHIS was created by J. Gregar at Argonne National Laboratory. Coal Samples were obtained from the Argonne Premium Coal Sample Program, managed by K.S. Vorres.

1. R.E. Winans, R.G. Scott, P.H. Neill, G.R. Dyrkacz, and R. Hayatsu, Fuel Proc. Techn. 12, 77 (1986).
2. R.E. Winans, R.G. Scott, P.H. Neill, G.R. Dyrkacz, R.L. McBeth, and R. Hayatsu, Proc. Int. Conf. on Coal Sci. 687 (1985).

Figure 1. Averaged mass spectra of d_{10}-anthracene – maleic anhydride adduct(I).

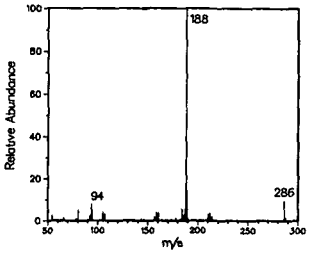

Figure 2. Total ion pyrogram of d_{10}-anthracene maleic anhydride adduct(I)

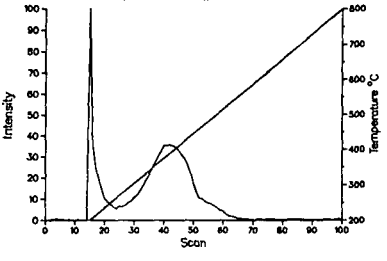

Figure 3. Selected ion pyrograms relative to the standard for APCS #2, subbituminous coal

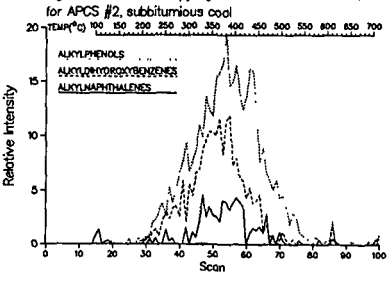

Figure 4. Selected ion pyrograms relative to the standard for APCS #1, medium volatile bituminous coal

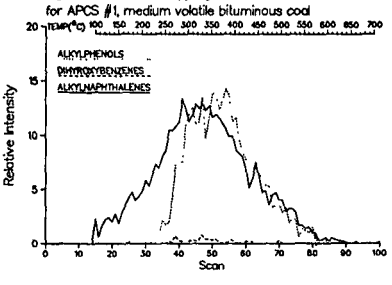

Figure 5. Selected ion pyrogram relative to the standard for APCS #2, subbituminous coal, duplicates.

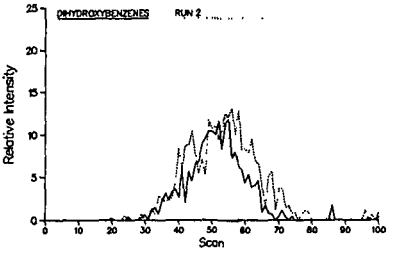

Figure 6. Selected ion pyrogram relative to the standard for APCS #2, subbituminous coal, duplicates

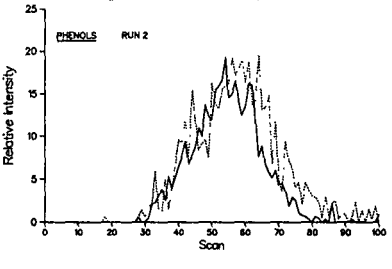

Presented at the 35th ASMS Conference on Mass Spectrometry and Allied Topics
May 24-29, 1987, Denver, CO

A COMPARISON OF THE METHODS OF MEDIUM RESOLUTION SELECTED ION RECORDING (SIR) AND MULTIPLE REACTION MONITORING (MRM) WHEN APPLIED TO THE ANALYSIS OF STERANES AND TRITERPANES IN CRUDE OIL EXTRACTS,

G.E. Harriman (1), R. Owen, V.C. Parr, O. Weir, D. Wood
VG Tritech, Crewe Road, Wythenshawe, Manchester, England.
1. Geochem Laboratories, Chester, England.

The characterisation of crude oil extracts, yielding information on source, maturation, migration and decomposition is traditionally carried out by an investigation into the presence of certain biomarkers. Steranes and triterpanes, which are present in the low pg/ul range, are examples of such. A fingerprint of oil is obtained when the m/z 217 and 191 fragments, common to each class of compound respectively, are monitored using medium resolution selected ion recording. At this resolving power (2-3000) interfering components in the oil, especially n-alkanes, are rendered insignificant and sample clean-up becomes unnecessary. However further information on relative abundancies of specific steranes and triterpanes necessitates the use of standard solutions to elucidate expected retention times. Alternatively, more specific mass spectrometrical methods may be utilised. One such method is to monitor the molecular ions for each component. A different approach is to monitor specific metastable reactions occuring in the first field free region of a double focussing instrument.

These latter two methods of improving selectivity are evaluated and compared using the VG TS-250 mass spectrometer.

Experimental

All analyses were carried out using a HP5890 gas chromatograph coupled directly to a VG TS250 tri-sector mass spectrometer. Samples were injected splitless in dichloromethane onto a 25m bonded phase OV-1 column.

1. SIR

   The molecular ions and fragments of C26 to C31 steranes and triterpanes were monitored at both 500 and 2000 R.P.

   Masses monitored:-

217.1956	sterane fragment	191.1800	triterpane fragment
358.36	C26 sterane	356.3443	C26 triterpane
372.3756	C27 sterane	372.360	C27 triterpane
386.3912	C28 sterane	384.3760	C28 triterpane
400.4069	C29 sterane	398.3912	C29 triterpane
414.422	C30 sterane	412.4069	C30 triterpane
428.4382	C31 sterane	426.4225	C31 triterpane

   The cycle time at 500 resolution was 0.94s. Sampling time was 50ms/channel. At 2000 resolving power the m/z 207.0329 column bleed peak was added as a lock mass, thereby increasing cycling time to 1.04s.

2. Multiple reaction monitoring The reaction between the molecular ion and the fragment (m/z 217.2 or m/z 191.18 as appropriate) was monitored for each of the C26 to C31 steranes and triterpanes. The total cycle time was 0.84s. Sampling time was 50ms per reaction.

Sterane traces for a terrestrial oil.

Note the absence of response for the C30 component as expected in an oil of this type. The SIR traces show a significant response.

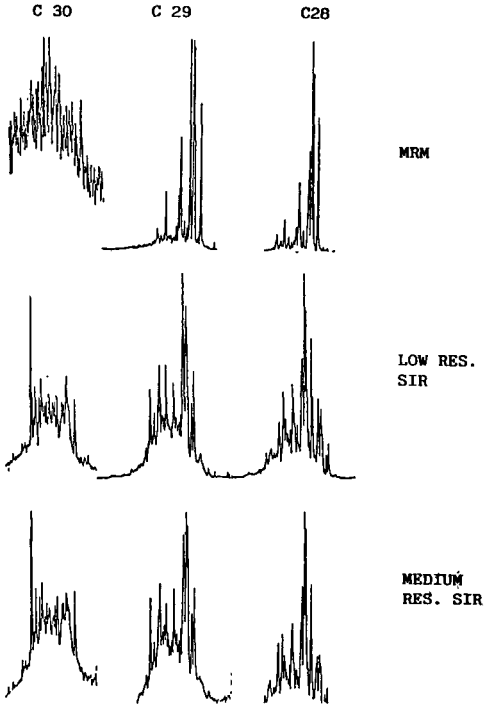

Analysis of Results

The three chromatograms above are indicative of the results obtained. The increase in resolution from 500 to 2000 in SIR led to little improvement in background or selectivity. This is evidenced by the corresponding MRM trace which shows a reduction in the number of peaks, improved selectivity and almost total elimination of the "hump" background. The extra peaks in the SIR trace are probably due to the carbon 13 isotope peak of the methyl loss species from the next eluting sterane in the series. Eliminating this response requires approximately 40-50,000 R.P. which is impractical in any sector instrument when switching masses in a GC time frame.

Discussion

The VG TS-250 displayed excellent suitability to the above analyses. The speed and controlability of the air cored electromagnet enabled magnet switching for the SIR experiments in time scales consistent with capillary column peak widths.

The tri-sector geometry gave artefact free linked scan data. The second ESA removed ions formed inside the electromagnet which may have been detected by a conventional double focussing mass spectrometer.

Conclusion

Multiple reaction monitoring on the VG TS-250 gave the best combination of sensitivity and selectivity in the analysis of biomarkers in oil. Detection limits in the low picogram levels were obtained. Medium resolution SIR suffered from interferences, the elimination of which requires unreasonably high resolution.

Presented at the 35th ASMS Conference on Mass Spectrometry and Allied Topics
May 24-29, 1987, Denver, CO

CHEMICAL IONIZATION - PROTON EXCHANGE MASS SPECTROMETRIC IDENTIFICATION OF ALKYL BENZENES, TETRALINS, AND INDANS IN A COAL-DERIVED JET FUEL

David J. Miller and Steven B. Hawthorne
University of North Dakota Energy Research Center
Box 8213 University Station
Grand Forks, North Dakota 58202

The lack of appropriate standards and the similarity of EI spectra shown by isomeric alkyl benzenes, indans, and tetralins often makes the identification of specific isomers impossible. Chemical ionization-proton exchange (CIPE) mass spectrometry using methanol-d_1 as a reagent gas aids in their identification by determining the number of unsubstituted aromatic positions. After chemical ionization of the aromatic ring (i.e., addition of D^+), only the aromatic hydrogens undergo exchange for deuterium. The number of deuterium exchanges observed allows one to assign the degree of alkyl substitution on the aromatic ring.

A Hewlett Packard model 5985B gas chromatograph/mass spectrometer *equipped with a dual electron impact/chemical ionization source was used to* obtain all of the mass spectra reported. Methanol-d_1 reagent was introduced directly into the source through a 1/16 in. o.d. stainless steel tube running through the heated transfer block collinear with the chromatographic column. Source parameters and reagent pressure were optimized by introducing m-diisopropylbenzene at a constant rate into the source through the direct insertion probe and maximizing the intensity of the (M+6) ion that is formed from the addition of D^+ and the exchange of all four aromatic hydrogens for deuterium. GC separations were performed with a Hewlett Packard 5890 gas chromatograph equipped with a 60 m x 0.25 mm i.d. DB-5 fused-silica capillary column (J & W Scientific, Folsom, CA).

Figure 1 shows the spectra obtained from CIPE analysis of the eight isomers of C_3 alkylbenzenes. While the EI spectra of all eight C_3 benzenes (except for n-propylbenzene) are virtually indistinguishable, CIPE spectra show that trimethyl, methylethyl, and propyl isomers can easily be identifies. Propylbenzenes show a pseudomolecular ion at (M+7) which corresponds to ionization by D^+ and the exchange of five aromatic protons for deuterium. Methylethylbenzenes and trimethyl benzenes show psuedomolecular ions at (M+6) and (M+5) respectively. These ions represent ionization and exchange of four (methylethyl) and three (trimethyl) aromatic protons for deuteriums. CIPE spectra also provide information on the positions of the alkyl substitution. For example, ortho and para disubstituted alkyl benzenes show a base peak (100% relative intensity) at the mass representing the exchange of all aromatic protons compared to an intensity of 30-40% for the meta-disubstituted benzenes.

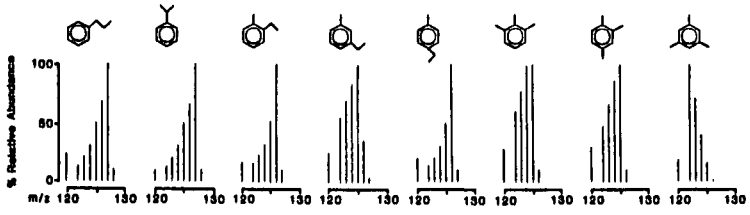

Figure 1. Chemical ionization-proton exchange mass spectra of C_3 alkylbenzene isomers with CH_3OD reagent gas.

CIPE was used to identify alkyl benzenes, tetralins, and indans in the aromatic fraction of a coal-derived jet fuel. Gas chromatographic/mass spectrometric (EI) analysis of the aromatic fraction of the jet fuel showed that this fraction (57 wt%) was composed of mainly alkyl substituted benzenes, indans, and tetralins, but few specific isomers could be identified. CIPE analysis allowed additional classification of over 50 alkyl benzene, indan, and tetralin isomers based on the degree of aromatic substitution.

Credit

This work was performed under Contract No. DE-AC22-87PC90016 For the U.S. Department of Energy, Pittsburgy Energy Technology Center.

Presented at the 35th ASMS Conference on Mass Spectrometry and Allied Topics
May 24-29, 1987, Denver, CO

HYDROCARBON TYPE ANALYSIS OF JET FUEL WITH GAS CHROMATOGRAPHY/MASS SPECTROMETRY

M.J. Gehron and R.A. Yost
Department of Chemistry, University of Florida
Gainesville, Florida 32611

Hydrocarbon type analysis (HTA) is widely used to evaluate the chemical composition of many petroleum and shale-derived products. For jet fuels, knowledge of hydrocarbon composition is very important for the design, performance, and cost of operation of today's high performance jet engines. Other important considerations of HTA of jet fuels is correlation of composition and physical parameters such as engine component wear, combustion efficiency, and density. Presently the methods used for HTA of jet fuels (ASTM 2789 gasoline range and ASTM 2425 diesel fuel range) are limited by the restricted boiling point range of the ASTM methods. Further more these methods have limited availability due to the decline of the designated instrumentation (CEC model-102).

We have developed a GC/MS method for HTA which is based on the current ASTM calibration matrices. The method employs a short-column (3 m x 0.25 mm x 1.0 µm thick film) DB-5 capillary which is interfaced to a Finnigan TSQ45 GC/MS and INCOS data system. Advantages of this method include employment of present day GC/MS instrumentation which is widely available and simple GC injection for sample introduction. Additionally, a resulting simulated distillation profile is obtained which provides information on the boiling point distribution or carbon number distribution of components comprising each jet fuel. Figure 1 illustrates such profiles for the six high density jet fuels studied. Determination of the classical summation ions (1,2) for each hydrocarbon type (paraffinic, cycloparaffinic, dicycloparaffinic, aromatic, indane/tetralinic, and naphthalenic) are obtained using mass chromatography quantitation, Figure 2. Results of this quantitation are subjected to the ASTM 2789 calibration matrix using a BASIC program which calculates the volume percent of each hydrocarbon type. Results of such an analysis of the six jet fuels studied are compared to actual ASTM 2789 results in Table I. The current ASTM method and

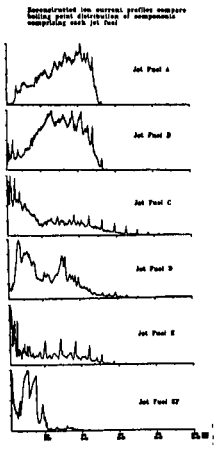

Figure 1 Chromatographic simulated distillation of fuels.

TABLE I

Comparison of GC/MS and ASTM Hydrocarbon Type Analyses
Experimental High Density Jet Fuels A-E
Simulated High Density Jet Fuel SF
in Volume Percent*

Jet Fuel	Paraffins	Cycloparaffins	Dicycloparaffins	Aromatics	Indanes/Tetralins	Naphthalenes
A	11.2 (10.7)	16.9 (16.6)	28.7 (26.4)	19.8 (11.4)	29.8 (29.8)	9.6 (3.8)
B	7.8 (9.3)	36.2 (41.8)	23.8 (28.6)	2.4 (2.8)	8.8 (8.8)	0 (0)
C	18.2 (14.3)	23.6 (26.3)	29.8 (26.6)	12.4 (12.3)	14.4 (14.8)	1.8 (2.3)
D	2.8 (1.3)	22.8 (28.6)	56.6 (56.0)	8.4 (7.2)	11.3 (13.1)	0.9 (0.9)
E	67.1 (70.8)	8.8 (17.3)	11.9 (2.1)	10.3 (7.6)	1.7 (1.4)	0.2 (0.1)
SF	11.0 (12.1)	23.1 (26.7)	28.7 (32.7)	2.8 (3.7)	4.1 (3.6)	0.3 (0.1)
Precision Fuel E	0.485	5.918	1.246	1.670	0.428	19.828

* Parenthesis indicate ASTM results

calibration matrices are based on magnetic sector MS and microburette (batch inlet) sample introduction, therefore, these results indicate the feasibility of performing HTA using current ASTM calibration matrices with quadrupole MS and introduction of sample by GC. Since the method incorporates GC introduction, studies were performed to investigate potential problems with component discrimination. Results indicate that Grob splitless injections are more reproducible then split injections and that at a specific minimum injection port temperature (220°C) component discrimination is greatly reduced if not eliminated.

The use of GC sample introduction and modern MS technology for HTA offers many avenues for improvements over classic HTA methods. For example, the use of longer GC columns can permit total fuel analysis (separation, identification and quantification of at least 95% of the components present at 0.5% volume). The use of tandem mass spectrometry (MS/MS) offers the opportunity to not only monitor fragment ions of a given hydrocarbon type, but also to indicate corresponding parent ions indicative of the molecular weight distribution of these ions. An example of this is shown in Figure 3 in which Aromatic 150, a specific boiling point cut of a purified aromatic mixture, is analyzed using MS/MS parents of m/z 105 and 119, characteristic daughter ions of aromatic compounds. From each parent scan we may perform mass chromatography of molecular ions which give a distinct distribution of molecular weights. Preliminary results indicate that paraffinic and cycloparaffinic compounds do not respond in these parent scans. Additionally parent scans were performed using daughter ions specific for paraffinic hydrocarbon types. No response was obtained from the Aromatic 150 for parents of paraffinic daughter ions.

This research was sponsored by Wright-Patterson Air Force Base - Fuels Division contract No. F33615-85-C-2508 through United Technologies - Pratt & Whitney.

1. Ralph Brown. Anal. Chem. 1955, 23, 430-437.

2. American Society of Testing Materials, ASTM 2789-81 and ASTM 2425, Annual Book of ASTM Standards, 1967.

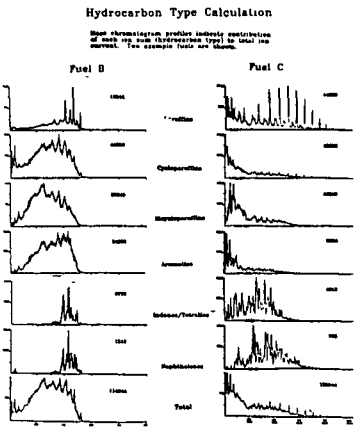

Figure 2 Mass chromatograms of the classic summation ions for ASTM 2789.

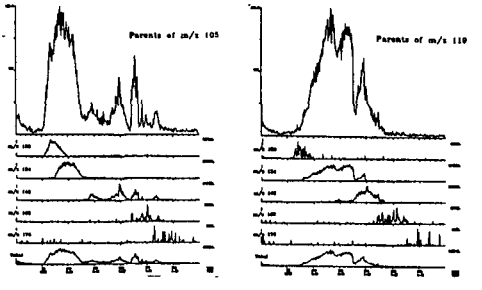

Figure 3 GC/MS/MS of Aromatic 150, with parents of m/z 105 and 119 daughters and mass chromatograms of parent ions.

Presented at the 35th ASMS Conference on Mass Spectrometry and Allied Topics
May 24-29, 1987, Denver, CO

Isotopic Determination of Calcium by Thermal Ionization Using a VG 354E Mass Spectrometer*

T. R. Mueller and R. L. Walker,
Oak Ridge National Laboratory,
Oak Ridge, TN 37831

Mass spectrometry is called upon for the isotopic analysis of calcium by a large number of disciplines. Our work has, to date, been focaused chiefly on support of isotopic enrichment programs. We have analyzed samples enriched by calutron and by ion exchange methods.

This report is addressed mainly to the development of a method for the analysis of enriched and normal samples by thermal emission techniques. The success of our method lies chiefly in the ability to eliminate interferences from species arising from both organic and inorganic contaminants. The first ionization potential for calcium is 6.09 V, a value well below that of all common organic species. The most troublesome inorganic contaminant is potassium. Isobaric interference occurs at mass 40, where K-40 contributes about one part per ten thousand to the Ca-40 measurement for equal amounts of K and Ca. However, if precautions are not taken to limit the K in the sample,the system pressure may rise to a level that interferes with the transport of Ca ions from the source region. During analysis, we attempt to maintain the source pressure at or below 1-micro-Pascal.

Potassium interference arises from several sources--the sample itself, contamination during handling and loading, and from the Re filaments. Most of our samples have been relatively free of K. The effects of K in the filaments is reduced to acceptable levels by thermal baking prior to loading with sample. Only the side filaments are loaded with sample. The center filament is covered with teflon tape during the loading and drying steps. Typically, each side filament receives 1 microgram of Ca from an aqueous, 1-2 M nitric acid medium. The samples are dried in air by passing about 0.6A through the filaments.

Analysis is done in a semi-automatic mode. Variability in the amount of K present makes it difficult to establish an automatic start-up procedure for computer control. Rather, the operator controls warm-up and focus, turning control over to the computer for peak finding and data acquisition.

With a few modifications, the software supplied by VG Isotopes, Ltd., works fairly well for uranium analysis. For use with lower masses, we have had to make extensive alterations in it. The dispersion of 354 mm, coupled with limited compliance of the Hall probe compensation circuit of the spectrometer, requires a different operational philosophy than that envisioned by their programmers. Careful examination of their statistical procedures also revealed excessive smoothing of the data. Provisions for data storage on an HP9133H (20 mB Winchester) were added. The data are recovered and transmitted to a Digital Equipment Corp., PDP-11/23 computer for processing by established programs.

Results with samples enriched in isotopes 44 and 48 showed excellent agreement with those obtained with the instrument used typically for stable isotopes analysis in our laboratory. Precision of measurement for the major isotope is 0.01 to 0.02%, RSD. With the VG354, sensitivity and precision are improved. The large dispersion of the instrument makes it impossible to utilize the multi-collector system with calcium; all calcium data were obtained with a peak-jumping procedure.

*Research sponsored by the U. S. Department of Energy, Office of Basic Energy Sciences, under Contract DE-AC05-84OR21400 with Martin Marietta Energy Systems, Inc.

Presented at the 35th ASMS Conference on Mass Spectrometry and Allied Topics
May 24-29, 1987, Denver, CO

NEGATIVE IONS IN INDUCTIVELY COUPLED PLASMA MASS SPECTROMETRY, J. E. Fulford and E. S. K. Quan, SCIEX®, 55 Glen Cameron Road, #202, Thornhill, Ontario, Canada, L3T 1P2.

Elemental and isotopic analysis using ICP-MS has focussed mainly in the detection of positive ions sampled from the ICP. Negative ions have received relatively little attention although some work on the halogens (1) and sulfur has been reported (2).

In the negative mode electron affinite species are observed primarily as singly charged atomic ions and some atoms, which are less electron affinite ((e.g.) Cr, Mn, Re) are observed as oxide, dioxide, trioxide and tetroxide species. (The oxygen originates in the H_2O and HNO_3 solvents used to dissolve the samples.) These observations suggest that polyatomic ions may be more of an interference problem in the negative mode than in the positive mode. These polyatomic species could reside in the plasma or they may be formed by fast reactions in the interface region between the atmospheric pressure plasma and the mass spectrometer vacuum chamber (10^{-5} to 10^{-6} torr).

The ion kinetic energies were measured for negative ions using retarding potential methods (3). Unlike positive ions, the negative ions did not show the increase in kinetic energy with mass (constant velocity source) which is expected from the free jet expansion (4). The negative ion energies were slightly negative with respect to ground and the energy distributions were approximately 1 volt at full width half maximum. These observations suggest that the negative ions observed in this work do not originate directly from the plasma but rather by reactions and recombinations which occur in the free jet expansion after the skimmer orifice.

While the process of formation for negative ions is different than that for positive ions, the effect of plasma parameters is very similar in both cases; as the aerosol flowrate is increased, the ion signal attains a local maximum within a similar flow range as that for positive ions (5). Linear calibration curves can be achieved for negative ions and typical sensitivities and detection limits are shown in Table 1.

Table 1: SENSITIVITIES AND DETECTION LIMITS FOR NEGATIVE AND POSITIVE IONS IN ICP-MS

Ion	Sensitivity (cps/ppm)	Detection Limit (3σ, ppb)
Cl^-	55000	1
Cl^+	900	5
F^-	60000	110*
F^+	-	+
Br^-	34000	2
Br^+	7500	1
I^-	100000	6
I^+	300000	0.01
$S(HSO_4^-)$	85	700
S^+	90	100
$P(PO_3^-)$	300	200
P^+	10000	20
Se^-	86	700
Se^+	6000	1

Notes

Background in negative mode is currently 1000 counts sec^{-1} (cps); for positive mode background is 10 cps.

* $^{18}OH^-$ in the background spectrum
\+ H_3O^+ in the background spectrum

The major advantage of the negative ion mode is presently in its capability to detect fluorine (as F^-) since in the positive mode, F^+ is interfered by the H_3O^+ ion ($>10^6$ cps) in the background spectrum. At this time the detection limits for most other elements are as good or better in the positive ion mode.

References

(1) G. H. Vickers, D. A. Wilson and G. M. Hieftje, Federation of Analytical Chemistry and Spectroscopy Societies, paper 192, (1986).

(2) D. J. Douglas, G. Rosenblatt, E. S. K. Quan and J. B. French, 6th International Symposium on Plasma Chemistry, paper B-5-6, (1983).

(3) J. A. Olivares and R. S. Houk, Appl. Spectrosc. 39, 1070, (1985). (1985).

(4) J. E. Fulford and D. J. Douglas, Appl. Spectrosc., 40, 971, (1985).

(5) G. Horlick, S. H. Tan, M. A. Vaughan, and G.A. Rose, Spectrochim. Acta, 40B, 1555,

Presented at the 35th ASMS Conference on Mass Spectrometry and Allied Topics
May 24-29, 1987, Denver, CO

SCINTILLATION-TYPE ION DETECTION FOR INDUCTIVELY COUPLED PLASMA MASS SPECTROMETRY

L. Q. Huang, Shiuh-Jen Jiang and R. S. Houk*
Ames Laboratory-USDOE and Dept. of Chemistry
Iowa State University, Ames, IA 50011

Inductively Coupled Plasma Mass Spectrometry (ICP-MS) has become an important new technique for elemental and isotopic analysis (1). In all the ICP-MS instruments constructed to date, the ion signals are monitored by an electron multiplier, which is generally of the Channeltron variety (2). Although good analytical performance can certainly be obtained with Channeltron electron multipliers, they do have several undesirable characteristics as detector for ICP-MS. A Channeltron has a limited lifetime of approximately 1 year under normal analytical use. The response of a Channeltron is only linear up to count rates of approximately 1×10^6 counts/s; above this value, calibration curves tend to droop. Deviation from linear response at high count rates particularly limits the concentration range over which either very large or very small isotope ratios may be determined and can be a source of error when isotope dilution is employed for quantitation.

The scintillation device depicted by items J-L in Figure 1 is an alternate ion detector for mass spectrometry. Its operation is based upon the following sequence of events. Ions from the mass analyzer (G) strike the negative target (J) and generate secondary electrons. These electrons are accelerated from the target to a thin metal film coated on the surface of a scintillator (K). The film thickness is chosen so that the secondary electrons can penetrate the film and deposit energy in the scintillator, which then luminesces at visible wavelengths that are sensed by the photomultiplier (L). This device is often referred to as a Daly detector after its inventor (3). A scintillation-type detector offers some potential advantages in the problem areas identified above for Channeltron electron multipliers. In the present work, this detector shows a linear range up to 3×10^6 counts/s, yields isotope ratios with precisions that are generally close to those expected from counting statistics, shows no gain fatigue after scanning across an intense peak, and yields signal stability of ± 5% relative standard deviation over two hours. These performance figures are better than those obtained previously with this particular instrument using a Channeltron electron multiplier as a detector. Detection limits and sensitivities obtained with the scintillator detector were similar to those obtained with a Channeltron. The scintillator detector also does not require rejuvenation or replacement as a Channeltron does.

The performance of the scintillator detector is either comparable or superior to that of a Channeltron electron multiplier with the particular ICP-MS instrument used. Additional improvements in the performance of the scintillator detector could be possible by further reduction of the background pressure or by offsetting both the target and PMT above or below the centerline of the sampler, skimmer, and mass analyzer.

Acknowledgement

The Ames Laboratory is operated for the US Department of Energy by Iowa State University under Contract No. W-7405-Eng-82. This research was supported by the Director for Energy Research, Office of Basic Energy Sciences.

References

1. R. S. Houk, Anal. Chem. 58, 97A-105A (1986).
2. E. Kurz, Am. Lab. 11(3), 67-82 (1979).
3. N. R. Daly, Rev. Sci. Instrum. 31, 264-267 (1960).

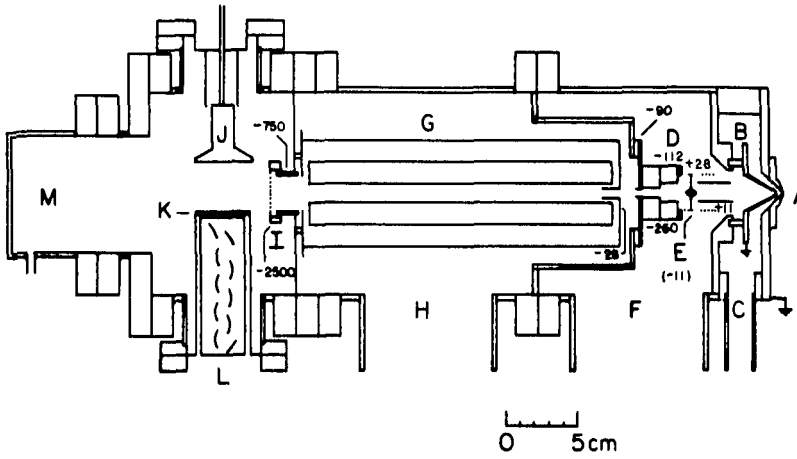

Figure 1. Schematic diagram of MS (ICP not shown): A - sampler, B - skimmer, C - port to rotary pump, D - ion lens (voltage setting listed), E - photon baffle, F - port to diffusion pump (1600 L s^{-1}), G - quadrupole mass analyzer, H - port to diffusion pump (800 L s^{-1}), I - exit lens (voltage settings listed), J - Al target, K - Al coated scintillator, L - PMT, M - turbomolecular pump (150 L s^{-1}).

Presented at the 35th ASMS Conference on Mass Spectrometry and Allied Topics
May 24-29, 1987, Denver, CO

REDUCING MATRIX EFFECTS IN INDUCTIVELY COUPLED PLASMA MASS SPECTROMETRY (ICP-MS),

D. Douglas, A. Boorn, J. Fulford, G. Gillson, K. Halligan and S. Tanner, SCIEX®, 55 Glen Cameron Road, #202, Thornhill, Ontario, Canada, L3T 1P2.

It has generally been reported in the literature that ICP-MS is more susceptible to non spectroscopic interelement interferences ("matrix effects") than ICP emission spectroscopy. Mostly suppression but in a few cases enhancement of analyte signals by a high (0.1%) concentration of concomitant elements has been observed. This has been reported for both the SCIEX® (1) and VG (2) commercial systems and at least one "homemade" system (3). A variety of mechanisms have been proposed to account for these observations, including (1) shifts of ionization equilibria in the ICP, (2) diffusion effects in the ICP, (3) plasma cooling in the supersonic expansion, (4) scattering effects in the molecular beam and (5) electron neutral collision effects in the interface. Each of these mechanisms can account for some of the observed effects but none can account for all. In this work we provide computational and experimental evidence for an alternate mechanism which can account at least qualitatively for the observed effects; space charge effects in the ion optic region.

The observed matrix effects are strongly dependent on ICP operating conditions. Table I shows analyte suppression observed for 0.2% Na and 0.5% Fe for analytes of varied mass. The operating conditions were ICP power 1200W, coolant flow 12 $Lmin^{-1}$, auxillary flow 1.0 $Lmin^{-1}$, aerosol gas flow 0.85 $Lmin^{-1}$ and sampler to load coil spacing 15 mm. Most noticeable in these data are the mass effects: light analytes (e.g. Li) suffer greater suppresion than heavy analytes (e.g. U), and the heavier matrix (Fe) cause greater suppression than the lighter. Similar results have been reported by Tan and Horlick (1).

The ion current measured to the first lens element (1st cylinder of a 3 cylinder Einzel lens) is 10^{-4} to 10^{-5}A. Space charge becomes significant for this lens at $\sim 10^{-9}$A. The ion optics then is strongly space charge affected. This is supported by computer calculations of the ion trajectories which show that total ion currents of $\sim 10^{-6}$A can markedly change the focussing properties of the ion optics. Furthermore, the computer modelling shows that light ions are defocussed more than heavy ions by the space charge.

The observed ion density in the ICP is ca. $1X10^{15}$ cm^{-3}. It is easily calculated that nebulising a 0.1% Na or 1% U solution increases this ion density by only $\sim 1X10^{13}$ cm^{-3} i.e. a negligible change, and this is in accord with direct measurements of the electron density. Despite the fact that the ICP ion density is unperturbed by these matrices it is found that the ion current downstream of the skimmer increases by ca. X5 when these solutions are nebulised. The reasons for this are poorly understood but appear to be due to selective loss of argon ions relative to metal ions in the interface or between the skimmer and first lens element. This may be due to fast recombination of Ar through the dimer ($Ar_2^+ + e \longrightarrow Ar + Ar$) or through resonant charge transfer of fast Ar to to thermal background argon to give a thermal argon ion which is then lost to the ion beam. This leads to the following proposed mechanism for the observed matrix effects:

(1) Ar^+ is selectively lost from the ion beam.
(2) Addition of a matrix changes the total ion current.
(3) The space charge and hence focal properties of the optics change with total current.
(4) Analyte signals change with the changed focal properties.

This mechanism appears to account for the observed mass effects and also for the variation of matrix effect with ICP parameters. Any change in the ICP conditions which increases the ratio of Ar^+ to M^+ (e.g. higher power, lower aerosol flowrate, more dilute solutions) keeps the total ion current more constant and hence reduces analyte suppressions.

It has been found here that a modification to the ion optics can reduce the suppressions of analyte signals. The modification consists of moving the 1st Einzel cylinder closer to the skimmer base and running the Einzel in the alternate mode ($(E_1E_2E_3)$ = (-130V,-15V,-130V)). With this modification, the ratios of ion signals with and without a 1% matrix of Na, Fe or U are shown in Table II. It is also found that with this arrangement the ion current to the lens system remains more constant (within $\pm 10\%$) providing additional support for the mechanism discussed above. With the reduced suppressions and ability to run high dissolved solids solution (up to 1%) detection limits for trace elements in solids are improved. Table III shows detection limits for 4 rare earth elements in solid U run as a 0.4% solution.

Presented at the 35th ASMS Conference on Mass Spectrometry and Allied Topics
May 24-29, 1987, Denver, CO

References

(1) S. H. Tan and G. Horlick, J. Anal. Atomic Spectrosc. in press 1987.
(2) R. F. Browner, *presented at the 1987 Winter Conference on Plasma Spectrochemistry*, Lyon, France, January 1987.
(3) J. A. Olivares and R. S. Houk, Anal. Chem. 58, 20, 1986.

TABLE I
SUPPRESSION WITH 0.2% Na or 0.5% Fe MATRIX

		0.2% Na	0.5% Fe
ANALYTE	Li	-19%	-12%
	Mn	-12%	-20%
	Pr	- 8%	-25%
	U	- 5%	-15%

TABLE II
RATIO OF SIGNAL WITH/WITHOUT MATRIX
MATRIX (1%)

		Na	Fe	U
ANALYTE	Mg	-	0.96	0.93
	Co	0.87	0.85	0.88
	In	0.98	0.99	0.99
	Th	0.88	0.97	1.06

TABLE III
DETECTION LIMITS IN URANIUM ng gm^{-1} (3σ, 10 seconds)

Element	Detection Limit
La	1.4
Pr	1.6
Sm	3.4
Gd	3.8

Presented at the 35th ASMS Conference on Mass Spectrometry and Allied Topics
May 24-29, 1987, Denver, CO

Inductively Coupled Plasma Mass Spectrometric Determination of Molybdenum in Wheat and Rice Flours Using Stable Isotope Dilution

E.S. Beary and P.J. Paulsen, National Bureau of Standards, Center for Analytical Chemistry, Gaithersburg, MD 20899

Inductively coupled plasma mass spectrometry (ICP-MS) has been developed into a high sensitivity technique (sub ppb detection limits) when analyzing solutions containing less than 1% total solids. Stable isotope dilution is potentially the most precise and accurate means of quantification with ICP-MS.

Molybdenum (Mo) has been determined in Wheat and Rice Flour Standard Reference Materials (SRM 1567a and 1568a respectively) by ICP-MS isotope dilution without chemical separation. Samples of 1.5 grams were spiked with ^{97}Mo so that the ratio of 97/98 = 1.5. The spiked samples were dissolved in $HNO_3/HClO_4/HF$, equilibrated and evaporated to dryness. The residues were redissolved in 30 grams of 1% NH_4OH. These solutions were introduced into the ICP-MS nebulizer at a rate of 0.2 mL/min. Isotopic ratio measurements of pure Mo were made to calibrate the mass bias of the ICP-MS. Comparison of Mo isotopic ratios in unspiked flour samples confirmed the absence of molecular interferences at the isotopes selected for ratio measurements (97/98 Mo).

The spike calibration was also used to assess the capabilities of the ICP-MS since concentrations can be adjusted to give optimum precision and accuracy in the ratio measurements. Three separate natural solutions were prepared using weighed portions of high purity Mo metal. Each piece was dissolved in dilute HNO_3, followed by saturated NH_4OH and diluted to a precisely known concentration by weight. Aliquots of each natural (A, B and C) were used to calibrate the spike. Table I shows the results of the spike calibration. The overall precision was 0.36% rsd.

Table 1
97 Molybdenum Spike Calibration Using Three Natural Mo Solutions

Sample	Spike Conc. µg/g	Ave. Spike Conc. µg/g
1A	7.3555	
2A	7.3486	7.3413
3A	7.3379	
4A	7.3232	
1B	7.3083	
2B	7.2751	7.2917
1C	7.2979	
2C	7.3022	7.3000
	Ave. A, B, C	7.3110

The average Mo concentrations in the wheat and rice flours were 0.504 µg/g and 1.523 µg/g respectively. The standard deviations were 0.004 (0.79% rsd) for the wheat flour and 0.002 (0.15% rsd) for the rice flour (Table 2). A realistic accuracy statement is indicated, however, based on twice the measurement precision plus the uncertainties due to the spike calibration and blank correction. The average blank was 0.0037 µg.

Table 2
Mo in Wheat Flour and Rice Flour by ICP-MS Isotope Dilution

	Wheat Flour µg/g		Rice Flour µg/g
1.	0.504	1.	1.523
2.	.501	2.	1.523
3.	.500	3.	1.520
4.	.511	4.	1.525
5.	.504		
	Ave: .504 µg/g (0.79% rsd)		1.523 µg/g (0.15% rsd)
	± 0.013 µg/g		± 0.011 µg/g

The wheat and rice flours analyzed are renewal Standard Reference Materials. These ID ICP-MS values for Mo are currently being pooled with data from Neutron Activation and ICP-Emission for the certification of Mo in these materials.

Presented at the 35th ASMS Conference on Mass Spectrometry and Allied Topics
May 24-29, 1987, Denver, CO

MATRIX CONSIDERATIONS IN THE ANALYSIS OF NONCONDUCTING POWDERS BY GLOW DISCHARGE MASS SPECTROMETRY.

S.L. Tong and W.W. Harrison, University of Virginia, Charlottesville, VA 22901

The glow discharge finds increasing use as a spectroscopic source in analytical chemistry. Its primary advantages are (1) the ability to generate quite simply an atomic population for sensitive analytical analyses, and (2) the generally nonselective nature of this atomization step. GDMS has to date been applied primarily to metals and alloys. We present here our first efforts to show the utility of GDMS to compacted materials. A molecular sample incorporated into a pressed conducting powder matrix can create a complex plasma environment. Of concern is the atomic/polyatomic mix of sputtered particles and the extent to which the plasma energetics can dissociate the molecular ions.

The ability to analyze samples directly in the solid state eliminates the need for the often difficult and time-consuming sample dissolution steps. GDMS sample disk or pin electrodes can be formed quickly and analyzed within minutes for elemental composition. Relative sensitivity factors fall mainly within a factor of 3 and absolute sensitivities are well into the ppb region. Potential applications include soils, sediments, minerals, and ores.

EXPERIMENTAL

The glow discharge instrument is built around a Balzers quadrupole, multiplier, and preamp. A direct insertion probe takes the analytical sample into the source chamber. An argon discharge runs at 0.8 torr, 1.7 KV, and 1.4 mA. A Tracor MCA accululates the ion counts, controlled by an HP 9816 computer. Several host matrices were studied, including graphite, Cu, Ag, Al, and Ta. 5-10% mixes of the sample with a host matrix gave suitable electrodes.

RESULTS AND DISCUSSION

The ideal matrix would provide good discharge characteristics while contributing minimal spectral lines. However, even monoisotopic elements produce such species as MAr, MO, MSi, etc. The discharge gas lines can also cause interferences. Graphite has poor sputtering yields and tends to form many plasma combinations. Aluminum has certain advantages, particularly in the upper mass ranges. Tantalum offers a high mass matrix that interferes with relatively few elements. We have run SCo-1 geological standard in Ta and examined all analytical peaks and background contributions. In, addition more detailed studies have been made of certain selected regions, such the rare earths. We have also prepared mixtures of rare earth oxides in Ta to determine relative sensitivity and oxide contributions. Figure 1 shows a mixture of 14 rare earths at 110 ppm for each element. The insert shows a compilation of RSF's for each element, calculated against Tb (taken as 1.00). The tight range of sensitivities shows the nonselective nature of GDMS. An examination of the isotope ratios indicates that oxide formation is small, giving little interference at these levels. However, at sub-ppm concentrations, oxide formation can be significant and must be carefully considered. The quadrupole instrument in this study cannot separate such interferences. As shown by Table I, it would require a reasonable amount of resolution to remove the overlapping lines and at these higher resolution settings, the ion throughput of the instrument is reduced, thus affecting sensitivity.

Presented at the 35th ASMS Conference on Mass Spectrometry and Allied Topics
May 24-29, 1987, Denver, CO

RARE EARTH MIXTURE IN TANTALUM

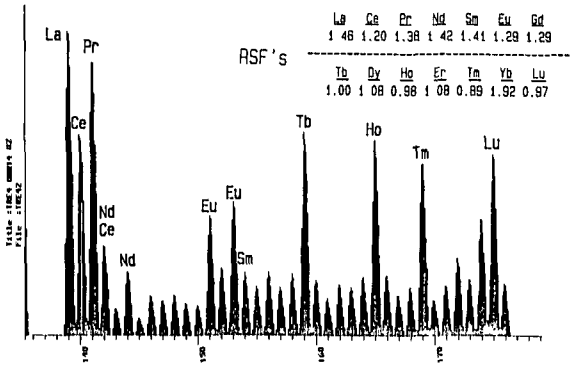

Figure 1. Spex-Mix rare earth mixture. Each element is present at 110 ppm.

Although GDMS interferences are in general quite low compared to other techniques, they can create problems at times. Examination of isotopic patterns will often reveal an unobstructed isotope for analytical use, but monoisotopic elements present particular problems. The use of EXPERT data systems to strip out projected interferences has been used in other techniques (e.g., ICPMS). High resolution instruments may solve the problem, but only at great cost. The desired approach would be to prevent or minimize polyatomic formation by creative discharge chemistry.

Table I. Resolution (M/M) Required to Separate Rare Earth Oxides From Nominal Atomic Lines

TYPICAL RARE EARTH OXIDE INTERFERENCES

Element	Isotope	MO Interference	Req. Resol.
Ba	134	Sm-150	8, 434
Ba	138	Sm-154	6, 973
La	139	Gd-155	7, 170
Ce	140	Gd-156	7, 122
Pr	141	Gd-157	7, 256
Nd	146	Dy-162	8, 587
Eu	151	Er-167	9, 540
Sm	154	Er-170	9, 147
Gd	156	Yb-172	8, 800
Tb	159	Lu-175	8, 323
Ho	165	Ta-181	7, 950

Presented at the 35th ASMS Conference on Mass Spectrometry and Allied Topics
May 24-29, 1987, Denver, CO

TRACE ANALYSES IN SEMICONDUCTOR MATERIALS, HIGH PURITY METALS AND NUCLEAR MATERIALS BY GLOW DISCHARGE MASS SPECTROMETRY;

HALL D J AND ROBINSON K; VG ISOTOPES LIMITED, ION PATH, ROAD THREE, WINSFORD, CHESHIRE CW7 3BX, UK

OBJECTIVE

This paper summarises some recent applications of Glow Discharge Mass Spectrometry highlighting results in areas that have been difficult or impossible to achieve with existing mass spectrometric techniques. Analytical benefits include excellent quantitation even in the absence of standards due to freedom from matrix effects and spectral interference.

APPLICATIONS

i. High Purity Metals

A patented cryo-cooled source has enabled low melting point solids such as indium and gallium to be analysed directly as the solid. Table 1 summarises a NO-STANDARDS analysis using the VG 9000 GDMS with chemical analyses on a characterised gallium sample. Agreement to within a factor of 3 is confirmed. Figure 2 shows the excellent precision achieved at ppb concentration levels on a high purity gallium sample. The speed of analysis is illustrated in table 2 showing analysis of a high purity indium sample where detection limits around 2ppb are achieved using integration times of 1 minute per element. Sub ppb detection limits are achievable by using slightly longer integration times.

TABLE 1

The Analysis of a 'Characterised' Gallium Sample
Comparison of VG 9000 Results with Quoted Data

Element	Quoted ppm weight	GDMS ppm ion beam ratio
Si	4.16	3.54
Ti	0.42	1.39
Cr	0.58	0.24
Mn	0.84	0.41
Fe	8.4	11.
Ni	0.41	0.43
Cu	0.91	0.44
Zn	1.74	0.67
Sn	0.43	0.40
Sb	0.43	0.17
Pb	0.43	0.53

*GDMS VALUES WITHOUT ANY STANDARDISATION

TABLE 2

TRACE ELEMENT ANALYSIS
ANALYSIS OF HIGH PURITY INDIUM
Concentration from Ion Beam Ratios

Element	Observed Conc (ppm)	Element	Observed Conc (ppm)
F 19	< 0.0035	Ni 58	< 0.0140
Mg 24	< 0.0027	Ag 107	< 0.0030
Al 27	0.0023	Cd 110	< 0.0133
Si 28	0.1547	Cd 111	< 0.0274
P 31	< 0.0022	In 113	MATRIX
S 32	< 0.0024	In 115	MATRIX
Ca 44	< 0.1009	Sn 119	< 0.0178
Cr 52	< 0.0018	Sb 121	0.0160
Mn 55	< 0.0013	Sb 123	0.0105
Fe 56	0.0230	Te 125	0.0453
Ni 60	< 0.0050	Tl 205	0.0984
Cu 63	< 0.0022	Pb 206	0.0116
Zn 66	< 0.0055	Bi 209	< 0.0015

24 ELEMENTS ANALYSED IN 24 MINUTES
DETECTION LIMITS AROUND 2 PPB ON MAJOR ISOTOPES
< COUNT RATE LIMITED LOD
< BACKGROUND LIMITED LOD

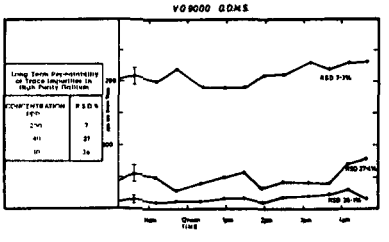

VG 9000 GDMS

Sub ppb detection limits in Gallium matrix
Integration time 5mins/element

ELEMENT	VG 9000 CONCENTRATION ppm ion beam ratio
Na	< 0.0005
Fe	< 0.0009
As	< 0.0006

< background limited LOD

FIGURE 2

ii. Transition Elements in Semiconductor Materials

Detection of these elements at sub ppm levels is extremely difficult in some matrices by traditional mass spectrometric techniques such as SSMS and SIMS.

Primarily due to spectral overlap with either dimer molecules or doubly charged ions. The problem is overcome in the VG 9000 due to two attributes:

1. dimer and doubly charged species occur only at ppm equivalent concentration levels (opposed to % concentrations in SSMS and SIMS).

2. mass resolution of around 6000 can be obtained with good transmission and hence sensitivity.

Presented at the 35th ASMS Conference on Mass Spectrometry and Allied Topics
May 24-29, 1987, Denver, CO

Figure 3 shows illustrations of ppb determinations of Fe in semiconductor grade SILICON and Cu in CADMIUM TELLURIDE. Similar spectra with freedom from spectral interference are obtained for the other transition elements in each of these matrices.

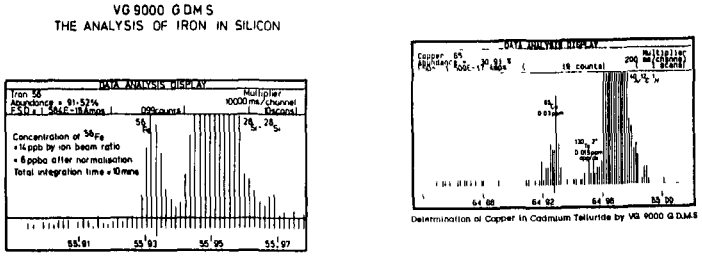

FIGURE 3

iii. Insulating Materials

The analysis of insulating materials can be illustrated by reference to the analysis of NBL-98 series standard U_3O_8 powders. These consist of a 30 element suite varying in concentration from 60 ppb to more than 700 ppm.

Pin electrodes were prepared by compaction with high purity graphite in approximately 3:1 proportions by weight: as analysis by GDMS is performed by ratioing impurity ion beams direct to the matrix (U^{238} in this case), the quantity of binding material used need not be known accurately, greatly simplifying preparation procedures.

Concentrations for each of the 30 elements were determined by measuring ion beam ratios, impurity against matrix, using an integration time of 12 seconds per element.

Figure 4 shows log/log plots of VG 9000 ion beam ratio concentrations v NBL provisional certified concentrations for a suite of elements, which are typical. Excellent correlation is obtained over a wide concentration range; sub ppm detection limits are obtained for most elements, which are limited by the blank.

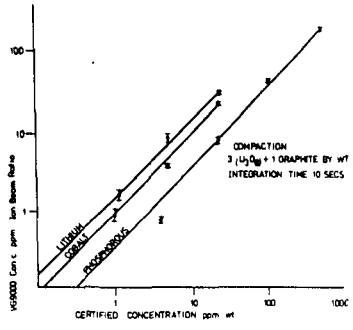

FIGURE 4

CONCLUSIONS

Glow Discharge Mass Spectrometry utilising a DC glow discharge source and high resolution mass analyser enables the direct analysis of solids at major minor and trace (ppb) concentrations. The combination, of freedom for matrix effects and spectral interference enable determinations, which are impossible to achieve by other techniques.

The high level of precision and accuracy obtained even in the absence of standards make it suitable for applications in both high purity and complex matrix analyses.

ENHANCEMENT OF ION YIELD IN RESONANCE IONIZATION MASS SPECTROMETRY WITH CW LASERS

D. C. Parent, B. L. Fearey, R. A. Keller, and C. M. Miller
Los Alamos National Laboratory, Los Alamos, NM 98545

In this communication we present the results of recent experiments aimed at enhancing the ion yield and increasing the resolution in Resonance Ionization Mass Spectrometry (RIMS) using cw lasers. These experiments are the continuation of previous work on Lu in our laboratory (Ref. 1), where Lu was ionized via a 1+1 scheme (one photon to resonance + one photon to ionize) using a single-frequency dye laser. It was observed that high ion signals (and high S/N) were obtained with only modest resolution of the hyperfine components of the resonant transition. The increase in linewidth is due to power broadening of the resonant transition, as high photon fluxes are necessary for the ionization step, the ionization cross section being generally much smaller than the absorption cross section. This loss of resolution must be eliminated if one wishes to do atomic spectroscopy or isotopically selective ionization.

To minimize this power broadening, we have used two cw lasers. A tunable dye laser of low irradiance, to provide selectivity in the resonant step without power broadening, is combined with a high irradiance argon ion laser, to efficiently ionize. The lasers were counterpropagated through the source of a magnetic sector mass spectrometer and focused between the sample filaments. The dye laser spot size was ~100 μm in diameter and the argon ion laser was ~130 μm in diameter. The sample was a solution of Lu and U (~1 μg each) dried on a Re filament, which was heated to ~1200°C to atomize the Lu.

In the first set of experiments, the dye laser was scanned over the hyperfine structure of the resonant transition ($^2D^\circ_{3/2} \leftarrow {}^2D_{3/2}$, 22125 cm^{-1}). Spectra were taken at different dye laser powers with and without the argon ion laser (~11 to 12 kW/cm^2). Four of these spectra are shown in Figure 1. Spectrum (a) is taken with the dye laser alone at low irradiance (5.5 W/cm^2). Spectrum (b) is the same as (a) with the addition of the argon ion laser. Note the large increase in the ion signal and improvement in the S/N ratio with the addition of the Ar^+ laser. (When the dye laser irradiance was further reduced, no ion signal above thermal background was observed with the dye laser alone, but signals of 1 to 6 thousand ions/second were seen with the addition of the argon ion laser.) Spectra (c) and (d) are with full dye laser power (~480 W/cm^2). In spectrum (c) (dye laser alone) the peaks are not as well resolved as in spectrum (d) (dye and argon ion lasers). This decrease in the apparent linewidth is presently under investigation.

In a second set of experiments, the degree of enhancement of the ion yield was determined by measuring the ion signal with and without the argon ion laser for various irradiances of the dye and argon ion lasers. The dye laser frequency was set to the maximum of the (5,5) hyperfine component at 22124.4 cm^{-1}. The enhancement, defined as

$$\text{Enhancement} = \frac{\text{Ion Signal (both lasers)} - \text{Ion Signal (dye laser)}}{\text{Ion Signal (dye laser)}}$$

is shown in Figure 2 as a function of argon ion laser irradiance for three fixed values of the dye laser irradiance. The enhancement decreases inversely with the dye laser irradiance, due to increased competition for ionization between the dye and argon ion lasers. At the lowest dye laser irradiance (5.6 W/cm^2) and highest argon ion laser irradiance (~12 kW/cm^2) the enhancement is almost 700. The nonlinear power dependence of the enhancement on the argon ion laser irradiance is also under investigation.

These experiments show that the use of a non-resonant laser in the ionization step greatly increases the ion yield and S/N ratio, increasing sensitivity and permitting the reduction of linewidths of the hyperfine components. This will prove to be a useful technique in measurements of low abundance species and in atomic spectroscopy.

Ref. 1. C. M. Miller, R. Engleman, Jr., and R. A. Keller, *J. Opt. Soc. Am.* B **2** (1985) 1503.

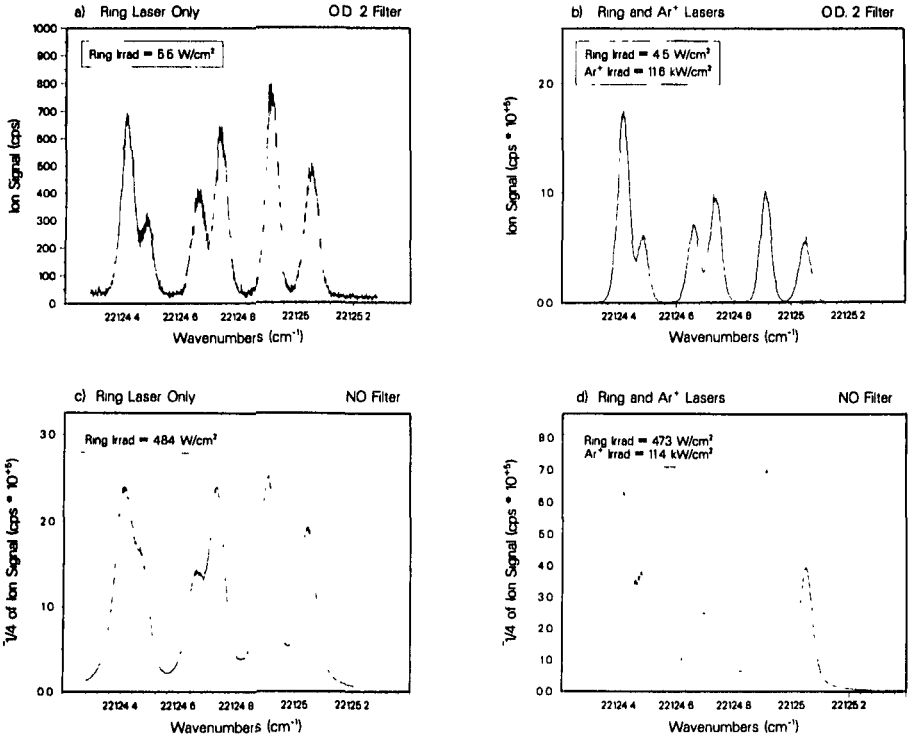

Figure 1. Spectra of the ^{175}Lu transition at 22125 cm^{-1}. The irradiances of the ring dye and argon ion lasers are given for each spectrum.

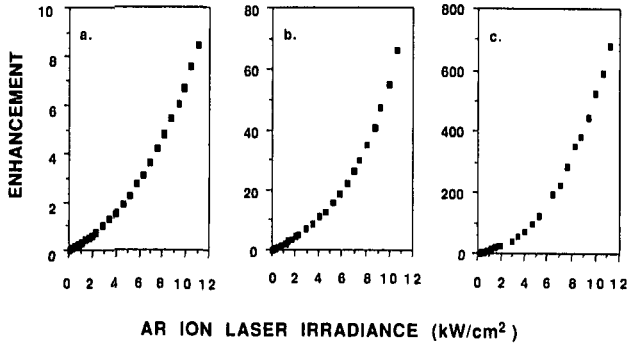

Figure 2. Enhancement of the Lu ion yield as a function of argon ion laser irradiance for fixed values of the ring dye laser irradiance, a) 643 W/cm^2, b) 65 W/cm^2, and c) 5.6 W/cm^2.

Presented at the 35th ASMS Conference on Mass Spectrometry and Allied Topics
May 24-29, 1987, Denver, CO

FAB MS STUDIES OF FORMATION AND STABILITIES OF GASEOUS POLYNUCLEAR LANTHANIDE OXIDES

Ishenkumba A. Kahwa[1], Thomas C.-Y. Hsieh[2], David W. Evans[3], Krishna M. Pamidimukkala[3], Roger A. Laine[3], and Joel Selbin[1]
Department of Chemistry[1], Food Science[2] and Biochemistry[3],
Louisiana State University & LSU Agricultural Center
Baton Rouge, LA 70803, U.S.A.

Previously we reported the detection of lanthanide (Ln) polynuclear polyoxo cluster species such as $Ln_3O_4^+$, $Ln_5O_7^+$, $Ln_6O_9^+$, $Ln_7O_{10}^+$ and $Ln_9O_{13}^+$ [1,2] in a FAB mass spectrometer. Inter-lanthanide cation coupling in these species occurs readily yielding statistical combinations such as $Tm_{3-n}Y_nO_4^+$, $Tm_{4-n}Y_nO_6^+$, $Tm_{5-n}Y_nO_7^+$, $Tm_{6-n}Y_nO_9$, n=0-6 [1]. With trivalent group IIIA elements Ga participated in the oxide cluster formation process yielding $GdGaO_3^+$. Other members either poisoned the entire oxide formation process(In^{3+}) or simply did not participate in it (Al^{3+}).

Besides novelty, the discovery of these oxides leads to interesting questions concerning their structure, stability, spectroscopy and potential applications in view of their unusual oxidation states and coordinative unsaturation. Frequently, yttrium clusters having odd numbers of yttrium atoms (odd clusters) are more abundant than those with even numbers (even clusters) in FAB MS spectra of yttrium compounds [1,2]. It was therefore interesting to determine stability trends among the various yttrium clusters and their fragmentation patterns in order to assess the implications of the unusual oxidation states and coordinative unsaturation of yttrium to the physical and chemical properties of the clusters.

A triple stage quadrupole TSQ70 Finnigan Mat mass spectrometer with FAB MS capability was used to obtain daughter ion spectra of various yttrium clusters. The fragmentation information obtained from averages of at least 20 scans for each set collision energy is summarized in Scheme 1. The signals for $Y_6O_9^+$ and $Y_9O_{13}^+$ were too low. YO^+ fragmented to Y^+ but the YO^+ intensity was 100% in the collision energy range 30 to 170eV.

Fragmentation of $Y_7O_{10}^+$, $Y_5O_7^+$ and $Y_4O_6^+$ yielded predominantly the ion $Y_3O_4^+$ in the collision energy range 30 to 170eV (collision offset -30V to -170V in scheme shown below). At low collision energies these large clusters yielded solely $Y_3O_4^+$ or $Y_3O_4^+$ and small amounts of YO^+ ($Y_5O_7^+$in the case of $Y_7O_{10}^+$). The even clusters were generally obtained at large collision energies along with odd clusters probably as a result of random fragmentation. The species Y^+ was produced only by even clusters, despite their higher O:Y atomic ratio.

The odd clusters are thus prominent in the daughter ion spectra of all parent ion oxide clusters because they are the more thermodynamically and kinetically favored products. Specifically, they are more resistant to collision induced fragmentation and do not require ionization to be detected since they are formed with an intrinsic positive charge.

The even clusters have a larger O:Y atomic ratio compared to odd clusters. In agreement with this observation the cluster $Y_2O_3^+$ with an O:Y atomic ratio of 3:2 is less stable than the cluster $Y_2O_2^+$ having an O:Y ratio of 2:2. The daughter ion spectrum of $Y_2O_3^+$ at 30eV has YO^+ (61%), $Y_2O_2^+$ (100%) and $Y_2O_3^+$ (32%) whereas that of $Y_2O_2^+$ has YO^+ (20%) and $Y_2O_2^+$ (100%). At 110eV all $Y_2O_3^+$ is fragmented but $Y_2O_2^+$ shows up with an intensity of 38% reflecting its greater thermodynamic stability.

These observations suggest important covalent contributions exhibiting directional geometric preferences which are more favorable in odd clusters and $Y_2O_2^+$ rather than even clusters and Y_2O_3. Large clusters show less tendency to fragmentation as expected from momentum transfer processes.

Acknowledgements: I. A. Kahwa (from Chemistry Department, University of Daressalaam, P.O. Box 35061, Daresalaam, Tanzania) thanks the U.S. Government (Fulbright Program) and LSU for financial assistance. Purchase of the TSQ70 mass spectrometer was supported by NIH grant #SSS-1(E)1S10RR-02803-01.

References:

1) I. A. Kahwa, T. C.-Y. Hsieh, R. A. Laine and J. Selbin, Inorg. Chim. Acta(1987) (in press); and Ibid, 118, 179 (1986).
2) I. A. Kahwa, T. C.-Y. Hsieh, R. A. Laine and J. Selbin, 34th ASMS Annual Conference on Mass Spectrometry and Allied Topics, p.148 (1986).

Presented at the 35th ASMS Conference on Mass Spectrometry and Allied Topics
May 24-29, 1987, Denver, CO

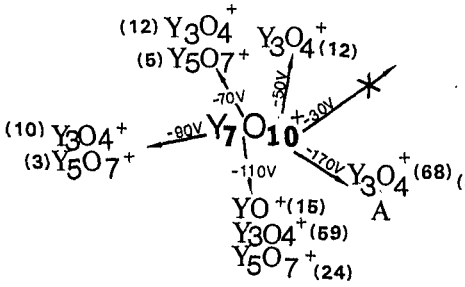

Parent ion intensity 100% throughout.

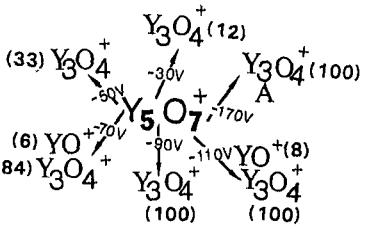

Parent ion intensity 100% up to -7 0V; 67% (-90V), 29% (-110V), 6% (-170V)

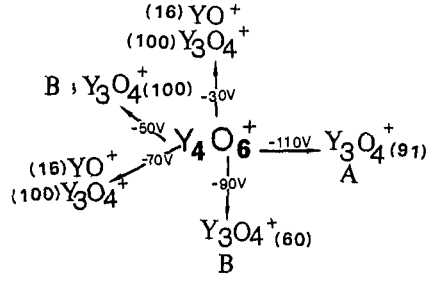

Parent ion intensity 66% (-30V), 50% (-50V), 51% (-70V), 32% (-90V) 28% (-110V)

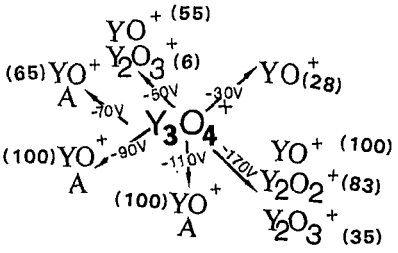

Parent ion intensity 100% up to -70V; 71% (-90V), 73% (-110V), 20% (-170V).

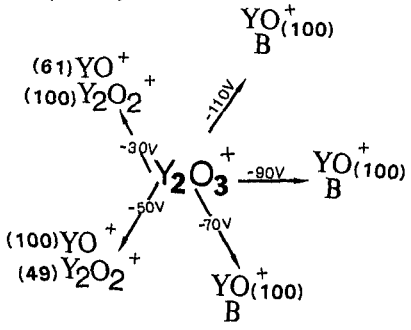

Parent ion intensity 32% (-30V), 19% (-50), 17% (-70), 11% (-90V), 0% (-110V).

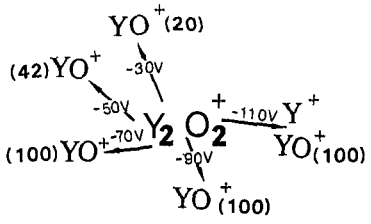

Parent ion intensity 100% up to -70V; 99% (-90V), 38% (-110V).

Scheme 1. A = ions YO^+, $Y_2O_2^+$, $Y_2O_3^+$, $Y_3O_4^+$, $Y_4O_6^+$, $Y_5O_7^+$, $Y_6O_9^+$ or $Y_7O_{10}^+$; series continuing to parent ion; B as in A but including Y^+. Parentheses enclose relative intensity. See text.

Presented at the 35th ASMS Conference on Mass Spectrometry and Allied Topics
May 24-29, 1987, Denver, CO

LEAD ISOTOPE RATIO ANALYSIS OF THE SACKLER BRONZES

Barnes, I.L., Chase, W.T., Holmes, L.L., Joel, E.C.*
Meyers, P., and Sayre, E.V.
Conservation Analytical Laboratory
Smithsonian Institution
Washington, DC 20560

The Arthur M. Sackler Collections contain approximately 400 early Chinese bronze ceremonial vessels of various types and shapes, mostly attributed by art historians to the Shang, Western Zhou and Eastern Zhou dynasties dating from 1300 to 221 B.C. Historically, the vessels reflect the various social and political periods as well as the religious periods of ancient China. The study of the bronze vessels in this collection, to include lead isotope ratio measurements, elemental anlaysis and structural examination, was carried out in collaboration with the Brookhaven National Laboratory, the Freer Gallery of Art, the Metropolitan Museum of Art, and the Arthur M. Sackler Foundation (1).

In view of the fact that the vessels are not from known excavations, information was needed to infer the origins of the objects, and whether similar vessels had similar origins. The initial aim of the project was to obtain detailed characteristics for each object, such as composition and structural details from which the method of fabrication including casting and joining techniques could be inferred; to evaluate these characteristics in conjunction with art historical evidence to establish or confirm details of Chinese bronze casting technology; and to help resolve questions of attribution. Eighty percent of the vessels were found to contain between 2 and 25% lead. This is a sufficiently high level to conclude that lead was probably an intentional addition to the metal alloy. Thus, lead isotope measurements should relate to the sources of lead used in their formation. However, unlike previous studies undertaken on European artifacts and their known mining and manufacturing areas, the ore data needed to determine or infer provenance was not available.

Overall, the lead isotope ratios obtained on the Sackler vessels are exceptional in terms of their diversity and spread in magnitude. The general conclusion is that Chinese leads tend to lie beyond the ranges usually encountered in most Western leads. Our observation on leads from early Chinese bronze vessels tends to confirm this.

When the data is divided according to the three periods to which the vessels were attributed, one observes some pronounced chronological changes. The distribution of points for the Shang dynasty vessels almost covers the entire range of isotope ratios encountered in this study (2). Clearly a great variety of leads were used during the Shang period. The use of the low ratio leads was very much dying out during the Western Zhou period, since relatively few vessels have low or intermediate lead isotope ratios. By the time of the Eastern Zhou dynasty, the occurrence of lead with low or immediate isotope ratios within the Sackler vessels becomes almost non-existent. Also the clustering in the high range is very tight. One could infer that during the Eastern Zhou period, lead from only a few related sources were used in these vessels. There is very good correlation between lead isotope results and chronology.

Further refinement of the data consists of a multivariate statistical approach using the principle components procedure developed at Brookhaven National Laboratory, which employs all three ratios to determine the characteristic vectors. The application further subdivided the isotopic

data into well-defined groups that also show good correlation to the chronological and art historical information. The data separated into eight major groups. A ninth group, whose resolution is difficult to display, and some small tentative groups designated A, B, C, and D, contain only a few specimens. These were not plotted. Figure 1 summarizes the lead groups, the distribution of the vessels for each period, and the group attribution as stated by the art historians involved in this study.

The results obtained to date would encourage one to believe that a close agreement in lead isotopes between objects would indeed indicate that the probability is high that they were made from lead from related sources. However, there is more to be learned about metals production and their use in early cultures. Nevertheless, the results provide good evidence that lead isotopes can significantly supplement structural and stylistic evaluations in the inference of origins and the relationships between similar objects. We hope to extend our measurements to include vessels of the Han and later dynasties in the near future.

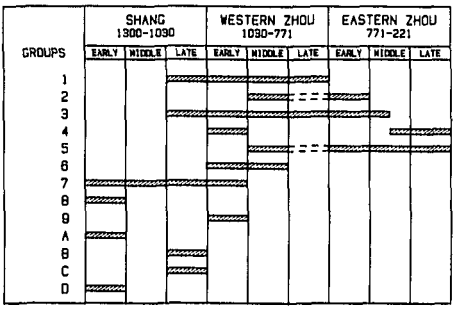

FIGURE 1. Distribution of Chinese Bronze Vessels According to Attribution and Lead Isotope Ratio Groups.

REFERENCES

1. Barnes, I.L., Chase, W.T., Holmes, L.L., Joel, E.C., Meyers, P., Sayre, E.V., Beginning of the Use of Metals and Alloys, Robert Maddin, Editor, MIT Press, in press.

2. Deal, E.C., "Use of Lead Isotopes in Archaeological Studies", 33rd Annual Conference on Mass Spectrometry and Allied Topics, San Diego, May 26-31, 1985, pp. 66-67.

Presented at the 35th ASMS Conference on Mass Spectrometry and Allied Topics
May 24-29, 1987, Denver, CO

ION CLUSTERS OF LITHIUM AND TIN EMITTED FROM LIQUID METAL ION SOURCE

Yahachi SAITO*, Makoto WATANABE, Takayuki HAGIWARA, Masahiro INOUE, Satoshi NISHIGAKI and Tamotsu NODA

Department of Electrical and Electronic Engineering, Toyohashi University of Technology, Toyohashi 440, Japan
* Department of Applied Physics, Nagoya University, Nagoya 464, Japan

During the last several years new cluster generation and detection methods have been developed. There are generation methods where the clusters have already been charged when they leave the place of formation: ion beam sputtering and liquid metal ion source. With other methods such as nozzle beam expansion and gas evaporation, neutral clusters are formed. In either case, small clusters can exist in various sizes, with certain clusters containing a definite number of atoms (magic number) showing a pronounced intensity in mass spectra. Small multiply-charged clusters, M_n^{z+}, are unobservable in mass spectra because the repulsive Coulomb forces between z charges cause rapid dissociation unless the cluster size exceeds a critical size, $n_{cri}(z)$. In the present study, we focused our attention to the magic numbers and the critical sizes of charged Li and Sn clusters emitted from a liquid metal ion source(LMIS).

An LMIS used in the present experiment is equipped with a reservoir for source material and with an emitter tip, which can be heated by electron bombardment. The detailed construction of the LMIS has already been described elsewhere.[1] Pure metals were used as the source material. The emitter tip was made of a tungsten wire for Li and of a nichrome wire for Sn. The mass distribution was measured with a single focusing magnetic analyzer.

1. Lithium

Figure 1 shows a mass spectrum of Li clusters from the LMIS at I_t = 50 μA, where I_t is the total emission current. Singly charged clusters containing up to 19 atoms were observed, but multiply charged clusters were never detected. Ion intensity as a function of cluster size shows local maxima at n = 7, 9, 13 and 19, compared with the neighboring clusters. The clusters which are abundant in mass spectra are assumed to be relatively more stable. Since species from LMIS are alrady in charged states in the process of cluster formation, information on the stability of charged clusters is obtained from the LMIS mass spectra without troublesome problems of size-dependent ionization cross-section and fragmentation.

These magic numbers are only partially explained by the electronic shell structure based on a spherical jellium model, which is successfully applied to interpreting the magic numbers of Na and K clusters.[2] According to this model, the cluster gains higher binding energy per atom and thus becomes more stable than others when the number of valence electrons in a cluster coincides with the shell closing number, 2, 8, 18, 20,... On the other hand,

atom packing consideration predicts magic numbers at n = 7, 13, 19, 55,... The latter model explains the observed magic numbers except for n = 9. The present result indicates that not only the electronic structure but also the geometric structures must be taken into account to explain the observed magic numbers.

2. Tin

Figure 2 shows a mass spectrum obtained at I_t = 2 μA. Not only singly charged clusters but multiply charged clusters were also observed. Clusters containing up to 7, 13 and 10 atoms for singly, doubly and triply charged clusters, respectively. Ion intensity of singly charged clusters as a function of cluster size shows discontinuous variations(steps) at n = 4 and 6. This feature can also be found in a mass spectrum of Si clusters from LMIS.[1] These magic numbers are commonly found for Si, Ge and Sn clusters.

The observed critical sizes were $n_{cri}(2) = 3$ and $n_{cri}(3) = 4$. The value of $n_{cri}(z)$ for Sn_n^{z+} reported so far are 3 for z = 2, 19(or 13) for z = 3, and 9 for z = 4.[3] The value of $n_{cri}(2)$ agrees with that already reported by other authors. On the other hand, the value of $n_{cri}(3) = 4$ found here is the smallest. Critical sizes estimated from the classical Rayleigh limit are $n_{cri}(2) = 3.7$ and $n_{cri}(3) = 8.4$. Although the macroscopic quantity was used for these small systems, the calculated critical sizes agree fairly well with the observed ones.

References
1) T. Noda et al.: Advances in Mass Spectrometry 1985 (John Wiley & Sons, New York, 1986) part B, p. 1531.
2) W. D. Knight et al.: Phys. Rev. Lett. 52(1984) 2141.
3) P. Joyes and J. Van de Walle: J. Phys. B 18(1985) 3805.

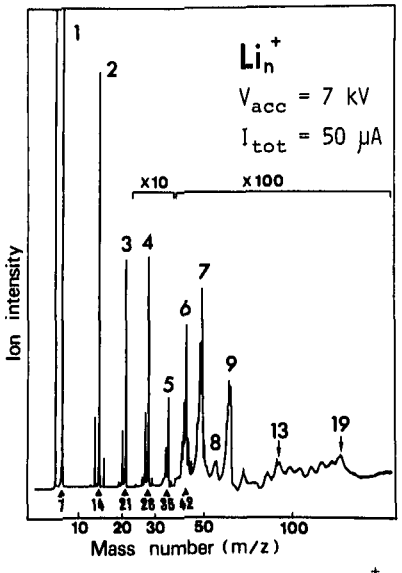

Fig. 1 Mass spectrum of Li_n^+.

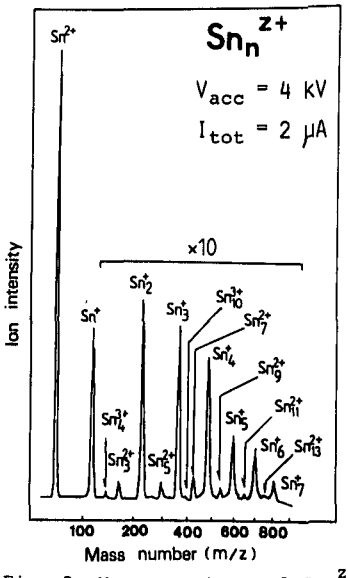

Fig. 2 Mass spectrum of Sn_n^{z+}.

Presented at the 35th ASMS Conference on Mass Spectrometry and Allied Topics
May 24-29, 1987, Denver, CO

LONG TERM GAIN LOSS IN CHANNEL ELECTRON MULTIPLIERS, MEASUREMENTS WITH TWO CEMs FOR MASS SPECTROMETRY APPLICATIONS

Peter F. Somssich
GTE Electrical Products Corp.
Lighting Research and Engineering
Danvers, Massachusetts 01923

Abstract

Applications involving a combination mass spectrometer/CEM for which gain stability over long periods of testing and actual operation is essential, demand reliable information on gain loss as a function of time and useage. Due to the large investment in time and resources very few works have been published reporting just such information as the result of actual testing on these devices. Where earth satellites and space exploration probes for in situ monitoring of nearby planet atmospheres are concerned, this kind of information is invaluable. However, even when routinely used in a laboratory environment, knowledge of the useful life of a CEM is important especially when the device has seen more than one user and application. Our particular application involved using a mass spectrometer with a CEM detector to measure gas components in a nearby planet atmosphere. Prior to the probe beginning its analysis, many years of space travel and testing would elapse. With this situation in mind, the Max Planck Institute for Nuclear Physics in Heidelberg, FRG, conducted a series of extensive tests using two Bendix CEMs (now marketed by Galileo): 4028 and 4700.

Experimental Conditions and Results of Tests

In preparation for the gain life tests, both CEMs were extensively documented to determine their characteristics and their optimal operating parameters(1,2). The tests were conducted in a vacuum chamber that contained a mass spectrometer and the CEM to be tested(Fig.1). A leak valve allowed for the introduction of different gases and a series of orifices, gitter and faraday cups allowed for the monitoring of both the CEM input flux as well as the corresponding output signals either in the pulse counting mode or the current mode. Fig.2 shows a typical CEM history of the CEM electron gain as a function of the total accumulated pulse counts(4,5,6,7). In the beginning each CEM experiences a cleanup phase which is associated with the process of cleaning of the CEM's surfaces in a vacuum. After this phase a long extended period is expected during which the gain remains relatively stable until at about 10^{11} Accumulated Pulse Counts(APC), a gradual and permanent gain loss is observed. The testing of the 4028 CEM was accomplished by introducing an Ar+ ion flux of 8000 C/sec into the CEM at 2400 V operating voltage which was in the counting plateau. Testing of the 4700 CEM on the other hand used an ion flux of 625000 C/sec and a voltage of 2800V. Fig.3 ,which also includes the typical CEM history
of Fig.2, show the results of our measurements. The 4028 CEM measurements began at approx. 10^{9} APC at which point the gain began decreasing. Unfortunately the test had to be concluded after only 5 days of operation. During that period however, while the gain did recover slightly from its initial losses it was not possible to predict a trend either up or down. This CEM lost approx. 25 % of its initial gain after the five days (equivalent to about 0.0013 Coulomb of output charge. Whether this gain was due to a late cleanup phase or a prophetic sign of gain losses to come, could not be determined. The 4700 CEM on the other hand was monitored for over 165 days (equivalent to 2.2 Coulomb of output charge. Measurements showed that from approx. 3X 10^{10} ACP (first data point) the gain, while declining closely approximated the CEM history curve up to about 10^{11} ACP. From there on until the test conclusion at 10^{12} ACP it continued to decline at approx. the same rate which was much less than would have been expected according to the CEM history. The higher gain 4700 showed more stability and lost only about 33% of its original gain when the test concluded. Fig.3 also show data taken by John Pantazis(3) using

a E1300 CEM specially designed by Detector Technology which has some similiarity with the 4028. The gain data would seem to indicate that from about 10^9 ACP on this device is similar to the CEM history curve. On the other hand there is no obvious explanation for the jump in the gain from 10^8 ACP to 10^9 ACP.

Bibliography
1)Somssich P.,34th ASMS Conf., Cincinnati,Ohio (1986()
2)Somssich P.,Diplomarbeit,University of Heidelberg,FRG(1976)
3)Pantazis J.,Emmanuel College, unpublished
4)Kurz E.,Channel Electron Multiplier,American Lab.(March 1979)
5)Galileo Electro-Optics Corp.
6)Rosenbauer H.,unpublished (1978)
7)McComas D.J.&Bame S.J.,Rev.Sci.Instr.55(4)1984

Many thanks to the Max Planck Institute for Nuclear Physics in Heidelberg,FRG,in particular Dr.R.Nord and Dr.D.Krankowsky. I would also like to thank GTE Sylvania,in particular Dr.V.Meyer and C.Gean.

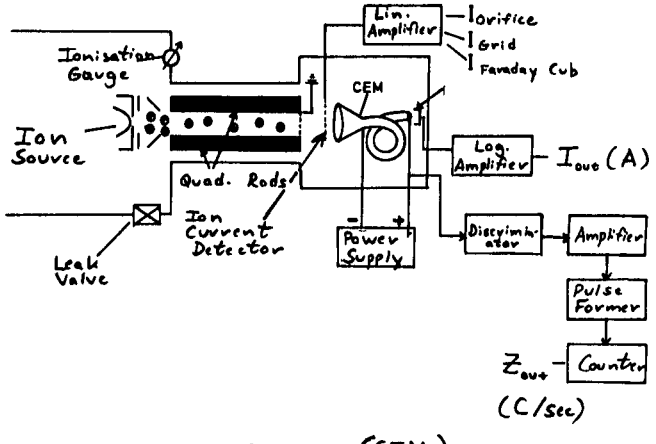

Fig. 1 Testing Set-up (CEM)

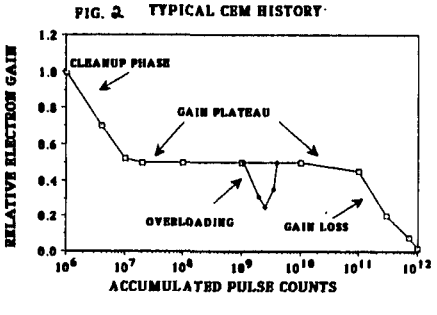

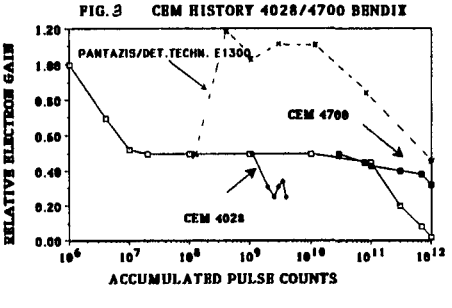

Presented at the 35th ASMS Conference on Mass Spectrometry and Allied Topics
May 24-29, 1987, Denver, CO

AN ISOTOPE DILUTION CAPILLARY COLUMN GC/MS METHOD FOR THE ACCURATE DETERMINATION OF SERUM CHOLESTEROL

M. J. Welch, A. Cohen, P. Ellerbe, R. Schaffer, L. T. Sniegoski, E. White V
Center for Analytical Chemistry, National Bureau of Standards,
Gaithersburg, MD 20899.

A definitive method for serum cholesterol[1] previously developed to provide an accuracy base for the evaluation of routine clinical methods used cholesterol-d_7 as the labeled material added as an internal standard, packed-column gas chromatography for sample introduction to the mass spectrometer and magnetic switching between the labeled and unlabeled ions being measured. With our GC/MS system converted to capillary columns, the unlabeled cholesterol was significantly separated from the internal standard, a situation which adds considerable imprecision to the measurements of the ratio of the intensities of the labeled and unlabeled ions. It was impractical to revert to packed columns for cholesterol measurements. Therefore a modified and improved method using a cholesterol-$^{13}C_3$ as the internal standard has been developed.

Experimental Briefly, the method consists of the following steps: A known weight of cholesterol-$^{13}C_3$ is added to a known weight of serum. Ethanol and 8.9 M potassium hydroxide are added and the mixture is held at 37° C for 3 hours to hydrolyze all cholesterol esters. The cholesterol is extracted with hexane and, after evaporation of the hexane, converted to a trimethylsilyl ether with bis-trimethylsilylacetamide (BSA). The derivative in excess BSA is injected onto a 15 meter FSOT DB-5 column, operated at 290°. The column is directly interfaced to a single focussing magnetic sector mass spectrometer operated in the electron impact mode. As the cholesterol-TMS peak elutes into the mass spectrometer, the intensities of the molecular ions of the unlabeled and labeled derivative are alternately measured. The number of intensity measurements which can be made using magnetic switching across a peak from a capillary column is too small for accurate measurement. An alternate means of switching[2] was developed that involved displacement of the ion beam with a dc voltage between two deflection plates located immediately in front of the detector slit, making it possible to rapidly switch the ion beam several mass units. As with the old method, each sample is measured twice in succession and these are bracketed by measurements of two standards whose unlabeled/labeled ratio bracket that of the sample. These standards consist of known weights of the labeled cholesterol and SRM 911a Cholesterol certified to be 99.8% pure. The weight ratio of the sample is found by linear interpolation of the measured intensity ratio between the two standard ratios. The measurements are repeated on a second day with the standards in reverse order The calculated weight ratios from the two days measurements are required to agree within 0.5%; if they do not a third measurement is made.

Results Results from remeasurement of cholesterol in SRM 909 (lyophilized human serum) and some 1985 survey sera from the College of American Pathologists (CAP) are shown in Table 1. Three sets of samples were independently prepared. Every sample in a given set was spiked from one solution of labeled cholesterol as were the standards used to measure that set. Errors which may contribute to set-set differences are reduced by this spiking technique. Confirmatory measurements on a subset of samples from the three sets were made to demonstrate the absence of bias in the ID/MS measurements. These results are summarized in Table 2. The results did not change significantly when either chromatographic or mass spectrometric conditions were changed; thus the likelihood of a measurement interference is small. However, one more set of confirmatory measurements, using ammonia CI and measurement of the $(M+_NH_4\text{-TMSOH})^+$ ions at 386 and 389 will be made for further confirmation.

The mean result for cholesterol in SRM 909 was 0.2% lower than was measured using the old method approximately one year earlier. Results from previous measurements dating back to 1980 suggest that the cholesterol concentration in this freeze-dried material may be decreasing slowly with time. The new method has better precision than does the old method, as well as greater specificity because of the use of capillary columns.

This new method is now being used to certify cholesterol concentrations in some freeze-dried and frozen reference serum pools at normal and elevated levels.

Table 1

CHOLESTEROL CONCENTRATIONS IN MMOLES/L*G

Pool	Set	# of Samples	Mean Concentrations Set	Pool	CV(%) Sample Means	Set Means
SRM 909	1	6	4.3320	4.3334	0.12	0.03
	2	6	4.3341			
	3	6	4.3341			
CAP C10	1	2	25.157	25.134	0.15	0.13
	2	2	25.110			
CAP C11	1	2	25.415	25.444	0.14	0.13
	2	2	25.480			
	3	2	25.438			

Table 2

CONFIRMATORY MEASUREMENTS

Sample Means [Mmoles/(L*G)]

Pool	# of Samples	A	B	% Diff. from A	C	% Diff. from A
SRM 909	6	4.3322	4.3396	0.17	4.3335	0.03
CAP C10	1	25.187	25.134	-0.21	25.190	0.01
CAP C11	2	25.445	25.472	0.11	25.439	-0.02
		Mean Difference		0.11		0.02

A - Principal measurements using molecular ions at m/z 458 and 461 and a 15 m DB-5 column.

B - Confirmatory measurements using fragment ions at m/z 329 and 332 and a 15 m DB-5 column.

C - Confirmatory measurements using molecular ions at m/z 458 and 461 and a 30 m DB-17 column.

References

1. Cohen, A., Hertz, H. S., Mandel, J., Paule, R. C., Schaffer, R., Sniegoski, L. T., Sun, T., Welch, M. J., and White V, E. Clin. Chem. 1980, 26, 854-860.

2. Meiselman, S., Ellerbe, P., Welch, M. J., and White V, E., Presented at the 34th Annual Conference on Mass Spectrometry and Allied Topics, Cincinnati, OH, June 8-13, 1986.

Presented at the 35th ASMS Conference on Mass Spectrometry and Allied Topics
May 24-29, 1987, Denver, CO

POSITIVE AND NEGATIVE ION CHEMICAL IONIZATION MASS SPECTROMETRY (NH_4^+ AND OH^-) FOR THE IDENTIFICATION OF PYRROLIZIDINE ALKALOIDS IN EUPATORIUM SPECIES:

H. Hendriks, H.J. Huizing and A.P. Bruins, State University, Dept. of Pharmacy, Groningen, The Netherlands.

Hepatoxic and carcinogenic pyrrolizidine alkaloids in phytopharmaca, herbal teas, food and cattle forage are a cause of poisoning, disease and cattle losses. On the other hand, the PA indicine-N-oxide undergoes trials for use as an antineoplastic agent. Within the scope of a study of antitumor compounds in higher plants the presence of PAs in Eupatorium species is investigated. The combination of PICI and NICI in GC/MS of trimethylsilyl derivatives of PAs offers a rapid tentative structure elucidation (1).

PYRROLIZIDINE ALKALOIDS

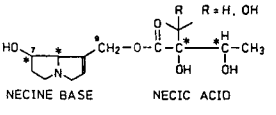

PICI with NH_4^+ gives abundant MH^+ ions. Cleavage of the ester bond at C_9 produces a fragment ion which further decomposes by elimination of the functional group at C_7, i.e. loss of TMSOH, acetic acid, tiglic acid, angelic acid etc. The positive fragment ions at m/z 220 and 120 in Figure 1 thus correspond with the necine base portion of the alkaloid.

NICI with OH^- cleaves ester bonds, generating carboxylate anions that provide a direct indication of the esterifying acids in PAs. Thus the ion at m/z 393 in Figure 1 is the tris-TMS echimidic anion. The presence of an acetoxy group at the carbon atom of echimidic acid gives rise to carboxylate anions at m/z 363 (di-TMS derivative) and

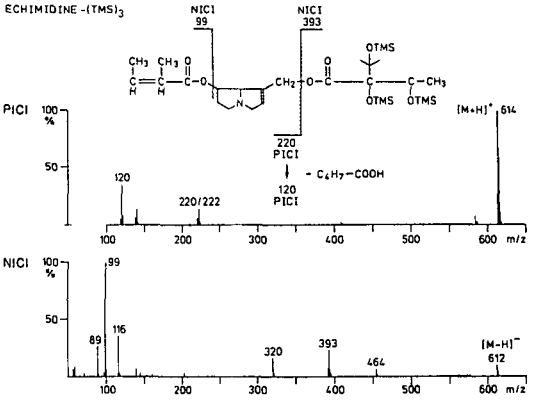

Figure 1 . Mass spectra of compound j (Figure 3)

m/z 59 the acetate ion. Such an acetyl derivative of echimidic acid has not been reported before in the PAs from Eupatorium species. Extracted ion current profiles of carboxylate ions are very helpful in the identification of ester alkaloids having a common esterifying acid, see Figure 2. Total ion current profiles of positive and negative ion chemical ionization GC/MS (NH_4^+ and OH^-) in Figure 3 show approximately equal sensitivity and profile in the region of interest between scan numbers 500 and 800.

In summary, PICI and NICI afford complementary mass spectral information and a rapid insight into the presence of PAs in plant material. It should be noted however, that mass spectrometry alone cannot differentiate between stereoisomeric PAs.

1. H.J. Huizing et al., Biomed. Env. Mass Spectrom. 13, 293 (1986).

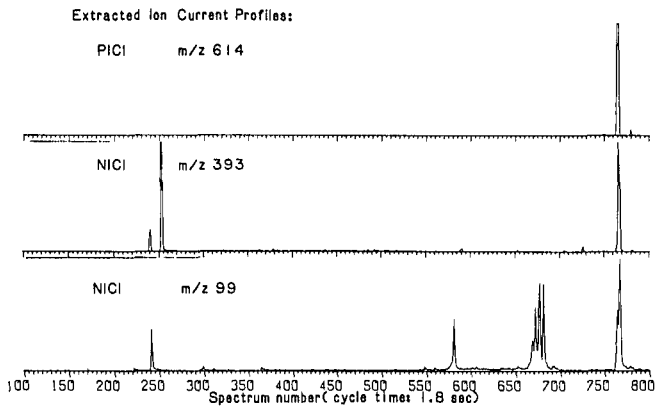

Figure 2

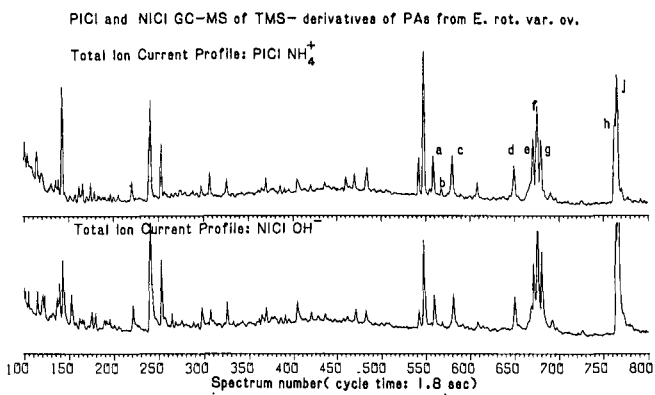

Figure 3

Presented at the 35th ASMS Conference on Mass Spectrometry and Allied Topics
May 24-29, 1987, Denver, CO

IDENTIFICATION OF CANNABIDIOL METABOLITES IN HUMAN URINE

D.J. Harvey[1] and R. Mechoulam[2]

(1) *University Department of Pharmacology, South Parks Road, Oxford, OX1 3QT, UK, and (2) The Hebrew University, Jerusalem, Israel.*

Introduction

Cannabidiol (CBD) is a non-psychotropic, natural cannabinoid from Cannabis sativa L. which is showing promise as a clinical drug for anticonvulsant therapy. Although its metabolism has been studied in several animal species (1), metabolism in humans does not appear to have been investigated. This paper reports the results of a study of the metabolism of CBD in a patient treated with a high dose of this drug.

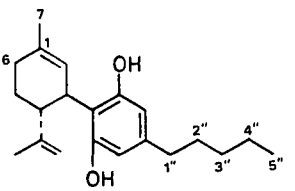

Cannabidiol (CBD)

Methods

Urine samples (1.5 l) were obtained from a dystonic patient treated with the drug at a dose of 600 mg daily. Metabolites were extracted with ethyl acetate (3 X 300 ml) and half of the extract was derivatized directly for GC/MS studies. The other half was chromatographed on Sephadex LH-20 in chloroform and chloroform/methanol mixtures, prior to derivatization, as described previously (2). The fractions eluting with 35-70 ml of chloroform and the first 50 ml of 10% methanol in chloroform were examined. Metabolites in all examined fractions were converted into TMS, [$^2H_9$]TMS, methyl ester/TMS or methyloxime/TMS derivatives, or were reduced with lithium aluminium deuteride prior to TMS ether formation. These derivatives were examined by GC/MS using a VG 12B mass spectrometer interfaced to a Varian 2440 gas chromatograph and to a VG 2050 data system. Additional processing was achieved with a VG 11/250 data system. The GLC column was 2m x 2mm 3%, SE-30 on 100-120 mesh Gas Chrom Q and spectra were recorded at 25 eV.

Results

Metabolites were identified by their ability to form appropriate derivatives and by comparison with published data (3). Prominent ions having structures a and b (retro-Diels-Alder cleavage) were useful in localizing the positions of the metabolically added groups.

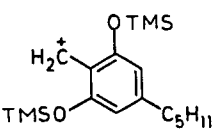

a

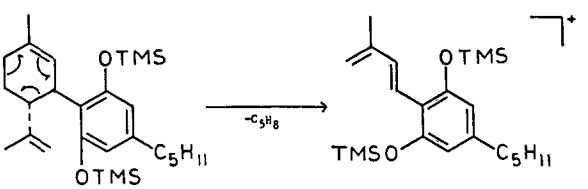

b

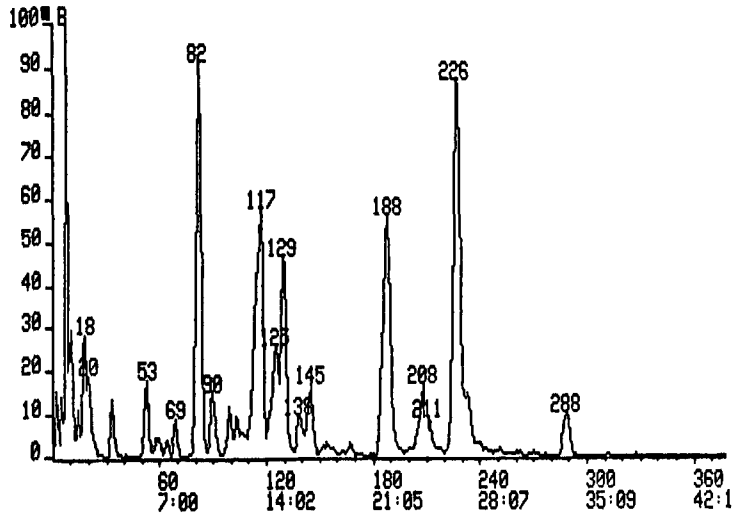

Fig. 1. Ion chromatogram (m/z 300 - 700) of metabolites of CBD separated on a 3% SE-30 packed column. Compounds identified are (indicated by scan number): 8) CBD, 33) cannabinol, 48) 4",5"-bis,nor-CBD-3"-oic acid, 53) 7-hydroxy-CBD, 69) CBD-7-oic acid, 82) 1"-hydroxy-CBD-7-oic acid plus an unidentified metabolite, 90) 6-hydroxy-bis,nor-CBD-3"-oic acid, 99) 7-hydroxy-bis,nor-CBD-3"-oic acid, 115) 2"-hydroxy-CBD-7-oic acid plus an unidentified metabolite (scan 117), 125) 3"-hydroxy-CBD-7-oic acid, 129) 4"-hydroxy-CBD-7-oic acid, 145) unidentified metabolite, 188) cholesterol, 226) CBD O-glucuronide.

Fig. 1 shows the profile of metabolites obtained directly from the urine and separated on a SE-30 packed column as TMS derivatives. Thirteen metabolites together with unchanged CBD (peak 1) and its glucuronide conjugate (peak 16) were identified. These metabolites were mainly hydroxylated derivatives of CBD-7-oic acid with hydroxy groups in the side-chain and terpene portion of the molecule (see figure legend). CBN-7-oic acid itself (peak 6) and its precursor alcohol (peak 5) were present in low concentration. Metabolites formed by the beta-oxidation pathway were also identified in low concentration; the most common had lost two carbon atoms from the side-chain. These were 4",5"-bis,nor-CBD-3"-oic acid (peak 4) and its 6- and 7-hydroxy derivatives (peaks 8 and 9 respectively).

Conclusions

Metabolism of CBN in humans thus appears to be similar to that observed earlier in mice, rats and guinea pigs although the ratios of the various metabolites were different.

References

1. D.J. Harvey and W.D.M. Paton, Rev. Biochem. Toxicol., 1984, 6, 221.
2. D.J. Harvey, B.R. Martin and W.D.M. Paton, J. Pharm. Pharmacol., 1977, 29, 482.
3. D.J. Harvey, Mass Spectrom. Rev., 1987, 6, 135.

Acknowledgements

This work was supported by grants from the Wellcome Trust and NIDA.

Presented at the 35th ASMS Conference on Mass Spectrometry and Allied Topics
May 24-29, 1987, Denver, CO.

SIMULTANEOUS DETERMINATION OF URINARY C-18 OXYGENATED STEROIDS AS ETIOLACTONE DERIVATIVES BY SELECTED ION MONITORING:

Connie Chan and Stanley Ulick; Dept. of Medicine,
Mt. Sinai School of Medicine of the City University of New York,
and the Veterans Administration Hospital, Bronx, NY 10468.

The mammalian adrenal cortex secretes two major corticosteroid hormones which arise from adjacent zones of the gland and are regulated independently by different stimulating factors. This anatomical and functional arrangement of the adrenal cortex, known as functional zonation, is normally maintained despite a common precursor cell for both zones and a common steroidogenic mechanism for the first half of the biosynthetic pathway. In the course of examining the urinary steroid profile by GC/MS in a disorder known as primary aldosteronism, a major unknown component was found in the unconjugated urinary neutral steroid fraction, subsequently identified as 18-hydroxycortisol [1], a structural hybrid combining the functional groups of the two major biologically active corticosteroid hormones, aldosterone and cortisol.

The hypothesis that 18-hydroxycortisol arose because of a defect in functional zonation permitting access of cortisol to the corticosterone methyl oxidase of the aldosterone biosynthetic pathway was tested by looking for, and finding the completely oxidized product of cortisol by this cytochrome P450 angular methyl oxidase, 18-oxocortisol [2]. The latter was found to be a mineralocorticoid agonist [3], probably contributing to the clinical manifestations of mineralocorticoid excess in the two hypertensive disorders in which the cortisol C-18 oxidation pathway is expressed [4].

For the quantitative assessment of the pathway it was desirable to measure the normal products as their urinary tetrahydro metabolites, aldosterone 18-hydroxycorticosterone and the aberrant ones arising from C-18 oxidation of cortisol, namely, 18-hydroxy and 18-oxocortisol. We investigated the TMS derivatives of the 18,20 cyclic hemi-ketal forms as well as the MO TMS derivatives. The latter afforded more reproducible quantitation when an unnatural isomer of tetrahydroaldosterone was used as internal standard because of a tendency to yield tautomeric forms if the C-20 ketone was not converted to a methoxime (Figure 1). A somewhat more convenient method, however, made use of the ability of periodic acid simultaneously to convert C-18 oxygenated steroids with an α-ketol side chain to γ-lactones and when applied directly to urine to effect the oxidative cleavage of glucuronides at the C-3 position. This procedure had the advantage of eliminating the need for enzymatic hydrolysis of the urinary steroid conjugates (Figure 2). In an example of a patient with primary aldosteronism, application of these methods revealed the quantitative importance of C-18 oxidation pathway in that its metabolites were considerably more abundant than those of cortisol whose metabolites normally predominate in human urine.

Presented at the 35th ASMS Conference on Mass Spectrometry and Allied Topics
May 24-29, 1987, Denver, CO

References

1. Chu M.D. and Ulick S.: Isolation and identification of 18-hydroxycortisol from the urine of patients with primary aldosteronism. J. biol. Chem. 257 (1982) 2218-2224.

2. Ulick, S., Chu M.D. and Land M.: Biosynthesis of 18-oxocortisol by aldosterone-producing adrenal tissue. J. biol. Chem. 258 (1983) 5498-5502.

3. Ulick S., Land M. and Chu M.D..: 18-Oxocortisol, a naturally occuring mineralocorticoid agonist. Endocrinology 113 (1983) 2320-2322.

4. Ulick S.: Evidence for defective functional zonation in adrenocortical hypertensive syndromes in man. Symposium in Adrenal Cortex in Hypertension. Raven Press, New York, Vol. 27 (1986) pp. 357-361.

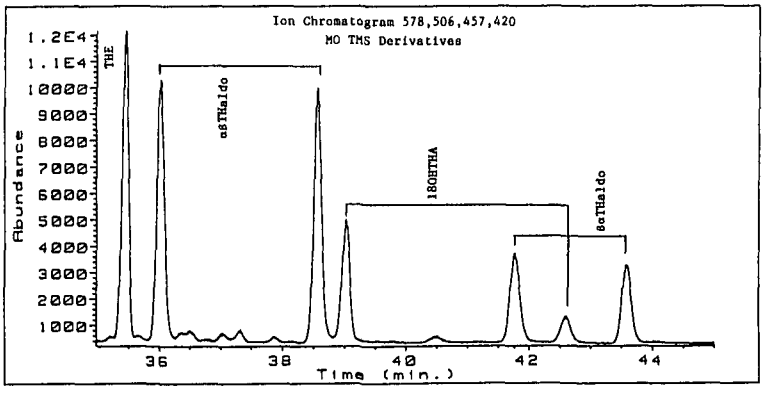

Figure 1

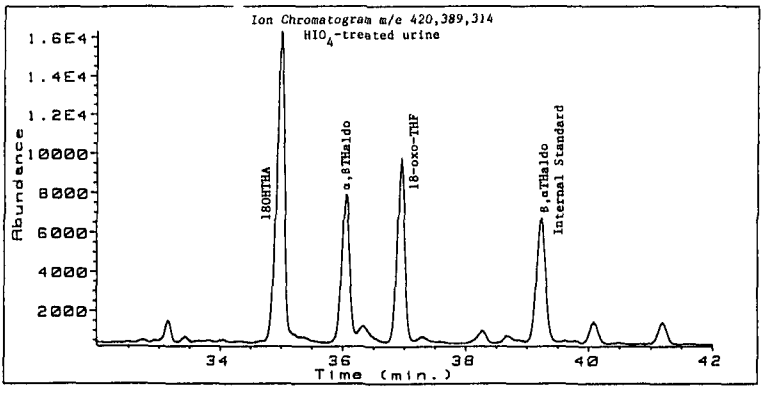

Figure 2

Presented at the 35th ASMS Conference on Mass Spectrometry and Allied Topics
May 24-29, 1987, Denver, CO.

DETERMINATION OF GLUTAMINE TURNOVER BY ISOTOPE DILUTION GC/MS

W.H. Schaefer, I.A. Blair, C.K. Reddy, R. Geer, N.N. Abumrad
Department of Pharmacology and Surgery,
Vanderbilt University, Nashville, Tenn. 37232

INTRODUCTION

Glutamine is the most abundant free amino acid in the body. It is a non-essential amino acid that can act as a substrate for both protein and carbohydrate synthesis. Glutamine plays a pivotal role many biosynthetic pathways such as the purine nucleotide cycle. It is necessary to completely elucidate its metabolism in order to fully understand its role physiologic and pathophysiologic states. The 5-carbon backbone is distributed into a number of different pools making it difficult to follow. However, the availability of ^{15}N-labelled glutamine at both the 2 and 5 positions provides the opportunity to monitor glutamine turnover by mass spectrometry. Further, by providing ^{15}N-substrate it is possible to monitor both utilization and subsequent biotransformation to glutamic acid and urea. We report the development of methodology for the determination of ^{15}N-incorporation into arterial glutamine, glutamic acid and urea subsequent to infusion of ^{15}N-ammonium chloride in an animal model.

RESULTS AND DISCUSSION

Glutamine was analyzed by conversion to its tris-trimethylsilyl derivative. Silylation was carried out by heating in bis-trimethylsilyltrifluoroacetamide (BSTFA) at 80°C. The mass spectrum of the ^{14}N-glutamine derivative showed major ions at m/z 362 (M), 347 (M-CH_3), 245, 156, 128, 73. The derivative of 2-^{15}N-glutamine showed major ions at m/z 363 (M), 348 (M-CH_3), 246, 156, 129, 73 and the derivative of 5-^{15}N-glutamine showed major ions at m/z 363 (M), 348 (M-CH_3), 246, 157, 128, 73. Selected ion monitoring analysis using capillary column gas chromatography allowed incorporation of ^{15}N into glutamine to be determined as follows. Monitoring ions m/z 245(^{14}N), 246 (^{15}N) allowed total incorporation to be determined, while monitoring ions m/z 156 (^{14}N), 157 (5-^{15}N) allowed incorporation into 5-^{15}N to be determined. Plasma samples were extracted by a modification of the procedure of Segal et al. (1).

Glutamic acid was analyzed by conversion to its tris-trimethylsilyl derivative as described above. The mass spectrum of the ^{14}N-derivative showed major ions at m/z 363 (M), 348 (M-CH_3), 246, 156, 128, 73 and the ^{15}N-derivative showed major ions at m/z 364 (M), 349 (M-CH_3), 247, 157, 129, 73 (Figure 1). Selected ion monitoring analysis of m/z 246 (^{14}N), 247 (^{15}N) allowed incorporation of ^{15}N- to be determined. Work-up and gas chromatography was carried out as described above.

Urea was analyzed by conversion to its pentafluoropropionyl (PFP), bis-TMS derivative. PFP derivatization was carried out by heating in PFP anhydride/ethyl acetate for 80° for 10 min and TMS derivatization as described above. The mass spectrum of the ^{14}N-derivative showed major ions at m/z 350 (M), 335 (M-CH_3), 231, 116, 73 and the ^{15}N-derivative showed major ions at m/z 351 (M), 336 (M-CH_3), 232, 116, 117, 73. Selected ion monitoring analysis of m/z 231 (^{14}N), 232 (^{15}N) (Figure 2) allowed incorporation of ^{15}N to be determined. Work-up and gas chromatography was carried out as described above. Ammonia utilization was determined by conversion of plasma ammonia to glutamic acid using ketoglutarate and glutamate dehydrogenase. ^{15}N content of the ammonia was then determined by analysis of the glutamic acid as described above.

Infusions of ^{15}N-ammonium chloride (100mg bolus then 0.075 mmol/kg/min) into a peripheral vein of a dog were carried out. Sampling was carried out in a femoral artery. Incorporation of ^{15}N into both the 2-N and 5-N of glutamine and into urea was observed. A minor incorporation into glutamic acid at later time point was also observed.

REFERENCE

1. Nissim, I., Yudkoff, M and Segal S. J. Biol. Chem.: 260 (1985) 13955.

ACKNOWLEDGEMENT

Supported by NIH grant AM 26657-061A.

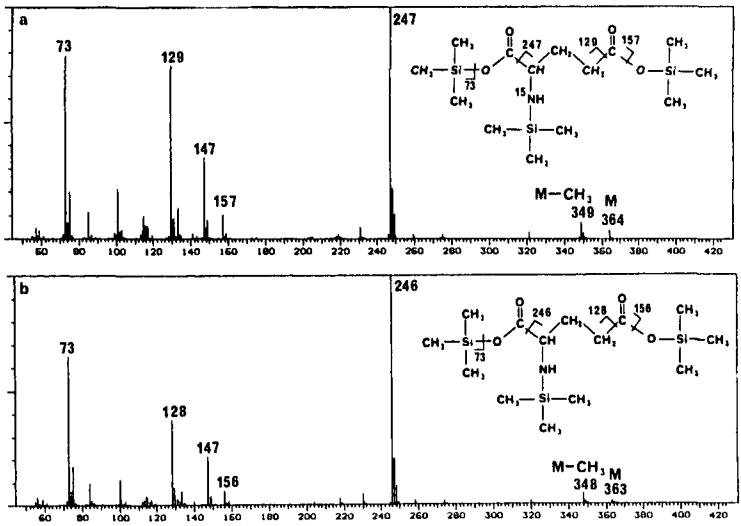

Figure 1. Electron impact mass spectra of the tris-TMS derivatives of a) ^{15}N-glutamic acid b) Glutamic acid.

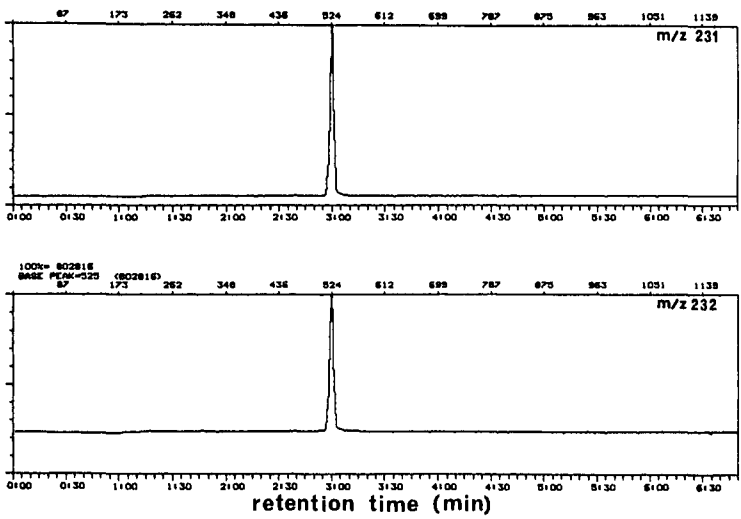

Figure 2. Selected ion current profile for plasma urea of the PFP, bis-TMS derivative.

Presented at the 35th ASMS Conference on Mass Spectrometry and Allied Topics
May 24-29, 1987, Denver, CO.

QUALITATIVE SCREENING OF ORGANIC ACIDS IN URINE BY A NEW DESORPTION/IONIZATION METHOD: K+ IONIZATION OF DESORBED SPECIES (K+IDS). D. B. Kassel, C. C. Sweeley, and J. Allison, Departments of Chemistry and Biochemistry, Michigan State University, East Lansing, MI, 48824.

The desorption/ionization method K+IDS (K+ Ionization of Desorbed Species) has been utilized for the analyses of thermally labile compounds and mixtures[1]. In the analysis of "non-volatile" species, a typical K+IDS mass spectrum contains both molecular weight and abundant structural information in the form of K+ adducts of the intact molecule and its thermal degradation products. For compounds (M) that exhibit some volatility, such as organic acids and small fatty acids, the K+IDS mass spectra yield only molecular weight information; i.e. only $(M+K)^+$ ions. Thus, mixtures of these compounds can be analyzed. The $(M+K)^+$ ions for each component yield a "molecular weight profile" of the mixture. Recently, a "two-filament" design has been implemented in this technique, improving the performance in two ways: 1. Better overlap between the temporal profiles for analyte desorption and alkali ion emission is achieved, increasing sensitivity; and 2. Quantification for mixture analysis is improved.

We are investigating the utility of K+IDS as a rapid approach for screening organic acidurias in urine. In this work, we have found that the use of Na+ emitters, i.e. Na+IDS, yields a method that is more sensitive than K+IDS. Organic acids are isolated from urine by conventional methodology. Once lyophilized, the organic acid components are not derivatized (as would be done for GC or GC/MS analysis), but are dissolved in an appropriate solvent. A few drops of this solution are placed onto the Na+IDS probe and the analysis performed. The emitter is rapidly heated to a temperature of approximately 1000°C. Desorption of intact molecules and Na+ ions occurs, forming $(M+Na)^+$ adducts. The result is a molecular weight profile representative of the components of the mixture. The urinary organic acid profiles thus generated, for a healthy and disease-state individual, are compared in Figures 1 and 2. All peaks in the mass spectra are $(M+Na)^+$ adducts of the individual organic components. The patient suffering from Maple Syrup Urine Disease (MSUD) shows abnormally high excretion of the hydroxyvaleric acids ($[M+Na]^+$ at m/z 141), consistent with data obtained from gas chromatographic (GC) analysis. In the control urine, the major component is hippuric acid ($[M+Na]^+$ at m/z 202), the results again being consistent with GC data. Simulated molecular weight profiles of the urinary organic acidurias are generated from available GC and GC/MS data and compared with the Na+IDS spectra. These comparisons assist in determining how closely the Na+IDS mass spectra parallel the true organic acid compositions.

We find that Na+IDS analysis of organic acid mixtures in urines can be used to distinguish between various disease-states. While such molecular weight profiles obviously do not provide as much information as full GC/MS analyses, the technique is exceedingly rapid. No derivatization step is required, and the Na+IDS spectrum can be generated in less than a minute. The utility of the method depends on the type of information desired.

1. D. Bombick and J. Allison: *Anal. Chem.*, **59**, 458 (1987).

Presented at the 35th ASMS Conference on Mass Spectrometry and Allied Topics
May 24-29, 1987, Denver, CO

Na+IDS Mass Spectrum of MSUD Organic Acids

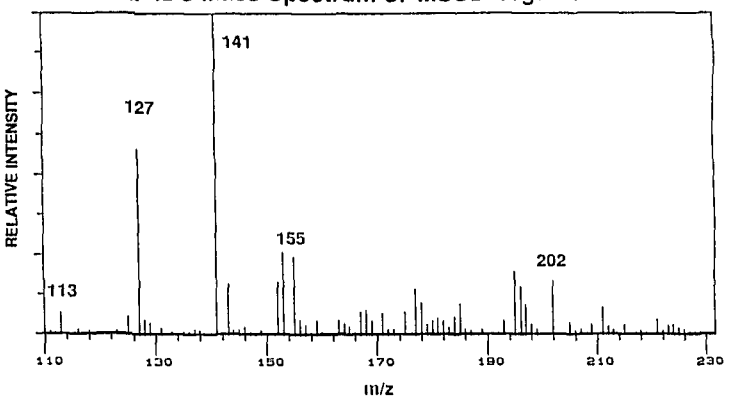

m/z $(M+Na)^+$	Organic Acids	*Relative Concentration
113	Lactic, Oxalic	49
127	2-hydroxy, and 3-hydroxybutyric,	394
141	*2-hydroxyisovaleric, Succinic, 3-hydroxyisovaleric	611
155	Glutaric, 2-hydroxy-3-methylvaleric	100
202	Hippuric	82

*Obtained from integration of peaks from GC-only data

Na+IDS Mass Spectrum of Control Urine

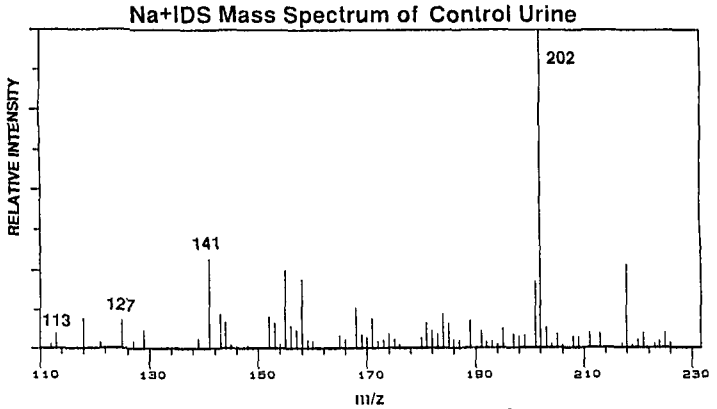

m/z $(M+Na)^+$	Organic Acids	*Relative Concentration
113	Lactic, Oxalic	61
127	2-hydroxy, and 3-hydroxybutyric, 2-hydroxy, and 3-hydroxyisobutyric	68
141	3-hydroxyvaleric, succinic, 3-hydroxyisovaleric	74
202	Hippuric	352

Presented at the 35th ASMS Conference on Mass Spectrometry and Allied Topics
May 24-29, 1987, Denver, CO

A METHOD FOR THE DETERMINATION OF ENDOGENOUS LACTIC AND PYRUVIC ACIDS, AND ENDOGENOUS AND ^{13}C-LABELLED 3-HYDROXYBUTYRIC AND ACETOACETIC ACIDS IN ORGAN PERFUSATES BY SIM-GCMS:

O.A. Mamer and J.A. Montgomery, The Biomedical Mass Spectrometry Unit, McGill University, 1130 Pine Ave. West, Montreal, Canada, H3A 1A3; and: C. Des Rosiers, S. Desrochers and H. Brunengraber, Research Center, Notre-Dame Hospital, 1560 East Sherbrooke, Montreal, Canada H3T 1A8.

The metabolism of lactic (L), pyruvic (P), 3-hydroxybutyric (HB) and acetoacetic (AA) acids was studied in isolated rat liver with the infusion of 3,4-$^{13}C_2$-labelled AA in amounts small enough not to disturb physiological equilibria. Aliquots of the circulating perfusate taken before and after the infusion were analyzed with a low resolution EI SIM-GCMS method described here.

P and AA are reduced in situ with sodium borodeuteride (BD) to 2-^2H-L and 3-^2H-HB respectively to distinguish them from endogenous L and HB. 2,3,3,3-$^2H_4$-L and 2,2,3,4,4,4-$^2H_6$-HB are used as internal standards. The acids are extracted into ether (1), and the TMS derivatives are admitted to the mass spectrometer via large-bore capillary GC inlet. The instrument used was a ZAB 2F-HS operated at 70 eV with flat-topped peaks having true baseline resolution. Ions monitored for HB are the m/z 117, 118, 119, 120 and 121 fragments produced respectively by: endogenous HB, endogenous AA reduced by BD, $^{13}C_2$-HB produced by endogenous reduction of $^{13}C_2$-AA (HB**), $^{13}C_2$-AA reduced by BD (AA**), and $^2H_6$-HB internal standard. The lactate set is similarly analyzed. The 5 fragmentogram areas collected for both the L and the HB sets (Fig 1) are corrected for natural abundance heavy isotope inclusion and for isotopic impurities in endogenous and administered substrates, internal standards and BD. These corrections are made with a small computer to solve 5 linear equations in 5 unknowns of the type:

$$a_{1-5}v + b_{1-5}w + c_{1-5}x + d_{1-5}y + e_{1-5}z = f_{1-5}$$

Application of a program written in Basic to effect the required corrections for the data represented in Fig. 1 produces the corresponding concentrations listed below. Copies of this program may be obtained by writing to the speaker.

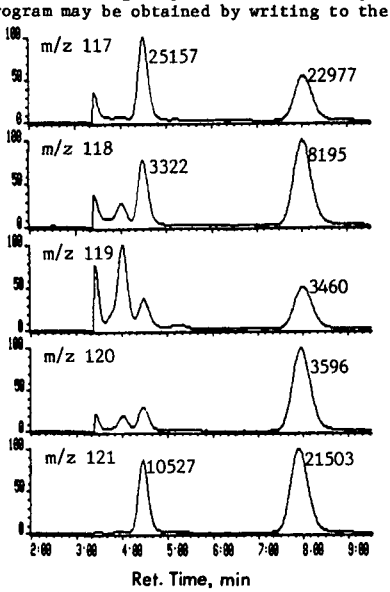

Fig. 1 SIM traces of fragments m/z 117, 118, 119, 120 and 121 represented at right in the analysis of rat liver perfusate after infusion of 3,4-^{13}C AA. The peak with RT 4.5 min is lactate, and the peak at 7.9 min is 3-hydroxybutyrate.

Acid Concentrations
From Data of Fig. 1

ACID	CONC (mg/L)
L	24.62
P	0.47
HB	10.97
AA	2.48
HB**	0.49
AA**	1.02

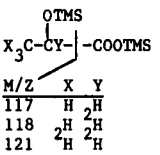

M/Z	X	Y
117	H	2H
118	2H	2H
121	2H	2H

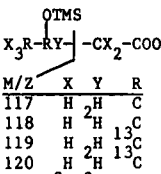

M/Z	X	Y	R
117	H	2H	C
118	H	2H	13C
119	H	2H	13C
120	H	2H	13C
121	2H	2H	C

A series of samples of sera and perfusates were analyzed for HB and AA by this method and by enzymatic assays for the purpose of comparing their results. Figure 2 illustrates the correlation between the present method and the enzymatic assays for these acids. Very much better correspondence is noted for AA in this study than in a earlier report using a similar approach based upon recoveries of incremental additions of synthetic AA to physiological fluids (2).

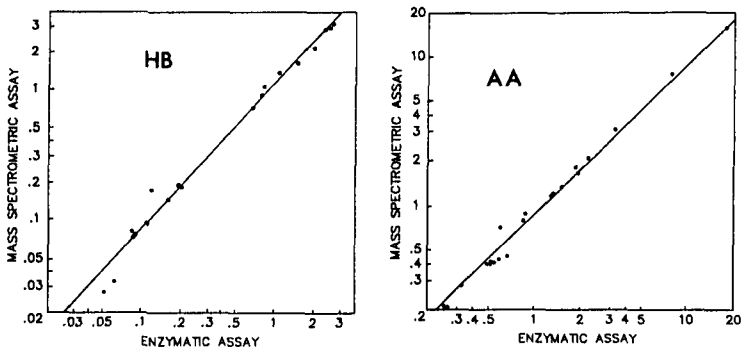

Fig. 2 Correlation of HB and AA concentrations determined by this method with those found with enzymatic assay of mixed samples of sera and organ perfusates.

1. B.F. Gibbs, K. Itiaba, O.A. Mamer, J.C. Crawhall and B.A. Cooper, Clin. Chim. Acta, 38, 447 (1972).

2. O.A. Mamer, Biomed. Environ. Mass Spectrom., in press.

Presented at the 35th ASMS Conference on Mass Spectrometry and Allied Topics
May 24-29, 1987, Denver, CO

ESSENTIAL OIL FROM THE UNICORN-PLANT (*PROBOSCIDEA LOUISIANICA*): IDENTIFICATIONS BY MASS SPECTROMETRY AND ALLELOCHEMICAL ACTIVITY

Waller, G. R.[1], Riffle, M. S.[1,2] and Murray, D. S.[2]
Depts. of Biochemistry[1] & Agronomy[2]
Oklahoma State University
Stillwater, OK 74078

Sgaramello, R. P.
International Flavors and Fragrances
Union Beach, NJ

The unicorn-plant (*Proboscidea louisianica* (Mill.) Thell.) is an annual broadleaf weed of the family *Martyniaceae*, found in the cotton growing areas of Texas and Oklahoma, and has been found to reduce cotton yields up to 83%. This viscid, pubescent plant is difficult to control with conventional herbicides, and often hand labor or spot treatment with more concentrated herbicides is used. It can reach heights of one meter and the canopy spread is approximately two meters. We have obtained evidence that the effect of allelochemicals upon the cotton plant can be a contributing factor when unicorn-plant is grown in the presence of cotton. Leaves and stems of the unicorn-plant were inhibitory in the bioassay as described below on cotton growth by 31%, roots 27%, and pods 35%. In an attempt to isolate a fraction of the components that might be inhibitory, essential oil was selected. The plant has an objectionable odor and relatively high content of essential oil. This was isolated by steam distillation of the leaves, stems, pods, and roots of the unicorn-plant for 5 hr. The pot residue was acidified with 2 N HCl and steam distilled for 5 hrs. The condensates were treated with NaCl to saturation, extracted with ethyl ether, dried over anhydrous Na_2SO_4 and evaporated to dryness under N_2. The normal and HCL-treated essential oils were tested for their allelochemical activity against cotton seeds and were analyzed by CGC/MS/DA using the MS-50 set at a resolution of 2,000. The Kratos mass spectrometer was equipped with a Varian Model 3700 gas chromatograph containing an OV-1 fused silica column 50 m x 0.32 mm and the samples were analyzed using a 1.0 µl injection with the splitter turned off, the oven at 50°C, which was programmed at 2°C/min to 225°C and held for 60 min using a He Flow of 0.5 ml/min. The data were acquired and analyzed using a Kratos DS-55 data system. Identifications were based on the comparison of known with unknown spectra and visual interpretation of the fragmentation patterns.

The MS-50 profile of the essential oils required approximately 140 min and 3,500 spectra for each sample and the results indicated that between 150-220 compounds were detected. From this mixture the following unknown peaks were identified from the normal essential oil: vanillin (Fig. 1), perillyl acetate, Δ-cadinene (Fig. 2), α-bisabolol, traxolide, 2-methyl-1,4-naphthoquinone, 9, 10-anthracenedione-(1-hydroxy-2(or 3)-hydroxymethyl), hexadecanoic acid, with small amounts of 6-methyl-5-hepten-2-one and piperitenone with the remaining compounds being mostly terpenes, terpenoids, and hydrocarbons. In the HCl-treated steam distillate the identities confirmed were vanillin (Fig. 1), phenylethyl alcohol, *p*-cymen-9-ol, trimethylcyclohexanone, dodecanoic and hexadecanoic acids, and tentatively 2-ethylbenzimidazole.

The bioassays were conducted by dissolving the essential oil in methanol and placing 2 ml of this mixture on two layers of 9 cm Whatman No. 1 filter paper in a petri dish. After methanol evaporation, 10 cotton seeds were placed between the layers of filter paper, 3 ml of distilled water was added, and the covered dish placed in a Ziploc bag to prevent loss of volatiles. They were incubated at 29°C for 72 hrs, and then the measurements of the radicle length were made. Each sample was used to treat at least 40 seeds. Table 1 shows the results of the bioassay against cotton using unicorn-plant steam distillates. Table 2 shows the bioassay results of some pure compounds both as individuals and as synergistic mixtures (Table 3) on the radicle length of cotton.

This preliminary data presents some mass spectral data on the identification of the compounds present in the essential oils, their inhibitory action, and some effects of the individual compounds of the unicorn-plant on cotton radicle growth.

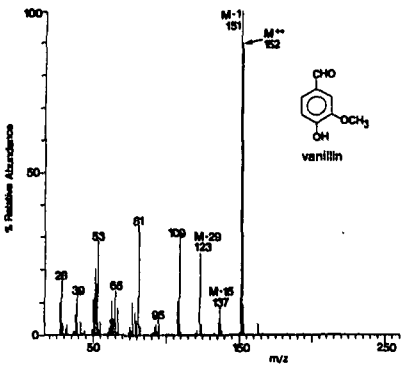

Figure 1. Mass Spectrum of Vanillin from the Essential Oil of the Unicorn-Plant.
Column background subtracted; Retention time: 39.3 min; Scan No. 980.

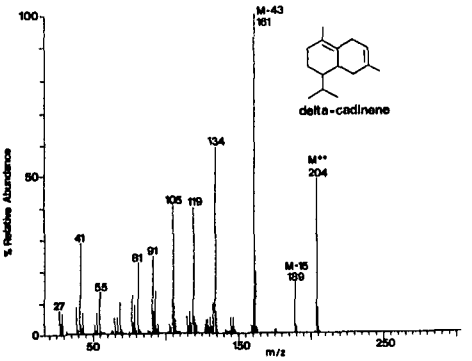

Figure 2. Mass Spectrum of Δ-Cadinene from the Essential Oil of the Unicorn-Plant.
Column background subtracted; Retention time: 79.33 min; Scan No. 1907.

Table 1. Inhibitory Effects of Steam Distillates of the Unicorn-Plant on Cotton Radicle Growth

Distillate	Concentration	Inhibition Toward Cotton
	mg/dish	%
Control	-	0
Steam Dist of		
Leaves	3.18	27 *
Roots	0.52	8
Pods	2.22	37 *
Acidic Steam Dist of		
Leaves	2.96	7
Pods	0.62	15 *
Roots	0.76	8

*Significantly different at a level of 95% confidence.

Table 2. Effect of Pure Compounds at 1 mMConcentration Identified in the Essential Oil of the Unicorn-Plant (UCP) on Cotton Radicle Growth

Compound	% Inhibition, 1 mM
Control	0
Vanillin	20 *
Phenyl ethyl alcohol	14
Δ-Cadinene	5
6-Methyl-5-hepten-2-one	17
UCP Essential Oil (Normal)[a]	9

[a]Assume an average MW of 200 for making the concentration.
*Significantly different at a level of 95% confidence.

Table 3. Effects of Pure Compounds at 2 mM Concentrationin a Synergistic Study from Unicorn-Plants on Cotton Radicle Growth

Control	% Inhibition
Control	0
Vanillin + Vanillin	18 *
Vanillin + Phenyl ethyl alcohol	12
Vanillin + Δ-Cadinene	18 *
Vanillin + 6-Methyl-5-hepten-2-one	12
Vanillin + UCP Essential Oil (normal)[a]	15

[a]Assume an average MW of 200 for making 2 mM concentration.
*Significantly different at a level of 95% confidence.

Presented at the 35th ASMS Conference on Mass Spectrometry and Allied Topics
May 24-29, 1987, Denver, CO

ANALYSIS OF CYCLODEXTRINS BY FAB/MS FAB/MS/MS AND THERMOSPRAY HPLC/MS:

R. D. Voyksner, F. P Williams, D. L. Koble, and H. H. Seltzman, Research Triangle Institute, P O. Box 12194, Research Triangle Park, NC 27709

Introduction

Cyclodextrins are cycloamyloses, composed of six, seven, or eight α-1,4 linked D-glucopyranose units in the form of a toroid with a hydrophobic interior. These compounds non-covalently bind other molecules within the cavity and can subsequently react with the bound molecule exhibiting many characteristics of enzymes. Cyclodextrins have been shown to scavenge acetylcholinesterase inhibitors such as the organophosphorous poison, soman, in vitro thus protecting this esterase In an effort to increase this soman scavenging activity, modified cyclodextrins were synthesized. This paper presents FAB/MS, FAB/MS/MS and thermospray HPLC/MS data used to

- verify structure and check purity
- differentiate between isomers
- identify products from reaction of cyclodextrins with soman

Experimental

The FAB samples were prepared by mixing 1 μL of a 1 μg/μL water solution containing the cyclodextrin with about an equal amount of matrix The FAB/MS analysis was performed on a VG ZAB-E operated at 10 kV accelerating potential with an Ion Tech FAB gun operated at 8 kV (1 mA) using xenon gas The instrument was normally scanned from m/z 300 to 2000 at 20 s/decade Both positive ion and negative ion spectra were acquired

FAB/MS/MS analysis was performed in a similar manner as above except the instrument was operated in the MIKES mode. The magnet was tuned to the $[M-H]^-$, $[M+H]^+$ or $[M+H-DEA]^+$ ion and helium collision gas was added to the second field free region to attenuate the main beam by 30-40%.

Thermospray HPLC/MS was used to analyze the product mixture from the reaction of BCD and soman. The HPLC was operated using a C_{18} 15 cm column with a solvent system consisting of 10% acetonitrile and 90% water (0.1 M ammonia acetate) at a flow of 1 mL/min. The Finnigan MAT thermospray interface was operated at a vaporizor temperature of 96°C and a source temperature of 280°C Negative ion detection was employed due to its superior sensitivity over positive ion detection for the cyclodextrins. The Finnigan MAT 4600 MS was scanned from 500-1800 (2 sec) during the analysis.

Results and Discussion

FAB/MS was used to analyze 31 synthetically modified cyclodextrins. The FAB/MS conditions were optimized for β-cyclodextrin (BCD) in an effort to obtain the best possible sensitivity and the most structural information. The sensitivity for BCD analyzed by FAB/MS decreased in the various matrices as follows: diethanolamine (DEA) > 50/50 dithioerythritol/dithiothreitol > 50/50 DEA/glycerol > thioglycerol > glycerol > triethanolamine The addition of salts, acidic or basic modifiers to the matrix did not improve the FAB/MS sensitivity. The various modified cyclodextrins analyzed using a DEA matrix exhibited $[M-H]^-$ and/or $[M+H+DEA]^+$ ions in positive ion detection and $[M-H]^-$ in negative ion detection. In some cases $[M+Na]^+$ ion were observed due to residual sodium in the sample or probe. Usually fragmentation was limited, and only observed in a fraction of the samples. The fragment ions detected were usually less than 10% relative intensity and mostly identified as [M-synthetic modifier + $H]^+$, and $[BCD+H]^+$ or in negative ion [M - synthetic modifier - $H]^-$ and $[BCD - H]^-$. Analyzing the cyclodextrins with another FAB matrix or modifier did not change the extent of fragmentation.

Thermospray HPLC/MS conditions were optimized on BCD. Thermospray proved most sensitive for BCD when ammonium acetate buffer (0 1 M) was present using negative ion detection. The negative ion spectra showed $[M-H]^-$ ions. Positive ion detection (about a factor of 5-10 less sensitive) showed $[M+H]^+$ and $[M+Na]^+$ ions Thermospray negative ion mass spectra of the chemically modified BCD only exhibited $[M-H]^-$ ions.

FAB/MS/MS analysis of the cyclodextrins proved successful in producing fragment ions indicative of the synthetic modification to the cyclodextrin. The fragment ion observed were from the cleavage of the synthetically introduced substituents from the glucopyranose ring and simple losses of water. The FAB/MS/MS spectra of the $[M-H]^-$ ion for C-2-$NH_2CH_2CH_2NHCH_2CH_2NH$-BCD and C-6-$NH_2CH_2CH_2NHCH_2CH_2NH$-BCD could be used to distinguish between these isomers. The ratios of ion intensities between the loss of water to the loss of the synthetic modification differed with substitution. The ratio of ion intensities for C-2 and C-6 linkages were 1.1 and 3.9, respectively.

The reaction of soman with BCD resulted in the formation of two new products of about equal quantity (based by HPLC/RI). The FAB/MS spectra of the reaction mixture indicated the presence of the soman-BCD complex (mw 1296). The FAB/MS spectra showed a $[M-H]^-$ ion at m/z 1295 and $[M+H+DEA]^+$ and $[M+Na]^+$ ions at m/z 1402 and 1319, respectively. The FAB/MS/MS spectrum of the $[M-H]^-$ ion exhibited fragment ions due to the loss of H_2O, $PO_2(CH_3)CH(CH_3)C(CH_3)_3$ and $PO_3(CH_3)CH(CH_3)C(CH_3)_3$. The FAB/MS analysis also indicated the presence of a diphosphonylated-BCD exhibiting an $[M+Na]^+$ ion at m/z 1481. Thermospray HPLC/MS analysis of the reaction mixture chromatographically separated the reaction products permitting acquisition of individual mass spectra (Figure 1). The spectra acquired were identical for the two products. No diphosphonylated-BCD was detected. Isomeric products are possible given the three reactive positions on BCD (2,3,6) and combinations with the four chiral forms of soman.

Acknowledgements

The authors thank J. Hines and P. Blau for developing the HPLC separation.

This research was supported by U. S. Army Medical Research and Development Command Contract No. DAMD17-84-C-4101 and by the Analytical and Chemical Science Unit of Research Triangle Institute.

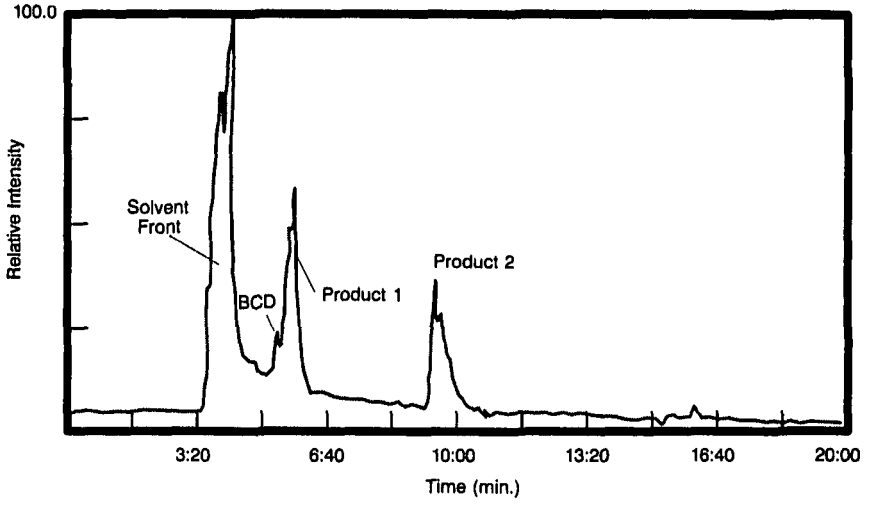

Figure 1. Thermospray HPLC/MS total ion current chromatogram showing the separation of the soman-BCD mixture.

Presented at the 35th ASMS Conference on Mass Spectrometry and Allied Topics
May 24-29, 1987, Denver, CO

DIRECT LIQUID INTRODUCTION (DLI) HIGH PERFORMANCE LIQUID CHROMATOGRAPHY-MASS SPECTROMETRY (HPLC-MS) AND THERMOSPRAY HPLC-MS OF BENZO(A)PYRENE (B(A)P) METABOLITES

J. Greaves and R. H. Bieri
Virginia Institute of Marine Science
College of William and Mary
Gloucester Point, Virginia 23062

The Elizabeth River, Virginia, is highly polluted, primarily with polynuclear aromatic hydrocarbons (PAH). Most of these compounds entered the river as a result of spillage and accidents at a wood preserving facility. A variety of diseases have been reported in fish from this river, including gill hyperplasia, fin erosion, integumental lesions, immune dysfunction, and cataracts. The diseases are not equally distributed among the different fish in the river with, for instance, the majority of cataracts occurring in the weakfish, Cynoscion regalis, and croaker, Micropongonias undulatus. These variations and the knowledge that the metabolites of PAH pass through highly reactive stages that may be mutagenic and carcinogenic has lead to the initiation of studies on PAH metabolites that are reported below. Vertebrate metabolism of PAH, of which B(a)P has been the most extensively investigated, involves hydroxylation, which may be at multiple sites and often associated with the formation of epoxides, followed by a conjugation stage which includes the formation of glucuronides and sulfates. The conjugates are then excreted, frequently in the bile.

Because of the lability of the compounds and the impracticality of analyzing conjugated metabolites by any other method, HPLC-MS has been investigated as an analytical method that will provide chromatographic separation and structural information. Both DLI and thermospray interfaces have been used for the analyses. For the DLI a 1 mm i.d. x 25 cm long C_{18} microbore HPLC column was used for all analyses. When thermospray was used samples were analyzed both with and without an HPLC column, the latter being a 4.6 mm i.d. x 10 cm long C_{18} column. Elution solvents were acetonitrile/water or acetonitrile/0.1M ammonium acetate. Solutions of B(a)P standard metabolites were prepared in methanol in the 100 ng-1 µg/µl range. The compounds used were: 1-, 3-, 7-, 9- and 11-hydroxy-benzo(a)pyrene; benzo(a)pyrene-trans-4,5-,-trans-7,8- and -trans-9,10-dihydrodiols, benzo(a)pyrene-r7,t8,t9,c10-, r7,t8,c9,t10-, r7,t8,c9,c10- and r7,t8,t9,t10-tetrahydrotetrols; benzo(a)pyrene-9-sulphate; benzo(a)pyrene-1, -3, -6, -7, and 9-glucuronides; and 7-glucuronyl-8-hydroxy-7,8-dihydrobenzo(a)pyrene.

Because of frequent clogging, the DLI interface was modified by enlarging the originally 5 µm aperture to 10 µm. In addition, a supplementary roughing pump was placed so as to act on the source block itself directly opposite the DLI probe. The vacuum port normally occupied by the gas chromatographic interface was used to accommodate this pump line. Increasing the diameter of the aperture in the DLI probe removed the clogging problem, frequently allowing continuous operation over an 8 h period. Replacing the cryogenic pump by a rotary vane pump that removed the vapor directly from the ionizing region of the source provided higher pumping speed within the ionizer and eliminated the need to keep a supply of liquid nitrogen.

DLI produced characteristic spectra for the non-conjugated metabolites when negative chemical ionization was used. Monohydroxy-B(a)P and B(a)P-dihydrodiols gave molecular or quasimolecular anions, but the B(a)P-tetrahydrotetrols were subject to more extensive fragmentation. Anions frequently encountered were m/z 302, m/z 286, m/z 284, m/z 268 and m/z 267. Fragmentation usually involved loss of water and/or hydrogen, and in certain instances was isomer specific; thus, for the B(a)P 4,5-dihydrodiol there was a fragment at m/z 254 that may have arisen from the elimination of a CO fragment from the ring after a quinone had been formed. In addition, for the B(a)P-tetrahydrotetrols if the hydroxy groups at the 8 and 9 positions were orientated in the same plane an intense ion occurred at m/z 258. The spectra changed as the source/desolvation temperature was raised (175°C-275°C, 25° increments) with increased fragmentation occurring. These changes in fragmentation caused major alterations in the spectra. For example, for B(a)P-trans-4,5-dihydrodiol the m/z 254 ion which is absent at 200°C is a dominant ion at 275°C, and for B(a)P-trans-9,10-dihydrodiol the molecular ion m/z 286 decreases from carrying almost 70% of the ion current at 200°C to 6% of the current at 275°C, with a double hydrogen abstraction apparently giving the m/z 284 ion which increases in an inverse relationship with m/z 286. 250°C was found to be a useful working temperature despite the reduced

molecular anions because below 225°C chromatographic integrity of some compounds was lost due to deposition on, and re-evaporation from, the source. The conjugated metabolites did not show molecular anions when DLI was used. Ionization efficiencies and therefore detection limits varied widely. For example, the 7,8- and 9,10-isomers ionization efficiencies were comparable while the 4,5-dihydrodiol had an ionization efficiency that was approximately ten times lower. For B(a)P-9,10-dihydrodiol and B(a)P-r7,t8,c9,t10-tetrahydrotetrol, the limits were less than 10 ng on column, using full scanning.

Initial experiments with spiked bile and DLI HPLC-MS have shown that B(a)P-9,10-dihydrodiol can be recovered from the bile. Spectra from such extracts have been obtained with only 12 ng of the metabolite being injected on column (assuming 100% recovery). The spectra obtained are not influenced by the biological matrix.

Because of the lack of molecular or other high mass ions for the conjugated metabolites, a thermospray HPLC-MS interface was investigated. This technique has allowed molecular or quasi-molecular anions to be observed for the B(a)P sulfates at m/z 347, for the mono-hydroxy glucuronides at m/z 444, and for 7-glucuronyl-8-hydroxy-7,8-dihydro-B(a)P at m/z 461. Considerable variability in the thermospray spectra has been encountered with molecular or quasi-molecular ions varying from being absent to occurring at 60% of the base peak intensity. A major fragment at m/z 267 is always noted. This ion corresponds to $[B(a)P-O]^-$. Experimental procedures such as source temperature, probe conditions and use of the discharge electrode have been varied systematically, but reproducible spectra have not been obtained. Until reliably reproducible spectra can be obtained, thermospray HPLC-MS will not be a useful technique for these compounds.

Presented at the 35th ASMS Conference on Mass Spectrometry and Allied Topics
May 24-29, 1987, Denver, CO

ANALYTICALLY USEFUL COLLISION REGIMES IN MS-MS

D A CATLOW, E CLAYTON, JOHN J MONAGHAN AND J H SCRIVENS
IMPERIAL CHEMICAL INDUSTRIES PLC, RUNCORN, HEATH, CHESHIRE, UK, WA7 4QD

The existing ad-hoc method of establishing collision conditions by increasing the collision gas pressure till the precursor ion intensity is reduced by some arbitrary figure appears to be a satisfactory procedure when operating at high collision energies (K.ev range). It did not appear to us to be a satisfactory way of achieving reproducible conditions when using instruments (QQQ/BEQQ/EBQQ etc) which operate at low collision energy. We, therefore, decided to carry out a systematic study of the effects of varying the parameters (collision energy, gas type and gas pressure) which determine the nature of the collision induced spectrum.

Because our instrument supplies an ICI corporate MS-MS service, we examine samples of wide-ranging chemical and biological origins. Our main aim in carrying out this work, therefore, was to establish for different chemical classes and different ionisation methods, sets of collision conditions which provided us with the maximum amount of analytically useful information. Thus when considering an EI molecular ion of any compound, we would like to obtain a daughter ion spectrum of that molecular ion identical to the normal EI spectrum, or at least similar enough to be recognised by a library search procedure. In addition we hoped, for every class of compound studied, to find a set of "robust" conditions where the collision induced spectrum was insensitive to slight variation of the collision energy and gas pressure. Three examples are described in this paper

The parameters measured in a BEQQ type instrument (VG ZAB-HSQ) were

Gas : Argon, xenon, helium, nitrogen and others.

Pressure : 0-10 mtorr (precisely measured using an Edwards ION 7 gauge).

Energy : 0-500 ev.

Ionisation : EI, CI, FAB.

while the chemical classes studied included aldehydes, amides, amines, esters, ethers, hydrocarbons, oximes, peptides, phends and sulphones.

The EI spectrum of a representative aliphatic hydrocarbon, tetradecane, shows a weak molecular ion, abundant low mass alkyl ions and very weak high mass alkyl ions. To identify it from the daughter ion spectrum of its molecular ion at m/z 198, we need to see the same features, as in the EI spectrum. It should be noted, however, that neither an experienced mass spectroscopist nor a library search procedure uses every ion in an EI spectrum to identify a compound. Thus the absence of several EI fragments from the collision induced spectrum should not prevent identification.

This proved to be the case for tetradecane where regardless (almost) of the gas used, daughter ion spectra identified as tetradecane by library searching were found over a wide energy range at low pressure but this energy window narrowed rapidly with increasing gas pressure.

The EI spectrum of butyl salicylate is characterised by a molecular ion at m/z 194, loss of butene to m/z 138, loss of butanol to m/z 120 followed by successive losses of C=O to m/z 92 and m/z 64, and alkyl ions at m/z 41/43/57. We studied these features in the daughter ion spectra of m/z 194 and found that we needed to operate at

gas pressure $\leq$ 2 mtorr (argon or xenon)
collision energy $\geq$ 40 ev (argon or xenon),

Octylbenzene shows an EI molecular ion at m/z 190 a characteristic m/z 91/92 ratio, alkyl ions and ions formed by cleavage of the alkyl chain (m/z 105, m/z 133). To reproduce these features in the daughter ion spectrum of m/z 190 pushes us again towards low pressure $\leq$ 1 mtorr and high energy ($\sim$ 100 ev). Comparison of the EI spectrum with a daughter ion spectrum of m/z 190 obtained using

gas pressure 0.5 mtorr xenon
collision energy 100 ev

suggests that a better fit would be obtained by reducing the m/z 190 abundance and this can easily be achieved by some fine tuning of the collision conditions, eg a slight increase in gas pressure, use of a heavier collision gas etc.

We have found that, for our analytical purposes, the most appropriate collision regimes vary considerably from one class of compound to another. In fact it is not uncommon to find that one collision regime cannot provide all of the chemical information we require. We have found this to be particularly so in the case of the FAB-MS-MS of peptides where one set of ions yields the high mass sequence ions and another is needed to pick up the low mass ions.

Our work, involving an exhaustive study of the effect on CID spectra of varying gas type, gas pressure and collision energy, that for the chemical classes studied, robust, reproductible and analytically useful collision regimes can be obtained. In addition, our results indicate that the CID spectrum of the EI molecular ion of an individual component in a complex mixture can, by correct choice of collision condition, be made to reproduce the EI spectrum of that component.

Presented at the 35th ASMS Conference on Mass Spectrometry and Allied Topics
May 24-29, 1987, Denver, CO

THE DETERMINATION OF 1,3 SULTONES IN ANIONIC SURFACTANTS BY TANDEM MASS SPECTROMETRY

T G BLEASE, D A CATLOW, E CLAYTON, J J MONAGHAN AND J H SCRIVENS
IMPERIAL CHEMICAL INDUSTRIES PLC, RUNCORN HEATH, CHESHIRE, UK, WA7 4QD

INTRODUCTION

Sultones, which are cyclic esters of hydroxy sulphonic acids, are skin sensitisers and, as such, undesirable components in detergent formulations. These sultones may be formed from alpha olefin sulphonates under bleaching conditions. The detection of these compounds at ppm levels in detergent formulations is a difficult analytical problem. Tandem mass spectrometric techniques have been used to obtain the selectivity required for this analysis with an objective of establishing ppm detection levels with no sample pretreatment.

The anionic detergent system employed in this study was a complex mixture of alcohol ether sulphates of general formulae, typical of many commercial formulations

$RO(CH_2CH_2O)_pSO_3^-Na^+$ $\qquad$ $R = C_nH_{2n+1}$ (n = 13, 15)

p is a distribution with an average value of 3.

The sultone standards used were 1-tetradecene 1,3 sultone [A] and 2-chloro tetradecane 1,3 sultone [B].

A

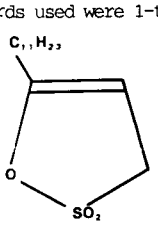

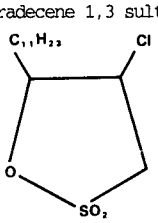

B

Existing methods of analysis involve a number of analytical steps: extraction, followed in many cases by a concentration stage and various methods of separation and detection. They are all working near the limits of their specificity and interference is a common concern.

EXPERIMENTAL DETAILS

Tandem Mass Spectrometry

All experiments were carried out using a VG ZAB QQ hybrid mass spectrometer of BEQQ geometry. The collision conditions employed were 25 eV collision energy and Argon at 1.2m Torr as the collision gas. All samples were introduced via a solids probe ramped from ambient to ~250°C. Negative chemical ionisation employing NH_3 was used as an ionisation method since

a) The sultones gave intense M^- ions together with a peak at m/z 80. Chloro sultones give a strong dehydrochlorination peak at $(M-HCl)^-$

b) The major components of the detergent matrix would not be expected to ionise under these conditions.

Daughter ion spectra of m/z 274 obtained from the C14, 1,3 sultone and the chloro C14 1,3 sultone showed the common structure of this ion. Of particular interest are the m/z 80 ion, SO_3^-, and the 133 ion which is given by

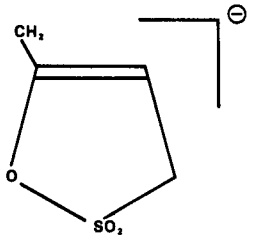

Daughter ion spectra of m/z 274 (at a precursor ion resolution of ~2000) in matrix samples showed that, for a target sultone such as A, the required sensitivity and specificity could easily be obtained.

To obtain a general method, it was recognised that the presence of the m/z 133 ion should be common to all 1,3 sultones and therefore experiments were carried out to obtain parent ion spectra of this ion with a view to establishing such a method. A parent ion spectrum of m/z 133 for the surfactant spiked with 10ppm of the C14 1,3 sultone is shown. Based on the signal to noise level a sub ppm detection limit could be expected.

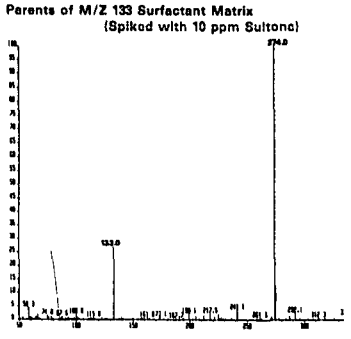

Preliminary work has also shown that parent ion scanning of m/z 80, SO_3^-, promises to produce an analytical method specific for both 1,3 and 1,4 sultones.

CONCLUSIONS

1 The combination of a selective ionisation method (-ve CI) and daughter ion scans obtained using tandem mass spectrometric techniques provides a selective and sensitive method for determining known sultones in anionic surfactant matrices. Selective reaction monitoring could give even lower detection levels (if required).

2 Parent ion scans of m/z 133 provides a general method for screening for 1,3 sultones in these surfactants. Little interference is observed and sub ppm detection levels have been shown. The use of parent ion scans of m/z 80 should enable us to make this a general method for both 1,3 and 1,4 sultones.

3 The method involves no sample preparation, is extremely fast (no chromatographic separation is involved) and provides the sensitivity and selectivity required.

Presented at the 35th ASMS Conference on Mass Spectrometry and Allied Topics
May 24-29, 1987, Denver, CO

"Internal Energy and Site of Protonation - Variables Which Affect Low Energy Collisional Activation MS/MS Analysis"

Boehringer Ingelheim Pharmaceuticals, Inc.
90 East Ridge, P.O. Box 368
Ridgefield, Connecticut 06877

Gordon Hansen, Frank Hatch, Victor Fuchs, Kurt Freter

The systematic classification of the types of fragmentation reactions observed for even electron (EE) ions upon collisional activation dissociation (CAD) experiments have been reported by F. W. McLafferty[1] and R. G. Cooks et al.[2]. These basic fragmentation pathways can be utilized for structure elucidation studies along with the assumption that CAD spectra are solely dependent on ion structure and are independent on parent ion internal energy. High energy (>1 kev) CAD spectra are generally reported to be independent of presursor ion internal energy[3]. However, in two studies, charge stripping CAD spectra were found to be strongly dependent on ion internal energy and possibly angular momentum[4,5].

In contrast, low energy (5-100 ev) CAD spectra may exhibit considerable dependence on ion internal energy resulting from the method of ion formation [6,7,8]. Our previous results suggested that chemical ionization reagent gas selection source pressure and repeller voltage can contribute to ion internal energy and affect daughter ion spectra. We have extended our initial studies with an investigation of the high energy and low energy CAD mass spectra of a series of multifunction compounds, 1,3-Dihydro-[4-[4-(3-indolyl) piperidino]alkyl]-2H-benzimidazolones, of the general structure I.

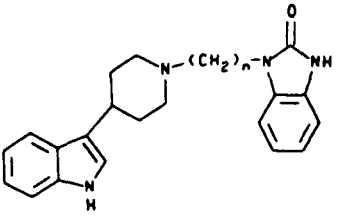

Results and Discussion

All experiments were carried out on a Kratos MS80-RFAQQ hybrid mass spectrometer. High energy CAD spectra were obtained at 4 KV (Ecm ≈ 40 ev) with a B/E linked scan, helium collision gas and 30% beam attenuation. Low energy CAD spectra were obtained at 30 ev (Ecm ≈ 4 ev) in the hybrid mode with argon collision gas and 30% beam attenuation. CH_4, i-C_4H_{10} and NH_3 CIMS reagent gas systems (0.5 torr) were employed to produce MH^+ species of varying internal energy and possible variations in initial "site of protonation". All samples were introduced by direct probe.

The high energy B/E daughter ion scan (a) and the low energy QQ daughter ion scans obtained with i-C_4H_{10} (b) and NH_3 (c) for the n=6 analogue are given in Figure 1. The B/E scan produces fragments that can be interpreted as the products of a "four-centered" reaction mechanism originating at the piperidino nitrogen (a) or the benzimidozolone nitrogen (b), Figure 2. The simple cleavage reactions observed are expected for high energy CAD and were independent of the CI reagent gas employed for ionization, i.e. precursor ion internal energy. The high energy CAD spectra were very similar to the 70 ev electron impact mass spectra suggesting that the lowest ionization potential site in a multifunctional compound may direct the most intense fragmentation pathways. As the methylene chain length is increased (n=2,4,6) the intensity of the charge migration product,* in Figure 2, drops to zero after being the base peak for n=2 and 4. This reflects a steric requirement for the formation of a stabilized benzimidozolone ion and the facile loss of neutral secondary amine from an EE ion dependent on product ion stability.

The low energy CAD spectra are significantly different from the high energy B/E scan spectra and they exhibit a strong dependency on ion internal energy resulting from the exothermicity of proton transfer reaction. For values of n=2 and 4, the charge migration ion * Figure 2, dominates the low energy CA spectra for all 3 CI reagent gases studied. An intense alpha-cleavage product (m/z=213) was observed for the CH_4 and i-C_4H_{10} systems but not for NH_3. The base peak in low energy CAD spectra of the n=6 analogue can best be explained as a rearrangement product (Figure 3.II) resulting from protonation on the indole nitrogen and formation of the indolium ion followed by charge migration and loss of neutral indole. This mechanism is supported by an experiment carried out with a D^+ ionization system (C_6D_6 and CH_4) and CAD MS/MS analysis of the MD^+ parent. The deuterium was not incorporated in the m/z=300 ion which would be expected if D^+ transfer occurred at the piperidino nitrogen.

1. F. W. McLafferty, Organic Mass Spectrom. 15, 1980, 114.
2. M. Sigaby, R. Day, R. Cooks, Organic Mass Spectrom. 14, 1979, 273 and 556.
3. M. Kim, F. McLafferty, JACS, 100, 1978, 3279.
4. M. Jarrold, A. Illies, N. Kirchner, M. Bowers, Organic Mass Spectrom., 18, 1983, 388.
5. A. Harrison, Organic Mass Spectrom., 22, 1987, 186.
6. S. Nacson, A. Harrison, W. Davidson, Organic Mass Spectrom. 6, 1986, pg 317.
7. H.I. Kenttamaa, Organic Mass Spectrom. 20, 1985, pg 703.
8. G. Hansen, F. Hatch, 34th ASMS Conf. 1986, pg 85.

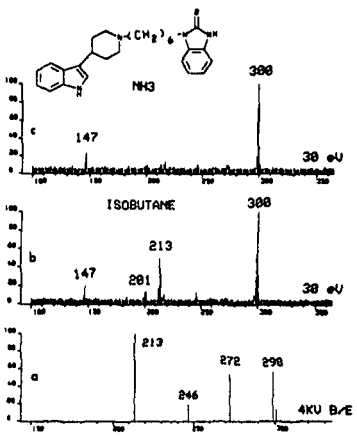

FIG. 1

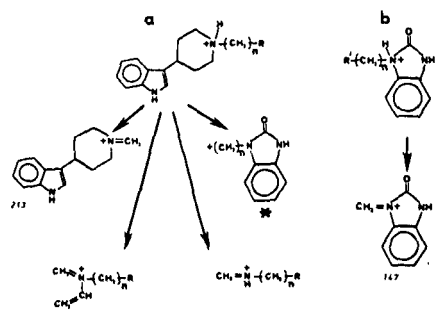

FIG. 2

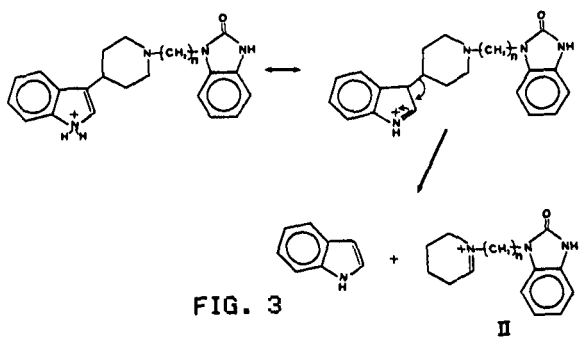

FIG. 3

Presented at the 35th ASMS Conference on Mass Spectrometry and Allied Topics
May 24-29, 1987, Denver, CO

COMPARISON OF ION STRUCTURES USING THREE METHODS FOR COLLISION-INDUCED DISSOCIATION*

J.M.Curtis, A.G.Brenton and J.H.Beynon
University College,Swansea SA2 8PP, Wales, U.K.

R.K.Boyd
Atlantic Research Laboratory, National Research Council,
1411 Oxford Street, Halifax, N.S., Canada B3H 3Z1.

Use of C.I.D. spectra to characterise and compare ion structures is now well established. Any such method should possess at least the following properties:
(i) spectra should be reproducible, to within useful limits, on a given instrument (both on a given day and on different occasions);
(ii) inter-laboratory comparability of spectra, obtained using nominally identical experimental conditions, should be similarly acceptable;
(iii) the spectra should display the maximum possible discrimination between ions of similar structures.

The present work was intended to investigate point (iii), and thus inevitably became involved in point (i); no attempt at point (ii) was made here. The $C_5H_8^{+\cdot}$ ions were chosen as a suitable test-case, since previous work has shown that some isomers are readily distinguished via CID spectra, while others are not (see (1) for an excellent account). In addition, there remains extant in the literature (2) a question as to the identity of the $C_5H_8^{+\cdot}$ fragment ions formed by EI of limonene, and this provides an example of the more important applications of such techniques.

The three techniques investigated here are;
(a) CID at keV energies (MIKES technique);
(b) energy-resolved CID (4-150 eV) in a RF-only quadrupole collision cell (ERCID);
(c) dissociative charge-stripping spectra, obtained free of interferences from processes corresponding to (a) by subjecting the product dications to a second collision to effect electron capture (3) (DCS/EC);

The instruments used were a VG Analytical ZAB-Q hybrid (4), for techniques (a) and (b), and a VG Analytical ZAB-2F modified (5) by addition of a second electric sector and used for techniques (a) and (c). Technique (a) (MIKES) performed well with respect to point (i) above, but displayed limited structural discrimination (point (iii)). The ERCID spectra displayed acceptable reproducibility on a given day, but spectra obtained on different days showed disappointingly large variability while still retaining such qualitative distinctions as were found. The DCS/EC technique was anticipated to prove irreproducible (point (i)), but in fact the performance in this regard was comparable with that of MIKES provided reasonable precautions were taken.

A notable feature of this investigation was the very large volume of data generated. In order to reduce this to manageable levels while comparing the structure discrimination characteristics of the techniques, the library comparison algorithms of a GC/MS datasystem (Finnigan-MAT Incos) were exploited. The figure shows the results of comparing CID spectra of $C_5H_8^{+\cdot}$ isomers with that from the fragment ion of limonene. The superior discrimination of the DCS/EC technique thus becomes apparent. A full account of this work will be published shortly.

(1) Dass et al., Org.Mass Spectrom. 21 (1986) 741.
(2) Harris et al., Org.Mass Spectrom. 14 (1979) 265.
(3) Kingston et al., Org.Mass Spectrom. 20 (1985) 546.
(4) Harrison et al., I.J.M.S.I.P. 74 (1986) 13.
(5) Rabrenovic et al., I.J.M.S.I.P. 52 (1983) 175.

*NRCC No. 27658

Presented at the 35th ASMS Conference on Mass Spectrometry and Allied Topics
May 24-29, 1987, Denver, CO

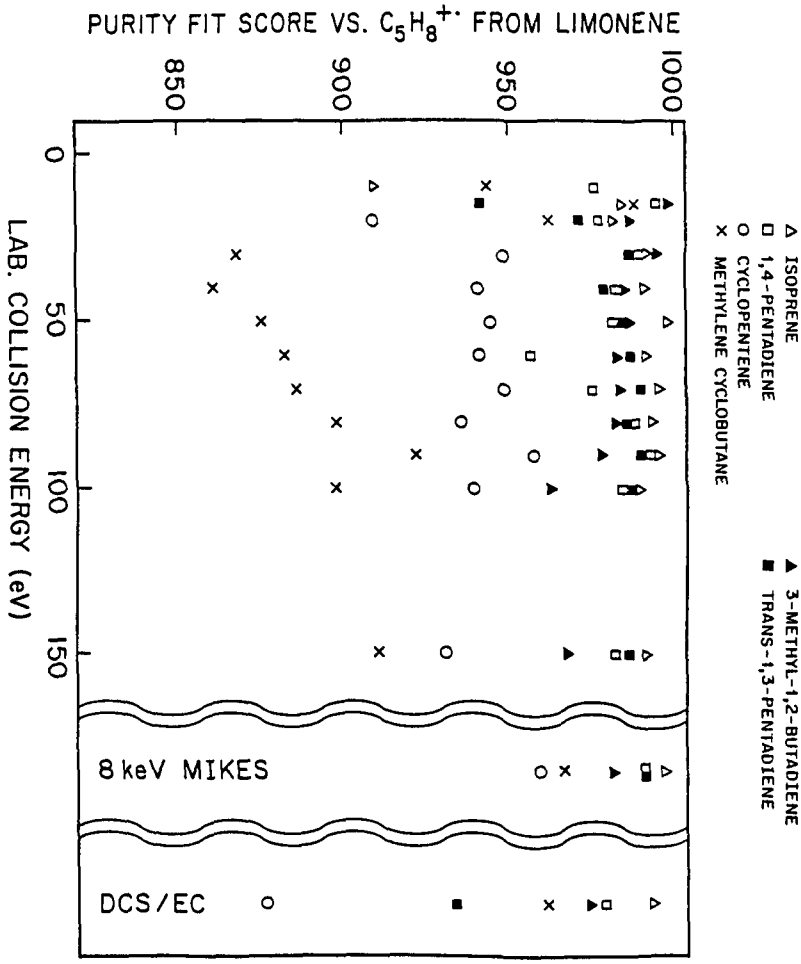

Presented at the 35th ASMS Conference on Mass Spectrometry and Allied Topics
May 24-29, 1987, Denver, CO

PREIONIZATION EFFECTS IN MASS SPECTROMETRY OF AZOXYBENZENES*

D.S.Waddell and N.J.Bunce
Dept. of Chemistry and Biochemistry,
University of Guelph, Guelph, Ontario, Canada N1G 2W1.

R.K.Boyd
Atlantic Research Laboratory, National Research Council,
1411 Oxford Street, Halifax, N.S., Canada B3H 3Z1

A routine purity check by GC/MS, of some synthetic substituted azoxybenzenes (see below), led to the conclusion that the compounds were

AZOXYBENZENE 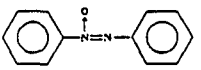

in fact the corresponding azobenzenes (desoxy-azobenzene). This conclusion was at variance with NMR data, which clearly indicated distinguishable rings. This discrepancy led to a thorough investigation of the mass spectrometric behaviour of these compounds, as an extension of the established work of Bowie et al.(1). It was found that the intensity ratio of the ions at m/z 198 ($M^{+\cdot}$) and m/z 182 ($(M-O)^{+\cdot}$, same as molecular ion of azobenzene) was a strong function of source temperature, source history and sample level (Fig.1). The conditions used in the original GC/MS analyses were such that the ion at m/z 182 predominated.

This ion at m/z 182 was observed by Bowie et al.(1), who confirmed its atomic composition to be $(M-O)^{+\cdot}$ by accurate mass measurement, but did not comment further on this unusual fragmentation. We have confirmed the atomic composition, and investigated the origins of this ion by tandem mass spectrometry (VG Analytical ZAB-Q hybrid instrument (2)). No signal corresponding to formation of fragment ions of m/z 182 could be observed, under any experimental conditions, when $M^{+\cdot}$ from azoxybenzene was induced to dissociate. The conditions included 8 keV collisions (MIKES technique) with helium and other collision gases, as well as collisions with a similar range of target gases (including xenon) in the collision quadrupole at energies in the range 5-200 eV. On the other hand, the C.I.D. spectra of the ion at m/z 182 were indistinguishable from the corresponding spectra of the molecular ion of azobenzene.

These observations can be rationalised on the basis of reduction of the azoxybenzene on active sites of the ion source prior to electron ionisation. The effect of sample size (Fig.1) reflects saturation of the available active sites. This behaviour is similar to that observed for EI of nitronaphthalene by Beynon et al.(3), who showed that the $(M-30)^{+}$ ion was the molecular ion of aminonaphthalene, formed in such a preionisation reduction. Subsequently it has been repeatedly shown (4-8) that aromatic nitro compounds undergo even more extensive reduction under CI conditions. We have extended this conclusion to the azoxybenzenes, using techniques of GC/MS (Fig.2) and tandem mass spectrometry. A full account of this work has been submitted for publication.

(1) Bowie et al., Aust.J.Chem. 20 (1967) 1601.
(2) Harrison et al.,I.J.M.S.I.P. 74 (1986) 13.
(3) Beynon et al.,I.J.M.S.I.P. 2 (1969) 291.
(4) Maquestiau et al.,Org.Mass Spectrom. 14 (1979) 117.
(5) Brophy et al.,Org.Mass Spectrom. 14 (1979) 201.
(6) Harrison et al.,Org.Mass Spectrom. 15 (1980) 284.
(7) Yinon et al.,Org.Mass Spectrom. 16 (1981) 264.
(8) Quilliam et al.,Spectrosc.Int.J. 3 (1984) 33.

* NRCC No. 27660

Presented at the 35th ASMS Conference on Mass Spectrometry and Allied Topics
May 24-29, 1987, Denver, CO

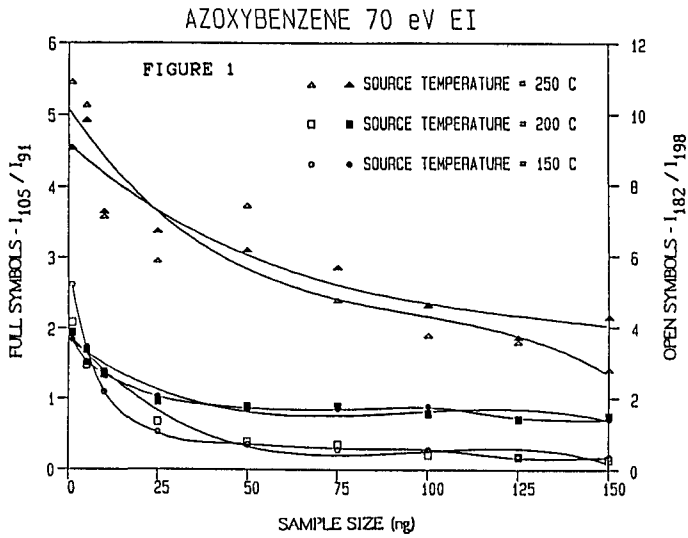

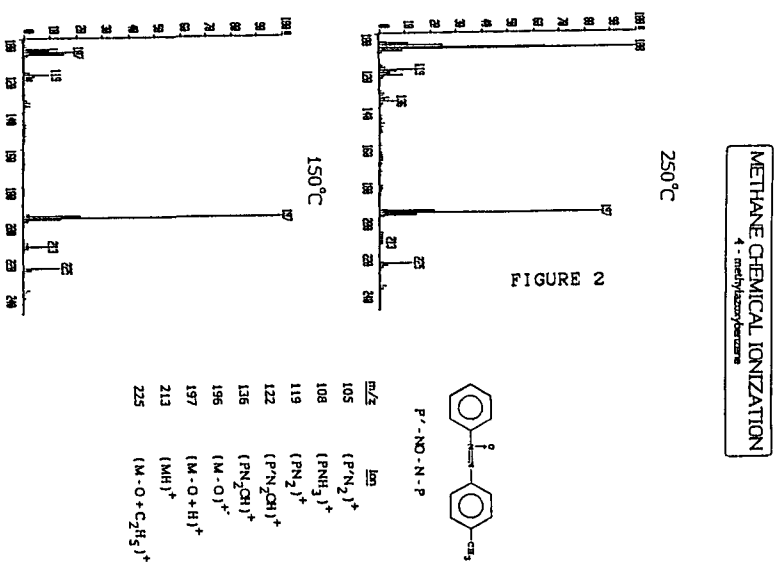

Presented at the 35th ASMS Conference on Mass Spectrometry and Allied Topics
May 24-29, 1987, Denver, CO

Anomalous Energy Release from a Distonic $C_3H_6O^{+\cdot}$ Ion.

C.E. Hudson,[a] D.J. McAdoo[a] and J.C. Traeger[b]
[a]Marine Biomedical Institute, University of Texas Medical Branch, Galveston, Texas 77550
[b]Department of Chemistry, La Trobe University, Bundoora, Victoria 3083, Australia

Distonic ions of the type I have frequently been proposed as intermediates in the fragmentation of $C_nH_{2n}O^{+\cdot}$ and $C_nH_{2n}O_2^{+\cdot}$ ions.

$$\dot{C}H_2CH_2CH{=}\overset{+}{O}H$$

I

It is desirable to directly characterize such intermediates to enhance our understanding of the relation between structure and properties and to provide a check on the proposed mechanisms. We have generated I from 3-alkoxypropanals.

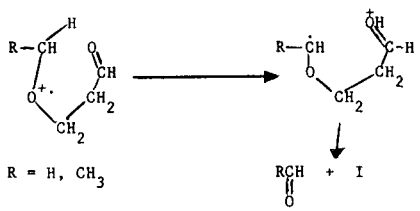

The metastable ion spectrum of I shows only an H· loss. The CAD spectrum, also dominated by H· loss, is similar to that of $CH_3CHCH{=}OH$ (II), except that I gives a larger peak at m/z 43 (12%) vs 2% from II.

AE (I) from $CH_3OCH_2CH_2CHO$[a]	948 ± 1.0 kJ/mole
Estimated internal thermal energy of precursor	15 ± 10
Energy difference between products and precursor	963 ± 11
Estimated H_f of precursor	-319 ± 5
$\Delta H°_f$ (products)	644 ± 16
$\Delta H°_f$ (CH_2O)	-(-113)± 1
$\Delta H°_f$ ($CH_2CH_2CH{=}OH$)	757 ± 17
compare ΔH_f (II)[2]	661
$\Delta H°_f$ (I)	757 ± 17
AE (58→57) -AE (58)[b]	108 ± 8
Transition state energy for fragmentation of I	865 ± 25
AE (58→57) from $CH_2{=}CHCH_2OH$ (III)[b]	1009 ± 5
ΔH_f ($CH_2{=}CHCH_2OH$)	-148
Transition state energy for fragmentation of III	861 ± 5

a. Photoionization
b. Electron impact, first field free region of MS9

It is very much a surprise to find then that the energy released in the fragmentation of I is 0.66 ± 0.09 kJ/mole while it is 15 ± 1 kJ/mole for II and III. The CAD spectra of the products of the 58→57 metastable transitions from I, II and III are very similar to each other and to an authentic spectrum of the propanoyl ion from $(C_2H_5)_2CO$. All three spectra differ from the CAD spectrum of protonated acrolein formed in a chemical ionization source by their higher intensity of m/z 42, lower intensity of m/z 55 and 56, and much lower intensity of m/z 31. The difference in energy release does not seem to be due to either a difference in reaction threshold energies or daughter ion structure. The difference cannot be due to different reacting configurations. To produce $C_2H_5CO^+$ +

H·, only two reacting configurations are possible namely $C_2H_5CHO^{+\cdot}$ and $C_2H_5C{=}OH$. However, both of these ions fragment by H. loss with $T_{\frac{1}{2}}$ = 15-16 kJ/mole.

In previous work we established that the m/z 42 peak in the CAD spectrum of $C_2H_5CO^+$ represents the loss of the terminal methyl.[2] Deuterium located in the methyl group is lost upon collision while deuterium in the methylene is retained in this CAD daughter. The ratio of 42 to 43 in monodeuterated ions thus indicate the proportion having D in the methyl and methylene. This ratio is as follows in the 59⟶58 metastable transition of O deuterated precursors: $CH_3\dot{C}HCH{=}\overset{+}{O}D$ 5.7, $C_2H_5C{=}OD$ 5.0, $CH_2{=}CHCH_2OD$ 6.0, $CH_2CH_2CH{=}OD$ 3.2. Thus all the above ions have deuterium content in their methyl groups well above the statistical 1.5. However, these data do not sample those ions losing the hydrogen originally attached to oxygen, a process that will later be shown to be critical. The most economical explanation of this is that the H on O is transfered to the terminal carbon in the step immediately preceeding fragmentation:

$$C_2H_5\dot{C}{=}\overset{+}{O}D \longrightarrow CH_3\dot{C}HCH{=}\overset{+}{O}D \longrightarrow \dot{C}H_2CH_2CH{=}\overset{+}{O}D \longrightarrow CH_2DCH_2CH{=}O^{+\cdot} \longrightarrow CH_2DCH_2C{\equiv}O^+ \;+\; H^\bullet$$

Since all the ions pass through I, it is hard to understand why I should show such a much smaller release of energy.

The resolution of this dilemma is not completely clear at present, but the spectra of deuterated forms of I in spectrometers sampling decomposition at differing ion lifetimes provide important clues.

D/H Loss Ratios

Spectrometer	$\dot{C}D_2CH_2CH{=}\overset{+}{O}H$	$\dot{C}H_2CD_2CH{=}\overset{+}{O}H$	$\dot{C}H_2CH_2CD{=}OH^+$	$\dot{C}H_2CH_2CH{=}\overset{+}{O}D$
DuPont 21-491[a]	0.32	0.30	0.16	0.05
MS 50 TA[b]	0.09	0.01	0.008	1.09

a. First field free region b. Third field free region

The results are so radically different that the ratio for $CH_2CH_2CH{=}OD$ was determined in the first field free region of the MS 50 TA. The result is 0.03, completely consistent with the DuPont first field free region results which are similar to results for other $C_3H_6O^{+\cdot}$ ions that have been examined.[3,4] The energy release measurements can be made conveniently only in the third field free region of the MS 50 TA. The results for I-O-d show that $T_{\frac{1}{2}}$ for the H · loss process is 15.4 kJ/mole which is the same as the other $C_3H_6O^{+\cdot}$ ions. The anomalous result is from the D· loss with $T_{\frac{1}{2}}$ = 0.71 kJ/mole. The CAD spectrum of this daughter, although quite noisy, is clearly more similar to the $C_2H_5CO^+$ spectrum than to the $CH_2{=}CHCH{=}\overset{+}{O}H$ spectrum.

The low energy release from I then stems from a process that is prominent only at long reaction times involving loss of the hydrogen originally on oxygen, a process less important in the other $C_3H_6O^{+\cdot}$ decompositions. Both decompositions produce $C_2H_5CO^+$ as the daughter.

1. J.L. Holmes and F.P. Lossing, J. Am. Chem. Soc., 102, 1591-1595 (1980).
2. D.J. McAdoo and C.E. Hudson, Org. Mass Spectrom., 18, 466-473 (1983).
3. D.J. McAdoo and D.N. Witiak, J. Chem. Soc. Perkin II, 770-773 (1981).
4. F. Turecek, V. Hanus and T. Gaumann, Int. J. Mass Spectrom. Ion Proc., 69, 217-231 (1986).

Presented at the 35th ASMS Conference on Mass Spectrometry and Allied Topics
May 24-29, 1987, Denver, CO

Study of the Radiative Relaxation Rates of Halobenzene Radical Cations

Hun Young So and Robert C. Dunbar, Case western Reserve University, Cleveland, Ohio 44106

Under the low enough pressure for collisions to be infrequent, a vibrationally excited molecule should relax toward ambient temperature by infrared fluorescence. The relaxation rates of various ions have been reported using the techniques of pressure variation,two color laser, pulsed laser, and chopped laser. In this work,the sequential two photon dissociation observed with cations having high fluorescence quantum yield will be described and the radiative relaxation rates of the ions measured by using the chopper laser technique will be discussed. Among the nine halobenzene cations only fluorobenzene, 1,3,5-trifluorobenzene, 1,3,5-trichlorobenzene and hexafluorobenzene gave enough observable two photon dissociation to carry out the chopper rate dependence measurement.

Since the first observation of the sequential two-photon dissociation by Freiser and Beauchamp, most sequential photodissociation studies have concentrated on cations having no radiative relaxation from their excited electronic states. The efficiency of the sequential two photon process is expected to be lower with cations having high fluorescence quantum yield. The reported unity fluorescence quantum yield of the first excited state of hexafluorobenzene cation implies that the sequential two photon absorption of this ion should not occur.

Maier and others have explored wide variety of halobenzene ions to detect the emission spectrum with electron impact excitation. Sixteen halobenzene cations are known so far which relax from the lowest excited electronic states through the fluorescence channel. The reason why some of the ions did not yield enough dissociation in the present experiments can be found from the transition energies between their two low lying electronic states. Spectroscopic information on the 0-0 electronic transition energies of these cations can be obtained from the ionization energies measured by photoelectron spectroscopy and gas phase emission data. These are summarized in Table 1 with the wavelength of the 0-0 emission bands observed from emission spectra. By comparing the energy gap between the ground and the first excited states of the cations, it is clear that the ions which did not yield observable dissociation have a larger energy gap between the $\tilde{X}$ and $\tilde{B}$ state than the irradiating photon energy given by our laser source. To observe the two photon dissociation within the time scale of seconds, with less than 1 W of laser power, an ion must have a strong allowed $\tilde{X}$-$\tilde{B}$ transition at the given laser wavelength. The failure to observe photodissociation with tetra- and pentafluorobenzene ions provide a confirmation that the observed photodissociation truly goes through the electronic excited state, which is not necessary in a simultaneous two photon process.

Though the $\tilde{X}$ to $\tilde{B}$ transition energy of 1,3,5-$C_6H_3F_3^+$ cation is slightly higher than the irradiating laser energy the observed extent of dissociation was enough to carry out the measurement of the chopper rate dependence. This is considered due to rotational hot band transitions from the rotational manifold of the ground electronic state, though the involvement of vibrationally hot ions unrelaxed after the electron impact formation of the ions cannot be totally excluded.

Maier, Leach and others have measured the fluorescence quantum yields of the hexafluorobenzene cation and 1,3,5-trifluorobenzene cations by the photoelectron-photon and the photoion-photon coincidence techniques. According to one of the measurements, the two ions have unity fluorescence quantum yields within their B electronic state manifold where the ions were pumped in the present experiment. The observation of the sequential two photon dissociation for these ions through states of unity fluorescence quantum yields is contradictory, because fluorescence deexcitation of the excited state will block the subsequent internal conversion processes following the first photon excitation. The reported quantum yield must be lower than unity value reported from the coincidence measurements. Even one percent of internal conversion would not be contradictory to the observation of photodissociation with ions of high fluorescence quamtum yields.

The radiative dissipation rates of the internal energy by photoexcited halobenzene cations are listed in Table 1. Figure 1 represents a typical observed chopper rate dependence of an ion. The first noticeable trend among those ions is that the relaxation rates of fluorobenzene ions are faster than the chlorobenzene ions with the same number of substituted halogens. This may correlate with the fact that there is increasing charge localization on the ring going from chlorobenzene ion to fluorobenzene ion. The HOMO of chlorobenzene molecule has substantial charge density on the chlorine as well as the ring carbons, while there is very little contribution of the fluorine atomic orbital in the HOMO of the

fluorobezene molecule. Thus ionizing chlorobenzene is expected to result in less charge localization than fluorobenzene. This large charge separation of the fluorobenzene cations is considered to be responsible for its faster relaxation compared with the chlorinated analog. The trihalogenated cations show 3 or 4 times greater relaxation rates than the monohalogenated cations. This result suggests that the C-X modes give good radiative cooling.

The relaxation rate of hexafluorobenzene cation appeared to be slower than expected from the rates of mono- and trihalobenzene cations. The surprisingly low relaxation rate of the hexafluorobenzene cation may reflect different infrared radiative properties, or may arise from a difference in dissociation thermochemistry. This rate is apparently faster that that of benzene, chlorobenzene or fluorobenzene cations but smaller than the trifluorobenzene cation.

Reference

R. C. Dunbar, J.-H. Chen, H. Y. So and B. Asamoto; J. Chem. Phys., 86, 2081 (1987)

Table 1. The difference of ionization energies of X and B states of halobenzene radical cations from PES and the wavelength of 0-0 transition bands from emission spectra. The observed radiative relaxation rates are listed on last column

Cations	δE(X-B), eV	λ_0, nm	Φ_F	Photon Energy, eV	Relaxation Rate, s^{-1}
$C_6H_5Cl^{\cdot+}$	2.23			2.54	5
$C_6H_5F^{\cdot+}$	2.60			2.71	14
1,2-$C_6H_4F_2^{\cdot+}$	2.84				
1,3-$C_6H_4F_2^{\cdot+}$	2.8		0.006		
1,4-$C_6H_4F_2^{\cdot+}$	2.94				
1,3,5-$C_6H_3Cl_3^{\cdot+}$	1.91	649.0	0.41	2.40	20
1,3,5-$C_6H_3F_3^{\cdot+}$	2.73	457.3	1.00	2.71	40
1,2,4,5-$C_6H_2Cl_4^{\cdot+}$	2.99	409.2	0.61		
$C_6HF_5^{\cdot+}$	2.86	433.2	0.98		
$C_6F_6^{\cdot+}$	2.66	462.9	1.00	2.71	26

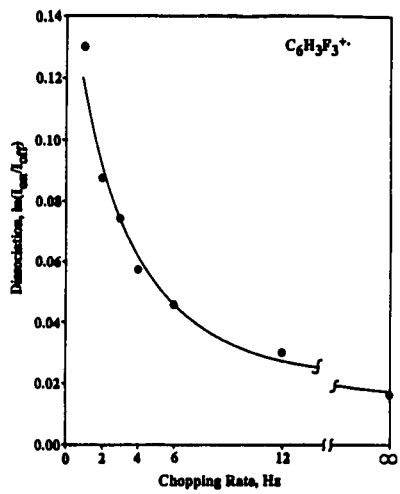

Presented at the 35th ASMS Conference on Mass Spectrometry and Allied Topics
May 24-29, 1987, Denver, CO

MOLECULAR STRUCTURE ELUCIDATION USING RESONANCE ENHANCED MULTIPHOTON IONIZATION/FRAGMENTATION. M. V. Johnston, G. R. Kinsel, K. R. Segar, and T. C. Chang, Department of Chemistry and Biochemistry, University of Colorado, Boulder, CO 80309-0215

Resonance enhanced multiphoton ionization/fragmentation (REMPI/F) can be thought of as a two step process where a parent ion is created and then photodissociated. Normally, the parent ion alone can be efficiently produced using a low laser intensity. As the intensity is increased, the parent ion and its daughters can absorb additional photons to cause extensive fragmentation. Most applications of REMPI/F have been in the low intensity limit where soft ionization is achieved. Recently, there has been interest in using REMPI/F fragmentation patterns at higher laser intensities for structure elucidation. Our goal has been to understand the details of fragment ion formation within the REMPI/F process and in particular the wavelength dependence of fragment ion abundances.

An important aspect of fragment ion formation in REMPI/F is that the internal energy of parent ions undergoing photodissociation is small. For an ensemble of parent ions produced by two photon ionization, the maximum spread of internal energies is given by the difference between the energy of two photons and the ionization energy (Figure 1). When the parent ion subsequently absorbs additional photons, this relative energy spread is maintained. In a one color REMPI/F experiment, changes in the laser wavelength affect both the relative spread and the average internal energy of parent ions undergoing photodissociation. Wavelength dependent changes in fragment ion formation can be illustrated with the hypothetical breakdown graph in Figure 2. When a "low" energy photon is absorbed, energy region B is accessed on the breakdown graph and "low" energy daughter ions represented by D_1^+ are abundant. When a "high" energy photon is absorbed, energy region C is accessed and only the higher energy fragments represented by D_2^+ are abundant. Thus, the low energy fragmentation pathway is enhanced when a low energy photon is used. This behavior is analogous to collision induced dissociation where low energy pathways are enhanced over higher energy processes when low collision energies are used. An example of this effect is shown in Figure 3 for p-cresol. At 286 nm, m/z 80 is strongly abundant in the REMPI/F mass spectrum. At 266 nm, its abundance relative to other fragment ions is diminished.

It is incorrect to assume that the trend illustrated above for low vs. high energy photons in REMPI/F will always be observed. In fact, it is sometimes necessary to use a higher energy photon to enhance the occurence of low energy processes. Consider Figure 2 again. Let region A correspond to the parent ion internal energy distribution upon absorption of one "low" energy photon and region C correspond to the distribution upon the absorption of a second photon of the same energy. In this case, no fragments are produced upon the absorption of one photon and only the high energy fragments (D_2^+) are produced upon the absorption of a second photon. Thus, low energy fragments are not observed in the mass spectrum at any laser intensity. However, if a higher energy photon is absorbed and the one photon parent ion distribution is given by region B, then the low energy fragments are efficiently produced. Therefore, the wavelength trend is reversed: a higher energy photon is required to enhance the production of low energy fragments. This effect is shown in Figure 4 for p-chloroaniline. At 266 nm, "low" energy fragments corresponding to the loss of Cl· and HNC are strongly abundant. At 290 nm, these ions are not observed.

This work shows that REMPI/F fragmentation patterns can be strongly wavelength dependent. This aspect must be kept in mind if REMPI/F mass spectra are to be used for structure elucidation. Furthermore, it is likely that "low" energy fragment ions will be observed only over a limited wavelength region since photons that are too high or too low in energy will result in "high" energy fragments being preferentially produced.

Presented at the 35th ASMS Conference on Mass Spectrometry and Allied Topics
May 24-29, 1987, Denver, CO

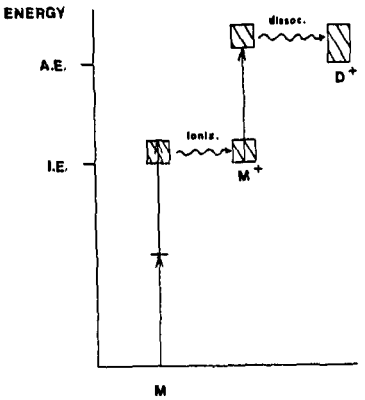

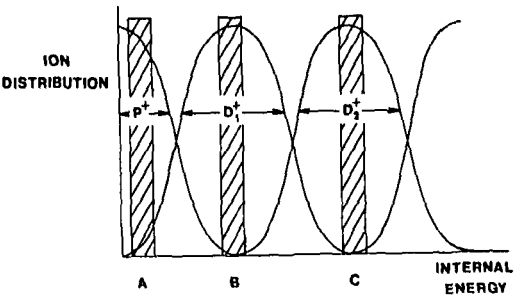

Figure 1 Figure 2
Shaded regions indicate ion internal energy distributions. (see text).

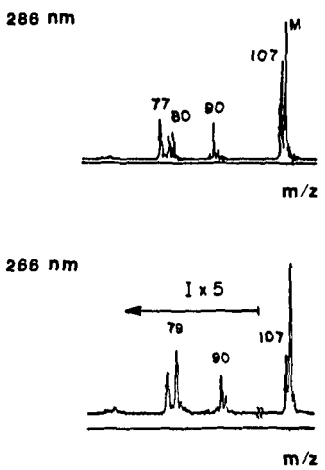

Figure 3 - REMPI/F
mass spectra of p-cresol.
top - 286 nm, bottom - 266 nm

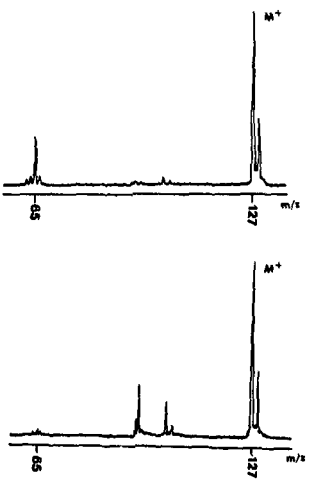

Figure 4 - REMPI/F
mass spectra of
p-chloroaniline.
top - 290 nm, bottom -
266 nm

Presented at the 35th ASMS Conference on Mass Spectrometry and Allied Topics
May 24-29, 1987, Denver, CO

NON-RESONANT MULTIPHOTON IONIZATION/FRAGMENTATION PATTERNS OF N-SUBSTITUTED ANILINES

Jeffrey A. Zimmerman and Rebecca M. O'Malley
University of South florida, Tampa, Florida 33620

The multiphoton ionization/fragmentation patterns for aniline have been studied by a number of groups (1-4). Schlag et al. used a time-of-flight reflectron to identify the major decomposition reactions occurring when ionization is initiated at 266 nm. The well-known metastable decomposition of the molecular ion, $C_6H_5NH_2^{+\cdot} \longrightarrow C_5H_6^{+\cdot} + CNH$, has also been investigated at 266 nm (3-4). This study of several N-substituted anilines, N-methylaniline, N-dimethylaniline, N-ethylaniline, and N-diethylaniline, was initiated to observe what effect N-substitution will have on the fragmentation patterns. The spectra were obtained using a time-of-flight mass spectrometer at wavelengths of 266 nm (near resonant), 532 nm and 355 nm (non-resonant).

Comparison of the electron impact spectra of aniline and the N-substituted anilines indicates a difference in the major fragmentation routes. In aniline the most intense fragment ion corresponds to the loss of CNH from the molecular ion to form $C_5H_6^{+\cdot}$. In contrast the most intense fragments formed in the N-substituted anilines are resonant stabilized ions formed by the loss of H$^\cdot$ from the methyl substituted and $CH_3^\cdot$ and $C_2H_5^\cdot$ from the ethyl and diethyl substituted anilines. All the N-substituted anilines have an intense m/z = 77 ($C_6H_5^+$) corresponding to the loss of the substituent amine group. The N-substituted spectra are very similar, but can be differentiated from each other by their molecular ions. The resonant spectra at 266 nm have many similarities to electron impact showing the same major ions, however smaller mass ions at m/z = 27 (possibly $C_2H_3^+$) in the ethyl substituted spectra and m/z = 42 and 44 (possibly $C_2NH_4^+$ and $C_2NH_6^+$) in the disubstituted spectra appear to be characteristic of the substituent group and contribute more to the spectra than in electron beam. Other low mass ions at m/z = 12, 24, 36, 37, 50, etc. are also observed and become more intense as laser pulse power is increased. These ions are characteristic of other substituted benzene systems.

The non-resonant spectra at 532 nm of aniline contain very little molecular ion, no $C_5H_6^{+\cdot}$, (the metastable decomposition product at 266 nm) and a large amount of $C_3NH_2^+$ (m/z = 52) along with other small mass ions including CNH_2^+ (m/z = 28). In contrast to this the ethyl substituted anilines both show no molecular ions but a small ($M^{+\cdot} - CH_3^\cdot$) ion in the ethyl substituted and a small ($M^{+\cdot} - CH_3^\cdot$) and ($M^{+\cdot} - C_2H_5^\cdot$) for the diethyl substituted. The methyl substituted anilines contain no molecular ion. All the spectra have high intensity ions at m/z = 12, 24, 39 and 51 which appear to be characteristic of the benzene ring in addition to other ions possibly originating from the substitution and were seen in the 266 nm spectra (m/z = 27, 42 and 44). In the N-diethylaniline and to a lesser extent in the N-ethylaniline spectra m/z = 29, (probably $C_2H_5^+$) distinguishes these systems from the methyl substituted ones. At higher pulse energies the spectra resemble each other more so than at low pulse energies, but still retain ions characteristic of their substitution. Similar observations are made for the non-resonant spectra at 355 nm, except for the observation of small molecular ions in N-diethyl and N-ethylaniline. In N-diethylaniline a ($M^{+\cdot} - C_2H_4$) ion is observed at 355 nm.

One possible route to the formation of the ions that originate from the substitution could be the ionization of neutrals in the intense laser flux. Production of carbon neutrals from fluorobenzene have been observed by Grant et al. (5) and small neutrals have been shown to be possible precursors to smaller mass ions by Martin (6). To model neutral amine fragments we choose a number of substituted amines. These are not exact duplicates of the neutrals that are formed in the fragmentation process, but contain an extra hydrogen. Results of multiphoton ionization at 532 nm have shown that even at high laser pulse energies these amines produce no $C^{+\cdot}$ or $C_2^{+\cdot}$, but undergo fragmentations similar to those observed in the N-substituted anilines (($M^{+\cdot} - H^\cdot)^+$, ($M^{+\cdot} - CH_3^\cdot)^+$, ($M^{+\cdot} - C_2H_2^\cdot)^+$). This would seem to indicate that the small mass ions in the N-substituted spectra which appear to be characteristic of the substitution are not produced by ionization of neutral species formed from the substituent group atoms during the ionization/fragmentation process.

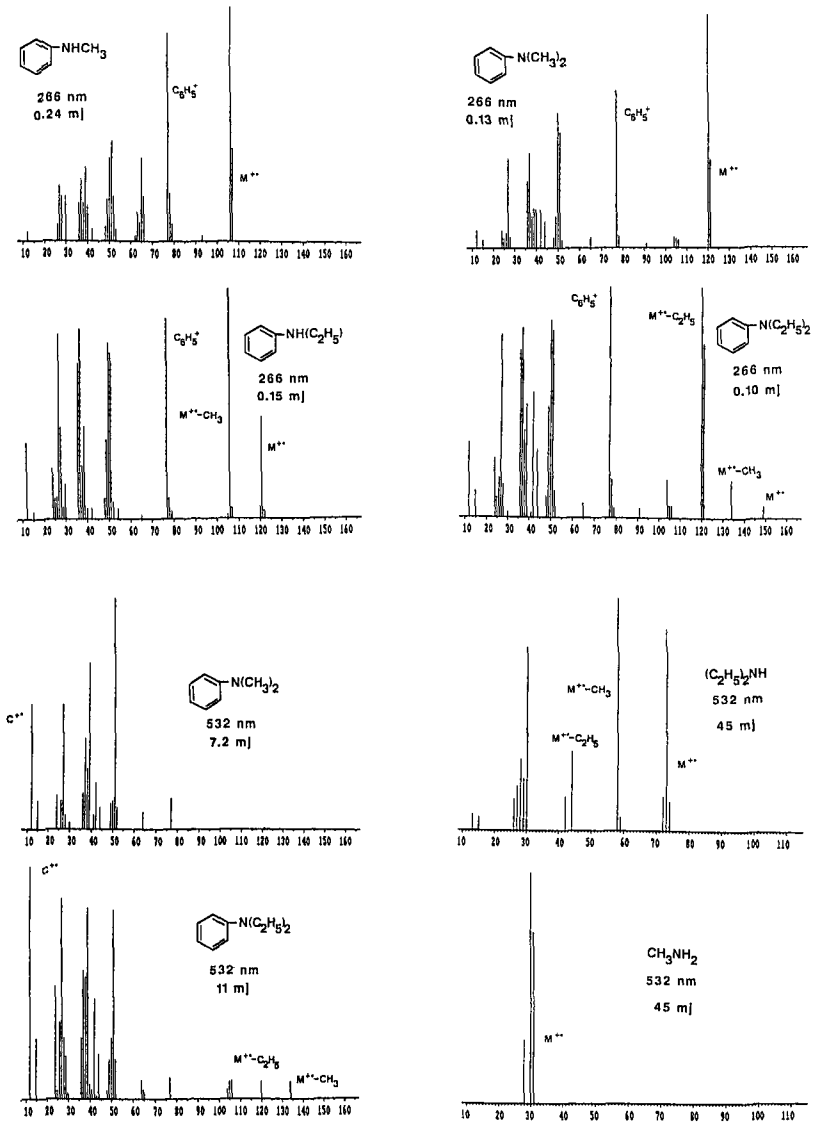

1. H. Kuhlewind, H.J. Neusser and E.W. Schlag, J. Chem. Phys. 82, 5452 (1985).
2. R. Proch, D.M. Rider and R.N. Zare, Chem. Phys. Lett., 81, 430 (1981).
3. T. Baer and T.E. Carney, J. Chem. Phys., 76, 1304 (1982).
4. J.A. Zimmerman, R.M. O'Malley and J.E. Weinzierl, Int. J. Mass Spectrom. and Ion Processes (1987), in press.
5. R.L. Whetten, K.J. Fu, R.S. Tapper and E.R. Grant, J. Phys. Chem. 87, 1484 (1983).
6. W.B. Martin and R.M. O'Malley, unpublished results.

Presented at the 35th ASMS Conference on Mass Spectrometry and Allied Topics
May 24-29, 1987, Denver, CO

INFRARED MULTIPHOTON DISSOCIATION OF THE NITROBENZENE CATION

Mehdi Moini and John R. Eyler

Department of Chemistry, University of Florida
Gainesville, Florida 32611

The nitrobenzene molecular cation has been the subject of extensive studies in recent years. Photoelectron photoion coincidence (PEPICO) spectrometry studies of the dissocation dynamics of energy-selected nitrobenzene cations have been published by two groups [1,2]. The appearance energies reported by Panczel and Baer are shown on the left side of Figure 1. Based on their results, the authors concluded that part of the NO^+ and all of the $C_6H_5O^+$ products are formed by dissociation from the ground electronic state of $C_6H_5NO_2^+$. On the other hand, it was argued that dissociation to produce $C_6H_5^+$ takes place from an excited electronic state. The AE's reported by Nishimura et al. are shown on the right side of Figure 1. Based on their results these authors concluded that near threshold the formation of NO^+ is probably preceeded by nitro-nitrite isomerization. They also concluded that all aspects of nitrobenzene ion dissocation can be explained adequately by statistical theories in spite of the complexity of the reaction dynamics.

The IRMPD of the nitrobenzene cation was thus studied in order to investigate its fragmentation mechanism and to determine which fragment ions were produced from the ground electronic state. Nitrobenzene ions were trapped in an FTICR analyzer cell [3] and subjected to gated irradiation from a continuous wave (cw) infrared laser with a wavelength of 10.28 u. Mass spectra for ions trapped for 300 ms without and with laser irradiation are shown in Figure 2a and 2b, respectively. The two peaks in Figure 2a with m/z 107 and m/z 93 are the result of ion/molecule reactions of the parent ion with nitrobenzene neutral and represent loss of O and NO, respectively. However, as can be seen in Figure 2b, IRMPD resulted in production of $C_6H_5O^+$ (m/z 93) as the most abundant fragment ion, but also some $C_5H_5^+$ (m/z 65) and NO^+ (m/z 30). The intensity of $C_6H_5NO^+$ (m/z 107) was essentially the same with and without laser irradiation, indicating that this ion is produced solely by an ion/molecule reaction. Ejection of this ion from the cell during the irradiation period had almost no effect on other fragments, indicating that it does not undergo IRMPD. No $C_6H_5^+$ (m/z 77) ion was observed, although this ion has an AE which is the same as [2] or even 0.15 eV lower than [1] $C_5H_5^+$.

When $C_6H_5O^+$ was ejected during the course of laser irradiation no $C_5H_5^+$ was produced, indicating that $C_6H_5O^+$ is the precursor of $C_5H_5^+$ by some mechanism, dissociative or reactive. However, increased irradiation time of either the parent ion or of $C_6H_5O^+$ which was itself produced by IRMPD from the parent did not increase the relative intensity of the $C_5H_5^+$ fragment significantly. Thus the remaining $C_6H_5O^+$ ions do not absorb ir radiation. Also, no $C_5H_5^+$ was observed when $C_6H_5O^+$, which was formed by IRMPD, was allowed to react with background nitrobenzene molecules, eliminating the possibility of an ion/molecule formation mechanism.

Thus one concludes that the production of $C_6H_5O^+$ and NO^+ by infrared multiphoton dissociation of the nitrobenzene cation indicates that these ions are produced from high vibrational levels of the ground electronic state of the ion. The mechanism of formation of these ions is different from that of $C_6H_5^+$, which is either produced directly from an excited electronic state or from the ground state via a pathway whose activation energy exceeds that of $C_6H_5O^+$, NO^+ and $C_5H_5^+$ by > ca. 0.2 eV, which is inconsistent with existing appearance energies. The results of this study also suggest that two different types of $C_6H_5O^+$ ions are produced by IRMPD, one stable with respect to dissociation and the other undergoing further fragmentation to give $C_5H_5^+$ on a > 100 us time scale. Figure 3 summarizes these results.

Presented at the 35th ASMS Conference on Mass Spectrometry and Allied Topics
May 24-29, 1987, Denver, CO

REFERENCES

1. M. Panczel and T. Baer, Int. J. Mass Spectrom. Ion Phys., 58 (1984) 43.
2. T. Nishimura, P.R. Das and G.G. Meisels, J. Chem. Phys., 84 (1986) 6190.
3. G. Baykut, C.H. Watson, R.R. Weller and J.R. Eyler, J.Am.Chem.Soc., 107 (1985) 8036.

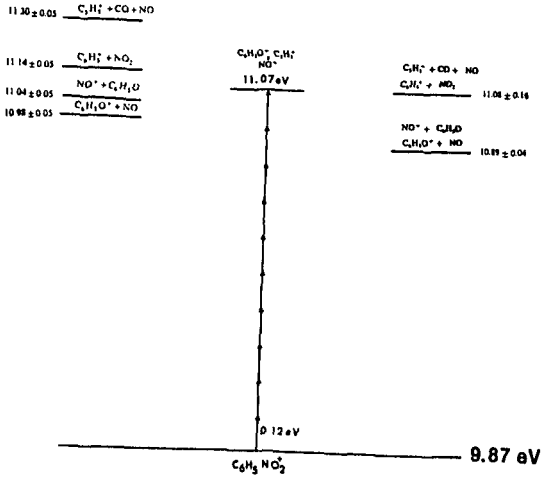

Figure 1

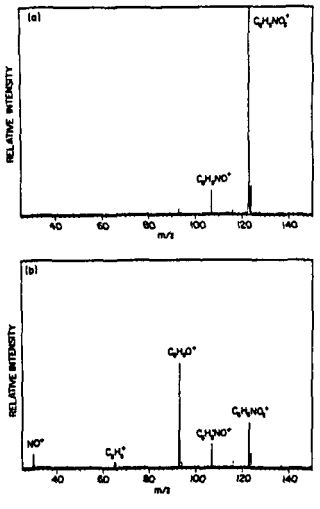

Figure 2

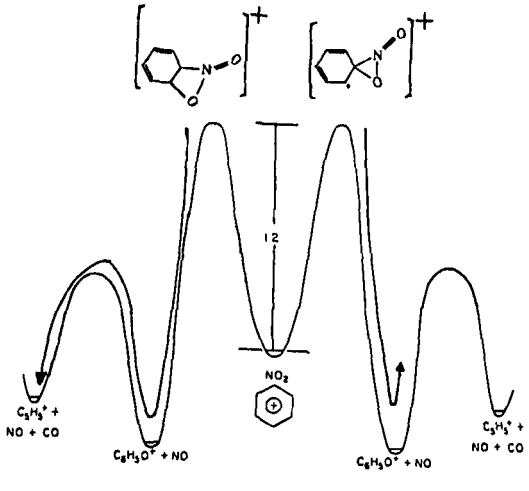

Figure 3

Presented at the 35th ASMS Conference on Mass Spectrometry and Allied Topics
May 24-29, 1987, Denver, CO

PHOTODISSOCIATION SPECTROSCOPY OF SEVERAL $C_5H_6^+$ ISOMERIC IONS

B. Asamoto, The Standard Oil Co., Cleveland, Ohio 44128; R. C. Dunbar, Case Western Reserve University, Cleveland, Ohio 44106

Photodissociation spectra were obtained in the ICR ion trap for the $C_5H_6^+$ ions from five isomeric neutral C_5H_6 precursors (Figure 1). It is clear from the distinct spectra obtained that interconversion of the non-decomposing ions does not occur; the spectra are sufficiently characteristic to distinguish the various structures. The spectral profile is similar for the cyclopentadiene and 2-methyl-1-butene-3-yne isomers, but they are clearly differentiated by the order-of-magnitude difference in cross section (Dissociation scale for cyclopentadiene is X 10). The location of the PDS peaks is in excellent accord with the PES spectra of the corresponding neutral compounds, suggesting retention of the neutral structure upon ionization in all cases.

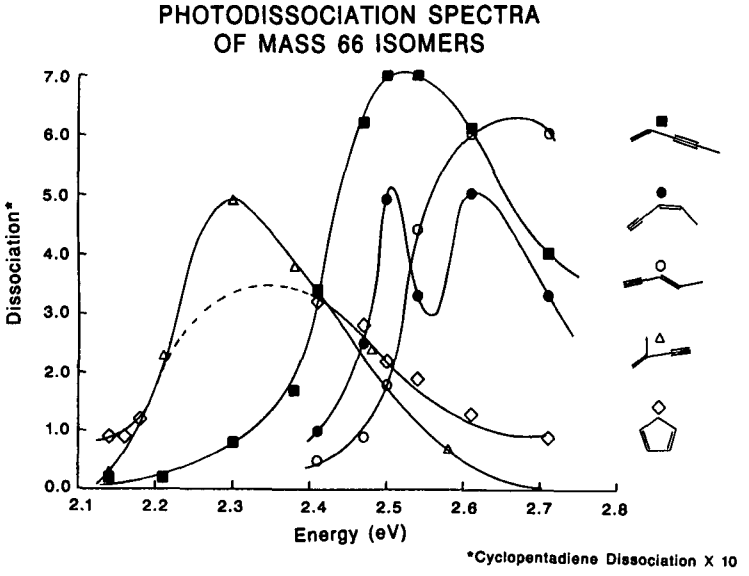

Figure 1

Fragment $C_5H_6^+$ ions were formed by low energy electron impact ionization of phenol, aniline, and thiophenol. A double resonance pulse, used to eject the parent ions, had the added effect of forming additional $C_5H_6^+$ ions by CID; therefore, the total population of ions which we were

observing was derived from both CID and electron impact. Photodissociation spectra of ions from the three precursors were similar (Figure 2). Based on the spectral profile and low cross section, the four acyclic structures were ruled out and the fragment ions were assigned the cyclopentadiene ion structure. This agrees with recent work by PIPECO[1] and charge-stripping mass spectrometry[2]. Partial PDS spectra were obtained for the aniline, phenol, and thiophenol parent ions and were in accord with expectations from the PES spectra.

MINDO/3 and MNDO calculations were carried out for a Koopmans' theorem comparison with the π-π transition energies of the $C_5H_6^+$ ions. Both of these calculations gave substantially better values than previous SPINDO calculations. The MNDO results were within about 0.1 eV of the experimental values for the transition energies of the ene-ynes.

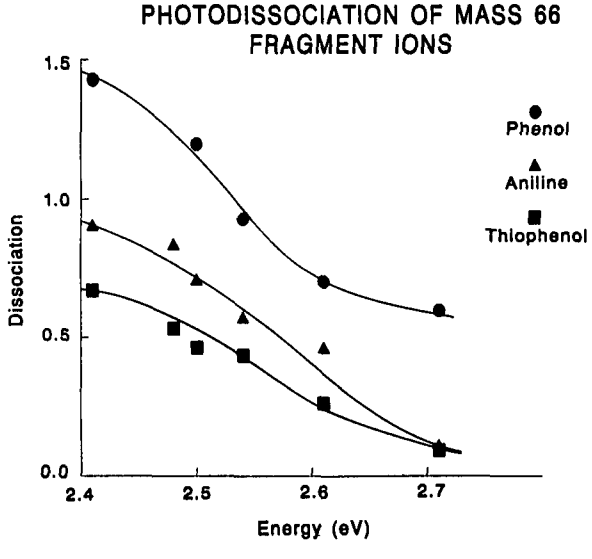

Figure 2

References

1. T. Baer and T. E. Carney, J. Chem. Phys., 1982, 76, 1304.

2. R. Flammang, P. Meyrant, A. Maquestiau, E. E. Kingston, J. H. Beynon, Org. Mass. Spectrom., 1985, 20, 253.

Presented at the 35th ASMS Conference on Mass Spectrometry and Allied Topics
May 24-29, 1987, Denver, CO

A NEW APPROACH TO ION DISSOCIATION IN MS-MS

Marvin L. Vestal; Department of Chemistry
University of Houston, Houston, TX 77004.

The standard approach to fragmenting ions in MS-MS is to collide them with neutral gas molecules. Recently collisions with surfaces and laser photodissociation have also been explored as alternatives, but none of these techniques provides the extensive, reproducible fragmentation produced directly by electron impact ionization of neutrals. Recently "soft" ionization techniques such as FAB and thermospray have been developed which are applicable to many large molecules not sufficiently volatile for EI. Unfortunately, these new techniques often yield little structurally significant fragmentation, and conventional CID MS-MS has also often failed to provide sufficient fragmentation for structural elucidation. In the present work a novel quadrupole cell has been designed which provides a practical method for accomplishing Electron Induced Dissociation (EID) of ions. This device can be used with either quadrupole or magnetic analyzers. Theoretical estimates of performance indicate that at least 20% of an ion beam of m/z 1000 should be dissociated and that the efficiency should increase at higher masses. This approach has the additional advantage, as in conventional EI, that the fragmentation pattern should be weakly dependent on the experimental parameters. Thus, reproducible fragmentation patterns should be obtained, and generation of a useful data base of EID spectra for both volatile and nonvolatile compounds may become practical. Furthermore, the RF only quadrupole discriminates against the copius quantites of low mass ions produced from residual gas in the vacuum system. This quadrupole EID system has been installed on a VG 70 SEQ using the configuration shown schematically in Figures 1 and 2.

Theoretical studies indicate that the proposed approach is feasible, but the first prototype produced only a few milliamps of electron current before it self-destructed. The input power required to produce several hundred milliamps of electrons at an energy of several hundred volts is on the order of 500 watts. Adequate means for coupling the large amount of heat generated across the vacuum barrier was not included in the intial design, and serious over-heating occurred before the useful range of electron currents was reached. While it is clear that some redesign of the apparatus will be required before the feasibility of this approach can be demonstrated experimentally, we are confident that EID will provide the ultimate answer to obtaining useful structural information on high mass, nonvolatile molecules by MS-MS.

Acknowledgement: This work was supported in part by a grant from the Texas Advanced Technology Research Project.

Presented at the 35th ASMS Conference on Mass Spectrometry and Allied Topics
May 24-29, 1987, Denver, CO

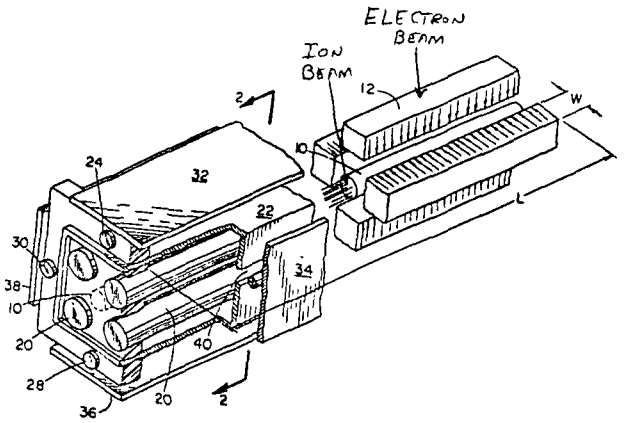

Figure 1. Schematic diagram of quadrupole EID cell showing the intersection of four sheets of electrons with an axial ion beam.

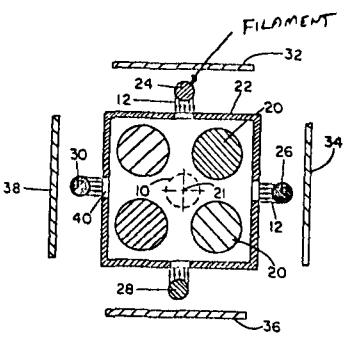

Figure 2. Cross sectional view of the EID cell. The ion beam travels perpendicular to the plane of the figure.

Presented at the 35th ASMS Conference on Mass Spectrometry and Allied Topics
May 24-29, 1987, Denver, CO

DISSOCIATION OF $CS_2^{+\cdot}$ IONS FORMED IN CHARGE-EXCHANGE REACTIONS OF CS_2^{2+} IONS

C.J.Reid, F.M.Harris and J.H.Beynon

Mass Spectrometry Research Unit, University College of Swansea,
Swansea SA2 8PP, U.K.

The electron capture induced decomposition (ECID) method, developed [1] in this Laboratory, is a novel way of exciting and dissociating ions within a field-free region of a double-focussing mass spectrometer. Some or all of the excitation energy of a singly-charged ion $M^{+\cdot}$ is derived from the charge-exchange reaction involving the doubly-charged ion M^{2+} i.e.

$$\underset{\longrightarrow}{M^{2+}} + G \longrightarrow \underset{\longrightarrow}{M^{+\cdot}} + G^{+\cdot} \qquad (1)$$

$\underset{\longrightarrow}{M^{2+}}$ represents the doubly-charged ion having a translational energy of several kilo-electron volts and G an atom of a collision gas. If ground-state to ground-state transitions are involved, the energy defect, ΔE, of the reaction is

$$\Delta E = IE(M^{+\cdot}) - IE(G) \qquad (2)$$

where $IE(M^{+\cdot})$ is the ionization energy of $M^{+\cdot}$ and IE(G) is the ionization energy of G. For a given projectile ion M^{2+} it follows that ΔE is dependent on the type of collision gas used. It might be expected, for example, that Xenon (IE(G) = 12.1 eV) will provide more internal energy than Helium (IE(G) = 24.6 eV). It is surprising, therefore, that the results of an ECID study of $C_6H_6^{2+}$ ions [1,2] and of doubly-charged ions of some methyl pyridines [3] showed that the use of Helium as collision gas is most likely to result in singly-charged ions having high internal energies.

The purpose of the investigation reported in this paper was to study the ECID process for a tri-atomic ion to see if it shows the same general trend as that observed for polyatomic ions. CS_2^{2+} was chosen for several reasons.

(a) The current of CS_2^{2+} ions obtainable from a conventional EI source is relatively high (16% of the base peak in the mass spectrum).
(b) The energy levels of $CS_2^{+\cdot}$ have been well characterised by photoelectron spectroscopy.
(c) Three distinct fragmentation reactions of excited $CS_2^{+\cdot}$ ions give rise to fragment ions $CS^{+\cdot}$, $S^{+\cdot}$ and $S_2^{+\cdot}$ which are well separated in a translational-energy spectrum. Further the threshold levels for all the fragmentation reactions have been calculated [4,5].
(d) Branching ratios when state-selected $CS_2^{+\cdot}$ ions dissociate have been measured [4].

Results were obtained using a ZAB-2F mass spectrometer with collision gases being introduced into a gas cell located at the intermediate focal plane. Fragment-ion spectra were obtained by scanning the voltages applied to the electric-sector plates. The relative abundances of the fragment ions obtained for different collision gases are shown in Fig.1.

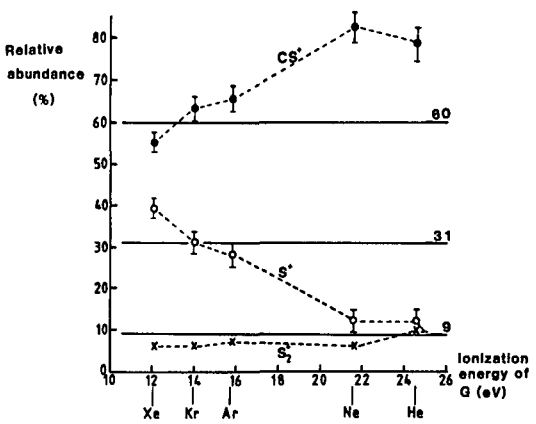

Fig. 1 Relative abundances of fragment ions when excited $CS_2^{+\cdot}$ ions, formed in charge-transfer collisions with atoms G, dissociate.

In a previous investigation [4] it was shown that $CS_2^{+\cdot}$ ions excited to the $\tilde{C}^2\Sigma_g^+$ state could dissociate to yield $CS^{+\cdot}$ and $S^{+\cdot}$ fragment ions in the ratio 58 : 42. Those excited to the $\tilde{D}^2\Pi_u^+$ state, on the other hand, dissociated to give three fragment ions $CS^{+\cdot}$, $S^{+\cdot}$ and $S_2^{+\cdot}$ having relative yields 60 : 31 : 9. It can be seen from Fig.1 that, for all target gases, $S_2^{+\cdot}$ is observed and thus at least some of the $CS_2^{+\cdot}$ ions in all cases are excited to the $\tilde{D}$ state. For XE, Kr and Ar targets it is seen that the relative yields are approximately those observed from state-selected $CS_2^{+\cdot}$ in the $\tilde{D}$ state [4] but the agreement for Ne and He is not as good.

To excite the $CS_2^{+\cdot}$ ions to the $\tilde{D}$ state requires considerable energy in the case of some of the gases used. For He, for example, ΔE ~ -7.3 eV and a further 6.8 eV is required to excite the ion to the $\tilde{D}$ state. This must come from the translational energy of the CS_2^{2+} ion and will result in an energy shift of the fragment-ion peaks. Energy-shift values for the $S_2^{+\cdot}$ fragment ions are shown in Table 1.

Table 1 Energy shifts of $S_2^{+\cdot}$ fragment-ion peaks and the corresponding shifts in excited $CS_2^{+\cdot}$ ions

Collision gas (G)	Energy defect to reach $\tilde{D}$ state (eV)	Energy shift of $S_2^{+\cdot}$ peak (eV)	Energy shift of excited $CS_2^{+\cdot}$ ions (eV)
He	14.2	16 ± 3	19 ± 3
Ne	11.2	12 ± 3	14 ± 3
Ar	5.4	11 ± 3	13 ± 3
Kr	3.6	8 ± 3	9 ± 3
Xe	1.7	5 ± 3	6 ± 3

It can be seen that the shift increases as the endothermicity of the reaction increases. The agreement between the measured values and those expected is not good and may be due to translational energies imparted to the target atoms in the collisions. As discussed briefly below, the charge-transfer reactions leading to excited states of $CS_2^{+\cdot}$ probably take place at small impact parameters.

We deduce, therefore, that for all the target gases used most of the excited $CS_2^{+\cdot}$ ions resulting from the charge-transfer reactions are in the D state. The energy to reach that state, in excess of the ΔE resulting from the charge transfer itself, is obtained from a reduction in the translational energy of the ions. Charge-transfer reactions which are exothermic are usually explained in terms of a 'curve-crossing' mechanism where potential energy curves for M^{2+} + G cross with those for $M^{+\cdot}$ + $G^{+\cdot}$. For reactions of large endothermicity the curves can only approach one another at high internal energies (and small separation between M^{2+} and G) where the state density is probably much larger and curve crossing is more likely to give rise to excited states. Whilst the mechanism is still not entirely clear the present work confirms that highly excited singly-charged ions can result from charge-transfer reactions of large endothermicity.

References

1. K.Vékey, A.G.Brenton and J.H.Beynon, Int.J.Mass Spectrom. and Ion Proc. 70, 277 (1986).
2. K.Vékey, A.G.Brenton and J.H.Beynon, J.Phys.Chem., 90, 3569 (1986).
3. J.M.Curtis, K.Vékey, A.G.Brenton and J.H.Beynon, Org.Mass Spectrom. 22, 289 (1987).
4. B.Brehm, J.H.D.Eland, R.Frey and A.Küstler, Int.J.Mass Spectrom. and Ion Phys. 12, 213 (1973).
5. M.J.Hubin-Franskin, D.Huard and P.Marmet, Int.J.Mass Spectrom. and Ion Phys. 27, 263 (1978).

Presented at the 35th ASMS Conference on Mass Spectrometry and Allied Topics
May 24-29, 1987, Denver, CO

GC/MS ANALYSIS OF n-ALKYLBENZTHIOPHENES IDENTIFIED IN ARABIAN HEAVY ASPHALTENES, PYROLYSIS OIL

By E. J. Gallegos

Introduction

A homologous series of n-alkylbenzthiophenes extending from C_{10} to C_{30} has been identified in the pyrolysis oil of Arabian Heavy asphaltenes. Within each homolog there are at least 22 resolved isomers. The mass spectra of these isomers typically show relatively intense molecular ions with base peaks at m/z 147, 161, or 175. Genesis of the benzthiophenes is rationalized on the basis of sulfur reacting with homologous series of n-alkylbenzenes which are also present in the Arabian Heavy pyrolysis oil.

Experimental

Pyrolysis GC/MS data were obtained using a 60-meter DB-1 fused silica column from J&W Scientific in a 5700A Hewlett-Packard gas chromatograph. The column was coupled directly to the source of a VG ZAB mass spectrometer. A Finnigan INCOS computer system was used for instrument control and data acquisition.

Results and Discussion

Preliminary evidence for the presence of a homologous series of n-alkylbenzthiophenes came from the repeat pattern of fragment ions at m/z 147, 161, and 175. The presence of sulfur in these fragment ions was confirmed at M/ΔM 10,000 mass resolution using GC/MS multiple ion detection (MID) methods.

This singlet, 92, doublet, 106, multiplet, 120, pattern across the C_{14} to C_{17} n-alkylbenzene homologs (Figure 1) is strikingly similar to the singlet, 147, doublet, 161, and multiplet, 175, pattern found for the n-alkyl benzthiophenes (Figure 2). This suggests that the n-alkylbenzthiophenes are generated directly from n-alkylbenzene--sulfur reactions during diagenesis. Figure 3 shows the $C_{15}H_{18}S$ benzthiophenes isomers.

Reflux experiments at 150°C with 1-phenyltetradecane and small amounts of 1-phenylhexadecane and sulfur in the presence of V_2O_5 yielded detectable amounts of phenyl-n-decylthiophene (MW 300), n-dodecylbenzthiophenes (MW 302), phenyl-n-dodecylthiophenes (MW 328), benzthiophenyl-n-octylthiophene (MW 328), tetrahydrodibenzthiophene (MW 188), diphenylthiophene (MW 236), n-nonylthiophene (MW 210), and many other as yet unidentified thiophene derivatives.[3]

Conclusions

Multiple isomer homologs of n-alkylbenzthiophenes and n-alkylbenzenes have been identified in Arabian Heavy asphaltnes pyrolysis oil and in the Arabian Heavy crude itself.

The close similarity between the molecular ion and fragment ion mass chromatograms of the n-alkylbenzenes and n-alkylbenzthiophenes suggests that the latter is formed from the former through reaction with sulfur in some form. Further, this is a secondary reaction during maturation of the oil when contact with sulfur is made.

These data support the concept of secondary reaction of sulfur with alkylbenzenes to form benzthiophenes directly during maturation.

Reference

1. DeRoo, Johan, and Hodgson, G. W., Chemical Geology 22 (1978) 71-78.

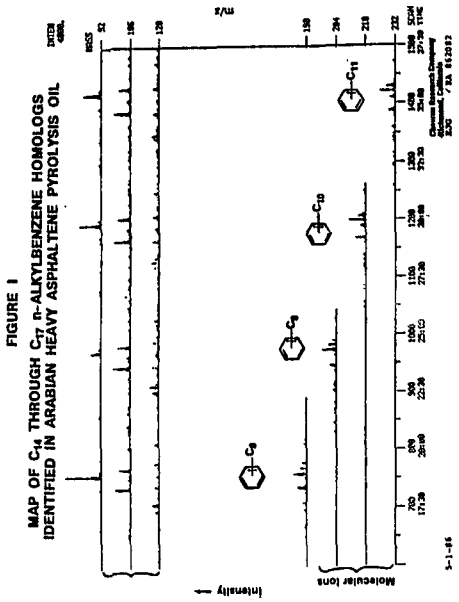

FIGURE 1
MAP OF C_{14} THROUGH C_{17} n-ALKYLBENZENE HOMOLOGS IDENTIFIED IN ARABIAN HEAVY ASPHALTENE PYROLYSIS OIL

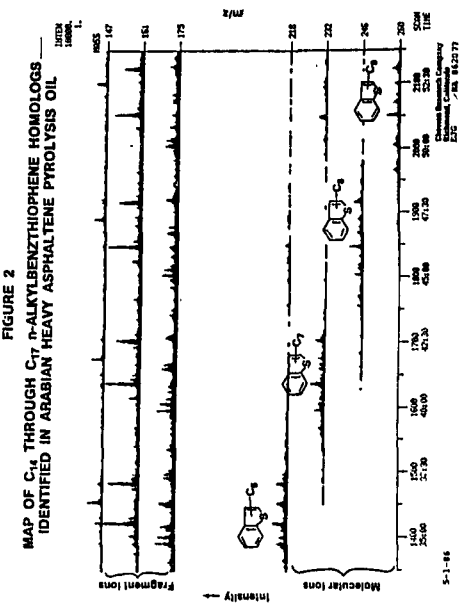

FIGURE 2
MAP OF C_{14} THROUGH C_{17} n-ALKYLBENZTHIOPHENE HOMOLOGS IDENTIFIED IN ARABIAN HEAVY ASPHALTENE PYROLYSIS OIL

FIGURE 3
MASS CHROMATOGRAMS OF MOLECULAR AND FRAGMENT IONS DUE TO THE $C_{18}H_{18}S$ n-ALKYLBENZTHIOPHENE HOMOLOG

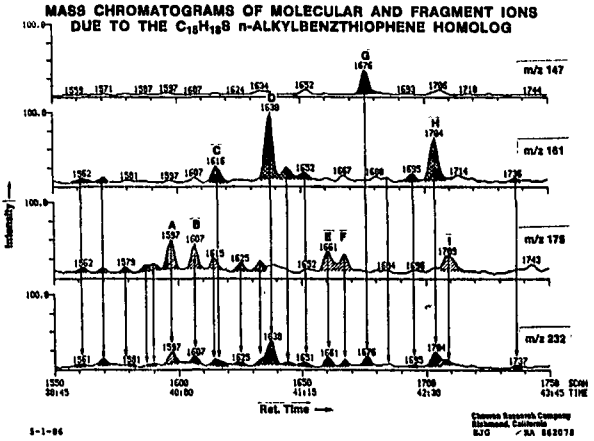

Presented at the 35th ASMS Conference on Mass Spectrometry and Allied Topics
May 24-29, 1987, Denver, CO

ANALYSIS OF COMPLEX SURFACTANT MIXTURES

F.M. Bockhoff, K.M. Shaw, P.A. Budinger, B. Asamoto
Standard Oil Research Center
4440 Warrensville Rd., Warrensville Hts., OH 44128

A. Mass Spectral Techniques for Surfactant Analysis

1. Analysis of Nitrogen Containing Neutral Surfactants

The positive FAB-MS spectrum gives an intense protonated molecular ion at m/z=370 The negative FAB-MS spectrum was contains a weak (M-1)- peak and considerable fragmentation. The largest fragment ion corresponds to the loss of an alkyl chain from the molecular ion. The positive TSP spectrum gives a single ion at m/z=298 corresponding to loss of a nitrogen substituent. The negative TSP spectrum, like the negative FAB-MS spectrum, contains a weak (M-1)- ion and considerable fragmentation. In addition, an unknown peak is present at m/z=384. The positive LD/MS spectrum contains strong (M+1)+ and (M+Na)+ ions at masses 370 and 392, respectively. The negative LD/MS spectrum does not exhibit a molecular ion species. In conclusion, these types of molecules give excellent molecular species spectra in the positive mode in both FAB-MS and LD/MS. We did not obtain positive molecular ion species by TSP or negative molecular ion molecular species by any of the techniques.

2. Analysis of Nitrogen and Sulfur Containing Neutral Surfactants

The positive FAB-MS spectrum contains a strong protonated molecular ion at m/z=434. The negative FAB-MS spectrum contains fragment ions at m/z=418 and m/z=292 that correspond to loss of substituent groups from the nitrogen. The positive LD/MS spectrum has a weak (M+H)+ at m/z=434. It also has fragments at m/z=312 and m/z=184 that are from the loss of one and two nitrogen substituents, respectively. The addition of KBr to the sample resulted in a strong (M+K)+ peak at m/z=472. The negative ion LD/MS spectra contains fragments at m/z=418 ans m/z=292 corresponding to losses of nitrogen substituents. No molecular species are observed. In conclusion, LD/MS exhibited strong positive and negative molecular species.

3. Branched Alkyl Alcohol

The positive FAB-MS spectrum is unusual because it contains an (M-H)+ ion at m/z=241. It also contains a large fragment ion at m/z=225 corresponding to (M-17)+. The negative FAB-MS spectrum is very weak and contains ions at (M-H)-, (M-3H)-, and (M-17)-. The positive LD/MS spectrum contains a weak (M+H)+ at m/z=243 and fragments (M-1)+ and (M-17)+ at m/z=241 and m/z=225, respectively. However, when KBr is added to the sample a strong (M+K)+ peak is observed at m/z=281. The negative ion LD/MS spectrum gives primarily an (M-1)- peak. In conclusion, an excellent method for obtaining molecular species on alkyl alcohols is with LD/MS.

B. Analysis of Surfactant Packages

1. Laboratory Detergent

IR done on the whole sample showed the presence of sodium triphosphate ($Na_5P_3O_{10}$) and an unknown carboxylic acid. NMR on the whole sample showed the presence of alkyl aryl sulfonates. FAB-MS on the whole sample observed an alkylbenzene sodium sulfonate species having alkyl chain lengths of 2-14, with a maximum at C11. A dimer series was also observed in the FAB-MS spectrum. A series of extractions were performed on the sample in the hopes of isolating individual compound types. The acetone solubles contained alkyl aryl sulfonates and a carboxylic acid (by IR and NMR). The water solubles contained sodium tripolyphosphate ($Na_5P_3O_{10}$) and sodium carbonate (Na_2CO_3) by IR. The solvent insolubles contained sodium pyrophosphate ($Na_4P_2O_7$) by IR.

2. Commercial Nonionic Surfactant Package

A commercial nonionic surfactant package was analyzed for total composition. GC/MS and NMR done on the solvent showed that the primary ingredient was (+) limonene (90 mole%) with numerous other minor components. The solvent apparently was from a citrus source. NMR also indicated that a phenolic ethylene oxide condensate was present at about 8 mole%. An EDAX elemental analysis of the sample showed the presence of sulfur, which indicated that another component was present in the sample. The solvent was stripped from the sample and IR on the residue showed the presence of an ester carbonyl. NMR and positive FAB-MS on the residue determined that the phenolic ethylene oxide condensate was para-nonyl-phenyl-ethoxy-alcohol, with an average of six ethoxy units. There was also an unknown m/z=445 peak in the positive FAB-MS spectrum. The negative FAB-MS spectrum contained a strong ion at m/z=421, which strongly indicated the presence of a MW=422 component. This would also be consistent with the explanation that the m/z=445 ion in the positive FAB-MS spectrum was due to sodium attachment to the MW=422 component. In an attempt to isolate the unknown component, a 2:1 methanol/water extraction was done on the solvent stripped extract. Two layers were produced and NMR showed that both layers contained the ethylene phenol condensate. EDAX analyses of both layers showed that only the bottom layer contained sulfur. The top layer NMR spectrum was subtracted from the bottom layer NMR spectrum and a spectrum of the unknown was obtained. The NMR resonances combined with the knowledge that sulfur and an ester was present led to the conclusion that the unknown was had a sulfosucinate structure. The MW of 422 obtained from FAB-MS gave dioctylsulfosuccinate as a likely candidate. The NMR of a genuine sample of dioctylsulfosuccinate was found to match the NMR spectrum of the unknown, proving that the assignment was correct. The assignment of the unknown molecular weight by FAB-MS was the key to solving the unknown structure.

3. Commercial UV Inhibitor Package

The Material Safety Data Sheet for a commercial UV inhibitor package lists its composition as 15-20% alkylphenol, 45-55% ester, and 25-35% organotin compound. GPC (gel permiation chromatography) was done on the sample and indicated the presence of at least six components. In order to determine which of the GPC peaks contained tin, GPC/ICP was done with the ICP set to monitor tin. The first two eluting GPC peaks were found to contain tin. The GPC separated peaks were collected and IR and NMR was run on each peak. The first peak was found to be tin complexed with a thiolester, the second and third peaks were thiolester compounds, and the fourth peak contained p-alkylphenols. 119-Sn NMR (spin 1/2) was done on the whole sample. The proton decoupled tin NMR spectrum indicated the presence of a large number of tin compounds. Each peak in the spectrum represents a different tin compound in the decoupled mode. The majority of resonances were in the 40-80 ppm range. All tin compounds in this chemical shift range are quaternary species. Another tin NMR spectrum was obtained where the protons adjacent to the tin were allowed to couple. What was observed were very broad unresolved resonances. This occurred because the large number of tin compounds in the mixture were coupled with many protons adjacent to the tin. This is strong evidence that alkyl chains are directly bonded to the tin. A thermospray MS spectrum was obtained on the sample and confirmed the presence of a number of tin components. The m/z=529 ion might be protonated $(C_4H_9)_2$-Sn-$(SCH_2COOC_4H_9)_2$. The m/z=473 ion might be the protonated analog of the MW=528 structure with one acid group instead of a butyl ester. Positive LD/MS done on the sample also shows the presence of the MW=472 component. The large m/z=359 ion is believed to be a fragment resulting from the loss of two butyl groups. A positive LD/MS spectrum was also obtained in the presence of ammonium hydroxide. The spectrum obtained was strikingly similar to the positive TSP spectrum. The negative LD/MS spectrum shows a large number of tin containing ions, most of which appear to be fragment ions. An m/z=471 was observed that could be the (M-1)- from the MW=472 component observed in the positive spectrum. An m/z=545 is also seen that could be the (M-1)- from the MW=546 component observed in the positive TSP spectrum. The base peak at m/z=415 is from the loss of butyl from the m/z=472 component.

Presented at the 35th ASMS Conference on Mass Spectrometry and Allied Topics
May 24-29, 1987, Denver, CO

Detailed Characterization of High MW Saturates by FDMS and ^{13}C NMR

Thomas Aczel, L.W. Dennis, S.D. Reynolds
Exxon Research and Engineering Co.

Knowledge of saturates composition is essential in many fossil fuel processes and applications. Most methods now in use involve electron impact, high voltage, compound type analyses that were developed more than 30 years ago. These methods have several excellent features, including ease of operation and high reproducibility. On the other hand, they yield only limited information and their accuracy is in question. The need is thus evident for the development of improved methodology, based not on fragmentation but on molecular ion analysis, as already developed for aromatics and polars (high resolution, low voltage methods).

Molecular ion analysis is not limited to an a-priori established data set; it determines both type and carbon number distribution; it is easier to quantify as there are no interferences among components and calibration coefficients are predictable. Among available molecular ion methods we selected field desorption mass spectrometry (FDMS), mainly because it is applicable to both distillate and resid (non-volatile) saturates. Its advantages also include a high degree of reproducibility and the possibility of extension to aromatics and polars. Disadvantages, such as loss of light components, generally with boiling points lower than 650F, and complex instrumentation can be obviated by the use of field ionization for the lighter components and by careful standardization of instrumental operations.

The approach has been proved highly successful for both distillate and resid saturates. Experimental conditions included the use of in-house prepared emitters, 50-60 scans per charge, and computerized calculation programs. The latter integrate the scans; carry out isotope corrections, calculate odd mass residuals (generally below 2 or 3 percent, indicating that we are indeed dealing with molecular ions); determine the carbon number, compound type distribution; and calculate atomic C_jH_j average MW, average Z number, etc. A high field magnet allows mass detection to MW 3000.

Data obtained on distillate fractions show good agreement with conventional type analyses and with distillation data; data obtained on resid saturates show satisfactory results from C_{20} to C_{170}.

A particularly useful approach is to integrate the carbon number, compound type analyses from FDMS with ^{13}C NMR data, as shown below. This technique allows the deconvolution of some of the NMR data and yields much more detailed compositional information than what would be derived from MS or NMR alone.

Presented at the 35th ASMS Conference on Mass Spectrometry and Allied Topics
May 24-29, 1987, Denver, CO

FDMS PLUS NMR YIELD EXTENSIVE CHARACTERIZATION OF GAS OIL AND RESID SATURATE FRACTIONS

PARAMETERS DETERMINED/ESTIMATED		
NMR	MS	NMR + MS
• C IN NAPHTHENIC RINGS + C IN METHYLENES α TO NAPHTHENIC RINGS	• C IN NAPHTHENIC RINGS	• C IN NAPHTHENIC RINGS • C IN METHYLENES α TO NAPHTHENIC RINGS
• C IN LONG SIDECHAINS + PARAFFINS	• C IN PARAFFINS	• C IN PARAFFINS • C IN LONG SIDECHAINS
• C IN METHYLS (MAX) + TERMINAL + BRANCHED + ON NAPHTHENIC RINGS • C IN "OTHER" SIDE-CHAINS, EX PARAFFINS (NMR + MS)	• C IN NAPHTHENIC SIDE-CHAINS	• AVERAGE SIDECHAIN LENGTH ON NAPHTHENIC RINGS + TOTAL + EX METHYL • AVERAGE NUMBER OF SIDE-CHAINS

It can be safely concluded that FDMS has a very significant potential for the characterization of distillate and resid saturates. Further development will include evaluating the accuracy of the equal sensitivity assumption now used, development of high resolution techniques, and the use of internal standards to monitor the fraction of sample analyzed.

Presented at the 35th ASMS Conference on Mass Spectrometry and Allied Topics
May 24-29, 1987, Denver, CO

APPLICATIONS OF SUPERCRITICAL FLUID CHROMATOGRAPHY-MASS SPECTROMETRY IN THE ANALYSIS OF FOSSIL FUELS

E. K. Chess, H. T. Kalinoski, B. W. Wright, H. R. Udseth, and R. D. Smith

Chemical Sciences Department, Pacific Northwest Laboratory, Richland, WA 99352

In recent years an active growth in the variety of applications of supercritical fluid chromatography (SFC) in the field of analytical chemistry has occurred. Because the physical properties of a supercritical fluid (e.g., low viscosity, high diffusivity, and reasonable solubility, etc.) impart characteristics to the supercritical mobile phase intermediate to those of a liquid and a gas, SFC has allowed the separation of some components of complex mixtures that were not amenable to gas chromatography (GC) or high performance liquid chromatography (HPLC). Conventional detectors used for SFC, such as ultraviolet (UV) absorption and flame ionization (FID), have worked very well with supercritical mobile phases such as CO_2, but do not perform as well for polar-modified fluids, which may contain up to 20 volume-percent of a polar modifier, such as 2-propanol. Mass spectrometry (MS) has provided a sensitive detector for capillary and packed column SFC that can readily accommodate polar-modified fluids and provide a more information-rich spectral output than most other types of detectors.

SFC has been applied to the analysis of fossil fuels through various approaches during the past five years. Of the 100 citations found in a library search of the Energy Research Abstracts data base (1981 through 1986) for the term "supercritical fluid chromatography", 76 citations involved research that employed a detector other than a mass spectrometer. For example, capillary column SFC-FID has been used in the analyses of petroleum- and coal-derived mixtures[1,2,3] and in the analysis of diesel fuels.[4] Hydrocarbon types found in petroleum liquids have been quantified by packed-column SFC-FID.[5] Polynuclear aromatic hydrocarbons (PAH) from extracts of diesel particulates[6] and carbon black (studied in our laboratory) have been identified by SFC-UV detection. Analytical-scale supercritical fluid extraction (SFE), combined with on-line capillary GC, has been applied to the analyses of the extractable materials from air particulate matter and coal tar.[7] SFC introduction of samples to Fourier-transform infrared spectrometers has been used to study nonvolatile materials derived from coal.[8,9] Capillary SFC-FID has recently been utilized for simulated distillation of high boiling petroleum fractions having atmospheric equivalent boiling points of less than 1426°F.[10]

The application of SFC-MS to the analysis of fossil fuels has been demonstrated primarily in our laboratories at Pacific Northwest Laboratory. One primary emphasis of our research programs involving fossil fuels analysis has been to develop supercritical fluids and chromatographic columns that can be used for the characterization of higher-molecular-weight (above 250 amu) and polar components of fossil fuels. Our research indicates that supercritical carbon dioxide is a relatively poor solvent for PAH and polar-substituted PAH, and needs (at a minimum) to be modified with the addition of a few percent of a polar solvent, such as isopropanol, in order to solvate polar fossil fuels. Another primary emphasis has been the development of the SFC-MS interface and flow restrictor technology. Successful interfaces have been developed for coupling capillary columns to both quadrupole[11] and magnetic sector mass spectrometers[12]; a unique high flow rate interface for coupling packed microbore columns to a quadrupole instrument has also been developed[13]. Our state of interface development is now such that SFC-MS can be used to analyze high-molecular-weight compounds that extend somwhat beyond that which can be analyzed by GC-MS. The extension to components at even lower volatility is now being realized with the application of polar-modified fluids.

A variety of fossil fuels, including diesel fuels, diesel fuel sediments, coal-derived liquids, and porphyrins have been analyzed by SFC-MS and related techniques. The diesel sediments were examined by supercritical fluid extraction using ammonia as the extracting fluid, followed by on-line tandem mass spectrometric analysis using a triple quadrupole mass spectrometer and collision induced dissociation. This analysis showed that the sediment material that had formed in "bad" diesel fuel was composed primarily of alkyl indoles, alkyl carbazoles, and polymeric pyrrole structures.[4] Boiling point fractions of coal-derived liquids have been examined by DFI-MS and by SFC-MS. The analyses produced average molecular weight distribution data that was comparable to that produced by low voltage direct-probe MS for fractions with boiling points less than 800°F. There was evidence for discrimination against the higher molecular weight species in the DFI-MS data for the higher boiling point fractions, but we believe that this discrimination results from poor solubility of the components of these fractions in the supercritical fluid, and not from discrimination inherent to the instrumental design.

SFC-MS has the potential to make major contributions to fossil fuel analysis. In order for the potential to be more fully realized, more knowledge about the ionization characteristics of unconventional CI reagents, such as polar-modified fluids, is needed. In addition, the phenomenon of solute nucleation in the SFC-MS interface region for nonvolatile compounds during expansion requires more study. With this knowledge will come better interface designs. What this area of research needs most of all, however, is more active participants who can apply MS detection to some of the analyses already being performed by SFC, which will lead to more rapid progress in the area. The commercial availability of SFC instrumentation appears to be stimulating such participation.

Literature Cited

1. Lee, M. L. 1986. Characterization of Coal Macerals by High Resolution Supercritical Fluid Chromatography, Annual Report. PB-87-102158/XAB, National Technical Information Service, Springfield, Virginia.

2. Lee, M. L. 1985. Separation of Large Coal Molecules Using High-Resolution Supercritical Fluid Chromatography, Final Report. PB-86-132842/XAB, National Technical Information Service, Springfield, Virginia.

3. Campbell, R. M., and M. L. Lee. 1986. Supercritical Fluid Fractionation of Petroleum- and Coal-Derived Mixtures. Anal. Chem. 58:2247-2251.

4. Wright, B. W., H. T. Kalinoski, A. J. Kopriva, H. R. Udseth, and R. D. Smith. 1986. Characterization of Navy Fuels Using Supercritical Fluid Analytical Methodologies, Final Report. Defense Technical Information Service, Alexandria, Virginia.

5. Norris, T. A., and M. G. Rawdon. 1984. Determination of Hydrocarbon Types in Petroleum Liquids by Supercritical Fluid Chromatography with Flame Ionization Detection. Anal. Chem. 56:1767-1769.

6. Jinno, K., T. Hoshino, R. Hondo, M. Saito, and M. Senda. 1986. Identification of Polycyclic Aromatic Hydrocarbons in Extracts of Diesel Particulate Matter by Supercritical Fluid Chromatography Coupled with an Ultraviolet Multichannel Detector. Anal. Chem. 58:2696-2699.

7. Wright, B. W., S. L. Frye, D. G. McMinn, and R. D. Smith. 1987. On-Line Supercritical Fluid Extraction-Capillary Gas Chromatography. Anal. Chem. 50:640-644.

8. Taylor, L. T. 1987. Identification of Nonvolatile Coal Derived Products via Chromatography Coupled with On-Line FTIR Detection, A Quarterly Technical Report. DOE/PC/70799-T8, National Technical Information Service, Springfield, Virginia.

9. Pariente, G. L., and P. R. Griffiths. 1986. Supercritical Fluid Extraction of Coal: Apparatus and Characterization Techniques. Proceedings of the Pittsburgh Conference and Exposition on Analytical Chemistry and Applied Spectroscopy. Pittsburgh Conference, Atlantic City, NJ.

10. Schwartz, H. E., R. G. Brownlee, M. M. Boduszynski, and F. Su. 1987. Simulated Distillation of High-Boiling Petroleum Fractions by Capillary Supercritical Fluid Chromatography and Vacuum Thermal Gravimetric Analysis. Anal. Chem. 59:1393-1401.

11. Wright, B. W., H. T. Kalinoski, H. R. Udseth, and R. D. Smith. 1986. Capillary Supercritical Fluid Chromatography-Mass Spectrometry. HRC&CC 9:145-153.

12. Chess, E. K., H. T. Kalinoski, B. W. Wright, and R. D. Smith. 1987. Development and Evaluation of Supercritical Fluid Chromatography-Mass Spectrometry for Polar and High-Molecular-Weight Coal Components, Annual Report. PNL-6140, Pacific Northwest Laboratory, National Technicial Information Service, Springfield, Virginia.

13. Smith, R. D., and H. R. Udseth. 1987. Mass Spectrometer Interface for Microbore and High Flow Rate Capillary Supercritical Fluid Chromatography with Splitless Injection. Anal. Chem. 59:13-22.

Presented at the 35th ASMS Conference on Mass Spectrometry and Allied Topics
May 24-29, 1987, Denver, CO

SUPERCRITICAL FLUID CHROMATOGRAPHY/MASS SPECTROMETRIC (SFC/MS) ANALYSIS OF WAXES

David J. Miller and Steven B. Hawthorne
University of North Dakota Energy Research Center
Box 8213 University Station
Grand Forks, North Dakota 58202

Supercritical fluid chromatography/mass spectrometric analysis of a variety of waxes (natural, petroleum, coal-derived, and synthetic) have been performed using direct introduction of the capillary SFC column effluent into the ion source of a Hewlett Packard 5985B GC/MS. Depending upon the source, waxes can be composed of a large variety of compounds including saturated hydrocarbons (paraffin and microcrystalline waxes), esters formed from even-numbered straight-chain C_{12}-C_{36} alcohols and carboxylic acids (natural waxes), triglycerides (bayberry wax) and long-chain carboxylic acids (acid montan wax).[1-3]

Standard compounds and wax samples were dissolved in chloroform (ca. 10 mg/ml) and injected via a 0.5 ul sample loop and a splitter onto a 10 m x 50 um DB-5 (0.2 um film thickness) chromatographic column (J & W Scientific, Folsom, CA). Carbon dioxide was pressure programmed from 75 atm (2 minute hold) to 175 atm at 25 atm/min and then at 5 atm/min to 290 atm. The column was held at 125 ^{o}C. In order to maintain supercritical conditions over the entire length of the column, an outlet restrictor was fabricated by sealing the end of the column and then grinding it to obtain a gas flow of 1-2 ml/min.[4]

Chemical ionization mass spectra were obtained under SFC/MS conditions for a number of standard compounds. Representative spectra for n-alkanes, alcohols, carboxylic acids, esters, diglyceride esters, and triglyceride esters are shown in Figure 1.

Methane chemical ionization MS of alkanes gave base peaks for pseudomolecular ions at $(M-1)^+$ and characteristic methylene losses. The alcohol standards showed a base peak at $(M-1)^+$ as well as ions at $(M-17)^+$ resulting from the loss of water from the protonated parent. Carboxylic acids showed base peaks at $(M+1)^+$ with a less intense peak at $(M-1)^+$. The relative intensity of the $(M-1)^+$ peak increased with the acid chain length.
Monoesters had pseudomolecular ions at $(M+1)^+$ and at $(M-1)^+$. The base peak for each monoester was at $(A+H)^+$ where A is the parent acid. An additional fragment at $(MH-ROH)^+$ was observed for each monoester (R is the attached alkyl group). All of the di- and triglycerides showed low intensity pseudomolecular ions at $(M-1)^+$. Diglycerides showed $(M-17)^+$ ions resulting from the loss of water from the protonated parent. The base peak for diglycerides was an ion formed by the loss of one carboxylic acid from the protonated parent. Triglycerides exhibit this same loss to produce the base peak.

An example of the application of SFC/MS to waxes is shown in Figure 2. Bayberry wax was analyzed and found to consist of free carboxylic acids (C_{14}, C_{16}, and C_{18}), diglycerides including dimyristin (MM), a mixed diglyceride formed with one palmitate and one myristate group (MP), dipalmitin (PP), and triglycerides including trimyristin (MMM), a mixed triglyceride containing two myristate and one palmitate group (MMP), a mixed triglyceride containing one myristate and two palmitate groups (MPP), and tripalmitin (PPP). SFC/MS was also used to identify C_{20} to C_{100} alkanes in microcrystalline and Fischer-Tropsch waxes, C_{12} to C_{24} carboxylic acids in a coal-derived montan wax, and esters and diesters ranging in molecular weight from 592 to 958 in beeswax.

Credit

This work was performed under Cooperative Agreement No. DE-FC21-83FE60181 and DE-FC21-86MC10637 for the U.S. Department of Energy, Office of Fossil Energy.

Presented at the 35th ASMS Conference on Mass Spectrometry and Allied Topics
May 24-29, 1987, Denver, CO

Referneces

1. J.F. Lawrence, J.R. Iyengar. B.D. Page and H.B.S. Conacher, J. Chromatogr.,236,403, (1982).

2. A.P. Tulloch, Cosmet. Perfum.,89,53 (1974).

3. A.P. Tulloch, J. Am. Oil Chem. Soc.,50, 367 (1973).

4. E.J. Guthrie and H.E. Schwartz,J. Chromatogr. Sci.,24, 236 (1986).

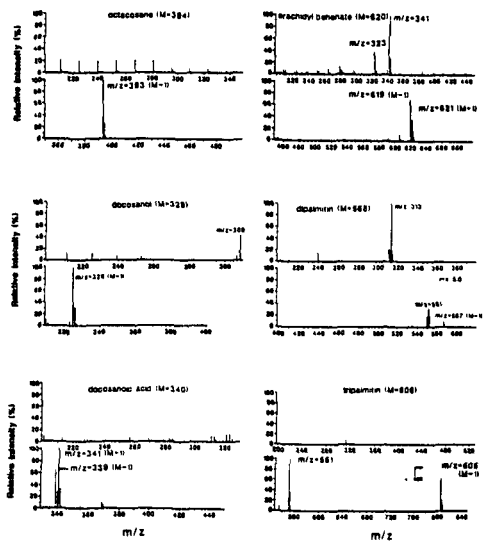

Figure 1. SFC/MS methane chemical ionization mass spectra of representative standards.

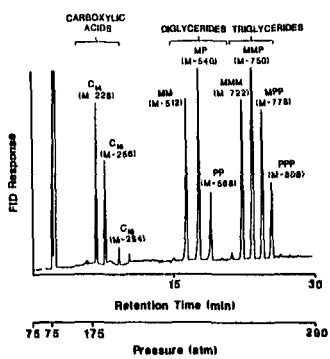

Figure 2. SFC/FID chromatogram of bayberry wax.

Presented at the 35th ASMS Conference on Mass Spectrometry and Allied Topics
May 24-29, 1987, Denver, CO.

Liquid Chromatography - Mass Spectrometry of Pesticides and Butyltin Compounds

Thomas A. Bellar and William L. Budde

U. S. Environmental Protection Agency, Cincinnati, OH 45268

The objective of this work was to develop a broad spectrum liquid chromatography/mass spectrometry (LC/MS) method for the simultaneous identification and measurement of a variety of non-volatile toxic organic compounds that may be present in drinking water, surface water, or groundwater. By broad spectrum, we mean a method that is capable of identifying and measuring a wide variety of non-volatile compounds using standardized conditions that are as simple and rugged as possible. By method, we mean a complete analytical method including extraction and concentration procedures, chromatography and mass spectrometry conditions, identification and measurement instructions, and quality control and reporting requirements.

Some of the compounds considered for inclusion in this method are shown in Table 1. All of these compounds are pesticides or pesticide metabolites that are considered a potential threat to the environment.

Table 1. Compounds Considered for Inclusion in a Broad Spectrum LC/MS Method for Analysis of Water Samples

Pesticide (metabolite) name	MW	quantitation ion	Chemical class
alachlor, Lasso	269	270	N-substituted amide (Cl)
aldicarb, Temik	190	208	carbamate (S)
aldicarb sulfone	222	240	carbamate (S)
aldicarb sulfoxide	206	207	carbamate (S)
ANTU	202	203	N-substituted thiourea (S)
atrazine-DA	187	188	triazine (Cl)
BPMC	207	225	carbamate
carbaryl	201	219	carbamate
carbofuran	221	222	carbamate
carboxin sulfoxide	241	268	N-substituted amide (S)
coumafuryl	298	299	lactone, keto, and hydroxy
cyanazine, Bladex	240	241	triazine (Cl)
diuron	232	233	N-substituted urea (Cl)
fenamaphos sulfoxide	319	171	
fluometuron	232	233	N-substituted urea (F)
linuron, Lorox	248	249	N-substituted urea (Cl)
methiocarb	225	243	carbamate (S)
methomyl, Lannate	162	163	carbamate (S)
metribuzin-DA		200	triazine (S)
monuron	198	199	N-substituted urea (Cl)
oxamyl	219	163	carbamate (S)
pronamid metabolite		274	
propachlor, Ramrod	211	212	N-substituted amide (Cl)
propham	179	180	carbamate
propoxur	209	210	carbamate
rotenone	394	395	keto, multi-ether
siduron	232	233	N-substituted urea
warfarin	308	309	lactone, keto, and hydroxy
zectran, Mexicarbate	222	223	carbamate

The water extraction procedures evaluated were a liquid-liquid extraction with methylene chloride, and a solid phase extraction using cartridges containing reverse phase liquid chromatography packing materials. The separation method selected was gradient elution high performance LC with a conventional reverse phase 25 cm x 4.6 mm ID column and a flow rate of 1.1 mL/min. The initial solvent composition was 80% water, containing 0.1 M ammonium acetate, and 20% acetonitrile. The final composition, after 33 minutes and elution of all compounds, was 50% water/acetonitrile. The eluate was directed through a Vestec thermospray interface to a Finnigan 4500 mass spectrometer. The mass spectrometer was operated with the filament off, ammonium acetate being the ionizing reagent. The spectrometer was scanned from 160-400 amu with a two second cycle time in the positive ion mode.

The candidate analytes were added to reagent water at an mean level of 13 parts per billion (3.6 - 50 micrograms per liter), extracted, and a portion of the extract in methanol injected into the LC/MS system. The system was calibrated using a single point external standard at the expected concentration level (assuming 100 % recovery). Quantitative measurements were made by integrating the abundance of the quantitation ions shown in Table 1 over the LC peaks. Each compound was extracted and analyzed a minimum of five times with each method. Four butyl tin compounds, which are used in marine paints as anti-fouling agents, did not respond to ammonium acetate ionization and were deleted from the potential analyte list.

With liquid-liquid extraction, the grand mean recovery of all compounds in Table 1 was 71% with a mean relative standard deviation of 11%. With the solid phase extraction, the grand mean recovery of all compounds in Table 1 was 76% with a mean relative standard deviation of 17%. Three of the compounds gave unacceptably low recoveries with the liquid-liquid extraction, and seven of the compounds gave unacceptably low recoveries with the solid phase extraction. There was variation in recovery among the different solid phase extraction cartridges, but all available data was used to calculate statistics for this paper.

We believe this method can be improved by selection of an appropriate internal standard, by automation of certain aspects, by selection of the most consistently performing solid phase extraction cartridge, and by use of a thermospray interface with greater stability, especially in the gradient controller.

Presented at the 35th ASMS Conference on Mass Spectrometry and Allied Topics
May 24-29, 1987, Denver, CO

FORENSIC COMPARISON OF EXPLOSIVES BY THERMOSPRAY/LIQUID CHROMATOGRAPHY/MASS SPECTOMETRY

D.W. Berberich, Department of Chemistry, University of Florida, Gainesville, Florida 32611, D.D. Fetterolf, Forensic Science Research Unit, FBI Academy, Quantico, Virginia 22135

The increase in terrorist activity in recent years has generated the need for improved analytical methods which can accurately identify explosives. The majority of current techniques for the analysis of explosives involve HPLC with non-specific detection. For more selectivity, mass spectrometry (MS) has been combined with HPLC for the detection of explosives usually with the DLI-HPLC-MS or HPLC with off-line CI-MS detection. Thermospray/ Liquid Chromatography/Mass Spectrometry (TSP/LC/MS) surmounts the inherent difficulties of DLI and off-line techniques by providing a direct, sensitive, and selective method for the analysis of explosives.

We have investigated the application of TSP/LC/MS to the separation and identification of commercial and military explosives. All experiments were performed with a Vestec TSP attached to a Finnigan-MAT Triple Quadrupole (TSQ 45). The liquid chromatographic separation was performed using dual Gilson Model 302 pumps and a C-18 column (Supelco 5 mm x 15 cm, 5 um packing). The column was operated using a premixed isocratic mobile phase consisting of 60/40 methanol (Burdick and Jackson)/0.10 M ammonium acetate (Aldrich) aqueous buffer with a flow rate of 1.5 mL/min. These conditions resulted in retention times of just over two minutes for common explosives, permitting rapid analysis. This is approximately 10 times faster than the separation reported using a 25 cm column with solvent programing (1). A typical separation is shown by the reconstructed ion chromatogram (RIC) and ion chromatograms in Figure 1. The ions at m/z 226 and 241 correspond to TNT $[M-H]^-$ and Tetryl $[M-NO_2]^-$, respectively. The ions at m/z 281, 355, 375 correspond to the acetate adduct $[M+CH_3COO]^-$ of RDX, HMX, and PETN, respectively.

Currently there are three modes of ionization available for use with the TSP interface: thermospray (filament-off), filament-on, and discharge ionization. With TNT as the reference compound, a sensitivity ratio of 1:3:1.4, with respect to base peak intensity, was observed in the negative ionization modes, respectively. The effect of the various ionization modes on the resulting negative ion mass spectrum of TNT are shown in Figure 2.

The ability of explosive compounds to capture electrons has been documented (2). One of the major distinctions between the three ionization modes for TSP is that with filament-off ionization there is no external source for the production of electrons. Both filament-on and discharge ionization have an external source of electrons which can produce thermal electrons. Therefore, the relative lack of sensitivity in the TSP(filament-off) mode may be attributed to the absence of thermal electrons which may contribute to filament-on and discharge ionization modes. The lack of thermal electrons in the TSP mode also accounts for different ions being observed in the various mass spectra of TNT. With TSP ionization, the most abundant ion for the TNT spectra is m/z 226 $[M-H]^-$, while in the other ionization modes the most abundant ion is m/z 227 $[M]^-$ due to electron capture by the highly electronegative nitro groups. The TSP was operated in the filament-on ionization mode which yielded unique spectra for the following explosive compounds: RDX; HMX; TNT; DNT; PETN; NG; DPA; MMAN; and Tetryl.

Presented at the 35th ASMS Conference on Mass Spectrometry and Allied Topics
May 24-29, 1987, Denver, CO

Developing a method of analysis for identifying post-blast residues is of equal utility as the characterization of unexploded materials. In order to evaluate the effectiveness of TSP(filament-on)/LC/MS for residue analysis, a number of improvised explosive devices were constructed and detonated under controlled conditions. The reconstructed ion chromatograms in Figure 3 were obtained from an acetone-wash of the end cap from a pipebomb. The presence of DPA shown in the positive ion trace and the presence of NG in the negative ion trace are indicative of the use of a double-based smokeless powder.

The data presented here demonstrates the applicability of TSP(filament-on)/LC/MS for the analysis and characterization of explosives and explosive residues. Chromatographic operating conditions permitted analysis of common explosives in just over two minutes. Negative ionization proved to be very sensitive for a large number of explosive compounds, while providing the high selectivity required to discriminate against interferents. Most of the explosives yielded only negative ion spectra, which exhibited a strong $[M+CH_3COO]^-$; however, additives in double based smokeless powders also yielded positive ion spectra.

References

1) Voyskner,R.D. and Yinon,J., Journal of Chromatography, 1983, 46, 45.
2) Chamberlain,A.T. and Marlow,J.S., Journal of Chromatographic Science, 1977, 15, 29.

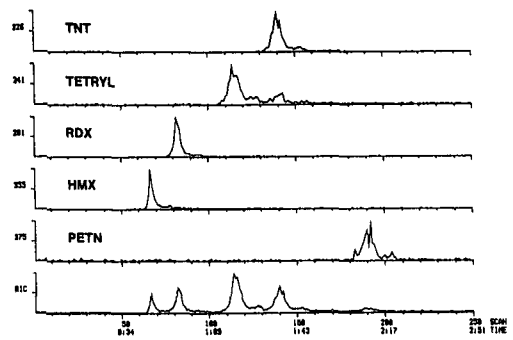

Figure 1. Ion chromatograms and reconstructed ion current (RIC) for negative ion TSP(filament-on)/LC/MS analysis of a standard explosive mixture.

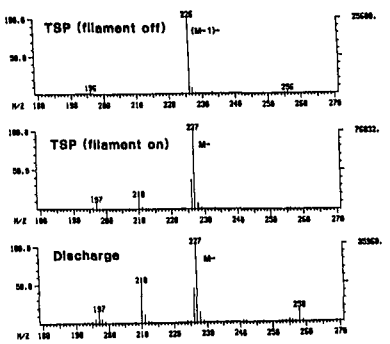

Figure. 2. Negative ion TSP/LC/MS spectra of TNT with different ionization modes.

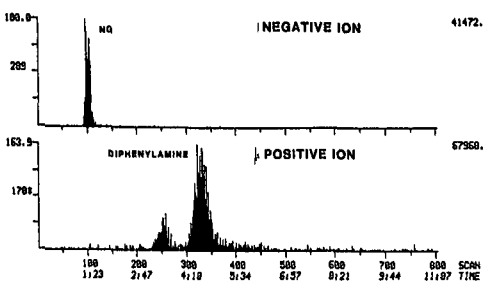

Figure 3. Reconstructed positive and negative ion chromatograms for smokeless powder residue.

Presented at the 35th ASMS Conference on Mass Spectrometry and Allied Topics
May 24-29, 1987, Denver, CO

Applications of High Resolution Mass Measurements in Thermospray LC-MS

L. Baczynskyj and G.E. Bronson,
Physical and Analytical Chemistry Research,
The Upjohn Company, Kalamazoo, MI 49001

The purpose of this study was to evaluate the accuracy and precision of exact mass measurements in the thermospray ionization technique. Two methods of determining the exact masses were used: the peak-matching technique and the magnetic scanning technique.

Experimental.

All experiments were performed on the Kratos MS80 RFA high resolution mass spectrometer using the Vestec-Kratos interface. The accelerating voltage was 4 kV. A Varian 5560 liquid chromatograph with a variable wavelength UV detector in line with the vaporizer was used. For peak-matching, the solution of the unknown and the reference mixture were pumped directly into the ion source. For magnetic scanning, the reference mixture was added after the UV detector.

Results and Discussion.

A. Peak-matching.

A solution of erythromycin dissolved in 0.1 M aqueous ammonium acetate-acetonitrile (4:1) was pumped simultaneously with a solution of PEG-600 in the same solvent system. The masses of interest were bracketed by two reference peaks and the resolution was set to 7,500. The exact masses of the following ions were determined: (M+H) at m/z 734, (M+H-H_2O) at m/z 716 and at m/z 558. The standard derivation for five measurements for each of these ions were 3.0, 1.2 and 2.3 ppm. The (M+H) ions of two unknown cyclic peptides at m/z 719 and 721 gave a standard derivations of 0.3 and 0.9 ppm. An equimolar mixture of cytidine, uridine, inosine, guanosine, thymidine and adenosine was prepared and the (M+H) ions of the nucleosides were mass measured. For cytidine, thymidine and adenosine excellent agreement between the measured and theoretical masses were found (less than 2 ppm). However for uridine and inosine errors of 60 and 30 ppm were found. This was due to the interference of the ^{13}C isotopic peaks of cytidine and adenosine respectively. For this reason the component mixture was reported by HPLC and full high resolution spectra obtained.

B. Magnetic scanning.

The high resolution mass spectra of the eluting components were obtained under the following conditions: 3 sec./dec. exponential scans from m/z 520 to 124. The calibrant (PEG 400) was added after the UV detector using a syringe pump. Under these conditions the accuracy of the measurements varied from 50 to 290 ppm. All errors were positive. Loop injections of pure components gave similar errors. After careful consideration of the experimental conditions it was concluded that the 44 dalton gaps between the major peaks of PEG are too large. For this reason a mixture of PEG, PEG-monomethyl and PEG-dimethyl ether were prepared. Using this mixture as markers, the accuracy of the mass measurements improved considerably. Thus for 12 scans across the LC peak corresponding to adenosine the RMS error on the m/z 268 (M+H) ion was 16.4 ppm. Whereas for inosine (M+H) at m/z 269, the RMS error for seven scans was 16.8. The abundances of the (M+H) ions for these two cases were quite different. In addition several pure components (lincomycin, spectinomycin, synthetic peptide of (M+H)420) were mass measured under the same conditions but using loop injections. For the (M+H) at m/z 407 of lincomycin 36 mass determinations showed a total RMS error of 11.2. Similarly 36 mass measurements of the (M+H) of the peptide at m/z 420 had a total RMS error of 10.1 ppm. Finally the (M+H) of spectinomycin at m/z 333 was mass measured. The total RMS error for 60 scans was 14.2 ppm.

Conclusions.
High resolution mass measurements in the thermospray ionization mode by the peak-matching technique gives good accuracy and precision. PEG or PPG can be used as reference markers. Large amounts of sample are necessary. Exact mass measurements can also be performed by scanning the magnetic field. However new marker mixtures are needed. PEG + PEG-monomethyl- and di-methyl-ethers can be used. The RMS errors are 12-16 ppm.

Presented at the 35th ASMS Conference on Mass Spectrometry and Allied Topics
May 24-29, 1987, Denver, CO

GC/FTIR/MS AND LC/MS ANALYSIS OF NITROSOBENZENE DECOMPOSITION PRODUCTS

R. Thomas Solsten, Hideji Fujiwara, and Stephen J. Wratten
Monsanto Company, Life Sciences Research Center
700 Chesterfield Village Parkway, Chesterfield, Missouri 63198

Metabolic transformations of anilines and their acylated derivatives have been a subject of continuing interest to our group because of the important herbicidal properties of several chloroacetanilides. A recent publication described the GC/MS identification of 2,6-diethylnitrosobenzene,1, as a rat metabolite of several chloroacetanilides and reported that 1 was a mutagen in the Ames salmonella assay. We found this interesting since our own studies of 2,6-diethylnitrosobenzene indicated that it is unstable at room temperature and decomposes in the injector of a gas chromatograph to produce a variety of compounds some of which are isomeric to 1.

DECOMPOSITION OF 2,6-DIETHYLNITROSOBENZENE AT ROOM TEMPERATURE

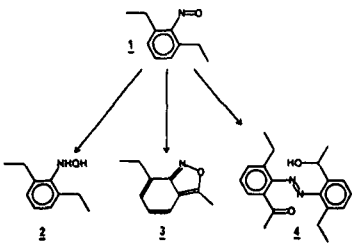

DECOMPOSITION OF 2,6-DIETHYLNITROSOBENZENE IN THE GAS CHROMATOGRAPH

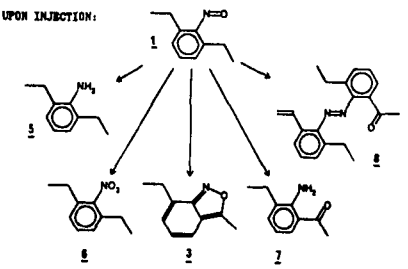

The decomposition products were characterized by LC/MS, NMR, HRMS, and GC/FTIR/MS along with comparison to synthetic standards. A series of alkyl-substituted standards were prepared to ascertain the mechanism of nitrosobenzene decomposition and the effect of substituents on nitrosobenzene stability. The results suggest that the decomposition is initiated by a 1,5 H shift from the alkyl side chain to the oxygen atom followed by a series of rearrangements, cyclizations, and radical trapping to produce the observed products.

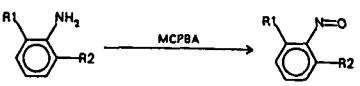

R1	R2	REL. STABILITY
Et	Et	- - -
Et	Me	- -
Me	Me	+
Me	OMe	-
Me	CF3	-
Me	t-Bu	- -
Me	n-Bu	- - -
Et	H	+

Subtle changes in the alkyl side chain frequently produced dramatic differences in the overall decomposition rate. For example, 2,6-dimethylnitrosobenzene was remarkably stable while the corresponding diethyl analog was completely decomposed after 24 hours at room temperature. LC/MS proved to be the best method for following the decomposition of each nitrosobenzene at room temperature and in most cases provided an intense protonated molecular ion with minimal fragmentation.

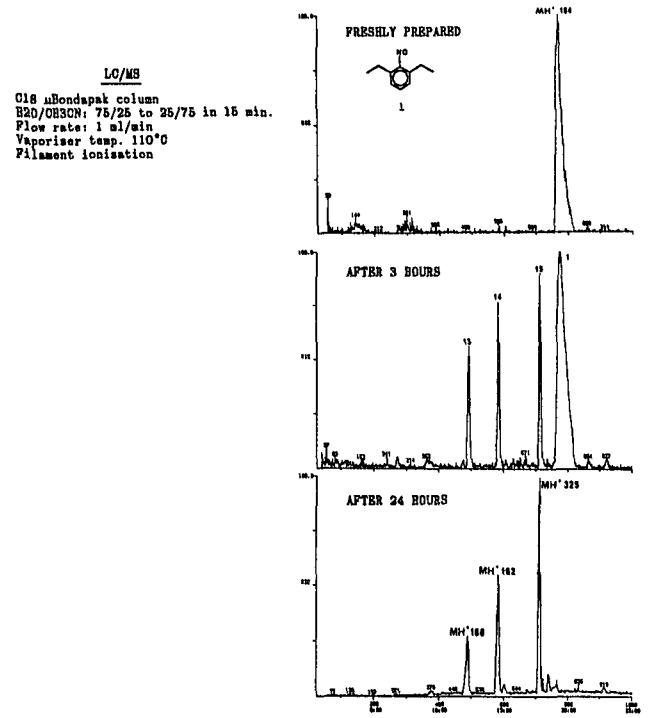

The assertion that nitrosobenzenes are formed during the in-vitro metabolism of chloroacetanildes is questionable since the previous investigators relied on GC/SIM/MS analysis for metabolilte identification. We have demonstrated that GC/MS is not an appropriate analytical method for such alkylated nitrosobenzenes. LC/MS appears to be a better technique for metabolic studies of chloroacetanilides since thermal decomposition is minimal. The instability of 2,6-diethylnitroso benzene at room temperature also obfuscates the results of the Ames assay which generally requires incubation of the analyte for several days at 37 degrees Centigrade. The observed mutagenicity ascribed to 1 may be due to compounds 2, 3, 4, or from p-hydroxydiethylaniline which is known to arise from rearrangement of the hydroxylamine 2.

1. E.C. Kimmel, J.E. Casida, and L.O. Ruzo, J. Agric. Food Chem. 34, 157-161 (1986)

Presented at the 35th ASMS Conference on Mass Spectrometry and Allied Topics
May 24-29, 1987, Denver, CO

IMPURITY DETERMINATION IN A RENIN INHIBITOR PEPTIDE USING THERMOSPRAY LC/MS

by

F. W. Crow, K. D. Evans, K. S. Manning and R. H. Robins

In developing drug candidate assays it is important to characterize all of the impurities which may be present. This is done to understand the chemistry and to develop methods to limit impurity levels. One relies heavily on liquid chromatography in the impurity determination process. One must verify that all of the impurities have been separated from each other and the bulk drug.

On-line thermospray LC/MS aids in the rapid identification of LC peaks without prior isolation and allows evaluation of the quality of the chromatographic separation by verifying the identity of peaks, determining misassigned or overlapping peaks and obtaining semiquantitative data for unresolved peaks.

Renin is important in regulating blood pressure. Angiotensin is broken down by renin into angiotensin I, which is converted into angiotensin II, which in turn causes constriction of blood vessels resulting in elevated blood pressure. A renin inhibitor blocks this cascade, thus regulating blood pressure. The structure of this Renin Inhibitor Peptide (RIP) is very similar to the structure of the region in angiotensin which is acted upon by renin. The peptide back-bone is similar. The 'C' and 'N' termini are protected to avoid enzymatic digestion. The difference is that RIP lacks the amide bond whose cleavage is catalyzed by renin. Therefore, RIP can bind to renin, but will not be release since the amide bond is not broken. The synthesis takes place in a stepwise fashion starting from one end of the molecule and adding each amino acid one at a time.

The thermospray spectrum of RIP is reasonably simple. It is dominated by the protonated molecule ion and contains some small fragment ions. In a typical analysis 20 mg of sample is injected on-column. The impurities we are looking at range from 1.0% to less than 0.1% of the total.

The spectrum of impurity L' demonstrates that data is easily obtained on impurities at the level of 0.5 - 1.0%. Similarly the spectra of impurities M and M' demonstrate full scan sensitivities at levels of less than 0.1%. This corresponds to less than 20 ng of compound injected on-column.

The spectra obtained for M/M' also demonstrate on of the most powerful aspects of the on-line thermospray LC/MS experiment. Mixture peaks can be easily detected and resolved due to the different molecular weights of the components. Using this method we determined the molecular weights and tentative structures of over 26 different species.

This provides us with an understanding of the impurity chemistry earlier in the development process. Thus allowing more time to devote to controlling those impurities. It aids in the chromatographic development by: a) giving an indication of the number of species which one is dealing with, b) aiding in detecting overlapping chromatographic peaks, c) verifying the identity of peaks by more than just retention time, d) discovering hidden peaks under other major peaks, even the bulk drug itself, and e) determining if further chromatographic development needs to be done to further resolve the peaks, as was the case in this study.

We have demonstrated that on-line thermospray LC/MS has the sensitivity, dynamic range and selectivity to provide molecular weight information in pharmaceutical impurities analyses for peptide like species.

Presented at the 35th ASMS Conference on Mass Spectrometry and Allied Topics
May 24-29, 1987, Denver, CO

Synthesis

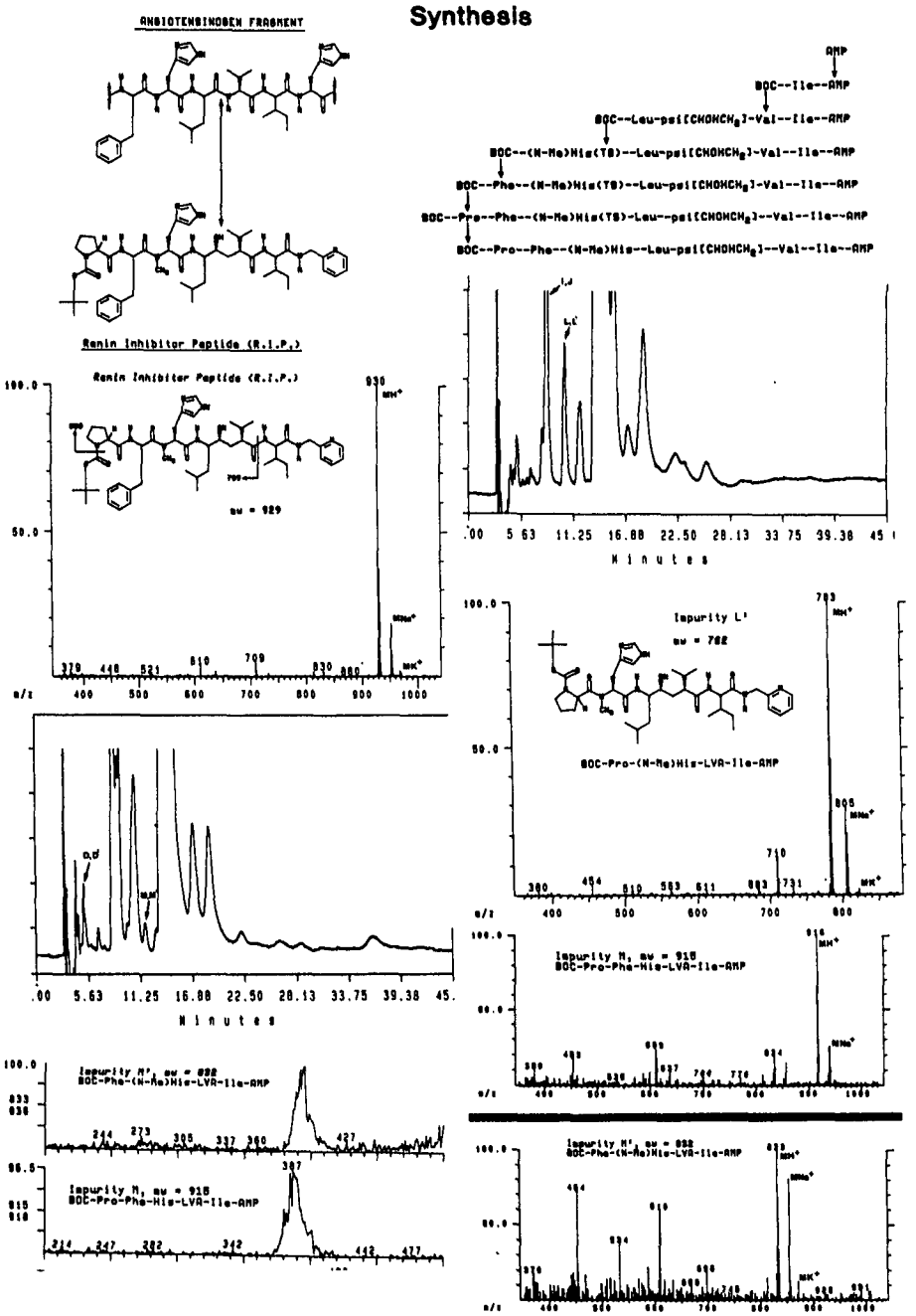

Presented at the 35th ASMS Conference on Mass Spectrometry and Allied Topics
May 24-29, 1987, Denver, CO

THERMOSPRAY LC/MS OF TRIGLYCERIDES,

R. A. Sanders & B. A. Charpentier; The Procter & Gamble Company, Winton Hill Technical Center, 6071 Center Hill Road, Cincinnati, OH 45224 and C. H. Vestal, Vestec Corporation, 9299 Kirby Drive, Houston, TX 77054

INTRODUCTION: Chromatographic profiling of triglycerides is an important analytical procedure in the food industry. Gas chromatography has been used for many years to provide the "carbon number profile" of complex triglyceride mixtures. As the name implies, GC methods have focused on distinguishing triglycerides of different carbon numbers. The number and position of carbon-carbon double bonds is not easily obtained from intact triglyceride mixtures by gas chromatography. Such information is available from GC of the methyl esters, but the method is lengthy and throws away information concerning the distribution of fatty acids in the intact glycerides. More recently, liquid chromatography (LC) has been used to profile intact triglycerides. Such procedures can readily distinguish between triglycerides on the basis of molecular weight and level of unsaturation. This work presents an on-line mass spectrometric method for identifying the components in the liquid chromatographic triglyceride profile.

EXPERIMENTAL: Liquid chromatography/mass spectrometry was performed using a Beckman liquid chromatograph consisting of three 112 pumps and a 421 controller connected via a Vestec Thermospray interface (Figure 1) to a Hewlett-Packard 5970A mass selective detector (MSD). The chromatographic columns were two Beckman Ultrasphere 5u (25 cm x 0.46 mm). Acetonitrile and methylene chloride were HPLC grade from American Burdick and Jackson (Muskegon, MI). Mono-, di and triglyceride standards were obtained from NuChek Prep, Inc., (Elysian, MN).

Samples were run both by direct injection (column out) and by passage through the columns. For direct injection, the solvent used was 60:40 v/v acetonitrile:methylene chloride. For chromatography, samples were run either isocratically (standards) using 60:40 v/v acetonitrile:methylene chloride or with a gradient (mixtures) going from 35-55% methylene chloride in acetonitrile in 40 minutes. Solvent flow rate was 1 mL/min. Samples were dissolved in methylene chloride prior to injection. In order to obtain sufficient ionization of the samples in these organic solvents, all samples were run in the filament-on mode.

RESULTS & DISCUSSION: Figure 2 displays the thermospray mass spectrum of the standard 1,2-dipalmitoyl-3-oleoyl-glycerine (PPO) obtained under the conditions described above. Figure 3 shows the origin of the (parent - $RCO_2)^+$ ions which are also characteristic of electron ionization spectra of triglycerides[1]. Since the MSD mass range is limited to less than 800 daltons, it is important that the diglyceride region of the spectrum is so clearly delineated -- in this case with PP^+ and PO^+ ions completely describing the fatty acid content of the molecule. A lower molecular weight molecule, trimyristolein - 716 daltons, allows observation of behavior in the molecular ion region (Figure 4). In this case (parent $+H)^+$ is observed in addition to (parent - $RCO_2)^+$. However, as known from CI studies of triglycerides, protonated triglycerides are not stable species in general. Triglycerides with no carbon-carbon double bond do not produce an observable protonated molecule under the LC/MS conditions used here.

Figure 5 displays an HPLC profile (evaporative analyzer detector) from a low erucic acid, rapeseed oil (Canola). The corresponding thermospray LC/MS chromatogram is shown in Figure 6. In a few minutes of LC/MS analysis and interpretation time, confirmation was obtained for triglyceride peak identifications which had required many hours by off-line techniques (peak collection followed by solids probe CI/MS). The spectrum of peak #8 is shown in Figure 7 to be POL where O represents oleic acid and L indicates linoleic.

CONCLUSIONS: Thermospray LC/MS is shown, in this work and others[2], to be an effective tool for on-line identification of triglycerides separated by reverse-phase HPLC. The combination of high resolution separations based on level of unsaturation as well as carbon chain length with MS fragmentation that specifies the three fatty acid components is a powerful one for triglyceride profiling applications.

REFERENCES:

1) M. Barber, T. O. Merren & W. Kelley, Tetrahedron Letters, 1063, 1964.

2) H. Kim & N. Salem, Jr., Anal. Chem., 59, 722, 1987.

Presented at the 35th ASMS Conference on Mass Spectrometry and Allied Topics
May 24-29, 1987, Denver, CO

Figure 1

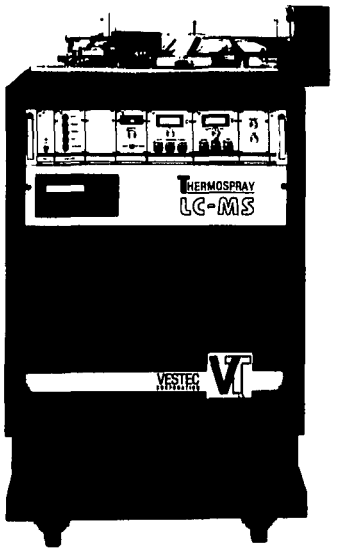

Figure 2

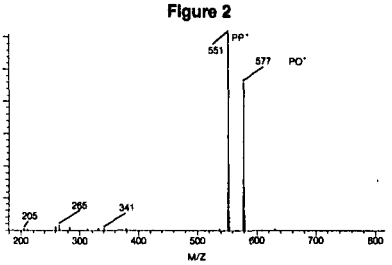

Figure 3

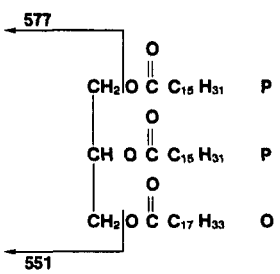

Figure 4

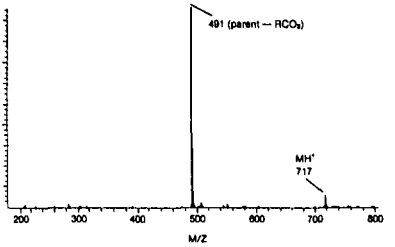

Figure 5

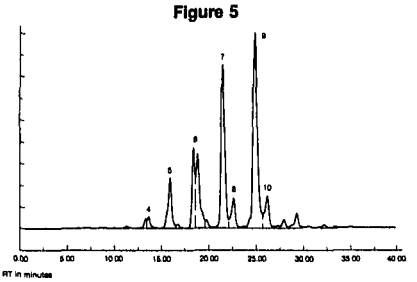

Figure 6

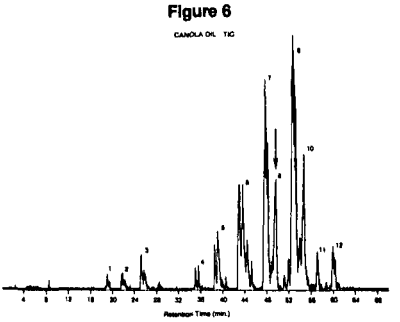

Figure 7

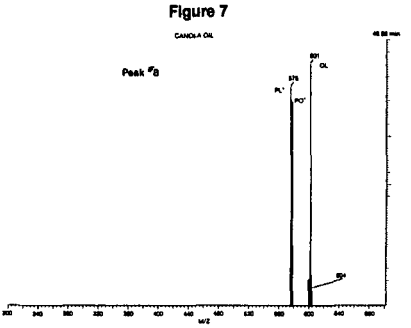

Presented at the 35th ASMS Conference on Mass Spectrometry and Allied Topics
May 24-29, 1987, Denver, CO

THE CHARACTERIZATION OF CAROTENOIDS AND RETINOIDS BY HPLC-MS-MS

Paul E. Farrow, Richard F. Taylor, Lauren M. Yelle
Arthur D. Little, Inc.
Acorn Park
Cambridge, Massachusetts 02140

The important role of carotenoids and retinoids in foods in protection from chemical carcinogenesis is becoming better understood. Work is currently under way to determine the relative distributions of these compounds in various foods. HPLC (LC) methods have been developed for these compounds in food extracts, and in conjunction with UV diode array detection and the availability of standards, identifications are made. Confirmation of these assignments by mass spectrometry is essential, as well as the identification of other carotenoid/retinoid species present.

The methods described in part here have been developed to confirm the identification of several carotenoids using a combination of LC-MS and LC-MS-MS. A group of related carotenoids were chosen as a study base. A standard solution of bixin, echinenone, canthaxanthin, and α and β-carotene was analyzed by LC-UV-MS under the conditions specified in Figure 1. A typical EI spectrum obtained for β-carotene is shown in Figure 2. MS-MS conditions such as collision energy and gas cell pressure were optimized using standard β-carotene. The daughter ion spectra for the molecular ion of each carotenoid was obtained. An example of a typical daughter ion spectrum of β-carotene is shown in Figure 3.

Food extracts were initially analyzed by LC-UV-MS full scanning to determine the presence of carotenoid species for which standards are not available. The extracts contain high levels of matrix compounds such as fatty acids, with carotenoids being minor components. This makes obtaining clean spectra of the compounds of interest difficult. In an effort to eliminate such interferences, selected ion recording (SIR) on the molecular ions was performed. This method, however, still has interferences associated with it. The use of LC-MS MRM (multiple reaction monitoring) was evaluated by monitoring transitions unique to each carotenoid species. LC-MS MRM was determined to be the method of choice for confirming the identity of these carotenoids due to its enhanced sensitivity and increased specificity over the other methods examined. Due to the complexity and structural similarity of these carotenoids, chromatographic separation was determined to be necessary for analysis of these food extracts. Thus, a combination of retention time data and mass spectral information is used.

In addition to the MRM technique, neutral loss experiments (e.g., M-92; toluene) on carotene related standards were carried out. This method proved to be applicable for "class specific" identification.

During the course of this work, the daughter ion spectra of α and β carotene were examined. The spectra showed characteristic differences giving, to our knowledge, the first reported qualitative mass spectral data of this type capable of distinguishing between these two isomers. In addition to moving belt EI, plasmaspray LC-MS has given preliminary data on these types of compounds, providing an alternate LC-MS technique. Figure 4 is a plasmaspray spectrum of β-carotene; further work using this LC-MS technique is underway.

Presented at the 35th ASMS Conference on Mass Spectrometry and Allied Topics
May 24-29, 1987, Denver, CO

EXPERIMENTAL CONDITIONS

Instrumentation	• *Waters HPLC model* 600 solvent delivery system • VG 70 SEQ hybrid mass spectrometer, 11-250J data system
HPLC conditions	• Partisil ODSIII 10μm column • 60% $CH_3OH/H_2O \longrightarrow$ 100% CH_3OH in 15 mins. Hold 30 mins. • 1 ml/min flow rate • 365 nm wavelength • 0.1 AUFS
LC-MS Interface	• *VG moving belt (polyimide)* • 1.2 cm/sec belt speed • nozzle temp: 270°
MS conditions	• 40eV electron ionization • source temp: 260°
MS-MS conditions	• 50eV collision energy • Argon gas at 5×10^{-7} mbar

Figure 1

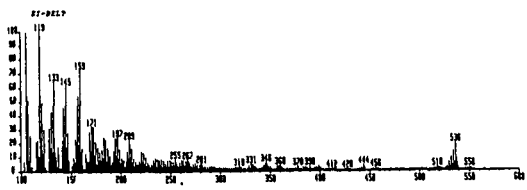

Figure 2

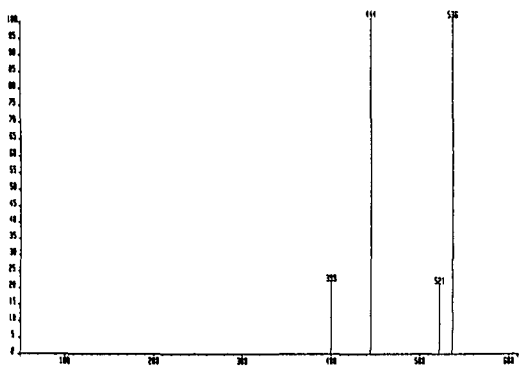

Figure 3

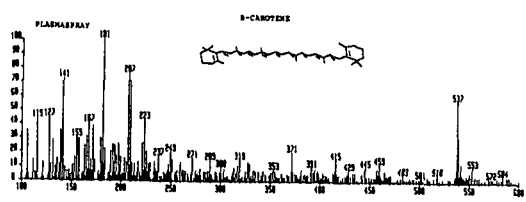

Figure 4

Presented at the 35th ASMS Conference on Mass Spectrometry and Allied Topics
May 24-29, 1987, Denver, CO

SEPARATION AND IDENTIFICATION OF ACETYLATED MONOGLYCERIDES BY REVERSED-PHASE HIGH PERFORMANCE LIQUID CHROMATOGRAPHY/MASS SPECTROMETRY USING A MOVING BELT INTERFACE.

Ramon L. Espino, Robert Weinkam and Brett R. Nelson, Section of the Analytical Chemistry, Biopharmaceutical Research, Allergan Inc., Irvine, California 92715

INTRODUCTION

A reversed-phase high performance liquid chromatography/mass spectrometry (LC/MS) method, using a moving-belt interface, is described for the separation and identification of individual palmitate and stearate monoglycerides, mono- and di-acetylated monoglycerides. The materials were resolved into six major components and two minor isomers,and the chemical structure of each component was determined. The separation was achieved with isocratic elution using reversed-phase columns and a 90/8/2 (by volume) acetonitrile, water and methanol mobile phase. The compounds were detected by a combination of UV detector and mass spectrometer, which provided reproducible chromatograms reported herein. The total ion chromatogram obtained in the EI^+ and CI^+ modes allowed identification of the peaks of interest in the UV chromatogram.

High Performance Liquid Chromatography/ Mass Spectrometry (LC/MS)

The mass spectra was obtained on a VG 7070E-HF mass spectrometer equipped with a LC/MS belt interface and a EI/CI source. Electron impact (EI^+) and chemical ionization (CI^+) spectra were produced at 70eV and 50eV, with a source pressure of about 1 X 10^{-6} and 2 x 10^{-5} mBar, respectively. The source temperature was set at 250°C. The spray depositor temperature was at 350°C and the nose-heater at 1.0 Amp. Ammonia gas was used as the reagent gas. The chromatography was obtained with a LKB 2150 pump (Bromma, Sweden) and a Rheodyne 2175 injector (Cotati, CA.). The separation was achieved using a 3.9-mm X 150-mm Novapak® 5μ column from Waters Associates (See Figure 2) and a 4.6-mm X 250-mm Ultremex® 5μ column from Phenomenex (Palos Verdes, CA) with the mobile phase previously outlined with a 1.0 mL/min flow rate (See Figures 1 to 4.

RESULTS

Mass spectral identification was obtained using HPLC/MS. Electron impact and ammonia chemical ionization were utilized to elucidate the structural fragmentation and the molecular weight. The results clearly show the presence of four sets of of chemical entities: palmitate/stearate monoglycerides, mono-acetylated monoglycerides, two isomeric mono-acetylated monoglycerides, and di-acetylated monoglicerides. A list of the chemical structures separated and identified are listed in Table I.

CONCLUSION

High performance liquid chromatography/ mass spectrometry (LC/MS) with a moving belt interface have been used to separate and elucidate the chemical structures of palmitate/stearate mono-, and di-acetylated monoglycerides. The moving belt interface has proven particularly useful for analyzing these monoglycerides. Electron impact and ammonia chemical ionization provided fragment ions which detailed structural information as well as molecular ion species. This detection technique may alleviate difficulties associated with HPLC of lipids using UV detectors as the universal detector. The moving belt interface is a powerful HPLC development tool to obtain structural information, as evidenced in this study. The sensitivity of the technique is compound dependent, the total lipid mixture is in the low μg level at full scan.

We believe that the LC/MS belt interface can be used to analyze other lipids and this should prove valuable specially for compositional and metabolic studies of biological systems.

Presented at the 35th ASMS Conference on Mass Spectrometry and Allied Topics
May 24-29, 1987, Denver, CO

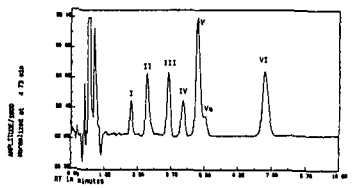

Figure 1. Separation of mono- and di-acetylated monoglycerides standard mixture using a Novapak® column. The mobile phase was 90/8/2 (by volume) acetonitrile, water and methanol at a 2.0 mL/min flow rate Absorbance was measured at 210 nm

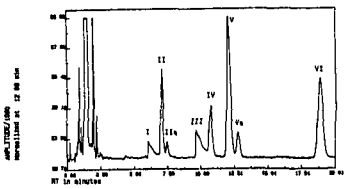

Figure 2. Separation of mono- and di-acetylated monoglycerides standard mixture using a Ultremex® column The mobile phase was 90/8/2 (by volume) acetonitrile, water and methanol at a 2.0 mL/min flow rate . Absorbance was measured at 210 nm.

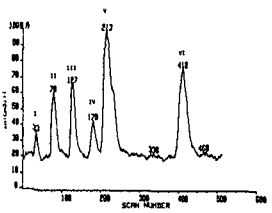

Figure 3. Total ion chromatogram of mono- and di-acetylated monoglycerides standard mixture using a Novapak® column. The mobile phase was 90/8/2 (by volume) acetonitrile, water and methanol at a 2.0 mL/min flow rate

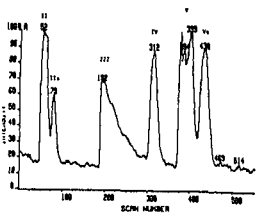

Figure 4. Total ion chromatogram of mono- and di-acetylated monoglycerides standard mixture using a Ultremex® column. The conditions were the same as Figure 4.

TABLE I

Components and Structures

Components

Peak	Name
I	Palmitate monoglyceride
II	Palmitate monoacetylated monoglyceride
IIa	Palmitate monoacetylated monoglyceride isomer
III	Stearate monoglyceride
IV	Palmitate diacetylated monoglyceride
V	Stearate monoacetylated monoglyceride
Va	Stearate monoacetylated monoglyceride isomer
VI	Stearate diacetylated monoglyceride

Structural Formulas

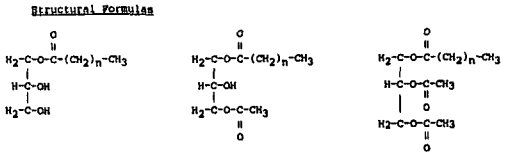

(1) n = 14
(3) n = 16

(2) n = 14
(5) n = 16

(4) n = 14
(6) n = 16

Presented at the 35th ASMS Conference on Mass Spectrometry and Allied Topics
May 24-29, 1987, Denver, CO

THERMOSPRAY/MASS SPECTROMETRY AND THERMOSPRAY/MS/MS OF DOXYLAMINE AND PYRILAMINE METABOLITES

W.A. Korfmacher, L.D. Betowski[1], C.L. Holder and R.K. Mitchum[1]

National Center for Toxicological Research, Jefferson, AR 72079 and
[1]USEPA, Las Vegas, NV 89114

INTRODUCTION

The antihistamine, doxylamine succinate, N,N-dimethyl-2-[1-phenyl-1-(2-pyridinyl)ethoxy]ethanamine succinate, a component of the drug Bendectin®, has been subjected to several studies regarding its safety and its metabolic products. Bendectin® was prescribed to pregnant women as an antinausea drug, but is no longer sold in the United States because of concerns that it might cause birth defects. Pyrilamine maleate, an ethylenediamine-type drug, belongs to a class of antihistamines that is used most frequently in prescription and non-prescription cold, allergy, and sleep aids. Pyrilamine may replace methapyrilene, a structural analog, which has been removed from the United States drug marketplace because it was shown to be a rat hepatocarcinogen. Pyrilamine maleate has also been shown to cause unscheduled DNA synthesis in primary cultures of rat hepatocytes.

Investigators at the National Center for Toxicological Research (NCTR) have conducted studies in the distribution and metabolism of doxylamine and pyrilamine in laboratory animals (1-3). Korfmacher and coworkers (4-7) have demonstrated that desorption chemical ionization mass spectrometry (DCIMS) is very useful for the analysis of doxylamine and pyrilamine and their metabolites. The DCIMS method has the disadvantage that the samples must be purified by HPLC before analysis. Thermospray (TSP) is a recently developed mass spectrometric ionization technique that shows great potential for the analysis of thermally labile compounds. In addition, TSP is an ideal MS ionization technique for direct liquid chromatography/mass spectrometry (LC/MS) analysis of samples. Therefore, the utility of TSP/MS for the analysis of doxylamine and pyrilamine and their metabolites was investigated.

In this work, we describe the use of TSP/MS for the analysis of pyrilamine and doxylamine and several of their metabolites obtained from rat and monkey metabolism studies. TSP/MS was found to provide excellent mass spectral results for these compounds. The utility of TSP/MS/MS was also investigated. TSP/MS/MS was found to provide additional analytical data for these samples and was successfully used for the direct analysis of a "cage wash" metabolite sample which has not undergone an HPLC purification step.

EXPERIMENTAL

Standard Compounds

Doxylamine and pyrilamine were obtained from commercial suppliers and found to be greater than 99% pure by HPLC. Doxylamine N-oxide was prepared as described by Holder et al. (6). Pyrilamine N-oxide and N-desmethyl-pyrilamine were synthesized as described in Korfmacher et al. (5). The structure of these compounds was confirmed by mass spectrometry and nuclear magnetic resonance spectroscopy.

Metabolites

Fischer 344 rats were dosed by gavage with either pyrilamine maleate or doxylamine succinate as described elsewhere (2,3,5,6). Urine and feces were collected from the animals using techniques described by Nony and coworkers (8,9). At the end of the test period, the cages were washed and the washings were saved and analyzed separately. Separation and purification of the metabolite extracts was performed using HPLC methodology described by Holder et al. (6). The doxylamine N-oxide metabolite was obtained from a rhesus monkey dosed with doxylamine as described by Slikker et al. (1).

Thermospray/Mass Spectrometry (TSP/MS)

Thermospray/mass spectrometry (TSP/MS) and TSP/MS/MS analysis was performed using a Finnigan MAT (San Jose, CA) 4500 Triple Stage Quadrupole (TSQ) mass spectrometer with a Vestec Corp. (Houston, TX) thermospray inlet system. Ten microliter volumes of the sample were flow injected into the TSP/MS system using a flow rate of 1.3 mL/min with aqueous 0.1 M ammonium

acetate/methanol (96:4 v/v) as the thermospray buffer solution. The ionizer pressure was typically adjusted to 1.4 x 10^{-5} torr and the vaporizer (tip) and jet temperatures were 219°C and 224°C, respectively. A collision energy of 20 eV was used for the collision-activated dissociation (CAD) experiments with argon set to 1.0 mtorr as the collision gas.

RESULTS AND DISCUSSION

For both doxylamine and doxylamine N-oxide, the base peaks of the TSP mass spectra were the $[MH]^+$ ion, with no fragment ions observed for doxylamine and only two significant fragment ions ($[MH-O]^+$ and $[MH-CH_2O]^+$) for doxylamine N-oxide. TSP/MS/MS analysis of the $[MH]^+$ ions for these compounds produced analytically significant fragment ions. TSP/MS/MS analysis of the m/z 287 ion of the doxylamine metabolite was especially useful for identifying the compound as the N-oxide metabolite.

Similar results were obtained for the TSP/MS and TSP/MS/MS analysis of pyrilamine and pyrilamine N-oxide. Again, the base peak of the TSP mass spectra for the standard compounds was the $[MH]^+$ ion and TSP/MS/MS analysis of the $[MH]^+$ ion produced characteristic fragment ions. TSP/MS/MS analysis of the m/z 302 ion from the pyrilamine N-oxide metabolite provided strong additional evidence for its identity.

Using TSP/MS alone, it would be difficult to distinguish between the N-desmethylpyrilamine and the O-dealkylated pyrilamine isomers, but TSP/MS/MS analysis of the $[MH]^+$ ion for each compound provided a clear method for differentiating these metabolites. TSP/MS analysis of a metabolite extract which was not purified by HPLC was also performed; TSP/MS/MS analysis of the m/z 272 ion from this extract provided a daughter ion spectrum that was used to identify the metabolite in this sample as O-dealkylated pyrilamine.

The TSP mass spectrum of a mixture of two doxylamine glucuronide metabolites resulted in $[MH]^+$ ions for the two metabolites. The daughter ion spectrum of the $[MH]^+$ ion included two fragment ions which aided the identification of this compound as a doxylamine glucuronide metabolite.

CONCLUSIONS

TSP/MS and TSP/MS/MS have been shown to be useful methods for the analysis of doxylamine and pyrilamine metabolites including two glucuronide metabolites of doxylamine. Analysis of biologically-derived metabolites provided spectra essentially identical to those obtained for authentic standards. In most cases, the combination of TSP/MS and CAD of the $[MH]^+$ ion provided almost unambiguous identification of the metabolite in the sample.

ACKNOWLEDGEMENTS

We thank J.O. Lay (NCTR) for helpful discussions. The authors are also grateful to W. Slikker, Jr. (NCTR) for providing the rhesus monkey metabolite sample. The authors also thank J. Cmarik (NCTR) for helping in the synthesis of the pyrilamine standards.

REFERENCES

1. W. Slikker, Jr., C.L. Holder, G.W. Lipe, W.A. Korfmacher, H.C. Thompson, Jr. and J.R. Bailey, J. Anal. Toxicol. 10, 87 (1986).
2. H.C. Thompson, Jr., A.B. Gosnell, C.L. Holder, P.H. Siitonen, K.L. Rowland and J.L. Cmarik, J. Anal. Toxicol. 10, 18 (1986).
3. C.L. Holder, H.C. Thompson, Jr., A.B. Gosnell, P.H. Siitonen, W.A. Korfmacher, C.E. Cerniglia, D.W. Miller, D.A. Casciano and W. Slikker, Jr., J. Anal. Toxicol., in press.
4. W.A. Korfmacher, C.L. Holder, J.P. Freeman, R.K. Mitchum and A.B. Gosnell, Org. Mass Spectrom. 20, 435 (1985).
5. W.A. Korfmacher, C.L. Holder, A.B. Gosnell and H.C. Thompson, Jr., J. Anal. Toxicol. 10, 142 (1986).
6. C.L. Holder, W.A. Korfmacher, W. Slikker, Jr., H.C. Thompson, Jr. and A.B. Gosnell, Biomed. Mass Spectrom. 12, 151 (1985).
7. E.B. Hansen, Jr., C.E. Cerniglia, W.A. Korfmacher, D.W. Miller and R.H. Heflich, Drug Metab. Dispo. 15, 97 (1987).
8. C.R. Nony, J.L. Martin and M.C. Bowman, J. Anal. Toxicol. 7, 49 (1983).
9. M.C. Bowman, C.R. Nony,, S.M. Billedeau, J.L. Martin, J.C. Thompson, Jr. and L.K. Lowry, J. Anal. Toxicol. 7, 55 (1983).

Presented at the 35th ASMS Conference on Mass Spectrometry and Allied Topics
May 24-29, 1987, Denver, CO

THE ANALYSIS OF DESULFO GLUCOSINOLATES USING THERMOSPRAY LC/MS

L.R.Hogge, D.W.Reed and E.W. Underhill

Plant Biotechnology Institute, National Research Council,
Saskatoon, Sask. S7N 0W9 Canada

Introduction:

Glucosinolates, possessing the general formula $R\text{-}C(\text{-}S\text{-}C_6H_{11}O_5)\text{=}N\text{-}O\text{-}SO_3^-$, are present in all Cruciferae many of which are economically valuable as vegetable and oilseed crops in the food industry. In vegetable crops the enzymatic breakdown products of glucosinolates are important flavor components but with oilseed crops these components reduce the quality of the oil and meal produced in the crushing process.
This laboratory is involved in research aimed at the production of Brassica spp. that contain little or no glucosinolates. In many cases it is also important to know the specific glucosinolates present as not all generate toxic aglycones. Therefore a reliable method for the separation and identification of these compounds is necessary.
Gas chromatography/Mass spectrometry (GC/MS) of the pertrimethylsilyl ethers of these compounds has been the method of choice for this analysis because of its excellent chomatographic resolution and sensitivity. Unfortunately not all glucosinolates are stable or derivatize completely using this method.
Recently a liquid chromatography method was developed for the separation of glucosinolates which prompted the authors to investigate the feasibility of using thermospray LC/MS for the analysis of these compounds. A description of this investigation is presented below.

Experimental:

Desulfoglucosinolates were produced from either commercially obtained glucosinolates (Aldrich and Calbiochem) or glucosinolates isolated in this laboratory from known cruciferous plants. The LC method was based upon the separation of glucosinolates as their desulfo-anologs prepared using a commercial sulfatase preparation (1).
LC separation of the glucosinolates was achieved using a 4.6 mm X 12.5 cm Whatman C18 Partisphere column. A linear gradient elution was used with 0.1M ammonium acetate and acetonitrile (0-33% acetonitrile) at a flow rate of 1 ml/min.. Thermospray LC/MS was performed using a Model 3300 Finnigan mass spectrometer retrofitted with a Vestec thermospray interface. The thermospray source temperature was 265 degrees.The mass spectrometer was scanned from mass 125 to mass 450 every 1.5 seconds.

Results and Discussion:

The feasibility of thermospray LC/MS was investigated by recording and studying both the positive and negative ion spectra of several glucosinolates. Table 1 shows the intensities of the protonated and deprotonated molecular ions obtained for the desulfoglucosinolates investigated. Molecular ions for 4-hydroxybenzyl and 3-indolylmethyl glucosinolates were not observed.
All the positive ion spectra have two common ions of high intensity. These ions at mass 180 and 214 indicate the presence of the glucose and the thio-glucose moiety respectively. The ion at m/z 180 is likely formed from the glucosyl-ammonia adduct whereas the ion at m/z 214 is most likely formed from the sulphur containing analog + 2 hydrogens as has been reported in the ammonia CI spectra of these compounds (2).
Diagnostic ions of the general formulae $(R\text{-}C\text{=}N\text{-}OH + H + NH_3)^+$, and $(R\text{-}C(\text{=}N\text{-}OH)\text{-}S+2H)^+$ were found in the spectra of all the glucosinolates investigated, with the exception of allyl and 3-butenyl. These ions may also be formed in the thermospray ionization of allyl and butenyl, however they would not be detected in this investigation as the mass spectrometer was not scanned below mass 125 in order to avoid the ammonium and acetate cluster ions. This is substantiated in the spectrum of 3-butenyl by the ion at mass 132 corresponding to $(CH_2\text{=}CH\text{-}CH_2\text{-}CH_2\text{-}C(\text{=}N\text{-}OH)\text{-}S+2H)^+$. Figure 1a, the positive ion spectrum of 2 hydroxy-3-butenyl, shows the diagnostic ions at m/z 130 and 148 indicating the mass of the

R group as well as the ions at 180 and 214 indicating the presence of the glucosyl and thioglucosyl moieties.
The negative ion spectra also have 2 common diagnostic ions of high intensity indicating the presence of the glucosyl and thioglucosyl moieties. The ion at mass 195 is most likely formed from cleavage of the thioglucosyl moiety, whereas mass 221 is postulated to have the structure $(C_6H_{11}O_5\text{-}S\text{-}C{\equiv}N)^-$. Ions of the general formula $(R\text{-}C(=NOH)\text{-}S)^-$ are present in all the spectra studied. Figure 1b shows the presence of these ions in the negative ion spectra of 2-hydroxy-3-butenyl.
Figure 2 shows the positive ion total ion chromatogram (TIC) obtained from the LC/MS analysis of the glucosinolates obtained from a leaf extract of Brassica juncea var. Cutlass. The glucosinolates identified are indicated by the labels on the individual peaks in the TIC. The negative ion TIC was very similar in appearance. Identifications were made by comparision of the positive and negative ion spectra with reference spectra. As butyl and pentyl glucosinolates were not available, tentative identifications were made by studying the spectra obtained in the plant extract.

References:

1. I. Minchinton, J. Sang, D. Burke and R.J.W. Truscott, J. Chromatogr., 247, 141 (1982)
2. J. Eagles, G.R. Fenwick, R. Gremlin and D. Rakow, Biomed. Mass Spec., 8, 265, (1981)

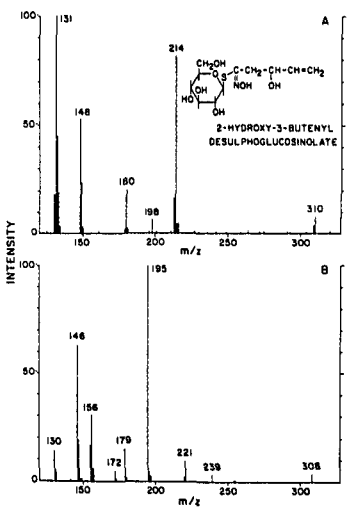

Figure 1. Positive and negative thermospray spectra of 2-hydroxy-3-butenyl DSGS.

Table 1. INTENSITIES OF POSITIVE AND NEGATIVE MOLECULAR IONS FOR THE DESULFOGLUCOSINOLATES INVESTIGATED

GLUCOSINOLATE	POS. ION $(M+H)^+$ m/z (%)	NEG. ION $(M-H)^-$ m/z (%)
ALLYL	280 (8)	278 (6)
BUTENYL	294 (7)	292 (2)
3-ME. SULPHINYL PROP.	344 (1)	342 (-)
PHENYL ETHYL	344 (6)	342 (0.5)
4-HYDROXY BENZYL	360 (-)	358 (-)
2-HYDROXY-3-BUTENYL	310 (5)	308 (3)
3-INDOLYLMETHYL	371 (-)	369 (-)

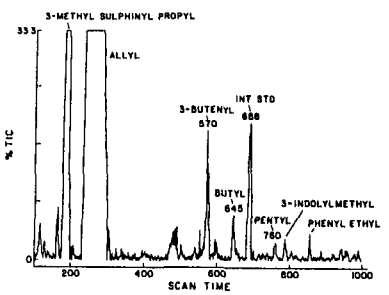

Figure 2. TIC for thermospray LC/MS analysis of leaf extract of Brassica Juncea var. Cutlass.

Presented at the 35th ASMS Conference on Mass Spectrometry and Allied Topics
May 24-29, 1987, Denver, CO

THE USE OF THERMOSPRAY LC/MS FOR THE CHARACTERIZATION OF SURFACTANTS

PAUL C. GOODLEY THE HEWLETT-PACKARD COMPANY,
1601 CALIFORNIA AVE., PALO ALTO, CA 94304

Surfactants or surface active agents are a special group of organic compounds which have properties for wetting or lowering the surface tension of other materials. The surfactants are formulated into numerous products of washing compounds, softners, shampoos, printing inks, agricutural chemicals and many other products.

Analytical techniques for the analysis and the identifications of these nonvolatile and thermally labile surface active agents often require lengthy separations or isolation. Subsequent molecular identification ususlly consist of comparing the the retention time on a chromatogran of an unknown to the retention time of a standard known compound. Modern techniques of UV/VIS and NMR are usually required to asist the confirmation of the idenity provided the components have been separated sufficently for those techniques.

However, liquid chromatography combined with thermospray mass spectrmetry (TS/LC/MS) is directly applicable to both the sepration and molecular identification of many of the thermally-labile and nonvolatile surfactants. Nonionic surfactants such as poly-ethoxynonylphenol, acetylenic glycols and polyethoxylated (ETO) glycols are a partial list which are applicable to the TS/LC/MS technique.

When a sample of nonionic surfactant, laural alcohol-ETO, was analyzed using the techniques of UV/VIS or refractive index as the LC detector, no useful information was obtained about the molecular character or the number components nor the number of ETO adducts in the sample matrix. Figure 1 shows a total ion trace (TIC) and the extracted ion profile of the same nonionic surfactant, analyzed using thermospray LC/MS as the separation and detection technique. No attempts were made to optimize the chromatography nor were any prior analysis made using standards to characterize the retention times of similiar samples.

The mass spectra from the single analysis produced a strong [M+NH4]+ ion as the base peak for each lauryl-ETO oligomer and decreased by 44 amu as the chromatographic run progressed in time. Extracted ion profiles were used to " pull out" the oligomers at the 44 amu intervals, which were unresolved by the chromatographic column. As shown in Figure 1, the ETO oligomers ranged from 17 to 2 and eluted in decreasing order from the GPC acryliamide column. (SHODA-DENCO DE-613) Even though the oligomer contrubution at n=17 approached the minimum detection limit, it serves to demonstrate the power of the TS/LC/MS technique for the analysis of polymeric type surfactants.

Ionic surfactants such as aromatic sulfonated salts can also be analyzed by thermospray LC/MS as the anion which is dissociated in aqueous solutions. Figure 2 shows the TIC and the mass spectrum of p-chlorobenzene sulfonate using the mass spectrometer's negative mode of detection. The presence of the chlorine atom is readily confirmed by the isotopic ratio of the 191,193 ions and the subsequent chlorine loss to yield the ion at 156; 35 amu from the parent at 191. Other surfactants such as xylene sulfonate, benxene sulfonate and saturated linear sodium sulfate salts were successfully analyzed using the thermospray filament-on technique.

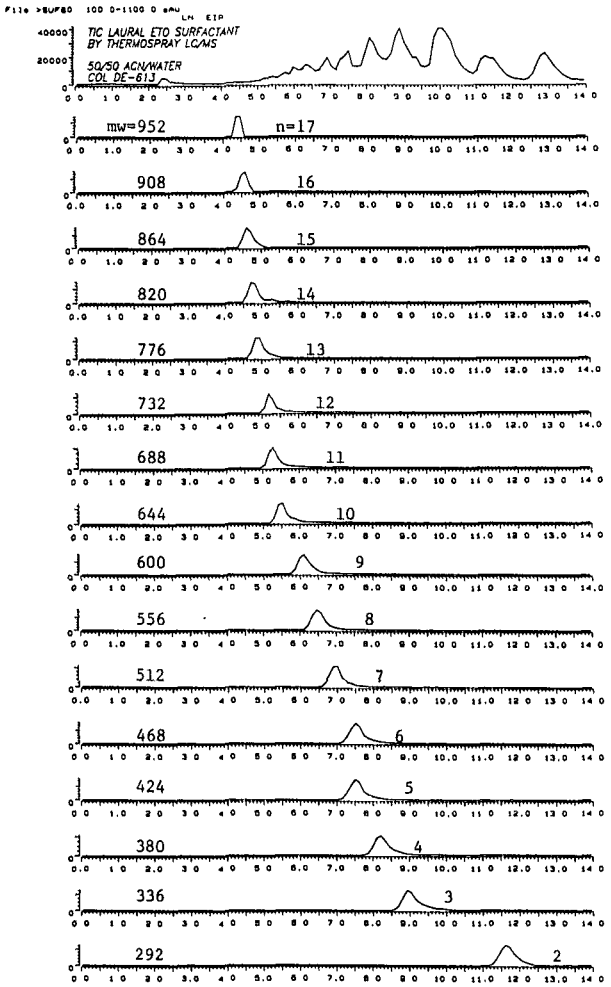

Figure 1. TS/LC/MS Lauryl ETO Adducts

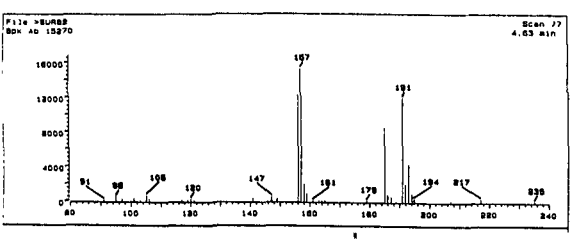

Figure 2. p-Chlorobenzene Sulfonate

Presented at the 35th ASMS Conference on Mass Spectrometry and Allied Topics
May 24-29, 1987, Denver, CO

CONTINUOUS FLOW FAST ATOM BOMBARDMENT - A NEW LC-MS TECHNIQUE

Alison E Ashcroft & John R Chapman

Kratos Analytical, Barton Dock Road, Urmston, Manchester, M31 2LD, UK

Introduction

Experiments described by Caprioli et al (1) have demonstrated that the introduction of a sample in a continuous flow of solvent through a length of silica capillary provides an alternative but equally acceptable method of liquid surface renewal in FAB-MS. An advantage of this technique is that a wide range of solvents may be used (for example, water, methanol, acetonitrile, toluene) unlike conventional FAB-MS where a solvent of suitable volatility (glycerol, thioglycerol) is mandatory.

The sample appears in the ion source in a concentrated volume over a relatively short period of time, and the system does not show any memory effects unless severely overloaded. The technique is highly reproducible, as determined by measurement of the peak areas for repeat injections of the same sample.

Thus continuous flow FAB-MS offers a suitable basis for the development of a viable LC-MS technique, as verified by preliminary invesitgations (2,3). LC-FAB-MS is achieved by positioning an LC column in between the place of sample introduction and the probe tip. The LC column can have a conventional internal diameter (1,2 or 4.6mm) in which case it is necessary to split the flow after the column to direct the required volume (2-10µl per minute) to the probe tip, while the remainder can be recycled or directed to an alternative detector. Alternatively, a micro HPLC column (<1mm id) can be used, in which case the flow rate through the column is compatible with the mass spectrometric requirements.

Experimental

A Kratos Analytical MS50FS equipped with a Kratos Analytical Continuous Flow FAB probe and an Ion Tech FAB gun was used for this work. A Brownlee MPLC pump was employed to deliver solvents at the flow rates specified in the text. A small proportion of the solvent system (approx 5%) should consist of a traditional FAB matrix. All separations illustrated were achieved with pre-column addition of glycerol, as the matrix did not affect significantly the elutropic strength of the solvent system. Post-column addition can be used if required.

Results & Discussion

LC-FAB-MS using a continuous flow probe has been employed to separate a variety of mixtures. The high sensitivity in general of FAB for peptides makes this method eminently suitable for peptide separations.

The chromatogram shows the separation of four peptides - angiotensins II and III, and leucine and methionine enkephalins, acheived by use of a 1mm x 15cm ODS HPLC column and a gradient elution of 5-60% aqueous methanol (with a constant 5% glycerol and 0.1% trifluoroacetic acid) over 30 minutes. A flow rate of 60µl per minute was maintained, with a 1:12 split after the column to divert 5µl per minute to the source. Spectra from two of the four components are presented, showing protonated molecular ions. Instrumental stability was maintained throughout the gradient elution.

Other peptides studied include analogues of the neuropeptide Thyrotropin Releasing Hormone, bradykinins and dipeptides.

Experiments have been carried out with micro-LC columns. For example, a separation of monocyclic B-lactam antibiotics has been achieved with a 0.22mm x 30cm slurry packed ODS column and an eluent of 80% aqueous methanol (plus 5% glycerol) flowing at a rate of 5µl per minute directly through the continuous flow FAB probe. This methodology offers a highly convenient means of separating and detecting low sample levels by LC-MS.

Conclusion

LC-FAB-MS in conjunction with a continuous flow probe offers a viable, complementary alternative to existing LC-MS interfacing techniques. It has been used successfully for a variety of peptide separations and has been shown to be suitable for thermally labile samples such as B-lactams. Data from both microbore and micro LC columns have been presented.

Acknowledgement

(1) Prof J Knox and I Grant, Department of Chemistry, Edinburgh University, UK for provision of micro-LC column and useful discussions.

References

(1) R M Caprioli, T Fan, J S Cottrell, Anal. Chem., (1986) 58, 2949

(2) A E Ashcroft, J R Chapman, J S Cottrell, J. Chromatogr., (1987) 394, 15

(3) D W Hutchinson, A R Woolfitt, K R Jennings, A E Ashcroft, Organic Mass Spectrometry. (1987), 22 304.

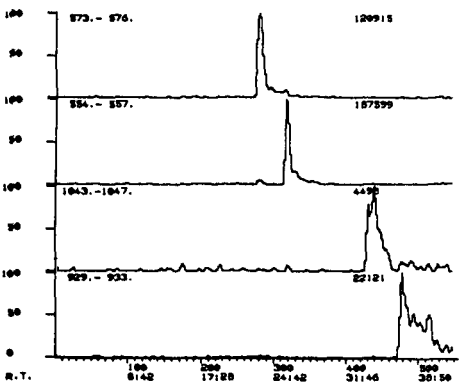

LC-FAB-MS: Peptide mixture 1mm x 15cm ODS

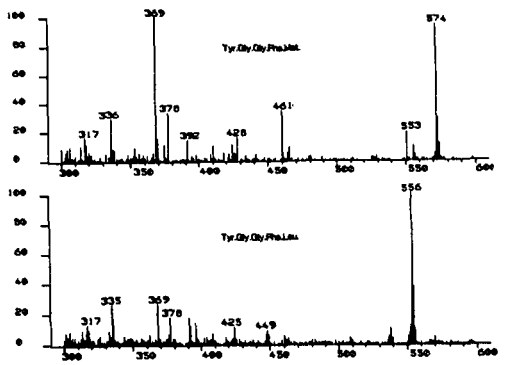

LC-FAB-MS: Peptide mixture - Leucine enkephalin (mw 555)
Methionine enkephalin (mw 573)

Presented at the 35th ASMS Conference on Mass Spectrometry and Allied Topics
May 24-29, 1987, Denver, CO

AN EVALUATION OF THE CONTINUOUS FLOW FAB PROBE AS A HPLC-MS INTERFACE

Bateman,R.H.,Jones,D.J.,*Krolik,S.T.
VG Analytical Ltd, Floats Rd, Wythenshawe, Manchester M23 9LE

Dynamic FAB is the most recent of HPLC-MS interfaces(1,2). In principle, the technique offers the potential of higher sensitivity than is currently available from other soft ionisation alternatives such as thermospray, Plasmaspray and moving belt.
Evaluation studies have revealed a number of significant features for useful application.
On column reproducibility
Chromatographic separation
Analysis of mixtures
Suppression of matrix interference
The probe can only handle approximately 5ul per minute of most eluents. However, the higher ionisation efficiency of the technique effectively compensates for the low flow capacity of the interface. (Tis technique is especially suited to packed fused silica LC columns.)

Relative sensitivity for different ionisation techniques at different flow rates

Sample: Gramicidin-s (mol wt 1141)

Ionisation technique	2ml/min	1ml/min	0.5ml/min	0.1ml/min	50ml/min
Thermospray	$2x10^{-12}$	$1x10^{-13}$	-	-	-
Plasmaspray	$4x10^{-12}$	$8x10^{-12}$	$2x10^{-12}$	-	-
Moving Belt/FAB	$2x10^{-12}$	$4x10^{-12}$	$8x10^{-12}$	$1x10^{-11}$	-
Dynamic FAB	$1x10^{-11}$	$2x10^{-11}$	$4x10^{-11}$	$2x10^{-10}$	$4x10^{-10}$

Relative sensitivity for different ionisation techniques amenable to interfacing to HPLC

Sample: Gramicidin-s (mol wt 1141)

Ionisation technique	Range of flow rates	Optimum flow rates	Sensitivity at optimum flow rates
Thermospray	1 - 2ml/min	1.5 - 2ml/min	10^{-12}
Plasmaspray	0.4 - 1.2ml/min	0.6 - 1ml/min	10^{-11}
Moving Belt/FAB	0.1 - 1.0ml/min	0.3 - 0.5ml/min	10^{-11}
Dynamic FAB	2 - 10µl/min	2 - 3µl/min	10^{-8}

MULTI-INJECTION MALTOTRIOSE

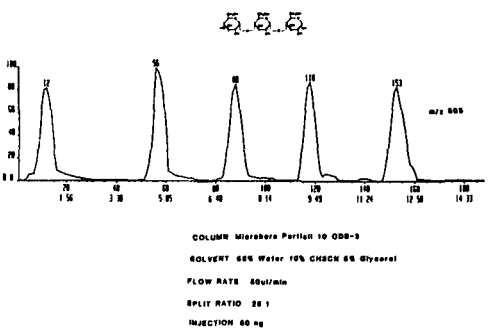

CYTIDINE DEOXYADENOSINE MIXTURE

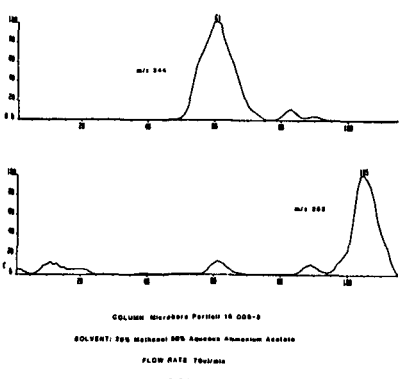

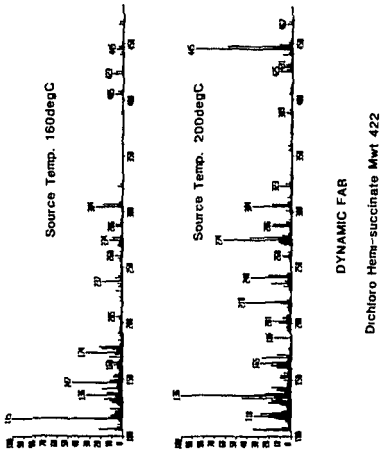

DYNAMIC FAB

Dichloro Hem-succinate Mwt 422

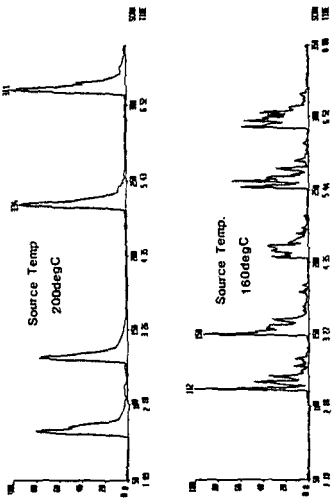

DYNAMIC FAB

Repetitive Injections Hemi-succinate

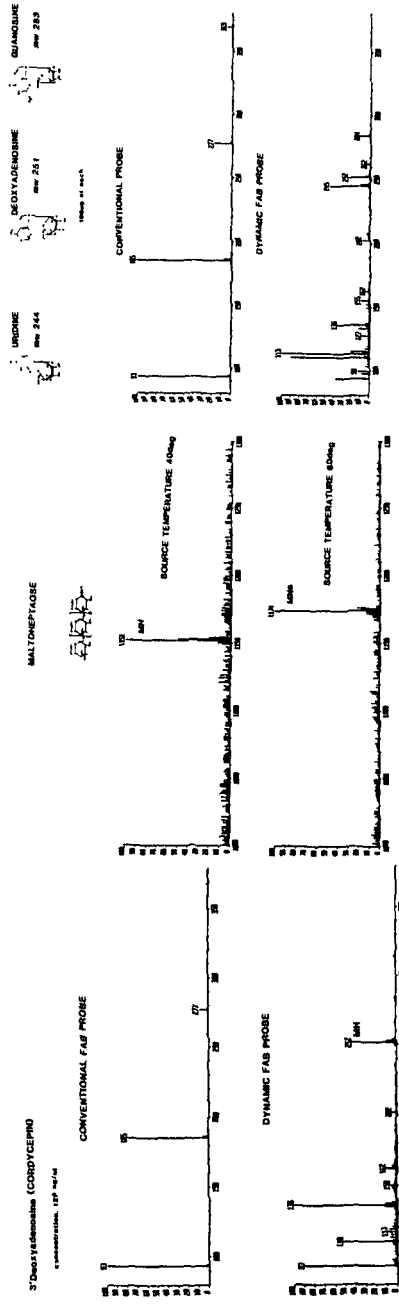

Presented at the 35th ASMS Conference on Mass Spectrometry and Allied Topics
May 24-29, 1987, Denver, CO

COMPARISON OF MOVING BELT/FAB, THERMOSPRAY AND CONTINUOUS FLOW FAB PROBE HPLC/MS TECHNIQUES FOR THE ANALYSIS OF PEPTIDES:

R. D. Voyksner and F. P. Williams, Analytical and Chemical Sciences, Research Triangle Institute, P. O. Box 12194, Research Triangle Park, NC, 27709, K. Tyczkowska, School of Veterinary Medicine, North Carolina State University, Raleigh, NC 27695.

HPLC/MS shows great promise in specific and sensitive detection of peptides in the molecular weight range of 1000-4000. Analytical procedures based on HPLC/MS should overcome problems associated with:

- Matrix interferences and salt interferences associated with direct probe techniques (i.e., FAB/MS)
- Extensive clean-up procedures necessary for probe techniques
- Loss of sensitivity using MS/MS alone or high resolution MS (for high molecular weight)
- Off-line HPLC techniques.

Three HPLC/MS techniques (continuous flow FAB, FAB-moving belt, and thermospray) were compared to FAB/MS for the analysis of gramicidin-S, renin substrate, γ-endorphin, and β-endorphin.

The three HPLC/MS techniques were compared to FAB/MS to determine spectral similarity, sample sensitivities, and degree of background noise. The FAB/MS spectra were acquired using thioglycerol (1 µL) and 1 µL of the peptide solution (80% H_2O, 19% MeOH, and 1% TFA) on the probe tip. The instrument (VG ZAB-E) was operated at 10 kV with the Ion Tech FAB gun operating at 8 kV (1 mA) using xenon gas. The instrument was operated between 2000 and 4000 resolution using positive ion detection. FAB/MS produced $[M+H]^+$ ions for each peptide. Estimated detection limits were compound dependent, ranging from approximately 1 ng for gramicidin-S to 800 ng for β-endorphin under full scan MS operation. In many cases, the HPLC/MS interface technique was less sensitive than FAB/MS, especially for the higher molecular weight test compounds. However, FAB/MS exhibited the most intense background ion current of the techniques evaluated (especially at lower masses). A summary of the individual techniques compared to FAB/MS is presented below.

- Continuous Flow FAB Probe

The continuous flow FAB probe (Research Triangle Institute, Research Triangle Park) was operated at 5 µL/min using 80% water, 13% acetonitrile and 7% glycerol. The probe used 0.06 mm ID fused silica to transfer the sample (1 µL) from the injector to the probe tip. The instrumental conditions were the same as for the FAB/MS analysis.

The continuous flow probe exhibited less background noise, identical spectra and similar sensitivity compared to FAB/MS. The analysis of higher molecular weight compounds by the continuous flow FAB probe resulted in poorer sensitivity, undoubtedly due to the decreased ion formation when glycerol, rather than thioglycerol, is employed. A thioglycerol matrix was determined to provide the best sensitivity in FAB/MS. The technique appears suitable for on-line HPLC/MS provided separations can be performed in the 1-5 µL/min. range.

- FAB Moving Belt

The VG moving belt interface was operated using 80% methanol in water with and without buffers at 1 mL/min. The effluent was spray deposited onto a Kaptron® belt moving at 2.5 cm/min. The instrumental conditions were the same as for the FAB/MS analysis.

The FAB moving belt interface exhibited poorer ion currents above molecular weight 1700 than FAB/MS. The lower molecular weight compounds (i.e., gramicidin-S) showed similar ion currents to FAB/MS. Current research seeks ways to increase the ion yield for the higher molecular weight molecules on the FAB moving belt interface. For example, the addition of ammonium acetate (0.1 M) and 1% glycerol to the solvent system increased the ion currents for leu-enkephlin, gramicidin-S, and renin substrate by a factor of 5-10 over the ion currents observed in only 80% methanol in water. The moving belt interface is also compatible with conventional HPLC separation methods for peptides.

- Thermospray HPLC/MS

Thermospray spectra were acquired using a mobile phase of 100% methanol or acetonitrile/water (45/55) with 0.01 M TFA at a flow of 1.0 mL/min. The Finnigan interface was operated with a vaporizor temperature of 92°C and a source temperature of 290°C. The Finnigan-MAT 4600 was operated in full scan mode (500-1800 daltons) using positive ion detection.

The thermospray interface showed sensitivities comparable to FAB/MS for the range of peptides analyzed. The thermospray spectra were simple, exhibiting $[M+H]^+$ and $[M+xNa]^+$ (x=1-3) ions, as well as their doubly charged ions. The negative ion spectra exhibited $[M-H]^-$ ions and the $[M-2H]^{-2}$ and $[M-3H]^{-3}$ ions (Figure 1). Additionally, thermospray showed little background noise compared to FAB/MS. The thermospray spectra exhibited intense (usually the base peak) doubly charged ions permitting the detection of peptides (such as ß-endorphin) beyond the single charged ion mass range of the instrument. Thermospray is also compatible with conventional HPLC methodology for the separation of peptides.

This comparison of the three techniques indicates thermospray exhibits the best combination of sensitivity and HPLC compatibility for detection of picomolar quantities of peptides.

Acknowledgement

The authors wish to thank K. Stachowiak, Dept. of Chemistry, University of Houston, TX, for the negative ion thermospray data. This research was supported by the National Institute on Drug Abuse, grant No. 1R01 DAC 4202-01.

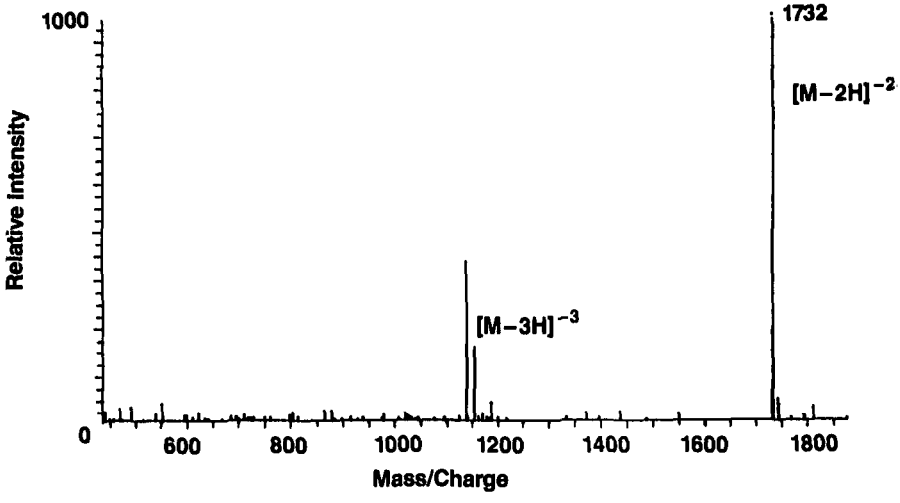

Figure 1. Thermospray mass spectrum of 2 nm of ß-endorphin (mw 3463).

Presented at the 35th ASMS Conference on Mass Spectrometry and Allied Topics
May 24-29, 1987, Denver, CO

STUDIES OF NATURAL PRODUCTS BY PACKED COLUMN SFC/MS

A.J. Berry, D.E. Games, I.C. Mylchreest, J.R. Perkins and S. Pleasance,
Department of Chemistry, University College, P.O. Box 78, Cardiff CF1 1XL
Wales

Packed column supercritical fluid chromatography (SFC) has advantages over high-performance liquid chromatography (LC) in that analysis time and method development is faster, low wavelength ultraviolet detection can be more readily used and chromatographic efficiencies and detection limits are better. In addition, high purity samples can be readily isolated and, because the gas volumes generated from the mobile phases are lower than in LC, SFC/MS is easier to effect than LC/MS. A criticism of SFC has been that it could only be used for non-polar involatile compounds, however, in early papers in the area, it was demonstrated that polar involatile molecules could be handled by the technique [1]. We have found that by use of polar modifiers e.g. methanol and methoxyethanol with carbon dioxide, the technique can be used for the analysis of a wide range of polar compounds [2].

In our studies of natural products by packed column SFC/MS, we have used two types of interface. One involves use of our Finnigan MAT or VG Analytical moving belt interfaces with a modified Finnigan MAT spray deposition device, which is linked to a Hewlett-Packard 1084 B liquid chromatograph modified for SFC [2,3]. This system enables ultraviolet and mass spectrometric detection to be performed in series and conventional EI and CI mass spectra can be obtained from solutes with good retention of chromatographic integrity. The second system utilizes a modified Finnigan MAT thermospray source operated in the filament-on mode [4]. Once again ultraviolet and mass spectrometric detection are performed in series and approximately 50% of the chromatographic eluent is handled by the mass spectrometer ion source. Good retention chromatographic integrity is obtained with the interface and if methanol is used as a modifier for the carbon dioxide then solvent moderated CI type spectra are obtained at low ng injected on column levels for full scan spectra. When carbon dioxide alone is used as the mobile phase, EI type spectra are obtained, presumably by a charge exchange ionization process.

Mixtures of PTH amino acids have been run on both interfaces. With the moving belt system, EI spectra are obtained and detection limits were better than we had previously obtained by LC/MS for these compounds [5]. Thermospray filament-on SFC/MS gave simple spectra consisting almost exclusively of $[M+1]^+$ ions. Figure 1 shows the computer reconstructed TIC trace obtained by thermospray filament-on SFC/MS of a mixture of PTH amino acids. The technique has also been found to be useful for studies of N-acetyl-N,O-permethylated peptides.

We have found packed column SFC/MS particularly useful for studies of crude extracts containing natural products. Our approach consists of initially making field desorption mass spectral measurements on the crude extracts to provide molecular weight profiles. This serves as a check for sample loss or decomposition during SFC/MS. SFC/MS measurements are then made on both types of interface. The EI data from the moving belt is structura-ly very informative, whilst the thermospray filament-on spectra provide confirmation of molecular weight. The technique has been applied in studies of indole alkaloids from Catharanthus roseus and milbemycins from fermentation extracts. Application of SFC/MS enables ready location of new compounds, which are isolated by semi-preparative SFC for further structural study.

We believe that packed column SFC/MS has considerable potential for the identification of known, and location of, new natural products. The technique is easier to use than LC/MS, gives better detection limits and method development is easier and faster. In addition, SFC enables high purity samples to be readily isolated for further structural study.

Presented at the 35th ASMS Conference on Mass Spectrometry and Allied Topics
May 24-29, 1987, Denver, CO

1. J.C. Giddings, M.N. Meyers, L. McLaren and R.A. Keller, Science, 1968, 162, 67.
2. A.J. Berry, D.E. Games and J.E. Perkins, J. Chromatogr., 1986, 363, 147.
3. A.J. Berry, D.E. Games and J.R. Perkins, Anal Proc., 1986, 23, 451.
4. A.J. Berry, D.E. Games and J.R. Perkins, Biomed. Environ. Mass Spectrom., 1987, in press.
5. D.E. Games and E.D. Ramsey, J. Chromatogr., 1985, 323, 67.

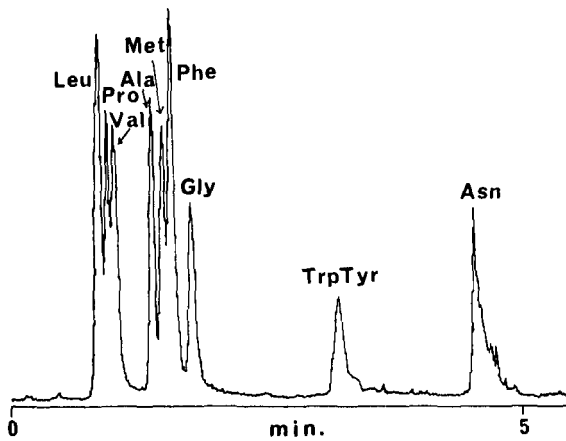

Figure 1 TIC trace obtained by filament-on SFC/MS from a mixture of PTH amino acids. *Sperhisorb 5μm; mobile phase : CO_2 + CH_3OH* programmed from 5% CH_3OH to 20% CH_3OH over 7 min.; flow rate : $3cm^3min^{-1}$ for 1 min. then $4cm^3min^{-1}$; oven : 75°C; column pressure : 319 bar; vaporizer : 160°C; jet : 140°C.

Presented at the 35th ASMS Conference on Mass Spectrometry and Allied Topics
May 24-29, 1987, Denver, CO

ANALYSIS OF PTH AMINO ACIDS BY THERMOSPRAY LIQUID CHROMATOGRAPHY - MASS SPECTROMETRY

Lily Yang and Christina Hsieh Vestal
Vestec Corporation, 9299 Kirby Drive, Houston, Texas 77054

Edman degradation, the classical technique for peptide sequencing yields phenylthiohydantion (PTH) derivatives which have been successfully chromatographed using a variety of elution protocols. PTH amino acids are usually detected at 254 nm using a UV detector. However, detection of either 254 nm or at their absorption maximum of 269 nm may suffer interference from impurities. The PTH derivatives are more volatile than free amino acids, and their retention properties are favorable for good separation without the use of special columns or complex mobile phase additives.

A series of PTH amino acid standards were studied using a Vestec model 201 Dedicated Thermospray LC-MS system on line with a Perkin-Elmer LC-75 UV detector. The HPLC separations were performed on a 5 µm C18-PTH amino acid column with a 5 µm PTH amino acid guard column. Solvent A was 0.1 M ammonium acetate (pH 5.0)/acetonitrile 70/30, and solvent B was 0.1 M ammonium acetate (pH 5.0)/acetonitrile 50/50. Separation of a mixture of 23 PTH amino acids was accomplished using 100% A for 5 minutes, then a 22 minute linear gradient from 100% A to 100% B. Both columns used were thermostated at 50° C. The flow rate was 1.2 mL/min.

Figure 1 shows the total ion chromatogram for analysis of 23 PTH-amino acids, 1.0 nanomole per compound injected on column while scanning m/Z 175 - 500 in 3 seconds and using filament-off ionization which gives the best signal-to-noise ratio. All of the compounds elute within 30 minutes, and the cycle time for the separation was 35 minutes. Although many of these compounds have the same nominal molecular masses, those which do are well separated. All of the PTH amino acids analyzed showed good quality mass spectra with intense protonated molecular ions. Little or no significant fragmentation was observed except for PTH-glutamic acid and PTH-PTC-lysine which show losses of HCOOH, H_2O, H_2S, and aniline. Typical examples are shown in Figure 2. Figure 3 shows the mass chromatograms of some of these PTH amino acids for 2.0 picomole injected on column under selected ion monitoring (SIM).

Results for these 23 PTH amino acids obtained using the thermospray filament-off mode of ionization and positive ion detection are summarized in Table I. Instrumental limits of detection by thermospray LC-MS are in the 0.2-8 picomole range using SIM (calculated as three times average noise, and using the mass chromatograms of the protonated molecular ions). These are generally somewhat lower than by UV detector at 254 nm.

The mass spectra and the detection limits for PTH-cysteic acid, PTH-aspartic acid, PTH-glutamic acid, and PTH-PTC-lysine may be improved using the negative ion mode of thermospray ionization as reported previously by Unger and Warrack.

Presented at the 35th ASMS Conference on Mass Spectrometry and Allied Topics
May 24-29, 1987, Denver, CO

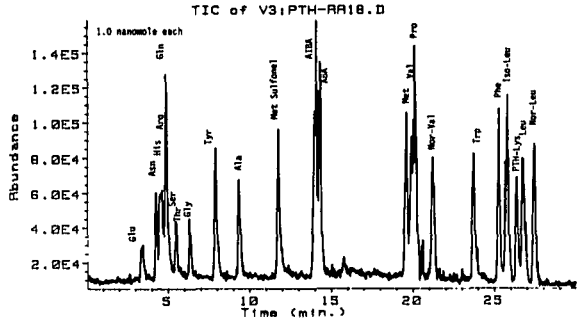

Figure 1. Total ion chromatogram of 23 PTH amino acids.

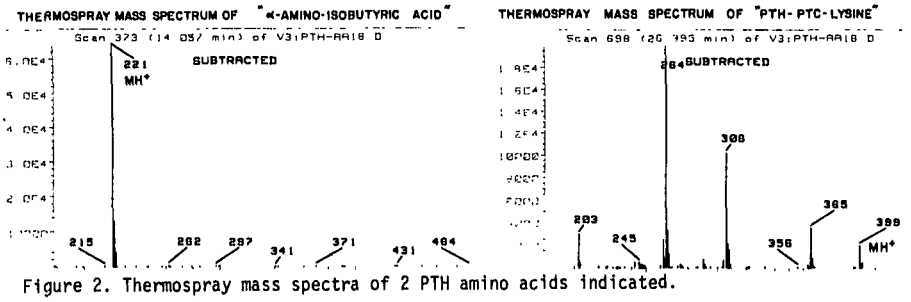

Figure 2. Thermospray mass spectra of 2 PTH amino acids indicated.

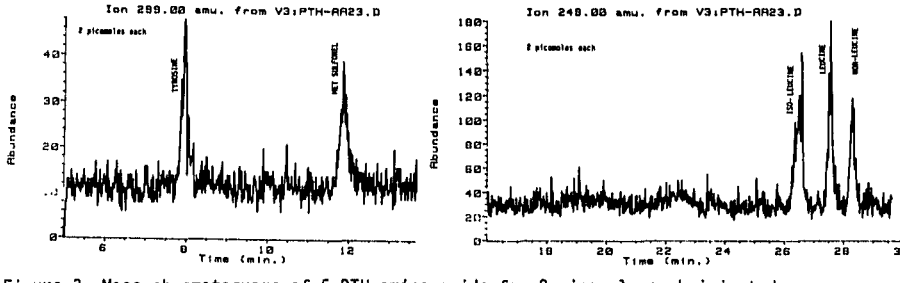

Figure 3. Mass chromatograms of 5 PTH amino acids for 2 picomole each injected on a C18 column by selected ion monitoring.

Table I. Summary of 23 PTH amino acids.

PTH-Amino Acid	MW	RT(min)	SIM Detection Limits(picomole)
Glu	264	3.2	8
Asn	249	3.9	2
His	272	4.2	4
Arg	291	4.3	8
Ser	222	4.5	8
Gln	263	4.5	1
Thr	236	5.3	8
Gly	192	5.9	4
Tyr	298	7.3	1
Ala	206	8.7	1
Met Sulfonel	298	10.8	1
AIBA	220	12.9	0.2
ABA	220	13.1	0.4
Met	266	18.8	0.5
Val	234	19.1	0.2
Pro	232	19.4	0.2
Nor-Val	234	20.6	0.3
Trp	321	23.2	1
Phe	282	24.8	0.5
Iso-Leu	248	25.4	0.3
PTC-Lys	398	26.1	4
Leu	248	26.5	0.3
Nor-Leu	248	27.3	0.3

Presented at the 35th ASMS Conference on Mass Spectrometry and Allied Topics
May 24-29, 1987, Denver, CO

THERMOSPRAY ANALYSIS OF ACHROMOPHORIC AND CHROMOPHORIC GLUTATHIONE CONJUGATES

Mark F. Bean, Sharon Pallante Morell, Deanne Dulik, and Catherine Fenselau
The Johns Hopkins University School of Medicine, Baltimore, MD

Reduced Glutathione (GSH), the major non-protein thiol constituent of cells, plays a key role in detoxification of electrophilic xenobiotics. Recent reports implicate glutathione conjugates in the development of resistance to antineoplastic agents. In contrast conversion of conjugates to free thiols via cysteine-β-lyase can result in greater toxicity of the substrate. These chemically and thermally unstable polar metabolites can be analyzed by GCMS only after extensive derivatization. Characterization by Fast Atom Bombardment or Plasma Desorption gives reliable molecular weight information but few diagnostic fragments, and can be hampered by the presence of sample contaminants and salts.

Thermospray LC-MS is an attractive technique for the analysis of glutathione conjugates for several reasons: 1) Detection is independent of UV chromophoric moieties, 2) The analysis of complex mixtures of non-volatile, structurally similar compounds is possible with minimal sample manipulation, and 3) It provides not only molecular weight information but also structurally useful fragmentation yielding a sequence of ions diagnostic for the presence of glutathione conjugates.

Solvent conditions for optimal HPLC are not always the same as for optimal Thermospray ionization. Thermospray has best sensitivity at 1.2 to 1.3 ml/min flow rates, whereas some HPLC separations require 0.8 ml/min. We have found that certain antineoplastic nitrogen mustards and their GSH conjugates react with H_2O and acetate in the Thermospray plume, and that molecular ions are best produced in 50% acetonitrile solvent systems. Temperature sensitive glutathione conjugates that give poor spectra in aqueous ammonium acetate, yield more intense molecular ions with increasing percentages of acetonitrile. The high amount of organic solvent often necessary for good molecular ion intensity will preclude the chromatographic separation of these extremely polar compounds. To succeed with optimal hplc separation as well as thermospray ionization, we have introduced a third pump and a micro needle valve/T post-column. The advantages are: 1) Additional organic modifier or buffer may be added to the HPLC effluent to yield optimum ionization, and 2) The flow into the MS ion source may be adjusted to its optimum of 1.2 ml/min.

Our protocol for the analysis of glutathione conjugates calls for 35-60% acetonitrile in the mobile phase if one is making direct injections through only a guard column. These conditions produce excellent spectra but negate the possibility of chromatography since polar GSH conjugates are not retained on the column. Our solution to the dilemma was to add the necessary solvent post-column via an additional pump and metering T-valve. Enhanced molecular ion intensity under these conditions may in part be due to altered solvent - sample interactions in the source, and in part may be related to the much lower optimum vaporizer temperatures that are possible with increasing organic solvent concentrations (B.P. of acetonitrile = 81.6°C). This protocol provides class characteristic fragment ions related to the cleavage of glutamic acid from the GLU-CYS-GLY conjugates. Thus intense ions at $(MH-129)^+$, m/z 147, and m/z 129/130 provide excellent indication of the presence of a glutathione conjugate in complex biological mixtures. The intense ions at m/z 179 in the glutathione spectra do not appear in conjugates since the thiol ether linkage to cysteine is not easily broken ($m/z\ 179 = CYS - GLY - H)^+$.

Presented at the 35th ASMS Conference on Mass Spectrometry and Allied Topics
May 24-29, 1987, Denver, CO

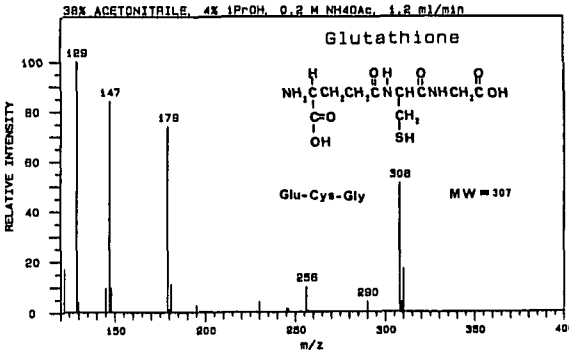

Ions chacteristic of GSH:
MH^+ = 308
m/z 129, 147
$(MH-GLU)^+$ = 179

Ions characteristic of GSH conjugates:
$(MH-129)^+$
m/z 129, 147

Post-column addition of MeCN:
LC-MS TIC of a mixture of Haloalkane glutathione adducts
1 = Dichlorovinyl-GSH
2 = Chlorotrifluoro-GSH
3 = Hexafluoropropyl-GSH

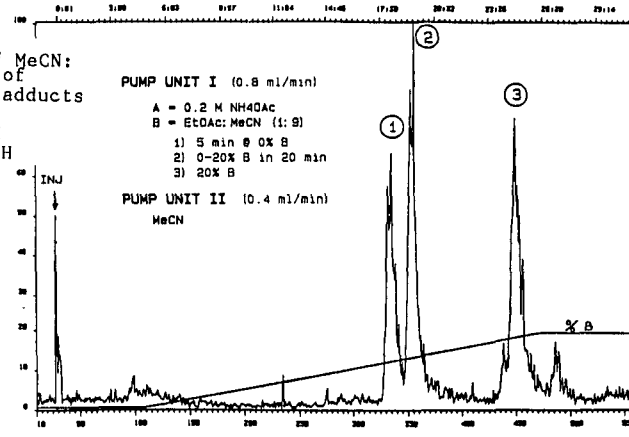

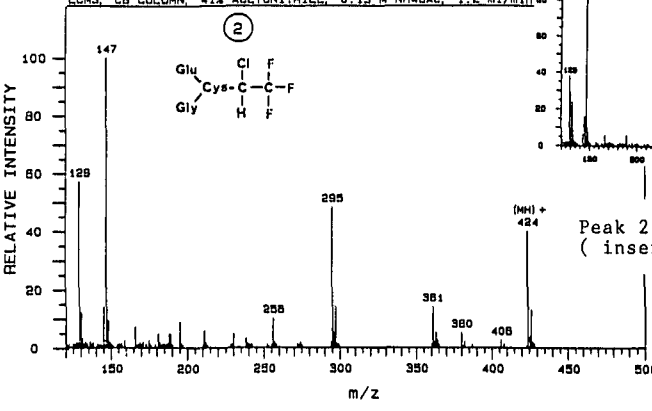

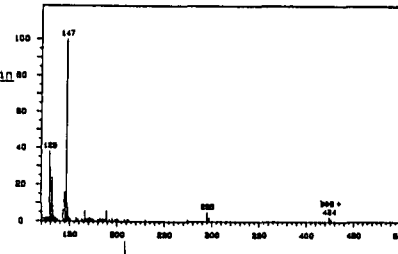

Peak 2 with post-column MeCN
(insert is without MeCN)

Presented at the 35th ASMS Conference on Mass Spectrometry and Allied Topics
May 24-29, 1987, Denver, CO

CHARACTERIZATION OF RADIATION INDUCED DAMAGE TO POLYADENYLIC ACID USING LIQUID CHROMATOGRAPHY-TANDEM MASS SPECTROMETRY.

A.J.Alexander[1], A.F.Fuciarelli[2], P.Kebarle[1] and J.A.Raleigh[2]
[1]Department of Chemistry, University of Alberta, Edmonton, Canada T6G 2G2.
[2]Department of Radiobiology, Cross Cancer Institute, 11560 University Avenue, Edmonton, Alberta, Canada T6G 1Z2.

Due to the high proportion of water in cells, 60-70% of cell inactivation by ionizing radiation has been attributed to hydroxyl radical attack on biomolecules such as DNA. Studies have shown the utility of HPLC-MS for the detection of modified nucleosides in enzymatic digests of tRNA (1) and for the analysis of nucleosides present in urine (2). However, most HPLC-MS interfaces produce abundant pseudo molecular ions but few fragment ions. Although this is beneficial in terms of overall sensitivity, only limited structural information is obtained. Tandem mass spectrometry (MS/MS) is a means of overcoming this inherent lack of specifity whilst maintaining good sensitivity (3). In this study HPLC-MS/MS, based on direct nebulization into an atmospheric pressure chemical ionization (APCI) source, has been used to identify molecular products resulting from radiation damage to a model nucleic acid, polyadenylic acid.

Polyadenylic acid was irradiated in aqueous solution at neutral pH to a dose of 1000 Gy and then enzymatically hydrolysed to the mononucleoside level prior to analysis. The products were separated using a Supelco LC-18-S column with an eluent of 10% methanol in 20 mM ammonium formate buffered to pH 4 with formic acid. The exit of the UV detector was connected directly to a heated nebulizer HPLC-MS interface. The APCI reagent ions were NH_4^+ clustered with water, ammonia and methanol. HPLC-MS and HPLC-MS/MS spectra were obtained using a Sciex Taga 6000E triple-Q MS.

The radiation induced products R- and S-8,5-cycloadenosine (peaks 4 @ 13), 8-hydroxyadenosine (peak 18), α -adenosine (peak 8) and adenine (peak 6) were positively identified by comparison of MS/MS spectra and retention times with those of authentic standards. HPLC peaks corresponding to 8-hydroxyadenine (peak 7) and 4 amino-5-formylamino-6-(ribosyl)aminopyrimidine (peak 1) were also identified by MS/MS. These assignments could not have been made on the basis of the primary APCI spectra alone. The MS/MS spectra consist of the base containing fragment $(BH+H)^+$ as the major ion, together with a number of lesser intensity ions all of lower mass. The fragments divide into two groups, those derived from the base moiety B and those from the sugar S. The mass and relative intensities of these ions provide a useful MS/MS "fingerprint".

1. Edmonds, C.G.; Vestal, M.L.; McCloskey, J.A.; Nucleic Acids Res., 1985, 13, 8197-8206.
2. Esmans, E.L.; Geboes, P.; Luytens, Y.; Alderweireldt, F.C.; Biomedical Mass Spectrom. 1985, 12, 241-245.
3. McLafferty, F.W.; (Ed) "Tandem Mass Spectrometry", Wiley, N.Y. 1983.

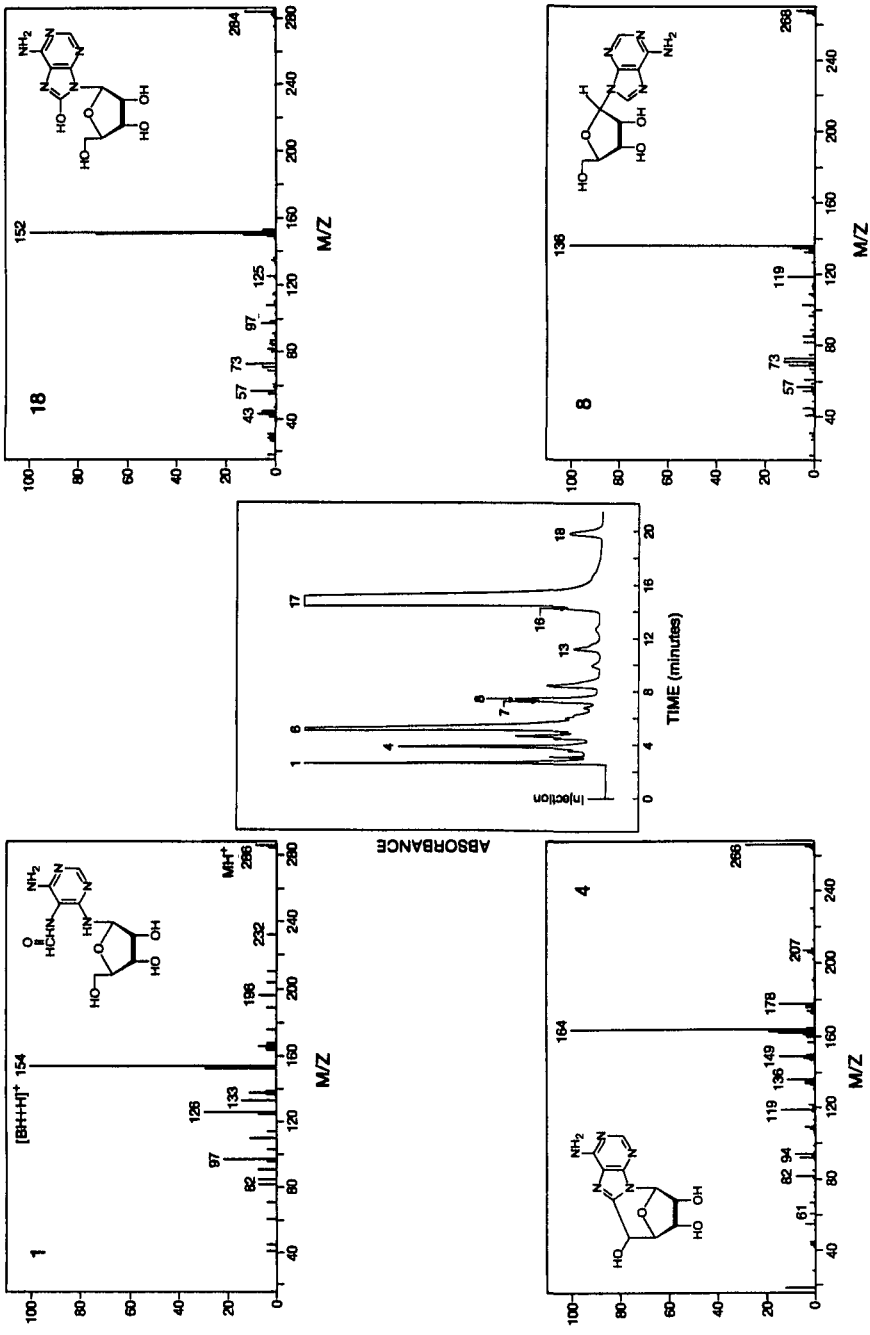
18
152
294
8
136
268
ABSORBANCE
TIME (minutes)
Injection
1
[B+H+H]+ 154
MH+ 266
4
164
266
M/Z

Presented at the 35th ASMS Conference on Mass Spectrometry and Allied Topics
May 24-29, 1987, Denver, CO

THERMOSPRAY LC/MS ANALYSIS OF POLYUNSATURATED PHOSPHOLIPID MOLECULAR SPECIES AFTER ETHANOL EXPOSURE.

H.Y. Kim[1], T.F. Taraschi[2], J.W. Karanian[1] and N.Salem, Jr.[1]
1. Lab. of Clinical Studies, Bldg 10, Rm 3C-218, DICBR, NIAAA, Bethesda, MD 20892
2. Dept. of Pathology, Thomas Jefferson University School of Medicine, Philadelphia, PA 19017

It is generally accepted that ethanol exerts its pharmacological effect through alterations in the physical properties of plasma membranes. These changes including, for example, membrane fluidity may be directly related to the level of polyunsaturated fatty acids esterified to phospholipids. Several reports have shown that ethanol can alter the levels of polyunsaturates but the degree and direction of these changes probably depend upon the ethanol dose, route of administration, duration of exposure, tissue studied and species.

In order to evaluate these changes in phospholipids at the molecular species level, thermospray LC/MS was employed. We have previously demonstrated that thermospray LC/MS provides a rapid and efficient technique for determining the molecular species present in the major lipid classes. Calibration curves for several molecular species of phosphatidylcholine (PC) showed linearity but had different response factors. Although the absolute amount of each species can be determined in this way, it is not generally applicable since relatively few standards are currently available. Efforts to prepare standards by partial synthesis were severely limited by autooxidation of polyunsaturated fatty acids containing more than two double bonds.

For many biological analyses, the relative distribution of various molecular species may provide the information required. With the thermospray technique, this can be readily calculated from the intensities of diglyceride ions obtained in the full mass range scanning mode. These ions are generally intense and unique for each phospholipid species. Due to varying response factors of different species, the area percent of these ions does not represent the absolute distribution. However, changes in molecular species distributions after pharmacological intervention still can be addressed by comparing the area percent figures. Reproducibility of this technique was evaluated using bovine liver phosphatidylinositol (PI). Molecular species were separated using an Altex Ultrasphere-ODS column (4.6mm x 7cm, 5u) and a mobile phase of methanol: hexane:ammonium acetate 500:25:30 (1 mL/min) (Figure 1). Six molecular species were determined in six repeated injections of bovine liver-PI by measuring the area percent of diglyceride ion peaks obtained by full mass range scanning. The result showed that the precision is in the 5 to 10 percent range. This approach was subsequently employed for the study of changes in membrane phospholipid species after ethanol feeding. It has been demonstrated that membrane tolerance to ethanol can be observed in lipid bilayers prepared from phospholipids isolated from alcoholic rats fed a liquid diet (1). This suggests that alterations in phospholipid composition are responsible for membrane tolerance. Molecular species analysis of the liver microsomal PI fraction isolated from alcoholic rats showed decreases in all 20:4w6 species and increases in other w-6 species compared to PI from the pair-fed control (Table 1). Di-18:1 species were also increased. The results obtained by GC analysis were also consistent. The loss of 20:4w6 species was not observed in all such paired samples, but the increase in other w-6 species appeared to be a reliable indicator of ethanol exposure.

Alternatively, thermospray technique was employed in conjunction with normal phase separation (Figure 2). Using this approach, the pre-separation step into each phospholipid class was eliminated. Also, changes in molecular species distribution can be simultaneously estimated for all the phospholipid classes in a single run. For di-14:0-PS and 16:0,18:1-PS, a linear relationship between the response ratio and amount ratio was observed, suggesting quantitative analysis of changes in molecular species distribution is possible. Further studies including dose and time dependent ethanol effects on phospholipid composition is now in progress using the thermospray technique with on-line reversed or normal phase separation, with or without internal standards.

1. T.F. Taraschi, J.S. Ellingson, A. Wu, R. Zimmerman and E. Rubin. Proc. Natl. Acad. Sci. USA, 83, 9399 (1986).

Presented at the 35th ASMS Conference on Mass Spectrometry and Allied Topics
May 24-29, 1987, Denver, CO

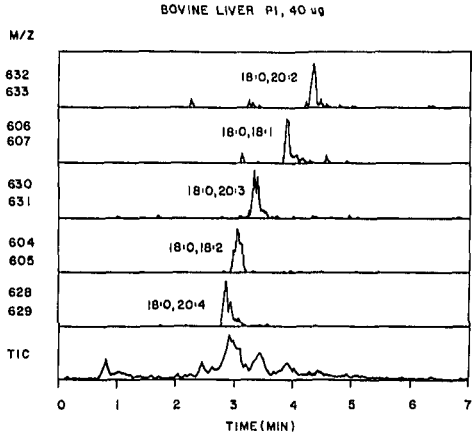

Figure 1. Molecular species of bovine liver PI separated on a reversed phase column. Diglyceride ions representative of each species are presented with the total ion current.

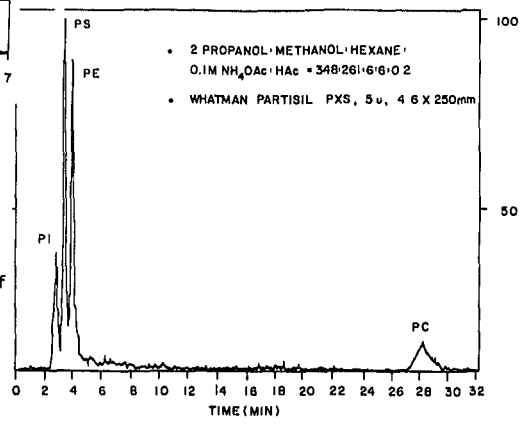

Figure 2. Separation and detection of phospholipid classes by normal phase HPLC/thermospray mass spectrometry. The flow rate was 1 mL/min.

Table I. Alterations in the molecular species distribution of rat liver microsomal phosphatidylinositol after ethanol exposure

Thermospray LC/MS			GC		
Molecular Species[a]	Control	Ethanol[b]	Fatty Acid	Control	Ethanol
18:0, 20:4w6	72.6	61.9	16:0	3.7	2.6
16:0, 20:4w6	4.3	1.4	18:0	41.9	42.5
18:1, 20:4w6	4.0	2.6	18:1	2.4	3.7
18:0, 18:2w6	3.5	6.6	18:2w6	1.3	1.9
18:1, 18:2w6	2.2	3.6	20:3w6	1.1	2.1
18:0, 20:3w6	4.3	7.8	20:4w6	42.6	38.4
18:0, 22:5w6	0.8	2.5	22:3w3	0.8	1.2
18:1, 18:1	3.9	6.8	22:5w6	0.8	1.9
18:0, 18:1	3.6	4.1	22:6w3	1.5	1.6
18:0, 22:6w3	1.0	2.0			
Total 20:4w-6 species	80.9	65.9			
Total other w-6 species	10.8	20.5	Total minor w-6	3.2	5.9

a. data are expressed as area percent based on diglyceride ions produced by thermospray LC/MS and do not represent the absolute percentages of each species.
b. Ethanol exposure was by means of 35 days of a liquid diet.

Presented at the 35th ASMS Conference on Mass Spectrometry and Allied Topics
May 24-29, 1987, Denver, CO

QUANTITATION BY LCMS OF NEUROPEPTIDES ISOLATED BY IMMUNOAFFINITY CHROMATOGRAPHY FROM SPINAL CORD

C. A. Lisek, J. Bailey, D. Lucas, T. L. Yaksh, and I. Jardine,
Depts. of Pharmacology and Neurosurgical Research,
Mayo Clinic, Rochester, MN 55905; and
M. A. McDowall and D. C. Smith,
VG Masslab, Ltd., Altrincham,
Cheshire, WA14 5RZ, United Kingdom

Neuropeptides are important biologically active molecules which play significant roles as neurotransmitters in the brain and spinal cord. These peptides are usually detected by radioimmunoassay (RIA), which affords high sensitivity of analysis but lacks complete specificity (Table 1). In principle, the combination of such immunological methods with the sensitivity and specificity of mass spectrometry should provide an optimal analytical methodology for endogenous neuropeptides. The strategy of this comprehensive approach is detailed below (Fig. 1).

[d_8-Phe^8]-methionine (met) enkephalin, [d_8-Phe^8]-substance P, [d_8-Phe^6]substance K, and [d_8-Phe^6, d_4-Ala^{18}]-VIP were synthesized from the tert-butoxycarbonyl (Boc) derivatives of d_8-phenylalanine and d_4-alanine via solid phase peptide synthesis, then purified by reverse phase HPLC.

Six to ten rat sacral spinal cords were weighed and sufficient 0.1 N HCl was added to produce a final concentration of 0.05 g/ml. The mixture was then boiled for 10 min, homogenized with a Polytron homogenizer, and the resultant homogenate (extract) was concentrated in vacuo. Yields: 85-91% for authentic methionine enkephalin, substance P, and VIP.

An aliquot of the concentrated HCl extract from rat sacral spinal cord was assayed for substance P (SP) activity by RIA using I^{125}-SP. A phosphate buffered saline (PBS) solution (0.05 M phosphate, 0.9% NaCl, pH 6.5) of the extract was then applied to a column containing rabbit polyclonal antibodies immobilized on cyanogen bromide-activated Sepharose 4B. The eluate was collected and assayed by RIA using I^{125}-SP to check the binding capacity of the column. After washing the column with PBS buffer and distilled water, substance P was eluted with 20% aqueous formic acid. The formic acid fractions from several runs were pooled and lyophilized, and a small aliquot was assayed by RIA for SP activity. Yield 100 pmol (10 rats).

Methionine enkephalin and substance P were analyzed by combined HPLC/thermospray mass spectrometry. The MH^+ and MNa^+ ions were selectively monitored. The results of SIM analyses are summarized in Table 2. HPLC conditions: HP Hypersil ODS (100 x 2.1 mm, 5 µm) column, 42% B (met-enkephalin) or 58% B (SP) (A: 0.1% TFA in H_2O, B: 0.1% TFA in 60% AcCN/H_2O), 0.6 ml/min, 10 and 20 µl injections. Thermospray conditions: source temp 250°C, vaporizer temp 370°C, chamber temp 425°C. Calibrants: polyethylene glycol 600 (0.1 mg/ml) and polypropylene glycol 1000 (0.5 mg/ml) in 0.1 M NH_4OAc for met-enkephalin and SP, respectively.

Methionine enkephalin and substance P were analyzed by dynamic liquid FAB mass spectrometry in the absence of an HPLC column. The results are summarized in Table 3. Liquid FAB conditions: 0.1% TFA and 10% glycerol in 50% MeOH/H_2O, 5-7 µl/min, 100 nl fixed volume injections, probe tip temp 60-70°C.

A strategy for the analysis of endogenous neuropeptides has been presented. The limits of detection of RIA, dynamic liquid FAB SIM MS, and thermospray SIM MS analyses of neuropeptides are 6-170 fmol, 1-2 pmol, and 100 pmol, respectively. RIA analysis affords the highest sensitivity but lacks the specificity of the MS techniques. Thermospray MS analysis is the least sensitive approach but is more compatible with standard HPLC methodology than liquid FAB. However, with recent advances in micro-HPLC technology, dynamic liquid FAB may prove to be the method of choice for the analysis of endogenous neuropeptides.

Acknowledgements

This research was supported by NIH grant GM32928 and by the Mayo Foundation.

Presented at the 35th ASMS Conference on Mass Spectrometry and Allied Topics
May 24-29, 1987, Denver, CO

Fig. 1 STRATEGY FOR ANALYSIS OF ENDOGENOUS NEUROPEPTIDES

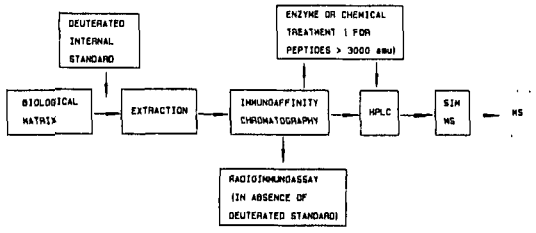

Table 1 RIA ANALYSIS OF ENDOGENOUS NEUROPEPTIDES

NEUROPEPTIDE	LIMIT OF DETECTION (PMOL)	CROSS REACTIVITY
METHIONINE ENKEPHALIN	170	[ARG6]-MET ENKEPHALIN (~ 30%) [ARG6,PHE7]-MET ENKEPHALIN (~30%) [ARG6,GLY7,LEU8]-MET ENKEPHALIN (NONE) METORPHINAMIDE (TRACE) B-ENDORPHIN (NONE)
SUBSTANCE P	10	OXIDIZED SUBSTANCE P (100%) SUBSTANCE K (<10%)
VIP	6	NONE KNOWN

Table 2 THERMOSPRAY SIM MS ANALYSIS OF NEUROPEPTIDES

NEUROPEPTIDE	LIMIT OF DETECTION (PMOL)	SIGNAL/NOISE
METHIONINE ENKEPHALIN	100	5/1
SUBSTANCE P	100	4/1

Table 3 DYNAMIC LIQUID FAB SIM MS ANALYSIS OF NEUROPEPTIDES

NEUROPEPTIDE	LIMIT OF DETECTION (PMOL)	SIGNAL/NOISE
METHIONINE ENKEPHALIN	2	5/1
SUBSTANCE P	1	5/1

Presented at the 35th ASMS Conference on Mass Spectrometry and Allied Topics
May 24-29, 1987, Denver, CO

Factors Controlling Ion Transfer in a Dual Cell Fourier Transform ICR

J.P. Honovich, S.P. Markey, T.-C.L. Wang, M.-C. Shih
Laboratory of Clinical Science, National Institute of Mental Health
Bethesda, Maryland 20892.

The FTMS/ICR mass spectrometer has proven itself to be an excellent mass analyzer. Unfortunately its need to operate at low pressures (< 10^{-7} torr) interferes with the use of many of the new techniques developed to analyze high mass compounds such as laser desorption (LD). In order to deal with the large pressure burst after each laser shot, Nicolet has introduced the differentially pumped dual-cell FTMS/ICR mass spectrometer. Ions are produced in the high pressure source cell and then transferred electrically through a small conductance limit to a low pressure analyzer cell for high resolution analysis. The technique promises to be both a simple and elegant method. We have investigated several experimental factors involved in using this approach effectively.

Electron Impact (EI): In order to optimize the inherent transfer efficiency and to model the transfer process for LD ions, we have investigated the transfer of EI-produced ions. Ions produced by electron impact in the high pressure source cell can be transferred to the analyzer cell by grounding a conductance limit in two types of experimental sequences. One is the transfer during the 5 ms ionization event where ions are allowed to randomize between cells. This procedure was used in the mechanical alignment of the ICR cell with respect to the magnetic field - an alignment which can effect the transfer efficiency by one to two orders of magnitude.

The second is a gated transfer, in which a packet of ions is produced and trapped in the source cell and then transferred to the analyzer by grounding the conductance limit for a specific time. This gated transfer sequence is best suited to investigate transfer times and efficiencies. Figure 1 shows the result of consecutive experiments which monitor the ion population in the analyzer cell as a function of the ion transfer time (time that the conductance limit is grounded). The time difference between successive maxima reflect the transfer time, while the diminishing maxima are a result of transfer losses as the ion packet shuffles between cells. By investigating a range of masses at various trapping potentials, it is possible to fit the transfer frequencies to an equation from the literature (1). Another set of experiments involves increasing the pressure to vary the ion density. Figure 2 shows that at low ion density (low pressure), ion transfer can be very efficient (> 90%, lower curve) while high ion densities (high pressure, upper curve) results in proportionally high losses on each transit through the conductance limit. Once the high ion density curve has been reduced the losses parallel those of the low density curve (low pressure).

Laser Desorption: Analogous to the EI results above, by grounding the conductance limit after firing the laser, high mass ions can be transferred to the analyzer region in a time-dependent manner as shown in Figure 3. Extrapolation of EI results discussed above predicted an arrival time of ~400 μsec. in contrast to the observed 1000 μsec This discrepancy can be rationalized by the fact that the ions were produced at the probe tip in a field free region and not at the center of the cell as in EI. Additionally, we have observed that ions with kinetic energy are able to penetrate through the conductance limit and be trapped in the analyzer. Figure 4B below shows that PEG 1500 ions are transmitted into the analyzer cell even when the conductance limit is not grounded and kept at 2 volts. It has been found that a barrier of 2-10 volts is required to stop these ions from penetrating into the analyzer cell. Thus, these are ions which must have been kinetically excited by the laser desorption process. Another factor is that in the FTMS-2000, the laser beam strikes the probe at an oblique angle (Fig. 5). Thus, the position where ions are generated is highly dependent upon horizontal probe position. Since ions will follow magnetic field lines, some probe positions allow transfer through the small (2 mm) conductance limit (Fig. 4B) while others will not (Fig. 4A), although they will contribute to source cell signal. Consequently, precise horizontal probe insertion dramatically influences the ability to transfer ions and effectively utilize the analyzer cell for high resolution.

Reference

1. C. Giancospro, F R. Verdun, J.-F. Muller, Int. J. Mass Spectrom. Ion Processes 72, 63 (1986).

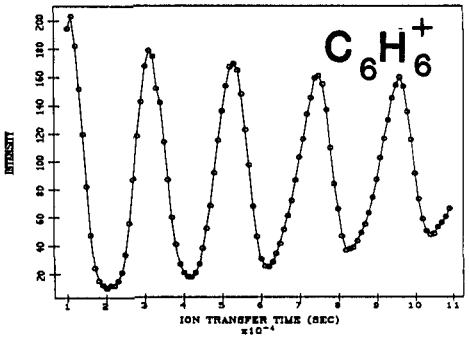

Figure 1

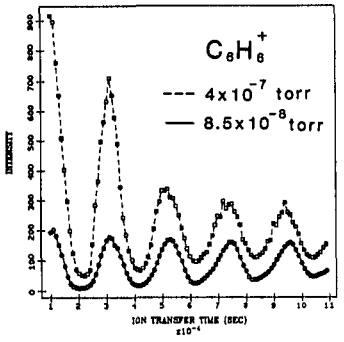

Figure 2

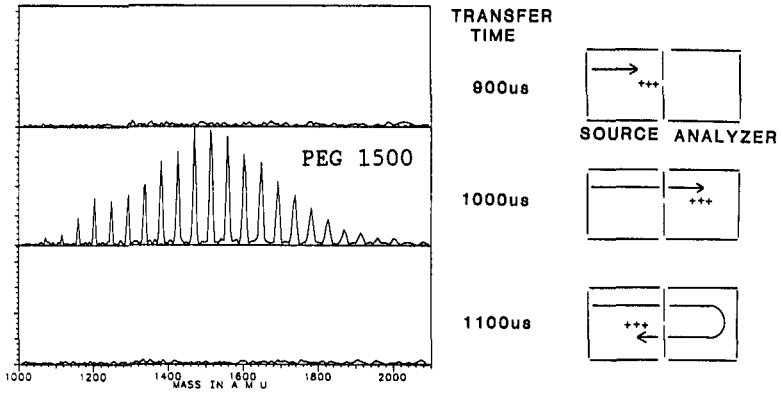

Figure 3.

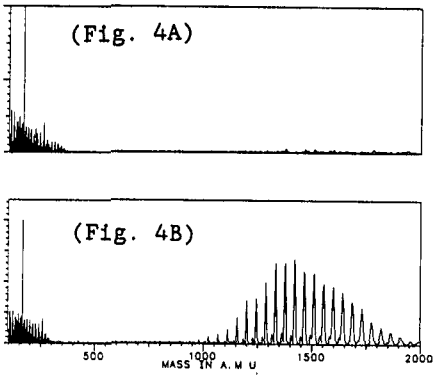

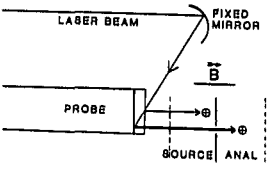

(Fig. 5)

Presented at the 35th ASMS Conference on Mass Spectrometry and Allied Topics
May 24-29, 1987, Denver, CO

IMPROVED ION TRAP PERFORMANCE WITH NEW CI AND MS/MS SCAN FUNCTIONS

M. Weber-Grabau, P. E. Kelley, J. E. P. Syka,
S. C. Bradshaw, Finnigan MAT, San Jose, California
J. S Brodbelt, Purdue University, West Lafayette, Indiana

The capability of the three-dimensional quadrupole ion trap to store ions has long been recognized and applied (1,2). The recent development of the mass-selective instability mode of operation, in combination with a light buffer gas, has significantly improved sensitivity and resolution (3). In this mode, the ion trap is operated with RF voltages only along the q-axis of the stability diagram. The buffer gas, at pressures around 10^{-3} torr, serves to cool the ions towards the center of the device. Helium is most commonly used, but hydrogen has the same basic effect. Therefore, an ion trap is easily coupled to a gas chromatograph, with the helium or hydrogen carrier gas used as buffer gas.

Due to its nature as an ion storage device, the ion trap allows the use of the time domain to perform experiments that, with conventional quadrupole or magnetic sector instruments, require specific ion sources or multiple analyzers. Operation in chemical ionization (CI) mode (4) and MS/MS mode (5) with daughter yields of typically 30-100% are possible with the same basic analyzer and relatively little extra hardware; the nature of the result spectrum depends mainly on the scan function.

Reaction mechanisms in positive ion CI include charge transfer, hydride abstraction and proton transfer. The first step in a CI experiment is the creation of a reagent ion population, $[R^+]$. The reagent ions are then consumed by reactions with analyte neutrals The number of product ions, P^+, formed depends on the initial reagent ion concentration, the sample concentration or partial pressure [M], the reaction rate and the reaction time. In order to avoid either space-charging the trap (when very much sample is present) or not producing enough product ions (when very little sample is present), we have developed a scan function in which reagent gas ionization time and reaction time are automatically optimized in realtime to produce a desired number of product ions The adjustment is based on a fast TIC or CI response measurement preceding the analytical scan (Fig. 1). From the rate equation, and with the reaction time set proportional to the reagent gas ionization time, t, it can be shown that

$$[P^+] = a \times [M] \times t^2$$

This expression is used to normalize the measured peak intensities to obtain a result proportional to the sample concentration. With the automatic reaction control scan function, CI/GC/MS spectra can be obtained at low concentration levels (Fig. 2); also, differences in reaction rates are compensated for, improving S/N ratios for compounds with low reaction rates.

We recently have modified the Ion Trap Mass Spectrometer (ITMS) to allow the combined application of DC and RF voltages to the ring electrode. This has resulted in scan functions with greatly improved sensitivity in Selected Ion Monitoring (SIM) and MS/MS modes.

A single mass can be isolated in the ion trap when, after ionization, the RF and DC potentials are adjusted so that the mass is near the apex of the stability diagram at q=0.78, a=0.15 (Fig. 3). After the RF voltage has been set, the DC voltage is pulsed on for less than one millisecond. When returning to the RF-only mode, only the selected (parent) mass is still stored. After the CID step, the daughter spectrum is acquired (Fig. 4).

Optimum storage efficiency in EI mode is achieved when the sample is ionized at low RF voltages (q≈0.05 for *m/z* 500). The number of ions stored is proportional to the exposure, i.e., the product of emission current and ionization time. Although on the order 10^6-10^7 ions can be stored, space-charge repulsion leads to resonance frequency shifts and line broadening (making MS/MS experiments difficult) as well as loss of resolution during mass analysis, when the number of ions exceeds 10^4-10^5. Thus, the need to stay out of the realm of space charge may result in the storage of very few ions for a low-abundance peak.

In the DC/RF mode, the total charge in the trap is reduced after all masses but one are ejected. Moreover, temporary storage at the stability diagram apex appears to have a spatial focussing effect. As a result, resolution is achieved in the CID and mass analysis steps even at greatly increased exposures. Fig. 5 illustrates the use of combined DC and RF voltages for the MS/MS analysis of *m/z* 231, a minor peak in the mass spectrum FC-43.

Without the MS/MS step, moving a mass to an apex of the stability diagram somewhat resembles the way a standard quadrupole instrument is operated (Fig. 3), except that ions remain stored. Multiple ionization/isolation steps are possible to accumulate ions of a selected mass. While the full-scan sensitivity

of the ion trap in RF-only mode is comparable to that of a quadrupole instrument in SIM, RF/DC operation provides a significant improvement in sensitivity for selected ions (Fig. 6), in particular in the presence of background.

References:

1. P. H. Dawson, N. R. Whetten, U.S. Patent No 3,527,939 (1970)
2. J. F. J. Todd, R. F. Bonner, in: Dynamic Mass Spectrometry, Vol. 4, Heyden, London 1976
3. G. C. Stafford, P. E. Kelley, D. R. Stephens, U.S. Patent No. 4,540,884 (1985)
4. J. S. Brodbelt, J. N. Louris, R. G. Cooks, Anal. Chem. 59(9), 1278-85 (1987)
5. J. N. Louris, R. G. Cooks, J. E. P. Syka, P. E. Kelley, G. C. Stafford, J. F. J. Todd, *in press*

CI Automatic Reaction Control Scan Function

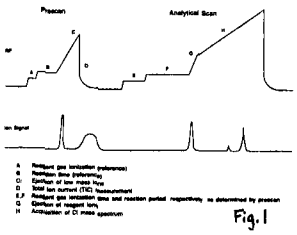

Fig. 1

MS/MS With RF/DC Parent Isolation

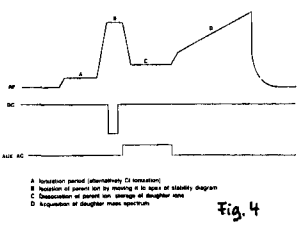

Fig. 4

RF/DC Single Ion Monitoring Scan Function

6a

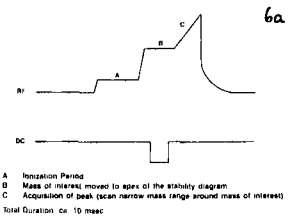

100 pg Methyl Stearate (mw = 298), CH_4 CI with ARC

2a

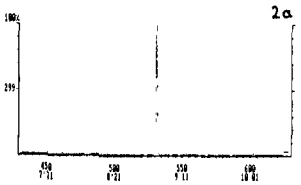

FC43, *m/z* 205-280 with 100 Fold Increased Ionization

5a

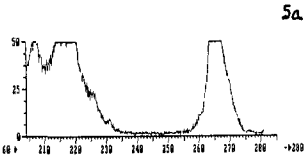

10 pg Methyl Stearate, *m/z* 298

6b

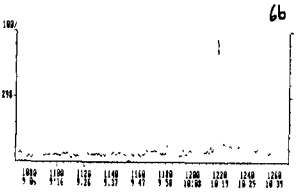

Fig. 6

100 pg Methyl Stearate, CH_4 CI Full Spectrum

2b

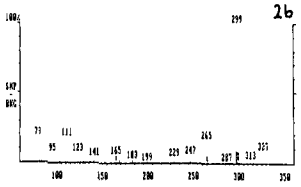

Fig. 2

RF/DC Isolation Of *m/z* 231 (<0.5% Of Base Peak)

5b

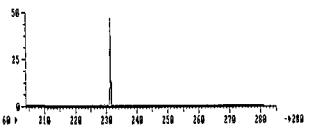

Daughters Of *m/z* 231 · 100% Conversion Efficiency

5c

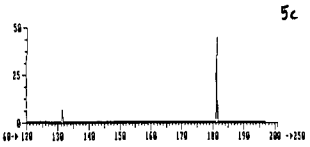

Fig. 5

ITMS Configuration

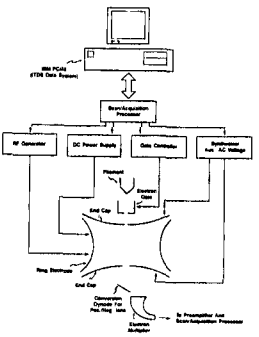

Fig. 7

Stability Diagram for the Ion Trap

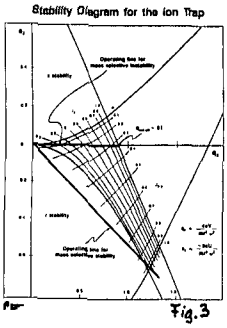

Fig. 3

Presented at the 35th ASMS Conference on Mass Spectrometry and Allied Topics
May 24-29, 1987, Denver, CO

ULTRAHIGH RESOLUTION FT-ICR-SPECTROMETRY

M. Bamberg, M. Allemann* and K. P. Wanczek

Inorganic Chemistry, University, D-28 Bremen, West-Germany
(*) Spectrospin AG, CH-8117 Fällanden, Switzerland

The ultrahigh resolution experiments were carried out with an ICR spectrometer with a magnet of 7.02 T field strength and 8.9 cm room temperature bore. A Spectrospin Aspect 3000 Minicomputer controls the instrument. Two cylindrical ICR cells, with solid respectively with perforated side plates for better pumping were used. To reach the lowest possible pressure a new vacuum system was constructed. It consits of two compartments: The UHV-system consisted of a combination of an ion getter pump and titanium sublimation pump. These ultrahigh vacuum pumps are backed up by a high-vacuum system consisting of oil diffusion pump with high performance cold trap. Both units are connected via a separation valve. This allows the ICR cell region to be pumped separately. The base pressure was below 10^{-12} mbar, which allows inlet pressures in the range of 5×10^{-12} mbar. Because of their low masses and high resonance frequencies oxygen and argon were used as sample gases.
The optimisation of all instrumental parameters had to be carefully established prior to the ultrahigh resolution experiments.
The resolution is defined as[1]:

$$m / \Delta m(FWHH) = \omega / \Delta\omega(FWHH) = 0.264\ e\ B\ T / m$$

In order to achive the attainable highest resolution the absorption-mode of operation of the spectrometer was chosen[1].
The resolution is inversely proportional to mass m/e and directly proportional to magnetic field strength B and observation duration of the transient T. In contrast to sector field mass spectrometers it is not depending on constructive and geometrical features as slit widths and other focussing means. It is possible to reach resolutions better 10^4 times better than in sector field mass spectrometers.
An increase of resolution depends mainly on the mean free time between collisions, which limits the observation of the transient. Therefore the pressure must be as low as possible. Furthermore the excitation of the ions for detection has to be controlled carefully, the resulting cyclotron trajectory of ions are of importance when considering the intensity, the resolution and the effective cyclotron frequencies of the measured mass peak.
In order to reach a good signal to noise ratio, the excitation energy should be selected so as to attain the highest peak intensities. Depending on constructive features of the ICR cell, the optimum ion trajectory is between 55% (perforated side plates) and 70 % (solid side plates) of the cell radius. Excitation energies forcing ions to exceed this cyclotron orbit will diminish the resolution and further cause a shift of the effective resonance frequency of a few Hertz. It could not be determind whether inhomogenities of the magnetic or electric fields

cause this limitation. Ion orbits of smaller radius are not effecting the resolution.
At the pressure below 2×10^{-10} mbar no peak width deterioration can be observed, even at ionisation pulses of 40 sec, because the number of ions is so small. This is true even for small ion orbits, where space charge effects are strong[2]. Thereby a large range of excitation energies for high resolution experiments is possible.
A limitation of resolving power caused by the influence of small magnetic field inhomogenities was determined experimentely. Location of the ICR cell 1 cm away from the center of the homogeneous region of the magnetic field causes a field change of $\Delta B = 1.11 \times 10^{-5}$ T. However the resolution for Ar^+ was still at least 2×10^8! This field error is averaged by the fast cyclotron motion of the ions[3].
The best possible mass resolution could be obtained only at the lowest pressures. Slight pressure increase causes an immediate decrease of resolution, the transient becomes shorter. Compared to the influence of the pressure, there was a wide range for selection of other instrumental parameters such as trapping plate potentials, excitation energy, delay times between the various pulses.

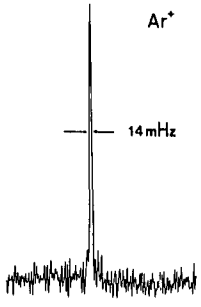

Fig. 1.

Ar^+-Peak
m / Δm(FWHH)
<200,000,000

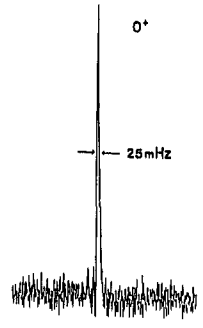

Fig. 2.

O^+-Peak
m / Δm(FWHH)
<300,000,000

The aquisation time for the Ar^+ spectrum (Fig. 1) was 80 sec and 100 sec for O^+ (Fig. 2). The number of ions for one scan produced within the ICR cell is approximately 5000. The peaks shown are recorded without spectrum averaging in a single scan.

Acknowledgment

Financial support by the Deutsche Forschungsgemeinschaft is gratefully acknowledged.

References

1. A. G. MARSHALL, M. B. COMISAROW, G. PARISOD, J. Chem. Phys. 71, 4434 (1979)
2. T.-C. L. WANG, A. G. MARSHALL, Int. J. Mass Spectrom. Ion Proc. 68, 287 (1986)
3. M. B. COMISAROW, in H. HARTMANN, K. P. WANCZEK (Eds.), Ion Cyclotron Resonance Spectrometry, Vol. 2, Springer-Verlag, Berlin, 1982

Presented at the 35th ASMS Conference on Mass Spectrometry and Allied Topics
May 24-29, 1987, Denver, CO.

LASER DESORPTION FOURIER TRNASFORM MASS SPECTROMETRIC ST UDY OF OLIGOPEPTIDES IN THE PRESENCE AND ABSENCE OF COLLISION ACTIVATED DISSOCIATION

Cathy Liub-Chii Yang, Chemistry Department, University of California, Riverside, CA 92521

INTRODUCTION

Collision Activated Dissociation (CAD) has been applied to many different methods of mass spectrometry[1-4] such as Fast Atom Bombardment Mass Spectrometry(FABMS), and Field Desorption Mass Spectrometry(FD/MS). It was concluded by many researchers[1-4] that the positive ion spectra obtained by FABMS or FDMS in the presence of CAD can only be a complementary source for oligopeptide sequencing. Secondary ion mass spectrometry[5] was used to study oligopeptides and the spectra revealed convincing information to sequence oligopeptides. Recently, the positive ion spectra obtained by LD/FTMS in the presence of CAD[6] revealed encouraging results. Authors suggested that subtracting every adjacent peak in the positive ion spectra to select the ions corresponding to the cleavages between the oligopeptides' backbone.

Here, a different methodology is proposed to sequence oligopeptides by using the positive and negative ion spectra obtained by LD/FTMS in the presence of CAD with water.

EXPERIMENTAL SECTION

Laser desorption mass spectra were obtained by a Nicolet FTMS-1000 Fourier transform mass spectrometer at 3 Tesla, equipped with a Tachisto Model 215G CO_2 TEA gas laser. For the spectra reported here, the laser delivered 0.3J per 40 nsec pulse at 10.6 um. The laser beam centered at a 5.08 cm^3 cell made of 80% transmissive stainless steel after passing through a zinc selenide window and a 4 in. focal length zinc selenide focusing lens to bring it to focus to just before the stainless steel sample probe tip. Trapping voltages were set at 1V and -1V to obtain the positive and negative ion spectra. A bandwidth of 1.3 MHz corresponds to a lower mass cutoff at m/z 30 amu and a sweeping rate of 400Hz/us were employed. 32K data points, augmented by 32K zeroes prior to Fourier transformation, were obtained yielding average mass resolution 3,000 to 5,000 (50% valley definition). The water vapor pressure was maintained at a static pressure of 8*10(-8) torr. Total pressure of the system was maintained at a pressure of 1*10(-7) torr.

RESULTS AND DISCUSSION

Figure 1 reveals a typical example of the effect of CAD on the spectra obtained by LD/FTMS. Figure 1 (a) reveals only two peaks corresponding to the cleavages of t-BOC-tetraproline's backbone, and Figure 2 (b) reveals all the Z terminus ions corresponding to the cleavages between the t-BOC-tetraproline's backbone.

Table I lists all the oligopeptides examined in this work. The examined oligopeptides categoried into two groups First, both positive and negative ion spectra revealed the same series of A and/or Z terminus ions. Second, the positive and negative ion spectra revealed different series of A or Z terminus ions.

First category of oligopeptides revealed three types of characteristic fragmentation patterns in the spectra obtained by LD/FTMS in the presence of CAD. The first type, both positive and negative ion spectra consistently revealed the A or Z terminus ions. The second type, both positive and negative ion spectra consistently revealed the Z terminus ions. Figure 2 is a typical example of the second type of fragmentation patterns. The third type, both positive and negative ion spectra consistently revealed the A terminus ions.

This phenomenon can be used to sequence an oligopeptide directly by selecting the ions corresponding to the cleavages of the oligopeptides' backbone from both positive and negative ion spectra. This phenomenon was found in the spectra obtained by SIMS[5], but was not found in the spectra obtained by photodissociation FTMS[7] and FABMS[8].

ACKNOWLEDGEMENT

Cathy L.C. Yang acknowledges Dr. Charles L. Wilkins and Kenton Dunbar for discussing this work.

The support of Grant GM 30604-05 is greatly appreciated.

Presented at the 35th ASMS Conference on Mass Spectrometry and Allied Topics
May 24-29, 1987, Denver, CO

REFERENCES

1. Neumann, G.M., Derrick, P.J., Aust. J. Chem., 1984, 37, 2261-2277.
2. Higuchi, T., Maruyama, Y., Int. J. Mass Spectrom. Ion Phys., 1983, 46, 423-426.
3. Morris, H.R., Panico, M., Barber, B., Bordoli, R.S., Sedgewick, R.D , Tyler, A., Biochem. Biophys. Res. Commun., 101, 1981, 623-631.
4. Roepstorff, P., Hojrup, P., Moller, J., Biomed. Mass Spectrom., 12, 1985, 181-189.
5. Seki, S., Kambara, H., Naoki, H., Org. Mass Spectrom., 20, 1985, 18-24.
6. Cody, R.B., Amster, I.J., McLafferty, F.W. Proc. Natl. Acad. Sci., 82, 1985, 6367-6370.
7. Bower, W.D., Delbert, S.S., Hunter, R.L., McIver, R.T., J. Am. Chem. Soc., 1984, 106, 7288-7289.
8. Konig, W.A., Aydin, M., Schulze, U., Rapp, U., Hohn, M., Pesch, R., kalikhevitch, Int. J. Mass Spectrom. Ion Proc., 46, 1983, 403-406.

TABLE I

Gly-His-Gly-OH	Penta-Glycine
Hexa-Gly-OH	t-BOC-tetra-Proline
Tetra-phenylalanine	Asp-Gly-OH
Glu-Glu-OH	Leu-Gly-Phe-OH
Penta-Alanine	Leu-Alanine
Gly-Phe-Ala-OH	Ala-Glu-Lys-Ala-Ala-OH
Glu-Tyr-OH	Trp-Met-Asp-Phe-OH
Lys-Cys-Thr-Cys-Cys-Ala-OH	Bradykinin
Angiotensin II.	

Figure 1: Laser desorption Fourier transform mass spectra of t-BOC-tetraproline (a) in the absence of CAD (b) in the presence of CAD.

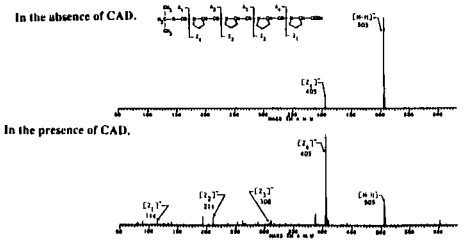

Figure 2: Laser desorption Fourier transform mass spectra obtained in the presence of CAD for angiotensin II (a) positive ion spectrum (b) negative ion spectrum.

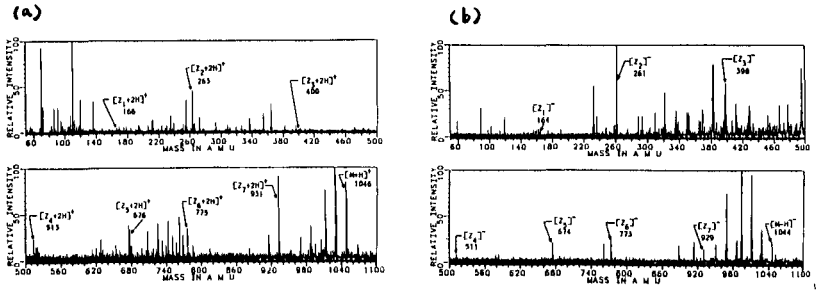

Presented at the 35th ASMS Conference on Mass Spectrometry and Allied Topics
May 24-29, 1987, Denver, CO

^{252}Cf PLASMA DESORPTION FOURIER TRANSFORM ION CYCLOTRON RESONANCE MASS SPECTROMETRY IMPROVEMENT IN ION TRAPPING EFFICIENCIES

S.K. Viswanadham[a], R.R.Weller[b], C.S. Giam[a,b], and D.M. Hercules[a]

[a]Department of Chemistry and
[b]Department of Industrial Environmental Health Sciences
University of Pittsburgh
Pittsburgh, PA 15261

^{252}Cf plasma desorption has shown the ability to ionize samples in the mass range above 25,000 amu. Detection of the desorbed ions has been accomplished by time-of-flight analysis, providing a complete mass spectrum for each desorption event. FT-ICR mass spectrometic techniques provide a better alternative since they do not suffer from poor resolution and the mass discrimination of high mass ions that is inherent to time-of-flight analysis.

Early ^{252}Cf PD-FT-ICR-MS was characterized by low signal-to-noise ratios attributed to poor ion trapping efficiencies[1]. Greatly improved spectra have been obtained by alterations in the source-sample-cell geometries (see Fig. 1). The most improved spectra were obtained with the source and sample immediately adjacent to the trapping plate (either just outside or inside through a 1.5 cm hole). Improved trapping efficiencies (though still estimated to be very low) resulted in the decrease of ion accumulation times from 30 to 2 minutes. Signal-to-noise ratios have also improved by a factor of up to 300. Trapping voltage studies suggest that a 1 to 3 V potential produces the best results.

Excellent spectra were obtained for CsI, N,N,N-trimethyl-p-aminophenolate, 18-crown-6 ether, tetrapentylammonium bromide (TPAB, Fig. 2), chloropyrifos (Fig. 3), and bromophos (Fig. 4). Expected isotopic distributions were observed. TPAB showed structurally significant fragmentation. 18-crown-6, bromophos, and chloropyrifos spectra showed one or more pseudo-molecular ions corresponding to $(M+H)^+$, $(M+Li)^+$, $(M+Na)^+$, or $(M+K)^+$. A cationized dimer corresponding to $(2M+Na)^+$ was observed for chloropyrifos.

[1]R. R. Weller, S.K. Viswanadham, M.A. Sheetz, C.S. Giam, and D.M. Hercules, presented at ASMS 34 Annual Conference. Cincinnati, OH, June 8-13, 1986.

Source-Cell Configurations: ^{252}Cf PD-FT-ICR-MS

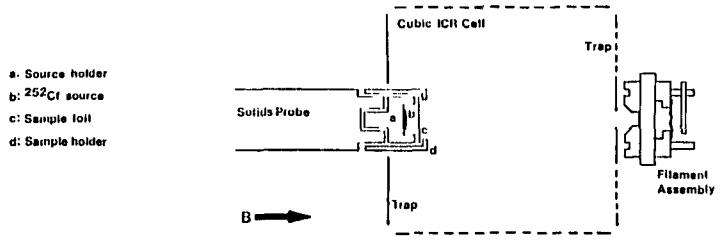

Figure 1

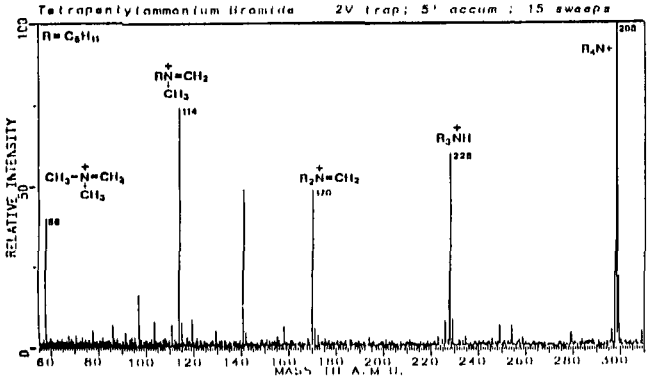

Figure 2

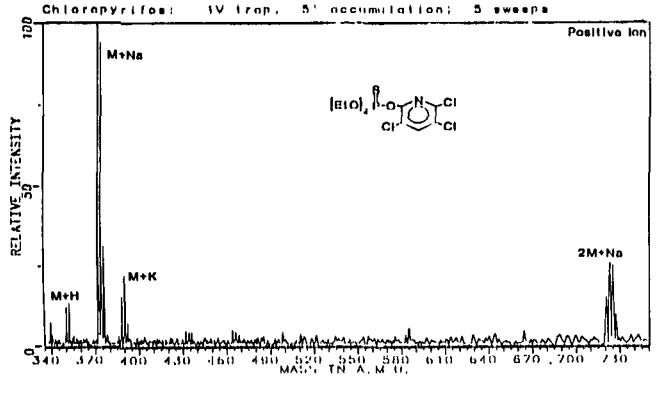

Figure 3

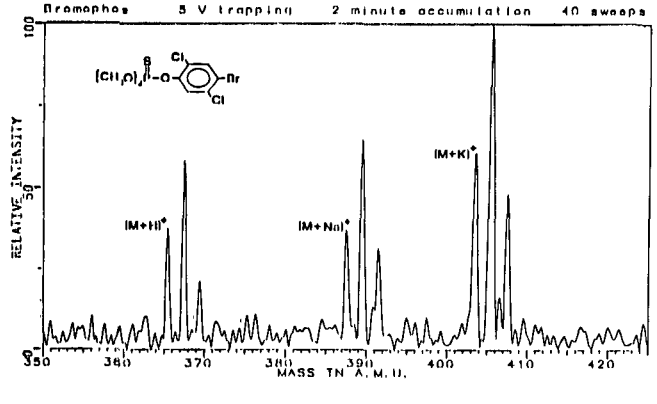

Figure 4

Presented at the 35th ASMS Conference on Mass Spectrometry and Allied Topics
May 24-29, 1987, Denver, CO.

APPLICATION OF FTICR SPACE CHARGE CORRECTIONS TO ACCURATE MASS MEASUREMENTS

Jon T. Meek, William G. Millen, Thomas J. Francl, Gerald W. Stockton, Michael L. Thomson and Richard S. Wayne, American Cyanamid Company, Agricultural Division, P.O. Box 400, Princeton, NJ 08540

INTRODUCTION

The utility of FTICR for making accurate mass measurements has been limited by the need to keep the ion space charge constant for both the calibration and the sample analysis. Typical sample introduction techniques can produce a wide range of ion densities in the ICR cell which will result in frequency shifts that invalidate the previous calibration. Our initial accurate mass investigations were consistent with calculations by Francl, et. al.[1] which predicted that space-charge-induced frequency shifts should be independent of mass. An investigation was initiated to determine if a lock mass could be used to correct for these frequency shifts.

The mass calibration equation was obtained from the Lorentz force equation by assuming that the electric field in the ICR cell is radially directed (perpendicular to B):

$$m = qB/2\pi f + qE/4\pi^2 rf^2$$

This is similar to the equation derived by Ledford et. al.[2] The derivative of this equation was used to predict how an observed mass would shift with changes in the electric field within the ICR cell:

$$dm = qdE/4\pi^2 rf^2$$

EXPERIMENTAL

These experiments were performed on an FTICR at the Agricultural Research Division of American Cyanamid. The distingushing features of this instrument include a 7 Tesla magnet and an advanced data system. The system was operated in the electron impact (EI) mode of ionization and samples were introduced with a heated solids probe.

Data were obtained by digitizing single transients for 262 ms at 2 MHz (512k data points) with a 12 bit ADC. Accurate frequency measurements were made by a "Zoom" transform algorithm[3] using a 16x zero fill at each observed frequency with a gaussian fit to the top half of each peak. The FTICR is calibrated by fitting the observed frequencies from tris(perflouroheptyl)-s-triazine to the calibration equation:

$$m = C_0/f + C_1/f^2 + C_2$$

where C_0 is a measure of the magnetic field, C_1 of the effective electric field and C_2 should be the mass of an electron since we are using atomic masses instead of ionic masses in our mass table.

Space-charge-induced frequency shifts which were generated during the analysis of a sample were corrected by using a lock mass to either 1) calculate the change in the electric field term of the calibration equation using:

$$\Delta C_1 = \Delta m\ f^2$$

or 2) by shifting all frequencies in the mass spectrum by the difference between the observed and calibration frequencies of the lock mass:

$$\Delta f = f_{obs} - f_{cal}$$

The accurate masses calculated from the corrected data were used to determine elemental compositions and the resulting errors compared to uncorrected data.

RESULTS

Table I shows raw and corrected data for series of scans from samples of pendimethalin and hexabromobenzene which were introduced on a solids probe.

CONCLUSIONS

The use of a lock mass will correct for space-charge-induced frequency shifts in an FTICR over a broad mass range. It was demonstrated that the accurate mass capabilities of an FTICR can be significantly improved (average and RMS errors 1ppm or less below m/z=556) by using a lock mass to correct for these frequency shifts.

1/ T.J. Francl, M.G. Sherman, R.L. Hunter, M.J. Locke, W.D. Bowers and R.T. McIver, Jr. Int. J. Mass Spectrom. Ion Proc. 1983, 54, 189-199.

2/ E.B. Ledford, Jr., D.L. Rempel and M.L. Gross, Anal. Chem. 1984, 56, 2744-2748.

3/ T.J. Francl, R.L. Hunter and R.T. McIver, Jr. Anal. Chem. 1983, 55, 2094-2096.

TABLE I - BETWEEN SCAN ACCURATE MASS ERRORS

FORMULA	MASS	# of Scans	RAW DATA Avg.Error (Std Dev) ppm		SPACE CHARGE CORRECTED Avg.Error (Std Dev) ppm	
Pendimethalin ($C_{13}H_{19}N_3O_4$)						
$C_7H_7N_2$	119.060923	6	2.1	(1.6)	-0.03	(0.15)
$C_7H_8N_3$	134.071822	4	3.7	(0.8)	0.33	(0.11)
$C_8H_{10}N_2$	134.084398	4	3.7	(0.8)	0.35	(0.10)
$C_8H_8N_3$	146.071822	5	3.4	(1.7)	0.29	(0.29)
$C_9H_{10}N_2$	146.084398	4	4.1	(0.9)	0.38	(0.13)
$C_9H_{10}N_2O$	162.079313	8	2.0	(1.8)	-0.35	(0.24)
$C_8H_7N_2O_2$	163.050753	5	3.6	(1.8)	0.08	(0.17)
$C_8H_9N_3O$	163.074562	4	4.8	(1.1)	0.67	(0.24)
$C_{10}H_{13}NO$	163.099714	3	4.3	(0.3)	-0.35	(0.36)
$C_9H_9N_3O_2$	191.069477	8	2.7	(2.2)	-0.15	(0.25)
$C_9H_{10}N_3O_3$	208.072216	8	2.5	(2.3)	-0.51	(0.49)
$C_{11}H_{14}N_3O_4$	252.098431	4	6.0	(1.4)	-0.39	(0.35)
Lock mass at m/z = 168.988823 (C_3F_7).						
Hexabromobenzene						
$C_6Br_4{}^*Br_0$	387.67334	5	-1.4	(0.61)	-0.38	(0.75)
$C_6Br_3{}^*Br_1$	389.67130	9	-1.5	(0.45)	-0.19	(0.56)
$C_6Br_2{}^*Br_2$	391.66925	9	-1.3	(0.51)	0.01	(0.40)
$C_6Br_1{}^*Br_3$	393.66721	9	-1.0	(0.50)	0.33	(0.40)
$C_6Br_0{}^*Br_4$	395.66516	6	-1.8	(1.1)	-0.63	(0.90)
$C_6Br_4{}^*Br_1$	468.58963	9	-1.3	(0.85)	0.27	(0.45)
$C_6Br_3{}^*Br_3$	470.58759	9	-2.0	(0.79)	-0.4	(0.68)
$C_6Br_2{}^*Br_3$	472.58554	9	-1.6	(0.75)	0.02	(0.43)
$C_6Br_1{}^*Br_4$	474.58350	9	-0.95	(0.86)	0.66	(0.52)
$C_6Br_5{}^*Br_1$	547.50797	9	-2.2	(1.3)	0.24	(1.2)
$C_6Br_4{}^*Br_2$	549.50592	9	-1.8	(0.45)	0.09	(0.77)
$C_6Br_3{}^*Br_3$	551.50388	9	-0.99	(0.71)	0.88	(0.81)
$C_6Br_2{}^*Br_4$	553.50183	9	-1.8	(0.45)	0.09	(0.65)
$C_6Br_1{}^*Br_5$	555.49979	9	-1.6	(0.73)	0.5	(1.1)
Lock mass at m/z=263.987106 (C_5NF_{10})						

A 1Hz error is 1.1ppm at m/z=120 and 5ppm at m/z=550.
$^*Br = {}^{81}Br$

Presented at the 35th ASMS Conference on Mass Spectrometry and Allied Topics
May 24-29, 1987, Denver, CO

Improved Peak Shapes from a Modified FTMS Cubic Cell Incorporating Segmented Trap Plates

Don L. Rempel, Midwest Center for Mass Spectrometry, Department of Chemistry, University of Nebraska, Lincoln, NE 68588-0362

The difficulty in designing an ideal trap for use in a Fourier transform mass spectrometer is the achievement of both a quadrupolar electric field for spatially invariant ion cyclotron frequencies and uniform excitation and detection fields for no z-mode excitation and no signal harmonics. The pursuit of ideal quadrupolar electric fields leads one to the use of a hyperbolic trap. However, the demand for a simple excitation field requires parametric mode operation (1) which makes wideband excitation waveform design difficult.

An alternative approach emphasizes that the cubic trap already performs modestly well and that only improvement is needed. Here, it is shown that segmented trap plates (2) can be used to adjust the trap electric fields for improved performance. The trap plates were segmented by introducing a 0.0127-m diameter circular gap, centered on the z-axis, to electrically isolate a disk from the remaining outer segment of each trap plate of a 0.0254-m cubic trap constructed with 304 SS. The disk was held at 0.958 V. The outer segment was held at 0.985 V for normal operation and 1.704 V for compensated operation. Other conditions were a 1.2-Tesla magnetic field; 1.0×10^{7}-Torr benzene pressure; 150-nA, 2.5-mS, 50-eV electron beam; a 0.345-volt b-p by 700-μs rf burst excitation; and a 444.9-ms observation time. Data was taken from the m/z = 78 ion.

To gain insite into the operation of the trap with segmented plates, computations were performed by using a model that assumes a low amplitude rf burst excitation and insignificant ion-ion or ion-neutral interactions on the time scale of excitation and detection so that the computations in ref. 3 of excited cyclotron orbit radius and ion signal amplitude of each ion apply. In addition, it was assumed that each ion moves harmonically with incommensurate frequencies over a cylinder coaxial to the z-axis. Then the observable signal contribution occurs at an average cyclotron frequency as approximated by the effect of the trap electric field radial component that has been averaged over the cylinder. The weighted signal contributions of 1000 representative ions were accumulated to form a calculated peak shape. The effect of finite observation time was taken into account.

For the normal cubic trap, the peak shapes are doublets for essentially all excitation times (160 μs to 1260 μs) for which signals are observed. The increase in peak separation with increasing trap voltage suggests that the effect is electric in origin. Collisions modify the z-mode amplitude distribution of the ions initially formed along the z-axis, as shown in Fig. 1. The maximum of the peak shifts over 70 Hz in 4.0 s. This change is anticipated by the calculated peaks in Figs. 2 and 3, where postulated initial and 300 K thermal z-mode amplitude distributions were used. Experimentally, the doublet disappears with large ion populations or long observation times.

For the compensated cubic trap, the peak is unified. As shown in Fig. 4, the peak shape remains constant in a repeat of the experiment shown in Fig. 1. The shift in the peak controid is less than or equal to 0.1 Hz for the conditions used here. At an ionization-to-excitation delay of 1.0 ms, compensation improves the signal-to-noise ratio by over a factor of two.

Literature Cited

1. D.L. Rempel, E.B. Ledford and M.L. Gross, (submitted).
2. S.K. Huang and D.L. Rempel in **Proceedings of the 34th Annual Conference on Mass Spectrometry and Allied Topics**, 1986, 167.
3. D.L. Rempel, S.K. Huang and M.L. Gross, **Int. J. Mass Spectrom. Ion Proc.**, 70 (1986) 163.

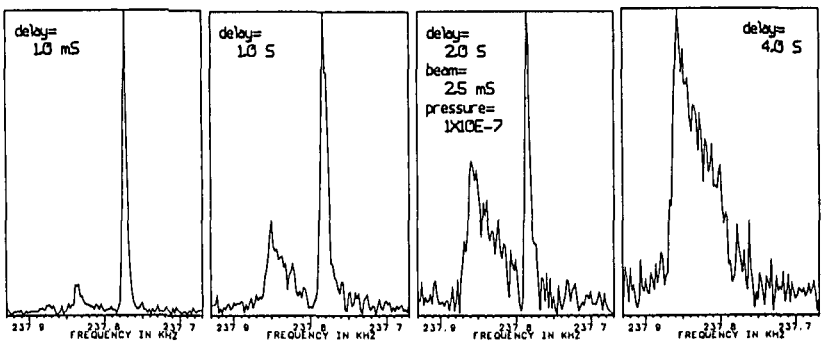

Figure 1. Evolution of peak shape in a normal cubic trap.

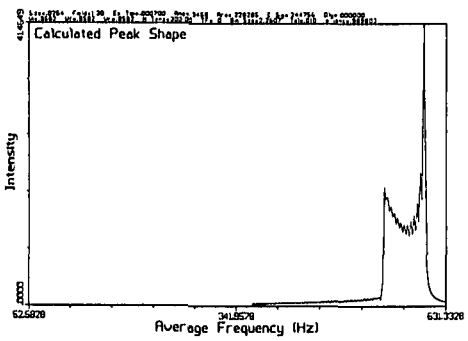

Figure 2. Calculated peak shape assuming a z-mode amplitude distribution that would be formed during the ionization period.

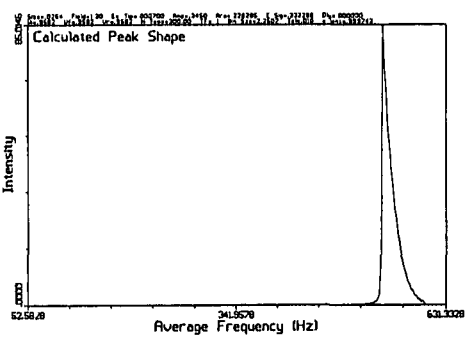

Figure 3. Calculated peak shape assuming a thermal z-mode amplitude distribution.

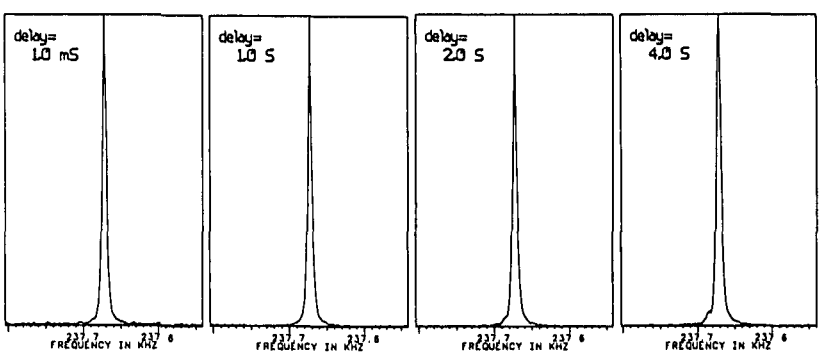

Figure 4. Evolution of peak shape in a compensated cubic trap.

Presented at the 35th ASMS Conference on Mass Spectrometry and Allied Topics
May 24-29, 1987, Denver, CO

EFFECTIVENESS OF VELOCITY COMPACTION FOCUSING FOR IMPROVING THE RESOLVING POWER OF A CONVENTIONAL TOF MASS SPECTROMETER*

M. L. Muga
TOFTEC
P.O. Box 12877
Gainesville, FL, 32604

Velocity Compaction (VC) ion focusing in a pulsed time-of-flight (TOF) mass spectrometer (MS) selectively accelerates the ions in an iso-mass packet in such a manner as to give all ions a nearly equal final drift velocity. In this way the spatial distribution of ions within the iso-mass packets is "frozen" and peak-to-peak adjacent-mass ion packets continue to separate during the final drift period with minimal overlap. Velocity compaction ion focusing was primarily developed to extend the useful mass range above 1000 amu, thereby taking advantage of the efficient heavy mass transmission characteristics of the straight path TOF mass spectrometer. The new ion focusing technique can, however, be used effectively for improving the performance in the lower mass range that is covered typically by the conventional (i.e. constant energy acceleration) TOF mass spectrometer.

Thus application of a VC acceleration stage after a conventional first stage extraction and short drift path as shown in Fig. 1 should enhance the overall mass resolving power.

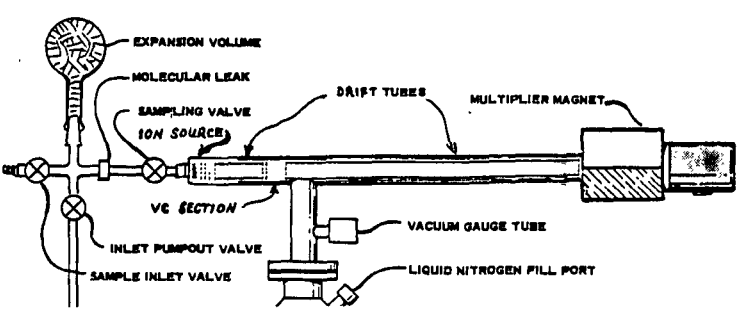

Figure 1) Cut away drawing of time-of-flight tube showing relative positions of first stage drift, velocity compaction acceleration stage and final drift region.

Computer generated ion flight times for such a design were undertaken based on a CVC, Inc. instrument with electron impact (EI) ion source. This ion source is characterized by a four grid extraction and acceleration unit with grid spacings of 0.20 cm, 0.17 cm, 0.37cm and 0.55 cm. respectively, beginning with the ion formation region. The original dimensions and grid spacings in the ion source were retained in the calculations but the initial drift distance was shortened to 15 cm. followed by a deceleration grid placed 0.2 cm after the initial drift tube. The overall flight path was lengthened from 40 cm to 1.0 meters in some cases and 1.2 meters in others. A slight improvement in resolving power for the longer flight paths was indicated.

The length of the velocity compaction section chosen was varied between 3 and 4 cm. in order to gauge the extent of the voltage swings needed to effect velocity compaction. The shorter this distance, the higher are the voltage swings needed to bring about the velocity compaction focusing. The maximum voltage rise, applied to the variable acceleration grid which is attached to the final drift tube, was less than 2000 volts and typical flight times of 45 microseconds for mass 500 amu were obtained. Results indicate that a resolving power ($M/\Delta M|_{fwhm}$) of about 2000 at mass 500 amu can be attained. By correcting the spectrum peak heights for known isotopic abundances the expected spectrum for Hg^+ could be generated as shown in Fig. 2.

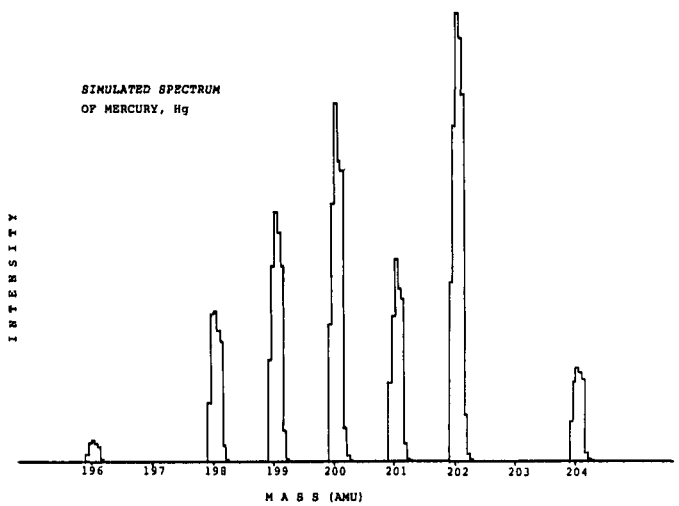

Figure 2) Expected Spectrum of Mercury, Hg, from Computer Generated Flight Times Based on Velocity Compaction Ion Focusing in Mid-Flight.

Modification of a used time-of-flight instrument is currently underway in order to test the validity of these computer generated flight time spectra.

* Supported in part by the Department of Health and Human Services Public Health Service Small Business Innovation Research (SBIR) Phase II Program, Grant No. MH39422-02, National Institute of Mental Health.

Presented at the 35th ASMS Conference on Mass Spectrometry and Allied Topics
May 24-29, 1987, Denver, CO

CAPILLARY GAS CHROMATOGRAPHY / ICR-MASS SPECTROMETRY USING AN EXTERNAL ION SOURCE AND A NOVEL ION TRANSFER SYSTEM

P. Caravatti, P. Grossmann, P. Kofel,
M. Allemann, H.P. Kellerhals

Spectrospin AG, Industriestrasse 26,
8117 Faellanden/Zurich, Switzerland

Fourier Transform Mass Spectrometry (FTMS), a rapidly developing technique (1 - 7) is applied increasingly to studies of analytical importance. New ionization methods and coupling techniques such as static and liquid SIMS (8 - 9), FAB (10), GC/MS and LC/MS turned out to be very successful in the field of conventional mass spectrometry. Therefore a strong demand exists to use these ionization methods also in combination with FTMS.

The most important problem with FTMS that hampered the use of these techniques is the requirement that FTMS must be operated at low pressure. This pressure limitation arises because mass resolution is proportional to the ion transient signal duration. Recently, three methods have been described to circumvent this pressure limitation:

Construction of a tandem quadrupole ICR (11), the double cell design (12) and a FTMS instrument with an external ion source without a quadrupole ion transfer system (13).

One of the most useful tools for complex mixture analysis is the combination of Gas Chromatography with Mass Spectrometry (GC MS). In this work we present the experimental set up of our GC/FTMS system with external ion source.

Several test mixtures were investigated with this GC - FTMS configuration. Broad band spectra and high resolution spectra were taken from the GC eluents. Broad band spectra interpretation is helped by library search programs using the NBS mass spectra library. Typical resolution achieved in the high resolution mode is about 180'000 for m/z 57. First sensitivity measurements indicate a detection limit in the picogram range for high resolution mode (S/N = 20:1 for 100 picogram undecane) and low nanogram range for broad band mode.

At present this sensitivity is inferior compared to conventional mass spectrometers, but system improvements already started will improve the achieved sensitivity.

References

1. R.T. McIver, American Laboratory, Nov. 1980
2. K.P. Wanczek, Int. J. Mass Spectrom. Ion Proc. **60** (1984), 11.
3. M.B. Comisarow, Anal. Chim. Acta **178** (1985), 1 - 15
4. R.B. Cody, J.A. Kinsinger , S. Ghaderi, I.J. Amster, F.W. McLafferty, Ch.E. Brown; Anal. Chim. Acta **178** (1985), 43 - 66
5. N.M.M. Nibbering in: Advances in Mass Spectrometry (Ed.J.F.J. Todd), p. 417-435, John Wiley & Sons, 1986
6. D.A. Laude, C.L. Johlman, R.S. Brown, D.A. Weil, Ch.L. Wilkins; Mass Spectrometry Reviews **5** (1986), 107 - 166
7. D.H. Russell, Mass Spectrometry Reviews 1986, **5**, 167 - 189
8. Secondary Ion Mass Spectrometry, Springer Series in Chemical Physics, Vol. 9 (1979), Vol 19 (1982), Vol. 25 (1983), Vol. 36 (1984)
9. E. de Pauw, Mass Spectrometry Reviews 1986, **5**, 191 - 212: Liquid matrices for secondary ion mass spectrometry
10. R.M. Caprioli: Fast-atom-bombardment Mass Spectrometry: Applications to Solution Chemistry, in Specialist Periodical Report Mass Spectrometry, Vol. 8 (1985), 184 - 209

11. R.T. McIver, R.L. Hunter, M.S. Story, J. Syka and M. Labunsky, Proc. 31st Annu. Conf. Mass Spectrom. Allied Top., 1983, Boston.

12. R.L. Settine, J.A. Kisinger, S. Ghaderi, Europ. Spec. News, **58**, (1985), 16

13. P. Kofel, M. Allemann, H.P. Kellerhals, K.P. Wanczek, Int. J. Mass Spec. Ion Proc. **65** (1985), 97 - 103.

Presented at the 35th ASMS Conference on Mass Spectrometry and Allied Topics
May 24-29, 1987, Denver, CO

INJECTION OF IONS FROM AN EXTERNAL ION CAGE INTO AN ICR CELL

P. Kofel*, M. Allemann, Hp. Kellerhals
Spectrospin AG, Industriestr. 26, CH-8117 Faellanden/Zurich (Switzerland)
and **K.-P. Wanczek**
University of Bremen, Inorganic Chemistry, NW 2, D-2800 Bremen (West Germany)
(*) Present address: University of Waterloo, Dept. of Chemistry, Waterloo, Ont., N2L 3G1, Canada

An ICR spectrometer with a single cell design (i.e ion generation and ion detection in the same cell) has the disadvantage that high gas loads decrease the mass resolution of the instrument drastically. Several ways to overcome this limitation have been proposed during the last few years: the tandem quadrupole FTMS [1], the external ion source with electrostatic lenses [2,3] and the dual cell FTMS [4]. Common to all these new developments is that ion generation and ion detection are separated in space, allowing differential pumping of the two regions.

The advantage of the dual cell design over the two other approaches is that the ions can be accumulated in the ion source cell, which in principle allows a lower partial pressure detection limit. However the dual cell design with the ion source directly beside the ICR detection cell has several disadvantages. There is still a considerable gas flow through the ion transfer hole, limiting the pressure differential Because of the higher pressure in the source cell the ions diffuse relatively fast in radial directions, which decreases the number of ions that can be transferred to the detection cell. Additionally, access to the ion source region is still poor.

An external ion source capable of storing the ions during the ionization period combines the advantages of external ion source and dual cell, increasing the theoretical partial pressure detection limit by at least one order of magnitude [5]

Experiments were performed on a CMS 47 ICR spectrometer [6]. The external ion cage was mounted to the main vacuum system on the opposite side to the ICR cell, e.g. no differential pumping was applied. Fig. 1 shows schematically the arrangement of the electrodes. The ion cage was located about 10 cm outside the magnet in a stray field of 0.15 T. The ions produced in the ion cage were trapped by the combined action of the magnetic stray field and an electric trapping field applied between the end plates and the cylinder of the ion cage. Ions were transferred from the ion cage to the ICR cell by "opening" the extraction plate E, i.e. by pulsing the plate to a lower potential than the cylinder of the ion cage. The ions are guided by the magnetic field only. Trapping of the ions in the ICR cell was achieved by "opening" and "closing" the trapping plate T in the same way.

Fig. 2 shows the dependence of transfer efficiency on transfer energy. The potential difference between ion cage and ICR cell was kept constant: V_K-V_C = 0 3 V. As clearly can be seen, the transfer is much more efficient with a few eV of kinetic energy. The maximum in Fig. 2 corresponds to a transfer efficiency of 12%. This was determined by recording the relative intensity of ions produced in the ICR cell using identical ionization conditions For the measurements of Fig. 2 the extraction potential as well as the time between "opening" the extraction plate and "closing" the trapping plate were optimized for each measurement.

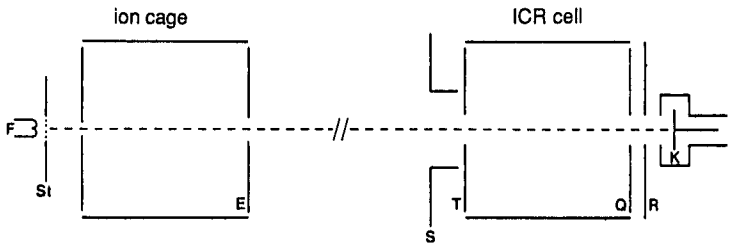

Fig. 1 Experimental arrangement of external ion cage and ICR cell. The ion cage traps on the same principle as the ICR cell, but in the much weaker (stray) field of 0.15 T.

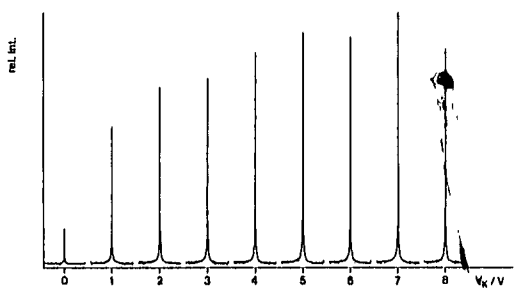

Fig. 2 Relative abundance of m/z=78, $C_6H_6^+$, as a function of transfer energy.

The magnetic ion cage used in this study was operated in the stray field of the superconducting magnet only. This, however, is not the ion cage of choice for a differentially pumped system. As the pressure is increased and the ion cage is moved away from the magnet to allow differential pumping, the trapping time in the ion cage is reduced rapidly. For a differentially pumped system either an additional magnet has to be used, or another storing principle, e.g. r.f. electrical fields or space charge trapping.

References:

[1] R T. McIver, R.L. Hunter and W.D. Bowers, Int. J. Mass Spectrom. Ion Processes, 64 (1985) 67.

[2] P. Kofel, M. Allemann, Hp Kellerhals and K.-P. Wanczek, Int. J. Mass Spectrom. Ion Processes, 65 (1985) 97; P. Kofel, M. Allemann, Hp Kellerhals and K.-P. Wanczek, Int. J. Mass Spectrom. Ion Processes, 72 (1986) 53.

[3] J.M. Alford, P.E. Williams, D.J. Trevor and R.E. Smalley, Int. J. Mass Spectrom. Ion Processes, 72 (1986) 33.

[4] R L. Settine, J.A. Kinsinger and S. Ghaderi, European Spectroscopy News, 58 (1985) 16.

[5] P. Kofel, Thesis, Bremen (FRG), 1987; P. Kofel, M. Allemann, Hp. Kellerhals and K.-P. Wanczek, Int. J. Mass Spectrom. Ion Processes, to be published.

[6] Spectrospin AG, Faellanden, Switzerland.

Presented at the 35th ASMS Conference on Mass Spectrometry and Allied Topics
May 24-29, 1987, Denver, CO

WINDOWED EXCITATION SIGNALS FOR FTMS

D. Alan Hanna, R. Bradford Spencer, and Seth Goodman
Nicolet Instrument Corporation
5225-1Verona Road
Madison, Wisconsin 53711-0508

Windowing is a commonly used technique in Fourier transform analysis of data. It is accomplished by multiplying the sequence of data values by a series of values defined by a window function. The window function typically rises smoothly from zero to some maximum value, and then smoothly falls back to zero. The purpose of windowing is to reduce artifacts in the spectrum produced. These arise from two sources: the finite length of the data sample, and the sampling of the data at discrete points.

The finite length of the sample has the result that the spectrum obtained is the convolution of the "true" spectrum with the transform of the time window which defines the interval. The transform of the time window has the familiar sin(x)/x form, and is the shape that the spectrum of a pure-frequency time-domain signal takes, when the signal is sampled for a finite time. As the time interval is lengthened, the frequency peak narrows, but retains the sin(x)/x shape. For a more complex spectrum, the same effect holds: the computed spectrum is the convolution of the true spectrum with sin(x)/x.

The discrete sampling results in signals of all frequencies mapping into the region $0 \leq f \leq f_s/2$, where f_s is the frequency at which the data is sampled. This is the **Nyquist** relationship, and $f_s/2$ is the **Nyquist frequency**. To unambiguously determine the spectrum, the frequencies observed must fall in the region defined above. Even then, distortion can arise, because the infinitely-extending tails of the sin(x)/x function can cause wrap-around of signal at the ends of the interval.

In analysis, window functions are used to alter the shape of the convoluting lineshape, to remove its most prominent artifact-generating features: the sidelobes of the function, and the relatively slow fall-off of these lobes away from the function center. This requires a tradeoff: the central peak of the function is broadened.

In Fourier Transform Infrared (**FTIR**) Analysis, window functions are used in another way. An infrared interferogram is essentially a symmetric function of pathlength difference: one side of the interferogram duplicates the information contained in the other side. Because of this, it is possible to acquire and process an asymmetric interferogram, and still obtain a proper spectrum. The advantage of this is that, for the same number of acquired points, higher resolution may be obtained. (In **FTIR**, pathlength difference is the analogue of time in frequency analysis: signals acquired to greater pathlength differences have higher resolution, due to the narrowing of the convoluting function.) To properly transform the data, proper weighting of the points must be made. If the interferogram is windowed with a function which passes smoothly through the zero-path-length-difference point of the interferogram, and has a value of 1/2 at this point, each data value is properly weighted. (there would otherwise be spectral distortion.)

SWIFT (Stored Waveform, Inverse Fourier Transform) excitation functions created without any phase shifting are exactly symmetric functions. Thus, it seems reasonable that the same technique used in analysis of **FTIR** interferograms may be used beneficially in **SWIFT** synthesis. That is, it should be possible to select an asymmetric portion of a **SWIFT** function, window it in the same manner as is done in **FTIR** analysis, and obtain an asymmetric **SWIFT** excitation function with the same characteristics. For a given number of points, this function would yield higher resolution in the excitation spectrum. Since one of the prime reasons for using **SWIFT** is to be able to selectively excite ions according to their mass/charge ratio, this would represent an improvement in non-phase-shifted **SWIFT** performance.

This work reports the results of investigation of this idea, using several potential window functions. The functions used were:

Triangle	**Sine Ramp**
Cosine	**Blackmann**
Double Cosine	

The cosine window is one cycle of a cosine, starting at its minimum, and shifted up by one, to join with a "boxcar" function. The Double cosine is two such cosines, joined together so that the maximum of the first, shifted upwards by one, connects with the minimum of the second, shifted up by three. The sine ramp is the sum of a sine and a simple ramp, and the Blackmann is a combination of cos(x) and cos(2x), similarly shifted. All but the triangle are connected to a boxccar function; the triangle rises to a maximum and then falls to zero at the other

end. Each function must meet the criterion that its value at the point corresponding to the center of the starting symmetric SWIFT function must be 1/2 its maximum value.

The investigation was done by generating a SWIFT waveform from a starting "desired" excitation spectrum containing several features useful for showing the effects on the final spectrum due to the finite time window and the applied intensity-correcting window. The process used was

Generate a desired excitation spectrum
Inverse Fourier transform this to a symmetric SWIFT function
Apply the window being tested
Apply a Blackmann window, for additional smoothing
Fourier transform the resulting windowed SWIFT function
Examine the resulting spectrum

The two windowing operations could be reversed, with no effect on the result. The Blackmann windowing was symmetric with the original symmetric SWIFT function.

The results are illustrated in Figure 1, which shows the starting spectrum and the best resulting spectrum. The best results, considering both side lobes and resolution, was for the cosine window, shifted by 1/4. Larger shifts resulted in pronounced artifacts, which are regarded as undesireable. (Shifting by 1/4 is the same as dropping 1/4 of one side of the symmetric SWIFT function, and extending the other side an equivalent number of points.)

Conclusion

The examined process does work. Its maximum benefit would occur if the SWIFT waveform were sampled completely asymmetrically. In this case, resolution would be doubled. The best results correspond to dropping 1/2 of one side, corresponding to a 50% resolution improvement.

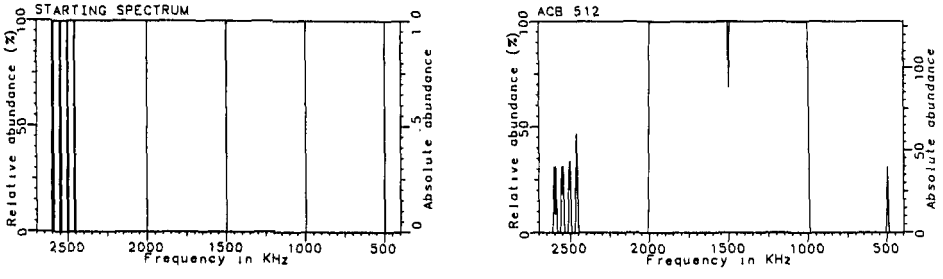

Figure 1. Starting Spectrum and Spectrum from Cosine Window @ 1/4 Asymmetry

Presented at the 35th ASMS Conference on Mass Spectrometry and Allied Topics
May 24-29, 1987, Denver, CO

High Temperature Mass Spectrometry at Enhanced Sensitivity and at High Resolution (3000)

Guenter Wagner and Bernd Laser, Finnigan MAT GmbH, D-2800 Bremen, West Germany

Mass spectrometers with high temperature Knudsen cell inlet systems have been used in the past to

- study thermodynamic activities of alloys or pure systems to establish phase diagrams,
- determine partial pressures of elemental systems,
- quantify enthalpies of sublimation or condensation,
- measure the high temperature equilibrium constants of alloy systems,
- determine ionization efficiencies and ion appearance potentials of solids,
- study the thermochemical behaviors of vapor phase solids and liquids, and to
- investigate the permeability of solids under high temperature conditions.

Generally, the instruments used in such investigations have been sector or quadrupole type mass spectrometers with low resolving power and, frequently, also with rather low sensitivity. Experimental procedures and results quite often have suffered from these deficiencies. Quantitative results did not comply with theory for reasons of background interferences and for reasons of insufficient detection limits.

Any high temperature environment like a Knudsen cell inlet system generates considerable background pressures. Background mass lines will interfere with the analyte mass lines at low mass spectrometric resolution. At low resolution, the very small ion intensities of high melting point materials with accordingly low vapor pressures are superimposed by background and are no longer detectable.

Many years of experience with high temperature Knudsen cell inlet systems has led to development of a new High Temperature Mass Spectrometry System. This instrument combines a Knudsen cell inlet system capable of a maximum temperature of 3000°K with a magnetic type mass spectrometer employing an extended geometry/stigmatic focusing analyzer system of high ion transmission, with ion counting detection, and resolution variable from m/ m = 250 to 4000.

This instrument provides new capabilities for the investigation of high temperature materials systems. With its mass multiplet resolving power and high sensitivity the detection limits for low vapor pressure high melting point materials are as low as 10^{-9} mbar partial pressure in the Knudsen cell. Melting point determinations of pure systems can be demonstrated to comply within $\pm 1^{\circ}$ K with values reported in the literature, and vapor pressure curves for the different isotopes of an element will coincide completely. Quantitative isotope ratio determinations, including minor isotopes, can be demonstrated for high melting point elements like Nickel with all the isotopes resolved from background mass lines.

The instrument's software and hardware supports difficult applications by providing

- safe peak detection and digitization linear over a wide dynamic range,
- safe mass calibration, accurate to a few millimass units, for multiplet resolved data acquisition with unambiguous mass peak identification.

The software allows for automatic temperature control, data acquisition and transformation of ion intensity/temperature data into -Lgt (I*T) over 1000/T vapor pressure curves.

Presented at the 35th ASMS Conference on Mass Spectrometry and Allied Topics
May 24-29, 1987, Denver, CO

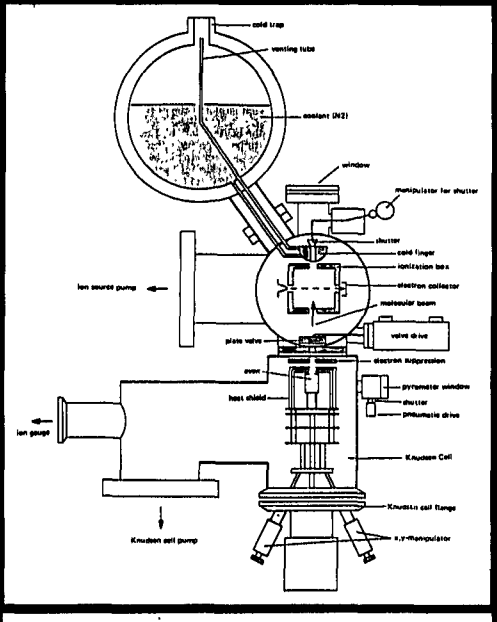

Knudsen Cell Arrangement With Cryo Trap, Ion Source And Pyrometric Temperature Measurement

Nickel Isotopes, Evaporated At 1496°K Temperature Of Knudsen Cell, And Resolved From Background

Analytical Parameters

Resolution M/ΔM 2300
Electron Emission 1 mAmp
Acceleration Voltage 10000 Volts
Vapor Pressure of Nickel
5×10^{-5} Torr
SEM Dynode Voltage 1800 Volts
SEM Gain 2.5×10^{6}

Isotope Pattern

	(mV)	(Atom %)	(Atom % Literature)
^{58}Ni	180.33	66.41	67.76
^{60}Ni	69.36	25.54	26.16
^{61}Ni	3.52	1.29	1.29
^{62}Ni	10.04	3.69	3.66
^{64}Ni	8.28	3.05	1.16

Presented at the 35th ASMS Conference on Mass Spectrometry and Allied Topics
May 24-29, 1987, Denver, CO

HIGH MASS ANALYSES USING QUADRUPOLE INSTRUMENTATION: R. Madden, R.T. Brackmann, S.N. Ketkar, F. Poeppel, Extrel Corporation, Pittsburgh, PA 15238.

The mass range of quadrupole devices can be extended by a combination of reduction of operating frequency, increase of power and reduction of quadrupole rod diameters. The resulting increase in the upper mass limit is more useful if the ion source and the transport ion optics are optimized to suit the ionization mode.

The most successful ion sources for production of high mass ions use bombardment of high energy ions or atoms (FAB) on a liquid matrix containing the sample of interest. The ions ejected from the liquid matrix have a wide energy spread which is not suitable for a mass spectrometer, thus resulting in broad mass peaks. Moreover, due to the linear nature of the quadrupole structure, the directly reflected fast ions, photons and metastables remain unfiltered and give rise to an untunable offset on the detector signal.

We report here the combined use of a linear energy analyzer and an off axis detector to overcome the above mentioned ill effects.

Figure 1 shows a schematic of the total quadrupole system employed in this study. It consists of an Extrel Model 7-162-8 quadrupole operated with C-50-S5 electronics. The energy analyzer is an Extrel Model 616-2 Bessel Box. A Phrasor Scientific Cs ion gun produces high energy ions in the range of 5-10 keV. CsCl in a 50/50 matrix of methanol/glycerol was used as the sample. CsCl clusters of the type $Cs(CsCl)_n$; n=1...21 were detected with the present setup.

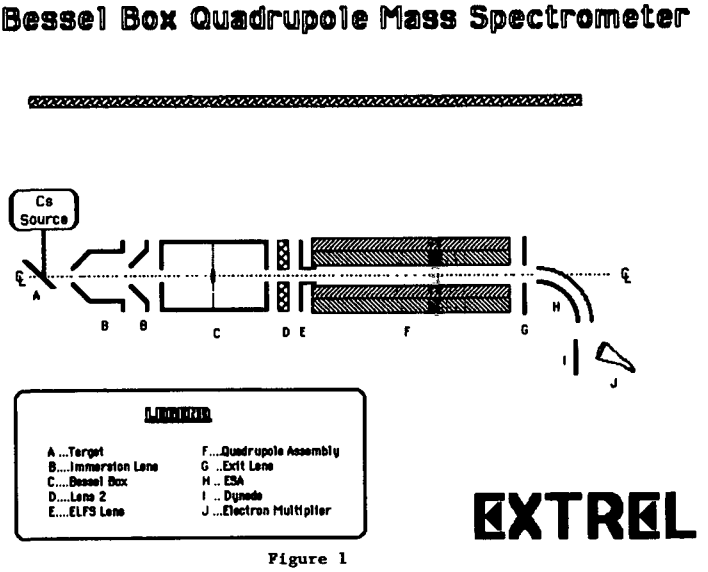

Figure 1

Figure 2 shows a spectra of $Cs(CsCl)_{19}$ at a nominal mass of 3335 amu with unit resolution. The individual peaks displayed are due to the isotope of Cl and are 2 amu apart. The upper mass limit of the system is 4000 amu. However, the intensity of the clusters of the type $Cs(CsCl)_n$ for n>20 drops off very rapidly.. Figure 3 shows a cluster $Cs(CsCl)_{21}$ at a nominal mass of 3671 amu.

In conclusion, we have demonstrated the capability of a quadrupole mass spectrometer system to operate, with unit resolution, up to 4000 amu. Work is in progress to extend the upper mass limit.

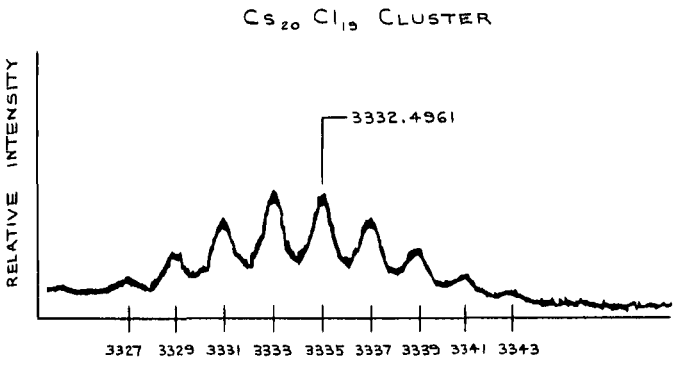

Figure 2

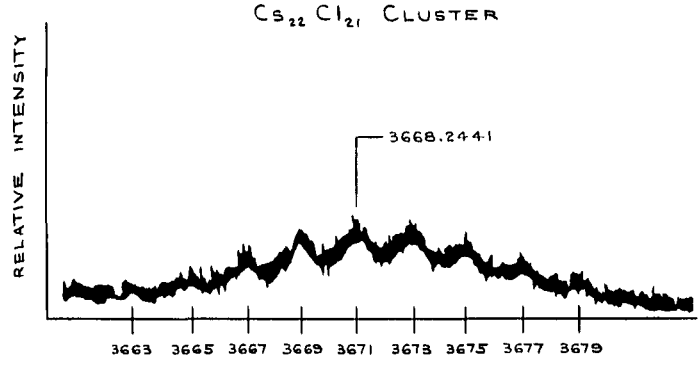

Figure 3

Presented at the 35th ASMS Conference on Mass Spectrometry and Allied Topics
May 24-29, 1987, Denver, CO

EI/FAB SPECTRA ACQUISITION WITH A MODIFIED EI SOURCE IN A VG-ZAB-2F

C.J. Metral PRI-NCI-FCRF P.O. Box B 21701

INTRODUCTION

Implementation of the DIP GUN (Phrasor Scientific) on KRATOS MS80[1,2,3] has shown that it is possible to acquire EI/FAB and CI/FAB spectra by simply modifying a standard EI or CI source. Unfortunately, on VG instruments this is complicated by the 5/16" solids probe inlet which is not big enough to maintain the high voltage needed at the nozzle tip; the entire vacuum interlock for the probe must be replaced. The alternative presented here makes use of the saddle field gun present in most VG instruments coupled with some simple modifications of the souce and the DCI probe tip. These modifications include clearing the FAB beam path by removing or shaving one of the collimating magnets and opening a hole at the base of the source exit plate. In addition, one needs to modify the DCI probe tip by removing the filament and placing a stainless steel tip in its place.

Some of the more obvious advantages of the combined source are ease of calibration and exact mass measurements without contamination of the matrix. Additional advantages include the wider variety of samples that one is able to handle and the capability of acquiring EI/FAB spectra without a matrix over a wide range of temperatures by supplying controlled heat via the DCI tip contacts. There is some evidence of characteristic EI/FAB spectra where the fragmentation is not a superposition of FAB and EI patterns. For some of these compounds the need to operate in the EI/FAB mode suggest that the ionization cross section of the FAB process is low and they are thermally unstable. To produce a spectrum the neutrals must first be desorbed followed by EI ionization. The performance evaluation of the combined source has been carried out with many different compounds some of which are not typical FAB analytes.

INSTRUMENT MODIFICATIONS

As illustrated in figures 1 and 2 the major modifications are in the source exit plate and the DCI probe tip. In addition, one must remove or shave the bottom collimating magnet and the trap guard inside the source block.

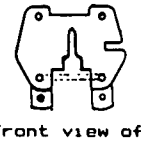

Figure 1. Front view of source exit after modifications.

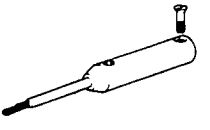

Figure 2. DCI probe tip after spotwelding a stainless steel target.

OPERATING NOTES

Although it is possible to obtain EI/FAB spectrum with the modifications shown above, after a while the temperature in the source reaches 160°C making it difficult to use volatile matrices. One can use other matrices such as sorbitol, phosphoric acid, dithioerythritol, dithiosorbitol, etc., or no matrix at all. Because of heating capabilities there is no need to prepare magic bullet and a simple water or methanol solution of the isomers suffices. To permit the use of volatile matrices one needs to reduce the filament current. This is done by turning the RV2 potentiometer in the source emission control board.

WARNING: put instrument in standby when turning RV2

This pot sets the maximum current through the filament which normally reads 5 Amps. For EI/FAB operation a setting of 3.8-4.2 Amps is sufficient. To reduce the filament current further the tungsten filament must be replaced by thoriaded iridium which operates below 4 amps. Finally, a simple means of controlling the FAB contribution to the spectrum is reducing the gun power, or alternatively, reducing the electron energy.

SPECTRA ACQUISITION

In addition to the EI and FAB modes of operation this source can be used for thermal desorption EI, EI/FAB; and liquid SIMS of compounds which are

liquids below 600°C such as phosphoric acid, polyethers, small peptides, organic acids, high molecular weight hydrocarbons, etc. Certain classes of compounds yield spectra only in the EI/FAB mode of operation as shown in one of the captions below. Exact mass measurements are readily made with the P.M.U. using PFK or any other reference. The spectra below illustrate some of these points clearly.

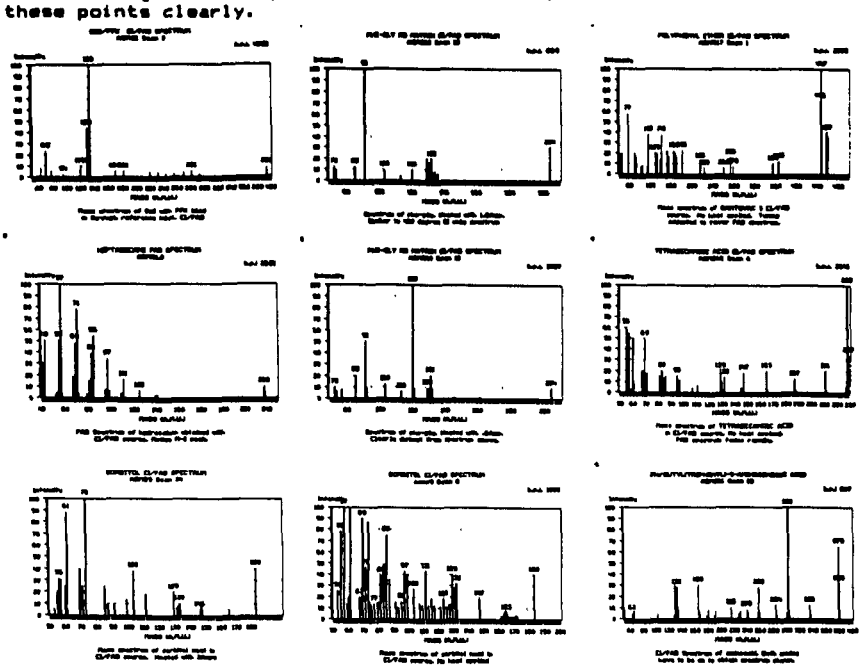

CONCLUSIONS

A simple modification of the EI source of a VG-ZAB permits the acquisition of EI/FAB spectra thereby enhancing the application of the instrument. the capability of heating the FAB target allows a single tip to be used for liquid SIMS, EI/FAB, FAB, EI, and desorption EI. Tuning parameters and source conditions can be manipulated to bias a spectrum towards FAB or EI. There is strong evidence of unique EI/FAB spectra for some compounds, possibly revealing new information. At the present it seems that a mechanism for these EI/FAB processes suggests the desorption of neutrals with little or no ions, followed by EI IONIZATION. The heating of the source, although a disadvantage, does not present a problem. Finally, it must be said that there is a factor of 3 or less loss of sensitivity in the FAB mode vs. the standard FAB source. Also, this EI/FAB source can not be used for CI/FAB.

1. K. Jaysihulu, R.Day, C. Metral, J. Wemerling, and M. Madis 33rd ASMS Conf., San Diego, 1985 p. 510
2. J. Perel, J. Mahoney, C. Metral Pitt. Conf. & Expo. 1986 No. 861
3. C.J. Metral and R.A. Day Anal. Lett., 19(1&2), 217-227 (1986)

Presented at the 35th ASMS Conference on Mass Spectrometry and Allied Topics
May 24-29, 1987, Denver, CO

INSTRUMENTAL MODIFICATIONS TO A MODULAR CHROMATOGRAPHY/SIMS INSTRUMENT

R. A. Flurer, G. C. DiDonato, K. L. Duffin, and K. L. Busch
Department of Chemistry, Indiana University, Bloomington, IN 47405

The use of mass spectrometry in combination with chromatography is a powerful technique for the analysis of complex mixtures. While GC/MS and LC/MS are now established techniques, the combination of mass spectrometry with the planar forms of chromatography, such as thin layer chromatography and electrophoresis, has just recently been demonstrated [1-3]. Over the past two years, we have constructed a chromatography/secondary ion mass spectrometer (SIMS) and demonstrated its applications to the separation and analysis of mixtures. The need for several changes in the design of the original instrument have become apparent. The purpose of this paper is to describe such changes, and the justifications for them, in detail.

The original instrument used a cesium primary ion gun based on a thermionic emission source. Although the spot size could be narrowed to 0.1 mm diameter, the shape and diameter of the spot could change as the source aged, or as the pressure in the vacuum chamber varied. To circumvent such problems, a gallium liquid metal ion gun has been installed (FEI instruments). Molten gallium is coated onto the tip of a fine emission needle of 0.1 micrometer end diameter. A negative potential of 7 to 12 kV is applied to a counterelectrode, drawing positively-charged gallium ions away from the needle in a process of field emission. A steady stream of gallium ions is emitted from this point source through a beam-defining aperture and into an ion optical column. The ion optics include an octupole stigmator that lads in the focus of the beam and also provides the ability to raster the beam across a small area of the surface without the loss of spatial resolution. With the depth of field specified for the instrumental configuration, a raster distance of up to 1 cm can be used. Beam diameters for the gallium gun are specified as narrow as 0.5 micrometers; one to ten micron resolution is in accord with the spatial resolution needs of the chromatograms and electrophoretograms that are analyzed. A beam current of as high as 1 A/cm^2 can be achieved. Typically, the source is operated with primary ion current densities of about 10^{-4} A/cm^2. This primary ion flux is sufficient to melt the phase transition matrix in the chromatogram [2], but does not seem to cause excessive dissociation of the organic molecules. Differential pumping of the liquid metal ion gun is necessary to maintain a two order of magnitude difference in pressure between the field emission source and the main chamber of the instrument, which can reach a pressure as high as 5 x 10^{-6} torr.

A major modification to the instrument is the addition of an automated sample stage capable of introduction into the vacuum system of chromatograms (or other samples) that measure up to 15 cm on a side (Figure 1). The sample vacuum chamber is therefore much larger than the original source housing, and fitted with removable glass windows both for ease of sample access and to monitor the operation of the system. Provision is made for concomitant fluorescence detection of the spots on the chromatogram. Pumping capacity in the previous system was limited, and a large diffusion pump was added to the system. Sample changeover times now require about ten minutes. The need for such pumping capacity was not expected in the original design. However, as the samples became larger in size, and the variety of solvents added to the system more diverse, the original pumping capacities were exceeded, and sample changeover times lengthened.

The new sample chamber is also enlarged to accommodate the automatic translation stages. These are vacuum-compatible designs of translators originally designed as laser positioners (Burleigh Instruments). Two stages are necessary for movement of the chromatogram through the point of instrument focus in x and y axes. The piezoelectric translators are capable of linear motion of up to 8.25 inches, with 1 micron resolution, and a slew rate of 5 s/cm. This resolution and scanning speed are compatible with the requirements of a chromatographic imaging analysis. The translation stages are also equipped with position encoders that enable an independent assessment of position that can be linked with the mass spectrometric data across the entire xy field. Spatial calibration on the chromatogram itself

(other than an initial position determination) is not required.

The mass spectrometer and the data system are also undergoing modification. Extension of the mass range of the quadrupole to m/z 3500 range is underway. This additional capability places greater demands on the data system in terms of the amount of information that must be processed, stored, and displayed. Sufficient DAC resolution to assign peak masses accurately requires two scan modes, a wide range scan, and a more accurate scan across a narrower mass range. Data compression is necessary in order not to overload the data storage capabilities of the system. Processing of the data for display is carried out with the ASYST system.

1. J. W. Fiola, G. C. DiDonato, and K. L. Busch, Rev. Sci. Instrum., 57 (1986) 2294.
2. G. C. DiDonato and K. L. Busch, Anal. Chem., 58 (1986) 3231.
3. K. L. Busch, Trends Anal. Chem., 6 (1987) 95.

Figure 1

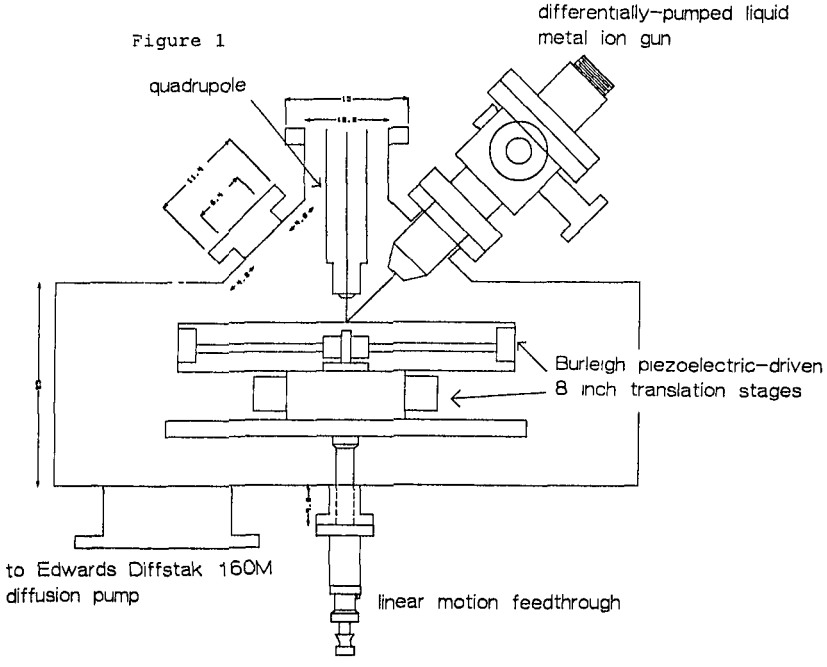

Presented at the 35th ASMS Conference on Mass Spectrometry and Allied Topics
May 24-29, 1987, Denver, CO

A MICRO-VOLUME CURIE-POINT PYROLYZER FOR RAPID, HIGH RESOLUTION CAPILLARY GC/MS

Henk L.C. Meuzelaar, William H. McClennen, and Yongseung Yun
University of Utah, Biomaterials Profiling Center
391 S. Chipeta Way, Suite F, Salt Lake City, Utah 84108

There are many examples of the use of analytical pyrolysis (Py) to apply the powerful GC/MS technique to complex nonvolatile samples, including synthetic polymers, geopolymers and biopolymers. Py-GC/MS has impressive specificity for the analysis of polymer structure and investigation of thermal stability properties. The technique has been extensively applied to coal science both as a tool for structure elucidation and to study the initial products evolved in thermal processes such as liquefaction, gasification and combustion. Finally, in biodetection work where the amount of sample may be severely limited, the potential sensitivity of Py-GC/MS is also of importance.

As in all high resolution GC applications the sample injection technique is crucial. In Py-GC/MS the chromatographic resolution can be particularly limited by the width of peaks produced by pyrolyzers with long (several seconds) heating times or large dead volumes. Cryofocussing of products on the capillary column can be of value but adds some complexity to the process.

Our objective was to develop a low dead volume pyrolyzer for fast and simple analysis of nonvolatile samples by capillary GC/MS. Our approach has been to use Curie-point pyrolysis with disposable ferromagnetic filaments and easily replaceable glass pyrolysis tubes to minimize the amount of sample and the dead volume of the injector and maximize the ease, speed and efficiency of the analysis.

These experiments were performed on a Tracor 560 gas chromatograph equipped with a 15 m X 0.32 i.d. column coated with 0.25 um of DB-5 (J&W Scientific). A Fischer 0310 Curie-point pyrolysis power supply operating at 1.5 kW and 1 MHz was used for the pyrolyses. The mass spectrometer was the Finnigan MAT 700 Ion Trap Detector (ITD) with version 3.01 software operating on an IBM PC-XT.

As shown in Figure 1, critical elements of our design include the use of a 1.5 mm i.d. Pyrex glass pyrolysis tube which uses the variation of the split ratio to further adjust between the optimization of sensitivity and resolution. Amounts ranging from 0.8 to 25 ug of the samples dissolved and/or finely suspended in methanol were placed on the ferromagnetic filaments and allowed to dry. The filament was then drawn into the pyrolysis tube. Typical He carrier gas column flow was 2.8 ml/min. The sample injection was performed by inserting the pyrolysis tube into the preheated injector, sealing the o-ring, shutting off the injector backflush, and firing the pyrolyzer for 0.6 to 2.0 sec within 10 to 40 sec. after initial insertion.

For these experiments, using the standard open split interface and transfer line on the ITD, the open split vent was simply closed briefly to pressurize the tail of the column and minimize exposure of the column stationary phase to air during the sample change. The GC was programmed from 30 or 40 to 250 or 280°C at 15 or 20°C/min and data acquired in full scans from m/z 50 to 240 at 2 or 4 scans/s or, in one case, m/z 50 to 112 at >6 scans/s.

The examples demonstrate the wide product boiling range, high sensitivity, short analysis time, and high resolution capabilities of this pyrolysis inlet. In a coal sample (not shown) phenols, aromatic and alicyclic hydrocarbons and alkenes and alkanes through the range of C_5 to C_{29} were observed. A portion of the polystyrene pyrogram (Figure 2) shows the base of the main product styrene expanded X64 to show its s/n greater than 200 for 78 ng and 2-methylstyrene (at time 1:50) as an impurity of approx. 0.4%. The sample of a bacteria (Figure 3) and of albumin protein (Figure 4a) indicate the wealth of chemical information which can be used to characterize materials in an analysis which takes as little as 5 to 10 min. And finally, the expanded high scan rate chromatograms of the albumin sample (Figure 4b) clearly show the high GC resolution afforded by the low-dead volume and flash pyrolysis to give peaks often less than 1 s wide.

The authors are indebted to Drs. Pete Snyder (CRDEC) and Paul Kelley (Finnigan MAT) for providing samples as well as some of the hardware and software used in these experiments. Moreover, the expert technical assistance of Wally Maswadeh (pyrolyzer construction) and Janell Bunger (Py-GC/MS analyses) is gratefully acknowledged.

Presented at the 35th ASMS Conference on Mass Spectrometry and Allied Topics
May 24-29, 1987, Denver, CO

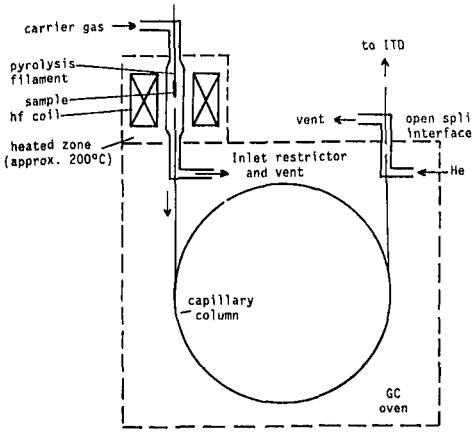

Figure 1. Highly schematized experimental design.

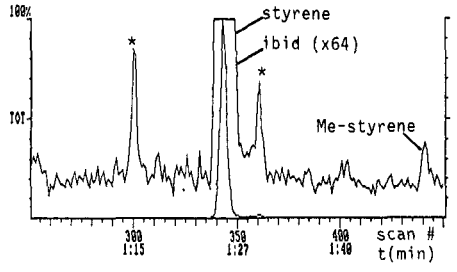

Figure 2. Partial pyrogram of polystyrene sample (78 ng) showing high sensitivity (S/N ratio of styrene monomer peak approx. 250:1).

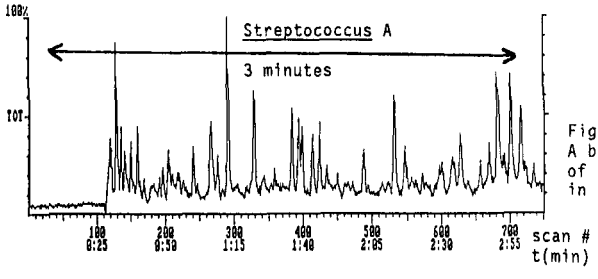

Figure 3. Pyrogram of Streptococcus A bacteria demonstrating possibility of obtaining detailed Py-GC pattern in less than 3 minutes.

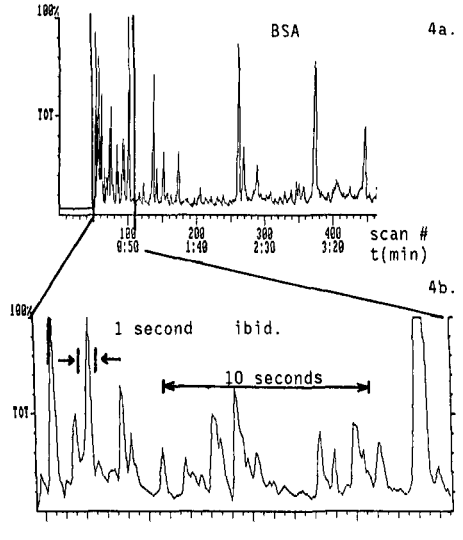

Figure 4. Partial pyrogram of protein sample (BSA). Note narrow peak widths in expanded baseline plot.

Presented at the 35th ASMS Conference on Mass Spectrometry and Allied Topics
May 24-29, 1987, Denver, CO

THE GALILEO PROBE MASS SPECTROMETER

H. B. NIEMANN, D. N. HARPOLD, J. E. COOLEY, AND S. H. WAY
NASA/GODDARD SPACE FLIGHT CENTER, GREENBELT, MD

PROJECT GALILEO, SCHEDULED FOR LAUNCH IN NOV. 1989, WILL SEND A SPACECRAFT CONSISTING OF AN ORBITER AND ENTRY PROBE TO JUPITER TO EXPLORE THE PLANET, ITS ATMOSPHERE AND ITS MOONS. THE PROBE, AFTER WITHSTANDING AN ENTRY SPEED OF 48 KM/SEC, DESCENDS INTO THE PLANET'S TURBULENT, HYDROGEN-RICH ATMOSPHERE TAKING SCIENTIFIC MEASUREMENTS DOWN TO A PRESSURE OF MORE THAN 10 EARTH ATMOSPHERES. THE ORBITER CARRIES THE PROBE DURING THE 6 YEAR INTERPLANETARY FLIGHT AND THEN CIRCLES THE PLANET FOR 20 MONTHS. COMPLIMENTING THE PROBE DATA, THE ORBITER'S 11 SCIENTIFIC INSTRUMENTS WILL STUDY THE MAGNETOSPHERE, IONOSPHERE, ATMOSPHERE, AND SURFACE PROPERTIES OF JUPITER AND ITS SATELLITE.

THE PROBE SEPARATES FROM THE ORBITER 150 DAYS BEFORE THE JUPITER ENCOUNTER. DURING THE PROBE'S SUBSONIC 60 MINUTE PARACHUTE DESCENT, SCIENCE INSTRUMENTS ASSESS THE STRUCTURE AND COMPOSITION OF THE ATMOSPHERE, DETERMINE THE LOCATION AND STRUCTURE OF THE CLOUDS, AND MEASURE LIGHTNING, RADIO EMISSIONS, AND ENERGY ABSORPTION. THE PROBE TRANSMITS THESE DATA TO THE ORBITER FOR RELAY TO THE EARTH'S TRACKING STATIONS.

THE OBJECTIVE OF THE GALILEO PROBE MASS SPECTROMETER EXPERIMENT IS TO DETERMINE THE CHEMICAL AND ISOTOPIC COMPOSITION OF THE JOVIAN ATMOSPHERE AS A FUNCTION OF ALTITUDE FORM 0.1 BAR TO AT LEAST 10 BAR. ATMOSPHERIC GASES WILL BE DETECTED AND THEIR MIXING RATIOS WILL BE DETERMINED OVER A NOMINAL MASS RANGE FROM 1 TO 52 AMU WITH OCCASIONAL MEASUREMENTS FROM 1 TO 150 AMU.

THE JOVIAN ATMOSPHERE IS COMPRISED PRIMARILY OF 90 PERCENT HYDROGEN AND 10 PERCENT HELIUM; IT ALSO INCLUDES MINOR AMOUNTS ($\sim 10^{-3}$ TO 10^{-10}) OF THE NOBLE GASES NEON, ARGON, KRYPTON, AND XENON AS WELL AS NON-INERT GASES LIKE H_2O, CH_4, NH_3, H_2S, C_2H_2, PH_3, HCl, HF, AND CO AS WELL AS OTHER TRACE CONSTITUENTS. THE MASS SPECTROMETRY MEASUREMENTS OF THESE GASES WILL AID IN UNDERSTANDING OF THE PROCESSES INVOLVED IN THE FORMATION OF THE SOLAR SYSTEM. FOR EXAMPLE, THE COSMIC ABUNDANCES OF KRYPTON AND XENON ARE POORLY DEFINED, SO THE MASS SPECTROMETER OFFERS THE FIRST OPPORTUNITY TO MEASURE THESE ELEMENTS IN A SINGLE UNDISTURBED RESERVOIR. THE RESULTS CAN BE USED TO CALIBRATE A VERY LARGE MASS OF DATA ON NOBLE GAS ABUNDANCES IN METEORITES, THE EARTH, AND THE INNER PLANETS.

THE MASS SPECTROMETER SENSOR IS A HYPERBOLIC ROD QUADRUPOLE WITH 15 CM LONG RODS, A DUAL FILAMENT ELECTRON IMPACT ION SOURCE, AND A CONTINUOUS CHANNEL

SECONDARY ELECTRON MULTIPLIER. THE ION SOURCE PRESSURE RANGE IS FROM 10^{-13} TO 10^{-4} MBAR AND THE SPECTROMETER HAS A DYNAMIC RANGE OF 10^{8}.

THE MEASUREMENT STRATEGY INVOLVES DIRECT MEASUREMENT OF THE SPECIES, USE OF FRAGMENTATION PATTERNS AT DIFFERENT ELECTRON ENERGIES, AND CHEMICAL ENRICHMENT CELLS FOR INCREASED DETECTION OF ATMOSPHERIC TRACE CONSTITUENTS.

THE SAMPLE INLET SYSTEM CONSISTS OF TWO FULLY SELF-CONTAINED UNITS WHICH OPERATE IN TIME SEQUENCES AS THE PROBE DESCENDS THROUGH THE ATMOSPHERE. BOTH UNITS CONTAIN A HIGH PRESSURE FLOW SYSTEM WHOSE GAS INLET SIDE IS PLACED NEAR THE APEX OF THE PROBE, AND WHOSE EXIT PORTS ARE PLACED AT THE MINIMUM PRESSURE POINT INSIDE THE PROBE. INLET AND OUTLET PORTS ARE SEALED BY METAL-CERAMIC DEVICES AND KEPT UNDER VACUUM PRIOR TO ENTRY. FIGURE 1 IS A CUT AWAY VIEW OF INSIDE THE PRESSURIZED HOUSING SHOWING THE SUBASSEMBLIES OF THE EXPERIMENT.

A SMALL FRACTION OF THE ATMOSPHERIC GAS IS CONDUCTED THROUGH PRESSURE REDUCING CAPILLARY LEAKS INTO THE IONIZATION REGION OF THE ION SOURCE FOR DIRECT SAMPLE ANALYSIS. A PORTION OF THE ATMOSPHERIC GAS ALSO FLOWS INTO THE ENRICHMENT CELLS WHERE NOBLE GAS MEASUREMENTS AND TRACE GAS SAMPLE ENRICHMENTS ARE MADE. (FIGURE 2).

NON-EVAPORABLE GETTERS AND A SPUTTER ION PUMP ESTABLISH A FLOW OF SAMPLE GAS THROUGH THE ION SOURCE AT A PARTICULAR PRESSURE WHEN A SAMPLING DEVICE IS OPENED. THE INSTRUMENT IS BEING BUILT AT GODDARD SPACE FLIGHT CENTER; IT WEIGHS APPROXIMATELY 12 KILOGRAMS AND CONSUMES ABOUT 25 WATTS OF POWER.

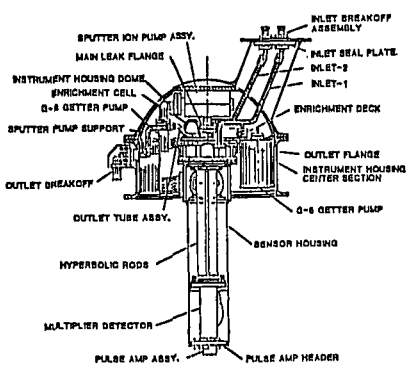

FIGURE 1: CROSS SECTIONAL VIEW OF QPMS WITH LOWER HOUSING REMOVED.

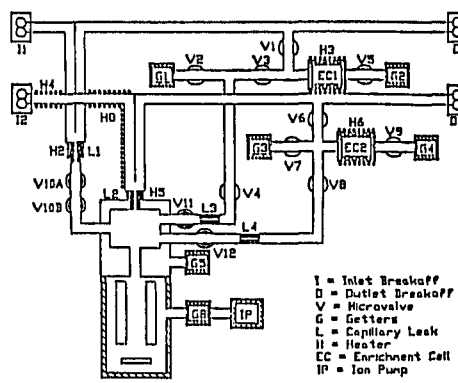

FIGURE 2: SCHEMATIC OF SAMPLE INLET SYSTEM

Presented at the 35th ASMS Conference on Mass Spectrometry and Allied Topics
May 24-29, 1987, Denver, CO

ANALYSIS OF THE REFLECTRON PRINCIPLE BY 252-Cf DESORPTION MASS SPECTROMETRY IN A LOW VOLTAGE REGIME

P.W. Geno and R.D. Macfarlane; Department of Chemistry
Texas A&M University, College Station, Texas 77843

In the past several years there has been a renewed interest in time-of-flight mass spectrometry (TOF) as a method of mass analysis for particle-induced desorption techniques. One approach to improving the resolution in TOF is the use of the Mamyrin reflectron (1,2). The reflectron is an electrostatic reflector that compensates for the distribution of velocities of ions of the same mass. The reflectron principle has been applied to 252-Cf-PDMS (3) and SIMS (4) with reported resolutions of 6000 to 10,000. These values are significantly lower than theoretically predicted. Our approach to studying the sources of resolution loss in the reflectron is to operate in a low voltage regime. Operating at low voltages would have the advantage of increased sensitivity to small changes in reflectron parameters making it an ideal method of studying reflectron performance.

The 252-Cf plasma desorption mass spectrometer used in this study is shown in Fig. 1, and has been described in detail elsewhere (5). This system has three modes of operation; traditional non-reflecting mode (zero-order), non-focusing reflection mode (first-order) and velocity focusing mode (second-order). Novel to our approach to a linear reflectron geometry is a CsI conversion dynode detector (see Fig. 1). This detector consists of an aluminum plate coated with CsI. As the reflected ions are accelerated into the dynode, conversion electrons are produced which are accelerated and then detected by the CEMA detector at the right side of the figure.

We have found that the velocity focusing conditions are different from those calculated by Mamyrin (1) and are best determined experimentally. In this determination, deceleration and reflection voltages are selected which are close to the Mamyrin parameters. The acceleration voltage is then varied in small increments around the acceleration voltage of interest. A plot of the TOF of a selected ion (here $^{6}Li^{+}$) as a function of the inverse square root of the acceleration voltage results in a straight line. Fig. 2 shows one of these plots for 100 V acceleration, 115.5 V reflection and 63, 68 and 73 V deceleration. If the line has a positive slope the reflectron is undercompensating and the deceleration voltage is increased. If the line has a negative slope, the reflectron is overcompensating and the deceleration voltage is decreased. At the velocity focusing condition the slope of the line is zero. We have found that a more efficient methos of establishing velocity focusing is to monitor the line-shape of the H^{+} ion peak (see Fig. 3). At the focusing conditions, the resolution and initial kinetic energy contribution to the line shape are minimized.

Fig. 4 shows $^{6}Li^{+}/^{7}Li^{+}$ spectra acquired in zero-, first-, and second-order modes at 40 V acceleration. The first-order spectrum has a slight increase in resolution over the zero order spectrum due to an increased flight-path length. The second-order spectrum shows a decrease in FWHM as well as an increased separation in TOF giving a significant resolution enhancement. Although the integrated intensity of the $^{6}Li^{+}$ peak is reduced in spectrum (c), the peak channel intensity is improved due to peak narrowing. Fig. 5 shows a comparison bradykinin spectra acquired at (a) 17 kV in zero-order mode and (b) 500 V in second-order mode. Resolution of the $(M+H)^{+}$ peaks are comparable. Some of the smaller peaks are narrower at the lower acceleration voltage. An interesting feature of this figure is the shift in TOF of the broad peak produced by metastable fragment ions. These ions have the same velocity as the parent ion (but lower mass and kinetic energy) and as a result are reflected in the deceleration region.

This work has demonstrated that a Mamyrin reflectron can be operated in a low voltage regime. Future work will involve investigating parameters which affect resolution such as alignment and reflectron voltage stability. This work was supported by the NSF (CHE-8604609) and the Robert A. Welch Foundation (A-258).

1) B.A.Mamyrin, V.I.Karataev, D.V. Shmikk and V.A.Zagullin, Sov. Phys. JETP, 37 (1973) 45.
2) B.A.Mamyrin and D.V. Shmikk, Sov. Phys. JETP, 49 (1979) 762.
3) S.Della-Negra and Y.LeBeyec, Int. J. Mass Spectrom. Ion Processes, 61 (1984) 21.
4) E.Niehuis, T.Heller, H.Feld and A.Benninghoven, in A.Benninghoven (Ed.), Ion Formation from Organic Solids, Vol. III, Springer-Verlag, Berlin,1986.
5) P.W.Geno and R.D.Macfarlane, (accepted for publication in Int. J. Mass Spectrom. Ion Processes).

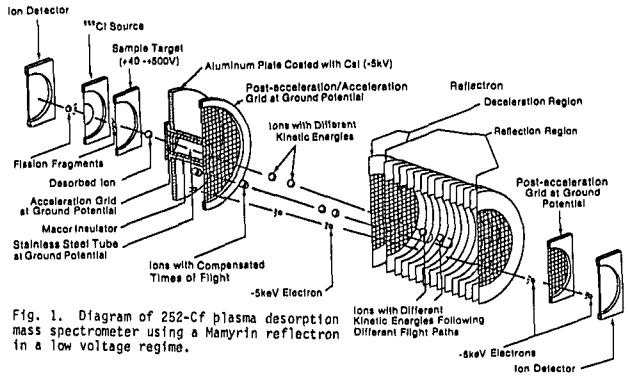

Fig. 1. Diagram of 252-Cf plasma desorption mass spectrometer using a Mamyrin reflectron in a low voltage regime.

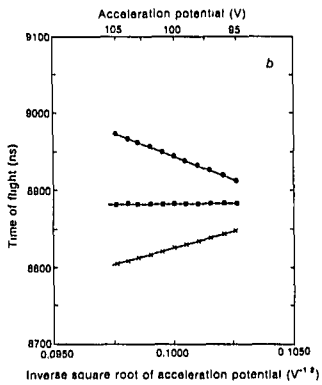

Fig. 2. Establishment of the velocity focusing condition for +100 V acceleration.

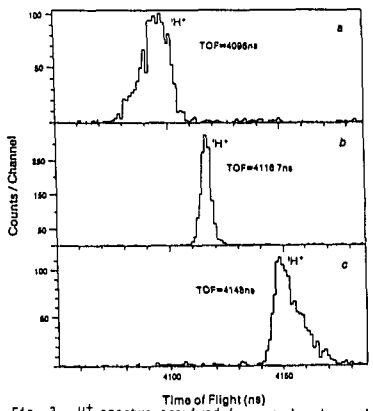

Fig. 3. H^+ spectra acquired in second-order mode at +100 V acceleration, 115.5 V reflection and (a) 63 V, (b) 68 V and (c) 73 V deceleration.

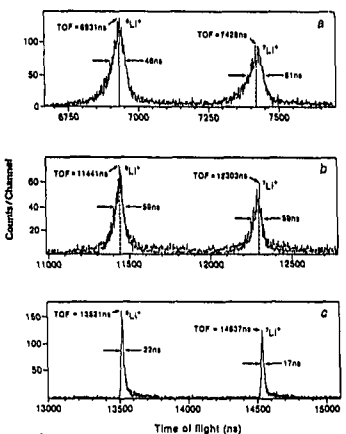

Fig. 4. $^6Li^+/^7Li^+$ spectra at 40 V acceleration acquired in (a) zero, (b) first and (c) second order modes.

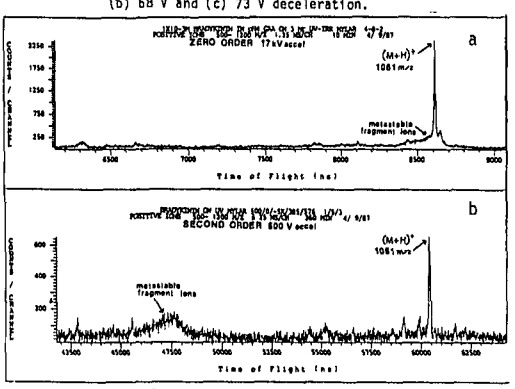

Fig 5. Bradykinin spectra acquired in (a) zero-order mode with 17KV acceleration and (b) second-order mode with 500 V acceleration.

Presented at the 35th ASMS Conference on Mass Spectrometry and Allied Topics
May 24-29, 1987, Denver, CO

COMPUTER MODELING OF SECONDARY ION TRAJECTORIES IN A SIMS/TSQ MASS SPECTROMETER

Bryan L. Bentz and Richard E. Honig

David Sarnoff Research Center
Princeton, New Jersey 08543-5300

The ELectron Optics Program "ELOP" developed at the David Sarnoff Research Center has been used to model secondary ion trajectories in a "static SIMS" instrument designed in our laboratory for organic surface analysis. The program, which operates on an IBM 3081 mainframe computer, computes three-dimensional trajectories of charged particles in electric and magnetic fields. It has been used in the present study to optimize electrode shapes and potentials for the transport and collection of low-energy, polyatomic ions sputtered from a large surface area by keV primary ions.

To achieve high overall ion detection sensitivity in static SIMS, it is desirable to extract as many desorbed ions as possible. To this end, the angular emission pattern and kinetic energy distribution of sputtered polyatomic ions need be considered when analyzer optics are designed. For a cosine distribution of emitted ions, approximately 6.7% of the total secondary ion current, N_T, falls within a cone formed by an emission half-angle, Θ, of 15° ($N(\Theta) = 0.5N_T(1 - \cos 2\Theta)$). 25% of the total emitted current falls within an emission half-angle of 30°. Assuming a Maxwellian distribution of initial kinetic energies peaking at 2 eV, the number of ions with energies of 2 eV or less is approximately 20% of the total emitted. 42% of the ions have energies less than twice the peak energy, i.e., 4 eV in our example. Because of these relatively low initial kinetic energies, moderate electric field strengths at the sample surface are sufficient to provide efficient extraction. Ion collection from a one-cm^2 sample area, large by conventional standards, was studied here as this provides high integrated ion signal intensities. The ion transfer optics must deliver secondary ions to the mass analyzer within its entrance area and angular acceptance limitations. Ion optical calculations will help achieve this goal.

The secondary ion transfer system is made up of the following regions: a one-cm^2 sample area from which the sputtered ions are extracted by two specially shaped electrodes; additional acceleration in a two-element cylindrical lens; x- and y-deflection electrodes for "dynamic emittance matching"; a two-element cylindrical lens for deceleration and focusing; a 90° spherical electrostatic analyzer (ESA) for energy selection; and a set of aperture electrodes for deceleration and beam injection into a Finnigan MAT triple stage quadrupole (TSQ) mass spectrometer.

Each of these regions was computer-modeled as a separate problem whereby trajectory coordinates and energies at the exit boundary of each problem were stored in a file which, in turn, served as input data for trajectory simulations in the next region. In this manner, a composite drawing of ion trajectories from the sample to the mass analyzer could be obtained. All the regions mentioned above are presented in rotational ("ZR") symmetry, with the exception of the x- and y-deflection plates which had to be modeled in planar "XY" symmetry. Three-dimensional trajectories were computed and evaluated for each region.

Figure 1 shows the geometric configuration of the electrodes drawn to scale and potentials for the transmission of 200 u, positive secondary ions emitted on-axis with 5 eV initial energy. 5 eV ions were chosen for this study since this kinetic energy window includes 82% of the desorbed particles. The calculations show that for secondary ions with lower initial energy the beam envelope is slimmer, and for secondary ions with higher initial energy it is wider. As already mentioned, large-area ion extraction is required to obtain high analytical sensitivity in static SIMS. Figure 2 shows computer-modeled trajectories of principal rays of secondary ions emitted from an extended source, 1 cm in diameter. As described in the figure, placement of x- and y-deflection plates with their "center of deflection" at the crossover shown makes it possible for all ions originating from an extended sample area to be directed onto the spectrometer axis. An example of this dynamic emittance matching scheme is given in Figure 3 which shows computer-modeled trajectories of 5 eV secondary ions emitted 5 mm off-axis in the xz plane. Application of an appropriate voltage to the x-deflection plates has brought the secondary ions back to the spectrometer axis, enabling them to pass through the remaining optics to enter the quadrupole mass filter. Without the dynamic emittance deflection, the ions from off-axis sample locations would be lost in the deceleration tube lens in front of the ESA.

Presented at the 35th ASMS Conference on Mass Spectrometry and Allied Topics
May 24-29, 1987, Denver, CO

FIGURE 1

Computer-Modeled Trajectories of On-Axis Secondary Ions

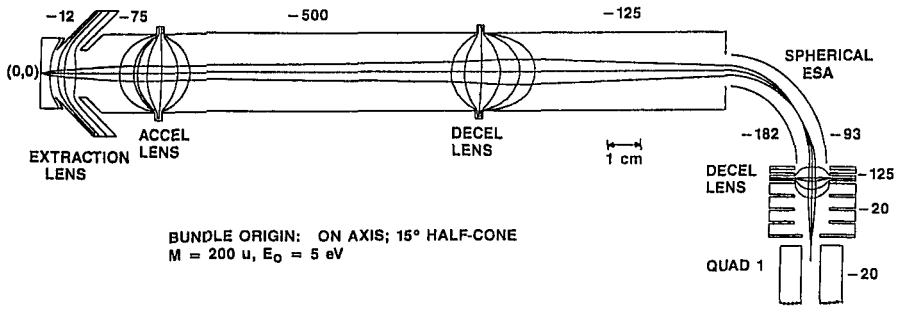

FIGURE 2

Computer-Modeled Trajectories of Principal Rays of Secondary Ions Emitted from an Extended Source

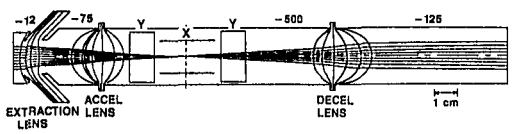

ORIGIN OF IONS: 1.25, 2.5, 3.75, and 5 mm ABOVE AND BELOW THE AXIS

M = 200 u, E_0 = 5 eV

Trajectories were calculated up to the entrance plane of the spherical electrostatic analyzer and in the absence of dynamic emittance deflection voltages.

X and Y deflection plates are placed with their "center of deflection" (dashed line) at the crossover shown above. This makes it possible for all ions originating from an extended sample area to be directed onto the spectrometer axis.

FIGURE 3

Computer-Modeled Trajectories of Off-Axis Secondary Ions

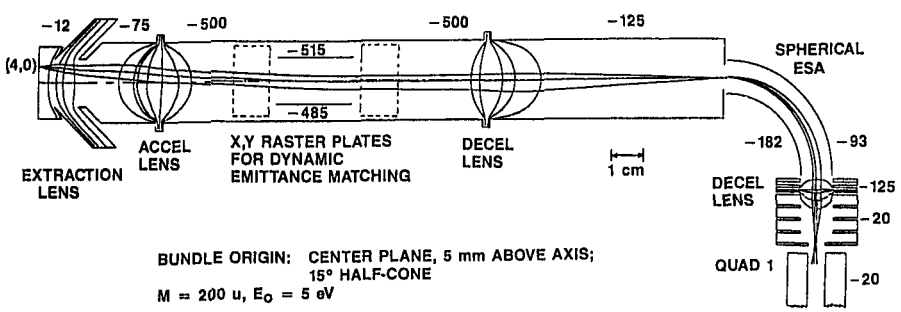

Presented at the 35th ASMS Conference on Mass Spectrometry and Allied Topics
May 24-29, 1987, Denver, CO

NEW SCAN MODES REVEALED BY A SYSTEMATIC EVALUATION OF MULTISTAGE MS EXPERIMENTS

J.C. Schwartz and M. Vincenti
Chemistry Department, Purdue University, W. Lafayette, IN 47907

A.P. Wade and C.G. Enke
Chemistry Department, Michigan State University, E. Lansing, MI 48824

The number of analyzing stages incorporated into mass spectrometers is continuously increasing. Development of pentaquadrupole, 4-sector, and hybrid instruments, as well as FT instruments and ion traps makes an increasing number of possible scan modes available. A system for delineating all possible scan modes for a given number of analyzer stages is presented here. As a consequence of these investigations, a new MS/MS scan mode was perceived. This new scan is also presented and examples of its performance are given.

A recent paper presenting several new MS/MS/MS scan modes proposed the symbolism in Figure 1 to represent the various scan types.[1] A morphological analysis can be performed on this symbolism to obtain the representations of all possible scan modes for an n stage experiment. This method applies the management science techniques of "morphological charts (MC)" and "analysis of interconnected decision areas (AIDA)" by establishing a set of selection rules in order to logically filter out any redundant or nonsensical symbol combinations in a set of symbolisms. For example, Figure 2 shows all symbol combinations for the expression of a two analyzer scan mode. The morphological analysis eliminates all but four of the 32 possibilities. The remaining four symbols represent the well known parent, daughter, reaction monitoring, and constant neutral loss experiments.

Further consideration of the symbol O ➡ O reveals that it can represent not only the constant neutral loss (or gain) scan, but a new type of scan in which <u>any</u> fixed relationship between parent (m1) and daughter (m2) masses may be defined, i.e. m2 = f(m1). The constant neutral loss (or gain) scan is just a single member of this class of experiments which can be referred to as functional relationship scans. See Figure 3. In this case, the particular function is m2 = m1-k, where k = m3. For demonstration of the scan, two chemical systems are investigated. The first system utilizes the scan function m2 = (m1+1)/2 to detect all symmetrical proton-bound dimers produced by a mixture of five amines in a CI source. After undergoing CAD, only symmetrical proton-bound dimers produce a daughter which satisfy this relationship. Figure 4a shows the CI mass spectrum indicating the presence of all the symmetrical and unsymmetrical proton bound dimers. Figure 4b shows the functional relationship spectrum displaying exclusively the symmetrical species. The second system recognizes Diels-Alder adducts in a mixture of adducts which are comprised of dienes and dienophiles of equal mass by utilizing a scan function m2 = (1/2)m1. CAD causes these ionized adducts (m1) to undergo a retro Diels-Alder (RDA) reaction to produce daughter ions (m2) at half their mass. Figure 5a shows the EI mass spectrum indicating presence of symmetrical and unsymmetrical Diels-Alder adducts. Figure 5b is the functional relationship scan displaying three of the possible four symmetrical products. The adduct ZZ does not show an efficient RDA process due to other more favorable decomposition pathways. The peak at m/z 158 is a false positive which simply fragments to give a m/z 79 ion.

Although simple scan functions have been investigated here, it is clear that the functional relationship scan can be used as a highly specific scan type and custom designed searches for groups of compounds.

The morphological analysis of the 64 possible symbolisms for a MS/MS/MS experiment produces 8 unique and useful scan types. All of these scans were listed in the previous reference[1] and most have been implemented. In general, the analysis proves that for n stages of analysis there are 2^n unique and useful mass spectral scan modes.

1 Louris, J.N.; Wright, L.G.; Cooks, R.G.; Schoen, A.E. <u>Anal. Chem.</u> 1985, 57, 2918.

Presented at the 35th ASMS Conference on Mass Spectrometry and Allied Topics
May 24-29, 1987, Denver, CO

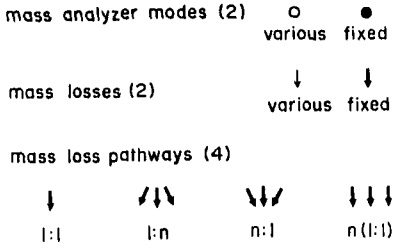

Figure 1

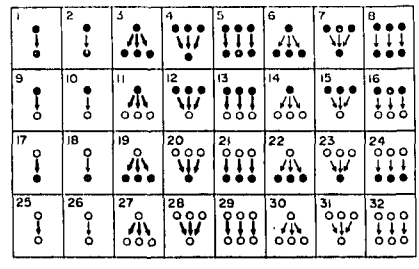

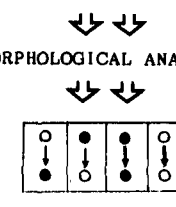

Figure 2

$m_1^+ \rightarrow m_2^+ + m_3$

	m_1^+	m_2^+	m_3	SYMBOL
REACTION MONITORING	CONSTANT	CONSTANT	CONSTANT	
DAUGHTER	CONSTANT	SCANNED	SCANNED	
PARENT	SCANNED	CONSTANT	SCANNED	
CONSTANT NEUTRAL LOSS (OR GAIN)	SCANNED	SCANNED	CONSTANT	
FUNCTIONAL RELATIONSHIP	SCANNED	SCANNED	SCANNED	

Figure 3

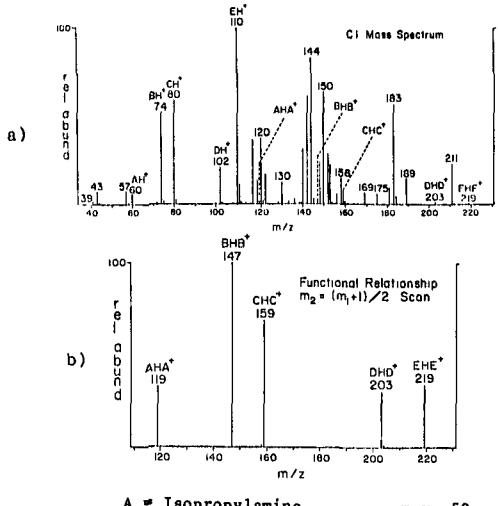

A = Isopropylamine m.w. 59
B = Sec-Butylamine m.w. 73
C = Pyridine m.w. 79
D = n-Hexylamine m.w. 101
E = 2-Methoxypyridine m.w. 109

Figure 4

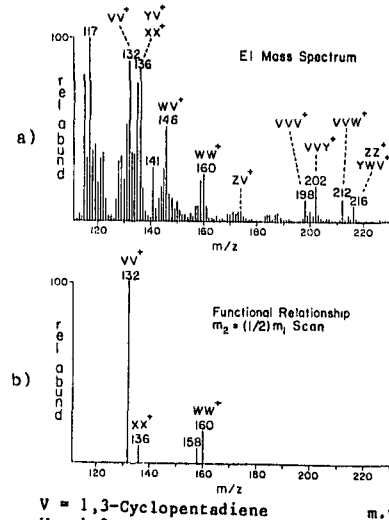

V = 1,3-Cyclopentadiene m.w. 66
W = 1,3-cyclohexadiene m.w. 80
X = 1,3-pentadiene m.w. 68
Y = crotonaldehyde m.w. 70
Z = 1,3-cyclooctadiene m.w. 108

Figure 5

Presented at the 35th ASMS Conference on Mass Spectrometry and Allied Topics
May 24-29, 1987, Denver, CO

A TOF-FTMS SYSTEM FOR PROBING HIGH MASS ANALYSIS BY FT-ICR METHODS

C.D. HANSON, M.E. CASTRO AND D.H. RUSSELL
TEXAS A&M UNIVERSITY, COLLEGE STATION, TX 77843

The development of an ion excitation scheme for ion cyclotron resonance (ICR) compatible with Fourier transform data analysis methods has greatly increased the analytical utility of the method. Owing to the high resolution and sensitivity of the technique, the potential utility of FTMS for the analysis of large biomolecules was recognized early.[1] Two different approaches for interfacing high pressure source regions with ICR systems have been presented,(i) the dual cell approach as introduced by Nicolet Instruments and (ii) the external ion source such as McIver's tandem quadrupole FT-ICR and Wanczek's external ion source. Such systems are difficult to evaluate because the signals measured give relative abundance of the ions trapped in the cell, and it is not easy to relate these relative values to absolute numbers of ions in the cell. Absolute measurements are important because sensitivity and mass resolution are directly dependant upon the number of ions trapped. As a first approach to investigating the issues related to the trapping and detection efficiencies of FT-ICR we have constructed a prototype time-of-flight/FTMS apparatus (figure 1)

An integral part of this instrument is a two-dimensional deflection quadrupole.[2] This novel interface permits multiple high pressure sources and/or detectors to be used on-line with a high vacuum FT-ICR analyzer. This lensing element increases the flexibility for investigating the problems incurred in high mass FTMS. The two-dimensional quadrupole has a broad energy bandpass with a high transmission, minimizing ion loss and maximizing sensitivity. Because this interface permits multiple high pressure sources to be connected on line with the FTMS analyzer region, the lens assembly can be used to evaluate the use of different ion sources and structural probe methods for analyzing and characterizing large peptides and related systems.

The utility of external ion sources for analyzing large involitle, thermally labile organic molecules has been demonstrated, e.g., bovine insulin and horse cytochrome C have been analyzed.[3] However, the experimental results indicate limits in the resolution of high mass ions due to the finite duration of the time-domain image current signal. Preliminary investigations indicate that this limitation is due to ion losses which occur as a result of unstable ion trajectories and/or the inability to effectively trap the ions in the ICR cell. In the case where ions are produced external to the magnetic field and directed into the ion cell, the effects of scattering the ion beam into the X-Y plane by field inhomogeneities must be considered. Due to the paramagnetic susceptibility of 304 and 316 stainless steel, the field lines of the solenoid magnet are perturbated forming bottlenecks at the ion cell apertures (figure 2a). Since the magnetic field lines are redirected into the X-Y plane, the trajectories of ions through the perturbated magnetic field will be deflected and the ions will gain kinetic energies in the X-Y plane. According to our model a magnetic bottleneck of the type described above will have its strongest effect on ions entering the cell close to the entrance aperture, accelerating them in the X-Y plane and reflecting them away from the orifice prior to entering the ICR cell. Only ions which are entering the center of the aperture will experience the weakest magnetic field effects and enter the ion cell. Owing to the second bottleneck at the rear trap plate, ions of low mass which are more strongly effected by the magnetic field gradients will be deflected and no longer have acceptable angular trajectories to pass through the exit orifice. This results in low mass ions being magnetically trapped in the ICR cell, whereas high mass ions are less sensitive to the magnetic field gradients and therefore exit the ion cell prior to electrostatic trapping.

Detailed measurements of ion partitioning in a dual-cell are consistent with the concept of magnetic inhomogeneities having large effects on ion trapping and detection.[4] To test our model, ion partitioning experiments were preformed in a stainless steel dual cell. In these experiments, ion partitioning resulted in no detectable signal from the ions transported from the source region to the analyzer region. In order to investigate the effect of magnetic inhomogeneities on transporting ions, the stainless steel trap plates were replaced with trap plates constructed of oxygen free copper. Since oxygen free copper has a weak diamagnetic susceptibility 2500 times less than that of stainless steel, the effect of the magnetic inhomogeneities should be greatly reduced (figure 2b). Once the magnetic inhomogeneities were removed by replacing the stainless steel plates with oxygen free copper, 50% of the ions produced in the source region were trapped and detected in the analyzer region after allowing

equal partitioning between the two regions. Based on these results, the presence of magnetic inhomogeneities caused by the magnetic susceptibility of the stainless steel, deflects the ions being transported between the two regions of the dual cell, leading to ion loss prior to detection.

[1] C.L. Wilkins and M.L. Gross Anal. Chem.1981,53,1661A
[2] H.D. Zeman Rev. Sci. Inst. 1977,48,1079
[3] D.F. Hunt *et al.* Proc. Natl. Acad. Sci.,1987,84,620
[4] E.L. Kerley, C.D. Hanson and D.H. Russell to be submitted.

FIG. 1

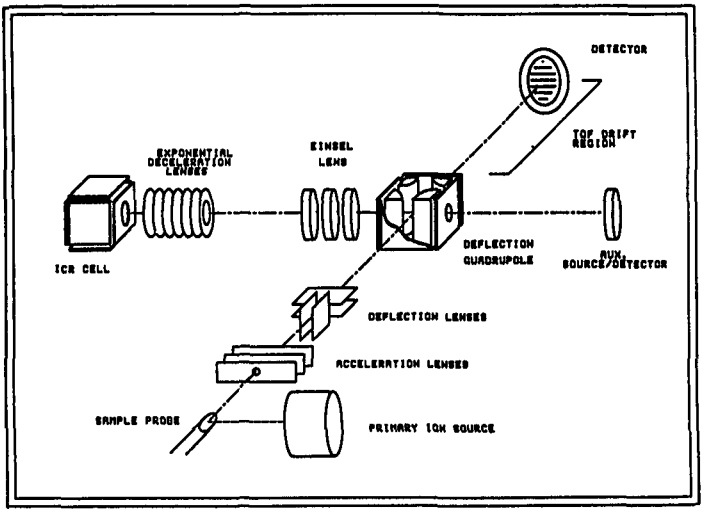

FIG. 2

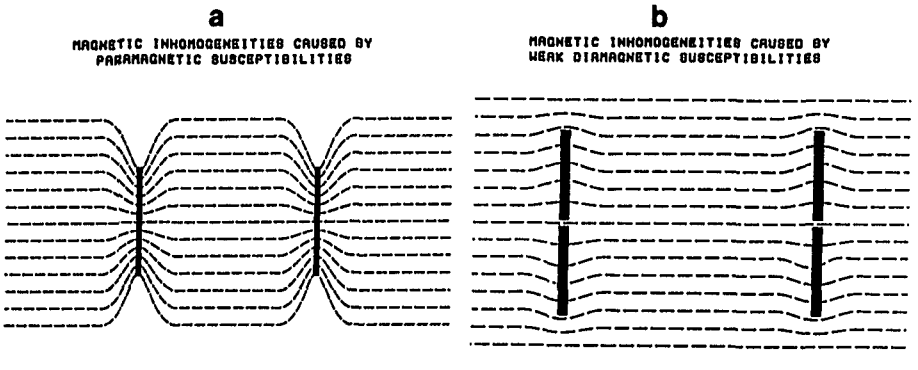

INDEX

OF

AUTHORS

ABBAS, H K 935
ABBAS, S A 858
ABBOTT, F S 455
ABBOTT, F S 11
ABDEL-MAKSOUD, H M 959
ABERTH, W 944
ABERTH, W 717
ABERTH, W 860
ABUMRAD, N N 1024
ACKERMANN, B L 417
ACKERMANN, B L 560
ACZEL, T 1066
ACZEL, T 377
ADAMS, J 227
AICHELE, D G 134
AICHELE, D G 127
ALAI, M 74
ALBERT, R H 393
ALEXANDER, A J 1106
ALKALAY, D 502
ALKALAY, D 505
ALLEMAND, P 576
ALLEMANN, M 1130
ALLEMANN, M 1128
ALLEY, C C 132
ALLISON, J 1026
ALLISON, J 733
ALLISON, J 799
AMY, J 279
ANDEREGG, R J 574
ANDEREGG, R J 830
ANDEREGG, R J 542
ANDERSON, S 584
ANDRZEJEWSKI, D 522
ANNAN, M 682
ANONICK, P K 492
APFFEL, A 440
APLIN, R T 429
APLIN, R T 431
APPELHANS, A D 737
ARBOGAST, B 713
ARMENTROUT, P B 670
ASAMOTO, B 1056
ASAMOTO, B 1064
ASHCROFT, A 642
ASHCROFT, A E 1094
ASHCROFT, A E 638
ASMUS, P A 961
AVERY, M 516
AVIENTE, V 791
AXELROD, B 580
BABCOCK, L M 600
BABCOCK, L M 582
BACZYNSKYI, L 397
BACZYNSKYI, L 1076
BAER, T 349
BAER, T 725
BAER, T 840
BAHR, U 88
BAILEY, S L 690
BAILLIE, T A 271
BAILLIE, T A 465
BAKER, P F 743
BAKER, P F 506
BALDONI, J M 476
BALICKI, M D 235
BALL, L M 149
BALLARD, K D 572
BAMBERG, M 1116
BANDURRAGA, M M 825
BARBER, M 642
BARBER, M 3
BAREFOOT, A C 413
BARLOW, S E 353
BARNES, I L 1010
BAROFSKY, D F 856
BAROFSKY, D F 310
BAROFSKY, D F 292
BAROFSKY, E 310
BARONAVSKI, A P 86
BARONAVSKI, A P 185
BARRY, R M 602
BARTMAN, C 138
BARTMAN, C 678
BASS, N 944
BASZIS, S R 823
BATEMAN, R H 415
BATEMAN, R H 1096
BATEMAN, R H 253
BAUMAN, N 385
BAX, M 502
BAYKUT, G 598
BAYKUT, G 96
BAYKUT, G 387
BEAN, M 1104
BEARY, E S 1000
BEATO, B D 969
BEAUGRAND, C 209
BEAUGRAND, C 345
BEAUGRAND, C 239
BEAVIS, R 68
BEAVIS, R 890
BEAVIS, R 195
BEAVIS, R C 652
BECCHI, M 956
BEHBEHANI, A L 371
BEL, P 544
BELAND, F A 705
BELL, D 540
BELLAR, T A 1072
BENCSATH, F A 29
BEND, J R 512
BENNETT, B D 568
BENNICH, H 528
BENNINGHOVEN, A 167
BENNINGHOVEN, A 169
BENNINGHOVEN, A 296
BENOIT, F M 144
BENSON, D 100
BENTZ, B L 1148

BENTZ, B L 221
BERBERICH, D W 1074
BERG, J 41
BERRY, A J 648
BERRY, A J 1100
BERTRAND, M J 399
BETOWKSI, L D 1088
BETOWSKI, L D 453
BEXON, J J 263
BEXON, J J 787
BEYNON, J H 207
BEYNON, J H 229
BEYNON, J H 1042
BEYNON, J H 1060
BHARGAVAA, A K 878
BIEMANN, K 570
BIEMANN, K 78
BIEMANN, K 556
BIEMANN, K 548
BIER, M E 279
BIER, M E 223
BIERBAUM, V M 353
BIERBAUM, V M 325
BIERI, R H 1034
BILL, J C 142
BIRNBAUM, L S 701
BJARNASON, A 335
BLAIR, I A 488
BLAIR, I A 1024
BLAIR, I A 508
BLAKELY, W F 900
BLAKLEY, C R 634
BLEASE, T G 1038
BLEASE, T G 179
BLETSOS, I V 169
BLETSOS, I V 167
BOCKHOFF, F M 1064
BOESL, U 538
BOESL, U 191
BOESL, U 626
BOLBACH, G 755
BOLBACH, G 753
BOLGAR, M S 478
BONDAROVICH, H A 361
BOORN, A 998
BORDAS-NAGY, J 793
BORNSTEIN, D 854
BOTT, P A 253
BOWEN, R D 850
BOWER, J E 339
BOWER, J E 337
BOYD, R K 1044
BOYD, R K 1042
BOYD, R K 229
BOYD, R K 123
BOZORGZADEH, M H 606
BOZORGZADEH, M H 395
BRACKMANN, R T 1136
BRADFORD, D 773
BRADSHAW, S C 775
BRADSHAW, S C 1114
BRENNAN, P J 72
BRENTON, A G 207
BRENTON, A G 1042
BRENTON, A G 229
BREWER, S J 942
BRICKER, D L 183
BRICKHOUSE, M D 211
BRINEGAR, C 54
BRODBELT, J S 343
BRODBELT, J S 1114
BRONSON, G E 1076
BROWN, N K 530
BROWN, R 1004
BROWN, R S 832
BROWN, R S 642
BROWN-BOOTH, L 269
BROWNER, R F 409
BRUINS, A P 1018
BRUMLEY, W C 393
BRUNENGRABER, H 1028
BUCHANAN, M V 25
BUCHANAN, M V 70
BUCHNER, J D 245
BUDDE, W L 1072
BUDDE, W L 371
BUDINGER, P A 1064
BUDZIKIEWICZ, H 749
BUEDEL, T A 111
BUNCE, N J 1044
BURKA, L T 701
BURKES, L J 650
BURLINGAME, A L 860
BURLINGAME, A L 944
BURLINGAME, A L 717
BURLINGAME, A L 876
BURNS, F B 389
BURSEY, J 100
BURSEY, J T 111
BURTON, R 11
BUSCH, K L 1140
BUSCH, K L 19
BUSCH, K L 852
BUSCH, K L 979
BUSH, E 463
BUTLER, L C 161
BYCROFT, B 3
BYRD, G D 449
CAIXACH, J 125
CALDWELL, G W 514
CALLAHAN, J H 436
CALLAHAN, J H 185
CALLAHAN, J H 312
CALLERY, P S 498
CALLERY, P S 496
CALLERY, P S 622
CALLERY, P S 684
CAMPANA, J E 813
CAPRIOLI, R M 566
CAPRIOLI, R M 640

CAPRIOLI, R M 676
CARAVATTI, P 1128
CARDENAS, D 161
CARDINALI, F L 365
CARDINALI, F L 690
CARR, S A 830
CARR, S A 933
CARR, S A 542
CARRASQUILLO, A 145
CARRUTHERS, R A 950
CASTLE, L W 844
CASTLEMAN, A W 187
CASTLEMAN, A W 612
CASTRO, M E 1152
CATLIN, D H 674
CATLOW, D 1038
CATLOW, D A 1036
CATLOW, D A 179
CEJA, P C 279
CERNY, R L 82
CERNY, R L 757
CESSNA, G 678
CESSNA, G 138
CHAMBERS, R J 739
CHAN, C 1022
CHANG, C K 482
CHANG, T C 1050
CHAPMAN, J R 1094
CHARALAMBOUS, P M 916
CHARALAMBOUS, P M 1004
CHARPENTIER, B A 1082
CHASE, W T 1010
CHEN, L 632
CHEN, T 856
CHENG, M T 616
CHENG, P-S 676
CHESS, E K 1068
CHHEDA, G B 878
CHIARELLI, M P 23
CHILDS, R 950
CHIPMAN, G R 614
CHIU, K S 115
CHOWDHURY, A K 590
CHRISTENSEN, S B 933
CHRISTIE, W H 929
CLARY, D C 668
CLAYTON, E 1036
CLAYTON, E 179
CLAYTON, E 1038
CLOTHIER, R 261
COATES, M L 500
COBURN, T T 977
CODY, R B 783
CODY, R B 664
CODY, R B 779
CODY, R B 259
COGGIOLA, M J 731
COHEN, A 1016
COLGROVE, S G 377
COLLE, E 686
CONE, C 361
CONTOS, D A 809
CONWAY, D C 965
CONZEMIUS, R J 926
COOK, K D 544
COOK, K D 745
COOK, K J 473
COOKS, R G 769
COOKS, R G 279
COOKS, R G 343
COOKS, R G 223
COOLEY, J E 1144
COOPER, W M 484
CORNISH, T 725
COSSON, J P 952
COSTELLO, C E 864
COSTELLO, C E 1
COSTELLO, C E 78
COSTELLO, C E 870
COTTER, R J 827
COTTER, R J 735
COTTER, R J 715
COTTER, R J 90
COTTRELL, J 66
COTTRELL, J S 251
COTTRELL, J S 308
COUTANT, J E 417
COUTANT, J E 560
COVEY, T R 536
CRAGOE, E J 526
CRAIG, A G 528
CRAIG, A G 578
CRAWFORD, D W 927
CRAWFORD, J L 411
CRAWFORD, R W 977
CREASY, W R 592
CREECH, J 546
CRIDDLE, R S 520
CROW, F W 1080
CROWLEY, J 700
CURTIS, J E 237
CURTIS, J M 1042
CURTIS, J M 229
CURTIS, M D 924
CZUCZWA, J M 134
D'AGOSTINO, P A 147
DAGUE, B 640
DAHL, D A 257
DAHL, D A 737
DAMODER, R 287
DANIEL, P F 959
DAS, B C 952
DAS, P R 711
DASS, C 558
DASS, C 316
DASS, C 963
DAVIDSON, W C 900
DAY, R A 568
DE KANEL, J 151
DE MAACK, F 952

DE WIT, J S M 512
DE WIT, J S M 419
DECKER, K 534
DEHARENG, D 347
DEINZER, M 713
DEINZER, M 886
DELANEY, T E 650
DELLA-NEGRA, S 755
DELLA-NEGRA, S 753
DELMORE, J E 257
DELMORE, J E 737
DEMAIO, W 423
DEMIREV, P 715
DEMIREV, P 90
DENNIS, L W 1066
DEPRUN, C 753
DEPRUN, C 755
DEPUY, C H 325
DEPUY, C H 353
DEROOS, F L 127
DEROOS, F L 134
DES ROSIERS, C 1028
DESIDERIO, D M 316
DESIDERIO, D M 558
DESIDERIO, D M 963
DESROCHERS, S 1028
DETERDING, L J 225
DEVANT, G 345
DEVANT, G 209
DEVANT, G 239
DHEANDHANOO, S 586
DIDONATO, G C 1140
DIDONATO, G C 852
DIDONATO, G C 979
DIELMANN, G 630
DIERS, J 658
DIETRICH, A M 149
DINO, J 554
DINO, J 197
DINO, J J 898
DIXON, J 580
DIXON, R R 429
DIZDAROGLU, M 900
DJURIC, Z 705
DOBB, D E 161
DOHERTY, S J 19
DOMON, B 864
DOMON, B 1
DONNELLY, J R 821
DONNELLY, J R 105
DONNELLY, J R 161
DONNELLY, J R 102
DORN, S B 306
DOUGLAS, D 998
DOYLE, R J 910
DRINKWATER, D E 201
DU, S 1
DUBAY, G R 438
DUCHAMP, D J 397
DUFFIN, K L 1140
DUFFIN, K L 19
DULAK, J G 136
DULIK, D 1104
DUNBAR, R C 1056
DUNBAR, R C 44
DUNBAR, R C 920
DUNBAR, R C 1048
DUNFORD, R 275
DURFEE, S L 357
DUTTA, S P 878
DZIDIC, I 967
DZIDIC, I 235
ECKENRODE, B A 241
ECKENRODE, B A 277
ECKER, E M 461
EGGER, H 502
EL-SAYED, M A 48
ELLEFSON, R E 922
ELLERBE, P 1016
ELLIOTT, G 642
ENGSTROM, A 528
ENKE, C C 1150
ENKE, C G 241
ENKE, C G 373
ENKE, C G 375
ENS, W 68
ENS, W 195
EPSTEIN, P S 924
ERICKSON, E 277
ERRINGTON, S G 431
ESPINO, R 1086
EVANS, J E 959
EVANS, K D 1080
EVANS, M J 399
EVANS, R J 981
EVANS, S 251
EYLER, J R 598
EYLER, J R 96
EYLER, J R 1054
EYLER, J R 43
EYLER, J R 387
FALICK, A M 318
FALLON, T 942
FAN, T 640
FAN, T 566
FARMER, P B 765
FARRAR, J M 672
FARROW, P E 1084
FASSETT, J D 52
FAST, D M 690
FAST, D M 365
FAULK, J 920
FAULL, K F 107
FAULL, K F 467
FEAREY, B L 1006
FEAREY, B L 904
FEISTNER, G J 692
FEISTNER, G J 107
FEISTNER, G J 467
FEIZI, T 950

FELD, H 296
FENESELAU, C 74
FENG, R 838
FENG, R 201
FENN, J B 723
FENN, J B 33
FENNESSEY, P V 17
FENSELAU, C 866
FENSELAU, C 1104
FERGUSSON, G J 634
FETTEROLF, D D 1074
FIELD, F H 29
FIELD, F H 321
FIES, W J 767
FIFER, E K 705
FIGUERAS, A 125
FISHER, J R 425
FISHER, S 876
FITE, W L 741
FLEET, G J W 429
FLESCH, G D 795
FLORY, D A 157
FLORY, D A 471
FLURER, R A 1140
FOLTZ, R L 696
FOLTZ, R L 698
FORBES, R 918
FORSTER, H J 461
FRAISSE, D 940
FRAISSE, D 956
FRAISSE, D 125
FRANCL, T J 1122
FRANCOM, P 698
FRASER-MONTEIRO, M 349
FREAS, R B 185
FREAS, R B 604
FREEMAN, H S 155
FREEMAN, J P 255
FRETER, K 1040
FREY, R 538
FRIEDRICH, B 584
FU, E W 480
FUCHS, V 1040
FUCIARELLI, A F 1106
FUERST, R 111
FUJII, T 27
FUJII, T 709
FUJIWARA, H 219
FUJIWARA, H 1078
FUKUDA, E K 622
FUKUDA, E K 490
FULFORD, J 998
FULFORD, J E 994
FURLONG, J J P 727
FUTRELL, J 584
FUTRELL, J H 58
GABLING, R-H 777
GALE, P J 221
GALLAGHER, R 610
GALLEGOS, E J 1062
GAMES, D E 1100
GAMES, D E 648
GANGULY,A K 954
GARDNER, J H 445
GARLAND, W A 490
GARLAND, W A 622
GARRETT, D A 409
GARRETT, J H 119
GARRETT, J H 121
GARRETT, J H 363
GARTEIZ, D A 636
GARVIE, C 494
GASKELL, S J 552
GASKELL, S J 504
GAUDRY, D 505
GAUDRY, D 502
GEELHAAR, L A 684
GEER, R 1024
GEHRON, M J 991
GEIDNER, R M 707
GELLENE, G I 84
GENO, P W 1146
GETEK, T A 443
GHADERI, S 779
GHISELLI, G 269
GIAM, C S 1120
GIAM, C S 894
GIBLIN, D E 231
GIBSON, B 944
GIBSON, B W 876
GIBSON, B W 318
GIBSON, B W 66
GILLECE-CASTRO, B 860
GILLEN, G 281
GILLIAM, J M 624
GILLSON, G 998
GLISH, G L 291
GLISH, G L 852
GLISH, G L 771
GOERINGER, D E 929
GOLDSTEIN, D B 107
GOLIK, J 438
GOODLEY, P C 1092
GOODMAN, S 1132
GOODMAN, S D 779
GOPINATHAN, M B 512
GORDON, L 401
GOTLIN, R W 17
GRABOWSKI, J J 351
GRANGE, A H 292
GRAUL, S T 805
GRAUL, S T 211
GRAY, B W 142
GREATHEAD, R J 900
GREAVES, J 1034
GREEN B N 3
GREEN, B N 540
GREEN, B N 142
GREEN, J P 13
GREEN, L W 98

GREENE, F T 249
GREENFIELD, J C 473
GREER, F M 942
GREGG, H 379
GREGG, H R 971
GRESE, R P 729
GRIFFIN, D 886
GRIFFIN, P R 550
GRIFFISS, M 876
GRIGSBY, R D 383
GRIMSRUD, E P 247
GRIMSRUD, E P 329
GROENEWOLD, G S 438
GROOPMAN, J D 763
GROSS, M L 801
GROSS, M L 82
GROSS, M L 844
GROSSMAN, P 1128
GROSSMAN, S 217
GROTEMEIER, H 538
GROTEMEYER, J 191
GROTEMEYER, J 626
GUENAT, C 554
GUENAT, C 197
GUENAT, C R 149
GUENAT, C R 898
GUEVREMONT. R 862
GUNAT, C 739
GUT, J 868
HACHEY, D L 269
HADDON, W F 359
HAGIWARA, T 1012
HAIL, M E 294
HAKANSSON, P 41
HAKANSSON, P 751
HAKANSSON, P 298
HALL, D J 916
HALL, R 255
HALLIGAN, K 998
HALLOS, B 819
HAMMOND, I 403
HANDA, M 359
HANEY, C A 155
HANKINSON, D J 799
HANNA, D A 259
HANNA, D A 1132
HANSEN, G 1040
HANSON, C D 1152
HARADA, K 884
HARBOL, K L 721
HARDEN, L 119
HARDEN, L H 121
HARDY, M 74
HARPOLD, D N 1144
HARPOOTLIAN, H 473
HARRIMAN, G E 987
HARRIS, F M 207
HARRIS, F M 1060
HARRIS, R E 171
HARRISON, A G 846
HARRISON, W W 931
HARRISON, W W 1002
HART, K J 375
HART, K J 373
HARTMAN, T G 475
HARTMAN, T G 320
HARVEY, D J 1020
HARVEY, D J 530
HATCH, F 1040
HATTON, C K 674
HAUER, C R 54
HAWTHORNE, S B 989
HAWTHORNE, S B 1070
HAYDEN, F G 492
HAYES, M 502
HEADLEY, J V 369
HEATH, J 403
HEDIN, C M 105
HEIN, R 783
HEIN, R E 259
HEITHMAR, E M 161
HELLER, D 866
HELLER, T 296
HEMLING, M E 830
HEMLING, M E 542
HENDRIKS, H 1018
HENION, J 432
HENION, J 15
HENION, J D 434
HENION, J D 654
HENRY, K D 391
HENSHAW, J M 161
HER, G R 874
HERCULES, D M 167
HERCULES, D M 169
HERCULES, D M 1120
HERD, C R 582
HERNANDEZ, O 512
HEROLD, D A 459
HEROLD, D A 492
HETTICH, R L 70
HIGASHIMORI, K 508
HIGUCHI, T 644
HILEMAN, F 815
HILL, R H 690
HILLENKAMP, F 88
HILLMAN, D C 161
HILPERT, L R 811
HINDENLANG, D M 233
HINSHAW, J V 159
HINSON, J A 453
HITES, R A 327
HITES, R L 267
HO, C-T 320
HOFMEISTER, G E 719
HOGGE, L R 1090
HOLDER, C L 484
HOLDER, C L 1088
HOLLAND, J F 241
HOLLAND, J F 958

HOLLAND, J F 302
HOLLAND, J F 277
HOLLER, J S 690
HOLLER, J S 365
HOLMAN, R W 231
HOLMAN, R W 801
HOLMAN, R W 848
HOLMES, J L 793
HOLMES, J L 840
HOLMES, L L 1010
HOLWITT, E 900
HOMOLYA, J 100
HOMOLYA, J B 111
HONIG, R E 1148
HONOVICH, J P 1112
HOOD, R 700
HOOD, R J 896
HORNER, L M 823
HORWITZ, J P 896
HOUK, R S 926
HOUK, R S 996
HOUK, V N 759
HOUNSELL, E F 950
HOWALD, W N 465
HOWARD, S 584
HSIEH, T C 1008
HSU, B-H 151
HSU, C S 177
HSU, S H 434
HSU, W N 155
HUANG, L 996
HUANG, L 926
HUANG, S D 92
HUANG, S K 213
HUDSON, C E 1046
HUDSON, C E 836
HUGHES, H 504
HUIZING, H J 1018
HUNDLEY, J 459
HUNT, A M 550
HUNT, D F 54
HUNT, D F 76
HUNT, D F 550
HUNT, D F 660
HUNT, J E 275
HUNT, J E 39
HUNT, S L 215
HUTCHINSON, D W 638
IANNUCCI, R 502
IKONOMOU, M 37
INAGAMI, T 508
INFANTE, R 145
INOUE, M 1012
ISAACS, S G 132
ISHII, D 644
ISHIKAWA, K 975
ITAGAKI, Y 644
JACOBSON, D B 658
JAIN, R K 858
JAJOO, H K 488
JALONEN, J 747
JAMES, J C 476
JAMIESON, G C 868
JAMIESON, W D 123
JAOUEN, D 209
JAOUEN, D 345
JAOUEN, D 239
JARDINE, I 1110
JARDINE, I 80
JARDINE, I 72
JARROLD, M F 337
JARROLD, M F 339
JAYASIMHULU, K 109
JENNING, K R 427
JENNINGS, K R 610
JENNINGS, K R 638
JENNINGS, K R 850
JIANG, K 318
JIANG, L 310
JIANG, S 996
JIMBA, H 27
JOAN, P S 125
JOEL, E C 1010
JOHLMAN, C L 785
JOHNSON, J L 128
JOHNSON, J V 294
JOHNSON, J V 773
JOHNSON, J V 971
JOHNSON, R E 41
JOHNSON, R S 556
JOHNSTON, M V 405
JOHNSTON, M V 193
JOHNSTON, M V 1050
JONES, A D 469
JONES, A D 694
JONES, D 415
JONES, D 1096
JONSSON, G 751
JONSSON, G 298
JORGENSON, J W 419
JUE, S G 463
JUNK, G 516
KABALKA, G W 850
KAHWA, I A 1008
KAISER, M F 498
KALINOSKI, H T 1068
KALINOSKI, H T 646
KAMAR, A 237
KAMBARA, H 407
KAMENSKY, I 528
KAMENSKY, I 578
KAMINSKI, H 538
KANDA, P 564
KANTER, E 275
KAPPATOS, D 958
KARANIAN, J W 457
KARAS, M 88
KASSAHUN, K 455
KASSEL, D B 733
KASSEL, D B 1026

KATONA, V R 134
KATRITZKY, A R 96
KATTA, V 441
KATTA, V 31
KATZ, R N 321
KAUFMAN, D G 898
KAYGANICH, K 447
KE, J 860
KEBARLE, P 1106
KEBARLE, P 300
KEBARLE, P 37
KEESEE, R G 187
KEESEE, R G 612
KEFEL, P 1128
KELLER, R A 1006
KELLERHALS, H 1130
KELLERHALS, H P 1128
KELLEY, P E 263
KELLEY, P E 9
KELLEY, P E 1114
KELLEY, P E 771
KELLEY, R B 469
KELLY, P 773
KELLY, S L 151
KEMPFF, M B 896
KENNERLEY, S 367
KENTTAMAA, H I 331
KEOUGH, T 825
KETKAR, S N 245
KETKAR, S N 1136
KETKAR, S N 741
KHANDELWAL, J K 13
KHEMANI, L 505
KIDWELL, D A 436
KILGORE, W W 694
KILLMER, L 510
KIM, H Y 1108
KING, F L 931
KING, G S 401
KING, G S 403
KINGSTON, R G 207
KINSEL, G R 1050
KINSEL, G R 405
KINSEL, G R 193
KINSINGER, J A 104
KINTER, M 492
KINTER, M 459
KIRK, D 409
KISER, R W 721
KITSON, F G 936
KLEBE, R J 564
KLEIMAN, R 518
KLEIN, A J 823
KLEIN, P D 269
KNAPP, D R 572
KNAPP, D R 7
KNOLL, H 21
KOBAYASHI, T 644
KOBLE, D L 1032
KOCH, S A M 703
KOFEL, P 1130
KORFMACHER, W A 453
KORFMACHER, W A 1088
KORFMACHER, W A 484
KORFMACHER, W A 705
KOYANAGI, G K 199
KREMER, J H 181
KRIER, C 347
KROLIK, S T 140
KROLIK, S T 1096
KUBOTA, E 644
KURLICK, N 113
KUTSCHERA, W 275
LABUDDE, J 488
LAFORTUNE, F 195
LAFORTUNE, F 890
LAFORTUNE, F 68
LAFORTUNE, F 652
LAINE, R A 858
LAINE, R A 1008
LAMPE, F W 425
LAN, L 377
LANFORD, R E 564
LARAMEE, J 713
LASER, B 1134
LATTIMER, R P 172
LATTIMER, R P 171
LAUER, R 823
LAUKIEN, F 918
LAUKIEN, F H 781
LAWSON, A M 950
LAY, J O 484
LAY, J O 255
LAY, J O 453
LE BEYEC, Y 755
LE BEYEC, Y 753
LEARY, J A 888
LEARY, J A 719
LEBO, J 128
LEDOUX, K A 476
LEE, E 432
LEE, E D 15
LEE, E D 654
LEE, E D 434
LEE, M S 421
LEE, T D 35
LEE, Y C 74
LEGEL, M A 927
LEGGESSE, K 35
LEITCH, C A 62
LEPAGE, P 940
LEVY, R H 465
LEWIS, S 261
LEWTAS, J 809
LEYH-NIHANT, B 347
LI, L 243
LI, M 1
LI, X 341
LI, Y G 795
LIAO, C L 795

LIAO, Q-J 480
LIEBMAN, C P 314
LIEBMAN, S A 181
LIFSHITZ, C 791
LIGHT, K J 733
LIGON, W V 306
LIM, H K 696
LIM, H K 698
LIN, S-N 676
LINDEN, H B 21
LINDQUIST, S-E 41
LINHARDT, R J 72
LINNOILA, M 457
LIPKA, J 66
LISEK, C A 1110
LITTLE, J L 411
LIU, Y-M 688
LOCKE, L A 451
LOGAN, T 111
LOH, S Y 391
LOI, C M 463
LOO, J A 727
LOPEZ, H 965
LORQUET, J C 347
LOURIS, J N 769
LUBMAN, D M 243
LUBMAN, D M 56
LUBMAN, D M 92
LUNDIN, R E 359
LYNN, R K 494
LYON, P A 215
LYS, I 735
MACDONALD, R G 98
MACFARLANE, R D 1146
MADDEN, R 1136
MAHONEY, J F 35
MAIN, D E 652
MAJOR, H 415
MALATESTA, A 177
MALCHOW, R D 711
MALHOTRA, R 731
MALIK, J M 219
MALLIS, L M 265
MALTBY, D A 650
MAMANTOV, G 314
MAMER, O A 686
MAMER, O A 1028
MANDELBAUM, A 854
MANNING, K S 1080
MARBURY, G D 153
MARBURY, G D 739
MARCH, R 333
MARCH, R E 237
MARCH, R E 199
MARGESON, J 100
MARKEY, S P 1112
MARKS, L 269
MARNETT, L J 700
MARSHALL, A G 632
MARSHALL, A G 914
MARSHALL, A G 938
MARSHALL, A G 656
MARTIN, B 688
MARTIN, L B 906
MARTIN, S A 78
MARTIN, W 866
MARTIN, W B 50
MARTINEZ, R I 586
MASON, R S 610
MASUCCI, J A 514
MASUDA, K 884
MATTA, K L 858
MATUSZAK, K P 294
MATZ, G 163
MAYERNIK, J A 894
MAYOL, R F 488
MCADOO, D J 836
MCADOO, D J 1046
MCALLISTER, R 100
MCBETH, R L 985
MCCLENNEN, W 789
MCCLENNEN, W H 1142
MCCLOSKEY, J A 878
MCCLURE, T D 743
MCCLURE, T D 506
MCDONALD, J R 592
MCDOWALL, M A 1110
MCELVANY, S W 803
MCELVANY, S W 86
MCFADDEN, W H 636
MCFADDEN, W H 536
MCGAUGHEY, J 100
MCGRAW, J M 690
MCLAFFERTY, F W 201
MCLAFFERTY, F W 838
MCLAFFERTY, F W 391
MCLAFFERTY, F W 727
MCLEAN, M A 157
MCLUCKEY, S A 291
MCLUCKEY, S A 771
MCLUCKEY, S A 852
MCNEIL, M 72
MECHOULAM, R 1020
MECKSTROTH, W 662
MECKSTROTH, W K 596
MEEK, J T 1122
MEEKER, J E 694
MEISELS, G G 203
MEISELS, G G 205
MELLY, S J 351
MENG, C K 723
MENG, C K 33
MESTDAGH, H 209
MESTDAGH, H 345
METRAL, C J 1138
MEUZELAAR H L C 1142
MEYERS, P 1010
MILLEN, W G 1122
MILLER, C D 363
MILLER, C M 904

MILLER, C M 1006
MILLER, D J 989
MILLER, D J 1070
MILLER, P E 977
MILLINGTON, D S 650
MILNE, T A 981
MILTON, D J 367
MIOTTO, J 502
MIOTTO, J 505
MIROCHA, C J 935
MISSLER, S R 973
MISSLER, S R 604
MISSLER, S R 813
MITCHELL, D 427
MITCHELL, D 850
MITCHUM, R K 1088
MITCHUM, R K 821
MITCHUM, R K 105
MITCHUM, R K 161
MITROVICH, S 136
MIWA, B J 490
MIZUNA, T 644
MOINI, M 1054
MOINI, M 598
MOJESKY, M T 912
MOKOTOFF, M 480
MONAGHAN, J J 1036
MONAGHAN, J J 3
MONAGHAN, J J 1038
MONAGHAN, J J 179
MONTGOMERY, J A 1028
MONTGOMERY, J A 686
MOORE, B L 825
MOORE, C B 425
MOORE, W 640
MOORE, W T 566
MORALES, A 300
MORGAN, S 187
MORIN, N 239
MORISON, D S 574
MORRIS, H R 942
MORROW, J C 840
MORROW, J C 349
MORTON, T H 797
MORTON, T H 608
MOSER, H 882
MUELLER, T R 993
MUGA, M L 1126
MUKAI, F 534
MULLEN, S L 914
MUNSLOW, W D 821
MUNSLOW, W D 105
MUNSON, B 602
MUNSON, B 618
MUNSTER, H 749
MURPHY, C 866
MURPHY, R C 5
MURPHY, R C 60
MURRAY, D S 1030
MUSSELMAN, B D 482
MUSSELMAN, B D 302
MUSSER, S M 496
MYLCHREEST, I C 648
MYLCHREEST, I C 1100
NASHED, N 217
NEEDHAM, L L 690
NELSON, B 1086
NELSON, H H 86
NELSON, H H 803
NEWCOME, B H 241
NG, C Y 795
NG, K 620
NGUYEN, N T 283
NIBBERING, N M M 323
NIBBERING, N M M 355
NIEDENZU, K 912
NIEDERHUT, W 526
NIEDERHUT, W J 102
NIEDERHUT, W N 813
NIEHUIS, E 296
NIELSEN, P 751
NIELSEN, P F 298
NIEMANN, H B 1144
NISHIGAKI, S 1012
NISHIMURA, T 205
NISHIMURA, T 203
NISHIOKA, M G 809
NIWA, Y 975
NODA, T 1012
NOGAR, N S 904
NORDMAN, B 440
NOURSE, B 373
NUNN, N J 105
NUWAYSIR, L M 832
O'BRIEN, R J 292
O'DONNELL, J E 249
O'HARA, M 700
O'KEEFE, A 592
O'LEARY, I A 473
O'MALLEY, R M 50
O'MALLEY, R M 1052
OCCOLOWITZ, J L 624
ODOM, R W 94
OGDEN, S 888
OH, M S 977
OHMICHI, N 791
OLBERDING, E L 486
OLESIK, S 840
OLIVARES, J A 646
OLIVARES, J A 283
OLTHOFF, J K 735
OLTHOFF, J K 90
ORLANDO, R 618
ORTH, R G 815
OSTERMAN, R M 634
OU, D W 532
OWEN, R 987
OWENS, G D 650
OZTURK, F 598
PACHUTA, R R 331

PACK, T W 155
PALAZZOLO, M 100
PALLANTE-MORELL, S 1104
PALMER, P T 373
PALMER, P T 375
PALOMINO, E 896
PAMIDI, K M 858
PAMIDIMUKKALA, K M 1008
PAN, S-S 496
PANESAR, S 455
PANG, H M 56
PANNELL, L K 217
PAPA, V M 532
PAPAYANNOPOULOS, I A 548
PARDO, R 275
PARENT, D C 1006
PARKER, C E 419
PARKER, C E 701
PARKER, C E 512
PARR, V C 987
PASSARELLA, R 612
PASTEL, M J 476
PATEL, S 361
PATKIN, A J 159
PATRZYC, H B 878
PATTERSOM, T 138
PATTERSON, B W 269
PATTERSON, D G 132
PATTERSON, T 678
PAULSEN, P J 1000
PAWLOSKY, R 935
PAWLOWSKI, T M 432
PEDERSEN, S F 719
PELLERITE, M J 215
PEREIRA, W E 117
PEREL, J 35
PERKINS, D D 409
PERKINS, J R 648
PERKINS, J R 1100
PESCH, R 630
PETERMAN, P H 128
PIATEK, B 620
PIKE, A W 17
PINKSTON, J D 650
PISERCHIO, M 425
PIZZITOLA, V 165
PLATTNER, R D 518
PLATTNER, R D 520
PLEASANCE, S 648
PLEASANCE, S 1100
POEPPEL, F 1136
POEPPEL, F 289
POEPPEL, F 136
PORCH, R 100
PORCH, R L 111
PORTER, C J 504
PORTER, C J 140
PORTER, C J 552
POTTER, D W 453
PRAMANIK, B N 711
PRAMANIK, B N 954
PRELL, G D 13
PRESSER, D 285
PRILL, G E 369
PRITCHETT, T 113
PROVOST, L R 147
QIAN, F 1
QUAN, E S K 994
QUARLES, J M 965
QUIRKE, J M E 969
QURESHI, N 715
RACHLINT, E 878
RAIA, J C 967
RALEIGH, J A 1106
REDDY, A M 902
REDDY, C K 1024
REDDY, G S 842
REDDY, G S 880
REDMAN, E W 797
REED, D W 1090
REENTS, W 662
REID, C J 1060
REILLY, M 552
REILLY, M 504
REINER, E J 819
REINER, J 892
REINHOLD, V 870
REINHOLD, V N 872
REINHOLD, V N 874
REISER, R W 413
REMACLE, F 347
REMPEL, D L 1124
RETTENMEIER, A W 465
REYNOLDS, J D 745
REYNOLDS, S D 1066
RHEE, C K 171
RIDGE, D P 662
RIDGE, D P 588
RIDGE, D P 596
RIFFLE, M S 1030
RIVERA, J 125
ROACH, J A G 393
ROBAUGH, D A 249
ROBBINS, E F 532
ROBERTS, G D 933
ROBERTS, G D 542
ROBERTS, G D 830
ROBERTS, W L 872
ROBINS, R H 1080
ROBINS, R H 961
ROBINSON, K 1004
ROBOZ, J 958
ROCKWOOD, A 584
ROCKWOOD, A L 31
ROCKWOOD, A L 441
RODACY, P J 389
ROEPSTORFF, P 751
ROEPSTORFF, P 298
ROLANDO, C 239
ROLANDO, C 209

ROLANDO, C 345
ROMANOWSKI, G 777
ROMINGER, K L 461
ROSEN, J D 320
ROSEN, J D 475
ROSEN, R T 320
ROSEN, R T 475
ROSENBERG, I E 524
ROSENBERRY, T L 872
ROSS, M M 86
ROSS, M M 436
ROSS, M M 312
ROSTAD, C 117
ROWE, M 904
ROWLAND, C N 161
RUBIN, I B 25
RUDEWICZ, P J 636
RUDEWICZ, P J 536
RUEGG, F C 52
RUNNALLS, N 401
RUNNALLS, N 403
RUSSELL, D H 265
RUSSELL, D H 834
RYAN, P A 367
SACK, T M 817
SAITO, Y 1012
SAKAIRI, M 407
SAKASHITA, C O 696
SALEHPOUR, M 275
SALEHPOUR, M 39
SALEM, N 457
SALEM, N 1108
SALGADO, J G 125
SANDERS, R A 1082
SANTANDER, P J 680
SANTIAGO, N 145
SANTIKARN, S 870
SANTIKARN, S 872
SANTIKARN, S 874
SARRE, P J 46
SAUTER, D 136
SAVE, G 41
SAVORY, J 459
SAYRE, E V 1010
SCANLAN, G S 72
SCHAEFFER, R 1136
SCHAEFFER, R 165
SCHAFFER, R 1016
SCHILDCROUT, S M 707
SCHLAG, E W 538
SCHLAG, E W 191
SCHLAG, E W 626
SCHLUNEGGER, U P 237
SCHNEIDER, K 892
SCHOELLER, D A 62
SCHRAM, K H 902
SCHRAM, K H 880
SCHRAM, K H 743
SCHRAM, K H 506
SCHREINER, A F 906
SCHRODER, E 749
SCHROEDER, E 630
SCHUELER, B 890
SCHUELER, B W 94
SCHULTEN, H -R 171
SCHULTZE, P 908
SCHUMACHER, P M 381
SCHWARTZ, J 1150
SCHWARTZ, T R 128
SCOBLE, H A 78
SCOTT, A I 680
SCOTT, R G 985
SCRIVENS, J H 427
SCRIVENS, J H 1038
SCRIVENS, J H 179
SCRIVENS, J H 1036
SCUDDER, P 950
SEARS, L J 329
SEARS, L J 247
SEDGWICK, R D 233
SEGAL, A 534
SEGALL, H J 469
SEGAR, K R 405
SEGAR, K R 1050
SEIBER, J N 469
SELBIN, J 1008
SELGREN, S F 84
SELTZMAN, H H 1032
SGARAMELLO, R P 1030
SHABANOWITZ, J 76
SHABANOWITZ, J 550
SHABANOWITZ, J 54
SHABANOWITZ, J 660
SHALER, T A 608
SHAO, J D 795
SHAO, J-D 349
SHARP, T R 680
SHARP, T R 628
SHAW, G J 522
SHAW, K M 1064
SHIBATA, D 580
SHIEL, D A 367
SHIH, M-C 1112
SHIMANSKAS, C 620
SHIRATSUCHI, K 884
SHOHET, L 779
SHOMO, R E 938
SHUL, R J 612
SIEGEL, M M 385
SIETSEMA, W K 445
SIM, P G 123
SIMMS, J R 825
SIN, C H 56
SLATTER, J G 11
SLIVON, L E 381
SMIECINSKI, R F 161
SMITH R G 823
SMITH, D 688
SMITH, D 946
SMITH, D C 233

SMITH, D C 1110
SMITH, G G 842
SMITH, R D 787
SMITH, R D 1068
SMITH, R D 646
SMITH, R D 263
SMITH, R D 283
SMITH, R W 512
SNIEGOSKI, L T 449
SNIEGOSKI, L T 1016
SNOW, T A 175
SNYDER, A P 789
SNYDER, A P 181
SO, H Y 1048
SODERSTROM, E 41
SOLCH, J G 121
SOLCH, J G 363
SOLCH, J G 119
SOLOMON, J J 534
SOLSTEN, R T 1078
SOMERVILLE, A C 967
SOMMERS, B 520
SOMSSICH, P F 1014
SOPCHYSHYN, F C 98
SOVOCOOL, G W 102
SOVOCOOL, G W 105
SOVOCOOL, G W 821
SPENCER, R B 1132
SPENGLER, B 88
SPITELLER, G 892
SQUIRES, R R 805
SQUIRES, R R 211
ST.JOHN, G A 731
STACE, A J 666
STACK, R J 520
STAFFORD, G 769
STAFFORD, G 279
STAFFORD, G C 263
STAFFORD, G C 775
STAMS, D A 797
STANDING, K G 68
STANDING, K G 890
STANDING, K G 753
STANDING, K G 195
STANDING, K G 652
STANLEY, J S 817
STANLEY, M S 19
STAUFFER, D B 391
STECZKO, J 580
STEGER, J 100
STEMMLER, E A 327
STENE, D O 5
STIRCHAK, E 886
STOCKTON, G W 1122
STODDART, S 361
STONE, J A 594
STONE, J A 341
STRATTON, R D 445
STRAUB, K 494
STRIFE, R J 9
STRIFE, R J 445
STROBEL, F 588
STROBEL, J 662
STUHLER, J D 486
STULTS, J T 302
STULTS, J T 948
SUBRAMANYAM, B 684
SUEPER, C V 127
SUMMERTON, J E 886
SUN, Y 946
SUNDQVIST, B 578
SUNDQVIST, B 64
SUNDQVIST, B 298
SUNDQVIST, B 751
SUNDQVIST, B 41
SUNNER, J 37
SUNNER, J 300
SUWANRUMPHA, S 471
SUZUKI, M 884
SWACKHAMER, D L 267
SWAIN, D 233
SWEETMAN, B J 508
SWENBERG, J A 703
SYKA, J E P 775
SYKA, J E P 1114
SYKA, J E P 767
TABET, J C 739
TABUCCHI, R 576
TACKETT, J R 922
TAGUCHI, V Y 819
TAKAYAMA, K 715
TAKEDA, N 884
TAKEDA, T 884
TAMIRI, T 854
TAMURA, M 508
TANAKA, C 115
TANG, S-Y 151
TANG, X 68
TANG, X 652
TANG, X 890
TANG, X 195
TATEMATSU, A 884
TAYLOR, D M 775
TAYLOR, J W 335
TAYLOR, L C E 308
TAYLOR, M L 121
TAYLOR, M L 363
TAYLOR, M L 119
TAYLOR, P 62
TAYLOR, R F 1084
TAYLOR, W S 600
TECKLENBURG, R E 183
TEMBREULL, R 243
TERWILLIGER, D T 371
TETLER, L 3
TETLER, L W 642
THEOBALD, F 749
THIBAULT, P 399
THOMSON, M L 1122
TIERNAN, T O 121

TIERNAN, T O 363
TIERNAN, T O 119
TODD, G D 690
TODD, G D 365
TODD, J F J 787
TODD, J F J 263
TODD, J F J 189
TODD, P J 304
TODD, P J 314
TOLUN, E 963
TOLUN, E 189
TOMER, K B 419
TOMER, K B 554
TOMER, K B 701
TOMER, K B 197
TONDEUR, Y 813
TONDEUR, Y 526
TONDEUR, Y 102
TONG, S L 1002
TOSS, M M 185
TOU, J C 287
TOWNSEND, R R 74
TRAEGER, J C 1046
TRAFTON, W 584
TRAHEY, N M 927
TRAVIS, J C 52
TRIEBE, F M 823
TRUDELL, J R 868
TSARBOPOULOS, A 80
TSONG, I S T 829
TSOUPRAS, G 576
TURLINGTON, J M 153
TURNER, M J 703
TUSCHALL, J R 153
TWISS-BROOKS, A B 391
TWOREK, H A 878
UDSETH, H R 646
UDSETH, H R 1068
ULICK, S 1022
UNDERHILL, E W 1090
UNGER, S E 478
UPDEGRAFF, D 357
UY, M 866
VALIGA, R E 929
VALLADIER, P 700
VAN BREEMEN, R B 546
VAN BREEMEN, R B 906
VAN DOREN, J M 353
VAN DORSSELAER, A 940
VANLANGENHOVE, A 115
VANLEYEN, D 169
VANLEYEN, D 167
VANNESS, F F 121
VANNESS, G F 119
VARMA, R S 850
VATH, J E 570
VENTURA, F 125
VERDUN, F R 938
VESTAL, C H 130
VESTAL, C H 1082
VESTAL, C H 1102
VESTAL, M L 1058
VESTAL, M L 417
VESTAL, M L 634
VESTAL, R E 463
VICKERS, R 830
VISWANADHAM, S K 1120
VONNAHME, T L 105
VOORHEES, K J 357
VOYKSNER, R D 1032
VOYKSNER, R D 562
VOYKSNER, R D 155
VOYKSNER, R D 1098
VRBANAC, J J 7
VRBANAC, J J 447
WADDELL, D S 1044
WADE, A 1150
WADE, A P 373
WADE, A P 375
WAGEL, D 119
WAGEL, D J 121
WAGNER, D A 682
WAGNER, G 1134
WAGONER, D 100
WALDEN, T L 900
WALKER, R J 52
WALKER, R L 993
WALLER, G R 1030
WALLS, F 66
WALLS, F C 318
WALTER, K 191
WALTER, K 538
WALTER, K 626
WANCZEK, K P 1130
WANCZEK, K P 1116
WANCZEK, K P 21
WANCZEK, K P 777
WANG, B H 727
WANG, D T 819
WANG, J-S 524
WANG, R 715
WANG, R 451
WANG, T 856
WANG, T H 983
WANG, T-C L 1112
WARD, S R 825
WARNER, C D 801
WARRACK, B M 478
WARREN, C D 870
WARSHAWSKY, D 109
WASKELL, L 66
WATANABE, M 1012
WATSON, C H 387
WATSON, C H 96
WATSON, J T 482
WATSON, J T 948
WATSON, J T 277
WATSON, J T 447
WAY, S H 1144
WAYNE, R S 1122

WEAVER, C 688
WEBB, J 876
WEBER-BRABAU, M 1114
WEBER-GRABAU, M 263
WEBER-GRABAU, M 769
WEBER-GRABAU, M 9
WEDDLE, G H 596
WEERASINGHE, C A 451
WEIDOLF, L 432
WEIDOLF, L 15
WEIDOLF, L O G 654
WEIL, D A 104
WEIL, D A 783
WEINKAM, R 1086
WEINTRAUB, S T 564
WEIR, O 987
WEISS, G 538
WEISS, M 163
WEITZ, C J 467
WELCH, M J 1016
WELLER, D 886
WELLER, R R 1120
WELLER, R R 894
WENCLAWIAK, B W 908
WESDEMIOTIS, C 201
WESDEMIOTIS, C 838
WESTMORE, J B 195
WESTMORE, J B 890
WESTON, W L 17
WHITE, E 449
WHITE, E 811
WHITE, E 1016
WICKHAM, T J 610
WIEDERHOLD, M 532
WILDER, D R 411
WILKINS, C L 832
WILKINS, C L 785
WILLIAM, J C 874
WILLIAMS, E R 727
WILLIAMS, F P 562
WILLIAMS, F P 1098
WILLIAMS, F P 1032
WILLIAMS, P 64
WILLIAMS, P 281
WILLIAMS, T D 574
WILLOUGHBY, R C 289
WILLOUGHBY, R C 245
WILLOUGHBY, R C 136
WILLS, M R 459
WILSON, S B 950
WINANS, R E 985
WINBOROUGH, M 678
WINTER, C K 469
WISE, M B 807
WISHNOK, J S 761
WITEK, D J 465
WITTROCK, A 461
WONG, C 379
WONG, C M 971
WONG, L K 480
WONG, S F 33
WOOD, D 987
WOOD, G W 882
WOODWARD, D 128
WOOLFITT, A R 638
WRATTEN, S J 1078
WRIGHT, B W 1068
WRIGHT, J L C 862
WRONKA, J 596
WRONKA, J 918
WRONKA, J 662
WU, W N 514
WYSOCKI, V H 223
WYTENBURG, W J 594
XIANGYU, J 688
XU, R 795
YAKSH, T L 1110
YAMASAKI, R 876
YANG, C L C 1118
YANG, L 130
YANG, L 1102
YANG, X-L 612
YATES, J R 76
YAZDANPARAST, R 580
YELLE, L M 1084
YERGEY, A L 425
YERGEY, J A 457
YOFFE, J A 142
YOST, R A 773
YOST, R A 421
YOST, R A 789
YOST, R A 991
YOUNG, A 333
YOUSSEFI, M 785
YU, Z 944
YUN, Y 1142
ZABRANSKY, B 275
ZEBRE, L E 719
ZENG, C-H 1
ZHA, Q 203
ZHA, Q 205
ZHANG, M-Y 201
ZHANG, M-Y 838
ZHAO, M 480
ZHONGRUI, Z 946
ZHU, N-Z 550
ZIDAROV, D 399
ZIESEL, J -P 791
ZIMMERMAN, J A 1052
ZIMMERMAN, M L 127
ZITRIN, S 854
ZORETIC, P A 739

Presented at the 35th ASMS Conference on Mass Spectrometry and Allied Topics
May 24-29, 1987, Denver, CO

Chemometrics for Everyone

A Workshop Sponsored by the
Computer Applications Interest Group

The purpose of this workshop was to provide an introduction to the field of multivariate statistical analysis applied to chemistry, otherwise known as chemometrics, and examine specific applications of chemometrics to mass spectrometry. Approximately one hundred persons were present at the beginning of the workshop. The workshop began with the introduction of the three panelists, Robert Meglen (University of Colorado, Denver), Charles Wilkins (U. of California, Riverside), and Paul Peterman (U.S. Fish & Wildlife Service, Columbia, MO).

Dr. Meglen provided an excellent introduction to chemometrics in general. The focus of his statements was that the ability of the machine to create data often surpasses the capacity of traditional reduction techniques. Also, as the number of dimensions to an experiment increases, so also does the inability of viewer to comrehend the results. The answer to such cases of "data overload" is to apply multivariate statistical techniques to the data. Such techniques effectively reduce the number of significant components to a level that is useful and comprehensible to a normal human being. Dr. Meglen's presentation concluded with an impressive series of computer-generated graphics which, despite some awkward moments at the slide projector, elicited sighs of envy from many members of the audience.

Dr. Wilkins discussed his work with pattern recognition techniques applied to mass spec library searches. His work has recently been focused on the marriage of GC/IR and GC/MS to form a GC/IR/MS instrument. Such a hybrid system results in an increase in the amount of data that must be correlated. Software has been written to match GC elution peaks from both detectors, perform normal library searches on each peak using libraries appropriate to each method of detection, and then cross-correlate the results to produce a composite prediction. The procedure was illustrated with a number of examples, showing that the GC/IR/MS results were superior to either detection medthod when considered alone.

Mr. Peterman concluded the workshop with an example of chemometrics applied to real-life chemical problems. In a study conducted in cooperation with the Canadian Wildlife Service, a principal components analysis (PCA) approach known as SIMCA (Soft Independent Modeling by Class Analogy) was used to study dioxin residue levels in hazardous waste and herring gull eggs. In the first study, isotope ratios for the three largest ions in the molecular clusters of dioxins and furans were submitted to the SIMCA program to determine variability from theoretical values. The technique was found to provide a simple method for determining contamination due to presence of mixtures of chlorinated compounds. In the study of herring gull eggs, SIMCA was used to determine if dioxin residue profiles were similar at different geographical locations or if trends could be detected.

Presented at the 35th ASMS Conference on Mass Spectrometry and Allied Topics
May 24-29, 1987, Denver, CO

APPLICATIONS OF MS/MS TO ENVIRONMENTAL PROBLEMS

A Workshop Sponsored by the
Environmental Applications Interest Group

This workshop was organized to examine the use of tandem mass spectrometers (MS/MS) for the analysis of environmental samples. Both the advantages and limitations of this technique were discussed. Featured speakers included Joe Campana (University of Nevada), Roger Hayes (Midwest Center for Mass Spectrometry), Nicholas Kurlich (Enviresponse, Inc.), Mary Sisak (Ashland Petroleum), and Scott McLuckey (Oak Ridge National Laboratory). In addition, many in the audience contributed to the discussions following each of the presentations.

Joe Campana compared GC/MS, GC/HRMS, and GC/MS/MS for the analysis of dioxin and found a minimum of interference when GC/MS/MS was employed, even when mixtures containing 1000-fold more arochlor were tested. Discussion ensued about the relative merits of GC/MS/MS and GC/HRMS. Campana stated that extremely good mass resolution would be needed for GC/HRMS to approach the capabilities of GC/MS/MS for the analysis of dioxins in complex sample matrices.

Roger Hayes showed the utility of MS/MS for the rapid survey of complex mixtures for the presence of dioxins. He used a solids probe for sample introduction. It was summarized that MS/MS is good for the rapid analysis of targeted compounds.

Nick Kurlich discussed his experience with MS/MS sampling of ambient indoor air. These studies employed a commercial triple quadrupole instrument equipped with an atmospheric pressure ionization source. He suggested that most of the problems he encountered using this instrument were with sampling and ionization, and not with MS/MS.

Mary Sisak has used a similar triple quadrupole instrument to monitor ambient air, as well as volatiles in soils. On this particular commercial instrument, she viewed the cryogenic pumps used on the ionization source as a problem because they limited the actual time the instrument could be operated to 4-8 hours. Her experience suggested that the lower limits of detection were in the low parts-per-billion range using the atmospheric pressure ionization source. This particular source was better for polar compounds, whereas the low pressure chemical ionization source was better for a wider range of compounds. Saturation problems occurred when analyte concentrations were high, but again, these are source problems, not MS/MS problems. The overall method was viewed as difficult to assess for quality assurance/quality control purposes. Overall, she agreed that the technique was best suited for the rapid screening of targeted compounds and not for continuous monitoring.

Scott McLuckey described a new hybrid MS/MS instrument for rapid, high specificity environmental monitoring consisting of a quadrupole mass filter and time-of-flight analyzer. The advantages of this instrument is that it is relatively simple and has higher ion transmission (e.g., higher sensitivity) than a triple quadrupole; however mass resolution was lower than that of a triple quadrupole.

In summary, all of the speakers agreed that MS/MS has a number of advantages for detecting targeted compounds in environmental situations, including speed, high specificity, and high selectivity. At present, techniques for atmospheric sampling are a limiting factor for direct MS/MS analysis of air and better ionization sources are needed.

Submitted by:

Michelle V. Buchanan, chairman
Scott A. McLuckey

Presented at the 35th ASMS Conference on Mass Spectrometry and Allied Topics
May 24-29, 1987, Denver, CO

COMPUTERIZED ION OPTIC DESIGN MADE EASY

A Workshop of the Ion Physics and Instrumentation Interest Group

This workshop was organized to discuss use and abuse of currently available ion optics design and analysis programs. The workshop started off with three discussion leaders sharing their insights, experiences, and prejudices on the subject with the approximately 70 attendees.

The first speaker, Peter Todd from Oak Ridge National Laboratory, presented remarks for first-time users The central theme of his discussion was that the value of an ion optics program is related to the user's knowledge of the physics of ion optics. Knowledgeable users generally find that these programs are a real boon in their work. However, the novice user is often trapped and misled because of misunderstandings about the fundamental physics of ion optics. Todd felt the novice should read suggested references first before plunging into a modeling effort. Moreover, Todd shared a personal set of rules and perspectives for ion optics design. The most notable rule was "If you have a serious ion optics problem get an expert in ion optics to help you".

The second speaker, Jeff Wyatt from the Naval Research Laboratory, continued this theme with interpretations of electrostatic mirror designs obtained via the SIMION PC/AT program. Wyatt reminded the audience that the Laplace equation governs traffic in the ion optics arena. Thus in the absence of radial voltage gradients, horizontal voltage gradients must be linear or zero. This means that even poorly designed electrostatic reflectors will tend to have linear fields near their central axis whether or not the designer actually wanted them. Wyatt also showed ion trajectories in the vicinity of electrostatic grids. His point was to demonstrate that grids are really collections of many small lens elements that can and often do affect ion trajectories.

The third speaker, Jim Delmore from the Idaho National Engineering Laboratory, discussed the use of ion optics programs to assist in the analysis of experimental observations. Delmore's discussion example involved using the SIMION PC/AT program to confirm that three experimentally observed anomalous mass peaks were caused by ion production (via electron bombardment) on the first three lens elements of his instrument.

A business meeting was then chaired by Scott McLuckey of Oak Ridge National Laboratory. Lists of possible subjects for future symposia and workshops were created as well as a list of potential feature lecture speakers.

The remainder of the workshop was dedicated to demonstrations of SIMION PC/AT Version 3.0 by Tony Appelhans and David Dahl of the Idaho National Engineering Laboratory. Tony conducted a first time SIMION user class for approximately 30 people. Dave and about 20 current SIMION PC/AT users discussed the program's new features and assorted ion optics war stories. The workshop lasted about an hour longer than scheduled due to audience interest.

Respectfully submitted:

David A. Dahl

Presented at the 35th ASMS Conference on Mass Spectrometry and Allied Topics
May 24-29, 1987, Denver, CO

Fundamentals Workshop

Ionic Clusters: methods of generation and reactions.
Chairman: Michael T. Bowers

After a busy morning and afternoon for participants interested in fundamentals, a workshop on the above topic was held from 7 - 9.30 pm. on the Tuesday evening of the conference. About 12 short presentations, interspersed by discussion, covered a wide range of topics, mostly on metal clusters with a few on rare gas clusters.

Techniques and instrumentation used in the production of clusters, such as FTICR and expansion sources, were discussed but the major problems identified was that of trying to obtain quantitative information on the reactivity of metal clusters. A growing area of interest is in the occurrence of reactions on the surfaces of clusters to which a few speakers referred.

At its peak, the number of participants was in the region of 60-70 and although the number fell as the evening wore on, there were always enough to sustain a useful discussion. Perhaps because the subject is still relatively young, the workshop was used primarily to exchange information rather than to engage in controversial discussion: the latter will doubtless arrive when more is known of the problems involved in generating clusters and measuring their reactivity.

Presented at the 35th ASMS Conference on Mass Spectrometry and Allied Topics
May 24-29, 1987, Denver, CO

WORKSHOP

MS/MS CAD Database: Instrument Design and Operation Apposite to CAD Dynamics

Organizers: Richard I. Martinez (NBS) and R. Graham Cooks (Purdue U.)

(Attendance: ca. 180)

The purpose of this Workshop was to examine options for working toward a practical, standardized CAD spectral database for XQQ instruments (QQQ, BEQQ, etc.), and to discuss technical details of instrument design and/or operation essential to the successful development of such a database.

To provide a focus for the Workshop discussion, R.I. Martinez (NBS) presented an overview of published works which indicated that very different CAD spectra are observed for the same molecule on different QQQ instruments; i.e., the relative intensities measured in different QQQ instruments for any one pair of progeny ions differed by factors ranging into the hundreds, even though the same nominal operating conditions were supposedly used in each of the QQQ instruments. This suggests that current instrument designs and/or the choice of parameter settings provide a distorted view of the molecular dynamics of the CAD process (because of scattering losses due to poor ion containment within Q2, fringing fields between Q2/Q3, etc.). Hence, one observes instrument-DEPENDENT CAD spectra. He suggested that one could probably measure instrument-INDEPENDENT CAD spectra under kinetically-correct operating conditions. Workshop participants who use XQQ instruments agreed to participate in the NBS Round-Robin to provide a zeroth order assessment of which instrument designs are kinetically well behaved.

The following report is a summary of written comments submitted by the following participants:

R.K. Boyd (NRC, Canada); R.G. Cooks (Purdue U.); C.G. Enke (Michigan State U.); J. Fulford (SCIEX); J.H. Futrell (U. of Delaware); F. deMaack (Nermag); R.I. Martinez (NBS); F.W. McLafferty (Cornell U.); J.J. Monaghan (ICI); T.H. Pritchett (EPA); J.A.G. Roach (FDA); R. Schaeffer, S. Dheandhanoo, and S. Ketkar (EXTREL); A.E. Schoen (Finnigan); R.A. Yost, J.V. Johnson, and M. Hail (U. of Florida).

The key MS/MS parameters which can cause the relative intensities measured in different QQQ instruments for various progeny ions to differ significantly are:

(1) the number of collisions undergone by a "parent" ion within Q2, a parameter usually characterized in terms of "target thickness" [(actual path length traversed by the ion in its oscillatory trajectory through the gas target) x (effective number density of the CAD target gas)], and the type of target gas (influences the extent of energy transfer) ;
(2) the duration of the interaction between the "parent" ion and the target gas, which is determined by the collision energy for "parent" ions entering Q2;
(3) the energy level of the analyzing quadrupole Q3 relative to that of Q2 which, because of the translational energy distribution of the "progeny" fragment ions, determines whether or not some progeny ions can enter Q3;
(4) the Mathieu parameter q_z (rf voltage of Q2) and restrictive interquadrupole apertures of diameter <1.4 r_o, because of mass-dependent focusing effects which determine how effectively parent/daughter ions can be contained within Q2 for emittance (transmission) into Q3; and
(5) the type of detector used [Daly detector, Channeltron (with or without conversion dynode), etc.] because of differences in mass-dependent conversion gain.

When probed with crossed-beam apparatus, the reaction dynamics of the CAD process are found to be dependent on the internal energy, collision energy, choice of collision gas (deposited energy), scattering angle, and energy of the product ions. Hence, unless the dynamics are taken into account, results in XQQ instruments will be highly instrument dependent, even though reproducible conditions can be established for analytical purposes {with few exceptions, measurements for any given ion within any one XQQ instrument exhibit long-term (9-month interval) reproducibility (precision) to within ±10%; one lab reported this precision for 3 different XQQ instruments (QQQ, BEQQ, EBQQ)}.

One example was cited to emphasize the need for proper accounting of CAD dynamics in XQQ instruments: for perfluorotributylamine, the relationship $E_{daughter} = (m_{daughter}/m_{parent})^n E_{parent}$, between the kinetic energy of the m/z 264 fragment ion ($E_{daughter}$) and that of the m/z 414 "parent" ion (E_{parent}), changes from n= 1 to n= 2 as the Ar gas target thickness is increased: hence, the choice of Q3 pole bias (rod offset) and target thickness will significantly affect the intensity measured for the m/z 264 fragment ion relative to that of other fragment ions.

Major classes of MS/MS experiments: (i) Mixture Analysis [quantitation with or without prior separation (speciation)] and (ii) Structure Elucidation ["isolated" neat compound (prior separation)]. For (i), precision within any one XQQ instrument is critical, and goal is to maximize sensitivity for characteristic daughter ions; need different "standardized" conditions for different substructure classes to compensate for differences in CAD dynamics. For (ii), goal is to maximize number of structurally-significant daughter ions. For both (i) and (ii) it would be very helpful to identify each MS/MS peak according to the collision energy and target thickness required to produce it; this would provide the input necessary for an intelligent program to qualitatively predict a spectrum [cf. presence/absence algorithms [see (b) below]].

For the identification of unknowns, some Government agencies are required by statute to match the spectrum of an unknown to that of a pure standard sample or to a "standard spectral library", following strict criteria for matching the relative ion intensities [presence/absence algorithms [see (b) below] for daughter ions would not suffice for this type of work]. Hence, such agencies need standardized operating conditions and a standard reference library (database) for CAD spectra.

A proposal was made that if all manufacturers were to fully characterize their instruments with respect to the key MS/MS parameters, it may become possible to obtain correction factors with which each type of instrument could be adjusted (following some protocol) to give the same CAD spectra within reasonable limits. If such an approach were to succeed, it might resolve statutory problems faced by Government agencies which use a variety of XQQ instruments from different manufacturers.

Summary of some of the proposals made for conceptually-different CAD databases [symbols designate how each type of proposed database can potentially be utilized: EY (EN)= can (cannot) elucidate structure of <u>unknown</u> compound <u>not</u> included in database; QY (QN)= can (cannot) quantitate <u>unknown</u> compound <u>not</u> included in database]:

(a) EY/QY- Kinetically-correct (single-collision conditions) CAD database of absolute cross sections for the CAD of ionic substructures measured under standardized operating conditions (may have to use different standardized conditions for different substructure classes to compensate for differences in CAD dynamics)

(b) EY/QN- Collect complete MS/MS "map" (all the daughters of all the parents) under single-collision conditions and relatively high collision energy; database based on the presence (bona fide neutral loss) or absence of ion signal at particular combinations of parent and daughter masses (correspond to specific ion substructures); spectrum matching algorithms that weight the presence/absence of peaks more and the relative ion abundances less yield better daughter spectrum matches than the algorithms borrowed from matching normal mass spectra.

(c) EN/QN- Analytically useful (but not necessarily kinetically-correct) reference spectra to be used within either one single XQQ instrument or within many XQQ instruments of the same model (one manufacturer) operated under identical, standardadized conditions.

(d) EN/QN- Based on current knowledge, prescribe pseudo-standard conditions (e.g., 70 eV for electron impact ionization), and collect a very large number of contributed CAD "reference" spectra (masses and abundances) from all types of XQQ instruments; statistical analysis will provide a basis for a search algorithm for structure elucidation ("quality index", etc.), and for fine-tuning the standardization rules as our knowledge grows.

Presented at the 35th ASMS Conference on Mass Spectrometry and Allied Topics
May 24-29, 1987, Denver, CO

WORKSHOP

NEW TECHNIQUES FOR DESORPTION IONIZATION OF LIQUID SAMPLES

Several new methods for the desorption ionization of samples contained in liquid matrixes were discussed, including continuous flow FAB, subambient LSIMS, and thermally assisted FAB. The purpose of the workshop was to have an active discussion of these techniques among those currently using them so that experiences could be exchanged and also to provide others present additional information. The total attendance at the meeting was in the range of 250-300 people.

The continuous flow FAB probe was discussed both from an operational and performance point of view. The method generally provides decreased background, increased sensitivity, and decreased ion suppression effects relative to the 'standard' FAB method. It was stressed that the best performance was obtained when a thin liquid film was achieved on the probe tip from the proper balance of liquid flow rate, pumping efficiency and heat. For most instruments, flows of 5-10 µL/min and temperatures of about 40-70 C produced stable operation. It was found that a number of users had employed several different types of solvent systems, including water containing 5% glycerol and completely organic solvents such as toluene. Temperature adjustments were necessary to achieve stability with different solvent systems. Parameters such as probe tip design and shape, and orientation of the probe in the instrument are not considered to be major factors in obtaining stability or optimum performance, although it is recognized that some of these factors may differ from instrument to instrument. The nature of the tip surface is believed to play a significant role in obtaining stability with easily wettable surfaces being best. Contamination of the source was not found to be a major problem. Several users reported cleaning their source not more often than either a CI or EI source. A number of laboratories reported continuous operation of the probe for 6-8 hours with no apparent deleterious effect on the performance of the probe or the mass spectrometer.

Subambient LSIMS was discussed in view of the extended duration of the signal produced when the temperature of the liquid matrix was maintained at about 2°C. Using a coolable probe, signals could be maintained for 30 min or more in many cases. Thus, liquid solvents such as thioglycerol and tetraglyme could be readily used. The spectra were also characterized by a decrease in the background relative to that normally seen with FAB. Several others in attendance also have seen similar results using several methods of cooling the probe tip.

Thermally assisted FAB is a technique where substances which are normally too immobile to act effectively as a FAB matrix are heated to a fluid state using a heatable probe. Spectra were successfully obtained using aqueous solutions of saccharides such as fructose and glucose. Spectra are charcterized by intense molecular ion species from the analyte and decreased matrix cluster ions which are normally seen in FAB when glycerol or a similar liquid is used.

Submitted by Richard M. Caprioli
Workshop organizer

Presented at the 35th ASMS Conference on Mass Spectrometry and Allied Topics
May 24-29, 1987, Denver, CO

PROBLEMS IN APPLICATIONS OF RIMS TO ISOTOPE RATIO MEASUREMENTS

Isotope Ratio Interest Group Workshop

Resonance ionization mass spectrometry (RIMS) has intrigued isotope ratio practitioners since the early eighties because of its potential for high elemental selectivities and sensitivities. However, the technique has yet to be applied widely. The purpose of this workshop was to review the development of RIMS techniques and identify factors of particular concern for isotope ratio measurement.

The speakers were all from laboratories well experienced with RIMS and they discussed the RIMS processes systematically from atom formation to ion detection, as follows: Atomization, L.J. Moore; Multiphoton Ionization, C.M. Miller; and Detection, J.D. Fassett. Larry Moore discussed three mechanisms for generation of atomic vapours: thermal, ion sputterred, and laser ablated. Thermal vaporization yielded the narrowest energy distributions, but sputterring or ablation were much better matched to the duty cycles of pulsed lasers. Both sputterring and ablation yielded sufficient ground state populations; for example, 65% for Fe by ion sputterring. Some important applications of RIMS to surface analysis of semiconductors were identified.

Charley Miller reviewed many practical excitation schemes for a wide variety of elements as atomic vapours. He identified some of the pitfalls, which generally have solutions. In cw excitations, optically-induced redistributions of magnetic substate populations and weak branchings to intermediate metastable states can alter peak height ratios and lineshapes. Hyperfine splittings can enhance excitation of one isotope more than another; this is usually avoided by use of laser bandwidths $\geq 1\ cm^{-1}$. In pulsed excitations, amplified spontaneous emission can cause unwanted population of intermediate states and degradation of selectivity. Most of these pitfalls can be avoided by judicious selection of excitation schemes and adjustment of laser parameters such as power and focal volume. More details were presented in the poster sessions by Brian Fearey (RPA 27) and Denise Parent (RPC 41).

Jack Fassett discussed detection techniques for RIMS, and mentioned that one of the advantages of cw lasers is that the detection methods are identical to those used for thermal ionization, and hence are well developed. For pulsed laser ionization, either transient digitizers or pulse counters must be used. Currently available digitizers do not have the resolution or data processing speed for direct single ion pulses, for example the bit resolution of an 8 bit digitizer decreases to only ~4 bits for a 100 MHz frequency signal. For single detector magnetic sector systems, the signal may be stretched out with a high input impedance amplifier and recorded with a transient digitizer. For time-of-flight systems, pulse counting with time-to-digital convertors or gated counters may be used for weak signals, and transient recorders for strong signals (~1000 ions/pulse). However, the mass resolution of time-of-flight spectrometers deteriorates at higher signal strengths. Poisson statistics can be used to test for absence of dead time errors in pulse counting. More details were presented in the symposium on Lasers and Mass Spectrometry on Monday by Jack Fassett (MOC 1145) and Larry Green (MOF 515).

In summary, resonance ionization mass spectrometry can be applied to many practical analyses, but its acceptance is slow because most isotope ratio laboratories are accustomed to and equipped for chemical purification/thermal ionization methods.

Attendance at the workshop was good, ~50, but time restrictions limited the discussions. Phil Hemberger elicited suggestions for a symposium topic next year, and most attendees supported a multidisciplinary isotope ratio session.

L.W. Green

Presented at the 35th ASMS Conference on Mass Spectrometry and Allied Topics
May 24-29, 1987, Denver, CO

REPORT OF THE BIOMEDICAL APPLICATIONS INTEREST GROUP MEETING

The biomedical applications interest group meeting was held immediately following the workshop on desorption ionization of liquid samples. The main purpose of the meeting was to provide members with an opportunity to discuss and make suggestions for topics they would like to have covered at the next ASMS meeting. In particular, this included suggestions for a plenary lecture, symposia and workshops.

It was suggested by several of the members that a plenary lecture be given in the general aspects of molecular biology, particularly as it may be applied to areas of interest to members of ASMS. It was stressed that this should be a presentation by a teacher and skilled lecturer who will be able to provide a grasp of basic concepts to those not skilled in the art of applications of molecular biology to modern biomedical research.

Several symposium topics were suggested. The first suggestion was to have a session devoted to continuous flow FAB. Speakers would present a diverse number of applications and techniques involving this method of sample introduction using FAB. At least one talk could be directed at aspects concerning the art and practice of successfully using the technique. A second symposium suggestion was to broaden the scope of the first by including other types of liquid capillary interfaces which are used either as separation devices or introduction devices that are connected directly to a mass spectrometer. Third, several members thought that a symposium based on the quantitative analysis of peptides derived from biological sources would be of great value. Presentations would include both applications as well as practical aspects of achieving good precision and accuracy.

Two workshop suggestions were made. The first would be based on the approaches for combining capillary zone electrophoresis and mass spectrometry. From indications at this meeting, it was thought that there will be several groups who would be submitting papers next year and that a workshop discussing principles, problems, and applications would be timely. A second suggestion would involve a detailed discussion of the techniques involved in the quantitation of peptides derived from biological sources. It was stressed that this might include a tutorial-like discussion led by one or more of the people in the field who have been successful in this area.

Finally, members were, and are, encouraged to write the Vice-President for Programs or myself with further suggestions concerning the ASMS meeting next year. Our interest group represents many members with a wide diversity of interests and talents. Your views, concerns, and expectations regarding the program for next year are vital inputs.

Submitted by Richard M. Caprioli

Presented at the 35th ASMS Conference on Mass Spectrometry and Allied Topics
May 24-29, 1987, Denver, CO

Computer Applications Interest Group Business Meeting

This year's interest group business meeting followed the "Chemometrics for Everyone" workshop. A number of delays forced the workshop to unprecedented lengths, and by the time the business meeting came to order, the audience had thinned considerably. Those who remained were heartily congratulated.

The interest group chairman began by announcing that the much awaited ASMS bulletin board system (BBS) is now operational and eagerly awaiting business. The telephone number for the new board, christened "SpecNet", is (816) 363-5199. Baud rates of 300/1200 are supported. If problems are encountered when attempting to access SpecNet, please call Jon Onstot at (816) 753-7600. The board currently supports public and private message sections, a bulletin section for society related news, and file upload/ download capabilities. As the BBS is still in its infancy, suggestions for additional features were solicited. Responses included an electronic job opportunity section, a database of academic laboratories and a database of current products from the various instrument manufacturers.

Ideas were also solicited from the audience for future workshop topics, but the sleepy faces in the crowd indicated that further discussions would be fruitless. The chairman asks that persons wishing to see a particular topic discussed at next year's conference please leave a message on SpecNet, or contact me personally.

Respectfully submitted,

Jon Onstot
Computer Applications Group Chairman

Presented at the 35th ASMS Conference on Mass Spectrometry and Allied Topics
May 24-29, 1987, Denver, CO

ENVIRONMENTAL INTEREST GROUP REPORT
DENVER 1987

The Environmental Interest Group held its annual meeting prior to the workshop on "Applications of MS/MS to Environmental Problems". A report on this workshop is included in this volume. The meeting was attended by about 100 people. A number of subjects were suggested for workshops and/or symposia for next year, including:

- Applications of supercritical fluid and liquid chromatography with mass spectrometry
- Analysis of closed environments (e.g., indoor air, submarines, space vehicles)
- Atmospheric ionization and other ionization techniques for air monitoring
- Analysis of targeted compounds
- Quality control data for quantitative measurements
- What does EPA do with priority pollutant data?

A number of suggestions were offered with respect to organizing future meetings. One person suggested that the full three hour period for poster sessions was too long for authors to be present. It was thought that an hour and a half would be more reasonable, with the poster displayed for the full three hours. It was also suggested that the poster sessions end at noon so the authors could have lunch and attend afternoon sessions.

It was thought that the poster sessions should be organized so only half of the posters in one session be on one topic. This would make it easier to attend both the oral presentations and the poster session at the same time.

Another comment was that the meeting topics should be grouped together so people would not have to stay the entire week of the meeting. This was countered by others who argued that they like having the meeting organized as it is at present, so they could take advantage of learning about progress in a variety of areas.

Submitted by:

Michelle V. Buchanan
Oak Ridge National Laboratory

Presented at the 35th ASMS Conference on Mass Spectrometry and Allied Topics
May 24-29, 1987, Denver, CO

Report on Fundamentals Interest Group Meeting

The meeting was held towards the end of the Workshop on clusters on the evening of Tuesday, 26 May 1987 with approximately 35 persons in attendance.

Four subjects were proposed for symposia. Because of the proximity of the meeting to various institutions in the region of San Francisco, there was substantial support for a symposium centred on Synchrotron Radiation and Photoionisation Phenomena and, in view of the subject matter of the workshop, it was to be expected that there was almost equal support for a symposium on Cluster Ions. There was only slightly less support for a more general symposium on The Interaction of Theory and Experiment in Gas Phase Ion Chemistry, a subject proposed from the chair in view of representations made by several members of the Fundamentals Interest Group who were unable to attend the meeting. If one takes these representations into account, the level of support for all three symposia was very similar. Somewhat lower support was given to a suggestion of a symposium on Interstellar Chemistry although (see below) this might form a suitable subject for a workshop.

It was recognised that the meeting was not necessarily representative of the views of the Fundamentals Interest Group as a whole since some (inexplicably ?) chose not to attend the Workshop on Cluster Ions. Furthermore, it was also recognised that subject matter proposed by other interest groups would influence the final choice of topics and speakers just as at the Denver meeting, care was taken to avoid overlap between the Fundamentals Symposium and that on Lasers in Mass Spectrometry. Nevertheless, there was strong support for at least two half-day symposia sponsored by the Fundamentals Interest Group.

Three plenary speakers were discussed, the final choice of whom will depend on the choice of subjects for symposia. On a show of hands at the meeting, the speakers were placed in the following order: Y T Lee (chemical dynamics), L Radom (theory of ionic structures), J Tröe (kinetics of ion-molecule reactions).

Two titles were suggested for workshops, Cold Ions and Interstellar Chemistry, and in view of the lively discussion in several fundamental sessions, there might still be some interest in a workshop in Internal Energy Effects in ionic reactions

K R Jennings

Presented at the 35th ASMS Conference on Mass Spectrometry and Allied Topics
May 24-29, 1987, Denver, CO

ISOTOPE RATIO INTEREST GROUP REPORT

This year's interest group meeting followed a workshop on Resonance Ionization Mass Spectrometry, convening on May 28, 1987. Approximately fifty people attended the workshop and meeting.

The workshop, "Problems in Practical Applications of RIMS to Isotope Ratio Mass Spectrometry," covered the problems and caveats associated with RIMS. It was organized by Lawrence W. Green and gave an excellent overview of the methodology.

The discussion following the workshop centered on two topics:
1. Suggestions for next year's program.
2. How to attract greater interest, participation, and appreciation of the Isotope Ratio Interest Group.

A symposium in which applications of isotope ratio mass spectrometry in Life, Earth, and Physical sciences are presented was recommended. Two workshops were suggested - "The Status and Future of Standards in Elemental and Isotopic Analysis," which would be of general interest outside the Isotope Ratio Interest Group, and "A Manufacturer/User Forum" to discuss the present capabilities of commercial isotope ratio instruments and future areas of instrument development.

The Group agreed that it is important to open active lines of communication within our Group and to attract the attention and interest of those from other areas of inorganic mass spectrometry and instrumentation. As a first step towards this goal, I will initiate a news letter and a mailing list that will be distributed within our Group and to those in related fields. Those who wish to be included on the mailing list may write to me. The participation of investigators from disciplines such as geology and atmospheric science would be a valuable asset to our Group and to future ASMS conferences. The Group hopes to encourage and stimulate such participation.

P. H. Hemberger
Isotope Ratio Interest
Group Chairman

Presented at the 35th ASMS Conference on Mass Spectrometry and Allied Topics
May 24-29, 1987, Denver, CO

Interest Group: Qualitative Organic Analysis

This group met at 1.00 p.m. on Tuesday, May 26th. About fifty persons attended.

The question of symposia and/or workshops for the 1988 ASMS meeting was discussed at length. It was clear from an almost unanimous show of hands that symposia are unpopular, insofar as there is no time for discussion. Several suggestions were made for arrangements which should give rise to a greater exchange of ideas. One such is described below.

Proposed items for future consideration were:

(a) The present role of isotopes in mass spectrometric studies;

(b) The increasing use of ion-molecule and ion-radical complexes as stable intermediates in both unimolecular and bimolecular gas phase ion studies.

The second title is not precise, but Dr. D. McAdoo who proposed the subject will be assisting J.L. Holmes in sharpening the focus of what could prove to be a stimulating series of presentations and which would include ample discussion time.

Before the meeting adjourned it was proposed that this interest group be renamed "Physical-Organic Mass Spectrometry". It was concluded that this indeed expressed more adequately the concerns of those present. Hereafter this shall be the title for this group.

The meeting adjourned at 2.15 p.m.

Suggested format for discussion-workshop.

(i) Morning: Authors would have five minutes to state the key finding or proposal which is illustrated by their poster presentation.

(ii) Afternoon: Posters available for inspection. Authors present for part of the time (?).

(iii) Evening: Group discussion, centred about the poster presentations.

Comments: For this to be successful, the selected central topic for the workshop would have to be quite well defined; much would depend upon the individual who acted as discussion leader/coordinator at the evening session. The number of posters should perhaps not exceed fifteen?

Submitted by: J.L. Holmes

Presented at the 35th ASMS Conference on Mass Spectrometry and Allied Topics
May 24-29, 1987, Denver, CO

QUANTITATIVE ORGANIC ANALYSIS INTEREST GROUP

The quantitative organic interest group held a workshop entitled "Quantitative analysis of lipid derived mediators". The major focus of the workshop was to present realistic approaches to the analysis of these complex, thermally labile substances. Three major groups of arachidonic acid metabolites were discussed together with a section on phospholipids with particular reference to platelet activating factor.

Dr. Bob Murphy from the University of Colorado began the workshop with a discussion of some of his elegant work on the analysis of lipoxygenase metabolites of arachidonic acid. He illustrated the use of ^{18}O-labelled internal standards that can be employed to overcome the enormous problems involved in the synthesis of deuterated standards. He further discussed his desulfurization procedure for the analysis of sulfidopeptide leukotrienes.

Dr. Ian Blair from Vanderbilt University discussed some of his recent work on the quantitative analysis of epoxygenase products of arachidonic acid. He showed the difficulties involved in the separation of the different isomers. He illustrated how it was possible to carry out quantitative determinations of a mixture of all four possible epoxides. The carboxylic acids were converted to pentafluorobenzyl ester derivatives and analyzed by GC/MS using negative ion chemical ionization detection. He demonstrated that separation of the individual isomers could be achieved by hydrogenation of the unsaturated lipid to the corresponding saturated epoxide. Further specificity of analysis was achieved by observing the fragmentation pattern under negative ion conditions.

Dr. Keith Clay from the University of Colorado described his recent work on the analysis of platelet activating factor. He showed how the acyl group can readily migrate subsequent to removal of the phosphocholine moiety to the 3 position in the case of ether lipids and to both the 3 and 1 position for acyl lipids. He showed that sensitivity of analysis was greatly improved by the use of negative ion chemical ionization mass spectrometry. He further showed that pentafluorobenzoyl derivatives readily captured thermal electrons in the gas phase to give intense M^- ions. This contrasted with pentafluorobenzyl derivatives of the leukotrienes and epoxides. They underwent heterolytic cleavage reactions to give intense M-PFB ions.

Dr. Jim Vabanac from the Medical University of South Carolina illustrated the use of tandem mass spectrometry on a Nermag R30-10 TSQ for the quantitative analysis of prostanoids. His presentation focussed on the quantitative analysis of thromboxane B_2. He demonstrated that the use immunoaffinity chromatography in combination with short capillary columns and MS/MS allowed a rapid throughput of samples. He also described his attempts at causing specific fragmentation of negative ions using collisional activation.

In conclusion, it was evident that negative ion chemical ionization afforded the most sensitive method for the analysis of lipid derived mediators. However, the advent of MS/MS techniques raises the possibility that electron impact methods in combination with collisional activation will have utility in situations where there is a relatively higher abundance of the analyte. Over 100 members took part in what turned out to be a very lively workshop.

Subsequent to the workshop an Interest Group Meeting was held. Several suggestions were received for Workshops next year: 1) Quantitative analysis of peptides. 2) In search of the ultimate sensitivity for quantitative analysis. One suggestion was received for a Symposium: Structural characterization of unknown biomolecules.

Submitted by:

Ian A. Blair, Ph.D.
Vanderbilt University

Presented at the 35th ASMS Conference on Mass Spectrometry and Allied Topics
May 24-29, 1987, Denver, CO

ASMS INTEREST GROUP ON SOLIDS AND SURFACE ANALYSIS

WORKSHOP REPORT

"Static Secondary Ion Mass Spectrometry of Organic Molecules"

The workshop was held on Thursday evening, May 28, from 7-9 p.m. About twenty people attended. The purpose of this workshop was to address the following questions:

In what cases is SIMS useful and when should SIMS not be attempted?
Can masses greater than 5K be observed by static SIMS?
What is known about the sensitivity of SIMS on various instruments using quaternary ammonium salts as test compounds?
If a unique instrument could be built, what would it consist of to obtain maximum sensitivity and resolution?
What (if anything) hinders SIMS from being as widely used as FABMS?

After a brief introduction by David Kidwell (NRL) about the purpose of the workshop several speakers gave informal discussions on instrument design and on questions related to mechanisms of ion production in FABMS.

K. Bush (U. Indiana) presented his design for a scanning SIMS instrument to analyze materials on chromatography media. The advantages of such an instrument are: the separation power of chromatography and the detection capability of mass spectrometry. Bush emphasized that for optimum performance in his quadrupole based system, a liquid matrix must be applied to the chromatography medium to allow high primary ion beam currents and thus high secondary ion currents. The matrix must be in the liquid phase only during ion bombardment and solidify at other times to minimize diffusion and loss of chromatographic separation.

K. Standing (U. Manitoba) presented his time of flight instrument which uses a reflectron design. With this instrument, resolution of better than 8K Daltons has been demonstrated. No post acceleration is used and yet detection of masses >10K Daltons have been observed with a 10 KeV secondary ion beam energy.

A. Benninghoven (U. Munster) distinguished his design for a time of fight from that of Standing in having mass separation in the primary ion gun and post acceleration. Primary ion mass separation allows all the primary ions in the primary pulse to arrive simultaneously. This decreases the spectral background by minimizing time spread in the resulting secondary ion pulse.

P. Todd (Oak Ridge) discussed some of the inconsistencies in the ion diffusion model of surface renewal in FABMS. Todd brought-out that diffusion of molecules in glycerol is too slow to provide surface renewal. Therefore, in the high primary ion currents used in FABMS, the surface layer should be quickly removed and the bulk concentration examined. Several models of surfactant character to molecules influencing the FABMS spectra were called into question.

In examining instrument designs for static SIMS analysis, a time of flight instrument design of the reflectron type, with a post acceleration conversion dynode is desirable. For dynamic SIMS or FABMS, with the higher secondary ion currents, any mass analyzer can be used. No sensitivity comparisons were made on any test compounds for the instrumental types examined. Hindrance in the use of static SIMS arises from the low secondary ion fluxes produced which necessitates TOF analyzers.

Since there was a general agreement among participants that there is no difference between the analytical capabilities of static SIMS and FABMS, the workshop next year will concentrate on mechanisms of ion formation and/or imagining of organic molecules from biological materials. The development of hardware and software will be emphasized in the imaging of biological materials.

Presented at the 35th ASMS Conference on Mass Spectrometry and Allied Topics
May 24-29, 1987, Denver, CO

Young Mass Spectrometrists Interest Group Report

The Young Mass Spectrometrists Interest Group was involved with two functions this year. The first was the traditional Sunday evening get-together. In the first part of this meeting, Burnaby Munson led off with a discussion of the history of ASMS. He told entertaining stories of "palace revolts" and of how the society and the conference have evolved over the years. Specifically the major changes in the meeting that were discussed included the increasing attendance (and the effect on the meeting site), changing emphasis/fields of interest (inorganic to biomedical), and the advent and increasing popularity of poster sessions. Next, Graham Cooks spoke about research, and mass spectrometry/instrumental research in particular, in a very enlightening and thought-provoking presentation. He concluded with a brief discussion of the present structure of ASMS (the Society and the Conference) and of ways in which young mass spectrometrists can get involved. After some discussion and a beer break, a general meeting of the Interest Group was held, which comprised the second part of this function. Ideas were solicited for Interest Group functions at the 1988 ASMS Conference. After some discussion, the consensus was that there should be a workshop organized on proposal writing. Members of academic, industrial, and government laboratories agreed that all could benefit from such a workshop. The preliminary plan is that senior members of ASMS could share their experiences after some general principles on the subject were presented, possibly by a professional. Other workshop ideas that were mentioned included discussion of careers, postdoctoral positions, and scheduling of athletic events at ASMS Conferences. It was agreed that this Sunday evening function is an excellent opportunity for young mass spectrometrists to meet and share experiences before the main conference begins, and this tradition should be continued. Many young mass spectrometrists, for whom this was their first ASMS conference, especially benefitted from the information given in Graham Cooks' talk on the society and the meeting, and it was suggested by many that this become an annual event.

The second function sponsored by this Interest Group was a workshop on the preparation, editing, and review of scientific manuscripts. A panel of four editors of relevant journals (Catherine Fenselau - Biomedical and Environmental Mass Spectrometry, Klaus Biemann - Analytical Chemistry, Mike Bowers - International Journal of Mass Spectrometry and Ion Processes, and John Holmes - Organic Mass Spectrometry) was assembled. After some introductory remarks by Professor Holmes (whose idea this workshop topic was) on general do's and don't's of manuscript preparation and on the functions and responsibilities of the author, editor, and reviewer there was a lively question-and-answer period. The discussions ranged from how to deal with seemingly unfair reviews to the relative advantages and disadvantages of rapid communications versus full papers. This workshop served not only to educate younger mass spectrometrists on manuscript preparation and how to deal with editors and reviewers but also helped to reduce some of the often adversarial feelings that can exist between the corresponding parties in the manuscript publication process.

Both of the meetings were well-attended and the discussions served as evidence of many interested and enthusiastic young mass spectrometrists.

Submitted by

Mark Ross

Mark Ross

Presented at the 35th ASMS Conference on Mass Spectrometry and Allied Topics
May 24-29, 1987, Denver, CO

ASMS Education Committee Report

ASMS once again sponsored a series of short courses on the weekend preceding the Annual Conference. As in prior years, course evaluations received from the students indicated that the courses were very successful, with most students achieving their goals. This year's short courses and organizers were as follows:

Interpretation of Mass Spectra - James Kelley
Quantitative Mass Spectrometry - Alfred Yergey
Electronics of Mass Spectrometry - Christie Enke
Fourier Transform Mass Spectrometry - Robert McIver, Jr.

As one of the few committees in ASMS, a prime charge to the newly constituted Education Committee was to develop a mission statement for the educational role of ASMS and, therefore, the purview of the Education Committee. The adopted mission statement is:

> The mission of the ASMS Education Committee is to inform, educate, and promote understanding at all levels about the science and practice of mass spectrometry.
>
> In carrying out this responsibility, ASMS has the role of educating non-specialists about the benefits of mass spectrometric data to their research, of educating new mass spectrometrists on proper use of the technique and the data it generates, and of providing continuing education for all mass spectrometrists.
>
> To fulfill this role, the Education Committee will develop approaches and instructional materials to accomplish its mission and to foster activities which will increase the awareness, knowledge, and quality-of-practice of the science of mass spectrometry.

To obtain input on the priority of various educational activities which the Society might undertake, a workshop was held on Educating the Masses on Masses. Topics for discussion included: The ASMS Role in Education; Continuing Education of ASMS Members; Education of the Scientific Community In the Science of Mass Spectrometry; and ASMS Responsibility for Research Ethics Issues. A large part of the discussion focussed on the support ASMS provides for local discussion groups and the educational role that these discussion groups can undertake. It was recommended that ASMS supply names of potential speakers and ideas for discussion topics at local meetings. It was recommended that educational materials be provided to local discussion groups, so they can provide short courses and other educational activities.

There was considerable interest and opinion expressed on mass spectrometric education provided in university and industrial environments. It was recommended that ASMS assist or encourage university educators to provide more instruction in mass spectrometry. As a starting point, it was recommended that ASMS survey universities to ascertain what is currently being taught about mass spectrometry, and which institutions are providing such instruction on a regular basis. It also would be important to determine what instructional materials are being used in courses in universities, as well as in the many courses that are being taught in industrial environments.

It was recommended that ASMS encourage ACS to include more mass spectrometry training in ACS approved curricula and encourage ACS to stimulate mass spectrometry education in the university system. It was the sense of the attendees at the workshop that the symposium on state-of-the-art research in mass spectrometry was very worthwhile and should be continued in the future, with a regular rotation through the research of the different interest groups in ASMS.

The introductory short courses on Interpretation of Mass Spectra and Quantitative Mass Spectrometry should continue to be offered on a regular basis. In addition, advanced topic short courses should be offered with a rotational schedule, so that each year

several different short courses are offered. The courses of highest priority to the workshop attendees were: MS/MS, Practical CI, LC/MS, and FAB. This priority reflected current desires, combined with knowledge of those courses which had recently been taught and, therefore, should be moved to a later date on a rotational schedule.

At a meeting of the Education Committee, whose membership is Ann Goetz, Paul Goodley, Al Yergey and Harry Hertz, the following activities were given priority for the coming year: organizing a second symposium on State-of-the-Art Research in Mass Spectrometry and a workshop on the research ethics issues associated with credibility of data. Furthermore, the following major assignments were taken on by members of the ASMS Education Committee:

Exploring the possibility of putting classic books in mass spectrometry on laser discs -- Al Yergey

Conducting a survey on educational materials available for instruction in mass spectrometry -- Paul Goodley

Proposing ASMS outreach activities in basic mass spectrometric education (e.g., videotapes and brochures) -- Ann Goetz; and

Education by way of short courses -- what should be offered -- where and when? -- Harry Hertz

The Education Committee will be making a proposal for carrying out these activities to the ASMS Board of Directors during the course of this year.

Respectfully submitted,

Harry S. Hertz

Presented at the 35th ASMS Conference on Mass Spectrometry and Allied Topics
May 24-29, 1987, Denver, CO

BUSINESS MEETING OF THE AMERICAN SOCIETY FOR MASS SPECTROMETRY

Marriott Hotel City Center
Denver, Colorado
May 27, 1987

The meeting was called to order at 10:45 a.m. by President Meisels. Harry Hertz was appointed as the parliamentarian for the meeting.

Robert McIver presented the Secretary's report. The minutes of last year's Business Meeting are contained in the Proceedings of the 34th Annual Conference. It was moved, seconded and approved by those in attendance that the minutes of the meeting be accepted as printed. The Secretary then announced the proposed amendment to Article IV of the ASMS Constitution was passed by a ballot vote of 593 in favor, 155 opposed. Paul Goodley was appointed to serve for one year as the third member-at-large with responsibility for measurements and standards.

McIver announced the results of the 1987 election. The new Secretary is Susan T. Weintraub, the Vice President for Arrangements is Gary L. Glish, and the Member-at-Large with responsibility for the Bound Volume is Willard W. Harrison. The other candidates - W. D. Jamieson, Philip S. Berger, and Douglas P. Ridge - were acknowledged and applauded by the members.

McIver then announced the winners of the 1987 ASMS Student Travel Awards. They are Rowland S. Annan, Kevin D. Ballard, Ionnis V. Bletsos, Mark D. Brickhouse, Paul W. Geno, Stephen L. Howard, I. A. Kahwa, Edgar D. Lee, Mike S. Lee, C.-K. Meng, Roger S. Mercer, Marina Rincon, Hun Young So, John R. Yates III, and Emirgul Tolum. Each awardee received a $300.00 stipend, payable in cash or equivalent airfares or hotel accommodations.

McIver concluded his report by stating that it was his sad duty to inform the membership of the passing away of Thomas J. Francl.

Treasurer Kelsey D. Cook began his report by stating that ASMS has assets totaling $302,345. The SIMS Conference held in Washington, D.C. had a surplus of $6,400. The Board has allocated $3,000 of this for a SIMS symposium next year at the San Francisco Annual Conference, and the remainder will be used as seed money for the next international SIMS conference held in the U.S. around 1991. Cook reviewed the ASMS Balance Sheet as of April, 1987. He emphasized that the Board has come very close to making each ASMS activity self supporting. There were no questions from the floor. It was moved, seconded and approved by the membership that the Treasurer's report be accepted.

Catherine E. Costello, Vice President for Arrangements, began her report by saying that attendance at the Annual Meeting has set a new record. She said that since many members had expressed displeasure with overlapping the meeting each year with the Memorial Day weekend, the schedules have been arranged so there are no overlaps for the next three meetings. Next year the Annual Meeting will be held in San Francisco at the Hilton Hotel from June 5-10. In 1989 we will meet in Toronto at the Royal York Hotel from May 21-26. The 1990 Annual Conference will be held in Tucson, Arizona at two hotels, the Westin La Paloma and the Ventana Canyon. Even though these hotels are five miles apart, the Tucson site has excellent facilities and provides a welcome change of pace from the downtown, urban settings used previously.

Ronald A. Hites, Vice President for Programs, acknowledged the work of this year's Program Review committee (Ian Blair, Michelle Buchanan, Richard Caprioli, Graham Cooks, Catherine Costello, Gary Glish, Gerry Meisels, and John Onstot). This committee sorted the abstracts according to topic and each abstract was read by two members of the committee. This year at the Annual Conference there are 6 plenary talks, 62 symposia talks, 166 oral presentations, and 439 poster presentations for a total of 673. There were 66 submitted abstracts that were not included in the final program. Some members commented that there should be an appeals procedure established next year so that an author has an opportunity to revise the abstract. Also, there was support for the idea of expanding the poster sessions as needed so that all members have an opportunity to present their work.

Charles N. McEwen, Member-at-Large in charge of the Bound Volume, reported that extended abstracts were submitted for 91% of the papers presented last year in Cincinnati. There were 2550 copies of the Bound Volume printed, and each was 1290 pages long. Unfortunately many foreign members did not receive their copies because the shipping agent lost them.

Christie G. Enke, Member-at-Large for educational activities, described his responsibilities as coordinator for the Short Courses and the Fall Workshop. This year there were four ASMS Short Courses, Interpretation of Mass Spectra, Quantitative Mass Spectrometry, Fourier Transform Mass Spectrometry, and Electronics of Mass Spectrometry. Total attendance at the Short Courses was around 100. This year the topic of the Fall Workshop is "Mass Spectrometric Approaches to the Analysis of Biopolymers." It is being organized by Chuck McEwen and will be held in Boston on October 29-30.

In the President's report, G. G. Meisels focused on three fundamental issues facing the Society. First, he stated that he would like ASMS to be the mainstream organization for those who make their living by mass spectrometry. The Annual Conference focuses on the research interests of the members, and educational needs are addressed by activities such as the Short Courses. The ASMS Fall Workshop has been very successful as a special topics meeting where specialists can gather to discuss recent advances in a field. Meisels noted that several other small mass spectrometry meetings have become established over the years. He then announced that one of the these, the Asilomar Conference on Mass Spectrometry, has decided to become an affiliate of ASMS as of July 1, 1987.

A second issue facing the Society is the format of future Annual Conferences. As the Society continues to grow in membership and the number of papers presented, it becomes more and more difficult to have just three parallel oral sessions. Meisels opened the floor for discussion of this issue. When asked how many members needed to present a paper in order to attend the conference, a show of hands indicated that about 25% did need to present a paper, and for about 75% it didn't matter. After further discussion, a straw vote showed there was very broad support (20:1) for keeping the number of oral sessions the same and increasing the number of poster presentations as the meeting grew.

The third issue addressed by Meisels was the length of term of the Vice President for Programs, President and Past President. Presently one person serves successive two-year terms at each of these positions. He said that this has been discussed by the Board because some feel that six years is too long a commitment. Catherine Fenselau commented that the Board should consider decoupling the job of VP Programs and President. Frank Field commented that the six year term was important for continuity and that it did not seem that onorous to him. Graham Cooks spoke in favor of changing the term so that more people could become involved with the Board.

Meisels then announced the 1987 ASMS Research Awards. This year there were twenty research proposals submitted and reviewed by an outside panel of experts. Susan V. Olesik from the Department of Chemistry, Ohio State University, is the winner of the VG Instruments Research Award for her proposal "Supercritical Fluid-Electrospray Ionization Mass Spectrometry." W. Alan Wolstenholme made the presentation on behalf of VG Instruments. Robert E. Finnigan presented the Finnigan Research Award to Philip J. Brucat of the Department of Chemistry, University of Florida. Dr. Brucat's proposal was titled "Fluorescence Spectroscopy in the Time Domain: The Properties of Optically Excited Nitrogen Dioxide."

Finally, Meisels expressed his appreciation to retiring Board members Catherine Costello, Robert McIver, and Chuck McEwen for their work on behalf of ASMS. The meeting was adjourned at 12:46 p.m.

Respectfully submitted,

Robert T. McIver, Jr.
Secretary

Presented at the 35th ASMS Conference on Mass Spectrometry and Allied Topics
May 24-29, 1987, Denver, CO

Revised July 6, 1987

AMERICAN SOCIETY FOR MASS SPECTROMETRY

CONSTITUTION AND BYLAWS

ARTICLE I. NAME

The name of this Society shall be "The American Society for Mass Spectrometry".

ARTICLE II. PURPOSE

It is the purpose of this Society to promote and disseminate knowledge of mass spectrometry and allied subjects.

ARTICLE III. MEMBERSHIP

Membership in the American Society for Mass Spectrometry shall be open to any individual, or with approval of the Board of Directors, to any corporate entity with a bona-fide interest in mass spectrometry.

ARTICLE IV. MANAGEMENT

The management of the Society shall be vested in the Board of Directors which shall consist of the following members: the officers of the Society hereafter listed, three elected members-at-large, and the immediate Past-President.

The Officers of the Society shall be:

President
Vice President for Programs, who shall be President-Elect of the Society
Vice President for Arrangements
Secretary
Treasurer

ARTICLE V. DUTIES OF OFFICERS

Section 1. The President shall be the chief executive officer of this Society; he shall preside at all meetings of the members and directors; he shall have general and active management of the business of this Society; he shall see that all orders and resolutions of the Board of Directors are carried out; he shall execute all bonds, mortgages, and all contracts of this Society and cause or direct the affixing of the corporate seal thereto; he shall have general superintendence and direction of all other officers of this Society and see that their duties are properly performed; he shall submit a report of the operations of the Society for the fiscal year to the Board of Directors and members at the annual meeting, and from time to time shall report to the Board of Directors all matters within his knowledge that may affect this Society; he shall be 'ex-officio' a member of all committees except the Nominating and Audit Committees and shall have the power and duties and management usually vested in the office of President in a corporation; he shall appoint all committees, except as may be otherwise provided; and he shall send, or cause to be sent by the Secretary, notices of any meetings of the Board of Directors.

Section 2. The Vice President for Programs shall be vested with all the powers and shall perform all the duties of the President during the absence of the latter and shall have such other duties as may, from time to time, be determined by the Board of

Directors. The same shall be true of the Vice President for Arrangements who shall be next in the line of succession. In the event that the President shall be absent at any meeting, the Vice President for Programs shall preside, and if neither is present at a meeting, the Vice President for Arrangements shall preside.

Section 3. The Secretary or a deputy appointed by the President shall attend all meetings of the Board of Directors and all general meetings of the Society and act as a clerk thereof; he shall record all votes and minutes of all proceedings; he shall perform such other duties as may be prescribed by the Board of Directors or the President; and he shall be the custodian of the corporate seal and all of the books and records of the Society except as may be otherwise provided.

Section 4. The Treasurer shall have charge of the funds of the Society and shall deposit them in the name of the Society in depositories designated by the Board of Directors; he shall arrange for the payment of all valid Society bills and debts from Society funds, and shall make a complete and accurate report of the finances of the Society at each annual meeting of the members, or at any other time upon request, to the Board of Directors.

ARTICLE VI. DUTIES AND POWERS OF THE BOARD OF DIRECTORS

Section 1. The property and business of the Society shall be managed by the Board of Directors.

Section 2. In addition to the general powers of the Board of Directors by virtue of their office, the powers and authority expressly given by law, by terms of the Charter of this Society, and elsewhere in these Bylaws, the following specific powers are expressly conferred on the Board of Directors: To purchase or otherwise acquire for the Society any property, right or privilege which it is authorized to acquire at such price or consideration and upon such terms as they deem expedient; To appoint, to remove or suspend subordinate agents or servants, to determine their duties and affix their salaries; To remove or suspend any subordinate officer or servants; To determine who shall be authorized on behalf of the Society to sign bills, notices, receipts, acceptances, endorsements, checks, releases, contracts and any other instruments; To delegate any of the powers of the Board to any standing committee, special committee, or to any officer or agent of the Society, with such powers as the Board may deem fit and proper to grant; Generally to do all such lawful acts and things as are not by law, or by Charter, or by these Bylaws directed or required to be done by members of the Board of Directors.

Section 3. Any action which may be taken at a meeting of the Board of Directors, may be taken without a meeting by a letter ballot sent by and filed with the Secretary of the Society and provided all members of the Board of Directors file ballots.

Section 4. In the event that the office of any elected officer or member of the Board of Directors shall become vacant, the Board of Directors shall immediately fill the vacancy for the remainder of the unexpired term; however, no member who thus fills a vacancy in the office of Vice President for Programs shall automatically succeed to the Presidency, but the Society shall in such event elect its next President. A President who vacates office before the conclusion of his term shall not retain membership on the Board of Directors as Past-President as described in Article IV.

Section 5. The ballot of the election to membership on the Board of Directors of the Society shall be by closed, written ballot.

Section 6. Any member shall be eligible to hold office in the Society.

ARTICLE VII. FIDELITY BONDS

The Board of Directors may require such officers or agents to be bonded as it shall deem necessary; for any amount or amounts as it may deem requisite, at the expense of the Society.

ARTICLE VIII. LOCATION

The principal office of this Society shall be located in the City of Pittsburgh, Commonwealth of Pennsylvania.

ARTICLE IX. DISSOLUTION

In the event of either voluntary or involuntary dissolution of the Society, the funds or assets of the Society, remaining after discharging all just debts of the Society or its officers in the name of the Society, shall be distributed without encumbrances to a non-profit group, organization or institution of learning engaged in the field of mass spectrometry within the contemplation of Section 170 (c) (2) of the Internal Revenue Code (1954). The selection of the recipient or recipients shall be made by the majority of the Board of Directors in office at the time of dissolution but in no event shall the assets be distributed to any member or members of the Society.

ARTICLE X. SOCIETY SEAL

The Society shall have a seal, upon which shall be inscribed the name of the Society, the year of its creation, and the word "Pennsylvania", the state of the Society's incorporation.

ARTICLE XI. AMENDMENTS

Section 1. A proposed amendment to the Constitution and Bylaws of the Society, signed by at least three members of the Board of Directors or by fifty members of the Society must be submitted to the Secretary at least fifteen weeks before the regular annual business meeting at the Annual Conference of the Society. The Secretary shall send or cause to be sent the proposed amendment to each member within a reasonable time and at least prior to thirty days before the Annual Conference. After the amendment has been discussed at that meeting, the Secretary will send a letter ballot on the proposed amendment as amended at the meeting to all Society members; if two-thirds of the votes obtained by letter ballot within six weeks are in favor of the proposed amendment, it shall be adopted.

Section 2. The Board of Directors shall also have the power to amend the Bylaws by a two-thirds vote of its membership.

Section 3. The Board of Directors is authorized to renumber articles and sections of the Constitution and Bylaws to correspond with any changes that may be made.

Section 4. Proceedings for removal of members of the Board of Directors shall be conducted as outlined above for amendments to the Constitution (Article XI, Section 1). If the request for removal is supported by two-thirds of the letter ballots received within six weeks, the Board member or members in question shall be removed from office and a replacement selected by the Board of Directors in accordance with Article VI, Section 4.

ARTICLE XII. ARCHIVIST

The Board of Directors shall appoint a Society Archivist whose duties shall be the collation and preservation of all documents deemed to be of historical interest. All records will be reproduced on microfilm from time to time and all of the original documents will be reviewed by the Archivist before they are disposed of. The Archivist shall report his activities to the Board of Directors annually and will report them to the general membership whenever appropriate.

The Archivist shall be nominated by the President and appointed to office by a two-thirds vote of the Board of Directors. The incumbent shall be reviewed annually and may be reappointed at the pleasure of the Board.

Expenses incurred by the Archivist on Society business shall be reimbursed.

Presented at the 35th ASMS Conference on Mass Spectrometry and Allied Topics
May 24-29, 1987, Denver, CO

BYLAWS

1. MEMBERSHIP

1.1 Application for membership shall be made in writing, on a form to be specified by the Board of Directors. The membership year shall commence January 1 and end December 31.

1.2 Membership becomes effective upon receipt by the Treasurer of dues and a properly executed application.

1.3 Failure to pay dues by four (4) weeks prior to the Annual Conference shall result in the requirement to pay nonmember registration fees for the Annual Conference in that year. Membership in the Society shall lapse if in arrears dues are not paid by December 31. Payment of current dues shall suffice for reinstatement; however, payment of nonmember registration will reinstate membership for that year.

1.4 Membership may be terminated without prejudice by written notice to the Secretary.

1.5 Members of record shall be defined as those members who have paid their dues prior to December 31 the preceeding year and new members who have paid their dues prior to February 1 the present year.

1.6 Every member of record as of February 1 shall have the right to vote and to hold office.

1.7 The books, accounts and records of the Society shall be open for inspection to any member of the Board of Directors at any time. Members of the Society may upon written request to the Board of Directors, inspect such books, accounts and records of the Society at such reasonable times as the Board of Directors may designate.

1.8 The Secretary will prepare or cause to be prepared at least one annual membership report to the Board of Directors.

1.9 Members whose dues are in arrears shall not receive the Abstracts from the Annual Conference.

2. COLLECTIONS AND DISBURSEMENTS

2.1 Membership classes and dues within such classes shall be determined by the Board of Directors.

2.2 The Board of Directors is authorized to determine separately a fee for each general meeting to cover the expenses of holding the meeting. Payment of this fee is a requirement for attendance.

2.3 Disbursements shall be made by approval of a majority of the Board of Directors. Disbursements in excess of $5000.00 shall be made by check signed by two members of the Board.

2.4 The fiscal year of the Society shall be from January 1 to December 31.

2.5 The Treasurer will prepare or cause to be prepared an annual financial report to the Board of Directors.

3. TERMS OF OFFICE AND ELECTION

3.1 The elected officers and directors-at-large shall hold office for a term of two years, except as otherwise provided in Article VI of the Constitution, with their term year commencing on July 1 and ending June 30.

3.2 The President shall appoint a Nominating Committee consisting of five members representing diverse areas in mass spectrometry. He shall not be a member of this committee. This selection shall be approved by the Board of Directors by a two-thirds vote. Two or three of this committee will be appointed each year for two-year terms. It shall nominate candidates, normally two, for each of three offices to be filled in alternate years according to the following rotation:

Even Years - Vice President for Program

- Treasurer

- Member-at-large, who shall serve in the capacity of Coordinator for Educational Affairs

- Member-at-large, who shall serve in the capacity of Coordinator for Measurements and Standards

Odd Years - Vice President for Arrangements

- Secretary

- Member-at-large, who shall serve in the capacity of Editor of the Conference Proceedings.

The committee will report in writing to the Board of Directors before June 30 each year. These reports will include a statement of each candidate's consent to serve and a professional resume for each candidate. Each slate of candidates and the resumes will be distributed to the members by the Secretary before September 15.

3.3 Any Society member can nominate another member for any office except President by submitting to the Secretary before January 15 of the election year:

a. signatures of at least 50 Society members endorsing the nomination;
b. signed statement of the nominee indicating his agreement to hold office if elected;

c. professional resume of the nominee.

3.4 The election results shall be made known at the next annual business meeting and the new officers shall assume office as specified in paragraph 3.1 of the Bylaws.

4. COMMITTEES AND INTEREST GROUPS

4.1 Standing Committees. The standing committees of the Society shall be a Nominating Committee as described in section 3.2 of the Bylaws, and an Education Committee as described below.

4.2 Education Committee. This committee is responsible for fostering the further education in mass spectrometry of users and practitioners of the method. The Committee has five members. A chairman and three members are appointed by the President of the Society, with the approval of the Board. The elected Board member-at-large with responsibility for educational matters shall be an 'ex-officio' member of the Committee and serve as liaison with the Board.

4.3 Committee on Measurements and Standards. This committee is responsible for matters related to measurements and standards in mass spectrometry. The committee has five members. A chairman and three members are appointed by the President of the Society, with the approval of the Board. The elected Board member-at-large who serves in the capacity of Coordinator for Measurements and Standards shall be an 'ex-officio' member of the committee and serve as laison with the Board.

4.4 Other Committees. The President shall appoint such committees and interest group coordinators as are necessary to accomplish the purpose of the Society. The terms of all appointments shall not exceed the term of office of the President, who may

terminate a committee at any time. Members and chairpersons may be reappointed by the incoming President.

4.5 Interest Groups. Such groups are responsible for advising the Board and especially the Vice President for Programs on matters of special concern in subject areas and serve as a resource in the development of the program of the Annual Conference. Interest groups are established and dissolved at the discretion of the President, with the advice and approval of the Board. They are led by Coordinators, who are appointed by the President of the Society with the approval of the Board. Coordinators chair meetings of participants at the Annual Conference who share in the interest area.

5. MEETINGS

5.1 The Society shall meet at least once a year in order to present scientific papers and conduct business. Fifty members shall constitute a quorum for the transaction of business.

5.2 The time and place of the general meeting shall be determined by the Board of Directors.

5.3 Meetings of the Board of Directors may be called by the President or, in his absence, by the Vice President for Programs. Alternatively, two-thirds of the Board of Directors may call a meeting by written request to the President. Five directors shall constitute a quorum of the Board of Directors.

5.4 A simple majority of those present shall be required to pass any motion at any meeting of the members or Board of Directors, unless otherwise provided (see Article VI, Section 3).

5.5 Each Director shall be entitled to two weeks notice of any meeting of the Board of Directors.

5.6 Notice of the annual general meeting shall be sent to each member at least thirty days before the meeting.

5.7 The President shall, in response to a petition bearing the signatures of not fewer than twenty members and requesting that the Board of Directors consider a specified question, place this item on the agenda of the first meeting of the Board of Directors which is scheduled to convene on a date not preceeding the thirtieth day following receipt of the petition. The member whose signature appears first on the petition shall be entitled to two weeks notice of such meeting, and the same member or a member designated by him shall be entitled to attend such meeting and discuss the specified question with the Board of Directors.

5.8 Whenever any notice is required to be given by the provisions of the Bylaws, a waiver thereof in writing, signed by the person or persons entitled to such notices whether before or after the time stated therein, shall be equivalent to the required notice.

5.9 The President may appoint any member of the Society, not a member of the Board of Directors, to be parliamentarian for the duration of a given business meeting.

6. COMPENSATION

6.1 No member of the Board of Directors of the Society shall receive salaries or fees for his services.

6.2 Members of the Board of Directors of the Society shall be reimbursed for all reasonable expenses incurred in connection with their official duties.

7. MISCELLANEOUS

7.1 The financial records of the Society shall be audited at least once within the term of office of the Treasurer.

7.2 The business of the Society shall be conducted in accordance with the latest edition of Roberts' Rules of Order unless otherwise specified herein.

Presented at the 35th ASMS Conference on Mass Spectrometry and Allied Topics
May 24-29, 1987, Denver, CO

The following creation was the winning entry in the ASMS Unknown Search '87. It was presented by the Metastable Tabernacle Choir, at the Flying W Ranch, May 27, 1987.

The Thirteen Days of ASMaS

Proposed by: Colleen Rostad
Rearranged by: Fred McLafferty

On the first day of ASMaS my mentor gave to me,
A copy of McLafferty.
On the second day of ASMaS my mentor gave to me,
Two filaments.
On the third day of ASMaS my mentor gave to me,
Three blown boards.
On the fourth day of ASMaS my mentor gave to me,
Four turbo pumps.
On the fifth day of ASMaS my mentor gave to me,
Five gold O-rings.
On the sixth day of ASMaS my mentor gave to me,
Six sexy sectors.
On the seventh day of ASMaS my mentor gave to me,
Seven pumps a sucking.
On the eighth day of ASMaS my mentor gave to me,
Eight filthy samples.
On the ninth day of ASMaS my mentor gave to me,
Nine power glitches.
On the tenth day of ASMaS my mentor gave to me,
Ten high mass daughters.
On the eleventh day of ASMaS my mentor gave to me,
Eleven heads a crashing.
On the twelfth day of ASMaS my mentor gave to me,
Twelve unknown ions.
On the thirteenth day of ASMaS my mentor gave to me,
Thirteen grants a milking.

LAWRENCE E ABBEY
GEORGIA TECH
CHEMISTRY DEPT
ATLANTA GA 30332
PHONE: 404 894 4061

WILLIAM H ABERTH
UC SAN FRANCISCO
PHARMACEUTICAL CHEM
SAN FRANCISCO CA 94143
PHONE: 415 476 4895

BRADLEY L ACKERMANN
MERRELL DOW PHARMACEUTICAL
2110 E GALBRUITH RD
CINCINNATI OH 45215
PHONE: 513 948 6081

ROBERT A ADAMS
3480 TANBARK CT NE

ATLANTA GA 30319
PHONE: 404 255 4817

JOSEPH B ADDISON
GOVERNORS STATE UNIV
COLL OF ARTS & SCI
UNIVERSITY PK IL 60466
PHONE: 312 534 5000

MEHRSHID ALAI
856 W NELSON ST

CHICAGO IL 60657
PHONE:

KENNETH M ALDOUS
NY STATE HEALTH DEPT
WADSWORTH CENTER
ALBANY NY 12201
PHONE: 518 473 0030

N E ALEXANDER
NIH
BLDG 13 ROOM 3W13
BETHESDA MD 20892
PHONE: 301 663 9085

ALEX R ALLAN
MT SINAI HOSPITAL
BOX 156
NEW YORK NY 10128
PHONE: 212 650 7729

CHARLES ALLGOOD
DEPT OF CHEMISTRY
UNIV OF DELAWARE
NEWARK DE 19716
PHONE: 302 451 2917

HAMDY ABDEL-MAKSOUD
257 EAST COTTAGE ST

DORCHESTER MA 02125
PHONE: 617 642 0188

LINDA D ABRAMS
1511 RAVEN RUN DR

MECHANICSVILL VA 23111
PHONE: 804 359 1900

THOMAS ACZEL
EXXON R/E
ROUTE 22 EAST
ANNANDALE NJ 08801
PHONE: 201 730 2231

HOLLY FORTNUM ADAMSONS
DEPT OF CHEMISTRY BOX 10
MICHIGAN STATE UNIV
EAST LANSING MI 48824
PHONE: 517 353 6376

MOHAMMED S AHMED
DEPT OF CHEMISTRY
CASE WESTERN RESERVE UNIV
CLEVELAND OH 44106
PHONE: 216 368 3599

MARK ALASANDRO
DUPONT
EXPERIMENTAL STATION
WILMINGTON DE 19808
PHONE:

R T ALESSANDRO
ENVIROMENTAL TEST CERT CORC
284 RARITAN CENTER PARKWAY
EDISON NJ 08818
PHONE: 201 225 6725

E D ALFORD
BROWN & WILLIAMSON
PO BOX 35090
LOUISVILLE KY 40232
PHONE: 502 568 7680

RAY H ALLEN
R H ALLEN CO
PO BOX 27
BOULDER CO 80306
PHONE: 303 442 2141

MAHENDER REDDY ALLIRI
UNIV OF ARIZONA
DEPT OF PHARM SCIENCES
TUCSON AZ 85721
PHONE: 602 626 4072

ROBERT M ABERNATHEY
MS G740
LOS ALAMOS NAT'L LAB
LOS ALAMOS NM 87544
PHONE: 505 667 9810

FRED P ABRAMSON
GEORGE WASHINGTON UNIV
PHARMACOLOGY DEPT
WASHINGTON DC 20037
PHONE: 202 676 2946

JEANETTE ADAMS
ROUTE 8

LINCOLN NE 68506
PHONE: 402 472 3507

SOMASUNDARAM SAM ADDANKI
109 NASHUA LANE

BOWIE MD 20716
PHONE:

DANIEL G AICHELE
BATTELLE
505 KING AVE
COLUMBUS OH 43201
PHONE:

RICHARD ALBERT
ETC CORP
4806 HUNTERS GLEN DR
PLAINSBORO NJ 08536
PHONE: 609 275 8645

LOUIS ALEXANDER
ENTERS FOR DISEASE CONTRO
1600 CLIFTON RD
ATLANTA GA 30333
PHONE:

DAVID ALKALAY
CIBA-GEIGY CORP
444 SAWMILL RIVER RD
ARDSLEY NY 10502
PHONE: 914 478 3131

CYNTHIA C ALLEY
CTRS FOR DIS CONTROL
TOXICOLOGY C17-1814
ATLANTA GA 30333
PHONE: 404 452 4144

JOHN ALLISON
MICHIGAN STATE UNIV
CHEMISTRY DEPT
EAST LANSING MI 48824
PHONE: 517 353 4513

LAURA A ALLISON
CONOCO INC
R&D EAST
PONCA CITY OK 74603
PHONE: 405 767 2761

C ANTHONY ALTAR
CIBA-GEIGY CORP

SUMMIT NJ 07901
PHONE: 201 277 5650

M M ANBAR
181 HALWILL DR

SNYDER NY 14226
PHONE: 716 831 2328

DAVID J ANDERSON
GEOLOGY 541
INDIANA UNIV
BLOOMINGTON IN 47405
PHONE: 812 335 1005

WILLIAM R ANDERSON
LEHIGH UNIV
MUDD BLDG 6
BETHLEHEM PA 18015
PHONE: 215 758 3465

ROLAND S ANNAN
DEPT OF CHEMISTRY
NORTHEASTERN UNIV
BOSTON MA 02115
PHONE: 617 437 2794

BRIAN ARBOGAST
ENVIRONMENTAL SCI CTR
WENIGER HALL
CORVALLIS OR 97331
PHONE:

SALEH ARGHESTANI
HAH RM 20
DEPT OF CHEMISTRY
LINCOLN NE 68588
PHONE: 402 472 5554

KENNETH ARMOCK
MI DEPT OF AGRICULTURE
1615 S HARRISON ROAD
EAST LANSING MI 48823
PHONE: 517 373 6410

KEIJI G ASANO
401 GALLAHER VIEW RD #79

KNOXVILLE TN 37919
PHONE: 615 574 4884

NICK ALMASY
MI DEPT OF AGRICULTURE
1615 S HARRISON ROAD
EAST LANSING MI 48823
PHONE: 517 373 6410

V O ALTEMOSE
CROSS ST

CAMPBELL NY 14821
PHONE:

ROBERT J ANDEREGG
101 MILL CREEK RD
APT 304
ANDIMORE PA 19003
PHONE: 207 581 1171

SCOTT L ANDERSON
CHEMISTRY DEPT
SUNY
STONY BROOK NY 11794
PHONE: 516 632 7915

D A ANDRZEJEWSKI
FDA
200 C STREET SW HFF-426
WASHINGTON DC 20204
PHONE: 202 245 8478

ALEX APFFEL
HEWLETT-PACKARD
1601 CALIFORNIA AVE
PALO ALTO CA 94304
PHONE: 415 857 1501

STEPHEN AREDISIAN
SOUTHERN ILLINOIS UNIV
473 WINCHESTER PLACE
BELLEVILLE IL 62221
PHONE: 618 235 2332

GEORGES M ARGOUD
DEPT OF MEDICINE
UNIV OF NEW MEXICO HOSPITA
ALBUQUERQUE NM 87131
PHONE: 505 277 4657

PETER ARROWSMITH
IBM
MS K32 803D
SAN JOSE CA 95120
PHONE: 408 927 2520

ROBERT W ASHMORE
DEPT OF PHARMACOLOGY
EXPERIMENTAL THERAPEUTICS
WASHINGTON DC 20307
PHONE: 301 427 5273

MICHAEL F ALMOND
KRATOS ANALYTICAL
535 E CRESENT
RAMSEY NJ 07446
PHONE: 201 825 7500

JON AMSTER
UNIV OF CALIFORNIA
DEPT OF CHEMISTRY
IRVINE CA 92717
PHONE: 714 856 6780

BRIAN K ANDERSON
ROSS LABORATORIES
625 CLEVELAND AVE
COLUMBUS OH 43215
PHONE: 614 119 7345

STEPHEN ANDERSON
400 WOLLASTON AVE E-3

NEWARK DE 19715
PHONE: 302 451 1118

VINCENT ANICICH
2800 MONTROSE AVENUE
No 1
LA CRESENTA CA 91214
PHONE:

ANTHONY D APPELHANS
EG&G IDAHO INC
PO BOX 1625
IDAHO FALLS ID 83415
PHONE: 208 526 0862

JANET AREY
AIR POLLUTION RES CTR
UNIV OF CALIFORNIA
RIVERSIDE CA 92521
PHONE: 714 787 3502

PETER B ARMENTROUT
DEPT OF CHEMISTRY
UNIV OF CALIFORNIA
BERKELEY CA 94720
PHONE: 415 642 4428

BRUCE K ASAMOTO
STANDARD OIL RESEARCH
4440 WARRENSVILLE CTR ROAD
CLEVELAND OH 44128
PHONE: 216 581 5776

GRAHAM ATKIN
VG INSTRUMENTS INC
32 COMMERCE CENTER
DANVERS MA 01923
PHONE:

JOHN W AULD
37748 SUNNYDALE

LIVONIA MI 48154
PHONE: 313 897 1395

PIERRE J AUSLOOS
NAT'L BUR OF STAN
CTR FOR CHEM PHYSICS
WASHINGTON DC 20234
PHONE: 301 975 2500

E R AUSTIN
IFDC
PO BOX 2040
MUSCLE SHOALS AL 35660
PHONE: 205 764 8365

MICHAEL J AVERY
IOWA STATE UNIV
113 SPEDDING
AMES IA 50011
PHONE: 515 294 6615

RUSSELL J AYERS
FOOD & DRUG ADMINISTRATION
1560 E JEFFERSON
DETROIT MI 48207
PHONE: 313 226 6129

LUCIA M BABCOCK
CHEMISTRY DEPT
CHOPPIN HALL
BATON ROUGE LA 70803
PHONE: 504 388 3239

LUBO BACZYNSKYJ
THE UPJOHN CO
301 HENRIETTA
KALAMAZOO MI 49001
PHONE: 616 385 7401

TOMAS BAER
UNIV NORTH CAROLINA
CHEMISTRY DEPT
CHAPEL HILL NC 27514
PHONE: 919 966 5433

DONALD A BAFUS
617 ELM

NEWTON KS 67114
PHONE:

G L BAFUS
1504 S 23RD

BLUE SPRINGS MO 64015
PHONE: 816 966 5000

THOMAS A BAILLIE
UNIV OF WASHINGTON
MEDICINAL CHEMISTRY
SEATTLE WA 98195
PHONE: 206 545 2468

E S BAKER
ROCKWELL HANFORD
200 WEST 234-5
RICHLAND WA 99352
PHONE: 509 373 3872

PETER F BAKER
UNIVERSITY OF ARIZONA
COLLEGE OF PHARMACY
TUCSON AZ 85721
PHONE: 602 626 4072

RANDALL J BAKER
MARION LABS INC
PO BOX 9627
KANSAS CITY MO 64134
PHONE: 816 966 5000

TIMOTHY R BAKER
28 GILBERT STREET

WATERTOWN MA 02172
PHONE: 617 437 4696

C R BALDOCK
114 OGONTZ LANE

OAK RIDGE TN 37830
PHONE: 615 483 6779

JOHN M BALLARD
CELANESE RESEARCH
86 MORRIS AVE
SUMMIT NJ 07901
PHONE: 201 522 7570

KEVIN D BALLARD
MED UNIV OF SC
PHARMACOLOGY DEPT
CHARLESTON SC 29401
PHONE: 803 792 2471

ANNIE BALLATORE
813 COLQUITT

HOUSTON TX 77006
PHONE:

MARK BAMBACHT
AMOCO CORP
PO BOX 400
NAPERVILLE IL 60566
PHONE: 312 420 5230

SHERA BANBURY
MASSTRON INC
6595 ODELL PLACE
BOULDER CO 80301
PHONE: 303 530 7778

L J BARABAS
MORTON CHEMICAL DIV
PO BOX 2184
GREENVILLE SC 29602
PHONE: 803 244 5351

WAYNE M BARAN
100 E STREAMWOOD BLVD

STREAMWOOD IL 60107
PHONE: 391 3380

ROBERT J BARBUCH
MERRELL DOW PHARMACEUTICAL
PO BOX 68470
INDIANAPOLIS IN 46268
PHONE: 317 873 4856

MISTY BARKLEY
29 BACK DR

EDISON NJ 08817
PHONE: 201 819 8589

ROBERT M BARKLEY
CIRES
CAMPUS BOX 449
BOULDER CO 80309
PHONE: 303 492 1158

STEPHEN E BARLOW
CHEMISTRY DEPT
UNIV OF COLORADO
BOULDER CO 80309
PHONE: 303 492 7396

I L BARNES
NBS
A-23 PHYSICS
GAITHERSBURG MD 20899
PHONE: 301 975 4100

RAMON M BARNES
CHEMISTRY DEPT
GRC TOWERS
AMHERST MA 01003
PHONE: 413 545 2294

DOUGLAS F BAROFSKY
DEPT OF AGRICULTURAL CHEM
OREGON STATE UNIV
CORVALLIS OR 97331
PHONE: 503 754 2906

ELISABETH BAROFSKY
DEPT OF AG CHEMISTRY
OREGON STATE UNIV
CORVALLIS OR 97331
PHONE: 503 754 2906

ROBERT P BARRON
FDA-CTR DRUGS & BIOLOGICS
HFN-160/DSDDP
ROCKVILLE MD 20857
PHONE: 301 496 9020

CHRISTOPHER M BARSHICK
DEPT OF CHEMISTRY
UNIV OF VIRGINIA
CHARLOTTESVLL VA 22901
PHONE: 804 924 7180

CANDACE D BARTMAN
EXTREL CORP
PO BOX 11512
PITTSBURGH PA 15238
PHONE: 412 963 7530

LOUISETTE J BASA
GENENTECH INC
460 PT SAN BRUNO BLVD
S SAN FRAN CA 94080
PHONE: 415 266 2057

LEWIS M BASS
DEPT OF CHEMISTRY
MILLERSVILLE UNIV
MILLERSVILLE PA 17551
PHONE: 717 872 3764

CHARLENE W BAYER
6276 ROSECOMMON DRIVE

NORCROSS GA 30092
PHONE: 404 894 3825

JAN M BEANE
IOWA STATE UNIV
85A GILMAN HALL
AMES IA 50011
PHONE: 515 294 5958

ALFRED J BEATTIE
E I DUPONT
EXPERIMENTAL STA
WILMINGTON DE 19898
PHONE: 302 772 2240

MARY D BECK
1252 QUARRY LANE
CLAYTON ENV SCI INC
PLEASANTON CA 94566
PHONE: 415 426 2600

W B BARRETT
730 ST JOHNS PL

DALLASTOWN PA 17313
PHONE: 301 771 4950

REGINA M BARRY
2805 NORMANDY CT

NEWARK DE 19713
PHONE: 302 451 2917

MICHAEL J BARTELS
TOXICOLOGY LAB
1803 BLDG
MIDLAND MI 48674
PHONE: 517 636 9057

JOHN BARTMESS
CHEMISTRY DEPT
UNIV OF TENNESSEE
KNOXVILLE TN 37996
PHONE: 615 974 6578

B B BASCHKIN
2 CAPTAINS LANE

RYE NY 10580
PHONE: 914 835 3506

ILORA BASU
INDIANA UNIVERSITY
SPEA, GEOLOGY 541
BLOOMINGTON IN 47405
PHONE: 812 335 6246

M GOKHAN BAYKUT
5051 ALTON PKWY #118

IRVINE CA 92714
PHONE:

ELLYN S BEARY
NAT'L BUR OF STAN
BLDG 222 RM A 353
GAITHERSBURG MD 20899
PHONE: 301 975 4138

DEBRA J BECK
ONEIDA RESEARCH
ONE HALSEY ROAD
WHITESBORO NY 13492
PHONE: 315 735 3050

CHRISTOPHER H BECKER
SRI INTERNATIONAL
M S PS091
MENLO PARK CA 94025
PHONE: 415 859 5130

V M BARRINGER
4604 EMMACYN DR

SUMMERFIELD NC 27358
PHONE: 919 292 7100

T L BARRY
FDA
850 3RD AVE
BROOKLYN NY 11232
PHONE: 718 965 5722

GREG J BARTLING
1014 RIVERVIEW TERRACE

NEW MRTNSVLL WV 26155
PHONE: 304 455 4400

P L BARTNER
SCHERING CORP
60 ORANGE
BLOOMFIELD NJ 07003
PHONE: 201 429 3989

BRENDA P BASILE

18314 ELMDON
HOUSTON TX 77084
PHONE: 713 492 2510

MARK R BAUER
BATTELLE
505 KING AVE
COLUMBUS OH 43201
PHONE: 614 424 3913

MARK F BEAN
DEPT OF PHARMACOLOGY
JOHNS HOPKINS SCH OF MED
BALTIMORE MD 21205
PHONE: 301 955 6961

BRIAN DAVID BEATO
3751 SW 20TH AVENUE
APT 132
GAINESVILLE FL 32607
PHONE: 904 335 0631

DONALD D BECK
GENERAL MOTORS RESEARCH
PHYSICAL CHEMISTRY DEPT
WARREN MI 48098
PHONE: 313 986 1291

LARRY D BECKER
USGS-NWQ%
5293-B WARD RD
ARVADA CA 80004
PHONE:

CARL F BECKNER
FINNIGAN MAT
355 RIVER OAKS PKWY
SAN JOSE CA 95134
PHONE: 408 433 4800

A A BEDNARCZYK
NAARDEN INTERNATL
10 PAINTERS MILL RD
OWINGS MILLS MD 21117
PHONE: 301 363 2550

THOMAS D BEHYMER
INDIANA UNIV
541 GEOLOGY BLDG
BLOOMINGTON IN 47405
PHONE: 812 335 1217

WILLIAM R BEHYMER
USI INDUSTRIAL CHEMICAL
1275 SECTION ROAD
CINCINNATI OH 45237
PHONE:

ROSS C BEIER
COVTERL, USDA
PO DRAWER G E
COLL STN TX 77841
PHONE: 409 260 9411

JON L BEIHOFFER
DENVER FEDERAL CENTER
BOX 25227
DENVER CO 80225
PHONE:

ROBERT G BEIMER
S-CUBED
3398 CARMEL MTN ROAD
SAN DIEGO CA 92121
PHONE:

PETER BEL
UNIVERSITY OF TENNESSEE
DEPT OF CHEMISTRY
KNOXVILLE TN 37996
PHONE: 615 974 8679

JOHN BELAND
EBMUD/LAB SERVICES
PO BOX 24055
OAKLAND CA 94623
PHONE: 415 465 3700

RONALD L BELANGER
1899 MAPLE HILL ST

YORKTWN HGHTS NY 10598
PHONE: 914 335 6208

MICHAEL G BELL
LOS ALAMOS NATL LAB
PO BOX 1663/K484
LOS ALAMOS NM 87545
PHONE: 505 667 7134

SUZANNE C BELL
LOS ALAMOS NAT'L LABORATOR
MS K484
LOS ALAMOS NM 87545
PHONE: 505 667 5889

V E BELL
HOFFMANN-LAROCHE INC

NUTLEY NJ 07110
PHONE: 201 235 2852

THOMAS H BELLUS
2027 HOYT AVENUE
No 1
SEATTLE WA 98201
PHONE: 206 476 8090

F A BENCSATH
THE ROCKEFELLER UNIV
1230 YORK AVENUE
NEW YORK NY 10021
PHONE: 212 570 8852

J G BENDORAITIS
MOBIL RESEARCH & DEV

PAULSBORO NJ 08066
PHONE: 609 423 1040

BRIAN D BENNETT
CHEMISTRY DEPT
UNIV OF CINCINNATI
CINCINNATI OH 45220
PHONE:

BRYAN L BENTZ
DAVID SARNOFF RES CTR
CN 5300
PRINCETON NJ 08543
PHONE: 609 734 2015

WOLFGANG BENZ
HOFFMANN-LAROCHE INC
KINGSLAND ST
NUTLEY NJ 07110
PHONE: 201 235 3786

DAVID W BERBERICH
1930 SW 14TH TERRACE

GAINESVILLE FL 32608
PHONE: 904 375 8922

PETER J BERG
MAYO ENDOCRINE RES
5-164 W JOSEPH
ROCHESTER MN 55905
PHONE: 507 285 5097

PHILIP S BERGER
TEKNIVENT CORP
11684 LILBURN PARK
ST LOUIS MO 63132
PHONE: 314 994 0500

STEVEN R BERGER
HEWLETT-PACKARD CO
1601 CALIFORNIA AVENUE
PALO ALTO CA 94304
PHONE: 415 857 1501

JACK BERGES
CENREF LABS
PO BOX 68/695 N 7TH ST
BRIGHTON CO 80601
PHONE: 303 659 0497

ALICE M BERGMANN
SUNY @ BUFFALO
DEPT OF CHEMISTRY
BUFFALO NY 14214
PHONE: 716 831 3016

LYLE E BERGQUIST
2676 E OTEROPL #11

LITTLETON CO 80122
PHONE: 303 796 0835

R E BERKLEY
133 MONTCLAIR CIRCLE

DURHAM NC 27713
PHONE: 919 541 2439

PATRICIA BETHEL
2433 BYRON STREET

BERKELEY CA 94702
PHONE: 415 843 0215

LEON D BETOWSKI
EPA-EMSL
QUAL ASSURANCE DIV
LAS VEGAS NV 89114
PHONE: 702 456 8165

JOSEPH R BIANCHINE
VP MEDICAL RES & DEV
AMERICAN CRITICAL CARE
WANKEGAN IL 60085
PHONE: 312 473 3000

KLAUS BIEMANN
MIT
CHEMISTRY 56-010
CAMBRIDGE MA 02139
PHONE: 617 253 7221

D M BIER
WASHINGTON UNIV
METABOLISM
ST LOUIS MO 63110
PHONE: 314 362 6923

MARK E BIER
CHEMISTRY BLDG
BOX 333
W LAFAYETTE IN 47907
PHONE: 317 494 6898

VERONICA M BIERBAUM
UNIV OF COLORADO
CHEMISTRY DEPT
BOULDER CO 80309
PHONE: 303 492 7081

J E BILLER
MIT
CHEMISTRY 56-025
CAMBRIDGE MA 02139
PHONE: 617 253 7232

STEPHEN S BILLETS
US EPA EMSL-QAD
PO BOX 15027
LAS VEGAS NV 89114
PHONE: 702 798 2232

DANIEL BINDER
WATER RESEARCH LABORATORY
910 DUBLIN ROAD
COLUMBUS OH 43215
PHONE: 614 222 7691

ROBERT C BINIAKEWITZ
CHAMPION INT'L CORP
WEST NYACK ROAD
WEST NYACK NY 10994
PHONE: 914 578 7208

GEORGE M BIRD
SUN CHEMICAL CORP
631 CENTRAL AVE
CARLSTADT NJ 07072
PHONE: 201 933 4500

ASGEIR BJARNASON
UNIV OF WISCONSIN-MADISON
1101 UNIVERSITY AVE
MADISON WI 53706
PHONE: 608 262 4561

SADOR S BLACK
E R SQUIBB & SONS
PO BOX 191
NEW BRUNSWICK NJ 08903
PHONE: 201 519 2800

IAN A BLAIR
PHARMACOLOGY DEPT
VANDERBILT UNIV
NASHVILLE TN 37232
PHONE: 615 322 2094

CALVIN R BLAKLEY
2007 WILDERNESS PT DR

KINGWOOD TX 77339
PHONE: 713 796 9677

JULIE A BLANCKAERT
6103 E LONG CIRCLE N

ENGLEWOOD CO 80112
PHONE: 303 796 7504

WILLIAM E BLANTON
1042 MIDLAND ST

BRIGHTON CO 80601
PHONE: 303 659 0497

IOANNIS V BLETSOS
DEPT OF CHEMISTRY
UNIV OF PITTSBURGH
PITTSBURGH PA 15260
PHONE: 412 624 2799

KARL BLOM
2805 NORMANDY CT

NEWARK DE 19713
PHONE: 302 772 7328

LYNN J BLUETT
XEROX CORPORATION
800 PHILLIPS RD 139-64A
WEBSTER NY 14580
PHONE: 716 422 3179

FRANK M BOCKHOFF
STANDARD OIL CO
4440 WARRENSVILLE CTR ROAD
CLEVELAND OH 44128
PHONE: 216 581 5838

RICHARD BOGAR
NORTHWEST & ALASKA FISH ENVIRON CONSERVATION DIV
SEATTLE WA 98112
PHONE:

CORRINE L BOGERT
CT6707 RALSTON RD
ARVADA CO 80002
PHONE: 303 421 3130

VINCE BOJAN
1155 ZION RD

BELLEFONTE PA 16823
PHONE: 814 353 0600

MARK S BOLGAR
SQUIBB INST FOR MED RES
PO BOX 4000
PRINCETON NJ 08540
PHONE: 609 921 5429

KEVIN B BOLGER
US EPA
CENTRAL REGIONAL LAB
CHICAGO IL 60605
PHONE: 312 353 4676

DANIEL D BOMBICK
WRIGHT STATE UNIV

DAYTON OH 45435
PHONE: 513 873 2340

KRISTI E BONAPARTE
1611 LORNA DR

HENDERSON NV 89015
PHONE: 702 739 3142

HENRY A BONDAROVICH
C/O IFF
1515 HWY 36
UNION BEACH NJ 07735
PHONE: 201 264 4500

WILLIAM BONE
FINNIGAN MAT
1383 PICCARD DRIVE
ROCKVILLE MD 20850
PHONE: 301 948 1067

E J BONELLI
HP SCIENTIFIC INSTR
1601 CALIFORNIA AVE
PALO ALTO CA 94304
PHONE: 415 857 6028

RICCARDO BONI
NIH NIMH SECT ON ALAN BIOC
BLDG 10 RM 3D40
BETHESDA MD 20892
PHONE: 301 496 2151

JEANNE BONURA
ANALYTICAL TECHNOLOGIES
2113 S 48TH STREET #107
TEMPE AZ 85282
PHONE: 602 438 1530

WILLIAM J BOULDIN
DOW CHEMICAL CO
OCD-ENV SER-SOUTH
FREEPORT TX 77541
PHONE: 409 238 5219

WILLIAM D BOWERS
17 WILD GOOSE CT

NEWPORT BEACH CA 92663
PHONE: 714 856 6780

MOHAMMED BOZORGZADEH
DEPT OF CHEMISTRY
UNIV OF NEBRASKA
LINCOLN NE 68588
PHONE: 402 472 3507

RICHARD T BRACKMANN
EXTREL CORP
PO BOX 11512
PITTSBURGH PA 15238
PHONE: 412 963 7530

JOEL C BRADLEY
CAMBRIDGE ISOTOPES LAB INC
20 COMMERCE WAY
WOBURN MA 01801
PHONE: 617 938 0067

VERNON O BRANDT
ETHYL TECHNICAL CENTER
BOX 14799
BATON ROUGE LA 70898
PHONE: 504 768 5837

ALAN BREAU
2714 FOX HARBOR DR

INDIANAPOLIS IN 46227
PHONE: 317 276 4382

GARY B BREWSTER
THE COCA-COLA CO
MAIL CODE TEC 6
ATLANTA GA 30301
PHONE: 404 676 3668

FRED W BRILL
105 N MARION DRIVE

GOLDSBORO NC 27530
PHONE: 919 731 5200

JULIET H BORTHWICK
2416 RAINTREE COURT

PLANO TX 75074
PHONE: 214 578 8912

JAMES H BOURELL
1548 BRENTWOOD CT

WALNUT CREEK CA 94595
PHONE: 415 930 6028

RAY BOWMAN
MASSTRON INC
6595 ODELL PLACE
BOULDER CO 80301
PHONE: 303 530 7778

LESLIE BRACEWELL
UNIV OF COLORADO-BOULDER
CB 215
BOULDER CO 80309
PHONE: 303 492 1151

ANNE BRADBURN
5215 PINEBROOK DR
APT D
INDIANAPOLIS IN 46254
PHONE: 317 293 0164

DEVIN K BRAIN
PROCTER & GAMBLE
IVORYDALE TECH CENTR
CINCINNATI OH 45217
PHONE: 513 627 5661

W E BRASELTON
MICHIGAN STATE UNIV
PHARMACOLOGY DEPT
EAST LANSING MI 48824
PHONE: 517 355 7441

J THOMAS BRENNA
IBM
DEPT T43-257-2
ENDICOTT NY 13760
PHONE: 607 755 1363

MARK BRICKHOUSE
2601 SOLDIERS HOME RD #103

W LAFAYETTE IN 47906
PHONE: 317 463 1379

ROD A BRITTEN
84 WEST MARIPOSA ST

ALTADENA CA 91001
PHONE: 818 354 3520

DAVID BOSTWICK
GEORGIA INST OF TECH
CHEMISTRY DEPT
ATLANTA GA 30332
PHONE: 404 894 4061

MICHAEL T BOWERS
UNIV OF CALIFORNIA
CHEMISTRY DEPT
SANTA BARBARA CA 93106
PHONE: 805 961 2893

ARTHUR J BOYER
PPG INDUSTRIES INC
ENVIRONMENTAL SCI CTR
PITTSBURGH PA 15238
PHONE: 412 963 5874

DONALD E BRACKEN
NJ STATE DEPT OF HEALTH
PUB HEAL & ENVIR LABS
TRENTON NJ 08625
PHONE: 609 984 0646

JAMES G BRADLEY
JET PROPULSION LAB
MS 11-116
PASADENA CA 91109
PHONE: 818 354 4215

STEVEN K BRANCH
TRACER TECHNOLOGIES INC
20 ASSEMBLY SQUARE DR
SOMERVILLE MA 02145
PHONE: 617 964 4800

L L BRAYTON
PO BOX 5075, STN A

CHAMPAIGN IL 61820
PHONE: 217 333 2545

DAVID BRENT
BURROUGHS WELLCOME
3030 CORNWALLS
RES TRI PK NC 27709
PHONE: 919 248 4235

PHILIP R BRIGGS
HARVARD UNIVERSITY
CHEMISTRY DEPT
CAMBRIDGE MA 02138
PHONE: 617 495 1903

JENNIFER S BRODBELT
BOX 335, CHEMISTRY BLDG
PURDUE UNIV
W LAFAYETTE IN 47906
PHONE: 317 494 5264

HARRY O BROTHERTON
CHEMISTRY DEPT
NORTHEAST LOUISIANA UNIV
MONROE LA 71209
PHONE: 318 342 4136

C L BROWN
CALIFORNIA STATE UN
CHEMISTRY DEPT
LOS ANGELES CA 90032
PHONE: 213 224 3613

ROBERT D BROWN
110 WINDBRIDGE DRIVE

WEST CHESTER PA 19380
PHONE: 215 363 0402

SHARON M BROWN
IFF R&D
1515 HWY 36
UNION BEACH NJ 07735
PHONE: 201 264 4500

PHILIP J BRUCAT
UNIV OF FLORIDA
DEPT OF CHEMISTRY
GAINESVILLE FL 32611
PHONE: 904 392 2006

JOHN MICHAEL BUCHANAN
8319 GARFIELD COURT

SPRINGFIELD VA 22152
PHONE: 703 642 6723

JOHN P BUCK
900 PARKVIEW LANE

MUKWONAGO WI 53149
PHONE: 414 363 3475

THOMAS L BUELT
HARRIS ENV TECH INC
627 ROSE ST
LINCOLN NE 68501
PHONE: 402 475 5968

S S BULUSU
US ARMY ARDC
ENERG MAT DIV
DOVER NJ 07801
PHONE: 201 724 6450

DAVID J BURINSKY
ORTHO PHARMACEUTICAL
RTE 202; PO BOX 300
RARITAN NJ 08869
PHONE: 201 218 6275

SUSAN A BROTHERTON
EMS LABORATORIES
7901 W MORRIS
INDIANAPOLIS IN 46231
PHONE: 317 243 8305

CHARLES E BROWN
DEPT OF BIOCHEMISTRY
MED COLL OF WISCONSIN
MIKWAUKEE WI 53226
PHONE: 414 257 8436

ROBERT S BROWN
950 LINDEN ST APT B-22

RIVERSIDE CA 92507
PHONE: 714 787 4740

MARILYN L BROWNAWELL
320 ROBERTS LN

SCOTCH PLAINS NJ 07076
PHONE: 201 463 0003

DOMINIQUE BRUMENT
DELSI INSTRUMENTS
10 KINGSBRIDGE ROAD
FAIRFIELD NJ 07006
PHONE: 201 227 7690

MICHELLE V BUCHANAN
OAK RIDGE NAT'L LAB
BLDG 4500-S
OAK RIDGE TN 37831
PHONE: 615 576 6690

THOMAS J BUCKLEY
NBS
BLDG 222 B-348
GAITHERSBURG MD 20899
PHONE: 301 975 2560

ALEXANDER M BUKO
ABBOTT LABS
ABBOTT PARK DEPT 417 AP9
ABBOTT PARK IL 60064
PHONE: 312 937 2082

ZORA E BUNN
PO BOX 12313
2 TRIANGLE DRIVE
RES TRI PK NC 27709
PHONE: 919 549 0611

RICHARD BURKE
IT CORPORATION
5103 OLD WILLIAM PENN HWY
EXPORT PA 15632
PHONE: 412 731 8806

ROBERT P BROUGHAM
DELSI INSTRUMENTS
10 KINGSBRIDGE ROAD
FAIRFIELD NJ 07006
PHONE: 201 227 7690

JOHNIE C BROWN
CHEMISTRY DEPT
UNIV OF WISCONSIN
MADISON WI 53706
PHONE: 608 262 3449

SHARON BROWN
23 NASSAU ROAD

VERONA NJ 07044
PHONE: 201 429 4211

RICHARD F BROWNER
SCH OF CHEMISTRY
GEORGIA INST OF TECH
ATLANTA GA 30332
PHONE: 404 894 4020

ROBERT J BRUNFELDT
R J BRUNFELDT CO
PO BOX 2066
BARTLESVILLE OK 74005
PHONE: 918 336 4467

JAMES D BUCHNER
EXTREL CORP
PO BOX 11512
PITTSBURGH PA 15238
PHONE: 412 963 7530

WILLIAM L BUDDE
EPA
26 W ST CLAIR ST
CINCINNATI OH 45268
PHONE: 513 569 7309

DAVID A BULPETT
US ARMY METERIALS TECH LAB
ATTN: SLCMT-OMP
WATERTOWN MA 02172
PHONE: 617 923 5649

LARRY BURCHFIELD
FINNIGAN MAT
355 RIVER OAKS PARKWAY
SAN JOSE CA 95134
PHONE: 214 775 3279

A L BURLINGAME
UNIV OF CALIFORNIA
PHARMCEUTICAL CHEM
SAN FRANCISCO CA 94143
PHONE: 415 476 5641

FRANK B BURNS
SANDIA NAT'L LABS
DIV 1821
ALBUQUERQUE NM 87185
PHONE: 505 846 5689

JOAN T BURSEY
RADIAN CORPORATION
PO BOX 13000
RES TRI PK NC 27709
PHONE: 919 481 0212

KENNETH L BUSCH
CHEMISTRY DEPT
INDIANA UNIV
BLOOMINGTON IN 47401
PHONE: 812 335 2081

GERRY W BUTTLER
MONSANTO CO
MAIL CODE U4C
ST LOUIS MO 63167
PHONE: 314 694 4213

RONALD BUXTON
ENGINEERING SCIENCE
600 BANCROFT WAY
BERKELEY CA 94710
PHONE: 415 841 7353

DALE K CABBINESS
CONOCO INC
PO BOX 1267
PONCA CITY OK 74603
PHONE: 405 767 4478

JOHN B CALLAGHAN
680 FRANKLIN STREET

DENVER CO 80218
PHONE: 303 399 3747

E L CALLIS
LOS ALAMOS NATIONAL LAB
MAIL STOP G740
LOS ALAMOS NM 87545
PHONE: 505 667 9868

CLAY S CAMPBELL
FINNIGAN MAT
355 RIVER OAKS PKWY
SAN JOSE CA 95134
PHONE: 408 433 4800

THOMAS W CAMPBELL
8009 HILLRISE DRIVE

AUSTIN TX 78759
PHONE: 512 458 7587

ROBERT BURPEE
PPG IND INC
PO BOX 31
BARBERTON OH 41203
PHONE: 216 848 4161

MAURICE M BURSEY
UNIV NORTH CAROLINA
CHEMISTRY DEPT 045A
CHAPEL HILL NC 27514
PHONE: 919 962 4403

ERNIE D BUSH
VA MEDICAL CENTER
500 W FORT ST
BOISE ID 83702
PHONE: 208 336 5100

S E BUTTRILL
CHAS EVANS & ASSOC
301 CHESAPEAKE DRIVE
REDWOOD CITY CA 94063
PHONE: 415 369 4567

JOHN T BYCHOWSKI
FIREMAN'S FUND
ENVIRONMENTAL LAB
PETALUMA CA 94952
PHONE: 707 778 4193

THOMAS CAIRNS
US FDA
1521 W PICO BLVD
STUDIO CITY CA 90015
PHONE: 213 252 7571

JOHN H CALLAHAN
NAVAL RESEARCH LABORATORY
CODE 6112 CHEMISTRY DIV
WASHINGTON DC 20375
PHONE: 202 767 3551

DOUGLAS CAMERON
WESTERN RESEARCH CTR
PO BOX 3395
LARAMIE WY 82071
PHONE: 307 721 2365

JAMES A CAMPBELL
PACIFIC NORTHWEST LABS
329 BLDG/300 AREA
RICHLAND WA 99352
PHONE: 509 376 0899

DAVID C CANADA
MARTIN MARIETTA CORP
PO BOX P MS 446
OAK RIDGE TN 37831
PHONE: 615 574 9764

D G BURROWS
NORTHWEST & ALASKA
FISHERIES CENTER
SEATTLE WA 98112
PHONE: 206 442 5660

PETER C BUSCEMI
ATF-NATL LAB CENTER
1401 RESEARCH BLVD
ROCKVILLE MD 20850
PHONE: 301 294 0410

GORDON F BUTLER
554 RED ROCK

WADSWORTH OH 44281
PHONE: 216 336 9675

W H BUTTRILL
1616 MEETING HOUSE LANE

ANNAPOLIS MD 21401
PHONE: 301 757 1854

GARY D BYRD
NAT'L BUR OF STAN
A 113 CHEMISTRY
GAITHERSBURG MD 20899
PHONE: 301 975 3116

GARY CALDWELL
MCNEIL PHARMACEUTICAL

SPRING HOUSE PA 19477
PHONE: 215 628 5537

PATRICK S CALLERY
UNIV OF MARYLAND
20 N PINE ST
BALTIMORE MD 21201
PHONE: 301 328 2980

JOSEPH E CAMPANA
QUALITY ASSURANCE LAB
UNIV OF NEVADA
LAS VEGAS NV 89119
PHONE: 702 739 3142

SCOTT CAMPBELL
VG INSTRUMENTS
1008 BRISTOL LANE
MODESTO CA 95350
PHONE: 209 545 8105

RAUL CANEZ
ALCON LABS
6201 S FREEWAY
FORT WORTH TX 76115
PHONE: 817 551 4703

RICHARD J CAPP
3038 PITCHFORK LN

MCKEES ROCKS PA 15136
PHONE: 412 777 8372

JOHN H CAPPIS
LOS ALAMOS SCI LAB
INC-7 MS-J514
LOS ALAMOS NM 87544
PHONE: 505 667 4498

RICHARD M CAPRIOLI
UNIV OF TEXAS HSC
ANALTYICAL CHEM CTR
HOUSTON TX 77225
PHONE:

H S CARDEN
5361 BIGGER RD

KETTERING OH 45440
PHONE: 513 865 3789

MICHAEL D CARDENAS
T EDISON TECH CENTER
11131 ADAMS RD
FRANKSVILLE WI 53126
PHONE: 414 835 1544

DANIEL B CARDIN
UNION OIL RESEARCH
376 S VALENCIA ROOM M-101
BREA CA 92621
PHONE: 714 528 7201

JO CARLIN
MERCK SHARP & DOHME
RESEARCH LABORATORY
RAHWAY NJ 07065
PHONE: 201 574 5920

TIMOTHY J CARLIN
MOBIL RES & DEV CORP
RESEARCH DEPT
PAULSBORO NJ 08066
PHONE: 609 423 1040

STEVEN A CARR
SMITHKLINE & FRENCH
L-940, SWEDELAND RD
SWEDELAND PA 19479
PHONE: 205 270 6650

ANTONELLA N CARRARO
UNIV OF TEXAS MED BRANCH
610 TEXAS AVE
GALVESTON TX 77550
PHONE: 409 761 6576

JOHN E CARROLL
MATTSON INSTRUMENTS
1001 FOURIER COURT
MADISON WI 53719
PHONE: 608 831 5515

DONNA SUE CARTER
INDIANA UNIVERSITY
DEPT OF CHEMISTRY
BLOOMINGTON IN 47405
PHONE: 812 335 6246

JOEL A CARTER
107 WINDSONG RD

CLINTON TN 37716
PHONE: 615 574 2447

ALLEN M CARY
FINNIGAN MAT
355 RIVER OAKS PKWY
SAN JOSE CA 95134
PHONE: 408 483 4800

L F CASABONA
TELEDYNE-ISOTOPES
50 VAN BUREN AVE
WESTWOOD NJ 07675
PHONE: 201 664 7070

HOWARD H CASPER
DEPT OF VETERINARY SCIENCE
NORTH DAKOTA STATE UNIV
FARGO ND 58105
PHONE: 701 237 7529

CAROLYN J CASSADY
12567 BROODMOOR

OVERLAND PARK KS 66209
PHONE: 716 753 7600

SHEILA A CASSIDY
ROY F WESTON INC
256 WELSH POOL RD
LIONVILLE PA 19353
PHONE: 215 524 0180

GENE CASSIS
WATERS ASSOCIATES
34 MAPLE STREET
MILFORD MA 01757
PHONE: 617 478 2000

LYLE W CASTLE
UNIV OF NEBRASKA-LINCOLN
DEPT OF CHEMISTRY
LINCOLN NE 68588
PHONE: 402 472 3507

P M CASTLE
778 CEDARWOOD DR

PITTSBURGH PA 15235
PHONE: 412 256 2090

ALBERT W CASTLEMAN
PENNSYLVANIA STATE UNIV
CHEMISTRY DEPT
UNIVERSITY PK PA 16802
PHONE: 814 865 7242

MAURO E CASTRO
DEPT OF CHEMISTRY
TEXAS A&M UNIV
COLLEGE STN TX 77843
PHONE: 409 845 8839

LARRY C CATTRAN
HEWLETT PACKARD
1601 CALIFORNIA AVE
PALO ALTO CA 94304
PHONE: 415 857 6118

STEVEN P CEPA
ABBOTT LABS
D 417 AP-9
ABBOTT PARK IL 60064
PHONE: 312 937 7534

RONALD L CERNY
CHEMISTRY DEPT
MCMS
LINCOLN NE 68588
PHONE: 402 472 3507

GREGORY CESSNA
EXTREL CORP
PO BOX 11512
PITTSBURGH PA 15238
PHONE: 412 963 7530

J W CHAI
DEPT OF CHEMISTRY
HOWARD UNIVERSITY
WASHINGTON DC 20059
PHONE:

BRIAN CHAIT
ROCKEFELLER UNIV
1230 YORK AVE
NEW YORK NY 10021
PHONE: 212 570 8849

JOHN A CHAKEL
GENENTECH INC
460 PT SAN BRUNO
SO SAN FRAN CA 94080
PHONE: 415 266 1239

WALTER S CHAMBERLIN
1001 CEDRO CT

LOS ALAMOS NM 87544
PHONE: 505 667 2054

DANIEL Y K CHAN
METPATH LABORATORY
1300 E TOUHY AVENUE
DES PLAINES IL 60018
PHONE: 312 635 4700

CHERNG CHANG
MONSANTO RESEARCH CORP
PO BOX 32
MIAMISBURG OH 45342
PHONE: 513 865 4162

SHAW F CHANG
3M CENTER
BLDG 270-35-05
ST PAUL MN 55144
PHONE: 612 733 7947

PETER J CHANTRY
WESTINGHOUSE
RES & DEV
PITTSBURGH PA 15235
PHONE: 412 256 1001

DENNIS M CHARKOWSKI
UNIV OF IOWA
PHARMACOLOGY DEPT
IOWA CITY IA 52242
PHONE: 319 335 7956

PHILIPPE CHASTAGNER
E I DUPONT
SAVANNAH RIVER LAB
AIKEN SC 29808
PHONE: 803 725 3293

NANCY WU CHEN
COOK CTY OFF OF THE
MEDICAL EXAMINER
CHICAGO IL 60612
PHONE: 312 666 0500

EDWARD K CHESS
BATTELLE NWST LABS
PO BOX 999
RICHLAND WA 99352
PHONE: 509 376 2234

TINA M PAWLOWKSI CHICHILA
427 WARREN RD

ITHACA NY 14850
PHONE: 607 255 6555

C L CHAN
E LOS ANGELES COLLEGE
CHEMISTRY DEPT
MONTEREY PARK CA 91754
PHONE: 213 265 8650

KELVIN W CHAN
SYNTEX RESEARCH
3401 HILLVIEW AVE
PALO ALTO CA 94304
PHONE: 415 855 5660

RUTH CHANG
CA STATE DEPT OF
HEALTH SERVICES
BERKELEY CA 94704
PHONE: 415 540 3003

SHAW F CHANG
RIKER LABS 3M CO
3M CENTER BLDG 270-35-05
ST PAUL MN 55144
PHONE: 612 733 7947

RICHARD CHAPMAN
FINNIGAN MAT
355 RIVER OAKS PKWY
SAN JOSE CA 95134
PHONE: 408 433 4800

JUDI CHARLES
HAZARDOUS MATERIALS LAB
2151 BERKELEY WAY
BERKELEY CA 94704
PHONE: 415 525 2486

DALE A CHATFIELD
SAN DIEGO STATE UNIV
CHEMISTRY DEPT
SAN DIEGO CA 92182
PHONE: 619 265 5806

PAUL H CHEN
ENVIRONMENTAL SCI & ENGIN
PO BOX ESE
GAINESVILLE FL 32602
PHONE: 904 371 1985

GIRISH B CHHEDA
ROSWELL PAK MEM INST
666 ELM ST
BUFFALO NY 14263
PHONE: 716 845 2388

MINGJIEN CHIEN
GIVANDAN CORP
125 DELAWANNA AVE
CLIFTON NJ 08817
PHONE: 201 365 8580

CONNIE K CHAN
40-22 77 STREET

ELMHURST NY 11373
PHONE: 212 367 7879

HELEN CHANDLER
IT CORP
304 DIRECTORS DR
KNOXVILLE TN 37923
PHONE: 615 690 3211

S Y CHANG
BURROUGHS WELLCOME CO
ORGANIC CHEMISTRY
RES TRI PK NC 27709
PHONE: 919 248 3360

TED T CHANG
AMERICAN CYANAMID
1937 W MAIN ST
STAMFORD CT 06904
PHONE: 203 348 7331

DALE L CHAPPELOW
CORE LAB-LITTON
8210 MOSLEY ROAD
HOUSTON TX 77075
PHONE: 713 943 9776

BONNIE A CHARPENTIER
PROCTER & GAMBLE CO
6071 CENTER HILL RD
CINCINNATI OH 45224
PHONE: 513 659 7654

CHIA T CHEN
11616 FLINTS GRV LN

GAITHERSBURG MD 20878
PHONE: 202 523 7174

MICHAEL T CHENG
STAUFFER CHEMICAL CO
1200 SOUTH 47TH ST
RICHMOND CA 94804
PHONE: 415 527 8998

MICHAEL P CHIARELLI
2205 S 10TH STREET
NO 107
LINCOLN NE 68502
PHONE: 402 372 3507

D M CHINN
FINNIGAN MAT
5088 ESTHER DR
SAN JOSE CA 95124
PHONE: 408 433 4800

JOHN W CHINN
CHEMISTRY DEPT
UNIV OF TEXAS
AUSTIN TX 78712
PHONE: 512 471 7344

DIANE CHO
FINNIGAN MAT
355 RIVER OAKS PKWY
SAN JOSE CA 95134
PHONE: 408 433 4800

ABUL KASEM CHOWDHURY
UNIVERSITY OF CALIFORNIA
DEPT OF CHEMISTRY
RIVERSIDE CA 92521
PHONE: 714 787 4740

RAY CHRISTOPHER
4415 NORWALK DR #18

SAN JOSE CA 95129
PHONE: 408 946 4848

HENRY CHUNG
R J REYNOLDS TOBACCO
BOWMAN GRAY TECH CTR
WINSTON-SALEM NC 27102
PHONE: 919 773 4939

KEITH L CLAY
UNIV OF COLORADO
PHARMACOLOGY DEPT
DENVER CO 80262
PHONE: 303 394 8759

MICHAEL T CLEARY
SIGNAL RESEARCH CTR
50 UOP PLAZA
DES PLAINES IL 60016
PHONE: 312 391 3448

MIDGE COATES
CHEMISTRY DEPT
UNIV OF CALIFORNIA
RIVERSIDE CA 92521
PHONE: 714 787 4740

JOHN T CODY
QUALITY CONTROL DIV
AIR FORCE DRUG TESTING LAB
BROOKS AFB TX 78235
PHONE: 512 536 2961

ALLEN I COHEN
SQUIBB INST MED RES
PO BOX 191
NEW BRUNSWICK NJ 08903
PHONE: 201 545 2686

GARY R CHIPMAN
AMOCO CORP
AMOCO RES CTR
NAPERVILLE IL 60566
PHONE: 312 420 5248

F E CHOU
334 OVERBROOK RD

BALTIMORE MD 21212
PHONE: 301 391 9116

JEFF CHRISTENSON
NICOLET INSTRUMENTS
5225-1 VERONA ROAD
MADISON WI 53711
PHONE: 608 271 3333

MICHAEL CHU
4915F PROSPECTOS DR
TRIANGLE LAB
RES TRI PARK NC 27713
PHONE: 919 544 5720

LILLIAN CHURCHILL
SIGNAL RESEARCH CTR
50 EAST ALGONQUIN ROAD
DES PLAINES IL 60017
PHONE: 312 391 3170

MICHAEL P CLAY
CUMMINS ENGINE COMPANY
MAIL CODE 20650
COLUMBUS IN 47202
PHONE: 812 377 8676

S D CLEMANS
STERLING WINTHROP
COLUMBIA TURNPIKE
RENSSELAER NY 12144
PHONE: 518 445 8139

RONALD L COCHRAN
ASHLAND CHEMICAL CO
PO BOX 2219
COLUMBUS OH 43216
PHONE: 614 889 4642

ROBERT B CODY
NICOLET INST CO
5225-1 VERONA RD
MADISON WI 53711
PHONE: 608 271 3333

M J COHEN
PCP INC
2155 INDIAN ROAD
W PALM BEACH FL 33409
PHONE: 305 683 0507

KIN S CHIU
205 ALEWIFE BROOK PARKWAY

CAMBRIDGE MA 02138
PHONE: 617 661 3111

CAROL S CHOW
CHEMICAL WASTE MNGMT
150 WEST 137TH STREET
RIVERDALE IL 60627
PHONE: 312 841 8360

W H CHRISTIE
OAK RIDGE NAT'L LAB
PO BOX Y BLDG 9735
OAK RIDGE TN 37831
PHONE: 615 574 2455

T Z CHU
FINNIGAN CORP
355 RIVER OAKS PKWY
SAN JOSE CA 95134
PHONE: 408 433 4800

JAMES D CIUPEK
MONSANTO CO U1C
800 N LINDBERGH BLVD
ST LOUIS MO 63167
PHONE: 314 694 1678

FREDERICK J CLAYTON
JOHN E EGAN LAB
METRO SANITARY DIST
SCHAUMBURG IL 60193
PHONE: 312 529 7700

ANDREW J CLIFFORD
DEPT OF NUTRITION
UNIV OF CALIFORNIA
DAVIS CA 95616
PHONE: 916 752 3376

ARTHUR B CODDINGTON
UNIV OF ILLINOIS
BOX 51-1 NOYES LAB
URBANA IL 61801
PHONE: 217 333 2545

MICHAEL J COGGIOLA
SRI INTERNATIONAL
333 RAVENSWOOD AVE
MENLO PARK CA 94025
PHONE: 415 859 3045

K H COLBERG
AMERICAN CAN CO
TECH SER
BARRINGTON IL 60010
PHONE: 312 381 1900

BRUCE N COLBY
PACIFIC ANALYTICAL
1989-B PALOMAR OAKS WAY
CARLSBAD CA 92009
PHONE: 619 931 1766

SHELLEY J COLDIRON
5116 SCHUBERT STREET
AMES IA 50010
PHONE: 515 292 5888

STEVEN G COLGROVE
RAINTREE APTS No 1321
3300 ROLLINGBROOK DRIVE
BAYTOWN TX 77521
PHONE: 713 425 5784

GEORGE J COLLINS
FINNIGAN MAT
355 RIVER OAKS PKWY
SAN JOSE CA 95134
PHONE: 408 433 4800

JENNIFER A COLLINS
BIO-ANALYTICAL TECHNOLOGIENRL
2356 N LINCOLN
CHICAGO IL 60614
PHONE: 312 880 6900

RICHARD J COLTON
CODE 6170
WASHINGTON DC 20375
PHONE: 202 767 2671

C M COMBS
99 ALEXANDER DR
MERIDEN CT 06450
PHONE: 203 284 6000

CONRAD CONE
IFF R&D
1515 HIGHWAY 36
UNION BEACH NJ 07735
PHONE: 201 264 6500

PATRICK A CONLON
5 FRESNO ST
BARNEGAT NJ 08005
PHONE: 201 666 6644

JOHN D CONNELL
KRATOS SCIENTIFIC
603 ROSE CT
LISLE IL 60532
PHONE: 312 529 7510

GERALD R CONNER
INFICON LEYBOLD
6500 FLY ROAD
E SYRACUSE NY 13057
PHONE: 315 437 0377

MICHAEL J CONNOLLY
227 N WHITE ROCK RD
HOLMES NY 12531
PHONE: 914 855 5065

DENISE A CONTOS
1802 ASHLAND AVE
COLUMBUS OH 43212
PHONE: 614 424 3281

D C CONWAY
TEXAS A&M UNIVERISTY
CHEMISTRY DEPT
COLLEGE STN TX 77843
PHONE: 209 845 4034

R J CONZEMIUS
1211 GARFIELD AVE
AMES IA 50010
PHONE: 515 294 5822

CHARLES J COOK
8301 DITZLER
RAYTOWN MO 64138
PHONE: 816 997 5541

G L COOK
8220 E GARFIELD M-15
SCOTTSDALE AZ 85257
PHONE: 602 994 3326

H D COOK
WESTINGHOUSE
BAPL
WEST MIFFLIN PA 15122
PHONE: 412 476 5424

J CARTER COOK
VG INSTRUMENTS INC
430 MALL BLVD
SAVANNAH GA 31406
PHONE: 217 333 2545

KELSEY D COOK
CHEMISTRY DEPT
UNIV OF TENNESSEE
KNOXVILLE TN 37996
PHONE: 615 974 8019

R GRAHAM COOKS
PURDUE UNIVERSITY
CHEMISTRY DEPT
W LAFAYETTE IN 47907
PHONE: 317 494 5262

CHARLES B COOPER
UNIV OF DELAWARE
PHYSICS DEPT
NEWARK DE 19711
PHONE: 302 451 2666

CHARLES V COOPER
NIOSH
4676 COLUMBIA PKWY
CINCINNATI OH 45226
PHONE: 513 841 4241

DON A COOPER
RT 2 BOX 302
PURCEVILLE VA 22132
PHONE: 703 285 2583

W J COOPER
FLORIDA INTERNL UNIV
DRINKING WATER RES CTR
MIAMI FL 33199
PHONE: 305 559 3049

JOHN CORNELIUS
FINNIGAN MAT
355 RIVER OAKS PARKWAY
SAN JOSE CA 95134
PHONE: 408 433 4800

TIM CORNISH
U OF NC AT CHAPEL HILL
CHEMISTRY DEPT
CHAPEL HILL NC 27514
PHONE:

CATHERINE E COSTELLO
MIT
CHEMISTRY 56-029
CAMBRIDGE MA 02139
PHONE: 617 253 7224

DONNA B COSULICH
LEDERLE LABORATORIES
MIDDLETOWN RD
PEARL RIVER NY 10965
PHONE: 914 735 5000

ROBERT J COTTER
JOHNS HOPKINS UNIV
MID ATLANTIC MS LAB
BALTIMORE MD 21205
PHONE: 301 955 3431

J E COTTON
2512-102 AVE NE

BELLEVUE WA 98004
PHONE: 237 5399

THOMAS COVEY
FINNIGAN MAT
355 RIVER OAKS PARKWAY
SAN JOSE CA 95134
PHONE: 408 433 4800

JEFFREY S CRAIN
AMES LAB-USDOE
IOWA STATE UNIV
AMES IA 50011
PHONE: 515 294 3887

DAVID CRAWFORD
US DOE
NEW BRUNSWICK LABORATORY
ARGONNE IL 60438
PHONE:

WILLIAM R CREASY
CHEMISTRY DIV
CODE 6110
WASHINGTON DC 20375
PHONE: 202 767 2398

JAN R CROWLEY
WAYNE STATE UNIV
435 CHEMISTRY
DETROIT MI 48202
PHONE: 313 577 3073

ZORAH F CURRY
866 BONNIE GLEN DR

MARIETTA GA 30067
PHONE: 404 424 2411

MARIA-LOURDES DAHL
MONSANTO
800 N LINDBERGH
ST LOUIS MO 63167
PHONE: 314 694 5754

PAUL DANIELLO
2384 HALFMOON DR
APT 1
ST LOUIS MO 63114
PHONE: 304 428 1325

G D DAVES
LEHIGH UNIV
CHEMISTRY DEPT
BETHLEHEM PA 18015
PHONE: 215 861 3471

M W COUCH
RESEARCH SERVICES
VA MEDICAL CTR
GAINESVILLE FL 32602
PHONE: 904 374 6059

J WAYNE COWENS
GCDC ROOM 371
RPMI
BUFFALO NY 14263
PHONE: 716 845 3563

PAMELA F CRAIN
UNIV OF UTAH
311A SKAGGS HALL
SALT LAKE CTY UT 84112
PHONE: 801 581 5581

LINDA CRAWFORD
SERCO LABORATORIES
1931 WEST COUNTY ROAD C2
ST PAUL MN 55113
PHONE: 612 636 7173

FRANK W CROW
THE UPJOHN CO
UNIT 7832-259-12
KALAMAZOO MI 49001
PHONE: 616 323 4344

JEFFREY G CUMMISKEY
EI DUPONT DE NEMOURS INC
EXPERIMENTAL STA E353/237
WILMINGTON DE 19898
PHONE: 307 772 7653

JEAN CZUCZWA
BATTELLE COLUMBUS DIV
505 KING AVENUE
COLUMBUS OH 43201
PHONE:

JIM DAHLGRAN
BORG WARNER CHEMICAL
PO BOX 68
WASHINGTON WV 26181
PHONE: 304 863 7325

PRADIP R DAS
SCHERING-PLOUGH CORP
60 ORANGE STREET
BLOOMFIELD NJ 07003
PHONE: 201 429 3977

ARTHUR DAVIDSON
DEA WESTERN FIELD LAB
PO BOX 36075
SAN FRANCISCO CA 94102
PHONE: 415 556 0951

JOHN COUTANT
MERRELL DOW PHARM
2110 E GALBRAITH RD
CINCINNATI OH 45215
PHONE: 513 948 7884

JOHN COWPAR
VG INSTRUMENTS INC
300 BROAD ST
STAMFORD CT 06901
PHONE: 203 332 4546

A G SKIP CRASKE
240 ALPHA DRIVE
PO BOX 11512
PITTSBURGH PA 15238
PHONE: 412 963 7530

RICHARD W CRAWFORD
LLNL
PO BOX 808
LIVERMORE CA 94550
PHONE: 415 422 6309

CATHERINE ANN CROWDER
7038 KINZALOW DRIVE

KNOXVILLE TN 37909
PHONE: 615 584 7797

JAMES E CURLETT
STATE OF ARIZONA
1207 WEST 10TH PL
TEMPE AZ 85281
PHONE: 602 257 2369

DAVID A DAHL
6300 NORTHSIDE CIRCLE

IDAHO FALLS ID 83401
PHONE: 208 526 9915

HOWARD S DANACEN
966 HUNGERFORD DR
UNIT 9B
ROCKVILLE MD 20850
PHONE: 301 279 2214

CHHABIL DASS
STOUT NEUROSCIENCES
MASS SPEC LAB
MEMPHIS TN 38163
PHONE: 901 528 5488

THOMAS A DAVIDSON
HELIUM OPERATIONS
BUREAU OF MINES
AMARILLO TX 79101
PHONE: 806 376 2368

TIM DAVIDSON
3051 MARSHALL APT 5

CINCINNATI OH 45220
PHONE: 513 475 4312

MARGARET R DAVIS
261 ROCHELLE AVENUE

PHILADELPHIA PA 19128
PHONE: 215 768 3081

WILLIAM E DAVIS
NOR-AM CHEMICAL CO
PO BOX 5130
N MUSKEGON MI 49445
PHONE: 616 744 4711

ROBERT DAY
5A BROOKSIDE DRIVE

DRYDEN NY 13053
PHONE: 607 755 8312

MARK A DEARTH
GEOLOGY 541
INDIANA UNIV
BLOOMINGTON IN 47405
PHONE: 812 335 6246

JOHN A DEFEVER
14469 ELLEN DR

LIVONIA MI 48154
PHONE: 313 554 6824

DANA E DEJOHN
WARNER LAMBERT
PO BOX 1047
ANN ARBOR MI 48106
PHONE: 313 996 7135

W JOHN DELANEY
39 BITTERWOOD LA

THE WOODLANDS TX 77381
PHONE: 713 292 2431

WILLIAM DEMAIO
914 GRANT AVE

IRWIN PA 15642
PHONE: 713 749 2675

CHARLES H DEPUY
UNIV OF COLORADO
CHEMISTRY DEPT
BOULDER CO 80309
PHONE: 303 492 7652

JOHN P DAVIES
217-6 NIMITZ DR

W LAFAYETTE IN 47906
PHONE: 317 494 5264

W D DAVIS
R D 5
COUNTY FARM ROAD
BALLSTON SPA NY 12020
PHONE:

ENRICO DAVOLI
UNL - DEPT OF CHEMISTRY
HAMILTON HALL RM 29
LINCOLN NE 68588
PHONE: 602 472 3507

LINDA K DEAN
INDIANA UNIVERSITY
CHEMISTRY DEPT
BLOOMINGTON IN 47405
PHONE: 812 335 3436

B A DEBARBIERI
37 WARREN ST
APT 3A
NUTLEY NJ 07110
PHONE: 201 235 2852

MAX L DEINZER
OREGON STATE UNIV
AGRICUL CHEM DEPT
CORVALLIS OR 97331
PHONE: 503 754 2906

DON C DEJONGH
FINNIGAN CORP
355 RIVER OAKS PKWY
SAN JOSE CA 95134
PHONE: 408 433 4800

SHERRI-SUE DELBERT
CHEMISTRY DEPT
MICHIGAN STATE UNIV
EAST LANSING MI 48824
PHONE: 517 353 5215

BRUCE R DEMARK
PROCTER & GAMBLE
MIAMI VALLEY LABS
CINCINNATI OH 45247
PHONE: 513 245 2572

HENRY L DEQUASIE
215 MEADOWOOD ROAD SW

FAIRVIEW TN 37062
PHONE: 615 322 2094

DEAN V DAVIS
UNOCAL SCIENCE & TECH DIV

BREA CA 92621
PHONE: 714 528 7201

WILLIAM DAVIS
ATOM SCIENCES
114 RIDGEWAY CTR
OAK RIDGE TN 37830
PHONE: 615 483 1113

RICHARD A DAY
UNIV OF CINCINNATI
CHEMISTRY DEPT
CINCINNATI OH 45221
PHONE: 513 475 3673

THOMAS A DEAN
WAYNE STATE UNIVERSITY
175 CHEMISTRY
DETROIT MI 48202
PHONE: 313 577 3080

JAMES J DECORPO
NAVAL SEA SYS COMM
CODE 56YB
WASHINGTON DC 20362
PHONE: 202 692 5307

DAVID A DEIS
2450 DUNSWORTH DR

COLUMBUS OH 43085
PHONE: 614 227 3854

MICHAEL J DEKREY
CONOCO INC RE 228
PO BOX 1267
PONCA CITY OK 74603
PHONE: 405 767 2945

JAMES E DELMORE
R #7 BOX 54

IDAHO FALLS ID 83401
PHONE: 208 526 2820

ALFRED J DEOME
ALLIANCE TECH CORP
213 BURLINGTON RD
BEDFORD MA 01730
PHONE: 617 275 9000

FRED L DEROOS
TWIN CITY TESTING CORP
662 CROMWELL AVE
ST PAUL MN
PHONE:

DOMINIC DESIDERIO
UNIV OF TENNESSEE
RM A218 COLEMAN BLDG
MEMPHIS TN 38163
PHONE: 901 528 5488

LISA DETTER
DEPT OF CHEMISTRY
BOX 390
W LAFAYETTE IN 47907
PHONE: 317 494 5462

SEKSAN DHEANDHANOO
EXTREL CORP
240 ALPHA DR
PITTSBURCH PA 15238
PHONE: 412 963 7530

V H DIBELER
56 N. PENNA AVE
P O BOX 151
BETHANY BEACH DE 19930
PHONE:

GERD DIELMANN
FINNIGAN MAT
355 RIVER OAKS PKWY
SAN JOSE CA 95134
PHONE: 408 433 4800

L A DIETZ
1124 MOHEGAN RD

SCHENECTADY NY 12309
PHONE:

ROBERT L DITTRICH
RALSTON PURINA CO
900 CHECKERBOARD SQUARE
ST LOUIS MO 63164
PHONE: 314 982 3416

A S DOAN
GODDARD SPC FLT CTR
CODE 615
GREENBELT MD 20771
PHONE: 301 286 7511

D L DOERFLER
307 CROYDON LANE

MANCHESTER MO 63021
PHONE: 314 537 6756

MALCOLM DOLE
110 WOOD ROAD M-1

LOS GATOS CA 95030
PHONE: 408 354 0478

ANTHONY J DESTEFANO
NORWICH EATON PHARM
PO BOX 191
NORWICH NY 13815
PHONE: 607 335 2603

JOS SIMON DEWIT
NIEHS
RESEARCH TRIANGLE PARK
RES TRI PARK NC 27709
PHONE: 919 541 5709

FRANK DIAS
NUTRA SWEET CO
601 E KENSINGTON
MT PROSPECT IL 60056
PHONE: 312 506 2363

L L DICKERSON
2005 S HIGBEE

IDAHO FALLS ID 83401
PHONE: 208 526 3035

ANDREA M DIETRICH
UNIV OF N CAROLINA
ENVIR SCI & ENGIN
CHAPEL HILL NC 27514
PHONE: 919 966 3862

JOHN J DINO
5706 LOYAL AVENUE

DURHAM NC 27713
PHONE: 919 541 2964

MARY A DITUSA
1975 NOTTINGHAM LANE

WHEATON IL 60187
PHONE: 312 653 2792

ROY L M DOBSON
PROCTER & GAMBLE CO-MVL
BOX 39175
CINCINNATI OH 45247
PHONE: 513 245 2046

LINDA DOHERTY
CHEMISTRY DEPT
MICHIGAN STATE UNIV
EAST LANSING MI 48824
PHONE: 517 353 6767

BRUNO M DOMON
MIT
DEPT OF CHEMISTRY RM 56-01
CAMBRIDGE MA 02139
PHONE: 617 253 7237

LEESA DETERDING
MCMS
UNIV OF NEBRASKA
LINCOLN NE 68588
PHONE: 402 472 3507

PATRICIA H DHAHIR
ELI LILLY & CO
WISHARD MEMORIAL HOSPITAL
INDIANAPOLIS IN 46202
PHONE: 317 261 4807

J R DIAS
UNIV OF MISSOURI
CHEMISTRY DEPT
KANSAS CITY MO 64110
PHONE: 816 276 2284

GERALD C DIDONATO
CHEMISTRY DEPT
INDIANA UNIVERSITY
BLOOMINGTON IN 47401
PHONE: 812 335 3436

DONNA K DIETRICH
2441 W LINCOLN AVE #31

ANAHEIM CA 92801
PHONE:

MARY M DIRR
PROCTER & GAMBLE
11810 E MIAMI RIVER ROAD
CINCINNATI OH 45247
PHONE: 513 245 2258

MICHAEL F DIXON
GALILEO ELECTRO-OPTICS
GALILEO PK
STURBRIDGE MA 01518
PHONE: 617 347 9191

DAVID W DODSWORTH
BRISTOL-MYERS CO
PO BOX 4755
SYRACUSE NY 13221
PHONE: 315 432 2265

STEVE DOHERTY
CHEMISTRY DEPT
INDIANA UNIV
BLOOMINGTON IN 47405
PHONE: 812 335 3436

JOSEPH R DONNELLY
734 STRAWBERRY PL

HENDERSON NV 89015
PHONE: 702 798 2299

FRANKLIN G DOOLITTLE
DEPT OF CHEMISTRY
WASHINGTON STATE UNIV
PULLMAN WA 99163
PHONE: 509 335 1707

STEVEN B DORN
GEN'L ELEC CORP
R&D BLDG K-1 RM2A40
SCHENECTADY NY 12301
PHONE: 518 387 6419

RALPH C DOUGHERTY
FLORIDA STATE UNIV
CHEMISTRY DEPT
TALLAHASSEE FL 32306
PHONE: 904 644 5725

ROBERT C DRAKE
3020 RIMROCK DR

LAWRENCE KS 66046
PHONE: 913 864 3223

DONALD DRINKWATER
240 BAKER LABORATORY
CORNELL UNIVERSITY
ITHACA NY 14853
PHONE: 507 255 3731

KEVIN DUFFIN
CHEMISTRY BLDG
INDIANA UNIV
BLOOMINGTON IN 47405
PHONE: 812 335 3436

WAYNE K DUHOLKE
THE UPJOHN CO

KALAMAZOO MI 49002
PHONE:

MICHAEL A DUNCAN
DEPT OF CHEMISTRY
UNIV OF GEORGIA
ATHENS GA 30602
PHONE: 404 542 1998

JOCELYN C DUNPHY
INDIANA UNIVERSITY
CHEMISTRY DEPT
BLOOMINGTON IN 47405
PHONE: 812 335 3436

ANTHONY N DURYEA
701 ALPHA DR

PITTSBURGH PA 15238
PHONE: 412 963 7262

J WALLACE DOONG
7319 LONGVINE

HOUSTON TX 77072
PHONE: 713 660 0901

MARIE G DORVIL
1085 NW 117TH STREET

MIAMI FL 33168
PHONE: 305 325 2675

TAD DOURDEVILLE
WATERS CHROMATOGRAPHY
DIV OF MILLIPORE
MILFORD MA 01757
PHONE: 617 478 2000

PETER A DREIFUSS
W R GRACE CO
WASHINGTON RESEARCH CTR
COLUMBIA MD 21044
PHONE: 301 531 4504

D L DROPKIN
3408 MORNINGSIDE DR

RALEIGH NC 27607
PHONE: 919 541 2323

MAUREEN DUFFY
CAMBRIDGE ISOTOPE LABS INC
20 COMMERCE WAY
WOBURN MA 01801
PHONE: 617 938 0067

ROBERT C DUNBAR
CASE WESTERN RESERVE
CHEMISTRY DEPT
CLEVELAND OH 44118
PHONE: 216 368 3712

LOREN L DUNHAM
2831 MARINA DR

ALAMEDA CA 94501
PHONE: 408 988 7136

RICHARD DUNPHY
ORTHO PHARMACEUTICAL
ROUTE 202 PO BOX 300
RARITAN NJ 08869
PHONE:

ROBERT C DUTKY
SPECTRAL COMPUTING
14112 NEW HAMPSHIRE AVE
COLESVILLE MD 20904
PHONE: 301 384 5305

R CAMERON DOREY
DEPT OF CHEMISTRY
WICHITA STATE UNIV
WICHITA KS 67208
PHONE: 316 689 3120

DOUGLAS DOSTER
MORTON/THIOKOL
1275 LAKE AVE
WOODSTOCK IL 60098
PHONE: 805 338 1800

ROBERT J DOYLE
NAVAL RESEARCH LAB
CODE 6110
WASHINGTON DC 20375
PHONE: 202 767 3551

RUSSELL C DREW
VIKING INSTRUMENTS CORP
103-B CARPENTER DRIVE
STERLING VA 22170
PHONE: 703 689 2214

GEORGE R DUBAY
PM GROSS/CHEMICAL LAB
DUKE UNIVERSITY
DURHAM NC 27706
PHONE: 919 684 2414

D L DUGGER
114 LEOLEIS DR

MARLBORO MA 01752
PHONE: 617 466 2764

MARK DUNCAN
NINCDS/NIH
BLDG 10 RM 3D40
BETHSEDA MD 20892
PHONE: 301 496 2151

GORDON H DUNN
JILA/NBS
UNIV OF COLORADO
BOULDER CO 80309
PHONE: 303 492 7824

R J DUPZYK
LLL
PO BOX 808 L-396
LIVERMORE CA 94550
PHONE: 415 422 6611

DANIEL M DYE
AIZA CORP
950 PAGE MILL ROAD
PALO ALTO CA 94303
PHONE: 415 494 5302

JOHN DYKINS
DEPT OF CHEMISTRY
UNIV OF PENNSYLVANIA
PHILADELPHIA PA 19104
PHONE: 215 989 8164

JOSEPH E DZIEDZIC
FMC CORP
PO BOX 8
PRINCETON NJ 08540
PHONE: 609 452 2300

BRIAN ECKENRODE
CHEMISTRY DEPT
MICHIGAN STATE UNIV
EAST LANSING MI 48824
PHONE: 517 353 5215

KENNETH W EDGELL
BIONETICS CORP
16 TRIANGLE PARK DR
CINCINNATI OH 45246
PHONE: 513 771 0448

MARTHA EIDNES
HENKEL CORP
2330 CIRCADIAN WAY
SANTA ROSA CA 95405
PHONE: 707 575 7155

F A ELDER
237 JUDSON ST

WEBSTER NY 14580
PHONE: 422 3179

CLAUDIA H ELKINS
STAUFFER CHEMICAL
EASTERN RESEARCH CENTER
DOBBS FERRY NY 10522
PHONE: 914 693 1200

WILLIAM H ELLIOTT
ST LOUIS UNIV
BIOCHEMISTRY DEPT
ST LOUIS MO 63104
PHONE: 314 577 8150

RUSSELL ENGBRECHT
PUGET SOUND NAVAL SHIPYARD
CODE 134.3
BREMERTON WA 98314
PHONE:

PAUL S EPSTEIN
3260 CREEK

ANN ARBOR MI 48104
PHONE: 313 344 1770

PAUL P DYMERSKI
GAMUT
9616 NORTHRIDGE CT
RICHMOND VA 23235
PHONE: 804 272 8587

R E EBY
955 W OUTER DRIVE

OAK RIDGE TN 37830
PHONE: 615 483 1829

JAMES P EDASERY
72-31 LITTLENECK PWY

GLEN OAKS NY 11004
PHONE: 212 650 7909

CHARLES G EDMONDS
UNIV OF UTAH
COLLEGE OF PHARMACY
SALT LAKE CTY UT 84112
PHONE: 801 581 5581

W NOEL EINOLF
PHILIP MORRIS USA
RESEARCH CENTER
RICHMOND VA 23261
PHONE: 804 274 2530

JAMES F ELDER
R J REYNOLDS TOBACCO
R & D DEPT
WINSTON-SALEM NC 27102
PHONE: 919 773 4941

ROBERT E ELLEFSON
MONSANTO RESEARCH CO
MOUND LAB R171
MIAMISBURG OH 45342
PHONE: 513 865 3791

WILLIAM B EMARY
DEPT OF CHEMISTRY
BOX 402
W LAFAYETTE IN 47907
PHONE: 317 464 6898

ROGER E ENGLAND
800 BUCHANAN STREET

ALBANY CA 94710
PHONE: 415 486 3519

JOHN A ERAS
2020 W BEVERLY BLVD

LOS ANGELES CA 90057
PHONE: 213 974 4647

ISMET DZIDIC
1220 BARTLETT
NO 2
HOUSTON TX 77006
PHONE: 713 493 7766

M W ECHO
WINCO
PO BOX 536
IDAHO FALLS ID 83402
PHONE: 208 526 2327

LARRY EDEN
MARION LABS INC
PARK B
KANSAS CITY MO 64134
PHONE: 816 966 5000

JIMMIE G EDWARDS
UNIV OF TOLEDO
CHEMISTRY DEPT
TOLEDO OH 43606
PHONE: 419 537 2111

BRIAN EITZER
541 GEOLOGY BLDG
INDIANA UNIV
BLOOMINGTON IN 47405
PHONE: 812 335 5976

VINCENT A ELDER
MARY KAY COSMETICS
PO BOX 152231
IRVING TX 75015
PHONE: 214 638 6750

ALLAN J ELLGREN
BOC GROUP
100 MOUNTAIN AVE
MURRAY HILL NJ 07974
PHONE:

EDGAR M EMERY
285 OLD ROAD

PORT READING NJ 07064
PHONE: 201 225 6700

CHRISTIE G ENKE
MICHIGAN STATE UNIV
CHEMISTRY DEPT
EAST LANSING MI 48824
PHONE: 517 535 4511

ERIC ERICKSON
CHEMISTRY DEPT
MICHIGAN STATE UNIV
EAST LANSING MI 48824
PHONE: 517 353 5215

MITCHELL D ERICKSON
ARGONNE NAT'L LAB
9700 S CASS AVENUE
ARGONNE IL 60439
PHONE:

STEVE ERICKSON
COLORADO SCHOOL OF MINES
DEPT OF CHEMISTRY
GOLDEN CO 80401
PHONE:

JAMES S ERSKINE
DOW CHEMICAL
B-1219
FREEPORT TX 77541
PHONE: 409 238 3244

THOMAS J ESKEW
MAAS INC
1155 ZION RD
BELLEFONTE PA 16823
PHONE: 814 353 0600

RAMON ESPINO
10372 BRYAN STREET
RIVERSIDE CA 92505
PHONE: 714 354 5954

KURT L ETTENHOFER
BENDIX ESD
1400 TAYLOR AVE
BALTIMORE MD 21284
PHONE: 301 321 5330

BARBARA EVANS
23 LLOYD ST
WINCHESTER MA 01890
PHONE: 617 642 0188

C A EVANS
CHARLES EVANS & ASSOC
301 CHESAPEAKE DR
REDWOOD CITY CA 94063
PHONE: 415 369 4567

DANIEL EVANS
152 DAVEY LABORATORY
BOX 31
UNIV PARK PA 16802
PHONE: 814 863 3583

JAMES E EVANS
E KENNEDY SHRIVER CT
200 TRAPELO RD
WALTHAM MA 02254
PHONE: 617 642 0188

JAMES V EVANS
MILES LABORATORIES
ANALYTICAL RESEARCH
ELKHART IN 46515
PHONE: 219 262 7762

ROBERT J EVANS
SOLAR ENERGY RES INST
1617 COLE BLVD
GOLDEN CO 80401
PHONE: 303 231 1384

KERRY EVEN
4501 ERSKINE RD
HEWLETT-PACKARD
CINCINNATI OH 45242
PHONE: 513 891 9870

J W EWING
1701 LEXINGTON DR
LYNCHBURG VA 24503
PHONE:

JOHN R EYLER
UNIV OF FLORIDA
CHEMISTRY DEPT
GAINESVILLE FL 32611
PHONE: 904 392 0532

BARBARA L FABRICANT
OWENS CORNING FIBERGLASS
PO BOX 415
GRANVILLE OH 43023
PHONE: 614 587 7360

C DAVID FADA
2213-235TH PL SE
BOTHELL WA 98021
PHONE: 206 486 4167

I S FAGERSON
UNIV MASSACHUSETTS
CHENOWETH LAB
AMHERST MA 01003
PHONE: 413 545 2278

HENRY M FALES
NAT'L INST OF HEALTH
BLDG 10, ROOM 7N 318
BETHESDA MD 20892
PHONE: 301 496 2135

A M FALICK
SCH OF PHARMACY
PARMACEUTICAL CHEM
SAN FRANCISCO CA 94143
PHONE: 415 476 5160

TSENG-PU FAN
UNIV OF HOUSTON
CHEMISTRY DEPT
HOUSTON TX 77004
PHONE:

PENG FANG
PO BOX 113
MCINTOSH AL 36553
PHONE: 205 944 2201

JAMES M FARRAR
UNIV OF ROCHESTER
DEPT OF CHEMISTRY
ROCHESTER NY 14627
PHONE: 716 275 5834

JOHN E FARRELL
SIX HASTING ROAD
YARDVILLE NJ 08620
PHONE: 609 585 8908

KAREN FARRELL
NORTH SHORE SANITARY DIST
RUSSELL ROAD
GURNEE IL 60031
PHONE: 312 623 6060

PAUL FARROW
ARTHUR D LITTLE INC
15 ACORN PARK
CAMBRIDGE MA 02140
PHONE: 617 864 5770

JACK D FASSETT
NBS
BLDG 221 RM A21
GAITHERSBURG MD 20899
PHONE: 301 975 4109

DOUGLAS FAST
CENTERS FOR DISEASE CONTRO
BLDG C17 ROOM 1814
ATLANTA GA 30333
PHONE: 404 452 4144

JIM FAULK
CASE WESTERN RESERVE UNIV
CHEMISTRY DEPT
CLEVELAND OH 44106
PHONE: 216 231 2609

KYM F FAULL
STANFORD UNIVERSITY
PSYCHIATRY DEPT
STANFORD CA 94305
PHONE: 415 497 7205

KENNETH D FAUST
ROCKY MTN ANALYTICAL LAB
4955 YARROW ST
ARVADA CO 80002
PHONE: 303 421 6611

GOTTFRIED FEISTNER
DEPT OF PSYCHIATRY
STANFORD UNIV MEDICAL CTR
STANFORD CA 94305
PHONE: 415 723 7073

RONG FENG
CHEMISTRY DEPT
BAKER LAB
ITHACA NY 14853
PHONE: 607 256 3731

CATHERINE C FENSELAU
UNIVERSITY OF MARYLAND
CHEMISTRY DEPT
BALTIMORE MD 21228
PHONE:

ROBERTO FERNANDEZ
412 DAVIS ROAD
PO BOX 3326
PASADENA TX 77501
PHONE: 713 477 6841

WILLIAM FIES
155 CHEROKEE WAY

PORTOLA VLLY CA 94025
PHONE: 408 433 4800

H H FINEGOLD
RD 1, BOX 165

DALLASTOWN PA 17313
PHONE:

JOHN W FIOLA
48 CAROL DRIVE

DEDHAM MA 02026
PHONE: 617 275 5444

JAMES R FISHER
1000 W AARON DRIVE I-8

STATE COLLEGE PA 06803
PHONE: 814 863 1333

MICHAEL FLANAGAN
ACUREX CORP
405 CLYDE AVE BLDG 12
MOUNTAINVIEW CA 94039
PHONE: 415 964 3200

BRYAN L FEAREY
LOS ALAMOS NATL LAB
ISOTOPIC & NUC CHEM GRP 7
LOS ALAMOS NM 87545
PHONE: 505 667 4534

JACK R FELKEY
TMS ANALYTICAL
6376 MORENCI TRAIL
INDIANAPOLIS IN 46268
PHONE: 317 291 5697

JOHN B FENN
ENGINEERING DEPT
YALE UNIV
NEW HAVEN CT 06520
PHONE: 203 432 4379

ANNA M FERGUSON
THERMODYNAMICS RES
ZACHRY BLDG
COLLEGE STATI TX 77843
PHONE: 409 845 4940

DEAN D FETTEROLF
FED BUREAU OF INVESTIGATIO
FORENSIC SCIENCE RESEARCH
QUANTICO VA 22135
PHONE: 703 640 6131

RONALD FIETKAU
TEXAS A&M UNIVERSITY
CHEMISTRY DEPT
COLLEGE STA TX 77843
PHONE:

SAUL W FINK
UNIVERSITY OF HOUSTON
DEPT OF CHEMISTRY
HOUSTON TX 77004
PHONE: 713 749 2646

DERRY L FISHEL
KENT STATE UNIV
CHEMISTRY DEPT
KENT OH 44242
PHONE: 216 672 2978

WADE L FITE
EXTREL CORP
240 ALPHA DR
PIITSBURGH PA 15238
PHONE: 412 963 7530

GERALD D FLESCH
IOWA STATE UNIV
AMES LAB
AMES IA 50011
PHONE: 515 294 3887

VERNON J FEIL
USDA-MRRL
STATE UNIV STATION
FARGO ND 58105
PHONE: 701 237 5771

JERRY FELSHER
140 RIDGE ROAD

NEW CITY NY 10956
PHONE: 914 634 8905

PAUL V FENNESSEY
UNIV OF COLORADO
MED CTR C232
DENVER CO 80262
PHONE: 303 394 7286

G J FERGUSSON
124 NASSAU PLACE

CLAREMONT CA 91711
PHONE: 714 626 8258

FRANK H FIELD
ROCKEFELLER UNIV
1230 YORK AVE
NEW YORK NY 10021
PHONE: 212 570 8848

MICHAEL S FILIGENZI
ENSECO/CAL LABS
2544 INDUSTRIAL BLVD
W SACRAMENTO CA 95616
PHONE: 916 372 1393

ROBERT E FINNIGAN
FINNIGAN MAT
355 RIVER OAKS PKWY
SAN JOSE CA 95134
PHONE: 408 433 4800

DIXIE L FISHER
ALLERGAN PHARMACEUTICALS
ANALYTICAL CHEMISTRY
IRVINE CA 92715
PHONE: 714 752 4500

JOHN J FITZGERALD
ETC
284 RARITAN CENTER PWY
EDISON NJ 08837
PHONE: 201 225 6716

DON FLORY
UNIV OF HOUSTON
DEPT OF CHEMISTRY
HOUSTON TX 77004
PHONE:

RICK A FLURER
DEPT OF CHEMISTRY
INDIANA UNIV
BLOOMINGTON IN 47405
PHONE: 812 335 3436

RODGER L FOLTZ
UNIV OF UTAH
CTR HUMAN TOXICOLOGY
SALT LAKE CTY UT 84112
PHONE: 801 581 5117

G O FOSS
FARRELL ROAD

NEWTOWN CT 06470
PHONE: 203 834 6343

H G FOUDA
PFIZER INC
DRUG METABOLISM
GROTON CT 06340
PHONE: 203 441 4647

DAVID F FRALEY
903 SARBROOK DR

CINCINNATI OH 45231
PHONE: 513 627 6412

JAMES C FRANKLIN
141 CUMBERLAND VIEW

OAK RIDGE TN 37830
PHONE: 615 574 2284

ROYAL B FREAS
DEPT OF CHEMISTRY
UNIV OF HOUSTON
HOUSTON TX 77004
PHONE: 713 749 4630

LOUIS C FREES
INFICON LEYBOLD
6500 FLY ROAD
E SYRACUSE NY 13057
PHONE: 315 437 0377

SCOTT B FRENCH
ICI AMERICAS
BIOMED RESEARCH DEPT
WILMINGTON DE 19897
PHONE: 302 575 2275

CARL FREY
DRAGOCO INC
PO BOX 261
TOTOWA NJ 07511
PHONE: 201 256 3850

DENIS L FOERST
HEWLETT-PACKARD S/D
1601 CALIFORNIA AVE
PALO ALTO CA 94304
PHONE: 415 857 6025

ROBERT A FORBES
BRUKER INSTRUMENTS
MANNING PARK
BILLERICA MA 01821
PHONE: 617 667 9580

KIRK B FOSTER
11549 HARLAN STREET

BROOMFIELD CO 80020
PHONE: 303 966 2429

ROBERT E FRAAS
28 FOUNTAIN CIRCLE

RICHMOND KY 40475
PHONE: 606 624 1292

THOMAS J FRANCL
AGRICULTURAL RES DIV
AMERICAN CYANAMID CO
PRINCETON NJ 08690
PHONE: 609 799 0400

BLAIR A FRASER
FDA
BOB/DBB/8800
BETHESDA MD 20892
PHONE: 301 496 1840

DONNAJEAN A FREDEEN
DEPT OF CHEMISTRY
UNIV OF BRIDGEPORT
BRIDGEPORT CT 06601
PHONE: 203 576 4439

KELLY D FREGIEN
UNIV OF MINN HOSP
GC-MS LAB
MINNEAPOLIS MN 55455
PHONE: 612 373 8772

ROBERT S FREUND
AT&T BELL LABS
600 MOUNTAIN AVE
MURRAY HILL NJ 07974
PHONE: 582 3865

MARGARET A FRISCH
IBM RESEARCH CENTER
PO BOX 218
YORKTWN HGTS NY 10598
PHONE: 914 945 1037

THEODORE L FOLK
227 WASHINGTON AVE

CUYAHOGA FALL OH 44221
PHONE: 216 796 4217

JOHN B FOREHAND
A H ROBINS INC
1211 SHERWOOD AVE
RICHMOND VA 23220
PHONE:

NORMAN G FOSTER
2719 ROBINWOOD LANE

DENTON TX 76201
PHONE: 817 387 4840

ARMEL FRADIN
UCHSC DEPT OF PHARMACOLOGY
BOX C236
DENVER CO 80262
PHONE: 303 394 8937

D J FRANK
8790 C ALLISON DRIVE

WESTMINSTER CO 80005
PHONE: 303 966 7855

WILLIAM FRASURE
ANALYTICAL SPECIALTIES
326 MARION AVE
ST LOUIS MO 63119
PHONE: 314 962 8648

J P FREEMAN
1500 ROCK

PINE BLUFF AR 71602
PHONE: 501 541 4369

BEN S FREISER
PURDUE UNIVERSITY
CHEMISTRY DEPT
W LAFAYETTE IN 47907
PHONE: 317 494 5270

NELSON M FREW
WOODS HOLE OCEAN INS
FYE BUIDLING
WOODS HOLE MA 02543
PHONE: 617 548 1400

STEPHEN W FROELICHER
DOW CHEMICAL
1707 BLDG
MIDLAND MI 48674
PHONE:

EMIL W FU
SANDOZ INC
59 ROUTE 10
E HANOVER NJ 07936
PHONE: 201 386 8121

JOHN D FUHRMAN
MONSANTO UZI
800 N LINDBERGH BLVD
ST LOUIS MO 63167
PHONE: 314 694 4238

PHILLIP T FUNKE
E R SQUIBB
PO BOX 4000
PRINCETON NJ 08540
PHONE: 609 921 4993

RAYMOND L FURNER
NEUROSCIENCES PROG
UNIV OF ALABAMA
BIRMINGHAM AL 35294
PHONE: 205 934 2443

DOUGLAS A GAGE
MICHIGAN STATE UNIV
MASS SPEC FACILITY
E LANSING MI 48824
PHONE: 517 353 0612

THEODORE J GALEN
17625 EL CAMINO REAL

HOUSTON TX 77058
PHONE: 713 483 4641

GUY GALLELLO
2200 IVY LANE

FINDLAY OH 45840
PHONE: 419 423 3526

ERNEST L GARNER
NAT'L BUR STANDARDS
BLDG 221 ROOM B362
GAITHERSBURG MD 20899
PHONE: 301 975 2002

SIMON J GASKELL
DEPT OF MEDICINE, 826E
BAYLOR COLLEGE OF MEDICINE
HOUSTON TX 77030
PHONE:

R A GEHLBACH
5150 EAST 65

INDIANAPOLIS IN 46220
PHONE: 317 849 4990

ROGER G FUELSTER
US GOV'T DEA
NORTH CENTRAL LAB
CHICAGO IL 60607
PHONE: 312 353 3640

HIDEJI FUJIWARA
MONSANTO CO
AA1F
CHESTERFIELD MO 63198
PHONE: 314 537 6271

ED FURLONG
SPEA LABORATORY
ROOM 541 GEOLOGY
BLOOMINGTON IN 47401
PHONE: 812 335 1217

JEAN H FUTRELL
DEPT OF CHEMISTRY
UNIV OF DELAWARE
NEWARK DE 19716
PHONE: 302 451 1247

DIANE S GALE
PEDIATRIC METABOLISM
BOX 3028
DURHAM NC 27710
PHONE: 919 684 3729

KENNETH L GALLAHER
STANDARD OIL CO
4440 WARRENSVILLE RD
CLEVELAND OH 44128
PHONE: 216 581 5826

J RUSSEL GANT
PERKIN ELMER CORP
761 MAIN AVE
NORWALK CT 06859
PHONE:

C GENE GARRETT
TEXAS INSTRUMENTS
PO BOX 655621/MS 938
DALLAS TX 75265
PHONE: 214 995 4748

DANIEL GAUDRY
CIBA-GEIGY
444 SAW MILL RIVER RD
ARDSLEY NY 10502
PHONE: 914 337 0897

MICHAEL J GEHRON
DEPT OF CHEMISTRY
UNIV OF FLORIDA
GAINESVILLE FL 32611
PHONE: 904 392 0515

RALPH W FUHRHOP
618 HOLLYWOOD PLACE

WEBSTER GROVE MO 63119
PHONE: 314 275 7272

ELAINE K FUKUDA
HOFFMAN LAROCHE
340 KINGSLAND ST
NUTLEY NJ 07110
PHONE: 201 235 2019

JORGE FURLONG
DEPT OF CHEMISTRY
BAKER LABORATORY
ITHACA NY 14853
PHONE: 607 255 3731

WILLIAM G GABODA
BETZ LABORATORIES
4636 SOMERTON RD
TREVOSE PA 19047
PHONE: 215 355 3300

P JANE GALE

DAVID SARNOFF RES CTR
PRINCETON NJ 08443
PHONE: 609 734 3053

EMILIO J GALLEGOS
CHEVRON
PO BOX 1627
RICHMOND CA 94804
PHONE: 415 620 4113

W A GARLAND
DEPT DRUG METABOLISM

NUTLEY NJ 07110
PHONE: 201 235 2137

DANIEL GARTEIZ
FINNIGAN MAT
355 RIVER OAKS PWY
SAN JOSE CA 95134
PHONE: 408 433 4800

M L GAY
6-H RIDGE RD

GREENBELT MD 20770
PHONE: 301 498 0245

DAVID L GEIGER
2502 CROSS COUNTRY ROAD

FAIRBORN OH 45324
PHONE: 513 255 2631

PAUL R GEISSLER
EXXON CHEMICAL CO
PO BOX 241
BATON ROUGE LA 70821
PHONE: 504 359 4644

GARY L GERMANN
1101 CRESCENT DRIVE

SPRINGFIELD IL 62704
PHONE: 217 782 8389

BENJAMIN Y GIANG
STAUFFER RESEARCH
1200 SO 47TH ST
RICHMOND CA 94804
PHONE: 415 231 1118

GRAHAM GIBSON
4 ELENA COURT M

MEDFORD NJ 08055
PHONE: 609 654 1862

CHARLES GILKER
CORNELL UNIV MED COLL
1300 YORK AVE
NEW YORK NY 10021
PHONE: 212 472 4841

GREG GILLEN
DEPT OF CHEMISTRY
ARIZONA STATE UNIV
TEMPE AZ 85281
PHONE: 609 965 4236

TODD A GILLESPIE
UNIV OF FLORIDA
LEIGH HALL BOX 122
GAINESVILLE FL 32611
PHONE: 904 392 0515

R E GLICK
FLORIDA STATE UNIV
CHEMISTRY DEPT
TALLAHASSEE FL 32306
PHONE: 904 644 4824

DAVID R GODWIN
NDRC LABORATORIES INC
3553 MILLER PARK DRIVE
GARLAND TX 45042
PHONE: 241 276 2986

MILTON W GOHEEN
1211 KNOLLWOOD CT

RICHLAND WA 99352
PHONE: 509 376 3358

GREGORY I GELLENE
DEPT OF CHEMISTRY
UNIV OF NOTRE DAME
NOTRE DAME IN 46556
PHONE: 219 239 7837

TIM GETEK
DEPT OF CHEMISTRY
UNIV OF HOUSTON
HOUSTON TX 77004
PHONE: 713 749 2675

DARYL GIBLIN
DEPT OF CHEMISTRY
UNIV OF NEBRASKA
LINCOLN NE 68588
PHONE: 402 472 3507

JEAN LUC GIGUET
DELSI INSTRUMENTS
10 KINGSBRIDGE ROAD
FAIRFIELD NJ 07006
PHONE: 201 227 7690

ROBERT A GILL
XEROX CORP
800 PHILLIPS RD
WEBSTER NY 14580
PHONE: 716 422 3571

KEITH T GILLEN
SRI INTERNATIONAL
333 RAVENSWOOD AVE
MENLO PARK CA 94025
PHONE: 415 859 3250

K A GINGERICH
TEXAS A&M UNIVERSITY
CHEMISTRY DEPT
COLLEGE STN TX 77843
PHONE: 409 845 2431

ROBERT M GLIDDEN
US FDA
10 W 35TH STREET
CHICAGO IL 60616
PHONE: 312 886 7074

DOUGLAS E GOERINGER
OAK RIDGE NAT'L LAB
PO BOX Y BLDG 9735
OAK RIDGE TN 37831
PHONE: 615 574 2452

A A GOLDBERG
115 LIVINGSTON AVE

EDISON NJ 08820
PHONE: 201 906 6814

PAUL W GENO
DEPT OF CHEMISTRY
TEXAS A & M UNIV
COLLEGE STN TX 77843
PHONE: 409 845 1939

SAHBA GHADERI
IBM
5600 COTTLE RD
SAN JOSE CA 95123
PHONE:

BRADFORD W GIBSON
DEPT OF PHARMACEUTICAL CHE
UNIV OF CALIFORNIA
SAN FRANCISCO CA 94143
PHONE: 415 476 5320

PHYLLIS W GILBERT
THE CLOROX CO
7200 JOHNSON DRIVE
PLEASANTON CA 94566
PHONE: 415 847 6601

BETH GILLECE-CASTRO
2035 9TH AVE
UNIV OF CALIFORNIA
SAN FRANCISCO CA 94116
PHONE: 415 476 5129

P W GILLES
UNIV OF KANSAS
CHEMISTRY DEPT
LAWRENCE KS 66045
PHONE:

ANNE B GIORDANI
1429 KEARNEY

ANN ARBOR MI 48104
PHONE: 313 996 5017

GARY L GLISH
OAK RIDGE NATL LAB
PO BOX Y
OAK RIDGE TN 37831
PHONE: 615 574 2456

ANN G GOETZ
HOFFMANN-LAROCHE
BLDG 71
NUTLEY NJ 07110
PHONE: 201 235 2058

WENDY GOLDBERG
MERCK ISOTOPES
PO BOX 2000
RAHWAY NJ 07065
PHONE: 201 574 4207

PAUL C GOODLEY
HEWLETT PACKARD
SCI INST DIV
PALO ALTO CA 94304
PHONE: 415 857 6194

GREGORY V GOODRIDGE
NATIONAL MED SVCS INC
2300 STRATFORD AVE
WILLOW GROVE PA 19090
PHONE: 215 657 4900

LEO A GORMAN
VG INSTRUMENTS
134 JUNEDALE DR
CINCINNATI OH 45218
PHONE: 513 825 1790

JOSEPH J GRABOWSKI
DEPT OF CHEMISTRY
HARVARD UNIV
CAMBRIDGE MA 02138
PHONE: 617 495 4130

WILLIAM L GRADY
114 SPRINGHOUSE ROAD

SAVANNAH GA 31419
PHONE: 912 238 7779

PETER W GRAVES
DETECTOR TECHNOLOGY
PO BOX K-300
BROOKFIELD MA 01506
PHONE: 617 867 4030

WESLEY A GRAY
MEDICAL SCHOOL
CASE WESTERN RESERVE UNIV
CLEVELAND OH
PHONE:

LARRY A GREEN
708 UNION ROAD

MICKLETON NJ 08056
PHONE: 609 423 1040

STEVE H GREENHOUSE
51 SCHUYLER AVE
APT 3 G
STAMFORD CT 06902
PHONE: 203 348 7331

JOSEPH F GREER
CIBA GEIGY
BLDG J RM J210
SUMMIT NJ 07901
PHONE: 201 277 7143

GEORGE W GOODLOE
1359-A HAMPTON DRIVE

AUBURN AL 36830
PHONE: 205 826 5066

S M GORDON
IITRI
CHEMISTRY DIVISION
CHICAGO IL 60616
PHONE: 312 567 4374

JOHN D GORSUCH
GENCORP
RESEARCH DIV
AKRON OH 44305
PHONE: 216 798 4025

DONALD G GRACZYK
ARGONNE NAT'L LAB
CHEMICAL TECHNOLOGY DIV
ARGONNE IL 60439
PHONE: 312 972 4460

ANDREW H GRANGE
935 SE 16TH AVE
NO 10
PORTLAND OR 97214
PHONE: 503 690 1084

CHARLES L GRAY
RICERCA INC
PO BOX 1000
PAINESVILLE OH 44077
PHONE: 216 357 3343

MICHAEL GRAYSON
3433 BLUFFVIEW DR

ST CHARLES MO 63303
PHONE: 314 233 2541

ROBERT L GREENALL
9329 HARDY DR

OVERLAND PARK KS 66212
PHONE: 913 236 3881

R CLIVE GREENOUGH
29 LYNWOOD DRIVE

MILLDALE CT 06467
PHONE: 203 288 3518

HUGH GREGG
LLNL
PO BOX 808 L-310
LIVERMORE CA 94550
PHONE: 415 423 7501

DENNIS GOODPASTURE
675 BROOKSEDGE BLVD

WESTERVILLE OH 43081
PHONE: 614 891 3344

GWEN D GORETSAS
HEWLETT-PACKARD
2025 LARPENTEUR
ST PAUL MN 55113
PHONE: 612 641 9500

SOHRAB HABIBI GOUDARZI
1113 STATE ST
APT 1R
LAFAYETTE IN 47905
PHONE:

H H GRADE
GENERAL ELECTRIC CO
R&D CENTER
SCHENECTADY NY 12301
PHONE: 518 387 6419

SUSAN T GRAUL
427 S RIVER RD #34

W LAFAYETTE IN 47906
PHONE: 317 743 9690

JOHN W GRAY
GALILEO ELEC-OPTICS
GALILEO PARK
STURBRIDGE MA 01518
PHONE: 617 347 9191

JOHN GREAVES
SCH OF MARINE SCIENCE
COLLEGE OF WM & MARY
GLOUCESTER PT VA 23062
PHONE: 804 642 7247

FRANK T GREENE
MIDWEST RESEARCH INST
425 VOLKER BLVD
KANSAS CITY MO 64110
PHONE: 816 753 7600

GARY GREER
VESTEC CORP
9299 KIRBY DR
HOUSTON TX 77054
PHONE: 713 796 9677

JOHN M GREGSON
SEWPCP LAB, SAN FRANCISCO
2350 42ND AVE
SAN FRANCISCO CA 94116
PHONE: 415 648 6882

RICHARD P GRESE
UNIV OF NEBRASKA LINCOLN
MIDWEST CTR FOR MASS SPEC
LINCOLN NE 68588
PHONE: 402 472 3507

RONALD D GRIGSBY
NIPER
PO BOX 2128
BARTLESVILLE OK 74005
PHONE: 918 337 4376

QUIRINUS G GRINDSTAFF
MARTIN MARIETTA
Y-12 PLANT
OAK RIDGE TN 37831
PHONE: 615 574 0679

MICHAEL L GROSS
UNIV OF NEBRASKA
CHEMISTRY DEPT
LINCOLN NE 68588
PHONE: 402 472 2794

FREDERICK W GROTHKOPP
1958 MCPHERSON

RICHLAND WA 99352
PHONE: 509 375 3131

ROBERT M GRUVER
PENN STATE UNIV
BORLAND BLDG
UNIVERSITY PA PA 16802
PHONE: 814 863 2966

CHRISTIAN GUENAT
NIEHS
PO BOX 12233
RES TRI PK NC 27709
PHONE: 919 541 2964

DAVID M GUIDO
THE UPJOHN CO
7234-25-11
KALAMAZOO MI 49001
PHONE: 616 385 5461

DONALD F GURKA
US EPA/QAD
944 EAST HARMON
LAS VEGAS NV 89102
PHONE:

RAY F HAACK
4049 VIA MAYISOL
APT 118
LOS ANGELES CA 90042
PHONE: 818 354 6568

DONALD A GRIFFIN
OREGON STATE UNIV
AGRICULTURAL CHEM
CORVALLIS OR 97331
PHONE: 503 754 2906

CASEY C GRIMM
DEPT OF CHEMISTRY
FLORIDA STATE UNIV
TALLAHASSEE FL 32306
PHONE: 904 644 6484

GEORGE GRINS
7011 BLACKBERRY DR

ARLINGTON TX 76016
PHONE: 817 467 0211

MARVIN F GROSTIC
7207 S 27TH

SCOTTS MI 49088
PHONE: 616 323 2804

IAN GROVE
VG INSTRUMENTS
32 COMMERCE CENTRE
DANVERS MA 01932
PHONE: 203 322 4546

BRIDGET P GUCCIONE
GENCORP
ANALYTICAL RESEARCH
AKRON OH 44305
PHONE: 216 798 4028

J G GUERRERA
27 MIRIAM DRIVE

MATAWAN NJ 07747
PHONE:

RICHARD J GUIDOBONI
NORTHERN ANAL LAB
7 TOPSFIELD DR
NASHUA NH 03062
PHONE: 603 673 1420

JOHN P GUTE
6414 GLENGARRY

WHITTIER CA 90606
PHONE: 613 699 0405

DAVID L HACHEY
BAYLOR COLL OF MED
PEDIATRICS DEPT
HOUSTON TX 77030
PHONE: 713 799 6002

PATRICK R GRIFFIN
10-5 COPELEY HILL

CHARLOTESVILL VA 22903
PHONE: 804 924 7994

ERIC P GRIMSRUD
CHEMISTRY DEPT
MONTANA STATE UNIV
BOZEMAN MT 59717
PHONE: 406 994 5418

GARY GROENEWOLD
BOX 804

IDAHO FALLS ID 83402
PHONE: 208 526 2803

A A GROTE
NIOSH
4676 COLUMBIA PKWY
CINCINNATI OH 45226
PHONE: 513 841 4308

J B GRUTKA
659 LANDAU AVE

JOLIET IL 60432
PHONE:

ALBERT E GUDAT
HEWLETT PACKARD
W120 CENTURY ROAD
PARAMUS NJ 07653
PHONE:

H Y GUH
PFIZER INC
EASTERN POINT RD
GROTON CT 06340
PHONE:

WILSON M GULICK
MICH TECH UNIV
CHEM & CHEM ENGIN
HOUGHTON MI 49931
PHONE: 906 487 2296

JAMES W GUTHRIE
1119 UPLAND DRIVE NE

ALBUQUERQUE NM 87112
PHONE: 505 846 4266

MURRAY HACKETT
CLSES EPA
6201 CONGDON BLVD
DULUTH MN 55804
PHONE: 208 720 5766

WILLIAM F HADDON
WRRC, USDA
800 BUCHANAN
ALBANY NY 94710
PHONE: 415 486 3693

JEAN HADLEY
UNIV OF COLORADO-HSC
4200 E 9TH AVE
DENVER CO 80262
PHONE: 303 394 8961

LYNN R HAGEMAN
NESTLES FOODS QAL
809 COLLINS ROAD
MARYVILLE OH 43040
PHONE: 513 644 8133

MARK E HAIL
301 LEIGH HALL
UNIV OF FLORIDA
GAINESVILLE FL 32611
PHONE: 904 392 0515

DAVID J HAJDASZ
DEPT OF CHEMISTRY BOX 468
PURDUE UNIV
W LAFAYETTE IN 47907
PHONE: 317 494 7446

ROBERT J HALE
TENNESSEE EASTMAN CO
B-150 RESEARCH
KINGSPORT TN 37662
PHONE: 615 229 3066

PATRICIA M HALL
BALL CORP
1509 S MACEDONIA AVE
MUNCIE IN 47302
PHONE: 317 747 6564

THOMAS HAMERLY
DETECTOR TECH INC
PO BOX K300
BROOKFIELD MA 01506
PHONE:

CARL G HAMMAR
M-368 STARLING LOVING
DEPT OF PATHOLOGY
COLUMBUS OH 43210
PHONE: 614 293 4587

MYNARD C HAMMING
232 VIRGINIA AVE

PONCA CITY OK 74601
PHONE: 405 765 4190

CHRISTINE V HAMPTON
3997 E SUNWIND DR

OKEMOS MI 48864
PHONE:

OWEN W HAND
DEPT OF CHEMISTRY BOX 473
PURDUE UNIV
W LAFAYETTE IN 47907
PHONE: 317 494 5264

CAROL A HANEY
204 TRAILS END CT

RALEIGH NC 27614
PHONE: 919 737 3746

ALAN HANNA
2514 PRAIRIE ROAD

MADISON WI 53711
PHONE: 608 271 3333

ROBERT E HANNAH
2840 NESTLING RD

PHILADELPHIA PA 19154
PHONE: 215 278 7434

R J HANRAHAN
UNIV OF FLORIDA
NUCLEAR SCIENCE
GAINESVILLE FL 32611
PHONE: 904 392 1442

GORDON E HANSEN
BOEHRINGER-INGELHEIM
RES & DEV CTR
RIDGEFIELD CT 06877
PHONE: 203 748 4200

JEFFREY W HANSEN
71 LINCOLN AVE

FAIR LAWN NJ 07410
PHONE: 201 666 6644

STUART HANSEN
HEWLETT-PACKARD CO
1601 CALIFORNIA AVE
PALO ALTO CA 94304
PHONE: 415 857 7271

CURT HANSON
TEXAS A&M UNIVERSITY
DEPT OF CHEMISTRY
COLLEGE STATI TX 77801
PHONE:

JACK HANSON
FINNIGAN MAT
355 RIVER OAKS PARKWAY
SAN JOSE CA 94034
PHONE:

KIMBERLY G HANZELKA
MARTIN MARIETTA ENERGY SYS
PO BOX Y
OAK RIDGE TN 37831
PHONE: 615 574 6535

HISAKO HARA
JOHNS HOPKINS SCH OF MED
725 N WOLFE ST
BALTIMORE MD 21205
PHONE: 301 955 3022

KEVIN L HARBOL
DEPT OF CHEMISTRY
UNIV OF KENTUCKY
LEXINGTON KY 40506
PHONE: 606 257 6957

GARY C HARBOUR
THE UPJOHN CO
7000 PORTAGE RD (1140-230-
KALAMAZOO MI 49001
PHONE: 616 323 5200

DWAYNE HARDIN
RADIAN CORPORATION
8501 MOPAC BLVD
AUSTIN TX 78766
PHONE: 512 454 4797

D R HARDY
NAVAL RESEARCH LAB
CODE 6180
WASHINGTON DC 20375
PHONE: 202 767 3559

KIM HARICH
VIRGINIA TECH
DEPT OF BIOCHEMISTRY
BLACKSBURG VA 24061
PHONE:

R L HARLESS
701 WHITE OAK DR

CARY NC 27511
PHONE: 919 541 2248

ALAN D HARMON
MCCORMICK & CO
RES & DEV LABS
HUNT VALLEY MD 21031
PHONE: 301 667 7458

PETER E HAROLDSEN
BAYLOR COLLEGE MEDICINE
ONE BAYLOR PLAZA
HOUSTON TX 77030
PHONE:

D N HARPOLD
GODDARD SPC FLT CTR
CODE 615
GREENBELT MD 20771
PHONE: 301 286 8054

JUDITH C HARRIS
ARTHUR D LITTLE INC
15-310 ACORN PARK
CAMBRIDGE MA 02140
PHONE: 617 864 5770

MARK HARRISON
UNIV OF COLORADO HSC
4200 EAST 9TH AVE BOX C232
DENVER CO 80262
PHONE: 303 394 4287

HASKELL V HART
SHELL DEVELOPMENT CO
PO BOX 1380
HOUSTON TX 77251
PHONE: 713 493 7725

MARK A HARTWIG
HEWLETT PACKARD
1200 E DIEHL RD
NAPERVILLE IL 60566
PHONE: 312 357 8800

T MICHAEL HARVEY
VG INSTRUMENTS
PO BOX 12554
RES TRI PK NC 27709
PHONE: 919 942 8405

CAROLINE HATTON
DEPT OF PHARMACOLOGY
UCLA SCH OF MEDICINE
LOS ANGELES CA 90024
PHONE: 213 206 6656

CHARLES R HAUER
DEPT OF CHEMISTRY
UNIVERSITY OF VIRGINIA
CHARLOTESVILL VA 22901
PHONE: 804 924 7994

RUTH HAWLEY-FEDDER
LLNL
L-310
LIVERMORE CA 94550
PHONE: 415 422 6328

TERRENCE M HARPER
AMERICAN ANAL LABS, INC
100 LINCOLN ST
AKRON OH 44308
PHONE: 216 535 3232

WILLIAM L HARRINGTON
RCA LABORATORIES
DAVID SARNOFF RES CT
PRINCETON NJ 08540
PHONE: 609 734 2415

ROBERT E HARRIS
BOX 41022

BRECKSVILLE OH 44141
PHONE: 216 447 5369

ROBERT H HARRISON
BROWARD SHERIFFS OFFICE
CRIME LABORATORY
FT LAUDERDALE FL 33301
PHONE:

KEVIN J HART
DEPT OF CHEMISTRY
MICHIGAN STATE UNIV
EAST LANSING MI 48824
PHONE: 517 353 5215

D J HARVAN
701 W CORNWALLIS ROAD

DURHAM NC 27707
PHONE: 919 544 5729

J RONALD HASS
TRIANGLE LABORATORIES
PO BOX 13485
RES TRI PK NC 27709
PHONE: 917 544 5729

RICKY L HATTON
PO BOX 15609

HATTIESBURG MS 39404
PHONE: 601 264 9320

JERRY HAWKINS
1155 TECH OPS DIV
DLPSI
MCCLELLND AFB CA 95652
PHONE:

THOMAS G HAYDEN
VANDERBILT UNIV MED CTR N
DEPT OF PATHOLOGY/CLIN TOX
NASHVILLE TN 37232
PHONE: 615 332 2609

TIMOTHY W HARPER
985 S LINCOLN ST

KENT OH 44240
PHONE: 216 325 2511

GAIL HARRIS
NICOLET INSTRUMENTS
5225-1 VERONA ROAD
MADISON WI 53711
PHONE: 608 271 3333

C BRETT HARRISON
EXTREL CORP
PO BOX 11512
PITTSBURGH PA 15238
PHONE: 412 963 7530

WILLARD W HARRISON
UNIV OF VIRGINIA
CHEMISTRY DEPT
CHARLOTTESVLL VA 22901
PHONE: 804 924 3435

THOMAS G HARTMAN
252 BOUNDARY AVENUE

STATEN ISLAND NY 10306
PHONE: 201 932 9686

PAUL HARVATH
BUICK MOTOR DIV
BLDG 85, DIV 46-83
FLINT MI 48550
PHONE: 313 236 0241

FRANK W HATCH
BOEHRINGER INGELHEIM
90 EAST RIDGE
RIDGEFIELD CT 06877
PHONE: 203 748 4200

SUSAN HATTOX
BOEHRINGER INGELHEIM
175 BRIAR RIDGE RD
RIDGEFIELD CT 06877
PHONE: 203 748 4200

R L HAWKS
5429 31ST STREET NW

WASHINGTON DC 20015
PHONE: 301 443 5280

DAVID A HAYES
12400 MOSSY BARK TRAIL
AUSTIN TX 78750
PHONE: 512 454 4797

JOHN M HAYES
INDIANA UNIV
BIOGEOCHEM LABS
BLOOMINGTON IN 47405
PHONE: 812 335 5610

MARION E HAYES
GALILEO ELCTRO-OPTICS
GALILEO PARK
STURBRIDGE MA 01518
PHONE:

MICHAEL J HAYES
CIBA-GEIGY CORP
444 SAW MILL RIVER ROAD
ARDSLEY NY 10502
PHONE: 914 478 3131

ROGER HAYES
UCHSC
4200 E 9TH AVE C232
DENVER CO 80262
PHONE: 303 394 8961

MARK J HAYWARD
649 NORTH 7TH STREET
NO 1
LAFAYETTE IN 47901
PHONE: 317 423 6898

KELLY HEAD
META-TRACE
13715 RIDER TRAIL N
EARTH CITY MO 63045
PHONE: 314 298 8566

BRYAN HEARN
305 LEIGH HALL
DEPT OF CHEMISTRY
GAINESVILLE FL 32611
PHONE: 904 392 4892

JOHN HEARN
FINNIGAN MAT
355 RIVER OAKS PKWY
SAN JOSE CA 95134
PHONE: 408 433 4800

EUGENE C HEATH
HARRIS LABS
PO BOX 80837
LINCOLN NE 68501
PHONE: 402 476 2811

H D HECK
CIIT
PO BOX 12137
RES TRI PK NC 27709
PHONE: 919 541 2070

WILLIAM L HECKLE
2312 FAIRVIEW AVENUE

CINCINNATI OH 45219
PHONE: 513 721 0198

CLYDE HEDIN
1020 WOODBRIDGE DR

LAS VEGAS NV 89108
PHONE: 702 798 2492

DAVID L HEIKES
FDA
1009 CHERRY
KANSAS CITY MO 64106
PHONE: 816 374 5524

RICHARD E HEIN
NICOLET INSTRUMENTS
5225 VERONA RD
MADISON WI 53711
PHONE: 608 271 3333

CURT E HEINE
DEPT OF CHEMISTRY
MICHIGAN STATE UNIV
EAST LANSING MI 48824
PHONE: 517 353 6767

THOMAS M HEINZE
1701 EAST 10TH STREET

PAWHUSKA OK 74056
PHONE:

DAVID N HELLER
JOHNS HOPKINS UNIV
725 N WOLFE ST
BALTIMORE MD 21205
PHONE: 301 955 6961

STEPHEN R HELLER
USDA-ARS, ASRI-MDCL
ROOM 56 BLDG 007
BELTSVILLE MD 20705
PHONE: 301 344 1709

WILLIAM G HELLIER
2105 SEAGULL CT

PITTSBURGH CA 94565
PHONE: 415 427 4513

ROBERT HELLMANN
WESTINGHOUSE MATERIALS CO
PO BOX 398704
CINCINNATI OH 45239
PHONE: 513 738 6551

PHILIP H HEMBERGER
LOS ALAMOS NAT'L LAB
GROUP CLS-1, MS G740
LOS ALAMOS NM 87545
PHONE: 505 667 9903

MARK E HEMLING
SMITH KLINE & FRENCH L-940
PO BOX 7929
PHILADELPHIA PA 19101
PHONE: 215 270 6549

M J HENCHMAN
BRANDEIS UNIV
CHEMISTRY DEPT
WALTHAM MA 02254
PHONE: 617 861 4028

JEFFREY R HENDEL
1804 MURIEL COURT

PRINCETON NJ 08540
PHONE: 201 225 5600

T R HENDERSON
5609 DON FELIPE CT SW

ALBUQUERQUE NM 87105
PHONE: 505 831 1111

WILLIAM A HENDERSON
1268 CRESTHAVEN DR

SILVER SPRING MD 20903
PHONE:

JACK D HENION
CORNELL UNIVERSITY
EQUINE DRUG TESTING
ITHACA NY 14850
PHONE: 607 256 6556

KENT D HENRY
BAKER LABORATORY BOX 215
CORNELL UNIVERSITY
ITHACA NY 14853
PHONE: 607 255 3726

RICHARD A HEPPNER
APPLIED SCIENCE DIV
2771 N GAREY AVENUE
POMONA CA 91767
PHONE: 714 593 3581

GUOR-RONG HER
HARVARD SCH OF PUBLIC HLTH
DEPT OF NUTRITION
BOSTON MA 02115
PHONE: 617 732 0632

CHARLES R HERD
LOUISIANA STATE UNIV
CHEMISTRY DEPT
BATON ROUGE LA 70803
PHONE: 504 388 6658

MARK H HERMANSON
SPEA
INDIANA UNIV
BLOOMINGTON IN 47405
PHONE: 812 335 1005

HARRY S HERTZ
NBS
A309 CHEMISTRY
GAITHERSBURG MD 20899
PHONE: 901 975 3145

ROBERT HETTICH
OAK RIDGE NATL LAB
BLDG 4500-S MS-120
OAK RIDGE TN 37831
PHONE: 615 574 4867

BRUCE J HIDY
BATTELLE LABS
505 KING AVE
COLUMBUS OH 43201
PHONE: 614 424 4591

CHARLES E HIGNITE
IBM BLDG E35-013
DEPT E35
SAN JOSE CA 95120
PHONE:

FRED D HILEMAN
MONSANTO U1F
800 N LINDBERGH BLVD
ST LOUIS MO 63167
PHONE: 314 694 1275

JOHN C HILL
1501 HARVEY ROAD
PENTHOUSE
COLLEGE STN TX 77840
PHONE:

LAURENCE R HILPERT
NAT'L BUR STAN
BLDG 222 RM A-113
WASHINGTON DC 20234
PHONE: 301 963 7370

DAVID S HIRANO
ANATEC LAB INC
435 TESCONI CIRCLE
SANTA ROSA CA 95401
PHONE: 707 526 7200

GLEN HERMAN
OCCIDENTAL CHEM CO
LONG RD
GRAND ISLAND NY 14072
PHONE:

DAVID A HEROLD
UNIV OF VIRGINIA
PATHOLOGY DEPT
CHARLOTTESVLL VA 22908
PHONE: 804 924 5691

RICHARD F HERZOG
9221 W BROWARD BLVD
NO 2304
PLANTATION FL 33324
PHONE:

DENNIS L HEURING
TMS ANAL SERVICES
6376 MORENCI TRAIL
INDIANAPOLIS IN 46268
PHONE: 317 291 5697

GARY M HIEFTJE
INDIANA UNIVERSITY
DEPT OF CHEMISTRY
BLOOMINGTON IN 47405
PHONE: 812 335 2189

TETSUO HIGUCHI
JEOL
11 DEARBORN ROAD
PEABODY MA 01960
PHONE:

DAVID R HILKER
NEW YORK STATE HEALTH DEPTMIT
WADSWORTH CTR FOR LAB & RECHEMISTRY 56-016
ALBANY NY 12201
PHONE: 518 474 1675

JOSEPH F HILLER
DOW CHEMICAL CO
574 BLDG
MIDLAND MI 48667
PHONE: 517 636 2126

GEORGE W HIME
15501 SW 106 AVE

MIAMI FL 33157
PHONE: 305 549 7347

RONALD A HITES
INDIANA UNIV
SPEA 410 H
BLOOMINGTON IN 47405
PHONE: 812 335 0193

JOSEPH HERMAN
STUART PHARMACEUTICALS

WILMINGTON DE 19897
PHONE: 302 575 8219

G R HERTEL
UNIV CENTRAL FLORIDA
CHEMISTRY DEPT
ORLANDO FL 32816
PHONE: 305 275 2246

KENNETH R HESS
FRANKLIN & MARSHALL COLLEG
DEPT OF CHEMISTRY
LANCASTER PA 17604
PHONE: 717 291 4123

R ANTHONY HICKS
E I DUPONT -SRP
BLDG 232-H RM 114
AIKEN SC 29808
PHONE: 803 557 8375

PETER M HIERL
UNIV OF KANSAS
CHEMISTRY DEPT
LAWRENCE KS 66044
PHONE: 913 864 3019

D L HILDENBRAND
SRI INTERNATIONAL

MENLO PARK CA 94025
PHONE: 415 859 3436

JAMES AMHERST HILL
CAMBRIDGE MA 02139
PHONE: 617 253 7236

RANDY G HILLIARD
BROWARD SHERIFFS OFFICE
CRIME LABORATORY
ST LAUDERDALE FL 33301
PHONE:

DAVID M HINDENLANG
ALLIED CORP
PO BOX 1021R
MORRISTOWN NJ 07960
PHONE: 201 361 5139

JOSEPH A HNATOW
TMA/ERG
117 N FIRST ST
ANN ARBOR MI 48104
PHONE: 313 662 3104

VEI-SHI HO
MI DEPT OF NAT RESOURCES
ENVIRONMENTAL LAB
LANSING MI 48912
PHONE: 517 373 2197

CHARLES H HOCART
UNIV OF UTAH
311A SKAGGS HALL
SALT LAKE CIT UT
PHONE: 801 581 5581

MICHAEL K HOFFMAN
US DEPT OF AGRICULTURE
300 12TH STREET SW
WASHINGTON DC 20250
PHONE: 202 447 7623

DAVID HOLKEBOER
INFICON L-H INC
6500 FLY RD
E SYRACUSE NY 13057
PHONE: 315 437 0377

WILLIAM E HOLLINGSWORTH
DEPT OF CHEMISTRY
CAMPUS BOX 215
BOULDER CO 80302
PHONE:

JAMES R HOLTSCLAW
HONEYWELL INC
M/S 665-M
CLEARWATERR FL 33546
PHONE: 813 579 6226

ROBIN J HOOD
CHEMISTRY DEPT
75 CHEMISTRY
DETROIT MI 48202
PHONE: 313 577 2046

EVAN C HORNING
11610 STARWOOD DR

HOUSTON TX 77024
PHONE: 713 799 4721

ROBERT S HOUK
IOWA STATE UNIV
CHEMISTRY DEPT
AMES IA 50011
PHONE: 515 294 9462

STEPHEN LEE HOWARD
DEPT OF CHEMISTRY
UNIV OF DELAWARE
NEWARK DE 19716
PHONE: 302 451 1247

J R HOBBS
DOT/TSC
CODE 48
CAMBRIDGE MA 02142
PHONE: 617 494 2534

ALFRED T HODGSON
LAWRENCE BERKELEY LAB
MS 70-110A
BERKELEY CA 94720
PHONE: 415 486 5301

CARL HOGBERG
6901 BRYN MAWR DR

AUSTIN TX 78723
PHONE: 512 458 7587

J F HOLLAND
MICHIGAN STATE UNIV
BIOCHEMISTRY DEPT
EAST LANSING MI 48824
PHONE:

ROBERT W HOLMAN
DEPT OF CHEMISTRY
756 HAMILTON HALL
LINCOLN NE 68588
PHONE: 402 472 3507

RICHARD E HONIG
99 DEMPSEY AVE

PRINCETON NJ 08540
PHONE: 609 921 7824

JOHN J HOPPE
VACUMETRICS INC
2261-#1 PALMA DR
VENTURA CA 93003
PHONE: 805 644 7461

MARJORIE G HORNING
BAYLOR COLL MEDICINE
RM 826 E
HOUSTON TX 77030
PHONE: 713 465 6249

K R HOUSTON
413 FOREST OAKS LANE

LAKE JACKSON TX 77556
PHONE: 409 297 5814

J R HOYLAND
DURYEA ASSOCIATES
701 ALPHA DRIVE
PITTSBURGH PA 15238
PHONE: 412 963 7262

D L HOBROCK
8736 MALTBIE RD

CENTERVILLE OH 45459
PHONE: 513 865 4064

HENRY T HOFFMAN
22 VANDER VEER DR

LAWRENCEVILLE NJ 08648
PHONE: 609 292 3950

JOE HOHMANN
NICOLET INSTRUMENT CORP
5225-1 VERONA ROAD
MADISON WI 53711
PHONE: 608 271 3333

JAMES S HOLLER
CENTER DISEASE CNTRL
TOXI BRANCH C17-1814
ATLANTA GA 30333
PHONE: 404 452 4144

GALE A HOLMES
DOW CHEMICAL CO
BLDG B-1219
FREEPORT TX 77541
PHONE: 409 238 7814

JEFF P HONOVICH
NIMH BLDG 10-3D40

BETHESDA MD 20014
PHONE: 301 496 2151

JOSEPH P HOPPESCH
BORG-WARNER RESEARCH
WOLF & ALGONQUIN RDS
DES PLAINES IL 60018
PHONE: 312 827 3131

STEVAN R HORNING
DEPT OF CHEMISTRY BOX 477
PURDUE UNIV
W LAFAYETTE IN 47907
PHONE:

WILLIAM N HOWALD
DEPT OF MEDICINAL CHEMISTR
UNIV OF WASHINGTON
SEATTLE WA 98195
PHONE: 206 543 6439

DAVID W HOYT
FINNIGAN MAT
355 RIVER OAKS PKWY
SAN JOSE CA 95134
PHONE: 408 433 4800

MARILYN P HOYT
6 HOWELL DRIVE

ANDOVER MA 01810
PHONE: 617 258 3083

THOMAS C HSIEH
DEPT OF FOOD SCIENCE
LOUISIANA ST UNIV
BATON ROUGE LA 70803
PHONE: 504 388 5193

FONG FU HSU
DEPT OF MEDICINAL CHEMISTR
UNIV OF UTAH
SALT LAKE CTY UT 84112
PHONE:

ROGER S H HSU
CORNELL UNIVERSITY
DRUG TESTING & TOXICOLOGY
ITHACA NY 14850
PHONE: 607 255 6555

LE QUN HUANG
984 PAMMEL CT

AMES IA 50011
PHONE: 515 294 3887

W C HUBBARD
NIH NCI
DEPT OF HEALTH & HUMAN SVC
FREDERICK MD 21701
PHONE: 301 496 5660

GREGORY L HUDSON
ENVIRONMENTAL LABORATORIES
103 S LEADBETTER ROAD
ASHLAND VA 23227
PHONE: 804 798 1589

BARBARA HUGHES
US EPA
DENVER FEDERAL CENTER
DENVER CO 80225
PHONE:

HELEN HUGHES
DEPT OF MED RM 826E
BAYLOR COLL OF MED
HOUSTON TX 77030
PHONE: 713 799 4721

HOYING L HUNG
CHEMISTRY DEPT
NORTHWESTERN UNIV
EVANSTON IL 60201
PHONE: 312 491 5514

JERRY D HRIBAR
G D SEARLE & CO
4901 SEARLE PKWY
SKOKIE IL 60077
PHONE: 312 982 7505

BIH-HSIUNG HSU
DEPT MEDICINAL CHEMISTRY
COLLEGE OF PHARMACY
GAINESVILLE FL 32610
PHONE: 904 392 3421

FRANCIS S HSU
PHILIP MORRIS USA
PO BOX 26583
RICHMOND VA 23261
PHONE: 804 274 2641

HUA CHING HU
11 BENFORD DR

PRINCETON JCN NJ 08550
PHONE: 609 452 2300

SUNKWEI HUANG
ADAMANTECH INC
1501 BLUEBALL AV
LINWOOD PA 19061
PHONE: 215 358 5115

F G HUDDA
36 PERRY AVE

LATHAM NY 12110
PHONE: 518 387 6665

JAMES E HUDSON
ALCON LABORATORIES
PO BOX 6600
FORT WORTH TX 76115
PHONE: 817 551 8113

C G HUGHES
UNIV OF KENTUCKY
TOBACCO & HEALTH
LEXINGTON KY 40506
PHONE: 606 257 9318

JOHN M HUGHES
HEWLETT-PACKARD CO
PO BOX 58019
SANTA CLARA CA 95052
PHONE: 408 988 7289

DONALD F HUNT
UNIV OF VIRGINIA
CHEMISTRY DEPT
CHARLOTTESVLL VA 22901
PHONE: 804 924 3610

TACHENG HSIEH
SANDOZ CROP PROTECTION
ANAL CHEMISTRY
CHICAGO IL 60611
PHONE: 312 670 4823

C SAM HSU
EXXON RES & ENGIN
CLINTON TOWNSHIP
ANNANDALE NJ 08801
PHONE: 201 730 7228

J P HSU
9210 CHADDSFORD

SAN ANTONIO TX 78250
PHONE: 512 522 2228

FRANCIS Y HUANG
12821 WEST GOLDEN LANE

SAN ANTONIO TX 78249
PHONE: 512 699 9090

LEE HUBBARD
CIBA-GEIGY CORP AG DIV
PO BOX 18300
GREENSBORO NC 27419
PHONE: 919 292 7100

CHARLES E HUDSON
MARINE BIOMEDICAL INST
200 UNIVERSITY BLVD
GALVESTON TX 77550
PHONE: 409 761 2939

B MASON HUGHES
1065 CAMARGO

BALLWIN MO 63011
PHONE: 314 694 1466

DAVID B HUGHES
34 LANGHORNE CR

NEWPORT NEWS VA 23606
PHONE: 804 599 4795

SUSAN V HUMMEL
US ENVIRONMENTAL PROT AGNC
P O BOX 16602
ARLINGTON VA 22215
PHONE: 703 557 7324

JERRY E HUNT
CHEM DIV 200 C173
ARGONNE NAT'L LAB
ARGONNE IL 60439
PHONE: 312 972 3517

SHARON HUNT
3M CENTER
BLDG 201-1W-29
ST PAUL MN 55144
PHONE: 612 733 2533

JOHN G HUNTINGTON
9679 YUKON CT

BROOMFIELD CO 80020
PHONE:

JIM HURST
FINNIGAN MAT
355 RIVER OAKS PKWY
SAN JOSE CA 95134
PHONE: 408 433 4800

NIAN-ZHOU HZU
DEPT OF CHEMISTRY
UNIVERSITY OF VIRGINIA
CHARLOTTESVIL VA 22901
PHONE: 804 924 7994

ELAINE C IGO
134 GROVE STREET

MELROSE MA 02176
PHONE: 800 538 7067

RAFAEL N INFANTE
CATHOLIC UNIV
CHEMISTRY DEPT
PONCE PR 00732
PHONE: 809 844 4150

A P IRSA
BROOKHAVEN NATL LAB
CHEMISTRY DEPT
UPTON NY 11973
PHONE: 516 282 4326

S C ISRAEL
UNIV OF LOWELL
CHEMISTRY DEPT
LOWELL MA 01854
PHONE: 617 452 5000

J M JACKSON
MARTIN MARIETTA
ENERGY SYSTEMS INC
PADUCAH KY 42001
PHONE: 502 444 6311

LEROY JACOBS
WAL INC
6385 W 52ND AVE #5
ARVADA CO 80002
PHONE: 303 278 2506

R L HUNTER
ION SPEC CORP
ONE LONGSTREET
IRVINE CA 92720
PHONE: 714 261 7743

W T HUNTRESS
JET PROPULSION LAB
L83-301
PASADENA CA 91109
PHONE: 818 354 8275

ALAN E HUTCHINGS
BARBEAU-HUTCHINGS INC
10 S FRANKLIN TPK
RAMSEY NJ 07446
PHONE:

MR A IDELSON
ICON SERVICES
19 OX BOW LANE
SUMMIT NJ 07901
PHONE:

CARL F IJAMES
DEPT OF CHEMISTRY
UNIV OF CALIFORNIA
RIVERSIDE CA 92521
PHONE: 714 787 4740

L L INGRAM
PO DRAWER FP

MISSISSIPPI S MS 39762
PHONE: 601 325 3102

ROBERT K ISENSEE
ONEIDA RES SERVICE
ONE HALSEY ROAD
WHITESBORO NY 13492
PHONE: 315 736 3050

PHILLIP ISSENBERG
UNIV OF NEBRASKA
EPPLEY INST
OMAHA NE 68105
PHONE: 402 559 4473

THOMAS C JACKSON
EASTMAN KODAK
RESEARCH LABS
ROCHESTER NY 14650
PHONE: 716 477 8515

DENLEY JACOBSON
NORTH DAKOTA STATE UNIV
DEPT OF CHEMISTRY
FARGO ND 58105
PHONE: 701 237 8811

R TRACY HUNTER
1 NORTH 14TH STREET

RICHMOND VA 23219
PHONE: 804 786 4898

H E HURST
UNIV OF LOUISVILLE
MED SCHOOL
LOUISVILLE KY 40292
PHONE: 502 588 5291

PAUL M HYDE
LSUMC
BIOCHEMISTRY DEPT
NEW ORLEANS LA 70112
PHONE: 504 568 6585

CHARLES R IDEN
SUNY-STONY BROOK
PHARMACOLOGY DEPT
STONY BROOK NY 11794
PHONE: 516 246 2298

ANDREAS J ILLIES
CHEMISTRY DEPT
AUBURN UNIV
AUBURN AL 36849
PHONE: 205 826 4043

SAM E INSALACO
O.H.M. CORP
PO BOX 551
FINDLAY OH 45839
PHONE: 419 423 3526

ILEANA ISERN-FLECHA
PO BOX 3242

BOCA RATON FL 33427
PHONE: 305 998 3058

DAVID WANG IVERSON
DELSI INSTRUMENTS
10 KINGSBRIDGE ROAD
FAIRFIELD NJ 07006
PHONE: 201 227 7690

THOMAS J JACKSON
1614 RICHFOREST

RICHARDSON TX 75081
PHONE: 214 851 8456

SOHAIL JAHANI
RD 6 ROBISNON LANE

KLAPPINGERS F NY 12590
PHONE: 914 221 2485

SOHAIL JAHANI
RD 6
ROBINSON LANE
NY 12590
PHONE: 914 221 2485

ALAN T JAMES
EXXON PRODUC. RES.
PO BOX 2189
HOUSTON TX 77001
PHONE: 713 965 4158

JOHN JANZER
MATTSON INSTRUMENTS
PO BOX 1109
PLUMSTEADVILL PA 18949
PHONE: 215 766 0751

J A JARRELL
11 HYDE STREET

NEWTON HGHLND MA 02161
PHONE: 617 478 2000

STEVE JEFFERTS
JILA/ U OF COLORADO
CAMPUS BOX 440
BOULDER CO 80309
PHONE: 303 492 7873

NANCY JEAN JENSEN
MCMS

LINCOLN NE 68588
PHONE: 402 472 3507

BRIAN A JEROME
OAK RIDGE NAT'L LAB
BLDG 3550
OAK RIDGE TN 37831
PHONE: 615 574 6167

XIANG-YU JIANG
318 PHARMACY BLDG
PURDUE UNIV
W LAFAYETTE IN 47907
PHONE: 317 494 1449

EMILE C JOEL
2408 17TH PLACE SE

WASHINGTON DC 20020
PHONE: 301 921 2781

BRUCE JOHNSON
FINNIGAN CORP
355 RIVER OAKS PARKWAY
SAN JOSE CA 95134
PHONE: 408 433 4800

HEMANT KUMAR JAJOO
VANDERBILT UNIV
DEPT OF CHEMISTRY
NASHVILLE TN 37332
PHONE: 615 322 2094

GENE C JAMIESON
ZOECON CORP
975 CALIFORNIA AVE
PALO ALTO CA 94304
PHONE: 415 354 3459

CHARLES H JARBOE
UNIV OF LOUISVILLE
PHAMACOLOGY & TOX
LOUISVILLE KY 40292
PHONE: 502 588 5158

MARTIN F JARROLD
AT&T BELL LABS
1E313
MURRAY HILL NJ 07974
PHONE:

JIM JEFFERY
CALIF STATE DEPT OF JUSTICCTR FOR HEALTH SCIENCES
BUR OF FORENSIC SVC
SACRAMENTO CA 95820
PHONE: 916 739 5136

T E JENSEN
5574 CASTLETON DR

W BLOOMFIELD MI 48033
PHONE: 313 322 4598

KE JIANG
UC SAN FRANCISCO
MASS SPECTRO LAB
SAN FRANCISCO CA 94143
PHONE: 415 476 4893

SHIOW-JEN JIN
CASE WESTERN RES UNIV
10701 EAST BLVD
CLEVELAND OH 44106
PHONE: 216 791 3800

JEROME JOHEMKO
FINNIGAN CORP
355 RIVER OAKS PARKWAY
SAN JOSE CA 95134
PHONE:

BRUCE M JOHNSON
PFIZER INC
CENTRAL RESEARCH
GROTON CT 06340
PHONE: 203 441 3789

GEORGE JAKUBOWSKI
TRAVENOL LABORATORIES
6301 LINCOLN AVE
MORTON GROVE IL 60053
PHONE: 312 965 4700

DALE JANSEN
WATERS
DIVISION OF MILLIPORE
MILFORD MA 01757
PHONE: 617 478 2000

IAN JARDINE
MAYO CLINIC
PHARMACOLOGY DEPT
ROCHESTER MN 55905
PHONE: 507 284 4178

KOKA JAYASIMHULU
UNIV OF CINCINNATI
700 MORGAN HALL
CINCINNATI OH 45219
PHONE: 513 872 6349

D J JENDEN
PHARMACOLOGY DEPT
LOS ANGELES CA 90024
PHONE: 213 825 6694

ALFRED H JENSON
662 ARBOR VALLEY

CAMPBELL HALL NY 10916
PHONE: 201 934 9000

SHIUH-JEN JIANG
AMES LAB-USDOE
IOWA STATE UNIV
AMES IA 50011
PHONE: 515 294 3887

JILL M JOBBINS
1400 MILTON AVE

SOLVAY NY 13209
PHONE: 315 487 4311

CAROLYN JOHLMAN
PHILLIPS PETROLEUM CO
RESEARCH & DEVELOPMENT
BARTLESVILLE OK 74004
PHONE: 714 787 4740

BRUCE P JOHNSON
TENNESSEE EASTMAN CO
BLDG 231
KINGSPORT TN 37662
PHONE: 615 229 5651

CARL G JOHNSON
123 FYE LABORATORY
WOODS HOLE OCEAN INST
WOODS HOLE MA 02543
PHONE: 617 548 1400

JAN JOHNSON
DEPT OF STATE POLICE
BUR OF FORENSIC SCIENCES
SPRINGFIELD IL 62704
PHONE: 217 782 7430

KENNETH L JOHNSON
3600 BENTON STREET
No 33
SANTA CLARA CA 95051
PHONE: 408 247 1663

ROBERT L JOHNSON
119 HOLLOWOAK CT

CARY NC 27511
PHONE: 919 248 4353

MURRAY V JOHNSTON
DEPT OF CHEMISTRY
CAMPUS BOX 215
BOULDER CO 80309
PHONE: 303 492 5033

E G JONES
SYSTEMS RESEARCH LAB
RES APPLICATIONS DIV
DAYTON OH 45440
PHONE: 513 426 6000

TAMMY L JONES
2743 TAYLOR

N LAS VEGAS NV 89030
PHONE: 802 798 2144

GREGORY A JUNGCLAUS
MIDWEST RES INST
425 VOLKER BLVD
KANSAS CITY MO 64110
PHONE: 816 753 7600

LONNIE G JUSTICE
HEWLETT PACKARD
675 BROOKSEDGE BLVD
WESTERVILLE OH 43081
PHONE: 614 891 3344

MARY FRANCES KAISER
20 N PINE ST
UMAB PHARMACY SCHOOL
BALTIMORE MD 21201
PHONE: 301 328 2982

CHRIS JOHNSON
UNIV OF COLORADO - HSC
DEPT OF PHARMACOLOGY
DENVER CO 80262
PHONE: 303 394 8961

JODIE V JOHNSON
UNIV OF FLORIDA
314 LEIGH HALL
GAINESVILLE FL 32609
PHONE: 904 392 0515

P E JOHNSON
HUMAN NUTRITION LAB
BOX 7166 UNIV STATN
GRAND FORKS ND 58202
PHONE: 701 795 8416

W H JOHNSON
UNIV OF MINNESOTA
PHYSICS DEPT
MINNEAPOLIS MN 55455
PHONE: 612 624 0802

A DANIEL JONES
FAC FOR ADVANCED INSTR
9 HUTCHISON HALL
DAVIS CA 95616
PHONE: 916 752 0284

F E JONES
536 24TH SW

MIAMI OK 74354
PHONE: 918 542 9801

KURIAKOSE T JOSEPH
6030 PARKLAND DR

CORPUS CHRIST TX 78413
PHONE:

GREGOR A JUNK
US DOE
AMES LAB
AMES IA 50011
PHONE: 515 294 9488

ISHENKUMBA A KAHWA
CHEMISTRY DEPT
LOUISIANA STATE UNIV
BATON ROUGE LA 70803
PHONE: 504 388 5811

RAYMOND E KAISER
3382 PEPPERMILL
APT 2B
W LAFAYETTE IN 47906
PHONE: 317 497 1099

ERIC K JOHNSON
FINNIGAN MAT
355 RIVER OAKS PARKWAY
SAN JOSE CA 95134
PHONE: 408 433 4800

JUDITH A JOHNSON
STERLING-WINTHROP RESEARCH
81 COLUMBIA TURNPIKE
RENSSELAER NY 12144
PHONE: 518 445 8247

RICHARD S JOHNSON
MIT
CHEMISTRY 56-016
CAMBRIDGE MA 02139
PHONE: 617 253 7236

MARK JOHNSTON
NICOLET INSTRUMENTS
5225-1 VERONA ROAD
MADISON WI 53711
PHONE: 608 271 3333

CHRISTOPHER S JONES
MONTANA STATE UNIV
DEPT OF CHEMISTRY
BOZEMAN MT 59717
PHONE: 406 994 5420

GILBERT G JONES
AMOCO RESEARCH CTR MSB-5
PO BOX 400
NAPERVILLE IL 60566
PHONE: 312 420 5773

CHARLES M JUDSON
UNIV OF KANSAS
CHEMISTRY DEPT
LAWRENCE KS 66044
PHONE: 913 864 3223

JEANETTE JURUSIK
NYS DEPT OF HEALTH
WCL&R
ALBANY NY 12201
PHONE: 518 474 1675

MARY FRANCES KAISER
UMAB PHARMACY SCHOOL
20 N PINE ST
BALTIMORE MD 21201
PHONE: 301 328 2982

ROBERT G KALEY
MONSANTO
800 N LINDBERGH
ST LOUIS MO 63167
PHONE: 314 694 8558

HENRY T KALINOSKI
BATTELLE PACIFIC NW LABS
PO BOX 999
RICHLAND WA 99352
PHONE: 509 376 1656

JOHN DE KANEL
DIV OF PARI-MUTUEL WAGERIN
1350 NW 12TH AVE ROOM 507
MIAMI FL 33136
PHONE: 305 325 2671

J J KARLINER
CIBA-GEIGY CORP
ANALYTICAL DEPT
ARDSLEY NY 10502
PHONE: 914 478 3131

DANIEL B KASSEL
333 CHEMISTRY BLDG
DEPT OF CHEMISTRY
EAST LANSING MI 48824
PHONE:

ROBERT N KATZ
ROCKEFELLER UNIV
BOX 253
NEW YORK NY 10021
PHONE: 212 570 8674

G L KEARNS
1504 SAN CARLOS BAY DRIVE

SANIBEL ISLND FL 33957
PHONE:

ROBERT G KEESEE
THE PENNSYLVANIA STATE UNI
152 DAVEY LAB
UNIV PARK PA 16802
PHONE: 814 863 3574

MICHAEL A KELLEY
98 COPPER MINE ROAD

FARMINGTON CT 06032
PHONE: 203 274 5461

SHARON L KELLY
RORER GROUP
800 BUSINESS CENTER DR
HORSHAM PA 19034
PHONE: 215 628 6738

MARIANNE KEMPFF
WAYNE STATE UNIV
75 CHEMISTRY BLDG
DETROIT MI 48202
PHONE: 313 577 3072

GEORGE J KALLOS
DOW CHEMICAL CO
BLDG 574
MIDLAND MI 48640
PHONE: 517 636 5340

ARTHUR KANT
139 WOODRIDGE RD

WAYLAND MA 01778
PHONE:

TOM KARNS
UNIV OF OKLAHOMA
CHEMISTRY DEPT
NORMAN OK 73019
PHONE: 405 325 2843

PATRICK E KASTL
DOW CHEMICAL USA
TOXICOLOGY
MIDLAND MI 48640
PHONE: 517 636 2060

KENJI KAWAOKA
EASTMAN KODAK CO
ATD B-82 KP
ROCHESTER NY 14620
PHONE: 716 477 6733

RONALD KEEFE
INTERNATIONAL PAPER CO
PO BOX 797
TUXEDO PARK NY 10987
PHONE: 914 351 2101

PAUL R KELLER
PROCTER & GAMBLE
11520 REED HARTMAN
CINCINNATI OH 45241
PHONE: 513 530 3045

PAUL E KELLEY
FINNIGAN MAT
355 RIVER OAKS PKWY
SAN JOSE CA 95134
PHONE: 408 433 4800

LEONID KELNER
10401 GROSVENOR DR #1101

ROCKVILLE MD 20852
PHONE: 703 530 2374

ERIC J KEMPSTER
2178 POMPEY-FABIUS ROAD

FABIUS NY 13063
PHONE: 315 413 2221

M S KAMINSKY
SURFACE TREATMENT SCI I
906 SOUTH PARK AVE
HIMSDALE IL 60521
PHONE:

IZET M KAPETANOVIC
PRECLIN PHARM SEC EPILEPSY
NINCDS, NIH
BETHESDA MD 20892
PHONE: 301 496 6777

STEVEN KASS
DEPT OF CHEMISTRY
UNIV OF MINNESOTA
MINNEAPOLIS MN 55455
PHONE: 612 625 7513

VISWANATHAM KATTA
DEPT OF CHEMISTRY
UNIV OF HOUSTON
HOUSTON TX 77004
PHONE: 713 749 2675

KATHLEEN A KAYGANICH
DEPT OF CHEMISTRY
MICHIGAN STATE UNIV
EAST LANSING MI 48824
PHONE: 517 353 0612

JOSEPH B KEENAGHAN
FINNIGAN MAT
1383 PICCARD DR
ROCKVILLE MD 20850
PHONE: 301 948 1067

JAMES A KELLEY
NIH
NCI LAB MED CHEM
BETHESDA MD 20892
PHONE: 301 496 3597

RONALD BRUCE KELLEY
U OF C DAVIS
DEPT OF ENVIRONMENTAL TOXI
DAVIS CA 95616
PHONE: 916 752 2541

PAUL C KEMPER
DEPT OF CHEMISTRY
UNIV OF CALIFORNIA
SANTA BARBARA CA 93106
PHONE: 805 961 2673

J M KENNISH
UNIV OF ALASKA
CHEMISTRY DEPT
ANCHORAGE AK 99508
PHONE: 907 786 1236

DONALD V KENNY
1350 KING AVE APT 102

COLUMBUS OH 43201
PHONE:

HILKKA KENTTAMAA
PURDUE UNIV
CHEMISTRY DEPT
W LAFAYETTE IN 47907
PHONE: 317 494 6898

EDWARD H KERNS
BRISTOL MYERS CO
2404 PENNSYLVANIA AVE
EVANSVILLE IN 47721
PHONE: 812 429 8225

MOHAN KHARE
EA ENGINEERING SCI & TECH
15 LOVETON CIRCLE
SPARKS MD 21152
PHONE: 301 771 4950

BRET KIEFABER
532 BODEN WAY

OAKLAND CA 94610
PHONE: 415 832 3543

HEE-YONG KIM
261 CONGRESSIONAL LANE
#308
ROCKVILLE MD 20852
PHONE: 301 496 4900

FRED L KING
DEPT OF CHEMISTRY
MCCORMICK ROAD
CHARLOTTESVLL VA 22901
PHONE: 804 924 7180

DONNA J KINNEY
RD 1 BOX 309

W. SAND LAKE NY 12196
PHONE: 518 474 1675

JAMES A KINSINGER
MASSTRON INC
6595 ODELL PLACE
BOULDER CO 80301
PHONE: 303 530 7778

MICHAEL KINTER
DEPT OF PATHOLOGY
CLINICAL LABS BOX 168
CHARLOTTESVLL VA 22908
PHONE: 804 924 9204

LLOYD KENT
105 RIVERDALE BLVD

PEMPTON LAKES NJ 07442
PHONE: 201 867 4100

CHRISTINE N KENYON
451 HOMER AVENUE

PALO ALTO CA 94301
PHONE: 408 447 7952

SUHAS KETKAR
EXTREL CORP
PO BOX 11512
PITTSBURGH PA 15238
PHONE: 412 963 7530

WARREN LEE KIDD
3213 MONTERREY BLVD

BATON ROUGE LA 70814
PHONE: 504 925 5012

W E KILLINGER
W R GRACE & CO
RESEARCH DIV
COLUMBIA MD 21044
PHONE: 301 531 4479

HYUN SOOK KIM
UNIV OF CALIFORNIA
CHEMISTRY DEPT
SANTA BARBARA CA 93106
PHONE: 805 961 2673

ROY W KING
UNIV OF FLORIDA
CHEMISTRY DEPT
GAINESVILLE FL 32611
PHONE: 904 392 0592

GARY R KINSEL
CAMPUS BOX 215
UNIV OF COLORADO
BOULDER CO 80309
PHONE: 303 492 8516

T H KINSTLE
BOWLING GREEN ST UNIV
CHEMISTRY DEPT
BOWLING GREEN OH 43403
PHONE: 419 372 2658

JEFFREY P KIPLINGER
5414 WAYNE STREET

RALEIGH NC 27606
PHONE: 919 683 6076

RICHARD H KENT
REG FORENSIC LAB
27 WOODLAND RD
PAINESVILLE OH 44077
PHONE: 216 325 9517

THOMAS W KEOUGH
9896 BARNSLEY CT

CINCINNATI OH 45242
PHONE: 513 245 2486

J K KHANDELWAL
MT SINAI MED SCHOOL
PHARMACOLOGY DEPT
NEW YORK NY 10029
PHONE: 212 650 5603

DAVID KIDWELL
NAVAL RES LAB
CODE 6170
WASHINGTON DC 20375
PHONE: 202 767 3575

LEWIS B KILLMER
325 N EDGMONT ST

MEDIA PA 19063
PHONE: 215 270 6656

BRENDA J KIMBLE
AMPHION ASSOCIATES
PO BOX 1608
LAFAYETTE CA 94549
PHONE: 415 372 8260

SHERRILL KING
W R GRACE & CO
CRYOVAC DIV
DUNCAN SC 29334
PHONE: 803 433 2559

ROBIN KINSER
PHILIP MORRIS USA
RESEARCH CENTER
RICHMOND VA 23261
PHONE: 804 274 5905

MICHAEL KINTER
BOX 168
UNIV OF VA MEDICAL CTR
CHARLOTTESVLL VA 22901
PHONE:

MARION C KIRK
SOUTHERN RES INST
2000-9TH AVE S
BIRMINGHAM AL 35255
PHONE: 205 323 6592

NADIA D KIRZECKY
AMER CYANAMID CO
PO BOX 400
PRINCETON NJ 08540
PHONE: 609 799 0400

F G KITSON
3 HARTFORD PLACE

NEWARK DE 19711
PHONE: 302 772 3543

PETER D KLEIN
6608 FANNIN AVE
RM 601
HOUSTON TX 77030
PHONE: 713 799 6001

DANIEL R KNAPP
MED UNIV S CAROLINA
PHARMACOLOGY DEPT
CHARLESTON SC 29425
PHONE: 803 792 2471

W B KNIGHTON
FRANKLIN & MARSHALL
CHEMISTRY DEPT
LANCASTER PA 17604
PHONE: 717 291 4124

CATHY J KOLANOWSKI
2144 TANSEL ROAD

INDIANAPOLIS IN 46234
PHONE: 317 274 3220

RICHARD W KONDRAT
CHEMISTRY DEPT
UNIV OF CALIFORNIA
RIVERSIDE CA 92521
PHONE: 714 787 5287

MARK E KOSLIN
9803 FREMONT AVE

MONTCLAIR CA 91763
PHONE: 714 593 3581

JAROSLAV KRAMAR
HEWLETT-PACKARD
SCIENTIFIC INSTRUMENTS DIV
PALO ALTO CA 94304
PHONE:

MARY J KREEK
ROCKEFELLER UNIV
1230 YORK AVE
NEW YORK NY 10021
PHONE: 212 570 8248

ROBERT W KISER
9-CP BLDG
UNIV OF KENTUCKY
LEXINGTON KY 40506
PHONE: 606 257 4622

MICHAEL KLANECKY
443 WRIGHT STREET
NO 307
LAKEWOOD CO 80228
PHONE: 303 966 4788

KEITH S KLINE
5840 LAKETON DRIVE
APT E
INDIANAPOLIS IN 46220
PHONE: 317 576 0319

GARY D KNERR
411 N ALMON
NO 523
MOSCOW ID 83843
PHONE: 208 885 6756

FRITZ J KNORR
SURFACE SCIENCE LABS
465 NATIONAL AVE
MTN VIEW CA 94043
PHONE: 415 962 8780

ERIC W KOLODZIEJ
MONSANTO CO
800 N LINDBERGH
ST LOUIS MO 63167
PHONE:

WALTER A KORFMACHER
NCTR
BIOCHEM TOX DIV
JEFFERSON AR 72079
PHONE: 501 541 4108

JAMES G KOSTELC
MONSANTO CO
MAIL ZONE BB2I
CHESTERFIELD MO 63198
PHONE: 314 537 6218

S W KRASNER
METRO WATER DIST
WATER QUALITY BRANCH
LA VERNE CA 91750
PHONE: 714 593 7474

GERHARD M KRESBACH
NORTHEASTERN UNIV
BARNETT INSTITUTE
BOSTON MA 02115
PHONE: 617 437 2794

PETER T KISSINGER
BIOANALYTICAL SYS
2701 KENT AVE
W LAFAYETTE IN 47906
PHONE: 317 463 4527

E R KLEIN
6608 FANNIN AVE
SUITE 601
HOUSTON TX 77030
PHONE: 713 799 6183

STEVEN E KLOHR
2339 YEAGER ROAD #4

W LAFAYETTE IN 47906
PHONE: 317 494 1467

T C KNIGHT
2370 S BRENTWOOD ST

LAKEWOOD CO 80227
PHONE: 303 977 4241

CHARLES KOCH
HEWLETT PACKARD
503 LARKSPUR AVE
CORONA DEL MA CA 92625
PHONE:

MICHAEL G KOLOR
71 MET KEATON DR

PEARL RIVER NY 10965
PHONE: 914 735 8622

RICHARD A KORNFELD
BATTELLE COLUMBUS DIV
505 KING AVENUE
COLUMBUS OH 43201
PHONE: 614 424 3934

KAREN KOTZ
RD#1 BOX 57

NESHANIC NJ 08853
PHONE:

JOHN M KRECISZ
SCA CHEMICAL SERVICES
11700 S STONY ISLAND
CHICAGO IL 60617
PHONE: 312 646 5700

THOMAS KRICK
UNIV OF MINNESOTA
BIOCHEMISTRY DEPT
ST PAUL MN 55108
PHONE: 612 624 7715

THAIYA KRISHNAMURTHY
RES DIRECTORATE
CHEM RES DEV & ENG CTR
APG MD 21010
PHONE: 301 671 2255

JANA L KROTTINGER
CONOCO INC
PO DRAWER 1267
PONCA CITY OK 74603
PHONE: 405 767 2954

W F KUHN
PHILIP MORRIS USA
RESEARCH CENTER
RICHMOND VA 23261
PHONE: 804 274 3918

S D KUMAR
RADIAN CORP
PO BOX 9948
AUSTIN TX 78766
PHONE: 512 454 4797

PHILLIP A KUYKENDALL
FINNIGAN MAT
355 RIVER OAKS PKWY
SAN JOSE CA 95134
PHONE: 408 433 4800

JACQUES L LABROSSE
BALZERS
8 SAGAMORE PARK RD
HUDSON NH 03051
PHONE: 603 889 6888

LARRY LAFLEUR
NCASI
PO BOX 458
CORVALLIS OR 97339
PHONE: 503 754 2015

S T LAI
69 SCANTIC DRIVE

E LONGMEADOW MA 01028
PHONE:

JOHN G LAMBERTON
REICHHOLD CHEMICALS
PO BOX 1433
PENSACOLA FL 32596
PHONE: 904 433 7621

LES LAMPARSKI
DOW CHEMICAL
BLDG 57408, L-233
MIDLAND MI 48667
PHONE:

MICHAEL J KRISTO
CHEMISTRY DEPT
MICHIGAN STATE UNIV
EAST LANSING MI 48824
PHONE: 517 353 5215

FRANCIE M KUBIAK
MILES LABORATORIES
1127 MYRTLE ST BOX 40
ELKHART IN 46514
PHONE: 219 262 7979

BOB KULAWY
ONEIDA RES SVC INC
ONE HALSEY RD
WHITESBORO NY 13492
PHONE: 315 736 3050

KAREN KUOPPALA
9680 HARISON ST

THORNTON CO 80229
PHONE: 303 252 0408

JAMES N KYRANOS
191 BILLINGS RD

NORTH QUINCY MA 02171
PHONE: 617 479 9352

IRWIN LADD
UNION CARBIDE CORP
1 SUNSET DR
GROTON/HUDSON NY 10520
PHONE:

C ROBERT LAGERGREN
2110 HOWELL AVE

RICHLAND WA 99352
PHONE: 509 373 3872

SHIH-TSE JASON LAI
25815 SOUTHBROOK

EL TORO CA 92630
PHONE: 714 770 0039

STEPHEN A LAMMERT
FINNIGAN MAT
355 RIVER OAKS PKWY
SAN JOSE CA 95134
PHONE: 408 433 4800

FRED W LAMPE
PENN STATE UNIV
152 DAVEY LAB
UNIVERSITY PK PA 16802
PHONE: 814 865 6553

KYLE J KROHA
23 E LAKESHORE DRIVE
No 7
CINCINNATI OH 45237
PHONE: 812 335 3436

DOUGLAS W KUEHL
EPA
6201 CONGDON BLVD
DULUTH MN 55804
PHONE: 218 720 5558

NARAYAN KUMAR
AMERICAN WATER WORKS
1115 S ILLINOIS ST
BELLEVILLE IL 62220
PHONE: 618 235 3600

NICHOLAS J KURLICK
ENVIRESPONSE INC
GSA RARITAN DEPOT BLDG 209
EDISON NJ 08837
PHONE: 201 906 6872

GILLES LABELLE
CAMBRIDGE ISOTOPE LABS
20 COMMERCE WAY
WOBURN MA 01801
PHONE: 617 938 0067

A L LAFLEUR
16 WALL STREET

ARLINGTON MA 02174
PHONE: 617 253 3499

WILLIAM M LAGNA
11209 SANDYVALE ROAD

BRADSHAW MD 21021
PHONE: 301 671 3729

ROGER A LAINE
BIOCHEMISTRY DEPT
LOUISIANA STATE UNIV
BATON ROUGE LA 70803
PHONE:

CAROLEJEAN H LAMOUREUX
METABOLISM & RADIATION
RESEARCH LABORATORY
FARGO ND 58105
PHONE: 701 237 5771

DONALD P LAND
CHEMISTRY DEPT
UNIV OF CALIFORNIA
IRVINE CA 92717
PHONE: 714 856 6780

HERBERT H LAND
ETTC-TOXICON
3213 MONTERREY BLVD
BATON ROUGE LA 70814
PHONE: 504 925 5012

RUSSELL F LANG
US DEPT OF COMMERCE
NOAA/AOML
MIAMI FL 33149
PHONE: 305 361 4387

MARK A LAPACK
ANALYTICAL LABS
DOW CHEMICAL CO
MIDLAND MI 48640
PHONE: 517 636 6329

EDMUND A LARKA
6818 WOODHILL TRAIL

EDEN PRAIRIE MN 55344
PHONE: 612 625 3053

R KAZMER LATVEN
AMERICAN BIOTEST LAB
3350 SCOTT BLVD BLDG 15
SANTA CLARA CA 95054
PHONE: 408 727 5525

M T LAUG
ARGONNE NATIONAL LAB
PO BOX 2528
IDAHO FALLS ID 83401
PHONE: 208 526 7311

J H LAUTERBACH
BROWN & WILLIAMSON TOBACCOSKCL TOXICOLOGY DEPT
1600 W HILL ST
LOUISVILLE KY 40232
PHONE: 502 568 7567

DIANE J LAWVER
1922 LANKA LANE

CO SPRINGS CO 80915
PHONE: 303 636 5966

SAM D LE
2020 W BEVERLY BLVD

LOS ANGELES CA 90057
PHONE: 213 974 4647

EDWARD B LEDFORD
624 PEACH ST
PO BOX 80837
LINCOLN NE 68501
PHONE: 402 475 7640

DOROTHY C LANE
WESTERN RESEARCH INST
PO BOX 3395
LARAMIE WY 82071
PHONE: 307 821 2267

H G LANGER
DOW CHEMICAL
PO BOX 400
WAYLAND MA 01778
PHONE: 617 651 9634

JAMES A LARAMEE
AG CHEMISTRY
OREGON STATE UNIV
CORVALLIS OR 97331
PHONE: 503 754 2906

BARBARA S LARSEN
DUPONT
EXPERIMENTAL STATION E228
WILMINGTON DE 19898
PHONE: 302 772 4876

JAMES M LAU
120 W. CENTURY RD

PARAMUS NJ 07653
PHONE:

DIRK LAUKIEN
BRUKER INSTRUMENTS INC
MANNING PARK
BILLERICA MA 01821
PHONE: 617 667 9580

DAVID W LAW
1075 FIRST AVENUE
KG OF PRUSSIA PA 19406
PHONE: 215 962 7673

JACKSON O LAY
NAT'L CTR FOR TOX RESEARCH
HFT-184R
JEFFERSON AR 72079
PHONE: 501 541 4364

JOHN J LEARY
PFIZER INC
EASTERN POINT RD
GROTON CT
PHONE:

EDGAR D LEE
CORNELL UNIV
EQUINE DRUG TESTING
ITHACA NY 14850
PHONE: 607 255 6555

JACK LANG
MARTIN-MARIETTA ENERGY SYS
DEPT 513 MS 2229
PIKETON OH 45661
PHONE: 614 289 2331

PATRICK LANGVARDT
DOW CHEMICAL CO
1803 BLDG
MIDLAND MI 48640
PHONE: 517 636 1108

BARBARA LARKA
6818 WOODHILL TRAIL

EDEN PRAIRIE MN 55344
PHONE: 612 641 9485

ROBERT P LATTIMER
B F GOODRICH R & D
9921 BRECKSVILLE RD
BRECKSVILLE OH 44141
PHONE: 216 447 5369

DAVID LAUDE
UC RIVERSIDE
DEPT OF CHEMISTRY
RIVERSIDE CA 92521
PHONE:

FRANK H LAUKIEN
4 TROWBRIDGE PLACE
APT 4C
CAMBRIDGE MA 02138
PHONE: 617 864 2181

JULIE K LAWRENCE
1320 1/2 W EDWARDS

SPRINGFIELD IL 62704
PHONE: 217 782 7430

JOSEPH LAZAR
1006 N MONROE ST

WILMINGTON DE 19801
PHONE:

JULIE A LEARY
MASS SPECTROMETRY LAB
COLL OF CHEM
BERKELEY CA 94720
PHONE: 415 642 0701

MIKE S LEE
CHEMISTRY DEPT
LEIGH HALL 356
GAINESVILLE FL 32611
PHONE: 904 392 0515

TERRY D LEE
CITY OF HOPE
IMMUNOLOGY DEPT
DUARTE CA 91010
PHONE: 818 966 3211

MICHAEL G LEGENDRE
USDA APHIS NMRAL
3505 25TH AVE
GULFPORT MS 39505
PHONE: 601 863 8124

CATHERINE LEH
227 APACHE WAY

TEWKSBURY MA 01876
PHONE: 617 851 4876

CHRIS P LEIBMAN
UT STATION
PO BOX 16433
KNOXVILLE TN 37916
PHONE: 615 574 2455

ROBERT E LEMIEUX
1211 SHERWOOD AVE

RICHMOND VA 23220
PHONE: 804 257 2389

S R LEONE
UNIV OF COLORADO
JILA CAMPUS BOX 440
BOULDER CO 80309
PHONE: 303 492 5128

STEVEN K LEUNG
3401 LA GRANDE BLVD

SACRAMENTO CA 95823
PHONE: 916 428 1193

DOUGLAS E LEWIS
BIO-ANALYTICAL TECHNOLOGIE
2300 CHILDREN'S PLAZA
CHICAGO IL 60614
PHONE: 805 644 7461

SHARON G LIAS
NAT'L BUR OF STANDARDS

GAITHERSBURG MD 20899
PHONE: 301 921 2439

MARK LICHTENWALNER
NAT'L MED SERVICES INC
2300 STRATFORD AVENUE
WILLOW GROVE PA 19090
PHONE: 215 657 4900

JANET M LEE-WUEBBELS
12270 CHESAPEAKE

FLORISSANT MO 63033
PHONE: 314 694 1273

KASSU LEGESSE
BECKMAN RESEARCH INST
DIV OF IMMUNOLOGY
DUARTE CA 91010
PHONE:

JIM LEHMAN
DEPT OF CHEMISTRY
ARIZONA STATE UNIV
TEMPE AZ 85287
PHONE: 602 965 6193

ROGER J LEIBRAND
HEWLETT-PACKARD
1601 CALIFORNIA AVE
PALO ALTO CA 94304
PHONE: 415 857 6127

FRANK LEMUNYON
4414 NW 79TH TERRACE

KANSAS CITY MO 67151
PHONE:

KHINGKAN LERTRATANANGKOON
UNIV OF TEXAS MED BRANCH
DEPT OF PHARM & TOXIC J-31
GALVESTON TX 77550
PHONE: 409 761 1561

MILTON I LEVENBERG
ABBOTT LABS
DEPT 418, AP9
ABBOTT PARK IL 60064
PHONE: 312 937 2080

SYDELL LEWIS
ROHM & HAAS
8838 CREFELD STREET
PHILADELPHIA PA 19118
PHONE: 215 248 9065

L M LIBBEY
OREGON STATE UNIV
DPT FOOD SCI/TECH
CORVALLIS OR 97331
PHONE: 503 754 4636

J G LIEHR
UNIV OF TEXAS
MEDICAL BRANCH
GALVESTON TX 77550
PHONE: 409 761 1561

H F LEFEVRE
LEFEVRE ENGINEERING
2945 BURRVILLE RD
FORT RECOVERY OH 45846
PHONE: 419 375 4104

A M LEGRAND
WESTINGHOUSE NFD
PO DRAWER R
COLUMBIA SC 29250
PHONE: 803 776 2610

THOMAS A LEHMAN
PO BOX 435

N NEWTON KS 67117
PHONE: 316 283 2500

THOMAS LEIKER
BUR OF RECLAMATION M/C 152
DENVER FEDERAL CTR
DENVER CO 80225
PHONE: 303 236 4290

R ESPINOSA LENIZ
1200 N QUEEN ST
NO 402
ARLINGTON VA 22209
PHONE: 703 237 1733

RICHARD G LETT
PITTSBURGH ENERGY TECH CTR
USDOE
PITTSBURGH PA 15236
PHONE: 412 675 5805

STEVEN B LEVERY
THE BIOMEMBRANE INST
201 ELLIOTT AVE W
SEATTLE WA 98119
PHONE: 206 285 1309

LIANG LI
UNIV OF MICHIGAN
CHEMISTRY DEPT
ANN ARBOR MI 48109
PHONE: 313 747 2881

DANIEL J LIBERATO
HOFFMAN-LAROCHE INC
DEPT OF DRUG METABOLISM
NUTLEY NJ 07110
PHONE:

JERROLD M LIESCH
MERCK INSTITUTE
R80 M223
RAHWAY NJ 07065
PHONE: 201 574 5546

KAREN J LIGHT
MICHIGAN STATE UNIV
DEPT OF CHEMISTRY
E LANSING MI 48824
PHONE: 517 353 6495

W V LIGON
GENERAL ELECTRIC COD
R&D CENTER
SCHENECTADY NY 12301
PHONE: 518 385 8647

WILLIAM LIJINSKY
NCI FREDERICK CANCER
RESEARCH FACILITY
FREDERICK MD 21701
PHONE: 301 695 1221

H K LIM
CTR FOR HUMAN TOXICOLOGY
38 SKAGGS HALL
SALT LAKE CTY UT 84112
PHONE: 801 581 5119

DENIS C K LIN
ENSECO
214 DEEPDALE DR
MIDDLETONN NJ 07748
PHONE:

DING-PING LIN
3967 IVERNESS LANE
W BLOOMFIELD MI 48033
PHONE: 313 855 6196

SECHOING LIN
WARNER-LAMBERT/PARKE-DAVIS
188 HOWARD AVE
HOLLAND MI 49424
PHONE: 616 392 2375

SHEN NAN LIN
3751 GRENNOCH
HOUSTON TX 77025
PHONE: 713 972 5614

KENNETH A LINCOLN
2016 STOCKBRIDGE AVE
REDWOOD CITY CA 94061
PHONE: 415 369 7481

N C LING
THE SALK INSTITUTE
BOX 85800
SAN DIEGO CA 92138
PHONE: 619 453 4100

RICHARD W LINTON
CHEMISTRY DEPT
UNIV OF N CAROLINA
CHAPEL HILL NC 27514
PHONE: 919 962 2303

CAROL A LISEK
MAYO CLINIC
PHARMACOLOGY DEPT
ROCHESTER MN 55905
PHONE: 504 284 4224

ANITA KAY LISTER
PURDUE UNIVERSITY
CHEMISTRY DEPT
W LAFAYETTE IN 47906
PHONE: 317 494 5264

DOROTHY LITTLE
FRICK CHEMICAL LAB
ROOM 25
PRINCETON NJ 08540
PHONE: 609 452 3928

JAMES L LITTLE
TENN EASTMAN (KODAK)
BLDG 150
KINGSPORT TN 37662
PHONE: 615 229 3066

DUANE LITTLEJOHN
NICOLET INSTRUMENTS
5225-1 VERONA ROAD
MADISON WI 53711
PHONE:

JAMES F LITTON
LOCKHEED MISSILES & SPACE
0/48-92 B/195B
SUNNYVALE CA 94088
PHONE: 408 756 3646

NORMAN W LIU
SEARLE RES LAB
4901 SEARLE PKWY
SKOKIE IL 60077
PHONE: 312 982 8847

RAY H LIU
CRIMINAL JUSTICE
UNIV OF ALABAMA
BIRMINGHAM AL 35226
PHONE: 205 934 2069

YA-MEI LIU
MDCH, PHARMACY BLDG
PURDUE UNIVERSITY
W LAFAYETTE IN 47907
PHONE: 317 494 1449

H A LLOYD
NIH
BLDG 10 RM 7N312
BETHESDA MD 20892
PHONE: 301 496 3376

JOHN R LLOYD
FINNIGAN MAT
355 RIVER OAKS PKWY
SAN JOSE CA 95134
PHONE:

HSI H LO
PERKIN-ELMER
APPLIED SCIENCE DIV
POMONA CA 91767
PHONE: 714 593 3581

LYNETTE LOBMEYER
DEPT OF PHARMACOLOGY
UNIV OF COLORADO
DENVER CO 80262
PHONE: 303 394 8961

JOHN LOGSDON
9909 HOYT WAY
WESTMINSTER CO 80020
PHONE: 303 421 6611

STANTON LOH
BAKER LAB
CORNELL UNIV
ITHACA NY 14853
PHONE: 607 256 3726

MICHAEL LOMBARSKI
E I DUPONT
POLYMER PRODUCT DEPT
WILMINGTON DE 19828
PHONE: 302 772 2420

JOSEPH A LOO
CHEMISTRY DEPT
BAKER LAB
ITHACA NY 14853
PHONE: 607 255 3731

LAZARO LOPEZ
SUBURBAN LAB, INC
4140 LITT DRIVE
HILLSIDE IL 60162
PHONE: 312 544 3260

VIORICA LOPEZ-AVILA
ACUREX CORP
485 CLYDE AVE
MNTN VIEW CA 94039
PHONE: 415 961 5700

HARVEY LOUCKS
HEWLETT-PACKARD
SCIENTIFIC INSTRUMENTS
PALO ALTO CA 94304
PHONE: 415 857 6989

JAMES J LOVAS
PO BOX 490

REDONDO BEACH CA 90277
PHONE: 213 974 4647

DAVID M LUBMAN
CHEMISTRY DEPT
UNIV OF MICHIGAN
ANN ARBOR MI 48109
PHONE: 313 764 1669

WILLIAM J LUKSEMBURG
CALIFORNIA ANAL LABS
2544 INDUSTRIAL BLVD
W SACRAMENTO CA 95691
PHONE: 916 372 1393

MICHAEL LUTZ
CHEMISTRY DEPT
UNIV OF CALIFORNIA
IRVINE CA 92717
PHONE: 714 856 5682

LESLIE T LYTLE
4305 MINUTEMAN DR

CINCINNATI OH 45245
PHONE: 606 572 2280

JOHN L MACDONALD
RALSTON PURINA CO
3RS CHECKERBOARD SQ
ST LOUIS MO 63164
PHONE: 314 982 3038

JAMES M MADSON
MCDONNELL DOUGLAS
DEPT 223 BLDG 110
ST LOUIS MO 63166
PHONE: 314 233 2544

DONALD F MAGIN
PHILIP MORRIS R&D
BOX 26583
RICHMOND VA 23261
PHONE: 804 274 4153

KENNETH O MAHLER
SGE INC
2007 KRAMER LANE
AUSTIN TX 78758
PHONE:

EDWARD D LOUGHRAN
LOS ALAMOS NAT'L LAB
PO BOX 1663
LOS ALAMOS NM 87545
PHONE: 505 667 4894

NORMAN LOW
HEWLETT-PACKARD
1601 CALIFORNIA AVE
PALO ALTO CA 94304
PHONE: 415 857 7381

CLAUDE A LUCCHESI
NORTHWESTERN UNIV
DEPT OF CHEMISTRY
EVANSTON IL 60201
PHONE: 312 491 3479

HENRY E LUMPKIN
1600 DEEP WOOD DR

ROUND ROCK TX 78681
PHONE: 512 255 8386

PAUL LYNE
2532 VAN HISE AVENUE

MADISON WI 53705
PHONE: 608 262 1845

ABDUL MABUD
108-7 MARRIED STUDENT CT

W LAFAYETTE IN 47906
PHONE: 317 494 5262

RONALD D MACFARLANE
TEXAS A&M UNIVERSITY
CHEMISTRY DEPT
COLLEGE STN TX 77843
PHONE: 409 845 2021

C W MAGEE
RCA LABORATORIES

PRINCETON NJ 08540
PHONE: 609 734 2519

PAUL MAHAFFY
CODE 615-1
GODDARD SPACE FLIGHT CTR
GREENBELT MD 20771
PHONE: 301 286 8184

JOHN MAHONEY
PHRASOR SCIENTIFIC
1536 HIGHLAND AVE
DUARTE CA 91010
PHONE: 213 357 3201

JOHN N LOURIS
CHEMISTRY DEPT
BOX 589
W LAFAYETTE IN 47907
PHONE: 317 494 6898

HANS-JORG LQUE
ASTON-LAB CHEM DEPT
PURDUE UNIVERSITY
W LAFAYETTE IN 47907
PHONE: 317 494 6898

ROBERT LUDICKY
MORTON THIOKOL INC
1275 LAKE AVE
WOODSTOCK IL 60098
PHONE: 815 338 1800

WILLIAM R LUSBY
USDA
BLDG 467 BARC-EAST
BELTSVILLE MD 20705
PHONE: 301 344 2389

PHILIP A LYON
3M COMPANY
CORPORATE RESEARCH
ST PAUL MN 55144
PHONE: 612 736 3525

TABER MACCALLUM
PO BOX 689

ORACLE AZ 85623
PHONE: 602 792 2156

ROBERT J MADDEN
EXTREL CORP

PITTSBURGH PA 15238
PHONE: 412 963 7530

VINCE MAGGIO
CENTER FOR DISEASE CONTROL
1600 CLIFTON RD
ATLANTA GA 30333
PHONE:

NELS H MAHLE
DOW CHEMICAL CO
574 BLDG
MIDLAND MI 48640
PHONE: 517 636 9691

G J MAINS
301 E REDBUD DR

STILLWATER OK 74074
PHONE: 405 624 5941

GREGORY MAISEL
1931 WEST COUNTY ROAD C-2
ST PAUL MN 55113
PHONE: 612 636 7173

SIMIN D MALEKNIA
MASS SPEC LAB
WELCH 1-408C
ASUTIN TX 78712
PHONE: 512 471 7344

MATTHIAS MANN
YALE UNIVERSITY
DEPT OF CHEM ENG
NEW HAVEN CT 06520
PHONE: 203 432 4379

PAUL MARCELL
UNIV OF COLORADO MED CTR
BOX B-170 UCHSC
DENVER CO 80262
PHONE:

ALVIN B MARCUS
6 BAYARD ROAD
APT 859
PITTSBURGH PA 15213
PHONE: 412 624 8406

JAY A MARK
HUNTINGTON BCH POLICE
2000 MAIN STREET
HUNTINGTON BC CA 92648
PHONE: 714 536 5682

HENRY A MARSH
5901 S RICE
BELLAIRE TX 77396
PHONE: 703 432 2683

DON J MARSHALL
197 NORTH RD
BEDFORD MA 01730
PHONE: 617 263 2936

LEROY B MARTIN
NCSU
DEPT OF CHEMISTRY
RALEIGH NC 27695
PHONE: 919 737 2942

STEPHEN J MARTIN
RUSKA LABS INC
PO BOX 742688
HOUSTON TX 77274
PHONE: 713 975 0547

TAPAN KANTI MAJUMDAR
PURDUE UNIVERSITY
103-16 W STATE STREET
W LAFAYETTE IN 47907
PHONE: 317 743 9795

LARRY MALLIS
CHEMISTRY DEPT
UNIV OF IOWA
IOWA CITY IA 52242
PHONE: 319 335 1381

J J MANURA
SCIENTIFIC INSTR SERVICES
ROUTE 179
RINGOES NJ 08551
PHONE: 201 788 5550

ANGELA M MARCELLI
99 SIEBERLING ST
GENERAL TIRE CO
AKRON OH 44329
PHONE: 216 798 3375

RICHARD K MARCUS
CHEMISTRY DEPT
CLEMSON UNIVERSITY
CLEMSON SC 29631
PHONE: 803 656 5011

SANFORD P MARKEY
NIMH NIH
BLDG 10-3D40
BETHESDA MD 20892
PHONE: 301 496 2151

PHILIP G MARSH
OCCIDENTAL CHEMICAL CORP
TECHNOLOGY CTR
GRAND ISLAND NY 14072
PHONE: 716 773 8453

EDWIN MARTI
WIS STATE LAB OF HYGIENE
465 HENRY MALL
MADISON WI 53713
PHONE: 608 262 4523

LOUIS MARTIN
CIBA GEIGY
556 MORRIS AVENUE
SUMMIT NJ 07901
PHONE: 201 277 7143

WILLIAM B MARTIN
814 POWERS ST
BALTIMORE MD 21211
PHONE: 301 955 6961

J O MALBICA
ICI AMERICAS INC
BIOMEDICAL RES LAB
WILMINGTON DE 19897
PHONE: 302 575 2268

DAVID A MALTBY
PEDIATRIC METABOLISM
BOX 3028
DURHAM NC 27710
PHONE: 919 684 2036

DEAN MARBURY
19 PINNACLE ROAD
DURHAM NC 27705
PHONE: 919 544 5729

D T MARCOVICH
AFDTL BROOKS AFB
AFDTL (#930)
BROOKS AFB TX 78223
PHONE:

PETER J MARINELLI
PURDUE UNIVERSITY
BOX 618 CHEMISTRY BLDG
W LAFAYETTE IN 47906
PHONE: 317 494 7446

TERRY D MARRIOTT
RICE UNIV
CHEMISTRY DEPT
HOUSTON TX 77251
PHONE: 713 527 8101

ALAN G MARSHALL
CHEMISTRY DEPT
120 W 18TH AVE
COLUMBUS OH 43210
PHONE: 614 292 3446

JERRY D MARTIN
212 FRANK WEST CIRCLE
STOCKTON CA 95206
PHONE: 209 983 1340

STEPHEN A MARTIN
MIT
BLDG 56-035
CAMBRIDGE MA 02139
PHONE: 617 253 7233

RICHARD I MARTINEZ
A147 CHEMISTRY
NAT'L BUR OF STANDARDS
GAITHERSBURG MD 20899
PHONE: 301 975 2516

DAVID MARTINSEN
AMERICAN CHEMICAL SOCIETY
1155 16TH STREET NW
WASHINGTON DC 20036
PHONE: 202 452 2110

IAN J MASSEY
SYNTEX
3401 HILLVIEW AVE
PALO ALTO CA 94304
PHONE: 415 855 6156

W RODNEY MATHEWS
THE UPJOHN CO
BIOPOLYMER CHEM 7240-25-11
KALAMAZOO MI 49001
PHONE: 616 385 7507

DWIGHT E MATTHEWS
CORNELL UNIV MED COLLEGE
DIV ENDOCRIN & METABOLISM
NEW YORK NY 10021
PHONE: 212 472 4841

KENNETH P MATUSZAK
UNIV OF FLORIDA
401 LEIGH HALL
GAINESVILLE FL 32611
PHONE: 904 392 0515

RALPH J MAY
GENERAL ELECTRIC
BLDG K-1 RM 2A40
SCHENECTADY NY 12308
PHONE: 518 387 6419

HOWARD T MAYFIELD
AIR FORCE ENG & SVC CENTER
HQ AFESC/ROVC STOP 21
TYNDALL AFB FL 32403
PHONE: 904 283 4297

JERRY MCCLEARY
PERKIN-ELMER
2771 NORTH GAREY AVE
POMONA CA 91767
PHONE: 714 593 3581

JAMES A MCCLOSKEY
UNIV OF UTAH
COLLEGE OF PHARMACY
SALT LAKE CTY UT 84112
PHONE: 801 581 5581

ASHLEY L MCCORMACK
UNIVERSITY OF VIRGINIA
CHEMISTRY DEPT
CHARLOTTESVIL VA 22901
PHONE: 804 979 7629

ROB MARUYAMA
ADOLPH COORS CO
MAIL #BC600
GOLDEN CO 80401
PHONE:

JOHN A MASUCCI
217 DIANE AVE
HATBORO PA 19040
PHONE: 215 628 5539

SHARON MATLOCK
233 NORTH THIRD AVENUE
APT A
MANVILLE NJ 08835
PHONE: 201 225 6700

MARY JANE I MATTINA
CHEMISTRY DEPT
EMORY UNIV
ATLANTA GA 30322
PHONE: 404 727 6625

G G MATZ
BRUKER INSTRUMENTS INC
MANNING PARK
BILLERICA MA 01821
PHONE: 617 667 9580

RAYMOND E MAY
7652 COOLFIELDS WAY
SACRAMENTO CA 95828
PHONE: 916 362 5332

SUEANN MAZER
1430 CENTRAL PARK AVE
KETTERING OH 45409
PHONE: 513 229 2806

CRAIG A MCCLELLAND
M&M/MARS, INC
HIGH STREET
HACKETTSTOWN NJ 07840
PHONE: 201 852 1000

THOMAS D MCCLURE
UNIVERSITY OF ARIZONA
PHARMACEUTICAL SCI
TUCSON AZ 85721
PHONE: 602 626 3434

TERRENCE MCCORMICK
LINDEN-CHROMASSPEC
PO BOX 3451
PRINCETON NJ 08540
PHONE: 609 921 5439

FLOYD C MASELES
UNIV OF TEXAS
2.204A WELCH HALL
AUSTIN TX 78712
PHONE: 512 471 5484

RON MATHERLY
BAKER PERFORMANCE CHEMICAL
3920 ESSEX LN
HOUSTON TX 77027
PHONE:

MICHAEL B MATTAMMAL
111 GRECC
VA MEDICAL CENTER
ST LOUIS MO 63125
PHONE: 314 481 0400

JEAN E MATUSIK
FOOD & DRUG ADMN
GAITHERSBURG MD 20878
PHONE: 202 245 1371

R K MAULDIN
CELANESE FIBERS
PO BOX 32414
CHARLOTTE NC 28232
PHONE: 704 554 3134

JANET A MAYERNIK
A724 CRABTREE HALL
UNIV OF PITTSBURGH
PITTSBURGH PA 15261
PHONE: 412 624 5576

DAVID J MCADOO
62 LE BRUN COURT W
GALVESTON TX 77551
PHONE: 409 761 2939

WILLIAM MCCLENNEN
BIOMATERIALS PROFILING CTR
391 S CHIPETA WAY SUITE F
SALT LAKE CTY UT 84108
PHONE: 801 581 8431

GARY A MCCLUSKY
WARNER LAMBERT CO
PO BOX 1047
ANN ARBOR MI 48106
PHONE: 313 996 7525

J M MCCREA
PO BOX 172
MONROEVILLE PA 15146
PHONE: 412 242 0448

D A MCCRERY
BLDG B1219
DOW CHEMICAL-TX OPERATIONS
FREEPORT TX 77541
PHONE: 409 238 3244

RICHARD A MCDONIE
UNION CARBIDE TECH CTR
BLDG 770 ROOM 118
S CHARLESTON WV 25303
PHONE: 304 747 4591

JOYCE E MCFADDEN
AZS CORP
762 MARIETTA BLVD
ATLANTA GA 30318
PHONE: 404 873 1851

J H MCGLOTTEN
SCHERING CORP
GALLOPING HILL ROAD
KENILWORTH NJ 07033
PHONE: 201 558 5881

JEFFREY M MCGUIRE
HERCULES INC
RESEARCH CENTER
WILMINGTON DE 19894
PHONE: 302 995 3294

KEITH B MCKELLOP
BOEHRINGER INGELHEIM
RES & DEV
RIDGEFIELD CT 06877
PHONE: 203 748 4200

MATTHEW A MCLEAN
UNIV OF HOUSTON
DEPT OF CHEMISTRY
HOUSTON TX 77004
PHONE: 713 749 2646

GREG MCMANEMIN
MERCK & CO RESEARCH
PO BOX 2000
RAHWAY NJ 07065
PHONE: 201 574 7057

CATHERINE J MCNEAL
TEXAS A&M UNIVERSITY
CHEMISTRY DEPT
COLLEGE STN TX 77843
PHONE: 409 845 2355

GINA M MEAGHER
COMMERCIAL TESTING
490 ORCHARD ST
GOLDEN CO 80401
PHONE: 303 278 9521

KENNETH E MCCULLOH
10304 ST ALBANS DR
BETHESDA MD 20814
PHONE: 301 530 1617

STEPHEN W MCELVANY
CHEMISTRY DIV/CODE 6111
NAVAL RESEARCH LAB
WASHINGTON DC 20375
PHONE: 202 767 2398

WILLIAM H MCFADDEN
FINNIGAN MAT
355 RIVER OAKS PKWY
SAN JOSE CA 95134
PHONE: 408 433 4800

STEVEN R MCGOWN
DEPT OF BIOCHEMISTRY
PS II
STILLWATER OK 74075
PHONE: 405 624 6202

D J MCINTOSH
UNIV OF ALASKA
INST MARINE SCIENCE
FAIRBANKS AK 99775
PHONE: 907 474 6731

H S MCKOWN
393 EAST DRIVE
OAK RIDGE TN 37830
PHONE: 615 574 2454

SCOTT A MCLUCKEY
OAK RIDGE NAT'L LABORATORY
BLDG 9735
OAK RIDGE TN 37831
PHONE: 615 574 2454

WALTER J MCMURRAY
YALE UNIV SCH OF MEDICINE
333 CEDAR STREET
NEW HAVEN CT 06510
PHONE: 203 785 4525

RUSSELL D MCNIECE
AQUALAB INC
2621-130 RIDGEPOINT DRIVE
AUSTIN TX 78754
PHONE: 512 928 8905

J C MEANS
UNIV OF MARYLAND
CHESAPEAKE BIOL LAB
SOLOMONS MD 20688
PHONE: 301 326 4281

R N MCDONALD
KANSAS STATE UNIV
CHEMISTRY DEPT
MANHATTAN KS 66506
PHONE: 913 532 6680

CHARLES N MCEWEN
DUPONT COMPANY
CENTRAL RES DEPT
WILMINGTON DE 19898
PHONE: 302 772 2952

DONALD D MCFALL
PPG INDUSTRIES
PO BOX 31
BARBERTON OH 44203
PHONE: 216 848 4161

J M MCGUIRE
ATHENS ENVIRONMENTAL
RESEARCH LABORATORY
ATHENS GA 30613
PHONE: 404 546 3185

ROBERT T MCIVER
UNIV OF CALIFORNIA
CHEMISTRY DEPT
IRVINE CA 92717
PHONE: 714 856 6085

FRED W MCLAFFERTY
CORNELL UNIVERSITY
CHEMISTRY DEPT
ITHACA NY 14853
PHONE: 607 255 4699

JOHN MCMAHON
2670 WILLOW WOOD DR
ERIE PA 16506
PHONE: 814 838 3293

RICHARD MCNAUGHT
GENERAL FOODS CORP
TECHNICAL CTR
WHITE PLAINS NY 10625
PHONE: 914 335 6806

J H MCREYNOLDS
SUNY MEDICAL SCHOOL
BIOPHYSICAL SCIENCE
BUFFALO NY 14214
PHONE: 716 831 3245

WILMA K MECKSTROTH
OHIO STATE UNIV
944 BRICE ROAD
REYNOLDSBURG OH 43068
PHONE: 614 366 3321

PATRICK W MEEHAN
RADIAN CORP
8501 MOPAC BLVD
AUSTIN TX 78766
PHONE:

GERRY G MEISELS
UNIV OF NEBRASKA
1223 OLDFATHER HALL
LINCOLN NE 68588
PHONE: 402/472-6262

G E MELLEN
935 HUGHES DR

ST ALBANS WV 25177
PHONE: 304 727 8126

JIM MERDINK
AM DRUG TESTING LABS
BUILDING 10
SANTA CLARA CA 95054
PHONE: 408 727 5525

CLIMACO J METRAL
309 BOXFORD COURT

FREDERICK MD 21701
PHONE: 301 695 1226

MICHAEL MEYERS
NICOLET INSTRUMENTS
5225-1 VERONA ROAD
MADISON WI 53711
PHONE: 608 271 3333

JOSEF MICHL
5404 WESTERN HILLS DRIVE

AUSTIN TX 78731
PHONE: 512 471 1782

DAVID MICKUNAS
14-A CEDAR LANE

HIGHLAND PARK NJ 08904
PHONE:

MICHAEL J MIILE
ENSECO/CAL LABS
2544 INDUSTRIAL BLVD
SACRAMENTO CA 95691
PHONE: 916 756 7419

WILLIAM G MILLEN
AMERICAN CYANAMID
PO BOX 400
PRINCETON NJ 08540
PHONE: 609 799 0400

JON R MEEK
AMERICAN CYANAMID
PO BOX 400
PRINCETON NJ 08540
PHONE: 609 799 0400

ERIC G MELANSON
FINNIGAN MAT INSTITUTE
4450 CARVER WOODS DR
CINCINNATI OH 45242
PHONE: 513 891 2100

BENNETT MELNICK
TRAVENOL LABS INC
6301 N LINCOLN AVE
MORTON GROVE IL 60645
PHONE: 312 965 4700

MARCIA MEREDITH
6858 GAWANDA ST ROAD

HAMBURG NY 14075
PHONE: 716 649 9515

H L MEUZELAAR
BIOMATERIALS PROFILING
391 S CHIPETA WAY
SALT LAKE CTY UT 84108
PHONE: 801 581 8431

SEYMOUR MEYERSON
650 N TIPPECANOE ST

GARY IN 46403
PHONE: 219 938 1933

JOHN A MICHNOWICZ
HEWLETT PACKARD
1601 CALIFORNIA AVE
PALO ALTO CA 94304
PHONE: 415 857 5481

BRIAN S MIDDLEDITCH
UNIV OF HOUSTON
BIOCHEMISTRY DEPT
HOUSTON TX 77004
PHONE: 713 749 4845

RICHARD M MILBERG
UNIV OF ILLINOIS
SCH OF CHEM SCIENCES
URBANA IL 61801
PHONE: 217 333 2545

CHARLES M MILLER
MS J-514
LOS ALAMOS NATL LAB
LOS ALAMOS NM 87545
PHONE: 505 667 4546

T K MEHRHOFF
14120 82ND AVE N

SEMINOLE FL 33542
PHONE: 813 541 8769

S J MELFORD
DEPAUL UNIVERSITY
CHEMISTRY DEPT
CHICAGO IL 60614
PHONE: 312 341 8180

CHIN-KAI MENG
YALE UNIVERSITY
9 HILLHOUSE AVE
NEW HAVEN CT 06520
PHONE: 203 432 4335

GUY L MERRILL
24 SOUTHBURY RD

CLIFTON PARK NY 12065
PHONE: 518 393 6611

V D MEYER
CTRGTE LIGHTING PRODUCTS
100 ENDICOTT ST
DANVERS MA 01923
PHONE: 617 777 1900

I I MICHAEL
AFGL-PHG

HANSCOM AFB MA 01731
PHONE: 617 377 2433

DUANE L MICKELSON
THE UPJOHN CO
LOC 1140-230-2
KALAMAZOO MI 49001
PHONE: 616 323 4031

CARL H MIDGETT
US TOBACCO CO
800 HARRISON ST
NASHVILLE TN 37202
PHONE: 615 244 5270

JEFFREY ROBERT MILLARD
CHEMISTRY DEPT
INDIANA UNIV
BLOOMINGTON IN 47405
PHONE: 812 335 7723

DAVID J MILLER
UNIV OF NORTH DAKOTA ERC
PO BOX 8213
GRAND FORKS ND 58202
PHONE: 701 777 5107

DAVID L MILLER
EG&G IDAHO INC
PO BOX 1625
IDAHO FALLS ID 83415
PHONE: 208 526 1856

LELAND V MILLER
UNIV OF COLORADO
HEALTH SCIENCE CTR C232
DENVER CO 80262
PHONE: 303 394 8126

TOM A MILNE
SERI
1617 COLE BLVD
GOLDEN CO 80401
PHONE: 303 231 1440

DONALD M MINTZ
1633 S MARY AVENUE

SUNNYVALE CA 94087
PHONE: 415 493 4000

LAURA A MITACEK
DU PAGE COUNTY CRIME LAB
501 NORTH COUNTY FARM ROAD
WHEATON IL 60187
PHONE: 312 682 7817

STEVE MOCK
MONTANA STATE UNIV
GAINES HALL
BOZEMAN MT 59717
PHONE: 416 994 5419

JAMES MONCUR
LOCKHEED
3251 HANOVER ST
PALO ALTO CA 94304
PHONE: 415 424 2533

RICHARD M MONTGOMERY
243 EAST GLEN AVE

RIDGEWOOD NJ 07450
PHONE: 914 357 2000

DENISE S MOORE
R J REYNOLDS TOBACCO
BOWMAN GRAY TECH CTR
WINSTON-SALEM NC 27102
PHONE: 919 773 4938

WILLIAM T MOORE
ANALYTICAL CHEM CENTER
UT MED SCHOOL
HOUSTON TX 20708
PHONE: 713 792 5612

DEBORAH MILLER
UNION CARBIDE
BLDG 770-318
S CHARLESTON WV 25303
PHONE: 304 747 4463

DAVID S MILLINGTON
DEPT OF PEDIATRICS
BOX 3028
DURHAM NC 27710
PHONE: 919 684 2036

ROBERT D MINARD
PENN STATE UNIV
152 DAVEY LAB
UNIV PARK PA 16802
PHONE: 814 865 2202

CHESTER J MIROCHA
DEPT PLANT PATHOLOGY
UNIV OF MINNESOTA
ST PAUL MN 55108
PHONE: 612 625 8772

RONALD K MITCHUM
US EPA
PO BOX 15027
LAS VEGAS NV 89114
PHONE: 702/798-2103

MEHDI MOINI
CHEMISTRY DEPT
UNIV OF FLORIDA
GAINESVILLE FL 32611
PHONE: 904 392 4892

KARIN MONSON-KIRLAND
ICI AMERICAS INC
BMRD L-215
WILMINGTON DE 19897
PHONE: 302 575 2277

ARTHUR MOORE
BOX 269

LITTLETON CO 80220
PHONE: 303 794 2601

JOHN A MOORE
DOW CORNING CORP
3901 S SAGINAW RD
MIDLAND MI 48640
PHONE: 517 496 5711

SHARON PALLANTE MORELL
JOHNS HOPKINS UNIV
PHARMACOLOGY DEPT
BALTIMORE MD 21205
PHONE: 301 955 6961

DENNIS A MILLER
MICH TECH UNIV
CHEM & CHEM ENGIN
HOUGHTON MI 49931
PHONE: 906 487 2059

FRANK D MILLS
USDA, ARS, AG ENV QUAL INS
BLDG 306, RM 114, BARC-EAS
BELTSVILLE MD 20705
PHONE: 301 344 1903

JAMES MING
NASA/GODDARD SPACE CENTER
CODE 313.2
GREENBELT MD 20771
PHONE: 301 286 5289

STEPHEN R MISSLER
TEXACO
PO BOX 425
BELLAIRE TX 77401
PHONE: 713 432 2687

KEI MIYANO
F A I HUTCHINSON HALL
ROOM 9
DAVIS CA 95611
PHONE: 916 752 6272

MARK TWINING MOJESKY
DEPT OF CHEMISTRY
CHEM/PHYS BLDG ROOM 4
LEXINGTON KY 40506
PHONE: 606 257 6957

FRED MONTGOMERY
BALZERS
508 LEE ST
CEDAR HILL TX 75104
PHONE: 214 291 2968

CATHERINE A MOORE
DEPT OF CHEMISTRY
UNIV OF CALIFORNIA
IRVINE CA 92717
PHONE: 714 856 5682

LARRY J MOORE
ATOM SCIENCES INC
114 RIDGEWAY CTR
OAK RIDGE TN 37830
PHONE: 615 483 1113

JOHN J MORELLI
309 S AIKEN AVENUE
APT 4
PITTSBURGH PA 15232
PHONE: 412 624 8303

DAVID MORISON
UNIV OF MAINE AT ORONO
473 AUBERT HALL
ORONO ME 04469
PHONE: 207 581 1187

WILLIAM J MORRIS
FDA
RM 500 US CUSTOMS HOUSE
DENVER CO 80202
PHONE: 303 844 4915

SANDRA L MORT
POLLUTION CONTROL SYSTEMS
C R 550 S BOX 17
LA OTTO IN 46763
PHONE: 219 637 3137

PAUL D MUDGETT
308-C PERSHING

COLLEGE STN TX 77840
PHONE: 409 693 0724

THEODORE R MUELLER
OAK RIDGE NAT'L LAB
PO BOX Y
OAK RIDGE TN 37831
PHONE: 615 574 2454

C E MULLER
4139 BELLAIRE BLVD

HOUSTON TX 77025
PHONE: 713 665 2115

DAVID J MUNCH
US EPA
26 WEST ST CLAIR STREET
CINCINNATI OH 45268
PHONE: 513 569 7945

STANLEY MURAKAMI
SYNTEX CORP
3401 HILLVIEW AVENUE
PALO ALTO CA 94304
PHONE: 415 855 5692

ROBERT C MURPHY
UNIV OF COLORADO
MEDICAL CENTER
DENVER CO 80262
PHONE: 303 394 8962

BRIAN D MUSSELMAN
JEOL USA INC
11 DEARBORN RD
PEABODY MA 01960
PHONE:

KENT MORRILL
TENN EASTMAN CO
B150
KINGSPORT TN 37662
PHONE: 615 229 3066

G H MORRISON
CORNELL UNIVERSITY
CHEMISTRY DEPT
ITHACA NY 14853
PHONE: 607 256 3614

THOMAS H MORTON
UNIV OF CALIFORNIA
CHEMISTRY DEPT
RIVERSIDE CA 92521
PHONE: 617 495 4022

MANFRED MUELLER
FINNIGAN MAT
355 RIVER OAKS PKWY
SAN JOSE CA 95134
PHONE: 408 433 4800

M LUIS MUGA
TOFTEC
PO BOX 12877
GAINESVILLE FL 32604
PHONE: 904 472 2668

MOHAMMAD M MUMTAZ
PREVENTATIVE MEDICINE
COMMUNITY HEALTH F-17
GALVESTON TX 77550
PHONE: 409 761 4661

BURNABY MUNSON
UNIV OF DELAWARE
CHEMISTRY DEPT
NEWARK DE 19716
PHONE: 302 451 2340

SANDRA MURAWSKI
11781 ROSE LN APT D

CINCINNATI OH 45246
PHONE: 513 530 3749

JOHN S MURRAY
4227 WOODLAND DR

INDIANAPOLIS IN 46254
PHONE: 317 243 8305

STEVE MUSSER
DEPT MCPG
UNIV OF MARYLAND
BALTIMORE MD 21201
PHONE: 301 328 2982

FRANK MORRIS
HOLLY OAK TERRACE
301 MAPLE AVE
WILMINGTON DE 19809
PHONE: 302 575 8410

J CHARLES MORROW
UNIV OF NORTH CAROLINA, CH
DEPT OF CHEMISTRY
CHAPEL HILL NC 27514
PHONE: 919 962 1271

NEIL MOSESMAN
SUPELCO INC
SUPELCO PARK
BELLEFONTE PA 16823
PHONE: 814 359 3441

SANDRA L MUELLER
ABBOTT LABS
D-417 AP9
ABBOTT PARK IL 60064
PHONE: 312 937 2081

STEVEN L MULLEN
NIH/MSU MASS SPEC FACILITY
BIOCHEMISTRY BLDG
E LANSING MI 48824
PHONE: 517 353 0612

IN K MUN
1 APPLE COURT

NANUET NY 10954
PHONE: 212 305 1230

EDMOND MURAD
AF GEOPHYSICS LAB
PHK
HANSCOM AFB MA 01731
PHONE: 617 377 3176

CONSTANCE M MURPHY
JOHNS HOPKINS UNIV
725 N WOLFE STREET
BALTIMORE MD 21205
PHONE: 301 955 6961

E E MUSCHLITZ
UNIV OF FLORIDA
CHEMISTRY DEPT
GAINESVILLE FL 32611
PHONE: 904 392 9619

CARL MYERHOLTZ
HEWLETT-PACKARD LABS
1651 PAGE MILL RD
PALO ALTO CA 94304
PHONE: 415 857 3752

LESTER MYERS
MASON & HANGER
PO BOX 30020
AMARILLO TX 79177
PHONE: 806 381 4208

N N NARASIMHACHARI
MEDICAL COL VIRGINIA
PSYCHIATRY DEPT
RICHMOND VA 23298
PHONE: 804 786 5360

CHAD C NELSON
311A SKAGGS HALL
UNIV OF UTAH
SALT LAKE CTY UT 84114
PHONE: 801 581 5582

ROBERT J NELSON
NORTHEASTERN UNIV
CHEMISTRY DEPT
BOSTON MA 02115
PHONE: 617 437 5069

DONI R NEUFELD
3942 CLAUS CIRCLE

BATON ROUGE LA 70809
PHONE: 504 926 4311

JOHN C NEWTON
LAW LIV NAT'L LAB
L-310
LIVERMORE CA 94550
PHONE: 415 422 6892

HAI NGUYEN
ALLERGAN INC
2525 DUPONT DR
IRVINE CA 92715
PHONE: 714 955 6867

LAWRENCE NIELSEN
UNION CAMP CORP
PO BOX 6941
LAWRENCEVILLE NJ 08648
PHONE: 609 896 1200

JOHN A NIKORA
B F GOODRICH CENTER
CHEMISTRY DIVISION
AVON LAKE OH 44012
PHONE: 216 933 0288

ALBERT J NITOWSKI
63 GALPIN STREET

NAGATUCK CT 06770
PHONE: 203 723 3495

SUSAN NAKAMA
HUNTINGTON BCH POLICE
2000 MAIN ST
HUNITNGTON BC CA 92648
PHONE:

DAVID NEAL
PROCTER & GAMBLE
MIAMI VALLEY LABORATORIES
CINCINNATI OH 45247
PHONE: 513 245 2258

HERB NELSON
NAVAL RESEARCH LAB
CODE 6110
WASHINGTON DC 20375
PHONE: 202 767 3686

SIDNEY D NELSON
UNIV OF WASHINGTON
DEPT MEDICINAL CHEM
SEATTLE WA 98195
PHONE: 206 543 1419

BRUCE NEWCOME
CHARLES EVANS & ASSOC
301 CHESAPEAKE DR
REDWOOD CITY CA 94063
PHONE: 415 369 4567

KENNETH T NG
CIBA-GEIGY CORP
444 SAW MILL RIVER ROAD
ARDSLEY NY 10502
PHONE: 914 478 3131

ROBERT A NICHOLAS
TECHNICAL CTR
ANHEUSER-BUSCH INC
ST LOUIS MO 63118
PHONE: 314 577 2909

HASSO B NIEMANN
NASA GODDARD SPACE
FLIGHT CTR
GREENBELT MD 20771
PHONE: 301 344 8706

TOSHIHIDE NISHIMURA
UNIV OF NEBRASKA
524 HAMILTON HALL
LINCOLN NE 68588
PHONE: 402 472 3517

ROY W NOBLE
MONSANTO CO
MAIL CODE U1F
ST LOUIS MO 63167
PHONE: 513 694 1272

GENE J NANDREA
US FDA
500 US CUSTOMS HOUSE
DENVER CO 80202
PHONE: 303 844 4915

JIM NEILSEN
THE UPJOHN CO
301 HENRIETTA
KALAMAZOO MI 49009
PHONE:

PAUL R NELSON
DEPT OF CHEMISTRY
GEORGIA TECH
ATLANTA GA 30332
PHONE: 404 894 4070

VINCENT P NERO
TEXACO INC
BOX 509
BEACON NY 12508
PHONE: 914 831 3400

A S NEWTON
1665 THOUSAND OAKS

BERKELEY CA 94707
PHONE: 415 486 5040

KWOKEI J NG
SCHERING CORP
60 ORANGE STREET B-6-139
BLOOMFIELD NJ 07003
PHONE: 201 429 4213

WARREN NIEDERHUT
504 ZUBER AVE

HENDERSON NV 89015
PHONE: 702 739 3142

A O NIER
UNIV OF MINNESOTA
PHYSICS/ASTRONOMY
MINNEAPOLIS MN 55455
PHONE: 612 624 6804

MARCIA G NISHIOKA
BATTELLE COL LABS
RM 7238
COLUMBUS OH 43201
PHONE: 614 424 4964

JIM NOONAN
OHIO STATE UNIV
1935 COFFEY ROAD
COLUMBUS OH 43210
PHONE: 614 422 4299

PETER NORBERG
TEKNIVENT CORP
11684 LILBURN PARK ROAD
ST LOUIS MO 63146
PHONE: 314 994 0500

ERIC J NORMAN
1044 SUNWOOD CT

CINCINNATI OH 45231
PHONE: 513 521 8378

CURT NORWOOD
EPA ERL
SOUTH FERRY ROAD
NARRAGANSETT RI 02882
PHONE: 401 789 1071

ANNE D O'DONNELL
13651 LAMON

CRESTWOOD IL 60445
PHONE: 312 291 8346

REBECCA M O'MALLEY
UNIV OF S FLORIDA
CHEMISTRY DEPT
TAMPA FL 33620
PHONE: 813 935 8120

R W ODOM
301 CHESAPEAKE DRIVE

REDWOOD CITY CA 94063
PHONE: 415 369 4567

ANTHONY OKEEFE
9555 DISTRIBUTION AVE
WESTERN RESEARCH CORP
SAN DIEGO CA 92121
PHONE: 619 578 5885

IRVING A OLEARY
THE UPJOHN CO
UNIT 7256-126-2
KALAMAZOO MI 49001
PHONE: 616 385 4579

JAMES OLTHOFF
JOHNS HOPKINS SCH OF MED
PHARMACOLOGY DEPT
BALTIMORE MD 21205
PHONE: 301 955 6961

J DOUGLAS OPTHOFF
CLAYTON ENVIRONMENTAL
CONSULTANTS
NOVI MI 48050
PHONE: 313 344 1770

PETER D NORBERG
TEKNIVENT CORP
11684 LILBURNN PARK RD
ST LOUIS MO 63146
PHONE: 314 994 0500

JAMES D NORMAN
T107 N F D C
TENN VALLEY AUTHORITY
SHEFFIELD AL 35660
PHONE: 205 386 2390

BOBETTE D NOURSE
PURDUE UNIVERSITY

W LAFAYETTE IN 47907
PHONE: 317 494 5271

J T O'DONOVAN
FINNIGAN INSTRUMENTS
1383 PICCARD DR #100
ROCKVILLE MD 20850
PHONE: 301 948 1067

JOHN L OCCOLOWITZ
LILLY CORPORATE CTR
DEPT MC525
INDIANAPOLIS IN 46285
PHONE: 317 261 4713

TERESA ODOM
FINNIGAN MAT
355 RIVER OAKS PKWY
SAN JOSE CA 95134
PHONE: 408 433 4800

EDWARD L OLBERDING
MERRELL-DOW PHARMACEUTICAL
9550 ZIONSVILLE RD
INDIANAPOLIS IN 46268
PHONE: 317 873 7149

SUSAN OLESIK
OHIO STATE UNIV
DEPT OF CHEM
COLUMBUS OH 43210
PHONE: 614 422 2251

BRUCE ONISKO
STAUFFER CHEMICAL CO
1200 S 47TH STREET
RICHMOND CA 94804
PHONE: 415 231 1058

MICHAEL ORBANOSKY
8141 CLANTON G C T

SACRAMENTO CA 95828
PHONE: 916 682 2012

BOB NORDMAN
HEWLETT-PACKARD CO
1601 CALIFORNIA AVE
PALO ALTO CA 94304
PHONE: 415 857 1501

D J NORTHINGTON
WEST COAST ANAL SERVICE
9840 ALBURTIS AVE
SANTA FE CA 90670
PHONE: 213 948 2225

LYDIA NUWAYSIR
3725 CRANFORD AVE
APT #43 SOUTH
RIVERSIDE CA 92507
PHONE: 714 787 4740

JOHN R O'LEAR
CHEMISTRY BLDG
BOX 652
W LAFAYETTE IN 47906
PHONE: 317 494 5262

GEORGE ODELL
RD #6 ROBINSON LANE

WAPPINGERS FA NY 12590
PHONE: 914 221 2485

SHERRI OGDEN
CHEMISTRY DEPT
UNIV OF CALIFORNIA
BERKELEY CA 94720
PHONE: 415 642 0701

RONALD G OLDHAM
3038 ORCHARD HILL

SAN ANTONIO TX 78230
PHONE: 512 494 5213

KEITH L OLSON
GM RESEARCH
ANALYTICAL CHEMISTRY
WARREN MI 48090
PHONE: 313 986 0827

JON D ONSTOT
MIDWEST RES CTR
425 VOLKER BLVD
KANSAS CITY MO 64110
PHONE: 816 753 7600

RON ORLANDO
DEPT OF CHEMISTRY
UNIV OF DELAWARE
NEWARK DE 19716
PHONE: 302 451 2917

DENNIS J ORR
FINNIGAN MAT
355 RIVER OAKS PKWY
SAN JOSE CA 95134
PHONE: 408 433 4800

CHARLES M OSBURN
OSBURN INSTRUMENT SERVICES
THISBE RANCH
SPARKS NV 89431
PHONE: 702 343 1116

FEZA OZTURK
CHEMISTRY DEPT
LEIGH HALL
GAINESVILLE FL 32611
PHONE: 904 392 4892

STEVEN J PACHUTA
3M
CORPORATE RESEARCH LABS
ST PAUL MN 55144
PHONE: 612 736 1922

RODNEY P PAGE
ARCO
388 ULTIMO AVENUE
LONG BEACH CA 90814
PHONE:

JOSEPH C PAN
ROY F WESTON INC
256 WELSH POOL ROAD
LIONVILLE PA 19353
PHONE: 215 524 0180

R C PANDEY
XECHEM, INC
DIV OF LYPHOMED INC
ROSEMONT IL 60018
PHONE: 312 390 1626

VINCENT M PAPA
RES RESOURCES CTR M/C 937
835 S WOOD
CHICAGO IL 60612
PHONE: 312 996 4853

DENISE PARENT
NAVAL RESEARCH LAB
CODE 6110
WASHINGTON DC 20375
PHONE:

STEVEN PARKHURST
DOW CHEMICAL
EVS-620 BLDG
MIDLAND MI 48640
PHONE: 517 636 5429

ROBERT G ORTH
RT 1 BOX 658A
CEDAR HILL MO 63016
PHONE: 314 694 1271

REBECCA OSTERMAN
2475 GRAY FALLS DR #618
HOUSTON TX 77077
PHONE: 713 796 9677

C F PACHUCKI
GENERAL ELECTRIC CO
KNOLLS ATOM POW LAB
SCHENECTADY NY 12301
PHONE: 518 393 6611

TERRY W PACK
229 S WOODCREST ST
DURHAM NC 27703
PHONE: 919 541 6678

PETER T PALMER
CHEMISTRY DEPT
MICHIGAN STATE UNIV
EAST LANSING MI 48824
PHONE: 517 353 5215

SHU-TEH PAN
7720 LORRAINE AVE #102
STOCKTON CA 95210
PHONE: 209 957 3405

EDWARD K PANG
GTE PRODUCTS CORP
100 ENDICOTT STREET
DANVERS MA 01923
PHONE: 617 777 1900

I A PAPAYANNOPOULOS
M.I.T.
RM 56-012 CHEM DEPT
CAMBRIDGE MA 02139
PHONE: 617 253 7237

CAROL E PARKER
NIEHS
PO BOX 12233
RES TRI PARK NC 27709
PHONE: 919 541 5008

N H PARSONS
GENERAL ELECTRIC CO
PO BOX 2908
LARGO FL 34294
PHONE: 813 541 8417

DAVID OSBORNE
DATACHEM
520 WAKARA WAY
SALT LAKE CTY UT 84108
PHONE: 801 584 3260

EDWARD B OVERTON
5536 RIVERBEND DRIVE
BATON ROUGE LA 70820
PHONE: 504 388 8521

ROBIN ROUSH PACHUTA
3255 COACHMAN RD
APT 332
EAGAN MN 55121
PHONE:

F G PADRTA
ENGINEERED MATERIAL RES CT
50 E. ALGONQUIN RD
DES PLAINES IL 60017
PHONE: 312 391 3175

KRISHNA M PAMIDIMUKKALA
LOUISIANA STATE UNIV
DEPT OF BIOCHEMISTRY
BATON ROUGE LA 70803
PHONE: 504 388 5228

R J PANCIROV
10 SHADYLAWN DR
MADISON NJ 17940
PHONE: 201 932 8256

LEWIS K PANNELL
NIH
BLDG 8 ROOM B2A-23
BETHESDA MD 20892
PHONE: 301 496 4055

DAVID M PAREES
AIR PRODUCTS & CHEM
PO BOX 538
ALLENTOWN PA 18105
PHONE: 215 481 5794

DANIEL PARKER
TEKNIVENT CORP
11684 LILBURN PARK RD
ST LOUIS MO 63146
PHONE: 314 994 0500

LES G PARTRIDGE
TMA/NORCAL
2030 WRIGHT AVENUE
RICHMOND CA 94804
PHONE: 415 235 2633

ROSE PASSARELLA
152 DAVEY LABORATORY
BOX 83
UNIV PARK PA 16802
PHONE: 814 863 3583

SUBHA M PATEL
1573 WASHINGTON VALLEY RD
BRIDGEWATER NJ 08807
PHONE: 201 264 4500

PAT PATTERSON
EXCALIBUR TECHNOLOGIES
122 TULANE S E
ALBUQUERQUE NM 87106
PHONE:

J F PAULSON
AFGL-LID
HANSCOM AFB MA 01731
PHONE: 617 861 3124

ROBERT J PAWLOSKY
UNIV OF MINNESOTA
495 BORLAUG HALL
ST PAUL MN 55104
PHONE: 612 625 2751

MICHAEL A PEAT
CHEMWEST ANAL LABS
600 W NORTH MARKET BLVD
SACRAMENTO CA 95834
PHONE: 916 923 0840

M B PENNINGTON
6407 LONGVIEW
SHAWNEE KS 66218
PHONE: 816 997 4187

JULIUS PEREL
PHRASOR SCIENTIFIC
1536 HIGHLAND AVE
DUARTE CA 91010
PHONE: 818 357 3201

CORTES L PERRY
PO BOX 4325
HUNTSVILLE AL 35815
PHONE: 205 881 1921

PAUL H PETERMAN
1 ROLLINGWOOD WEST DRIVE
ROUTE 5
COLUMBIA MO 65202
PHONE: 314 875 5399

MICHAEL J PASTEL
LEDERLE LABORATORIES
BLDG 65 ROOM 126
PEARL RIVER NY 10965
PHONE: 914 735 5000

ADAM PATKIN
PERKIN-ELMER
761 MAIN AVENUE
NORWALK CT 06859
PHONE: 203 762 6804

JOSE A PAULINO
CORBOX 682 CHEMISTRY DEPT
PURDUE UNIVERSITY
LAFAYETTE IN 47907
PHONE: 317 742 1121

DAVID PAULY
TWIN CITY TESTING CORP
662 CROMWELL AVENUE
ST PAUL MN 55114
PHONE: 612 641 9485

DAVID A PEAKE
PROCTER & GAMBLE
IVORYDALE TECH CTR
CINCINNATI OH 45217
PHONE: 513 627 7584

RANDALL E PEDDER
UNIVERSITY OF FLORIDA
BOX 431 LEIGH HALL
GAINESVILLE FL 32611
PHONE: 904 392 0515

DANIEL PENTEK
YALE UNIV
CHEMICAL INSTR CTR
NEW HAVEN CT 06511
PHONE: 203 432 3935

DEBORAH D PERKINS
SCH OF CHEMISTRY
GEORGIA TECH
ATLANTA GA 30332
PHONE: 404 894 4051

DONALD L PERRY
8155 JEFFERSON HWY
APT 703
BATON ROUGE LA 70804
PHONE: 504 928 0232

DAVID W PETERSON
HEWLETT-PACKARD CO
1601 CALIFORNIA AVE
PALO ALTO CA 94304
PHONE:

SIDDHARTH M PATEL
GOODYEAR TIRE & RUBBER CO
735 CLIFFSIDE DR
AKRON OH 44313
PHONE: 216 796 5158

DONALD G PATTERSON
CTR FOR DISEASE CONT
TOXICOLOGY BRANCH
ATLANTA GA 30333
PHONE: 404 452 4176

PAUL J PAULSEN
NBS
BLDG 221 RM A25
WASHINGTON DC 20234
PHONE: 301 921 2781

RAPHE PAVLICK
WESTON INC
3360 BETTY LANE
LAFAYETTE CA 94549
PHONE: 209 957 3405

DAN S PEARCE
1580 TARRYTOWN
SAN MATEO CA 94402
PHONE: 415 857 7448

H E PENA
215 RIO VISTA DR
ST CHARLES MO 63303
PHONE: 314 982 5404

ROBERT J PERCHALSKI
PHARMATEC INC
PO BOX 730
ALACHUA FL 32615
PHONE: 904 462 1210

RICHARD E PERRIN
MOUNTAIN ROUTE 100
JEMEZ SPRINGS NM 87025
PHONE: 501 667 4498

ROBERT K PERTUIT
PPG INDUSTRIES
PO BOX 1000
LAKE CHARLES LA 70602
PHONE:

DEANNA L PETERSON
3347 FEDERAL BLVD
DENVER CO 80211
PHONE: 303 794 7127

GLENN S PETERSON
25 BIRCH MEADOW DR

WATERTOWN CT 06795
PHONE:

DANIEL PHELPS
AMOCO PRODUCTION CO
PO BOX 3385
TULSA OK 74102
PHONE: 918 660 3129

LAWRENCE R PHILLIPS
19820 COCHRANE WAY

GAITHERSBURG MD 20879
PHONE: 301 496 4570

ADRIAN PIKE
FINNIGAN MAT
355 RIVER OAKS PARKWAY
SAN JOSE CA 95134
PHONE: 303 988 5557

JAMES W PINSON
AMER LABS & RESEARCH
1008 SOUTHEAST CR
HATTIESBURG MS 39402
PHONE: 601 264 9320

MATTHEW V PISERCHIO
3420 PLAZA DRIVE

STATE COLLEGE PA 16801
PHONE: 814 863 1333

IRENE PLAKUNOV
15 NORTHWICK DR

ROCHESTER NY 14617
PHONE: 716 338 8594

CHESTER E PLUCINSKI
18354 W 58TH PLACE #D

GOLDEN CO 80403
PHONE: 303 966 7593

S M POLING
263 S CHESTER AVE

PASADENA CA 91106
PHONE: 818 796 0239

JOHN A POLTA
HENKEL RESEARCH CORP
2330 CIRCADIAN WAY
SANTA ROSA CA 95407
PHONE: 707 575 7155

R J PETERSON
FIRMENICH INC
PO BOX 5880
PRINCETON NJ 08540
PHONE: 609 452 1000

EVAN T PHILLIPPO
USDA FSIS EASTERN LAB
PO BOX 6085
ATHENS GA 30605
PHONE: 404 546 3144

W C PHILLIPS
1108 FRANK DR

CHAMPAIGN IL 61821
PHONE:

J DAVID PINKSTON
MIAMI VALLEY LABS
PROCTER & GAMBLE
CINCINNATI OH 45247
PHONE: 513 245 2269

E G PIOTROWSKI
ERRC USDA
600 E MERMAID LN
PHILADELPHIA PA 19118
PHONE: 215 233 6487

H O PITTS
1370 CLAREMONT DR

BOULDER CO 80303
PHONE: 303 966 4106

BRUCE E PLASHKO
A E STALEY CO
BLDG 63
DECATUR IL 62525
PHONE: 217 421 2563

FRED O POEPPEL
110 PARKER ROAD

SARVER PA 16055
PHONE: 412 782 3884

LAWRENCE P POLLACK
15321 DELPHINIUM LANE

ROCKVILLE MD 20853
PHONE: 703 750 3000

STEVEN C POMERANTZ
DEPT MEDICINAL CHEMISTRY
311A SKAGGS HALL
SALT LAKE CTY UT 84112
PHONE: 801 581 5582

G A PETZINGER
9 LAMBERT STREET

WOODBRIDGE NJ 07095
PHONE: 718 965 5722

DENNIS R PHILLIPS
UNIVERSITY OF UTAH
311A SKAGGS HALL
SALT LAKE CTY UT 84112
PHONE: 801 581 5581

MARY JANE PHINNEY
PO BOX 1446

ANGLETON TX 77515
PHONE: 713 796 9677

J L PINKUS
75 CLEVELAND ROAD

WELLESLEY MA 02181
PHONE: 617 720 6400

ALBERT J PIRONE
ICI AMERICAS INC
ROOM C-120 B
WILMINGTON DE 19808
PHONE: 302 575 8385

VINCE PIZZITOLA
EXTREL CORP
PO BOX 11512AITH RD
PITTSBURGH PA 15238
PHONE: 412 963 7530

RONALD D PLATTNER
NORTHERN REG LAB
1815 N UNIVERSITY ST
PEORIA IL 61604
PHONE: 309 685 4011

THOMAS R POFAHL
KRAFT INC
801 WAUKEGAN RD
GLENVIEW IL 60025
PHONE: 312 998 3619

CHARLES W POLLEY
ARCO CHEMICAL CO
3801 W CHESTER PIKE
NEWTOWN SQ PA 19073
PHONE: 215 359 2440

BING T POON
WALTER REED ARMY
INST OF RESEARCH
WASHINGTON DC 20307
PHONE: 301 427 5426

JIM POPPITI
FINNIGAN MAT
1383 PICCARD DRIVE
ROCKVILLE MD 21797
PHONE: 301 948 1067

RICHARD F PORTER
CORNELL UNIVERSITY
CHEMISTRY DEPT
ITHACA NY 14853
PHONE: 607 256 3483

THOMAS C POTTER
MOBIL RESEARCH & DEV

PAULSBORO NJ 08066
PHONE:

ROGER E POWERS
DEPT OF CHEMISTRY
UNIV OF PENNSYLVANIA
PHILADELPHIA PA 19104
PHONE: 215 898 8164

DAVID PRESSER
MATTSON INSTRUMENTS INC
1001 FOURIER CT
MADISON WI 53717
PHONE: 608 831 5515

PHILIP C PRICE
UNION CARBIDE
TECH CTR 770-120
S CHARLESTON WV 25303
PHONE: 304 747 5594

D G PRITCHARD
UNIV OF ALABAMA
MICROBIOLOGY DEPT
BIRMINGHAM AL 35294
PHONE: 205 934 6023

JOHN DAVID PRYNE
PROCTER & GAMBLE
6100 CENTER HILL ROAD
CINCINNATI OH 45224
PHONE: 513 659 2543

ZHA QINGMEI
642 HAMILTON HALL
UNIV OF NEBRASKA
LINCOLN NE 68588
PHONE: 402 472 3517

ELLIOT M RACHLIN
651 EAST BIRCHFIELD LANE
APT 7U
MURREY UT 84107
PHONE: 801 581 5415

MICHAEL A POQUETTE
UW HOSPITAL TOXICOLOGY LAB
600 HIGHLAND AVE
MADISON WI 53792
PHONE: 608 263 7029

BARBARA S PORTZ
U OF CO HEALTH SCI CTR
GI DIV BOX B158
DENVER CO 80262
PHONE: 303 394 7287

LINDA POULTER
UCSF
SCHOOL OF PHARMACY S926
SAN FRANCISCO CA 94143
PHONE: 415 476 5249

B N PRAMANIK
SCHERING CORP
60 ORANGE ST
BLOOMFIELD NJ 07003
PHONE: 201 429 3993

BILL PRICE
HEWLETT-PACKARD
PO BOX 105005
ATLANTA GA 30339
PHONE: 404 980 7412

R B PRIME
IBM (H20/025)
5600 COTTLE ROAD
SAN JOSE CA 95193
PHONE: 408 256 6167

THOMAS H PRITCHETT
US EPA
V8 EPA-ERT
EDISON NJ 08829
PHONE:

HARLAN G PULSIPHER
420 EAST 600 NORTH

BRIGHAM CITY UT 84302
PHONE: 801 863 3303

ALLEN QUICK
UNIV OF COLORADO HSC
4200 EAST 9TH AVE BOX C232
DENVER CO 80262
PHONE: 303 394 7287

BARBARA D RADECKI
BASF CORPORATION
1419 BIDDLE AVE
WYANDOTTE MI 48192
PHONE: 313 246 6324

RANDALL LAMARR PORCH
LABRADIAN CORP
PO BOX 13000
RES TRI PARK NC 27709
PHONE: 919 481 0212

THOMAS POTTER
GC/MS LABORATORY
UNIV OF MASSACHUSETTS
AMHERST MA 01003
PHONE: 413 545 3505

DAVID H POWELL
ENVIRON SCI & ENGIN
PO BOX ESE
GAINESVILLE FL 32602
PHONE: 904 332 3318

BIKASH PRAMANIK
HOWARD HUGHES MEDICAL
UT HEALTH SCI CTR
DALLAS TX 75235
PHONE: 214 689 5017

JOSEPH F PRICE
4043 FAUNSDALE DRIVE

MONTGOMERY AL 36109
PHONE: 205 261 2739

JOHN F PRINCE
3576 PINE CONE CIR

WALDORF MD 20601
PHONE:

BERTHA L PROCTOR
UNIV OF TEXAS
ENV SCIENCE
RICHARDSON TX 75080
PHONE: 214 690 2970

JAMES W PYPER
LLNL
PO BOX 808 L-310
LIVERMORE CA 94550
PHONE: 415 422 7311

B A RABY
1547 ARATA COURT

SAN JOSE CA 95125
PHONE: 408 294 6718

GIL RADOLOVICH
MIDWEST RESEARCH INST
425 VOLKER BLVD
KANSAS CITY MO 64110
PHONE: 816 753 7600

THOMAS P RADUS
BETTIS LABS 14D
PO BOX 79
W MIFFLIN PA 15122
PHONE: 412 476 5824

GREGORY S RAHN
ONEIDA RES SERVICE
ONE HALSEY ROAD
WHITESBORO NY 13492
PHONE: 315 736 3050

HARRI G RAMJIT
MERCK & CO
28-1F SUMMNEY TOWN PIKE
WEST POINT PA 19486
PHONE: 215 661 5305

SCOTT RANDO
RR 1
BOX 98-31
SHOHOLA PA 18458
PHONE: 717 296 7309

CARL E RECHSTEINER
CHEVRON RES CORP
POB 1627 RM 41-3240
RICHMOND CA 94802
PHONE: 415 620 5095

DOUGLAS REED
SEARLE R&D
4901 SEARLE PKWY
SKOKIE IL 60077
PHONE: 312 982 4530

WILLIAM REENTS
AT&T BELL LABS
ROOM 1A-320
MURRAY HILL NJ 07974
PHONE: 201 582 2097

MARC H REILLY
BAYLOR COLLEGE OF MEDICINE
CENTER FOR EXP THERAPEUTICS
HOUSTON TX 77030
PHONE:

R F REITER
13422 BROKEN BR CT

CHANTILLY VA 22021
PHONE: 703 378 6020

DON L REMPEL
UNIV OF NEBRASKA
CHEMISTRY DEPT
LINCOLN NE 68588
PHONE: 402 472 3507

FRANK M RAFFO
430 COOPER STREET
APT 2F
WOODBURY NJ 08096
PHONE: 609 853 9053

ASIT RAKSIT
CORNELL UNIVERSITY
DEPT OF CHEMISTRY
ITHACA NY 14853
PHONE: 607 255 0567

L S RAMOS
DEPT OF CHEMISTRY
BG 10
SEATTLE WA 98195
PHONE: 206 543 8888

LEO RAPHAELIAN
ARGONNE NATL LAB
9700 S CASS AVE
ARGONNE IL 60439
PHONE: 312 972 6937

SUSAN J REDDING
1315 S KNOX CT

DENVER CO 80219
PHONE: 303 934 4435

DWIGHT REED
FORENSIC SCI SERVICE
PO BOX 449
SANTA ANA CA 92702
PHONE: 714 834 3073

DAVID R REESE
GT ENVIRONMENTAL LABS
4 MILL STREET
GREENVILLE NH 03048
PHONE: 603 878 2500

VERNON N REINHOLD
HARVARD SCH OF PUBLIC HEALTH
BOSTON MA 02115
PHONE: 617 732 0631

GARY A REITZ
UNIVERSITY OF TEXAS
CHEMISTRY DEPT
AUSTIN TX 78712
PHONE: 512 471 3480

MICHAEL E RENNEKAMP
ONEIDA RESEARCH SERVICES
2756 BELLA VIA AVE
COLUMBUS OH 43229
PHONE: 614 882 8288

LEO RAFTOGIANIS
FINNIGAN MAT
355 RIVER OAKS PKWY
SAN JOSE CA 95134
PHONE: 408 433 4800

JAMES C RAMAGE
VG INSTRUMENTS
32 COMMERCE CENTRE
DANVERS MA 01923
PHONE:

ROWLAND RANDALL
UNIV OF WISCONSIN
BIOCHEMISTRY DEPT
MADISON WI 53706
PHONE:

DAVID B READER
CAMBRIDGE ISOTOPE LABS
20 COMMERCE WAY
WOBURN MA 01801
PHONE: 617 938 0067

G SUDHAKAR REDDY
DEPT OF CHEMISTRY
UTAH STATE UNIV
LOGAN UT 84322
PHONE: 801 750 1624

LORI L REED
AQUA TECH ENV CSLT INC
6878 S STATE RT 100
MELMORE OH 44845
PHONE: 419 397 2659

JAMES P REILLY
DEPT OF CHEMISTRY
INDIANA UNIV
BLOOMINGTON IN 47405
PHONE: 812 335 1980

ROBERT W REISER
E I DUPONT
EXPERIMENTAL STATION
WILMINGTON DE 19898
PHONE: 302 772 1434

DON K REMLING
3246 CURTIS CIRCLE

PLEASANTON CA 94566
PHONE: 415 484 2408

JOHNNY D REYNOLDS
3932 PAPERMILL SQUARE
APT H
KNOXVILLE TN 37919
PHONE: 615 974 8679

W W RICE
121 W MAIDEN LANE

OAK RIDGE TN 37830
PHONE:

DOUGLAS P RIDGE
UNIV OF DELAWARE
CHEMISTRY DEPT
NEWARK DE 19711
PHONE: 302 451 1197

PIERO RINALDO
YALE UNIV SCH OF MED
NS-393A DEPT HUMAN GEN
NEW HAVEN CT 06510
PHONE: 203 785 4475

RUSSELL D RING
BASF CORP
1419 BIDDLE AVE
WYANDOTTE MI 48192
PHONE: 313 246 6325

ANASTASIA RIZWANIUK
HOECHST-ROUSSEL
ROUTE 202-206 NORTH
SOMERVILLE NJ 08876
PHONE: 201 231 2652

EUGENE F ROBBINS
UNIV OF ILLINOIS
RES RESOURCES CTR M/C 937
CHICAGO IL 60680
PHONE: 312 996 7462

DWIGHT F ROBERTS
ENVIR SCI & ENGIN
PO BOX ESE
GAINESVILLE FL 32602
PHONE: 904 332 3318

DONALD H ROBERTSON
S.A.T.D.
MATERIALS SCIENCE BRANCH
NATICK MA 01760
PHONE: 617 651 5535

JOHN ROBOZ
MT SINAI SCH OF MED
1 GUSTAVE LEVY PL
NEW YORK NY 10029
PHONE: 212 650 7382

HENRY RODRIGUEZ
460 PT BRUNO BLVD

S SAN FRAN CA 94080
PHONE: 415 266 1252

DAVID RICK
DOW CHEMICAL CO
1803 BUILDING
MIDLAND MI 48674
PHONE: 517 636 8235

AIDAN RIDLEY
2996 24TH ST

BOULDER CO 80302
PHONE: 303 939 9882

MARINA E RINCON
784 LAUREL WALK "D"

GOLETA CA 93117
PHONE: 805 685 1973

NELSON H RISSER
LANCASTER LABORATORIES
2425 NEW HOLLAND PIKE
LANCASTER PA 17601
PHONE: 717 656 2301

DON J RIZZO
GENERAL FOODS CORP
555 SO BROADWAY
TARRYTOWN NY 10591
PHONE: 914 335 6807

RONNY C ROBBINS
2403 ROTH

EDGEWOOD MD 21040
PHONE: 671 4253

GERALD D ROBERTS
SMITHKLINE & FRENCH LABS
1500 SPRING GARDEN ST
PHILADELPHIA PA 19101
PHONE: 215 270 6660

RUSSELL ROBINS
THE UPJOHN CO
7832-259-12
PORTAGE MI 49008
PHONE:

ALAN L ROCKWOOD
DEPT OF CHEMISTRY
UNIV OF HOUSTON
HOUSTON TX 77004
PHONE: 713 749 2162

BRIAN A ROGERS
GILLETTE RES INST
1413 RESEARCH BLVD
ROCKVILLE MD 20850
PHONE: 301 738 0206

DOUG E RICKERT
CHEM INDUS INST TOXI
PO BOX 12137
RES TRI PK NC 27709
PHONE: 919 541 2070

TIM L RILEY
3552 CREEKSIDE DR

ANN ARBOR MI 48105
PHONE: 313 996 4046

KENNETH L RINEHART
UNIV OF ILLINOIS
CHEM 454 ROGER ADAMS
URBANA IL 61801
PHONE: 217 333 0627

JAMES RITTER
34 BLAKESLEE ST

BRISTOL CT 06010
PHONE: 203 589 5370

JOHN A G ROACH
FDA
HFF-424
WASHINGTON DC 20204
PHONE: 202 245 1371

CHRIS R ROBERTS
UNIV OF COLORADO
DEPT OF CHEM & BIOCHEM
BOULDER CO 80309
PHONE: 303 492 7396

WILLIAM L ROBERTS
CASE WESTERN RES UNIV
DEPT OF PHARMACOLOGY
CLEVELAND OH 44106
PHONE: 216 368 3495

DOUGLAS W ROBINSON
PENNWALT
900 FIRST AVE
KG OF PRUSSIA PA 19406
PHONE: 215 337 6563

RICHARD S RODGERS
158 S MARKET ST

EPHRATA PA 17522
PHONE: 717 738 0326

STEPHEN P ROGERS
1535 N HORNE ROAD
#110
MESA AZ 85203
PHONE: 602 244 3711

PETER F ROGERSON
ANALYTICAL SERVICES BRANCH
US GEOLOGICAL SURVEY
ARVADA CO 80002
PHONE: 303 236 5345

DENNIS K ROHRBAUGH
125 FAIRMONT DR
BEL AIR MD 21014
PHONE: 301 671 2366

WILLIAM K ROHWEDDER
USDA
N REGIONAL RESEARCH
PEORIA IL 61614
PHONE: 309 685 4011

DONALD J ROKOP
LANL
BOX 1663
LOS ALAMOS NM 87545
PHONE: 505 667 7796

TRACY ROLD
1693 GENEVA CIRCLE
LONGMONT CO 80501
PHONE: 303 776 7096

PETER ROLLER
NIH
NCI
BETHESDA MD 20892
PHONE: 301 496 1323

JOHN M ROMAN
NCI-FCRF
PROGRAM RESOURCES
FREDERICK MD 21701
PHONE: 301 698 1226

LUSHAN RONG
35 NOYES LABORATORY BOX 518
UNIV OF IL CHEMISTRY DEPT
URBANA IL 61801
PHONE: 217 333 2545

DEBRA J ROSANO
JUDITH RD
PEABODY MA 01960
PHONE: 617 777 8977

T L ROSE
97 BARTLETT HILL RD
CONCORD MA 01742
PHONE:

JOSEPH D ROSEN
DEPT FOOD SCIENCE
COOK COLLEGE
NEW BRUNSWICK NJ 08903
PHONE: 201 932 9667

ROBERT T ROSEN
CTR FOR ADVANCED FOOD TECH
COOK COLLEGE
NEW BRUNSWICK NJ 08903
PHONE: 201 932 8306

IRA ROSENBERG
BRISTOL-MYERS CO
5 RESEARCH PARKWAY
WALLINGFORD CT 06492
PHONE: 203 284 6333

MARK M ROSS
CODE 6110
NAVAL RES LAB
WASHINGTON DC 20375
PHONE: 202 767 3148

COLLEEN E ROSTAD
US GEOLOGICAL SURVEY
WRD
ARVADA CO 80002
PHONE: 303 236 3616

ARLENE ROTHWELL
PURDUE UNIVERSITY
CHEMISTRY DEPT
W LAFAYETTE IN 47907
PHONE: 317 494 5469

SUSAN ROTTSCHAEFER
1195 HART LANE
HARTSVILLE PA 18974
PHONE: 215 270 7948

TIM ROY
MOBIL OIL
TOXICOLOGY DIV
PRINCETON NJ 08540
PHONE: 609 737 5509

MELVIN D ROZEBOOM
DAILY ANALYTICAL LABS
1621 CANDLETREE DR
PEORIA IL 61614
PHONE: 309 692 5252

ADELE L ROZEK
465 W DOMINION DR
UNIT 306
WOOD DALE IL 60191
PHONE: 312 670 4824

MARTIN A RUDAT
DUPONT
TEXTILE FIBERS
WILMINGTON DE 19898
PHONE: 302 772 2634

PATRICK J RUDEWICZ
FINNIGAN MAT
355 RIVER OAKS PARKWAY
SAN JOSE CA 95134
PHONE: 408 433 4800

DAVID H RUSSELL
TEXAS A&M UNIV
CHEMISTRY DEPT
COLLEGE STN TX 77843
PHONE: 409 845 3345

JOHN W RUSSELL
BRISTOL MYERS
PHARMACEUTICAL R&D
EVANSVILLE IN 47721
PHONE: 812 429 8384

MORLEY E RUSSELL
NORTHERN ILLINOIS UNIV
CHEMISTRY DEPT
DEKALB IL 60115
PHONE: 815 753 6881

JOHN M RUTH
PO BOX 450
COLLEGE PARK MD 20740
PHONE: 301 344 3136

PHILIP W RYAN
PACIFIC ANALYTICAL
1989-B PALOMAR OAKS WAY
CARLSBAD CA 92009
PHONE: 619 931 1766

ROBERT J RYBA
STANDARD OIL INDIANA
PO BOX 400
NAPERVILLE IL 60566
PHONE: 312 420 5966

F M SAAD
MICHIGAN PUB HEALTH
3500 N LOGAN ST
LANSING MI 48909
PHONE: 517 335 8076

F E SAALFELD
5510 VENTNOR LANE
SPRINGFIELD VA 22151
PHONE: 202 696 4101

THOMAS M SACK
MIDWEST RESEARCH INST
425 VOLKER BLVD
KANSAS CITY MO 64110
PHONE: 816 753 7600

STEVE SAKALOW
FINNIGAN MAT
355 RIVER OAKS PARKWAY
SAN JOSE CA 95134
PHONE:

MEHRAN SALEHPOUR
ARGONNE NATL LAB
200 CHM
ARGONNE IL 60439
PHONE: 312 972 3517

VINCENT G SALTAMACH
COLUMBIA UNIV
BOX 555 HAVEMEYER
NEW YORK NY 10027
PHONE: 212 280 2165

MADELINE P SAMPSON
12110 HUNTINGTON PK

HOUSTON TX 77099
PHONE: 713 527 8101

PHILLIP E SANDERS
UNIV OF ILLINOIS
VET MED BASIC SCI BLDG 162
URBANA IL 61801
PHONE: 217 244 1571

SITTHIVET SANTIKARN
HARVARD SCH OF PUB HEALTH
DEPT OF NUTRITION
BOSTON MA 02115
PHONE: 617 732 0632

G G SANZONE
VIRGINIA POLYTECH
CHEMISTRY DEPT
BLACKSBURG VA 24061
PHONE: 703 961 5492

JANICE R SAUCERMAN
BRISTOL-MYERS USPNG
2404 PENNSYLVANIA AVE
EVANSVILLE IN 47721
PHONE: 812 429 7914

M D SCAMUFFA
1343 CREEKFORD CIRCLE

SUGARLAND TX 77478
PHONE: 713 776 6038

RON SADECKY
UNIV OF COLORADO
CHEM & BIOCHEM DEPT
BOULDER CO 80309
PHONE: 303 492 1159

C OKADA SAKASHITA
UNIVERSITY OF UTAH
38 SKAGGS HALL
SALT LAKE CTY UT 84112
PHONE: 801 581 5117

LARRY SALLANS
PPG INDUSTRIES INC
PO BOX 31
BARBERTON OH 44203
PHONE: 216 848 4161

MARY E SALYAN
THE BIOMEMBRANE INST
201 ELLIOTT AVE W
SEATTLE WA 98119
PHONE: 206 285 1309

PAUL C SAMSON
ALLIED-SIGNAL INC
ENG MATERIALS RES CTR
DES PLAINES IL 60017
PHONE: 312 391 3378

ROBERT A SANDERS
PROCTER & GAMBLE CO
6071 CENTER HILL RD
CINCINNATI OH 45224
PHONE: 513 659 7865

IVAN SANTOS
2670 BRANDON RD

COLUMBUS OH 43221
PHONE: 614 488 3626

I M SARASOHN
DUPONT
KINSTON PLANT
KINSTON NC 28501
PHONE: 919 522 6468

ANDREW D SAUTER
2356 AQUA VISTA

HENDERSON NV 89015
PHONE: 702 454 7884

GALE F SCANLAN
MAYO CLINIC
738 GUGGENHEIM
ROCHESTER MN 55901
PHONE: 507 284 4213

KOZO SAITO
UNIV OF PITTSBURGH
DEPT OF CHEMISTRY BOX 43
PITTSBURGH PA 15260
PHONE: 412 624 8304

ELAINE SALADINO
VARIAN ASSOCIATES
1801 BITTERSWEET LANE
MT PROSPECT IL 60056
PHONE: 312 698 5580

G E SALSER
17 ARTHUR PLACE

YONKERS NY 10701
PHONE: 201 894 6266

R H BARRY SAMPLE
INDIANA UNIV SCH OF MED
DEPT OF PATHOLOGY
INDIANAPOLIS IN 46223
PHONE: 317 274 7641

JOHN M SANDERS
RICERCA INC
PO BOX 1000
PAINESVILLE OH 44077
PHONE: 216 357 3349

GARY L SANTEE
EASTMAN KODAK
150 BELMEADE ROAD
ROCHESTER NY 14617
PHONE: 716 722 3194

JEFFREY SANTROCK
GENERAL MOTORS RESEARCH
BIOMEDICAL SCIENCE DEPT
WARREN MI 48090
PHONE: 313 986 1672

F G SATKIEWICZ
JOHN HOPKINS UNIV
APL
LAUREL MD 20707
PHONE: 301 792 6247

PHIL SAVICKAS
DOW CHEMICAL CO
BLDG 574
MIDLAND MI 48640
PHONE: 517 636 8728

M D SCANLON
57 MARIEMONT AVE

BUFFALO NY 14220
PHONE: 716 631 0360

WILLIAM SCHAEFER
DEPT OF PHARMACOLOGY
VANDERBILT UNIVERSITY
NASHVILLE TN 37221
PHONE:

RICHARD SCHAEFFER
EXTREL CORP
PO BOX 11512
PITTSBURGH PA 15238
PHONE: 412 963 7530

MARLENE E SCHAPS
EXXON PRODUCTION RESEARCH
PO BOX 2189
HOUSTON TX 77252
PHONE: 713 965 7623

MARTIN SCHAUER
UNIV OF COLORADO
JOINT INST FOR LAB ASTROPHCEHS
BOULDER CO 80309
PHONE: 303 492 7762

RICHARD H SCHEEL
MICH PUBLIC HEALTH
EPIDEMIOLOGY STUD DIV
LANSING MI 48909
PHONE: 517 335 8349

THOMAS A SCHEHL
DE MAO-1
KENNEDY SPACE CENTER
CAPE KENNEDY FL 32899
PHONE: 305 867 3080

STEVEN M SCHEIFERS
31 GOLDEN AVENUE
APT 23B
BATTLE CREEK MI 49015
PHONE: 616 961 2096

S E SCHEPPELE
BARTLESVILLE ENERGY
TECHNOLOGY CENTER
BARTLESVILLE OK 74003
PHONE: 918 337 4414

KEVIN L SCHEY
3554 A CHAUNCEY ST E DR
LAFAYETTE IN 47905
PHONE: 317 494 5264

S M SCHILDCROUT
YOUNGSTOWN STATE UNIV
CHEMISTRY DEPT
YOUNGSTOWN OH 44555
PHONE: 216 742 7114

ALLEN W SCHINSKY
11326 LOVELAND
LIVONIA MI 48150
PHONE: 313 344 1770

ANDREW SCHKUTA
CAMBRIDGE ANAL ASSOC
1106 COMMONWEALTH
BOSTON MA 02215
PHONE: 617 232 2207

JOHN J SCHLAGER
903 15TH AVE N E
ROCHESTER MN 55904
PHONE:

CHARLES E SCHMIDT
PETC-DOE
PO BOX 10940
PITTSBURGH PA 15236
PHONE:

JOHN G SCHMIDT
BRISTOL-MYERS CO
2404 PENNSYLVANIA
EVANSVILLE IN 47721
PHONE: 812 429 8225

R J SCHMITT
SRI INTERNATIONAL
333 RAVENWOOD AVE
MENLO PARK CA 94025
PHONE: 415 859 5579

H K SCHNOES
UNIV OF WISCONSIN
BIOCHEMISTRY DEPT
MADISON WI 53706
PHONE: 608 262 0650

WILLIAM C SCHNUTE
FINNIGAN CORP
355 RIVER OAKS PKWY
SAN JOSE CA 95134
PHONE: 408 433 4800

ROBERT J SCHOCK
2305 WESTBURY ROAD
LANSING MI 48906
PHONE: 419 647 4196

DALE A SCHOELLER
UNIV OF CHICAGO
BOX 223
CHICAGO IL 60637
PHONE: 312 702 6561

ALAN E SCHOEN
1867 INDIAN CREEK CT
SAN JOSE CA 95148
PHONE: 408 946 4848

DONALD M SCHOENGOLD
3655 STORRIE CT
LAS VEGAS NV 89103
PHONE: 702 739 3142

DONALD L SCHOOLEY
MILES LABORATORIES
PO BOX 932
ELKHART IN 46515
PHONE: 219 262 7804

DAVID M SCHRADER
CHEMISTRY DEPT
MARQUETTE UNIV
MILWAUKEE WI 53233
PHONE: 414 224 3332

MAUREEN A SCHRADER
814 BROADWAY B
INDIANAPOLIS IN 46202
PHONE: 317 274 3220

KARL H SCHRAM
UNIV OF ARIZONA
COLLEGE OF PHARMACY
TUCSON AZ 85721
PHONE: 602 626 5630

E M SCHREIBER
22 FAIRFIELD CT
PITTSBURGH PA 15201
PHONE: 412 624 3113

J M SCHROEER
ILLINOIS STATE UNIV
PHYSICS DEPT
NORMAL IL 61761
PHONE: 309 438 5193

JOSEPH N SCHROEPFER
3M
3M CENTER
ST PAUL MN 55144
PHONE: 612 733 6288

LEONARD SCHRONK
WYETH LABS
ROOM C084
PHILADELPHIA PA 19101
PHONE: 215 341 2565

ADAM J SCHUBERT
ARCO PETROLEUM PRODUCTS
1801 SEPULVEDA
CARSON CA 90745
PHONE: 213 548 8000

MARILYN SCHWARTZ
UC SAN FRANCISCO
S OF PHARMACY, S926
SAN FRANCISCO CA 94143
PHONE: 415 476 2582

HUBERT A SCOBLE
MIT
CHEMISTRY DEPT
CAMBRIDGE MA 02139
PHONE: 617 253 7229

RICHARD SCOTT
ACUREX CORP
405 CLYDE AVENUE
MTN VIEW CA 94039
PHONE: 415 961 9298

KIM SEGAR
UNIV OF COLORADO
CAMPUS BOX 215
BOULDER CO 80309
PHONE: 303 492 6958

MUSTAFA I SELIM
DEPT OF CHEMISTRY
MURRAY STATE UNIV
MURRAY KY 42071
PHONE: 502 762 2584

ROBERT SERFASS
DEPT OF FOODS & NUTRITION
105 MACKAY HALL
AMES IA 50011
PHONE: 515 294 3570

JEFFREY SHABANOWITZ
UNIV OF VIRGINIA
CHEMISTRY DEPT
CHARLOTTESVLL VA 22901
PHONE: 804 924 7994

LAMAAT M SHALABY
DUPONT EXPER STA
AGRICULTURAL DEPT
WILMINGTON DE 19898
PHONE: 302 772 3481

LIESA A SHANAHAN
HONEYWELL INC
600 N E 2ND ST
HOPKINS MN 55343
PHONE: 612 931 6983

WILLIAM G SCHULZE
MILLER BREWING CO
3939 W HIGHLAND BLVD
MILWAUKEE WI 53108
PHONE: 414 931 3643

K E SCHWARZ
HP SCIENTIFIC INSTR
1601 CALIFORNIA AVE
PALO ALTO CA 94304
PHONE: 415 857 6056

JUDITH SCOTT
IONSPEC
17851 ARBOR LANE
IRVINE CA 92715
PHONE:

JOE SEARS
CHEMISTRY DEPT
MONTANA STATE UNIV
BOZEMAN MT 59717
PHONE: 406 994 4801

ROSALIND SEGESTA
9837 MINT STREET
BATON ROUGE LA 70809
PHONE: 504 388 6770

ATISH D SEN
DEPT OF PHYSICS & ASTRONOMY
UNIV OF WYOMING
LARAMIE WY 82071
PHONE: 307 766 6150

KENNETH SETCHELL
CHLDN'S HOSPITAL MED CTR
CLINICAL MASS SPECTROMETRY
CINCINNATI OH 45229
PHONE: 513 559 8442

CEDRIC H SHACKLETON
OAKLAND CHDN'S HOSP
747 52ND STREET
OAKLAND CA 94609
PHONE: 415 428 3604

TOM SHALER
UC RIVERSIDE
CHEMISTRY DEPT
RIVERSIDE CA 92521
PHONE:

JIAN-DONG SHAO
DEPT OF CHEMISTRY
UNIV OF NORTH CAROLINA
CHAPEL HILL NC 27514
PHONE: 919 962 7577

JAE C SCHWARTZ
3554 A CHAUNCEY CT E DR
LAFAYETTE IN 47905
PHONE: 317 494 6898

ESTON SCHWECKE
HUNTINGTON BCH POLICE
2000 MAIN ST
HUNTINGTON BC CA 92648
PHONE:

R G SCOTT
ARGONNE NATIONAL LAB
D-200
ARGONNE IL 60439
PHONE: 312 972 3529

DON SEDGWICK
ALLIED CORP
CORPORATE TECHNOLOGY
MORRISTOWN NJ 07960
PHONE: 201 455 2977

WILLIAM E SEIFERT
UNIV OF TX MED SCH
ANALYTICAL CHEMISTRY
HOUSTON TX 77225
PHONE: 713 792 5612

DILIP K SENSHARMA
UCLA
CHEMISTRY DEPT
LOS ANGELES CA 90024
PHONE: 213 825 9810

SATINDER K SETHI
TRAVENOL LABS
6301 LINCOLN AVE
MORTON GROVE IL 60053
PHONE: 312 965 4700

FRANCIS J SHALA
353 DERBY DOWNS RD
NEWARK OH 43055
PHONE: 614 587 7233

LARRY SHAMPINE
BRISTOL MYERS CO PRDD
5 RESEARCH PKWY
WALLINGFORD CT 06492
PHONE: 203 284 6422

A G SHARKEY
321 OLD ENGINEERING HALL
UNIV OF PITTSBURGH
PITTSBURGH PA 15260
PHONE: 412 624 8878

T E SHARP
LOCKHEED RES LAB
3251 HANOVER
PALO ALTO CA 94304
PHONE: 415 424 2528

PAUL W SHEARER
HERCULES INC
RESEARCH CENTER
WILMINGTON DE 19894
PHONE: 302 995 3258

DENISE A SHEPPERD
39 BITTERWOOD CIR

WOODLANDS TX 77381
PHONE:

SCOTT SHERMAN
1395 ENGLEWOOD

ST PAUL MN 55104
PHONE: 612 644 9637

MING-CHUEN SHIH
6820 MARBURY ROAD

BETHESDA MD 20817
PHONE:

STEPHEN SHRADER
SHRADER ANAL LAB
3814 VINEWOOD
DETROIT MI 48208
PHONE: 313 894 4440

JOANNA SHULSKY
OSHA ANLAYTICAL LAB
1781 SOUTH 300 WEST
SALT LAKE CTY UT 84115
PHONE:

MELVIN W SIEGEL
ROBOTICS INSTITUTE
CARNEGIE-MELLON UNIV
PITTSBURGH PA 15213
PHONE: 412 578 8802

MARY LOU SIGSBY
1008 BRAYTON CT

RALEIGH NC 27606
PHONE:

LAURENCE SILLY
JOHNS HOPKINS UNIV
725 N WOLFE ST
BALTIMORE MD 21205
PHONE: 301 955 6961

THOMAS R SHARP
DEPT OF CHEMISTRY
CTR FOR CHEM CHAR & ANAL
COLLEGE STN TX 77843
PHONE: 409 845 8404

EDWARD W SHEEHAN
1100 SALK HALL
PHARMACOLOGY & TOXICOLOGY
PITTSBURGH PA 15261
PHONE: 412 648 8575

JAMES SHERFINSKI
NICOLET INSTRUMENTS
5225-1 VERONA ROAD
MADISON WI 53711
PHONE: 608 271 3333

WILLIAM R SHERMAN
WASHINGTON UNIV
SCHOOL OF MEDICINE
ST LOUIS MO 63110
PHONE: 314 362 7013

CHARLES J SHIMANSKAS
CIBA-GEIGY CORP
444 SAW MILL RIVER ROAD
ARDSLEY NY 10502
PHONE: 914 478 3131

ANIL K SHUKLA
DEPT OF CHEMISTRY
UNIV OF DELAWARE
NEWARK DE 19716
PHONE: 302 451 1118

GARY D SIDES
1732 TAHITI LANE

ALABASTER AL 35007
PHONE: 934 9151

EMIL G SIEGMUND
US FDA
1521 W PICO BLVD
LOS ANGELES CA 91042
PHONE: 213 252 7592

KENNETH W SIGVARDSON
EI DUPONT DE NEMOURS INC
EXPERIMENTAL STA E353-239
WILMINGTON DE 19898
PHONE: 302 772 7522

A H SILVER
1 OVERBROOK PLACE

HILLSDALE NJ 07642
PHONE: 201 943 7100

JOHN SHAW
FDA (HFF-426)
200 C ST SW
WASHINGTON DC 20204
PHONE: 202 472 9144

TRACI SHELL
MONSANTO RESEARCH CORP
PO BOX 32
MIAMISBURG OH 45342
PHONE: 513 865 4752

PAUL L SHERMAN
MONSANTO - U1F
800 N LINDBERGH BLVD
ST LOUIS MO 63167
PHONE: 314 694 3519

JENTAIE SHIEA
MONTANA STATE UNIV
CHEMISTRY DEPT
BOZEMAN MT 59717
PHONE: 406 994 4801

RONALD SHOMO
CHEMISTRY DEPT BOX 169
OHIO STATE UNIV
COLUMBUS OH 43210
PHONE: 614 292 4214

RANDY SHUL
765 EAST MAIN ST

BRIDGEWATER NJ 0880
PHONE:

MARSHALL M SIEGEL
LEDERLE LABS
AMERICAN CYANAMID
PEARL RIVER NY 10965
PHONE:

JAMES SIGNORELLI
PEPSICO RESEARCH CENTER
100 STEVENS AVE
VALHALLA NY 10595
PHONE: 914 742 4633

LAURENCE SILLY
JOHNS HOPKINS UNIV
SCHOOL OF MEDICINE
BALTIMORE MD 21205
PHONE: 301 955 3022

R W SILVERMAN
UNIV OF CALIFORNIA
PHARMACOLOGY DEPT
LOS ANGELES CA 90024
PHONE: 213 825 5448

BERND R SIMONEIT
OREGON STATE UNIV
COLL OF OCEANOGRAPHY
CORVALLIS OR 97331
PHONE: 503 754 2155

JOHN SIMPSON
UNIV OF COLORADO-HSC
4200 E 9TH AVE
DENVER CO 80302
PHONE: 303 394 8937

MARY E SISAK
ASHLAND PETROLEUM
843 TENTH AVE
HUNTINGTON WV 25701
PHONE:

LAURENCE E SLIVON
BATTELLE LABS
505 KING AVE
COLUMBUS OH 43201
PHONE: 614 424 4274

ARTHUR SMITH
TEKNIVENT
11684 LILBURN PARK RD
ST LOUIS MO 63146
PHONE: 314 994 0500

DANNE E SMITH
36 STONE RUN ROAD

BEDMINSTER NJ 07921
PHONE: 201 685 7555

DAVID LEE SMITH
MEDICINAL CHEM DEPT
PURDUE UNIV
W LAFAYETTE IN 47907
PHONE: 317 494 6094

JAMES S SMITH
7A GRACE'S DRIVE

COATESVILLE PA 19320
PHONE: 215 692 5770

PAUL V SMITH
FDA LAB
10 WEST 35TH STREET
CHICAGO IL 60616
PHONE: 312 886 7074

ROBERT F SMITH
ROUTE 5
BOX 136
MURPHY NC 28906
PHONE: 704/837-7086

D S SIMONS
NBS
BLDG 222 RM A121
GAITHERSBURG MD 20899
PHONE: 301 975 3903

RAJESH SINGHI
ENVIRO RESEARCH INC
4 VALENE RD
EDISON NJ 08820
PHONE: 201 769 8918

JOHN SLAYBACK
ONEIDA RESEARCH SERVICES
ONE HALSEY ROAD
WHITESBORO NY 13492
PHONE: 315 736 3050

JAMES SLOVINSKI
12537 W FIRST PLACE

LAKEWOOD CO 80228
PHONE: 303 236 5132

CHARLES A SMITH
17669 SAN VICENTE

FNTN VALLEY CA 92708
PHONE: 714 896 5280

DAVID E SMITH
1230 PATTEN

LOS ALTOS CA 94022
PHONE: 408 433 4800

GARMON BROOKS SMITH
US EPA
PO BOX 1198
ADA OK 74820
PHONE: 405 332 8800

JOHNNY SMITH
TVA
2314 NORWOOD BLVD
FLORENCE AL 35630
PHONE: 205 386 2371

PHILIP C SMITH
NATL INST OF HEALTH
BLDG 37, ROOM 2C04
BETHESDA MD 20892
PHONE: 301 496 2090

RONALD G SMITH
MONSANTO AG PRODUCTS
700 CHESTERFLD VILLAGE PKWPO BOX 2226
ST. LOUIS MO 63198
PHONE: 314 537 6275

WILLIAM J SIMONSICK
DUPONT MARSHALL RES LAB
3500 GRAYS FERRY AVE
PHILADELPHIA PA 19146
PHONE: 215 339 6269

KATHLEEN E SINGLETON
SOUTHERN RESEARCH INST
PO BOX 55305
BIRMINGHAM AL 35255
PHONE: 205 323 6592

GARY M SLEMP
1311 COOK ST #307

DENVER CO 80206
PHONE:

REIN SMIT
VESTEC CORP
9299 KIRBY DRIVE
HOUSTON TX 77089
PHONE: 713 796 9677

CHERYL A SMITH
MULTI TECH LABORATORIES
320 TESCONI CIRCLE UNIT R
SANTA ROSA CA 95401
PHONE: 707 544 5570

DAVID H SMITH
ORNL MARTIN MARIETTA
PO BOX Y BLDG 9735
OAK RIDGE TN 37831
PHONE: 615 574 2454

GRANT GILL SMITH
UTAH STATE UNIV

LOGAN UT 84322
PHONE:

MICHAEL W SMITH
7379 RT 32

COLUMBIA MD 21044
PHONE: 301 531 4479

RICHARD D SMITH
BATTELLE-NW
BLDG 329 AREA 300
RICHLAND WA 99352
PHONE: 509 376 0723

CHARLES R SNELLING
EXXON R&D LABS
BATON ROUGE LA 70821
PHONE: 504 359 8361

L T SNIEGOSKI
NAT'L BUR OF STAN
BLDG 222 RM A361
GAITHERSBURG MD 20899
PHONE: 301 975 3133

JOHN D SNYDER
700 HAWLEY ROAD

MASON MI 48854
PHONE:

JOSEPH G SOLCH
8370 HEILMAN DR

NEW CARLISLE OH 45344
PHONE: 513 873 2202

RICHARD T SOLSTEN
MONSANTO CO AA1F
LIFE SCIENCES RES CTR
CHESTERFIELD MO 63198
PHONE: 314 537 6272

PETER F SOMSSICH
36 RAVINE ROAD

AMHERST NH 03031
PHONE: 617 777 1900

G W SOVOCOOL
3155 HIGHVIEW DR

HENDERSON NV 89015
PHONE: 702 798 2212

STEVEN P SPENCE
USGS-NWQL
5293B WARD RD
ARVADA CA 80002
PHONE:

G N SPOKES
US TESTNG
1415 PARK AVE
HOBOKEN NJ 07030
PHONE: 201 792 2400

ROBERT R SQUIRES
CHEMISTRY DEPT
PURDUE UNIV
W LAFAYETTE IN 47907
PHONE: 317 494 7322

VASSILIS STAMOUDIS
GEOCHEM & ENVIRON INSTRU
ER-203
ARGONNE IL 60439
PHONE: 312 972 7637

TIMOTHY A SNOW
CONOCO R&D
PO BOX 1267
PONCA CITY OK 74603
PHONE: 405 767 5563

INGVAR E SODAL
6595 ODELL PLACE
SUITE M
BOULDER CO 80301
PHONE: 303 530 7778

BRUCE H SOLKA
7813 W ROSEDALE

CHICAGO IL 60631
PHONE: 312 567 5290

B D SOLTMANN
1909 BRIDGEPORT DR

RALEIGH NC 27609
PHONE: 919 847 0744

BAN-HUAT SONG
6810 NEWLIGHT COURT

FT WASHINGTON MD 20744
PHONE: 301 249 4000

GLENN E SPANGLER
BENDIX ESD
1400 TAYLOR AVE
BALTIMORE MD 21284
PHONE: 301 321 5261

ROBERT B SPENCER
5121 FLAMBEAU RD

MADISON WI 53705
PHONE: 608 271 3333

ROBERT L SPRAGGINS
3663 S SHERIDAN D-16

DENVER CO 80235
PHONE: 303 989 3855

ALLAN E STAFFORD
800 BUCHANNAN ST

ALBANY NY 94710
PHONE: 415 486 3657

JEFFREY A STAMP
153 E LITTLE CANADA ROAD
#219
ST PAUL MN 55117
PHONE: 612 624 1295

A PETER SNYDER
CHEMICAL RES DEV & ENG CTR
SMCCR-RSL
ABERDEEN P GD MD 21010
PHONE: 301 671 2416

STEPHEN A SOKOLOW
1901 VALPARAISO

MENLO PARK CA 94025
PHONE: 415 324 2222

JEROME J SOLOMON
NEW YORK UNIV MED CTR
ENVIRONMENTAL MEDICINE
TUXEDO PARK NY 10987
PHONE: 914 351 4398

NANCY SOMERS
101-5 RAL
DEPT OF CHEMISTRY
URBANA IL 61820
PHONE: 217 333 0655

JUDY SOPHIANOPOULOS
2994 MCCULLY DR, NE

ATLANTA GA 30345
PHONE: 404 939 6526

DAVID N SPEIS
ETC CORP
PO BOX 7808
EDISON NJ 08818
PHONE: 201 225 6759

J A SPHON
FDA
HFF-426
WASHINGTON DC 20204
PHONE: 202 472 9144

RUSSELL C SPREEN
ICI/STUART PHARMACEUTICALS
RT 202 & MURPHY ROAD
WILMINGTON DE 19897
PHONE: 302 575 3999

GEORGE STAFFORD
FINNIGAN MAT
355 RIVER OAKS PKWY
SAN JOSE CA 95134
PHONE: 408 433 4800

C G STANDARD
STERLING CO
PO BOX 1311
TEXAS CITY TX 77592
PHONE: 409 942 3519

JOHN STANLEY
MIDWEST RESEARCH INST
425 VOLKER BLVD
KANSAS CITY MO 64110
PHONE: 816 753 7600

MICHELE S STANLEY
CHEMISTRY DEPT BOX 267
INDIANA UNIV
BLOOMINGTON IN 47405
PHONE: 812 335 3436

DAVID T STANTON
UNIROYAL CHEMICAL CO
ELM STREET
NAUGATUCK CT 06770
PHONE: 203 723 3684

DOUGLAS B STAUFFER
GEORGETOWN UNIV MED CTR
DEPT OF RADIOLOGY
WASHINGTON DC 20904
PHONE:

JAMES L STAUFFER
UNIV OF UTAH
311 A SKAGGS HALL
SALT LAKE CTY UT 84112
PHONE: 801 581 7532

RALPH STEARNS
MERCK & CO
PO BOX 2000 RY80L109
RAHWAY NJ 07065
PHONE: 201 574 5253

W L STEBBINGS
3M COMPANY
201-BS-05
ST PAUL MN 55144
PHONE: 612 733 4891

JOHN D STEIN
GENERAL ELECTRIC
1334 KATHY CT
LIVERMORE CA 94550
PHONE: 415 862 4317

URS STEINER
FINNIGAN CORP
355 RIVER OAKS PKWY
SAN JOSE CA 95134
PHONE: 408 433 4800

ELIZABETH A STEMMLER
106 HIGH POINT LANE

OAK RIDGE TN 37830
PHONE: 615 574 4867

DANNY O STENE
4200 EAST 9TH
UNIV OF CO HEAL SCI CTR
DENVER CO 80226
PHONE: 303 394 8937

JAMES L STEPHENSON
2402 OMEGA ROAD

RICHMOND VA 23228
PHONE: 804 359 1900

MYRON STEPHENSON
US EPA
PO BOX 377
HULL GA 30646
PHONE: 404 546 1456

RICHARD STEPNOWSKI
CHEMISTRY DEPT
MICHIGAN STATE UNIV
EAST LANSING MI 48824
PHONE: 517 353 6495

FREDERICK A STEVIE
AT&T BELL LABS
ROOM 2C-070
ALLENTOWN PA 18103
PHONE: 215 439 7169

D W STEWART
675 BEACH AVE

ROCHESTER NY 14612
PHONE:

DWIGHT D STIFF
5700 BUNKER HILL STREET
NO 804
PITTSBURGH PA 15206
PHONE: 412 648 8575

R N STILLWELL
10 DANIELS DRIVE

BEDFORD MA 01730
PHONE: 617 239 0128

W G STILLWELL
MIT
APPLIED BIOLOGICAL SCIENCE
CAMBRIDGE MA 02139
PHONE: 617 253 3118

JAMES J STOFFEL
BATTELLE-NW
BLDG 320 AREA 300
RICHLAND WA 99352
PHONE: 509 376 2142

MARTIN STOGNIEW
PO BOX 25

BLOOMING GROV NY 10914
PHONE:

PAUL W STOKER
4505 MARYLAND PARKWAY
UNIV OF NEVADA, ERC, QAL
LAS VEGAS NV 89119
PHONE: 702 739 3142

HOWARD A STORMS
GENERAL ELECTRIC CO
M/C V08
PLEASANTON CA 94566
PHONE: 415 862 4527

MICHAEL STORY
FINNIGAN MAT
355 RIVER OAKS PWY
SAN JOSES CA 95134
PHONE: 408 433 4800

STEVEN J STOUT
AMERICAN CYANIMID
AGRICULTURAL DIV
PRINCETON NJ 08540
PHONE: 609 799 0400

JUSTIN G STRAH
PFIZER INC

GROTAN CT 06340
PHONE: 203 441 4024

JOHN W STRAND
7715 FLANDERS DRIVE

SAN DIEGO CA 92126
PHONE: 619 578 6766

DARYL P STRANDBERGH
8924 PERRIN

LIVONIA MI 48150
PHONE: 313 344 1770

LARRY STRATTAN
US EPA
DENVER FEDERAL CTR
DENVER CO 80225
PHONE:

KENNETH M STRAUB
SMITH KLINE & FRENCH LABS
MAIL CODE L 711
SWEDELAND PA 19479
PHONE: 215 270 6163

ROBERT J STRIFE
MIAMI VALLEY LABS
PROCTER & GAMBLE
CINCINNATI OH 45247
PHONE: 513 245 2655

SUSAN E STRONG
HEWLETT PACKARD
1601 CALIFORNIA AVE
PALO ALTO CA 94304
PHONE: 415 857 7890

G P STURM
NAT'L INST FOR PETRO
AND ENERGY RES
BARTLESVILLE OK 74005
PHONE: 918 337 4314

BABU SUBRAMANYAM
20 N PINE ST
SCH OF PHARM DEPT OF MED
BALTIMORE MD 21201
PHONE: 301 328 2982

H R SULLIVAN
ELI LILLY CO
RESEARCH LABS
INDIANAPOLIS IN 46285
PHONE: 276 4631

TERRY L SUMPTER
DEPT OF CHEMISTRY
UNIV OF TENNESSEE
KNOXVILLE TN 37996
PHONE: 615 974 6578

SOMCHAI SUWANRUMPHA
DEPT OF CHEMISTRY
UNIV OF HOUSTON
HOUSTON TX 77004
PHONE: 713 743 2675

DEBORAH L SWACKHAMER
SCH OF PUBLIC HEALTH
MAYO BLDG BOX 197 U OF MIN
MINNEAPOLIS MN 55455
PHONE: 612 626 0435

JEFFREY D SWEATLOCK
PURDUE UNIVERSITY
CHEMISTRY DEPT
W LAFAYETTE IN 47907
PHONE: 317 494 5262

BRIAN J SWEETMAN
VANDERBILT UNIV
PHARMACOLOGY DEPT
NASHVILLE TN 37232
PHONE: 615 322 2094

FREDERICK STROBEL
UNIVERSITY OF DELAWARE
DEPARTMENT OF CHEMISTRY
NEWARK DE 19716
PHONE: 302 451 1197

JOHN T STULTS
MICHIGAN STATE UNIV
CHEMISTRY DEPT
EAST LANSING MI 48824
PHONE: 517 353 6767

DAVID L STYRIS
205 CRAIGHILL

RICHLAND WA 99352
PHONE: 509 376 1907

KIM SUKWHA
US EPA
CHICAGO IL 60605
PHONE:

RICHARD E SULLIVAN
26461 MONTECITO LANE

MISSION VIEJO CA 92691
PHONE: 213 933 5991

TUNG SUN
USDA-FSIS
PO BOX 6085
ATHENS GA 30604
PHONE: 404 546 3571

ROBERT K SUZUKI
25 HICKORY PLACE
APT H-4
CHATHAM NJ 07928
PHONE: 201 380 8520

ROBERT SWAIM
FINNIGAN MAT
PO BOX 5997
KINGWOOD TX 77325
PHONE: 713 360 2740

CHARLES C SWEELEY
MICHIGAN STATE UNIV
BIOCHEMISTRY DEPT
EAST LANSING MI 48824
PHONE: 517 353 3257

DAVID R SWENSON
JOINT INST FOR LAB ASTRO
BOX 440
BOULDER CO 80309
PHONE: 303 492 7763

J M STRONG
13103 BLUHILL RD

SILVER SPRING MD 20906
PHONE: 301 496 4116

CATHERINE M STUPAK
BALZERS
8 SAGAMORE PARK RD
HUDSON NH 03051
PHONE: 603 889 6888

T C K SU
SMU
CHEMISTRY DEPT
N DARTMOUTH MA 02747
PHONE: 617 999 8235

CLINT SULFRIDGE
158 WADDELL CIRCLE

OAK RIDGE TN 37830
PHONE: 615 574 2438

R L SUMMERS
E I DUPONT DE NEMOURS
BOX 347
LA PORTE TX 77571
PHONE: 713 470 3464

YIPING SUN
DEPT MEDICINAL CHEMISTRY
SCH OF PHARMACY
W LAFAYETTE IN 47907
PHONE: 317 494 1449

H J SVEC
IOWA STATE UNIV
CHEMISTRY DEPT
AMES IA 50011
PHONE: 515 294 6486

ADRIAN SWANSON
INTERPOLL, INC
4500 BALL ROAD NE
CIRCLE PINES MN 55014
PHONE: 612 786 6020

KEVIN M SWEENEY
6500 CREEKWOOD CT

MOBILE AL 36609
PHONE: 205 470 3243

DENNIS F H SWIJTER
HAIR PRODUCTS & CHEMICALS
2085 ASTER RD
MACUNGIE PA 18062
PHONE: 215 481 4629

JOHN SYKA
FINNIGAN MAT
355 RIVER OAKS PKWY
SAN JOSE CA 95134
PHONE: 408 433 4800

VINCENT TABONE
FINNIGAN CORP
355 RIVER OAKS PKWY
SAN JOSE CA 95134
PHONE: 408 433 4800

KOLI TAGHIZADEH
BIOMATERIALS PROFILING CTR
391 S CHIPETA WAY
SALT LAKE CIT UT 84108
PHONE: 801 581 8431

YULIN TAN
DOE
ENVIRON MEAS LAB
NEW YORK NY 10014
PHONE: 212 620 3481

SHENG-YUH TANG
RORER CENTRAL RESEARCH
BLDG #2
HORSHAM PA 19044
PHONE: 215 962 3354

LESTER TAYLOR
BURROUGHS WELLCOME
3030 CORNWALLIS ROAD
RES TRI PK NC 27709
PHONE: 919 248 3218

WILLIAM S TAYLOR
LOUISIANA STATE UNIV
CHEMISTRY DEPT
BATON ROUGE LA 70810
PHONE: 504 388 6658

RICHARD M TEETER
203 DEL VALLE CIRCLE

EL SOBRANTE CA 94803
PHONE:

JOSEPH TERRELL
CLAYTON ENV CONSULTANTS
22345 ROETHEL DR
NOVI MI 48050
PHONE: 313 344 1770

CHARLES A THOMAS
LEYBOLD-HERAEUS
VACUUM PRODUCTS INC
EXPORT PA 15632
PHONE: 412 327 5700

DEBORAH A SZARO
26 WALNUT STREET

FOXBORO MA 02035
PHONE: 617 253 1806

M W TABOR
18 JUNEFIELD AVE

CINCINNATI OH 45218
PHONE: 513 872 4830

TSONG-LIN TAI
20530 ANZA AVE APT 7

TORRANCE CA 90503
PHONE: 213 371 0405

CALVIN K TANAKA
ENSECO-CAL LAB
2544 INDUSTRIAL BLVD
W SACRAMENTO CA 95691
PHONE: 916 372 1393

ARNOLD R TAYLOR
CONOCO INC
1000 S PINE/PO BOX 1267
PONCA CITY OK 74603
PHONE: 405 767 4736

M L TAYLOR
175 BREHM LABORATORY
WRIGHT STATE UNIV
DAYTON OH 45435
PHONE: 513 873 2203

RON TECKLENBURG
TEXAS A&M UNIVERSITY
DEPT OF CHEMISTRY
COLLEGE STN TX 77843
PHONE: 409 845 0613

DAVID TEPLOW
CALTECH
DIV OF BIOLOGY, 147-75
PASADENA CA 91125
PHONE: 818 356 3628

D T TERWILLIGER
6350 OAK CREEK DR

CINCINNATI OH 45247
PHONE: 513 385 8825

DAVID W THOMAS
SRI INTERNATIONAL
ROOM AB-011
MENLO PARK CA 94025
PHONE: 415 859 3787

P A SZCZEPANIK-VANLEEUWEN
UNIV OF IL AT CHICAGO
SCH OF PUB HEALTH
CHICAGO IL 60680
PHONE: 312 966 2927

JUANITA R TACKETT
MONSANTO RESEARCH CORP
PO BOX 32
MIAMISBURG OH 45342
PHONE: 513 865 3790

C R PETE TALLEY
E I DUPONT
EXPERIMENTAL STATION
WILMINGTON DE 19898
PHONE: 302 772 2142

K K TANAKA
YALE UNIVERSITY
HUMAN GENETICS
NEW HAVEN CT 06510
PHONE: 203 785 2659

JAMES W TAYLOR
UNIV OF WISCONSIN
CHEMISTRY DEPT
MADISON WI 53706
PHONE: 608 262 4561

PAUL A TAYLOR
2544 INDUSTRIAL BLVD

W SACRAMENTO CA 95691
PHONE: 916 372 1393

PIERRE TECON
1131 SHERMAN AVE

MENLO PARK CA 94025
PHONE: 408 946 4848

TERRYANN N TERNES
MARTIN MARIETTA ENERGY SYS
BLDG 9995 MS 01
OAK RIDGE TN 37831
PHONE: 615 574 2354

TONY THEOHARIDES
WALTER REED ARMY INSTITUTE
DEPT OF PHARMACOLOGY
WASHINGTON DC 20317
PHONE: 301 427 5295

DEBORAH A THOMAS
3500 SUTHERLAND AVE
H202
KNOXVILLE TN 37919
PHONE: 615 584 4835

FAIRWELL THOMAS
NIH
BLDG 10 RM 7N115
BETHESDA MD 20892
PHONE: 301 496 6508

QUENTIN THOMAS
FINNIGAN INSTITUTE
4450 CARVER WOODS ROAD
CINCINNATI OH 45242
PHONE:

FREDERICK A THOME
R J REYNOLDS TOBACCO
BOWMAN GRAY TECH CTR
WINS-SALEM NC 27102
PHONE: 919 773 4936

JOHN J THOMPSON
ALLIED CHEMICAL
20 PEABODY ST
BUFFALO NY 14210
PHONE: 716 827 6374

KELLY R THORNBURG
MIDWEST RESEARCH INST
425 VOLKER BLVD
KANSAS CITY MO 64110
PHONE: 816 753 7600

SANDRA J TILLIN
USDA-WRRC
800 BUCHANAN ST
ALBANY CA 94710
PHONE: 415 486 3139

PAUL R TITUS
ILLINOIS DEPT OF STATE POLUCHSC
BUREAU OF FORENSIC SCIENCE
JOLIET IL 60432
PHONE: 815 727 5301

LASZLO TOKES
SYNTEX RESEARCH
3401 HILLVIEW AVE
PALO ALTO CA 94304
PHONE: 415 855 5713

KENNETH B TOMER
NIEHS
PO BOX 12233
RES TRI PARK NC 27709
PHONE: 919 541 2965

STEPHEN S TONG
CORNING GLASS WKS
SULLIVAN PK FR-18
CORNING NY 14831
PHONE: 607 974 3363

H R THOMAS
SUBURBAN LABS INC
4140 LITT DT
HILLSIDE IL 60162
PHONE: 312 544 3260

TIMOTHY THOMAS
CHEMISTRY DEPT
UNIV OF MISSOURI
KANSAS CITY MO 64110
PHONE: 816 276 1555

JEFF THOMPSON
HUNTINGTON BCH POLICE
2000 MAIN ST
HUNTINGTON BC CA 92648
PHONE:

RICHARD M THOMPSON
BATTELLE LABS
505 KING AVE
COLUMBUS OH 43201
PHONE: 614 424 4620

JOHN R THORP
HEWLETT-PACKARD
10535 HARWIN
HOUTON TX
PHONE:

EDMUND TING
LA COUNTY SHERIFF
CRIMINALISTICS LAB
LOS ANGELES CA 90057
PHONE: 213 974 4647

SUSAN S TJOA
4200 E 9TH AVE C232
DENVER CO 80262
PHONE: 303 394 8175

EMIRGUL TOLUN
UTCHS
STOUT NEUROSCIENCE LAB
MEMPHIS TN 38163
PHONE: 901 528 5488

YVES G TONDEUR
UNIV OF NEVADA, LAS VEGAS
ENVIRONMENTAL RES CTR
LAS VEGAS NV 89119
PHONE: 702 739 3142

PAUL C TOREN
MONSANTO CO
800 N LINDBERGH BLVD
ST LOUIS MO 63167
PHONE:

MICHAEL J THOMAS
BIOCHEMISTRY DEPT
BOWMAN GRAY SCH MED
WINSTON-SALEM NC 27103
PHONE: 919 748 2313

MICHAEL M THOMASON
SOUTHERN RES INST
2000 9TH AVENUE SOUTH
BIRMINGHAM AL 35255
PHONE: 205 323 6592

JOHN THOMPSON
UNIV OF COLORADO
SCHOOL OF PHARMACY
BOULDER CO 80309
PHONE:

MICHAEL L THOMSON
AMERICAN CYANAMID
AGRICULTURAL DIV
PRINCETON NJ 08540
PHONE: 609 799 0400

THOMAS O TIERNAN
WRIGHT STATE UNIV
BREHM LAB
DAYTON OH 45431
PHONE: 513 873 2202

G S TINT
EAST ORANGE VA HOSP

EAST ORANGE NJ 07019
PHONE: 201 676 1000

PETER J TODD
OAK RIDGE NAT'L LAB
PO BOX Y BLDG 9735
OAK RIDGE TN 37831
PHONE: 615 574 2455

ALBERT D TOMASSIAN
PERKIN-ELMER CORP
2771 N GAREY AVENUE
POMONA CA 91767
PHONE: 714 593 3581

HUAYI TONG
MIDWEST CTR FOR MASS SPEC
UNIV OF NEBRASKA
LINCOLN NE 68588
PHONE:

ANIBAL TORRES
SK&F LABORATORIES
PO BOX 2700
GUAYAMA PR 00654
PHONE: 809 864 4545

JOHN P TOTH
PESTICIDE RESEARCH LAB
UNIV OF FLORIDA
GAINESVILLE FL 32611
PHONE: 904 392 1978

JOSEPH A TRAINA
BERLEX LABORATORIES
110 E HANOVER AVE
CEDAR KNOLLS NJ 07927
PHONE: 201 540 8700

CHI KIM TRANG
MONSANTO CO
800 N LINDBERGH BLVD
ST LOUIS MO 63167
PHONE: 314 694 4441

JOHN R TROOST
EIRA INC
161 JAMES DR W, STE 100
ST ROSE LA 70087
PHONE: 504 469 0333

B P TSAI
UNIV OF MINNESOTA
CHEMISTRY DEPT
DULUTH MN 55812
PHONE: 218 726 7585

ANTHONY TSARBOPOULOS
MAYO CLINIC
DEPT OF PHARMACOLOGY
ROCHESTER MN 55905
PHONE: 507 284 2565

ROBERT L TUCKER
CLOROX CO
7200 JOHNSON DR
PLEASANTON CA 94566
PHONE: 415 847 6651

ANDERS TUNLID
INST FOR APPLIED MICROBIOL
UNIVERSITY OF TENNESSEE
KNOXVILLE TN 37932
PHONE: 615 675 9523

MAX J TURNER
CIIT
PO BOX 12137
RES TRI PK NC 27709
PHONE: 919 541 2070

KRYSTYNA TYCZKOWSKA
SCHOOL OF VET MED, NCSU
4700 HILLSBOROUGH ST
RALEIGH NC 27606
PHONE:

JAMES C TOU
DOW CHEMICAL CO
ANALYTICAL LAB
MIDLAND MI 48640
PHONE: 517 636 2551

THOMAS M TRAINOR
ENVIRONMENTAL RES & TECH
33 INDUSTRIAL WAY
WILMINGTON MA 01887
PHONE: 617 657 4290

MICHAEL L TREHY
MONSANTO U4G
800 N LINDBERGH BLVD
ST LOUIS MO 63167
PHONE: 314 694 1515

ROBERT L TROTTIER
LOCTITE CORP
705 N MOUNTAIN RD
NEWINGTON CT 06111
PHONE: 203 278 1280

ROBERT TSAI
LOCTITE PUERTO RICO
PO BOX 669
SABANA GRANDE PR 00747
PHONE: 809 873 6500

K Y TSERNG
CLINICAL PHARMACOLOGY
VA MEDICAL CTR
CLEVELAND OH 44106
PHONE:

WILLIAM O TUCKER
ROUTE 7
BOX 198
CLINTON TN 37716
PHONE: 615 574 2419

JERRY A TURBETT
TURBETT ASSOC
PO BOX 352
BOULDER CO 80306
PHONE: 303 442 4838

JOHN R TUSCHALL
NORTHROP SERVICES
PO BOX 12313
RES TRI PK NC 27709
PHONE: 919 549 0611

HAROLD R UDSETH
BATTELLE NORTHWEST
PO BOX 999
RICHLAND WA 99352
PHONE: 509 376 1656

WILLIAM F TRAGER
UNIV OF WASHINGTON
MEDICINAL CHEM
SEATTLE WA 98195
PHONE: 206 543 7025

VINH THI TRAN
ROY F WESTON INC
256 WELSH POOL ROAD
LIONVILLE PA 19353
PHONE: 215 524 0180

JOANN TRIMBLE
UNIV OF TENNESSEE
COLEMAN BLDG, RM 2A09
MEMPHIS TN 38163
PHONE: 901 528 5488

JEAN-LUC TRUCHE
HEWLETT-PACKARD
SCIENTIFIC INSTRUMENTS DIV
PALO ALTO CA 94304
PHONE: 415 857 1501

RUSHUNG TSAO
DEPT OF CHEMISTRY
UNIV OF CALIFORNIA
RIVERSIDE CA 92521
PHONE: 714 787 5287

MICHAEL TUCKER
FINNIGAN CORP
355 RIVER OAKS PARKWAY
SAN JOSE CA 95134
PHONE: 408 433 4800

ALBERT TUINMAN
DEPT OF CHEMISTRY
UNIV OF TENNESSEE
KNOXVILLE TN 37996
PHONE:

CRAIG R TURNER
4320 ARLINGTON CIRCLE #1E

LIVERPOOL NY 13090
PHONE: 315 425 5100

W J TUTING
507 SHIRLEEN LANE

MINE HILL NJ 07801
PHONE: 201 227 7690

MARK UHRICH
FINNIGAN MAT
355 RIVER OAKS PKWY
SAN JOSE CA 95134
PHONE: 408 433 4800

STANLEY ULICK
VA HOSPITAL
130 W KINGSBRIDGE RD
BRONX NY 10468
PHONE: 212 367 7879

ROGER UPHAM
TWIN CITY TESTING CO
662 CROMWELL AVE
ST PAUL MN 55114
PHONE: 612 641 9486

O MANUEL UY
JOHNS HOPKINS UNIV APL
JOHNS HOPKINS ROAD
LAUREL MD 20707
PHONE: 301 953 5334

PAUL P VALLON
ESTEE LAUDER INC
125 PINE LAWN RD
MELVILLE NY 11747
PHONE: 516 531 1500

GARY J VANBERKEL
OAK RIDGE NATIONAL LAB
PO BOX X
OAK RIDGE TN 37831
PHONE: 605 574 4884

ROY W VANDERHAAR
1540 SWALLOW ST.

NAPERVILLE IL 60565
PHONE: 312 420 5240

ERIK VANKUIJK
MONTANA STATE UNIV
108 GAINES HALL
BOZEMAN MT 59717
PHONE: 406 994 5378

JAMES VATH
MIT
RM 56-016
CAMBRIDGE MA 02139
PHONE: 617 284 8700

CHRISTINA H VESTAL
VESTEC CORP
9299 KIRBY DRIVE
HOUSTON TX 77054
PHONE: 713 796 9677

DOM VICCHIO
NIH
ROOM 136, BLDG 6
BETHESDA MD 20982
PHONE:

STEVE E UNGER
SQUIBB INST FOR MEDICAL
RESEARCH
PRINCETON NJ 08543
PHONE: 609 921 4987

BERNARD L UPSHULTE
DASCOMB RESEARCH PARK
PO BOX 3100
ANDOVER MA 01810
PHONE: 617 475 9030

AUSRINE K VALAITIS
AMERICAN INST DRUG DETECT
9665 ALLEN AVE
ROSEMONT IL 60018
PHONE: 312 678 2113

LUNN VANATTA
2932 SEYMOUR DR

DALLAS TX 75229
PHONE: 214 579 2331

RICHARD B VANBREEMEN
DEPT OF CHEMISTRY BOX 8204
NORTH CAROLINA STATE UNIV
RALEIGH NC 27695
PHONE: 919 737 2942

G G VANDERVELDE
5715 LAWN DRIVE

WESTERN SPRGS IL 60558
PHONE: 312 841 8360

AGNES VANLANGENHOVE
ENSECO INC
205 ALEWIFE BROOK PKWY
CAMBRIDGE MA 02138
PHONE: 617 611 3111

CAROL VELSKO
LLNL
PO BOX 808, L-232
LIVERMORE CA 94550
PHONE: 415 423 6256

MARVIN L VESTAL
VESTEC
9299 KIRBY DRIVE
HOUSTON TX 77054
PHONE: 713 749 2675

RICHARD VICKERS
5 GOLFERS WAY SOUTH

THORNDALE PA 19372
PHONE: 215 384 9349

BILLY T UPCHURCH
1213 BLUEBIRD DRIVE

VIRGINA BEACH VA 23451
PHONE: 804 431 0415

MICHAEL J URBAN
RD 1 BOX 167-F

JACKSON NJ 08527
PHONE: 201 225 2225

J L VALENTINE
ORAL ROBERTS UNIV
SCHOOL OF MEDICINE
TULSA OK 74170
PHONE: 918 493 8134

GARY J VANBERKEL
OAK RIDGE NALT LAB
PO BOX X
OAK RIDGE TN 37831
PHONE: 615 574 4884

W J VANDENHEUVEL
MERCK SHARP & DOHME
RESEARCH LABORATORY
RAHWAY NJ 07065
PHONE: 201 574 5443

SCOTT W VANETTEN
160 MILLERICK AVE

LAWRENCEVILLE NJ 08648
PHONE: 201 225 6795

JAMES P VANNOY
1281 BROCKETT ROAD
50-I
CLARKSTON GA 30021
PHONE: 404 939 2910

WILLIAM J VERRET
6608 HORNWOOD

HOUSTON TX 77074
PHONE: 713 954 6766

M M VESTLING
CHEMISTRY DEPT
SUNY COLL @ BROCKPORT
BROCKPORT NY 14420
PHONE: 716 395 5594

NANCY E VIEIRA
NICHD, LTPB
BLDG 6, RM 136
BETHESDA MD 20205
PHONE: 301 496 5531

S K VISWANADHAM
CHEMISTRY DEPT
BOX 10
PITTSBURGH PA 15260
PHONE: 412 624 8302

DAVID W VONENDT
CAL-MSC
SMITHSONIAN INSTN
WASHINGTON DC 20560
PHONE: 202 287 3721

ROBERT D VOYKSNER
204 TRAIL'S END CT

RALEIGH NC 27614
PHONE: 919 541 6697

BRUCE F WAGNER
IT CORPORATION
312 DIRECTORS DRIVE
KNOXVILLE TN 37923
PHONE: 615 690 3211

L C WAGNER
2030 TOWNGATE DRIVE

GARLAND TX 75041
PHONE: 214 995 2294

MICHAEL R WAKEFIELD
1211 BURNHAM DRIVE

SAN JOSE CA 95132
PHONE: 408 756 3236

RAYMOND L WALKER
ORNL MARTIN MARIETTA
PO BOX Y BLDG 9735
OAK RIDGE TN 37831
PHONE: 615 574 2449

BING HUANG WANG
CHEMISTRY DEPT
BAKER LABORATORY
ITHACA NY 14853
PHONE: 607 255 3731

JIA-SHEN WANG
CLAIROL INC
2 BLACHLEY RD
STAMFORD CT 06922
PHONE: 203 357 5089

WAYNE WARGO
2316 SWANSEA RD

COLUMBUS OH 43216
PHONE: 614 227 3456

T S VISWANATHAN
8409 WEST 90TH ST

OVERLAND PARK KS 66212
PHONE: 913 236 3881

KENT J VOORHEES
COLORADO SCH MINES
CHEMISTRY DEPT
GOLDEN CO 80401
PHONE: 303 273 3616

JAMES VRBANAC
MED UNIV OF SC
PHARMACOLOGY DEPT
CHARLESTON SC 29425
PHONE: 803 792 2471

DAVID A WAGNER
49 SYMPHONY ROAD
APT 24
BOSTON MA 02115
PHONE: 617 722 3000

ERIK WAHLIN
UNIV OF COLORADO
JOINT INST FOR LAB ASTROPH
BOULDER CO 80309
PHONE: 303 492 7763

LARRY S WAKEMAN
EASTMAN KODAK RESEARCH
BLDG 82
ROCHESTER NY 14650
PHONE: 716 722 4738

GEORGE R WALLER
OKLAHOMA STATE UNIV
BIOCHEMISTRY DEPT
STILLWATER OK 74078
PHONE: 405 624 6199

J L WANG
BECKMAN INDUSTRIAL
4141 PALM STREET
FULLERTON CA 92635
PHONE: 714 447 2337

RONG WANG
BIOPHYSICS BLDG B-11
725 N WOLFE STREET
BALTIMORE MD 21205
PHONE: 301 955 6961

CHARLES D WARNER
DEPT OF CHEMISTRY
HASTINGS COLLEGE
HASTINGS NE 68901
PHONE: 402 462 2402

KEVIN J VOLK
1676 SW 16TH ST

GAINESVILLE FL 32608
PHONE: 904 376 4559

PAUL VOUROS
NORTHEASTERN UNIV
INST CHEMICAL ANAL
BOSTON MA 02115
PHONE: 617 437 2840

P A WADSWORTH
814 CHEVY CHASE CIR

SUGAR LAND TX 77478
PHONE: 713 491 4754

GUENTER WAGNER
FINNIGAN MAT
355 RIVER OAKS PKWY
SAN JOSE CA 95134
PHONE: 408 433 4800

AUSTIN L WAHRHAFTIG
UNIV OF UTAH
CHEMISTRY DEPT
SALT LAKE CTY UT 84112
PHONE: 801 581 6048

KENNETH M WALKER
BROWN & WILLIAMSON TOBACCO
PO BOX 35090
LOUISVILLE KY 40232
PHONE: 502 568 7986

FRED WALLS
PHARM CHEMISTRY
UNIV OF CALIFORNIA
SAN FRANCISCO CA 94143
PHONE: 415 476 4894

JEFF S I WANG
ABBOTT LABS
D-418 ABBOTT PARK
N CHICAGO IL 60064
PHONE: 312 937 2082

T HELEN WANG
PENNZOIL PRODUCTS CO
TECHNOLOGY DIV
WOODLANDS TX 77387
PHONE: 713 363 8049

BETHANNE WARRACK
SQUIBB INST FOR MED RES
PO BOX 4000
PRINCETON NJ 08543
PHONE: 609 921 5439

PHIL WARREN
FINNIGAN MAT
355 RIVER OAKS PKWY
SAN JOSE CA 95134
PHONE: 408 433 4800

JAMES R WARRING
NICOLET INSTRUMENTS CORP
5225-1 VERONA RD
MADISON WI 53711
PHONE: 608 271 3333

MARVIN ALAN WATKINS
4917-F DANA DRIVE

RALEIGH NC 17606
PHONE: 919 541 2964

JAN WATSON
ROCKWELL INTERNATIONAL
ROCKY FLATS PLANT
GOLDEN CO 80401
PHONE: 303 966 7976

CLARA WEBB
DOW CHEMICAL CO
B-1222 BLDG
FREEPORT TX 77541
PHONE: 409 238 2924

LISA SMITH WEBB
ROUTE 6 TOPSIDE ROAD
APT 82-D
LOUISVILLE TN 37777
PHONE: 615 970 3462

G H WEDDLE
FAIRFIELD UNIV
CHEMISTRY DEPT
FAIRFIELD CT 06430
PHONE: 203 254 4000

LEO A WEIBEL
HAZLETON LABS
PO BOX 7545
MADISON WI 53707
PHONE: 608 241 7654

SUSAN T WEINTRAUB
UT HEALTH SCI CTR
7703 FLOYD CURL DR
SAN ANTONIO TX 78284
PHONE: 512 567 4043

MARK WEISS
BRUKER INSTRUMENTS
MANNING PARK
BILLERICA MA 01821
PHONE: 617 667 9580

ROBERT W WARREN
SUN REFINING & MFG
ARD
MARCUS HOOK PA 19061
PHONE: 215 447 1814

JUNE WASCHE
4770 PENNYROYAL RD

FRANKLIN OH 45005
PHONE: 513 772 2818

CLIFFORD H WATSON
LEIGH HALL BOX 554

GAINESVILLE FL 32611
PHONE: 904 376 5816

DAVID WATT
1044 BELVEDERE LANE

SAN JOSE CA 95129
PHONE:

GORDON W WEBB
770 STIMSON

IDAHO FALLS ID 83402
PHONE: 208 526 3048

BILL D WEBER
IBM CORP
D/12W, B/630, Z/E70
HOPEWELL JUNC NY 12533
PHONE:

LAL WEERASINGHE
SMITHKLINE BECKMAN
1600 PAOLI PIKE
WESTCHESTER PA 19380
PHONE: 215 251 7489

DAVID A WEIL
NICOLET INSTRUMENTS
5225 VERONA ROAD
MADISON WI 53711
PHONE: 608 271 3333

C R WEISENBERGER
OHIO STATE UNIV
CHEMISTRY DEPT
COLUMBUS OH 43210
PHONE:

JAMES C WEISSHAAR
UNIV OF WISCONSIN
DEPT OF CHEMISTRY
MADISON WI 53706
PHONE: 608 262 0266

VIRGIL L WARREN
18534 LIPPITZANER

CYPRESS TX 77433
PHONE:

BRUCE A WASILCHUK
DEPT OF CHEMISTRY
NORTHEASTERN UNIV
BOSTON MA 02115
PHONE: 617 437 2794

J THROCK WATSON
DEPT BIOCHEMISTRY
MICHIGAN STATE UNIV
EAST LANSING MI 48824
PHONE: 517 353 0855

JAMES G WATT
FINNIGAN CORP
355 RIVER OAKS PKWY
SAN JOSE CA 95134
PHONE: 408 433 4800

HUGH M WEBB
3746 SAN REMO DR

SANTA BARBARA CA 93105
PHONE: 805 961 4252

MICHAEL WEBER-GRABAU
FINNIGAN MAT
355 RIVER OAKS PWY
SAN JOSE CA 95134
PHONE: 408 433 4800

ANNEMARIE WEGMANN-SZENTE
STANFORD UNIV
CHEMISTRY DEPT
STANFORD CA 94305
PHONE: 415 497 2859

ROBERT J WEINKAM
ALLERGAN PHARM
2525 DUPONT DR
IRVINE CA 92715
PHONE: 714 955 6713

T J WEISMANN
106 SHORT ST

PITTSBURGH PA 15237
PHONE: 412 434 5824

KENNETH J WELCH
SC JOHNSON & SON INC
ANAL R&D STA MS 056
RACINE WI 53403
PHONE: 414 631 2993

MICHAEL J WELCH
NAT'L BUR OF STAN
RM A-113 BLDG 222
GAITHERSBURG MD 20899
PHONE: 301 921 2153

STEVEN WERNLUND
50 NOTTINGHAM WAY

SOMERSET NJ 08873
PHONE: 201 873 5861

JAY Y WESTCOTT
UNIV OF CO HSC
BOX B-133 CVP DEPT
DENVER CO 80262
PHONE: 303 394 7524

CHARLES WESTON
ENVIRONMENTAL TEST & CERT
284 RARITAN CENTER PKWY
EDISON NT 08818
PHONE: 201 225 6784

CONRAD WHEELER
3235 VICENTE STREET
APT #6
SAN FRANCISCO CA 94116
PHONE: 415 561 2635

DAVID C WHITE
INST FOR APP MICROBIOLOGY
10515 RESEARCH DR
KNOXVILLE TN 37932
PHONE: 615 675 9520

FREDERICK A WHITE
RENSSELAER POLY INST
NUCLEAR ENG DEPT
TROY NY 12181
PHONE: 518 270 6398

JOANNE O WHITNEY
131 TERESITA BLVD

SAN FRANCISCO CA 94127
PHONE: 415 566 7755

MARGARET E WICKHAM
MIDWEST RES INST
425 VOLKER BLVD
KANSAS CITY MO 64110
PHONE: 816 753 7600

RICHARD A WIELESEK
UNIV OF OREGON
CHEMISTRY DEPT
EUGENE OR 97403
PHONE: 503 686 4641

ROBERT R WELLER
GRAD SCH OF PUBLIC HEALTH
DEPT OF IEHS
PITTSBURGH PA 15261
PHONE: 412 624 3113

CHRYS WESDEMIOTIS
BOX 441 BAKER LABORATORY
CORNELL UNIV
ITHACA NY 14853
PHONE: 607 255 3731

DAVID G WESTMORELAND
ROHM & HAAS CO
727 NORRISTOWN RD
SPRING HOUSE PA 19477
PHONE: 215 641 2033

H R WETHERELL
MSP LAB
714 SO HARRISON
EAST LANSING MI 48823
PHONE: 517 337 6191

HERBERT G WHEELER
SOUTHWEST RESEARCH INST
6220 CULEBRA ROAD
SAN ANTONIO TX 78284
PHONE: 512 684 5111

EARL L WHITE
R J REYNOLDS TOBACCO CO
BOWMAN GRAY TECH CTR
WINSTON-SALEM NC 27102
PHONE: 919 773 4015

KEVIN D WHITE
FDA
HFF-426
WASHINGTON DC 20204
PHONE: 202 245 1371

N F WHITTAKER
NIH
BLDG 8 RM 62A-21
BETHESDA MD 20892
PHONE: 301 496 4055

ROBERT L WIECZOREK
100 DEFOREST AVENUE
TECHNICAL CTR
EAST HANOVER NJ 07936
PHONE: 201 884 4000

JAMES T WILDER
SIMSPEC
1474 FIELDCREST CIR
PLEASANT HILL CA 94523
PHONE: 415 229 0325

BERND WENCLAWIAK
DEPT OF CHEMISTRY
UNIV OF TOLEDO
TOLEDO OH 43606
PHONE: 419 537 2664

DAVID WESLEY
ASHLAND PETROLEUM CO
PO BOX 391
ASHLAND KY 41101
PHONE: 606 329 3333

ALAN F WESTON
OCCIDENTAL CHEMICAL
360 RAINBOW BLVD S BOX 72
NIAGRA FALLS NY 14302
PHONE: 716 286 3607

JEFF R WETZLER
WESTINGHOUSE-BETTIS
PO BOX 79
WEST MIFFLIN PA 15122
PHONE: 412 476 5839

J W WHEELER
10019 REDDICK DRIVE

SILVER SPRING MD 20901
PHONE: 202 636 6910

EDWARD WHITE
NBS
A113 CHEMISTRY
GAITHERSBURG MD 20899
PHONE: 301 921 2153

CRAIG M WHITEHOUSE
220 PLEASANT PT RD

BRANFORD CT 06405
PHONE:

JOSEPH K WICHMANN
WALLACE LABS
HALF ACRE ROAD
CRANBURY NJ 08512
PHONE: 609 655 6630

DANIEL R WIEDERIN
IOWA STATE UNIV
29 SPEDDING HALL
AMES IA 50011
PHONE: 515 294 3387

ZBIGNIEW A WILK
CHEMISTRY DEPT BOX 56
UNIV OF PITTSBURGH
PITTSBURGH PA 15260
PHONE: 412 624 8304

BRUCE E WILKES
ENVIRONMENTAL ANALYTICAL
5176 CRYSTAL DRIVE
CROSS LANES WV 25313
PHONE: 304 776 2730

JOANN WILKINSON
S-CUBED
3398 CARMEL VALLEY RD
SAN DIEGO CA 92138
PHONE: 619 453 0060

EVAN WILLIAMS
BAKER LAB
DEPT OF CHEMISTRY
ITHACA NY 14853
PHONE: 607 256 3731

TODD D WILLIAMS
CHEMISTRY DEPT
AUBERT HALL
ORONO ME 04469
PHONE: 207 581 1169

ROSS C WILLOUGHBY
EXTREL
240 ALPHA DRIVE
PITTSBURGH PA 15238
PHONE: 412 963 7530

ROGER T WILSON
USDA FSIS MWL
PO BOX 5080
ST LOUIS MO 63115
PHONE: 314 263 2686

WILLEM WINDIG
CRDEC
AMCCOM, SMCCR-SL
APG MD 21010
PHONE: 301 671 2416

PAUL WINKLER
3254 BEECHWOOD DR

LAFAYETTE CA 94549
PHONE: 415 283 0403

MARCUS B WISE
OAK RIDGE NAT'L LAB
P O BOX X
OAK RIDGE TN 37831
PHONE: 615 574 4867

STANLEY WOJINSKI
15555 NE 33RD

REDMOND WA 98075
PHONE: 206 788 7045

PERRY S WILKES
FDA
60 EIGHTH ST NE
ATLANTA GA 30309
PHONE: 404 347 4002

DALE A WILLCOX
218 W CHESTNUT ST

MACUNGIE PA 18062
PHONE: 215 481 7977

FRED P WILLIAMS
RESEARCH TRIANGLE INST
PO BOX 12194
RES TRI PK NC 27709
PHONE: 919 541 6699

TYLON O WILLINGHAM
YORK RESEARCH CONSULTING
938 QUAIL ST
DENVER CO 80219
PHONE: 303 233 1513

JOHN M WILSON
DEPT OF PHARMACY
UNIV OF MASS MED CTR
WORCESTER MA 01605
PHONE: 617 856 4926

RANDALL E WINANS
ARGONNE NATL LAB
CHEMISTRY DIV
ARGONNE IL 60439
PHONE: 312 972 7479

BRIAN WINGER
PURDUE UNIVERSITY
2601 SOLDIERS HM RD#16
W LAFAYETTE IN 47907
PHONE: 317 494 5264

DAVID L WINMILL
HERCULES INC
RESEARCH CENTER
WILMINGTON DE 19894
PHONE: 302 995 3267

JOHN S WISHNOK
MIT
APPLIED BIOLOGICAL SCI
CAMBRIDGE MA 02139
PHONE: 617 253 6795

MARTA H WOLFE
SHRINERS HOSP

GALVESTON TX 77550
PHONE: 409 761 6575

CHARLES L WILKINS
UNIV OF CALIFORNIA
CHEMISTRY DEPARTMENT
RIVERSIDE CA 92521
PHONE: 714 787 3518

JIM WILLEY
8194 FLOWER COURT

ARVADA CO 80005
PHONE:

PETER WILLIAMS
ARIZONA STATE UNIV
CHEMISTRY DEPT
TEMPE AZ 85287
PHONE: 602 965 4107

ROBERT D WILLIS
ATOM SCIENCES
114 RIDGEWAY CTR
OAK RIDGE TN 37830
PHONE: 615 483 1113

MARK WILSON
BALZERS
8 SAGAMORE PARK RD
HUDSON NH 03051
PHONE: 603 889 6888

JAMES WINDAK
406 KEECH

ANN ARBOR MI 48103
PHONE: 313 996 8325

C R WINKELMAN
1570 SIMMONS DR

CLEARWATER FL 33516
PHONE: 813 447 7157

MARY WINSBOROUGH
EXTREL CORP
240 ALPHA DR
PITTSBURGH PA 15238
PHONE: 412 963 7530

RICHARD J WNUK
UPJOHN CO
301 HENRIETTA ST
KALAMAZOO MI 49001
PHONE: 616 385 7918

ROBERT R WOLFE
SHRINERS HOSPITAL
METABOLISM UNIT
GALVESTON TX 77550
PHONE:

W ALAN WOLSTENHOLME
VG INSTRUMENTS
13840 WEST OAK GLEN RD
VALLEY CENTER CA 92082
PHONE: 619 749 9306

WILLIAM W WONG
MEDICAL TOWERS BLDG
SUITE 601
HOUSTON TX 77030
PHONE: 713 799 6187

KARL V WOOD
PURDUE UNIV
FUELS ANAL LAB
W LAFAYETTE IN 47907
PHONE: 317 494 7357

JOHN W WOODS
8 RICHARDS RD

LYNNFIELD MA 01940
PHONE: 617 246 0040

CHARLES J WRIGHT
1210 MAJESTIC WAY

WEBSTER NY 14580
PHONE: 716 477 6733

LYNN H WRIGHT
US EPA
EMSL MD-78
RES TRI PARK NC 27711
PHONE: 919 541 2951

JEFF R WYATT
NRL
CODE 6110
WASHINGTON DC 20375
PHONE: 202 767 3244

MARK YANCEY
BATTELLE
505 KING AVE
COLUMBUS OH 43201
PHONE:

SONG-CHENG YANG
NIMH
BLDG 10 3040
BETHESDA MD 20892
PHONE:

SUSAN K YEAGER
LOCKHEED MISSILE & SPACE CC
O/48-92, B/195B
SUNNYVALE CA 94088
PHONE: 408 756 3236

CARLA M WONG
NASA M/S 244-7
AMES RESEARCH CENTER
MOFFETT FIELD CA 94035
PHONE: 415 694 4294

G M WOOD
2 LITTLE BLUFF RD

NEWPORT NEWS VA 23606
PHONE: 804 865 2466

NEVILLE WOOD
BASF ARC

RES TRI PK NC 27709
PHONE:

J R WOOLSTON
RCA LABORATORIES

PRINCETON NJ 08540
PHONE: 609 734 3108

ELAINE WRIGHT
1329 HENRY ST APT 1B

BERKELEY CA 94709
PHONE: 415 528 4220

JOHN WRONKA
DEPT OF CHEMISTRY
NORTHEASTERN UNIV
BOSTON MA 02115
PHONE: 617 437 4513

VICKI H WYSOCKI
CHEMISTRY DEPT
BOX 482
W LAFAYETTE IN 47907
PHONE: 317 494 6898

CATHY L C YANG
DEPT OF CHEMISTRY
UNIV OF CALIFORNIA
RIVERSIDE CA 92521
PHONE: 714 787 4740

JOHN R YATES
DEPT OF CHEMISTRY
MCCORMICK RD
CHARLOTTESVLL VA 22901
PHONE: 804 924 7994

GEORGE YEFCHAK
CHEMISTRY DEPT
MICHIGAN STATE UNIV
EAST LANSING MI 48824
PHONE: 517 353 5215

LAN K WONG
UNIV OF PITTSBURGH
SCHOOL OF PHARMACY
PITTSBURGH PA 15261
PHONE: 412 648 8553

JOE M WOOD
230 SHEETZ ST
APT 7
W LAFAYETTE IN 47906
PHONE: 713 743 8408

PAUL L WOOD
CIBA GEIGY
556 MORRIS AVE
SUMMIT NJ 07901
PHONE: 201 277 5741

DEREK WORKMAN
CHEMISTRY BOX 826
PURDUE UNIVERSITY
W LAFAYETTE IN 47907
PHONE:

LARRY G WRIGHT
DOW CHEMICAL USA
BLDG 734
MIDLAND MI 48640
PHONE: 517 636 4893

WU-NAN WU
MCNEIL PHARMACEUTICAL
WELSH & MCKEAN RDS
SPRING HOUSE PA 19477
PHONE: 215 628 5562

GEORGE F YAMNITZKY
NORTH CENTRAL LABORATORY
ROOM 500
CHICAGO IL 60607
PHONE: 312 353 3640

LILY YANG
VESTEC CORP
9299 KIRBY DRIVE
HOUSTON TX 77054
PHONE: 713 796 9677

RAZIEH YAZDANPARAST
BIOCHEMISTRY DEPT

W LAFAYETTE IN 47907
PHONE: 317 494 1622

LAUREN M YELLE
ARTHUR D LITTLE INC
15 ACORN PARK
CAMBRIDGE MA 02140
PHONE: 617 864 5770

RICHARD O YELTON
FINNIGAN CORP
4450 CARVER WOODS DRIVE
CINCINNATI OH 45242
PHONE: 513 891 2100

JAMES A YERGEY
NIAAA/LCSNIH
BLDG 10 RM 3C218
BETHESDA MD 20892
PHONE: 301 496 4900

GLENN YOSHIMURA
4336 MAIN

SKOKIE IL 60076
PHONE: 312 793 4767

STEVEN E YOUNG
2455 THADDEUS DR

MOUNTAIN VIEW CA 94043
PHONE: 415 859 4806

CASEY K YU
RHO-CHEM CORP
425 ISIS
INGLEWOOD CA 90301
PHONE: 213 776 6233

T Y YU
PETROLITE CORP
TRETOLITE DIVISION
ST LOUIS MO 63119
PHONE: 314 961 3500

ELLEN M YUREK
DEPT OF CHEMISTRY
MICHIGAN STATE UNIV
EAST LANSING MI 48824
PHONE: 517 353 6767

DANIEL W ZAHAREVITZ
4702 SHARON ROAD

CAMP SPRINGS MD 20748
PHONE: 301 496 4116

LEAH E ZEBRE
925 CHERRY ST

WHEATON IL 60187
PHONE: 312 260 9883

ZHONGRUI ZHOU
DEPT OF MED CHEM & PHARM
PURDUE UNIVERSITY
W LAFAYETTE IN 47907
PHONE: 317 494 1449

ANDREW J YENCHA
SUNY-ALBANY
CHEMISTRY DEPT
ALBANY NY 12222
PHONE: 518 442 4416

W D YONEKAWA
NIH
BLDG PARK 5, RM 445
BETHESDA MD 20892
PHONE: 301 496 6777

RICHARD A YOST
UNIV OF FLORIDA
CHEMISTRY DEPT
GAINESVILLE FL 32611
PHONE: 904 392 0557

TIM L YOUNGLESS
CHEVRON CHEMICAL CO
1862 KINGWOOD DR
KINGWOOD TX 77339
PHONE: 713 359 6541

KYUNG YU
AFAMRL-THA
AREA B BLDG 79
A F BASE OH 45433
PHONE: 513 255 2704

MARC YUDKOFF
CHDN'S HOSP OF PHIL
1 CHILDREN'S CTR
PHILADELPHIA PA 19104
PHONE: 215 596 9412

M F ZABIELSKI
UNITED TECH RES CTR
SILVER LANE, MS 30
EAST HARTFORD CT 06108
PHONE: 203 727 7431

JULIE A ZALIKOWSKI
JAMES H MONTGOMERY ENG
555 N WALNUT
PASADENA CA 91101
PHONE: 818 796 9141

QINGMEI ZHA
DEPT OF CHEMISTRY
642 HAMILTON HALL
LINCOLN NE 68588
PHONE: 402 472 3517

NIAN-ZHOU ZHU
DEPT OF CHEMISTRY
UNIV OF VIRGINIA
CHARLOTTESVIL VA 22901
PHONE: 904 924 7994

ALFRED L YERGEY
NIH
BLDG 6 RM 136
BETHESDA MD 20205
PHONE: 301 496 5531

MATTHIAS YOONG
6904 DOVE STREET

VENTURA CA 93003
PHONE: 818 787 7380

SO HUN YOUNG
DEPT OF CHEMISTRY
CASE WESTERN RESERVE UNIV
CLEVELAND OH 44106
PHONE:

M J YOUSSEFI
UNION CARBIDE
PO BOX 670
BOUND BROOK NJ 08805
PHONE: 201 563 5075

MING L YU
IBM RESEARCH CENTER
PO BOX 218
YORKTOWN HGHT NY 10598
PHONE: 914 945 2564

YONGSEUNG YUN
BIOMATERIALS PROFILING CTR
UNIV OF UTAH
SALT LAKE CTY UT 84108
PHONE: 801 581 8431

JEFF ZADOROZNY
CLAYTON ENV CONSULTANTS
22345 ROETHEL DR
NOVI MI 48050
PHONE: 313 344 1770

RICHARD G ZAYLSKIE
USDA AG RES SERVICE
STATE UNIV STATION
FARGO ND 58105
PHONE: 701 237 5771

MEI-YI ZHANG
BOX 285
BAKER LABORATORY
ITHACA NY 14853
PHONE: 607 255 3731

ANTHONY K ZIBERNA
FINNIGAN MAT INSTITUTE
4450 CARVER WOODS DR
CINCINNATI OH 45242
PHONE: 513 891 2100

BARBARA ZIELINSKA
STATEWIDE AIR POLLUTION
RESEARCH CTR
RIVERSIDE CA 92521
PHONE:

DEBORAH L ZINK
MERCK SHARP & DOHME
PO BOX 2000 R80M-223
RAHWAY NJ 07065
PHONE: 201 574 7207

DOUGLAS ZOOK
MONTANA STATE UNIV
DEPT OF CHEMISTRY
BOZEMAN MT 59717
PHONE: 406 994 5419

KIMBERLY J ZILIS
ROCKY MOUNTAIN ANALYTICAL
4955 YARROW ST
ARVADA CO 80002
PHONE: 303 421 6611

JOSEPH A ZIRROLLI
DEPT OF PHARMACOLOGY C236
UCHSC
DENVER CO 80262
PHONE: 303 394 8961

ROSALIE M ZUBYK
230 SUMMIT HOUSE
WEST CHESTER PA 19382
PHONE: 302 772 4536

JEFFREY ZIMMERMAN
14401 HELLENIC DRIVE B6
TAMPA FL 33613
PHONE: 813 974 3778

JAMES J ZOLDAK
MDS ADVANCED ANALYTICS
2 DUNDEE PARK
ANDOVER MA 01810
PHONE: 617 942 1093

FRANK ZULESKI
STUART PHARMACUETICALS
ICIA
WILMINGTON DE 19897
PHONE:

FRANK S ABBOTT
FAC OF PHARMACEUTICAL SCI
UNIV OF BRITISH COLUMBIA
VANCOUVER, BC V6T 1W5
PHONE: 604 228 2566

ANTHONY ALEXANDER
DEPT CHEMISTRY
UNIVERSITY OF ALBERTA
CANADA, T6G 2G2
PHONE: 403 432 3502

COLIN ALLISON
UNIV OF WATERLOO
DEPT OF CHEMISTRY
WATERLOO ONTARIO N2L 3G1
PHONE: 519 885 1211

GUY P ARSENAULT
RR 2
MIDDLE ROAD
KINGSTON ONT K7L 5H6
PHONE: 613 545 7484

TERRENCE ASHE
ESSO PETROLEUM CANADA
PO BOX 3022
SARNIA ONTARIO N7T 7M1
PHONE: 519 339 2970

RONALD C BEAVIS
PHYSICS DEPT
UNIV OF MANITOBA
WINNIPEG MAN R3T 2N2
PHONE: 204 942 9358

F M BENOIT
HEALTH-WELFARE DEPT
ENVIRONMENTAL HEALTH
OTTAWA ONTARIO K1A 0L2
PHONE:

M J BERTRAND
UNIV OF MONTREAL
CHEMISTRY DEPT
MONTREAL QUEBEC H3C 3J7
PHONE:

RON F BONNER
SCIEX
55 GLENCAMERON RD
THORNHILL ONT L3T 1P2
PHONE: 416 881 4646

CLAUDE BOURDONNAIS
VG INSTRUMENTS
5929 TRANSCANADIONNE
ST LAURENT QUEBEC H4M 2P1
PHONE: 514 744 5519

ROBERT K BOYD
ATLANTIC RES LAB
NATIONAL RES COUNCIL
HALIFAX NS B3H 3Z1CANADA
PHONE:

ALAIN R CASSISTA
ENVIRONMENT CANADA
867 LAKESHORE PO BOX 5050
CANADA L7R 4A6
PHONE:

SIU C CHAN
FOOTHILLS HOSP LAB MED DEP
1403-29ST NW
CANADA T2N 2T9
PHONE:

SWAPAN K CHOWDHURY
DEPT OF CHEMISTRY
UNIV OF ALBERTA
EDMONTON ALBERTA T6G 2G2
PHONE: 403 432 3205

MELVIN B COMISAROW
UNIV BRIT COLUMBIA
CHEMISTRY DEPT
VANCOUVER BC V6T 1Y6
PHONE: 604 228 3494

RONALD CORKUM
BARRINGER MAGENTA LTD
304 CARLINGVIEW DR
CANADA
PHONE: 416 675 3870

PIERRE L COULOMBE
ANALYTECH
742 MOONEY'S BAY PL
OTTAWA ONTARIO K1V 9R2
PHONE:

IAIN H CROCKER
BOX 496
DEEP RIVER
ONTARIO K0J 1P0
PHONE: 613 584 3311

DOUG CROSBY
SHELL CANADA LTD
OAKVILLE RESEARCH CTR
OAKVILLE ONTARIO L6J 5C7
PHONE: 416 827 1141

PAUL A D'AGOSTINO
275 11TH STREET NE
MEDICINE HAT
ALBERTA T1A 6A8
PHONE:

W R DAVIDSON
SCIEX INC
55 GLENCAMERON RD
THORNHILL ONT L3T 1P2
PHONE: 416 881 4646

PETER H DAWSON
NAT'L RESEARCH COUNCIL
MICROSCTRUCTURAL SCIENCES
OTTAWA ONTARIO K1A 0R6
PHONE: 613 993 9369

DONALD J DOUGLAS
SCIEX INC
55 GLENCAMERON RD STE 202
CANADA
PHONE: 416 881 4646

DAVID A DURDEN
PSYCHIATRIC RES DIV
A114 CMR BLDG
SASKATOON SASK S7N 0W0
PHONE: 306 933 6912

RICHARD W EDOM
COLL OF PHARMACY
UNIV OF SASKATCHEWAN
SASKATOON SASK S7N 0W0
PHONE: 306 966 6370

GUENTER K EIGENDORF
UNIV BRIT COLUMBIA
CHEMISTRY DEPT
VANCOUVER BC V6T 1Y6
PHONE: 604 228 3235

M J EVANS
CHEMISTRY DEPT
UNIV OF MONTREAL
MONTREAL QUE H3C 3J7
PHONE: 514 343 6884

LAFORTUNE F
UNIV OF MANITOBA
PHYSICS DEPT
CANADA
PHONE: 204 474 9358

JIM FEDORA
ESSO PERTROLEUM CANADA
RESEARCH DIVISION
SARNIA ONT N7T 7M1
PHONE:

H PETER FISCHER
PETRO CANADA
RES & DEV DEPT
MISSISSAUGA ONT L5K 1A8
PHONE: 416 896 6790

I P FISHER
PETROCANADA
RESEARCH & DEVELOP
SHERIDAN PK ONT L5K 1A8
PHONE: 403 220 5890

J B FRENCH
4 THORNBANK RD
THORNHILL ONT L4J 2A2
PHONE: 416 667 7706

MYRA GORDON
1209 RICHMOND ST
APT 612
LONDON ONT N6A 3L7
PHONE:

ALEX G HARRISON
UNIV OF TORONTO
CHEMISTRY DEPT
TORONTO ONT M5S 1A1
PHONE: 416 978 3577

ALAN M HOGG
UNIV OF ALBERTA
CHEMISTRY DEPT
EDMONTON ALBERTA T6G 2G2
PHONE: 403 432 5577

BOB JAKOBSON
RAYONICS SCIENTIFIC
585 CANARCTIC DRIVE
CANADA
PHONE: 416 736 1600

JAMES KAPRON
DEPT OF CHEMISTRY
MCMASTER UNIV
HAMILTON ONTARIO L8S 4M1
PHONE: 416 525 9140

PAUL KEBARLE
UNIV OF ALBERTA
CHEMISTRY DEPT
EDMONTON ALBERTA T6G 2G2
PHONE: 403 432 3469

GREG KOYANAGI
TRENT UNIVERSITY
DEPT OF CHEMISTRY
ONTARIO K91 7B8
PHONE:

BENJAMIN P LAU
HEALTH & WELFARE CAN
FOOD RESEARCH
OTTAWA ONTARIO K1A 0L2
PHONE: 416 993 4994

CLAUDE J FORTIN
LAB DE POLICE SCIENTIFIQUE
1701 PARTHENAIS, 5TH FL
MONTREAL QUE H2K 3S7
PHONE: 514 873 2704

JOHN FULFORD
SCIEX
55 GLENCAMERON ROAD
THORNHILL ONTARIO L3T 1P2
PHONE: 416 881 4646

LAWRENCE W GREEN
ATOMIC ENERGY OF CAN
CHALK RIVER NUC LAB
CHALK RIVER ONT K0J 1J0
PHONE: 613 584 3311

J M HARTWELL
CIL INC
2101 HADWEN RD
MISSISSAUGA ONT L5K 2L3
PHONE: 416 823 7160

LAWRENCE R HOGGE
NAT'L RES COUNCIL
110 GYMNASIUM RD
SASKATOON SASK S7N 0W9
PHONE: 306 975 4193

W D JAMIESON
NRC
1411 OXFORD ST
HALIFAX NS B3H 3Z1
PHONE: 902 426 8279

KELEM KASSAHUN
PHARMACEUTICAL SCIENCES
UNIV OF BRITISH COLUMBIA
VANCOUVER BC V6T 1W5
PHONE: 604 228 5946

PETER KOFEL
UNIV OF WATERLOO
DEPT OF CHEMISTRY
CANADA
PHONE: 519 888 4591

J R KRAUSE
UNIV OF OTTAWA
CHEMISTRY DEPT
OTTAWA ONTARIO K1N 9B4
PHONE: 613 564 4039

D L LEWIS
DEPT OF AGRICULTURE
TOXICOLOGY LAB
EDMONTON ALBERTA T6H 4P2
PHONE: 403 436 8410

M G FOSTER
ZENON ENVIRONMENTAL
845 HARRINGTON CT
BURLINGTON ONT L7N 3P3
PHONE: 416 639 6320

HUGH A GILLIS
NAT'L RESEARCH COUNCIL
1411 OXFORD ST
HALIFAX NS B3H 3Z1
PHONE: 902 426 9736

ROGER GUEVREMONT
NRC OF CANADA
1411 OXFORD ST
NOVA SCOTIA B3H3Z1
PHONE: 802 426 6406

JOHN HEADLEY
ALBERTA ENVIRON CTR
CHEMISTRY WING
VEGREVILLE ALBERTAT0B 4L0
PHONE: 403 632 6761

JOHN L HOLMES
UNIV OF OTTAWA
CHEMISTRY DEPT
OTTAWA ONTARIO K1N 9B4
PHONE: 613 231 2239

KAZIK JEDRZEJCZAK
77 QUEBEC AVE APT 2132
CANADA M6P 2T4
PHONE: 416 767 9857

C W KAZAKOFF
UNIV OF OTTAWA
CHEMISTRY DEPT
OTTAWA ONTARIO K1N 9B4
PHONE: 614 231 4039

GEORGE J KOVES
CTR OF FORENSIC SCIENCE
TOXICOLOGY
TORONTO ONT M7A 2G8
PHONE:

D A LANE
31 DE VERE GDNS
TORONTO ONTARIO M5M 3E6
PHONE: 416 667 4965

FREDERICK P LOSSING
UNIV OF OTTAWA
CHEMISTRY DEPT
OTTAWA ONTARIO K1N 9B4
PHONE: 613 564 4039

ANNETTE M LOVETT
VG INSTRUMENTS CANADA INC
2 SILVER AVE
CANADA M6R 3A2
PHONE: 416 533 2381

ORVAL MAMER
MCGILL UNIV
1130 PINE AVE WEST
MONTREAL QUEBEC H3A 1A3
PHONE:

ROBERT MASSE
INRS-SANTE
245 BLVD HYMNS
PTE CLAIRE QUEBEC H9R 1G6
PHONE: 514 253 2832

D L MCGILLIVRAY
UNIV OF VICTORIA
CHEMISTRY DEPT
VICTORIA BC V8W 2Y2
PHONE: 604 721 7183

T B MCMAHON
DEPT OF CHEMISTRY
UNIV OF WATERLOO
WATERLOO ONT N2L 3G1
PHONE: 519 888 4591

W F MILES
MASS SPEC LAB
LAB SERVICES DIV
OTTAWA ONTARIO K1A 0C5
PHONE: 613 995 4907

JANE MONTGOMERY
BIOMEDICAL MASS SPEC
1130 PINE AVE W
MONTREAL QUE H3A 1A3
PHONE: 514 392 6716

RONALD B NEW
CHEMISTRY DEPT
UNIV OF WINDSOR
WINDSOR ONT N9B 3P4
PHONE: 519 253 4232

GUY PAQUETTE
QUEBEC MIN OF ENVIRONMENT
2700 EINSTIN
CANADA G1P 3W8
PHONE: 418 643 8225

OMER PELLETIER
5 BERNIER

CANADA
PHONE: 613 954 0302

D B MACLEAN
MCMASTER UNIVERSITY
CHEMISTRY DEPT
HAMILTON ONTARIO L8S 4M1
PHONE: 416 525 9140

RAYMOND E MARCH
TRENT UNIVERSITY
CHEMISTRY DEPT
PETERBOROUGH ONT K9J 7B8
PHONE: 705 748 1361

L J MCBURNEY
DCIEM
PO BOX 2000
DOWNSVIEW ONT M3M 3B9
PHONE: 416 635 2130

DOUGLAS E MCINTYRE
HEWLETT-PACKARD CANADA
6877 GOREWAY DR
MISSISSAUGA ONT L4V 1M8
PHONE: 416 678 9430

ROGER MERCER
80 ST GEORGE STREET

TORONTO ONTARIO M5S 1A1
PHONE: 416 445 5248

JACK M MILLER
BROCK UNIV
CHEMISTRY DEPT
ST CATHERINES ONT L2S 3A1
PHONE: 416 688 5550

J E MORGAN
MORGAN SCHAFFER CORP
5110 COURTRAI AVE
MONTREAL QUE H3W 1A7
PHONE: 514 739 1967

F I ONUSKA
CCIW-AMRS
PO BOX 5050
BURLINGTON ONT L7R 4A6
PHONE: 416 637 4635

E R PAQUIN
MINISTERE AGRICULTURE
2700 RUE EINSTEIN
SAINTE FOY QUE G1P 3W8
PHONE: 418 651 2175

D W PRIDDLE
UNIV OF TORONTO
CHEMISTRY DEPT
TORONTO ONTARIO M5S 1A1
PHONE: 416 978 5088

GREG MALIS
LAB SERVICES BLDG #22
ROOM B5
OTTAWA ONTARIO K1A 0C6
PHONE:

ANDRE MARTINEAU
2485 NAPOLEON

BROSSARD QUEBEC J4Y 1Y5
PHONE: 514 253 2832

DOUG MCCLURE
RCM POLICE FORENSIC LAB
PO BOX 8885
OTTAWA ONTARIO K1G 3M8
PHONE: 613 993 0645

ADAM MCMAHON
UNIV OF TORONTO
DEPT OF CHEMISTRY
TORONTO M551A1 ONTCANADA
PHONE: 416 978 3571

F Y MESSIER
ENV QUEBEC
850 BOUL VANIER
QUEBEC H7C 2M7
PHONE: 514 873 3072

ALEXANDER A MOMMERS
CHEMISTRY DEPT
UNIV OF OTTAWA
OTTAWA ONTARIO K1N 9B4
PHONE: 613 564 4039

HANSPETER MOSER
UNIV OF WINDSOR
DEPT OF CHEMISTRY
WINDSOR ONT N9B 3P4
PHONE: 519 253 4232

HENRIANNA Y PANG
ROOM 1149A MED SCI BLDS
DEPT OF MED GENETICS
TORONTO ONTARIO M5S 1A8
PHONE: 416 978 8184

J R PARE
1300 GIROUARD EST, STE 6

SAINT HYACINTHE QCJ2S 2Y1
PHONE: 514 773 6419

GRANT PRILL
ALBERTA ENV CENTER
BAG 4000
CANADA TOB-4L0
PHONE:

M A QUILLIAM
MCMASTER UNIVERSITY
CHEMISTRY DEPT
HAMILTON ONTARIO L8S 4M1
PHONE: 416 525 9140

MARK L J REIMER
CHEMISTRY DEPT
UNIV OF MANITOBA
WINNIPEG MANITOBA R3T 2N2
PHONE: 204 474 9761

JEAN-PIERRE SCHMIT
UNIV OF QUEBEC
CHEMISTRY DEPT
MONTREAL PQ H3C 3P8
PHONE: 514 282 3048

GREG SLATTER
PHARMACEUTICAL SCIENCES
UNIV OF BRITISH COLUMBIA
VANCOUVER BRIT COLV6T 1N5
PHONE: 604 228 5946

J A STONE
QUEEN'S UNIVERSITY
CHEMISTRY DEPT
KINGSTON ONTARIO K7L 3N6
PHONE: 613 525 2615

V Y TAGUCHI
ONTARIO MIN ENVIRONMENT
125 RESOURCES ROAD
REXDALE ONTARIO M9W 5L1
PHONE: 416 248 3755

J B WESTMORE
UNIV OF MANITOBA
CHEMISTRY DEPT
WINNIPEG MAN R3T 2N2
PHONE: 204 474 9761

GORDON W WOOD
UNIV OF WINDSOR
VICE PRESIDENT ACADEMIC
WINDSOR ONTARIO N9B 3P4
PHONE: 519 253 4232

LOUIS RAMALEY
DALHOUSIE UNIVERSITY
CHEMISTRY DEPT
HALIFAX NS B3H 4J3
PHONE: 902 424 3305

R T RYE
CONCORDIA UNIV
CHEMISTRY DEPT
MONTREAL QUEBEC H3G 1M8
PHONE: 514 848 3344

DAVID B SERGEANT
DEPT FISH & OCEANS
GLFRB
BURLINGTON ONT L7R 4A6
PHONE:

RICHARD W SMITH
CHEMISTRY DEPT
MCMASTER UNIV
HAMILTON ONTARIO L8S 4M1
PHONE: 416 525 9140

JAN A SUNNER
DEPT OF CHEMISTRY
UNIV OF ALBERTA
EDMONTON ALBERTA T6G 2G2
PHONE: 403 432 3502

XUEJUN TANG
DEPT OF PHYSICS
UNIV OF MANITOBA
WINNIPEG MANITOBA R3T 2N2
PHONE:

JONATHAN WONG
CHILDERNS HOSPITAL
BIOCHEM DISEASE LAB
VANCOUVER V6H 3V4
PHONE: 604 875 2307

RAGHAV YAMDAGNI
UNIV OF CALGARY
CHEMISTRY DEPT
CALGARY ALB T2N 1N4
PHONE: 403 220 5890

NEIL REID
SCIEX
55 GLENCAMERON RD
CANADA L3T 1P2
PHONE:

R W SADLIER
12 BAL HARBOUR DR
GRIMSBY ONT L3M 4P9
PHONE:

BORI I SHUSHAN
SCIEX
55 GLENCAMERON RD
THORNHILL ONT L3T 1P2
PHONE: 416 881 4646

KENNETH STANDING
UNIV OF MANITOBA
PHYSICS DEPT
WINNIPEG MANITOBA R3T 2N2
PHONE: 204 474 9358

JAN E SZULEJKO
DEPT OF CHEMISTRY
UNIV OF WATERLOO
WATERLOO ONT N2L 3S1
PHONE: 519 885 1211

ALAN VIAU
383 COLE RD
CANADA
PHONE: 519 836 0189

S K WONG
UNIV WESTERN ONTARIO
CHEMISTRY DEPT
LONDON ONTARIO N6A 5B7
PHONE: 519 679 2796

ALEX B YOUNG
DEPT OF CHEMISTRY
UNIV OF TORONTO
TORONTO M5S 1A1
PHONE: 416 978 3571

GUNTER ALLMAIER
INST F ANAL CHEMISTRY
UNIV OF VIENNA
A-1090 VIENNA
AUSTRIA

EMANUELE ARLANDINI
FARMITALIA-CERBA
VIA GRACCHI, NO 35
MILANO
ITALY

MICHAEL A BALDWIN
UNIVERSITY OF LONDON
SCHOOL OF PHARMACY
LONDON WC1N 1AX
ENGLAND

R H BATEMAN
VG ANALYTICAL
FLOATS ROAD
MANCHESTER M23 9LE
ENGLAND

ALFRED BENNINGHOVEN
PHYSIKALISCHES INST
UNIV MUNSTER
4400 MUNSTER
WEST GERMANY

KIRIT H BHATT
PHARMACOLOGY/TOXICOLOGY
UNIV OF KUWAIT
SAFAT
KUWAIT 13110

A J BOERBOOM
A DURER STR 25-2

1077 LT AMSTERDAM
NETHERLANDS

RENE N BOTTER
CEN SACLAY DPC

CEDEX
FRANCE

A P BRUINS
STATE UNIVERSITY
PHARMACY DEPT
9713-AW GRONINGEN
NETHERLANDS

ROD BUCHANAN
KRATOS ANALYTICAL
BARTON DOCK RD
ENGLAND M31 2LD

R T APLIN
DYSON PERRINS LAB
OXFORD UNIVERSITY
OXFORD OX1 3QY
ENGLAND

P J ARPINO
ECOLE POLYTECHNIQUE
LAB CHIM ANAL PHYS
91128 PALAISEAU
FRANCE

MICHAEL BARBER
U M I S T
CHEM DEPT
MANCHESTER
UK

CLAUDE BEAUGRAND
NERMAG
49 QUAI DU HALAGE
RUEIL MALMAISON
F 92500 FRANCE

A J BERRY
DEPT OF CHEMISTRY
UNIVERSITY COLLEGE
CARDIFF CF1 1XL
UNITED KINGDOM

JOHN C BILL
207 CREWE ROAD

CHESHIRE
ENGLAND

ROBERT S BORDOLI
VG ANALYTICAL LAB
FLOATS ROAD
MANCHESTER M239LE
ENGLAND

CHARLES J W BROOKS
UNIV OF GLASGOW
CHEMISTRY DEPT
GLASGOW G12 8QQ
SCOTLAND

DR D BRUMENT
NERMAG
49 QUAI DU HALAGE
F 92500
FRANCE

PROF H BUDZIKIEWICZ
INST. ORG. CHEM.
GREINSTR. 4
5000 KOELN 41
WEST GERMANY

T R ARIYARATNE
TANDEM ACCELERATOR LAB
UNIV OF UPPSALA
UPPSALA
SWEDEN

ALLISON ASHCROFT
KRATOS ANALYTICAL
BARTON DOCK RD
ENGLAND M31 2LD

DAMIA BARCELO
ENVIRONMENTAL CHEM DEPT
JORGE GIRONA SALGADO 18-26
SPAIN

EMILIO BENFENATI
BIOMEDICAL MASS SPEC UNIT
INSTITUTO MARIO NEGRI
MILANO 20157
ITALY

J H BEYNON
17 COLTSHILL DRIVE
MUMBLES
SWANSEA SA3 4SN
GREAT BRITAIN

WALTER BLACKSTOCK
GLAXCO GROUP RESEARCH
PHYSICAL CHEMISTRY DEPT
MIDDLESEX UB6 OHE
ENGLAND

PETER BOTT
VG ANALYTICAL
FLOATS ROAD
MANCHESTER
ENGLAND M23 9LE

M C TEN NOEVER DE BROUW
TNO-CIVO
PO BOX 360
3700 AJ ZEIST
NETHERLANDS

CURT BRUNNEE
FINNIGAN MAT
BARKHAUSENSTR 2
D-2800 BREMEN 10
WEST GERMANY

JOHN CANTLE
VG INSTRUMENTS
ROAD 3, WINSFORD
CHESHIRE
UK

PABLO CARAVATTI
SPECTROSPIN AG
INDUSTRIESTRASSE 26
8117 FAELLANDEN
SWITZERLAND

JEAN CESARIO
SEAIN - Bat 91
CEN/SACLAY
CEDEX
FRANCE

ROLANDO CHRISTIAN
9 RUE DE LA PRAIRIE
ANTONY
PARIS 38
FRANCE

MAGDA M CLAEYS
UNIV INSTELL ANTWERP
PHARMACY DEPT
B-2610 WILRIJK
BELGIUM

DR DAVID C CLARY
UNIVERSITY OF CAMBRIDGE,
UNIV CHEM LAB
CAMBRIDGE CB2 1EW
UK

MALCOLM CLENCH
UVG TRITECH
CREWE ROAD
MANCHESTER
UK

KEITH R COMPSON
FAISAN
1 PADDOCK BROW
CHESHIRE
U.K.

J S COTTRELL
KRATOS
BARTON DOCK RD
MANCHESTER M31 2LD
ENGLAND

ANTHONY G CRAIG
DEPT OF IMMUNOLOGY
BIOMEDICAL CENTER
S-75123 UPPSALA
SWEDEN

ROLF DARSKUS
BIOCONTROL GMBH
PO BOX 16 30
D-6500 MAINZ
W GERMANY

B C DAS
S N NERMAG
49 QUAI DE HALAGE
RUEIL MALMAISON
92500 FRANCE

T S DAVIS
VG ANALYTICAL
FLOATS ROAD
MANCHESTER
ENGLAND M23 9LE

F F DEGREVE
CEGEDUR PECHINEY
CENTRE DE RECHERCHES
38340 VOREPPE
FRANCE

PROF G DEMORTIER
DEPT OF PHYSICS
FNDP
B5000 NAMUR
BELGIUM

J J DEUTSCH
21 HAMASORERET
RACHEL ST
JERUSALEM
ISRAEL

G L DEVANT
NERMAG
49 QUAI DU HALAGE
F 92500
FRANCE

STEPHEN DOWN
MASS SPECTROMETRY DATA CTR
ROYAL SOC OF CHEMISTRY
NOTTINGHAM NG7 2RD
UNITED KINGDOM

J D DROWART
VRIJE UNIV BRUSSELS
PLEINLAAN 2
B-1050 BRUSSELS
BELGIUM

A M DUFFIELD
UNIV NEW SOUTH WALES
CLINIC PHARMACOLOGY
KENSINGTON NSW
AUSTRALIA 2033

KUBOTA E
JEOL
1418 NAKAGAMI AKISHIMA
TOKYO 196
JAPAN

GERRY ELLIOTT
KRATOS ANALYTICAL
BARTON DOCK ROAD
MANCHESTER
ENGLAND

HANS P EPPLER
BALZERS AG
FL9496 BALZERS
BALZERS
LIECHTENSTEIN

E E ESMANS
UNIV ANTWERPEN
ORGANISCHE SCHEIKUND
B-2020 ANTWERPEN
BELGIUM

CATHERINE E EVANS
UNIVERSITY COLLEGE CARDIFF
PO BOX 78
U.K. CF11XL

R F EVANS
QUEENSLAND UNIV
CHEMISTRY DEPT
ST LUCIA QNLAND 40
AUSTRALIA

SID EVANS
KRATOS
BARTON DOCK ROAD
MANCHESTER M31 2LD
ENGLAND

S M FACCHETTI
CCR-EURATOM
RADIOCHEMISTRY DIV
21020 ISPRA-VARESE
ITALY

P B FARMER
MRC TOXICOLOGY UNIT
WOODMANSTERNE RD
SURREY SM5 4EF
ENGLAND

M A FERREIRA
DEPT OF CHEMISTRY
FAC OF SCIENCES
1294 LISBON CODEX
PORTUGAL

ROBERT W FINNEY
SPECTROSCOPY BLDG 10 RM 12
BRITISH PETRO RESEARCH CTR
MIDDX TW16 7LN
UNITED KINGDOM

HANS FORSTER
BOEHRINGER INGELHEIM
6507 INGELHEIM
IRHEIN
FRG

DANIEL J FRAISSE
SPEC DE MASSE
SCA-CNRS
69390-VERNAISON
FRANCE

H G FRANK
UNIV TUEBINGEN
INST TOXIKOLOGIE
D 7400 TUEBINGEN
FED REP GERMANY

RUDIGER FREY
BRUKER FRANZEN ANALYTIK Gm
KATTENTURMER HEERSTR 122
D-2800 BREMEN 61
WEST GERMANY

MARLIN FRIESEN
IARC/CIRC
150 COURS A THOMAS
69372 LYON
FRANCE

TOSHIHIRO FUJII
NAT'L INST FOR ENVIRONMENT STUDIES
IBARAKI 305
JAPAN

JEAN F GAL
UNIV DE NICE
CAMPUS VALROSE
NICE 06034 CEDEX
FRANCE

DAVID E GAMES
UNIVERSITY COLLEGE
CHEMISTRY DEPT
CARDIFF CF1 1XL
WALES

T T GAUMANN
EPFL-ECUBLENS
INST DE CHIMIE PHYS
CH-1015 LAUSANNE
SWITZERLAND

CHRIS F GELIJKENS
PARKLAAN 78

B-2700 ST-NIKLAAS
BELGIUM

E E GELPI
RD GUINARDO 5 7

08024 BARCELONA
SPAIN

MICHAEL GEORGIEFF
INST FUR ANESTHESIOLOGIE
KLINIKUM MANNHEIM
6800 MANNHEIM
FED REP GERMANY

DR H GLEISPACH
ABT FUR MASSENSPEKTROMETRIE
UNIV KINDERKLINIK
A 8036 GRAZ
AUSTRIA

RUDIGER GOHLKE
GSG MEG-UND ANALYSENGERATE
VERTRIEBSGESELLSCHAFT MBH
7500 KARLSRUHE 41
BUNDSREPUBLIK D

SIMON GOSS
PHYSICAL CHEMISTRY
LA TROBE UNIV
VICTORIA 3083
AUSTRALIA

VALERIE GOULD
VG MASSLAB
TUDOR ROAD
CHESHIRE
UK

BRIAN GREEN
VG ANALYTICALD
FLOATS ROAD
MANCHESTER M23 9LE
ENGLAND

DAVID T GREEN
PPF INT'L LTD
KENNINGTON ROAD
KENT TN240LT
UK

FIONA GREER
M-SCAN LTD
SILWOOD PARK
ASCOT
ENGLAND SL5 7P2

I K GREGOR
CHEMISTRY SCHOOL
UNIV OF NSW
KENSINGTON NSW 203
AUSTRALIA

PETER GROSSMANN
SPECTROSPIN AG
INDUSTRIESTRASSE 26
CH-8117 FALLANDEN
SWITZERLAND

JUERGEN GROTEMEYER
INST F PHYSIKALISCHE CHEMIE
TECHNISCHE UNIV MUNCHEN
8046 GARCHING
WEST GERMANY

LUTZ GROTJAHN
GBF
MASCHERODER WEG 1
D-3300 BRAUNSCHWEI
W GERMANY

STEPHEN GUYAN
VG ANALYTICAL
FLOATS ROAD
MANCHESTER
UK

KARLEUGEN HABFAST
FINNIGAN MAT
BARKHAUSEN STR 1
2800 BREMEN
W GERMANY

ROBERT J HAGEMANN
CEN FAR/SEA
BP No 6
ROSES CEDEX
FRANCE

JOHN M HALKET
DEPT CHEMICAL PATHOLOGY
QUEEN CHARLOTTES HOSPITAL
LONDON W6 OXG
ENGLAND

DAVID J HALL
VG ISOTOPES LTD
ION PATH, ROAD THREE
CW7 3BX ENGLAND

FRANK M HARRIS
UNIV COLL OF SWAMSEA
SINGLETON PARK
SWANSEA SA2888
UK

D J HARVEY
OXFORD UNIVERSITY
PHARMACOLOGY DEPT
OXFORD OX1 3QT
ENGLAND

YUTAKA HASHIMOTO
NIPPON KAYAKU CO LTD
31-12 SHIMO 3-CHOME
TOKYO 115
JAPAN

FRANZ HILLENKAMP
INST F BIOPHYSIK
UNIV FRANKFURT
D-6000 FRANKFURT
WEST GERMANY

EDMOND DE HOFFMANN
PL PASTEUR 1 BOX 17

LOUVAIN-LA-NEUVE
B-1348 BELGIUM

M A HOURIEH
PO BOX 686

ALEPPO
SYRIA

W A HUBER
BALZERS AG

FL 9496 BALZERS
LIECHTENSTEIN

A H JACKSON
UNIVERSITY COLLEGE
CHEMISTRY DEPT
CARDIFF CF1 1XL
WALES

KEITH R JENNINGS
UNIV OF WARWICK
GIBBET HILL ROAD
COVENTRY CV4 7AL
ENGLAND

GUNNAR JONSSON
TANDEM ACCELERATOR LAB
UNIV OF UPPSALA
UPPSALA S 75121
SWEDEN

THOMAS KAISER
P O BOX 68

ENNETMOOS NW
SWITZERLAND

ZEEV KARPAS
NRCN
PO BOX 9001
BEER-SHEVA
ISRAEL 84190

K G HEUMANN
UNIV REGENSBURG
CHEMISCHES INSTITUT
D-84 REGENSBURG
WEST GERMANY

KENZO HIRAOKA
YAMANASHI UNIVERSITY
FACULTY ENGINEERING
KOFU 400
JAPAN

A J HOLLAND
M-SCAN LTD
SILWOOD PARK SUNNINGHILL
BERKSHIRE
ENGLAND SL5 7PZ

ZHOU HUA
ANALYSIS & RES CTR
ZHONGSHAN UNIV
GUANGZHOU
P R OF CHINA

SABURO ISHII
JEOL LTD
NAKAGAMI CHO 1418
TOKYO 196
JAPAN

J E JALONEN
UNIV OF TURKU
CHEMISTRY DEPT
20500 TURKU 50
FINLAND

KE JIANG
PO BOX 934

BEIJING
PR CHINA

DANIEL JOULAIN
P ROBERTET ET CIE
B.P. 100
06333 GRASSE
FRANCE

H H KAMBARA
HITACHI LTD
ADVANCED RESEARCH LAB
TOKYO 185
JAPAN

CONCETTA KASCHERES
RUA DR ANTONIO HOSSRI 388

SOA PAULO 13100
BRAZIL

TONY HICKSON
VG INSTRUMENTS
3 TUDOR ROAD
CHESHIRE
U.K.

M G HODGES
BP INTERNATIONAL
SUNBURY-ON-THAMES
MIDDLESEX
TW15 2BJ UK

P T HOLLAND
RUAKURA AG RES CTR

HAMILTON
NEW ZEALAND

ZHOU HUA
ANALYSIS & RESEARCH CENTER
ZHONGSHAN UNIVERSITY
GUANGZHOU
PRC (CHINA)

Y I ITAGAKI
JEOL LTD
AKISHIMA
TOKYO 196
JAPAN

HUW A JAMES
WATER RESEARCH CTR
PO BOX 16 HENLEY RD
MARLOW BUCKS
ENGLAND

D D JONES
VG ANALYTICAL
FLOATS ROAD
MANCHESTER
ENGLAND M23 9LE

ALINE JUERY
C E A SERVICES R C P
BP 12
FRANCE

IVAN KAMENSKY
PO BOX 15045

S-75215 UPPSALA
SWEDEN

SUE KENNERLEY
KRATOS ANALYTICAL
BARTON DOCK RD
ENGLAND M31 2LD

GRAHAM KILPATRICK
INTERION LTD
46 ASHSTEAD ROAD
MANCHESTER M33 3PX
ENGLAND

HANS KNOF
AM FORSTTEICH 15/17

D-2000 NORDERSTEDT
WEST GERMANY

WILLIAM LAUWERS
JANSSEN PHARMACEUTIC
TURNHOUTSE BAAN 30
B-2340 BEERSE
BELGIUM

PIET A LECLERCQ
EINDHOVEN UNIV TECH
PO BOX 513
5600-MB EINDHOVEN
NETHERLANDS

CHAVA LIFSHITZ
HEBREW UNIV
PHYSICAL CHEM DEPT
JERUSALEM
ISRAEL

MICHAEL W LINSCHEID
SPEKTROCHEM
BUNSEN-KIRCHHOFF
D-4600 DORTMUND 1
W GERMANY

NORMAN LYNAUGH
VG MASSLAB
ALTRINCHAM
CHESHIRE
ENGLAND

J K MACLEOD
AUSTRALIA NAT UNIV
RES SCHOOL OF CHEM
CANBERRA ACT 2600
AUSTRALIA

A I MALLET
INSTITUTE OF DERMATOLOGY
ST THOMAS HOSPITAL
LONDON EI1 7EH
ENGLAND

PETER MARCUS
ISRAEL ATOMIC ENERGY COMM
NRC NEGEN
BEER-SHEVA 84-190
ISRAEL

M S KIM
SEOUL NATIONAL UNIV
CHEMISTRY DEPT
SEOUL 151
KOREA

TAPIO KOTIAHO
BIOLOGINKUJA 7

02150 ESPOO
FINLAND

A M LAWSON
CLINICAL RES CENTRE
HARROW
LONDON HA1 3UJ
ENGLAND

ANDRE P DE LEENHEER
STATE UNIV OF GENT
RIJVISSCHEPARK 18
B-9710 GENT
BELGIUM

CLAES LINDBERG
PHARMACOKINETICS LAB
AB DRACO
LUND S-22100
SWEDEN

P A LONGEVIALLE
ICSN CNRS

YVETTE
FRANCE

F DE MAACK
NERMAG
49 QUAI DU HALAGE
F 92500
FRANCE

MARTYN MACPHERSON
BP RESEARCH CTR
CHERTSEY ROAD
MIDDLESEX TW16 7LN
ENGLAND

A A MANDELBAUM
TECHNION
CHEMISTRY DEPT
HAIFA 32000
ISRAEL

K M MARNELA
TAMPERE UNIV
PO BOX 607
33101 TAMPERE 10
FINLAND

GRAHAM S KING
ICI PLANT PROTECTION DIV
METAB & RESIDUE SECTION
BRACKNELL BERK
ENGLAND

S S KROLIK
VG ANALYTICAL
FLOATS ROAD
MANCHESTER M23 9LE
ENGLAND

YVON LEBEYEC
INSTITUT DE PHYS NUCLAIRE

FRANCE

IVOR LEWIS
DEPT OF CHEMISTRY
KING'S COLLEGE LONDON
LONDON WC2R 2LS
ENGLAND

H BERNHARD LINDEN
PO BOX 61 03 07

D-2800 BREMEN 61
W GERMANY

J C LORQUET
DEPT OF CHEMISTRY
UNIV LIEGE
B-4000 LIEGE 1
BELGIUM

ALLAN MACCOLL
UNIVERSITY COLLEGE
CHEMISTRY DEPT
LONDON WC1H 0AJ
ENGLAND

HILARY MAJOR
VG ANALYTICAL
FLOATS ROAD
MANCHESTER M23 9LE
UK

M F MAQUIN
SOCIETE ROUSSEL UCLAF
SPECTROMETRIE DE MASSE
93230 ROMAIVILLE
FRANCE

ALLEMANN MARTIN
SPECTROSPIN AG
INDUSTRIESTRASSE 26
8117 FAELLANDEN
SWITZERLAND

ISAMU MATSUMOTO
INST HUMAN GENETICS
KANAZAWA MED UNIV
ISHIKAWA 920-02
JAPAN

HAJIME MATSUSHIMA
HAMAMATSU UNIV SCH OF MEDI
3600 HANDA-CHO

JAPAN

GERHARD MATZ
TECHNICAL UNIV OF HAMBURG
HARBURGER SCHLOSSTR 20

W GERMANY

OLIVIER MAULAT
NERMAG
49 QUAI DU HALAGE
F 92500
FRANCE

M A MCDOWELL
VG MASSLAB
3 TUDOR ROAD
ALTRINCHAM
ENGLAND WA14SR2

J B MCKINNON
VG ISOTOPES
ION PATH ROAD 3
CHESHIRE
UK

RUSSELL G MCLOUGHLIN
15 VIVIAN STREET

IVANHOE VIC
3079 AUSTRALIA

G G MELLERIO
UNIVERSITY OF PAVIA
C G S LAB MS
27100 PAVIA
ITALY

BRIAN J MILLARD
KRATOS
BARTON DOCK RD
MANCHESTER M31 2LD
ENGLAND

J J MOMIGNY
UNIV DE LIEGE
INST DE CHIMIE
B-4000 LIEGE
BELGIUM

JOHN J MONAGHAN
ICI C&P GROUP
PO BOX 8
CHESHIRE WA7 4OD
UNITED KINGDOM

JOERG MONIG
GSF-INST FUR TIEFLAGERUNG
THEODOR-HEUSS-STR 4

FRG

E E MONTER
ZEISIGWEG 6

D5653 LEICHLINGEN
WEST GERMANY

COLIN MOORE
KRATOS ANALYTICAL
BARTON DOCK RD
ENGLAND M31 2LD

H R MORRIS
IMPERIAL COLLEGE
BIOCHEMISTRY DEPT
LONDON SW7 2AZ
ENGLAND

J D MORRISON
LA TROBE UNIVERSITY
PHYSICAL CHEMISTRY
MELBOURNE VIC 3083
AUSTRALIA

JOHN MYATT
ICI C&P GROUP
PO BOX 8 THE HEATH
CHESHIRE WA7 4QD
ENGLAND

IAIN C MYLCHREEST
UNIVERSITY COLLEGE CARDIFF
PO BOX 78
CARDIFF
UK CF1 1XL

ULRICH NEUERT
WERTHERSTR 163

4800 BIELEFELD 1
WEST GERMANY

N M NIBBERING
JANSHOF 39

1391-XK ABCOUDE
NETHERLANDS

EWALD NIEHUIS
PHYS INST UNIV MUNSTER
DOMAGHSTR 75
4400 MUNSTER
F R GERMANY

FRANKLIN NIELSON
INSTITUTE OF MOLECULAR BIONATL CHEM LAB FOR INDUSTRY
ODENSE UNIVERSITY
5230 ODENSE M
DENMARK

YOSHIO NIWA
YATABE IBARAKE 305
JAPAN

TAMOTSU NODA
TOYOHASHI UNIV OF
TECHNOLOGY
TOYOHASHI 440
JAPAN

J J OGDEN
BRIT NUCLEAR FUELS
BLDG 202 MASS SPEC
CHESTER CHIGER
UK

YOKO OHASHI
DEPT OF BIOCHEM FAC OF MED1RSC
UNIV OF TOKYO
TOKYO 113
JAPAN(113)

CATHERINE ORLEY
B P 8
VILLEJUIT 94800
FRANCE

R R OWEN
VG ANALYTICAL
FLOATS ROAD
MANCHESTER
ENGLAND M23 9LE

JANET OXFORD
GLAXO GROUP RESEARCH
BIOCHEM PHARMACOLOGY
HERTFORDSHIRE
UK

V C PARR
VG ANALYTICAL
FLOATS ROAD
MANCHESTER
ENGLAND

BEATRICE PELLI
CONS NAX DELLA RICERCHE
AREA DI RECERCA DI PADOVA
35020 CAMIN
ITALY

JOHN R PERKINS
UNIVERSITY COLLEGE CARDIFF
PO BOX 78
CARDIFF
UK CF1 1XL

REINHOLD PESCH
FINNIGAN MAT
BARKHAUSEN STR 2
2800 BREMEN
W GERMANY

T I PLATZNER
NRCN
PO BOX 9001
BEER SHEVA
ISRAEL

STEPHEN PLEASANCE
UNIVERSITY COLLEGE CARDIFF
PO BOX 78
CARDIFF CF1IXL
UK

CHRIS J PORTER
VG ANALYTICAL
FLOATS ROAD
MANCHESTER
ENGLAND M23 9LE

PATRICK POWERS
16 MORETON AVENUE
HARPENDEN
HERTS AL5 2ET
ENGLAND

JOHN PRATT
KRATOS ANALYTICAL
BARTON DOCK RD
ENGLAND M31 2LD

M P PRZYBYLSKI
UNIV MAINZ
INST ORG CHEMIE
D-6500 MAINZ
WEST GERMANY

JOHN A RACE
VG ANALYTICAL LTD
FLOATS ROAD
MANCHESTER M23 9LE
ENGLAND

EDWARD D RAMSEY
MIN OF AGRICULTURE FOOD &
HALDIN HOUSE OLD BANK OF
NORWICH
UK NR2 4SX

UWE RAPP
AMD INTECTRA GMBH
EKLEIN KOHREN 36
D-2833 BECKELN
WEST GERMANY

GUY RICART
UNIV OF LILLE
UER CHIMIE BAT C4
D'ASCO CEDEX
FRANCE

WILHELM J RICHTER
CIBA GEIGY
K 127.508
CH-4002 BASEL
SWITZERLAND

GAVIN C RIDER
VG INSTRUMENTS
CHARLES AVENUE
WEST SUSSEX
ENGLAND

W W RIEPE
BERBAU-FORSCHUNG GMB
FRANZ-FISCHER-WEG 61
D-4300 ESSEN 13
WEST GERMANY

JOSEP RIVERA
MASS SPECTROMETRY LAB/CSIC
J GIRONA SALGADO 18-26
SPAIN

J D ROBINSON
VG ANALYTICAL
FLOATS ROAD
MANCHESTER
ENGLAND

PETER ROEPSTORFF
ODENSE UNIVERSITY
DEPT OF MOLECULAR BIOLOGY
DK 5230 ODENSE M
DENMARK

FRANZ W ROLLGEN
INST PHYSICAL CHEM
UNIV OF BONN
D-5300 BONN
W GERMANY

KEITH ROLLINS
VG MASSLAB LTD
3 TUDOR ROAD
CHESHIRE
ENGLAND

YAHACHI SAITO
NAGOYA UNIVERSITY
DEPT OF APPLIED PHYSICS
NAGOYA 464
JAPAN

MINORU SAKAIRI
HITACHI ADVANCED RESEARCH
1-280 HIGASHI-KOIGAKUBO
TOKYO-TO 185
JAPAN

P J SARRE
UNIVERSITY OF NOTTINGHAM
DEPT OF CHEMISTRY
NOTTINGHAM
UK

GORAN SAVE
TANDEM ACCELERATOR LAB
UPPSALA UNIV
UPPSALA S 75121
SWEDEN

G G SCHADEN
FACHBER
PHARMAZIE D UNIV
D-3550 MARBURG
WEST GERMANY

EGMONT SCHALLER
HOLZWEG 7

D-7803 HEUWEILER
W GERMANY

U P SCHLUNEGGER
UNIVERSITAT BERN
INSTIT ORGAN CHEMIE
CH-3012 BERN
SWITZERLAND

PROF HELMUT SCHWARZ
INSTITUT FUR ORGANISCHE
TECHNISCHE UNIVERSITAT BERR
D1000 BERLIN 12

JAMES SCRIVENS
CHICI PETROCHEMICALS
ESEARCH DEPT
WILTON CLEVELAND
ENGLAND TS6 8JE

DR G SEROSSE
NERMAG
49 QUAI DU HALAGE
F 92500
FRANCE

YUKIO SHIMIZU
KOGAI-SHIGEN
KENKYUSHO
IBARAKI 305
JAPAN

R D SMITH
THE LITTLE HOUSE
BOVINGDON GREEN
HERTS HP3 OLD
ENGLAND

B P STIMPSON
AERE HARWELL
INSTR & APPLIED
OXFORDSHIRE OX11 0
ENGLAND

RAFFAELE TABACCHI
UNIV DE NEUCHATEL
INST DE CHIMIE
CH-2000 NEUCHATEL
SWITZERLAND

JOHN F J TODD
UNIV CHEM LABORATORY
UNIV OF KENT
KENT CT2 7NH
UK

GERHARD TRESSL
HEWLETT PACKARD
HERREN BERGERSTR 110
703 BOEBLINGEN
W GERMANY

M M TSUCHIYA
4 37 27 KUGAYAMA
SUGINAMI KU
TOKYO 168
JAPAN

PIRJO VAINIOTALO
UNIV OF JOENSUU
DEPT OF CHEMISTRY
SF-80101 JOENSUU
FINLAND

G L B VANDERPEYL
DSM RESEARCH BV
DEPT FA/SO
6160 MD GELEEN
THE NETHERLANDS

ULRICH J G SEYDEL
FORSCHUNGSINSTITUT
BIOPHYSICS DIV
D-2061 BORSTEL
FED REP GERMANY

FRANCOIS Y SIMONDET
L'AIR LIQUIDE CRCD
BP 126
JOUY EN JOSAS
78350 FRANCE

GERHARD SPITELLER
UNIVERSITY OF BAYREUTH (WGUNIV OF SUSSEX
POSTFACH 10 12 51
D-8580 BAYREUTH
WEST GERMANY

STEFAN STROMBERG
UNIVERSITY OF LUND
BIOCARB.AB
LUND S-22370
SWEDEN

AKIRA TATEMATSU
MEIJO UNIVERSITY
PHARMACY FACULTY
NAGOYA 468
JAPAN

J C TRAEGER
LA TROBE UNIVERSITY
PHYSICAL CHEMISTRY
BUNDOORA VIC 3083
AUSTRALIA

C W TSANG
APPLIED SCIENCE
HONG KONG POLYTECH
KOWLOON
HONG KONG

HAROLD TUDGE
KRATOS ANALYTICAL
BARTON DOCK RD
ENGLAND M31 2LD

SOPHIE VAJTA
32 RUE DE GOMETZ

BURES-SUR-YVETTE
91440 FRANCE

ALAIN VANDORSSELAER
CNRS INST OF NEUROCHEMISTRINST DE QUIMICA BIO-ORGANI
5,RUE B PASCAL
67084 STRASBOURG
FRANCE

PETER SHEPHERD
JOHN WILEY & SONS
BAFFINS LANE
CHICHESTER
ENGLAND P0191UD

CHARLES SMITH
VG ANALYTICAL
TUDOR ROAD
CHESHIRE
ENGLAND

A J STACE
DEPT OF CHEMISTRY
BRIGHTON BN192J
UK

MAKOTO SUZUKI
MEIJO UNIVERSITY
PHARMACY FACULTY
NAGOYA 468
JAPAN

J P THENOT
LERS
SYNTHELABO
75013 PARIS
FRANCE

PIETRO TRALDI
CONS NAX DELLA RECERCHE
AREA DI RECERCA DE PADOVA
35020 CAMIN
ITALY

GEORGES TSOUPRAS
INSTITUT DE CHIMIE
AV DE BELLEVAUX 51
2007 NEUCHATEL
SWITZERLAND

P J TURNER
VG MICROMASS LTD
ION PATH
WINSFORD CHESHIRE
ENGLAND

DR J VANDERGREEF
CIVO-TNO
PO BOX 360
3700 AJ ZEIST
NETHERLANDS

FRANCESC VENTURA
J GIRONA SALGADO 18-26
08034 BARCELONA
SPAIN

PAUL VIGNY
INSTITUTE CURIE
11 RUE P ET M CURIE
75231 PARIS CEDEX
FRANCE

ADAM VINCZE
ISRAEL INST BIOL RES
PO BOX 19
NESS ZIONA 70450
ISRAEL

DR J VINK
ORGANON INT'L BV
PO BOX 20
OSS 5340 BH
NETHERLANDS

RAVERDINO VITTORIO
HEWLETT-PACKARD
150 RTE DU NANT D'AVRIL
GENEVE
SWITZERLAND

KEITH WADDELL
VG ANALYTICAL
FLOATS ROAD
MANCHESTER
UK

CLIFF WAKEFIELD
KRATOS ANALYTICAL
BARTON DOCK RD
ENGLAND M31 2LD

KARL PETER WANCZEK
PARKALLEE 197

D-2800 BREMEN
WEST GERMANY

ERNST WEBER
FINNIGAN MAT GMBH
BARKHAUSEN STR 2

FRG

PATRICK WEHRUNG
UNIV DE STRASBOURG
DEPT DE CHIMIE
F-67008 STRASBOURG
FRANCE

ADRIAN WEISZ
DEPT OF CHEMISTRY
TECHNION-ISRAEL INST OF TE
32000 HAIFA
ISRAEL

S A WIKSTROM
HUDDINGE UNIV HOSP
RESEARCH CENTER F68
S-14186 HUDDINGE
SWEDEN

GARY D WILLETT
DEPT OF PHY CHEM
UNIV OF N.S.W.
N.S.W. 2033
AUSTRALIA

DAVID WILLIAMS
VG ANALYTICAL LTD
FLOATS ROAD
MANCHESTER
UK

DUDLEY H WILLIAMS
CAMBRIDGE UNIVERSITY
LENSFIELD ROAD
CAMBRIDGE CB2 1EW
ENGLAND

HERMANN WOLLNIK
UNIVERSITY GIESSEN
H BUFF RING 16
6300 GIESSEN
WEST GERMANY

DAVID WOOD
52 POISEBROOK ROAD
OFFERTON
CHESHIRE SK2 5JF
ENGLAND

CHRISTOPHER WOODWARD
VG ANALYTICAL
FLOATS RD
MANCHESTER
ENGLAND

ZIRO YAMAIZUMI
NAT'L CANCER CENTER INST
BIOLOGY DIV
TOKYO 104
JAPAN

JEHUDA YINON
WEIZMANN INSTITUTE
ISOTOPE RESEARCH
REHOVOT 76100
ISRAEL

L F ZERILLI
GRUPPO LEPETIT
VIA DURANDO 38
20158 MILANO
ITALY

MARKUS ZOLLINGER
TALSTRASSE 28

ZOLLIKERBERG
SWITZERLAND